GİRESUN UNIVERSITY
TECHNICAL SCIENCES VOCATIONAL SCHOOL

INTERNATIONAL TECHNOLOGICAL SCIENCES And DESIGN SYMPOSIUM 27-29 June 2018

PROCEEDING BOOK

www.itesdes.org
info@itesdes.org
itesdes2018@gmail.com
+90 454 310 10 00
15 55 - 14 77 - 15 70

ITESDES 2018

1. INTERNATIONAL TECHNOLOGICAL SCIENCES AND DESIGN SYMPOSIUM

27-29 June 2018 - Giresun/TURKEY

PROCEEDING BOOK

ISBN: 978-975-2481-10-7

Published on 13/11/2018

Editor: Aysun TÜRKMEN
Editorial Asistants: Erhan İŞLER, Elif Sultan AKPINAR, Mehmet KONAL
Language Editor: Birkut GÜLER, Özgür TOMAK
Cover Design: Recep GELEGEN
Layout: Ercan ÇİMŞİR, Sercan KÜLCÜ

Address: Giresun University, Gazi Paşa Campus, Technical Sciences Vocational School, 28049, Giresun/TURKEY
E-mail : itesdes2018@gmail.com

ITESDES 2018

27-29 June 2018

Giresun University, Giresun - TURKEY

HONORARY CHAIR

Prof. Dr. Cevdet COŞKUN
Rector of Giresun University

SYMPOSIUM CHAIR

Prof. Dr. Aysun TÜRKMEN
Technical Sciences VHS Director

SYMPOSIUM ORGANIZING COMMITTEE & SECRETARIAT

Assoc. Prof. Dr. Can ALAŞALVAR	Lect. Muhammet Anıl KAYA	Lect. Ahmet Mustafa ÖZTÜRK
Asist. Prof. Dr. Kenan BÜYÜKKAYA	Lect. Nurdan KUMAŞ ŞENOL	Lect. Elif Sultan AKPINAR
Asist. Prof. Dr. Muaffak SARIOĞLU	Lect. Mehmet KONAL	Lect. Alparslan TÜFEKÇİ
Lect. Ali Osman ELMAS	Lect. Halil KÖYMEN	Lect. Özgür TOMAK
Lect. Recep GELEGEN	Lect. Sercan KÜLCÜ	Lect. Birkut GÜLER
Lect. Erhan İŞLER	Lect. Ercan ÇİMŞİR	

SCIENTIFIC COMMITTEE

Prof. Dr.	A. Fevzi BABA	Marmara University - TURKEY
Prof. Dr.	A. Yalçın TEPE	Giresun University - TURKEY
Prof. Dr.	Abdalla Uba ADAMU	Bayero University - NIGERIA
Prof. Dr.	Ahmet KUBAŞ	Namık Kemal University - TURKEY
Prof. Dr.	Ali Kemal AYAN	Ondokuz Mayıs University - TURKEY
Prof. Dr.	Andrey G. KOSTIANOY	Russian Academy of Science - RUSSIA
Prof. Dr.	Ata Yakup KAPTAN	Ondokuz University - TURKEY
Prof. Dr.	Birol ELEVLİ	Ondokuz Mayıs University - TURKEY
Prof. Dr.	Branislav ZİVKOVİC	Belgrade University - SERBIA
Prof. Dr.	Elif Neyran SOYLU	Giresun University - TURKEY
Prof. Dr.	Emilija Nenezic	University of Montenegro - MONTENEGRO
Prof. Dr.	Gülcan SEÇKİN	Gazi University - TURKEY
Prof. Dr.	Gürsel ÇOLAKOĞLU	Karadeniz Technical University - TURKEY
Prof. Dr.	Hüseyin YILMAZ	Yıldız Technical University - TURKEY
Prof. Dr.	İhsan AKYURT	Giresun University - TURKEY
Prof. Dr.	İsmail AYDIN	Karadeniz Technical University - TURKEY
Prof. Dr.	İsmail USTA	Marmara University - TURKEY
Prof. Dr.	Kemal YILDIRIM	Gazi University - TURKEY
Prof. Dr.	Lubos HES	Technical University of Liberec - CZECH REPUBLIC
Prof. Dr.	M. Serkan SOYLU	Giresun University - TURKEY
Prof. Dr.	Mehmet AKBULUT	Selçuk University - TURKEY

Prof. Dr.	Mehmet TÜFEKÇİ	Avrasya University - TURKEY
Prof. Dr.	Metin YÜKSEK	Marmara University - TURKEY
Prof. Dr.	Mustafa CİN	Giresun University - TURKEY
Prof. Dr.	Mustafa SOYLAK	Erciyes University - TURKEY
Prof. Dr.	Mustafa TÜRKMEN	Giresun University - TURKEY
Prof. Dr.	Mustafa TÜZEN	Gaziosmanpaşa University - TURKEY
Prof. Dr.	Naci İSPİR	Atatürk University - TURKEY
Prof. Dr.	Nazmi POLAT	Ondokuz Mayıs University - TURKEY
Prof. Dr.	Nehat BEKJIRI	Tetova University - MACEDONIA
Prof. Dr.	Savaş CANBULAT	Kastamonu University - TURKEY
Prof. Dr.	Sema PALAMUTÇU	Pamukkale University - TURKEY
Prof. Dr.	Semra ÇOLAK	Karadeniz Technical University - TURKEY
Prof. Dr.	Serdar SALMAN	Marmara University - TURKEY
Prof. Dr.	Sermin ÖRNEKTEKİN	İstanbul Ayvansaray University - TURKEY
Prof. Dr.	Şahin ALBAYRAK	Berlin Technical University - GERMANY
Prof. Dr.	Şahlan ÖZTÜRK	Nevşehir University - TURKEY
Prof. Dr.	Şevket Metin KARA	Ordu University - TURKEY
Prof. Dr.	Uğur KÖLEMEN	Giresun University - TURKEY
Prof. Dr.	Vladimir PESİC	Montenegro University- MONTENEGRO
Prof. Dr.	Vedat CEYHAN	Ondokuz Mayıs University - TURKEY
Prof. Dr.	Yusuf GÜVEN	Mersin University - TURKEY
Assoc. Prof. Dr.	Abdigani HALILOV	Yusuf Balasagun Milli University - KYRGYZSTAN
Assoc. Prof. Dr.	Ahmet DALKIRAN	Selçuk University - TURKEY
Assoc. Prof. Dr.	Aslı YURDİGÜL	Manas University - KYRGYZSTAN
Assoc. Prof. Dr.	Ayhan KARA	Giresun University - TURKEY
Assoc. Prof. Dr.	Ayşegül ÇEBİ	Giresun University - TURKEY
Assoc. Prof. Dr.	Bahadır KOZ	Giresun University - TURKEY
Assoc. Prof. Dr.	Cenk DEMİRKIR	Karadeniz Technical University - TURKEY
Assoc. Prof. Dr.	Ersin TEMEL	Giresun University - TURKEY
Assoc. Prof. Dr.	Eşref DEMİR	Giresun University - TURKEY
Assoc. Prof. Dr.	Eva Marguí	University of Girona - SPAIN
Assoc. Prof. Dr.	Hamza ÇINAR	Gazi University - TURKEY
Assoc. Prof. Dr.	İlkay KOCA	Ondokuz Mayıs University - TURKEY
Assoc. Prof. Dr.	Kemal YILDIZLI	Ondokuz Mayıs University - TURKEY
Assoc. Prof. Dr.	Mehmet Lütfi HİDAYETOĞLU	Selçuk University - TURKEY
Assoc. Prof. Dr.	Murat AYDIN	Karadeniz Technical University - TURKEY
Assoc. Prof. Dr.	Mükrimin Şevket GÜNEY	Giresun University - TURKEY
Assoc. Prof. Dr.	Yasemin ŞİŞMAN	Ondokuz Mayıs University - TURKEY
Assoc. Prof. Dr.	Yusuf YURDİGÜL	Manas University - KYRGYZSTAN
Dr. Lecturer	Aleksandra SRETERQVİC	Belgrade University - SERBIA

Dr. Lecturer	Duygu BALPETEK KÜLCÜ	Giresun University - TURKEY
Dr. Lecturer	Elif TOPALOĞLU	Giresun University - TURKEY
Dr. Lecturer	Erdoğan AKMAN	Manas University - KYRGYZSTAN
Dr. Lecturer	Murat YOLCU	Giresun University - TURKEY
Dr. Lecturer	Onur Özdal MENGİ	Giresun University - TURKEY
Dr. Lecturer	Özgür HASANÇEBİ DEMİRKAN	Giresun University - TURKEY
Dr. Lecturer	Özlem TUNÇ DEDE	Giresun University - TURKEY
Dr. Lecturer	Selin KARAİBRAHİMOĞLU	Giresun University - TURKEY
Dr. Lecturer	Şerifali DEĞİRMENÇAY	Giresun University - TURKEY
Dr. Lecturer	Ülkü BAYKAL	Giresun University - TURKEY
Dr. Lecturer	Volkan BAŞER	Giresun University - TURKEY
Dr. Lecturer	Yasemin BARAN	Giresun University - TURKEY
Dr. Lecturer	Zuhal YOLCU	Giresun University - TURKEY
Dr. Lecturer	Zülüf ÖZTUTGAN	Giresun University - TURKEY
Dr.	Aikaterini ANASTASOPOULOU	Hellenic Center for Marine Research - GREECE
Dr.	Ali TURAN	Giresun University - TURKEY
Dr.	Mohamed HABİLA	King Saud University - SAUDI ARABIA
Dr.	Niyazi AYHAN	Manas University - KYRGYZSTAN
Dr.	Regina JAMANKULOVA	Manas University - KYRGYZSTAN
Dr.	Semiv BELLO	Olabisi Onabanjo University - NIGERIA
Dr.	Usman İbrahim ABUBAKA	Bayero University - NIGERIA

INVITED SPEAKERS	
Prof. Dr. Andrey G. KOSTIANOY Russian Academy of Sciences, RUSSIA	Satellite Monitoring of Essential Climate Variables Related to The Ocean
Prof. Dr. Mustafa SOYLAK Erciyes University, TURKEY	Some Applications Of Nanotechnology in Analytical Chemistry
Ahmet GÖÇMEZ TUBITAK - Defense Industry Development Institute, TURKEY	Leading Company in National Munition Design: Tübitak Sage
Marcin STOKLOSA NITREX Co. , POLAND	Technological Advantages Of Controlled Ferritic Nitrocarburizing
Utku İNAN Tamçelik Isıl İşlem Sanayi ve Ticaret A.Ş., TURKEY	Heat Treatment Applications at Defence Industry
F. Semih ÖZKAN Manager – Powertrain NVH, Ford Otosan, TURKEY	Analytical Sign-Off Roadmap For Powertrain Development

In the past, the products that day-to-day people put forth for the purpose of living their lives gave birth to industrialization in time, and industrialized societies became stronger day by day. However, industrialization has not been considered as an ultimate factor and the continuity of developments has forced industrialization to move forward. In this context, today's societies have entered a transition period from the industrial society to the information society. The changes that can be considered the most important elements in this transition process are the changes that take place in the field of technology.

The changes that have taken place in the field of technology have been spread to every area of our lives even though it made society felt out of place by the acceptance of by the society in the early periods. As a matter of fact, computers which are one of the most fruitful fruits of technological developments have entered our lives and network technologies that provide computers, additional equipment of these devices, multimedia technologies and data communication have been used intensively in all areas of our lives. Education which is on the field of use is the only area in which there are a rapid change and development in the methods and forms of use as well as being remarkable with the speed of transition from classical to modernity. In particular, the combination of educational software with traditional methods is remarkable in terms of the use of technology in education.

However, it is not possible to say that the elements mentioned always progress in the desired manner. As a matter of fact, everything about technological developments and keeping

up with them has not progressed as expected. One of the educational structures that toke its toll, is design education. The fact that developments in design education do not occur at the desired speed is a condition that can not be attributed to the lack of development. It is seen that there is a necessity to utilize computers at different stages of the design education when the structure is examined but it is seen that the fact that the universities do not have enough equipments in this sense until the near term makes sufficient development in the mentioned area .

Today, the necessity of using technology in an educational sense has been recognized, and the use of information technology in this direction has become widespread, and the opportunities that have arisen due to the increase of productivity have made the use of technology widespread in arts and sciences. This has opened the way for an invitation to leave the places of traditional drawings to modern drawing methods and tools. One of the areas where the change mentioned became effective is undoubtedly the design. Studies conducted in the fields of planning and design show that the use of information technology in education has become more necessary than a luxury today.

We greet and welcome you with warm feelings to discuss those necessities at this symposium organized by Giresun University, Vocational School of Technical Sciences.

Editor

Prof. Dr. Aysun TÜRKMEN

CONTENTS

Peak-to-Average Power Ratio Reduction for Partial Transmit Sequences using Partical Swarm Optimization Algorithm in Wavelet Packet Modulation	Wisam Hayder MAHDİ, Necmi TAŞPINAR
Failure Situations in The Off-Grid Photovoltaic Solar Panel Systems	Kenan YANMAZ
MECHANICAL, INDUSTRIAL ENGINEERING AND MATERIAL SCIENCE (ORAL PRESENTATIONS)	765-1120
Flow Characteristics of Swirling Coaxial Impinging Air Jets: An Experimental Investigation	Burak MARKAL
A Study on Microstrucutre and Mechanical Properties of DP 450 and IF 7314 Steels by Using Resistance Spot Welding	Fatih HAYAT, Cihangir Tevfik SEZGİN, Burak DİNDAR, Numan Berke KOŞUN, Muhammet ŞİMŞEK
Microstructure and Mechanical Properties of Al2024-SiC Nanocomposites	A. Hasan KARABACAK, Aykut ÇANAKÇI, Temel VAROL, Fatih ERDEMİR
Analysis of Weldability of IF 7314 and DP 600 Steels by Using Resistance Spot Welding	Fatih Hayat, Cihangir Tevfik Sezgin, Halil Gümüşten, Onur Daşçı
Numerical Analysis of the Effect of Turbulators to Heat Transfer of a Pellet Fuelled Boiler	Bilal SUNGUR, Bahattin TOPALOĞLU
MHD Natural Convection in Square Enclosure Having Linearly Heated Adjacent Walls	Birol ŞAHİN
Consodilation and Investigation of Properties of Hydroxyapatite-316L Stainless Steel Composites	Serdar ÖZKAYA, Aykut ÇANAKÇI, Temel Varol, A.Hasan KARABACAK, Müslim ÇELEBİ, Fatih ERDEMİR
Production and Characterization of Al-SiC Composites by Mechanical Milling	Doğan ŞİMŞEK, İjlal ŞİMŞEK, Dursun ÖZYÜREK
Microstructure and Dry Sliding Wear Behaviour of Al+2% Graphite Alloy Reinforced with Different Al_2O_3 Content	Doğan ŞİMŞEK, İjlal ŞİMŞEK, Musa YILDIRIM, Dursun ÖZYÜREK
Investigation of Mechanical and Macrostructural Properties of AA2024 and AA 5754 Plates Joined by Friction Stir Spot Welding	Damla UŞAR, Sevgi TOSUN, Betül ÖZTÜRK, Yılmaz TAŞOVA, Yahya BOZKURT. Serdar SALMAN
Effect of Oil Flow Rate, Contact Pressure and Sliding Speed on the Wear Properties of Zn-15Al-3Cu Alloy	Ali Paşa HEKİMOĞLU, Temel SAVAŞKAN
Effect of Heat Treatment on the Microstructure and Hardness Development of 1.2080 Cold Work Tool Steel	Fatih HAYAT, Cihangir Tevfik SEZGİN, Samet KURTULDU, Nurettin AYDIN, Ebubekir HACI
Effect of Heat Treatments on S 235 Steel	Fatih HAYAT, Cihangir Tevfik SEZGİN, Berfu ATICI, Tuğba EKİNCİ
Evaluation of Low Alloyed Ribbed Construction Steels Produced Via Tempcore Process According to TS 708 Standard	Erhan DOĞAN, Gürel ÇAM
A Proposition for Using Heat Pump Unit to Integrate Cooling, Heating and Refrigerating Functions	Faraz AFSHARI, Farzad AFSHARI
Analysis of Academic Publications in the Field of Industrial Engineering in Turkey	Ayca ÖZCEYLAN, Eren ÖZCEYLAN, Cihan ÇETİNKAYA, Barış ÖZKAN
Investigation of the Effect of Consumables on Product Quality in Submerged Arc Welded Pipe Production	Özlem Pınar ÖNDER GÜNBAY, Gürel ÇAM

Handle Properties of Woven Pique Fabrics Produced From Mechanical Recycled Cotton Fibers	Leman ATİKER, Nilgün ÖZDİL, Arif Taner ÖZGÜNEY, Kadri IŞILAY, Turhan AVDAN
Liquid Moisture Transport: Usage Of R-Pet Instead Of Conventional Pet	Mehdi HATAMLOU, Gamze SÜPÜREN MENGÜÇ, Arif Taner ÖZGÜNEY, Nilgün ÖZDİL
Luxury Animal Fiber/Cotton Blends: Sustainable, Profitable, Niche Production	Gamze SÜPÜREN MENGÜÇ , Nilgün ÖZDİL, Faruk BOZDOĞAN
BBSpecial: Thermochromic Textile Product Designs For Babies	Öykü DEGIGOĞLU, Kayhan TOPLU, Serhat KARAKAYA, Arif Taner ÖZGÜNEY
Comparison of The Activities Classical and Nano Chemicals on Different Finishing Processes of Cotton Fabrics	Eylen Sema DALBAŞI
Photochromic Textiles	E. Perrin AKÇAKOCA KUMBASAR, Seniha MORSÜMBÜL
Effect of Pique Pattern Printing on Thermal and Handle Properties of Fabrics	Serhat KARAKAYA, Gamze SÜPÜREN MENGÜÇ, Arif Taner ÖZGÜNEY, Nilgün ÖZDİL, Gonca ÖZÇELİK KAYSERİ
Needle Puncture Resistance of Fabric Layers used for Micrometeoroids and Orbital Debris (MMOD) Protection	Emrah TEMEL
The Use Of Different Clay Types For Adsorption Of Reactive Dyes From Textile Wastewater	Nuriye KERTMEN, Emriye Perrin AKÇAKOCA KUMBASAR, Saadet YAPAR
Use of Natural Fibers in Composite Reinforcement	Hatice AKTEKELİ, Deniz DURAN
A Comparison on Physical Properties of Ring-, Compact- And Compact Siro- Spun Yarns Produced from Different Fibers	Memik Bünyamin Üzümcü, Burak Sarı, Nida Oğlakcıoğlu, Hüseyin Kadoğlu
Time-dependent Strength Change of Absorbable Surgical Sutures Held in Mucosal Medium	Deniz MİZMİZLİOĞLU, Emrah TEMEL, Faruk BOZDOĞAN
Investigating Abrasion Resistances of Denim Fabrics Including Different Chenille Weft Yarns	Hüseyin Gazi TÜRKSOY, Sibel KAPLAN, Sümeyye ÜSTÜNTAĞ, Sinem BİLGİN YÜCEL
Effects of Water and Fertilizer - Saving Agrotextile Material on Biomass Production and Photosynthesis in Lettuce under Drought Stress	İlhan ÖZEN, Gamze OKYAY, Abdullah ULAŞ
TEXTILE TECHNOLOGY (POSTER PRESENTATIONS)	1478-1545
Surface Roughness and Friction Characteristics of Denim Fabrics	Gonca ÖZÇELİK KAYSERİ, Gamze SÜPÜREN MENGÜÇ, Nilgün ÖZDİL
Defects in Denim Washing And Solutions	Ayşegül KÖRLÜ
High Strength Braiding Ropes for Different Applications	Pınar ÇELIK, Tuba BEDEZ UTE, Hüseyin KADOGLU
Time-dependent Strength Change of Emergency Tent Fabric after UV Exposure	Emrah TEMEL, Faruk BOZDOĞAN, Deniz MİZMİZLİOĞLU
Smart Textiles: A General Perspective	Merve TÜREMEN, Aslı DEMIR
A Review on the use of Estabragh (Milkweed) Fibers in Nonwoven Applications	MohammadAmin SARLİ, Deniz DURAN
The Usage of Natural Antimicrobials in Textiles	Tülay GÜLÜMSER, Ebru BOZACI

Regional Transformation Parameters Determined with Geographic Information Systems Approach: Giresun Example	Ulku KIRICI YILDIRIM, Yasemin SISMAN
Accessibility of Urban Living Quality Indicators; a Case Study of Giresun	Aziz SISMAN, Ridvan ERTUGRUL YILDIRIM, Atakan KARACA
Estimating Compressive Strength of Rock Using Geographically Weighted Regression	Cem YAYLAGÜL, Bülent TÜTMEZ
Smart Cities and Transportation	Elif ALDANMAZ, Aziz ŞİŞMAN
Digitization of Cadastral Sheets by Polynomial Transformation Methods	Yasemin SISMAN, Ulku KIRICI YILDIRIM
Long Term Monitoring of Giresun Province and Perimeters by Using Remote Sensing	Mehmet Ali DERELİ, Nizar POLAT, Mehmet Ali UĞUR, Mustafa YALÇIN
High Resolution DSM Generation with Low Cost UAV	Nizar POLAT, Murat UYSAL, Mehmet Ali DERELİ
INTERIOR DESIGN, ARCHITECTURE, LANDSCAPE, FURNITURE DESIGN, FURNITURE INDUSTRY (ORAL PRESENTATIONS)	1949-1995
Form, Material and Symbol: Iconic Architecture in Built Environment	Burcu KÖSE KHIDIROV, Bilge KÖSE, Ahmet KÖSE
Three Dimensional Modelling In Landscape Architecture Teaching	Deryanur DİNÇER, Türker OĞUZTÜRK
R&D and Technological Knowledge in SMEs: Furniture Industry in Samsun Region	Seval MUTLU ÇAMOĞLU
Determination of Recreational Area Usage Potential of Rize Province Coastal Ridge	Banu BEKCİ, Merve ÜÇOK, Hasan Yılmaz
INTERIOR DESIGN, ARCHITECTURE, LANDSCAPE, FURNITURE DESIGN, FURNITURE INDUSTRY (POSTER PRESENTATIONS)	1996-2008
Transforming Landscapes	Hasan YILMAZ, Banu BEKCİ, Merve ÜÇOK
ORAL PRESENTATIONS	2009-2076
How Do You Save The World Design? "Analysis of an Artist Project about What the Design is"	Aylin GÜNGÖR
A Semi Automatic Windows Which Prevent to Poison Carbon Monoxide and Other Toxıc Gases	Mehmet Senan YILMAZ
Examining and Reinterpreting Fashion Design Samples of Leading Designers of Futurism	Nurdan KUMAŞ ŞENOL, Ali Osman ELMAS
World War I (1914-1918) Examination of Women's Garment Fashion and Reinterpretation with Digital Programs	Nurdan KUMAŞ ŞENOL, Çiğdem ÖZDEMİR
The Extraordinary Biosorption Potential of Vetiver Grass Grown in Giresun	Derya EFE, Bengü ERTAN

ANALYTICAL, ANORGANIC, ORGANIC, PHYSICAL, BIO, ENVIRONMENTAL CHEMISTRY

ORAL PRESENTATIONS

Specification of BTEX (Benzene, Toluene, Ethylbenzene, Xylenes (o+p+m) VOC (Volatile Organic Component) In Giresun Province Seasonally With The Help of Passive Sampling and Evaluation of Their Effects on Human Health

Alev ELKAYA [1*], Aysun TÜRKMEN [2]

[1] Giresun University, Instıtute of Science, Chemistry Department, Giresun, Turkey; alevkara28@hotmail.com

[2] Giresun University, Instıtute of Science, Chemistry Department, Giresun, Turkey; aturkmen72@hotmail.com

[*] **Corresponding Author:** alevkara28@hotmail.com

Abstract

Benzene, toluene, ethyl benzene, xylenes (BTEX) are the most hazardous volatile organic components for health. (Lee and Coll., 2001; Leovic and Coll., 1998). They have both short and long term negative effects on health. In this study it is aimed to quantify the BTEX (Benzene, toluene, ethyl benzene, xylenes) levels in outdoor environment in Giresun Province with the help of passive sampling. The passive sampling was carried out by placing coconut charcoal passive sampling tubes in 9 areas starting from Güre to Aksu in Giresun Province. These sample were left outdoor environments which were differ in heights and usage of heating resource such as coal or natural gas in March-April. The samples were desorbed in laboratory. Through the extract sampling, the active carbons were resolved and the evaluations were done with GC-MS spectrometer. The differentiation of BTEX-VOC in stations were output via ANOVA test. In Giresun, the result where the stations were not taken into consideration in general were Benzene: 1,301±0,195; Toluene: 2,104±0,069; Ethylbenzene: 0,243±0,055; m-p Xylenes: 0,342±0,038; o-Xylene0,222±0,039 in ppm.

Key Words: Giresun, Air Pollution, Volatile Organic Components (VOC), BTEX, Outdoor Environments.

1. Introduction

In recent years due to industrialization and increase in human activities, the great variety of environmental pollution has been born therefore many hazardous substances has been venting into the atmosphere. The fuels used for heating, hazardous gases emission of the vehicles and other pollutive factors are causing air pollution.

The pollutive gases in the atmosphere are specified through passive sampling. These sampler are generally disk or cylindrical tubes. The aim of the passive sampling is based on the diffusion through differentiation of the pollutant concentration. The target quantified pollutant is sampled with adsorption method in a selected chemical environment (Yeşilyurt and Akcan, 2001).

1.1. Effects of Fossil Fuels

The main source of air pollutants in cities are the gas emissions of fossil fuels which are used in heating and power generation, vehicles as solid fuels. The most common air pollutants in cities and nearby are sulphur dioxide (SO_2), nitrogen oxide (NO or NO_2, generally named as NOX), carbon monoxide (CO), ozone (O_3), suspended solid content (PM) and lead (Pb). The usage of fossil based solid fuels is a significant source for the pollutants. Especially with the start of heating season, the air pollution increases. Low qualified coal usage, unsuitable fuelling systems, implementation of incorrect burning techniques and inadequate operational maintenance of the boilers are in the main reasons of air pollution caused by heating in winter season (Keçebaş, and Coll. 2010).

1.2. The Effect of Coal

Usage of coal as a energy generation resource causes environmental pollution considerably. Gases such as carbon dioxide, carbon monoxide, sulphur oxide, nitrogen oxide which are the results of coal consumption and solid particles such as ash and various hydrocarbon compounds are the main reasons for air pollution.

1.3. The Effect of Natural Gas

Natural Gas is the easiest flammable gas and has the best combustion efficiency. Even though SO_2 and PM emissions is significantly low, nitrogen oxide (NO_X) emission which is the most hazardous pollutant can be seen, Accordingly, in heating using natural gas instead of coal etc. reduces the hazardous gas emissions significantly (Mao and Coll., 2005).

Giresun is located in Blacksea Region in Turkey. The population of the city is 437.393. (www.nufusu.com/il/giresun-nufusu). The source of income is hazelnut trade. The settlement due to the geographic position is mostly in the coastal region. On a contrary the provided opportunity of natural gas usage, most of neighbourhood uses coal as a heating resource.

The gases which are caused as a result of industrial activities and fuels (such as coal, wood etc.) that are used by locals for heating purpose leads a perceptible air pollution. In addition to this, because of heavy traffic as the coastal road of the city is also used by nearby cities, the exhaust gases are considered as air pollutant factors.

The purpose of the study wass to evaluate the pollution level and quantify the BTEX-VOC (Benzene, Tolune, Ethylbenzene, Xylene (o+m+p)) in air in Giresun Province with the help of passive sampling which were specified in areas where natural gas and coal were used.

2. Material and Method

2.1 The Place of Study

Giresun Province is neighbour with Trabzon and Gümüşhane in west, Ordu in south, Erzincan and Sivas in southwest and its north is surrounded by Black sea. The study was conducted between March 15th and April 15th 2018, in total 28 stations which are located in coastal and interior areas of the 9 selected neighbourhoods were specified. The sample areas were the places that uses coal and natural gases as heating source.

The specified areas were; Aksu, Industrial area, Kumyalı, Güre, Yeniyol, Giresun City Centre, Teyyaredüzü, City Castle Area, Çıtlakkale. The stations that the samples were left are shown in Figure 2.1

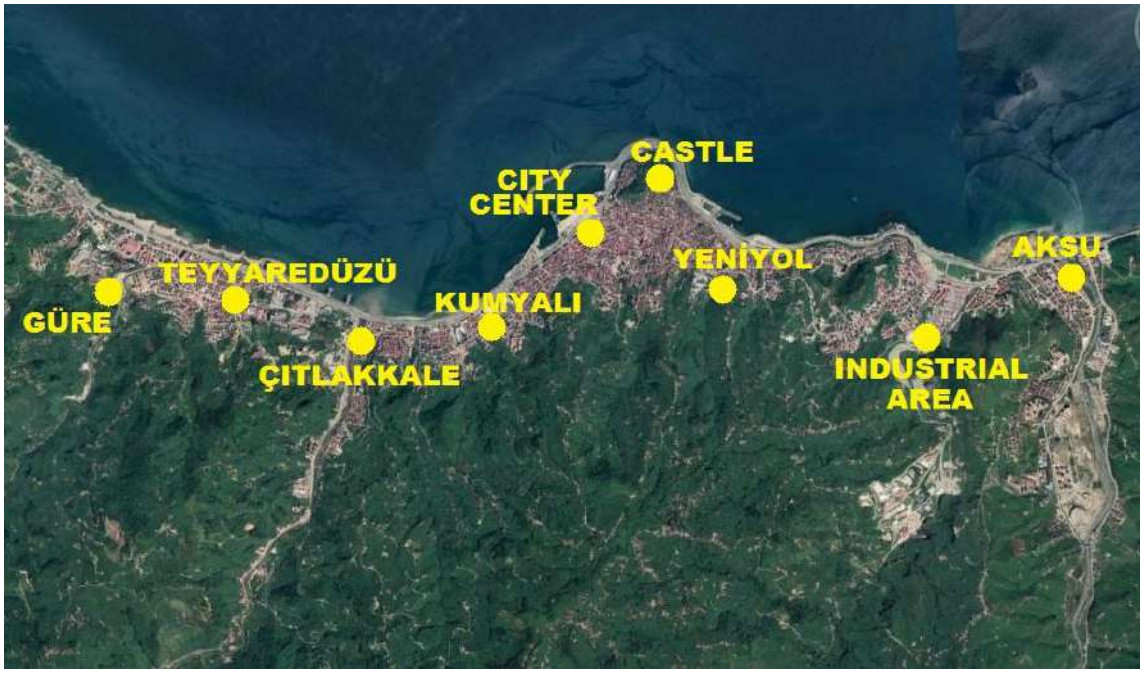

Figure 2.1. The stations that the Volatile Organic Components (VOC) samples were taken in Giresun.

2.2 Climate and Meteorology in Giresun

As the mountains run parallel to coastline, there are 2 different kind if climate region in the province. In the coastline, the climate is warm and rainy.

Table 2.1. Average wind speed, temperature, humidity, total amount of precipitation (Giresun Regional Directorate of Meteorology, 2018).

Months	Avg. Wind Speed (m/sec)	Avg. Temperature (°C)	Avg. Humidity (%)	Total Amount of Precipitation (kg/m^2)
March	1.6	11.9	69.9	128.6
April	1.5	12.9	69.8	45.8

2.3. Collection of Samples and Preparation for Analysis

With the help of passive sampling tubes, the pollutant which were in the form of gas were collected. In Drager Orsa 5 Passive sampling tube, coconut based active charcoal were used as sorbents. The two sides of the tubes were closed with cellulose acetate filters and they were left to the outdoors.

Figure 2.2. Drager Orsa 5 Passive Sampling Tube (www.frontline-safety.co.uk)

The substances of sampling tubes were transposed to suitable sized vials for desorption and were added 2 ml carbon disulfide (CS_2) which was the solution for desorption. The vials were closed with screw cap right after. Thereafter with the help of ultrasonic bath the desorption process of the samples were conducted. The extracted which were desorbed were transposed to the sample vials (In this way the active carbons were resolved.). The vials were closed with silicon/PTFE sealing ring and screw cap. To be analyzed they were placed to the gas chromatography.

2.4. The Equipment

2.4.1 The Reagents and Materials Used in Gas Chromatography

- **GC Column:** DB-VRX;60m x 0,25mm x 1,40um film (www.agilent.com)
- **Detector:** Fire Ionization Detector (FID)
- **Detector Gases:** High-purity dry air and Hydrogen for FID
- **Carrier Gas: High-purity** Helium to carry the samples in all chromatographic systems

2.5. Statistical Analysis

The one-way analysis of variance was conducted through ANOVA test, in the conditions where the differentiation were significant statistically, Post-Hoc Test (Tukey) were applied (Şenocak, 1998, Özdamar, 1999). The analysis of the statistics was carried out with SPSS Package.

3. Research Findings

In the study which was carried out in Giresun Province between March 15th and April 15th the average concentration of Volatile Organic Components in the stations are shown in the tables.

Table 3.1. The Average Concentrations of Volatile Organic Components in the Stations

The Stations	Benzene	Toluene	EthylBenzene	m-p Xylene	o- Xylene
Güre interior area	1,116±0,151^{abcd}	1,145±0,152^{ab}	0,097±0,013^{a}	0,147±0,007^{abc}	0,128±0,011^{ab}
Güre coastal area	1,820±0,051^{abcde}	1,220±0,010^{abc}	0,233±0,003^{a}	0,340±0,010^{abcd}	0,240±0,010^{ab}
Teyyaredüzü interior area	*	*	*	*	*
Teyyaredüzü coastal area	0,533±0,172^{ab}	0,713±0,007^{ab}	0,013±0,013^{a}	0,077±0,003^{abc}	0,037±0,019^{a}
Kumyalı coastal area	2,657±0,057^{de}	2,400±0,000^{abcdef}	0,327±0,015^{a}	0,510±0,006^{cd}	0,387±0,003^{ab}
Kumyalı interior area	0,267±0,128^{ab}	0,583±0,007^{a}	0,113±0,012^{a}	0,100±0,020^{abc}	0,123±0,009^{ab}
City Center coastal area	**4,357±0,035^{f}**	**7,823±0,047^{h}**	**0,907±0,363^{b}**	**1,023±0,071^{e}**	**0,500±0,218^{a}**
City Center interior area	0,346±0,321^{abcd}	1,295±0,225^{abcde}	0,043±0,025^{a}	0,096±0,056^{abc}	0,087±0,067^{a}
Giresun Castle interior area	*	*	*	*	*
Giresun Castle coastal area	**0,017±0,007^{a}**	**0,280±0,127^{a}**	**0,003±0,003^{a}**	**0,000±0,000^{abc}**	**0,010±0,000^{ab}**
Industrial interior area	1,693±0,026^{bcde}	2,898±0,032^{bcdeg}	0,295±0,019^{a}	0,400±0,105^{abcd}	0,310±0,023^{ab}
Industrial coastal area	*	*	*	*	*
Aksu interior area	*	*	*	*	*
Aksu coastal area	2,207±0,047^{cde}	3,223±0,026^{fg}	0,390±0,130^{a}	0,330±0,010^{abcd}	0,090±0,046^{a}
Çıtlakkale interior area	0,997±0,902^{abcd}	2,203±0,030^{cdef}	0,327±0,009^{a}	0,487±0,003^{bcd}	0,417±0,007^{ab}
Çıtlakkale coastal area	1,460±0,710^{abcde}	3,267±0,015^{fg}	0,390±0,050^{a}	0,687±0,009^{de}	**0,500±0,010^{b}**
Yeniyol interior area	2,903±0,003^{ef}	2,687±0,012^{ef}	0,080±0,040^{a}	0,227±0,083^{abcd}	0,027±0,009^{a}
Yeniyol coastal area	0,872±0,127^{abc}	1,300±0,271^{abcd}	0,190±0,073^{a}	0,368±0,144^{abcd}	0,263±0,110^{ab}

*:can not read.
Table should be viewed from top to bottom for ANOVA.
Each vertical column was analyzed in terms of statistics.

The acquired averages concentration values in the study are shown in Table 3.1. The bold written values show the highest values, the underlined values shows the lowest values.

When the stations are ignored, the total average is (for BTEX) respectively Benzene: 1,301±0,195; Toluene: 2,104±0,069; Ethylbenzene: 0,243±0,055; m-p Xylenes: 0,342±0,038; o-Xylene: 0,222±0,039 in ppm.

When analyzed statistically, there are significant differences between Benzene and Toluene values ($p < 0.05$). Between Yeniyol interior area and City Center Coastal area, there is no statistically significant difference ($p > 0,05$).

In the Ethyl benzene concentrations, there is no statistically significant difference in values except City Center Coastal area ($p > 0,05$). The highest concentration value was found at the City Center Coastal Station.

When analyzed statistically, there were significant differences between the stations in m-p-o Xylene concentrations ($p < 0.05$). The highest concentration value was found at the City Center Coastal Station. The highest values for o-Xylene were found at Çıtlakkale Coastal area and City Center Coastal Stations.

4. Results and Discussion

In the literature reviews; the study that Küçükaçıl and his colleagues done in 2015 in thermal power plant in Kütahya examined VOC the seasonal distribution (summer-winter). The concentrations were collected using passive samplers from 109 different stations.

In winter, the highest standard deviation values were 0.57 (benzene), 0.76 (toluene), 0,59 (n- decane), 0,73 (n-decane) and 0,84 (n-dodecane); in summer the highest standard deviation values were, 0,89 (n-decane), 1,25 (n-hexane), 1,30 (n-undecane), 1,28 (toluene) and 1,78 (n-dodecane). In general, the total VOC concentration in winter were higher than in summer. Higher UOB rates was quantified in the city centre and the districts where the heavy traffic was seen in Kütahya. In addition, in the study the carcinogenic risk ratios which are caused as a result of exposing to Benzene concentrations for a long time for each sample areas were estimated, the rates showed changes between $2,2.10^{-5}$ - $3,65.10^{-8}$ in winter; $5,36.10^{-6}$ - $2,12.10^{-7}$ in summer. In both seasons, the estimated risk ratio in the %80 of the sample stations exceed the 1.10^{-6} risk ratio which is stated and accepted by EPA.

In the study that Buczynka and his colleagues carried out in Antwerp, Belgium in 2009 BTEX measurements was done, before and after main track-renewal, in the areas where the heavy traffic was seen. It was aimed to improve the air quality by reducing the traffic lane.

From this point of view, before the main-track renewal project in 2003, BTEX avg. concentrations had been; benzene 1,6, toluene 7, ethyl benzene 0,9, m+p xylene 2,3, o-xylene 0,9. After the main track-renewal project, in 2005 the levels were; benzene 2,5, toluene 9,5, ethyl benzene 1,6, m+p xylene 3,4, o-xylene 1,3 ppb. The acquired results showed that reducing the traffic lane increased the traffic jam thus increased the emission levels coming out from the vehicles.

In the study that Karaca, F. was carried out on Historical Peninsula in İstanbul in 2012, the average rates of benzene, toluene, ethyl benzene, m+p xylene and o-xylene respectively were; 0,61 µg m^3, 5,18 µg m^3, 0,38 µg m^3, 1,04 µg m^3 ve 0,7 µg m^3; the average rates in winter respectively were; 1,03 µg m^3, 3,11 µg m^3,0,20 µg m^3, 0,52 µg m^3 ve 0,36 µg m^3.

Table 4.1. Toxicity Values for Volatile Organic Compounds BTEX (US EPA, 1998a,b)

Chemical	**Referance Dose (mg/kg/day)**	**Cancer Factor $(mg/kg/day)^{-1}$**	**US EPA Cancer Classification**
Benzene	$8.57x10^{-3}$	$2.73x10^{-2}$	A (carcinogenic)
Toluene	$1.14x10^{-1}$	-	-
Ethylbenzene	$2.86x10^{-1}$	-	-
Xylene	$2.86x10^{-2}$	-	-

In the study that was carried out in Giresun, with specified stations, where natural gases and coal was used and had heavy traffic, dense population and industrialization, effects of BTEX air pollutants, which is considered as Volatile Organic Components (VOC) that have the hazardous effects on health, was analyzed. As it can be seen in Table 3.1., the acquired average values, the highest Benzene concentration was found in City Center coastal area and the lowest was in Giresun Castle coastal area. The highest Toluene concentration value was found in City Center coastal area and; the lowest was in Giresun Castle coastal area. The highest Ethyl Benzene concentration value was in City Center coastal area; the lowest was in Giresun Castle coastal area. The highest o-m-p Xylene concentration values was found in City Center coastal area and the lowest was in Giresun Castle coastal area.

As the study is planned to be continued in other seasons, we are of the opinion that we can obtain more determining information on the scope.

Acknowledgement: This study was supported by Giresun University, BAP (FEN-BAP-A-160317-44)

References

Periodicals:

Buczynska, A.J.,Krata, A., Stranger, M., Godoi, A.F.L., Kontozova-Deutsch, V., Bencs, L., Naveau, I., Roekens, E., Grieken, R.V. (2009). ‘’Atmospheric BTEX-concentration in an area with intensive street traffic’’, Atmospheric Environment, 43, pp.311-318.

Keçebaş, A., Gedik, E., Kayfeci, M., (2010). Machine Technologies and Electronics Journal Volume: 7, No: 3, 2010 (23-30).

Lee Sc, Lam S, Faı Hk, (2001). Characterization of UOBs, ozone, and PM10 emissions from office equipment in an environmental chamber. Build. Environ. 36:837-842.

Leovıckw, Whitaker Da, Northeim C., Sheldonls (1998). Evaluation of test method form ensuring indoor air emission from dry-process photo copiers. J. Air Waste Manage. Assoc. 48:915-923.

Mao, X., Guo, X., Chang, Y., Peng, Y., (2005). “Improving Air Quality in Large Cities by Substituting Natural Gas for Coal in China: Changing Idea and Incentive Policy Implications”, Energy Policy, 33, 307-318.

Books:

Şenocak, M., 1998. Biostatistics. Istanbul Univ., Cerrahpaşa Medical Faculty Publishing Fascicule No: 214 pg 314, İstanbul.

Özdamar, K., 1999. Biostatistics with SPSS. Kaan Bookstore Publishing pg 454, Eskişehir.

Yeşilyurt, C., and Akcan, N., (2001). TR The Ministry of Health Refik Saydam Sanitation Centre Presidency, Directorate of Environmental Health Research " Monitoring Methodologies of Air Quality and Sample Criteria".

Symposium, Congress, Paper:

Karaca, F., (2012). "Study on BTEK Surface Diffusion Profile on Historical Peninsula in İstanbul" Fatih University, Department of Environmental Engineering, İstanbul.

Küçükaçıl, G., Üzmez, Ö., Arı, A., Gaga, E., (2015, October). 6th National Air Pollution and Control Symposium, "The areal and Seasonal Distributions of Volatile Organic Components (VOG) in Thermal Power Stations in Kütahya", İzmir.

Other Sources:

Giresun Regional Directorate of Meteorology 2018.

URL-1:https://www.frontline-safety.co.uk/drager-orsa-5-passive-sampling-tube, (Date of access: 10 June 2018).

URL-2:https://www.nufusu.com/il/giresun-nufusu, (Date of access: 10 June 2018).

URL-3:https://www.agilent.com/store/en_US/Prod-122-1564/122-1564, (Date of access: 01 March 2018).

Electrochemical Characterization of CO-Releasing Manganese-Imidazole Complexes

Mutlu SÖNMEZ ÇELEBİ*, Elvan ÜSTÜN, Songül KIRLAK

Ordu University, Faculty of Science and Arts, Department of Chemistry, 52200, Ordu, Turkey.

* **Corresponding Author:** mutlucelebi@odu.edu.tr

Abstract

As important catalysts, metal carbonyl complexes have received considerable attention in recent years owing to their ability to store and transport carbon monoxide that have been proven to function as antiinflammatory, antiapoptotic or antiproliferative agents. In this study, $[Mn(CO)_3(bpy)L]PF_6$ type novel manganese complexes have been characterized electrochemically and related to CO-releasing properties.

Keywords: CORMs, Manganese complexes, Imidazole ligands, Electrochemistry.

1. Introduction

As important catalysts, metal carbonyl complexes have received considerable attention in recent years owing to their ability to store and transport carbon monoxide that have been proven to function as antiinflammatory, antiapoptotic or antiproliferative agents (Mancuso 2004; Üstün et al. 2016). Since the discovery of nickel tetracarbonyl more than a century ago, metal carbonyls have played a very important role in pharmaceutical chemistry. These complexes are now established as useful biomolecules. CO has been known as toxic since ancient times, because the CO binds to empty coordination site of hemoglobin to form carbonmonoxy hemoglobin (COHb) and impairs oxygen transport to tissue. On the other hand, CO is produced endogenously as a by-product during degradation of hemoglobin and COHb levels of up to 10% are asymptomatic (Romão et al. 2012). With the emerging evidence that small amounts of CO produced by the organism is a key element in life processes, the search for compounds which would release CO at specific sites with a controllable and tunable rate was initiated. Thus, the synthesis of molecules or metal complexes which release CO for therapeutic purposes has been of great interest in recent years.

The availability of "CO-releasing molecules" (CORMs) that are compatible with a physiological environment not only has excellent prospects for biological or medicinal purposes but would also impact on organometallic chemistry. An obvious choice for CO-releasing molecules is transition metal complexes with one or more carbon monoxide ligands. CORMs should be reasonably soluble in water, be non-toxic prior and after decomposition or have a controlled release of CO and the follow up product(s) should be known (simple CO exchange or further reactions). Eventual CO-ligands may not interact with the bio-systems. Furthermore, a factor which also applies to main group element CO releasers, potential targeting is desirable. Considering the aqueous environment of application, reasonable aqueous stability, hence, not a very rapid CO release, is a base.

In this study, $[Mn(CO)_3(bpy)L]PF_6$ type novel manganese complexes have been characterized electrochemically and related to CO-releasing properties. Chemical structures of the complexes are presented in Figure 1.

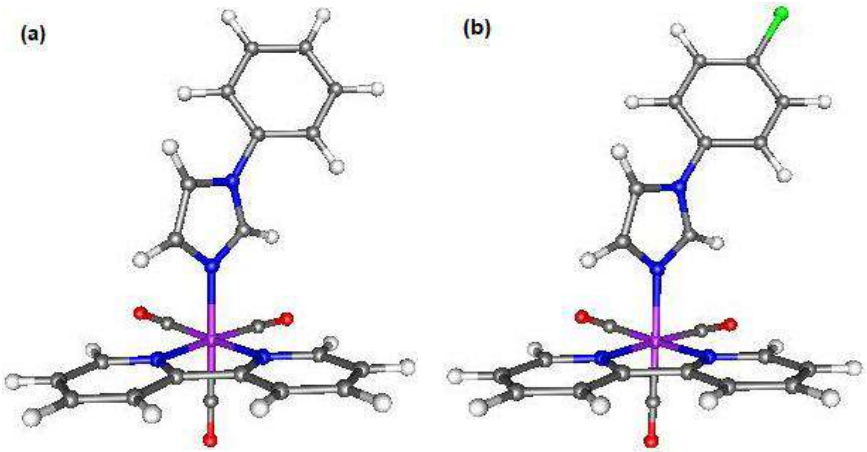

Figure 1. Chemical structures of (a) $[Mn(CO)_3(bpy)(1\text{-phenylimidazole})]PF_6$ and (b) $[Mn(CO)_3(bpy)(1\text{-}(4\text{-klorophenyl})imidazole)]\ PF_6$ complexes.

2. Materials and Methods

Cyclic voltammograms (CVs) of the compounds were recorded using a CHI Model 600E Potentiostat with 3-electrode configuration. The working electrode was a pencil graphite electrode (PGE) with a diameter of 0.5 mm. A Pt wire was used as the counter electrode and a saturated calomel electrode (SCE) was used as the reference electrode.

The complex molecules were dissolved in acetonitrile and tetra-n-butylammonium perchlorate (TBAP) was used as the supporting electrolyte. Analytical concentration of the solutions was 4.0 mM for each molecule. All the electrochemical experiments were performed after purging a sufficient amount of pure nitrogen gas to the solutions in order to remove the dissolved oxygen.

3. Results and Discussion

CVs of $[Mn(CO)_3(bpy)(1\text{-phenylimidazole})]PF_6$ and $[Mn(CO)_3(bpy)(1\text{-}(4\text{-klorophenyl})$ imidazole)] PF_6 complexes are given in Figure 2 and Figure 3 respectively. We also recorded the CVs of the complexes at different scan rates and observed that the nature of the voltammograms did not change with scan rate (not shown). Moreover, the peak currents were all linearly dependent on scan rate, confirming the cyclic voltammogram arises from an adsorbed species.

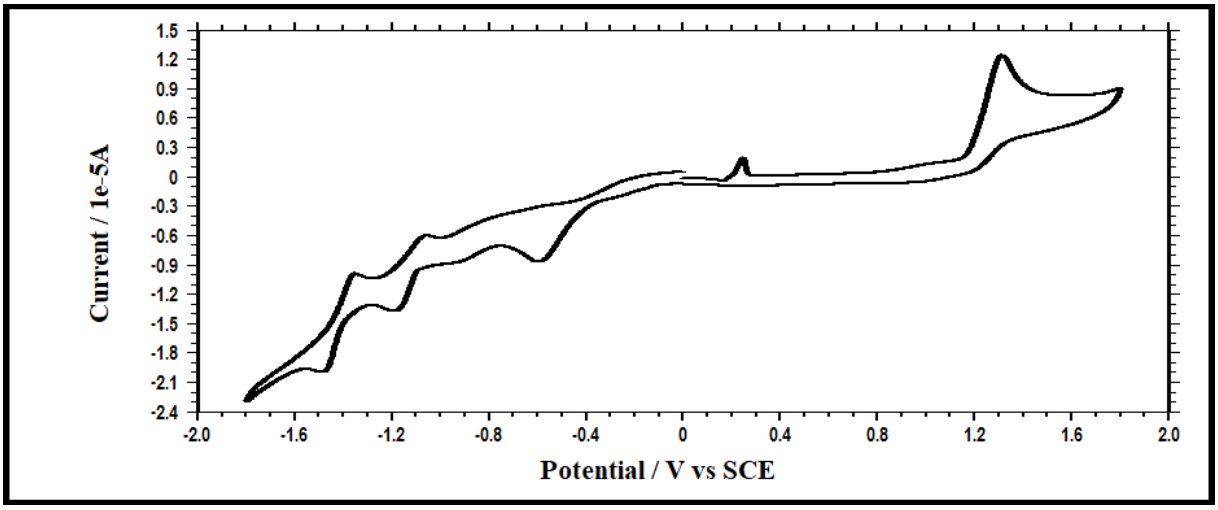

Figure 2. CV of 4.0 mM solution of $[Mn(CO)_3(bpy)(1\text{-phenylimidazole})]PF_6$ complex containing 100 mM TBAP in acetonitrile. Scan rate = 50 mV s^{-1}

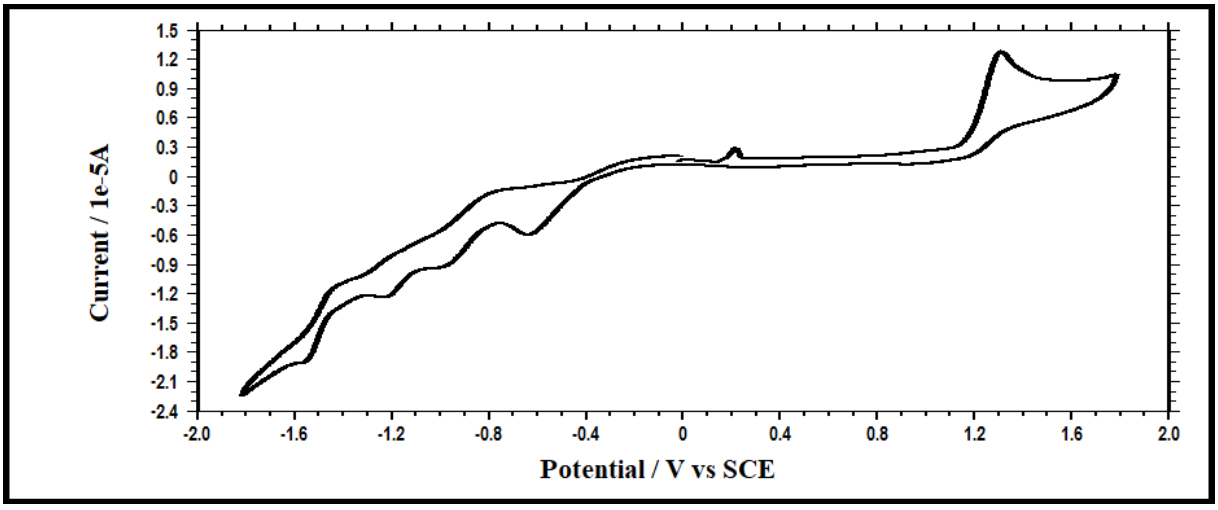

Figure 3. CV of 4.0 mM solution of $[Mn(CO)_3(bpy)(1\text{-}(4\text{-klorophenyl})\ imidazole)]PF_6$ complex containing 100 mM TBAP in acetonitrile. Scan rate = 50 mV s^{-1}

As clearly seen from the voltammograms, both compounds show an irreversible oxidation peak around +1.30 V. As the potentials are quite close to each other, the peaks look almost unaffected by differentiating the ligands and therefore should be attributed to the metal center of the complexes rather than the ligand sites. These oxidation peaks are assigned to the monoelectronic oxidation of Mn(I) to Mn(II). Additionally, both compounds feature complicated oxidation and reduction peaks at the negative potential region. This behavior is assigned to ligand based oxidation/reduction of the complex molecules as the position of the peaks are obviously affected by altering the substituents on the ligands coordinating the metal.

Finally, we compared the CVs of the complexes before and after irradiation of the complex solution with UV light (366 nm) to relate the electrochemical behavior to CO release. For this purpose, we recorded CVs of $[Mn(CO)_3(bpy)(1\text{-phenylimidazole})]PF_6$ and $[Mn(CO)_3(bpy)(1\text{-}(4\text{-klorophenyl})imidazole)]\ PF_6$ before and after irradiation with UV light for 20 min (Figure 4).

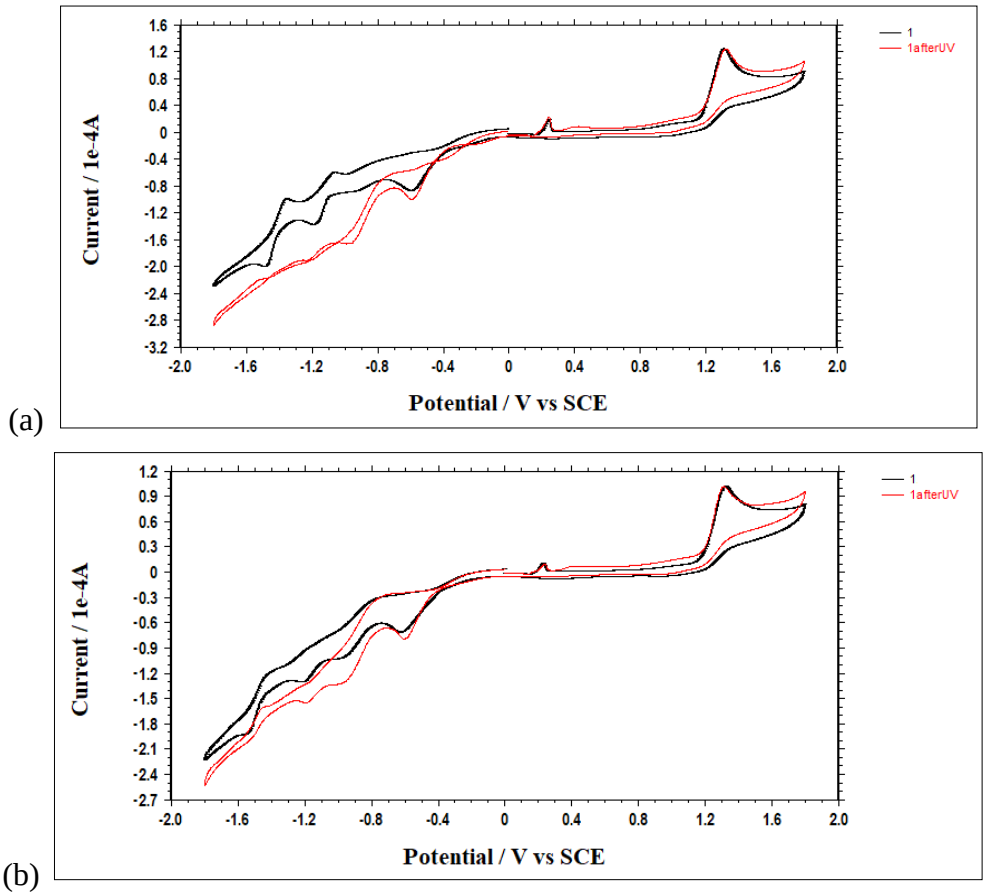

Figure 4. CVs of (a) $[Mn(CO)_3(bpy)(1\text{-phenylimidazole})]PF_6$ (b) $[Mn(CO)_3(bpy)(1\text{-}(4\text{-klorophenyl})$ $imidazole)]PF_6$ before (black) and after (red) irradiation with UV light (366 nm) for 20 min. (Scan rate = 50 mV s^{-1})

It is clearly seen from Figure 4 that after irradiation of the complexes with UV light, presumably due to the release of the CO contained in the molecule, the peaks in the negative potential region are significantly affected while the oxidation peaks in the positive region remains unchanged. This behavior also confirms the assignment of the peaks at negative potentials to the ligand sites of the molecules.

Acknowledgement

This work was supported by the Scientific Research Projects Coordination Department of Ordu University (ODUBAP) with grant number: HD-1601.

References

Mancuso, C. (2004) "Heme Oxygenase and Its Products in the Nervous System." *Antioxidants & Redox Signaling* 6(5): 878–87. http://www.liebertonline.com/doi/abs/10.1089/ars.2004.6.878.

Romão, C.C., Blättler, W.A., Seixas, J.D. and Bernardes, G.J.L. (2012) "Developing Drug Molecules for Therapy with Carbon Monoxide." *Chemical Society Reviews* 41(9): 3571–83.

Üstün, E., Çol Ayvaz, M., Sönmez Çelebi, M., Aşcı, G., Demşr, S. and Özdemir, İ. (2016) "Structure, CO-Releasing Property, Electrochemistry, DFT Calculation, and Antioxidant Activity of Benzimidazole Derivative Substituted $[Mn(CO)_3(Bpy)L]PF_6$ type Novel Manganese Complexes." *Inorganica Chimica Acta* 450: 182–89.

New Solid State Type Potentiometric Zinc Ion-Selective Sensor Based on Ion-Imprinted Polymer

Nurşen DERE

Giresun University, Science&Arts Faculty, Chemistry Department, Giresun /Turkey

Corresponding Author: nursen_1988@windowslive.com

Abstract

The ion selective sensors are as an alternative to the expensive methods, therefore, their high selectivity, low detection limits, short response time, low cost, wide operating range, high accuracy and precision, simple design, no damage to the analysed material [1-2]. The IIPs are used in ion selective sensor construction [3]. In this study; the zinc ion-imprinted polymer (IIP) was synthesized by suspension polymerization by using Zn(II) ion, methacrylamide, methacrylic acid and ethylene glycol dimethacrylate as the template, functional monomers and cross-linker respectively. The resultant Zn(II)-imprinted polymer was used as ionophore in the PVC membrane to obtain a selective potentiometric response towards Zn(II) ions. A new solid-state type potentiometric sensor was developed for Zn(II) sensing. The proposed sensor exhibited a selective Nernstian response towards Zn^{2+} ion for 2 months without any considerable divergence in potentials. The response time of the sensor was considerably short. The developed sensor was effectively performed in the wide pH range. The sensor was successfully used as an indicator electrode in the potentiometric titration of Zn(II) ions.

Keywords: Zinc, Ion imprinted polymer, Ion-selective sensor, Potentiometry.

1. Introduction

Zinc is one of the most important essential trace elements in human nutrition. Zinc involves in human body very important roles for biological systems and plays an essential role in the production of cell division and the genetic materials. Zinc is procurable in many foodstuffs with plant or animal sources. Deficiency of the zinc affects a lot of people in the world and cause many diseases including nausea, electrolyte imbalance, lethargy, and anemia. On the other hand, drinking water contains trace amounts of Zn(II) ions, especially when stored in the metal containers. Industrial activities and toxic waste sites can increase the zinc pollution of the local water recourses to levels that may cause health problems [4-6].

Molecular imprinting method for obtaining more selective polymeric particles is a rapidly evolving technique for preparing the molecularly imprinted polymers (MIPs) with high affinity for the target molecule. The molecular imprinting method is referred to in the literature as a key-lock model. The conception of the ion imprinting method appears to be similar to the molecular imprinting method. The difference between the polymers obtained by the ion imprinting method and the MIPs is that ions and generally metal ions are used instead of molecules as a template [7-10]. Many metal IIPs have been prepared including alkaline [11] and transition elements [12], noble [13] and heavy metals [14], actinides [15], and lanthanides [16]. The ion-imprinted polymers (IIP) are used in artificial reception, solid phase extraction (SPE), catalysis facilitation, chromatographic separation, membrane separation, and sensor construction.

In this study; new solid state type potentiometric Zinc ion-selective sensor based on ion-imprinted polymer(IIP) has been developed for Zn(II) sensing. The proposed sensor was also used for the determination of Zn(II) contents of some environmental water samples.

2. Material and Method

2.1. Reagents and Solutions

Methacrylamide, ethylene glycol dimethacrylate (EGDMA), polyvinyl alcohol (PVA), methacrylic acid (MAA), azobisisobutyronitrile (AIBN), methanol, toluene, ethanol, high molecular weight polyvinylchloride (PVC), tetrahydrofuran (THF), o-nitrophenyl octyl ether (NPOE), dioctyl sebacate (DOS), dibutyl phthalate (DBP), potassium tetrakis (4-chlorophenyl) borate (KTpClPB), disodium ethylenediaminetetraacetate dihydrate (EDTA-Na_2) and graphite

were purchased from Sigma-Aldrich. Epoxy resin (Ultrapure SU 2227) and hardener (Desmodur RFE) were obtained from Victor and Bayer AG, respectively. The solvents and all other salts used in the study were supplied by Merck. The ionophore was synthesized and purified following the procedures are given in the literature [17].

2.2. Apparatus

The EMF measurements were achieved by a high-input impedance multi-channel potentiometer device designed in our laboratory and supported by a computer program. Throughout the measurements, Basi-MF-2079-RE-5B model Ag/AgCl electrode was used as reference electrode. Shimadzu (model AUX220) brand analytical balance was used for weighing operations. The deionized water was obtained from a Sartorius Stedim (Ariium 611UV) ultra-deionized water (18.3 MΩ) device. Perkin Elmer AAS instrument (Model Analyst 400) was used in the spectroscopic zinc determinations. The pH values of the solutions were adjusted by using a Jenway 3040 model Ion Analyser. Thermogravimetry analysis (TGA) was carried out using SII O-Extar 6000 thermal analyzer. Hitachi SU 1510 model instrument was used for Scanning Electron Microscopy (SEM) analysis of the polymers.

2.3. Synthesis of the Zn(II)-imprinting polymer

The Zn(II)-imprinted polymer (Zn-IP) was synthesized by following the method described below with the use of $[Zn_2(\mu\text{-maa})_3(maa)]_n$ complex, AIBN and EGDMA[14]. The preparation process of the polymers and the removal of Zn(II) ions are representatively shown in Fig. 1.

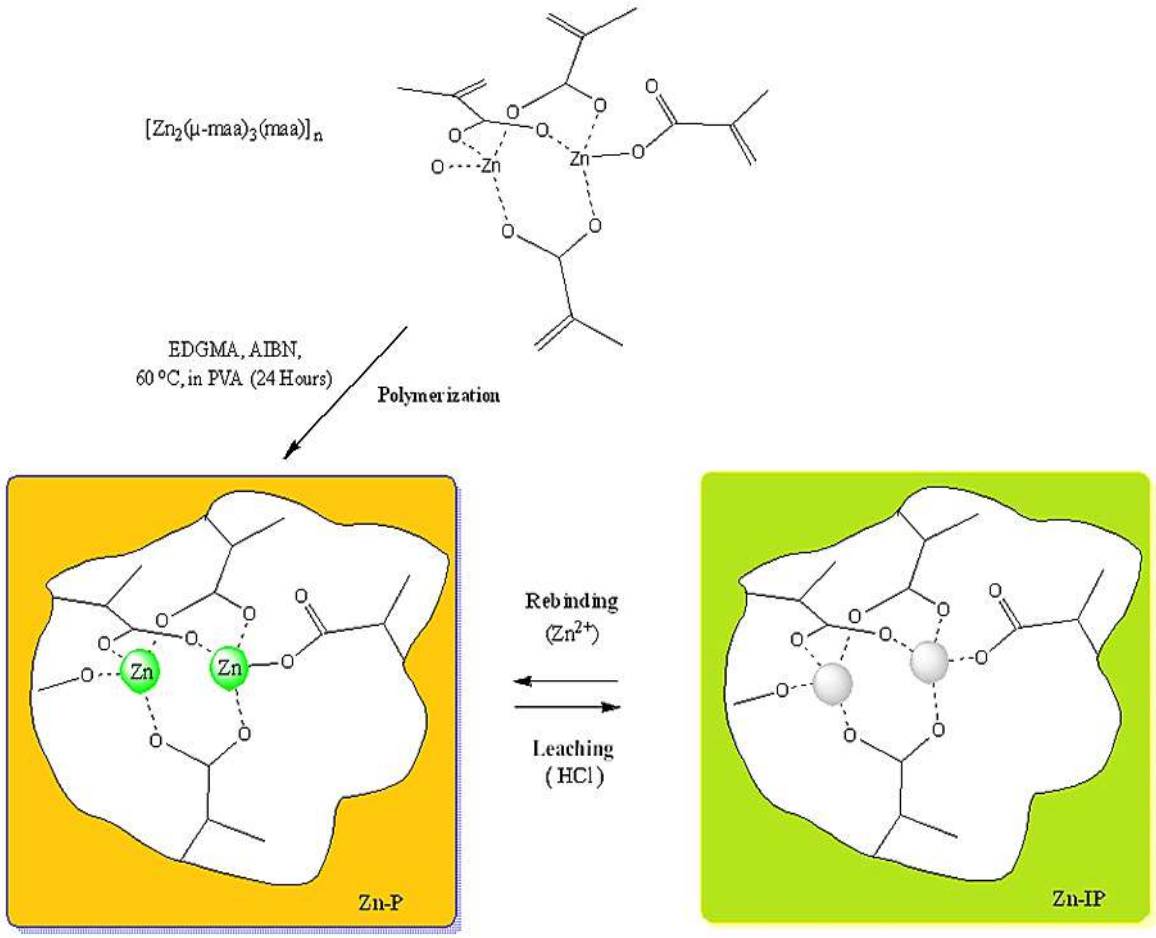

Figure 1. Schematic representation of the Zn(II)-imprinted polymer (Zn-IP) preparation process.

2.4. Preparation of the Zn^{2+}-selective sensor

The Zn^{2+}-selective PVC membrane sensor was prepared according to the procedures described in literature a work [2]. The preparation of the sensor has occurred in two steps. At the first step, a solid contacts mixture consisting of, epoxy and hardener was prepared in THF. A copper wire was dipped into this mixture a few times to obtain a coating and allowed to stand a day in room temperature. At the second step, ion selective membrane cocktail consisting of 4% (w/w) Zn-IP, 26% (w/w) PVC, 69% (w/w) plasticizer and 1% (w/w) KTpClPB was prepared in 2.5 mL THF. The surface of the solid contacts obtained at the first step was coated with this ion selective membrane dipping into the cocktail. The sensor was left to be dried at laboratory conditions a day. Later, the potentiometric performance characteristics of the sensor were investigated.

3. Results and Discussion

Characterization of IIPs is the important stage of their synthesis. For this purpose, characterization studies of the polymer particles were achieved by a number of techniques such as SEM, TGA and the obtained results are summarized below.

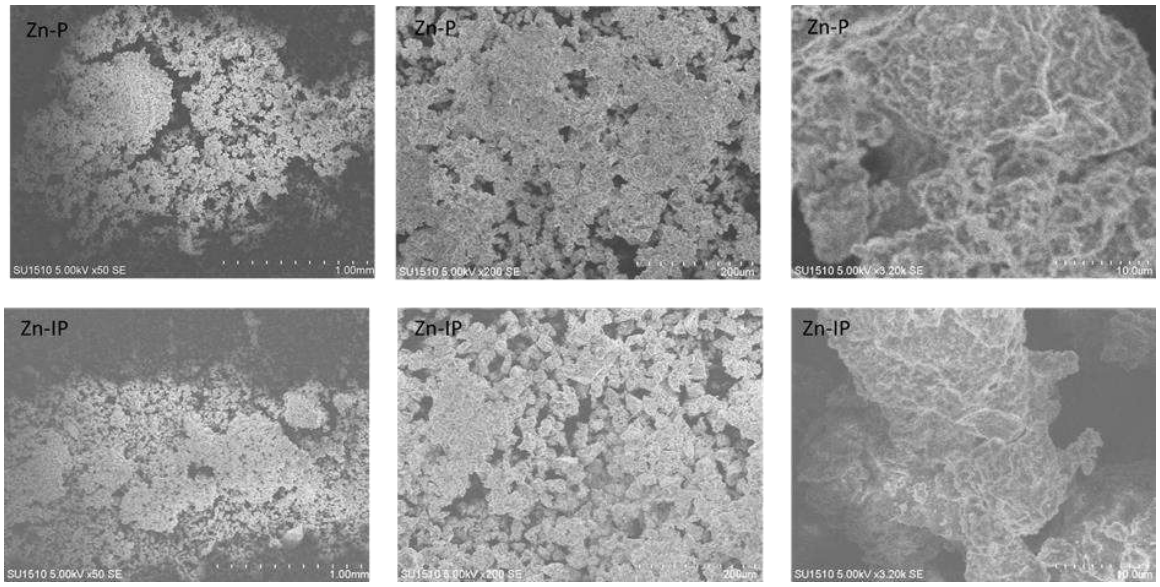

Figure 2. SEM images of the polymer particles (up: Zn(II) containing polymer (Zn-P), down: Zn(II)-imprinted polymer (Zn-IP)).

The surface morphologies of the Zn-P and Zn-IP were investigated by SEM, and the relevant SEM micrographs were depicted in Fig. 2. The Zn-P and Zn-IP particles are substantially small in size, and have taken on a dust form. Moreover, an enhanced surface area was observed from the SEM images of the Zn-IP than Zn-P. Consequently, from the potentiometric results; the relatively porous surfaces of the Zn-IP possess the suitable interaction sites and specific cavities for Zn^{2+} ions.

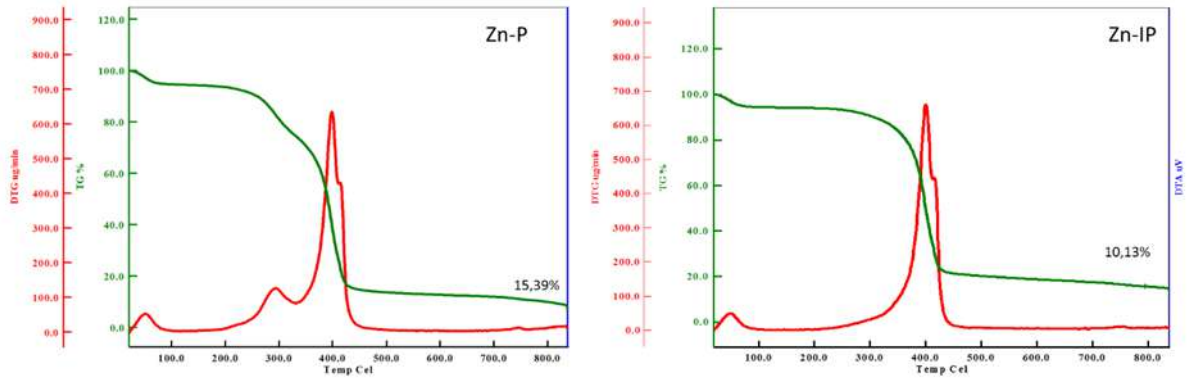

Figure 3. TGA curves of the polymers (left: Zn-P, right: Zn-IP).

Thermal behaviors of polymers before and after leaching were obtained by performing TGA at a heating rate of 10°C/min from 30 to 810°C. The TGA curves are shown in Fig. 3. Evidently, the Zn-P and Zn-IP showed different char yields of 15.39 % and 10.13%, respectively. Therefore, the char yield of Zn-P is much higher than that of Zn-IP, which clearly shows the removal of Zn(II) ions from the polymer.

Influences of the membrane composition are significantly affects potentiometric responses of the ion selective electrode. Therefore, the influnces to study the potentiometric response, the sensitivity of the Zn^{2+}-selective sensor on the potentiometric performances, the plasticizer (NPOE, DOS, DBP) and lipophilic additive (KTpClPB) were investigated, and the results summarized in Table 1. As shown in Table 1, the membrane prepared based on NPOE as optimum membrane exhibited better potentiometric performances in the ways of the linear range of 10^{-1}–10^{-5} mol/L and detection limit of $8.6x10^{-6}$ mol/L.

Table 1. Membrane compositions and potentiometric behaviors of Zn^{2+}-selective sensors.

No	Composition of Membrane (% w/w)						Potentiometric Behavior		
	PVC	NPOE	DOS	DBP	KTClPB	IIP	Slope (mV/decade)	Linear range (mol/L^{-1})	Detection limit (mol.L^{-1})
I	26	69	-	-	1	4	28.1	10^{-1}-10^{-5}	$6.86x10^{-6}$
II	26	-	69	-	1	4	27.4	10^{-1}-10^{-5}	$4.25x10^{-5}$
III	26	-	-	69	1	4	26.3	10^{-1}-10^{-4}	$7.72x10^{-5}$

The potentiometric response of the proposed sensor was monitored as a function of Zn^{2+} concentration in the range 10^{-7} to 10^{-1} mol/L. The potentiometric response and calibration graph of the sensor are shown in Fig. 4. and Fig. 5., respectively. As can be seen from Figures, the sensor membrane are shows a near-Nernstian behavior of a slope (28.1 mV/decade, R^2: 0.99) over a wide concentration range of 10^{-1}–10^{-5} mol/L and a lower detection limit of $6.86x10^{-6}$ mol/L.

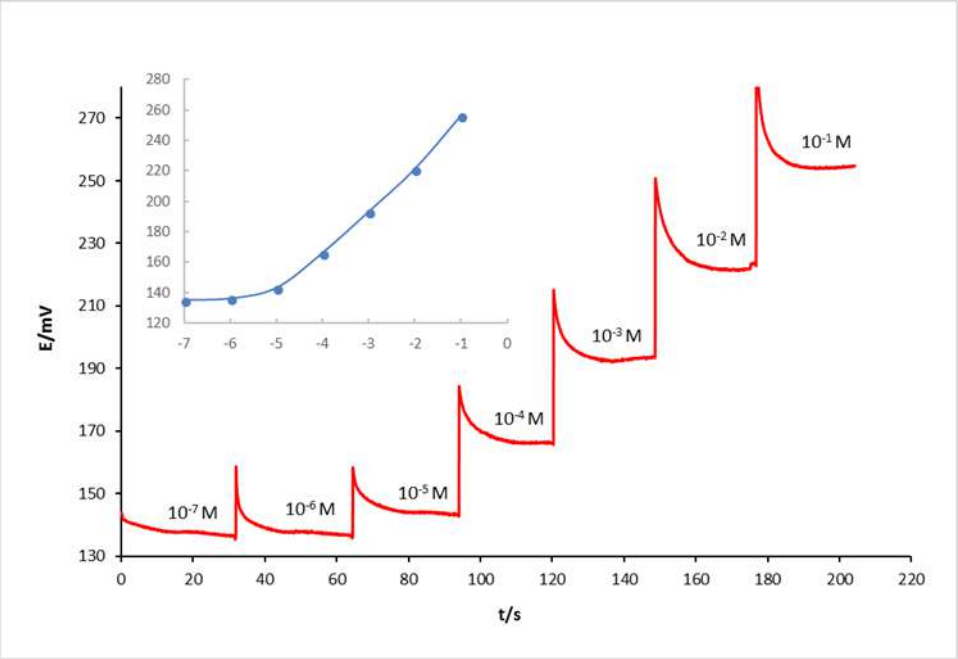

Figure 4. Dynamic potential response of the Zn^{2+}- selective sensor

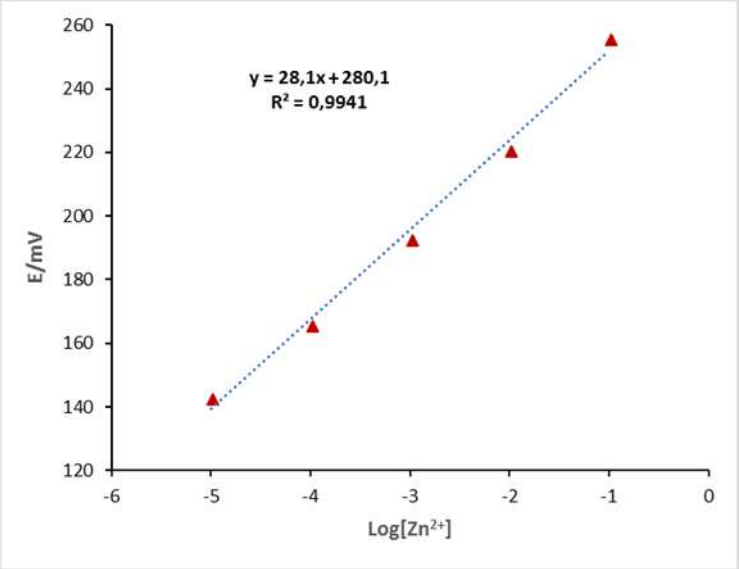

Figure 5. Calibration curve of the Zn^{2+}-selective sensor

Lifetime, working pH range and temperature range are important features that affect the performance of the ion selective sensors. In order to determine the lifetime of the Zn^{2+}-selective sensor, the potentiometric measurements were taken on certain days. The pH effect on the sensor response has been examined, optimum temperature range of the sensor determined, and the obtained results are shown in Table 2.

Table 2. Potentiometric performance characteristics of the prepared Zn^{2+}-selective sensor

Linear range, mol.L^{-1}	Slope(mV)	Response time, s	Detection limit, mol.L^{-1}	Lifetime, week	Working pH range	Temperature range, °C
10^{-1}-10^{-5}	28.1±2.4	10-15	6.86x10^{-6}	8-10	4-7	10-35

3.1. Analytical Applications

The proposed sensor was used as an indicator electrode in the potentiometric titration of 10 mL of 10^{-3} M $Zn(NO_3)_2$ with 10^{-3} M EDTA solution in order to display the applicability of the proposed Zn^{2+}-selective sensor in real life. A typical titration curve is shown in Fig. 6., which shows that the endpoint of the titration can be accurately determined using the Zn^{2+}-selective sensor.

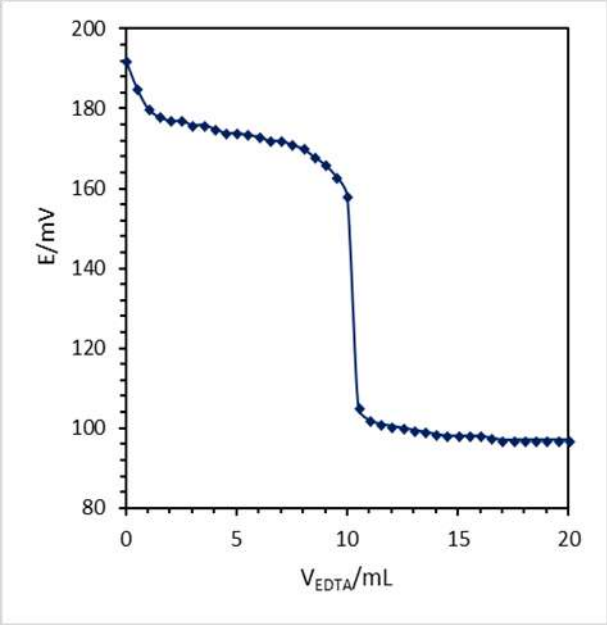

Figure 6. Potentiometric titration curve of 10^{-3} M Zn(II) with 10^{-3} M EDTA

The prepared Zn^{2+}-selective sensor was also applied to determine the Zn^{2+} contents of some water samples. In order to validate the potentiometric method, the AAS method was used as reference technique for evaluation of the accuracy, precision and reliability of the obtained results. The paired t-test was performed for the statistical analysis of data. The obtained results were compared with those measured by AAS, the relative error and the t value are summarized in Table 3. Therefore, it can be concluded that the method applying the proposed sensor is a satisfactory agreement in comparison with the AAS method.

Table 3. Comparative analysis results obtained from the proposed sensor and AAS for the determination of Zn^{2+} contents in real water samples (for N = 3 at the 95% confidence level).

Water type	Potentiometric method*	AAS*	E_{ra}**	t-test***
				1.140
River	0.014±0.002	0.013±0.001	3.586	
Spring	0.021±0.005	0.021±0.002	2.018	
Tap	0.025±0.003	0.024±0.001	2.544	
Waste	0.348±0.019	0.336±0.006	4.568	

*The average values of three determinations ± standard deviation.
**The relative error for the potentiometry versus AAS.
***Calculated t value is 1.140 by a paired t-test, the theoretical values of t is 3.182 (p = 0.05).

Acknowledgment

I would like to thank my advisor, Dr. Murat Yolcu, for her valuable support and guidance for conducting this research. I also would like to thank Dr. Zuhal Yolcu from Giresun University for supplying us with complex ($[Zn_2(\mu\text{-maa})_3(maa)]_n$) substances.

References

Isildak I, Covington A. K., Electroanal. (1993), 5, 815-824.

Isildak I., Yolcu M., Isildak O., Demirel N., Topal G., H. Hosgoren H., Microchim. Acta (2004), 144, 177-181.

Bojdi M. K., Behbahani M., Najafi M., Bagheri A., Omidi F., Salimi S., Electroanal. (2015), 27, 2458-2467.

Dong, Y., Ogawa, T., Lin, D., Koh, H. J., Kamiunten, H., Matsuo, M., & Cheng, S., (2006). Molecular mapping of quantitative trait loci for zinc toxicity tolerance in rice seedling (Oryza sativa L.), Field Crops Research. 95(2-3), 420-425.

Pohl, P., Sergiel, I., & Prusisz, B. (2011), Direct analysis of honey for the total content of Zn and its fractionation forms by means of flame atomic absorption spectrometry with solid phase extraction and ultrafiltration approaches, Food Chemistry. 125(4), 1504-1509.

Kaur, S., Walia, T. P. S., & Mahajan, R. K. (2008), Comparative studies of zinc, cadmium, lead and copper on economically viable adsorbents, Journal of Environmental Engineering and Science, 7(1), 83-90.

G. Vlatakis, L. I. Andersson, R. Muller, K. Mosbach, (1993), Drug assay using antibody mimics made by molecular imprinting, Nature. 361, 645-647.

K. Haupt, K. Mosbach, (2000), Molecularly imprinted polymers and their use in biomimetic sensors, Chem. Rev. 100, 2495-2504.

S. J. Li, W. K. Li, M. X. Zheng, J. M. Zhang, (2008), Rationally designing molecularly imprinted polymer toward a high specific recognition byusing a stoichiometric self-assembly, Polym. Plast. Technol. 47, 936-942.

P. Y. Chen, R. Vittal, P. C. Nien, G. S. Liou, K. C. Ho, (2010), A novel molecularly imprinted polymer thin film as biosensor for uric acid, Talanta. 80, 1145-1151.

H. R. Rajabi, M. Shamsipur, S. M. Pourmortazavi, (2013), Preparation of a novel potassium ion imprinted polymeric nanoparticles based on dicyclohexyl 18C6 for selective determination of K^+ ion in different water samples, Mat. Sci. Eng. C-Mater. 33, 3374-3381.

B. Godlewska-Zylkiewicz, E. Zambrzycka, B. Lesniewska, A. Z. Wilczewska, (2012), Separation of ruthenium from environmental samples on polymeric sorbent based on imprinted Ru(III)-allyl acetoacetate complex. Talanta. 89, 352-359.

S. Daniel, P. E. J. Babu, T. P. Rao, (2005), Preconcentrative separation of palladium(II) using palladium(II) ion-imprinted polymer particles formed with different quinoline derivatives and evaluation of binding parameters based on adsorption isotherm models, Talanta. 65, 441-452.

N. N. M. Yusof, T. Kobayashi, Y. Kikuchi, (2016), Ionic Imprinting Polymers Using Diallylaminomethyl-Calix[4] Resorcinarene Host for the Recognition of Pb (II) Ions, Polym. Polym. Compos. 24, 687-694.

F. F. He, H. Q. Wang, Y. Y. Wang, X. F. Wang, H. S. Zhang, H. L. Li, J. H. Tang, (2013), Magnetic Th(IV)-ion imprinted polymers with sa-lophen schiff base for separation and recognition of Th(IV), J. Radioanal. Nucl. Ch. 295, 167-177.

M. Moussa, V. Pichon, C. Mariet, T. Vercouter, N. Delaunay, (2016), Potential of ion imprinted polymers synthesized by trapping approach for selective solid phase extraction of lanthanides, Talanta. 161, 459-468.

Z. Yolcu, PhD Thesis, (2011). Synthesis of Cu(II) and Zn(II) complexes containing vinyl group and investigation of metal ion imprinting properties of their polymers Ondokuz Mayıs University, Institute of Science, Samsun, Turkey.

Characterization, Vibrational and NMR Spectroscopic Study of (Z)-N-(3,4-Dimethylisoxazol-5-Yl)-4-((2-Hydroxy-4 Methoxybenzylidene)Amino)Benzenesulfonamide Molecule

Cihan ŞEN [1], Saliha ALYAR [2*], Hamit ALYAR[3], Mustafa Tuğfan BİLKAN[4], Ümmühan ÖZMEN ÖZDEMİR[5]

[1] Çankırı Karatekin University, Faculty of Science, Department of Chemistry, Çankırı, Turkey; cihanfen212@gmail.com

[2] Çankırı Karatekin University, Faculty of Science, Department of Chemistry, Çankırı, Turkey; saliha@karatekin.edu.tr

[3] Çankırı Karatekin University, Faculty of Science, Department of Physics, Çankırı, Turkey; halyar@karatekin.edu.tr

[4] Çankırı Karatekin University, Faculty of Science, Department of Physics, Çankırı, Turkey; mtbilkan@karatekin.edu.tr

[5] Gazi University, Faculty of Science, Department of Chemistry, Ankara, Turkey; ummuhan@gazi.edu.tr

[*] **Corresponding Author:** saliha@karatekin.edu.tr

Abstract

In this work, the molecular structure of (Z)-N-(3,4-dimethylisoxazol-5-yl)-4-((2-hydroxy-4-methoxybenzylidene)amino)benzenesulfonamide was investigated by using Fourier transform infrared spectroscopy (FT-IR), 1H, 13C, NMR spectroscopies. The FT-IR, of compound was recorded at room-temperature and discussed assisted with B3LYP/6-311G(d,p) level of theory along with scaled quantum mechanics force field (SQM-FF) method. Furthermore, 1H and 13C NMR analyses were performed at B3LYP/6-311++G(d,p) theory level using gauge including atomic orbital (GIAO) method and compared with the experimental findings. Calculations were performed using the Gaussian 09 program with density function theory (DFT).

Keywords: DFT, FT-IR, NMR, SQM, Sulfonamides

1. Introduction

Sulfonamides were the first drugs found to act selectively and could be used systematically as preventive and therapeutic agents against various diseases (Mandell et al., 1996; Nogrady, 1988). Later on, many thousands of molecules containing the sulfanilamide structure have been created yielding formulations with greater effectiveness and less toxicity. Sulfa drugs are still widely used for conditions such as acne and urinary tract infections, and are receiving renewed interest for the treatment of infections caused by bacteria resistant to other antibiotics. Also, a number of other activities, some of which have been recently observed, include endotelin antagonism, anti-inflammatory activity, tubular transport inhibition, insulin release, carbonic anhydrase and saluretic actions (Wolff, 1996).

In the present study, vibrational band assignment of (Z)-N-(3,4-dimethylisoxazol-5-yl)-4-((2-hydroxy-4-methoxybenzylidene)amino)benzenesulfonamide were calculated using B3LYP/6-311++G(d,p) theory level. 1H and 13C NMR analyses were performed at B3LYP/6-311++G(d,p) theory level using gauge including atomic orbital (GIAO) method.

2. Experimental

Sulfisoxazole and 2-hydroxy-4-methoxybenzaldehyde were added to a 20 mL ethanol solution and stirred at room temperature for 15 minutes, then refluxed for 24 hours under reflux. The resulting yellow-orange precipitate was filtered and washed with ethanol. The product was dried and crystallized from ethanol.

Yield 72%; Melting point: 218-220 0C. Elemental analysis results for C19H19N3O5S (%): (Calcd.) C, 56.85; H, 4.77; N, 10.47; S, 7.99 (Found): C, 56.55; H, 4.70; N, 10.25; S, 7.80.

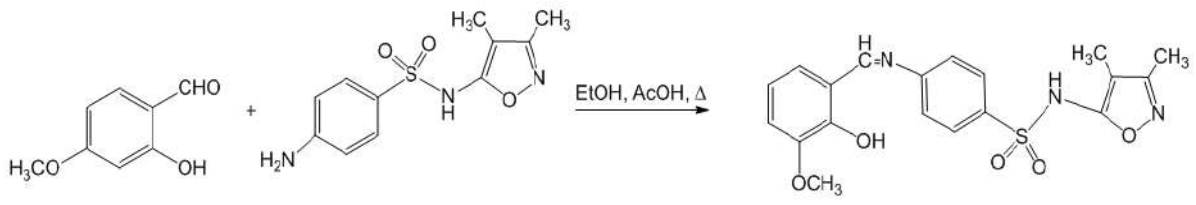

Figure 1.

3. Material and Method

The geometry of (Z)-N-(3,4-dimethylisoxazol-5-yl)-4-((2-hydroxy-4-methoxybenzylidene)amino)benzenesulfonamide was fully optimized without any constraint with the help of an analytical gradient procedure implemented within the Gaussian 09 program (Frish et al., 2009). All the parameters were allowed to relax and all the calculations converged to an optimized geometry which corresponds to a true energy minimum as revealed by the lack of imaginary values in the wave number calculations. The molecular geometry optimizations, vibrational frequency calculations, performed with the Gaussian 09 software package by using DFT/B3LYP approaches. Optimized molecular structure of studied compound given in Fig.1. The vibrational band assignments were performed at B3LYP/6-311++G (d,p) theory level combined with scaled quantum mechanics force field (SQMFF) methodology. Each vibrational modes of the studied compound were characterized by their potential energy distributions (PED) which were calculated by using SQM-FF program (SQM, 2013). HOMO-LUMO analysis, reactivity descriptors and nonlinear optical properties of (E)-1-(4-flourobenzylidene)urea studied with same level of theory. 1H and 13C NMR analyses were performed at B3LYP/6-311++G(d,p) theory level using gauge including atomic orbital (GIAO) method.

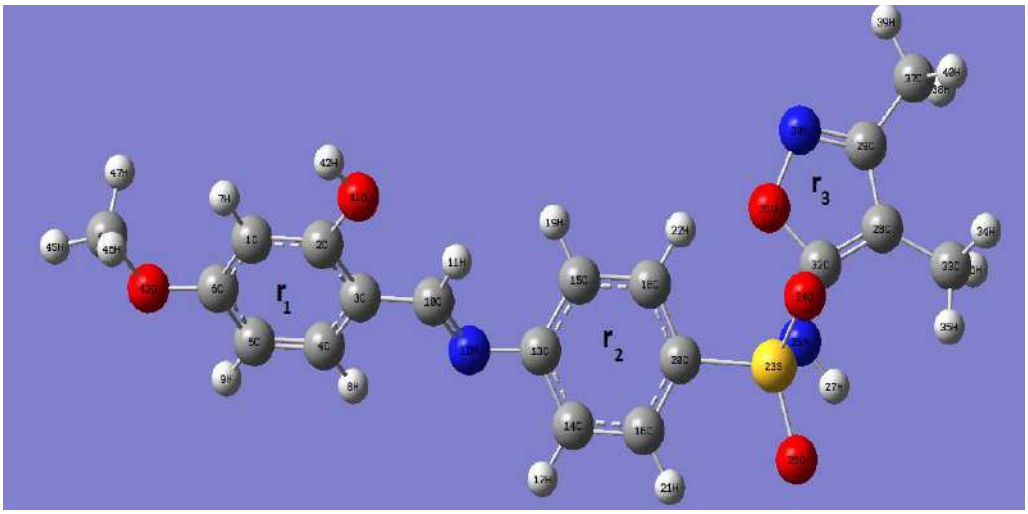

Figure 2. Molecular structure of (Z)-N-(3,4-dimethylisoxazol-5-yl)-4-((2-hydroxy-4-methoxybenzylidene)amino)benzenesulfonamide obtained by B3LYP/6-311++G(d,p) method

4. Results and Discussion

4.1 Vibrational Band Assignment

Vibrational frequencies and corresponding vibrational assignments of (Z)-N-(3,4-dimethylisoxazol-5-yl)-4-((2-hydroxy-4-methoxybenzylidene)amino)benzenesulfonamide have been investigated theoretically. DFT/B3LYP is provides acceptable vibrational wave numbers for organic molecules. Vibrational frequencies of (Z)-N-(3,4-dimethylisoxazol-5-yl)-4-((2-hydroxy-4-methoxybenzylidene)amino)benzenesulfonamide were calculated at the DFT levels with B3LYP (Becke-Lee-Yang-Parr three parameters) hybrid functional (Lee at al.,1988). The vibrational band assignments were performed at B3LYP/6-311++G(d,p) theory level combined with scaled quantum mechanics force field (SQMFF) methodology to compare the experimental and calculated vibrational frequencies of the title compounds. The vibrational modes were assigned on the basis of PED analysis using SQM program. The visual check for the vibrational band assignments were also performed by using Gauss-View program.

Table 1. Assignment of fundamental vibrations of (Z)-N-(3,4-dimethylisoxazol-5-yl)-4-((2-hydroxy-4-methoxybenzylidene)amino)benzenesulfonamide by normal mode analysis based on SQM force field calculations using selective scaled B3LYP/6-311++G(d,p)

Exp.			PED
FT-IR	UnscaledFreq.	ScaledFreq.	Description (%)
3705	3679	3591	υ (OH) (100)
3100	3510	3216	υ (NH) (100)
	3250	3112	υ_s $(CH)_{r1}$ (100)
	3249	3110	υ_s $(CH)_{r2}$ (91)
2985	3247/3232/3224	3108/3094/3086	υ_{as} $(CH)_{r2}$ (98)
	3234	3095	υ_{as} $(CH)_{r1}$ (100)
	3220	3087	υ (C1H) (99)
	3189/3112	3052/2978	υ $(CH_3)_{r1}$ (91)
	3158/3123/3098	3022/2989/2965	υ_{as} $(CH_3)_{r3}$ (84)
	3107	2974	υ (C10H) (100)
	3051/3037	2920/2907	υ_s $(CH_3)_{r3}$ (100)
	3038	2908	υ_s $(CH_3)_{r1}$ (85)
1614	1682	1667	υ (C10=N12) (55)
	1672/1636	1650/1616	υ $(CC)_{r1}$ (45)
	1650	1632	υ (C32N) (49) + υ (C32C28) (12)
	1626/1619/1456	1609/1602/1433	υ $(CC)_{r2}$ (65)
	1569/1501/1205	1542/1502/1175	γ $(CH_3)_{r1}$ (40)
	1543/1533/1530	1535/1524/1519	β $(CH)_{r3}$ (34)
	1542/1535	1534/1528	β $(CH_3)_{r1}$ (21)
	1537	1532	β $(CCH)_{r2}$ (85)
	1488	1477	υ (C29N)(37) + υ (C29C37)(22)
	1477	1456	υ $(CC)_{r1}$ (36) +γ $(CH_3)_{r1}$ (30)
	1476/1464	1450/1444	γ $(CH_3)_{r3}$ (51)
	1454	1426	υ $(CC)_{r3}$ (36) + υ (C32N)(37)
	1436	1412	υ $(CC)_{r1}$ (13) + β (CCH11) (15) + β (N12CH) (13)
	1403	1386	υ $(CC)_{r1}$ (73)

υ, streching; υ_s, symmetric stretching; υ_{as}, asymmetricstretching; β, in-planebending; γ, out of planebending

Exp.			PED
FT-IR	UnscaledFreq.	ScaledFreq.	Description (%)
	1371	1362	$\upsilon\ (CC)_{r2}$ (73)
	1356	1321	$\beta\ (CCH)_{r2}$ (45)
	1347	1320	$\beta\ (CCH)_{r1}$ (45)
	1341	1314	β (C32NH) (53)
1339	1340	1337	$\upsilon_{as}\ (SO_2)$ (42)
1255	1262	1249	υ (O C6) (41)
1151	1146	1130	$\upsilon_{s}\ (SO_2)$ (48)
968	975	956	υ (SN) (55) + υ (CS) (18)+ $\upsilon\ (CC)_{r2}$ (10)
829	835	827	υ (CS) (41) +$\gamma\ (CCC)_{t2}$ (25)

ν, stretching; νs, symmetric stretching; νas, asymmetricstretching; β, in-planebending; γ, out ofplanebending

In order to enable assignment of the observed peaks, we have analyzed the all vibrational frequencies and compared our calculated results of the investigated compound with their experimental ones. The experimental frequencies are listed together with calculated frequencies in Tables 1. The calculated values of vibrations show good agreement with the experimental results as seen in Table 1.

4.1.1. O-H Vibrations

In the OH region, very strong and broad band occur at 3600 – 3400 cm−1. Two OH stretching mode observed at 3705 cm^{-1} in the FT-IR spectrum for (Z)-N-(3,4-dimethylisoxazol-5-yl)-4-((2-hydroxy-4-methoxybenzylidene)amino)benzenesulfonamide. These band calculated at 3591cm^{-1}.

4.1.2. N-H Vibrations

The N-H stretching vibration of secondary amine groups of some aliphatic or aryl sulfonamides occurs in the region 3300–3200 cm^{-1}. The strong bands at 3100 cm-1 in the FT-IR spectrum assigned as the N-H stretching vibration. This band theoretically calculated at 3216 cm^{-1}.

4.1.3. C-H Vibrations

The aromatic C-H stretching vibrations were normally found between 3100 and 2900 cm-1. The bands observed at 2985 cm−1 in the FTIR spectrum were assigned to C-H stretching vibrations. These bands theoretically calculated at 3112-3095 cm-1.

4.1.4. C-N Vibrations

Silverstein et al. assigned C–N stretching absorption in the region 1342-1266 cm^{-1}. The spectra of benzene and benzoic acid substituted compounds show the band in the region 1260-1210 cm^{-1}. In analogy with the previous work, the band appears at 1242 cm^{-1} in FTIR spectrum and 1237 cm^{-1} in FT Raman spectrum of 5A2HBA are assigned to C–N stretching mode of vibration. Theoretically calculated at 1255cm^{-1}.

4.1.5. C-C Vibrations

The bands between 1650-1400 cm^{-1} in benzene derivatives were assigned to C-C stretching vibrations. In the present study, the frequencies observed in the FT-IR spectrum at 1581, 1493 and 1451 cm^{-1} have been assigned to C-C stretching vibrations. The same vibrations appear in the FT Raman spectrum at 1546, 1494 and 1448 cm^{-1}. The theoretically predicted frequencies at 1541, 1495 and 1450 cm^{-1} are in excellent agreement with experimental data.

4.2. NMR Spectra

The NMR spectrum (1H-13C) of the molecule was measured in DMSO. Theoretical NMR calculations were performed in the DMSO phase using the B3LYP / 6- 311G ++ (d, p) theory. The marking of ^{13}C was made using an equilibrium linear relationship proposed by Blanco et al. (Blanco et al., 2006). The equation suggested by Silva et al. was used to obtain the chemical shift values for ^{1}H (Silva et al., 2008).

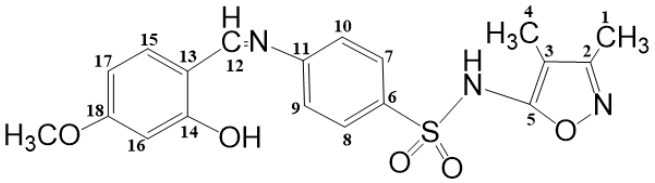

Fig.3.

Table 2. Experimental and calculated 13C NMR and 1H NMR chemical shifts (ppm) for (Z)-N-(3,4-dimethylisoxazol-5-yl)-4-((2-hydroxy-4-methoxybenzylidene)amino)benzenesulfonamide

Assignment	*Compound*	
	δ(exp.)	*δ(exp.)*
C1	10.76(CH3)	10.75
C2	166.04	166.41
C3	128.61	124.95
C4	6.35CH3)	6.34
C5	161.64	163.58
C6	156.70	156.71
C7	124.18	128.61
C8	129.13	129.13
C9	116.61	101.28
C10	124.94	122.52
C11	161.91	161.63
C12	192.40(CN=N)	191.58
C13	122.96	116.64
C14	150.91	134.87
C15	119.37	107.89
C16	148.42	104.75
C17	119.64	107.75
C18	118.04	132.69
C19	56.54(OCH3)	56.10
H1	2.07	2.07
H4	1.65	1.65
H3	-	-
OCH3	3.83	3.81
H7	7.15	7.33
H8	7.23	7.79
H9	7.43	7.52
H10	7.55	6.58
H12	8.97	8.90
H15	6.89	7.56
H16	-	6.46
H17	6.57	6.50
H18	7.80	-
NH	11.1	10.98
OH	12.5	13.64

^{1}H NMR spectrum of (Z)-N-(3,4-dimethylisoxazol-5-yl)-4-((2-hydroxy-4-methoxybenzylidene)amino)benzenesulfonamide; The protons H1, H4, H12 and OCH_3 were observed at 2.07 ppm, 1.65 ppm, 8.97 ppm and 3.83 ppm and calculated at 2.07 ppm, 1.65 ppm, 8.90 ppm and 3.81 ppm, respectively. The signal of the phenolic OH group observed at 12.50 ppm was calculated at 13.64 ppm. The signal of the N-H group observed at 11.10 ppm was calculated at 10.98 ppm. At the range of δ 6.57-7.80 ppm, the signals belong to the aromatic Ar-H protons.

In the ^{13}C NMR spectrum of (Z)-N-(3,4-dimethylisoxazol-5-yl)-4-((2-hydroxy-4-methoxybenzylidene)amino)benzenesulfonamide; The carbon signals C1, C4, C12 and OCH_3 were observed at 10.76 ppm, 6.35 ppm, 192.40 ppm and 56.54 ppm, respectively, and were calculated at 10.75 ppm, 6.34 ppm, 191.58 ppm and 56.10 ppm, respectively. δ in the 101.28-166.41 ppm region, the signals belong to aromatic Ar-C carbons.

References

Blanco, F., Alkorta, I., Elguero, J., (2007). Statistical analysis of 13C and 15N NMR chemical shifts from GIAO/B3LYP/6-311++G** calculated absolute shieldings. Magn. Reson. Chem. ,45,797-800.

Frisch, M. J. et al., Gaussian 09: Revision B.01 Gaussian Inc., Wallingford, CT, 2009.

Lee, C., Yang, W., and Parr, R. G., (1988). Development of the Colle-Salvetti correlation-energy formula into a functional of the electron density. Phys. Rev B., 37, 785-789.

Mandell, G.L., Petri, W.A., Hardman, J.G., Limbird, L.E., Molinoff, P.B., Ruddon, R.W., Gilman, A.G., (1996). Goodman's and Gilman's the Pharmacological Basis of Therapeutics., New York :McGraw-Hill.

Nogrady, T., (1988).Medicinal Chemistry, New York: Oxford University press.

Silva, A.M.S., Sousa, R.M.S., Jimeno, M.L., Blanco, F., Alkorta, I., Elguero, J., (2008). Experimental measurements and theoretical calculations of the chemical shifts and coupling constants of three azines (benzalazine, acetophenoneazine and cinnamaldazine). Magn. Reson. Chem. ,46, 859-864.

SQM version1.0, Scaled Quantum Mechanical, 2013 GreenAcres Road, Fayetteville, Arkansas 72703.

Wolff, M.E., (1996). Burger's Medicinal Chemistry and Drug Discovery.Laguna Beach: Wiley.

Synthesis of bioesters from waste sunflower oil biodiesel using a biocatalytic route

Bahar Gürkaya Kutluka, Togayhan Kutluk[1,2], *Nurcan Kapucu[1.2]

[1] Department of Chemical Engineering, Kocaeli University, 41380 Kocaeli, Turkey

[2] Alternative Fuels R&D Center, Kocaeli University, 41040 Kocaeli, Turkey

*** Corresponding Author:** bgurkaya@gmail.com

Abstract

Nowadays studies on the production of biolubricants have been increased. Biolubricant production can be carried out by enzyme and chemical catalysis. Enzyme catalyzed reactions are more environmentally friendly because they occur mild conditions than chemical catalyzed reactions. Enzyme catalyzed studies are limited. The amount of catalyst and mixing are important parameters for the cost of the reaction. Therefore in this study, effects of temperature (35-55 0C) and mixing rate (200-500 rpm) on enzymatic transesterification of waste sunflower oil (WSO) biodiesel (fatty acids methyl esters (FAMEs,)) and trimethylolpropane (TMP) were examined for the biolubricant production. Also two types of immobilized lipases (Thermomyces lanuginosus (TL) and Candida antarctica (CA)) were used in this reaction. Experiments were implemented that 50 ml conical flasks on magnetic stirrer with 1/3 TMP/FAME molar ratio, 5% TL or 1% CA lipase contents during 72h reaction time. According to experimental results clearly specified that 45 °C temperature and 500 rpm mixing rate are optimum conditions for both lipases. The maximum FAME conversions were obtained as 83% and 97% in the presence of TL and CA lipases, respectively.

Keywords: biolubricant, *Candida antarctica*, fame, lipase, *Thermomyces lanuginosus*, waste sunflower oil

1. Introduction

The protection of materials and energy is important for the operation of mechanical systems. The main reason for the power loss is the friction in these systems and can be reduced by lubrication. The lubricants function as friction inhibiting substances. Facilitates smooth functions, maintains reliable machine functions and reduces frequent malfunctions. Today, increasing global crude oil prices, global oil shortage, and global concern about environmental pollution have raised the concern about the development and use of environmentally friendly lubricants from alternative sources (Chowdhury et al 2013). Compared to mineral oils, their low toxicity and fast biodegradability as well as their low thermal properties make it very important to reduce loss from use. Although mineral oil based hydraulic fluids are still cost-effective, they are an oil-derived product, so prices have been rising over the years. Although the technical properties of biolubricants used as sources of vegetable oils are good enough to compete with mineral oils, their thermal stability and low temperature behavior are major disadvantages (Akerman ve diğ. 2011). They are also susceptible to hydrolysis and have a high tendency to oxidation. These disadvantages are disappears the substitution of glycerin with other polyol alcohols (especially TMP), the removal or replacement of polyunsaturated fatty acids, or the addition of additives (Schneider, 2006). The main reaction shows in figure 1. The transesterification method is widely used in the production of biodegradable products. In this method, the glycerol in the vegetable oil is replaced by another polyol alcohol such as trimethylolpropane, neopentyl glycol or pentaerythritol. The product obtained in this way is semisynthetic and has a biodegradable structure (Bremmer and Plonsker, 2008). Transesterification reactions can be carried out chemically or enzymatically. While sodium methylate is used as a chemical catalyst, different micrororganisms may be preferred as enzyme sources in liposomal reactions. According to many researches, the temperature is very high and the time is short in the reactions that take place by chemical catalysis. The lipase enters the reaction with catalysts at lower temperatures for longer periods of time. In addition, fatty acids or fatty acid methyl esters may be used instead of oils. (Salimon et al., 2010). By using waste oils as a raw material in the production of biolubricants, it is possible to reduce both environmental problems and production costs. Our country has about 950 thousand tons of liquid, 550 thousand tons of margarine, 200 thousand tons of feed, paint and soap industry needs, including 1.7 million tons of vegetable oil consumption. It is estimated that about 350 thousand tons of vegetable waste oil is produced as a result of the oil consumption obtained by the oil refining process (Kutluk, 2013). Waste sunflower oils (WSO) can be considered as

alternative raw materials for this purpose with properties such as cheap, environmental pollution reduction, conversion to a high added value product, etc. The studies that carried out with environmentally friendly enzymatic processes used biodegradable waste oils as raw materials in the production ofbiolubricant , are limited. In a study that carried out acid catalyzed fatty acid methyl ester production from the waste frying oil., the produced methyl esters isolated from the medium were continuously fed to the medium at vacuum pressure, and the content of TMP fatty acid triester products was up to 87.5% using base catalyzed (KOH) high temperature transesterification, and after the purification steps 99.6% pure TMP triester was obtained (Wang et al., 2014). Biolubricant production with rapeseed fatty acid methyl esters and 1-hexadecane in iso-octane solvent medium was investigated with waxy liposomes (*Mucor miehei*), and the equilibrium conversion increased from 90% to 83% when the byproduct methanol was allowed to leave the medium (Hallberg et al., 1999). Another study examining the production of palm oil esters by transesterification in the presence of liposomal RM IM catalyst in a palm oil and oleyl alcohol solvent environment resulted in an ester content of 80%. Properties such as ester density, refractive index, surface tension, iodine value, acid value, saponification value are also measured according to ASTM standards (Keng et al., 2009). In this study, the biolubricant production was investigated with the transesterification of WSO biodiesel and TMP using enzyme catalysts, the effect of temperature and mixing rate were examined on the production.

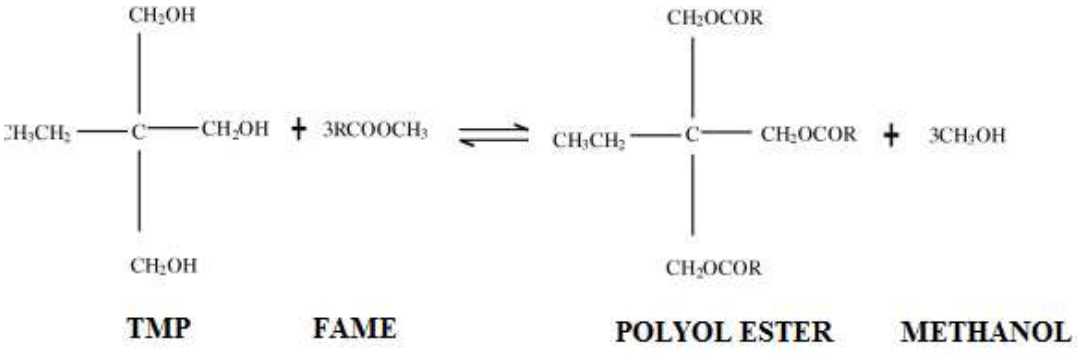

Figure 1. Esterification reaction between FAME and TMP

,

2. Material and Method

2.1. Materials

WSO was collected from local restaurants in Kocaeli/TURKEY. TL and CA as a gift from NovoNordisk. All other chemical which were used in experiments were purchased from Merck and Sigma-Aldrich.

2.2. WSO's Fame production and analysis

Transesterification reaction was kept according to our previous studies (Kutluk 2013). Fame content was determined by an Agilent 7820 GC analysis system equipped with a flame ionization detector (FID) and a 30m x 320µm x 0.25µm capillary column (CARBOWAX 20M). The system was calibrated using the internal standard methyl heptadecanoate according to EN 14103. FAME conversion was determined to the following equation:

$$\text{FAME conversion (\%)} = \frac{(\sum A) - AEI}{AEI} \text{x} \frac{CEI \text{x} VEI}{m} \text{x} 100 \quad (1)$$

∑AI=total peak area from the $C_{14:0}$ to $C_{24:1}$

AEI = total peak area of the methylheptadeconoate

CEI = concentration, in mg/mL of methylheptadeconoate solution

VEI= volume,in mL, of methylheptadeconoate solution

M=massi in mgi of the sample

2.3. Bioester production

Transesterification reactions were implemented that 50 ml open flasks on magnetic stirrer with FAME/TMP molar ratio 3/1, 72 h reaction time and lipase content 1% and 5% for CA and TL, respectively. The effect of temperature (35-45 °C) and mixing rate (200-500 rpm) were examined on the production.

3. Results and Discussion

3. Results

3.1. Effect of reaction temperature on transesterification

Enzymes are sensitive to temperature changes affecting proteins due to their protein structure. The increase in the rate of reaction is directly proportional to temperature. But above an optimum point it starts falling and stops completely. The effect of temperature on the transesterification reaction of FAME with TMP in the presence of TL and CA and are shown in figure 2 and figüre 3 respectively.Results are clearly shows that 45°C is optimum temperature for both lipases and the highest FAME conversions (83% and 98%) were achieved at this temperature. Above the temperature lipases were degredate because of their protein structures.

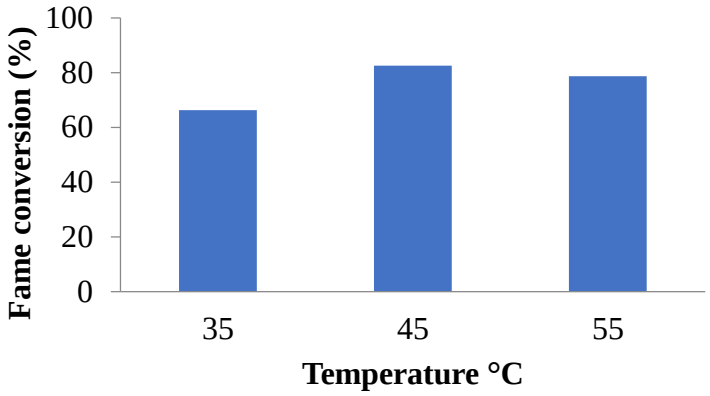

Figure 2. Effect of temperature on transesterification reaction in the presence of TL

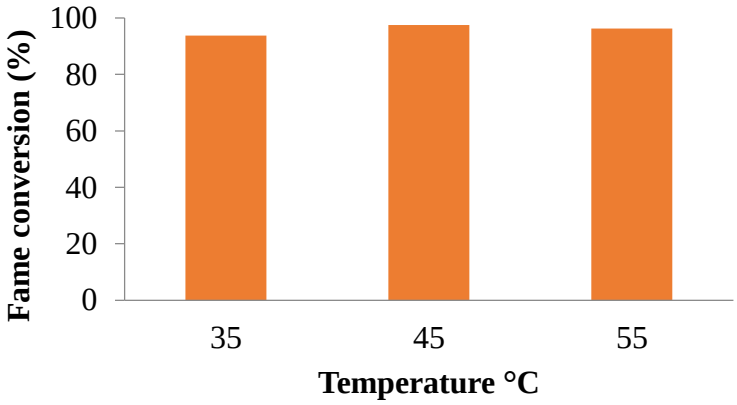

Figure 3. Effect of temperature on transesterification reaction in the presence of CA

3.2. Effect of mixing rate on transesterification

It is also a problem of confusion that the immobilized lipase at low mixing speeds cannot be homogeneously dispersed in the liquid phase, or at high speed is directed upward from the container walls and sticking and sticking out of the liquid phase. The effect of mixing rate on the transesterification reaction of FAME with TMP in the presence of TL and CA and are shown in figure 4.and figüre 5, respectively. Mixing speeds below 400 rpm are insufficient to attain the inter-phase mass transfer constraints according to the results obtained for the esterification reaction. It appears that this barrier has been exceeded at 500 rpm for TL. On the other hand, no significant effect on the reaction for all mixing speeds studied in the precense of CA. The highest FAME conversions (83% and 98%) were achieved at 500 rpm with TL and CA, respectively.

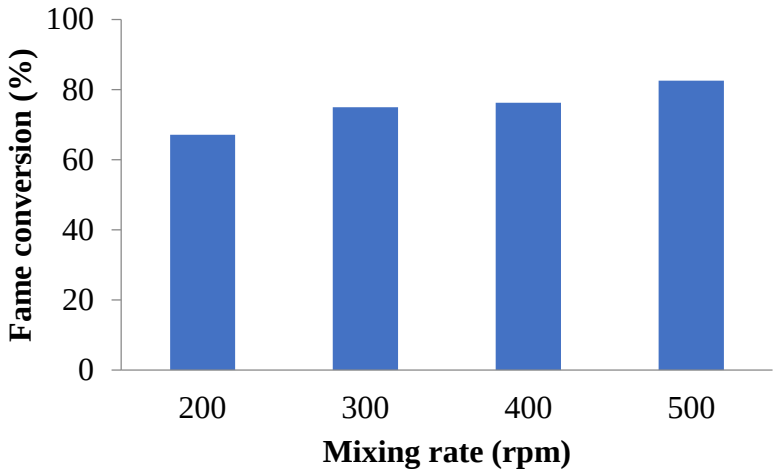

Figure 4. Effect of mixing rate on transesterification reaction in the presence of TL

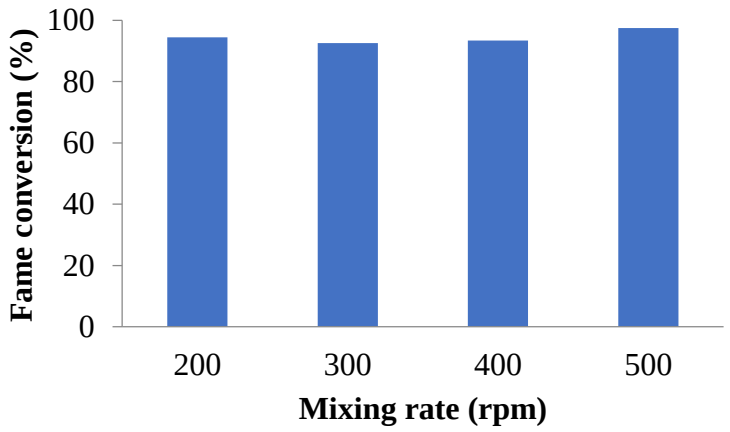

Figure 5. Effect of mixing rate on transesterification reaction in the presence of CA

4. Conclusion

This study emphasize that TMP esters synthesized from waste sunflower oil biodiesel using a biocatalytic route environmentally friendly process. Conformance that the experimental studies the maximum FAME conversions 83% and 97% and were obtained in the presence of TL and CA lipases, respectively. More work has to be done to optimize the process conditions. Our investigations are still going on.

Acknowledgement

We thank to Novo Nordisk for presenting Lipozyme TL IM (TL) and Novozyme 435 (CA). This study was granted by The Scientific and Technological Research Council of Turkey (TUBITAK) (Project No. 217M525)

References

Åkerman C. O., Hagström A. E. V., Mollaahmad M. A., Karlsson S., Hatti-Kaul R.,(2011). Biolubricant synthesis using immobilised lipase: Process optimisation of trimethylolpropane oleate production, Process Biochemistry, 46, 2225–2231.

Bremmer, B. J., Plonsker, L.,(2008). Bio-Based Lubricants-A Market Opportunity Study Update. 1st ed., United Soybean Board, Omni Tech International, USA

Chowdhury A., Mitra D., Biswas D., (2013). " Synthesis of Biolubricant Components from Waste Cooking Oil Using a Biocatalytic Route", Wiley Online Library, DOI 10.1002/ep.11866.

Hallberg M. L., Wang D., Härröd M. (1999). Enzymatic Synthesis of Wax Esters from Rapeseed Fatty Acid Methyl Esters and a Fatty Alcohol, Journal Of The Amerıcan Oıl Chemısts Socıety, Vol 2, 182-187.

Keng P.S. Basri M. , Zakariaa M.R.S., Abdul Rahman M.B., Ariff A.B. , Abdul Rahman R.N.Z., Sallehd A.B. (2009). Newly synthesized palm esters for cosmetics Industry Industrial Crops And Products 29, 37–44.

Kutluk T.,(2013). Bitkisel Atık Yağlardan Tutuklanmış Lipaz Katalizli Biyodizel Üretimi, Yüksek Lisans Tezi, Kocaeli Üniversitesi, Fen Bilimleri Enstitüsü, Kocaeli.

Salimon J., Salih N., Yousif E.,(2010). Review Article-Biolubricants: Raw materials, chemical modifications and environmental benefits, European Journal of Lipid Science Technology, 112, 519–530.

Schneider, M. P.,(2006). Plant-oil-based lubricants and hydraulic fluids. Journal of Science and Food Agricultural, 86, 1769–1780.

Wang E., Ma X., Tang Z., Yan R., Wang Y., Riley W. W., Reaney M. J. T., (2014). Synthesis and oxidative stability of trimethylolpropane fatty acid triester as a biolubricant base oil from waste cooking oil, Biomass and bioenergy

Assessment of water quality of Kop Stream (Çoruh Basin) by using heavy metal pollution index

Özlem TUNÇ DEDE [1*], Melike SEZER [2], Volkan OSKAY[3]

[1] University, Faculty, Department, City, Country; e-mail 1Giresun University, Environmental Engineering Department, Giresun, Turkey; ozlem@tuncdede.com

[2] State Hydraulic Works (DSI) Regional Directorate of Trabzon, Department of Quality Control and Laboratory, Trabzon, Turkey; melikesezer@dsi.gov.tr

[3] State Hydraulic Works (DSI) Regional Directorate of Trabzon, Department of Quality Control and Laboratory, Trabzon, Turkey; cmosvolki@gmail.com

[*] **Corresponding Author:** ozlem@tuncdede.com

Abstract

Water quality is important for public health and aquatic life. Technological developments and increase in human population are the main factors effecting the quality of water resources. Among the water pollutants, the heavy metals can accumulate in the environment and may cause toxic and harmful effects in aquatic life and also human life. Thus, proper assessment of water quality is inevitable for well-management of water resources and sustainability. Heavy metal pollution index (HPI) method can be used for the effective assessment of water quality according to heavy metal contents. This method is based on assigning a rating or weightage (Wi) values for each parameter which shows the composite influence of each element on the overall water quality. The rating value is between 0 and 1 and it reflects the importance of individual quality considerations. In this study, the water quality of Kop Stream, which is the main stream in Çoruh Basin, was investigated with respect to heavy metal contamination. Water were collected for one-year period in 2017 and 21 trace metals were analyzed. The concentrations of the elements were evaluated according to Surface Water Quality Regulation, Turkey. While most of the samples were under the average annual values given in the standard; especially iron and aluminum exceed the limit values at some points. All data obtained were used to calculate the heavy metal pollution index value.

Keywords: Heavy metal, index, Kop stream, trace metal, water quality.

1. Introduction

Water quality is an important health issue due to limited resources of freshwater in the world. The growth of population, urban expansion and technological improvements effect the water quality. Various kinds of pollutants can enter water through different ways. Among these pollutants, heavy metals are one of the major contaminants due to their non-degradable properties. They are toxic, can accumulate human body and effects the nervous system. They have also harmful effects in aquatic life. Thus, proper assessment of the water quality according to heavy metal pollution is very important (Dede, 2016, Reza and Singh, 2010; Prasad and Bose, 2001).

Water Quality Index (WQI) can be calculated via quick and simple methodology and shown as a single number. It can describe the overall quality of water bodies. By using WQI, water quality can be express in a comprehensible manner: «very good, good, poor». Method of heavy metal pollution index (HPI) assigns a weightage (Wi) for individual heavy metal parameter which shows the composite influence of each heavy metal on the overall water quality (Equation 1). (Dede, 2016, Reza and Singh, 2010; Prasad and Bose, 2001).

$$HPI = \sum_{i=1}^{n} Q_i W_i / \sum_{i=1}^{n} W_i \qquad (1)$$

where;

Qi: sub-indices
Wi: unit weightage
n: number of parameters

Unit weightage (W_i) can be calculated by taking inverse of standard limit values (S_i). Its value changes between 0 and 1. Sub-indices (Qi) can be calculated by using equation 2:

$$Q_i = \sum_{i=1}^{n} \frac{\{M_i(-)I_i\}}{S_i - I_i} * 100 \qquad (2)$$

where; Mi is the monitored value, I_i is the ideal value in µg/L and n is number of parameters. In this study, the ideal values, I_i, was assumed as zero for all element. In general, the value of critical pollution index is taken as 100.

2. Material and Method

This study covers the investigation of heavy metal pollution in Kop Stream (Bayburt, Turkey). Kop Stream is located in Bayburt, Çoruh Basin (Figure 1). Kop Stream is generally used for human consumption and irrigation purposes. It is open to pollution due to human activities, agricultural activities (pesticides and fertilizers) and mining activities (URL-1).

Figure 1. Kop Stream, Bayburt, Turkey (Google Maps).

Water samples were collected from Kop Stream at one station every month over the period from February 2017 to July 2017. The samples were collected in 1 L plastic bottles and preserved by adding 1 mL of 1:1 diluted nitric acid. Bottles were sealed tightly and transported to the DSI Water Analysis Laboratory. All procedures were followed in accordance with "Standard Methods 1060 Collection and Preservation of Samples" (Eaton and Clescen, 2005). Heavy metal analyses were carried out according to the EPA 200.8 method by using ICP-MS (Inductively Coupled Plasma-Mass Spectrometry) (EPA, 1994).

3. Results and Discussion

Analysis of 15 parameters (Pb, Zn, Cr, Mn, Fe, Cu, Co, Ni, Al, As, B, Ti, V, Ba and Sn) were done during experimental period and the minimum, maximum values and standard deviation of analysis results were listed in Table 1.

Table 1. The minimum and maximum values of parameters analyzed for Kop Stream sample, corresponding maximum values given in Turkish Surface Water Quality Regulation (URL-2**)**

Parameters	Limit Values (µg/L)	Min Value (µg/L)	Max Value (µg/L)	Annual Average Value (µg/L)	Standard Deviation
Lead (Pb)	14	0,63	4,25	1,65	1,33
Zinc (Zn)	231	8,64	95,23	57,08	41,61
Chromium (Cr)	142	2,08	12,21	5,73	3,48
Manganese (Mn)	500	2,07	50,18	26,25	20,56
Iron (Fe)	101	16,66	939,31	308,53	373,42
Copper (Cu)	3,1	1,4	11,76	8,51	4,79
Cobalt (Co)	2,6	1,02	3,15	1,96	1,09
Nickel (Ni)	34	0,43	40,23	12,13	14,48
Aluminum (Al)	27	5,49	574,63	248,92	246,62
Arsenic (As)	53	0,71	2,38	1,55	1,18
Bor (B)	1472	0,13	332,37	127,71	137,94
Titanium (Ti)	42	1,1	25,86	9,26	11,22
Vanadium (V)	97	1,19	3,48	2,25	0,99
Barium (Ba	680	1,72	122,94	73,04	43,38
Tin (Sn)	13	1,45	7,33	4,42	2,94

The results were evaluated according to the maximum values given in Turkish Surface Water Quality Regulation (Table 1). It was determined that 3 parameters (Fe, Cu and Al) exceeded the limit values given in the Turkish regulation. Iron and aluminum are among the most abundant elements in Earth's crust. Exposure to high amounts of these elements may cause health problems in human.

Heavy metal pollution index (HPI) were calculated by using the mean concentrations. All calculated index and unit weightage values were listed in Table 2. The index values were found above critical pollution level, 100, which means the station is polluted with heavy metals. The results showed that HPI model gave reasonable results in comparison to individual results.

Table 2. HPI values for KOP Stream

Parameters	Mean concentration value (Mi) (µg/L)	Standard limit value (Si) (µg/L)	Unit weightage (Wi)	Sub-index (Qi)	Wi*Qi	HPI
Lead (Pb)	1,65	14	0,0714	11,79	0,84	
Zinc (Zn)	57,08	231	0,0043	24,71	0,11	
Chromium (Cr)	5,73	142	0,0070	4,04	0,03	
Manganese (Mn)	26,25	500	0,0020	5,25	0,01	
Iron (Fe)	308,53	101	0,0099	305,48	3,02	
Copper (Cu)	8,51	3,1	0,3226	274,52	88,55	
Cobalt (Co)	1,96	2,6	0,3846	75,38	28,99	
Nickel (Ni)	12,13	34	0,0294	35,68	1,05	160
Aluminum (Al)	248,92	27	0,0370	921,93	34,15	
Arsenic (As)	1,54	53	0,0189	2,91	0,05	
Bor (B)	127,71	1472	0,0007	8,68	0,01	
Titanium (Ti)	9,25	42	0,0238	22,02	0,52	
Vanadium (V)	2,25	97	0,0103	2,32	0,02	
Barium (Ba	73,04	680	0,0015	10,74	0,02	
Tin (Sn)	4,42	13	0,0769	34,00	2,62	

References

Dede, O.T., (2016), Application of the Heavy Metal Pollution Index for Surface Waters: A Case Study for Çamlıdere. Hacettepe J. Biol. & Chem., 44 (4), 499-504.

Eaton, A. D. and Clescen, L. S.,(2005), Standart Methods for the Examination of Water and Waste Water (STMD), American Public Health Association (APHA), USA.

EPA 200.8., 1994, Determination of Trace Elements in Waters and Wastes by Inductively Coupled Plasma-Mass Spectrometry [PDF document]. Retrieved from Online Web site: https://www.epa.gov/sites/production/files/2015-08/documents/method_200-8_rev_5-4_1994.pdf

Reza R. and Singh, G. (2010), Heavy metal contamination and its indexing approach for river water. Int. J. Environ. Sci. Tech., 7 (4), 785-792.

Prasad, B. and Bose, J.M., (2001), Evaluation of the heavy metal pollution index for surface and spring water near a limestone mining area of the lower Himalayas. Environmental Geology, 41, 183-188.

URL-1: Çevre ve Şehircilik İl Müdürlüğü, Bayburt İli 2016 Yılı Çevre Durum Raporu [PDF document]. Retrieved from Online Web site: http://webdosya.csb.gov.tr/db/ced/editordosya/Bayburt_icdr2016.pdf

URL-2: Yerüstü Su Kalitesi Yönetmeliği, 2012, Resmi Gazete:30.11.2012-Sayı:29797 [Online document]. Retrieved from Online Web site: http://www.mevzuat.gov.tr/Metin.Aspx?MevzuatKod=7.5.16806&MevzuatIliski=0&sourceXmlSearch=

Electrocatalytic Oxidation of Formic Acid on Pt Nanoparticles Supported on Conducting Polymer Nanocomposite

Ayşe Nur YILMAZ*, Mutlu SÖNMEZ ÇELEBİ

Ordu University, Faculty of Science and Arts, Department of Chemistry, 52200, Ordu, Turkey.

* **Corresponding Author:** ayse61nur61@hotmail.com

Abstract

Preparation and characterization of a Pt-based catalyst supported on poly(vinylferrocenium)-poly(pyyrole) conducting polymer composite (Pt@PVF-PPy) was described for electrocatalytic oxidation of formic acid. Pt precursor was aqueous solution of K_2PtCl_4 and electrochemical and chemical reduction methods were compared for optimum catalyst performance. Other experimental parameters such as polymer film thickness and Pt loading were also optimized with respect to the formic acid oxidation peak current values.

Keywords: Conducting Polymers, Poly(vinylferrocene), Poly(pyrrole), Formic Acid Electrooxidation.

1. Introduction

In today's world, polymers are irreplaceable materials in the fields of science and technology. Their unique features such as light weight, high stability and mechanical resistance make them useful for improvement of advanced technological systems (Chen et al., 2017). Conducting polymers which are also referred to as "synthetic metals" have the unique advantage of carrying both metal-like and polymer-like properties such as conductivity, magnetism, flexibility, processability and low toxicity. Among these polymers, polypyyrole (PPy), polyaniline (PANI) and polythiophene (PTh) and their derivatives are widely investigated (Çelebi and Yılmaz, 2018).

PPy, which can very easily be deposited on any electrode material via electrochemical deposition has many attractive properties such as high conductivity, excellent redox activity, easy processability, good thermal and electrochemical stability, low toxicity, etc. Poly(vinylferrocenium) (PVF) is a redox type conducting polymer which is preferred as a mediator in many catalytic reactions (Akgül et al., 2012; Çelebi et al., 2008; Erden et al., 2015). Electrode surfaces can simply be modified with a PVF film via physical or electrochemical methods such as dip coating, droplet evaporation, oxidative deposition or cyclic voltammetric deposition.

Fuel cells, which produce electrical energy with relatively low emissions are considered as one of the most promising alternative power sources to the traditional systems (Çelebi 2016; Antolini, 2009). Polymer based support materials are widely used in low-temperature fuel cells in order to improve their electrocatalytical performance, durability and efficiency. Due to their unique properties such as gas and water permeability and proton and electron conductivity, conducting polymers are regarded as ideal catalyst supports. However, further development is still required for commercialization (Sharma and Pollet, 2012). Recently, conducting polymers have been widely used as catalyst supports for metal nanoparticles (Yin et al., 2017; Bai et al., 2015; Sapurina et al., 2016).

Combining redox polymers, with a conjugated conducting polymer overcomes limitations associated with the relatively low conductivity of the redox polymer compared to its conjugated analogue. For example, replacing PVF or PPy with a PVF/PPy hybrid improves the electronic conductivity of the PVF film while eliminating insufficient exposure of PPy to the electrolyte due to relatively low porosity (Tian et al., 2015).

Herein, we describe utilization of PVF-PPy composite as support material for facile synthesis of Pt@PVF-PPy catalyst for electrooxidation of formic acid. Influence of

experimental conditions on the performance of the catalyst system was studied via cyclic voltammetry of formic acid solution in acidic medium. The prepared catalyst was also compared with Pt@PVF catalyst which was previously developed for formic acid electrooxidation (Çelebi and Pekmez, 2017).

2. Materials and Methods

Electrochemical experiments were recorded with CHI 600E electrochemical workstation. A three electrode system glass cell was used with a platinum disc electrode (Pt, 2 mm in diameter) as the working electrode. Silver/silver chloride (Ag/AgCl) and saturated calomel electrodes (SCE) were used as reference electrodes in methylene chloride and aqueous media respectively. A platinum (Pt) wire was used as the counter electrode.

3. Results and Discussion

The preparation route of the Pt@PVF-PPy catalyst was comprised of three facile stages: (i) electrochemical formation of PVF-PPy composite film on the electrode surface, (ii) loading $PtCl_4^{-2}$ complex ions to the polymer composite matrix via cyclic voltammetry, (iii) chemical or electrochemical reduction of the $PtCl_4^{-2}$ complex. The experimental preparation conditions were optimized by recording the cyclic voltammograms (CVs) of 0.5 M HCOOH solution containing 0.5 M H_2SO_4 and comparing the formic acid oxidation peak current values.

Electrochemical formation of PVF-PPy composite film on the electrode surface was carried out by cyclic voltammetry from a solution containing 20 mM pyyrole (Py) monomer, 2.0 mg/mL PVF polymer and 100 mM TBAP (Figure 1a). Blank voltammogram of the resulting film in 0.5 M H_2SO_4 clearly indicates the existence of PVF (oxidation at 0.45 V and reduction at 0.29 V vs. SCE) and PPy (oxidation at 1.0 V vs. SCE) (Figure 1b).

(a) 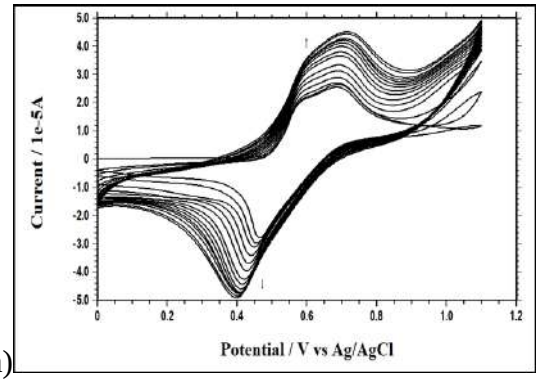

(b) 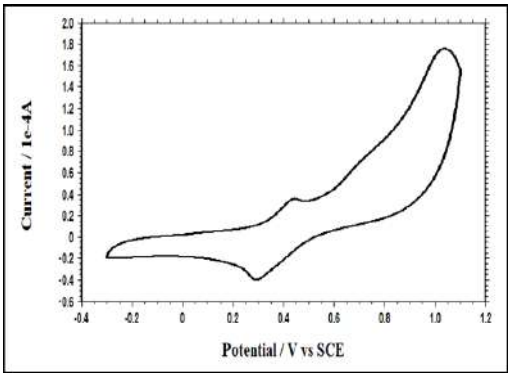

Figure 1. (a) Growth of PVF-PPy composite film by cyclic voltammetry from a solution containing 20 mM Py, 2.0 mg/mL PVF and 100 mM TBAP; (b) CV of PVF-PPy film recorded in 0.5 M H_2SO_4. Scan rate: 100 mV s^{-1}

3.1. Influence of thickness of polymer composite film

Polymer film thickness was controlled by the number of cycles during the deposition of the polymer composite film. In order to investigate the influence of the polymer film thickness, Pt@PVF-PPy catalyst was prepared using polymer composites with different thicknesses and the performance of the catalysts were compared. Figure 2 presents influence of polymer composite film thickness on the oxidation peak current values of formic acid. As clearly seen from the figure, a thin PVF-PPy composite film prepared using 15 cyclic voltammetric cycles is optimal.

(a) 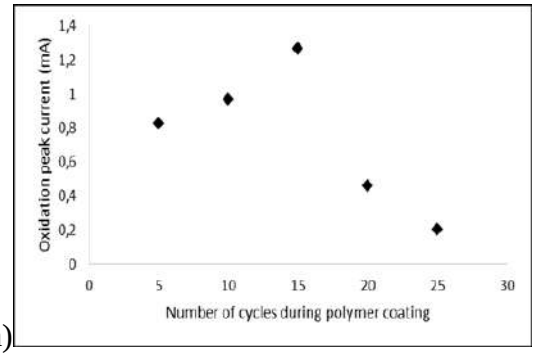

(b) 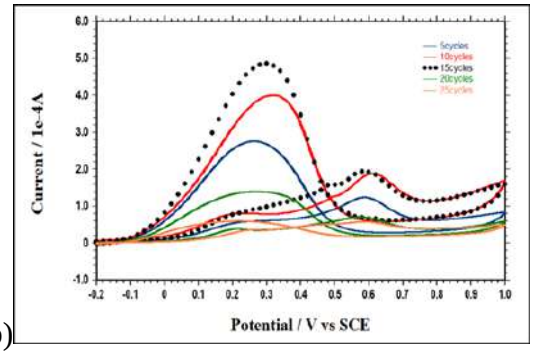

Figure 2. (a) Influence of polymer composite film thickness on the oxidation peak current values of formic acid; (b) Corresponding CVs recorded in 0.5 M HCOOH+0.5 M H_2SO_4. Scan rate: 50 mV s^{-1}

3.2. Influence of amount of $PtCl_4^{2-}$ complex immobilized into the polymer composite

Amount of the Pt complex immobilized into the polymer composite film was definitely the most important parameter influencing the performance of the Pt@PVF-PPy catalyst system.

In order to optimize the amount of Pt in the catalyst, CVs of formic acid solution were recorded with catalyst systems prepared using various amounts of the $PtCl_4^{2-}$ complex. The amount of Pt was controlled by number of cycles during cyclic voltammetric deposition of the complex from 2.0 mM K_2PtCl_4 solution and comparison of the oxidation peak current values of formic acid for various Pt loadings revealed an optimal cycle number of 80 during cyclic voltammetry.

3.3. Comparison of electrochemical and chemical methods for the reduction of $PtCl_4^{2-}$ complex

Electrochemical and chemical reduction methods were both studied and compared for the reduction of $PtCl_4^{2-}$ complex immobilized into the polymer composite film. Electrochemical reduction was performed by constant potential electrolysis method in 0.5 M H_2SO_4 solution. Influence of both reduction potential and reduction time on the oxidation peak current of formic acid were studied and the optimum conditions were determined as -0.3 V (vs. SCE) for electrolysis potential and 5 min for electrolysis time.

Hydrazine was used as the reducing agent for the chemical reduction of the Pt complex and the reduction was carried out by simply holding the $PtCl_4^{2-}$ incorporated PVF-PPy composite film in stirred 0.1 M hydrazinium hydrate solution. The optimum reduction time for chemical reduction process were found as 30 min. When the performance of the two reduction methods was compared towards electrooxidation of formic acid, chemical reduction was chosen as the preferred reduction method by means of oxidation peak current (Figure 3).

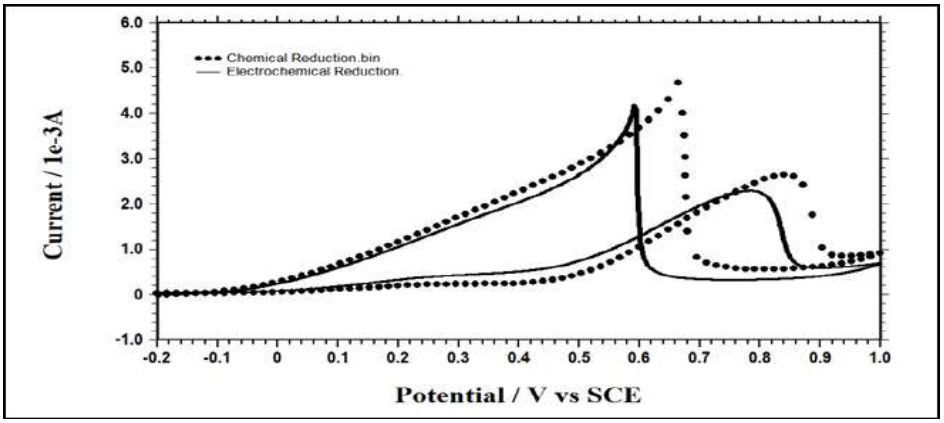

Figure 3. CVs of 0.5 M HCOOH + 0.5 M H_2SO_4 solution recorded with Pt@PVF-PPy catalyst prepared by chemical (•••) and electrochemical (—) reduction methods. Scan rate: 50 mV s^{-1}

3.4. Performance of the Pt@PVF-PPy catalyst prepared under optimum conditions

Figure 4 presents CV of 0.5 M HCOOH solution recorded with the Pt@PVF-PPy catalyst prepared under optimum conditions.

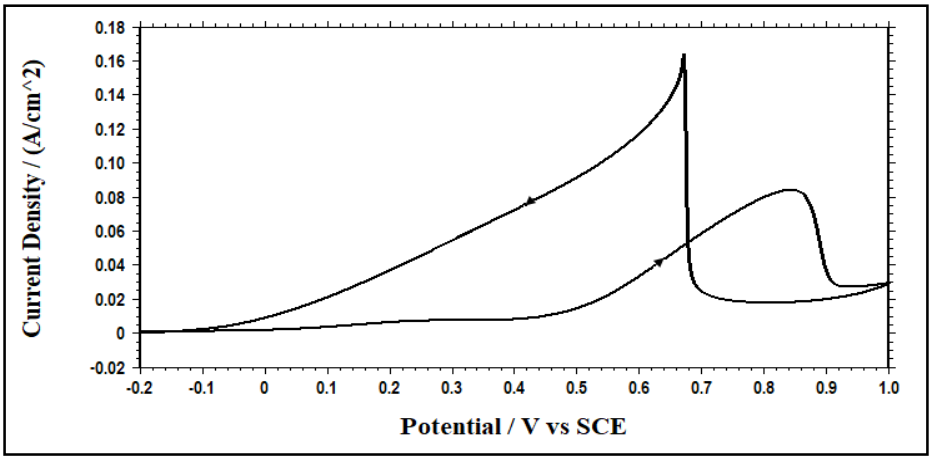

Figure 5. CV of 0.5 M HCOOH + 0.5 M H_2SO_4 solution recorded with Pt@PVF-PPy catalyst prepared under optimum conditions. Scan rate: 50 mV s^{-1}

As a conclusion, facile synthesis of a Pt based electrocatalyst was described using PVF-PPy conducting polymer composite as the support material. Three simple steps were followed during the preparation route: electrodeposition of the polymer composite film onto the electrode material, incorporation of Pt complexes into the polymer matrix via cyclic voltammetric scans in K2PtCl4 solution, and reduction of Pt complexes. Optimum experimental conditions were determined according to the performance of the catalyst towards electrochemi-cal oxidation of formic acid.

Acknowledgement

This work was supported by the Scientific Research Projects Coordination Department of Ordu University (ODUBAP) with grant number: TF-1616.

References

Akgül E., Gülce A. and Gülce H. (2012). Electrocatalytic oxidation of methanol on poly(vinylferrocene) modified Pt electrode. J. Electroanal. Chem., 668, 73-82.

Antolini E. (2009). Carbon supports for low-temperature fuel cell catalysts. Appl. Catal. B Environ., 88, 1-24.

Bai Z., Zhang Q., Lv J., Chao S., Yang L. and Qiao J. (2015). A Facile Preparation of Palladium Catalysts Supported on Hollow Polypyrrole Nanospheres for Ethanol Oxidation. Electrochim. Acta. 177, 107-112.

Chen W., Weimin H., Li D., Chen S. and Dai Z. (2017). The Preparation Approaches of Polymer/graphene Nanocomposites and their Appilcation Research Progress as Electrochemical Sensors. J New Mat. Elect. Sys., 221, 205-221.

Çelebi M.S. and Yılmaz A.N. (2018). PVF-PPy Composite as Support Material for Facile Synthesis of Pt@PVF-PPy Catalyst and Its Electrocatalytic Activity Towards Formic Acid Oxidation. J New Mat. Elect. Sys., 221, 157-162.

Çelebi M.S., Pekmez K., Özyörük H. and Yıldız A. (2008). Preparation and physical/electrochemical characterization of Pt/poly(vinylferrocenium) electrocatalyst for methanol oxidation. J. Power Sources, 183, 8-13.

Çelebi M.S. in Advanced Electrode Materials, Edited by A. Tiwari, F. Kuralay, and L. Uzun, Wiley-VCH, Weinheim, p. 397 (2016).

Çelebi M.S. and Pekmez K. (2017) Electrooxidation of Formic Acid Using Pt Nanoparticles Supported on Conducting Poly(Vinylferrocene) Polymer Support. Hacettepe J. Biol. & Chem., 45, 351-358.

Erden P.E., Kaçar C., Öztürk F. and Kılıç E. (2015). Amperometric uric acid biosensor based on poly(vinylferrocene)-gelatin-carboxylated multiwalled carbon nanotube modified glassy carbon electrode. Talanta. 134, 488-495.

Sapurina I., Stejskal J., Šedenková I., Trchová M., Kovárová J., Hromádková J., Kopecká J., Cieslar M., El-Nasr A.A. and Ayad M.M. (2016). Catalytic activity of polypyrrole nanotubes decorated with noble-metal nanoparticles and their conversion to carbonized analogues. Synth. Met., 214, 14-22.

Sharma S. and Pollet B.G. (2012). Support materials for PEMFC and DMFC electrocatalysts - A review. J. Power Sources, 208, 96-119.

Tian W., Mao X., Brown P., Rutledge G.C. and Hatton T.A. (2015). Electrochemically Nanostructured Polyvinylferrocene/Polypyrrole Hybrids with Synergy for Energy Storage. Adv. Funct. Mater., 25, 4803-4813.

Yin F., Wang D., Zhang Z., Zhang C. and Zhang Y. (2017). Synthesis of mesoporous hollow polypyrrole spheres and the utilization as supports of high loading of Pt nanoparticles. Mater. Lett., 207, 225-229.

$[Mn(CO)_3(bpy)L]PF_6$ Type New CO-Releasing Molecules with Benzimidazole Derivative Ligands

Elvan ÜSTÜN[1*], Mutlu SÖNMEZ ÇELEBİ[2], Songül KIRLAK[3]

[1]Ordu University, Faculty of Arts and Science, Department of Chemistry, Ordu, Turkey; elvanustun@odu.edu.tr
[2]Ordu University, Faculty of Arts and Science, Department of Chemistry, Ordu, Turkey; mutlucelebi@odu.edu.tr
[3]Ordu University, Faculty of Arts and Science Department of Chemistry,Ordu,Turkey; songulkirlak@hotmail.com

[*] **Corresponding Author:** elvanustun@odu.edu.tr

Abstract

Carbon monoxide (CO) which is known as “silent killer” due to its poisoning and toxic effects, converts hemoglobin (Hb) to carboxyhemoglobin (COHb) and hinders the oxygen-carrying capacity of Hb. In fact, CO is naturally produced in living organisms by the action of heme oxygenase enzymes, which catalyze the degradation of heme and generate CO, biliverdin and ferrous iron. Endogenous increment of the CO amount in a tissue shows beneficial effects in numerous pathophysiological situations. Therefore, exogenous CO supplement is being accepted as an effective therapeutic way. Safe transmission of appropriate amount of CO to the tissue is crucial. Therefore, CO-releasing molecules (CORMs) became a reliable way out and metal carbonyl complexes are among the most promising candidates for this mission. Here, insights into bioactivity of CO, administration and detection of releasing properties of CO-releasing molecules are reviewed.

Keywords: CO-Releasing Molecules, Manganese Complexes, Metal Carbonyls, CORMs

1. Introduction

Paracelsus, who is known as the father of modern pharmacology, says, “Poison is in everything, and no thing is without poison. The dosage makes it either a poison or a remedy.” The recent studies about carbon monoxide (CO) confirms Paracelsus’s idea. CO, which is odorless, tasteless and colorless, known as a toxic gas. CO binds to hemoglobin to form carboxyhemoglobin with an affinity 240 times higher than that of oxygen and hinders oxygen transport to the organs/tissues (Tavares et al., 2012). This is the primary reason of the toxicity of CO. On the other hand, CO is one of the three byproducts of the degradation of heme by enzyme heme oxygenase (Figure 1) and the levels of carboxyhemoglobin of up to 10% are asymptomatic (Romão et al., 2012). On the contrary, CO is locally produced in the tissue of the disease sites (Alberto and Motterlini, 2007). This production of CO in healing processes is the basic approach for the usage of CO as a new gasotransmitter (Wu and Wang, 2005). Although the role of CO in therapeutic applications has not been entirely elucidated, it could be related to the activity of heme oxygenase enzyme (Dulak et al., 2008; Sawle et al., 2005). CO has been shown anti-apoptotic (Parfenova et al., 2006), anti-inflammatory (Otterbein et al., 2000) and vasodilator (Foresti et al., 2004) effects and many papers about the investigations in anticancer (Üstün et al., 2017), antioxidant (Üstün et al., 2016), antibacterial (McLean et al., 2013) etc. activities of CO have been published.

Temporally and spatially transportation of CO to tissue with controllable quantity is the main problem of this issue. It is necessary to use a carrier for release CO in a controlled manner, because of the toxicity of CO inhalation. The molecules that are capable of delivering exogenous CO to tissue in a controlled fashion are define as CO-releasing molecules (CORMs) (Motterlini et al., 2002). Metal carbonyl complexes have been suggested to be good candidates as CORMs even if many organic molecules like oxalates and carboxylates have been tested (Wang et al., 2014). Many metal carbonyl complexes have recently synthesized and analyzed for this aim.

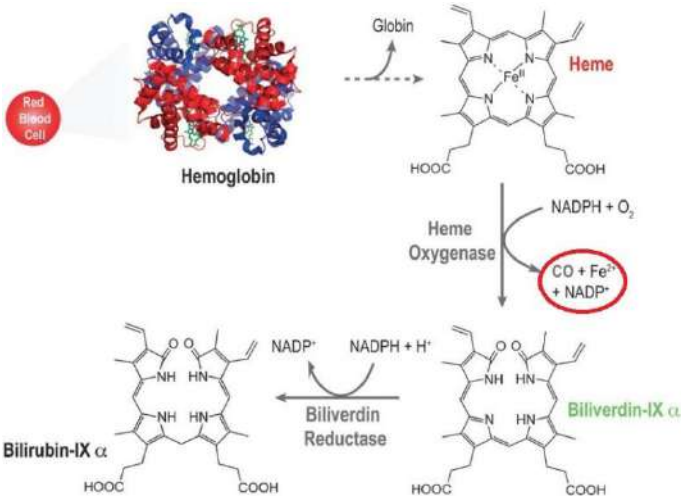

Figure 1. Hemoglobin degradation process

CO can be released from CORM through a ligand exchange reaction (Dördelmann et al., 2011), enzyme-triggering reaction (Botov et al., 2013), and an activatable redox (Jimenez et al., 2015). In order to achieve CO-releasing from these kind of reactions, the CORMs have to exposed a chemical pushing effect like pH, temperature in tissue. However, light sensitivity of metal carbonyl complexes can be an alternative way for providing CO-releasing. Photoactive CORMs that are stable in dark but can release CO by illumination with UV or visible light with certain wavelength have defined as photoCORMs (Schatzschneider, 2010). On the other hand, new papers that included polymeric and nano material carriers for transport and deposit CO have published recently (Bohlender et al., 2014).

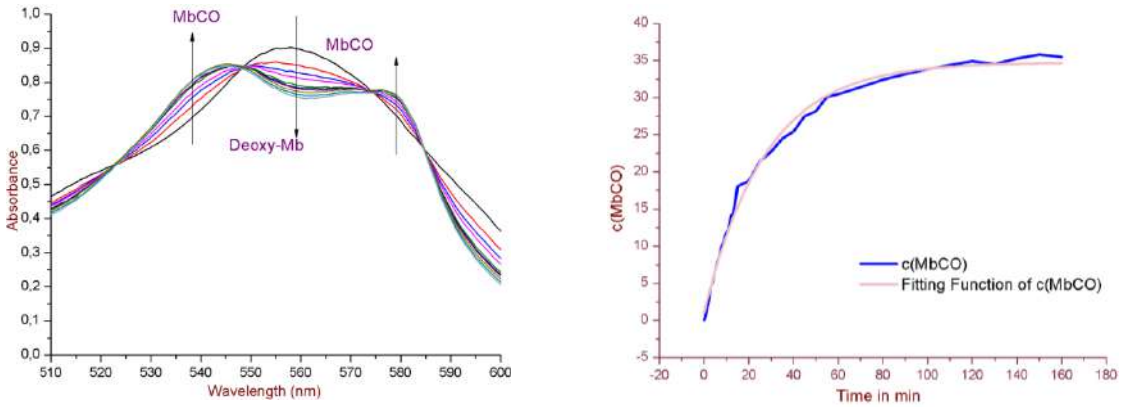

Figure 2. a) Change of absorption of myoglobin with the irradiation at 366 nm UV light for a solution of CORM in PBS (pH = 7.4) in the presence of myoglobin and sodium dithionite under Argon

atmosphere as monitored by UV/Vis spectroscopy. **b)** Change of carboxymyoglobin concentration in myoglobin-assay procedure and drawn fitting function

The CO-releasing could be detected by myoglobin-assay (Gonzalez et al., 2011). The amount of released CO have assessed by measuring of the conversion of deoxy-myoglobin to carboxymyoglobin (Figure 2). After commercial myoglobin converts to deoxy-myoglobin with excess $Na_2S_2O_4$, carboxymyoglobin occurs with interaction of deoxy-myoglobin and CORMs. The molar absorbance of deoxy-myoglobin reads at 540 nm, while carboxymyoglobin has two strong absorbance at 540 nm and 577 nm, and this absorbance dependence makes CO-releasing measurable and detectable.

2. Results and Discussion

The researches on CO as a new therapeutic agent have continued with an increasing attention since the beginning of 2000s. Recent studies are generally about synthesis/characterization of the best CO-releasing molecule, analyzing the bioactivities of new complexes, improving new methods for safe CO transfer and enlightening the mechanism of action of CO/CORMs in body.

$[Mn(CO)_3(bpy)L]PF_6$ type complexes were characterized by ^1H NMR, ^{13}C NMR, IR and LCMS. The absorbance maxima and molar extinction coefficients of complexes were determined in dimethylsulfoxide. One broad band was observed for complexes 370s nm with low intensity

For confirming the dark stability and the light sensitivity of complexes, the absorbance at the selected wavelength both in myoglobin solution (510 nm: isobestic point; 540 nm and 577 nm: MbCO maxima, 557 nm: deoxy-Mb maxima) and in DMSO was measured for 16 h and the absorbance of the complex molecule was measured for a reliable period with UV exposure. CO-releasing properties of the complexes were identified by myoglobin-assay. Total released CO, CO equivalents, the percentage released CO and half-life ($t_{1/2}$) were determined with UV-Visible Spectrophotometer at 1 min intervals. The $t_{1/2}$ in this study is defined as the time taken for compounds to release 50% of the total CO ligand present per molecule.

The CO-releasing properties of the CORMs should be discussed in two parts: i) totally released CO and ii) half-life of releasing. Either instant CO concentration or sustainable CO-releasing might become important in possible therapeutic applications. The location and the number of substituted groups can change the CO-releasing properties. The half-life results are

compatible with conjugation capacities of substituted groups. Ortho- and para-substituted groups in promote to electron flow which strengthen the Mn-CO back-bonding and induce to augmentation of half-life.

Acknowledgement

Support of Ordu University Scientific Project Coordination Department (ODUBAP, Project No: HD-1601) is gratefully acknowledged.

References

Alberto, R., Motterlini, R., (2007). Chemistry and biological activities of CO-releasing molecules (CORMs) and transition metal complexes. Dalton Trans., 1651-1660.

Bohlender, C., Gläser, S., Klein, M., Weisser, J., Thein, S., Neugebauer, U., Popp, J., Wyrwa, R., Schiller, A., (2014). Light-triggered CO release from nanoporous non-wovens. J Mater Chem B, 2, 1454-1463.

Botov, S., Stamellou, E., Guttentag, M., Alberto, R., Neudörfl, J.M., Yard, B., Schmalz, H.G., (2013). Synthesis and Performance of Acyloxy-diene-Fe$(CO)_3$ Complexes with Variable Chain Lengths as Enzyme-Triggered Carbon Monoxide- Releasing Molecules. Organometallics, 2, 3587-3594.

Dördelmann, G., Pfeiffer, H., Birkner, A., Schatzschneider, U., (2011). Silicium dioxide nanoparticles as carriers for photoactivatable CO-releasing molecules (PhotoCORMs). Inorg Chem, 50, 4362-4367.

Dulak, J., Deshane, J., Jozkowicz, A., Agarwal, A., (2008). Heme oxygenase-1 and carbon monoxide in vascular pathobiology: Focus on angiogenesis. Circulation, 117, 231-241.

Foresti, R., Hammad, J., Clark, J.E., Johnson, T.R., Mann, B.E., Friebe, A., Green, C.J., Motterlini, R., (2004). Vasoactive properties of CORM-3, a novel water-soluble carbon monoxide-releasing molecule. Br J Pharmacol, 142, 453-460.

Gonzalez, M.A., Fry, N.L., Burt, R., Davda, R., Hobbs, A., Mascharak, P.K., (2011). Designed iron carbonyls as carbon monoxide (CO) releasing molecules: Rapid CO release and delivery to myoglobin in aqueous buffer, and vasorelaxation of mouse aorta. Inorg Chem, 50, 3127-3134.

Jimenez, J., Chakraborty, I., Mascharak, P.K., (2015). Synthesis and Assessment of CO-Release Capacity of Manganese Carbonyl Complexes Derived from Rigid-Diimine Ligands of Varied Complexity. Eur J Inorg Chem, 30, 5021-5026.

McLean, S., Begg, R., Jesse, H.E., Mann, B.E., Sanguinetti, G., Poole, R.K., (2013). Analysis of the bacterial response to Ru$(CO)_3$Cl(Glycinate) (CORM-3) and the inactivated compound identifies

the role played by the ruthenium compound and reveals sulfur-containing species as a major target of CORM-3 action. Antioxid Redox Signal., 19, 1999-2012.

Motterlini, R., Clark, J.E., Foresti, R., Sarathchandra, P., Mann, B.E., Green, C.J., (2002). Carbon monoxide-releasing molecules: characterization of biochemical and vascular activities. Circ Res, 90, E17-E24.

Otterbein, L.E., Bach, F.H., Alam, J., Soares, M., Lu, H.T., Wysk, M., Davis, R.J., Flavell, R.A., Choi, A.M.K., (2000). Carbon monoxide has anti-inflammatory effects involving the mitogen-activated protein kinase pathway. Nat Med, 6, 422-428.

Parfenova, H., Basuroy, S., Bhattacharya, S., Tcheranova, D., Qu, Y., Regan, R.F., Laffler, C.W., (2006). Glutamate induces oxidative stress and apoptosis in cerebral vascular endothelial cells: contributions of HO-1 and HO-2 to cytoprotection. Am J Physiol Cell Physiol, 290, C1399-C1410.

Romão, C.C., Blättler, W.A., Seixas, J.D., Bernardes, G.J.L., (2012). Developing drug molecules for therapy with carbon monoxide. Chem Soc Rev., 41, 3571.

Sawle, P., Foresti, R., Mann, B.E., Johnson, T.R., Green, C.J., Motterlini, R., (2005). Carbon monoxide-releasing molecules (CO-RMs) attenuate the inflammatory response elicited by lipopolysaccharide in RAW264.7 murine macrophages. Br J Pharmacol, 145, 800-810.

Schatzschneider, U., (2010). Photoactivated biological activity of transition-metal complexes. Eur J Inorg Chem, 1451-1467.

Tavares, A.F.N., Nobre, L.S., Saraiva, L.M., (2012). A role for reactive oxygen species in the antibacterial properties of carbon monoxide-releasing molecules. FEMS Microbiol Lett., 336, 1-10.

Üstün, E., Çol Ayvaz, M., Sönmez Çelebi, M., Aşci, G., Demir, S., Özdemir, I., (2016). Structure, CO-releasing property, electrochemistry, DFT calculation, and antioxidant activity of benzimidazole derivative substituted $[Mn(CO)_3(bpy)L]PF_6$ type novel manganese complexes. Inorganica Chim Acta, 450, 182-189.

Üstün, E., Özgür, A., Coşkun, K.A., Demir Düşünceli, S., Özdemir, İ., Tutar, Y., (2017). Anticancer activities of manganese-based photoactivatable CO-releasing complexes (PhotoCORMs) with benzimidazole derivative ligands. Transit Met Chem., 42, 331-337.

Wang, D., Viennois, E., Ji, K., Damera, K., Draganov, A., Zheng, Y., Dai, C., Merlin, D., Wang, B., (2014). A click-and-release approach to CO prodrugs. Chem Commun, 50, 15890-15893.

Wu, L., Wang, R.U.I., (2005). Carbon Monoxide : Endogenous Production , Physiological Functions, and Pharmacological Applications. Pharmacological Reviews, 57, 585-630.

$[Mn(CO)_3(2,2\text{-bipyridyl})(4\text{-methoxybenzylbenzimidazole})]PF_6$ Complex As A New CO-Releasing Molecules

Tuğba TECİR[1], Elvan ÜSTÜN[2*], Serpil DEMİR DÜŞÜNCELİ[3], İsmail ÖZDEMİR[4]

[1]Ordu University, Faculty of Arts and Science, Department of Chemistry, Ordu, Turkey; tugba_tecir52@hotmail.com

[2] Ordu University, Faculty of Arts and Science, Department of Chemistry, Ordu, Turkey; elvanustun@odu.edu.tr

[3]İnönü University, Faculty of Arts and Science, Department of Chemistry, Malatya, Turkey; sdemir44@gmail.com

[4]İnönü University, Faculty of Arts and Science, Department of Chemistry, Malatya, Turkey; ismail.ozdemir@inonu.edu.tr

[*]**Corresponding Author:** elvanustun@odu.edu.tr

Abstract

Metal carbonyl complexes are important milestones in development of organometallic chemistry and have found a wide variety of applications since the first synthesized complex. One of the most important recent area of using these complexes is storage and transfer of carbon monoxide. $[Mn(CO)_3(2,2\text{-bipyridyl})(4\text{-methoxybenzylbenzimidazole})]PF_6$ as a new CO-releasing molecule was synthesized. We have investigated metal-to-ligand charge transfer (MLCT) transitions with DFT/TDDFT calculations with ORCA package program with BP86 functional.

Keywords: CO-Releasing Molecules, Manganese Complexes, Metal Carbonyls, CORMs

1. Introduction

Metal carbonyls are an important type of organometallic complex that have found a wide variety of applications since the first synthesized complex (Vessieres et al., 1999). Although early metal carbonyls were mostly used as catalyst (Gross and Ford, 1982), pharmaceutical applications of recent carbonyl complexes have accelerated the researches. Several practical applications of these complexes have been tested for probes in polymerization processes (Lees, 1983), labeling of biomolecules (Metzler-Nolte, 2001), and exploitation of solar energy (Balzani et al., 1996). Recently, one of the most important area of using these complexes is storage and transfer of carbon monoxide (Mann, 2012; Mann and Motterlini, 2007; Johnson et al., 2007).

Carbon monoxide (CO) is a well-known toxic gas. CO interference with oxygen transport in blood due to its binding to heme iron centers in hemoglobin is an important contributor to CO toxicity (Üstün et al., 2017). In fact, there are regularly certain amounts of CO in healthy tissue. It is endogenously produced during the degradation process of heme proteins by enzyme heme oxygenase. It is also known that CO rate in healing process is much more than that of accepted routine (Romão et al., 2012). Exogenously applied CO exerts potent therapeutic agent (Alberto and Motterlini, 2007). Metal carbonyl complexes are most promising candidates for deposit and transport carbon monoxide.

Myoglobin assay is the most commonly used method for measuring CO-releasing properties of carbonyl complexes. UV-Vis Spectrophotometer principally bases it on following the transformation of deoxymyoglobin to carbonmonoxy-myoglobin (Motterlini et al., 2012). Electronic transitions of molecules are the major landmark to make decision for proper wavelength of UV lamp. A photoCORM which has maxima on longer wavelength (preferably visible region) of UV spectra could be stimulated with a lower energy UV-lamp and is more advantageous for possible therapeutic.

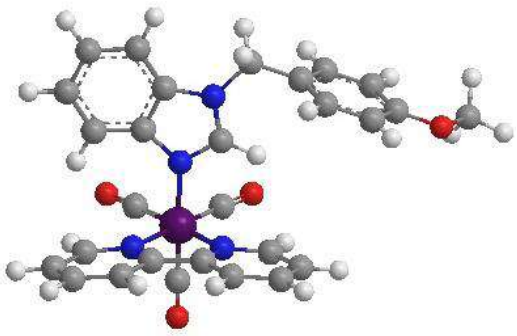

Figure 1. Chemical structures of $[Mn(CO)_3(2,2\text{-bipyridyl})(4\text{-methoxybenzylbenzimidazole})]PF_6$

In this study, $[Mn(CO)_3(2,2\text{-bipyridyl})(4\text{-methoxybenzylbenzimidazole})]PF_6$ complex was synthesized and investigated metal-to-ligand charge transfer (MLCT) transitions with DFT/TDDFT calculations with ORCA package program with BP86 functional.

2. Calculation Method

DFT/TDDFT calculations for full unconstrained geometry optimizations and electronic transitions were carried out with ORCA version 2.8 using the exchange functional according to Becke and the correlation functional suggested by Perdew, hereafter called BP (Neese, 2009), with the resolution-of-the-identity (RI) approximation, a TZV basis set, the tightscf and grid4 options (van Lenthe et al., 1994; van Lenthe et al., 1996; Weigend and Ahlrichs, 2005). The COSMO solvation model was used for analyzing the solvent effects on all calculations. Scalar

Table 1. Energies (between 300-600 nm), oscillation strengths (fosc), main orbital contributions and important singlets of $[Mn(CO)_3(2,2\text{-bipyridyl})(4\text{-methoxybenzylbenzimidazole})]PF_6$ with TDDFT/BP86 in gas phase

States	Molecular orbitals			Main transitions
3	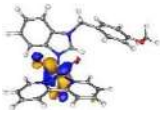 HOMO-2	593.3 nm (% 42.5)	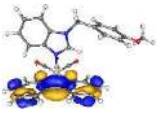 LUMO	 MLCT(f_{osc}:0.0318)
4	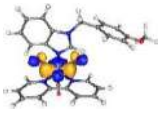 HOMO-3	552.4 nm (% 85.9)	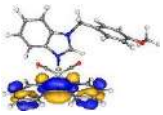 LUMO	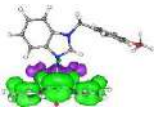 MLCT(f_{osc}:0.0110)
12	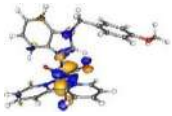 HOMO-1	431.0 nm (% 68.0)	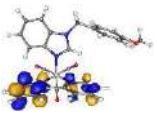 LUMO+2	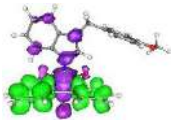 MLCT(f_{osc}:0.0207)
14	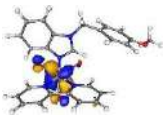 HOMO-2	394.8 nm (% 34.9)	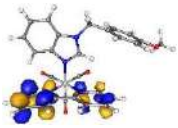 LUMO+2	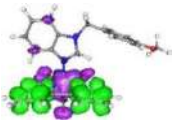 MLCT(f_{osc}:0.0822)
15	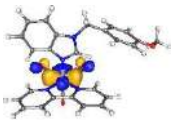 HOMO-3	393.3 nm (% 74.9)	 LUMO+2	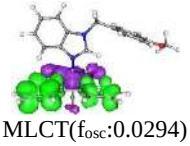 MLCT(f_{osc}:0.0294)
21		351.4 nm (% 62.8)		

	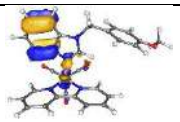 HOMO-5		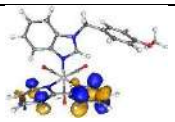 LUMO+1	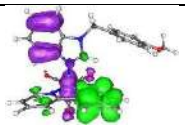 MLCT(f_{osc}:0.0374)
23	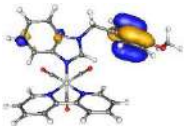 HOMO-6	341.2 nm (% 37.6)	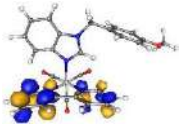 LUMO+2	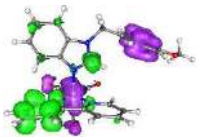 MLCT(f_{osc}:0.0315)
24	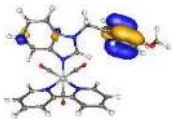 HOMO-6	340.1 nm (% 48.2)	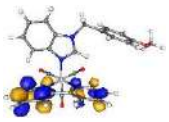 LUMO+2	 MLCT(f_{osc}:0.0250)

relativistic effects were treated using the Zeroth Order Regular Approximation (ZORA) formalism (Goerigk and Grimme, 2011). To speed up the calculations TZV/J auxiliary basis set was used.

3. Results and Discussion

Irradiation into the low-lying metal-to-ligand charge transfer (MLCT) bands, which belong to transitions from the metal to the lowest p* orbital of the ligand, may give rise to photo-dissociation of carbonyl ligand and this is, in fact, the main mechanism of CO release with UV-light. An understanding of photochemistry of transition metal compounds requires knowledge of the properties of molecular orbitals, spectra and appropriate excited states. Density functional theory (DFT) and time-dependent DFT approach (TDDFT) plays a crucial role in characterization of the excited states coordination complexes. Furthermore, applications of TDDFT approaches have recently been reported on transition metal complexes and got good results. Structures and electronic transitions predicted with the popular BP86 functional are no worse or in many cases are even slightly better than those predicted by the hybrid B3LYP functional.

Tungsten compounds containing aromatic ligands usually exhibit intense metal-to-ligand charge transfer (MLCT) transitions in UV-Vis spectrum. Electronic transitions and contributor molecular orbitals were analyzed with the aim of providing the participation to spectra bands in different solvents. Only strong transitions with an oscillator strength >0.01 are reported and contributions >10% are listed in Table 1. HOMO of molecule intensively consists of transition metal orbitals while LUMO is formed completely from bpy orbitals, thus the HOMO-LUMO

transition is a kind of MLCT which is expected to occur theoretically, but this transition could not be observed in UV-spectra practically because of weak oscillation strength. Electronic states with highest oscillating force are state 14 and state 21.

Acknowledgement

Support of Ordu University Scientific Project Coordination Department (ODUBAP, Project No: B-1808) is gratefully acknowledged.

References

Alberto, R., Motterlini, R., (2007). Chemistry and biological activities of CO-releasing molecules (CORMs) and transition metal complexes. Dalton Trans., 1651-1660.

Balzani, V., Juris, A., Venturi, S., Campagna, S., Serroni, S., (1996). Luminescent and Redox-Active Polynuclear Transition Metal Complexes. Chem. Rev., 96, 759-833.

Goerigk, L., Grimme, S., (2011). A thorough benchmark of density functional methods for general main group thermochemistry, kinetics, and noncovalent interactions. Phys. Chem. Chem. Phys., 13, 6670-6688.

Gross, D.C., Ford, P.C., (1982). Nucleophilic Activation of Coordinated Carbon Monoxide. 3.l Hydroxide and Methoxide Reactions with the Trinuclear Clusters $M_3(CO)_{12}$ (M = Fe, Ru, or Os). Implications with Regard to Catalysis of the Water Gas Shift Reaction. Inorg. Chem., 21, 1704-1706.

Johnson, T.R., Mann, B.E., Teasdale, I.P., Adams, H., Foresti, R., Green, C.J., Motterlini, R., (2007). Metal carbonyls as pharmaceuticals? $[Ru(CO)_3Cl(glycinate)]$, a CO-releasing molecule with an extensive aqueous solution chemistry. Dalton Trans., 1500–1508.

Mann, B.E., (2012). CO-Releasing Molecules: A Personal View. Organometallics, 31(16) 5728–5735

Mann, B.E., Motterlini, R., (2007). CO and NO in medicine. Chem. Commun., 4197–4208.

Metzler-Nolte, N., (2001). Labeling of Biomolecules for Medicinal Applications Bioorganometallic Chemistry at Its Best. Angew. Chem. Int. Ed., 40, 1040-1043.

Motterlini, R., Clark, J.E., Foresti, R., Sarathchandra, P., Mann, B.E., Green, C.J., (2002). Carbon monoxide-releasing molecules: characterization of biochemical and vascular activities. Circ Res, 90, E17-E24.

Neese, F., (2009). Prediction of molecular properties and molecular spectroscopy with density functional theory: From fundamental theory to exchange-coupling. Coord. Chem. Rev. 253, 526-563.

Neese, F., (2012). The ORCA program system. WIREs Comput Mol Sci, 2, 73–78.

Romão, C.C., Blättler, W.A., Seixas, J.D., Bernardes, G.J.L., (2012). Developing drug molecules for therapy with carbon monoxide. Chem Soc Rev., 41, 3571.

Üstün, E., Düşünceli, S.D., Özdemir, İ., (2017). [$Mn(CO)_3$(bpy)(N-2-chlorobenzylbenzimidazole)]OTf complex as a new photoactivatable CO-releasing molecule. Bulgarian Chemical Communications, 49(I), 50-56.

Van Lenthe, E., Baerends, E.J., Snijders, J.G., (1994). Relativistic total energy using regular approximations. J. Chem. Phys., 101, (1994) 9783.

Van Lenthe, E., van Leeuwen, R., Baerends, E.J., Snijders, J.G., (1996) Int. J. Quantum Chem., 57,281.

Vessieres, A., Salmain, M., Brossier, P., Jaouen, G., (1999). Carbonyl metallo immuno assay: a new application for Fourier transform infrared spectroscopy. Journal of Pharmaceutical and Biomedical Analysis, 21, 625–633.

Weigend, F., Ahlrichs, R., (2005). Balanced basis sets of split valence, triple zeta valence and quadruple zeta valence quality for H to Rn: Design and assessment of accuracy. Phys. Chem. Chem. Phys., 7, 3297.

Increasing Indoor Air Quality; Ionizer or HEPA Filter?

Serden BASAK [1*], Kazım Onur DEMİRARSLAN [2]

[1] Artvin Çoruh University, Sağlık Bilimleri Fakültesi, İş Sağlığı ve Güvenliği Bölümü, Artvin, Turkey; serdenbasak@artvin.edu.tr

[2] Artvin Çoruh University, Engineering Faculty, Environmental Engineering, Artvin, Turkey; onurdemirarslan@artvin.edu.tr

[*] **Corresponding Author:** serdenbasak@artvin.edu.tr

Abstract

Indoor Air Quality (IAQ) refers to the air quality within and around buildings and structures, especially as it relates to the health and comfort of building occupants. IAQ can be affected by gases (including carbon monoxide, radon, volatile organic compounds), particulates or microbial contaminant that can induce adverse health conditions. Source control, filtration and the use of ventilation to dilute contaminants are the primary methods for improving indoor air quality in most buildings. Poor IAQ has two types of effects on human health : Immediate effects or Long term effects. Carbon dioxide (CO_2) is one of the important parameter that determines indoor air quality and can be measured quickly. As the number and activity of people in indoor increases, the amount of carbon dioxide increases too and the air begins to become polluted. The best option to clean the indoor air is opening a windows if possible. However, Some of today's buildings do not have pop-up windows. At this point technology is engaged and usually offers us two different choices to increase the IAQ. One of them is ionizers and the second one is HEPA and active carbon filters. In this study, the comparison of an ionizer and an air purifier with HEPA and active carbon filters were used to reduce the amount of CO_2. To determine CO_2 level a CO_2 meter (PCE) was used. As result, the ionizer does not have significant effect to decrease CO_2 level

Keywords: Indoor Air, Quality, CO_2, Ionizer, HEPA filter

1. Introduction

All living beings need oxygen in the atmosphere in order to survive. People have to breathe 4.76 m3 of atmosphere air for 1 m^3 of oxygen (Ertürk, 2017). The concept of air quality has emerged for clean air needs. The indoor air quality is related to the cleaning of the air inhabited in living spaces. Fresh air can be described as air where no more than 80% of people who do not have any known pollutants above the harmful concentration levels determined by the competent authorities and who inhale this air feel any dissatisfaction with the quality of the air. Houses, workplaces, schools, etc. In recent years, there has been a growing concern about the cleanliness of indoor air (Dönmez, 2002). Humans have encountered internal air problems since the day they found fire. The man who learns to remove the smoke from a hole in the cave ceiling has had to deal with internal air problems in the next millennium. Employees working in the construction of the Egyptian pyramids were found to have more respiratory illnesses than those working outside, and the Romans discovered heating from the floor to allow for smoke-free heating. In the 11^{th} century, Ibn al-Haldun pointed out that air pollution would cause diseases in his book Mukaddime (URL-1). Today, human beings, who spend most of their lives indoors, are cut off directly from the natural environment and exposed directly to pollutants in the indoor environment. As a result, there are health problems and discomforts called Indoor Building Syndrome, Patient Building Syndrome and Building Related Diseases which are caused by direct indoor environment and air (URL-2). In studies on the status and evaluation of indoor air quality, it is often necessary to consider the temperature, relative humidity, air velocity, carbon dioxide (CO_2), breathable suspended particulate matter (PM), volatile organic compounds (VOC), nitrogen oxides (NOx), carbon monoxide parameters such as ozone (O_3), sulfur dioxide (SO_2), radon, formaldehyde (HCHO), bacteria count are measured (URL-2). Examples of other polluting gases include carbon monoxide, particulates (such as cigarette smoke, spray gasses), organic vapors, nitrogen oxides, sulfur dioxide, microorganisms, ozone, fibers, formaldehyde, sulphate and the like. mentioned. Despite the small proportions of these gases, the damages to building residents, building materials or contents are very large. Therefore, these pollutants must be removed from the environment (Aslan, 1997).

The indoor air quality in closed spaces concerns the cleaning of the indoor air. Because of the different expectations and different perceptions of people in terms of indoor air quality in these volumes, it is not realistic to set definite limits for indoor air quality. In order to clarify this, ASHRAE 62-1989, 2001 and 2004 introduced an acceptable indoor air quality standard (Ertürk, 2017). According to these standards, the amount of oxygen in the air is very important.

The amount of oxygen in closed spaces may be at least 11% and the rate of carbon dioxide may be 3%. The lower limit of oxygen in people's work activities should be around 17% to 18%. A person weighing 68 kg breathes 12 m3 (14.4 kg) of air for 24 hours (Ertürk, 2017).

In this study, possible changes in the amount of CO_2 in two different environments were measured using two indoor air quality enhancers with HEPA and ionizer. In addition, $PM_{2.5}$ measurements were also performed to support the study. As a result, it is desired to eliminate the deficiency in the literature. In addition, HEPA and ionizer indoor air quality enhancement devices on the market have been shown to have any effect on CO_2.

2. Material and Method

The study was carried out in two stages. Firstly, in the first stage, the HEPA filter was operated 8.5 hours in a room with a volume of 33.5 m^3 and at the same time CO_2 and temperature measurements were made. CO_2 and temperature measurements were made with PCE-AC3000 (Germany). At the same time $PM_{2.5}$ measurements were also carried out to support the study. In the second stage, an aquarium with a volume of 100 l was used for ionizer filter and the time-dependent change in the amount of CO_2 contained therein was examined.

2.1. HEPA Filters

It is called filter for equipment or materials which are used to separate unwanted gas, vapor or other particles in the air. All filters are manufactured in such a way as not to allow the slightest leakage (URL-3). HEPA filters are named after the words "High Efficiency Particulate Air Filter" (Anil et al., 2007). The HEPA filter is a filter that has 85% or more efficiency, which can remove air from the air up to 0.3 microns. The numerical value in front of HEPA filter types also increases the dust and particle retention value. In fact, HEPA-like filters have been developed against radioactive particles in room air in the United States in the 1940s and are differentiated after World War II (URL-4).

2.2. Ionizer Filters

Ionizer filters are used to clean air in enclosed spaces. Such devices also help to retain particles as small as 0.01 microns in diameter. This diameter also includes pollen, bacteria, allergens and dust, many of which can lead to respiratory problems. Compared to the HEPA

filter, it does not have any physical filter. The ionizer works by emitting negative charged ions into the air. These ions attract ions that are considered positively charged, such as allergens, dusts, and bacteria, and remove them from the environment (URL-5).

3 . Results and Discussion

CO_2, temperature and $PM_{2.5}$ measurements were performed at two different times in a room with a volume of 33.5 m^3. The first measurements were made by running the filter in the second measurements made without running the HEPA filter. All these measurement results are given in Figure 1.

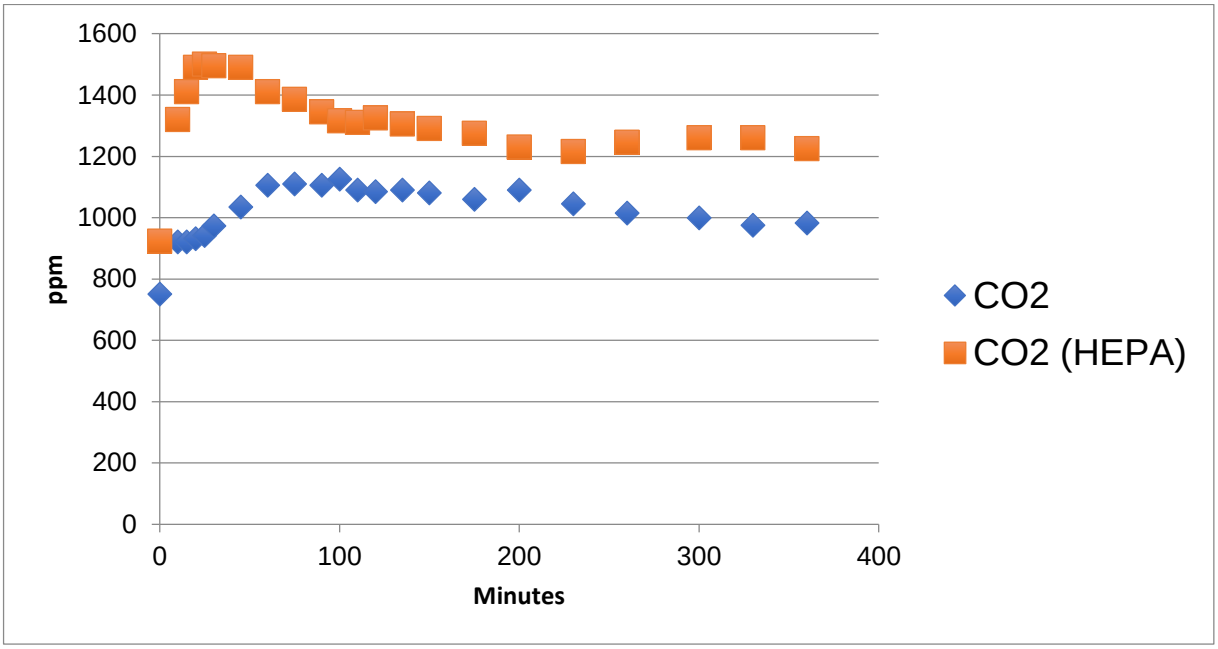

Figure 1. HEPA filter experiment results

The reason for the lower CO_2 amount in the experiment without the HEPA filter is that the air was windy that day and therefore the air comes to the room under the door. From the results, it can be seen that there is no effect on the CO_2 between the operation of the filter and the operation of the filter. However, when $PM_{2.5}$ measurements were taken, it was determined that the result of filtration without HEPA filter was 26 $\mu g/m^3$ and that this concentration decreased to 9 $\mu g/m^3$.

In the ionizer experiment, a closed and external air isolation environment of 100 l volume was established. First, the amount of CO_2 in the environment was fixed, then the first

measurement was made and the ionizer filter was operated to continue the measurement. The experimental results are given in Figure 2.

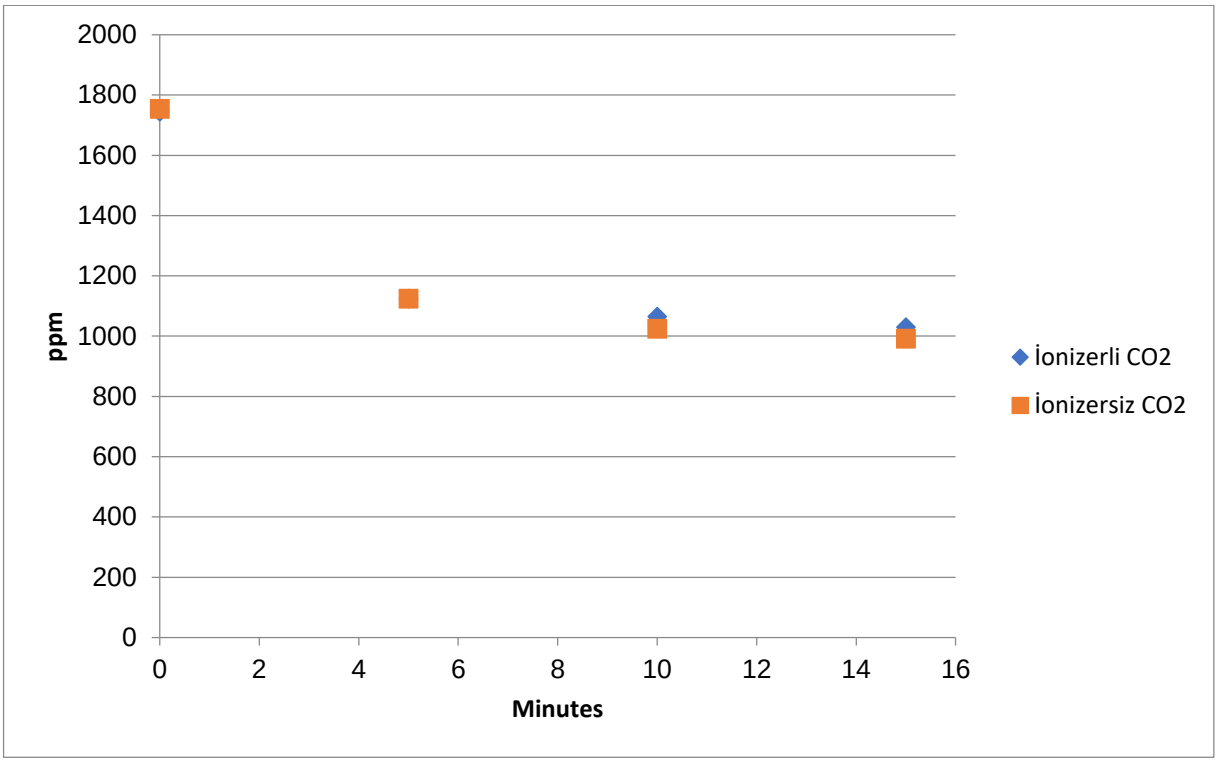

Figure 2. Ionizer experiment results

When Figure 2 is examined, it can be clearly seen that the ionizer has no effect on CO_2 emissions.

Humans spend close to 80% of their time in indoor spaces such as home, school, workplace, shopping center. In this case, the pollutants in the air can be exposed more. There are many devices in the market that will increase the quality of the indoor air and advertising to people. It is stated in these advertisements that the devices will significantly improve indoor air quality. However, in this study it was understood that the two devices commonly found in the market did not have any effect on CO_2. The only solution to reduce CO_2 concentration indoors is to ventilate the room. However, during ventilation, outdoor air pollutants may enter the interior, further reducing the air quality of the environment. Although according to occupational health and safety regulations, air conditioning and ventilation equipments, should be checked periodically and cleaning of the devices should be done at certain intervals, but in practice this issue can be neglected. If it is not done periodically, especially the air conditioners can cause various diseases such as legionnaire disease. There are several ways to improve indoor air quality, but choosing the most suitable one will be more economical and healthier.

References

Anıl, O.B., Mobedi, M., Özerdem, M.B., (2007), Hastane hijyenik ortamlarının klima ve havalandırma sistemleri, VIII. Ulusal Tesisat Mühendisliği Kongresi, http://www1.mmo.org.tr/resimler/dosya_ekler/1df9e625f8a9517_ek.pdf

Aslan, D.E., (1997), İç Hava Kalitesi Kontrolü, III. Ulusal Tesisat Mühendisliği Kongresi ve Sergisi, http://mmoteskon.org/wp-content/uploads/2014/12/1997-05.pdf.

Dönmez, O., (2002), İç Hava Kalitesi, Yüksek Lisans Tezi, İstanbul Teknik Üniversitesi, Fen Bilimleri Enstitüsü, İstanbul.

Ertürk, M., (2017), Yatılı okul yatakhanelerinde iç hava kalitesi probleminin araştırılması ve yeni bir sistem geliştirilmesi, Sakarya Üniversitesi Fen Bilimleri Enstitüsü Dergisi, 21 (5), 851-859.

URL-1, Bulgurcu, H., Havalandırma ve İç Hava Kalitesi, http://deneysan.com/Content/images/documents/havalandirma-1_46167331.pdf

URL-2, Bulut, H., İnsan Yoğunluklu Toplu Yaşam Ortamlarında İç Hava Kalitesinin Analizi, http://eng.harran.edu.tr/~hbulut/iklim2011.pdf

URL-3, Bulgurcu, H., Havalandırma Filtreleri, http://deneysan.com/Content/images/documents/havalandirma-3_63272884.pdf

URL-4, http://www.havalandirmatoztoplamasistemleri.com/detay/25/hepa-filtre-cesitleri/

URL-5, https://homeairguides.com/about-air-purifiers/what-is-an-air-ionizer-how-does-an-ionizer-work/

ANALYTICAL, ANORGANIC, ORGANIC, PHYSICAL, BIO, ENVIRONMENTAL CHEMISTRY

POSTER PRESENTATIONS

Spektroscopic Analysis, HOMO-LUMO Energies and Nonlinear Optical Properties of 2-Chloro-5-Nitrobenzyl Alcohol

Engin KAYALI[1], Hamit ALYAR [2*], Saliha ALYAR [3], Mustafa Tuğfan BİLKAN[4]

[1] Çankırı Karatekin University, Faculty of Science, Department of Physics, Çankırı, Turkey; enginkayali71@karatekin.edu.tr

[2] Çankırı Karatekin University, Faculty of Science, Department of Physics, Çankırı, Turkey; halyar@karatekin.edu.tr

[3] Çankırı Karatekin University, Faculty of Science, Department of Chemistry, Çankırı, Turkey; bilalcangul@gmail.com

[4] Çankırı Karatekin University, Faculty of Science, Department of Physics, Çankırı, Turkey; saliha@karatekin.edu.tr

[*] **Corresponding Author:** halyar@karatekin.edu.tr

Abstract

In this work, the structure of 2-Chloro-5-Nitrobenzyl Alcohol is optimized using density functional theory (DFT) method. The molecular geometry and vibrational band assignments are calculated using B3LYP/6-311++G(d,p) level of theory. The overestimations of the calculated wave numbers are corrected by the aid of scaled quantum mechanics force field methodology. The computational frequencies are found to be in good agreement with the experimental frequencies. Nonlinear optical properties such as polarizability, polarizability of anisotropy, first static hyperpolarizability of 2-Chloro-5-Nitrobenzyl Alcohol were calculated with same level of theory. Furthermore, HOMO–LUMO molecular orbital energy difference were calculated at the stationary point on the energy surface. All calculations performed with Gaussian 09, Gauss View 5.0 and SQM 1.0 software.

Keywords: DFT, FT-IR, HOMO-LUMO energies, NLO

1. Introduction

Benzyl Alcohol is commonly used in pharmaceutical products as an antimicrobial preservative at levels of 3-5% (Kibbe, 2000). It is well established when exposed to air, benzyl alcohol oxidizes slowly to benzaldehyde and subsequently to benzoic acid. The chemical oxidation of benzyl alcohol to benzaldehyde has been widely studied (Korcek et. al., 1972; Abend et.al., 2004; Choudhary et. al.; 2003). The use of aromatic alcohols has been restricted to their antimicrobial activity. That is probably because these molecules have been reported to cause aggregation of proteins, and are hence not ideal candidates as protein stabilizers. Protein aggregation not only has an adverse effect on the functionality of a protein but can also trigger a severe immune response in some patients (Demeule at. al., 2006; Moore and Lepperd, 1980; Schernthaner, 1993).

In this study, vibrational band assignment of 2-Chloro-5-Nitrobenzyl Alcohol were calculated using B3LYP/6-311++G(d,p) theory level. Also, nonlinear optical properties (NLO) and HOMO-LUMO molecular orbital energies studied with same level of theory.

2. Material and Method

The geometry of 2-Chloro-5-Nitrobenzyl Alcohol was fully optimized without any constraint with the help of an analytical gradient procedure implemented within the Gaussian 09 program (Frish et al., 2009). All the parameters were allowed to relax and all the calculations converged to an optimized geometry which corresponds to a true energy minimum as revealed by the lack of imaginary values in the wave number calculations. The molecular geometry optimizations, vibrational frequency calculations, performed with the Gaussian 09 software package by using DFT/B3LYP approaches. Optimized molecular structure of studied compound given in Fig.1. The vibrational band assignments were performed at B3LYP/6-311++G (d,p) theory level combined with scaled quantum mechanics force field (SQMFF) methodology. Each vibrational modes of the studied compound were characterized by their potential energy distribution (PED) which were calculated by using SQM-FF program (SQM, 2013). Nonlinear optical properties (NLO) and HOMO-LUMO molecular orbital energies studied with same level of theory.

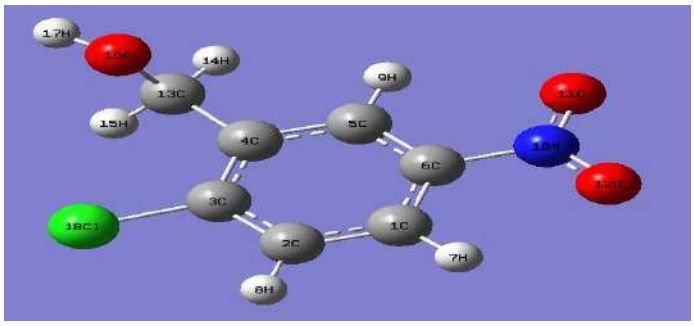

Figure 1. Molecular structure of 2-Chloro-5-Nitrobenzyl Alcohol obtained by B3LYP/6-311++G(d,p) method

3. Results and Discussion

3.1 Vibrational Band Assignment

Vibrational frequencies and corresponding vibrational assignments of 2-Chloro-5-Nitrobenzyl Alcohol have been investigated theoretically. DFT/B3LYP is provides acceptable vibrational wave numbers for organic molecules. Vibrational frequencies of 2-Chloro-5-Nitrobenzyl Alcohol were calculated at the DFT levels with B3LYP (Becke-Lee-Yang-Parr three parameters) hybrid functional (Lee at al.,1988). The vibrational band assignments were performed at B3LYP/6-311++G(d,p) theory level combined with scaled quantum mechanics force field (SQMFF) methodology to compare the experimental and calculated vibrational frequencies of the title compounds. The vibrational modes were assigned on the basis of PED analysis using SQM program. The visual check for the vibrational band assignments were also performed by using Gauss-View program.

Table 1. Assignment of fundamental vibrations of 5-amino-2-hydroxybenzoic acid by normal mode analysis based on SQM force field calculations using selective scaled B3LYP/6-311++G(d,p) (Experimental values taken from Ramachandran, 2013)

Mod.	FT-IR	FT-Raman	6-311++G(d,p)	Potential energy Distributions (P.E.D.)
υ1	3509s	-	3744	υ(OH) (100)
υ2	3090m	3087	3087	υ_s (CH) (98)
υ3	-	-	3076	υ_{as} (CH) (98)
υ4	2901m	2896	3068	υ_{as} (CH) (99)
υ5	-	-	2920	υ_{as} (CH_2) (100)
υ6	-	-	2882	υ_s (CH_2) (100)
υ7	1789w		1653	υ_{as} (NO_2) (37) + υ_{as} $(CC)_{ring}$ (27)
υ8	1714w		1613	υ_{as} $(CC)_{ring}$ (35) + υ_{as} (NO_2) (17)
υ9		-	1594	υ_{as} $(CC)_{ring}$ (35) + υ_{as} (NO_2) (32)
υ10		-	1510	δ (CH_2) (52)
υ11	1584m	1612w	1475	$\delta(CH)_{ring}$ (69)
υ12	1513vs	1575m	1456	w(CH_2) (89)
υ13	-	1514m	1425	w(CH_2) (84)
υ14	-	-	1397	υ (CN) (67)
υ15	-	1420m	1369	tw(CH_2) (84)
υ16	1340vs	1347s	1301	tw(CH_2) (34) + $\delta(CH)_{ring}$ (21)
υ17	-	-	1287	δ (CH_2) (30) + β (OH) (26)
υ18	-	-	1246	δ (CH_2) (32) + β (OH) (20)
υ19	-	-	1219	δ $(CCC)_{ring}$(42) + β (OH) (30)
υ20	-	-	1165	δ $(CCH)_{ring}$(68)
υ21	-	1194s	1132	υ (CN) (45) + δ $(CCH)_{ring}$(22)
υ22	1184s	-	1076	υ (CCl) (28) + δ $(CCC)_{ring}$(43)
υ23	-	-	1062	δ $(CH)_{ring}$ (63)
υ24	-	1096s	1015	υ (CO) (78)
υ25	-	1070s	982	υ (CO) (54)
υ26	1027vs	1038s	945	ρ(CH_2) (67)
υ27	-	-	933	υ (CN) (30) + $\beta(CH)_{ring}$ (26)
υ28	-	-	853	$\beta(CH)_{ring}$ (26)

ν: bond stretching, δ: in-plane angle bending, β: out-of-plane angle bending,τ: torsion, sci: scissoring, ρ:rocking, w: waging, as: antisymmetric and s: symmetric

Mod.	FT-IR	FT-Raman	6-311++G(d,p)	Potential energy Distributions (P.E.D.)
υ29	903s	925s	825	δ $(CCC)_{ring}$(68) + sci (NO_2) (81)
υ30	-	-	754	τ(CH) (31) + τ(CCCC) (25) + τ(CCNO) (12)
υ31	794s	805m	740	τ(CH) (28) + τ(CCCC) (21) + τ(CCNO) (13)
υ32	740s	-	708	δ $(CCC)_{ring}$(68)
υ33	-	712m	615	τ(CH) (34) + τ(CCCC) (26) + τ(CCCCl) (18)
υ34	600w	612m	577	δ (CCC)(42) + δ (CCN)(15)
υ35	-	-	538	υ(CCl) (16) + δ (CNO)(40)
υ36	-	-	522	τ(CH) (37) + τ(CCCC) (26)
υ37	491m	482wv	465	$\beta(CH)_{ring}$ (42)
υ38	-	-	391	δ (CCC)(38) + δ (CNO)(16)
υ39	-	-	352	τ(CCCN) (34) + τ(CCCC) (17)
υ40	-	336vw	315	δ (CCC)(46)
υ41	-	296vw	277	τ(CCOH) (34) + τ(CH_2 OH) (17)
υ42	-	-	245	τ(CCCCl) (27) + τ(CH_2 CC) (19)
υ43	-	211vw	206	τ(OH) (51)
υ44	-	-	193	δ (CCN)(64)
υ45	-	149vw	136	τ(CCNO) (42)
υ46	-	112vw	94	τ(CCCCl) (35)
υ47	-	-	58	τ(CCCO) (42) + τ(CH_2 CC) (14)
υ48	-	-	55	τNO_2 (91)

ν: bond stretching, δ: in-plane angle bending, β: out-of-plane angle bending,τ: torsion, sci: scissoring, ρ:rocking, w: waging, as: antisymmetric and s: symmetric

In order to enable assignment of the observed peaks, we have analyzed the all vibrational frequencies and compared our calculated results of the investigated compound with their experimental ones. The experimental frequencies are listed together with calculated frequencies in Tables 1. The calculated values of vibrations show good agreement with the experimental results as seen in Table 1.

3.1.1. O-H Vibrations

In the OH region, very strong and broad band occur at 3600 – 3400 cm^{-1}. Two OH stretching modes are observed at 3442 cm-1 and 3718 cm-1 in the FT-IR spectrum for studied compound. This band calculated at 3744 cm-1.

3.1.2. C-H Vibrations

The aromatic C-H stretching vibrations were normally found between 3100 and 2900 cm-1. Accordingly, in the title compound, asymmetric and symmetric stretching vibrations were observed at 3090 cm-1 and 2901cm-1 in the FT-IR spectrum whereas, in the FT-Raman, it is at 3087cm-1 and 2896cm-1, respectively. Theoretically, this vibration is calculated at 3087 and 3068 cm-1.

3.1.3. C-Cl Vibrations

The C-Cl stretching gives generally strong bands in 770-505 cm-1 region. The sharp FT-IR and FT-Raman bands at 600 cm-1 and 612cm-1, respectively observed in the spectrum of the title compound are assigned to C-Cl is stretching vibration. Theoretically, this vibration is calculated at 538 cm-1.

3.1.4. C-C Vibrations

The bands between 1650-1400 cm-1 in benzene derivatives were assigned to C-C stretching modes. Accordingly, in the present study, the C-C vibrations of the title compound were observed at 1584 and 1714 cm-1 in the FT-IR spectrum and the FT-Raman spectrum observed at 1612 cm-1. Theoretically, this vibration was calculated at 1613 cm-1 and 1594 cm-1.

3.2. HOMO-LUMO Molecular Orbital Energies

Both the Highest Occupied Molecular Orbital (HOMO) and the Lowest Unoccupied Molecular Orbital (LUMO) are the main orbital taking part in chemical reaction. The HOMO energy characterizes the ability of electron giving, the LUMO characterizes the ability of electron accepting, and the gap between HOMO and LUMO characterizes the molecular chemical stability. Energies of HOMO, LUMO and their orbital energy gaps were calculated by B3LYP/6-311G++(d,p) method. The 3D plots of the frontier orbitals are shown in Fig. 2.

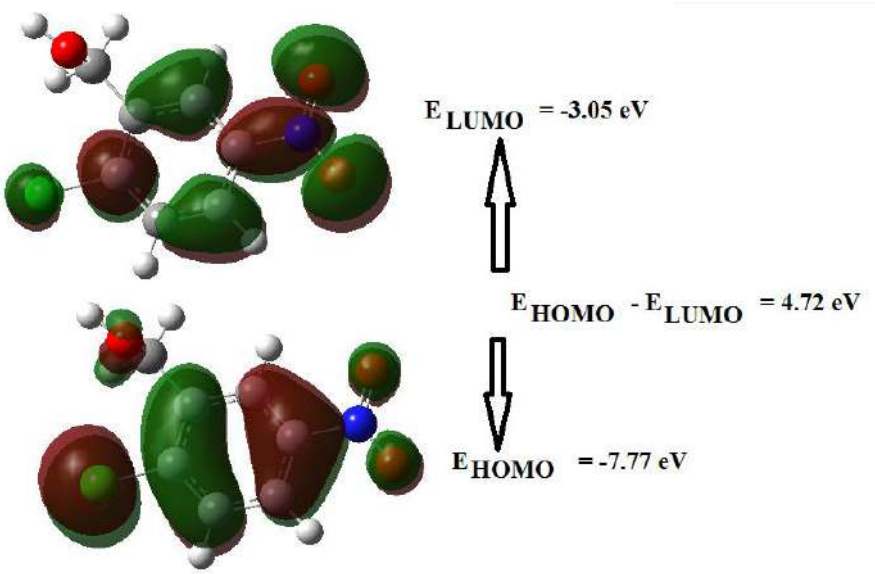

Figure 2. Molecular orbital surfaces and energy levels for the HOMO and LUMO of 2-Chloro-5-Nitrobenzyl Alcohol

3.3. Nonlinear optical properties (NLO)

Optical wave manipulation is one of the future technologies for optical processing. It has various applications in fiber-optic communications and optoelectronics which makes it an increasingly important topic among electrical engineers. The calculations of total static dipole moment(μ) static polarizability (αave) and first static hyperpolarizability (βtot) from the Gaussian output as follows:

$$\mu = (\mu x2 + \mu y2 + \mu z2)^{1/2} \quad (1)$$

$$\langle\alpha\rangle = 1/3\ (\alpha xx + \alpha yy + \alpha zz\ )$$

$$\beta tot = [(\beta xxx + \beta xyy + \beta xzz)^2 + (\beta yyy + \beta yzz + \beta yxx)^2 + (\beta zzz + \beta zxx + \beta zyy)^2]^{1/2}$$

Table 2. The electric dipole moment μ (D), the mean polarizability <α> (a.u.) and the first hyperpolarizability βtot (a.u.) of 2-Chloro-5-Nitrobenzyl Alcohol by DFT B3LYP/6-311++G(d,p) method

Parameter	B3LYP	Parameter	B3LYP
μ_x	2.59	$ß_{xxx}$	-59.64
μ_y	-2.99	$ß_{xxy}$	40.27
μ_z	0.14	$ß_{xyy}$	-66.72
M	3.96	$ß_{yyy}$	40.11
α_{xx}	154.04	$ß_{xxz}$	-1.83
α_{xy}	4.39	$ß_{xyz}$	3.78
α_{yy}	115.76	$ß_{yyz}$	11.19
α_{xz}	-2.86	$ß_{xzz}$	27.27
α_{yz}	-2.94	$ß_{yzz}$	-40.60
α_{zz}	63.56	$ß_{zzz}$	-0.51
<α>	111.12	β_{tot}	107.14

The computations show that, the first static hyperpolarizability of 2-Chloro-5-Nitrobenzyl Alcohol is 107.14 a.u. (0.925x10-30 esu). This value is 2.48 times larger than that of urea (0.3728x10-30 esu).

References

Abend, A. M., Chung, L., Bibart, R. T., Brooks, M., McCollum, D. G, (2004), Concerning the stability of benzyl alcohol: Formation of benzaldehyde dibenzyl acetal under aerobic conditions, J.Pharm. Biomed Analysis, 35, 957–962.

Choudhary, V. R., Chaudhari, P. A., Narkhede, V. S., (2003), Solvent-Free liquid phase Oxidation of benzylalcohol to benzaldehyde by molecular Oxygen using non-noble transition metal containing hydrotalcite-like solid catalysts, Catal. Commun,. 4, 171–175.

Demeule, B., Gurny, R., Arvinte, T.,(2006), Where disease pathogenesis meets protein formulation: renal deposition of immunoglobulin aggregates, Eur. J. Pharm. Biopharm., 62, 121–130.

Frisch, M. J. et al., Gaussian 09: Revision B.01 Gaussian Inc., Wallingford, CT, 2009.

Kibbe, A. H.,(2000), Handbook of Pharmaceutical Excipients, Washington, American Pharmaceutical Association.

Korcek, S., Chenier, J. H. B., Howard, J.A., Ingold, K.U., (1972), Absolute Rate constants for Hydrocarbon Autoxidation.XXI. Activation Energies for propagation and the correlation of propagation Rate constants with carbon-hydrogen Bond strengths, Can. J. Chem., 50, 2285–2297.

Lee, C., Yang, W., and Parr, R. G., (1988). Development of the Colle-Salvetti correlation-energy formula into a functional of the electron density. Phys. Rev B., 37, 785-789.

Moore, W. V., Leppert, P., (1980), Role of aggregated human growth hormone (hGH) in development of antibodies to hGH, J. Clin. Endocrinol. Metab., 51, 691–697.

Ramachandran, S., Velraj, G., (2013), DFT, FT-IR and FT-Raman Investigations of 2-chloro-5-nitrobenzyl alcohol. Rom. Journ. Phys., Vol. 58, No. 3–4, P. 305–317.

Schernthaner, G., (1993), Immunogenicity and allergenic potential of animal and human insulins, Diabetes Care, 16, (Suppl. 3) 155–165.

SQM version1.0, Scaled Quantum Mechanical, 2013 GreenAcres Road, Fayetteville, Arkansas 72703.

ECOLOGY, BIOLOGY, MARITIME SCIENCES

ORAL PRESENTATIONS

Investigation of the Effect of Magnetic Field on Forgetfulness: Trabzon Province Example

Galip Safa AKTÜRK[1], Nurhan GÜMRÜKÇÜOĞLU[1*], Ogün UZUN[1]

[1] Karadeniz Technical University, SHMYO, Trabzon, Turkey; galipsafa_AKTURK@hotmail.com

[1]Karadeniz Technical University, SHMYO, Trabzon, Turkey;ngumrukcuoglu@ktu.edu.tr

[1]Karadeniz Technical University, SHMYO, Trabzon, Turkey;Ogunuznn97@gmail.com

[*] **Corresponding Author:** ngumrukcuoglu@ktu.edu.tr

Abstract

The MRI working principles that using nowadays is based on magnetic field. In these days, one of the most used techniques of diagnosis is MRI.The purpose of this study is the effect of magnetic field on dementia. The research has been conducted by surveys on 41 MRI personnels in Trabzon province hospitals. Before the survey, the personal informations, health statuses, living facilities, hereditary diseases and the dementia disease possibilities of the relatives has been collected and recorded of the personnels. Withal personnels without any dementia triggering problem has been passed to second phase. In second phase, mini mental condition examination, reasoning function examination, arithmetic skill and abstraction skill examination has been applyed to personnels. During the examination, the conversations that will be used in fourth phase has been talked and visual objects has been shown to personnels. In third phase, some images has been shown and at the end of the phase, personnels had quized by visual memory test. For the last and fourth phase, has taken two weeks break. And later, personnels has been questioned with the second phase. Information received by recording and long-term effect on amnesia as a result of exposure to magnetic fields of MRI which operates according to the test results was investigated on a small scale.As a result, the dementia of MRI personnel was examined by Mini-mental condition examination, examination of reasoning function, arithmetic skill, abstraction skill tests and test results fits with possible and possible forgetfulness dementia criteria.

Key Words: Magnetic field, Dementia, MRI personnel, Forgetfulness

1. Introduction

Magnetic resonance imaging is a medical method used to distinguish certain anatomical structures from other structures and identify healthy and diseased tissues by using radio waves in the magnetic field obtained by using a large powerful magnet. Magnetic resonance is known to be used in laboratory surveys outside the health field and in tests in the construction industry**.**

Forgetfulness can be defined as the loss of memory or the inability to find the registered information in his head. Although it is a normal part of the aging process, it can also be a symptom of diseases and certain conditions, or it can appear as a side effect of drugs (Wiliam, 2016). The brain is one of the most complex parts of the body, responsible for the extremely complex processes, such as the storage and subsequent reuse of memories. The memoirs are extremely important because they are the foundation of learning. In a deeper sense, memories help us to enrich our lives, to connect our emotions more, to establish relationships with others, and to reveal our identities (Kirshner, 2017). Common causes of forgetfulness include aging, side effects from medications, trauma, vitamin deficiencies cancer in the brain and brain infections, as well as various other disorders and diseases. Stress, overwork, restlessness and persistent distractions can interfere with short-term memory (Hrenchir, 2015, https://www.docdoc.com/info/condition/forgetfulness/).

The purpose of this study was to determine the effect of the magnetic field on forgetfulness and the forgetfulness test was applied to the MR personnel working in the hospitals

.2. Material and Method

The research was carried out in 4 hospitals randomly selected from the province of Trabzon A total of 30 MRI personnel, 20 female and 10 male, participated in the study of forgetfulness test. The test staff consists of Mental Analysis test (orientation, knowledge about himself and his environment, awareness of current events, attention, short-term memory and learning, long-term memory, reasoning, abstraction-abstract thinking ability, complex visual perception and structuring skill, praxi skill), Reasoning Test, Arithmetic Skill Test, Culture level test, and personal questions (http://www.itfnoroloji.org/semi2/ mentalmuayene.html). The effect of the magnetic field on forgetfulness test was done on 30 MRI staff, age average,

equivalent to the cultural level, and sample 30 people who did not have any unforeseen risk not working anywhere, including MRI. Analyzes were scored based on sample subjects.

2.1. Findings

In the tests performed to determine the effect of the magnetic field on forgetfulness, the MRI staff was scored forgetfulness score of 100 and ranked as 100 highest and 1 lowest. As a result of the analyzes made, averages of the total points out of the 100 scoring points made to the guestions were taken. For example, the average score of the selected people is calculated as 6.85. The MRI staff who were tested for forgetfulness had an average level of forgetfulness of 6.85 to 10 points, 3. Level forgetful, a score of 10-20 points of 2. Level forgetful, and those above 20 were considered to be 1. Level forgetful.
The working time of the test personnel was calculated according to the test data and it was analyzed that it varied between 1 month and 252 months (Table 1).

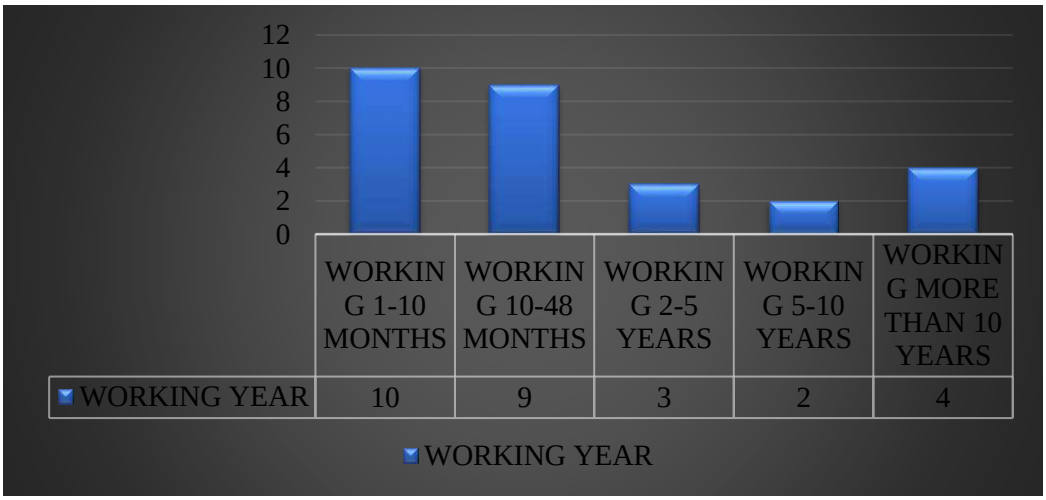

Figure 1. MRI Personnel Distribution by Working Year

It has been noted that the randomly selected 30 persons are not specified in the working environment and year, and that these persons are not working more. Thus, it is aimed to remove the depression and fatigue factor related to the work and to get better results. The average age of the tested personnel was found to be 20.56 (Table 2).

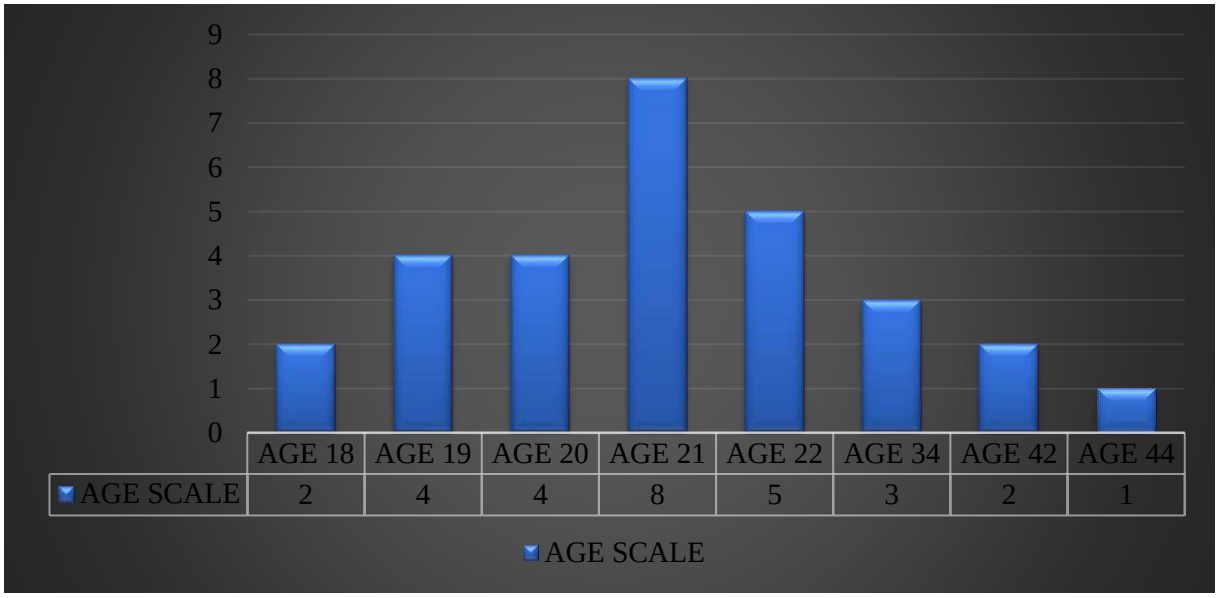

Figure 2. MRI Personnel Distribution by Age

According to this average, it was tried to Keep the average age of the selected people as equivalent. Thus, it was concluded that age has not an effect on forgetfulness. The rate of forgetfulness of the personnel performing. The test was calculated and varied between 4.45 and 23.15 points. The average of the results of the analysis of 30 randomly selected tests was taken and the average was 6.85, Level 3 was forgetful.

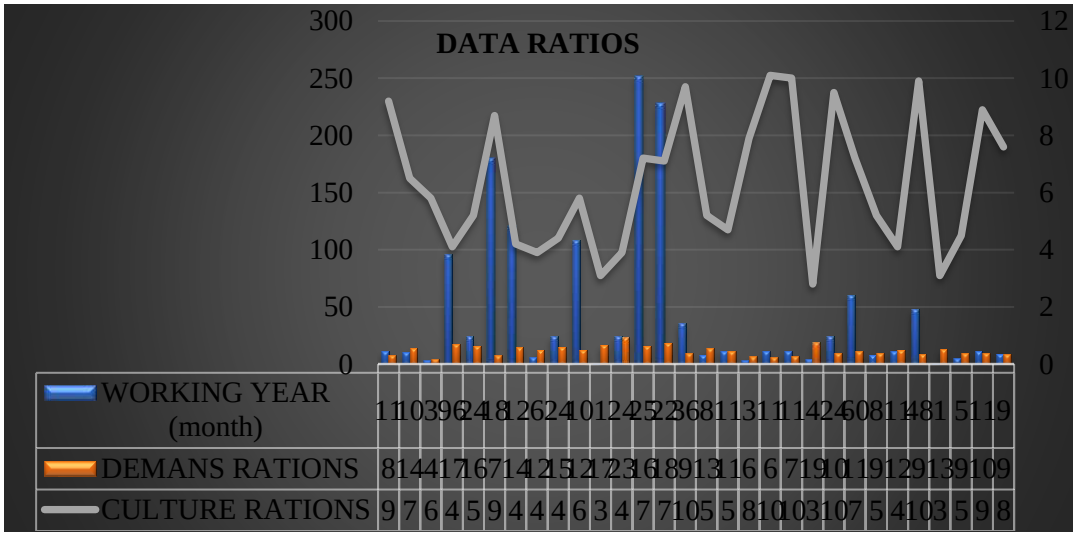

Figure 3. MRI Personnel Distribution by Working Year, Dementia and Culture Level

During the evaluation, it is necessary to include the social and cultural situation of the person in the account for orientation and information about him as much as for general information. (Table 3).

3. Results and Discussion

For the attention function, a series of 5 digit numbers can be counted at the lower normal limit. But if the person can only repeat the series of 4 digit numbers, this might be a slight forgettable. The inability of the person to repeat these numbers can be caused by not being impaired in the instant memory but not in the concentration skill. Deterioration in the mental control function also depends on the person's concentration difficulty and the deterioration of the mental trail (step-by-step tracing of the mind). The fact that the patient is able to say fewer words than a normal person at his / her age and educational level shows us that he has difficulty in maintaining attention and creating internal strategies.

As a result of this study, according to the tests performed, the MR personnel reached to the point that they are experiencing short-term memory deficits according to the study year, age and culture levels but it has come to the conclusion that these problems are diminishing as they move away from magnetic field exposure. In this study, the effect of MR on forgetfulness is the starting point of the investigation, and it is planned to repeat it on a larger mass and in detail in the proceeding processes.

References

Hrenchir, T. (2015). Top 8 Causes of Forgetfulness Online website: https:// www. newsmax.com/FastFeatures/Memory-Forgetfulness-Causes-Health/2015/03/11/id/629575/

Kirshner, H. S. (2017). Approaches to intellectual and memory impairments. In: Daroff RB, Fenichel GM, Jankovic J, Mazziotta J. C. eds. Bradley's Neurology in Clinical Practice. 6th ed.

Öktem, Ö. Mental Durum Muayenesi. http://www.itfnoroloji.org/semi2/mentalmuayene.html

Philadelphia, Pa: Elsevier Saunders; 2012:chap https://www.docdoc.com/info/condition/forgetfulness/

Wiliam, C., (2016). What is forgetfulness? Online website: https:// www. healthgrades. Com /right-care /brain-and-nerves /forgetfulness

Adsorption Properties Of *Urtica Dioica* On Colour Removal Of Malachite Green

Bengü ERTAN[1*], Derya EFE[1]

[1*]GiresunUniversity, Espiye Vocational School, Giresun, Turkey; bengu.ertan@giresun.edu.tr

[1]Giresun University, Espiye Vocational School, Giresun, Turkey; derya.efe@giresun.edu.tr

[*]**Corresponding Author:** bengu.ertan@giresun.edu.tr

Abstract

Synthetic dyes have been widely used in many industries. Wastewater discharged at the end of the processes pollutes clean water resources. It is harmful for living organism. They also give negative effects on biological activities such as bacterial growth and photosynthesis. Malachite green is one of them and it is mutagenic, carcinogenic and genotoxic. Therefore it is important to apply the efficient water treatment before disposal of the wastewater. Several methods have been developed for the removal of dyes such as advanced oxidation processes, photocatalysis, membrane filtration, coagulation, ion exchange and adsorption. Adsorption is the efficient method and biosorption materials are preferred because they are both cheap and environmentally friendly. *Urtic adioica* was used as an adsorbent in this study. Effects of pH, temperature, contact time and amount of adsorbent were examined. 89.74% of colour removal yield was obtained as pH 6.0, at 40°C,contact time of 120 min and biosorbent amount: 0.1 g. Isotherm studies show that the process fitted with Freundlich isotherm model and the kinetic data showed that the decolourization process followed the pseudo second order model. As a result of the work, it has been revealed that *Urtica dioica* can be used as an alternative for the removal of colour from wastewater.

Keywords: Malachite green, Adsorption, Wastewater, Synthetic dyes.

1. Introduction

Synthetic dyes have been widely used in many industries such as textile, paper, plastic, cosmetic, food and leather processing (Azhar et al., 2005; Garg et al.,2004). Wastewater discharged at the end of the processes pollutes clean water resources. It is harmful for living organism. They also give negative effects on biological activities such as bacterial growth and photosynthesis(Allen and Koumanova, 2005). Malachite green is one of them and it is mutagenic, carcinogenic and genotoxic (Sandra et al. 1999; Hu et al. 2006; Kumar et al. 2008). Therefore it is important to apply the efficient water treatment before disposal of the wastewater. Several physical and chemical methods have been developed for the removal of dyes such as advanced oxidation processes, photocatalysis, membrane filtration, coagulation, ion exchange and adsorption (Zhou et al., 2015). Adsorption is commonly used due to its efficiency and simplicity (Gupta et al., 2002). Biosorption materials are preferred because they are both cheap and environmentally friendly. They also contain chitin, glucan, protein, mannan, melanine and lipid fractions and it can provide potential binding sites for pollutants (Bowman and Free, 2006). Stinging nettle (Urtica dioica) was used as a biosorbent in this study.

Stinging nettle (*Urtica dioica L.*), the plant which have found in Black Sea region as large populations is very rich in terms of chemical constituents and has been used as herbal medicine, food/feed, fibre and cosmetic sector for many centuries (Ayan et al., 2006). Stinging nettle fibre has good absorbent characteristics; good anti-static, thermoregulatory and transpiration characteristics, non-lignified cell wall, soft and resistant fibres with low specific weight. In fig 1(c), stinging nettle fibres are located between the outer bark (epidermis) and the central woody core, arranged in bundles held together with gummy substances called pectin. (Virgilioa et al., 2015).

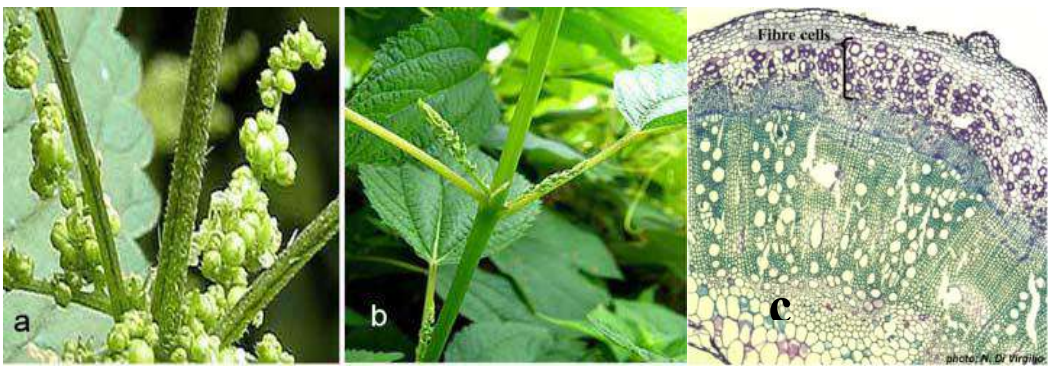

Figure 1.Female (a) and male (b) flowering stinging nettle (U. dioica) (c) cross section of stinging nettle stem (original magnification, 5×). Fixation ,paraffin and methacrylate resin embedding.

2. Material and Method

2.1. Preparing the biosorbent and dye solution

Urtica dioica, collected from this region(Black Sea), was washed with water then deionized water, dried 80°C for 48 h in oven to remove the moisture then ground and passed through a 0.5 mm sieve.

The stock solution of malachite green was prepared $1gL^{-1}$with DDW using malachite green oxalate from Sigma Aldrich. The physical and chemical properties of malachite green were seen in Table 1.

Table 1. Some physical properties of malachite green

Specification	Malachite green
Common name	Malachite green
Other name	Aniline green; Basic green 4; Diamond green B; Victoria green B
IUPAC name	4-[(4-dimetilaminofenil)fenil-metil-N,N dimetilanilin
Chemical formula	$C_{23}H_{25}ClN_2$
Molecular weight (g mol^{-1})	364.91
Solubility in water(g l^{-1}) in 298 K	40
Colors at different pH	Green-blue in water ,Yellow < pH 2 ,Green between pH 2-11.8 , Colourless> pH 13.8
λmax (nm)	618
Molecular structure	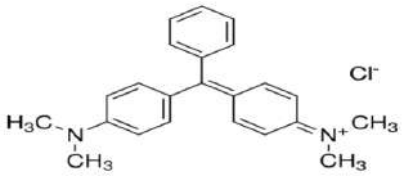

2.2. Adsorption Experiments

The adsorption experiments were performed after adding (0.05-0.3) g of adsorbent, pH of solution (2-8), contact time (15-120) min and temperature (25- 50)°C.

Biosorbent was poured into the dye solution and incubated for 2 h at room temperature (25°C) and 200 rpm in incubator shaker. The sample was centrifuged to remove the adsorbent then analyzed by uv-visible spectrophotometry to determinate the dye concentration.

2.3. Adsorption kinetic

The kinetic process can be premeditated by conducting a different set of adsorption experiments at constant temperature and variable time (15-150 min).

2.4. Adsorption isotherm

Isotherm studies were performed using batch system containing 50 mL of varied concentrations of dye solution (30-200 mgL^{-1}), a fixed amount of biosorbent (0.1 g).

3. Results and Discussion

3.1. Effect of pH

pH is the most important parameter on adsorption. The pH of the solution influences the charge of adsorbent surface and charge of dye molecule. The adsorption was increased with an increase in pH from 2 to 6 (see Figure 2). It can be explained that the adsorbent surface becomes more negative at the higher pH value due to hydroxyl ions. Therefore, more electrostatic attraction occurs between positively charged of protonated carboxylic group cationic dyemolecules and negatively charged of adsorbent (Garg et al., 2003).pH value of more than 8 was not investigated because of the instability of dye colour.

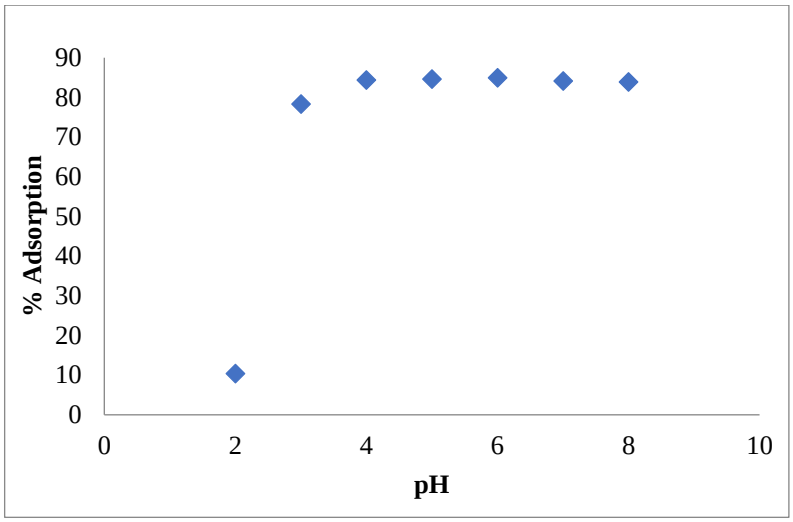

Figure 2.The pH effect on the adsorption of malachite green by *Urticadioica.*

3.2. Effect of adsorbent dose

The effect of adsorbent dose on adsorption was investigated between 0.05-0.3 g, seen Figure 3. 0.1 g of adsorbent is enough to adsorption and more than 0.1 g, % adsorption value was decrease moreover *Urtica dioica* was left its own colour on the media.

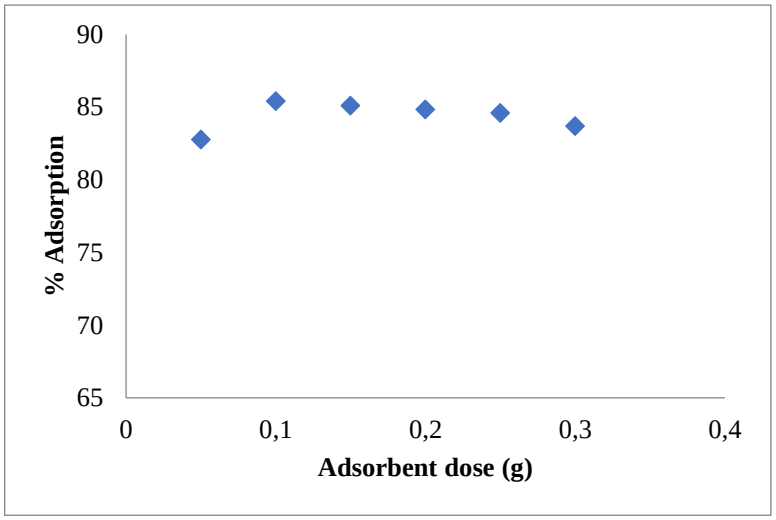

Figure 3. The effect of adsorbent dose on the adsorption of malachite green by *Urtica dioica*.

3.3. Effect of contact time

As seen in Figure 4, adsorption occurs fast, removal of dye was nearly completed in 80 min and 85.56% removal at an equilibrium time of 2 h. It is because of availability of surface charge.

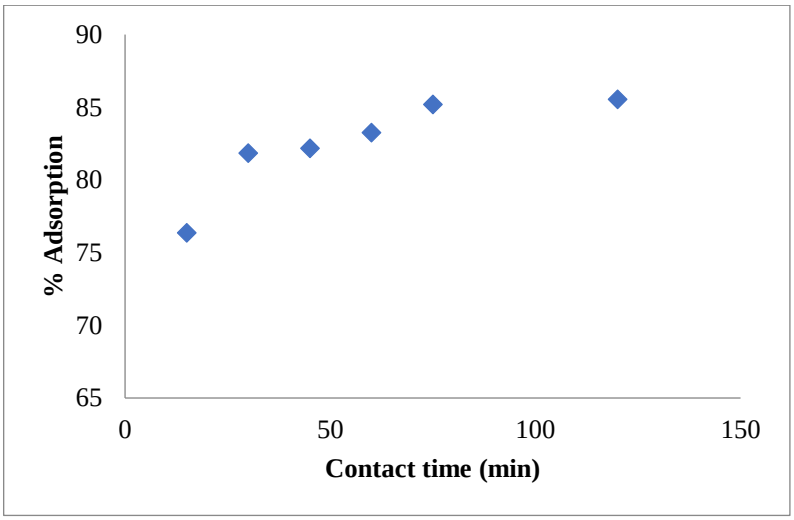

Figure 4. The effect of contact time on the adsorption of malachite green by *Urtica dioica*.

3.4. Effect of temperature

The temperature effect was investigated at 25, 30, 40 and 50°C. Optimum adsorption value was obtained 89.74% at 40°C.

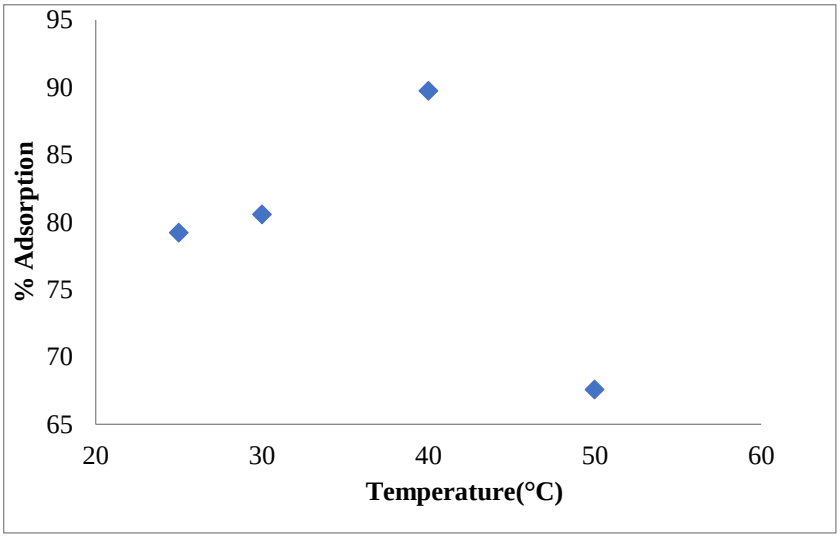

Figure 5. The effect of temperature on the adsorption of malachite green by *Urtica dioica*.

3.5. Adsorption isotherms

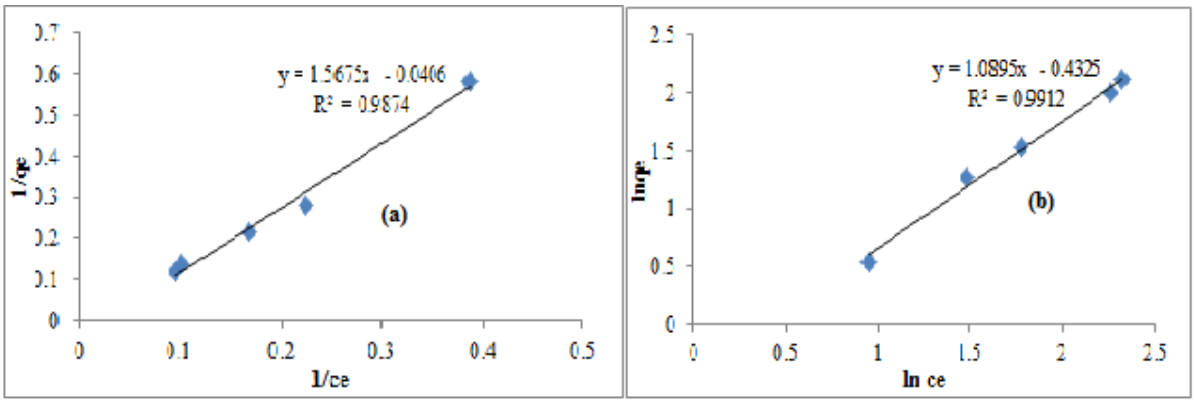

Figure 6. The linear plots of Langmuir isotherm (a) and Freundlich isotherm (b) for adsorption of Malachite green onto *Urtica dioica.*

As seen Figure 6, it is concluded the equilibrium data fit well with Freundlich isotherm model, the R^2 value of 0.9912.

3.6. Adsorption kinetics

The pseudo-second kineticmodel is assumed that the rate-limiting step can be adsorption involving valence forces with sharing or exchange of electrons between adsorbent and dye (Ho and Mckey, 1998). According to Figure 7 the pseudo-second order model was appropriately explained the kinetics.

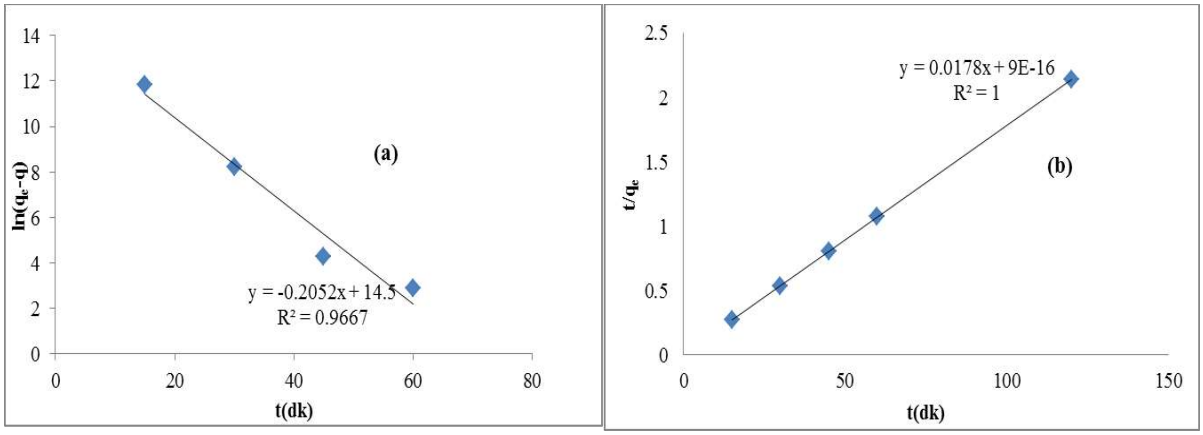

Figure 7. The linear plots of pseudo first-order model (a) and pseudo second-order model for the adsorption of malachite green onto *Urtica dioica*.

4. Conclusion

Urtica dioica used as an adsorbent in this study was mainly lignocellulosic. It is non-toxic, easy to access, cheap and found worldwide.

The isotherm model of Freundlich was better than Langmuir model and the adsorption follows the kinetics of pseudo second-order model. Maximum adsorption capacity was 24.63 mg/g.

Thus it is suggested that *Urtica dioica* can be used as an alternative adsorbent for decolourization of wastewater.

References

Allen, S.J., Koumanova, B., (2005) Decolourisation of water/wastewater using adsorption. J. Univ. Chem. Technol. Metall. 40, 175–192.

Azhar, S.S., Liew, A.G., Suhardy, D., Hafiz, K.F., Hatim, M.D.I., (2005) Dye removal from aqueous solution by using adsorption on treated sugarcane bagasse. J. Appl. Sci. 2 (11), 1499.

Garg, V.K., Kumar, R., Gupta, R., (2004) Removal of malachite green dye from aqueous solution by adsorption using agro-industry waste: a case study of Prosopis cineraria. Dyes Pigm. 62,1.

Garg, V.K., Gupta, R., Yadav, A.B., Kumar, R., (2003) Dye removalfrom aqueous solution by adsorption on treated sawdust. Bioresour. Technol. 89 (2), 121.

Hu, Z.G., Zhang, J., Chan, W.L., Szeto, Y.S.,(2006) The sorption of acid dye onto chitosan nanoparticles. Polymer. 47: 5838–5842.

Kumar, A., Prasad, B., Mishra, I.M.,(2008) Adsorptive removal of acrylonitrile by commercial grade activated carbon: kinetics, equilibrium and thermodynamics. J. Hazard Mater. 152: 589–600.

Sandra, J.C., Lonnie, R.B., Donna, F.K., Daniel, R.D., Louis, T., Frederick, A.B.,(1999) Toxicity and metabolism of malachite green and leuco malachite green during short-term feeding to Fischer 344 rats and B6C3F1 mice. Chem-Biol Interact. 122:153–170.

Zhou, Y., Min, Y., Qiao H., Huang, Q., Wang, E. and Ma, T., (2015) Improved removal of malachite green from aqueous solution using chemically modified cellulose by anhydride. Int. J. Biol. Macromol., 74: 271-277.

Gupta, V.K., Jain, C.K., Chandra, S. and Agarwal, S., (2002) Removal of Lindane and Malathion from Waste Water Using Bagasse fly Ash, a Sugar Industry Waste.Water Research, 36, 2483-2490.

Bowman, S.M., Free, S.J., (2006) The structure and synthesis of the fungal cell Wall, Bioessays 28, 799-808.

Virgilioa, N. Di, Papazogloub, E.G., Jankauskienec, Z., Lonardod, S. Di, Praczyke, M., Wielgusze, K., (2015) The potential of stinging nettle (Urtica dioica L.) as a crop with multiple uses", Industrial Crops and Products 68, 42–49.

Ayan, A.K.,Çalışkan,Ö.,Çırak, C., Isırganotu (Urtica spp.)'nun ekonomik önemi ve tarımı (2006) J. of Fac. of Agric., OMU 21(3): 357-363.

Ho, Y. S.; McKay, G., (1998) Kinetic models for the sorption of dye from aqueous solution by wood. Process Saf. Environ. Prot., 76,183–191.

Chromosome abnormalities in Meristematic Cells of Root Tips of *Vicia faba* L. after the different treatments of 18F-FDG and Statistical Comparative

Didem GOKSOY[1], Yasemin PARLAK[1*], Bahattin BOZDAĞ[2], Ali ÖZDEMİR[3], Ahmet MUTLU[1], Gul GUMUSER[1], Elvan SAYIT[1], Canan OZDEMIR[2]

[1]*Celal Bayar University, Department of Nüclear Medicine, School of Medicine,Manisa, Turkey;*
[2]*Celal Bayar University, Science and Art Faculty, Biology Department, Manisa, Turkey;*
[3]*Celal Bayar University, Science and Art Faculty, Mathematics Department, Manisa, Turkey;*

[*] **Corresponding Author:** yasemin.gultekin@hotmail.com

Abstract

The cytological effects of 18F-FDG which used in the oncological imaging, have been studied using root meristems of *Vicia faba* L. Seeds of the plant were kept in 18F-FDG standart for different time period as control during 1/12, 1/4, 2, 3, 4, 5, 6, 12 and 24 hours. Seeds which treated with 18F-FDG were germinated and the root tips obtained were prepared for microscopic examination and some abnormalities, as fish bone chromosome, chromosome dispersion, chromosome adherence, chromosome breaking, bridge chromosome, chromosome shrinking, ring chromosome were observed. Abnormalities were seen at each treated depended on the time periods except at 24 hour treatment. Mitotic activity and abnormalities were particularly low in roots after 2 hours of treatment. A lot of micronucleus in interphase cell were seen at the different hours of treatment. The results obtained were evaluated statistically.

Key words: Abnormalities, chromosome, 18F-FDG, *vicia*, statistical

1. Introduction

Since the middle of 1995, 18F-FDG PET scanning of the body has been a clinical tool for the evaluation of various cancers. Fludeoxyglucose (18F) is used in medicine in patients with confirmed cancer or suspected cancer; It is used in the molecular imaging method to determine the cardiological diseases and to diagnose neurological disorders and inflammatory diseases and infectious diseases whose cause is unknown (Fatangare and Svatoš 2016). Molecular imaging is the visualization, characterization and measurement of biological functions at the molecular and cellular level in living organisms. Molecular imaging techniques using radioisotopes allow the visualization of functional and phenotypic changes in pathological conditions. Radionuclides used in practice are low atomic numbers and short half-life elements. It is the most preferred radionuclide in routine studies due to the relative long half life (110 minutes) (18F) when compared to other positron emitters. Thus changes in tissue level (18F) - FDG involvement (decrease-increase, no involvement) reflect altered glucose metabolism in different pathological conditions such as cancer. This allows the assessment of abnormal glucose metabolism during the pathological process. Following the first synthesis in 1970, the first FDG-PET imaging was performed as molecular imaging in 1976. The clinical effect of (18F) FDG, which has been in use since the early 1980s, has been recognized around the world, particularly in Europe, and today there is considerable experience with the use of (18F) FDG (Henry et al .2003).

There are still a few unanswered questions in this field. First of all, it is known that FDG causes cytotoxicity in hypoxic tumor cells (Lampidis et al., 2006; Kurtoglu et al., 2007).

Recently,FDG has attracted the attention of plant scientists as it has been used as a tracer for in vivo imaging in plants (Partelováetal., 2014; Meldauetal., 2015).

Various chemical substances used in the fields of medicine, biology and agriculture can negatively affect living things beside their positive effects. In this study, we aimed to examine effects of 18F-FDG treatments in different time periods on root tip cells of *Vicia faba*.

2. Material and Method

Seeds of *Vicia faba* were used in the study. Seeds were kept in 18F-FDG 1/12, 1/4, 2, 3, 4, 5, 6, 12 and 24 hours. Then, seeds were washed by distilled water and germinated in Petri dishes at 20–25°C. After fixation of root tips, they were put in 70% ethyl alcohol. Stock root tips were stained by the Feulgen method (Darlington and La Cour 1976) and were made ready

for microscopic examination. Homologous areas were chosen on these preparations for cytogenetic examination; the cells in these areas were counted and the numbers of mitotic cells were also detected. Chromosomal abnormalities were detected in the cells counted. The preparations were photographed with a motorized Leica DM 3000 microscope (Leica Microsystems, Wetzlar, Germany).

3. Results and Discussion

In this study, the effect of 18F-FDG on mitotic cell division in the root tip of *Vicia faba* which is the pure germ line of broad bean was investigated. At the end of the study, it has been observed that 18F-FDG standard treatment on the seeds at different time periods increased mitotic cell division according to control group. The highest increase was observed at the 2 hour of treatment. Mitotic activity and abnormalities were particularly low in roots after 2 hours of treatment.

It has been observed that 18F-FDG caused various chromosomal as abnormalities fish bone chromosome, chromosome dispersion, chromosome adherence, chromosome breaking, bridge chromosome, chromosome shrinking, ring chromosome at different stages of mitotic division and different time periods (Figure 1 A-F).

The most observed abnormality was chromosome dispersion, fish bones chromosome and chromosome breaking. Fish bones chromosome, chromosome dispersions and chromosome adherence were observed all treatment hours except to 24 hour treatment time. All chromosomal abnormalities were identified as the highest level at 2-hour treatment, while the lowest chromosomal abnormalities were identified at 1/12 and 1/4 hours treatment. In addition, a lot of micronucleus in interphase cell were seen especially at the 24 hours of treatment (Figure 1: A-F, Figure 2, Table I).

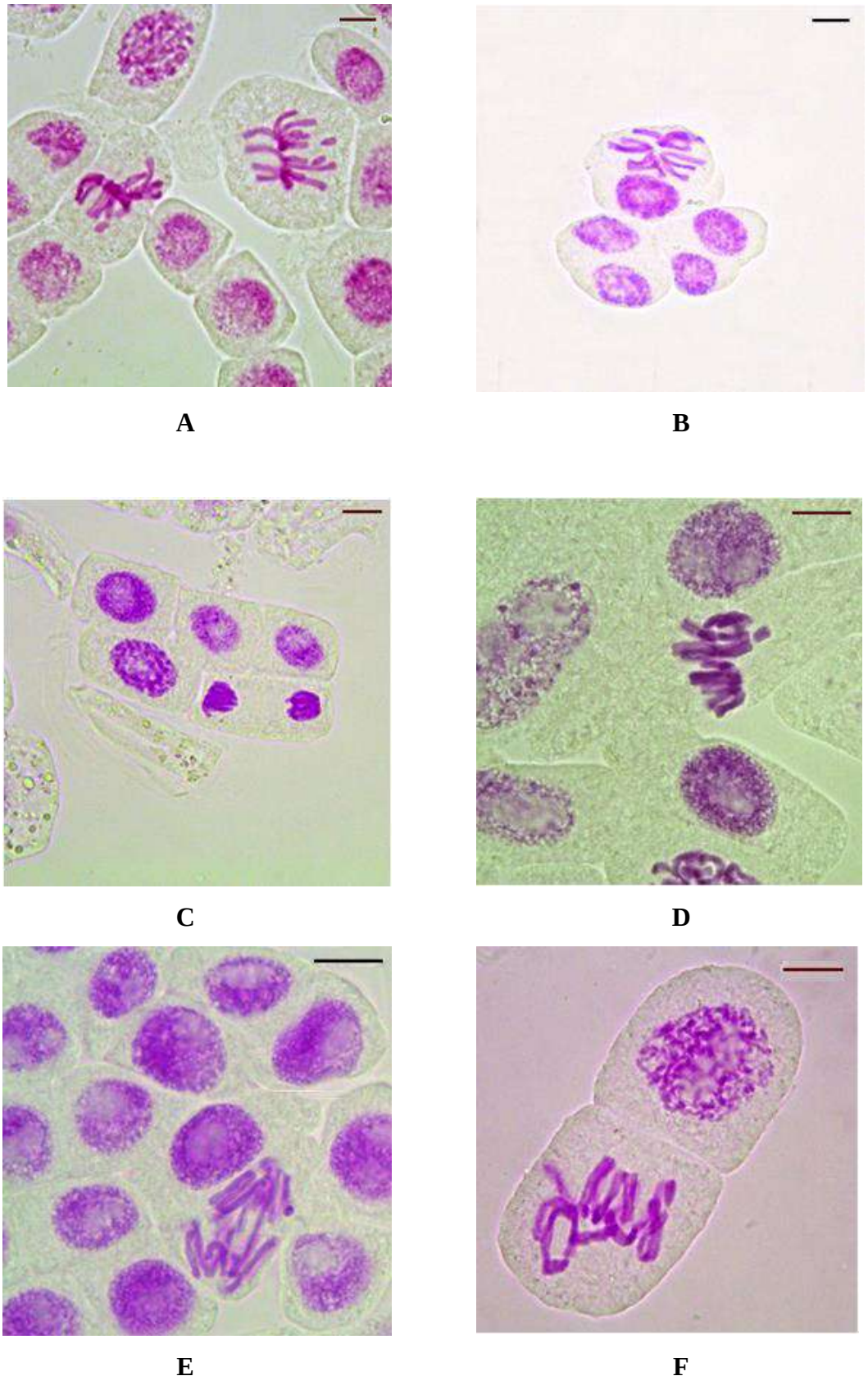

Figure 1. Chromosomal abnormalities produced by 18-FDG in *V. faba*. Fish Bone (A); Chromosome dispersion (B); Chromosome shrinkage (C); Chromosome breaking (A, D); Chromosome adherence (A, D, F); Bridge chromosome (E); Ring chromosome (F)

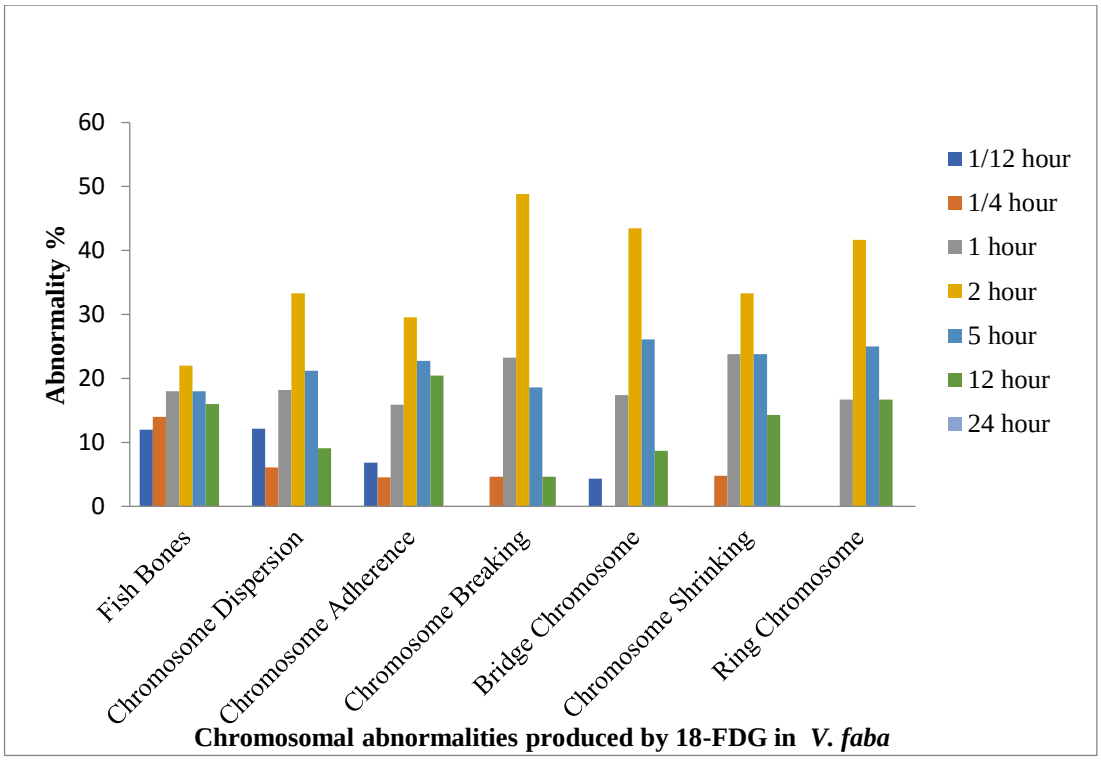

Figure 2. Types and proportions of chromosomal abnormalities and the percentage of total abnormalities produced by the different treatments of 18-FDG in *V. faba* root.

Table I. Types and proportions of chromosomal abnormalities and the percentage of total abnormalities produced by the different treatments of 18-FDG in *V. faba* root.

Treatment Time (Hour)	**Chromosomal abnormalities produced by 18-FDG (%)**						
	Fish Bones	**Chromosome Dispersion**	**Chromosome Adherence**	**Chromosome Breaking**	**Bridge Chromosome**	**Chromosome Shrinking**	**Ring Chromosome**
1/12	12.00	12.12	06.82	00.00	04.35	00.00	00.00
1/4	14.00	06.06	04.55	04.65	00.00	04.76	00.00
1	18.00	18.19	15.91	23.26	17.39	23.81	16.67
2	22.00	33.33	29.55	48.84	43.48	33.33	41.67
5	18.00	21.21	22.73	18.60	26.09	23.80	25.00
12	16.00	09.09	20.45	04.65	08.70	14.29	16.67
24	00.00	00.00	00.00	00.00	00.00	00.00	00.00

4. Discussion

In present study, cytogenetic effects of 18F-FDG on meristematic cells of root tips belonging to the plant (*Vicia faba*) have been investigated. Seeds of the plant, prepared were kept in 18F-FDG for different time period as control during, 1/12, 1/4, 2, 3, 4, 5, 6, 12 and 24 hours.

In present study it was determined that 18F-FDG was caused to some chromosomal abnormality at the *Vicia faba* as fish bones chromosome adherence, chromosome dispersions, chromosomal adherence, bridge chromosome, chromosome breaking, chromosome shrinking, ring chromosome. Similarly, it has been reported that uranium and copper chloride have caused to some chromosomal abnormality on root tip cells of *Vicia faba* and *Vicia hirsute*. It has been determined that the frequency of mitotic cell division were affected by uranium depending on the different treating time and uranium led to chromosomal abnormalities in the *V. faba* and *V. hirsuta* cells (Ozdemir et al., 2008 ; İnceer et al., 2003). In other study, the results pointed out that increase of the lead (PbCl2) concentrations cell division was decreased, several mitotic anomalies such as c mitosis, lagging chromosomes, multipolar anaphases and chromosome bridges on root tip cells of lentil (*Lens culinaris* Medik.) (Kıran & Sahin 2005).

In similar, the researchers found similar results for uranium concentration. In the them study, the growth of seedling was considerably stimulated by uranium tailings at high concentrations rather than at low concentrations. The results revealed that nuclease (RNase) activity were stimulated at low uranium tailings lixivium concentrations and inhibited at high concentrations. As the concentrations of uranium tailings lixivium became higher, the inhibitory effect increased. So, the uranium tailings have complex effects on nuclease activity (Yi, et al., 2007).

In another, study, it was determined that effect of the cadmium chloride

in the pure germ line of *Vicia faba* were evaluated in relation to the chromosomal abnormalities and rate of cell division. Seeds grown in the nutrient medium for 48 hours containing different concentrations of cadmium chloride showed different genotoxic effects such as polyploidy, multipolarity, chromosomal bridge with fragments, lagging chromosome and micronuclei. Relative division rate (RDR) was decreased with increasing cadmium concentration (Parween et al., 2011).

Radioactive elements can pass to plants through soil and then can reach people. Studies about the role of transition metals in soil and plants are not sufficient enough (Kasianenko & Kulieva 2002). There are reports about copper, zinc, lead and chrome that pointed out the result

of causing to cytogenic effect on *Allium cepa* root tips (Arambasic et al., 1995). Leonard et al., (1983) reported that mercury compounds were effect spindle fibers at the time of cell division on the plant as *Vicia faba* and *Allium cepa*.

In this study, we intended to determine cytogenetic effect of 18F-FDG used in medicine in patients with confirmed cancer or suspected cancer on the root tip cells of *Vicia faba* whose the seeds are widely consumed by people as food.

References

Arambasic, M.B., S. Bjelic and G.S. Subakov. 1995. Acute toxicity of heavy metals (Copper, Lead, Zinc), phenol and sodium on Allium cepa L., Lepidium sativum L. Daphnia magna St. comparative ınvestigations and the practical applications. Wat. Res. 29: 497-503.

Darlington, C.D. and L.F. La Cour. 1976. The Handling of Chromosomes. Allen and Unwin.

Fatangare A. , Svatoš A. (2016), Applications of 2-deoxy-2-fluoro- D-glucose (FDG) in Plant Imaging: Past, Present, and Future , Front. Plant Sci. 7:483. doi: 10.3389/fpls.2016.00483

İnceer, H., S. Ayaz, O. Beyazoğlu and E. Entürk. 2003. Bakır klorür'ün Helianthus annuus (L.) kök ucu hücreleri üzerine sitogenetik etkileri. Turkish Journal of Biology, 27: 43-46.

Kasianenko, A.A. and G.A. Kulieva 2002. Ecological consequences of depleted uranium use in ammunition. Bulletin of Russian Peoples' Friendship University. Series Ecology and Life Safety-Moscow, Publishing House of RPFU, 6, 90-99.

Kıran, Y. and A. Sahin. 2005. The effects of the lead on the seed germination, root growth and root tip cell mitotic divisons of Lens culinaris Medik. G.U. Journal of Science, 18(1): 17-25.

Henry W.D. Yeung, Ravinder K. Grewal, MD, Mithat Gonen, Heiko Schöder, and Steven M. Larson (2003) Patterns of 18F-FDG Uptake in Adipose Tissue and Muscle: A Potential Source of False-Positives for PET. J Nucl Med November 1, 2003 vol. 44no. 11 1789-1796.

Leonard, A., P. Jacqued and R. Lauverys. 1983. Mutagenicity and teratogenicity of mercury compounds. Mutat. Res., 114: 1-8.

Meldau,S.,Woldemariam,M.G.,Fatangare,A.,Svatos,A.,and Galis,I.(2015). Using2-deoxy-2-[18F]fluoro-D-glucose([18F]FDG)to study carbon allocation in plants after herbivore attack. BMCRes. 8:45. doi:10.1186/s13104-01 5-0989-z

Özdemir, C., F.S. Erees and S. Çam, S. 2008. Cytogenetic effects of uranium on root tip cells of Vicia faba L.

Botanica Lithuanica, 14(3): 155-158. Partelová,D.,Uhrovˇcík, J.,Lesný,J., Horník, M.,Rajec,P., Kováˇc,P., etal.(2014).Application of positron emission tomography and 2-[18F] fluoro-2-deoxy-D- glucose for visualization and quantification of solute transportin plant tissues. Chem.Pap. 68, 1463–1473.doi:10.2478/s11696-014-0609-8

Parween T., S. Jan, Mahmooduz zafar, M.P. Sharma, A. Mujib and T. Fatma. 2011. Genotoxic impact of cadmium on root meristem of Vicia faba L. Russian Agricultural Sciences, 37(2): 115-119.

Lampidis,T.J ,Kurtoglu, M., Maher, J.C., Liu, H., Krishan, A., Sheft,V., et al.(2006). Efficacy of 2-halogen substituted D-glucose analogs in blocking glycolysis and killing “hypoxic tumor cells. *Cancer Chemother. Pharmacol.* 58, 725–734. doi:10.1007/s00280-006-0207-8.

Yi, S., R. Wang, T. Feng, Y. Xiang and Zhou. 2007. Effects of uranium tailings lixivium on early growth of Vicia faba. Journal of Hunan University of Science & Technology (Natural Science Edition) -04: 113-116.

A Perspective for Sewage Sludge Management in Turkey

Ozge KOKSAL[1*], Nurdan Gamze TURAN[2], Yuksel ARDALI[3]

[1]Ondokuz Mayıs Unıversity, Engineering Faculty, Department of Environmental Engineering, Samsun, Turkey; ozgekoksal8@gmail.com

[2]Ondokuz Mayıs Unıversity, Engineering Faculty, Department of Environmental Engineering, Samsun, Turkey; gturan@omu.edu.tr

[3]Ondokuz Mayıs Unıversity, Engineering Faculty, Department of Environmental Engineering, Samsun, Turkey; yuksel.ardali@omu.edu.tr

[*]**Corresponding Author:** ozgekoksal8@gmail.com

Abstract

Industrialization rapidly developing technology and population growth cause various environmental problems over the world. Treatment sludge management is one of these environmental problems. The collection, handling and transport and disposal of all kinds of sludge resulting from the treatment of drinking water, municipal and industrial wastewater, are necessary to protect the environment. Turkey has taken important steps with new regulations from the legal aspects and identified priority areas in environmental issues in recent years. Sludge management is in the priority work area on the list. In this study, sewage sludge management in Turkey was examined. In addition, related problems are investigated in detail. Future management strategies and solution proposals are also presented.

Keywords: Sewage sludge, waste management, wastewater.

1. Introduction

Sewage sludge can be described as the solid or semi-solid residue left over after the treatment of wastewater. It can be described as the by-product, yet it shall be treated as a waste in the process of wastewater treatment in the literature [4]. It is one of the most important hazardous solid wastes generated from the wastewater treatment processes. It is a complex emulsion of a lot of organic chemical compounds and solid particles as well as high concentration of water and heavy metals. Wastewater treatment plant is a facility in which a composition of diverse processes (i.e., physical, chemical and biological) are used to removal pollutants. The waste residue created during these treatment processes is known as sewage sludge. Sewage sludge production currently results in various environmental topics in many developed and developing nations. Rapidly industrialization and boosted population with the extensive growth of urban zones has also increased concerns in relation to it disposal [5]. The inappropriate disposal or insufficient treatment of sewage sludge could lead serious environmental problem and human health impacts. Hence, a diversity of effective sludge treatment technologies have been developed to eliminate the hazardous compounds and reduce its negative impacts, due to its raising production quantity over the world [6]. Previously, the disposal of excessive sewage sludge has been undertaken through traditional methods; including incineration, landfilling or ocean dumping. However, a boost in related environmental fears and hard laws has led to these disposal options being altered by biological methods (i.e., composting, aerobic and anaerobic digestion) [5].

In Europe, 40% of sewage sludge generated is disposed of in landfill plants, 37% in agricultural use, 11% in incineration and 12% by different means. In Europan Union countries, 18% of domestic sewage sludge is disposed of in landfill plants, 23% by thermal methods, 45% by use in soil, 7% by composting and the other 7% by other methods. On the other hand in the USA, 45% of domestic sludge is disposed of in landfill and incineration plants, 21% in agricultural use, 12% in landscape use and 2% for soil remediation purposes [2].

In our country, highly significant parts performed by legal arrangements during the European Union accession process have been taken and priority areas on the environment have been stated. The regulations have been put into place within the framework of Environment Law number 2872 and its linked Water Pollution Control Regulation, Urban Wastewater Treatment Directive, Regulation on Landfill of Waste, Regulation on Soil Pollution Control and Point Source Contaminated Sites, Regulation on the use of Domestic and Urban Sewage Sludge in Soil as well as Regulation on Waste Incineration and Waste Management.

There is not enough knowledge about sewage sludge rates in Turkey and a lot of countries. From past to present, these issues have brought about various problems. The purpose of this study, the quantities and resources of sewage sludge generated in Turkey were examined. Besides future management strategies and solution proposals are also presented.

2. Sewage sludge generation in Turkey

A wastewater treatment plant is a central unit of the municipal wastewater system. It receives polluted wastewater from the urban area, originated from various supplies including domestic, industrial, commercial, hospital and agricultural in the form of water, human excreta, personal care products, detergents, disinfectants, and sediments etc. Although many variations of wastewater treatment plants exist, most of the facilities usually have the following steps: preliminary treatment and secondary treatment. A typical layout of a conventional wastewater treatment plants is shown in Figure 1 [7].

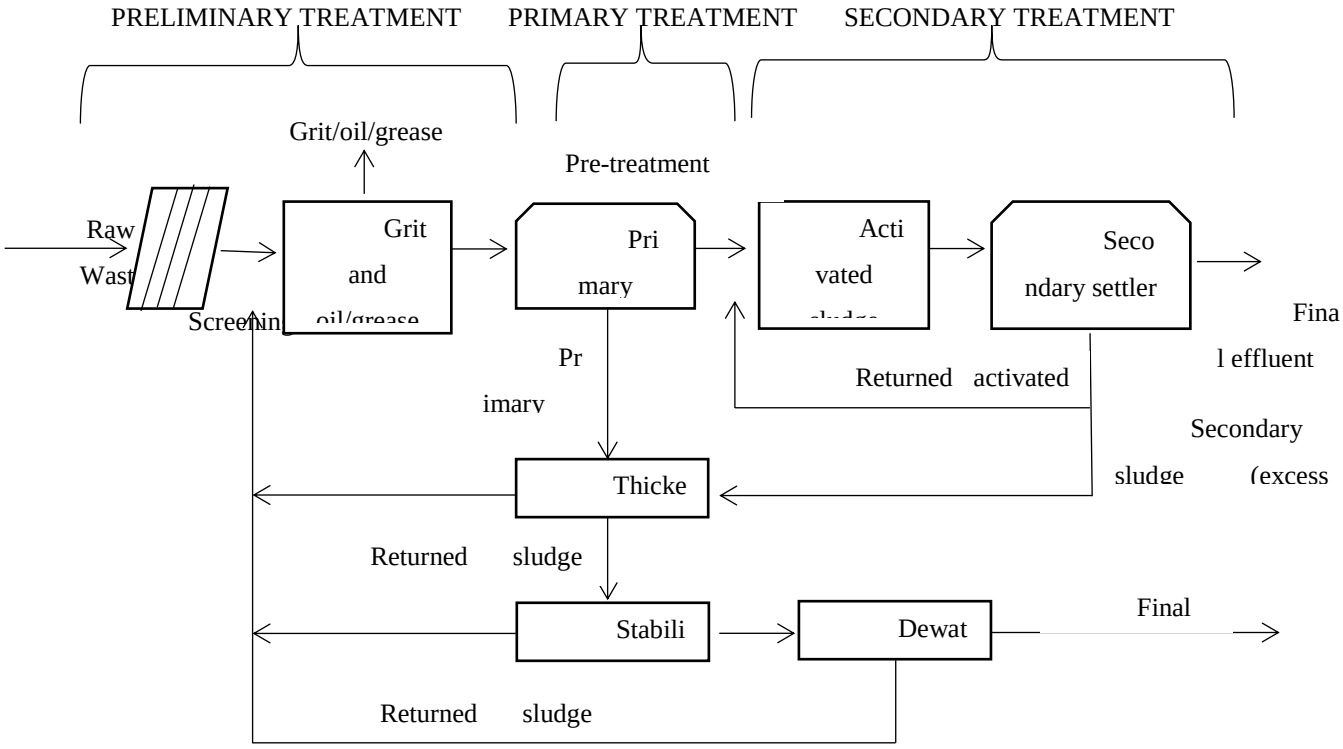

Figure 1. The treatment of municipal wastewater and the production of sewage sludge [7].

The primary stage removes 50-70% of the total suspended solids in the raw wastewater and the sludge occurred at this stage is called primary sludge. The secondary treatment is a

biological process involving utilization of microbes to stabilize organic constituents and to remove non-colloidal solids. In Turkey, municipal wastewaters treat by using 1% of natural treatment, 23% of physical treatment, 31% of biological treatment and 44% of advanced treatment processes. The amount of treated wastewater in the municipal wastewater treatment plants of Turkey is shown in Figure 2.

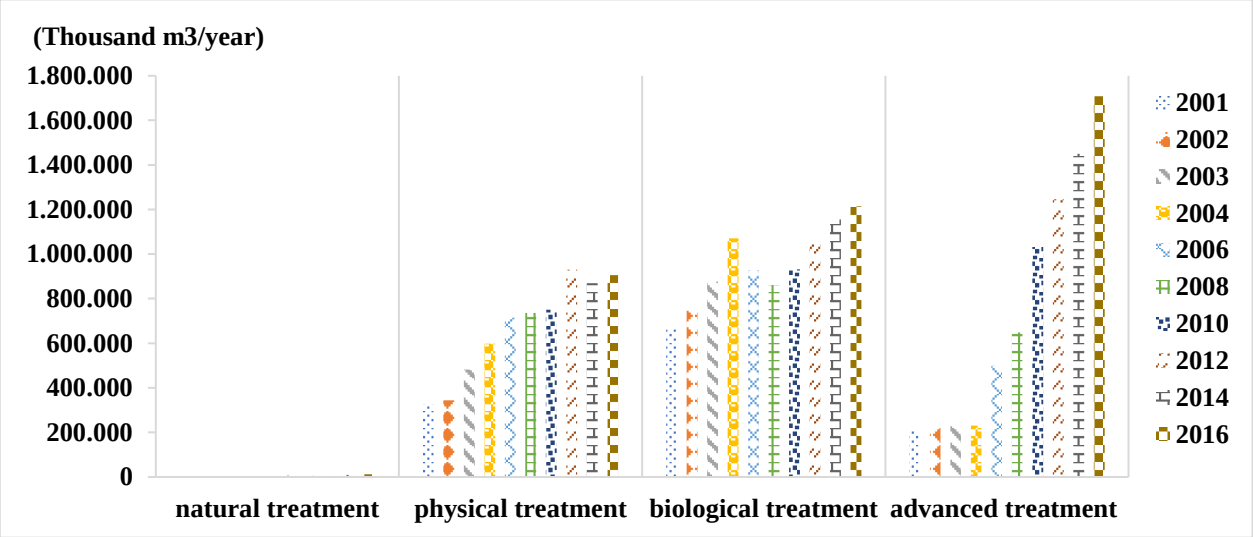

Figure 2. The amount of treated wastewater in the wastewater treatment plants of Turkey
(thousand m^3/year).

According to Figure 2, municipal wastewaters treat by using 1% of natural treatment, 23%of physical treatment, 31% of biological treatment and 44% of advanced treatment processes. In 2016, Figure 3. is indicated the amount of sewage sludge percentages by disposal and recovery methods of Turkey.

Sewage sludge refers to scented and semi-viscous waste that contains solids at the rate of 0.25-12% depending on the applied treatment processes. Sewage sludge that is occurred at diverse steps in the treatment plant has specific characteristics such as solid concentration and biological degradability. Table 1. demonstrates the composition of domestic sewage sludge in different regions of Turkey.

Table 1. Characteristics of sewage sludge generated in various regions in Turkey [2].

City Kayseri	Bursa (East)	Bursa (West)	Mersin (Tarsus)	Istanbul (Paşakoy)	Samsun (Bafra)	Ankara	Eskişehir
Item, Sludge Dewatered	Anaerobic stabilization ponds	Anaerobic stabilization ponds	Activated sludge	Dewatered sludge	Dewatered sludge	Dewatered sludge	Dewatered sludge
pH	**7.09**	**6.99**	**6.25**	**8.01**	**6.24**	**6.08**	**5.73**	**6.43**
Conductivity	**1.86**	**2.38**	**-**	**-**	**10.67**	**3.63**	**5.57**	**6.29**
(dS/m)	**52.8**	**52.1**	**69.55**	**-**	**79.4**	**55.2**	**80.5**	**61.6**
TVS (%)	**4.91**	**4.25**	**15.77**	**74.48**	**11.6**	**23.2**	**16.9**	**17.8**
TS (%)	**2.48**	**2.07**	**5.80**	**-**	**7.81**	**3.73**	**5.23**	**4.49**
TN (%)	**0.41**	**0.24**	**-**	**-**	**0.86**	**0.72**	**0.46**	**1.05**
TP (%)	**-**	**-**	**6.7**	**8.96**	**-**	**-**	**-**	**-**
C/N	**448**	**202**	**56.9**	**174.89**	**35.2**	**96.7**	**197**	**415**
Ni (mg/kg)	**28**	**353**	**103.9**	**356.73**	**119**	**271**	**163**	**1345**
Cu (mg/kg)	**2278**	**7451**	**701.8**	**839.14**	**543**	**4900**	**1268**	**1927**
Zn (mg/kg)	**4114**	**586**	**60**	**396.5**	**19.7**	**128**	**85.3**	**380**
Cr (mg/kg)	**126**	**73.3**	**< 30**	**42.021**	**43.3**	**146**	**58.8**	**301**
Pb (mg/kg)	**1.69**	**1.70**	**< 0.1**	**1.805**	**0.53**	**4.43**	**0.80**	**4.33**
Cd (mg/kg)	**-**	**-**	**-**	**502.19**	**-**	**-**	**-**	**0.53**
Mn (mg/kg)	**0.25**	**0.24**	**-**	**-**	**0.31**	**0.22**	**0.14**	**-**
K (%)	**-**	**-**	**-**	**-**	**-**	**-**	**-**	**038**
Ca (%)	**-**	**-**	**-**	**-**	**-**	**-**	**-**	**-**
Na (%)	**-**	**-**	**-**	**-**	**-**	**-**	**-**	**-**
Fe (%)	**-**	**-**	**-**	**0.14**	**-**	**-**	**-**	**-**

As can be seen from the table, characteristics of sewage sludge change per region treatment unit and season. Sewage sludge which is occurred as a result of wastewater treatments includes some inorganic compounds; phosphor, nitrogen and recoverable organic carbon. Furthermore, the heavy metals in its composition (Kd, Ni, Cr) and persistent organic compounds (pesticides, dioxins, PCB etc.) refer to hazardous characteristics to the sewage sludge [2].

3. Sewage sludge management in Turkey

The main goals of sludge treatment process are to reduce the total weight and volume in order to facilitate transportation and additional treatment, to stabilize the material through the destruction of pathogenic microorganisms, elimination of unpleasant odors, reduction of volatile solid content for safer disposal. Some stabilization methods such as anaerobic digestion also offer opportunity for energy recovery [7].

According to Turkish Statistics Institue (TurkStat) data for 2016, approximately 299.296 tons of sludge is generated in Turkey. 31% of sewage sludge is burned for energy recovery, 27% of them is disposed in sanitary landfills, 20% of them is disposed in open dumping area, 2% of them is dumped onto land without any control, 6% of them is used for ecological proposals, 3%of them is used in agriculture and 11% of them is temporarily dumped. The amount of sewage sludge by disposal and recovery methods of Turkey are given in Table 2 and Figure 3 as the numeral and rational, respectively.

Table 2. Amount of sewage sludge by disposal and recovery methods, (TurkStat) 2016(1)

Methods	**Amount of sewage sludge (tons)**
Incineration with energy recovery	93 940
Disposal in controlled landfill sites	83 005
Disposal in municipal dumping sites	62 733
Dumping onto land	7 023
Land treatment resulting in benefit to agriculture or ecological improvement	19 470
Agricultural use	9 261
Other(2)	33 125
Total	**299 296**

TurkStat, Municipal Wastewater Statistics, 2016
(1) Data on sludge amount is in dry matter
(2) Includes sludge amounts temporarily stored, buried, etc.

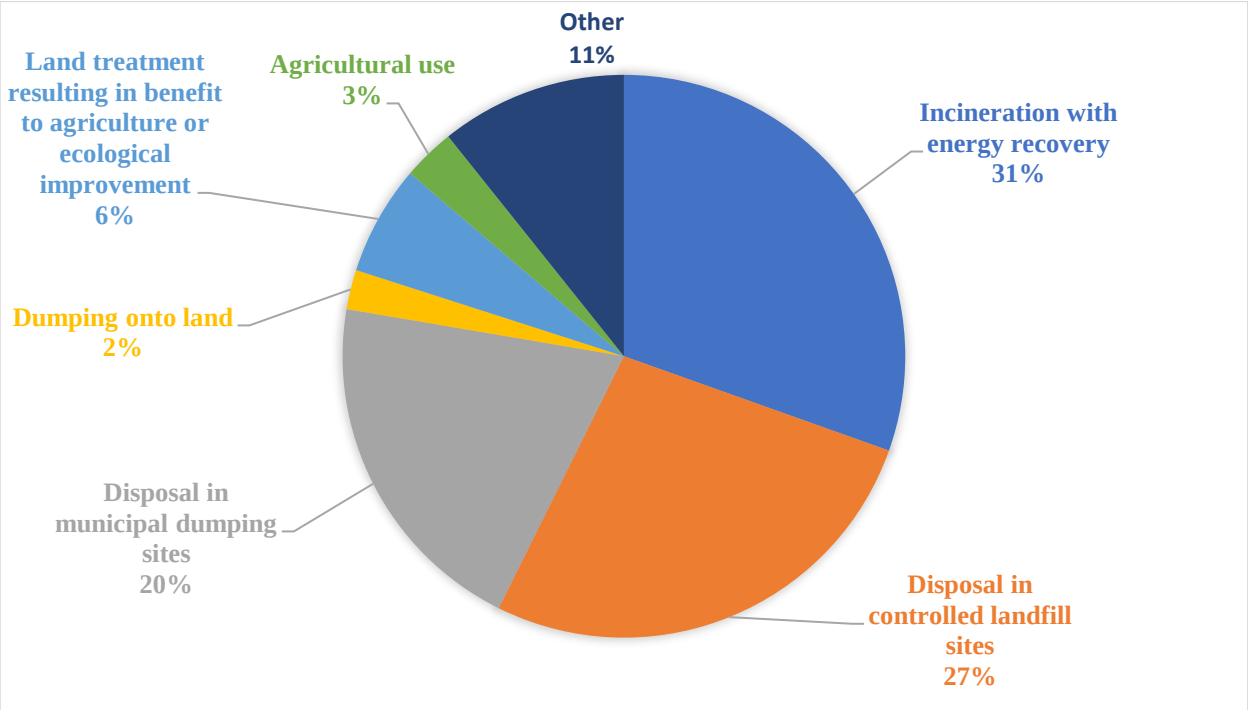

Figure 3. Amount of sewage sludge by disposal and recovery methods, (TurkStat) 2016[(1)]

In Turkey, anaerobic digestion is generally used in order to recover energy from municipal sewage sludge. However, it would not be sufficient to take into account only current technologies for sustainable sludge management. For this purpose, it is necessary to compare different methods with one another according to various criterion [2]. To realize energy or heat recovery from sewage sludge, biochemical (anaerobic digestion, gasification) and thermal (incineration, pyrolysis, supercritical water gasification) methods can be employed. In the anaerobic digestion and supercritical water gasification methods, sludge drying is not required. To have a high yield with incineration, gasification and pyrolysis methods, the water content of sludge needs to be reduced. In terms of energy recovery heat is generated by incineration, bio-oil by pyrolysis and biogas by anaerobic digestion and supercritical water gasification [2]. Nowadays, there are two main parts for sewage sludge management, namely organic recycling and recycling of the energy and material as shown in Figure 4 [1].

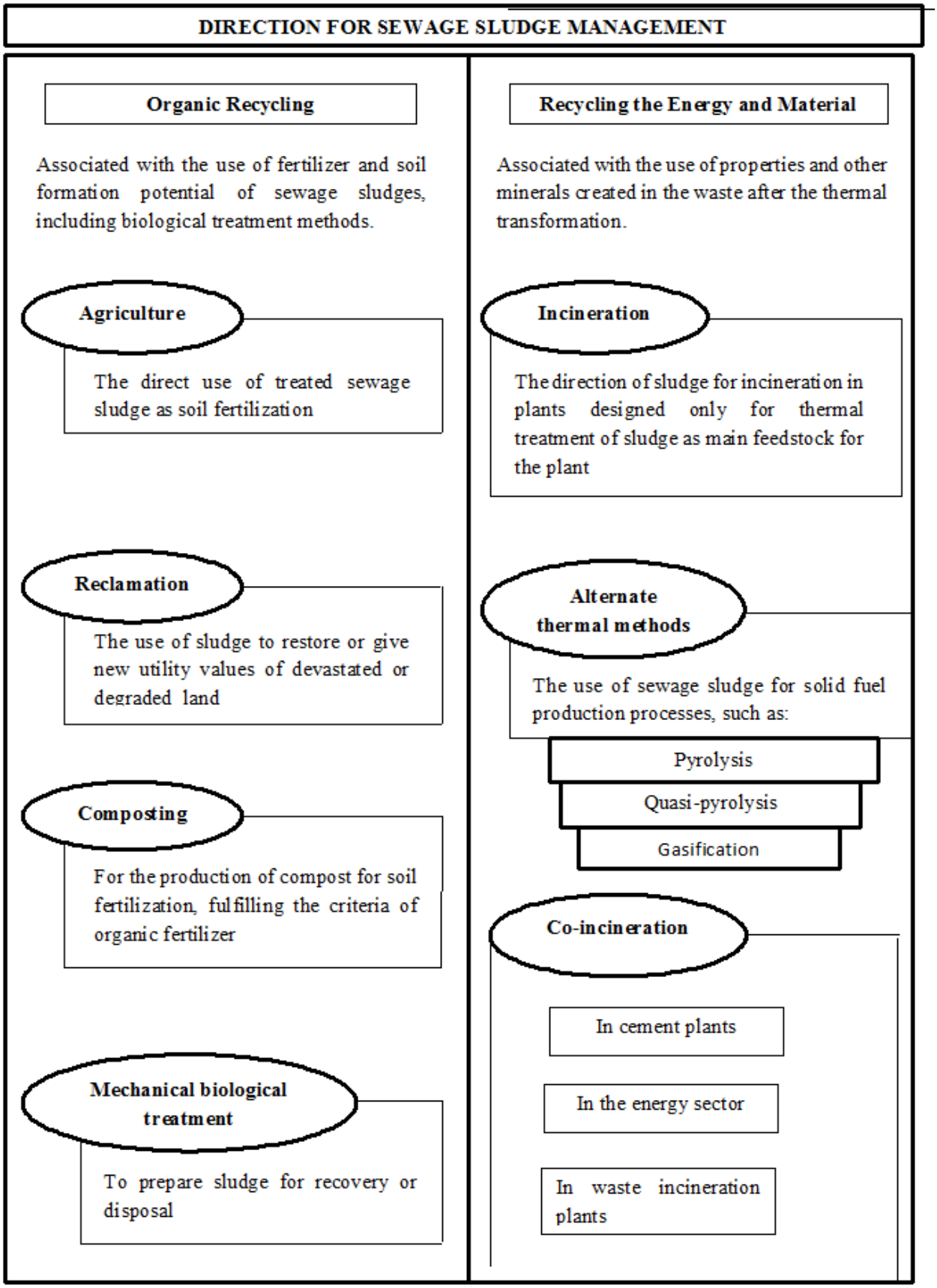

Figure 4. The main strategies of sewage sludge disposal.

4. Conclusions

The management of sewage sludge is becoming an issue of growth importance. The rapid growing of population and the fast rate of urbanization create serious challenges to the sustainable development. In the wake of lesser land-fill sites and stringent disposal regulations, a shift is required from conventional disposal to advanced valorization strategies. The production and consumption levels which rapidly increasing day by day, result in increased amount of wastewater and consequently amount of sludge which needs to be treated. In present, sewage sludge disposal methods are not sufficient with respect to treatment efficiency and released greenhouse gas emissions. Therefore, alternative methods should be identified for sustainable sewage sludge management. Sewage sludge management process should be developed separately for each treatment plant. Only then it is possible that management methods will be ecologically and economically justified. Comprehensive chemical characteristics together with toxicity characteristics are essential for the development of methods concerning sewage sludge management.

References

Kacprzak M., Neczaj E., Fijalkowski K., Grobelak A., Grosser A., Worwang M., Rorat A., Brattebo H., Almas A., Singh B. R., 2017. Sewage Sludge Disposal Strategies For Sustainable Development, *Environmental Research*, 156, 39-46.

Adar E., Karatop B., İnce M., Bilgili M. S., 2016. Comparison of Methods for Sustainable Energy Management with Sewage Sludge in Turkey Based on SWOT-FAHP Analysis, *Renewable and Sustainable Energy Reviews*, 62, 429-440.

Cieślik B. M., Namieśnik J., Konieczka P., 2015. Review of Sewage Sludge Management: Standarts, Regulations and Analytical Methods, *Journal of Cleaner Production*, 90, 1-15.

Fijalkowski K., Rorat A., Grobelak A., Kacprzak M. J., 2017. The Presence of Contaminations in Sewage Sludge – The Current Situation, *Journal of Environment Management*, 203, 1126-1136.

Anjum M., Al-Makishah N. H., Barakat M. A., 2016. Wastewater Sludge Stabilization Using Pre-Treatment Methods, *Process, Safety and Environmental Protection*, I02, 615-632.

Liu G., Song H., Wu J., 2015. Thermogravimetric Study and Kinetic Analysis of Dried Industrial Sludge Pyrolysis, *Waste Management*, 41, 128-133.

Syed-Hassan S. S. H., Wang Y., Hu S., Su S., Xiang J., 2017. Thermochemical Processing of Sewage Sludge to Energy and Fuel: Fundamentals, Challenges and Considerations, *Renewable and Sustainable Energy Reviews*, 80, 888-913.

Effects Of Pumice Amendment On Compost Quality İn İndustrial Sludge Composting

Nurdan AYCAN[1*], Nurdan Gamze TURAN[2]

[1]Ondokuz Mayıs Üniversity, Dept. of Environmental Engineering, Samsun, Turkey
[2]Ondokuz Mayıs Üniversity, Dept. of Environmental Engineering, Samsun, Turkey

*** Corresponding Author:** nurdann.aycan@gmail.com

Abstract

In this study, the pilot-scale co-composting of industrial sludge and pumice with three different rates was conducted for 13 weeks to evaluate the effects of compost quality. The results indicated that all of three additives could adequately buffer pH, considerably reduce ammonia and enhance organic matter degradation. Particularly, pumice amended treatment showed the least nitrogen loss by 19.13%. The results of the study showed that pumice as amendment material is an effective material for composting of industrial sludge. The best combination of industrial sludge and pumice is suggested as a rate of 40% pumice and 60% industrial sludge to improve the quality od compost.

Keywords: Treatment sludge; sludge management; composting; natural amendments; pumice.

1. Introduction

The sludge is an unavoidable by-product arising from wastewater treatment processes (Bratina et al., 2016). Sludge production have increased with the industrialization, population growth and rapid development of urbanization. Management of sewage and industrial sludge is a significant problem all over the world (Mymrin et al., 2014).

Industrial sludge contains more hazardous materials than sewage sludge such as heavy metals, organic pollutants and pathogens (Wu et. Al., 2015; Islam et al., 2017). The qualities and quantities of industrial sludge depend on origin and treatment processes. Improper management of industrial sludge lead to environmental and health risks (Silva et al., 2011).

Lots of sludge treatments techniques are used to eliminate the hazardous constituent and mitigate its negative impacts (Silva et al., 2011). The most common sludge treatment techniques are landfill, composting, incineration and pyrolysis (Arif et al., 2018). Among them, composting is an applicative and low-cost technique for converting sludge into a safe and usable product (Wong et al., 2017; Jain et al., 2018). However, a high moisture content and a low particle size affect the dynamics of the composting process (Barrena et al., 2014). Thus, the sludge should be mixed with dry material.

The aim of the study is to investigate the effects of pumice on industrial sludge composting. For the experiments, in-vessel composting systems were constructed as pilot scale. The variations of pH, electrical conductivity, moisture content, ammonia nitrogen, nitrate nitrogen and total nitrogen were analyzed during the process. At the end of the process, the results were compared to compost quality ciriteria.

2. Materials and methods

Industrial sludge was obtained from an industrial wastewater treatment plant (Samsun, Turkey). The characteristics of the indsutrial sludge is presented in Table 1.

Table 1. The characteristics of industrial sludge

Parameters	Value	Method
pH	8.26	TSISO 10390
Lead (Pb^{2+}), mg/L	<0.01	EPA 200.7
Zinc (Zn^{2+}), mg/L	0.653	EPA 200.7
Copper (Cu^{2+}), mg/L	3.152	EPA 200.7
Total organic carbon (TOC), mg/kg	151300	TS 12089 EN 13137

Sulphate (SO_4^{2-}), mg/L	139.81	SM 4500 (SO_4^{2-}) E
Selenıum (Se^{2-}), mg/L	0.404	EPA 200.7
Crom (Cr^{6+}), mg/L	0.275	EPA 200.7

The pumice purchased from Soylu Mining Co. Inc. (Nevşehir, Turkey). The physicochemical properties of pumice are listed in Table 2.

Table 2. The physicochemical properties of pumice

Compounds	**Weight (%)**
Na_2O	3.65
Al_2O_3	12.27
SiO_2	73.44
CaO	0.96
$TıO_2$	0.10
K_2O	4.37
Fe_2O_3	1.2
SO_3	0.08

The composting process was conducted in closed bench-scale reactor with an inner width of 25 cm, lenght of 40cm and height of 25 cm. Forced aeration was supplied by the air pump. Fresh air was pumped into the reactor from the bottom through perforation pipes fitted as parallel (Fig. 1).

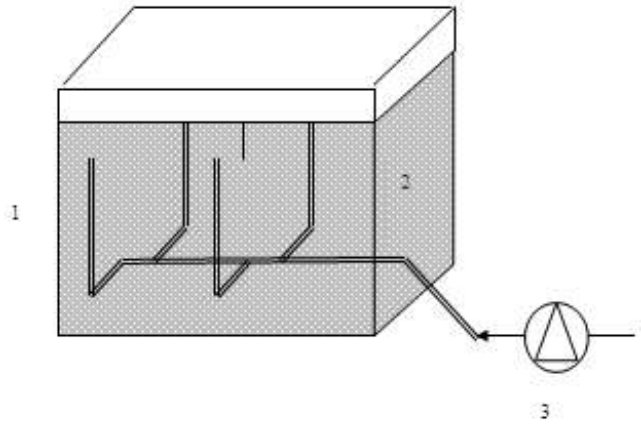

Figure 1. Schematic view of pilot composting systems (1) composting unit, (2) sludge mixture, (3) ventilation pump

Industrial sludge and pumice were mixed at different ratios as volume. Mixture ratios are given in Table 3. For each treatment, 25 L of the mixture was prepared and composted for 100 days. Sampling was carried out weekly during the process.

Table 3. Mixture ratios for this study

System no	**Mixture rates**
System 1	10% Pumice + 90% Industrial Sludge
System 2	25% Pumice + 75% Industrial Sludge
System 3	40% Pumice + 60% Industrial Sludge

3. Results and discussion

Figure 2 presented the change of the pH during composting process. The pH values varied between 6.5-8.0 during the process. At the beginning of the composting process, the pH values was found as about 8.0. It decreased from 3rd week to 7th week. Then, it increased approximately 7.5 of pH. These fluctuations are thought to be due to the rapid breakdown of organic matter into organic acids in the first weeks (Haug, 1993). The optimum pH value for the mature compost is 6.5-7.2 (WERL, 2000). Accordingly, at the end of the composting process, the pH values of all systems are compatible with the mature compost pH.

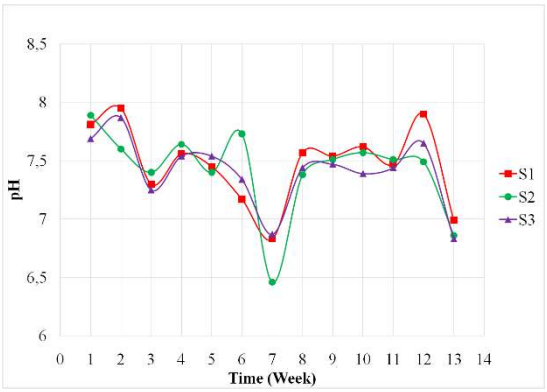

Figure 2. Effect of pumice on pH

At the beginning of the composting process, the electrical conductivity values of the systems varied between 0.6-0.8 mS/cm. The electrical conductivity values decreased depending on the acidity in the first weeks. The highest electrical conductivity value was found in the system S1 (System 1; 10% pumice + 90% industrial sludge). In all systems, the electrical conductivity values began to decrease after 8 weeks (Figure 3).

According to Penwarn (2002), the compost maturity grade of <1 mS/cm is "very good", the compost maturity grade of 1-2 mS/cm is "medium", and the compost maturity grade is 2-3 mS/cm is considered "salty". At the end of the process, the electrical conductivity values of the composts obtained in all pumice operated systems are in "very good" class.

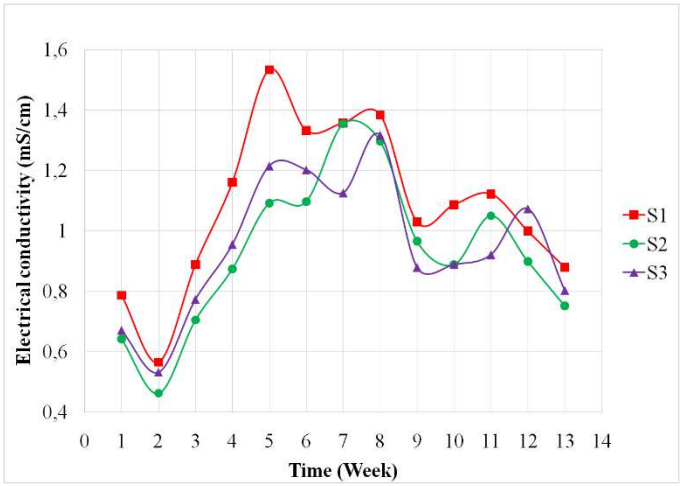

Figure 3. Effect of pumice on electrical conductivity

In all composting systems, moisture content values changed between 50-60% during the process. At the beginning of the process, moisture content values were close to 60%. It was measured approximately 50% at the end of the process.

The optimum moisture content value for composting is given 50% in the literature (Haug, 1993). As shown in Figure 4, although there were minor changes in the moisture content during the process, the moisture content values at the end of the process were optimum in all pumice-operated systems.

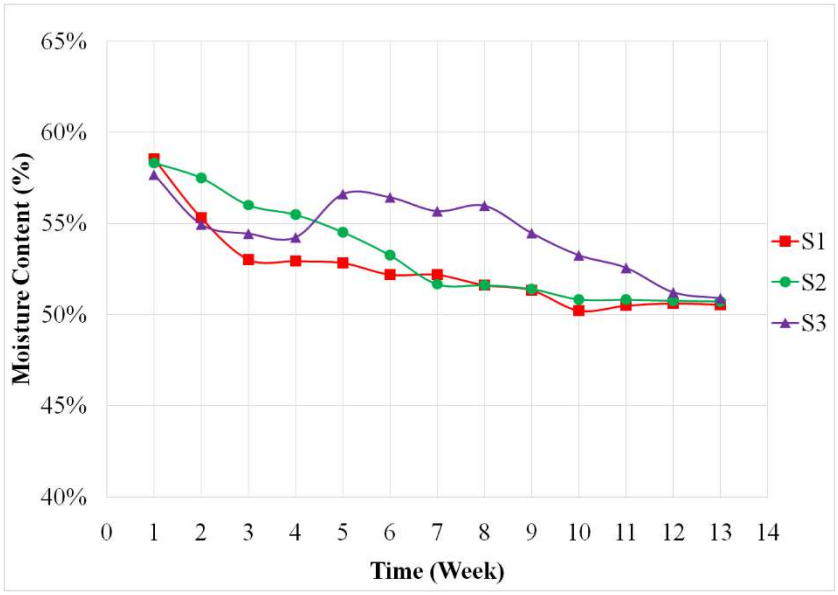

Figure 4. Effect of pumice on moisture content

According to the compost quality criteria, the ammonium nitrogen (NH_4^+-N) value must be within the range of 75-500 mg/L (WERL, 2000). At the end of the composting process, the ammonium nitrogen (NH_4^+-N) values of the composts obtained from the systems were 294.21

mg/L for S1 (System 1; 10% pumice + 90% industrial sludge), 252.21 mg/L for S2 (System 2; 25% pumice + 75% industrial sludge) and 222.52 mg/L for S3 (System 3; 40% pumice + 60% industrial sludge). Accordingly, all systems using pumice have mature compost standards in terms of ammonium nitrogen (NH_4^+-N) parameter (Figure 5).

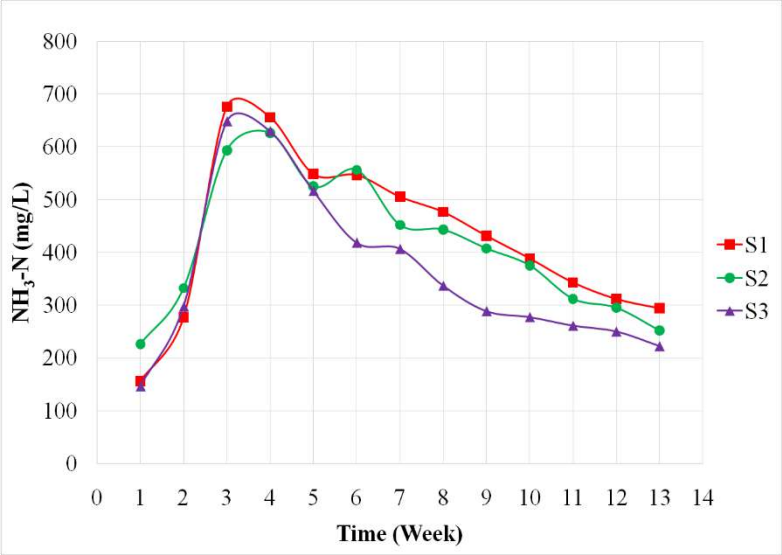

Figure 5. Effect of pumice on ammonium nitrogen (NH_4^+-N)

Nitrate nitrogen (NO_3^--N) values of the composting systems increased only in the first week. Then, its concentration decreased until the end of the process. Figure 6 shows the changes in nitrate nitrogen (NO_3^--N) in all systems. The compost quality according to nitrate nitrogen (NO_3^--N) concentration in composting processes is evaluated by the ratio of nitrate nitrogen (NO_3^--N) concentration to ammonium nitrogen (NH_4^+-N) concentration. The ammonium nitrogen (NH_4^+-N)/ nitrate nitrogen ratio (NO_3^--N) should be within the range of 0.5-3.0 for mature compost (WERL (2000). Accordingly, the ratios of ammonium nitrogen (NH_4^+-N)/ nitrate nitrogen (NO_3^--N) of the composts are in the range of 0.5-3.0. Therefore, all systems containing pumice provide the necessary value for mature compost. The ratios obtained at the end of the process; 2.55 for the S1 (System 1; 10% pumice + 90% industrial sludge), 2.25 for the S2 (System 2; 25% pumice + 75% industrial sludge) and 2.99 for the S3 (System 3; 40% pumice + 60% industrial sludge).

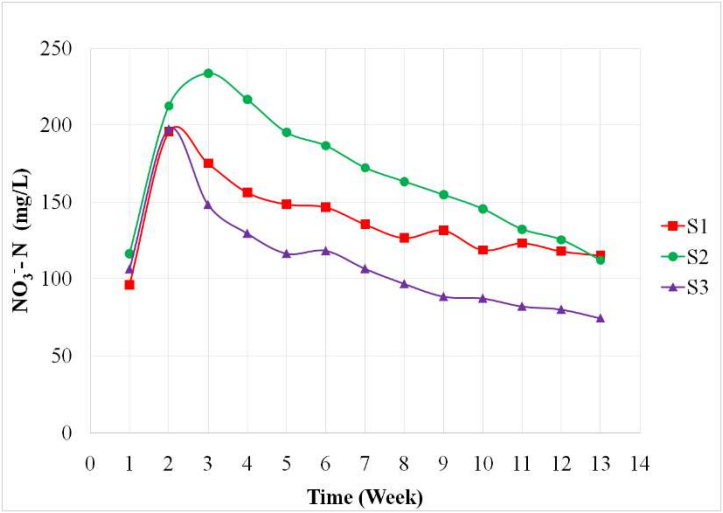

Figure 6. Effect of pumice on nitrate nitrogen (NO_3^--N)

The total nitrogen values of the systems are approximately 4.46% at the beginning of the process. The change of the total nitrogen concentration during the composting process is shown in Figure 7. As can be seen in Figure 7, a steadily decreasing curve was observed at the total nitrogen concentrations during the process. At the end of the process, the minimum nitrogen loss carried out in the system of S3 (System 3; 40% of pumice + 60% industrial sludge), and the maximum nitrogen loss occurred in the system of S1 (System 1; 10% of pumice + 90% industrial sludge).

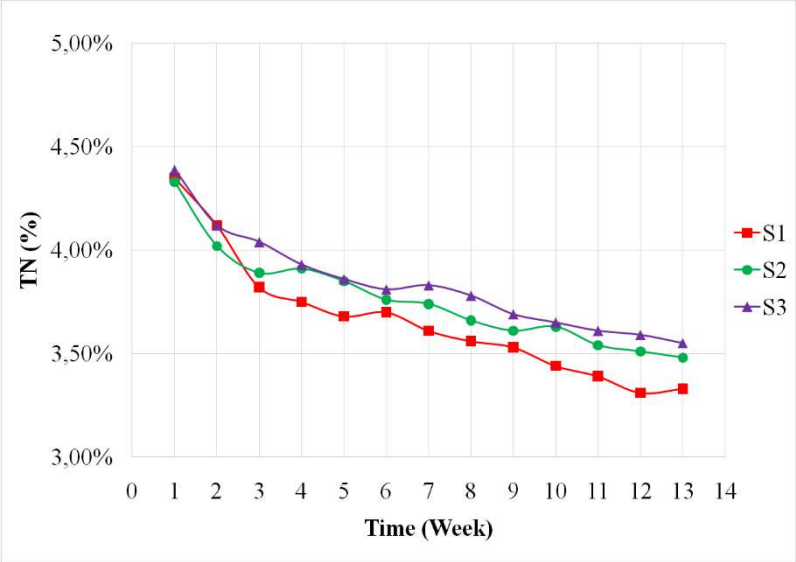

Figure 7. Effect of pumice on total nitrogen (TN)

4. Conclussions

To improve the compost quality, a pilot scale co-composting system with industrial sludge and pumice carried out in this study. Three different mixture ratios were tested and system performances are compared. The main conclusions from the study are as follows:

- The moisture content of the industrial sludges is very high for composting.
- Pumice can be used as a suitable additive material for industrial sludge composting.
- Pumice is an easy available and economical material.
- The use of pumice in the composting process has improved compost quality.

References

Arif, M. S., Riaz, M., Shahzad, S. M., Yasmeen, T. and Buttler, A. (2018). Fresh and composted industrial sludge restore soil functions in surface soil of degraded agricultural land, Science of The Total Environment, Volumes 619–620, Pages 517-527.

Barrena, R., Font, X., Gabarrell, X. and Sánchez, A. (2014). Home composting versus industrial composting: Influence of composting system on compost quality with focus on compost stability**,** Waste Management, Volume 34, Issue 7, Pages 1109-1116.

Bratina, B., Šorgo, A., Kramberger, J., Ajdnik, U. and Šafarič, R. (2016). From municipal/industrial wastewater sludge and FOG to fertilizer: A proposal for economic sustainable sludge management, Journal of Environmental Management, Volume 183, Part 3, Pages 1009-1025.

Haug, R. T. (1993). The Practical Handbook of Compost Engineering, Lewis Publishers, Florida.

Islam, M. S., Ahmed, M. K., Raknuzzaman, M., Habibullah-Al-Mamun, M. and Kundu, G. K. (2017). Heavy metals in the industrial sludge and their ecological risk: A case study for a developing country, Journal of Geochemical Exploration, Volume 172, Pages 41-49.

Jain, M. S., Daga, M. and Kalamdhad, A.S. (2018). Composting physics: A degradation process-determining tool for industrial sludge, Ecological Engineering, Volume 116, Pages 14-20.

Mymrin, V., Ribeiro, R. A. C., Alekseev, K., Zelinskaya, E. and Catai, R. (2014). Environment friendly ceramics from hazardous industrial wastes, Ceramics International, Volume 40, Issue 7, Part A, Pages 9427-9437.

Penwarn, W. (2002). Quality Compost, Educations Seminers, Petrik Technology & Approach, Petrik Laboratories, Inc., USA.

Robledo-Mahón, T., Aranda, E., Pesciaroli, C., Rodríguez-Calvo, A. and Calvo C. (2018). Effect of semi-permeable cover system on the bacterial diversity during sewage sludge composting, Journal of Environmental Management, Volume 215, Pages 57-67.

Silva, M.A.R., Testolin, R.C., Godinho-Castro, A.P., Corrêa, A.X.R. and Radetski C.M. (2011). Environmental impact of industrial sludge stabilization/solidification products: Chemical or ecotoxicological hazard evaluation?, Journal of Hazardous Materials, Volume 192, Issue 3, Pages 1108-1113.

WERL. (2000). Compost Quality in America, Technical Document, New York State Association of Recyclers, pp, 30-42, Woods End Research Laboratory, Inc., USA.

Wong, J. W. C., Wang, X. and Selvam, A. (2017). Improving Compost Quality by Controlling Nitrogen Loss During Composting, Current Developments in Biotechnology and Bioengineering, Book chapter:4, Pages 59-82.

Wu, Q., Cui, Y., Li, Q. and Sun, J. (2015). Effective removal of heavy metals from industrial sludge with the aid of a biodegradable chelating ligand GLDA, Journal of Hazardous Materials, Volume 283, Pages 748-754.

Application Of Brush Type Fish Passage To Hydroelectric Power Plant And Monitoring Of Fish Pass Efficiency With Pit Tag Sysytem

Bülent VEREP [1*], Serhat KÜÇÜKALİ [2], Davut TURAN[1], Ahmet ALP[3], Tanju MUTLU[4], Cüneyt KAYA[1]

[1]Univ. of Recep Tayyip Erdogan, Fac. of Fisheries, 53100, Rize-Turkey; bulent.verep@erdogan.edu.tr
[2]Çankaya Univ., Fac. of Eng., Civil Engineering Department, Ankara-Turkey; kucukali@cankaya.edu.tr
[3]Kahramanmaraş Sütçüimam Univ., Fac. of Agriculture, Maraş-Turkey; aalp@ksu.edu.tr
[4]Univ. of Recep Tayyip Erdogan, Voc. School of Techical Sciences, Rize-Turkey; tanju.mutlu@erdogan.edu.tr

[*] **Corresponding Author:** bulent.verep@erdogan.edu.tr

Abstract

Since the Eastern Black Sea region has an important potential in terms of river resources in our country, hydroelectric power plants have been in service in many rivers in the region in recent years. While the contribution of these plants to the country's economy is important, the environmental impacts of the construction phase and the hydrological and ecological effects of the river basin, where the dam is in operation, are getting more and more important. This study focuses on the existing fish migration in a hydroelectric power plant built on Iyidere. The fish passing performance of the present vertical slotted fish pass which has been transformed into a brush type fish pass, which is known to be newly used in Europe and known as fish friendly, has been examined. For this purpose, fish species caught electroshock around the fish passages were monitored by electromagnetic tags. With the 2 antenna PIT Tag monitoring system installed on the fish pass, the fish species living in the river basin were followed upwards through the fish pass of the related hydroelectric power plant and the brush type fish passage structure performance was determined. During the study, 450 fish belonging to 5 different species were tagged and it was determined that all species used fish gates.

Keywords: fish pass, hydro-electric power, fish, PIT tag.

1. Introduction

Our presentation is about application of brush type fish passage to hydroelectric power plant and Monitoring of fish pass efficiency with PIT tag system. Since the Eastern Black Sea region has an important potential in terms of river resources in our country, hydroelectric power plants have been in service in many rivers in the region in recent years. While the contribution of these plants to the country's economy is important, the environmental impacts of the construction phase and the hydrological and ecological effects of the river basin, where the dam is in operation, are getting more and more important.

This study focuses on the existing fish migration in a hydroelectric power plant built on Iyidere. The fish passing performance of the present vertical slotted fish pass which has been transformed into a brush type fish pass, which is known to be newly used in Europe and known as fish friendly, has been examined.

As you know, Fish migrate in short and long range for food, reproduce, sheltering, escaping from predators and due to change in environmental conditions and water quality. Since hydroelectric power plants, which meet the needs of electricity by utilizing water power, are installed on the rivers, the roads of the creatures who use the waterway are unfortunately closed. Therefore, the fish passages serve as a bridge in the upstream and downstream movements of the fish. Fish use fish passages like human across the stream for the sustainability of food chain in stream.

Turkish freshwater fish fauna are very rich and have 368 species, 31 families and 16 orders. Dominant species is from Cypriniformes order (247 species) and family of Cyprinidae (188 species). Others are Nemacheliidae (39 species), Salmonidae (21 species), Cobitidae (20 species), Gobiidae (18 species). In Turkish freshwater fish fauna is also very rich in terms of endemism, because it has 153 endemic species and nowadays non-native species are getting more and more as 28 species due to climate changing (Çiçek et al., 2005).

If we want to give some information about fish pass status of big dams, reservoirs or regulators and Small Hydropower Plants, It can be said that all big dams have no passage, 35 reservoirs or regulators (R&R) have fish passage of the 176 R&R but most of small hydropower plants have fish pass (URL 1; Çelebi, 2014) (Table 1).

Table 1. The Dam, Res&Reg and SHP numbers and fish passage status in Turkey

Type	Number	Fish passage status	Private or Governmental
Dam	592	No	G
Res/Reg	176	35	G
SHP	413	Most of them	P

In Turkey, most of small hydro power plants prefer pool and weir type fish pass. But It can be seen other type fish pass in some projects like vertical slot and denyl type fish pass (Özcan, 2016; Vigneus and Larinier, 2002) (Figure 1). But a fish passage types of brush so far not been applied in Turkey. This study as the project brush-type fishway is the first application in Turkey.

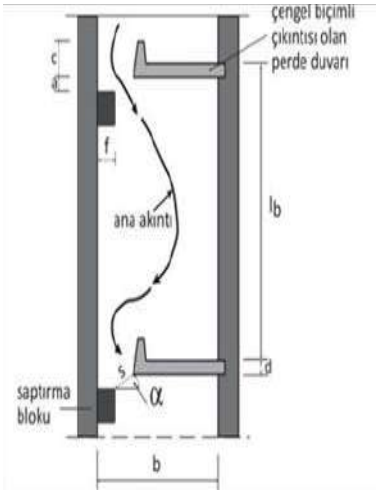

a-Vertical slot

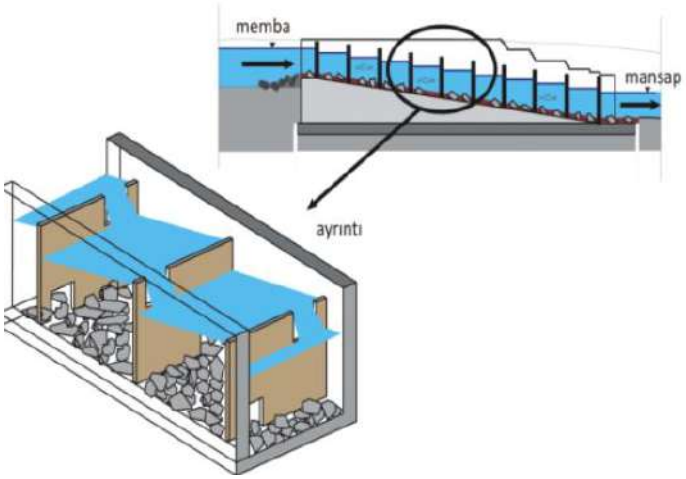

b-Pool and Weir with orifice

c-Brush type

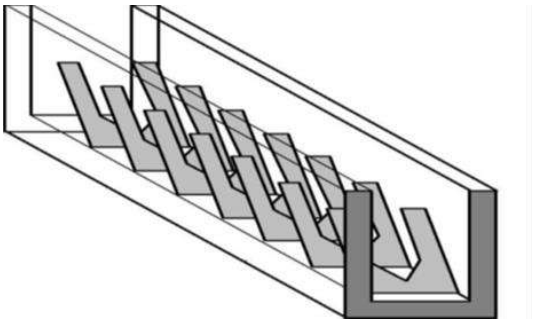

d-Denyl type

Figure 1. Fish passage types used by hydro power plants in Turkey (Tüfek, 2009)

The problems of fish passage in Turkey in general can be divided into 2 groups according to their structural and functional. Structural problems include wrong target species selection, unsuitable fish pass type choices and non-consideration of downstream fish migration. Functional problems are the incorrect design of the entrance of fish passages, the lack of water in a sufficient amount and the high slope of the fish passage structure (Verep and Turan, 2015; Verep et. al., 2016; Küçükali et al., 2017; Verep et. al., 2017).

And also some problems of Turkish fish passage of small hydropower plants in turkey are;

- Most of the fish pass structures are pool-weir and they have high current velocity (V>2 m/s) in the orifice slots,
- Passability of small and weak swimming capacities fish were not taken into account
- Inlet and outlet of the fish passages were not adequately designed for fish traceability
- Dynamic upstream water levels were ignored.
- If flow regime is supercritical, our fish passages are not functional. Because no pool and fast flow for small and weak fish to pass.
- Some fish passages designed inadequately in terms of upstream inlet for fish traceability.

In Yeşilırmak River Basin, a Project has been done and it contains pool&weir fish pass, and in general small fish caught in the Project area as shown in this presentation., that's why the pool&weir type fish pass is not appropriate for this basin (Verep et. al., 2017).

2. Material and Methods

Within the scope of this project, a field study was carried out in the Iyidere Akarsu in the eastern Black Sea rivers (Figure 2). İyidere River Basin in the Eastern Black Sea in Turkey, with a basin area of 1053 km^2; 40°20'0.76" E longitude and 40°59'34.36" N latitudes and 40°37'29.63 "E longitude and 40 ° 39'3.82" N latitudes and the total length of the stream is 53 km. The Incirli regulator and hydroelectric power generation plant located in the town of Kalkandere was taken into operation on 25 May 2011. Incirli HEPP's has 25.2 MW installed power and a tunnel of 6 Km long. The regulator has a drainage area of 895 km^2 and a net gross

of 63 m and a net reduction of 47 m are provided to the powerhouse from the regulator. There are 3 vertical axis Francis turbines in the powerhouse.

At this point, we recommend brush type fish pass and prepared a research project to try Turkey conditions in the basin of İyidere river on the eastern black sea region of Turkey. In this river basin are very rich in terms of SHP. In a SHP with pool weir type, fish passage will be converted to brush type and thus, the efficiency of the fish pass will be determined in this project.

On the base of a rectangular or trapezoidal cross-section, brush blocks or mixing elements are arranged as a roughness element in the hydraulic direction.

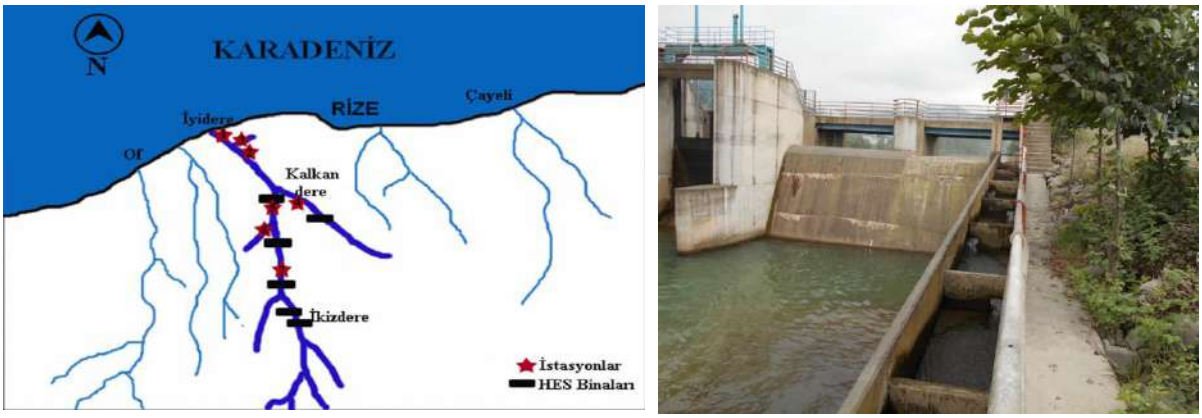

Figure 2. Study area and SHP

The brush block consists of a bunch of brushes, each containing 5 to 8 elastic brushes. While working with oval plastic brushes of sizes 4 mm-6 mm (average 5 mm) until 2010, instead of these, round plastic brushes of 6 mm diameter were used as of 2011. The brush block is made of brush bundles made of plastic or similar material and placed in the holes of a perforated carrier plate. The carrier plate and thus the brush block is mounted on a standard trapezoidal base plate of 300 mm wide, cut or welded in various rectangular, half or full trapezoidal, triangular or rhombic shapes. The brush block is screwed directly into the bottom of the canal or fixed on the individual concrete basement. A sensitive base substrate is placed around the brush pack. The length of the reed on the carrier plate normally corresponds to 47 cm.

The figurative fish passage structure examined under the project is located in the fish zone of the cyprinids. The maximum permissible speed of this zone is 1.8 m / s and the limit value for the amount of energy broken in unit volume is 150 W / m3. In the Incirli HEPP, the orifices

of the pool-orifice fish passage that existed prior to this study did not allow the passage of small and weak fishes due to water jetting. Within the scope of the project, the existing pooled-orifice fish passage in the Incirli HEPP, which is operated in the basin of Iyidere River, has been converted to brush type fish passage. Photographs related to the conversion of brush type fish pasture to the existing fish crossing in Incirli HEPP are presented in Figures. The construction of the brush type fish crossing was completed in as little as 4 days. The completion of the construction in such a short time is the reason why the materials are prefabricated in the factory and there is no concrete cast during construction. The reason for the diagonal arrangement of the brush blocks is that in such a sequence the flow is constantly transversally provided to the mixture and momentum transfer to the lateral direction. Pools were formed between brush groups by grouping brush blocks. The height of the fish passage is 5 m. The rectangular cross-section of the fish cross has a bottom slope of 10%, a channel width of 1.1 m, and a total length of 46.17 m. A total of 166 brushblocks and 45,973 brushes were placed in the desired order in the fish passages. River stones (up to a maximum of 0.16 m in diameter) were placed in the canal bed to create low velocity and turbulent microhabitat. This natural structure is thought to be beneficial to move upwards with species with low swimming performance (eg. rockfish).

Flow and turbulence measurements were performed primarily in the study. During the reed fish transition, uniform flow conditions occur and flow is in the river regime. The uniform flow depth within the fish passage way was measured by a liminometer which was placed in the micro ADV measurement system.

The concept of fish passage efficiency is concerned with both qualitative and quantitative evaluations. The productivity of a fish pass is considered a qualitative concept; this includes checking whether the system provides satisfactory passage for the target species under the flow conditions observed during the migrating period. In this study, the biotelemetry method was applied to determine the effectiveness of the fish pass. For this purpose, 2 antennas were placed on the lower section and upper part of the fish pass. The antennas are connected to a receiver, which is routed over the fish pass. The fish caught from the creek section at the bottom of the fish pass are marked. The tagged fishes were detected by the antenna as they passed through the square shaped antennas and their brand numbers and transit times were automatically recorded in the receivers.

The fishes to be watched telemetrically in the study were caught by electroshock devices below the fish passage during the migration season. The fish caught are labeled with PIT tags, stunned with appropriate anesthetic agents. The numbers of the tags placed on the body of the fish are read in the pistol and the fish species, size and other characteristics are recorded,

whichever fish is to be placed. PIT tags with electromagnetic properties are placed in small holes in the abdominal cavity of the fish with the tag gun. Since the holes are small, sewing is not necessary and it is healing shortly. Then, in clean, oxygenated water, the fish will settle within 15-20 minutes. The healthy fish are separated from the fish, and they are expected to pass through the fish passage. At the entrance and exit of the fish pass, the fish passing through the square antennas are detected and the PIT tag numbers of the fish are stored in the sensor device.

The Iyidere river basin could be considered rich in fish species before the establishment of hydroelectric dams. About 12-15 kinds of fish species were mentioned. But nowadays, the river basin where 6 different small hydro power plants operate seems to be considerably weakened in terms of fish species. In this study, 6 different species have been intensively caught, tagged and included for monitoring. During the study which lasted approximately 18 months, 372 species of fish were labeled in different species. 100 of these fishes have found the entrance of the fish pass and reached the fish pass.

3. Results and Discussion

Table 2. Efficiency of fish pass according to fish species

Species	Number of tagged fish	Fish number of detected with entrance antennas	Attractiveness performance (%) (AP)	Fish number of detected with exit antennas	Fish pass performance or efficiency (%) (EP)
Trout	55	28	50.91	19	67.86
Spirlin	97	33	34.02	20	60.61
Barbel	99	17	17.17	11	64.71
Barb	18	5	27.78	5	100.00
Chub	40	8	20.00	7	87.50
Goby	65	8	12.31	4	50.00
Total	372	100	26.88	66	66

The most important factor in migrating fish in the study area is the water temperature. Since the optimum water temperature conditions occur between March and May, thats why fish migrations occur in these months. 100 of the 372 tagged fish were able to reach the fish passage. To examine the species of fish that can find the fish passage: The species composition of the

fish that finds the fish passage is as follows; 33 spirlin, 28 trout, 17 barbel, 8 chub, 8 goby and 5 barb.

Two types of performance are examined when the effectiveness of a fish passage is determined. These are the passing of the fish passage and the other is attractiveness of fish pass that the shows to be able to find the entrance of fish pass. In this study, the percentage of fish reaching the lower part of the passageway was evaluated as attractiveness. The number of fish perceived on the upper antenna of the fish passage is called the fish passage performance. The attractive performance of the fish passage is calculated on the ratio of the number of fish that can find the fish passage to the number of all labeled fish. so it can be said that 26.88 percent of the tagged fishes were able to find the fish passage (Table 2). On the other hand, the efficiency of the fish passage is defined as the ratio of the number of fish that can find the entrance to the fish pass to the number of fish that pass the exit antennas of fish passage. That is to say, 66 percent of the efficiency of the Incirli fish pass in which the work was carried out. 66 percent of the fish that could find the fish passage were able to pass through the fish passage. In terms of fish species, activity was highest in 100% of Barb, followed by Chub with 87.5% followed by trout with 67.86%, Barbel with 64.71% and Spirlin with 60.61%. It has a low percentage of activity, such as 50%, although there are abundant goby species (Table 2).

References

[1] URL-1: http://www.dsi.gov.tr, (Date of access: 12 Mart 2018).

[2] Çelebi, R. 2014, Balık geçitleri ve Türkiye'de mevcut durumu [PDF document]. Retrieved from Symposium Notes Online Web site: http://www. http://sue.sdu.edu.tr/assets/uploads/sites/74/files/ramazan-celebi-sunum-18072014.pdf

[3] Özcan, Ç. B., (2016). Balık Geçiti, Balık Göçü Yapıları: Tasarım, Boyutlandırma ve İzleme, Devlet Su İşleri, (Translated from): Fischaufstiegsanlagen und fi schpassierbare Bauwerke – Gestaltung, Bemessung, Qualitätssicherung, Deutsche vereinigung für Wasserwirtschaft, Abwasser und Abfall e.V.

[4] Çiçek, E., Birecikligil, S.S., and Fricke, R. (2005). Freshwater fishes of Turkey: a revised and updated annotated checklist, BIHAREAN BIOLOGIST 9 (2): 141-157.

[5] Vigneus, E., and Larinier, M. (Eds.). (2002). Fishways: biological basis, design criteria and monitoring, . Food and Agriculture Organization of United Nations, Cemagref and CSP.

[6] Verep B., Turan D. (2015). "Fish Passages Examples From the Stream of Eastern Blacksea Region of Turkey", FISH PASSAGE 2015: international conference on river connectivity best practices and innovations, groningen, hollanda, 22-25 Haziran 2015, vol.1, no.1, pp.56-56.

[7] Verep B. , Küçükali S., Turan D. , Alp A. (2016). "A critical analysis of existing fish pass structures at small hydropower plants in Turkey", International Conference on River Connectivity: Fish Passage 2016, Amherst, A.B.D., 17-25 Haziran 2016, vol.1, no.11, pp.1-1.

[8] Küçükali S., Verep B. , Turan D. , Alp A., Mutlu T. , Özelçi D., et al., (2017)."An investigation of the hydrodynamic and fish behavior characteristics of the brush-type fish passage: Iyidere (Turkey) field study", Fish Passage 2017: International Conference on Engineering and Ecohydrology for Fish Passage, Corvallis, Oregon, A.B.D., 19-21 Haziran 2017, vol.2017, no.1, pp.143-143.

[9] Verep B. , Akin Ş., Şahin C. , (2017)."The Dam Effects on the Distributions of Fish Assemblages and Water Quality on Yeşilırmak River (Turkey) using Principle Component Analysis", Fish Passage 2017: International Conference on Engineering and Ecohydrology for Fish Passage, Corvallis, Oregon, A.B.D., 19-21 Haziran 2017, vol.2017, no.1, pp.53-53.

[10] Tüfek Ö.M. (2009). Balık Geçitleri: Tasarım, Boyutlandırma ve İzleme, Devlet Su İşleri, (Translated from): Fish passes: design, dimensions and monitoring, FAO-2002, 111s.

Prestudies for the Wastewater Reuse in Green Areas

Saba FATTAHİ[1*], Mustafa SAĞLAM[2], Yüksel ARDALI[1]

[1]Ondokuz Mayis University, Engineering Faculty, Department of Environment Engineering, Atakum, 55200, Turkey.
[2]Ondokuz Mayıs University, Agricultural Faculty, Department of Soil Science and Plant Nutrition, Atakum, 55200, Turkey

[*]**Corresponding Author:**yüksel.ardali@omu.edu.tr

Abstract

Domestic effluents may contain important nutrients for agricultural crop development, and reusing this effluent on irrigation can reduce the potable water demand, recycle nutrients, and decrease effluent discharges on water bodies. The use of treated municipal wastewater for farming irrigation has been a popular and old practice in agriculture. Due to water restrictions and rising water use in recent years, especially in agricultural sector and increasing pressure on freshwater resources in water-deficit regions, using of non-conventional water sources or lower-quality water resources has been considered as a solution for water requirements in agricultural sector. This study evaluated the changes on physical, chemical characteristics of a purified wastewater, the yield and the quality of grass after cultivation with treated wastewater on irrigation. In this study, the use of treatment of domestic wastewater and the physical and chemical analyses of treated wastewater were taken into account. Petri dishes method was used in this experiment and based on Petri's experiments with four replicates and 11 base factors (treated wastewater (a)) and four models of golf grass seed (Lolium perenne topgun, Poa pratensis geisha, Festuca rubra com, Festuca rubra sergei (b)).This study was carried out in four randomized design experiments, and 25 seeds per petri dishes were planted and added to the aluminium plates with the addition of treatment water at different concentrations of the peters. Based on the static rules, after germination time for each seed was completed and at the end of the work, data and results were obtained using a MSTAT-C package based on a randomized factorial or completely randomized analysis of variance. Considering the results and the data obtained and taking into account the interaction between germination speed and germination strength and length of bud, root length and fresh weight of bud and root fresh weight and taking into account the mean square and with considering that all factors are significant at a probability level of 1%, for each analysis, the average Duncan Table was prepared. As a result based on analysis of variance of MSTAT-C package and taking into account the interaction between treated and grass concentrations and according to the average Duncan table lolium perenne topgun with the highest data were considered the most suitable and best lawn for golf course and Poa pratensis geisha with very low germination rate and are not suitable for golf courses.

Keywords: wastewater treatment, golf course, grass, irrigation, reused water

1. Introduction

In many arid and semi-arid countries, water is increasingly scarce; as a result, specialists are thought to provide new water sources, which is effective on agricultural development. Water consumption has increased with increasing world population and rising health levels (Azarpira et al., 2013; Alizadeh et al., 2011). Agriculture is the largest user of water with about 75% of freshwater being currently used for irrigation (Prathapar, 2000). The use of treated municipal wastewater for farming irrigation has been a popular and old practice in agriculture. Due to water restrictions and rising water use in recent years, especially in agricultural sector and increasing pressure on freshwater resources in water-deficit regions, using of non-conventional water sources or lower-quality water resources has been considered as a solution for water requirements in agricultural sector. Wastewater is one of the lower-quality water resources. Also nonconventional water sources, especially treated municipal wastewaters represent complementary supply sources that may be substantial in regions affected by extreme scarcity of renewable water resources (Mousavi and Shahsavari, 2014; Mousavi et al., 2013; Galavi et al., 2009; Al-Jasser, 2011). Therefore, use of treated municipal wastewaters is introduced to prevent environment pollution and as a source for irrigation in agriculture (Scott et al., 2000; Oweis et al.,2000). The successful development of this reliable water resource depends upon close examination and synthesis of elements from infrastructure and facilities planning, wastewater treatment plant sitting, treatment process reliability, economic and financial analysis, water utility management, and public acceptance (Azarpira et al., 2014; Friedel et al., 2000; Jimenez, 2005; Fonseca et al., 2007; Mohammad et al., 2007; Choukr-allahand Hamdy, 2008). Asgari et al. (2007) reported that total dry matter and leaf area index of maize statistically affected with using treated municipal wastewater, in this study, maximum dry matter and leaf area index were obtained of the treatment that was irrigated with wastewater.

The crisis of water scarcity is one of the challenges facing the world today. Restriction of water resources has attracted researchers to the principled use of unconventional waters such as saline waters and urban and industrial wastewater. Due to the development of cities and increased water use, a large amount of wastewater is produced, which can be considered as a valuable resource in increasing the vegetation cover. Provided that it’s proper use is accompanied by proper wastewater treatment. Correct use of urban wastewater, in addition to the expansion of vegetation, prevents environmental pollution on the one hand, and on the other hand, having nutrient elements, in addition to reducing the pollution of surface water and

groundwater, reduces the cost of using chemical fertilizers (Abedi Kupaii et al., 1982). This is why water resources and cheap fertilizers are being considered and wastewater and wastewater treatment projects are being implemented on a large scale in industrialized and developing countries. As cities grow and their population grows, and the expansion of industries and factories, the issue of environmental pollution and the reduction of natural resources is increasingly important. Undoubtedly, urban environmental protection should be sought in the best use of industry and technology and related pollutants to protect the climate (Miller, 1984). Water scarcity in arid and semi-arid areas is one of the limiting factors in the development of green space. Increasing population growth and increasing environmental pollution require solutions to water scarcity, one of which is the reuse of sewage (Ghaneian et al., 2000).

In most countries with water scarcity, sewage sludge can be the cheapest and most accessible water source for irrigation due to the richness of the plant's elements. The use of refined wastewater for direct consumption of beverages has not yet been scientifically recognized for economic and psychological reasons, but if the reuse of treated wastewater and its transmission to the urban network, especially for irrigation of green spaces and industrial use since 1928 in the United States. In countries like Japan, Brazil, and Arabic countries facing dehydration, the use of wastewater for urban and agricultural use is increasing day by day. There is a lot of research about the effects of irrigation with sewage in some countries of the world. According to the research, irrigation with sewage can lead to losses, on the other hand, the need for irrigation in arid and semi-arid regions of the world, the presence of some of the high consumption and low consumption requirements of the plant in these waters and the prevention of pollution Habitats are benefiting from the reuse of these waters (Matouq, 2008).

2. Materials and Methods

The purpose of reuse of treated urban wastewater is to irrigate agriculture, fields, and green areas and determine the effect on the soil and vegetation. For this, treatments used by the Samsun metropolitan municipality golf course will be investigated in determining the effects on the lawn and soil of treated water and drinking water one irrigation techniques will be used: irrigation with treated wastewater. This experiment was carried out with petri method of raising grass seed, with four repetitions. In total, 44 petri dishes were germinated. The samples shall be collected with disinfected plastic bottles during the test period. Chemical analyses have been carried out for the characterization of treated water used in this study. In this study, the use of

treatment of domestic wastewater and the physical and chemical analyses of treated wastewater were taken into account, the initial values were found as pH= 7.32, EC=1463, BOD_5= 24 mg/l, COD=18 mg/l, NO_3-N=<0.1 mg/l, NO_2=<0.1 mg/l, T=19.6°C, dissolved oxygen=5.61 mg/l, total nitrogen=0.050 mg/l, total phosphorus=0.70 mg/l, NH_4-N= <0.1 mg/l, and suspended solid=0.262 mg/l. In this experiment, 9 cm sterile petri dishes were used with petri dye paper (Paper tray inside 9 cm sterile petri dishes). This study was carried out in four randomized design experiments, and 25 seeds per petri were planted and added to the aluminium plates with the addition of treatment water at different concentrations of the peters. The seeds were kept in an incubator at 25 ± 1 °C. Based on the static rules, after germination time for each seed was completed and at the end of the work, data and results were obtained using a MSTAT-C package based on a randomized factorial or completely randomized analysis of variance. Based on Petri's experiments with four replicates and 11 base factors (treated wastewater (a)) and four models of golf grass seed (Lolium perenne topgun, Poa pratensis geisha, Festuca rubra com,Festuca rubra sergei (b)) and interactions between them (a*b), either randomized or completely randomized design, and factorial based on the following method done.

3. Results

Considering the results and the data obtained and taking into account the interaction between germination speed and germination strength and length of bud, root length and fresh weight of bud and root fresh weight and taking into account the mean square and with considering that all factors are significant at a probability level of 1%, for each analysis, the average Duncan table was prepared (Table-1).

Table 1. Statistical analysis for the interaction between germination speed and germination strength and length of bud, root length and fresh weight of bud and root fresh weight

V.K	S.D	Germination speed		Germination strength		Sprout length	
		K.O.	F Value	K.O.	F Value	K.O.	F Value

Purification Water	10	279.16	23.41**	139.66	6.57**	0.5620	6.01**
Grass Types	3	12530.31	1051.16**	18935.41	892.11**	75.11	802.92**
Purification Water × Turf Types	30	145.39	12.19**	112.61	5.30**	0.8730	9.33**
Error	132	11.92		21.22		0.0940	
General	175	----------	----------	----------			
CV%		6.61	6.77	5.55			

V.K	S.D	Root length		Fresh weight buds		Root fresh weight	
		K.O.	F Value	K.O.	F Value	K.O.	F Value
Purification Water	10	10	0.3680	7.52**	1.16	10.15**	0.7410
Grass Types	3	3	33.64	686.77**	177.23	1545.81**	340.11
Purification Water × Turf Types	30	30	0.2680	5.47**	1.58	13.85**	1.54
Error	132	132	0.0490		0.1150		0.2830
General	175	175	----------	----------	----------		
CV%			9.61	6.50	7.99		

Germination Speed: According to the average Duncan table, the festuca rubra com. Longfellow grass is 90% refined at 84.75 a, freshwater with 85.50 a maximum germination and festuca rubra sergei 90%, treated wastewater with 24.75 and minimum data and speed Germination (Table-2).

Table-2. Average Duncan tables for germination speed in four grasses

Germination Speed										Av.
%100	%90	%80	%70	%60	%50	%40	%30	%20	%10	Fresh water

Lolium perenne topgun	62.00 def	50.00 ijklm	68.75 bcd	64.50 de	54.25 ghijk	46.50 lmno	59.00 efg	51.50 hijkl	48.75 jklmn	55.50 fghij	57.50 fgh	56.20 B
Poa pratensis geisha	43.50 mnopq	35.00 rstu	41.00 opqr	47.75 klmno	29.75 tuv	28.75 uv	36.50 qrst	37.25 pqrs	32.00 stu	33.75 stu	28.75 uv	35.82 D
Festuca rubra com.Longfellow	73.25 bc	84.75 a	74.00 b	73.25 bc	73.25 bc	73.50 bc	74.25 b	69.00 bcd	68.00 bcd	66.50 cd	85.50 a	74.11 A
Festuca rubra sergei	44.00 mnop	24.75 v	43.00 mnopq	56.00 fghi	45.25 lmno	42.00 nopqr	44.25 lmnop	42.75 mnopq	45.00 lmno	37.50 pqrs	45.50 lmno	42.73 C
Average	55.69 B	48.63 D	56.69 B	60.38 A	50.63 CD	47.69 D	53.50 BC	50.13 D	48.44 D	48.31 D	54.31 B	

Germination strength: According to the average Duncan table in the grass, lolium perenne topgun in freshwater with 93.75 a and 40% of refined wastewater with 92.00 ab are maximum germination capacity of grass and poa pratensis geisha in treated wastewater is 50%, 60% and 60% with 33. 75 and 36.00 have the lowest germination strength (Table-3).

Table-3. Germination strength in four grasses

	Germination strength											
	%100	%90	%80	%70	%60	%50	%40	%30	%20	%10	fresh water	Av.
Lolium perenne topgun	90.75 abc	81.00 cdef	88.75 abcd	85.50 abcdef	79.25 def	81.25 cdef	92.00 ab	82.00 bcdef	85.00 abcdef	87.50 abcde	93.75 a	86.07 A
Poa pratensis geisha	52.75 jkl	42.50 mno	46.25 lmn	54.50 jkl	36.00 o	33.75 o	41.00 mno	43.00 mno	38.75 no	41.00 mno	38.50 no	42.55 C
Festuca rubra com. Longfellow	82.50 bcdef	90.07 abc	82.13 bcdef	84.50 abcdef	76.75 fg	81.00 cdef	87.25 abcde	83.00 bcdef	78.50 ef	86.00 abcdef	90.00 abc	83.79 A
Festuca rubra sergei	49.75 klm	57.00 ijk	53.00 jkl	69.00 gh	65.00 hi	54.00 jkl	61.25 hij	64.25 hi	64.50 hi	62.00 hij	58.00 ijk	59.80 B
Average	68.94 BC	67.64 BC	67.53 BC	73.38 A	64.25 CD	62.50 D	70.38 AB	68.06 BC	66.69 BCD	69.13 AB	70.06 AB	

Sprout length: According to the average Duncan table in the grass, lolium perenne topgun in fresh water with 6.82 b and 80% of treated wastewater, the maximum length of

germination and poa pratensis geisha in 60% of refined waste with 3.36 have the lowest germination length Assigned (Table-4).

Table-4. Sprout length in four grasses.

	Sprout length											
	%100	%90	%80	%70	%60	%50	%40	%30	%20	%10	Fresh water	Av.
Lolium perenne topgun	6.78 bc	5.27 jkl	7.34 a	6.32 cdef	5.96 efgh	6.53 bcd	5.20 kl	5.70 hij	5.07 l	6.81 bc	6.82 b	6.16 B
Poa pratensis geisha	3.65 mn	3.38 n	3.67 mn	4.07 m	3.36 n	3.41 n	3.55 n	3.44 n	3.64 mn	3.60 n	3.53 n	3.57 D
Festuca rubra com. Longfellow	6.47 bcd	6.57 bcd	6.48 bcd	6.53 bcd	6.54 bcd	6.21 defg	6.46 bcd	5.98 efgh	6.57 bcd	6.19 defg	6.37 bcde	6.40 A
Festuca rubra sergei	5.70 hij	5.76 ghi	5.64 hijk	5.80 ghi	5.88 fghi	5.49 ijkl	6.57 bcd	6.34 bcde	5.78 ghi	6.37 bcde	5.60 hijk	5.90 C
Average	5.65 ABC	5.25 D	5.78 A	5.68 ABC	5.44 BCD	5.41 CD	5.44 BCD	5.36 CD	5.26 D	5.74 AB	5.58 ABC	

Root length: According to the average Duncan table, lolium perenne topgun in 10% and 80% of treated wastewater with 3.43a and 3.45a had the highest root length and in poa pratensis geisha grass in freshwater and 10% refined waste with 0.527 minimum root length (Table-5).

Table-5. Root length in four grasses

	Root length											
	%100	%90	%80	%70	%60	%50	%40	%30	%20	%10	Fresh water	Av.
Lolium perenne topgun	2.84 b	2.40 bcdef	3.45 a	2.51 bcde	2.66 bc	2.47 bcde	2.47 bcde	2.37 bcdef	2.14 defgh	3.43 a	2.66 bc	2.67 A
Poa pratensis geisha	0.660 l	0.735 l	0.745 l	0.647 l	0.665 l	0.685 l	0.762 l	0.755 l	0.640 l	0.527 l	0.630 l	0.6775 D
Festuca rubra com. Longfellow	2.19 cdefgh	2.22 cdefg	2.45 bcdef	2.16 defgh	2.28 cdefg	2.06 efghijk	2.56 bcd	2.37 bcdef	2.40 bcdef	2.55 bcd	2.48 bcde	2.34 B
Festuca rubra sergei	1.74 hijk	1.66 ijk	1.61 k	1.66 jk	1.97 fghijk	1.83 ghijk	2.48 bcde	2.13 defghi	1.73 hijk	2.12 defghij	2.28 cdefg	1.93 C
Average	1.85 BC	1.75 C	2.06 AB	1.74 C	1.89 BC	1.76 C	2.07 AB	1.91 BC	1.73 C	2.16 A	2.01 AB	

Fresh weight buds: According to the average Duncan table, had the highest fresh weight in grass, lolium perenne topgun in freshwater, 50% and 80%, and 100% treated wastewater

with 8.35, 8.66, 8.42 and 8.34. And in the grass of poa pratensis geisha in 10% of treated wastewater with the lowest fresh weight of 2.27 (Table 6).

Table-.6. Fresh weight buds in four grasses

	Fresh weight buds											
	%100	%90	%80	%70	%60	%50	%40	%30	%20	%10	Fresh water	Av.
Lolium perenne topgun	8.34 a	6.69 bc	8.42 a	6.59 bcd	6.59 bcd	8.66 a	6.75 b	5.65 efghi	6.24 bcdef	6.52 bcd	8.35 a	7.16 A
Poa pratensis geisha	2.42 l	2.45 l	2.49 l	2.33 l	2.65 l	2.26 l	2.40 l	2.31 l	2.51 l	2.27 l	2.31 l	2.40 D
Festuca rubra com. Longfellow	6.24 bcdef	5.49 fghij	5.59 efghi	5.49 fghij	5.68 efghi	6.20 bcdef	5.62 efghi	5.55 fghi	5.92 defgh	5.61 efghi	6.00 cdefg	5.76 B
Festuca rubra sergei	4.83 jk	5.93 defgh	5.50 fghij	5.04 ijk	5.24 hijk	5.66 efghi	6.31 bcde	6.17 bcdef	5.31 ghijk	5.61 efghi	4.73 k	5.48 C
Average	5.45 ABC	5.14 CDEF	5.50 AB	4.86 F	5.04 DEF	5.69 A	5.27 BCDE	4.92 F	4.99 EF	5.01 EF	5.35 BCD	

4. Conclusion

Based on analysis of variance of MSTAT-C package and taking into account the interaction between treated and grass concentrations and according to the average Duncan Table Lolium perenne topgun with the highest data in germination rate and germination strength and length of bud and length root and fresh weight of bud and fresh weight of root were considered the most suitable and best lawn for golf course. And grass Festuca rubra com. Longfellow was considered as the second proper lawn. The grass Poa Pratensis Geisha with very low germination rate and germination strength and root length and germination, and fresh germ and root grass are not suitable for golf courses.

References

Abedi-Koupai, J., B. Mostafazadeh-fard, M. Afyuni and M. R. Bagheri., (2003). Effect of treated wastewater on soil chemical and physical properties in an arid region, *Journal of Plant Soil and Environment*, 52(82): 335-344.

Azarpira, H., Behdarvand, P., Dhumal, K. and Pondhe, G., (2013). Phytoremediation of municipal wastewater by using aquatic plants, *Advances in Environment Biology*, 7(14): 4649-4654.

Alizadeh, M.R., Dabbaghi, A., Rahimi-Ajdadi, F., Rezaei, M. and Rahmati, M.H., (2011). Effect of salinity and irrigation regimes on the internode physical variations, *Australian Journal of Crop Science*, 5(12):1595-1602

Al-Jasser, A.O. (2011). Saudi wastewater reuse standards for agricultural irrigation: Riyadh treatment plants effluent compliance. Journal of King Saud University – *Engineering Sciences*, 23: 1-8.

Azarpira, H., Dhumal, K. and Pondhe, G., (2014). Application of Phycoremediation Technology in the Treatment of Sewage Water to Reduce Pollution Load, *Advances in Environment Biology*, 8(7): 2419- 2423.

Choukr-allah, R. and Hamdy, A. (2008). Wastewater treatment and reuse as a potential water resource for irrigation, *Salinity and plant nutrition laboratory BP 773*, Agadir, Morocco.

Friedel, J.K., Langer, T., Siebe, C. and Stahr, K. (2000). Effects of long-term wastewater irrigation on soil organic matter, soil microbial biomass and its activities in central Mexico, *Biology Fertilise Soils*, 31: 414-421.

Fonseca, A.F., Herpin, U., Paula, A.M., Victória, R.L. and Melfi, A.J. (2007). Agricultural use of treated sewage effluents: agronomic and environmental implications and perspectives for Brazil, Scientia Agricola.

Jimenez, B. (2005). Treatment technology and standards for agricultural wastewater reuse: a case study in Mexico, *Journal of Irrigation and Drainage*, 54: 23-33.

Ghanayan, Mt., et al. (2000) Sewage study and possibility of reuse of effluent in Kish Island, Proceedings of the 3rd National Conference on Health (Volume 1), Kerman University of Medical Sciences and Health Services.

Galavi, M., Jalali, A., Mousavi, S.R. and Galavi, H. (2009). Effect of treated municipal wastewater on forage yield, quantitative and qualitative properties of sorghum (S. bicolor Speed feed), *Asian Journal Plant Science*, 8: 489-494.

Miller, JT (1984), Living in the Environment Translation of Majid Makhdoom, *Tehran University of Science publication*

Matouq,M. (2008), The potential for reusing treated municipal wastewater for irrigation in the Hashemite Kingdom of Jordan, *International Journal of Water*, 4, 105-120.

Mousavi, S.R., Galavi, M. and Eskandari, H. (2013), Effects of treated municipal wastewater onfluctuation trend of leaf area index and quality ofmaize (Zea mays), *Water Science Technology*, 67(4): 797-802.

Mousavi, S.R. and Shahsavari M. (2014), Effects of Treated Municipal Wastewater on Growth and Yield of Maize (Zea mays), Biological Forum – *An International Journal*, 6(2): 228-233.

Mohammad, R.M.J., Hinnawi, S. and Rousan, L. (2007), Long term effect of wastewater irrigation of forage crops on soil and plant quality parameters, *Desalination*, 215: 143-152.

Oweis, T., Zhang, H. and Pala, M. (2000), Water use efficiency of rained and irrigated bread wheat in a Mediterranean environment, *Agronomy Journal*, 92: 231- 238.

Prathapar, S.A. (2000), Water shortages in the 21st century. In: The Food and Environment Tightrope, Cadman H. (ed), Australian Centre for International Agricultural Research, Canberra, 123 Australia, pp. 125-133.

Scott, C.A.J., Zarazúa, A. and Levine, G. (2000). Urban-wastewater reuse for crop production in the water-short Guanajuato river basin, Mexico, *International Water Management Institute*, P O Box 2075, Colombo, Sri Lanka.

A Research on *Lactococcus garvieae* Infection Observed in Rainbow Trout (*Oncorhynchus Mykiss*)

Fikri BALTA[1*] Zeynep DENGİZ BALTA[2]

[1] Recep Tayyip Erdoğan Üniversitesi, Su Ürünleri Fakültesi, Su Ürünleri Yetiştiriciliği Bölümü, Rize, Türkiye.
[2]Recep Tayyip Erdoğan Üniversitesi, Fen Bilimleri Enstitüsü, Su Ürünleri Anabilim Dalı, Rize, Türkiye.

[*] **Corresponding Author:** fikri.balta@erdogan.edu.tr

Abstract

In this study, fish were sampled from 12 different fish farms in Eastern Black Sea Region between January 2014 and September 2017. It was isolated hundred bacteria isolates from diseased rainbow trout (*Oncorhynchus mykiss*). All isolates identification were carryed out by using conventional biochemical tests, api 20 strep tests and PCR tests. ATCC 43921 reference strain was used as a positive control. According to results of the api 20 strep test, it was determined that 68 isolates from 100 bacterial isolates were *Lactococcus garvieae*. The PZR test was confirmed by using the pLG-1 and pLG-2 reference genes (16S rRNA) specific for the *L. garvieae* species. As a result of the study, it was confirmed that there were 68 *L. garvieae* from 100 strains isolated from rainbow trout. The antibiotic susceptibility test results showed that *L. garvieae* isolates were resistant %100 to streptomycin, sulfamethoxazole and sulfamethoxazole+trimethoprim, 94.2% to ampicillin, 72.5% to oxytetracycline, 55.07% to erythromycin and 43.5% to oxolinic acid, 26.09% to enrofloxacin, % 20.3 doxycycline, 8,7% to amoxicillin and florphenicol. The most effective antibiotic was found to be florfenicol, amoxicillin, doxisicline and enrofloxacin.

Keywords: *Lactococcus garvieae*, api 20 strep, 16S rRNA, PCR, antimicrobial agents

1. Introduction

Lactococcosis is a worldwide septicemic fish disease characterized by bilateral exophthalmia and caused by the bacteria *Lactococcus garvieae* (Austin and Austin, 1999; Kusuda and Salati, 1999). *Lactococcus garvieae* has been isolated as causative agent of disease, yellowtail (*Seriola quinqueradiata*), eels (*Anguilla anguilla*), rainbow trout (*Oncorhynchus mykiss*), tilapia (*Oreochromi*s sp.), kingfish (*S. Lalandi*), mullet (*Mugil cephalus*), Giant freshwater prawn (*Macrobrachium rosenbergii*). In addition to aquatic animals, *L. garvieae* has been isolated from other homoiothermic and poikilothermic animals such as cows, buffalos, cats and dogs. *L. garvieae* is also a zoonotic pathogen, occurring rarely and with a low virulence in human infections. This disease infects farmed fish during the summer when the water temperature exceeds 20°C (Tsai et al., 2013**)**. There appears to be pronounced variation in disease signs, İncluding exophthalmia and distended abdomen (these are also common features with BKD), Hemorrhaging in the eye (this is a characteristic of ERM), Haemorrhaging in the opercula and at the base of the fins, and on the surface (this could be confused with vibriosis), and darkening of the skin. Moribund fish swim erratically just below the surface of the water. Yellowtails were damaged in the liver, kidney, spleen and intestine, and there was a concomitant accumulation of ascitic fluid in the peritoneal cavity. Marin fish is present a pronounced enteritis, pale livers and blood in the peritoneal cavity (Austin and Austin, 1999; Austin and Austin, 2007).

In Turkey, *L. garvieae* was first isolated in 2001 after an outbreak on rainbow trout farms (Cagırgan and Tanrıkul, 1995; Diler et al., 2002; Altun et al., 2004). Since then, infections have been repeatedly occurring, in the cultivated rainbow trout in dam lakes and concrete pools especially in the warm summer months.

1. Material and Method

1.1. Fish Samples

Fish were sampled from 12 different fish farms in Eastern Black Sea Region between Jane 2014 and September 2017. *L. garvieae* isolates were collected from trout farms in different geographic areas (Trabzon, Rize, Artvin, Gümüşhane, Kayseri, Sivas, Ordu). Sixty-eight isolates were isolateded on TSA from different organs (kidney, spleen, eye and liver) of the diseased rainbow trouts with lactococcosis. All isolates were stored in 15-20% glycerol

containing tryptic soy broth (TSB, Merck) at -80°C. For analyses, they were inoculated on tryptic soy agar (TSA, Merck) and incubated at 25°C for 18 h.

1.2. Bacteria Identification

Biochemical tests were performed with the api 20 Strep kits (bioMe ´rieux). *Lactococcus garvieae* ATCC 43921 was used as the reference strain. Specific primers to identify *L. garvieae*, pLG-1 (5′-CATAACAATGAGAATCGC-3′) and pLG-2 (5′-GCACCCTCGCGGGTTG-3′), were used (Collins et al., 1989). PCR amplification of *L. garvieae* was carried out according to Zlotkin et al. (1998).

1.3. PCR Protocol

A PCR-based protocol was developed for *L. garvieae* identification. The primers were used in a PCR protocol that included a denaturation step at 94°C for 3 min, followed by 35 cycles of denaturation at 94°C for 1 min, annealing at 55°C for 1 min and extension at 72°C for 1.5 min, ending with a 10 min extension step at 72°C. As results, only *L. garvieae* isolates, regardless of their origin, amplified a fragment of 1100 bp in size, which indicated that the developed protocol was specific for the agent (Zlotkin et al., 1998).

1.4. Antimicrobial Sensitivity Test

Antimicrobial susceptibility tests of the *L. garvieae* isolates were determined by the standard disk diffusion method on Müller-Hilton agar (Merck) plates, by using the eleven antibiotics. The plates were incubated at 25°C for 20 h. The following antibiotic disks (Oxoid) were used: oxytetracycline, doxisicline, oxolinic acid, sulfamethoxazole, ampicillin, amoxiclin, florfenicol, streptomycin, enrofloxacin, erythromycin and sulfamethoxazole-trimethoprim. The antibiotic disks were placed on the Müller-Hilton agar by using a disc dispenser. The Clinical and Laboratory Standards Institute (CLSI, 2008; 2013**)** were used for the evaluation of the results. Reference strain streptococcus aureus was used as quality a control in the antimicrobial susceptibility tests.

2. Results and Discussion

2.1. Clinical Semptoms

Fish present clinical symptoms such as lethargy, anorexia, melanosis, erratic swimming, uni- or bilateral exophthalmia, hemorrhages in the ocular zone, perianal area, fins and anal prolapsus. Lactococcosis usually causes acute outbreaks that affect a large number of fish, and can produce mortalities between 10% and 80%.

*2.2.*Biochemical, cultural and physiological characteristics of *L. garvieae*

L. garvieae is a facultatively anaerobic, non-motile, catalase negative and oksidase negative, non-spore forming, Gram positive ovoid coccus, occurring in pairs and short chains, and it produces α-haemolysis on blood agar (BA). It grows at 10-45 °C in media containing 0% and 6.5% sodium chloride (NaCl). According to the results of the API 20 sterp test, the differences were determined to be in the sugar test.

Api 20 strep profile of our *L. garvieae* isolates showed 7143115, 7143515 and 7143555, while standart *L. garvieae* (ATCC43921) showed 7143115.

2.3. PCR test results

The PCR assay resulted in the amplification of a band of 1,100 bp in size that was detected for all *L. garvieae* strains tested, including the *L. garvieae* ATCC 43921 reference strain. The PCR test was confirmed by using the pLG-1 and pLG-2 reference genes (16S rRNA) specific for the *L. garvieae* species. As a result of the study, it was confirmed that there were 68 *L. garvieae* from 100 strains isolated from rainbow trout.

2.4. Treatment

These study, the highest incidence of resistance was to sulfamethoxazole, streptomycin and sulfamethoxazole-trimethoprim (100%), ampicillin (94.2), oxytetracycline (72.5%), followed by erythromycin (55.07%), oxolinic acid (43.5%), enrofloxacin (26.09%), doxisicline (20.3), but all isolates were less resistant to amoxiclin and florfenicol (8.7%). The most effective antibiotic was found to be florfenicol, amoxicillin, doxisicline and enrofloxacin.

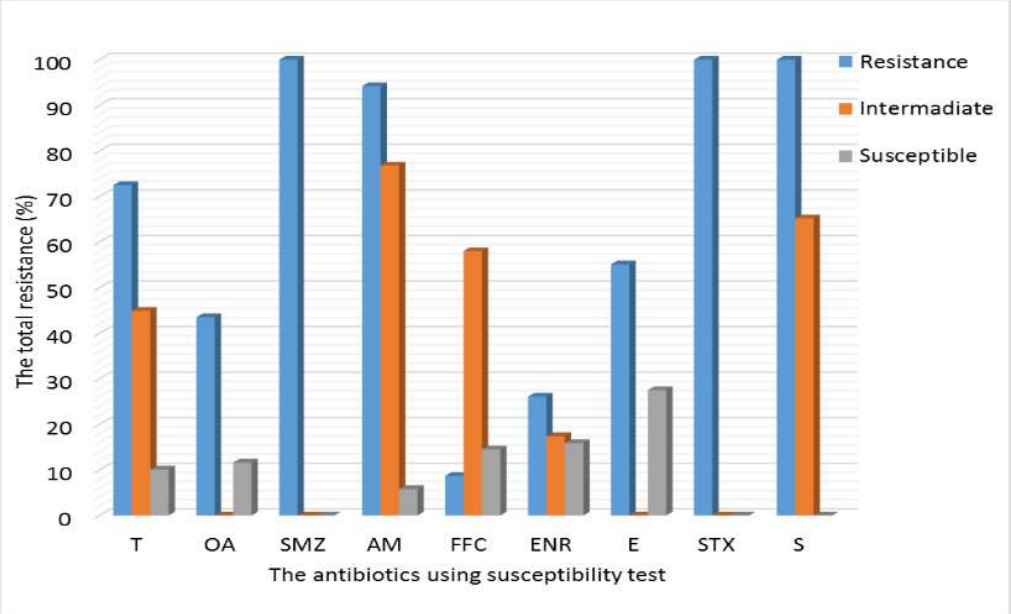

Figure 1. Antibiotic susceptibility profiles of *L. garvieae* isolates. T: Oxytetracycline, OA: Oxolinic acid, SMZ: Sulfamethoxazole, AM: Ampicillin, FFC: Florfenicol, ENR: Enrofloxacin, STX: Trimethoprim - Sulfametoxazole,E: Erythromycin, S: Streptomycin, DO: Doxycycline, AX: Amoxicillin.

2.5.Control

In recent years, adjuvanted vaccines have been developed with different mineral oils. They have been tested in laboratory and field trials, anesthetizing fish and inoculating them intraperitoneally. Complete protection is usually reached 3-week post-vaccination with simple bacterins and 4-5-week post-vaccination with oiladjuvanted vaccines. Protection remains for a period of 3-4 months with bacterins and 4-5 months with adjuvanted vaccines. It has been reported that the optimal time for vaccination is when fish weight approximately 50 g and water temperature is around 12-14°C. Recent studies evaluating the effect of the inclusion of different adjuvants in the vaccine formulation for rainbow trout have been demonstrated that the inclusion of a non-mineral oil adjuvant yielded a good protection four weeks after vaccination and conferred protection for 4-8-month post-vaccination, obtaining RPS values of 83.3% (Ravelo et al., 2006, Altun et al., 2010).

Referans

Altun, S., Diler, O. and Adiloglu, A.K. (2004). Genotyping of Lactococcus garvieae strainsfrom rainbow trout (Oncorhynchus mykiss) by16S rDNA sequencing. *Bull. Eur. Ass. Fish Pathol.*, 24:119-125.

Altun, S., Kubilay, A., Ekici S., Didinen, B.I. and Diler O., (2010). Oral Vaccination Against Lactococcosis in Rainbow Trout (Oncorhynchus mykiss) Using Sodium Alginate and Poly (lactide-co-glycolide) Carrier. *Kafkas Univ Vet Fak Derg*, 16 (Suppl-B), 211-217.

Austin, B. and Austin, D.A. (1999). BacterialFish Pathogens: Disease in Farmed and Wild Fish, 3rd ed. Springer-Praxis, Chichester, UK.

Austin, B. and Austin, D.A. (2007). BacterialFish Pathogens: Disease in Farmed and Wild Fish, 4th ed. Springer-Praxis, Chichester,UK.

Cagırgan, H. and Tanrıkul, T.T. (1995). A new problem Enterococcus-like Infection in Rainbow Trout (*Oncorhynchus mykiss*) Farms in Turkey (in Turkish). *Veteriner Kontrol ve Arastirma Enstitusu Dergisi*, *33*, 9-19.

CLSI (2008). Performance Standards for Antimicrobial Disk and Dilution Susceptibility Tests for Bacteria İsolated From Animals; Approved Standa-Third Edition. CLSI document M31-A3. Vol. 38, No.8, Wayne, PA.

CLSI (20013). Performance Standards for Antimicrobial Susceptibility Testing; Twenty-Third Informational Supplement. CLSI document M100-S23. Vol. 33, No.1, Wayne, PA.

Collins, M.D., Ash, C., Farrow, J.A.E., Wallbanks, S. and Williams, A.M, (1989). 16S ribosomal ribonucleic acid sequences analysis of lactococci and related taxa. Description of *Vagococcus fluvialis* gen. nov., sp. nov. *J. Appl. Bacteriol.* 73, 433-437

Diler, O., Altun, S., Adiloglu, A.K., Kubilay, A. and Isikli, B.I. (2002). First occurence of streptococcosis affecting farmed rainbow trout(Oncorhynchus mykiss) in Turkey. *Bull. Eur.Ass. Fish Pathol.*, 22:21-26.

Kusuda, R. and Salati, F. (1999). *Enterococcus seriolicida* and *Streptococcus iniae*. pp. 303-317. In: P.T.K. Woo, D.W. Bruno (eds.). Fish Diseases and Disorders Viral, Bacterial and Fungal Infections, vol. 3. CABI Publ.

Ravelo, C., Magarinos, B., Herrero, M.C., Costa, L., Toranzo, A.E. and Romalde, J.L., (2006). Use of adjuvanted vaccines to lengthen the protection against lactococcosis in rainbow trout (Oncorhynchus mykiss). *Aquaculture*, 251, 153-158.

Tsai, M.A., Wang, P.C., Yoshida, T., Liaw, L.L. and Chen, S.-C. (2013). Development of a sensitive and specific LAMP PCR assay for detection of fish pathogen *Lactococcus garvieae. Dis. Aquat. Org*., 102, 225–235.

Zlotkin, A., Eldar, A., Ghittino, C. and Bercovier, H. (1998). Identification of *Lactococcus garvieae* by PCR. *J Clin Microbiol*, 36, 983-5.

A Study On Wound Healing Potential Of The Antioxidant Effective *Halopteris Scoparia* (Brown Algae) Sauvageau Extract

Adem GÜNER[1*], N. Ülkü KARABAY YAVAŞOĞLU[2]

[1]Giresun University, Faculty of Science and Lecture, Department of Biology, Giresun-Turkey; ademeguner@gmail.com

[2]Ege University, Faculty of Science, Department of Biology, Izmir-Turkey; ulku.karabay@ege.edu.tr

[*] **Corresponding Author:** ademeguner@gmail.com

Abstract

Wound healing is the process of repair and regeneration following injury in tissues. This progression involves a series of well-orchestrated cellular and molecular processes. The aim of this study was to determine the possible wound healing in parallel to the antiangiogenic effect of *H.scoparia* methanol extracts. *H.scoparia* was collected from the coastline of Urla, Izmir, in April 2012. The samples were washed and maintained in a refrigerator at -20°C. Wound healing activity determined by CytoSelectTM 24-Well Wound Healing Assay Kit (Cell Biolabs, INC). Fibroblast cells (2–5x10^4) were seeded in the plates and incubated for 24 and 48 h at 37±1◦C. Cells were stained with DAPI and Giemsa for 5 min. *In vivo* anti-angiogenic conducted by the HET-CAM (Hen's Egg Test Chorio- Allantoic-Membrane) method. Fertilized eggs were placed in an incubator at 37±1◦ C and 58±2% hum. for 5 days. After, the eggs were opened on the snub side, sample dissolved in DMSO was placed onto it as 1mg/mL. Then, the time for the appearance of each of the endpoints (hemorrhage, vascular lysis, and coagulation) were monitored. The *H.scoparia extract* induced proliferation and/or migration of fibroblasts up to 76±4 % compared to control cells in wound healing assay. However, HET-CAM results show that methanol extract has no anti-angiogenic or weak effect in all treated dose (300, 600 and 900 mg/mL). It is revealed that wound healing potential of *H.scoparia* can be used as a potential agent in the healing of chronic/external wounds.

Keywords: Wound healing, HET-CAM assay, algae

1. Introduction

Between the marine plants, the macroalgae are preferred for many area, such as in the food industry, animal feeding, medicine, pharmacy, and for fertilizer. These macroalgae are an abundant source of the food compounds (Nigam and Pandey, 2009). The main agar, alginate, and carrageenan substance of seaweeds are used as thickening agents. Also, there is a noteable order of secondary metabolites in present use or development. These seaweed derivatives have emerged in recent years as a rich and important source of natural bioactive compounds and so, the production and applications of these bioproducts have been used as a potential agent in the medical industry (Chapman, 1970; Pereira, 2011).

Wound healing is a complex of biochemical actions leading to the restoration of structural and functional integrity with the strengthening of healthy tissues. *In vitro* wound healing tests have been studied by researchers for many years to calculate cell polarity, remodeling of tissue matrix or cell proliferation, migration rates of different cells and culture conditions. However, wound healing tests are a relatively inexpensive and simple method by which endothelial cell migration can be accomplished with tools readily available to most biologists (Cynthia, 2008).

The present study was firstly conducted to evaluate *in vitro* angio/antiangiogenic activity of *H.scoparia* methanol extracts.

2. Materials and methods

2.1. Seaweed material

H.scoparia was collected at a depth of 1-2 m, in a region of high light intensity, from the coastline of Urla, Izmir, in April 2012 and was identified by one of the authors (A. Sukatar). Voucher specimens (number: 40796) were deposited in the Hydrobiology Laboratory of Ege University, Faculty of Science, Department of Biology. The samples were washed three times with tap water to remove salt, epiphytes and sand attached to the surface, then carefully rinsed with fresh water, and maintained in a refrigerator at -20°C.

2.2. Preparation of extracts

Algal samples were dried at 45°C. Powdered material (108 g) was extracted with methanol (Met) (purity ≥ 99.9%, Merck, Darmstadt, Germany) at room temperature in an ultrasonic bath (3 x 1 L of solvent, 40°C, 24 h). The combined extracts were evaporated separately under reduced pressure by using Rotary evaporator (Heidolph300 LabroRota, Germany) to dryness and were obtained 3902 mg from the extracts.

2.3. HET-CAM (Hen's egg test chorioallantoic membrane) irritation test

Irritation effects of samples was carried out on fertile Leghron chicken eggs weighing 50-60 gr obtained from commercial sources (Lezita, İzmir, TURKEY) by using HET-CAM method modified of Kishore et al. (2008). Fertilised hens' eggs were placed into an incubator with conveyor rotation system at 37±1°C and 80±2% humidity for 5 days. On day 5, the eggs were opened on the snub side sucked off through a hole on the pointed side and then a round piece of shell (3-4 cm diameter) was removed carefully with forceps. After that, 300 µl of the freshly prepared sample at 0.5 and 1 mg/ml concentration that dissolved in DMSO (0.05%) (0.5 and 1 mg/ml) was applied to the CAM. The irritation severity (IS) for a period of up to 5 min was scored as:

$$IS = [(301-h) \times 5]/300 + [(301-l) \times 7]/300 + [(301-c) \times 9]/300 \quad (1)$$

where, h is the time of vascular hemorrhage occurred; l is the time of first vascular lysis occurred; and c is the time of first vascular coagulation occurred. Irritation classification based on IS: 0.0–0.9, non-irritation; 1.0–4.9, slight irritation; 5.0–8.9, moderate irritation; and 9.0–21.0, severe irritation. Also, 0.9% NaCl as negative control and 0.1N NaOH as positive control at the concentration of 300 µL were also tested. For every test compound, 5 eggs were utilized. All samples were tested in triplicate at different times.

2.4. Wound Healing Assay

Wound healing activity determined by CytoSelectTM 24-Well Wound Healing Assay Kit (Cell Biolabs, INC). Fibroblast cells ($2–5x10^4$) were seeded in the plates and incubated for 24 and 48 h at 37±1°C. Cells were stained with DAPI and Giemsa for 5 min.

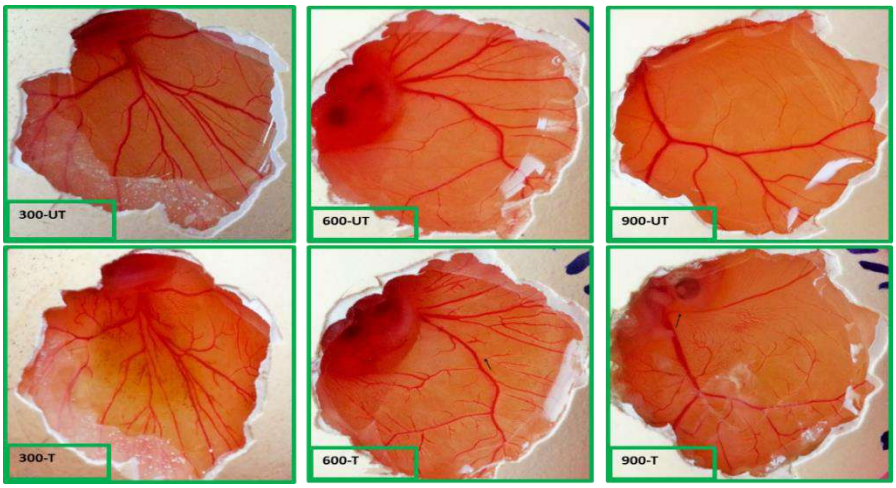

Fig. 1 Photographs illustrating of the potential irritation or toxicity on vascularization before exposure to the test samples (0 min) and after the exposure for up to 5 min by HET-CAM assay. UT: before traetment, T: after treatment.

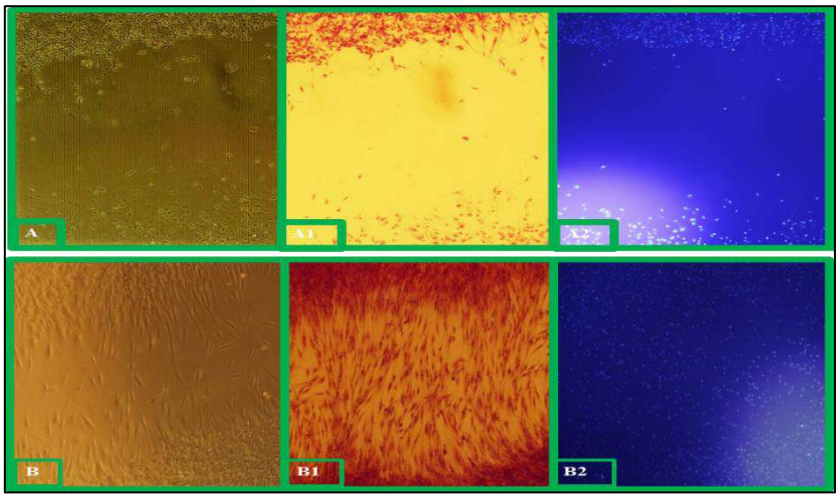

Fig.2 Photographs illustrating of the wound healing scracth assay for 48 h. A: control, A1: Giemsa dye, A2: DAPI dye; B: extract treatment, B1: Giemsa dye, B2: DAPI dye.

3. Result and Discussion

Traditional herbal medicines have been intensively favored for primary health care in many area. Especially, many active chemicals isolated from algae important contribution to the development of the many new drugs for the treatment of many diseases (Burtin, 2003). The present study is the first report to demonstrate the wound healing and irritation efficacy of edible *H. scoparia*.

In the angiogenesis process, endothelial growth factor inhibitors, endothelial cell signal transduction inhibitors, inhibitors of endothelial cell proliferation and inhibitors of endothelial

bone marrow precursor cells are used as targets (*Chung and Ferrara, 2011*). According to the anti-irritant HET-CAM test, methanol extract had no lead to any irritation at the 300 mg/mL with IS value of 0.03±0.01, 600 and 900 mg/mL extracts caused a slight irritation with weak lysis on the CAM after 5 min, respectively 1.2±0.03 and 1.4±0.02 (Fig. 1). However, when we were evaluated angiogenic activity of extract, it induced proliferation and/or migration of fibroblasts up to 76±4 % compared to control cells in wound healing assay (Fig. 2). There are limited studies on wound healing of macroalgae. But, algae active compounds such as alginate, carotenoid, and flavonoids proven to be contributors to the wound healing processes (Lee et al., 2009).

In conclusion, given that the extracts does not cause any irritation and has the antimicrobial with antioxidant effect (unpublished data), wound healing potential of *H. scoparia*, especially in the proliferative phase, can be considered as a valuable therapeutic agent to regeneration chronic/external wounds.

References

Burtin, P., (2003). Nutritional value of seaweeds. Electron J Environ Agric Food Chem, 2, 498–503.

Chapman, V.J., (1970). Seaweeds and their uses, 2nd edn. Methuen, London, 304 p.

Chung, A.S. and Ferrara, N., (2011). Developmental and pathological angiogenesis, Annu Rev Cell Dev Biol., 27, 563–584.

Cynthia, A., and Reinhart-K., (2008). Chapter 3:Endothelial Cell Adhesion and Migration. Methods in Enzymology, Volume 443.

Lee, W.R., Park, J.H., Kim, K.H., et al., (2009). The biological effects of topical alginate treatment in an animal model of skin wound healing. Wound Repair Regen. 17, 505–10.

Nigam, P.S., Pandey, A., (2009). Production of bioactive secondary metabolites: Biotechnology for agro-industrial residues utilization. 1 st ed. Springer, Netherlands, pp 129–145.

Pereira, L., (2011). A revıew of the nutrıent composıtıon of selected edıble seaweeds. In: Pomin VH, editors. Seaweed: Ecology, Nutrient Composition and Medicinal Uses. Nova Science Publishers Inc, Nova lorque, pp 15-47.

Detection of *bla*$_{NDM}$ and *bla*$_{KPC}$ in *Klebsiella pneumoniae* Isolates

Ayşegül SARAL[1]*, Esma AKYILDIZ[2] , Azer ÖZAD DÜZGÜN[3] , Tuba KÖSE[4] , Fatih Şaban BERİŞ[5]

[1]Artvin Coruh University, Faculty of Health Sciences, Department of Nutrition and Dietetics, Artvin, Turkey
[2]Recep Tayyip Erdogan University, Molecular Biology and Genetic Laboratory, Rize, Turkey
[3]Gumushane University, Faculty of Engineering and Natural Sciences, Department of Genetics and Bioengineering, Gümüşhane, Turkey
[4] Fatih State Hospital, Microbiology Laboratory, Trabzon, Turkey
[5]Recep Tayyip Erdogan University, Faculty of Arts and Sciences, Department of Biology, Rize, Turkey

* **Corresponding Author:** asaral@artvin.edu.tr

Abstract

Klebsiella pneumoniae is a rapidly spreading nosocomial pathogen in hospitals worldwide. It is difficult to eradicate infections caused by *K. pneumoniae*, which carry genes for resistance to the majority of antimicrobial drugs, including carbapenems. NDM (New Delhi Metallo β-lactamases) is Class B Metallo β-lactamases and hydrolyses all β -lactams except aztreonam. KPC (*K. pneumoniae* carbapenemase) is Class A β-lactamases and hydrolyses cephalosporins, penicillins, monobactams, and carbapenems. The purpose of this study was to investigate the presence of *bla*$_{NDM}$ and *bla*$_{KPC}$ among *Klebsiella pneumoniae* isolated from Fatih General State Hospital in Turkey. A total of 40 isolates of *K. pneumoniae* were used in this study. VITEK 2 Compact system was used for identification and antibiotic susceptibility testing of isolates. Antibiotic susceptibility testing results were interpreted using EUCAST Version 8.0. Genomic DNA used as a template for PCR assays was made with using boiling method. 40 *K. pneumoniae* isolates were screened for *bla*$_{NDM}$ and *bla*$_{KPC}$ by PCR. PCR amplification was performed using the PCR conditions determined in previous studies. According to antibiotic resistance test results; Isolates were resistant to piperacillin/tazobactam (45%), ceftazidime (85%), meropenem (15%), amikacin (2.5%), gentamicin (27.5%), ciprofloxacin (70%), and trimethoprim/sulfamethoxazole (65%). *bla*$_{NDM}$ and *bla*$_{KPC}$ were found in 1and 2 isolates, respectively. *bla*$_{NDM}$ and *bla*$_{KPC}$ had been identified previously in *K. pneumoniae* strains isolated from Turkey. As a result of this study, it can be said that the presence of *bla*$_{NDM}$ and *bla*$_{KPC}$ in these isolates continues to cause problems in the clinical settings.

Keywords: *Klebsiella pneumoniae*, Antibiotic resistance, *bla*$_{NDM}$ and *bla*$_{KPC}$.

1. Introduction

Antibiotic resistance in Gram-negative bacteria is a major problem worldwide. β-lactam antibiotic resistance is often provided by β-lactamases, including extended spectrum β-lactamases (ESBLs), plasmid mediated AmpC β-lactamases and carbapenemases. Clinical isolates of *Klebsiella pneumoniae* are known to harbor a wide variety of β-lactamases and are naturally resistant to ampicillin and amoxycillin. β-lactam antibiotics are commonly used in the treatment of infections caused by this bacterium. The emergence and rapid spread of drug-resistant *K. pneumoniae* isolates has become a serious clinical problem (Iraz et al., 2015).

β-lactamases are classified into four molecular classes, A, B, C, and D, based on conserved and distinguishing amino acid motifs. Classes A, C, and D include enzymes that hydrolyze their substrates by forming an acyl enzyme through an active site serine, whereas class B β-lactamases are metalloenzymes that utilize at least one active-site zinc ion to facilitate β-lactam hydrolysis (Bush and Jacoby, 2010).

Class B metallo-β-lactamases (MBLs) hydrolyze almost all β-lactam antibiotics except monobactams. MBLs include BcII, CcrA, IMP, VIM, SPM, BlaB, NDM, GIM, SIM, DIM, TMB, Bla2, KHM, Sfh, ImiS, CphA, AsbM1, L1, FEZ, BJP, AIM, THIN-B, GOB, CAU, CAR, SMB, POM and CRB11 (Palzkill, 2013). NDM is a novel MBL enzyme, and its variants are the latest carbapenemases to be recognized and reported worldwide. NDM confers resistance to all β-lactam antibiotics with the exception of aztreonam (Fomda et al., 2014). NDM-1 was first identified in a carbapenem-resistant *K. pneumoniae* strain from the urine sample of a Swedish patient of Indian origin who traveled to New Delhi. Since then, more than 40 countries have reported NDM-producing isolates (Iraz et al., 2015).

Klebsiella pneumoniae carbapenemases (KPCs) are one of the class A carbapenemases and are generally plasmid-encoded enzymes. KPC hydrolyze β-lactams of all classes including the carbapenems. KPC hydrolyze penicillins and first generation cephalosporins more efficient than carbapenems, oxyiminocephalosporins, monobactam and cephamycins (Upadhyay et al., 2014). *K. pneumoniae* carbapenemases (KPCs) have been reported worldwide (Lee et al., 2015).

The aim of this study was to characterize the susceptibility profile and investigate presence of bla_{NDM} and bla_{KPC} in *K. pneumoniae* collected from Fatih State Hospital in Turkey.

2. Material and Method

2.1. Bacterial Strains

40 clinical strains of *K. pneumoniae* were collected from the clinical samples of the patients from Fatih State Hospital in Turkey between October 2017 and March 2018. Identification of the strains was confirmed to the species level by using the automatic system VITEK 2 (bioMerieux, Durham, NC, USA) according to the manufacturer's instructions.

2.2. Antimicrobial Susceptibility Testing

Antimicrobial susceptibility tests were performed by the VITEK 2 Compact system (bioMerieux, Durham, NC, USA), and the results were interpreted according to the EUCAST Version 8.0. The following antibiotics were used; piperacillin/tazobactam, ceftazidime, meropenem, amikacin, gentamicin, ciprofloxacin, and trimethoprim/sulfamethoxazole.

2.3. DNA extraction

Genomic DNA used as a template for PCR assays was obtained from bacterial suspension grown overnight in Luria Broth with shaking incubator at 37^0C. Bacterial suspension was centrifuged at 13000 r.p.m. for 5 min. Pellet was suspended in 500 ml distilled water and subsequently boiled in a water bath for 10 min. Debris was centrifuged at 13000 r.p.m. for 5 min. Five hundred microlitres of supernatant was used as the template for PCR assays (Copur Cicek et al., 2013).

2.4. Detection of *bla*$_{NDM}$ and *bla*$_{KPC}$ genes

All isolates were tested for the presence of the *bla*$_{NDM}$ and *bla*$_{KPC}$ genes. Primers used for detection for *bla*$_{NDM}$: *bla*$_{NDM}$ F (5'-TGG AAT TGC CCA ATA TTA TGC -3') and *bla*$_{NDM}$ R (5'-TCA GCG CAG CTT GTC GGC CAT GC -3'); for *bla*$_{KPC}$: *bla*$_{KPC}$F (5'-CGT TCT TGT CTC TCA TGG CC -3') and *bla*$_{KPC}$R (5'-CCT CGC TGT GCT TGT CAT CC -3') (Iraz et al., 2015). A single reaction mixture contained: 5µl of genomic DNA, 20pM of each primer, 10 µl reaction buffer (Promega), 3 µl 25mM $MgCl_2$, 200mM of dNTPs and 1.5 of U GoTaq Flexi Polymerase (Promega) in a final volume of 50 µl.

PCR amplification condition was as follows: initial denaturation at 95^0C for 5 min followed by 35 cycles of 45 s at 95^0C, 45 s at 54^0C for bla_{NDM}, and 52^0C for bla_{KPC} and 1 min at 72^0C, with a final extension of 10 min at 72^0C. All PCR results were analyzed on 1% agarose containing 0.5 µg/mL ethidium bromide and subsequently visualized under UV light.

3. Results and Discussion

K. pneumoniae is an opportunistic pathogen that causes community- and hospital-acquired infections such as bloodstream and urinary tract infections and pneumonia [18]. Today, carbapenems are the most potent antimicrobial agents used in the treatment of serious infections caused by multiresistant Gram-negative bacteria. However, carbapenem resistance in Enterobacteriaceae is emerging in all parts of the world. In this study susceptibility profile and presence of bla_{NDM} and bla_{KPC} in *K. pneumoniae* strains was investigated.

A total of 40 non-duplicate clinical *K. pneumoniae* strains were collected from Fatih State Hospital in Turkey over a 6-month period. All isolates were tested for susceptibility to seven antimicrobials by the VITEK 2 Compact system (bioMerieux, Durham, NC, USA). The frequency of resistance of fourty clinical isolates to each antibiotics tested was determined. Resistance to piperacillin/tazobactam (45%), ceftazidime (85%), meropenem (15%), amikacin (2.5%), gentamicin (27.5%), ciprofloxacin (70%), and trimethoprim/sulfamethoxazole (65%) was observed (Table 1). The lowest resistance rates were for meropenem (15%), amikacin (2.5%). The highest resistance rate was observed for ceftazidime (85%).

Table 1. Antibiotic susceptibility test results of 40 *K. pneumoniae* strains

Antibiotics	R (n)	R%	S (n)	S%	I (n)	I%
Piperacillin/tazobactam	18	45	12	30	10	25
Ceftazidime	34	85	2	5	4	10
Meropenem	6	15	30	75	4	10
Amikacin	1	2.5	31	77.5	8	20
Gentamicin	11	27.5	27	67.5	2	5
Ciprofloxacin	28	70	6	15	6	15
Trimethoprim/sulfamethoxazole	26	65	14	35	0	0

All 40 *K. pneumoniae* isolates tested for susceptibility to antibiotics were screened for the presence of bla_{NDM} and bla_{KPC}. bla_{NDM} and bla_{KPC} were found in 1 and 2 isolates, respectively. bla_{NDM} and bla_{KPC} harboring three isolates were found to be resistant to meropenem.

Carbapenems such as imipenem and meropenem are used in the United States and elsewhere to treat very sensitive Gram negative nosocomial pathogens. *K. pneumoniae* has caused worldwide concern due to its ability to produce ESBL. Carbapenems have been the preferred drugs for the management of infections caused by ESBL producing *K. pneumoniae*. In recent years, the spread of carbapenem resistant Enterobacteriaceae (CRE), especially *K. pneumoniae*, has become a major global health problem and has become a clinical challenge for physicians (Spagnolo,et al., 2014). Also, Epidemics caused by carbapenem resistant Klebsiella species have begun to be reported increasingly in our country (Demiray et al., 2017).

NDM is a novel MBL enzyme, and its variants are the latest carbapenemases to be recognized and reported worldwide. NDM-1 was first identified in a carbapenem-resistant *K. pneumoniae* strain from the urine sample in 2008. Since then, more than 40 countries have reported NDM-producing isolates (Iraz et al., 2015). Many studies have been reported NDM producing *K. Pneumoniae* isolates from Turkey (Gokmen et al., 2016; Kilic and Baysallar, 2015; Iraz et al., 2015). In this study, bla_{NDM} in *K. pneumoniae* strain isolated from a hospital in Turkey were detected.

Klebsiella pneumoniae carbapenemases (KPCs) are one of the class A carbapenemases and hydrolyze penicillins and first generation cephalosporins more efficient than carbapenems, oxyiminocephalosporins, monobactam and cephamycins (Upadhyay et al., 2014). Although known as one of the most common carbapenemases globally, KPC has been reported from Turkey rarely. KPC producing *K. Pneumoniae* from Turkey was first reported in 2014 (Labarca et al., 2014). The presence of KPC producing *K. Pneumoniae* strains in this study may indicate that these strains also began to spread in Turkey.

Acknowledgement

This work was supported by Gumushane University Research Fund Grants BAP-18.S5119.03.02.

References

Iraz, M., Özad Düzgün, A., Sandallı, C., Doymaz, M. Z., Akkoyunlu, Y., Saral, A., Peleg A. Y., Özgümüş, O. B., Beriş, F. Ş., Karaoğlu, H., and Çopur Çiçek, A. (2015). Distribution of β-Lactamase Genes Among Carbapenem-Resistant *Klebsiella pneumoniae* Strains Isolated From Patients in Turkey. Annals of Laboratory Medicine, 35(6), 595-601.

Bush, K., and Jacoby, G. A. (2010). Updated Functional Classification of β-Lactamases. Antimicrobial Agents and Chemotherapy, 54(3), 969-976.

Palzkill, T. (2013). Metallo-β-lactamase structure and function. Annals of the New York Academy of Sciences, 1277, 91-104.

Fomda, B. A., Khan, A., and Zahoor, D. (2014). NDM-1 (New Delhi metallo beta lactamase-1) producing Gram-negative bacilli: Emergence & clinical implications. The Indian Journal of Medical Research, 140(5), 672-678.

Upadhyay, S., Ranjan Sen, M., and Bhattacharjee A. (2012). Identification and Characterization of Carbapenem Hydrolysing β-lactamase–KPC among *Enterobacteriaceae*: A report from North India. Asian Journal of Medical Sciences, 3, 11-15.

Lee, C. R., Lee, J. H., Park, K. S., Kim, Y. B., Jeong, B. C., and Lee, S. H. (2016). Global Dissemination of Carbapenemase-Producing *Klebsiella pneumoniae*: Epidemiology, Genetic Context, Treatment Options, and Detection Methods. Frontiers in Microbiology, 7: 895.

Copur Cicek, A., Saral, A., Ozad Duzgun, A., Cizmeci, Z., Kayman, T., Balci, P. O., Dal, T., Firat, M., Yazici, Y., Sancaktar, M., Ozgumus, O. B., and Sandalli, C. (2013). Screening of Class 1 and Class 2 Integrons in Clinical Isolates of *Pseudomonas aeruginosa* Collected from Seven Hospitals in Turkey: A Multicenter Study. Open Journal of Medical Microbiology, 3, 227-233.

Spagnolo, A., Orlando, P., Panatto, D., Perdelli, F., and Cristina, M. (2014). An overview of carbapenem-resistant *Klebsiella pneumoniae*: epidemiology and control measures. Reviews in Medical Microbiology, 25(1), 7-14.

Demiray, T., Aydemir, Ö., Kılıç, Ü., Yılmaz, K., Köroğlu, M., and Altındiş, M. (2017). Karbapenem Dirençli *Klebsiella pneumoniae* İzolatlarında Karbapenemaz Saptanmasında Karbapenemaz İnaktivasyon Testinin Kullanımı. Türk Mikrobiyoldji Cemiyeti Dergisi, 47(2), 78-82.

Guven Gokmen, T., Nagiyev, T., Meral, M., Onlen, C., Heydari, F., and Koksal, F. (2016). NDM-1 and rmtC-Producing *Klebsiella pneumoniae* Isolates in Turkey. Jundishapur Journal of Microbiology, 9(10), e33990. http://doi.org/10.5812/jjm.33990

Kilic, A., and Baysallar, M. (2015). The First *Klebsiella pneumoniae* Isolate Co-Producing OXA-48 and NDM-1 in Turkey. Annals of Laboratory Medicine, 35(3), 382-383.

Labarca, J., Poirel, L., Özdamar, M., Turkoglü, S., Hakko, E., and Nordmann, P. (2014). KPC-producing *Klebsiella pneumoniae*, finally targeting Turkey. New Microbes and New Infections, 2(2), 50-51.

Determination of Antimicrobial and Antioxidant Activities of Some Vinegar Samples Commercially Sold in Turkey

Ayşe Gül CANİKLİOĞLU[1]*, Sinem AYDIN[2]

[1]Giresun University, Faculty of Education, Department of Primary Education, Giresun, Turkey, aysegulcaniklioglu@gmail.com

[2]Giresun University, Faculty of Arts and Sciences, Department of Biology, Giresun, Turkey, sinem.aydin@giresun.edu.tr

* **Corresponding Author:** aysegulcaniklioglu@gmail.com

Abstract

In this study, the antimicrobial and antioxidant activities of gilaburu (*Viburnum opulus* L.), apple (*Malus domestica* L.), artichoke (*Cynara scolymus* L.) and hawthorn (*Crataegus* spp.) vinegars which are commercially sold in Turkey were investigated. The antimicrobial activities of the samples were identified by using disc diffusion method on eight different bacteria and three different yeasts. As a result of these studies, it was determined that all samples had antimicrobial activity but the activity of gilaburu vinegar was higher than the others. Also the antioxidant activities of the studied samples were identified by using DPPH radical scavenging activity, total fenolic content, total flavonoid content, ABTS radical scavenging activity, and determination of total antioxidant capacity methods. According to the results, the highest total phenolic content was found in the artichoke vinegar (344.54±0.004 µg GAE/mL) and the lowest total phenolic content was found in the gilaburnu vinegar (46.86±0.002 µg GAE/mL). The highest and the lowest total flavonoid contents were obtained in hawthorn vinegar (387.30±0.001 µg QE/mL) and gilaburu vinegar (104.80±0.0004 µg QE/mL), respectively.

Keywords: Gilaburu, Apple, Artichoke, Hawthorn, Vinegar, Antimicrobial, Antioxidant

1. Introduction

Vinegar is a fermented product recognized by people for centuries and utilized for many various purposes. The oldest known use of vinegar is dates back 10,000 years ago (Tan, 2005; Johnston and Gaas, 2006). Flavored vinegar has been commercially manufactured and sold for about 5000 years. The Babylonians manufactured and sold fruit, honey and malt sweetened vinegar until the 6th century (Tan, 2005). By the 10th century, Sung Tse utilized sulfur and vinegar for hindering infections as handwashing material (Chan et al., 1993; Tan, 2005).

Currently, vinegar is utilized in many areas. It is utilized for the preparation of foodstuffs such as mayonnaise, tomato paste and mustard, flavoring agent for salads, disinfecting agent in especially for fresh vegetables and fruits because of having antimicrobial effects (Plessi, 2003; Tan, 2005; Solieri and Giudici, 2009).

In vinegar production, initially sugar in food turn into alcohol in anaerobic conditions. The manufactured alcohol is oxidized via acetic acid bacteria (AAB) to acetic acid and water under aerobic circumstances (Aktan and Kalkan, 1998).

Due to each country has different unique products, different vinegar types are produced in worldwide (e.g. rice vinegar in China and in Japan, traditional balsamic vinegar in Italy (Guizani and Mothershaw, 2006). Lately, different fruit and vegetable vinegars have sold on the world market (Shahidi et al., 2008).

In the present survey, the antimicrobial and antioxidant activities of gilaburu (*Viburnum opulus* L.), apple (*Malus domestica* L.), artichoke (*Cynara scolymus* L.) and hawthorn (*Crataegus* spp.) vinegars which are commercially sold in Turkey were explored.

2. Material and Method

2.1. Providing of the samples

The gilaburu (Biotama), apple (Çukurova'dan lezzetler), artichoke (Hel-Kim) and hawthorn (Hel-Kim) vinegars utilized in the studies were purchased from different herb shops in Giresun.

2.2. Microorganisms

Microorganisms used during the study are provided from Giresun University Medicine Faculty and Arts and Sciences Faculty Microbiology Laboratory culture collection. In this study as Gram (+) bacteria species, *Staphylococcus aureus* (ATCC 29213), *Enterococcus faecalis* (ATCC 29212), *Bacillus subtilis* (ATCC 6633), *Gordonia rubripertincta*; and as Gram (-) bacteria species, *Proteus vulgaris* (ATCC 13315), *Klebsiella pneumoniae* (ATCC 700603), *Enterobacter aerogenes* (CMM 2531) and *Salmonella enterica* (ATCC 14028) are used. In addition as yeast species, *Candida albicans* (FMC 17), *Candida tropicalis* (ATCC 13803) and *Candida parapsilosis* (ATCC 22019) are used.

2.3. Determination of Antimicrobial Activities of Plant Waters

For each vinegar, 30 mL of the sample was sterilized by passing through 0.45 µM filters. Each sample was applied on the studied microorganisms by using disc diffusion method. For bacteria in Müller Hinton Broth (MHB), for yeasts in Sabouraud Dextrose Broth (SDB) overnight cultures were prepared and 200 µL of suspension containing 10^8 CFU/mL of bacteria-yeast (prepared by measuring in a spectrophotometer at a concentration of 10^8 CFU/mL according to 0.5 McFarland standard) was spread over the Müller Hinton Agar (MHA) (for bacteria) and Sabouraud Dextrose Agar (SDA) (for yeast). Sterile discs with a diameter of 6 mm were placed on the MHA (for bacteria) and SDA (for yeasts) and 2 of the discs on the petri were impregnated with 20 µL of different vinegar samples and only 1 of them was treated with sterile diluted water (negative control), streptomycin and tetracycline (for bacteria) and nystatin (for yeasts) were added as positive control on the same petri. After incubation of the cultured petri dishes for 1 hour in the refrigerator, the bacteria were incubated at 37 ° C for 24 hours and the fungi at 27 ° C for 48 hours. The inhibition zones were measured in millimeters (Murray et al., 1995). The tests were carried out three times.

2.4. Determination of Antioxidant Activities of Plant Waters

2.4.1. Total Phenolic Content

Total phenolic contents of vinegar samples were determined by the procedure of Slinkard and Singleton (1977) using gallic acid standard. 0.1 mL vinegar sample (diluted 1:5 ratio) and 4.5 mL distilled water were mixed. Then, 0.1 mL Folin–Ciocalteu reagent (previously diluted 3- fold with distilled water) was put into the mixture. After 3 minutes, 0.3 mL Na2CO3 (2%) was added. The absorbance was measured at 760 nm, after incubating the mixture for 90 min. The quantity of the total phenolic compounds was denoted as µg of gallic acid equivalent (GAE)/mL. The tests were carried out three times.

2.4.2. Total Flavonoid Content

Total flavonoids of vinegars were determined by the method of Zhishen et al. (1999). 0.25 mL vinegar sample (diluted 1:5 ratio) was added to 1.25 mL distilled water followed by 75 µL $NaNO_2$ (%5) and incubated for 5 min. Afterwards, 150 µL $AlCl_3.6H_2O$ (%10) was added to the mixture and then incubated for 5 min, the reaction mixture was treated with 0.5 mL NaOH (1M) and 725 µL distilled water. Absorbance was read spectrometrically at 510 nm. The amount of total flavonoid compounds was calculated as µg of catechin equivalents (CE)/mL. The tests were carried out three times.

2.4.3. Total Antioxidant Capacity

Total antioxidant capacity of the vinegar samples were defined by the method of Prieto et al. (1999). Absorbance was measured at 695 nm. The results were calculated as µg of ascorbic acid equivalents (AAE)/mL. The tests were carried out three times.

2.4.4. DPPH Radical Scavenging Activity

DPPH radical scavenging activity of vinegars was determined by 1,1- diphenyl- 2- picryl- hydrazyl (DPPH) (Blois, 1958). Appropriate dilution series (50- 200 µg/mL) were prepared for vinegars. 0.75 mL of each solution was added to 1.5 mL of DPPH. The mixture was stirred vigorously and allowed to stand in the dark at the room temperature for 30 min. Absorbance was measured at 517 nm with a Shimadzu 1240 UV–Vis spectrophotometer. The tests were carried out three times. BHT and Rutin used as standards. The DPPH radical scavenging activity was calculated using the following equation:

% inhibition: $[(A_0-A_1)/A_0]X100$ (1)

A_0: Absorbance of the control

A_1: Absorbance of the sample

2.4.5. ABTS Radical Scavenging Activity

ABTS radical scavenging assay was carried out mixing 150 µL vinegar (50-200 µg/mL) with 2850 µL of the $ABTS^{\cdot+}$ solution for 2 h in a dark condition. The absorbance was taken at 734 nm using the spectrophotometer. This scavenging generates a decline in the absorbance at 734 nm (Arnao et al., 2001). The tests were carried out three times. The ABTS radical scavenging activity was calculated using the following equation:

% inhibition: $[(A_0-A_1)/A_0]X100$ (2)

A_0: Absorbance of the control

A_1: Absorbance of the sample

3. Results and Discussion

3.1. Antimicrobial Activity

As a result of the antimicrobial activity studies, the vinegar samples did not show any effect on *E. faecalis* but it was also determined that they formed zone diameters in the range of 7-17 mm against the other bacteria. The largest zone diameters for each vinegar sample were measured against *S. aureus* (Figure 1).

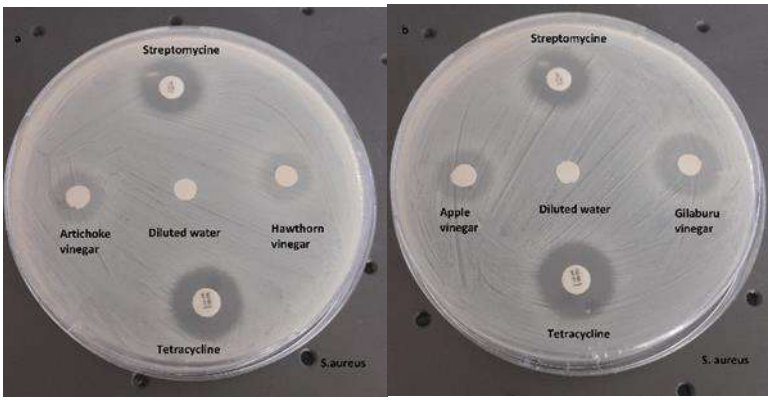

Figure 1. Antimicrobial activities of artichoke - hawthorn (a), apple - gilaburu (b) vinegars on *S. aureus*

Antimicrobial activity of the studied vinegars are shown in Table 1. It has also been observed that some vinegars have the same size as the antibiotics used as the control group and some of them formed larger zones than the antibiotics. The results indicated that some of the studied vinegar samples worked as the same as standard antibiotics, and some were even more effective than streptomycine or tetracycline (Table 1).

Table 1. Inhibition zones of vinegars, standard antifungal and antibiotics

Microorganisms		Inhibition Zone Diameters (mm)							
		Apple water	Gilaburu water	Artichoke water	Hawthorn water	Diluted water	Str.	Tet.	Nis.
Gram (+) bacteria	*B. subtilis*	8	7	8	8	-----	20	10	U
	S. aureus	13	17	12	14	-----	15	16	U
	E. faecalis	------	-----	-----	-----	-----	----	18	U
	G. rubripertincta	10	12	8	9	-----	20	16	U
Gram (-) bacteria	*E. aerogenes*	9	10	7	7	-----	20	12	U
	S. enterica	9	12	11	9	-----	14	15	U
	P. vulgaris	10	12	10	10	-----	22	10	U
	K.pneumoniae	10	12	10	10	-----	18	8	U
Yeasts	*C. albicans*	23	34	24	21	-----	U	U	22
	C. tropicalis	9	10	9	17	-----	U	U	23
	C. parapsilosis	34	36	29	27	-----	U	U	23

Str: Streptomycine, Tet: Tetracycline, Nis: Nystatin, U: Untested, (-): No inhibition

In addition, vinegar samples were found to have high antifungal activity. The largest zone diameters were measured when vinegar samples were applied on *C. parapsilosis* (Figure 2).

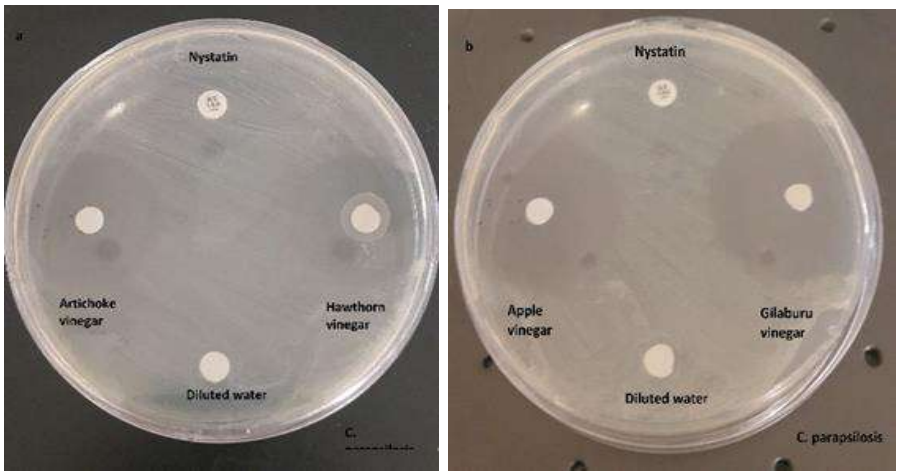

Figure 2. Antifungal activities of artichoke - hawthorn (a), apple - gilaburu (b) vinegars on *C. parapsilosis*

3.2. Antioxidant Activity

The antioxidant activities of the studied samples were identified by using DPPH radical scavenging activity, total fenolic content, total flavonoid content, ABTS radical scavenging activity, and determination of total antioxidant capacity methods.

Total phenolic content, total flavanoid content and total antioxidant capacity of vinegars were presented in Table 2. The highest total phenolic and flavonoid contents were found in apple vinegar and the lowest total phenolic and flavonoid contents were found in gilaburu vinegar. Total antioxidant capacity of the vinegars increases in the following order: Gilaburu vinegar< Hawtorn vinegar< Apple vinegar < Artichoke vinegar.

Table 2. Total phenolic content, total flavanoid content and total antioxidant capacity of the vinegars

Vinegar sample	Total Phenolic Content (µg GAE/mL)	Total Flavonoid Content (µg CE/mL)	Total Antioxidant Capacity (µg AAE/mL)
Gilaburu vinegar	46.36±0.002	104.8±0.0004	47.5±0.007
Hawtorn vinegar	189.54±0.0002	192.11±0.0003	386.25±0.017
Apple vinegar	237.27±0.0002	387.3±0.001	988±0.011
Artichoke vinegar	344.54±0.004	188.46±0.002	1116.25±0.0014

DPPH radical scavenging activity of the vinegars is given in Figure 3. The highest and the lowest activities were observed in apple and gilaburu vinegars, respectively. All the vinegar samples were exhibited higher activity than standards (BHT and Rutin) at 1000 µg/mL (except gilaburu vinegar).

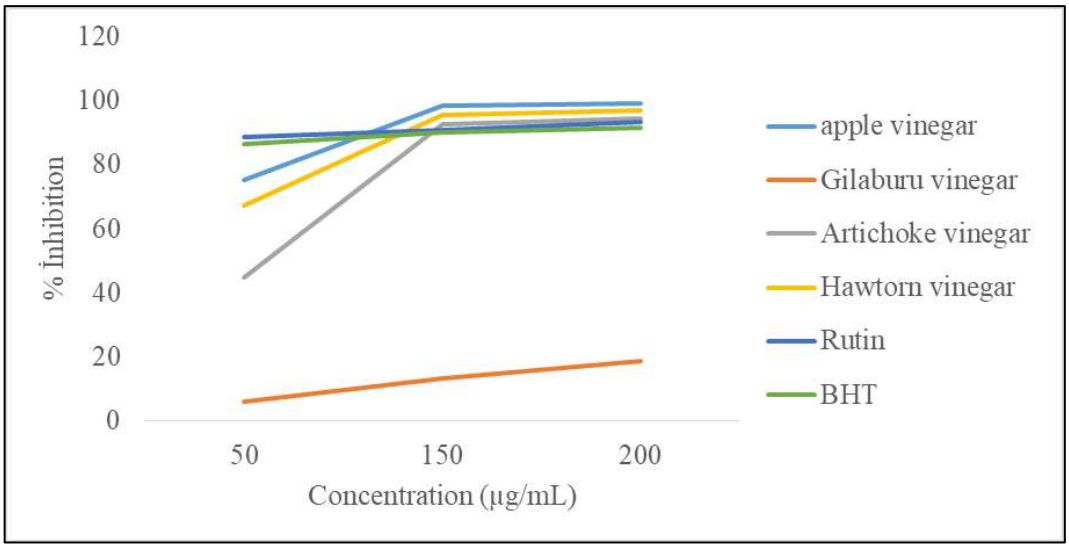

Figure 3. DPPH radical scavenging activities of the vinegars (% inhibition)

ABTS radical scavenging activity of vinegars are illustrated in Table 3. Gilaburu vinegar had no activity. The highest activity was found in hawtorn vinegar.

Table 3. ABTS radical scavenging activity (%inhibition) of the vinegars

Vinegar	Concentration (µg/mL)	ABTS scavenging activity (% inhibition)
Gilaburu vinegar	50	No Activity
	100	No Activity
	150	No Activity
	200	No Activity
Hawtorn vinegar	50	9.59±0.0006
	100	26.76±0.0014
	150	47.06±0.002
	200	63.62±0.015
Apple vinegar	50	5.98±0.016
	100	21.5±0.019
	150	38.3±0.024
	200	51.23±0.022
Artichoke vinegar	50	No activity
	100	11.37±0.006
	150	21.3±0.002
	200	25.56±0.0009
Rutin	50	88.64±0.61
	100	89.61±0.88
	150	90.89±0.60
	200	93.40±1.07
BHT	50	86.39±1.57
	100	88.02±1.42
	150	90.05±0.50
	200	91.67±1.02

Investigations have shown that the highest antimicrobial activity is achieved with gilaburu vinegar, especially the antifungal activity of this sample is very high. However, in antioxidant activity tests, gilaburu vinegar samples showed the lowest activity at all tested parameters.

When the results of the antibacterial activity of the gilaburu fruit extract in the studies performed by Arslan et al. (2018) are examined, the extract has antibacterial activity at varying rates on the test microorganisms; but not antifungal activity. In our study, it was determined that antifungal activity of gilaburu vinegar is much higher than antibacterial activity.

The antimicrobial activity of the different extracts obtained from Gilaburu has also been tested in different studies. Burnaz et al. (2007) reported that chloroform and methanol extracts from *Viburnum opulus* exhibit antimicrobial activity. Hızlısoy (2009) found that fruit extract of Gilaburu collected from Kayseri showed antimicrobial activity on *S. aureus*, *E. coli* and *P. aeruginosa* bacteria. Again in a similar study, the activity of *V. opulus* extracts on *S. aureus* and *S. epidermidis* has been determined (Bubulica et al., 2012). Our studies also confirm the results in the literature. The largest zone diameters were measured against *S. aureus* during antibacterial activity tests with gilaburu vinegars.

In some studies, it has been reported that some *Viburnum* species have a high abundance of polyphenols that protect human health from the negative effects of oxidants (Česonienėet et al., 2010; Kraujalytė et al., 2013). In another study, Şeker et al. (2016) reported that the total phenolic content and radical scavenging activity values of gilaburu fruit pod added cakes, increased in proportion to the level of fruit pudding addition.

Zhu et al. (2004) investigated the antimicrobial activities of chloroform, ethyl acetate and n-butanol extracts of artichoke leaves in a study. They found that extracts showed higher activity against fungi than bacteria. In the same study, the phenolic contents of the extracts were also found to be quite high.

Vamanu et al. (2011) also found that the total phenolic, total flavonoid, and total antioxidant capacities of artichoke ethanol extracts were changed to the percentage of ethanol (25-50-75-97%). In our study, the results obtained from the artichoke vinegar tests of the relevant parameters were calculated to be quite high.

Elhan (2014), found that apple vinegar had antimicrobial activity against many bacteria and he also found that the antimicrobial activity increased as the concentration of the vinegar increased.

Karadeniz et al. (2004), calculated total flavonoid and phenolic content of various apple methanol extract grown in Turkey as the equivalent of quercetin and they determined that phenol contents were higher than those of flavonoids. In our study, the total phenolic content value of apple vinegar was 237.27 ± 0.0002 (µg GAE / mL), while the total flavonoid content value was determined as 387.3 ± 0.001 (µg KE / mL).

Tadic et al. (2008) revealed that hawthorn fruit extracts showed antimicrobial activity on *Micrococcus flavus*, *Bacilus subtilis* and *Lysteria monocytogenes* from Gram (+) bacteria, but no activity against *Candida albicans*. In our study, the widest zone diameter of hawthorn vinegar was measured against *S. aureus* from Gram (+) bacteria by 14 mm. Also, the zone diameter against *C. albicans* was determined as 21 mm.

Liu et al. (2010) showed that hawthorn extracts possess highly potent antioxidant activity against DPPH, hydroxyl radicals and lipid peroxidation in their study. The results of the DPPH experiment conducted with the hawthorn vinegar in our study also support this situation. Hawthorn vinegar DPPH result is determined as higher than standard antioxidants BHT and routine.

4. Conclusion

Vinegar is manufactured by different production methods around the world. In our research, antimicrobial and antioxidant activities of apple, gilaburu, artichoke and hawthorn vinegars were explored. When all the results obtained are taken into account; the most effective antimicrobial activity was found in gilaburu vinegar, but the highest antioxidant activities were different in different parameters. The highest activity for DPPH radical scavenging activity and total flavonoid content has been found in apple vinegar, for ABTS radical scavenging activity it has been found in the artichoke vinegar and for total phenolic and total antioxidant capacity it has been found in artichoke vinegar. It is seen from the results of all investigations that, changings in the sources of the vinegars, change the antimicrobial and antioxidant activities they show .

Since ancient times, vinegar is a product used as a flavor enhancer in foods and vinegar compounds can also be used as natural medicines in the treatment of many diseases as well. Scientific studies on this topic are increasing rapidly all over the world in recent years. In Turkey, vinegar consumption is increasing, especially wine vinegar. However, studies on the therapeutic effects are very few. With this study, we can lead another studies about the different

contents of vinegars and encourage the use of natural products in solving various health problems.

References

Aktan, N., and Kalkan, H. (1998). Sirke teknolojisi. Ege Üniversitesi Basımevi, İzmir.

Arnao, M. B., Cano, A. and Acosta, M. (2001). The hydrophilic and lipophilic contribution to total antioxidant activity. Food Chemistry, 73, 239- 244.

Arslan, M., Erbil, N. and Murathan, Z. T. (2018). Ardahan ve çevresinde yabani olarak yetişen gilaburu meyve ekstraktının antimikrobiyal, antioksidan ve antimutajenik aktivitelerinin araştırılması. Gümüşhane Üniversitesi Fen Bilimleri Enstitüsü Dergisi, 8 (1), 18-25.

Blois, M. S. (1958). Antioxidant determinations by the use of a stable free radical. Nature, 26, 1199-1200.

Bubulica, M. V., Anghel, I., Grumezescu, A. M., Saviuc, C., Anghel, G. A., Chifiriuc, M. C., Gheorghe, I., Lazar, V., and Popescu, A. (2012). In vitro evaluation of bactericidal and antibio film activity of *Lonicera tatarica* and *Viburnum opulus* plant extracts on Staphylococcus strains. Farmacia, 60 (1), 80-91.

Burnaz, N. (2007). Chemical composition and biological activity of extracts of *Viburnum opulus* ve *V. orientale* plants, Karadeniz Teknical University, Institue of Science, Trabzon.

Calfee, R. C., and Valencia, R. R. (1991). APA guide to preparing manuscripts for journal publication. Washington, DC: American Psychological Association.

Česonienė, L., Daubaras, R., Venclovienė, J. and Viškelis, P. (2010). Biochemical and agrobiological diversity of *Viburnum opulus* genotypes. Central European Journal of Biology, 5 (6), 864–871.

Chan, E, Ahmed, T. M., Wang, M., and Chan, J. C. M. (1993). History of medicine and nephrology in Asia. American Journal of Nephrology, 14, 295-301.

Elhan S., 2014. Investigation of the usage of different vinegar type and Concentration for disinfection of salad componenents, Atatürk University, Institue of Science, Erzurum.

Guizani, N. And Mothershaw, A. (2006). Fermentation: general principles. In: Hui, Y. H. (eds), Handbook of food science, technology and engineering. Taylor & Francis, London.

Hızlısoy, H. (2009).Investigation of antimicrobial effect of gilaburu on various microorganisms, Erciyes University, Institue of Medical Sciences, Kayseri.

Johnston, C. S., and Gaas C. A. (2006). Vinegar: medicinal uses and antiglycemic effect. Medscape General Medicine, 8(2), 61-83.

Karadeniz, F., Burdurlu, H. S., Koca, N., and Soyer, Y. (2005). Antioxidant activity of selected fruits and vegetables grown in Turkey. *Turkish Journal of Agriculture and Forestry*, *29*(4), 297-303.

Kraujalytė, V., Venskutonis, P. R., Pukalskas, A., Česonienė, L. and Daubaras, R. (2013). Antioxidant properties and polyphenolic compositions of fruits from different European cranberrybush (*Viburnum opulus* L.) genotypes. Food Chemistry, 141, 3695–3702.

Liu, P. Z., Kallio, H., Lu, D. G., Zhou, C. S., Ou, S. Y., and Yang, B. R. (2010). Acids, sugars, and sugar alcohols in chinese hawthorn (*Crataegus* spp.) fruits. Journal of Agricultural and Food Chemistry, 58, 1012–1019.

Murray, P. R., Baron, E. J., Pfaller, M. A., Tenover, F. C. and Yolke, R. H. (1995). Manual of clinical microbiology. ASM Press, Washington, DC.

Plessi, M. (2003). Vinegar. In: Caballero, B., Trugo, L. C., and Finglas P. M. (eds), Encyclopedia of food sciences and nutrition. Academic Press, Oxford.

Prieto, P., Pineda, M., and Aguilar, M. (1999). Spectrophotometric quantitation of antioxidant capacity through the formation of a phosphor molybdenum complex: Specific application to the determination of vitamin E. Analytical Biochemistry, 269, 337–341.

Shahidi, F., McDonald, J., Chandrasekara, A. and Zhong, Y. (2008). Phytochemicals of foods, beverages and fruit vinegars: chemistry and health effects. Asia Pacific Journal of Clinical Nutrition, 17, 380-382.

Slinkard, K., and Singleton, V. L. (1977). Total phenol analysis: automation and comparison with manual methods. American Journal of Enology and Viticulture, 28, 49-55.

Solieri, L. and Giudici, P. (2009). Vinegars of the world. Springer, Berlin.

Şeker, I. T. Ertop, M. H. and Hayta, M. (2016). Physicochemical and bioactive properties of cakes incorporated with gilaburu fruit (*Viburnum opulus*) pomace. Quality Assurance and Safety of Crops and Foods, 8 (2), 261-266.

Tadic, V. M., Dobric, S., Markovic, G. M., Dordevic, S. M., Arsic, I. A., Menkovic, N. R., and Stevic, T. (2008). Anti-inflammatory, gastroprotective, free-radical-scavenging, and antimicrobial activities of hawthorn berries ethanol extract. Journal of Agricultural and Food Chemistry, 56, 7700–7709.

Tan, S. C. (2005). Vinegar fermentation, Louisiana State University, Institue of Science, Louisiana.

Vamanu, E., Vamanu, A., Nita, S., and Colceriu, S. (2011). Antioxidant and antimicrobial activities of ethanol extracts of *Cynara scolymus* (*Cynarae folium*, Asteraceae family). Tropical Journal of Pharmaceutical Research, *10*(6), 777-783.

Zhishen, J., Mengcheng, T., and Jianming, W. (1999). The determination of flavonoid contents in mulberry and their scavenging effects on superoxide radicals. Food Chemistry, 64, 555-559.

Zhu, X., Zhang, H. and Lo, R. (2004). Phenolic compounds from the leaf extract of artichoke (*Cynara scolymus* L.) and their antimicrobial activities. Journal of Agricultural and Food Chemistry, *52*(24), 7272-7278.

The Impact of Natural Disasters and Environmental Pollution on Agricultural Lands

Uğur SERENCAM[1] Betül GIDIK[2]* Hüseyin SERENCAM[3]

[1]Bayburt University, Faculty of Engineering, Department of Civil Engineering, 69000 Bayburt, Turkey; userencam@bayburt.edu.tr

[2] Bayburt University, School of Applied Science, Department of Organic Farming Managemant, 69000 Bayburt, Turkey; betulgidik@bayburt.edu.tr

[3] Bayburt University, Faculty of Engineering, Department of Food Engineering, 69000 Bayburt, Turkey; hserencam@bayburt.edu.tr

* **Corresponding Author:** betulgidik@bayburt.edu.tr

Abstract

Turkey is a country in which frequent natural disasters take place in many applications, among which are earthquakes, floods and landslides. These disasters are experienced to be the most common ones. In addition, environmental pollution, which is resulted from the increase in population, natural disasters and industrialization, becomes a growing environmental problem in Turkey. The country is an agricultural land. It is, therefore, both natural disasters and environmental pollution could cause the eradication of fertile land in the setting. Disasters, including floods, landslides and wind erosion to name a few, are quite effective in the depletion of rich soils. 79.4% of the soil of Turkey is exposed the erosion. Also one billion ton soil is transported per year because of the erosion. Furthermore, soil pollution, stemming from heavy metals, pesticides and industrial wastes, also might result in the exhaustion of efficient agricultural land. In this study, it is aimed to describe how to reduce the adverse effects of natural disasters and environmental pollution on efficient farming areas.

Keywords: Agriculture, Natural disasters, Environmental pollution, Heavy metals.

1. Introduction

Soil; is occurred by air, water, organic matter and some rock products (Ergene 1993). Turkey is an agricultural country, for this reason soil is one of the most important sources. Nowadays, fertile soil are decreasing due to various reasons. Natural disasters such as erosion, floods and earthquakes, as well as environmental wastes, heavy metals and pesticides, that are increasing due to population growth and industrialization, cause the depletion of fertile soils (Doelsch 2005; Syed 2005).

Erosion is known as the natural disaster that caused the most damage to the soil. 24 billion tons of soil disappear by the ground of erosion on the earth (Çepel 1998, AGM 2007). Turkey is exposed to soil erosion is high or very high level of 79.4%, Africa, Europe and North America or by the order of 22, 17 and 6 times more likely occur erosion. For this reason the fertile agricultural lands are affected negatively. According to TUIK data; in our country erosion is observed in about 75% of agricultural lands, in addition, annually 90 million tonnes of plant, 500 million tonnes of fertile agricultural land and 1.4 billion tonnes of land are lost (TUIK 2015). One of the natural disasters that cause the loss of fertile agricultural land is also flood and it is often experienced due to the geographical features of our country and the unconscious use of forests. It also leads to loss of life and property damage as well as loss of fertile land and cultivated areas (Perlin 1989). Heavy metal pollution, by accumulating in the soil and especially in the fields of agricultural production, is becoming a problem for human and animal health (Doelsch 2005).

2.1. Efficient Effect to Fertile Soil of Soil Pollution and Natural Disasters

The soil pollution is occurred by the various affect as biological, physical, chemical and geological. On the other hand the main causes of soil contamination are wastes, incorrect or over-fertilizer applications, the use of improper agricultural techniques, and the accumulation of heavy metals in the soil.

The soil structure and characteristics are severely deteriorated in regions where urbanization is rapd, in this case, poor use of land, contamination of soil due to inadequate infrastructure and pollution caused by construction are playing a role.

Wrong agricultural practices also have negative effects on the soil. Chemical fertilizers and pesticides, which are used unconsciously in large quantities especially in agricultural activities, have a negative impact on environmental pollution (Karaca and Turgay 2012).

Especially chemical fertilizers and pesticides, which are used unconsciously in large quantities in agricultural activities, have a negative impact on environmental pollution (Aydemir ve İnce 1988; Kızıloğlu 1995; Kızıloğlu ve Bilen 2000).

The most common heavy metals contaminated to the soil are Cd, Cr, Hg, Pb, Cu and Zn (Albering 1999). Natural disasters are defined as natural disasters that cause social, economic, physical and environmental losses on people and settlements and stop normal life and interrupt daily activities (Ergünay 1996; Karancı 2006).

Turkey, is exposed to various natural disasters such as meteorological characteristics in terms of features and tectonic formation by geological structure, topography. Natural disasters coming to the cause damage to life and property as well as some economic damages. These economic losses count in the disappearance of settlements and the reduction of fertile agricultural land. Such damages are caused by natural disasters especially, such as landslides, floods and floods, erosion, earthquakes.

Earthquake is occured in our country, more than developed countries and among the most common natural disasters in our country are seismic erosion. It is known that the erosion of fertile soil is caused by the loss of and it is largely dangerous (Ergünay 1996, Gülkan 1999, Erpul and Saygın 2012). The negative effects of forests erosion caused by, unconsciously destroying forests causes erosion in grassland and meadow use to be damaged in misguided or non-agricultural activities (Çepel 1998). Another reason for the loss of fertile land is the mistakes made during the processing of the soil. Some studies show that soil treatment is associated with soil organic carbon and P content, and that correct treatment improves soil fertility, while erroneous treatment results in yield and crop loss (Çepel 1998; Heckrath ve ark. 2005; Anonymous 2005a).

2.2. Measures to be Taken for the Protection of Fertile Agricultural Land

In order to contribute to the economy of our country, which is an agricultural country, and to sustain agricultural activities, it is necessary to protect the productive agricultural land. Damaged or lost fertile land, causes agricultural activities and agricultural products to decline, import dependence on some agricultural products, and damage to the country's economy. For all these reasons, the protection of fertile agricultural land is necessary. It may be possible to protect the fertile soil by don't use out of purpose use and to existing agricultural land. Furthermore, the use of fertilizers and pesticides used in agricultural production must be controlled. In order to prevent heavy metal pollution from various wastes, industrial waste and

domestic wastes should not be left directly to the nature and proper treatment plants should be established. Farmers carrying out agricultural activities may be able to protect the fertile soil by using appropriate agricultural practices such as irrigation, sowing and fertilization by training, and by using the suitable equipment (Mikayilov and Acar 1998). New practices must be made to prevent environmental pollution. The environmental pollution that occuret by he decrease of the forests leads to natural disasters such as erosion and flooding. Forest land needs to be expanded to prevent such natural disasters from destroying fertile land. Proper areas should be forested to protect the fertile soil from the damage of natural disasters such as erosion and flood (Yücel 1995). It is possible to protect from the harmful effects of natural disasters, such as erosion and flood by forming meadow and pasture areas, too.

3. Results and Discussion

Turkey is an agricultural country and agricultural products occupy an important place in the national economy (Atıcı ve Kurt 2007). However, natural disasters such as environmental pollution, erosion, flood and earthquake, and misapplication, cause the damaged or reduction of fertile agricultural land. Some measures are needed to protect these lands. For our country, the need of efficient agricultural land and the existing fertile areas should be determined. Fertile land is sometimes used in non-agricultural activities, it must be protected by preventing this use. It is also important for agricultural activities to be carried out with appropriate tools and equipment and using of organic fertilizers in order to protect fertile soils.

To avoid soil pollution, industrialization should be as far away from agricultural land as possible. In addition by establishing appropriate treatment systems environmental pollution should be prevented and fertile land use in agricultural activities should be analyzed at regular intervals. If chemical pollution is detected, measures should be taken according to the contamination rate of the pollutant and the pollution rate (Mikayilov ve Acar 1998).

Efforts should be made to prevent natural disasters, which are the most impacts of the disappearance of efficient land. It is especially important to protect from erosion by afforestation. It is known that some species of trees are rooted in roots and marshes with a length of 100 km in a 1 m^3 bedrock, 90 tons in one hectare area and 40 tons in a beech forest in a spruce forest (Çepel 1995). Presence or absence of forest; it changes the amount of water held in the atmosphere, underground or in the ground. This is affected that respectively; erosion frequency, ecosystem functions, water quantity (Çolak ve ark. 2010). For all these reasons, the increase in afforestation and forest areas is necessary both for the prevention of environmental

pollution and some natural disasters, as well as for the protection of fertile land which is very important in agricultural activities. Besides these, it is very important to organize trainings on environmental protection and agricultural activities.

References

AGM, (2007), Ağaçlandırma ve Erozyon Kontrolü Seferberliği Eylem Planı (2008-2012), T. C. Çevre ve Orman Bakanlığı, Ankara.

Anonymous, (2005a). Soil Pollution. Palestinian National İnformation Centre. Elektronik (Online) Erişim, http://www.pnic.gov.ps/english/Environment/Environment_Pollution-1.html#Soil%Pollution.

Albering, J.H., van Leuson, S.M., Moonen, E.J.C., Attogewerff, J.A., Kleinjans, J.C.S., (1999). Human health risk assessment: A case study involving heavy metal soil contamination after the flooding of river meuse during the winter of 1993-1994. Environmental Health Perfectives, 107(1): 1-13.

Atıcı, C. ve Kurt, F. (2007) "Türkiye"nin Dış Ticareti ve Çevre Kirliliği: Çevresel Kuznets Eğrisi Yaklaşımı", Tarım Ekonomisi Dergisi, 13(2): 61-69.

Aydemir, O., İnce, F., (1988). Bitki Besleme, Dicle Üniv. Eğitim Fak., Yay. No: 2, Diyarbakır.

Çepel, N., (1995), Yok Ettiğimiz Ormanlarımız Kaybolan Fonksiyonel Değerler ve Zamanımızın Orman Ölümleri, TEMA Vakfı Yayınları. Yayın No:2, Genişletilmiş 3. Basım, İstanbul.

Çepel, N., (1998). Çevre ve İnsan, Akdeniz Yayıncılık A. Ş.,İstanbul.

Çolak, A. H., Kırca, S., Rotherham, I., D., İnce, A., (2010), Restoration and Rehabilitation of Deforested and Degraded Forest Landscapes in Turkey, ISBN: 978-605-393-049-5, İstanbul.

Doelsche, E., Saint Macary H., Van Kerchove V., (2005). Sources of very heavy metal content in soils of volcanic island (La Reunion). Journal of Geochemical Exploration, in press, corrected prof, avilable on line 7 Nov.2005.

Doelsche, E., Van de Kerchove, V., Saint Macary H., (2005). Heavy metal content in soils of Reunion (Indian Ochean). Geoderma, in press, corrected prof. Available online 24 October 2005.

Ergene, A., (1993). Toprak Biliminin Esasları, Atatürk Üniv. Yay. No:586, Zir. Fak. Yay. No:267, Ders Kitapları Serisi No:42.

Ergünay, O. (1996). "Türkiye'de Afet Zararlarının Azaltılması Konusunda Yapılan ve Yapılması Gereken Çalışmalar Hakkında Rapor" Afet İşleri Genel Müdürlüğü , Ankara.

Erpul, G., Deviren Saygın, S., (2012). Ülkemizdeki Toprak Erozyonu Sorunu Üzerine: Ne Yapmalı?. Toprak Bilimi ve Bitki Besleme Dergisi. 1(1), 26 - 32.

Gülkan P., (1999) "Afetlere Karşı Hazırlıklı Olma: Planlama ve Yapı Denetimi", Deprem Güvenli Konut Sempozyumu, Ankara.

Heckrath, G., Djurhuus, J., Quine, T. A., Van Oost, K., Govers, G. And Zhang, Y., (2005). Landscape and Watershed Processes. Journal Environmental Quality. 34:312-324.

Karaca, A., Turgay, O.C. (2012). Toprak Kirliliği. Toprak Bilimi ve Bitki Besleme Dergisi. 1(1), 13 – 19.

Karanci N., (2006). "Afetlerle Yaşamak yada Afet Yaşamamak", 14. Ulusal Psikoloji Kongresi, Eylül.

Kızıloğlu, F. T. ve Bilen, S., (2000). Çevre Kirliliği, Atatürk Üniv. Zir. Fak. Yay. No:220.

Kızıloğlu, T., Toprak Mikrobiyolojisi ve Biyokimyası, (1995). Atatürk Üniv. Zir. Fak. Yay. No:180.

Mikayilov, F. D., Acar, B., (1998). Toprak ekosistemlerinde kirleticilerin taşınım mekanizmasının incelenmesi ve odellenmesi, Ekoloji Çevre Derg., 7(28): 20-23.

Perlin, J., (1989), A Forest Journey: The Role of Wood in the Development of Civilization, Harvard University Press, Cambridge, Massachusetts, London, England, ISBN: 0—674-30892-1.

Syed, Ibrahim B., (2005). Pollution. Islamic Research Foundation International, Inc. 7102 W. Shefford Lane Louisville, KY 40242-6462, USA Elektronik (Online) Erişim, http://www.irfi.org/articles/articles_51_ 100/pollution.htm.

TUİK (2015), http://www.tuik.gov.trErişim Tarihi : 06.08.2016/ 15.43.

Yücel, M., (1995). Çevre Sorunları, Çukurova Üniv. Zir. Fak. Yay. No: 109, Ders Kitapları, Yay. No:28.

Examination of Preparation to Be Performed Before Sea Trial

Yusuf GENÇ[1*], Murat ÖZKÖK[2]

[1]Ordu University, Fatsa Vocational Higher School, Vessel Construction Program, Ordu, Turkey; E-mail: yusufgenc55@yahoo.com

[2]Karadeniz Technical University, Surmene Faculty of Marine Sciences, Naval Architecture and Marine Engineering, Trabzon, Turkey; E-mail: muratozkok@ktu.edu.tr

[*] **Corresponding Author: y**usufgenc55@yahoo.com

Abstract

In this study, what has to be done before the cruise has been examined in order to perform the sea trial of a ship came to the delivery stage more regularly. First the things to be done are listed and explanations have been made about them. The model of the sea trial implementation process obtained within this scope has been transformed into a questionnaire and 20 engineers and captains experienced in navigation have been received opinion. It has been asked to these persons how and in what direction the implementation process model contributes the sea trial if carried out before the cruise. As a result, it is understood that the ratio of those who say that the improvement process model will have a high level of positive contribution to the sea trial is 45% while 25% of those who think that it will be very high. By this means, it is determined that the preparations to be made before the sea trial are important and will contribute to perform the cruise more ordinate.

Keywords: Plannig, Sea trial, Ship, Shipbuilding

1. Introduction

It is necessary to check for whether a ship that has been created having passed through challenging stages throughout the duration of its construction carries the necessary provisions on topics like security, maneuvering, equipment, and adequacy. For this reason, ships that have come to the end of their production phases are going on sea trial. Along with the tests to be done on the sea trial showing differences, the International Maritime Organization (IMO) sees conducting, turning, zig-zag, and stopping maneuvers as imperative to identify whether ships larger than 100 meters have the capacity for adequate maneuvering (IM0 Circular, 2002). Many more tests are conducted during sea trial along with these tests that the IMO made mandatory. It is very important in terms of both the shipyard and the ship owner that sea trial passes orderly and without problem. This is why the planning conducted prior to the sea trial needs to have been prepared well.

A plan has been created in the scope of this study for the preparations necessary prior to the sea trial for the ship. This study considers the minimization of issues that are experienced or may be experienced prior to and at the moment of the sea trial. The amount of time spent on this sea trial may be shortened in this respect, and it may be possible for the total cost to be reduced. While these tests and trials conducted in the shipyard are carried out under the supervision of ship representatives and the class, they will at the same time help the persons who will be the personnel of the ship in the future to get to know the vessel. During the tests, a ship that is newly in its construction phase is the property of the shipyard and carries the flag of the manufacturing state because it has not yet been delivered to the property owner (Aktan, 1995).

The sea trials are generally done in our country on the coastal section on which the shipyard is found. Because there are generally no ship traffic problems in the conducting of sea trial tests in the Aegean and Mediterranean seas, no time problems will occur in the conducting of these trials. However, especially the Marmara Sea is a place where problems are experienced in terms of the experiences of sea trial because of the straits vessel traffic and harbour traffic experienced in the gulf region which has developed industry.

Figure 1 shows the instantaneous photograph taken from Marine Traffic, in which each color of the Marmara Sea represents a separate type of vessel. Considering substantially heavy ship traffic, it is understood that conducting test sea trial trials is difficult in the region of the Tuzla and Yalova shipyards.

Figure 1. Marine traffic of Marmara and Bosphorus (URL-1, 2018)

The ships coming to the Marmara Sea are examined in two sections, indirect and direct passing vessels. Ships that pass through the Turkish Bosporus without stopping at ports in the Marmara Sea are called direct passing vessels, and ships that come to unload cargo at the ports found within the Marmara Sea are called indirect passing vessels (Kılıç, 2009). With its annual vessel activity of approximately 125,000 the Marmara Sea traffic volume at levels close to the Strait of Dover and much more than channels like the Suez and Panama canals (Altan, 2014).

1.1 Turkish Straits Vessel Traffic

Turkish Channels: It is defined as the coastal strip of the Istanbul Bosporus, the Çanakkale Dardanelles, and the Marmara Sea that surround this area with the transit areas of vessels (Official Gazette, 1998). The volume of ship traffic in the Turkish Bosporus is gradually increasing. In 1936 when the Montreux Convention was signed, an average 4,500 ships cross the Turkish Bosporus each year. However, it is known that this figure has reached 50,000 in recent years (Altan, 2014). Turkish channels are waterways that have high accident and pollution risk because of dangerous cargo and tanker traffic (Essiz and Dagkiran, 2017).

The Istanbul Bosporus is one of the busiest waterways in the world. Approximately 132 vessels pass the Bosporus each day. This number is around 2,000 per day with local vessel traffic (Akten, 2004).

The table shows the indirect and direct ship passing between the years of 2006-2016 for the Istanbul Bosporus (URL-2, 2017).

Table 1. Bosphorus vessel passages between the years of 2006 and 2016

Years	Total number of vessels	Total gross Tonnage	Direct passing	Indirect passing
2006	54.880	475.796.880	31.880	23.000
2007	56.606	484.867.696	31.826	24.780
2008	54.396	515.639.614	31.762	22.634
2009	51.422	514.656.446	32.297	19.125
2010	50.871	505.615.881	28.668	22.203
2011	49.798	523.543.509	27.938	21.860
2012	48.329	550.526.579	27.345	20.984
2013	46.532	551.771.780	26.577	19.955
2014	45.529	582.468.334	26.212	19.317
2015	43.544	565.216.784	25.243	18.301
2016	42.553	565.282.287	26.050	16.503

2. Material and Method

A ship whose harbor acceptance tests have concluded and all commissioning processes have been completed is ready to set out for sea trial. Sea trials can last anywhere from 36 to 48 hours under normal conditions. The importance is great of the preparations that must be conducted prior to the sea trial because the deferral of the delivery date of a ship that has passed into the delivery phase can be precluded and the cost of the sea trial is high. For this reason, attention should be shown to tending to the necessary preparations in terms of not experiencing problems in the setting out to the ship on the day and time of setting out on the sea trial.

- **Optaining necessary permisions for sea trial**

Before ships leave the harbor in which they reside, they must obtain a harbor exit document from the port authorities to which the harbor is connected. However, vessels that will set out to sea trial are exempt from harbor exit documentation because they are not yet registered. In addition to this, the relevant shipyard must get permission by applying to the port authority for the ship to be able to set out for sea trial. The shipyard must indicate on the

application it will submit in writing to the port authority the total number of persons who will set out on the sea trial on the vessel along with their names, last names, and T.R. ID numbers.

- **Invitation to sea trial relevant persons from the outside**

Invitations are planned prior to the sea trial for the purpose of ensuring the participation on time in the sea trial of many people, primarily including the representatives of the class institution in which the shipyard operates. Because for the machinery and equipment used on the ship (main machinery, generator, cooler, etc.), the service engineers need to participate in the sea trial too. No matter how tested machinery and equipment are in the accompaniment of service engineers under prior to the sea trial, the intervention of authorized service engineers in the relevant equipment will be more beneficial in the mishaps that may occur during the sea trial. For this reason, the prolonging of the duration of the sea trial can be prevented with solutions produced in the short term in accompaniment with service engineers, and the sea trial cost can be reduced accordingly.

- **Determination of shipyard staff for sea trial**

First, those who will be setting out on the sea trial should be designated among the project workers (manager, chef, captain, engineer, etc.) who were responsible in the production of the vessel. Especially the engineers that are responsible for the ship in the areas of pipe outfitting and electricity absolutely have to be on the ship. Additionally, personnel with sea trial experience should be prioritized. Those who monitor the work done on the vessel should be designated among the workers and subcontractor firm employees who worked in the manufacture of the ship. The fastest and most reliable intervention that can be made for mishaps that may occur in a ship during the sea trial can be carried out by workers in the production of the vessel.

- **Supplying to vessel that to be used food, fuel, etc during sea trial**

Before the process of taking the ship from the harbor into the open sea begins, the oil, fuel, and water necessary for the duration of the sea trial and adequate provisions need to be purchased for the ship. No matter what is necessary after the ship is taken into open water, can only be transported to under limited conditions and with small boats.

- **Investigation of weather forecast reports**

Meteorology information is important during the stage of identifying the day of the sea trial. The necessary sensibility should be shown in terms of both security and of being able to shorten the total amount of time to be spent on the sea trial for a ship that is to set out for the first time on a sea trial, and a date should be specified based on this. A sea trial to be conducted in poor weather conditions will also negatively affect personnel and decrease the work performance.

- **Preparation of vessel for sea trial condition with ballas operation**

The ship whose necessary preparations have been completed for the sea trial and that has been supplied needs to be taken out into the open sea at least 12-24 hours before the day of the sea trial. Because the depth of the harbor in which the shipyard is found may not be deep enough and thus the necessary load limits cannot be attained on the sea trial. In addition to this, tug boat service is necessary for the ship to shove off from the port, and it might not be possible to get this service when it is requested.

- **Determining tests that will be done at the same time during sea trial**

The tests (like the separator alarm test / anchor tests) that can be done in the same time slot but that won't affect one another during sea trial must be specified. A reduction in the total duration of time spent can be ensured in this respect by conducting tests simultaneously rather than consecutively.

- **Organizing coordination and communication during sea trial on vessel**

It is important that arrangements be made, having taken the necessary steps prior to the sea trial on issues like the work distribution, coordination, and communication on the sea trial in terms of being able to complete the sea trial in the planned duration of time. In this respect, losses of time that may be experienced can be precluded.

- **Determining division of work for tests that will be done at the same time**

While more than one test is conducted in the same time slot during the sea trial, the division of work must have been done among the personnel. In this respect, time loss can be prevented by conducting the tests simultaneously rather than asynchronously, and this can contribute to the reduction of the total duration of the sea trial. What is important here is that the tests that are planned in the same time slot have been well specified. The tests must not affect one another throughout the duration they are conducted.

- **Determining staff shift time and distrubition of work**

Shift times and distributions must be made by setting out on the sea trial with an adequate number of personnel. The objective here is to prevent the occurrence of errors by personnel working long hours. The errors made during the sea trial can lead to the relevant test being redone or a subsequent test not being held, and all tests to be held immediately after are affected.

- **Preparation of tests to be carried out at the same time during sea trial**

While any test continues to be conducted on the sea trial, the preparations for a subsequent test must be carried out so as to preclude unnecessary losses of time. The importance of the communication and coordination between personnel is great here. It is rather important for the duration of time lasting until a subsequent test when the relevant test ends be able to be reduced. Additionally, the people on the ship knowing what the subsequent test will be will remove any uncertainty during the conducting of the test.

- **Coordination and communication on the vessel**

The correspondences that will take place between the relevant people throughout the sea trial on the ship should be made in an uninterrupted fashion using systems of communication that are wireless or internal (such as telephones or announcement systems). In the necessary situations, the captain should provide information to the personnel by announcing what a subsequent test is. Experiencing coordination and communication deficiencies will negatively affect the sea trial.

2.1. Examination of the Plan of Work to be Conducted Before and During the Sea Trial

The improvement process model has been prepared and displayed in Figure 2 for the sea trial with regard to topics that are thought to contribute to the planned and orderly conduct of the sea trial and that have been explained above. Later, this process was asked to 20 experts in the field, being converted to a survey format.

Statements of opinion were asked of these people on the topic of whether the acquired processes would have a contribution to the ability to more orderly implement the sea trial of the ship and to the ability to shorten the amount of time spent for the sea trial. While providing statements of opinion to expert individuals, they were asked to choose one of five options that were ranked as very low, low, moderate, high, and very high and to additionally indicate their views with regard to the topic, if they had any. The completed surveys were examined, and the rates of responses (very low, low, moderate, high, and very high) were calculated as percentages.

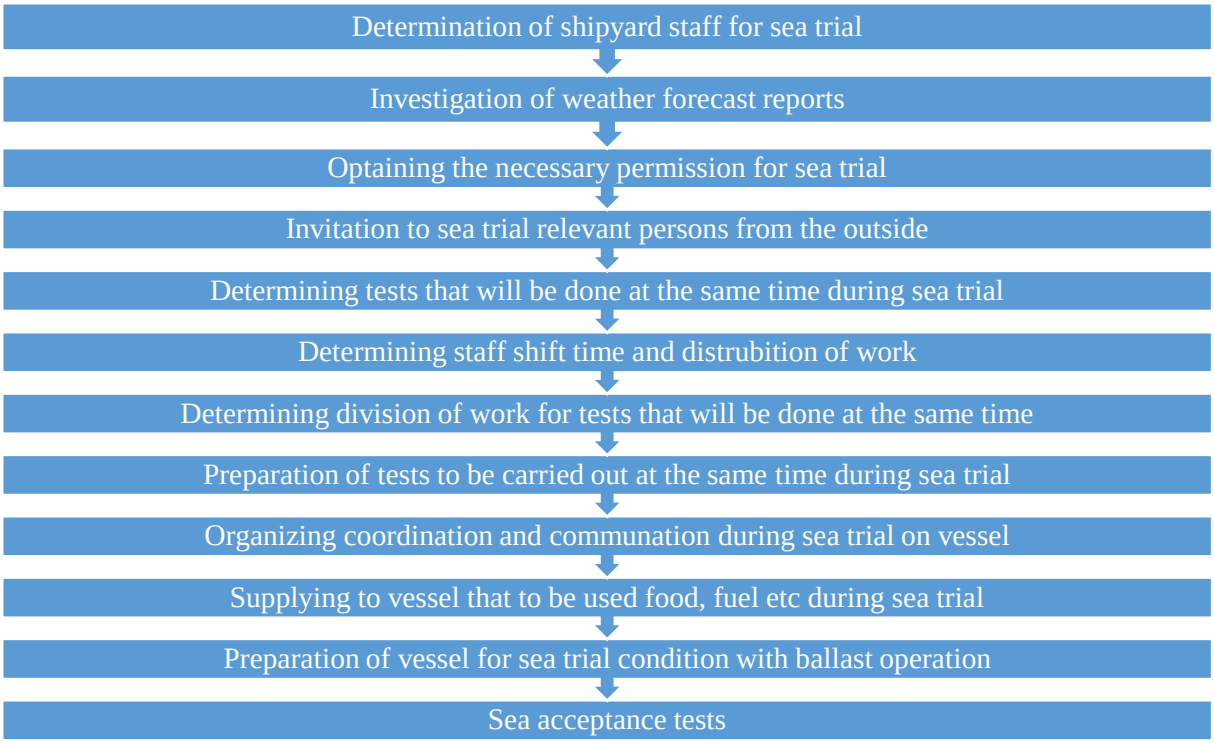

Figure 2. Improvement process for sea trial

3. Results and discussions

The survey study created using the sea trial improvement process model (Figure 2) was asked to experts, and the findings obtained from this survey are shown below.

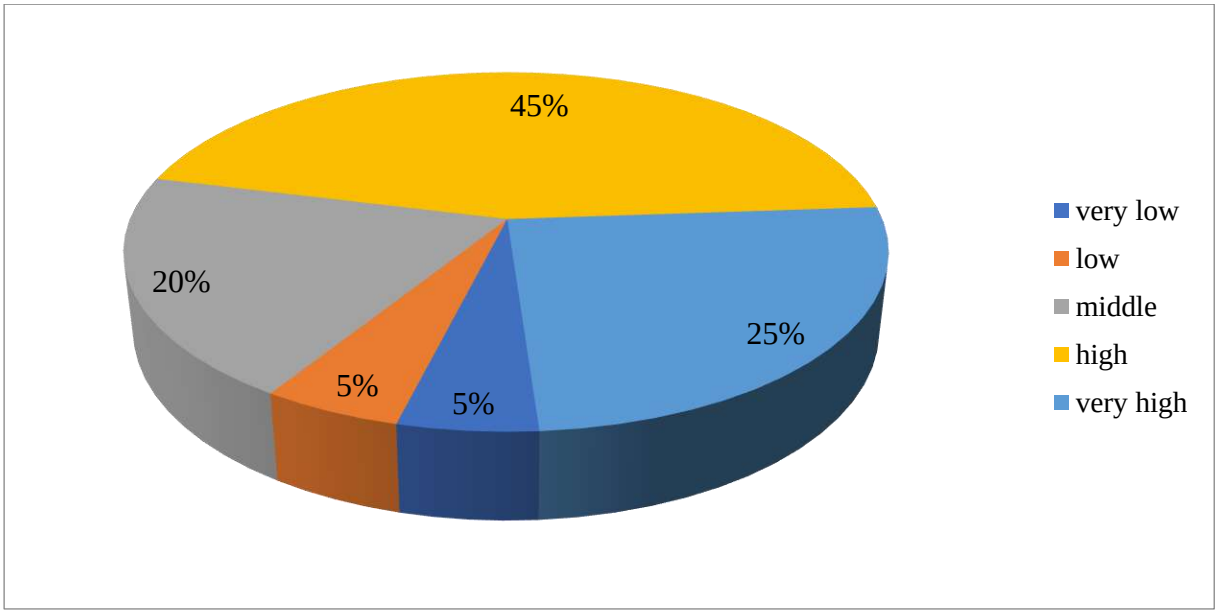

Figure 3. Importance distribution of the improvement process

In the conducted survey, the rate of those who said that the contribution of the pre-sea trial improvement process on the sea trial will be low or very low was determined to be 5%. While those who said its contribution would be moderate was at the level of 20%, the rate of those asserting the position that it would be high was 45%. It was revealed that the rate in this survey of those who adopted the view that it has a very high contribution was 25%.

4. Conclusions

This study mentions the intense vessel traffic experienced in the Marmara Sea and discusses what the plans are that need to be devised prior to the sea trial and how they should be made in terms of the more orderly and systematic advancement of the sea trial in fully manufactured ships that will set out on the sea trial in shipyards in relation to this.

The survey prepared regarding the planning that needs to be done prior to the sea trial was asked to experts. As a result of the survey, the conclusion was reached that the conducted planning was high at a rate of 45% and very high at a rate of 25% of the ability to orderly implement the sea trial of the conducted planning and of the contribution to the ability to shorten the amount of time spent for the sea trial. In addition to this, while those that say its contribution could be at a moderate level are at a level of 20%, it was determined that those saying it will be low or very low is at a level of 5%. Therefore, it is understood that the importance of the planning that must be done prior to the sea trial is high. For this reason, it is seen that serious preparation and conducting the necessary planning prior to the sea trial at shipyards can positively contribute to the process.

References

Aktan, N., (1995). *Gemilerin Liman ve Deniz Tecrübelerinin Planlanması*, Yüksek Lisans Tezi, İstanbul Teknik Üniversitesi, Fen Bilimleri Enstitüsü, İstanbul.

Akten, N., (2004). Analysis of Shipping Casualties in the Bosphorus, *The Journal of Navigation*, 57, 345-356.

Altan, T., (2014). *Marmara Denizi Trafik Akışı ve Trafik Düzeninin Analizi*, Yüksek Lisans Tezi, İstanbul Teknik Üniversitesi, Fen Bilimleri Enstitüsü, İstanbul.

Essiz, B., Dagkiran, B., (2017, September). Accidental Risk Analyses of the Istanbul and Canakkale Straits, *World Multidisciplanary Earth Sciences Symposium*, (pp. 1-8). Prague, Czech Republic.

IMO Circular MSC/Circ., (2002). Explanatory Notes to the Standarts for Ship Manoeuvrability, International Maritime Organization, 1053.

Kılıç, A., (2009). Marmara Deniz'inde Gemilerden Kaynaklanan Egzoz Emisyonları, *BAÜ FBE Dergisi*, 11,2, 124-134.

Resmi Gazete, (1998). Türk Boğazları Deniz Trafik Düzeni Tüzüğü, Başbakanlık Basımevi 23515(Mükerrer), 2.

URL-1, https://www.marinetraffic.com/en/ais/home/centerx:28.7/centery:40.7/zoom:9. (15 Mayıs 2018).

URL-2, https://atlantis.udhb.gov.tr/istatistik/gemi_gecis.aspx. (10 Mart 2017).

Urban problems and sustainable urbanization strategies in Turkey

Kasım Atmaca[1*], N. Gamze Turan[2], Nevzat Beyazıt[3]

[1] Ondokuz Mayıs University, Engineering Faculty, Dept. of Environmental Engineering, 55200, Samsun, Turkey
[2] Ondokuz Mayıs University, Engineering Faculty, Dept. of Environmental Engineering, 55200, Samsun, Turkey
[3] Ondokuz Mayıs University, Engineering Faculty, Dept. of Environmental Engineering, 55200, Samsun, Turkey

[*] **Corresponding Author:** kasim.atmaca@omu.edu.tr

Abstract

The environmental problems have an important place within the context of sustainable development debate due to the globalization and internationalization all over the world. There is a high level of consensus between the developed and developing countries in regard to the level of sensitivity for environment, however, the types of the environmental problems that are faced and their economic, social and cultural characteristics are considerably different. The fundamental factors of the environmental problems in developed countries are rapid development and industrilization, whereas, the environmental problems of the developing countries are derived from low income level, unplanned urbanization and industrilization and inappropriate land use decisions. The differences in these dimensions directly affect the policies of each group of countries.

The most important problems of developing countries can be summarized as follows; insufficient economic growth and unemployment, poverty, rapid population growth, migration, rapid and unplanned urbanization, environmental pollution, inadequacy of infrastructure and services and deterioration of natural resources. Turkey has some problems that are similar to those of other developing countries such as rapid population growth and urbanization, environmental pollution and deterioration of natural resources.

The aim of this study, to investigate the urban problems and sustainable urbanization strategies in Turkey. To achieve this, the paper will address two main objectives: the first considers basic environmental problems, the second discusses the urbanization strategies.

Keywords: Keyword one, Keyword two, Keyword three.

1. Introduction

Until 2030, the world's rural population is expected to remain largely static, while the urban population is projected to grow by 1,5 billion people. By 2030, 60% of the global population will live in cities. Over 90% of that urban growth will ocur in cities and towns of the developing world.

The urbanization of the global population has fundamental ramifications for the economy, society and the environment. Urban centres currently cover only a small part of the world's land surface-0,51% of the total land area. However, urban areas will expand significantly during the next two to three decades. Based on the current trends, urban land cover will increase by 1,2 million km^2 by 2030, nearly tripling global urban land area between 2000 and 2030 (Jiboye, 2005; Osasona et al., 2007).

Cities cover a small part of the world, but their physical and ecological footprints are much larger. Cities accounted for 82% of global GDP in 2014 (3) and by 2025 this will rise to an estimated 88% . There will be 230 new cities by then, all in middle income countries (UN-Habitat, 2007).

Urbanization may be defined as the movement of population from rural to urban areas, the growth of cities in number and size and the increase of the share of urban population in total population. Such a definition should not overlook the fact that urbanization entails at the same time a transformation in the structure of economy and proceeds in parallel with a certain change in human behaviour at least in theory. Especially, the characteristics of urbanization in developing economies differ widely from those in already developed and industrialized nations (UNFPA, 2007)

2. Urbanization in Turkey

Turkey is a country in the process of development, and of a rapid population growth. The economy is predominantly based on agriculture, and a great majority of its population is rural. In Turkey, between 1927 and 1950, a great percentage of Turkish population remained rural. After 1950, urbanization has become accelerated, but the rural character of the population has not been reversed or changed susbstantially. In the other words, urbanization has been a phenemonen of last twenty years. If the existing conditions will continue to prevail and there is no doubt that they will a greater migration flow from the villages to cities will be expected (Oladunjoye, 2005).

Urban population in Turkey was reported as 58749346 in 2016, according to the World Bank collection of development indicators, compiled from officially recognized sources.

Figure 1: Urban population growth in Turkey

Rural population in Turkey was reported at 20763080 in 2016, according to the World Bank collection of development indicators, compiled from officially recognized sources.

Figure 2: Rural population in Turkey

3. Urbanization Problems in Turkey

3.1 Air Pollution

The air is an essential ingredient for our wellbeing and a healthy life. Unfortunately polluted air is common throughout the world (EPHA,2009) specially in developed countries from 1960s. (Kan, 2009). Polluted air contains one, or more, hazardous substance, pollutant, or contaminant that creates a hazard to general health (Health and Energy, 2007).

The main pollutants found in the air such as, particulate matter, PAHs, lead, ground-level ozone, heavy metals, sulphur dioxide, benzene, carbon monoxide, and nitrogen dioxide (European Public Health Alliance, 2009). Air pollution in cities causes a shorter lifespan for city dwellers (Progressive Insurance, 2005). According to Mishra (2003) rapid growth in urban population, increasing industrilization, and rising demands for energy and motor vehicles are the worsening air pollution levels. The other factors, such as poor environmental regulation, less efficient technology of production, congested roads, and age and poor maintenance of vehicles, also add to the problem. Air pollution is caused of ill and death by natural and man-made sources, major man-made sources of ambient air pollution include tobacco smoke, combustion of solid fuels for cooking, heating, home cleaning agents, insecticides industries, automobiles, power generation, poor environmental regulation, less efficient technology of production, congested roads, and age and poor maintenance of vehicles. The natural sources include incinerators, and waste disposals, forest and agricultural fires (European Public Health Alliance, 2009).

In Turkey, the provincial centers having annual maximum, minimum and average PM and SO_2 concentartions are given in Figure 3 and Figure 4, respectively.

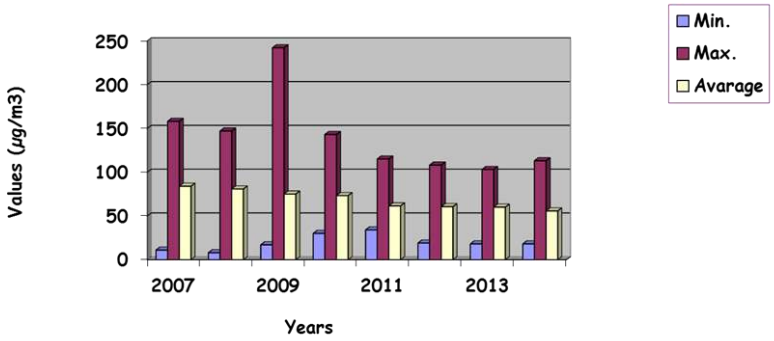

Figure 3.

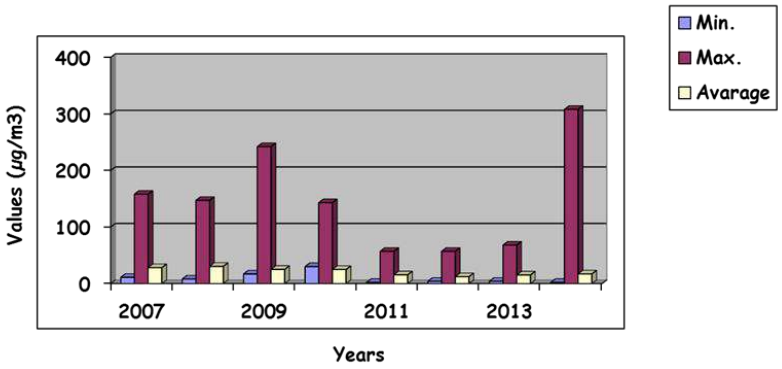

Figure 3.

3.2. Water Pollution

The water is essential ingredients for wellbeing and a healthy life. Unfortunately polluted water and air are common throughout the world (European Public Health Alliance, 2009). The WHO states that one sixth of the world's population, approximately 1.1 billion people do not have Access to safe water and 2.4 billion lack basic sanitation (European Public Health Alliance, 2009). Polluted water consists of Industrial discharged effluents, sewage water, rain water pollution (Ashraf et al, 2010) and polluted by agriculture or households cause damage to human health or the environment (European Public Health Alliance, 2009). This water pollution affects the health and quality of soils and vegetation (Carter, 1985). Some water pollution effects are recognized immediately, whereas others, dont show up for months or years (Ashraf et al, 2010). Estimation indicates that more than fifty countries of the world with an area of twenty million hectares area are treated with polluted or partially treated polluted water (Hussain et al, 2001) including parts of all continents and this poor quality water causes health hazard and death of human being, aquatic life and also disturbs the production of different crops (Ashraf et al, 2010; Scipeeps, 2009). In fact, the effects of water pollution are said to be the leading cause of death for humans across the globe, moreover, water pollution affects our oceans, lakes, rivers, and drinking water, making it a widespread and global concern (Scipeeps, 2009). The untreated industrial and municipal wastes have created multiple environmental hazards for mankind, irrigation, drinking and sustenance of aquatic life. The drainage water contains heavy metals in addition to biological contaminations.

3.3. Soil Pollution

Addition of substances which adversely affect the quality of soil or its fertility is known as soil pollution. Generally polluted water also pollute soil. Solid waste is a mixture of plastics, cloth, glass, metal and organic matter, sewage, sewage sludge, building debris, generated from households, commercial and industries establishments add to soil pollution. Fly ash, iron and steel slag, medical and industrial wastes disposed on land are important sources of soil pollution. In addition, fertilizers and pesticides from agricultural use which reach soil as run-off and land filling by municipal waste are growing cause of soil pollution. Acid rain and dry deposition of pollutants on land surface also contribute to soil pollution (Khan, 2004).

3.4. Noise Pollution

Noise is one of the most common pollutant. Noise by definition is “sound without value” or “any noise that is unwanted by the recipient”. Noise in industries such as stone cutting and crushing, steel forgings, loudspeakers, shouting by hawkers selling their wares, movement of heavy transport vehicles, railways and airports leads to irritation and an increased blood pressure, loss of temper, decrease in work efficiency, loss of hearing which may be first temporary but can become permanent in the noise stress continues. It is therefore of utmost importance that excessive noise is controlled. Noise level is measured in terms of decibels (dB). WHO (World Health Organization) has prescribed optimum noise level as 45 dB by day and 35 dB by night. Anything above 80 dB is hazardous.

4. Sustainable Urbanization Strategies in Turkey

Sustainability adds new dimensions to urbanization. Conversely, urbanization, depending upon its pace, natüre and patterns, may create numerous problems or opportunities that will need special treatment. Therefore, sustainable urbanization is the maximization of economic efficiency in the use of resources including air, water and soil, maintaining natural resources stocks at or above their present level, ensuring social equity in the distribution of development benefits and costs, and avoidance of unnecessary foreclosure of future development options.

When applied to the field of urban development, it is assumed that sustainable urbanization can be secured only when master planning is directed to minimize travel needs, to promote public transportation, to conserve fertile agricultural lands, to avoid wasting other

sensitive and non-renewable ecological resources and to enhance energy savings in building designs and layouts. This would require certainly carrying out sustainability in city planning practices through regional resource inventories, vertical and horizontal coordination among all public authorities and private entities involved in regional resource management and the development of renewable resource strategies.

Most of the countries in the Mediterranean Basin were not able to realize the principles formulated in the Agenda 21, particularly with respect to sustainable urbanization. Turkey is not an exception to such an observation. Urban development is considerably influenced there qualitatively and quantitatively by rapid urbanization. Urbanization has been not only rapid, but also one-directional, unbalanced and disorderly. It operates to increase the rate of unemployment and underemployment in major cities and to inflate the informal sector. Rapid urbanization is also characterized since 1950 by a rapid increase in the number of squatter dwellings that surrounded the major cities (Knight, 1993).

5. Conclusion

Nearly half the worlds population now lives in urban settlement. Urban offers the lure of better employment, education, health care and culture; and they contribute disproportionately to national economies. However, current worldwide urbanization presents important challenges of urban poverty, megacities, social deterioration and environmental degradation. Rapid urbanization in many developing countries worldwide has become a major concern because of its detrimental effects on environment. To reverse urban environmental degradation in most developing countries such as Turkey, it is essential to understand and specify the factors that perpetuate the lack of appropriate preventive and curative environmental actions. As a result, there should be a strategic framework of action prepared by local planners based on the core principles of sustainable development.

References

Ashraf, M.A., Maah, M. J., Yusoff, I. & Mehmood, K. (2010). Effects of Polluted Water Irrigation on Environment and Health of People in Jamber, District Kasur, Pakistan, International Journal of Basic & Applied Sciences, 10 (3), pp. 37-57.

Carter, F. W. (1985). Pollution Problems in Post –War Czechoslovakia, Transactions of the Institute of British Geographers, 10(1), pp. 17-44.

European Public Health Alliance, (2009). Air, Water Pollution and Health Effects.

Health and Energy, (2007). Air Pollution Health Efects.

Holland, W.W., Bennett, A.E., Cameron, I.R., Florey , C.V., Leeder, S.R., Shilling, R.S.F., Swan, A. V. &Waller, R.E. (1979). Health Effects of Particulate Polltion: Reappraising the Evidence. Am Journal Epidemiol, 110 (5), pp. 525-659. Scruton, R. (1996).

Hussain, I., Raschid, L., Hanjra, M. A., Marikar, F. & van der Hoek, W. (2001). A Framework for Analyzing Socioeconomic, Health and Environmental Impacts of Wastewater Use in Agriculture in Developing Countries, IWMI

Jiboye A. D. (2005). "Globalization and the Urban Growrh Process in Nigeria". In,W. Fadare et al. (EDS). Proceedings of the Conference on Globalization, Culture and the Nigerian Built Environment. Vol. II. Obafemi Awolowo University , Ile-Ife, Nigeria.

Kan, H. (2009). Environment and Health in China: Challenges and Opportunities Environmental Health Perspectives, 117 (12), pp. A530-A531.

Khan, S.I. (2004). Dumping of Solid Waste: A Threat to Environment.

Knight R.V. (1993)."Sustainable Development-Sustainable Cities" International Social Science Journal, Vol.45 pp, 35-54.

Mishra, V. (2003). Health Effects of Air Pollution, Background Paper for Population-Environment Research Network (PERN) Cyberseminar, December 1-15.

Osasona C., Ogunshakin L. &Jiboye A. (2007). "The African Woman's Right to Security through Sanitation. From the Dwelling Unit to the Neighborhood". Conference Proceeding on, Right to Live in Africa. Trieste, 9-10 November. University of Trieste, Italy.

Progressive Insurance, (2005). Pollution Impact on Human Health

Scipeeps, (2009). Effects of Water Pollution.

UN-Habitat, (2007). Milestones in the Evolution of Human Settlements Policies. 1976-2006. State of the World Cities. Report 2006/2007. The MDGs and Urban Sustainability. 30 Years of Shaping the Habitat Agenda. U.K. Earthscan.

UNFPA (2007). State of the World Population 2007, Unleasing the Potential of Urban Growth. New York. United Nations Population Fund.

Investigation of Antioxidant Capacity and Anti-Tyrosinase Activity of *Parmotrema perlatum* and *Protoparmeliopsis muralis* Lichens

Sinem AYDIN [1*], Kadir KINALIOĞLU [2]

[1] Giresun University, Faculty of Science and Arts, Department of Biology, Giresun, Turkey; sinem.aydin@giresun.edu.tr

[2] Giresun University, Faculty of Science and Arts, Department of Biology, Giresun, Turkey; kadir.kinalioglu@giresun.edu.tr

[*] **Corresponding Author:** sinem.aydin@giresun.edu.tr

Abstract

In this research, antioxidant and anti-tyrosinase activities of water, ethanol and chloroform extracts of *Protoparmeliopsis muralis* and *Parmotrema perlatum* lichen species. Antioxidant ability of the extracts were revealed by different methods such as total phenolic content, total flavonoid content, metal chelating activity, trolox equivalent antioxidant capacity and copper reducing antioxidant capacity (CUPRAC). Whereas the highest total phenolic content was determined in the ethanol extract of *P. perlatum* lichen; the lowest total phenolic content was determined in the ethanol extract of *P. muralis* lichen. Lichen extracts were exhibited lower metal chelating activity than Etilen Diamine Tetra Asetic Acid (EDTA). Anti-tyrosinase activity of the extracts were also investigated. Only ethanol extract of the both lichens showed tyrosinase inhibition. According to the results, it is concluded that *P. muralis* and *P. perlatum* lichens could be an alternative to synthetic antioxidant and antityrosinase agents.

Keywords: Lichen, Antioxidant capacity, Tyrosinase inhibitor.

1. Introduction

Antioxidants retard or prevent oxidation of oxidizable substrates. Antioxidants might be synthesized such as reduced glutathione (GSH) and superoxide dismutase (SOD) or taken as dietary antioxidants. Plants have long been an alternative to exogenous (i.e., dietary) antioxidants. It is thought that two-thirds of the world's plants posssess medicinal value and nearly all of these possess superb antioxidant capacity (Kasote et al., 2015).

Tyrosinase enzyme is distributed in plants, microorganisms and animals. The generation of melanin in the human body impacted or decrease by various mechanisms such as anti-oxidation, tyrosinase inhibition and melanin inhibition of migration from cell to cell. Lately, tyrosinase inhibitors have been utilized in cosmetics and depigmenting agents for hyperpigmentation (Verma et al., 2008).

Lichens are symbiotic associations consists of a fungi and an algae or a blue-green algae. Lichens have been utilized as traditional medicines in worldwide for centuries (Shibata e al., 1948). Lichens synthesize many of secondary metabolites which are often structurally unique to lichens. These lichen secondary substances have many bioactivities, such as antitumour, antibacterial, anti-fungal, antiviral, antiinflammatory and antioxidant activities (Luo et al., 2009).

The present study describes the determination of the antioxidant, antioxidant and anti-tyrosinase activities of water, ethanol and chloroform extracts obtained from *Protoparmeliopsis muralis* and *Parmotrema perlatum* lichens were investigated.

2. Material and Method

2.1. Collection of the Lichens

P. muralis and *P. perlatum* specimens were collected from the following locations and the collected samples were dried in laboratory conditions. It was authenticated by Kadir KINALIOĞLU. Some examples of these lichen samples are stored in the herbarium of the Biology Department, Faculty of Arts and Science, Giresun University.

P. muralis: Trabzon, Araklı, Kızılkaya plateau, 2222 m.

P. perlatum: Giresun, Merkez, Boztekke village 22 m.

P. muralis and *P. perlatum* lichens is seen in Figure 1 and Figure 2, respectively.

Figure 1. *P. muralis*

Figure 2. *P. perlatum*

2.2. Preparation of The Lichen Extracts

Dried lichen samples were powdered in blender and extracts were obtained using water, ethanol and chloroform solvents. Lichen samples were weighed to 30 g and subjected to Soxhlet extraction separately in 300 mL of distilled water, 300 mL of ethanol and 300 mL of chloroform solvents. Extracts were stored at -80 ºC until analysis proceeded (Kumar et al., 2012).

2.3. Determination of Antioxidant Activities of Lichen Extracts

2.3.1. Total Phenolic Content

Total phenolic content of lichen extracts was determined by the procedure of Slinkard and Singleton (1977) using gallic acid standard. 0.1 mL lichen extract and 4.5 mL distilled water were mixed. Then, 0.1 mL Folin–Ciocalteu reagent (previously diluted 3- fold with distilled water) was put into the mixture. After 3 minutes, 0.3 mL Na_2CO_3 (2%) was added. The

absorbance was measured at 760 nm, after incubating the mixture for 90 min. The quantity of the total phenolic compounds was denoted as µg of gallic acid equivalent (GAE)/mL. The tests were carried out three times (Slinkard and Singleton, 1977).

2.3.2. Total Flavonoid Content

Total flavonoid content of lichen extracts was determined by the method of Zhishen et al. (1999). 0.25 mL extract was added to 1.25 mL distilled water followed by 75 µL $NaNO_2$ (%5) and incubated for 5 min. Afterwards, 150 µL $AlCl_3.6H_2O$ (%10) was added to the mixture and then incubated for 5 min, the reaction mixture was treated with 0.5 mL NaOH (1M) and 275 µL distilled water. Absorbance was read spectrometrically at 510 nm. The amount of total flavonoid compounds was calculated as µg of catechin equivalents (QE)/mL. The tests were carried out three times (Zhishen et al., 1999).

2.3.3. Total Antioxidant Capacity

Total antioxidant capacity of the lichen extracts was defined by the method of Prieto et al. (1999). Absorbance was measured at 695 nm. The results were calculated as µg of ascorbic acid equivalents (QE)/mL. The tests were carried out three times (Prieto et al., 1999).

2.3.4. CUPRAC Activity

250 µL of aqueous $CuCl_2$ solution, 250 µL of neocuprine solution in alcohol and 250 µL of aqueous NH 4Ac buffer (pH 7.0) were mixed and 250 µL of the extract was added. After 30 min, the absorbance of the mixture was measured at 450 nm. The result is given as an absorbance-concentration plot (Özyürek et al., 2009).

2.3.5. Trolox Equivalent Antioxidant Capacity

Trolox equivalent antioxidant capacities of lichen samples were made according to the method developed by Arnao et al. (Arnao et al., 2001). Solutions of 7.4 mM ABTS and 2.6 mM potassium persulfate in water were prepared. These solutions were allowed to stand in the dark for 12-16 hours with stirring. This mixture of methanol was then added. The absorbance of this solution is read at 734 nm and the absorbance of the $ABTS^+$ cation is 0.700 ± 0.02. 2850 µL of

the prepared ABTS solution was added and 150 µL of lichen extract was added and the resulting mixture was allowed to stand in the dark for 2 hours and the absorbance was measured at 734 nm. Trolox was used as a standard substance in the study. The equivalent antioxidant capacity of the trolox was calculated as µg Trolox/g lichen from the standard graphical equation of trolox. The tests were done in triplicate.

2.3.6. Metal Chelating Activity

Lichen extratcts and standard (EDTA) were prepared at concentrations of 250-1000 µg/mL. 500 µL of lichen extracts added to 1.6 mL of distilled water. Then, 0.05 mL of $FeCl_2$ was added and the mixture was allowed to stand for 30 minutes. Then, 0.1 mL of ferrozine was added and incubated for another 10 min and the absorbance was measured at 562 nm. Results are calculated from the following equation (Loizzo et al., 2012).

$$\% \text{ Activity} : [(A_0-A_1)/A_0]x100 \quad (1)$$

A_0=Absorbance of the control

A_1= Absorbance of the sample

2.4. Anti-Tyrosinase Activity

Anti-tyrosinase activities of lichen extracts prepared at different concentrations were determined according to the method of Vanni et al. (Vanni et al., 1990). The IC_{50} value is the amount of substance that causes 50% inhibition and the low IC_{50} value indicates that the tyrosinase inhibitory activities of the extract or standards are high.

$$\% \text{ Activity} : [(A_0-A_1)/A_0]x100 \quad (2)$$

A_0=Absorbance of the control

A_1= Absorbance of the sample

3. Results and Discussion

3.1. Antioxidant Activity

3.1.1. Total Phenolic and Flavonoid Contents of the Extracts

Total phenolic and flavonoid contents of the extracts were given in Table 1. The highest phenolic content was determined in the ethanol extract of *P. perlatum* and the lowest phenolic content was determined in the water content of *P. muralis.* Extracts of *P. perlatum* exhibited higher total phenolic content than extracts of *P. muralis.*

While the highest total flavonoid content was obtained in the ethanol extract of *P. muralis*, the total flavonoid content was obtained in the water extract of *P. perlatum*. *P. muralis* demonstrated higher total flavonoid content than *P. perlatum*.

Table 1. Total phenolic and flavonoid contents of the extracts

Lichen Extract	**Total Phenolic Content (µg GAE/g lichen)**	**Total Flavonoid Content (µg QE/g lichen)**
Water extract of *P. muralis*	18.29±0.006	39.90±0.008
Ethanol extract of *P. muralis*	200.97±0.002	275.14±0.020
Chloroform extract of *P. muralis*	156.76±0.002	180.38±0.010
Water extract of *P. perlatum*	45.65±0.005	13.95±0.005
Ethanol extract of *P. perlatum*	468.32±0.014	89.27±0.018
Chloroform extract of *P. perlatum*	203.23±0.032	88.35±0.007

Rankovic et al. (2011) found that the total phenolic content of the acetone extract of *Lecanora muralis* (synonym of *P. muralis*) as 43.19 ± 1.085 µg pyrocatechol equivalent (Rankovic et al., 2011). In our current study, different results were obtained due to the different solvents used and the standard antioxidant used. In an another study, the total phenolic content of *L. muralis* was determined as 50.93 ± 1.191 µg pyrocatechol / mg extract (Paul and Singh, 2014), while in another study the same total phenolic content was found as 74.66 ± 0.09 mg gallic acid equivalent/g dry weight (Valadbeigi and Raskhi, 2015).

Rankovic et al (2011) determined the total flavonoid content of the acetone extract of *Lecanora muralis* as 34.56 ± 1.074 µg rutin equivalent (Rankovic et al., 2011). While Kosanic

et al. (2014) found that the total flavonoid content of *L. muralis* as 39.91 ± 1.066 µg rutin equivalent/mg extract (Kosanic et al., 2014), Valadbeigi and Raskhi were found the total flavonoid content of *L. muralis* as 74.78 ± 0.07 mg catechin equivalent/g dry weight (Valadbeigi and Raskhi, 2015). Patil et al. (2011) calculated the total flavonoid content of the *P. perlata* (synonym of *P. perlatum*) lichen as 6.89 ± 0.07 mg quercetin equivalent/g lichen (Patil et al., 2011).

3.1.2. Total Antioxidant Activity of the Extracts

Total antioxidant activity of the extracts was demonstrated in Table 2. The highest total antioxidant capacity was found in ethanol extract of *P. muralis* whereas the lowest total antioxidant capacity was found in water extract of *P. perlatum*. *P. muralis* demonstrated higher total antioxidant capacity than *P. perlatum*.

Table 2. Total antioxidant activity of the extracts

Lichen Extract	Total Antioxidant Capacity (µg AAE/g lichen)
Water extract of *P. muralis*	69.45±0.49
Ethanol extract of *P. muralis*	246.55±0.77
Chloroform extract of *P. muralis*	166.59±1.00
Water extract of *P. perlatum*	22.11±1.17
Ethanol extract of *P. perlatum*	146.81±1.21
Chloroform extract of *P. perlatum*	86.85±0.21

Rahman et al. (2014) identified the total antioxidant capacity of the methanol extract of *P. perlata* as the ascorbic acid equivalent of 1.3 mg / mL^{-1} ascorbic acid equivalent (Rahman et al., 2014). In our study, total antioxidant capacities of water, ethanol and chloroform extracts of *P. perlatum* lichen were found as 22.11 ± 1.17, 146.81 ± 1.21 and 86.85 ± 0.21 µg ascorbic acid equivalents/g, respectively. Leela and Iyer (2016) found that the total antioxidant capacity (% inhibition) of *P. perlata* as 39% (Leela and Iyer, 2016).

3.1.3. CUPRAC Activity

CUPRAC activity results of the extracts were given in Table 3. When the results are examined, it is seen that *P. perlatum* lichen has higher CUPRAC activity than *P. muralis* lichen. The lichen extracts showed lower activity than the BHT used as standard.

Tablo 3. CUPRAC activity of the extracts

Lichen	Concentration (µg/mL)	Absorbance
Water extract of *P. muralis*	250	0.223±0.007
	500	0.301±0.015
	750	0.354±0.006
	1000	0.409±0.006
Ethanol extract of *P. muralis*	250	0.284±0.013
	500	0.316±0.011
	750	0.390±0.010
	1000	0.434±0.021
Chloroform extract of *P. muralis*	250	0.192±0.005
	500	0.209±0.004
	750	0.275±0.017
	1000	0.314±0.012
Water extract of *P. perlatum*	250	0.264±0.014
	500	0.338±0.019
	750	0.435±0.025
	1000	0.509±0.008
Ethanol extract of *P. perlatum*	250	0.205±0.017
	500	0.300±0.023
	750	0.435±0.022
	1000	0.505±0.014

Chloroform extract of *P. perlatum*	250	0.420±0.004
	500	0.526±0.035
	750	0.602±0.014
	1000	0.766±0.041
BHT	250	0.643±0.008
	500	0.695±0.015
	750	0.805±0.017
	1000	0.882±0.001

To the best of our knowledge, there isn't any study related to *CUPRAC* activity of *P. muralis* and *P. perlatum* lichens.

3.1.4. Trolox Equivalent Antioxidant Capacity

Trolox equivalent antioxidant capacity of the extracts were demonstrated in Table 4. The highest and lowest trolox equivalent capacities of the studied lichen extracts were determined in chloroform extract of *P. perlatum* lichen and water extract of *P. perlatum* lichen, respectively.

Table 4. Trolox equivalent antioxidant capacity of the extracts

Lichen Extract	**Trolox Equivalent Antioxidant Capacity (µg troloks/g lichen)**
Water extract of *P. muralis*	91.20±0.013
Ethanol extract of *P. muralis*	213.10±0.033
Chloroform extract of *P. muralis*	155.34±0.055
Water extract of *P. perlatum*	61.48±0.010
Ethanol extract of *P. perlatum*	107.70±0.001
Chloroform extract of *P. perlatum*	335.63±0.001

To the best of our knowledge, there isn't any study related to trolox equivalent antioxidant capacity of *P. muralis*.

In the literature, there are studies about trolox equivalent antioxidant capacity of *P. perlatum* lichen is performed. Hara et al. (2011) examined the trolox equivalent antioxidant capacity of *Parmotrema chinense* (synonym of *P. perlatum*) and it was found that trolox

equivalent antioxidant capacity of *P. chinense* as 158 µmol/L (Hara et al., 2011). In our study, TEAC values were higher than the current literature. This situation is thought to be caused by the collection of studied lichens from different geographies.

3.1.5. Metal Chelating Activity of the Extracts

Metal chelating Activity of the extracts were illustrated in Table 5. The activity of *P. muralis* lichen was not observed in the water and ethanol extracts, whereas 1.4% and 3.01% inhibition was found in the chloroform extract. No activity was found in the water and chloroform extract of the *P. perlatum* lichen, whereas activity of 15.26% and 32.09% was found in the ethanol extract. Compared with the two lichen samples in terms of metal chelating activities, *P. perlatum* lichen was found to be more effective.

Table 5. Metal chelating activity of the extracts

Lichen Extract	Concentration (µg/mL)	% Activity
Water extract of *P. muralis*	250	NA
	500	NA
	750	NA
	1000	NA
Ethanol extract of *P. muralis*	250	NA
	500	NA
	750	NA
	1000	NA
Chloroform extract of *P. muralis*	250	1.4±0.23
	500	1.57±0.45
	750	2.44±1.59
	1000	3.01±2.01
Water extract of *P. perlatum*	250	NA
	500	NA
	750	NA
	1000	NA
Ethanol extract of *P. perlatum*	250	15.26±0.306
	500	19.73±0.346
	750	22.75±0.273
	1000	32.09±0.170

Chloroform extract of *P. perlatum*	250	NA
	500	NA
	750	NA
	1000	NA
EDTA	250	94.56±4.54
	500	96.33±0.91
	750	96.90±1.51
	1000	97.68±2.06

To the best of our knowledge, there isn't any study related to metal chelating activity of *P. muralis* and *P. perlatum*.

3.2. Anti-Tyrosinase Activity

Table 6 summarizes anti-tyrosinase activity of the extracts. Both of ethanol extracts of lichen species showed tyrosinase inhibition activity, whereas no activity was observed in other lichen extracts.

Table 6. Anti-tyrosinase activity of the extracts

Lichen	**Concentration (µg/mL)**	**% inhibition**	**IC_{50}**
Ethanol extract of *P. muralis*	0.00001	7.83±2.02	
	0.001	13.33±1.52	
	0.01	14.83±4.64	3.191±0.057
	10	16.33±1.89	
Ethanol extract of *P. perlatum*	0.00001	6.83±3.78	
	0.001	7.66±2.25	
	0.01	13.16±3.78	2.862±0.049
	10	13.66±1.52	
Kojic Acid	0.00001	70.83±0.90	
	0.001	79.68±1.56	
	0.01	89.06±1.56	1.868±0.443
	10	91.66±0.90	

There isn't any literatüre about anti-tyrosinase activity of the *P. muralis* lichen. However, *P. chinense* lichen was studied and it was reported that this Lichen have no tyrosinase inhibition (URL-1). As a result of our studies, it has been determined that the ethanol extract of *P. perlatum* lichen exhibits low anti-tyrosinase activity.

Acknowledgement

This study was supported by Giresun University BAP (FEN-BAP-C-140316-02).

References

Arnao, M. B., Cano, A., and Acosta, M. (2001). The hydrophilic and lipophilic contribution to total antioxidant activity. Food Chemistry, 73, 239-244.

Hara, K., Endo, M., Kawakami, H., Komine, M., and Yamamoto, Y. (2011). Anti-oxidation activity of ethanol extracts from natural thalli of lichens. Mycosystema, 30 (6), 950-954.

Kasote, D. M., Katyare, S. S., Hegde, M. V., and Bae, H. (2015). Significance of antioxidant potential of plants and its relevance to therapeutic applications. International Journal of Biological Sciences, 11(8), 982-991.

Kosanic, M., Seklic, D., Markovic, S., and Rankovic, B. (2014). Evaluation of antioxidant, antimicrobial and anticancer properties of selected lichens from Serbia. Digest Journal of Nanomaterials and Biostructures, 9 (1), 273-287.

Kumar, S., Dhankhar, S., Arya, V. P., Yadav, S., and Yadav, J. P. (2012). Antimicrobial activity of *Salvadora oleoides* Decne. against some microorganisms. Journal of Medicinal Plants Research, 6 (14), 2754-2760.

Leela, K., and Iyer, P. (2016). Extraction and application of secondary metabolites from *Parmelia perlata*. Asian Journal of Biological and Life Sciences, 5 (2), 211-216.

Loizzo, M. R., Tundis, R., Bonesi, M., Menichini, F., Mastellone, V., Avallone, L., and Meninchini, F. (2012). Radical scavenging, antioxidant and metal chelating activities of *Annola cherimola* Mill. peel and pulp in relation to their total phenolic and total flavonoid contents. Journal of Food Composition and Analysis, 25, 179-184.

Luo, H., Yamamoto, Y., Kim, J. A., Jung, J. S., Koh, Y. J., and Hur, J. S. (2009). Lecanoric acid, a secondary lichen substance with antioxidant properties from *Umbilicaria antarctica* in maritime Antartica (King George Island). Polar Biology, 32(7), 1033-1040.

Özyürek, M., Bektaşoğlu, B., Güçlü, K., and Apak, R. (2009). Measurement of xanthine oxidase inhibition activity of phenolics and flavonoids with a modified cupric reducing antioxidant capacity (CUPRAC) method. Analytica Chimica Acta, 636, 42-50.

Patil, B. S., Adhikrao, G. V., Subhash, T. S., Ramesh, K. C., and Umesh, A. A. (2011). Insulin secretagogue, alpha-glucosidase and antioxidant activity of some selected spices in spreptotocin-induced diabetic rats. Plant Food for Human Nutrition, 66, 85-90.

Paul, S., and Singh, A. R. J. (2014). An antioxidant and bioactive compound studies of *Parmelia perlata*, *Ganoderma lucidum* and *Phellinus igniarus*- supplementary drug. Asian Journal of Pharmaceutical Technology&Innovation, 2 (7), 13-22.

Prieto, P., Pineda, M., and Aguiler, M. (1999). Spectrophotometric quantition of antioxidant capacity through the formation of a phosphor molybdenum complex: specific application to the determination of Vitamin E. Analytical Biochemistry, 269, 337-341.

Rahman, H., Vijaya, B., Ghosh, S., Pant, G., and Sibi, G. (2014). In vitro studies on antioxidant, hypolipidemic and cytotoxic potential of *Parmelia perlata*. American Journal of Life Sciences, 2 (6-1), 7-10.

Rankovic, B. R., Kosanic, M. M., and Stanojkovic, T. P. (2011). Antioxidant, antimicrobial and anticancer activity of the lichens *Cladonia furcata*, *Lecanora atra* and *Lecanora muralis*. BMC Complementary and Alternative Medicine, 11 (97), 1-8.

Shibata, S., Ukita, T., Tamura, T., and Miura, Y. (1948). Relation between chemical constitutions and antibacterial effects of usnic acid and derivatives. The Japanase Medical Journal, 1, 152–55.

Slinkard, K., and Singleton, V. L. (1977). Total phenol analysis: automation and comparison with manual methods. American Journal of Enology and Viticulture, 28, 49-55.

URL-1:
http://indianlichenology.com/pdfFiles/1%20Chapter%20Medicinal%20lichens%20of%20India.pdf (Date of access: 04 April 2017).

Valadbeigi T., and Raskhi, S. (2015). GC-MS analysis and anticancer effect against MCF-7 and HT-29 cell lines and antioxidant, antimicrobial and wound healing activities of plant-derived compounds. Journal of Basic Research in Medical Sciences, 2 (4), 1-11.

Vanni, A. Gastaldi, D., and Giunata, G. (1990). Kinetic investigations on the double enzymatic activity of the tyrosinase mushroom. Annali Di Chimica, 80, 35-60.

Verma, N., Behera, B. C., Sonone, A., and Makhija, U. (2008). Lipid peroxidation and anti-tyrosinase inhibition by lichen symbionts grown in vitro. African Journal of Biochemistry Research, 2(12), 225-231.

Zhishen, J., Mengcheng, T., and Jianming, W. (1999). The determination of flavonoid contents in mulberry and their scavenging effects on superoxide radicals. Food Chemistry, 64, 555-559.

Antioxidant Properties of Various Extracts of *Dianthus orientalis*

Kadriye ÖZCAN

Giresun University, Engineering Faculty, Genetic and Bioengineering Department, Giresun, Turkey

Abstract

Free radicals, especially oxygen free radicals or reactive oxygen species are active oxygen compounds generated by oxidation reactions of exogenous factors. These reactive species may oxidize proteins, lipids or DNA and can initiate degenerative/chronic diseases including, cancer, diabetes and cardiovascular disease. Antioxidants are substances that when present at low concentrations with respect to oxidizable substrates, inhibit or delay the oxidation process. Therefore, antioxidants have a vital role in the maintenance of human health and prevention of disease caused by free radicals. Due to the benefits of antioxidants, in this study, the antioxidant properties of *Dianthus orientalis* obtained from Gümüşhane was investigated. The antioxidant capacity of plant extracts were evaluated by free radical scavenging assays (DPPH and ABTS). The amount of total phenolics and flavonoid content in extract were determined according to Folin-Ciocalteu and $AlCl_3$ colorimetric method, respectively. As a results, the ethanol extract exhibited high total phenolic and flavonoid contents, 399.51±0.8 GAE/g extract and 145±0.3 QUE/g extract, respectively. Furthermore free radical scavenging assays showed in ethanol and methanol extract had high properties as 61.38±0.1 and 13.23±0.3 trolox equivalent, for ABTS and DPPH, respectively. Consequently, it is predicted that *Dianthus orientalis* has potency to be used as a natural antioxidant agent.

Keywords: ABTS, Dianthus orientalis, DPPH, TPC, TFC

1. Introduction

The genus Dianthus contains about 300 species, spreading in temperate and cold zones of the Northern Hemisphere (Hsieh et al., 2004). In Turkey, where 33 out of 76 Dianthus species is endemic and which of them are reported (Hamzaoglu et al., 2015). Dianthus species are medicinal plants belonging to the family Caryophyllaceae and are reported to be used as anti-inflammatory, diuretic, immune system enhancer and expectorant among the population. They are used in the treatment of urinary infection, boils, menopause, gonorrhea, cough and cancer in traditional treatment because of their beneficial biological effects The antimicrobial, pro-apoptotic, antioxidant and antidiabetic effects of dianthus species were found to be beneficial because of their beneficial flavonoid and steroid compounds (Hsieh et al., 2004; Nho et al., 2012; Yu et al., 2012; Kazeem and Ashafa, 2015).

In this study, total phenolic, flavanoid and antioxidant capacity of *Dianthus orientalis* collected from Gumushane extracts were investigated.

2. Material and Method

2.1. Extraction

The plant materials were extracted with each solvent (ethanol, methanol and ethylacetate) at 37 °C 125 rpm during 24 h. The extracts were filtered using filter paper and then concentrated under vacuum at 40 °C using a Rotary evaporator. The residues obtained were stored in a freezer at -20 °C until further tests.

2.2. Total phenolic contents

The total amount of phenolic substance in the extract was determined according to the Folin-Ciocalteu method (Slinkard and Singleton, 1977) with the small changes we mentioned in our previous study (Ozcan and Acet, 2018). The absorbance was measured at 750 nm with micro plate absorbance reader (iMarkTM 1681135, BioRad). The total phenolic content was calculated as Gallic acid equivalents (GAE) in milligram per gram of extract (mg GAE/g extract).

2.3. Total flavanoid contents

Total flavonoid content of the extract was determined according to $AlCl_3$ colorimetric method (Moreno et al., 2000) with some minor modification we mentioned in our previous study (Ozcan and Acet, 2018). The total flavonoid content was calculated in milligrams of rutin equivalents (RE) per gram of extract.

2.4. ABTS assay

The 2, 2-azinobis-3- ethylbenzothiazoline-6-sulfonic acid (ABTS) free radical caption scavenging activity was determined using a spectrophotometric method (Re et al., 1999) with minor modifications. Briefly, 80 µl sample and 160 µl ABTS solution mixed and waited at 6 minutes. The mixture was measured at 750 nm and the antioxidant capacity of each extract was calculated as trolox equivalents (TE) (mg TE/g extract).

2.5. DPPH assay

The effect of the plant extracts on 1, 1-diphenyl-2-picrylhydrazyl (DPPH) radical was determined using a spectrophotometric method (Kirby and Schmidt, 1997) with minor modification. Briefly, 125 µl of the plant extract was added to 125 µl 0.1 mM DPPH. The mixture was waited 45 minutes and measured at 490 nm. The antioxidant capacity of each extract was calculated as trolox equivalents (TE) (mg TE/g extract).

2.5. Statistical analyses

All the analyses were carried out in triplicate. The data was recorded as mean ± standard deviation and analysed by SPSS (version 11.5 for Windows 2000, SPSS Inc.). Oneway analysis of variance was performed by ANOVA procedures. $P<0.05$ was accepted as significant.

3. Results and Discussion

Aerial parts of *Dianthus orientalis* various extracts have been investigated in this study. Extraction yields, total phenolic and flavonoid contents of the extracts were shown in Table 1. The highest yield of extract was methanol (12.11%) and followed by ethanol (10.5%) and ethyl acetate (3.46%), respectively. The total phenolic content of extracts exhibited variable values

ranged from 399.51 to 290.15 mg GAE/g extract as shown in Table 1. Especially, the ethyl acetate extracts have had the highest level of phenolic content as 399.51 mg GAE/g extract. In a study conducted with the methane and aqueous extracts of *Dianthus superbus*, the total phenolic content content was determined as 590 and 690 mg gallic acid equivalent / 100 g sample, respectively (Cai et al., 2004). In the different studies, the total phenolic content of *Dianthus superbus* was determined as 2404 mg gallic acid equivalent / 100 g extract (Gau et al., 2011) and the total phenolic content of *Dianthus carmelitarum* dimethyl sulfoxide extract was determined as 853.9±19.4 mg GAE/100g extract (Turan et al., 2017).

Total flavonoid contents of plant extracts determined from three different solvents ranged from 102 to 145 mg RE/g extract as shown Table 1. The highest level of the value observed in ethyl acetate extracts similar to total phenolic. It was not observed a correlation between yield % of plant extracts and amounts of total phenolic/flavonoid contents (Table 1). In a study, the total flavonoid content of Dianthus superbus aqueous extract was determined as 327 mg rutine equivalent / 100 g extract (Gou et al., 2011), while in another study *Dianthus carmelitarum* total flavanoid content was determined as 636.5 ± 13.1 mg RE extract (Turan et al., 2017).

Table 1. Total phenolics and flavanoids of the plant extracts

Extracts	% Yield	Total Phenolics (GAE Equivalent)	Total Flavanoid (RE Equivalent)
Ethanol	10.25	290.15±2.3^{c}	102±0.2^{c}
Methanol	12.11	376.23±3.1^{b}	133±0.5^{b}
Ethyacetate	3.46	399.51±0.8^{a}	145±0.3^{a}

Antioxidant activity of the extracts was detected by different methods such as DPPH and ABTS. DPPH radical scavenging activity was found to be maximum in ethanol extract (13.23 mg TE /g extract) and minimum in the ethylacetate extract (8.93 mg TE /g extract). All DPPH activity assay results were summarized Table 2. Antioxidant activity as determined by ABTS assay was detected the highest in ethyl acetate extract (61.38 mg TE /g extract) and minimum in ethanol extract (21.52 mg TE /g extract). ABTS radical scavenging activity of extracts was displayed at Table 2. The antioxidant activity values obtained in the study are consistent with the literature data. It is thought that the differences between the plant species used, the climatic

characteristics of the area where the plant is collected, the type of solvent used or the extraction method may be different.

Table 2. Antioxidant properties of the plant extracts.

Extracts	ABTS (Trolox Equivalent)	DPPH (Trolox Equivalent)
Ethanol	21.52± 1.0^{c}	13.23±0.3^{a}
Methanol	50.11±0.8^{b}	12.33±0.4^{b}
Ethyacetate	61.38±0.1^{a}	8.93±0.1^{c}

This study has demonstrated that extracts of *D. orientalis* were rich in terms of total phenolic, flavonoid content; the species have significant antioxidant activity in all of the tested methods. The extracts might have therapeutic effects such as prevent radical attacks. As a result, *D. orientalis* might be recommended as a new potential source of natural antioxidants and pharmacological areas.

References

Cai, Y., Luo, Q., Sun, M. and Corke, H. (2004). Antioxidant activity and phenolic compounds of 112 traditional Chinese medicinal plants associated with anticancer. Life Sciences, 74, 2157-2184.

Gou, J., Zou, Y. and Ahn, J. (2011). Enhancement of antioxidant and antimicrobial activities of Dianthus superbus, Polygonum aviculare, Sophora flavescens, and Lygodium japonicum by pressure-assisted water extraction. Food Science and Biotechnology, 20(1), 283-287.

Hamzaoglu, E., Koc, M., Buyuk, I., Aksoy, A. and Soydam-Aydin, S. (2015). Presence of *Dianthus roseoluteus* Velen. (*Caryophyllaceae*) in Turkey and a new species: *Dianthus macroflorus* Hamzaoglu. Systematic Botany, 40, 208-213.

Hsieh, P.W., Chang, F.R., Wu, C.C., Wu, K.Y., Li, C.M., Chen, S.L. and Wu, Y.C. (2004). New cytotoxic cyclic peptides and dianthramide from *Dianthus superbus*. Journal of Natural Products, 67, 1522-1527.

Kazeem, M.I. and Ashafa, A.O.T. (2015). *In-vitro* antioxidant and antidiabetic potentials of *Dianthus basuticus* Burtt Davy whole plant extracts. Journal of Herbal Medicine, 5, 158-164.

Kirby, A.J. and Schmidt, R.J. (1997). The antioxidant activity of Chinese herbs for eczema and of placebo herbs. Journal of Ethnopharmacology, 56, 103-108.

Moreno, M.I., Isla, M.I, Sampietro, A.R. and Vattuone, M.A. (2000). Comparison of the free radical-scavenging activity of propolis from several regions of Argentina. Journal of Ethnopharmacology, 71, 109-114.

Nho, K.J., Chun, J.M. and Kim, H.K. (2012). Ethanol extract of Dianthus chinensis L. induces apoptosis in human hepatocellular carcinoma HepG2 cells in vitro. Evidence-Based Complementary and Alternative Medicine, Article ID: 573527, doi: 10.1155/2012/573527.

Ozcan, K. and Acet, T. (2018). In vitro antioxidant and antimicrobial activities of the five different solvent extracts of *Centaurea pulcherrima* var. *freynii* from Turkey. Fresenius Environmental Bulletin, 27, 4047-4051.

Re, R., Pellegrini, N., Proteggente, A. Pannala, A., Yang, M. and Rice-Evans, C. (1999). Antioxidant activity applying an improved ABTS radical cation decolorization assay. Free Radical Biology and Medicine, 26, 1231-1237.

Slinkard, K. and Singleton, V.L. (1977). Total phenol analyses: automation and comparison with manual methods. Am J Enol Viticult, 28, 49-55.

Turan, I., Demir S., Aliyazicioğlu, R., Misir, S. and Aliyazicioğlu, Y. (2017). Investigation of Antioxidant and Cytotoxic Properties of *Dianthus carmelitarum* Extract. GUSTIJ, 1, 41-50.

Yu, J.Q., Yin, Y., Lei, J.C., Zhang, X.Q., Chen, W., Ding, C.L., Wu, S., He, X.Y., Liu, Y.W. and Zou, G.L. (2012). Activation of apoptosis by ethyl acetate fraction of ethanol extract of Dianthus superbus in HepG2 cell line. Cancer Epidemiology, 36, 40-45.

Effects of Pumice Amendment on Compost Quality in Industrial Sludge Composting

Nurdan AYCAN DÜMENCİ[1*], Nurdan Gamze TURAN[2]

[1]Ondokuz Mayıs Üniversity, Dept. of Environmental Engineering, Samsun, Turkey; nurdann.aycan@gmail.com
[2]Ondokuz Mayıs Üniversity, Dept. of Environmental Engineering, Samsun, Turkey; gturan@omu.edu.tr

***Corresponding Author:** nurdann.aycan@gmail.com

Abstract

In this study, the pilot-scale co-composting of industrial sludge and pumice with three different rates was conducted for 13 weeks to evaluate the effects of compost quality. The results indicated that all of three additives could adequately buffer pH, considerably reduce ammonia and enhance organic matter degradation. Particularly, pumice amended treatment showed the least nitrogen loss by 19.13%. The results of the study showed that pumice as amendment material is an effective material for composting of industrial sludge. The best combination of industrial sludge and pumice is suggested as a rate of 40% pumice and 60% industrial sludge to improve the quality od compost.

Keywords: Treatment sludge; Sludge management; Composting; Natural amendments; Pumice.

1. Introduction

The sludge is an unavoidable by-product arising from wastewater treatment processes (Bratina et al., 2016). Sludge production have increased with the industrialization, population growth and rapid development of urbanization. Management of sewage and industrial sludge is a significant problem all over the world (Mymrin et al., 2014).

Industrial sludge contains more hazardous materials than sewage sludge such as heavy metals, organic pollutants and pathogens (Wu et. Al., 2015; Islam et al., 2017). The qualities and quantities of industrial sludge depend on origin and treatment processes. Improper management of industrial sludge lead to environmental and health risks (Silva et al., 2011).

Lots of sludge treatments techniques are used to eliminate the hazardous constituent and mitigate its negative impacts (Silva et al., 2011). The most common sludge treatment techniques are landfill, composting, incineration and pyrolysis (Arif et al., 2018). Among them, composting is an applicative and low-cost technique for converting sludge into a safe and usable product (Wong et al., 2017; Jain et al., 2018). However, a high moisture content and a low particle size affect the dynamics of the composting process (Barrena et al., 2014). Thus, the sludge should be mixed with dry material.

The aim of the study is to investigate the effects of pumice on industrial sludge composting. For the experiments, in-vessel composting systems were constructed as pilot scale. The variations of pH, electrical conductivity, moisture content, ammonia nitrogen, nitrate nitrogen and total nitrogen were analyzed during the process. At the end of the process, the results were compared to compost quality ciriteria.

2. Materials and methods

Industrial sludge was obtained from an industrial wastewater treatment plant (Samsun, Turkey). The characteristics of the indsutrial sludge is presented in Table 1.

Table 1. The characteristics of industrial sludge

Parameters	Value	Method
pH	8.26	TSISO 10390
Lead (Pb^{2+}), mg/L	<0.01	EPA 200.7
Zinc (Zn^{2+}), mg/L	0.653	EPA 200.7
Copper (Cu^{2+}), mg/L	3.152	EPA 200.7
Total organic carbon (TOC), mg/kg	151300	TS 12089 EN 13137

Sulphate (SO_4^{2-}), mg/L	139.81	SM 4500 (SO_4^{2-}) E
Selenıum (Se^{2-}), mg/L	0.404	EPA 200.7
Crom (Cr^{6+}), mg/L	0.275	EPA 200.7

The pumice purchased from Soylu Mining Co. Inc. (Nevşehir, Turkey). The physicochemical properties of pumice are listed in Table 2.

Table 2. The physicochemical properties of pumice

Compounds	Weight (%)
Na_2O	3.65
Al_2O_3	12.27
SiO_2	73.44
CaO	0.96
$TıO_2$	0.10
K_2O	4.37
Fe_2O_3	1.2
SO_3	0.08

The composting process was conducted in closed bench-scale reactor with an inner width of 25 cm, lenght of 40cm and height of 25 cm. Forced aeration was supplied by the air pump. Fresh air was pumped into the reactor from the bottom through perforation pipes fitted as parallel (Fig. 1).

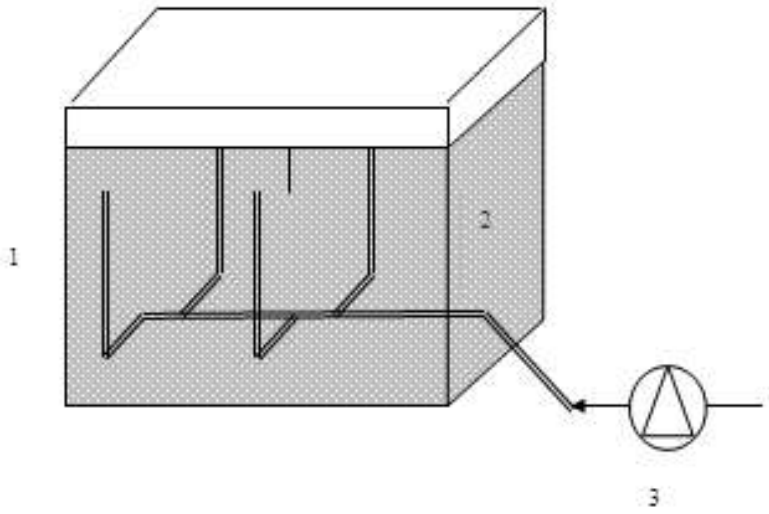

Figure 1. Schematic view of pilot composting systems (1) composting unit, (2) sludge mixture, (3) ventilation pump

Industrial sludge and pumice were mixed at different ratios as volume. Mixture ratios are given in Table 3. For each treatment, 25 L of the mixture was prepared and composted for 100 days. Sampling was carried out weekly during the process.

Table 3. Mixture ratios for this study

System no	Mixture rates
System 1	10% Pumice + 90% Industrial Sludge
System 2	25% Pumice + 75% Industrial Sludge
System 3	40% Pumice + 60% Industrial Sludge

3. Results and discussion

Figure 2 presented the change of the pH during composting process. The pH values varied between 6.5-8.0 during the process. At the beginning of the composting process, the pH values was found as about 8.0. It decreased from 3rd week to 7th week. Then, it increased approximately 7.5 of pH. These fluctuations are thought to be due to the rapid breakdown of organic matter into organic acids in the first weeks (Haug, 1993). The optimum pH value for the mature compost is 6.5-7.2 (WERL, 2000). Accordingly, at the end of the composting process, the pH values of all systems are compatible with the mature compost pH.

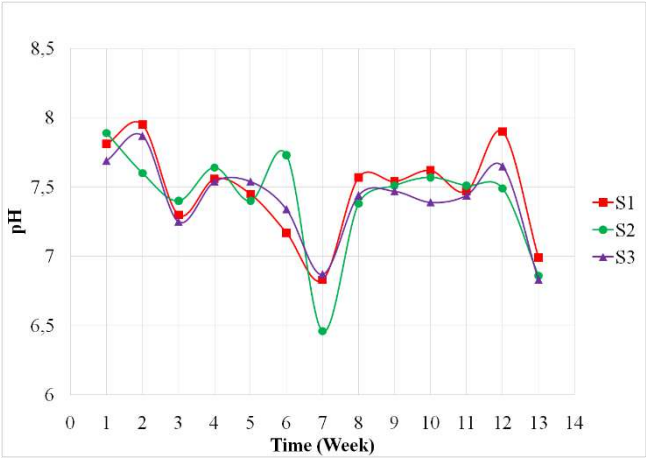

Figure 2. Effect of pumice on pH

At the beginning of the composting process, the electrical conductivity values of the systems varied between 0.6-0.8 mS/cm. The electrical conductivity values decreased depending on the acidity in the first weeks. The highest electrical conductivity value was found in the system S1 (System 1; 10% pumice + 90% industrial sludge). In all systems, the electrical conductivity values began to decrease after 8 weeks (Figure 3).

According to Penwarn (2002), the compost maturity grade of <1 mS/cm is "very good", the compost maturity grade of 1-2 mS/cm is "medium", and the compost maturity grade is 2-3 mS/cm is considered "salty". At the end of the process, the electrical conductivity values of the composts obtained in all pumice operated systems are in "very good" class.

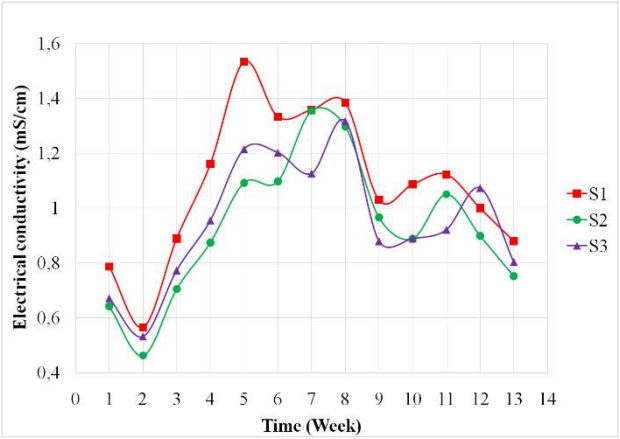

Figure 3. Effect of pumice on electrical conductivity

In all composting systems, moisture content values changed between 50-60% during the process. At the beginning of the process, moisture content values were close to 60%. It was measured approximately 50% at the end of the process.

The optimum moisture content value for composting is given 50% in the literature (Haug, 1993). As shown in Figure 4, although there were minor changes in the moisture content during the process, the moisture content values at the end of the process were optimum in all pumice-operated systems.

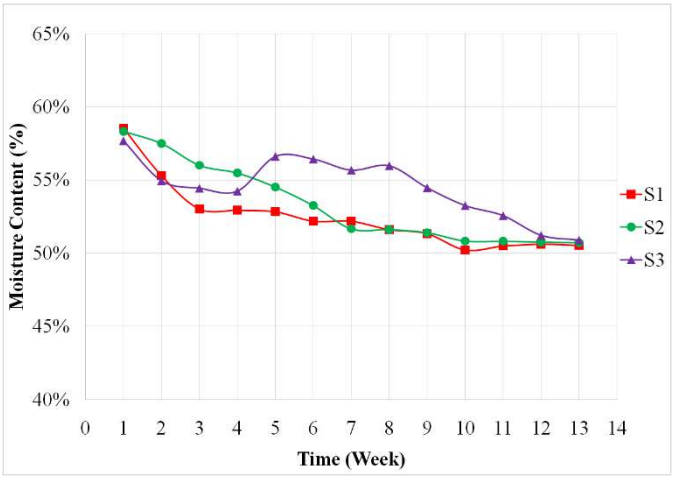

Figure 4. Effect of pumice on moisture content

According to the compost quality criteria, the ammonium nitrogen (NH_4^+-N) value must be within the range of 75-500 mg/L (WERL, 2000). At the end of the composting process, the ammonium nitrogen (NH_4^+-N) values of the composts obtained from the systems were 294.21 mg/L for S1 (System 1; 10% pumice + 90% industrial sludge), 252.21 mg/L for S2 (System 2; 25% pumice + 75% industrial sludge) and 222.52 mg/L for S3 (System 3; 40% pumice + 60% industrial sludge). Accordingly, all systems using pumice have mature compost standards in terms of ammonium nitrogen (NH_4^+-N) parameter (Figure 5).

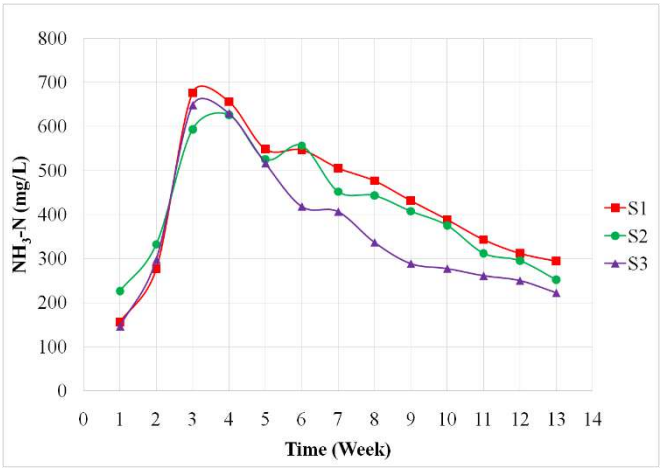

Figure 5. Effect of pumice on ammonium nitrogen (NH_4^+-N)

Nitrate nitrogen (NO_3^--N) values of the composting systems increased only in the first week. Then, its concentration decreased until the end of the process. Figure 6 shows the changes in nitrate nitrogen (NO_3^--N) in all systems. The compost quality according to nitrate nitrogen (NO_3^--N) concentration in composting processes is evaluated by the ratio of nitrate nitrogen (NO_3^--N) concentration to ammonium nitrogen (NH_4^+-N) concentration. The ammonium nitrogen (NH_4^+-N)/ nitrate nitrogen ratio (NO_3^--N) should be within the range of 0.5-3.0 for mature compost (WERL (2000). Accordingly, the ratios of ammonium nitrogen (NH_4^+-N)/ nitrate nitrogen (NO_3^--N) of the composts are in the range of 0.5-3.0. Therefore, all systems containing pumice provide the necessary value for mature compost. The ratios obtained at the end of the process; 2.55 for the S1 (System 1; 10% pumice + 90% industrial sludge), 2.25 for the S2 (System 2; 25% pumice + 75% industrial sludge) and 2.99 for the S3 (System 3; 40% pumice + 60% industrial sludge).

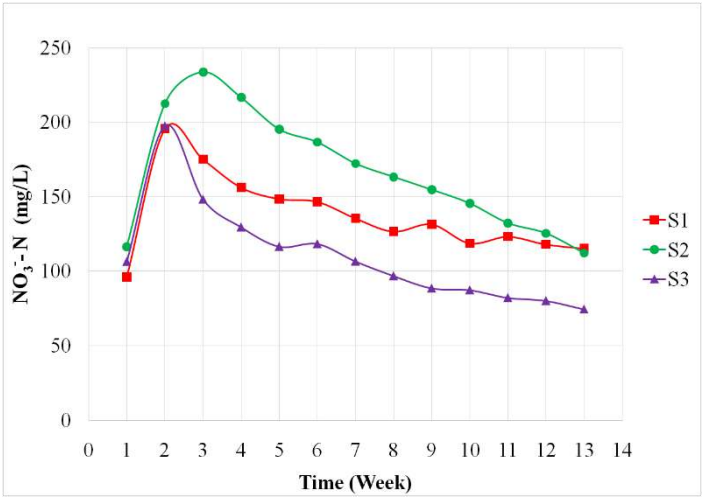

Figure 6. Effect of pumice on nitrate nitrogen (NO_3^--N)

The total nitrogen values of the systems are approximately 4.46% at the beginning of the process. The change of the total nitrogen concentration during the composting process is shown in Figure 7. As can be seen in Figure 7, a steadily decreasing curve was observed at the total nitrogen concentrations during the process. At the end of the process, the minimum nitrogen loss carried out in the system of S3 (System 3; 40% of pumice + 60% industrial sludge), and the maximum nitrogen loss occurred in the system of S1 (System 1; 10% of pumice + 90% industrial sludge).

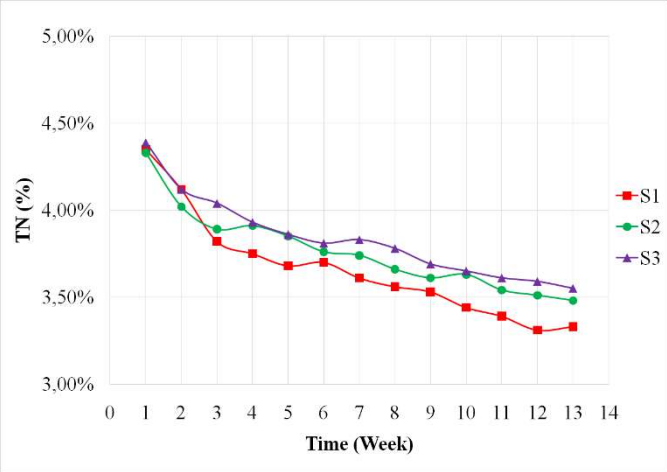

Figure 7. Effect of pumice on total nitrogen (TN)

4. Conclussions

A pilot scale co-composting system with industrial sludge and pumice carried out to improve the compost quality in this study. Three different mixture ratios were tested and system performances are compared. The main conclusions from the study are as follows:

- The moisture content of the industrial sludges is very high for composting.
- Pumice can be used as a suitable additive material for industrial sludge composting.
- Pumice is an easy available and economical material.
- The use of pumice in the composting process has improved compost quality.

References

Arif, M. S., Riaz, M., Shahzad, S. M., Yasmeen, T. and Buttler, A. (2018). Fresh and composted industrial sludge restore soil functions in surface soil of degraded agricultural land, Science of The Total Environment, Volumes 619–620, Pages 517-527.

Barrena, R., Font, X., Gabarrell, X. and Sánchez, A. (2014). Home composting versus industrial composting: Influence of composting system on compost quality with focus on compost stability, Waste Management, Volume 34, Issue 7, Pages 1109-1116.

Bratina, B., Šorgo, A., Kramberger, J., Ajdnik, U. and Šafarič, R. (2016). From municipal/industrial wastewater sludge and FOG to fertilizer: A proposal for economic sustainable sludge management, Journal of Environmental Management, Volume 183, Part 3, Pages 1009-1025.

Haug, R. T. (1993). The Practical Handbook of Compost Engineering, Lewis Publishers, Florida.

Islam, M. S., Ahmed, M. K., Raknuzzaman, M., Habibullah-Al-Mamun, M. and Kundu, G. K. (2017). Heavy metals in the industrial sludge and their ecological risk: A case study for a developing country, Journal of Geochemical Exploration, Volume 172, Pages 41-49.

Jain, M. S., Daga, M. and Kalamdhad, A.S. (2018). Composting physics: A degradation process-determining tool for industrial sludge, Ecological Engineering, Volume 116, Pages 14-20.

Mymrin, V., Ribeiro, R. A. C., Alekseev, K., Zelinskaya, E. and Catai, R. (2014). Environment friendly ceramics from hazardous industrial wastes, Ceramics International, Volume 40, Issue 7, Part A, Pages 9427-9437.

Penwarn, W. (2002). Quality Compost, Educations Seminers, Petrik Technology & Approach, Petrik Laboratories, Inc., USA.

Robledo-Mahón, T., Aranda, E., Pesciaroli, C., Rodríguez-Calvo, A. and Calvo C. (2018). Effect of semi-permeable cover system on the bacterial diversity during sewage sludge composting, Journal of Environmental Management, Volume 215, Pages 57-67.

Silva, M.A.R., Testolin, R.C., Godinho-Castro, A.P., Corrêa, A.X.R. and Radetski C.M. (2011). Environmental impact of industrial sludge stabilization/solidification products: Chemical or ecotoxicological hazard evaluation?, Journal of Hazardous Materials, Volume 192, Issue 3, Pages 1108-1113.

WERL. (2000). Compost Quality in America, Technical Document, New York State Association of Recyclers, pp, 30-42, Woods End Research Laboratory, Inc., USA.

Wong, J. W. C., Wang, X. and Selvam, A. (2017). Improving Compost Quality by Controlling Nitrogen Loss During Composting, Current Developments in Biotechnology and Bioengineering, Book chapter:4, Pages 59-82.

Wu, Q., Cui, Y., Li, Q. and Sun, J. (2015). Effective removal of heavy metals from industrial sludge with the aid of a biodegradable chelating ligand GLDA, Journal of Hazardous Materials, Volume 283, Pages 748-754.

Biotechnological Applications of Image Analysis: An Example of Asteriscus and Lapillus Otolith Measurements in Juvenile Cyprinid Species

Derya BOSTANCI[1], Serdar YEDİER[1]*, Seda KONTAŞ[2] and Nazmi POLAT[3]

[1] Ordu University, Department of Molecular Biology and Genetics, Ordu, Turkey

[2] Ordu University, Department of Fisheries Technology Engineering, Ordu, Turkey

[3] Ondokuz Mayıs University, Department of Biology, Samsun, Turkey

* **Corresponding Author:** *serdar7er@gmail.com*

Abstract

Otolith studies base on the morphometric measurements have increased in importance for fish identification and discrimination species with using the image analysis programs. We have tested the availability of asteriscus and lapillus otoliths for interspecific discrimination even at such small sizes and also to determine the suitability of ImageJ and Digimizer image analysis programs, which are widely used in the field of fisheries, in such small samples. In the current study, we examined juvenile fish with a quite small total length of *Cyprinus carpio* and *Cyprinion macrostomum*. Afterward, each of the fish's otolith characters such as area, length, perimeter, and width were measured using ImageJ and Digimizer image analysis programs. There was no statistically significant difference between the right and left otolith pairs in both lapillus and asteriscus from *C. carpio* and *C. macrostomum*. Asteriscus have a higher discrimination potential for lapillus and the use of asteriscus in species discrimination in cyprinid fish will give better results. The results of the current study indicated that the ImageJ software is a more sensitive program than the Digimizer program in lapillus samples but Digimizer is a more sensitive program than ImageJ in asteriscus samples. According to the species discrimination data were obtained with the two programs, they showed maximum discrimination even in very small samples examined. Since the selection of an image analysis program used in both fisheries and different areas is very important for the success of the study, it is necessary to choose a program according to size, structure and literature suitability of the samples which are examined in the study.

Keywords: Otolith, Fisheries, Interspecific discrimination, ImageJ, Digimizer.

1. Introduction

Advancing technology by increasing its development day by day enables the emergence of more powerful computers and image analysis programs to work with the best performance (Schneider et al., 2012). Biotechnology enables this technology to be used most effectively in the world of science (Vecht–Lifshitz and Ison, 1992). Image analysis is an indispensable tool for researchers who need to obtain accurate quantitative information from their samples (Joyce-Loebl, 1985). Image analysis programs to speed up the operations of traditional microscopic methods in several areas, allowing time-consuming work to be performed in a short time and at the same time more accurate (Goins and Reedy, 2000). The advent of new video technology and increasingly powerful computers allow application of this technique to a very large range of methodologies. Nowadays image analysis programs are widely used in many fields such as medicine, pharmacy, biology, architecture, agriculture, industry, and fisheries.

Otoliths are bony structures that are found in pairs inside the fish's inner ear and they give information about their lives. There are three different otolith pairs, varying in size and shape (Tuset et al., 2008). These are lapillus, sagitta, and asteriscus. They are influential in vital events of many fish, especially balance and hearing senses. Otolith studies base on the morphometric measurements have increased in importance for fish identification and discrimination fish species and populations with using the image analysis systems and software programs (Bostanci et al., 2015). All these morphological otolith characters such as area, length, perimeter, and width can use in fisheries studies and the characters were also considered to be an index for specific discrimination and identified for freshwater and marine fish species (Tuset et al., 2003).

The Cyprinidae are the largest freshwater fish family, collectively called cyprinids, that includes *Cyprinus carpio* and *Cyprinion macrostomum*. The family includes an estimated 220 genera with 2420 species (Nelson, 2006). They have a wide geographic distribution and many species with high morphological diversity make their taxonomic distinction difficult (Howes, 1991). Turkey has 385 freshwater fish species and 206 of these fish species are members of the Cyprinidae family (Froese and Pauly, 2018). The Cyprinidae family, which is the most popular member of the Turkish freshwater fish fauna, has an important place for Turkish fish fauna.

In the current study, we examined juvenile fish with a quite small total length of *C. carpio* and *C. macrostomum*. We have tested the availability of asteriscus and lapillus otoliths for interspecific discrimination even at such small sizes and also to determine the suitability of ImageJ and Digimizer image analysis programs, which are widely used in the field of fisheries, in such small samples.

2. Material and Method

Cyprinus carpio (Common carp) samples were collected from Ordu (Kabalak pond) and *Cyprinion macrostomum* (Kangal fish) samples were collected from Sivas (Kangal Balıklı Çermik Thermal Spring) (Figure 1).

Figure 1. Sampling locations.

The samples were brought to the hydrobiology laboratory of Ordu University Molecular Biology and Genetics Department and other operations were performed in this lab. Total length was measured to the nearest 0.1 cm for each *Cyprinus carpio* and *Cyprinion macrostomum* species and individuals of the same size group were included in the study (Figure 2). Because the fish samples are quite small, sex discrimination could not be done. In this work, we have already studied only juvenile individuals.

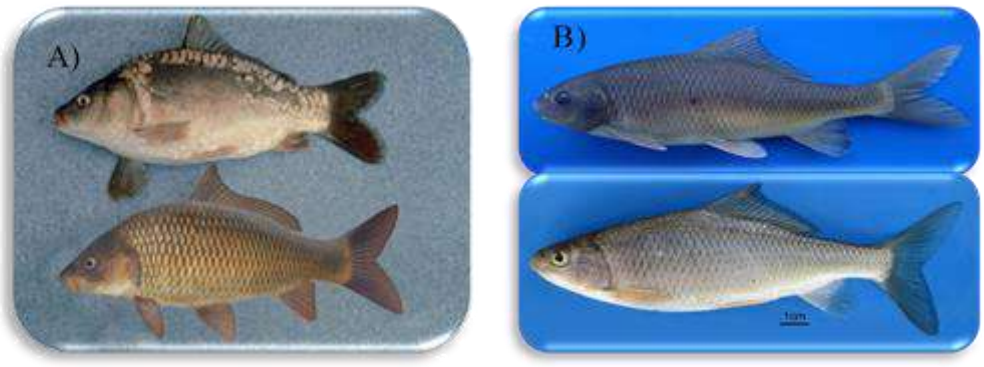

Figure 2. *Cyprinus carpio* (A) and *Cyprinion macrostomum* (B) (Froese and Pauly, 2018).

Otoliths which are asteriscus and lapillus were removed from the fish samples suitable for examination. Undamaged and cleaned left and right otoliths were evaluated. Each otolith pair is photographed by the Leica S8APO microscope and computer-connected camera system (Figure 3). Afterward, each of the fish's otolith characters such as area, length, perimeter, and width was measured using ImageJ and Digimizer image analysis programs (Figure 4).

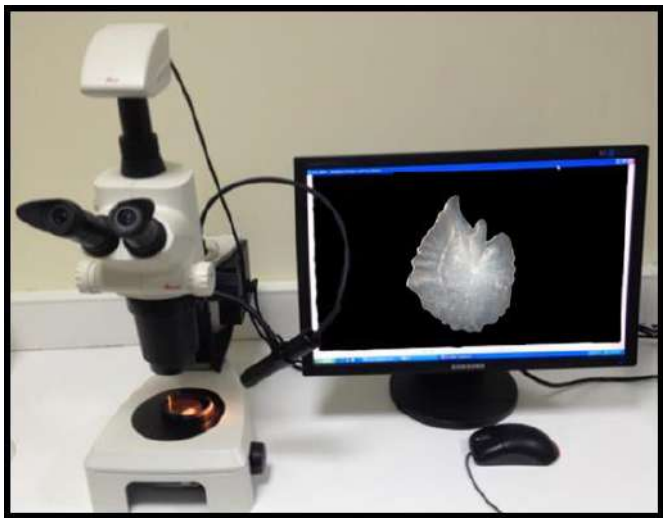

Figure 3. Leica S8APO microscope and computer-connected camera system.

All statistical analyzes were done with the SPSS program (Ver. 21). The differences between the right and left otoliths of the species were calculated by paired t test. The difference between the program measures was calculated by t test. Canonical discrimination analysis was used for species discrimination.

Figure 4. The interface for image analysis programs.

3. Results and Discussion

In the current study, right and left asteriscus and lapillus otoliths of juvenile fish samples were examined from Sivas and Ordu. *Cyprinus carpio* and *Cyprinion macrostomum* otoliths are photographed by the Leica S8APO microscope and computer-connected camera system. The size, width, area, and perimeter of the right and left asteriscus and lapillus otoliths of these two fish species were measured by the same researcher using both the Digimizer and the ImageJ programs. The obtained values were recorded in the catalogs.

In *C. carpio*, the right and left lapillus otolith characters were measured by Digimizer and ImageJ programs. There was no statistically significant difference between *C. carpio* right and left lapillus otolith characters measured by Digimizer program (P>0.05) (Table 1). However, a significant difference was found between the left and right lapillus otolith area values measured by the ImageJ program (P<0.05) (Table 1).

Table 1. Comparison of the characters of right and left lapillus otolith pairs in *Cyprinus carpio* obtained by both image analysis programs.

Variables	Side	Applications	Mean	SE	StDev	Min.	Max.	P Values	Paired t Test
Area	Left	Digimizer	0.1866	0.0079	0.0209	0.1624	0.2063	0.767	0.057
	Left	ImageJ	0.1900	0.0081	0.0213	0.1660	0.2100		
	Right	Digimizer	0.1899	0.0081	0.0213	0.1626	0.2113	0.925	0.038*
	Right	ImageJ	0.1910	0.0080	0.0213	0.1670	0.2100		
Width	Left	Digimizer	0.4178	0.0090	0.0238	0.3887	0.4451	0.868	0.082
	Left	ImageJ	0.4200	0.0089	0.0237	0.3920	0.4480		
	Right	Digimizer	0.4247	0.0093	0.0245	0.3891	0.4522	0.939	0.088
	Right	ImageJ	0.4237	0.0088	0.0234	0.3930	0.4460		
Length	Left	Digimizer	0.5877	0.0126	0.0333	0.5502	0.6155	0.885	0.075
	Left	ImageJ	0.5903	0.0127	0.0335	0.5530	0.6230		
	Right	Digimizer	0.5907	0.0125	0.0330	0.5504	0.6231	0.932	0.086
	Right	ImageJ	0.5923	0.0128	0.0340	0.5550	0.6220		
Perimeter	Left	Digimizer	1.7431	0.0415	0.1099	1.6194	1.8371	0.526	0.255
	Left	ImageJ	1.7064	0.0375	0.0993	1.5880	1.7940		
	Right	Digimizer	1.7786	0.0419	0.1109	1.6114	1.9742	0.156	0.052
	Right	ImageJ	1.6943	0.0362	0.0958	1.5870	1.7900		

In *C. macrostomum*, the right and left lapillus otolith characters were measured by Digimizer and ImageJ programs. There was no statistically significant difference between *C. macrostomum* right and left lapillus otolith characters measured by Digimizer program (P>0.05) (Table 2). However, a significant difference was found between the left and right lapillus otolith area and length values measured by the ImageJ program (P<0.05) (Table 2).

Table 2. Comparison of the characters of right and left lapillus otolith pairs in *Cyprinion macrostomum* obtained by both analysis programs.

Variables	Side	Applications	Mean	SE	StDev	Min.	Max.	P Values	Paired t Test
Area	Left	Digimizer	0.1811	0.0078	0.0207	0.1579	0.2027	0.984	0.280
	Left	ImageJ	0.1813	0.0073	0.0194	0.1600	0.2010		
	Right	Digimizer	0.1801	0.0075	0.0199	0.1569	0.1980	0.760	0.027*
	Right	ImageJ	0.1833	0.0075	0.0197	0.1620	0.2030		
Width	Left	Digimizer	0.4120	0.0094	0.0248	0.3822	0.4368	0.244	0.062
	Left	ImageJ	0.4271	0.0080	0.0212	0.3940	0.4580		
	Right	Digimizer	0.4088	0.0089	0.0237	0.3813	0.4330	0.037*	0.062
	Right	ImageJ	0.4389	0.0089	0.0237	0.4120	0.4650		
Length	Left	Digimizer	0.5975	0.0115	0.0304	0.5583	0.6324	0.805	0.114
	Left	ImageJ	0.5933	0.0123	0.0325	0.5570	0.6220		
	Right	Digimizer	0.6038	0.0123	0.0326	0.5662	0.6360	0.641	0.030*
	Right	ImageJ	0.5956	0.0120	0.0318	0.5580	0.6240		
Perimeter	Left	Digimizer	1.7621	0.0411	0.1087	1.6380	1.9179	0.642	0.760
	Left	ImageJ	1.7343	0.0410	0.1086	1.6060	1.8840		
	Right	Digimizer	1.7572	0.0376	0.0995	1.6369	1.8500	0.690	0.928
	Right	ImageJ	1.7359	0.0360	0.0951	1.6310	1.8250		

Using Digimizer and ImageJ programs, a discrimination analysis was performed according to *Cyprinus carpio* and *Cyprinion macrostomum* lapillus otolith characters. For *C. carpio*, using the lapillus otolith data both programs discriminated 100% and 85.7% for *C. macrostomum*. A total of 92.9% is distinguished (Table 3; Figure 5). According to the discriminant analysis, both images were effective in separating the species in the same manner in the analytical.

Table 3. Results of cross-validation for classifying *Cyprinus carpio* and *Cyprinion macrostomum* using the lapillus otolith character values.

Classification Results[a]						
	Groups	Predicted Group Membership				Total
		C. carpio Digimizer	*C. carpio* ImageJ	*C. macrostomum* Digimizer	*C. macrostomum* ImageJ	
Original %	*Cyprinus carpio* Digimizer	100	0	0	0	100
	Cyprinus carpio ImageJ	0	100	0	0	100
	Cyprinion macrostomum Digimizer	0	0	85.7	14.3	100
	Cyprinion macrostomum ImageJ	0	0	14.3	85.7	100
a. 92.9 % of original grouped cases correctly classified.						

There was no statistically significant difference between measurements of *C. carpio* lapillus otoliths obtained by two analysis programs used in the study (P>0.05) (Table 1). Although these two image analysis programs have been successful at the same rate in the discrimination analysis, a statistical difference was found between *C. macrostomum* right lapillus otolith width measured by these two programs (P<0.05) (Table 2). There was no statistical difference between the other lapillus otolith measurements (P>0.05) (Table 2).

When the mean lapillus otolith width value of the *C. macrostomum* obtained by both image analysis programs was examined, it was determined that both the right and left otolith data were higher by the ImageJ program (Table 2). This indicates that the ImageJ program is more accurate than the Digimizer program, especially in measuring the lapillus otolith width.

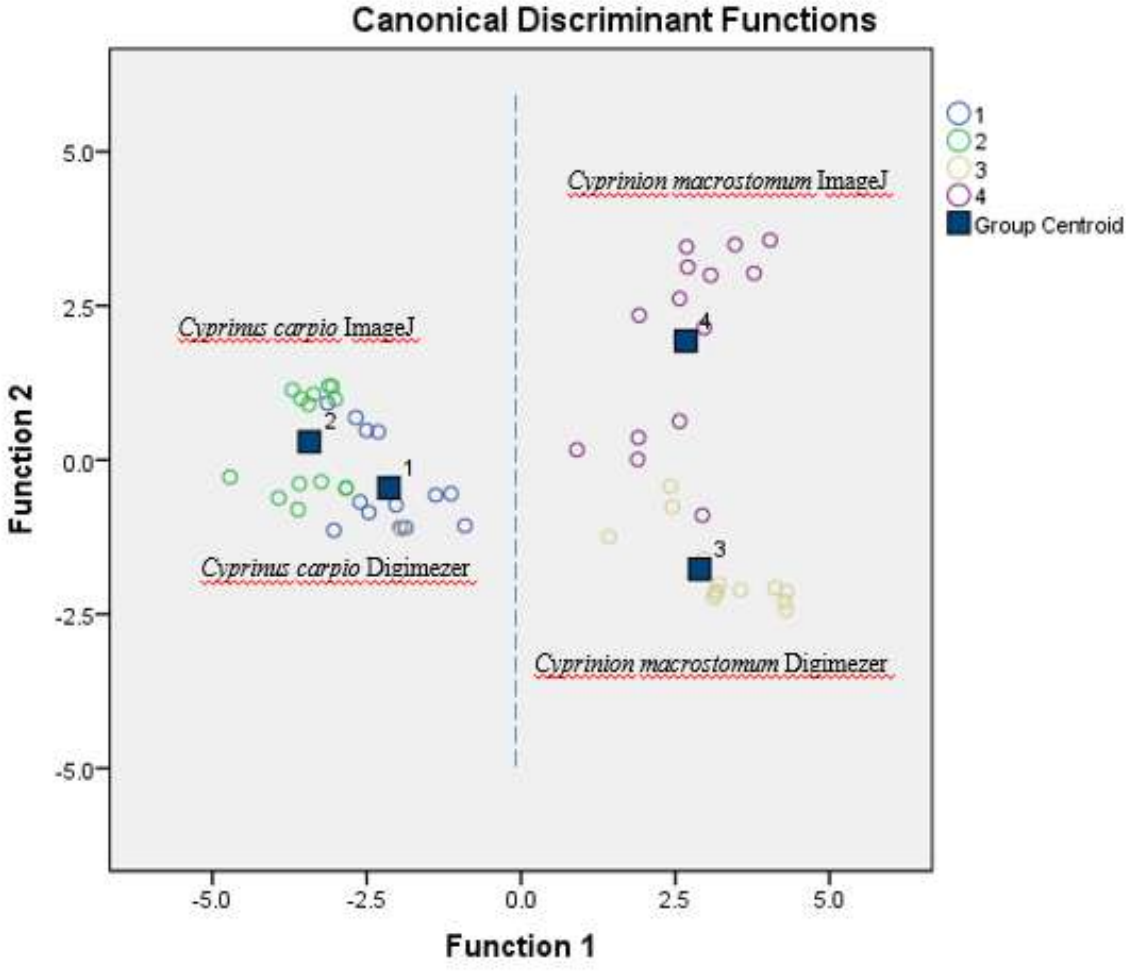

Figure 5. Discrimination of the species formed as a result of evaluating lapillus otoliths of these two species by analysis of different image analysis programs.

In *C. carpio*, the right and left asteriscus otolith characters were measured by Digimizer and ImageJ programs. There was no statistically significant difference between *C. carpio* right

and left lapillus otolith characters values measured by Digimizer and ImageJ programs (P>0.05) (Table 4).

Table 4. Comparison of the characters of right and left asteriscus otolith pairs in *Cyprinus carpio* obtained by both analysis programs.

Variables	Side	Applications	Mean	SE	StDev	Min.	Max.	P Values	Paired t Test
Area	Left	Digimizer	0.2645	0.0119	0.0314	0.2262	0.2972	0.902	0.814
	Left	ImageJ	0.2666	0.0109	0.0287	0.2290	0.2970		
	Right	Digimizer	0.2656	0.0111	0.0293	0.2252	0.2972	0.956	0.972
	Right	ImageJ	0.2664	0.0109	0.0288	0.2280	0.2980		
Width	Left	Digimizer	0.5427	0.0142	0.0375	0.4927	0.5815	0.677	0.472
	Left	ImageJ	0.5349	0.0117	0.0308	0.4980	0.5720		
	Right	Digimizer	0.5473	0.0138	0.0364	0.4917	0.5874	0.563	0.424
	Right	ImageJ	0.5367	0.0111	0.0294	0.4950	0.5650		
Length	Left	Digimizer	0.6811	0.0212	0.0562	0.6271	0.7803	0.594	0.350
	Left	ImageJ	0.6671	0.0140	0.0370	0.6250	0.7000		
	Right	Digimizer	0.6740	0.0162	0.0430	0.6256	0.7315	0.702	0.166
	Right	ImageJ	0.6656	0.0141	0.0374	0.6240	0.6990		
Perimeter	Left	Digimizer	2.1458	0.0709	0.1875	1.9008	2.4052	0.063	0.788
	Left	ImageJ	1.9707	0.0422	0.1115	1.8360	2.1020		
	Right	Digimizer	2.1537	0.0697	0.1844	1.9051	2.4055	0.077	0.070
	Right	ImageJ	1.9906	0.0447	0.1182	1.8340	2.1070		

In *C. macrostomum*, the right and left asteriscus otolith characters were measured by Digimizer and ImageJ programs. There was no statistically significant difference between *C. macrostomum* right and left asteriscus otolith characters measured by Digimizer and ImageJ programs (P> 0.05) (Table 5).

Table 5. Comparison of the characters of right and left asteriscus otolith pairs in *Cyprinion macrostomum* obtained by both analysis programs.

Variables	Side	Applications	Mean	SE	StDev	Min.	Max.	P Values	Paired t Test
Area	Left	Digimizer	0.2618	0.0114	0.0301	0.2203	0.2909	0.869	0.609
	Left	ImageJ	0.2591	0.0110	0.0290	0.2200	0.2910		
	Right	Digimizer	0.2597	0.0125	0.0330	0.2205	0.3003	0.897	0.700
	Right	ImageJ	0.2574	0.0116	0.0308	0.2210	0.2920		
Width	Left	Digimizer	0.5495	0.0116	0.0307	0.5134	0.5840	0.770	0.094
	Left	ImageJ	0.5446	0.0117	0.0310	0.5060	0.5860		
	Right	Digimizer	0.5549	0.0122	0.0323	0.5155	0.5844	0.948	0.120
	Right	ImageJ	0.5537	0.0129	0.0342	0.5030	0.5870		
Length	Left	Digimizer	0.7194	0.0170	0.0450	0.6528	0.7769	0.771	0.181
	Left	ImageJ	0.7267	0.0179	0.0472	0.6530	0.7730		
	Right	Digimizer	0.7064	0.0166	0.0438	0.6529	0.7769	0.976	0.076

	Right	ImageJ	0.7071	0.0165	0.0437	0.6520	0.7730		
Perimeter	Left	Digimizer	2.2630	0.0535	0.1414	2.1211	2.4303	0.049*	0.560
	Left	ImageJ	2.1114	0.0428	0.1134	1.9830	2.2160		
	Right	Digimizer	2.2721	0.0552	0.1460	2.1116	2.4392	0.029*	0.154
	Right	ImageJ	2.0967	0.0429	0.1136	1.9500	2.2360		

Using Digimizer and ImageJ programs, a discrimination analysis was performed according to *Cyprinus carpio* and *Cyprinion macrostomum* asteriscus otolith characters. For *C. carpio* and *C. macrostomum*, using the lapillus otolith data both programs discriminated 100%. A total of 100% is distinguished (Table 6; Figure 6). According to the discriminant analysis, both images were effective in separating the species in the same manner in the analytical.

Table 6. Results of cross-validation for classifying *Cyprinus carpio* and *Cyprinion macrostomum* using the asteriscus otolith character values.

Classification Results[a]						
	Groups	Predicted Group Membership				Total
		C. carpio Digimizer	*C. carpio* ImageJ	*C. macrostomum* Digimizer	*C. macrostomum* ImageJ	
Original %	*Cyprinus carpio* Digimizer	100	0	0	0	100
	Cyprinus carpio ImageJ	0	100	0	0	100
	Cyprinion macrostomum Digimizer	0	0	100	0	100
	Cyprinion macrostomum ImageJ	0	0	0	100	100
a. 100 % of original grouped cases correctly classified.						

There was no statistically significant difference between measurements of *C. carpio* asteriscus otoliths obtained by two analysis programs used in the study (P>0.05) (Table 4).

Although these two image analysis programs have been successful at the same rate in the discriminate analysis, a statistical difference was found between the measurements of both right and left asteriscus otolith perimeter of *C. macrostomum* measured by these two programs (P<0.05) (Table 5). There was no statistical difference between the other asteriscus otolith measurements (P>0.05) (Table 5).

When the mean asteriscus otolith perimeter value of the *C. macrostomum* obtained by both image analysis programs was examined, it was determined that both the right and left otolith data were higher by the Digimizer program (Table 5). This indicates that the Digimizer program is more accurate than the ImageJ program, especially in measuring the asteriscus otolith perimeter.

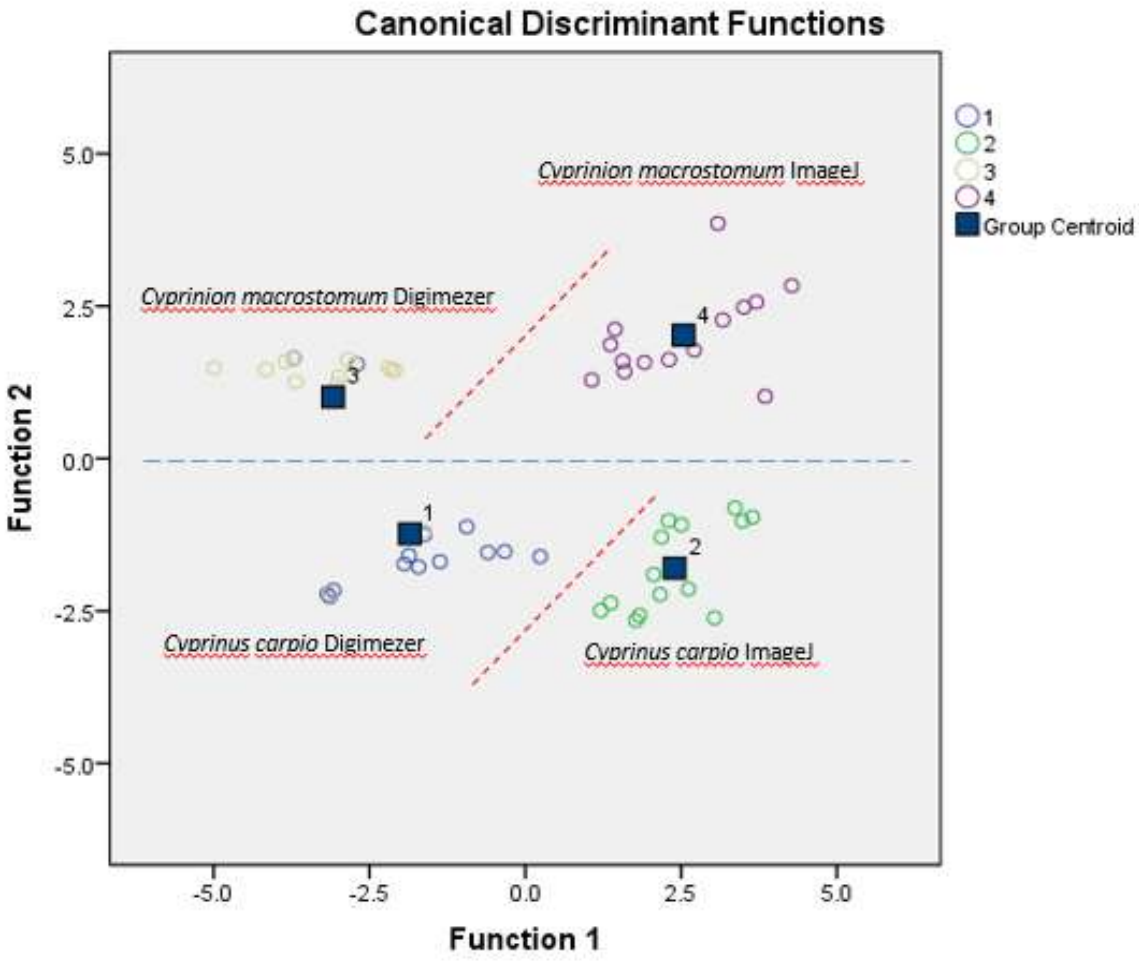

Figure 6. Discrimination of the species formed as a result of evaluating asteriscus otoliths of these two species by analysis of different image analysis programs.

Asteriscus have a higher discrimination potential than lapillus otoliths in these Cyprinid fish. The use of asteriscus gives better results in species discrimination in Cyprinid fish. This prediction is consistent with the data of the other studies such as Kontas & Bostanci (2015), Yilmaz et al., (2015), and Omar & Amohamed (2016).

The reasons for choosing image analysis programs to be applied in studies may differ between researchers. However, they can be classified as such cost of the program, computer suitability, ease of use, interface appearance and output types.

Since the selection of an image analysis program used in both fisheries and different areas is very important for the success of the study; therefore, it is necessary to choose program according to size, the structure of the samples. Literature suitability and sensitivity of the program should be prioritized when choose the programs.

Acknowledgement

We would like to thank Furkan Coşkun for having kindly supplied the *Cyprinion macrostomum* specimens in this study.

References

Bostanci, D., Polat, N., Kurucu, G., Yedier, S., Kontas¸ S., and Darcin, M. (2015). Using otolith shape and morphometry to identify four *Alburnus* species (*A. chalcoides, A. escherichii, A. mossulensis and A. tarichi*) in Turkish inland waters. J. Appl. Ichthyol. 31, 1013-1022.

Froese, R., and Pauly, D. (2018). FishBase. World Wide Web electronic publication.www.fishbase.org, version (20/06/2018).

Goins, E., and C. L. Reedy. 2000. Digital image analysis in microscopy for objects and architectural conservation. *Objects Specialty Group Postprints*, Vol. 7. American Institute for Conservation Objects Specialty Group. Washington, D. C.:AIC. 122–33.

Howes G J. Systematics and biogeography: an overview. In: Winfield I J,Nelson J S, eds. Cyprinid Fishes: Systematics, Biology and Exploitation. London: Chapman and Hall, 1991. 1–33.

Joyce-Loebl (Firm), (1985). Image Analysis: Principles and Practice. Joyce-Loebl, Gateshead, England, pp: 250.

Kontas, S., and Bostanci, D. (2015). Morphological and Biometrical Characteristics on Otolith of *Barbus tauricus Kessler*, 1877 on Light and Scanning Electron MicroscopeInt. J. Morphol., 33(4): 1380-1385.

Nelson J S, ed. Fishes of the World. New York: John Wiley and Sons Inc., 2006.

Omar, A. M., and Amohamed, S. K. (2016) Comparative morphological studies on the otoliths (ear stones or crystals) in some marine and fresh water fishes. Int J Fish Aquat Stud 4:512–517.

Schneider, C. A., Rasband, W. S. and Eliceiri, K. W. (2012). NIH Image to ImageJ: 25 years of image analysis. Nat Methods 9:671- 675.

Tuset, V. M., Lombarte, A., González, J. A., Pertusa, J. F. and Lorente, M. J. (2003). Comparative morphology of the sagittal otolith in *Serranus* spp. J. Fish Biol., 63(6): 1491-504.

Tuset, V. M., Lombarte, A. and Assis, C. A. (2008). Otolith atlas for the western Mediterranean, north and central eastern Atlantic. Sci. Mar., 72(Suppl. 1): 7-198.

Vecht-Lifshitz, S. E. and Ison, A. P. (1992). Biotechnological applications of image analysis: Present and future prospects. J. Biotechnol. 23:1-18.

Yilmaz, S., Yazicioglu, O., Yazici, R. and Polat, N. (2015). Relationships between fish length and otolith size for five cyprinid species from Lake Ladik, Samsun, Turkey. Turkish Journal of Zoology, 39: 438-446.

Analysis Of Mosses And Soil Along Giresun-Samsun Highway In Turkey During 2006-2017

Bahadır KOZ

Giresun University, Department of Mathematics and Science Education, Giresun, Turkey

Corresponding Author: bahadirkoz@yahoo.com; Bahadir.koz@giresun.edu.tr

Abstract

The heavy metal analysis of mosses and soil in the Black Sea region of Turkey was determined using ICP-MS (Inductively Coupled Plasma – Mass Spectrometer)spectrometry method. The technique of moss analysis provides a surrogate, time-integrated measure of metal deposition from the atmosphere to terrestrial systems. It is easier and cheaper, less prone to contamination and allows a much higher sampling density than conventional precipitation analysis. A qualitative moss analysis showed that the samples contained Vanadium, Chromium, Mangenese, Iron, Cobalt, Nickel, Copper, Zinc, Lead. While the mean concentration values of V, Cr, Mn, Fe, Co, Ni, Cu, Zn, and Pb in the moss samples collected from city centers are 27.94, 15.85, 270.50, 5355.48, 7.91, 52.98, 35.18, 78.80 and 17.60, mg/kg, respectively. In general, the concentration of Vanadium, Chromium, Mangenese, Iron, Cobalt, Nickel, Copper, Zinc and Lead in mosses decreased between 2006 and 2017. Since this study was a heavy metal analysis along the highway, evaluation of this elements with their potential hazards for ecology and human was briefly discussed.

KeyWords: Moss, Heavy metals, Traffic, ICP-MS, Black Sea Region.

1. Introduction

Efficient and flexible transport systems are an important part of the world's economy and thus, life quality. Nevertheless, road traffic is an important negative factor regarding air quality, noise and land consumption [1].

Heavy metals originate from both natural and anthropogenic sources in the environment. In the atmosphere, natural sources of these elements are volcanic eruptions, cosmic and terrestrial dusts, vegetation fires and salt spray from the oceans. Anthropogenic sources include emissions from different industrial plants (steel and non-ferrous metallurgy, smelters, alloying plants, petrochemical industry, fertiliser plants, coal power plants, industrial and home furnaces) and motor traffic. The amount of heavy metal originating from natural sources in the atmosphere is small as compared with the anthropogenic flux of these elements [2].

The USEPA highlights 21 toxic substances that can mainly be assigned to road traffic. Some heavy metals are among them (e.g. Pb, Cu, Cd, Zn.) (US Government, 2001). The number of licensed motor vehicles in Turkey has increased by nearly 75% in the last 10 years, which is reflected by a similar annual increase of the average road performance. The situation in Turkey reflects the situation in most countries of the world. Thus, the monitoring of airborne metals in the urban environment has become an essential part of environmental planning and control programs in many parts of the world. Biomonitoring is a technique using organisms or biomaterials to obtain information on certain characteristics of the biosphere [3]. Mosses have been well studied as tools for the biomonitoring of the atmospheric pollution. Mosses have no root system or cuticle layer; hence, mineral adsorption occurs over their entire surface. Therefore, mosses are excellent biomonitors for trace elements in air [4]. Mosses are used as sensitive bioindicators of heavy metal contamination. They accumulate large amounts of these elements in their tissues [5, 6].

In 1990 lead-free gasoline was made compulsory in the United States of America and Canada. In 1993, Austria was the first European country with a similar legislation and other states followed this example [1]. Due to an increasing awareness of environmental pollution, the rates of Pb emissions and ambient air concentrations have been decreased dramatically inWestern and Central Europe since the late 1970s [7].

It is observed that there has been a decreasing consumption rate of lead oil since 2001 compared to consumption rate of lead oil, lead-free oil and LPG in vehicles. In recent years, LPG is substituted for normal and lead oil. When the data published in2003 is investigated, lead oil, LPG and lead-free oil have consumption rates of 25, 36 and 39%, respectively, in

consumption distribution of oil and oil equivalent LPG [8]. When the data published in 2018 is investigated, lead oil, diesel, lead-free and LPG oil have consumption rates of 0, 33.8, 26.7 and 39.1%, respectively, in consumption distribution of oil and oil equivalent LPG [9]. Vehicles in the country, the use of leaded gasoline was banned in 2007 year.

The aim of this study (1) is to determine the change in heavy metal concentrates in the mosses along the Giresun-Samsun highway in Turkey for the last 11 (2006-2017) years. In this paper, we report on the temporal trends (2006-2011) of heavy metal concentrations in mosses. As the emissions of these heavy metals have declined across Europa in recent decades [10], We wait that, the concentartions of these metals in mosses have declined too. In particular, we expected a marked decline in the lead concentrations in mosses due to the introduction of unleaded petrol.

2. Materials and methods

2.1. Study area

Research area is located in Turkey's eastern Black Sea region, which receives the most rainfall in Turkey. The length of the Giresun-Samsun highway is 500 km. There are 3 province and 9 borough in region. Mosses are bioindicators for environmental pollution; therefore they are scarcely present in the polluted areas [11]. Therefore only a limited number of moss samples could be collected. The fact that we could not find abundant number of moss samples in the region might be an indication that the region could be polluted by environmental factors. The region of Savas Village of Artvin province was selected as control regions as they are far from heavy traffic and human disturbances

2.2. Sampling and preparation

Moss and soil samples were collected from 8 centers and 15 center intervals along Giresun-Samsun highway located in the Eastern Black Sea of Turkey (Table 1).The map of the studied region is given in (Fig. 1). The samples were collected in August 2017. Then, the samples were put temporarily in polythene bags. Some important notes such as the features of the habitat where the moss samples were collected, altitude, and sampling date were recorded. The collected samples were put in bags shortly after they were brought back to the laboratory. The macroscopic and microscopic investigations of the samples were made with a stereo microscope. They were identified by using The Moss Flora Britain and Ireland [12], Die Moos-

und Farnpflanzen Europas [13], Flora dei Muschi D'Italia [14], and The Bryophyte Flora of Israel and Adjacent Regions [15] reference publications.

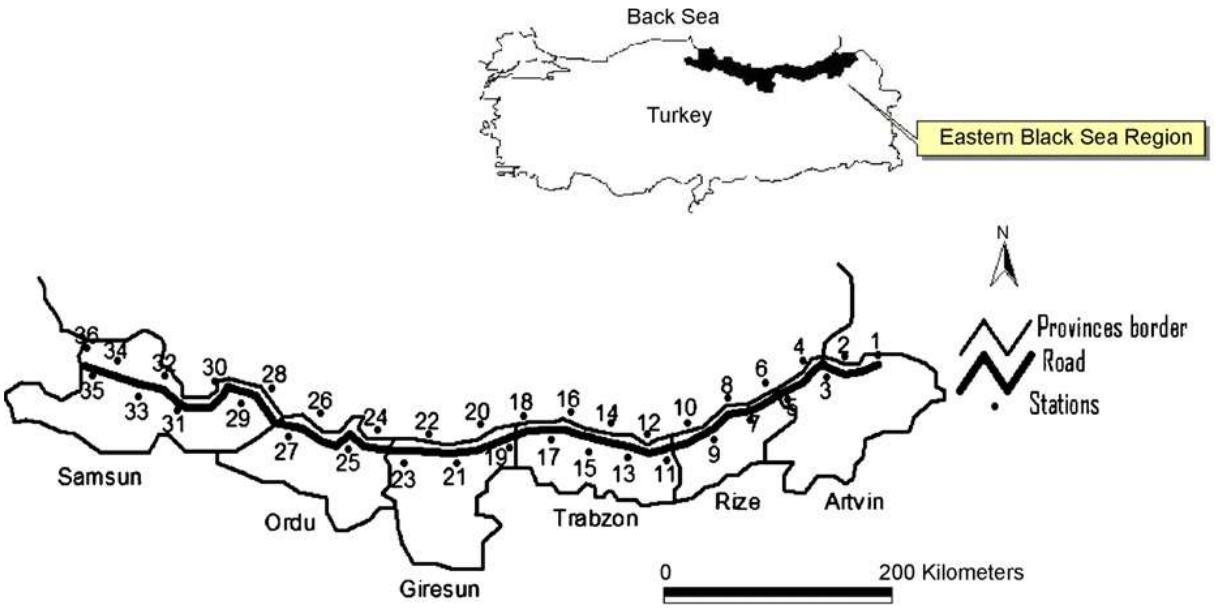

Figure 1. Map of sampling area. (25) Giresun. (26) Bulancak. (27) Piraziz. (28) Gulyalı. (29) Ordu. (30) Persembe. (31) Fatsa. (32) Unye. (33) Terme. (34) Carsamba. (35) Tekkekoy and (36) Samsun

Table 1. Site description of the stations along Giresun-Samsun Highway

Location	Species of Moss	Average vehicle number (2006)	Average vehicle number (2016)	Population (2005)	Population (2017)
Giresun	*Eurhyncnium striatum*	19351	27001	83686	134937
Giresun-Bulancak	*Plagiothecium succulentum*	11463	22408		
Bulancak	*Leucodon sciuroides*	11354	19074	32182	65024
Bulancak-Piraziz	*Scleropodium purum*	11463	18359		
Piraziz-Gülyalı	*Scleropodium purum*	8235	16350		
Gülyalı-Ordu	*Homalothecium sericeum*	7984	17344		
Ordu	*Ctenidium molluscum*	23456	30966	112525	213582
Ordu-Perşembe	*Hypnum cupressiforme*	10430	19838		
Perşembe-Fatsa	*Ctenidium molluscum*	8646	14726		
Fatsa	*Brachythecium mildeanum*	8875	20929	63721	117526
Fatsa-Ünye	*Ctenidium molluscum*	9402	16332		
Ünye	*Ctenidium molluscum*	9847	20640	61552	125722
Terme	*Homalothecium sericeum*	9342	21093	25052	71196
Terme-Çarşamba	*Leucodon sciuroides*	8424	19504		
Çarşamba	*Brachythecium albicans*	13245	32084	49189	137576
Çarşamba-Tekkeköy	*Brachythecium mildeanum*	14977	27769		
Tekkeköy-Samsun	*Amblystegium varium*	35716	47303		
Samsun	*Hypnum cupressiforme*	40004	62683	363180	625890
Kavak-Samsun	*Tortella fragilis*	9750	30833		

During the laboratory process to evaporate remaining water, all samples were dried for 24 h at 85 °C in a Heraeus furnace and then ground in a SPEX mill. To reduce particle size effect, the obtained powder was sieved using a 400 mesh sieve and then stirred for 25 min to a well mixed sample. In order to have the elemental composition, all samples were analyzed by ICP-MS spectrometry.

2.3. Inductively coupled plasma mass spectroscopy (ICP-MS) analysis

One gram of the sample was digested with 6 ml of nitric acid and 2 ml of hydrogen peroxide in a microwave digestion system (CEM MARSX, 240/50, USA). The residue was then diluted with deionized water in 10 ml volumetric flaks [16]. The samples were filtered through a 0.45 □m filter prior to analysis. Calibration standards were prepared from a multi-element standard (Merck, Darmstadt, Germany). Percent recoveries were 93 for Ni, 104 for Cu, 113 for Cr, 102 for Zn, 91 for Cd, and 115 for Pb. Samples were analyzed three times for heavy metals using an ICP-MS (BRUKER 820-MS, Germany) as mg.kg-1 wet weight [16]. The working conditions of instrument featured in this study are shown in Table 2.

Table 2. ICP-MS working conditions

Parameters	Settings	Parameters	Settings
Plasma flow	18.0 (l/min)	Corner lens	-193 (volt)
Auxiliary flow	1.80 (l/min)	Left mirror lens	45 (volt)
Nebulizer flow	0.90 (l/min)	Right mirror lens	33 (volt)
Sheath gas	0.15 (l/min)	Bottom mirror lens	38 (volt)
CRI gas He	160 (ml/min)	Entrance lens	-1 (volt)
CRI gas H_2	100 (ml/min)	Fringe bias	2.5 (volt)
RF power	1.40 (kW)	Entrance plate	-39 (volt)
Sampling depth	6.5 (mm)	Pole bias	0 (volt)
Pump rate	4 (rpm)	Scan mode	Peak hopping
Stabilization delay	15 (s)	Dwell time	20 (ms)
Spray chamber	3 (^{O}C)	Points per peak	1
First extraction lens	-1 (volt)	Scans/Replicate	50
Second extraction lens	-180 (volt)	Replicates/Sample	3
Third extraction lens	-226 (volt)		

3. Results

Concentrations of elements in the moss samples collected along Giresun-Samsun highway are shown in Table 3. The mean concentrations values of V, Cr, Mn, Fe, Co, Ni, Cu, Zn, and Pb were 27.94, 15.85, 270.50, 5355.48, 7.91, 52.98, 35.18, 78.80 and 17.60, respectively. As expected, it has been observed that the concentrations of the elements in moss samples collected from the control region were much lower than those collected from the measurement sites.

Table 3. Heavy metal concentrations in the mosses samples collected (mg/kg)

ample Number	Species of Moss	Location	V (mg/kg)	Cr (mg/kg)	Mn (mg/kg)	Fe (mg/kg)	Co (mg/kg)	Ni (mg/kg)	Cu (mg/kg)	Zn (mg/kg)	Cd (mg/kg)	Pb (mg/kg)
1	*Eurhynchium striatum* (Hedw.) Schimp.	Giresun Merkez	25.47	16.72	354.48	4662.15	8.10	35.00	35.58	124.34	0.11	24.13
2	*Scleropodium purum* (Hedw.)Limpr.	Bulancak-Giresun	26.92	9.33	221.90	3366.02	5.56	23.96	29.18	49.99	1.13	9.37
3	*Plagiothecium succulentum*(Wils.)Lindb.	Bulancak-Giresun	20.65	13.75	254.90	4120.65	6.58	47.29	30.30	90.87	N.D.	18.65
4	*Leucodon sciuroides* (Hedw.) Schwaegr.	Bulancak	20.39	19.30	265.93	4373.89	7.65	45.74	28.74	98.87	N.D.	22.13
5	*Scleropodium purum* (Hedw.)Limpr.	Piraziz-Bulancak	20.65	12.27	237.44	3877.53	6.50	50.33	27.86	90.44	N.D.	10.67
6	*Scleropodium purum* (Hedw.)Limpr.	Piraziz-Gülyalı	23.17	21.84	216.43	3967.13	6.37	49.08	29.55	50.50	N.D.	13.45
7	*Homolothecium sericeum* (Hedw.)B.S.G.	Ordu-Gülyalı	36.12	7.36	279.16	3717.02	6.39	25.52	29.32	46.72	N.D.	9.93
8	*Ctenidium molluscum* (Hedw.)Mitt.	Ordu Merkez	32.22	7.78	410.36	4417.94	7.43	38.75	27.54	56.61	0.21	7.26

9	*Hypnum cupressiforme*Hedw.	Perşembe-Ordu	33.61	9.06	208.66	4075.12	6.09	36.57	27.42	117.06	N.D.	14.28
10	*Eurhynchium striatulum(Spruce)B.S.G.*	Perşembe-Fatsa	33.61	9.06	208.66	4075.12	6.09	36.57	27.42	117.06	N.D.	14.28
11	*Ctenidium molluscum* (Hedw.)Mitt.	Perşembe-Fatsa	26.79	14.78	250.32	4461.93	7.30	49.87	38.76	78.44	N.D.	19.85
12	*Brachythecium mildeanum (Schimp.)Milde*	Fatsa	29.38	19.35	260.48	5375.02	8.76	58.95	49.03	60.75	N.D.	26.54
13	*Ctenidium molluscum* (Hedw.)Mitt.	Ünye-Fatsa	21.68	20.14	238.61	5047.36	7.74	62.40	47.86	90.98	N.D.	14.56
14	*Ctenidium molluscum* (Hedw.)Mitt.	Ünye Merkez	6.94	7.40	155.23	4571.10	6.55	56.39	8.66	12.65	N.D.	3.71
15	*Homolothecium sericeum* (Hedw.)B.S.G.	Terme	33.65	22.08	274.56	6493.03	9.84	65.12	11.20	70.20	N.D.	8.76
16	*Leucodon sciuroides* (Hedw.) Schwaegr.	Terme-Çarşamba	32.93	18.71	253.76	4984.92	8.23	60.92	34.13	56.74	N.D.	7.56
17	*Bryum albicans* (Hedw.)B.S.G.	Çarşamba Merkez	30.56	19.54	270.75	6783.90	8.33	64.30	20.30	98.65	N.D.	17.49
18	*Bryum mildeanum* (Schimp.) Milde	Çarşamba-Tekkeköy	24.34	20.23	249.07	6483.90	7.55	58.37	30.85	80.70	N.D.	22.37
19	*Pleurozium schreberi*(Brid.) Mitt.	Çarşamba-Tekkeköy	21.52	37.25	263.49	4222.44	7.03	56.27	30.39	64.49	N.D.	6.69
20	*Amblystegium varium*(Hedw.) Lindb.	Samsun-Tekkeköy	32.32	17.40	318.54	7403.86	9.65	78.30	30.65	120.40	N.D.	37.85
21	*Eurhynchium striatum* (Hedw.) Schimp.	Samsun Merkez	33.11	10.10	352.35	8722.09	11.47	77.74	114.78	54.91	0.53	7.84

22	*Hypnum cupressiforme* Hedw.	Samsun Merkez	38.54	13.83	365.94	9386.72	13.78	68.27	50.55	90.90	N.D.	56.79
23	*Tortella fragilis* (Hook.&Wils.)Limpr.	Samsun-Kavak	38.23	17.39	310.54	8587.40	9.10	73.05	49.08	90.33	N.D.	30.80
Average			**27.94**	**15.85**	**270.50**	**5355.48**	**7.91**	**52.98**	**35.18**	**78.80**		**17.60**
Max.-Min Values			**38.54-6.94**	**37.25-7.36**	**410.36-155.23**	**9386.72-3366.02**	**13.78-5.56**	**78.3-23.96**	**114.78-8.66**	**124.34-12.65**		**56.79-3.71**

N.D.= Not Dedected

The average concentrations of elements collected from centers are relatively higher than those both center intervals and control region as shown Table 4. Heavy metals are emitted to the environment from different sources, such as transportation, industrial activities, fossil fuels, agriculture, urbanization and other human activities. While the average concentration values of V, Cr, Mn, Fe, Co, Ni, Cu, Zn and Pb in the moss samples collected from city centers were 25.51, 16.02, 284.54, 5239.57, 8.09, 52.03, 25.86, 74.58 and 15.71 $mg.kg^{-1}$; those in the moss samples from city center intervals were 28.03, 16.32, 250.82, 4885.02, 7.15, 50.60, 33.05, 81.76 and 16.45 $mg.kg^{-1}$,those in the moss samples from control region were 5.01, 15.07, 209.17, 2908.40, 3.62, 34.57, 11.84, 23.76 and 3.22 $mg.kg^{-1}$, respectively. The average concentrations of heavy metals in the center and center intervals are very close.

Table 4. The average concentrations and ranges of elements in mosses collected from centrums. centrum intervals and control regions.

	V (mg/kg)	Cr (mg/kg)	Mn (mg/kg)	Fe (mg/kg)	Co (mg/kg)	Ni (mg/kg)	Cu (mg/kg)	Zn (mg/kg)	Pb (mg/kg)
Centrum Average Range	25.51	16.02	284.54	5239.57	8.09	52.03	25.86	74.58	15.71
Centrum interval Average Range	28.03	16.32	250.82	4885.02	7.15	50.60	33.05	81.76	16.45
Control region Average Range	5.01 9.17-0	15.07 20.25-13.17	209.17 290.67-146.57	2908.40 3847.71-2110.39	3.62 4.68-2.64	34.57 46.32-28.85	11.84 13.88-9.42	23.76 29.91-19.79	3.22 3.61-2.63

3. Discussion

According to the Table 1, the number of vehicles in Turkey was 12,227,393 in 2006 increased to 21,090424 in 2017. The population of Turkey was 69,729,967 in 2006, increased to 80,810525in 2017 [9]. Nevertheless, the vanadium, chromium, manganese, iron, cobalt, nickel, copper, zinc, cadmium, lead concentration in mosses decreased significantly across region between 2006 and 2017. A similar situation is seen in europe [17, 18].

Although the mean concentration values of all elementsin the samples collected from the city centers are relatively higher than those from the center intervals, the difference between mean values of Pb was observed to benot so high. This might be explained that the city centers and the center intervals are quite close together in the studied area since the urbanization becomes dense near the coast. As can be seen from the figure, moss samples collected from Samsun show higher Pb levels, and also two other maps show the same trend. The main sources of lead are the combustion of lead gasoline, waste incineration and industry. Lead is known to induce reduced cognitive development and intellectualperformance in children, and increased blood pressure and cardiovascular disease in adults [19].

The source of copper and zinc is brake and tires [20]. Cu, Zn and Co is released from cars and trucks [21]. Chromium, Manganese, Iron and Nickel are also present in the earth crust. People living near hazardous waste sites containing these heavy metals may be exposed to high levels of these chemicals. Acute toxicity of cobalt may be observed as effect on the lungs including asthma and pneumonia. The International Agency for Research on Cancer (IARC) has determined that cobalt and chromium is a possible carcinogen to humans [22]. When breathing very high levels of chromium in air, it can damage the lungs, stomach and intestines. The most common adverse health effect of nickel in humans is an allergic reaction. Major sources of exposure are auto exhaust, fertilizers, industrial waste and combustion of fuel oil [23].

The present results were compared with literature data in Table 5. As seen from the table, the present results are quite higher than the measurements taken from different countries in Europe. It could be attributed that the environmental pollution is a much more serious problem in Turkey. According to the Table 5; Finland, France, Germany and Romania on a downward trend in heavy metal concentrations are also seen in Turkey. The most important reason for the state to ban the use of leaded gasoline in vehicles in Turkey, emphasizing the vehicle inspection by government and rising environmental awareness is growing.

Table 5. Comparison of the elemental concentration results (mg/kg) with literature data. (References: V. Cr. Fe. Ni. Cu. Zn=[17]; Cd and Pb = [18])

	V(mg/kg)	Cr(mg/kg)	Mn(mg/kg)	Fe(mg/kg)	Co(mg/kg)	Ni(mg/kg)	Cu(mg/kg)	Zn(mg/kg)	Cd(mg/kg)	Pb(mg/kg)	Year	References
Finland	3.36	1.47		357		1.70	5.07	35.9	0.26	9.9	1990	[17]
Finland	1.24	1.06		210		1.38	3.38	27.6	0.12	3.0	2000	[17]
France	2.46	3.16		549		1.94	5.30	32.4	0.20	8.8	1995	[17]
France	2.89	1.69		654		2.30	6.40	40.4	0.20	5.7	2000	[17]
Germany	2.87	1.83		561		2.38	9.13	50.2	0.31	12.9	1990	[17]
Germany	1.06	0.91		343		1.13	7.14	41.0	0.21	4.6	2000	[17]
Romania	12.53	10.85		5114		8.41	18.42	69.1	1.02	35.1	1990	[17]
Romania	7.99	8.46		2518		3.35	21.56	79.6	0.46	14.4	2000	[17]
Sarp-Samsun highway		52.2	790.5	40090	11.6	17.2	267.5	175.5	0	39.1	2006	[24]
Giresun-Samsun highway	27.94	15.85	270.50	5355.48	7.91	52.98	35.18	78.80	0.36	17.60	2017	Present study

The lead concentration in mosses decreased significantly between 2006 and 2017. Because; in cars, the use of leaded gasoline was banned in Turkey since 2007 [9]. Gasoline lead additives have been the key emission source of lead over the last decades. Pb pollution is correlated with urbanization and thedensity of the human population. The main target for Pb toxicity inboth adults and children is the nervous system. Exposure to Pb mayalso result in anemia. At high levels of exposure, lead can severelydamage the brain and kidneys in adults or children and ultimatelycause death [25].

Vanadium can cross the brood-brain barrier. Toxicity is manifest especially after inhalation; symtoms include green tongue and diarrhea, cramps [26]. Chromium is essential element, required for carbohydrate and lipid metabolism and it is deficiency may be associated to cardiovascular disease [27]. Toxicity of Mangenese in polluted working environments leads to manganism, a neurological disease [28].

Cadmium enters the environment because of human activities, mainly concerning its industrial use and waste disposal. The main source of human exposure is food, but tabocco smoke is important also [29].

Cobalt is an essential element as an integral part of Vitamin B_{12} and is therefore essential for folate and fatty acid metabolism. Toxicity from excess cobalt leads to cardiomyopathy with damage to heart muscle due to anoxia [29].

Copper is essential for the functioning of many metalloproteins and enzymes and it also plays a role in regulation of gene expression. It is required for growth, defense bone strenght, blood cell production, iron transport and metabolism. Toxicity from excess copper is very rare, mainly from contaminated water: It causes gastrointestinal problems [29].

Nickel is a cofactor for some enzymes, urease and others [30]. It is involved in the metabolism of methionine, vitamin B_{12}, folate and therefore it is suggested that it may be essential. Toxicity also leads to anemia and decreased growth. Sensitive individuals may react to low doses.

Zinc is an essential nutrient, present in all tissues of the human body; It is a structural components of over 300 enzymes, important for metabolism of all macromolecules. Excess zinc derives from pollution. Symptoms of acute poisoning are nausea, vomiting, diarrhea, lethargy and fever. Chronic exposure should interfere with copper status and immune response interfering with reproduction [31].

Higher and lower levels of the other elements were dedected, in moss samples, when compared to substrate concentrations. These differing levels are directly relatable to

morphological and anatomical features of moss, such as metal absorbing abilities, surface area, high cell membrane permeabilty, pH, additives, elemental concentrations in the atmosphere, humidity, direction of dominating wind and other climatic conditions have various effects on metal concentration in moss [23].

4. Conclusions

The moss surveys in east Black Sea of Turkey during the period 2006-2017 have increased the knowledge about the location of significant heavy metal emissions sources, the extent of the areas polluted by these sources and the changes of the deposition with time. Heavy metal concentrations in the region have fallen considerably in 2017 compared to 2006. Mosses proved well in many fields of environmental control. The results showed that the elemental concentartions in the samples collected from the center intervals. This could be attributed to the traffic density, urbanization, industrial activities, fossil fuels consumed by the population and the human activities. Higher or lower levels of the elements were dedected in moss samples, when compared to substrate concentrations. These differing levels are directly relatable to morphological and anatomical features of mosses.

Finally we like to say that bryophytes which are mostly small in size, are essentially for the integral understanding and control of the present state and future development of our environment.

Acknowledgements

This research was supported by Foundation of Giresun University, Giresun, Turkey.

References

[1] Dockery, D.W. 2001. Epidemiological evidence of cardiovascular effects of particulate air pollution, *Environmental Health Perspective*, 109, 483–486.

[2] Markert, B.A., Breure, A.M., Zechmeister, H.G. 2003. *Bioindicators&Biomonitors, Principles, Concepts and Applications.* London, 334.

[3] Wolterbeek, B. 2002. Biomonitoring of trace element air pollution: principles, possibilities and perspectives, *Environmental Pollution*, 120 (1), 11–21.

[4] Lee, S.L. Li, X.D. Zhang, G. Zhang, L. Qi, S.H. Peng, X.Z., 2005. Biomonitoring of trace metals in the atmosphere using moss (*Hypnum plumaeforme*) in the Nanling Mountains and the Pearl River Delta Southern China, *Atmospheric Environment*, 39, 397–407.

[5] Grodzinska, K., Szarek-Lukaszewska, G. 2001. Response of mosses to the heavy metal deposition in Poland—an overview, *Environmental Pollution*, 111, 443–451.

[6] Uyar, G. Ören, M. İnce, M. 2007. Atmospheric heavy metal deposition in Düzce Province by using mosses as biomonitors, *Fresenius Environmental Bulletin*, 16, 145–153.

[7] Massadeh, A.M. Snook, R.D. 2002. Determination of Pb and Cd in road dusts over the period in which Pb was removed from petrol in the UK, *Journal of Environmental Monitoring*, 4, 567–572.

[8] http://www.cevreorman.gov.tr/moz (February 15, 2006).

[9] http://www.tuik.gov.tr (February 28, 2018)

[10] Ilyin, I., Travnikov, O. 2005. Modelling of Heavy Metal Airborne Pollution in Europa: Evaluation of the Model Performance.EMEP/MSC-E Technical Report8/2005. Meteorological Synthesizing Centre-East, Moscow, Russian Federation. Available from:

[11] Zechmeister, H. G., Grodzinska, K., & Szarek-Lukaszewska, G. 2003. *Bryophytes*. In B. A. Markert, A.M. Breure, & H. G. Zechmeister (Eds.), Bioindicators/biomonitors (principles, assessment, concepts) (pp. 329–374). Amsterdam: Elsevier.

[12] Smith, A. J. E. 2004. *The moss flora of Britain and Ireland*. Edinburgh: Cambridge University Press.

[13] Frey,W., Frahm, J. P., Fischer, E., & Lobin,W. 1995. *Die Moos und Farnpfanzen Europas*. Stuttgart: G. Fischer.

[14] Pedrotti, C. C. (2001). Flora Dei Muschi D'İtalia. Rome: Antonia Delfino Editore.

[15] Herrnstadt, I., Heyn, C. C., Bischler, H., & Jovet-Ast, S. 2004. *The bryophyte flora of Israel and adjacent regions*, Jerusalem: Israel Academy of Sciences and Humanities.

[16] Türkmen.M., Dura, N. 2016. Assessment of heavy metal concentrations in fish from south western black sea, *Indian Journal of Geo Marine Science*, 45(11), 1552-1559

[17] Harmens, H., Norris, D.A., Koerber, G.R., Buse , A., Steinnes, E., Ruhling, A. 2007. Temporal trends in the concentration of arsenic, chromium, copper, iron, nickel, vanadium and zinc in mosses across Europe between 1990 and 2000, *Atmospheric Environment*, 41, 6673-6687.

[18] Harmens, H., Norris, D.A., Koerber, G.R., Buse, A., Steinnes, E., Ruhling, A. 2008. Temporal trends (1990-2000) in the concentration of cadmium, lead, and mercury in mosses across Europa, *Environmental Pollution*, 151, 368-376.

[19] Communities of the European Commission, (2002) Commission Regulation (EC) 221/2002 of 6 February 2002 amending regulation (EC) No.466/2002 setting maximum levels for certain contaminants in foodstuffs. Official journal of the European Communities. Brussels, 6 February 2002.

[20] Zechmeister, H.G., Hohenwallner, D., Riss, A., Hanus-Illnar, A. 2005. Estimation of element deposition derived from roadtraffic sources by using mosses, *Environmental Pollution*, 138, 238-249.

[21] Garg, B.D., Cadle, S.H., Mulawa, P.A., Groblicki, P.J., Laroo, C. and Parr, G.A. 2000. Brake wear particulate matter emissions. *Environmental Science and Technology*, 34, 4463-4469.

[22] IARC, 1993. IARC Monographs on the Evaluation of Carcinogenic Risks to Humans, Vol. 58, Lyon, France.

[23] Koz, B., Cevik, U., Ozdemir, T., Duran, C., Kaya, S., Gundogdu, A. and Celik, N. 2008. Analysis of mosses along Sarp-Samsun highway in Turkey, *Journal of Hazardous Materials*, 153, 646-654.

[24] Koz, B., Cevik, U., Bulut, V.M., Kaya, S., Gundogdu, A., Celik, N. 2013. Heavy metal analysis by moss species in the Black Sea region of Turkey. *Fresenius Environmental Bulletin*, 22, 1287-1295.

[25] Agency for Toxic Substances and Disease Registry (ATSDR), 2008. Division of Toxicology, Clifton Road, NE, Atlanta, GA, available at:

[26] Mukherjee, B., Patra, B., Mahapatra, S., Banerjee, P., Tiwari, A., Chatterjee, M. 2004. Vanadium-An elementof atypical biological significance, *Toxicology Letters*, 150, 135-143.

[27] World Health Organization, 1988a. Environmental Health Criteria 58- Chromium. Geneva: WHO.

[28] World Health Organization, 1980b. Environmental Health Criteria-Mangenese. Geneva: WHO.

[29] World Health Organization, 1992. Environmental Health Criteria- Cadmium. Geneva: WHO.

[30] World Health Organization, 1991a. Environmental Health Criteria- Nickel. Geneva: WHO.

[31] World Health Organization, 2001a. Environmental Health Criteria- Zinc. Geneva: WHO.

Biogas As A Renewable Energy And The Factors Affecting The Biogas Production

Ersin TEKE[1], Özlem TUNÇ DEDE[2*], Mükrimin Şevket GÜNEY[3]

[1] Giresun University, Faculty of Engineering, Mechanical Engineering Department, Giresun, Turkey; ersinteke28@hotmail.com

[2] Giresun University, Faculty of Engineering, Environmental Engineering Department, Giresun, Turkey; ozlem@tuncdede.com

[3] Giresun University, Faculty of Engineering, Mechanical Engineering Department, Giresun, Turkey; guney80@gmail.com

[*] **Corresponding Author:** ozlem@tuncdede.com

Abstract

Renewable energy sources are an integral part of the world and important for sustainable development and clean environment. The possibility of depletion of fossil-based energy resources requires efficient and widespread use of renewable energy resources as well as efficient use of available resources. Different sources of renewable energy are available, such as; biomass, solar, hydro power, wind energy and geothermal energy. Among the renewable energy sources, the use of organic wastes (biomass) is getting important for environmental and energy optimization. Biogas, a colorless and odorless gas, is produced during anaerobic fermentation of organic wastes. Biogas contents mainly methane, carbon dioxide and small amount of hydrogen sulphur, nitrogen and hydrogen. The percentages of these matters change with content of organic materials. Animal wastes (manure, wastes of slaughter house, etc.), plants and agricultural wastes (stubble, corncob, sugar beet leaves, grass, etc.), domestic and industrial organic wastes (sewage and bottom sludge, waste of paper and food industry, etc.) which have high organic contents can be used for the production of biogas. Since biomass energy is an inexhaustible resource, it is seen as an appropriate and important source of energy because it can be obtained everywhere, especially for rural areas. In this study, the factors affecting the production of biogas, the equivalent potential energy value of biogas and its place in the country's economy has been investigated.

Keywords: Agricultural waste, animal waste, biogas, energy source.

1. Introduction

Renewable energy sources are important for sustainable development. They are an integral part of the world and necessary for clean environment. Because fossil-based energy resources are limited in the world, researchers tend to find alternative renewable energy resources like biomass, solar, hydro power, wind energy and geothermal energy. Among them, the use of organic wastes (biomass) is getting important for environmental and energy optimization. Biogas is a colorless and odorless gas and produced during anaerobic fermentation of organic wastes. The main constituents of biogas are methane (40-70%), carbon dioxide (30-60%) and small amount of hydrogen sulphur (0-3%), nitrogen and hydrogen. The amounts of these constituents depend on the composition of organic materials in biomass. Different sources of wastes which have high organic contents such as animal wastes (manure, wastes of slaughter house, etc.), plants and agricultural wastes (stubble, corncob, sugar beet leaves, grass, etc.), domestic and industrial organic wastes (sewage and bottom sludge, waste of paper and food industry, etc.) can be used for the production of biogas (Ilkılıç and Deviren, 2011; Kılıç 2011; URL-1). This study covers the equivalent potential energy value of biogas, its place in the renewable energy resources and the factors affecting the production of biogas.

2. Material and Method

Biogas technology enables both energy production from organic wastes and the disposal of wastes to the soil improvement It is an important technology that can supply clean and environmentally friendly energy. The calorific value of biogas is 4700-5000 kcal/m^3. 1 m^3 biogas is equal to 0.62 L of gas oil, 1.46 kg charcoal, 12.3 kg cow dung cake and 4.70 kWh electrical energy (Kılıç, 2011; URL-1).

Different sources of organic wastes can be used for the production of biogas. The biogas productivity and the produced methane percentages of different biomass sources were compared in Table 1.

Table 1. The biogas productivity values and methane% of some biomass sources (URL-1)

Source	Biogas productivity (L/kg)	Methane (%v)
Cow manure	90-310	65
Chicken manure	310-620	60
Hog manure	340-550	65-70
Corn wastes	380-460	59
Grass	280-550	70
Leaf	210-290	58
Algae	420-500	63
Activated sludge	310-800	65-80

3. Results and Discussion

Biogas is a colorless, odorless, light and bright blue flame burning gas obtaining from the fermentation of organic wastes under anaerobic conditions. There are three main stages in biogas formation: hydrolysis, acid formation and methane production. In the first step, biomass wastes are hydrolyzed to fatty acids, glycerol, monosaccharaides, peptides and amino acids via microbial enzymes. These substances are converted to low-molecular weight substances like acetic acid by acid-forming (acetogenic) bacteria. In the last step, these low molecular weight substances are converted to methane and carbon dioxide by methanogenic bacteria (Ilkılıç and Deviren, 2011; Kılıç, 2011).

Because biogas formation proceeds via microbiological effects, every condition affects the microbial environment should be considered during biogas formation. The bacteria Temperature is an important parameter during the biogas formation. It effects the metabolic rate, ionization and equivalents and nutrient solubility. Three different temperature ranges, psychrophilic or ambient temperature (< 25°C), mesophilic (25-40°C) and thermophilic (45-60°C) region, are important for the growth of bacteria (acidogens and methanogens) and biogas production. Generally, biogas plants work in mesophilic range, sometimes especially in winter season, it can work in psychrophilic range (15-20°C). Regarding to thermophilic region, it is not economic due to requiring too much energy to reach high temperatures (Ilkılıç and Deviren, 2011; Uzodinma et al., 2007). pH is another parameter that effect the growth of bacteria. The optimum pH changes between 6.6-7.6 during anaerobic fermentation. pH less than 6.2 has a toxic effect on bacteria and diminish even stop methane formation. pH level depends on the

amount of fatty acid, bicarbonate alkalinity and amount of carbon dioxide. The other important parameter is C:N (Carbon/Nitrogen) Ratio. Carbon is used as a raw material for energy production and nitrogen is an essential element for the growth of bacteria. This ratio should not exceed 25-30:1 or less than 10:1. Higher nitrogen means formation of ammonia which negatively affect biogas formation. Organic loading load is daily amount of organic material loaded to unit volume (m^3) of the bioreactor. It should be kept at optimum level for stable pH levels. The other important parameters are hydraulic retention time, mixing, existence of mineral ions, heavy metals and detergents (Ilkılıç and Deviren, 2011; Kılıç, 2011).

Biogas can be used in combustion directly and/or converted to electrical energy. While biogas can be directly used in gasoline engines without any additives, the use after purification of methane content is another way. When using the biogas in diesel engines, it needs to be mixed with diesel in certain ratios (18-20%). Liquid fertilizer is a sub-product of biogas plants and can be used in agricultural areas as in liquid form or after drying (Kılıç, 2011; URL-1).

Turkey has approximately 120 million tone petroleum equivalent biomass capacity (Kılıç, 2011). In Turkey, among renewable energy resources, biomass encompasses 1.48% and 1241.1 GWh of total renewable energy (Karagöl and Kavaz, 2017). In the world, while 80% of biogas facilities is located in China, 10% is in India, Nepal and Thailand. In Europe, Germany is the country with the highest production rate with 2,200 facilities. Italy follows Germany with 70 biogas plants.

Biomass is a cheap and environmentally friendly energy and manure renewable resources. It provides waste recovery and eliminates odor problems. It can grow almost everywhere and suitable for energy efficiency in every scale. However; low cycle efficiency, competition for agricultural areas and high moisture contents are the main disadvantages (Kılıç, 2011).

References

Kılıç, F.C., (2011). Biyogaz Önemi, Genel Durumu ve Türkiye'deki Yeri, Makale, Mühendis ve Makina, 52(617), 94-106.

Ilkılıç, C. and Deviren, H., (2011). Biyogazın Üretimi ve Üretimi Etkileyen Faktörler, 6th International Advanced Technologies Symposium (IATS'11), Elazığ, Turkey.

Karagöl, E.T. and Kavaz, İ., (2017). Dünya'da ve Türkiye'de Yenilenebilir Enerji [PDF document]. Retrieved from Online Web site:
https://setav.org/assets/uploads/2017/04/YenilenebilirEnerji.pdf

Uzodinma, E.O.U., Ofoefule, A.U., Eze, J.I. and Onwuka, N.D., (2007). Optimum mesophilic temperature of biogas production from blends of agro-based wastes, Trends in Applied Sciences Research, 2(1), 39-44.

URL-1: http://www.yegm.gov.tr/yenilenebilir/biyogaz.aspx (Date of access: 25 July 2018).

Renewable Energy Resources: Wave Energy

Özlem TUNÇ DEDE [1*], Mükrimin Şevket GÜNEY [2]

[1] Giresun University, Faculty of Engineering, Environmental Engineering Department, Giresun, Turkey; ozlem@tuncdede.com

[2] Giresun University, Faculty of Engineering, Mechanical Engineering Department, Giresun, Turkey; guney80@gmail.com

[*] **Corresponding Author:** ozlem@tundede.com

Abstract

Renewable energy is energy that is generated from natural processes that are continuously replenished. This includes sunlight, geothermal heat, wind, tides, water, and various forms of biomass. This energy cannot be exhausted and is constantly renewed. Approximately three-quarters of the earth's surface are covered by lakes, seas, and oceans, which offer various renewable energy sources. Generally, the energy potentials of oceans are classified in five groups: wave energy, tidal energy, ocean thermal energy, ocean current energy, and salinity gradient energy. Among this group, wave energy can be obtained from wave surface directly or wave pressure under the surface. In many parts of the world, the wind is so regular and continuous that it will constantly create waves. The wave energy conversion subject is new, essential, and in development stage. Many kinds of technology have been projected to use wave energy and designed to be installed on the coast and offshore. However, wave energy technologies differ according to the wave they interact with and adapt to and the energy they turn the wave energy. Although the waves have a big energy potential and clean energy, it might be difficult to establish the initial system because of inherently changeable behavior of ocean environments. In this study, wave energy as a renewable energy sources have been discussed.

Keywords: Clean energy, ocean, renewable energy, wave.

1. Introduction

Renewable energy is an energy that is generated from natural processes that are continuously replenished. Wind, sun, geothermal heat, ocean waves and tides, and biomass are the main sources of renewable energy sources. About three-quarters of the earth's surface are covered by lakes, seas, and oceans, which offer various renewable energy sources for example, thermal energy from ocean and mechanical energy from waves and tides. Ocean thermal energy from sun's heat can be obtained as warming of surface water by sun's heat and creation of thermal energy due to temperature differences between surface and the deep. Mechanical energy from waves and tides can be converted to electrical energy by using mechanical devices (Güney, 2015; URL-1).

Wave energy are new, essential, and in development stage and can be obtained from wave surface directly or wave pressure under the surface. In many parts of the world, the wind is so regular and continuous that it will constantly create waves. Many kinds of technology have been projected to use wave energy and designed to be installed on the coast and offshore. The wave energy technologies vary according to the wave they interact and the energy that the wave energy is converted. Although the waves have a big energy potential and clean energy, it might be difficult to establish the initial system because of inherently changeable behavior of ocean environments (Güney, 2015; URL-1).

2. Material and Method

Renewable energy resources provide approximately 12% of world's energy consumption (URL-2). The main renewable energy sources were listed in Table 1 (Hoogwijk and Graus, 2008; Johansson, 2004; URL-1).

Table 1. Renewable energy resources

Resource
Hydropower
Biomass energy
Solar energy
Wind energy
Geothermal energy
Ocean energy

Among the renewable energy resources, ocean energy encompasses tidal, wave and ocean thermal energy and have a considerable potential for production of energy (Drew et al., 2009). Total worldwide potential of wave energy is estimated to be about 2 TW of electricity (Hoogwijk and Graus, 2008).

3. Results and Discussion

Wave energy is a clean, unlimited energy resources and has a great energy potential. However, it needs some cost during initial investment. Establishment of initial systems may have some difficulties due to inherent change of ocean conditions. Thus, wave energy devices should be made strong enough in order to survive ocean environment.

In general, three types of applications are possible for conversion of wave energy (URL-1).

1. Shoreline applications
2. Near shore applications
3. Offshore applications

Shoreline Applications

Maintenance and construction of shoreline devices are easier than other applications. Energy production structures are either fixed or buried on the coast and no need for deep water connections or long underwater electrical cables. Because the waves are weakened as they pass through shallow waters, they are less likely to be damaged under extreme conditions. However, these types of applications have some limitations such as coastline geometry and geology, tidal level and coastal protection (Drew et al., 2009; URL-1).

Oscillating water column (OWC), TAPered CHAnel (TAPCHAN) and Pendular are the main types of shoreline applications (Figure 1).

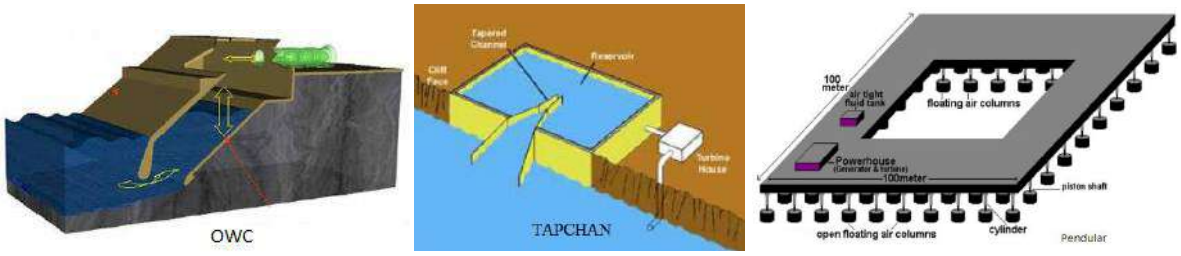

Figure 1. Shoreline applications (URL-1)

Near Shore Applications

"Near shore devices are defined as devices with relatively shallow water" (Drew et al., 2009). The applications are carried out in water depths of 10-25 meters. In order to supply a stationary base during oscillation, devices are generally attached to a seabed. The disadvantage of this kind of systems is limited energy potential due to weakened waves in shallow water (Drew et al., 2009; URL-1).

Osprey and wosp 3500 are the main types of near shore applications (Figure 2).

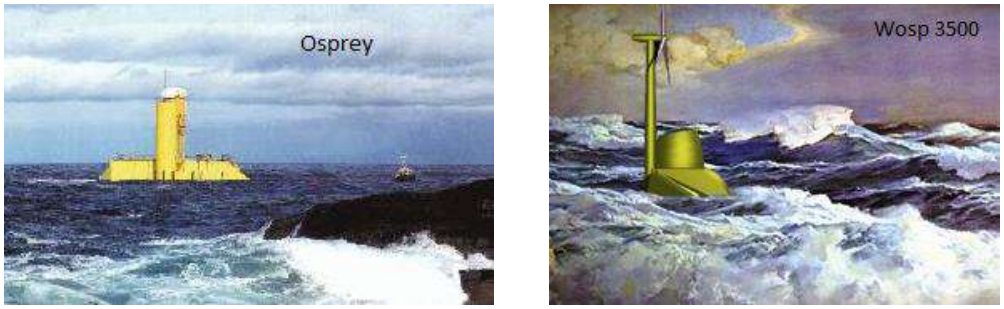

Figure 2. Near Shore applications (URL-1)

Offshore Applications

Offshore applications are carried out in water depths of more than 40 meters. Deep water waves have high energy content and this provides greater amount of wave energy. However, such systems require long electrical cables. The construction and maintenance of offshore devices are difficult. They need to be designed in order to survive under hard conditions which means extra cost (Drew et al., 2009; URL-1).

McCabe wave pump, OPT wave energy converter (WEC) and pelamis are the main types of offshore applications (Figure 3).

Figure 3. Offshore applications (Jackson and Boxx, 2012; URL-1)

Wave energy is one of the most promising renewable energy resources. However, the use conversion technologies are still in development stage. When using the technologies for wave energy conversion, environmental impacts should also be considered.

References

Drew B., Plummer A. R., and Sahinkaya M.N., (2009). A review of wave energy converter technology. Proceedings of the Institution of Mechanical Engineers Part A Journal of Power and Energy, 223(8), 887-902.

Guney, M.S., (2015). Wave Energy Conversion Technologies. Journal of Naval Science and Engineering, 11(2), 25-51.

Hoogwijk, M. and Graus, W., (2008), Global potential of renewable energy sources: a literature assessment. Retrieved from:
https://www.researchgate.net/publication/237576106_Global_Potential_of_Renewable_Energy_Sources_a_Literature_Assessment

Jackson, G. and Boxx, R., 2012, Persistence and Survival in Entrepreneurship: The Case of the Wave Energy Conversion Corporation of America, New England Journal of Entrepreneurship, 15(1), 1-8.

Johansson, T.B. et al, (2004), The potentials of renewable energy [PDF document] Retrieved from:http://ren21.net/Portals/0/documents/irecs/renew2004/The%20Potentials%20of%20Renewable%20Energy.pdf

URL-1: http://www.yegm.gov.tr/teknoloji/dalga.aspx (Date of access: 26 July 2018)

URL-2: https://www.americangeosciences.org/critical-issues/faq/how-much-world-energy-consumption-and-electricity-generation-renewable-energy (Date of access: 26 July 2018)

Evalution of Biochemical Properties of Immobilized Glucose Isomerase Isolated from *Anoxybacillus gonensis*

Züleyha AKPINAR[1*], Hakan KARAOĞLU[1], Fatih Şaban BERİŞ[2], Derya EFE[3]

[1] Recep Tayyip Erdogan University, Faculty of Fisheries and Aquatic Science, Department of Basic Sciences, Rize, Turkey, z.akpinar0@gmail.com, hakan.karaoglu@erdogan.edu.tr

[2]Recep Tayyip Erdogan University, Faculty of Art and Science, Department of Biology, Rize, Turkey, fatihberis@gmail.com

[3] Giresun University, Espiye Vocational School, Department of Medicinal and Aromatic Plants, Giresun, Turkey, deryayanmis@yahoo.com

[*] **Corresponding Author:** z.akpinar0@gmail.com

Abstract

Xylose isomerase (d-xylose ketol-isomerase E.C 5.3.1.5) catalyzes the isomerization of D-xylose to xylulose on the first step of xylose metabolism. Xylose isomerase is also known as glucose isomerase (GI) because of involving in the reversible isomerization of glucose to fructose. This isomerization reaction is important to produce high fructose corn syrup (HFCS) used in the food industry. Many researchers have been studied about efficiently immobilization of GI to produce cheaper. Immobilization of enzymes has advantages such as reuse, separation from product and continuous operation. However, it can be observed that immobilization process can change the biochemical properties of enzymes. In this study, GI was purified from thermophilic *Anoxybacillus* sp. by heat-shock, anion exchange and hydrophobic interaction chromatography, respectively. The purified enzyme was immobilized on cross-linked chitosan beads and biochemical properties of immobilized GI were determined. Optimum activity was observed at 85◦C and pH 6.5, respectively. The relative activity was decreased to 10% after 5 reactions.

Keywords: Glucose isomerase, Thermophilic, Immobilization, Chitosan

1. Introduction

The most commonly used group for producing biotechnological enzymes in microorganism groups is thermophilic microorganisms due to their enzymes that can catalyze biochemical reactions at very high temperatures (Demain et al., 1981). Thermophilic enzymes; are more stabile and active against pH changes and high temperatures, exhibit optimum activity at higher temperatures than the optimum growth temperatures of microorganisms and do not allow microorganism contamination in the environment at high temperatures, they significantly increase the diffusion rates and solubilities of the materials involved in the reaction, thus allowing more product formation (Banglish et. al., 2002; Burg, 2003). DNA polymerase, amylase, xylanase, chitinase, cellulase, protease, lipase and glucose isomerase are only a few of the industrially used thermophilic enzymes (Xu, 2014).

Glucose isomerase, which is widely used in the food industry among many thermophilic enzymes which are of commercial importance, has become the focus of many scientists (Chen et al., 1979; Blow et al., 1992). Glucose isomerase (D-xylose ketol-isomerase E.C 5.3.1.5) catalyzes the isomerization of D-xylose to D-xylulose and D-glucose to D-fructose (GI requires divalent cations such as $Mg^{2+,}$ Co^{2+} or Mn^{2+} for maximum activity (Chen, 1980; Bogumil et al., 1993; Patine et al., 1999; Demirel et al., 2006; Bhosale et al., 1996; Karaoglu et.al, 2013). Known inhibitors of GI are xylitol, arabitol, sorbitol, mannitol, xylose and tris. Although Mg^{2+} is a better activator than Co^{2+}, it is necessary for the Co^{2+} enzyme to remain stable in the desired quaternary structure. This enzyme is one of the three most used enzymes in the world (Anon, 1993; Karaoglu et al., 2013; Yanmis et al., 2014). Glucose isomerase, which isomerize glucose to fructose in the production of High Fructose Corn Syrup (HFCS), has an industrially importance. Since, HFCS is largely used in beverage industry, bakery products, various cereal products, dairy products pickled products, processed foods and vegetables, soap, tomato sauces, canned goods (Deraadt et al., 1994). The first criterion to consider when presenting an enzyme for industrial use is how economical the production and use of the enzyme is. Many researchers have been studied about efficiently immobilization of GI. Because the most efficient method of economical production of GI for industrial applications is the immobilization (Cabral and Kennedy, 1991; CRA, 1994; Bickerstaff, 1997; Brady and Jordan, 2009). In the light of this information, Immobilization of enzymes has advantages such as reuse, separation from product and continuous operation. However, it can be observed that immobilization process can change the biochemical properties of enzymes. In this study, GI was purified from thermophilic *Anoxybacillus sp*. by heat-shock, anion exchange and hydrophobic interaction chromatography,

respectively. The purified enzyme was immobilized on cross-linked chitosan beads and biochemical properties of immobilized GI were determined.

2. Material and Method

2.1. Transformation of pETG2GI into *E.coli* BL21(DE3) Strains

In our previous studies, glucose isomerase from *A.gonensis* was cloned to pET28a^{+} expression vector and new recombinant plasmid was named as pETG2GI. Recombinant pETG2GI plasmid was transformed to *E. coli* strain BL21(DE) strains by standard calcium chloride transformation protocol (Bor et al., 1992; Karaoglu et al. 2013).

2.2. Production of GI

The pETG2GI containing colonies were inoculated at 37 °C in 400 ml of LB medium containing 0,05 mg/ml of kanamycin and incubated till 0,8 optical density. Subsequently, incubation was continued for 4 more hours after induction with 1 mM IPTG. After incubation, cells precipitated by centrifugation were solubilized in 100 mM of MOPS buffer and after, sonicated by sonicator. The crude extract was obtained by cleaning by centrifugation (Karaoglu et. al., 2013; Yanmis et. al., 2014).

2.3. Purification of AgoGI

Heat-Shock Application, DEAE-Sepharose Ion Exchange Column and Phenyl-Sepharose Hydrophobic Interaction Column Chromatography were used to purify *A. gonensis* GI (AgoGI) from the resulting cell lysate. Cell extract obtained by disintegration with sonicator was incubated at 70 °C for 15 min. Denatured proteins were removed by centrifugation. DEAE-Sepharose fast flow was used as column material for ion exchange chromatography. The assay was performed using a Biologic Lp System (Bio-Rad) instrument. Phenyl-Sepharose fast flow (Sigma) was used as a column material for hydrophobic interaction chromatography. The assay was performed using a Biologic Lp System (Bio-Rad) instrument. The amount of protein of the enzyme solution was calculated and in order to calculate GI activity, the enzyme was reacted by diluting 5 times for every steps. The GI activity of enzyme solution was calculated Unit (Karaoglu et. al., 2013)

2.4. Immobilization of GI

At the first step, chitosan beads were prepared. 400 mg of chitosan was weighed and dissolved in 20 ml of 5% acetic acid solution. This solution was transferred into a chromatography column and dropwise into the 1 M NaOH solution. The composed beads were filtered and washed with pure water to remove excess amount of NaOH. Then, 2.5% glutaraldehyde prepared in 100 mM MOPS buffer solution (pH 7) was added to the washed beads and left to incubate for 4 hours for immobilization enzyme to chitosan beads. The beads were washed 10 times with distilled water to remove unbound glutaraldehyde. The purified GI is added to the beads and mixed for 12 hours at room temperature.Subsequently, the mixture was washed with 100 mM MOPS buffer and enzymes not bound to the beads were removed from the medium (Keskin et al., 2017).

2.5. Determination of optimum conditions and kinetic parameters of immobilized AgoGI

The reactions were carried out between 30 °C and 100 °C for optimum temperature and pH 5 and pH 10 for optimum pH, respectively. In order to calculate the kinetic parameters of the enzymes, a serial reaction was carried out at 85 °C and pH 6.5, which was determined by increasing the substrate concentration up to 700 mM. Michaelis-Menten constant (K_m) and maximum velocity (V_{max}) values; was calculated using the OriginPro 8.1 analysis program from the Michaelis-Menten chart plotted as the amount of fructose released in μmol/min (Karaoglu et al., 2013).

3. Results and Discussion

After the gene of GI from *A. gonensis* that was in pET28a(+) was expressed in *E.coli* BL21 (DE3) strain, the enzyme was successfully purified with heat schock, ion-exchange, and hydrophobic column chromatography techniques. The results were given in Table 1. The SDS-PAGE imaginations were given in Figure1 for purified GI from every purification steps. As it is seen in the purification table, all purification applications were successful. After purification, the specific activity of the enzyme increased from 8,41 to 20,64 μmol/min/mg protein, while the enzyme was purified 2,45 fold with 72,1% yield.

Table1. Purification Table for GI obtained from every purification steps

PURIFICATION STEPS	Total Volume (ml)	Protein (mg/ml)	Total Protein (mg)	Activity (µmol/dk/µl)	Total Activity (µmol/dk)	Specific Activity (µmol/dk/mg protein)	Yield	Fold
Cell Extract (A)	28	7,18	201,0	0,0605	1694	8,41	100,0	1,00
Heat-shock App. (B)	26,2	5,33	139,8	0,0615	1611,3	11,53	95,1	1,37
Ion Exchange C. C. (C)	24	3,62	86,9	0,0565	1356	15,60	80,0	1,85
Hydrofobic I.C.C. (D)	33	1,91	63,0	0,0370	1221	20,64	72,1	2,45

Figure 1. The SDS-PAGE imagination of purified GI from every purification steps.

The purified enzyme was successfully immobilized on the chitosan beads. The determination of the optimum temperature was performed. The best working temperature of the immobilized enzyme was determined as 85 °C (Grafic 1). According to Karaoglu et al. (2010), the optimum working temperatures of wild type and recombinantly produced *A. gonensis* GI were found to be 85 °C (Karaoglu et al., 2013). In this case, the optimum working temperatures of immobilized enzymes and free enzymes are the same.

After immobilization of the enzymes to any matrix, different changes can occur on the surface of enzyme because of the different charge distribution of the matrix surface and the interaction of the enzyme with the matrix. These changes can cause differences between the optimum working pH values of the immobilized enzyme and the free enzyme. In this study, the maximum working pH value of the immobilized enzyme was found to be as 6.5 (Grafic 2). Similarly, according to the study performed by Karaoglu et al. (2010), the optimum pH value of free enzyme was 6.5. Immobilization of the enzyme on chitosan beads did not cause any changes in the enzyme's optimum pH values.

As a result of analysis, the K_m value of the enzyme was calculated as 134,18±3.69 mM and the V_{max} value as 64,94±0,48 µmol/min/mg protein. As a result of calculations made with this data, kcat value is calculated as 206,9071/sec. The value of catalytic activity, kcat/K_m, was calculated as 1.54 (Grafic 3). The gene encoding *A. gonensis* GI was cloned into an expression vector and the enzyme was recombinantly produced by Karaoglu (2013). K_m value of the free enzyme is 138.37 mM, while the K_m value of the immobilized enzyme is determined as 132.11 mM. When the V_{max} value of the free enzyme was calculated as 40.51, the V_{max} value of the immobilized enzyme was calculated as 65.46 µmol/min/mg protein in our study. Immobilization of enzymes often causes changes in the K_m and V_{max} values of the enzymes. In this study, however, a significant change in the kinetic parameters of the immobilized enzyme did not occur. In other words, AgoGI has been successfully immobilized on chitosan beads without any significant change in kinetic parameters (Table 2).

Table 2. The Kinetic parameter comparison of free enzyme and immobilized enzyme.

Glucose Isomerase	K_m (mM)	V_{max}(µmol/min/ mg protein)	References
AgoG2GI (WildType)	146,08±9,50	43,72±1,01	Karaoğlu (2010)
AgoG2GI (Recombinant)	138,37±7,63	40,51±0,81	Karaoğlu (2014)
Immobilized AgoGI	132,11±3.7	65,46±0,55	(This study)

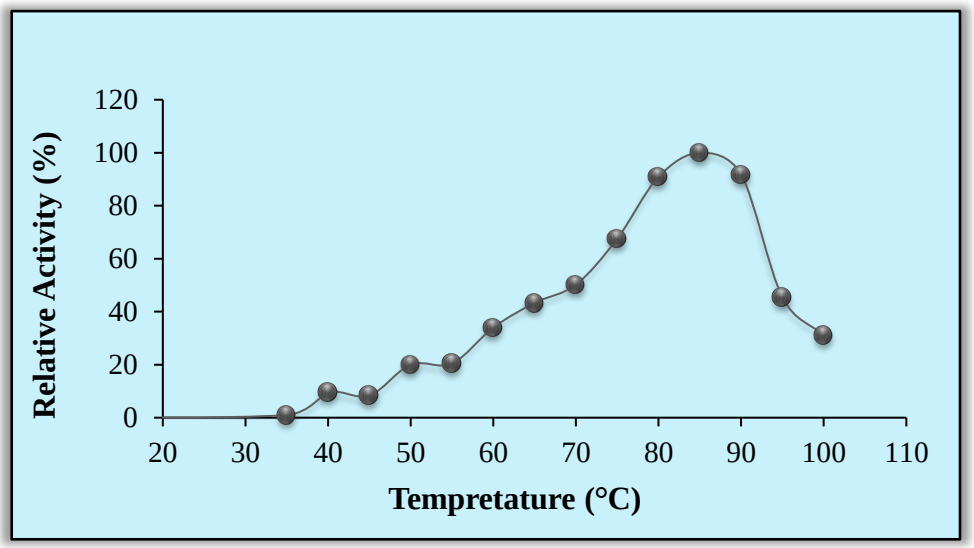

Figure 1. Effect of temperature on activity of the immobilized AgoGI

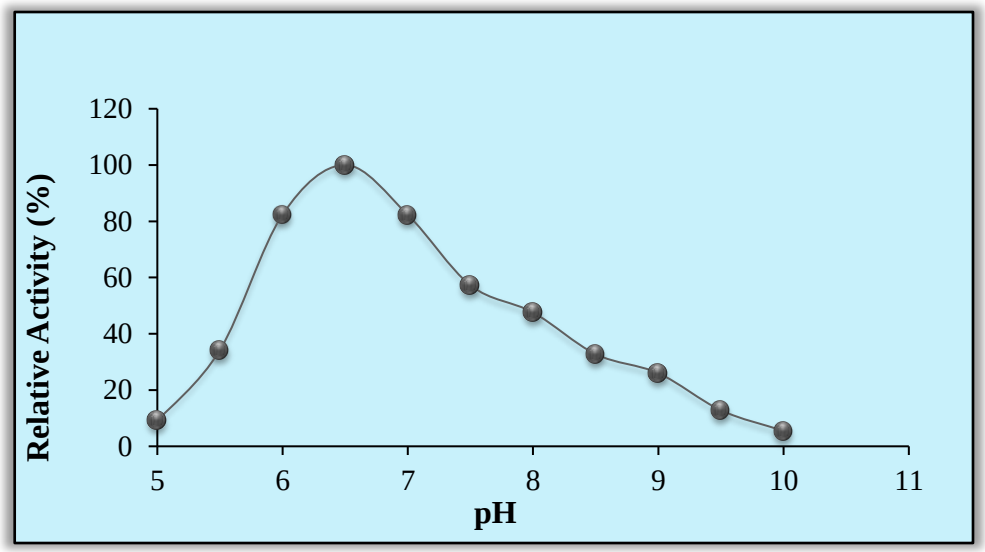

Figure 2. Effect of pH on activity of the immobilized AgoGI

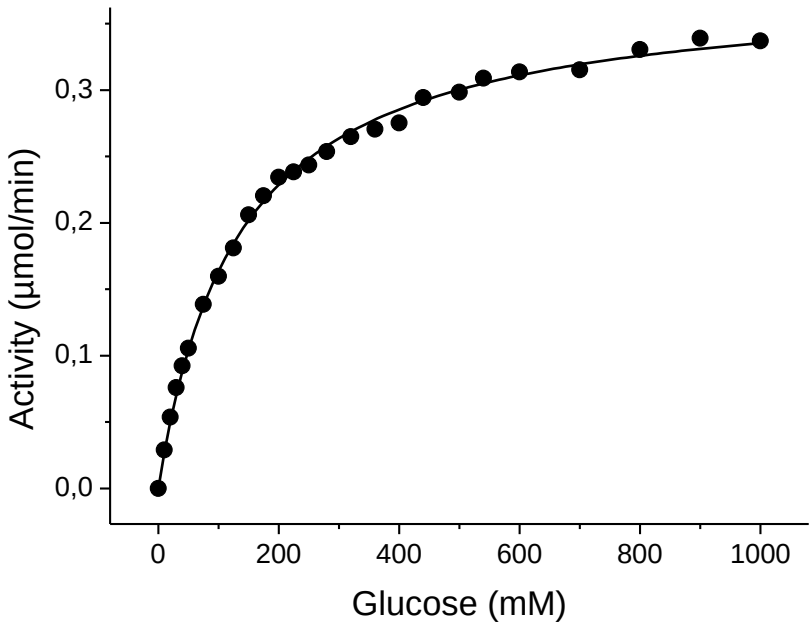

Figure 3. Kinetic Parameters of Immobilized AgoGI

Acknowledgement

I am gratefull Merve Kızaklı for her contribution. This study was supported by Rize Recep Tayyip University due to Project coded as BAP-2014.103.01.03.

References

Anon. (1993). Multifunctional sweeteners. Baking and Snack. 15 (4), 31-34.

Bandlish, R.K., Hess, J. M., Epting, K.L., Vieille, C. (2002). Glucose to Fructose Conversion at High Temperatures with Xylose (Glucose) Isomerases from Streptomyces Murinus and to Hyperthermophilic Thermotoga Species. Biotechnology and Bioengineering, 80(2),185–194.

Bhosale, S. H., Rao, M. B., and Deshpande, V. V. (1996). Molecular and industrial aspects of glucose isomerase Archive of Microbiological Rewievs, 60, 280-300.

Bickerstaff, G.F. (1997). Immobilization of Enzyme as the 21 st Century Begins. Immobilization of Enzyme and Cells, Humana Press, Totowa, New Jersey, 1;1-13.

Blow, D. M., Collyer, C. A., Goldberg J. D. ve Smart, O. S. (1992). Structure and mechanism of D-xylose isomerase. Faraday Discuss. (93): 67-73.

Bogumil, R., Kappl, J., Huttermann, C. ve Witzel, H. (1993). Xand Q-band EPR studies on the two Mn12-substituted metal-binding sites of D-xylose isomerase. European Journel of Biochemistry, 213, 1185–1192.

Bor, Y. C., Moraes, C., Lee, S.-P., Crosby, W. L., Sinskey, A. J., and Batt, C. A. (1992). Cloning and sequencing the Lactobacillus brevis gene encoding xylose isomerase. Gene 114:127–131.

Brady, D. and Jordan, J. (2009). Advances in enzyme immobilisation. Biotechnol Letters, 31;1639–1650.

Burg, B.V.D. (2003). Extremophiles as a source for novel enzymes. Current Opinion in Microbiology, 6: 213-218.

Burg, B.V.D. (2003). Extremophiles as a source for novel enzymes. Current Opinion in Microbiology, 6, 213-218

Cabral, J.M.S. and Kennedy, J.F. (1991). Covalent and coordination immobilization of proteins. In: Protein immobilization. Fundamentals and Applications (Taylor, R. F., ed.), Marcel Dekker, New York, NY, 73–138.

Chen, P., Anderson, A.W. and Han, Y.W., 1979. Production of Glucose Isomerase by Streptomyces flavogriseus. Applied Environmental Microbiology, 37,324–331.

Chen, W. P. (1980). Glucose İsomerase. Process Biochemistry, 15, 30–35.

CRA. 1994. Corn refining, the process, the products. Corn Refiners Association Inc.

Demain, A.L. and Solomon, N.A. (1981). In industrial microbiology and the advent of genetic engineering. Scientific American, Freeman and Company. San Francisco, 3-14.

Demirel, G., Özçetin, G., Şahin, F., Tümtürk, H., Aksoy, S., Hasırcı, N. (2006). Semi-interpenetrating Polymer Networks (IPNs) for Entrapment of Glucose Isomerase. Reactive & Functional Polymers, 66, 389–394.

Deraadt, A., Ebner, M., Ekhart, C. W., Fechter, M., Lechner, A., Strobl, M. ve Stutz, A. E. (1994). Glucose İsomerase (EC 5.3.1.5) as a reagent in carbohydrate synthesis: success and failures with

the isomerisation of nonnatural derivatives of D-Glucose into the corresponding 2-Ketoses. Catalysis Today, 22, 549–561.

Guisan, J.M. (2006). Method in biotechnology: İmmobilization of Enzymes and Cells. Humana Press, 450

Karaoglu, H., Yanmis, D., Sal, A., S., Celik, A., Canakci, S., Belduz, A., O. (2013). Biochemical characterization of a novel glucose isomerase from Anoxybacillus gonensis G2T that displays a high level of activity and thermal stability. Journal of Molecular Catalysis B: Enzymatic, 97, 215–224.

Keskin S., Ertunga N., Bektas, K. (2017). Covalent Immobilization of α-Amylase from Thermophilic Geobacillus sp. TF14 on Chitosan Beads. Sakarya University Journal of Science, 21(6), 1342-1348.

Xu H., Shen D., Wu X.Q., Liu Z.W., and Yang Q.H. (2014). Characterization of a mutant glucose isomerase from Thermoanaerobacterium saccharolyticum. Genetics and Molecular Biology of Industrial Organisms, 41, 1581-1589.

Yanmis D., Karaoglu H., Colak N.D., Sal F.A., Canakci S., and Belduz A.O. (2014). Characterization of a novel xylose isomerase from Anoxybacillus gonensis G2T. Turkish Journal of Biology, 38, 586-592.

Yanmis D., Karaoglu H., Colak N.D., Sal F.A., Canakci S., and Belduz A.O. (2014). Characterization of a novel xylose isomerase from Anoxybacillus gonensis G2T. Turkish Journal of Biology, 38, 586-592.

Actual Fish Fauna of İyidere Stream, Rize-Turkey

Davut TURAN [1*], Cüneyt KAYA [1], Esra BAYÇELEBİ [1] Bülent VEREP [1]

[1] Recep Tayyip Erdoğan University, Faculty of Fisheries, Rize, Turkey; dvtturan@yahoo.com; cnytkaya@yahoo.com; doganeesra@gmail.com; bulent.verep@erdogan.edu.tr

[*] **Corresponding Author:** dvtturan@yahoo.com

Abstract

İyidere is an 80 kilometres long stream that flows through the Ovit Mountain to the southeastern Black Sea in İyidere district. Fieldworks were carried out between 2004 and 2018 in order to reveal the fish fauna of the İyidere Stream. Fish samples from 10 stations in the Rize province were collected and assessed systematically. Five hydroelectric power plants were built on the stream. Before these hydroelectric power plants were established, 14 species (*Lampetra lanceolata, Liza aurata, Mugil cephalus, Ponticola rizensis, Salmo coruhensis, S. rizeensis, Squalius orientalis, Chondrostoma colchium, Alburnoides fasciatus, Barbus tauricus, Capoeta banarescui*, *Rutilis frisii, Alburnus derjugini, Cobitis splendens*) were identified according to previous studies. As a result, after the establishment of the hydroelectric power plants, a serious reduction in the population density of all species was observed. However, *Rutilus frisii* and *Cobitis splendens* were not found again.

Keywords: Biodiversity, fish fauna, İyidere Stream, Anatolia

1. Introduction

Although there is no big river in the Rize province, there are many coastal streams along the shore. The most important of these streams are Fındıklı, Fırtına, Hemşin, Çayeli, Taşlıdere and İyidere. İyidere is an 80 kilometres long stream that flows through the Ovit Mountain to the southeastern Black Sea in İyidere district. Thirteen (*Lampetra lanceolata* (Kux & Steiner 1972), *Liza aurata* (Risso 1810), *Mugil cephalus* (Linaeus 1758), *Neogobius kessleri* (Günther 1861), *Salmo trutta labrax* (Pallas 1811), *Leuciscus cephalus* (Linnaeus 1758), *Chondrostoma colchium* (Kessler 1899), *Alburnoides bipunctatus* (Bloch 1758), *Barbus taurucus escherichi* (Berg 1917), *Capoeta tinca* (Heckel 1843), *Rutilis frisii* (Nordmann 1840), *Chalcalburnus chalcoides* (Güldenstaedt 1772), *Cobitis splendens* (Erkakan et al. 1999)) fish species belonging to 6 families have been reported (Kutrup, 1994; Turan, 2003, Verep et al. 2005). Bayçelebi et al. (2017) also reported 14 species from İyidere (see. Table 1) based on fish materials collected between April 2004 and April 2014.

In this study, the effects of five hydroelectric power plants, which were established after 2005 in Iyidere Stream (see Table 1), on fish fauna were investigated and current taxonomic positions and their stock densities of the determined species were reviewed.

Table 1. Hydroelectric Plants on İyidere

Name of the company	Name of the station	License Date	License Duration
Zorlu doğal elektrik üretimi Inc.	ZORLU HPP	1950-1955	30
Sanko Inc.	CEVİZLİK HPP	11.08.2010	-
Sanko Inc.	YOKUŞLU HPP	14.09.2006	49
Sanko Inc.	KIZILAĞAÇ HPP	30.12.2012	-
Laskar Enerji üretim Inc.	İNCİRLİ HPP	24.08.2005	-
Mertler enerji Inc.	SARAY HPP	31.03.2014	-

2. Material and Method

Fish samples were caught at 6 different sampling sites in İyidere Stream (Figure 1) with pulsed DC electro-fishing equipment, cast net and gill net between 2004 and 2018. Fish samples were fixed in 4% formalin and transferred to the laboratory for morphological investigation. We also followed Turan (2003) and Bayçelebi et al. (2017) for identification.

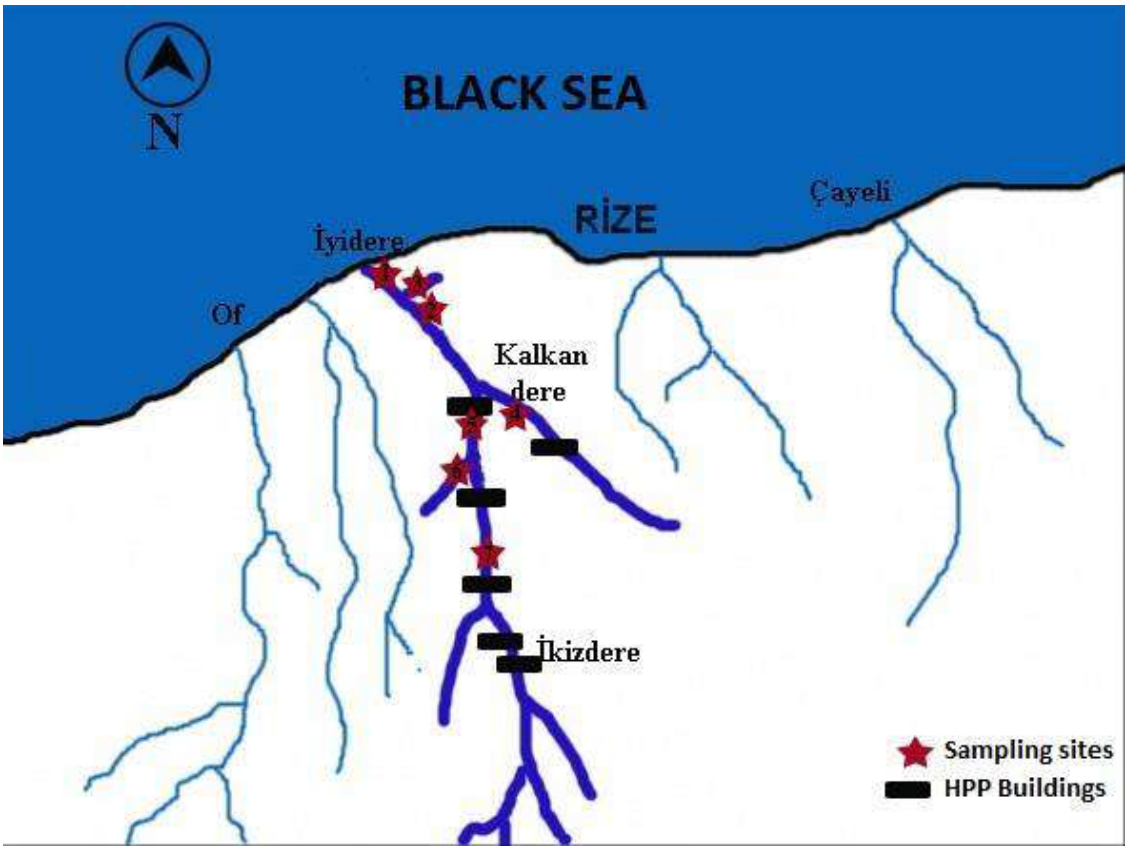

Figure 1. Sampling sites and HPP buildings on the İyidere Stream

3. Results and Discussion

In this study, it has been determined that there are 14 different fish species in the İyidere Stream. Our taxonomic results support Bayçelebi et al. (2017)'s taxonomic findings.

We have not found *Rutilus frisii* and *Cobitis splendens* in the İyidere stream and its tributaries in recent years.

We could not observed *Capoeta banarescui* and *Chondrostoma colchicum* in the main stream, although they were previously identified in İyidere where is the HPP established. But we found both species in two different restricted tributaries of the İyidere stream.

In addition to this, it was found that the *Lampetra lanceolata* species, which was known to be distributed up to 15 km inland from the mouth of the river, has been found to be distributed only a few km inland from the mouth of the river. In this study and in previous studies, no exact

stock determination was provided. However, considering the abundance of fish in previous studies, significant decrease in the number of individuals in the unit area was observed.

Furthermore, all other species have had reduction in their stock density.

3.1. *Lampetra lanceolata* Kux & Steiner, 1972

Figure 2. General apparence of *Lampetra lanceolata*

3.2. *Salmo coruhensis* Turan, Kottelat & Engin, 2010

Figure 3. General apparence of *Salmo coruhensis*

3.3. *Salmo rizeensis* Turan, Kottelat & Engin, 2010

Figure 4. General apparence of *Salmo rizeensis*

3.4. *Ponticola rizensis* (Kovacic & Engin, 2008)

Figure 5. General apparence of *Ponticola rizensis*

3.5. *Mugil cephalus* Linnaeus, 1758

Figure 6. General apparence of *Mugil cephalus*

3.6. *Chelon auratus* (Risso,1810)

Figure 7. General apparence of *Chelon auratus*

3.7. *Cobitis splendens* Erk'akan, Atalay-Ekmekçi & Nalbant, 1998

Figure 8. General apparence of *Cobitis splendens*

3.8. *Barbus tauricus* Kessler, 1877

Figure 9. General apparence of *Barbus tauricus*

3.9. *Chondrostoma colchicum* Derjugin, 1899

Figure 10. General apparence of *Chondrostoma colchicum*

3.10. *Squalius orientalis* Heckel, 1847

Figure 11. General apparence of *Chondrostoma colchicum*

3.11. *Rutilus frisii* (Nordmann, 1840)

Figure 12. General apparence of *Rutilus frisii*

3.12. *Alburnoides fasciatus* (Nordmann, 1840)

Figure 13. General apparence of *Alburnoides fasciatus*

3.13. *Alburnus derjugini* Berg, 1923

Figure 14. General apparence of *Alburnus derjugini*

3.14. *Capoeta banarescui* Turan, Kottelat, Ekmekçi & Imamoglu, 2006

Figure 15. General apparence of *Capoeta banarescui*

In parallel with the increasing energy demand in Turkey, the importance of renewable and cheap hydroelectric power plants (HPPs) has increased. As a result of the structure of hydroelectric power plants, some of the streams are removed from the natural river bed. Depending on the seasons, some amount of water is released from the reservoirs. These systems are estimated to have adverse effects on the ecological balance. Fish and other aquatic organisms play an important role in this balance. In order to maintain their generations, fish migrate during the specific months. These migrations are possible by flowing water from the river bed and planning the design of fish passages in accordance with the natural life. Thus, fishes in the environment will be able to survive together with HPPs. However, in our observations, it was determined that the number of individuals in the unit area decreased significantly. Serious studies are needed on the stock structure of fish species in these areas. In this wise, the impact of HPPs on fish species and stocks will be explained in detail.

Acknowledgement

We would like to thank to Tanju Mutlu, Akif Er and Şeyda Kumtepe for assistance in the field.

References

Bayçelebi, E., Kaya, C., and Turan, D., (2017). Rize İli'nin Güncel Balık Faunası, Journal of Anatolian Environmental&Animal Sciences, 43-46.

Kutrup B., (1994). Trabzon Yöresindeki Tatlısu Balıklarının Taksonomisi ve Ekolojik Özellikleri Üzerine Araştırmalar (Doktora Tezi), K.T.Ü. Fen Bilim. Enst., Trabzon, 64.

Turan D., (2003). Rize ve Artvin Yöresindeki Tatlısu Balıklarının Sistematik ve Ekolojik Yönden İncelenmesi. Phd thesis. İzmir: Ege Üniversitesi Fen Bilimleri Enstitüsü.

Verep, B., Şahin, C., and Turan, D., (2005). İyidere (Trabzon)'nin Fiziko-Kimyasal Açıdan Su Kalitesinin Belirlenmesi, EKOLOJİ, 14 (34), 26-35.

ECOLOGY, BIOLOGY, MARITIME SCIENCES

POSTER PRESENTATIONS

Investigation of Antimicrobial Activities of Various Solvent Extracts of Endemic *Achillea teretifolia* (Civan Perçemi) from Gümüşhane

Tuba ACET

1Gümüşhane University, Faculty of Engineering and Natural Sciences, Department of Genetic and Bioengineering, Gümüşhane, TURKEY,

Abstract

In this study, I investigated antimicrobial activities of *Achillea teretifolia* (endemic) plants which using by rural people as a folk medicine in Gümüşhane. These plants were collected from Gümüşhane, have extreme climate conditions and difficult habitat, during flowering time (July) and dried. The plant materials (10 g) were extracted with 200 ml each solvents (ethanol, methanol and ethyl acetate) at 37 °C 125 rpm during 24 h. The extracts were filtered and then concentrated. Disk diffusion method was used for determine antimicrobial activity. Fourteen microorganisms were preferred to detect the activity. 10 mg/ml stock solution was prepared by plant extract dissolved in DMSO. Then extract impregnated discs were put on petri dishes with inoculated test organisms (0.5 McFarland). After this treatment petri dishes were incubated at 37 °C and 25 °C for bacteria and yeast, respectively. Afterwards 2 days incubation, inhibition zone around the discs was measured as millimetre. As a positive control chloramphenicol was used equal concentration with samples. Finally, the extracts exhibited antimicrobial activity against to at least one test organisms. Ethanol extract of flower has exhibited significant antimicrobial activity on *Candida albicans* with 18 mm inhibition zone. Ethyl acetate extract of flower has shown strong antimicrobial activity on *Bacillus cereus* with 11 mm inhibition zone. Consequently, it has believed that *Achillea teretifolia* might have potency to be used as a natural antimicrobial agent.

Keywords: Antimicrobial, Ethanol, Methanol, Ethyl acetate, *Achillea teretifolia*

1. Introduction

The *Achillea* genus has 49 species (58 taxa) occurring in five sections and 24 of them are endemic in Turkey (Güner et al, 2012). Not only in Turkey but also around world *Achillea* species is an important biological resource in folk medicine against most of health problems. According to literature, some *Achillea* extracts exhibit rich pharmacologic activities such as anti- oxidant, anticancer (Bali et al, 2015), antimicrobial (Karaalp et al, 2009), wound healing (Akkol et al, 2011), antidiabetic (Conforti et al, 2005), anti- inflammatory (Küpeli et al, 2007), antihypertensive, and antihyperlipidemic properties (Asgary et al, 2000).

Although, there are some reports about this plant's antimicrobial properties, this is the first report demonstrating the potential anti- microbial effect of *Achillea teretifolia* plants which collected from Gümüşhane, Artabel area. As we already know that plants can accommodate their land by using more and different kind of seconder metabolites like phenolic and flavonoids, they have a big role on radical scavenger systems and effect on microorganisms. In addition, plants can store these kinds of metabolites in stems or flowers. Because of that, we investigated of antimicrobial activities of various solvent extracts of endemic *Achillea teretifolia* (Civan Perçemi) from Gümüşhane which using by rural people as a folk medicine.

2. Material and Method

2.1. Collection of Plant material:

This research was carried out in Gümüşhane University, Department of Genetic and Bioengineering Research Lab. Plant samples were collected from Gümüşhane Artabel Natural Park, Beşgöller around, 2800-3000 m. during flowering time (July). The plant aerial parts were chopped, dried and powdered. The plant materials (20 g) were extracted with 400 ml each solvent at 37 °C 125 rpm during 24 h. The extracts were filtered using Whatman filter paper (No: 1) and then concentrated under vacuum at 40 °C using a Rotary evaporator. The residues obtained were stored in a freezer at -20 °C until further tests.

2.2. Preparation of the extracts:

The plant materials (10 g) were extracted with 200 ml each solvents (ethanol, methanol and ethyl acetate) at 37 °C 125 rpm during 24 h. They air-dried and finally ground plant samples extracted by using solvents. Extracts were in filtered by using filter paper and solvent evaporated under vacuum.

2.3. Antimicrobial Activity:

Disk diffusion method was used for determine antimicrobial activity. Fourteen microorganisms were preferred to detect the activity. 10 mg/ml stock solution was prepared by plant extract dissolved in DMSO. Then extract impregnated discs were put on petri dishes with inoculated test organisms (0.5 McFarland).

After this treatment petri dishes were incubated at 37 °C and 25 °C for bacteria and yeast, respectively. Afterwards 2 days incubation, inhibition zone around the discs was measured as millimetre. As a positive control chloramphenicol was used equal concentration with samples.

3. Results and Discussion

The extracts exhibited antimicrobial activity against to at least one test organisms (Table 1-2). Ethanol extract of flower has shown the highest antimicrobial activity on *Candida albicans* with 18 mm inhibition zone. Ethyl acetate extract of flower has shown strong antimicrobial activity on *Bacillus cereus* with 11 mm inhibition zone. Therefore, it has believed that *Achillea teretifolia* might have potency to be used as a natural antimicrobial agent.

According to the previous studies, we found that ethanol extracts of plant flowers exhibited high amount of fenolic and flavanoid content compare to others. So, there might be a positive correlation between antimicrobial activity and phenolic/flavanoid content.

This is the first report demonstrating from Gümüşhane Artabel Area, the potential antimicrobial effects of *A. teretifolia* extracts. Further investigations about the extracts in animal models are needed for additional understanding of in vivo activity.

Our in vitro results show that the extracts, especially ethanol and ethly acetate extract of flowers could be used as antimicrobial agents.

Table 1. Disc diffusion zones of plant stem extract

Plant Part		Microorganisms	Ethanol	Methanol	Ethyl Acetate	Positive Control (Chloramphenicol)
Stem	Gram (+) bacteria	*B. cereus*	8	7	9	20
		MRSA	-	-	-	15
		L. monocytogenes	-	-	9	18
	Gram (-) bacteria	*K. pneumoniea*	7	7	7	18
		E. coli	8	8	8	13
		V. parahaemolyticus	-	8	9	11
	Yeast/	*C. albicans*	8	9	9	-

Table 2. Disc diffusion zones of plant flower extract

Plant Part		Microorganisms	Ethanol	Methanol	Ethyl Acetate	Positive Control (Chloramphenicol)
Flower	Gram (+) bacteria	*B. cereus*	9	-	**11**	20
		MRSA	7	-	-	15
		L. monocytogenes	-	-	9	18
	Gram (-) bacteria	*K. pneumoniea*	-	7	7	18
		E. coli	-	8	8	13
		V. parahaemolyticus	-	7	8	11
	Yeast/	*C. albicans*	**18**	-	9	-

Acknowledgement

This work was financially supported by the Scientific Research Project Coordination Unit of Gümüşhane University (Project code: 16.F5119.02.01).

References

Akkol, E. K,, Koca, U., Pesin, I., and Yilmazer, D., (2011). Evaluation of the wound healing potential of *Achillea biebersteinii* Afan. (Asteraceae) by in vivo excision and incision models. Evidence-Based Complementary and Alternative Medicine, 2011, 474026.

Asgary, S., Naderi, G. H., Sarrafzadegan, N., Mohammadifard, N., Mostafavi, S., and Vakili, R., (2000). Antihypertensive and antihyperlipidemic effects of *Achillea wilhelmsii.* Drugs Experiment of Clinical Research, 26, 89- 93.

Bali, E. B., Açık, L., Elçi, P., Sarper, M., Avcu, F., and Vural, M., (2015). In vitro anti- oxidant, cytotoxic and pro- apoptotic effects of *Achillea teretifolia* Willd extracts on human prostate cancer cell lines. Pharmacognosy Magazine, 44, 308-315.

Conforti, F., Loizzo, M. R., Statti, G. A., and Menichini, F., (2005). Comparative radical scavenging and antidiabetic activities of methanolic extract and fractions from *Achillea ligustica* ALL. Biological and Pharmaceutical Bulletin, 28,1791- 4.

Karaalp, C., Yurtman, A. N., and Yavasoglu, N. U., (2009). Evaluation of anti- microbial properties of *Achillea L.* flower head extracts. Pharmacotical Biology, 47,86- 91.

Küpeli, E., Orhan, İ., Küsmenoğlu, Ş., and Yeşilada, E., (2007). Evaluation of anti- inflammatory and anti- nociceptive activity of five anatolian Achillea species. Turkish Journal of Pharmaceutical Science, 4, 89- 99.

Books:

Güner, A., Akyıldırım, B., Alkayış, M. F, Çıngay, B., Kanoğlu, S. S., and Özkan, A. M., (2012). Türkçe bitki adları. In: Güner A, Aslan S, Ekim T, Vural M, Babaç MT, editors. Türkiye Bitkileri Listesi (Damarlı Bitkiler). İstanbul: Nezahat Gökyiğit Botanik Bahçesi ve Flora Araştırmaları Derneği Yayını.

Effects of Shipyards on Environment

Muhammet BORAN[1*], Nigar ALKAN[2]

[1]Karadeniz Technical University, Faculty of Marine Sciences, Department of Maritime Transportation and Management Engineering, Trabzon, Turkey; mboran@ktu.edu.tr

[2]Karadeniz Technical University, Faculty of Marine Sciences, Department of Fisheries Technology Engineering, Trabzon, Turkey: anigar@gmail.com

[*] **Corresponding Author:** mboran@ktu.edu.tr

Abstract

In this study, the effects of the activities carried out on shipyards were determined. A shipyard is a facility for shipbuilding, repair, maintenance, and shipbreaking. Some shipyards also manufacture offshore oil and gas drilling platform. Because shipyards are located on the water, pollution created by shipyard activities can fall into the water directly or be carried in by runoff. Activities that are gradually generating environmental pollution in shipyard; welding operation, surface treatment operation include painting and coating, abrasive blasting operations, ship repair and maintenance. Surface treatment is among the most environmentally hazardous process in shipyard. Ship maintenance and repair will be generating of dangerous waste of oil, hydraulic fluids and lubricants, thinners, acid and anti-freeze. Sewage of shipyard employee also causes environmental pollutions.

Key Words: Shipyard, environmental pollution, water pollution, ship building, ship repairing.

1. Introduction

The shipbuilding and repair industry builds and repairs ships, barges, and other large vessels, whether self-propelled or towed by other craft. Ship construction and ship repairing have many industrial processes in common (EPA, 1997). The main inputs at shipyards are steel plate, energy and labor. Large quantities of steelwork may be stockpiled, prior to shot blasting to remove oxidized layers and application of primer coat. The activities can occur in the open air or in purpose built facilities (EBRD, 2008). There are several wastes and pollutants being released during shipbuilding and ship repairing processes. The volume of these wastes and pollutants create a huge amount with major risk on environmental and ecological point of interest. Modern and environmentally friendly production techniques reduce the volume of wastes that effects the environment (Bilgili ve Çelebi, 2013). This is crucial for the protection of environment from pollutants originating from shipyards.

Steel and other metals, paints, solvents as much as means of grinding and sandblast residues, are strongly related to the raw materials used by the shipbuilding and repairing industry. A large variety of chemicals for the preparation and finishing of the surfaces are in use, such as the de-greasing solvents, acid and alkaline cleaning agents, metal covering solutions (Papaioannou, 2003).

In shipbuilding industry more activities have been doing in open air environment, and secondly most activity near by the waterfront location. This is clearly defining the potential pollutants to go directly into the aquatic environment. Hence those been raised more pollution and give significant impact to the environment (Mohamed, 2013).

Shipyards generate large quantities of wastes that cause environmental pollution. The main propose of this study is to reveal the effects of shipyards to the environment.

2. Material and Method

This manuscript reviews available studies on the effects of shipyards to the environment. This includes different kind of facilities.

3. Results and Discussion

The shipyard processes such as construction, maintenance and repairing activity creates a tremendous amount of pollution to the environment. The construction phase in shipyard is a significant number of processes which are constituted with significant changes to the environment (Mohamed, 2003). Various types of solid, liquid and gaseous form of wastes are known as the outcome of shipbuilding and ship repair processes. Solid wastes to be generated as a result of ship construction and ship repair are, metal wastes, used welding electrodes and scrap material, welding slag, steel ball, packing wastes, wood, metal and so on. Liquid wastes from shipyards are domestic process wastewater hydraulic machine oils, cutting (Boron) oils, sewage and bilge water. Pipe workshop and in the plant and warm-up activities can cause air pollution (Bas et al., 2007). These contaminants may affect water, air and soil unless preventive actions are considered. The effect of these contaminants on workers health is as important as the environmental effect (Celebi et al., 2009).

Polluting activities, involved in ship building and ship repairing facilities are cleaning and de-greasing, preparation for painting, paints of metallic parts, vessel construction with use of fiber glass, scrapping and operational emissions (Papaioannou, 2003).

A large variety of chemicals for the preparation and finishing of the surfaces are in use, such as the de-greasing solvents, acid and alkaline cleaning agents, metal covering solutions. Solvents are commonly used to formulate both bottom paints and coatings used for topside applications such as corrosion resistance. Furthermore, particles, lubricants solutions and resins waste, metal containing sludge, paint color or polishing residues are considered to be the usual pollutants (Papaioannou, 2003; EBRD, 2008).

Painting and coating waste can account for more than 50% of total dangerous waste generated at shipyard. Both activity use significant number of chemicals that hazardous or flammable, such as thinner or solvent, and activity release significant air pollutants including lead, particulate matter, volatile organic compound copper, zinc and the waterfront locations of shipyards increase the potential for pollutants to reach bodies of water. Many of the coatings used on hulls contain anti-fouling heavy metals, such as copper and zinc. Paints containing tributyltin (TBT) are used as anti-fouling paint in the past. TBT is now banned globally but still remains as a hazardous substance on the hull of older vessels and is a concern during maintenance and servicing of hulls in shipyards. The metals are toxins added to marine coatings to prevent marine organisms from building up on ship hulls, which reduces speed and fuel

efficiency. When ships hull is prepared for painting, the first stage typically is pressure washing to remove any marine growth on the hull and/or to remove old paint. This wash water characteristically contains high levels of heavy metals from the removed paints (Mohamed, 2003; EBRD, 2008).

Maruyama at al. (1983) discussed by determining PCB concentrations in sediment, in water, and in biological samples. PCBs were detected in all samples, in which much higher concentrations, more than 10 μg/g, were found in three sediment samples where located near the shipyard drains. They found out that the results strongly suggest that the shipbuilding is primarily responsible for the PCB pollution in Nagasaki Bay.

Noise coming from shipyards has a great influence on the nearby surrounding areas, decreasing with increasing distance from the shipyards and almost disappearing beyond a given distance (Chung et al., 2011). Workers in shipyard may exposed to continuous sound levels of between 85 dbA to 105 dbA (Mohamed, 2013).

Shipyards generate large quantities of wastes, management of which assume prime importance owing to the extent of pollution. Pollution prevention is the best sought out method for reducing pollution. Many options are available for reducing the extent of pollution from shipyard processes most of them being source reduction methods (Papaioannou, 2003).

In general there is already a large potential in the shipbuilding industry for eliminating much of the environmental stress by adopting new technologies and materials which are optimized for better product and environmental performance, as well as by implementing new design processes that pay respect to life-cycle thinking. As a start, with freight rates being historically low, combined with the current over-capacity of ships, retrofitting of already existing and cost-effective technologies could be an opportunity for otherwise financially challenged, but technologically advanced, shipyards and shipping companies to reduce their fuel consumption and gain an economic advantage in the industry (Papaioannou, 2003).

There are several different function that occur at shipyards. Each of shipyards creates their own unique set of potential environmental problems. Pollution can occur simultaneously with the variety of operation at shipyards.

References

Baş, B., Ölmez, T., Tünay, Ö., Kabdaşlı, I. and Kabdaşlı S., (2007). Bir tersanenin kirlilik profilinin oluşturulması ve atık azaltımı için örnek çalışma. *6. Ulusal Kıyı Mühendisliği Sempozyumu*, İzmir 2007.

Bilgili, L. ve Çelebi U.B., (2013). An innovative method establishment for a green shipyard concept. *2nd International Conference on Sustainable Intelligent Manufacturing* (SIM), Lisbon, Portugal.

Celebi, U.B., Akanlar, F.T. and Vardar, N., (2009). Chemicals and hazardous wastes generated by shipyard production and their effects on human health at workplace. *Fresenius Environmental Bulletin*, 18(10), 1901-1908.

Chung, j.W., Lee, M.E. and Lee, H.D., (2011). Characteristics of environmental pollution related with public complaints in an industrial shipbuilding complex, Korea. *Environ. Monit. Assess*., 177, 73–84.

EPA, (1997). Profile of the Shipbuilding and Repair Industry, EPA Office of Compliance, EPA/310-R-97–008.

European Bank for Reconstruction and Development (EBRD). Environmental and Social Policy May 2008. Performance Requirement 2: Labour and Working Conditions. Retrieved from http://www.ebrd.com/enviro/ tools/index.htm.

Maruyama, K., Sahrul, M., Tanabe, S. and Tatsukawa, R. (1983). Polychlorinated biphenyl pollution from shipbuilding in Nagasaki Bay, Japan. *Ecotoxicology and Environmental Safety*, 7 (5), 514-520.

Mohamed, H.S., (2003). Environmental management in shipbuilding industry, Bachelor Environmental & Occupational Health and Safety, Faculty of health School of Health Science, The University of Newcastle, Australia.

Papaioannou, D., (2003). Environmental implications, related to the shipbuilding and ship repairing activity in Greece, *Pomorski zbornik* 41 (1), 241-252.

PHYSICS AND STATISTICS

ORAL PRESENTATIONS

Molecular Structure and Spectroscopic Properties of 5-amino-2-hydroxybenzoic acid

Hamit ALYAR [1*], Bilal CANGÜL [2], Saliha ALYAR[3]

[1] Çankırı Karatekin University, Faculty of Science, Department of Physics, Çankırı, Turkey; halyar@karatekin.edu.tr

[2] Çankırı Karatekin University, Faculty of Science, Department of Physics, Çankırı, Turkey; bilalcangul@gmail.com

[3] Çankırı Karatekin University, Faculty of Science, Department of Chemistry, Çankırı, Turkey; saliha@karatekin.edu.tr

[*] **Corresponding Author:** halyar@karatekin.edu.tr

Abstract

In this work, the structure of 5A2HBA is optimized using density functional theory (DFT) method. The molecular geometry and vibrational band assignments are calculated using B3LYP/6-311++G(d,p) theory level The overestimations of the calculated wave numbers are corrected by the aid of scaled quantum mechanics force field methodology. The computational frequencies are found to be in good agreement with the experimental frequencies. 1H and 13C shielding tensors for 5A2HBA are calculated with GIAO/DFT/B3LYP/6-311++G(d, p) methods in DMSO. All calculations performed with Gaussian 09, Gauss View 5.0 and SQM 1.0 software.

Keywords: IR, NMR, DFT, B3LYP

1. Introduction

5-amino-2-hydroxybenzoic acid (5A2HBA) is the active component of sulfasalazine. Soluble in water and slightly soluble in alcohol but insoluble in ethanol. It is an anti-inflammatory drug that is used to treat inflammation of the digestive tract (Crohn's disease) and mild to moderate ulcerative colitis (Muthu and Paulraj, 2011). It is used in the synthesis of other organic compounds including pharmaceuticals. Synthesis and other investigations on the title compound and its derivatives have been carried out by many researchers. The role of a new H_2S-releasing mesalamine derivative (5-amino-2-hydroxybenzoic acid) has been reported (Distrutti et al., 2006).

In this study, vibrational band assignment of 5A2HBA were calculated using B3LYP/6-311++G(d,p) theory level. Also, ^{1}H and ^{13}C shielding tensors for 5A2HBA are calculated with GIAO/DFT/B3LYP/6-311++G(d,p) methods in DMSO.

2. Material and Method

The geometry of 5-amino-2-hydroxybenzoic acid was fully optimized without any constraint with the help of an analytical gradient procedure implemented within the Gaussian 09 program (Frish et al., 2009). All the parameters were allowed to relax and all the calculations converged to an optimized geometry which corresponds to a true energy minimum as revealed by the lack of imaginary values in the wave number calculations. The molecular geometry optimizations, vibrational frequency calculations, performed with the Gaussian 09 software package by using DFT/B3LYP approaches. Optimized molecular structure of studied compound given in Fig.1. The ^{1}H and ^{13}C NMR chemical shifts of the title compound were calculated in DMSO using the GIAO method. The vibrational band assignments were performed at B3LYP/6-311++G (d,p) theory level combined with scaled quantum mechanics force field (SQMFF) methodology. Each vibrational modes of the studied compound were characterized by their potential energy distribution (PED) which were calculated by using SQM-FF program (SQM, 2013).

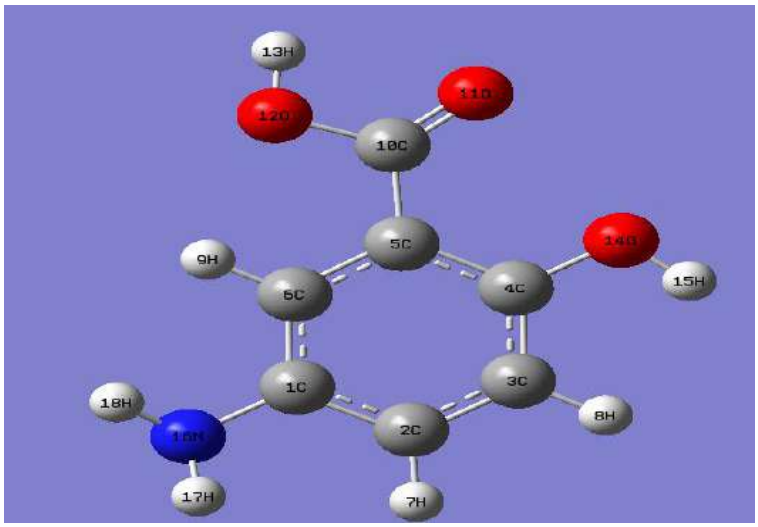

Fig.1 Molecular structure of 5-Amino-2-hydroxybenzoic aid obtained by B3LYP/6-311++G(d,p) method

3. Results and Discussion

3.1 Vibrational Band Assignment

Vibrational frequencies and corresponding vibrational assignments of 5-amino-2-hydroxybenzoic acid have been investigated theoretically. DFT/B3LYP is provides acceptable vibrational wave numbers for organic molecules. Vibrational frequencies of 5-amino-2-hydroxybenzoic acid were calculated at the DFT levels with B3LYP (Becke-Lee-Yang-Parr three parameters) hybrid functional (Lee at al.,1988). The vibrational band assignments were performed at B3LYP/6-311++G(d,p) theory level combined with scaled quantum mechanics force field (SQMFF) methodology to compare the experimental and calculated vibrational frequencies of the title compounds. The vibrational modes were assigned on the basis of PED analysis using SQM program. The visual check for the vibrational band assignments were also performed by using Gauss-View program.

Table 1. Assignment of fundamental vibrations of 5-amino-2-hydroxybenzoic acid by normal mode analysis based on SQM force field calculations using selective scaled B3LYP/6-311++G(d,p) (Experimental values taken from Muthu and Paulraj, 2011)

Mode	Exp. [XX]				PED
	FT-IR	FT-Raman	Unscaled Freq.	Scaled Freq.	Description (%)
48	3718	3737	3826	3677	υ (O14-H) (100)
47	3442	3690	3778	3631	υ (O12-H) (100)
46	3429	3629	3656	3515	υ_{as} (NH_2) (100)
45	3384	3180	3562	3424	υ_{s} (NH_2) (100)
44	3098	3088	3203	3066	υ (C6-H) (100)
43	3083	3059	3169	3034	υ_{s} (CH) (99)
42	2974	3021	3149	3014	υ_{as} (CH) (100)
41	1797	1769	1794	1789	υ (C=O) (85) + β (C18-OH) (5)
40	1650	1666	1668	1642	υ $(CC)_{ring}$ (56) + sci (NH_2) (33)
39	1619	1608	1655	1611	υ $(CC)_{ring}$ (58) + β (NH_2) (16)
38	1581	1548	1630	1583	υ $(CC)_{ring}$ (63) + β (COH15) (10)
37	1493	1494	1539	1498	υ $(CC)_{ring}$ (26) + υ (C4-O) (10) + β (CCH) (40)
36	1451	1448	1470	1435	υ $(CC)_{ring}$ (35) + β (CCH) (19) + β (CNH) (11) + β (CCN) (10)
35	1376	1389	1374	1334	υ $(CC)_{ring}$ (26) + υ (C5C10) (12) + υ (C-O12) (10) + β (CO-H13) (18) + β (COC) (10)
34	1352	1361	1346	1316	υ $(CC)_{ring}$ (27) + β (CO-H13) (18) + β (COC) (13) + β (CO-H15) (26)
33	1314	1312	1335	1301	υ $(CC)_{ring}$ (10) + υ (C4-O) (10) + β (CCH) (53) + β (CO-H15) (10)
32	1266	1281	1294	1263	υ (C4-O) (42) +υ $(CC)_{ring}$ (31)
31	1242	1237	1282	1255	υ (CN) (35) +υ $(CC)_{ring}$ (10) + β (CCH) (17) + β (CO-H13) (10)
30	1190	1194	1200	1164	υ $(CC)_{ring}$ (12) + β (CO-H15) (32) + β (CCH) (36) + β (CO-H13) (10)
29	1133	1158	1181	1146	υ $(CC)_{ring}$ (22) + υ (C5-C10) (10) + β (CCH) (44) + β (CO-H13) (18)
28	1117	1100	1154	1127	υ $(CC)_{ring}$ (15) + υ (C-O12) (15) + β (CCH) (23) + β (CO-H15) (17) + β (CO-H13) (10)
27	1087	1092	1107	1075	υ $(CC)_{ring}$ (24) + β (NH_2) (60)
26	1029	1036	1054	1042	υ (CO) (35) +υ $(CC)_{ring}$ (16) + β (CCH) (18) + β (CCC) (17)
25	948	962	944	919	υ $(CC)_{ring}$ (42) + υ (CN) (13) + υ (C5-C10) (12) + β (CCC) (10)
24	929	-	933	913	γ (CH) (85)
23	886	870	902	883	γ (CH) (82)
22	811	857	818	804	γ (CH) (75)

Table 1. Continued

21	796	810	801	792	υ (C – O14)(26) + υ $(CC)_{ring}$ (21) + υ (CN) (12) + β (CCC) (19)
20	772	751	796	785	β (CCH) (39) + T(CCCO)(27)+ τ(OCCH)(12)
19	714	742	735	724	υ $(CC)_{ring}$ (19) + υ (C10-O12) (12) + υ (C5-C10) (10) + β (CCC) (20) + β (CO_2) (16)
18	687	704	700	692	τ$(CCCC)_{ring}$(40) + τ$(CCCH)_{ring}$(21)+ τ(CCCO)(10)+ τ(OCOH)(10)
17	684	662	664	663	υ (CO)(10) + β (CO_2) (24) + β $(CCC)_{ring}$ (17) + β (C5-CO_2) (14)
16	641	596	618	604	γ (CNH_2) (83)
15	570	588	573	561	γ (OH13) (77)
14	560	542	543	542	β (C5C10-O12) (18) + β (CC-O14) (23) + β (CO_2) (10)
13	539	521	536	527	τ(CCO-H13)(26)+ τ$(CCCH)_{ring}$(21)+ τ$(CCCC)_{ring}$(10)
12	485	497	485	480	υ $(CC)_{ring}$ (20) + υ (CN)(16) + β $(CCC)_{ring}$ (40)
11	464	-	430	427	τ$(CCCC)_{ring}$(45) + τ$(CCCH)_{ring}$(20) + τ(CCC-O11)(14) + τ(CCO-H13)(13)
10		422	402	400	υ (C5-C10)(20) + β (CC-O14) (26) + β (CC-O11) (23)+ β $(CCC)_{ring}$ (15)
9		-	388	389	β $(CCC)_{ring}$ (10) + β (CC-N) (31) + β (CC-O12) (23) + β (CC-O11) (10)
8		354	360	358	τ$(CCCC)_{ring}$(10) + τ(CCCO)(28) + τ(CCCN)(22) + τ(CCHN)(10)
7		-	314	313	υ $(CC)_{ring}$ (10) + υ (CC) (11) + β $(CCC)_{ring}$ (11) + β (CC-O14) (28) + β (CCN) (26)
6		280	300	294	τ (CCO-H15) (96)
5		216	239	234	τ (CCNH) (99)
4		173	196	197	β $(CCC)_{ring}$ (64) + β (CCO) (16) + β (CCN) (10)
3		-	164	164	τ$(CCCC)_{ring}$(30) + τ (CCCN)(21) + τ (CCCO)(20)
2		-	116	116	τ$(CCCC)_{ring}$(40) + τ (CCCO)(32)
1		-	20	20	τ (CCCO)(96)

ν, *stretching*; νs, *symmetric stretching*; νas, *asymmetric stretching*; β, *in-plane bending*; γ, *out of plane bending*; δ, *scissoring*; ω, *wagging*; ρ, *rocking*; t, *twisting*; τ, *torsion*

In order to enable assignment of the observed peaks, we have analyzed the all vibrational frequencies and compared our calculated results of the investigated compound with their experimental ones. The experimental frequencies are listed together with calculated frequencies in Tables 1. The calculated values of vibrations show good agreement with the experimental results as seen in Table 1.

O-H Vibrations

In the OH region, very strong and broad band occur at 3600 – 3400 cm^{-1}. Two OH stretching modes are observed at 3442 cm^{-1} and 3718 cm^{-1} in the FT-IR spectrum for 5A2HBA. This vibration observed at 3737 and 3690 cm^{-1} at Raman spectrum. These bands calculated at 3677 and 3631 cm^{-1}. These results suggest that one OH stretching possibly include in the formation of intra molecular hydrogen bonding.

C-H Vibrations

The aromatic C-H stretching vibrations were normally found between 3100 and 2900 cm^{-1}. The bands observed at 2974 and 3083 cm^{-1} in the FTIR spectrum and 3021 and 3059 cm^{-1} in the FT-Raman spectrum were assigned to C-H symmetric stretching vibrations. Similarly, the band observed at 3098 cm^{-1} in the FTIR spectrum and 3088 cm^{-1} in the FT-Raman spectrum was assigned to C-H asymmetric stretching vibration.

C-N Vibrations

Silverstein et al. assigned C–N stretching absorption in the region 1342-1266 cm^{-1} (Silverstein et al., 1981). The spectra of benzene and benzoic acid substituted compounds show the band in the region 1260- 1210 cm^{-1}. In analogy with the previous work, the band appears at 1242 cm^{-1} in FTIR spectrum and 1237 cm^{-1} in FT Raman spectrum of 5A2HBA are assigned to C–N stretching mode of vibration. Theoretically calculated at 1255cm^{-1}.

C-N Vibrations

The bands between 1650-1400 cm^{-1} in benzene derivatives were assigned to C-C stretching vibrations. In the present study, the frequencies observed in the FT-IR spectrum at 1581, 1493 and 1451 cm^{-1} have been assigned to C-C stretching vibrations. The same vibrations appear in the FT Raman spectrum at 1546, 1494 and 1448 cm^{-1}. The theoretically predicted frequencies at 1541, 1495 and 1450 cm^{-1} are in excellent agreement with experimental data.

3.2. ^{1}H and ^{13}C Spectral Analysis

Chemical shift values were calculated in ppm scale with reference to TMS molecule. Aromatic carbons gave signals with chemical shift values ranging from 86 to 123 ppm in the overlying regions of the spectrum. Because of the lesser degree of chemical screening on C10, it gave a greater chemical shift value. The chemical shift values of the H atoms were obtained at a very low level (≤ 8 ppm). The chemical shift values of the total of H and C atoms are given in Table 2.

Table 2. The experimental ^{13}C and ^{1}H NMR chemical shifts (ppm) together within the calculated data for 5-amino-2-hydroxybenzoic acid in DMSO-d_6 (Experimental values taken from Muthu and Paulraj, 2011)

Atom	Exp.	B3LYP/6-311++G(d,p)
C10	143.80	144.13
C5	86.90	82.67
C6	89.30	88.98
C1	109.50	106.35
C2	93.40	90.60
C3	96.70	96.78
C4	123.40	120.44
H9	8.16	7.04
H7	6.47	5.73
H8	6.71	6.01
H16	6.91	6.09
H15	3.48	3.50
H17	4.49	4.50
H18	4.32	4.16

References

Distrutti, E., Sediari, L., Mencarelli A., Renga, B., Orlandi, S., Russo, G., Caliendo, G., …et al., (2006). 5-amino-2-hydroxybenzoic acid and 4-(5-thioxo-5h[1,2]dithiol-3yl)-phenyl ester (atb-429), a hydrogen sulfide-releasing derivative of mesalamine, exerts antinociceptive effects in a model of postinflammatoryhypersensivity. J. Pharmacol Exp. Ther. ,319, 447-458.

Frisch, M. J. et al., Gaussian 09: Revision B.01 Gaussian Inc., Wallingford, CT, 2009.

Muthu, S.and Paulraj, E. I., (2011). Molecular structure, spectroscopic (FT-IR, FT-Raman, NMR) studies and first-order molecular hyperpolarizabilities of 5-amino-2-hydroxybenzoic acid (5A2HBA) by ab initio HF and density functional method. J. Chem. Pharm. Res., 3(5), 323-339.

Lee, C., Yang, W., and Parr, R. G., (1988). Development of the Colle-Salvetti correlation-energy formula into a functional of the electron density. Phys. Rev B., 37, 785-789.

SQM version1.0, Scaled Quantum Mechanical, 2013 GreenAcres Road, Fayetteville, Arkansas 72703.

Silverstein, R.M., Bassler, G.C., Morrill, T.C., (1981). Spectrometric Identification of Organic Compounds. New York: Wiley.

Crystal structure and Hirshfeld surface analysis of (E)-2,6-di-tert-butyl-4-{[2-(2,4-dinitrophenyl)hydrazinylidene]methyl}phenol

Cemile BAYDERE[1*], Sevgi KANSIZ[2], Necmi DEGE[3]

[1*]Ondokuz Mayıs University, Faculty of Arts and Sciences, Department of Physics, Samsun, Turkey; cemle28baydere@hotmail.com

[2]Ondokuz Mayıs University, Faculty of Arts and Sciences, Department of Physics, Samsun, Turkey; sevgi.koroglu@omu.edu.tr

[3]Ondokuz Mayıs University, Faculty of Arts and Sciences, Department of Physics, Samsun, Turkey; necmid@omu.edu.tr

[*] **Corresponding Author:** cemle28baydere@hotmail.com

Abstract

The molecular structure of (E)-2,6-di-tert-butyl-4-{[2-(2,4-dinitrophenyl)hydrazinylidene]methyl}phenol that formulated as $C_{21}H_{26}N_4O_5$ was determined by single-crystal X-ray diffraction. The crystal structure orthorhombic space group *Pnma*, with parameters a=18.7651(10) Å, b=6.9193(4) Å, c=17.259(1) Å, V=2240.9(2) Å^3, Z=4. In the crystal structure, intermolecular O—H···O hydrogen bond link molecules into a three-dimensional network. Also**,** there is an intramolecular O—H···O hydrogen bond present, forming an S(6) ring motif. Crystal Explorer program was used to determine remarkable interactions in the crystal. Hirshfeld surface analysis and two dimensional fingerprint plots have been investigated.

Keywords: Crystal structure, Hirshfeld surfaces, Schiff base, dinitrobenzene, X-ray.

1. Introduction

Schiff-bases are considered as an important class a versatile tool among organic compounds. They have wide applications in analytical chemistry, in medicine and in biological processes including antifungal, antibacterial and anticancer activities (Przybylski *et al.*, 2009). Schiff base ligands are considered privileged ligand since has also played an important role in the development of coordination and supramolecular chemistry (Moroz *et al.*, 2012; Sen *et al.*, 2018). This kind of ligands have a chelating structure to coordinate metal ions through the imine nitrogen and another group to form complexes (Moroz *et al.*, 2008; Moroz *et al.*, 2010). The complexes of Schiff bases have wide range of utilization in various areas of science such as in pharmaceutical, agriculture and industrial chemistry (Anis *et al.*, 2013; Sen *et al.*, 2018).

Thus, in this study, we designed a type of Schiff base with a sterically hindered phenol group to give (E)-2,6-di-tert-butyl-4-{[2-(2,4-dinitrophenyl)hydrazinylidene]methyl}phenol. We performed the characterization, the crystal structure and Hirshfeld surface analysis of the title Schiff base compound.

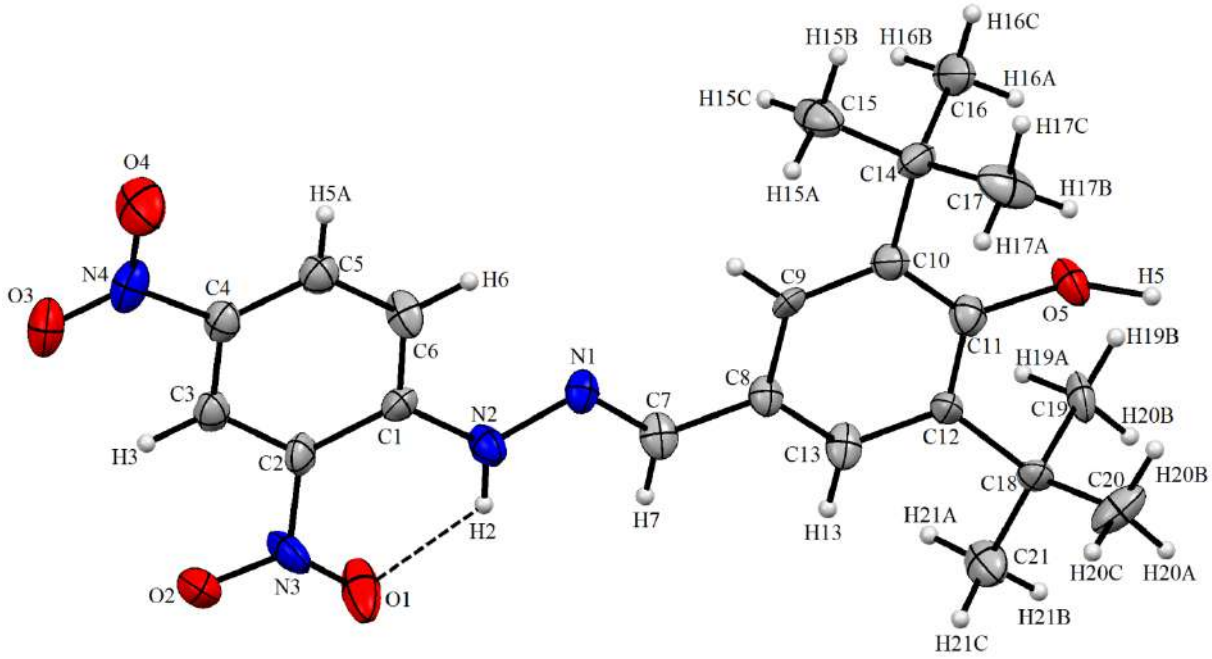

Figure 1. The molecular structures of the title compund showing the atom-numbering scheme.

2. Material and Method

The crystallographic measurements of $C_{18}H_{17}N_5O_2$ was performed on STOE IPDS 2 (*Stoe Imaging Plate Diffraction System II)* diffractometer with graphite-monochromatized Mo*K*α radiation (λ = 0.71073 Å). Data integration and reduction were performed with X-AREA (Stoe and Cie, 2002). Absorption correction (μ = 0.09 mm^{-1}) was made by the integration method with X-RED (Stoe and Cie, 2002). The SHELXT (Sheldrick, 2015a) software package was used for structure solution. All non-hydrogen atoms were refined anisotropically by the full-matrix least squares using SHELXL (Sheldrick, 2015b). ORTEP-3 for Windows (Farrugia, 2012) was used to preparation the figures. To prepare material for publication, WinGX (Farrugia, 2012) and publCIF (Westrip, 2010) software were used. All H atoms were positioned geometrically and refined using a riding model, restraining the bond lengths at 0.93 Å for aromatic C─H and 0.96 Å for other C─H atoms. For the hydrogen bondings analysis, the PLATON (Spek, 2003) software was used. Details of the crystal data, data collection and refinement process are listed in Table 1.

Crystal Explorer 17.5 (Turner *et al.*, 2017) was used to obtain the Hirshfeld surface and to analysis the interactions in the crystal. Also, the analysis of the associated two dimensional fingerprint-plot with Hirshfeld surface provide a appropriate tools of quantifying the interactions within the crystal structures.

Table 1. Crystal data and structure refinement parameters for the title compound.

Crystal Data	
Chemical Formula	$C_{21}H_{26}N_4O_5$
Formula weight (a.k.b.)	414.46
Temperature (K)	296
Crystal system	Orthorhombic
Space group	*Pnma*
Unit cell parameters	
a ≠ b ≠ c (Å)	18.7651 (10), 6.9193 (4), 17.259 (1)
Crystal size (mm)	0.22 × 0.15 × 0.11
Volume, V ($Å^3$)	2240.9 (2)
Z	4
μ (mm^{-1})	0.09
F_{000}	880

Calculated density (Mg/m^3)	1.228
Data collection	
Diffractometer	STOE IPDS 2
Wavelength (Å)	0.71073
θ range for data collection (˚)	$1.6 \leq \theta \leq 25.5$
Index ranges	
h_{min}, h_{max}	-22, 22
k_{min}, k_{max}	-8, 8
l_{min}, l_{max}	-20, 20
Measurement method	*ω* scan
Reflections collected	14854
Independent reflections	2270
Observed reflections [$I > 2\sigma(I)$]	912
Absorption correction	Integration
T_{min}, T_{max}	0.982, 0.994
R_{int}	0.105
Refinement	
Refinement method	SHELXL17/1
Parameters	178
$R[F^2 > 2\sigma(F^2)]$	0.071
$wR(F^2)$	0.215
GooF = S	0.96
$\Delta\rho_{min}$, $\Delta\rho_{max}$ ($e/Å^3$)	-0.16, 0.39

3. Results and Discussion

X-ray diffraction study of (E)-2,6-di-tert-butyl-4-{[2-(2,4-dinitrophenyl) hydrazinylidene] methyl}phenol has been carried out and the data obtained are presented in Table 1. The crystal structure of the compound, crystallized in a orthorhombic space group *Pnma*, with Z=4 for the formula unit, '$C_{21}H_{26}N_4O_5$'. A perspective view the compound is shown in Fig. 1 that shows one intramolecular (N2─H2···O1) hydrogen bond (Table 2).

Table 2. Hydrogen bonding geometry for the compound (Å, ˚).

D─H···A	*D*─H	H···A	*D*···A	*D*─H···A
N2─H2···O1	0.86	1.96	2.583 (8)	129
O5─H5···O1^{i}	0.82 (2)	2.28 (5)	2.782 (7)	120 (4)

Symmetry codes: (i) x+1/2, y, -z+3/2.

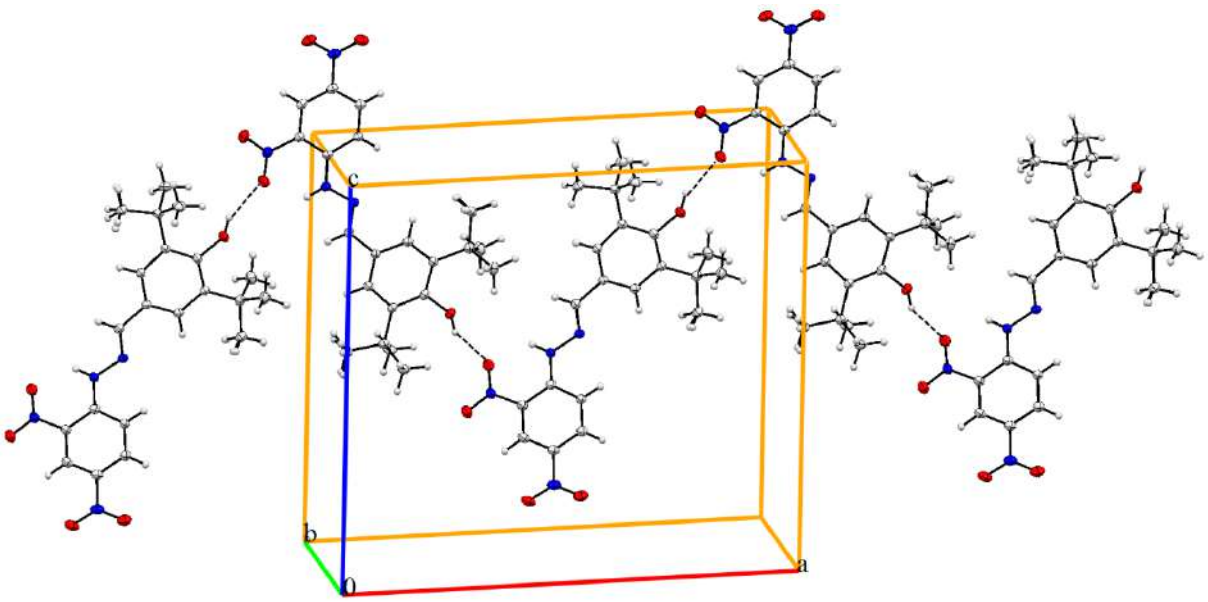

Figure 2. A partial view of the crystal packing of the title compound. Dashed lines denote the intermolecular O─H···O hydrogen bonding.

We used the Hirshfeld surface to get an idea of the presence of hydrogen bonds and intermolecular interactions in the crystal structure of compound and two-dimensional fingerprints calculated using the Crystal Explorer program (Turner *et al.*, 2017).

The maps of d_{norm}, d_i and d_e on molecular Hirshfeld surfaces were shown in Fig. 3 for the title compound. The red spots over the surface indicate the inter-contacts involved in strong hydrogen bonds and interatomic contacts (Aydemir *et al.*, 2018; Gümüş *et al.*, 2018; Kansız and Dege, 2018). The red spots on the d_{norm}, d_i and d_e surfaces of the compound correspond to N—H···O intramolecular and O—H···O intermolecular hydrogen bond interactions. The Hirshfeld surfaces were performed using a standard (high) surface resolution with the three-dimentional d_{norm} surfaces mapped over a fixed colour scale of -0.179 (red) to 2.255 (blue) Å. The red spots identified in Fig. 4 correspond to the near-type H···O contacts resulting from hydrogen bond O─H···O.

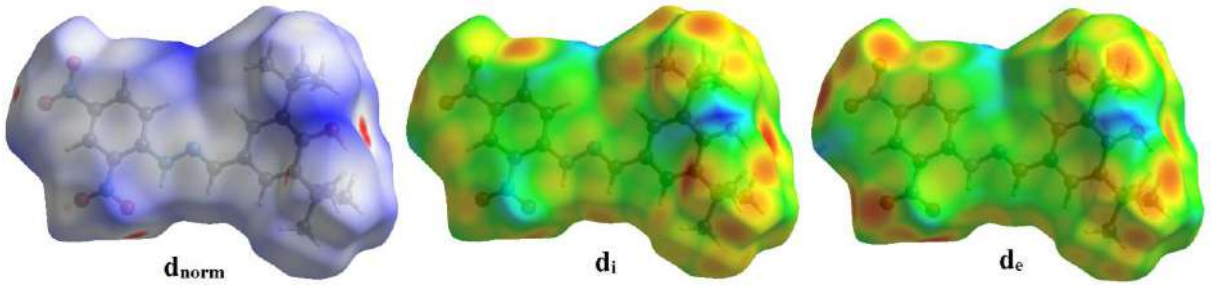

Figure 3. The Hirshfeld surface of the title compound mapped with d_{norm}, d_i and d_e.

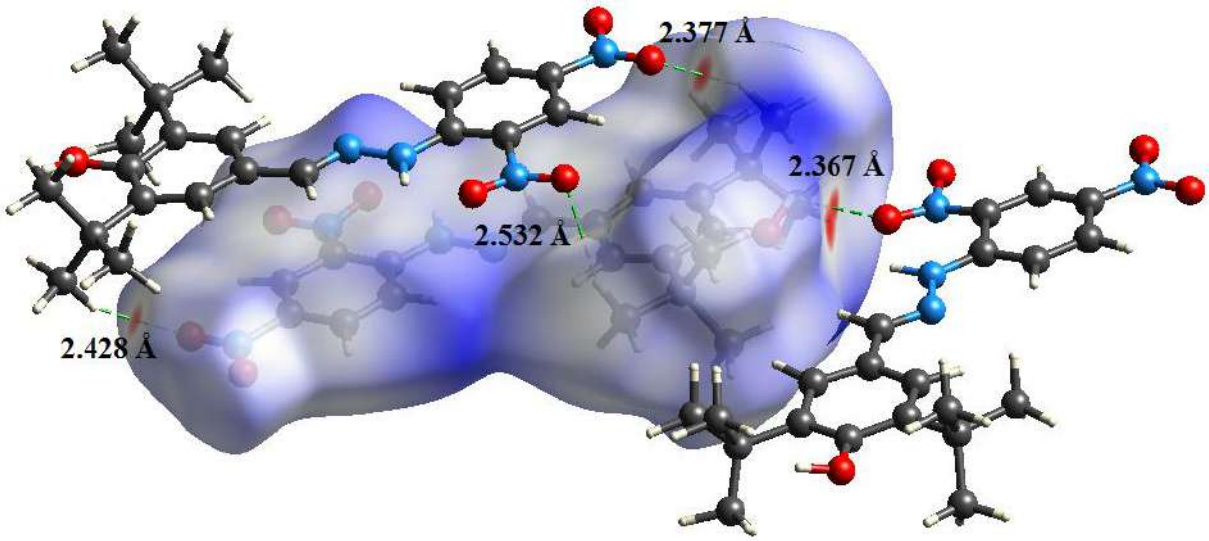

Figure 4. d_{norm} mapped on Hirshfeld surfaces for visualizing the intermolecular interactions of the title compound.

Fig. 5 shows the two-dimensional fingerprint of the sum of the contacts contributing to the Hirshfeld surface represented in normal mode. The graph shown in Fig. 6 (H···H) shows the two-dimensional fingerprint of the (di, de) points associated with hydrogen atoms. It is characterized by an end point that points to the origin and corresponds to de + di ~ 2.5 Å, which indicates the presence of the H···H contacts in this study (47.2%). Two symmetrical points at the top, bottom left and right with de + di ~ 2.5 Å indicate the presence of the H···O/O···H (30.6%) contacts. These data are characteristic of O─H···O hydrogen bond. The graph shown in Fig. 6 (H···C/C···H) shows the contact between the carbon atoms inside the surface and the hydrogen atoms outside the surface of Hirshfeld and vice versa. The analysis of this graph shows two symmetrical wings on the left and right sides (7.2%). Further, there are C···N/N···C (4.5%), C···C (4.1%) and H···N/N···H (4.1%) contacts.

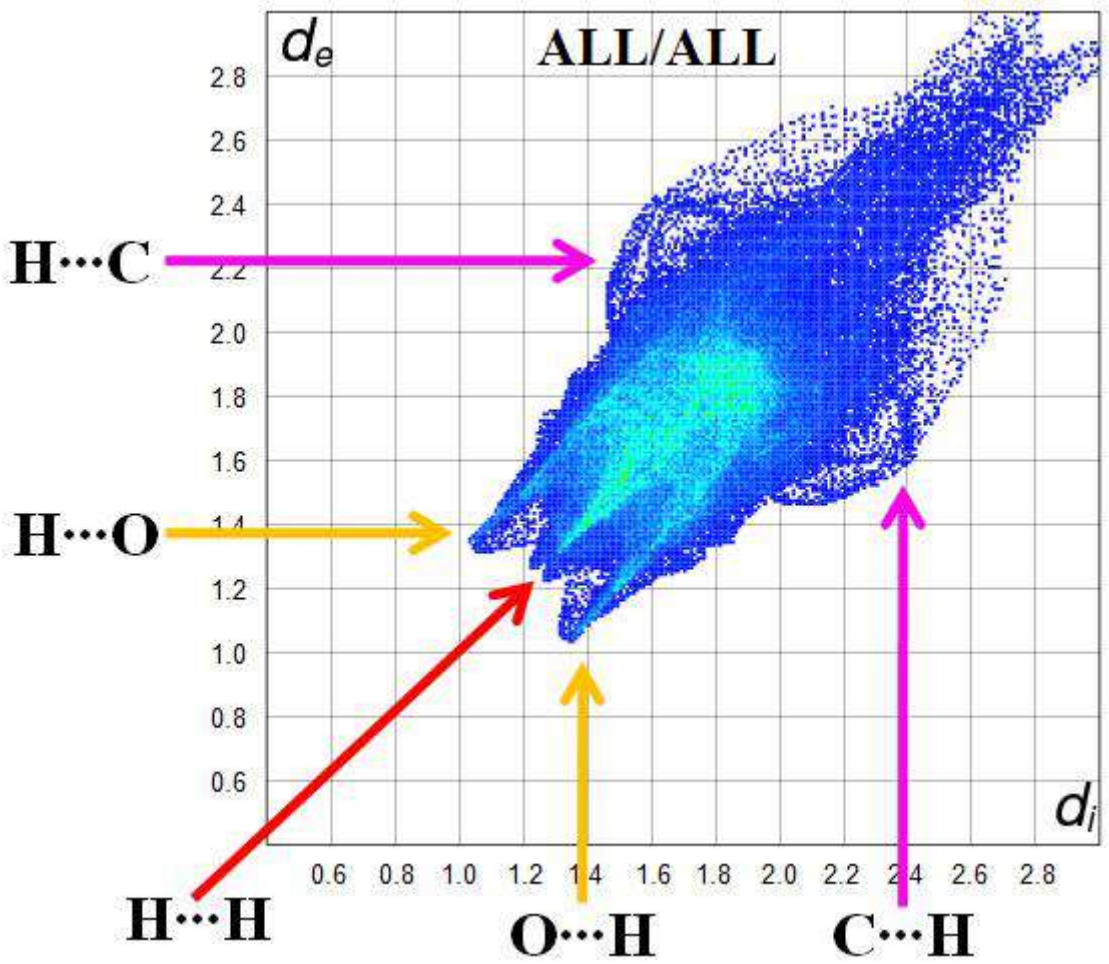

Figure 5. Fingerprint of the title compound.

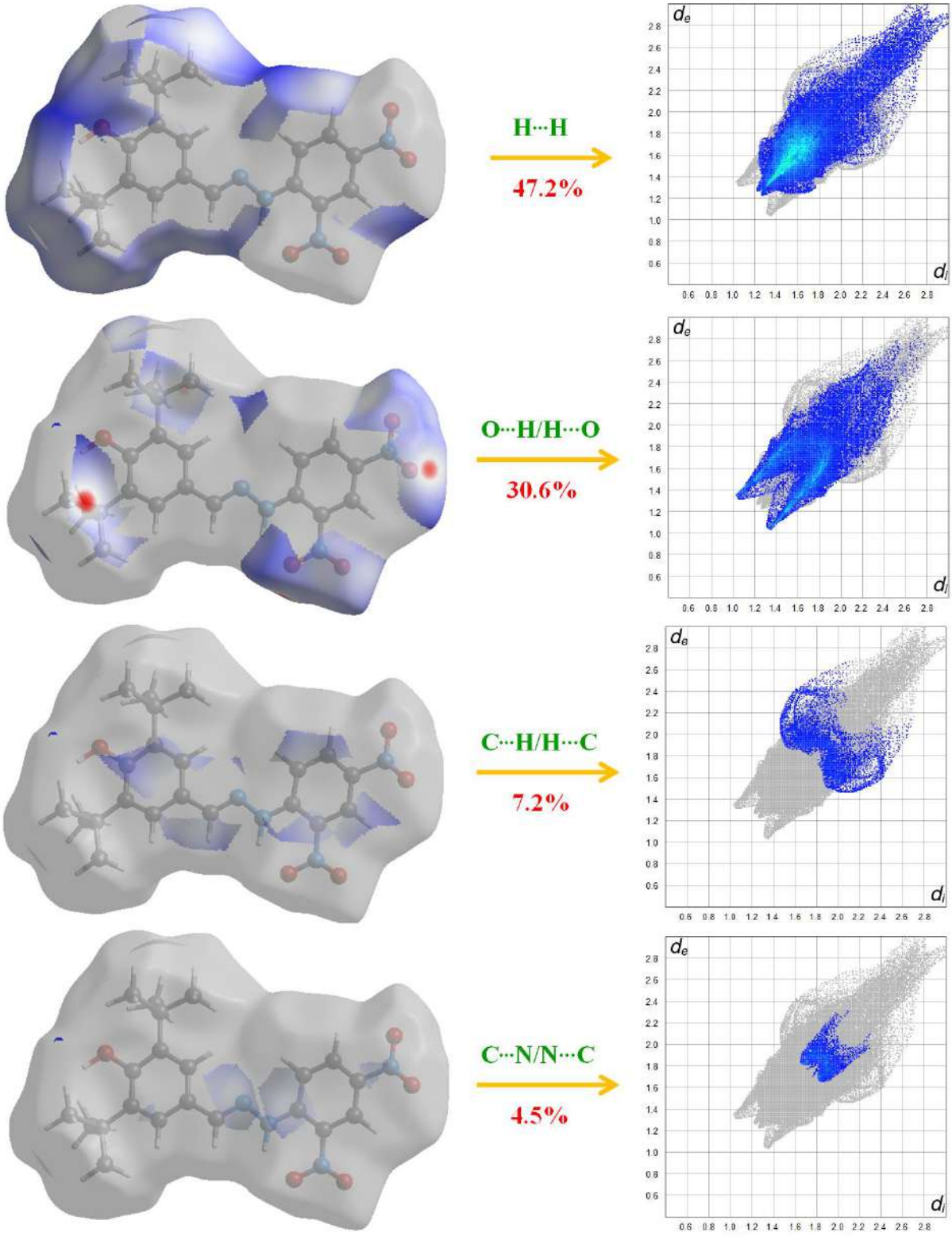

Figure 6. Two-dimensional fingerprint plots with a d_{norm} view of the H···H (47.2%), H···O/O···H (30.6%), H···C/C···H (7.2%), and C···N/N···C (4.5%) contacts in the title compound.

The view of the three-dimensional Hirshfeld surface of the title compound plotted over electrostatic potential energy in the range -0.065 to 0.065 a.u. using the STO-3G basis set at the Hartree–Fock level of theory. In Fig. 7, the O─H···O hydrogen-bond donors and acceptors are shown as blue and red areas around the atoms related with positive (hydrogen-bond donors) and negative (hydrogen-bond acceptors) electrostatic potentials, respectively.

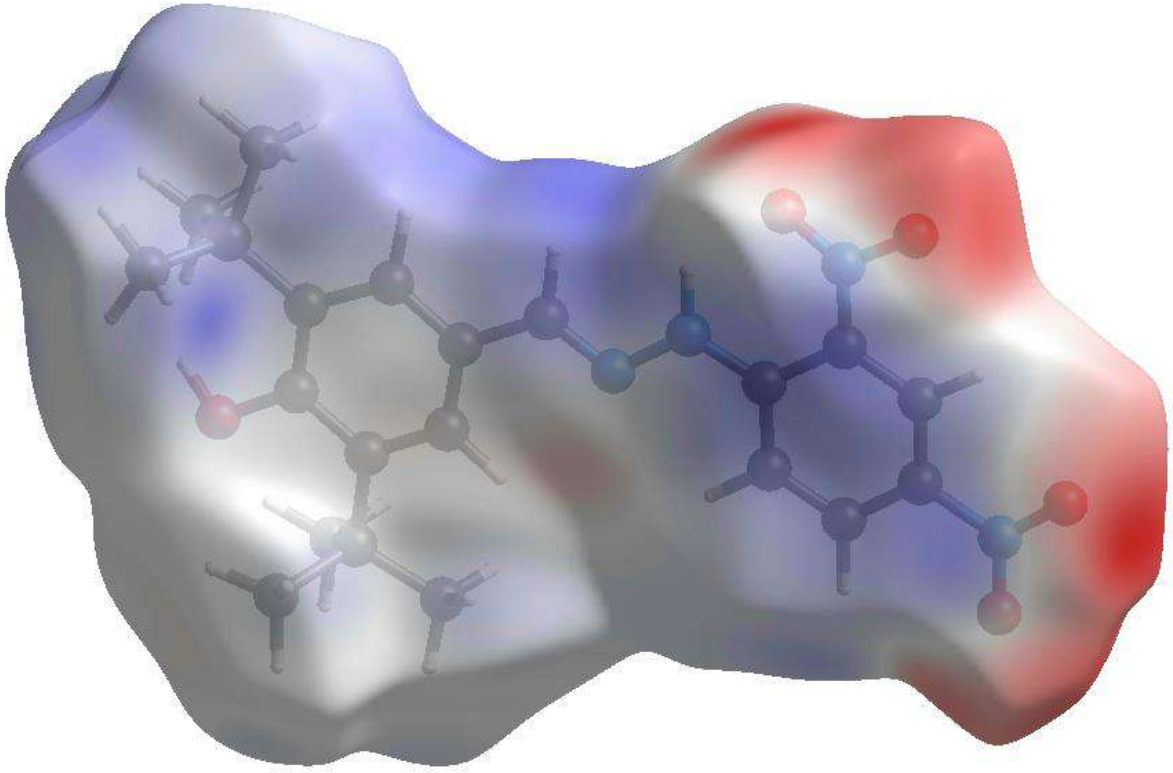

Figure 7. The view of the three-dimensional Hirshfeld surface of the title compound plotted over electrostatic potential energy.

$C_{21}H_{26}N_4O_5$ compound was characterized by single crystal X-ray diffraction technique and Hirshfeld surface analysis. In the crystal, O─H···O hydrogen bonds link the molecules into supramolecular chains propagating along the a-axis direction. Hirshfeld surface analyses and two dimensional fingerprint plots have been used to analyse the intermolecular interactions present in the crystal. The Hirshfeld surface analysis of the crystal structure specifies that the most important contributions for the crystal packing are from H···H (47.2%), H···O/O···H (30.6%), H···C/C···H (7.2%) and C···N/N···C (4.5%) interactions (Fig. 6).

References

Anis, I., Aslam, M., Noreen, Z., Afza, N., Hussain, A., Safder, M. and Chaudhry, A. H. (2013). A Review (part a) – General Applications of Schiff Base Transition Metal Complexes. Int. J. Curr. Pharm. Res. 5, 21-24.

Aydemir, E., Kansiz, S., Gumus, M. K., Gorobets, N. Y. and Dege, N. (2018). Crystal structure and Hirshfeld surface analysis of 7-ethoxy-5-methyl-2-(pyridin-3-yl)-11,12-dihydro-5,11-methano[1,2,4]triazolo[1,5-c][1,3,5]benzoxadiazocine. Acta Cryst. E74, 367–370.

Farrugia, L. J. (2012). WinGX and ORTEP for Windows: an update. J. Appl. Cryst. 45, 849–854.

Gümüş, M. K., Kansız, S., Aydemir, E., Gorobets, N. Y. and Dege, N. (2018). Structural features of 7-methoxy-5-methyl-2-(pyridin-3-yl)-11,12-dihydro-5,11-methano[1,2,4]triazolo[1,5-c][1,3,5]benzoxadiazocine: Experimental and theoretical (HF and DFT) studies, surface properties (MEP, Hirshfeld). Journal of Molecular Structure, 1168, 280-290.

Kansız, S. and Dege, N. (2018). Synthesis, crystallographic structure, DFT calculations and Hirshfeld surface analysis of a fumarate bridged Co(II) coordination polymer. Journal of Molecular Structure, 1173, 42-51.

Moroz, Y. S., Demeshko, S., Haukka, M., Mokhir, A., Mitra, U., Stocker, M., Müller, P., Meyer, F. and Fritsky, I. O. (2012). Regular high-nuclearity species from square building blocks: A triangular 3 × [2 × 2] Ni12complex generated by the self-assembly of three [2 × 2] Ni4molecular grids. Inorg. Chem., 51, 7445–7447.

Moroz, Y. S., Kulon, K., Haukka, M., Gumienna-Kontecka, E., Kozłowski, H., Meyer, F. and Fritsky, I. O. (2008). Synthesis and structure of [2 x 2] molecular grid copper(II) and nickel(II) complexes with a new polydentate oxime-containing Schiff base ligand. Inorg. Chem, 47, 5656–5665.

Moroz, Y. S., Szyrweil, L., Demeshko, S., Kozłowski, H., Meyer, F. and Fritsky, I. O. (2010). One-Pot Synthesis of a New Magnetically Coupled Heterometallic Cu 2Mn2 [2 × 2] Molecular Grid. Inorg. Chem., 49, 4750-4752.

Przybylski, P., Huczynski, A., Pyta, K., Brzezinski, B. and Bartl, F. (2009). Biological properties of Schiff bases and azo derivatives of phenols. Current Organic Chemistry, 13, 124-148.

Sen, P., Kansiz, S., Dege, N., Iskenderov, T. S. and Yildiz, S. Z. (2018).). Crystal structure and Hirshfeld surface analysis of 4-[4-(1H-benzo[d]imidazol-2-yl)phenoxy]phthalonitrile monohydrate. Acta Cryst. E74, 994–997.

Sen, P., Kansiz, S., Golenya, I. A. and Dege, N. (2018). Crystal structure and Hirshfeld surface analysis of N,N'-bis(3-tert-butyl-2-hydroxy-5-methylbenzylidene) ethane-1,2-diamine. Acta Cryst. E74, 1147–1150.

Sheldrick, G. M. (2015a). SHELXT – Integrated space-group and crystal-structure determination. Acta Cryst. A71, 3–8.

Sheldrick, G. M. (2015b). Crystal structure refinement with SHELXL. Acta Cryst. C71, 3–8.

Spek, A. L. (2003). Single-crystal structure validation with the program PLATON, J. Appl. Cryst. 36, 7-13.

Stoe & Cie (2002). X-AREA and X-RED32. Stoe & Cie GmbH, Darmstadt, Germany.

Turner, M. J., MacKinnon, J. J., Wolff, S. K., Grimwood, D. J., Spackman, P. R., Jayatilaka, D. and Spackman, M. A. (2017). Crystal Explorer Ver. 17.5. University of Western Avustralia, Pert.

Westrip, S. P. (2010). *publCIF: software for editing, validating and formatting crystallographic information files.* J. Appl. Cryst. 43, 920-925.

Vibrational Assignments, Electronic Properties and Reactivity Descriptors of (E)-1-(4-flourobenzylidene)urea

Fatih AKYILDIZ [1], Hamit ALYAR [2*], Saliha ALYAR[3]

[1] Çankırı Karatekin University, Faculty of Science, Department of Physics, Çankırı, Turkey; fatihakyildiz@gmail.com

[2] Çankırı Karatekin University, Faculty of Science, Department of Physics, Çankırı, Turkey; halyar@karatekin.edu.tr

[3] Çankırı Karatekin University, Faculty of Science, Department of Chemistry, Çankırı, Turkey; saliha@karatekin.edu.tr

[*] **Corresponding Author:** halyar@karatekin.edu.tr

Abstract

Schiff base organic molecules are of fundamental importance and have got a large number of applications in biological and industrial fields.

In this study, the structure of (E)-1-(4-flourobenzylidene)urea is optimized using density functional theory (DFT) method. Thevibrational band assignments are calculated using B3LYP/6-311++G(d,p) level of theory combined with scaled quantum mechanics force field methodology. The computational frequencies are found to be in good agreement with the experimental frequencies. HOMO-LUMO analysis, reactivity descriptors and nonlinear optical properties of (E)-1-(4-flourobenzylidene)urea studied with same level of theory. All calculations performed with Gaussian 09, Gauss View 5.0 and SQM 1.0 software.

Keywords: B3LYP, DFT, IR, NMR, SQM

1. Introduction

The >C=NH-group is present in Schiff base organic molecules are of fundamental importance. They have got extensive application in biological and industrial fields. Schiff bases with a potential pharmaceutical use were synthesized (Charles, 1955). Schiff bases have been reported for their biologic properties, such as anti-bacterial, anti-fungal, anti-inflammatory, analgesic, anti-convulsant, anti-tubercular, anti-cancer, anti-oxidant and anti-helmintic activities (Mounika et al. 2010; Venkatesh, 2011; Kiraz et al. 2009; Sondhi, et al. 2006).

In the present study, vibrational band assignment of (E)-1-(4-flourobenzylidene)urea were calculated using B3LYP/6-311++G(d,p) theory level. Also, HOMO-LUMO analysis, reactivity descriptors and nonlinear optical properties of (E)-1-(4-flourobenzylidene)urea studied with same level of theory.

2. Material and Method

The geometry of (E)-1-(4-flourobenzylidene)urea was fully optimized without any constraint with the help of an analytical gradient procedure implemented within the Gaussian 09 program (Frish et al., 2009). All the parameters were allowed to relax and all the calculations converged to an optimized geometry which corresponds to a true energy minimum as revealed by the lack of imaginary values in the wave number calculations. The molecular geometry optimizations, vibrational frequency calculations, performed with the Gaussian 09 software package by using DFT/B3LYP approaches. Optimized molecular structure of studied compound given in Fig.1. The vibrational band assignments were performed at B3LYP/6-311++G (d,p) theory level combined with scaled quantum mechanics force field (SQMFF) methodology. Each vibrational modes of the studied compound were characterized by their potential energy distribution (PED) which were calculated by using SQM-FF program (SQM,2013). HOMO-LUMO analysis, reactivity descriptors and nonlinear optical properties of (E)-1-(4-flourobenzylidene)urea studied with same level of theory.

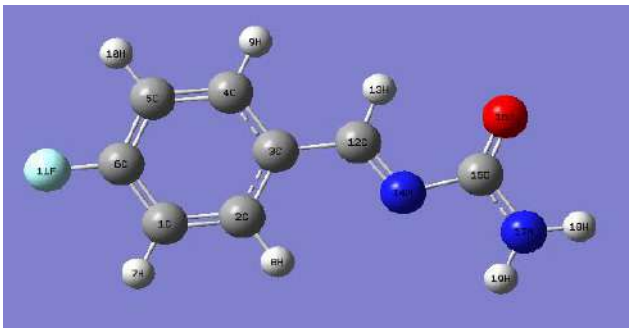

Fig.1 Molecular structure of (E)-1-(4-flourobenzylidene)urea obtained by B3LYP/6-311++G(d,p) method

3. Results and Discussion

3.1 Vibrational Band Assignment

Vibrational frequencies and corresponding vibrational assignments of (E)-1-(4-flourobenzylidene)urea have been investigated theoretically. DFT/B3LYP is provides acceptable vibrational wave numbers for organic molecules. Vibrational frequencies of (E)-1-(4-flourobenzylidene)urea were calculated at the DFT levels with B3LYP (Becke-Lee-Yang-Parr three parameters) hybrid functional (Lee et al.,1988). The vibrational band assignments were performed at B3LYP/6-311++G(d,p) theory level combined with scaled quantum mechanics force field (SQMFF) methodology to compare the experimental and calculated vibrational frequencies of the title compounds. The vibrational modes were assigned on the basis of PED analysis using SQM program. The visual check for the vibrational band assignments were also performed by using Gauss-View program.

Table 1. Assignment of fundamental vibrations of (E)-1-(4-flourobenzylidene)urea by normal mode analysis based on SQM force field calculations using selective scaled B3LYP/6-311++G(d,p) (Experimental values taken from Tracy et al., 2018)

Mod.	FT-IR	Un Scaled	Scaled	Potential energy Distributions (P.E.D.)
51	-	3998	3678	υ_{as} (NH_2) (100)
50	3462	3852	3543	υ_{s} (NH_2) (100)
49	3089	3417	3143	υ_{s} (CH) (98)
48	-	3410	3137	υ_{as} (CH) (99)
47	3062	3399	3127	υ_{as} (CH) (99)
46		3368	3098	υ_{as} (CH) (99)
45	2922	3269	3007	υ (C12H) (37)
44	1714	1852	1703	υ (CN) (25) + υ (CO) (67)
43	1666	1827	1680	υ (CN) (30) + υ (CO) (45) +sci (NH_2) (18)
42	1581	1801	1656	$\upsilon(CC)_{ring}$ (85)
41	-	1778	1635	$\upsilon(CC)_{ring}$ (89)
40	1531	1770	1628	υ (CO) (63) +sci (NH_2) (22)
39	1483	1688	1552	β (CCH) (76)
38	-	1574	1448	$\upsilon(CC)_{ring}$ (67) + β (CCH) (26)
37	1346	1546	1422	β (NCH) (26)
36	1309	1504	1383	υ (CN) (48) + β (NCH) (26)
35	-	1465	1347	β (CCH) (82)
34	-	1376	1265	$\upsilon(CC)_{ring}$ (75)
33	-	1342	1234	$\upsilon(CC)_{ring}$ (42) + υ (CC) (35)
32	1201	1333	1226	υ (CF) (57) + $\upsilon(CC)_{ring}$ (21) + $\beta(CCH)_{ring}$(18)
31	1143	1293	1189	υ (CF) (48) + $\upsilon(CC)_{ring}$ (20) + $\beta(CCH)_{ring}$(23)
30	-	1224	1126	β (CNH_2) (76)
29	-	1220	1222	$\upsilon(CC)_{ring}$ (35) + $\beta(CCH)_{ring}$(40)
28	-	1203	1106	γ (CH) (68)

ν: bond stretching, β: in-plane angle bending,γ: out-of-plane anglebending,τ: torsion, sci: scissoring, w: waging, t: twist as: antisymmetric and s: symmetric

Table 1. Continued

Mod.	FT-IR	Un Scaled	Scaled	Potential energy Distributions (P.E.D.)
27	1008	1168	1074	γ (CH) (69)
26	-	1135	1044	γ (CH) (68)
25	929	1133	1042	$\beta(CCC)_{ring}$ (59)
24	891	1033	950	υ (CC) (65)
23	831	985	906	γ (CH) (68)
22	-	970	892	γ (CH) (68)
21	804	943	867	$\beta(CCC)_{ring}$ (46) + β (CCN) (23)
20	-	879	808	τ(CCCH) (34) + τ(CNCN) (28) + τ(CNCO) (17)+ τ(NCNH) (15)
19	-	861	792	υ (CF) (35) + β (CCC)(42)
18	677	813	747	τ(CCCC) (26) + τ(CCCH) (34)
17	634	719	661	$\beta(CCC)_{ring}$ (42) + β (OCN) (27)
16	-	701	644	$\beta(CCC)_{ring}$ (43) + β (OCN) (26)
15	-	686	631	w(NH_2) (62)
14	-	646	594	t(NH_2) (73)
13	518	610	261	β (CCN) (32) + β (NCN) (18) + β (NCO) (13)
12	-	581	534	τ(CCCC) (35) + τ(CCCH) (28)
11	-	551	506	$\beta(CCC)_{ring}$ (44) + β (NCN) (20) + β (NCO) (25)
10	-	482	443	τ(CCCC) (27) + τ(CCCH) (19) + τ(CCCF) (19) + τ(HCCF) (12)
9	-	437	402	β (CCF) (30) + β (CCC) (22) + β (NCN) (10)

ν: bond stretching, β: in-plane angle bending,γ: out-of-plane anglebending,τ: torsion, sci: scissoring, w: waging, t: twist as: antisymmetric and s: symmetric

In order to enable assignment of the observed peaks, we have analyzed the all vibrational frequencies and compared our calculated results of the investigated compound

with their experimental ones. The experimental frequencies are listed together with calculated frequencies in Tables 1. The calculated values of vibrations show good agreement with the experimental results as seen in Table 1.

N-H Vibrations

The N−H stretching vibration appears strongly and broadly in the region 3500–3300 cm^{-1}. In this study, the amino group stretching vibration is observed at very strong band at 3462 cm^{-1} in FT-IR spectrum. The wavenumber calculated at 3678 and 3543 cm^{-1} assigned to the N-H vibration of the title molecule.

C=O Vibrations

The carbonyl vibrations bands in ketones normally show strong intensity and are expected in the region 1715–1680 cm−1. The strong band observed at 1714 cm−1 in FT-IR were assigned to the carbonyl stretching vibration of the studied molecule. This band theoretically calculated at 1703 cm-1.

C-H Vibrations

The aromatic C-H stretching vibrations were normally found between 3100 and 2900 cm-1. Experimental C-H stretching vibrations were also observed at 3089, 3062 and 2922 cm-1. These bands theoretically calculated at 3143, 3137, 3127 and 3098 cm-1.

3.2. HOMO-LUMO Molecular Orbital Energies

Both the Highest Occupied Molecular Orbital (HOMO) and the Lowest Unoccupied Molecular Orbital (LUMO) are the main orbital taking part in chemical reaction. The HOMO energy characterizes the ability of electron giving, the LUMO characterizes the ability of electron accepting, and the gap between HOMO and LUMO characterizes the molecular chemical stability. The energy gap between the HOMOs and LUMOs called as energy gap. It is a critical parameter in determining molecular electrical transport properties since it is a measure of electron conductivity. Energies of HOMO, LUMO and their orbital energy gaps were calculated by B3LYP/6-311G++(d,p) method. The 3D plots of the frontier orbitals are shown in Fig. 2.

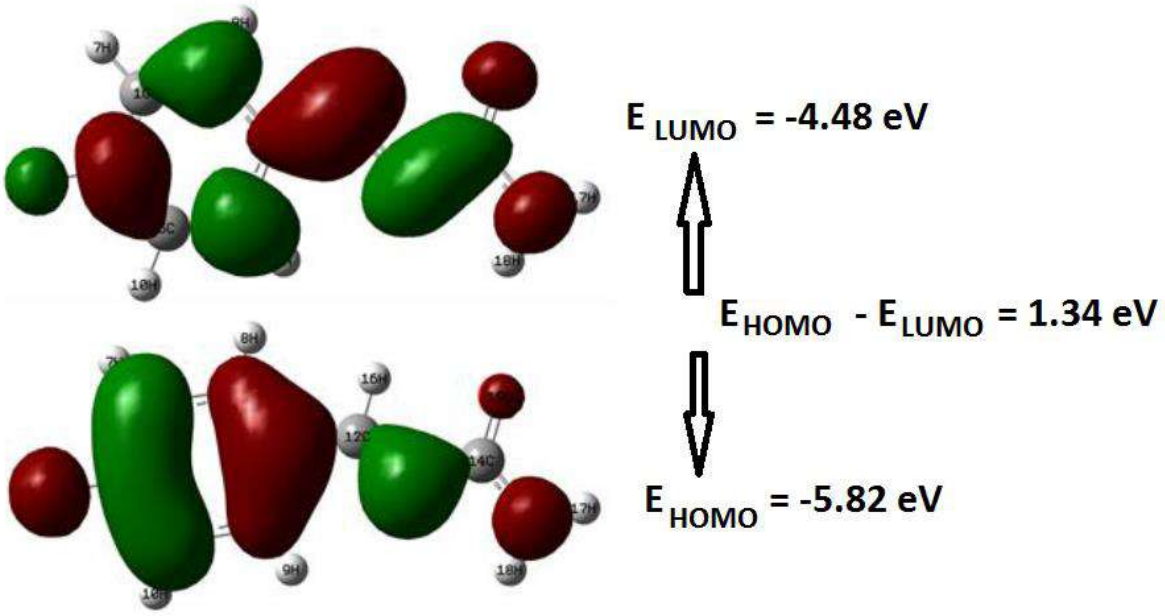

Fig. 2. Molecular orbital surfaces and energy levels for the HOMO and LUMO of (E)-1-(4-flourobenzylidene)urea

3.3. Nonlinear Optical Properties (NLO)

Optical wave manipulation is one of the future technologies for optical processing. It has various applications in fiber-optic communications and optoelectronics which makes it an increasingly important topic among electrical engineers. The calculations of total static dipole moment(μ) static polarizability (α_{ave}) and first static hyperpolarizability (β_{tot}) from the Gaussian output as follows:

$\mu = (\mu x2 + \mu y2 + \mu z2)^{1/2}$

$<\alpha> = 1/3\ (\alpha xx + \alpha yy + \alpha zz\ )$

$\beta_{tot} = [(\beta xxx + \beta xyy + \beta xzz)^2 + (\beta yyy + \beta yzz + \beta yxx)^2 + (\beta zzz + \beta zxx + \beta zyy)^2]^{1/2}$

Table 2. The electric dipole moment μ (D), the mean polarizability <α> (a.u.) and the first hyperpolarizability βtot (a.u.) of 2-Chloro-5-Nitrobenzyl Alcohol by DFT B3LYP/6-311++G(d,p) method

Parameter	B3LYP	Parameter	B3LYP
μ_x	-3.98	$ß_{xxx}$	1342.60
μ_y	-0.10	$ß_{xxy}$	774.35
μ_z	-0.53	$ß_{xyy}$	-148.57
μ_{tot}	4.01	$ß_{yyy}$	170.55
α_{xx}	279.30	$ß_{xxz}$	-149.53
α_{xy}	-10.43	$ß_{xyz}$	42.90
α_{yy}	125.22	$ß_{yyz}$	-24.69
α_{xz}	-3.59	$ß_{xzz}$	9.19
α_{yz}	0.08	$ß_{yzz}$	14.9
α_{zz}	69.19	$ß_{zzz}$	-56.75
$<\alpha>$	157.90	β_{tot}	1556.37

The computations show that, the first static hyperpolarizability of (E)-1-(4-flourobenzylidene)urea is 107.14 a.u. (0.925x10-30 esu). This value is 36 times larger than that of urea (0.3728x10-30 esu).

References

Charles, D. Lowry, Jr., (1955). Stabilization of waxes. U.S. 2,715,073.

Frisch, M. J. et al., Gaussian 09: Revision B.01 Gaussian Inc., Wallingford, CT, 2009.

Kiraz, A., Yıldız, M., Dülger, B., (2009), Synthesis and Characterization of Crown Ethers. Asian J. Chem. 21, 6, 4495-4507.

Lee, C., Yang, W., and Parr, R. G., (1988). Development of the Colle-Salvetti correlation-energy formula into a functional of the electron density. Phys. Rev B., 37, 785-789.

Mounika,K., Pragathi, A., Gyanakumar,C., (2010). Synthesis¸ Characterization and Biological Activity of a Schiff Base Derived from 3-Ethoxy Salicylaldehyde and 2-Amino Benzoic acid and its Transition Metal Complexes. J. Sci. Res. 2 (3), 513-524.

Sondhi, S.M., Singh, N., Kumar, A., Lozach, O., Meijer, L., (2006), Synthesis, anti-inflammatory, analgesic and kinase (CDK-1,CDK-5 &GSK-3) inhibition activity evaluation of benzimidazole /benzoxazole derivatives and some Schiff's bases. Bio-organic & MedicinalChemistry, 14(11), 3758–3765.

SQM version1.0, Scaled Quantum Mechanical, 2013 GreenAcres Road, Fayetteville, Arkansas 72703.

Tracy, J., Dhandapani, A., Bharanidharan, S., (2018), Nonlinear optical investigation of (E)-1-(4-flourobenzylidene)urea using theoretical calculations. Int. J. Adv. Chem., 6 (1) (2018) 26-36.

Venkatesh, P., (2011), Synthesis, characterization and antimicrobial activity of various schiff bases complexes of Zn (II) and Cu (II) ions. Asian J Pharm Hea Sci. 1(1),8–11.

3D Printers And Application Fields

Nazım ÇABUK[1*], Senem ÇABUK[2]

[1] Ankara University, Graduate School of Natural and Applied Science, Department of Physics Engineering, TURKEY. nacabuk@ankara.edu.tr

[2] Ankara University, Graduate School of Natural and Applied Science, Department of Astronomy and Space Science,TURKEY. secabuk@ankara.edu.tr

[*] **Corresponding Author:** nacabuk@ankara.edu.tr

Abstract

In this research, we investigate the presence of three dimensional printer technology, past daily development, and applications in science and technology. “3D Printers and Applications” is a research in which we deal with details of the history, structure and equipment, software, usage areas and applications of 3D printers, which have become an indispensable part of science, industry, technology and innovation. Cost analysis is also considered in this project study which gives reasons about the necessity of 3D printers, types according to usage areas and structures, mechanical, electrical, electronic elements, 3D printer compatible modeling software, system requirements and output formats for these software. Applications have been made using the latest release printers of various brands.

Keywords: 3D printer, Reprap, Stereolithography, Fused Deposition Modeling, Selective Laser Sintering, Polyjet, filament, .stl, .obj, .wrml, .ply, Polylactic Acid, Polyamide, CAD.

1. Introduction

Human beings have felt the need to visualize the knowledge they produce in every period of history from the beginning of history to the present day. As the information outputs change, the writing tools and languages also change. For example, today, classic items have been replaced by digital pens, the location of the paper, touch screens and printers are replaced by 3D printers. 3D printers are the most advanced of concrete output tools. 3D printing is a technique that works with the additive used in the production of parts produced by adding layers until the final shape is obtained. The advantages of 3D printing are the cost reduction of prototypes and the faster production process of complex shapes (Mičieta et al., 2016).

The majority of 3D printer manufacturers are concentrated to develop and sell machines of high precision and small size. On the other hand, the market of machines where large parts are produced with low precision is also highly developed (Stopka et al., 2017).

2. Types of 3D Printers

Three-dimensional printers are evaluated according to their printing techniques.

- Stereolithography (SLA) Method: Stereolithography (SLA) is a new technology based on layered manufacturing, the most common among all three-dimensional production techniques. Because of the SLA's layer formation mechanism, complex parts can be manufactured directly in a short time without metal molds which will replace the pattern in the casting.

Figure 1. Production by SLA method

- Fused Deposition Modeling (FDM) Method: The thermoplastic material used in this technique is in the form of a filament. Usually 1.75 - 3 mm wire thickness is used. During 3D printing, the material in the form of wire is melted by passing a 0.4 mm diameter mold and the production is carried out by axial movement. By stacking the layers on top of each other, the object is created.

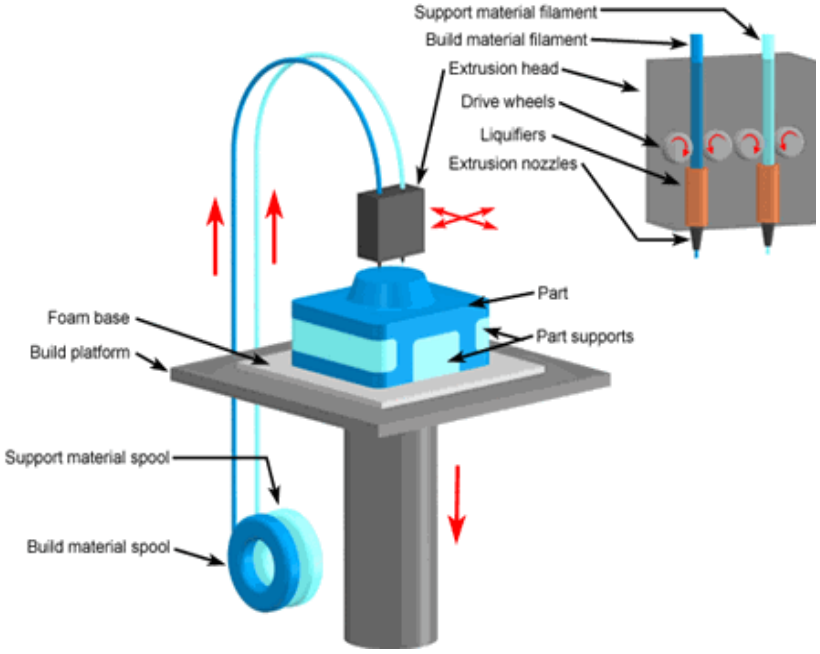

Figure 2. Basic parts of FDM devices

- Selective Laser Sintering (SLS) Method: Selective Laser Sintering is a process of ın Layer Production = LM, that allows the production of complex 3D parts by combining the successive layers of powder material on top of each other (Kruth et al., 2001). Solidification is achieved by processing selected areas using thermal energy provided by a focused laser beam (Kruth et al., 1996).

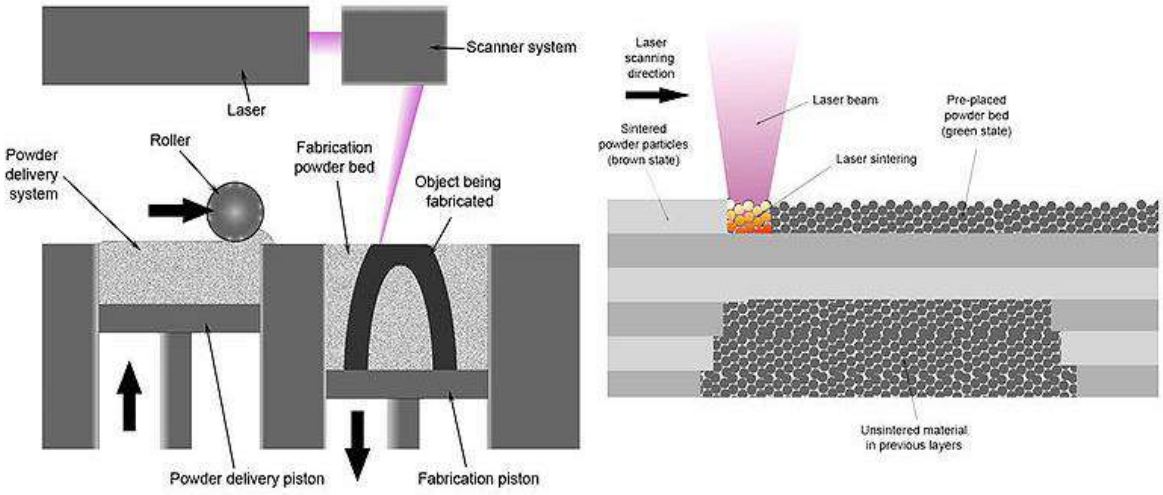

Figure 3. Production by SLS method

- Polyjet Method: This method is similar to Ink-jet technology. The sprayer adheres the powder in the right places by sending a thin film layer of ultraviolet light on the cross-section of the layer. The gaps to be supported between the layers are again sprayed with powder.

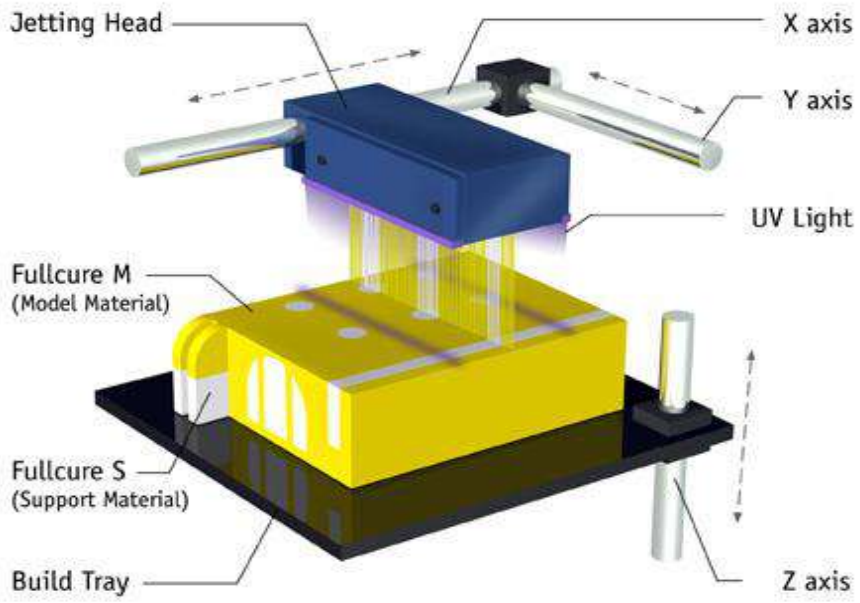

Figure 4. Basic parts of Polyjet devices

- 3-Dimensional Printing (3DP) Method: 3D printing (3DP) technology has been in existence for over 30 years. 3DP is often referred to as rapid prototyping and sometimes as "Contour Manufacturing" (Anjum et al., 2017).ASTM defines Additive Manufacturing as a "layer on layer" (ASTM, 2015).

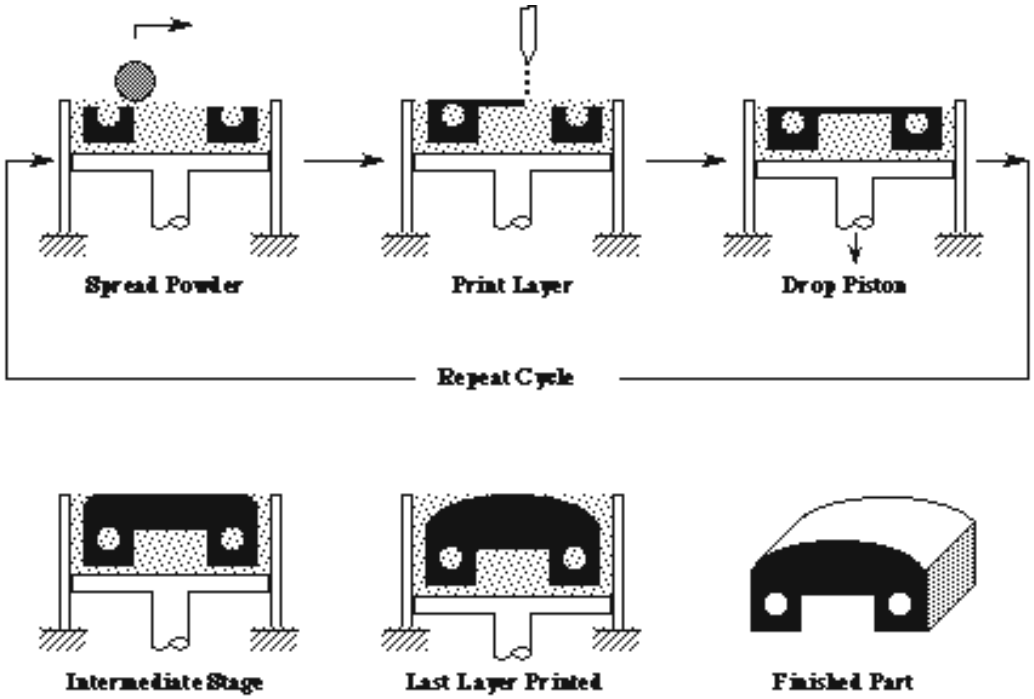

Figure 5. Production stages with 3DP method

3. Hardware of 3D Printers

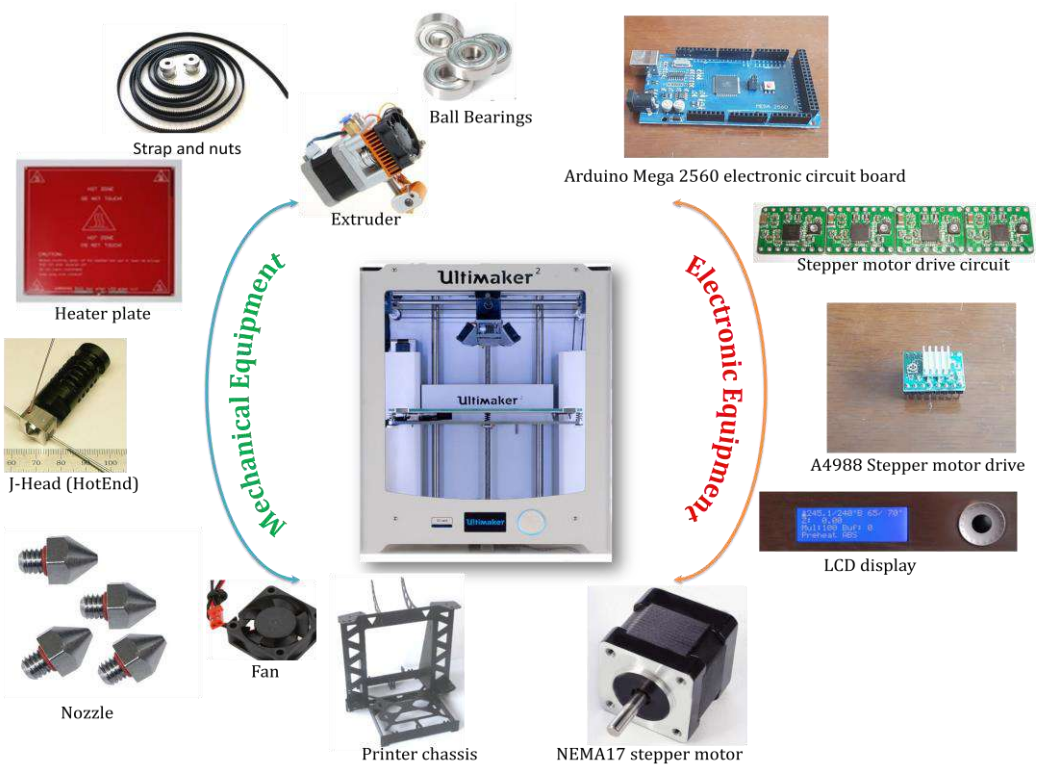

Figure 6. The basic elements of a 3D printer

Filaments can be selected from different materials according to the desired product. There are 3 kinds of flaments:

a. ABS (Acrylonitrile Butadiene Styrene): It is a light but hard thermoplastic polymer which is used frequently in industry.

b. PLA (Polylactic Acid): PLA is a bioplastic derived from natural and edible sources such as corn starch, sugar cane. It disappears more quickly in nature than in other plastics.

c. NYLON - PA (Polyamide): It is a more flexible, durable and lightweight filament than ABS and PLA. Nylon filament layers adhere better to each other than PLA and ABS.

Figure 7. Examples of PA and PLA materials

In order for the filaments to take the desired shape, some physical conditions need to be adapted. These conditions are given in Table 1.

Table 1. Physical conditions to be provided according to filament types.

Filament Type	Exturuder Temperature (°C)	Table Temperature (°C)
ABS	220-235	80-110
PLA	180-200	20-50
PA	200-220	20-50

4. Results and Discussions

In 1900, the effort to digitize the atom that began with Max Planck was a breakthrough in the quantum world, and atomic data were sent to electrical signals by mathematical

modeling, and then electronic science was able to present these electrical signals to the service of science and thus humanity with a full mathematical modeling. not only the emergence of abstract samples such as data storage units (such as flash disks and memory cards), but also the invention of the latest 3D printer, which is capable of producing digital, storable, concrete outputs. 3D printers, which are the best examples of electronic science to talk to the renewed world by means of computer software, have enabled production of prototypes or spare parts in space and physics research. In addition, medicine, education, engineering, reverse engineering, industry, food, chemistry and biophysics and areas such as each day in the creation of a new design has revolutionized the contribution.

In industrial applications, it is possible to match the limit of production with the 3D printer with the innovation limit of the sector in which it is used. In addition, every day new designs are added to the 3D printer, which provides the user with every imaginable strength needed according to the user's imagination and the limited usage area.

In the first versions, the studies started with reservations in the sense of cost can be easily obtained from the market with many brands and models at the price that the home user can easily reach when needed. Therefore, the issue to be discussed for 3D printers is not cost. The focus of today's development work on 3D printers is print quality and durability. As a matter of fact, the factories established for mass production of high value-added products in many sectors have now been replaced by a table-sized 3D printer.

References

Periodicals:

Anjum, T., Dongre, O., Misbah F. ve Nanyam N. (2017). Purview of 3DP in the Indian Built Environment Sector, Creative Construction Conference 2017, CCC 2017, 19-22 June 2017, Primosten, Croatia.

ASTM, (2015). ASTM F2792-12a, Standard Terminology for Additive Manufacturing Technologies, West Conshohocken: ASTM International, 2009.

Kruth, J.P., Wang, X., Laoui, T. ve Froyen, L. (2001). Lasers and Materials in Selective Laser Sintering, Proc. Int. Conf. on Laser Assisted Net Shape Engineering.

Kruth, J.P., Van Der Schueren, B., Bonse ve J.E., Morren, B. (1996). Basic powder Metallurgical Aspects in Selective Metal Powder Sintering, Annals of the CIRP Vol. 45/1.

Mičieta, B., Biňasova, V. ve Markovič, J. (2016). Advances İn Sustainable Energy Efficient Manufacturing System, MM Science Journal, pp. 918-926.

Stopka, M., Kohar, R., Gramblicka, S. ve Madaj, R. (2017). Dynamical Analysis of 3D Printer's Powertrain, TRANSCOM 2017: International scientific conference on sustainable, modern and safe transport, Procedia Engineering 192 (2017) 845 – 850.

Investigation of Structural, Spectral of Cobalt–Nalidixic Acid Complex with Pyridine

Tuğba AYCAN [1*], Filiz ÖZTÜRK [2], Serkan DEMİR [3], Hümeyra PAŞAOĞLU [4]

[1] Ondokuz Mayıs University, Faculty of Arts and Sciences, Physics department, Samsun, Turkey; tugba.aycan@omu.edu.tr

[2] Ondokuz Mayıs University, Blacksea Advanced Technology Research and Application Center, Samsun, Turkey; filiz.ozturk@omu.edu.tr

[3] Giresun University, Faculty of Engineering, Department of Industrial Engineering, Giresun, Turkey; serkan.demir@giresun.edu.tr

[4] Ondokuz Mayıs University, Faculty of Arts and Sciences, Physics department, Samsun, Turkey; hpasa@omu.edu.tr

[*] **Corresponding Author:** tugba.aycan@omu.edu.tr

Abstract

The mixed–ligand title complex, $[Co(nal)_2(py)_2]\cdot 4H_2O$ (1) (nal=anion of nalidixic acid, py=pyridine), was synthesis and comparatively investigated by focusing on their supramolecular architectures. Its structural properties were characterized by X–ray diffraction technique (XRD) and Fourier transform infrared spectroscopy (FT–IR), UV–Vis spectroscopy and Thermal analysis. It has been observed that complex has crystallized in the monoclinic space group P 2/c. The Co(II) ion has ideal octahedral geometry surrounded by two oxygen atoms of keto and carboxyl groups bonded as chelate from nalidixate, two nitrogen atoms from two pyridine ligands. The monomer are connected by C–H···O and π–π interactions to form sheet structures. The FT–IR investigation of the complex was performed within the mid–IR region, mainly focusing on the characteristic vibrations of nalidixic acid and pyridine moieties by considering ligand behavior in the case of complex formation. Ultra–violet (UV)–visible spectral analysis and Differential Thermal Analysis (DTA) were carried out to understand optical and thermal properties.

Keywords: Nalidixic acid, Pyridine, Single crystal XRD, IR spectroscopy, UV–Vis spectroscopy, Thermal analysis.

1. Introduction

Quinoline has important biological activities. For example, the benzimidazole ring addition to the 4–position exhibits antimicrobial and antifungal activity. The addition of a triazole ring to the 3–position in the 2–chloro–quinoline derivatives enhances the antimicrobial and antifungal activity. The addition of the trifluoromethyl group to the 7–position and the 8–position influences the biological activity. On the other hand, it is well known that the N–alkyl added to the 3–position on the quinolones shows strong antimicrobial, antioxidant activities. There are also antimicrobial and antituberculosis activity by the addition of oxazole and isoxazole into the quinine. Most highly effective quinolone antimicrobials contain the trifluoromethyl group or fluorine atom which binds to the quinoline ring. Trifluoromethyl or fluorine on the quinolone also changes such as basicicity or acidity parameters. In fact, the dipole moment of the molecule and the reactivity and stability of neighboring groups changes.

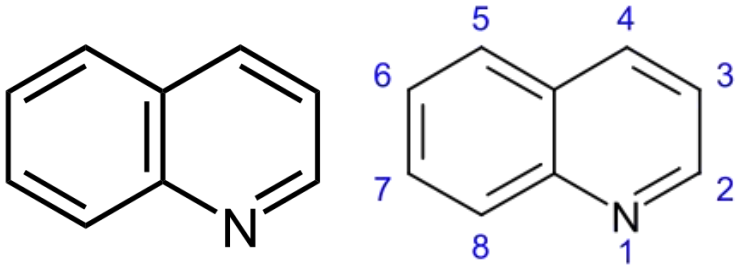

Figure 1. General structure of quinolin

In general, quinoline derivatives are extremely useful in the treatment of various diseases such as urinary tract infections, soft tissue infections, respiratory tract infections, bone–joint infections, typhoid fever, sexually transmitted diseases, prostatitis, community–acquired pneumonia, acute bronchitis and sinusitis (Arjmand et al., 2014; Balaji et al., 2013; Fernández-Galleguillos et al., 2014). Synthetic quinolone is the first of antibiotics. Synthetic quinolone antibiotics were discovered by George Lesher et.al. in the 1960s as a by–product of chloroxine production and were developed in 1963 for the treatment of urinary tract infections. Since 1967 it has been used for different treatments. The structure of nalidixic acid is shown in Figure 2 (Aggarwal et al., 2011; Emmerson et al., 2003).

2. Material and Method

2.1. Synthesis

Nalidixic acid was also dissolved (1 mmol, 0.23 g) into pyridine, followed by dropwise addition of an aqueous solution of CoCl2.6H2O (1 mmol, 0.24 g). The pink colored solution was filtered off and allowed to crystallize at 25 °C. and orange crystals were obtained after 1–2 months.

2.2. Materials and Instrumentation

Simultaneous TG, DTG and DTA curves were obtained in nitrogen atmosphere at 10 K/min heating rate in the platinum pats, in the range of temperature 20–1000 °C by using TA DMAQ800 thermal analyser in OMU–KITAM laboratory. The UV–Visible spectra of title compound was recorded at room temperature in aqua solution on a Unicam UV–Vis spectrophotometer working between 200 and 1100 nm. The absorption spectra of title complex was drawn using VISION*collect* Software. XRD data was collected using a Stoe IPDS diffractometer at 296 K by graphite monochromatic MoK_α radiation (λ=0.71073 Å). The crystal structure was analyzed by direct methods and all non–hydrogen atoms were refined anisotropically by full matrix least–squares methods using the program SHELX97 (Sheldrick, 1992). WinGX (Farrugia, 1999), ORTEP–3 for Windows (Farrugia, 1997) and MERCURY (Macrae et al., 2006) software were used for molecular drawings and other materials. Crystal data and structure refinement parameters for $[Co(nal)_2(py)_2]\cdot 4H_2O$ are given in Table 1.

Table 1. Crystal data and structure refinement parameters for $[Co(nal)_2(py)_2]\cdot 4H_2O$.

Formula	$C_{34}H_{36}CoN_6O_9$
Formula weight	731.62
Temperature(K)	293
Radiation, λ(MoK_α)	0.71073
Crystal system	Monoklinik
Space group	*P*2/c
a, b, c(Å)	22.853(7), 8.4859(18), 19.517(6)
α, β, γ (°)	90, 114.78(2), 90
Volume ($Å^3$)	3436.2(17)
Z	4
Calculated density (g cm^{-3})	1.414
μ(mm^{-1})	0.56

F(000)	1524
Crystal size (mm)	0.72, 0.393, 0.17
θ range (º)	2.0–26.5
Index ranges	$-28 \leq h \leq 28, -10 \leq k \leq 10, -24 \leq l \leq 24$
Measured Reflections	22052
Independent reflections	7129
Reflections observed [$I \geq 2\sigma(I)$]	3233
Data/restrains/parameters	7129/4/472
Goodness–of–fit on F^2	0.76
Final *R* indices [$I \geq 2\sigma(I)$]	R_1= 0.043; wR_2= 0.081
R indices (All data)	0.071

3. Results and Discussion

3.1. Crystal and Molecular Structure of the Complex

The geometric parameters of $[Co(nal)_2(py)_2]\cdot 4H_2O$ (Hnal=nalidixic acid and pyr=pyridine) complex are given in Table 2. Co(II) ion is coordinated to Co(II) metal through the nalidixate oxygen atom and the pyridine nitrogen atom in the structure in the center of symmetry (Figure 2). The coordination environment of the cobalt atom is defined as slightly distorted octahedral. The equatorial plane of the octahedral geometry forms the oxygen atoms of two nalidixic acids while the two pyridine ligands form the axial plane. The unit cell has four lattice water molecules.

Table 2. Selected bond distances (Å) and bond angles (º) for complex and nalidixic acid.

$[Co(nal)_2(py)_2]\cdot 4H_2O$		Hnal(Gangavaram et al., 2012)	Hnal (DFT/B3LYP/6311G)
Bond lengths (Å)			
Co–O1	2.077(2)	–	–
Co–O2	2.024(2)	–	–
Co–O4	2.053(2)	–	–
Co–O5	2.026(2)	–	–
Co–N5	2.196(3)	–	–
Co–N6	2.220(3)	–	–
C1–O2	1.261(3)	1.333	1.368
C1–O3	1.243(3)	1.208	1.246
C3–O1	1.258(3)	1.264	1.254
C13–O5	1.264(3)	1.333	1.368
C13–O6	1.232(3)	1.208	1.246
C15–O4	1.264(3)	1.264	1.254
Bond angles (º)			
O2–Co–O1	86.83(8)	O1–Co–N6	98.79(17)
O2–Co–O4	93.38(8)	O4–Co–O5	88.03(8)
O2–Co–O5	178.38(9)	O4–Co–N5	87.98(9)
O2–Co–N5	88.79(9)	O4–Co–N6	90.77(9)
O2–Co–N6	91.48(9)	O5–Co–N5	90.47(9)

O1–Co–O4	177.50(9)	O5–Co–N6	89.28(9)
O1–Co–O5	91.72(8)	N5–Co–N6	178.73(10)
O1–Co–N5	89.54(9)	–	–

The bond length Co1–N5 (2.196(3) Å) ve Co1–N6 (2.220(3) Å) forming the axes of the octahedral geometry is longer than the bond length Co1–O1 (2.077(2) Å), Co1–O2 (2.024(3) Å), Co1–O4 (2.053(2) Å) and Co1–O5 (2.026(2) forming the equatorial axis. It also supports that the Co (II) centered compound has octahedral geometry in Table 2. In the literature, there is no single crystal X–ray study of mixed ligand complexes with cobalt metal with octahedral geometry. Therefore, it is a study to be used as a reference. The compound has two nalidixate anions. These nalidixate anions are bound to the cobalt metal from the carboxyl and keto groups. The C–O bond lengths (C1–O2=1.261(3) Å; C13–O6=1.264(3) Å) of the carboxyl group bound to the metal were significantly shorter than that of the free C–O bond length (1.333 Å) (Gangavaram et al., 2012), while (C1–O3) 1.243 Å bond length was extended according to the free Hnal. (Gangavaram et al., 2012). Because the length of the bond is shortened when the –COOH group that coordinate to the metal is deprotone. So C=O that have the double bond character is delocalized and increases the bond length. As shown in Table 2, the bond length increases with the weakening of the double bond character of the keto group. The RMS value of the mixed ligand complex was 0.023. These value indicates that the cobalt metal deviates slightly from the plane.

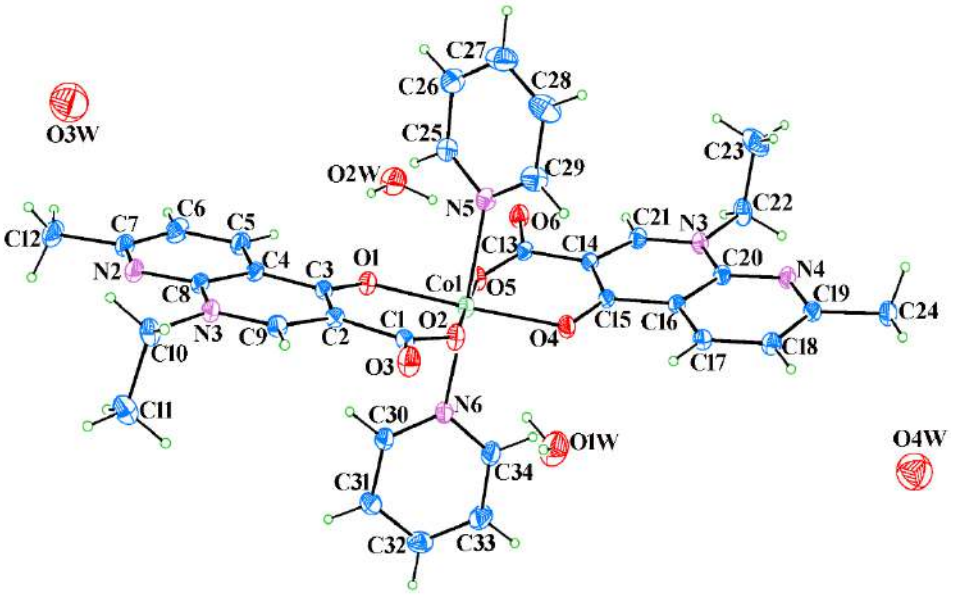

Figure 2. The molecular structure of $[Co(nal)_2(py)_2]\cdot 4H_2O$ complex

Table 3. Hydrogen bond geometry (Å, º) for the complex

D–H···*A*	*D*–H	H···*A*	*D*···*A*	*D*–H···*A*
C10–H10A···O3^{i}	0.97	2.52	3.434 (1)	157
C22–H22B···O6^{ii}	0.97	2.48	3.307 (1)	144
C27–H27···O1W^{iii}	0.93	2.45	3.303 (1)	152
O2W–H2WA···O1	0.85	2.37	3.201 (1)	165
O2W–H2WB···O5	0.85	2.47	2.821(1)	105
O1W–H1WB···O3^{iv}	0.85	2.04	2.868 (1)	164

Symmetry code: (i) –x+2,y,-z+3/2; (ii) –x+1,y,-z+1/2; (iii) x,-y,z-1/2; (iv) x,-y+1,z+1/2

The crystalline packaging of the title compound is achieved by intramolecular and intermolecular bonds. Hydrogen bond geometry is given in Table 3. O1W–H1WB···O3^{iv} and O2W–H2WB···O5 bonds between the O atoms of the carboxyl group of nalidixic acid and the O atoms of the lattice water molecule are bonded with hydrogen bonds. These monomeric structures form the 1D polymeric structure in the [001] direction with the C(9) chains (Figure 3). Similarly, the 2D polymeric structure is formed by adding the hydrogen bonds between O3W and O4W lattice water in (101) plane and resulting in $R_8^8(22)$ synthons at (n_1+½, ½, n_2+½ n_1 and n_2 =0 or integer) positions (Figure 4). In addition, with participating to packing of C–H···O bonds, 3D supramolecular structure is formed (Figure 5). π–π interactions play also an important role in the formation of a 3D supramolecular structure.

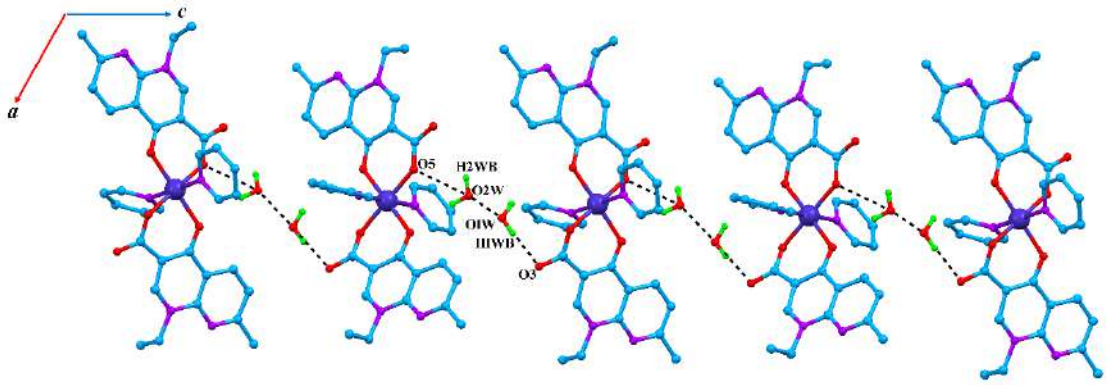

Figure 3. The 1D polymeric structure of O–H···O hydrogen bonds for the complex formed by the C (9) chains (Non–relevant H atoms were omitted for clarity)

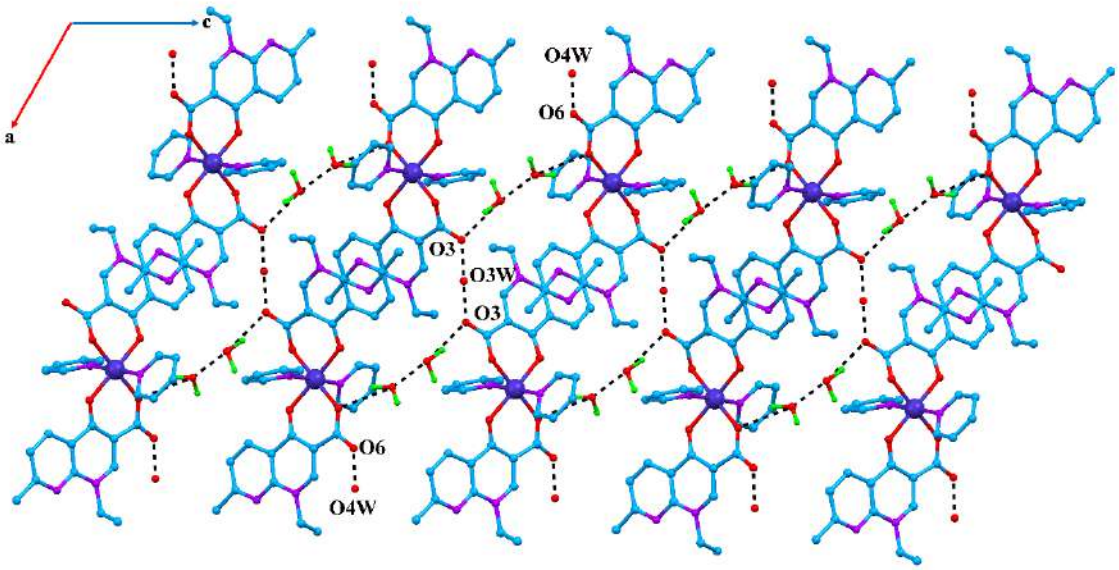

Figure 4. 2D planar structure generated by the hydrogen bonds of the lattice water molecules for the complex (Non–relevant H atoms were omitted for clarity)

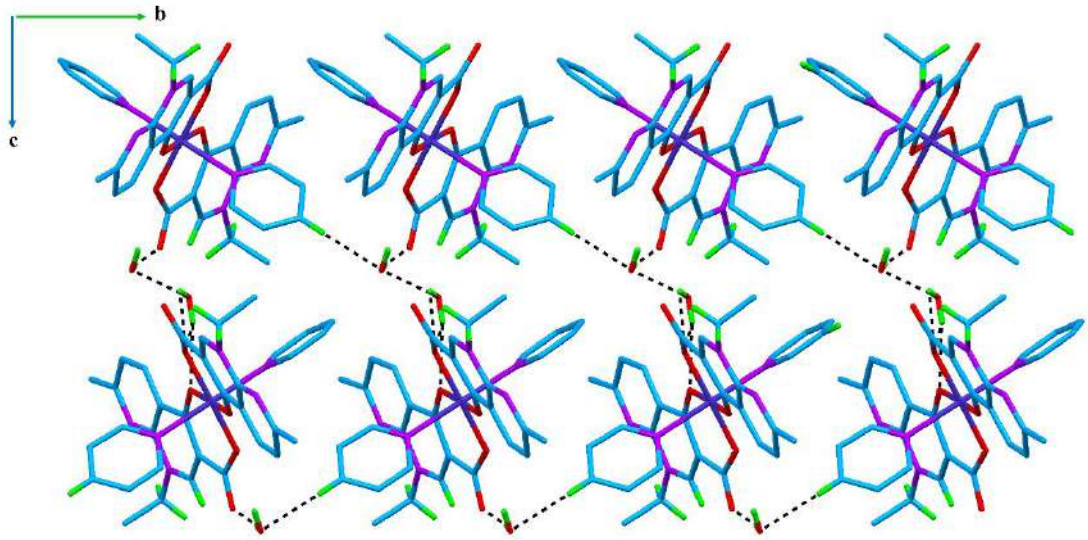

Figure 5. 3D supramolecular structure of the complex formed by C27–H27 ⋯ O1W bonds

3.2. IR spectra

When the IR spectrum of the complex is examined, characteristic and strong peaks in the range 4000–400 cm^{-1} are observed. The IR spectrum of the complex is given in Figure 6.

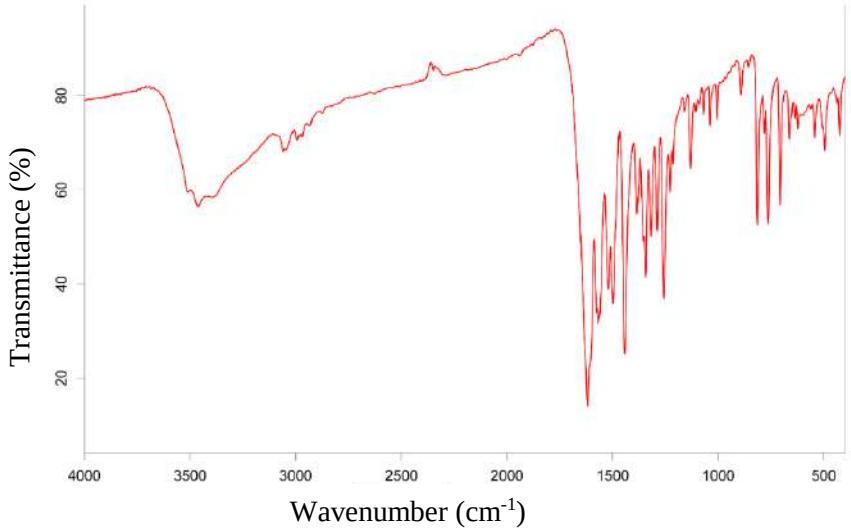

Figure 6. Experimental IR spectrum of complex

The peaks seen at 3499 cm^{-1} and 3437 cm^{-1} are due to the stretching vibrations of the crystal lattice $\nu(H_2O)$. While stretch peaks of CH_3 and CH_2 are observed in the range of 3019–2933 cm^{-1} in the free ligand, they are seen in the range of 3016–2898 cm^{-1} in the Co(II) complex (Table 4). The peaks of 1820 cm^{-1}, 1797 cm^{-1}, 1718 cm^{-1} in the IR spectra of nalidixic acid are assigned to the v(C=O) and v(C=O) stretching vibrations while v(C=O) stretching vibration at 1652 cm^{-1} is originated. Because of the formation of the Co (II) complex and the coordination of nalidixic acid from the oxygen atoms to the metal, the strong stretching vibrations of the C=O group are shifted to 1699 cm^{-1} and are observed as a broad peak.

Table 4. Characteristic vibration peaks for Co(II) complex and nalidixic acid

Assignment	Hnal (cm^{-1})	$[Co(nal)_2(py)_2]\cdot 4H_2O$ (cm^{-1})
$\nu(H_2O)$	–	3509,3462,3390
$\nu(CH)_{pyr}$ (ligand)	–	3342
$\nu(CH)_{pyr}$	3075	3060
$\nu(CH_3)+\nu(CH_2)$	3019–2933	2994,2968,2932
$\nu(CO)+\nu(C=O)_{pyr}$	1820,1797,1718	1619
$\nu(C=O)_{COOH}$	1652	
$\nu(C=C)_{nal}$	1606z	1605
$\nu_{as}(COO)^-$	–	1567
$\nu(C=O)_{pyr}$	1573,1556	1575
$\nu(C=N)_{pyr}$	1530	1520
$\nu(C=N)_{pyr}$	1503	1498

ν(CC)	1457	1443
δ(OH)	1416	–
$\nu_s(COO)^-$	–	1385
$\delta_s(CH_3)+\delta(CH)$	1392, 1377, 1361, 1355	1355
$\delta_{as}(CH_3)+\nu(CC)$	1337,1306,1290,1240	1344,1318,1289,1258
$\beta(CH)_{pyr}$	1152,1148	1160,1130

3.3. UV–Vis Spectra

The UV–Vis spectrum of the complex and nalidixic acid was recorded in DMF and in the range of 190–1100 nm. The UV–Vis spectrum of nalidixic acid has characteristic absorption bands (Neugebauer et al., 2005). The bands observed in the range 204–257 nm are from the π→π* transition of the aromatic ring. The calculated value of the π→π* transition is observed in the range of 202–259 nm for the free ligand, while the complex is observed in the range of 203–252 nm (Figure 7). The maximum of 337 nm and 339 nm observed in the experimental UV–Vis spectrum of nalidixic acid and complex is due to the transition of n → π *, respectively. The band observed in the visible region of the complex originates from the d–d transition (638 and 496 nm). These bands correspond to $^4T_{1g}(F)\rightarrow {}^4A_{2g}(F)$ ve $^4T_{1g}(F)\rightarrow {}^4T_{1g}(P)$ transitions (Raman et al., 2004).

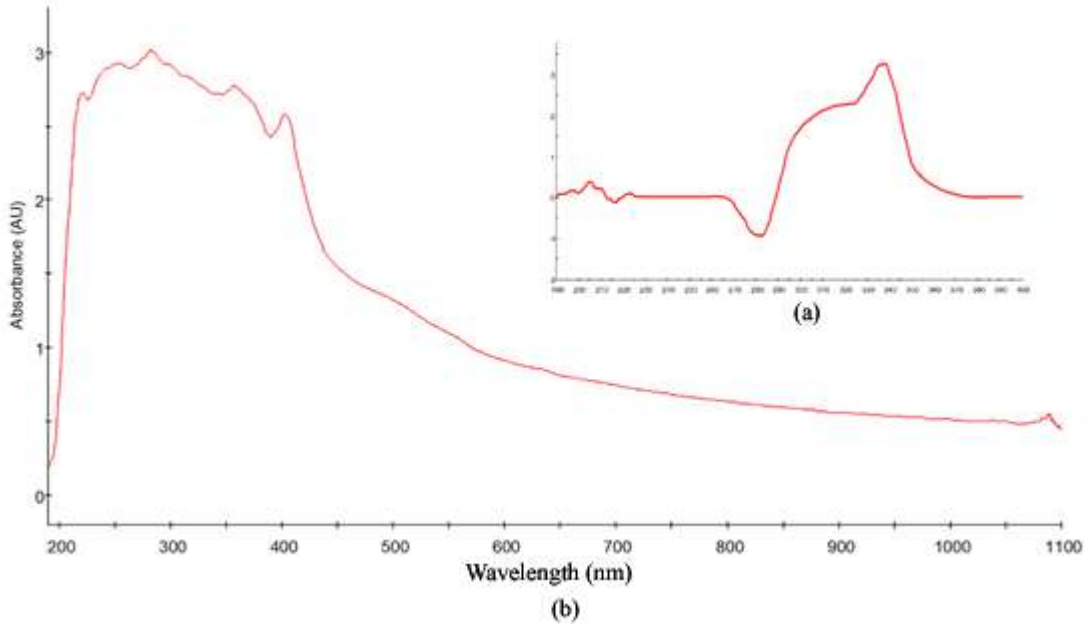

Figure 7. Experimental UV–Vis spectrum of (a) Nalidixic Acid and (b) The complex

3.4. Thermal Analysis

The thermal analysis curve of $[Co(nal)_2(py)_2]\cdot 4H_2O$ complex is given in Figure 8. In the temperature range of 20–318 °C, four moles of free water molecules and two moles of pyridine ligand are endothermically degraded. A total reduction of 30.51% occurs in these two steps (DTGmax: 75, 145 and 173 °C; calcd: 31.46%). The remaining organic product decomposes some of the structure of Nalidixic acid with a strong decomposition in the 318–377 °C temperature range and these decomposition continues to 995 °C. As a result of these degradations, the conversion to CoO is carried out (total loss of mass: exp: 88.71%; calcd: 89.76%).

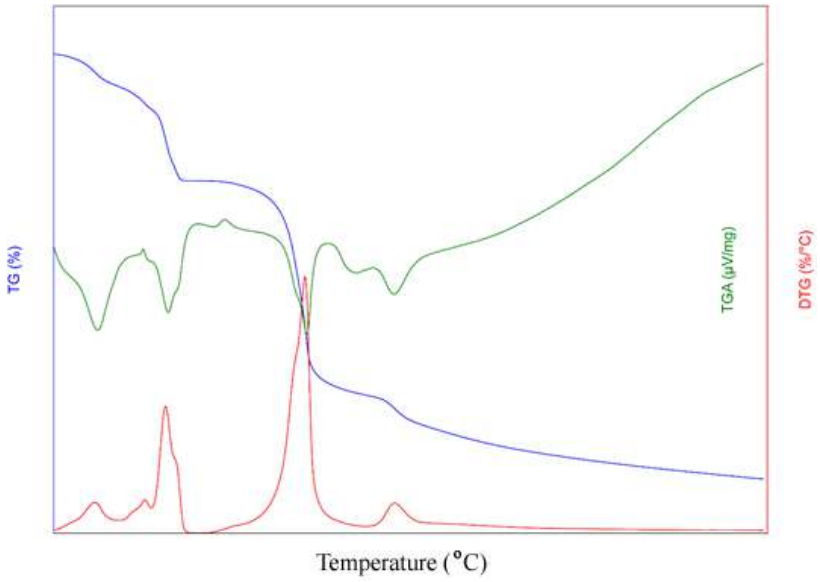

Figure 8. Thermogravimetric curves of the complex (TG, DTG and DTA)

Acknowledgement

Financially, Ondokuz Mayıs University has supported this study (Project No: PYO.FEN.1904.15.022).

References

Aggarwal, N., Kumar, R., Dureja, P. and Khurana, J. (2011). Synthesis, antimicrobial evaluation and QSAR analysis of novel nalidixic acid based 1, 2, 4-triazole derivatives. *European journal of medicinal chemistry*, *46*(9), 4089-4099.

Arjmand, F., Yousuf, I., Afzal, M. and Toupet, L. (2014). Design and synthesis of new Zn (II) nalidixic acid–DACH based Topo-II inhibiting molecular entity: Chemotherapeutic potential validated by its in vitro binding profile, pBR322 cleavage activity and

molecular docking studies with DNA and RNA molecular targets. *Inorganica Chimica Acta, 421*, 26-37.

Balaji, G., Rajesh, K., Priya, R., Iniyavan, P., Siva, R. and Vijayakumar, V. (2013). Ultrasound-promoted synthesis, biological evaluation and molecular docking of novel 7-(2-chloroquinolin-4-yloxy)-4-methyl-2H-chromen-2-one derivatives. *Medicinal Chemistry Research, 22*(7), 3185-3192.

Emmerson, A. and Jones, A. (2003). The quinolones: decades of development and use. *Journal of Antimicrobial Chemotherapy, 51*(suppl_1), 13-20.

Farrugia, L. J. (1997). ORTEP-3 for Windows-a version of ORTEP-III with a Graphical User Interface (GUI). *Journal of Applied Crystallography, 30*(5), 565-565.

Farrugia, L. J. (1999). WinGX suite for small-molecule single-crystal crystallography. *Journal of Applied Crystallography, 32*(4), 837-838.

Fernández-Galleguillos, C., Saavedra, L. A. and Gutierrez, M. (2014). Synthesis of new 3-(2-chloroquinolin-3-yl)-5-phenylisoxazole derivatives via click-chemistry approach. *Journal of the Brazilian Chemical Society, 25*(2), 365-371.

Gangavaram, S., Raghavender, S., Sanphui, P., Pal, S., Manjunatha, S. G., Nambiar, S. and Nangia, A. (2012). Polymorphs and cocrystals of nalidixic acid. *Crystal Growth & Design, 12*(10), 4963-4971.

Macrae, C. F., Edgington, P. R., McCabe, P., Pidcock, E., Shields, G. P., Taylor, R., . . . Streek, J. v. d. (2006). Mercury: visualization and analysis of crystal structures. *J. Appl. Crystallogr., 39*(3), 453-457.

Neugebauer, U., Szeghalmi, A., Schmitt, M., Kiefer, W., Popp, J. and Holzgrabe, U. (2005). Vibrational spectroscopic characterization of fluoroquinolones. *Spectrochim Acta A Mol Biomol Spectrosc., 61*(7), 1505-1517. doi:10.1016/j.saa.2004.11.014

Raman, N., Ravichandran, S. and Thangaraja, C. (2004). Copper (II), cobalt (II), nickel (II) and zinc (II) complexes of Schiff base derived from benzil-2, 4-dinitrophenylhydrazone with aniline. *Journal of Chemical Sciences, 116*(4), 215-219.

Sheldrick, G. (1992). *SHELXS-97 and SHELXL-97*. Germany,: University of Gottingen.

Synthesis, spectroscopic, structural characterization and magnetic studies of copper(II)-sulfamethazine complex with N-(2-hydroxyethyl)-Ethylenediamine

Filiz ÖZTÜRK[1,*], Tuğba AYCAN[2]

[1]Karadeniz Advanced Technology Research and Application Center, Ondokuz Mayıs University, Samsun, Turkey; filiz.ozturk@omu.edu.tr

[2]Department of Physics, Faculty of Arts and Sciences, Ondokuz Mayıs University, Samsun, Turkey; tugba.aycan@omu.edu.tr

[*] **Corresponding Author:** filiz.ozturk@omu.edu.tr

Abstract

2([Cu(hydeten)$_2$]·smz$_2$)·na·5H$_2$O (Hsmz: sulfamethazine, hydeten: N-(2-hydroxyethyl)-Ethylenediamine and na; nicotinamide) complex has been synthesized and the techniques used for the characterization have been single crystal X-ray diffraction, IR, EPR and UV-vis. The title complex crystallizes in monoclinic system with space group P2$_1$/c with a = 8.3424(2) Å, b = 39.3072(9) Å, c = 14.2053(4) Å, β= 106.274(2)°, V = 4471.5(2) Å^3 and Z = 2. The copper(II) center is surrounded by four nitrogen atoms and one oxygen atoms from hydeten ligands and exhibits a distorted square-pyramidal geometry ($\tau = 0.23$). The vibrational investigation has been carried out on the basis of some characteristic IR bands of complex. The powder EPR spectra of Cu(II) complex at room and liquid nitrogen temperature were recorded. Based on EPR and optical absorption studies, spin-Hamiltonian and bonding parameters have been calculated, indicate the presence of the unpaired electron in the $d_{x^2-y^2}$ orbital.

Keywords: Sulfamethazine; X-ray crystal structure; EPR, IR

1. Introduction

Sulfonamides were the first effective chemotherapeutic agents used systematically for the avoiding and treatment of bacterial infections in humans. Aromatic sulfonamide derivatives and their metal complexes possess many applications, in addition to antibacterial activity such as diuretic, antiglaucoma or antiepileptic drugs, among others (Corradi et.al., 1994; Ferrer et.al., 1990), like antifungal activity and, in many cases, metal-ligand complexes have a higher biological activity than single ligand complexes (Barboiu et.al., 1996; Bellú et.al., 2005).

It is used to treatment of bacterial diseases in human and veterinary medical that sulfanamide group is a drug Sulfamethazine (Hsmz; Figure 1) (Tiwari et.al., 1984; Maury et.al., 1985). Sulfamethazine is an anti-infective agent with antimicrobial activity similar to other sulfo drugs (Giuseppetti et.al., 1994; Nakai et.al., 1984). As a continuation of these studies, we synthesized and characterized a complex that four N-(2-hydroxyethyl)-ethylenediamine and four sulfamethazine ligands surrounding two copper ions.

In this study, Cu(II) complex with X ray diffraction, elemental analyses, EPR, UV-vis and FT-IR was characterized.

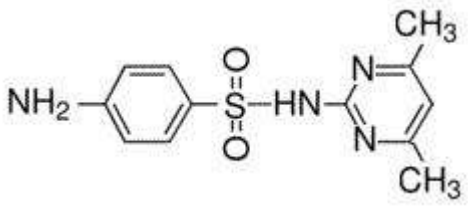

Figure 1. Sulfamethazine (Hsmz)

2. Material and Method

2.1. Synthesis of 2([Cu(hydeten)$_2$]·smz$_2$)·na·5H$_2$O

Aqueous solution (20 mL) of $CuCl_2 \cdot 6H_2O$ (2 mmol) was added to an aqueous solution (20 mL) of sulfamethazine (4 mmol). Then, precipitates were filtered and washed. Methanol solution(20 mL) with hydeten (4 mmol) and na (4 mmol) were added into methanol solutions of these precipitates under stirring. The solution was heated to around 60ºC with stirring for 2 h, then filtered and the mixture was allowed to crystallize at room temperature. After about four week, dark blue single crystals of the compound were obtained.

2.2. Physical measurements and Crystal Structure Determination

All chemicals were purchased from commercial sources and used without further purification. The FT-IR spectra with KBr technique were recorded in a Bruker Vertex 80V spectrometer in the mid-IR region (4000-400 cm^{-1}). The spectra was converted in to transmittance using Bruker OPUS software. The powder and solution samples EPR spectra was recorded by a Varian E-109C model spectrometer X-band EPR spectrometer with a magnetic field modulation frequency of 100 kHz. The *g* values were obtained by comparison with *g*=2.0036 of standard sample Cu^{2+}. UV-vis absorpsion spectrum of complex were registired at room temperature in DMF solution on a Unicam UV–Vis spectrophotometer working between 200 and 900 nm.

XRD data was collected using a Stoe IPDS diffractometer at 296 K by graphite monochromatic MoK_α radiation (λ=0.71073 Å). Data reduction: Stoe X-RED (Stoe ve Cie, 2002), Cell refinement: Stoe X-AREA (Stoe ve Cie, 2002), Data collection: Stoe X-AREA (Stoe ve Cie, 2002). By direct methods analysed the crystal structure and all Cu, C, O and N atoms were refined anisotropically using the program SHELXL-2014 (Sheldrick, 2014). Molecular figures were drawn by using ORTEP-3, MERCURY software. Crystal data and structure refinement parameters for $[Co(nal)_2(py)_2]\cdot 4H_2O$ are given in Table 1.

Table 1. Crystal data and structure refinement parameters for 2([Cu(hydeten)$_2$]·smz$_2$)·na·5H$_2$O.

Formula	$C_{70}H_{114}Cu_2N_{26}O_{18}S_4$
Formula weight	1859.15
Temperature(K)	298
Radiation, λ(MoK$_\alpha$)	0.71073
Crystal system	Monoclinic
Space group	$P2_1/c$
Unit cell dimensions	
***a, b, c*(Å)**	8.3424 (2), 39.3072 (9), 14.2053 (4)
α, β, γ (°)	90, 106.274 (5), 90
Volume (Å^3)	4471.5 (2)
Z	2
Calculated density (Mg.m^{-3})	1.381
***μ*(mm^{-1})**	0.65
***F*(000)**	1956
Crystal size (mm)	0.60 × 0.29 × 0.12
***θ* range (°)**	1.5- 26.4
Index ranges	$-10 \le h \le 10$ $-48 \le k \le 48$ $-17 \le l \le 17$
Measured Reflections	46331
Independent reflections	16870
Reflections observed [$I \ge 2\sigma(I)$]	11075
Absorption correction	Integration
Refinement method	Full matrix least-squares on F^2
Data/restrains/parameters	16870/14/1047
Goodness-of-fit on F^2	0.97
Final *R* indices [$I \ge 2\sigma(I)$]	R_1= 0.068; wR_2= 0.175
***R* indices (all data)**	0.117
$\Delta\rho_{max}$; $\Delta\rho_{min}$ (eÅ^{-3})	0.61; -0.44

3. Results and Discussion

3.1. Molecular structure

The title compound (Fig.2) consists of discrete four smz^{1-} anions, two [Cu(hydeten)$_2$]$^{2+}$ complex cations, one na and five lattice waters molecules. Cu1 cation is coordinated with two hydeten ligands, which while one has a tripodal conformation, the other acts as bidentate ligand through the two N atoms. The other Cu2 also has same coordination. The geometric values describing the coordination polyhedron of Cu(II) ions, according to τ values defined by Addison, et al. (1984) correspond to slightly distorted square pyramidal environment and τ (τ = (β-α)/60) values have found 0.23 to two Cu(II) ions (Addison, 1984). Here, β and α are the largest bond angles of the atoms coordinated to around of the metal (Table 1). While the equatorial position of the distorted square pyramidal geometry is constructed by the nitrogen

atoms of hydeten ligands, the oxygen atom of it is the axial sites of square pyramidal geometry. It is noted that O1 and O3 in axial positions are weakly bonded to Cu1 and Cu2 ions, respectively, when compared to nitrogen atoms in equatorial plane (Table 2). Hydeten ligands that is five-coordinated to the copper metal are found barely in the literature. When we examine the compounds with four or six-coordination, the Cu-N bond lengths of the complex are in good agreement with the corresponding distances in the literature that is reported for: $[Cu(hydeten)_2Pt(CN)_4]$ [Cu–N3: 2.029(4) Å, Cu–N4: 2.070 (4) Å] and $[Cu(NCS)_2(hydeten)]$ [Cu-N3:2.013(3) Å, Cu-N4: 2.000(3) Å] (Karadağ et.al., 2009; Paşaoğlu et.al., 2005).

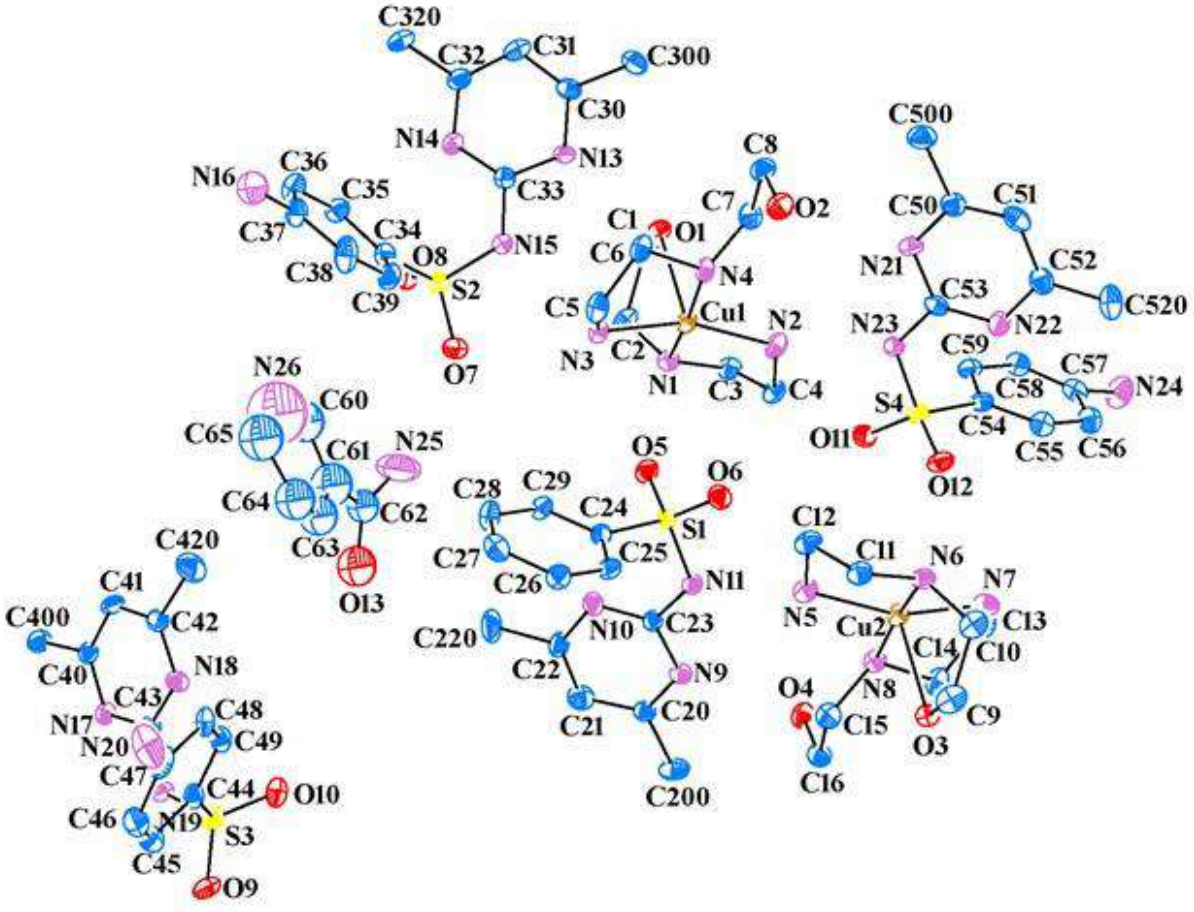

Figure 2. *The molecular view of 2([Cu(hydeten)$_2$]·smz$_2$)·na·5H$_2$O given with the atom labelling drawn in Ortep-3. Hydrogen atoms and water molecules were omitted for simplify.*

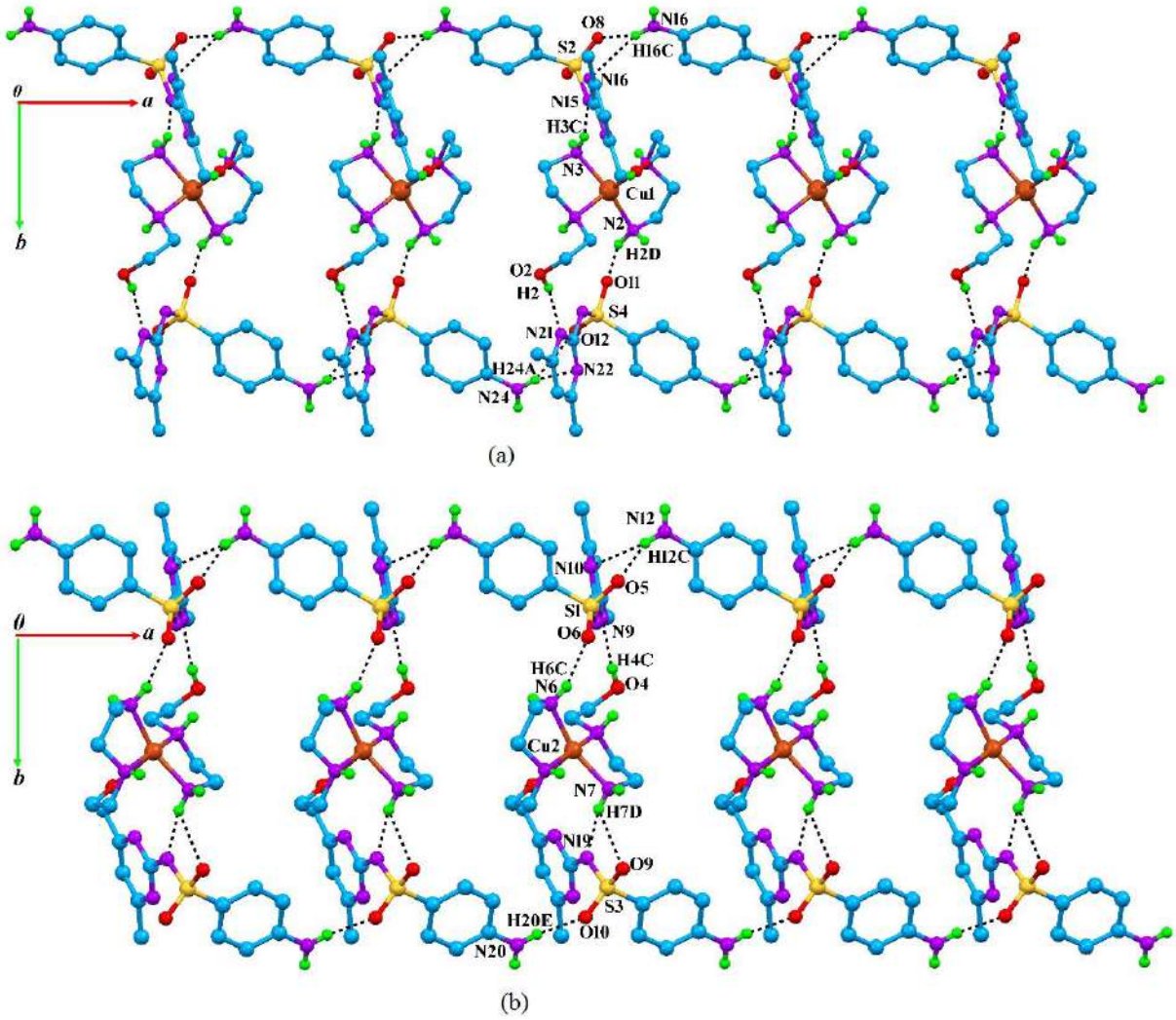

Figure 3. *1D polymeric ribbons formed by connecting (a) $[Cu(hydeten)2]^{2+}$ (involving Cu1) cation and smz2 and smz4 anions (b) $[Cu(hydeten)2]^{2+}$ (involving Cu2) cation and smz1 and smz3 anions by H-bonds in [100] direction.*

Table 2. *Selected bond distances (Å) and angles (º) of the complex and similar structure reported in the literature.*

	Complex	$Ni(dien)_2]\cdot(smz)_2$(Bulut and et.al.,2015), $[Cu(C4H12N2O)_2]\cdot(ClO4)_2$ (Chastain and et.al., 1973)		Complex	$[Cu(C4H12N2O)_2]\cdot(ClO4)_2$ (Chastain and et.al., 1973)
Bond lengths (Å)			Bond angles (º)		
Cu1-N1	2.030(8)	2.036(3)	N2-Cu1-N3	158.4(4)	166.0
Cu1-N2	2.037(2)	2.012(4)	N2-Cu1-N4	96.0(3)	95.0
Cu1-N3	2.004(9)	2.041(3)	N4-Cu1-N3	86.3(3)	84.9
Cu1-N4	2.020(8)	2.018(4)	N2-Cu1-N1	85.7(4)	84.8
Cu1-O1	2.330(7)	2.419(3)	N1-Cu1-N3	95.0(3)	98.7
Cu2-N5	2.022(8)	-	N1-Cu1-N4	172.1(4)	165.7
Cu2-N6	2.010(9)	-	N2-Cu1-O1	110.1(4)	89.6
Cu2-N7	1.991(9)	-	N3-Cu1-O1	91.2(3)	76.6
Cu2-N8	2.023(9)	-	N4-Cu1-O1	93.3(3)	96.6
Cu2-O3	2.308(7)	-	N1-Cu1-O1	78.9(3)	97.7
N11-C23	1.368(13)	1.374(3)	N7-Cu2-N6	158.7(4)	-
N11-S1	1.573(8)	1.568(2)	N7-Cu2-N5	95.6(3)	-
N15-C33	1.372(13)	-	N7-Cu2-N8	85.8(4)	-
N15-S2	1.584(9)	-	N6-Cu2-N5	85.4(4)	-
N19-C43	1.373(14)	-	N6-Cu2-N8	95.8(3)	-
N19-S3	1.591(9)	-	N5-Cu2-N8	172.9(4)	-
N23-C53	1.385(12)	-	N7-Cu2-O3	92.1(3)	-
N23-S4	1.567(8)	-	N6-Cu2-O3	108.8(3)	-
			N5-Cu2-O3	78.9(3)	-
			N8-Cu2-O3	94.2(3)	-

The title complex has a lot of inter-molecular and intra-molecular hydrogen bonds due to donor and acceptor groups of hydeten and smz, these hydrogen bonds is important to form the supramolecular structure (Table 3). The discrete $[Cu(hydeten)_2]^{2+}$ cation (involving Cu1) and smz2 and smz4 anions are connected by H-bonds involving N-H···O and N-H···N interactions resulting in $R_2^1(6)$ synthons, $R_2^2(13)$ synthons and $R_2^1(6)$ synthons (Etter , 1990; Bernstein, 1995) (Figure 3(a)). Similarly, the discrete $[Cu(hydeten)_2]^{2+}$ cation (involving Cu2) and smz 1 and smz 3 anions are connected by H-bonds resulting in $R_2^1(6)$ synthons, $R_2^2(13)$ synthons, $R_2^1(6)$ synthons and C(8) chains. (Figure 3(b)).

Table 3. *Hydrogen bonding geometry of 2([Cu(hydeten)$_2$]·smz$_2$)·na·5H$_2$O.*

D-H···A	D-H	H···A	D···A	D-H···A
C8—H8B···O4^{i}	0.97	2.56	3.469 (13)	156
N1—H1···N12^{iii}	0.98	2.54	3.428 (16)	150
N1—H1···O5	0.98	2.42	3.126 (11)	129
N2—H2C···O3W	0.89	2.21	2.969 (14)	143
N2—H2D···O11	0.89	2.24	3.038 (13)	149
N3—H3C···N15	0.89	2.10	2.960 (12)	163
N3—H3C···O7	0.89	2.66	3.183 (12)	119
N3—H3D···O5	0.89	2.40	3.061 (11)	131
N4—H4···O4W	0.98	2.00	2.970 (13)	169
N5—H5···N24^{iv}	0.98	2.56	3.424 (16)	147
N5—H5···O12	0.98	2.41	3.113 (11)	129
N6—H6C···O6	0.89	2.20	3.017 (12)	152
N6—H6D···O2W	0.89	2.17	2.950 (14)	146
N7—H7C···O12	0.89	2.37	3.033 (11)	131
N7—H7D···N19^{v}	0.89	2.07	2.937 (13)	163
N8—H8···O5W^{vi}	0.98	2.00	2.969 (12)	170
N12—H12D···N10^{iv}	0.86	2.41	3.216 (15)	156
N12—H12D···O5^{iv}	0.86	2.60	3.227 (14)	130
N16—H16C···N14^{iv}	0.86	2.56	3.320 (17)	149
N16—H16C···O8^{iv}	0.86	2.54	3.220 (17)	137
N20—H20D···O13^{iv}	0.86	2.08	2.90 (2)	159
N20—H20E···O10^{iv}	0.86	2.20	2.987 (17)	152
N24—H24A···N22^{iii}	0.86	2.48	3.268 (16)	153
O1—H1C···N13	0.93	2.16	2.656 (11)	113
O2—H2···N21	0.82	2.02	2.776 (13)	152
O3—H3···N17^{v}	0.93	2.19	2.665 (11)	111
O4—H4C···N9	0.82	1.97	2.751 (12)	159
N25—H25B···O7	0.86	2.12	2.84 (2)	141
O5W—H5WB···N11^{vii}	0.91 (3)	2.00 (4)	2.902 (12)	171 (19)
O5W—H5WB···O6^{vii}	0.91 (3)	2.6 (3)	3.251 (11)	127 (25)
O5W—H5WA···O11^{vii}	0.92 (3)	2.02 (12)	2.819 (11)	145 (17)
O4W—H4WA···O6	0.90 (3)	1.94 (3)	2.835 (11)	173 (8)
O4W—H4WB···N23	0.89 (3)	2.03 (4)	2.903 (12)	165 (8)

Symmetry codes: (i) x−1, y, z−1; (iii) x+1, y, z; (iv) x−1, y, z; (v) −x+1, y+1/2, −z+2; (vi) −x+1, y+1/2, −z+1; (vii) −x, y+1/2, −z+1.

In addition, the nicotinamide ligand between smz2 and smz3 is ligated to each other via hydrogen bonds to make progression of 1D tape formation (Figure 4), resulting in hydrogen bonded wavy chains in [010] directions (Figure 5) (Beatty, 2003).

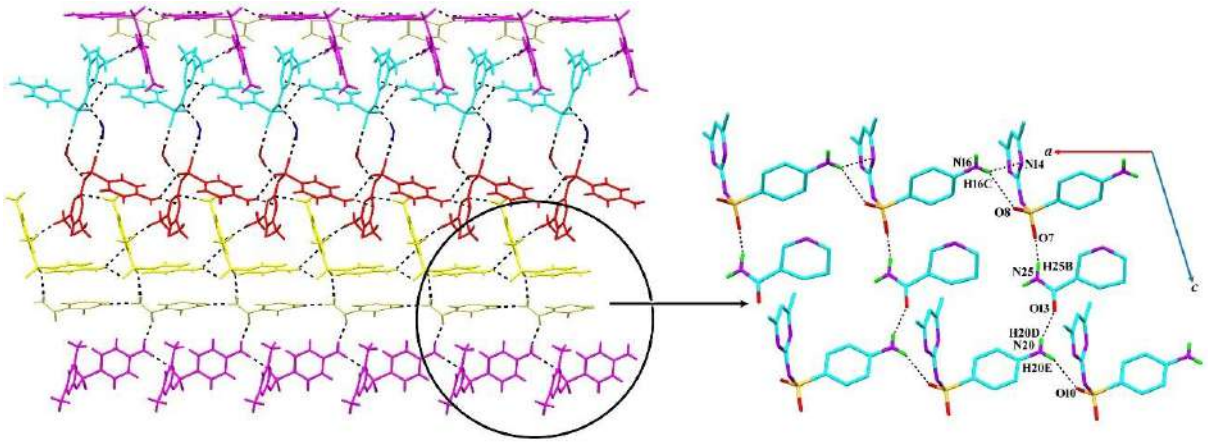

Figure 4. *2D supramolecular structure formed with progressing of 1D pseudo-rectangular-shaped structure (the nicotinamide ligand is bridging between smz2 and smz3). Hydrogen atoms have been omitted for clarity.*

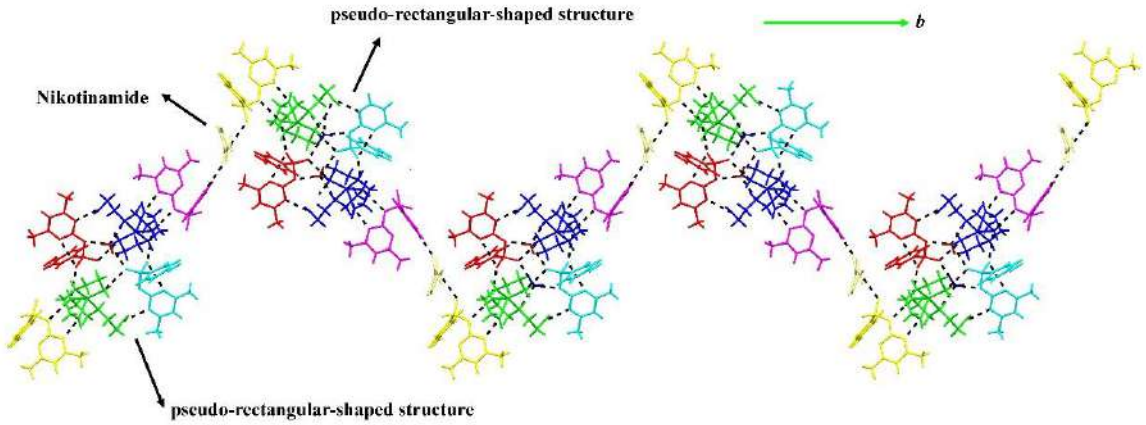

Figure 5. *The view in a direction of 2D wavy chains formed in [010] direction by hydrogen bonds.*

3.2. UV and EPR study

In the UV-vis spectrum of the copper complex which was taken in DMF at room temprerature has observe a strong band at around 320 nm (31250 cm^{-1}), a shoulder at 400 nm (25000 cm^{-1}) and a broad band at 596 nm (16778.5 cm^{-1}). The broad band at 596 nm is designated to $d_{xy} \rightarrow d_{x^2-y^2}$ transition of Cu^{2+} ion in a penta coordinated square–pyramidal symmetry (C4v) (Mohan ve ark, 1988; Hathaway and Tomlinson, 1970). The EPR spectra of

copper(II) compound at room temperature and liquid nitrogen temperature were recorded (Fig. 6). Copper complexes with five coordination may either a square pyramidal or trigonal bipyramidal structure (Addison et.al., 1984; Styka et.al., 1978). In this case the ground states will be $d_{x^2-y^2}$ or d_{z^2} respectively (Barbucci et.al., 1977). The EPR spectra of Cu(II) complex in the polycrystalline state at 298 K show only one broad signal at g_{iso} = 2.07 and the spectra of complex in DMF at 77 K show with three g values g_1 (g_y=1.98), g_2 (g_x=2.05), and g_3 (g_z=2.20) that indicate rhombic distortion in the geometry and tetragonally elongated square pyramids copper(II) ion environment, that is a characteristic of much of the Cu(II) complexes in solution (Styka et.al., 1978; Kopel et.al., 2003; John et.al., 2003). Results obtained of the EPR analysis is in fairly good agreement with the copper geometries obtained from the crystal structures (τ = 0.23).

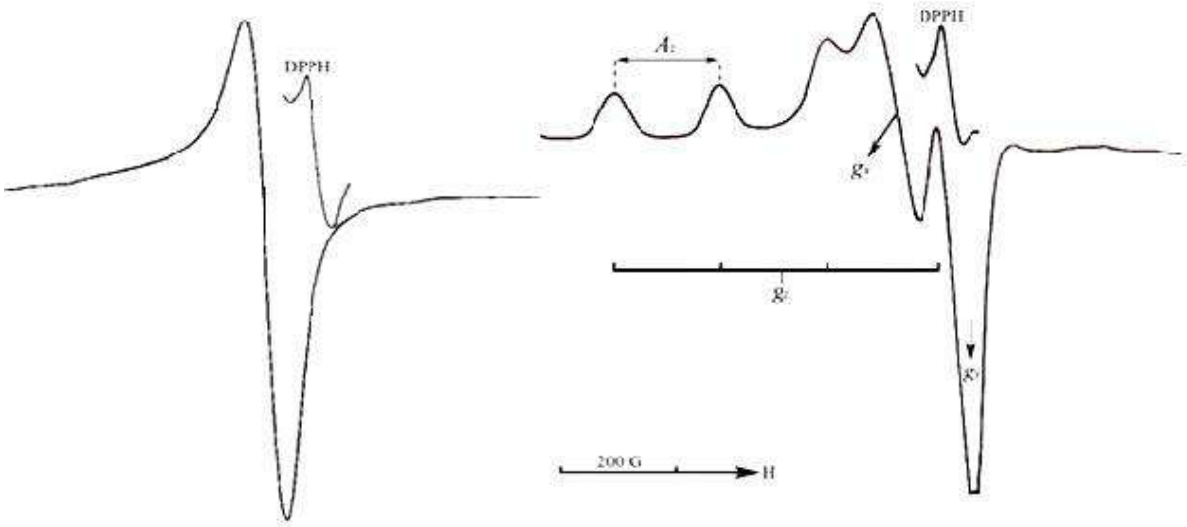

Figure 6. (a) The powder EPR spectrum at room temperature of complex, **(b)** The EPR spectrum in DMF solution of complex.

The g values obtained from the spectrum appear to be $g_3 \rangle g_2 \rangle g_1$ (Table 4). The g values are related by the expression: $R = (g_2 - g_1)/(g_3 - g_2)$. When R is greater than one which the d_{z^2} is the predominant ground state and when R is less than one which the $d_{x^2-y^2}$ is the predominant ground state. In this study, the calculated of R (0.46) values shown that $d_{x^2-y^2}$ is the ground state and copper (II) complex is recommend a distorted square based pyramidal geometry. It is agreement with UV and XRD (Philip et.al., 2005; El-Sonbati et.al., 2003).

It is seen that the copper complex with the elongated-square pyramid environment is almost axially to the g and A values obtained from the EPR spectrum (John et.al., 2003; Philip et.al., 2005; El-Sonbati et.al., 2003).

Table 4. EPR and bonding parameters of 2([Cu(hydeten)$_2$]·smz$_2$)·na·5H$_2$O.

	This work	[Cu(L2)2,2'-biby)] (John et.al., 2003)	[Cu(dptsc)(μ-N$_3$]$_2$ (Philip et.al., 2005)
$g_{//}/g_z(g_3)$	2.20	2.194	2.1961
g_x (g_2)	2.05	2.055	2.0631
g_y (g_1)	1.98	2.034	1.9868
g_{av} *(77K)*	2.076	2.099	2.0820
giso (solid)	2.07	2.690	2.0638
$A_{//}/A_z(G)$	172	170	175

3.3. FT-IR Vibrational Spectra

The title complex may have stretching OH modes in 3523 cm^{-1} being originated from OH group of lattice water (Uçar et.al., 2009). There are the $\upsilon_{as}(NH_2)$ and $\upsilon_s(NH_2)$ vibration peaks for three different ligands that is smz anions, hydeten ligands and nicotinamide. These peaks are assigned at 3439 cm^{-1} and 3347 cm^{-1} for smz, at 3389 cm^{-1} and 3161 cm^{-1} for na and 3271 cm^{-1}, 3244 cm^{-1} and 3217 cm^{-1} for hydeten. The OH stretching originate from hydeten ligands are observed at 3334 cm^{-1} in the complex spectrum, while it is observed at 3325 cm^{-1} in the free hydeten spectrum. These shift is arisen from coordinating to metal as well as to do hydrogen bond of hydroxyl group in the hydeten. Because of the deprotonation of the –SO_2NH– moiety, the peak for the sulfonamide (N–H) group in the free ligands at around 3125 cm^{-1} are not observed in the spectrum of the complex (Hossain et.al., 2007). The asymmetric SO_2 and symmetric SO_2 stretching vibrations of smz ions generally appear in the region 1390-1290 cm^{-1} and 1190-1120 cm^{-1}, respectively (Bulut et.al., 2015; Öztürk et.al., 2015). In complex, the $\upsilon_{as}(SO_2)$ and $\upsilon_s(SO_2)$ vibrations appears at 1375 cm^{-1}, 1311 cm^{-1} and 1132 cm^{-1}, respectively, this value is corresponding with literature (Bulut et.al., 2015; Öztürk et.al., 2015).

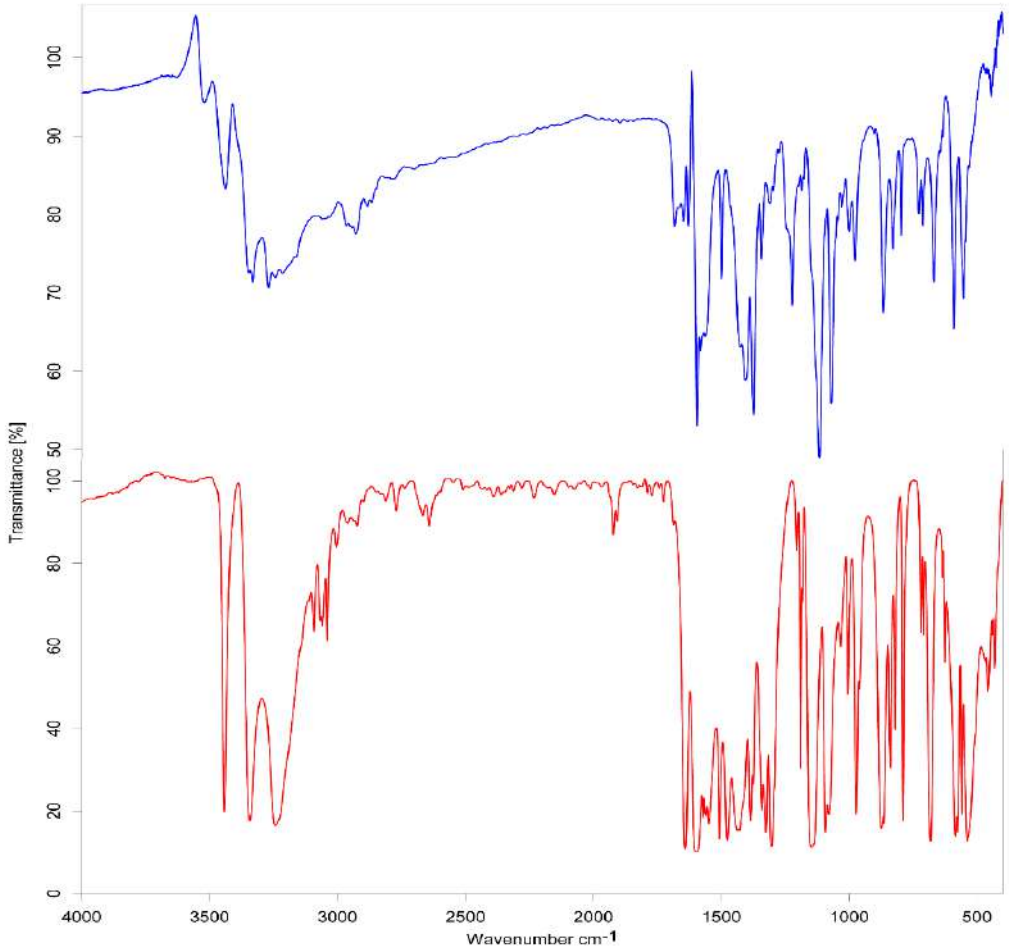

Figure 7. IR spectrum of the compound (blue line), IR spectrum of sulfamethazine (red line)

Table 5. Characteristic FT-IR bands of 2([Cu(hydeten)$_2$]·smz$_2$)·na·5H$_2$O complex at room temperature (cm^{-1}).

Assignments	Hydeten (Uçar et.al., 2007)	smz	na	[Hg(smz)$_2$(DMF)$_2$] (Hossain et.al., 2007)	Complex
ν(H$_2$O)	-	-	-	-	3523m
ν_{as}(NH$_2$)(smz)	-	3442	-	3457	3439s
ν_{as}(NH$_2$)(na)	-	-	3368	-	3389sh
ν_s(NH$_2$)(smz)	-	3342	-	3360	3347s
ν(OH)	3325	-	-	-	3334s
ν_{as}(NH$_2$)+ν(NH) (hydeten)	3218m	-	-	-	3271s,3244s
ν_{as}(NH$_2$)(hydeten)	-	-	-	-	3217

$v_s(NH_2)$(na)	-	-	3163	-	3161
v(CH)(aromatic)	-	3094,3067, 3059,3039	3060	-	3061,3031
$v(CH_3)$(smz)	-	3003,2963, 2922	-	-	2967, 2930
$v_{as}(CH_2)$(hydeten)	2947s	-	-	-	2945
$v_{as}(CH_2)$(hydeten)	2832s	-	-	-	2884,2869
υ(C=O)	-	-	1697,1679	-	1684
$v_{as}(SO_2)$	-	1368,1303	-	1373, 1292	1375,1311
$v_s(SO_2)$	-	1146	-	1194	1132
v(CO)	1067s	-	-	-	1072
v(MN)	-	-	-	-	446

Acknowledgement

We would like thank to Ondokuz Mayıs University Research Fund (PYO.FEN.1904.12.019) for financial support.

References

Addison A. W., Rao T. N., Reedijk J., van Rijn J., Verschoor G. C. (1984). Synthesis, structure, and spectroscopic properties of copper(II) compounds containing nitrogen–sulphur donor ligands; the crystal and molecular structure of aqua[1,7-bis(N-methylbenzimidazol-2′-yl)-2,6-dithiaheptane]copper(II) perchlorate. Journal of the Chemical Society, Dalton Transactions 7, 1349-1356.

Barbucci R., Bencini A., Gatteschi D. (1977). Electron spin resonance spectra and spin-Hamiltonian parameters for trigonal-bipyramidal nickel (I) and copper (II) complexes. Inorg. Chem. 16, 2117-2120.

Barboiu M., Cimpoesu M., Guran C., Supuran C.T. (1996). 1,3,4-Thiadiazole Derivatives. Part 91. Synthesis and Biological Activity of Metal Complexes of 5-(2-Aminoethyl)-2-Amino-1,3,4-Thiadiazole. Metal Base Drugs, 3, 227-232.

Beatty A.M. (2003). Open-framework coordination complexes from hydrogen-bonded networks: toward host/guest complexes. Coordination Chemistry Reviews 246, 131-143.

Bernstein J., Davis R.E., Shimoni L. and Chang N.L. (1995). Patterns in Hydrogen Bonding: Functionality and Graph Set Analysis in Crystals. Angew Chem Int Edit 34, 1555-1573.

Bellú S., Hure E., Trapė M., Trossero C., Molina G., Drogo C., Wiliams P.A.M., Atria A.M., Acevedo J. C. M., Zacchino S., Sortino M., Campagnoli D., Rizzotto M. (2005). Synthesis, structure and antifungal properties of Co(II)–sulfathiazolate complexes. Polyhedron 24, 501-509.

Bulut I., Ozturk F. and Bulut A. (2015). Synthesis, structural and electrochemical properties of nickel(II) sulfamethazine complex with diethylenetriamine ligand. Spectrochim Acta A Mol Biomol Spectrosc. 138, 138-145.

Chastain Jr. R. and Dominick T.L. (1973). Crystal structure of bis[N-(2-hydroxyethyl)ethylenediamine]copper(II) perchlorate, $[Cu(C_4H_{12}N_2O)_2](ClO_4)_2$. Inorganic Chemistry 12, 2621-2625.

Corradi A.B., Gozzoli E., Menabue L., Saladini M., Battaglia L.P., Sgarabotto P. (1994). Palladium(II) complexes of N-sulfonylamino acids. Part 1. Solid-state behaviour of binary and ternary 2,2′-bipyridine-containing systems. J. Chem. Soc., Dalton Trans., 0, 273-278.

El-Sonbati A. Z., Al-Shihri A. S. and El-Bindary A. A. (2003). Polymer Complexes. XLIII. EPR, Spectra, and Stereochemical Versatility of Novel Copper(II)Polymer Complexes. Journal of Inorganic and Organometallic Polymers 13, 99-108.

Etter M.C. (1990). Encoding and decoding hydrogen-bond patterns of organic compounds. Accounts of Chemical Research 23, 120-126.

Ferrer S., Borraś J., Garcia-Espană E. (1990). Complex formation equilibria between the acetazolamide ((5-acetamido-1,3,4-thiadiazole)-2-sulphonamide), a potent inhibitor of carbonicanhydrase, and Zn(II),Co(II), Ni(II) and Cu(II) in aqueous and ethanol-aqueous solutions. J. Inorg. Biochem. 39, 297-306.

Giuseppetti G., Tadini C., Bettinetti G. P. (1994). 1:1 Molecular complex of trimethoprim and sulfametrole. Acta Crystallogr. C50, 1289–1291.

Hathaway B.J., Tomlinson A.A.G. (1970). Copper(II) ammonia complexes. Coord. Chem. Rev. 5, 1-43.

Hossain G. G., Amoroso A., Banu A., Malik K.(2007). Syntheses and characterisation of mercury complexes of sulfadiazine, sulfamerazine and sulfamethazine. Polyhedron 26, 967-974.

Karadağ A., Şenocak A., Önal İ., Yerli Y, Şahin E. and Başaran A.C. (2009). Preparation, structural, magnetic and thermal properties of two heterobimetallic cyano-bridged nickel(II)–copper(II)/platinum(II) coordination polymers. Inorganica Chimica Acta 362, 2299-2304.

Maury L., Rambau J., Pauvert B., Lasserre Y., Berge G., Audran M. J. (1985). Physicochemical and structural study of sulfamethazine. Pharm. Sci. 74 422-426.

Mohan M., Gupta M.P., Chandra L., Jha N.K. (1988). Synthesis, characterization and antitumour properties of some metal(II) complexes of 2-pyridinecarboxaldehyde 2′-pyridylhydrazone and related compounds. Inorg. Chim. Acta 151, 61-68.

Nakai H., Takasuka M., Shiro M.J. (1984). X-Ray and infrared spectral studies of the ionic structure of trimethoprim–sulfamethoxazole 1 : 1 molecular complex. Chem. Soc., Perkin Trans. 2, 1459–1464.

Öztürk F., Bulut İ. and Bulut A. (2015). Structural, spectroscopic, magnetic and electrochemical studies of monomer N-substituted-sulfanilamide copper (II) complex with 2, 2′-bipyridine Spectrochimica Acta Part A: Molecular and Biomolecular Spectroscopy 138, 891-899.

Paşaoğlu H., Karadağ A., Tezcan F. and Büyükgüngör O. (2005). [N-(2-Hy-droxy-ethyl)ethyl-enedi-amine-κ3N,N′,O]-cis-bis-(iso-thio-cyanato-κN)copper(II), Acta Crystallographica Section C: Crystal Structure Communications 61, 93-94.

Philip V., Suni V., Kurup M. R. P., Nethaji M. (2005). Novel binuclear copper(II) complexes of di-2-pyridyl ketone N(4)-methyl, N(4)-phenylthiosemicarbazone: Structural and spectral investigations. Polyhedron 24 1133-1142.

John R. P., Sreekanth A., Kurup M. R. P., Usman A., Ibrahim A. R., Fun H.-K. (2003). Spectral studies and structure of a 2-hydroxyacetophenone 3-hexamethyleneiminyl thiosemicarbazonate(-2) copper(II) complex containing 1,10-phenanthroline. Spectrochimica Acta Part A 59, 1349-1358.

Sheldrick G.M. (2014) SHELXL2014, program for crystal structure refinement. University of Gottingen, Germany

Stoe & Cie (2002) X-AREA (version 118) and X-RED (version104). Stoe & Cie, Darmstadt.

Styka M.C., Smierciak R.C., Beinn E.L., Desimone R.E., Passariello J.V. (1978). Copper (II) complexes containing a 12-membered macrocyclic ligand. Inorg. Chem. 17,82-86.

Tiwari R. K., Haridas M., Singh T. P. (1984). Structure of 4-amino-N-(4,6-dimethyl-2-pyrimidinyl)benzenesulphonamide (sulfadimidine), $C_{12}H_{14}N_4O_2S$. Acta Crystallogr. C40 655-657.

Uçar İ., Karabulut B., Bulut A., Büyükgüngör O. (2007). Synthesis, crystal structure, Cu2+ doped EPR and voltammetric studies of bis[N-(2-hydroxyethyl)ethylenediamine]zinc(II) squarate monohydrateJournal of Physics and Chemistry of Solids 68(1), 45-52.

Uçar İ., Bozkurt E., Kazak C., Bulut A. (2009). Structural characterization and EPR spectral studies on mononuclear copper (II) complex of saccharin with ethylnicotinate. Spectrochimica Acta Part A: Molecular and Biomolecular Spectroscopy 72, 11-16.

Structure 2-(2 solution of -((2,6-dichlorophenyl)amino)phenyl)acetic acid

Necmi DEGE[1*] and Sevgi KANSIZ[2]

[1*]Ondokuz Mayıs University, Faculty of Arts and Sciences, Department of Physics, Samsun, Turkey; necmid@omu.edu.tr

[2]Ondokuz Mayıs University, Faculty of Arts and Sciences, Department of Physics, Samsun, Turkey; sevgi.koroglu@omu.edu.tr

[*] **Corresponding Author:** necmid@omu.edu.tr

Abstract

Single-crystal X-ray measurements were carried out using STOE IPDS II diffractometer with graphite-monochromated Mo Ka radiation (λ= 0.71069 Å). Intensity data were collected at 296°C. The crystal structure was solved using direct methods and refined by means of a fullmatrix least-squares procedure. All programs used for the solution, refinement and display of the structures are included in the WinGx program package. X_Area and X_Step Softwares were applied for data collection, data reduction and cell refinement. Programs SHELXT and SHELXL were used to solve and to refine structures, respectively.

In the crystal structure of the title compound, 2-(2-((2,6-dichlorophenyl)amino)phenyl)acetic acid, diclofenac acid [C_{14} H_{11} Cl_2 N_1 O_2], is two-dimensional hydrogen-bonded supra-molecular complex. An Ortep III view of the molecule of is shown below. Single crystal of the molecular structure synthesized and crystallizes monoclinic form, space group C 2/c with a = 20.2338 Å, b = 6.9908 Å, c = 20.0551 Å, α = 90° β = 109.537°, γ = 90°, V = 2673.5 $Å^3$.

Keywords: diclofenac acid; X-ray difraction; acetic acid

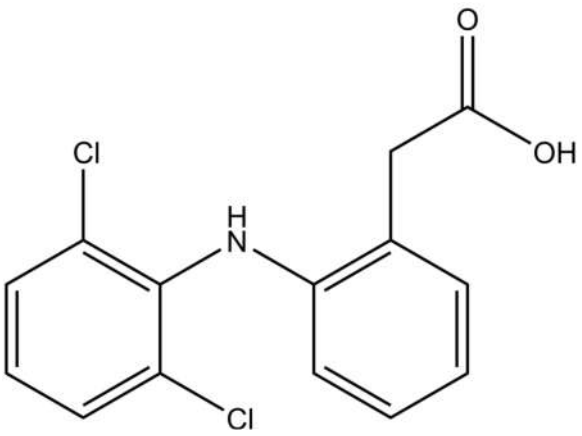

1. Introduction

Diclofenac, 2-[(2,6-dichlorophenyl)amino]phenylacetic acid (Fig. 1), is an excellent nonsteroidal anti-inflammatory drug and is mainly used in the treatment of rheumatoid arthritis and other rheumatoid disorders. It is a good example of a drug that is often prepared as a controlled-release formulation. Diclofenac has numerous solid forms, including the acid and various diclofenac salts. The exemplary diclofenac acid crystal forms include its monoclinic forms, in space group P2i/c. which is recrystallized from methanol by slow evaporation, and in C2/c, which is recrystallized from acetone (Castellari & Ottani, 1997). Diclofenac acid also exists in an orthorhombic form in space group Pcan, which is recrystallized from hot methanol by slow evaporation.

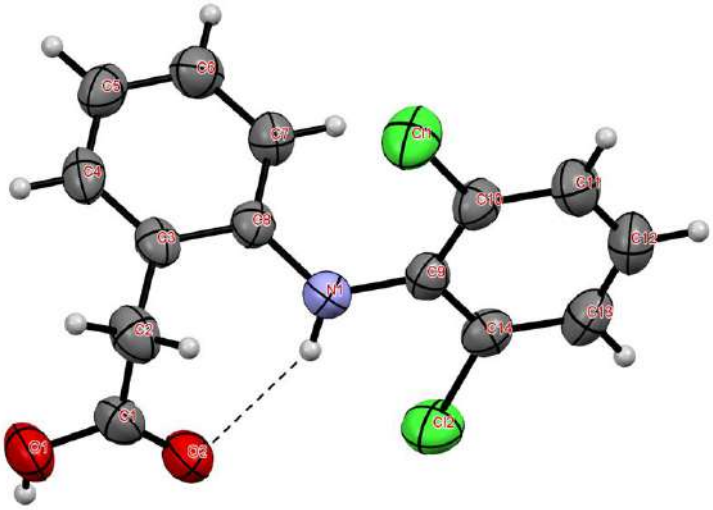

Figure 1. The molecular structures of the title compund showing the atom-numbering scheme.

2. Material and Method

The crystallographic measurements of $C_{14}H_{11}Cl_2NO_2$ was performed on STOE IPDS 2 (*Stoe Imaging Plate Diffraction System II)* diffractometer with graphite-monochromatized Mo*K*α radiation (λ = 0.71073 Å). Data integration and reduction were performed with X-AREA (Stoe and Cie, 2002). Absorption correction (μ = 0.48 mm^{-1}) was made by the integration method with X-RED (Stoe and Cie, 2002). The SHELXT (Sheldrick, 2015a) software package was used for structure solution. All non-hydrogen atoms were refined anisotropically by the full-matrix least squares using SHELXL (Sheldrick, 2015b). ORTEP-3 for Windows (Farrugia, 2012) was used to preparation the figures. To prepare material for

publication, WinGX (Farrugia, 2012) and publCIF (Westrip, 2010) software were used. All H atoms were positioned

Table 1. Crystal data and structure refinement parameters for the title compound.

Crystal Data	
Chemical Formula	$C_{14}H_{11}Cl_2NO_2$
Formula weight (a.k.b.)	296.14
Temperature (K)	296
Crystal system	Monoclinic
Space group	*C2/c*
Unit cell parameters	
$a \neq b \neq c$ (Å)	20.2338 (13), 6.9908 (4), 20.0551 (12)
β (°)	109.537 (5)
Volume, V (Å^3)	2673.5 (3)
Z	8
μ (mm^{-1})	0.48
F_{000}	1216
Calculated density (Mg/m^3)	1.471
Data collection	
Diffractometer	STOE IPDS 2
Wavelength (Å)	0.71073
θ range for data collection (˚)	$2.1 \leq \theta \leq 26.0$
Index ranges	
h_{min}, h_{max}	-24, 24
k_{min}, k_{max}	-8, 8
l_{min}, l_{max}	-21, 24
Measurement method	ω scan
Reflections collected	7295
Independent reflections	2625
Observed reflections [$I > 2\sigma(I)$]	1631
Absorption correction	Integration
R_{int}	0.037
Refinement	
Refinement method	SHELXL17/1
Parameters	177
$R[F^2 > 2\sigma(F^2)]$	0.043
$wR(F^2)$	0.089

GooF = S	0.93
$\Delta\rho_{min}$, $\Delta\rho_{max}$ (e/Å^3)	-0.16, 0.24

geometrically and refined using a riding model, restraining the bond lengths at 0.93 Å for aromatic C─H and 0.97 Å for other C─H atoms. For the hydrogen bondings analysis, the PLATON (Spek, 2003) software was used. Details of the crystal data, data collection and refinement process are listed in Table 1.

Crystal Explorer 17.5 (Turner *et al.*, 2017) was used to obtain the Hirshfeld surface and to analysis the interactions in the crystal. Also, the analysis of the associated two dimensional fingerprint-plot with Hirshfeld surface provide a appropriate tools of quantifying the interactions within the crystal structures.

3. Results and Discussion

X-ray diffraction study of 2-(2 solution of -((2,6-dichlorophenyl)amino)phenyl)acetic acid has been carried out and the data obtained are presented in Table 1. The crystal structure of the compound, crystallized in a monoclinic space group *C2/c*, with Z=8 for the formula unit, '$C_{14}H_{11}Cl_2NO_2$' (Fig. 1).

Table 2. Hydrogen bonding geometry for the compound (Å, ˚).

D─H···A	*D*─H	H···A	*D*···A	*D*─H···A
N1─H1A···O2	0.82 (3)	2.23 (3)	2.948 (3)	147 (2)
O1─H1···O2^{i}	0.82	1.83	2.651 (3)	177

Symmetry codes: (i) -x+1/2, -y+5/2, -z+1.

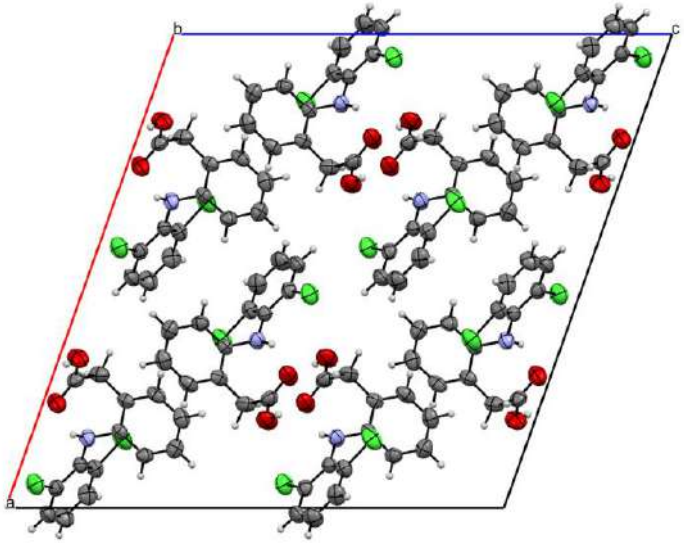

Figure 2. A partial view of the crystal packing of the title compound.

We used the Hirshfeld surface to get an idea of the presence of hydrogen bonds and intermolecular interactions in the crystal structure of compound and two-dimensional fingerprints calculated using the Crystal Explorer program (Turner *et al.*, 2017).

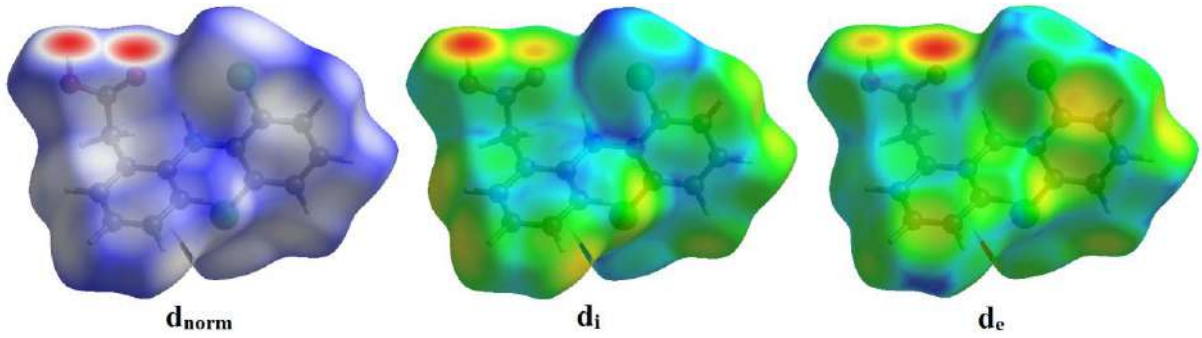

Figure 3. The Hirshfeld surface of the title compound mapped with d_{norm}, d_i and d_e.

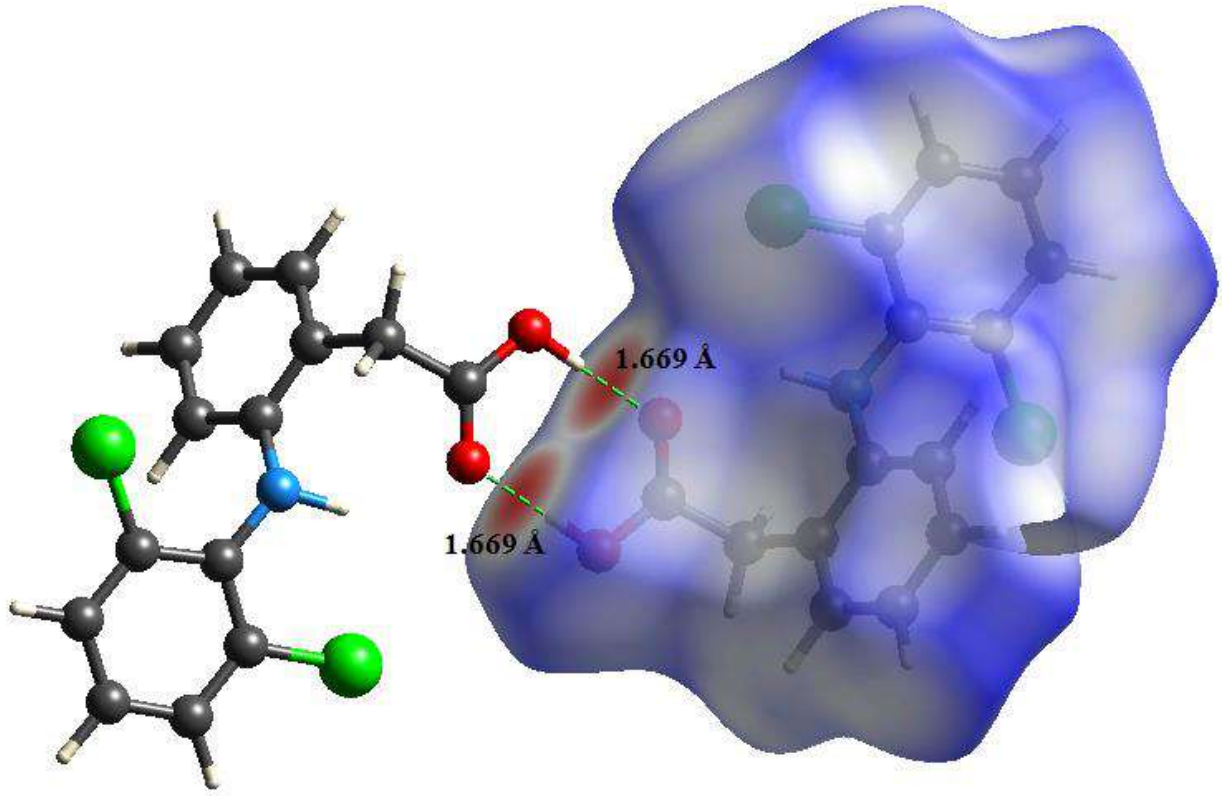

Figure 4. d_{norm} mapped on Hirshfeld surfaces for visualizing the intermolecular interactions of the title compound.

The maps of d_{norm}, d_i and d_e on molecular Hirshfeld surfaces were shown in Fig. 3 for the title compound. The red spots over the surface indicate the inter-contacts involved in strong hydrogen bonds and interatomic contacts (Aydemir *et al.*, 2018; Gümüş *et al.*, 2018; Kansız and Dege, 2018; Sen *et al.*, 2018). The red spots on the d_{norm}, d_i and d_e surfaces of the compound correspond to N—H···O intramolecular and O—H···O intermolecular hydrogen bond interactions. The Hirshfeld surfaces were performed using a standard (high) surface resolution with the three-dimentional d_{norm} surfaces mapped over a fixed colour scale of -0.732 (red) to 1.194 (blue) Å. The red spots identified in Fig. 4 correspond to the near-type H···O contacts resulting from hydrogen bond O─H···O.

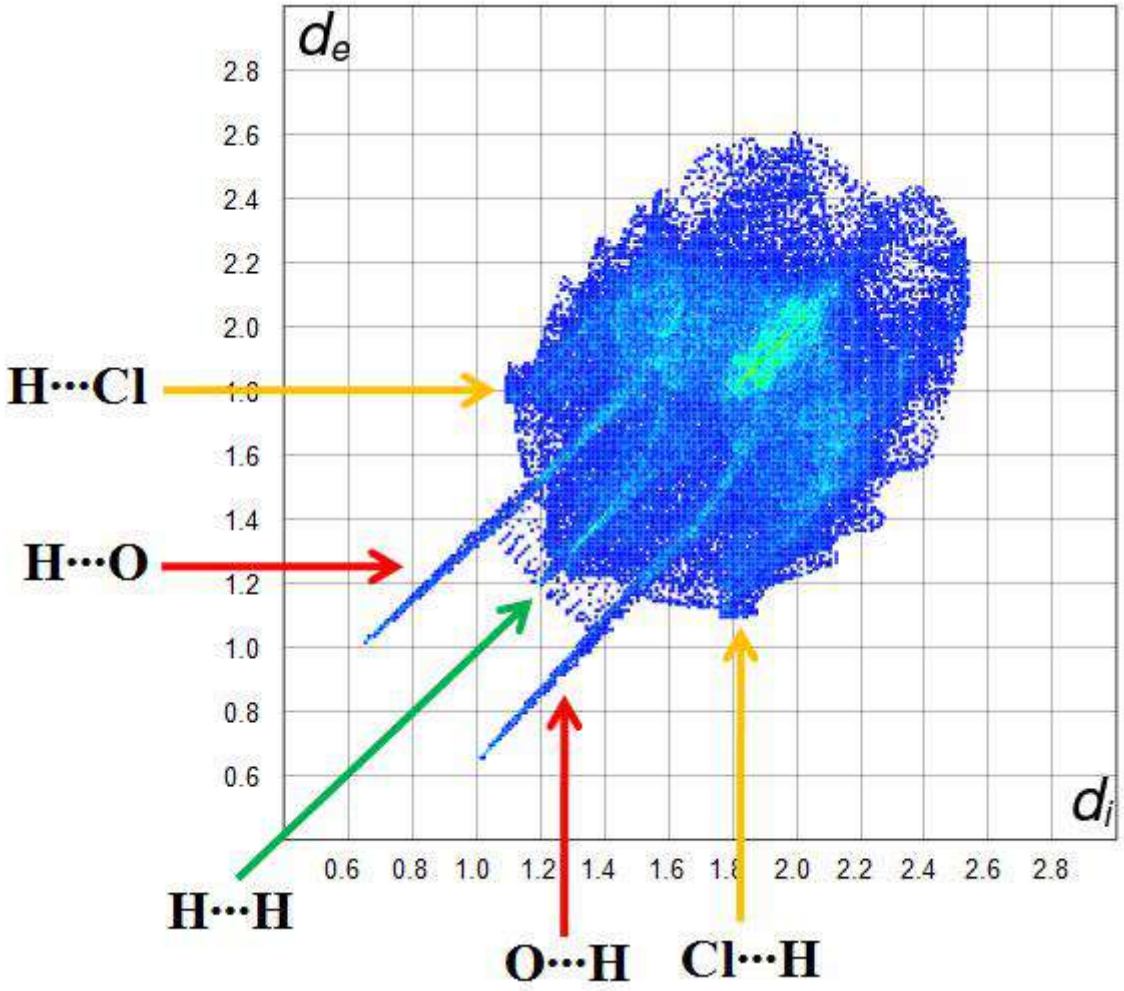

Figure 5. Fingerprint of the title compound.

Fig. 5 shows the two-dimensional fingerprint of the sum of the contacts contributing to the Hirshfeld surface represented in normal mode. The graph shown in Fig. 6 (H···H) shows the two-dimensional fingerprint of the (di, de) points associated with hydrogen atoms. It is characterized by an end point that points to the origin and corresponds to de = di = 1.2 Å, which indicates the presence of the H···H contacts in this study (32.9%). The graph shown in Fig. 6

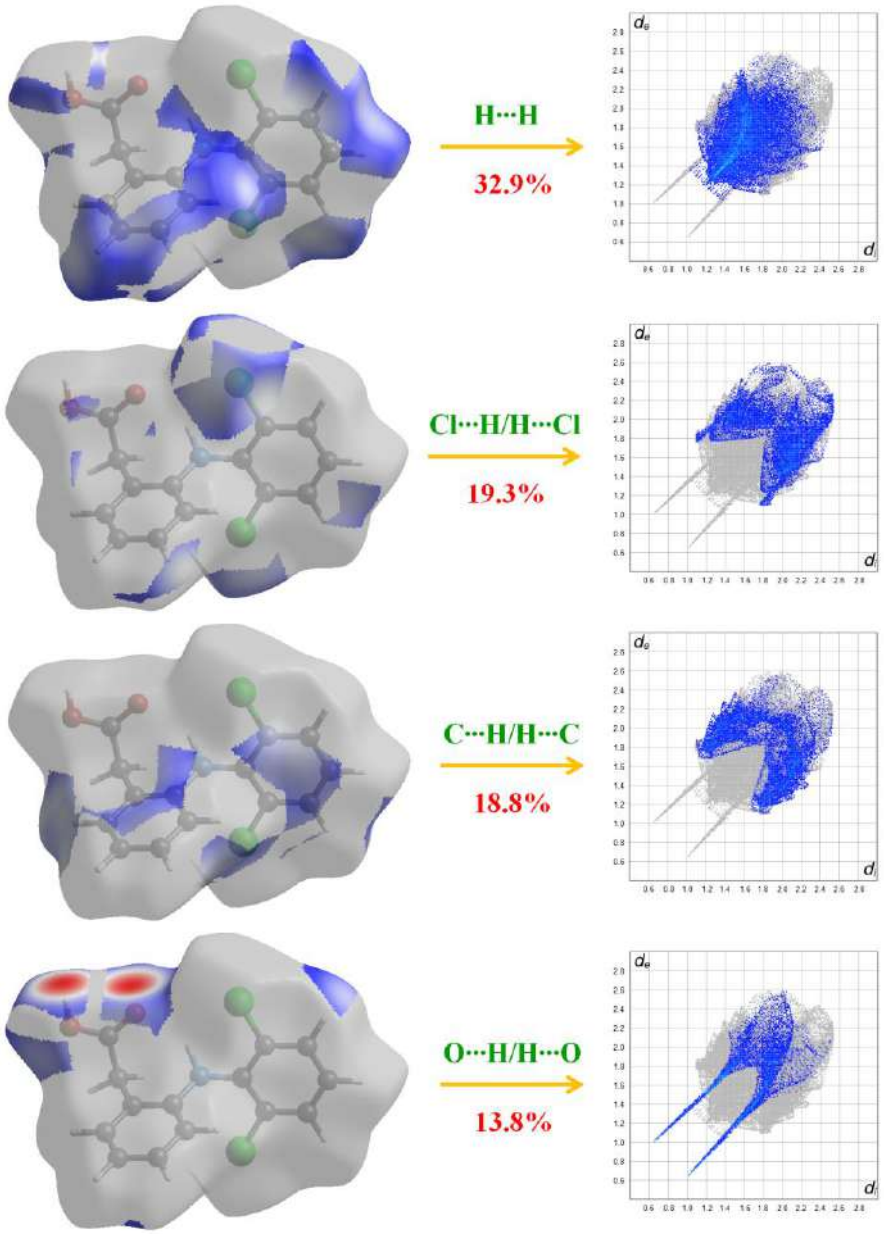

Figure 6. Two-dimensional fingerprint plots with a d_{norm} view of the H···H (32.9%), Cl···H/H···Cl (19.3%), H···C/C···H (18.8%), and O···H/H···O (13.8%) contacts in the title compound.

(H···C/C···H) shows the contact between the carbon atoms inside the surface and the hydrogen atoms outside the surface of Hirshfeld and vice versa. The analysis of this graph shows two symmetrical wings on the left and right sides (18.8%). Two symmetrical points at the top, bottom left and right with de + di ~ 1.7 Å indicate the presence of the H···O/O···H (13.8%) contacts. These data are characteristic of O─H···O hydrogen bond.

The view of the three-dimensional Hirshfeld surface of the title compound plotted over electrostatic potential energy in the range -0.083 to 0.213 a.u. using the STO-3G basis set at the Hartree–Fock level of theory. In Fig. 7, the O─H···O hydrogen-bond donors and acceptors are shown as blue and red areas around the atoms related with positive (hydrogen-bond donors) and negative (hydrogen-bond acceptors) electrostatic potentials, respectively.

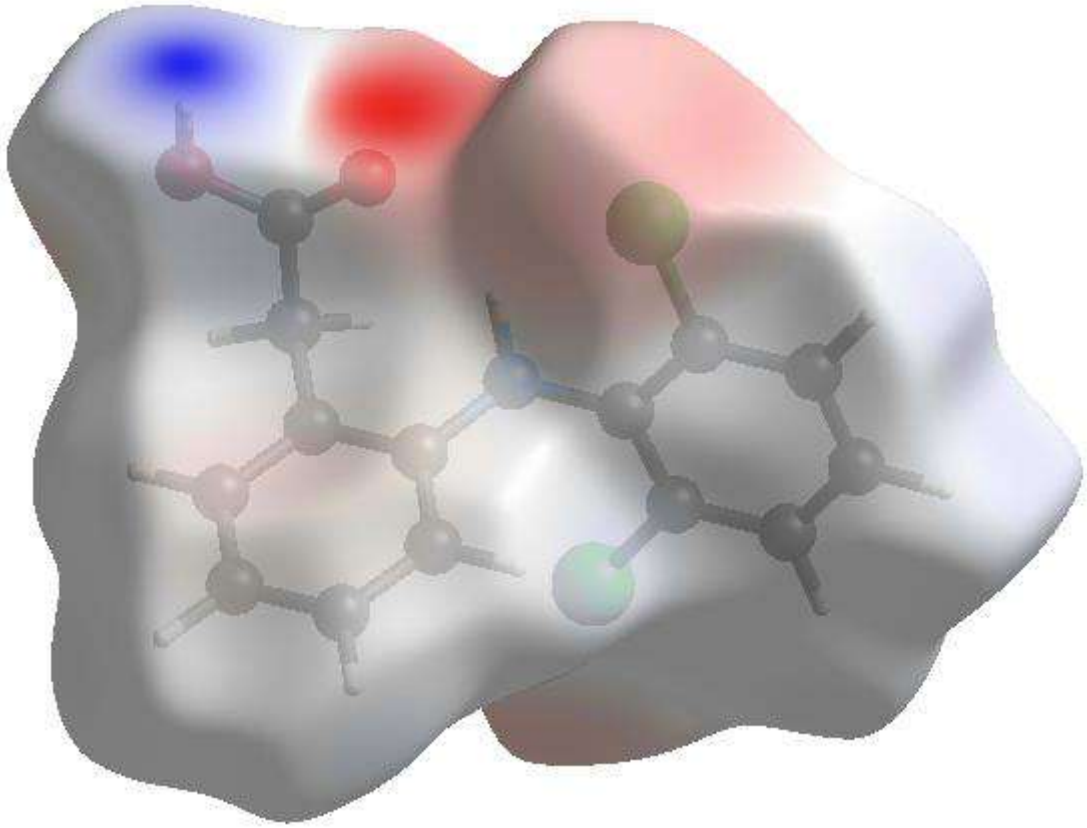

Figure 7. The view of the three-dimensional Hirshfeld surface of the title compound plotted over electrostatic potential energy.

$C_{14}H_{11}Cl_2NO_2$ compound was characterized by single crystal X-ray diffraction technique and Hirshfeld surface analysis. In the crystal, O─H···O hydrogen bonds link the molecules into supramolecular chains propagating along the a-axis direction. Hirshfeld surface analyses and two dimensional fingerprint plots have been used to analyse the

intermolecular interactions present in the crystal. The Hirshfeld surface analysis of the crystal structure specifies that the most important contributions for the crystal packing are from H···H (32.9%), Cl···H/H···Cl (19.3%), C···H/H···C (18.8%) and O···H/H···O (13.8%) interactions (Fig. 6).

References

Aydemir, E., Kansiz, S., Gumus, M. K., Gorobets, N. Y. and Dege, N. (2018). Crystal structure and Hirshfeld surface analysis of 7-ethoxy-5-methyl-2-(pyridin-3-yl)-11,12-dihydro-5,11-methano[1,2,4]triazolo[1,5-c][1,3,5]benzoxadiazocine. Acta Cryst. E74, 367–370.

Castellari. C., Ottani, S. (1997). Acta Cryst. C53, 794-797.

Farrugia, L. J. (2012). WinGX and ORTEP for Windows: an update. J. Appl. Cryst. 45, 849–854.

Gümüş, M. K., Kansız, S., Aydemir, E., Gorobets, N. Y. and Dege, N. (2018). Structural features of 7-methoxy-5-methyl-2-(pyridin-3-yl)-11,12-dihydro-5,11-methano[1,2,4]triazolo[1,5-c][1,3,5]benzoxadiazocine: Experimental and theoretical (HF and DFT) studies, surface properties (MEP, Hirshfeld). Journal of Molecular Structure, 1168, 280-290.

Kansız, S. and Dege, N. (2018). Synthesis, crystallographic structure, DFT calculations and Hirshfeld surface analysis of a fumarate bridged Co(II) coordination polymer. Journal of Molecular Structure, 1173, 42-51.

Sen, P., Kansiz, S., Golenya, I. A. and Dege, N. (2018). Crystal structure and Hirshfeld surface analysis of N,N'-bis(3-tert-butyl-2-hydroxy-5-methylbenzylidene) ethane-1,2-diamine. Acta Cryst. E74, 1147–1150.

Sheldrick, G. M. (2015a). SHELXT – Integrated space-group and crystal-structure determination. Acta Cryst. A71, 3–8.

Sheldrick, G. M. (2015b). Crystal structure refinement with SHELXL. Acta Cryst. C71, 3–8.

Spek, A. L. (2003). Single-crystal structure validation with the program PLATON, J. Appl. Cryst. 36, 7-13.

Stoe & Cie (2002). X-AREA and X-RED32. Stoe & Cie GmbH, Darmstadt, Germany.

Turner, M. J., MacKinnon, J. J., Wolff, S. K., Grimwood, D. J., Spackman, P. R., Jayatilaka, D. and Spackman, M. A. (2017). Crystal Explorer Ver. 17.5. University of Western Avustralia, Pert.

Westrip, S. P. (2010). *publCIF: software for editing, validating and formatting crystallographic information files*. J. Appl. Cryst. 43, 920-925.

Electrical Properties of Ag/Rubrene/n-GaP Schottky Diode

Ümmühan AKIN*

Selçuk University, Faculty of Science, Department of Physics, Konya, Turkey; uakin@selcuk.edu.tr

* **Corresponding Author:** uakin@selcuk.edu.tr

Abstract

Organic materials have attracted great attention due to their potential applications in micro- and optoelectronic devices such as solar cells (Peumans et al., 2003), organic light emitting diodes (Okumoto et al., 2006), field effect transistors (Malenfant et al., 2002), diodes (Yüksel et al., 2013), and so on. Particularly, most interest has been focused on organic/inorganic semiconductor contact. Because, the contact between organic layers and metal electrodes is one of the most important factors in determining the organic device performance (Sinha and Mukherjee, 2015). Therefore, the choice of organic material is very important. Rubrene among organic materials is one of the promising organic semiconductors due to its high electrical conductivity and mobility for device applications (Tuğluoğlu et al., 2015), and there are many works on the effect of rubrene organic semiconductor material (Tuğluoğlu et al., 2015; Chen et al., 2016; Guan et al., 2013; Yoon et al., 2011). However, the current-voltage (I-V) characteristic information of Ag/rubrene/n-GaP structure at the room temperature is still unknown. Therefore, the goal of this study is to determine the electrical parameters of Ag/rubrene/n-GaP Schottky diode via I-V measurements at the room temperature and to investigate the potential use of rubrene organic material for GaP based micro- and optoelectronic devices. The measured I-V characteristics of the device exhibit a good rectification behavior at the room temperature. The electronic parameters such as the ideality factor and the barrier height are determined from the experimental data using standard current-voltage analysis method.

Keywords: Rubrene, GaP, Schottky diode, electrical properties.

1. Introduction

In recent years, organic semiconductor materials have received a great deal of attention due to their remarkable properties in organic electronic devices (Jacobs and Moulé, 2017; Leitherer et al., 2017; Wang et al., 2017; Schwarze et al., 2016). In particular, they are very suitable materials for producing low-cost and flexible devices (Sinha and Mukherjee, 2015). Among these materials, rubrene ($C_{42}H_{28}$) has been one of the promising organic semiconductors owing to its high electrical conductivity and high mobility (Sinha and Mukherjee, 2015; Tuğluoğlu et al., 2015). Therefore, it has taken its place in technological applications such as organic light emitting diodes (OLEDs) (Choukri et al., 2006), organic photovoltaic cells (OPVs) (Chan et al., 2007), organic field effect transistors (OFETs) (Kim et al., 2007), organic-inorganic heterojunctions (He et al., 2017) and Schottky barrier diodes (Karadeniz et al., 2013). The Schottky barrier diodes are one of the simplest metal-semiconductor (MS) contact devices in the semiconductor technology and its electrical properties (Rhoderick and Williams, 1988) can be modified by a suitable organic semiconductor layer inserted between the metal and semiconductor (Barış et al., 2013). For this reason, many researchers have recently studied different organic semiconductor materials as interlayer to modify the electronic properties of metal-semiconductor contact (Gupta and Singh, 2005; Şimşir et al., 2012; Aydoğan et al., 2010). For example, the electronic properties of Au/PEDOT/n-GaAs Schottky diode have been analyzed by Aydın et al. (Aydın et al., 2011) and they have been modified with a thin layer of poly (3,4-ethylenedioxithiophene)-block-poly (ethylene glycol) in propylene carbonate (PEDOT) film. Yüksel et al. (Yüksel et al., 2013) studied the electronic properties of the perylene-diimide (PDI)/n-Si Schottky diode from their current-voltage (I-V) characteristics at varying temperature ranges from 75 to 300 K and determined effect of the temperature on some junction parameters such as ideality factor (n), barrier height (Φ_B), series resistance (R_S). It has been seen that the organic perylene-diimide on the n-Si substrate has indicated a good rectifying behavior at all temperatures. Furthermore, Güllü et al. (Güllü et al., 2010), Güllü and Türüt (Güllü and Türüt, 2010), and Aydoğan et al. (Aydoğan et al., 2010) reported that the non-polymeric organic compounds known as Congo Red, Orange G, and Orcein, exhibits the rectifying I-V characteristics and the ideality factor and barrier height values of prepared Schottky diode are greater than those of the conventional metal/semiconductor structures. In addition to these organic materials, the effect on the electrical properties of rubrene organic material for electronic devices has been investigated (Tuğluoğlu et al., 2015; Karadeniz et al., 2013; Barış

et al., 2013). The device parameters of Al/rubrene/n-GaAs Schottky diode have been investigated by means of current-voltage measurements in the temperature range 100-300 K by Tuğluoğlu et al. (Tuğluoğlu et al., 2015). It has been found that the ideality factors decreased and the barrier heights increased with increasing temperature. This observed behavior has been attributed to the barrier inhomogeneity at the rubrene/n-GaAs interface (Tuğluoğlu et al., 2015). Karadeniz et al. (Karadeniz et al., 2013) have fabricated an Al/p-Si and Al/rubrene/p-Si Schottky diode and they have analyzed the forward I-V characteristics of the diodes according to the standard thermionic emission theory. They have observed that the electrical parameters of the Al/rubrene/p-Si Schottky diode are remarkably higher than those obtained for Al/p-Si diode. To investigate the interface effect of rubrene organic material on different semiconductor materials, in this present work, an Ag/rubrene/n-GaP Schottky barrier diode was fabricated and the current-voltage characteristics of diode was measured at the room temperature. The electronic parameters such as the ideality factor and the barrier height was determined from the experimental data using standard current-voltage analysis method.

2. Experimental Procedure

In this study, we have used an n-type (S-doped) GaP semiconductor wafer with (100) surface orientation, 0.0375 Ω cm resistivity and 400 μm thickness and it was supplied from University Wafer Inc. The GaP wafer was initially chemically cleaned with trichloroethylene and aceton and methanol for 3 min by ultrasonic vibration and then rinsed by ultrasonic vibration in DI water for 3 min. Thereafter, the wafer was cleaned $3H_2SO_4 + H_2O_2 + H_2O$ for 60 s, then rinsed by ultrasonic vibration in DI water. The final cleaning step diluted HF:H_2O (1:10) for 30 s, and dried by N_2 (%99,99). Immediately after surface cleaning, indium (In) metal with a purity of 99.99% was thermally evaporated on the whole back surface of the wafer with a thickness of 1500 Å under vacuum of approximately $5x10^{-6}$ Torr. Then, it was annealed at 350 °C for 3 min in vacuum to obtain a low resistivity ohmic contact. Next, the Rubrene organic material (5,6,11,12-tetraphenylnaphthacene) purchased from Sigma Aldrich was coated on the GaP semiconductor wafer by a spin coating method to form the rubrene organic film. Then, Schottky contacts were deposited on this organic film with a diameter of 2 mm using a metal shadow mask by evaporating 99.99% purity silver with a thickness of 1500 Å. The schematic diagram of the prepared device is shown in Figure 1. The current-voltage (I-V) measurements of the prepared diode were performed by a Keithley 2410 sourceMeter at 300 K.

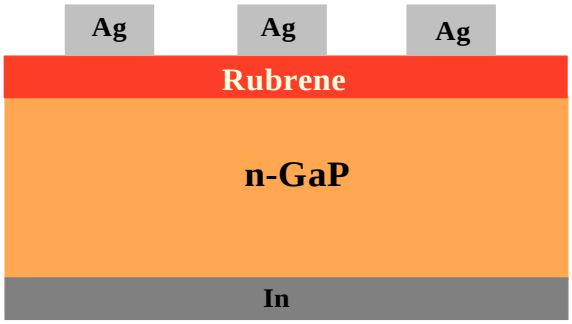

Figure 1. Cross-sectional view of Ag/Rubrene/n-GaP Schottky device.

3. Results and Discussion

For forward bias of V > 3kT/q, the current-voltage (I-V) characteristics of a Schottky diode can be analyzed in the frame of thermionic emission model using the following relation (Sze and Ng, 2007):

$$I = I_0 \left[e^{\left(\frac{qV}{nkT}\right)} \right] \quad (1)$$

where I_0 is the saturation current and is given by

$$I_0 = AA^*T^2 exp\left(-\frac{q\Phi_{B0}}{kT}\right) \quad (2)$$

Also, n is the diode ideality factor, Φ_{B0} is the Zero-Bias Schottky barrier height, q is the electronic charge, A is the diode area, A^* is the effective Richardson constant (98.2 A/cm^2K^2 for n-GaP), T is absolute temperature and k is the Boltzmann constant. The Figure 2 shows the semi-logarithmic I-V characteristic of the Ag/rubrene/n-GaP Schottky diode at room temperature. As can be seen from the Figure 2, the Schottky contact has good rectifying behavior.

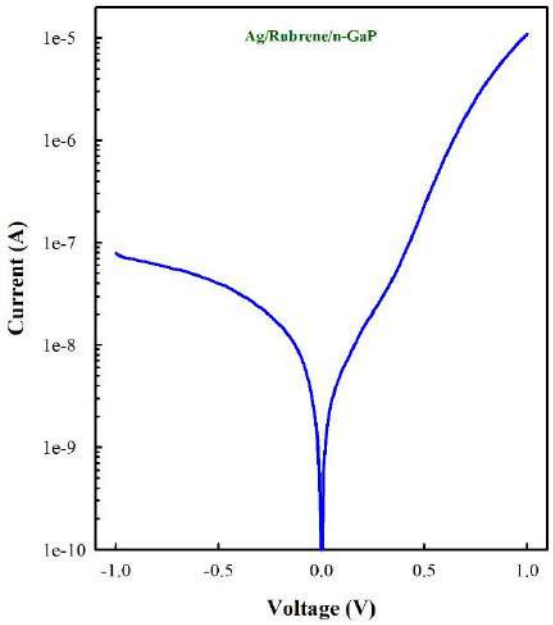

Figure 2. I-V characteristic of the Ag/Rubrene/n-GaP Schottky diode for 300 K.

The saturation current (I_0) value of diode was determined as 2.72717x10^{-09} A from the linear portion intercept of log I-V at V = 0. Also, the ideality factor (n) of the prepared diode can be determined from the slope of linear region of the forward bias ln I-V characteristic as

$$n = \frac{q}{kT}\left(\frac{dV}{d(lnI)}\right) \quad (3)$$

On the other hand, the Schottky barrier height (Φ_{B0}) can be obtained from equation (2) as

$$\Phi_{B0} = \frac{kT}{q}\ln\left(\frac{AA^{*}T^{2}}{I_0}\right) \quad (4)$$

and the values of ideality factor and the Schottky barrier height for the Ag/rubrene/n-GaP diode are 4.78 and 0.834 eV, respectively.

In Schottky diodes, series resistance (R_S) is also one of the important parameters that determine the electrical properties of diode and this parameter can be evaluated from a method developed by Cheung and Cheung (Cheung and Cheung, 1986). According to this method, the forward bias current-voltage characteristics due to the thermionic emission theory of MS contacts can be expressed as

$$I = I_0 \left[exp\left(\frac{qV - IR_S}{nkT}\right)\right] \quad (5)$$

where IR_S is the voltage drop across the series resistance of diode. If I_0 saturation current is substituted in equation (5), the applied voltage (V) can be obtained as

$$V = IR_S + n\Phi_B + \frac{nkT}{q}\ln\left(\frac{I}{AA^*T^2}\right) \quad (6)$$

By differentiating the equation (6) with respect to I and rearranging, the equation (7) is find that

$$\frac{dV}{d\ln(I)} = \frac{nkT}{q} + IR_S \quad (7)$$

A plot of $\frac{dV}{dln(I)}$ versus I will be linear and the slope of graph gives R_S series resistance and the intercept of graph on the current axis gives $\frac{nkT}{q}$. To obtain Φ_B barrier height of diode, Cheung and Cheung defined a function as

$$H(I) = V - \left(\frac{nkT}{q}\right)\ln\left(\frac{I}{AA^*T^2}\right) = n\Phi_B + IR_S \quad (8)$$

If it is drawn a graph of $H(I)$ according to I, the series resistance (R_S) and the barrier height (Φ_B) can be easily found. In Figure 3, it has been given the plots of $dV/dln(I)$ and $H(I)$ versus I for Ag/rubrene/n-GaP Schottky diode at room temperature.

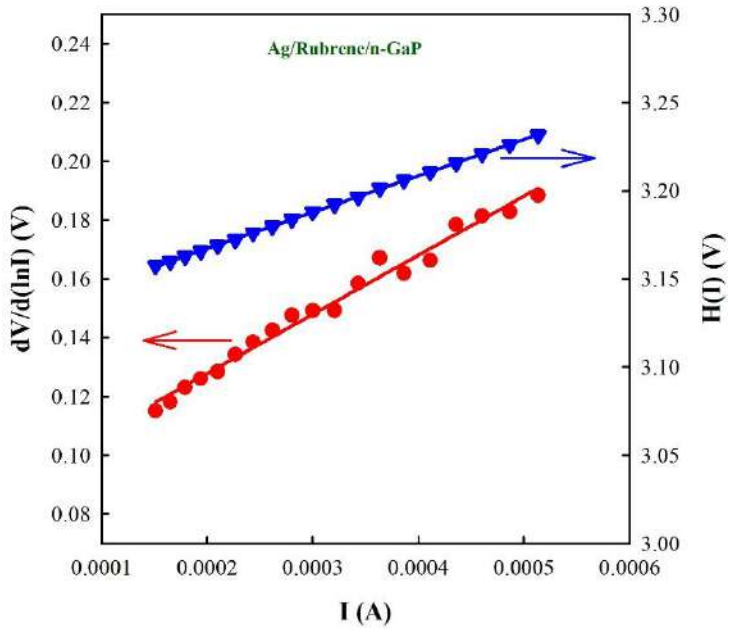

Figure 3. $dV/d\ In(I)$-I and $H(I)$-I characteristics of Ag/Rubrene/n-GaP Schottky diode.

As can be seen from the plot of $dV/d\ In(I)$ versus I, the curve show a good linearity and the ideality factor (n) and the series resistance (R_S) have been determined from Figure 3. However, the plot of $H(I)$ versus I has been shown similar behavior and the series resistance (R_S) and the barrier height (Φ_B) have been found. The values of diode parameter determined by different methods for an Ag/rubrene/n-GaP Schottky barrier diode have been listed in Table 1. As can be seen from the Table 1, the values obtained by different methods are in good agreement with each other. The ideality factor value for room temperature (n = 4.78) was found greater than those reported for Al/rubrene/p-Si Schottky diode structures by Karadeniz et al. (Karadeniz et al., 2013), as 1.51, depending on the Al contact thickness. This high n value can be attributed to the presence of the interfacial layer, the lateral inhomogeneous barrier height distributions and the native oxide layer at metal-semiconductor interface. On the other hand, at the room temperature, the value of barrier height (0.834 eV) is higher than reported at same study (0.771 eV).

Table 1. Diode parameters determined by different methods for an Ag/Rubrene/n-GaP Schottky device.

	Parameters	Ag/Rubrene/n-GaP (In this work)	Al/Rubrene/p-Si (Karadeniz et al.,2013)
I-V	I_0 (A)	2.72717×10^{-9}	---
	n	4.78	1.51
	Φ_B (eV)	0.834	0.771
dV/d(lnI)-I	n	4.78	3.21
	R_S (Ω)	8685	1874.5
H(I)-I	Φ_B (eV)	0.814	0.692
	R_S (Ω)	8746	1764.7

4. Conclusion

In the presented study, it has been investigated the forward I-V characteristic of Ag/rubrene/n-GaP Schottky diode at the room temperature. The prepared device has shown a good diode behavior at the room temperature. The diode parameters such as the ideality factor, the barrier height and the series resistance have been determined in the frame of the thermionic emission theory. The values of saturation current, ideality factor and barrier height have been found as 2.72717×10^{-9} A, 4.78 and 0.834 eV, respectively. Also, it has been

observed that the values of diode parameter determined by different methods are in good agreement with each other.

Acknowledgments

The author thanks Dr. Ö. Faruk YÜKSEL from Selçuk University and Dr. Nihat TUĞLUOĞLU from Giresun University for their contributions in this study.

References

Aydın M. E., Soylu M., Yakuphanoglu F., and Farooq W. A., (2011). Controlling of electronic parameters of GaAs Schottky diode by poly(3,4-ethylenedioxithiophene)-block-poly(ethylene glycol) organic interlayer. Microelectronic Engineering, 88, 867-871.

Aydoğan Ş., İncekara Ü., Deniz A. R., and Türüt A., (2010). Extraction of electronic parameters of Schottky diode based on an organic Indigotindisulfonate Sodium (IS). Solid State Communications, 150, 1592-1596.

Aydoğan Ş., İncekara Ü., Deniz A. R., and Türüt A., (2010). Extraction of electronic parameters of Schottky diode based on an organic Orcein. Microelectronic Engineering, 87, 2525-2530.

Barış B., Yüksel Ö. F., Tuğluoğlu N., and Karadeniz S., (2013). Double barrier heights in 5,6,11,12-tetraphenylnaphthacene (rubrene) based organic Schottky diode. Synthetic Metals, 180, 38-42.

Chan M. Y., Lai S. L., Fung M. K., Lee C. S., and Lee S. T., (2007). Doping-induced efficiency enhancement in organic photovoltaic devices. Applied Physics Letters, 90, 023504.

Chen L., Deng J., Gao H., Yang Q., Kong L., Cui M., and Zhang Z., (2016). Ellipsometric study and application of rubrene thin film in organic Schottky diode. Applied Surface Science, 388, 396-400.

Cheung S. K., and Cheung N. W., (1986). Extraction of Schottky diode parameters from forward current-voltage characteristics. Applied Physics Letters, 49, 85-87.

Choukri H., Fischer A., Forget S., Chénais S., Castex M.-C., Adès D., Siove A., and Geffroy B., (2006). White organic light-emitting diodes with fine chromaticity tuning via ultrathin layer position shifting. Applied Physics Letters, 89, 183513.

Guan Z., Wu R., Zang Y., and Yu J., (2013). Small molecule dye rubrene doped organic bulk heterojunction solar cells. Thin Solid Films, 539, 278-283.

Güllü Ö., and Türüt A., (2010). Electrical analysis of organic dye-based MIS Schottky contacts. Microelectronic Engineering, 87, 2482-2487.

Güllü Ö., Kilicoglu T., and Türüt A., (2010). Electronic properties of the metal/organic interlayer/inorganic semiconductor sandwich device. Journal of Physics and Chemistry of Solids, 71, 351-356.

Gupta R. K., and Singh R. A., (2005). Fabrication and characteristics of Schottky diode based on composite organic semiconductors. Composites Science and Technology, 65, 677-681.

He X., Chow W., Liu F., Tay B., and Liu Z., (2017). MoS_2/Rubrene van der Waals heterostructure: Toward ambipolar field-effect transistors and inverter circuits. Small, 13, 1602558.

Jacobs I. E., and Moulé A. J., (2017). Controlling molecular doping in organic semiconductors. Advanced Materials, 29, 1703063.

Karadeniz S., Barış B., Yüksel Ö. F., and Tuğluoğlu N., (2013). Analysis of electrical properties of Al/p-Si Schottky contacts with and without rubrene layer. Synthetic Metals, 168, 16-22.

Kim K., Kim M. K., Kang H. S., Cho M. Y., Joo J., Kim J. H., Kim K. H., Hong C. S., and Choi D. H., (2007). New growth method of rubrene single crystal for organic field-effect transistor. Synthetic Metals, 157, 481-484.

Leitherer S., Jäger C. M., Krause A., Halik M., Clark T., and Thoss M., (2017). Simulation of charge transport in organic semiconductors: A time-dependent multiscale method based on nonequilibrium Green's functions. Physical Review Materials, 1, 064601.

Malenfant P. R. L., Dimitrakopoulos C. D., Gelorme J. D., Kosbar L. L., Graham T. O., Curioni A., and Andreoni W., (2002). N-type organic thin-film transistor with high field-effect mobility based on a N,N′-dialkyl-3,4,9,10-perylene tetracarboxylic diimide derivative. Applied Physics Letters, 80, 2517-2519.

Okumoto K., Kanno H., Hamada Y., Takahashi H., and Shibata K., (2006). Green fluorescent organic light-emitting device with external quantum efficiency of nearly 10%. Applied Physics Letters, 89, 063504.

Peumans P., Yakimov A., and Forrest S. R., (2003). Small molecular weight organic thin-film photodetectors and solar cells. Journal of Applied Physics, 93, 3693-3723.

Rhoderick E. H., and Williams R. H., (1988). Metal-semiconductor contacts (2nd ed.). Oxford, England: Clarendon Press.

Schwarze M., Tress W., Beyer B., Gao F., Scholz R., Poelking C., Ortstein K., Günther A. A., Kasemann D., Andrienko D., and Leo K., (2016). Band structure engineering in organic semiconductors. Science, 352, 1446-1449.

Şimşir N., Şafak H., Yüksel Ö. F., and Kuş M., (2012). Investigation of current-voltage and capacitance-voltage characteristics of Ag/perylene-monoimide/n-GaAs Schottky diode. Current Applied Physics, 12, 1510-1514.

Sinha S., and Mukherjee M., (2015). A comparative study about electronic structures at rubrene/Ag and Ag/rubrene interfaces. AIP Advances, 5, 107204.

Sze S. M., and Ng K. K., (2007). Physics of semiconductor devices (3rd ed.). Hoboken, New Jersey, United States of America: John Wiley & Sons.

Tuğluoğlu N., Çalışkan F., Yüksel Ö. F., (2015). Analysis of inhomogeneous barrier and capacitance parameters for Al/rubrene/n-GaAs (100) Schottky diodes. Synthetic Metals, 199, 270-275.

Wang X., Zhang J., Chen Y., and Chan P. K. L., (2017). Molecular dynamics study of thermal transport in a dinaphtho[2,3-b:2′,3′-f]thieno[3,2-b]thiophene (DNTT) organic semiconductor. Nanoscale, 9, 2262-2271.

Yoon Y., Kim S., Lee H., Kim T., Babajanyan A., Lee K., and Friedman B., (2011). Characterization of rubrene polycrystalline thin film transistors fabricated using various heat-treatment conditions. Thin Solid Films, 519, 5562-5566.

Yüksel Ö. F., Tuğluoğlu N., Gülveren B., Şafak H., and Kuş M., (2013). Electrical properties of Au/perylene-monoimide/p-Si Schottky diode. Journal of Alloys and Compounds, 577, 30-36.

Yüksel Ö. F., Tuğluoğlu N., Şafak H., Nalçacıgil Z., Kuş M., and Karadeniz S., (2013). Analysis of temperature dependent electrical properties of Au/perylene-diimide/n-Si Schottky diodes. Thin Solid Films, 534, 614-620.

COMPUTER AND COMMUNICATION

ORAL PRESENTATIONS

Fuzzy Logic Based Decision Support System for Broadcaster on Twitch

Ercan ATAGÜN [1*], Murat KORKMAZ[2], Tunahan TİMUÇİN[3], İbrahim YÜCEDAĞ[4]

[1] Duzce University, Graduate School Of Natural And Applied Sciences, Computer Engineering, Duzce, Turkey;ercan-atagun@hotmail.com

[2] Duzce University, Graduate School Of Natural And Applied Sciences, Computer Engineering, Duzce, Turkey;muratkorkmaz30@hotmail.com

[3] Duzce University, Graduate School Of Natural And Applied Sciences, Computer Engineering, Duzce, Turkey;t.timucin01@gmail.com

[4] Duzce University, Graduate School Of Natural And Applied Sciences, Computer Engineering, Duzce, Turkey;yucedagi@gmail.com

[*] **Corresponding Author:** ercan-atagun@hotmail.com

Abstract

Social media is at the forefront of the fields that science and technology are developing. The expansion of social media and internet bandwidth has enabled the emergence of a live broadcast platform. Twitch is one of the most important platforms that serves this area in particular.Especially in the playground, Twitch appeals to millions of users around the world.The large number of users using this platform, the need to analyze the data coming from these users, necessitated the application of artificial intelligence techniques.One of the most important of these artificial intelligence techniques is the Fuzzy Logic approach.In this paper, it is aimed to make an estimation of the audience size which can be addressed according to the characteristics of the users who broadcast on Twitch and those who consider broadcasting or studying with Fuzzy Logic.

Keywords: Fuzzy Logic, Decision Support System, Twitch

1. Introduction

The use of social media is becoming widespread in many places around the world. With the development of Internet connection technologies, social media content has begun to differ. Especially the increase in internet bandwidth is changing the behaviors of social media content producers. After the development of video-based social media content, live broadcast platforms are gaining importance. The content produced in live broadcasting platforms serves in many fields such as education, commercial, military and health. Since live broadcasting platforms have become increasingly widespread, analysis studies in this area have gained importance. In this study, the live broadcast platform Twitch was analyzed and a recommendation system was proposed to the content producers.

The statistics on Twitch, which is a live broadcasting platform, emerge as the area that needs to be done. According to the Twitch 2017 report, 355 billion minutes Twitch channels were followed, while more than 2 million unique monthly publishers were generated, while the winners of this platform increased by 223%. All figures show a growth of 25% in 2016 compared to 2016 and continue to operate in more than 60 countries around the world.

In recent years, live streaming platforms have been used for educational purposes through video. These processes are used as a practical and easily accessible method for non-professional trainers. The social benefits that Twitch brings out of the new communities and which people come to these environments have been emphasized (Hamilton et al., 2014).

Rapidly growing live streaming platforms continue to grow with viewers. The basic follow-up motivations of viewers have been the subject of research. In a study, it was concluded that topics such as social interaction, community sense, meeting new people, entertainment, information search and lack of external support in real life were aimed at monitoring Twitch (Hilvert et al., 2018).

In another study, the potential of live broadcasting technology and the features required to improve learning from instructors at different levels of expertise have been addressed. By selecting a game, the potentials in the in-game performance have been measured and the potentials of the channel, which live in certain conditions, have been addressed. In addition, the characteristics of the novices in the live broadcasting environment and the characteristics of the learning were determined. It has been studied that live broadcasting technology can improve learning and provide the most appropriate conditions for students to learn (Katherine et al., 2017).

In this study, a decision support system will be proposed to be popular with new content producers by taking advantage of the basic features of content producers in the Twitch platform. The data set of the study consists of the basic features of the live broadcast channels that produce content. Content manufacturers have a direct link to popular features. These links have an effect on the different levels of popularity of each feature. These complex connections require the use of the Fuzzy Logic approach in the study.

Logic basically started with Aristotle approach. In all cases, Aristotle used the concepts of True or False. This logic approach has been used for many years and is still used. However, it has been found that these rationales have shortcomings in terms of specifying needs. In the studies done, everything could not be expressed by binary logic such as ”Exist”, ”None” or ”True”, ”False”. Thus, the fuzzy logic approach, in which uncertain ones can be expressed, has emerged (Timuçin et al., 2017).

The first Fuzzy Logic approach was announced in 1956 during a conference in the US. Lotfi A. Zadeh published the Fuzzy Logic approach with his article published in this conference (Zadeh, 1965). This approach, which is closer to the human thought system, produces more accurate results in identifying real situations. The human thought system is used fundamentally 0.2, 0.6. instead of certain expressions. Fuzzy Logic approach, in which the intermediate values have gained meaning, was found to be the most suitable method for this study.

2. Material and Method

In this study, Fuzzy Logic approach is used. The data set of the study was obtained using TwitchAPI. The data set of the study was collected by providing a TwitchAPI connection with the C # programming language. Collected data is in JSON format and C # language methods are used for normalization. The collected data were made meaningful to pass through the Fuzzy logic controller after the normalization process. The application was created using MATLAB. As the fuzzy inference method, the clarification method shown in Figure 1 was determined as Mamdani. The method used by Mamdani and called the mean of the maximum (MOM - mean of maximum) is a direct result of fuzzy cluster and membership function operations with fuzzy logic.

Figure 1. Basic Structure of Fuzzy Logic Controller

Blurring is defined as the process of converting the values that are the input information of the study to a human language language such as Slow, Normal, Fast. After the blur, a new set of values that are converted to this new language is delivered to the Decision Making Center. The Decision Making Center develops inferences similar to the implications of people against events and situations. The Decision Center establishes the rules and sets these rules. These stored rules are delivered to the Rinsing Unit. Rinse Converts the unit to values that can be detected by computer systems. The resulting output values are used to serve the final purpose of the study.

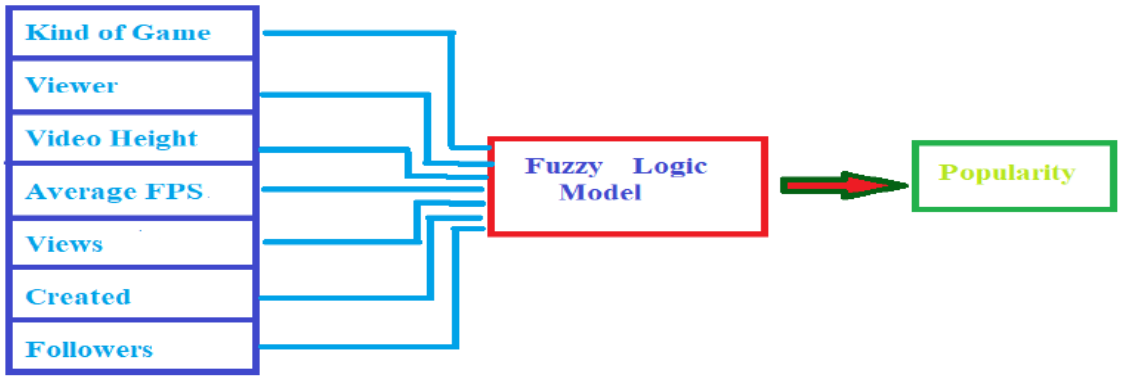

Figure 2. Fuzzy Logic Structure

Figure 2 shows the fuzzy logic structure, which is adapted to the input data and output data in this study. To determine the main characteristics of the live broadcasting platform channels, which are very watched and less watched. It is to provide a decision support system to the channel users who want to find the similarities in the data classes and want to be popular.

In the study, the type of the game played in the channel is PS KindofGame, the channel's instant view average ”Viewer ight, the screen size of the channel ın VideoHeight”, the average Frame Per Second (FPS) value of the channel AverageFPS “, the total number of views of the channel is Views, the channel's broadcast history “Created”, the number of followers of the channel, “Followers ”, has been determined according to the input data. When determining the characteristics of these data, a Member Degree was assigned for each parameter. It is used to determine the degree to which an input value belongs to a human language term with the help of this assigned Membership Degree.

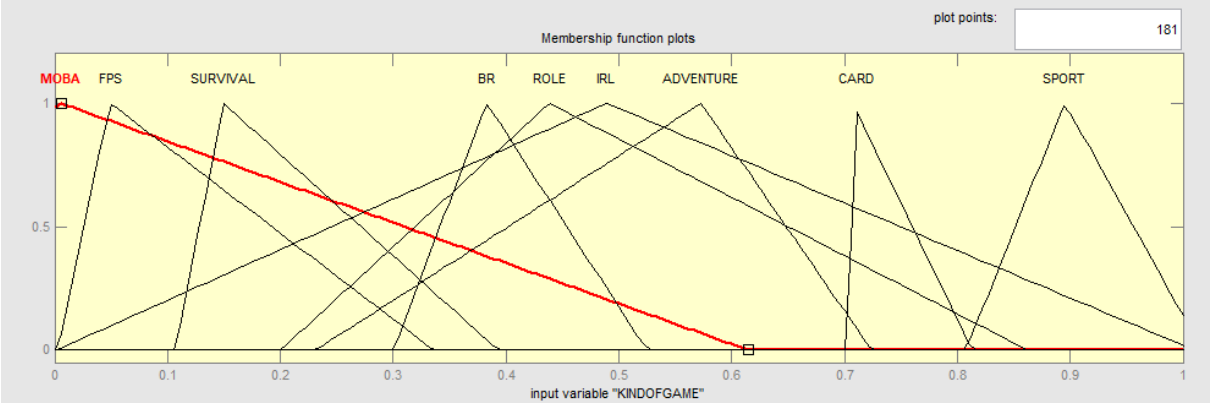

Figure 3. KindofGame Membership Function

For KindofGame 9 game types have been determined. These are FPS (First Person Shooter), Survival, MOBA (Multiplayer online battle area), BR (Battle Area), ROLE (Role Action), IRL (In Real Life), Adventure, Card, Sport.

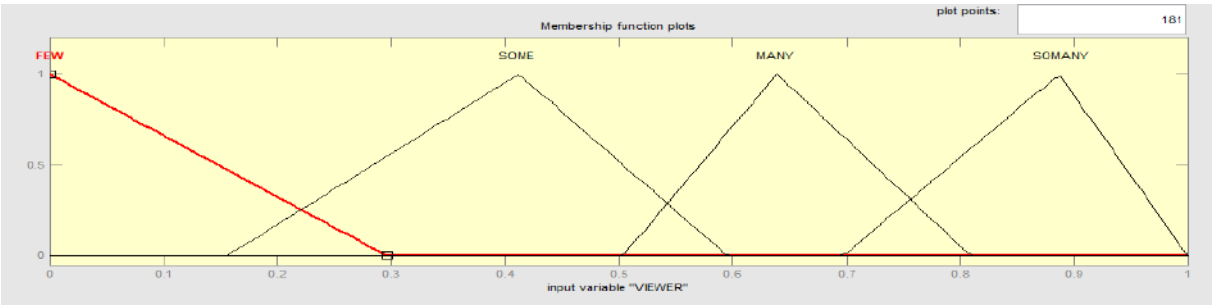

Figure 4. Viewer Membership Function

The number of views has been assigned as Less, More, Too, Too Much.

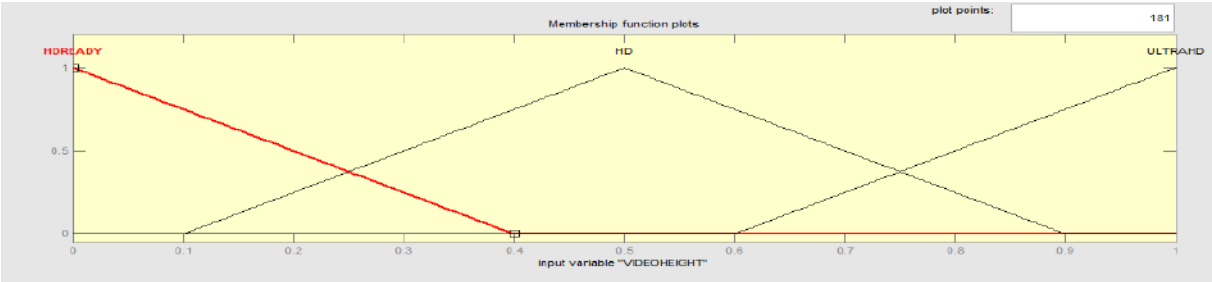

Figure 5. VideoHeight Membership Function

Screen size membership ratings are set to HDReady, HD, and UltraHD.

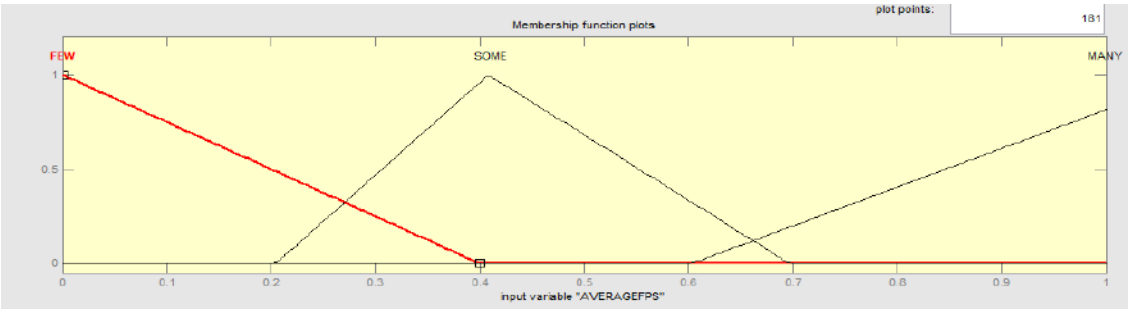

Figure 6. AverageFPS Membership Function

Average FPS values were determined as low, medium and high.

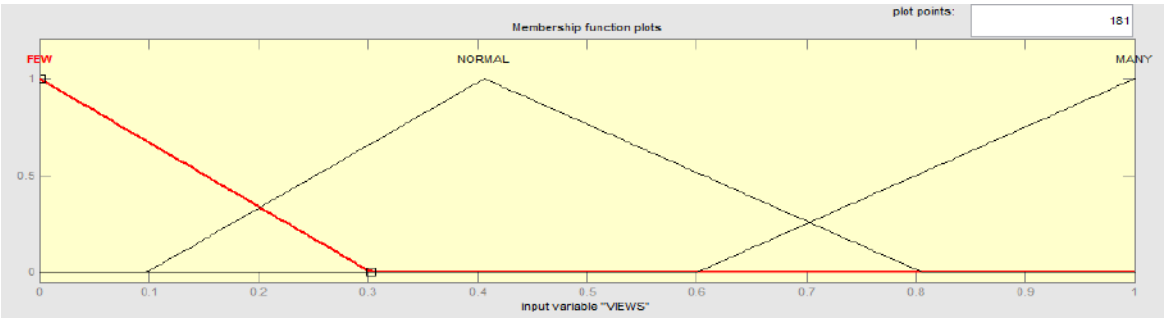

Figure 7. Views Membership Function

If the number of views is in the data set, the membership ratings are set as Az, Normal, and Multi.

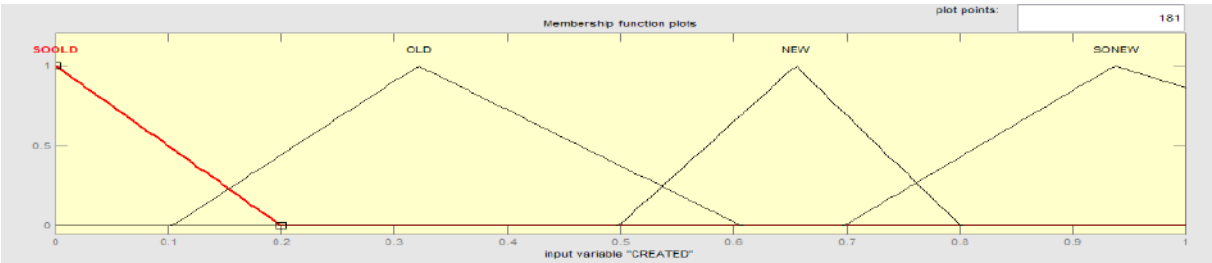

Figure 8. Created Membership Function

Very old, old, new, very new membership levels are determined in the input information about the broadcast history.

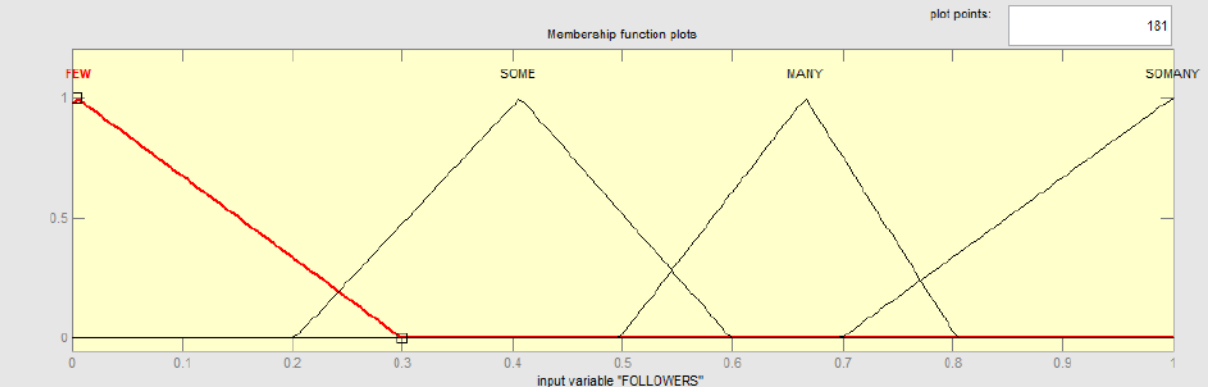

Figure 9. Followers Membership Function

In the input information about the tracker information, the membership degrees are set to Low, A little, Very, Very Over.

3. Results and Discussion

The data obtained by normalization process after data pre-processing will be transferred according to the determined label values. Instant viewing 0-100: Low, 100-500: Moderate, 500-5000: High, 5000+ Very High; Screen Quality 720p: HDReady, 900p: HD, 1080p: UltraHD; Average FPS: 0-30: Low, 30-60: Medium, 60+: High; Past Views: 0-1000000: Low, 1000000-10000000: Normal, 10000000+: High; Publishing History (Created): 2018,2017: Very new, 2016,2015: New, 2014,2013: Old, 2012,2011: Very old; Follower: 0-500: Low, 500-1000: Normal, 1000-100000: High, 100000+: Very.

Output classes are classified as popular, popular, and very popular. These input values have been passed through Fuzzy Controller. Then, it is aimed to obtain popularity class based on the rule table. The number of rules is calculated by multiplying all the input data determined as input. For optimum operation, this number of rules must be as low as possible and is expected to verify the result optimally. The total number of rules used in this study is 27. The results obtained by the Decision Making Unit according to the rules determined in the rule table are assigned to the Popularity output parameter after passing through the Rinse Unit. These values will be aimed at finding answers to the question about the status of being popular with the live broadcast content producer. The output parameters shown in Fig. 10 are

intended to determine the popularity level in the maintenance of features that the content generating channels have.

Table1. Rule Table

If (KINDOFGAME is FPS) and (VIEWER is FEW) and (VIDEOHEIGHT is ULTRAHD) and (AVERAGEFPS is MANY) and (VIEWS is SOME) and (CREATED is SOOLD) and (FOLLOWERS is FEW) then (POPULARITY is LITTLEPOPULARITY) (1)
If (KINDOFGAME is BR) and (VIEWER is SOMANY) and (VIDEOHEIGHT is ULTRAHD) and (AVERAGEFPS is FEW) and (VIEWS is FEW) and (CREATED is SONEW) and (FOLLOWERS is SOMANY) then (POPULARITY is LITTLEPOPULARITY) (1)
If (KINDOFGAME is BR) and (VIEWER is MANY) and (VIDEOHEIGHT is HD) and (AVERAGEFPS is SOME) and (VIEWS is MANY) and (CREATED is OLD) and (FOLLOWERS is MANY) then (POPULARITY is SOMEPOPULARITY) (1)
If (KINDOFGAME is IRL) and (VIEWER is FEW) and (VIDEOHEIGHT is ULTRAHD) and (AVERAGEFPS is FEW) and (VIEWS is FEW) and (CREATED is SOOLD) and (FOLLOWERS is SOMANY) then (POPULARITY is LITTLEPOPULARITY) (1)
If (KINDOFGAME is IRL) and (VIEWER is MANY) and (VIDEOHEIGHT is ULTRAHD) and (AVERAGEFPS is FEW) and (VIEWS is MANY) and (CREATED is SOOLD) and (FOLLOWERS is MANY) then (POPULARITY is SOMEPOPULARITY) (1)
If (KINDOFGAME is IRL) and (VIEWER is SOMANY) and (VIDEOHEIGHT is HD) and (AVERAGEFPS is FEW) and (VIEWS is MANY) and (CREATED is SOOLD) and (FOLLOWERS is SOMANY) then (POPULARITY is SOPOPULARITY) (1)
If (KINDOFGAME is MOBA) and (VIEWER is SOME) and (VIDEOHEIGHT is HDREADY) and (AVERAGEFPS is FEW) and (VIEWS is FEW) and (CREATED is SOOLD) and (FOLLOWERS is FEW) then (POPULARITY is LITTLEPOPULARITY) (1)
If (KINDOFGAME is MOBA) and (VIEWER is MANY) and (VIDEOHEIGHT is ULTRAHD) and (AVERAGEFPS is MANY) and (VIEWS is SOME) and (CREATED is SONEW) and (FOLLOWERS is FEW) then (POPULARITY is SOPOPULARITY) (1)
If (KINDOFGAME is MOBA) and (VIEWER is MANY) and (VIDEOHEIGHT is ULTRAHD) and (AVERAGEFPS is MANY) and (VIEWS is MANY) and (CREATED is SONEW) and (FOLLOWERS is FEW) then (POPULARITY is SOMEPOPULARITY) (1)
If (KINDOFGAME is SURVIVAL) and (VIEWER is MANY) and (VIDEOHEIGHT is HDREADY) and (AVERAGEFPS is MANY) and (VIEWS is SOME) and (CREATED is NEW) and (FOLLOWERS is FEW) then (POPULARITY is LITTLEPOPULARITY) (1)
If (KINDOFGAME is SURVIVAL) and (VIEWER is MANY) and (VIDEOHEIGHT is ULTRAHD) and (AVERAGEFPS is MANY) and (VIEWS is SOME) and (CREATED is NEW) and (FOLLOWERS is FEW) then (POPULARITY is SOPOPULARITY) (1)
If (KINDOFGAME is SURVIVAL) and (VIEWER is MANY) and (VIDEOHEIGHT is ULTRAHD) and (AVERAGEFPS is FEW) and (VIEWS is SOME) and (CREATED is NEW) and (FOLLOWERS is FEW) then (POPULARITY is SOMEPOPULARITY) (1)
If (KINDOFGAME is CARD) and (VIEWER is FEW) and (VIDEOHEIGHT is HDREADY) and (AVERAGEFPS is MANY) and (VIEWS is FEW) and (CREATED is SOOLD) and (FOLLOWERS is FEW) then (POPULARITY is LITTLEPOPULARITY) (1)
If (KINDOFGAME is CARD) and (VIEWER is FEW) and (VIDEOHEIGHT is HDREADY) and (AVERAGEFPS is MANY) and (VIEWS is SOME) and (CREATED is SOOLD) and (FOLLOWERS is SOMANY) then (POPULARITY is SOMEPOPULARITY) (1)
If (KINDOFGAME is SPORT) and (VIEWER is FEW) and (VIDEOHEIGHT is HDREADY) and (AVERAGEFPS is MANY) and (VIEWS is SOME) and (CREATED is SOOLD) and (FOLLOWERS is SOMANY) then (POPULARITY is LITTLEPOPULARITY) (1)
If (KINDOFGAME is SPORT) and (VIEWER is SOME) and (VIDEOHEIGHT is ULTRAHD) and (AVERAGEFPS is MANY) and (VIEWS is SOME) and (CREATED is SONEW) and (FOLLOWERS is SOMANY) then (POPULARITY is SOMEPOPULARITY) (1)
If (KINDOFGAME is ROLE) and (VIEWER is FEW) and (VIDEOHEIGHT is ULTRAHD) and (AVERAGEFPS is MANY) and (VIEWS is SOME) and (CREATED is SONEW) and (FOLLOWERS is FEW) then (POPULARITY is LITTLEPOPULARITY) (1)

Low Popular, Popular and Very Popular variables that belong to the output class mentioned here are the first listed content producer channels on the Twitch homepage. TwitchAPI connection is provided with C # programming language and data for hours of N = 7 are determined for all days of the week. These data were stored in the text file and kept on the local computer. These data were then prepared for MATLAB application development by pre-processing data.

After all the data were collected together, the technical specifications received for each live broadcast content channel were matched to the level of popularity. The specifications of the content generator channel are given in the table below. The data in the table are given together with the data format which was obtained first and the state of the data after preprocessing.

As an example, the first content in Table 1 is a game channel FPS type of game, 1080p worth of the screen to provide images, with an average of 90 FPS, 3000000 total monitoring, since 2012 and 450 followers, while the value of the popularity value was found to be 0.282. These values indicate that there is a less popular channel as measured by the rule table. Also shown in Table 1 is given by calculating the Popularity values of the other channels.

Table 2. Output Value Obtained According to Input Values

KindofGame	Viewer	VideoHeight	Average FPS	View	Created	Followers	Popularity
FPS	90 (FEW)	1080p (ULTRAHD)	90 (MANY)	3000000 (SOME)	2012 (SOOLD)	450 (FEW)	0.282 (LITTLEPOPULAR)
Sport	750 (SOME)	1080p (ULTRAHD)	80 (MANY)	4000000 (SOME)	2017 (SONEW)	150000 (SOMANY)	0.562 (SOMEPOPULAR)
MOBA	3000 (MANY)	1080p(ULTRAHD)	75 (MANY)	3500000 (SOME)	2018SONEW	320(FEW)	0.703 (SOPOPULAR)
IRL	6000 (SOMANY)	900p (HD)	30 (FEW)	12000000 (MANY)	2012 (SOOLD)	120000 (SOMANY)	0.834 (SOPUPLAR)
CARD	95 (FEW)	720p (HDREADY)	70 (MANY)	900000 (FEW)	2011 (SOOLD)	180 (FEW)	0.178(LITTLEPOPULAR)

In card games, followers and total viewing affect the popularity. This situation makes the interaction with the user very important. Screen quality in sports games and the introduction of the new publication required a positive advantage. In the Role games, instant follow-up and the number of followers are related to the popularity. In adventure games, the situation is slightly different. The history of viewing is quite high and the display quality is high. The MOBA is a new channel-type content generator, and a high FPS value is important. While each input value mentioned here is meaningful together, its effect on the result class is different. In this study, decision support system has been prepared for content producers who want to reach the masses by determining the basic features required to be popular in the live broadcasting platform. Thanks to this proposed system, it will take into account the need to have content to be popular with live broadcast channels or new content producers who have not yet entered the broadcast. The current system leads to a positive acceleration in the way of popularity by making the least monitored channels the main features as well. This study will produce more optimal results using more data sets. In order to improve the existing system, the content produced by the channels will also produce more optimum results by considering other features such as audio and video. A broader rule table will produce more usable and predictable results.

References

Hamilton W.A., Garretson O., Kerne A. (2014) Streaming on Twitch: Fostering participatory communities of play within live mixed media. Proceedings of the 32nd Annual ACM conference on human factors in computing systems (2014), Dept. of Computer Science and Engineering1,Dept. of Sociology2,Texas A&M University, College Station, Texas USA.

Timuçin T, Korkmaz M, Yücedağ İ, Biroğul S, Fuzzy Logic Based Product Selection with SQL Query Method in Computer Industry, International Academic Research Congress, October 2017 Alanya, ANTALYA

Zadeh, L. A. (1965). Fuzzy Set, Information and Control. 8, 338-353.

Ganesh, M. K. S., & Thanushkodi, K. (2015). An efficient software cost estimation technique using fuzzy logic with the aid of optimization algorithm. International Journal of Innovative Computing, Information and Control, 11(2), 587-597.

Mamdani, E. H., & Assilian, S. (1993). An experiment in linguistic synthesis with a fuzzy logic controller. In Readings in Fuzzy Sets for Intelligent Systems (pp. 283-289).

Zorah Hilvert-Bruce, James T. Neill, Max Sjöblom, Juho Hamari (2018), Social motivations of live-streaming viewer engagement on Twitch , Computers in Human Behavior, July 2018, Pages 58-67

Katherine Payne, Mark J.Keith, Ryan M.Schuetzler, Justin ScottGiboney, (2017), Examining the learning effects of live streaming video game instruction over Twitch, Computers in Human Behavior Volume 77, , Pages 95-109, December

B Gültekin, S Biroğul, İ Yücedağ, (2015), İşe Alım Süreci Aday Ön Tesbitinde Bulanık Mantık Tabanlı SQL Sorgulama Yönteminin İncelenmesi, Düzce Üniversitesi Bilim ve Teknoloji Dergisi 3 (1)

ME Bayrakdar, S Bayrakdar, İ Yücedağ, A Çalhan, (2015), Bilişsel Radyo Kullanıcıları için Bulanık Mantık Yardımıyla Kanal Kullanım Olasılığı Hesabında Farklı Bir Yaklaşım, , Düzce Üniversitesi Bilim ve Teknoloji Dergisi 3 (1), 3.

L Sabah, I Yücedag, C Yalcin, (2017), Earthquake Hazard Analysis For Districts Of Düzce Via Ahp And Fuzzy Logic Methods, Cognitive Systems 2 (1)

MŞ Biçen, A Çalhan, İ Yücedağ, (2016), Kablosuz Heterojen Algılayıcı Ağlarda Bulanık Mantık Tabanlı Ağ Geçidi Seçimi, Düzce University Journal of Science and Technology 4 (2)

Kablosuz Heterojen Algılayıcı Ağlarda Bulanık Mantık Tabanlı Ağ Geçidi Seçimi

MŞ Biçen, A Çalhan, İ Yücedağ, (2016), Düzce University Journal of Science and Technology 4 (2)

URL-1: https://www.twitch.tv/year/2017/((Date of access: 21 Mayıs 2018).

Visual Object Detection with Deep Learning

Murat KORKMAZ[1*], İbrahim YÜCEDAĞ[2]

[1] Duzce University, Computer Engineering, Duzce, Turkey

[2] Duzce University, Computer Engineering, Duzce, Turkey

[*] **Corresponding Author:** muratkorkmaz30@hotmail.com

Abstract

Object Detection is the process of the classify objects and find their location in the image and show object's position with the bounding box. Object detection which is important part of image processing has variety of uses like security and medical imaging. Because of several factors like classify object, shape deformation and partial occlusion, object detection is difficult subject and need numerous training data. On the other hand especially in recent years, thanks to data which is increasing very rapidly and using of graphic processing unit(GPU) for the computation, deep learning has become very importance and achieved very successful results in many research area. The performance of visual targeting algorithms based on the deep learning approach has also improved significantly. In this paper, it is aimed to introduce the target detection algorithms which use deep learning approach and analyze them in detail to reveal their differences.

Keywords: Deep Learning, Visual Object Detection, Machine Learning.

1. Introduction

Visual object detection is process of classify an object in image or video and show the object in image or video with bounding box. Visual object detection has variety of uses area like human-computer interaction, medical imaging and it is crucial part of image processing (Felzenszwalb et all., 2010).

Feature extraction, which is done by the expert for the classify object rightly does not give expected results all the time. Like the suitability of the extracted feature and deformity of given shape, some factors have bad effects on the accuracy of the system. On the other hand with the developing technology using of the GPUs for the machine learning area and incredible growing sizes of training data, using of deep learning for image recogniton provided reduce the bad effect of the manually feature extraction. Deep learning has been the most preferred method in recent years, especially in areas such as image recognition, voice recognition, natural language processing, and achieving very high performance rates(LeCun et all.,2015; Goodfellow et all.,2016).

Deep Learning is the process of feature extraction automatically by computer instead of by expert. Deep learning need numerous data to extract features appropriately. The number of training data has positive correlation with the success of the system but it has negative correlation with the study time. With the more data, the more appropriate the classification will be performed by the computer but the training time will be longer.

In the chapter 2 we will see convolutional neural network and in the chapter 3 we will detailed the region based convulutional neural network(R-CNN), Fast R-CNN and Faster R-CNN algorithms which are visual object detection algorithms based deep learning. We will show the difference between those algorithm.

2. Convolutional Neural Network Architecture

Convolutional neural network(CNN) architecture regarded as a main architecture of deep learning and it is used for image classification mostly. CNN is consist of different layers and those are; convolutional, pooling, fully connections layers(LeCun and Bengiu, 1995). Convolutional layer which is give the name to this architecture is the most important layer . In this layer we obtain a feature map with a n x n kernel used on image with the predefined stride lenght. After that layer, we use rectifier linear unit to normalize variables between 0 and

255(Krizhevsky et. All, 2012). In the pooling layer we reduce the feature maps width and heights with the pre defined n x n kernel size. Fully connection layer has connections with the all activations of the layer before itself.

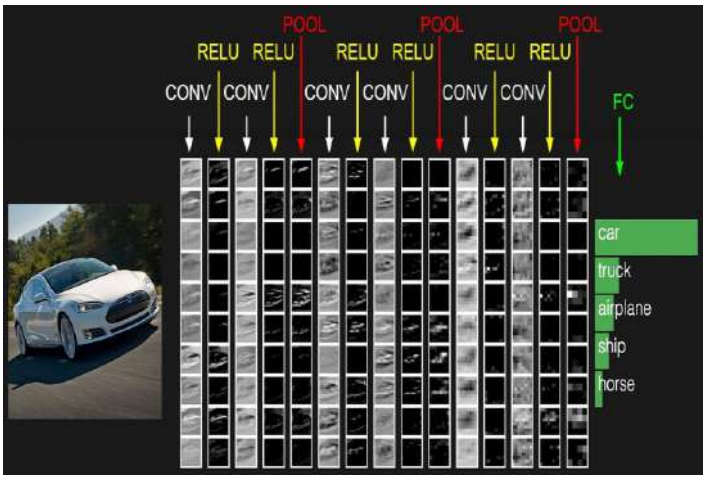

Figure 1. CNN Architecture.

3. Visual Object Detection Algorithm Based Deep Learning

3.1. Region-based Convolutional Neural Network

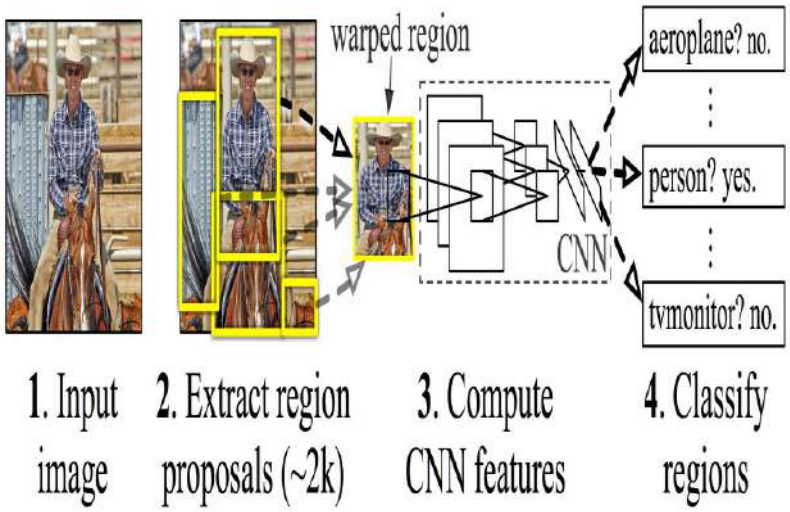

Figure 2. R-CNN Architecture(Girshick et all.,2014).

Region based convolutional neural network technique consist of 3 stage. First stage is use selective search algorithm(Uijlings et all.,2013) which is the algorithm of image segmantation to produce approximately 2000 region proposal. Second stage is apply CNN for

all region of interest(RoI) one by one. The last stage is using support vector machines(Cortes et all., 1995) to classify output of CNNs and using linear regression if the roi has object(Girshick et all.,2014).

3.2. Fast R-CNN

R-CNN is the important algorithm for the visual object detection but it has some disadvantages. First, applying a separate convolutional neural network process to each of the approximately 2000 regions obtained after the selective search is quite disadvantageous in terms of time and resources. It is also disadvantageous to produce new models by using support vector machines after the CNN. Fast R-CNN method aims to eliminate these two disadvantages of the R-CNN method.

Instead of using approximately 2000 separate convolutional neural network, convolutional neural network is used just one time for the entire image. Then it is produced regions by applying selective search to the last convolutional feature map of this neural network. After that process, using a max pooling layer, which called RoI pooling, for the obtain fixed-length vector and use it in fully connection layer. After fully connection layer obtained 2 layer, one of then is the softmax probability for K class and another one is the 4 real number for the position of one of the K class. Use of the Softmax method also avoided the use of 2000-3000 separate support vector machines in the R-CNN structure (Girshick, 2015).

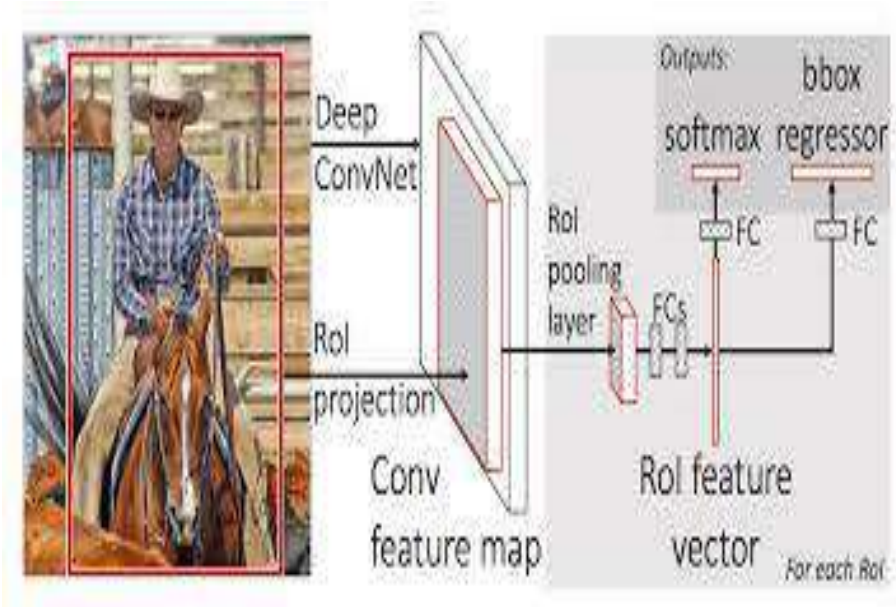

Figure 3. Fast R-CNN Architecture(Girshick, 2015).

3.3. Faster R-CNN

The Fast R-CNN method can eliminate some of the disadvantages of the R-CNN's method, but it is insufficient to overcome all of its disadvantages. The biggest disadvantage of the Fast R-CNN method is the process of determining the regions using the selective search method. To change this disadvantaged situation a neural network is designed instead of using selective search algorithm.

This neural network, which is called the region-proposal network, is aimed to create a n x n sliding window to the last convolutinal attribute map layer, mentioned in the structure of Fast R-CNN-and apply it to the entire layer. Then it is hold the objectness score, which is hold the information about whether the anchor boxes in sliding windows or not, if anchor boxes were exist its also would hold the their positions. Sections with a score above a certain value are defined as regions.

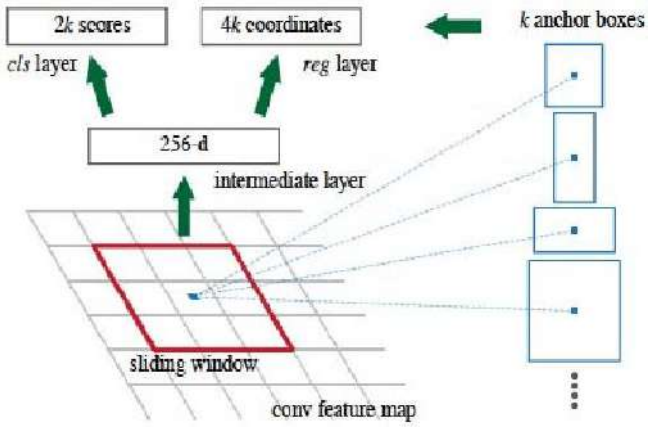

Figure 4. Region Proposal Network(Ren et all.,2015)

After the regions are determined by RPN, RoI Pooling, which is mentioned in the structure of Fast R-CNN, fully connection and then softmax and bounding box regressor operations are applied to regions. With the use of neural networks instead of selective search, the determination of regions has significantly improved both speed and accuracy results. (Ren et all.,2017)

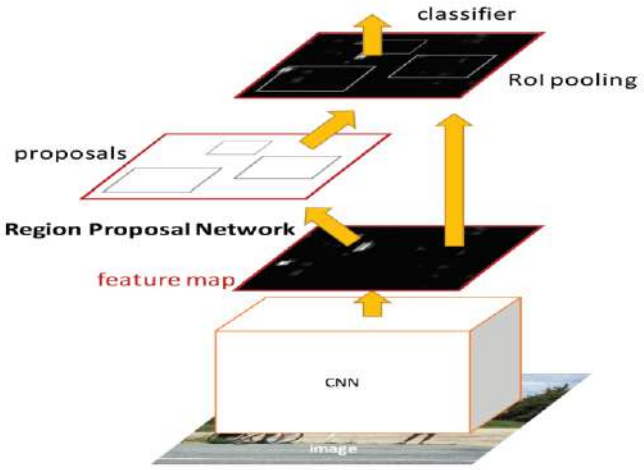

Figure 5. Faster R-CNN Architecture(Ren et all.,2015)

4. Conclusion

Table 1. Comparison of Models(Lei et all, 2016).

	R-CNN	**Fast R-CNN**	**Faster R-CNN**
Test time per image	50 second	2 second	**0.2 second**
Acceleration	1x	25x	**250x**
mAP(VOC 2007)	66.0	**66.9**	**66.9**

Thanks to deep learning, the accuracy of image recognition and object detection algorithms is significantly increased. In this study R-CNN, Fast R-CNN and Faster R-CNN algorithms were examined and the results are given at table 1. As can seen from the table 1, Faster R-CNN is better than the other methods because it aiming to eliminate the shortcoming of the previous methods. Only a few of the deep learning-based visual target detection methods which were develop later, got significantly better result from Faster R-CNN.

References

Cortes, C., & Vapnik, V. (1995). Support-vector networks. Machine learning, 20(3), 273-297.

Felzenszwalb, P. F., Girshick, R. B., McAllester, D., & Ramanan, D. (2010). Object detection with discriminatively trained part-based models. IEEE transactions on pattern analysis and machine intelligence, 32(9), 1627-1645.

Girshick, R., Donahue, J., Darrell, T., & Malik, J. (2014). Rich feature hierarchies for accurate object detection and semantic segmentation. In *Proceedings of the IEEE conference on computer vision and pattern recognition* (pp. 580-587).

Girshick, R. (2015). Fast r-cnn. In *Proceedings of the IEEE international conference on computer vision* (pp. 1440-1448).

Goodfellow, I., Bengio, Y., Courville, A., & Bengio, Y. (2016). Deep learning (Vol. 1). Cambridge: MIT press.

Krizhevsky, A., Sutskever, I., & Hinton, G. E. (2012). Imagenet classification with deep convolutional neural networks. In Advances in neural information processing systems (pp. 1097-1105).

LeCun, Y., & Bengio, Y. (1995). Convolutional networks for images, speech, and time series. The handbook of brain theory and neural networks, 3361(10), 1995.

LeCun, Y., Bengio, Y., & Hinton, G. (2015). Deep learning. Nature, 521(7553), 436.

Lei, F., Karpathy, A., Johnson, J.(2016) Spatial Localization and Detection [PDF document]. Retrieved from Lecture Notes Online Web site: http://cs231n.stanford.edu/slides/2016/winter1516_lecture8.pdf

Ren, S., He, K., Girshick, R., & Sun, J. (2017). Faster R-CNN: towards real-time object detection with region proposal networks. IEEE transactions on pattern analysis and machine intelligence, 39(6), 1137-1149.

Ren, S., He, K., Girshick, R., & Sun, J. (2015). Faster r-cnn: Towards real-time object detection with region proposal networks. In Advances in neural information processing systems (pp. 91-99).

Uijlings, J. R., Van De Sande, K. E., Gevers, T., & Smeulders, A. W. (2013). Selective search for object recognition. International journal of computer vision, 104(2), 154-171.

QR Code Supported Web-Based Student Attendance System

Osman DUMAN[1*], Baki GÖKGÖZ[1]

[1]Gümüşhane University, Department of Computer Technology Vocational School of Torul, Gümüşhane, Türkiye

[*]**Corresponding Author:** oduman@gumushane.edu.tr

Abstract

Mobile phones are irreplaceable for our daily lives. We carry out many activities using mobile phones. This study presents a mobile application developed for mobile phones. This application provides taking class attendance through a mobile application. The attendance is taken by scanning a QR code by the students over the mobile application for a certain period. The QR code is projected on screen by the instructor after logging in the web-based system. Hence the attendance process which is a time taking burden for the instructor can be easily and quickly realized. Student-based, class-based, and instructor based reports can be generated through this system.

Keywords: Classroom attendance, QR code, mobile programming, web programming

1. Introduction

Many universities in our country make attendance to classes obligatory basing on student affairs regulations. This obligation is at 70% rate for theoretical and 80% rate for practical lectures for Gümüşhane University. Taking and processing attendance is the responsibility of lecturers. Traditionally, lecturers take attendance manually. The students sign their names on the attendance sheet prepared by the lecturer or they write their names on a blank sheet the name of the lecture written on the top.

Studies conducted in the literature for maintaining attendance can be classified as follows: Studies where biometric data are used or not, internet based and having central database, and local studies. Some studies which are internet based and having central database are exemplified as follows. RIFD (Radio Frequency Identification) ultra-high frequency (UHF) reader devices put at the entrance of classrooms. Using these devices make contact-free attendance possible (Çakır and Kaygısız, 2011). In this developed system, hardware costs are an important burden. In another study made by using RIFD technology, the attendance is taken by reading the labels distributed to students by the help of RIFD reader devices. At the same time, the attendance situation can be shown to students with the aid of a screen placed on the doors (Pala, 2008). In another study with RIFD, a reader based application and an RIFD card were developed and the lecturer and students scan their cards to take attendance. Data is collected platform-free with the help of web services (Sezdi and Tüysüz, 2018). A web-based mobile application was developed for checking student attendance, and attendance was taken through the mobile application by showing the classrooms according to the student location information (Bilen et. al, 2015). An attendance system was developed with the aid of a NFC (Near Field Communication) based mobile application (Baykara et. al, 2017). An attendance system was developed using QR code. Class, lecturer, date and hour information were coded into this QR code and the attendance was taken. Moreover, to detect fake attendance the location service information was used and the system was integrated to the Moodle system (Masalha and Hirzallah, 2014). Attendance is automatically performed on the mobile application using a mobile device that supports this technology with a beacon device with Bluetooth low energy (BLE) technology. The limitation of the system is the necessity of having a device with BLE support (Bayılmış and Özdemir, 2016). Following are some of the studies that have internet and central database where biometric data are used. A cloud-based attendance system has been developed through video streaming. The video image has been authenticated by face

recognition algorithm (Mittal et. al, 2017). Fingerprint based student attendance system has been developed. In the study made using Arduino platform does not use internet and common database. However, the use of a biometric data such as a fingerprint prevents the use of fake signature (Turan and Karakuzu, 2017).

2. Barcode QR Code Technology

Today, barcodes provide data storage for optical readers. Widely used barcodes are linear barcodes. It is widely used in products for shopping. A two-dimensional development of a linear barcode has allowed the development of a data matrix that allows us to store more data. The QR code technology was developed in 1994 for the purpose of tracking the automotive production process and then standardized by ISO (ISO/IEC 18004: 2000/2006). It has been used for the first time in the field of pharmacy in our country (Acartürk, 2012).

When we look at the barcode types used today, 4 types of barcode are widely used. These are EAN/UPC barcodes. EAN (European Article Numbering) is used in European countries; UPC (Universal Product Codes) is used in America and Canada. Code 39 is able to encode all the letters of the alphabet big. Encoding begins and ends with the * character (Figure 1). PDF 417 stores two-dimensional data and can store over 2000 characters. Today, some airline companies use it in printed boarding passes (Figure 2). INTERLEAVED 2 OF 5, shortly ITF, is used in industrial applications (Figure 3). It stores numerical data (Dokucu, 2014).

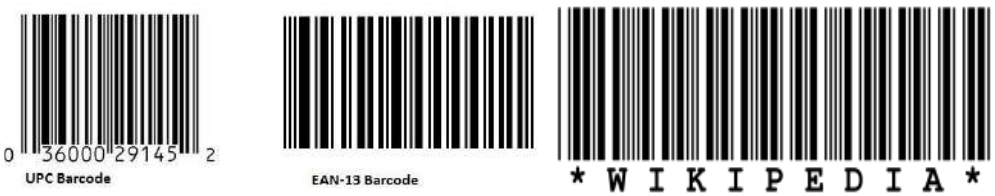

Figure 1. UPC/EAN, Code 39 Barcode examples (Deveci, 2011; URL-1)

Figure 2. A boarding pass example with PDF 417 (Nergiz, 2010)

Figure 3. A barcode example having ITF-14 (URL-2) and QR code example.

3. Application

A two-stage application was developed in this study. The mobile app was developed using AppInventor for the Android platform. The second phase of the application was developed with the php language on the Linux web server. Mysql 5.6 was used as the database. The application was made using “osmanduman.com” domain name and hosting service.

3.1. Web Application

The lecturer enters the system by entering the registration number and password through the website. The lessons given during the active period are listed after the introduction (Figure 4). From here they can choose the lecture they want to take attendance for, see the class list and the course attendance status. After the selection of the course for attendance the information goes to the entrance page where it records the date, the class, the time and the section (Figure 5). When the course information is recorded, it is associated with a randomly generated 12-digit singular code. The QR code containing this code is generated (Figure 5).The lecturer ensures that the square code appears on the screen from the projection device. Students log in to the mobile application they have installed on their phones and scan the code reflected on the screen to complete the attendance. The instructor completes the attendance process by clicking on the finish button under the QR code. Thus attendance is turned off via the mobile application. The instructor can see from the course list page the list of students entering the course, how many weeks the students are coming (Figure 6) and with which browser on which date and with which IP address the student did the attendance process (Figure 7).

Figure 4. Instructor page.

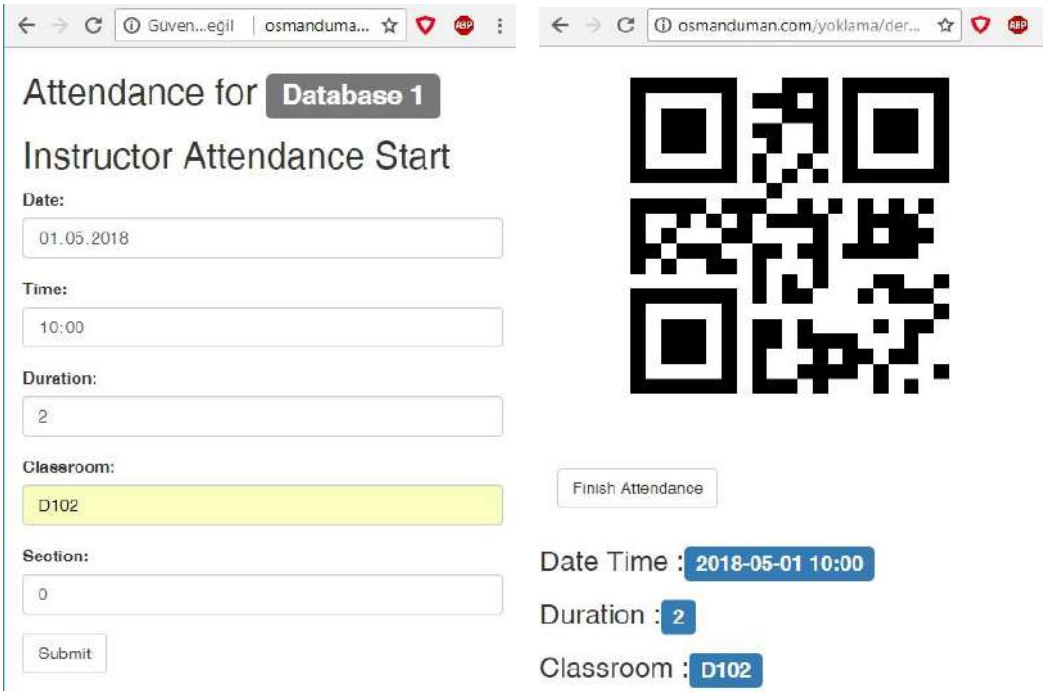

Figure 5. Instructor attendance start page and QR code page

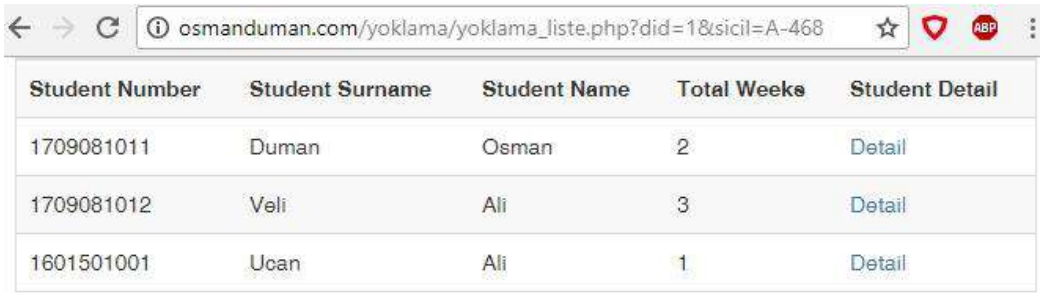

Figure 6. Page showing how many weeks the student has attended the class

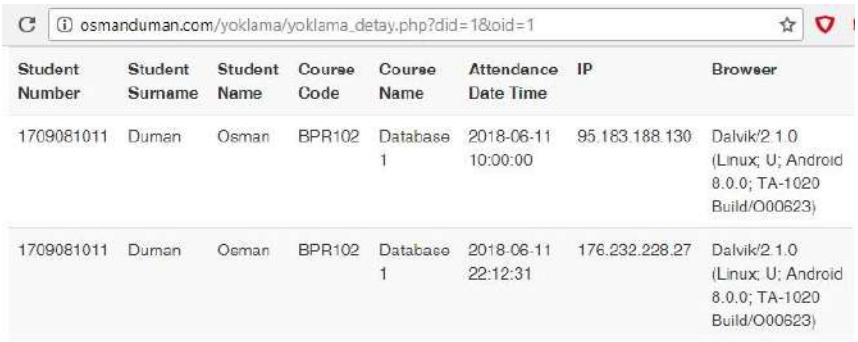

Student Number	Student Surname	Student Name	Course Code	Course Name	Attendance Date Time	IP	Browser
1709081011	Duman	Osman	BPR102	Database 1	2018-06-11 10:00:00	95.183.188.130	Dalvik/2.1.0 (Linux; U; Android 8.0.0; TA-1020 Build/O00823)
1709081011	Duman	Osman	BPR102	Database 1	2018-06-11 22:12:31	176.232.228.27	Dalvik/2.1.0 (Linux; U; Android 8.0.0; TA-1020 Build/O00823)

Figure 7. Page showing the dates the student attend the class

3.2. Mobile Application

The students open the mobile application and enter the student number and password as the user name on the entrance page and enters the system. If they are not registered to the system, they register on the registration page (Figure 8). After logging in to the system, the attendance screen opens (Figure 8). On this screen, the attendance is completed by scanning the QR code and receiving the location information. The data sent through the mobile application is transferred to the database developed through the web application.

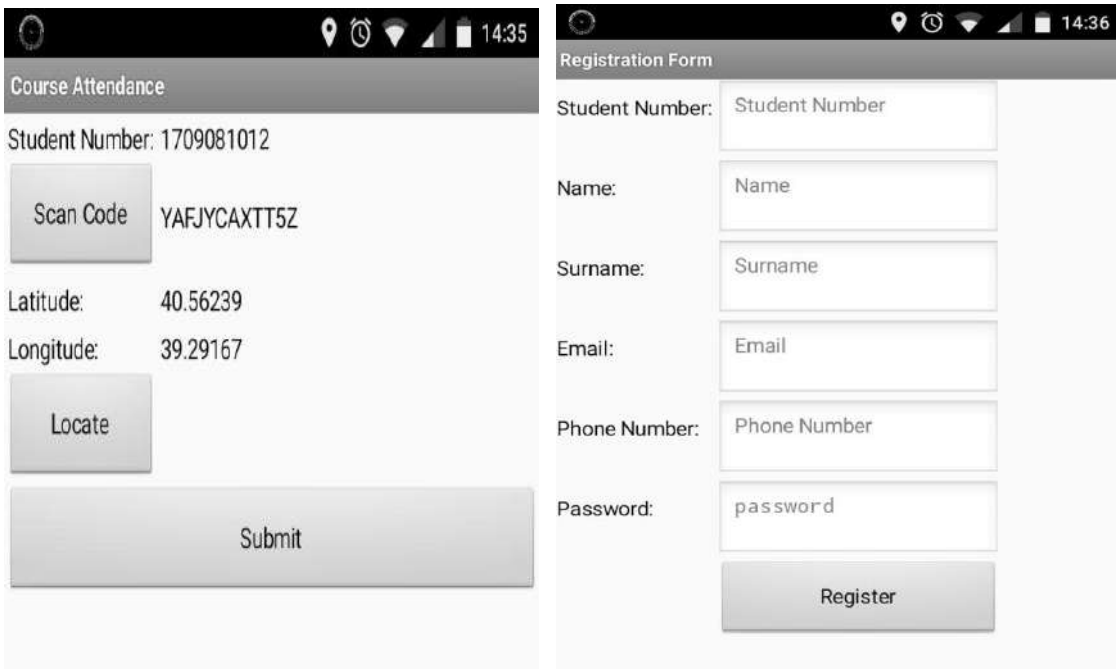

Figure 8. Attendance page and student registration page

4. Conclusion and Suggestions

In this study, it is ensured that mobile phones which are rapidly becoming popular today are used as an auxiliary tool in the education and training process. The attendance process, which is necessary for the lecturers and students, has been completed in real time via mobile phones. Taking attendance and storing it in the database facilitates processes such as absentee detection, easy creation of reports, saving from unnecessary paper overload. During the attendance, by taking the location, IP, browser information, signing for someone else is tried to be prevented. The limitation of the study is the necessity of writing the application for the Android platform as well as for the IOS platform. The use of the Android operating system on mobile devices is 80.99 % as of May 2018 in our country (URL-3). The use of the IOS operating system is 17.44 % as of May 2018 in our country (URL-4). If the application is also developed for the IOS platform as the database is being shared, it can be successfully applied at 98% without additional cost.

References

Acartürk, C., (2012, Şubat). Barkod Teknolojilerinin Eğitimde Kullanımı: Bilişsel Bilimler Çerçevesinde bir Değerlendirme. *XIV. Akademik Bilişim Konferansı (AB 2012),* Uşak: Uşak Üniversitesi.

Bayılmış, C., Özdemir, M., (2016). Bluetooth Düşük Enerji Teknolojisine Sahip İşaretçi ve Akıllı Telefon Temelli Öğrenci Yoklama Sistemi. *Bilişim Teknolojileri Dergisi,* (9)3,249-254.

Bilen, M., Yiğit, T., ve Işık A. H., (2015, Şubat). KNN Algoritması Tabanlı Mobil Devam Takip Yazılımı, *XVII. Akademik Bilişim Konferansı* (AB 2015), Eskişehir: Anadolu Üniversitesi.

Baykara, M., Gürtürk, U., ve Karakaya E., NFC Tabanlı Akıllı Mobil Yoklama Sistemi. *2nd International Conference on Computer Science and Engineering,(UBMK'17)*(s. 937-941).Antalya Türkiye.

Çakır, A., ve Kaygısız, H. B., (2011, May). Kablosuz Öğrenci Yoklama Kontrol Sistemi. *6th International Advanced Technologies Symposium, (IATS'11)*(s. 33-35). Elazığ: Fırat University.

Deveci, M. S., (2011). Barkod Tanıma ve Barkod Çeşitleri. Retrieved from: https://mehmetsalihdeveci.net/2011/03/08/barkod-tanima-ve-barkod-cesitleri/

Dokucu, D.,(2014). Barkod Tipleri. Retrieved from: http://www.netdelojistik.com/2014/08/barkod-tipleri.html

Masalha F.,Hirzallah, N., (2014). A Students Attendance System Using QR Code. *(IJACSA) International Journal of Advanced Computer Science and Applications,* (5) 3, 75-79.

Nergiz, A.,(2010). THY, Biniş Kartlarının Tasarımını Yeniledi. Retrieved from: https://www.havayolu101.com/2010/10/28/thy-binis-kartlarinin-tasarimini-yeniledi/

Mittal, A., Khan, F. S., Kumar, P., and Choudhury, T., (2017, August). Cloud Based Intelligent Attendance System through Video Streaming. *International Conference On Smart Technologies For Smart Nation, (SmartTechCon2017)*(p. 1352-1357). Bengaluru: REVA University.

Pala, Z.,(2008, Nisan). RFID Teknolojisi ile e-Yoklama Uygulaması. *II. Uluslararası Bilgisayar ve Öğretim Teknolojlleri Sempozyumu.* İzmir: Ege Üniversitesi.

Sezdi, E., ve Tüysüz E.,(2018). Elektronik Bilgi Sistemleri Tabanlı Öğrenci Yoklama Kontrol Sistemi. *Bilgi Yönetimi Dergisi*, (1) 1, 23-31.

Turan, Z., ve Karakuzu C., Student Attedance System Based on Fingerprint. *2nd International Conference on Computer Science and Engineering,(UBMK'17)*(s. 967-971).Antalya Türkiye.

URL-1: https://help.gototags.com/article/code-39-barcode/ , (Access Date: 1 June 2018).

URL-2: http://www.barcodelabelcreator.com/barcodelabelcreator/itf-14.html, (Access Date: 1 June 2018).

URL-3: http://gs.statcounter.com/os-market-share/mobile/turkey#monthly-200901-201805, (Access Date: 1 June 2018).

URL-4: http://gs.statcounter.com/os-market-share/mobile/ww#monthly-200901-201805 , (Access Date: 1 June 2018).

Examining Database Optimization Using Database Management System Models in a Mobile Application

Baki GÖKGÖZ[1], Osman DUMAN[2], Menşure KOLÇAK[3]

[1]Gümüşhane University, Department of Computer Technology Vocational School of Torul, Gümüşhane, Türkiye
[2]Gümüşhane University, Department of Computer Technology Vocational School of Torul, Gümüşhane, Türkiye
[3]Atatürk University, Faculty of Economics and Administrative Sciences, Department of Economics, Erzurum, Türkiye

[*]**Corresponding Author:**bakigokgoz@gumushane.edu.tr

Abstract

Today, with the rapid development and change experienced in information technologies, the amount of data that needs to be stored by users has reached a very large size. Horizontal scaling of large data sets is difficult to use the relational database model. As a result, NoSQL database models emerged towards the end of 2009. Large data sets can be stored with the NoSQL DBMS model. Database transactions of systems with high data communication traffic such as Facebook and twitter can be performed easily and quickly. Today, mobile devices, especially mobile phones, are used extensively. In this study, performance comparison using relational database model and NoSQL database model was done for application developed for mobile device in Android Studio environment. The results are shared and based on these results, the best method for database optimization is recommended.

Keywords: NoSQL, Mobile Application, Relational Database, Database Management Systems, SQLite, CouchBase Lite

1. Introduction

Generally, in the world of information, it is important to hide the data and to access these data quickly when there is a need. Today, with the rapid development and change experienced in information technologies, the amount of data that needs to be stored by users has reached a very large size. In 2000, social networks such as Web 2.0 technology and similar web applications have entered the life of mankind. This situation is known as the main reason for the increase of internet data.

The relational database model that stores and processes data on the Internet is used for over 40 years (Codd, 1970). The use of the relational database model is difficult when large data sets are scaled horizontally. As a result, NoSQL database models emerged towards the end of 2009. With the NoSQL DBMS model, large datasets can be stored in a single file. In this context, relational databases as well as non-relational database management systems are used in databases where processes such as reading and writing are heavily used. Non-relational database management systems (NoSQL) with performance and flexibility features have become preferred by world-renowned companies such as Google, Facebook and Amazon (Gökşen, 2015). In general, any database that is not a Relational Database Management System (RDBMS) supports things that do not have a specific order. NoSQL data warehouse does not conform to ACID specifications (atomicity, consistency, isolation, and durability), and high availability and support for large data sets can be provided in horizontally scaled environments (Tiwari, 2011).

NoSQL data models are divided into four subcategories: key-value, chart, document, and column database. The key-value accelerates database read and write operations. The diagram allows the database nodes to be navigated easily through links. The column database provides the ability to perform extensive query and data analysis on applications with associated columns aggregated in a column family (Ünalır, and others , 2015).

There are many differences between relational and non-relational databases. These differences can be summarized in three main points (Al Hinai, 2016): scaling, type of collections and consistency.

Scaling: Relational database systems are vertically scaled to accommodate more data sets. NoSQL database systems are horizontally scaled to accommodate more data sets. As the amount of data increases in relational database systems, more hardware is needed.

Type of Collections: Relational database systems use interrelated structured tables for data storage. NoSQL database systems deal with semi-structured or unstructured data sets that are not related to each other. Depending on this situation, NoSQL database systems affect performance in a positive way (Hammes, and others, 2016).

Consistency: Consistency is a condition of ACID and CAP theorems (Brewer, 2000). All users see the consistency of the data. If any inconsistent data occurs in the operations on the database, it is necessary to undo the whole operation.

When comparing relational databases with NoSQL databases according to the nine-faceted feature, they achieved the following results (Mohamad, and others, 2014):

Transaction Reliability: Relational databases that work with ACID rules outperform NoSQL databases at this point.

Data Model: Relational databases processes are modeled mathematically. The columns are well defined and the associated data are stored in rows in the same structure. This is a well-organized data model. NoSQL uses the techniques that allow categorization to be used as a data model. The most obvious distinction is that it does not use tables as a storage structure. This is effective when managing unstructured data such as Word, pdf, images and video.

Scalability: While relational databases can be scaled vertically, NoSQL databases can be scaled horizontally. The problem that vertical growth brings with it is more hardware.

Cloud: Relational databases do not support full content in the data search and it is difficult to scale the data beyond a limit. NoSQL databases are flexible for unstructured, semi-structured, or structured data.

Big Data Handling: Since the data in the relational databases grow vertically, this can lead to new servers and performance problems. NoSQL does not have performance problems because it is designed for large data.

Data Warehouse: Data stored in relational databases is increasing over time and trying to overcome this problem through OLAP, data mining and statistical operations. NoSQL is not designed to be a data warehouse, and designers are focused on high performance and scalability.

Complexity: The data in the relational database must be transformed into tables by users. When data-table mismatch occurs, the structure of the database may become complicated. NoSQL databases do not have this problem because of their ability to store unstructured, semi-structured, or structured data.

Crash Recovery: Log files and ARIES algorithms are also used to prevent data loss that can occur in relational databases. However, this depends on the frequency of data recovery and backup in NoSQL databases.

Security: Relational databases support many security services because they are widely used. Again, there are many studies about security because relational database is used very long time. NoSQL database systems, as opposed to relational database methods, do not have a new and long history, so new work is being done for security problems.

In this study, it was aimed to compare the performance of the CouchBase Lite NoSQL database in the Android Studio environment with the SQLite relational database used as embedded in mobile devices. CouchBase Lite, a variant of the NoSQL database used in practice, is very similar to key-value storage.

2. Methods and Materials

In this study, which aims to compare the performance of SQLite and CouchBase Lite databases, Windows 10 and 64 Bit version is used as the operating system. Android Studio 3.1.2 was used as the development environment. The code part of the work was developed in the Java programming language. The application developed for this study uses SQLite and CouchBase Lite databases. Performed database operations; adding data, listing data, updating data and deleting data. Performance comparison between relational database systems and NoSQL database systems has been made. The findings are comparatively shared in Table 1 and Table 2. In addition, the developed application interface is shown in Fig 1.

Figure 1. Improved application interface.

3. Findings and Discussion

In this study, which is performed to determine database performance on mobile devices, transactions were performed with 10000 and 20000 records, respectively. The operations were repeated with 3 iterations and an average value was calculated.

Table 1. Performance data for 10000 records (millisecond).

Number of experiments	Add Record		Bulk Data Listing	
	CouchBase Lite	SQLite	CouchBase Lite	SQLite
1	605	1302	7541	5245
2	513	1520	7293	5105
3	491	1321	7626	5312
Average	536,3	1381	7786,6	5087,6

Table 1. Performance data for 20000 records (millisecond)

Number of experiments	Add Record		Bulk Data Listing	
	CouchBase Lite	SQLite	CouchBase Lite	SQLite
1	1225	3120	15321	11746
2	1003	3112	15227	12021
3	989	3225	14921	11956
Average	1072,3	3152,3	15156,3	11907,6

4. Results and Suggestions

In general, it has been observed that the SQLite database, which is a relational database model, is better than the NoSQL database model in terms of performance. It has been understood that the Relational Database Model will be a more optimal option for institutions when processing large amounts of data in the tomb.

Contrary to what is generally known, this study has a different conclusion. In other words, according to the literature, NoSQL database is weaker than Relational Database in terms of performance. The reason for this may be that the queries written are simple. In addition, in systems where larger data are processed, this comparison can yield better results.

References

Al Hinai A. H. (2016). A Performance Comparison of SQL and NoSQL Databases for Large Scale Analysis of Persistent Logs Department of Information Technology.

Brewer, E. A. (2000). Towards robust distributed systems (abstract). Proceedings of the Nineteenth Annual ACM Symposium on Principles of Distributed Computing - PODC '00, 7-19.

Codd, E. F. (1970). A relational model of data for large shared data banks. Communications of the ACM Commun. ACM, 13(6), 377-387.

Dayne H., Medero H., and Mitchell. H. (2014) "Comparison of NoSQL and SQL Databases in the Cloud. "Comparison of NoSQL and SQL Databases in the Cloud!: Paper 12. AIS Electronic Library (AISeL). SAIS 2014 Proceedings. http://aisel.aisnet.org/sais2014/12.

Eken, S., Kaya, F., Sayar, A., and Kavak, A. (2014). " Document-Based NoSQL Databases: MongoDB and CouchDB horizontal scalability comparison", 7. Engineering and Technology Symposium.

Gökşen, Y. (2015). "Changes in Data Sizes in Data Base Management Systems: NoSQL", Journal of Information Technologies, 8-3.

Mohamed M, A., Altrafi O, G. and Ismail M, O. (2014). Relational vs. NoSQL Databases: A Survey. International Journal of Computer and Information Technology, 3 (3), 598-601.

Tiwari, S. (2011). Using Oracle Berkeley DB as a NoSQL Data Store . http://www.oracle.com/technetwork/articles/cloudcomp/berkeleydb-nosql-323570.html

Ünalır, T.O., İnan, E., Yöngül, B., Olca, E., Şentürk, F., and Mostafapour, V. (2015). "A Hybrid Data Architecture Recommendation for Data Intensive Information Systems", 9th National Software Engineering Symposium.

A Comparison of Performance Metrics of Turkish Twitter Messages Using Text Representations

Abdullah Ammar KARCIOĞLU[1*], Tolga AYDIN[1], Gülşah Tümüklü ÖZYER[1]

[1]Ataturk University, Department of Computer Engineering, Erzurum, Turkey

[*]**Corresponding Author:** ammar.karcioglu@atauni.edu.tr

Abstract

With the development of technology and the spread of the internet all over the world, social media platforms have evolved over time so that people can be aware of the changes happening in the world at any moment, and that everyone can share their own thoughts. Twitter, one of the most used social media platforms around the world, has become one of the most important parts of everyday life. With twitter, users share their own feelings and thoughts to create important data sources that can be used in sentiment analysis work on the social media in the field of data mining. In this study, which is implemented in python programming language, sentiment analysis was performed by using text representations in turkish twitter messages that users shared. The aim of the study, the performance effects of Bag-of-Words(BOW) model weighted by Tf-Idf and semantic relation based Word2Vec model are compared on sentiment analysis. In this study, which applied 3 different models, in the third model, the highest accuracy percentage was obtained with 66.40% by applying Random Forest algorithm to Word2Vec model. The results obtained using the machine learning algorithms from the scikit-learn library compared the performance metrics and provided the literature contribution to turkish natural language processing studies.

Keywords: Twitter, Sentiment Analysis, Text Representation, Word2Vec

1. Introduction

According to twitter statistics (Aslam, 2018), with 100 million users per day and more than 500 million tweets per month, users share their feelings and thoughts with the whole world quickly and reliably. Twitter; has become one of the most important social media platforms day by day because of the number of daily users and the amount of sharing made. Thanks to its large data set, it has become an important source for researchers on sentiment analysis studies(Gemci ve Peker, 2013). Unlike other text with long content, twitter messages are limited to 140 characters, so twitter is called a microblogging service (Kim et al., 2010).

Over time, becoming an important social media platform of twitter, it has caused researchers to change their workspaces, thanks to its large data set. In the past, the researchers focused on the structure of twitter and performed some studies. Then they performed studies on extracting semantic information from the twitter data and contributed to the study of sentiment analysis in social media(Kim et al., 2010).

In the literature on sentiment analysis; a corpus was created from the comments of users with different interests and sentiment analysis was performed on this data set. Purpose of this; contribute to the field of opinion mining and develop a model on sentiment classification with a formed corpus. They performed a linguistic analysis study mainly using the n-gram method (Pak et al., 2010).

In another study of twitter sentiment analysis, it has been shown that POS (Part of Speech) features may not be useful for sentiment analysis in the field of microblogging(Kouloumpis et al., 2011). It has been shown that using hashtags to collect training data in the study produces successful results in positive and negative data. In addition, it has been described that the method of producing better results using better training data may depend on the characteristics of the features. As a result, it has been shown that when the features of microblog services are added, the success rate may decrease(Kouloumpis et al., 2011).

In some studies on semantic analysis on twitter, it has been shown how twitter messages are concentrated under which topic names by using semantic relationship from twitter contents by using PLSA and LDA methods(Kim et al., 2010). They also presented a vector space model that learns text representations that find meaningful information in order to derive a semantic relationship in sentiment analysis using LSA and LDA methods(Maas et al., 2011). The model's probabilistic basis gives a theoretically verified technique for the induction of the word vector

as an alternative to the overwhelming number of commonly used matrix factorization-based techniques.

Topic modeling methods such as LSA, PLSA and LDA have been developed in the literature(Alghamdi, 2015). However, Word2Vec (Mikolov et al., 2013a and 2013b), one of the semantic relation-based methods developed by Mikolov and his colleagues, aimed to extract meaningful information on texts.

Because of the lack of natural language processing studies in the literature on Turkish language and also because there is not a lot of studies based on semantic relation in Turkish, it is aimed to perform sentiment analysis study by applying text representation methods to positive and negative labeled Turkish twitter messages. In this study, it has been shown that by using the text representation methods, good results are produced in the classification of sentiment analysis in labeled turkish twitter messages. Moreover, it has been shown that these text representations and classification algorithms will produce successful results in sentiment analysis studies. For each feature extraction method using Tf-Idf and Word2Vec (unlike LDA and PLSA methods), performans metrics were compared using Linear SVM, Logistic Regression, KNN, Decision Tree and Random Forest algorithms.

The rest of this article is organized as follows. Chapter 2 describes our materials and methods. In this section, data set, preprocessing steps on data, root retrieval, text representation methods and classifiers are shown. Chapter 3 shows our findings as a result of study. Section 4 describes our study results and the study we plan to do in the future.

2. Material and Method

In our study, three different models were developed using different text representation methods. All basic classifiers were trained in the same data set, but different text representation methods were applied. First model as given in the section 2.1.1., each machine learning algorithm was applied by feature extracting by Tf-Idf text representation method and the results are obtained. Second model as given in the section 2.1.2., Word2Vec text representation method was applied. However, twitter messages were represented by the average of word embeddings. In the third model; The Word2Vec method was used. However, in this model, messages were represented by the average of the weighted word embeddings.

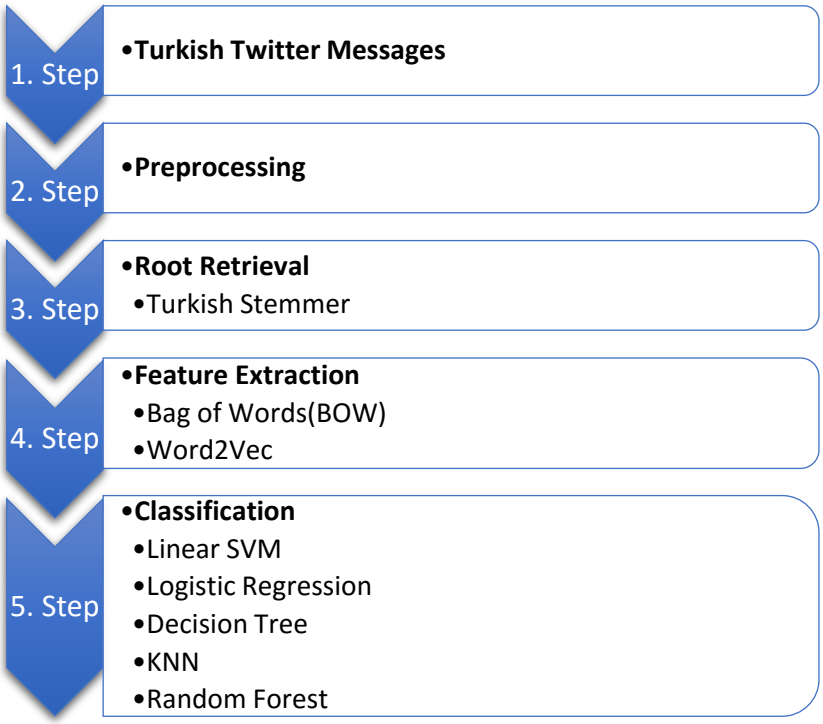

Figure 1. The Model of System

2.1. Text Representations

Text representations are very important for lexical features used in twitter sentiment analysis studies. Recent studies have shown that intensive, low-dimensional and real-valued word embedding provide competitive performance for twitter sentiment classification(Ren et al., 2016).

2.1.1. Bag of Words(BOW)

The Tf-Idf (Term Frequency - Inverse Document Frequency) model is one of the popular approaches to text representation in natural language processing. Tf-Idf creates a vector space model of the text by weighting the text to show how important the word in the text is in the document (Salton, 1988).

Pang and his colleagues pioneered in the field of bag-of-word(BOW) where each word was represented as a vector (Ren et al., 2016-14). The BOW model has some problems, such as limited classification performance due to the high size of the text representation and the

inability to catch the semantic relation between the words. In this study, The representation adopted by this work is the bag-of-words weighted by Tf-Idf.

2.1.2. Word2Vec

Word2Vec, which is one of the most commonly used models for generating word vectors, is implemented with two models described as "skip-gram (SG)" and "continuous bag-of-words (CBOW)" (Nakov et al., 2016).

The Word2Vec model, which succeeded in finding semantic relations between words, was developed by Mikolov and his colleagues (Mikolov et al., 2013a and 2013b). This model, which is basically a shallow artificial neural network, has an input layer, a projection layer and an output layer that allows to find words that are close to each other.

In this study, default parameter values of Word2Vec model were used. A 300-dimensional "wiki-tr" corpus (Grave, 2017) with 416051 words developed by Bogazici University was used for the training of the Turkish data set. In addition, since there was no previously trained vector in the study, a 300-dimensional vector was initially chosen.

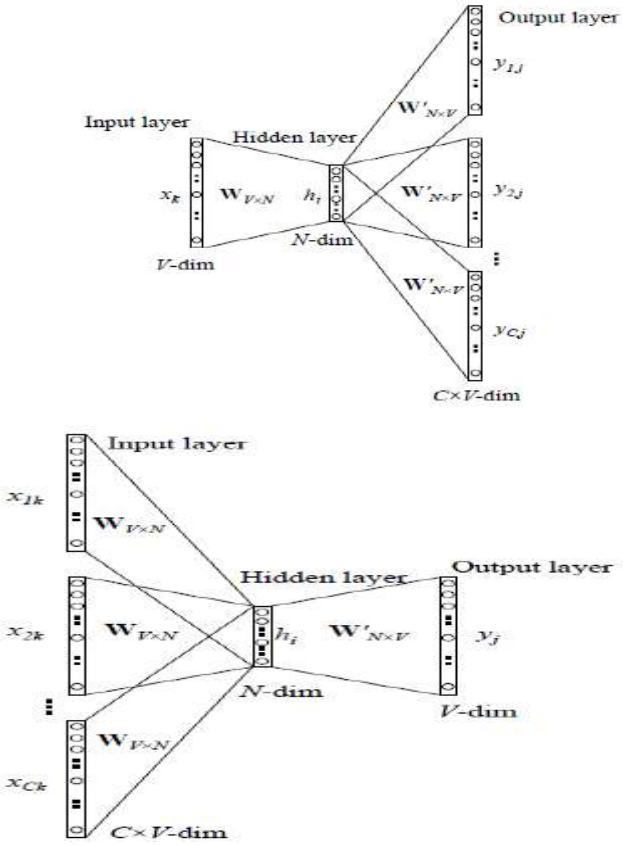

Figure 2. Models of CBOW and Skip-Gram (Rong, 2014)

2.2. Data Set

As shown in Figure 3, the training of our Turkish twitter data with positive and negative label and emoji based, which is 80% training data and 20% test data, was performed in itself and the results were compared.

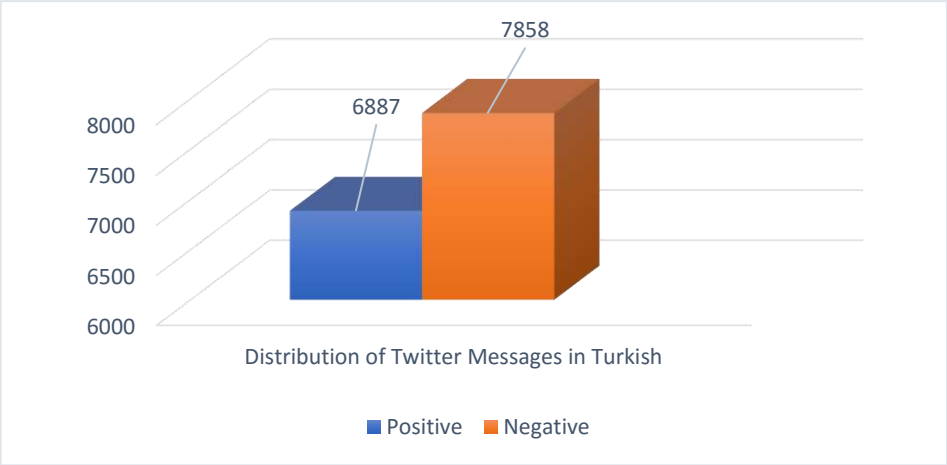

Figure 3. Distribution of Labeled Turkish Twitter Messages

2.3. Data Preprocessing

Before feature extracting of our data set, we processed the data set in one of the natural language processing steps, the data preprocessing step. We removed the hashtags that begin with the "#" character, the username that begins with the "@" character, all the digits, punctuations and image marks, and URL addresses in our data set. After completing these operations, we performed a tokenize operation. As the final stage; we removed the stop words and obtained the cleaned data set.

2.4. Root Retrieval

One of the natural language processing processes is root retrieval processing. We have completed rooting using the Turkish Stemmer library (Tunçelli, 2015), which is developed in the python programming language, to root retrieval of our pre-processed data set.

2.5. Classifiers

In this work, which is performed in the python programming language, the success metrics of the results obtained using the machine learning algorithms in the scikit-learn library(Pedregosa et al., 2011) are compared. The parameter values of the selected algorithms are described below.

2.5.1. Linear SVM

Linear SVM was originally formulated for binary classification(Tang, 2013). The SVM classifies by constructing an N-dimensional hyperplanar that best separates the data into two categories(Mitchell, 1997). The support vector machine is a supervised learning method that produces input-output mapping functions from a labeled set of training data(Wang, 2005). We performed our work by selecting the default values of the algorithm.

2.5.2. Logistic Regression

Logistic regression is the most common method used to model binary response data. When the response is binary, it typically takes the form of 1/0, with 1 generally indicating a success and 0 a failure. However, the actual values that 1 and 0 can take vary widely, depending on the purpose of the study(Hilbe, 2011). We performed our work by selecting the default values of this algorithm.

2.5.3. Decision Tree

A decision tree can be used as a model for a sequential decision problems under uncertainty. A decision tree describes graphically the decisions to be made, the events that may occur, and the outcomes associated with combinations of decisions and events(URL). Decision tree models include such concepts as nodes, branches, terminal values, strategy, payoff distribution, certain equivalent, and the rollback method(URL). The parameter values of our decision tree were chosen as (criterion = "gini", random_state = 100, max_depth=100, min_samples_leaf=8).

2.5.4. KNN

A more sophisticated approach, k-nearest neighbor (KNN) classification, finds a group of k objects in the training set that are closest to the test object, and bases the assignment of a label on the predominance of a particular class in this neighborhood(Wu et al., 2008).

There are three key elements of this approach: a set of labeled objects, e.g., a set of stored records, a distance or similarity metric to compute distance between objects, and the value of k, the number of nearest neighbors(Wu et al., 2008). The neighbor number of the algorithm in our study was choosen as 3.

2.5.5. Random Forest

Random forest is an algorithm for classification developed by Leo Breiman that uses an ensemble of classification trees(Díaz-Uriarte and De Andres, 2006). Random forests are an effective tool in prediction. Because of the Law of Large Numbers they do not overfit. Injecting the right kind of randomness makes them accurate classifiers and regressors(Breiman, 2001). We performed our work by selecting the default values of the algorithm.

3. Results and Discussion

After applying the preprocessing and rooting operations, which are natural language processing steps, to our dataset and then we compared the machine learning algorithms after feature extracting of our data. We defined our performance metrics as accuracy and average recall.

As a result of the study, we have achieved the highest accuracy percentage of 66.40% in the third model we created with Word2Vec model. We have also shown that two different Word2Vec models we have developed can increase accuracy and average recall values in most of the algorithms we implemented.

In the study(Çoban et al, 2015) performed by Çoban and his colleagues, the highest success in the BOW model was achieved with 62.48%. However, with the BOW model we have developed, we have achieved the highest accuracy percentage of 65.18% in the BOW model by increasing their accuracy percentage by 4.32%. In addition,increasing their the highest accuracy percentage, we also achieved the highest accuracy percentage by 66,40% in our work.

Table 1. Results of The First Model

Classifiers	Accuracy	Average Recall
Tf-Idf+Linear SVM	**%65,18**	%60,14
Tf-Idf+Logistic Reg.	%64,10	%59,56
Tf-Idf+Decision Tree	%59,66	%54,51
Tf-Idf+KNN	%57,04	%55,73
Tf-Idf+Random Forest	%63,12	%58,82

Table 2. Process Time of The First Model

Classifiers	Process Time(sec)
Tf-Idf+Linear SVM	**4,701**
Tf-Idf+Logistic Reg.	12,451
Tf-Idf+Decision Tree	11,087
Tf-Idf+KNN	8,781
Tf-Idf+Random Forest	33,286

As shown in Table 2, the lowest processing time was obtained with Linear SVM in the sentiment analysis study in the BOW model weighted Tf-Idf, while the highest processing time was obtained by Random Forest algorithm. In the first stage, the highest accuracy rate and lowest processing time were obtained by Linear SVM.

Table 3. Results of The Second Model

Classifiers	Accuracy	Average Recall
Word2Vec+Linear SVM	%51,20	%50,10
Word2Vec+Logistic Reg.	%63,14	%62,72
Word2Vec+Decision Tree	**%66,12**	%65,47
Word2Vec +KNN	%65,77	%65,15
Word2Vec+Random Forest	%65,92	%65,75

Table 4. Process Time of The Second Model

Classifiers	Process Time
Word2Vec+Linear SVM	3,954
Word2Vec+Logistic Reg.	**0,257**
Word2Vec+Decision Tree	2,273
Word2Vec +KNN	13,654
Word2Vec+Random Forest	1,383

As shown in Table 4, in our second model using word2Vec, the lowest processing time was obtained with KNN. Using linear regression, we achieved a low process time and a accuracy rate close to the highest accuracy rate**.**

Table 5. Results of The Third Model

Classifiers	Accuracy	Average Recall
Word2Vec+Linear SVM	%51,28	%50,10
Word2Vec+Logistic Reg.	%63,51	%62,86
Word2Vec+Decision Tree	%66,18	%65,48
Word2Vec +KNN	%65,92	%65,30
Word2Vec+Random Forest	**%66,40**	%65,31

Table 6. Process Time of The Third Model

Classifiers	Process Time
Word2Vec+Linear SVM	3,911
Word2Vec+Logistic Reg.	**0,232**
Word2Vec+Decision Tree	2,916
Word2Vec +KNN	13,572
Word2Vec+Random Forest	1,500

As shown in Table 6, with the Word2Vec model, which was averaged by Tf-Idf-weighted word placements, the lowest processing time was obtained by Linear Regression in the third model, while the highest processing time was obtained by KNN. Using Random Forest algorithm, low process time and highest success rate were obtained.

4. Conclusions and Recommendations

In this study, which is sentiment analysis study using nltk library of python programming language in Turkish natural language processing, we compared accuracy and average recall percentages by using different text representations for sentiment analysis study on twitter, which is one of the social media platforms. We have shown that better results can be achieved using the Word2Vec model, which is based on the semantic relationship, and that machine learning algorithms can be used effectively in sentiment analysis studies. We have also shown that by developing the used Word2Vec model, we can produce better results in itself. In order to achieve better results in our future studies, we aim to do the following studies;

- ✓ Working on a larger data set and increasing the number of labels in data.
- ✓ Working on data sets that are specific to a keyword.
- ✓ To develop a larger size corpus that can be used in Turkish natural language processing.
- ✓ To achieve higher accuracy by adding other algorithms more suitable to the models used.

References

Alghamdi, R., & Alfalqi, K. (2015). A survey of topic modeling in text mining. Int. J. Adv. Comput. Sci. Appl.(IJACSA), 6(1).

Aslam, S., January 1, 2018. Twitter by the Numbers: Stats, Demographics & Fun Facts. It was taken from https://www.omnicoreagency.com/twitter-statistics/ on 10/01/2018.

Breiman, L. (2001). Random forests. Machine learning, 45(1), 5-32.

Çoban, Ö., Özyer, B., & Özyer, G. T. (2015, May). Sentiment analysis for Turkish Twitter feeds. In Signal Processing and Communications Applications Conference (SIU), 2015 23th (pp. 2388-2391). IEEE.

Díaz-Uriarte, R., & De Andres, S. A. (2006). Gene selection and classification of microarray data using random forest. BMC bioinformatics, 7(1), 3.

Gemci, F., & Peker, K. A. (2013, November). Extracting Turkish tweet topics using LDA. In Electrical and Electronics Engineering (ELECO), 2013 8th International Conference on (pp. 531-534). IEEE.

Grave, E, 3 May 2017. Pre-trained word vectors. It was taken from https://github.com/mmihaltz/word2vec-GoogleNews-vectors on 15/12/2017.

Hilbe, J. M. (2011). Logistic regression. In International Encyclopedia of Statistical Science (pp. 755-758). Springer Berlin Heidelberg.

Kim, T. Y., Min, M., Yoon, T., & Lee, J. H. (2010). Semantic Analysis of Twitter contents using PLSA, and LDA. In SCIS & ISIS SCIS & ISIS 2010 (pp. 189-192). Japan Society for Fuzzy Theory and Intelligent Informatics.

Mikolov, T., Chen, K., Corrado, G., & Dean, J. (2013). Efficient estimation of word representations in vector space. arXiv preprint arXiv:1301.3781.

Mikolov, T., Sutskever, I., Chen, K., Corrado, G. S., & Dean, J. (2013). Distributed representations of words and phrases and their compositionality. In Advances in neural information processing systems (pp. 3111-3119).

Mitchell T. M., Machine Learning. McGraw-Hill Science, 1997.

Nakov, P., Ritter, A., Rosenthal, S., Sebastiani, F., & Stoyanov, V. (2016). SemEval-2016 task 4: Sentiment analysis in Twitter. In Proceedings of the 10th International Workshop on Semantic Evaluation (SemEval-2016) (pp. 1-18).

Pedregosa, F., Varoquaux, G., Gramfort, A., Michel, V., Thirion, B., Grisel, O., ... & Vanderplas, J. (2011). Scikit-learn: Machine learning in Python. Journal of machine learning research, 12(Oct), 2825-2830.

Ren, Y., Wang, R., & Ji, D. (2016). A topic-enhanced word embedding for twitter sentiment classification. Information Sciences, 369, 188-198.

Rong, X. (2014). word2vec parameter learning explained. arXiv preprint arXiv:1411.2738.

Salton, Gerard, and Christopher Buckley. "Term-weighting approaches in automatic text retrieval." Information processing and management 24.5 (1988): 513-523.

Tang, Y. (2013). Deep learning using linear support vector machines. arXiv preprint arXiv:1306.0239.

Tunçelli, O., 11 Jan 2015. Turkish Stemmer for Python. It was taken from https://github.com/otuncelli/turkish-stemmer-python on 12/01/2018.

URL: http://treeplan.com/chapters/introduction-to-decision-trees.pdf

Wang, L. (Ed.). (2005). Support vector machines: theory and applications (Vol. 177). Springer Science & Business Media.

Wu, X., Kumar, V., Ross Quinlan, J. et al. Knowl Inf Syst (2008) 14: 1. https://doi.org/10.1007/s10115-007-0114-2

Xie, W., Zhu, F., Jiang, J., Lim, E. P., & Wang, K. (2016). Topicsketch: Real-time bursty topic detection from twitter. IEEE Transactions on Knowledge and Data Engineering, 28(8), 2216-2229.

Multivalued Quantum Logic Circuits: Some New Suggestions and Applications

Mikail Doğuş KARAKAŞ[1*], Azmi GENÇTEN[2]

[1] Department of Computer Technology, Vocational School of Design, Amasya University, Amasya, Turkey; mdkarakas@amasya.edu.tr

[2] Department of Physics, Faculty of Arts and Sciences, Ondokuz Mayıs University, Samsun, Turkey; gencten@omu.edu.tr

[*] **Corresponding Author:** mdkarakas@amasya.edu.tr

Abstract

A dit is a d−dimensional ($d \geq 3$) classical unit. Its equivalence in quantum information is qudit (quantum dit). In classical and quantum information, it is called as multivalued logic. For example, three level quantum systems of spin−1 are called as qutrits. As there exist d−dimensional state space in qudit states, they have advantages in the storage and processing of quantum information. Therefore, multivalued quantum logic gates and circuits are of interest in quantum information processing. First, in this study, basic principles of multivalued quantum logic gates are presented. Then, some multivalued quantum logic circuits are suggested and applied to qutrit states

Keywords: Quantum information processing, multivalued quantum logic, qutrit, ququart.

1. Introduction

In quantum information processing qubits or in general qudits are used instead of bits. A d−dimensional (d≥3) unit of information in quantum information is called qudit (Proctor and Kendon 2016). In classical and quantum information, it is used as multivalued logic gate (Muthukrishnan and Stroud 2000; Brennen, et al. 2005; Bullock, et al. 2005). Three level quantum system (d=3) can be obtained from magnetic quantum spin numbers of spin−1 (Çorbaci, et al. 2016). Four level quantum systems of spin−3/2 (d=4) are called as ququarts (Di and Wei 2013). In multivalued logic systems, there exist d−dimensional state space. So they have advantages in the storage and processing of quantum information. In quantum information processing, multivalued quantum logic gates and circuits are of interest (Khan and Perkowski 2007; Karakaş and Gençten 2018; Parasa and Perkowski 2015).

In this study, some multivalued quantum logic circuits are suggested and applied to some qudit states. In section 2, theoretical background is presented for multivalued quantum logic gates and cırcuits. A new implementation of SWAP logic circuit for two qudit states is presented in section 3. Then, this circuit is applied to two qutrit states. Also, a superdense coding circuit is suggested and applied for two− qutrit entangled states in section 3. The conclusion of the study is given in section 4.

2. Theory

A qudit is d dimensional (d≥3) unit of information in quantum information. Then, a qutrit is a three level quantum system. As shown in Table 1, Zeeman levels of spin−1 electron or nucleus are referred as qutrit.

Table 1. Single qutrit states for spin−1

m_I	1	0	-1
qutrit	$\|0\rangle = \begin{pmatrix}1\\0\\0\end{pmatrix}$	$\|1\rangle = \begin{pmatrix}0\\1\\0\end{pmatrix}$	$\|2\rangle = \begin{pmatrix}0\\0\\1\end{pmatrix}$

A general expression for Hadamard gate of qudits is given as (Karakaş and Gençten 2018)

$$H_{(d)} = \frac{1}{\sqrt{d}} \sum_{1,j=0}^{d-1} e^{i2\pi j1/d} \left| j \right\rangle \left\langle 1 \right| \tag{1}$$

So, the matrix representation of one qutrit Hadamard gate can be written as (Çorbaci, et al. 2016).

$$\mathrm{H} = \frac{1}{\sqrt{3}} \begin{pmatrix} 1 & 1 & 1 \\ 1 & c & c^2 \\ 1 & c^2 & c \end{pmatrix}. \tag{2}$$

Where $c = e^{i\frac{2\pi}{3}}$, $c^2 = e^{-i\frac{2\pi}{3}} = c^*$. By applying this Hadamard gate, superpositions of single qutrit states are found as given in Table 2.

Table 2. The superpositions of single qutrit states.

qutrit, $\left\|a\right\rangle$	$\mathrm{H}\left\|a\right\rangle$
$\left\|0\right\rangle$	$(\left\|0\right\rangle + \left\|1\right\rangle + \left\|2\right\rangle)/\sqrt{3}$
$\left\|1\right\rangle$	$(\left\|0\right\rangle + c\left\|1\right\rangle + c^2\left\|2\right\rangle)/\sqrt{3}$
$\left\|2\right\rangle$	$(\left\|0\right\rangle + c^2\left\|1\right\rangle + c\left\|2\right\rangle)/\sqrt{3}$

For two spin−1 system such as SI (S=1, I=1) spin system, nine two-qutrit states of $\left|00\right\rangle, \left|01\right\rangle, \left|02\right\rangle, \left|10\right\rangle, \left|11\right\rangle, \left|12\right\rangle, \left|20\right\rangle, \left|21\right\rangle$ and $\left|22\right\rangle$ are obtained by direct products of single qutrit states. Two qutrit CNOT gates can be found by using the ternary addition of qutrit states:

$$CNOT_a(T)\left|a,b\right\rangle = \left|a, b \oplus a\right\rangle \tag{3}$$

$$CNOT_b(T)\left|a,b\right\rangle = \left|a \oplus b, b\right\rangle \tag{4}$$

These two−qutrit CNOT gates are 9x9 matrices and they can be written in Dirac notation as following:

$$CNOT_a(T) = |00\rangle\langle 00| + |01\rangle\langle 01| + |02\rangle\langle 02| + |10\rangle\langle 11| + |11\rangle\langle 12| + |12\rangle\langle 10| + |20\rangle\langle 22| + |21\rangle\langle 20| + |22\rangle\langle 21| \quad (5)$$

$$CNOT_b(T) = |00\rangle\langle 00| + |01\rangle\langle 11| + |02\rangle\langle 22| + |10\rangle\langle 10| + |11\rangle\langle 21| + |12\rangle\langle 02| + |20\rangle\langle 20| + |21\rangle\langle 01| + |22\rangle\langle 12| \quad (6)$$

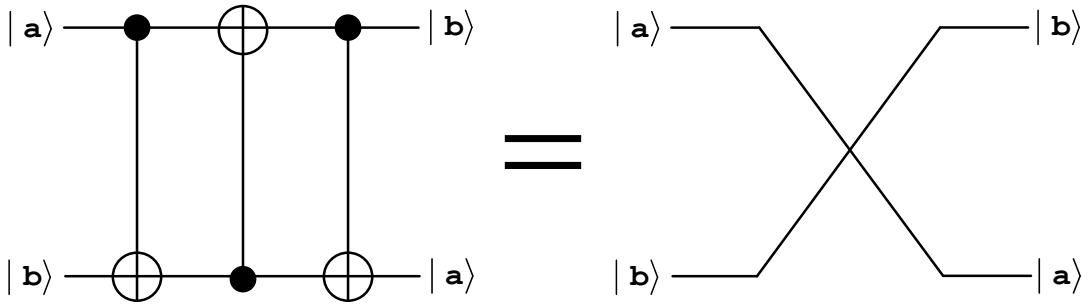

Figure 1. SWAP logic gate for two qubits.

By using the SWAP logic gate two quantum states are exchanged as shown in Figure 1. This circuit can be used only for two qubit states. For this circuit, following equation is used.

$$SWAP = CNOT_a CNOT_b CNOT_a = \begin{pmatrix} 1 & 0 & 0 & 0 \\ 0 & 0 & 1 & 0 \\ 0 & 1 & 0 & 0 \\ 0 & 0 & 0 & 1 \end{pmatrix} \quad (7)$$

By using this equation, two−qubit states are exchanged as following:

$$SWAP|ab\rangle = |ba\rangle \quad (8)$$

3. Results and Discussion

The SWAP logic gate for two qubit states is given in Figure 1. This is not valid for two qudit states. Different implementations of SWAP logic gate for two qudit states are suggested in the literature (Garcia-Escartin and Chamorro-Posada 2013). Here a new implementation of SWAP logic gate for two qudit states is suggested as shown in Figure 2. This implementation can be expressed as following:

$$\left[\left(-I\right)\otimes I\right]CNOT_a\left[I\otimes\left(-I\right)\right]CNOT_b\left[I\otimes\left(-I\right)\right]CNOT_a \tag{9}$$

In this equation $I = U_{00}$. By using this equation, two−qudit states are exchanged as following:

$$CNOT_a\left|a,b\right\rangle = \left|a,a\oplus b\right\rangle \tag{10}$$

$$\left[I\otimes\left(-I\right)\right]\left|a,a\oplus b\right\rangle = \left|a,-a\oplus -b\right\rangle \tag{11}$$

$$CNOT_b\left|a,-a\oplus -b\right\rangle = \left|a\oplus -a\oplus -b,-a\oplus -b\right\rangle = \left|-b,-a\oplus -b\right\rangle \tag{12}$$

$$\left[I\otimes\left(-I\right)\right]\left|-b,-a\oplus -b\right\rangle = \left|-b,a\oplus b\right\rangle \tag{13}$$

$$CNOT_a\left|-b,a\oplus b\right\rangle = \left|-b,a\oplus b\oplus -b\right\rangle = \left|-b,a\right\rangle \tag{14}$$

$$\left[\left(-I\right)\otimes I\right]\left|-b,a\right\rangle = \left|b,a\right\rangle \tag{15}$$

Then, for two qudit states

$$SWAP\left|ab\right\rangle = \left|ba\right\rangle \tag{16}$$

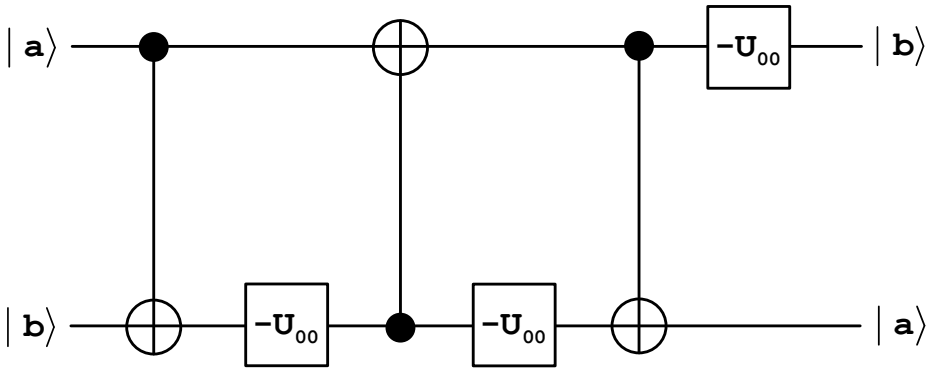

Figure 2. A new implementation of SWAP logic gate for two qudit states.

For two qutrit states matrix representation of this SWAP logic gate can be expressed in Dirac notation as following:

$$\begin{aligned} SWAP(T) = {} & \left|00\right\rangle\left\langle 00\right| + \left|01\right\rangle\left\langle 10\right| + \left|02\right\rangle\left\langle 20\right| + \left|10\right\rangle\left\langle 01\right| + \left|11\right\rangle\left\langle 11\right| \\ & + \left|12\right\rangle\left\langle 21\right| + \left|20\right\rangle\left\langle 02\right| + \left|21\right\rangle\left\langle 12\right| + \left|22\right\rangle\left\langle 22\right| \end{aligned} \tag{17}$$

Application of this SWAP logic gate to two qutrit states are presented in Table 3.

Table 3. Application of SWAP logic gate to two qutrit states.

Input, $\|ab\rangle$	$\|00\rangle$	$\|01\rangle$	$\|02\rangle$	$\|10\rangle$	$\|11\rangle$	$\|12\rangle$	$\|20\rangle$	$\|21\rangle$	$\|22\rangle$
Output, $SWAP(T)\|ab\rangle = \|ba\rangle$	$\|00\rangle$	$\|10\rangle$	$\|20\rangle$	$\|01\rangle$	$\|11\rangle$	$\|21\rangle$	$\|02\rangle$	$\|12\rangle$	$\|22\rangle$

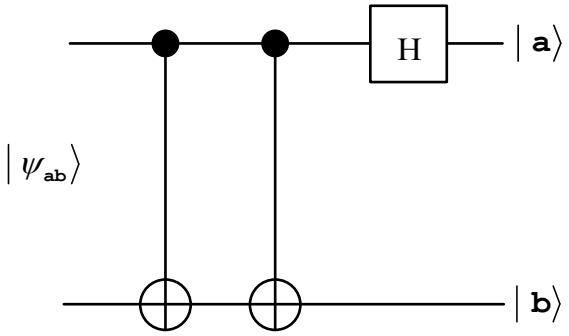

Figure 3. Quantum Circuit for superdense coding of two-qutrit entangled states.

Table 4. Superdense coding for two−qutrit entangled states.

Input, $\|\psi_{ab}\rangle$	Output, $\|ab\rangle$
$(\|00\rangle + \|11\rangle + \|22\rangle)/\sqrt{3}$	$\|00\rangle$
$(\|01\rangle + \|12\rangle + \|20\rangle)/\sqrt{3}$	$\|01\rangle$
$(\|02\rangle + \|10\rangle + \|21\rangle)/\sqrt{3}$	$\|02\rangle$
$(\|00\rangle + c\|11\rangle + c^2\|22\rangle)/\sqrt{3}$	$\|10\rangle$
$(\|01\rangle + c\|12\rangle + c^2\|20\rangle)/\sqrt{3}$	$\|11\rangle$
$(\|02\rangle + c\|10\rangle + c^2\|21\rangle)/\sqrt{3}$	$\|12\rangle$
$(\|00\rangle + c^2\|11\rangle + c\|22\rangle)/\sqrt{3}$	$\|20\rangle$
$(\|01\rangle + c^2\|12\rangle + c\|20\rangle)/\sqrt{3}$	$\|21\rangle$
$(\|02\rangle + c^2\|10\rangle + c\|21\rangle)/\sqrt{3}$	$\|22\rangle$

For two−qutrit entangled states (Çorbaci, et al. 2016), superdense coding can be performed by using the suggested superdense coding circuit given in Figure 3. For this circuit, following equation is used:

$$\left|ab\right\rangle = \left(H_3 \otimes E_3\right)\left[CNOT_a^2(T)\left|\psi_{ab}\left(Q\right)\right\rangle\right]. \quad (18)$$

By using this equation, two−qutrit states are obtained from the two−qutrit entangled states as given in Table 4. In this Table two−qutrit entangled states are taken from our study (Çorbaci, et al. 2016).

4. Conclusion

In this study, first, theoretical background is presented for multivalued quantum logic gates and cırcuits. Then, a new implementation of SWAP logic circuit for two qudit states is presented. This circuit is applied to two−qutrit states and expected SWAP operation is achieved. Also, a superdense coding circuit is suggested for two−qutrit entangled states. By applying this circuit, expected superdense coding is performed for two−qutrit entangled states.

References

Brennen, G. K., O'Leary D. P., and Bullock S. S.. 2005. "Criteria for Exact Qudit Universality." Physical Review A - Atomic, Molecular, and Optical Physics 71(5), 052318.

Bullock, S. S., O'Leary D. P., and Brennen Gavin K.. 2005. "Asymptotically Optimal Quantum Circuits for D-Level Systems." Physical Review Letters 94(23): 230502. https://link.aps.org/doi/10.1103/PhysRevLett.94.230502.

Çorbaci, S., Karakaş M. D., and Gençten A.. 2016. "Construction of Two Qutrit Entanglement by Using Magnetic Resonance Selective Pulse Sequences." Journal of Physics: Conference Series 766(1): 012014. http://stacks.iop.org/1742-6596/766/i=1/a=012014?key=crossref.02ca399829cfe05174acdbbc3c3371f5.

Di, Y. M., and Wei H. R.. 2013. "Synthesis of Multivalued Quantum Logic Circuits by Elementary Gates." Physical Review A - Atomic, Molecular, and Optical Physics 87(1), 012325.

Garcia-Escartin, J. C., and Chamorro-Posada P.. 2013. "A SWAP Gate for Qudits." Quantum Information Processing 12(12): 3625–31.

Karakaş M. D., and Gençten A.. 2018. "Construction of Two−Ququart Quantum Entanglement by Using Magnetic Resonance Selective Pulse Sequences." Zeitschrift für Naturforschung A, Volume 73, Issue 10, Pages 911–918. https://doi.org/10.1515/zna-2017-0441.

Khan, M.H.A., and Perkowski M. A.. 2007. “GF(4) Based Synthesis of Quaternary Reversible/Quantum Logic Circuits.” In 37th International Symposium on Multiple-Valued Logic (ISMVL’07), , 11–11. http://ieeexplore.ieee.org/document/4215934/.

Muthukrishnan, A., and Stroud S.. 2000. “Multivalued Logic Gates for Quantum Computation.” Physical Review A - Atomic, Molecular, and Optical Physics 62(5): 052309–052301.

Parasa, V., and Perkowski M.. 2015. “Quantum Phase Estimation Using Multivalued Logic.” 2011 41st IEEE International Symposium on Multiple-Valued Logic 24(1–4): 224–29. http://ieeexplore.ieee.org/document/5954237/.

Proctor, T. J., and Kendon V.. 2016. “Hybrid Quantum Computing with Ancillas.” Contemporary Physics 57(4): 459–76.

Solving of The Traveling Salesman Problem For Turkey By Simulated Annealing Algorithm Using Metaheuristic Approach

Mustafa Furkan KESKENLER [1*], Eyüp Fahri KESKENLER [2]

[1] Atatürk University, Engineering Faculty, Computer Engineering, Erzurum, Turkey; mfkeskenler@gmail.com
[2] Recep Tayyip Erdoğan University, Engineering Faculty, Material Science And Nanotechnology Engineering, Rize, Turkey; keskenler@gmail.com

[*] **Corresponding Author:** mfkeskenler@gmail.com

Abstract

Traveling salesman problem (TSP), commonly used NP-Hard problems, is one of the problems that contributed greatly to development of computer science. The aim of problem is to find the shortest tour starting from the city where a salesman is located and returning to the starting city after visiting each city only once. Distance between cities is considered as top view and distances are calculated according to the coordinates. This process can not be calculated at polynomial time. That is, the number of cities increases, calculation period exceeds reasonable calculation times considerably. Because of this, different approaches are needed. This problem is calculated about some countries and results are shared. In this study, the shortest tour distance based on eighty one city located in Turkey is calculated using Metaheuristics algorithm. According to the coordinates of eighty one cities, distance of the shortest tour calculated is 77 and these cities are arranged to form the shortest tour. Simulated Annealing algorithm is used for this calculation. SA algorithm, which is one of stochastic search methods, is similar to the physical annealing process for solids. This algorithm is based on principle of heating the solids and then slowly cooling them. The annealing temperature is 1000 oC, the cooling rate (alpha) is 0.983, and the freezing point value (epsilon) is 0.001, in this study. Inversion method was used as perturbation function. In addition, some optimization studies have been made on SA algorithm and the calculation time has been reduced significantly. Solved TSP problem is widely used in airway transport, network establishment and cargo companies.

Keywords: TSP, Simulated annealing, Metaheuristic, Turkey, Optimization, NP-Hard.

1. Introduction

Data sets which are belong to various country and locations are used for Traveling Salesman Problem studing on computer sciences. Turkey that not being among this data sets has been added by using coordinate of 81 city in the study. Thus, the related problem has been solved over Turkey and it has been aimed that to be a referans source for the later studies.

Metaheuristics algorithms are a decision mechanism that works on these heuristic algorithms. So different heuristic methods can be used for a problem. Metaheuristic algorithms are used to decide which of these heuristic methods will be chosen and what values of the selected algorithm parameters will be (Dietrich and et al.). Metaheuristic methods are independent of the problem.

Solutions have been realized by using Simulated Annealing Algorithm. The working time has been accelerated by making several optimizations on Simulated Annealing Algorithm. Furthermore, optaining faster and more reliable results is aimed by occuring hybrid model with Genetic Algorithm.

2. Material and Method

Simulated annealing and genetic algorithm has been used on TSP cost for Turkey. Hybrid model is formed by coding Genetic algorithm in simulated annealing algorithm. Thus, better results have been obtained.

2.1. Traveling Salesman Problem - TSP

Traveling salesman problem (TSP), commonly used NP-Hard problems, is one of the problems that contributed greatly to development of computer science (Fernándeza and et al., 2018).

The aim of problem is to find the shortest tour starting from the city where a salesman is located and returning to the starting city after visiting each city only once (figure 1) (Ren and et al., 2018).

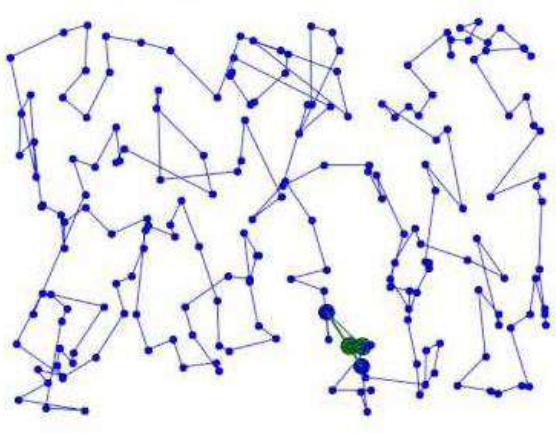

Figure 1. An example for Traveling Salesman Problem.

Distance between cities is considered as top view and distances are calculated according to the coordinates. This process can not be calculated at polynomial time (Wang, 2004). That is, the number of cities increases, calculation period exceeds reasonable calculation times considerably. Because of this, different approaches are needed.

This problem is calculated about some countries and results are shared (figure 2). In this study, the shortest tour distance based on eighty one city located in Turkey is calculated using Metaheuristics algorithm. The values given in table 1 are used in this calculation.

Figure 2. The number of centers used in other countries for the TSP problem.

Table 1. Turkey's cities and their coordinates.

Row Number	City	Latitude	Longitude	Row Number	City	Latitude	Longitude
1	ADANA	37	35,321333	42	KAHRAMANMARAŞ	37,585831	36,937149
2	ADIYAMAN	37,764751	38,278561	43	KARABÜK	41,2061	32,62035
3	AFYONKARAHİSAR	38,750714	30,556692	44	KARAMAN	37,17593	33,228748
4	AĞRI	39,626922	43021596	45	KARS	40,616667	43,1
5	AKSARAY	38,36869	34,03698	46	KASTAMONU	41,38871	33,78273
6	AMASYA	40,64991	35,83532	47	KAYSERİ	38,73122	35,478729
7	ANKARA	39,92077	32,85411	48	KIRIKKALE	39,846821	33,515251
8	ANTALYA	36,88414	30,70563	49	KIRKLARELİ	41,733333	27,216667
9	ARDAHAN	41,110481	42,702171	50	KIRŞEHİR	39,14249	34,17091
10	ARTVİN	41,18277	41,818292	51	KİLİS	36,718399	37,12122
11	AYDIN	37,856041	27,841631	52	KOCAELİ	40,85327	29,88152
12	BALIKESİR	39,648369	27,88261	53	KONYA	37,866667	32,483333
13	BARTIN	41,581051	32,460979	54	KÜTAHYA	39,416667	29,983333
14	BATMAN	37,881168	41,13509	55	MALATYA	38,35519	38,30946

15	BAYBURT	40,255169	40,22488	56	MANİSA	38,619099	27,428921
16	BİLECİK	40,056656	30,066524	57	MARDİN	37,321163	40,724477
17	BİNGÖL	39,062635	40,76961	58	MERSİN	36,8	34,633333
18	BİTLİS	38,393799	42,12318	59	MUĞLA	37,215278	28,363611
19	BOLU	40,575977	31,578809	60	MUŞ	38,946189	41,753893
20	BURDUR	37,461267	30,066524	61	NEVŞEHİR	38,69394	34,685651
21	BURSA	40,266864	29,063448	62	NİĞDE	37,966667	34,683333
22	ÇANAKKALE	40,155312	26,41416	63	ORDU	40,983879	37,876411
23	ÇANKIRI	40,601343	33,613421	64	OSMANİYE	37,213026	36,176261
24	ÇORUM	40,550556	34,955556	65	RİZE	41,02005	40,523449
25	DENİZLİ	37,77652	29,08639	66	SAKARYA	40,693997	30,435763
26	DİYARBAKIR	37,91441	40,230629	67	SAMSUN	41,292782	36,33128
27	DÜZCE	40,843849	31,15654	68	SİİRT	37,933333	41,95
28	EDİRNE	41,681808	26,562269	69	SİNOP	42,02314	35,153069
29	ELAZIĞ	38,680969	39,226398	70	SİVAS	39,747662	37,017879
30	ERZİNCAN	39,75	39,5	71	ŞANLIURFA	37,159149	38,796909
31	ERZURUM	39,9	41,27	72	ŞIRNAK	37,418748	42,491834
32	ESKİŞEHİR	39,776667	30,520556	73	TEKİRDAĞ	40,983333	27,516667
33	GAZİANTEP	37,06622	37,38332	74	TOKAT	40,316667	36,55
34	GİRESUN	40,912811	38,38953	75	TRABZON	41,00145	39,7178
35	GÜMÜŞHANE	40,438588	39,508556	76	TUNCELİ	39,307355	39,438778
36	HAKKARİ	37,583333	43,733333	77	UŞAK	38,682301	29,40819
37	HATAY	36,401849	36,34981	78	VAN	38,48914	43,40889
38	IĞDIR	39,887984	44,004836	79	YALOVA	40,65	29,266667
39	ISPARTA	37,764771	30,556561	80	YOZGAT	39,818081	34,81469
40	İSTANBUL	41,00527	28,97696	81	ZONGULDAK	41,456409	31,798731
41	İZMİR	38,41885	27,12872				

2.2. Simulated Annealing and Hybrid Model

Simulated Annealing algorithm is used for this calculation. SA algorithm is similar to the physical annealing process for solids (Mamano and Hayes, 2017). This algorithm is based on principle of heating the solids and then slowly cooling them.

The simulated annealing algorithm is based on finding the global minimum without the local minimum (Zhu, 2018). The simulated annealing algorithm uses Algorithm 1 to calculate the lowest cost for the TSP problem.

Genetic algorithm has been used to determine the first route in the simulated annealing algorithm. The combination of two algorithms was called hybrid model. hybrid model was coded according to the Algorithm 2.

```
Algorithm SIMULATED-ANNEALING
Begin
    temp = INIT-TEMP;
    place = INIT-PLACEMENT;
    while (temp > FINAL-TEMP) do
        while (inner_loop_criterion = FALSE) do
            new_place = PERTURB(place);
            ΔC = COST(new_place)  - COST(place);
            if (ΔC < 0) then
                place = new_place;
            else if (RANDOM(0,1) < e^(-(ΔC/temp))) then
                place = new_place;
        temp = SCHEDULE(temp);
End.
```

Algorithm 1. Pseudo code of simulated annealing for TSP problems (Simulated An.)

```
Algorithm SIMULATED-ANNEALING
Begin
    temp = INIT-TEMP;
    place = INIT-PLACEMENT;  →→→→→→→→→→→→→→Genetic Algorithm
    while (temp > FINAL-TEMP) do
        while (inner_loop_criterion = FALSE) do
            new_place = PERTURB(place);
            ΔC = COST(new_place)  - COST(place);
            if (ΔC < 0) then
                place = new_place;
            else if (RANDOM(0,1) < e^(-(ΔC/temp))) then
                place = new_place;
        temp = SCHEDULE(temp);
End.
```

Algorithm 2. Pseudo code of simulated annealing for TSP problems (Hybrid Model)

Parameter values for simulated annealing and genetic algorithm are given in figure 3.

```
//SA Parameters
double temperature = 1000.0;//Initial temperature
double alpha = 0.983;//Cooling rate
double epsilon = 0.001;//Freezing point
unsigned int numberOfIterationsPerTemperature = 1200;

//GA Parameters
int numberOfGenerations = 50;
int populationSize = 1040;
double crossoverRate = 0.95;
double mutationRate = 0.15;
```

Figure 3. Simulated Annealing & Hybrid Model (SA-GA) Parameters

3. Results and Discussion

Measurement Attributes;

- A computer used for performance measurements that is 2400 MHz core 2 duo – 4 thread CPU, 10 Gb RAM, SSD.
- Berlin52 and Turkey81 data sets are used in the Performance Measurements.
- The measurements were tested on different functions.

According to Simulated Annealing Algorithm appling on Berlin52 data set, it is resulted that the developed model gains 28.61% and 0.08% rates for time and cost, respectively (table2).

Table 2. Measurement results for TSP problem according to Berlin52 data set

	Simulated Annealing		**Hibrid Model – SA & GA**		
	Time (s)	Cost	Time (s)	Cost	Gain %
Executive Time 1	19.9	7542	24.3	7542	
Executive Time 2	20.8	7554	20.2	7544	Time: %28.61
Executive Time 3	33.3	7542	20.7	7542	
Executive Time 4	17.0	7583	19.5	7561	Cost: %0.08
Executive Time 5	48.1	7542	14.6	7542	
Average	**27.82**	**7552.6**	**19.86**	**7546.2**	

TSP problem has been applied firstly in Turkey81 data set and the cost has been found as 77. The rate of %68.62 for time and, 1.02% for cost gain is obtained owing to optimizate on Simulated Annealing Algorithm with improved hybrid model (table 3).

Table 3. Measurement results for TSP problem according to Turkey81 data set

	Simulated Annealing		**Hibrid Model – SA & GA**		
	Time (s)	Cost	Time (s)	Cost	Gain %
Executive Time 1	21.5	77	6.4	79	
Executive Time 2	37.3	77	11.8	77	
Executive Time 3	16.9	79	4.1	77	Time: %68.62
Executive Time 4	20.1	77	7.6	78	Cost: %1.02
Executive Time 5	17.0	82	5.5	77	
Average	**22.56**	**78.4**	**7.08**	**77.6**	

References

Dietrich, B. L., Escudero, L. F., Chance, F. Efficient reformulation for 0–1 programs: methods and computational results, Discrete Appl. Math. 42, 147-175.

Fernándeza, J.R., López-Camposb, J.A., Segadeb, A., Vilánb, J.A. (2018). A genetic algorithm for the characterization of hyperelastic materials, APPLIED MATHEMATICS AND COMPUTATION, 329 (2018) 239-250.

Mamano, N., Hayes, W.B., (2017). SANA: simulated annealing far outperforms many other search algorithms for biological network alignment, Bioinformatics, 33, 2156-2164.

Ren,Y., Zhang, C., Zhao, F., Xiao, H., Tian, G. (2018). An asynchronous parallel disassembly planning based on genetic algorithm, EUROPEAN JOURNAL OF OPERATIONAL RESEARCH, 269, 647-660.

Wang, R.L. (2004). Agenetic algorithm for subset sum problem, Neurocomputing, 57, 463-468.

Zhu, T., Chen, S., Zhu,W., Wang,Y. (2018). Optimization of sound absorption property for polyurethanefoam using adaptive simulated annealing algorithm, JOURNAL OF APPLIED POLYMER SCIENCE, 135, 46426.

Examination of Middle School Mathematics Teachers' Experiences of Using a Smart Phone

Cemalettin YILDIZ[1*]

[1]Giresun University, Faculty of Education, Department of Mathematics and Science Education, Giresun, Turkey;

[*] **Corresponding Author:** cemalyildiz61@gmail.com

Abstract

The purpose of this study is to reveal middle school mathematics teachers' experiences of using a smart phone. In the study, survey method was used. The study was carried out with 105 middle school mathematics teachers. As a data collection tool, a survey that consists of two sections was used. Percentages and frequencies were used in terms of analysis of the data. In addition, direct quotations from the opinions of teachers regarding their answers to questions in the survey were included. As a result of the study, it was determined that majority of the teachers use smart phones every day, have a good level of smart phones usage competencies, have been using smart phones at least for three years, and that they desire to improve themselves on using smart phones. In addition, it was revealed that a considerable number of teachers think that smart phones affect social life partially positive, believe that smart phones contribute to professional development positively, think that smart phones have advantages and disadvantages at an equal rate and experience difficulties in terms of running out of battery. Lastly, it was determined that considerable majority of the teachers use smart phones at least for an hour per day, use smart phones in the evenings mostly, learn how to use smart phones on their own, follow the developments related to smart phones and use smart phones mostly for taking pictures and to display them. In-service training activities for teachers can be organized by the Ministry of National Education on how to use smart phones more effectively.

Keywords: Middle school mathematics teachers, Smart phone, Teachers' use of a smart phone, Mobile technology.

1. Introduction

Technology is generally used as a general concept that includes all the technologies that people develop and use in their daily lives (Çepni, Ayvacı, & Bacanak, 2004). With the development of technology, significant changes have occurred in many tools and materials. One of these tools is the mobile phones that have become an important part of our lives. People first used mobile phones that were heavy and did not have much feature. The features of mobile phones have gradually increased with the advancement of technology. Smart phones have been formed through the development of mobile phones today's technology.

The smart phone is a mobile communication device designed with the addition of the features of Personal Digital Assistants which is a product of the computer world to the classic features provided by the mobile phone (Kaya, 2018). In addition to the features provided by ordinary mobile phones, smart phones can perform most of the operations that computers can do through mobile operating systems (Ada & Tatlı, 2013). The ease of use and the availability of many programs and applications that make life easier cause the widespread use of smart phones (Altundağ & Bulut, 2017). The fact that smart phones have many important features such as talk, messaging, camera, internet, use of social media, flashlight, calculator, notepad has recently made these devices quite attractive (Yusufoğlu, 2017). These features have led to the use of smart phones in almost every household.

Since the use of smart phones is generally evaluated in mobile phone usage, it is useful to divide the concept of mobile phone into two as "simple mobile phone" and "smart phone" (Çakır & Demir, 2014). Simple mobile phones are devices only for messaging and phone calls, while smart phones are smart devices with operating systems that function as computers (Minaz & Çetinkaya-Bozkurt, 2017).

According to statistics of "Household Information Technology Usage Survey" belongs to month of April 2016 by the Turkish Statistical Institute (TSI), there are mobile phone or smart phone in 96.9% of households (TSI, 2016). This finding shows that the use of mobile phones or smart phones has increased compared to 96.8% value of the year 2015 (TSI, 2015).

According to the results of "Deloitte Global Mobile Costumer Survey" which performed every year with the participation of many countries since 2012, it was determined in Turkey that smart phone usage was 67.0% in 2013, 86.0% in 2015, and 92.0% in 2017 (Deloitte, 2013, 2015, 2017). These findings indicate that smart phone usage has been increasing in recent years.

The change and development in informatics are is also experienced in smart phone technology. People may now have to use smart phones in their work, education and daily lives.

For this reason, smart phones are widely used by people of different age groups (Doğan & İlçin-Tosun, 2016; Park, Nam, & Cha, 2012; Şenel, 2016). Considering that there are individuals in the educational community among the people who use smart phones, it can be said that teachers have an important place among these individuals. The increasing use of smart phones among people has also raised the need to work on the effects of these devices on teachers. Besides, it is also an important issue from the sociological point of view to reveal the experiences of teachers on smart phones who shape future generations. For this reason, it is aimed to reveal the smart phone use experiences of mathematics teachers working in middle school in the current research. Current research will be guiding and informative for smart phone manufacturers and users towards teachers' use of smart phones. It is also considered that this study will be the basis of and will shed light on new studies through the changes such as adding new questions to the questionnaire used in the study and changing the sample.

2. Method

The survey method was used in the study. Survey studies are the researches that aim to collect data to determine certain characteristics of a group (Büyüköztürk, Çakmak, Akgün, Karadeniz, & Demirel, 2010). This method has been preferred in the present study since the object, event or individual that subjected to the study can be tried to be described as it is, and it can be studied on whole of the universe or a sample taken from it (Karasar, 2007).

2.1. Sampling

Criterion sampling method was used in this study. Individuals in the sample were selected according to the criteria of "working in a middle school and having a smart phone". The sample of the study consists of 105 middle school mathematics teachers working in public schools in the fall semester of 2017-2018 academic years. The teachers in the sample were subjected to the "Experiential Questionnaire on the Use of Smart Phones". Some demographic characteristics related to teachers obtained through surveys are presented in the tables below. Gender distributions of teachers are given in Table 1:

Table 1. Gender distributions of teachers

	f	%
Female	73	69.5
Male	32	30.5

When Table 1 is examined, it is seen that most of the teachers are female. The age ranges of teachers are presented in Table 2:

Table 2. The age ranges of teachers

	f	%
20-25	10	9.5
26-30	11	10.5
31-35	15	14.3
36 or more	69	65.7

When Table 2 examined, it is understood that a significant proportion of teachers are at least 36 years old. The service years of teachers are given in Table 3:

Table 3. Service years of teachers

	f	%
0-5	18	17.1
6-10	11	10.5
11-15	25	23.8
16-20	15	14.3
21 or more	33	31.4
Absent/No respond	3	2.9

When Table 3 is examined, it is seen that most of the teachers have at least 11 years of experience. The titles of the teachers are presented in Table 4:

Table 4. The titles of teachers

	f	%
Intern teacher	10	9.5
Teacher	77	73.3
Expert Teacher	16	15.2
Absent/No respond	2	1.9

When the Table 4 examined, it is understood that the number of intern and expert teachers is not much. The education levels of teachers are given in Table 5:

Table 5. Education levels of teachers

	f	%
Institute of Education (3 years)	3	2.9
Faculty of Education	71	67.6
Faculty of Arts and Sciences	20	19.0
M.D.	9	8.6
Ph.D.	0	0.0
Absent/No respond	2	1.9

When Table 5 is examined, it is seen that most of the teachers are graduates of education faculties. English language levels of teachers are presented in Table 6:

Table 6. English language levels of teachers

	f	%
Very weak	22	21.0
Weak	25	23.8
Moderate	30	28.6
Good	8	7.6
Very good	6	5.7
Absent/No respond	14	13.3

When Table 6 is examined, it is understood that more than half of the teachers have English language levels at moderate or lower levels.

2.2. Development and Implementation of Data Collection Tool

The "Experiential Questionnaire on the Use of Smart Phones" was developed by the researcher to determine the experience of using middle school mathematics teachers' smart phones. The questionnaire consists of two parts. In the first part of the questionnaire, there are 6 questions about the demographic characteristics of the teachers and 13 questions about the smart phone usage in the second part. Under these 13 questions, gaps were also left to allow teachers to write down their views on their answers to the questions. The studies in the literature were benefited during the question formation in the questionnaire (Balcı, Gölcü, & Öcalan, 2013; Çakır & Demir, 2014; Subramanian, 2009; Yaşar, 2013) and the opinions of two experts were taken. In addition, 50 teachers read the questions in the questionnaire during pilot application and the researcher made corrections on the issues that were not understood at the end of this reading process. Furthermore, two Turkish teachers were asked whether the questions were understandable or not, and then the questions were formed in their final version. The questionnaire was applied to the teachers during break times or during the free hours of the teachers.

2.3. Data Analysis

The data were analyzed by using descriptive analysis method. First, the data in the surveys were entered in the Excel table. Then, the frequency and percentage values were calculated for the answers given by the teachers to the questionnaire. The findings are presented in tables.

Direct quotations from teachers' answers are given under the tables. Since some of the questions in the questionnaire can be answered more than once, the total of the percentage values in some tables may exceed 100.0%. Besides, since some questions may not be answered by teachers and some questions may be marked by multiple choices, the total number of frequencies may be different from the total number of teachers.

3. Results

The frequencies of teachers' use of smart phones are given in Table 7:

Table 7. Frequencies of teacher's use of smart phones

	f	%
Everyday	74	70.5
Almost everyday	18	17.1
Several days a week	5	4.8
Several days per month	3	2.9
Never	3	2.9
Absent/No respond	2	1.9

When Table 7 considered, it is understood that the most of teachers use smart phone in "every day". Examples of teachers' statements towards the frequencies of smart phones use are as follows:

"K6: I use my smart phone every day to communicate with my friends on Facebook."
"K19: I use my smart phone every day to text on WhatsApp."
"K21: I use a smart phone every day to have call with my family."

Competencies of teachers on smart phones use are presented in Table 8:

Table 8. Competencies of teachers on smart phone use

	f	%
Very weak	3	2.9
Weak	6	5.7
Medium	30	28.6
Good	49	46.7
Very good	14	13.3
Absent/No respond	3	2.9

When Table 8 is examined, it is seen that teachers more consider themselves as "good" level in smart phone usage competency. Examples of teachers' competencies for using a smart phone are as follows:

"K4: The phone use competency of someone using a phone every day is already good."
"K8: I think my phone usage is good. Generally, when I encounter a problem, I can solve it myself."
"K13: I can use the applications on phone in a good way."

The frequency of whether the teachers want to improve themselves on smart phone use is presented in Table 9:

Table 9. The frequency of whether the teachers want to improve themselves on smart phone use

	f	%
Yes	53	50.5
No	47	44.8
Absent/No respond	5	4.8

When Table 9 examined, it is understood that most of the teachers want to improve themselves with the use of smart phones. Examples of teachers' expressions about whether they want to improve themselves in terms of using smart phones are as follows:

"K9: I want to improve myself because smart phones are developing as technology evolves and new features are added to smart phones. I want to improve myself to learn these features."
"K14: I don't want to improve myself because I think I can use smart phones enough."
"K17: Smart phones have many functions that make our daily life easier. I would like to improve myself to make more use of these facilities."

The opinions of teachers about the effects of smart phones on social life are presented in Table 10:

Table 10. The effects of smart phones on social life

	f	%
Negative effects	4	3.8
Partially negative effects	26	24.8
Non-effective	25	23.8
Partially positive effects	33	31.4
Positive effects	16	15.2
Absent/No respond	1	1.0

When Table 10 is examined, it is seen that approximately one third of the teachers stated that smart phones are "partially positive effects" on their social life of. Examples from the sentences of the teachers about the impacts on social life of smart phones are as follows:

"K1: Smart phones have partially positive effects on social media to communicate with people."
"K15: Does not affect social life because the smart phone is different, my social life is different."
"K38: Affects social life positively because it allows me to reach too many people quickly. It helps me to have information about different people"

According to the teachers, the effects of the smart phone on professional life are presented in Table 11:

Table 11. The effects of the smart phone on professional life

	f	%
I think that it definitely doesn't contribute.	10	9.5
I think it doesn't contribute.	20	19.0
I think it contributes.	57	54.3
I think that it definitely contributes.	11	10.5
No idea.	5	4.8
Absent/No respond	2	1.9

When Table 11 is examined, it is seen that a significant number of teachers think that smart phones have a positive contribution to their professional development. Examples from the teachers' sentences for the impact of smart phones on professional development are as follows:

"K3: I can do my research fast and at that moment. Since my access to information is fast, it is definitely useful for my professional development."
"K10: I think the contribution to our professional education is also positive in order to follow the developing technology."
"K27: I think that some programs that can be installed on smart phones have improved professional development."
"K55: I don't think it has anything to do with my professional development."

The durations of smart phone uses for teachers are presented in Table 12:

Table 12. The durations of smart phone uses by teachers

	f	%
Less than one year	7	6.7
1-2 years	23	21.9
3-4 years	42	40.0
5-6 years	21	20.0
More than 7 years	7	6.7
Absent/No respond	5	4.8

When Table 12 examined, it is understood that 66.7% of teachers use smart phones for "at least 3 years". Examples from the statements of the teachers about the durations of smart phones use are as follows:

"K5: I got my phone when I started to college. So, I've been using the smart phone for 8 years."
"K8: I've been using smart phones for about 7-8 years."
"K14: It's been 5-6 years since I started using the smart phone."

The durations of daily use of smart phones by teachers are presented in Table 13:

Table 13. The durations of daily use of smart phones by teachers

	f	%
Less than 1 hour	38	36.2
1-2 hours	43	41.0
3-4 hours	12	11.4
5-6 hours	6	5.7
More than 7 hours	2	1.9
Absent/No respond	4	3.8

When Table 13 examined, it is understood that 60.0% of teachers use smart phones at least one hour per day. Examples from the statements of teachers regarding the durations of daily use of smart phones are as follows:

"K1: Social media, search, messaging. 3-4 hours spends for these."
"K3: I spend 1 to 2 hours in a day on the phone, except for phone calls."
"K31: Sometimes it may be more than 5-6 hours. I use smart phone while studying."
"K39: I usually use my smart phone in my spare time. Sometimes I read books in electronic environment. It's like 7 hours in those times."
"K40: I spend most of the day through working. That's why I use the smart phone for 1 hour at most."

The times for teachers' uses of smart phones are presented in Table 14:

Table 14. The times for teachers' uses of smart phones

	f	%
Break times in school	6	5.7
After school	13	12.4
At night	61	58.1
In the evening	12	11.4
At weekends	2	1.9
In class when I need to search for something	4	3.8
Absent/No respond	7	6.7

When Table 14 is examined, it is seen that teachers mostly use their smart phones "in the evening". Examples from the teachers' sentences about the use of smart phones are as follows:

"K11: I use it in the evening because I have more free time in the evening."
"K15: It has been a habit to make surfing at night before going to bed. I can't sleep without doing."
. K19: After dinner, I use it to relax, to relieve fatigue."
"K50: I use in the class when I'm curious about something."

The teachers' learning ways of smart phone use are presented in Table 15:

Table 15. The teachers' learning ways of smart phone use

	f	%
By myself	87	82.9
From my family	20	19.0
From my friends	16	15.2
From my students	3	2.9

When Table 15 examined, it is understood that most teachers have learned to use the smart phone by themselves. Examples from the teacher's statements about learn ways to use smart phones are as follows:

"K3: I more learned smart phone by myself. I don't need much help."
"K9: I learned the smart phone on my own through using. I learned some of the features that I didn't know, from my friends and family."
"K44: I learned the smart phone through trial and error. Maybe I've asked my friends some things that I didn't know."

The frequencies of teachers to follow developments on smart phones are presented in Table 16:

Table 16. The frequencies of teachers to follow developments on smart phones

	f	%
Everyday	5	4.8
Almost everyday	13	12.4
Several times a week	16	15.2
Several times a month	18	17.1
Several times a year	23	21.9
Never	28	26.7
Absent/No respond	2	1.9

When Table 16 is examined, it is seen that approximately one third of the teachers follow the developments about smart phones. The examples from the teachers' sentences about the frequencies of following developments related to smart phones are as follows:

"K16: I try to keep developments about the smart phone even once a month."
"K24: I'm very interested in the smart phone. Therefore, I try to follow developments every day."
"K55: I look at smart phone developments several times in a month."
"K59: I'm not interested in the smart phone's software event, so I'm not following the developments."

The general opinions of teachers about the smart phone are presented in Table 17:

Table 17. The general opinions of teachers about the smart phone

	f	%
Very helpful	4	3.8
Helpful	43	41.0
Harmful	5	4.8
Very harmful	1	1.0
Equally helpful and harmful	48	45.7
Absent/No respond	4	3.8

When Table 17 examined, it is understood that most teachers' general opinions on the smart phone is "equally helpful and harmful". Examples from the teachers' statements about general opinions about smart phones are as follows:

"K29: Very useful who use it efficient."
"K32: I think both the loss and benefit is equal because if the person wants to use this tool very useful, the person can use it very useful or vice versa."
"K42: Both helpful and harmful because making research is easy. Communication is provided. But it is harmful when used other than its purpose especially for children."
"K48: I think it is very useful as long as it is used correctly. It is necessary to know how to use it right."

The problems that teachers face when using a smart phone are presented in Table 18:

Table 18. The problems that teachers face when using a smart phone

	f	%
Battery problems	60	57.1
Making addiction	42	40.0
Connection problems about internet	36	34.3
Spam	29	27.6
Personal security problems	27	25.7
Screen freeze	26	24.8
High internet fees	23	21.9
Foreign language problems	15	14.3
Storage problems	2	1.9
System errors	1	1.0

When Table 18 is examined, it is seen that teachers stated more problems due to "technical" features of smart phones. The examples from teachers' sentences towards the problems they encounter when using a smart phone:

"K6: It makes addiction because I use it actively."
"K18: There are certain problems after the phones have been used for a certain period. Especially the screen is freezing, and the battery gets low fast."
"K22: When the new version is released, the speed of the old version is decreasing. I have also a storage problem on my phone."
"K35: I don't understand some issues on the smart phone since I don't understand very good English."

The aims of teachers' use of smart phones are given in Table 19:

Table 19. The aims of teachers' use of smart phones

	Never		Rare		Sometimes		Usually		Always	
	f	%	*f*	%	*f*	%	*f*	%	*f*	%
1.To make research	7	6.7	14	13.3	33	31.4	39	37.1	12	11.4
2.For surfing	14	13.3	22	21.0	26	24.8	33	31.4	10	9.5
3.To make chat	27	25.7	18	17.1	18	17.1	32	30.5	10	9.5
4.To enter social sharing sites (facebook, twitter etc.)	12	11.4	17	16.2	14	13.3	39	37.1	23	21.9
5.To read materials such as books, newspapers or articles	7	6.7	15	14.3	33	31.4	37	35.2	13	12.4
6.To make an appointment with hospitals	23	21.9	31	29.5	27	25.7	9	8.6	15	14.3
7.To check the analyze results	47	44.8	30	28.6	16	15.2	5	4.8	7	6.7
8.To apply for examinations	28	26.7	20	19.0	25	23.8	18	17.1	14	13.3
9.For the application procedures	52	49.5	18	17.1	16	15.2	9	8.6	10	9.5
10.To learn the cooking recipe	34	32.4	11	10.5	18	17.1	33	31.4	9	8.6
11.To learn the wheatear forecast	9	8.6	19	18.1	24	22.9	37	35.2	16	15.2
12.To watch the TV	56	53.3	24	22.9	14	13.3	6	5.7	5	4.8
13.To make shopping	43	41.0	24	22.9	19	18.1	11	10.5	8	7.6
14.To download program, music, games or videos	24	22.9	27	25.7	25	23.8	20	19.0	9	8.6
15.For watching the film	46	43.8	30	28.6	16	15.2	8	7.6	5	4.8
16.To play the game	37	35.2	23	21.9	22	21.0	18	17.1	5	4.8
17.To listen to music	18	17.1	22	21.0	34	32.4	20	19.0	11	10.5
18.For distance learning	48	45.7	31	29.5	20	19.0	5	4.8	1	1.0
19.For electronic mail processing	26	24.8	15	14.3	21	20.0	26	24.8	17	16.2
20.For e-school operations	26	24.8	18	17.1	20	19.0	24	22.9	17	16.2
21.For online banking transactions	37	35.2	14	13.3	19	18.1	21	20.0	14	13.3
22.To make video talk	29	27.6	26	24.8	18	17.1	21	20.0	11	10.5
23.To watch educational videos	23	21.9	19	18.1	33	31.4	20	19.0	10	9.5
24.To translate to different languages or from different languages to Turkish.	38	36.2	17	16.2	28	26.7	14	13.3	8	7.6
25.To follow developments or innovations in the world	9	8.6	17	16.2	34	32.4	33	31.4	12	11.4
26.To communicate with people and share information at the same time	18	17.1	16	15.2	31	29.5	29	27.6	11	10.5
27.To take advantage of e-government facilities	26	24.8	24	22.9	31	29.5	16	15.2	8	7.6
28.To learn about trip or travel issues	18	17.1	21	20.0	35	33.3	18	17.1	13	12.4
29.To get tickets to transportation vehicles such as plane, bus etc.	30	28.6	22	21.0	29	27.6	15	14.3	9	8.6
30.To get tickets to entertainment environments such as cinema, theater and so on.	42	40.0	30	28.6	19	18.1	11	10.5	3	2.9
31.To monitor economy or stock market news	50	47.6	24	22.9	18	17.1	8	7.6	5	4.8
32.To take note	27	25.7	26	24.8	23	21.9	19	18.1	10	9.5
33.To record voice	31	29.5	24	22.9	26	24.8	17	16.2	7	6.7
34.To record Video	19	18.1	22	21.0	26	24.8	23	21.9	15	14.3
35.To take or view a photo	10	9.5	10	9.5	17	16.2	40	38.1	28	26.7
36.To share photos online	19	18.1	15	14.3	23	21.9	27	25.7	21	20.0
37.For tasks and other list management (calendar, etc.)	27	25.7	23	21.9	22	21.0	26	24.8	7	6.7
38.To use the calculator	16	15.2	19	18.1	32	30.5	27	25.7	11	10.5
39.To look at the map	21	20.0	26	24.8	33	31.4	17	16.2	8	7.6
40.Cheating during the exam	93	88,6	5	4.8	4	3.8	2	1.9	1	1.0

When Table 19 examined, it is understood that 88.6% of the teachers never use smart phones to make "cheating during the exam", 29.5% of them rarely use to get "appointments at the hospital" and "distance learning", 33.3% of them sometimes use to "get information about travel or travel matters issues", 38.1% of them use to "take or view photos", and 26.7% of them use to always "to take or view the photos". Examples from the teacher statements about the aim of smart phone use are as follows:

"K2: I always use the smart phone to take picture or view picture."
"K9: I never use the smart phone to make cheating."
"K18: I rarely use my smart phone to make appointments from hospitals."
"K21: I occasionally use it to get information about a trip or travel."
"K24: I rarely use it for distance learning."
"K26: I occasionally use it to make cheating in exams."

4. Discussion, Conclusion and Recommendations

The findings obtained from this study that conducted to determine the experiences of middle school mathematics teachers on the use of smart phones are discussed with the literature and presented below.

It was revealed that many teachers use smart phones every day. This shows that teachers live in with smart phone very close. In addition, most of the teachers have been using smart phones for at least three years and following the developments about smart phone. Accordingly, it is understood that the smart phones, which have become an indispensable element of daily life, have been adopted by teachers. Şenel (2016) determined that pre-service English teachers were seeing mobile phones as "a part of life". Therefore, it is understood that smart phones are an important device for teachers to do daily and professional work.

Nearly half of the teachers (46.7%) found themselves good sufficient at smart phone use. In addition, 37.2% of the teachers found themselves to be sufficient at medium level or below the intermediate level. There can be said that one of the main reasons why some teachers see themselves as low sufficient for smart phones is the rapidly changing and evolving technology. The English level of teachers may have generated a sense of their partial disability in the use of smart phones. Seminars or courses can be organized by the Ministry of National Education to increase the level of sufficiency on smart phone use of teachers who have low sufficiency at smart phones to better levels. In addition, in-service training activities can be organized for teachers who have a foreign language problem while using a smart phone.

Most of the teachers want to improve themselves in the use of smart phones. This situation can be caused by such reasons as “accessing information in a short and easy way, making life easier, and catching the innovations brought by the age” (Özkan, 2010). Teachers wanting to develop themselves on the use of smart phones can be considered as a situation that has emerged in line with these needs.

When the intensity of using smart phones considered, it is understood that 41.0% of the teachers use smart phones 1-2 hours a day. Yusufoğlu (2017) determined that a significant number of university students use their smart phone for 4-6 hours a day. Minaz and Çetinkaya-Bozkurt (2017) revealed that the duration of using smart phones was 2-6 hours per day for university students. The fact that almost half of the teachers use a smart phone for 1-2 hours per day may be an indication that participants do not spend much time with smart phones in general. When the most used smart phone times were examined, it was revealed that 58.1% of the teachers used smart phones in the evenings. This finding shows that teachers prefer to use smart phones in the evening after leaving school.

It has been determined that 82.9% of teachers have learned to use smart phones by themselves. From this finding, it was concluded that most of the teachers learned to use smart phones on their own. In addition, it was found that families were most likely to help teachers in learning smart phones and then their friends and students respectively. In this context, it is understood that teachers learned to use smart phones from their families, friends, and students other than their efforts.

It has been revealed that a significant number of teachers think that the benefit and harm of smart phones is equal. This shows that teachers are aware of the benefits of smart phones as well as their harms. It is gratifying that teachers who take on the education of future generations are conscious of the use of current technologies. Only teachers who are conscious smart phone users can raise conscious students (Altundağ & Bulut, 2017). Therefore, it is of utmost importance that teacher’s use of smart phones in a conscious and controlled manner to be a model for their students and to have a healthy communication with students.

The responds of teachers on how smart phones affect social life concentrate on “partially positive effects”. However, the number of teachers who stated that smart phones have a negative impact on social life is not few. It was determined that approximately one fourth of the teachers stated that smart phones affect social life as “negative” or “partially negative”. Having negative aspects in terms of social aspect in addition to the positive aspects of smart phones prepares the basis for some negativities. The most important of these negativities expressed by the teachers is the addiction of smart phones. Roberts and Pirog (2013) stated that simple mobile phones,

Minaz and Çetinkaya-Bozkurt (2017), Pearson and Hussain (2016) and Soni, Upadhyay, and Jain (2017) stated that smart phones were making addiction. In addition, it is understood that they cannot give up these devices although teachers see smart phones as a threat to health. To reduce the addiction on smart phones, teachers in this situation should limit the use of smart phones and be cautious when using these devices. At the same time, awareness-raising activities related to smart phone addiction can be organized in schools.

It was revealed that a significant number of teachers think that smart phones have positive contributions to professional development. Therefore, it may be useful for teachers to use smart phones more to get information or do research for the lessons. In addition, teachers can be provided more detailed information about how smart phones can be used in lessons and sample applications can be shown. It was determined that the teachers' difficulties related to smart phones were more about technical problems. Yaşar (2013) determined that the problems faced by people related to smart phones are about "usability", "operating system", "connection", and "internet browser". It is recommended that companies that produce smart phones should take precautions to eliminate technical problems such as easy get low battery, freezing of the screen and system failures. In addition, it is recommended to use virus programs on smart phones to prevent from virus attacks and keep personal information secure.

It was found that teachers can use all the features of an average smart phone such as call, e-mail, messaging, management, social media, and connection. When the teachers' use of smart phones considered, it was determined that these devices more used to take pictures or view them. Therefore, it can be said that teachers see smart phones as more entertainment devices. Ellwood-Clayton (2003), Şenel (2016), Taylor and Harper (2003) stated that simple mobile phones and Yusufoğlu (2017) stated that smart phones used for entertainment purposes. It is thought that teachers are in such a perception since they can perform a significant part of the activities that they consider as fun in daily life with the help of smart phones. Another finding that draws attention to the use of smart phones by teachers is that some of the teachers emphasize that some teachers use smart phones for cheating. When it is considered that teachers should be a role model for their students, teachers are advised not to use smart phones for cheating.

In summary, it was seen that smart phones were widely used among teachers. In this context, it should be kept in mind that teachers who have important roles in the development of future generations should be sensitive about the conscious use of smart phones. At this point, in-service trainings can be provided to teachers on issues such as effective use of technology and technology literacy. In addition, teachers' experience of using smart phones can be

investigated by considering gender, age, year of service, title, and educational status. Finally, more detailed data can be obtained regarding the experiences of teachers in using smart phones through interviews and observations.

References

Ada, S., & Tatlı, H. S. (2013, Ocak). Akıllı telefon kullanımını etkileyen faktörler üzerine bir araştırma. XV. Akademik Bilişim Konferansı, Akdeniz Üniversitesi, Antalya.

Altundağ, Y., & Bulut, S. (2017). Aday sınıf öğretmenlerinde problemli akıllı telefon kullanımının incelenmesi. Abant İzzet Baysal Üniversitesi Eğitim Fakültesi Dergisi, 17(4), 1670-1682.

Balcı, Ş., Gölcü, A. A., & Öcalan, M. E. (2013). Internet usage patterns among university students. Journal of Selçuk Communication, 7(4), 5-22.

Büyüköztürk, Ş., Çakmak, K. E., Akgün, E. Ö., Karadeniz, Ş., & Demirel, F. (2010). Bilimsel araştırma yöntemleri (5. Baskı). Ankara: Pegem Akademi Yayıncılık.

Çakır, F., & Demir, N. (2014). Üniversite öğrencilerinin akıllı telefon satın alma tercihlerini belirlemeye yönelik bir araştırma. Dokuz Eylül Üniversitesi İktisadi ve İdari Bilimler Fakültesi Dergisi, 29(1), 213-243.

Çepni, S., Ayvacı, H. Ş., & Bacanak, A. (2004). Fen eğitimine yeni bir bakış: Fen, teknoloji, toplum. Trabzon: TOP-KAR Matbaacılık.

Deloitte. (2013). Turkey mobile consumer survey 2013. Retrieved from https://www2.deloitte.com/content/dam/Deloitte/tr/Documents/technology-media-telecommunications/tr_globalmobilesecurirtysurvey_infographic.pdf adresinden erişildi.

Deloitte. (2015). Deloitte global mobile consumer survey 2015: Turkey executive summary. Retrieved from https://www2.deloitte.com/content/dam/Deloitte/tr/Documents/technology-media-telecommunications/deloitte-global-mobil-kullanici-anketi-2015-f.pdf adresinden erişildi.

Deloitte. (2017). Deloitte global mobile consumer survey 2017: Turkey executive summary. Retrieved from https://www2.deloitte.com/content/dam/Deloitte/tr/Documents/technology-media-telecommunications/deloitte_gmcs_2017.pdf adresinden erişildi.

Doğan, U., & İlçin-Tosun, N. (2016). Lise öğrencilerinde problemli akıllı telefon kullanımının sosyal kaygı ve sosyal ağların kullanımına aracılık etkisi. Adıyaman Üniversitesi Sosyal Bilimler Enstitüsü Dergisi, 8(22), 99-128.

Ellwood-Clayton, B. (2003). Virtual strangers: Young love and texting in the Filipino archipelago of cyberspace. In K. Nyiri (Ed.), Mobile democracy: Essays on society, self and politics (pp. 225-239). Vienna: Passager Verlag.

Karasar, N. (2007). Bilimsel araştırma yöntemi (17. Baskı). Ankara: Nobel Yayın Dağıtım.

Kaya, A. (2018). Dünyanın en iyi akıllı telefonu 2018. 26 Ağustos 2018 tarihinde https://www.tech-worm.com/dunyanin-en-iyi-akilli-telefonu-2018/ adresinden erişildi.

Minaz, A., & Çetinkaya-Bozkurt, Ö. (2017). Üniversite öğrencilerinin akıllı telefon bağımlılık düzeylerinin ve kullanım amaçlarının farklı değişkenler açısından incelenmesi. Mehmet Akif Ersoy Üniversitesi Sosyal Bilimler Enstitüsü Dergisi, 9(21), 268-286. DOI: 10.20875/makusobed.306903.

Özkan, E. (2010). İlköğretim II. kademe öğrencilerinin bilgisayar-internet kullanım durumlarının değerlendirilmesi (Uşak ili örneği). (Yayınlanmamış yüksek lisans tezi). Afyon Kocatepe Üniversitesi, Sosyal Bilimler Enstitüsü, Afyon.

Park, S. Y., Nam, M. W., & Cha, S. B. (2012). University students' behavioural intention to use mobile learning: Evaluating the technology acceptance model. British Journal of Educational Technology, 43(4), 592-605.

Pearson, C., & Hussain, Z. (2016). Smart phone addiction and associated psychological factors. Addicta: The Turkish Journal of Addictions, 3, 193-207.

Roberts, J., & Pirog, S. (2013). A preliminary investigation of materialism and impulsiveness as predictors of technological addictions among young adults. Journal of Behavioral Addictions, 2(1), 56-62. DOI: 10.1556/JBA.1.2012.011.

Soni, R., Upadhyay, R., & Jain, M. (2017). Prevalence of smart phone addiction, sleep quality and associated behaviour problems in adolescents. International Journal of Research in Medical Sciences, 5, 515-519.

Subramanian, S. (2009). Dynamically adapting design and usability in consumer technology products to technology and market life cycles: A case study of smart phones. (*Unpublished master's thesis).* University of Florida, Massachusetts Institute of Technology, United States of America.

Şenel, M. (2016). Analysis of ELT students' perceptions as to mobile phones through metaphors. Kastamonu Education Journal, 24(4), 1749-1764.

Taylor, A. S., & Harper, R. (2003). The gift of the gab? A design oriented sociology of young people's use of mobiles. Journal of Computer Supported Co-operative Work, 12(3), 267-296.

Turkish Statistical Institute [TSI]. (2015). Household information technology usage survey, 2015. Retrieved from http://www.tuik.gov.tr/PreHaberBultenleri.do?id=18660 adresinden erişildi.

Turkish Statistical Institute [TSI]. (2016). Household information technology usage survey, 2016. Retrieved from http://www.tuik.gov.tr/PreHaberBultenleri.do?id=21779 adresinden erişildi.

Yaşar, Ö. (2013). Akıllı telefonların informal öğrenme için kullanımının incelenmesi. (Yayınlanmamış yüksek lisans tezi). Bahçeşehir Üniversitesi, Fen Bilimleri Enstitüsü, İstanbul.

Yusufoğlu, Ö. Ş. (2017). Smart phones as leisure activities and their impact on social life: A research on students of the university. Journal of the Human and Social Sciences Researches, 6(5), 2414-2434.

Effect of Inclusion of Delta Derivatives and Log Energy to MFCC Features on Text-independent Gender Recognition

Ergün YÜCESOY[1*], Vasif V.NABİYEV[2]

[1] Ordu University, Vocational School of Technical Sciences, Ordu, Turkey; yucesoye@hotmail.com

[2] Karadeniz Technical University, Department of Computer Engineering, Trabzon, Turkey;vasif@ktu.edu.tr

[*] **Corresponding Author:** yucesoye@hotmail.com

Abstract

In this study, a system automatically recognizing the speaker's gender independent of the text is presented. In the proposed system, the mel-frequency cepstral coefficients (MFCC) are used to represent the speech signals while the vector quantization (VQ) method is used to construct the gender models. In the study, one of the ten sentences of each of 8 male and 8 female speakers selected from the TIMIT dataset are used in the training of the system, and 10 sentences of each of 56 female and 112 male speakers are used in the test phase. In the study, feature vectors formed by combination of MFCC, delta derivatives and log energy are modelled by 5 different model sizes of 8, 16, 32, 64 and 128. Test results showed that the highest recognition rate is achieved as 98.57% in the modelling of features formed with the second order derivative of the first 20 MFCC (excluding 0th coefficient) and logarithmic energy parameters by the 64 centroids of vector quantization.

Keywords: Speech processing, Gender recognition, Vector quantization, MFCC

1. Introduction

Different levels of information is transmitted to the listener with the speech signal. At the beginning of this information is the message information delivered by means of words. The speaker's identity, mental state, gender, age and language are some of the information transmitted with the message. From this information, gender is one of the most prominent features of a conversation, and automatically recognized gender information is used directly or indirectly in many applications. Gender information can be used directly in the selection of products such as advertising, music, etc according to the gender of the person, and also used as a preliminary information in speech and speaker recognition systems (Harb and Chen, 2005; Bahari and Van Hamme, 2011). Gender preliminary information provide performance enhancement in automatic speech recognition systems by allowing the creation of gender-dependent models, in speaker recognition systems by limiting research space to same gender speakers (Neti and Roukos,1997; Abdulla et al., 2001). In this process, according to the used text the systems are divided into two, text dependent and text independent. In text dependent systems, all users speak the same text, while in text independent systems there are no restrictions on the text. The limited and known text greatly improves the performance of text dependent systems while reducing its flexibility. On the other hand, the systems independent of the text are flexible, but the increasing complexity with flexibility leads to a decrease in the recognition rate of the system.

As with all recognition systems, the input signal is first transformed into parameters called features. As a result of this step called feature extraction, unnecessary information is removed from the speech signal to obtain a compact form representing speech and speaker characteristics. Features extracted from the speech recordings of the known speaker are used in the training of the speaker models while those extracted from the unknown speakers are used in the test phase. During the test phase, the test data are compared with the trained speaker models and one match score is calculated. Then, according to these scores, it is decided that the test data belongs to the class.

One of the most important factors affecting recognition performance is the selection of features extracted from the speech signal. Some of the features used in speech-based recognition systems are fundamental frequency (F0), formant frequency, amplitude and bandwidth, linear predictive cepstral coefficients (LPCCs), and mel-scale cepstral coefficients (Narang and Gupta, 2015). Among these features, MFCC is the most widely used feature type and is used alone or in combination with various features in many studies, especially speech and speaker

recognition systems. In the study conducted by (Dhonde et al., 2017), The number of MFCC features and the effect of delta derivatives on speaker recognition were examined in detail. However, a similar study was not done on the recognition of the gender of the speaker. In this study, the number of MFCC features and the effect of delta derivatives and logarithmic energy parameters on gender recognition were investigated. While the vector quantization (VQ) approach was used to construct gender models in the study, the effect of gender models defined by different numbers of center points on the performance was also examined. The rest of the paper is organized as follows; the features used in the study and extraction procedure are presented in Chapter 2. Vector quantization approach used to construct gender models is presented in Chapter 3. The experimental results, and conclusions and suggestions are given in Chapter 4 and in Chapter 5 respectively.

2. Feature Extraction

The speech signal is analyzed by converting it into parametric values with less variability and more discriminative characteristics. There are various methods used to extract these values, called features, from the speech signal. These methods, called short-term analysis methods, are applied on the short parts of the speech signal where it is assumed to be stationary. At the end of the process, the scalar values obtained from each analysis part are combined to form the feature vector. In this study, Mel Frequency cepstral Coefficients, delta parameters and logarithmic energy parameters derived from these coefficients were used as feature vector.

In the first phase of the MFCC method, a pre-emphasis is made. With the pre-emphasis, the spectral energy is compensated by the reduction of high-frequency parts caused by the voice production mechanism. For this purpose, the speech signal is filtered by a high pass filter with transfer function $H(z) = 1 - a * z^{-1}$ $(0.9 \leq a \leq 1)$. The signal is then split into frames of 20-30 ms long, overlapping 20-50%. While this signal is assumed to be stationary within a short period of time, overlapping of certain parts of the frames will prevent the loss of information that may occur at the boundary. Then, a window function is applied to each frame to reduce the boundary discontinuity. For this purpose, the Hamming window given by $w(n) = 0.54 - 0.46 * \cos\left(\frac{2\pi n}{N-1}\right), 0 \leq n \leq N-1$ is usually used (Rabiner and Schafer, 1978). The spectrum of the signal is then estimated by calculating the discrete Fourier transform of each frame. The obtained spectrum is multiplied by a mel-scale filter set and passed to the mel-spectrum in which human non-linear frequency perception is represented. The mel-scale changes linearly

up to 1 kHz and logarithmically over 1 kHz which is by $f(mel) = 2595 * \log_{10}(1 + f_{hz}/700)$. Then, the logarithm function is applied to simulate the human perception of the loudness, and at the final stage, a discrete cosine transform is applied to the filter outputs to switch to the cepstral space where the fast and slow changing components of the signal are represented separately. The first k (12-13) of MFCC coefficients are usually used as features. Capstral coefficients well represent the local spectral properties of the analyzed frame. But, it does not represent dynamic properties that change over time. For this reason, the first and second derivatives of the cepstral coefficients are usually included in the feature vectors. These coefficients, called delta coefficients, is calculated by the expression $d_t = \frac{\sum_{n=1}^{N} n(c_{t+n} - c_{t-n})}{2\sum_{n=1}^{N} n^2}$. Where d_t is the delta coefficient calculated according to the static coefficients of $C_{t+N} - C_{t-N}$ and N is generally chosen as 2. The delta-delta coefficients are calculated in a similar way using delta coefficients instead of constant coefficients. In the study, logarithmic energy components calculated by expressing $E = \log \sum_{n=1}^{N} s_n^2$ are also included in the feature vector and the effect of this parameter on gender recognition success is also examined.

3. Gender Modeling with Vector Quantization

Vector quantization is a kind of data compression method that transforms a large vector space into a limited number of regions. In this method, the features obtained from each speaker are grouped into M discrete regions. These regions are represented by the central points called the code word. The codebooks created by the combination of the code words are stored in the database as the speaker model. There are various methods used to compress the set of N-point training vectors into the M codebook vectors (Kinnunen at al., 2011). Among these methods, K-means and LBG algorithms are the most popular methods and we preferred the LBG algorithm in our study (Linde at al., 1980). In the training phase of the developed system, the code books created with the features of known speakers are stored in the database together with gender information. In the test phase, the distances (Euclid) between the gender models and the features of the unknown speakers are calculated and the gender of the speakers are decided according to the average of this distances.

4. Experimental Results

The system developed in the study was tested with the TIMIT database. The TIMIT database consists of speech recordings of a total of 630 speakers, 438 male and 192 female, selected from 8 main dialect regions of the United States. In recordings made in a noiseless studio environment, each speaker spoke 10 sentences, two of them in common. 168 of the 630 speakers were assigned as the test set, and the rest as the training set. In the training of the system, the second records (SA2) of 8 male and 8 female speakers selected from the training set and in the testing of the system, the 1680 speech of 168 speakers given as the test set were used. In the study, zero MFCC coefficient (0), delta coefficients (d: delta and D: delta-delta) and logarithmic energy (e) parameters were added to different number of MFCC coefficients (M) and the effect of these parameters on gender recognition was investigated. In the study the effect of VQ model size on success was also examined. For this purpose, the feature vectors are defined in 5 different model sizes and the most suitable model size is determined as a result of the tests (Figure 1-5).

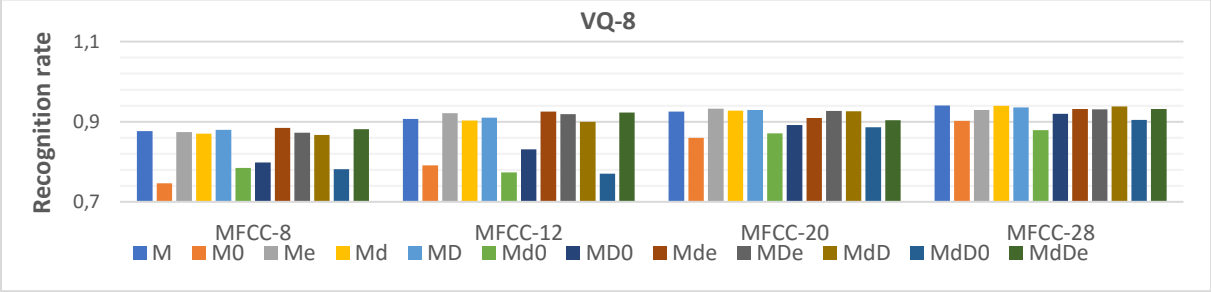

Figure 1. Gender recognition rate for the 8-point VQ model

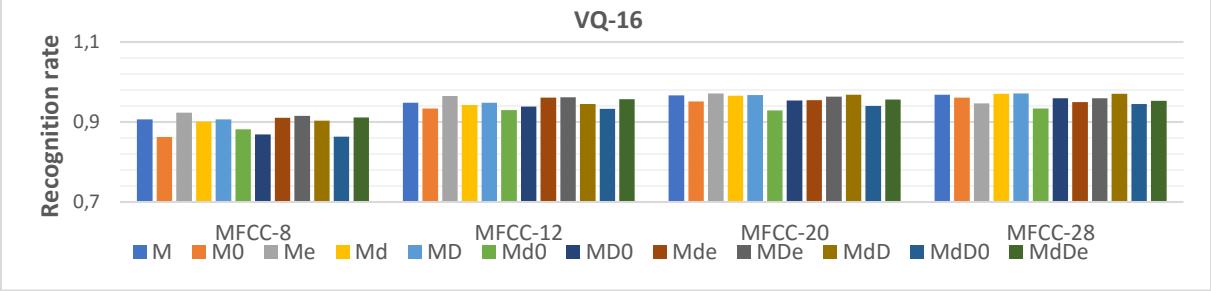

Figure 2. Gender recognition rate for the 16-point VQ model

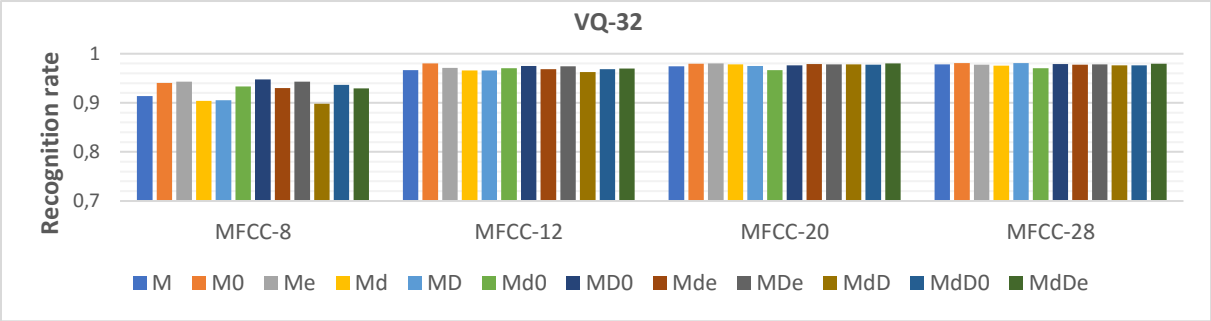

Figure 3. Gender recognition rate for the 32-point VQ model

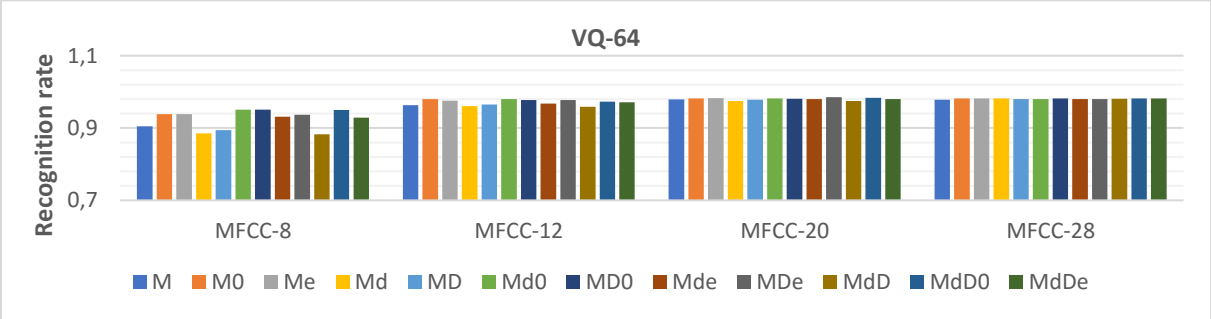

Figure 4. Gender recognition rate for the 64-point VQ model

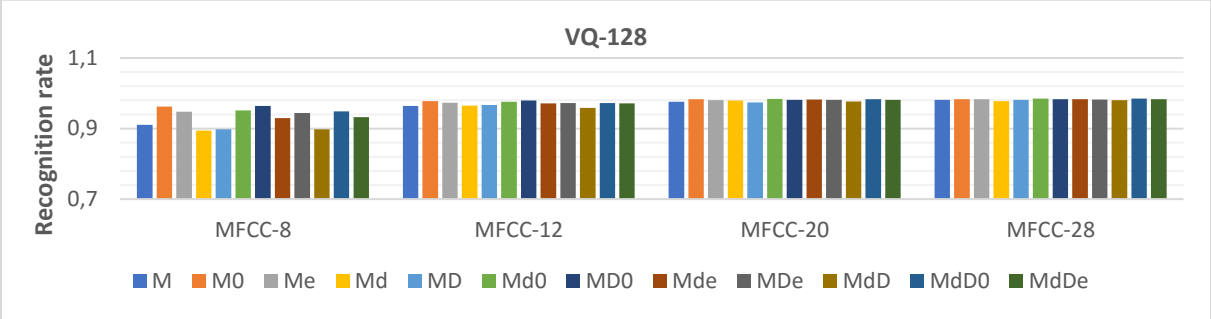

Figure 5. Gender recognition rate for the 128-point VQ model

The results showed that the increase in the number of MFCCs and VQ model size increased the gender recognition success but the increase after the MFCC number of 12 and the model size after 32 did not lead to a meaningful change in success. It was also found that delta and logarithmic energy parameters added to MFCC coefficients had no significant effect on success. In the test with 12 different feature sets and 5 different model sizes, the lowest gender recognition rate was obtained as 74.64% with 9 MFCC coefficients (inc. 0th) modeled with 8 point VQ model. The highest success rate was obtained as 98.57%, modeling of the features (MDe) formed by adding delta-delta and logarithmic energy parameters to the 20 MFCC coefficients with 64 point VQ model. However, considering the processing load depending on

the feature set and model size, the first 13 MFCC (inc. 0th) vector is selected as the optimum feature set, and the 32-point VQ model is selected as the optimum model size. The success rate of the gender recognition system based on these parameters is calculated as 98.03.

5. Conclusions and Recommendations

In this study, the MFCC coefficients, the delta coefficients derived from these coefficients, and the logarithmic energy parameter and the effects of VQ model size on gender recognition were examined. In the tests, the MFCC number and VQ model size have a significant effect on gender recognition, while the delta coefficients and the logarithmic energy parameters added to the MFCC coefficients have no significant effect on success despite increasing the process load. The optimal VQ model size for the developed gender recognition system is 32, and the first 13 MFCC coefficients (including 0th) are specified as the feature vector. The performance of the gender recognition system created with these parameters was calculated as 98.03%. In future studies it will be useful to investigate the effects of different features such as LPCC, PLP, fundamental frequency and formant frequency on gender recognition in addition to the MFCC coefficients.

References

Abdulla, W. H. and Kasabov, N.K., (2001). Improving speech recognition performance through gender separation, in Artificial Neural Networks and Expert Systems International Conference (ANNES) (pp. 218-222). Dunedin, New Zealand.

Bahari, M.H. and Van Hamme, H.,(2011, September). Speaker age estimation and gender detection based on supervised non-negative matrix factorization, Biometric Measurements and Systems for Security and Medical Applications (BIOMS), 2011 IEEE Workshop on (pp. 1-6). Milan, Italy.

Dhonde, S., Chaudhari, A., and Jagade, S. (2017). Integration of Mel-frequency Cepstral Coefficients with Log Energy and Temporal Derivatives for Text-Independent Speaker Identification. Proceedings of the International Conference on Data Engineering and Communication Technology (pp. 791-979). Singapore.

Harb, H., and Chen, L. (2005). Voice-based gender identification in multimedia applications. Journal of intelligent information systems, 24(2-3), 179-198.

Kinnunen, T., Sidoroff, I., Tuononen, M., and Fränti, P. (2011). Comparison of clustering methods: A case study of text-independent speaker modeling. Pattern Recogn. Lett., 32(13), 1604-1617.

Linde, Y., Buzo, A., and Gray, R. (1980). An algorithm for vector quantizer design. IEEE Transactions on communications, 28(1), 84-95.

Neti, C. and Roukos, S.,(1997, December). Phone-specific gender-dependent models for continuous speech recognition, Automatic Speech Recognition and Understanding Workshop (ASRU97) (pp. 192-198). Santa Barbara, CA, USA,

Narang, S., and Gupta, M. D. (2015). Speech Feature Extraction Techniques: A Review. International Journal of Computer Science and Mobile Computing, 4(3), 107-114.

Rabiner, L. R., and Schafer, R. W. (1978). Digital processing of speech signa: Prentice Hall.

Methods to Facilitate Current Literature Survey: Google Scholar, Web of Science and ResearchGate Example

Yasin KAYA[1*]

[1] Karadeniz Technical University, Faculty of Engineering, Department of Computer Engineering, Trabzon, Turkey; yasin@ktu.edu.tr

[*] **Corresponding Author:** yasin@ktu.edu.tr

Abstract

Accessing information in the world has become easier nowadays along with evolving technology. There are new opportunities provided by technology to keep up with current work of researchers in the field of study. In this study, three academic platforms widely used in the academic world are examined. These; Google Scholar, Web of Science and ResearchGate. The researchers use these three platforms for similar purposes that can be summarized as literature review, citation search, access to the work of other researchers, and identification of their published references. Google Scholar is able to scan without restriction on publication type and index (Conference proceedings, Journal paper, Book chapter, or Patent). Web of Science is the world's strongest citation index. It has about 12,000 journal and 55 million articles. Unlike the Google Scholar system, these indexed studies consist of higher-level journals papers and conference proceedings. ResearchGate is a platform for scientists, built by scientists. The purpose of the system is to collect researchers around the world under one roof.

Keywords: Literature Survey, Google Scholar, Web of Science, ResearchGate, Citetion Alert.

1. Introduction

Google Scholar ("Google Scholar," 2018) is one of the major academic search engines (Beel & Gipp, 2009). Academic search engines is considered as the search products that localize scientific information on the web (Ortega, 2014).

Google Scholar searches a wide range of academic fields. It is able to scan without restriction on publication type and index including peer-reviewed articles, theses, books, and abstracts from academic publishers, professional societies, pre-print sources, and universities (such as Conference proceedings, Journal paper, Book chapter, or Patent) (Anders, Evans, & Rrt, 2010).

A researcher can define an alert for the search result and Google Scholar sends an e-mail for this alert at defined time intervals. Likewise, when followed manuscript cited in any publication, Google Scholar sends an informational message.

Web of Science is the world's strongest citation index ("Web Of Science," 2018). It has about 12,000 journal and 55 million articles. Unlike the Google Scholar system, these indexed studies consist of higher-level journals papers and conference proceedings. The literature reviews in this index can be made using more criteria. For example, researchers can be search on a wide range of parameters such as work title, publication date, article, publication language, conference, author address, and funding organization. The system generates daily, weekly or monthly batch reports according to the search results and sends mail to the researchers. Similarly, a researcher can define a citation alarm for a publication.

Research Gate is a platform for scientists, built by scientists ("Research Gate," 2018). The purpose of the system is to collect researchers around the world under one roof. The mission of the system is to connect the world of science and get public to researches. Using the site, studies can be shared, contacts and collaborations can be made with researchers working on the same field, scientific questions and discussions can be started, job advertisements and appropriate job opportunities can be followed and statistical information about the studies can be obtained. A researcher can be add their works to the platform, or the system can automatically recognize the work and offer to the user. In this study, we mention the academic events provided by these three platforms.

2. Material and Method

The opportunities provided by these three platforms to academics will be discussed in this section.

2.1. Literature Review

Google scholar is like a specialized search engine for the Academy. A single search box can be used to search for all keywords, such as author names, article titles, or journals names. It can be applied directly to known Google search habits using this search box. However, when you want to search the literature by using Web of Science, you can determine many criteria such as database, author, journal, date range, title and summary keywords, etc. you want to scan. The searches in Web of Science cover the publications in this index. However, there is no database restriction on Google Scholar and ResearchGate. When searching in ResearchGate, filtering can be made according to the type of publication (journal, announcement notice, book, thesis, presentation, poster, etc.).

2.2. Author Statistics

Google Scholar shows only the author publications and the number of citations made in terms of date. Web of Science maintains the number of full text access of the author's publications and the number of citations in his own database. In this context, ResearchGate has the largest author statistics. ResearchGate records references to the author's works, full-text readings, full-text requests, number of question-answer discussions, etc., and finally a value named RG Score is calculated.

2.3. Alerts

Google Scholar Citations offer a simple way for academician to keep track of citations to their papers. The authors can be check who is citing their publications, graph citations over time, and compute several citation metrics ("Google Scholar," 2018). In addition, google scholar sends alerts to you when any of your posts are cited, new articles are added in a search criterion you previously saved, and a new publication of a researcher you follow is published. For example, to receive an alert email when a particular article is cited, you can search for the title of your paper, click on the "Cited by" link at the bottom of the search result; and then click on the envelope icon in the left sidebar of the search results page ("Google Scholar," 2018).

Similarly, an e-mail alert can be generated after a search in Web of Science. To do so, click on the "Create Alert" link on the left panel on the screen where the search result is listed ("Web Of Science," 2018).

Unlike these, you do not need to set any alerts about the citation alert in the ResearchGate system. Instant e-mails related to references made to your registered publications on the ResearchGate site are automatically sent ("Research Gate," 2018).

3. Results and Discussion

In this study, the opportunities provided by the three academic platforms in academic literature review are discussed: Google Scholar, Web of Science, and ResearchGate. Google Scholar automatically scans for broader publications. The Web of Science searches only the data in its local database. However, the journals and conferences in this database contain higher and more recognized academic journals than other platforms. Likewise, when evaluating the references, only the citations in their database are evaluated. ResearchGate is differentiating himself from the other platforms because it brings academicians together under one roof and provides an academic sharing platform.

References

Anders, M. E., Evans, D. P., & Rrt, M. (2010). Comparison of PubMed and Google Scholar Literature Searches. Respir Care.

Beel, J., & Gipp, B. (2009). Google Scholar ' s Ranking Algorithm : An Introductory Overview. 12th International Conference on Scientometrics and Informetrics (ISSI'09). https://doi.org/10.1109/RCIS.2009.5089308.

Google Scholar. (2018). Retrieved April 10, 2018, from http://scholar.google.com

Ortega, J. L. (2014). Academic Search Engines: A Quantitative Outlook. Academic Search Engines: A Quantitative Outlook. https://doi.org/10.1016/C2013-0-23226-8

Research Gate. (2018). Retrieved May 10, 2018, from http://www.researchgate.com

Web Of Science. (2018). Retrieved April 20, 2018, from http://webofknowledge.com

Reasons For The Emergence Of MOOCs, Historical Development and Types

Hakan ÖZCAN[1]*

[1] Gazi University, Computer Education and Instructional Technology, Master Student, Ankara, Turkey.

Corresponding Author: hakanozcan2007@hotmail.com

Abstract

MOOCs offer new opportunities for lifelong learning and continue to attract attention as a mass training center for people from all walks of life. The aim of this study is to contribute to the better understanding of MOOCs and to the place of individuals in their present and future educational preferences, giving them a holistic view of the reasons, historical development and types of MOOCs. In the research made as documentary screening model, "MOOC historical development and types" in ProQuest and "MOOC" key word were questioned in Yök Akademik and the information was collected by accessing the articles and theses in the databases. It is seen that MOOCs continue to be open education, MOOCs emerged due to the fact that traditional education institutions are inadequate in terms of increasing student needs, increasing the importance of lifelong learning by including the internet in every area of life and the change and transformation of new education paradigms in education. The MOOCs first started in 2008 as cMOOC, in 2011 the xMOOc and the hMOOC with both crawlers feature started in 2013. Although MOOCs started in 2008, they can not be said to have completed development. The types of MOOC's and the changes they make in education are addressed separately for future research.

Keywords: MOOC History Development and Types, MOOC.

* This paper was prepared through the graduate thesis of Gazi University Institute of Educational Sciences in 2018.

1.Introduction

It is almost impossible for the 21st century, when deprivation of information due to lack of information makes it feel better, to hold on to life without the lifelong learning of individuals. Individuals in the transformative and repulsive power of life can only be adapted to life-long learning by constant learning. In order to achieve this adaptation, there is a need for educational environments that enable lifelong learning. Some of these environments are MOOCs. With MOOCs, evolving in an evolutionary process everybody can get the training they need. MOOCs are. The reasons for the emergence of MOOCs, their historical development and their types will contribute to a better understanding of MOOCs and to the future of individuals by taking MOOCs in their training plans.

MOOCs by Educause (2013, p.1) "the mass of the lesson in theory that there is no limit in the record; generally open to the extent that anyone who wants free can join; learning activities are carried out online; a specific area and specific learning objectives ". With this definition, it is understood that MOOCs are massive, open (appealing to every scepter), online and lesson building. It will enable the development of the historical development of MOOCs and the understanding of the way to the MOOC varieties.

Interaction between people who are involved in the internet at every moment of life has been affected and these effects have been reflected in educational environments and new environments have been created (Kop & Hill, 2008). With the ever-increasing number of students, traditional education institutions are unable to meet their needs (Koutropoulos et al., 2012). The desire to reach all over the world, the technology and the models developed in accordance with it, have broadened the circle of lifelong learning, revealing new roles and more interactive structures at the mass level. (Dabbagh, 2005; de Waard et al., 2011; Kop, Fournier & Mak, 2011). These virtual structures, designed on the network, have brought the idea of learning livelihood into an innovative perspective that everyone in education can take advantage of, despite the stationary and limited nature of higher education. (Yuan & Powell, 2013). In this context, MOOCs are seen as a continuation of the educational support of the openness movement (Abelson, 2008; Johnstone, 2005; McKinney, Dyck & Luber, 2008), which represents every open, global and collaborative direction (Bonk, 2016).

The stages of the openness movement in education and the MOOCs appearing in the continuation are shown in the figure.

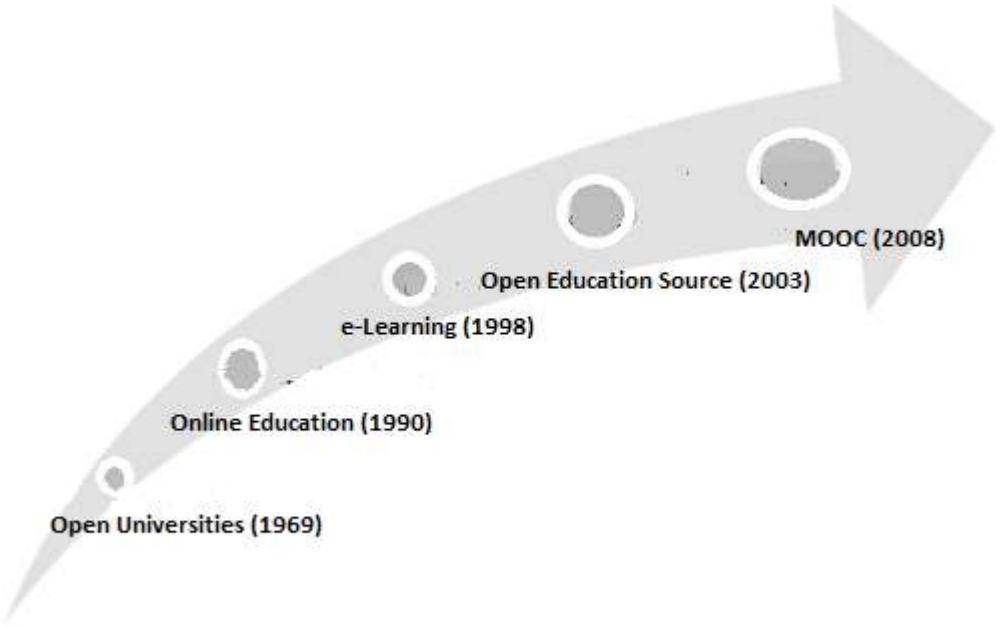

Firuge1.the important steps of the movement of clarity in education (Kalman, 2014)

(Ongulu, Akturk, Şahin, Hanoğlu & Dinçer, 2016) with the hybrids, which are composed of these two tidal assemblages, separated according to their pedagogical background and differences in practice (Rodriguez, 2012)

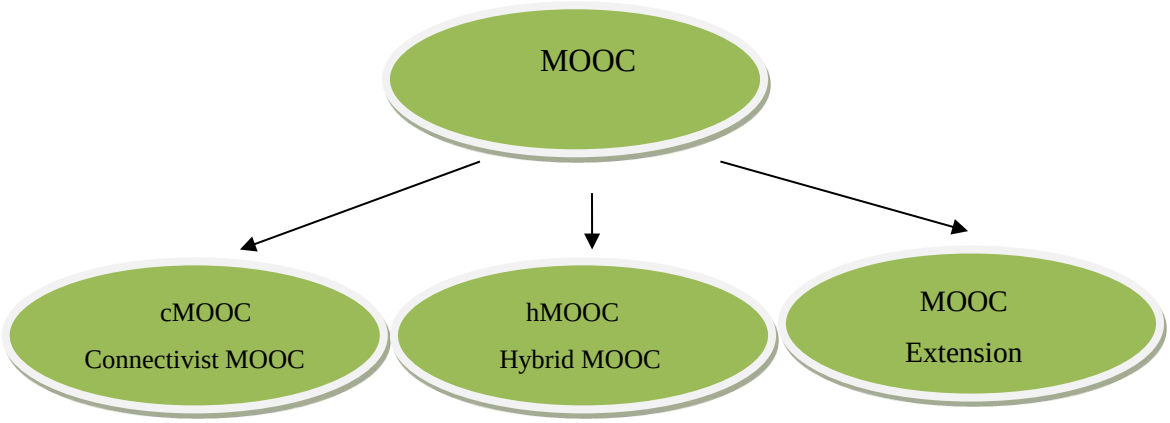

Figure 2.The important steps of the movement of clarity in education

MOOCs have started cMOOC with a course entitled "Contextual and Related Knowledge-CCK08" at George Siemens and Stephen Downes University of Manitoba (Siemens, 2013). In 2011, Sebastian Thrun and Peter Norving launched CSCE (Leckart, 2012) to teach CS221 coded artificial intelligence (AL). hMOOCs emerged in 2013 (Bozkurt, 2016).

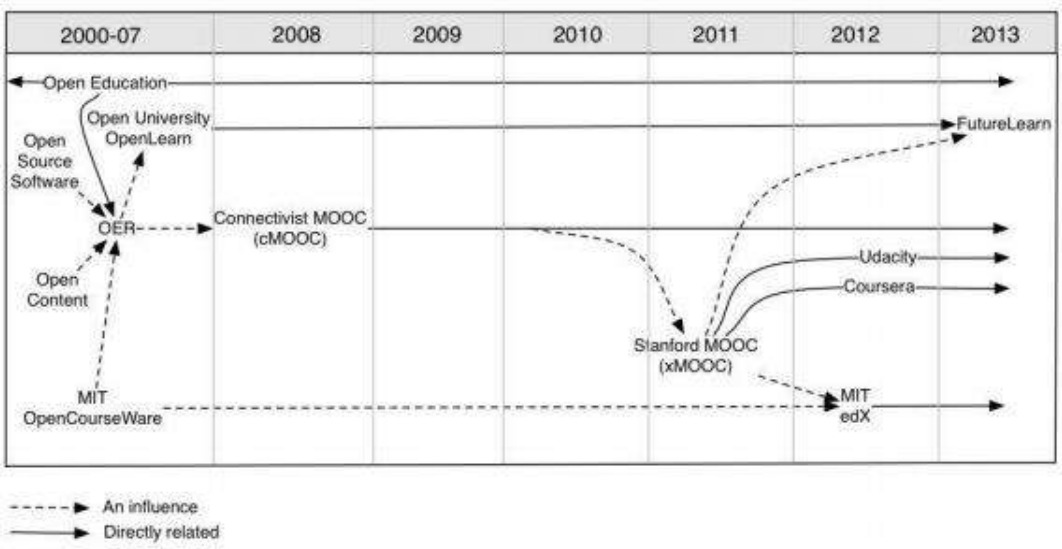

Figure 3. The emergence and development of Mass Open Online Lessons (Yuan & Powell, 2013).

Starting with the openness movement, cMOOC was introduced in 2008, followed by the process from the establishment of the traditional model xMOOC example and MOOC platforms in 2011 until 2015.

Connective MOOCs with English counterpart cMOOC are used with the letter "c" because they adopt the connective learning theory. cmooc; MOOCs, later known as xMOOC, which adopt more traditional approaches, are defined as XMOOC in the extended / extension words xMOOC as an extension of the traditional course system (Bozkurt, 2016).

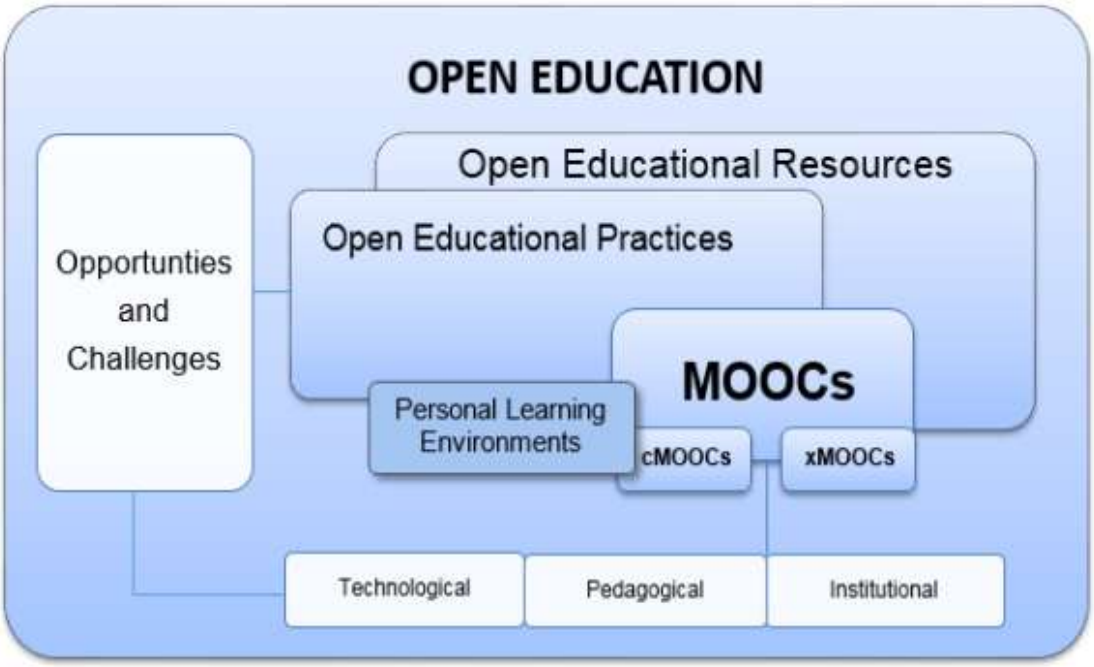

Figure 4. MOOC formation and types are shown (Saadatmand, 2017).

The research will provide a better understanding of the reasons for the emergence of MOOCs and their historical development and the need for species to be provided in the natural development process of MOOCs for lifelong learning.

2.Materyal Method

In this study, the probing method was used. Karasar (2005) examined the existing records and documents and expressed the data collection as documentary screening method In the research made as documentary screening model, "MOOC historical development and types" in ProQuest and "MOOC" key word were questioned in Yök Akademik and the information was collected by accessing the articles and theses in the databases. This method has been used since theses and articles emerging with key words in the study were examined.

3. Findings and Discussion

Due to the increasing number of students, the limited number of traditional educational institutions are inadequate in responding to needs. (Koutropoulos et al., 2012). The need for lifelong learning has increased with the involvement of the Internet in all areas of life, the role of educators and educators has shifted from learning to teaching to teaching institutions to share information on global networks (Dabbagh, 2005; de Waard et al., 2011; Kop, Fournier & Mak , 2011).Despite the traditional nature of higher education, open and distance learning and subsequent mass structures offer a fairer environment for equality in education (Yuan & Powell, 2013). The increase in educational costs can be attributed to the preference of MOOCs. (UT, 2014). The MOOCs have emerged as a result of different perspectives on openness movement and open source of lectures. (Yuan & Powell, 2015). A change in pedagogical approach and learning theory that has not been anticipated from open lectures has opened the way to the MOOC (Tekdal, Baz & Catlak, 2015). Again, changes in educational platforms have led to the formation of MOOCs (Saadatmand, 2017).

In 2008, c MOOC was launched by George Siemens and Stephen Downes (Siemens, 2013). In 2011, xMOOC (Leckart, 2012) to teach CS221 coded artificial intelligence and finally hMOOCs to feature both crawlers emerged in 2013 (Bozkurt, 2016). Some sources of MOOCs have been examined in two versions. Early-stage MOOCs "MOOC1.0" were able to transfer one-way information with tools such as short video, reading materials. Over time, this structure became social support 'MOOC2.0' (Soylev, 2017).

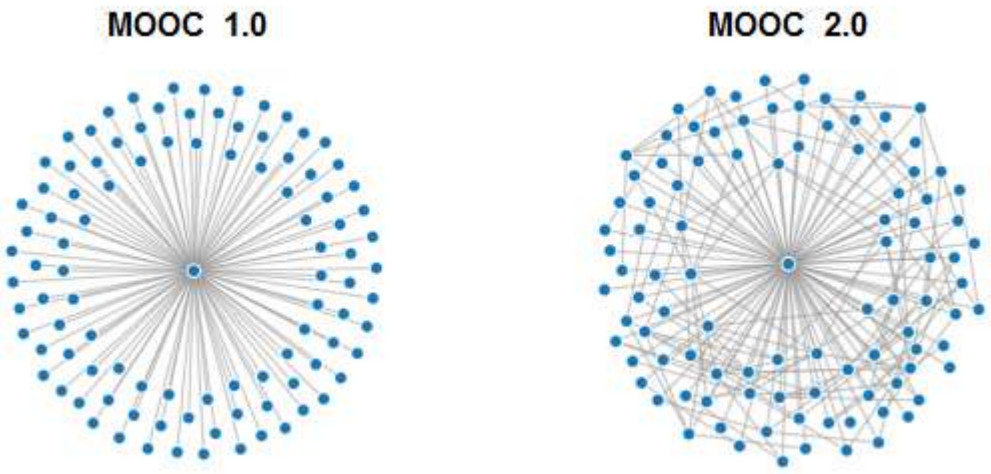

Figure 5. MOOC versions (Slathe, 2014).

As can be understood, MOOC 2.0 has more interaction. It can be argued that the active use of social media, intensification of mixed learning has increased interaction (Suen, 2014).

All MOOCs have the following characteristics when separated by their version or type. Self determination, diversity, openness, and interaction (Cabiri, 2012).

4. Conclusions and Recommendations.

MOOCs offer new opportunities for lifelong learning every day. Aydin (2017) found that MOOC's awareness was low in the research he conducted, which resulted in lack of language barriers, recognition and reputation. Increasing the use of MOOC depends on the understanding of the MOOC's tenets. Although MOOCs started in 2008, they cannot be said to have completed development. This evolution seems to continue because of the potential to change higher education (Saadatmand, 2017). The types of MOOC's and the changes they make in education are addressed separately for future research.

References

Abelson, H. (2008). The creation of OpenCourseWare at MIT. *Journal of Science Education and Technology, 17*(2), 164–174.

Aydin, C. H. (2017). Current status of the MOOC movement in the world and reaction of the Turkish higher education institutions. *Open Praxis*, *9*(1), 59-78.

Bonk, C. J. (2016). Keynote: What Is the State of E-Learning? Reflections on 30 Ways Learning Is Changing. Journal of Open, Flexible and Distance Learning, 20(2), 6-20.

Bozkurt, A. (2016). *Identifying interaction patterns and teacher-learner rolesin connectivist massive open online courses.* (Doctora dissertation). Retrieved from https://s3.amazonaws.com/academia.edu.documents/49218415/Baglantici_Kitlesel_Acik_Cevrimici_Derslerde_Etkilesim_Oruntuleri_ve_Ogreten-Ogrenen_Rollerinin_Belirlenmesi-Aras_BOZKURT.pdf?AWSAccessKeyId=AKIAIWOWYYGZ2Y53UL3A&Expires=1527439434&Signature=0ZUiBSZgCA9cEhMQPvIb2vyMjpQ%3D&response-content-disposition=inline%3B%20filename%3DBaglantici_Kitlesel_Acik_Cevrimici_Dersl.pdf

Bonk, C. J. (2016). Keynote: What Is the State of E-Learning? Reflections on 30 Ways Learning Is Changing. *Journal of Open, Flexible and Distance Learning*, *20*(2), 6-20

Cabiria, J. (2012, July). Connectivist learning environments: Massive open online courses. The 2012 World Congress in Computer Science Computer Engineering and Applied Computing, Las Vagas, July 16-19, 2012.

Dabbagh, N. (2005). Pedagogical models for E-Learning: A theory-based design framework. *International journal of technology in teaching and learning*, *1*(1), 25-44.

De Waard, I., Abajian, S., Gallagher, M. S., Hogue, R., Keskin, N., Koutropoulos, A., & Rodriguez, O. C. (2011). Using mLearning and MOOCs to understand chaos, emergence, and complexity in education. *The International Review of Research in Open and Distributed Learning*, *12*(7), 94-115.

Educause (2013). Seven things you should knowaboutMOOCs II. Educause learning initiative. http://net.educause.edu/ir/library/pdf/ELI7097.pdf (Erişim tarihi: 28.04.2018).

Johnstone, S. (2005). Open educational resources serve the world. *Educase Quarterly*, *28*(3), 15.

Kalman, Y. M. (2014). A race to the bottom: MOOCs and higher education business models. Open Learning: The Journal of Open and Distance Learning, 29(1), 514.

Karasar, N. (2005). Scientific research metod. Ankara: Nobel Publishing Distribution, 151-152.

Kop, R., & Hill, A. (2008). Connectivism: Learning theory of the future or vestige of the past? *International Review of Research in Open and Distance Learning*, *9*(3). Retrieved from http://www.irrodl.org/index.php/irrodl/article/view/523/1103

Kop, R., Fournier, H., & Mak, J. S. F. (2011). A pedagogy of abundance or a pedagogy to support human beings? Participant support on massive open online courses. *The International Review of Research in Open and Distributed Learning*, *12*(7), 74-93.

Koutropoulos, A., Gallagher, M. S., Abajian, S. C., de Waard, I., Hogue, R. J., Keskin, N. Ö., & Rodriguez, C. O. (2012). Emotive vocabulary in MOOCs: Context & participant retention. *European Journal of Open, Distance and E-Learning*, *15*(1).

Leckart, S. (2012). The Stanford education experiment could change higher learning forever. *Wired Magazine*, *20*, 122-128.

McKinney, D., Dyck, J. L., & Luber, E. S. (2008). iTunes University and the classroom: Can podcasts replace professors? *Computers & Education*, *52*, 617–623.

Ongulu,Aktürk, Çağrı & Dinçer (2015, Kasım). MOOC environments. Paper presented at the XVIII. Academic Computer Conference AB'2016, Aydın.

Rodriguez, C. O. (2012). MOOCs and the AI-Stanford Like Courses: Two Successful and Distinct Course Formats for Massive Open Online Courses. European Journal of Open, Distance and E-Learning. http://www.eurodl.org/?p=current&article&article=516#MobiMOOC (Erişim tarihi: 28.04.2018).

Saadatmand, M. (2017). A New Ecology For Learning: An Online Ethnographic Study of Learners' Participation and Experience in Connectivist MOOCs. *Helsinki Studies in Education.*

Salathe, M. (2014). MOOCs 2.0: Scaling One-on-One Learning. Retrieved 15 April 2016 from https://www.wired.com/insights/2014/09/moocs-2-0/

Siemens, G. (2013). Massive open online courses: Innovation in education. In McGreal, R., Kinuthia, W., & Marshall S. (Eds), *Open educational resources: Innovation, research and practice* (pp. 5–16). Vancouver: Commonwealth of Learning, Athabasca University.

Soylev, A. (2017). MOOCs 2.0: The Social Era of Education. *Turkish Online Journal of Distance Education*, *18*(2), 56-67.

Suen, H. K. (2014). Peer assessment for massive open online courses (MOOCs). *The International Review of Research in Open and Distributed Learning*, *15*(3).

Tekdal, M., Baz, F. C., & Catlak, S. (2015). Current MOOC Platforms at Online Education. *International Journal of Scientific and Technological Research*, *1*(2), 144-149.

Top Universities (UT), 2014 "Tuition Fees at the World's Top Universities". Retrieved 29 April 2016 from http://www.topuniversities.com/student-info/student-finance/tuitionfees-world's-top-universitiesYuan, L., & Powell, S. (2013). MOOCs and Open Education: Implications for Higher Education - A white paper, JISC CETIS (Centre for Educational Technology & Interoperability Standards). Retrieved from http://publications.cetis.ac.uk/2013/667.

Yuan, L., & Powell, S. (2013). MOOCs and Open Education: Implications for Higher Education - A white paper, JISC CETIS (Centre for Educational Technology & Interoperability Standards). Retrieved from http://publications.cetis.ac.uk/2013/667.

Yuan, L., & Powell, S. (2015). Partnership Model for Entrepreneurial Innovation in Open Online Learning. *eLearning Papers, 41(May)*, 1–9.

Prevention of Occupational Diseases of the White-Collar Workers through Computer-Assisted Exercise Model

Bulut KARADAĞ[1*], Yalçın ARI[2]

[1] Vakıf Participation Bank Inc., İstanbul, Turkey
[2] Vakıf Participation Bank Inc., İstanbul, Turkey

[*]**Corresponding Author :**bulut.karadag@vakifkatilim.com.tr

Abstract

A direct increase in the number of white collar employees has become with the enhancement of service industry in Turkey. White collar employees have caught some occupational diseases since their bodies are inactive for a long time. These illnesses cause some pain and edema in their hands, legs, back and neck. If the pains last for a long time, they leave some permanent damages during their old age. Continuity of the pains has also been a reason for losing their job. The workers being aware of these problems have pursued some sportive activities personally. Some of the workers are trying to get rid of these problems by doing exercises in gymnasiums after work or at the weekends. However, all of the employees don't have enough time and facilities to do exercise. In this study, the exercises they need to do are shown on the monitor with regular periods during the time white collar employees work in front of their computer and they are expected to do these exercises. The practices which the employee is asked to do while he/she is sitting or standing are shown with a video which comes up on the screen and stays there for a duration between two and five minutes. The exercise movements shown are for preventing occupational diseases which the white collar employees may have. The occupational diseases which may become in their bodies can be blocked thanks to these sportive activities.

Keywords: White Collar, Occupational Disease, Computer Assisted Exercise, Alternative Exercise.

1. Introduction

With the development of technology and service sector in the 21st century, the number of white-collar workers is also increasing. Up to 20 years ago, while occupational diseases are usually related to blue-collar workers, nowadays white-collar employees are also important. The concept of occupational disease is constitutionally defined by Article 14 of Law No. 5510 and is explained as follows; temporary or permanent illness, physical or mental disability that the insured has suffered due to the reasons for the work being undertaken or due to the nature of the work he has done or due to the conditions of his employment. *SSGSSK, 2006:Mad.14

The first person to have a scientific approach to occupational diseases in the world is considered the Italian clinician Ramazzini who lived in the 16th century. Bernardino Ramazzini, considered the father of worker health and work safety, explains the reason for writing the first occupational disease book, as "this is a coincidence and observation of my writing this book. The city I live in is quite crowded and the buildings are close to each other and high. The pits in which waste from the house is collected must be drained every three years. A person who makes pit emptying the house cleaning business was working so fast I was sitting on the stand and ambitious: "Why are you running so fast, it runs a bit slower and fatigue," I said. He then lifted his head up and looked at me with his bloody, fried, and scanty eyes: "Three or four hours in this business, he understands why I'm working so fast. I am going to be blinded even more here, so I want to finish my job, run the house, wipe my eyes and close it in a dark room." After this visit, I came across many blind people walking around the city. When I asked them, I saw them all who had done the same thing before. With this coincidence, I wanted to examine the health status of all employees. "(Özveri, 2002). This observation shows the seriousness of occupational diseases.

The first legal studies and regulations for the protection of workers against occupational accidents and occupational diseases started in the late 19th century. When the social insurance law is brought to the stage, the problems are primarily due to the social importance and the size of the issues, such as the prevalence of work accidents and occupational diseases. The working class, which is a class emerging with the industrial revolution, has begun to pay the price of social prosperity that emerged and developed with the Industrial Revolution. It has been observed that this situation does not coincide with social justice, and legal arrangements have been made for occupational accidents and occupational diseases. Despite legal regulations, in

all countries entering the industrialization process, the most important social problems, work accidents, technological developments have emerged as a trace. (Narter, 2015: 7)

The most important feature of occupational diseases hundred percent is avoidable. There are some responsibilities for employers to prevent occupational diseases. Occupational diseases can be avoided in enterprises when control methods are applied correctly and necessary risk management studies are done. When the employee is given the task, the employee's health and safety will be taken into account. In order to ensure proper working conditions for the employer; should provide training and information, determine the organization, provide the necessary tools and equipment, adapt health and safety measures to changing conditions, and work to improve the current situation. The employer is obliged to inform the employees, to provide training for the employees, to receive the opinions of the employees and to ensure their participation.

As seen in Table 1, Classification can also be done by taking into consideration factors such as the route of entry (skin, respiration and digestion), appearance and course of the disease (acute and chronic) and the region affected by the disease (local and systemic) in the examination and classification of occupational diseases.

Table 1. Classification of Occupational Diseases.

According to the organs that affected by occupational diseases;	According to the cause of the occupational disease;
· Respiratory system · Digestive system · Hematopoietic system · **Musculoskeletal system** · Excretory system · Hearing organ and system · Multiple organ effects	· Chemical reasons · **Physical causes** · Biological reasons · Powders

Occupational Musculoskeletal System Diseases

• The main complaint is pain in the upper extremities, neck, shoulders, wrists and belly.

• Physical and psychosocial factors are influential in musculoskeletal disorders.

Causes

• Unsuitable postures and movements

• Use of tools with ergonomic inadequacy

• Psycho-social problems

Musculoskeletal diseases are generally divided into upper extremity diseases (neck, shoulder, elbow, hand and wrist) and lumbar diseases.

Waist Diseases

• Tilting the body

• Fixed working position

• Repeated movements

Precautions

• Adhere to simple ergonomic rules

• Ensuring adequate rest

• Physical exercise trainings

Within the scope of this study, it is aimed to prevent the occupational diseases caused by white collar workers sitting in front of the computer continuously. At certain intervals, reminders made on the screen indicate what the employee needs to do. First of all, it is reminded that the work done by the body, head, arms and legs is in a position suitable to the characteristics of work done. With this reminder, the employee is expected to work in the proper body position. It is also intended to protect the worker against occupational illness by showing the exercise videos necessary for activating the unused muscles with the videos displayed on the screen and balancing the body functions that are used or not used too much.

2. Material and Method

2.1. Implementation

In order to be able to do this study, firstly, the videos to be shown were made. Figure 1 and Figure 2 show the desired exercise contents of white collar workers. After the videos are completed, a Figure 3 code block is placed in a "*.bat*" file for each video. In the example, Exercise.mp4 videos will run on Windows Media Player full screen and will automatically shut down after 15 seconds.

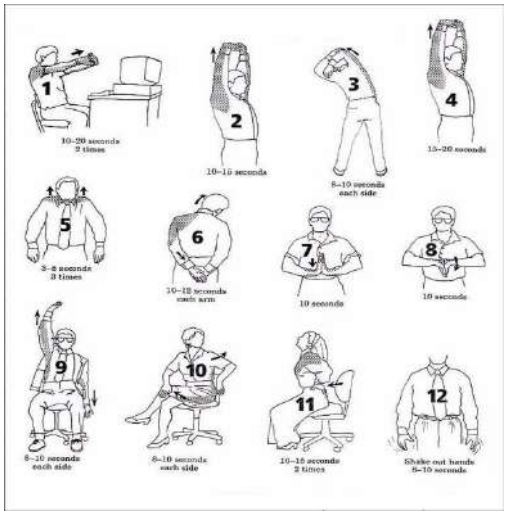

Figure 1. Exercises to do at the desk.

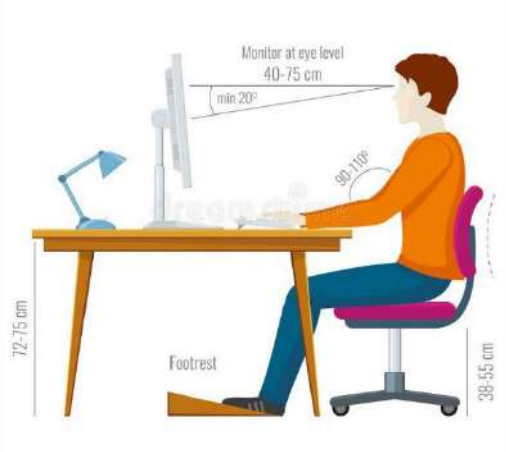

Figure 2. Sitting posture in office.

```
@ECHO OFF
start wmplayer "d:\Exercise.mp4" /fullscreen
timeout/t 15
taskkill /F /IM wmplayer.exe
exit
```

Figure 3. Code in the .bat file**.**

In the second step, the .bat file was created with the help of Task Scheduler as shown in figure 4 to ensure that it worked for certain periods. In the example, the prepared video "Exercise Video 1" was set to work every day at 10:00 AM.

The white collar staff who works in front of the computer watches the video automatically shown at 10:00 AM while continuing daily work. The exercise shown in this

video is expected to be done by the employee. Different exercise videos are shown at other hours of the day. At this point, the employee has followed the ergonomic rules throughout the day and has done some exercises.

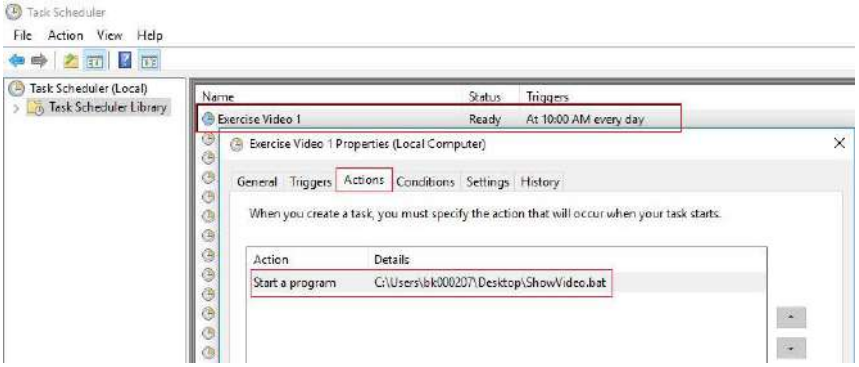

Figure 4. Scheduling the file.

3. Findings and Discussion

When statistics on occupational diseases are taken into consideration, the incidence of occupational diseases among white collar employees is very low. The reason for this is that white collar workers are suffering from ergonomic problems that arise during later ages. As a result, occupational illnesses during the working life are not reflected in the statistics. Table 2 shows the count of occupational diseases among white collar employees in some occupational groups in 2016.

Table 2. Distribution of the Number of Insured Having Work Accident and Exposure to Occupational Disease by Classification of Economic Activity and Gender, 2016

Classification of Economic Activity	Number of insured having occupational disease		
	Male	Female	Total
Computer programming. consulting and related activities	**0**	**0**	**0**
Information service activities	**0**	**0**	**0**
Financial services activities excluding insurance and pension funds	**0**	**1**	**1**
Insurance reinsurance and pension funds, except compulsory social security	**0**	**0**	**0**
Financial services and auxiliary activities for insurance activities	**0**	**1**	**1**

4. Results and Suggestions

As a result of this work, with the help of the videos displayed on the screen, the sitting posture of the white collar employees are reminded and the exercises are fulfilled. Prevention of occupational diseases that could occur in the coming years was ensured. The continuity of exercises is important to prevent occupational diseases. If a regular exercise program is applied, occupational diseases of white-collar workers will be prevented in later ages.

References

Haslegrave, C.M, (1994).“What do we mean by a working posture?”, Ergonomics.

Ilıman, E. Z. (2015). International Journal of Healthy Management and Strategies Research, 22, 23.

Internet: Özveri, M. (2002). Türkiye ve Dünyadaki Meslek Hastalıklarına ilişkin yasal düzenlemelere genel bir bakış, URL: http://muratozveri.net.

John, P. M. (2010). Windows Command Line Administration Instant Reference, Indianapolis, India: Wiley Publishing, Inc.

Narter, S. (2015). İş Kazası ve Meslek Hastalığında Hukuki ve Cezai Sorumluluk,Ankara: Adalet Yayınevi.

Statistics, URL: http://www.sgk.gov.tr/wps/portal/sgk/tr/kurumsal/istatistik

Sosyal Sigortalar ve Genel Sağlık Sigortası Kanunu (16.06.2006). No 5510, Resmi Gazete, 26200, 5, C: 45

Türkiye Cumhuriyeti Sosyal Güvenlik Kurumu, (2016). Work Accidents and Occupational Diseases

Electroencephalography (Eeg) Signals Analysed With K-Near Neighbor Algorithm (K-Nn) and Estimated of Epileptic Seizure

Adil KONDİLOĞLU[1*], Harun BAYER[2], Enes ÇELİK[3]

[1]Giresun University, Technical Sciences Vocational School, Computer Technology Department, Giresun; Turkey
[2]İnönü University, Akçadağ Vocatioal School, Computer Technology Department, Malatya; Turkey
[3]Kırklareli University, Babaeski Vocational School, Computer Technology Department, Kırklareli; Turkey

[*] **Corresponding Author:** adil.kondiloglu@giresun.edu.tr

Abstract

The epileptic seizure is a condition of deterioration of brain's normal activity which is temporarily happened abnormal electrical condition. When the epileptic seizure occurs, there is a temporary loss of consciousness or different symptoms in the patient. In this study, EEG signals of patients who have eyes open, eyes closed and epileptic seizures are used. 6900-line data set are generated each patient's 23-second EEG measurements to sample with 178 data samples per second, The k-NN algorithm is trained with 66% of the data set and is estimated with remaining part. Algorithm performance is analyzed by changing the neighbor value of k-NN algorithm and neighbor search algorithms. It is estimated at 73.0605% accuracy when the neighbor value of the algorithm is set to 1, 76.087% accuracy when it is set to 2, and 70.8866% accuracy when it is set to 3. Additionally, when the estimation is carried out using the cross-validation method, it is estimated that 73.913% accuracy for neighbor value 1, 76.5652 % accuracy for 2 and 72% accuracy for 3. In this study, epileptic seizure prediction from EEG signals and performance analysis of the algorithm are performed.

Keywords: Epilepsy, Machine Learning, k-Nearest Neighbor, Cross Validation.

1. Introduction

Epilepsy is a disorder in which the normal activity of the brain is impaired as a result of an abnormal condition that temporarily occurs in the nerve cells of the brain. Temporary loss of consciousness during the seizure adversely affects the daily lives of patients. Drug and electrical treatment methods are applied to prevent nöbetlin.

The health field is a field in which many data such as patient information, disease information and treatment process are found and many studies are being made using these field machine learning algorithms. Many studies have been done with epilepsy patient data and EEG signals using machine learning algorithms.

In this study, attributes were created using EEG data and patient information, and the generated data were used with support vector machines to measure the classification performance (Avşar, 2009).

In another study, features were derived from EEG signals using wavelet transforms, support vector machines were trained using some classes of signal data, and seizure predictions were made with 97.5% accuracy (Nergiz ve ark., 2014).

In another study, migraine diagnosis was made with artificial neural networks and support vector machines by performing transformations on EEG signals (Akben ve ark., 2010).

From machine learning algorithms, k-NN algorithms are algorithms that classify neighbors in terms of their properties and are used in many health-related works and achieve successful results.

In a study on Chronic Obstructive Pulmonary Disease (COPD) prediction, the disease was estimated with 100% accuracy using the k-NN algorithm using 26 features extracted from the photoplethysmographic signals (Örenç ve ark., 2017).

In another study, 7 features were selected from 34 featured datasets of Mesothelioma patients with the help of Genetic Algorithm and the classification performance of k-NN algorithm increased from 96% to 100% (Albayrak ve Albayrak, 2016).

In this study, EEG signals are classified with k-NN algorithm which is used in many studies and successful results are obtained and seizure prediction is done.

2. Material and Method

The K-NN algorithm was obtained from the UCI machine learning database for EEG data of epileptic patients for training and testing procedures. In a study conducted, EEG data were examined using the data and prediction errors and correlational techniques (Andrzejak ve ark., 2001). The data set used in the study was generated using EEG data from five patients. The generated data set contains 100 single-channel EEG signals each of 23.6 seconds. Each second is divided into 178 pieces and each piece is sampled with 12 bits. In total, 11500 lines of data with 178 features are created. In the dataset 179. In particular, the EEG signal is categorized using numbers 1-5. EEG signal recorded in patient number one grade seizure, EEG signal recorded in area number two class tumor, EEG signal recorded in non-tumor area in grade three, EEG signal recorded in eyes of class number four patient patients, eyes of class five patients open represents the recorded EEG signal. In the study, the data set obtained by extracting the second and third class data from EEG signals obtained from the brain tumorous and non-tumorous regions of the data set is used. The properties of the generated dataset are shown in Table 1.

Table 1. Data set properties.

Attribute Name	Attribute Value
X1	-2047 - 2048
X2	-2047 - 2048
. .	-2047 - 2048
.	
X178	-2047 - 2048
y(sınıf)	1,4,5

In Table 1, the IBK algorithm is used from the k-NN algorithms of the WEKA program to perform operations on the data set whose properties and property values are shown.

2.1. k-NN Algorithm

The k-NN algorithm is based on determining the class to which new observational values belong by using training data whose classes are specific (Özkan, 2013). The classification is made by considering the classes of data that are closest in distance to the selected number by k

value. The Euclidean distance formula shown in Eq. (1) is used to determine the distance of the test data from the training data (Özkan, 2013).

$$d(i, j) = \sqrt{\sum_{k=1}^{p}(x_{ik} - x_{jk})^2} \quad (1)$$

With the formula shown in Eq. (1), the distances of the test data are calculated for each feature of the training data. Considering the classes of the closest distance data as the number of neighbors determined by the k value, the most repeated class is considered as the class of the test data.

Apart from the method of selecting the repetition class that repeats the most, the Weighted Voting method is one of the methods used for class selection. First, the weighted distance values for each training data of the test data are calculated using the formula shown in Eq. (2) (Özkan, 2013).

$$d(i, j)' = \frac{1}{d(i,j)^2} \quad (2)$$

The expression d (i, j) shown in Eq. (2) is the Euclidean distance value. The weighted distance values of the data belonging to the same class are summed and the weighted distance values of each class are obtained by taking the classes of the least weighted distance values into account in the value specified by k value. As a result of the operations, the class with the lowest weighted distance value is accepted as the class of test data.

3. Findings and Discussion

Algorithm-based classification studies were carried out in two stages. In the first stage, the data set is divided into 66% training data and 34% test data and classification is performed.

In the second step, cross-validation is performed and classification is made. The data set is divided into 10 parts and each piece is used as test data and the remaining 9 pieces are used as training data. The classification process is completed by obtaining the average value of the classification operation results for each part that is separated. We also examine the effects of performance by changing k values for each stage. The correct classification performances of the algorithms are shown in Table 2.

Table 2. Algorithm results.

Attribute Name		%66 Train, %34 Test	Cross Validation
IBk	k=1	%73.0605	% 3.913
	k=2	%76.087	%76.5652
	k=3	%70.8866	%72

In Table 2, when the value of k is set to 3 in the classification result of the IBk algorithm, it is seen that the classification result falls. The algorithm performs the classification with the highest accuracy when referring to 2 neighboring properties during classification. As a result of the classification, the confusion matrix showing the true and false values of the state of the test data and the classification data for 66% training-34% test and 10-part cross-validation for k = 2 is as shown in Figure 1.

%66 eğitim - %34 test verisi

```
=== Confusion Matrix ===

   a   b   c   <-- classified as
 661  70  41 |   a = 1
   0 444 352 |   b = 4
   0  98 680 |   c = 5
```

Çapraz Doğrulama

```
=== Confusion Matrix ===

    a    b    c   <-- classified as
 2008  181  111 |    a = 1
    2 1287 1011 |    b = 4
    5  307 1988 |    c = 5
```

Figure 1. IBK Algorithm Confusion Matrices.

The error matrix is shown in Figure 2 as the distinction of the given algorithm to the classes on the classification plane.

Figure 2. IBk Algorithm Test Data Class Separation.

In Figure 2, the classifications for the k = 2 value indicate classes with red colors 1, blue colors 4, and green colors 5. The plane shows the x-axis test results, the y-axis algorithm's

estimation results. Correctly classified data are accumulated on the (0,0), (4,4) and (5,5) coordinates of the plane. Incorrect classifications are outside these coordinates.

3.1. ROC Analysis

In the decision making process, one of the methods used to determine the discrimination of the test is the ROC (Receiver Operating Characteristic) curve method. The ROC curve is based on statistical decision theory and was used in electronic signal definitions and radar problems early in the 1950s (Tomak ve Bek, 2010). Today, ROC analysis is a method used to determine the performance of diagnostic tests applied in different clinical situations, to evaluate the accuracy of statistical models such as logistic models and linear classification analysis. In the coordinate system where the ROC curve is to be formed, the true positive value of the diagnostic test on the Y axis is the false positive value on the X axis. The ROC curve is drawn by combining the corresponding positive and false positive points at each cut-off point.

The area under the ROC curve determines the accuracy of the test in distinguishing between patients and non-ill persons. The expected value of the area under the ROC curve is 0.50 when the diagnostic test being studied has no discriminating ability. In a perfect test, the value of the field is 1.00 with zero false positive and zero false negative.

In the study, the values of the k-value of the IBK3 algorithm and the results of the test results are shown in Table 3 below the ROC curve.

Table 3. Areas under the ROC curve.

Attribute Name		%66 Train, %34 Test			Çapraz Doğrulama		
		Class 1	Class 4	Class 5	Class 1	Class 4	Class 5
IBk	k=1	0,916	0,683	0,798	0,926	0,686	0,801
	k=2	0,928	0,721	0,845	0,936	0,722	0,844
	k=3	0,936	0,742	0,862	0,941	0,737	0,859

The ROC curve for Class 1 results shown in Figure 1 and Figure 2 for k = 2 values of the ROC curve fields shown in Table 3 is shown as an example in Figure 3.

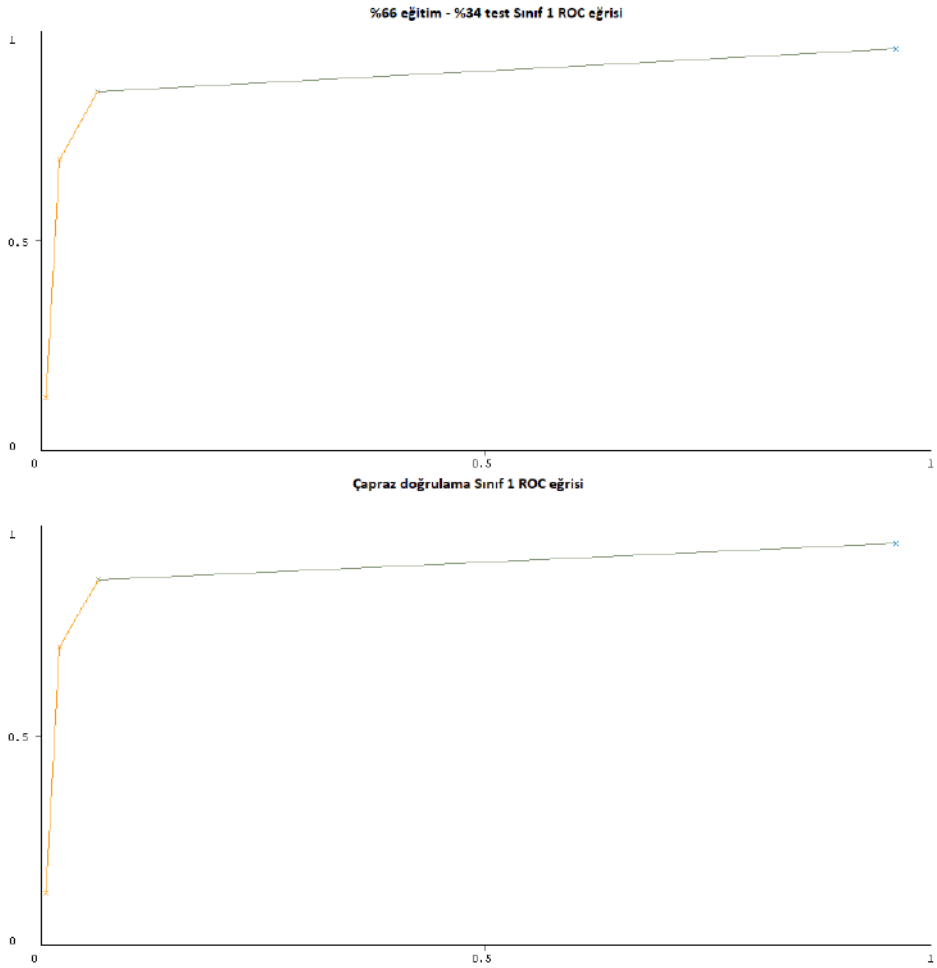

Figure 3. ROC curves for class 1.

4. Results and Suggestions

The estimated epileptic seizure was performed using EEG data in the study, and the k-NN algorithm performed high-order correct classification. Considering the ROC curriculum areas, it can be said that correct classification is made at the level of significance. It is also thought that the number of patients and the amount of data can be increased to increase the successful classification rate.

References

Avşar, E. (2009). *Tek–Sınıf Destek Vektör Makineleri Kullanılarak Epileptik EEG İşaretlerinin Sınıflandırılması*. Yüksek Lisans Tezi, İstanbul Teknik Üniversitesi, Fen Bilimleri Enstitüsü, İstanbul.

Mergiz, M., Özerdem, M. S., Akın, M. (2014). Dalgacık Dönüşümü Kullanılarak EEG İşaretlerinde Epileptik Nöbet Tespiti. *Tıp Teknolojileri Ulusal Kongresi*, (s. 70-73), Nevşehir.

Akben, S. B., Subaşı, A., Kıymık, M. K. (2010). EEG İşaretleri ile Migren Tanısında Yapay Sinir Ağları ve Destek Vektör Makineleri Sınıflandırma Yöntemlerinin Karşılaştırılması. *18.Sinyal İşleme ve İletişim Uygulamaları Kurultayı (SIU2010 – IEEE)*, (s. 637-640), Diyarbakır.

Örenç, S., Uçar, M. K., Bozkurt, M. R., Bilgin, C. (2017, October). A new approach for treatment of chronic obstructive pulmonary disease. *In Medical Technologies National Congress (TIPTEKNO)*, 2017 (pp. 1-4). IEEE.

Albayrak, M., Albayrak, A. (2016). Mezotelyoma Hastalığı Verilerinin Sınıflandırılmasında Genetik Algoritma ile Özellik Seçimi. *Tıp Teknolojileri Kongresi,* (s. 138-141), Antalya.

Andrzejak, R. G., Lehnertz, K., Mormann, F., Rieke, C., David, P., Elger, C. E. (2001). Indications of nonlinear deterministic and finite-dimensional structures in time series of brain electrical activity: Dependence on recording region and brain state. *Physical Review E*, 64(6), 061907. doi: 10.1103/PhysRevE.64.061907

Özkan, Y., (2013). *Madenciliği Yöntemleri* (2. basım). İstanbul: Papatya Yayıncılık Eğitim A.Ş.

Tomak, L., Bek, Y., (2010). İşlem karakteristik eğrisi analizi ve eğri altında kalan alanların karşılaştırılması. *Deneysel ve Klinik Tıp dergisi*, 27, 58-65.

Results Of Cryotherapy Treatments Estimated with Support Vector Machines and Decision Tree

Adil KONDİLOĞLU[1*], Harun BAYER[2], Enes ÇELİK[3]

[1]Giresun University, Technical Sciences Vocational School, Computer Technology Department, Giresun; Turkey
[2]İnönü University, Akçadağ Vocatioal School, Computer Technology Department, Malatya; Turkey
[3]Kırklareli University, Babaeski Vocational School, Computer Technology Department, Kırklareli; Turkey

[*] **Corresponding Author:** adil.kondiloglu@giresun.edu.tr

Abstract

Warts are hard and rough structure which is occured as result of infection of Human Papillomavirus which is generally locate top layer of skin. Warts generally occur in various parts of the body such as hands, feet, face in skin color. There are different type of methods such as operation, laser, elektrokroter, kriyo in wart treatment. The cryo among these methods have begun to be used in the treatment of skin diseases such as warts using with liquid nitrogen in the health field. In this study, results of treatment which is performed on cryotherapy are estimated using data of 90 different patients of wart. The support vector machine and decision tree algorithm of WEKA program are used for estimation. After the algorithms were trained with 66% of the data, the LibSVM with 87.0968% accuracy, the SMO algorithm with 90.3226% accuracy and the J48 algorithm with 93.5484% accuracy were predicted the treatment result. When the algorithms are trained using cross validation, the LibSVM algorithm with 86.6667% accuracy, the SMO algorithm with 92.2222% accuracy, and the J48 algorithm with 93.3333% accuracy were predicted the treatment result. In addition, the effect values of features and features that are effective in forecasting are estimated and the algorithm performances are compared according to the estimation results. With the study is aimed that effectively progress of the cryotherapy process and help successfully end of treatment process.

Keywords: Cryotherapy, Machine Learning, Support Vector Machine, Decision Tree

1. Introduction

Machine learning is used in many studies to model and infer the system in areas such as education, banking, social media, and health. In the field of health; many studies have been conducted in which machine learning algorithms have been used for various purposes such as diagnosis of diseases, successful completion of treatment period, cost analysis of treatment period. Decision tree algorithms and support vector machines are frequently used supervised learning algorithms for solving the classification problem through fast results and successful classification features. Successful inferences can be made for the system modeled by the appropriateness of training data and adequate training.

When the algorithms used for the classification problem are examined, the support vector machines are often used in many different classification problems. Support vector machines take place in the literature between efficient machine learning algorithms because of their high generalization performance, fast results in large volume data and successful classification performance (Ayhan ve Erdoğmuş, 2014).

In one study, support vector machines and decision tree algorithms were used to predict disease with liver disorders, breast cancer and heart disease datasets, and the predictive performances of the algorithms were compared (Ahmed K ve ark., 2013). As a result of the study, support vector machines estimated the liver disorders with 57,97%, breast cancer with 75% and heart diseases with 55,55% accuracy. Decision tree algorithms estimated the liver disorders with 57.97%, breast cancer with 75% and heart diseases with 55.55% accuracy. In addition, estimating the kernel function of the support vector machine and estimating the effect of the kernel function on the estimation are also studied.

In another study, training and test data sets were prepared using the data of 433 patients in Zonguldak Karaelmas University Medical Faculty Psychiatric Policlinic and classified for supportive vector machines and nighttime eating syndrome (Akşehirli Yılmaz ve ark., 2013). As a result of the study, the algorithm was classified as 91.52% for the training dataset and 86.14% for the training dataset.

In another study, 175 fibromyalgia patients and 176 healthy subjects were used to classify the disease with support vector machinery (Zontul ve ark., 2017). 15 features were used for 351 individuals and the data set was divided into 67% training and 33% test data. The SVC method of the Python sklern.svm library was used and also the classification operation was performed by dividing the data set into 10 parts. The result was classified with 85% accuracy.

Decision trees algorithms are simple learning algorithms that are easy to understand and show decision clarifications as well as decisions (Taşkın, 2014). Decision trees form a tree-like decision structure by dividing the data into small sized decision trees, using the induction method (Albayrak ve Yılmaz Koltan, 2009). The generated tree structure reveals the relationship between the data properties and also shows nonlinear relationships as well as linear relationships.

In a study on the prediction of heart disease; predictions were made with 99% accuracy using decision tree algorithms using patient data including blood sugar, cholesterol, smoking, chest pain type and electrocardiography (Masethe ve Masethe, 2014). It was determined that the decision tree and the chest pain type were important features in predicting the disease.

In another study, 89% accuracy classifications were made by decision tree algorithm using data of age, body mass index, family history of diabetes, systolic and diastolic blood pressure data of type-2 diabetics (Sayadi ve ark., 2017). It is seen that the diastolic blood pressure information in the first node in the tree model formed by the algorithm is the most important feature for classification and the age information in the second node is also the second important feature.

In another study, 11 features were extracted from the voice data of Parkinson's patients using the Basic Component Analysis tools, and predictions were made using decision tree algorithms using these properties (Aich ve ark., 2018). As a result of the study, algorithms are successful classification by 96.83%.

As supportive vector machines and decision tree algorithms in the literature, cryotherapy process is analyzed in two wart treatments and the conclusions are made based on the algorithm results.

2. Material and Method

Support vector machines and decision tree algorithms for cryotherapy treatment for training and testing procedures have been obtained from the UCI machine learning database for patient data. A system design has been made to select the wart treatment method by using fuzzy logic and Apriori algorithms with the mentioned data (Khozeimeh ve ark., 2017; Khozeimeh ve ark., 2017). The dataset used contains data from 90 wart patients treated with cryotherapy. The characteristics of patient data are shown in Table 1.

Table 1. Patient characteristics.

Number	Attribute Name	Attribute Value
1	Response to treatment	1-Yes, 0-No
2	Gender	Male, Female
3	Age	15-67
4	Time elapsed before treatment(month)	0-12
5	The number of warts	1-12
6	Types of wart	1-Common, 2-Plantar, 3-Both
7	Surface area of the warts (mm^2)	4-750

As seen in Table 1, the patient's data consist of 6 features except the response to the treatment process. The features; Feature No. 1 is the treatment result, Feature No. 2 is the patient's gender, Feature No. 3 is the patient's age, Number 4 is the time from the onset of the feature to treatment, Number 5 is the number of warts, Number 6 is the wart type, and Number 7 is the surface area of the warts.

In the study, libSVM and SMO are used as support vector machines of WEKA program, and j48 algorithm is used as decision tree algorithms.

2.1. Support Vector Machines

Support vector machines are a classification method with the help of linear or nonlinear functions. Support vector machines are often used to separate the data into two classes or to separate them into more classes.

2.1.1. Linear separation of data

It is possible to draw an infinite grain function to separate the two classes. The aim is to determine the function that will make the most appropriate way. Functions in multidimensional space are expressed as hyperplanes. The data set is expressed as {xi, yi}, i = 1, ... n if we consider n sets of training data that will divide the dataset linearly into two classes. It shows the number of elements n and y ∈ {-1, + 1} class labels.

The most suitable hyperplanes that will share the two classes of data are the ones with the largest gap between them. These hyperplanes identified for the classes are named support vectors. The linear hyperplane drawn in the middle of the support vectors takes the name of the

optimal hyperplane that separates the two classes (Özkan, 2013). Can be expressed as shown in Equation (1) in terms of hyperplane points.

$$w^T x + b = 0 \quad (1)$$

In equation (1), w^T and x are vector quantities, w^T is the weight vector and $w = \{w_1, w_2, ..., w_n\}$. In the equation, x is the point on the line and b is the slope (Küçüksille ve Ateş, 2013). The boundary hyper-planes of the classes are as expressed by Eqs. (2) and Eq. (3).

$$w^T x_i + b > 0, \; y=+1 \quad (2)$$

$$w^T x_i + b > 0, \; y=-1 \quad (3)$$

$$y_i(w^T x_i + b) - 1 \geq 0 \quad \forall i \quad (4)$$

Equation (2) and Equation (3) are obtained from Equation (4).

2.1.2. Nonlinear separation of data

The data may not always be separated by linear planes. The data of other classes may have fallen into the boundary planes of the classes. In case that the data are not separated by a linear plane, the solution is created by adding the loose variables ξi, which are non-negative and error, to the optimization model (Özkan, 2013).

The optimal hyperplane using the loose variable is shown in Eq. (5), and the boundary hyperplanes as shown in Eq. (6) and Eq. (7).

$$y_i(w^T x_i + b) \geq 1 - \xi_i \quad (i=1,2,\ldots n), \; \xi_i \geq 0 \quad (5)$$

$$w^T x_i + b \geq 1 - \xi_i, \; y=+1 \quad (6)$$

$$w^T x_i + b \leq -1 + \xi_i, \; y=-1 \quad (7)$$

ξi is the distance from Xi to the loose variable Xi. In case of indivisibility, the value of ξi is $0 \leq \xi i < 1$ and the value of ξi in case of incorrect classification, $\xi i \geq 1$ (Küçüksille ve Ateş, 2013). Equation (8) is obtained by adding the additional C variable to the formulas for situations that prevent linear separation.

$$L(w, \xi) = \frac{1}{2} w^T w + C(\sum_{i=1}^{n} \xi i)^k \quad (8)$$

The C variable in Eq. (8) is chosen by the user and is an integer value that provides the condition C> 0 and affects the border width. In the case of complete linear non-separability, the problem is solved using the expression in Eq. (5).

3. Decision Tree Algorithms

Decision tree algorithms; decision nodes, leaves, and branches that go to these leaves by creating tree structure algorithm to classify. Decision trees have been developed with methods such as entropy, classification, regression and memory based classification.

The decision tree algorithms are algorithms based on ID3 and C4.5 entropy. The J48 decision tree algorithm is used in the WEKA program as the counterpart of the C4.5 decision tree algorithm, which is the improved version of the ID3 decision tree algorithm. The J48 algorithm performs classification using entropy and normalization. It also provides decision trees for numerical qualities.

3.1. Entropy and Gain Measurement

The amount of uncertainty in a system is called entropy (Özkan, 2013). When the probabilities of n data and data are given as $P = \{p_1, ..., p_n\}$, a data set $\{a_1, ..., a_n\}$, the total uncertainty of the data set is calculated by the formula shown in Eq. (9).

$$H(S) = -\sum_{i=1}^{n} p_i \log_2(p_i) \quad (9)$$

Approaching the uncertainty value to 1 means increasing the uncertainty of the system, while approaching 0 means decreasing uncertainty.

Considering the attribute values that will classify the data set into classes, there are probabilities of cluster and P_T class values including T class values $\{C_1, C_2, ..., C_k\}$. (Özkan, 2013). The probability value for the class values is expressed as $p_i = \frac{|Ci|}{|T|}$ and the average probability value is as shown in Equation (10).

$$H(T) = -\sum_{i=1}^{n} p_i \log_2(p_i) \quad (10)$$

If the class property T is divided into subclasses T_1, T_2, ..., Tn, depending on the non-class X property values, Ti is considered as the weight average of the information required to determine the class of an item. (Özkan, 2013). The information required to determine the class of an element of T is computed as shown in Eq. (11).

$$H(X,T) = \sum_{i=1}^{n} \frac{|Ti|}{|T|} H(Ti) \qquad (11)$$

The gain criterion is used to measure the information obtained by dividing T data by X. The gain criterion is calculated as shown in Equation (12).

$$Kazanç(X, T) = H(T) - H(X,T) \qquad (12)$$

In Equation (11), the gain having the highest value of the X attributes calculated as the gain criterion is selected as the branch node. The tree structure of the data set is created by applying the same operations to the other attributes.

In the case of numerical values, the class values are sorted first and the median value of the sorted values is taken as the threshold value. Processes are performed taking into account the case where entropy and gain values of the tree structure are smaller, equal or larger than the threshold value.

4. Findings and Discussion

Classification studies with algorithms were done in two steps. In the first stage, the data set is divided into 66% training data and 34% test data and classification is performed.

In the second step, cross-validation is performed and classification is made. The data set is divided into 10 parts and each piece is used as test data and the remaining 9 pieces are used as training data. The classification process is completed by obtaining the average value of the classification operation results for each part that is separated. The correct classification values of the algorithms are shown in Table 2.

Table 2. Algorithm results.

Attribute Name	Percentage of successful classification	
	%66 Train, %34 Test	Cross Validation
LibSVM	%87.0968	%94.4444
SMO	%90,3226	%92.2222
J48	%93.5484	%93.3333

As shown in Figure 4, the confusion matrix showing the true and false values of the classification data and the state of the test data for the 66% training-34% test and the 10-part cross-validation results in the classification results of the algorithms specified in Table 2.

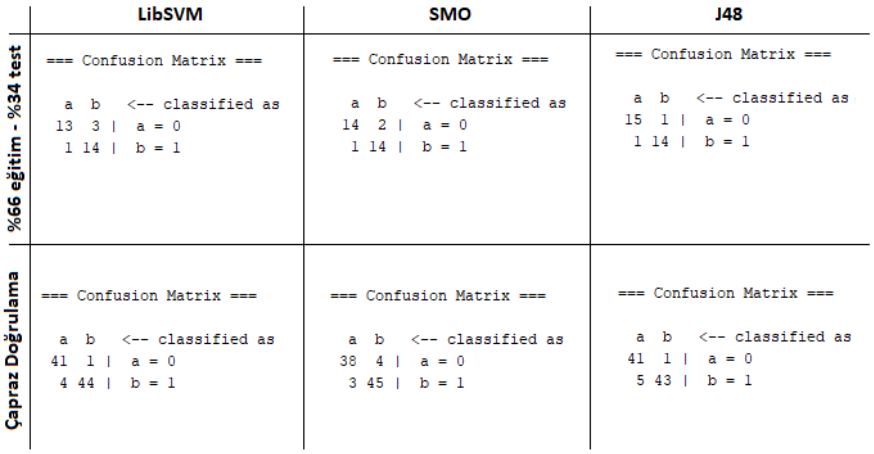

Figure 4. Confusion Matrices of Algorithms.

Figure 4 shows the decision tree generated by the J48 algorithm, which shows the error matrices.

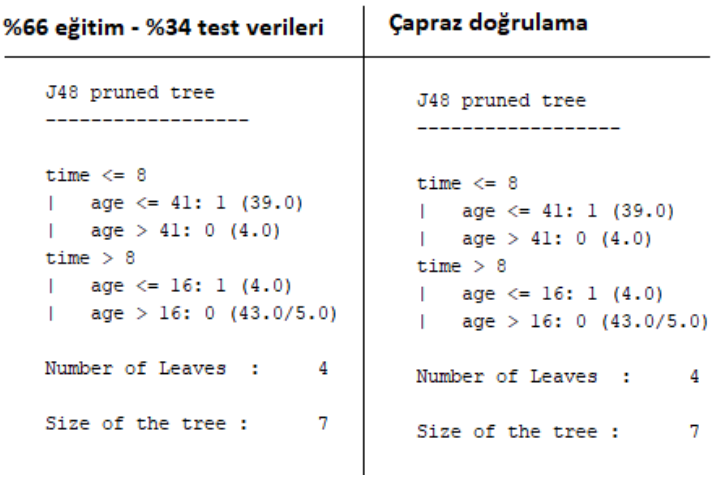

Figure 5. J48 algorithm decision tree.

Figure 5 shows the tree structures constructed by the J48 algorithm with 34% test data and 10 parts cross-validation results. When the constructs are examined, there is a time feature on the root node of the tree and an age feature on the sub node. Considering the nodes of the decision tree, it is understood that time and age are important characteristics for classification.

5. Results and Suggestions

In the study, the estimation of wart disease was made using some data of patients and in general the classification algorithms performed high-order correct classification. The study was conducted using specific characteristics of a number of patients. It is possible to increase the classification rate by increasing the amount of data and types. In addition, there are many inherent variables such as nutrition, genetic factors, blood pressure that can affect the treatment process of patients and there are many external factors such as stress, fatigue and air temperature. Control of the effects of all factors on the patient can directly affect the treatment process as well as affect the health status. The effects of these factors on the patient may be due to the difficulty of studying predictability.

References

Ayhan, S , Erdoğmuş, Ş . (2014). Destek Vektör Makineleriyle Sınıflandırma Problemlerinin Çözümü İçin Çekirdek Fonksiyonu Seçimi. *Eskişehir Osmangazi Üniversitesi İktisadi ve İdari Bilimler Dergisi*, 9 (1), 175-201. Retrieved from http://dergipark.gov.tr/oguiibf/issue/5712/76473

Ahmed K, A., Aljahdali, S., Hussain, S. N., (2013). Comparative Prediction Performance with Support Vector Machine and Random Forest Classification Techniques. *International Journal of Computer Applications,* 69(11). doi: 10.5120/11885-7922

Akşehirli Yılmaz, Ö., Ankaralı, H., Aydın, D., Saraçlı, Ö., (2013). Tıbbi Tahminde Alternatif Bir Yaklaşım: Destek Vektör Makineleri. *Turkiye Klinikleri J Biostat*, 5(1),19-28.

Zontul, C , Hayta, E , Zontul, M , Taş, A , Siliğ, Y . (2017). Destek Vektör Makineleri ile Fibromiyalji Sendromu Sınıflaması. *Acta INFOLOGICA*, 1 (2), 92-98. Retrieved from http://dergipark.gov.tr/acin/issue/33868/357404

Taşkın, G . (2014). Veri Madenciliğinde Karar Ağaçları ve Bir Satış Analizi Uygulaması. *Eskişehir Osmangazi Üniversitesi Sosyal Bilimler Dergisi*, 6 (2), 221-239. Retrieved from

http://dergipark.gov.tr/ogusbd/issue/10987/131495

Albayrak, A. S., Yılmaz Koltan, Ş., (2009). Veri Madenciliği: Karar Ağacı Algoritmaları ve İMKB Verileri Üzerine Bir Uygulama. *Süleyman Demirel Üniversitesi İktisadi ve İdari Bilimler Dergisi*, 14 (1), 31-52. Retrieved from http://dergipark.ulakbim.gov.tr/sduiibfd/article/view/5000122495/5000112800

Masethe, H. D., Masethe, M. A. (2014, October). Prediction of heart disease using classification algorithms. *In Proceedings of the world congress on Engineering and Computer Science* (Vol. 2, pp. 22-24).

Sayadi, M., Zibaeenezhad, M., & Ayatollahi, S. M. T. (2017). Simple Prediction of Type 2 Diabetes Mellitus via Decision Tree Modeling. *International Cardiovascular Research Journal*, 11(2).

Aich, S., Younga, K., Hui, K. L., Al-Absi, A. A., Sain, M. (2018, February). A nonlinear decision tree based classification approach to predict the Parkinson's disease using different feature sets of voice data. *In Advanced Communication Technology (ICACT), 2018 20th International Conference on* (pp. 638-642). IEEE.

Khozeimeh, F., Alizadehsani, R., Roshanzamir, M., Khosravi, A., Layegh, P., & Nahavandi, S. (2017). An expert system for selecting wart treatment method. *Computers in biology and medicine*, 81, 167-175.

Khozeimeh, F., Jabbari Azad, F., Mahboubi Oskouei, Y., Jafari, M., Tehranian, S., Alizadehsani, R., Layegh, P. (2017). Intralesional immunotherapy compared to cryotherapy in the treatment of warts. *International journal of dermatology*, 56(4), 474-478. doi: 10.1111/_jd.13535

Kavzoğlu, T., Çölkesen, İ. (2010). Destek vektör makineleri ile uydu görüntülerinin sınıflandırılmasında kernel fonksiyonlarının etkilerinin incelenmesi. *Harita Dergisi*, 144(7), 73-82.

Özkan, Y., (2013). *Madenciliği Yöntemleri* (2. basım). İstanbul: Papatya Yayıncılık Eğitim A.Ş.

Küçüksille, E , Ateş, N . (2013). Destek Vektör Makineleri ile Yaramaz Elektronik Postaların Filtrelenmesi. *Türkiye Bilişim Vakfı Bilgisayar Bilimleri ve Mühendisliği Dergisi*, 6 (1), Retrieved from http://dergipark.gov.tr/tbbmd/issue/22246/238807

Investigation of Russian Internet Newspapers From The Age-Friendly Web Site Criteria

Niyazi AYHAN[1*]

[1]Kyrgyz-Turkish Manas University, Faculty of Communication, PR and Advertisingt, Bishkek, Kyrgyzstan; niyaziayhan@mail.ru

[*]**Corresponding Author:** niyaziayhan@mail.ru

Abstract

New media offers multimedia with all the features of traditional media. It is interesting to researchers who make communication studies because of their characteristics such as spreading among users and integrating social life. New media has been changes in the field of journalism as well as in many areas. The newspapers continued their activities due to their low costs in the new media channel. However, some problems are encountered in using the new media for middle age population. The American National Institute On Aging has set the Age Friendly Web Site Criteria to get the most out of these problems. The study focuses on the Russian press in order to provide these criteria for the newspapers published in the new media channel. Literature was presented about new media, Russian Internet Journal and age- friendly web criteria in this context. Later on, newspaper of the Russian State Rosiskaya Gazeta and Moskovskiy Komsomolets were subjected to content analysis based on these criteria. There have been some conclusions about whether the newspapers provided the Age Friendly Web Site Criteria. It has been found that the rate of providing the Age Friendly Web Site Criteria of Russian internet newspapers is over 80 percent. Rosiskaya Gazeta is the newspaper that provides the most age- friendly Web Site Criteria.

Keywords: New Media, Russian Internet Journal, Age Friendly Web Site Criteria, Rosiskaya Gazeta, Moskovskiy Komsomolets

1. Introduction

The new media is the continuation of the conventional media. New media has brought many innovations in terms of access to information. These innovations have also greatly influenced the field of journalism. New media provides an opportunity to communicating with more audiences by low-cost. New media contains all the features of traditional media and it presents multi media environment . New media attracts the attention of audiences with such reasons.

The new media is a media based on information technology. In this context, it is expected that new media users have the ability to use information technologies. However, the middle and elderly population faces some problem about having possession.These problems are set in front of them to medium and old population in the use of new media.Many works are being done to reduce most of the obstacles and for the elderly population to benefit more from the new media. Age Friendly Website Criteria one of the studies of National Institue on Aging .The National Institue on Aging has recommended some criteria for middle and elderly people to using new media. This criterion is to design the readability of the text, to provide information for elderly people, to the similarity of other media texts, to the ease of browsing the web. This study focuses on the mentioned criteria to what extent the government centered newspapers broadcast on the Russian new media channel bear these criteria. In this context, the contents were analyzed Rosisaya Gazeta and Moskovskiy Komsomolets based on the elderly Friendly Website Criteria. Content analysis was performed over a total of 38 criteria. some results have been reached as a result of analysis

In this study reached the end result to Rosiskaya Gazeta is provide the criterionn the most elderly-friendly Web Site Criteria. However, Moskovskiy Komsomolets provides the criterion in the web site and it is quite high. Russian newspapers that broadcast on the new media channel provide the most Text Design Criteria. And at least the Information Regulation Criteria. Generally, it has been determined that the rate of achieving the Age Friendly Web Site Criteria is % 80.15. This data is the result of the elderly population's ease of use of internet newspapers.

2. New Media and Internet Journalism

Researchers in various fields of social sciences have introduced the concept of new media in the 1970s. The concept of the new media has undergone a number of changes and the internet has been spreading throughout the whole of the 1990's with the use of broad masses (Thompson, 1995:25). Today, the concept is generally used in the form of traditional media such as newspapers, radio TVs, etc., as well as new communication technologies. New media is formed on interaction and virtuality. New media users meet a new field that transcends time and space limitations. The new media is separated from the traditional media. These properties can be explained by the concepts of interaction, mass unification and asynchronism. The indirect interaction of the traditional media between the receiver and the transmitter has been actively involved in the audience. there is indirect interaction between the receiver and the transmitter in the traditional media, the viewer is actively involved in the new media communication. Another feature of the new media is related to the concept of mass unification. Disenfranchisement can be explained as the publication of the traditional media to specific groups in the new media instead of broadcasting to the whole mass. Another feature of the new media is the asynchrony feature.

The same urgency requirement in traditional media does not exist in the new media. The audience has the opportunity to access the contents of the new media. Communication takes place in one direction in traditional media, there is a mutual interaction in the new media. The mass is important in traditional media publishing. However, in the new media publishing, the individual is important (Yurdigül - Zinderen, 2102:83-85).

The development of new communication technologies has influenced the field of journalism. In this context, the Internet has allowed the spread of existing mass media. new media has become a medium in which information is reproduced and presented in new formats (Çakır, 2007:125). Online journalism publishing has created a presentation style in this unique environment. This presentation is in the form of more rhetoric and persuasive elements. Traditional newspapers aimed at increasing the circulation of newspapers by increasing the attention of readers to increase page visits. (Işık - Koz, 2009:171).

In addition, the new media journalism has begun to attract great attention, thanks to itfeatures such as audio, design, image, video format.

3. New Media Environment and Internet Journalism in Russia

Internet access began in 1995 in Russia. Up to this year, internet was used by limited people in Russia. Internet access was opened to all Russia In June 1995, by company "Russia-On-Line" (ROL) (Mashkova, 2006:18). The path of limitlessness has been opened. in values and behavior norms (Gorny, 2206:28). The Internet has led to a change in social life in Russia after the totalitarian regime. New media continued to develop With the spread of the Internet in Russia. First of all It has increased web versions of printed newspapers. Then only newspapers and news portals were published on the web. The first newspaper to broadcast on the internet is Uchitelya Gazeta In 1995. Shortly afterwards national newspapers like Izvestiya and Aif started online broadcasting since 1996 (Murzakulova, 2008:70-71). In the same year Ros Business Consulting website and national news service sites started their activities. But the socio- political project news site with the first professional structure is Gazeta.ru. Therefore 1999 year is period of professional network media in Russia (Mashkova, 2006:18).

Internet journalism was a web version of printed newspapers until 2000 in Russia. Postfactum.ru, ORT, Kommersant in August 2000, and NTV-Ntv.ru in September started publishing on the web (Mashkova, 2006:18).

Newspapers, blogs, photo galleries and breaking news were added after 2000. Today, Russian internet newspapers have a faster, better quality and more interactive quality than web versions of printed newspapers (Murzakulova, 2008: 71). There was a decrease in the circulation of printed newspapers in Russia when 2009-2010. This situation has attracted newspapers to the internet. The Vedomosti newspaper is one of the online-oriented newspapers because it can not receive 140,000 circulation. The monthly audience figures of leading news sites in Russia are as follows:

mail.ru/novosti.ru has 10.5 million visitors per month, yandex / novosti 9.8 million and rambler novosti.ru 6.5 million visitors. The rapid growth and spread of the Internet has also led to the growth of news agencies. In this context, the most visited news agency site is ria.ru (6.9 million) (Pankin, 2011:21).

Rossiyskaya Gazeta (российская газета), which is one of the newspapers examined in the scope of the study, It started publishing in 1990. The newspaper is the state broadcasting organ. It is published 5 days a week. Today, it continues its publications in printed format and internet. The newspaper Moskovskiy Komsomolets (Московский комсомолец), another of the newspapers examined, has been published since 1919. One of the newspapers examined is the Moskovskiy Komsomolets (Московский комсомолец) . The newspaper has been published

since 1919. Newspapers are published daily. It is a state broadcasting organ. It is also published in print and internet.

Internet journalism is being used more than traditional newspaper publishing in Russia as it is all over the world. The most common reason for this is that multimedia, interactivity, free.

4. Aging and Age Friendly Web Site Criteria

The declining fertility rate is the most fundamental variable of the population structure (Altıparmak, 2009:159). The decrease in the fertility rate causes the increase of the elderly population. It is expected that this ratio will be 20% of the total population over the age of 65 in the EU countries (Dönümcü, 2006:43). This data is constantly being revised by international organizations. However, the common view is that the elderly population is increasing in the world (Akyazı - Kara, 2017:1352).

Aging is the process in which the body is forced to perform its basic functions. (Öksüzokyar et al, 2016:34). Aging also brings mental and perception problems. The elderly population can not adapt to new technologies In this process. There are some difficulties in using elderly population technologies. the elderly population must be provided with internet compatibility. It is important to do the work for it.

According to Holzinger, Searle and Nischelwitzer, elderly individuals face many obstacles when they use information technology. The most important of these obstacles are cognitive, motivation (fear, belief, etc.), physical (thinking), and perception (sight, hearing etc.). In addition, there are differences in the use of information technology among elderly individuals such as learning time, speed of implementation, error rate, recall and subjective satisfaction. (Akyazı - Kara, 2017:1355).

The National Institute on Aging has published a booklet called Making Your Web Site Senior Friendly to minimize these problems, The National Institute on Aging has listed elderly friendly website criteria. These criteria are in the form of designing readability of text, information presentation, similarity to other media texts, ease of navigation on the web, ease of control of the website. (www.nlm.nih.gov).

These criteria are an important data quality within the business lines that operate on the internet, whose target population is the middle and elderly population. Sanner stated that most of the middle and elderly people should not ignore the internet in this context.

Sanner's attention to the web sites that can be noticed by the target criteria of the mass of the target is middle aged and elderly individuals (Sanner, 2004:20).

5. Material and Method

The main framework of the study is the National Institute on Aging's criteria for making Your Website Senior Friendly. The criteria other than visual perception were not included in the study. The study was carried out only on 38 criteria related to visual perception The work of Akyazı and Kara (2017) Bilişim Çağının Haber Kaynağı Olarak İnternet Gazetelerinin Yaşlı Dostu Web Sitesi Kriterleri Açısından Karşılaştırmalı Analizi has set an example for studying.

The aim of the study was to determine the extent to which the Russian state-run newspapers published in the new media circles met the criteria of the Age Friendly Web Site. For this purpose, it is applied to content analysis method which is from quantitative studies. Frequency and categorical analysis techniques were applied to content analysis techniques. In this context, numerical, percentage and proportional values of units and items are presented by frequency analysis technique. categorical analysis technique is grouped by criteria.

5.1. Universe and Sampling

The universe of the work is state-centered newspapers that take place in the Russian press and broadcast on the new media channel. The sample of the work is Rossiskaya Gazeta and Moskovskiy Komsomolets. These newspapers are state-based newspapers broadcasting on the new media channel..

5.2. Findings of Work

Table 1. Criteria of information editing

	Rosiskaya Gazeta https://rg.ru	Moskovskiy Komsomolets http://www.mk.ru/news/
1. little space for news on the homepage	+	+
2 Serving a site map	-	-
3. place fewer ads on the main page	+	+

4. providing opportunities to close ads	-	+
5. provide the opportunity to return to the top of the page	+	+
6. homepage button	-	-

Information editing criteria is one of the age friendly web site criteria. There are six sub criteria in the information editing criteria. These criteria are little space for news on the homepage, serving a site map, place fewer ads on the main page, providing opportunities to close ads, provide the opportunity to return to the top of the page and homepage button.

In the context of the newspapers covered in the study, there were very few reports on the main page of both newspapers, websites only have title of news. However, neither the newspaper nor the site map was encountered. Both newspapers set the criterion of the place fewer ads on the main page ctiteria . In this context, an advertisement was found in Rossiskaya Gazeta while two ads were found in Moskovskiy Komsomolets. Rosiskaya Gazette does not offer the opportunity to close ads.

However, Moskovskiy Komsomolets offers this possibility. Both newspapers offered the opportunity to return to the top of the page. But there is no homepage button in the newspapers.

Table 2. Criteria of text design

	Rosiskaya Gazeta https://rg.ru/	Moskovskiy Komsomolets http://www.mk.ru/news/
1. leave enough white space on the page	+	+
2. leave space between paragraphs	+	+
3. leave space between clickable destinations (buttons, etc.)	+	+
4. using a character without snakes	+	+
5. using a non-condensed text style	+	+
6. use font size that will not make reading difficult	+	+
7. providing the ability to change the font size	-	-
8. using a bold text style	+	+
9. using large fonts or colors in titles	+	+
10. do not use words that consist entirely of upper case letters	+	+
11. do not use italic writing style	+	-
12. using left-aligned alignment	+	+
13. using a patternless background	+	+
14. using contrast (white background - black text)	+	+

The second criterion of the Age-Friendly Web Site is the Criteria of text design. There are fourteen sub-criteria under this criterion. These sub-criteria are Leave enough white space on the page, leave space between paragraphs, leave space between clickable destinations (buttons, etc.), using a character without snakes, using a non-condensed text style, use font size that will not make reading difficult, providing the ability to change the font size, using a bold text style, using large fonts or colors in titles, do not use words that consist entirely of upper case letters, do not use italic writing style, using left-aligned alignment, using a patternless background, using contrast (white background - black text).

Both newspapers have enough white space on the page and ith spaces between paragraphs and clickable destinations (buttons, etc.). The newspapers used without snakes and condensed writing style. This article is of a writing size that will not make it difficult to read the types. However, newspapers were not allowed to change the size of the text. Bold text style is used in newspaper texts. The titles are in large font and color. In both newspapers, all capital letters are not used. Moskovskiy Komsomolets appeared in italic font while Russkaya Gazeta had no italic writing style. The newspapers used left-aligned alignment. Both newspapers were found to have no background, texts were given in black text on a white background.

Table 3. Easy Access to Information Criteria

	Rosiskaya Gazeta https://rg.ru/	Moskovskiy Komsomolets http://www.mk.ru/news/
1. Using similar symbols	+	+
2. Do not use pop-up windows	+	+
3. News category	+	-
4. Using directional buttons (previous-next page, forward-back, etc.)	-	-
5. Ensure menus are opened with one click	+	+
6. Using menus that do not require scrolling	+	+
7. Using recognizable links	+	+
8. Highlight visited links	+	+
9. Using noticeable buttons	+	+
10. Do not use horizontal scrolling on the page	+	+

11. Do not use too much vertical scrolling on the page	-	-
12. Open new pages in same window	+	+
13. Using a search engine	+	+
14. Offer companion suggestions in the search engine	-	-
15. Providing contact information	+	+
16. Do not use moving content (floating slides, etc.)	+	+
17. Do not use ads in the middle of news text	+	+
18. Providing easy access to the destination (photo news, etc.)	+	+

It is the third criterion of the Age Friendly Web Site Criteria for Easy Access to Information. There are eighteen sub-criteria under this criterion. These sub-criteria are using similar symbols, do not use pop-up windows, news category, using directional buttons (previous-next page, forward-back, etc.), ensure menus are opened with one click, using menus that do not require scrolling, using recognizable links, highlight visited links, using noticeable buttons, do not use horizontal scrolling on the page, do not use too much vertical scrolling on the page, open new pages in same window, using a search engine, offer companion suggestions in the search engine, providing contact information, . do not use moving content (floating slides, etc.), do not use ads in the middle of news text and providing easy access to the destination (photo news, etc..

In the context of the newspapers covered in the study similar symbols were used in both newspapers and the use of pop-up windows which can prevent readers from accessing information, is not included in the newspapers. Moskovskiy Komsomolets does not inform the reader about this issue, while Rosiskaya Gazeta informs readers about what news categorization they have.

Navigator buttons are not included in the newspaper sites, menus are opened with one click and menus that do not require scrolling are used. This contributes to the easy access of news readers to the news. The newspapers used links that were recognizable by readers. As well as highlighting the links that readers have visited. Both newspapers use the same types of buttons that readers will notice. Horizontal shifts were not detected on the pageThe search button was found in newspapers,. There are no complementary suggestions in the search engine. Both newspapers provided news information about the newspaper or the web site. Readers were provided with the opportunity to easily reach photographs or newsletters with no moving content or scrolling. In addition, no advertising was found to prevent the reading of the news text.

Table 4. Providing Criteria

	Rosiskaya Gazeta https://rg.ru/	Moskovskiy Komsomolets http://www.mk.ru/news/	Total
Criteria of information editing Over 6 Criteria	3 %50	4 %66,6	%58.3
Criteria of text design Over 14 Criteria	13 %92,85	12 %85,71	% 89.28
Easy Access to Information Criteria Over 18 Criteria	15 %83,33	14 %77,77	% 80.55
Total of 38 criteria	31 %81.57	30 %78.74	% 80.15

3. Results and Discussion

There are some differences between the new media and the conventional media.

Conventional media have the ability to present information without the need of any ability of the viewer / reader. However, some of the talents for the audience / reader in the use of new media come to the forefront. The most important of these abilities is the use of information technology. In this context, aging is an obstacle to the use of new media National Institue on Aging) has set some criteria under the title of Age Friendly Web Site Criteria.

The Institute believes that these criteria will make it easier for the elderly population to use new media, and that the elderly population will have much easier access to information.

This study is based on the criteria of the National Institue on Aging Age Friendly Web Site. It focuses on the extent to which state-based newspapers in the Russian press, which broadcast on the new media channel, provide age-friendly web criteria.

Rosiskaya Gazeta and Moskovskiy Komsomolets were taken as samples and content analysis was applied based on the Age Friendly Web Site Criteria. In this context, numerical, percentage and proportional values of units and items are presented by frequency analysis technique. the criteria were grouped by the categorical analysis technique. As a result of the analysis some results have been reached.

To the extent that the newspapers provide the Age Friendly Web Site Criteria, the table 4 is presented. Accordingly, Moskovskiy Komsomolets 66.6 percent Rosiskaya Gazeta secured 50 percent respectively within the scope of the six-item information editing criteria. In the Text Design Criteria, 92.85 percent of Rosiskaya Gazeta and 85.71 percent of Moskovskiy Komsomolets are provided. In the context of easy access to information, Rosiskaya Gazeta maintained 83.33 percent and Moskovskiy Komsomolets 77.77 percent. When we look at the general collection, the newspapers that provided the most with the criteria of the Age Friendly Website were Rosiskaya Gazeta with 81.57 percent. The rate by which the Moskovskiy Komsomolets newspaper provided these criteria was 78.74%. The newspapers seem to provide the most Text Design Criteria (89.28 percent). The minimum criteria provided by the newspapers is the Information Regulation Criteria (58.3 percent). In general, it was determined that the percentage of state-based newspapers in the Russian press, which broadcast on the new media channel, is 80.15 percent to provide the Age-Friendly Web Site Criteria.

References

Altıparmak, Saliha (2009). Huzurevinde Yaşayan Yaşlı Bireylerin Yaşam Doyumu, Sosyal Destek Düzeyleri ve Etkileyen Faktörler, F.Ü.Sağ.Bil.Tıp Derg., 23 (3), 159-164.

Akyazı, Erhan. Kara, Tolga (2017). Bilişim Çağının Haber Kaynağı Olarak İnternet Gazetelerinin Yaşlı Dostu Web Sitesi Kriterleri Açısından Karşılaştırmalı Analizi, International Journal of Social Sciences and Education Research Online, 3(4), 1352-1363.

Çakır, Hamza (2007). Geleneksel Gazetecilik Karşısında İnternet Gazeteciliği, Sosyal Bilimler Enstitüsü Dergisi (22), 123-149.

Dönümcü, Şadiye (2006). Yaşlı Ve Sosyal Hizmetler, Türk Fiz. Tıb. Rehab. Derg. 42-46.

Gorny, E. (2006). A Creative History of The Russian Internet, University of London.

Işık, Umur. Koz, Konur Alp (2009). Cinsellik Üzerinden "Tık Ticareti": İnternet Haberciliği Üzerine Bir İnceleme, İletişim Kuram ve Araştırma Dergisi, (29), 168-188

Making Your Web Site Senior Friendly, https://www.nlm.nih.gov/pubs/checklist.pdf, (Date of access: 8 May 2018).

Mashkova, S.G. (2006). İnternet-Jurnalistika: Uçebnoe Posobie, Tambovskiy Gosudastvenniy Tehniçeskiy Universitet.

Murzakulova, G (2008). Farklı Toplumlarda İnternet Gazeteciliği: Rusya ve Türkiye İnternet Gazetelerinin Karşılaştırmalı Çözümlenmesi, Ankara University, Social Sciences Institute

Öksüzokyar, Muhammed Mustafa. Eryiğit, Saadet Çisen. Düzen, Kerime Öğüt. Mergen, Berna Erdoğmuş. Sökmen, Ülkü Nur. Öğüt, Serdal (2016). Biyolojik Yaşlanma Nedenleri ve Etkileri, Mehmet Akif Ersoy Üniversitesi Sağlık Bilimleri Enstitüsü Dergisi, 4(1), 34-41.

Pankin, A. (2011) Mapping Digital Media: Russia, Open Society Foundaions.

Sanner, Brigid McHugh (2004). Creating Age-Friendly Websites, The Journal on Active Aging, 20-24.

Thompson, J.B (1995). The Media and Modernity: A Social Theory of The Media, Polity Press, Cambridge.

Yurdigül, Yusuf. Zinderen, İ. Ethem (2012).Yeni Medyada Haber Dili (Ayşe Paşalı Olayı Üzerinden Geleneksel Medya ve İnternet Haberciliği Karşılaştırması), The Turkish Online Journal of Design, Art and Communication 2(3), 81-91.

Political Communication and Information Technologies: Giresun Example of Social Media Usages of Political Parties

Oğuz Han ÖZTAY[1], İrfan AKPINAR[1*]

[1]Giresun University, Vocational High School of Technical Sciences, Department of Electronic Automatization Programing of Radio and Television, Giresun, Turkey

[*] **Corresponding Author:** irfan.akpinar@giresun.edu.tr

Abstract

The media are regarded as the fourth power after legislative, execution, and judiciary in the democracies according to Liberal Pluralistic Approach Political parties are trying to make mass media in order to reach the target masses and the other parts of the society. Political parties and candidates are intensely using the Internet as a means of information technology. One of the most important means of social media platforms is for the political parties and candidates to use their messages to the voters. Today approximately 60 millions people use intensive internet in Turkey. Most of the internet users also use social media platforms. The most used social media platform is Facebook in Turkey. Moreover, Turkey is in the first fancies of Twitter in comparison to populations. In the study, the social media usages the political parties which are the Justice and Development Party, the Republican People's Party, and the Nationalist Action Party in Giresun. In the contest of this study, Twitter and Facebook accounts are analyzed using content analysismethodbetween March 15th and April First 2018.The results of this study show that social media are effective in the Giresun Political parties.

Keywords: Political Communication, Information Technologies, The Internet, Social Media.

1. Introduction

One of the most important assumptions of the way of administration, which is called democracy, is inauguration of people to be elected by the people. At this point, it is important candidates to be recognized by public, which has great importance at the point of choosing who is to be chosen. The authority is, person or political party, who is going to strive for public to recognize them. For this reason, these people need to introduce themselves to the public and persuade the public who will elect them.

The election resulted from the transfer of the voting application to the massive masses - such as making their own propaganda for election and selection, introducing themselves are nowadays called as *political communication* process. When examined from the point of view of the nature, it is an indisputable fact that it is a necessary element in today's political environment. Because of this, the individuals or parties in the political environment are obligated to promote their future services to public in means of their cultural values, their ideological sensitivities, and so on with political communication. In this respect, it is useful to talk about the types of communication methods mentioned in the single structure as political communication and the methods of political communication which can be used to reach the electors or public. Even there are some differents methods and ways in sense of political communication from past to current, nowadays; meetings and conferences, conferences, brochures, concerts, trips, e-mails, media messages, banners, posters, CD's, corporate newspapers, social media, etc., are used in political communication. In addition to changing or diversifying aspects such as roads, methods and practices, the dimensions of influence of all these communication paths are also different (Erdoğan, 1997: 190).

It is not wrong to say that these methods are day-to-day from the first democratic implementations, even though the definition of the political communication, or the diversification of communication means, is based on a recent past. Moreover, that will be a good idea to take the first steps of this process up to all the systems in the election of administrators. It is also possible to see that a number of definitions have been made about the political communication that can be attributed to such contradictions of the past. The first noteworthy definition of political communication was made by Chaffe. Chaffe defines political communication such; *"The role that communication plays in the political process"* (Tokgöz, 2008: 109), as defining politics and communication as a whole. It is possible to see a more systematic and profound approach in another definition made on this subject. Political communication in this related definition is *"the process of negotiating on the messages related*

to the execution of public policy and the change of leaders, press and citizens of any country" (Perloff, 1998: 8). In a different definition, the structure of political communication is defined as *"Public discourses on the way in which public resources are distributed and the way in which official authorities in the legislative, executive and judicial systems work and how they are implemented."* (Oktay, 2002: 22).

As the function political communication is examined, *communication*it seems to have included the general features of communication as mention at the concept. As a matter of fact, constructions such as receiver, transmitter, channel, message, feedback that are considered to be essential in terms of political communication process have a fundamental point in political communication as well as a feature that increases the influence of this communication (Dalkıran, 1995: 42).

It is possible to say that the emergence of a political communication structure in today's sense is based on the second half of the 1900's, although we base it on quite old ones. The Presidential elections that took place during the mentioned periods are accepted as a turning point in this respect. At this turning point, the existence of communication tools and the use of the means of communication are very important. However, there are also those who point out that the development of this issue is multiplet and according to these individuals, the important points in development are the great importance of political communication in opposition action groups as well as mass media (Oktay, 2002: 25). The presidential elections in the United States, where political communication is first used professionally, are also remarkable in terms of applied strategies. In the periodical political communication strategies, television commercials, negative political advertisements, the use of the internet, the use of social media in the internet reveals the dimensions of political communication (Doğan, 2002: 16).

Approaching political communication studies in terms of forms in Turkey seems to have a brief professional history as well as in the world. As a matter of fact, when the studies in this area are examined, the view that Mustafa Kemal, who is accepted as the founder of the new regime, immediately after the declaration of the republic, carried out political communication personally by himself is emphasized in studies. (Çakan, 2004: 302).However, in terms of the history in political communication at Turkish Republic, it is possible to emphasize that there is more deep-rooted structure of Mustafa Kemal compared to fellow contemporary leaders. Indeed, first political communication studies are began to change the system of government but not to change the party in power on elections. However, it is not possible to talk about a wide range of communications at specified time intervals in Turkey as in America. For this reason,

utilization of technological elements in communication activities has been limited and political communication has been mainly performed in direct expressions. It is known that besides the communication channel, the general knowledge level of the people enforces a communication based on direct narration (Çakan, 2004: 302). It is been observed progress of political communication development after the end of a difficult era for Turkey aligned with the progress with them. Internet has been added recently in means of media tools addition to such as radio, newspaper, banner, television. This area has progressed by sustaining its predecessors as the emerge of new technologies. The expressions of social media in the internet structure is the transformation of the communication activities in almost all fields to a structure in which the progress of the technological innovations is due to the progressive nature of the technological innovations nowadays. (Çambay, 2015).

Of course, the possibility of political parties not taking place on a platform where communication activities are used so intensely is undeniable. This has led to the necessity for political parties to be present at social media for political communication. At this point, it is possible to see that social media experts are recruited to almost all political parties when political party approaches are examined.

2. Method

This study will examine the social media use of local party branches in Giresun of ruling and main opposition parties in Turkey, the Justice and Development Party , the Republican People's Party and the Nationalist Movement Party.

The use of Facebook and Twitter, covering the two-week period between March 15th and April 1st, will be compared with the descriptive analysis technique. Findings obtained as a result of the comparison will be interpreted according to the social media usage practices of the local branches of the political parties in Giresun.

A descriptive analysis of the social media use of the political parties within the Giresun provincial organization is as follows.

The Justice and Development Party has posted 20 posts via Facebook within the specified time period. Those are; military operations in different Islamic geographies, visits of bureaucrats from abroad, party activities (meetings, congresses, conventions, rallies), Islamic blessed days and national holidays related posts.

The Justice and Development Party made a total of 33 posts via Twitter during the specified time period. Those are; military operations in different Islamic geographies, visits of bureaucrats from abroad, party activities (meetings, congresses, conventions, rallies), Islamic blessed days and national holidays related posts. However, the posts of military operations abroad within these posts are higher than Facebook posts.

Republican People's Party has posted 28 posts via Facebook within the specified time period. Facebook posts are, party meetings, social and cultural activities and neighborhood representative, villages, nursing homes, unions etc. meetings related ones.

Republican People's Party posted 27 posts via Twitter within specified time period. Those posts are, party meetings, social and cultural activities and neighborhood representative, villages, nursing homes, unions etc. meetings related ones.

Nationalist Movement Party posted 34 posts via Facebook within the specified time period. Facebook posts are; cross border military operations, visits of party representatives, convention and meetings, caucus, party activities (theater plays, youth branches visit), Islamic blessed days and national holidays related posts, the death of important people related to ideology and national holidays related.

Nationalist Movement Party posted 2 posts via Twitter during the specified time period. Those post are, martyrs and death of politically important people related posts.

3. Conclusion

It is possible to realize that local branches of political parties are not neglected once we study Turkey's three most popular and well-established political parties' activities related to political communication on social media channels and also they carry on activities on this channel. However, it is possible to see that the social media post numbers and also contexts of posts differ from each political party to other in both Facebook and Twitter. In this respect, when we evaluate the political communication activities of the parties in the stated circles, it is possible to reach the following results.

The ruling Justice and Development Party's, the ruling party, local branch posted, in-party activities and also nationally important visits, national and religious related posts and also related with international issues has been observed as the broadest post context between political parties. We can say that political party ranked second with their post count (53) has

more informative context or broader presence on social media compared to other political parties. This can be reconciled with the party's being ruling party. It is also an important factor in ensuring that people have knowledge of national and international issues through these posts. Moreover, the party local branch Twitter posts (33) are more than their Facebook posts (20). This means that Justice and Development Party Giresun Branch is more active at Twitter. The posts are posted via those two social media networks are aligned.

The main opposition party, the Republican People's Party, is ranked number one with the number of posts in social media which is 55. However, when the party's local branch's posts are examined, it is seen that in the general sense, there is no different content except for the activities within the party in the national specific sense. At this point, it can be said that the use of social media for the party is mainly used to inform party activities. It is also possible to reconcile the party's attitude is because of their being the main opposition party. However, it is also possible to mention that , in this respect there is lack of information on the ruling parties' incomplete / incorrect practices regarding the activities of governing. In addition to this, in terms of voters or followers, misinformation can be considered as a lack of information about national and international issues. When party posts are examined, it is seen that the two social media platforms provide a homogeneous use of close to each other. Posts posted via two social media platforms are similar. In this context, it is possible to say that there is no different posts in means of social media platforms.

When the posts of the Nationalist Movement Party are examined, it is seen that there is a low presence (36) compared to the other two political parties, and this presence is focused on Facebook account. This political party, like the ruling party, uses social media in order to provide information about the activities within the party in general, while referring to national and national elements which are not party activities. It is possible to state that the party's attitude towards this issue is incomplete presence compared to other political parties. It can also be said that there are few network-specific shares, and therefore there is no restricted posts, because these few posts in the Twitter account with fewer posts are the same as those in the other social media platform.

It seems that the parties involved in the political communication structure and the purposes of this work have been lacking in informing the general activities and informally using social media in this way, but with the exception of the Justice and Development Party in addressing international issues. The transmission of the analysis of the activities carried out on this issue and the way of informing the electors creates a conscious elector mass and also an

important move for being opposition party but it is neglected by the parties. Instead of posting related to activities of political parties posting informative posts on the activities of ruling or opposition parties will be more purposeful in means of political communication. This approach, consolidating the supporters and also helping floating voters to decide, will be beneficial for political parties.

References

Çakan, I. (2004), Konuşunuz Konuşturunuz, Tek Parti Döneminde Politikanın Etkin Silahı: Söz, İstanbul: Otopsi Yayınları.

Çambay, S. O. (2015),Bir Toplumsallaşma Aracı Olarak Yeni Medya: Kuramsal Bir Değerlendirme,Karabük: Karabük Üniversitesi Sosyal Bilimler Enstitüsü Dergisi, C. 5, S. 2.

Dalkıran, N. (1995), Siyasal Reklamcılık ve Basının Rolü İstanbul: Türkiye Gazeteciler Cemiyeti Yayınları.

Doğan, İ. (2002), Özgürlükçü ve Totaliter Düşünce Geleneğinde Sivil Toplum, İstanbul: Alfa Yayınları.

Erdoğan, İ. (1997), İletişim, Egemenlik, Mücadeleye Giriş, Ankara: İmge Yayınları.

Oktay, M. (2002), Politikada Halkla İlişkiler İstanbul: Derin Yayınları.

Perloff, R.M. (1998), Political Communication: Politics, Press, and Public in America. Mahwah: Lawrence Erlbaum Associates.

Tokgöz, O. (2008), Siyasal İletişimi Anlamak İstanbul: İmge Yayınları.

Use of Communication Technologies in Political Communication Process

Yusuf YURDİGÜL[1], Yelda KORKUT[2*]

[1]Manas University, Faculty of Communication, Department of Radio, Television and Cinema, Bişkek, Kırgızistan
[2]Atatürk University, Faculty of Communication, Department of Radio, Television and Cinema, Erzurum, Türkiye

Corresponding Author: yelda.korkut@atauni.edu.tr

Abstract

Communication technologies have great prominence as technologies that almost all disciplines in our day, especially communication, use. Political communication is one of them. Communication technologies that facilitate access to the masses are very important in the political communication process. Political communication practices that exist not only in the election period but also outside the election period need to be carried out effectively. In order for this process to be effective, it is advantageous for communication technologies to be actively and appropriately used by political actors. Because it is necessary to transfer the message correctly to the target group which is scattered in political communication. For this, using all communication technologies increases both the effect of the message and the expansion of the target mass. This article establishes a conceptual framework in the context of politics, communication, technology and political communication. In order to reveal these subjects, literature review method is used. In addition, the study will conduct a field survey to determine the use of communication technologies. As an example, the political parties in Erzurum are discussed. The questionnaire to be conducted on the politicians of the party provincial administration is the method to be used in the area survey of the work.

Keywords: Politics, Communication, Technology, Political Communication

1. Introduction

"Politics", a word of Arabic origin, means "horse training." In contrast, the word “policy” taken from the west is known to be of Greek origin. In Greek, the "police" is the name given to the city-states, while the word policy means "state-owned work". Kışlalı states that it is difficult to talk about the existence of a consensus among scientists on the subject of political science. For some, the issue is limited to only the "state". However, the majority consider a wider concept, which is "power". Remarking that the notion of power is a phenomenon that involves the power of making, implementing and enforcing the decision, Kışlalı also states that the issues concerning political science cover the political processes including power formation, power-sharing and use of political power. (Kışlalı, 1999: 17-18)

Politics has the characteristics of universality and continuity in terms of time and space. The essence of politics is a view of the distribution of values in society and a conflict of interest which is a power struggle. Politics is not only a conflict but a compromise. (Kapani, 1987: 19-21)

Communication is basically expressed in a process that the idea is coded in a symbolic form to be sent to the recipient by means of a suitable means, the receiver analyzes it as a new version of the original idea and gives feedback by providing a similar cyclic process. (Steward Smith, Denton, 2012: 29)

When we define politics as a compromise between different segments of society and the focuses of power on a common ground, we can refer to communication as a process of making common symbols, discussing and agreeing on them. The works in this context are carried out through politics and politics is carried out through communication. (Smith, 1990, s. 7)
Damlapınar and Balcı state that democracy, power, government, service, success / failure, trust / mistrust, scandal, polemic, and many other similar themes have been among the main problems of the political world so far, yet the main issue of today’s politics is “communication”. Because the success of the political system and the sustainability of this success in every democratic society depends on the effectiveness and deontology of the political communication process. (Damlapınar and Balcı, 2014: 26)

Once the definition of both disciplines is cleared, political communication can be defined more easily. As the concept of political communication encompasses two very comprehensive disciplines such as "politics" and "communication", it is not possible to make a single and limited definition. Another difficulty in defining the concept as a concept is that the political communication phenomenon and its process has undergone constant changes in its

historical development. Political communication applications starting with rhetoric and propaganda, increasing population, developing technology, historical and political processes have resulted in different definitions of political communication.

The concept of political communication and its application was born and developed in the United States after the Second World War and began to be widely used in Western Europe in the 1960s. (Topuz, 1991: 7) Political communication as a concept is defined in the Communication Dictionary as "An interdisciplinary academic field consisting of research on the relations between political processes and communication processes." (Mutlu, 1994: 199) Political communication is an interdisciplinary effort that takes advantage of the theoretical, philosophical and practical foundations of different disciplines including communication, political science, history, psychology, and sociology. (Miller and McKerrow, 2010: 61-62)

The concept of political communication is examined from different perspectives. Powell and Cowart describe political communication (Powell and Cowart, 2015: 19) in terms of campaign communication in the book "Political Campaign Communication". This is an approach that includes messages submitted by candidates and politicians, which are also related to the campaign except for election periods. They also state that the political communication, which is also defined as the working process that contributes to the exchange of ideas in the democratic process, is a strategic form of communication. This strategic communication may include a discussion between two people in a convention hall, a commercial telecasting from a broadcasting vehicle throughout the campaign period, or the works of a company employee for a pay rise.

In another definition, Perloff defines political communication in the book "Political Communication" as the process of exchanging and interpreting meaning in messages related to the conduct of a nation's leadership, the media, and the citizen's public policy. (Perloff, 2013: 8-11) There are many meanings in this definition. Firstly, according to Perloff, political communication does not occur automatically; this is a process. Media, which plays a critical role in modern political communication, needs to be at the center of the political communication process. Because the communication between political agents and the public is provided through the media. Second, three actors forming the golden triangle of political communication are the leaders, the media and the people. The third is the exchange and interpretation of messages, which are characteristic of political communication. Finally, there is the widespread belief that political communication is related to elections. But the most distinctive feature of political communication is related to messages. Messages are largely related to the management or conduct of public policies. Another one of the definitions that are worth evaluating in terms

of communication is; Siyasal It is a constant single or bidirectional communication effort of a political opinion or organ by taking the advantage of advertising, propaganda and public relations techniques according to the requirements of time and conjuncture in order to ensure public confidence and support in the political system in which it operates and then to become the power. (Uslu, 1996: 790)

Factors such as professionalization of political communication activities, the use of political campaigns by public agencies in public relations and the emergence of political advertising and political marketing activities nowadays require all communication techniques that Uslu has also expressed in his definition. Uslu also referred to the continuity, which means political communication includes not only the usual period of pre-election work but also a range of sustainable non-election work. The most important step of political communication that will make a difference today is that it needs to be used after the election as well.

According to Asa Briggs and Peter Burge, technology cannot be considered without economy and industrial revolution prioritized the notion of communication revolution, which is continuous and unending. The British pioneer of the publishing in the 19th and 20th centuries, Charles Knight redefined the victory over time and the distance firstly as the effect of railways and steamships, then as the world-wide-web effect of a dozen of new media like telegraph, phone, photo, movies, computers (Brigs and Burke, 2011: 113).

Developments in technological capacity for producing, recording, transmitting and converting messages from radio to videotexes are the most noticeable events for discovering communication. Books, radio, television, computers, satellite dishes, talk shows, street shows, advertisements, and political campaigns are cultural works that remind us that we are constantly communicating and increasing our capacity to communicate. (Pearce, 1989: 4) In this context, the technological developments offer the service of mankind the tools that make it easier to reach the masses and these developments change the communication methods and tools. This change and transformation are clearly seen in political communication as well.

These transformations are clearly seen in political campaigns which is an important factor in political communication. Perhaps the biggest transformation was in the field of technology in political campaigns. Technological advances as the use of radio in the 1920s and the use of television in the 1950s in American political campaigns are considered to be just the beginning. 1952 Eisenhower used spot announcement on television for the first time in his campaign. In 1960 John Kenndy used his own electoral probe. In 1972, George McGovern led the mass e-mail, and in the 1980 Jimmy Carter he addressed his voters via teleconference. 1984 Ronald Reagen used satellite broadcasting in rallies, and in 1988 promising messages were

conveyed to voters via videotapes. In 1992, former California Governor Edward G. Brown answered questions using his own 800 phone numbers. In 1996, candidates were in a hurry to be available on the internet. (Trent and Friedenberg, 2008: 13-14) In the 2000s, communication forms of social media such as web 2.0 based Facebook, YouTube, Twitter, and blog began to be used by the political agents. In the 2008 US presidential elections, Barack Obama reached the voters especially young people using social networking sites. (Aziz, 2014: 77) Thus, developing technology has changed the form and content of campaigns. Different ways of reaching more voters have been multiplied by technology and continue to multiply.

The political speeches, which started with an oral culture, continued with public opinion, banners, advertisements, and announcements. With the development of technology, political communication has increasingly entered the process of technicalization.

The radio, of course, has an older history than television. Policy environments looked for ways to take advantage of the radio which was found before the First World War and became widespread after the war. Firstly, the Americans, then the Soviets, the Germans, and then the Italians made the radio a propaganda tool. (Topuz, 1991: 131)

In 1928, the first major initiative in America came from President Hoover. Hoover was the rival candidate to New York Governor Al Smith and Hoover won the election by gaining great sympathy via radio broadcasts. The radio used in Britain in 1923 resulted in the success of the Labor Party. In France, Radio took place in the election campaigns for the first time in 1932. Germany was the first country to recognize the importance of radio in the political field. In 1933, as soon as Hitler came to power, the propaganda minister Göbbels who said "The most powerful propaganda means is the radio " was charged. (Topuz, 1991: 131-137) The first impressive political speeches from radio to home were made in Nazi Germany. In fact, after the First World War in the United States, especially the presidential Office took advantage of a new tool by speaking to the nation on the radio; for example, President Roosevelt told the New Deal which was the solution to the 1929 world economic crisis by addressing the "forgotten people" on the radio but the changing understanding of the nature of political speech was established in Nazi Germany. (Köker, 2007: 109) This new understanding means influencing, convincing and guiding the masses.

The development of television broadcasting in the United States after the Second World War brought about the political parties' use of television as a new means of communication for political purposes. First, in the United States on November 3, 1952, the speeches on television in the elections aroused interest. Eisenhower's work with BBDO and Young and Rubicam

advertising agency in the election speeches between General Eisenhower and Adlai Stevensons gave Eisenhower the election win. (Topuz, 1991: 56-58)

Therefore, it was necessary to wait for the 1952 US Presidential elections to see a real politician-advertiser cooperation. The presidential race between Eisenhower - Stevenson in 1952 took its place in the history of communication as being the first election of the cooperation politics and advertising. The selection techniques used during these elections also show clues of a new era of political communication. (Çankaya, 2015: 75)

The 2008 presidential election in the United States was the beginning of the digital revolution in political communication. Barack Hussein Obama became the first president to realize the possibilities of the websites in the process of creating political brands and communicating with the voter. For this reason, targeting the young population as the key voter, Obama made use of the Internet technology to include young people in politics and won the voters who voted for the first time. (Çankaya, 2015: 123-124) By using digital technology, especially after Obama, who won elections in the 2008 elections by creating election strategies over social networks, this new communication medium has begun to be used in other countries. Three important developments in the relationship between politics and social media draw attention: 2008 Presidential elections and Barack Obama, the Arab Spring which was influential in the Middle East and the Gezi Protests in our country. (Bostanci, 2014: 86)

Political communication aims to influence the preferences of voters during the election periods. Whether it is traditional or new, creating an agenda with all means of communication and following the agenda are necessary for the success of a campaign. In this context, political parties and leaders have to use the communication means and the media effectively. (Ölçer, 2016: 749) It is of great importance that communication means and media that are not valid only for the election period are effectively used outside the election period as well.

2.Material and Method

2.1. Method of the Study

A literature review was conducted to form the conceptual framework of the study. A survey was conducted with 100 political agents working in the party provincial organization of the Justice and Development Party, Nationalist Movement Party and the Republican People's Party in Erzurum. The data obtained by the scanning method were subjected to descriptive analysis with frequency and Anova analysis in SPSS program.

2.2. Limitations

While the conceptual framework of the study is limited to the concepts of Politics, Communication, Technology, and Political Communication, the field research is limited to the political agents working in the party provincial organization of the Justice and Development Party, Nationalist Movement Party and the Republican People's Party operating in Erzurum province. In the study, communication technologies are determined as radio, newspaper, television, and social networks that include Facebook, Twitter, and Instagram. The study was applied out of the election period.

2.3. Research Group

100 political agents working in the party provincial organization of the Justice and Development Party, Nationalist Movement Party and the Republican People's Party participated in the study.

2.4. Analysis

The data obtained by using face-to-face survey method were analyzed in SPSS program and descriptive evaluation was utilized. Frequency and Anova analyzes were applied.

3. Results and Discussion

The study was carried out with 100 political agents working in the provincial organization of the Justice and Development Party, Nationalist Movement Party and the Republican People's Party operating in Erzurum. Participants were asked three types of questions, including closed-ended questions, multiple-choice questions, and open-ended questions. These questions directed to the participants were classified under certain categories. Accordingly, the question categories asked to the participants, questions and the data obtained from the answers to the questions were evaluated under the following headings:

3.1.Demographic information questions

The participants were asked demographic questions aimed at acquiring information such as gender, age, education level. According to the information obtained, the tables showing the demographic status of the participants are given below.

Table 1. Gender

		Frequency	Percent	Valid Percent	Cumulative Percent
Valid	female	20	20,0	20,0	20,0
	male	80	80,0	80,0	100,0
	Total	100	100,0	100,0	

Table 2. Age

		Frequency	Percent	Valid Percent	Cumulative Percent
Valid	18-33	56	56,0	56,0	56,0
	34-49	35	35,0	35,0	91,0
	50-over	9	9,0	9,0	100,0
	Total	100	100,0	100,0	

Table 3. Education Status

		Frequency	Percent	Valid Percent	Cumulative Percent
Valid	0	1	1,0	1,0	1,0
	Primary	2	2,0	2,0	3,0
	Middle School	3	3,0	3,0	6,0
	High School	26	26,0	26,0	32,0
	Upper Secondary	20	20,0	20,0	52,0
	Bachelor's	43	43,0	43,0	95,0
	Postgraduate	5	5,0	5,0	100,0
	Total	100	100,0	100,0	

Among the demographic questions directed at the participants, factors such as gender, age, and educational status were asked considering they are important factors in using communication technologies. 20% of the participants were female and 80% were male. 56% of the participants were between the ages of 18 and 33, 35% were between the ages of 34-49 and 9% were aged between 50 and over. Looking at this age range, the 18-33 age range is particularly advantageous in terms of the use of new communication technologies. As for the education status, postgraduates constituted 43% and only 1 participant had no education.

3.2. Use of traditional communication tools

In this study, the use of newspapers, radio, and television from traditional communication tools that play an important role in getting political information was asked through multiple choice questions. At the same time, multiple choice questions were also asked regarding the use of these mass medium at the local level, which is also used as a means of political information distribution.

Table 4. Printed local newspaper

		Frequency	Percent	Valid Percent	Cumulative Percent
Valid	0	2	2,0	2,0	2,0
	everyday	38	38,0	38,0	40,0
	A few times a week	23	23,0	23,0	63,0
	Once a week	12	12,0	12,0	75,0
	Once a month	4	4,0	4,0	79,0
	Once in a few months	11	11,0	11,0	90,0
	never	10	10,0	10,0	100,0
	Total	100	100,0	100,0	

38% of the participants read printed local newspapers every day, while 10% of them never read it.

Table 5. Local internet newspaper

		Frequency	Percent	Valid Percent	Cumulative Percent
Valid	0	1	1,0	1,0	1,0
	everyday	48	48,0	48,0	49,0
	A few times a week	15	15,0	15,0	64,0
	Once a week	17	17,0	17,0	81,0
	Once a month	7	7,0	7,0	88,0
	Once in a few months	7	7,0	7,0	95,0
	never	5	5,0	5,0	100,0
	Total	100	100,0	100,0	

Compared to the printed newspaper, the Internet newspaper is read by 48% of the participants every day, while it is never read by 5%. The percentage of those who read the internet newspaper every day is higher than the ones who read printed newspaper.

Table 6. Printed national newspaper

		Frequency	Percent	Valid Percent	Cumulative Percent
Valid	0	2	2,0	2,0	2,0
	everyday	39	39,0	39,0	41,0
	A few times a week	25	25,0	25,0	66,0
	Once a week	7	7,0	7,0	73,0
	Once a month	11	11,0	11,0	84,0
	Once in a few months	6	6,0	6,0	90,0
	Never	10	10,0	10,0	100,0
	Total	100	100,0	100,0	

39% of the participants read printed national newspapers every day, while 10% of them never read it.

Table 7. National internet newspaper

		Frequency	Percent	Valid Percent	Cumulative Percent
Valid	0	1	1,0	1,0	1,0
	Everyday	51	51,0	51,0	52,0
	A few times a week	20	20,0	20,0	72,0
	Once a week	9	9,0	9,0	81,0
	Once a month	7	7,0	7,0	88,0
	Once in a few months	5	5,0	5,0	93,0
	Never	7	7,0	7,0	100,0
	Total	100	100,0	100,0	

51% of the participants follow national internet newspapers everyday, while 7% of them never follow them.

Table 8. National public radio

		Frequency	Percent	Valid Percent	Cumulative Percent
Valid	0	3	3,0	3,0	3,0
	Everyday	30	30,0	30,0	33,0
	A few times a week	15	15,0	15,0	48,0
	Once a week	19	19,0	19,0	67,0
	Once a month	10	10,0	10,0	77,0
	Once in a few months	11	11,0	11,0	88,0
	Never	12	12,0	12,0	100,0
	Total	100	100,0	100,0	

TRT, which is a national public radio station, is listened by 30% of the participants every day and it is not listened by 12% of the participants.

Table 9. Private news radios

		Frequency	Percent	Valid Percent	Cumulative Percent
Valid	Everyday	29	29,0	29,0	29,0
	A few times a week	21	21,0	21,0	50,0
	Once a week	12	12,0	12,0	62,0
	Once a month	13	13,0	13,0	75,0
	Once in a few months	10	10,0	10,0	85,0
	Never	15	15,0	15,0	100,0
	Total	100	100,0	100,0	

Private news radios are listened by 29% of the participants everyday, and they are not listened by 15% of them.

Table 10. Any local radio

		Frequency	Percent	Valid Percent	Cumulative Percent
Valid	0	2	2,0	2,0	2,0
	Everyday	18	18,0	18,0	20,0
	A few times a week	22	22,0	22,0	42,0
	Once a week	18	18,0	18,0	60,0
	Once a month	15	15,0	15,0	75,0
	Once in a few months	9	9,0	9,0	84,0
	Never	16	16,0	16,0	100,0
	Total	100	100,0	100,0	

Local radios are lower than the national public radio and national private radio channels in terms of listening rate. 18% of the participants listen to local radio every day and 16% never listen.

Table 11. National public TV

		Frequency	Percent	Valid Percent	Cumulative Percent
Valid	Everyday	52	52,0	52,0	52,0
	A few times a week	21	21,0	21,0	73,0
	Once a week	10	10,0	10,0	83,0
	Once a month	4	4,0	4,0	87,0
	Once in a few months	7	7,0	7,0	94,0
	Never	6	6,0	6,0	100,0
	Total	100	100,0	100,0	

National Public television is watched by 52% of the participants every day and is never watched by 6%.

Table 12. Private TV news channels

		Frequency	Percent	Valid Percent	Cumulative Percent
Valid	Everyday	61	61,0	61,0	61,0
	A few times a week	18	18,0	18,0	79,0
	Once a week	6	6,0	6,0	85,0
	Once a month	5	5,0	5,0	90,0
	Once in a few months	5	5,0	5,0	95,0
	Never	5	5,0	5,0	100,0
	Total	100	100,0	100,0	

Private TV news channels are watched daily by 61% of the participants and they are never seen by 5%.

Table 13. Local TV channels

		Frequency	Percent	Valid Percent	Cumulative Percent
Valid	Everyday	34	34,0	34,0	34,0
	A few times a week	19	19,0	19,0	53,0
	Once a week	18	18,0	18,0	71,0
	Once a month	12	12,0	12,0	83,0
	Once in a few months	7	7,0	7,0	90,0
	Never	10	10,0	10,0	100,0
	Total	100	100,0	100,0	

Local television channels are watched daily by 34% of the participants, while 10% of them never watch.

Table 14. Being a guest on any local radio program with your political identity

		Frequency	Percent	Valid Percent	Cumulative Percent
Valid	0	1	1,0	1,0	1,0
	never	68	68,0	68,0	69,0
	Hardly any	19	19,0	19,0	88,0
	rarely	4	4,0	4,0	92,0
	sometimes	4	4,0	4,0	96,0
	often	1	1,0	1,0	97,0
	always	3	3,0	3,0	100,0
	Total	100	100,0	100,0	

68% of the participants do not be guests on local radio programs.

Table 15. Giving an interview to a local newspaper with your political identity

		Frequency	Percent	Valid Percent	Cumulative Percent
Valid	never	38	38,0	38,4	38,4
	Hardly any	31	31,0	31,3	69,7
	rarely	13	13,0	13,1	82,8
	sometimes	11	11,0	11,1	93,9
	often	3	3,0	3,0	97,0
	always	3	3,0	3,0	100,0
	Total	99	99,0	100,0	
Missing	System	1	1,0		
	Total	100	100,0		

38% of respondents do not give interviews to local newspapers.

Table 16. Being a guest on a local TV program with your political identity

		Frequency	Percent	Valid Percent	Cumulative Percent
Valid	never	73	73,0	73,0	73,0
	Hardly any	16	16,0	16,0	89,0
	rarely	6	6,0	6,0	95,0
	sometimes	3	3,0	3,0	98,0
	often	1	1,0	1,0	99,0
	always	1	1,0	1,0	100,0
	Total	100	100,0	100,0	

73% of the participants do not be guests of the programs on local TV channels and 1% of them always participate in the programs.

3.3. The preferences of using communication tools and social media usage questions:

Table 17. Weekly internet usage

		Frequency	Percent	Valid Percent	Cumulative Percent
Valid	0	1	1,0	1,0	1,0
	1-10	31	31,0	31,0	32,0
	11-20	23	23,0	23,0	55,0
	21-30	16	16,0	16,0	71,0
	31-40	9	9,0	9,0	80,0
	41-50	6	6,0	6,0	86,0
	51-over	14	14,0	14,0	100,0
	Total	100	100,0	100,0	

31% of the participants have 1-10 hours, 23% have 11-20 hours, 16% have 21-30 hours, 9% have 31-40 hours, 6% have 41-50 hours, 14% have over 50 hours of internet usage.

Table 18. The preferences of using communication tools

		Frequency	Percent	Valid Percent	Cumulative Percent
Valid	0	1	1,0	1,0	1,0
	Computer	21	21,0	21,0	22,0
	Mobile phone	78	78,0	78,0	100,0
	Total	100	100,0	100,0	

When the participants were asked about their computer and mobile phone preferences from the communication tools, 78% answered the mobile phone as the first choice and 21% answered the computer as the first choice. 1% do not prefer either tool.

Table 19. The frequency of Facebook use

		Frequency	Percent	Valid Percent	Cumulative Percent
Valid	0	2	2,0	2,0	2,0
	Everyday	67	6,0	6,0	8,0
	A few times a week	8	3,0	3,0	11,0
	Once a week	7	7,0	7,0	18,0
	Once a month	7	7,0	7,0	25,0
	Once in a few months	3	8,0	8,0	33,0
	Never	6	67,0	67,0	100,0
	Total	100	100,0	100,0	

67% of participants use Facebook daily, 6% do not use Facebook.

Table 20. The frequency of Twitter use

		Frequency	Percent	Valid Percent	Cumulative Percent
Valid	Everyday	58	58,0	58,0	58,0
	A few times a week	12	12,0	12,0	70,0
	Once a week	3	3,0	3,0	73,0
	Once a month	4	4,0	4,0	77,0
	Once in a few months	3	3,0	3,0	80,0
	Never	20	20,0	20,0	100,0
	Total	100	100,0	100,0	

58% of the participants check on Twitter every day and 20% of them do not have a Twitter account.

Table 21. The frequency of Instagram use

		Frequency	Percent	Valid Percent	Cumulative Percent
Valid	0	1	1,0	1,0	1,0
	Everyday	60	60,0	60,0	61,0
	A few times a week	13	13,0	13,0	74,0
	Once a week	6	6,0	6,0	80,0
	Once a month	2	2,0	2,0	82,0
	Once in a few months	18	18,0	18,0	100,0
	Total	100	100,0	100,0	

60% of the participants are on Instagram every day, while 18% have Instagram account.

Table 22. Sharing political content on Facebook

		N	Mean	Std. Deviation	Std. Error
	Everyday	67	4,06	1,816	,222
	A few times a week	16	3,19	1,721	,430
	Once a week	2	1,00	,000	,000
	Once a month	5	2,00	1,000	,447
	Once in a few months	2	3,50	2,121	1,500
	Never	8	1,75	1,753	,620
	Total	100	3,56	1,914	,191
Model	Fixed Effects			1,763	,176

Table 23. Sharing political content on Twitter

		N	Mean	Std. Deviation	Std. Error
	Everyday	58	4,40	1,696	,223
	A few times a week	12	3,25	1,712	,494
	Once a week	3	3,00	2,000	1,155
	Once a month	4	2,00	,000	,000
	Once in a few months	3	2,33	1,528	,882
	Never	20	1,40	1,188	,266
	Total	100	3,46	1,972	,197
Model	Fixed Effects			1,583	,158
	Random Effects				,956

Table 24. Sharing political content on Instagram

		N	Mean	Std. Deviation	Std. Error
	0	1	2,00	.	.
	Everyday	60	3,48	1,855	,239
	A few times a week	13	2,69	1,494	,414
	Once a week	6	3,83	1,941	,792
	Once a month	2	3,00	1,414	1,000
	Once in a few months	18	1,39	1,195	,282
	Total	100	3,00	1,859	,186
Model	Fixed Effects			1,710	,171
	Random Effects				,632

4. Conclusion and Implications

Although changing and transforming political communication is interpreted as the process of creation, distribution, and perception of political information in advance, it is no

longer limited to a simple data exchange. Managing with a control on this process with the communication technologies developed in modern understanding is a more effective method. In this context, it is necessary to take an active role in this transformation in political communication by using communication technologies effectively. Because communication technologies are both one of the reasons for this process and they contain important tools to manage the process well.

In pre-modern societies, Canvassing has been used as an effective method and still continues. In the modern period politics, newspapers, books, radio, television, cinema, magazines and posters started to take an active role in the mass media of mass communication. The radio, newspaper and television which are among the communication tools that people can use to get informed about political events out of the election period transmit one-way messages. They do not see their receivers and have a closed structure. The viewer / reader / listener is in the passive position. Developments in electronic communications provide a cheap and easy way to deliver messages to more audiences. These new media networks launched by Barack Obama in the 2008 elections with social media is a new method used both during the election and the election period which is free of charge, interactive and exempt from geographic limitations. Highly costly political campaigns prepared and carried out by agencies during the election campaigns require serious budgets. In this era, this process can be carried out at no cost through social media.

The traditional means of communication, which are especially used in American election campaigns and spread all over the world, are an indispensable element in political communication. In addition, with new communication technologies, new media directs the use of political communication in the world. For this reason, all communication technologies should be used at the same time to communicate with the target audience who are locally dispersed. It is important to determine which tool is suitable for transmitting which message. Because each vehicle is not suitable for every message, each vehicle has its own characteristics. At the same time, the target audience is fed through different channels of communication and reaching them will make it easier to reach more people by using different communication technologies.

Among the results obtained in the study, television is the most preferred choice in getting political information. The use of local mass media for the dissemination of political information is insufficient. The use of social media accounts to close this gap may be effective. However, although social media accounts of the participants are available, there is no active use. It seems passive also in producing political messages. As a suggestion, trainings, seminars and courses can be organized in the provincial organizations of parties to ensure the adaptation

of political agents to new communication technologies. Especially communication technologies, which are the most important stakeholders of political communication, and the way to use them appropriately can be assisted by communication faculties and academics.

References

Aziz, A. (2014). *Siyasal İletişim*. İstanbul: Nobel Yayınları.

Bostancı, M. (2014). "Siyasal İletişim 2.0." *Erciyes İletişim Dergisi*, Akademia, 3(3), 84-96.11

Çankaya, E. (2015). *Siyasal İletişim Dünyada ve Türkiye'de*. (1.baskı). Ankara: İmge yayınları

Köker, E. (2007). *Politikanın İletişimi İletişimin Politikası*. (1.Baskı). Ankara: İmge yayınları.İstanbul: Kriter Yayınevi.

Kışlalı, T. (1999). *Siyaset bilimi.* Ankara: İmge Kitapevi.

Damlapınar Z.- Şükrü B,(2014). *Seçimler,Adaylar, İmajlar,* Literatürk academia

Miller, J. L., & McKerrow, R. E. (2010). History of political communication. Review of Communication, 10(1), 61-74.

Mutlu, E. (1994). *İletişim Sözlüğü.* Ankara: Ark Yayınları.

Ölçer, N. (2016). "1 Kasım 2015 genel seçimleri örneğinde siyasi parti liderlerinin Twitter kullanım pratikleri". *Gümüşhane Üniversitesi İletişim Fakültesi Elektronik Dergisi*, 4(2).

Özkan, N. (2014). *Seçim Kazandıran Kampanyalar*. (4. Baskı). İstanbul: MediaCat Kitapları.

Pearce, W. B. (1989). *Communication and the human condition*:SIU Press.

Perloff, R. M. (2013). *Political communication: Politics, press, and public in* America:Routledge.

Powell, L., & Cowart, J. (2015). *Political campaign communication: Inside and out*. Routledge.

Topuz, H. (1991). *Siyasal Reklamcılık: Dünya Ve Türkiye' den Örneklerle.* İstanbul.

Trent, J. S., & Friedenberg, R. V. (2008). Political campaign communication: Principles and practices. Rowman & Littlefield.

Explaining The Divorce Which Causes Certain Social Problems in Cartoons

Gülşah DOĞANAY[1*]

[1] Giresun University, Vocational High School of Technical Sciences, Department of Architecture and City Planning, Giresun, Turkey

[*] **Corresponding Author:** gulsah.doganay@giresun.edu.tr

Abstract

The cartoons address various subjects about people and society in an artistic and exaggerated manner and have a unique language of communication with its own aesthetic qualities hence are used in a variety of areas. The change in society and human relations has also caused changes in family structure. Increased urbanization with industrialization has encouraged migration from the village and the large family has given its place to elementary family. Social and economic changes have paved the way for some contemporary problems in the familial structures. One of these problems is the increase in divorce rates. As it is known, there are very different reasons for divorcing. The objective of this study is to explain some reasons for divorce in Turkey, as given in cartoons. In this context, some divorce reasons as represented in cartoons, were addressed. Cartoons are used mostly in politics, but also in all subjects that are of concern for the society. Cartoons can shake thoughts and beliefs of individuals due to their thought-provoking and humorous nature and catchy characteristic. The individual questions himself and his society in cartoon's specific language. Being able to question and be questioned are two of the most important human characteristics. Even without needing to use any language, the cartoons are powerful tools that can induce laughter and questions at the same time and for that very reason, the cartoon is a stance against all kinds of authority and power. In the scope of this study the divorce and its reasons in Turkey are examined by using such characteristics of the cartoons. This research is qualitative study and it is prepared using the descriptive method. The cartoons used in the study were drawn by İbrahim Çırak. This study aims at drawing attention to the ever-increasing divorce rates in Turkey and raise awareness based on gender equality. It is beyond doubt that replacement of traditional roles in family with an equalitarian understanding will facilitate co-existence of family members.

Keywords: Cartoon, Divorce, Design, Marriage, Art

1. Introduction

Divorce is a hyperdimensional and complex phenomenon. For this reason, different disciplines engage in extensive researches in this subject. The phenomenon of divorce affects not only individuals but also the society as a whole in various aspects such as psychological, social, economic etc. Presently, divorce has become an important issue in Turkey (Doğan, 2016, p. 992). Naturally, it is not fair to address the phenomenon of divorce as a problem. Nonetheless, increase in the divorce rates and corresponding changes in the society can be characterized as contemporary global problems. Marriage and divorce directly affect the changes in population and in family structures and indirectly affect the population size (Turkish Statistical Institute). For this reason increases in the divorce can in return cause certain familial and population problems. This study aims at drawing attention to increasing divorce rates in Turkey and its reasons through use of cartoons.

Divorce is a legal process where all marital bonds between the parties of a legally acknowledged marriage as husband and wife by a decision of a judge, reserving the rights concerning the children, if any which allow the parties to marry again, with others (Arıkan, 1996, p.33) It is legal termination of marriage. In this sense, it dissolves the marriage between the man and the woman through a legal decree allowing the parties to get married again (Turkish Statistical Institute, 2011, p.10). Naturally, there are countless reasons for divorcing. According to a study by SEKAM the leading reasons for divorce in Turkey are disloyalty (%24,5), physical abuse (%17,6), lack of love (%17,4) and additions such as alcohol abuse and gambling (%17,3), respectively.

The Turkish Civil Code numbered 4721 categorizes the reasons for divorce into two sub-groups as related to private or public interest.

Reasons Related to Private Interest:

1. Adultery
2. Attempt against one's life
3. Committing an offense and leading a disreputable life
4. Abandonment
5. Mental incapacity
6. Breakdown of marriage
7. Maltreatment, degrading treatment

Reasons Related to Public Interest:

If the bond of marriage has abolished irremediably due to any unpredictable reasons as a result of which the couple cannot be expected to share conjugal life, this is considered as a reason of public interest. Therefore, it can be stated that adultery, attempt against one's life, committing offense, abandonment, mental incapacity, leading a disreputable life, breakdown of marriage and degrading treatment can be considered as marital problems that lead to divorce. According to data from 2016 research by TÜİK, irresponsible and indifferent behavior ranks the first among all the problems that lead to divorce for both men and women in Turkey.

Among the reasons that damage the familial unity the most and hence resulting in divorce or domestic violence and breakdown of marriage: adultery, indifference, rudeness, irresponsibility, diminishing of love and mutual respect, anger, miscommunication, interventions by relatives, substance abuse and addictions, selfishness, poverty, ignorance, disproportional reactions, violation of privacy, intolerance, discontent are some of the main factors. It is even possible to posit that the number of problems equals the number of the unhappy families. As Tolstoy said: "Happy families are all alike; every unhappy family is unhappy in its own way" (Çayıroğlu, 2016, p.12).

In general, the families in crisis try to maintain their family union despite a multitude of problems before divorce. On the other hand, it is also a fact that the couples do not seek solutions to their marital problems or help until they are in a full-scale crisis and facing divorce. The fact that women consider miscommunication, economic problems, problems with the in-laws even domestic violence as a cross to carry for long years and they do not even think about divorce until domestic violence becomes life-threatening or until their husbands have an affair with other women indicates that women endeavor to maintain their marriage (Uçan, 2007, p.45). Irrespective of its actual reason, divorce causes certain problems for the individual and the society. There are many studies that highlight ever-increasing divorce rates in today's world. This study focuses on some reasons of divorce in Turkey as represented in cartoons.

Humor, in written form, develops in parallel to its times. Similarly, whether in the form of painting, sculpture, cartoon or graphics, the visual humor mirrors its age. Cartoon is one of the most important forms of visual humor. A cartoon is the drawn form of humor. As the number of definitions for humor is countless, the same applies for the cartoon (Yardımcı, 2010, p.27)

By going beyond the limits of humor, the cartoon has become rather popular in the academics in recent years. The academic studies on cartoons, especially in the fields of visual arts, education and communication sciences has been more frequently created in recent years.

According to Turkish Linguistic Society's definition, a cartoon is "*a humorous drawing that depicts any aspects of people's and society's life in an exaggerated, thought-provoking manner*". The cartoon is often associated with satire and critique. The goal of the cartoon, if anything, is to target the pressures of most powerful segments of the society on the others. For this reason, given its antagonistic, ever-questioning and unyielding characteristics, the cartoon creates a resistance against pressure and authoritarianism especially in societies where they occur (Erdem, 2007; as cited in Deniz, 2017, p.491).

What is Cartoon:

It is exaggerated drawings of people or objects. A cartoon is, first and foremost, humor. A drawing technique in the form of humor. Today, the cartoon is the art of humor in drwaing (Şenyapılı, 2003, p. 133).

The word cartoon derives from Italian "Caricare" which means "charging, conveying the grotesque". Cartoon is a product of enlightenment and first occurred in renaissance Italy (1946). Some people credit the term cartoon to Annibale Carraci, author of the book "Arti di Bologna / Arts of Bologna" whereas some others claim that Mosini, who penned the foreword of the same book, was the actual inventor of the term (Şenyapılı, 2003, p. 14-15)

What Does Cartoon Tell?

Trough criticism of different public personalities or institution, the cartoon allows public discussion of important social issues, unearthing or exposing problems which might be difficult to be discussed otherwise. "As a popular form of art, cartoon can directly interact with everyday citizen with masses regardless whether they have special interest in art or not. Despite evident lack of an integrative approach towards the drawing style and contents of the cartoon, it can be stated that we have a mass sensitivity towards cartoon-related publications" (Özsezgin, 1988; as cited in Öğüdü, 2011, p.19).

2. Objective

General objective of the present study is to draw attention to the divorce as a trending issue and to depict the divorce and its reasons in Turkey through cartoons. Humorous approach of cartoons as well as their function as intriguing visual elements allows it to influence popular

perception of issues and facilitate critical approach to social problems. In this study, various cartoons are used to depict some of the reasons behind increasing divorce rates. The rationale behind selection of the cartoons as well as the general objectives of the study were shaped by following questions:

1-What is divorce?

2- What are the reasons for divorce in Turkey?

3-Why the increase in divorce rates pose a problem?

4-What is cartoon?

4- What are the social effects of cartoon?

Visual arts have very high influence on individuals and masses. As a form of humor, the cartoon has the power to compel thoughts and laughter at the same time. For this reason, cartoon has been subjected to many studies in various fields such as sociological, political and educational areas. In addition to its humorous aspects, cartoon is a powerful tool for critical approaches and for this reason it was decided to underline, to highlight the phenomenon of divorcing by using cartoons.

3. Method

This study was designed as a qualitative research. A “qualitative research” is a method of academic study wherein qualitative data collection methods such as observations, interviews and document analysis are used in a qualitative process towards understanding perceptions and events in a realistic and integrative manner in their natural environment. (Yıldırım & Şimşek, 2016, p.41). The cartoons included in this study were interpreted by using content analysis method. The content analysis method is frequently used for visual elements such as paintings or television programs (Büyüköztürk, Kılıç Çakmak, Akgün, Karadeniz & Demirel, 2016, p. 250).

4. Findings and Interpretation

In this study, the cartoons depicting reasons for divorce in Turkey were interpreted. In addition to direct narration, connotative interpretation of the cartoons was also provided.

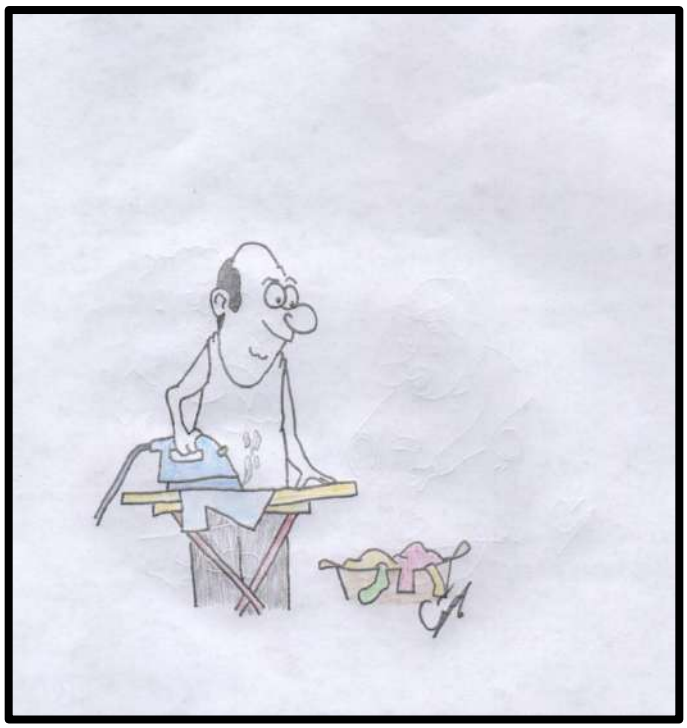

Cartoon 1. Regarding chores as a woman's duty

Narrative: This cartoon depicts a character: a man ironing clothes. The man is doing a chore contrary to social assent. He seems unhappy. He symbolizes loneliness and bachelorhood. In social perception, chores are women's duty. A divorced man is symbolized as a man doing chores hence a miserable man. The cartoon depicts a male character doing chores, which does not closely fit the traditional understanding of a man's job. The society perceives chores as a woman's duty. In fact, lack of sufficient meticulous attention to chores or asking for the man's help for doing chores can result in divorce.

Biological sex and gender are so closely correlated that it is very difficult, even impossible to dissociate them. The traditional culture of the society expects ***female*** behavior, thoughts, beliefs, appearance, attitude and perceptions from ***women*** and ***manly*** behavior, thoughts, beliefs, appearance, attitude and perceptions from men. The social perception defines limits for individual's identity and the social control does not allow the individual to breach those limits. This discrimination is considered as a main property of culture which functions to create a world where the individual can live **comfortably**. But unfortunately, this merely serves for creation of a world where traditional gender discrimination prevails. Environmental conditions and biological differences between the sexes, has made women more attached to house and guided them towards less physically demanding occupations and professions to a passive position before man and guided men towards social life/space, towards more physically demanding

professions and occupations hence towards an active position above women. Normally, man is the subject and the woman is the mere object (Vatandaş, 2007, p. 48).

Cartoon 2. Economic reasons

Narrative: Two characters appear in this cartoon: the woman is depicted as an irresponsible person who always goes to shopping whereas the man is the victim of woman's senseless expenses and struggling to meet the needs. In practice women are usually pressurized by their husbands and by the society in general for being economically irresponsible and for not managing the family finances properly. With a connotative interpretation, this cartoon depicts a man who is obliged to earn the bread and a woman who puts extra burden on the family finance with luxury and unnecessary expenses hence damaging the unity of the family. In this age of consumption frenzy, the divorce is caused by economic reasons in most cases. But most of the time, women are accused as usual suspects and are subjected to economic violence not only by their husbands but also by the society.

Researches indicate that women are continuously exposed to different forms of economic violence both in domestic and in public space. In domestic terms, a woman's participation to economy to generate income can be prevented by the husband, the children and even by the parents and relatives. In other cases, women are forced to work at jobs that they do not want or all of the money they earned can be taken away from them or be burdened with the

entirety of economic responsibility. Additionally, there are numerous types of economic violence that the women can face in their families. The women are considered to bear the chief responsibility for countless domestic chores required for reproduction of the family but are often disappointed by the treatment they receive in return. Some families even seek for ways to deprive women's inheritance rights and force women to waive them. In the case of divorce women often suffer economic violence in division of assets. Women's crystallized labor for years of hard work in the house is simply dismissed and become invisible in the event of divorce. Economic violence suffered by women is the most effective form of violence. Economic independence is directly linked to the strength to cope with circumstances that negatively affect the phycological and corporal well-being of the woman. Economic dependence is the weakest spot of woman that most exposes her to other forms of violence (Eşkinat, 2013, p. 292)

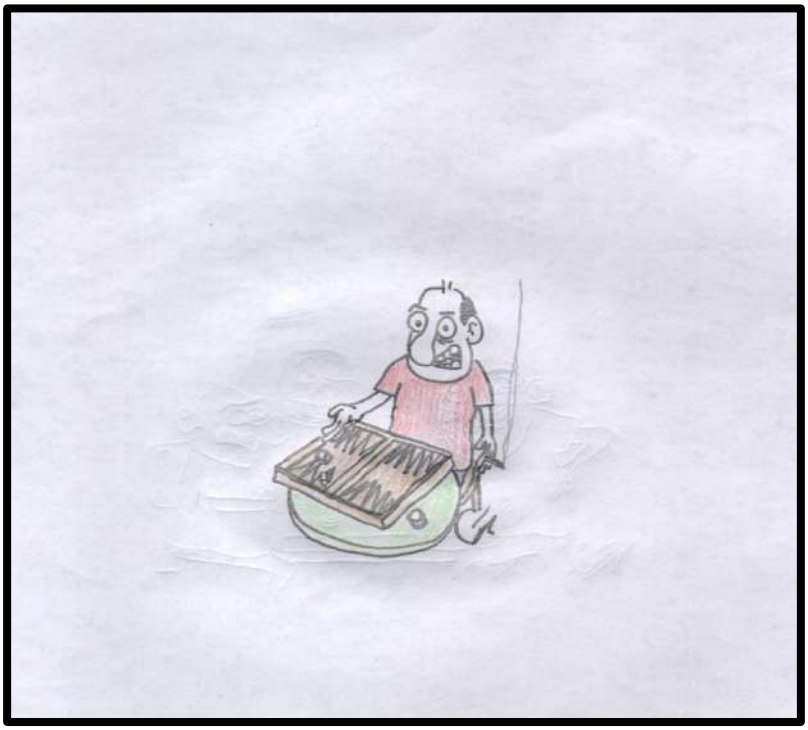

Cartoon 3. Gambling and Other Bad Habits

Narrative: There is only one character in this cartoon. This person is characterized as a gambler and ill-tempered. He is depicted as a man who gambles, chatters and swears all the time. Gambling is a bad habit that causes many social and familial problems. In cartoons, a gambler keeps losing money but believes that the lady luck will smile him soon. Getting lonelier and losing everyone he loves, the gambler cannot give up his habits on the belief that he is going

the win something someday. This cartoon tells us about the damages of the gambling to the family and highlights its importance as one of the reasons for divorce.

Gambling is a bad habit that starts as an occasional fun but quickly escalates into a raging menace that cause increasing losses and neglecting family, work and so on. One of the leading motives behind gambling is the bitter sweet excitement of the risk. When a gambler loses money, he tends to hide this out of guilt. Once started, a gambler plays down to the last dime. The gambler often ends up committing theft, fraud or embezzlement to pay his debts. Gambling is a predominantly male habit. It is a serious problem that affects the family life and causes divorce (Büyükkaragöz, 1993, p.76).

Cartoon 4. Underaged Marriage

Narrative: There are two characters depicted in this cartoon. First is a little girl playing with a teddy bear and the second is a much older man. Underaged marriage is a serious problem in many places in the world. This cartoon underlines this issue and draws attention to inappropriateness and negativity of underaged marriage. In a connotative light, the cartoon shows a frightened, timid little girl holding her teddy bear and a man, unmoved or troubled with the age of the girl. This cartoon underlines the inappropriateness of underaged marriage and criticizes social acknowledgement of and lack of sufficient social reaction against this issue. Underaged marriage cannot be accepted. This cartoon depicts the impacts of underaged marriage on the divorces.

"Kid brides" are little girls under eighteen, forced into marriage which is legitimized by the social sphere after marriage is blessed in a religious ceremony or in other words by "imams" performed upon consent of the parents of the kid.

The passage taken from Tarımeri gives a clear idea about the situation: "*Girls often become mothers under the age of 18 especially in Eastern and Southeastern Anatolia where underaged marriage is an everyday phenomenon. In Diyarbakır Maternity Hospital, which receives patients from all provinces in the region, 573 girls gave birth under the age of eighteen in the year 2010; the same number for the year 2011 was 520 and 193 kids became mothers in this hospital only in the first six months of this year. Approximately 20 thousand births are performed annually in this hospital and 20 kids of 13 years of age gave birth in this hospital.*" (Tarımeri, 2013, p.8).

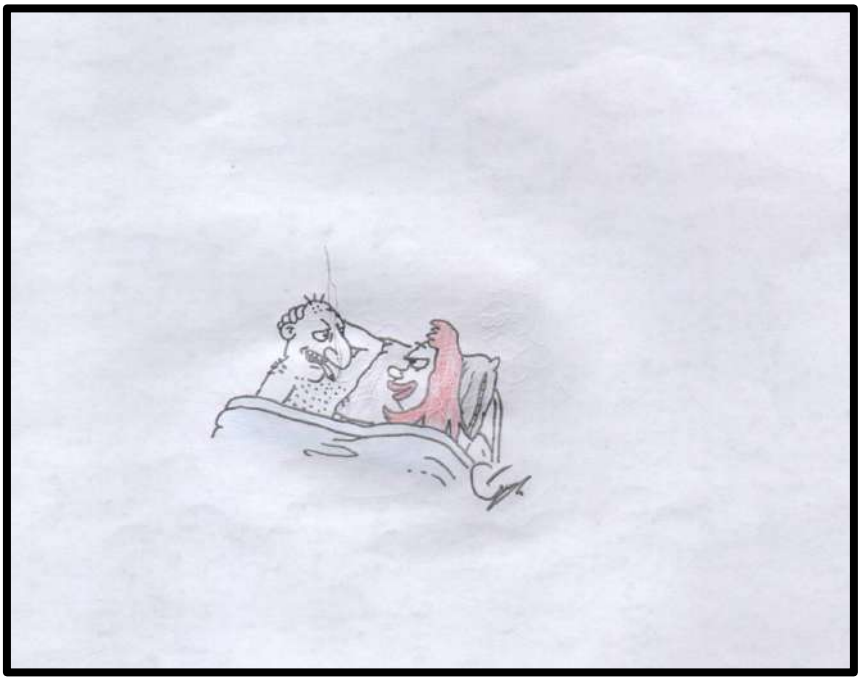

Cartoon 5. Sexual Problems

Narrative: Two characters appears in this cartoon. The man is depicted as sexually eager whereas the woman hides under the blanket and is angry about man's eagerness. This cartoon refers to the common "I have a headache" theme and similar jokes and underlines the importance of sexual activity in the marriage. In a connotative interpretation this cartoon tells us about the social convention that woman, who is dear jewel of the home, must not only do all the chores in the house but also satisfy the sexual needs of her husband. Also, it is suggested

that a happy marriage can be achieved through sexual harmony. Sexual problems have always been one of the chief reasons for divorce.

Sexual health, sexual equality requires fairness and respect. If gender inequalities and power imbalances can be positively transformed through good interpersonal relationships, sexual health will be positively affected. Sexual life should be free from forcing and exploitation. In some cases, sexuality could easily become the oppressive tool of the stronger on the weak. Sex can be the tool of oppression between the man and the woman, rich and the poor, employer and the employee, captor and captive. Sex must be based on mutual trust, consent, devotion and respect. Sexual relations should be dominated by love, sharing and mutual care. In a relationship of mutual love and respect, sex would be more satisfying. To achieve a sexually healthy status, all individuals, including the youth, should have life-long access to extensive sex education, sexual health information and services. To be sexually responsible, all individuals need to obtain necessary knowledge and information (Bozdemir & Özcan, 2011, p.40).

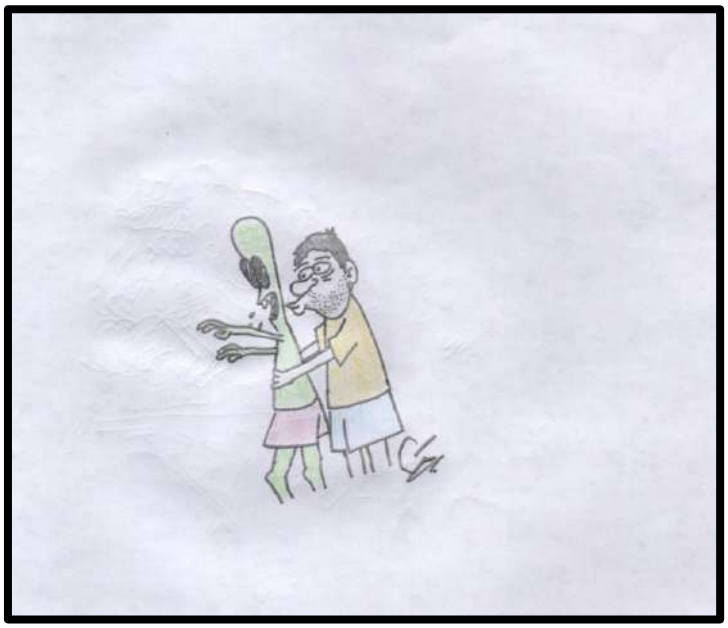

Cartoon 6. Foreign Woman (Immigrant Woman) and Second Wives Problem

Narrative: This cartoon depicts two characters. Man is the passionate, sexually eager character. “Alien” is panicked and frightened. Female is the object of desire while the man is the one “desiring”. The cartoon depicts the theme of “foreign woman”. The cartoon shows a female alien character which appears to be desiring to communicate with mankind and to know a new civilization is harassed by a male earthling. The drawing connotes the harassment

suffered by the refugee women in Turkey, that they are often taken as second and even third wives and the marriages that end for this reason.

According to a 2015 report by ORSAM the most noteworthy development in this regard is the fact that young and old, single and already married Turkish men take young Syrian women as their second wives. This occurs most intensively in Kilis, Şanlıurfa and Hatay provinces and causes dissidence in local people especially women. The divorce rates are sky-rocketing in these three provinces especially due to the issue of "Syrian Bride". The official record does not show any significant increase in marriages with Syrian women but the real numbers are extremely high. In fact, generally the Syrian marriages take place merely through religious ceremony. For instance in Kilis Province, it is asserted that approximately %20 of all divorces are originating from Syrian-bride-related problems. Women often complain pressure due to fear of losing their husbands and accuse Syrian people for enticing their husbands. Worst, there is an economic aspect to marriages with Syrian women. Men who wish to marry a young Syrian girl apply to intermediaries and pay a brokerage fee. A bride price is also paid to the family of the Syrian girl. Syrian families consider such marriages both as a way to gain money and to save their daughter's life. This problem is most frequent in Şanlıurfa and Kilis provinces. Yet another dimension of this problem involves exploitation of young kids. In fact, marriage with underaged Syrian girls is not a rare occasion.

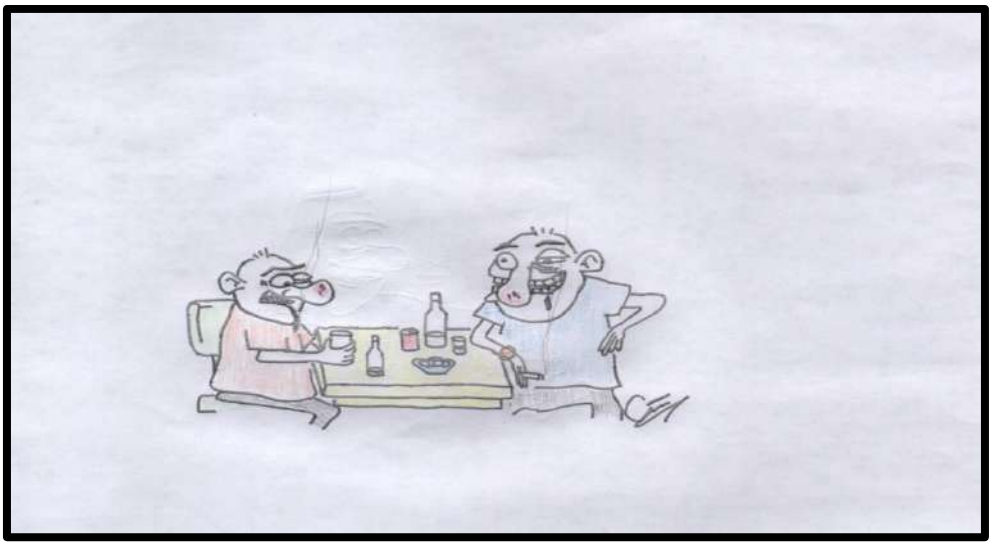

Cartoon 7. Alcohol Abuse

Narrative: This cartoon depicts two characters. Drunkards on the table without a care in the world is the chosen theme of the cartoon as a reflection of negative aspects of the alcohol addiction. The cartoon connotes times poorly spent on alcohol drinking instead of family and

shows us devastated personalities. The drawing tells about the negative impacts of alcohol abuse on the marriage.

According to World Health Organization any person whose alcohol abuse restricts the physical and psychological wellbeing and affects the interpersonal relationships and hinders performance of his/her social and economic duties is called an alcoholic (Büyükkaragöz, 1993, p.76).

Destruction of family structure through disturbance and violence means complete destruction of the family which is the nucleus of a society. According to a 2006 report by Turkish Statistical Institute, %12.2 of all divorces are caused by alcohol and gambling addiction. In the year 2008 a total number of 99.663 couples get divorced. When calculated over said percentage, the number of couples divorced due to alcohol abuse is 12.158. However, considering that alcohol can also be the root cause for other reasons of divorce such as irresponsibility and indifference to the livelihood of the house, disrespectful behavior, beating, maltreatment of wife and children, alcohol abuse actually have much more influence on divorces (Babuna, 2011, p.18).

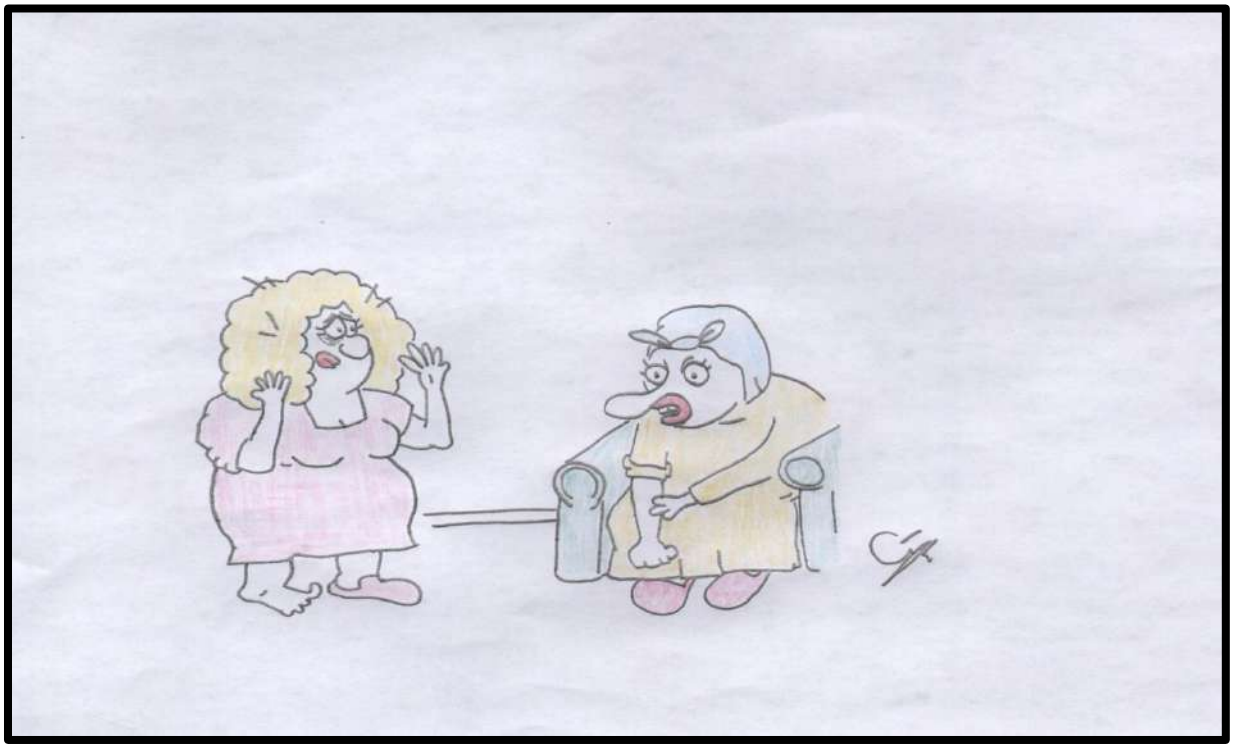

Cartoon 8. Domestic Violence and Problems with In-laws

Narrative: This cartoon depicts two characters. The daughter in-law is depicted as a tired woman who shuttles between chores and even loses one slipper on the route. Mother in-law, on the other hand, is depicted as a grumpy crone who even inflict violence to her daughter in-law.

In Turkish culture, an ideal woman should take care of her husband's parents and assume all responsibility for household chores without any complaints. This cartoon tells us about the domestic violence a woman suffers.

In traditional societies, internalization of gender roles would lead to the mentality that considers violence towards woman as a normal thing. Developments in mass communication systems, changes in mental patterns on gender roles, development of educational opportunities and women's economic freedom by extension has made the violence against women more visible and tore down the mentality that considers violence as a normal destiny for women hence triggered increase in divorce rates. In conclusion the reasons of divorce in Turkey includes domestic violence against women, economic dependence of women, difference between genders concerning gender roles, spousal abuse, parents' involvement and disruption in couples' relationships, addictions and economic problems (Günindiersöz, 2011, p.261).

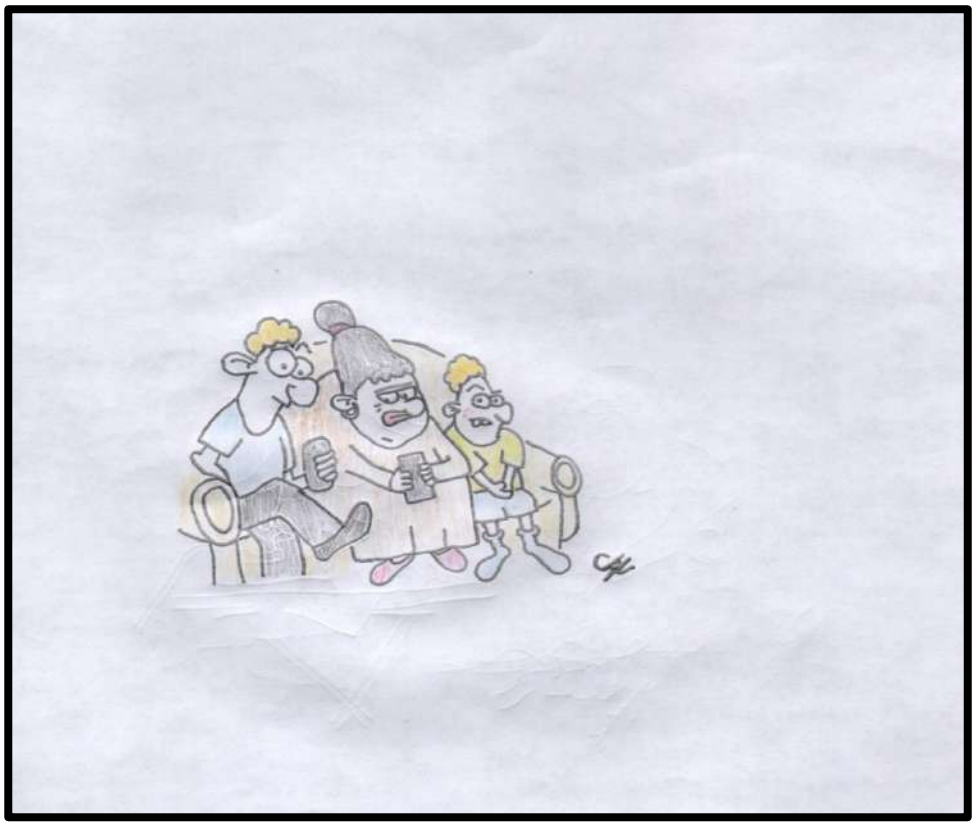

Cartoon 9. Communication and Social Media Addiction

Narrative: This cartoon depicts three characters, namely mother, father and child. This cartoon tells us about a family that do not have any communication despite being at the same place. Spending too much time with their phones, the parents fail to spend any time with their

child. Connotationally, the child is unsettled, as if he had a bad exam and he is actually happy that it was not noticed. On the other hand, the mother seems to follow lives of others on social media and is saddened by not having a similarly spectacular life. The father follows up exchange market and foreign currency exchange rates. The family has zero communication and interaction despite being at the same place. The cartoon underlines the misuse of social media and its impacts on breakdown of marriages.

With fast-paced developments in communication technologies, the mass communication tools have practically become a weapon to rule, guide and control the society. From warmongering news pieces to advertisements of food, the mass communication media decides what to think, what to eat and with whom to fight. Effectiveness of mass communication tools in convincing people and determining their agenda, brought power wars over the ownership of these tools. In fact, ownership of the mass media is an important factor for strengthening elf-legitimacy of owners of power and capital (Ünür, 2016, p.2).

Researches show that media affects families in various ways. First, privacy of family gets torn apart day by day. Behaviors and relationship formats that are not compatible with traditional Turkish family structures and culture is propagandized in media. In fact, the media is a prevailing factor in adultery. Therefore, the mesdia has various negative impacts on family (Küçükcan, as cited in Doğan, 2016, p.1).

A divorce study by ASAGEM, which was published in 2009, showed that intrafamilial communication problems ranks the first place among the reasons for divorce. Results of the study also suggests that media is an important factor that leads to lack of intrafamilial communication and hence to divorce (Doğan, 2016, p.8).

Studies allege that, by allowing people to share their entire life with the whole world, the social networking sites such as Facebook and Twitter abolish privacy and confidentiality and completely eliminate the sense of intimacy and deepen the envy. It is seen that the social networks and social media are extremely influential especially on digital natives and has complete control on their life styles, habits, entertainment and learning behavior. It would not be surprising to see copied minds after a certain period of time. For this reason, especially parents should question themselves whether they spend sufficient quality time with their children (Yıldız, 2012, p. 529).

5. Conclusion and Suggestions

Divorce is a significant global problem. There are many studies conducted on solutions against divorce because the divorce has impacts on social, economic, psychological and populational structure of individuals and of the society. Studies are focused on different solutions. Any reduction of divorce would depend on understanding the factors affecting it. For this reason, the reasons lying behind the rapid acceleration of divorce rates should be determined and preventive measures should be implemented.

As any other human problem, the divorce can be resulted from various reasons nowadays as any change in the world would lead to changes in human problems. The roles of individuals change; so does the family structure in the entire society. Any study on divorce that aims at presenting solutions, would need to consider the regional differences and influence of traditional and religious structures. In Turkey, reasons for divorce slightly differ by the geographical regions yet it can be said that main problems are the same for all regions. For instance, second-wife does not considered as a problem in rural areas but it does and it should pose a problem in industrialized, larger urban areas.

A divorce is the sum of flaws in marriages, lack of sufficient and effective communication and conflicts between the couple. A couple divorces when they cannot healthily overcome such obstacles. A divorce is not a problem in itself. Yet the reasons that accelerate the divorce rates so high do pose a problem. Naturally, unity of the family is of great importance yet individual happiness, physical and psychological health of individuals are more important than anything else. Therefore, studies should not strive to eliminate the divorce but should try to determine the reasons behind and suggest solutions for measures to be implemented. For instance we believe that governments have great responsibility in eliminating economic problems in preventing economic distress and in supporting families in economic distress which is one of the most significant factors that magnify stress in marriages. Elimination of economic problems and supporting women's economic independence are of great importance. It can be stated that women are more aware and more sensitive towards determining and providing for the economic needs of the family. In Turkish society, there are none or extremely rare examples of women spending away the family funds to their addictions such as gambling or alcohol abuse.

In this study we have addressed a selection of reasons of divorce in Turkey by using the critical language of cartoons. As a result, by combining the element of laughter of the cartoons, we aimed at underlining those reasons to raise awareness. A cartoon is a catchy, influential and striking medium. It is easy to remember their morals. A cartoon "sarcastically" makes its point. It challenges the power structures, social conventions and restrictions. For this reason cartoons

was selected medium to draw attention to divorce which is one of the global human problems of this age and time.

References

Arıkan, Ç. (1996). *People's attitudes towards divorce*. Republic of Turkey Prime Ministry Family Research Institute.

Arpacı, F. & Ersoy, A. F. (2007). Effects of women's employment on the quality of life of the family. *Journal of Social Policy Studies, 11*(11), 41-50.

Babuna, C. (2012) Alcohol Addiction and Health Problems, Alcohol Report. Istanbul. *Turkish Green Crescent Society*.

Büyüköztürk, Ş., Kılıç Çakmak, E. Akgün, Ö. E., Karadeniz , Ş., & Demirel , F. (2016). Scientific Research Methodology. Ankara. Pegem Publications (22nd Edition).

Büyükkaragöz, S. (1993). Harmful Habits and Educational Measures. Selçuk University Journal of Social Sciences Institute (2), 73-81.

Bozdemir, N. & Özcan, S. (2011). An overview of sexuality and sexual health. Turkish Journal of Family Medicine and Primary Care, *5*(4).

Çayıroğlu, Y. , (2016). Psycho-Social Dynamics of Family Breakdowns in Modern Times, Mehir Family Magazine, 3, 11-40.

Deniz, D. (2017). Representation of Women in Political Cartoons: 1950 Elections and Objectified Women. Karabük University Journal of the Institute of Social Sciences, *7*(2), 490-511.

Doğan, Ş. (2016). Attitudes Towards Divorce: An Attitude Scale for Factors that Increase the Divorce and Factors that Prevent the Divorce. Itobiad: Journal of the Human & Social Science Researches, *Itobiad: Journal of the Human & Social Science Researches, 5*(4).

Eşkinat, R. (2013). Economic Violence against Women in Turkey (Research Oriented Divorced Women). Journal of Social Science / Dumlupinar University Journal of Social Sciences , (37).

Ersöz, A. G. (2011). A Treatise on Relationship Between Divorce and Domestic Violence Against Women in Turkey. Sociology Conferences (43), 249-264.

İçuygu, A, (2016). Syrian refudees in Turkey. The Long Road Ahead.Transtlantic Council on Migration.Transaltlantic Council on migration Policy Institute.Brussels. Retrieved from http://www.migrationpolicy.org/resarc/syrina-refugeesturkey-long-road-ahead, 3(8).

Orhan, O. & Gündoğar, S. S. (Eds.). (2015). Impacts of Syrian Refugees on Turkey. Middle East Strategical Research Center.

Öğüdü, H. (2011). Cartoon analysis of Turkish political life: Akbaba magazine example (master's thesis) Selçuk University Social Sciences Institute, Konya.

Özkaya, C. Vatandaş, C. , Aydı M., Tekin, M., Can , B., Arabacı,C., & Çıtlak ,O. (2011). Families in Turkey (Structural Properties, Function and Changes of the Family, İstanbul: SEKAM Publication.

Şenyapılı, Ö. (2003). What's Cartoons Objects, Approaches, Styles; Who Draw Cartoons and Why? METU Development Foundation Publishing and Communication Inc. Publications.

Tarımeri, N. (2013). When Will We Forget? "Drama of "Kid Bride" Esra Nur, Imam Marriages and Irresponsive Responsibles.

The Turkish Civil Code, 4721. Retrieved from, www.yayin.adalet.gov.tr/dosyalar/pdf/tmkm.pdf

Turkish Statistical Institute (2016). Marriage and Divorce Statistics, Turkish Statistical Institute Retrieved from, www.tuik.gov.tr

Uçan, Ö. (2007). A Retrospective Evaluation of Women Applying to Crisis Center in Divorce Process. Ankara University Psychiatric Crisis Application and Research Center, Ankara.

Ünür, E. (2016). An Analysis of How Traditional Media Uses Social Media: Twitter Use in TV Series. Turkish Journal of Social Research / Social Researchers found Turkey Magazine *20* (1).

Varol, M. (2011). Alcohol Report. Istanbul. Turkish Green Crescent Society, İstanbul.

Vatandaş, C. (2007). Perception of gender and gender roles. Sociology Conferences, (35), 29-56.

Yardımcı, İ. (2010). The concept of humor and its place in art. Journal of Social Sciences, *3(2), 1-14.*

Yıldırım, A., & Şimşek, H. (2016). Qualitative Research Methods in Social Sciences (10th Edition).

Yıldız, A. K. (2012). The effect of social networking sites on the learning and understanding of privacy of digital natives, *13*(2), 529-542.

Energy Consumption Modelling Of Residential Sector of Turkey for Different Construction Materials

Gül Nihal GÜĞÜL [1*]

[1] Selcuk University, Faculty of Technology, Department of Computer Engineering,, Konya, Turkey, gul.gugul@selcuk.edu.tr

[*] **Corresponding Author:** gul.gugul@selcuk.edu.tr

Abstract

The Residential sector in Turkey accounts for about 30% of the total national energy consumption. In this study, heating energy consumption of a single detached house with different construction materials for seven cities of Turkey is modelled by means of simulations conducted by eQUEST software. Hourly climate data of Erzurum, Ankara, Izmir, Antalya, Trabzon, Şanlıurfa and Konya are obtained from General Directorate of Meteorology for 2015 and 2016. This data is converted into “bin” weather file format in order to be inserted into eQUEST. The results of simulations show that most energy efficient roof, wall and door construction material is wood for cold climates.

Keywords: Building Energy Simulation, Energy Saving, eQUEST, Cold Climate, Cold Climate

1. Introduction

The amount of energy consumed in residential sector has a significant share in final energy consumption that is about 22% (USDOE, 2010) in USA, about 30% in Turkey (ETKB, 2010). According to the sectorial energy consumption of Turkey, highest energy consumption after the industrial sector is caused by residential and services sectors and this consumption is continuously increasing as a results of increase in number of new building constructions (DEK-TMK, 2015). In last decade, area of single detached houses constructed in Ankara, Izmir and Istanbul are nearly 4 million m^2, 3,8 million m^2 and 3,8 million m^2 respectively (TUIK, 2015). Therefore, energy saving in residential sector of Turkey is of great importance.

Energy saving in residential sector can be accomplished by improvements on building envelope and supplying energy demand with renewable energy sources. Both of these methods results in reducing the fossil fuel consumption and associated emissions.

There are many studies in the open literature on reducing the energy consumption and associated emissions of residential sector. Many of these studies are conducted by modelling the energy demand of buildings using building energy simulation software's (DOE-2 (DOE2, 2015), EnergyPlus (USDOE, 2015), eQUEST (DOE2, 2015), TRNSYS (TRNSYS, 2015), ESP-r (ESRU, 2015)) and determining the amount of energy savings with the application of scenarios on envelope. Envelope improvement scenarios are conducted by retrofitting the building envelope or design ((Florides, et al., 2000); (Friess, et al., 2012); (Sozer, 2010); (Friedman, et al., 2014); (Tettey, et al., 2014); (Babaizadeh, et al., 2015); (Gustafsson, et al., 2016); (Ivanovic-Sekularac, et al., 2016); (Hurmekoski, et al., 2015); (Jayasinghe, et al., 2002)). Some of these studies also calculated associated reductions in emissions and conducted economic analysis in addition to envelope retrofits ((Bonakdar, et al., 2014); (Ashrafian, et al., 2016); (Özkan, et al., 2011); (Öztürk-Kerestecioğlu, et al., 2015)). In addition to this a few of these studies also compared brick and timber before and after construction stage ((Thomas, et al., 2018); (Sandanayake, et al., 2016)).

In this study, it is aimed to determine the heating energy demand of a single detached house for seven major cities of Turkey, namely Trabzon, Şanlıurfa, Ankara, Erzurum, Istanbul, Antalya and Izmir. A single detached house is modelled in eQUEST building energy simulation software by using meteorological data of each city obtained from General Directorate of Meteorology. The meteorological data obtained is converted into "bin" files to be inserted into eQUEST software by using "Elements" software that was developed by Big Ladder Software with the funding and collaboration of Rocky Mountain Institute (Big Ladder Software, 2016).

Then a standard house model is developed and different exterior wall materials are applied to the model for each city to determine the potential in energy savings in single detached houses constructed in seven major cities of Turkey. To the authors' best knowledge; there is no study that covers developing a heating energy model of a single detached house and applying climate data of seven cities of Turkey to this model for different envelope construction scenarios.

2. Methodology

This section provides information on the methodology followed during model development and simulations, data collection and energy efficiency results.

2.1. Characteristics of the Standard Model House

In this study a model house is developed as a standard to be used for each city. Standard house is single floor and single detached. Total heated area of the house is 200 m^2. Heating system is baseboard electricity system (heating set point 20 ºC). The construction of exterior wall of model house is wood with 1,25 cm fibre insulation. Ground of the house contacts to the earth and ground floor is made of 15 cm concentrate. 15% of each wall from floor to ceiling is made of windows that are 12 mm air filled 6 mm double clear glazing. Standard house has two outer doors made of Steel; Polyurethane one of which is facing to South second is to East. U values of constructions and materials of all current constructions are summarized in Table 1.

Table 1 U value of materials and constructions in standard model house

Case	Current Construction	U value of Const., W/$m^{2°}$-K
Roof Construction	Wood Standard Frame	0,164
Roof Insulation	No Insulation	
Wall Construction	Wood Standard Frame	0,319
Walls Insulation	1,25 cm fibre sheathing	
Door Material	Steel, Polyurethane	4,650
Ground Floor	Earth Contact	1,167
Window Glazing	Double 12 mm air filled 6 mm glazing	2,100
Window Frame	Aluminium	15,780

2.2. Climate Data

After the determination of constructions to be used in standard house, hourly climate data of cities with different climate zones (CZ) (BULUT, et al., 2007) namely as Trabzon (CZ:2),

Şanlıurfa (CZ:2), Ankara (CZ:3), Erzurum (CZ:5), Istanbul (CZ:2), Antalya (CZ:1) and Izmir (CZ:1) are obtained from General Directorate of Meteorology for 2015 and 2016. Then climate data obtained is converted into "bin" files by using "Elements" software (Big Ladder Software, 2016).

2.3. Modelling of the Standard House

The heating energy consumption model of the house is created by using the data given in section 2.1 and 2.2 in eQUEST simulation software environment. After completing the model, energy consumption for heating is estimated by eQUEST. Type of weather data used in this study is "bin" data. Meteorological data of each city obtained from General Directorate of Meteorology is converted into "bin" files by using "Elements" software that was developed by Big Ladder Software with the generous funding and collaboration of Rocky Mountain Institute (Big Ladder Software, 2016). Screenshot of the standard model house is shown in Figure 1.

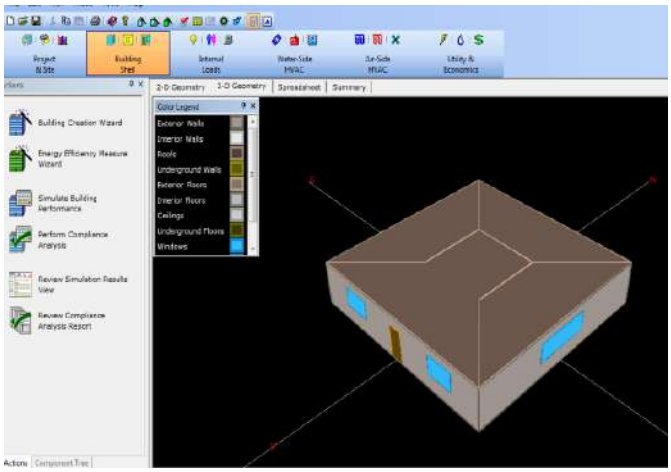

Figure 1. Screenshot of the standard model house

2.4. Wall Scenarios

After the model development is complete the wall materials listed in Table 2 are applied to the model for each city. Then energy consumption of house for each case is simulated in software and results are compared.

Table 2 U values of materials and constructions for suggested exterior wall improvement scenarios

Sce. Code	Suggested Construction	Suggested Insulation	U value of Const., W/m$^{2\circ}$-K
Reference House	Wood	No insulation	0,0099
W-1	20 cm concrete	5 cm polyisocyanurate	0,0068
W-2	15 cm concrete	5 cm polyisocyanurate	0,0068
W-3	10 cm concrete	5 cm polyisocyanurate	0,0068
W-4	20 cm concrete	No insulation	0,0144
W-5	15 cm concrete	No insulation	0,0150
W-6	10 cm concrete	No insulation	0,0150
W-7	Wood frame 60 cm	No insulation	0,0134
W-8	Double Standard Wood Frame	No insulation	0,0065
W-9	Wood frame 60 cm	5 cm polyisocyanurate	0,0069
W-10	Double Standard Wood Frame	5 cm polyisocyanurate	0,0042

In this study polyisocyanurate is used as insulation material due to its high performance calculated in a study conducted for cold climate homes (Güğül, 2018).

3. Results and Discussion

According to the simulation results, energy consumption for heating of the reference house is estimated as 0,87; 0,64; 4,08; 5,86; 1,71; 0,057 and 0,376 MWh/year by eQUEST, for Trabzon, Şanlıurfa, Ankara, Erzurum, Istanbul, Antalya and Izmir respectively. Therefore heating energy consumption per unit area is calculated as 4,35; 3,2; 20,4; 29,3; 8,55; 0,285 and 1,88 kWh/year- m^2 for Trabzon, Şanlıurfa, Ankara, Erzurum, Istanbul, Antalya and Izmir respectively. Estimated heating energy consumptions of the standard model house are shown in Table 3 and Figure 2 for each city and each wall scenario.

Table 3 Heating energy consumption (EC) of the house in each city (MWh/year) and energy saving (ES) compared to the reference house (%)

	Trabzon			**Şanlıurfa**			**Ankara**			**Erzurum**			**İstanbul**			**Antalya**			**İzmir**		
	EC	**ES, %**	**ES, MWh/yr**	**EC**	**ES, %**	**ES, MWh/yr**	**EC**	**ES, %**	**ES, MWh/yr**	**EC**	**ES, %**	**ES, MWh/yr**	**EC**	**ES, %**	**ES, MWh/yr**	**EC**	**ES, %**	**ES, MWh/yr**	**EC**	**ES, %**	**ES, MWh/yr**
Reference House (Wood)	0,87			0,64			4,08			5,86			1,71			0,057			0,376		
20 cm concrete, 5 cm Insulation	0,59	32	**0,28**	0,44	31	**0,20**	3,24	21	**0,84**	4,86	17	**1,00**	1,25	27	**0,46**	0,047	18	**0,01**	0,164	56	**0,21**
15 cm concrete, 5 cm Insulation	0,57	34	**0,30**	0,42	34	**0,22**	3,23	21	**0,85**	4,85	17	**1,01**	1,23	28	**0,48**	0,028	51	**0,03**	0,153	59	**0,22**
10 cm concrete, 5 cm Insulation	0,56	36	**0,31**	0,4	38	**0,24**	3,23	21	**0,85**	4,85	17	**1,01**	1,23	28	**0,48**	0,015	73	**0,04**	0,154	59	**0,22**
20 cm concrete, No Insulation	1,24	-43	**-0,37**	0,86	-34	**-0,22**	4,98	-22	**-0,90**	7,04	-20	**-1,18**	2,28	-33	**-0,57**	0,110	-92	**-0,05**	0,55	-46	**-0,17**
15 cm concrete, No Insulation	1,28	-47	**-0,41**	0,89	-39	**-0,25**	5,06	-24	**-0,98**	7,13	-22	**-1,27**	2,33	-36	**-0,62**	0,120	-110	**-0,06**	0,59	-57	**-0,21**
10 cm concrete, No Insulation	1,32	-52	**-0,45**	0,93	-45	**-0,29**	5,18	-27	**-1,10**	7,25	-24	**-1,39**	2,4	-40	**-0,69**	0,135	-137	**-0,08**	0,65	-73	**-0,27**
Wood frame 60 cm	0,82	6	**0,05**	0,6	6	**0,04**	3,93	4	**0,15**	5,69	3	**0,17**	1,63	5	**0,08**	0,047	16	**0,01**	0,342	9	**0,03**
Double Standard Wood Frame	0,58	33	**0,29**	0,41	36	**0,23**	3,25	20	**0,83**	4,85	17	**1,01**	1,26	26	**0,45**	0,015	73	**0,04**	0,204	46	**0,17**
Wood frame 60 cm	0,5	43	**0,37**	0,36	44	**0,28**	3,04	25	**1,04**	4,59	22	**1,27**	1,14	33	**0,57**	0,009	84	**0,05**	0,166	56	**0,21**
Double Standard Wood Frame	0,4	54	**0,47**	0,27	57	**0,36**	2,7	34	**1,38**	4,18	29	**1,68**	0,97	43	**0,74**	0,003	94	**0,05**	0,115	69	**0,26**

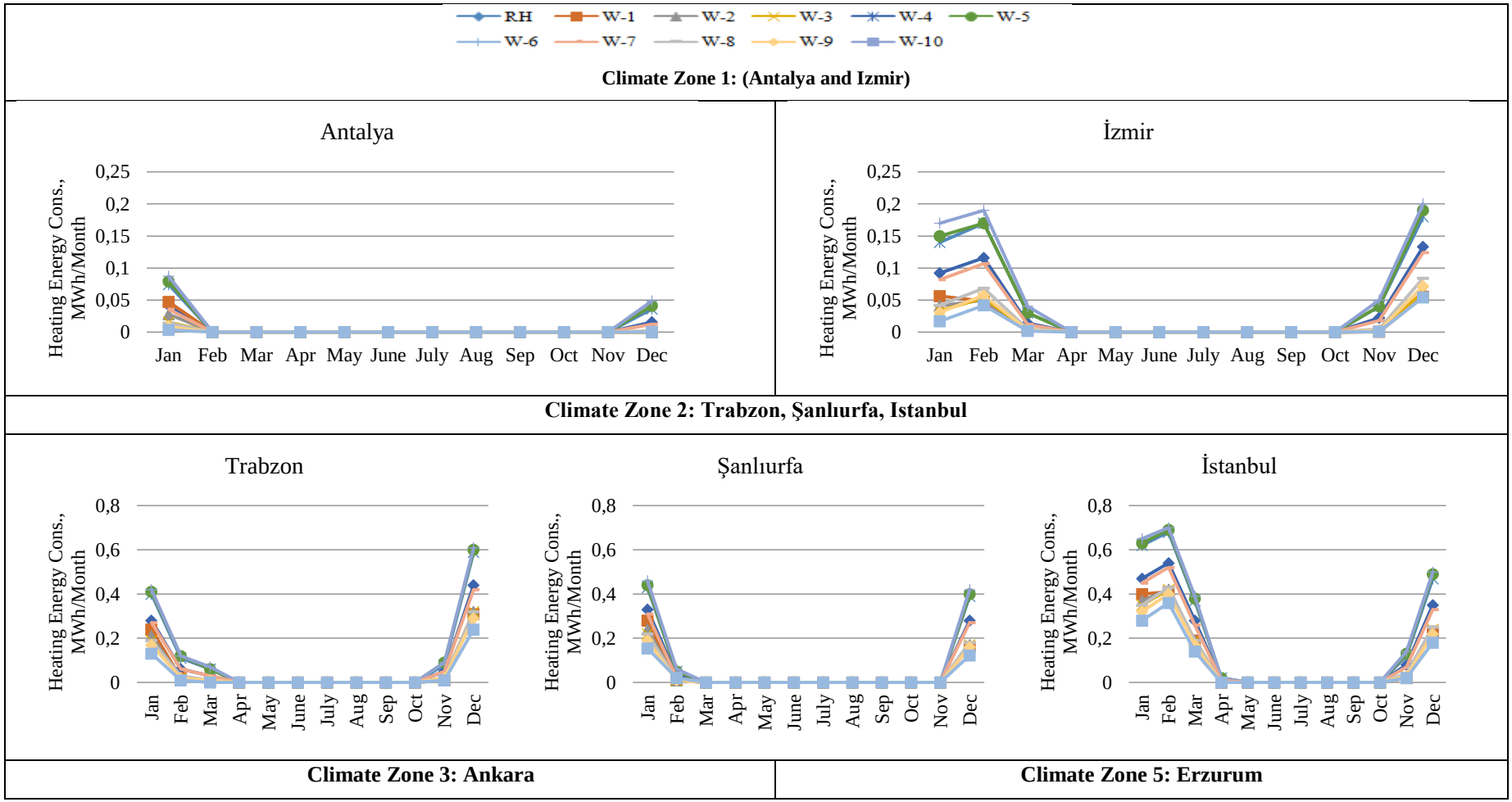
RH
W-1
W-2
W-3
W-4
W-5
W-6
W-7
W-8
W-9
W-10
Climate Zone 1: (Antalya and Izmir)
Antalya
İzmir
Heating Energy Cons., MWh/Month
0,25
0,2
0,15
0,1
0,05
0
Jan Feb Mar Apr May June July Aug Sep Oct Nov Dec
Climate Zone 2: Trabzon, Şanlıurfa, Istanbul
Trabzon
Şanlıurfa
İstanbul
0,8
0,6
0,4
0,2
0
Climate Zone 3: Ankara
Climate Zone 5: Erzurum

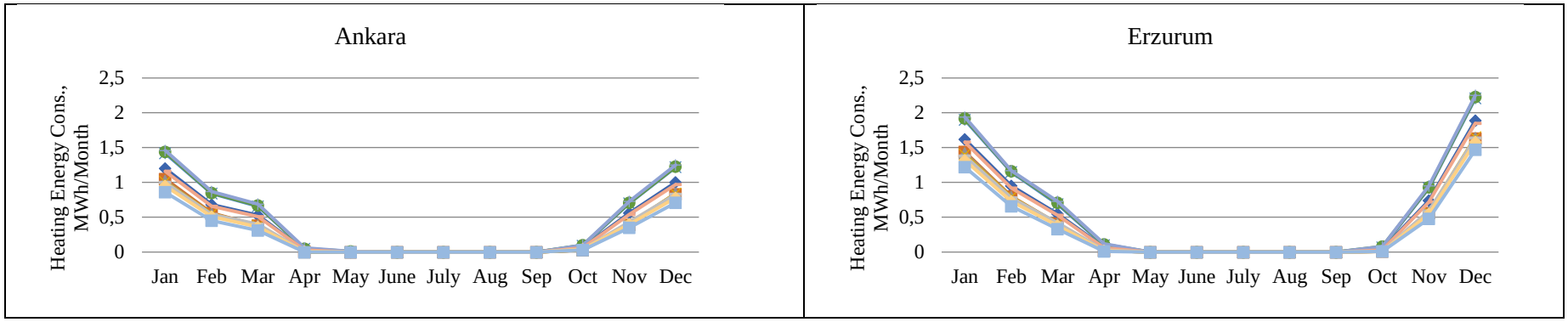

Figure 2 Heating energy consumption of the house in each city (MWh/Month) according to climate zones

According to Table 3 and Figure 2 most efficient wall construction for all cities is (W-10) Double Standard Wood Frame with 5 cm polyisocyanurate insulation. Application of W-10 wall on Climate Zone 1 cities, Antalya and Izmir, resulted in 96% and 69% energy saving respectively. The highest percentage obtained in Climate Zone 1 however amount of maximum energy saving is obtained in Climate Zone 5 city that is Erzurum.

Concrete walls without insulation (W-4, W-5, W-6) resulted in energy loss in all cities. Energy loss with the application of W-4, W-5 and W-6 scenarios in Erzurum Climate are 1,18 MWh/yr, 1,27 MWh/yr and 1,39 MWh/yr respectively whereas energy loss is only 0,05 MWh/yr, 0,06 MWh/yr and 0,08 MWh/yr in Antalya.

Concrete walls with 5 cm polyisocyanurate insulation (W-1, W-2, W-3) resulted in energy saving compared to reference house respectively with highest savings in climate zone 5. Maximum savings with the application of scenarios (W1 to W-10) are obtained in Erzurum which is the coldest city which shows that the colder the climate it's more efficient to construct efficient buildings.

Conclusion

In this study energy efficient wall materials for seven different cities of Turkey are investigated by using eQUEST simulation software. Most efficient wall construction for all cities is found to be Double Standard Wood Frame with 5 cm polyisocyanurate insulation (W-10). With the application of W-10 wall in Climate Zone 5 city that is Erzurum 1,68 MWh/year energy saving is obtained. This saving is equal to the annual heating energy consumption of the model standard house located in Istanbul and double of the annual heating energy consumption of the model standard house located in Trabzon.

Concrete walls without insulation resulted in energy loss in all cities. Concrete walls with 5 cm polyisocyanurate insulation resulted in energy saving compared to reference house. Maximum savings obtained with the application of scenarios (W1 to W-10) are in Erzurum which is the coldest city which shows that the colder the climate it's more efficient to construct efficient buildings. Application of W-10 wall on Climate Zone 1 cities, Antalya and Izmir, resulted in 96% and 69% energy saving respectively which have hot humid climates and heating system of the most of the residential houses are air conditioning that makes effective to reduce heating energy consumption which is parallel to electricity consumption in Climate Zone 1 cities. The highest percentage obtained in Climate Zone 1 however amount of maximum energy saving is obtained in Climate Zone 5 city that is Erzurum.

References

Ashrafian, T., Yilmaz, A. Z., Corgnati, S. P., & Moazzena, N. (2016). Methodology to define cost-optimal level of architectural measures for energy efficient retrofits of existing detached residential buildingsin Turkey. Energy and Buildings, 120, 58-77.

Babaizadeh, H., Haghighi, N., Asadi, S., Broun, R., & Riley, D. (2015). Life cycle assessment of exterior window shadings in residential buildings in different climate zones. Building and Environment, 90, 168-177.

Big Ladder Software. (2016). Elements. https://bigladdersoftware.com/projects/elements/

Bonakdar, F., Dodoo, A., & Gustavsson, L. (2014). Cost-optimum analysis of building fabric renovation in a Swedish multi-story residential building. Energy and Buildings, 84, 662–673.

Bulut, H., Büyükalaca, O., & Büyükalaca, O. (2007). Türkiye İçin Isitma Ve Soğutma Derece-Gün Bölgeleri. 16. Ulusal Isı Bilimi ve Tekniği Kongresi, (30 Mayıs-2 Haziran). Kayseri.

DEK-TMK. (2015, 4 21). Türkiye Enerji Denge Tabloları. Dünya Enerji Konseyi Türk Milli Komitesi Derneği: http://www.dektmk.org.tr/incele.php?id=MTAw#

DOE2. (2015). eQUEST Overview. DOE2: http://www.doe2.com/download/equest/eQUESTv3-Overview.pdf

eQUEST. (2016). the QUick Energy Simulation Tool. DOE2: http://www.doe2.com/equest/

ESRU. (2015, 01). ESP-r Overview. Energy Systems Research Unit: http://www.esru.strath.ac.uk/Programs/ESP-r_overview.htm

ETKB. (2010). ETKB. http://www.enerji.gov.tr/EKLENTI_VIEW/index.php/raporlar/raporVeriGir/61543/2

Florides, G., Kalogirou, S., Tassou, S., & Wrobel, L. (2000). Modeling of the modern houses of Cyprus and energy consumption analysis. Energy, 25 (10), 915–937.

Friedman, C., Becker, N., & Erell, E. (2014). Energy retrofit of residential building envelopes in Israel: A cost-benefit analysis. Energy, 77, 183-193.

Friess, W. A., Rakhshan, K., Hendawi, T. A., & Tajerzadeh, S. (2012). Wall insulation measures for residential villas in Dubai: A case study in energy efficiency. Energy and Buildings, 44, 26–32.

Gustafsson, M., Gustafsson, M. S., Myhren, J. A., Bales, C., & Holmberg, S. (2016). Techno-economic analysis of energy renovation measures for a district heated multi-family house. Applied Energy, 177, 108-116.

Gugul, G. N. (2018). Energy Simulation Study of Efficient Construction Materials for Cold Climate Homes. The 9th International Cold Climate Conference Sustainable new and renovated buildings in cold climates. Kiruna: Lund University.

Hurmekoski, E., Jonsson, R., & Nord, T. (2015). Context, drivers, and future potential for wood-frame multi-story construction in Europe. Technological Forecasting & Social Change, 99, 181–196.

Ivanovic-Sekularac, J., Cikic-Tovarovic, J., & Sekularac, N. (2016). Application of wood as an element of facade cladding in construction and reconstruction of architectural objects to improve their energy efficiency. Energy and Buildings, 115, 85–93.

Jayasinghe, M., Attalage, R., & Jayawardena, A. (2002). Thermal comfort in proposed three-storey passive houses for warm humid climates. Energy for Sustainable Development, 6 (1), 63-73.

Özkan, D. B., & Onan, C. (2011). Optimization of insulation thickness for different glazing areas in buildings for various climatic regions in Turkey. Applied Energy, 88, 1331-1342.

Öztürk-Kerestecioğlu, F., Tümer-Özkan, D. B., Hamamcıoğlu, C., Yerliyurt, B., Sakinç, E., & Hafizoğlu, T. (2015). Reducing Cooling and Heating Loads in Existing Residential Buildings in the Context of Building Envelope: Beykoz-Kanlıca. MEGARON , 10 (4), 451-469.

Sandanayake, M., Zhang, G., & Setunge, S. (2016). Environmental emissions at foundation construction stage of buildings e Two case studies. Building and Environment, 95, 189-198.

Sozer, H. (2010). Improving energy efficiency through the design of the building envelope. Building and Environment, 45 (12), 2581–2593.

Tettey, U. Y., Dodoo, A., & Gustavsson, L. (2014). Effects of different insulation materials on primary energy and CO2emission of a multi-storey residential building. Energy and Buildings, 82, 369-377.

Thomas, D., & Ding, G. (2018). Comparing the performance of brick and timber in residential buildings – The case of Australia. Energy and Buildings, 159, 136–147.

TRNSYS. (2015). http://sel.me.wisc.edu/trnsys

TUIK. (2015). TUIK Bölgesel Istatistikler. 6 7, 2012 tarihinde TUIK: http://tuikapp.tuik.gov.tr/Bolgesel/menuAction.do

USDOE. (2010). Chapter 2 : Residential Sector. 6 11, 2015 tarihinde Building Energy Data Book: http://buildingsdatabook.eren.doe.gov/ChapterIntro2.aspx

USDOE. (2015). USDOE EnergyPlus Energy Simulation Software. http://www.energyplus.gov/

COMPUTER AND COMMUNICATION

POSTER PRESENTATIONS

Design of Net Zero Emission on Grid Single Detached Dwelling: Ankara Case

Gül Nihal GÜĞÜL[1*]

[1]Selcuk University, Faculty of Technology, Computer Engineering Department, Konya, Turkey

[*] **Corresponding Author:** gul.gugul@selcuk.edu.tr

Abstract

Energy consumption in the residential sector of Turkey has a share of 30% that makes savings of great importance. In this study, a net zero-emission detached house is designed for Ankara, Turkey climate with the aim of reducing the residential energy consumption. The designed residence has 120 m^2 heated area. Exterior envelope constructions of the windows and walls are argon filled 3 layer glazing and polyiso insulation on the exterior wall and roof which are made of wood. In addition, window/wall ratio of the house is 50% in the south, 15% in the west and east, and 5% in the north side. These percentage values are found to be optimum as the result of simulations conducted. Under these conditions, the energy consumption for heating in Ankara province is estimated as 1970 kWh/year by eQUEST software. Heat gain from people, lighting and electrical devices are calculated as 12 kWh/day. The electricity consumption of the house is calculated as 7,76 kWh/day by using datasheets. It was found that a 4 kW capacity solar panel system was sufficient to meet the electricity and heating demand of the house during all seasons. The total cost of the system was obtained as 33.000 TL. For hot water supply, a solar energy system with 10 m^2 collector area was found to be sufficient and cost of this system was obtained as 7.000 TL from local firms. In this case, the housing met all energy demands with renewable systems and caused net zero greenhouse gas emissions.

Keywords: Net zero emission buildings, Zero energy buildings, Building Energy Simulation, Renewable energy

1. Introduction

The amount of energy consumed in residential sector has a significant share in total energy consumption. Residential sector has a share of about 22% in the USA and 30% in Turkey over total energy consumption. According to the sectorial energy consumption between 1990-2013 Turkey's highest energy consumption is caused by the housing and services sectors after the industrial sector and this consumption is continuously increasing. In Turkey, the amount of energy consumed in the residential sector is increasing in parallel with the rapid increase in population and the number of houses. For this reason, the energy savings to be made at residential sector is of great importance.

There are many studies conducted in literature to investigate the ways to decrease the energy consumption in residential sector. These studies investigate the potential of decrease by using renewable energy sources or by improving the envelope of buildings. Nowadays studies go a step further of decreasing the energy consumption to develop zero energy houses. There are many net zero energy consumption (NSET) buildings constructed around the world.

For instance in the United States, most of the high-performance buildings on the South Table Mountain campus of NREL (National Renewable Energy Laboratory), have reached the status of net zero energy consumption building (NSET). By combining the most advanced energy-efficient materials and renewable energy technologies, these buildings have become a model for sustainability (NREL, 2018). In addition to this in Singapore, which has a hot and humid climate, the building and construction authority (BCA) has shown the efficient use of energy by improving a building on the BCA Academy campus. An old building in the campus with building materials such as shading devices, light colors, vertical green walls, high performance glass and light wall systems has been converted into a net zero energy consumption (NSET) building (HPB Magazine, 2015). The first NSET building in Jamaica was opened on October 25, 2017 at the Mona campus of the University of Western India (UWI) under the auspices of the Institute for Sustainable Development (ISD) (UWI, 2017). The Rochester Institute of Technology (RIT) has built a training and research building of 88,000 gross ft2 in the Rochester, NY campus. The four-storey building contains office, laboratory, classroom and meeting area (Hu, 2016). Canada also has many net zero energy building projects. In 2010, Vancover built the first very high-quality residential building (net zero energy consumption (NSET)) for people in Southeast False Creek in Canada. In addition, as of July 2010, all new buildings in Vancouver had to comply with the LEED (Leadership in Energy and

Environmental Design) standard. The LEED rating system is an internationally recognized tool for evaluating green buildings. The certification levels offered by LEED are Certified, Silver, Gold and Platinum (City of Vancouver, 2018).

In this study, technological analysis of the methods that can be applied in an on-grid single detached house in the Ankara climate to minimize the energy consumption caused by the residences will be passed through with the design of a net zero energy emission house. Energy demand for the designed residence will be provided by renewable energy sources. In order to reach the Net Zero Emission House (NZEH) target, the dwelling is planned to use the lowest thermal conductivity materials in the market, energy efficient electric household appliances, three layers of glazing filled with argon gas. In addition design of the window and door directions is planned to be most beneficial from sunlight. Dwelling's electricity and heating demand will be supplied by the photovoltaic solar panels requirements, hot water demand will be supplied from solar-assisted systems.

2. Methodology

The whole electricity and heating demand of the house will be supplied by "Photovoltaic Systems". Photovoltaic systems can be on-grid or off-grid systems. In this study, an on-grid system is designed and surplus electricity is planned to be sold to the government.

In the study, firstly electricity demand of the dwelling is calculated by using the power value of electric appliances and their usage duration by using equation (1) and results are shown in Table 1.

$$Q_{elec} = (\sum_{i=1}^{8760} h \times P)/1000 \quad (1)$$

Q_{elec} : Energy demand for electrical appliances, kWh/year

i : Appliance

h : Usage duration, h

P : Power of the appliance, W

Then heat gain from electrical equipment, people and lighting is calculated according to sensible (SHG) and latent (LHG) heat gains of the appliances by using equation (2) and results are shown in Table 1.

$$Q_{HG} = (\sum_{i=1}^{8760} h \times P)/1000 \quad (2)$$

Q_{HG} : Heat gain, kWh/year

i : Appliance, people or lighting

h : Usage duration for appliances and lighting or presenting duration for people

P : Power of the appliance and lighting or heat emission from people according to activity, W

Hot water demand of the dwelling is supplied by solar domestic hot water system (SDHW). Four people thought to reside in the dwelling and according to literature four people consume minimum 150 kg hot water per day. Amount of daily hot water consumption (mhw) is assumed to be constant throughout the year. Energy demand to obtain 150 kg hot water per day is calculated by assuming mains water temperature equal to 100 cm underground soil temperature and hot water temperature is equal to 55 °C. Solar radiation data is an hourly data. Therefore calculations are made hourly. To calculate the hourly hot water consumption, a normalized domestic hot water profile is used (Duffie, et al., 2013). Then, required annual energy for DHW supply is calculated for each hour with equation (3).

$$Q_{hwa} = \left(\sum_{l=1}^{8760}(m_{hw-hourly} \times c \times \Delta T)\right) \quad (3)$$

Q_{hwa} : Energy demand for DHW supply, kWh/year

$m_{hw\text{- }hourly}$: Hourly hot water consumption, kg/day

c :Water essence, kWh/kg-°C

ΔT : Hot water temperature - Mains water temperature, °C

Heating demand of the dwelling is estimated by the model developed in eQUEST software. Heat gains of the dwelling are subtracted from estimated heating demand and final heating demand is calculated. Finally total energy demand of the house is calculated by summing the energy demand for electricity and heating to estimate the capacity of required photovoltaic panel that achieve the goal of NZEH. Then capacity of required SDHW system is estimated by energy demand for hot water. Developed NZEH is assumed to sell surplus electricity produced by PVP's to government because the PVP's are designed to provide the peak demand during winter in order to not effected by power cut.

3. Results and Discussion

Firstly heat gain of the dwelling is calculated according to sensible (SHG) and latent (LHG) gains and found as 12 kWh per day as shown in Table 1. In addition to this electricity consumption of the house is calculated as 7,76 kWh/day as shown in Table 1.

Table 1. Heat gain and electricity consumption of the house

Device name	Usage Duration, h/day	Rooms, W		Bath-WC, W		Kitchen, W		Heat Gain, W/day	Electric Cons., kW/day	Power
		SHG	LHG	SHG	LHG	SHG	LHG			
Refrigerator	24					180		4320	0,7	
Deep freeze	24					50		1200	0,5	
Oven	0,1					350	350	70	0,1	1000
Microwave	0,1					350	350	70	0,07	700
Exhauster	0,5					50		25	0,05	100
TV	3	40						120	0,15	50
Computer	2	40				40		160	0,1	50
Washing machine	0,5			500				250	0,5	1000
Dish machine	0,2					250	250	100	0,1	500
Vacuum cleaner	0,1	350						35	0,12	1200
Iron Steam	0,5	500	500					500	1	2000
Toast machine	0,1					700		70	0,07	700
Electric / Steam Cooker	2					500	500	1000	4	2000
Lighting	3	100						300	0,3	100
People	10	260	120					3800		
Total								12020	7,76	

Heating demand of the house is estimated by the model developed in eQUEST software and model is shown in Figure 1.

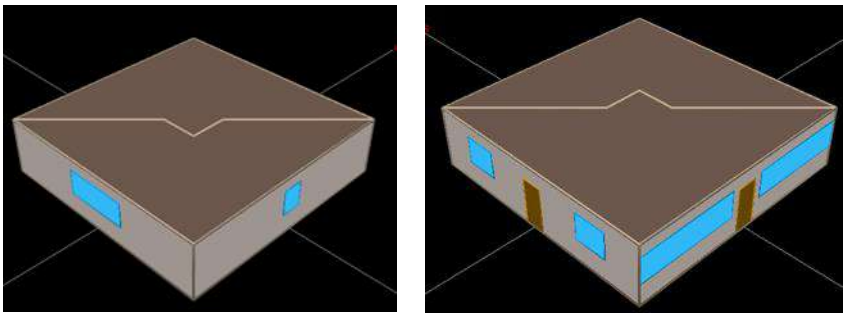

Figure 1 Model developed in eQUEST software

According to calculated heat gains and estimated heating demand overall heating demand which is found by subtracting gains from estimated heating demand is calculated daily and shown in Figure 2.

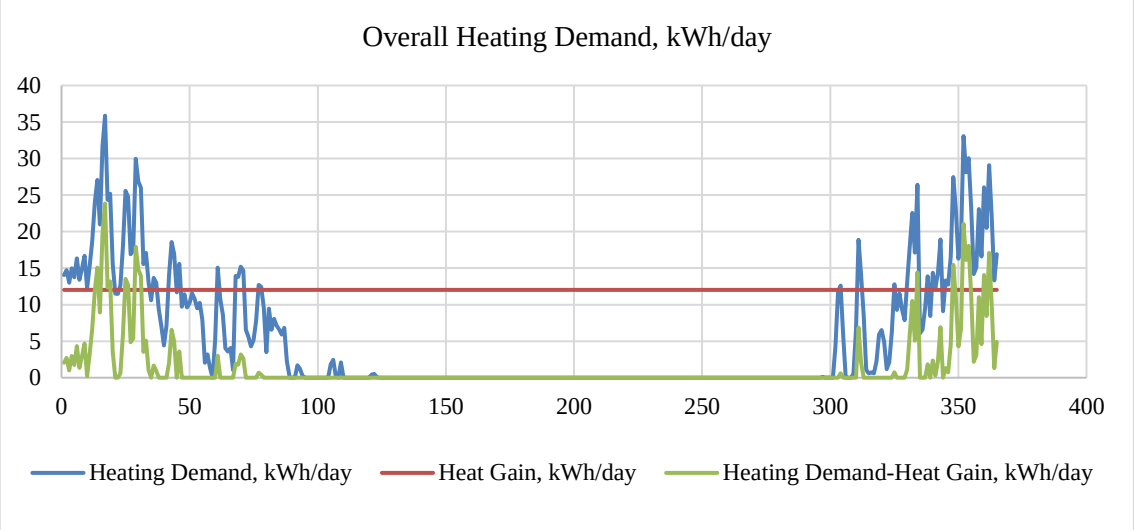

Figure 2 Overall Heating Demand

Then electricity demand of the house is added to overall heating demand and final energy demand that is going to be supplied by photovoltaic panels is calculated and result is shown in Figure 3.

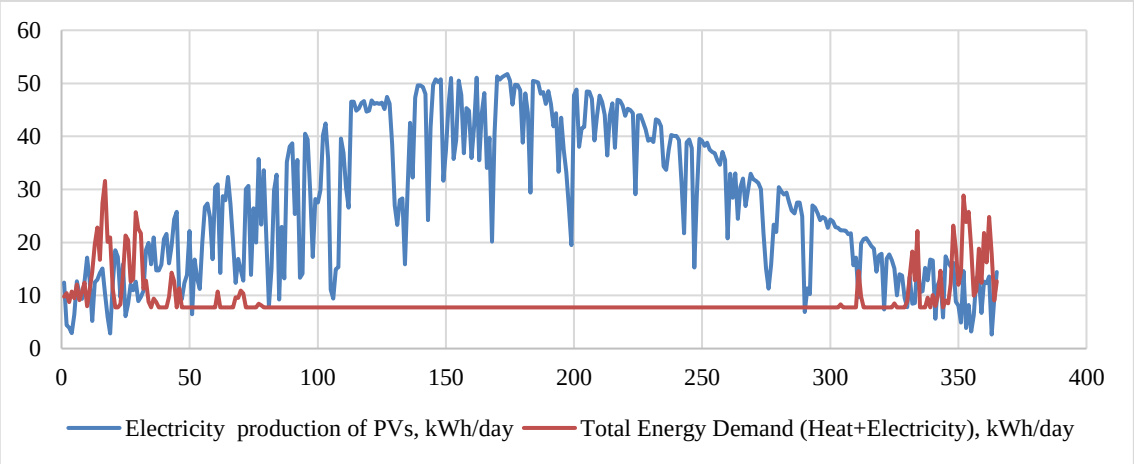

Figure 3 Total energy demand, kWh/day

According to daily energy demand, average energy demand of the house during January and February which are the coldest months is found as 12 kWh/day. Average sunshine duration of Ankara during January and February is 3,5 hours (General Directorate of Meteorology,

2018). Therefore a 4 kW PVP system can produce 14 kWh/day energy and can supply the energy demand of the house even during coldest months. 4 kW PVP system is composed of 16 photovoltaic panels and has 40 m2 area which is an available roof space for a single detached house. Cost of a 4 kW PVP is obtained from a local firm as 33,000 TL with an efficiency of 16% (Solar Dukkan). Electricity production of this system is calculated by using equation (4) in order to estimate the surplus electricity production that will be sold to the government.

$$EP_{pvp} = \left(\sum_{l=1}^{8760}(SR_{hourly} \times A \times \eta)\right) \quad (4)$$

EP_{pvp} : Electricity Production of PVP, kWh/year
SR_{hourly} : Hourly Solar Radiation, W
A : Area of PVP, m2
η: Efficiency of PVP, %

After calculating the hourly electricity production of PVP, daily electricity production is calculated by summing each days production then value of money obtained from selling surplus electricity is calculated by using equation (5).

$$SES = \left(\sum_{l=1}^{365}(SE \times EV \times DV)\right) \quad (5)$$

SES : Surplus electricity sold to the government, TL/year
SR : Amount of surplus electricity, kWh/day
EV : Value of electricity bought by government, $
DV : Value of USD Dollars in Turkey, TL/$

In Turkey value of produced electricity bought by government is 0,133 $. Daily electricity sold to the government is shown in Figure 4 and amount of total electricity found as 4325 TL/year.

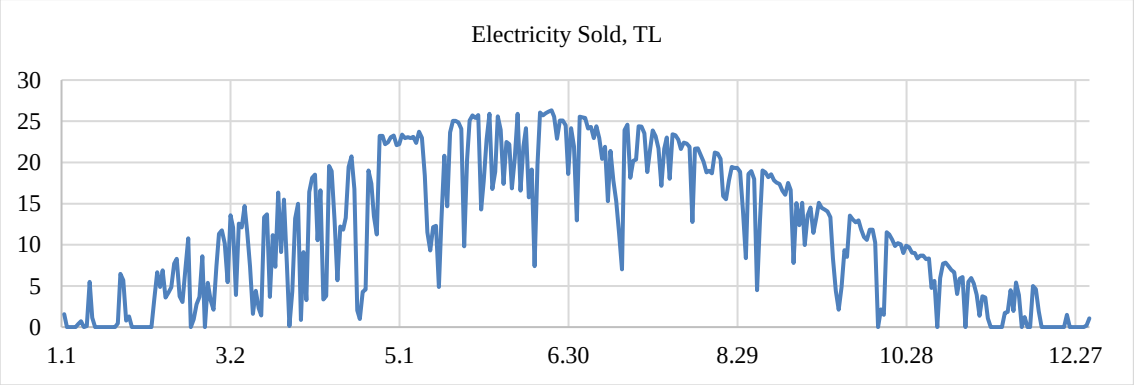

Figure 4 Daily electricity sold to the government, TL/day

Finally energy demand for hot water is calculated and found as 2481 kWh/year. Temperature of mains water is assumed to be the as the temperature of soil under 100 cm ground and hourly soil temperature is obtained from General Directorate of Meteorology. In order to compensate the domestic hot water demand 10 m2 SDHW system is required. Cost of system is obtained as 7000 TL from local firms. Therefore cost of whole system to meet «Net zero emission» standard is obtained as 40.000 TL.

4. Conclusion

In this study, technological analysis of the methods that can be applied in a single detached house in Ankara climate to minimize the energy consumption caused by the residences will be passed through with the design of a net zero energy emission house. Energy demand of the designed residence is provided by renewable energy sources. In order to reach the Net Zero Emission House (NZEH) target, the dwelling is planned to use the lowest thermal conductivity materials in the market, energy efficient electrical appliances, and three layers of glazing filled with argon gas. In addition design of the window and door directions is planned to be most beneficial from sunlight. Dwelling's electricity and heating demand is supplied by the photovoltaic solar panels, hot water demand is supplied from solar-assisted systems. Result of calculations show that heating energy consumption is estimated as 1970 kWh/year. Total heat gain is calculated as 12 kWh/day and the electricity consumption of the house is calculated as 7,76 kWh/day. It was found that a 4 kW capacity solar panel system was sufficient to meet the electricity and heating demand of the house during all seasons. The total cost of the system was obtained as 33.000 TL. For hot water supply, a solar energy system with 10 m^2 collector area was found to be sufficient and cost of this system was obtained as 7000 TL from local firms. In

this case, the housing met all energy demands with renewable systems and reached net zero greenhouse gas emissions with a 40.000 TL renewable energy system. Finally in case of selling surplus electricity to the government 4325 TL/year can be saved.

References

2 KW On Grid Solar Energy System, Solar Dukkan, (2018). URL:https://www.solardukkan.com/detay.php?ur_id=NTM2&ur_seo=2-kw-on-grid-gunes-enerjisi-sistemi--enerji-uretimi-1650tlsene, (Date of access: 1 March 2018).

About National Renewable Energy Laboratory, NREL, (2018). URL:https://www.nrel.gov/about/, (Date of access: 1 March 2018).

Green Buildings, City of Vancouver, (2018). URL:http://vancouver.ca/files/cov/gc2020-goal3.pdf, (Date of access: 17 March 2018).

Ming, H. Net-positive Building and Alternative Energy in an Institutional Environment, ACEEE Summer Study on Energy Efficiency in Building. - Monterey, California : 2016. pp 1-8.

Region's first Net Zero Energy Building to be constructed at The UWI, (2017) URL:https://www.uwi.edu/alumnionline/news-and-updates/latest-news/campus-news/mona/region-s-first-net-zero-energy-building-be-constructed, (Date of access: 22 January 2018).

Seasonal normal: Ankara, General Directorate of Meteorology, (2018) URL:https://www.mgm.gov.tr/veridegerlendirme/il-ve-ilceler-istatistik.aspx, (Date of access: 9 March 2018).

Duffie, J. A. and Beckman, W. A., (2013). Solar Engineering of Thermal Processes. New Jersey: Wiley.

Zero Energy Building @ BCA Academy: Singapore HPB Magazine (2015). URL: http://www.hpbmagazine.org/Case-Studies/Zero-Energy-Building--BCA-Academy-Singapore/, (Date of access: 2 February 2018).

ELECTRICAL AND ELECTRONICS ENGINEERING

ORAL PRESENTATIONS

Internet Based Smart Home Automation Application Using Microcomputer

Ahmet ÖZKAYA[1*], Muharrem MERCİMEK[2]

Yıldız Technical University, Electrical-Electronics Faculty, Control Automation Engineering, Istanbul, Turkey
[1]ozkaya.a@gmail.com
[2]mercimek@yildiz.edu.tr

[*]**Responsible Author:**ozkaya.a@gmail.com

Abstract
In this study we deal with design, development and management of a smart home automation application using microcomputers and control cards. The automation system is designed and developed to be work universally for broad applications such as control of home appliances and systems of air conditioning, water, electricity and natural gas. In this study we put emphasis on the control of lighting system and motorized curtains. Mainly, the algorithm is run automatically using the intensity information gathered from the environment. Also it can be managed with user commands. Data logging, use of Hyper Text Transfer Protocol (HTTP) communication protocols, server design and web application development are the tasks utilized constituently. Local and internet based communication protocols are both employed. In the realization of application in the study, Internet of Things (IoT) architecture and the Open Platform Communications - Unified Architecture (OPC-UA) protocol to assemble IoT concept on industrial systems are utilized.
Keywords: Smart home automation; internet of things; Microcomputer; Raspberry Pi; HTTP; OPC-UA.

1. Introduction

Smart house automation is a definition of routine operations in the daily life which are done automatically with the systems in the house. Smart home can be defined as a unified model of computer technology and communication. Smart home automation is being developed to facilitate life, to save energy and to ensure safety by considering people's original lifestyle (Süzen, 2013).

Technologies that are an integral part of daily life consist of three stages of development (Çayıroğlu, Erkaymaz, 2007). The first stage has been the development of all kinds of equipment to meet the needs and using them in daily life (Qin and friends, 2016). The second stage has been the remote control of these devices (Fırat, Fırat, 2017). The third stage is the control and programming of all devices via different communication paths from a single center or long distances (Gubbi and friends, 2013). Third stage is within the definition of smart home automation. IoT concept has entered our lives together with the industrial 4.0 trend in this third stage (Yılmaz, 2016; URL-1, 2018).

A microcomputer-based automation system consists essentially of a mainframe computer, environmental control units connected to it (sensors, relays, etc.) and software that performs the inspection between these two units. In this project, Raspberry Pi 3 (Maksimović and friends, 2014) is used as microcomputer, Arduino UNO module as microcontroller, camera, motors and relays are used as environmental control units.

In practice, it is automatically controlled by analyzed the light intensity of the environment or manually controlled by the user command received via the application on web. So that, the lighting and curtain opening / closing control is performed. In addition, the status of the lamp and the curtain are instantly saved in the database. This information can be seen by connecting to the web application on the microcomputer with any web browser.

The system is designed and manufactured to be managed from the computer, mobile devices and tablets via web application. HTTP is used as the communication protocol and OPC-UA (Leitner, Mahnke, 2006) protocol is also used for telemetrically monitoring the data. One of the important shortcomings of the IoT systems (Khan and friends, 2012) is that they can’t integrate with the current industrial systems. OPC-UA protocol is used in order to ensure connectivity of the industrial systems with IoT concept (URL-2, 2018).

2. Application

The camera connected to the microcomputer USB interface takes images from the external environment. This image is stored on the microcomputer and processed to determine the light intensity falling on the background in the image. The threshold of lighting decision is determined for reference to the lighting system. If the measured light intensity is greater than this threshold value, the lighting of the home is turned off. When the light intensity is less than the threshold value, the lighting of the home is turned on. It is provided to close the curtains when the lamp is turn on, and to open the curtains when the lamp is turned off. In addition to these requests determined by the image processing algorithm, the request can be made by the user, and if the user intervenes, user request is evaluated as dominant decision. The determined decision is sent to the server. The microcontroller connects to this server through the internet network and takes the related command and energizes the relay connected to the lamp. The lamp is switched on or off in this way. This information is also stored in a database on the microcomputer. Another microcontroller controls a motor drive circuit that turns on and off the curtains of the same room. It learns the command to open or close the curtain by connecting to the server, turns the curtain on or off by running the motor. It also sends status data of the curtain to the microcontroller and allows the relevant data to be stored in the database.

2. Structure of the System

The central software for home lighting automation, works on Raspberry Pi 3. Image processing algorithm and software are running on this microcomputer, and the database and server are also been on this microcomputer. Arduino UNO is the second basic tool used as hardware (Badamasi, 2014). The Arduino Ethernet Shield is the card used to connect the Arduino UNO to the internet, and these two cards were thought of as a single structure and were briefly referred to as microcontrollers. In addition, due to the high current drawn by the lighting elements, relay sets were used to keep the system free of this current and to isolate the system.

The system described above in its most basic form is detailed in the following sections. In the first part, the hardware connection structure of the system is discussed. In the second part, the software connection structure is emphasized.

2.1. The Hardware Connection Structure of the System

The link between microcomputer and microcontroller is provided by a digital processing line via a modem that manages the network. In previous versions, Raspberry Pi needed an ethernet connection for internet connection. However, the fact that the Raspberry Pi 3 is able to make a connection with the Wi-Fi connection removes the necessity of using an ethernet cable (Pampattiwar and friends, 2017). A USB camera is also connected to the microcomputer.

The microcontroller has three basic connections. One of these is the ethernet connection line that connect the modem and microcontroller each other. The other two are the direct current line that connect microcontroller with lighting control system and curtain control system. In cases where modem supports wireless networks, the microcontroller is also connected to the network via wireless connection, making necessary configurations in the modem. This eliminates the need for ethernet cable connections.

The hardware connection diagram of the system is shown in Figure 1.

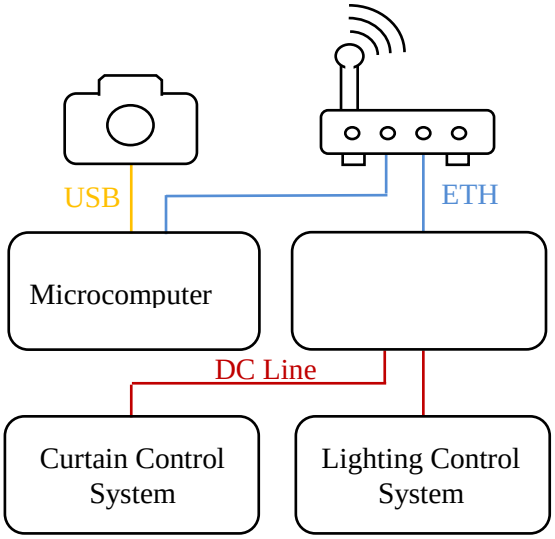

Figure 1. Hardware connection diagram.

Another part used in the project is the relay module which controlled the lamp. Using the relay module, with a voltage as low as 5 VDC can be switched high voltage lines such as 220 VAC. The general connection diagram of the lighting control system is shown in Figure 2.

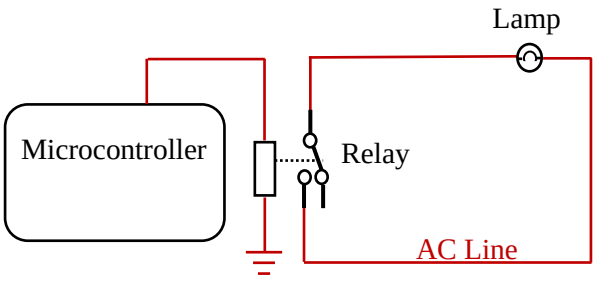

Figure 2. Connection diagram of lighting control system.

Stepping motors are used in applications requiring precise motion (Göktepe, Yavuz, 2016). As a function, it can move step by step to a specific desired position or rotate continuously in the desired direction. Because of this feature, in application, stepping motor was used to open and close the curtain at the desired distance.

To operate the step motors in the desired direction and speed, it should be apply pulses to the windings in a certain order. How many steps the motor takes depends on the applied these pulses. The pulses applied to the windings can be made simply by a switching system. The circuits that make this switching operation are called motor driver control circuits. Using these cards it is possible to operate the stepping motors at the desired speed and desired accuracy. Motor driver control card was used in this application. In Figure 3, the curtain control circuit is shown schematically.

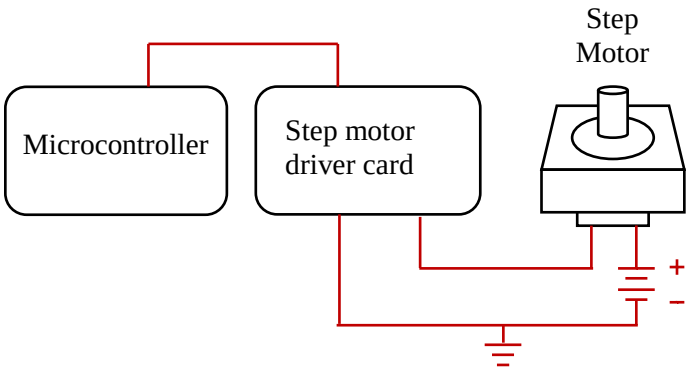

Figure 3. Connection diagram of curtain control system.

2.2. The Software Connection Structure of the System

The software that running on the microcomputer is as follows;

• Python programming language was used for generating commands by processing the image getting from the camera.

• SQLite database software language was used for saving the generated numerical data, commands and the current state of the system in the database.

• An Apache web server was installed to access the database via internet.

• A web interface was created using the CSS and ASP .NET software language to easily access and queries the created database.

• OPC-UA standard is used to provide secure data transfer. The OPC-UA standard refers to platform-independent software standards that use the same interface and allow data transfer between machines, systems, and devices in different manufacturers (Imtiaz, Jasperneite, 2013).

The software that running on the microcontroller are as follows;

• C software language was used for generate commands that received and processed data from the server.

• JSON data exchange format was used for sending the instant status of curtain and lamp to the server. JSON is a data identification form that is completely independent of programming languages but very similar to C-derived language spelling (Nurseitov and friends, 2009; URL-3, 2018).

The algorithm that generates the decision-making mechanism is shown in Figure 4, a similar algorithm was also run for curtain control system.

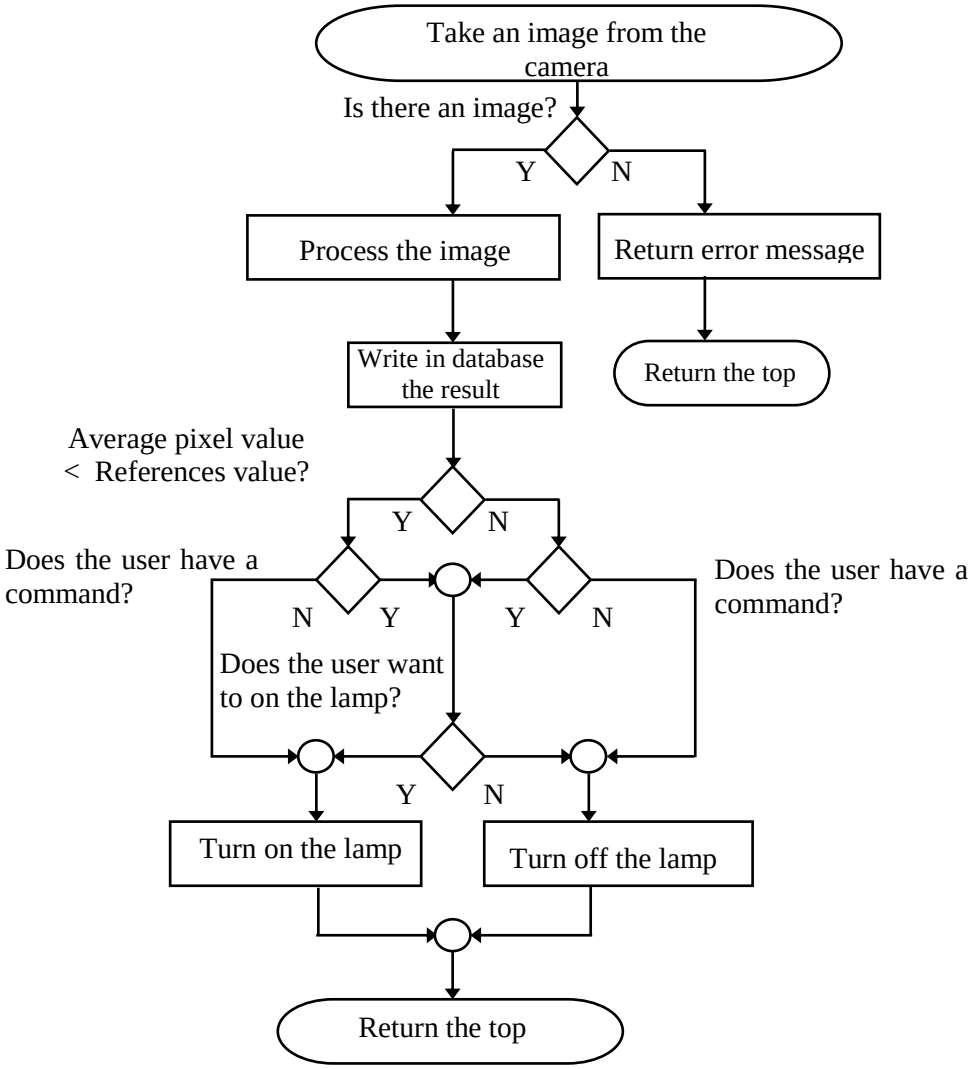

Figure 4. Diagram of decision-making mechanism.

The user connects to the server by entering the user name and password through the web application. It can send commands to the server and display current status. The operation steps of the server in Figure 5 are generally shown.

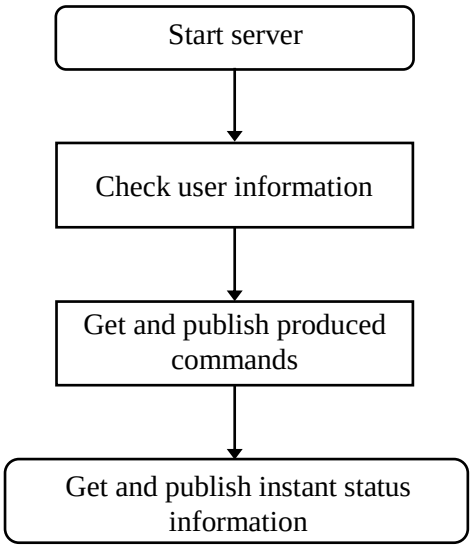

Figure 5. The operation steps of the server.

The flowchart of the software on microcontroller that executes the generated instructions is shown in Figure 6. Microcontroller software receives and executes commands from the server as well as sending instant situations to the server.

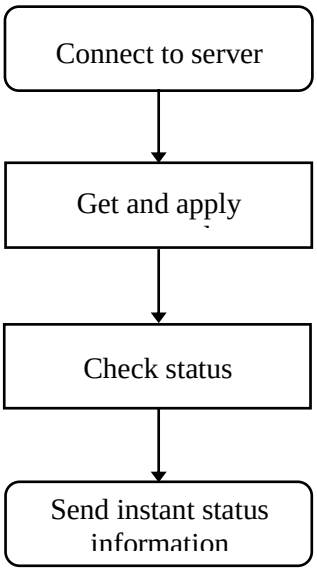

Figure 6. The flowchart of the software on microcontroller

3. Analysis

Application shows that the benefit provided by the system is obtained by turning off the lights when it is bright, rather than by opening the lights in the dark. The main reason for this is the opening of the lights when there is a need for light, but the forgetting or late closing of the lights when it reaches normal brightness level.

It has been observed that the system has low cost and low power consumption compared to its counterparts.

In addition, it showed that, the OPC-UA protocol can be used effectively in industrial systems to secure communication with the Internet of things concept that have entered our lives together with the industry 4.0 trend (Schleipen and friends, 2016).

4. Results

Application's design and software studies are presented on a sample scenario. Besides, most of the equipment used in home automation can be controlled with making some modifications on design and software. Images were taken at certain intervals from the camera and these images were processed instantaneously and used as input to the algorithm. The processed value was compared with the reference value previously determined by the user and the decision was made. This decision is the decision made in automatic mode. In addition, the user can make own decision by switching to manual mode.

Decisions were saved in the database as commands and broadcasted via the server. The microcontroller was connected to the server over the local network and takes commands and applied.

In addition, the status information has been sent to the server and saved on.

The connection of the server with the microcontroller is provided locally, and the connection to the web application is provided over the internet. In the project, OPC-UA data transfer standard is used in network connections. In this way, the data was transmitted and controlled in a safe manner. In this respect, this is an example for Industry 4.0 applications.

As a result, a compact product has been created that can perform the expected functions using a lot of software and hardware equipment.

Thanks

I thank Asst. Prof. Tarik Veli Mumcu for his support and knowledge from designing to finishing at every level of the project.

References

Süzen, A. A., (2013). Home automation for disabilities using kinect technology. SDU International Journal of Technological Science, 5(2).

Çayiroğlu, İ., Erkaymaz, H. (2007). Computer aided distance house by telephone line access). Pamukkale University Journal of Engineering Sciences, 13(3), 379-385.

Yılmaz, F. (2016). Revolution in Manufacturing Processes and Industry 4.0.

Maksimović, M., Vujović, V., Davidović, N., Milošević, V., & Perišić, B. (2014). Raspberry Pi as Internet of things hardware: performances and constraints. design issues, 3, 8.

Badamasi, Y. A. (2014). The working principle of an Arduino. In Electronics, computer and computation (icecco), 2014 11th international conference on (pp. 1-4). IEEE.

Pampattiwar, K., Lakhani, M., Marar, R., Menon, R. (2017). Home Automation using Raspberry Pi controlled via an Android Application.

Göktepe, M., & Yavuz, E. G. E. (2016). Control of stepper motors with optical sensors. Erciyes University Science Institute Journal, 22(1-2).

Imtiaz, J., Jasperneite, J. (2013, July). Scalability of OPC-UA down to the chip level enables "Internet of Things". In Industrial Informatics (INDIN), 2013 11th IEEE International Conference on(pp. 500-505). IEEE.

Schleipen, M., Gilani, S. S., Bischoff, T., & Pfrommer, J. (2016). OPC UA & Industrie 4.0-enabling technology with high diversity and variability. Procedia CIRP, 57, 315-320.

Leitner, S. H., Mahnke, W. (2006). OPC UA–service-oriented architecture for industrial applications. ABB Corporate Research Center.

Khan, R., Khan, S. U., Zaheer, R., Khan, S. (2012, December). Future internet: the internet of things architecture, possible applications and key challenges. In Frontiers of Information Technology (FIT), 2012 10th International Conference on (pp. 257-260). IEEE.

Gubbi, J., Buyya, R., Marusic, S., Palaniswami, M. (2013). Internet of Things (IoT): A vision, architectural elements, and future directions. Future generation computer systems, 29(7), 1645-1660.

Fırat, S. Ü., Fırat, O. Z. (2017). Sanayi 4.0 Devrimi Üzerine Karşılaştırmalı Bir İnceleme: Kavramlar, Küresel Gelişmeler ve Türkiye (A Comparative Study on the Industrial 4.0 Revolution: Concepts, Global Developments and Turkey). Toprak İşveren Magazine, (114), 10-23.

Qin, J., Liu, Y., & Grosvenor, R. (2016). A categorical framework of manufacturing for industry 4.0 and beyond. *Procedia Cirp*, *52*, 173-178.

Nurseitov, N., Paulson, M., Reynolds, R., Izurieta, C. (2009). Comparison of JSON and XML data interchange formats: a case study. Caine, 9, 157-162.

Bray, T. (2017). The javascript object notation (json) data interchange format.

URL-1: https://www.chip.com.tr/haber/nesnelerin-interneti-iot-nedir_64458.html (14 August 2016)

URL-2: http://opcturkey.com/kepserverex-2 (13 February 2017)

URL-3: http://www.json.org/json-tr (10 January 2018)

Determination of Connection Locations of FACTS Devices to Improve Power System Stability

Beytullah BOZALİ[1*], Ali ÖZTÜRK[2], Salih TOSUN[3]

[1]Duzce University, Duzce Vocational School, Department of Electricity and Energy, Düzce, Turkey; beytullahbozali@duzce.edu.tr
[2]Duzce University, Faculty of Engineering, Department of Electric and Electronic Engineering, Düzce, Turkey; aliozturk@duzce.edu.tr
[3]Duzce University, Faculty of Technology, Department of Electric and Electronic Engineering, Düzce, Turkey; salihtosun@duzce.edu.tr

[*]**Responsible Author:**

beytullahbozali@duzce.edu.tr

Abstract

In this study, thyristor controlled series compensators (TSCS) and static var compensator (SVC) effects on voltage stability of power systems were investigated. The studies were carried out on the IEEE 9 bus test system using simulation programs. TSCS and SVC effects on the voltage drops were examined with continuous power flow analysis method. Line stability index values and voltage stability index values of load busses were calculated. According to these values FACTS Devices connection points of power system were determined. After connecting Facts devices, load flow analysis were made by simulation programs. According to the results obtained from studies in improving the stability limit of the power system and reduce active power loss has been shown to have a significant impact of FACTS devices.

Keywords: Power System, Voltage Stability, FACTS Devices, TSCS, SVC

1. Introduction

Depending on the developing technology, electricity demands are also increasing day by day. The increase in energy demand forces power systems to work in regions close to the limits of stability. This situation leads to a reduction in stability limits so the importance of voltage stability has gained increasingly importance in recent years (Taylor, 1994). Voltage stability can be defined as ability to hold between certain limits of voltage amplitude values of load buses of a power system in all conditions (Yalçın, 1995).

Various methods are used to avoid voltage collapses, which is the most important problem in voltage stability. it is possible to increase the voltage stability limits by performing series and parallel compensation on the transmission lines and transformer control with tap changer (Dirik, 2006). It is ensured that the voltage values in the load buses are kept at the desired level thanks to transformer tap changer control (Balanathan, 1998). Transmission line serial reactance is compensated by serial compensation and in this way the maximum power limits of the transmission line can be increased. it is possible to keep the voltage values at the desired values by supplying and removing reactive power from the system.

As demand for electric energy increases, power systems become more complicated as well. Classical methods used to prevent voltage instability and collapse on growing and complex systems sometimes they can not meet the system needs(Gümüş and Yalçın, 2013). Thanks to flexible alternating current transmission system (FACTS) devices, voltage problems in complex and growing systems are solved more quickly and effectively. Besides, when FACTS devices are used properly, ensures the best use of available resources by increasing the stability limits of power systems(Mithulananthan, vd., 2005).

In this study firstly, the voltages, active and reactive power values of each buses, and transmitted power values are obtained with the PowerWorld simulation program to the example nine-bus power system. Then, using Matlab program and bus reduction method, line stability index and voltage stability index valuess were found. Thyristor-Controlled Series Compensation (TSCS) was connected to the weakest transmission line of the example nine bus transmission system according to line stability index values. And similarly Static Var Compensators (SVC) was connected to the weakest load bus of the example nine bus

transmission system according to voltage stability index values. Voltage stability, active and reactive losses in this power system were analyzed using the PowerWorld program under different scenarios. As a result, the FACTS devices connection points have been determined to improve the voltage stability and to minimize the active power losses.

2. Material and Method

2.1. FACTS Devices

FACTS devices which make up modern compensation methods, the use of these devices have gained great importance on account of response in a very short time, individual controllability of each phase, unbalanced loads can be compensated (TMMOB, 1999; Bayram, 1997). FACTS control responds faster than conventional controllers because of its power electronics base. These devices increase the stability limits of the transmission lines when properly used. FACTS have two main purposes. The first is to increase the power transfer capacities of the transmission systems and the second is to control the power flow on the transmission lines. At the same time FACTC devices are also used to ensure voltage stability (Hasanovic, 2000). Today, many power flow controllers have been developed under the name FACTS. The most common of these can be denoted as Static Var Compensator (SVC), Thyristor Controlled Series Capacitor (TCSC), Static Compensator (STATCOM), Unified Power Flow Controller (UPFC), Phase Shifting Transformer (PST) and Static Synchronous Series Capacitor (SSSC)

2.2. Static Var Compensator

The main task of the SVC is provide capacitive or inductive current to the bus depending on the control datas (IEEE, 1995). SVC allows to control the system voltage within the specified limits with reactive power control. The most well-known forms are the constant capacity thyristor controlled reactor (TCR) and the thyristor controlled capacitor (TSC). The simple structure of the SVC for voltage control is shown in Figure 1.

Working principle of SVC is based on obtaining shunt impedance with variable values depending on the calculated triggering angles of capacitorss and / or reactors. With appropriate triggering, a wide range of reactive power settings can be made on the bus from the maximum

capacitive reactive power value to the maximum inductive reactive power value (Arifoğlu, 2002). The inductance value determine Capacitive or inductive working status of the device. The value of inductance is determined by equation (1) (Canizares and Zeno, 1999).

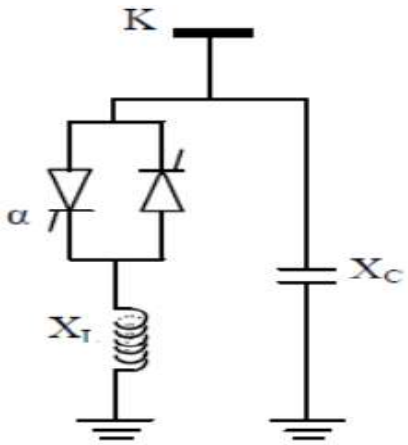

Figure 1. Basic Structure of SVC.

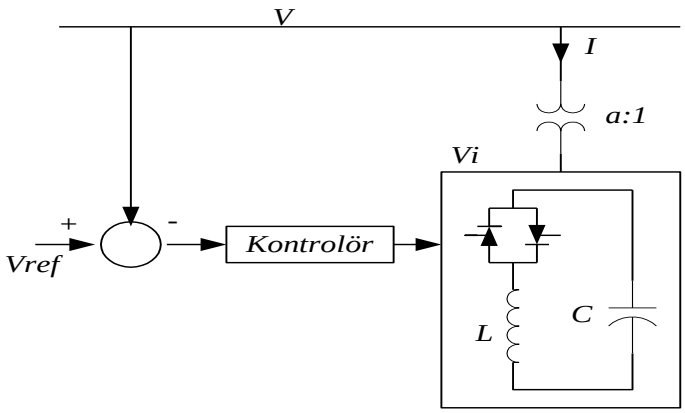

Figure 2. Schematic Model of SVC.

$$X_V = X_L \frac{\pi}{2(\pi-\alpha)+\sin 2\alpha} \quad (1)$$

In Equation 1, XL express the uncontrolled fundamental inductive reactance of the thyristor and α express the trigger angle (Canlzares and Faur, 1999; Taleb, vd., 2004). The total impedance of the controller is found by Equation (2).

$$X_e = X_C \frac{\pi / r_x}{\sin 2\alpha - 2\alpha + \pi(2-\frac{1}{r_x})} \quad (2)$$

In Equation 2, rx = Xc / XL gives the limits of the triggering angles and the limit values of the controllers, Xc is the capacitive reactance. The output power of the SVC is determined by the Equation (3). V is the voltage of the transmission line in equation 3,

$$Q_c = \frac{V^2}{X_v} - \frac{V^2}{X_c} \quad (3)$$

The voltage control characteristic of the SVC under continuous operation is also shown in Figure 3 (Canizares, 2000). V_{ref} shows the voltage value under normal load condition, B_{max} indicates availability of all capacities, B_{min} indicates that all capacities are deactivated. Depending on these, it is ensured that the current supplied to the system is inductive or capacitive. In this system the SVC controls the power system to which it is connected by acting as an adjustable reactive power source.

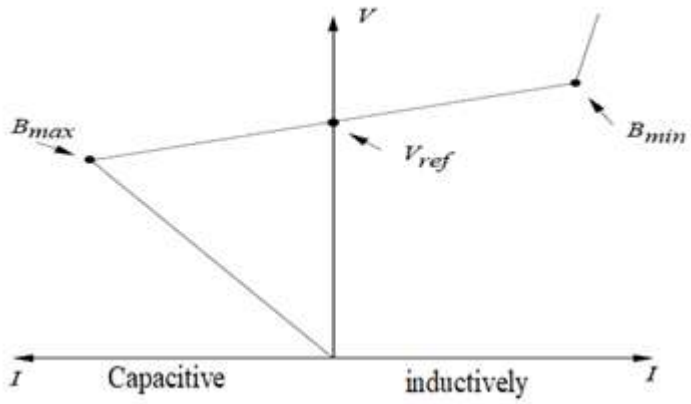

Figure 3. Typical Steady State V–I Characteristic of a SVC.

2.3. Thyristor Controlled Series Capacitor

TCSC is a typical serial FACTS device. TCSC configuration was shown in Figüre 4. TCSC uses a fixed capacitor (CF), thyristor controlled reactors (TCR) and a capacitor (C) connected in shunt with them (Tiwari and Sood, 2009). The reactance can change smoothly and quickly with the control of the triggering angles of the thyristors. TCSC can directly regulate power flow and allow system to work closer to line limit values. It can improve the dynamic performance and stability of the power system due to its fast and flexible ability. The X-I characteristic of the TCSC was shown in Figure 5. For stability and damping control, the TCSC usually operates in the capacitive region. This situation was shown in Figure5 ase ABC field (Larsen vd., 1993; Bowler vd., 1992; Medina vd., 2003).

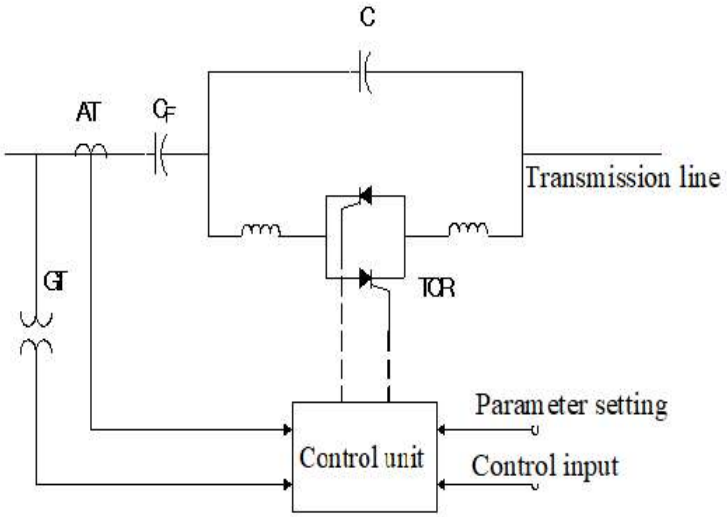

Figure 4. Modeling Circular of TCSC.

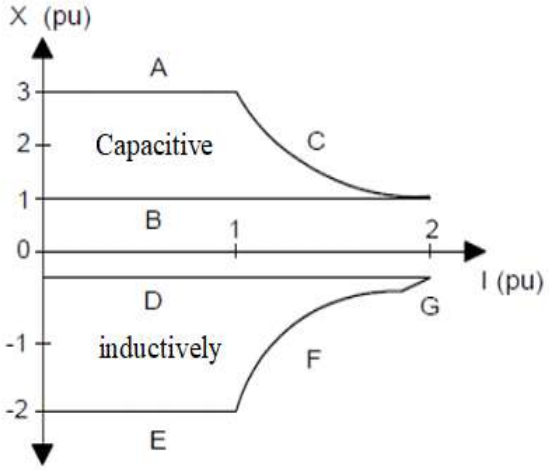

Figure 5. X-I Characteristic of TCSC.

In the Figure 5, A and E firing angle limit, B the situation where the thyristors are blocked, C maximum voltage limit, D thyristors are in full transmission region, F harmonic heating limiti, G Thyristor current limit (max.) are express respectively

3. Findings and Discussion

3.1. System Simülations and Results

Based on the proposed cogeneration price function and the avoided costs concerning the loss and upgrade of transmission lines, computer simulations are conducted. Details are given in the following.

3.2. System Description and Methodology

To illustrate the correctness and practicality of the proposed price function, computer simulations for an IEEE-9 bus system shown in Figure 6 are given. The system bus data and line parameters are listed in Tables 1 and 2, respectively.

Table 1. Bus Data (base case) Base=100MVA

Bus no.	Pg (PU)	Qg (PU)	PL (PU)	QL (PU)	Bus type
1	Swing	Swing	0.00	0.00	1
2	1.63	0.00	0.00	0.00	2
3	0.85	0.00	0.00	0.00	2
4	0.00	0.00	0.00	0.00	3
5	0.00	0.00	0.90	0.30	3
6	0.00	0.00	0.00	0.00	3
7	0.00	0.00	1.00	0.35	3
8	0.00	0.00	0.00	0.00	3
9	0.00	0.00	1.25	0.50	3

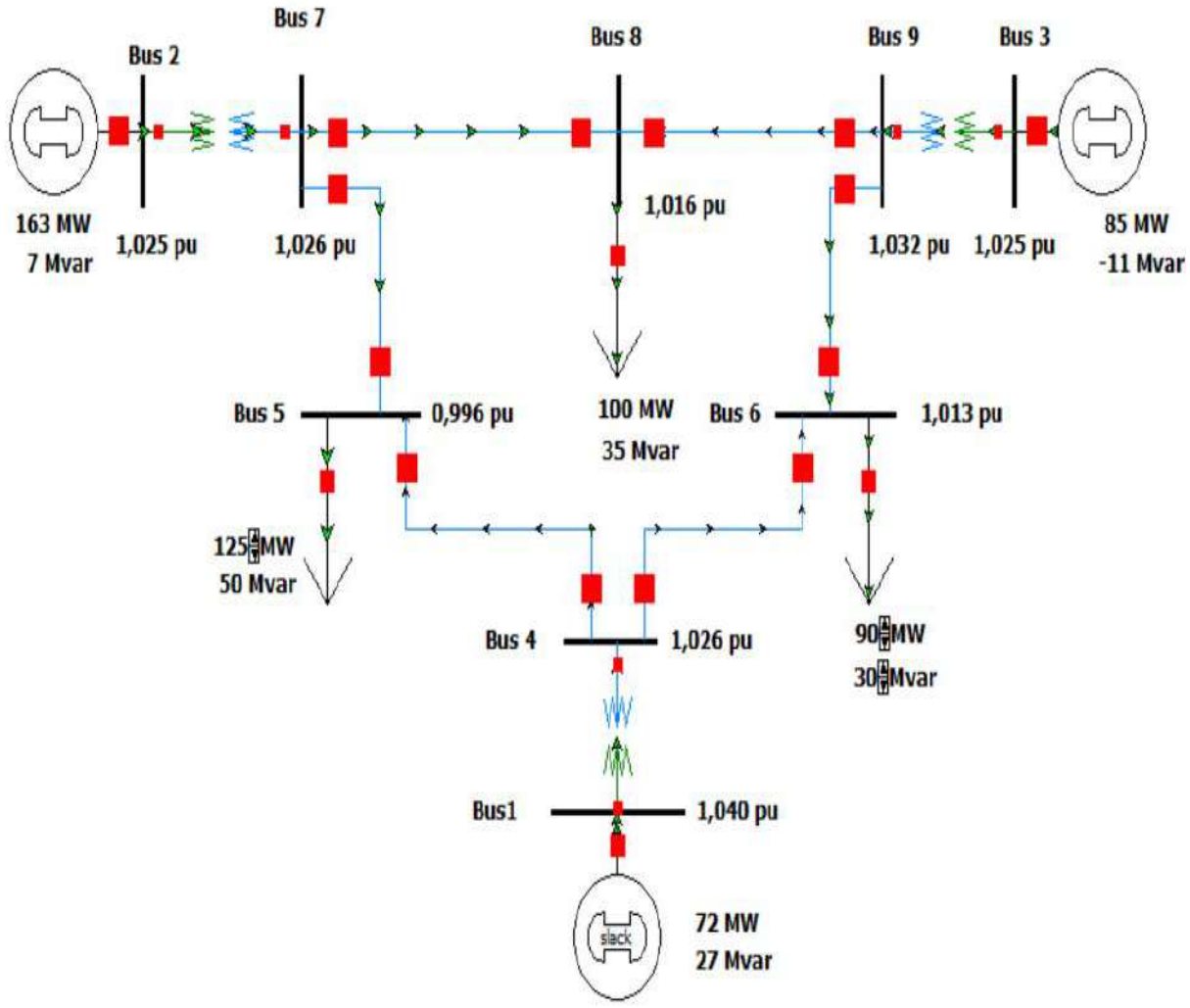

Figure 6. IEEE 9 Bus Model in Power World Simulator

Figure 6 to system with 9 buses and 3 generators. This particular test case also includes 3 two-winding transformers, 6 lines and 3 loads. The base kV levels are 13.8 kV, 16.5 kV, 18 kV, and 230 kV. The single-line diagram of the 9-bus case is shown below (Anderson and Fouad, 2003).

Table 2. Transmission Line Data 9 Bus System

Line no.	From_bus	To_bus	R	X	B
1	4	1	0.0000	0.0576	0.0000
2	2	7	0.0000	0.0625	0.0000
3	9	3	0.0000	0.0586	0.0000
4	5	4	0.0100	0.0850	0.1760
5	6	4	0.0170	0.0920	0.1580
6	7	5	0.0320	0.1610	0.3060
7	9	6	0.0390	0.1700	0.3580
8	7	8	0.0085	0.0720	0.1490
9	8	9	0.0119	0.1008	0.2090

Power flow analysis is called the backbone of power system analysis. Transient stability analysis of system fault analysis and its improvement is one of the basic problems in power system engineering. The single line diagram of IEEE 9 bus model is shown in figüre 6.

Table 3. Bus Data of IEEE 9 Bus Test System

Name	Nom kV	PU Volt	Volt (kV)	Angle (Deg)	Load MW	Load Mvar	Gen MW	Gen Mvar
1	16.5	1.04000	17.160	-0.00			71.63	27.02
2	18	1.02501	18.450	9.28			163.00	6.57
3	13.8	1.02501	14.145	4.67			85.00	-10.91
4	230	1.02580	235.935	-2.22				
5	230	0.99566	229.003	-3.99	125	50		
6	230	1.01268	232.916	-3.69	90	30		
7	230	1.02583	236.941	3.72				
8	230	1.01597	233.673	0.73	100	35		
9	230	1.03239	237.449	1.97				

Table 4. Power Flow List of IEEE 9 Bus Test System

From Bus	To Bus	Branch Device Type	MW From	Mvar From	MVA From	MW Loss	Mvar Loss
4	1	Transformer	-71.6	-23.9	75.5	0.0	3.12
2	7	Transformer	163.0	6.6	163.1	0.0	15.83
9	3	Transformer	-85.0	15.0	86.3	0.0	4.10
5	4	Line	-40.7	-38.7	56.1	0.26	-15.80
6	4	Line	-30.5	-16.5	34.7	0.17	-15.51
7	5	Line	86.6	-8.4	87.0	2.30	-19.69
9	6	Line	60.8	-18.1	63.5	1.35	-31.53
7	8	Line	76.4	-0.8	76.4	0.48	-11.51
8	9	Line	-24.1	-24.2	34.2	0.09	-21.18

3.3. Voltage and Line Stability Indexes of the Nine-Bus Test System

Active power loss values that obtained by power flow analysis for IEEE 9 Bus Test System are given in Table 5. Power System Analysis Toolbox (PSAT) simulation program was used in analyzes. According to these values, the serial TSCS was connected to the transmission line with the most power losses (Between 7 and 5 buses) so that trnasmission line losses were minimized. In the case of using the PSAT program, a graph of the bus voltage values was obtained by continuous power flow analysis for the IEEE 9 Bus Test System. Voltage values were shown in Figure 7. Due to the low voltage of the 5th bus, the SVC was connected to the 5th bus to increase and control the voltage values. SVC was selected between 2 and 15 MVAr power values.

Table 5. Power Losses IEEE 9 Bus Test System

From Bus	To Bus	Line	P Loss
9	8	1	0,00088
7	8	2	0,004753
9	6	3	0,013538
7	**5**	**4**	**0,023**
5	4	5	0,002575
6	4	6	0,001664
2	7	7	2,22E-16
3	9	8	0

1	4	9	0

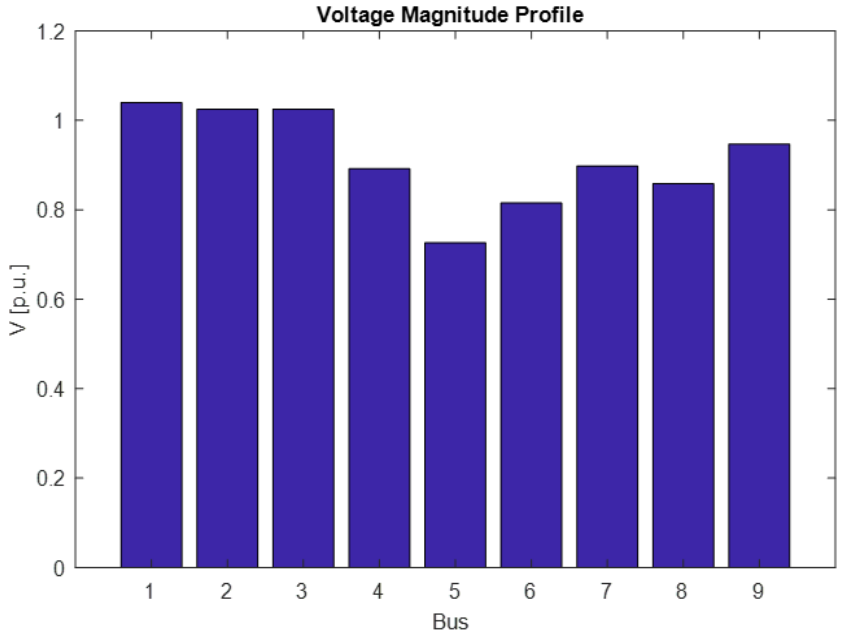

Figure 7. IEEE 9 Bus PSAT Simulator Voltage Values

3.4. Bus Voltage Values, After placing the FACTS Devices on the 9 Bus Test System

Table 6. Bus voltage Values , After TSCS

Bus No	%20		%40		%60		%80	
	Before placing the FACTS device	After placing the FACTS device	Before placing the FACTS device	After placing the FACTS device	Before placing the FACTS device	After placing the FACTS device	Before placing the FACTS device	After placing the FACTS device
1	1.04	1.04	1.04	1.04	1.04	1.04	1.04	1.04
2	1.025	1.025	1.025	1.025	1.025	1.025	1.025	1.025
3	1.025	1.025	1.025	1.025	1.025	1.025	1.025	1.025
4	1.0258	1.0246	1.0258	1.0262	1.0258	1.028	1.0258	1.03
5	0.99563	0.99316	0.99563	0.99702	0.99563	1.0014	0.99563	1.0063
6	1.0127	1.0109	1.0127	1.0124	1.0127	1.014	1.0127	1.0156
7	1.0258	1.0117	1.0258	1.0117	1.0258	1.0117	1.0258	1.0118
8	1.0159	1.006	1.0159	1.0062	1.0159	1.0063	1.0159	1.0065
9	1.0324	1.029	1.0324	1.0292	1.0324	1.0295	1.0324	1.0297

Real Power Losses [p.u.]	**0,04641**	**0,022027**	**0,04641**	**0,019891**	**0,04641**	**0,017996**	**0,04641**	**0,016471**
Reactive Power Losses [p.u.]	**-0,9216**	**-0,61061**	**-0,9216**	**-0,6438**	**-0,9216**	**-0,68036**	**-0,9216**	**-0,72076**

The TSCS was connected to the transmission line serially between bus number 5 and 4. So, the transmission line reactance becomes controllable between 20% and 80%. The results were given in Table 6. According to the results, active and reactive power losses have been reduced and it has been understood that it has a positive effect on the stability of voltage.

Table 7. Bus Voltage Values, After placing the SVCs on the 9 Bus Test System

Bus No	Before placing the FACTS device	SVC is worth 2 Mar	SVC is worth 4 Mar	SVC is worth 5 Mar	SVC is worth 8 Mar	SVC is worth 10 Mar	SVC is worth 15 Mar
1	1.04	1.04	1,04000	1,04000	1,04000	1,04000	1,04000
2	1.025	1.025	1,02500	1,02500	1,02500	1,02500	1,02500
3	1.025	1.025	1,02500	1,02500	1,02500	1,02500	1,02500
4	1.0258	1,02646	1,02714	1,02748	1,02851	1,02919	1,03092
5	0.99563	0,99743	0,99924	1,00015	1,00287	1,00470	1,00929
6	1.0127	1,01319	1,01373	1,01400	1,01481	1,01535	1,01671
7	1.0258	1,02622	1,02667	1,02689	1,02757	1,02802	1,02917
8	1.0159	1,01624	1,01660	1,01678	1,01732	1,01768	1,01859
9	1.0324	1,03256	1,03276	1,03286	1,03317	1,03338	1,03390
Real Power Losses [p.u.]	**0,04641**	**0,046**	**0,046**	**0,046**	**0,046**	**0,046**	**0,045**
Reactive Power	**-0,9216**	**-0,925**	**-0,928**	**-0,93**	**-0,934**	**-0,937**	**-0,945**

Losses [p.u.]				

SVC with different values between 2 MVAr and 15 MVAr was connected to number of 5 in the IEEE 9 bus test system. The results obtained were given in Table 7. According to the results, active power losses have been reduced and it has been understood that it has a positive effect on the stability of voltage.

3.5 Both SVC and TSCS connection status for IEEE 9 Bus Test System

Table 8. Bus Voltage Values, in case of 20% Serial Compensation (TSCS) and SVC Connected Together

Bus Number	Before placing the FACTS device	SVC 5 MVAr	SVC 10 MVAr	SVC 15 MVAr
1	1.04	1,04000	1,04000	1,04000
2	1.025	1,02500	1,02500	1,02500
3	1.025	1,02500	1,02500	1,02500
4	1.0258	1,02798	1,02958	1,03118
5	0.99563	1,00092	1,00515	1,00942
6	1.0127	1,01473	1,01601	1,01729
7	1.0258	1,02768	1,02890	1,03014
8	1.0159	1,01742	1,01838	1,01934
9	1.0324	1,03314	1,03366	1,03419
Real Power Losses [p.u.]	**0,04641**	**0,046**	**0,046**	**0,046**
Reactive Power Losses [p.u.]	**-0,9216**	**-0,956**	**-0,964**	**-0,97**

Table 9. Bus Voltage Values, in case of 40% Serial Compensation (TSCS) and SVC Connected Together

Bus Number	Before placing the FACTS device	SVC 5 MVAr	SVC 10 MVAr	SVC 15 MVAr
1	1.04	1,04000	1,04000	1,04000

2	1.025	1,02500	1,02500	1,02500
3	1.025	1,02500	1,02500	1,02500
4	1.0258	1,02839	1,02985	1,03132
5	0.99563	1,00146	1,00531	1,00920
6	1.0127	1,01541	1,01659	1,01778
7	1.0258	1,02868	1,03002	1,03136
8	1.0159	1,01818	1,01921	1,02024
9	1.0324	1,03343	1,03395	1,03448
Real Power Losses [p.u.]	**0,04641**	**0,047**	**0,047**	**0,046**
Reactive Power Losses [p.u.]	**-0,9216**	**-0,985**	**-0,992**	**-0,998**

Table 10. Bus Voltage Values, in case of 60% Serial Compensation (TSCS) and SVC Connected Together

Bus Number	Before placing the FACTS device	SVC 5 MVAr	SVC 10 MVAr	SVC 15 MVAr
1	1.04	1,04000	1,04000	1,04000
2	1.025	1,02500	1,02500	1,02500
3	1.025	1,02500	1,02500	1,02500
4	1.0258	1,02866	1,02994	1,03123
5	0.99563	1,00160	1,00498	1,00838
6	1.0127	1,01597	1,01704	1,01811
7	1.0258	1,02999	1,03146	1,03294
8	1.0159	1,01912	1,02023	1,02134
9	1.0324	1,03372	1,03425	1,03478
Real Power Losses [p.u.]	**0,04641**	**0,048**	**0,048**	**0,048**
Reactive Power Losses [p.u.]	**-0,9216**	**-1,017**	**-1,012**	**-1,028**

Table 11. Bus Voltage Values, in case of 80% Serial Compensation (TSCS) and SVC Connected Together

Bus Number	Before placing the FACTS device	SVC 5 MVAr	SVC 10 MVAr	SVC 15 MVAr
1	1.04	1,04000	1,04000	1,04000
2	1.025	1,02500	1,02500	1,02500
3	1.025	1,02500	1,0250	1,02500
4	1.0258	1,02865	1,02972	1,03079
5	0.99563	1,00105	1,00383	1,00662
6	1.0127	1,01634	1,01726	1,01818
7	1.0258	1,03172	1,03336	1,03501
8	1.0159	1,02029	1,02150	1,02272
9	1.0324	1,03401	1,03455	1,03509
Real Power Losses [p.u.]	**0,04641**	**0,051**	**0,05**	**0,05**
Reactive Power Losses [p.u.]	**-0,9216**	**-1,05**	**-1,055**	**-1,06**

In case of TSCS and SVC Connected Together for IEEE 9 bus Test System, the results were given in Table 8-11. SVCs with different power ratings, such as 5 MVAr, 10 MVAr, and 15 MVAr and TSCS rates from 20% to 80%. According to the obbtained results, If the SVC is 5 MVAr and TSCS is 20%, the power system can operate most stable, active and reactive power provides the best power transfer. As a result, by connecting the SVC and the TSCS to the connection points determined in the system, it is possible to provide much more stable operation of the system.

4. Conclusion and Suggestions

SVC was connected to number of 5 in the IEEE 9 bus test system and also the TSCS was connected to the transmission line serially between bus number 4 and 5. In this case, Active Power, Reactive Power and Angle values result were given in Table 12. According to these values, If 80% TSCS and SVC with 15 MVAr are connected to the system, voltage stability and power transfer will be positively affected, both voltage stability and power transfer will be improved.

Table 12. Power losses before and after inserting FACTS Devices

	Ploss	**Qloss**
Before placing the FACTS device	0.046	-0.0922
20% TSCS	0,047	-0,949
40% TSCS	0,047	-0,978
60% TSCS	0,049	-1,01
80% TSCS	0,051	-1,045
TSCS and SVC are connected together	0,045	-0,93

In this study, the effects of the transistor controlled series compensator (TSCS) and the static var compensator (SVC) controllers on the power system voltage stability were investigated. The studies have been done on the IEEE 9 bus test system. The effects of TSCS and SVC on voltage collapses were investigated using the continuous power flow analysis method. The stability index values of the lines and the voltage stability index values of the load buses were calculated. According to the results obtained by the study, it is seen that the FACTS devices have a significant effect on improving the stability limits of the power system and reducing active power losses.

The power loss values before and after placing FACTS devices were given in Table 12. As a result, the points to connect the FACTS devices to improve the stability of the system have been determined. Thanks to the FACTS devices, significant improvements have been achieved for power transfer and voltage stability.

References

Arifoğlu, U., (2002). *Güç Sistemlerinin Bilgisayar Destekli Analizi*, Alfa Yayınları, İstanbul.

Anderson, P. M., and Fouad, A. A., (2003). Power System Control and Stability, 2nd ed. New York: IEEE Press,

Balanathan, R., (1998). *Techniques to efficiently improve power system voltage stability*, Doctor thesis, The university of Auckland, New Zealand.

Bayram, M., (1997). *Reaktif Güç Kompanzasyonu*, ENTES, İstanbul,

Bağrıyanık, M., (1997). *Enerji iletiminde gerilim kararlı en uygun reaktif güçdesteklemelerinin incelenmesi*, İstanbul Teknik Üniversitesi Fen Bilimleri Enstitüsü, Doktora Tezi, 161 Sayfa.

Bowler, C., Larsen, E., Damsky, B., Nilsson, S., (1992). Benefits of thyristor-controlled series compensation, *CIGRE*, paper No. 14/37/38-04.

Canizares, C.A., Zeno T.F., (1999). Analysis of SVC and TCSC Controllers in Voltage Collapse, *IEEE Transactions on Power Systems*, Vol. 14, No. 1.

Canizares, C.A., (January 2000). *Power Flow and Transient Stability Models of FACTS Controllers for Voltage and Angle Stability Studies*. In Proc. of IEEE/PES Winter Meeting, Singapore.

Cutsem, TV, Vournas C, (1998). Voltage Stability of Electric Power Systems, *Power Electronics and Power System Series*, Kluwer.

Canlzares, C.A., Faur, Z.T., Analysis SVC and TCSC Controllers in Voltage Collapse, *IEEE Transactions on the power systems*, vol. 14, No. 1, February 1999, pp. 158-165.

Dirik, H. (2006). *STATCOM ve SSSC Denetleyicilerinin Güç Sistemi Gerilim Kararlılığı Üzerine Etkisinin İncelenmesi*. Yüksek Lisans Tezi, Ondokuz Mayıs Üniversitesi, Samsun, Türkiye,

Gümüş, T.E., and Yalçın, M.A., (2013). *Facts cihazlarının gerilim kararlılığına etkisinin incelenmesi*, SAÜ. Fen Bil. Der. 17. Cilt, 2. Sayı, s.1-6.

Hasanovic, A., (2000). *Modeling and Control of The Unified Power Flow Controller (UPFC)*, MA Thesis, West Virginia Uni.,

IEEE FACTS working group 15.05.15, "FACTS Application", December 1995.

Kaur, R., Kumar, D. (2016). Transient Stability Improvement of IEEE 9 Bus System Using Power World Simulator, *MATEC Web of Conferences 57, ICAET*, 01026 (2016), pp. 2,4.

Kaur, R., Kumar, Er. D., (January 2016). Transient Stability Analysis of IEEE 9 Bus System in Power World Simulator, *Ramandeep Kaur Int. Journal of Engineering Research and Applications*, ISSN: 2248-9622, Vol. 6, Issue 1, (Part - 2) January 2016, pp.35-39.

Larsen, E., Clark V., Miske K., Urbanek S., A., (1993). Characteristics and rating considerations of thyristor-controlled series compensation, *IEEE/PES Summer meeting*, paper no 93 SM 433-3 PWRD, Vancouver Canada, july 18-22.

Mithulananthan, N., Sode -Yome, A., and Acharya, N., (2005). *Application of FACTS Controllers in Thailand Power Systems*, School of Environment, Resources and Development Asian Institute of Technology, Thailand.

Milano, F., Vanfretti, L., Morataya, J. C., (2008). *An Open Source Power System Virtual Laboratory: The PSAT Case and Experience*, IEEE Transactions on Education, Vol. 51, No. 1, pp. 17-23, February.

Mallaiah B. and Ramana Reddy P., (2015). Voltage Stability Enhancement Through Optimization Techniques, Internet.

Medina, A., Ramos-Paz, A., Fuerte-Esquivel, C.R., (2003). *Swift computation of the periodic steady state solution of power systems containing tcscs*, Elsevier, Electrical Power and Energy Systems 25, 689–694.

Subramani, C., Dasch, S.S., Arun Bhaskar, M., Jagdeshkumar, M., (2009). *Simulation technique for voltage stability Analysis and contingency ranking in power systems*, International Journal of Recent Trends in Engineering, Vol 2, No. 5.

Taylor, W. (1994). *Power System Voltage Stability*, McGraw-Hill, New York.

TMMOB, TMMOB *Reaktif Güç Kompanzasyonu Seminer Notları*, İstanbul EMO, 1999.

Tiwari, P.K., Sood, Y.R., (2009) *Optimal Location Of Facts Devices İn Power System Using Genetic Algorithm*, Nature & Biologically İnspired Computing, 2009. Nabic 2009. World Congress On, Pages: 1034 – 1040.

Talebi, N., Ehsan, M., Bathaee, S.M.T., (2004). *Effects of SVC and TCSC Control Strategies on Static Voltage Collapse Phenomena*, IEEE Proceedings, Southeast Con, pp. 161 - 168, Mar.

Yalçın, M.A. (1995). *Enerji Sistemlerinde Gerilim Kararlılığının Yeni Bir Yaklaşımla İncelenmesi*, Doktora Tezi, İTÜ Elektrik-Elektronik Fakültesi, İstanbul.

Investigation of the Effects of Power Transformer Tap Changer Ratio Values on Power Systems Voltage Stability

Beytullah BOZALİ[1*], Ali ÖZTÜRK[2], Salih TOSUN[3]

[1]Duzce University, Duzce Vocational School, Department of Electricity and Energy, Düzce, Turkey; beytullahbozali@duzce.edu.tr
[2]Duzce University, Faculty of Engineering, Department of Electric and Electronic Engineering, Düzce, Turkey; aliozturk@duzce.edu.tr
[3]Duzce University, Faculty of Technology, Department of Electric and Electronic Engineering, Düzce, Turkey; salihtosun@duzce.edu.tr

[*]**Responsible Author:**
beytullahbozali@duzce.edu.tr

Abstract

The critical values of a power system are the boundary values of voltage stability. These are the values of the maximum active power that load busses can take and the values of voltage amplitude and angle of the busses in this condition. In this research, the voltage stability values in electric power systems are defined according to the tap chance values of under load tap changer transformers. So, the effects of the tap changes values on the voltage stability were examined. Transformer tap settings are used to hold the voltage against voltage changes at a specified reference value. At the same time the stability limit values are changed when voltage control. The studies were carried out on the IEEE 9 bus test system using simulation programs. The voltage stability limit values are determined for different transformer tap change ratio values. The results show that transformer tap change rate values changes have affected critical values.

Keywords: Power System , Voltage Stability, Power Transformer, Tap Changer

1. Introduction

Depending on the developing technology, electricity demands are also increasing day by day. The increase in energy demand forces power systems to work in regions close to the limits of stability. This situation leads to a reduction in stability limits so the importance of voltage stability has gained increasingly importance in recent years(Taylor, 1994). As demand for electric energy increases, power systems become more complicated as well. Classical methods used to prevent voltage instability and collapse on growing and complex systems sometimes they can not meet the system needs(Gümüş and Yalçın, 2013). Power system critical values are voltage stability limit values. Critical values of a power system is load bus active power value ,load bus voltage amplitude value and load bus angle value when the load bus has the highest active power value. Voltage stability can be defined as ability to hold between certain limits of voltage amplitude values of load buses of a power system in all conditions(Yalçın, 1995). Changes of loads in the power system cause unwanted voltage changes. Under Load Tap-Changer Transformers (ULTCT) are used to solve this problem. ULTCT are an important voltage regülatör and are systems that keep the voltage at the load bus at desired values thanks to automatic conversion rates (Dong vd., 2004). ULTCT have an important influence on the medium-term voltage stability problem. (Zhu vd., 2000) and (Vournas, 2002). Using the static analysis in the given references, they have shown that the ULTCT have the effect of increasing the maximum power transfer and improving the stability of the voltage.

Thanks to the tap changer ratios, it allows to keep the voltage in the load buses at the desired level (Balanathan,1998). ULTCT have believed to be able to remove or minimize ineffective voltage instabilities of power systems. Studies in the field of ULTCT were carried out to investigate the stability effects in the field of voltage stability (Bourgin vd.,1993; Glavitsch vd.,1981). Some studies in the literature were concern ULTCT with new models (Calovic, 1994; Liu vd., 1989). Other studies were concerned with the effects on voltage stability.

Transformer tap changer settings are used to hold the voltage against voltage changes at a specified reference value. At the same time, the stability limit values change when voltage control is performed. In this study firstly, the voltages, active and reactive power values of each buses, and transmitted power values are obtained with the PowerWorld simulation program to the example nine-bus power system. Than, Voltage stability limit values were determined according to the tap change ratio of ULTCT. Thus, the effects of the tap changer rate values on

the voltage stability were examined. The works were carried out using simulation programs on the IEEE 9 Bus Test System. The critical values of voltage stability for different transformer tap changer ratio values were determined by plotting P-V curve. As a result of the works, it has been seen that the critical values have also affected with the tap changer values of transformer.

2. Materyal ve Metotlar

2.1. Model of Transformer With TAP-Changer

When the system voltage level drops, it is necessary to tap change of transformer for the consumers who are connected to the secondary side. Adjustable transformers (tap-changers) are commonly used to adjust the voltage in power systems. There are two types depending on whether the tap changer is automatic or not. The transformer that automatically changes the tap when the load changes is called under load tap changer transformer (ULTC).

A transformer having a nominal conversion ratio can be represented by an impedance or admittance that is serially connected with an ideal auto-transformer as shown in Figure 1a. The parameters of the equivalent pi circuit were shown in Figure 1b.

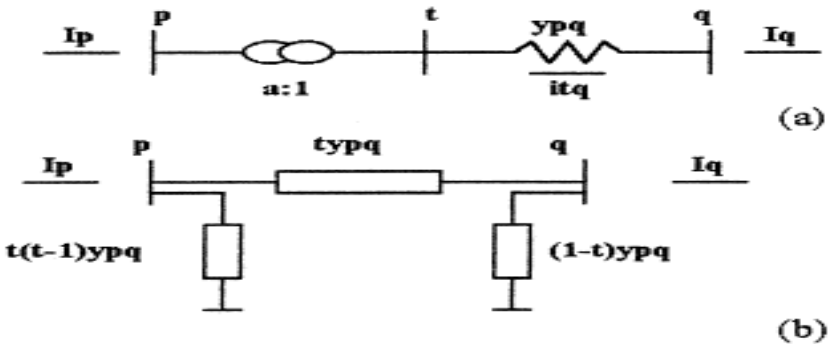

Figure 1. Tapped-changing transformer representations. (a) Equivalent circuit; (b) Equivalent pi circuit with parameters.

Non-nominal tap change ratio ('t' = 1 / a), the nominal unit value is the percentage deviation above or below the value. It usually ranges between 0.8 and 1.2. (t = 1 / a) and a is the conversion ratio of the ideal equivalent automatic transformer shown in figure 1. y_{pq} represents the serial admitans value of transformer in the Figure1. (El-Sadek vd., 1999).

2.2.Interrelation Between Loads Power and Tap-Changing Ratio at Different Load Voltages

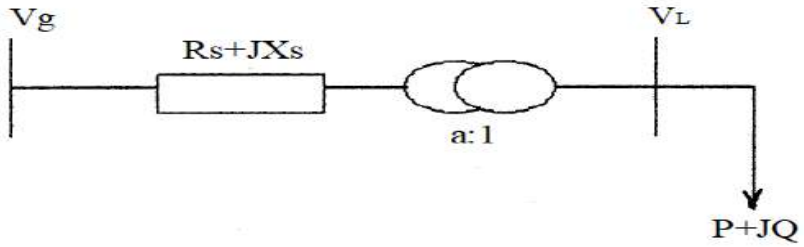

Figure 2. Thevenin's equivalent system.

The system in Figure 2 is used to examine the relationship between load power at different load voltages of tap changer transformer. Rs ohmic resistance value of transmission line, Xs inductive reactance value of transmission line, Vg source of line voltage value, VL voltage of load value, represents respectively inthe Figure 2

2.3. Stability Index

2.3.1. Continuous Case Voltage Stability

Static analyzes (load flow analyzes) of voltage stability are considered to be seen as a continuous state problem. Voltage stability is also called load stability. System and voltage stability can be examined with static analysis, although it is dynamic. In a power system under given operating point and disturbance conditions, if the voltages remain at or close to the equilibrium values after the disturbing effect, the voltage of this power system is stable (Cutsem and Vournas 1998). If the voltages after the disturbing effect are below the acceptable limits, the system is in the unstable region and voltage drop may ocur (Bağrıyanık, 1997).

The main cause of the instability is the inadequacy of the power system to meet the reactive power demand. Voltage instability normally occurs in heavily loaded systems. In reality, the voltage dependence depends on the relationship between power (P, Q) and voltage (V). The two-bus power system model was shown in Figure 3. The P-V curve for the two-bus transmission line was shown in Figure 4. Critical values of a power system is load bus active power value, load bus voltage amplitude value and load bus angle value when the load bus has the highest active power value. This point is called the critical load point of the system. Critical

values were shown on Figure 4. The upper part of the P-V curves that given Figure 4. reflects the normal steady-state operating region, while the lower region is the region corresponding to the voltage instability. More power demand from critical power leading to system instability (Kunder, 1993; Kundur, 1994; Kundur and Morison, 1997).

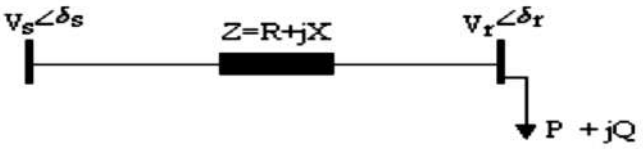

Figure 3. Two-bus power and voltage system model.

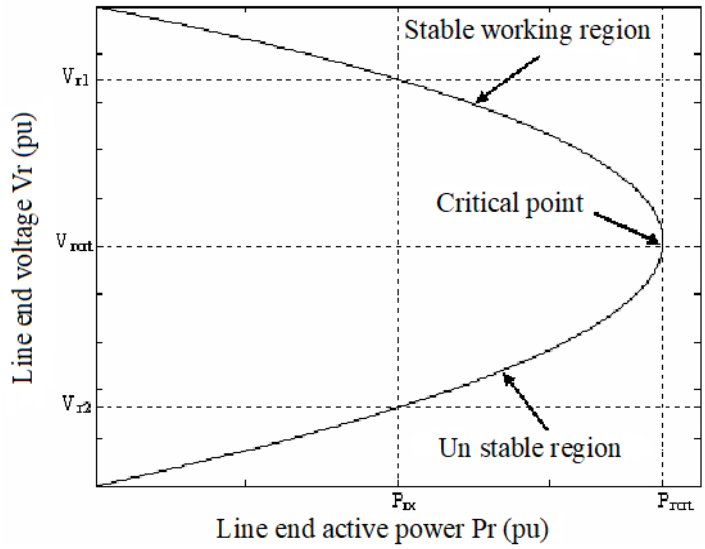

Figure 4. Transmission line P-V curve.

The voltage-loading parameter (V-λ) and relationship between active and reactive power of bus in the power system are expressed in Equation (1).

$$P_L = P_{L0}\,(1+\lambda) \qquad Q_L = Q_{L0}(1+\lambda) \tag{1}$$

P_{L0} and Q_{L0}, the initial active power and reactive power values, P_L and Q_L. the active power and reactive power values of the load, λ the maximum load parameter value are express in equation 1. Continuous power flow analysis are required to establish the relationship between the voltage and the maximum load parameter (V-λ).

3. Findings and Discussion

3.1. System Simülations and Results

Based on the proposed cogeneration price function and the avoided costs concerning the loss and upgrade of transmission lines, computer simulations are conducted. Details are given in the following.

3.2. System Description and Methodology

To illustrate the correctness and practicality of the proposed price function, computer simulations for an IEEE-9 bus system shown in Figure. 5 are given. The system bus data and line parameters are listed in tables 1 and 2, respectively.

Table 1. Bus data (base case) Base=100MVA

Bus no.	Pg (PU)	Qg (PU)	PL (PU)	QL (PU)	Bus type
1	Swing	Swing	0.00	0.00	1
2	1.63	0.00	0.00	0.00	2
3	0.85	0.00	0.00	0.00	2
4	0.00	0.00	0.00	0.00	3
5	0.00	0.00	0.90	0.30	3
6	0.00	0.00	0.00	0.00	3
7	0.00	0.00	1.00	0.35	3
8	0.00	0.00	0.00	0.00	3
9	0.00	0.00	1.25	0.50	3

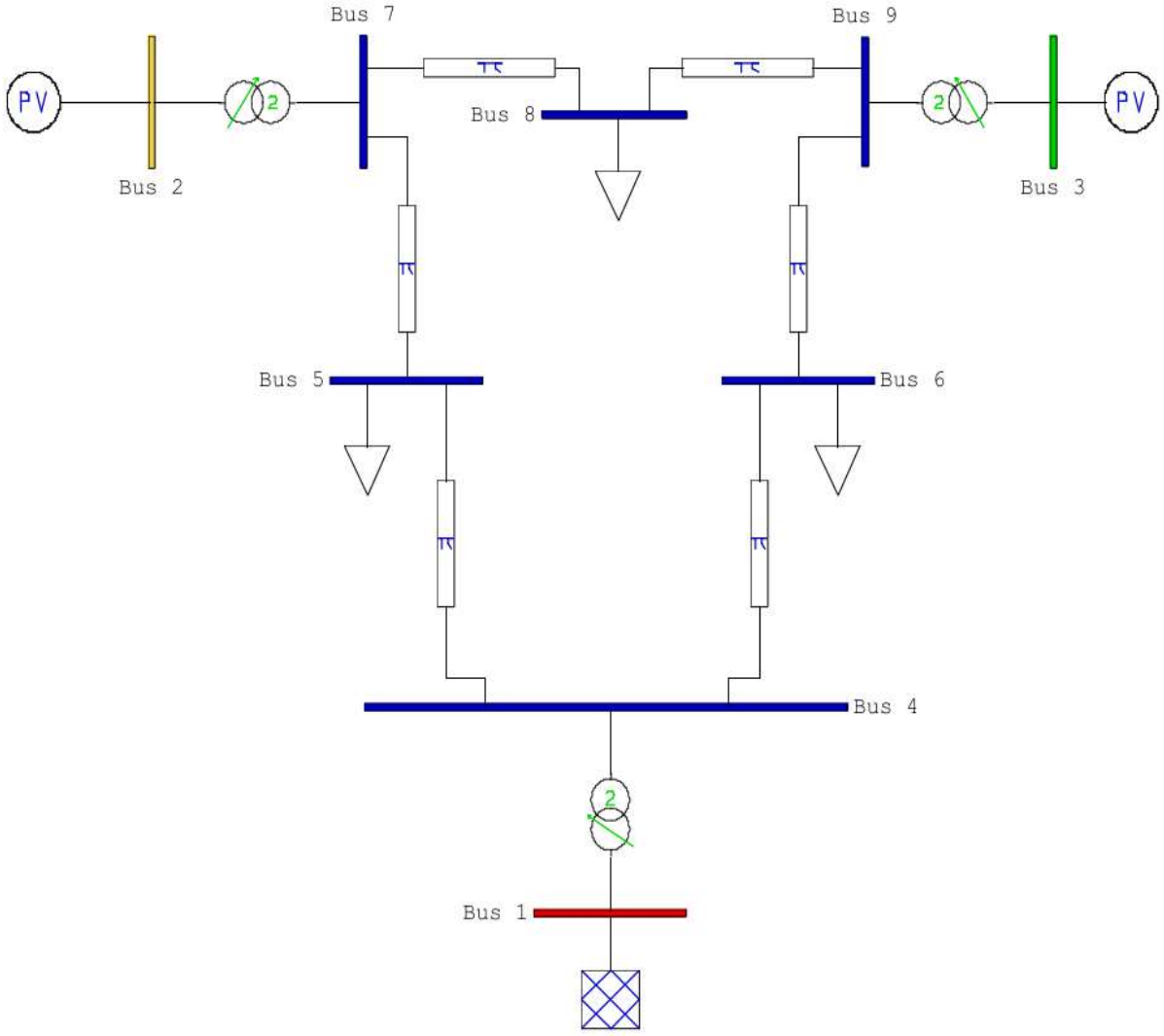

Figure 5. IEEE 9 Bus Model in PSAT simulator

Figure 5 to system with 9 buses and 3 generators. This particular test case also includes 3 two-winding transformers, 6 lines and 3 loads. The base kV levels are 13.8 kV, 16.5 kV, 18 kV, and 230 kV. The single-line diagram of the 9-bus case is shown below (Anderson and Fouad, 2003; Huang and Yeh, 2004).

Table 2. Transmission line data 9 bus system

Line no.	From_bus	To_bus	R	X	B
1	4	1	0.0000	0.0576	0.0000
2	2	7	0.0000	0.0625	0.0000
3	9	3	0.0000	0.0586	0.0000
4	5	4	0.0100	0.0850	0.1760

5	6	4	0.0170	0.0920	0.1580
6	7	5	0.0320	0.1610	0.3060
7	9	6	0.0390	0.1700	0.3580
8	7	8	0.0085	0.0720	0.1490
9	8	9	0.0119	0.1008	0.2090

Power flow analysis is called the backbone of power system analysis. Transient stability analysis of system fault analysis and its improvement is one of the basic problems in power system engineering. The single line diagram of IEEE 9 bus model is shown in Figure 5.

Table 3. Bus data of IEEE 9 bus model

Name	Nom kV	PU Volt	Volt (kV)	Angle (Deg)	Load MW	Load Mvar	Gen MW	Gen Mvar
1	16.5	1.04000	17.160	-0.00			71.63	27.02
2	18	1.02501	18.450	9.28			163.00	6.57
3	13.8	1.02501	14.145	4.67			85.00	-10.91
4	230	1.02580	235.935	-2.22				
5	230	0.99566	229.003	-3.99	125	50		
6	230	1.01268	232.916	-3.69	90	30		
7	230	1.02583	236.941	3.72				
8	230	1.01597	233.673	0.73	100	35		
9	230	1.03239	237.449	1.97				

Table 4. Power flow list of IEEE 9 bus system

From Bus	To Bus	Branch Device Type	MW From	Mvar From	MVA From	MW Loss	Mvar Loss
4	1	Transformer	-71.6	-23.9	75.5	0.0	3.12
2	7	Transformer	163.0	6.6	163.1	0.0	15.83
9	3	Transformer	-85.0	15.0	86.3	0.0	4.10
5	4	Line	-40.7	-38.7	56.1	0.26	-15.80
6	4	Line	-30.5	-16.5	34.7	0.17	-15.51
7	5	Line	86.6	-8.4	87.0	2.30	-19.69
9	6	Line	60.8	-18.1	63.5	1.35	-31.53
7	8	Line	76.4	-0.8	76.4	0.48	-11.51
8	9	Line	-24.1	-24.2	34.2	0.09	-21.18

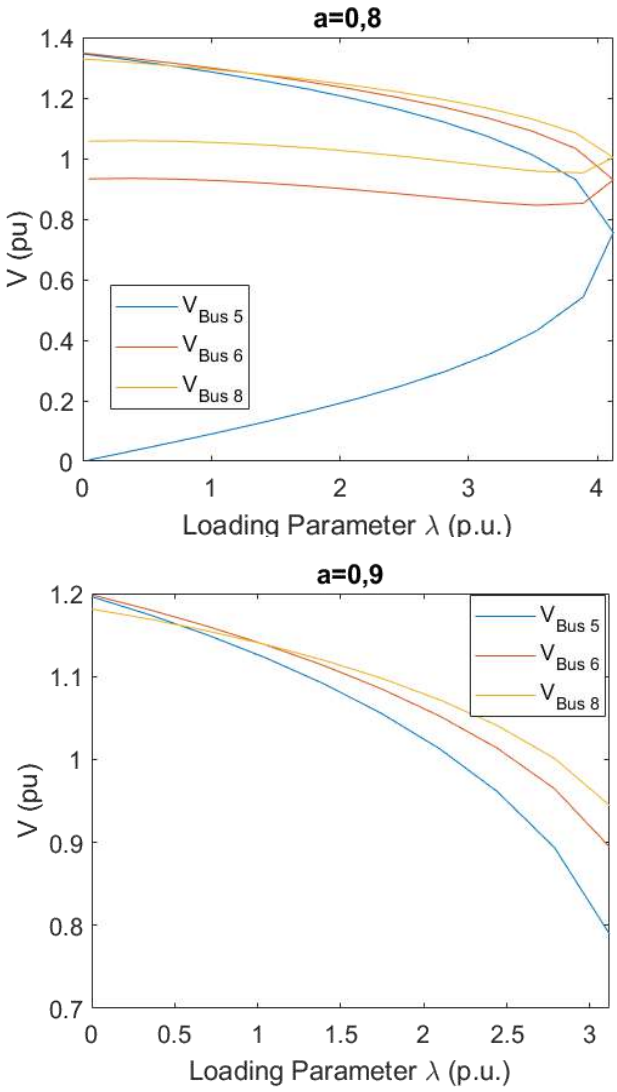

Figure 6. P-λ Curves For Power Systems With ULTCT for a = 0.8, a = 0.9

When continuous load flow is performed in the IEEE 9 bus test system in the PSAT environment the tap changer ratio of transformer 'a' is chosen as 0.8. In this case V_{Bus5}=0.75589, V_{Bus6} =0.92943, V_{Bus8} =1.00288 are calculated as critical values. The maximum load parameter value is 3.11845 under conditions where the tap changer value value 0.8. The change of P-λ when the tap changer ratio has 0.8 was shown in Figure 6.

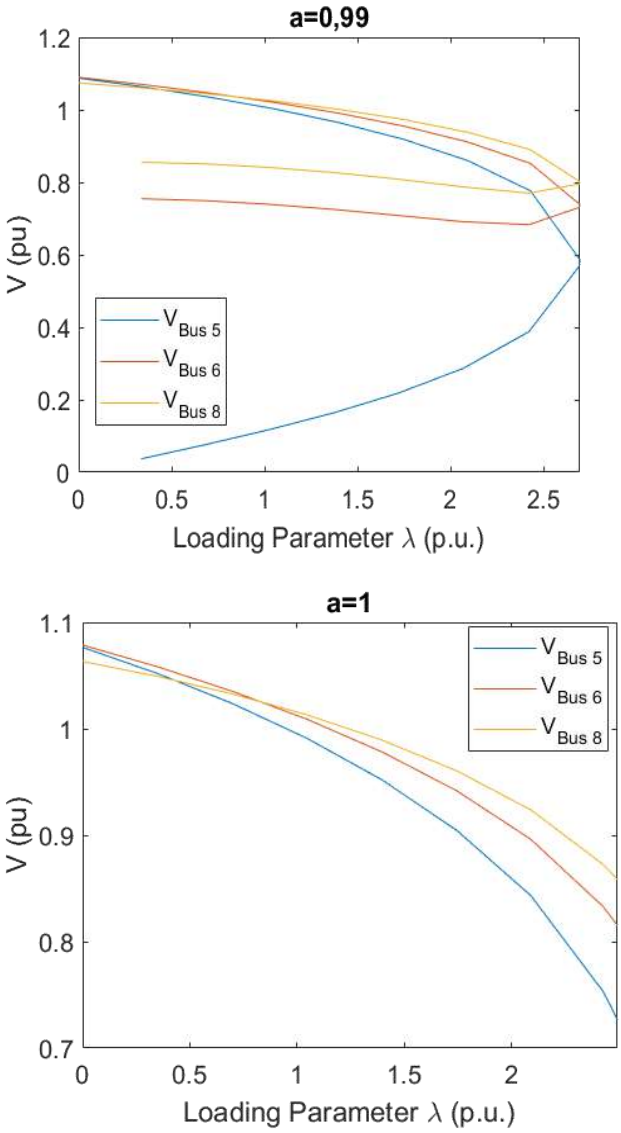

Figure 7. P-λ Curves For Power Systems With ULTCT for a = 0.99, a = 1

When continuous load flow is performed in the IEEE 9 bus test system in the PSAT environment the tap changer ratio of transformer 'a' is chosen as 0.99. In this case V_{Bus5}=0.56840, V_{Bus6} =0.73051, V_{Bus8} =0.79535 are calculated as critical values. The maximum load parameter value is 2.49325 under conditions where the tap changer value value 0.99. The change of P-λ when the tap changer ratio has 0.99 was shown in Figure 7.

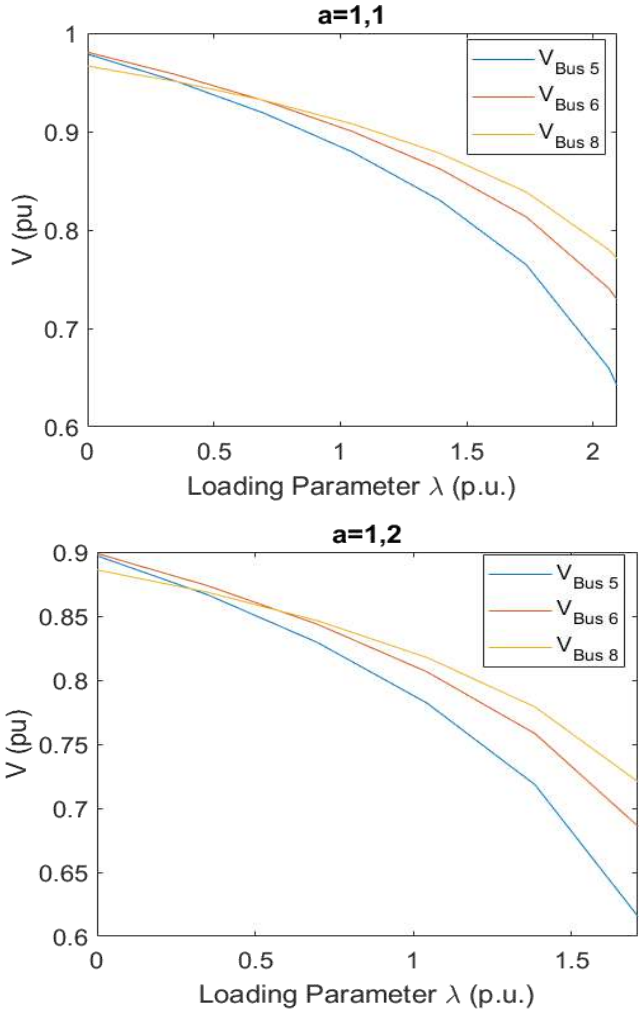

Figure 8. P-λ Curves For Power Systems With ULTCT for a = 1.1, a = 1.2

When continuous load flow is performed in the IEEE 9 bus test system in the PSAT environment the tap changer ratio of transformer 'a' is chosen as 1.1 In this case V_{Bus5}=0.64187, V_{Bus6} =0.72926, V_{Bus8} =0.77083 are calculated as critical values. The maximum load parameter value is 1.71079 under conditions where the tap changer value value 1.1. The change of P-λ when the tap changer ratio has 1.1 was shown in Figure 8.

Table 5. Critical Voltage Values at the Different Tap Changer Ratio Values for IEEE 9 Bus Test System

Different Tap Change Ratio Values (a)	Loading Parameter λ (pu)	Bus Critical Voltage Parameter		
		V Bus 5	V Bus 6	V Bus 8
0,8	4.12341	0.75589	0.92943	1.00288
0,9	3.11845	0.78951	0.89449	0.94466
0,99	2.69084	0.56840	0.73051	0.79535

1	2.49325	0.72619	0.81510	0.85824
1,1	2.09466	0.64187	0.72926	0.77083
1,2	1.71079	0.61568	0.68614	0.72074

Critical voltage Values were given in Table 5. at the different tap changer ratio values for IEEE 9 Bus Test System. When we examine these values, Increase of Tap changer ratio 'a' value leads to improved voltage stability but this situation negative is a situation in terms of the power transfer at the tranasmission line.

4. Conclusion and Suggestions

In this study, limit values of voltage stability were determined according to the tap changer ratio values of power transformers that can change stages under load. Thus, the effects of the tap changer rate values on the voltage stability were examined. Voltage stability limit values were determined for different transformer tap changer ratio values (a = 0,8, a = 0,9, a = 0,99, a = 1, a = 1,1, a = 1,2). When we look at these values, increase of tap changer rate value ('a') has been seen to improve in terms of voltage stability but these situations have ‘a’ negative effect on power energy transfer capacity.

As a result of the studies, it has been seen that the changes in the transformer tap changer values also affect the critical values. The change of tap changer rate of transformer is usually done by the operators. This situation causes some difficulties and disruptions in practice. Voltage changes are known at every hour of the day depending on the load density. Thus, tap changes must be done automatically by computer program. The bus voltage values increase due to capacitive effects or load reduction, in this case reactor connection is needed to reduce of bus voltage. The automatic tap changer setting will cause the reactor investments to decrease.

References

Abaci, K., Yalçin, M. A., Uyaroğlu, Y., And Gelberi H., (PDF document, 2014). Güç Sistemlerinde Kademe Değiştirici Transformatörlerin Kaotik Osilasyonlari, Retrieved from Lecture Notes Online Web Site: https://www.researchgate.net/profile/Kadir_Abaci/publication/229035893, pp. 3-4, (Erişim Tarihi: 27.04.2018).

Anderson, P. M., and Fouad, A. A., (2003). Power System Control and Stability, 2nd ed. New York: IEEE Press,

Balanathan R. (1998). Techniques to efficiently improve power system voltage *stability*, Doctor thesis, The university of Auckland, New Zealand.

Bağrıyanık, M. (1997). *Enerji iletiminde gerilim kararlı en uygun reaktif güçdesteklemelerinin incelenmesi*, İstanbul Teknik Üniversitesi Fen Bilimleri Enstitüsü, Doktora Tezi, 161 Sayfa.

Bourgin, F. G. Testud, B. Heilbronn, J. Versille, (1993). *Present practices and trends on the French power system to prevent voltage collapse,* IEEE Trans. Power Syst. 8 (3) (1993) 778.

Cutsem, TV., Vournas, C., (1998). *Voltage Stability of Electric Power Systems, Power Electronics and Power System Series*, Kluwer.

Canizares, C.A., (February 1999). On bifurcations voltage collapse and load Modelling, *IEEE Transactions on Power Systems*, Vol. 10, No.1, 512-522,

Claudio, A. Canizares, On bifurcations, voltage collapse and load modelling, *IEEE Trans. On Power Systems*, Vol.10, No. 1, pp.512- 522, February

Calovic, M.S., (1984). Modeling and analysis of under load tap changing transformer control systems, *IEEE Trans*. PAS 103 (7) (1984) 1909.

Dong, F. Chowdhury, B. H., Crow, M.L., Acar, L., (2004). *Impact of Load Tap Changing Transformers on Power Transfer Capability*, Electric Power Components and Systems, 32:1331–1346,

El-Sadek, M. Z., Mahmoud, G.A., Dessouky, M.M., Rashed, W.I., (1999). *Tap changing transformer role in voltage stability enhancement,* Electric Power Systems Research, vol. 50 pp. 115–118,

Gümüş, T.E., and Yalçın, M.A., (2013). *Facts cihazlarının gerilim kararlılığına etkisinin incelenmesi*, SAÜ. Fen Bil. Der. 17. Cilt, 2. Sayı, s.1-6.

Glavitsch, H., Baker, R., Guth, G., (1981). Stability improvement by static phase shifting or tap-changing transformers, *7th PSCE conference*, Lausanne, Switzerland, pp 1–8, July 1981.

Huang, Y.H. and Yeh, S. N. (2004). Cogeneration pricing based on avoided costs of power generation and transmission, *Journal of the Chinese Institute of Engineers*, 27:2, pp. 211-221, DOI:10.1080/02533839.2004.9670866

Kunder, P., (1993). *Power system stability and control*, Power System Engineering Series, Mc Graw Hill.

Kundur, P., (1994). *Power System Stability and Control*, New York: McGraw-Hill,

Kundur, P., and G.K., (1997). Morison, A review of defination and classification of stability problems in today's power systems, Panel Sension on Stability Terms and Defination, *IEEE PES Winter Meeting*, New York,

Kaur, R., Kumar, Er. D., (January 2016). Transient Stability Analysis of IEEE 9 Bus System in Power World Simulator, *Ramandeep Kaur Int. Journal of Engineering Research and Applications*, ISSN: 2248-9622, Vol. 6, Issue 1, (Part - 2) January 2016, pp.35-39

Liu, C.-C., Vu, K., (1989). Analysis of tap-changing dynamics and construction of voltage stability regions, *IEEE Trans*. Circuits Syst. 36 (4) (1989) 575.

Taylor, W., (1994). *Power System Voltage Stability*, McGraw-Hill, New York.

Vournas, C. D., (January 2002). On the role of LTCs in emergency and preventive voltage stability control, *IEEE Power Engineering Society Winter Meeting*, New York, NY,

Yalçın, M.A., (1995). *Enerji Sistemlerinde Gerilim Kararlılığının Yeni Bir Yaklaşımla İncelenmesi*, Doktora Tezi, İTÜ Elektrik-Elektronik Fakültesi, İstanbul

Zhu, T. X., Tso, S. K., and Lo, K. L., (2000). An investigation into the OLTC effects on voltage collapse, *IEEE Trans on Power Systems*, vol. 15, no. 2, pp. 515–521,

Abacı K., and Özer, Z., (Aralık 2006). Yük Altında Kademe Değiştirici Transformatörlerin Çok Katmanlı Yapay Sinir Ağı Tabanlı Online Kontrolu, *Elektrik-Elektronik- Bilgisayar Mühendisliği Sempozyumu*, *ELECO*, pp. 2.

Two Alternate Representations of The Electric Field of a Line Source

Mustafa KARA[1]

[1]*Ordu University, TBMYO,Electronic Communication, Ordu, Türkiye;*
email:mustafa.kara@odu.edu.tr

Abstract

In this study, electric field produced by a line source located on the z-axis is obtained in two different forms. Firstly, electric field is derived by using the vector potential, and represented by the zeroth order of second kind Hankel function. Secondly, to obtain the electric field the vector potential is approximated by evaluating the contour integral by the stationary phase point method which resulted in the approximate value of the Hankel function. Obtained electric field is plotted numerically in Matlab.

Keywords: Line Source, Vector Potential, Hankel Function, Stationary Phase Point Method.

1. Introduction

A wide variety of investigations on line source scattering have been carried out in diffraction theory. (Dangelmayr and Wright, 1985) studied on caustics generated by line sources in three-dimensional case, and interpreted the diffraction patterns around the caustics. Moreover, they compared the caustics by a line source with the ones generated by unconstrained waves. Applications of caustics in remote sensing are taken into consideration as well.

(Sanyal and Bhattacharyya, 1986) obtained a uniform asymptotic expansion (UAE) of Maliuzhinets' exact solution for incident plane wave diffraction by a half-plane with two face impedances. Their approach can be employed for an arbitrary line source incidence using a heuristic approach. (Tiberio et al, 1989) studied on the problem of evaluating the scattered field by an impedance wedge illuminated by a line source. In a study, where a two-dimensional problem is examined for the radiating field of a line source, (Kinoshita,1994) investigated the scattering of electromagnetic waves of a line source by a strip conductor. (Monounou et al., 2000) proposed a method which they called directive line source model (DLSM) for predicting the diffracted field generated by a sound wave incident on a half plane. That method can be applied to some types of radiations such as omnidirectional cylindrical and spherical waves, plane waves and waves of directional sources.(Volski and Vandenbosch, 2003) examined radiation patterns of electric and magnetic line sources located near the truncation of a semi-infinite grounded dielectric structure based on physical optics (PO) solutions. (Volski and Vandenbosch, 2003) suggested an efficient method calculating radiation pattern of an electric line source located on a semi-infinite grounded dielectric structure. (Umul, 2008) examined scattering of the radiated fields of a line source by a cylindrical parabolic reflector by employing the modified theory of physical optics (MTPO), and evaluated the reflected geometrical optical fields as well as the edge diffracted fields by asymptotic methods. (Umul, 2016) studied the diffraction of a line source field by a resistive half plane between isorefractive media. (Uslenghi, 2016) solved the boundary-value problem of the radiation of an electric or magnetic line source by a perfectly conducting half-plane located at the planar interface separating two isorefractive media. (Basdemir, 2016) investigated the scattered field by a conducting half plane between two isorefractive media for which a directive line source is used for illumination.

In this study we will obtain two forms of an electric line source field to be used alternately.

1. Theory

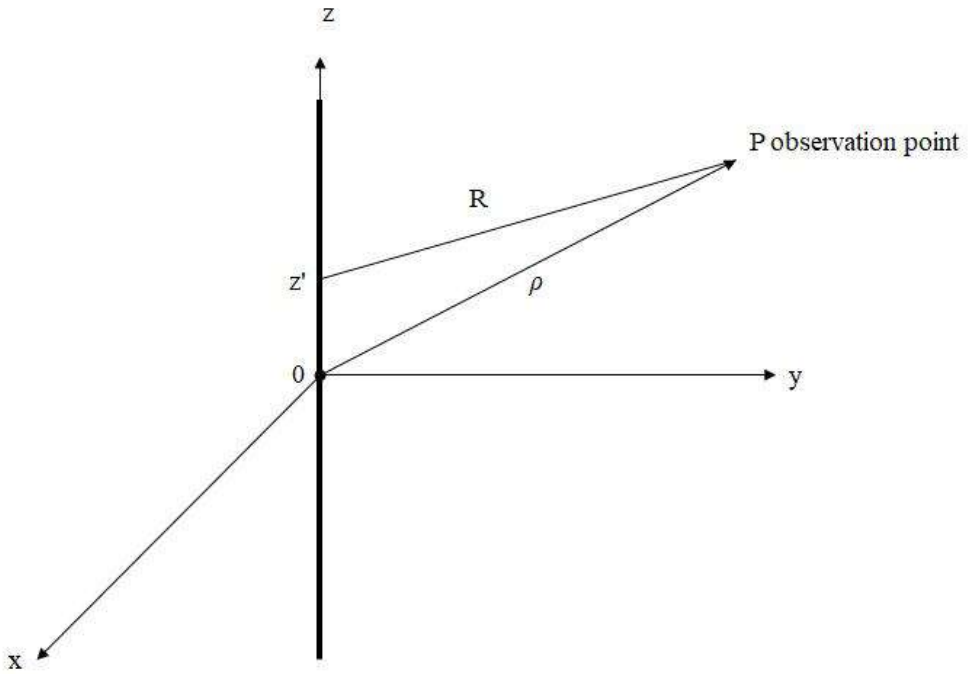

Figure 1. Line source located on the z-axis.

We start with the vector potential $\vec{A}$ as,

$$\vec{A} = \hat{e_z}\frac{\omega\mu_0 I_0}{4\pi}\iiint_{v'}\frac{e^{-jkR}}{R}dx'dy'dz', \quad (1)$$

Where $k = 2\pi/\lambda$ is the wave number, λ is the wavelength, $x' = 0,\ y' = 0,$ and $z' = [-\infty, \infty]$, as shown in Fig. 1, and

$$R = \sqrt{x^2 + y^2 + (z - z')^2}, \quad (2)$$

and

$$R = \sqrt{\rho^2 + (z - z')^2}. \quad (3)$$

ρ is the cylindrical coordinate. Letting $z - z' = \rho sinh\alpha$, we write, $dz' = \rho cosh\alpha\, d\alpha$, and, $\vec{A}$ becomes,

$$\vec{A} = \hat{e_z}\frac{\omega\mu_0 I_0}{4\pi}\oint_C e^{-jk\rho cosh\alpha}\, d\alpha. \quad (4)$$

Since zero-order of the second kind Hankel function, which is known as the Bessel function of the third kind, is written as,

$$H_0^{(2)}(k\rho) = \frac{j}{\pi}\oint_C e^{-jk\rho cosh\alpha} d\alpha. \quad (5)$$

$\vec{A}$ is reduced to,

$$\vec{A} = \hat{e_z} \frac{kZ_0}{4j} H_0^{(2)}(k\rho). \quad (6)$$

It is seen that a line source results in the Hankel function (Balanis, 1989). Therefore, one form of the electric field of the line source is written as,

$$\vec{E} = -j\omega\vec{A} = -\hat{e_z} \frac{\omega k Z_0}{4} H_0^{(2)}(k\rho). \quad (7)$$

For another form of the electric field, we will evaluate the vector potential asymptotically by using the stationary phase point method for which kρ>>1 is assumed. The integral of the form,

$$I = \int_a^b f(x) e^{jkg(x)} dx \quad (8)$$

is to be calculated where $f(x)$ and $g(x)$ are the amplitude and phase functions respectively. Taylor expansion of the phase function is written as,

$$g(x) = \sum_{n=0}^{\infty} \frac{g^{(n)}(x_s)}{n!} (x - x_s)^n \quad (9)$$

where x_s is the stationary phase point value of x. $f(x)$ and $g(x)$ can respectively be approximated as,

$$f(x) \cong f(x_s), \quad (10)$$

and

$$g(x) \cong g(x_s) + \frac{g'(x_s)}{1!}(x - x_s) + \frac{1}{2} g''(x_s)(x - x_s)^2. \quad (11)$$

Second term in $g(x)$ is zero by the definition of the stationary phase point method. Substituting these expressions in Eq. (8) we write,

$$I = f(x_s) e^{-jkg(x)} \int_{-\infty}^{\infty} e^{-jk\frac{1}{2}g''(x_s)(x-x_s)^2} dx \quad (12)$$

Using change of variable as,

$$\frac{y^2}{2} = \frac{jkg''(x_s)(x-x_s)^2}{2} \quad (13)$$

and

$$dx = \frac{dy\, e^{-j\frac{\pi}{4}}}{\sqrt{kg''(x_s)}} \quad (14)$$

The integral is rewritten as

$$I = f(x_s) e^{-jkg(x)} \frac{e^{-j\pi/4}}{\sqrt{kg''(x_s)}} \int_{-\infty}^{\infty} e^{-\frac{y}{2}} dy, \quad (15)$$

and

$$I = f(x_s) e^{-jkg(x)} \frac{e^{-j\pi/4}\sqrt{2\pi}}{\sqrt{kg''(x_s)}}. \quad (16)$$

For the expression of the vector potential amplitude function is unity, and the phase function $g(\alpha)$ is

$$g(\alpha) = cosh\alpha. \tag{17}$$

At the stationary phase point $g'(x)$ will be zero,

$g'(\alpha) = sinh\alpha$=0 where

$$sinh\alpha = \frac{e^{\alpha}-e^{-\alpha}}{2} \tag{18}$$

from which it is concluded that $\alpha = \alpha_s = 0$.

$$g''(\alpha_s) = cosh\alpha_s = 1, \tag{19}$$

$$cosh\alpha = \frac{e^{\alpha}+e^{-\alpha}}{2}, \tag{20}$$

$$\vec{A} = \hat{e_z}\frac{\omega\mu_0 I_0}{4\pi}\frac{\sqrt{2\pi}\, e^{-j\frac{\pi}{4}} f(x_s) e^{-jk\rho cosh\alpha_s}}{\sqrt{k\rho cosh\alpha_s}}, \tag{21}$$

and

$$\vec{A} = \hat{e_z}\frac{kZ_0 I_0 e^{-j\frac{\pi}{4}}}{2\sqrt{2\pi}}\frac{e^{-jk\rho}}{\sqrt{k\rho}}, \tag{22}$$

where $\frac{e^{-jk\rho}}{\sqrt{k\rho}}$ is the cylindrical wave factor. Finally electric field is obtained as,

$$\vec{E} = -j\omega\vec{A} = \hat{e_z}\frac{-j\omega kZ_0 I_0 e^{-j\frac{\pi}{4}}}{2\sqrt{2\pi}}\frac{e^{-jk\rho}}{\sqrt{k\rho}}, \tag{23}$$

and finally electric field is obtained as

$$\vec{E} = -j\omega\vec{A} = \hat{e_z}\frac{-\omega kZ_0 I_0 e^{j\frac{\pi}{4}}}{2\sqrt{2\pi}}\frac{e^{-jk\rho}}{\sqrt{k\rho}}. \tag{24}$$

which is the another well known representation of the electric field of a line source. In the plots of Eq. (24) electric field is normalized to ωkZ_0 for simplicity and the parameters λ=0.1, $\varphi\epsilon[0,2\pi]$ are considered. The same plots are obtained by means of Eq. (7) which is the other form of the electric field of the line source.

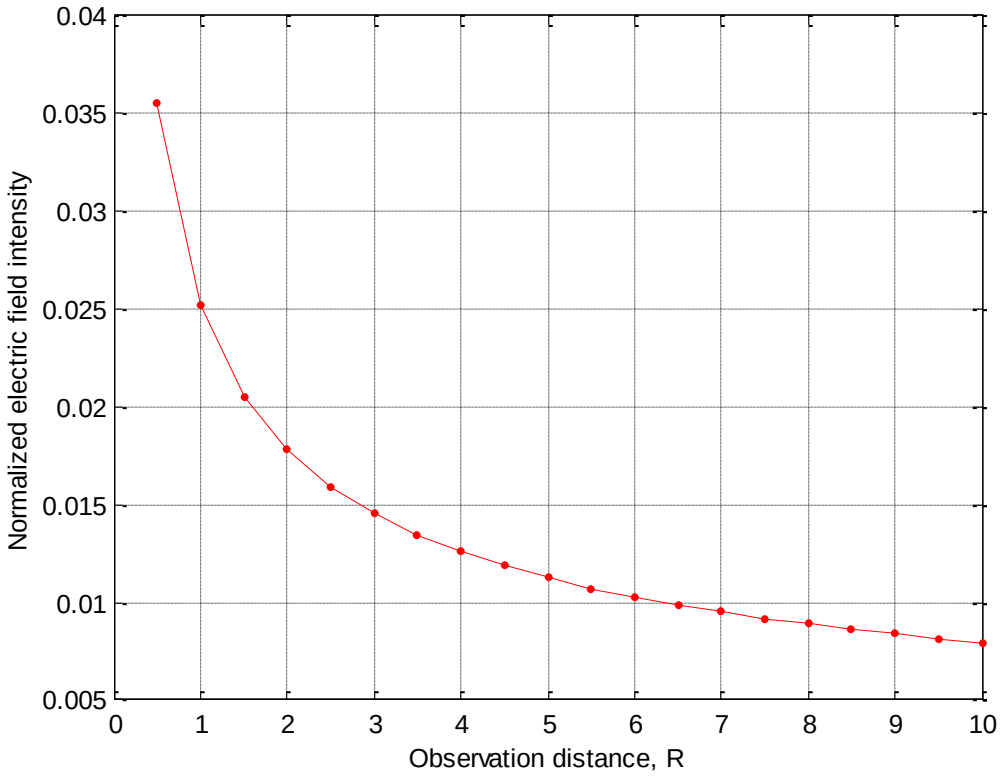

Figure 2. Normalized electric field variation of a line source with respect to R

Fig. 2 shows the electric field variation with respect to observation distance. As the distance increases electric field reduces due to the inverse proportionality between the field intensity and the square root of the distance.

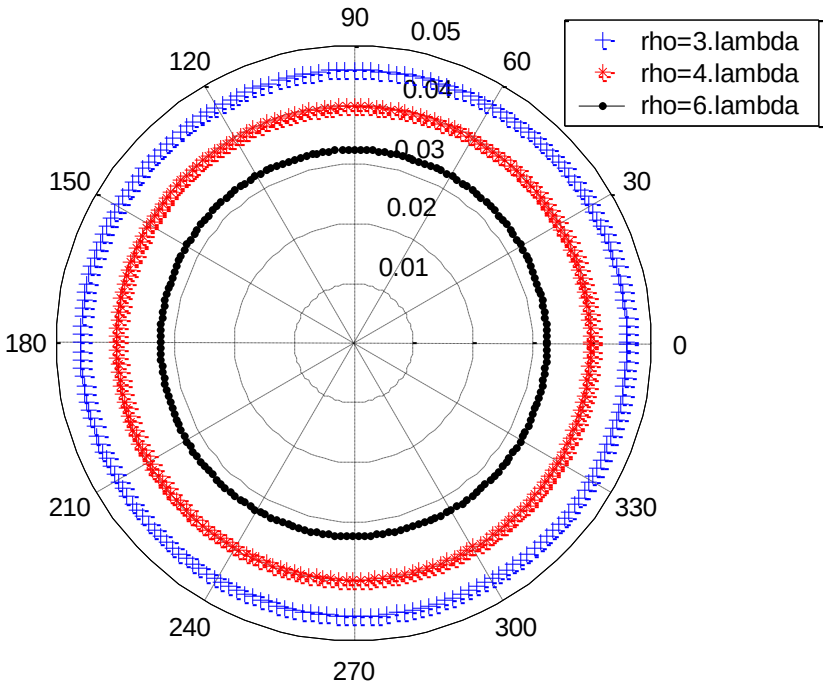

Figure 3. Normalized electric field variation of a line source with respect to φ.

Fig. 3 shows that electric field around the line source is cylindrical and is not dependent on φ due to the symmetry of the source. It can be seen that the field strength is inversely proportional with the observation distance R. As R goes to infinity, field strength approaches to zero.

2. Conclusion

In the present paper electric field of a line source is obtained by means of the vector potential. The derived expression which contains the zero-order Hankel function of the second kind is asymptotically evaluated by using the method of stationary phase point. Electric field of a line source is observed as a cylindrical wave around it which is an expected situation. Also, field strength behaved as a decaying function with respect to the observation distance. For the Matlab plots, both of the electric field representations derived in this study are used, and the same results are obtained exactly.

References

Balanis C. A., (1989), Advanced Engineering Electromagnetics, Wiley.

Basdemir, H. D., (2016), Directive line source scattering by a half-plane between two isorefractive media. *Optik*, 131, 124-131

DOI:10.1016/j.ijleo.2016.11.096

Dangelmayr, G., Wright, F. J. (1985). Caustics and diffraction from a line source. *Optica Acta*, 32, 441-462

http://dx.doi.org/10.1080/713821748

Kinoshita, T., (1994), Diffraction of electromagnetic waves from a line source by a conducting strip. *Electronics and Communications in Japan, 77, 14-23.*

Menounou, P., Vishniac, J. B., Blackstock, D. T., (2000), Directive line source model: A new model for sound diffraction by half planes and wedges. Journal of the Acoustical Society of America, 107,2973-2986

Sanyal, S., Bhattacharyya, A. K., (1986), Diffraction by a Half-Plane with Two Face Impedances Uniform Asymptotic Expansion for Plane Wave and Arbitrary Line Source Incidence. *IEEE Transactions on Antennas and Propagation*, 34, 718-723.

Tiberio, R., Pelosi, G., Manara, G., Pathak, P. H., (1989), High-frequency scattering from a wedge with impedance faces illuminated by a line source, part I: diffraction. *IEEE Transactions on Antennas and Propagation, 37, 212-218.*

Umul, Y. Z., (2008), Scattering of a line source by a cylindrical parabolic impedance surface. *Journal of Optical Society of America A*, 25, 1652-1659.

Umul, Y. Z., (2016), Diffraction of a line source field by a resistive half-plane between isorefractive media. *Optical Quantum Electronics*, 49:23.

DOI 10.1007/s11082-016-0883-5

Uslenghi, P.L.E., (2016), Radiation of a line source over a half-plane located at the interface between isorefractive media. *IEEE Antennas Wireless Propagation Letters*, 15, 356–357 DOI: 10.1109/LAWP.2015.2445857

Volski, V., Vandenbosch, G. A. E., (2003), Efficient integral equation formulation of diffraction at the edge of a truncated dielectric structure based on PO solutions: Application to the case of arbitrarily polarized line sources. *Radio Science, 38, 1031.*

DOI:10.1029/2001RS002483,

Volski, V., Vandenbosch, G., (2003), Radiation pattern of an electric line source located in a semi-infinite grounded dielectric slab calculated using expansion wave concept and geometrical theory of diffraction. *IEE Proceedings-Microwaves, Antennas and Propagation, 150, 70-76.* DOI: IO. 1049/ip-map:20030446

Examination of Parameters Affecting Indoor Air Pollutıon On A Sample Applıcatıon

Burcu KAPLI[1*]

[1] Giresun University, Engineering Faculty ,Giresun/TURKEY; burcu_kapli.enerji@hotmail.com

Corresponding Author: burcu_kapli.enerji@hotmail.com

Abstract

Although air pollution is generally considered to be outside, the air in our house or in our office may be polluted. There may be many factors that cause indoor air pollution. If the living space is on the side of a highway, or if there is a place to roast, if you are smoking nearby, all of them will cause indoor air pollution. Indoor air quality can cause immediate discomforts as well as permanent illnesses. Ensuring that our air is well ventilated and free from contaminants can enhance indoor air quality. In the work done, a sample is taken at the side of a motorway, and simple mass conservation equations are written to calculate the amount of pollution in each interior. The equations are solved with the MATLAB package program.

Key words: Interior, air pollution, ventilation

1. Introduction

In recent years, people are increasingly interested in problems caused by pollutant releases in the interior [Alexander and Klein 2003; Endregard et al 2010; Enserink 2013; Shao et al. 2016; Siddiqui et al 2012]. The reason for this is that indoor air quality is increasingly influencing human health. In many studies, the level of pollutants in the indoor environment has been found to be higher than that of the external environment. In addition, according to a survey conducted by the United Nations, 88% of a day's time is passing by the buildings [Robinson and Nelson, 1995]. Considering that people spend as much as 90% of their time in internal spaces and pollutants in these spaces can not be removed from the environment, it becomes clear that indoor air quality is an important and noticable issue. Pollutants from many sources that spill into the indoor environment cause acute and chronic health problems.

Pollutants that disrupt indoor air quality are caused by indoor and outdoor environment. People is main reason of indoor pollution sources. In addition to these, there are pollution sources as furniture, cleaning materials, cigarette smoke, stove smoke, tools and devices for various purposes, high toxics and volatile organic compounds (VOC), formaldehyde, UOB, paints and resins, and many substances such as cooking, photocopying machines and respirable suspension particles (eg PM2.5, PM10) etc. [Vural and Balanli, 2005]. Outside pollutants may be dust in the atmosphere, pollen, car exhausts and industrial pollutants. Contaminants in the ambient air adversely affect the indoor air quality, either with the incoming air or with the leaking outside air. As a result, people exposed to pollutants in environments with low indoor air quality experience various health problems and discomforts such as allergies, infections, poisoning and fatigue. For example; Volatile organic compounds (VOC) and formaldehyde in low constructions cause complaints about the characteristic nervous system such as drowsiness, headache and fatigue. In case of chronic exposure, they show carcinogenic effects. Continuous exposure to UOBs at low concentrations causes respiratory disease and asthma (Norback and Ark., 1995). Long-term particulate matter (PM) exposure has been associated with death from cardiovascular diseases [Liu and Zhai 2007]. In this study, parameters affecting air quality are examined. The effects of these parameters on human health are mentioned. The basic principles of ventilation based on the need for CO_2. In addition is explained. Mass conservation equations

have been written by taking measurements of CO_2 amounts in various environments such as housing and office classrooms.

2. Experimental Procedures

In every area of our life there are factors that cause air pollution in our living spaces. This can sometimes be the exhaust gas of cars, frying in cooking areas, and the fuels we use for heating purposes. In Europe and developed countries, the amount of CO in air in standard air quality is determined to be 10 mg/m^3 [Washington, DC, US 1991].

In 2011, the PM2.5 concentrations in Ontario showed an hourly change of 3.4 (mg/m^3) per cubic meter, in Sarnia with 10.5 mg/m^3. In Finland recently, carbon monoxide peak concentrations of up to 60 mg/m^3 (53 ppm) have been reported in municipal households operating in city gas. Environmental tobacco smoke in houses, offices, vehicles and restaurants has shown that the average 8-hour carbon monoxide concentration varies between 23-46 mg/m^3 (20-40 ppm) [Ontario Report 2011].

While eating at a restaurant on the side of the highway outside the city and away from the pollution; even when we safely leave our children to the playground, they are exposed to air pollution at certain rates.

The natural air passage between polluters and spaces is modelled by taking to a restaurant on a countryside highway as an example.

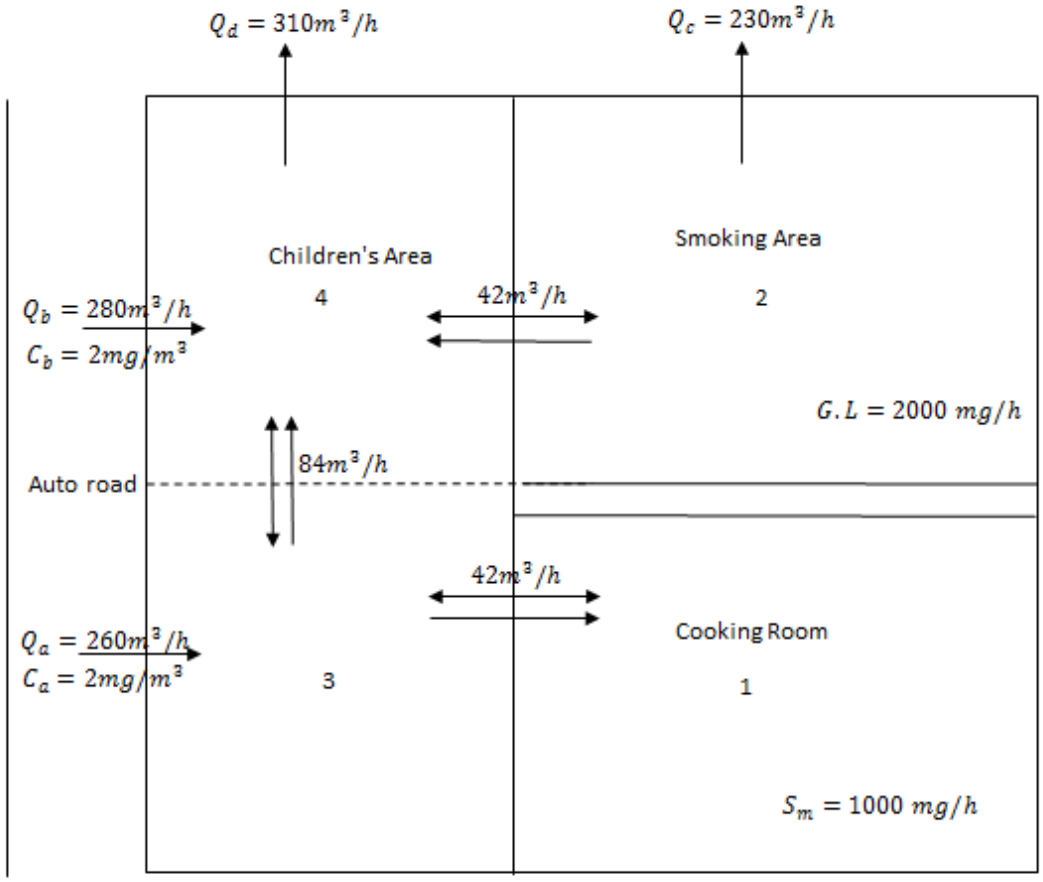

3. Experimental Results and Discussion

When steady-state mass equations are written for each room, the following equations were obtained.

$$0 = S_m + Q_a .C_3 + E_{31} (C_3 - C_1) \quad (1)$$

$$0 = G.L + E_{24} (C_4 - C_2) + (Q_a + Q_b - Q_d) .C_4 + Q_a .C_3 - Q_c .C_2 \quad (2)$$

$$0 = Q_a .C_a + E_{31} (C_1 - C_3) + E_{34} (C_4 - C_3) - Q_a .C_3 \quad (3)$$

$$0 = Q_b .C_b + E_{34} (C_3 - C_4) + E_{24} (C_2 - C_4) - Q_d .C_4 \quad (4)$$

The following Matrix equation is obtained;

$$\begin{Bmatrix} 42 & 0 & -302 & 0 \\ 0 & 272 & -260 & -272 \\ -42 & 0 & 386 & -84 \\ 0 & -42 & -84 & 436 \end{Bmatrix} \begin{Bmatrix} C_1 \\ C_2 \\ C_3 \\ C_4 \end{Bmatrix} = \begin{Bmatrix} 1000 \\ 2000 \\ 560 \\ 520 \end{Bmatrix}$$

When these sets of equations are solved with MATLAB package program;

$C_1 = 236.9327\ mg/m^3$
$C_2 = 47.2294\ mg/m^3$
$C_3 = 29.6397\ mg/m^3$
$C_4 = 11.5444\ mg/m^3$

The amount of carbon monoxide in the form of air is in mg/m^3 format. The results show that there is CO in the frying environment which may be harmful to human health. These results show us the importance of designing a good ventilation system and the transition between rooms.

Even in the child's playground there is reasonable amount of CO. If we write the factors that affect this;

0.1488	0.0041	0.1250	0.0266
0.0221	0.0048	0.0221	0.0072
0.0174	0.0006	0.0174	0.0037
0.0055	0.0006	0.0055	0.0037

$C_{4,\text{baking room}} = a_{41}^{-1} * W_{\text{baking room}}$ $\quad C_{4,\text{baking room}} = 0{,}0055 * 1000 = 5{,}5\ mg/m^3$

$\%\text{Baking room} = \frac{5{,}5\ mg/m^3}{11{,}5444\ mg/m^3} x100 = \%47$

It is observed that the most common cause of pollution in children's play area is frying are with the rate of 47%

$C_{4,\text{smokers}} = a_{42}^{-1} * W_{\text{smokers}}$ $\quad C_{4,\text{smokers}} = 0{,}0006 * 2000 = 1{,}2\ mg/m^3$

$\%\text{Smokers} = \frac{1{,}2\ mg/m^3}{11{,}5444\ mg/m^3} x100 = \%10$

The presence of a ventilation system that opens outdoors from the cigarette allowed area seems to have a less negative effect on air quality in the children's play area

$C_{4,outside\ air} = a_{4a}^{-1} * Q_a * C_a + a_{4b}^{-1} * Q_b * Q_a$

$C_{4,outside\ air} = 0.0055 * 2 * 260 + 0.0037 * 2 * 280 = 4{,}932\ \mathrm{mg/m^3}$

$\%\text{Outside air} = \frac{4{,}932\ \mathrm{mg/\ m^3}}{11{,}5444\ \mathrm{mg/m^3}} \text{x} 100 = \%42$

The suction of the children's play area from the outside, although it seems like an advantage, the highway is the second pollutant effect.

4. Conclusion;

We are exposed to polluted air in all areas of our life. As you can see in the study conducted, there is a large amount of CO in the ambient air even when eating at a restaurant away from the noise of the city on the highway.

If the ventilation design was well done; for example, if there was an independent ventilation directly opening out of the cooking chamber, the CO quantities would not be so high.

The main polluters in the children's play area were observed to be the frying room and the highway. Children who play innocently and away from dangers in the children's field are exposed to polluted air due to the cooking room and the car exhaust from cars.
Isolating the children's playground from the highway and making the frying area independent may be measures to reduce CO quantity. Another solution is to reduce the amount of CO in the children's play area with a good ventilation design.

As obvious in the study explained above, the lack of a good ventilation while designing an environment causes a lot of air pollution inside.

References

1. Alexander DA, Klein S (2003). Biochemical terrorism: Too awful to contemplate, too serious to ignore—Subjective literature review. British Journal of Psychiatry, 183: 491–497.

2. ROBINSON J, NELSON WC. National Human Activity Pattern Survey Data Base. United States Environmental Protection Agency, Research Triangle Park, 1995.

3. VURAL MS, BALANLI A. Yapı ürünü kaynaklı iç hava kirliliği ve risk değerlendirme de ön araştırma. Megaron YTÜ Mimarlık Fakültesi Dergisi. 1(1): 28-39, 2005.

4. NORBACK D, BJORNSSON E, JANSON C, WIDSTROM J, BOMAN G. Asthma and the indoor environment:the significance of emission of formaldehyde and volatile organic compounds from newly painted indoor surfaces. Occupational and Environmental Medicine. 52(69): 388-395, 1995.

5. Liu X, Zhai Z (2007). Inverse modeling methods for indoor airborne pollutant tracking: Literature review and fundamentals. Indoor Air, 17: 419–438.

6. Air quality criteria for carbon monoxide. Washington, DC. US Environmental Protection Agency, Office of Research and Development, 1991 (publication no. EPA-600/B-90/045F).

7. Air Quality in Ontaria Report 2011.

Evaluation of the Electromagnetic Field Levels in Ordu City Center for the Selected Base Stations' Coverage Areas

Mustafa Mutlu[1*], Çetin Kurnaz[2*]

[1]*Ordu University, Vocational School of Technical Sciences, Ordu, Turkey.*

[2]*Ondokuz Mayıs University, Department of Electrical and Electronics Engineering, Samsun, Turkey.*

[*] **Corresponding Author:** ckurnaz@omu.edu.tr

Abstract

In this study, electric field strength (E) measurements were conducted at six different base stations coverage areas in Ordu city center. E measurements were taken using Narda EMR-300 electromagnetic field meter in 100 kHz–3GHz frequency band. The maximum E (E_{max}) values and average E (E_{avg}) values were recorded at a total of 213 locations from different distances to base stations. The maximum mean E_{max} was calculated as 1.2326 V/m and the maximum mean E_{avg} value was calculated as 0.7416 V/m. These values are well below the limit values determined by International Commission on Non-Ionizing Radiation Protection (ICNIRP) and Turkey's Information and Communication Technologies Authority (ICTA). At the next stage of the study, the change of the E_{avg}s depending on the distance of the measurement locations to the base station was examined, and the probability density graph for E_{avg}s were obtained.

Keywords: Base station, Electric field strength (E), E measurements, EMR-300.

1. Introduction

Wireless communication systems are widely used today in most of the developed countries. A large portion of wireless communication is provided over cellular radio networks, and cellular (mobile) communications are among the indispensable parts of our lives (Çerezci ark, 2012). With this popularity for mobile communication, the number of base stations, which are the basic building blocks of mobile communication requests, is increasing day by day. Due to the fact that a large majority of the population in our country lives in the cities, existing base stations are inadequate to meet user demands (Engiz and Kurnaz, 2017). Since each base station can serve a limited number of users, the limited number of separated frequency bands can force operators to meet user demands. One of the solutions is to use the frequency band that a base station uses, another base station at a distance that does not cause interference, and reduce the coverage area of base stations (using micro and pico cell structures). However, in this case too, due to the decreasing base station output power, much more base station setup is needed to expand coverage. Thus, increasing base station numbers to meet user demands (high-speed data rate, access to the system from any desired location, etc.) is an unavoidable reality. As each base station is a source of electromagnetic fields (EMF), the number of base stations that are increased together with the number of base stations that are being exposed is also increasing (Kurnaz, 2018). Many places such as radio-TV transmitters, transmitters, high-voltage lines, transformers, mains voltage, radio broadcasts and Wi-Fi broadcast electromagnetic waves in places where urbanization is intense. With the increasing electromagnetic wave frequency, the energy of the electromagnetic wave increases and the harmful effects on the living are also growing. At low frequencies, the limit values set by the World Health Organization (WHO) are high and the limit values are lower at high frequencies. When the electromagnetic wave increases the cell temperature at low frequencies, the high frequency electromagnetic wave like X ray (tera Hz, penta Hz) warms (Miclaus and Bechet, 2007). The cell and causes the change in the molecular structure as well. When exposed to an electromagnetic wave, the amount of energy absorbed by the body tissues is measured by the Specific Absorption Rate (SAR) in W/kg. It is almost impossible to directly measure SAR as a parameter that varies from person to person. Instead of SAR, the electric field strength (V/m), magnetic field strength (A/m) and power density (W/cm^2), which can be easily measured and/or observed, are used at the boundary values of the electromagnetic wave. There are international standards and safety limit values on possible negative effects of electromagnetic waves (Mousa, 2011). These limit values

have been established by the International Commission for the Prevention of Non-Ionizing Radiation (ICNIRP), an international commission recognized by the WHO, who has been admitted to exposure to general public health 24 hours a day. Regarding the electromagnetic wave, each country sets limit values according to its own standards. Legislation on electromagnetic radiation in Turkey Information and Communication Technologies Authority (ICTA) is made by the ICTA, ICNIRP (the International Commission on Non-Ionizing Radiation Protection) from the limit values set by constitute the necessary regulations are based. The limit values for the electric field strength (E) determined by ICNIRP (ICNIRP, 1998) and ICTA (BTK, 2015) are given in Table 1.

Table 1. Limit values for electric field determined by ICNIRP and ICTA

Frequency Range(MHz)	Electric Field Intensity(V/m)	
	ICNIRP	BTK
0,010-0,15	87	65,25
0,15-1	87	65,25
1-10	87/f½	65,25/f½
10-400	28	21
400-2000	1,375f½	1,03f½
2000-60000	61	45,75

When table 1 is examined; limit values; 30.9 (V/m) for base stations operating at 900 MHz, 43.7 (V/m) for base stations operating at 1800 MHz, 45.75 (V/m) for 3G systems (2100 MHz and 2450 MHz) and Wi-Fi devices. These values are the total limit value of the environment and are four times the limit value of the media for a single device.

2. Material and Method

In this study, it was aimed to measure and evaluate the electromagnetic fields originating from the base stations in the Ordu city center, especially in the six districts where the population is crowded. The average and maximum values of the E were recorded in each of the 213 locations determined during six minutes. In addition, the altitude and coordinate values of

measurement locations are recorded by GPS. Electric field measurements were taken with Narda EMR-300 EMF meter (Anonim, 2016-1) and GPS measurements were taken with MAGELLAN SporTrak COLOR BN 895107 GPS (Anonim, 2016-1). The EMR-300 is shown in Figure 1 for the electromagnetic field gauge and in Figure 2 for the MAGELLAN SporTrak GPS. The EMR-300 was kept at a height of 150 cm from the floor, and the mobile phone on the personnel performing the measurement to prevent any electromagnetic fields was closed. At each measurement location, the EMR-300 is reset and the GPS device is set to see at least three satellites and the measurement is started. Electric field measurements were made by approaching the base station starting from the farthest point to the base station. An electric field probe (EP 2244/90.73) was used to measure the frequency range of 100 kHz to 3 GHz in the field measurements and the cellular system was selected for measurements between 10:^{00} and 15:^{00} where the data traffic was intense. The maximum (E_{max}) and mean (E_{avg}) values of the electric field strength, the distance from the base station to the measured position, and the azimuth and elevation angle of the base station antenna are recorded on Google Earth.

Figure 1. Narda EMR-300 electromagnetic field meter and electric field probe

Figure 2. GPS device used in measurements

Base stations and coverage areas for electric field measurements made in the Ordu city center are given in Figure 3.

Figure 3. Scope of base stations and measurement points in the city center of Ordu

3. Measurement Results and Evaluations

Electric field values recorded for six different base stations (ORMIG, ORMEH, ORDTU, SUBAM and OSINA) are given in fig 4. Using Figure 4, the electric field values in the Ordu city center can be visually evaluated easily. As can be seen from Figure 4, the highest electric field values are recorded in the Subaşı district and the lowest electric field values are recorded

in the Akyazı district. Statistical analyzes of the maximum and average value of the electric field measured in the neighborhoods according to the neighborhoods are given in Table 2.

Figure 4. Electric field measurement results for six different base stations in Ordu city center

Table 2. Statistical properties of measured field values

Location		E_{max} (V/m)	E_{ort} (V/m)
ORDTU	Average	0,6332	0,7416
	Standart Deviation	0,0496	0,4569
ORKAZ	Average	0,5947	0,6468
	Standart Deviation	0,4116	0,4513
ORMEH	Average	0,6450	0,3176
	Standart Deviation	0,6112	0,3293
ORMİG	Average	0,5557	0,2495
	Standart Deviation	0,5374	0,2767
OSİNA	Average	0,8050	0,3332
	Standart Deviation	0,5157	0,1929
SUBAM	Average	1,2326	0,6752
	Standart Deviation	1,3924	0,7788

As the power of the electromagnetic wave moves away from the donor, it decreases inversely with the distance of the distance. Figure 5 shows the variation of the electric field values measured at a total of 213 points around six base stations in Ordu city center with respect to the distance from the base station transmitting antenna (Mutlu and Çavdar, 2010).

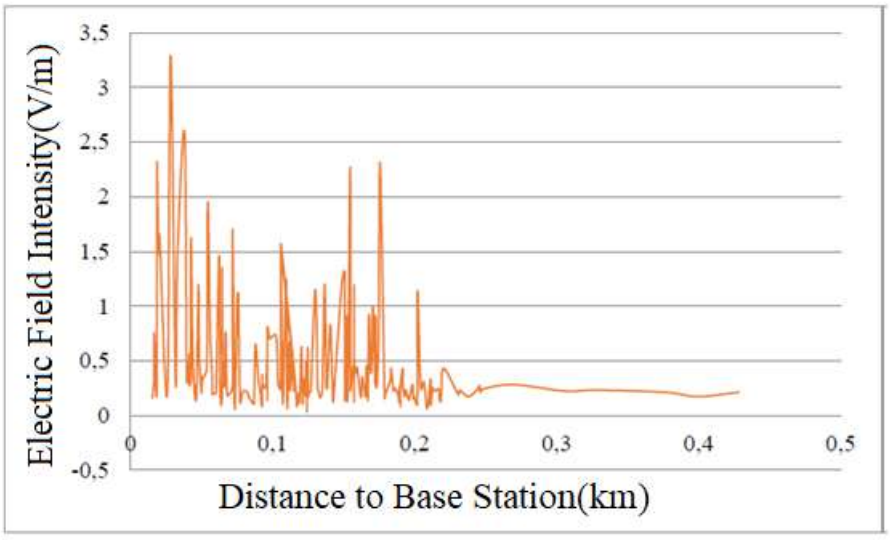

Figure 5. Change of mean electric field by distance to base station

Figure 6 shows the changes in mean electric field values according to the probabilities of arrival in the measurements made (Mutlu, 2010). It is easy to see how often the electric field values recorded from Figure 6 are repeated, the electric field changes between boundaries, and what the average of the measurements is.

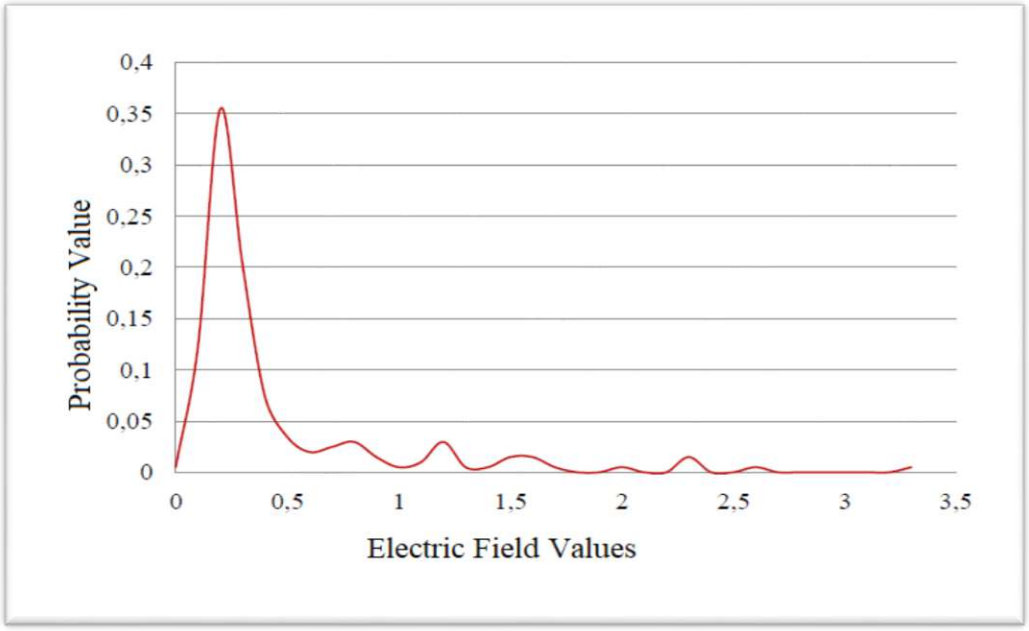

Figure 6. Probability density graph of mean electric field values

4. Conclusions and Recommendations

In this study, electric field values of six selected base stations were recorded in six districts in Ordu city center. The change of the electric field values, which are recorded in 213 locations in total, depending on the measurement location, base station distance, the range of electric field change and the probabilities are examined. From the results of the electric field measurement, it was determined which area the exposed electric field value is low/high. It is seen that the measured electric field values are well below the limit values determined by ICTA. Although exposure to base stations is low, exposure to mobile phones and SAR value in the body are also considered, so it is recommended to use earphones in mobile phone calls, keep conversation time short, and especially use social media more quickly.

References

Çerezci. O, Kartal. Z, Pala. K, Türkkan. A, (2012) "Elektromanyetik Alan ve Sağlık Etkileri", Bursa: Özsan Matbaacılık.

Engiz. B.K., Kurnaz. Ç, (2017) "Long-Term Electromagnetic Field Measurement and Assessment for a Shopping Mall", Radiation Protection Dosimetry, vol.175, no.3, pp.321-329.

Kurnaz. Ç, (2018) "An Empirical Modeling of Electromagnetic Pollution on a University Campus", Applied Computational Electromagnetics Society Journal, vol.33, no.1, pp.111-114.

Miclaus.S, Bechet. P, (2007) "Estimated and Measured values of the Radiofrequency Radiation Power Density around Cellular Base Stations", Environment Physics, vol. 52, no. 3–4, pp. 429–440.

Mousa. A, (2011) "Electromagnetic radiation measurements and safety issues of same cellular base stations in Nablus", Journal of Engineering Science and Technology Review, vol. 4, no. 1, pp. 35-42.

ICNIRP Guidelines, (1998) "Guidelines for Limiting Exposure to Time-Varying Electric, Magnetic, and Electromagnetic Fields (up to 300GHz)", International Commission on Non-Ionizing Radiation Protection, Health Physics 74 (4), pp.494-522.

BTK, (2015) "Elektronik Haberleşme Cihazlarından Kaynaklanan Elektromanyetik Alan Şiddetinin Uluslararası Standartlara Göre Maruziyet Limit Değerlerinin Belirlenmesi, Kontrolü ve Denetimi Hakkında Yönetmelikte Değişiklik Yapılmasına Dair Yönetmelik", 9 Ekim tarihli Resmi Gazete, sayı no.29497.

Anonim, (2016) http://www.narda-sts.us/pdf_files/Data Sheets /EMR 300_Data Sheet_Discontinued.pdf (Erişim tarihi: 01.06.2016).

Anonim, (2016-1) http://www.magellangps.com (Erişim tarihi: 02.06.2016).

Mutlu. M, Çavdar. İ, (2010) "GSM 900 Bandında COST-231 Walfisch-Ikegami Yönteminin Ordu iline Uyarlanması", Elektrik Elektronik Bilgisayar Mühendisliği Sempozyumu (ELECO'2010), 2-5 Aralık, Bursa.

Mutlu. M, (2010) "GSM 900 Bandında COST-231 Walfisch-Ikegami Yönteminin Ordu iline Uyarlanması", Yüksek Lisans Tezi KTÜ Fen Bilimleri Elektrik Elektronik Bölümü.

The Elimination of Harmonics in Solar Energy Systems

Alparslan TÜFEKÇİ[1], Onur Özdal MENGİ[2], Özgür TOMAK[1]

[1]Technical Sciences Vocational School of Giresun University, Giresun, Turkey,
alparslan.tufekci@giresun.edu.tr, ozgur.tomak@giresun.edu.tr
[2]Energy Systems Engineering, Giresun University, Giresun, Turkey ; onur.ozdal.mengi@giresun.edu.tr

Abstract

In this study, the problem of eliminating harmonics on loads fed by solar energy which is a renewable energy source is being discussed. Energy is obtained as a result of sunlight falling on solar panels. As the resultant energy is the dc voltage, the need to convert this energy into an appropriate one arises. Especially the alternating current loads must be fed appropriately. Power electronic arrangements, such as chopper and inverters, cause harmonics. Apart from this, nonlinear loads cause deterioration. For this reason, it is necessary to examine the harmonics that are occurring in the systems fed from the solar panels. Classification of harmonics, determination of its type and methods of destruction are discussed. Since the system works entirely independently from the network, the filters that are designed to solve the harmonic problems caused by it and the loads are gaining importance. It is necessary to develop these filters correctly and should not place an extra burden on the system. All the different filters designed for the study performed in MATLAB / Simulink environment have been tried, and the results are compared. The results obtained shed light on the problem of where and how to use which type of filter.

Keywords: Renewable energy source, filter, photovoltaic, harmonics.

1. Introduction

The definition of quality energy in electrical network systems can be given as waveform distortion in the current drawn from the network and changes in the voltage and frequency of the network. Even if voltage and frequency change, many electrical devices cannot detect this and are not sensitive to this. On the other hand, it is possible to measure very sensitive energy quality by the circuit elements controlled and developed by electronic circuits. There has been an increase in power quality problems due to non-linear loads that have recently become widespread. These non-linear loads lead to the formation of harmonics in the current or voltage components at frequencies other than the nominal frequency (50 Hz) in the network. Harmonics damage the circuit elements and electrical equipment designed according to the nominal frequency in case of exceeding the values determined by the standards, decreases the efficiency and causes additional losses. In order to minimize these losses, harmonic filters are connected to the circuit to reduce the harmonic levels and electrical energy is produced below the standard values.

2 2. Materıals and Methods

3 2.1. Solar Cells

Photovoltaic panels collect the rays coming from the sun and convert them from the rays into electrical energy. Photons on the panel break electrons from the surface of N-type silicon semiconductors. These free electrons from the orbit create an electrical field of approximately 0.5V in each panel. Free electrons are desired to be drawn by positively charged cavities on the P-type semiconductor surface. In this electrical field, when the flow of free electrons is completed on a load, the solar radiation is converted into electrical energy.

By connecting these photovoltaic panels in series or parallel, we increase the current and voltage values and thus the desired voltage values are reached. The efficiency of photovoltaic panels is proportional to the amount of light intensity coming to the panel. The more steep the sun's rays, the greater the amount of energy produced [1].

2.2. Harmonic

It is sufficient to calculate Total Harmonic Distortion (THD) if it is desired to express a wave or waveform with a single unit. Here we determine the amount of distortion by calculating the current or voltage THD value of the wave as follows [2].

$$THD=\frac{\sqrt{\sum_{k=2}^{k_{max}} Mk^2}}{M_1} \quad (1)$$

Where Mk is a unit with effective value M. shows the harmonic component. Mi is the effective value of the basic component.

$$\text{Efektif Değer}=\sqrt{\sum_{k=1}^{k_{max}} Mk^2}=M_1.\sqrt{1+THD^2} \quad (2)$$

Total Harmonic Distortion (THD) is a very important parameter for electrical circuits and it will be beneficial to determine and prevent loss power according to the results. The THD can give a positive result when calculating how much heat a distorted voltage wave applied to a load on the charge will generate [2].

2.3. PID Controller

PID Controller consists of block diagrams which are transferred through the system's proportional (P), integral (I) and derivative (D) operations. The parameters called P, I and D are formed by the combination of the initials of the (P) roportional, (I) integral and (D) erivative words [3].

If there is a proportional effect in the circuit; The parameter P, also called the proportional band, is the value of the control mechanism in the control device, which is inversely proportional to the gain amount, and acts to the control output by multiplying the error with a certain gain value.

If there is an integral effect on the circuit, it decreases the bandwidth by decreasing the damping by integrating the control output. In this way, the frequency response sits in a short time.

If there is a derivative effect in the circuit, it decreases the rise time and sitting time by performing the derivative of the control output by the derivative process.

2.4. Filters

In order to prevent the harmful effects of harmonics, it may not be sufficient to design a filter or filter. In addition to filter design, harmonic currents should be prevented. It is possible

to minimize the harmonic currents by connecting them in series or in parallel with R-L-C elements which should be added to the system for this purpose. [4]. In addition to the serial LC filter, it is possible to reduce harmonic currents significantly by means of parallel harmonic filters connected to the circuit. The harmonic filters to be connected to the circuit are as follows;

1) C type high pass filter
2) Dual tuned harmonic filter
3) High pass harmonic filter
4) Single-tuned harmonic filters

2.5. Inverters

The main task of the inverter is to convert a DC voltage to AC voltage. This is a symmetric sine wave, while making the transformation with equal amplitude and frequency is done intact. It is also desirable to obtain the output voltage with a low harmonic. The most commonly used inverter models are the switching frequency switching systems or PWM (Pulse Width Modulation), ie pulse width modulation techniques [5].

3. Results and Discussion

The system has been tested in an 30°C environment with 1000W / m2 light intensity. Soltech 1STH-215-P solar panels are used in this study. In each branch 40 solar panels are connected in series and 20 in parallel. In total, 800 solar panels were used. The DC voltage from the solar panels is converted into alternating current by an inverter. Thanks to the controller, output values are kept constant at 380V / 50Hz. The inverter is a standard 2-level 6-IGBT inverter. The classic PID controller is used for this inverter. Here, the voltage on the load is measured, then divided into components d and q using the abc-dq0 transformation. These components are controlled separately. d is trying to set the value of component 1 to q if it is q. The signals obtained at the output of the controllers are used as the input signal of PWM by converting them into the sine wave form with dq0-abc conversion. PWM signals are sent to IGBTs and 6 IGBTs are used. The controller also tries to keep the frequency value from the system at 50Hz using PLL (phase locked loop). Here, the d and q components are controlled using the PID controller. In the classical PID Kp=01, K_I=40 Kd=0,05 were selected. In the filter circuits the coil value is 1mH and the capacitor value is 22μF. In harmonic filters Qc = 20kVar is selected. Values were taken as constant in all simulation studies. In the system, it was tried

to create harmonic by using RL load. The first load has a value of 45kW / 20kVAr and the second has a value of 15kW. In addition, the sampling time of 2 μsn was selected for graphs [6].

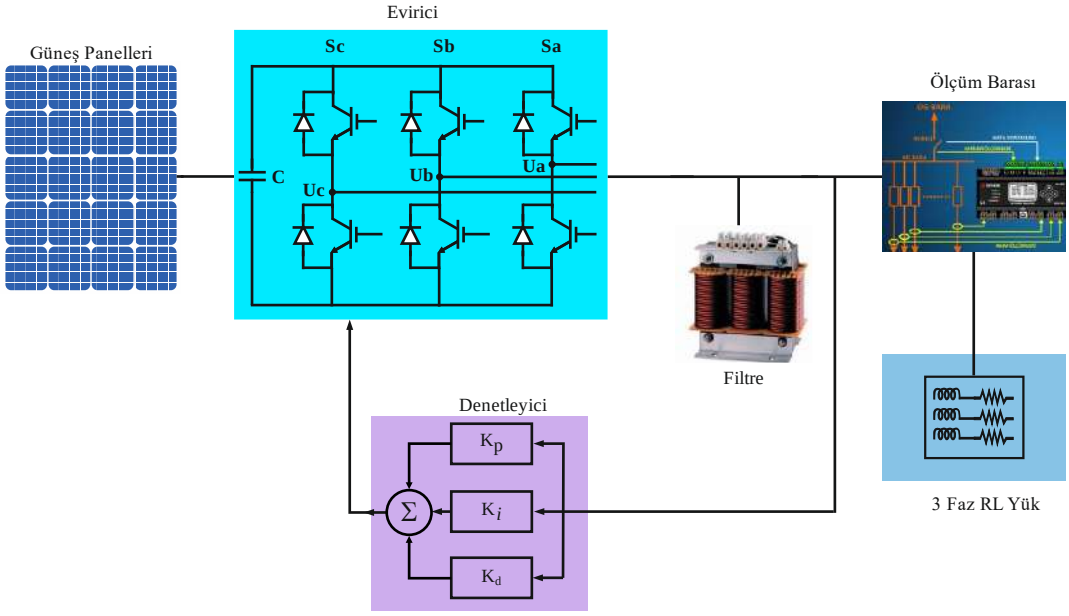

Figure 1. Single Line Diagram

3.1. Applying the PID Controller to the Circuit with LC Filter

When the variation of the load voltage is examined in the operation of classical PID with LC filters; The 380V voltage reaches 0.2 seconds and the fluctuation is less. Correspondingly, the d-q axis assembly has a lower current surge. When the FFT (Fast Fourier Transform) analysis is performed, the classical PID has a THD (Total Harmonic Distortion) ratio of 4.12% and is above the standard values. The modulation index of the

circuit is around 0.6 and the circuit produces continuous energy.

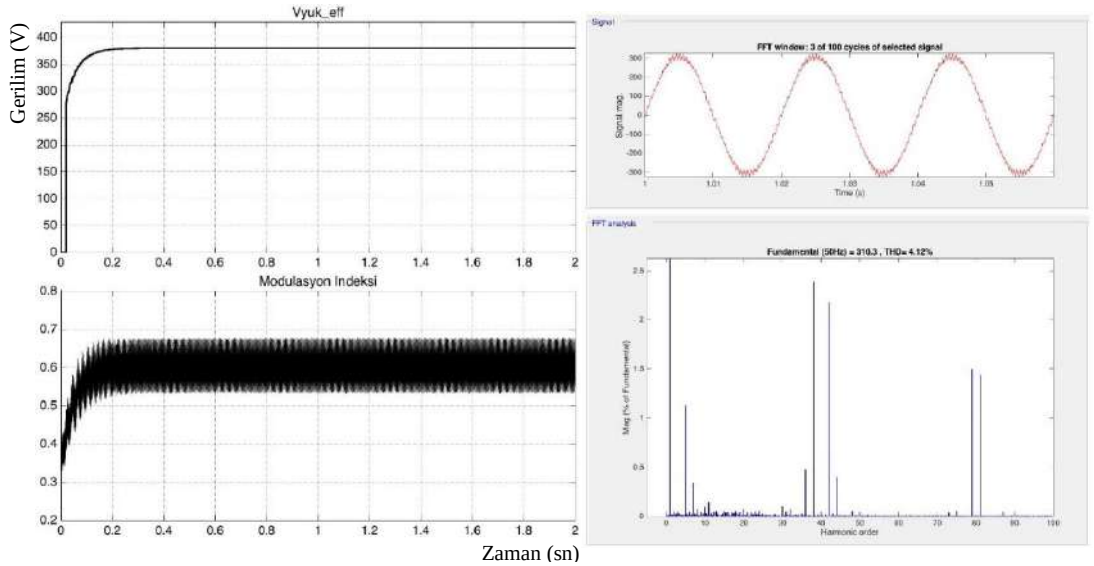

4 Figure 2. Output load, modulation index and THD graph in circuit with LC filter

5 3.2. Application of PID Controller to Circuit with Type C High Pass Harmonic Filter

When the load voltage change is examined in the study of classical PID with high pass filters of type C; The 380V voltage reaches 0.2 seconds and the fluctuation is very small. When the detailed FFT analysis is performed, the THD rate of classical PID is 2.92% and is below the standard values. The modulation index of the circuit is around 0.6 and the circuit produces continuous energy.

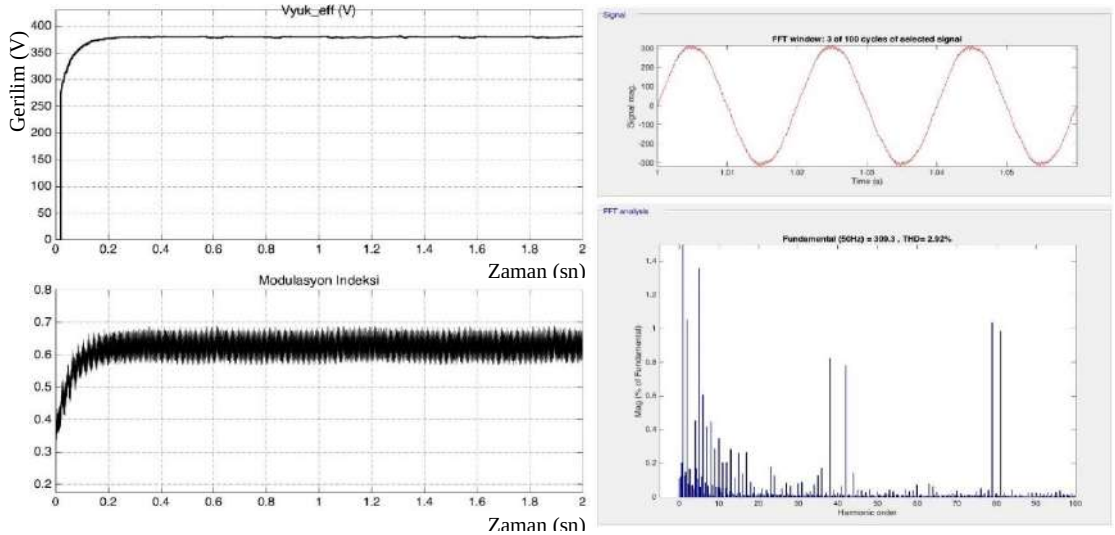

Figure 3. Output load, modulation index and THD graph in circuit with C type high pass harmonic filter

3.3. Application of PID Controller to the Circuit with High Pass Harmonic Filter

When the load voltage change is examined in the study of classical PID with high pass filters of type C; The 380V voltage reaches 0.2 seconds and the fluctuation is very small. When the detailed FFT analysis is performed, the rate of THD of the classical PID is 2,88% and is below the standard values. The modulation index of the circuit is around 0.6 and the circuit produces continuous energy.

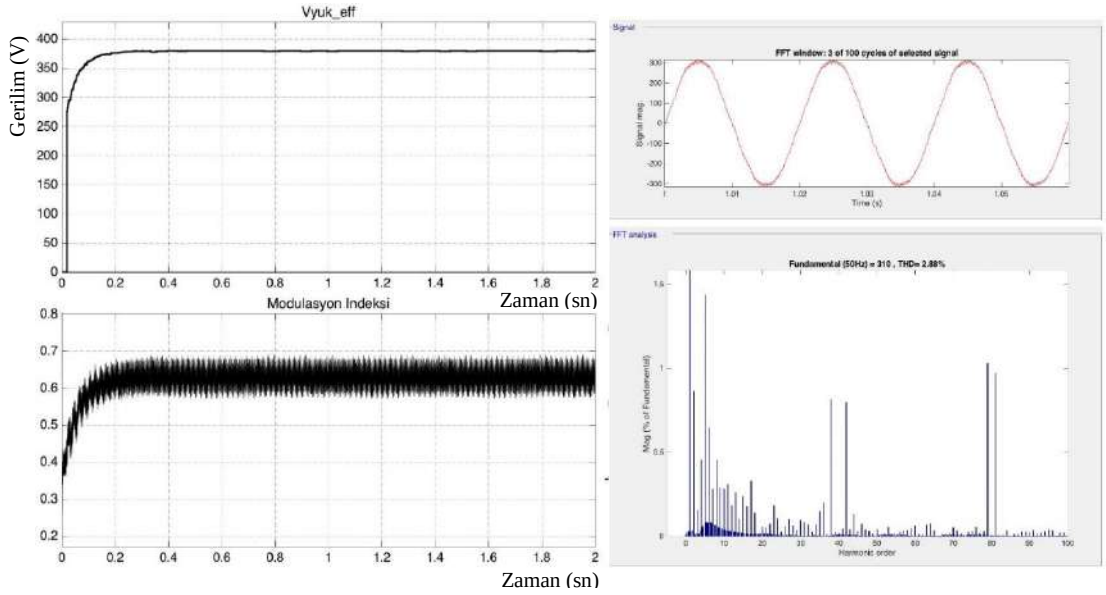

Figure 3. Output load, modulation index and THD graph in circuit with high pass harmonic filter

4. Result

Harmonics are one of the most common problems in electrical energy production. Harmonic filters are the easiest solution to reduce or decrease their harmonic currents. For this

reason, an LC filter and two harmonic filter applications were made and the TDH values were tried to be determined within the limit values. The results of the studies in the table below are given.

Table 1. FFT analysis results when filters and controllers are active

Controller and Filter Types	$V_{load\text{-}effective}$ (V)	V_{load} Phase-to-phase (V) Lowest-Highest voltage	THD value for $I_{r\ load}$ (%)	THD value for $V_{r\ load}$ (%)
PID Controller LC filter	379	550-560	3,91	4,12
PID Controller Type C High Pass Harmonic Filter	380,7	560-564	2,78	2,92
PID Controller **High Pass Harmonic Filter**	**380,9**	**550-565**	**2,74**	**2,88**

As seen in Table 1, when the inverter output is controlled by the PID controller and when the high-pass harmonic filter is applied in parallel to the circuit, the lowest voltage voltage between phase-phase is measured as 56V to 550V at the highest. When the detailed FFT analysis was performed, the THD value was 2.88% with high pass harmonic filter. When the THD values of both current and voltage values are examined, the circuit of the output voltage and current in the circuit with high-pass harmonic filter is the lowest, the least harmonic, and the lowest of the standard rates.

References

[1] Uyarel A. Yücel, Öz Etem Sait, 1987. Güneş Enerjisi ve Uygulamaları, Birsen Yayınevi,
[2] Arillaga J., Bradley D. A. and Bodger P. S., Power System Harmonies, John Wiley & Sons Ltd., Norwich. 1985.

[3] Benjamin C.K., 1991. Automatic Control System, Sıxth Edition Prentice Hall International Editions, Englewood Cliffs,
[4] Ay, S., "Alçak Gerilim Tesislerindeki Gerilim Harmonikleri Ve Filtre Tasarımı", Kaynak Elektrik Dergisi, Sayı: 95. 1996.
[5] Tadros, Y., Salama, S. ve Höf, R., "Three level IGBT Inverter". 23rd Ann. Power Electron. Specialists Conf., 1992.Tüfekçi, A. 2018 ."Yenilenebilir Enerji Sistemlerinde Harmonik Analizi", Giresun Üniversitesi Fen Bilimleri Enstitüsü, Yüksek Lisans Tezi,

A New Method of Ultrawideband Pulse Shaping

Meryem Filiz[1*]

[1] Erciyes University, Department of Science, Electrical and Electronic Engineering, Kayseri, Turkey;

[*]**Responsible Writer:** meryemf@gmail.com

Abstract

In this study, an effort was made to develop a new method for ultrawideband pulse shaping. Odd, even and derivative forms of Gaussian pulses are used. This paper aims to investigate ultrawideband pulse shaping methods and developed e new method by combining pulsers. Pulses have been examined for compatibility with the frequency mask issued by the Federal Communications Commission (FCC). In previous studies, the ultrawideband pulse splicing method was implemented by combining Gaussian Pulse Derivatives. In this study, Gaussian derivatives were tried to be combined using different methods and aimed to achieve better performance.

Keywords: Ultrawideband, pulse shaping, odd even pulses, Gaussian pulse derivatives, FCC.

1. Introduction

Ultra wideband pulse shapes are known as high-energy waveforms between 3.1 and 10.6 GHz (FCC ET, 2002). Ultra wideband wireless communication system is used for different purposes: i) radar, ii) ultrasound, iii) earthquake people search and so forth. Compared to wifi technology, Ultra wideband technology has significant advantages such as high energy content and equal strength in coverage area. Given these characteristics, it can be said that Ultra wideband is less harmful for human health than other technologies.

In Ultra wideband communication systems, the quality of communication increases by using the appropriate pulse. For this reason, a set of different techniqiues are used to shape the ultrawideband pulse. Gaussian pulses and their derivatives, Hermite polynomials, and Prolate Spherical pulses constitute the pulse shapes used for ultrawideband systems (Win, 2000; Zhang, 2003; Michael, 2002; Parr, 2003). The mathematical functions of these pulses, frequency spectrum energies, bandwidths are used in the design and shape of the pulse.

With Ultra wideband technology, the systems are spread over the frequency range in the large spectrum. It is important to suppress the intersymbol interference in this large spectrum. In 2002, the FCC identified the spectral distribution boundaries to be used by Ultra wideband systems with Equivalent Isotropically Radiated Power (EIRP).

Below is a table with the frequency values for the Ultra wideband for which the FCC commission has been set.

Table 1: Frequency values determined by the FCC

Frequency (MHz)	Indoor EIRPM (dBm)	Outdoor EIRPM (dBm)
<960	-41.3	-41.3
960-1610	-75.3	-75.3
1610-1990	-53.3	-63.3
1990-3100	-51.3	-61.3
3100-10600	-41.3	-41.3
>10600	-51.3	-61.3

2.1.Ultrawideband Pulse Shapes

The Gaussian pulse is the most commonly used pulse shapes in Ultra wideband. The equation in the time domain of the Gaussian pulse is shown below. Time t, σ2 and A respectively indicate pulse variance and amplitude.

$$x(t) = \frac{A}{\sqrt{2\pi\sigma^2}} e^{\left(-\frac{t^2}{2\sigma^2}\right)} \quad (1)$$

Showing the superscript as $^{(n)}$, the n derivation of the Gaussian pulse is expressed as:

$$x^{(n)}(t) = -\frac{n-1}{\sigma^2} x^{(n-2)}(t) - \frac{t}{\sigma^2} x^{(n-1)}(t) \quad (2)$$

Frequency analysis of time-domain pulses is done by Fourier transform. The pulse value obtained by Fourier transform of n^{th} derivation of Gaussian pulse is given below.

$$x_n(f) = A(j2\pi f)^n e^{\left(-\frac{(2\pi f\sigma)^2}{2}\right)} \quad (3)$$

Another impulse used in Ultra wideband communications is the Hermite Pulse. The equation in the time domain of Hermite pulses is shown as follows:

$$h_{e_n}(t) = (-\tau)^n e^{t^2/2\tau^2} \frac{d^n}{dt^n}(e^{-t^2/2\tau^2}) \quad (4)$$

Different Hermite polynomials are used in the literature. The following example shows Hermite polynomials:

$$\begin{aligned} h_{e0}(t) &= 1 \\ h_{e1}(t) &= \frac{t}{\tau} \\ h_{e2}(t) &= \left(\frac{t}{\tau}\right)^2 - 1 \\ h_{e3}(t) &= \left(\frac{t}{\tau}\right)^3 - 3\frac{t}{\tau} \\ h_{e4}(t) &= \left(\frac{t}{\tau}\right)^4 - 6\left(\frac{t}{\tau}\right)^2 + 3 \\ h_{e5}(t) &= \left(\frac{t}{\tau}\right)^5 - 10\left(\frac{t}{\tau}\right)^3 + 15\frac{t}{\tau} \\ h_{e6}(t) &= \left(\frac{t}{\tau}\right)^6 - 15\left(\frac{t}{\tau}\right)^4 + 45\left(\frac{t}{\tau}\right)^2 - 15 \\ h_{e7}(t) &= \left(\frac{t}{\tau}\right)^7 - 21\left(\frac{t}{\tau}\right)^5 + 105\left(\frac{t}{\tau}\right)^3 - 105\frac{t}{\tau} \end{aligned} \quad (5)$$

$$h_{e8}(t) = \left(\frac{t}{\tau}\right)^8 - 28\left(\frac{t}{\tau}\right)^6 + 210\left(\frac{t}{\tau}\right)^4 - 420\left(\frac{t}{\tau}\right)^2 + 105$$

Norman and Bo developed a new method based on power spectral density using even and odd pulses of Gaussian monocycle (Beaulieu and Hu, 2006). According to this, the frequency of a odd pulse, including the number of convoluted rectangular windows, is shown below:

$$P_n^o(f) = \frac{\tau^n}{2j}\{sinc^n[\tau(f - f_c) - sinc^n[\tau(f + f_c)]\} \qquad n = 1,2,3, \ldots \tag{6}$$

The time expression of the Gaussian odd pulse is given below:

$$p_n^o(t) = \sum_{m=0}^{n} \frac{n(-1)^{n-m}\left[\frac{t}{\tau} - \left(\frac{n}{2} - m\right)\right]^{n-1} \sin(2\pi f_c t)}{m!(n-m)!} \times U\left[\frac{t}{\tau} - \left(\frac{n}{2} - m\right)\right] \tag{7}$$

The equation for the time expression of the Gaussian even pulse is given below:

$$p_n^e(t) = \sum_{m=0}^{n} \frac{n(-1)^{n-m}\left[\frac{t}{\tau} - \left(\frac{n}{2} - m\right)\right]^{n-1} \cos(2\pi f_c t)}{m!(n-m)!} \times U\left[\frac{t}{\tau} - \left(\frac{n}{2} - m\right)\right] \tag{8}$$

The equation for the frequency expression of a Gaussian even pulse is given below:

$$P_n^e(f) = \frac{\tau^n}{2}\{sinc[\tau(f - f_c) - sinc^n[\tau(f + f_c)]\} \quad n = 1,2,3, \ldots \tag{9}$$

2.2.Techniques Used for Ultrawideband Pulse Design

Ultra wideband pulses are similar to noise. Ultrawideband system energy is spread over a very large bandwidth. Pulses have a very low energy and power density.

For Ultra wideband pulse production, producing a single and a short pulse is considered by using a traditional and basic approach. By varying pulse characteristics it is aimed to achieve the desired design criterion as a result of changing the characteristics of the energy in the frequency spectrum.Three basic characteristics of the energy mentioned below have to be considered.

- The desired band width of the given energy should be carefully defined and evaluated,
- The customized ultrawideband frequency should be within the spectrum and appropriate energy limits,
- The energy produced should be centered within the desired spectrum.

Pulses with very low spectral power density and high bandwidth cannot be detected by unauthorized systems. If the bandwidth is larger, the resolution, spacing and location will be effective. Thus, it is not necessary to use difficult and complicated algorithms and it is possible to make a prediction with good accuracy. High frequency is used when the pulses are high-power while low frequency is used for positioning, such as radar. The system used ultra wideband handles two design principles, amplitude and pulse width for impact generator in penetrating radar applications. Pulse width is determined when small objects are determined, and impact amplitude is influenced when objects are detected. In this way, pulses can collect various environmental information in different places.

Optimization is the best solution for a problem or function in terms of variables, constraints and goals. Sometimes the best solution is more than one. Ultra wideband pulse shaping optimization techniques are utilized. For example, Particle Swarm Optimization (PSO) has been used in the literature (Keshavarz, and frn., 2010). In 1995, Eberhart and Kennedy developed an optimization algorithm based on the behavior of animal species. They have analyzed animals, specifically fish and birds. Each solution represents a particle called as a bird. Birds send coordinates to the fitness function when searching food and, the results are evaluated based on the fitness function. In the Ultra wideband application, this optimization technique is used to select the most appropriate combination of Gaussian derivatives to increase pulse shaping performance.

3. Methods Used In the Previous Studies

Reza and Ben have studied the new wide spherical pulse functions used in ultra wideband communications. Using these classes of functions, they produced orthogonal pulses. Additionally, they terminated the inter-symbols interference. They used Pulse Position Modulation as the modulation technique that is suitable for these pulses (Reza and frn., 2003).

In the Giuseppe's study, orthogonal pulse-modulated Hermite pulses were used. Transciever the receiver pulseshapes are obtained with the cross correlation of Hermite pulses (Abreu, 2003).

Bo and Norman have compared the previously obtained pulse shapes, which provide the best performance in ultrawideband communication systems, in their work. Bit error rate (BER), multiple access interference and the required spectral propagation limits have been examined in that study. High-order Gaussian monocycle and prolate spherical function-pulses have been found to match spectral propagation masks without frequency shift. Frequency shifting and bandpass filtering are used to compensate for spectral masks of modified Hermite polynomial-based pulses. Accordingly, even and odd pulses of Gaussian monocyle provide a performance as good as prolate spherical function based pulses. Even and odd pulses of Gaussian monocycle is compared with the modified Hermit polynomial-pulses system models (Hu and Beaulieu, 2004).

Ultra wideband communication and compatibility is an important issue that needs to be examined. Interference should be avoided according to the appropriate pulse shape design. Yin and Hongbo have discussed the approximate spherical pulse functions in their work. The simple and straightforward mathematical expression of these pulses have been investigated to meet the power spectral limits of the FCC spectral mask (Yin and Hongbo, 2005).

Table 2: Comparative table of Ultra wideband impact shaping studies

Yazar Adı	Tarihi	Kullandığı Darbe Şekli	Kullandığı Method
Reza.S.Dilmaghani	2003	Prolate Spheriodal Pulses	New UWB Pulse Shaping
Giuseppe Thadeu Freitas de Abreu	2003	Hermite Pulses	Modulation Technique
Bo Hu	2004	Gaussian, Prolate Spheriodal, Hermite Pulses	New Design Method
Lu Yin	2005	Prolate Spheriodal Pulses	New Design Method
Igor Dotlic	2007	Gaussian Pulses	New Design Method
Cai Cheng-Lin	2008	Gaussian Pulses	New Design Method
Liu, Wenke	2008	Hermite Pulses	New Design Method

Hans W. Pflug	2008	Gaussian Pulses	New Design Method
Sayed Noorodin Keshavarz	2010	Gaussian Derivatives	Optimization Technique
Li LI	2011	Gaussian Derivatives	New Design Method
Imen Barraj	2013	Modified triangular	New Design Method
Meenu B Menon	2015	Gaussian Derivatives	Hibrit Approach
Ante Milos	2017	Gaussian ve Hermite Pulses	Pulse Shaper
B. A. Lagovsky	2017	Gaussian Pulses	Pulse Optimization

In this work with Igor and Ryuji, FCC has produced a new design method for full-band, non-linear ultrawideband pulses that provide spectral mask boundaries. This method uses convex programming in each iterative process step and updates the phase distribution of the objective function. This method can be easily modified in different orthogonal Ultra wideband pulse design problems with the help of mathematical structure. With this method, high spectral efficiency has been achieved with a large number of orthogonal pulse shapes (Dotlic and Kohno, 2007).

Cai and his team have investigated a new wave design method for ultrawideband wireless communication with the linear combination of Gaussian pulse derivatives. The scaling factor of Gaussian pulse derivates and derivative coefficient of the spread spectrum effect are considered in this study. According to the simulation results, the linear combination of Ultra wideband pulse was found to meet the indoor and outdoor FCC propagation mask rules and the BER performance was very good (Lin and frn, 2008).

Liu has developed a new method of pulse shaping based on orthogonal Hermite functions. The pulses obtained from the simulated results meet the FCC spectral mask and optimize the transmitted power spectrum. Also, the hardware implementation was simple. As a result, high power efficiency and pulse DC components are produced (Wenke and frn, 2008).

In the Hans's study, Ultra wideband pulse shape calculation method analysis for wireless communication used in the IEEE 802.15.4a standard has been reviewed (Pflug, 2008).

Sayed has been interested in Ultra wideband wireless communication by using the linear combination of Gaussian pulse derivatives. Scaling factor and scattered spectrum effect of differential coefficients are determined. The Gaussian pulse derivatives are combined in triplicate or multiplied with the construction method. It is desirable that the gain is the best with the weight coefficient. PSO optimization is used when the weight vector and scaling factor are

optimized. This optimization method is inspired by herd behavior. In the PSO algorithm, each individual searches for the best solution with swarm knowledge. Simulation results show better performance than single Gaussian derivative pulses. The single derivative pulses do not meet the FCC propagation mask very well. In this study, it is seen that the 4th and 5th Gaussian derivative is most suitable by optimizing the pulse shape and weight vector with PSO model. Thus, it has been analyzed that random Gaussian derivative combinations determined by optimization are better able to compute FCC boundaries than single derivative combinations (Keshavarz, 2010).

Li has have developed a two-stage ultrawideband pulse shaping method with Gaussian variants. First, the optimal combination of Gaussian derivatives was used to adapt the sidebands to the mask. Second, a bandpass filter was used (Li and frn, 2011).

Imen and Hatem produced a pulse by combining two triangular pulses. The first is characterized by the positive amplitude and the second by the smallest negative amplitude. The simulated impulse has a cross correlation magnitude of 0,97 for the main lobe of the reference pulse and 0.22 for the side lobes for a period of at least 0.5 ns. The Darbenin spectrum can be easily adapted to PSD mask (Barraj and frn, 2013).

Meeno and co-workers have attempted to use a hybrid approach for UWB pulse shaping (Meeno and frn,2015).

High-grade Gaussian and modified Hermite monocycle crests were used in Ante, Goron and Mladen works. Since UWB uses very short pulses, the filter technique that banded in the shape of these pulses is used. Efficiency has been gained in 89% in Gaussian, 62% in modified Hermite pulses (Milos and frn, 2017).

Lagovsky, Chikina have stated that it is necessary to develop UWB signal-based robots and other technical specifications for high-speed radio communication systems. UWB radar is used in geology and geophysics in remote sensing. Moreover, UWB is also used for breathing, heart beat, cardiovascular system and other systems in medicine. The quality and accuracy of the UWB mark affect these measurement results. Therefore, fast algorithms used in real time are developed (Lagovsky and Chikina, 2017).

4. Proposed Method

In this study, we propose a new method for Ultra wideband communication systems using Gaussian and derivative waveforms, and a development that will contribute to the UWB

communication system by achieving high performance pulses. The variance and derivative of the Gaussian pulse will be modified in the direction of achieving a pulse shape that matches the FCC mask as closely as possible and at the same time maximizes the bandwidth. The pulse will then be configured in accordance with the PSD's FCC masks. Optimization techniques will be used for the most appropriate Gaussian derivatives. Commonly used optimization techniques are:

• Artificial Intelligence Techniques that is an optimization technique developed by taking the neural network structure as an example. It is used in engineering applications and in different fields.

• PSO (Particle Swarm Optimization)

• Genetic Algorithm (GA) which is a basic GA -a random number generator, a conformity assessment unit, and genetic operator stages for reproductive, crossover and mutation operations. Genetic operators are used to develop solutions in successive generations.

• Tabu Research Algorithm (TRA) that is an intuitive research algorithm based on clever problem solving proposed by Fred Glover in 1986.

• Artificial bee colony algorithm (AB) inspired by bee behaviors. It was constructed according to the nutritional search methods of bees (Akay and Karaboğa, 2012).

This work will be done in MATLAB environment and the results will be evaluated in MATLAB environment. MATLAB code is written for Gaussian and its derivatives. Time and frequency shapes were obtained. Analyzes of power spectral density are continuing.What is more, Gaussian triangles are investifated 3's folds, 4's folds, 5's folds. The achievements of the coupons handled in this way are not very good, and efforts to improve are continuing. In this context, it is aimed to increase the performance by using appropriate optimization technique.

5. Results and Future Work

In this study ultra wideband impact shaping methods and compatibility with the limits in Table 1 were examined. These studies have been investigated in detail and are shown in Table 3. A new method will be developed by using optimization and combining technique which gives the best result and ultrawideband pulse shape suitable for FCC mask boundaries. By determining our future work in this way, it is planned to create an ultrawideband pulse shape with higher performance ratio as a result of a new method. The least squares evaluation function technique will be used to measure the impact performance of the new method.

Thanks

This work with FBT-07-10 project code number is supported by Erciyes University Scientific Research Projects Unit.

References

"Revision of Part 15 the Commission's rules regarding ultra-wideband transmission systems," FCC, ET Docket 98-153, 2002.

Win, M. Z. and Scholtz ,R. A., *"Ultra-wide bandwidth time-hopping spread-spectrum impulse radio for wireless multiple-access communications,"* IEEE Trans. Commun., vol. 48, pp. 679–691, Apr. 2000.

Zhang, J. T., Abhayapala, D. and Kennedy, R. A., *"Performance of ultrawideband correlator receiver using Gaussian monocycles"* in Proc. IEEE ICC 2003.

Michael, L. B., Ghavami, M., and Kohno, R., *"Multiple pulse generator for ultra-wideband communication using Hermite polynomial based orthogonal pulses"* in Proc. IEEE Conf. Ultra Wideband Systems and Technologies 2002, pp. 47–51.

Parr, B., Cho, B., Wallace, K., and Ding Z., *"A novel ultra-wideband pulse design algorithm"* IEEE Commun. Lett., vol. 7, pp. 219–221, May 2003.

Beaulieu, N. and Hu, B. A *'Pulse Design Paradigm for Ultra-Wideband Communication Systems'. IEEE Transactions on Wireless Communications*, VOL. 5, NO. 6, JUNE 2006

Keshavarz, S. N., Hamidi, M. and Khoshbin, H. *'A PSO-based UWB Pulse Waveform Design Method.*' *Second International Conference on Computer and Network Technology*. Iran

Reza, S., Ghavami, D. M., Allen, B., Aghvami, H. *'Novel UWB Pulse Shaping Using Prolate: Spheroidal Wave Functions,*' *IEEE 2003 International Symposium on Personal,Indoor and Mobile Radio Communication Proceedings* , London

Abreu, G. T. F., Mitchell, C. J. and Kohno, R. *'On the Design of Orthogonal Pulse-Shape Modulation for UWB Systems Using Hermite Pulses'*

Wu, X., Tian, Z., Davidson T. N., and Giannakis, G. B. *Optimal Waveform Design For UWB Radios*, USA.

Hu, B. and Beaulieu, N. C. *'Pulse Shaping in UWB Communication Systems', 2004.*

Yin, L., Hongbo, Z. *'UWB Pulse Design Using the Approximate Prolate SpheroidalWave Functions'. 2005 IEEE Internaional Symposium on Microwave, Antenna, Propagation and EMC Technologies for Wireless Communications Proceedings, 2005.*

Dotlic, I., Kohno, R. *'Design of the Family of Orthogonal and Spectrally Efficient UWB Waveforms', IEEE Journal of Selected Topics in Signal Processing, Vol. 1, No. 1, June 2007 21*

Lin, C. C., Hui L. X., Sheng, X. X. And Tao, W. H. *'A Novel UWB Pulse Design Method of Optimizig Combination with Differential Gaussian Pulse.' Ultrawideband and Ultrashort Impulse Signals*, 15-19 September, 2008, Sevastopol, Ukraine pp. 228-230

Wenke, L., Jianjun, L., Shuang, C. *'A Novel Pulse Shaping Method for Ultra-Wideband Communications', 2008.*

Pflug, H. W. *'UWB Pulse Shaping for IEEE 802.15.4a'.* the Netherlands, 2008.

Li, L., Wang, P., Wu, X., Zhang, J., '*Improved UWB Pulse Shaping Method Based On Gaussian Derivatives', 2011.*

Barraj, I., Trabelsi, H., Masmoudi, M. *'Power Spectral Density of Modified Hermite Pulses for M-ary Pulse Shape Modulation', 2013.*

Milos, A., Molnar, G. and Vucic, M. *'A Hybrid Approach for UWB Pulse Shaping',2017.*

B. A. Lagovsky and A. G. Chikina. Shape Optimization of UWB Pulses Russia *2017, Progress In Electromagnetics Research Symposium,*

Meenu, B., Menon, D., Gopakumar, A&N,. '*Spectral-Efficient UWB Pulse Shapers Generating Gaussian and Modified Hermitian Monocycles', 2013.*

Akay, B., Karaboğa D., *'A modified Artificial Bee Colony algorithm for real-parameter optimization'*, Information Sciences, 192, pp. 120–142, 2012.

Overview Work On Dna Cryptography

Gülcan YILDIZ[1], Büşranur KÜÇÜKUĞURLU[2], Doğan YILDIZ[3*]

[1] 1 Ondokuz Mayıs University, Engineering Faculty, Department of Computer Engineering, Samsun, Turkey; gulcan.ozer@omu.edu.tr

2 Gumushane University Faculty of Engineering and Natural Sciences, Department of Software Engineering, Gumushane, Turkey;

busra.kucukugurlu@gumushane.edu.tr

3 Ondokuz Mayıs University, Engineering Faculty, Department of Electrical-Electronics Engineering, Samsun, Turkey; dogan.yildiz@omu.edu.tr

[*] **Corresponding Author:** dogan.yildiz@omu.edu.tr

Abstract

Since security is one of the most important issues nowadays, the development of cryptography and cryptographic analysis are considered as areas of ongoing research. As traditional encryption systems become increasingly vulnerable to attack, the concept of DNA (Deoksiribo Nucleic Acid) cryptography has emerged as a new approach to creating reliable algorithms. The most important purposes of investigating DNA cryptography are to explore the DNA molecule and the properties of the reaction, to create the relevant theories, to explore possible progressive directions, to search for simple methods to understand DNA cryptography, and to lay the foundation for future progress. Parallelism in the DNA molecule and high storage capacity make this field efficient. DNA cryptography is still in the process of being developed and there are not many studies on this subject. In this study, some studies on DNA Cryptography in the literature have been examined.

Keywords: DNA, DNA cryptography, data security, steganography.

1. Introduction

The coded text generated by the encryption algorithm is similar to the biological structure of the DNA strand sequence in DNA cryptography, and utilizes this similarity.1 grams of DNA contains 1021 DNA bases, equivalent to 108 TB of DNA, which is why the high storage capacity of DNA is used. In addition, since parallel and fast calculation can be performed, it is advantageous to use instead of conventional cryptography methods (Popovici, 2010).

General information will be given about DNA cryptography, in Section 2. Summer of the work done in this area will be given in section 3.

2. General Information

2.1. DNA

The DNA, Deoxyribo Nucleic Acid, is a double-stranded helical molecule carrying genetic information. Each thread is based on 4 base cadisine: Adenine (A), Timin (T), Guanine (G) and Cytosine (C). Adenine (A) matches with 2 hydrogen bonds with Timin (T); Guanine (G) matches with 3 hydrogen bonds with Cytosine (C) in double-stranded structure (Anam, 2010).

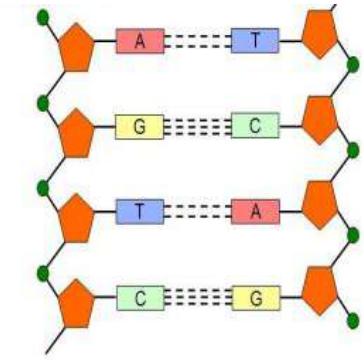

Figure 1. Bond structure of DNA bases (Soni, 2013)

2.2. DNA Cryptography

It was first suggested by L. Adleman in the 1990s. Adleman proved this technique by solving the seven-sided Hamilton Path Problem (Soni, 2013). Most commonly used DNA Cryptography techniques: PCR (Polymerized Chain Reaction), OTP (One Time Pad)

Algorithm, Substitution, XOR processing, Hybridization, Symmetric Key Cryptosystem using DNA, Asymmetric Key Crypto System. (Jacob, 2013).

2.3. PCR

PCR is the enzymatic synthesis of copies of a DNA fragment, directed by primers. In other words, this means that a desirable region of DNA is replicated in a short period of time from the cell (PCR machines).

In terms of encryption, encrypted messages can be solved if appropriate primers are found. This is quite difficult. Therefore, primers can serve as keys in encryption (Jeevidha, 2011).

2.4. OTP

The key generated for encryption in OTP is disposable. Every key used is destroyed once it is used for one time and a new key is generated for each new message (Alavi-Milani, 2012).

2.5. Logistic Map

Logistic map is a deterministic, random-like process with non-converging, restricted and nonlinear dynamic systems. Long-term random number sequences have a very important place in production, sampling, numerical analysis, decision making and heuristic optimization methods (Alataş, 2007). Logistics maps are used effectively in the encoding of images because of their sensitive dependence on initial conditions, random behavior and non-repetitive features. The logistic map is given by Equation (1).

$$X_{n+1} = \lambda X_n(1 - X_n) \quad (1)$$

Where, Xn ∈ (0,1) and λ are the system variables and parameters, respectively, and n is the number of iterations. Thus, taking a starting value x0 and a parameter k, {Xn} n∞ = 0 is

computed. The starting values and the λ value have a very important function in the logistic map. The degree to which the logistic map is affected by different λ values is shown in Fig. 2 by the bifurcation diagram. This is a compliment of the logistic map, as a λ function. The solution obtained for $0 \leq \lambda \leq 1$ is only a fixed point. For $1 < \lambda \leq 3$, there is also a fixed point. $3 < \lambda \leq 3.75$, the removal of the two-fold of the map is displayed. $3.75 < \lambda < 4$, the map becomes chaotic. Finally, in the case of $\lambda = 4$, chaos can be composed of various values ranging from 0-1.

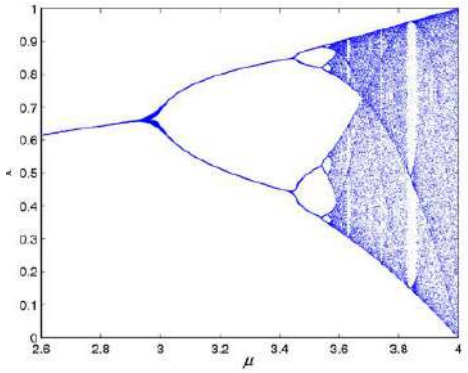

Figure 2. Bifurcation diagram (Liu, 2012)

2.6. Steganography

Steganography refers to "hidden text" in ancient Greek and is given to the science of hiding information (important: not encryption). The biggest advantage of steganography over cryptography is that someone who sees information is unaware that it is important information in what it sees, so it does not search for information. Whereas a coded message is interesting because of mystery, even if it is difficult to solve.

3. Related Works

In Soni et. al. (Soni, 2010) ve Terec et. al. (Terec, 2011) studies, symmetric and asymmetric DNA cryptography methods have been described. Symmetric algorithms are algorithms that use the same key for encryption and decryption operations. In asymmetric algorithms, the encryption key and the decryption key are different. The key that encrypts the key is public key and the key that decrypts the key is private key. According to symmetric encryption algorithms it is much more difficult to decipher the password.

In Alavi-Milani (Alavi-Milani, 2012) study, a DNA coding method has been developed with the help of a DNA_OTP sequence generated by using the random properties of the logistic map. The fact that numbers consisting of logistic maps are random and sensitive to the initial value generated from the key raises the security of the proposed algorithm. The flow diagram of the proposed method is given in Figure 3.

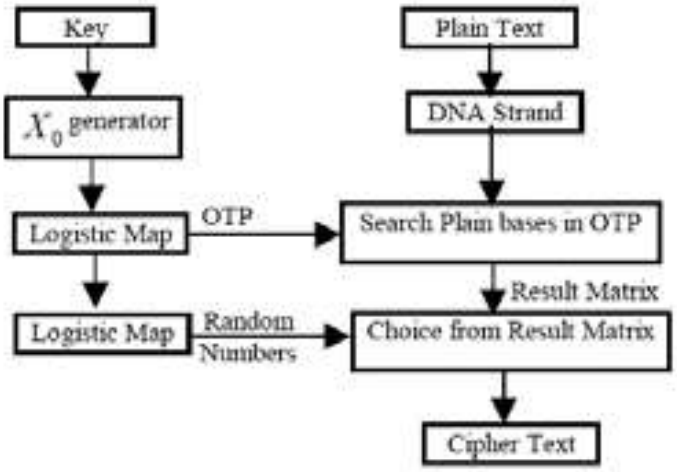

Figure 3. Flowchart of the proposed method (Alavi-Milani, 2012)

Goyat and Jain (Goyat, 2016) have suggested that the method is an effective DNA-based encryption method to provide more reliable data transmission. The algorithm basically consists of 2 steps: round key selection and message encryption stages.

In another study on DNA cryptography, a novel parallel coding technique published by Pramanik and Setua (Pramanik, 2012) is proposed using one-time-pad scheme, DNA molecular structure, the DNA hybridization technique, which certainly minimizes time complexity. A single-stranded DNA (ssDNA) can form double-stranded DNA (dsDNA) with other ssDNA chains complementary to each other, under certain conditions. In this process, called hybridization, double-stranded molecules are hybrids of fibers from different sources.

Majumdar and Sharma (Majumdar, 2014) have mentioned how they suggest new approach towards information security based on DNA cryptography in their study. This method of DNA-based encryption consists basically of 4 steps. These stages include generating and selecting a round key, encrypting the message, encoding the DNA and providing the data integrity.

The novelty of the method suggested by Wang et. al. (Wang, 2013) is to separate the message in order to solve the security problem of DNA steganography. Security analysis

expressed that DNA steganography can come from above the security problem on the basis of the proposed method, and then a message can be sent and hidden by an enemy.

Kumar and Singh (Kumar, 2011) declared that a data hiding algorithm was developed using DNA sequence and traditional steganography technique. By using steganography, they have described an algorithm consisting of hiding the data to the DNA sequences and sending the encoded DNA sequences to the recipient with a key.

Liu et al. (Liu, 2012) have proposed an RGB image encryption algorithm based on DNA coding combined with logistic functions in the study. The simulation results of the proposed algorithm show that the secret key has strong sensitivity and large space. In addition, it can counteract the statistical attack, comprehensive attack and is therefore suitable for encrypting RGB images. The flow diagram of the image encryption algorithm is shown in Figure 4.

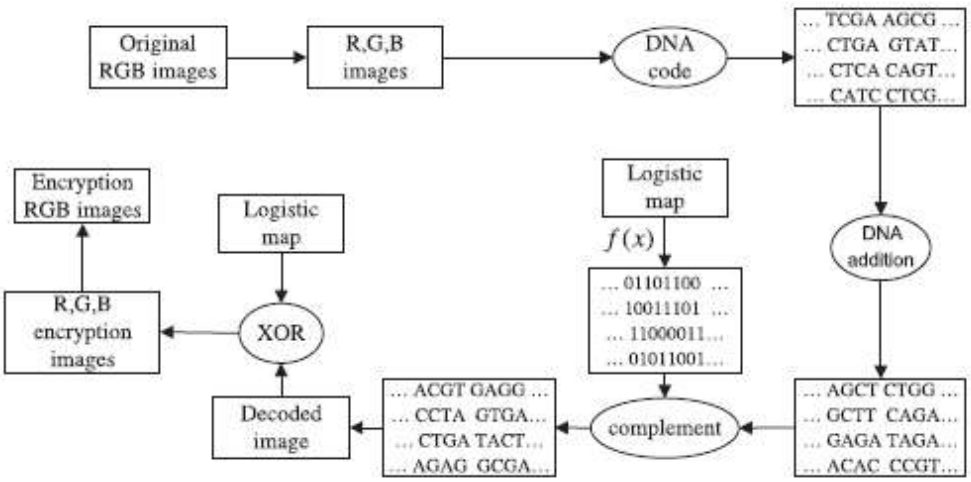

Figure 4: The flow diagram of the image encryption (Liu, 2012)

The security vulnerabilities of the study (Liu, 2012) were analyzed in the study of Ozkaynak and his colleagues (Ozkaynak, 2013). It has been shown that hidden parameters can be removed by using the selected clear text attack. Four different special images were used for the attack. All pixel values of these images are respectively 0, 85, 170 and 255 values. When the encrypted formats are examined, they have the same value for color components 85 and 170. After applying the key space reduction algorithm, it is seen that the key space falls from 256 to 16. As a result, it can be seen that the key values can be found exactly as a result of the brute force attack.

4. Conclusion

DNA cryptography is the art of preserving data using DNA sequences. DNA cryptography is a slightly new area of encryption performed by DNA computation. DNA is used as a message carrier in this area and biotechnology such as PCR is used as an application mechanism. Large-scale storage capacity and parallel computability of DNA molecules can be used effectively for encryption, authentication and authorization. DNA based cryptography is one of the effective methods of reaching secure data communications. It provides fast and parallel calculation for problems requiring high storage. DNA cryptography is a field that has openness and potential to work on. In this study, recent studies on DNA cryptography are examined.

References

Alataş, B., Akın, E., ve Özer, A. B. (2007). Kaotik Haritalı Parçacık Sürü Optimizasyon Algoritmaları.

Alavi-Milani, M. M. R., Pehlivan, H. ve Hosein-Pour, S., (2012). OTP (One Time Pad) tabanlı DNA şifreleme yöntemi. Akademik Bilişim, 12, 1-3.

Anam, B., Sakib, K., Hossain, M. ve Dahal, K., (2010). Review on the Advancements of DNA Cryptography. arXiv preprint arXiv:1010.0186.

Goyat, S. ve Jain, S., (2016). A secure cryptographic cloud communication using DNA cryptographic technique. In Inventive Computation Technologies (ICICT), International Conference on (Vol. 3, pp. 1-8). IEEE.

Jacob, G., ve Murugan, A., (2013). DNA based cryptography: An overview and analysis. International Journal of Emerging Science, 3(1), 36-42.

Jeevidha, S., Basha, D. M. S. ve Dhavachelvan, D. P., (2011). Analysis on dna based cryptography to secure data transmission. International Journal of Computer Applications (0975–8887), 29(8).

Kumar, D. ve Singh, S., (2011). Secret data writing using DNA sequences. In Emerging Trends in Networks and Computer Communications (ETNCC), 2011 International Conference on (pp. 402-405). IEEE.

Liu, L., Zhang, Q. ve Wei, X., (2012). A RGB image encryption algorithm based on DNA encoding and chaos map. Computers & Electrical Engineering, 38(5), 1240-1248.

Majumdar, A. ve Sharma, M., A New Approach Toward Information Security Based On Dna Cryptography.

Ozkaynak, F., Ozer, A. B. ve Yavuz, S., (2013). Security analysis of an image encryption algorithm based on chaos and DNA encoding. In Signal processing and communications applications conference (SIU), 2013 21st (pp. 1-4). IEEE.

Popovici, C., (2010). Aspects of DNA cryptography. Annals of the University of Craiova-Mathematics and Computer Science Series, 37(3), 147-151.

Pramanik, S. ve Setua, S. K., (2012). DNA cryptography. Electrical & Computer Engineering (ICECE), 2012 7th International Conference on. IEEE.

Soni, E. R., Soni, E. V. ve Mathariya, E. S. K, (2010). Innovative field of cryptography: DNA cryptography. In International Conference on Information Technology Convergence and Services.

Soni, R. ve Prajapati, G., (2013). A modern review on DNA cryptographic techniques. Int. J. Adv. Res. Comput. Sci. Softw. Eng, 3(7).

Terec, R., Vaida, M. F., Alboaie, L. ve Chiorean, L., (2011). DNA security using symmetric and asymmetric cryptography. International Journal of New Computer Architectures and their Applications (IJNCAA), 1(1), 34-51.

Wang, Z., Zhao, X., Wang, H. ve Cui, G., (2013). Information hiding based on DNA steganography. In Software Engineering and Service Science (ICSESS), 2013 4th IEEE International Conference on (pp. 946-949). IEEE.

A Study on Office Lighting in Educational Buildings

Özer ŞENYURT

Ordu University, Technical Sciences Vocational High School, Ordu, Turkey,

* **Corresponding Author:** zersenyurt@hotmail.com

Abstract

Lighting is defined as applying light to provide better visibility of the objects and the environment. Lighting of a space is realized by natural lighting and artificial lighting. Artificial lighting is preferred if natural lighting is inadequate. It is known that light has physiological and psychological influences on human being. Visual comfort conditions can be achieved with proper lighting. As a result of the design of correct illumination, work efficiency will increase, unnecessary tiredness, headache and pain, nervousness will lessen. For this reason, the right lighting increases working performance of employees in office environment and at the same time the physiological and psychological negative influences can be prevented. It is not possible to achieve a sufficient level of luminosity at every point of the space in accordance with the intended use. However, it is important to ensure the brightness level at working plane in the standards.

In this study, luminous levels were measured at certain times of the day with a Luxmeter at two office in Ordu University Vocational School of Technical Sciences. The results were interpreted with tables and graphs and compared with the light level standards. With the lighting design software Dialux, lighting designs of offices were carried out and the luminous values were compared with the actual measurements. It has been determined that light distributions and light levels are inadequate for actual measured values.

Keywords: Lighting, Lighting design, Luxmeter, Dialux.

1. Introduction

Lighting, natural and artificial light sources to ensure the most appropriate visual condition, is the application of light. Lighting should provide the visual comfort, visual performance and security of the people (Kesten D., 2006:6). Lighting comfort, is achieved by obtaining the intensity of illumination needed in the working environment without disturbing the eye in the appropriate light color (Sağlam Ş., 2006:1). With good lighting, eyesight is improved, and maintained, attention loss is reduced, motivation is increased. Moreover staffing increases, aesthetic feelings and comfort needs are met (Toylan H., 2008:7).

Light sources are achieveded into two category: natural and artificial. An example to the natural lighting is the one provided by the Sun. When natural lighting is inadequate, then artificial lighting takes place.

Applications where only the working plane is illuminated and other places are in the dark affect the visual comfort and reduce work efficiency (Sağlam Ş., 2006:26). Illumination does not only affect visual performance, but it is also effective on mental activities such as concentration, remembering, reasoning (Kılıç Ş.,2010:13).

It is necessary that this factors should be kept at certain values fort he work effiency eye health and visual comfort (Güvenkaya K.R. 2008:13). Different lighting intensities are needed depending on the intended use of working environment. With Standarts, it is described that how much must needed of lighting intensity is needed in every place.

If the natural light source is insufficient due to the direction of the illuminated environment, the artificial lighting can remain constant during the operation period. This causes significiant amount of energy loses. Depending on the change of daylight, the light intensity falls below or exceeds the desired level during the day. This stitutation significantly affects the luminous comfort in the working environment.

As in many official institutions, mostly fluorescent lamps are used in general purpose lighting in educational institutions. It is aimed to reach the desired lighting levels by using luminaires with fluorescent lamps produced in different sizes. If the homogeneous distribution of the light intensity is not achieved in the illumination of the space, insufficient lighting occurs. This causes to reduced visual comfort and environment performance. If comfort conditions are satisfied, the physiological and psychological performances of the employees will be maximized.

In order to make correctly and more economically the lighting that meets the requirements specified in the nowaday standards, computer-aided lighting design softwares are used. With these Softwares, it is also possible to improve of the existing illuminations by redesigning with computer. It is possible to take correct measures to improve energy and time saving. In additon, due to the continuous variation of daylight, It is easy to determine criteria on how to apply the daylight-dependent lighting control system in the office, both in terms of visual comfort conditions and energy saving in lighting.

2. Basic Concepts and Standards in Lighting

2.1. Lighting and Lighting Types

Lighting is to provide adequate lighting level and the most suitable seeing environment by utilizing natural and artificial light sources in order to make the environment and objects visible. The purpose of illumination is to increase visual comfort and visual performance. Good lighting should meet the physiological and psychological needs of people.

Two types of illumination are used for illumination of places as natural and artificial illumination. Natural Lighting is benefited from sun as a natural light source. For this purpose, to benefit from natural light windows are used. Artificial lighting is lighting made with artificial light sources in cases where daylight is inadequate.

2.2. Basic Concepts Related to Lighting

Luminous flux (ϕ); The amount of light emitted from the light source per unit of time, the unit is lumen (lm).

Efficiency factor (e); the ratio of the total light flux coming from a light source to the power of the source, the unit being lm/W.

Luminous intensity (E); unit is the amount of luminous flux that falls on the surface, its unit (lm/m^2) - Lux. Measured by luxury meter.

Luminance; It is the amount of light intensity coming from a light emitting surface.

The glare is called that of eyes temporarily can not see the objects due to external influences.

The color temperature is expressed in Kelvin (K) and indicates the light color of the light source. (Sağlam Ş., 2006:24).

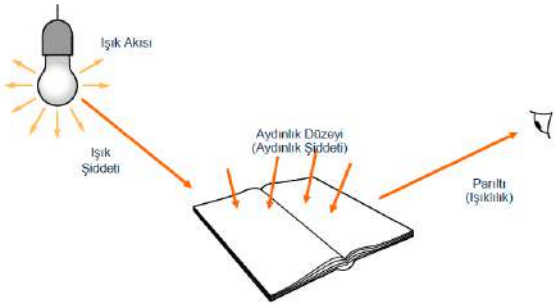

Figure 1 Basic concepts of lighting

2.3. Lighting Standarts

There are standards to improve human performance in the work areas, reduce operating, maintenance and repair costs of the lighting system and ensure quality lighting. The Illuminating Engineering Society of North America (IESNA) is the requirement of adhering to the criteria set out by the International Institute of Engineering Services (CIBSE) or the Commission Internationale de I'Eclairage (CIE). (Kılıç Ş.,2010:23)

The European standard prEN12464-1, given in Table 1, specifies lighting requirements for indoor workplaces that meet the requirements for visual comfort and performance. (Kesten D., 2006:7).

Table 1: Lighting requirements for tasks and activities in educational facilities

Interior Types by Task or Activities	Em (Lux)
Classrooms, tutorial rooms	300
Evening classes and classes for adult education	500
Auditorium	500
Writing board	500
Show table	500
Technical drawing classes	750
Practical classes and laboratories	500
Handicraft classes	500
Computer application classes	300
Training workshops	500

3. Physical Properties of Measured Offices, Measurement and Design

3.1. Physical Properties of Offices

The walls are light yellow and the reflection coefficient is 70%. Ceilings are white whitewash and reflection coefficient is 80%. Floors are mostly stone-coated and reflective

coefficient is 40%. The ceiling height is 2.80 m. The dimensions of the first office are 3.70 m x 3.85 m, 14,245 m^2 and it is in the north direction. The size of the second office is 3.70 m x 3.50 m, 12.95 m^2 and it is in the south direction. The working plane is 0.85 m. According to the values stated in the standards, it is seen that the offices should be illuminated by 300 lux luminous intensity.

The luminaires used in lighting are with 2x36W fluorescent light bulbs and electronic ballasts. Fluorescent bulbs are Philips brand; luminous flux 2500 lumens, Snow White 12000°K color temperature, life is 20000 hours.

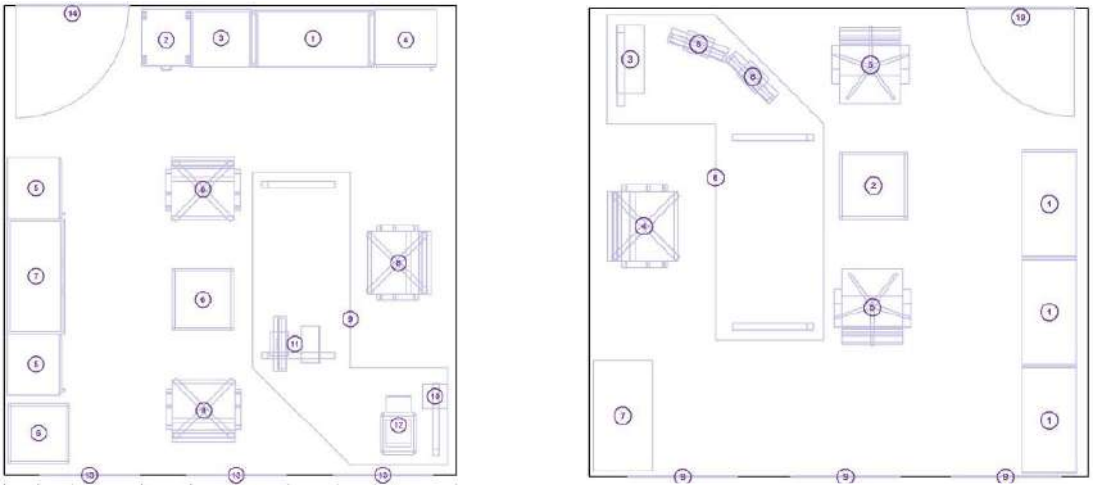

a) b)

Figure 2 Office object layout, a) First office, b) Second office

a) b)

Figure 3 3D views of offices with Dialux software, a) First office, b) Second office

3.2. Measurement Method and Measurements of Light Intensity

CEM/DT-1309 model digital luxury meter is used in the measurements. The photodetector of the luxury meter consists of a silicon photo diode and a spectral reactive filter.

The measuring range is automatic stage and the top stage is 40 kLux. The sampling rate is 1.5 per second. The measurements were received from June 12, 2017 to June 15, 2017. Sunrise at the specified time of 4:56 am, the sunset took place at 20:01. The weather report at the measurement dates has been different in the open air, closed and partly cloudy. The measurements were taken every day in the same way, periodically at intervals of one and a half hours, and seven measurement hours were determined and started at 09:00 and finished at 18:00.

The measurement was carried out at 4 different locations in offices. Measurements are made, it is only in daylight illumination and in the case of integrated lighting when the lamps are on. The values are shown in Figures 4, 5, 8 and 9.

Table 2 Weather conditions in the measurement date

Day / Hour		**09:00**	**10:30**	**12:00**	**13:30**	**15:00**	**16:30**	**18:00**
017	12.06.2017	Mixed	Mixed	Mixed	Mixed	Mixed	Mixed	Mixed
017	13.06.2017	Clear	Clear	Clear	Clear	Clear	Clear	Clear
017	14.06.2017	Mixed	Mixed	Mixed	Closed	Closed	Closed	Closed
017	15.06.2017	Closed	Mixed	Mixed	Mixed	Mixed	Mixed	Mixed

Weather during the measurement days; on Monday and Thursday the weather was partly cloudy. On Tuesday clear sky. On Wednesday partly cloudy untill noon, closed sky in the afternoon.

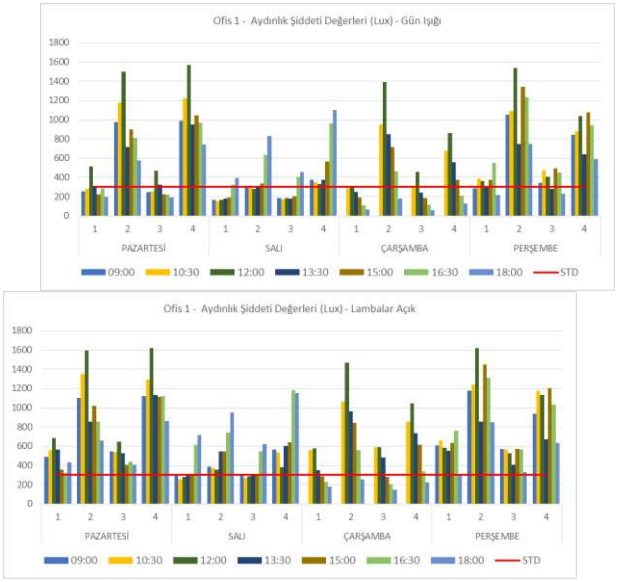

a) b)

Figure 4 Measurements of the luminous intensity of the first office a) Daylighting b) Integrated lighting

In the first office, measuring points 1 and 2 are on the working table. When the artificial lighting is not used at measuring point 1, it is below of the standard value (300 lux). Artificial lighting should be done continuously. Due to its proximity to the window, measuring point 2 has a luminous intensity well above the standard at any time of the day. Measurement point 3 reaches the standards only if artificial lighting is applied. The measuring point 4 has a luminous intensity well above the standard except for the day when the air is off. It is observed that artificial lighting was necessary in the closed sky. Besides it is concluded that depending on the weather condition and is quite unstable. This will increase the energy consumption. At the same time, it is certain that the employee will be physically uncomfortable when the light intensity exceeds the standards. Shading or regional light control is required.

a) b)

Figure 5 Measurements of the luminous intensity of the second office a) Daylighting b) Integrated lighting

In the second office, measuring points 1 and 2 are on the work table. In particular, measuring point 1 is below the standard values after 3 pm. Artificial lighting should be used in this case. This causes unnecessary lighting due to the uneven distribution of light intensity in the office and increases energy consumption. However, when all of the measurement days were taken into consideration, values above the standard were generally observed at other measurement points. Light control should be provided by shading instead of making artificial lighting. however, with the artificial illumination for measurement point 1, the standard values must be approached. But, this would be appropriate to provide by a daylight-dependent light control system.

3.3. Lighting Design of Offices with Dialux Program

Dialux 4.13 software is used in the lighting design of the offices. The design was simulated on the basis of the weather conditions on the measurement dates. In the computer design, object locations, planning data, lighting technique results, account points, study plane value curves, 3D images are take in the result reports.

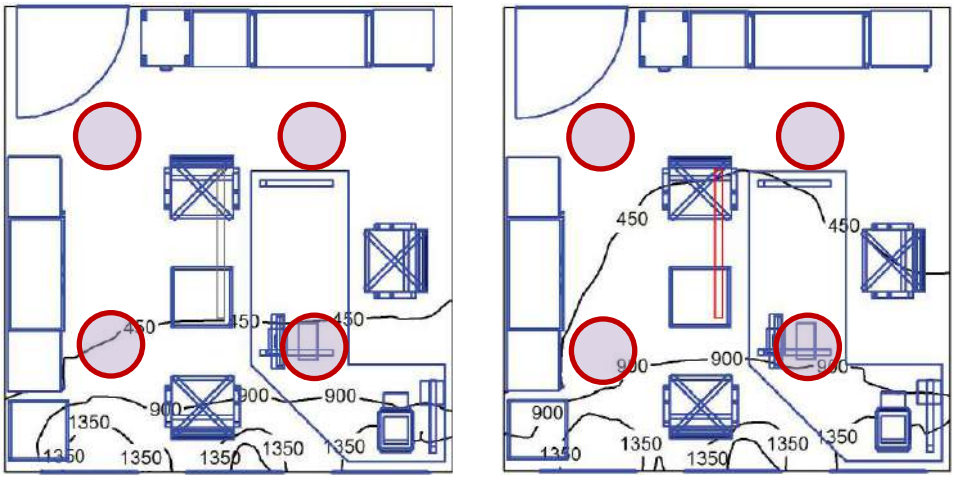

a) b)

Figure 6 First office measurement points and sample light distribution a) Natural b) Integrated

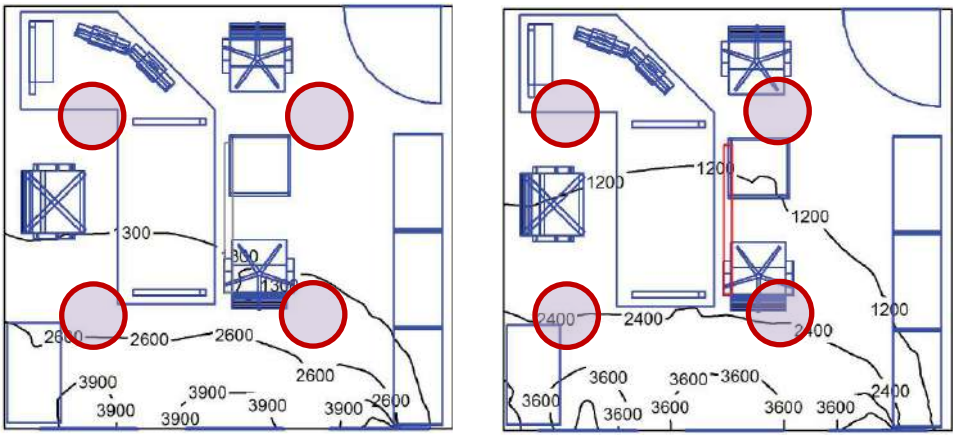

a) b)

Figure 7 Secondary office measuring points and sample light distribution a) Natural b) Integrated

Design parameters; Location: Ordu, longitude: 37,53 degrees, latitude 41 degrees, first office for North direction 243 degrees, second for office; The north direction is 63 degrees.

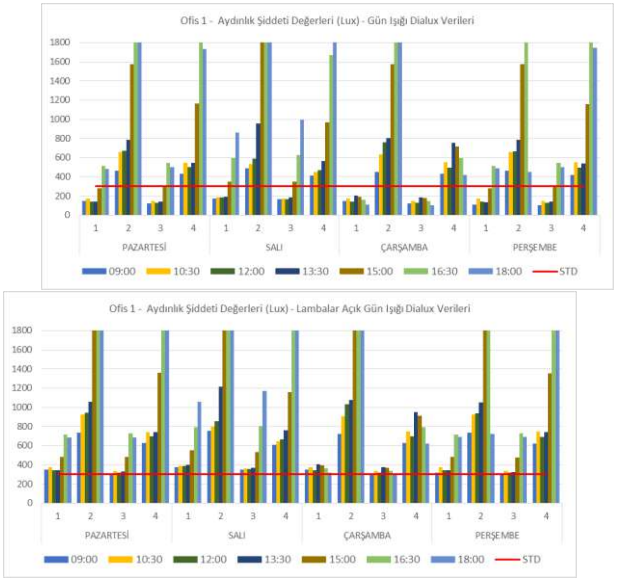

a) b)

Figure 8 The first office Dialux design luminous intensity values a) With daylight b) Integrated lighting

As it can be clearly seen from the Dialux design for the first office, it is seen that the light intensity at the measurement points 1 and 3 is above the standard values in the afternoon and it is very low in the morning hours. Moreover, it is clear that the level to be obtained at the measurement points 2 and 4 is much higher than the standards even in the case of natural lighting, and a continuously increasing luminous intensity is reached from the morning hours until the last measurement hour. When the integrated lighting is done, it is calculated that every measurement point will exceed the standard values at every hour of the day.

Shading is required at the measuring points 2 and 4, which are close to the window, and it is appropriate to use daylight-sensitive lighting automation in cases below the standard values obtained in closed weather conditions.

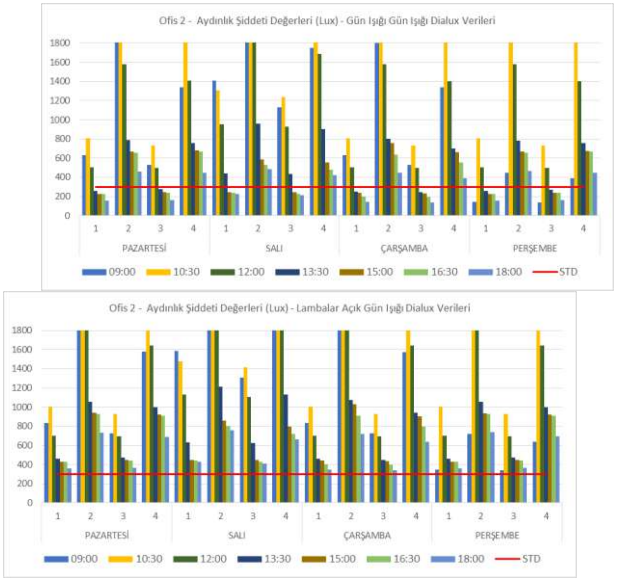

a) b)

Figure 9 The second office Dialux design luminous intensity values a) Daylighting b) Integrated lighting

The Dialux design for the second office clearly provides a luminous intensity above the standard values, even in the case of natural lighting, from the first hours of the day, but later in the day, the luminous intensity in the office decreases. The use of artificial lighting in the morning is unnecessary and it is appropriate to do it after a certain time in the afternoon. In case of integrated lighting, it is calculated that the standards will be exceeded. As in the first office, the high values obtained at the measuring points near the window indicate that natural lighting should be taken into the office by shading.

3.4. Comparison of Real Measurements and Dialux Designs

Generally, the values obtained from the actual measurements and the results of the Dialux design are very similar. Significantly, in Dialux designs, very high values are obtained at measuring points 2 and 4. The values obtained in the measurements were high but they were found to be quite small compared to the values found in the calculations. When the natural lighting values for the first office are examined, the values measured below the standards at the measurement points 1 and 3 are obtained similarly in Dialux designs. Dialux calculations and made in the measurement are clearly visible standard values will be achieved in the integrated lighting. For the second office, it is evident from the measurement and design calculation results that there is a similar situation as the evaluations for the first office.

Generally, the designs are similar to the actual measurement values. In order to ensure homogeneous distribution within the offices (300 Luxury), as specified in the standards,

considering the designs and actual measurement values, it is seen that shading should be done in areas close to the window and artificial illumination should be done at the intensty points when low values are obtained.

4. Results and Discussion

80 to 90% of human perception is carried out through the eye. Most of the fatigue caused by work conditions is due to eye strain. (Demirci H., 2008:15). When the glare is too much, the eyesight decreases, visual performance drops, and a feeling of unease and uneasiness occurs (Güvenkaya K.R. 2008:15). Poor lighting creates a troublesome working environment, weakens the nerves of the eye, and may even cause temporary or permanent blindness. Fatigue caused by bad lighting distracts itself causing morale and it nervous behavior (Kılıç Ş.,2010:9).

when lighting is well above the standards in the working environment, glare and discomfort will occur. Likewise, eye fatigue will be encountered as it will make it difficult to see at low light intensity. It is appropriate to design a daylight sensitive lighting control system. In order to meet the requirements of visual comfort during the periods of high light intensity, shading should be done on the windows, but the light level of the luminaires should be checked in the regions with low light intensity.

By controlling the artificial lighting, the energy distribution will be ensured and the distribution of the light will be more homogenous in the offices where the daylight is insufficient. However, due to the continuous variation of daylight, the control of the light should be done as a daylight sensitive lighting control. In order to provide both visual comfort conditions and lighting energy saving, sunlight sensitive lighting control systems will ensure the smooth distribution of light in offices.

References

Başkan B.T., (2014). Aydınlatma temel kavramları. *Aydınlatma Akademisi, T. Philips*.

Demirci H., (2008). *Bina Tasarımında Aydınlatma ve Renk Olgusunun Biyoharmoloji ve Biyosüreçaçısından İncelenmesi.* Fırat Üniversitesi Biyomühendislik Anabilim Dalı Yükseklisans Tezi, Elazığ.

Ganslands H., Hoffman H., (1992). *Handbook of lighting design*. Wiesbaden: ERCO Edition.

Giray E., (2009). *Dinamik Aydınlatma ve Uygulaması*. Yıldız Teknik Üniversitesi Fen Bilimleri Enstitüsü Elektrik Mühendisliği Anabilim Dalı Yüksek Lisans Tezi, İstanbul.

Güvenkaya K.R., (2008). *İlköğretim Dersliklerinde Aydınlatma Enerjisi Yönetimi Açısından Yönlere Göre Uygun Cephe Seçeneklerinin Belirlenmesi Üzerine Bir Yaklaşım*. İstanbul Teknik Üniversitesi Fen Bilimleri Enstitüsü Mimarlık Anabilim Dalı Doktora Tezi, İstanbul.

Kesten D., (2006). *Eğitim Binalarında Etkin Aydınlatma Tasarımının İncelenmesi Salvagny (Fransa) Şehir Okulu Örneği*. İstanbul Teknik Üniversitesi Fen Bilimleri Enstitüsü Mimarlık Yüksek lisans tezi, İstanbul.

Kılıç Ş., (2010). *Farklı Anlayışla Tasarlanmış İlköğretim Okullarının Aydınlatma Açısından Değerlendirilmesi; Kastamonu Gazipaşa Ve Merkez İlköğretim Okulları.* Karabük Üniversitesi Fen Bilimleri Enstitüsü Mimarlık Anabilim Dalı Yüksek Lisans Tezi, Karabük.

Kılıçarslan G.U., (2011). *Aydınlatma Tasarımı Kriterlerinin Hastane Mekânlarında İrdelenmesi*. Mimar Sinan Güzel Sanatlar Üniversitesi Fen Bilimleri Enstitüsü İç Mimarlık Anabilim Dalı Yüksek Lisans Tezi, İstanbul.

Özkaya M., Tüfekçi T., (2011). *Aydınlatma Tekniği*. İstanbul: Birsen Yayınevi.

Sağlam Ş., (2006). *Şebeke Bağlantılı Fotovoltaik aydınlatma Sisteminin Bulanık Mantık İle Kontrolü.* Marmara Üniversitesi Fen Bilimleri Enstitüsü Elektrik Eğitimi Anabilim Dalı Doktora Tezi, İstanbul.

Simons R.H., Bean A.R., (2001). *Lighting Engineering Applied Calculations*. Elsevier Ltd.

Ulusan G.N., (2012). *Eğitim Yapılarının Enerji Etkin Aydınlatma Açısından İncelenmesi: Kağıthane Anadolu Lisesi Örneği.* Mimar Sinan Güzel Sanatlar Üniversitesi Fen Bilimleri Enstitüsü İç Mimarlık Anabilim Dalı Sanatta Yeterlilik Tezi, İstanbul.

Automatic Arrhythmia Detection In Electrocardiogram Signal Using Smoothed Pseudo Wigner Ville Distribution And Artificial Neural Networks

Özgür TOMAK[1*], Birkut GÜLER[1], Alparslan TÜFEKÇİ[1]

[1]Technical Sciences Vocational School of Giresun University, Giresun, Turkey, ozgur.tomak@giresun.edu.tr, birkut.guler@giresun.edu.tr, alparslan.tufekci@giresun.edu.tr

Automatic Arrhythmia Detection In Electrocardiogram Signal Using Smoothed Pseudo Wigner Ville Distribution And Artificial Neural Networks

Abstract

Electrocardiogram (ECG) signals is an essential resource for arrhythmia detection. This study is aimed at automatic classification of ECG signals. The signal was first passed through preprocessing for the classification to be made with less error, For feature extraction, Wigner Ville distribution was used. To avoid interference in positive and negative regions of the spectrum, the signal has been restructured with the Hilbert transform. To get rid of cross-terms, smoothed pseudo-Wigner Ville distribution was preferred. After obtaining the energy and the variance based features which were obtained from this distribution, classification phase is reached. Artificial neural networks were used for the classification. Classification with artificial neural networks was done with the help of MATLAB toolboxes (Neural Network/Data Manager). Data to be used in this study was obtained from the Physionet database. Multi-layer feedforward neural network was trained and evaluated its performance in a set of ECG data.

Keywords: Electrocardiography, Smoothed Pseudo Wigner Ville, Artificial Neural Networks, Arrhythmia.

1. Electrocardiography (ECG)

The process of recording electrical activity in the heart is known as electrocardiography (ECG). It is frequently used to diagnose heart diseases. It is a method that is often used in the diagnosis of arrhythmia and is not likely to harm the patient. An ECG signal is basically a P wave, a QRS complex, and a T wave. The basic structure of an ECG is given in Figure 1.

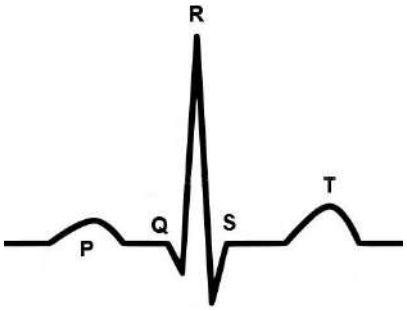

Figure 1. Basic structure of the ECG.

By briefly examining an ECG signal, the P wave reflects the depolarization of the atria. Under normal conditions, the stimulus exits the sinus node, first to the right and then to the left atrium is depolarized. The PR interval refers to the total time required for the depolarization of the atria, the atrioventricular (AV) knot, the sensory bundle, the branchial and purkinje fibers, to pass through the atrium. The QRS complex reflects the depolarization of the ventricles. Q wave is the first negative wave after the P wave, R wave is the first positive wave, and S wave is the negative wave after R. ST segment demonstrates electrically silent period between ventricular depolarization and repolarization. T wave reflects the repolarization of the ventricles. QT interval reflects the total time spent for ventricular depolarization and repolarization. The moving metal needle of the ECG device records electrical changes on a thermally sensitive, rotating paper. The paper rotation speed is usually set at 25 mm at the most. On the ECG paper there are small squares of 1X1 mm and large squares of 5X5 mm. In the horizontal plane 1 mm indicates 0.04 seconds and 5 mm indicates 0.2 seconds. Width of P wave is less than 0.11 second, amplitude less than 2.5 mm. Normal value for PR range is 0.12-0.20 second. The duration of the QRS complex (the time between the beginning of the Q wave and the end of the S wave) does not exceed 0.11 seconds. The duration of the T wave is 0.10 - 0.25 s. (İlerigelen ve Mutlu, 2014).

Many studies have been done on automatic ECG analysis today due to the importance of diagnosing heart diseases. Computer-assisted ECG analysis will help identify health problems in the area as well as help to identify heart conditions easier. Reyna and Fierro proposed using the Wigner Distribution Initiative Terms or cross terms to improve perception of ventricular late potentials(Reyna ve Fierro, 2011). The detection of ventricular late potentials is difficult because the amplitudes are very similar to the electrocardiographic noise levels and the spectral components overlap by both the broadband spectral band and the broad spectral band of the ECG signal. It has been found that the detection process is much easier by using this method. Branzila et al. Using the Wigner function, the noises in the ECG signals are cleared (Branzilla et al., 2012). Aqil et al. have examined comparatively many methods including the Wigner Ville transformation in determining the R peak point. (Aqil et al. 2015). Qaraqe et al. Analyzed ECG signals by combining heart rate variability (HRV), matching-tracking and Wigner-Ville distribution algorithms extracted from ECG, (Qaraqe et al., 2016). They have aimed at obtaining high time quality-frequency distribution of HRV signals and effective HRV features that represent situations that do not involve seizures and seizures.

If we look at the work done in this regard, the work to be done in this regard should be done in the form of appropriate feature identification and classification. The data used were obtained from the data selected from the MIT-BIH ECG arrhythmia database in the Physionet database. Data were sampled at 360 Hz(Goldberger et al., 2000). An ECG signal with important points from this database is shown in Figure 2.

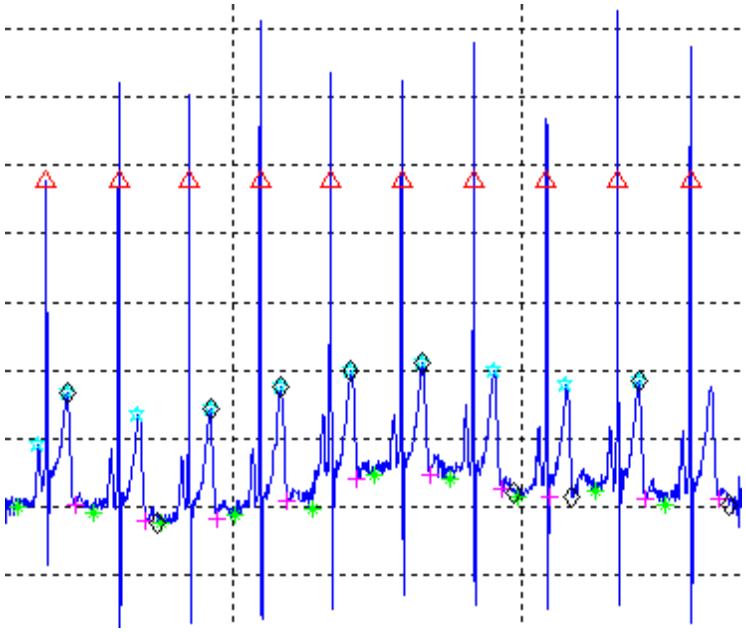

Figure 2. ECG signal (İmportant points are marked)

ECG signals may have time domain attributes as well as frequency domain attributes and classification processes.

2. Feature Extraction

With pre-processing, the signal is optimized for feature extraction. After that, the attributes are extracted from the ECG signals and these attributes are given as input to the artificial neural network for classification. The Wigner Ville Distribution is used for feature extraction.

2.1. Wigner Ville

The Wigner Ville Distribution with a time frequency distribution is shown in equation 1(Auger et al., 1996).

$$W_x(t,f) = \int_{-\infty}^{\infty} x\left(t+\frac{\tau}{2}\right)\, x^*\left(t-\frac{\tau}{2}\right) e^{-j\pi f\tau}\, d\tau \quad (1)$$

The discrete time equivalent is shown below.

$$W_x(nT,f) = 2T\, \sum_{l=-L}^{L} x\,(n+l)\; x^*(n-l)\, w(l)\, w^*(-l) e^{-j4\pi fl} \quad (2)$$

Where t is the sampling period and w is the symmetric, final analysis window.

The Wigner-Ville distribution is a distribution that shows time and frequency information on the same plane and is real-valued, preserving time-frequency shifts and providing many features that are desirable in time-frequency distributions.

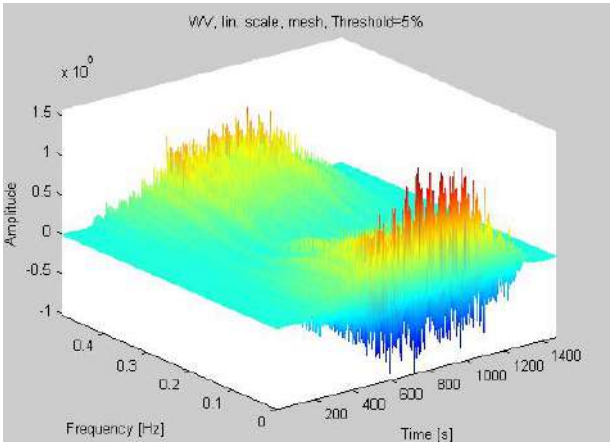

Figure 3. Wigner-Ville distribution of the ECG signal in Figure 2

We use the following method to avoid the noise in the negative and positive regions of the spectrum (Chouvarda et al., 2001).

$$z(n) = x(n) + jH[x(n)] \tag{3}$$

x(n) signal is preprocessed ECG signal and H[] is the Hilbert transformation. To improve the signal, a band-pass filter was applied, in which low-pass and high-pass filters were applied in succession to filter out the signal from the noise. The derivative operator has been applied to the QRS complex to become apparent and to suppress the P, T waves. The squaring operation makes the negative values positive and the small and large values become even more pronounced. Also, softening is done by integration process.

The Smoothed Pseudo Wigner-Ville distribution is used to get rid of the cross terms in the signal. this distribution is generally shown in the Equation 4(Auger et al., 1996).

$$SPW_x(t,v) = \int_{-\infty}^{\infty} h(\tau) \int_{-\infty}^{\infty} g(s-t)\, x\left(s+\frac{\tau}{2}\right)\, x^*\left(s-\frac{\tau}{2}\right) ds\, e^{-j2\pi v\tau} d\tau \tag{4}$$

Such a distribution is shown in Figure 4. We have come to the stage of classification with self-attributes based on the energy and variance properties obtained from this distribution.

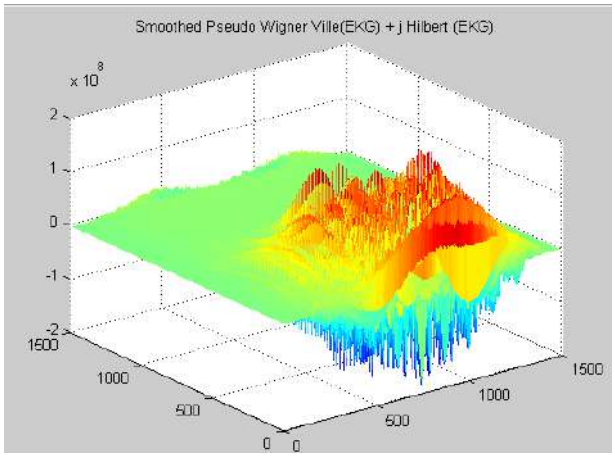

Figure 4. Smoothed Pseudo Wigner-Ville distribution of the ECG signal in Figure 2 arranged according to formula (3).

2.2. Classification

ANN is basically in the form of a directional network consisting of three layers, the input layer, the hidden layer and the output layer. The layers come from the neurons and the connections between the neurons are carried out by weight vectors. Each neuron (node), consists of three main parts: synapses (connections), collector and activation function.

The most important point in ANN is the learning rule. The Back-Propagation Algorithm (BPA) is a consultative learning algorithm aimed at minimizing the overall system error. Connection weights are randomly selected for startup and are updated to system error. Weight update starts at the output layer and advances backward(Özbay,1999). Classification with artificial neural networks was done with the help of the Toolbox (Neural Network / Data Manager, Figure 5) in Matlab.

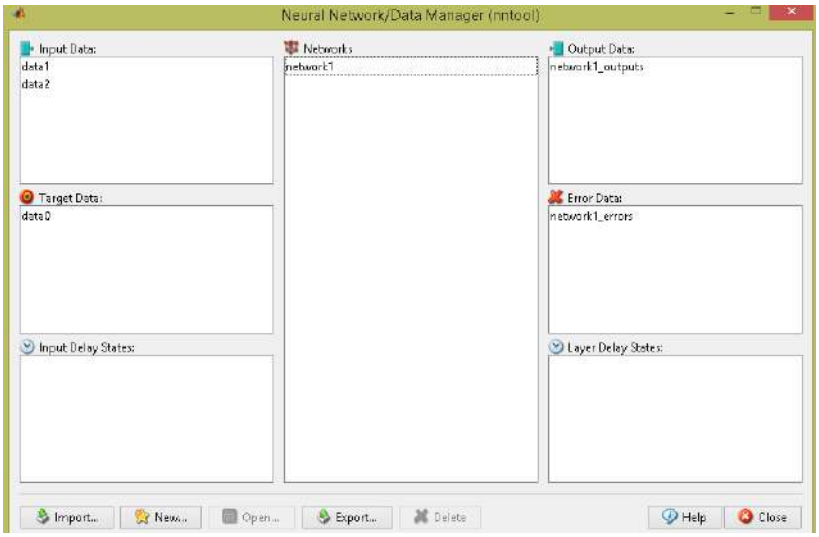

Figure 5. The Neural Network / Data Manager interface.

In the training phase, the artifacts of the artificial neural network are taken as input and the feature values of these artifacts are given as input. The input and output values are taught to the artificial neural network by inputting ECG signals from Physionet database as inputs and 0 and 1 as outputs. 0 or 1 values are obtained during the test operation. 1 is the value for the arrhythmia, 0 is the value for the normal signal. When we look at the classification obtained from the data selected from the MIT-BIH ECG arrhythmia database in the Physionet database, a 96.7% success was achieved.

3. Results and Suggestions

We call irregularities outside the normal range of motion in the heart as arrhythmia. Early and accurate diagnosis of arrhythmias is a very important step. Many studies are being conducted at this point and the success levels increase depending on the improvements in the possibilities of the technology.

In this study, the data selected from the MIT-BIH ECG arrhythmia database in the Physionet database were pre-processed and passed the classification stage with energy and variance-based self-extracting features obtained from the signal Smoothed Pseudo Wigner Ville distribution. Classification with artificial neural networks achieved a success rate of 96.7%. In this study, it is aimed to improve the self-qualifications and to increase the success rate by trying different classification methods.

References

Aqil, M., Jbari, A., & Bourouhou, A. (2015, November). Evaluation of time-frequency and wavelet analysis of ECG signals. In Complex Systems (WCCS), 2015 Third World Conference on (pp. 1-5). IEEE.
ISO 690

Auger, F., Flandrin, P., Gonçalvès, P., and Lemoine, O. (1996). Time-frequency toolbox. CNRS France-Rice University, 46.

Branzila, M., David, V., and Padole, C. (2012, October). ECG signal processing using wigner function. In Electrical and Power Engineering (EPE), 2012 International Conference and Exposition on (pp. 601-604). IEEE.

Chouvarda, I., Maglaveras, N., & Pappas, C. (2001). Adaptive time-frequency ECG analysis. In Computers in Cardiology 2001 (pp. 265-268). IEEE.

Goldberger, A. L., Amaral, L. A., Glass, L., Hausdorff, J. M., Ivanov, P. C., Mark, R. G., ... and Stanley, H. E. (2000). Physiobank, physiotoolkit, and physionet. Circulation, 101(23), e215-e220.

İlerigelen, B., and Mutlu, H. (2014). Ekg Kursu Kitapçığı.

Özbay, Y. (1999). EKG aritmilerini hızlı tanıma. Doktora Tezi, Selçuk Üniversitesi, Fen Bilimleri Enstitüsü, Konya.

Qaraqe, M., Ismail, M., and Serpedin, E. (2016, August). Combined matching pursuit and Wigner-Ville Distribution analysis for the discrimination of ictal heart rate variability. In Signal Processing Conference (EUSIPCO), 2016 24th European (pp. 2045-2049). IEEE.

Reyna, M. A., and Fierro, L. S. (2011, March). Using wigner distribution's cross terms to detect patterns of ventricular late potentials. In Health Care Exchanges (PAHCE), 2011 Pan American (pp. 28-28). IEEE.

Automatic Arrhythmia Detection Using Wavelet Transform and Boosted Tree Classification

Özgür TOMAK[1*], Birkut GÜLER[1], Alparslan TÜFEKÇİ[1]

[1]Technical Sciences Vocational School of Giresun University, Giresun, Turkey, ozgur.tomak@giresun.edu.tr, birkut.guler@giresun.edu.tr, alparslan.tufekci@giresun.edu.tr

Abstract

It can be said that heart diseases are one of the most common causes of death in the world. In this study, it was aimed for detection of the arrhythmia by automatic examination of the person's electrocardiography (ECG) records. In this process, features obtained from the wavelet method was classified by boosted tree method. The heartbeats were divided into seven different classes. Adaptive Boosting (AdaBoost) method was used to reduce the number of features, and it speeds up the signal processing process. This method is known as bringing together a lot of weak learners and creating powerful learners from this process. ST-Petersburg Institute of Cardiological Database has been preferred for analysis. Test and training accuracy was found in 12 channel ECG data. The method waas fast enough to detect real-time arrhythmia. MATLAB was used for all analyzes.

Keywords: Electrocardiogram (ECG), Discrete Wavelet Transform, AdaBoost, Classification.

1. Detection of Arrhythmia

Electrocardiography (ECG) is a widely used biomedical signal in the detection of heart diseases. Automatic diagnosis of arrhythmias provides early treatment. In this study, the coefficients from the discrete wavelet transform for the detection of arrhythmia were reduced by AdaBoost method, but more powerful features were obtained. These properties are classified using the Boosted Tree method. ST-Petersburg Institute of Cardiological Database was used in this study. These records belong to the patient group of 15 women and 17 men aged between 18 and 80 years. Analyzes were performed on 75 signals with a 12-channel length of 30 minutes. 176177 the heartbeat was mixed randomly and then used. The sampling frequency for each recording is 257 Hz. A sample data from the ST-Petersburg Institute Cardiology Database is given in Figure 1 (Goldberger et al., 2000).

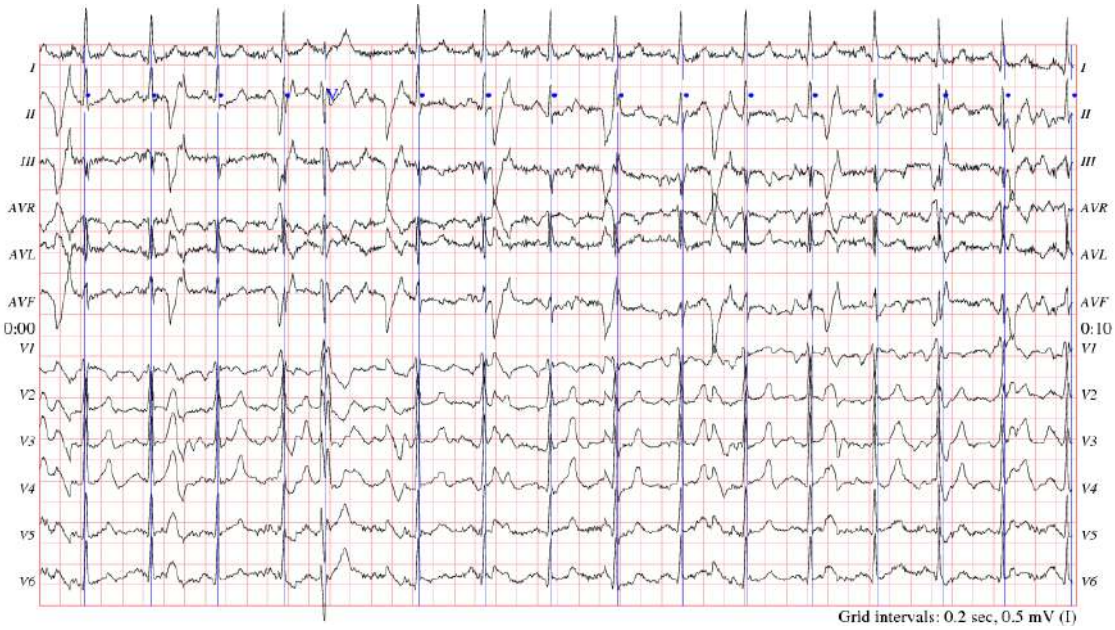

Figure 1. A sample data from the ST-Petersburg Institute Cardiology Database.

Determination of arrhythmia in ECG signal is an increasingly important research topic. The studies have been done in this subject in many different ways. Some of these studies are mentioned below.

Dokur et al. determined the properties of the ECG signal using Wavelet Transform and Fourier analysis. Artificial neural networks and genetic algorithms are used in the classification stage. Classification was done for 10 different arrhythmia types, with 99.4% success in wavelet

transform and 92.2% in Fourier transform. (Dokur et al., 1999). In their study, Zhao et al. Used the coefficients obtained by wavelet transform from each ECG signal as a feature. Then, they created feedback networks with autoregressive modeling and successfully classified 6 different arrhythmia types with Support Vector Machine (Zhao and Zhang 2005). Jiang et al. classified using the Support Vector Machine method with the properties obtained by using independent component analysis in the coefficients obtained from the wavelet transform and obtained 98.65% success rate (Jiang et al., 2006). Prasad and Sahambi used sym6 as a wavelet family and decomposed at level 4 and classified the results with artificial neural networks (Prasad and Sahambi, 200). Erdoğmuş and Pekçakar used db2 and db10 as wavelet families in their study and classified them in artificial neural networks using coefficients obtained by decomposing at level 4 (Erdoğmuş and Pekçakar, 2009).

2. Method Used

In particular, the coefficients obtained from the wavelet method are used. These features extracted from ECG signals are given as input to the Boosted Tree algorithm for classification.

2.1. Discrete Wavelet Transform

In Discrete Wavelet Transform; low-pass and high-pass filters are applied again through discrete processing, and data is reduced by filters on the resulting signals.

$$y_{high}[k] = \sum_n x[n].g[2k-n] \quad (1)$$

$$y_{low}[k] = \sum_n x[n].h[2k-n] \quad (2)$$

$$h[N-1-n] = (-1)^n g(n) \quad (3)$$

At each level, the values are calculated, where N is the number of current samples of x [n] (Vatansever et al.).

The names of the wavelet types and some of the wavelet functions are given in Figure 2.

The discrete wavelet analysis of the signal at level 5 with Db 6 wavelet is given in Figure 3. Multiresolution dyadic tree is given in Figure 4.

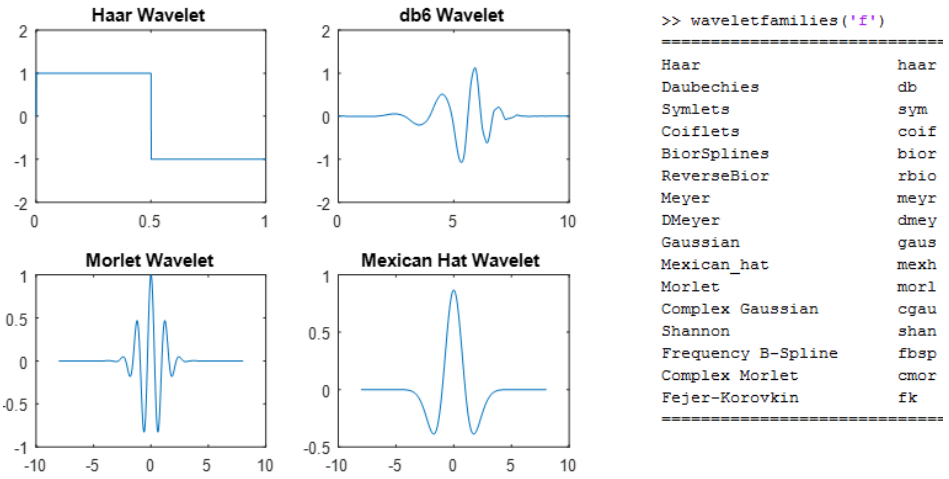

Figure 2. The names of the wavelet types and some of the wavelet functions

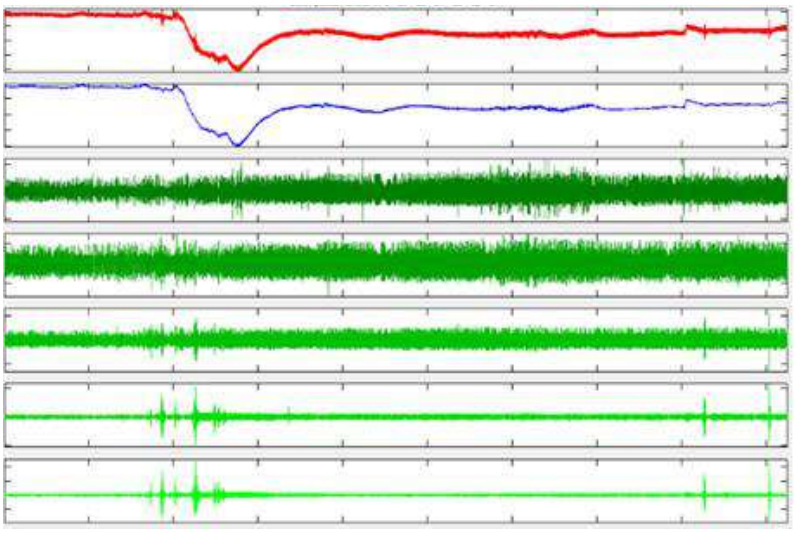

Figure 3. The discrete wavelet analysis of the signal at level 5 with Db 6 wavelet.

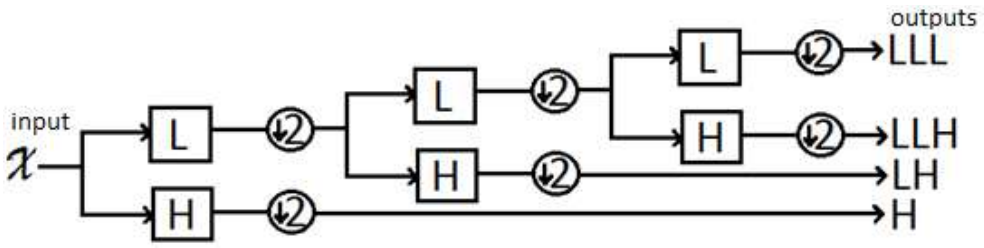

Figure 4. Multiresolution dyadic tree.

2.2. Boosted Tree Classification

Boosted Trees algortihm was preffered for classification. Adaptive Boosting (AdaBoost) was selected as Ensemble aggregation method. This method is known as bringing together a lot of weak learners and creating powerful learners from this process. The AdaBoost algorithm can be said to be the first useful algorithm in this area. AdaBoost is especially useful for classifications with many features. The AdaBoost training process reduces the size performance and improves the execution time by selecting features that are known to improve the model's performance. Being applicable, low memory usage and higher prediction speed are the reasons why it is preferred.

$$F_T(x) = \sum_{t=1}^{T} f_t(x) \quad (4)$$

Every f here is a weak learner who takes an x object as input and returns a value that indicates the class of the object. Each weaker learner produces an output hypothesis, $h(x_i)$, for each instance in the training set. At each iteration, a weak learner is selected and a coefficient α is assigned such that the classifier total learning error E {t} of the obtained step is reduced to a minimum.

$$E_t = \sum_i E[F_{t-1}(x_i) + \alpha_t h(x_i)] \quad (5)$$

Here, $F_{t-1}(x)$ is the classifier developed until the previous education stage. *E(F)* is the error function and $f_t\ (x) = \alpha_t\, h(x)$ is the weak student considered as an addition to the final classifier. In each iteration of the training process, each instance in the test set is assigned a weight w_t equal to the current error value $E\big(F_{t-1}\ (x_i)\big)$ on that sample.

Learning type is decision tree. Decision trees are one of the best choices for quick classification and are also easy to interpret. The number of learners was selected as 30, the learning rate was 0.1, and the maximum number of divisions was 20.

The heartbeats are divided into 7 different classes. These can be classified as normal beat, early ventricular contraction, atrial early beat, node beat, supraventricular beat, right branch

beat, and unidentified beat. 176177 heartbeats from the ST-Petersburg Institute Cardiology Database were mixed randomly, half used for training and half used for testing. In trainin part, 10 fold cross validation method is used. The coefficients obtained from 5th level decomposition of the signal with db1 wavelet function for 12 channels were transformed to stronger features by the AdaBoost method and classified using MATLAB with the Boosted Tree method. The obtained results are given in Table 1.

3. Results and Suggestions

The data that we use in the classification came from the ST-Petersburg Institute Cardiological Database and the data is composed of 176177 heart beats. Strong features were obtained from the coefficients obtained by Discrete Wavelet Method by AdaBoost method and classified by Boosted Trees method. The results obtained are successful for each channel and the method is fast enough to detect real-time arrhythmias. Reduction in the amount of data makes it easier to send through the net and process the signal.

	Training Accuracy	**Test Accuracy**
Channel 1	95.3	94.9
Channel 2	94.6	93.7
Channel 3	92.7	91.6
Channel 4	94.9	94.1
Channel 5	93.6	93.2
Channel 6	93.7	92.9
Channel 7	92.4	91.6
Channel 8	94.0	93.5
Channel 9	94.4	93.8
Channel 10	93.3	93.0
Channel 11	94.1	93.2
Channel 12	93.9	93.2

Table 1. Training and test accuracy results.

References

Goldberger, A. L., Amaral, L. A., Glass, L., Hausdorff, J. M., Ivanov, P. C., Mark, R. G., ... and Stanley, H. E. (2000). Physiobank, physiotoolkit, and physionet. Circulation, 101(23), e215-e220.

Dokur, Z., Olmez, T., and Yazgan, E. (1999). ECG waveform classification using the neural network and wavelet transform. In [Engineering in Medicine and Biology, 1999. 21st Annual Conference and the 1999 Annual Fall Meetring of the Biomedical Engineering Society] BMES/EMBS Conference, 1999. Proceedings of the First Joint (Vol. 1, pp. 273-vol). IEEE.

Zhao, Q., & Zhang, L. (2005, October). ECG feature extraction and classification using wavelet transform and support vector machines. In Neural Networks and Brain, 2005. ICNN&B'05. International Conference on (Vol. 2, pp. 1089-1092). IEEE.

Jiang, X., Zhang, L., Zhao, Q., and Albayrak, S. (2006, November). ECG arrhythmias recognition system based on independent component analysis feature extraction. In TENCON 2006. 2006 IEEE Region 10 Conference (pp. 1-4). IEEE.

Prasad, G. K., and Sahambi, J. S. (2003, October). Classification of ECG arrhythmias using multi-resolution analysis and neural networks. In TENCON 2003. Conference on Convergent Technologies for the Asia-Pacific Region (Vol. 1, pp. 227-231). IEEE.

Erdoğmuş, P., and Pekçakar, A. (2009). Dalgacık dönüşümü ile ekg sinyallerinin özellik çıkarımı ve yapay sinir ağları ile sınıflandırılması. Uluslararası İleri Teknolojiler Sempozyumu, 13-15.

Vatansever, F., Uysal, F., & Uzun, A. (2002). Ayrik Dalgacik Dönüşümü ile Gürültü Süzme. 338-342.

Experimental Investigation of Biogas Production in Organic Garbage Waste

Ferdi ÖZBILGIN[1], Ünsal AÇIKEL[2], Emre Aşkın ELIBOL[3], Serkan DEMIR[4], Ali YALÇIN[5], Halil ŞENOL[6]

[1]Giresun University, Engineering Faculty, Department of Electrical and Electronics Engineering, Giresun, Turkey; email: ferdi.ozbilgin@giresun.edu.tr

[2]Cumhuriyet University, Engineering Faculty, Department of Chemical Engineering, Sivas, Turkey; email: unsal.acikel@gmail.com

[3]Giresun University, Engineering Faculty, Department of Mechanical Engineering, Giresun, Turkey; email: emreaskinelibol@gmail.com

[4]Giresun University, Engineering Faculty, Department of Industrial Engineering, Giresun, Turkey; email: serkan.demir@giresun.edu.tr

[5]Süleyman Demirel University, Engineering Faculty, Department of Chemical Engineering, Isparta, Turkey; email: ali.yalcin@sdu.edu.tr

[6]Giresun University, Engineering Faculty, Department of Chemical Engineering, Giresun, Turkey; email: halilsenol@yahoo.com

Corresponding Author: halilsenol@yahoo.com

Abstract

Today, with increasing population, energy needs are increasing. Humanity has used natural energy resources until recent years. But the limited number of natural energy sources and the growing need for energy have led people to renewable energy sources. One of the renewable energy sources is biogas. Biogas is a gas mixture that can be produced from organic materials by anaerobic fermentation method. This gas mixture contains 50-65% methane, 35-45% carbon dioxide and trace amounts of reactive gases such as hydrogen sulphur, carbon monoxide. In this study, biogas was produced from domestic organic solid wastes. The rate of biogas produced was found to be 156 ml biogas/ g $_{\text{volatile solids}}$. Methane gas and % 56, 7 of the biogas produced are found. Total COD removal during anaerobic fermentation was found to be 45.48 %. The working temperature was also carried out under mesophilic conditions (about 39 ^{0}C). As a result of this study, the efficiency of anaerobic fermentation and biogas production process under mesophilic conditions has been experimentally proven.

Keywords: COD removal, biogas, anaerobic fermentation, methane

1. Introduction

Due to the increasing population of the world and our country, the energy demand also tends to increase continuously. This increase in energy consumption rapidly consumes the natural energy resources available. Right now our world's energy needs are 29% coal, 24,2% natural gas, 32,8% petroleum, 4,5% nuclear, 6.8% hydro and 2.7% from renewable energy sources. Energy demand in our country is 28.5% petroleum, 29,20% coal, 32,5% natural gas, 2,8% hydro, the remaining 7% renewable and other energy sources. Our country has limited reserves in terms of energy use and imports about 60% of its energy use from outside. But our country is renewable are very rich in terms of energy resources and are not sufficiently evaluated. Biogas energy is in the status of renewable energies and has a considerable potential in our country (Haak et al., 2016). As Turkey's average annual biomass potential estimated 109.4 million tonnes stopped. Our country is annually The waste in the forests is 5-7 million tons of biomass (shell, leaf, chip, branch, etc.) It indicated. This suggests that our country is extremely rich in organic wastes (Kaya et al., 2009).

Turkey's energy consumption is constantly increasing due to rapid economic development. Turkey 2000 and energy consumed between 2015 and 5 years between 2000 and 2010 it is in excess (Onurbaş and Turker, 2012). Buddha proves that energy consumption is increasing. For this reason, resources. An alternative source to these different energy sources is biogas. Because our country has a very favorable and rich source for biogas production (Sümer et al., 2016).

1.1. Biogas in Turkey

Turkey in the first study on biogas production in 1957 in the Soil and Water Research Institute It began. Some studies were carried out in the 1960s to establish pilot facilities in the State Farms It was established. As a result of this, the Ministry of Agriculture started in 1963 5 of them were in the Eskişehir Soil Water Research Institute, 2 of them were in the villages of Eskişehir a total of 8 biogas plants were set up, including biride çorum test station. These facilities inefficient results were obtained from some of the productive parts. Despite this, lack of technical staff, insufficient training of farmers The study was terminated due to reasons. However, in the aftermath of 1980, UNICEF biogas production studies supported by technical information were initiated by DPT. First work started at Muş-Alparslan State Production Farm by establishing a 35 m^3 plant. In the year of 2006, the responsibility for the project was granted

to the Soil Water Research Institute and the government 6, 8, 12 and 50 m^3 with credit a total of nearly 1000 biogas plants were established. In the 2000s, biogas production studies, especially those led by universities projects . In 2010, with the Republic of Turkey Ministry of Environment and Urbanization Germany for a biogas facility built with the Ministry of Environment, Nature Conservation and Nuclear Safety Signatures were thrown. 1,200 heads of livestock, energy demand will be met. At the same time, fermentation as a result of biogas production fertilizer, the plant meets the necessary sufficiency to grow plants on the farm land. As other biogas plants in our country, 5 units of 15 m^3 and 2 units of 22 m^3 in Kayseri, 15 m^3 1 in Konya, 22 m^3 in 1 gediz lake and 1 in 280 m^3 in Elazığ (Koçar et al., 2010)

In this study, biogas production from organic waste was experimentally investigated. COD removal during the anaerobic process has been investigated. The resulting biogas was analyzed with a portable methane gas meter.

2. Material and Method

2.1. Analyzes of dry matter and organic matter applied to domestic solid waste and cattle breeding

Dry matter analysis should be performed on almost all organic wastes as it contains moisture before the anaerobic fermentation process is started. In this view, the total solid ratio is determined. Randomly selected organic waste was mixed homogeneously. Dry matter analysis was then carried out. Each sample was weighed 2 grams on a precision scale and dried for about 48-72 hours so that no moisture remains inside the sample at 105 ° C. Drying process was done with porcelain crucible. First of all, the porcelain crucible was dried at 110 ° C for 6 hours in such a way that no moisture remains. The percentages of solids in the dried samples were thus determined. Then, these weighed dry samples were placed in a porcelain crucible and allowed to stand at 550 ° C for 2.5-3 hours in an ash oven. After the burning process was completed, samples were taken and allowed to cool in a desiccator. As a result, organic matter burns at this temperature and becomes volatile. The ash formed when lit was weighed gravimetrically and the amount of volatile matter was found (APHA,2005).

2.2. Anaerobic fermentation process

In this process, organic waste is mixed with cattle grains. The reason for this is the presence of methanogens in active form in the cattle herb. Experimental system for anaerobic fermentation experiments was prepared by mixing 1: 0, 2: 1, 1: 1, 1: 2, 0: 1 mixture ratios of

each reactor waste wastes and ground wastes. Accordingly, 2-necked bottles of 1000 ml were used as a bioreactor operating at cut-off. In total, 15 bioreactor biogas of 1000 ml were set up to be 10% each, with 3 recurrences. According to the exit pipe of the bioreactors, suitable silicone hose and 100 ml gas collecting bags were added at the end of this hose. In all experiments, the bioreactors were filled with 80% (ie 800 ml) substrate and water mixture and 20% remained empty. Because methane bacteria require a certain amount of air (ie, nitrogen gas) to produce biogas. In order to prevent gas escapes, the entrance and exit of the hoses are covered with tape. The pH of each reactor should be measured for the oxygen free dark fermentation process and then the pH should be adjusted with 8 M NaOH and 8 M H2SO4 buffer solutions prepared as far as the pH in this range if the pH is not in the range of 6.6 to 7.6, which is the requirement for reprocessing methane bacteria in the biogas formation it is made. The heating temperature was chosen as 40 ° C ± 2 ° C. Experiments were carried out on 3 floors, that is, 3 reactors were prepared simultaneously from each reactor. The heating process was done with the help of a water tank. The experiments were started and the reactors were mixed for 2-3 minutes on average in 12 hours. The amount of gas produced is measured by means of known biogas gas collecting bags. Anaerobic process continued until gas formation stopped. As a result, the gas formation rate of each dry substance is calculated as ml of biogas / g $_{\text{volatile solids}}$. Since methanogenic bacteria are light sensitive bacteria, each reactor is wrapped with aluminum foil during the biogas production stage to provide an anaerobic fermentation system by eliminating the light permeability of the reactors. Fermentation process lasted 70 days on average. At the end of the 70th day, the anaerobic process was finished and the biogas content and biogas content were calculated volumetrically.

2.3.COD analysis

One of the most important methods for determining the contamination rates of wastewater (domestic or industrial) is COI analysis. It contains the oxidation state of organic substances without the speed of biodegradation by oxidation of the material. In environmental pollution, KOI is a frequently expressed factor. A metod is obtained by determining the amount of organic substances in the wastewater in terms of the amount of oxygen required for chemical oxidation. The method is based on the principle that all organic materials can be oxidized in acidic environments with strong oxidizers. All KOI determinations in anaerobic fermentation were made according to APHA standard methods (APHA, 2005

Table 1. Values of Some Parameters Used in Experiments

Parametres	**Cattle manure**	**Organic garbage waste**
% C	32,5	51,45
% N	1,70	1,29
C/N	19,11	39,88
% solid matter	20,5	14,0
% volatile solid matter (% SM)	82,9	82,0
pH	7,2	4,3
% Moisture	79,5	86,0

Table 1 above gives the results of the analyzes made on organic waste wastes and cattle larvae. Analyzes were applied to fresh wastes.

3. Results and Discussion

Table 2. Biogas formation rates of different mixing ratios

Ratio of garbage waste/ cattle manure	**Biogas production (biogas/ g $_{\text{volatile solids}}$)**	**% COD removed**
1:0	112,0	42,20
2:1	156,0	45,48
1:1	123,5	44,29
1:2	125,9	40,59
0:1	135,1	43,33

In Table 2 above, the rates of biogas production of 5 different mass mixing ratios are given after 70 days. As can be understood from tablodan, the highest biogas formation rate belongs to the reactant prepared with 2: 1 mixture ratio. The lowest biogas formation value was found to be 1: 0 by weight. Among the possible causes of these different production rates are the consumption of C and N micronutrients of anaerobic bacteria at different rates. Similarly, the highest COD removal occurred in the 2: 1 reactor.

Table 3. Biogas content of different mixing ratios

Ratio of garbage waste/ cattle manure	Volume % CH_4 ratio	Volume % CO_2 ratio	H_2S ratio (ppm)
1:0	59,1	40,5	524
2:1	56,7	43,0	563
1:1	55,9	43,9	617
1:2	58,8	41,0	778
0:1	58,2	41,5	309

In table 3 above, the biogas content of 5 different litter / cattle sand mix ratios is given volumetrically. The highest methane content (in the 1: 0 mixture reactor) is seen. The lowest methane content is observed in a 2: 1 stirred reactor at a volume of 56.7%. The lowest value of H2S was found to be 309 ppm and the highest value was found to be 617 ppm.

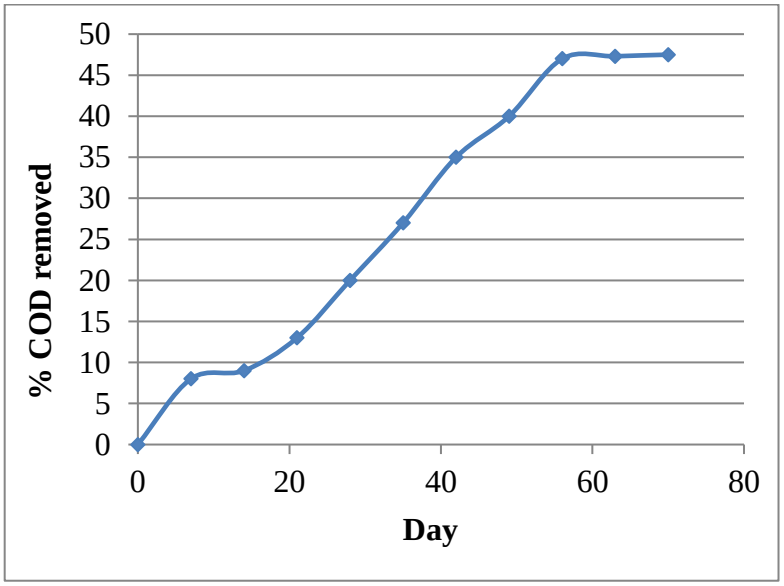

Figure 1. COD removal diagram for a 2: 1 mixture ratio reactor

Figure 1 above shows the CO_2 removal process of the reactant with a 2: 1 mixture ratio of waste to cattle. At the end of the 70th day, the total COD removal was approximately 45.48%.

Almost half of the organic substances in the organic waste are destroyed by anaerobic microorganisms.

Acknowledgement

This work was supported by the project M-740 by CÜBAP. Thanks to the relevant institution.

References

APHA, Standard Methods for the examination of water and wastewater, (2005). 21st Edition, , AWWA, WEF 2540 G.

Haak, L., Roy, R., and Pagilla, K. 2016. Toxicity and Biogas Production Potential of Refinery Waste Sludge for Anaerobic Digestion, Chemosphere, 144 (2016), 1170-1176.

Kaya, D., Çağman, S., Eyidoğan, M., Aydöne,r C., Çoban, V., and Tırıs M. (2009). Türkiye'nin Hayvansal Atık Kaynaklı Biyogaz Enerjisi ve Ekonomisi, Atık Teknolojileri Dergisi, 1: 48-51.

Koçar, G., Eryaşar, A., Ersöz, Ö., Arıcı, Ş., Durmuş, A. (2010). Biyogaz Teknolojileri, 1. St. Baskı, İzmir, Ege Üniversitesi Basımevi.

Onurbaş, A.A., and Türker, U. (2012). Status and Potential of Biogas Energy From Animal Wastes in Turkey, Renewable and Sustainable Energy Reviews, 16 (2012), 1557-1561.

Sümer, S.K., Kavdır, Y., and Çiçek, G. (2016). Türkiye'de Tarımsal ve Hayvansal Atıklardan Biyokömür Üretim Potansiyelinin Belirlenmesi, KSÜ Doğa Bilimleri Dergisi, 19 (4), 379-387.

Hiding an Encrypted Picture in an Image with LSB Method

Fatih DURMUŞ[1*], Ferdi ÖZBİLGİN[2], Serap KARAGÖL[3]

[1]Ondokuz Mayıs University, Engineering Faculty, Department of Electrical and Electronics Engineering, Samsun, Turkey; fatih.durmus@omu.edu.tr

[2]Giresun University, Engineering Faculty, Department of Electrical and Electronics Engineering, Giresun, Turkey; ferdi.ozbilgin@giresun.edu.tr

[3] Ondokuz Mayıs University, Engineering Faculty, Department of Electrical and Electronics Engineering, Samsun, Turkey; serap.karagol@omu.edu.tr

[*] **Corresponding Author:**
fatih.durmus@omu.edu.tr

Abstract

With the development of technology, the transmission of digital data in a secure manner becomes important. The stenography method is one of the oldest methods used in protecting information by hiding it in a carrier that can be text, voice, or an image. Steganography techniques rely mostly on storing a secret message inside an image file such as bmp, tiff, png, and jpg, in grey and RGB formats. Images may contain a wealth of information for industry and governments, and the falling of images into the wrong hands can lead to serious security problems. There are many techniques and algorithms used in Steganography such as F5, LSB, Java Steganography (JSteg), etc. In this study, a hidden image is applied to Vigenere and Seazer encryptions from primitive coding techniques and the obtained encrypted data is hidden in an image. Since steganography is used when transmitting the message text, primitive coding techniques are preferred. The size of the data along with the encrypted data is hidden in the blue component of the pixels in the image by the LSB (Least Significant Bit) method. MSE (Mean Squared Error) was used to determine the rate of change between the original image and the stegı image in which the encrypted data is hidden. Also, the degradation in image quality can be visually noticed by applying the histogram analysis This test shows a comparison between the original image and the stego image, using the histogram as a visual comparison tool.

Key Words: Hiding, Encryption, Steganography, LSB

1. Introduction

With the development of technology and electronic communication, data transfer, data storage and data processing are frequently performed. Simultaneously, there is an increase in the number of pirated software and people attacking and accessing stored information, especially in the data transfer stage. Data security has therefore become an important issue and means to counter these attacks and protect information. The first data protection began with the Caesar Cryptography Technique during the Second World War. However, in the following years, encryption was insufficient for security purposes and when communications were detected, it was possible to interrupt it without decrypting it. That is why steganography, a technique that conceals communication, was born.

Steganography is a long-standing science (Caldwell, 2003). The word itself means “hidden text” or “cursive writing” (Cummins et al., 2004). Steganography is the process by which any data can be transmitted to the recipient without allowing it to be understood by third parties. In a sense, this process can also be referred to as data hiding (Öksüzoğlu, 2013). The many types of data which can be hidden include a text file containing written information, a desired image file, and an audio file (Gopalan, 2003; Niimi et al., 2002; Sağıroğlu and Tunckanat, 2002; Shahreza, 2006; Sui and Luo, 2004; Tseng and Chang, 2004). The aim of data hiding is to conceal the data and prevent it from being noticed by third parties and to minimize the spoilage of the cover data in order to keep its integrity. At least the optimum rate is reached to ensure the highest data transmission with distortion (Atawneh, 2006; Singh et al., 2007).

The basic logic of steganography techniques is based on the principle of hiding the data in non-essential or non-critical sections of digital data file formats or where there may be an inability of human senses to perceive (Atıcı, 2007). A general steganographic system to be applied to the image is as in Figure 1. The data to hide is converted to stego-object by a data hiding function. It is recovered by the hidden data decoding function. Some of the most commonly used methods to hide data into the image are Least Significant Bit-LSB, some algorithms and transformations with masking, and filtering.

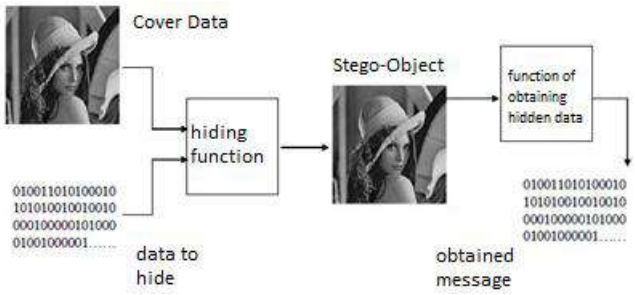

Figure 1. A General Steganography System

There are also many techniques to uncover this hidden data through data-hiding techniques. Therefore, it is desirable to improve the security of the data that is hidden by data encryption techniques. Caesar and Vigenere are known as primitive encryption techniques. Techniques such as DES (Data Encryption Standard) and AES (Advanced Encryption Standard) are known as modern encryption methods.

In this study, using the MATLAB programming language, the image in the extension file such as png and jpeg is encrypted by applying Vigenere encryption from the primitive encryption. An application that conceals the encrypted image by the LSB method in the blue pixel in the color image is developed.

2. Encryption and Steganography

In order to ensure the security of the image, the color codes are encrypted with the key and the encrypted codes are hidden by the LSB method in the blue color components of the image.

2.1. Encryption

Encryption is one of the most basic systems that provide information security in data transmission. The transmitted data is replaced by a system known to the party of the recipient. This system can be done by simple mathematical methods, but also by modern methods. This prevents data from being stolen by unwanted people (Yalman and Ertürk, 2008).

The encryption of the data and the decoding of the encrypted data are generally shown diagrammatically in Figure 2. The encrypted message is obtained by using the algorithm used for the information and encryption. This crypto data is passed through the general communication medium. Although the communication medium is low-cost, it is accessible to

unauthorized users. The actual message is obtained by the receiver using the crypto data and password key. Since crypto data is very different from the actual message, it is difficult for unauthorized users to obtain real data because they do not have a decryption key even if they access this data. (Akbal et al., 2010).

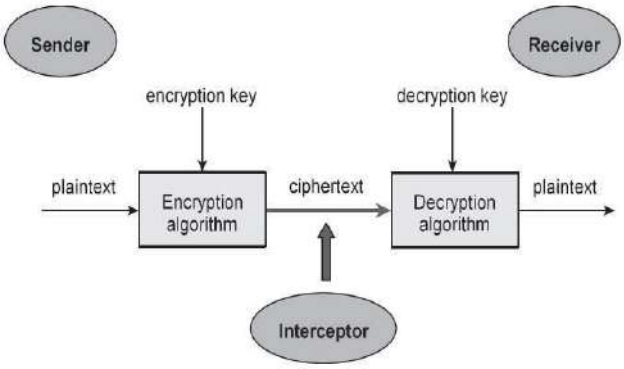

Figure 2. A General Encryption System

2.2. Hiding the Image

One of the most widely used methods of data hiding is to add it to the most insignificant bit of the image. The most insignificant bit of each byte of each pixel of the image is made by adding the data in the binary system. One-bit change will not make a visible difference to the eye.

In this study, the data in the encrypted and binary system is hidden in the lines of the blue pixel of the image. The size information of the data to be hidden is placed in the last bit of the blue pixel in the first line and it is hidden for the recipient to decode the data. In the algorithm, the encrypted data is inserted from the second row into the last bit of the blue pixel and hidden. This process continues until all bits in the encrypted data are hidden. The data placement algorithm was performed as in Figure 3. Since the encrypted data placed on the last bit is the same as the last bit of some pixels of the hidden picture, the change in the image was less than the data size.

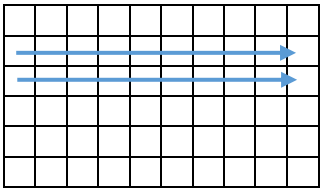

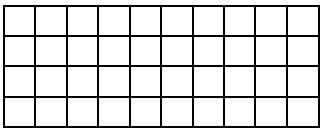

Figure 3. Data Hiding Algorithm

3. Findings and Discussion

In general, image steganography should place the content of a hidden message in the image so that the visual quality of the image cannot be changed. The lack of difference in the image after the data is hidden indicates the quality of the steganography algorithm. There are many methods such as MAD (Average Absolute Deviation), MSE (Percentage Mean Error), MAPE (Percentage of Average Absolute Error), MPE (Average Percent Error) which can be used to determine the rate of change in the carrier, or change rate. The MSE approach was used in this study because the frames of errors were taken and punished with great predictive errors. Calculation of MSE is given in Equation (1).

$$MSE = \frac{1}{M\ x\ N}\sum_{i=1}^{M}(P(i,j) - S(i,j))^2 \quad (1)$$

The MSE is the average of the sum of the squares of errors, the M and N row and column numbers, the P (i, j) cover data, and the S (i, j) stego object. The MSE value obtained in the calculations for the blue pixel is 0.0066. Since there was no change in the red and green pixels, the MSE value was zero.

In Figure 4, the original picture and the encrypted data are shown in the picture. The size of the encrypted data is 88,235 bytes. The hidden image has been delivered safely to the receiver. The receiver receiving the image obtains the data from the first row of the second column, determining the data size from the first row and retrieving the data from the last bits of the blue pixels in the direction of the arrow as in the algorithms of Figure 3.

Figure 4. (a) Original Image **(b)** Encrypted Image Hidden Image

Figure 5 shows the differenc ein the image created by taking the last bits of blue pixels. This data is converted to image data according to the number of bits in Figure 6. As seen here, the full image cannot be obtained without password information. The difficulty and complexity of the password will increase the security of the data.

In Figure 7, the effect of concealment on image distortion is shown by histogram analysis. In this case, the effect of encryption on this distortion is almost no level.

Figure 5. Difference between the original image and the encrypted data hidden image for the 88.235 byte image data in the algorithm used

Figure 6. (a) Image obtained without decryption **(b)** Image obtained by decryption

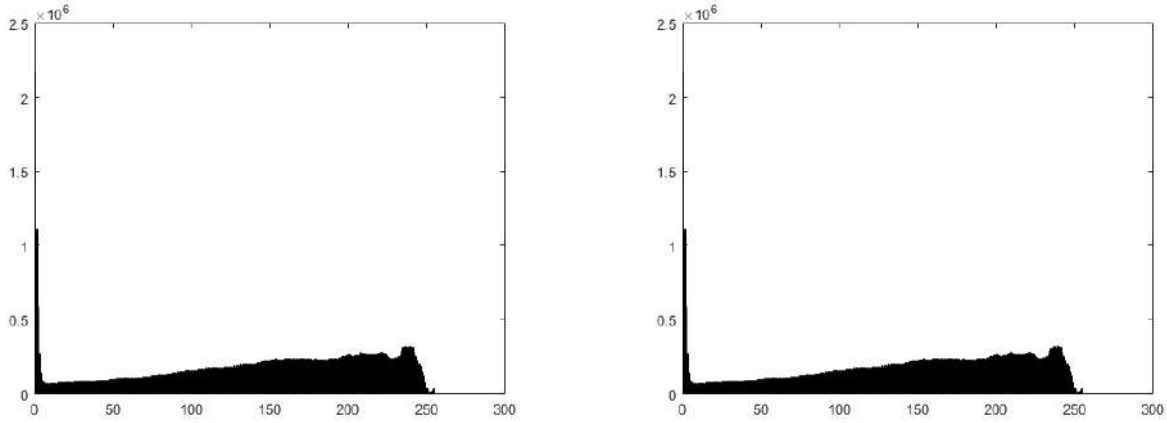

(a) **(b)**

Figure 7. (a) Histogram analysis of hiding created without encryption

(b) Histogram analysis of hiding created by encryption

4. Results and Recommendations

In this study, the image to be sent as a message using the MATLAB programming language is encrypted and hidden into an image by the method of adding the least significant bit. In this study, the image to be sent as a message using the MATLAB programming language is encrypted and hidden into an image by the method of adding the most meaningless bit. Data hiding was performed by inserting rows in the image. Since the encrypted data is only added to the last bit of blue pixels in the image, it will not be possible to detect the change with the eye.

The disadvantage of this study is that the size of the encrypted data to be hidden in the image is proportional to the size of the image. Larger data can be hidden within the image by

adding data compression or adding to the most meaningless second bit. Also, by applying modern cryptographic techniques, it may become safer to transmit data.

References

Atıcı, M. A. (2007). *Steganografik Yaklaşımların İncelenmesi, Tasarımı Ve Geliştirilmesi*, Yüksek Lisans Tezi, Gazi Üniversitesi, Ankara.

Caldwell, 2nd Lt. J. (2003). Steganography, *Crosstalk The Journal of Defense Software Engineering*, 25-27.

Cummins, J. Diskin, P. Lau and S. Parlett, R. (2004) *Steganography and Digital Watermarking*, School of Computer Science, The University of Birmingham.

Öksüzoğlu, S. (2013). Radyografik Görüntülere Veri Gizleme Uygulaması, *Sakarya Üniversitesi. Fen Bil. Der*. 17. Cilt, 2. Sayı, ss. 277-286.

Gopalan, K. (2003). Audio steganography using bit modification, *2003 InternationalConference on Multimedia and Expo*, 629-632, Baltimore, Maryland.

Niimi, M., Noda, H., Kawaguchi E. and Eason, R.O. (2002). High capacity and secure digital steganography to palette-based images, *Image Processing 2002. Proceedings 2002 International Conference 2:* 917-920, Rochester, New York, USA.

Sağıroğlu, S. ve Tunckanat, M. (2002). A Secure Internet Communication Tool, *Turkish Journal of Telecommunications*, 1(1):40-46.

Shahreza, S. (2006). Stealth steganography in SMS, *Wireless and Optical Communications Networks, 2006 IFIP International Conference*, Bangalore.

Sui, X.G. and Luo, H. (2004). A new steganography method based on hypertext, *Radio Science Conference*, 181-184, Qingdao, China.

Tseng, H.W. and Chang, C.C. (2004) Steganography using JPEG-compressed images, *The Fourth International Conference(CIT '04)*, 12- 17, China, Wuhan Computer and Information Technology.

Atawneh, S. (2006). A New Algorithm for Hiding Gray Images Using Blocks, *IEEE 2006, Information Systems Security*, Vol.15, Issue 6.

Singh, Kh. M., Singh, L. S., Singh, A. B. and Devi, Kh. S. (2007) Hiding Secret Message in Edges of the Images, *Information and Communication Technology Conferance*.

Yalman, Y. ve Ertürk, D. (2008). Sayısal Ses İçerisinde Gizli Veri Transferinin Kablosuz Ortamda Gerçekleştirilmesi, *Politeknik Dergisi*, 11(4): 319–327.

Akbal, T., Yalman, Y. ve Özcerit, A. T. (2010). Gerçek Zamanlı Sayısal Ses İçerisinde Sıkıştırılmış ve Şifrelenmiş Veri Transferi, *III. Ağ ve Bilgi Güvenliği Sempozyumu*, Ankara, Çankaya Üniversitesi.

Survey on 4.5G A1, A2 and A3 Packages Signal Quality on a University Campus

Yousif Ali RAJAB1[1*], Begüm KORUNUR ENGİZ[2],

[1] Ondokuz Mayis University, Faculty of Engineering, Department of Electrical and Electronics Engineering Samsun, Turkey , mail : *yousuf_ans88@yahoo.com* [2]

[*] **yousif ali rajab -rajab :** 15210231@stu.omu.edu.tr

Abstract

In order to summarize this study the aimed was to determining the downlink signal strengths of three cellular system operators (A, B, C) for 4.5G 800 MHz frequency (A1, A2, A3 packages) . To reach this goal measurements were conducted on Ondokuz Mayis University (OMU) Kurupelit Campus during seven hours in a day with 15 minutes sampling interval.The frequen- -cy spectrum between 791 MHz and 880 MHz was analyzed using SDR (software -defined radio) receiver [1].

Keywords: Signal strength measurements, SDR receiver, 4.5G, A1, A2, A3 packages

1. Introduction

A cellular mobile communication system consists of many cells, and a base station has placed a center of every cell. In cellular systems the situation of base station antenna square measure determined typically thus on make sure the best coverage space. In Turkey, presently 2G (second generation), 3G (second generation) and 4G (fourth generation) cellular systems square measure used, by suggests that of 3 totally different Cellular System (CS) operators named as Operator A, Operator Band Operator C. 900 Mc is employed by each Operator B and C, whereas 1800 Mc is employed by Operator A for 2G (GSM). All 3 operators use 2100MHz for 3G (UMTS) [2]. 4G is that the fourth generation of mobile communications standards. it's a successor of the 3G and provides ultra-broadband web access for mobile devices. The high information transfer rates create 4G networks appropriate to be used in USB wireless modems for laptops and even home web access. 4G capabilities LTE 800, LTE 900, LTE 1800, LTE2100, LTE 2600 [3] . Some recent client surveys show that a high level of satisfaction is powerfully correlated with signal strength. This study determines the downlink signal strengths of 3 cellular system operators (A, B, C) for 4.5G 800 MHz frequency (A1, A2, A3 packages).

2. Material and Method

All measurements had taken outdoor during 7 hours from 11:00 Am clock to 5:00 PM a clock on 20 November 2017 The total number of measurements were 27. measurements taken over a period of 30 minutes Each measurement would take ten minutes at a fixed location outside the restaurant of University Center Yasam Merkezi at Ondokuz mayis university in Samsun (latitude::41.3331438, longitude 36.2518264) .

This location as can see in fighure [1] has been selected because it is the best location for taking measurements because of direct line-of-sight several transmitters ((USB 2.0 TV Stick FM+DAB DVB-T SDR RTL2832U+ R820T)). [5] with antenna Which has the ability to cover from 25MHz to 1700MHz was used during the measurements.to cover The fourth generations band from 790 MHz to 1000 MHz. To receive the signal better, the antenna was installed vertically and placed at a height of 12 meters above sea level. The antenna connected to the dongle which is also connected to the laptop via a USB cable. Measurement controls, data acquisition, and analysis were realized with the MATLAB program .

Figure 1. Measurement Location

The system of measurement as explained consists of three main parts . first the antenna second the dongle and thrird is the labtob as we cane see in figure [2] .

Figure 2. The system of measurement

The antenna connected to the dongle which is also connected to the laptop via a USB cable. Measurement controls, data acquisition, and analysis were realized with the MATLAB program. in figure 1 we can see the whole low-cost measurement system which used in our

measurements. the task was to find the range of span between 790mhz to 820 MHz which are included three operators company (A-B and c) each one has 10 MHz and space between each operator 100 kHz.

3. Results and Discussion

Drive test measurement results that obtended from 11:00 am to 5:30 pm in one day was stored in PC for 2G, 3G and 4G systems using USB 2.0 TV Stick FM + DAB DVB-T SDR RTL2832U+ R820T are given in Fig 3 for each operator A, B,C , while results of each operator Separately can see it in fig 4 . can see clearly signal strengths of the three Operators Divided as follows Operator A which is stary from 790 MHz -801 MHz , Operator B which is stary from 801 MHz - 811 MHz , Operator C which is stary from 811 MHz - 820 MHz .

All these frequencies offer the fourth generation service to the users after drow all measurements the next step was to take operator A for all measurements and then we put them to gather using Matlab .as figure [4] Show operator B which its start from 801- MHz– 811MHz, we can see its have more intensity then operator A. İn onother hand operator C Noting that the intensity of users more than A but less than B operator.

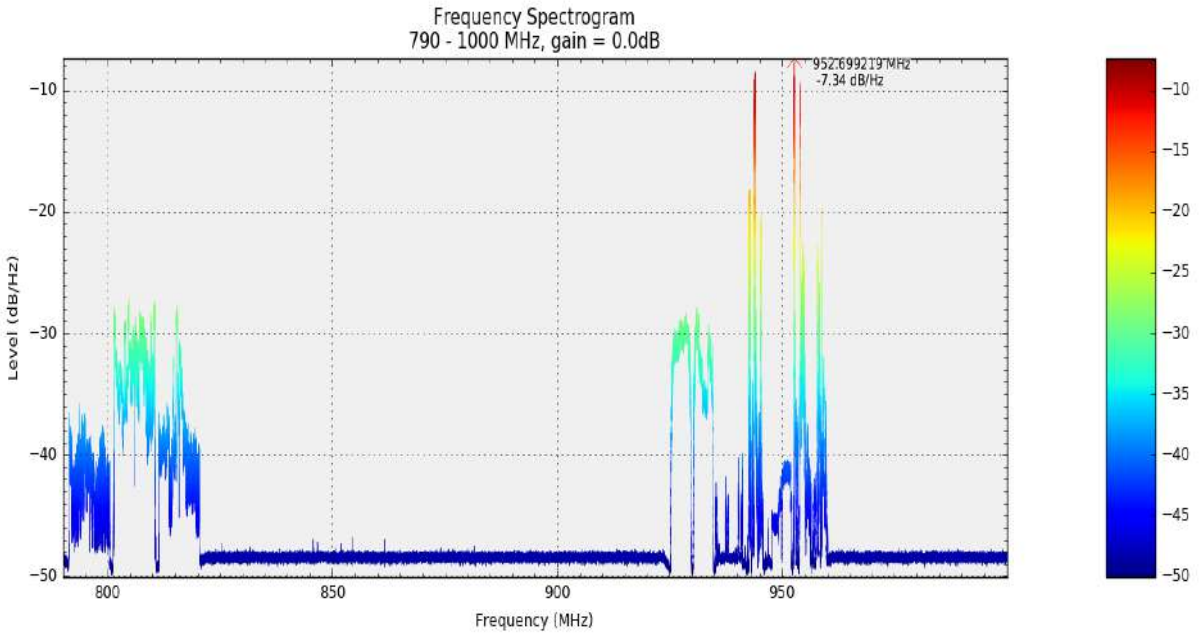

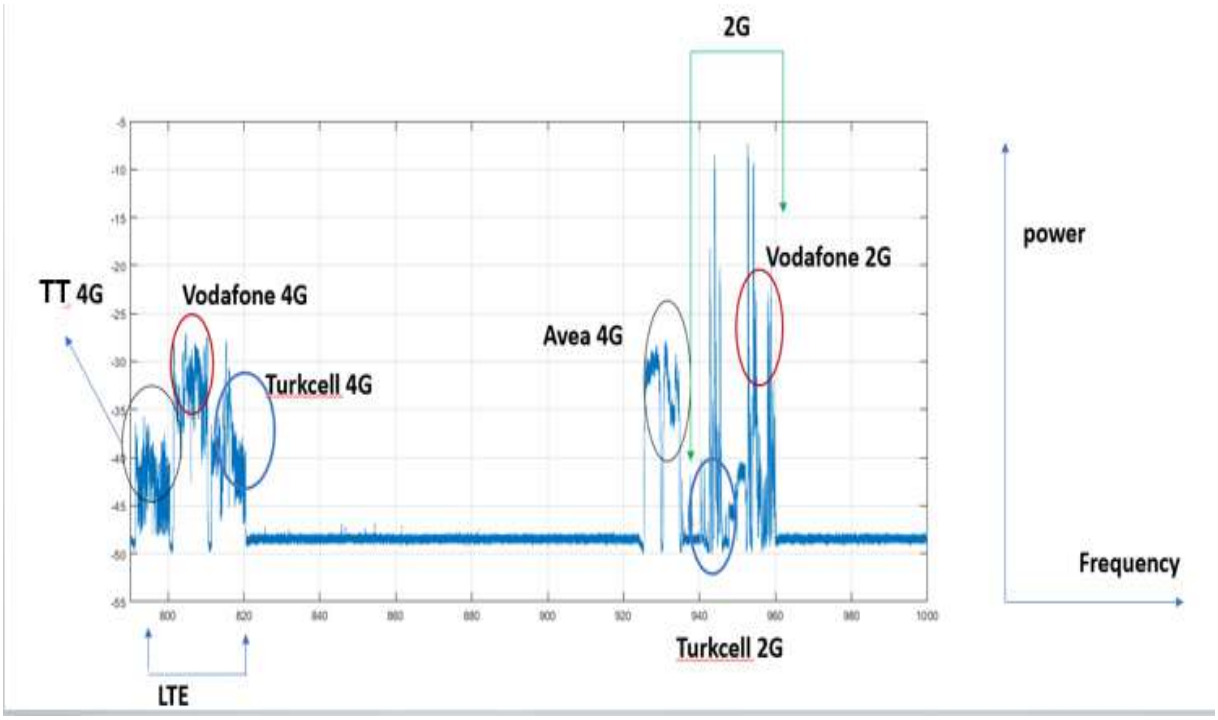

Figure 3. Signal strengths of the first measurement for Operators a) A b) B c) C

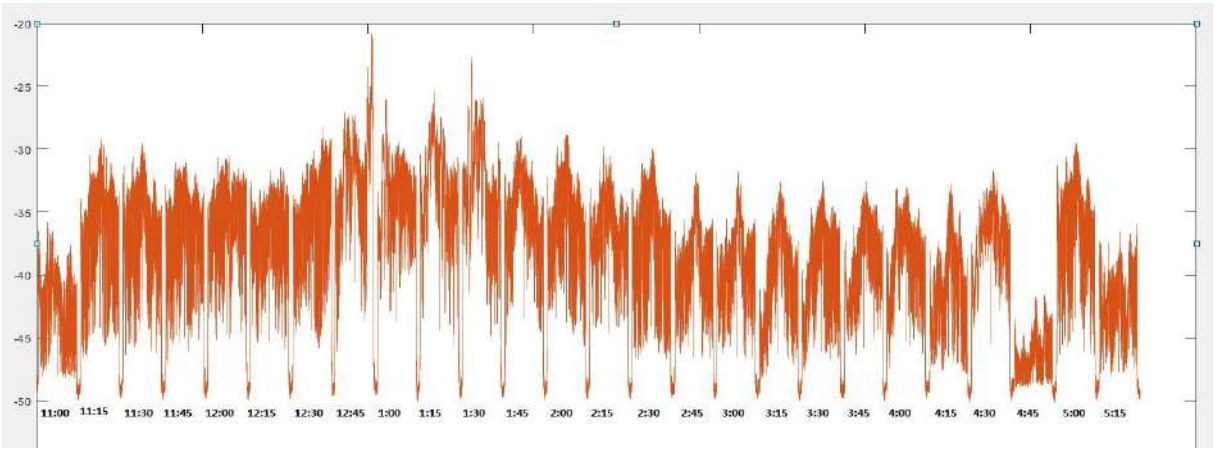

Operator A

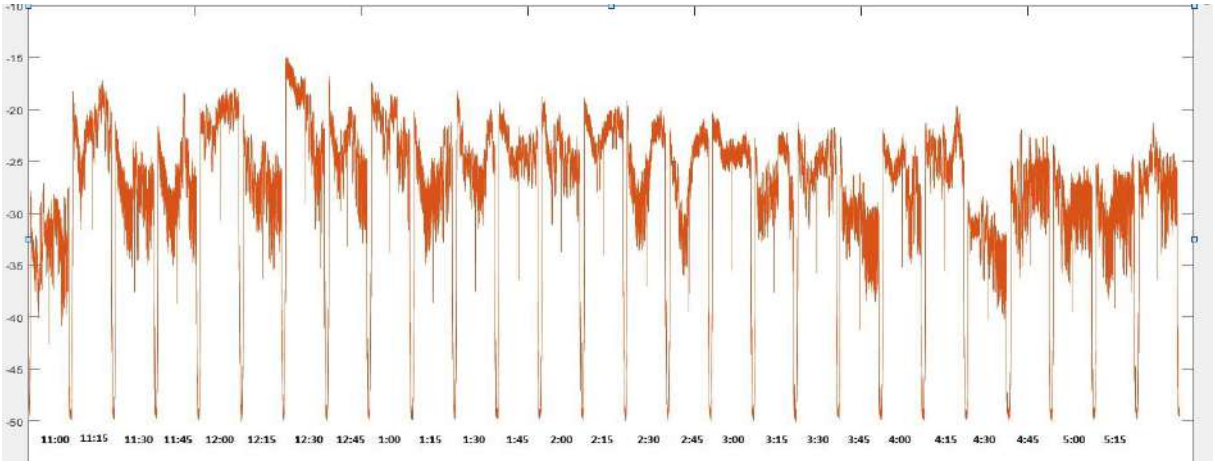

Operator B

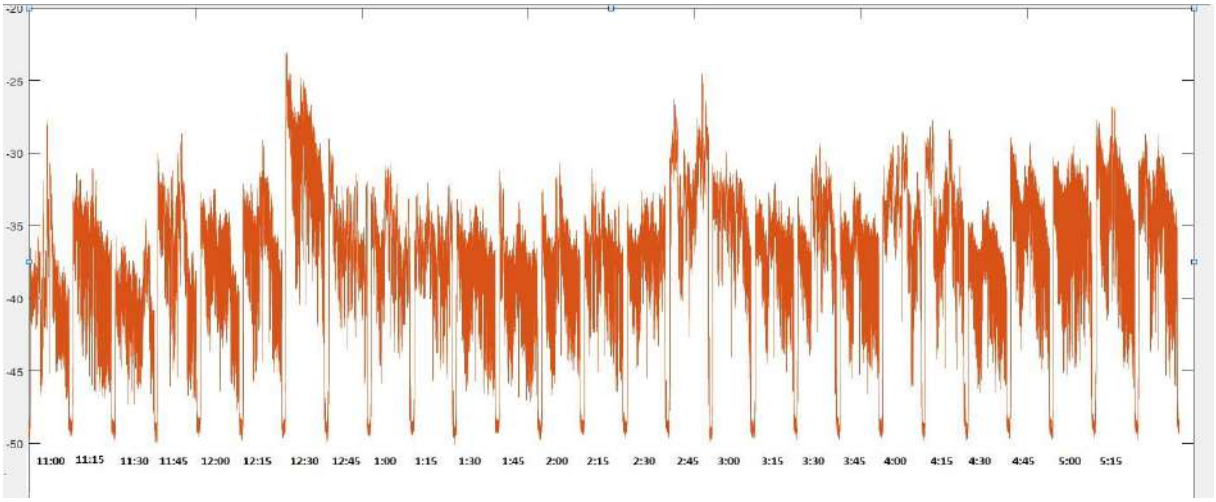

Figure 4. signal streanth of eagh operator

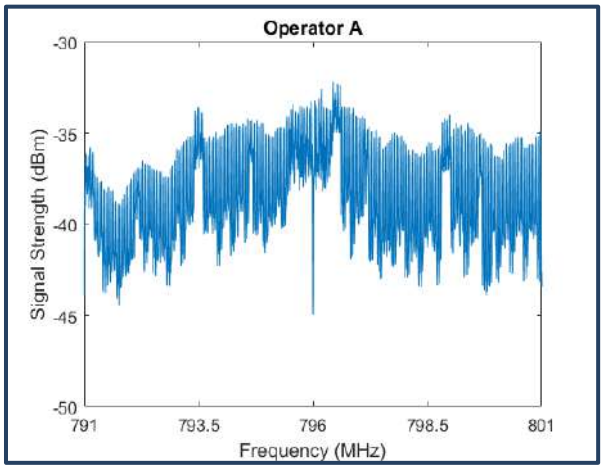

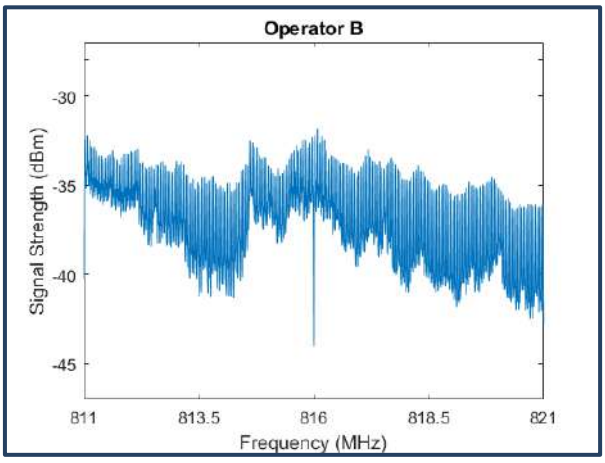

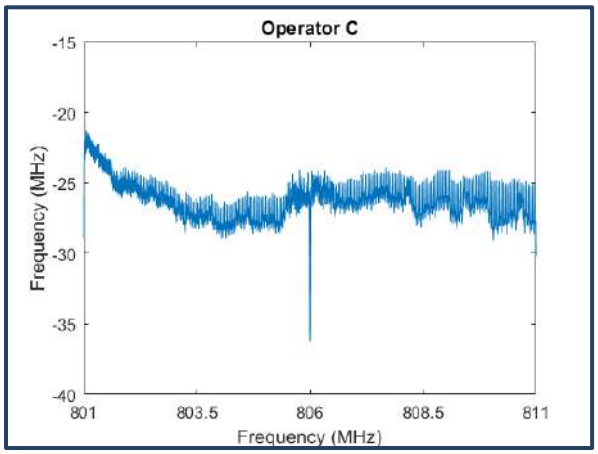

Figure 5. The maximum mean signal strengths

4 . Conclusion

According to measurement results; 4.5G signal strengths of Operator A vary between -21 dBm and -49 dBm. Operator B's and Operator C's signal strengths modification at intervals -23 dBm and -48 dBm, -15 dBm and -43 dBm severally. the maximum mean signal strengths calculated from twenty six measurements area unit - 32 dBm, -31 dBm and -21 dBm for Operator A, B and C severally. the measurement results show that the standard of 4.5G downlink signal is good for all operators. It is all over from the results that Operator C's signal quality is slightly higher than the others.

Acknowledgement

At this point I would like to thank my supervisor **Assistant Professor BEGÜM KORUNUR ENGİZ** who always helps me without tirelessness and continues to push me to be better.

References

Other Sources:

[1] Computer Science and Telecommunications Board, Wireless Technology Prospects and Policy Options. National Academy of Sciences, 2011. [Online]. Available: http://www.nap.edu/catalog.php?record id=13051# toc

[2] Savaş S., Topaloglu N., Ciylan B., Analysis of Mobile Communication Signal with Frequency Analysis Method, Gazi University Journal of Science, vol.25, no.2, pp.447-454, 2012.

[3] Ihttps://www.gsmarena.com/network-bands.php3?sCountry=TURKEY

[4] USB 2.0 Digital DVB-T DAB FM RTL2832U https://www.rtl-sdr.com/about-rtl-sdr/

Effects of Stator Slotting On Magnetic Field In BDFIM

Barış ÇAVUŞ[1*], Atabak NAJAFI[1]

[1]*Ondokuz Mayis University, Engineering Faculty, Electrical and Electronics Engineering, Samsun, Turkey;*

[*]**Responsible Writer:** baris.cavus@omu.edu.tr

Abstract

Brushless Doubly Fed Induction Machine (BDFIM) is a machine type that designed especially for offshore wind turbines applications. In recent years, due to the absence of brushes and slip rings the importance of BDFIM increases for wind energy production. In addition, it provides frequency control. BDFIM has a particular structure, for this reason the operating performance of BDFIM is not better than of other generator types. It has two stator windings and special nested loop squirrel cage rotor. One of the stator windings is control winding which has p_c pole pair and connects to power grid with power electronic converter. Other winding is power winding which has p_p pole pair and directly connects with power grid. Due to this structure, BDFIM has too many harmonics and the operating characteristic is below the desired level. Magnetic field analysis is required to be done to improve machine performance but this analysis is very difficult due to its complex structure. In this paper, BDFIM magnetic field has been analyzed and the influence of the slotting effect on the magnetic field and the machine performance has been examined.

Keywords: BDFIM, harmonic, magnetic field, slotting effect

1. Introduction

The Brushless Doubly Fed Induction Machine (BDFIM) becomes more important for wind energy generation, but this machine is not yet commercially produced (McMahon and others, 2006; Wang and others, 2016). Especially, after beginning of 21st century, the importance of the BDFIM has become even more important and academic studies have become more focused on this issue (Polinder and others, 2013). BDFIM has similar operation characteristics as other machines which are used for wind turbines such as DFIG (Carlson and others, 2006). In addition, BDFIM has high durability, reliability and low maintenance cost because of not having brushes and rings (Carroll and others, 2015). Additionally, it is low-speed machine, so gear box of BDFIM is smaller than other machine types (Strous and others, 2016).

It can be seen in Fig. 1, BDFIM has two stator (control and power) windings and these are magnetically uncoupled each other (Roberts, 2004). Control winding has p_c pole pair number and connects with power network via power electronic converter. With this converter, frequency of control winding can be changed, thus output voltage frequency can be kept constant. Power winding has p_p pole pair number and directly connects with power network. Rotor has a particial structure and it can be different from other types of rotor like reluctance and squirrel cage, but it is like squirrel cage and most appropriate for BDFIM (Wang and others, 2016). For BDFIM, strong cross-coupling between rotor and stator windings is essential to efficiency in BDFIM (Blazquez and others, 2009). Conventional cage rotor ensures low coupling with two stator windings separately, so cage nested loop rotors have been proposed for better coupling (Wang and Liu, 2016). Cage nested loop rotors have p_p+p_c nest and each nest has more than one short circuit loop. This special rotor design provides high coupling between rotor and control winding and between rotor and power windings separately.

Magnetic field of BDFIM is not simple because it has two stator windings. These windings produce magnetic field in air gap separately. These magnetic fields induce currents in rotor conductors and these currents produce magnetic field in air gap in addition to stator magnetic field. Two rotor currents induced by power and control winding have same frequency, thus BDFIM works in synchronous mode. Although there are other operating modes, the most suitable mode is the synchronous mode (Carlson and others, 2006). In addition, because of different structure of stator and rotor of BDFIM, air gap magnetic fields produced by both stator and rotor currents have many harmonics (Chen and others, 2014; Gorginpour and others, 2011). Though magnetic field in BDFIM is more difficult to understand, it has to be analyzed for better

understanding to working characteristics of BDFIM. In addition, this analysis is required for machine design (Strous and others, 2016).

Rotation speed of BDFIM depends on frequency and pole pair numbers of control and power winding;

$$n_r = \frac{60(f_p \mp f_c)}{p_p + p_c} \quad (1)$$

Here, f_p and f_c are frequencies of power and control windings, respectively.

It can be seen in (1), there is a correlation between rotation speed and f_c, therefore, if BDFIM runs as generator, f_c is used for constant output voltage frequency (Deng and others, 2009). In addition, p_p and p_c affect rotation speed.

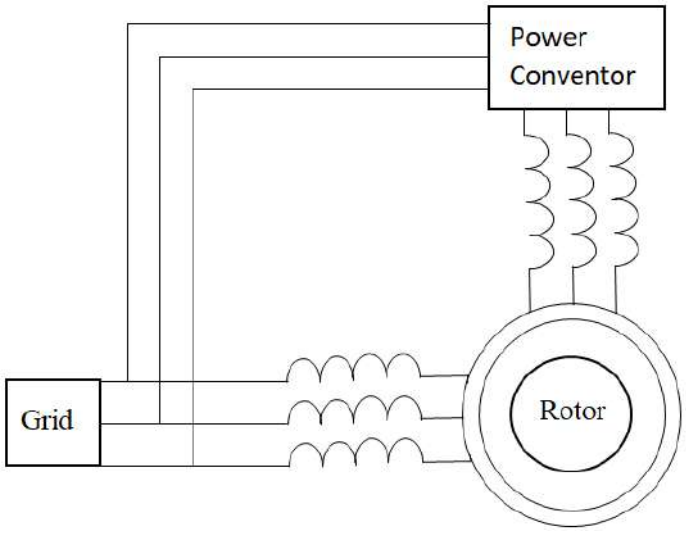

Figure 1. BDFIM structure.

Table 1. Parameters of BDFIM.

Number of phases	N_f	3
Axial length	l_s	1.6 m
Stator outer radius	r_{so}	1.5 mm
Stator inner radius	r_{si}	0.85 mm
Rotor outer radius	r_{ro}	0.65 mm
Rotor inner radius	r_{ri}	0.64 mm
Rated power	P	3.2 MW
Mechanical speed	f_m	6 Hz
Frequency (power winding)	f_{pe}	50 Hz
Frequency (control winding)	f_{ce}	10 Hz

If BDFIM is compared with other generator types for wind energy, working characteristics are not enough level in addition to high manufacturing cost and larger dimension of BDFIM (Wang and others, 2016). It means that design of BDFIM must be developed and the working characteristics should be improved on the desired level. In this paper, BDFIM magnetic field has been analyzed and the influence of the slotting effect on the magnetic field and the machine performance has been examined. When analyzing, machine parameters given in table 1 are used.

2. Analysis of Airgap Magnetic Field Distribution

From basic structure of BDFIM, machine has two stator windings and these windings are magnetically uncoupled each other. For this reason, design of stator structure is more complex and detailed. First of all, magnetic field and harmonics not taking into account slotting effect induced by stator windings should be known.

General form of air gap magnetic field of BDFIM induced from two stator windings and rotor conductors is,

$$B^r_{tot}(B^r,t) = \sum_{k_s} B^r_{s(k_s)} + \sum_{k_s}\sum_{k_r} B^r_{r(k_s,k_r)} \tag{2}$$

$B^r_{s(k_s)}$ is the stator magnetic field and $B^r_{r(k_s,k_r)}$ is rotor magnetic field. These magnetic fields have main and other harmonics (Carlson and others,2006). Here, k_s and k_r are harmonic orders of stator and rotor, respectively. To calculate $B^r_{s(k_s)}$, firstly, stator winding conductor distribution should be calculated as in (3).

$$C_{s,m}(\theta^s) = \frac{1}{2}\sum_{k_s=-\infty}^{\infty} C\cos(k_s\theta^s - \frac{k_s}{p}\beta_m) \tag{3}$$

$$C = \frac{1}{r_{si}}\frac{2}{\pi} n_c k_{qw(k_s)} pq \tag{4}$$

$$\beta_m = (m-1)\frac{2\pi}{N_{faz}},\ \forall\, m\ \in \{1{:}\,N_f\} \tag{5}$$

Here, r_{si} is inner radius of stator, n_c is number of conductors in a slot, p is number of pole pairs, q is number of slots per pole per phase and k_{qw} is winding factor which can be calculated in (6) (Pyrhönen and others, 2008). To calculate magnetic field of control and power windings, conductor distribution in (3) should be calculated for both windings.

$$k_w = \frac{\sin k_s \frac{q\alpha_u}{2}}{q \sin k_s \frac{\alpha_u}{2}} \quad (6)$$

To calculate air gap magnetic field, in addition to winding conductor distribution, stator currents should be calculated as in (7).

$$i_{s,m}(t) = \sqrt{2} I_s \cos(2\pi f_{se} t - \phi_m + \varphi_s) \quad (7)$$

$$\phi_m = (m-1)\frac{2\pi}{N_{faz}} \quad (8)$$

In (7), f_{se} is frequency and φ_s is phase shift for stator currents. After computing winding distribution and currents, air gap magnetic field induced by stator winding can be calculated in (9).

$$B_s^s(\theta^s, t) = \sum_{k_s} \frac{N_{faz}}{2} \frac{1}{k_s} r_{si} \frac{\mu_0}{l_g} C_{ks} \sqrt{2} I_s \cos(2\pi f_{se} t - k_s \theta^s + \frac{pi}{2} + \phi_m) \quad (9)$$

(9) can be applied to both stator windings separately. k_s harmonic orders can be found as (10) and (11) for power and control winding.

$$k_{s,power} = p_p(1 - 2nN_f) \quad (10)$$

$$k_{s,control} = p_c(2nN_f - 1) \quad (11)$$

Air gap magnetic field produced by both stator windings induces currents in rotor conductors and these currents produce magnetic field in air gap, too. Similar to stator magnetic field, to calculate rotor magnetic field, rotor conductor distribution must be calculated as in (12).

$$C_{r,nl}(\theta^r) = \frac{1}{2}(\underline{C}_{r,l(k_r)}) \cos(k_{r(}\theta^r - \beta_{r,n})) \quad (12)$$

$$\underline{C}_{r,l(k_r)} = -j \frac{1}{r_{ro}} \frac{2}{\pi} \sin\left(k_r \gamma_{r,l} \frac{\theta_{rp}}{2}\right) \cos(k_r \pi) \quad (13)$$

$$\beta_{r,n} = (n-1)\frac{2\pi}{N_y} \quad (14)$$

Here, r_{ro} is outer radius of stator, $\gamma_{r,l}$ is rotor loop span, θ_{rp} is rotor full nest pitch angle. Rotor current is;

$$i_{s,m}(t) = \sum_{k_s} \sqrt{2} I_{r,l(k_s)} \cos\begin{pmatrix} 2\pi f_{re(k_s)} t - k_s \phi_{r,n} \\ +\varphi_{r,l,k_s} \end{pmatrix} \quad (15)$$

$$\phi_m = (n-1)\frac{2\pi}{N_y} \quad (16)$$

From (12) and (15), rotor magnetic field can be expressed as (17)

$$B_r^r(\theta^r, t) = \sum_{k_s} \sum_{k_r} \sum_{l=1} \frac{N_{faz}}{2} \frac{1}{k_r} r_{ro} \frac{\mu_0}{l_{g,et}} \underline{C}_{r,l(k_r)} \sqrt{2} I_{r,l(k_s)} \cos(2\pi f_{re(k_s)} t - k_r \theta^r + \varphi_{r,l,k_s} - \frac{\pi}{2}) \quad (17)$$

Here, rotor harmonic orders can be expressed,

$$k_r \in k_s + nN_y \quad (18)$$

When the slotting effect of stator or rotor is taken into account, air gap permeance function should be considered. Thus, air gap magnetic field of stator with slotting effect can be computed as in (19);

$$B_s^s(\theta^s, t) = \sum_{k_s} \frac{\Lambda_{si}}{\Lambda_{s0}} \frac{N_{faz}}{2} \frac{1}{k_s} r_{si} \frac{\mu_0}{l_g} C_{ks} \sqrt{2} I_s \cos(2\pi f_{se} t - k_s \theta^s + \frac{pi}{2} + \phi_m) \quad (19)$$

Permeance function for stator;

$$\Lambda(\theta_s) = \Lambda_0 + \sum_{i=1}^{\infty} \Lambda_i \cos(2\pi i(\theta_s - \theta - \varphi_s)) \quad (20)$$

$$\Lambda_0 = \frac{\alpha_p \Lambda_{max} + (\pi - \alpha_p)\Lambda_{min}}{\pi} \quad (21)$$

$$\Lambda_i = \frac{2(\Lambda_{max} - \Lambda_{min})}{i\pi} \sin(i\alpha_p) \quad (22)$$

Here, α_p is teeth width. The rotor magnetic field with slotting effect can be calculated using air gap permeance function similarly to the stator magnetic field equations.

3. Simulation and Results

In this section, after expressing the airgap magnetic field distribution, the results are obtained by using the equations given previous section. In addition to analytic solution, 2D magnetic field distribution of BDFIM is obtained by using finite element method. As it can be seen in figure 2, airgap magnetic field distribution of BDFIM is smooth and regular. From structure of BDFIM, air gap magnetic field has more time and space harmonics. The distribution of the airgap magnetic field in which the harmonics are taken into account is shown in figure 3.

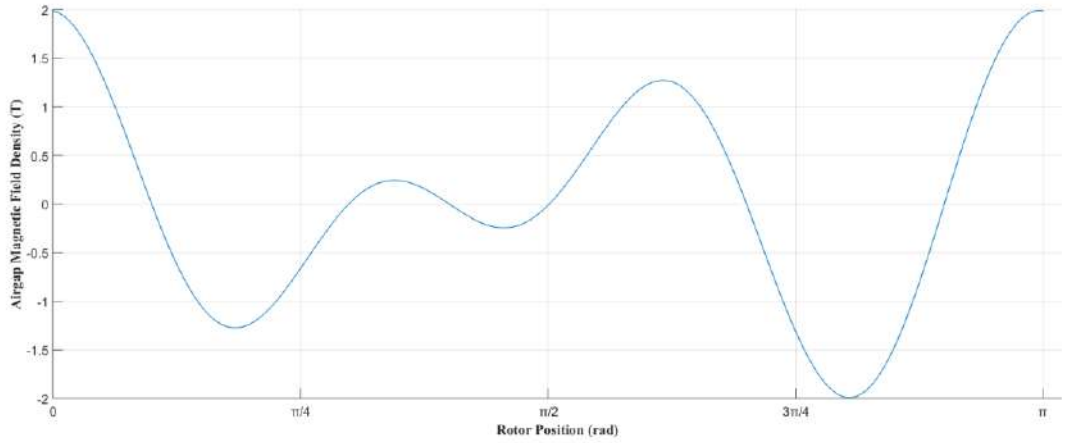

Figure 2. Main component of airgap magnetic field

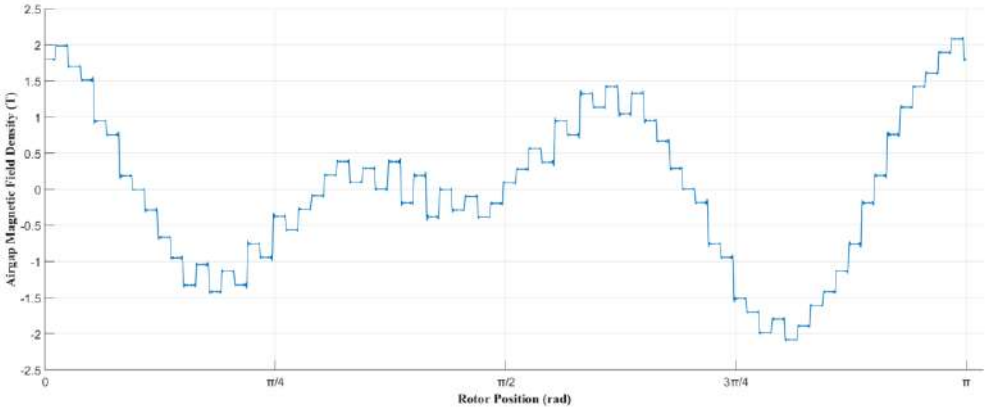

Figure 3. Airgap magnetic field with harmonic component

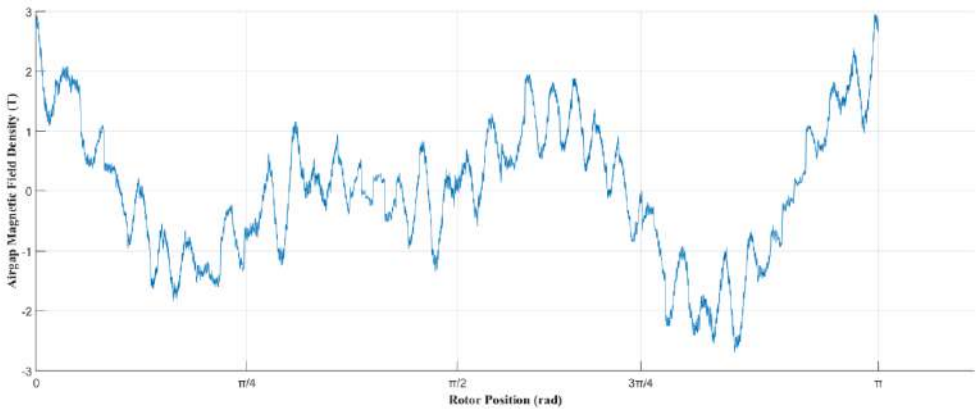

Figure 4. Airgap magnetic field with slotting effect

In addition to harmonics, slots have more a significant effect on the airgap magnetic field. If figure 4 is examined, it can be seen that the fluctuations in the magnetic field distribution increase and this is the effect of the slotting. Figure 5 represents 2-D magnetic field distribution of BDFIM and these fluctuations can be seen in figure 5 clearly.

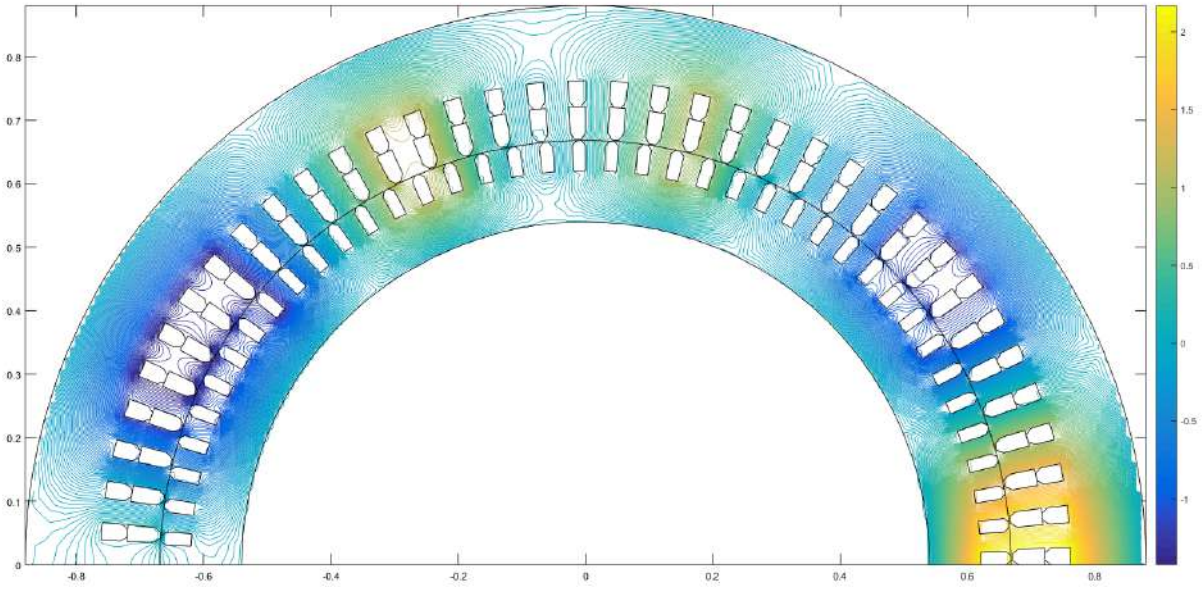

Figure 5. FEM 2-D BDFIM flux density distribution

4. Conclusion

BDFIM has a great potential for use in wind turbines but its performance is not desired level. Therefore, the magnetic field analysis of the BDFIM should be done in detail for good performance. However, BDFIM has different and complex structure and because of this, airgap magnetic field is result, design of BDFIM still continues to reduce these undesired effects.

Design of BDFIM should be further improved for better quality and efficient motor. For this purpose, like other factors in this issue, slotting effect must be expressed and this paper is prepared for this aim.

REFERENCES

Blazquez, F., Veganzones, C., Ramirez, D., Platero. C., (2009). Characterization of the Rotor Magnetic Field in a Brushless Doubly-Fed Induction Machine. *IEEE Transactions on Energy Conversion*, vol. 24, no. 3, pp. 599–607, Sep. 2009.

Carlson, R., Voltolini, H., Runcos, F. and Kuo-Peng, P., (2006). A performance comparision between brush and brushless doubly fed asynchronous generators for wind power systems. *Renewable Energy and Power Quality Journal*, vol. 1, no. 4, pp. 258-262.

Carroll, J., McDonald, A. and McMillan, D., (2015). "Reliability comparison of wind turbines with DFIG and PMG drive trains, *IEEE Trans. Energy Convers*., vol. 30, no. 2, pp. 663–670.

Chen, J., and Zhang, W., (2014). Harmonics in brushless doubly fed induction generator for torque ripple analysis and modeling, *IEEE Trans. Magn.*, vol. 50, no. 11, Art. no. 8203604.

Deng, X. M., Tan, G. J. and Zhang, X., (2009). Structure research and design of brushless doubly-fed machine," in *Proc. Asia-Pac. Power Energy Eng. Conf.*, pp. 1–4.

Gorginpour, H. Jandaghi, B. and Oraee, H., (2011). Time and space harmonics in brushless doubly-fed machine, in *Proc. 19th Iranian Conf. Elect. Eng. (ICEE)*, pp. 1–6.

McMahon, R. A., Wan, X., Abdi-Jalebi, E. Tavner, P., Roberts, P. C., and Jagiela, M., (2006). The BDFM as a generator in wind turbines, in *Proc. 12th Int. Power Electron. Motion Control Conf. (EPE-PEMC)*, Aug./Sep. 2006, pp. 1859–1865.

Polinder, H., Ferreira, J. A., Jensen, B. B., Abrahamsen, A. B., Atallah, K. and McMahon, R. A., (2013). Trends in wind turbine generator systems, *IEEE Journal of Emerging and Selected Topics in Power Electronics*, vol. 1, no. 3, pp. 174–185, Sept.

Pyrhönen, J., Jokinen, T. and Hrabovcová, V., (2008). *Design of Rotating Electrical Machines*, 1st ed. New York, NY, USA: Wiley.

Roberts, P. C., (2004). A study of brushless doubly-fed (induction) machines, Ph.D. dissertation, Univ. Cambridge, Cambridge, U.K., 2004.

Strous, T. D., Wang, X., Polinder, H, and Ferrira, J. A. B., (2016). Brushless doubly fed induction machines: magnetic field analysis, *IEEE Trans. Magn.*, vol. 52, no. 11, Art. no. 8108310.

Wang, X., Liu, D., Polinder, H., Lahaye, D. and Ferrira, J. A. B., (2016). Comparison of Nested-Loop Rotors in Brushless Doubly-Fed Induction Machines, 19th *International Conference on Electrical Machines and Systems (ICEMS)*, pp.1-6.

Wang, X., Strous, T. D., Lahaye, D., Polinder, H. and Ferrira, J. A. B., (2016). Harmonics Study of Nested-Loop Rotors in Brushless Doubly-Fed Induction Machines, *XXII International Conference on Electrical Machines (ICEM)*, pp. 371-377.

Wang, X., Strous, T. D., Lahaye, D., Polinder, H. and Ferrira, J. A. B., (2016). Modeling and Optimization of Brushless Doubly-Fed Induction Machines Using Computationally Efficient Finite Element Analysis, in *IEEE Transactions on Industry Applications*, vol 52, no.6.

Alternative approaches to expropriation in land acquisition for public investments

Volkan Baser[1]
[1]*Giresun University, Faculty of Engineering, Department of Geomatics Engineering, Giresun, Turkey*
volkan.baser@giresun.edu.tr

Abstract

Land acquisition for public investment is usually done through expropriation in our country. This method can bring great costs to the institution that will expropriate. Expropriation costs rise to the level of public investment costs and the applicability of the projects decreases, money and labor are lost. Moreover, the appraisal of the real estate to be expropriated does not reflect the reality and the citizen can be a victim. Privatized land owners and practicing institution can not benefit from the increase in the value of the public investment in the ending region.

The article 18 of 3194 numbered development law enacted in 1985 is related to Land Readjustment (LR). LR is an important technique to transform rural area to urban area and to carry out development plans for urbanization. The parcel owners in the project area have to abandon 40 % of their constructional area with LR. This situation is valid for new roads, streets, green lands, car parks, squares, police stations, playgrounds, primary school lands and religious places. In this study, the problems of land acquisition due to expropriation were emphasized and alternative solution based on LR was presented.

Keywords: Land Management, Expropriation, 3D Cadastre, Land Readjustment

1. Introduction

People have to produce, consume and make use of the goods they need in a social environment. This leads to the question of who and how to possess the goods needed. Property has, therefore, been the subject of both social conflicts and social regimes throughout history (Güriz, 1969).

It is known that natural resources are used collectively in antiquity where the human population on the earth is small and the concept of ownership does not occur. As the resources were diminishing, domestication and production and agricultural activities were discovered and the first steps taken to implement the property (Başer, 2014).

In modern societies, it is inevitable to introduce various restrictions on the use of immovable properties with zoning plans for the construction of regular and livable cities. These restrictions, of course, restrict the possibilities for saving the property on the property and thus constitute an interference with the property right (Akbulut, 2014). a significant amount of investment in infrastructure in order to improve the living standards of the rural and urban population in Turkey is carried out within the scope of development strategies. Due to the presence of factors such as population growth and technological developments, the administrations charged with fulfilling public services are increasingly in need of other resources as well as movable and immovable property. These requirements can be met not only by their own possibilities but also by the immovable property, which is sometimes the subject of private property, by the ownership of the property, when the property is beneficial. In our country this is usually achieved through expropriation (Kılıç, 2011; Arslanoğlu, 2013).

2. Expropriation

Expropriation is the process of transferring a part of the goods which are in private ownership or the whole of the goods to the public concerning the registration in case of public interest.

The application can be made without asking consent. That is why it is a challenge to realize public services and the most expensive, the longest, and perhaps the most noble, who can not be pleased with the failure of other more zoning-oriented zoning practices that protect the common interests of the community for public good purposes. You think the job is only technical; public institutions should feel the obligation to observe their attitudes in accordance with the principles of social and flawless responsibility (Ülger, 2010), if the expropriation, which has traditionally been done by mechanized people, requires a rigorous process management, and the smallest unit is the smallest unit. Because expropriation requires that immovable property owners have to abandon the property they are bound to with material and spiritual ties, they face long-term social problems such as migration and unemployment and are mostly victims (Türkoğlu, 2008).

Legal Structure in Expropriation

The expropriation was included in the 21st of the 1876 Constitution, 74th of the 1924 Constitution, 38th of the 1961 Constitution and 46th Article of the 1982 Constitution (Demirel, 2002). The 46th article of the constitution establishes the foundation of expropriation.

The expropriation proceedings are carried out according to the provisions of the expropriation law numbered 2942, which was enacted in 1983, and the Law on Amendment to the expropriation law numbered 4650 and 2001, which amended certain articles of this law.

Article 46, which entered into force in 2001 (Amended: 3.10.2001-4709 / 18 md.); "State and public legal entities; in the cases where the public interest requires, to expropriate all or part of the immovable property in private ownership in accordance with the principles and procedures indicated by law, and to establish administrative easements on them, provided that the real benefits are paid in advance. The expropriation fee is paid in cash and in advance with the incremental amount of cash that has been finalized. However, the implementation of agriculture reform is illustrated by the law on the payment of land for the expropriation of land for the purpose of enormous energy and irrigation projects and the realization of resettlement projects, the cultivation of new forests, protection of the coasts and tourism. In these cases, where the law may foresee payment in installments, the installment period may not exceed five years; in which case installments are paid equally. From the expropriated land, the price of those belonging to the small farmers who run the land directly is paid in advance. The highest interest shall be imposed on the installments foreseen in the second paragraph and for the unpaid expropriation compensation costs for any reason ".

3. Alternative Methods of Expropriation

Land Readjustment (LR)

Law No. 3194, which entered into force in 1985, concerns the 18th Land Readjustment (LR). With the LR, the parcel owners in the project area leave up to 40% of their usage at the end of the application free of charge for the value increase in the region. The abandoned part is called the areas separated by public services. These include roads, streets, green spaces, parking lots, squares, police stations, playgrounds for children, school areas as well as places of worship and primary education. (Uzun, 2009).

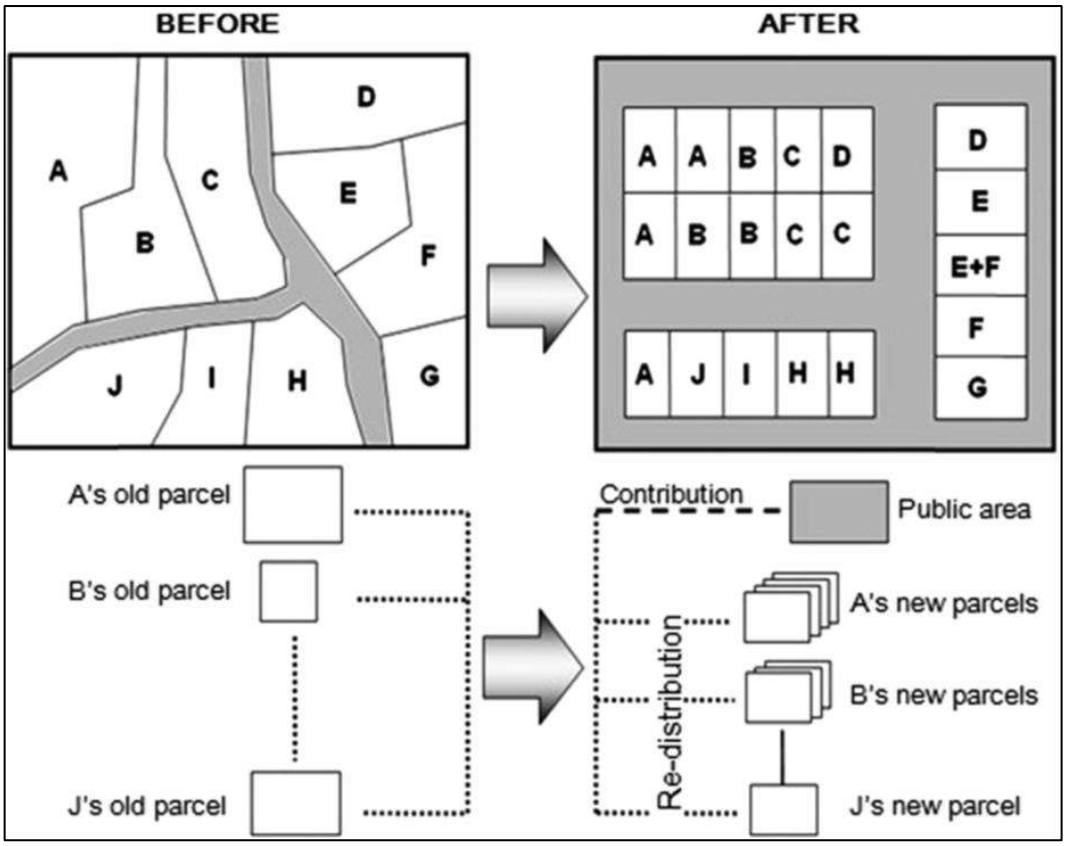

Figure 1. LR is old and new (Yomralıoğlu, 1993; Uzun and Celik, 2015).

3D Cadastre

Although objects are three-dimensional, cadastral systems are two-dimensional (Figure 2). For this reason, the rights and restrictions on the rights of the immovable in the vertical direction can not be shown and legal situations can not be recorded. The concept of 3D cadastre has been born to solve the problems arising from these confusions (Forrai and Kirschner, 2003). In this context, it is stated in many countries that the right of property extends from the center of the earth to the sky, that the boundaries of parcels are not vertical lines but vertical planes and extend to the earth's crust (Kalantari et al., 2008).

In our country, the third dimension of the property right has been tried to be solved by the Constitution and the Civil Code. ownership rights according to article 35 of the Constitution of the Republic of Turkey; "Everyone is entitled to ownership and inheritance. These rights may be restricted by law for public good purposes only. The use of the right of property can not be contrary to the benefit of society ". In Article 718 of the Civil Code, the content of immovable property; "The ownership on the land covers the air above and below the supply layers to the extent that it is beneficial for its use. Constructions, plants and resources are also included in the scope of this property, without any legal limitations "(Başer, 2014).

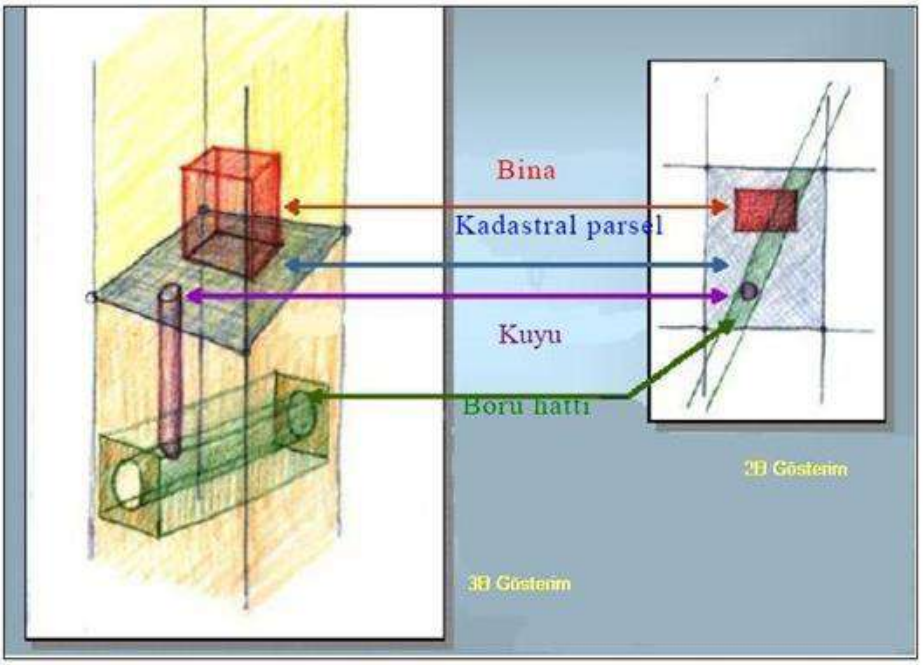

Figure 2. The 3D objects that are subject to registration (Forrai and Kirschner, 2003)

Increasing density on a limited scale nowadays causes different types of usage and legal objects to be overlaid, intertwined, or even more complex in the vertical dimension. This requires a clearer registration of 3D legal objects in the cadastre and a 3D geometric representation of the space where the rights are applied for a sustainable land administration. There is a growing tendency to use the underside of the surface of the land, particularly in areas of high population density. For this reason, the cadastre needs to be able to collect and manage vertical spatial information in order to be able to respond to increasing needs and to secure complex property rights effectively (Döner, 2009). In this context, high expropriation costs should be considered together with LR, 3D cadastre and floor ownership, which can be an alternative in the past.

Betterment Application

In Article 16 of the former Municipal Income Law No. 5237, betterment is explicitly stated. However, betterment has been lifted in the new municipal income law numbered 2464.

Studies show that the addition of the betterment application currently used in the private sector to the municipal income law is an important issue to be evaluated. The second important point is that the owners of the property benefit from the increase in the value of the parcels when the applicant passes through the region, whereas the expropriation institution can not benefit at all. It is evident that the implementation of this practice has created a value increase in the existing parcels. It will be correct to benefit not only the owners of the parcels but also the institution that will carry out the application at the same time.

4. Conclusions and Recommendations

When land acquisitions for public investments are made with expropriation, economic and social losses occur on behalf of the owners. Institutions are faced with budgetary constraints due to expropriation costs, and work is slow, time, money and labor are lost. LR, one of the

methods of implementation, is an application that can minimize these problems. With the LR application, up to 40% of the territory of the region where the public investment will be made can be provided free of charge for the increase in value resulting from the application. It should also be considered together with the LR floor ownership according to the type of public investment. Assessment of betterment practices will ensure that the public is free from the burden of expropriation. Also;

- Citizens are victims because the expropriation is an application made without the residence of the owners. All the parcel owners can not benefit from the gains brought by the public investment. With LR, this situation will partly come to an end.
- Since all the parcels in the edit region are affected equally, the blessing-balance balance will be achieved in some measure.
- Property complexity may be eliminated by generating zoning parcels that do not have a property problem around the roads opened by applying LR.
- If the application is carried out together with the floor ownership, the parcel with geometrically distorted, insufficiently insignificant, and structuring problem can be resolved.
- We should not make use of our betterment such as betterment application, but also to benefit from the increase in the value of the institution making the application. Real estate value increase tax should be evaluated in order to ensure the utilization of the immovable value to be generated by the application.

5. References

Akbulut, E., 2014. Kamulaştırmadan kaynaklı tam yargı davalarına danıştayın yaklaşımı ve alternatif çözüm önerisi.

Arslanoğlu, M. (2013). Acele kamulaştırma. Marmara Üniversitesi Hukuk Fakültesi Hukuk Araştırmaları Dergisi, 19(3), 203-224.

Başer, V., 2014. Kıyı ve Denizel Alanlarda Arazi Yönetimine Yönelik Sorunlar ve Çözüm Yaklaşımları, Karadeniz Teknik Üniversitesi, Fen Bilimleri Enstitüsü, Doktora Tezi, Trabzon.

Döner, F. ve Bıyık, C., 2009. Kadastroda Üçüncü Boyutun Kapsam ve İçeriği, XII. Türkiye Harita Bilimsel ve Teknik Kurultayı, Ankara.

Forrai, J., Kirschner, G., 2003. An Interdisciplinary 3D Cadastre Development Project in Practice, FIG Working Week, Paris.

Güriz, A., 1969. Teorik Açıdan Mülkiyet Sorunu, Ankara.

Kalantari, M., Rajabifard, A., Wallace, J. and Williamson, I., 2008. Spatially referenced legal property objects, Land Use Policy, 25, 2, 173-181.

Kılıç, O. (2011). Kamulaştırma davalarında arsa-arazi ayrımı. Akdeniz Üniversitesi Ziraat Fakültesi Dergisi, 24(1), 15-18.

Türkoğlu, İ., 2008. Petrol arama iletim faaliyetlerinde kamulaştırma ve problemler, Yüksek Lisans Tezi, *Karadeniz Teknik Üniversitesi Fen Bilimleri Enstitüsü*, Trabzon, 48-65.

Uzun, B., 2009. Using land readjustment method as an effective urban land development tool in Turkey. Survey Review, 41, pp. 57-70.

Uzun, B., Celik, N., 2014. Sustainable management of coastal lands: A new approach for Turkish coasts, Ocean & Coastal Management Volume: 95, pp. 53-62.

Ülger, N. E., 2010. Türkiye'de arsa düzenlemeleri ve kentsel dönüşüm, *Nobel Yayın Dağıtım*, İstanbul, 10-365.

Yomralioglu, T., 1993. A Nominal Asset Value-Based Approach for Land Readjustment and its Implementation Using Geographical Information Systems. Unpublished PhD Thesis. University of Newcastle Upon Tyne, UK.

Peak-to-Average Power Ratio Reduction for Partial Transmit Sequences using Partical Swarm Optimization Algorithm in Wavelet Packet Modulation

Wisam Hayder Mahdi [1] , Necmi Taşpınar[2]

[2]*Erciyes University, Engineering Faculty, Department of Electrical and Electronics Engineering, Kayseri, Turkey; taspinar@erciyes.edu.tr*

[*] **Corresponding Author:**

haiderwisam@yahoo.com

Abstract

Wavelet Packet Modulation (WPM) is a new scheme of choosing modulation scheme for transmission of multicarrier signal on wireless channel which helps in orthogonal wavelet base in place of sine functions. Though this modulation is over all similar to that of Multi-carrier code-division multiple access (MC-CDMA), it provides interesting additional features. Large Peak to Average Power Ratio (PAPR) of transmitted signal is the major drawbacks of the wavelet packet modulation (WPM) scheme. Utilizing the advantage of concentrating the energy to certain subspaces of the discrete wavelet transform, the performance of three methods to reduce PAPR in WPM is investigated. In general, the partial transmit sequence (PTS) technique is used to reduce PAPR. In this paper, we use the particle swarm optimization (PSO) algorithm to reduce the PAPR value of the PTS for WPM signals. The accomplishment of the particle swarm optimization (PSO) algorithm for Daubechies wavelets was compared with the primary WPM for different Daubechies wavelets, arbitrary search PTS for Daubechies wavelets and optimum PTS by computer simulations**.** In the simulations, WPM system has N=256 subcarriers and BPSK modulation was used. HPA is used with p= 0.5, 2 and IBO= 0,3,6 dB. Oversampling factor of the transmitted signal is L=4. In the simulations, the signal is transmitted over AWGN channel. The number of the phase factor is selected as W=2. WPM signals are randomly partitioned into V= 16 subblocks. In the simulations, the proposed system has better results than classical PTS system.

Keywords: Partial transmit sequence (PTS), peak-to-average power ratio (PAPR), wavelet packet modulation (WPM), particle swarm optimization (PSO).

1. Introduction

A multiplexing method avail a WPM (Wavelet Packet Modulation) where data containing bits regulate a place of orthogonal wavelet packet waveforms that are then consolidated into a single compound signal. WPM is a promising alternative to the popular Fast Fourier Transform (FFT) based Multi-carrier code-division multiple access (MC-CDMA). However, high peak to average power ratio (PAPR) that affects MC-CDMA is also a problem in WPM.

MC-CDMA may stand for Multi-carrier code division multiple accesses, a multiple access technology used in telecommunication systems based on OFDM. The large peaks increase the amount of inters modulation distortion resulting in an increase in the error rate. The average signal power must therefore be kept low to ensure that the transmitter amplifier operates in the linear region [4]. The survey of PAPR reduction in WPM can be summarized as follows: a multi-pass pruning method to reduce PAPR was proposed by Baro [5]. Zhang [6] suggested a threshold based method to reduce PAPR. Le et. al [7] derived upper bounds for the maximum PAPR for WPM transmission and based on these results wavelets that minimize PAPR are obtained. A novel adaptive companying transform scheme was prospective by Rostamzadeh to effectually declining the PAPR of OFDM and WPM signals [8]. Torun et. al [9] prospective a method to reduce the Peak-to-Average Power Ratio (PAPR) in the developmental Wavelet Packet Multi-carrier Modulation (WPM) system. A method works

on the principle that the PAPR of a multicarrier system can be adjusted by varying the phase-shifts of the subcarriers. Hence different PAPR values for the same information can be obtained by randomly altering the phases of the sub-carriers used to modulate the data. The WPM frame with the least PAPR is then identified and transmitted.

In this paper, we use the particle swarm optimization (PSO) algorithm to reduce the PAPR value of the PTS for WPM signals.

The paper is organized as follows: In Section II, the System model is described. In Section III, the wavelet packet modulation (WPM) and PAPR reduction of the WPC signals are described. In Section IV Classic PTS and PSO-PTS are introduced. In Section V, the simulation results are presented. In Section VI, conclusions are given.

2. Preliminaries

Figure 1 shows the system model that is used for the simulations. Firstly, we take input bit streams from the users are interleaved to eliminate burst error caused by the communication channel. Interpolate signals are epitomized with BPSK, and then PTS is adapted for PAPR diminution.

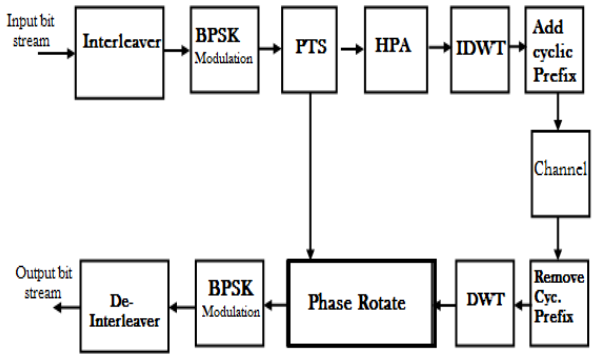

Figure 1: System Model.

The PTS requires side information, which has to be transmitted to get the original WPM signal in the system receiver. The cycle adjunct is then interpolated in the signal, that is intensify by the HPA to terminate the intersymbol interference (ISI) imitative from the communication channel. The cycle prefix is removed from the transmitted signal in the receiver. After the Discrete Fourier Transforms (DWT), phase rotation is applied to get the phase of the original MC-CDMA signal from the side information. Then BPSK demodulation is performed. Finally, each BPSK demodulated symbol is carried to the original place in the bit stream by the deinterleaver [3].

3. Wavelet Packet Modulation

In multi-carrier modulation we use a wavelet packet modulation (WPM) as a new type of intonation having high bandwidth utilization, unique convenience in the proficiency of anti-disturbing and multi-rate transmission. It is considered as a tough contender to Multi-carrier code-division multiple accesses (MC-CDMA).

3.1. Implementation of modulation

The simplified block diagram of the multicarrier communication system using wavelet packet transform is as shown in figure 2.

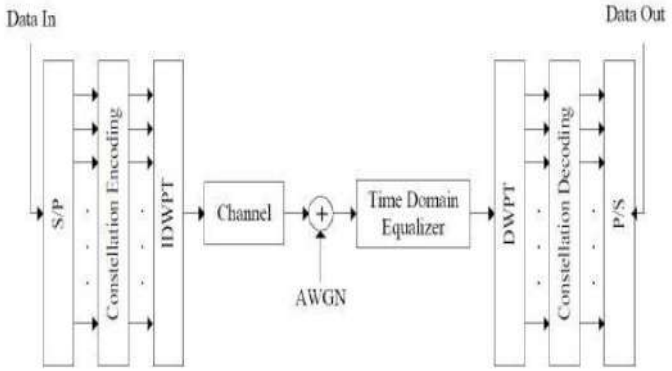

Figure 2: Block Diagram of WPM

The input data stream is divided into parallel lower data substreams by a serial to parallel (S/P) converter i.e. the data symbols design a block of N subcarriers that are first converted from serial to parallel to decrease symbol rate by a factor of N that is equal to the no. of sub-carriers. The signal transmitted on the channel is in the discrete domain, x[n], and is composed of successive modulated symbols, and each of this is constructed as the sum of M waveforms m[n] individually amplitude modulated with the constellation encoded symbol. So it can be expressed in the discrete domain as:

$$x[n] = \sum_{S} \sum_{m=0}^{M-1} a_{s,m} \varphi[n - sM]$$

Where $a_{s,m}$ is a intent encoded s^{th} data symbol regulate m^{th} the waveform T is denoting the sampling period, φm[k] is non-null only in the interval [0, LT − 1] for any m{0..M − 1}.

In an AWGN channel, the waveforms φm[k] should be cooperatively orthogonal to accomplish the lowest probability of defective symbol accommodation i.e. = δ[m − n] where represents a convolution operation and δ[j] = 1 if j = 0, and 0 otherwise. In MC-CDMA, the discrete functions φm[k] are the well-known M complex basis functions w[t]exp (j2π (m/M)kT) limited in the time domain by w[t] which is window function. These basis functions are sine-shaped waveforms that are equally spaced in the frequency domain, each having a bandwidth of 2π/M and are grouped in pairs of identical centric frequency and sometimes modulated by a complicated BPSK encoded symbol. In WPM, the subcarrier waveforms are attaining by applying the WPT. As in MC-CDMA, the inverse transform is apply to build the transmitted

symbol although the leading transform acquiesce recapture the data symbol transmitted. Since wavelet theory has part of its origin in filter bank theory, the processing of a signal into wavelet packet coefficients through WPT is usually referred as dissolution while the reverse operation is termed as fusion or reformation (i.e. from wavelet packet coefficients). The essential trait of the WPT is that the waveforms are elongated than the transform length. Consequently, WPM inhere a group of overlay transforms. As they overlay in time domain the starting of a later symbol is transmitted before the previous one(s) ends. The inter-symbol orthogonality is maintained as the waveforms are M-shifted orthogonally despite the overlap of consecutive symbols. Increased frequency domain localization can be made use provided by longer waveforms while the loss in system capacity is avoided that normally results from time domain spreading.

3.2. Peak average power ratio (PAPR) reduction of WPM

The PAPR of the base band transmitted signal x(t) is defined as the ratio of maximum power of the transmitted signal over the average power. The PAPR of MC-CDMA signal in analog domain can be represented as [2]:

$$PAPR = \frac{max_{0 \le t T_s} |X(t)|^2}{E(|X(t)|^2)}$$

Non-aligned distortion in HPA occurs in the analog domain, but the most of the signal processing operation for PAPR reduction occur in the digital domain. The PAPR of discrete time signal is given as [3]:

$$PAPR = \frac{max_n(|x(n)|^2)}{E(|x(n)|^2)}$$

Where, E (.) denotes ensemble average calculated over the duration of WPDM symbols. The Complementary Cumulative Distribution Function (CCDF) of the PAPR is one of the most frequently used performance measures for PAPR reduction techniques. The CCDF of the PAPR denotes the probability that the PAPR of data block exceeds a given certain value, and is expressed as follows [1]:

$$CCDF\ (PAPR0) = \Pr\{PAPR > PAPR0\}$$

From the central limit theorem it follows that for a large value of subcarriers N, the real and imaginary component of the multicarrier signal are modeled as a zero mean Gaussian distribution random variable with varianceσ^2. The amplitude of the MC-CDMA signal therefore has a Rayleigh distribution and its power distribution becomes a central chi-square

distribution with two degrees of freedom and zero mean [3]. The CCDF of the PAPR can be calculated as:

$$\Pr(PAPR \leq PAPR0) = 1 - (1 - e^{-PAPR0})^N$$

The distribution obtained by the conventional analysis, however, does not fit those of the PAPR of the MC-CDMA signals obtained by computer simulations, even for very large N. In [5], Van Nee and Prasad gave an empirical approximation:

$$CCDF(PAPR0) = 1 - (1 - e^{-PAPR0})^{\alpha N}$$

4. Classic PTS and PSO-PTS

PSO is called a population-based search algorithm that influenced by the performance of organic commonality that displayed both individual and social behavior; vis a vis of these communities are schools of fishes, flocks of birds, and swarms of bees. Members of such community chunk familiar ambition (e.g., finding food) that are realized by exploring its environment while interacting among them.

4.1. A basic PSO Algorithm

for every particle i = 1,2 ..., S **do**

Initialize the particle's position with a uniformly distributed random vector: $\mathbf{x}_i \sim U(\mathbf{b}_{lo}, \mathbf{b}_{up})$

Initialize the particle's best known position to its initial position: $\mathbf{p}_i \leftarrow \mathbf{x}_i$

if $f(\mathbf{p}_i) < f(\mathbf{g})$ **then**

update the swarm's most appropriate position: $\mathbf{g} \leftarrow \mathbf{p}_i$

Initialize the particle's velocity: $\mathbf{v}_i \sim U(-|\mathbf{b}_{up}-\mathbf{b}_{lo}|, |\mathbf{b}_{up}-\mathbf{b}_{lo}|)$

while a termination criterion is not met **do**:

for each particle i = 1, ..., S **do**

for each dimension d = 1, ..., n

do Pick random numbers: $r_p, r_g \sim U(0,1)$

Update the particle's velocity: $\mathbf{v}_{i,d} \leftarrow \omega\, \mathbf{v}_{i,d} + \varphi_p\, r_p\, (\mathbf{p}_{i,d}-\mathbf{x}_{i,d}) + \varphi_g\, r_g\, (\mathbf{g}_d-\mathbf{x}_{i,d})$

Update the particle's position: $\mathbf{x}_i \leftarrow \mathbf{x}_i + \mathbf{v}_i$

if $f(\mathbf{x}_i) < f(\mathbf{p}_i)$ **then**

Update the particle's best known position: $\mathbf{p}_i \leftarrow \mathbf{x}_i$

if $f(\mathbf{p}_i) < f(\mathbf{g})$ **then**

Update the swarm's most appropriate position: $\mathbf{g} \leftarrow \mathbf{p}_i$

The values b_{lo} and b_{up} are respectively the lower and upper boundaries of the search-space. The termination criterion can be the number of iterations performed, or a solution where the adequate objective function value is found [10]. The parameters ω, φp, and φg are chosen by the professional and control the behaviour and adequacy of the PSO technique.

4.2. PSO-PTS

PSO as an optimizer is used to solve the phase factor problem, which is shown as PSO process block in Fig 3 below. In PSO algorithm solution space of the problem is called particles, which is φ_k in the PTS based PSO scheme [11]. By moving the particles around in the search-space, the optimal solution of the phase problem will be reached. During the movement of the particles, each particle is characterized by two parameters: position and velocity [12]. The PSO algorithm evaluates particles with fitness value, which is PAPR the objective function. A solution space is randomly generated, which is a matrix of size S×K where S is the number of particles and K is the number of disjoint sub-block [13]. In other words, the solution space is a matrix its rows are $\varphi_1, \varphi_2, \ldots\ldots, \varphi_k$.

Since the PSO is an iterative algorithm, in the i^{th} iteration each particle can be described by its position vector $Y_{SK}^t = y_{S1}^t, y_{S2}^t, \ldots\ldots, y_{SK}^t$ and velocity vector is given as, $V_{SK}^t = v_{S1}^t, v_{S2}^t, \ldots\ldots, v_{SK}^t$ where $S\epsilon[1, S]$ and $Y_{SK}^t \epsilon R$ where R denotes the domain of the objective function. The PSO algorithm searches the solution space for the optimum solution by using iteration process. Each particle updates itself in every iteration by tracking two best positions. These are called the local best position, which is the best solution this particle achieved $p_{sk} = p_{s1}, p_{s2}, p_{s3}, \ldots . p_{sk}$ and the global best position can be given as

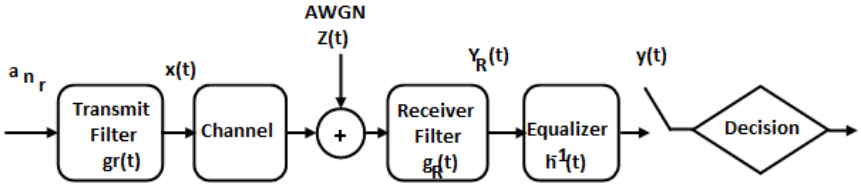

Figure 3: PAPR reduction techniques by using PSO based PTS weighing factor.

$p_{sk}^{g} = p_{s1}^{g}, p_{s2}^{g}, p_{s3}^{g}, \ldots\ldots, p_{sk}^{g}$ which the best position is obtained so far by any particle in the whole swarm. The updating process of the position and velocity of each particle can be expressed as

$$V_{SK}^{t+1} = wV_{SK}^{t} + C_1 r_1 (p_{sk}^{t} - Y_{SK}^{t}) + c_1 r_1 ((p_{sk}^{t})^{g} - Y_{SK}^{t})$$

$$Y_{SK}^{t+1} = Y_{SK}^{t} + V_{SK}^{t}$$

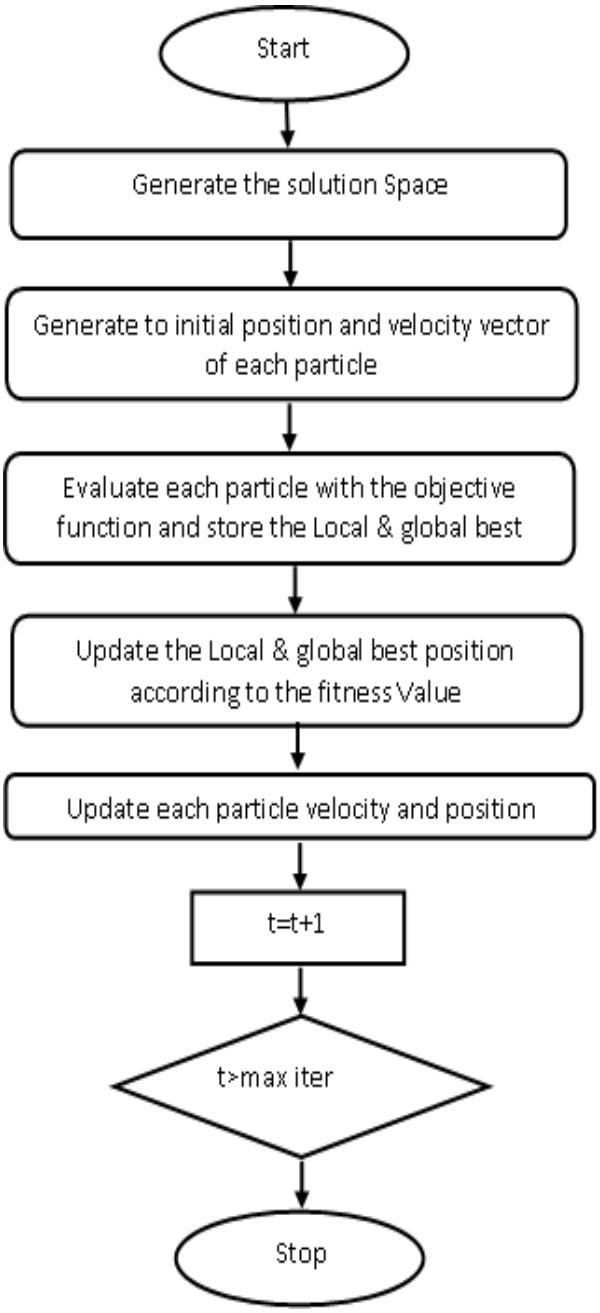

Figure 4: PSO-PTS Algorithm

Where, c_1 and c_2 are the acceleration terms [14]. The constant r_1 and r_2 are uniform distribution random numbers in the range of [0, 1]; w is the inertia factor.

5. Results

In the simulations, WPM system has N=256 subcarriers and BPSK modulation was used. HPA is used with p= 0.5, 2 and IBO= 0,3,6 dB. Oversampling factor of the transmitted signal is L=4. In the simulations, the signal is transmitted over AWGN channel. The number of the phase factor is selected as W=2. WPM signals are randomly partitioned into V= 16 subblocks.

In fig 5 shows CCDF vs PAPR using PSO-PTS for 8 user.

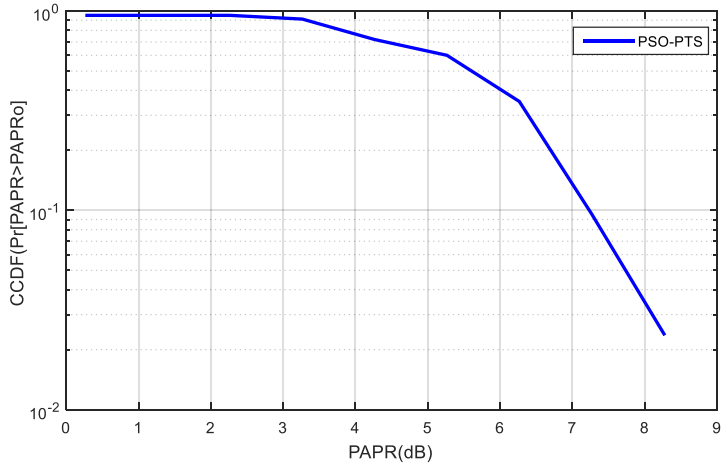

Figure 5: CCDF vs PAPR using PSO-PTS

In fig 6 shows BER vs SNR using PSO-PTS for 8 users.

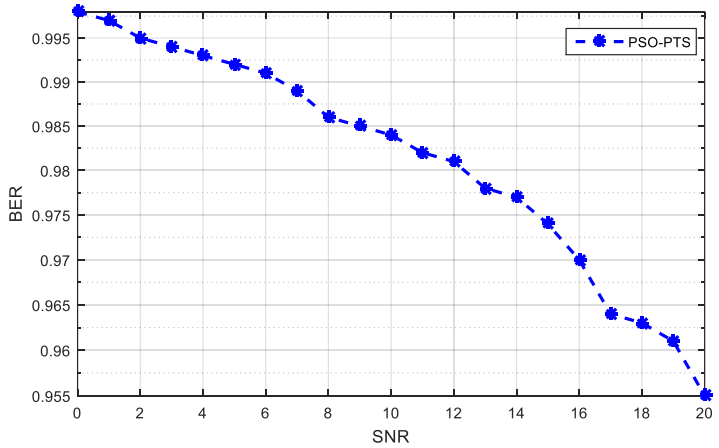

Figure 6: BER vs SNR using PSO-PTS.

In fig 7 shows CCDF vs PAPR using PSO-PTS and PTS.

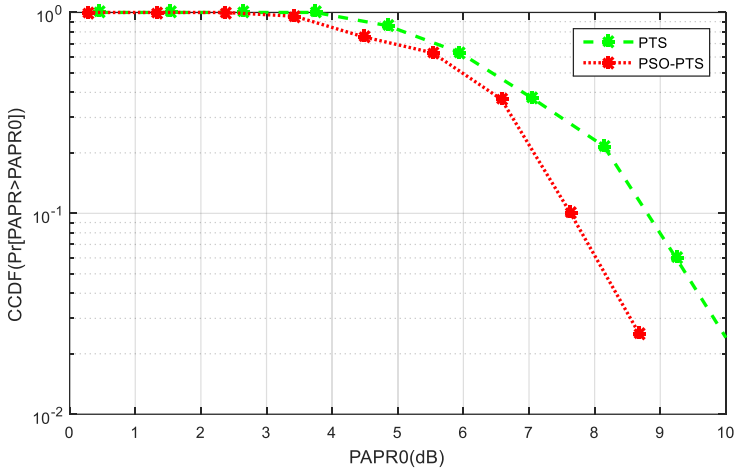

Figure 7: Performance comparison of PAPR vs CCDF.

In fig 8 representation the performance of BER vs SNR using PSO-PTS and PTS.

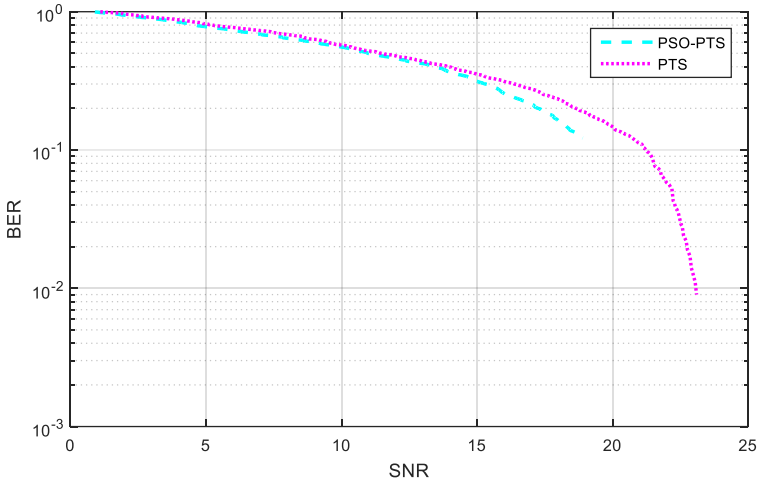

Figure 8: Performance comparison of SNR vs BER

6. Conclusion

The achievement of results, WPM starts us to wind up that this new modulation scheme is a feasible substitute to MC-CDMA to be considered for today's communication systems. WPM is kind of more perceptive than MC-CDMA to commonly find types of distortion due to non-ideal elements of the system. The main concern of WPM nevertheless resides in its skill to fulfill the wide range of fulfillment of tomorrow's ubiquitous wireless communications. PAPR reduction using particle swarm optimization (PSO) algorithm for PTS is proposed for wavelet packet modulation. In the result section we calculate CCDF vs PAPR using PSO-PTS and BER

vs SNR using PSO-PTS. Performance comparison also show in result section using PSO-PTS, PTS by plotting graph in single figure.

References

Berna Torun, M.K.Lakshmanan and H. Nikookar . (2010 September) ." Peak-to-Average Power Ratio Reduction of Wavelet Packet Modulation by Adaptive Phase Selection", *IEEE 21st Int*. Symposium on Personal, Indoor and Mobile Radio Communications.

D. Karaboga, (2005) .“An idea based on honey bee swarm for numerical optimization,” *Technical report-TR 06*, Erciyes University, Engineering Faculty, Computer Engineering Department.

A. R. Lindsey and J. C. Dill . (1995). “Wavelet packet modulation:A generalized method for orthogonally multiplexed communications,” in Proc.of the 27th Southeastern Symp. on System Theory, pp. 392-396.

A. Jamin and P. Mahonen. (2005 Mar). “Wavelet Packet Modulation for Wireless Communications,” *Wireless Communications and Mobile Computing Journal*, Vol. 5, No. 2, PP. 123-137.

M. Baro and J. Ilow, (2007 September) “Improved PAPR Reduction for Wavelet Packet Modulation using Multi-pass Tree Pruning,” *Proc. IEEE 18th Int. Symposium on Personal, Indoor and Mobile Radio Communications.*

Haixia Zhang, Dongfeng Yuan, Matthias Patzold, (2007), "Novel Study on PAPR Reduction in Wavelet Based Multicarrier Modulation System,*" Digital Signal Processing 17 PP. 272-279*.

N. T. Le, S. D. Muruganathan, and A. B. Sesay. (2008 September). “Peak-to-Average Power Ratio Reduction for Wavelet Packet Modulation Schemes via Basis Function Design,” *Proc. IEEE Vehicular Technology Conference*.

M. Rostamzadeh, V.T. Vakily , and M. Moshfegh.(2008). "PAPR Reduction in WPDM and OFDM System Using an Adaptive Threshold Companding Schems," *IEEE International Multi-Conference on System, Signals and Devices*.

Berna Torun, M. K. Lakshmanan and H. Nikookar, (2010 September)." Peak-to-Average Power Ratio Reduction of Wavelet Packet Modulation by Adaptive Phase Selection", *IEEE 21st Int. Symposium on Personal, Indoor and Mobile Radio Communications*.

Clerc, M. (2012), "Standard Particle Swarm Optimisation". HAL open access archive.

H. Bolcskei, D. Gesbert, and A. J. Paulraj. (2002 Feb). “On the capacity of OFDM-based spatial multiplexing systems, ”*IEEE Trans. Communi*., vol. 50, no. 2, pp. 225-234.

G. L. Stüber, J.R. Barry, S W Mclaughlin, Y.E Li, and M. Ann Ingram. (2004 Feb) “Broadband MIMO-OFDM Wireless Communications,” *IEEE Communications Magazine*, vol. 92, no. 2, pp. 271–294.

N. T. Hieu, S. W. Kim and H. G. Ryu .(2005Aug). “PAPR Reduction of the low complexity phase weighting method in OFDM Communication system,” *IEEE Transactions on Consumer Electronic*s, vol. 51,no. 3, pp. 776– 782, DOI: 10.1109/TCE.2005.1510483.

P. Mukunthan and P. Dananjayan. (2011 July). Modified PTS with FECs for PAPR reduction in MIMO-OFDM system with different sub blocks and subcarriers, *International Journal of Computer Science Issues*, vol. 8, Issue 4, no.2.

Failure Situations in The Off-Grid Photovoltaic Solar Panel Systems

Kenan YANMAZ

Giresun Univ., Vocational School of Technical Sciences, Giresun, Turkey; kenan.yanmaz@giresun.edu.tr

Corresponding Author: kenan.yanmaz@giresun.edu.tr

Abstract

The problems such as streak of lightning, short circuit failure and overload conditions are important for all electrical systems. In energy systems, the determination and prevention of failures and the selection of protective circuit elements are important. In this study, it was aimed to determine which elements in the systems damaged and how problems arise in case of a breakdown in the off-grid photovoltaic solar panel system where small strong loads were fed. We aimed to determine the correct protection policies according to the results obtained. The system model consisting of solar panels, batteries, inverter, filter and loads has been done with the simulations in Matlab/Simulink program, and the behavior of the system has been examined in detail by creating different failures. For the protection of the system, the necessary system design has been performed by determining the operations that could be done and the criteria of protection elements.

Keywords: Photovoltaic solar panel, Short circuit, Fault, Lightning.

1. Introduction

Solar energy is now widely used in many areas. For loads away from the grid, energy can be generated by means of systems that generate electricity from the sun (Labouret and Villoz, 2010). With these systems being cheap, their prevalence is increasing (Mengi and Altas, 2015). As these systems are becoming more widespread and the usage areas are expanding, the problems are increasing rapidly. In particular, faults due to ambient conditions affect the systems in different ways. The location, duration, type of the fault in the system and the condition of the consumers cause different types of faults. These fault situations cause problems in power electronics based devices such as rectifier, chopper, inverter, maximum power point monitor and battery charge regulator used in Photovoltaic Solar Energy Systems (PVSES) and their controllers (Krauter, 2006). This risks the safety of life and property of users (Enrique et al., 2013).

Temperature changes, humidity, seasonal effects, external living things, rain, hail, snow, floods and lightning effects, especially in the lightning strike situation has a significant effect on the systems. Lightning, which is a state of sudden load discharge, causes the systems to be exposed to an overcurrent and voltage in a short time and significant faults and fires may occur (Kasar and Tapre, 2018).

In studies on the subject in literature, papers that examine short circuit conditions for PV solar panels are frequently seen. These studies examine the electrical phenomena and results that occur when a direct solar cell is short-circuited (Mukherjee et al., 2014).

In another work done in real time in FGES designed as part of smart network, inverter current and voltage values are examined both phase to phase and phase to neutral in different fault situations and detailed in graphics (Katiraei et al., 2015).

In another study, fault types analysis was performed on an inverter with Voltage Space Vector based control algorithm. In this real-time study, the space Vector PWM algorithm works very well and the inverter performs remarkably (Zhang et al., 2017).

In a study conducted with a grid connected inverter, it was stated that the total harmonic distortion was low in the proposed system while system currents and voltage variations were examined in different fault situations (Yaai et al., 2013).

In this study, system behavior is investigated in case of failure of the loads fed by the off-grid photovoltaic solar panel system. After the failure of the system, the efficiency of the

Factional PI (FPI) controller, which is designed to keep the voltage of the loads at the desired level, is discussed with the efficient control system of the inverter. The results of the simulation study in MATLAB / Simulink environment and the effectiveness of the controller were examined in detail.

2. Material and Method

The simulated system consists of solar panels, inverters, controllers and loads. The main structure of the system is shown in Figure 1.

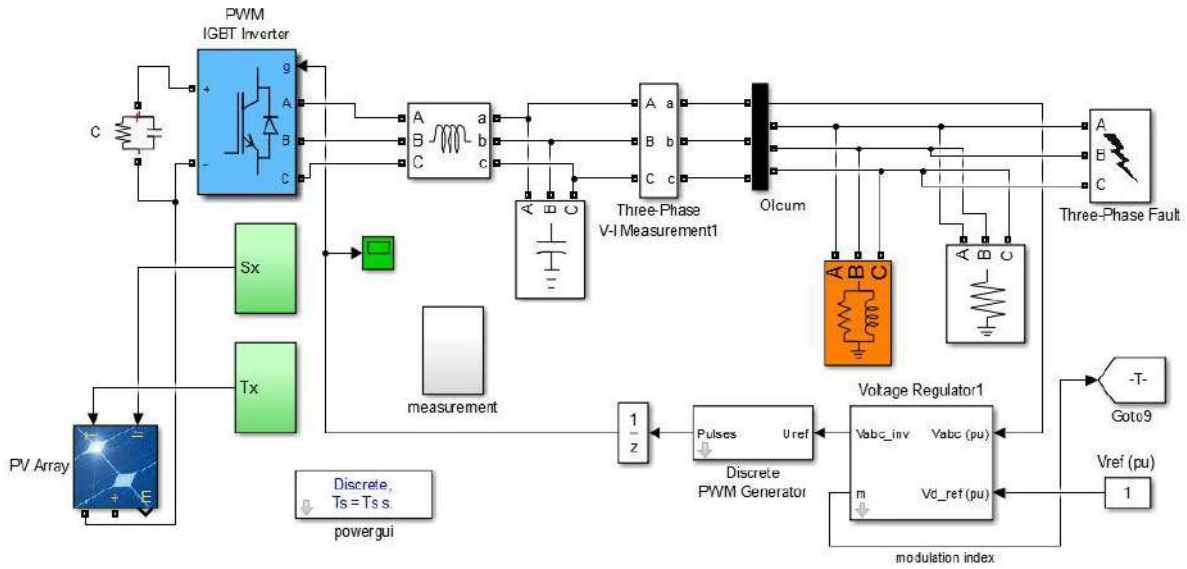

Figure 1. Main schema of the system

2.1. Photovoltaic Solar Panels

Solar cells are semiconductor materials that convert sunlight into electricity. PV solar cells are usually modeled by a current source, a diode connected in reverse parallel to it, and a resistor. Equivalent circuit model of a PV solar cell is shown in Figure 2 (Mengi, 2018).

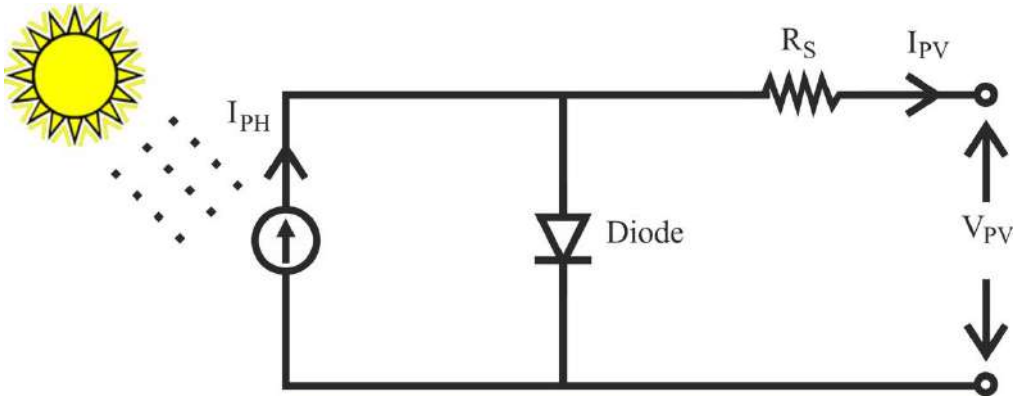

Figure 2. Equivalent circuit model of a PV solar cell.

The output voltage of the PV cell is as in Equation 1.

$$V_{PV} = \frac{N}{\lambda} ln\left(\frac{I_{SC}-I_{PV}+MI_0}{MI_0}\right) - \frac{N}{M} R_S I_{PV} \quad (1)$$

Here, M is parallel strings, λ is constant coefficient and depends upon the cell material, N is series cells per string, V_{PV} is cell output voltage (V), I_{PH} is photocurrent function of irradiation level and junction of temperature (A), I_{PV} is cell output current (A), I_{SC} is cell short circuit current (A), I_0 is reverse saturation current (A) and R_S is series resistance of cell (Ω).

2.2. Fractional PID Controller (PI$^{\lambda}$D$^{\mu}$)

For the first time, the fractional PID controller, which consists of a combination of PID control theory and fractional analysis, has been proposed by Podlubny. Podlubny has proved that it provides better results than classical PID by analyzing the dynamic response of the fractional control system (Podlubny, 1999).

PI$^{\lambda}$D$^{\mu}$ controllers are precisely tuned types of PID controllers. They work better than PID controllers. The best knowns are the descriptions of M. Caputo, Grunwald-Letkinov and Reimann-Liouville. PI$^{\lambda}$D$^{\mu}$ controller general block diagram is shown in Figure 3.

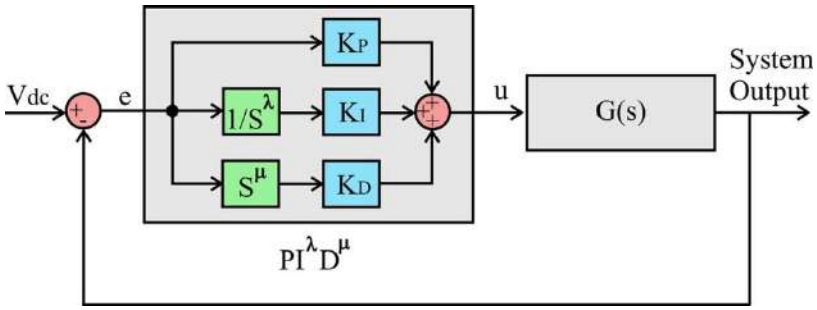

Figure 3. General block diagram of $PI^{\lambda}D^{\mu}$ controller.

System output, *C(s)*, is as seen in Equation 2.

$$c(s) = \frac{U(s)}{E(s)} = K_P + \frac{K_I}{s^{\lambda}} + K_D s^{\mu} \quad (2)$$

Here λ and $\mu \geq 0$. λ is the order of integration and μ is the order of differentiator. KP, KI and KD are the PID controller gains. U(s) and E(s) are the control and error signals, respectively. In this study, $PI^{\lambda}D^{\mu}$ controller software was performed by FOMCON Toolbox (Tepljakov et al., 2011).

3. Results and Discussion

The simulated system has a source consisting of 1200 units of 213W solar panel. Its installed capacity is 255kW. The system consists of solar panels, inverters, filters, loads, $PI^{\lambda}D^{\mu}$ controllers and measurement elements. The load consists of a 20kW / 10kVA RL load and a 10kW resistive load. Ambient conditions, temperature (T_x) and solar light (S_x) changes are shown in Figure 4. These situations affect the power of the solar panels and provide a realistic simulation.

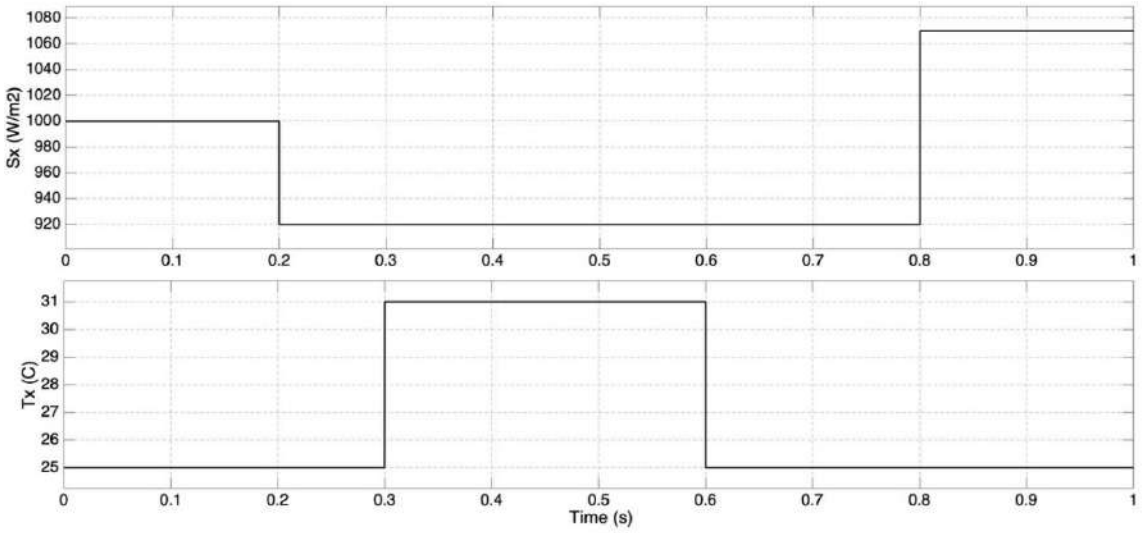

Figure 4. Sx and Tx changes

Figure 5 shows the change of current, voltage and power obtained from solar panels according to time. In this study, the sampling time is Ts = 1e-6s, and it is assumed that a short-circuit fault occurs on the load side in the range of T = 0.1 s and 0.12 s. In the meantime, there is a sudden increase in the current while the voltage decreases in the solar panels. There is a surge in power.

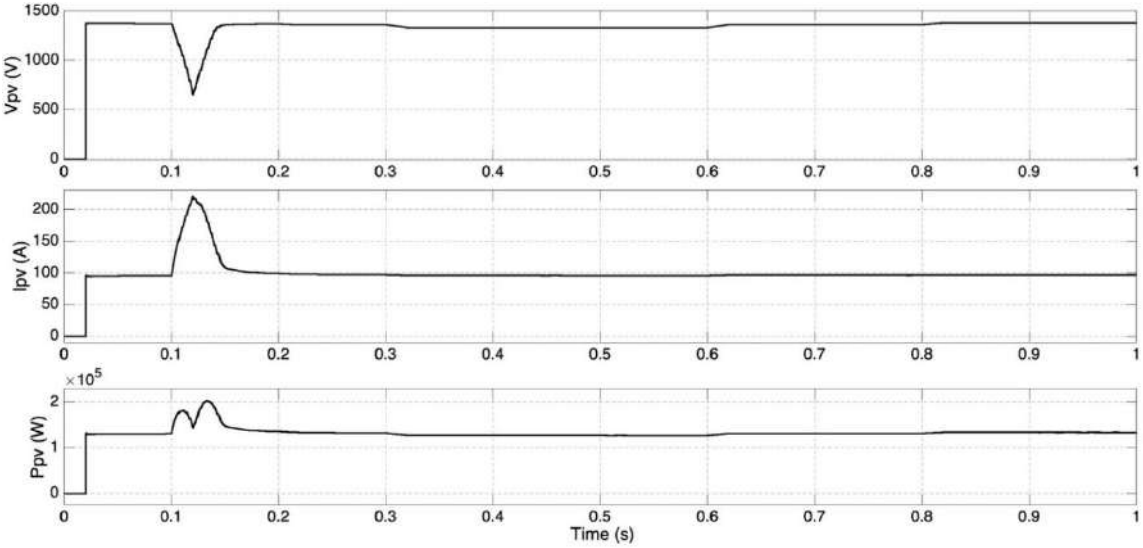

Figure 5. Current, voltage and power changes of solar panels.

Figure 6 shows the phase-to-phase and phase-to-neutral voltages on the load and the changes in the phase current on the load. As seen from these graphs, as a result of the effective operation of $PI^{\lambda}D^{\mu}$ controllers, the inverter is recovered after a malfunction in the system. The

controller controls the system correctly to ensure that the 380V / 50Hz phase-to-phase voltage on the loads. The voltage is in a clean sine wave form.

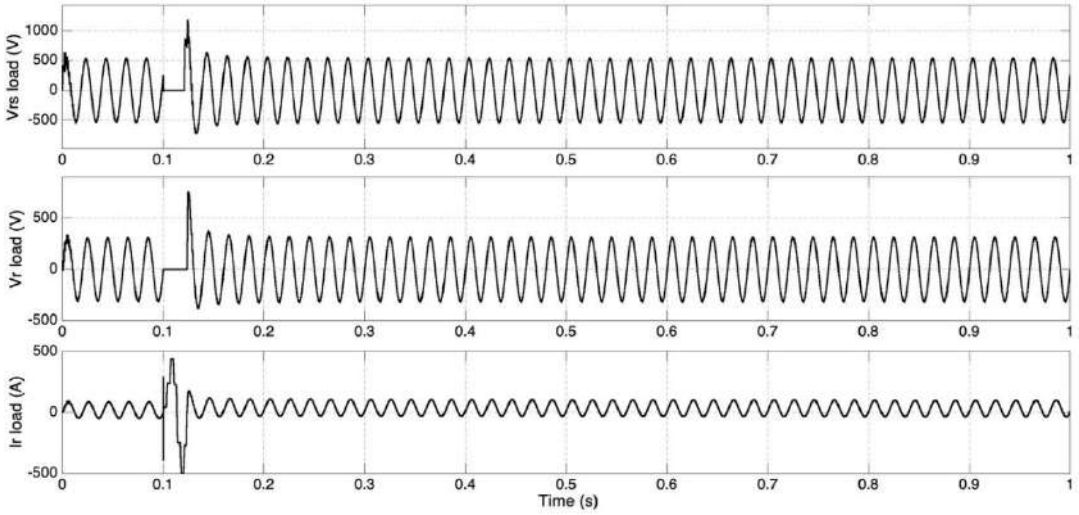

Figure 6. Phase-to-phase, phase-to-neutral voltages and phase current on the load

Figure 7 shows the phase-phase voltage waveform on the load. During the fault, a sudden increase occurs in the load voltage, followed by a sudden drop. This situation is quite short and at the same time, as a result of the efficient operation of the controller, the rapidly recovered system voltage is set to 380V.

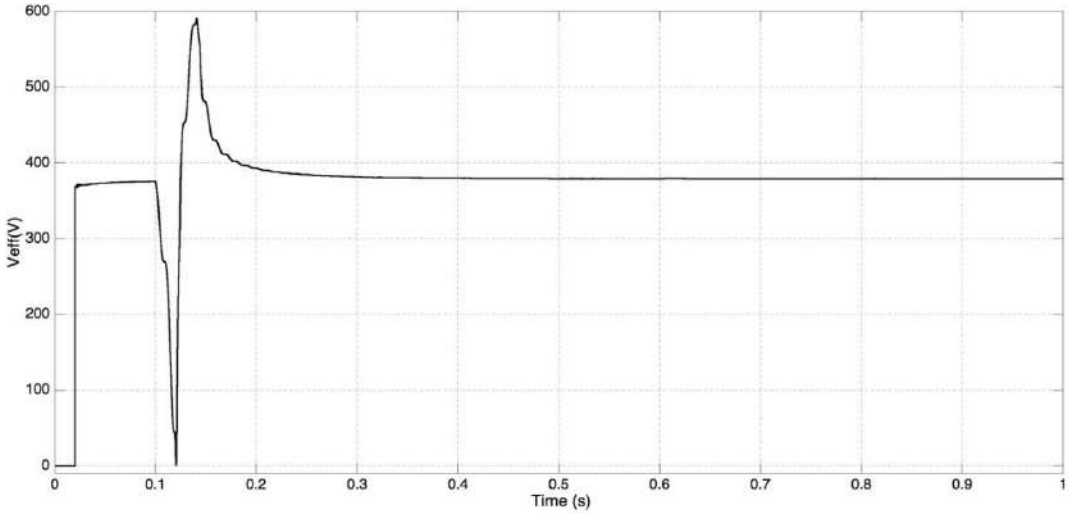

Figure 7. Phase-phase voltage waveform on the load.

In this study, the system is forced by a sudden change in the load side. As a result of the efficient operation of the controllers in the inverter, this situation is overcome and the required clean voltage is maintained.

References

Enrique, E. H., Zavanelli, W. A., and Ashtiani, S., (2014). Arc Flash Safety Concerns for Solar Panels. 2014 IEEE/IAS 50th Industrial & Commercial Power Systems Technical Conference, Fort Worth, TX, USA.

Kasar, K., and Tapre, P. C., (2018). A New Fast Detection Module for Short-circuit Current Detection in PV Grid system. Proceedings of the Second International Conference on Inventive Systems and Control (ICISC 2018), (pp. 468-472), Coimbatore, India.

Katiraei, F., Sun, C., and Enayati, B., (2015). No Inverter Left Behind: Protection, Controls, and Testing for High Penetrations of PV Inverters on Distribution Systems. IEEE Power and Energy Magazine, 13(2), 43-49.

Krauter, S. C. W., (2006). Solar Electric Power Generation – Photovoltaic Energy Systems. India: Springer.

Labouret, A., and Villoz, M., (2010). Solar Photovoltaic Energy. France: IET.

Mengi, O. O., and Altas, I. H, (2015). A New Energy Management Technique for PV Wind Grid Renewable Energy System. International Journal of Photoenergy, 2015, 1-21.

Mengi, O. O., (2018). A Five-Level H-Bridge STATCOM for Off-Grid PV Solar Farm Under Two Controllers PI and PI^{λ}-MPC Hybrid. International Journal of Photoenergy, 2018, 1-15.

Mukherjee, E., Sengupta, S., and Duttagupta, S. P., (2014). A heuristic approach of estimation of short-circuit current of a photovoltaic cell by Kalman filter. IEEE Global Humanitarian Technology Conference - South Asia Satellite (GHTC-SAS), Trivandrum.

Podlubny, I., (1999). Fractional-Order Systems and $PI^{\lambda}D^{\mu}$ – Controllers. IEEE Transactions on Automatic Control, 44(1), 208-214.

Tepljakov, A., Petlenkov, E., and Belikov, J. (2011). FOMCON: Fractional-order Modeling and Control Toolbox for MATLAB, 18th International Mixed Design of Integrated Circuits and Systems (MIXDES) Conference (pp. 684-689), Poland.

Yaai, C., Jingdong, L., Jinghua, Z., and Jin, S. (2013). Research on the Control Strategy of PV Grid-connected Inverter upon Grid Fault. International Conference on Electrical Machines and Systems, (pp. 2163-2167), Korea.

Zhang, X., Wang, F., Ji, W., Qiao, S., and Cao, Y., (2017). Fault Tolerant Control Method for Three-Level Photovoltaic Inverter Based on Redundant Voltage Space Vector. Proceedings of the 36th Chinese Control Conference, (pp. 9249-9253), China

MECHANICAL, INDUSTRIAL ENGINEERING AND MATERIAL SCIENCE

ORAL PRESENTATIONS

Flow Characteristics of Swirling Coaxial Impinging Air Jets: An Experimental Investigation

Burak MARKAL*

Recep Tayyip Erdogan University, Faculty of Engineering, Department of Energy Systems Engineering, Rize, Turkey

*Corresponding author: burak.markal@erdogan.edu.tr

Abstract
The present study experimentally investigates the fluid flow characteristics of a swirling coaxial impinging (swirling and round) air jet issuing from a nozzle having an inner circular flow passage and three outer swirling flow passages. Experiments have been conducted at different dimensionless nozzle-to-plate distances (H^* = 0.2, 0.4 and 0.6), and dimensionless flowrate ratios (Q^* = 0.1, 0.3 and 0.6) at a constant total flowrate of 1.66 x 10^{-3} m^3 s^{-1} (100 L/min). The distribution of the pressure coefficient (C_P) is obtained against the dimensionless radial distance (R^*) for each test condition. The results show that the flowrate ratio is a very important parameter influences the pressure distribution on the impingement plate. The magnitude of the pressure value at the stagnation point decreases with increasing flowrate ratio, and for Q^* = 0.6, the maximum value of the local wall pressure occurs at nearly R^* = 0.2. On the other hand, in the stagnation region, the magnitude of the local pressure values decreases with increasing nozzle-to-plate distance. For Q^* = 0.6, a significant subatmospheric region is obtained.

Keywords: pressure coefficient, swirling, coaxial, impinging jet.

1. Introduction

Impinging jet is one of the most effective heat transfer enhancement methods. Therefore, this technique is used effectively for heating and cooling applications such as drying of paper and textile, tempering of glass (Eiamsa-ard et al., 2015), cooling of electronic components and turbine blades (Yang et al., 2010), quenching of heated surfaces at nuclear reactors (Ahmed et al., 2017), etc. In a simple round impinging jet, there are basically three different flow regions (Eiamsa-ard et al., 2015) as a free jet region, an impingement region and a wall jet region. These flow regions are strongly depended on lots of geometrical and thermo-physical properties/conditions. In this regard; nozzle geometry, type and surface characteristics of the impingement plate, fluid type (liquid or gas), system configuration (impinging jet or free jet, confined or unconfined jet) are the main factors influence the flow structure. Therefore, in the jet literature, there are lots of studies having different purposes and characteristics.

Most of the studies are related to the impinging simple round/circular jets. In this context, Kim and Giovannini (2007) experimentally investigated a turbulent round air jet impinging on a square cylinder mounted on a flat plate. They experienced three-dimensional recirculation flow and stated that there was a good coherence between flow field and heat transfer distribution. Astarita and Cardone (2008) performed flow visualizations and heat transfer measurements for an impinging round jet on a rotating disk. They underlined the strong interaction between the turbulent jet and the laminar boundary layer over the disk. Duda et al. (2008) investigated the characteristics of a round jet issuing from a straight tube. They measured the velocity and turbulence intensity at the jet exit and employed smoke-wire visualization technique. They stated that when the jet exit-to-surface spacing increased from two to five, obvious effects could be seen, which were listed as stabilization of the flow, extension of the potential core and a reduction in vortex formation before impingement. Yakkatelli et al. (2010) focused on a single round jet through smoke-wire visualization technique. They used foamed aluminum heat sink as the impingement body. They concluded that increasing Reynolds number from a laminer to a turbulent jet lead the flow to penetrate the porous media more evenly and decreased the recirculation region at the exit of the foam. Tummers et al. (2011) performed detailed measurements with regards to the turbulent flow in the stagnation region of a single impinging jet and studied instantaneous flow reversals in the near wall region. They observed the flow reversals in a layer with approximately 0.2 mm thickness above the impingement plate and, stated that the relevant flow reversals were related to the small secondary vortices. Kalifa et al. (2016) experimentally investigated the flow and heat transfer characteristics of a round air jet through Particle Image Velocimetry (PIV) and Laser Doppler Velocimetry (LDV) techniques. They stated that the separation point approached to the jet axis with increasing nozzle-to-plate distance, and also concluded that the potential core length depended on nozzle-to-plate distance.

Some of the studies investigated flow characteristics of conventional impinging circular jets are summarized above. However, in classical circular or slot impinging jet flow, pressure distribution on the impingement surface has a maximum at the stagnation point (center of the plate) and then it suddenly decreases, as it is seen in Öztekin et al. (2012). In addition to pressure drop, similarly, Nusselt number shows the same behavior (Eiamsa-ard et al., 2015). However, this kind of flow or heat transfer behavior is not desired especially for some industrial applications such as

chemical vapour deposition and electronics cooling in which the uniformity of heat transfer is important in addition to intensity of it (Huang and El-Genk, 1998). To improve the radial uniformity on the impingement surface, the usage of swirling impinging jet has been proposed in the literature (Huang and El-Genk, 1998; Eiamsa-ard et al., 2015). The contribution of the swirl motion can provide a better advantage when the swirling flow is used in the coaxial jet configuration. However, after a literature survey, it is seen that the studies related to the swirling coaxial jet flow focus on free jet configurations and their relevant/possible applications such as flame stabilization, burners (design), mixing of fuel and oxidant, etc. A summary of these kinds of studies are given below.

Ribeiro and Whitelaw (1980) focused on the velocity characteristics in turbulent coaxial jets with and without swirl. They stated that coaxial jets without swirl reached the self-similar state earlier. Mahmud et al. (1987) experimentally and theoretically investigated the aerodynamics of free swirling coaxial jets ejected from a coal burner. They claimed that the flow pattern was significantly affected by the degree of swirl in primary and secondary jet regions. Lee et al. (2010) performed a study with regards to the shear perturbation in coaxial swirling jets. They underlined the importance of spreading rate of the shear layers at the jet exit. Adzlan and Gotoda (2012) experimentally explored the characteristics of vortex breakdown in the swirling coaxial jet with a density difference. They concluded that increasing centrifugal force in the jet with the vortex breakdown prevented the disappearance of the stagnation point at high values of the outer jet Reynolds number. Balakrishnan and Srinivasan (2017) paid attention to the reduction of the jet noise through the curved-vane type coaxial swirlers. They stated that the quantity of the shock cell and their spacing could be reduced via the swirling jets.

In the literature, there is only one study performed by Markal (2018) in which the heat transfer characteristics and the wall pressure distribution on the impingement plate in the case of swirling coaxial confined impinging turbulent air jets are investigated. The flow structure of the swirling coaxial jets are quite complex, and thus, new studies should be performed under different experimental conditions. Also, it should be noted that flow characteristics affect heat transfer on the impingement surface (Eiamsa-ard et al., 2015), and as stated by Baydar (1999), there is a linkage between the pressure distribution on the impingement plate and heat transfer coefficients. Therefore, the aim of the present study is to investigate experimentally the flow characteristics of

a swirling coaxial impinging air jet. In this regard, the distribution of the pressure coefficient on the impingement surface is obtained against the dimensionless radial distance for different dimensionless nozzle-to-plate distances and dimensionless flowrate ratios at a constant total flowrate.

2. Material and Method

The schematic representation of the experimental setup and the photograph of the test section are given in Fig. 1 and Fig. 2, respectively. The setup involves basically a screw compressor, an air tank, a filter and a dryer unit, pressure regulators, valves, rotameters and a test section. Air flow is provided via the compressor, and after an air tank, the flow passes through a filter and drier unit. Before the test section, there are two separate flowlines. One is connected to the inner circular passage of the nozzle and the other one is related to the outer swirling passages of the nozzle of which the photograph is seen in Fig. 3a. In each flow line, there are a precision pressure regulator (FESTO LRP-1/4-10 / 159502), a sensitive adjusting valve and a rotameter (Cole-Parmer GY-32461-60). By using these devices, the flowrate in each flow passage (inner circular and outer swirls) can be adjusted to the desired value, and thus, the parameter of flowrate ratio is used. As it is seen in Fig. 3a, the nozzle has an inner circular flow passage and three outer swirl passages. The nozzle is placed in a Delrin (acetal homopolymer resin) holder (see Fig. 3b). After exiting the outlets of the nozzle, the jet impinges on a circular plate with a diameter of 100 mm. On the impingement surface, pressure taps (0.5 mm diameter) have been generated by drilling the plate through the centerline of it. Firstly, the middle point (center) has been drilled. Then, the second taps on the right and left directions have been formed at 2.5 mm and 5 mm away from the first one, respectively. The other holes are formed 5 mm away from the second taps on each direction. There are twenty holes on the impingement surface; however, the circular plate is supported by bearings, and thus it can be rotated by 360 degrees. When the plate is rotated by 180 degrees, thirty nine readings (with 2.5 mm separations) could be performed due to the asymmetrical distribution of the pressure taps. All the pressure taps are connected to a scanning valve unit has multiple inlets but only one exit. The exit port is linked to a high precision manometer (Modus, MA2-0501). Geometrical details for the test section are given in Table 1.

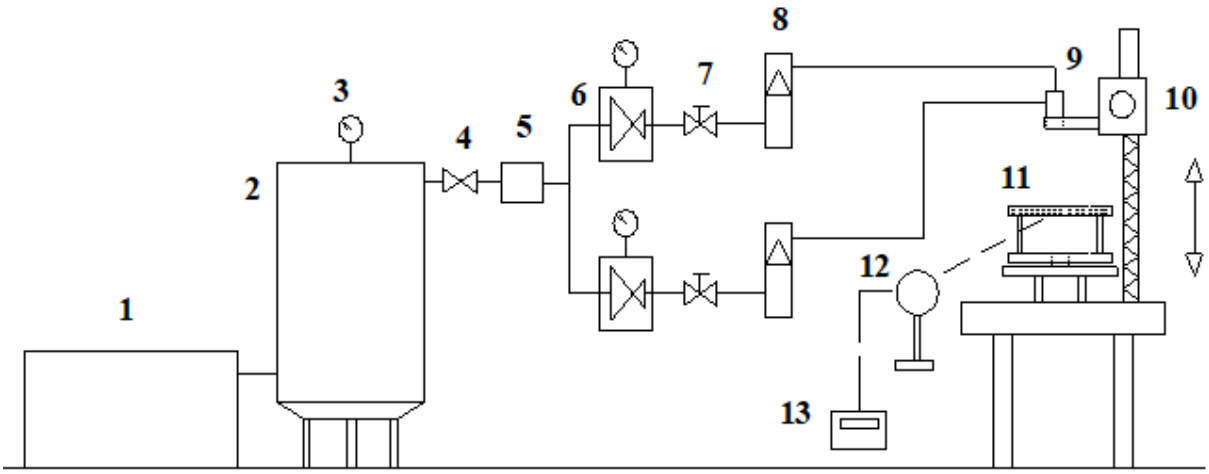

1- Compressor
2- Air tank
3- Manometer
4- Ball valve
5- Air filter and drier
6- Pressure regulator
7- Adjusting valve
8- Rotameter
9- Nozzle
10- Movement mechanism
11- Impingement plate
12- Scanning valve
13- Digital manometer

Figure 1. The schematic representation of the experimental setup

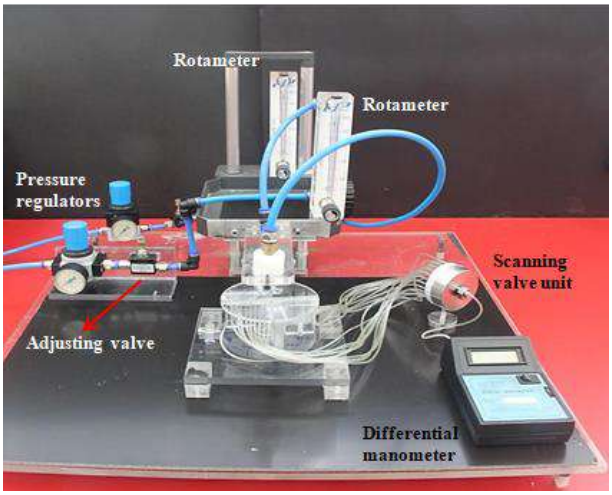

Figure 2. Photograph of the test section

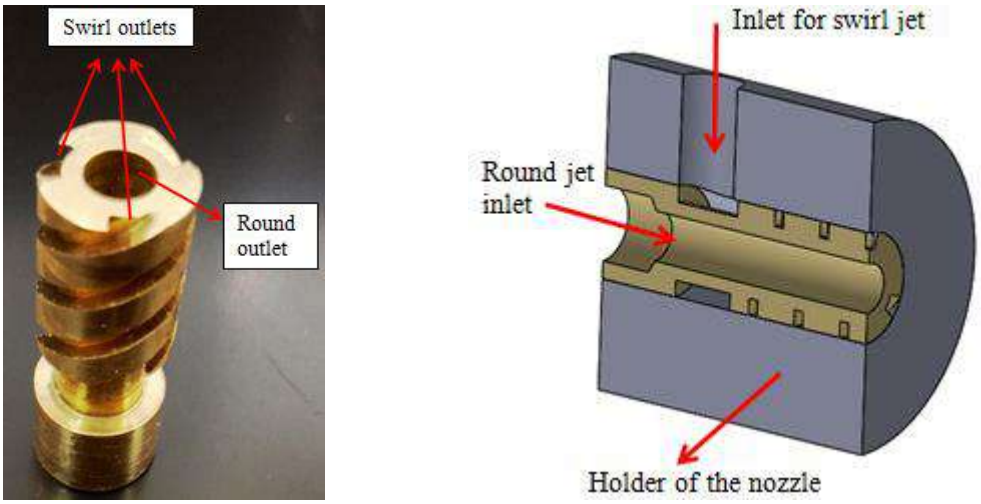

(a) (b)

Figure 3. The photograph (a) and placement of the nozzle (b)

Table 1. Geometrical details for the test section.

Nozzle inner diameter (for round jet exit)	4.5 mm
Impingement plate (surface) radius, r_o	50 mm
Round jet exit area, A_r	15.9 mm^2
Total swirl jet exit area, A_s	9 mm^2
Diameter of the nozzle holder	30 mm

The procedure followed in a test can be summarized as follow: Nozzle-to-plate distance and flowrate (for each line) are adjusted to the desired values. The flow is considered to have reached the steady state condition when the pressure distribution does not chance any further. Then, pressure differences are read by the manometer and, another relevant parameter is changed for the next test condition and the procedure is repeated. An uncertainty analysis has been performed according to the procedure proposed by Kline and McClintock (1953). The maximum uncertainty for the pressure coefficient, C_P, has been found to be less than ± 4.8%. The uncertainties related to the measurements (stems from devices) are obtained from the manufacturers' specification sheets (the codes of the devices are given above).

2.1. Data Reduction

As it is stated in the previous section, the nozzle has two types of outlets: one is round (an inner circular passage) and the other is swirl (three swirling passages). Therefore, the total area and the total flowrate are defined, respectively, as follows:

$$A_{tot} = A_s + A_r \tag{1}$$

$$Q_{tot} = Q_s + Q_r \tag{2}$$

where, A is the area, Q is the flowrate, while the subscripts of *tot*, *s* and *r* represent total, swirl and round, respectively. Reynolds number is defined as follows:

$$Re = \frac{u_m D_c}{v} \tag{3}$$

where, u_m is the mean velocity, D_c is the characteristic length (diameter) and the v is the kinematic viscosity, respectively. The mean velocity is calculated by dividing the total flowrate to the total cross sectional area, while the characteristic length is obtained by taking the square root of the total cross sectional area as in the following:

$$u_m = \frac{Q_{tot}}{A_{tot}} \tag{4}$$

$$D_c = \sqrt{A_s + A_r} \tag{5}$$

For the calculation of the characteristic length, the approach proposed by Muzychka and Yovanovich (2004) and Muzychka (2013) has been taken into consideration.

The flowrate ratio and the dimensionless nozzle-to-plate distance are determined, respectively, as follows:

$$Q^* = \frac{Q_s}{Q_{tot}} \tag{6}$$

$$H^* = \frac{H}{r_o} \tag{7}$$

where, H, is the distance between the exit of the nozzle and the impingement surface, and r_o is the radius of the impingement plate. For each experimental condition, the pressure distribution on the impingement plate is obtained, and the variation of the pressure coefficient with the dimensionless radial distance is presented. The pressure coefficient and the dimensionless radial distance are given respectively as follows:

$$C_p = \frac{2\Delta P}{\rho u_m^2} \tag{8}$$

$$R^* = \frac{r}{r_o} \tag{9}$$

where, ΔP is the pressure difference between the pressure taps and the ambient air, ρ is the density and r is the radial distance between the midpoint of any pressure tap and the midpoint of the impingement plate.

3. Results and Discussion

In the present study, experiments have been performed at different dimensionless nozzle-to-plate distances (H^* = 0.2, 0.4 and 0.6), and dimensionless flowrate ratios (Q^* = 0.1, 0.3 and 0.6)

at a constant total flowrate of 1.66 x 10^{-3} m^3 s^{-1} (100 L/min). The atmospheric air is used as the working fluid.

The variation of the dimensionless pressure coefficient with the dimensionless radial distance as a function of the dimensionless nozzle-to-plate distance for different values of the dimensionless flowrate ratio is given in Figs 4a to c. For all the flowrate ratios, in the stagnation region, the magnitude of the local pressure values decreases with increasing nozzle-to-plate distance. As it is also stated by Abdel-Fattah (2007) and Ozmen (2011), the reason can be explained as the jet spreading which causes a decrease in the kinetic energy at the jet center (due to increasing spacing).

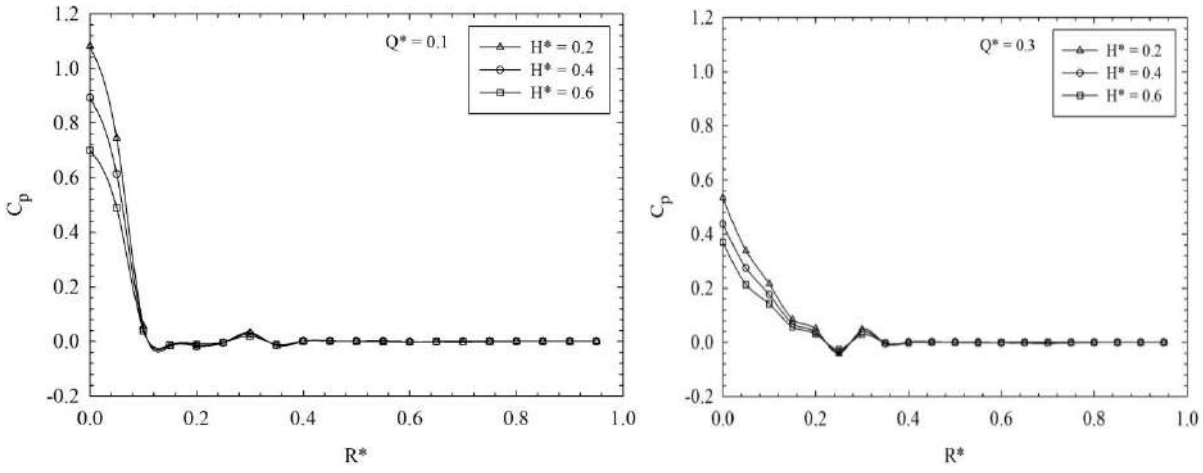

(a) (b)

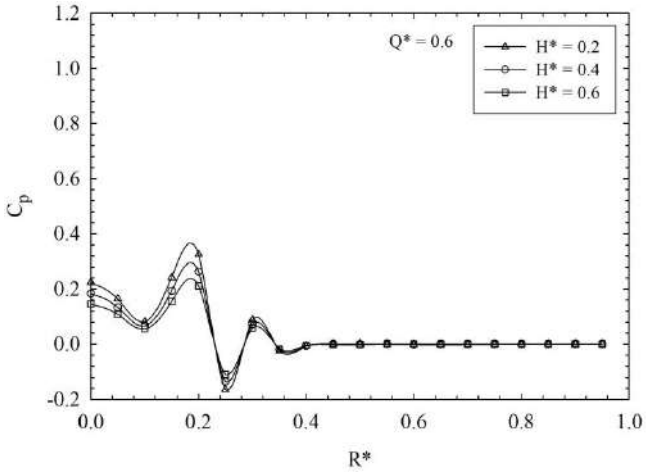

(c)

Figure 4. The variation of the dimensionless pressure coefficient with the dimensionless radial distance as a function of the dimensionless nozzle-to-plate distance for different values of the dimensionless flowrate ratio

Figures 5a to c show the variation of the pressure coefficient with the dimensionless radial distance as a function of flowrate ratio for different nozzle-to-plate distances. As it is seen in Fig. 5, the flowrate ratio plays a very important role on the pressure distribution. For all the nozzle-to-plate distances, similar behavior is obtained. The pressure coefficient peaks at the stagnation point (center of the plate) for Q^* = 0.1 and 0.3, and then decreases. Especially, for Q^* = 0.1, this decrement is quite obvious such that the pressure coefficient becomes (nearly) zero at R^* = 0.1. In other words, the jet pressure approaches to the atmospheric value shortly after the stagnation point. The pressure behavior in the case of Q^* = 0.1 resembles the one for simple circular or slot jet (see Baydar (1999) and Öztekin et al. (2012)). However, a significant variation takes place when the flowrate ratio increases. The magnitude of the pressure coefficient at the center of the impingement surface decreases obviously with increasing flowrate ratio. Increasing flowrate ratio means a decrease in the flowrate of the inner circular (round) passage. In other words, the jet spreads, and thus, the kinetic energy at the jet center diminishes. As a result, the local pressure at the center of the impingement plate decreases. In addition to the pressure coefficient at the center, the distribution of the pressure coefficient begins to change with increasing flowrate ratio. For Q^* = 0.3, the positive pressure region enlarges up to R^* = 0.2, and a slight subatmospheric region and a slight positive peak (secondary) appear on the surface. For Q^* = 0.6, obvious peaks appear in the distribution of the pressure coefficient such that the magnitude of the secondary peak (at nearly R^* = 0.2) is greater than the primary peak (at the center of the plate). Also, for Q^* = 0.6, a significant subatmospheric region occurs at approximately R^* = 0.25. For a better discussion of the physical phenomena, it can be mention about the general flow structure of a coaxial jet defined by Ko and Kwan (1976). According to Ko and Kwan (1976), in a conventional annular coaxial free jet, there are three different regions: Initial merging region, intermediate region and fully merged region. In the near field of the nozzle exit (in the initial merging region), primary and secondary mixing regions and potential cores appear. Balakrishnan and Srinivasan (2017) stated that the expressions of the Ko and Kwan (1976) can also be extended for coaxial swirl jets. In brief, the flow structure of the swirling coaxial jets are very complex, and also, for the impinging case (when an impinging

plate is used), the flow nature would be more complicated, as it is expected. As a result, there is a strong interaction between the different flow fields (multiple jets issuing from the nozzle) in a coaxial jet case. Fig. 5 represents this complexity. By increasing the effect of outer swirling jets, in other words, by increasing flowrate ratio, the distribution of the pressure coefficient on the impingement plate is completely changes. Ko and Kwan (1976) stated that there are peak values in each mixing regions, and the shear rate in these regions is the determining factor for these peaks. This is the probable reason of the peaks take place in the condition of $Q^* = 0.6$.

For $Q^* = 0.6$, a significant subatmospheric region appears as it is stated in the previous paragraph. The subatmospheric data indicates the existence of a recirculation region, and the pressure gradient becomes negative and positive in the subatmospheric region, and the positive pressure gradient separates the flow from the impinging surface (Obot and Trabolt, 1987; Ozmen, 2011). Baydar (1999) and Schafer et al. (1992) indicated that heat transfer improves at the leading and trailing edges of the recirculation region. Therefore, the obtained result is also very important for heat transfer applications.

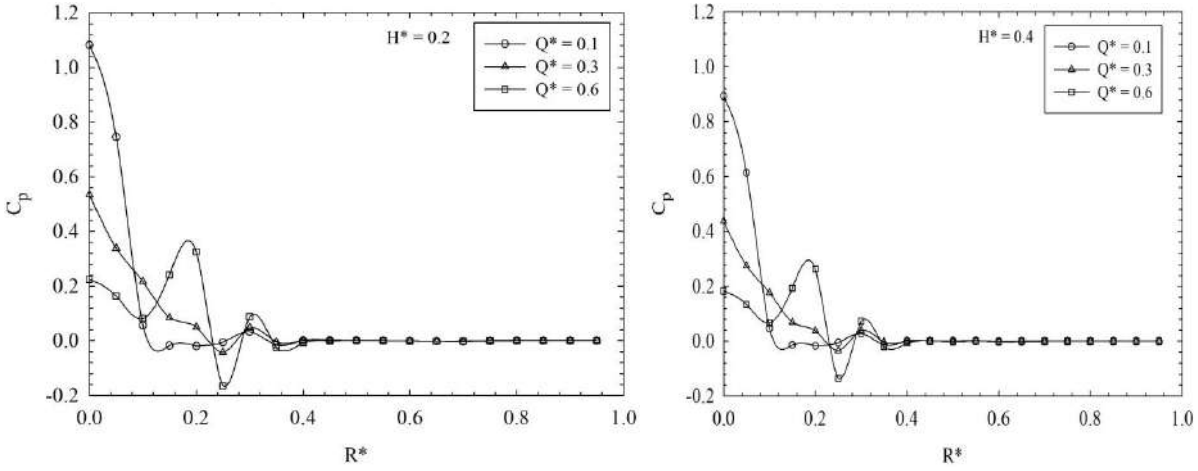

(a) (b)

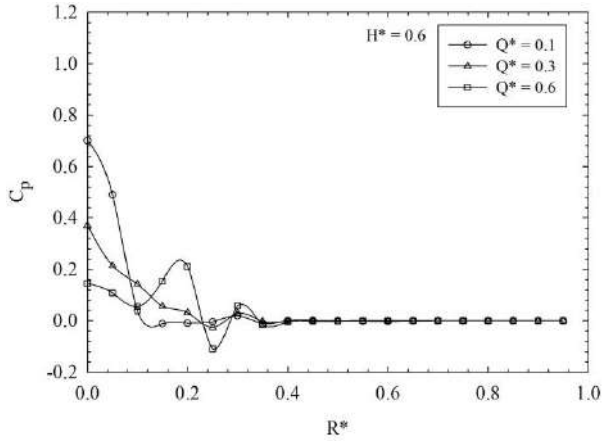

(c)

Figure 5. The variation of the dimensionless pressure coefficient with the dimensionless radial distance as a function of the dimensionless flowrate ratio for different values of the dimensionless nozzle-to-plate distance

4. Concluding Remarks

This study experimentally investigates the fluid flow characteristics of a swirling coaxial impinging (swirling and round) air jet. The main findings of the study can be summarized as in the following:

- For all the flowrate ratios, in the stagnation region, the magnitude of the local pressure values decreases with increasing nozzle-to-plate distance.
- Flowrate ratio plays a very important role on the pressure distribution. Contrary to Q^* = 0.1, for Q^* = 0.3, the positive pressure region enlarges up to R^* = 0.2, and a slight subatmospheric region and a slight positive peak (secondary) appear on the surface.
- For Q^* = 0.6, obvious peaks appear in the distribution of the pressure coefficient such that the magnitude of the secondary peak (at nearly R^* = 0.2) is greater than the primary peak (at the center of the plate). Also, for Q^* = 0.6, a significant subatmospheric region occurs at approximately R^* = 0.25.
- For future studies, new geometrical designs (for nozzles) can be taken into consideration.

References

Abdel-Fattah, A. (2007). Numerical and experimental study of turbulent impinging twin jet flow, *Experimental Thermal and Fluid Science*, 31, 1060–1072.

Adzlan, A., Gotoda, H. (2012). Experimental investigation of vortex breakdown in a coaxial swirling jet with a density difference, *Chemical Engineering Science*, 80, 174–181.

Ahmed, Z.U., Al-Abdeli, Y.M., Guzzomi, F.G. (2017). Flow field and thermal behaviour in swirling and non-swirling turbulent impinging jets, *International Journal of Thermal Sciences*, 114, 241-256.

Astarita, T., Cardone, G. (2008). Convective heat transfer on a rotating disk with a centred impinging round jet, *International Journal of Heat and Mass Transfer*, 51, 1562–1572.

Balakrishnan, P., Srinivasan, K. (2017). Jet noise reduction using co-axial swirl flow with curved vanes, *Applied Acoustics*, 126, 149–161.

Baydar, E. (1999). Confined impinging air jet at low Reynolds numbers, *Experimental Thermal and Fluid Science*, 19, 27-33.

Duda, J.C., Lagor, F.D., Fleischer, A.S. (2008). A flow visualization study of the development of vortex structures in a round jet impinging on a flat plate and a cylindrical pedestal, *Experimental Thermal and Fluid Science*, 32, 1754–1758.

Eiamsa-ard, S., Nanan, K., Wongcharee, K. (2015). Heat transfer visualization of co/counter-dual swirling impinging jets by thermochromic liquid crystal method, *International Journal of Heat and Mass Transfer*, 86, 600–621.

Huang, L., El-Genk, M.S. (1998). Heat transfer and flow visualization experiments of swirling, multi-channel, and conventional impinging jets, *International Journal of Heat and Mass Transfer*, 41, 583-600.

Kalifa, R.B., Hablib, S., Saïd, N.M., Bournot, H., Palec, G.L. (2016). Parametric analysis of a round jet impingement on a heated plate, *International Journal of Heat and Fluid Flow*, 57, 11–23.

Kim, N.S., Giovannini, A. (2007). Experimental study of turbulent round jet flow impinging on a square cylinder laid on a flat plate, *International Journal of Heat and Fluid Flow*, 28, 1327–1339.

Kline, S.J., McClintock, F.A. (1953). Describing uncertainties in single-sample experiments, *Mechanical Engineering*, 75, 3–8.

Ko, N.W.M. Kwan, A.S.H. (1976). The Initial Region of Subsonic Coaxial Jets, *Journal of Fluids Mechanics*, 73, 305 – 332.

Lee, W., Park, Y., Kwona, K., Taghavi, R. (2010). Control of shear perturbation in coaxial swirling turbulent jets, *Aerospace Science and Technology*, 14, 472–486.

Mahmud, T., Truelove, J.S., Wall, T.F. (1987). Flow characteristics of swirling coaxial jets from divergent nozzles, *Journal of Fluids Engineering*, 109, 275-282.

Muzychka, Y.S., Yovanovich, M.M. (2004). Laminar Forced Convection Heat Transfer in the Combined Entry Region of Non-Circular Ducts, *Journal of Heat Transfer*, 126, 54─61.

Muzychka, Y.S. (2013). Generalized Models for Laminar Developing Flows in Heat Sinks and Heat Exchangers, *Heat Transfer Engineering*, 34, 178-191.

Obot, N.T., Trabold, T.A. (1987). Impinging heat transfer within arrays of circular jets: part 1 – effects of minimum Intermediate and complete cross flow for small and large spacings, *J. Heat Transfer*, 109 872–879.

Özmen, Y. (2011). Confined Impinging Twin Air Jets at High Reynolds Numbers, *Experimental Thermal and Fluid Science*, 35, 355–363.

Öztekin, E., Aydin, O., Avci, M. (2012). Hydrodynamics of a turbulent slot jet flow impinging on a concave surface, *International Communications in Heat and Mass Transfer*, 39, 1631–1638.

Ribeiro, M.M., Whitelaw, J.H. (1980). Coaxial jets with and without swirl, *Journal of Fluid Mechanics*, 96, 769-795.

Schafer, D.M., Ramadhyani, S., Incropera, F.P. (1992). Numerical simulation of Laminar convection heat transfer from an in-line array of discrete sources to a confined rectangular jet, *Numerical Heat Transfer, Part A: Applications: An International Journal of Computation and Methodology, Transfer* 22, 121 – 141.

Tummers, M.J., Jacobse, J., Voorbrood, S.G.J. (2011). Turbulent flow in the near field of a round impinging jet, *International Journal of Heat and Mass Transfer*, 54, 4939–4948.

Yakkatelli, R., Wu, Q., Fleischer, A.S. (2010). A visualization study of the flow dynamics of a single round jet impinging on porous media, *Experimental Thermal and Fluid Science*, 34 1008–1015.

Yang, H.Q., Kim, T., Lu, T.J., Ichimiya, K. (2010). Flow structure, wall pressure and heat transfer characteristics of impinging annular jet with/without steady swirling, *International Journal of Heat and Mass Transfer*,53, 4092–4100.

A Study on Microstrucutre and Mechanical Properties of DP 450 and IF 7314 Steels by Using Resistance Spot Welding

Fatih Hayat[1], Cihangir Tevfik Sezgin[2*], Burak Dindar[3], Numan Berke Koşun[4], Muhammet Şimşek[5]

[1]Karabük University, Engineering Faculty, Metallurgy and Materials Engineering, Karabük, Turkey, fhayat@karabuk.edu.tr
[2]Kastamonu University, Cide Rıfat Ilgaz MYO, Welding Technology, Kastamonu,Turkey; ctsezgin@kastamonu.edu.tr
[3]Karabük University, Engineering Faculty, Metallurgy and Materials Engineering,Karabük,Turkey, bd.burakdindar@gmail.com
[4]Karabük University, Engineering Faculty, Metallurgy and Materials Engineering, Karabük, Turkey, berkem673@hotmail.com
[5]Karabük University, Engineering Faculty, Metallurgy and Materials Engineering, Karabük, Turkey, muhammet161994@gmail.com

[*] **Corresponding Author:** ctsezgin@kastamonu.edu.tr

Abstract

In this study, dissimilar weldability of IF 7314 and DP 450 Steel by using resistance spot welding (RSW) was investigated. Welded joint was cut as cross section.The sample was grinden with grinding paper as 120-400-800-1200. After the grinding process, the polishing was applied to sample. Each sample was etched with the nitrate solution that we prepared. After all operations microstructure of heat affect zone (HAZ), fussion zone was observed with optical microscope. Microhardness was observed . Tensile strength test was apllied to welded steel. It was observed that welding was successful.

Keywords: DP 450 steel, resistance spot welding, microstructure, IF 7314 steel, microhardness

1. Introduction

Steel is commonly used metal at automotive industry. Because of its using have got many reasons.The most important two things are automobile safety standards and reducing environmental pollution. These two main reason caused to improve many steel kinds. Two of these steels are IF (interstitial free) steels and dual phase (DP) steels.

These steels were designed to provide an excellent combination of drawability and mechanical strength based on their specific interstitial free (IF) metallurgy. These steels are hardened by adding manganese, silicon and phosphorous in solid solution to the ferrite. The metallurgy of IF steels optimizes their drawability (Arcelor, 2018).

Dual-phase steels are a high-strength low-alloy (HSLA) type of steel that occurs in the microstructure of the ferrite matrix in the dispersed state of the martensite. In other words, dual phase steels with two phases are called two dominant phases in the microstructure. These are ferrite and martensite (Toros,2013).

As the martensite ratio increases, the strength of the sheet increases and the formability feature decreases (Speich, 1993) . Formability increases as the ferrite ratio increases. So ductility increases.

It is one of the reasons why it is preferable to compete with light non-ferrous metals such as aluminum (Demir, 1997). Increased use in many car parts, such as wheel rim, seat frame, bumper, door panels, chassis, wheel covers, belt pulleys, etc (Pradhan, 1993).

Thanks to the welding, fasteners such as rivets and bolts are not used, making the vehicles lighter. One of the most important welding method is resistance spot welding (RSW). Low investment cost, fast manufacturin and low workmanship are the most important reasons for being preferred RSW. Table 1 shows the number of spot sources in vehicles belonging to various brands (Donders etc. 2005; Geißler, Hahn, 2011; Sonat, Doyum, 1999) . According to other welding methods, 85% resistance point welding is used in the formation of the vehicle body (Doruk etc. ,2016).

For these reasons, the effect of microstructure, tensile and hardness on the mechanical properties of DP 450 steel and IF 7314 steels in point resistance welded joints was investigated.

Table1. Spot Welding Numbers of Various Automotive Brands

Model of Vehicle	Number of RSW
Alfa Romeo Giulietta	3676
Volvo S60	3966
Citroen C4	3938
Saab 9-5 Sedan	4250
Honda CR-Z	4254
Opel Meriva	4533
Ford Grand C-MAX	5011
Fiat Linea	5031
Renault Latitude	5208
VW Sharan	5600
BMW 5 Series	5800

2. Material and Method

In this study, spot welding of IF 7314 steel was made with dual phase DP450 steel. For this purpose, the pieces were cut at the guillotine with dimensions of 100mm x 30 mm. After welding, the samples were cut in the disc (Cutting Machine) with Dispersion Oil and water. The samples were put in bakalite resin. Then, the sandpaper numbered as 200, 400, 600, 800, 1000, 1200, 2000 and 2500 was used respectively. It was then polished with diamonds paste and then etched with nital solution, dried with methanol. And then, microstructure images were taken at 50x, 100x, 200x, 500x, 1000x magnification.

Morover tensile strength test was carried out to the samples. Welding parmeters was shown in Table 2.

Table 2. Welding parameters

Ampers (kA)	Cycle
6	20
8	10
8	20
8	30
10	20
12	20

Chemical composition of both of steels were shown in Table 3. Mechanical properties of steels was seen in Table 4.

Table 3. Chemical compositions of steels

Steel	C	P	S	Mn	Si	Al	Cr
DP450	0,1	0,1	0,015	1,3	0,4	0,015	0,8
IF7314	0,08	0,03	0,03	0,4	-	-	-

Table 4. Mechanical properties of steels

Steels	Young Module (MPa)	Tensile Strenth (MPa)	Elongation (%)
DP 450	300	475	33
IF7314	210	290	38

3. Results and Discussion

3.1. Microstructure

Microstrcture of fussion zones were shown in Figure 1.

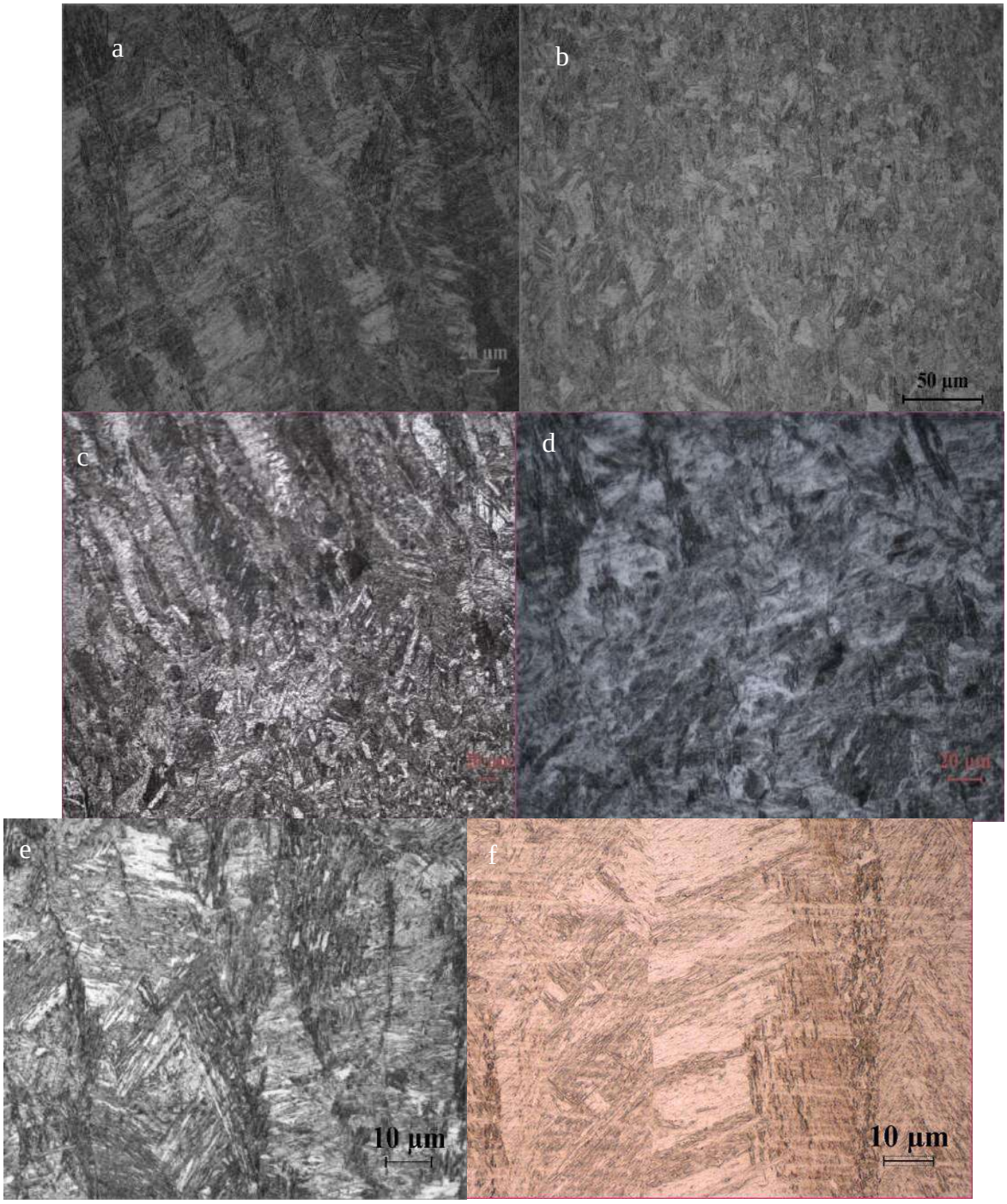

Figure 1. a)6 kA, 20cycle Fussion zone b) 8 kA, 10cycle Fussion zone c) 8 kA, 20cycle Fussion zone d) 8 kA, 30cycle Fussion zone e) 10 kA, 20cycle Fussion zone d)12 kA, 20cycle Fussion zone

As can be seen in Figure 1 fussion zone was occured by columnar grain. At resistance spot welding, cooling is faster than many welding methods, but cooling is more slowly as the heat input increases depending on the parameters in itself. When amperage and time increase cooling become slowly. Large columnar grain structure was observed in the weld zone because the fusion zone cools slowly. It could be said that martensite was occured at all of operations. Hardness of fussion zone was very high at every welding opertions. Martensite could be caused high hardness. DP450 steel was occured by ferrite and martensite. So the rate of ferrite dissolved in the austenite from main metal towards to the weld metal increases because of rapid cooling after welding process and therefore this may increase the martensite volume fraction (Demir and Elitaş, 2018).

3.2. Microhardness

Microhardness results was shown in Figure 2. At the same power when the cycle time was more and more hardness of fussion zone increased. 8 kA 30 cycles RSW operation had the highest hardness values as 473 HV. Avarage of fussion zone hardness was calculated as 441 HV fort his operation. And it could cause to occur martensite. So observation of the highest hardness values at 8 kA and 30 cycle operation can be explain with this reason. The rate of ferrite dissolved in the austenite from main metal towards to the weld metal increases because of rapid cooling after welding process and therefore this may increase the martensite volume fraction (Demir and Elitaş, 2018). This situation can explain to increase hardness of weld zone.

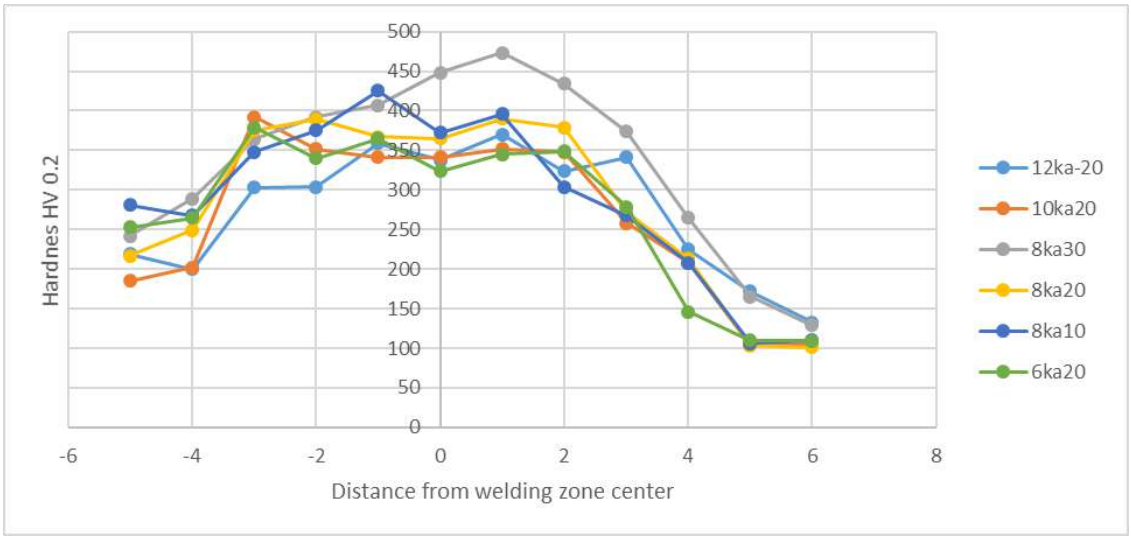

Figure 2. Microhardness results

The lowest hardness values were observing at base metals for each operations. Hardness of base metal of IF 7314 steel was lower than DP 450 steel. As it was expected situation. The highest hardness values were observing at fussion zone for each operations.

3.3. Tensile Strength Test

Tensile strength test results was shown in Table 5. Both of maximum stress and elongation values were too close for each operation. Maximum elongation was seen at operation 10 kA-20 cycle. But all stress and elongation results was lower than both of two base metals.

Table 5. Strength Test Results

Operation	Max Stress (MPa)	Elongation (%)
6 kA-20 cycle	120	15,4
8 kA- 10 cycle	120	7,5
8 kA- 20 cycle	121	8,4
8 kA- 30 cycle	119	7,5
10 kA- 20 cycle	124	7,9
12 kA- 20 cycle	122	7,8

4. Results and Discussion

- Fussion zone was occured by columnar grain. Because of rapid cooling it thought that martensite cold be occured in fussion zone

- The hardest zone was observed as 473 HVat fussion zone of metal was welded at 8 kA 30 cycle. Its average hardness value was 441 HV. This results thought that martensit could be occured in fussion zone.
- Maximum stress was observed at sample welded with 10 kA 20 cycle as124 MPa. But maximum stress of all samples are very close each other. Maximum strain was oberved at sample welded with 6 kA 20 cycle as 15,4%. Both tensile strength and elongation decreased at each operations according to values of base metals.

Referances

Demir, B., (1997), Çift fazlı çelik üretimi, çift fazlı çeliklerde martenzit hacim oranı ve morfolojisinin çekme özellikleri üzerine etkisi, Master Thesis, Gazi Üniversitesi, Ankara, Turkey.

Donders, S., Brughmans, M., Hermans, L., Tzannetakis, N. (2005) "The Effect of Spot Weld Failure on Dynamic Vehicle Performance," IMAC-XXIII, the 23rd InternationalModal Analysis Conference, Orlando.

Doruk, E., Pakdil, M., Çam, G., Durgun, İ., Kumru, U. C., (2016), Otomotiv Sektöründe Direnç Nokta Kaynağı Uygulamaları, Mühendis ve Makina, 673, 48-53.

Elitaş,M., Demir B., (2018). The effect of parameters on tensile properties of RSW junctions of DP1000 sheet metal, Engineering, Technology and Applied Science Research, 8(4), 3116-3120.

Geißler, G., Hahn, T. 2011, Process Development for Multi-Disciplinary Spot Weld Optimization With CAX-LOCO, LS-OPT and ANSA, 8th European Users Conference, Strasbourg, France.

Pradhan, R., (1993)"Continous Annealling Steel", ASM Metal Handbook Heat Treating Volume 4, The Materials Information Company, A.B.D., 135-160

Sonat, M., Doyum, A. B. 1999, Direnç Punto Kaynaklarının Ultrasonik Muayenesi, Kaynak Teknolojisi II. Ulusal Kongresi, TMMOB MMO, Ankara, Turkey.

Speich, G.R., (1993), Dual-phase steel, ASM Metal Handbook Properties and Selection Iron Steels and High Performance Alloys, Volume 1, The Materials Information Company, U.S.A..

Toros, S., (2013), TRIP800 çeliğinin şekillendirme kabiliyetinin incelenmesi ve modellenmesi, Doctoral Thesis, Niğde Üniversitesi, Niğde, Turkey.

URL-1: https://automotive.arcelormittal.com/europe/products/HYTSS/IF/EN (01.09.2018)

Microstructure and Mechanical Properties of Al2024-SiC Nanocomposites

A. Hasan KARABACAK[1*], Aykut ÇANAKÇI, Temel VAROL[1], Fatih ERDEMİR[1]

[1]Karadeniz Technical University, Metallurgy and Materials Engineering, Trabzon, TURKEY; hasankarabacak@ktu.edu.tr; aykut@ktu.edu.tr; tvarol@ktu.edu.tr; ferdemir@ktu.edu.tr

[*] **Corresponding Author:** hasankarabacak@ktu.edu.tr

Abstract

In this work, Al2024-SiC nanocomposites with different amount of SiC were produced by mechanical alloying method and hot pressing method. Al2024-SiC mixtures were milled with 8 hours in planetary ball mill under argon atmosphere at room temperature. To investigate the effect of SiC content on the properties of nanocomposites, the SiC content was changed 0, 1, 1.5, 2, 2.5 to 3 wt%. Than the milled powders were hot pressed at 560 ^{0}C for 3 hours under 500 MPa pressure to obtain the final samples. The change of microstructure, hardness, bending strength and tensile strength of Al2024-SiC nanocomposites with increasing SiC content were investigated. The uniform distribution, dispersion of SiC nano particles within the Al2024 matrix and fracture surfaces was examined by scanning electron microscopy (SEM). A maximum bending strength and tensile strength was obtained for 2 wt.% SiC reinforced Al2024 matrix nanocomposites. It was observed that the changes in hardness were conferred in relation to the SiC content. The results show that the increase in hardness values and reinforcement content plays a major role on the improvement of mechanical properties of the nanocomposites.

Keywords: Mechanical alloying, SiC, Nanocomposites, Microstructure, Strength.

1. Introduction

Particle reinforced metal matrix composites (MMCs) that provide advanced mechanical and physical properties combine the good aspects of both matrix and reinforcement materials. Aluminum alloys are the most commonly used materials for aircraft, automotive and military industries, even though many metals are used as matrix materials to develop new composites. High ductility, high stiffness, high strength to weight ratio and good corrosion resistance of Aluminum alloy are outstanding features for increasing their usability in the production of metal matrix composites or metal matrix nanocomposites[1-2]. Ceramics such as B4C, SiC, Al2O3 TiC are reinforced to aluminum and its alloys in order to develop properties such as mechanical strength, corrosion resistance and wear resistance [3]. On the other hand, the dynamic fracture toughness of the SiC particles reinforced aluminum matrix is higher than its static fracture toughness, but the volumetric rate of reinforcement increase is reduced[4]. SiC, a continuous networked ceramic, is a very promising material for use in semiconductor processing, nuclear fusion reactors, heat-sink plates, and high temperature thermo-mechanical applications because of their excellent chemical and thermal stability, high thermal conductivity, and good mechanical properties [5]. The development of metal matrix nanocomposites has recently been one of the most important advances in composite materials. Nanocomposites have developed mechanical properties that can be adapted to achieve the needs of specific applications. The mechanical alloying technique (MA) is the advanced production technique according to the results of previous studies [6]. In this production method, the powder particles are milled using ball collisions very fine particles and resulting in a homogeneous dispersion. MA method is a useful method for improving the distribution of reinforcement particles not only in composites but also in nanocomposites [7].

In the present work, in order to improve the mechanical properties of Al2024 alloy, the nano SiC particles were added to the matrix by mechanical alloying technique. Reinforced Al2024-SiC samples were prepared using a solid state route complemented with mechanical alloying techniques. The focus of this study is to explore the possibility of improving and mechanical properties of Al2024 alloys simultaneously. In this paper, the effect of reinforcement content on the mechanical properties on Al2024-SiC nanocomposites composites is presented.

2. Materials and Method

Al2024 alloy powders, nano SiC particles used as raw materials to fabricate the composites. The as-atomized Al2024 powders were supplied commercially with the chemical composition (in wt.%) of 4.85 Cu, 1.78 Mg, 0.385 Si, 0.374 Fe, 0.312 Mn, 0.138 Zn, 0.042 Cr, 0.005 Ti and Al (balance). Al2024 alloy powders with an average particle size of 50 μm were used as the matrix materials and SiC powders with an average particle size of 40 nm (Alfa Aesar, Germany) were used as the reinforcement material. Al2024 matrix powders and SiC particles (0, 1, 1.5, 2, 2.5 and 3 wt.%) were blended in a planetary ball-mill (Fritsch Gmbh, model ‘‘Pulverisette 7 Premium line’’) at room temperature using a tungsten carbide bowl and a high argon atmosphere for 8 h in order to break up the hard agglomerates. The milling medium was tungsten carbide balls with diameters of 10 mm. The ball-to-powder weight ratio and rotational speed were selected to be 10:1 and 400 rpm, respectively. The milling atmosphere was argon which was purged into a bowl before milling. Hot pressing was used for preparation of the Al2024-SiC composites. The microstructure, fracture surface and elemental distribution of cross-section of composites were investigated using Zeiss Evo LS10 scanning electron microscope. Local compositional analysis was conducted with an energy-dispersive X-ray spectroscopy (EDS). The microhardness of these composite samples was measured using the Binell hardness (HB) method under a load of 32 kg for a dwell time of 15 s. The bending and tensile strength test was performed using a MTS Universal Materials Testing Machine at room temperature. The crosshead speed was maintained at the speed of 0.3 mm/min. The geometry of bending and tensile test sample is 6 mm × 10 mm × 65 mm.

Table 1. Mechanical properties of the Al2024/SiC nanocomposite samples

Sample Code	Composition Al2024- SiC (%wt.)	Tensile Strength (MPa)	Bending Strength (MPa)	Hardness (BHN)
Al2024	100–0	202,0	279,2	101,6
S1	99–1	322,5	469,2	146,1
S1.5	98,5–1,5	337,9	598,7	147,1
S2	98–2	383,2	676,7	149,5
S2.5	97,5–2,5	195,5	573,9	153,3
S3	97-3	187,1	556,2	154,9

3. Results and Discussion

3.1. Microstructure

EDX analysis of Al2024 matrix composites reinforced with wt. 2% SiC (S2) nanoparticles are shown in the Fig 1. The most important factor in the fabrication of Al2024 matrix composites is the uniform dispersion of the reinforcements. As seen in the Fig.1 and Fig.2, the distribution of the reinforcing particles points to a tendency that a lot of particles are mostly placed in the particle boundary area. No macro porosity was observed in the Al2024 matrix composites and the distribution of the particles is not uniform in the matrix.

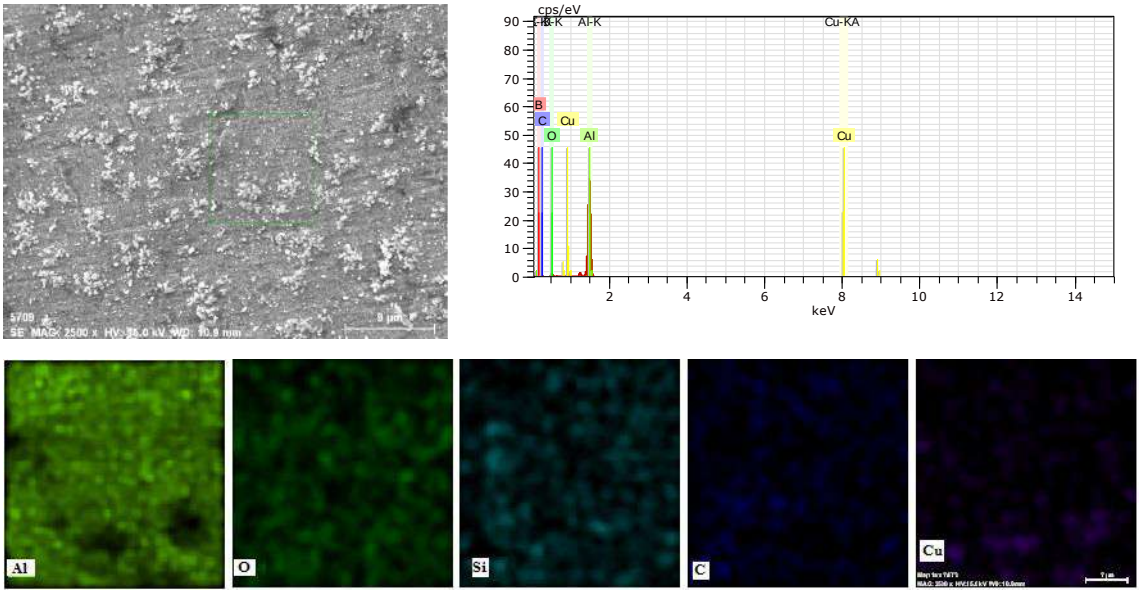

Fig.1. . EDX analysis of Al2024 matrix composites reinforced with wt. 2% SiC (S2) nanocomposite bulk sample.

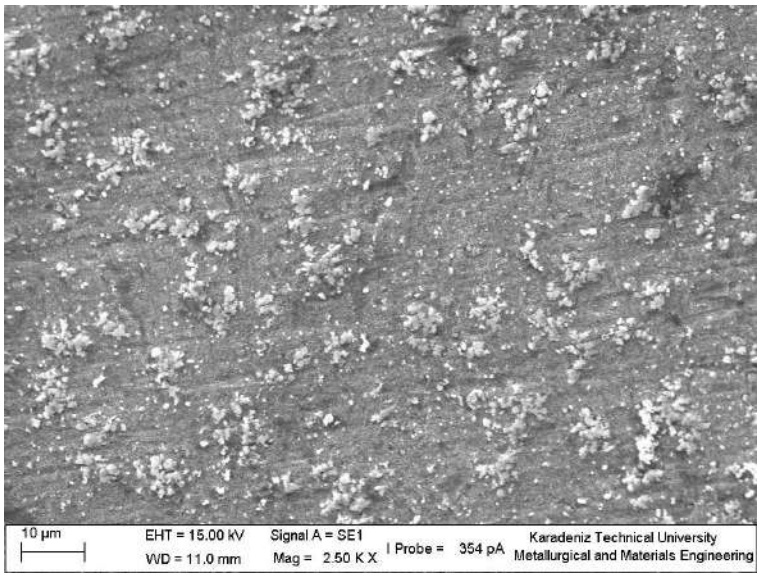

Fig.2. SEM image of S2 composite sample.

3.2. Tensile Strength

In the attempt to better evaluate mechanical properties of nanocomposites, tensile tests were conducted at room temperature and the results of tests are shown in Table 1. and in Figure 3. The reinforcement content can be determined to ceramic particle distribution in matrix alloys. Homogeneous distribution of reinforcement particles are observed in the medium reinforcement content. As the reinforcement content is increased, great number of reinforcement cluster are increased. This increase can be explained with the increasing in SiC content and homogeneous distribution. The increasing of tensile strength of SiC reinforcement particles is observed from Al2024 to S2 samples. After S2 sample the tensile strengths were rapidly decreased because decreasing homogeneous distribution of reinforcement particles in Al2024-SiC nanocomposites. So, the SiC particles agglomerates in matrix and these agglomerated areas decrease the mechanical properties of nanocomposite one of which is tensile strength.

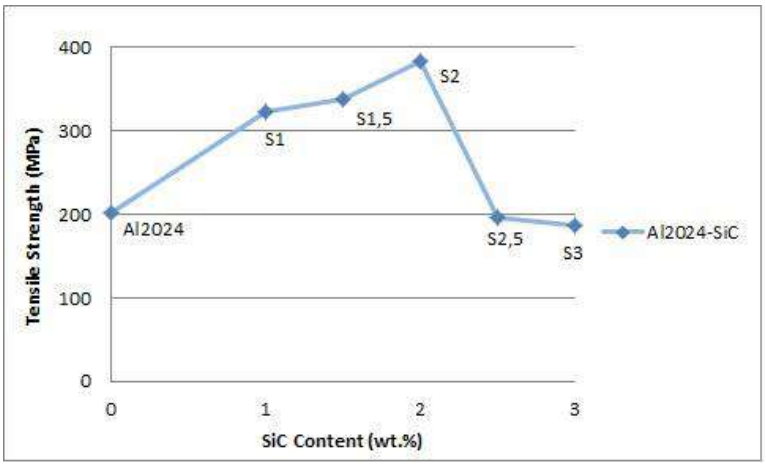

Fig.3. Tensile strength values of alloy and nanocomposite

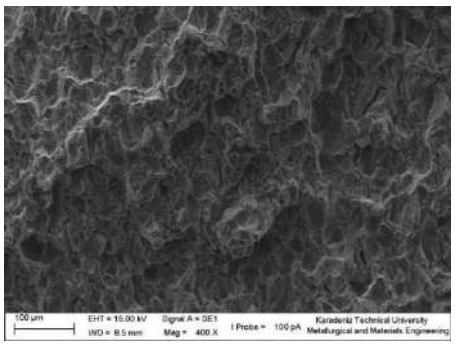

(a)

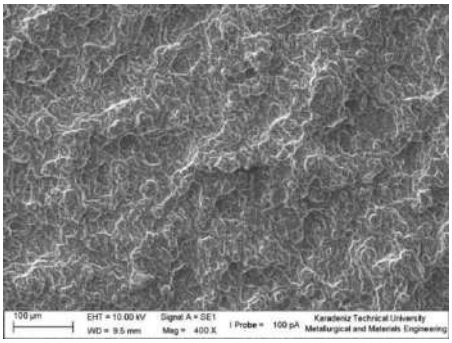

(b)

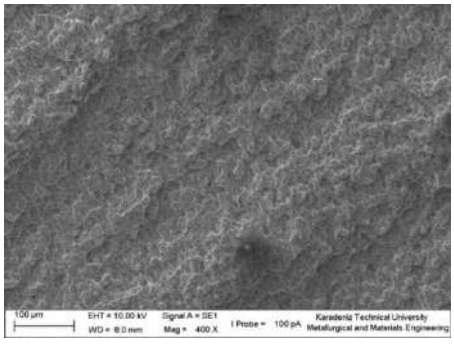

(c)

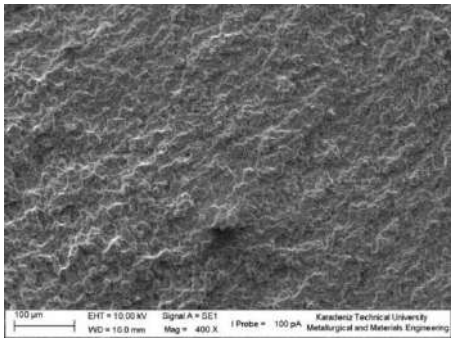

(d)

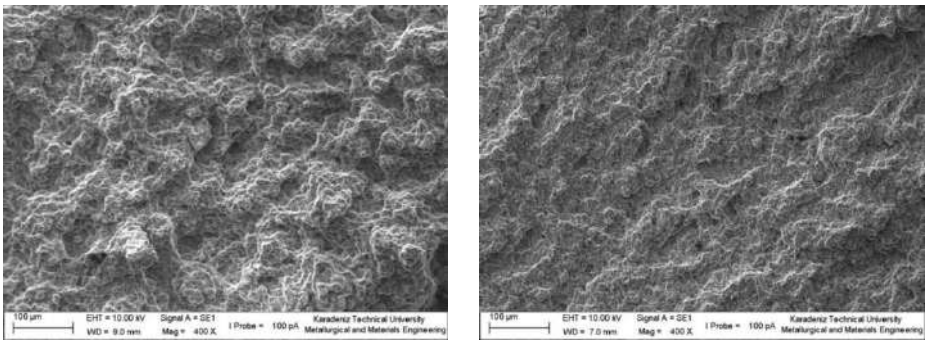

(e) (f)

Fig.4. SEM image of Al2024 (a), S1 (b), S1.5 (c), S2 (d), S2.5 (e) and S3 (f) fracture surface composite samples

3.3. Bending Strength

In the attempt to better evaluate mechanical properties of nanocomposites, bending tests were conducted at room temperature and the results of tests are shown in Table 1., in Figure 5 and in Figure 6. The reinforcement content can be determined to ceramic particle distribution in matrix alloys. Homogeneous distribution of reinforcement particles are observed in the medium reinforcement content. As the reinforcement content is increased, great number of reinforcement cluster are increased. This increase can be explained with the increasing in SiC content and homogeneous distribution. The increasing of tensile strength of SiC reinforcement particles is observed from Al2024 to S2 samples. After S2 sample the tensile strengths were rapidly decreased because decreasing homogeneous distribution of reinforcement particles in Al2024-SiC nanocomposites. So, the SiC particles agglomerates in matrix and these agglomerated areas decrease the mechanical properties of nanocomposite one of which is tensile strength.

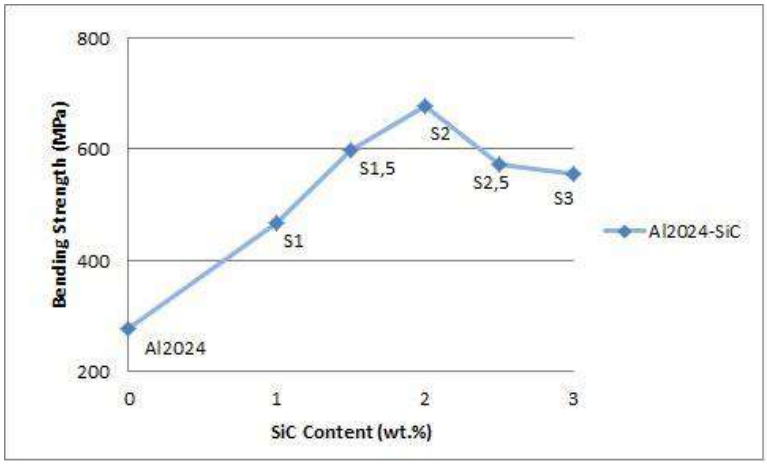

Fig.5. Bending strength values of alloy and nanocomposite

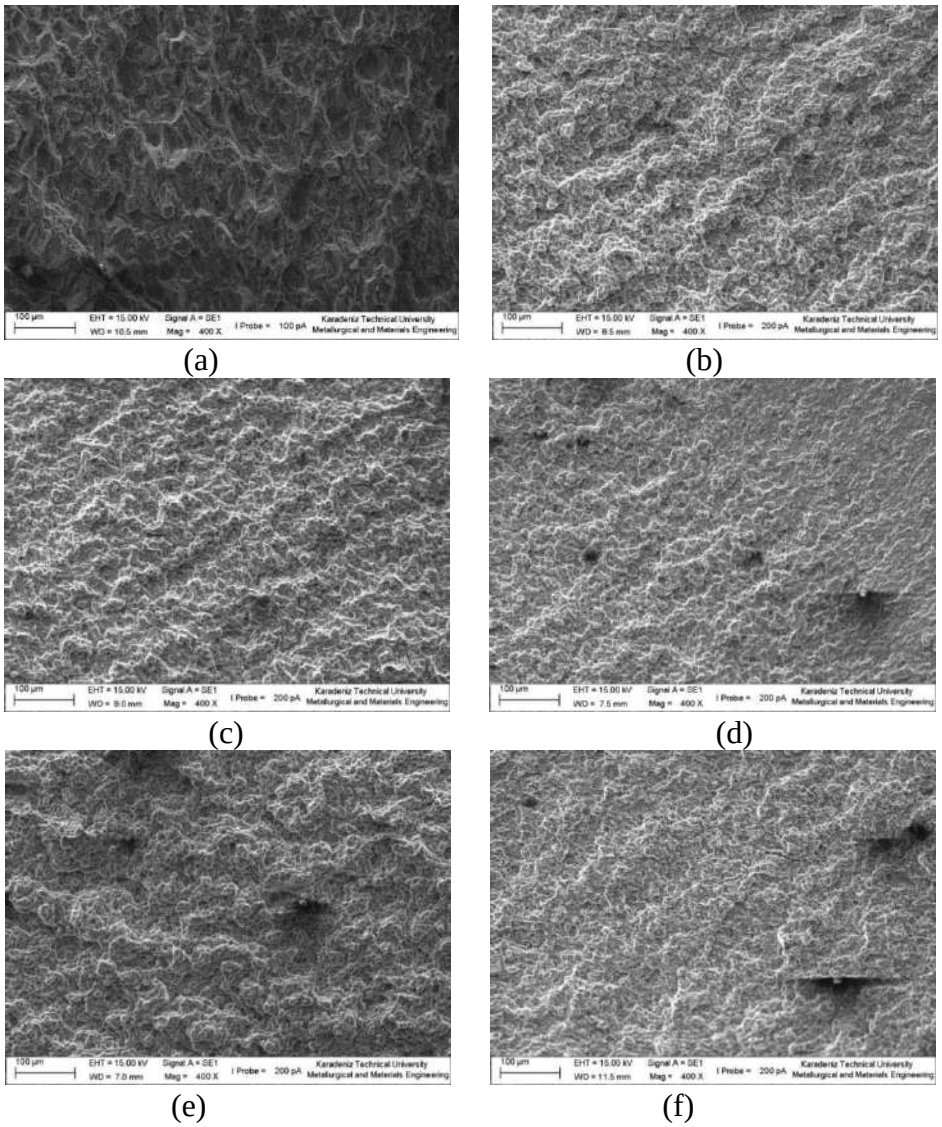

Fig.6. SEM image of Al2024 (a), S1 (b), S1.5 (c), S2 (d), S2.5 (e) and S3 (f) fracture surface composite samples

3.4. Hardness

The relation between the nanoparticle weight fraction and the HB values of Al2024-SiC nanocomposites is plotted in Fig.7. The hardness of the composites increased with increasing SiC particle weight fraction(Fig.7). The presence of hard SiC particles enhanced the work hardening rate of the matrix resulting in an increase in hardness. The hardness of S3 reinforced with SiC sample was 154.9 HB that was the highest hardness value.

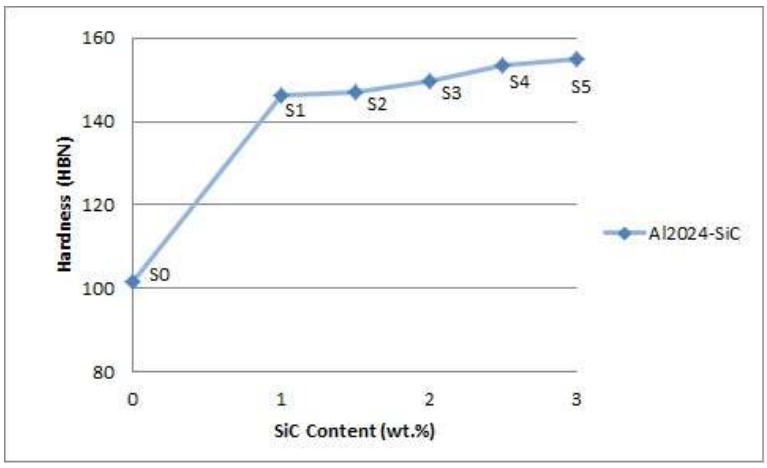

Fig.7. Brinell hardness values of Al2024-SiC nanocomposites

4. Conclusion

1. SiC nano particle added, Al2024 matrix nanocomposites were produced by mechanical alloying and hot-pressing method.
2. Microstructural examination showed that SiC distributions were homogeneous in the Al2024 alloy matrix.
3. Increase in reinforcement content resulted in increase in tensile strength of nanocomposite up to wt.%2 SiC, on the other hand after wt.%2 reinforcement they suddenly decrease.
4. Increase in reinforcement content resulted in increase in bending strength of nanocomposite up to wt.%2 SiC, on the other hand after wt.%2 reinforcement they suddenly decrease.
5. Increase in hardness of Al2024/SiC nanocomposites was observed with increase in SiC reinforcement content.

Referencs

Carreño-Gallardo, C. et al. (2014). Dispersion of silicon carbide nanoparticles in a AA2024 aluminum alloy by a high-energy ball mill, *Journal of Alloys and Compounds*, 586; S68–S72, 2014.

Sharifi, E., M. et al. (2011). Fabrication and evaluation of mechanical and tribological properties of boron carbide reinforced aluminum matrix nanocomposites, *Materials and Design*, 32; 3263–3271.

Kaczmar, J.W. et al. (2000). The production and application of metal matrix composite materials, *J Mater Process Technol*, 106; 58–67, 2000.

Erdemir, F. et al. (2015). Microstructural characterization and mechanical properties of functionally graded Al2024/SiC composites prepared by powder metallurgy techniques, *Trans. Nonferrous Met. Soc. China*, 25; 3569−3577.

Lım, K. Y. et al. (2014). Electrical properties of SiC ceramics sintered with 0.5 wt% AlN–RE2O3 [J]. *Ceramics International*, 40; 8885−8890.

Miracle, D.B., (2005). Metal matrix composites – from science to technological significance, *Compos Sci Technol*, 65; 2526–40.

Sharifi, E.M. et al. (2009). Fabrication of aluminum matrix hybrid nanocomposite by mechanical milling. *Int J Mod Phys B*, 23; 4825–32.

Analysis of Weldability of IF 7314 and DP 600 Steels by Using Resistance Spot Welding

Fatih Hayat[1], Cihangir Tevfik Sezgin[2*], Halil Gümüşten[3], Onur Daşçı[4]
[1]Karabük University, Engineering Faculty, Metallurgy and Materials Engineering, Karabük, Turkey, fhayat@karabuk.edu.tr
[2]Kastamonu University, Cide Rıfat Ilgaz MYO, Welding Technology, Kastamonu,Turkey; ctsezgin@kastamonu.edu.tr
[3]Karabük University, Engineering Faculty, Metallurgy and Materials Engineering,Karabük,Turkey, halilgumusten5@gmail.com
[4]Karabük University, Engineering Faculty, Metallurgy and Materials Engineering, Karabük, Turkey, odasci@karabuk.edu.tr

[*] **Corresponding Author:** ctsezgin@kastamonu.edu.tr

Abstract

In this study, mechanical properties and microstructure changing of DP 600 and IF 7314 steels dissimilar welding by using resistance spot welding (RSW) was analysied. Four different welding current and 3 different welding cycle numbers was used. Microstructure of heat affect zone (HAZ), fussion zone was observed with optical microscope. Microhardness was observed . Tensile strength test was applied to welded steel. It was observed that welding was successful.

Keywords: DP 600, resistance spot welding, IF 7314, weldability

1. Introduction

Steel is cheaper than many metals. Its amazing strength and plasticity combination makeit commonly used metal in the World. But increasing fuel cost and law about environmental pollution stopped automotive industry for producing heavy vehicles. High density of steel has become a problem. Manufacturer prefered low density metal like aluminium. Steel is 3 times heavier than aluminum in the same volume. Aluminum is a more expensive metal than steel. On the other hand, they are expected to produce best protection in case of an accident (Huin et.al.,2016). And the strength values of aluminum are not as high as steel. For these reasons, manfucaturer have to develop new steel types. İnterstitial steel (IF) is one of them.

Interstitial free (IF) steels with very low C and N contents have been successfully developed in order to perform specific or complex deep drawing operations in the automotive industry (Bayraktar et.al. 2007). The base material is designed using a basic vacuum-decarburized IF analysis stabilized with Ti and/or Nb. The individual strength classes are achieved by adding solid-solution-strengthening alloys (Voestalpine, 2016).

Dual-phase steels are a high-strength low-alloy (HSLA) type of steel that occurs in the microstructure of the ferrite matrix in the dispersed state of the martensite. Dual phase steel typically available in the tensile strength range of 450 to 980 MPa is widely used in today's car body manufacturing (Niobelcon, 2018). The volume fraction of hard martensite islands determines the strength of DP steel whereas the ductile ferrite matrix provides good formability (Niobelcon, 2018).

It is one of the reasons why it is preferable to compete with light non-ferrous metals such as aluminum (Demir, 1997). Increased use in many car parts, such as wheel rim, seat frame, bumper, door panels, chassis, wheel covers, belt pulleys, etc (Pradhan, 1993).

Resistance spot welding (RSW) is widely used in automotive industries. It is comparatively a clean process as it does not involve any filler material. The joint is occured with the application of pressure and heat. In the case of RSW, the flow of electric current causes heating. This heating further leads to an occurrence of localized melting and coalescence of a small volume of the material. This localized heat input is estimated as a product of squared value of weld current times

the electrical resistance of material to be welded. The electrical contact resistance of the material plays an important role in the nugget formation during spot welding (Gaoa et.al.).

It is difficult to monitor the nugget formation as the nugget is not directly exposed and exists between the electrodes.An average of 4,000 to 6,000 resistance spot welds are applied to the sedan vehicle bodies produced today (Doruk etc. ,2016). According to other welding methods, 85% resistance point welding is used in the formation of the vehicle body (Doruk etc. ,2016).

For these reasons, the effect of microstructure, tensile and hardness on the mechanical properties of DP 600 steel and IF 7314 steels in point resistance welded joints was investigated.

2. Material and Method

In this study, spot welding of IF 7314 steel was made with dual phase DP 600 steel. For this purpose, the pieces were cut at the guillotine with dimensions of 100mm x 30 x 3 mm. The lap joint welded parts (Fig.1) were exposed to tensile shear test.

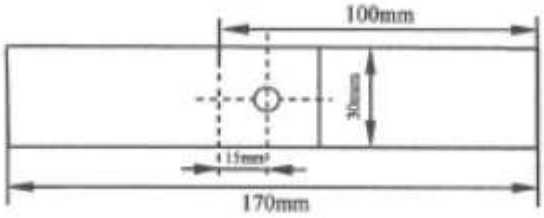

Figure 1. The Lap joint tensile sample RSW used in experiments

After welding, the samples were cut in the disc (Cutting Machine) with Dispersion Oil and water. The samples were put in bakalite resin. Then, the sandpaper numbered as 200, 400, 600, 800, 1000, 1200, 2000 and 2500 was used respectively. It was then polished with diamonds paste and then etched with nital solution, dried with methanol. And then, microstructure images were taken at 50x, 100x, 200x, 500x, 1000x magnification.

Morover tensile strength test was carried out to the samples. Welding parmeters was shown in Table 1.

Table 1. Welding parameters

Ampers (kA)	Cycle

6	20
8	10
8	20
8	30
10	20
12	20

Chemical composition of both of steels were shown in Table 2. Mechanical properties of steels was seen in Table 3.

Table 2. Chemical compositions of steels

Steel	C	P	S	Mn	Si	Al	Cu
DP 600	0,23	0,09	0,015	3,3	2	0,01	0,2
IF7314	0,08	0,03	0,03	0,4	-	-	-

Table 3. Mechanical properties of steels

Steels	Young Module (MPa)	Tensile Strenth (MPa)	Elongation (%)
DP 600	370	590	30
IF7314	210	290	38

3. Results and Discussion

3.1. Microstructure

Microstrcture of fussion zones were shown in Figure 1.

As can be seen in Figure 1 a fussion zone was occured by columnar grain (Rao et.al., 2017). 1 was the heat affect zone (HAZ) of DP 600, 2 was nugget form nd fussion zone, 3 was HAZ of IF 7314. It could be said that martensite was occured at all of operations. Cooling rate in weld metal was pretty high. This situation could block diffusion of carbon (Elitaş and Demir, 2018). So it could cause to occure martensite in fussion zone. Microhardness results was shown in Figure 2. These results strengthened idea of occuring martensite.

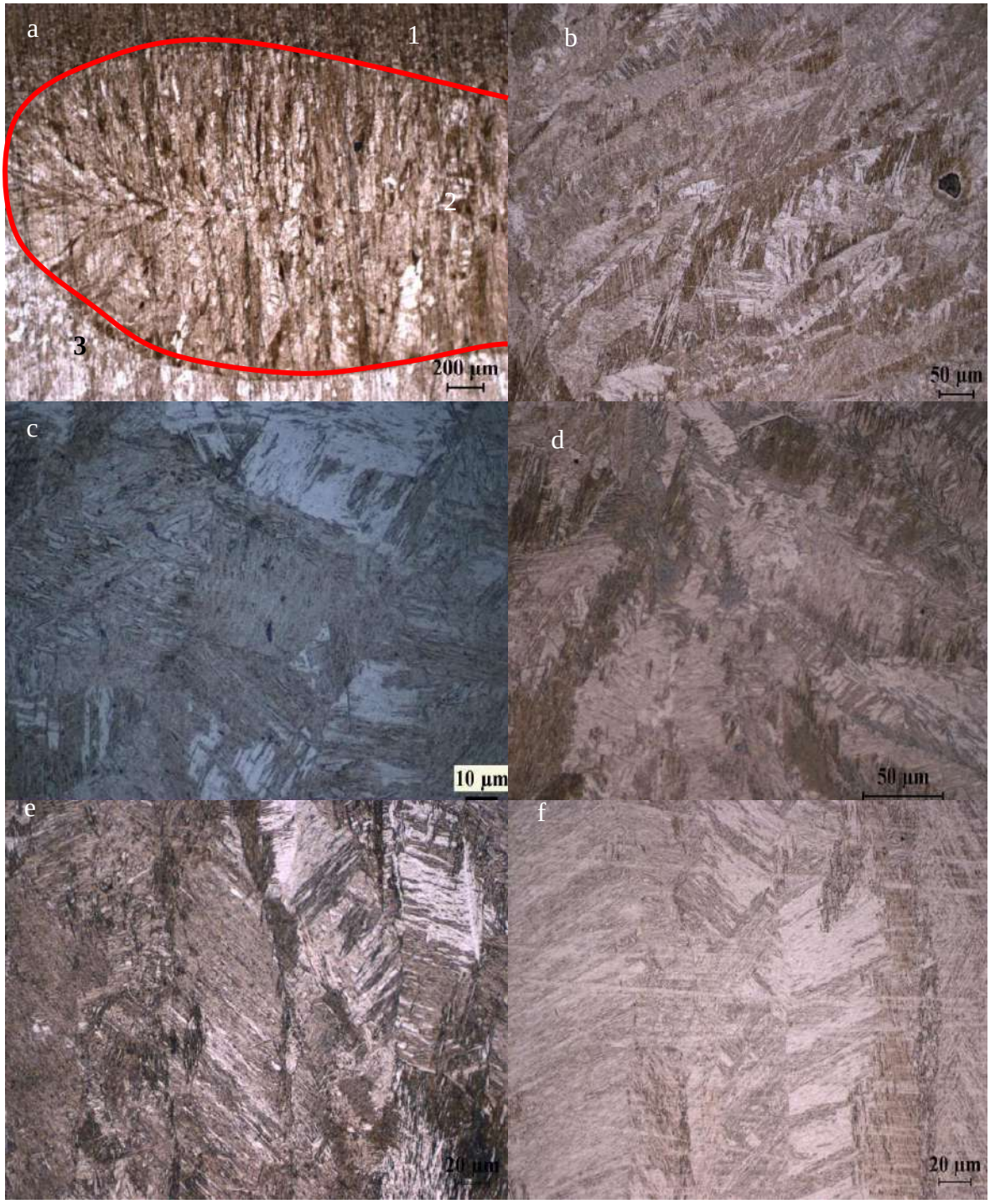
a
1
2
3
200 µm
b
50 µm
c
10 µm
d
50 µm
e
20 µm
f
20 µm

Figure 1. a)6 kA, 20cycle Fussion zone b) 8 kA, 10cycle Fussion zone c) 8 kA, 20cycle Fussion zone d) 8 kA, 30cycle Fussion zone e) 10 kA, 20cycle Fussion zone d)12 kA, 20cycle Fussion zone

3.2. Microhardness

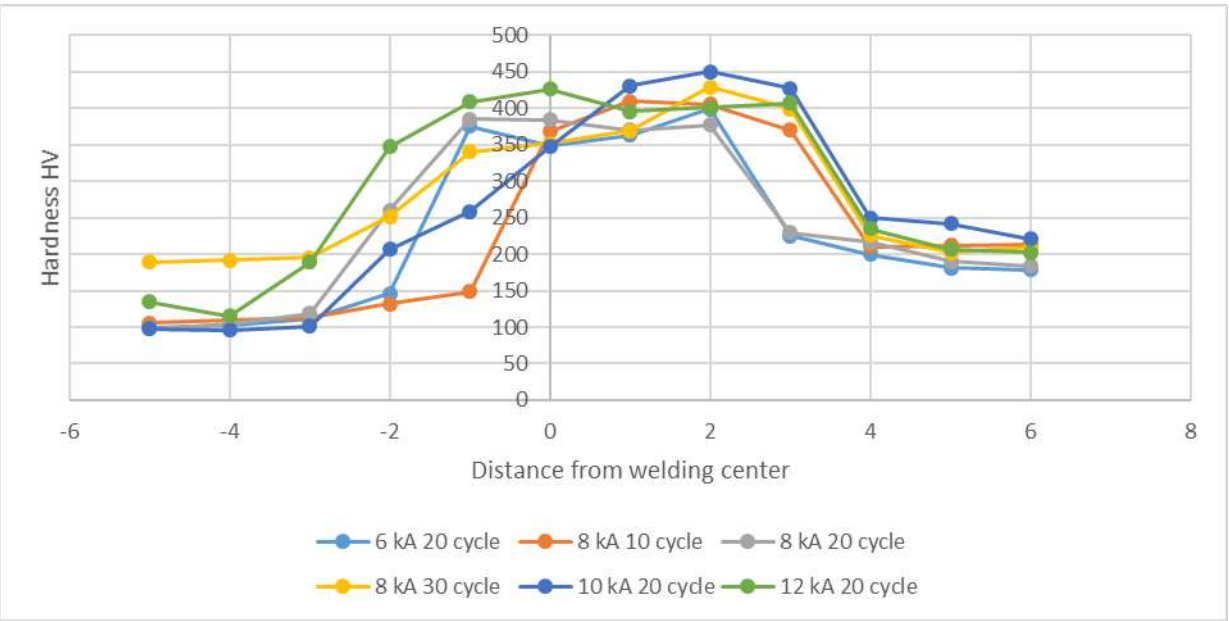

Figure 2. Microhardness results

Microhardness results was shown in Figure 2. At the same power when the cycle time was more and more hardness of fussion zone increased. The highest hardness values was seen at 10 kA 20 cycles RSW operation as 450 HV. Average hardness of fussion zone of this operation was 409 HV. The high values of hardness may be associated with the martensitic formations of alloy elements (Mn, Si, Cr, etc. that increase the hardena- bility in the chemical compositions of steels in states of rapid heating and cooling during the welding process (Hayat, 2011).

The lowest hardness values were observing at base metals for each operations. Hardness of base metal of IF 7314 was lower than DP 600. The highest hardness values were observing at fussion zone for each operations.

3.3. Tensile Strength Test

Tensile strength test results was shown in Table 5. Both of maximum stress and elongation values were too close for each operation. Maximum elongation was seen at operation 8 kA-20 cycle. But all stress and elongation results was lower than both of two base metals. The highest tensile strength value was observed at 8 kA- 10 cycle operation.

When the results in the same cycle were examined, it was observed that the tensile strength increased as the ampere increased. When the results in the same ampere (8 kA) were examined, the tensile strength decreases as the number of cycles increases. This is unexpected result. In literatüre, it was observed that the tensile strength of DP steels welding with RSW increases between 10 to 30 cycles (Hayat and Demir, 2009; Demir and Hayat, 2008; Hayat et.al.2005). In fussion zone heat is very high moreover melting occured in there. So chemical composition of DP and IF steels could be change at fussion zone and this situation could cause to meet these results.

Table 5. Strength Test Results

Operation	Max Stress (MPa)	Elongation (%)
6 kA-20 cycle	116	7,4
8 kA- 10 cycle	123	6,5
8 kA- 20 cycle	120	13,8
8 kA- 30 cycle	119	7,4
10 kA- 20 cycle	121	8
12 kA- 20 cycle	122	8,7

4. Results and Discussion

- Fussion zone was occured by columnar grain. It could be said that martensite was occured at all of operations.
- The hardest zone was observed at fussion zone of metal was welded at 10 kA 20 cycle as 450 HV. Alloy elements of DP 600 could be cause martensitic formation.
- Maximum stress was observed at sample welded with 8 kA 10 cycle as 123 MPa. But maximum stress of all samples are very close each other. And maximum strain was oserved at sample welded with 8 kA 20 cycle as13,8%.
- When the results in the same cycle were examined, it was observed that the tensile strength increased as the ampere increased at the same cycle number although the tensile strength decreases as the number of cycles increases at the same power.
- After the welding both tensile strength and elongation was observed to decrease at each operations.

Referance

Bayraktar E., Kaplan D, Devillers L., Chevalier J.P. (2007) Grain growth mechanism during the welding of interstitial free (IF) steels, Journal of Materials Processing Technology, 189. 114–125.

Demir, B., (1997), Çift fazlı çelik üretimi, çift fazlı çeliklerde martenzit hacim oranı ve morfolojisinin çekme özellikleri üzerine etkisi", Master Thesis, Gazi Üniversitesi, Ankara, Turkey.

Demir B.,Hayat F., (2008) Investigation of the spot welded junctions of the galvanize couted-uncouted DP 450 steel sheet, Proceedings of 12th International Materials Symposium, Denizli, Turkey

Doruk, E., Pakdil, M., Çam, G., Durgun, İ., Kumru, U. C., 2016. Otomotiv Sektöründe Direnç Nokta Kaynağı Uygulamaları, Mühendis ve Makina, 673, 48-53.

Elitaş,M., Demir B., (2018). The effect of parameters on tensile properties of RSW junctions of DP1000 sheet metal, Engineering, Technology and Applied Science Research, 8(4), 3116-3120.

Gaoa S., Lia Y., Yangb L., Qiub W. (2018) .Microstructure and mechanical properties of laser-welded dissimilar DP780 and DP980 high-strength steel joints Materials Science & Engineering A, 720, 117–129

Hui, T., Dancette S., Fabrègue D., Dupuy T., (2016), Investigation of the Failure of Advanced High Strength Steels Heterogeneous Spot Welds Metals 6, 111.

Hayat F., Acarer M., Demir B., Kaçar R., (2005). Çift-fazlı çeliklerin nokta direnç kaynağında martenzit hacim oranı ve kaynak zamanının kaynak kabiliyeti üzerine etkisi, 7th International Fracture Conferance Kocaeli Unıversıty, Kocaeli, Turkey.

Hayat F., Demir B., (2009). The effect of the weld time on dept intenıity factor and strength at RSW junctions of commercial DP 600 sheet steel , 5. Uluslararası İleriTeknolojiler Sempozyumu, Karabük, Turkey

Hayat F., (2011).Comparing properties of adhesive bonding resistance spot welding and adhesive weld bonding of coated and uncoated DP 600 steel, Journal Of Iron And Steeı. Research, Internatıonal, 18(9), 70-78.

Pradhan, R., (1993). “Continous Annealling Steel”, ASM Metal Handbook Heat Treating Volume 4, The Materials Information Company, A.B.D., 135-160

Raoa S.S., Chhibbera R., Arorab K.S., Shomeb M., (2017). Resistance spot welding of galvannealed high strength interstitial free steel, Journal of Materials Processing Technology, 246, 252–261

URL1:http://www.voestalpine.com/stahl/en/content/download/4680/file/Datasheet_HFIF_1608_EN.pdf?inLanguage=eng-GB

URL2:http://www.niobelcon.com/NiobelCon/resources/Advanced-metallurgical-concepts-for-DP-steels-with-improved-formability-and-damage-resistance.pdf

Numerical Analysis of the Effect of Turbulators to Heat Transfer of a Pellet Fuelled Boiler

Bilal SUNGUR[1], Bahattin TOPALOĞLU[1*]

[1]Ondokuz Mayıs University, Department of Mechanical Engineering, Samsun/Turkey

[*]**Corresponding author:** btopal@omu.edu.trr

Abstract

Energy consumption is increasing rapidly with the growth of the industry and a growing population in developing countries. Especially, the vast majority of energy used is imported in industry and homes, has led researchers to design more efficient systems, increasing the efficiency of existing systems and minimize energy losses. In this study, increasing the efficiency of pellet boiler with smoke tubes used for domestic heating has researched. In this context turbulators which have helical geometries inserted to smoke tubes of boiler and effects on heat transfer was investigated numerically. Calculations were performed at three-dimensional conditions and Fluent was used as the computational fluid dynamics software. In all cases, the RNG k-ε model was used for modeling the turbulent flow and the Finite rate/Eddy dissipation model was used for modeling the combustion. Temperature distribution and velocity vectors investigated according to the boiler with and without turbulators. Also, the effect of the usage of turbulators to the boiler efficiency investigated.

Keywords: Pellet boiler, Numerical modeling, Temperature distribution, Turbulator

1. Introduction

As the energy is expensive and the energy resources on the earth are gradually diminishing, the use of existing energy sources has become more important. In recent years different methods have been developed to save energy, especially in the energy sector. Heat exchangers are also one of the areas where energy is saved. Smoke tube boilers are also a heat exchanger used for heating purposes. The techniques used to increase the heat transfer in heat exchangers can be classified as active and passive methods. In active method, heat transfer happens with additional power to the fluid or environment which provides improvements in heat transfer, and in passive method, heat transfer happens without additional power. Increment of the surface areas increases the heat transfer. But with increasing surface, volume of the heat exchanger is growing. To prevent this, a turbulator inserted into the heat exchanger provides an increase on the heat transfer surface area and the heat exchangers volume will remain stationary. Turbulators placed into the tube increase the turbulence and improve the heat transfer. In other words, turbulators are devices which improve

the heat transfer between fluids at different temperatures. In the installed systems, increasing the efficiency of the existing system with passive heat transfer methods (demountable turbulators) is preferred rather than rebuild the entire system for heat exchangers or change necessary equipment's with new one.

Studies on biomass from alternative and renewable energy sources have gained great importance in recent years. Many developed countries see bioenergy as the main energy source for their future. For example; EU countries have set a target of 20% in 2020 for the biomass supply of energy consumption.

Biomass can be used in heating and industrial combustion systems. Boilers are widely used in many industries that require energy as well as being used for heating in residential areas. Energy efficiency in boilers depends on the quality of the combustion and the amount of energy transferred to the fluid (water). However, the emissions of flue gas depend on the quality of the burner, the design of the burner, the amount of pollutants in the fuel and the operating conditions of the combustion system.

Pellet fuels are one of the biomass energy sources and can be made from sawdust, wood chips, bark, waste, agricultural products, stems of crops, hazelnut, almond and walnut shells etc. These materials, compressed under high pressure after grinding and typically 6-8 mm in diameter, 10-11 mm in length, with a cylindrical structure and it's called with the name of pellet. Pellet fuel is a sustainable resource and has many advantages: reduces fossil fuel imports, contributes to the economy, leaves less waste after usage, and leads to exhaust emissions within acceptable limits.

Many researchers have realized research on the heat transfer effects of turbulators which are inserted in the pipes or tubes. Muthusamy et al. (2013) investigated the heat transfer, friction factor and thermal performance of conical turbulators with inner fins on flow direction and on the opposite flow direction experimentally. They stated that the turbulators inserted on the flow direction had better results. In order to increase the heat transfer in the concentric heat exchangers, Yıldız and Çakmak (2003) has placed straight-line injectors into the pipe inlet and experimentally investigated the resulting rotational flow. Lozza and Merlo (2001) investigated the effects of fins with the same kind of pipe but flat or wavy flap geometry on heat transfer in air-cooled condensers and liquid-phase coolers. Yakut and Sahin (2004) investigated experimentally the effect of coiled wire turbulators inserted to the tubes on the heat transfer and the friction factor. Kurtbaş et al. (2004)

placed into a pipe which is kept at constant heat, 62 mm wide and 1200 mm long, with different angles to the wings formed at different diameters and spacings on the sheet and experimentally examined their effect on heat and pressure loss. Karakaya and Durmuş (2013) experimentally investigated the effect of conical spring turbulators on the performance of the heat transfer and the pressure drop in a pipe. They observed that increasing the heat transfer increased the pressure losses and therefore an optimization should be made for pressure losses. Kahraman et al. [3] investigated experimentally and numerically the heat transfer performances of turbulators with two different fin gap (b=0.1 and 0.2 m) and three different angles (θ=30°, 45° and 60°). They reported that in all cases, using turbulators in tubes increased the Nusselt number. Akansu [4] analyzed numerically the effect of turbulators like porous-ring shaped on the heat transfer and the pressure drop. He used Fluent software in calculations. He used k-ω model as turbulence model and air as a fluid.

Some of the studies on numerical modeling of the solid fuel boilers are presented below.

Ahn and Kim (2014), designed a pellet fuelled boiler with 278 kW thermal power and then they carried out experiments and numerical simulation with this boiler. They used Fluent as CFD programme. They stated that the flame forms an arch from the second grate and this issue was predicted well by numerical simulations. Chaney et al. (2012) investigated the combustion performance and NO_x emissions optimization of 50 kW pellet boiler. They said that there are many parameters which can improve the combustion performance and NO_x emissions like primary and secondary air adjustment, secondary air inlet number etc. For modeling the gas phase they used Eddy Dissipation model and as a CFD program, they used Fluent program in their calculations. Chen et al. (2015) investigated the effect of flue gas recirculation experimentally and numerically in a 500 kW wood chip boiler. The FLIC code is used in the modeling of the bed, and the Fluent program is used in the modeling of the bed phase outside the bed. They noted that flue gas recirculation increased CO emissions, NOx and PM emissions, and reduced maximum flame temperatures. Collazo et al. (2012) simulated the domestic pellet boiler with CFD program and they used Finite rate/Eddy dissipation model for modeling the gas phase. They stated that the numerical results were in good agreement with the experimental results. As a result of the boiler analyses, they specified that the positions of water tubes and air inlet distributions were important factors which can cause the high emissions in such systems. Dong and Blasiak (2001) numerically analyzed the systems distributed the secondary air into to the boiler, which aims to reduce

emissions by more efficient combustion for 15 MW solid biomass-fired and 29 MW coal-fired boilers, respectively. They used Arrhenius finite-rate reaction mechanism and the Magnussen and Hjertager eddy-dissipation model to calculate the relationship between turbulence and chemistry. They took the biomass and coal gas reactions chemical data's directly adopted from the data generated by methane combustion reactions from the Fluent program and they stated that the numerical results were successful. Gómez et al. (2012) compared the heat transfer, temperature and species concentration of a domestic pellet boiler. As a result, they stated that the numerical results were in acceptable level of accuracy in comparison to experiments. Also, they numerically investigated the effect of water temperature on a pellet boiler and they showed that low water temperature increased the heat transfer.

In this study, the effects of heat transfer were investigated numerically by inserting helical turbulators to the smoke tubes of a 30 kW pellet-fueled boiler. In this context, a boiler with turbulators and without turbulators was investigated. Calculations were made for three-dimensional conditions. The results were evaluated by examining the temperature contours, the velocity vectors, the flue gas temperatures and the efficiencies.

2. Material and Method

Pellet fuel combustion occurs in four stages, like other solid fuels which are drying (evaporation of water), pyrolysis (separation of the volatile components), and combustion of volatile components and combustion of fixed carbon.

In the solution of combustion problems analytical, experimental and numerical methods can be applied. These methods can be applied separately, or they can be used together. Due to developments of powerful computers, numerical methods have been used quite often in recent years. In this study Fluent program was used as CFD program and therefore some information was given about the details of the submodels which were used in this program.

Various options are available for combustion modeling in Fluent program (Fluent, 2006). These are species transport model, non-premixed model, premixed model, partially premixed model, composition PDF model.

For the combustion modeling, species transport model was used in this study. In this model, the conservation of the species mass fractions is defined by the user contains a solution of chemical reactions. The reaction rates and the relationship of turbulence-reaction are taken into account with Arrhenius equation and/or Magnussen-Hjertager equations by the following models: laminar finite rate, finite-rate/eddy dissipation, eddy dissipation and eddy dissipation concept models (Fluent, 2006). Finite rate/Eddy dissipation model computes both the Arrhenius and the Eddy dissipation rates and uses the smaller value as the reaction rate. This model can be used to solve the problems as non-premixed combustion, premixed combustion, and partial premixed combustion.

In this study, volatile components of pellet fuel were modeled at a gas phase in a model boiler. The part of the fixed carbon was modeled by injecting carbon particles above the grate. Calculations were made at three-dimensional conditions. For modeling the turbulence RNG k-ε model, for modeling the combustion Finite rate/Eddy dissipation model and for modeling the radiation P1 approach were used. In reaction model, calculations were performed by entering the following equations into the program:

$$C_6H_6 + {}^{15}/_{2}\, O_2 \rightarrow 6CO_2 + 3H_2O \quad (1)$$

$$CH_4 + {}^{3}/_{2}\, O_2 \rightarrow CO + 2H_2O \quad (2)$$

$$H_2 + {}^{1}/_{2}\, O_2 \rightarrow H_2O \quad (3)$$

$$CO + {}^{1}/_{2}\, O_2 \rightarrow CO_2 \quad (4)$$

$$CO_2 \rightarrow CO + {}^{1}/_{2}\, O_2 \quad (5)$$

$$C < s > + O_2 \rightarrow CO_2 \quad (6)$$

Properties of pellet fuel was given in Table 1. The amount of moisture content in the fuel is considered by adding it to the gas phase. It is assumed that the volatile components consist of CO, CO_2, H_2, H_2O, light hydrocarbons (CH_4) and tar (C_6H_6) (Gómez et al., 2012).

Table 1. Properties of the pellet fuel

Proximate analyses	
Moisture [wt. %]	8.50
Ash [wt. %]	0.62
Fixed carbon [wt %]	16.20
Volatile matter [wt %]	74.68
Lower heating value [kJ/kg]	18330

Figure 1 shows the isometric view of the boiler and Figure 2 shows the gas passes. As can be seen, the combustion products are first passed directly through the combustion chamber (first pass) and come to the upper smoke chamber. Then, directed to 6 smoke tubes (second pass) and reached to bottom smoke chamber and exited from the chimney. The heat of the combustion products transfers to the water surrounding the smoke pipes by radiation and convection.

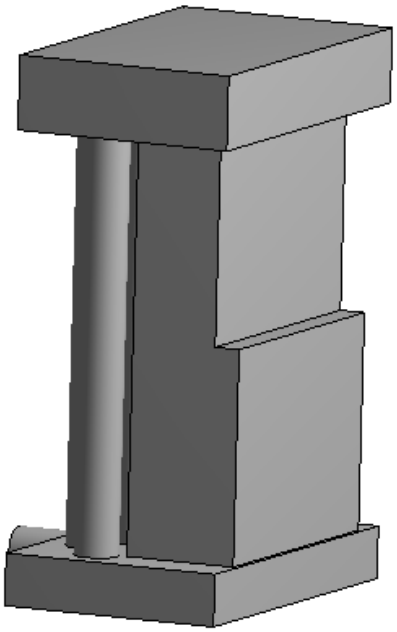

Figure 1. The isometric view of pellet boiler

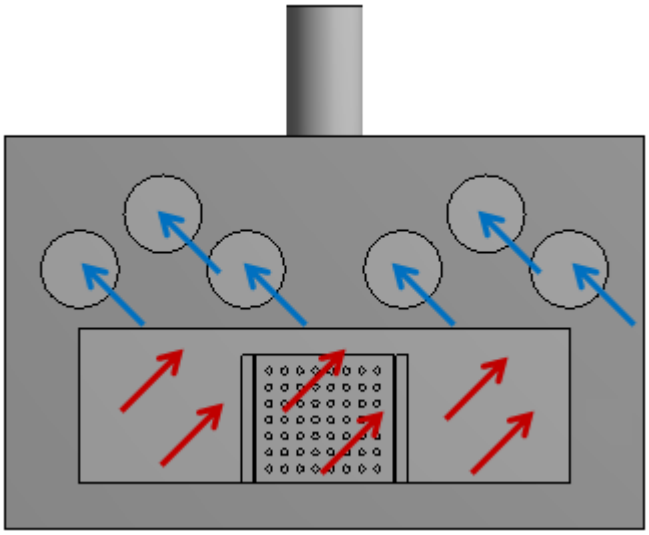

Figure 2. Gas passes; red arrow: gas exit from the combustion chamber, blue arrow: gas entering the smoke tube

In Figure 3, the helical turbulator geometry placed in the smoke tubes of the boiler is given. Figure 4 shows the top view of the boiler. As can be seen, there are six turbulators in total, one for each smoke tube.

Figure 3. The geometry of the helical turbulator

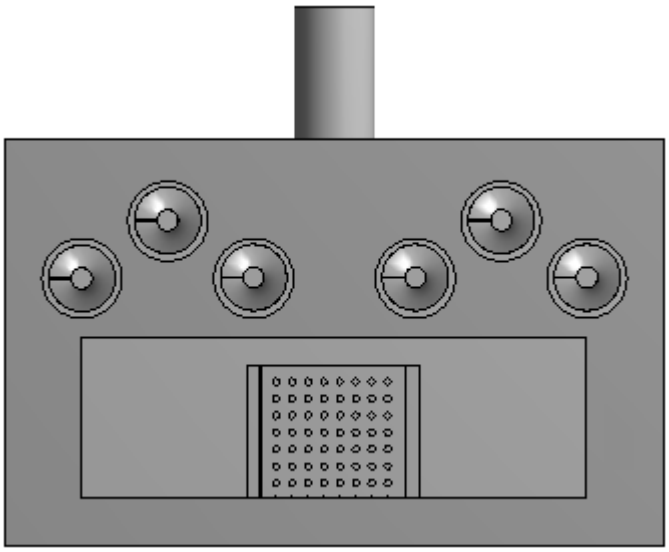

Figure 4. The top view of the boiler with turbulators in the smoke tubes

Both cases (with and without turbulators) are meshed with a similar grid structure and there are approximately 750 000 cells for each boiler.

All the calculations were made for the constant value of excess air coefficient λ=2. All surfaces in contact with water considered as the wall temperature of 353 K. Outlet region introduced as pressure outlet where atmospheric pressure prevails, air inlet and fuel inlet are introduced as velocity inlet. Iterations were continued up to the value of 10^{-6} for continuity and energy convergence criteria.

3. Results and Discussions

The temperature contours of pellet fuel combustion are shown in Figure 5. The temperature contours are given in three different views; the section of the center of the grate, the front smoke tubes, and the rear smoke tubes. As can be seen from the figure, in all cases flame temperatures reached to their maximum values in areas near to the grate, and temperatures decreased toward the exit because of the hot gases areas surrounded by water. In general, it is observed that the flame temperatures in the combustion chamber are around 1900 K in the areas close to the grate, and the temperature towards the upper smoke chamber is lower (about 1300 K) than the bottom parts. The gas temperatures towards the outlet region (from the grate section to the smoke tubes section) appear to be reduced by the effect of heat transfer. Especially, in the rear section of the smoke

tubes, boiler with turbulators, lower temperatures are occurred due to the increase of the heat transfer.

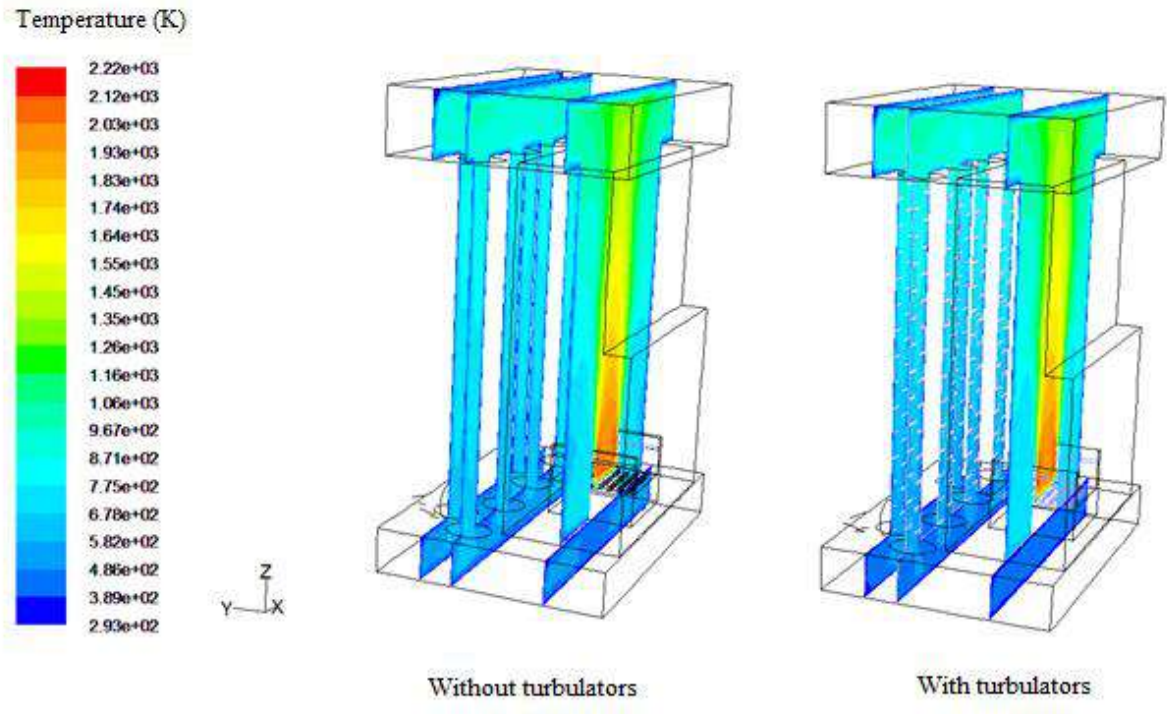

Figure 5. Temperature contours of pellet combustion

Figure 6 shows the velocity vectors. The combustion product gaseous are first passed directly through the combustion chamber (first pass) and come to the upper smoke chamber. Then, directed to 6 smoke tubes (second pass) and reached to bottom smoke chamber and exited from the chimney.

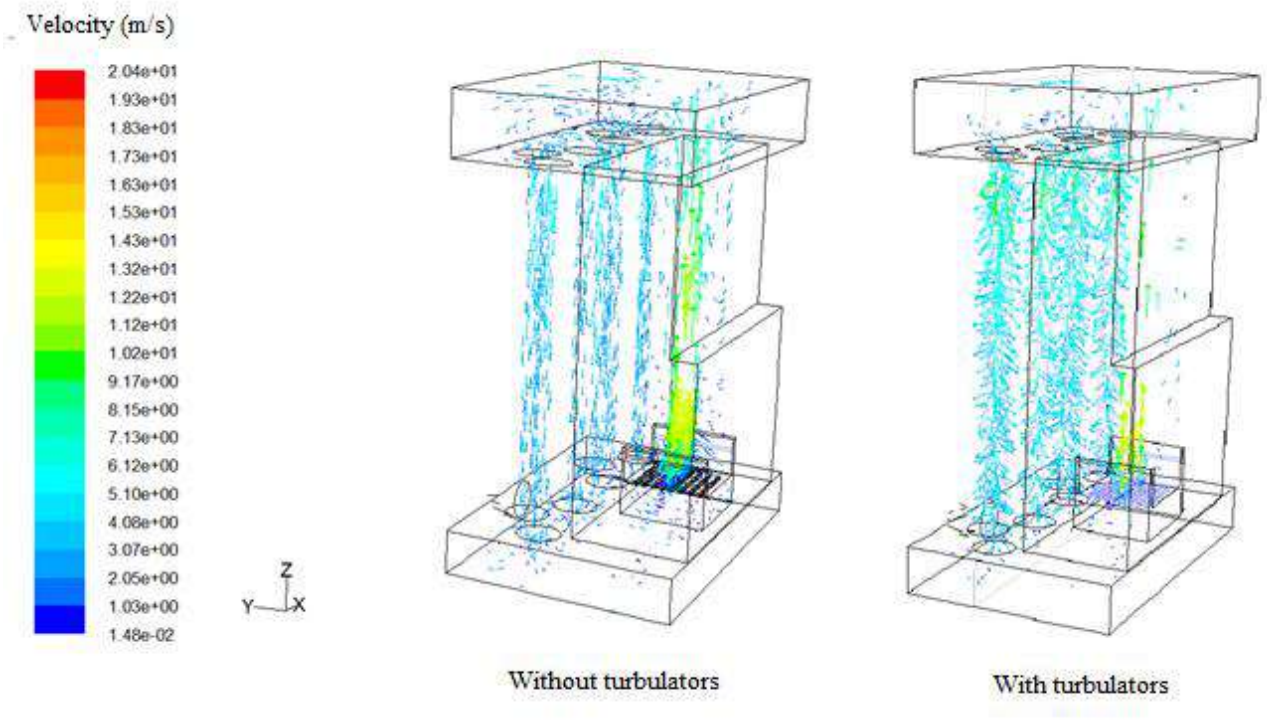

Figure 6. Velocity vectors of pellet combustion

In the situation of a boiler with turbulator, gas velocities show more complex movements instead of following a smooth path. This has a positive effect on heat transfer due to the increased path and mixing of flow.

The increase in heat transfer generally leads to an increase in pressure loss. In the case of boiler with turbulator, pressure loss was determined to be higher (40 Pa) than boiler without turbulator.

The efficiency of a boiler can be calculated with Eq.(7) as follows (Sungur et al., 2016), if losses are neglected except sensible heat of flue gases:

$$\eta = 1 - (1 + \lambda A_{sto})(T_{exh} - T_0)c_{p,exh} / H_U \quad (7)$$

In this equation λ is excess air coefficient, A_{sto} is stoichiometric air fuel ratio, $c_{p,exh}$ is specific heat of exhaust gases, T_{exh} is exhaust gas temperature, T_0 is ambient air temperature and H_U is lower heating value of the fuel.

According to this equation the exhaust gas temperatures can be used for comparison the boiler efficiency with and without turbulators. In the case of boiler without turbulator the exhaust gas temperature was 505.6 K, which was 433.8 K at boiler with turbulators. With these temperature values, the boiler efficiencies were 82.6% in the case of boiler without turbulator and 88.5% boiler with turbulator. Accordingly, helical turbulators inserted to the smoke tubes of the boiler increase the boiler efficiency approximately 6%.

4. Conclusions

In this study, the effects of heat transfer were investigated numerically by inserting helical turbulators to the smoke tubes of a 30 kW pellet-fueled boiler. In this context, a boiler with turbulators and without turbulators was investigated. Fluent 6.3 was used as the computational fluid dynamics software. In all cases, the RNG k-ε model was used for modeling the turbulent flow, the Finite rate/Eddy dissipation model was used for modeling the combustion and P1 radiation model was used for modeling the radiation. Calculations were made for three-dimensional conditions. The results were evaluated by examining the temperature contours, the velocity vectors, the flue gas temperatures and the efficiencies. In the situation of a boiler with turbulator, gas velocities show more complex movements instead of following a smooth path. This has a positive effect on heat transfer due to the increased path and mixing of flow. The increase in heat transfer generally leads to an increase in pressure loss. It was determined that pressure loss in the case of boiler with turbulator is higher than that without turbulator. The boiler efficiencies were 82.6% in the case of boiler without turbulator and 88.5% boiler with turbulator. Accordingly, helical turbulators inserted to the smoke tubes of the boiler increase the boiler efficiency approximately 6%.

References

Ahn J, Kim JJ. (2014). Combustion and heat transfer characteristics inside the combustion chamber of a wood pellet boiler. J Mech Sci Technol., 28, 789-795.

Akansu S.O. (2006). Heat transfer and pressure drops for porous-ring turbulators in a circular pipe, *Applied Energy*, 83, 280-298.

Chaney J, Liu H, Li J. (2012). An overview of CFD modelling of small-scale fixed-bed biomass pellet boilers with preliminary results from a simplified approach. Energ Convers Manage. 63:149-56.

Chen Q, Zhang X, Zhou J, Sharifi VN, Swithenbank J. (2015). Effects of Flue Gas Recirculation on Emissions from a Small Scale Wood Chip Fired Boiler. Energy Procedia. 66:65-8.

Collazo J, Porteiro J, Míguez JL, Granada E, Gómez MA. (2012). Numerical simulation of a small-scale biomass boiler. Energ Convers Manage. 64:87-96.

Dong W, Blasiak W. CFD modeling of ecotube system in coal and waste grate combustion. (2001) Energ Convers Manage.;42:1887-96.

Fluent. (2006). Fluent User's Guide.

Gómez MA, Comesaña R, Feijoo MAÁ, Eguía P. (2012). Simulation of the Effect of Water Temperature on Domestic Biomass Boiler Performance. Energies. 5:1044.

Kahraman N., Sekmen U., Çeper B., Akansu S.O. (2008). Boru içi akışlarda türbülatörlerin ısı transferine olan etkisinin sayısal incelenmesi, *Isı Bilimi ve Tekniği Dergisi*, 28(2), 51-59.

Karakaya H., Durmuş A. (2013). Heat transfer and exergy loss in conical spring turbulators, *International Journal of Heat and Mass Transfer*, 60, 756-762.

Kurtbaş İ., Gülçimen F., Durmuş A. (2004). Değişik tip kanatçıklar kullanarak sabit ısı akısına sahip bir ısı değiştiricisinin etkenliğini artırma, *Isı Bilimi ve Tekniği Dergisi*, 24(2), 117-125.

Lozza G., Merlo U. (2001). An Experimental Investigation of Heat Transfer and Frictio Losses of Interrupted and Wavy Fins for Fin-And-Tube Heat Exchangers, *International Journal of Refrigeration*, 24, 409-416.

Muthusamy C., Vivar M., Skryabin I., Srithar K. (2013). Effect of conical cut-out turbulators with internal fins in a circular tube on heat transfer and friction factor, *International Communications in Heat and Mass Transfer*, 44, 64-68.

Sungur B, Topaloglu B, Ozcan H. (2016). Effects of nanoparticle additives to diesel on the combustion performance and emissions of a flame tube boiler. Energy.;113:44-51.

Yakut K., Sahin B. (2004). The Effects of Vortex Characteristics on Performance of Coiled Wire Turbulators Used for Heat Transfer Augmentation, *Applied Thermal Engineering*, 24, 2427–2438.

Yıldız C., Çakmak G. (2003). Boru Girişinde Düzgün Sıralı Enjektörlü Türbülans Üretici Bulunan Isı Değiştiricilerinde Isı Geçişinin ve Basınç Düşümünün incelenmesi, *Termodinamik Dergisi*, 43(514), 32-37.

MHD Natural Convection in Square Enclosure Having Linearly Heated Adjacent Walls

Birol Şahin[1,*]

[1]*Recep Tayyip Erdogan University, Faculty of Engineering, Mechanical Engineering Department, Rize, Turkey*

[*]**Corresponding author:**

birol.sahin@erdogan.edu.tr

Abstract

Laminar steady state natural convection in square enclosure with magnetic field is analyzed numerically. Upper and left adjacent walls of the square enclosure are heated linearly while bottom wall is insulated. The other vertical wall is cooled. The solution is performed for various Rayleigh numbers and Hartmann numbers. The governing equations for steady state, two-dimensional, laminar natural convection flows with the Boussinesq approximation are discretized by SIMPLE algorithm using finite volume method (FVM). The results of the solutions are presented in form of streamlines, isotherms and average Nusselt numbers. It is found that heat transfer and fluid flow in square enclosure depend on Rayleigh numbers and Hartmann numbers.

Keywords: Magnetic field, Natural convection, Adjacent wall, Square enclosure.

1. Introduction

Natural convection in square enclosures have been studied by many authors. Natural convection applications have been used in many engineering areas such as nuclear reactor design, solar collectors, building design, thermal comfort, cooling of electronic equipment, etc. When the cavity is filled an electrically conducting fluid, magnetic field has an important role. Magnetic field is effect the fluid flow and heat transfer in the cavity. Natural convection heat transfer in rectangular cavities in the presence of magnetic field have been studied in recent years. Rudraiah et all (1995), studied numerically free convection of an electrically conducting fluid in a rectangular enclosure at the Prandtl number Pr=0.733, Grashoff number ranging from $2x10^4$ to $2x10^6$ and Hartmann number from 0 to 100. At the end of the study it is found that effect of the magnetic field was decreased the rate of convective heat transfer. Laminar, steady natural convection in a tilted square enclosure heated from below and cooled from top investigated by Pirmohammadi and Ghassemi (2009) in the presence of magnetic field. Sathiyamoorthy and Chamkha (2012) have investigated natural convection flow in a square cavity heated from below and left walls uniformly or linearly while the top and right walls cooled uniformly for different Hartmann numbers and Rayleigh numbers and inclination angle. Jani et all (2013), have studied numerically magneto-hydrodynamic free convection in a square cavity heated from below and cooled from other walls with an electrically conducting fluid for Prandtl number of 0.7. They found that convective heat transfer and fluid velocity are reduced with increasing magnetic field. Sathiyamoorthy and Chamkha (2010) have investigated natural convection flow of liquid gallium in a square cavity uniformly heated below and insulated from top while left and right wall heated linearly or uniformly cooled right wall with different inclination angles of magnetic field. They found that average Nusselt numbers are decreased with increasing values of the Hartmann numbers. Al-Salem et all (2012) have studied magneto hydrodynamic (MHD) mixed convection in a square cavity linearly heated bottom wall while left and right walls are adiabatic and sliding top wall is cooled uniformly. They found that lid direction is more effective on heat transfer and fluid flow. Son and Park (2017) investigated two dimensional laminar natural convection in the presence of magnetic field with an insulated square block in a square enclosure, heated from below and cooled from above while vertical walls are insulated. They found that the block size depends on the Hartmann number and Rayleigh number

conditions. Kherif et all (2016) have studied laminar steady natural convection heat transfer in an inclined rectangular enclosure including magnetic field heated from below and cooled from the adjacent top wall while the other walls insulated. They found that circulation and convection become stronger with increasing Grashoff numbers. Oztop et all (2009) investigated MHD buoyancy induced heat transfer and fluid flow in a square enclosure heated sinusoidally at bottom wall and uniformly cooled top wall. They obtained that heat transfer was decreased with increasing Hartmann number. Sheikhzadeh et all (2011) have investigated numerically steady magneto-convection heat transfer around a centrally located adiabatic body in a square enclosure for low Prantl numbers. Square enclosure heated left wall and cooled right wall while horizontal walls insulated well. They obtained that the increasing magnetic field is increased convection with increasing Prandtl number.

In this study, laminar, steady natural convection in the presence of magnetic field analyzed numerically in a square enclosure linearly heated left and upper adjacent walls and uniformly cooled right wall while bottom wall insulated for Rayleigh number ranging from 10^4 to 10^6 and Hartmann number from 0 to 50 and Prandtl number Pr=0.733.

2. Physical Model and Governing Equations

A schematic diagram of the square enclosure with coordinates and boundary conditions is shown in Fig. 1. Length and height of the enclosure are equal (L=H) for square geometry. Left and upper adjacent walls of the enclosure are heated linearly. Right wall is uniformly cooled while bottom wall is well insulated. It is considered that magnetic field effected in the horizontal direction uniformly on square enclosure. Working fluid is electrically conducted. Fluid properties are constant except density. The Boussinesq approximation is valid in the enclosure for buoyancy term. With these assumptions, steady two dimensional laminar continuity, momentum and energy equations (1-4) are as follows, respectively.

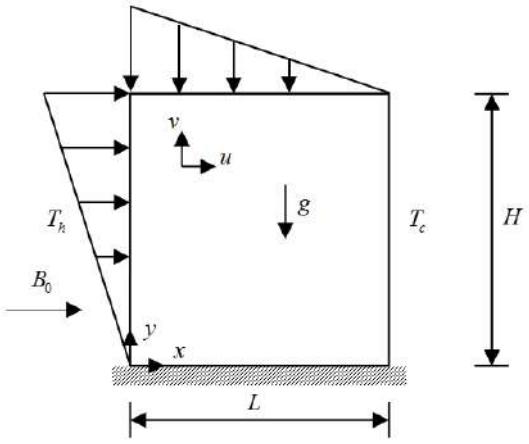

Figure 1. Schematic diagram of the problem.

$$\frac{\partial U}{\partial X}+\frac{\partial V}{\partial X}=0 \quad (1)$$

$$U\frac{\partial U}{\partial X}+V\frac{\partial U}{\partial Y}=-\frac{\partial P}{\partial X}+Pr\left(\frac{\partial^2 U}{\partial X^2}+\frac{\partial^2 U}{\partial Y^2}\right) \quad (2)$$

$$U\frac{\partial V}{\partial X}+V\frac{\partial V}{\partial Y}=-\frac{\partial P}{\partial Y}+Pr\left(\frac{\partial^2 V}{\partial X^2}+\frac{\partial^2 V}{\partial Y^2}\right)+RaPr\theta-Ha^2PrV \quad (3)$$

$$U\frac{\partial \theta}{\partial X}+V\frac{\partial \theta}{\partial Y}=\frac{\partial^2 \theta}{\partial X^2}+\frac{\partial^2 \theta}{\partial Y^2} \quad (4)$$

The non-dimensional parameters in above equations are:

$$X=\frac{x}{L},\qquad Y=\frac{y}{L},U=\frac{uL}{\alpha},\qquad V=\frac{vL}{\alpha},\qquad P=\frac{pL^2}{\rho\alpha^2},\qquad \theta=\frac{T-T_c}{T_h-T_c}$$

Where X and Y are the dimensionless coordinates of horizontal and vertical directions, U and V are the dimensionless velocity components, P is the dimensionless pressure and θ is the dimensionless temperature, respectively. Dimensionless numbers are given as follows;

$Ha=BL\sqrt{\frac{\sigma}{\rho v}}$, the Hartmann number

$Ra=\frac{g\beta(T_h-T_c)}{v\alpha}$, the Rayleigh number

$Pr=\frac{v}{\alpha}$, the Prandtl number

Boundary conditions are given as follows at non-dimensional form

On the left wall, U=V=0, $\theta = \frac{Y}{H}$

On the upper wall, U=V=0, $\theta = 1 - \frac{X}{L}$

On the right wall, U=V=0, $\theta = 0$

On the bottom wall, U=V=0, $\frac{\partial \theta}{\partial Y} = 0$

Local and average Nusselt number along the cold wall are given as follows, respectively.

$$Nu_y = -\frac{\partial \theta}{\partial X}\Big|_{X=L} \qquad Nu = \frac{1}{H}\int_0^H Nu_y dy$$

The governing equations are discretized by finite volume method using SIMPLE algorithm given by Patankar (1980). A Fortran program is developed to solve the discretized equations. Six different uniform grids are employed such as 20x20, 40x40, 80x80, 120x120, 160x160, 240x240 control volumes for grid refinement and 120x120 grids are chosen. In order to verify the present code, obtained results are compared with Pirmohammadi et all (2009) for different Rayleigh and Hartmann numbers that is shown in Table I. Obtained results are in good agreement with the literature results.

Table I. Comparison of the average Nusselt numbers between present study and Pirmohammadi et all (2009)

Ra	Ha	Nu	
		Present study	Pirmohammadi et all (2009)
		Nu	Nu
10^4	0	2.201	2.29
	10	1.932	1.97
	50	1.041	1.06
	100	1.005	1.02
10^6	0	8.994	8.9
	50	6.437	6.39
	150	2.641	2.64

The convergence criteria is

$$\frac{\sum_{i,j}\left|\varphi_{i,j}^{n+1} - \varphi_{i,j}^{n}\right|}{\sum_{i,j}\varphi_{i,j}^{n}} \le 10^{-5}$$

Where φ represents for average Nusselt numbers at right wall.

3. Results and Discussions

Numerical study is performed in a square cavity heated linearly adjacent walls in the presence of magnetic field. The results are obtained for Rayleigh number ranging from 10^4 to 10^6 and Hartman number ranging from 0 to 50 at the Prandtl number Pr=0.733. Figure 2 shows the isotherms and streamlines for different Rayleigh and Hartmann number. It is found that there is an upward flow near the heated adjacent walls and downward flow near the cold wall. A unicellular flow pattern is observed for all streamlines. Center of the unicellular pattern is displaced towards the center of the square cavity by increasing Hartmann number. Magnitude of the streamlines are decreased with increasing Hartmann number for fixed Rayleigh number. It is found that at high Rayleigh numbers center of the streamlines are moved to upper side of the right wall. For low Rayleigh number and high Hartmann number conduction heat transfer is dominant in the square enclosure. Isotherms are nearly perpendicular to linearly heated walls look like insulated wall approach. By increasing the Rayleigh number the convection is more dominant then magnetic field. The intensity of the isotherms are increased at linearly heated adjacent walls. When the Hartmann number increases isotherms become smoother.

Ra		Ha		
		0	25	50
10^4	ψ	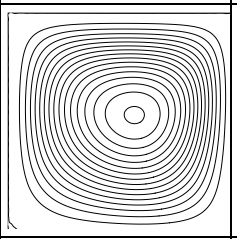	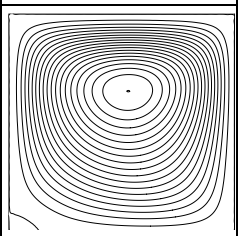	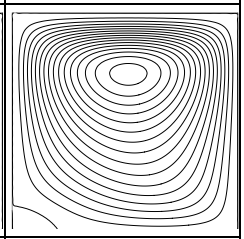
	θ	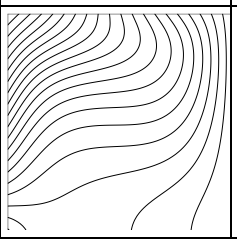	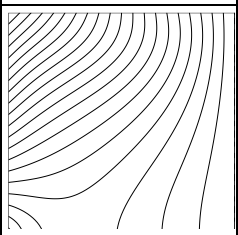	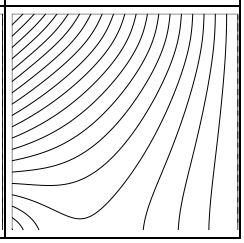

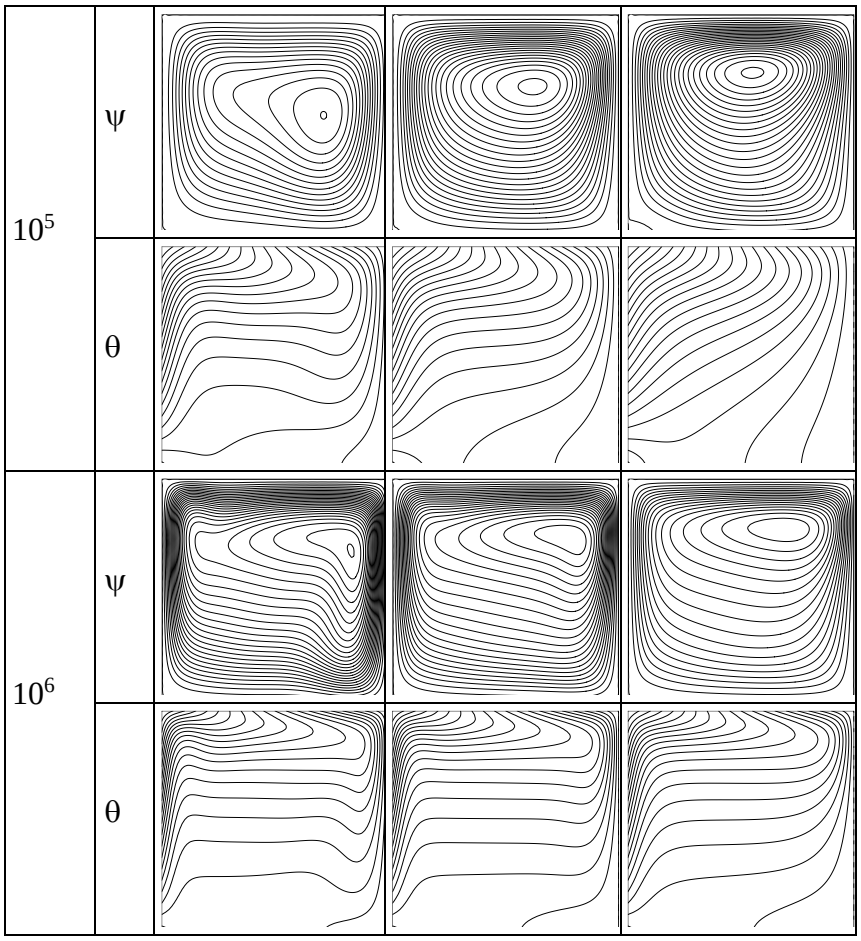

Figure 2. Streamlines and isotherms for different Rayleigh and Hartmann numbers.

Figure 3 shows the average Nusselt numbers of the right wall for different Rayleigh and Hartmann numbers. Bouyancy heat transfer is dominant for low Hartmann numbers and high Rayleigh numbers. Natural convection heat transfer is increased with increasing Rayleigh numbers and decreased with increasing Hartmann numbers. Conduction heat transfer and magnetic field are more dominant at high Hartmann numbers and low Rayleigh numbers. The highest heat transfer is occurred at high Rayleigh number in the absence of magnetic field, vice versa, the lowest heat transfer is occurred at low Rayleigh number in the presence of strong magnetic field. It is found that Nusselt numbers and heat transfer depend on the Rayleigh number and Hartmann number.

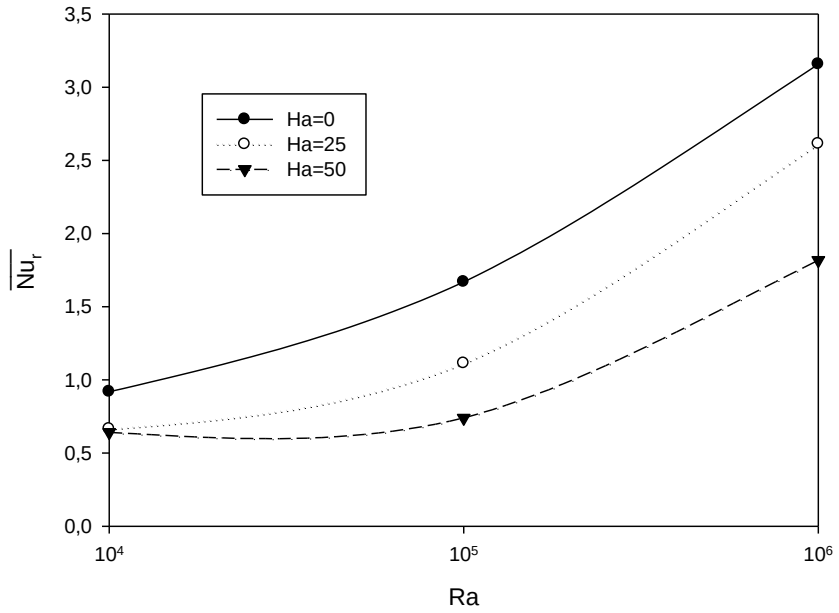

Figure 3. Variation of the average Nusselt numbers for different Rayleigh and Hartmann numbers.

4. Conclusions

It is investigated effect of linearly heated adjacent walls in a square enclosure in the presence of magnetic field for different Rayleigh and Hartmann numbers. The heat transfer and flow pattern are strongly depend on the magnetic field. It is found that magnetic field reduces the convective heat transfer. Natural convection heat transfer is increased with increasing Rayleigh numbers and decreased with increasing Hartmann numbers. In this study, a unicellular flow pattern is observed for all streamlines. Magnitude of the streamlines are decreased with increasing Hartmann number for fixed Rayleigh number. It was observed that according to the conventional temperature profile when the left and upper wall have linearly increasing and decreasing temperature profile respectively, the natural convection heat transfer is reduced.

5. References

Rudraiah, N., Barron, R.M., Venkatachalappa, M., Subbaraya, C.K., (1995). Effect of a magnetic field on free convection in a rectangular enclosure, *International Journal of Engineering Science*, Vol. 33(8), 1075-1084.

Pirmohammadi, M., Ghassemi, M., (2009). Effect of magnetic field on convection heat transfer inside a tilted square enclosure, *International Communications in Heat and Mass Transfer*, 36, 776-780.

Sathiyamoorthy, M., Chamkha, A.J., (2012). Natural convection flow under magnetic field in a square cavity for uniformly (or) linearly heated adjacent walls, *International Journal of Numerical Methods for Heat&Fluid Flow*, Vol. 22, No.5, 677-698.

Jani, S., Mahmoodi, M., Amini, M., (2013). Magnetohydrodynamic free convection in a square cavity heated from below and cooled from other walls, *World Academy of Science, Engineering and Technology, International Journal of Mechanical, Industrial Science and Engineering* Vol. 7, No.4, pp. 1-6.

Sathiyamoorthy, M., Chamkha, A.J., (2010). Effect of magnetic field on natural convection flow in a liquid gallium filled square cavity for linearly heated side wall(s), *International Journal of Thermal Science*, 49, 1856-1865.

Al-Salem, K., Öztop, H.F., Pop, I., Varol, Y., (2012). Effects of moving lid direction on MHD mixed convection in a linearly heated cavity, *International Journal of Heat and Mass Transfer*, 55, 1103-1112.

Son, J.H., Park, S., (2017). Numerical study of MHD natural convection in a rectangular enclosure with an insulated block, *Numerical Heat Transfer*, Part A, Vol. 7, No.10, 1004-1022.

Kherief, N.M., Berrahil, F., Talbi, K., (2016). Magneto-hydrodynamic flow in a two dimensional inclined rectangular enclosure heated and cooled on adjacent walls, *Journal of Applied Fluid Mechanics*, Vol.9, No.1, 205-213.

Oztop, H.F., Oztop, M., Varol, Y., (2009). Numerical simulation of magnetohydrodynamic buoyancy-induced flow in a non-isothermally heated square enclosure, *Communications in Nonlinear Science and Numerical Simulation*, 14, 770-778.

Sheikhzadeh, G.A., Fattahi, A., Mehrabian, M.A., (2011). Numerical study of steady magneto-convection around an adiabatic body inside a square enclosure in low Prandtl numbers, Heat Mass Transfer, 47, 27-34.

Pirmohammadi, M., Ghassemi, M., Sheikhzadeh, G.A., (2009). The effect of a magnetic field on buoyancy-driven convection in differentially heated square cavity, IEEE Trans. Magn., vol. 45, 407–411.

Patankar, S. V., (1980). Numerical Heat Transfer and Fluid Flow, New York, McGraw Hill.

Consodilation and Investigation of Properties of Hydroxyapatite-316L Stainless Steel Composites

Serdar ÖZKAYA[1], Aykut ÇANAKÇI[1], Temel Varol[1], A.Hasan KARABACAK[1], Müslim ÇELEBİ[1], Fatih ERDEMİR[1]

[1]Karadeniz Technical University, Engineering Faculty, Metallurgy and Materials Eng.Department, Trabzon, TURKEY, sozkaya@ktu.edu.tr

[*] **Corresponding Author:** sozkaya@ktu.edu.tr

Abstract

The aim of this study is production and investigation of properties of Hydroxyapatite (HA) matrix, 316L stainless steel powder reinforced biocomposites by powder metallurgy processes. The 316L powder ratio was changed from 0 to 2 wt%, to investigate the effect of 316L on the properties of HA/316L biocomposites. The composite powders were mixed in a planetary ball mill for 5 minutes to obtain homogenous distribution of 316L particles. Than the mixed powders were cold pressed under 600 MPa pressure, after that the green samples were sintered at 1200 ^{0}C for 2,5 hours under pure argon gas atmosphere. The density and porosity measurements were done by Archimed's method. The distribution of 316L particles and microstructural investigations were done using scanning electron microscopy. Moreover, the fracture toughness were investigated by using Vickers indentitation and Niihara fracture toughness formula. The investigations showed that, the density of samples are decreasing with increasing 316L powder amount. Moreover the fracture toughness were increased with increasing 316L content.

Keywords: Biomaterials, Biocomposite, Hydroxyapatite, 316L Stainless Steel, Powder metallurgy

1. Introduction

Introduction

Hydroxyapatite (HAp) is a calcium phosphate based material which is chemically very similiar to the natural bone. HAp has been widely used in the biomedical applications such as orthopedics, dental implants and at the other parts of human body because of it's mechanical properties and extremely high biocompatibiliy. One of the main applications of HA is that as coatings on metallic medical implants. Despite the advantages that HA presents, the brittle nature, and low fracture toughness of HA coating often result in rapid wear, and premature fracture of the coated layer. Hence, there is a need to improve the mechanical properties of the HA coatings without compromising the biocompatibility. Due to having good mechanical properties, some metallic materials like 316L stainless stell, titanium, platinium are being used as biomaterial. However, their corrosion ressistance are not enough to be used in long term in human body which is extremly agressive and acidic. Eventhough, these materials are suitable for short term using, the investigations showed that they are affecting the neighbour tissues in long term and they need to be taken of from body. Thus, the biomedical investigations are focused on new materials which have not only good corrosion and mechanical behaviours but also good biocompability. Most of these investigations are about coating the metallic materials with ceramics which have good biocompability such as SiC,TiC and Hydroxyapatite. The other subject area is about obtaining new materials by fabricating biocomposites. In this direction, two or more materials are being used to fabricate biocomposite. The main idea is compounding the superior behaviours of these materials such as "good biocompability" of one material, and "good mechanical behaviour" of the other material.

In this study our aim is fabrication of hydroxyapatite matrix, 316L stainless steel reinforced which is supposed to have good mechanical and biological properties. For this aim, the hydroxyapatite and 316L powders were milled in a planetary ball mill than compacted in a die which was followed by sintering process.Moreoever, mechanical and physical behaviours of fabricated samples were investigated.

Experimental Study

In the present work, hydroxyapatite powders (d50:42µm) were choosen as matrix and 316L SS powders (d50:40µm) were choosen as reinforcement material. The green samples were fabricated by powder metallurgy method. To obtain the green samples, the matrix and reinforcement powders were mixed in a planetary ball mill with different (0.25, 0.5, 1.5, 2 and 2.5 %wt) 316L SS contents for 3 minutes then they were hot pressed under argon gas atmposphere. The consolidation temperature was choosen as 560 ^{o}C and the pressure was 500 MPa. Then the green samples sintered under argon gass atmosphere at 1300 ^{o}C for 3 hours to obtain the bulk samples. The density measurements of biocomposite samples were done by Archimed's method and the investigations of microstructures were done by using stero microscope. The hardness measurements were done by using hardness Brinell measurement route. Moreoever the fracture toughness of bulk samples were obtained by using equation below;

$$K_{ıc}=(\in/(H\times P))/c^{\wedge}(3/2)$$

Where ∈: is the elastic modulus of HAp , H: Hardness Vickers, P: Applied load on Vickers measurement
c: Length of the crack

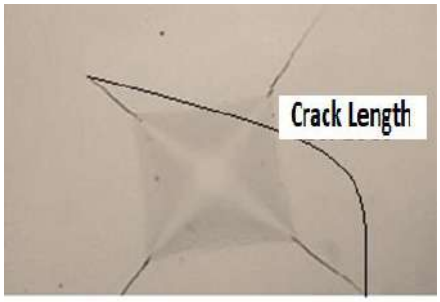

Figure 1. Illustration of crack length obtained from Vickers measurement

Results and Discussions

Microstructural Investigation

The microstructural images obtained from optical microscope are shown in Fig.2. In these figures the white areas are hydroxyapatite and the dark areas are 316L SS particles. As shown in figures the 316L SS powders were distributed homogenly in the matrix structure. Moreover, the matrix and reinforcement materials are compatible with each other so there is no lamination

between them. Additionally, because of the mechanical milling there is no agglomeration seen in the structure.

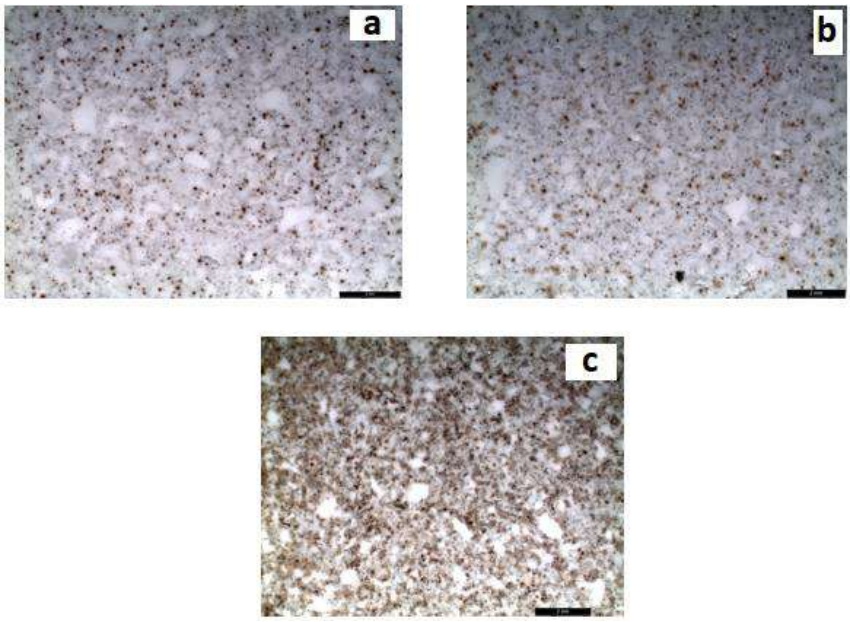

Figure 2. a)0.25 b)1 c) 2 wt % 316L SS

Density and Porosity Measurements

The density and porosity measurements showed that, the relative density of HAp-316L SS biocomposites were decreased with increasing 316L SS content. In other words, the porosities were increased with increasing 316L SS content. This increase in porosity can be explained by the adhere affect of 316L powders on compacting. As it was known, 316L SS powders are extremly hard particles so when the content of 316L increases, the compaction behaviour of composite powder decreases which also result as porosity in structure. When examine the Figure 3b, it is clear that the porosity decreases for 0.25wt% reinforced sample however it is always increasing for the other reinforcing ratios. This can be explained by the peak point of distribution rate of 316L in

hydroxapatite matrix. The maximum porosity was obtained for the 2wt% reinforced sample which is about 38 percentage.

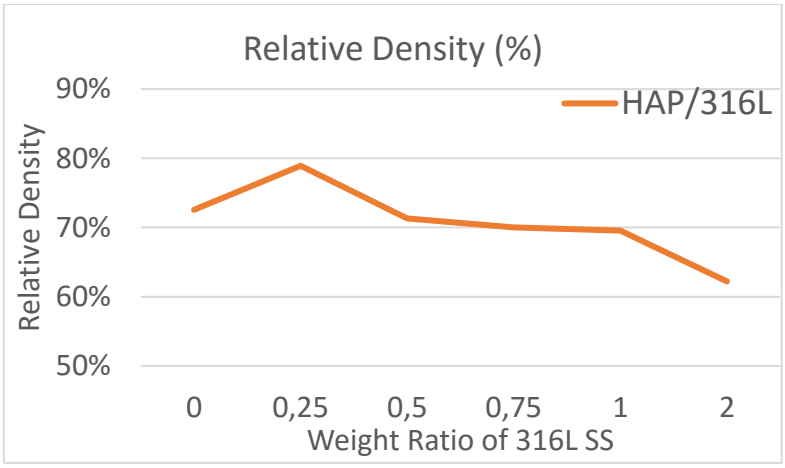

a)

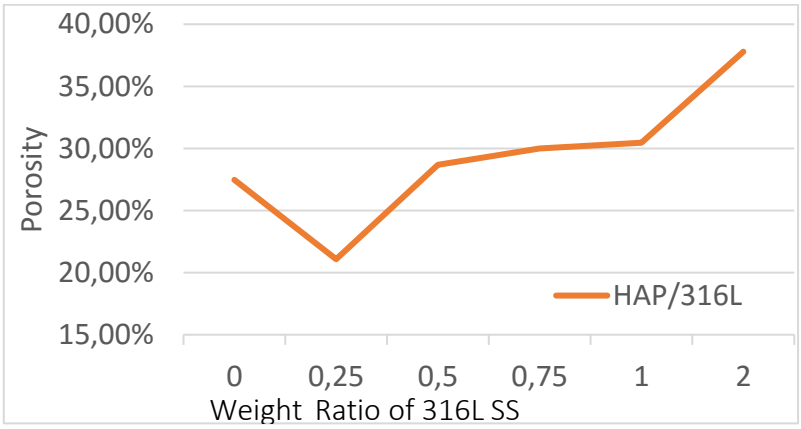

b)

Figure 3. a)Density and Porosity Graphics of Samples

Hardness and Fracture Toughness

The hardness and fracture toughness of samples as a result of increasing 316L content are shown in Figure 4. As shown in Fig.4a, Brinell hardness are decreasing with increasing 316L content. This decrease can be explained by the composite material theory. As known, the hydroxyapatite is a ceramic based material which is 4th material in hardness in literature. Thus, by additing 316L powders to the structure which is extremely softer then HAp, results in decrease in

hardness. The other reason of this decrease is, adverse affect on compacting which was also seen on density and porosites.

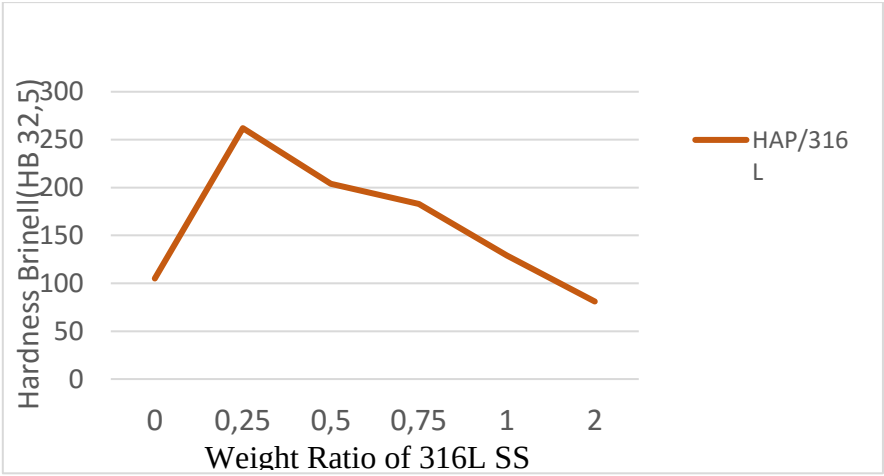

a)

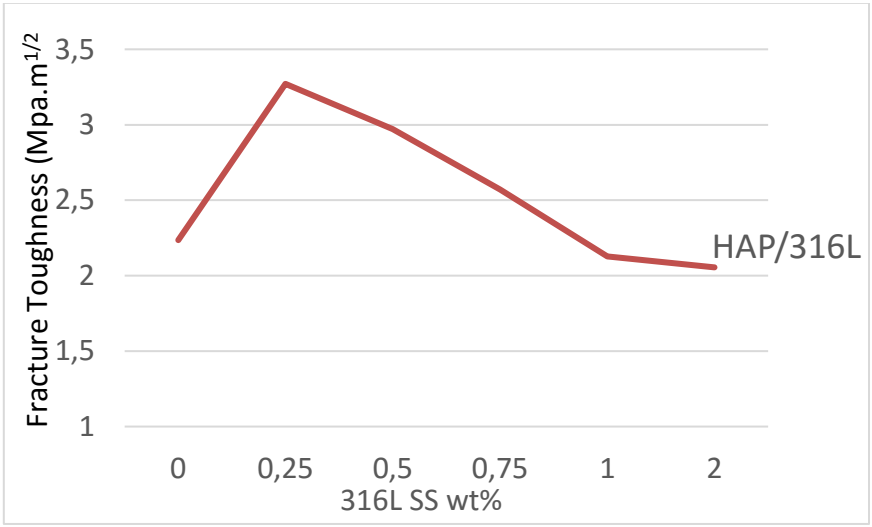

b)

Figure 4. a) Hardness measurements of samples changing with 316L content b)Fracture toughness of samples changing with 316L content

The fracture toughness measurements showed that the mechanical behaviours have the same slope of hardness and porosities. When examine the Fig.4b, it can be seen that highest fracture toughness was obtained for the sample include 2.5wt% reinforcement.

Conclusions

- Hydroxyapatie-316l SS biocomposites can be fabricate by powder metallurgy route.
- The mechanical behaviours can be developed by optimising the fabrication parameters.
- The highest fracture toughness was obtained fort he sample include 0.25wt% 316L sample.

References

Arifin, A., Sulong, A.B., Muhamad, N., Syarif, J., Ramli, M.I., 2014. Material processing of hydroxyapatite and titanium alloy (HA/ Ti) composite as implant materials using powder metallurgy: a review. Mater. Des. 55, 165–175.

Chenglin, C., Jingchuan, Z., Zhongda, Y., Shidong, W., 1999. Hydroxyapatite–Ti functionally graded biomaterial fabricated by powder metallurgy. Mater. Sci. Eng.: A 271, 95–100.

De Aza,P.N.,Pen˜ a, J.I.,Luklinska,Z.B.,Meseguer-Olmo,L.,2014. Bioeutectics ceramics forbiomedicalapplicationobtainedby laser floating zone method,Materials7, 2395–2410.

Huang, H., Wang, Z., Lu, J., Lu, K., 2015. Fatigue behaviors of AISI 316L stainless steel with a gradient nanostructured surface layer. Acta Mater. 87, 150–160.

Liu, D.-M., Yang, Q., Troczynski, T., 2002. Sol–gel hydroxyapatite coatings on stainless steel substrates. Biomaterials 23, 691–698.

Watari, F., Yokoyama, A., Omori, M., Hirai, T., Kondo, H., Uo, M., Kawasaki, T., 2004. Biocompatibility of materials and development to functionally graded implant for bio-medical application. Compos. Sci. Technol. 64, 893–908.

Younesi, M., Bahrololoom, M., 2010. Optimizations of wear resistance and toughness of hydroxyapatite nickel free stainless steel new bio-composites for using in total joint replacement. Mater. Des. 31, 234–243.

Production and Characterization of Al-SiC Composites by Mechanical Milling

Doğan ŞİMŞEK[1*], İjlal ŞİMŞEK[2], Dursun ÖZYÜREK[3]

[1] Bitlis Eren University, Technical Sciences Vocational School, Bitlis, Turkey,
[2] Karabuk University, TOBB Technical Sciences Vocational School, Karabuk,
[3] Karabuk University, Technology Faculty, Karabuk, Turkey

[*]**Corresponding author:** dsimsek@beu.edu.tr

Abstract

This study were investigated the effect of SiC amount and milling time on microstructure, density and hardness in the aluminum composites produced by mechanical milling. In the study, aluminum composites were mechanical milling at different times (30, 60, 90 and 120 min), adding SiC in different amounts (5%, 10%, 15% and 20%). A high chromium steel balls with a diameter of 6 mm, a ratio of 10:1 ball-powder and 2% stearic acid were used as milling component in the production of composites in a vibrating mill. The production of composite powders was carried out in an argon atmosphere. The composite powders produced were characterized using scanning electron microscopy, EDS analysis, optical microscope and powder size analyzer. As a result, it was observed that as the amount of added SiC and milling time increased, the powder size decreased and the hardness values increased. In addition, as the amount of added SiC increased, the densities of aluminum composites increased.

Keywords: Aluminum composite, mechanical milling, powder metallurgy, vibrating mill, SiC.

1. INTRODUCTION

Today, many industrial applications require materials with lower density (light) and higher rigidity and strength. Aluminum matrix composites (AMC) have become ideal materials for these requirements due to their various advantages (Prabhu et al. 2006; Torralba et al. 2002). Many researchers have used different production techniques to investigate AMCs, which can be produced using liquid or solid state techniques reinforced with hard particles such as carbides, oxides, and nitrides (Smagorinski et al. 1998). Different methods such as in-situ (in-situ nucleation) (Erek et al. 2017), spray (Sundararajan, 2017), and PVD (physical vapor deposition) have been used in these studies (Mortensen et al. 2002). Liquid state processes such as infiltration, squeeze casting, stir casting (Rajan et al. 1998), powder metallurgy (Yu et al. 2005), and spray deposition (Wannasin and Flemings, 2005) stand out among these methods. The powder metallurgy method is accepted to be a good method to produce metal matrix composites. Low treatment temperature is a significant advantage of the powder metallurgy (P/M) method compared to melting techniques (Arifin et al. 2014). Although the P/M method is accepted to be a good method to produce metal matrix composites, some problems are encountered in production of AMCs using this method (Zhao et al. 2014). One of the most significant problems encountered is the flocculation of particles added into the Al matrix and the non-homogeneous distribution of the ceramic reinforcement elements. Different methods are used to prevent such problems, one of which is the use of different mill types depending on the application's purpose (Suryanarayana, 2001).

In this study, commercially pure Al and SiC ceramic reinforcement element was mechanically milled with different amounts and different milling times using a mechanical vibration mill (in argon atmosphere). The purpose of the study was to investigate the effects of the different SiC amounts and milling times on the hardness, density and microstructure of the AMC mechanically milled using a vibration mill.

2. Materials and Method

The effects of different SiC amounts (5%, 10%, 15%, 20%) and milling times (30, 60, 90, 120 min) on AMCs milled in a vibration mill were investigated in this study. 99.5% pure and 53

µm gas atomized Al powder and 13 µm SiC powder were used to produce Al-SiC composite powders. A ball/powder ratio of 10:1 and 6 mm high-chrome steel balls in the vibration mill, and 2% stearic acid was used as the process control agent. The powder and ball charge was performed in argon environment for mechanical milling (MM). The composite powders produced were moved into glove box (under argon). Figure 1 shows the schematic view of the vibration mill used in experimental studies.

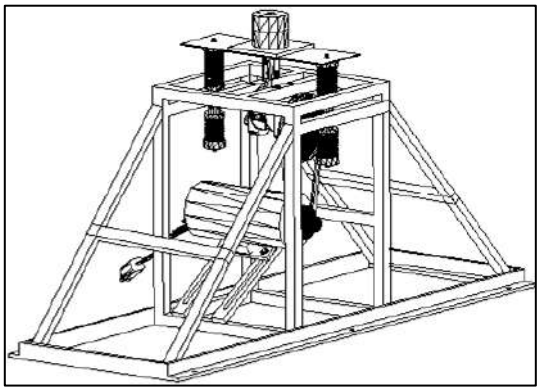

Figure 1. Schematic view of the vibration mill.

Powder size measurements and optical and scanning electron microscope examinations were performed to determine the powder size and shape depending on the MM time. The powders were cold-pressed under 630 MPa pressure to produce preformed composite parts. The preformed composite parts were sintered in argon environment at 560 °C for 30 minutes. Hardness measurements of the sintered aluminum composite parts were performed using an Affri universal hardness tester (HV2). Powder size analysis of the composite powders was performed using the laser technique in a Malvern Mastersizer-X device mixing the powders with distilled water and stirring for 5 minutes. Density measurements before and after sintering were performed using a density measurement kit on a Precisa XB 220A analytical balance.

3. Findings and Discussion

Figure 2 shows the change in powder size depending on milling time for Al-SiC composites produced in a vibration mill using different milling times.

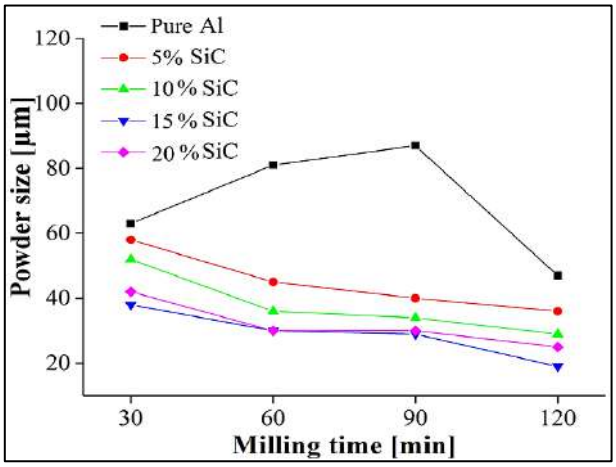

Figure 2. The change in powder size depending on milling time for Al-based composites mechanically milled using different milling times.

As shown in Figure 2, the pure aluminum powders mechanically milled for 30-90 min showed an increase in size (63-87 µm), while a decrease was observed in powder size (81 µm) when a milling time of 120 min was used. This is due to the enlargement of ductile metal powders with cold welding. Ductile powders which present a cold welding effect in the first stage of mechanical milling undergo deformation hardening in parallel with the increase in milling time, which causes them to fracture and shrink (Sankar and Singh, 1998). Powders in composites containing different amounts of SiC fracture and shrink due to constant milling effect. For this reason, the powder size in aluminum composites containing SiC decreases with increasing milling time. Similar results have been obtained in previous studies as well (Zhao et al. 2014; Simsek et al. 2018; Parvin et al. 2008). The powder size chart shows that the smallest powder size was obtained for the aluminum composites containing 15% SiC. Figure 3 shows the optical microscope images of the Al + 20% SiC composite powders mechanically milled in the vibration mill using different milling times.

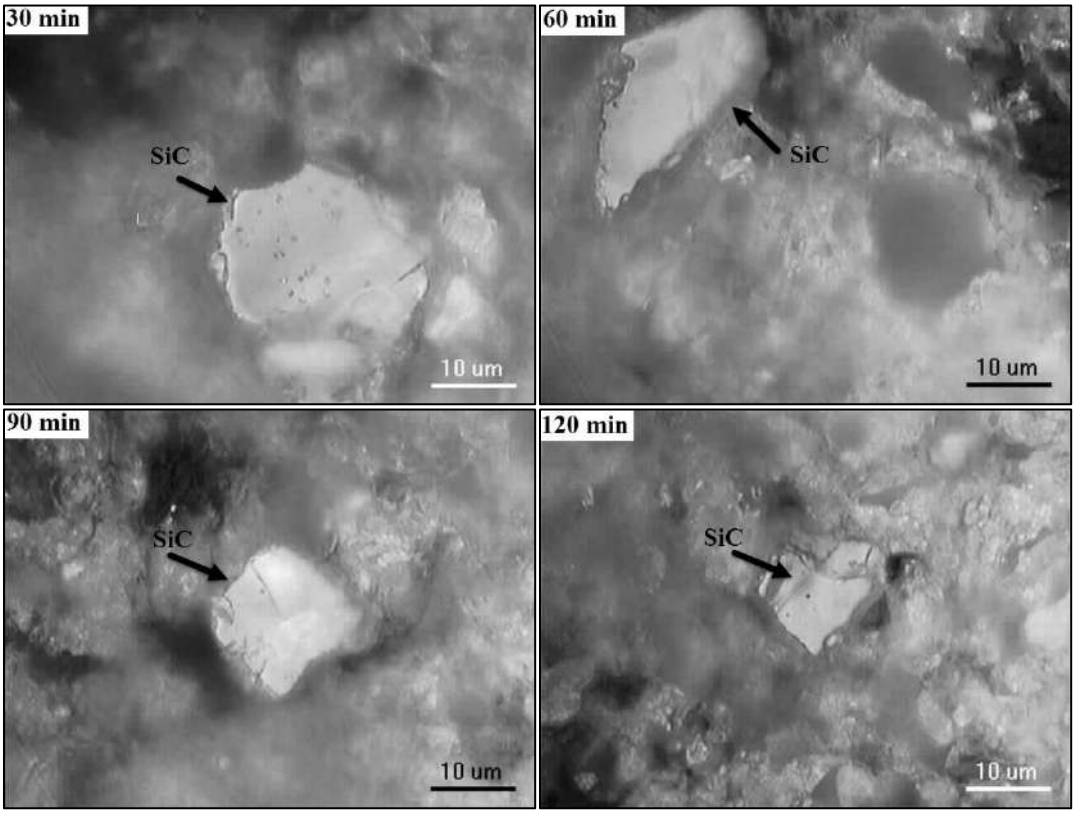

Figure 3. The optical microscope images of the AMCs containing 20% SiC mechanically milled using different milling times.

As evident from Figure 3, the optical microscope images of the aluminum composite powders containing 20% SiC showed a more coarse appearance after 30 min of mechanical milling compared to other mechanically milled composite powders. The SiC particles added to the matrix were observed to fracture and shrink more as a result of 120 min of MM compared to other milling times. One of the most significant problems encountered in the production of particle reinforced composite materials is the non-homogeneous distribution of the ceramic reinforcement elements (Campbell et al. 2016). It is a very common occurrence that reinforcement elements do not show a homogeneous distribution when short milling times are used. The increase in mechanical milling time allows for producing composite powders with a more homogeneous distribution. A relatively more homogeneous reinforcement material distribution has been achieved using longer milling times in a previous study (Zhao et al. 2014). Figure 4 shows the change in density (a) and hardness

(b) depending on milling time for Al-based composite materials mechanical milled using different milling times.

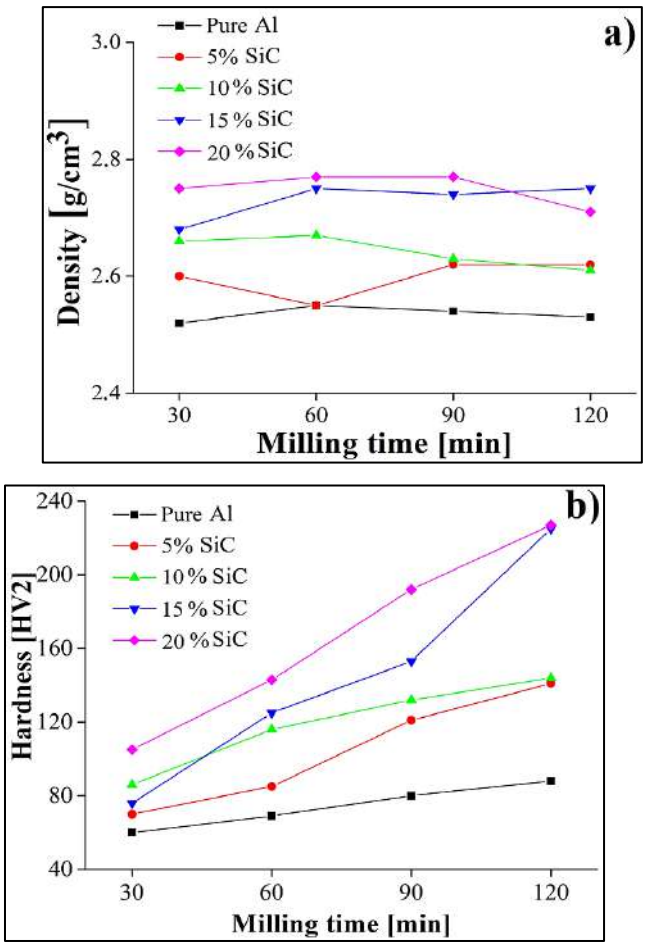

Figure 4. The change in density (a) and hardness (b) depending on milling time for AMCs mechanical milled using different milling times.

As shown in Figure 4.a, the density of pure aluminum powders was lower than the known density of aluminum (2.7 gr/cm^3) after the MM process. The composite materials containing 5%, 10%, and 15% SiC had increased density proportional to reinforcement material amount after 60 minutes of MM. In case of 90 minutes of MM, the composite materials containing 5% and 20% SiC once again displayed an increase in density, while the density of the pure Al and the composite materials containing 10% and 15% SiC decreased. Parvin et al. (2008) have reported that there was a decrease in density due to milling time, and the reason behind this decrease was the deformation

hardening caused by mechanical milling. The highest density value was obtained for the composite materials containing 20% SiC, whereas the lowest density value was obtained for the composite materials containing 5% SiC The density increased as the amount of SiC added to the matrix increased. This is a caused by the higher density of SiC compared to Al. The lowest hardness value was obtained for the pure aluminum as shown in Figure 4.b. The hardness value increased as the SiC amount added to the aluminum matrix and milling time increased. The lowest hardness value for the composite materials containing 20% SiC was 105 HV obtained after 30 minutes of milling, whereas the highest hardness value was 227 HV obtained after 120 minutes of milling. Zhao et al. (2014) have reported that powders which had not been deformed with MM were softer, the deformation increased with increasing milling time, and the hardness value increased in parallel. Figure 5 shows the SEM images and EDS results for the composites containing 10% SiC after 120 minutes of milling

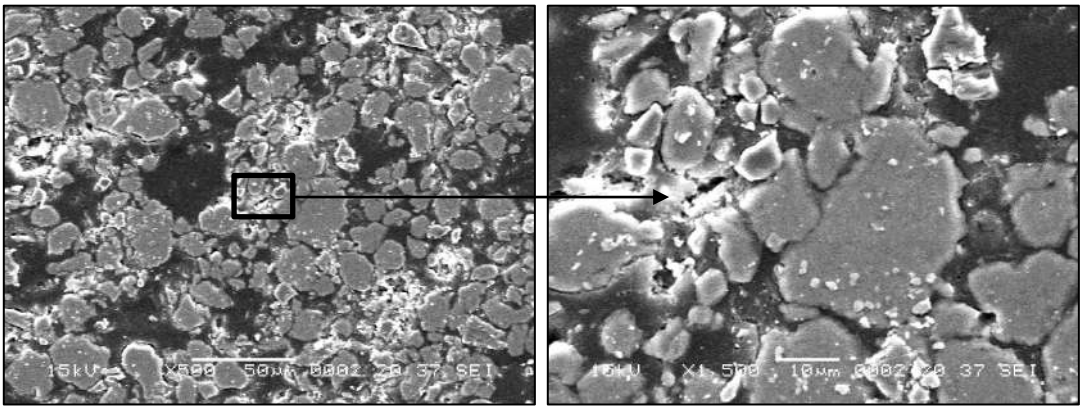

a)

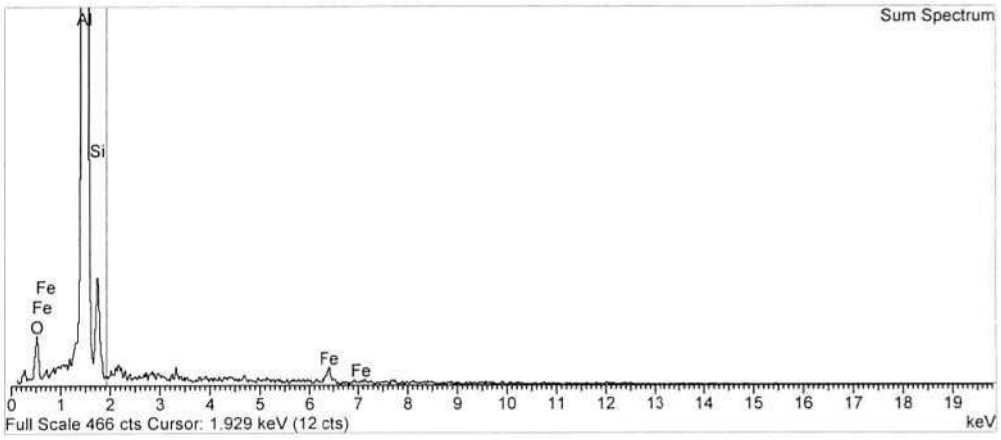

b)

Figure 5. The SEM images (a) and EDS results (b) for the AMCs containing 10% SiC after 120 minutes of milling.

The SEM images given in Figure 5.a shows that SiC particles (with sharp edges) within the matrix sunk into the matrix. The EDS analysis (Figure 5.b) showed that there was some staining (such as Fe) in the SiC reinforced Al composite materials produced using a vibration mill due to the milling equipment used. Although the MM process was performed in an atmosphere-controlled environment (argon environment), some O_2 staining was observed as well. During the milling process, constant crashes between ball-powder and ball-powder-milling chamber lead to clean surfaces on powders (within the milling chamber). Oxidation may occur on these clean surfaces due to the small amount of O_2 within argon or as a result of contact with atmosphere while taking the powders from the mill.

4. Results

The following results were obtained as a result of this study conducted to investigate the effects of the SiC amount and the mechanical milling time on SiC reinforced aluminum composites produced using a vibration mill.

The powder size of the composite powders produced by MM decreased with increasing mechanical milling time. Also, the powder size was observed to decrease with increasing amount of reinforcement phase (SiC). The smallest powder size was obtained for the composite material containing 20% SiC and milled for 120 min.

In general, the increase in the milling time led to a decrease in the density of the aluminum composites, albeit slightly. Also, the density of the composites was observed to increase in parallel with the increase in the amount of reinforcement element.

The hardness value of the composites produced by MM increased with the increasing amount of SiC. Also, the increase in the milling time led to an increase in hardness as well.

References

Arifin, A., Sulong, A. B., Muhamad, N., Syarif, J. and Ramli, M. I. (2014). Material Processing of Hydroxyapatite and Titanium Alloy (Ha/Ti) Composite as Implant Materials Using Powder Metallurgy: a review. *Materials & Design*, 55, 165-175.

Campbell, G. T., Raman, R. and Fields, R. J. (2016, August). Optimum Press and Sinter Processing For Aluminum/SiC Composites. *In Aluminum Powder Metallurgy Conference*.

Erek, H. B., Ozyurek, D. and Asan, A. (2017). Electrical Conductivity and Corrosion Performances of In Situ and Ex Situ AA7075 Aluminum Composites. *Acta Physica Polonica A*, 131(1), 153-155.

Mortensen, A., SanMarchi, C. and Degischer, H. P. (2002). Glossary of Terms Specific to Metal Matrix Composites. MMC-*Assess Thematic Network.*

Parvin, N., Assadifard, R., Safarzadeh, P., Sheibani, S. and Marashi, P. (2008). Preparation and Mechanical Properties of SiC-Reinforced Al6061 Composite By Mechanical Alloying. *Materials Science and Engineering: A*, 492(1-2), 134-140.

Prabhu, B., Suryanarayana, C., An, L. and Vaidyanathan, R. (2006). Synthesis and Characterization of High Volume Fraction Al–Al_2O_3 Nanocomposite Powders By High-Energy Milling. *Materials Science and Engineering: A*, 425(1-2), 192-200.

Rajan, T. P. D., Pillai, R. M. and Pai, B. C. (1998). Reinforcement Coatings and Interfaces ın Aluminium Metal Matrix Composites. *Journal of Materials Science*, 33(14), 3491-3503.

Sankar, R. and Singh, P. (1998). Synthesis of 7075 Al/SiC Particulate Composite Powders by Mechanical Alloying. *Materials Letters*, 36(1-4), 201-205.

Simsek, İ., Yıldırım, M., Tuncay, T., Ozyurek, D. and Simsek, D. (2018). Mekanik Alaşimlama/Öğütme Yöntemi İle Üretilen Al-SiC Kompozitlerin İncelenmesi. *Technological Applied Sciences*, 13(2), 165-171.

Smagorinski, M. E., Tsantrizos, P. G., Grenier, S., Cavasin, A., Brzezinski, T. and Kim, G. (1998). The Properties and Microstructure of Al-Based Composites Reinforced With Ceramic Particles. *Materials Science and Engineering: A*, 244(1), 86-90.

Sundararajan, *V. Aluminum Composites In Aerospace Applications.* http://satyameva-jayate.net/almmc.htm, (Erişim tarihi: 4.12.2017)

Suryanarayana, C. (2001). Mechanical alloying and milling. *Progress in materials science*, 46(1-2), 1-184.

Torralba, J. M., Velasco, F., Costa, C. E., Vergara, I. and Cáceres, D. (2002). Mechanical Behaviour of The Interphase Between Matrix and Reinforcement Of Al 2014 Matrix Composites Reinforced With (Ni_3Al) p. *Composites Part A: Applied Science and Manufacturing*, 33(3), 427-434.

Wannasin, J. and Flemings, M. C. (2005). Fabrication of metal matrix composites by a high-pressure centrifugal infiltration process. *Journal of Materials Processing Technology*, 169(2), 143-149.

Yu, P., Mei, Z. and Tjong, S. C. (2005). Structure, thermal and mechanical properties of in situ Al-based metal matrix composite reinforced with Al_2O_3 and TiC submicron particles. *Materials Chemistry and Physics*, 93(1), 109-116.

Zhao, N., Nash, P. and Yang, X. (2005). The Effect of Mechanical Alloying on SiC Distribution and The Properties of 6061 Aluminum Composite. *Journal of Materials Processing Technology*, 170(3), 586-592.

Microstructure and Dry Sliding Wear Behaviour of Al+2% Graphite Alloy Reinforced with Different Al_2O_3 Content

Doğan ŞİMŞEK[1*], İjlal ŞİMŞEK[2], Musa YILDIRIM[3], Dursun ÖZYÜREK[3]

[1] Bitlis Eren University, Technical Sciences Vocational School, Bitlis, Turkey,
[2] Karabuk University, TOBB Technical Sciences Vocational School, Karabuk,
[3] Karabuk University, Technology Faculty, Karabuk, Turkey

[*]**Corresponding author:** dsimsek@beu.edu.tr

Abstract

In this study, was investigated the microstructure and wear behaviors of aluminum composites reinforced different amounts (3%, 6%, 9% and 12%) Al_2O_3 and % 2 (% vol.) graphite. Within the scope of study, Al_2O_3 and graphite were added to Al matrix, and then mechanical alloyed for 60 minutes. Subsequently, the mechanical alloyed powders were pressed at 700 MPa, and sintered at 600 °C for 120 minutes. The produced aluminum composites were characterized by microstructure, scanning electron microscope (SEM + EDS), X-ray diffraction (XRD), density and hardness measurements. Afterwards, wear tests were carried out on a block on-ring type wear testing device, at sliding speed 0.2 ms^{-1}, under three different loads (10-20-30 N) and four different sliding distances (300-600-900-1200 m). As a result, the hardness and density of composites were observed to increase due to the increase in the amount of reinforcement in aluminum composites. The highest hardness and density values were obtained in composite material containing 12% Al_2O_3. As a result of the wear tests, the lowest weight loss was also obtained in composite containing 12% Al_2O_3.

Keywords: Al-Graphit-Al_2O_3 composite, wear, mechanical alloying.

1. INTRODUCTION

Aluminum matrix composites (AMC) are materials that are produced with reinforcement of different materials to aluminum matrix (Alizadeh and Taheri-Nassaj, 2012; Khorshid et al., 2010). Especially when high temperature is implemented, AMCs with reinforced Al_2O_3 provide good wear resistance (Prabhu et al., 2006). AMCs have high strength (Chawla ve Shen, 2001), low density (Bagherzadeh et al., 2015), better fatigue and wear resistance (Ozyurek et al., 2010; Ghanaraja et al., 2017). Thus, they are preferred in industrial sectors, particularly in aeronautics, defense, and automotive (Hesabi et al., 2006). These materials seem to be ideal materials, yet the high process costing limits the use of these materials. Even though there are many methods of production, the most used method is the mechanical alloying (MA), which is a method of formation

of new materials in the solid state. When it is compared to other particle reinforced composite manufacturing methods, there can be an AMC manufacturing with better mechanical qualities (Ozyurek et al., 2010). The MA process takes place in three stages: cold welding, strain hardening, and breakage. According to the Fogagnolo model (Fogagnolo et al., 2003), at the first stage of alloying, Al dusts take a shape of a flake with the high energy grinding effect occurred between ball-powder-container wall. As a result of cold welding in the ductile matrix phase, grain coarsening and diminution due to fracture in the brittle reinforcement phase occur. Therefore, in the following stages a composite structure is obtained by burying particles of the reinforcement phase in dusts forming the ductile matrix. In the progressive phase of the process, cold welded composite dusts break because of strain hardening. In the Al-C (graphite) alloy system, MA process is an important manufacturing method. In a study done by Chu (2001), it is determined that in the Al-C alloy system, small pieces of graphite transform to Al_4C_3 phase in the composition, and as for the bigger pieces of graphite, they stay as graphite cores that have not transformed in the structure. Besides in another study done by Bostan et al. (2004), it is stated that the MA process before sintering is not so effective in the formation of Al_4C_3 phase. In this study, the aim is to examine the effect of in situ Al_4C_3 phase and ex-situ Al_2O_3 reinforcement in composite materials that the different amounts of Al_2O_3 reinforcement in composite materials is added to Al-graphite matrix with using mechanical alloying method, to micro structural hardness and wear behaviors.

2. Materials and Method

In the experimental studies, commercially pure <50 μm aluminum and graphite powder (% volume) as matrix materials, <30 μm Al_2O_3 (% volume) as an element of reinforcement were used. 2% graphite and four different amounts of Al_2O_3 (3%, 6%, 9%, and 12%) were added to aluminum. Chemical composition of composite powders that were produced are given in Table 1.

Table 1. Chemical compositions of produced AMC powders

Element	Al (%vol.)	Graphite (%vol.)	Al_2O_3 (%vol.)
Al2Gr	98	2	---
+3Al_2O_3	95	2	3

+6Al_2O_3	92	2	6
+9Al_2O_3	89	2	9
+12Al_2O_3	86	2	12

Composite powders that were prepared in chemical composition given as in Table 1 were mechanically alloyed (MA) and cold extruded, and Ø10x8 mm sized raw samples were produced. During the MA process, a planetary mill was used. Composite powders prepared in a cell for stainless steel grinding were mechanically alloyed for 60 minutes with a 10 mm ball and with using 1:10 ball-powder ratio. Powders that were grinded during MA were waited for 10 minutes between 30 minute-long-periods for preventing powders from overheating. In the MA process, in order powders to not flocculate, 1 mL ethanol was used as a process control chemical. Composite powders that were produced were pre formed in the uniaxial hydraulic press (700 MPa). Zinc stearate was used as mold grease. Raw samples that were produced were sintered for 120 minutes in 600 °C and were cooled in an oven at room temperature. Samples prepared with applying standard metallographic procedures for microstructural examination were cauterized for 10-15 seconds with using 2 ml HF, 3 ml HCI, 20 ml HNO_3, 175 ml H_2O (Keller's) solution. Microstructural studies of cauterized composite materials were examined via a scanning electrode microscope (SEM+EDS). Also, produced composite materials were categorized with measuring X-ray diffraction (XRD), hardness, and density. Density measurements was done with Archimedes' principle. The average of density measurements on three samples was calculated. Vickers hardness was measured for 10 seconds as HV2. Hardness measurements was calculated with using three different samples from five different points. Wear tests were done according to ASTM G77 standard in the block-on-ring wear test mechanism. Tests were done with 0.2 ms^{-1} sliding speed, using three different weights (10 N, 20 N, 30 N) and four different sliding distance (300-1200 m). Before the wear tests, surfaces of the sample and ring were cleaned with alcohol. The wear tests were done for each parameter with 3 different samples, and the average weight loss and coefficient of friction were calculated. After the wear tests, active wear mechanisms were tried to be determined with examining the images of worn surfaces in SEM.

3. Findings and Discussion

SEM images of AMCs with different amounts of Al_2O_3 reinforced are given in Figure 1.

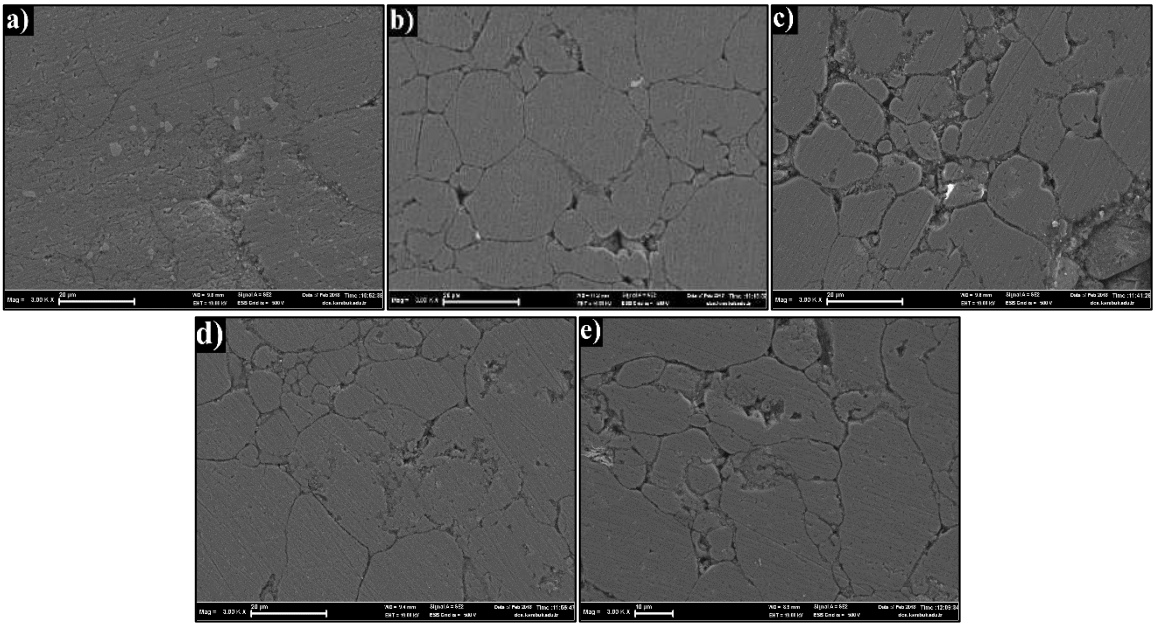

Figure 1. Microstructural SEM images of composite materials with different amounts of Al_2O_3 reinforced a) AlGr, b) 3% Al_2O_3, c) 6% Al_2O_3, d) 9% Al_2O_3, e) 12% Al_2O_3

Microstructural SEM images of composite materials with different amounts of Al_2O_3 reinforced given in the Figure 1 is examined, graphite (Gr) that scatter in the structure can be clearly seen. It can be understood that Al_2O_3 ceramic reinforcement in the alloy is generally concentrated in the grain boundary. This situation is because during 60 minutes mechanical alloying of the composite powders, aluminum pieces stick but does not get buried enough. In the study of Ozyurek et al. (2010), it is determined that with the effect of alloying, composite powders which were mechanically alloyed for 120 minutes were deformed enough, and hard Al_2O_3 pieces were buried to the matrix. Also, because Al_2O_3 pieces were buried well to Al pieces, they were more homogeneously scattered in the structure. XRD result of the composite material produced with 12% Al_2O_3 reinforcement is given in Figure 2.

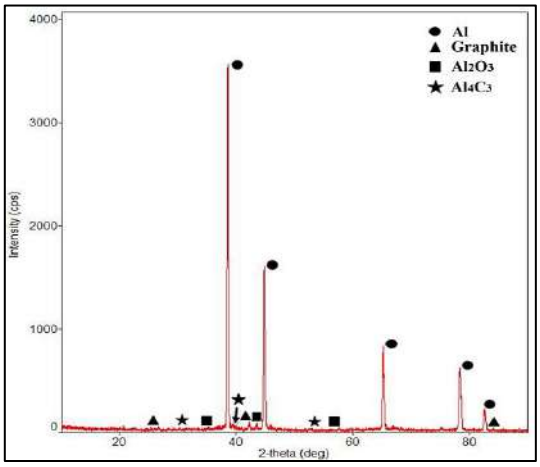

Figure 2. XRD result of the composite material produced with 12% Al_2O_3 reinforcement

When the XRD result of the composite material produced with 12% Al_2O_3 reinforcement given in Figure 2 is examined, it is seen that there is also Al_4C_3 compound in the composition of composite materials that are produced along with matrix phase of the composite material produced, Al, and graphite reinforcement phase, Al_2O_3. Formation of this compound in the structure is an expected situation. Formation reaction of Al_4C_3 and reaction temperature are given in Equation 1 and Equation 2 (Chu et al., 2001).

$$4Al + 3C \rightarrow Al_4C_3 \quad (1)$$

$$G° = -56600 + 10\ T\ (cal) \quad (2)$$

In here, $\Delta G°$ is Gibbs free energy, and T is reaction temperature in terms of Kelvin. In the temperature, which the sintering process is done (600 °C), according to Equation 2, Gibbs free energy is approximately -47870 cal. Therefore, it is an indication of the energy that is enough for formation of in-situ reactions in the temperature of the sintering process. In the study of Bostan et al. (2004), it is stated that in the Al-C system produced with mechanical alloying, Al_4C_3 compound is formed with sintering in the structure of the alloy in nano dimension. Along with this, in the study made by Chu et al. (2001) it is determined that small graphite pieces turn completely into Al_4C_3 phase, and bigger graphite pieces are seen in the structure as graphite cores that have not

transformed. The change in hardness and density of composite materials with different amounts of Al_2O_3 reinforced are given in Figure 3.

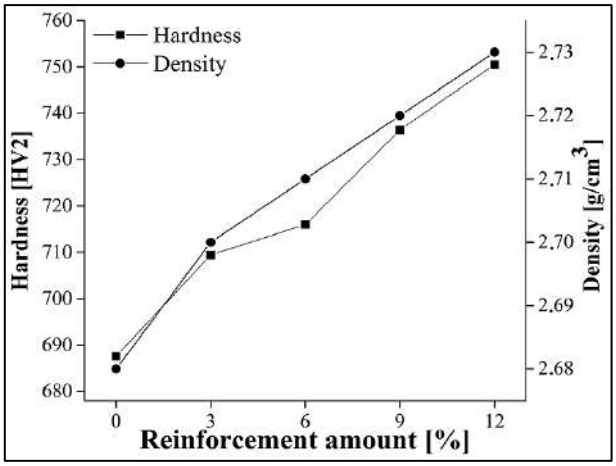

Figure 3. Change in hardness and density of composite materials with different amounts of Al_2O_3 reinforcement

When the density graph of composite materials with different amounts of Al_2O_3 reinforcement given in Figure 3 is examined, an increase in density depending on the amount of reinforcement is seen. While the lowest density is obtained 2.628 g/cm^3 in the material without reinforcement (Al%2Gr), the highest density is obtained 2.735 g/cm^3 in the sample with 12% Al_2O_3 reinforcement. This situation is because density of the reinforcement material (Al_2O_3) is higher than density of the matrix. In another previous study, similar results were obtained (Al-Mosawi et al., 2017). Again, when hardness results given in Figure 3 are examined, it is seen that with the increase of rate of reinforcement, hardness increases. The lowest hardness is obtained 687 HV from the Al%2Gr alloy without reinforcement the highest hardness is obtained 750 HV from the composite material with 12% Al_2O_3 reinforcement. It is understood that reinforcement of hard oxide (Al_2O_3) pieces to a relatively ductile matrix has a positive effect to hardness of the composite material. This condition makes a contribution to hardness of the composite material with increasing the resistance of the reinforcement material to plastic deformation of the matrix (Bharath et al., 2014). Weight losses and wear rates of composite materials with different amounts of Al_2O_3 reinforcement are given in Figure 4.

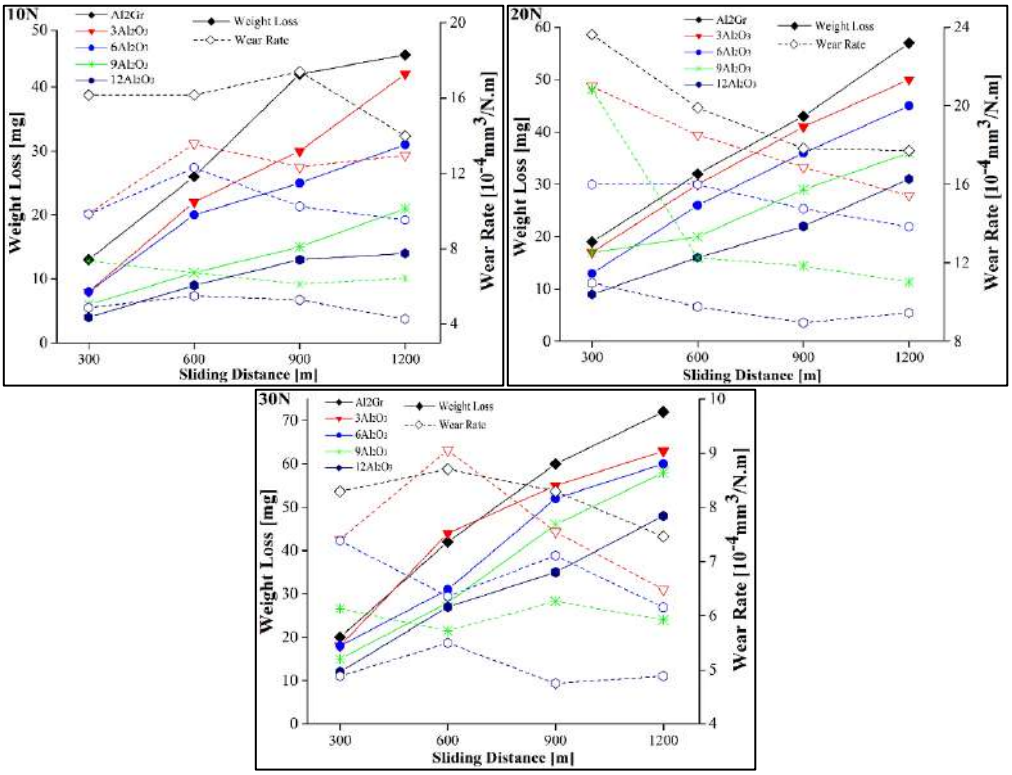

Figure 4. Weight losses and wear rates of composite materials with different amounts of Al_2O_3 reinforcement.

When the weight loss results given in Figure 4 are examined, it is seen that depending on the increase of Al_2O_3 amount in the Al2Gr matrix, there is a decrease in weight loss. Weight loss results that are obtained are supported by hardness results given in Figure 3. While the highest weight loss result is obtained from the sample with the lowest hardness (Al2Gr), the lowest weight loss is obtained from the sample with the highest hardness that is the composite material that consists 12% Al_2O_3 reinforcement. Again, when the wear rate graph given in Figure 4 is examined, it is seen that it leans to decrease even though there is fluctuation in wear rates. Increase in Al_2O_3 content in the matrix and glide distance are dominant factors in decrease of wear rate. The decrease in wear rate with the increase in reinforcement rate is because of the hardness of the reinforcement material. In the study made by Purohit et al. (2017), it is stated that wear rate decreases when the amount of hard reinforcement in aluminum matrix increases. Along with this, another reason for this situation is having 2% graphite in composite materials that are produced. The decrease in wear rate of hybrid

composites that contain graphite can attribute to collective effects of graphite and Al_2O_3 pieces in having a more resistant friction layer in the contact surface (Mahdavi and Akhlaghi,2011; Zhao at al. 2007). The fluctuation in this wear rate graph can be explained with the large piece that broke from the material during the wear becoming distant from the tribological system. When the graph of 30 N weight is examined, the sudden increase of weight loss of the composite material with 3% Al_2O_3 reinforcement on 600 m sliding distance shows this condition very clearly. Some previous studies support the obtained results [Ozyurek et al. 2010; Abouelmagd, 2004). Friction coefficients of composite materials with Al_2O_3 reinforcement at different rates are given in Figure 5.

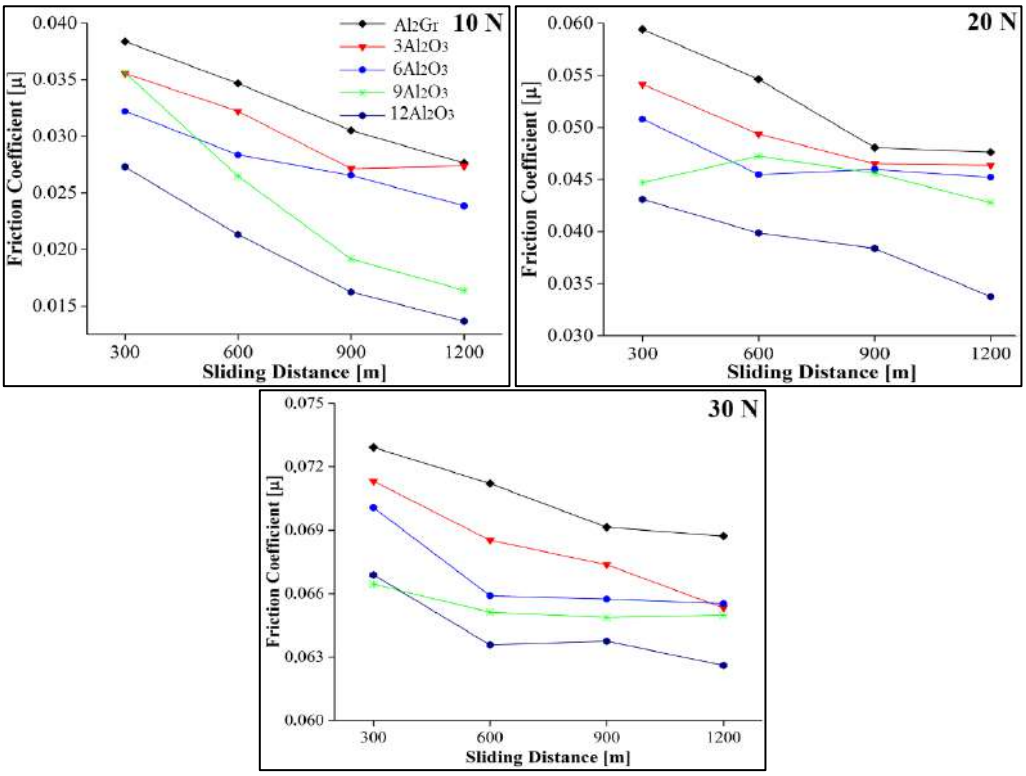

Figure 5. Friction coefficients of composite materials with Al_2O_3 reinforcement at different rates.

When the friction coefficients of composite materials with Al_2O_3 reinforcement at different rates given in Figure 5 are examined, with every weight there is a decrease in friction coefficient with an increase in sliding distance. With the increase in glide distance, the oxide layer that is formed with the effect of heat caused by the friction between the ring and the sample causes the friction coefficient to decrease. Again, as it can be understood from the graphs, depending on the

increase in reinforcement rates, the friction coefficient decreases. In the study of Ozyurek et al. (2010), similar results are obtained. Also, having graphite in the composition of composite materials causes the friction coefficient to decrease because the decrease in the friction coefficient arises from graphite content in the composition functioning as solid grease. In the study Baradeswaran and Perumal (2014) made, it is claimed that the graphite content decreases the friction coefficient; 5% graphite content in the AA 7075 alloy reduces the friction coefficient approximately 51%. Under the 20 N weight, it is observed that the friction coefficient of the composite material with the reinforcement 9% Al_2O_3 on 600 m sliding distance increases, and it decreases on longer distances. SEM images of wear surfaces of composite materials with different amounts of Al_2O_3 reinforcement under 30 N weight are given in Figure 6.

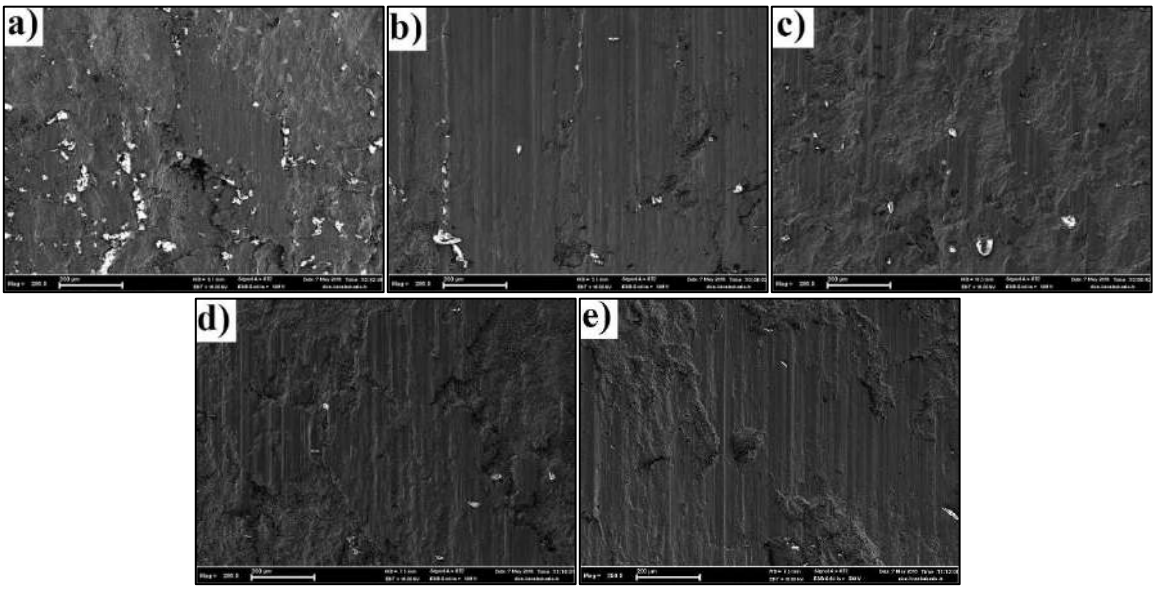

Figure 6. SEM images of worn surfaces of composite materials with different amounts of Al_2O_3 reinforcement under 30 N weight a) AlGr, b) 3% Al_2O_3, c) 6% Al_2O_3, d) 9% Al_2O_3, e) 12% Al_2O_3

When SEM images of worn surfaces given in Figure 6 are examined, deformation marks on the sample surface can clearly be seen. It is understood that the wear on the sample without Al_2O_3 is more than the other samples. Besides, in the same sample, oxidation (white areas) on the surface can clearly be seen. Depending on the increase of Al_2O_3 rate, it is observed that oxidation layer on the surface does not appear. It is understood that in all samples, some parts of the broken pieces

stuck to the surface again. It is observed that there is wear on the surfaces of the composite samples with 6% and 9% Al_2O_3 reinforcement. The friction coefficient under the 30 N weight given in Figure 5 support this situation. Pieces that are broken from the surface increasing the surface roughness causes friction coefficient to increase.

4. Results

Results obtained from the study that examines the wear behavior of composite materials with different amounts of Al_2O_3 reinforcement to Al-2Graphite matrix with the MA method are given below:

- It is determined that the Al_2O_3 reinforcement to the Al+Graphite matrix in Al-Graphite-Al_2O_3 composite materials does not display a homogeneous scattering in the structure; it especially concentrated in the grain boundary
- It is determined that in the XRD analysis result of Al-Graphite-12%Al_2O_3 composite materials, Al and Graphite forms Al_4C_3 compound in the composition.
- Hardness values of Al-Graphite-Al_2O_3 composite materials are obtained, and the highest hardness value is obtained from the composite material with 12% Al_2O_3 reinforcement with the increase of Al_2O_3 reinforcement in the matrix phase.
- Density values of Al-Graphite-Al_2O_3 composite materials are obtained with the increase in density of the composite material as Al_2O_3 reinforcement in the matrix phase increases, and the highest density value is obtained from the composite material with 12% Al_2O_3 reinforcement.
- According the wear test results, the highest weight loss is obtained from the Al-Graphite sample without reinforcement. It is determined that with the increase of Al_2O_3 reinforcement in the matrix, the weight loss decreases; the lowest weight loss is in the sample with 12% Al_2O_3 reinforcement.
- According the wear test results, the greatest friction coefficient is obtained from the Al-Graphite sample without reinforcement. It is determined that the friction coefficient decreases with the increase of Al_2O_3 reinforcement in the matrix, and the smallest friction coefficient is in the sample with 12% Al_2O_3 reinforcement.

References

Abouelmagd, G. (2004). Hot deformation and wear resistance of P/M aluminium metal matrix composites. *Journal of Materials Processing Technology*, 155, 1395-1401.

Alizadeh, A. and Taheri-Nassaj, E. (2012). Mechanical properties and wear behavior of Al–2 wt.% Cu alloy composites reinforced by B4C nanoparticles and fabricated by mechanical milling and hot extrusion. *Materials Characterization*, 67, 119-128.

Al-Mosawi, B. T., Wexler, D. and Calka, A. (2017). Characterization and mechanical properties of α-Al_2O_3 particle reinforced aluminium matrix composites, synthesized via uniball magneto-milling and uniaxial hot pressing. *Advanced Powder Technology*, 28(3), 1054-1064.

Bagherzadeh, E. S., Dopita, M., Mütze, T. and Peuker, U. A. (2015). Morphological and structural studies on Al reinforced by Al2O3 via mechanical alloying. *Advanced Powder Technology*, 26(2), 487-493.

Baradeswaran, A. and Perumal, A. E. (2014). Study on mechanical and wear properties of Al 7075/Al_2O_3/graphite hybrid composites. *Composites Part B: Engineering*, 56, 464-471.

Bharath, V., Nagaral, M., Auradi, V. and Kori, S. A. (2014). Preparation of 6061Al-Al_2O_3 MMC's by Stir Casting and Evaluation of Mechanical and Wear Properties. *Procedia Materials Science*, 6, 1658-1667.

Bostan, B., Ozdemir, A. T. and Kalkanli, A. (2004). Microstructure characteristics in Al-C system after mechanical alloying and high temperature treatment. *Powder metallurgy*, 47(1), 37-42.

Chawla, N. and Shen, Y. L. (2001). Mechanical behavior of particle reinforced metal matrix composites. *Advanced engineering materials*, 3(6), 357-370.

Chu, H. S., Liu, K. S. and Yeh, J. W. (2001). Damping behavior of in situ Al–(graphite, Al_4C_3) composites produced by reciprocating extrusion. *Journal of Materials Research*, 16(5), 1372-1380.

Fogagnolo, J. B., Velasco, F., Robert, M. H. and Torralba, J. M. (2003). Effect of mechanical alloying on the morphology, microstructure and properties of aluminium matrix composite powders. *Materials Science and Engineering: A*, 342(1-2), 131-143.

Ghanaraja, S., Ravikumar, K. S., Raju, H. P. and Madhusudan, B. M. (2017). Studies on Dry Sliding Wear Behaviour of Al_2O_3 Reinforced Al Based Metal Matrix Composites. *Materials Today: Proceedings*, 4(9), 10043-10048.

Hesabi, Z. R., Simchi, A. and Reihani, S. S. (2006). Structural evolution during mechanical milling of nanometric and micrometric Al_2O_3 reinforced Al matrix composites. *Materials Science and Engineering: A*, 428(1-2), 159-168.

Khorshid, M. T., Jahromi, S. J. and Moshksar, M. M. (2010). Mechanical properties of tri-modal Al matrix composites reinforced by nano-and submicron-sized Al2O3 particulates developed by wet attrition milling and hot extrusion. *Materials & Design*, 31(8), 3880-3884.

Mahdavi, S. and Akhlaghi, F. (2011). Effect of the graphite content on the tribological behavior of Al/Gr and Al/30SiC/Gr composites processed by in situ powder metallurgy (IPM) method. *Tribology Letters*, 44(1), 1-12.

Ozyurek, D., Tekeli, S., Güral, A., Meyveci, A., and Guru, M. (2010). Effect of Al_2O_3 amount on microstructure and wear properties of Al–Al_2O_3 metal matrix composites prepared using mechanical alloying method. *Powder Metallurgy and Metal Ceramics*, 49(5-6), 289-294.

Prabhu, B., Suryanarayana, C., An, L. and Vaidyanathan, R. (2006). Synthesis and characterization of high volume fraction Al–Al2O3 nanocomposite powders by high-energy milling. *Materials Science and Engineering: A*, 425(1-2), 192-200

Purohit, R., Qureshi, M. M. U. and Rana, R. S. (2017). The Effect of Hot Forging and Heat Treatment on Wear Properties of Al6061-Al_2O_3 Nano Composites. *Materials Today: Proceedings*, 4(2), 4042-4048.

Zhao, H., Liu, L., Hu, W. and Shen, B. (2007). Friction and wear behavior of Ni–graphite composites prepared by electroforming. *Materials & design*, 28(4), 1374-1378.

Investigation of Mechanical and Macrostructural Properties of AA2024 and AA 5754 Plates Joined by Friction Stir Spot Welding

Damla UŞAR[1], Sevgi TOSUN[1], Betül ÖZTÜRK[1], Yılmaz TAŞOVA[1], Yahya BOZKURT[1]. Serdar SALMAN [2*]

[1]Marmara University, Faculty of Technology, Department of Metallurgy and Materials Engineering, Kadıköy/İstanbul
[1,2]National Defense University, Rectorate of National Defense University, İstanbul, Turkey,

[*]**Sorumlu Yazar:** ssalman@marmara.edu.tr

Abstract

In this study, aluminum alloys which have important places in aviation and space industry are investigated their ability to weld with friction stir spot welding. The mechanical properties and the changes in the microstructure of the aluminum alloys used in the experiments were determined after welding process. Microhardness and tensile tests were carried out by taking samples in order to test them from welded materials. A suitable etching reagent was chosen to obtain the microstructure properties of the welded joints. The stir zone was examined under optical microscope. AA6061 powder's grain size was reduced and used as an intermediate layer for AA2024 and AA5754 plates. Mechanical tests and metallographic experiment results for welding zone of AA2024 and AA5754 specimen has compared both in low and high properties. Non-destructive radiographic inspection methods were used to control the discontinuity and defect of welded materials. Overall, the results show that satisfactory welds can be produced with these two alloys even when full mixing of the two alloys was not achieved in the in small square area. The products obtained from different materials are more important in the industry due to their technical and economic benefits.

Keywords: Friction Stir Welding, Aluminum alloys, Macrostructures, Aluminum powder

1. Introduction

People have discovered welded joints for the tools and equipments they need over the years. The continuous and unlimited increase of these needs is one of the leading causes of the advances in technology. Welding process has originated from the need to connect two metalic materials together [1]. It was later investigated that merely combining would not be enough and the researches were carried out so that the joining process can be performed without changing the material properties[2,3].

In line with the results of these researches, today's welding techniques are classified in two ways as fusion welding and solid state welding methods. In the fusion welding process, the fusion and the solidification by cooling in the molten state of the parts to be welded and the joined surfaces (to be welded) occurs. In solid state welding process, it is ensured that the parts to be welded are joined in solid state at a temperature below the fusion temperatures of the parts without fusion [4,5].

At the end of the 20th century, the friction stir welding (FSW), a solid state welding method improved by The Welding Institute (TWI), was used to provide connections for aluminum materials that are difficult to combine with other manufacturing methods. In the welding of the structures which are difficult to join, conditions such as the short process, no surface preparation of parts, automation convenience and etc. have led to the preference of the friction stir welding technique [6-8].

The friction stir spot welding method is suitable for many materials. However, the most important application area is to combine aluminum and aluminum alloys, which are both problematic and difficult to weld with other methods. This method, which can be applied very conveniently in all positions, combines aluminum alloys with very good mechanical properties [9].

2. Friction Stir Spot Welding

Any tool can be used as long as it can create the welding temperature on the material during welding process. If the material to be used is a soft material such as aluminum a tool kit made of H13 tool steel should be preferred, if it is a harder material, a tool such as Tungsten carbide should be preferred [10-13]. The friction stir spot welding method is carried out by moving the preferred mixer tool tip over the vertical axis at the midpoint of the materials placed on top of the prepared mold. The pin and shoulder parts of the welding tool move forward under the surface of the material and make a frictional heat [14,15]. With the energy of rotation and forward motion, the material starts to melt and the welding process is realized as the parts move into each other. A ring-shaped trace left by the tool pin on the material surface is formed with the forging pressure applied to the piece [16-18].

3. Material and Method

In this study, the appropriate welding parameters for the friction stir spot welding (FSSW) made by adding AA6061 powder between AA2024 and AA5754 parts were used. This welding method is mostly preferred in materials such as aluminum and copper.

Plates with a surface area of 25x100 mm, consisting of three different aluminum alloys, were assembled to combine with a FSSW in this study. The thickness of the AA2024 plate is 1.6 mm while the thickness of the AA5754 plate is 1.5 mm. Samples prepared for the experiments are shown in Figure 1.

Figure 1. Joined test samples

The aluminum materials used in the work are joined in different material combinations under certain parameters. AA6061 aluminum plate was converted into aluminum powder. AA6061 powder's grain size was reduced and used as an intermediate layer for AA2024-2024, AA5754-

AA5754, AA2024-AA5754 and AA5754-AA2024 plate couples. The chemical compositions and the mechanical properties of the aluminum alloys are given in Table 1 and Table 2 respectively.

Table 1. Aluminum alloys and chemical compositions.

Al Alloys	Fe	Si	Cr	Mn	Mg	Zn	Cu	Ti	Other	Al
AA 6061	0,5	0,6-1,0	0,1	0,2-0,8	0,8-1,2	0,25	0,6-1,1	0,1	0,15	Balance
AA 2024	0,5	0,5	0,1	0,3-0,9	1,2-1,8	0,25	3,8-4,9	0,15	0,15	Balance
AA 5754	0,4	0,4	0,1	0,5	2,6-3,6	0,2	0,3	0,15	0,15	Balance

Table 2. Mechanical properties of aluminum alloys

Al Alloys	Yield Strength (MPa)	Tensile Strength (MPa)	Elongation (%50)	Hardness (HB)
AA 6061	103-228	55-124	26	30
AA 2024	75	185	20	55
AA 5754	80-100	190-215	24	50-55

The basic benefits provided by the FSSW compared to conventional fusion welding processes can be summarized as reduction of porosity, microstructure change and process induced residual stresses and degradation. In these sectors the most commonly used aluminum alloys are 2024, 5754 and 6061.

The FSSW machine in the experiment is semi-automatic and used as a milling machine. The maximum spin speed of the machine used for welding is 2000 rpm. The milling machine works with the electric motor and transfers the rotational motion of the motor to the milling head shaft in the vertical head of the freewheel through the v-belt. The connection table of the milling machine is 1500 mm long. Machinery and welding equipments should be checked at regular intervals to obtain successful welding results. The speed parameter was set at 1500 rpm in the study. Milling machine used for the welding process is shown in Figure 2.

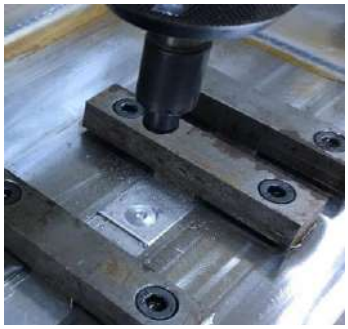

Figure 2. FSSW process.

The tool tip to be used for FSSW is designated from tool steel. The tool has been brought into the appropriate position for welding to take place. The length of the welding tool was 80 mm, the shoulder diameter was 10 mm and the pin diameter was 3 mm. The tool must be manufactured to the specified size so that the neck is suitable for the welding machine. To prevent the pin from impacting the milling table, the length of the welding tool must be less than the thickness of the part to be welded. The welding tool to be used in operation is given in Figure 3.

Figure 3. Welding tool.

The prepared AA6061 powder was placed between AA2024 plates of dimensions 25x100x1,6 mm and fixed to the milling machine in the forehead position. At a rotational speed of 1500 rpm, the vertically-acting welding tip is adjusted to sink one millimeter deep into the material in each second up to the shoulder level. The tool tip was quickly retracted after the pin had entered the 80% of the material thickness and remained in the waiting period for 10 seconds. The same operations were also carried out between sheets of AA5754, where AA6061 powder was used as the intermediate layer.

4. Test Results and Discussion

4.1. Tensile Test Results

Welding performance, quality of weld seam and microstructure properties of materials were investigated to be able to detect the material with the best mechanical properties among the welded joints. The results of the tensile test were used to compare the weldability of the materials. Based on this, the material which gives the best result of the tensile test have been determined. On the other hand, relationship between macroscopic studies of welded joints and the tensile test results was investigated.

In this study, the result of the friction stir spot welding tensile test using AA5754-AA6061-AA5754 materials (Figure 4) was lower than the result of the friction stir spot welding tensile test obtained by using materials AA2024 - AA6061 - AA2024 (Figure 5).

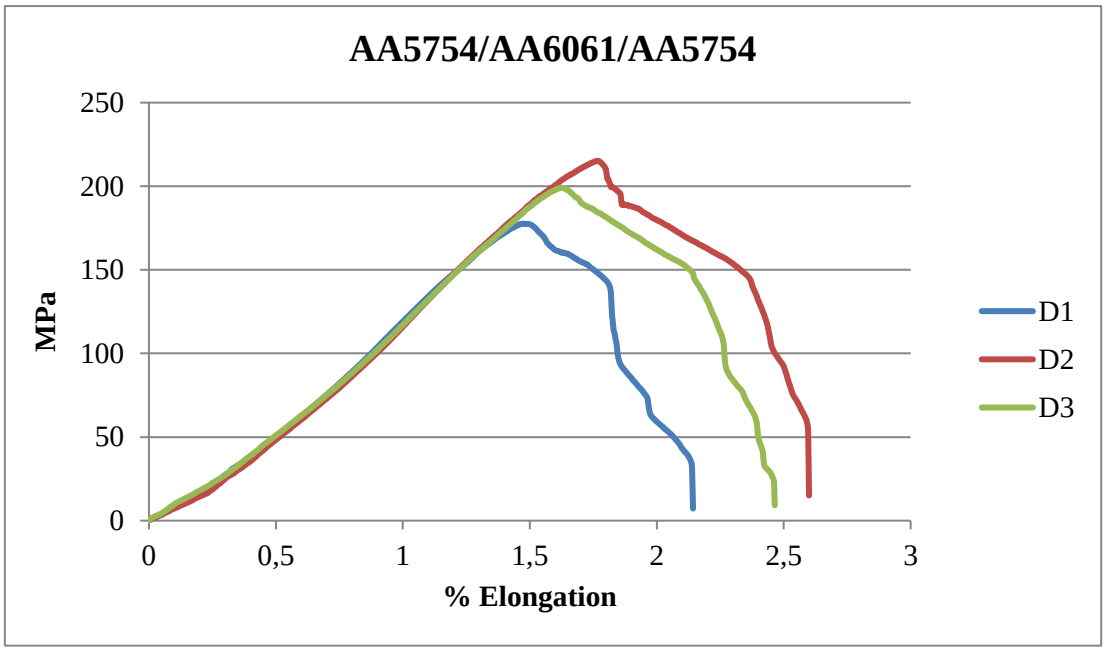

Figure 4. Tensile test results of AA 5754 - AA 6061 couples

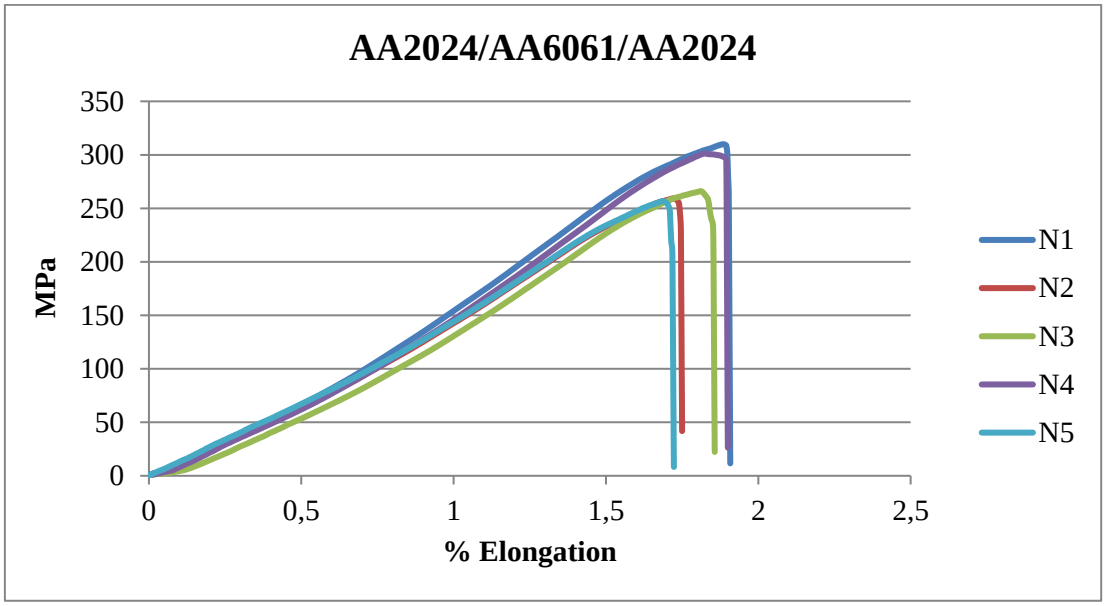

Figure 5. Tensile test results of AA 2024 - AA 6061 couples

In another study, the result of the FSSW tensile test using AA5754 - AA6061 - AA2024 materials (Series B) (Figure 6) was lower than the result of the friction stir spot welding tensile test obtained by using materials AA2024 - AA6061 - AA5754 (K series) (Figure 7).

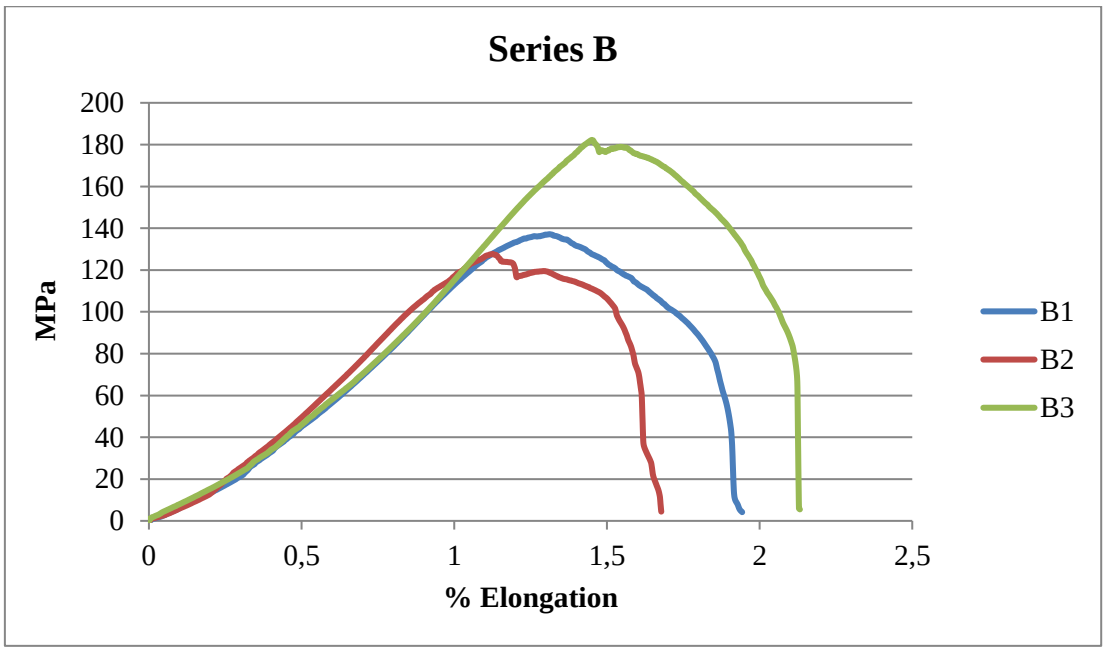

Figure 6. Tensile test results of AA 5754 – AA 6061 – AA 2024 series

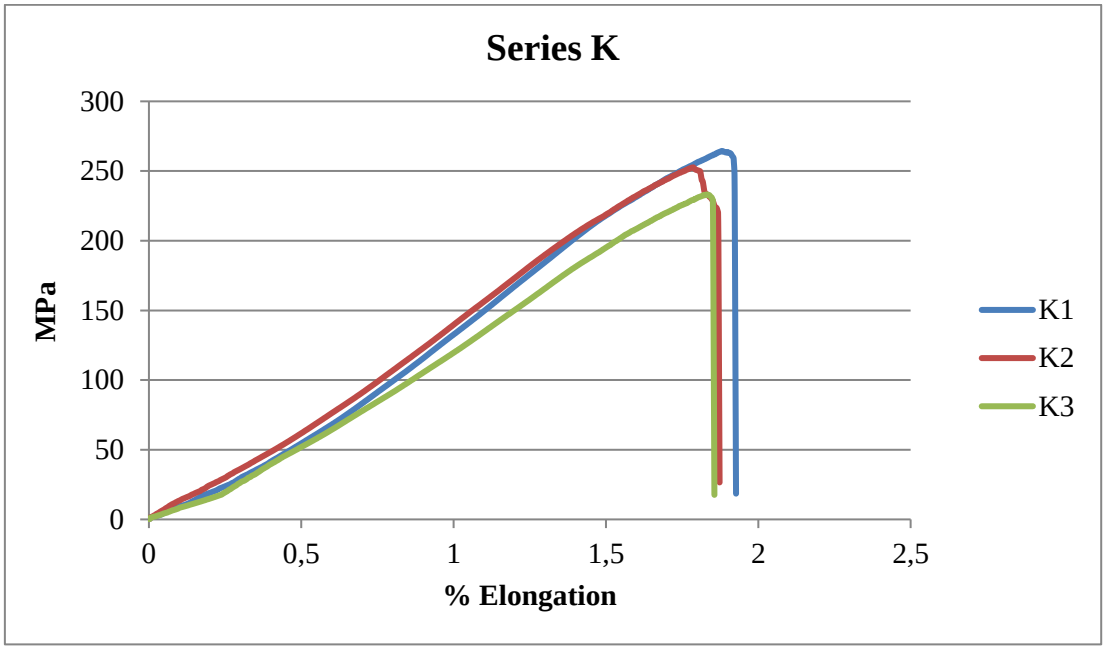

Figure 7. Tensile test results of 2024 – AA 6061 – AA 5754 series

4.2. Hardness Test Results

Vickers hardness measurements on welded joints showed a decrease in the hardness measurement results due to the temperature increase in the welded area, especially in HAZ (Table 3). In this study, the hardness values obtained from AA5754 - AA6061 - AA5754 materials are lower than the hardness values obtained from AA2024 - AA6061 - AA2024 materials according to the Vickers hardness measurement results obtained from the welding zone after the underwater FSSW process.

Table 3. Vickers Hardness Measurement Results from FSSW Samples at Three Critical Points

In another study, the hardness values of AA5754 - AA 6061 - AA2024 materials were almost equal to those of AA2024 - AA6061 - AA2024 materials according to the results of Vickers hardness measurements from the weld zone.

As the sample from AA2024 - AA6061 - AA5754 materials were damaged during cutting, the Vickers hardness measurement could not be made. Therefore, the hardness values obtained from samples taken from AA5754 - AA6061 - AA2024 materials can’t be compared.

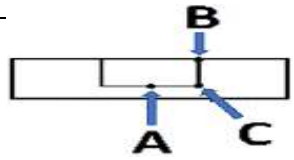	**Point A**		**Point B**		**Point C**	
1.Sample	HV	1432,4	HV	1394	HV	911
2.Sample	HV	1048,1	HV	1477	HV	979,7
3. Sample	HV	1002,8	HV	2818,7	HV	1066,1
4. Sample	HV	694,3	HV	699,2	HV	1270,4
5. Sample	HV	338,5	HV	297,4	HV	632,4
6. Sample	HV	474,9	HV	252,2	HV	404,7
7. Sample	HV	690,1	HV	956,5	HV	291,2
8. Sample	HV	1247,7	HV	257,4	HV	587,7
9. Sample	HV	992,4	HV	1037,6	HV	965,3
10. Sample	HV	1553,5	HV	730,9	HV	-
11. Sample	HV	676,1	HV	377,29	HV	473,3

Note: Because the 10th Cu sample was not subjected to adequate shearing and sanding, no microstructure appearance and hardness measurements were taken.

4.3. Examination of The Results of Radiographic Inspection

In this study, the radiographic images of 6 samples obtained from the FSSW using the AA 5754 - AA6061 - AA5754 materials shown in Figure 8 were compared. As a result of these comparisons, in the majority of 6 samples, the interposed AA6061 powder was found between the plates and outside the weld zone.

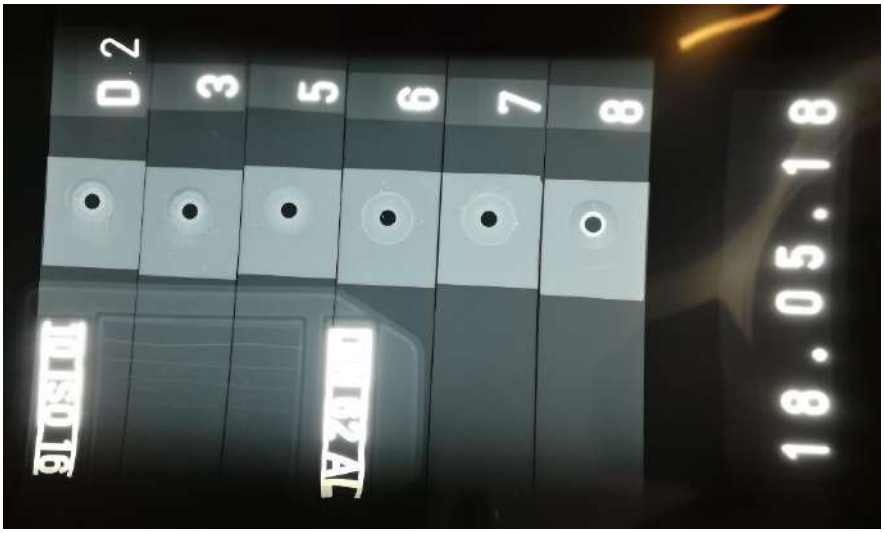

Figure 8. Radiographic examination image for AA5754 - AA6061 - AA5754 sheets

In this study, the radiographic images of 3 samples obtained from the friction stir spot welding made by using AA5754 - AA6061 - AA2024 materials were compared. As a result of these comparisons, it has been observed that the welded joint shows much better results than the welded connections underwater (Figure 9).

Figure 9. Radiographic examination image for AA5754 - AA6061 - AA2024 sheets

In this study, the radiographic images of 4 samples taken from a underwater friction stir spots welding using AA2024 - AA6061 - AA5754 materials shown in Figure 10 were compared. As a result of these comparisons, the desired results were obtained from the radiographic examination at a rate of approximately 50%.

Figure 10. Radiographic examination image for AA 2024 - AA 6061 - AA 5754 sheets

4.4. Macrostructure Studies

Metal microscope and visual inspection of welded joints has been provided. As a result of the examinations, weld defects such as void defects were not encountered in the welded connections.

In the microscopic image of the sample taken from the material as a result of the friction stir welding of the AA5754 - AA 6061 - AA2024 materials (Image 11), the trace of the welding tool tip is more visible than the other samples.

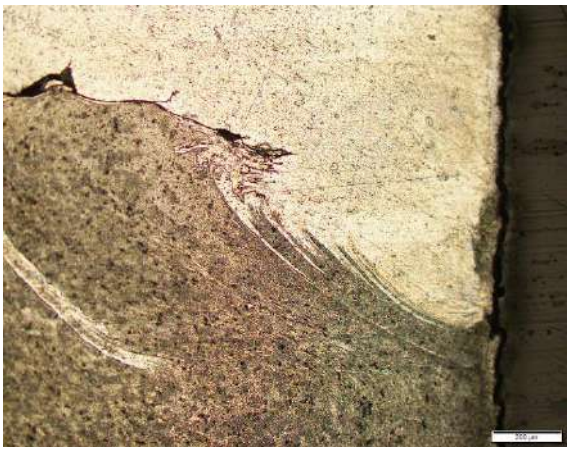

Figure 11. AA5754 - AA6061 - AA2024 series of macrostructure images taken from the junction points of the plates (10X)

It is difficult to obtain clear information due to erroneous (less) grinding of microscopic image of sample taken from material of friction stir welding results of AA 5754 - AA 6061 - AA 5754 (Fig. 12), and the blurring in the received images indicated the voids in the particle.

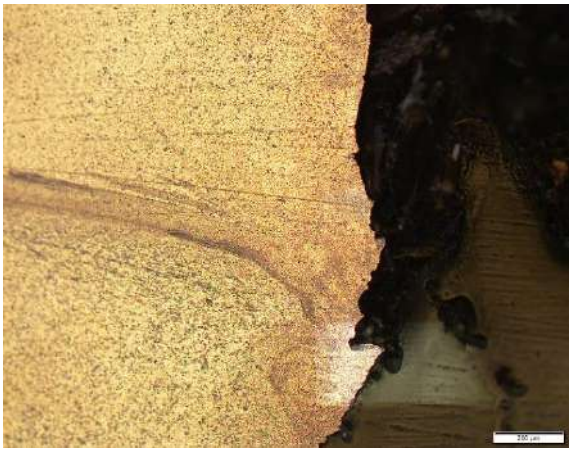

Figure 12. AA5754 - AA6061 - AA5754 series of macrostructure images taken from the junction points of the plates (10X)

The microscopic view of the sample taken from the material as a result of the friction stir welding of AA2024 - AA6061 - AA5754 materials (Fig. 13) produced a more prominent mark because the tip and rotation axis was held too much. Apart from this, there was no scattering in the used powder and the welding was good.

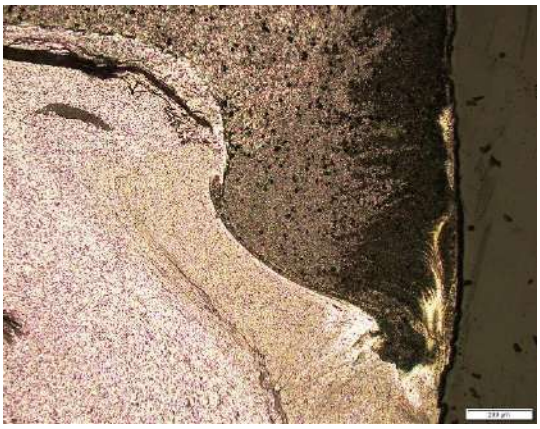

Figure 13. AA2024 - AA6061 - AA5754 series of macrostructure images taken from the junction points of the plates (10X)

Plates selected from the same material materials show a good merger in the HAZ region according to the microscopic images (Fig. 14) of the sample taken from the material of the friction stir welding of AA2024 - AA6061 - AA2024. The smudges that appear in the sample image are the residues of bakalite left on the material because they were bakalited two times and chemically exposed.

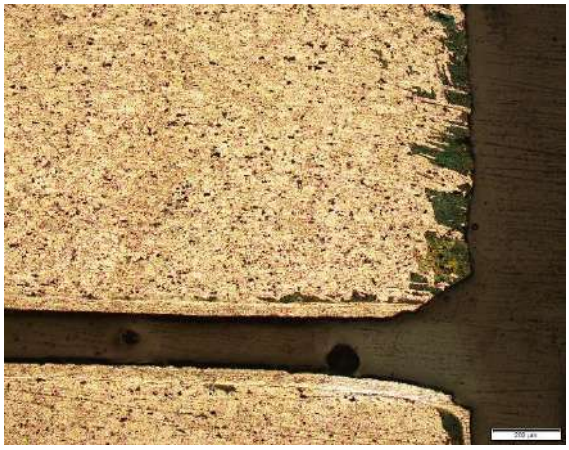

Figure 14. AA2024 - AA6061 - AA2024 series of macrostructure images taken from the junction points of the plates (10X)

5. Conclusions

Being one of the solid-state welding techniques, the FSSW located in the friction stir welding, has attracted attention as a new technique to replace the friction resistance welding, which is widely used in the automotive industry. Developments in this field show that materials used in many industries, such as the automotive sector, are suitable for lap welding joints. The applicability of the friction stir spot welding method to plastic materials as well as to the metal materials is a significant advantage over the friction resistance welding method. These studies have also shown that for the FSSW method, apart from the tool geometry, the welding tool has a significant effect on the tensile strength of the welded joint of the waiting time in the material.

It has been observed that aluminum alloy AA2024 - AA6061 - AA5754 materials were successfully combined with the friction stir spot welding.

References

[1] G. Çam: Sürtünme karıştırma kaynağı (SKK) :Al-alaşımları için geliştirilmiş yeni bir kaynak Teknolojisi, Mühendis ve Makine,46-541 (2005), pp. 30-39
[2] Anık,S.,1991: Kaynak Tekniği El Kitabı. Gedik Eğitim Vakfı, Türkiye.
[3] Tülbentçi,K.,1990: Mıg-Mag Eriyen Elektrod ile Gazaltı Kaynağı. Gedik Eğitim Vakfı Türkiye.
[4] Gerlich, A., Su, P., North,T. H., and Bendzsak, G. J., (2005). Friction stir spot welding of aluminum and magnesium alloys, Materials Forum 29, 290-294.
[5] Lathabai, S., Painter, M. J., Cantin, G. M. D., and Tyagi, V. K., (2006). Friction spot joining of an extruded Al-Mg-Si alloy, Scripta Materialia, 55, 899-902.
[6] url-1<www.metaluzmani.com> erişim tarihi = 24.05.2018
[7] url-2< www.muhendisbeyinler.net > erişim tarihi = 24.05.2018
[8] M. Aissani, S. Gachi,F. Boubenider, Y. Benkedda: Design and optimization of friction stir welding tool, Materials and Manufacturing Processes, 25-11, (2010), pp. 1199–1205.
[9] A. Kumar, L. Suvarna Raju: Influence of Tool Pin Profiles on Friction Stir Welding of Copper, Materials and Manufacturing Processes, 27, (2012), pp. 1414–1418.
[10] İpekoğlu, G., Çam, G., 2012: Farklı Al-Alaşımı Levhaların (AA6061/AA7075) Sürtünme Karıştırma Kaynağına Temper Durumunun Etkisi, TMMOB MMO Mühendis ve Makine Dergisi, 53, 40-47
[11] Kaçar, R., Ertek, H.E., Demir, H., Gündüz, S., 2011: Al-Cu-Al Malzeme Çiftinin Sürtünme Karıştırma Nokta Kaynak Kabiliyeti, Gazi Üniversitesi Mühendislik-Mimarlık Fakültesi Dergisi, 26, 349-357
[12] M. Boz, A. Kurt: The influence of stirrer geometry on bonding and mechanical properties in friction stir welding process, Materials & Design, 25-4, (2004), pp. 343–347.
[13] H. Badarinarayan, Y. Shi, X. Li, K. Okamoto: Effect of Tool Geometry on Hook Formation and Static Strength of Friction Stir Spot Welded Aluminium 5754-0 sheets, International Journal of Machine Tools & Manufacture, 49, (2009), pp. 814–823.
[14] S. Mandal, J. Rice: Experimental and Numerical Investigation of the Plunge Stage in Friction Stir Welding, Journal of Materials Processing Technology, 203, (2008), pp. 411–419.
[15] Y. Yang, P. Kalya, R. Landers, K. Krishnamurthy: Automatic Gap Detection in Friction Stir Butt Welding Operations, International Journal of Machine Tools & Manufacture, 48, (2008), pp.1161–1169.
[16] M. Melendez, W. Tang, C. Schmidt, J. C. McClure, A. C. Nunes, L. E. Murr: Tool Forces Developed during Friction Stir Welding, Nasa Technical Reports Server, (2003), Document ID: 20030071631.
[17] H. Okuyucu, A. Kurt, E. Arcaklioglu: Artificial neural network application to the friction stir welding of aluminum plates, Materials & Design, 28-1, (2007), pp. 78–84.
[18] A. Kumar, L. Suvarna Raju: Influence of Tool Pin Profiles on Friction Stir Welding of Copper, Materials and Manufacturing Processes, 27, (2012), pp. 1414–1418.

Effect of Oil Flow Rate, Contact Pressure and Sliding Speed on the Wear Properties of Zn-15Al-3Cu Alloy

Ali Paşa HEKİMOĞLU[1*], Temel SAVAŞKAN[2]

[1]Recep Tayyip Erdoğan University, Mechanical Engineering Department, Engineering Faculty, Rize, Turkey
[2]Haliç University, Mechanical Engineering Department, Engineering Faculty, Istanbul, Turkey

[*]**Corresponding author: a**li.hekimoglu@erdogan.edu.tr

Abstract

Wear properties of Zn-15Al-3Cu alloy were investigated at a range of oil flow rate (0.5-3cm^3), contact pressure (1–5 MPa), and sliding speed (0.5–2.5 ms^{-1}) for a sliding distance of 30,000 m using a block-on-disk type test machine. It was observed that the friction coefficient, working temperature and wear volume of the alloy decreased with oil flow rate. As the contact pressure increased, the friction coefficient of the alloy decreased, but its working temperature and wear volume increased. Sliding speed had no significant effect on the friction coefficient and wear volume of the alloy, but caused an increase in the working temperature. Wear surfaces of the alloy samples were examined using scanning electron microscopy (SEM). The area of the smeared surface layer increased with contact pressure, but decreased with oil flow rate. The results obtained from the wear tests are discussed in terms of microstructure and mechanical properties of the experimental alloy.

Keywords: Zn-15Al-3Cu alloy; Lubricated sliding; Wear test; Wear volume

1. Introduction

Zinc-based alloys were first developed in 1920s and used mainly for structural applications and decorative purposes (Goodwin and Ponikvar, 1980). Extensive research on these alloys has been resulted in the development of new bearing materials known as Alzen and ZA alloys (Gervais et al. 1980; Gervais et al. 1985; Lee et al. 1987; Skanazi et al., 1983). It has been reported that they have some advantages over the traditional bearing materials (Prasad, 2005; Delneuville, 1985; Lyon 1986). The most important advantages stated as good castability, low production cost, high wear resistance, high specific strength, good surface qualities, good embeddability, ideal tribological behavior in case of inadequate lubrication and high vibration damping capacity (Prasad, 2005; Delneuville, 1985; Lyon 1986). Despite these advantages, the strength of the zinc-based alloys is not adequate for some engineering applications. In order to overcome this disadvantage, research has been carried out on the strengthening of zinc-aluminum based alloys in recent years. These studies showed that the tensile strength and wear resistance of these alloys could be improved by changing the aluminum content and/or adding small amounts of copper (Savaşkan et al., 2003; Savaşkan et al. 2004; Savaşkan and Hekimoğlu, 2014; Hekimoğlu and Savaşkan, 2016). It has also been shown that addition of copper improves not only the strength of the alloys, but also their wear resistance. As a result of recent studies a number of ternary alloys (Zn-15Al-3Cu, Zn-25Al-3Cu, Zn-27Al-2Cu, Zn-40Al-2Cu, and Zn-75Al-3Cu) have been developed. Tribological properties of these alloys have been studied under different operating conditions. However, no work has been carried out on the lubricated friction and wear properties of Zn-15Al-3Cu alloy. It is known that the oil flow rate, pressure and sliding speed are important parameters for tribological applications of the bearing materials (Persson, 2000; Gahr, 1987; Bhushan, 2013). Therefore, the purpose of this study was to determine the effect of oil flow rate, contact pressure, and sliding speed on lubricated friction and wear properties of Zn-15Al-3Cu alloy.

2. Material and Method

Zn-15Al-3Cu was prepared by permanent mold casting using commercially pure aluminum (99.7 wt%), high-purity zinc (99.9 wt%), and an Al-50Cu master alloy. The alloy was melted in an electric furnace and poured into a conical-shaped steel mold at a temperature of approximately 600 °C. The chemical composition of the alloy was determined by atomic absorption analysis. Metallographic sample were prepared using standard techniques and etched with 2% Nital.

Microstructural examinations were performed with a scanning electron microscope (SEM). The density of the alloy was determined by Archimedes' method. The friction and wear properties of the alloy were investigated using a block-on-disk type machine. A photograph of this machine is shown in Fig. 1. The disc was made of SAE 1045 steel with a diameter of 200 ± 0.01 mm. It was hardened and tempered to obtain an average hardness of 50 ± 1 HRC. The surface of the disk was then ground and polished to obtain a roughness (Ra) lower than 1 μm. Friction and wear tests specimens with a size of 10 mm × 15 mm × 25 mm were prepared from the alloys. These tests were carried out at different flow rates, contact pressures, and sliding speeds for a sliding distance of 30.000 m. The values of the wear test parameters are given in Table 1. The friction force was determined using a load cell and the coefficient of friction of the alloys was calculated by dividing the friction force by the normal load. The rotational speed of the disk was adjusted by an electronic speed control unit and converted into sliding speed. The diameter of the sliding track on the disk surface was 150 mm. The temperature of the wear samples was measured with a copper–nickel thermocouple inserted in a hole at a distance of 1.5 mm from the rubbing surface. Each wear sample was ultrasonically cleaned and weighed before the wear tests using an electronic balance with an accuracy of 0.01 mg. The disk was cleaned with organic solvents before each test. The wear samples were cleaned in appropriate solvents and weighed to determine the mass loss after each test. The mass loss values of the wear specimens were converted into volume loss using the measured density of the alloy. The tests were performed at room temperature in air with a relative humidity of 70 ± 5%. The surface features of the wear samples were examined by SEM before and after the tests.

Fig. 1. A photograph of the block-on-disk type test machine

Table 1. The values of wear test parameters.

Oil flow rate (cm^3h^{-1})	Contact Pressure (MPa)	Sliding speed (ms^{-1})
0.25 1.0 1.5 2.0 2.5 3.0	6	2
1.0	1 2 3 4 5 6 7 8	2
1.0	6	0.5 1.0 1.5 2.0 2.5 3.0

3. Results and Discussion

Chemical composition of the experimental alloy is given in Table 2 and the microstructure of it is shown in Fig. 2. Microstructure of this alloy consisted of aluminum-rich α and ß, zinc-rich η and copper-rich ε phases. Formation of this microstructure was explained in papers published earlier (Savaşkan and Hekimoğlu, 2014; Hekimoğlu and Savaşkan, 2014; Hekimoğlu and Savaşkan, 2016).

Table 2. Chemical compositions of the experimental alloy

Alloy	Chemical composition (wt. %)		
	Zn	Al	Cu
Zn-15Al-3Cu	81,9	15,2	2,9

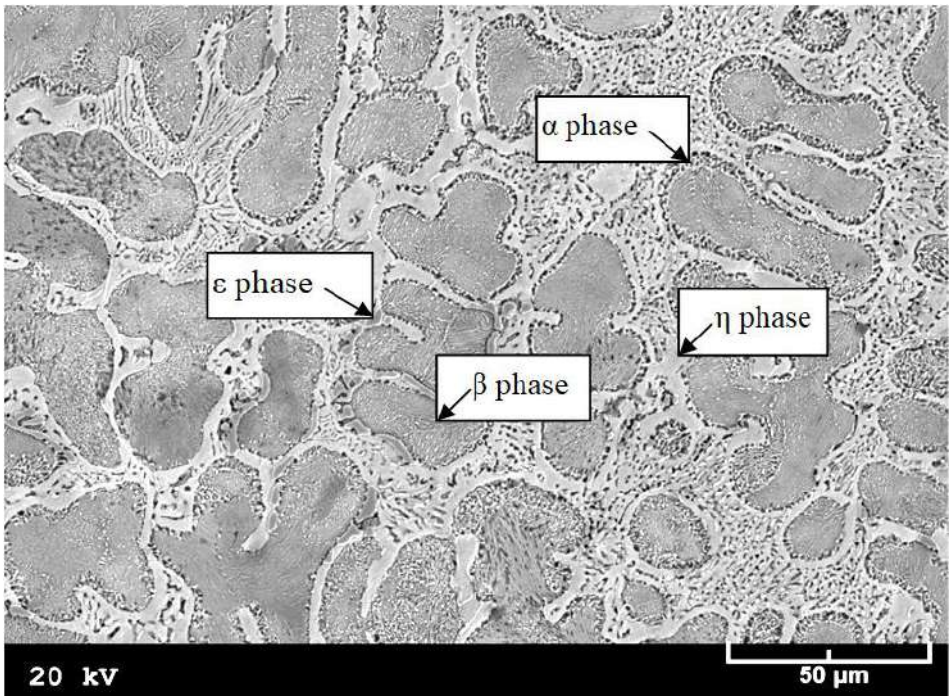

Fig. 2. SEM micrograph showing the microstructure of Zn-15Al-3Cu alloy

Friction coefficient, working temperature, and volume loss values of the alloys decreased continuously with increasing oil flow rate, Fig. 3. This may be related to the increase in the oil film thickness with increasing oil flow rate and thus decreasing metal-metal contact.

As the contact pressure increased, the friction coefficient of the alloy decreased, but their working temperature and wear volume increased, Fig. 4. This indicates that the wear tests were performed under hydrodynamic lubrication conditions. It is known that the friction coefficient decreases with increasing pressure in hydrodynamic lubrication conditions (Bican and Savaşkan, 2010). It is also known that as the pressure increases the thickness of oil film decreases (Bican and Savaşkan, 2010; Persson, 2000; Gahr, 1987; Bhushan, 2013). Decrease in oil film thickness can result in a decrease in friction coefficient by reducing the friction between oil molecules. The continuous increase in temperature and volume loss values may be due to the increase in friction force and frictional heating due to the increase in the metal-metal contact during running-in period.

It was observed that the temperature of the alloys increased continuously, but their friction coefficient and wear volume showed no significant change with sliding speed, Fig. 5. The increase in working temperature with increasing sliding speed can be explained in terms of centrifugal force acting on the lubricating oil. As the sliding speed increases, the centrifugal force acting on the lubricating oil increases, and this gives rise to an increase in the amount of oil removed from the disk surface. Both the decrease in the amount of lubricating oil and the increase in the friction between oil molecules can cause an increase in the working temperature. Increase in the working temperature

gives rise to a decrease in the viscosity of the oil. The decrease in the oil viscosity may balance the increase in the friction between oil molecules. This reduces the effect of sliding speed on the friction coefficient. It is known that in lubricated systems wear occurs mainly during running-in period due to metal-to-metal contact (Persson, 2000; Gahr, 1987; Bhushan, 2013). It is also known that the running-in period corresponds to a certain sliding distance rather than a running time. This means that increase in sliding speed decreases the time for running-in, but does not affect the sliding distance for this stage. Therefore, the wear volume is not expected to change considerably with sliding speed.

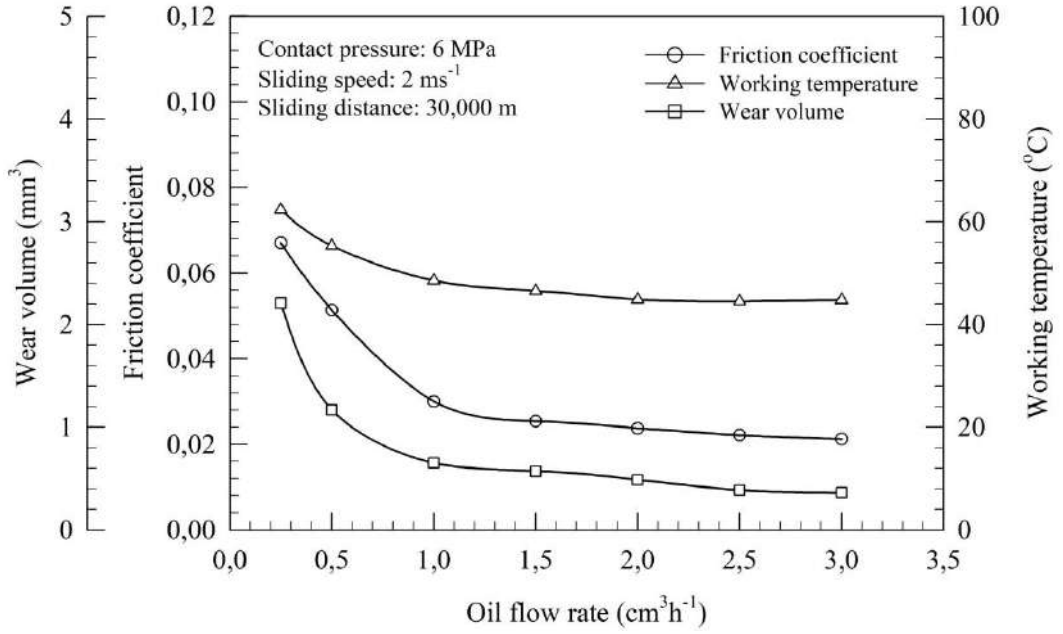

Fig. 3. Variations in the friction coefficient, working temperature, and wear volume of Zn-15Al-3Cu alloy with oil flow rate

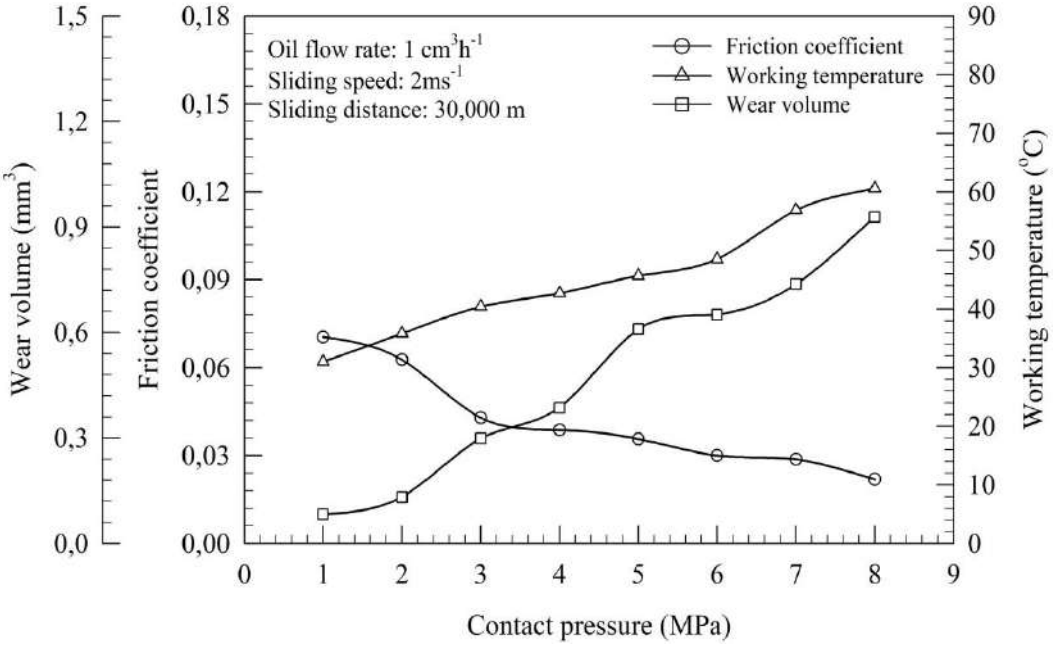

Fig. 4. Changes in the friction coefficient, working temperature, and wear volume of Zn-15Al-3Cu alloy with contact pressure

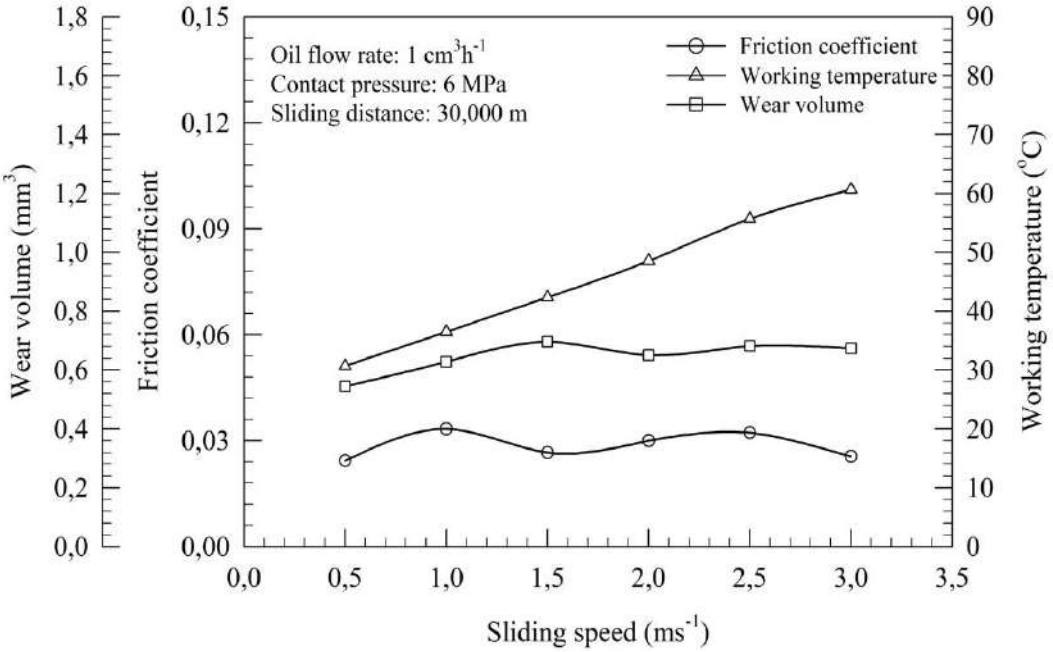

Fig. 5. Variations in the friction coefficient, working temperature and wear volume of Zn-15Al-3Cu alloy with sliding speed

The SEM images obtained from the worn surfaces of the samples tested at different oil flow rates, contact pressures and sliding speeds are shown in Fig. 6-12. These images show that the smeared area on the worn surface decreases with increasing oil flow rate, (Fig. 6-8), but increases with increasing

contact pressure, (Fig. 9 and 10). It was also observed that sliding speed has no significant effect on the wear surface of the alloys, (Fig. 11 and 12). These observations can be explained by the wear behavior of the samples. It is known that the smearing on the surface of the specimen occurs mainly during the running-in period (Halling, 1989; Savaşkan and Alemdağ, 2008; Hekimoğlu and Savaşkan, 2018). The increase in the oil flow rate shortens the period of metal-to-metal contact by accelerating the formation of oil film with sufficient thickness. The shortening in the duration of metal-to-metal contact results in a reduction in the amount of the wear volume. This may be the reason for the decrease in the smeared surface area of the wear samples with oil flow rate. The increase in the smeared surface area with pressure can be attributed to the increase in the contact area and wear rate during the running-in period (Halling, 1989; Hekimoğlu and Savaşkan, 2018). The sliding speed appeared to be not very effective on the appearance of worn surfaces, (Fig. 11 and 12). This may be attributed to the establishment of hydrodynamic lubrication in a shorter period of time by reducing the running-in period including boundary and mixed lubrication stages.

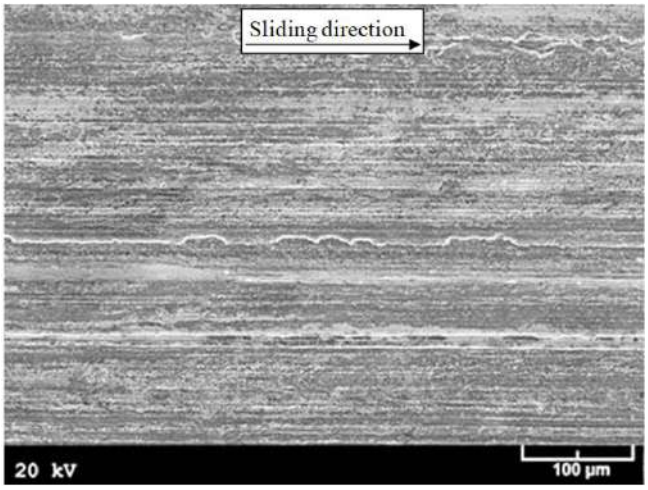

Fig. 6. SEM micrograph showing the surface of the wear samples of the alloy tested at an oil flow rate of 0.25 cm^3h^{-1} for 30.000 m (contact pressure = 6 MPa, sliding speed = 2 ms^{-1})

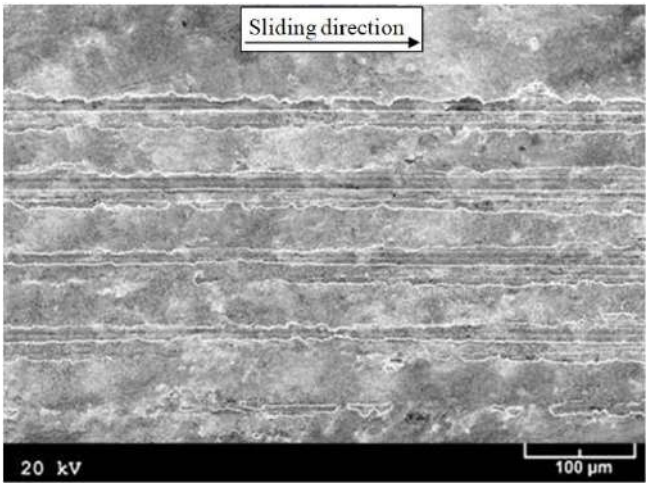

Fig. 7. SEM micrograph showing the surface of the wear sample tested at an oil flow rate of 1 cm^3h^{-1} for 30.000 m (contact pressure = 6 MPa, sliding speed = 2 ms^{-1})

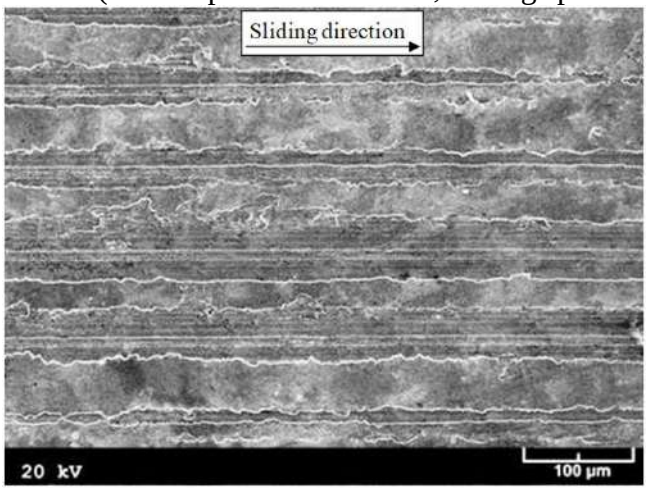

Fig. 8. SEM micrograph showing the surface of the wear sample tested at an oil flow rate of 3 cm^3h^{-1} for 30.000 m (contact pressure = 6 MPa, sliding speed= 2 ms^{-1})

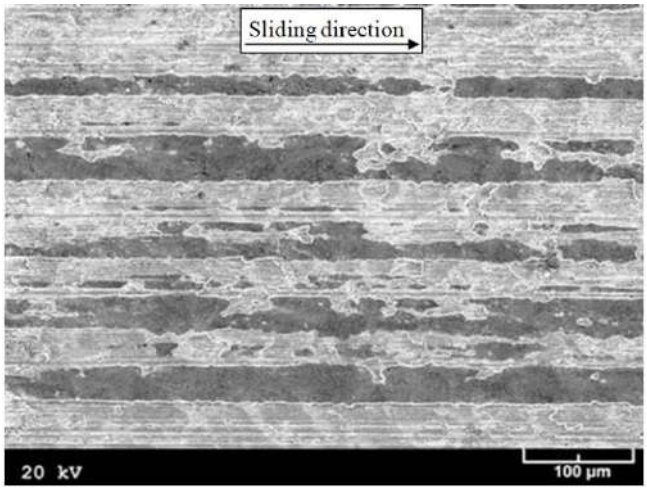

Fig. 9. SEM micrograph showing the worn surface of the sample tested at a constant contact pressure of 1 MPa for a sliding distance of 30.000 m (oil flow rate = 1 $cm^3 h^{-1}$, sling speed = 2 ms^{-1})

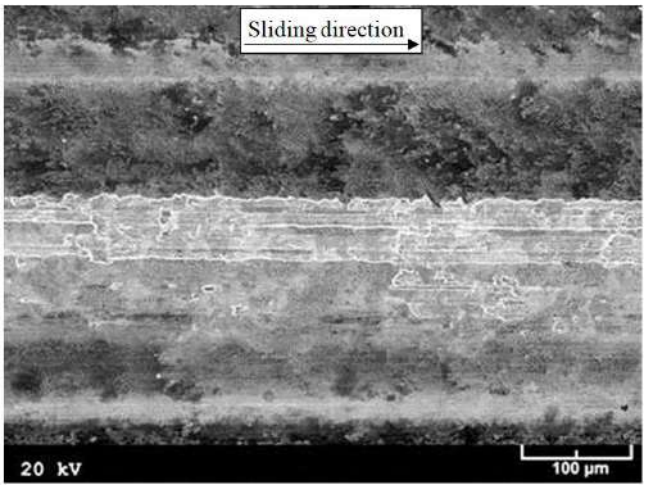

Fig. 10. SEM micrograph showing the surface of the wear sample tested at a contact pressure of 8 MPa for a sliding distance of 30.000 m (oil flow rate = 1 $cm^{-3}\,h^{-1}$, sling speed = 2 ms^{-1})

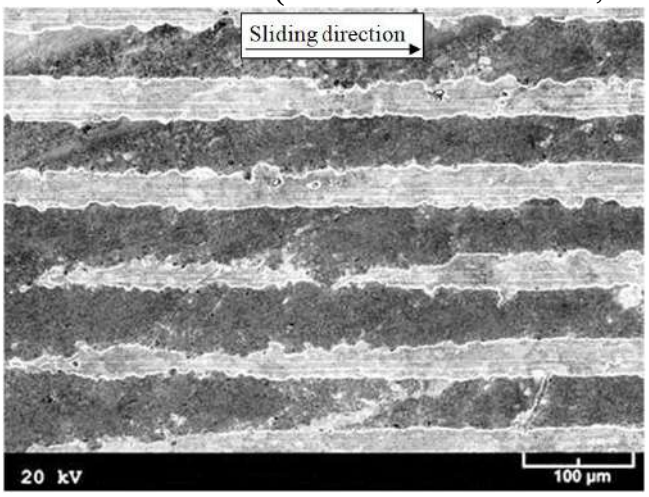

Fig. 11. Worn surface of the alloy sample tested at a sliding speed of 0.5 ms^{-1} for a sliding distance of 30.000 m (contact pressure = 6 MPa, oil flow rate = 1 $cm^3\,h^{-1}$)

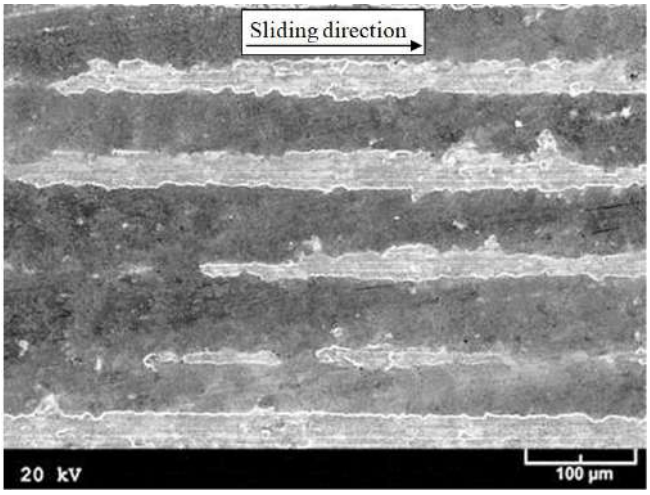

Fig. 12. Worn surface of the sample of the alloy tested at a sliding speed of 3 ms^{-1} for a sliding distance of 30.000 m (contact pressure = 6 MPa, oil flow rate = 1 cm^3 h^{-1})

4. Conclusions

The following conclusions are drawn from the work:

1. The friction coefficient, working temperature, and wear volume of Zn-15Al-3Cu alloy show a significant decrease with increasing oil flow rate.
2. Oil flow rate above 1cm^3h^{-1}, has no significant influence on the friction coefficient, working temperature and wear volume of Zn-15Al-3Cu alloy.
3. As the contact pressure increases, the friction coefficient of Zn-15Al-3Cu alloy decreases, but its wear volume and working temperature increase.
4. As the sliding speed increases, the working temperature of Zn-15Al-3Cu alloy increases, but its friction coefficient and wear volume show no significant change.
5. The area of smeared or adhered material on the worn surface of Zn-15Al-3Cu alloy decreases with oil flow rate, but increases with contact pressure. However, sliding speed has no significant effect on the smeared area.

Acknowledgement

This work was supported by the Karadeniz Technical University under a research contract (No. 2008.112.03.2).

References

Bhushan, B. (2013). Principles and Applications to Tribology (2nd ed.). New York: Wiley & Sons Ltd.

Bican, O. and Savaşkan, T., (2010). Influence of Test Conditions on the Lubricated Friction and Wear Behaviour of Al-25Zn-3Cu Alloy. Tribology Letters, 37, 175-182.

Delneuville, P., (1985). Tribological Behaviour of Zn-Al Alloys (ZA27) Compared with Bronze When Used as a Bearing Material with High Load and very Low Speed. Wear, 105, 283-292.

Gahr, K. H. Z. (1987). Microstructure and Wear of Materials. Amsterdam: Elsevier Science Publishing Company Inc.

Gervais, E., Levert, H. and Bess, M., (1980). The Development of a Family of Zinc-Based Foundry Alloys. American Foundrymen's Society Transaction, 88, 183-194.

Gervais, E., Barnhurst, R.J. and Loong, C.A., (1985). An Analysis of Selected Properties of ZA Alloys. Journal of Metals, 37, 11, 43-47.

Goodwin, F.E. and Ponikvar, A.L., (1989). Engineering Properties of Zinc Alloys (3d Ed.). USA:International Lead Zinc Research Organization.

Halling, J., (1989). Principles of Tribology. Great Britain: Macmillan Education Ltd.

Hekimoğlu, A. P. and Savaşkan, T. (2014). Structure and Mechanical Properties of Zn-(5-25)Al Alloys. International Journal of Materials Research, 105, 1084–1089.

Hekimoğlu, A.P. and Savaşkan, T., (2016). Lubricated Friction and Wear Properties of Zn-15Al-(1-5)Cu Alloys. Turkish Journal of Electromechanics & Energy. 1(2), 1-7.

Hekimoğlu, A.P. and Savaşkan, T., (2018). Lubricated Wear Characteristics of Zn–15Al–3Cu–1Si alloy and SAE 660 Bronze. Journal of the Faculty of Engineering and Architecture of Gazi University, 33(1), 145-154.

Lee, P.P., Savaşkan, T. and Laufer, E., (1987). Wear Resistance and Microstructure of Zn-Al-Si and Zn-Al-Cu Alloys. Wear, 117, 79-89.

Lyon, R., (1986). The Properties and Applications of ZA Alloys. The British Foundryman, 344-349.

Persson, B. N. J., (2000). Sliding Friction: Physical Principles and Applications (2nd ed.). Berlin: Springer.

Prasad, B.K., (2005). Sliding Wear Response of a Zinc-based Alloy and its Composite and Comparison with a Gray Cast Iron: Influence of Exeternal Lubrication and Microstructural Features. Materials Science and Engineering A, 392, 427-439.

Savaşkan, T. and Alemdağ Y., (2008). Effects of Pressure and Sliding Speed on the Friction and Wear Propertiefs of Al-40Zn-3Cu-2Si Alloy: A Comparative Study with SAE 65 Bronze. Materials Science and Engineering A, 496, 517-523.

Savaşkan, T., Hekimoğlu, A.P. and Pürçek, G., (2004). Effect of Copper Content on the Mechanical and Sliding Wear Properties of Monotectoid-Based Zinc-Aluminium-Copper Alloys. Tribology International, 37, 45-50.

Savaşkan, T., Purçek, G. and Hekimoğlu, AP., (2003). Effect of copper content on the mechanical and tribological properties of ZnAl27-based alloys. Tribology Letters, 15(3), 257-263.

Savaşkan, T. and Hekimoğlu, A. P. (2014). Microstructure and Mechanical Properties of Zn-15Al-Based Ternary and Quaternary Alloys. Materials Science and Engineering A - Structural Materials Properties Microstructure and Processing, 603, 52–57.

Skanazi, A.F., Pelerin, J., Coutsouradis, D., Magnus, B. and Meeus, M., (1983). Some Recent Developments in the Improvement of the Mechanical Properties of Zinc Foundry Alloys. Metallwissenschaft und Technik. 37(9), 898-902.

Effect of Heat Treatment on the Microstructure and Hardness Development of 1.2080 Cold Work Tool Steel

Fatih Hayat[1], Cihangir Tevfik Sezgin[2*], Samet Kurtuldu [3], Nurettin Aydın [4] , Ebubekir Hacı[5]

[1]Karabük University, Engineering Faculty, Metallurgy and Materials Engineering, Karabük, Turkey, fhayat@karabuk.edu.tr
[2]Kastamonu University, Cide Rıfat Ilgaz MYO, Welding Technology, Kastamonu,Turkey; ctsezgin@kastamonu.edu.tr
[3]Karabük University, Engineering Faculty, Metallurgy and Materials Engineering,Karabük,Turkey, skurtuldu@hotmail.com
[4]Karabük University, Engineering Faculty, Metallurgy and Materials Engineering, Karabük, Turkey, nrtaydin@gmail.com
[5]Karabük University, Engineering Faculty, Metallurgy and Materials Engineering, Karabük, Turkey, bkrhaci@gmail.com

[*] **Corresponding Author:** ctsezgin@kastamonu.edu.tr

Abstract

In this study, hardness of 1.2080,which is commercial name of steel, cold work tool steel was measured without heat treatment as 43.1 HRC. Samples were heated to 970 °C. They were cooled with water , oil and air. Their hardness was measured. Their microstructure was observed. Thenby these samples was tempered on 2 hours at 500 °C. The microstructure and and hardness was observed. The hardest sample was observed as oil quenced sample. Hardness of all samples was observed to decrease.

Keywords: 1.2080 steel, cold work tool steel, heat treatment

1. Introduction

Production of sheet metal parts that appeal to many sectors in manufacturing industry is realized by means of molds. These molds are also made of tool steel. For example, hole punches are made and used in different forms such as cylindrical heads and countersunk head. The punches are the elements that perform the drilling and cutting of the work piece in the mold and are made of high quality cold work tool steels and are hardened by hardening (Arslan, 2014).

1.2080 steel is an air/oil hardening cold-work alloy tool steel which has high carbon high chromium. The steel has approximately 2,1% C content (Uluköy etc., 2015) with have high carbon and high chromium. It displays excellent the abrasion and wear resistance Sadr etc.,2017). 2080 (X210Cr12) material is cold work steel with ledeburitic structure. It is a steel with high wear resistance and dimensional stability during heat treatment. Pressure resistance is high (Sağlammetal,2018; Arya,2018). It is suitable for high tensile cutting and punching tools, profile rolls, drawing and deep drawing molds, paper and plastic blades, scissors blades for thin sheets.

In this study, samples were heated to 970 °C. They were cooled with water , oil and air. Their hardness variation was observeed. Their microstructure was observed. Thenby these samples was tempered on 2 hours at 500 °C. The microstructure and and hardness was observed.

2. Material and Method

The samples were cut to a size of 50 x 50 mm and 16 mm in thickness. Microstructure and hardness values of non-heat-treated samples were then investigated. The samples were sanded with the abrasives 600, 800, 1000, 1200 respectively. Polishing was then carried out on the polishing machine by means of alumina (AL2O3). As the etching liquid, 2.5% nitric acid, 2.5% hydrochloric acid, 95% methanol (ethanol) was used in 100 ml and the microstructure images were obtained with the help of optical microscope.

Microstructure of original sample was shown in Figure 1.

As seen in the microstructure, the residual austenites are coarse-grained and spherical in the non-heat-treated sample. It is homogeneously distributed on the sample. It was observed that the carbides formed were slightly dispersed and coarse grained at the grain boundaries. The Rockwell hardness tester was 2.5 mm in diameter and 187.5 N was applied and the average hardness of 3 different points from the surface of the sample was measured as 43.1 HRC (400 HB).

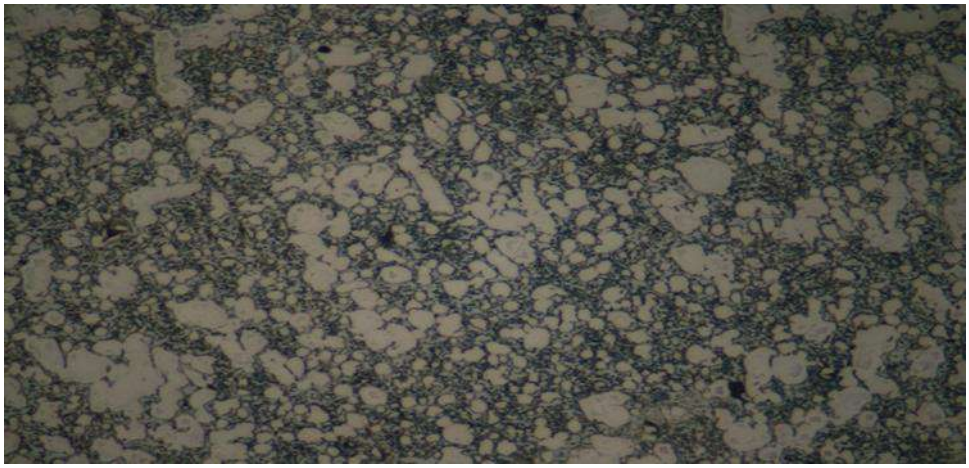

Figure 1. Microstructure of original sample (x 1000)

3. Results and Discussion

3.1. Samples heated at 970 ^{0}C

In Figure 2, austenitization temperature was increased to 970 ^{0}C in microstructure images and kept in heat treatment furnace for 2 hours. The parts removed from the furnace were then quenched by water cooling.

In the sample we applied quenching at the austenitization temperature, 1. carbide formation was realized with the effect of high carbon and chromium alloy elements. The residual austenites were slightly thinner in the structure and the carbides coalesced and the carbide coarse because of the austenitized samples. Carbon atoms during the heat treatment by spreading the austenite grain boundaries in these regions with the alloying elements to form chrome-rich carbides. The C atoms that did not form carbide and dissolved in the austenite cage during sudden cooling caused martensitic transformation. The average hardness value is 58,8 HRC.

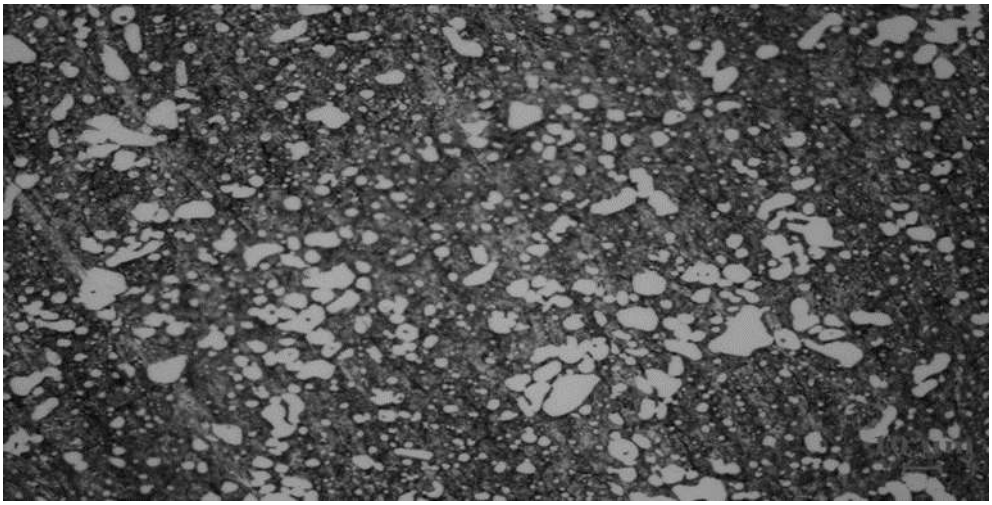

Figure 2. Microstructure of quenching with water after heated at 970 ^{0}C (x 1000)

In the microstructure images given in Figure 3, the austenitization temperature was increased to 970 ^{0}C and kept in the heat treatment oven for 2 hours. The parts removed from the oven were then oil quenched with instant cooling.

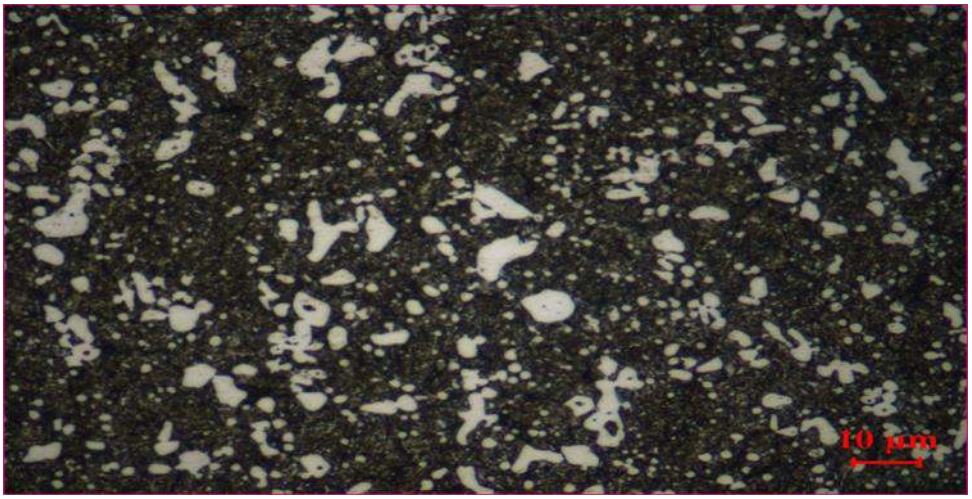

Figure 3. Microstructure of quenching with oil after heated at 970 ^{0}C

In the material that we apply the water quenching with the sudden cooling, the 1st carburetion is wrapped in the structure as a network and the residual austenites are spherical and they are distributed homogeneously. The residual austenites have irregular grain sizes. 1. The carbides spreading smoothly into the structure significantly increased the hardness of the material. The average hardness was 61,8 HRC.

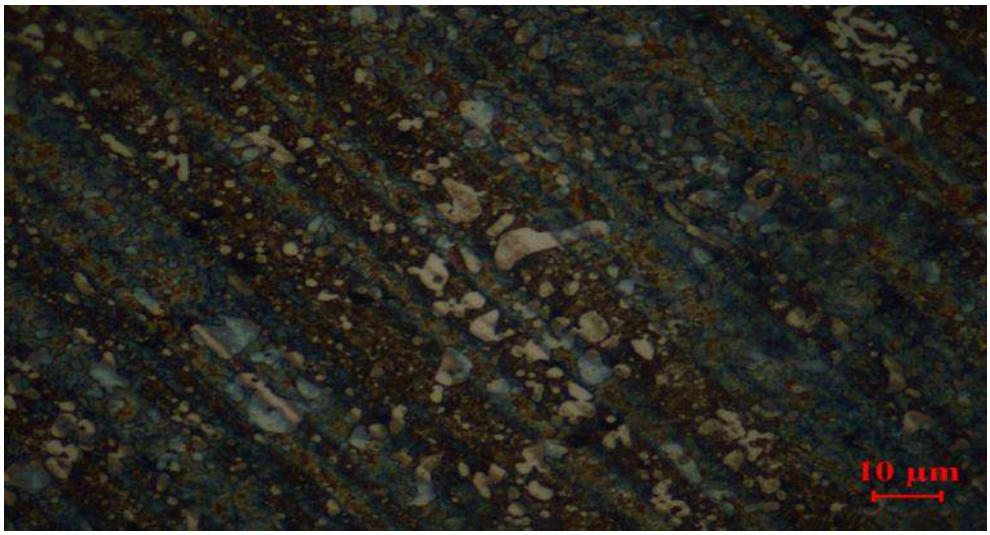

Figure 4. Microstructure of quenching with air after heated at 970 ^{0}C

As shown in Figure 4, the 1st carbides in the microstructure were observed in a small amount in the grain boundaries of the residual austenites as a result of the slow and controlled cooling. This is due to the fact that the carbon atoms in the structure do not form a high amount of carbide due to the fact that the cooling is not very fast. A small amount of carbide formation in the sample reduced the hardness of the material. The residual austenites appear to be coarse and spherical to the material. It is not a matter of martensite transformation. The average hardness was 54,7.

3.2. Samples heated at 500 ^{0}C after quenching

In the microstructure images shown in Fig. 5, austenitizing temperature was maintained in the oven for 2 hours, followed by tempering in 500 ^{0}C for 2 hours and then the hardness values were measured.

When the microstructure of the material which is tempered at high temperature after water quenching is observed, carbide roughing is observed. The coarse-grained carbides produced a reduction in the hardness of the material. It was observed that the coarse grained carbides were distributed evenly into the material. The average hardness value was observed as 50.5 HRC.

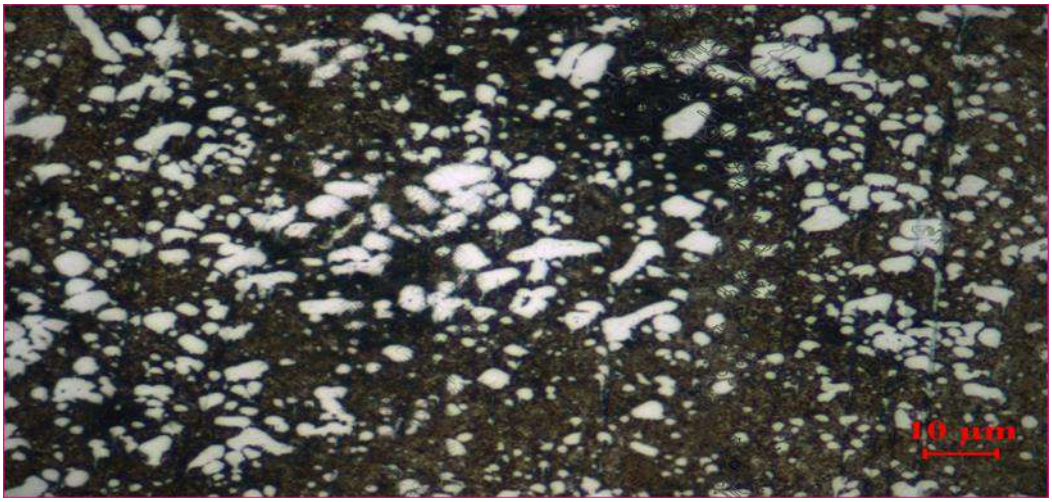

Figure 5. Microstructure of quenching with water sample be tempered in 500 ^{0}C

Figure 6 shows the microstructure of the tempering process for 2 hours at 500 ^{0}C of the oil quenching steel.

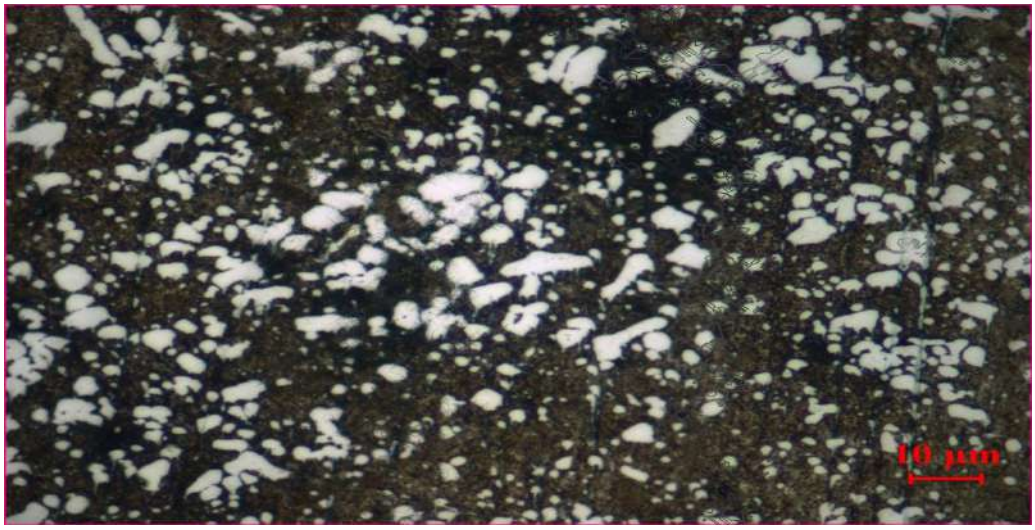

Figure 6. Microstructure of quenching with oil sample be tempered in 500 ^{0}C

In the microstructure shown in Figure 6, it is seen that residual austenites are formed around carbides in the sample which is tempered at 500 ^{0}C for 2 hours. When tempering at temperatures of 500 ^{0}C and above, it was determined that carbide amounts increased according to watered condition due to austenite decomposition and secondary carbide formation. Due to the high chromium content of our material, the carbides are clustered to form a second carbide. As the chromium is a ferrite-forming alloy element, the high addition of the structure to the structure narrows the austenite area of the steel. Since Ledeburitic cold work tool steels are used in tempered condition, maximum tool life is expected to reach 500 ^{0}C tempering temperature. It is also possible to increase the tool life by

homogenizing the carbide distribution and nitriding the material surface**.** Avarage hardness was observed as 57 HRC.

Figure 7 shows the microstructure of the tempering process for 2 hours at 500 ^{0}C of the air quenching steel.

As seen in the microstructure of Figure 7, if the cooling is slow and controlled, the residual austenites cover the structure and the carbide formation is observed to be very small. Avarage hardness was observed as 54,2 HRC.

Figure 7. Microstructure of quenching with air sample be tempered in 500 0C

4. Results and Discussion

- The highest hardness was observed at 970 °C by quencing with oil.
- After tempered at 500 °C, hardness of all samples decreased.
- The lowest hardness was observed that sample was carried out quenching with water and it was be tempered in 500 °C.

Referance

Uluköy A., Kaplan Y., Yıldız M., Çarık O., Onar V., Armağan E., Can A.Ç. (2015). The microstructure and hardness analysis of decarburization followed by boronizing AISI D3 tool steel, ICENS International Conference on Engineering and Natural Science, Skopje, Macedonia

Sadr P., Kolahdooz A., Eftekhari S.A., (2017). The effect of electrical discharge machining parameters on alloy DIN 1.2080 using the taguchi method and determinant of optimal design of experiments, Journal of Naval Architecture and Marine Engineering, 14 (1), 1447-64.

Arslan Y., (2014). DIN 1.2080 soğuk iş takım çeliği zımbalarda derin kriyojenik işlem ve temperlemenin alın aşınmasına etkisi, İleri Teknoloji Bilimleri Dergisi, 3 (1), 45-55.

URL1: http://www.saglammetal.com/tr/urun-detay/takim-celikleri/soguk-is-takim-celikleri/12080-cp10v-celik

URL2: http://www.aryametal.com/1.2080-X210Cr12-soguk-is-takimi-celikleri.html

Effect of Heat Treatments on S 235 Steel

Fatih Hayat[1], Cihangir Tevfik Sezgin[2*], Berfu Atıcı[3], Tuğba Ekinci[4]

[1]Karabük University, Engineering Faculty, Metallurgy and Materials Engineering, Karabük, Turkey, fhayat@karabuk.edu.tr
[2]Kastamonu University, Cide Rıfat Ilgaz MYO, Welding Technology, Kastamonu,Turkey; ctsezgin@kastamonu.edu.tr
[3]Karabük University, Engineering Faculty, Metallurgy and Materials Engineering,Karabük,Turkey, berfu.atc@gmail.com
[4]Karabük University, Engineering Faculty, Metallurgy and Materials Engineering, Karabük, Turkey, tuba.ek.t@gmail.com

[*] **Corresponding Author:** ctsezgin@kastamonu.edu.tr

Abstract

In this study, it was aimed to investigate the mechanical properties of S235 steelwhich was tempered 5 different temperatures. .The samples was holded at 200 ºC -400 ºC -600 ºC, 760ºC and 800 ºC temperature values. After the procedures applied with these parameters, the samples were cooled in air. Original samples and be applied heat treatment samples were tested by tensile strength test. Microstructure images were observed and their mechanical properties were determined. Three (3) steel pieces was used at tensile strength tests for each temperature

Keywords: S 235, heat treatment, microstructure, mechanical properties.

1. Introduction

S235 steel is one of structural steels. It is a non-alloy structural steel that is suitable for parts and machines of smaller thickness, which are besides welded and used statically or in just a slightly dynamical way. It is also used for various formed and welded parts, spurs, pins, levers, bolts, holders, and similar ones. This steel has a guaranteed weldability Costal etc. ,2018). Its yield strength is at least 235 MPa. Its tensile strength is between 360-770 Mpa for thickness between 3mm and 16mm (Azom,2018; Akçelik,2018)

St 235 steel is suitable for welding (Winczek, 2016; Winczek etc., 2018; and coating (Cebulski etc., 2017).

In this study, it was aimed to investigate the effect of heat treatment on the mechanical properties of 21 S235 steels.

Samples not subjected to heat treatment were subjected to tensile testing. Following the tensile test, all test samples were heat treated at different temperatures and times. For the determination and comparison of the yield and shrinkage values, separate tensile tests of the non-heat treated and applied samples were performed. It was determined as 760ºC-800ºC-900ºC and 200ºC-400ºC-600ºC. The samples were cooled in the air after the procedures applied with these parameters. After heat treatment applications, sanding and etching with 2% nital solution were performed. The microstructure images were examined and their mechanical properties were determined.

2. Material and Method

These steels are generally defined as unalloyed steel, the mechanical properties are mostly dependent on the amount of carbon, but the manganese, silicon, copper and sulfur elements resulting from the production raw materials and production forms, mainly nitrogen and phosphorus, are also highly effective

Chemical composion of s 235 steel was shown at Table1. Mechanical properties of S 235 was shown at Table 2.

Table 1. Chemical composition

C (Max)	N (Max)	P (Max)	Mn	S (Max)	Cu
0,17	0,012	0,035	1,4	0,035	0,55

Table 2. Mechanical properties

Diameter (mm)/ Thickness (mm)	10/16
Tensile Strength (MPa)	420-770
Yield Strength (Mpa)	300
Elongation (%)	9
Hardness (HB)	125-231

Heat treatments were carried out at 200 ° C, 400 ° C, 600 ° C, 760 ° C and 800 ° C . The annealing time is 60 minutes and the cooling is in the air. Following this process, microstructure images were taken and subjected to tensile test.

3. Results and Discussion

3.1. Microstructure

Figure 1, shows microstructure of original sample. Original sample consisted of ferrit and pearlite.

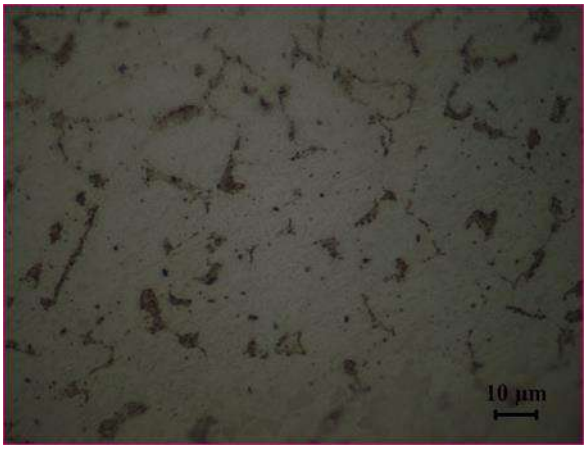

Figure 1. Microstructure of original sample

Figure 2 shows sample was tempered at 200 and 400 ° C. When temperature increased perlite grew. Figure 3a showed that pearlite volume decreased at 600 ° C. Grain boundry of ferrite became clear. Pearlite occured at grain boundry of ferrite. Figure 3b showed that pearlite volume increased again. All austenites, which consisted of 760 ° C, were transformed into perlite at room temperature.

This was result of cooling with air. Figure 5 showed that pearlite occured in room temperature. Black island showed pearlite and white matrix showed ferrite phase.

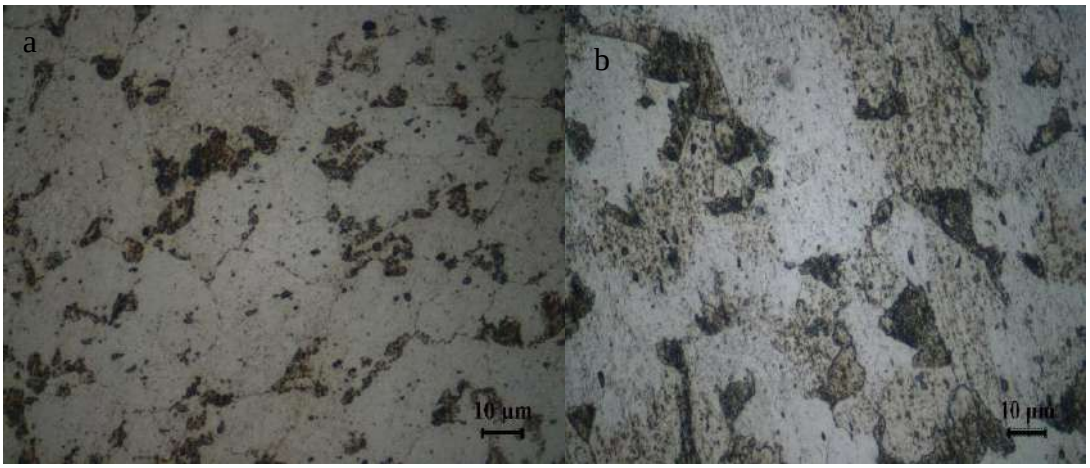

Figure 2. Microstructure of sample was tempered at a)200° C b)400 ° C

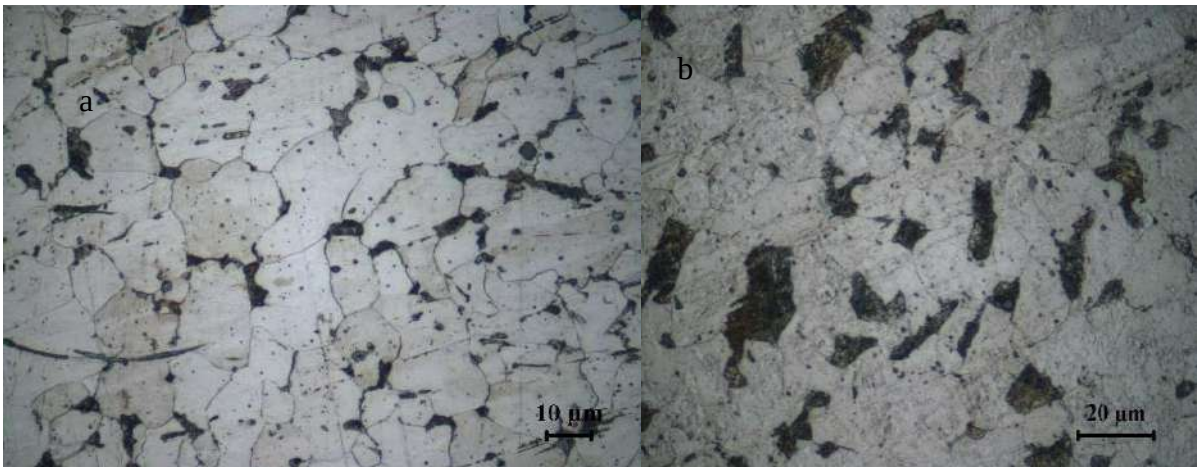

Figure 3. Microstructure of sample was tempered at a)600° C b)760 ° C

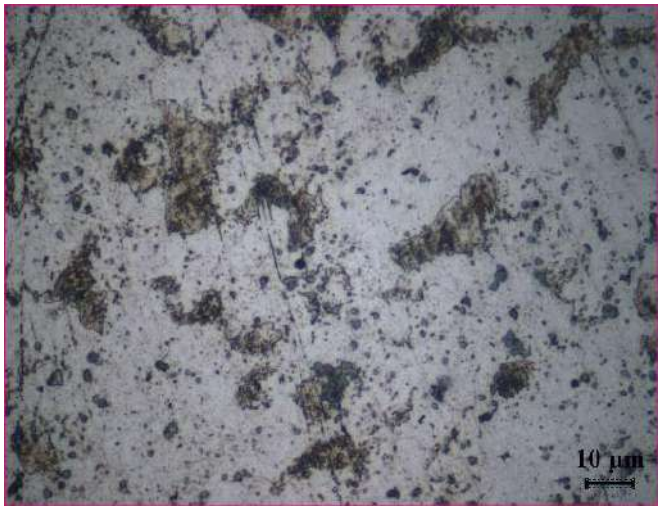

Figure 4. Microstructure of sample was tempered at 800° C

3.2. Tensile Strength Test

Table 3 showed results of tensile strength test. Yield strength and tensile strength of original sample was same with sample was tempered at 600 ° C. This results was maximum yield strength, too. Minimum yield strength was observed at sample was tempered at 800 ° C. Minimum tensile strength was observed at 400 ° C while minimum elongation was observed at 800 ° C. Maximum tensile strength was observed at 760 ° C and maximum.elongation was observed at 600 ° C.

Table 3. Tensile strength test results

Temperature ° C	Yield Strength MPa	Tensile Strength MPa	Elongation %
Room	280	418	30,8
200	264	423	31,1
400	227	332	25
600	280	418	31,3
760	277	428	26,2
800	213	333	18,3

4. Results and Discussion

- The highest tensile strength was observed at 760 °C. Minimum tensile strength was observed at 400 ° C
- The highest yield strength and maximum.elongation was observed at 600 ° C. It is same yield strength of original materials.
- For all microstructures of tempered sample they were consist of pearlite and ferrite in room temperature. Especially ferrite grain boundry was observed clearly at sample was tempered at 600 °C and pearlite was occured at these grain boundry. Pearlite volume increased until 600 °C. Volume of pearlite decreased at this temperature.

Referance

Košťál P., Moravčíková J., Sobrino D.R.D., Holubek R., (2018). On the effect of the cutting speed of a water jet abrasive cutting process on the surface morphology of the low carbon steel S235, Materials Science Forum, 919,92-100.

Winczek J., (2016). Modeling of heat affected zone in multipass GMAW surfacing S235steel element, Procedia Engineering, 136, 108 – 113

Cebulski J., Bęczkowski R., Pasek D., (2017). The use of TIG welding of forming a coating FeAl on the S235, 23rd International Conferance Engineering Mechanics, Svartska, Czech Republic.

Winczek J., Parkitny R., Makles K., Kukuryk M., (2018) Analytical model of stress field in submerged arc welding butt joint with thorough penetration, MATEC Web of Conferences 157,

Winczek J., Parkitny R., (2017).Modelling of Heat Affected Zone in Submerged arc Welding Butt Joint with Thorough Penetration, Procedia Engineering, 177, 241-246

URL1: http://www.akcelik.com.tr/dosyalar/kalite/Yap%C4%B1%20%C3%87elikleri/S235JR.pdf

URL2: https://www.azom.com/article.aspx?ArticleID=6022

Evaluation of Low Alloyed Ribbed Construction Steels Produced Via Tempcore Process According to TS 708 Standard

Erhan DOĞAN[1], Gürel ÇAM[2*]

[1] Net Haddecilik Industry Trade and Limited Company, 31900 Payas / Hatay, Turkey;
erhan.dogan@nethaddecilik.com.tr

[2] Iskenderun Technical University, Faculty of Engineering and Natural Sciences, Department of Mechanical Eng., 31200 İskenderun / Hatay, Turkey; gurel.cam@iste.edu.tr

[*]**Gürel ÇAM:** gurel.cam@iste.edu.tr

Abstract

The use of ribbed steel bars with high mechanical properties in the construction sector is currently increasing day by day. One of the processes to be used in order to increase the strength of ribbed steel bars without diminishing welding capability is the tempcore process.

In this study, low alloyed ribbed steel bars with different diameters were produced in a hot rolling mill both via conventional process and using tempcore process. The main purpose of this research is the examination of all the steel bars according to TS 708 and compare their mechanical properties. All the specimens extracted from low alloyed ribbed steels bars with different diameters produced by conventional and tempcore processes were tested and the results were evaluated according to TS 708. For instance, the tensile test results clearly indicated that the yield stress value of ribbed steel bar with a diameter of 8 mm produced with tempcore process, i.e., 496 N/mm^2, was significantly higher than that of the bar of the same diameter produced without tempcore process, i.e., 345 N/mm^2. The yield stress value of the bar produced using tempcore process is also reasonably higher than the minimum yield stress value specified in TS 708 standard, i.e., 420 N/mm^2. Moreover, the tensile and yield strength values of the ribbed steel bar for a given diameter increased significantly with the increase in quench period and water flow (i.e., amount of the water) used in tempcore process. On the other hand, this decreased the ductility of the steel. This study clearly indicated that the low alloyed construction steel bars produced by tempcore process comply with TS 708.

Keywords: Ribbed steel bars, Low alloyed steel, Hot rolling mill, Tempcore process, TS 708.

1. Introduction

In parallel with the technological developments in recent years reasonably high ductility and weldability as well as high yield strength and good bending properties are required from reinforced concrete steels. It is extremely expensive and difficult to achieve these desired properties in ribbed construction steels produced by using conventional methods in hot rolling mill. There are several processes in order to achieve desired properties in ribbed construction steels one of which is tempcore process [1].

Tempcore process is a special cooling process used in hot rolling mill. Fast cooling transforms the surface of the steel bar into martensite. After the quenching (fast cooling) martensitic zone up to a certain depth on the outside (outer periphery) of the steel is tempered by the heat of the core. In this way, low alloy steels with the desired mechanical properties can be produced in a hot rolling mill at a lower cost [2].

In the construction industry, production is made according to the standards of different countries in the world. When the standards are examined, it will be seen that the mechanical properties expected from the construction steel have increased over the years [3].

In this study, the mechanical properties of ribbed construction steels of various diameters produced by the tempcore process were investigated according to S420 quality of TSE 708 standard. low alloyed ribbed steel bars with different diameters were produced in a hot rolling mill both via conventional process and using tempcore process. The mechanical properties of all the steel bars produced were determined and evaluated according to TS 708. The results obtained from ribbed steel bars with different diameters produced by conventional and tempcore processes were also compared with each other. Moreover, the influences of quench period and water flow (i.e., amount of the water) used in tempcore process on the tensile and yield strength values of the ribbed steel bar for each diameter were also determined.

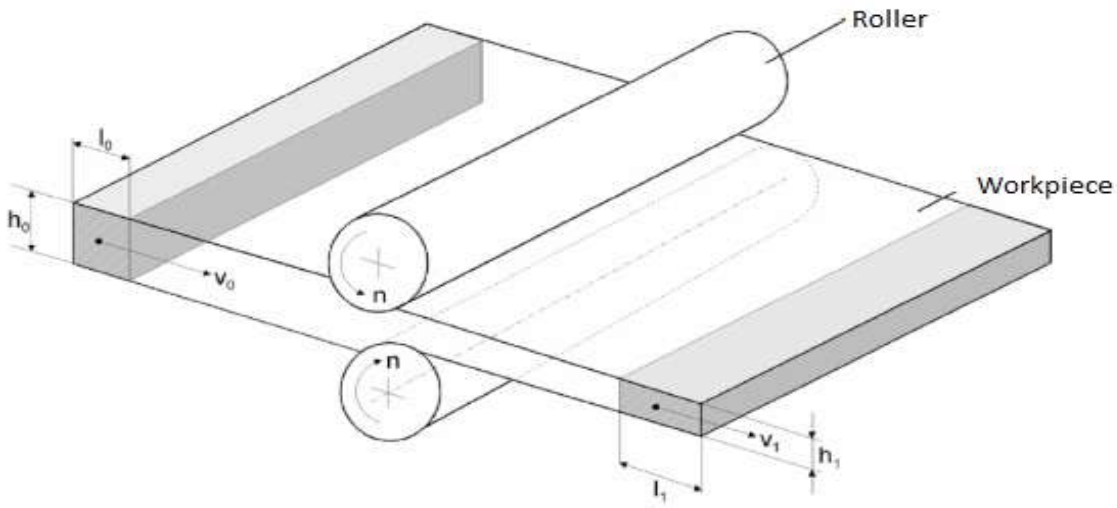

2. Material and Method

2. 1. Hot Rolling

Figure 1. Schematic illustration of a rolling process [5].

The forming process in which the thickness of the workpiece is reduced by the pressing forces produced by two rollers rotating in opposite directions is called rolling [4]. A rolling process is shown schematically in Figure 1 [5].

The majority of the rolling process is performed hot because of the large amount of deformation required. This process is called hot rolling. Hot rolled plates generally do not contain residual stresses and are isotropic. The thicknesses of the hot rolled products are not held at narrow tolerances and the workpiece surface has a characteristic oxide descale [4].

Steps of a rolling mill operation are as follows. Billets are placed in a hot furnace and kept in the furnace until a uniform temperature is reached. So that the metal will flow properly during rolling. The required rolling temperature for steel is around 1200 ^{o}C. This heating operation is called reheating. And the furnace where this process is done are called reheating furnace [4].

After reheating the ingot is transported to the rolling mill and rolled to one of the three intermediate forms called blum, bilet and slab. The blums are rolled futher to produce train railway, I, L and U profiles for structural shapes. Slabs are sent to flat product manufacture rolling mills and where plates or sheets are produced. And the billets are sent to bar rolling mills [4].

The billets are rolled in the stands and the construction steel is produced at the desired size in rolling mills. A hot rolling production flow is schematically shown in Figure 2. Constructional steel bars can be produced in sizes ranging from 8 mm to 50 mm in diameter.

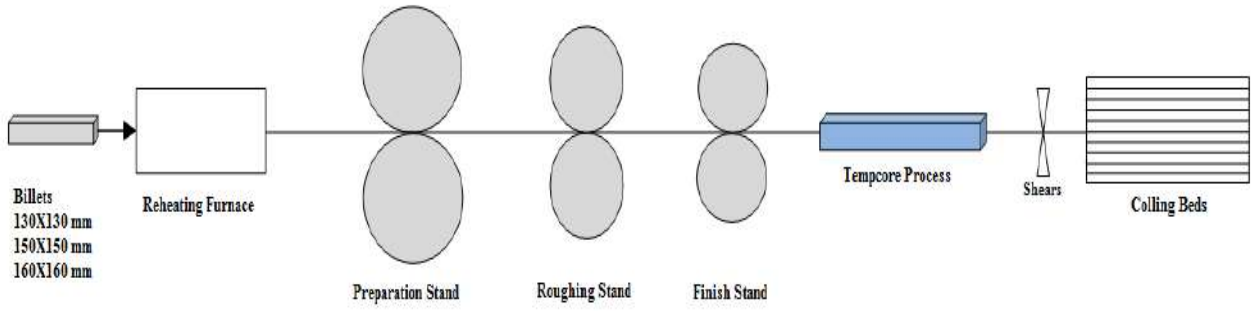

Figure 2. Hot Rolling Production Flow

2.2. Tempcore Process

The tempcore method is a self-tempering process in which the tempering of the fast cooled outer pheriphery is done by the temperature in the center of the bar following quenching at the finish rolling stand. The bar subjected to the tempcore method has to pass through three stages in this special heat treatment cycle as schematically shown in Figure 3 [2].

First stage is the application of cooling operation with accelerated quenching to the bar leaving the final rolling stand [2]

Second stage; the material leaving the fast cooling area is exposed to the ambient air up to the cooling platform. During this stage, the heat inside will cause the cooled surface to overheat [2].

Third step involves cooling the bar on the cooling platform to ambient temperature [2].

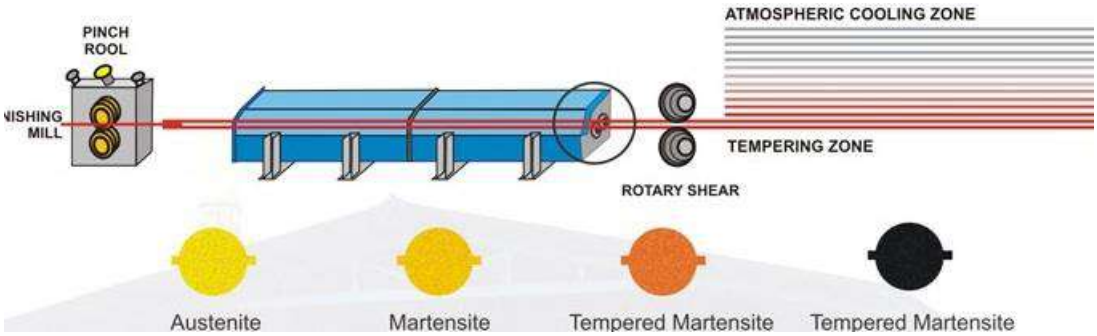

Figure 3. Phases of the tempcore process [2] .

During this process, a martensitic crust of a certain thickness on the surface is formed rapidly at the first step (Figure 4). The cooling efficiency must be such that the cooling rate of the part of the material surface up to a certain depth is higher than the critical martensitic cooling rate. The duration of this step depends on the depth of the desired martensitic crust. In the second stage, since the heat transfer coefficient of the air is small the temperature of the core of the bar reheats the surface crust due to the large temperature difference. The maximum temperature reached by the surface is called the tempering temperature. In this way, the martensitic surface is tempered to obtain high tensile strength material with an appropriate toughness [2].

Conventionally, when the surface temperature of the material reaches its maximum value, it is considered that the second step is completed. The duration of second step depends on largely the material diameter and the cooling conditions of the first step. At the second stage, the core remains austenitic, while the surface austenite turns into bainite. On the other hand, the bainite can be transformed depending on the austenite cooling conditions just below the tempered martensitic surface and the steel composition. At the third step, the remaining austenite undergoes semi isothermal transformation. A mixture of ferrite-perlite or ferrite-perlite-bainite is obtained depending on various factors [2].

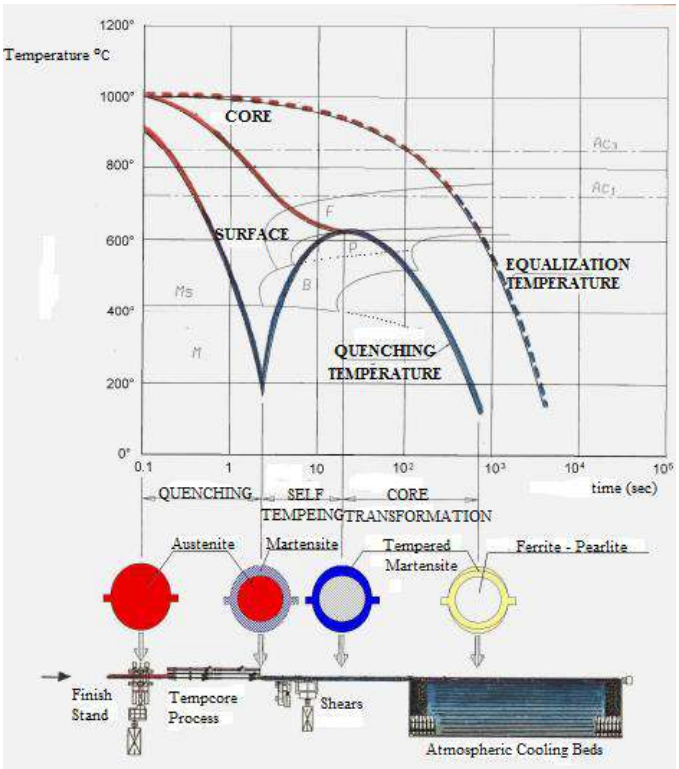

Figure 4. Time dependent microstructure-temperature relationship in tempcore process [3].

2.3. TS 708 Standard

This standard covers general and necessary specifications for the performance characteristics of weldable and non-weldable steel reinforcement manufactured and delivered in the form of bar, coils and rectilinear coils for use reinforced concrete structure [6]. Weldability depends on two properties: 1) carbon equivalent and 2) limiting the proportions of certain elements. According to TSE 708 standard, carbon equivalent (C_{eq}) and the highest value of each of the elements should not excess the values given in Table 1 [6].

Carbon equivalent (C_{eq}) should be calculated using the following equation [6].

$$C_{eq} = C + Mn/6 + (Cr + Mo + V)/5 + (Ni + Cu)/15 \quad (1)$$

Table 1. Chemical compositions (max. %) and carbon equivalent of selected class of steels [6].

Class of Steel	C [a]	S	P	N [b]	Cu	Carbon Equivalent
S 220	0,25	0,050	0,050	-	-	-
S 420	0,45	0,050	0,050	-	-	-
B 420 – B 500	0,22	0,050	0,050	0,12	0,80	0,50
Maximum deviation value in the product	0,02	0,005	0,005	0,002	0,05	0,02

[a] The maximum carbon value is allowed to be greater than 0,03% by mass, provided that the carbon equivalent is less than 0,02% by mass.

[b] If sufficient nitrogen binding elements are present, allow to contain higher nitrogen.

Mechanical properties of selected grades of constructional steel bars with different geometries according to TSE 708 standard are given in Table 2 [6].

Table 2. Mechanical properties of selected grades of constructional steel bars with different geometries [6].

Type	Planiform	Ribbed					Profiled [a]
Class	S 220	S 420	B 420B	B 420C	B 500B	B 500C	B 500A
Yield Strength (min) R_e (N/mm^2)	220	420	420	420	500	500	500
Tensile Strength (min) R_m (N/mm^2)	340	500	-	-	-	-	550
Tensile Strength / Yield Strength R_m/R_e	Min. 1,20	Min. 1,15	Min. 1,08	≥ 1,15 < 1,35	Min. 1,08	≥ 1,15 < 1,35	-
Experimental yield strength / Characteristic yield strength $R_{e\,act}/R_{e\,nom}$ (max)	-	1,30	-	1,30	-	1,30	-
Breaking Extension (min) A_5(%)	18	10	12	12	12	12	5

Total Elongation at max. Load (min) $A_{gt}(\%)$	-	-	5	7,5	5	7,5	2,5
Bending Angle (°)	180		-				
Bending Angle / Reverse Bending Angle	-		90/20				
[a] Manufactured by cold mechanical processing							

2.4. Low Alloy Ribbed Construction Steel Produced by Tempcore Process

The most important detail in producing construction steel is the chemical composition of the used billets (the starting material), which in turn determines the cooling period used in the tempcore process. The chemical composition of 150X150 mm billets, which was obtained from Isdemir and used to produce ribbed steel bars with different diameters in the hot rolling mill, is given in Figure 5. These billets were annealed in a reheat furnace and then hot rolled via the tempcore process and without tempcore process to produce ribbed construction steels with different diameters. The samples were extracted from all the produced ribbed steel bars and tensile test were conducted to determine the mechanical properties. The results obtained from the bars produced using tempcore process were compared with those obtained from the steel bars produced via conventional hot rolling. The mechanical test results were also analyzed according to TSE 708 standard.

MALZEME TEST BİLGİLERİ

İSKENDERUN DEMİR VE ÇELİK FABRİKALARI T.A.Ş.

İsdemir Kalite Kodu: 1.8420_01
Uluslararası Kalite Kodu: DIN 488-1
Sipariş No: 18100179902
Kütük Ölçüleri: 150x150x12000

Tarih : 28/03/2018
Plaka : 31V9651

Ağır. (Kg)	Döküm No	Tipi	Test No	Çap (mm)	MEKANİK ÖZELLİKLER ÇEKME TESTİ					Kimyasal Kompozisyon %, Pota Analizi												
					AkmaMuk.	Çekme Muk.	Uzama (%	Kesit Dar. (%)	Katlama	C	MN	P	S	SI								
2142	18112349	KÜTÜK	8112349450800	null						0.16	0.61	0.011	0.022	0.20								

Figure 5. Chemical composition of the billet used in this study.

3. Results and Discussion

The tempcore process has in general improved the mechanical properties of the ribbed construction steel bars. For instance, the stress-elongation curve of 8 mm diameter ribbed construction steel bar produced without tempcore process (via conventional hot rolling process) is given in Figure 6. On the other hand, Figure 7 illustrates the stress-elongation curve obtained from 8 mm diameter ribbed construction steel bar produced using tempcore process for comparison. As seen from these Figures, the yield stress value of 8 mm diameter ribbed construction steel bar produced via

conventional hot rolling process was 345 N/mm^2 whereas that of 8 mm diameter ribbed construction steel bar produced using tempcore process was 496 N/mm^2. This indicates that the yield stress value can be significantly increased by tempcore process for a given steel bar diameter.

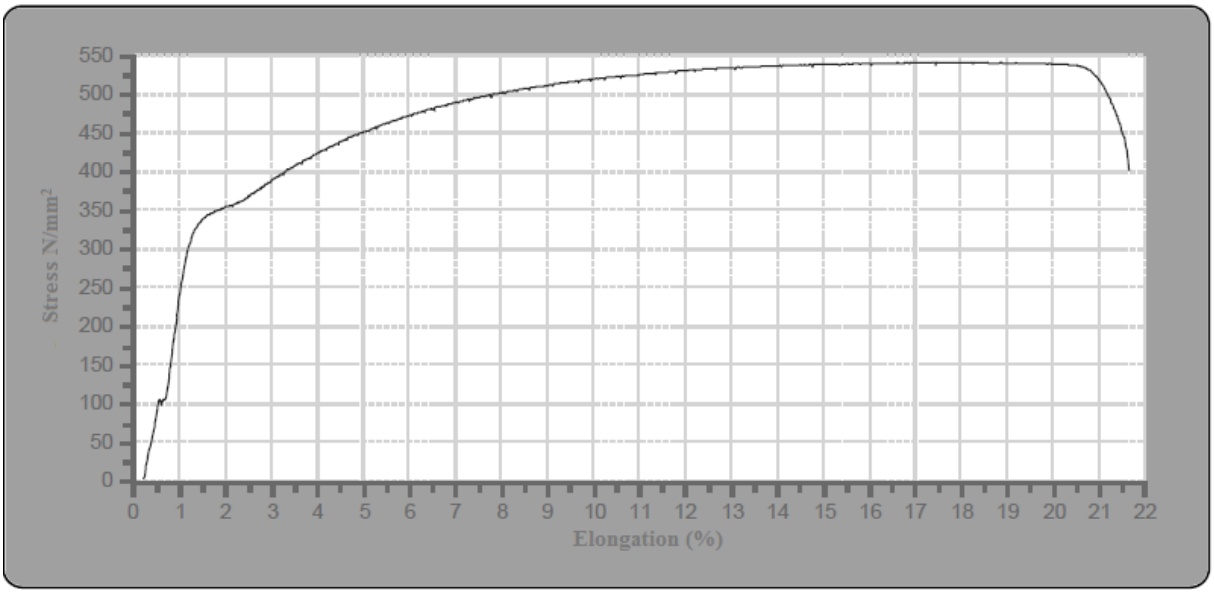

Figure 6. The stress-elongation curve of 8 mm diameter ribbed construction steel bar produced without tempcore process.

.

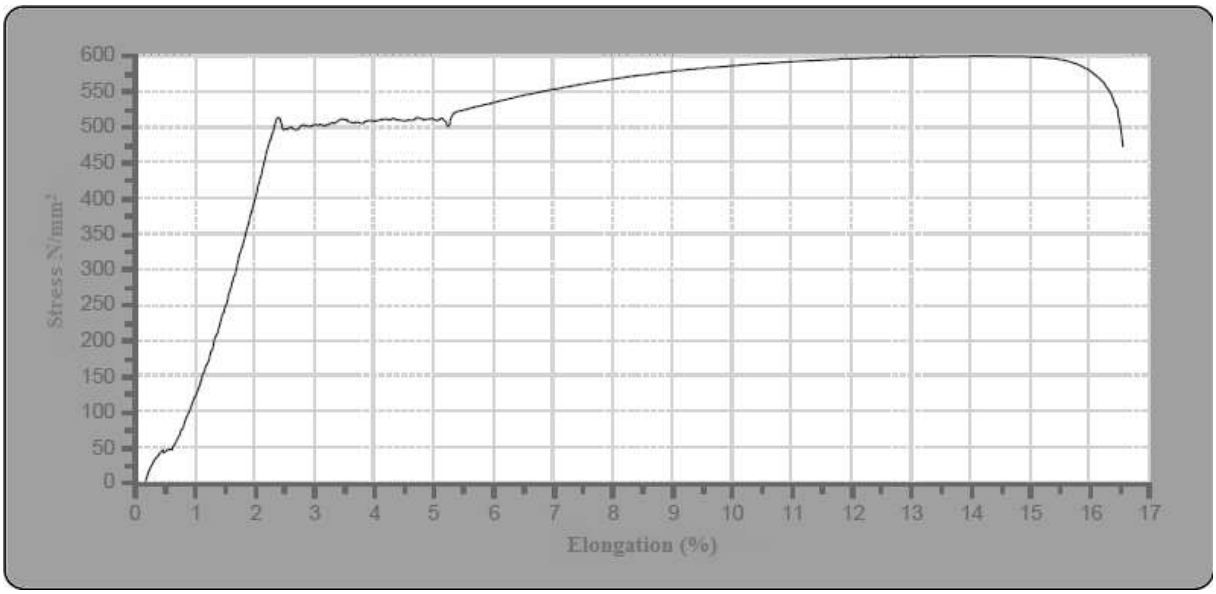

Figure 7. The stress-elongation curve of 8 mm diameter ribbed construction steel bar produced with tempcore process.

The tensile test results obtained from 8 mm diameter ribbed construction steel bars produced via conventional hot rolling process and tempcore process were also evaluated according to the quality S 420 of TSE 708 standard. Moreover, tensile strength/yield stress ratios are calculated as

follows for the bars produced without and with tempcore process, respectively, and the results are summarized in Table 3:

$$\frac{R_m}{R_e} = \frac{540{,}65}{345{,}35} = 1{,}56 \quad (2)$$

$$\frac{R_m}{R_e} = \frac{588{,}28}{496{,}58} = 1{,}18 \quad (3)$$

Table 3. Comparison of the tensile test results obtained from 8 mm diameter ribbed construction steel bars and their evaluation according to TSE 708 standard.

Type	Ribbed		
Class	TSE 708 S 420 Standard	Without Tempcore	With tempcore
Yield Stress (min) R_e (N/mm^2)	420	345,35	496,58
Tensile Strength (min) R_m (N/mm^2)	500	540,65	588,28
Tensile Strength / Yield Stress R_m/R_e	Min. 1,15	1,56 (2)	1,18 (3)
Experimental yield stress / Characteristic yield stress $R_{e\,act}/R_{e\,nom}$ (max)	1,30	1,54	1,18
Elongation (min) A_5(%)	10	21,6	19,7

As seen from Table 3, the yield stress (R_e) value of 8 mm diameter ribbed construction steel bar produced via conventional hot rolling process is below the minimum specified yield stress value in TSE 708 standard, i.e. 420 N/mm^2. The ratio of experimental yield stress to characteristic yield stress of ribbed steel bar produced without tempcore process is also greater than the maximum specified value of 1,30. On the other hand, the tensile test results of ribbed construction steel bar of 8 mm diameter produced via tempcore process comply well with TSE 708 standard.

Similarly, tensile tests were also conducted for ribbed steel bars with different diameters, namely 10 12, 14 and 16 mm, produced both by using conventional hot rolling and tempcore process. The results obtained are summarized in Table 4. The results clearly indicate that all the ribbed construction steel bars with various diameters produced via tempcore process in this study comply well with TSE 708 standard.

Table 4. Comparison of the tensile test results obtained from the ribbed steel bars with various diameters produced via conventional and tempcore processes and their evaluation according to TSE 708 standard.

Diameter	Ø10 mm		Ø12 mm		Ø14 mm		Ø16 mm	
Class	Without Tempcore	With Tempcore	Without Tempcore	With Tempcore	Without Tempcore	With Tempcore	Without Tempcore	With Tempcore
Yield Stress (min) R_e (N/mm^2)	317,05	473,29	348,26	498,57	364,74	487,73	314,68	479,32
Tensile Strength (min) R_m (N/mm^2)	474,81	561,7	544,61	599,66	531,17	581,09	474,26	594,23
Tensile Strength / Yield Stress R_m/R_e	1,49	1,18	1,56	1,20	1,45	1,19	1,50	1,23
Experimental yield stress / Characteristic yield stress $R_{e\,act}/R_{e\,nom}$ (max)	1,5	1,18	1,55	1,21	1,48	1,18	1,51	1,24
Elongation (min) A_5(%)	27,4	17,1	27	16,6	26	22	28,9	25,4

4. Conclusions

Low alloy steels have very good weldability but their mechanical properties are not within the desired levels. The mechanical properties (i.e., yield stress and tensile strength) of these steels can be increased without diminishing the ductility and weldability by producing them via tempcore process, owing to the tempered martensite formed on the surface. However, quench period and water flow (i.e., amount of the water) used in tempcore process should be optimized in order to produce ribbed steel bars having mechanical properties that comply with TSE 708 standard.

The results of this study showed that the ribbed construction steels which comply with TSE 708 standard cannot be produced via conventional hot rolling process. It was also clearly demonstrated

that ribbed construction steel bars complying with TSE 708 standard can be readily produced using tempcore process.

Acknowledgements

We would like to thank Mr. Mahmut KİRMİT, General Manager of Net Haddecilik Industry Trade and Limited Company, for his support and encouragement during the conduction this study. We would also like to thank Mr. A. Tolga ASLAN, Quality Control Supervisor of Net Haddecilik Industry Trade and Limited Company, for his continous support throughout this study.

References

[1] Uysal, A. (2002). *Beton Çelik Çubuklarının Çevrimsel Deformasyon Davranışının İncelenmesi.* Yüksek Lisans Tezi, İstanbul Teknik Üniversitesi, Fen Bilimleri Enstitüsü, İstanbul

[2] İkiz, B. (2009) *Sıcak Haddelemede Tempcore Prosesi*. Yüksek Lisans Tezi, Mustafa Kemal Üniversitesi, Fen Bilimleri Enstitüsü, Hatay

[3] Özsoy, D. (2001) İnşaat Çeliği ve Kontrollü Su Soğutma Yöntemi. *Mühendis ve Makine Dergisi*

[4] Groover, M.P. (2015) *Principles of Modern Manufacturing* (4th ed.) (pp. 387). Ankara: Nobel

[5] Erişir, E. (2012) Plastik Şekillendirme Yöntemleri [PDF Document] Kocaeli Üniversitesi, Metalurji Malzeme Mühendisliği. Retrieved from Lecture Notes Online Web site: http://metalurji.kocaeli.edu.tr/metal/files/DersNotlari/mmt407-06.pdf

[6] TSE. (2016) *Steel for the reinforcement of concrete - Reinforcing steel.* (pp. 1,4,5) Ankara: Turkish Standard Institute.

A Proposition for Using Heat Pump Unit to Integrate Cooling, Heating and Refrigerating Functions

Faraz Afshari[1*], Farzad Afshari[2],

[1]Erzurum Technical University, Department of Mechanical Engineering, 25240, Erzurum, Turkey; faraz.afshari@erzurum.edu.tr
[2]Azad University, Department of Agriculture Mechanization, Science and Research Branch, 14515/775 Tehran, Iran farzadafshari@srbiau.ac.ir

[*] **Corresponding Author:**
faraz.afshari@erzurum.edu.tr

Abstract

In this study, the possibility of using only one unit for cooling, heating and refrigerating purposes are discussed. Basically, air conditioning systems and refrigerators have approximately same working principle, but their thermodynamic behavior are different which will be compared in different ways. In the present study, one compressor as power element is used to handle combined system with three exchangers function as evaporator and condenser. Cooling and heating performance, efficiency and power consumption are some critical thermodynamic subjects will be evaluated in this investigation.

Keywords: Heat pump, Cooling, Heating, COP.

1. Introduction

Vapor compression heat pumps, cooling devices and refrigerators have same working principles but different usage. Heat pumps work in a steady state condition with approximately constant thermodynamic cycle, but refrigerators or freezers have variable thermodynamic cycles. Optimization of mentioned systems is directly related to the performance, efficiency, power consumption and environmental concerns. Hence, it is important to study the structure and characteristics of such systems in order to improve design, function and efficiency. Their cycle works in a manner that; heat is transferred from a low temperature source to a higher temperature sink by means of refrigerant that is circulated by means of a compressor. In some special cases, both cooling and heating applications can be employed together as applied in milk pasteurization (Ozyurt et al. 2004). In this section, a summary of previous studies on heat pump and freezer is presented from the literature. The refrigerant charge amount versus efficiency, power consumption and COP were analyzed to find out the optimal charge amount of the system (Corberan et al. 2008). Innovative refrigeration systems for food preservation, were discussed in a review study to identify the best available technologies (Aste et al. 2017). Magnetic refrigerant materials were described and their effects on refrigeration system were surveyed (Pecharsky et al. 1999). Mechanical components have been partially discussed to improve efficiency, compatibility, compact design and economy of the components including compressor (Sun, et al. 2010) evaporators and condensers (Bejarano et al. 2016). Numerical methodology on refrigeration cycle (Zsembinszki et al. 2016), refrigerant replacement with other alternative gases (Cabello et al. 2017), are some valuable studies with the aim of optimization of the refrigeration and air conditioning systems. In this study, the possibility of converting heat pump mode to freezer and working in two different modes at the same time is evaluated based on laboratory experiments. Cooling efficiency, COP, optimal charge amount, compressor working conditions and basic differences between a heat pump and refrigeration unit are discussed.

2. Material and Method

In the laboratory works, existing heat pump was converted to the refrigerator and also the possibility of converting a refrigerator to the heat pump was examined. Different experiments on the refrigerator and heat pump were performed to compare the performance and thermodynamic characteristics. In Fig. 1 scheme of the overall vapor compression cycles and the evaporator function as the main difference between a heat pump and cooling system have been displayed respectively.

Generally, compressor, condenser, evaporator, and expansion valve are primary parts in mentioned devices which render same duty. In the experiments, wind tunnel as evaporator of the heat pump was changed to a cube cooling chamber. Inlet and outlet side of wind tunnel was blocked and insulated. In the previous work carried out experimentally, air to air refrigerator parts were disassembled and installed out of refrigerators body and converted to a heat pump unit. Temperatures were measured by T-types thermocouples and pressures by Bourdon pressure gauges.

The refrigerant charge amount was increased gradually and obtained data were recorded for various experiments. A time interval as a very important parameter for the refrigerator cycle has been considered in the study and are presented in the diagrams in the next section. The chemical and physical properties of refrigerant R-134a (used refrigerant in this study) are presented in Tables 1.

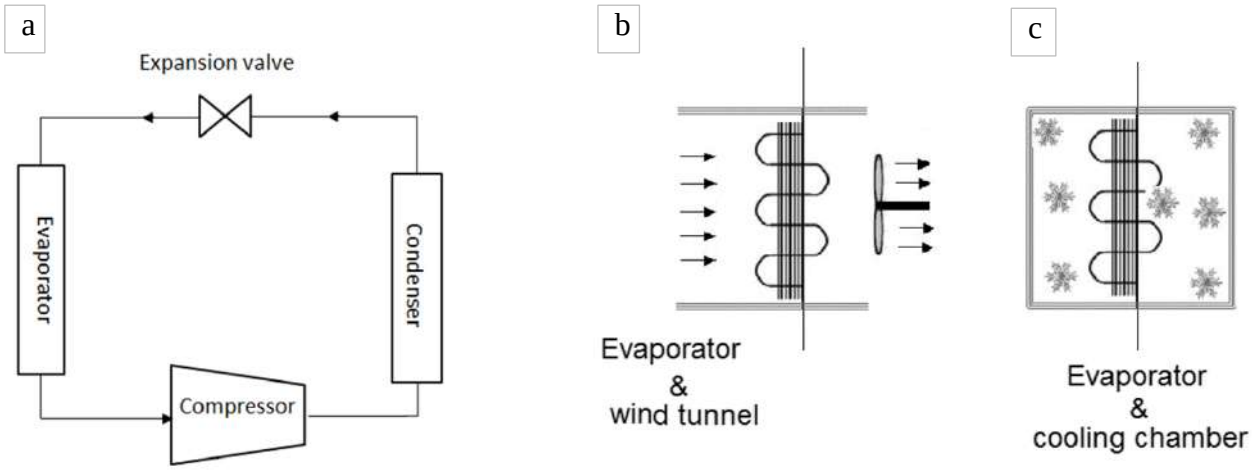

Figure 1. Scheme of the overall vapour compression cycles (a) Evaporator function in the heat pump unit or cooling systems (b) Evaporator function in the refrigerator (c)

Table 1. Refrigerant Properties

Refrigerant	R134a
Chemical formula	CH 2 FCF 3
Liquid density at 20°C (kg m^{-3})	1224.5

Liquid volume at 20°C (m^3 kg^{-1})	0.000816
Critical pressure (kPa)	4060.3
Critical temperature (°C)	101.08
ODP	0.0
GWP	1430

2.1. Analysis and Equations

The electromotor as driving force for the reciprocating compressor is employed to provide required mechanical energy. Electrical current, voltage and power consumption($\dot{W}_{comp}$) in the unit can be recorded via ampere meter and power meter. From the power rate, total power consumed in the system over the test time (t) is given as,

$$W_{total} = \dot{W}_{comp} \times t \quad (1)$$

The total heat transfer over the test time can be expressed as,

$$Q_{cond} = (\dot{m}_r h_2 - \dot{m}_r h_3) \times t \quad (2)$$

Where h_2 and h_3 are refrigerant enthalpy at condenser inlet and outlet and $\dot{m}_r$ is refrigerant flow rate. On the other side, heat transfer from the evaporator can be calculated by Eq. 3 and 4 for heat pump and refrigerator respectively:

$$Q_{evap} = \dot{m}_a c_{p,a}(T_{in,a} - T_{out,a}) \times t = (\dot{m}_r h_4 - \dot{m}_r h_1) \times t \quad (3)$$

$$Q_{evap} = m_a c_{p,a}(\Delta T_a) \times t = (\dot{m}_r h_4 - \dot{m}_r h_1) \times t \quad (4)$$

Where h_1 and h_4 are refrigerant enthalpy at evaporator outlet and inlet, ΔT_a is the temperature reduction of cooling chamber and m is the enclosed air mass inside cooling chamber of refrigerator.

Unlike the heat pump unit, the refrigerator has variable COP due to decreasing temperature of the evaporator over the cooling time when the compressor is running continuously. Consequently,

the cooling and heating COP (COP_L and COP_h) values of the refrigeration device should be calculated in specified times interval which are given as,

$$\mathrm{COP}_L = \frac{Q_{\mathrm{evap}}}{W_{comp}} \quad , \quad \mathrm{COP}_h = \frac{Q_{\mathrm{cond}}}{W_{comp}} \tag{5}$$

3. Results and Discussion

Experiments outcome and obtained results are analyzed and discussed in this section. For better understanding of the charge influence on the significant properties, including pressure, temperature and etc. the normalized refrigerant charge is used to explain results on the diagrams. Normalized value is the ratio of charge to optimal charge amount. In the Fig. 2, inlet and outlet pressures of the compressor with respect to the normalized charge are presented. The pressure of the refrigerant inside unit has a direct impact on the system and compressor function. As shown in the figures, with an increase in charge amount both inlet and outlet pressures increases as well as the pressure of the whole system (whether heat pump or refrigerator), which can be described by the increasing mass factor in the gas law. Working mode has also notable impact on the pressure. Heat pump results showed that, suction and discharge pressures are considerably more than that of refrigerator, which indicates higher thermal energy supply in the heat pump mode. In refrigerator mode, the compressor works in a more fluent state with low noises and also after a few seconds the system works more fluent than early seconds due to decreasing pressure of the system.

The internal temperatures of the compressors are highly effective on the performance of the compressor, and even, a high discharge temperature can give rise to failure of internal components due to material degradation or excessive thermal expansion. In the same manner, the compressor inlet and discharge temperature variations with respect to the refrigerant charge are shown in Fig. 3. With a comparison between obtained results, it is revealed that, compressor works in higher temperature in heat pump mode when compared to that of refrigerator. In addition, charge amount shows a negative impact on the temperature and causes a temperature drop in the compressor.

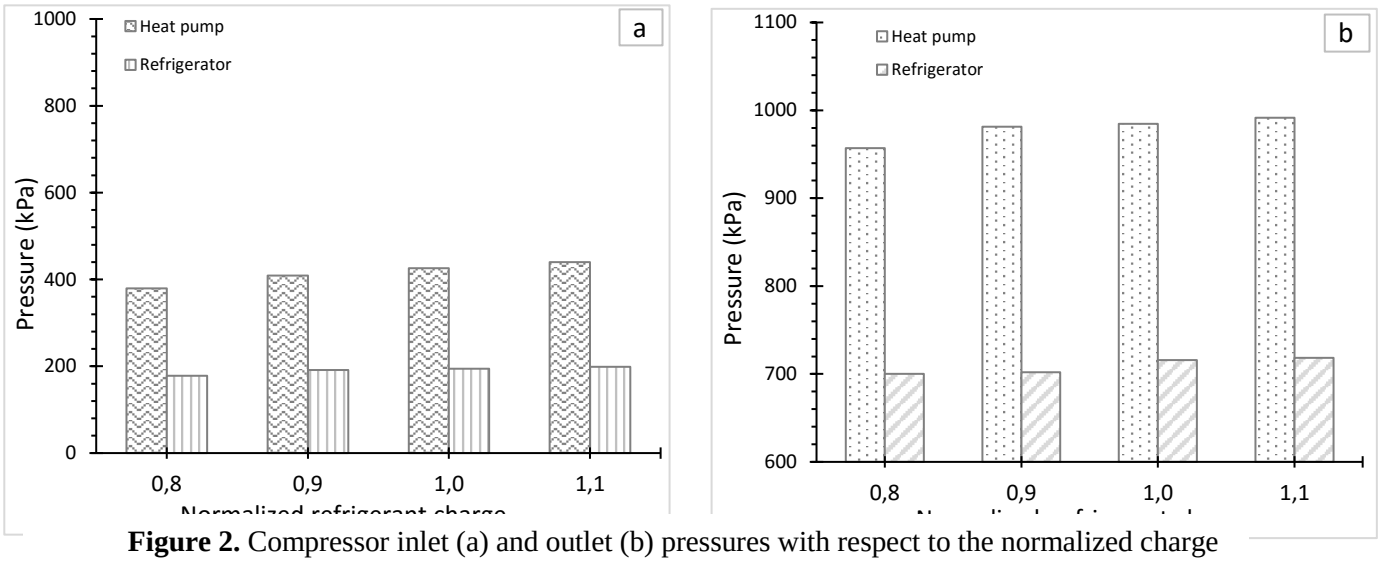

Figure 2. Compressor inlet (a) and outlet (b) pressures with respect to the normalized charge

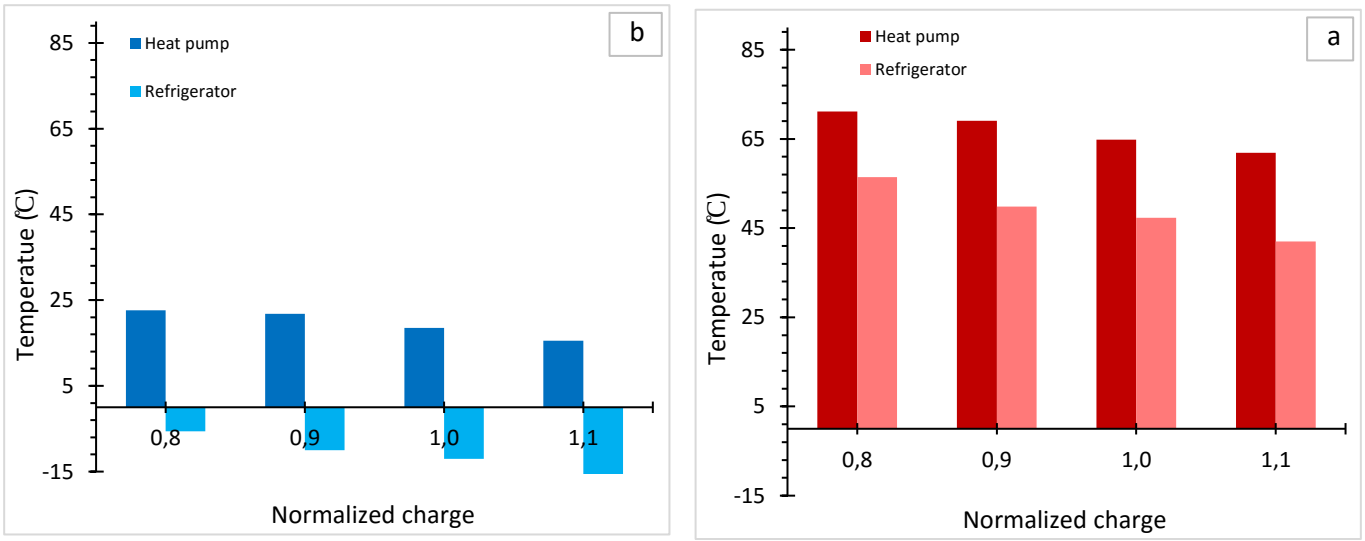

Figure 3. Compressor inlet (a) and outlet (b) temperatures with respect to the normalized charge

In the Fig. 4, COP_h values of the system are given with respect to the normalized charge amount at heat pump and refrigerator modes. Experiments demonstrate a large difference between COP of the heat pump and refrigerator. The reason for the low COP of the refrigerator is limited thermal energy which cause to a decrease in pressure, temperature and performance of the system. Because evaporator is installed in a closed box without access to environment heat energy.

In this regard, in refrigerators there is no need to operate continuously because the purpose is cooling the box and foods inside and so there is always electrical automatic on/ off device to switch the system to keep evaporator side in certain temperature.

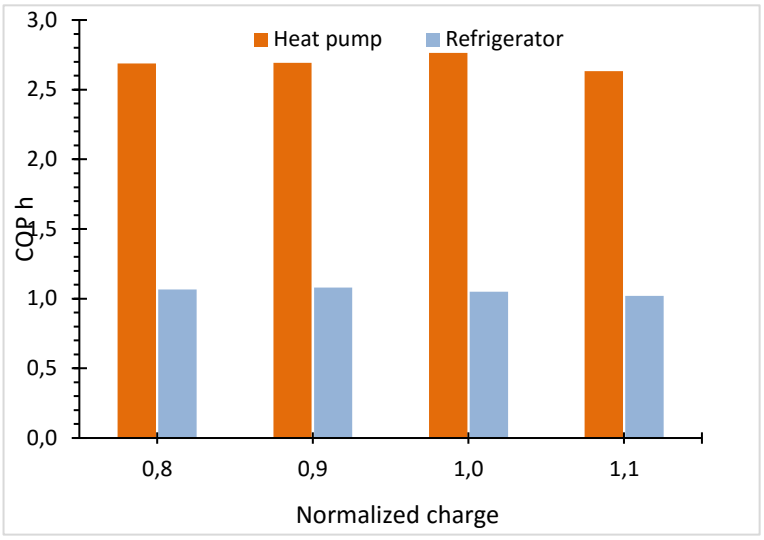

Figure 4. COP values versus normalized charge at two modes

As previously discussed refrigerator cycle varies over the operating time. Since the thermal energy in the box decreases when system is operating, power consumption of the electro motor-compressor unit falls down in refrigerator mode as shown in Fig. 5. The reason for this phenomena can be also described via pressure decrease of the whole system and less need for power over the compression process. On the other side, the heat pump power consumption results versus time is constant, which indicates a steady state operating condition.

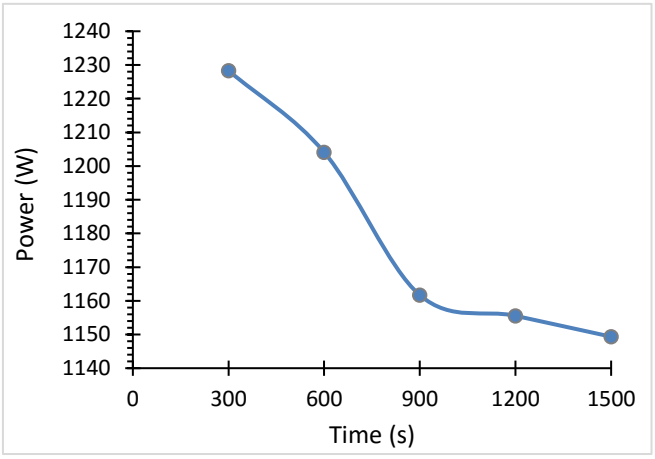

Figure 5. Power consumption of the refrigerator over the operating time

The compression ratio (absolute discharge pressure to absolute suction pressure) with respect to the charge is presented in Fig. 6 for two different modes. Discharge pressure is a function of

refrigerant characteristics and low-density refrigerants can be extremely compressed over the compression period. In fact, gases with an approximately low density don't show notable resistance to the compression applied by the compressor. In the figure, refrigerator compression is at a higher level than that of heat pump. Because the pressure of the cycle in refrigerator is low and the compression has been done efficiently.

Heat pumps are employed to operate in two different functions for cooling and heating as displayed in Fig. 7, which is so discussed in the literature. The function of the system is switched by using a shifting valve to reverse refrigerant circulating direction.

In another schematic figure, the main purpose of the study has been presented (Fig. 8). All functions including refrigerating, cooling and heating have been combined in the system, which works just by one compressor. In the normal refrigerators, electromotor-compressor unit is often in standby mode, but in the present design, the system may work continuously in desired modes.

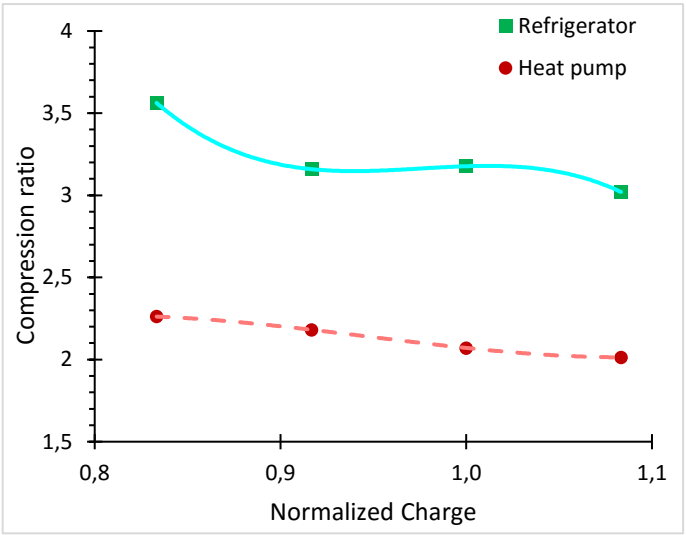

Figure 6. A comparison for compression ratio with respect to the charge amount in two modes

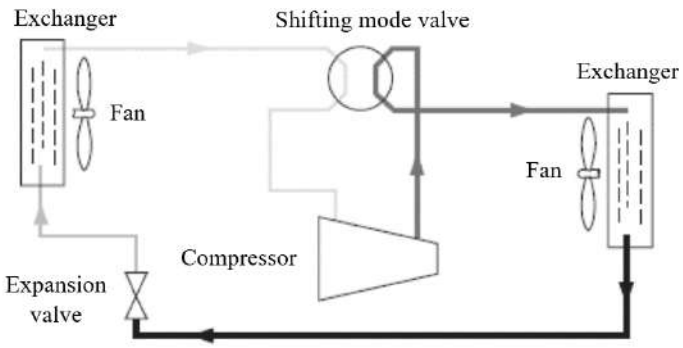

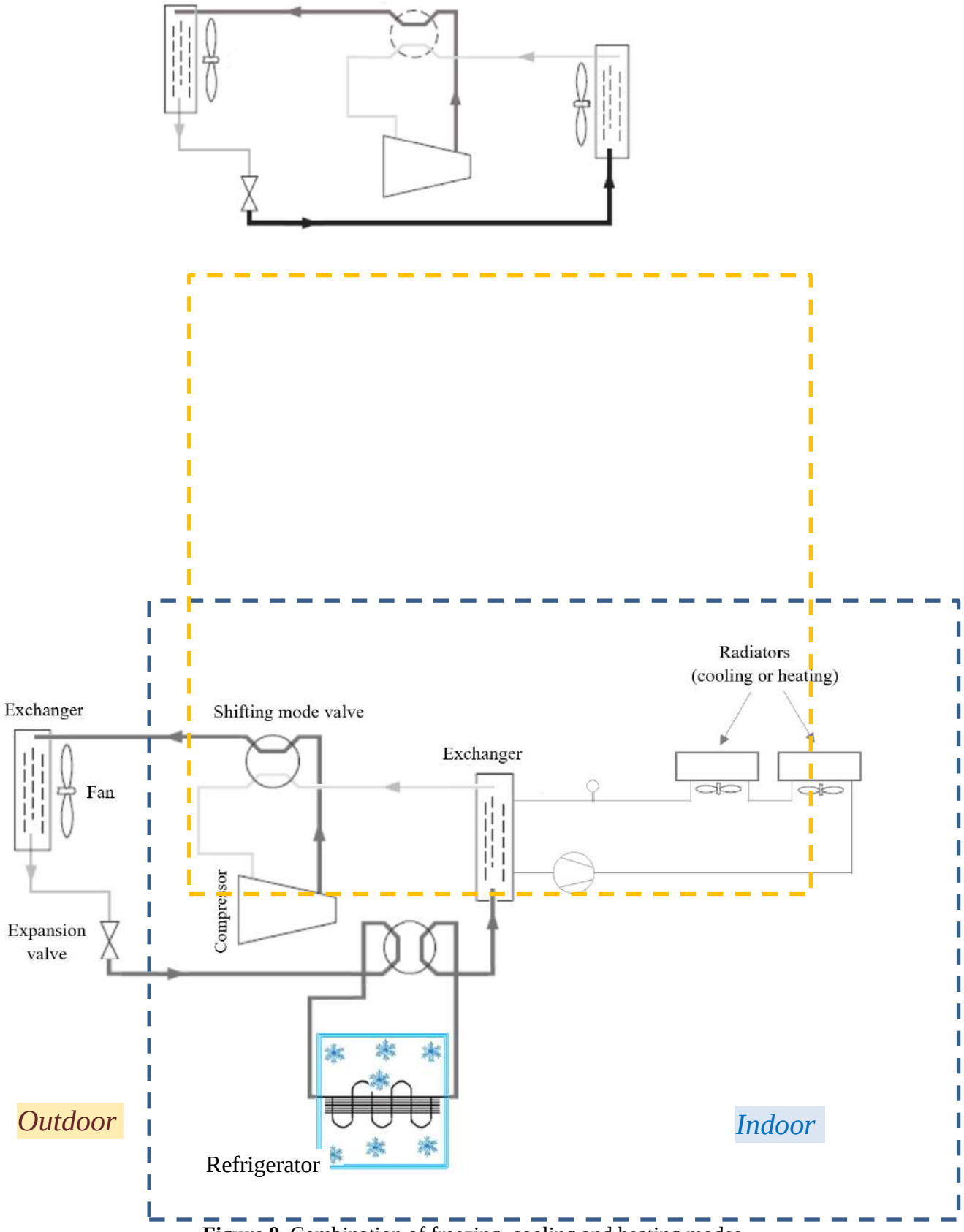

Figure 8. Combination of freezing, cooling and heating modes

4. Conclusion

The basic thermodynamic characteristics of a unit working in freezing, cooling and heating modes were analyzed using R134a, as circulating refrigerants. The main findings of the study can be summarized as follows;

It was revealed that, in a defined working condition heat pump thermodynamic characteristics are constant and the system operates with relatively constant power consumption. However, power consumption of refrigerators decreases over the operation time and also their thermodynamic properties and P-h cycle is variable. COP value was compared between two modes and it was concluded that, COP of the refrigerator is considerably lower than that of heat pump. Finally, proposed design of a systems was presented to evaluate the possibility of combining several functions in a unit. In the proposed design, radiators for heating or cooling purposes and a cooling chamber as a refrigerator were used in the system using just one compressor for whole unit.

Acknowledgement

This work has been inspired from the previous studies supported by Research Project Foundation (Project No. BAP-2013/105) of the Ataturk University. The authors also gratefully acknowledge Erzurum Technical University for support of the study.

References

Afshari, F. (2016). Gaz karışımları kullanan ısı pompalarının enerji ve ekserji verimlerinin deneysel olarak incelenmesi. Doktora Tezi, Atatürk Üniversitesi, Fen Bilimleri Enstitüsü, Erzurum.

Aste, N., Del Pero, C., Leonforte, F. (2017). Active refrigeration technologies for food preservation in humanitarian context–A review. *Sustainable Energy Technologies and Assessments*, 22, 150-160.

Bejarano, G., Rodriguez, D., Alfaya, J. A., Ortega, M. G., Castano, F. (2016). On identifying steady-state parameters of an experimental mechanical-compression refrigeration plant. *Applied Thermal Engineering*, 109, 318-333.

Cabello, R., Sanchez, D., Llopis, R., Catalaan, J., Nebot-Andres, L., Torrella, E. (2017). Energy evaluation of R152a as drop in replacement for R134a in cascade refrigeration plants. *Applied Thermal Engineering*, 110, 972-984.

Corberan, J. M., Martinez, I. O., Gonzalvez, J. (2008). Charge optimization study of a reversible water-to-water propane heat pump. *International Journal of Refrigeration*, 31(4), 716-726.

Ozyurt, O., Comakli, O., Yilmaz, M., Karslı, S. (2004). Heat pump use in milk pasteurization: an energy analysis, *Int. J. Energy Res.*, 28 (9), 833-846.

Pecharsky, V. K., Gschneidner Jr, K. A. (1999). Magnetocaloric effect and magnetic refrigeration. *Journal of Magnetism and Magnetic Materials*, 200(1-3), 44-56.

Sun, S., Zhao, Y., Li, L., Shu, P. (2010). Simulation research on scroll refrigeration compressor with external cooling. *International journal of refrigeration*, 33(5), 897-906.

Zsembinszki, G., de Gracia, A., Moreno, P., Rovira, R., Gonzalez, M. A., Cabeza, L. F. (2017). A novel numerical methodology for modelling simple vapour compression refrigeration system. Applied Thermal Engineering, 115, 188-200.

Analysis of Academic Publications in the Field of Industrial Engineering in Turkey

Ayca ÖZCEYLAN[1], Eren ÖZCEYLAN[2], Cihan ÇETİNKAYA[3], Barış ÖZKAN[4*]

[1] University of Gaziantep, Oğuzeli Vocational School, Gaziantep, Turkey
[2] University of Gaziantep, Industrial Engineering Department, Gaziantep, Turkey
[3] Adana Science and Technology University, Industrial Engineering Department, Adana, Turkey
[4] Ondokuz Mayis University, Industrial Engineering Department, Samsun, Turkey

[*]**Corresponding author:** baris.ozkan@omu.edu.tr

Abstract

Industrial Engineering is an engineering discipline that designs, improves, produces and controls complex systems in the globalized world. Data mining, which is also used in the field of industrial engineering as it is in many areas (health, banking, commerce, transportation, education, etc.), is one way of transforming data into meaningful information. The aim of this study is to determine the gaps in the literature by determining which topics and how often industrial engineers, working in Turkey, are dealing with using Data Mining and guide the engineers in this field. By using Scopus in the database prepared for this purpose, starting from 2018 necessary scans are carried out without making a year limit and 6613 data are obtained as a result of these scans. Several analyses are made on this data and these analyses are graphically displayed and interpreted. In this respect, the work is capable of enlightening the history of Industrial Engineering in Turkey.

Keywords: industrial engineering, data mining, industrial engineering publications.

1. Introduction

The emergence of concepts related to industrial engineering and widespread use of them began in the early 19th century. In this century, science and engineering developments have begun to be seen. Furthermore, as a result of utilizing steam power, the first Industrial Revolution was realized. With the formation of the industrial revolution, production systems that are more difficult to plan, organize, and direct which require special skills for management have begun to be developed. These production systems began to be more complicated than the old ones. The main advances in industrial engineering, as in many other engineering fields, began in World War II. These advances have become intertwined with the area knowns as operations research.

Today, the development of the competitive environment has accelerated the transformation of technology into products and services. For this reason, organizations today need to have systems that can work more efficiently and make the right decisions quickly in order to continue their activities. This situaiton increases the importance of industrial engineers who build and operate these systems

effectively. Therefore, with the development of new technologies, industrial engineers aimed at reducing the loss of time. Although there are many ways to accomplish this, this study will consider data mining practice.

Data mining is a data analysis technique that explores the relationships between large amounts of data, helps to find the connection between them and enables the capture of confidential information within the database systems (Kalikov, 2006). Today, data mining applications are widely used in many areas that need decision making. In this study, the main purpose is to determine the gaps in the literature by determining which topics and how often industrial engineers work in Turkey and guide the engineers in this field using data mining.

Industrial engineering raw materials are human, information, machinery, capital and time factors. Industrial Engineering is a professional group that develops and implements mathematical methods and techniques to ensure the most efficient use of these factors, and at the same time optimise them. In other words, the industrial engineers plan how much time, how much capital, how many people, and which technology can be used in production and manage this processes in an effective way.

In Turkey, industrial engineering was established by the Middle East Technical University and Istanbul Technical University in 1969 for the first time. Industrial engineering is one of the most popular and preferred professions especially among students in the last 20 years. Today in Turkey there are 78 universities which have Industrial Engineering departments, and about total 1000 instructors in this department. In the following table (Table 1) there are universities which give industrial engineering courses in Turkey.

Table 1. Universities that have Industrial Engineering Department

University Name			
1. Abdullah Gül University	21. Dumlupinar University	41. Istanbul Technical University	60. Nuh Naci Yazgan University
2. Adana Science and Technology University	22. Düzce University	42. Istanbul Commerce University	61. Okan University
3. Aksaray University	23. Erciyes University	43. Istanbul University	62. Ondokuz Mayis University
4. Alanya Alaaddin Keykubat University	24. Eskişehir Osmangazi University	44. Işik University	63. Middle East Technical University
5. Altinbaş University	25. Galatasaray University	45. İzmir University of Economy	64. Özyeğin University
6. Anadolu University	26. Gazi University	46. Kadir Has University	65. Pamukkale University
7. Ankara Yildirim Beyazit University	27. Gaziantep University	47. Karabük University	66. Piri Reis University
8. Antalya Bilim University	28. Hacettepe University	48. Karadeniz Technical University	67. Sakarya University
9. Atatürk University	29. Haliç University	49. Kirikkale University	68. Selçuk University
10. Atilim University	30. İhsan Doğramaci Bilkent University	50. Kocaeli University	69. Süleyman Demirel University
11.Bahçeşehir University	31. Istanbul Arel University	51. Koç University	70. Tobb Economy and Technology University
12.Balikesir University	32. Istanbul Aydin University	52. Kto Karatay University	71. Toros University
13.Başkent University	33. Istanbul Bilgi University	53. Maltepe University	72. University of Turkish Aeronautical Association
14. Bayburt University	34. Istanbul Gedik University	54. Manisa Celâl Bayar University	73. Turkish-German University
15. Beykent University	35. Istanbul Gelişim University	55. Marmara University	74. Uludağ University
16. Boğaziçi University	36. Istanbul Kültür University	56. Mef University	75. Üsküdar University
17. Çankaya University	37. Istanbul Medipol University	57. Namik Kemal University	76. Yalova University
18. Çukurova University	38. Istanbul Rumeli University	58. Necmettin Erbakan University	77. Yaşar University
19. Doğuş University	39. Istanbul Sabahattin Zaim University	59. Nişantaşi University	78. Yildiz Teknik University
20. Dokuz Eylül University	40. Istanbul Şehir University		

2. Literature Review

Data mining, which is used effectively in many areas, is one of today's most applied disciplines. It is one of the most frequently used methods by the institution and organization administrators thanks to its easy application and effective results as it finds more and more widespread usage area with each passing year. The data mining can be applied in the categories of education, commerce, engineering, banking and stock market, medicine and telecommunication. Within the scope of this study, the current studies related with educational data mining are investigated.

Romero and Ventura (2007) take into consideration data mining applications in the education between 1995-2005 and analyze the results. Baker and Yacef (2009) investigate the most outstanding studies that published between 1995-2005 and compare these studies with those that published in 2008 and 2009. Huang et al. (2009) perform an application in China Motor Corporation related with personnel educational training by using data minig and classify these data for future planning. Vialardi et al. (2009) apply data mining technique at the School of System Enginnering at Universidad de Lima in order to guide students in this department. Romero and Ventura (2013) review the current situation in educational data mining for the purpose of introducing it to researchers, instructors and students. Hegazi and Abugroon (2016) investigate studies related to data mining in higher education and compare these studies with each other. Bakhshinategh et al. (2018) survey the last ten years studies related with educational data mining and classify them according to some features.

3. Methodology

3.1. Data Mining

Data mining is a process that is carried out in order to extract valid, new, understandable and useful patterns from data arrays (Fayyad et al. 1996). data mining includes many disciplines such as artificial intelligence, fuzzy logic, machine learning, neural networks, and has become popular since the early 90s. Data mining process is divided into 5 steps by Fayyad et al. (1996). These steps are described in below:

- Selection: In this step the data that is predicted to be important is selected or created
- Preprocessing: The data is cleared, the missing data is completed, and new attributes are created in this step.

- Transformation: This step is the conversion of data to the appropriate format for different data mining methods.
- Data mining: Data mining methods are used in accordance with the determined objectives in this step.
- Interpretation: In this step it is interpreted that the patterns determined in the data mining phase whether contain enough information or not.

Data mining process that is proposed by Akpınar (2014) is as follows:

- Defining Problem
- Understanding of Data
- Preparing Data
- Building Model
- Selecting of Software
- Validaiton
- Interpretation

A data mining project can be different sizes from modeling a small series of data contained in an Excel spreadsheet to a project where hundreds of thousands of objects are used. According to size of project, the process can also change partly or majorly (Akpınar, 2014).

4. Results

There are many databases in the literature, however in this study Scopus is used in order to determine the gaps in the literature and guide the engineers in this field. Scopus is an academic database with a useful interface that compiles academic articles, authors and institutions in a very successful way. Some restrictions are imposed to the search, when using Scopus. These restrictions are: Affiliation country: Turkey, Affilition name: Industrial Engineering and Document type: Article, Conference Paper and Article in Press. As a result, 6613 articles and conference papers are conducted in total. In this 6613 results, the number of article rate is 75,5%, the number of conference paper rate is 23,7% and the number of article in press rate is 0,9%. In this section, various analyzes are made on 6613 data and the results of these analyzes are presented in order.

Firstly, the most and least used 50 words in Scopus are presented in Figure 2 and Figure 3, respectively. Key words include information from 1979 to 22.02.2018. These analyzes will help to

researchers to find the source of their reseach. The most preferred journals and conferences by researchers are analyzed and the results are given in Figure 4 and Figure 5 respectively. In Figure 5 and Figure 6, the instructors and universities that have maximum number of publications are listed. In figure 8, articles and conference papers rate is presented.

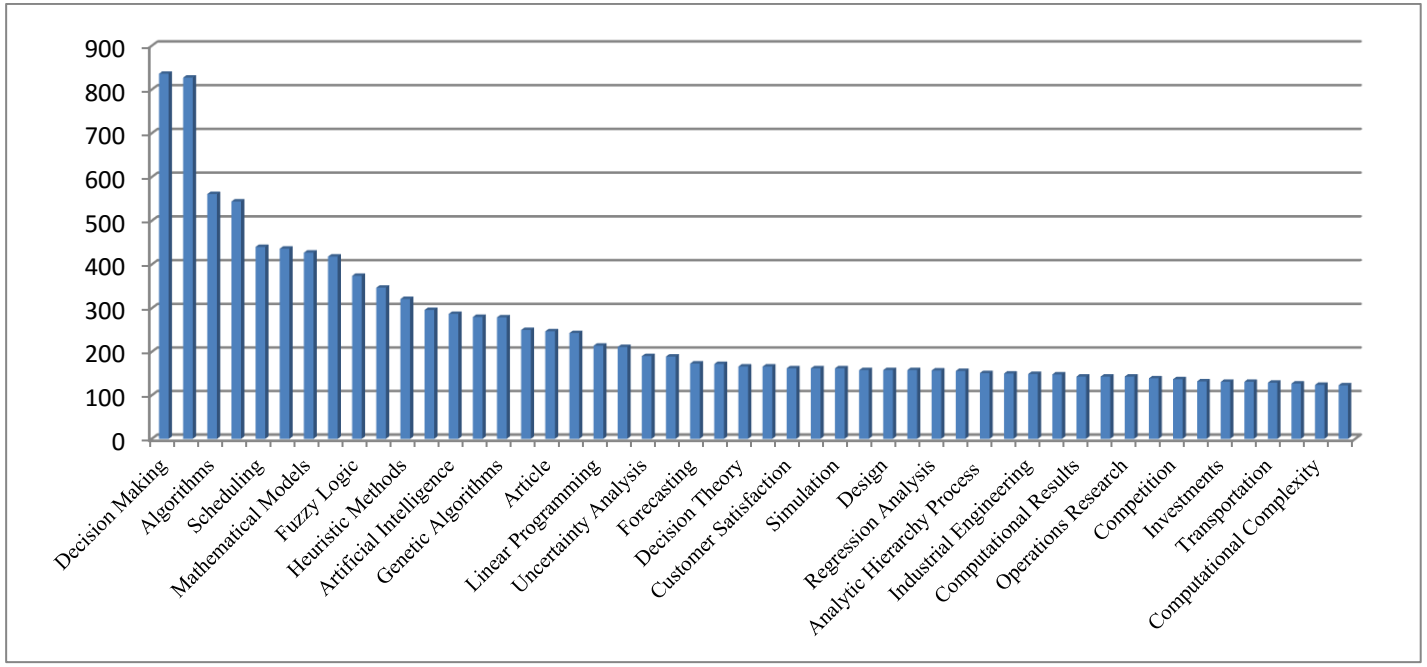

Fig. 1. The most commonly used key words in Scopus

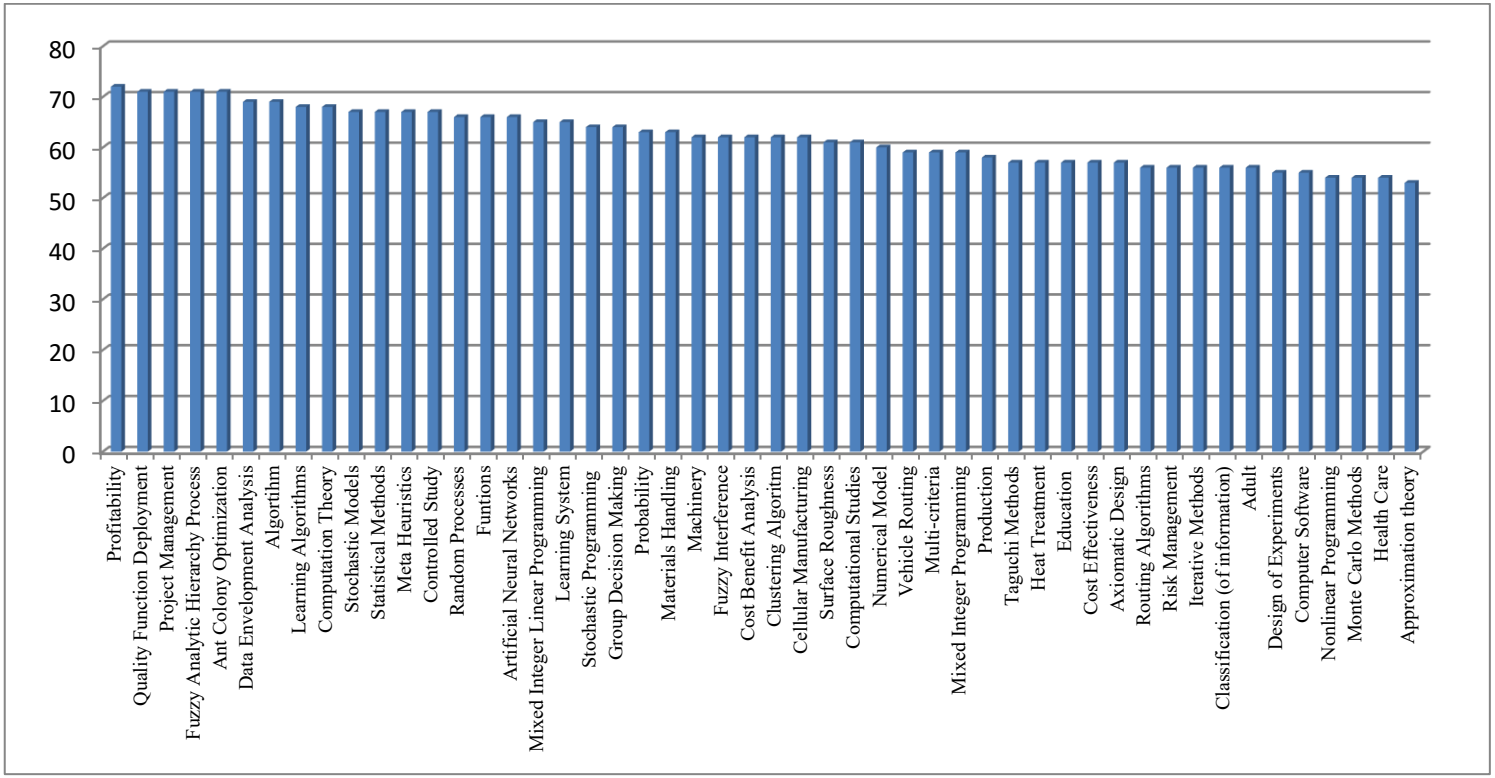

Fig. 2. The least used key words in Scopus

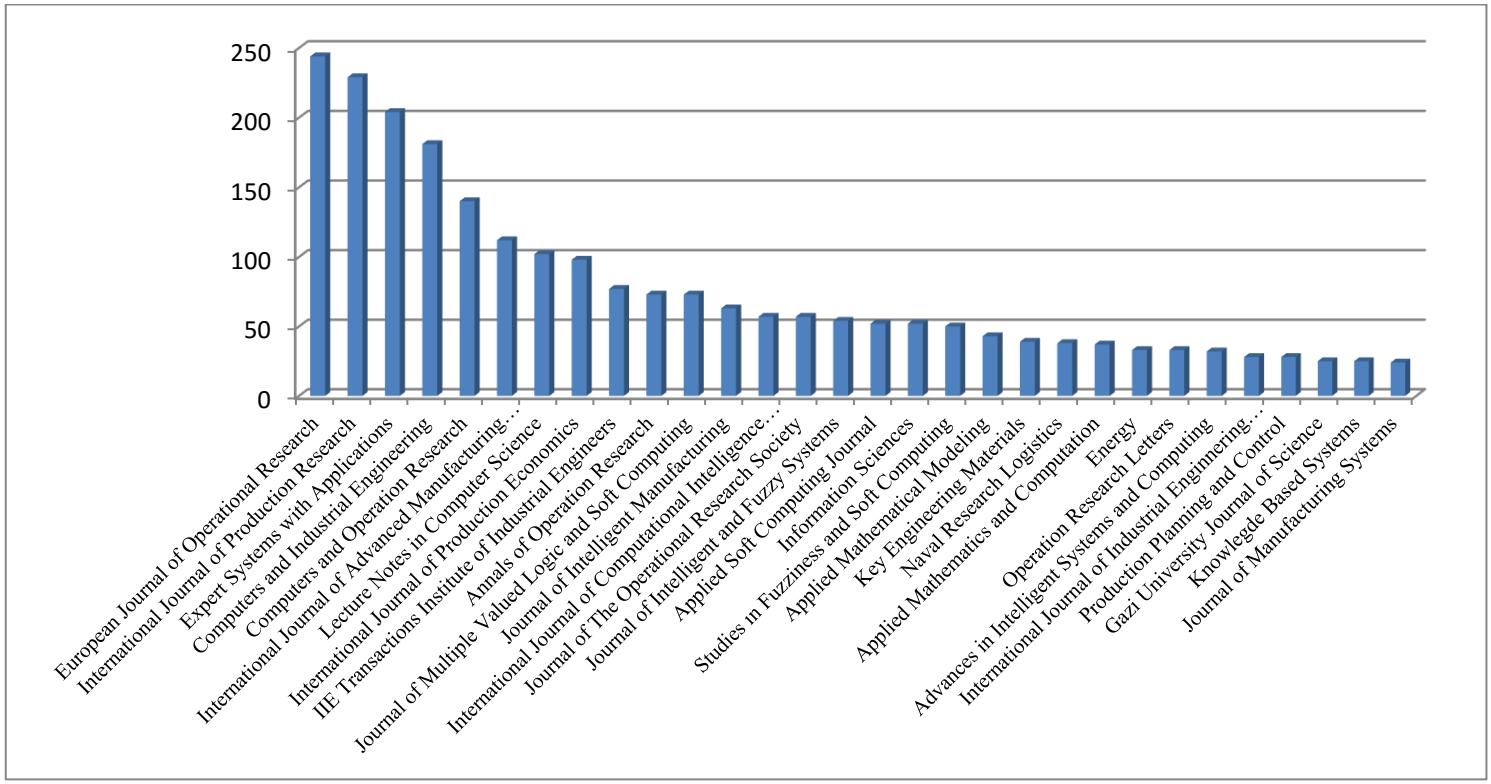

Fig. 3. The most preferred journals by researchers

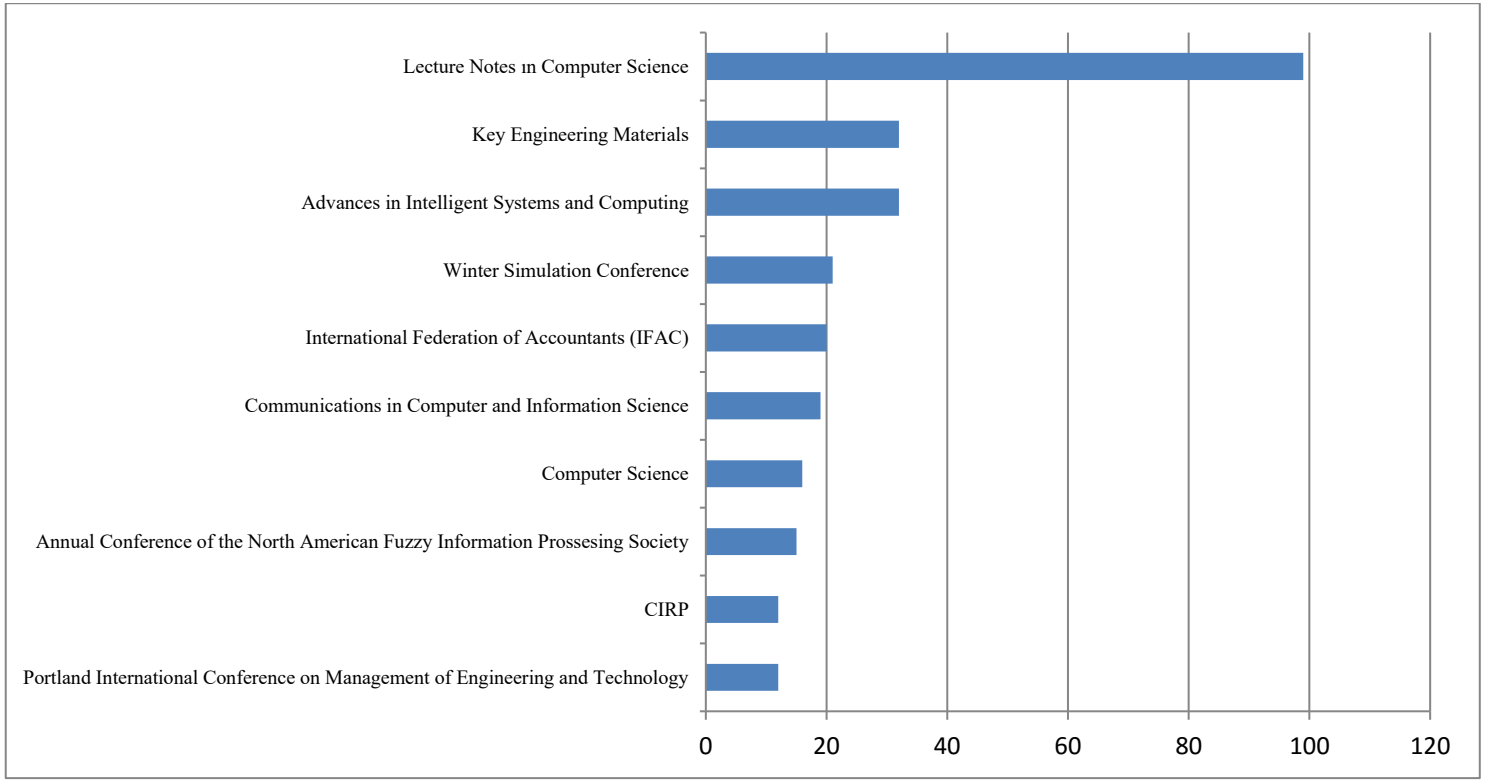

Fig. 5. The most preferred conferences by researchers

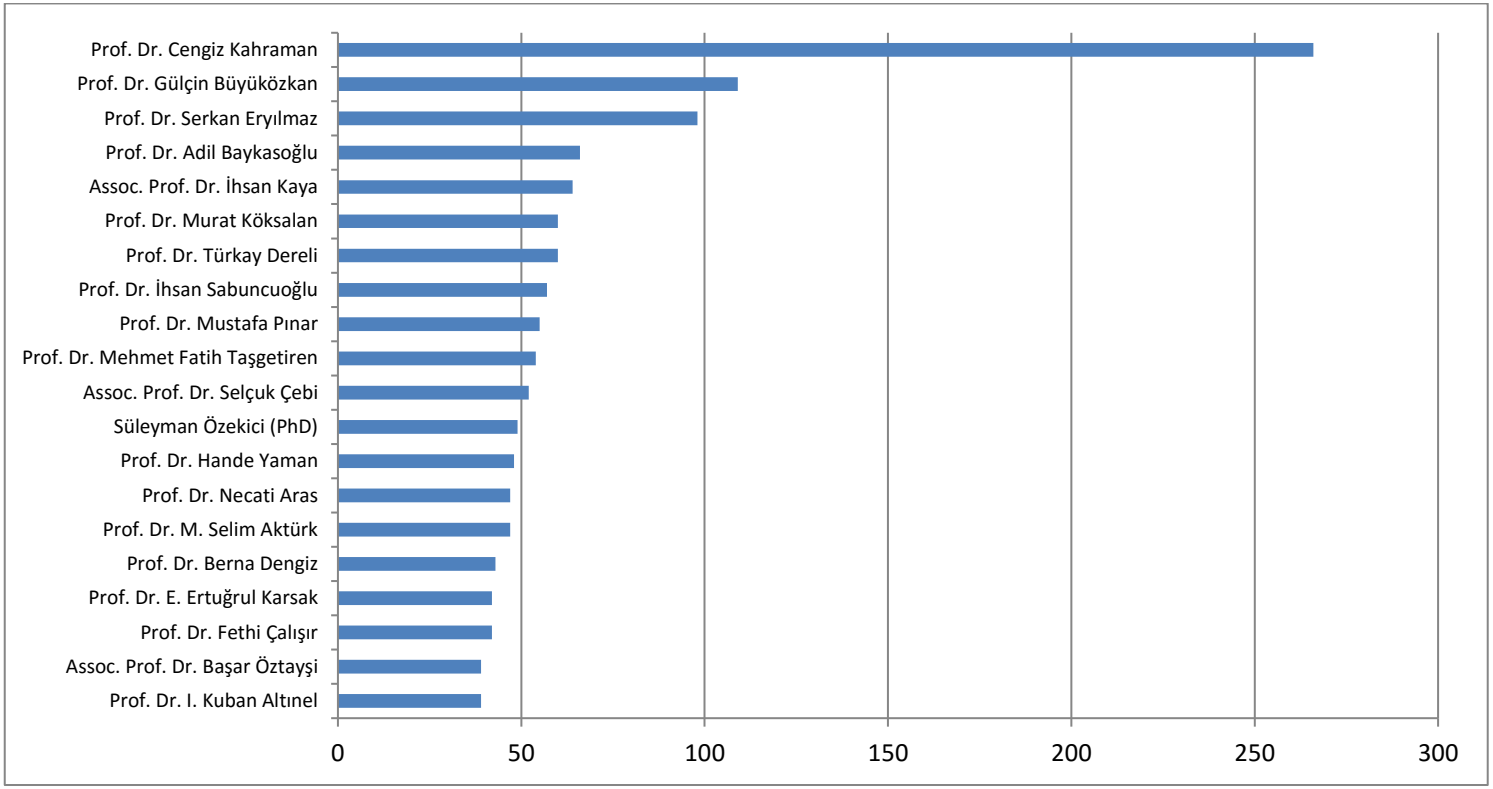

Fig. 6. The instructors who have maximum number of publications

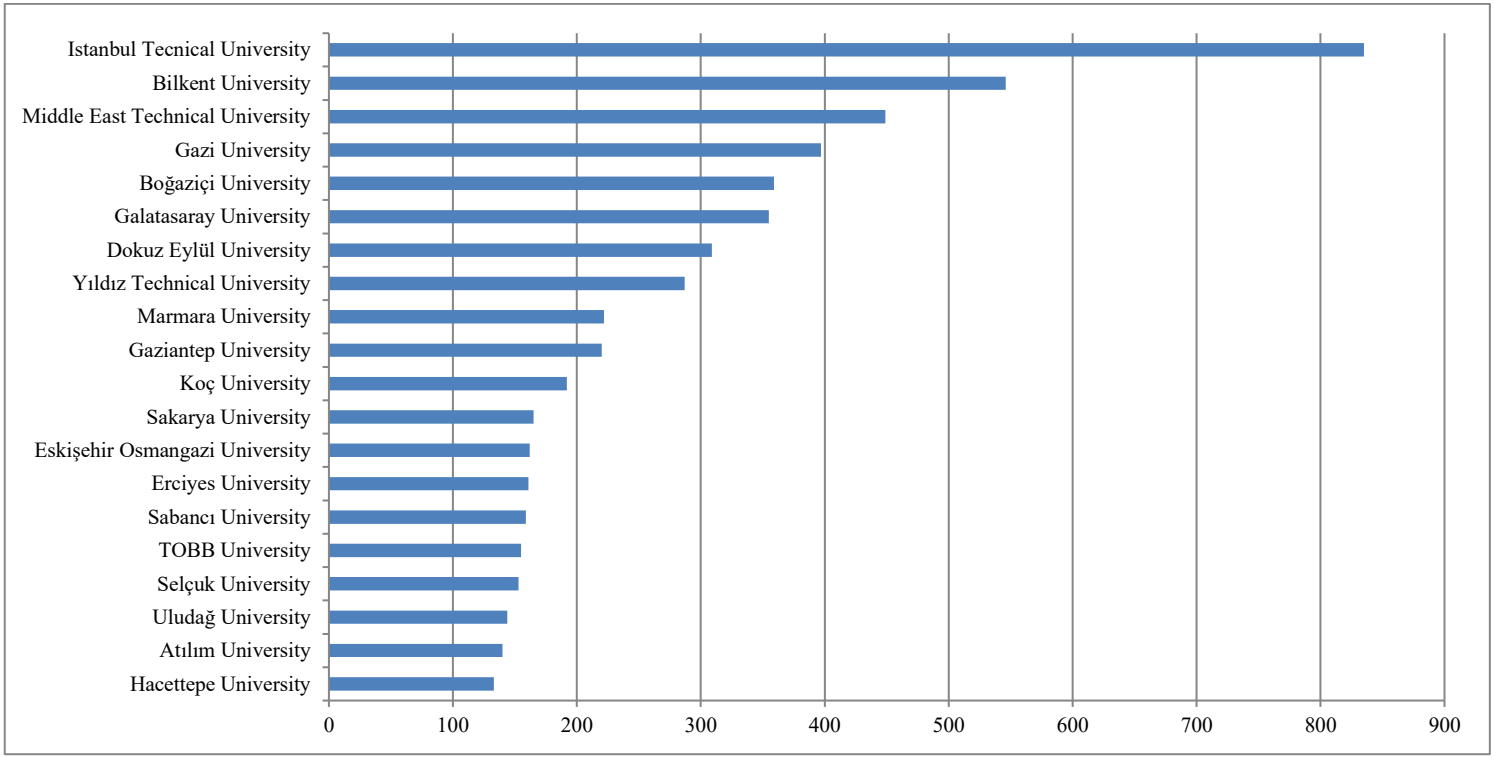

Fig. 7. Universities that have the highest number of publications

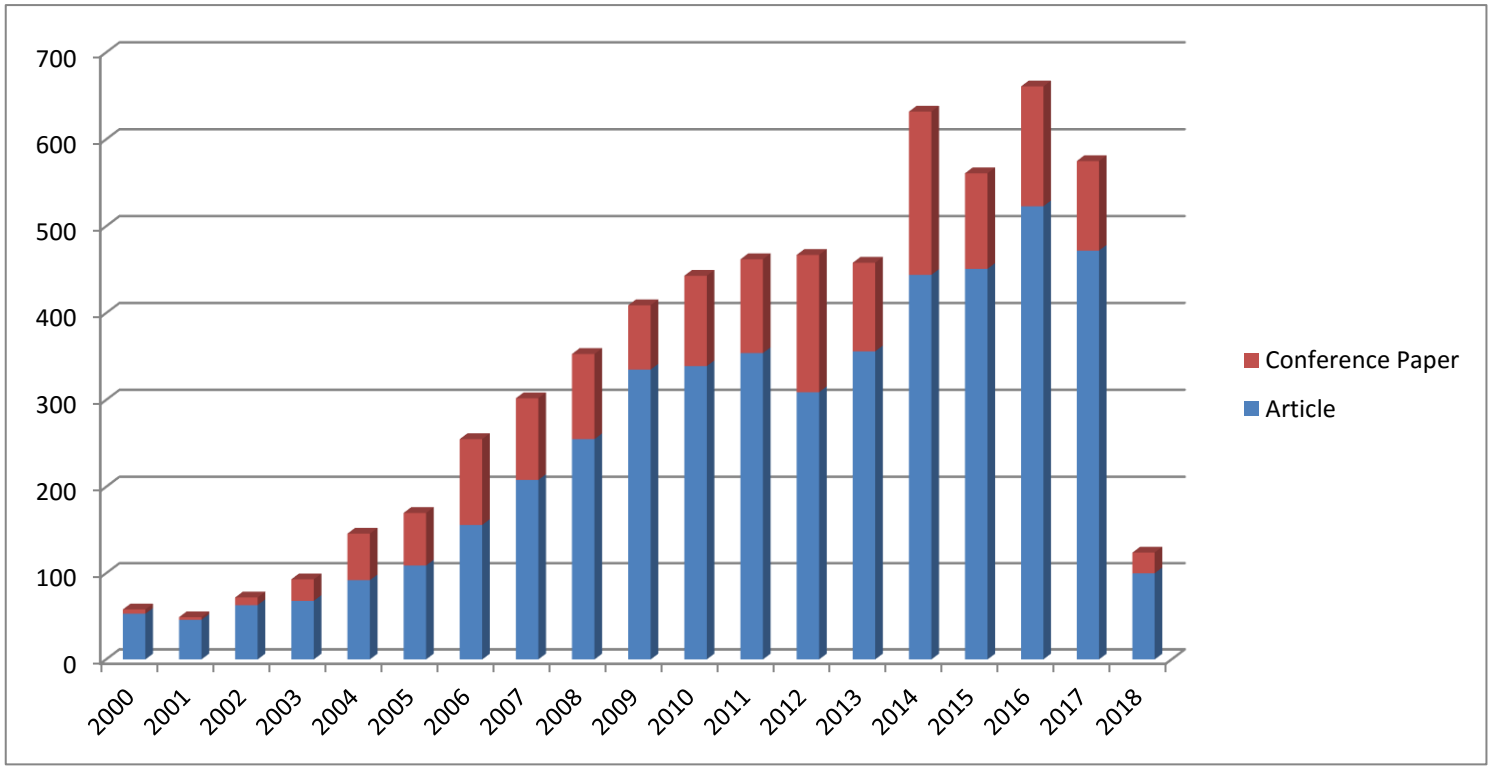

Fig. 8. Article and Conference paper rates between 2000-2018

5. Discussion and Conclusion

The data produced by computer systems is worthless alone. These data begin to make sense when they are processed for a specific purpose. Therefore, it is important to use techniques that can process large amounts of data. Data mining is one of these techniques which transform raw data into information or meaningful data.

This study examines the studies conducted by industrial engineers in Turkey from past to the present. For this purpose a comprehensive scaning is conducted in Scopus and 6613 data are obtained. Various analyzes are made with these data and results are presented in the previous section. It is thought that these analyzes will be very useful for training activities and will be used to create predictions for future researches.

References

Akpınar, H. (2014) "Data Veri Madenciliği Veri Analizi." İstanbul: Papatya Yayıncılık Eğitim.

Baker, R.S.J.D. and K. Yacef (2009) "The state of educational data mining in 2009: a review and future visions." Journal of Educational Data Mining 3–17.

Bakhshinategh, B. O. R. Zaiane, S. ElAtia, D. Ipperciel (2018) "Educational data mining applications and tasks: A survey of the last 10 years." Education and Information Technologies 23:537–553.

Fayyad, U., G. P.-Shapiro, P. Smyth (1996) "From data mining to knowledge discovery in databases." AI Magazine, 17: 37-54.

Hegazi, M.O., and M.A. Abugroon (2016) "The state of the art on educational data mining in higher education." International Journal of Computer Trends and Technology 31(1).

Huang, C.T., Lin, W.T., Wang, S.T., & Wang, W.S. (2009). "Planning of educational training courses by data mining: Using China Motor Corporation as an example." Expert Systems with Applications, 36: 7199–7209.

Kalıkov, A., (2006) "Veri Madenciliği ve Bir E-Ticaret Uygulaması." Yüksek Lisans Tezi, Gazi Üniversitesi, Fen Bilimleri Enstitüsü.

Romero, C. and S.Ventura (2007) "Educational data mining: A survey from 1995 to 2005." Expert Systems with Applications 33: 135–146.

Romero, C., and S. Ventura (2013) "Data mining in education." Wiley Interdisciplinary Reviews: Data Mining and Knowledge Discovery 3: 12–27.

Vialardi, C., J. Bravo, L. Shafti, A. Ortigosa (2009) "International Conference on Educational Data Mining Cordoba, Spain.

Investigation of the Effect of Consumables on Product Quality in Submerged Arc Welded Pipe Production

Özlem Pınar ÖNDER GÜNBAY[1,*], Gürel ÇAM[2]

[1] Tosçelik Spiral Pipe Product Industry and Limited Company, Osmaniye, TURKEY; ozlem.onder@toscelik.com.tr

[2] Iskenderun Technical University, Faculty of Engineering and Natural Sciences, Department of Mechanical Eng., 31200 İskenderun-Hatay, TURKEY; gurel.cam@iste.edu.tr

[*]**Corresponding author:** ozlem.onder@toscelik.com.tr

Abstract

The aim of this study is to conduct a detailed experimental investigation on the properties of spiral arc welded steel pipes produced by submerged arc welding technique using different consumable materials (i.e., same welding wire with different chemical compositions, different wire sizes and same coil with different chemical compositions). Submerged arc welding is a technique in which welding is formed under a protective powder layer. Spiral welded steel pipes are produced via this welding technique by joining from both sides (i.e., internal and external) at automatic welding stations. Proper welding parameters (i.e., welding current, arc voltage, wire feeding speed and welding speed) should be used to obtain defect-free weld seams. Moreover, the consumables used in submerged arc welding of steel pipes are very critical in order to increase production rate and competitiveness and to decrease production costs.

For this purpose, 7 different combinations were selected with different steel coils (API Spec 5L PSL2 X70 M) produced by different companies (namely Arcelor Mittal, Tisco, Shougang Jingtang and Shougang Quian'an) and different welding wire grades (namely S2Mo and S2MoTiB) and diameters (3.2 and 4.0 mm). Different weld parameters were determined for each combination and used in welding of these combinations. Mechanical tests and microstructural investigations were conducted to determine the effect of weld parameters and the consumables on the joint quality.

Moreover, production flow tests were done with the above mentioned materials to determine the suitability of the welded seams for repair. The results indicated that the welded steel pipes obtained using the steels plates produced by different companies do not have same mechanical properties, but their properties lie within the range of the API standard (API Spec 5L PSL2) requirements. It was also observed that the wire selection is more critical and the repair rates increase if the selection is not suitable and thus the standards cannot be met.

Keywords: Welding, Submerged arc welding, Welding consumables, Steel coil, Spiral welded pipe, Weld quality.

1. Introduction

The method of submerged arc welding is a sequence of physical and chemical events that occur under the granules of powder that can be understood from its name. By selecting appropriate welding parameters (welding current, arc voltage, wire feed speed, welding speed), faultless and good weld seams are obtained by this technique.

The submerged arc welding is a welding method of welding conducted under the protective dust cover of the welding base as schematically shown in Figure 1. Spiral welded steel pipes are widely welded internally and externally at automatic SAW stations by this technique.

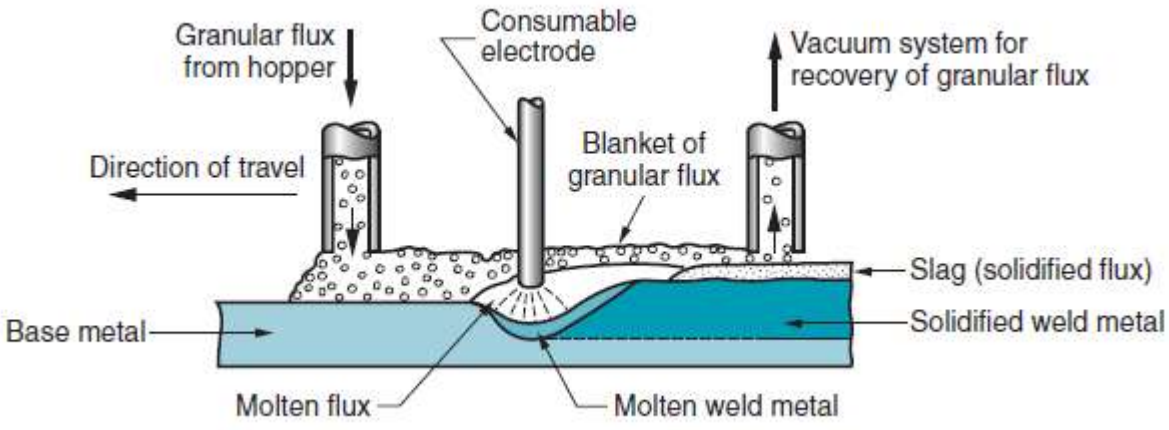

Figure 1. Principle of submerged arc welding [1]

As can be seen in Figure 1, the electrical arc is formed between the bare wire electrode and the metal to be welded. This is done by bringing the electrode close to the material and then quickly separating from it by a short distance. An electric arc is a discharge of electric current across a gap in a circuit. The electric energy from the arc thus formed produces temperatures of 5500 ^{o}C or higher, sufficiently hot to melt any metal. During arc welding the material is melted and some of it evaporates when the heat increase occurs. The source, which becomes more conductive by evaporation, facilitates and accelerates the movement of the atmosphere ions. In this way, the heat is further increased and the chain melting and solidification process is started [1-5].

In addition to these thermal events, welding dusts, which give a meaning to the underside weld, also play an active role on weld quality and strength, protecting the molten metal and hot weld seam from adverse effects of the atmosphere and, if necessary, contributing to welding seams such as an alloy element [4].

In this study; a detailed experimental investigation of the properties of welds obtained by using different consumable materials (same type of welded wire with different chemical properties, different wire sizes, same type of sheets with different chemical properties) was conducted in spiral arc welded spiral pipe production. Different weld parameters were determined for each combination and used in welding of these combinations. Mechanical tests and microstructural investigations were conducted to determine the effect of weld parameters and the consumables on the joint quality.

2. Material and Method

Different wire and sheet combinations have been used to determine the effects of consumable replacement. Table 1 summarizes the steels sheets and consumables which are used in welding trials. The results obtained from only the weld trials OZ-004 and OZ-006 will be discussed in this manuscript.

Table 1. Steels sheets and consumables used in this study.

No	Coil	Nominal Thickness	Procedure No	Subject	Wire Class	Wire Size (mm)			
1	ARCELOR	19.00mm	OZ-004	Wire Exchange Analysis	Lincoln S2Mo	4.00	3.2	4.00	3.2
2	ARCELOR	19.00mm	OZ-007		Lincoln S2Mo	4.00	4.00	4.00	3.2
3	ARCELOR	19.00mm	OZ-006		Oerlikon +Lincoln S2Mo	4.00	4.00	4.00	3.2
4	ARCELOR	19.00mm	OZ-008	Coil Exchange Analysis	GeKa S2MoTiB	4.00	4.00	4.00	4.00
5	ARCELOR	16.00mm	OZ-005		GeKa S2MoTiB	4.00	4.00	4.00	4.00
6	TISCO	19.00mm	OZ-009		GeKa S2MoTiB	4.00	4.00	4.00	4.00
7	SHOUGANG	19.00mm	OZ-010		GeKa S2MoTiB	4.00	4.00	4.00	4.00

For sheet material, X70M quality sheet from different manufacturers is selected whereas 3.2mm and 4mm thick S2Mo and S2MoTiB quality consumables were selected as welding wire in this study.

Various mechanical tests and microstructural investigations have been carried out to determine the effect weld parameters and the consumables on product performance characteristics.

2.1. Welding Parameters

Before starting the welding, the parameters of the submerged arc welding are determined. Verification of these parameters is done and records are kept. Weld Procedure Specification (WPS) is prepared and the welding trials were conducted according to the WPS prepared.

2.2. Electrical Parameters

Following electrical parameters are used in the current study:

Welding Current (I)

It is selected depending on the material (wall thickness (t) of the material to be welded) and wire diameter (Ø).

Welding Voltage (U)

It depends on the welding current. In addition, the type of powder used must be taken into account.

Welding Speed

It is selected according to welding current and welding voltage**.**

Current Type and Pole

In single-head welding operation, the internal and external welding current is DC.

In the welding with double head, inside and outside are 1st head DC, 2nd head AC.

In the three-head welding operation, the first head DC, the second head and the third head AC are inside and outside.

2.3. Welding Material Parameters

Welding Wire

Wire quality is selected for DC inside and outside depending on the material and for AC.

Welding Powder

The quality of the powder is selected depending on the quality of the material.

2.4. Geometric Parameters

2.4.1. Tandem System

Tandem system used in this study is shown in Figure 2.

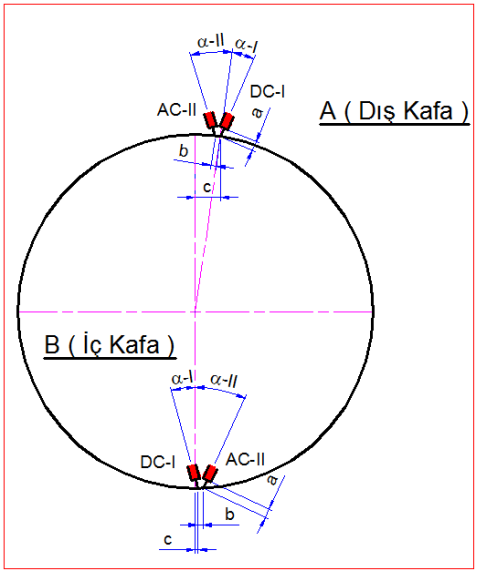

Figure 2. Tandem System [5].

Adjustment geometry of welding heads

DC - A AC - B	a	b	C	DC – I α I	AC – II α II

Welding Wire Diameter adjustment

inside / outside the head

2.4.2. Three Head System

Three head system used in this study is shown in Figure 3.

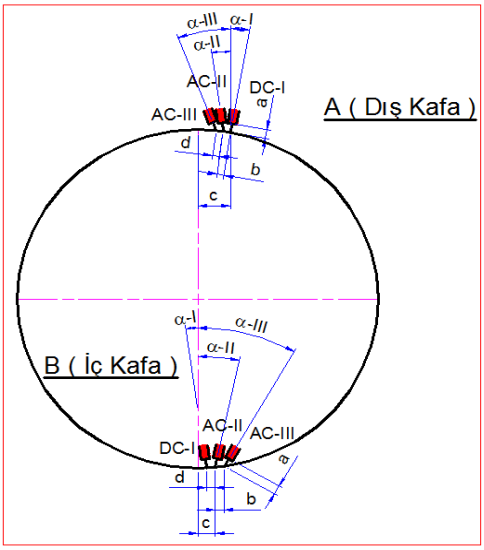

Figure 3. Three Head System [5].

Setting geometry of welding heads

outside inside	a (mm)			b (mm)	c (mm)	d (mm)	degree		
	DC (I)	AC (II)	AC (III)				α 1	α 2	α 3

Welded Wire Diameters

Inside / Outside Head

Welding Point Position (c)

It is the distance to the 6th and 12th clock points of the first welding head inside and outside.

Inside (c)

On the outside (c)

Wire Range (b and d)

Tandem and three heads are the distance between two wires.

For tandem (Figure 2)

Internal head (b) (d)

On the outside the head (b) (d)

For the three-head system (Figure 3)

Internal head (b) (d)

On the outside the head (b) (d)

Wire Height (a)

The distance between the welding nozzle and the material.

For tandem (Figure 2)

In the inside (a)

On the outside (a)

For the three-head system (Figure 3)

In the inside (a1), (a2), (a3)

On the outside (a1), (a2), (a3)

Wire Entry Angle (α)

It is the angle of the wire arrival direction with the normal at the welding point.

For tandem;

Inside and outside head 1st

Inside 2nd head

Outside 2nd head

For the three-head system;

Inside 1st, 2nd and 3th head

Outside 1st, 2nd and 3th head

2.5. Verification of Welding Parameters

2.5.1. Tensile Test

The Reject / Accept criterion applies to the relevant pipe manufacturing standard. This test specifically serves to verify the electrical parameters. The bending test is always carried out in every new production. In addition, this process is repeated with any parameters (A, V, welding speed, welding powder, welded wire) changed during manufacturing and the results are recorded.

2.5.2. Macro Inspection

Sections are taken from the weld, polished and etched. On this sample the welding geometry (height, width, depth of penetration and edge overlay) is measured and compared to the requested values. This inspection serves especially to verify the welding head settings. Care should be taken to ensure that the tailstock source is completely melted in the macro inspection.

2.5.3. Visual Inspection

During the welding process and after welding, the stitch form, evenness, burning is visually checked. This inspection serves to verify the general welding parameters.

2.5.4. Other Tests and Inspections

Other tests and examinations for the purpose of verifying other physical and chemical properties of the welding seam are also conducted. These tests and inspections are as follows: bending test, impact test, tear test, hardness test, radiographic examination, ultrasonic examination, magnetic examination, and hydrotest.

2.6. Welding Process Order

The orthogonal roles, top print roles (advocates) and resource heads in the SAW station are set. The selection of the welding parameters is done in accordance with the standard.

Verification of the welding parameters, the results of the predicted tests and examinations are evaluated. According to the results of these evaluations, the parameter values given in the standard are then changed. Transition to serial welding is permitted according to the result of verification test / examinations.

2.7. Welding Parameter Records

The resource parameters are registered for each resource transaction. The records are checked and stored.

3. Results and Discussion

This study is the part of a work (i.e., a detailed investigation) conducted to determine the effects of changing consumables on product quality of spiral submerged arc welded pipes using seven different wire and sheet combinations given in Table 1. In this paper, the results of only 2 different wire combinations will be discussed (namely Study 1, i.e., OZ-004, and Study 2, i.e., OZ-006.

In Study 1 (OZ-004), Arcelor X70M steel sheet was used and spiral submerged arc welded pipes were produced using Lincoln P223 powder and Lincoln S2Mo wire (external DC 4.0mm diameter wire, external AC 3.2mm diameter wire, internal DC 4.0mm, internal AC 3.2mm) according to API Spec 5L standard (Table 2).

Table 2. The consumables used in Study 1 (OZ-004).

No	Coil	Nominal Thickness	Procedure No	Subject	Wire Class	Wire Size (mm)			
1	ARCELOR	19.00mm	OZ-004	Wire Exchange Analysis	Lincoln S2Mo	4.00	3.2	4.00	3.2

As seen in Table 2, spiral welded pipes with the size of 1422,4 mm x 19,65 mm were produced in Study 1 using Arcelor Mittal coils. Pipe number 15S1100454 was produced for welding procedure qualification tests. All weld parameters and WPQR tests were carried out according to API Spec 5L 45th Edition.

In Study 2 (OZ-006), the internal AC is replaced by the internal DC. Thus, spiral submerged arc welded pipe production was conducted according to API Spec 5L standard using the Lincoln P223 powder and two different types of wire, namely Lincoln S2Mo (external DC 4.0mm diameter wire, external AC 3.2mm, internal DC 4.0mm) and Oerlikon SW-702Mo wire (internal AC 4.0mm).

Table 3. The consumables used in Study 2 (OZ-006).

No	Coil	Nominal Thickness	Procedure No	Subject	Wire Class	Wire Size			
3	ARCELOR	19.00mm	OZ-006	Wire Exchange Analysis	Oerlikon +Lincoln S2Mo	4.00	4.00	4.00	3.2

As seen in Table 3, spiral welded pipes with the size of 1422,4 mm x 19,65 mm were produced in Study 2 using Arcelor Mittal coils. Pipe number 15S2103715 was produced for welding procedure qualification tests. All welding parameters and WPQR tests were carried out according to API Spec 5L 45th Edition.

The Welding Procedure Specification (WPS) given in Figure 4 was prepared due to change of AC wire diameter and brand name of internal weld. In previous MPQT, the welding procedure has covered the use of 3,2 mm S2Mo wire with brand name Lincoln (Askaynak) in internal AC welding head. The wires for each welding head are given below for this procedure;

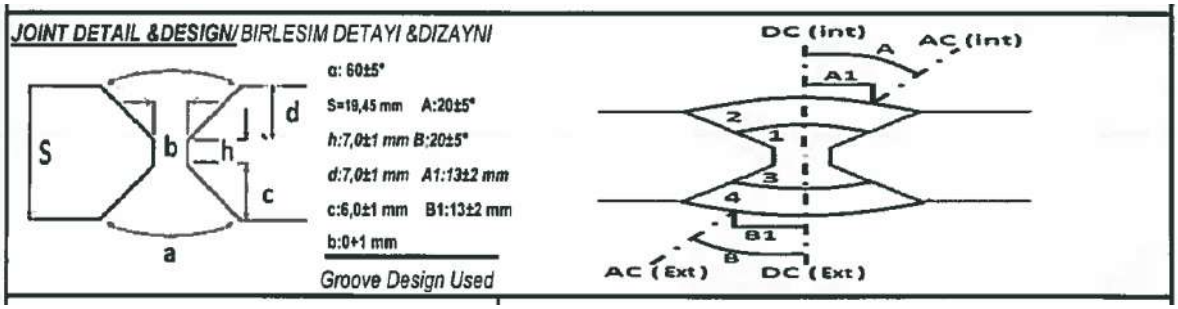

Figure 4. Welding Geometry / Combination Detail and Design

After welding visual inspection was carried out and optical microscopy was conducted on the metallography specimens extracted from both joints to evalute the weld profiles and weld geometries obtained. These investigations indicated that the weld geometries (height, width, depth of penetration and edge overlay) of the joints were in good agreement with the standard.

Moreover, tensile test specimens were extracted from 2 pipes produced as explained above and mechanical tests were carried out. According to API Spec 5L standard the yield and tensile strength values should be within the range of 485-635 N/mm^2 and 570-760 N/mm^2, respectively. Moreover, a set of three impact test specimens should be extracted from the pipes produced tested. And the result of impact test of each individual test piece should be about 75% of average value of three specimens. The required absorbed energy (toughness) value ranges from these pipes according to Pipe Body of PSL2 Pipe are given in Figure 5.

CVN Absorbed Energy Requirements for Pipe Body of PSL 2 Pipe

Specified Outside Diameter D mm (in.)	Full-size CVN Absorbed Energy min K_V J (ft·lbf)						
	Grade						
	≤ L415 or X60	> L415 or X60 to ≤ L450 or X65	> L450 or X65 to ≤ L485 or X70	> L485 or X70 to ≤ L555 or X80	> L555 or X80 to ≤ L625 or X90	> L625 or X90 to ≤ L690 or X100	> L690 or X100 to ≤ L830 or X120
> 1219 (48.000) to 1422 (56.000)	40 (30)	54 (40)	54 (40)	54 (40)	54 (40)	68 (50)	81 (60)
> 1422 (56.000) to 2134 (84.000)	40 (30)	54 (40)	68 (50)	68 (50)	81 (60)	95 (70)	108 (80)

Figure 5. CVN Absorbed Energy Requirements for Pipe Body of PSL2 Pipe

According to test results, in Run 1 (OZ-004), the yield strength value (i.e., 478 N/mm^2) obtained from Study 1 (OZ-004) was lower than the standard (minimum 485 N/mm^2), Table 4. On the other hand, other mechanical tests results (including bending and toughness tests) were within the ranges required by the standard as seen in Table 4. Moreover, as seen from the macrograph showing the cross-section of the joint (Table 4) the weld profile is good and NDT results were also acceptable according to the standard. It was also observed that the current values approached to minimum at the weld parameter changes.

On the other hand, all mechanical test results obtained from the pipe produced in Study 2 (OZ-006) were within the ranges required by the standard, Table 5. Moreover, the weld profile is good and NDT results were also acceptable according to the standard. It was, on the other hand, observed that the current values changed to maximum at the weld parameter changes. It was observed that the current values were changed to maximum at the weld parameter changes.

Table 4. The joint cross-section and mechanical test results of the pipe produced in Study 1 (OZ-004).

Tensile Test (Test Report Lab No: SAW PQR - Pipe No: 15S1100454)

Specimen No / Numune No	Width(mm) / Genişlik	Thickness(mm) / Kalınlık	Area(mm2) / Alan	Yield(N/mm2) / Yük	Ult. Un. Str.(N/mm2) / Stres	Type of Failure& Location / Kırılma Yeri ve Çeşidi
1 (transv)	38.1	19.6	746.76	556	687	Base Metal
2 (transv)	38.1	19.59	746.379	478	680	Base Metal

Guided Bend Tests (Test Report Lab No: SAW PQR - Pipe No: 15S1100454)

Specimen No / Numune No	Dimensions (mm) / Boyutlar(mm)		Jig Dia. / Jig Çap	Bending angle / Eğilme Açısı	Type / Türü	Result / Sonuç
1	38.1	19.45	75	180°	Face Bend	Satisfactory/Tatminkar
2	38.1	19.45	75	180°	Root Bend	Satisfactory/Tatminkar
3	38.1	19.45	75	180°	Face Bend	Satisfactory/Tatminkar
4	38.1	19.45	75	180°	Root Bend	Satisfactory/Tatminkar

Toughness Tests (Test Report Lab No: SAW PQR - Pipe No: 15S1100454)

Specimen No / Numune No	Notch Location / Çentik Yeri	Notch Type / Çentik Çeşidi	Test Temp. / Sıcaklık	6 / Boyutlar	Test Values / Test Değerleri(Joule)			
					1	2	3	Avarage
1	Kay./Weld	V type	-15	10x10	138	184	167	163
2	FL	V type	-15	10x10	188	129	128	148
3	FL+2	V type	-15	10x10	247	276	279	267
4	FL+5	V type	-15	10x10	436	325	345	369

Other Test/ Diğer Testler

Result-Satisfactory/ Sonuç : **Tatminkar/ Satisfactory**

Macro-Results/ Macro-Sonuçlar: **Tatminkar/ Satisfactory**

Hardness Test / Sertlik Testi **Tatminkar/ Satisfactory**

Other Test/ Diğer Testler

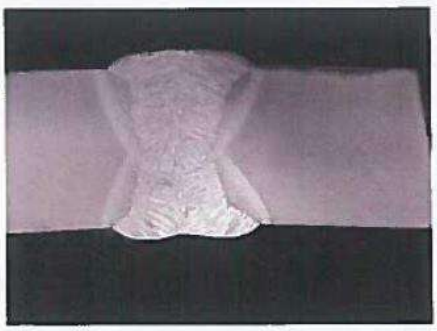

Pipe No : 15S1100454 Coil No:627569000 Heat No:61960 CE PCM:0,1567%

Table 5. The joint cross-section and mechanical test results of the pipe produced in Study 2 (OZ-006).

Tensile Test (Test Report Lab No: SAW PQR - Pipe No: 15S2103715)

Specimen No Numune No	Width(mm) Genişlik	Thickness(mm) Kalınlık	Area(mm2) Alan	Yield(N/mm2) Yük	Ult. Un. Str.(N/mm2) Stres	Type of Failure& Location Kırılma Yeri ve Çeşidi
1 (transv)	38.1	19.75	752.475	537	676	Base Metal
2 (transv)	38.1	19.77	753.237	540	673	Base Metal

Guided Bend Tests (Test Report Lab No: SAW PQR - Pipe No: 15S2103715)

Specimen No Numune No	Dimensions (mm) Boyutlar(mm)		Jig Dia. Jig Çap	Bending angle Eğilme Açısı	Type Türü	Result Sonuç
1	38.1	19.45	75	180°	Face Bend	Satisfactory/Tatminkar
2	38.1	19.45	75	180°	Root Bend	Satisfactory/Tatminkar
3	38.1	19.45	75	180°	Face Bend	Satisfactory/Tatminkar
4	38.1	19.45	75	180°	Root Bend	Satisfactory/Tatminkar

Toughness Tests (Test Report Lab No: SAW PQR - Pipe No: 15S2103715)

Specimen No Numune No	Notch Location Çentik Yeri	Notch Type Çentik Çeşidi	Test Temp. Sıcaklık	Dimensions Boyutlar	Test Values / Test Değerleri(Joule)			
					1	2	3	Avarage
1	Kay./Weld	V type	-15	10x10	157	104	122	128
2	FL	V type	-15	10x10	265	196	261	241
3	FL+2	V type	-15	10x10	310	450	292	351
4	FL+5	V type	-15	10x10	290	260	300	283

Other Test/ Diğer Testler

Result-Satisfactory/ Sonuç : **Tatminkar/ Satisfactory**
Macro-Results/ Macro-Sonuçlar: **Tatminkar/ Satisfactory**
Hardness Test / Sertlik Testi **Tatminkar/ Satisfactory**

Other Test/ Diğer Testler

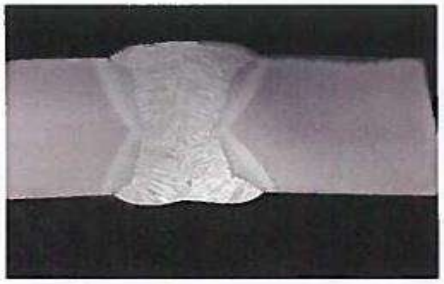

Pipe No : 15S2103715 Coil No:546926000 Heat No:65788 CE_{PCM}:0,164%

4. Conclusions

The results obtained in this study are as follows:

1) The most critical variation in weld parameters was found to be current. It was well observed that the high range of minimum and maximum current values increases the production cost of spiral arc welded pipes.
2) It was also observed that high current operation reduces machine efficiency
3) Mechanical test results were all in good agreement with the standard except the yield strength value of the pipe produced in Study 1.
4) The weld geometries ((height, width, depth of penetration and edge overlay) produced in both studies were in good agreement with the standard.
5) NDT results were also acceptable according to the standard.

Acknowledgements

We would like to thank TOSÇELİK SPIRAL PIPE Team, for their support and encouragement during the conduction this study. We would also like to thank Mr. Serdar GÜNBAY, Quality Control Supervisor of İSDEMİR, for his continuous support throughout this study.

References

[1] GROOVER M.P. ‘Modern İmalatın Prensipleri’, Nobel Akademik Yayıncılık Eğitim Danışmanlık Tic. Ltd. Şti, 4. Basımdan Çeviri, Ankara (2015).
[2] ANIK, S., ANIK, E.S., VURAL M. ‘1000 Soruda Kaynak Teknolojisi Cilt1’ Birsen Yayınevi, İstanbul (1993).
[3] LINCOLN ELECTRİC COMPANY. ‘’The Procedure Handbook of Arc Welding’’ Lincoln Electric Company 13 th Edition (December’94).
[4] ANIK, S. ‘’Kaynak Tekniği - Cilt2: Tozaltı Kaynağı ve Koruyucu Gazla Kaynak’’
[5] “Tosçelik Spiral Boru Üretim San. A.Ş. Eğitim Notları”, Osmaniye (2015).

Investigation of the Effect of Temperature and Flow Effect Rate on Thermal Performance in a Body-Pipe Type Heat Exchanger Using Cu_2O Nanofluid

İsmail HİLALİ [1], Harun ÇİFCİ [2*], Refet KARADAĞ[3]

[1] Harran University, Engineering, Mech. Eng., Şanlıurfa, Türkiye; email: ihilali@harran.edu.tr
[2] Harran University, Engineering, Mech. Eng., Şanlıurfa, Türkiye; email:haruncifci@harran.edu.tr
[3] Adıyaman University, Engineering, Mech. Eng., Adıyaman,Türkiye; email: refetkaradag@yahoo.com

[*] **Corresponding Author:** haruncifci@harran.edu.tr

Abstract

In this study, the effects of different fluid type, temperature and flow rate on the thermal performance of a body-pipe type heat exchanger were investigated numerically. Heat transfer performance for different flow rates and temperatures by using nanofluid that obtained by 2% volumetric concentration Cu_2O and water in heat exchanger which designed from aluminum body and copper pipes was compared with the analysis performed by pure water. The volumetric flow rates of fluids are 6 and 8 lt/min and the operating temperatures are 70-90℃, 10-30℃ for hot and cold fluids respectively. Thermal properties of nanofluid were calculated theoretically and analysis was performed via CFD program. According to the analysis results, heat transfer performance increased with temperature and flow rate increase in both nanofluid and pure water. As a result of the analysis, the output temperature of the hot Cu_2O nanofluid was 4.7℃ lower than the pure water for maximum temperature and flow rate and maximum heat transfer increment is calculated as %6.25.

Keywords: Heat Exchanger, Nanofluid, Volumetric Concentration, Temperature, Flow Rate.

1. Introduction

Today, heat exchangers are used in industrial and most engineering applications. Heat exchangers are devices that allow heat transfer between two different fluids without mixing. These devices include thermal power plants, chemical industry, heating and ventilation, air conditioning and cooling, automobile radiators, condenser systems and so on. There are many types of heat exchangers depending on the application areas; such as body tubular heat exchanger, plate heat exchanger, finned heat exchanger, regenerative heat exchanger. Body - pipe type heat exchangers are the most commonly used heat in the process industry. The body- pipe heat exchanger consists of parallel tubes arranged parallel to one another in the body pipe. Basic elements; pipes (or pipe bundles), body, two head heads, front and rear mirrors in which pipes are fixed, and baffle plates (also called baffle plates or curtains) that guide the flow in the body and support the pipes. One fluid flows through the pipes and the other fluid flows parallel or diagonally to the pipes on the body side.

The design and performance improvement of heat exchangers are underway. However, the low conductivity of the fluids used in the heat exchangers limits the high performance effect. Here, significant improvements in the performance of the heat exchangers can occur by improving the thermal properties of the working fluid. Today, traditional fluids such as water, ethylene glycol and oil are used in heat exchangers. Nanofluids are the new generation heat transfer fluids obtained by adding nano-sized solid particles (<100nm) to conventional heat transfer fluids such as water, oil and antifreeze (Choi (1995)).

In the literature, it is possible to find many studies aimed at increasing thermal performance by using nanofluids in heat exchangers. Madhesh and Kalaiselvam (2014) studied the effect of hybrid nanofluids prepared with copper-titanium (0.1-1% vol. concentration) and water on a heat exchanger. According to the results, the maximum heat transfer coefficient increase is 48.4%. SanthoshCibi *et al*. (2014) examined the effect of heat transfer on heat exchangers under laminate flow conditions using graphite nanofluids. Graphite nanoparticles were prepared in pure water at concentrations of 0.025%, 0.05%, 0.075%) and it was determined that the concentration of the graphite increased gradually with increasing concentration according to the experimental results. Researchers have reported that viscocity decreases as the particle concentration increases and the heat transfer coefficient increases as the flow rate increases. Nieh *et al*. (2014) investigated heat transfer performance in a vehicle radiator with using alumina, titania nanoparticles and nanofluids obtained with purified water and ethylene glycol (antifreeze). In the experiments, the effects of different nanoparticle concentration, different volumetric flows and different radiator inlet temperatures on the heat transfer capacity, pressure drop and pump power values were investigated. The researchers stated

that the highest heat transfer rate occurred in the alumina nanofluid after the experiments and the results showed that the maximum heat transfer with nanofluids increased by 25.6%, the pressure drop by 6.1%, the pump power by 2.5% and the radiator efficiency factor by 27.2%. Sohel *et al*. (2015) studied the cooling performances of nanofluids prepared with Al_2O_3 and water on mini-channel heat exchangers. Researchers have noted that the use of nanofluids reduces the heat exchanger temperature. Aliabadi *et al*. (2016) investigated the effects of Cu-water, Fe-water and Ag-water nanofluids on heat transfer and pressure losses in the serpentine heat exchanger were investigated. According to the results, the amount of heat transfer increased as the fluid flow increased. The highest heat transfer occurred in the cu-water nano fluid. the pressure loss increased slightly in comparison with pure water. Kumar *et al*. (2017) comprehended ZnO nanofluid provides better thermal performance than CeO_2 nano flow cube in the study of using CeO_2/water and ZnO nanofluids as a volume modifier of 0.5 - 2.0% in a heat exchanger. Diglio *et al*. (2018) investigated thermal performance of nanofluids prepared by nano-particles of 0.1% -1% ethylene glycol and water based silver, copper, aluminum, alumina, copper oxide, graphite and silicon oxide was numerically investigated. Researchers have found that the use of nanofluids reduces thermal resistance and emphasizes that the greatest heat transfer increase is in Ag nano fluid. Pourhoseini *et al*. (2018) examined the thermal performance of the silver-water nanofluid in the plate heat exchanger. According the results thermal conductivity value was 36.6% higher than pure water.

In this study, the effects of different fluid type, temperature and flow rate on the thermal performance of a body-pipe type heat exchanger were investigated numerically. Heat transfer performance for different flow rates and temperatures by using nanofluid that obtained by 2% volumetric concentration Cu_2O and water in heat exchanger which designed from aluminum body and copper pipes was compared with the analysis performed by pure water. According to the analysis results, heat transfer performance increased with temperature and flow rate increase in both nanofluid and pure water.

2. Material and Method

In this study, a body tube heat exchanger designed by mounting copper pipes with a diameter of 10 mm in an aluminum body with an outer diameter of 30 cm was designed. The heat exchanger was designed for passing cold fluid through the body and hot fluid through the pipe.

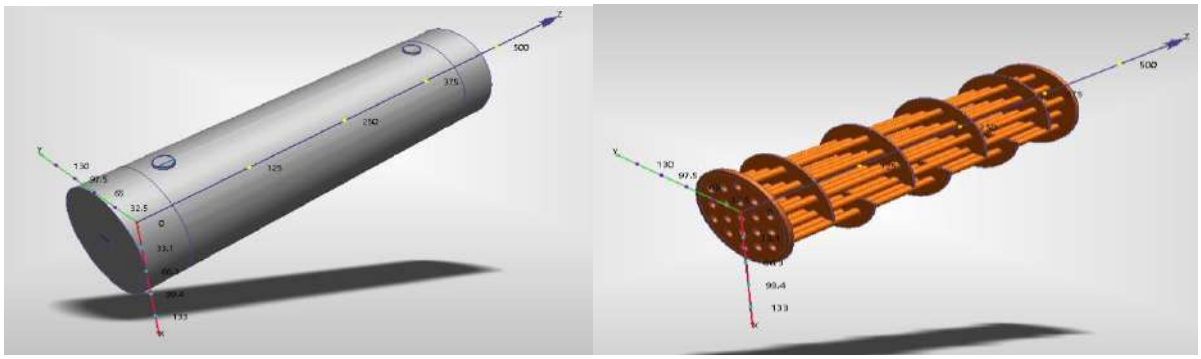

Figure 1. (a) Designed body-pipe heat exchanger image, (b) Heat exchanger inner part image

In the study, pure water and Cu_2O nanofluid were selected at a volumetric concentration of 2%. The thermal and physical properties of the nanofluid before the calculations are calculated using the equations obtained from the literature.

2.1. Calculation of Nano Fluid Volume Concentration

After the nanoparticles are identified, the amount of particulate required for each volumetric concentration is calculated with the following equations.

$$\emptyset = \frac{V_p}{V_T} \quad (1)$$

$$m_P = \rho_P V_P \quad (2)$$

In these equations, Ø, V_p, V_T, m_p and ρ_p mean volumetric concentration, particle volume, total volume, particle weight and particle density respectively.

2.2. Density and Specific Heat Calculation

Density and specific heat values are calculated by the following relations proposed by Pak and Cho (1998).

$$\rho_{nf} = (1-\emptyset)\rho_{bf} + \emptyset\rho_p \quad (3)$$

$$c_{p,nf} = (1-\emptyset)c_{p,bf} + \emptyset c_{p,p} \quad (4)$$

In these equations, nf, bf, and c_p mean nanofluid, base fluid and, specific heat respectively.

2.3. Heat Transfer Coefficient Calculation

There are many equations used in the literature for the calculation of the heat transfer coefficients of nanofluids. The most common equations in literature are:

2.3.1. Maxwell (1891) model

Effective heat transfer coefficient can be calculated from this equation.

$$k_{eff} = \frac{k_p+2k_f+(k_p-k_f)\emptyset}{k_p+2k_f-(k_p-k_f)\emptyset} \quad (5)$$

2.3.2. Yu and Choi (2003) model

$$k = \left[\frac{k_p+2k_{bf}+2(k_p-k_{bf})(1+\beta)^3+\emptyset}{k_p+2k_{bf}-(k_p-k_{bf})(1+\beta)^3\emptyset}\right] k_{bf} \quad (6)$$

Where β is the ratio of the nanolayer thickness to the original particleradius (β=0.1).

2.3.3. Murshed model

$$k_{nf} = \frac{1}{4}[(3\emptyset-1)k_p + (2-3\emptyset)k_{bf}] + \frac{k_{bf}}{4}\sqrt{\Delta} \quad (7)$$

$$\Delta = \left[(3\emptyset-1)^2\left(\frac{k_p}{k_{bf}}\right)^2 + (2-3\emptyset)^2 + 2(2+9\emptyset-9\emptyset^2)\left(\frac{k_p}{k_{bf}}\right)\right] \quad (8)$$

2.4. Viscosity Calculation

There are some equations from literature for calculate the viscosity of nanofluids.

2.4.1.Einsten model (Ø≤2 %)

$$\mu = \mu_{bf}(1 + 1{,}25\emptyset) \quad (9)$$

2.4.2.Timofeeva model

$$\mu_{nf} = (1 + 13{,}5\emptyset + 904{,}4\emptyset^2)\mu_{bf} \quad (10)$$

2.4.3. Brinkman model (≤ 4 % vol.)

$$\mu_{nf} = \mu_{bf}(123\emptyset^2 + 7{,}3\emptyset + 1) \quad (11)$$

2.5. Thermal and Physical Properties Tables of Nanoparticles, Water and Nanofluid

The thermal and physical properties of nanoparticles are given in Table 1. These values were obtained from the company where the material was purchased. For pure water and Cu_2O nanofluid the thermal and phsical properties are given in Table 1.

Table 1. Physical and thermal properties of Cu_2O nanoparticles used in the study

Nanoparticle properties				
Nanoparticle	Particle size (nm)	ρ (kg/m3)	Cp (J/kgK)	k (W/mK)
Cu_2O	16	6000	196,423	74

Table 2. Physical and thermal properties of Pure water and Cu_2O nanofluid

Nanofluid and water properties				
Fluid	ρ (kg/m3)	Cp (J/kgK)	k (W/mK)	μ (N.s/m2)
Pure Water	997	4179	0,613	1,373
Cu_2O Nanofluid	1097	3763	0,662	1,441

2.6. Numerical Study

The study was conducted on the CFD program in computer. Calculated thermal properties were added to the program and analyzed. The analysis was carried out for three different input-output temperature

values as 70-10, 80-20, 90-30 and 2 different flow rates as 0.1, 0.13 kg/s. Heat transfer calculations were performed after heat exchanger output temperature values were obtained.

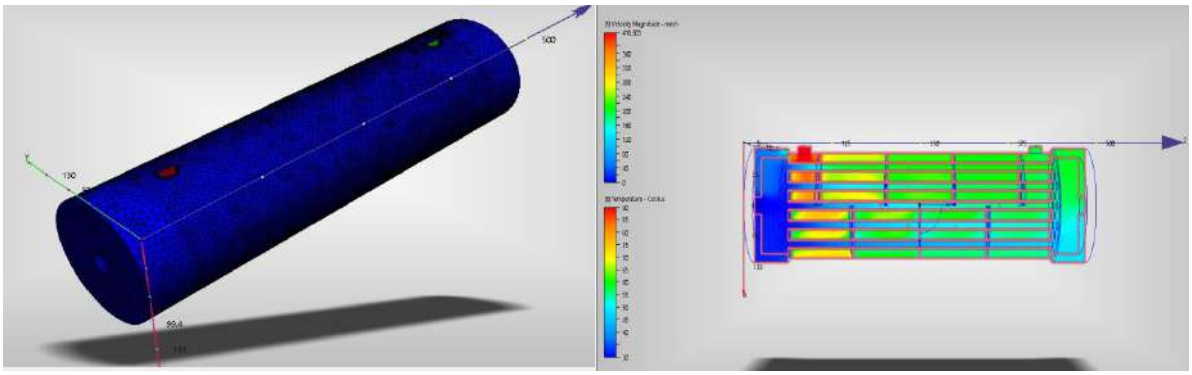

Figure 2. CFD analysis image: (a) Mesh image, (b) Analysis image

2.6. Heat Transfer Calculation

For heat transfer calculations this equation used was used.

$$\dot{Q} = \dot{m}_h Cp_h \left(T_{h,i} - T_{c,h}\right) \quad (12)$$

In this equation $\dot{Q}$, $\dot{m}_h$, Cp_h, $T_{h,i}$, $T_{c,h}$, mean heat transfer, hot fluid mass flow, specific heat, inlet and outlet temperatures respectively.

3. Results and Discussion

After numerical study, inlet and outlet temperatures for pure water and nanofluid were determined. Then heat transfer calculations were performed. The values that are found and calculated are given at Table 3 and Table 4.

Table 3. Input-outlet temperatures of pure water and total heat transfer amount.

Fluid	$T_{hot,inlet}$ (℃)	$T_{hot,out}$ (℃)	Mass Flow Rate $\dot{m}$(kg/s)	Specific Heat Cp (j/kgK)	Total Heat Transfer $\dot{Q}$ (W)
Pure Water	70	42,5	0,1	4179	11492,25
	70	45,3	0,13	4179	13418,77

	80	52,3	0,1	4179	11575,83
	80	55,3	0,13	4179	13418,77
	90	62,3	0,1	4179	11575,83
	90	65,3	0,13	4179	16515,41

Table 4. Input – outlet temperatures and total heat transfer amount of Cu_2O-water nano fluid.

Fluid	$T_{hot,inlet}$ (℃)	$T_{hot,out}$ (℃)	Mass Flow Rate ṁ(kg/s)	Specific Heat Cp (j/kgK)	Total Heat Transfer Q̇ (W)
Cu_2O Nanofluid	70	38,5	0,1	3743	11791,738
	70	40,7	0,13	3743	14258,645
	80	50,5	0,1	3743	11043,056
	80	53,5	0,13	3743	12896,044
	90	58,5	0,1	3743	11791,738
	90	60,7	0,13	3743	17549,102

The results in both fluids according to Tables. 3 and Table. 4 are as follows:

- Outlet Temperatures increased for both pure water and Cu_2O nano fluid by increasing the inlet temperature and mass flow rate.
- Heat transfer increased with increasing temperature for pure water and decreased with temperature increase for nanofluid.
- Heat transfer increased in both fluids with increasing flow.
- The highest heat transfer difference occurs at a temperature of 90℃ and a flow rate of 0.13 kg/s. The maximum increase in heat transfer is calculated as 6.25%.

As a result of this study, it was determined that nano fluid increased the heat transfer significantly. This work on body- pipe type heat exchanger increased the capacity of the heat exchanger. In this way, the heat exchanger surface area of the same heat transfer amount can be designed smaller.

References

Periodicals:

Aliabadi, M. K., Nouri, M., Sartipzadeh, O., Salami, M., (2016). Performance of Agitated Serpentine Heat Exchanger Using Metallic Nanofluids. Chemical Engineering Research and Design, 109, 53-64.

Brinkman, H. C., (1952). The Viscosity of Concentrated Suspensions and Solution. Journal of Chemical Physics, 20, 571–581.

Diglio, G., Roselli, C., Sasso, M., Channabasappa, U. J., (2018). Borehole Heat Exchanger with Nanofluids as Heat Carrier. Geothermics, 72, 112-123.

Kumara, V., Kumar, A., Ghosh, S. K., (2017). Characterization and Performance of Nanofluids in Plate Heat Exchanger, Materials Today: Proceedings, 4 , 4070–4078.

Madhesh, D., and Kalaiselvam, S., (2014). Experimental Analysis of Hybrid Nanofluid as a Coolant. Procedia Engineering, 97,1667–1675.

Murshed, S. M. S., Leong, K. C., Yang, C., (2005). Enhanced Thermal Conductivity of TiO_2–Water Based Nanofluids, International Journal of Thermal Sciences, 44, 367 – 373.

Nieh, H. M., Teng, T. P., Yu, C. C., (2014). Enhanced Heat Dissipation of a Radiator Using Oxide Nano Coolant. International Journal of Thermal Sciences, 77, 252-261.

Pak, B. C., and Cho, Y. I., (1998). Hydrodynamic and Heat Transfer Study of Dispersed Fluids with Submicron Metallic Oxide Particles. Exp. Heat Transf. 11,151–170.

Pourhoseini, S. H., (2018). Effect of silver-water nanofluid on heat transfer performance of a plate heat exchanger. Powder Technology. 33, 279-286

Santhoshcibi, V., Gokulraj, K., Kathiravan P., Rajeshkanna R., Ganesh, B., Sivasankaran, S., Vedhagirieswaran, V., (2014). Convective Heat Transfer Enhancement of Graphite Nanofluids in Shell and Tube Heat Exchanger. International Journal of Innovative Research in Science, Engineering and Technology, 3 (2).

Sohel, M. R., Saidur, R., Khaleduzzaman, S. S., Ibrahim, T. A., (2015). Cooling Performance Investigation of Electronics Cooling System Using Al_2O_3–H_2O Nanofluid. International Communications in Heat and Mass Transfer, 65, 89–93.

Yu, W., Choi, S. U. S., (2003). The Role of Interfacial Layers in The Enhanced Thermal Conductivity of Nanofluids: a renovated Maxwell model. Journal of Nanoparticle Research 5,167.

Books:

Maxwell, J. C., 1891. A Treatise on Electricity and Magnetism, unabridged 3rd ed., Clarendon Press, Oxford, UK,

Symposium, Congress, Paper:

Choi, U. S., and Eastman, J. A., (1995). Enhancing thermal conductivity of fluids with nanoparticles. International mechanical Engineering congress and exhibition, san Francisco, CA .

Other Sources:

A. Einstein, Investigation on Theory of Brownian Motion, first ed. Dover, New York, 1956.

Timofeeva, E. V., Routbort, J. L., Singh, D., (2009). Particle Shape Effects On Thermophysical Properties of Alumina Nanofluids, J. Appl. Phys. 106 (1), 014304.

Experimental Investigation of Thermal Storage Properties of Different Materials Using Solar Air Collector

İlhami ERCAN[1*], Hüsamettin BULUT[2], Yunus DEMİRTAŞ[3]

[1] *Harran University, Graduate School of Natural & Applied Sciences, Şanlıurfa, Turkey, ilhamiercan@outlook.com*
[2,] *Harran University, Mechanical Engineering Department, Şanlıurfa, Turkey*
[3] *Harran University, Mechanical Engineering Department, Şanlıurfa, Turkey*

[*]**Corresponding Author:** ilhamiercan@outlook.com

Abstract

Air conditioning systems have a high share of energy consumption in the world. Energy dependent countries such as Turkey need to develop different alternative solutions in order to reduce its energy consumption and to meet energy required for heating and cooling applications. Heat storage technologies are an important solution in terms of energy efficiency and energy sustainability. There are many different thermal storage methods, especially in solids, liquids and phase-change materials. In this study, thermal energy storage properties of Urfa stone and basalt stone were investigated experimentally under Şanlıurfa climate conditions. For this purpose, an insulated box where the stone is placed inside, an solar air collector, a fan and an experimental setup with the measuring devices have been used. Solar radiation, air inlet and outlet temperature, stone temperature and ambient temperature were measured and recorded by using a data logger. Air velocity was measured with an anemometer. The thermal energy storage potentials of the stones were determined according to the measurements recorded for different days and the time dependent temperature changes were examined. As a result of this study, it was determined that the thermal storage capacity of the basalt stone is higher than that of the Urfa stone. It has been also observed that the thermal storage potential of natural stones can be used in terms of energy efficiency in heating systems and in drying applications.

Keywords: Thermal storage, Urfa stone, basalt stone, solar air collector

1. Introduction

The use of renewable energy resources and the storage of energy have begun to gain importance due to the ever-decreasing fossil energy resources in the world and their negative effects on the environment. Energy storage is one of a solution for the problem of discontinuity and disconnection of renewable energy sources.

The energy storage is usually carried out as sensible and latent heat storage. In the sensible heat storage method, the sensible heat generated in the change of the temperature of the heat storage material is utilized. Heat storage can be done in liquid, solid, and hybrid materials with liquid and solid. The materials used in sensible heat storage are generally cheap and abundant. The latent heat is the heat that the material receives or gives during the phase change. In the latent heat storage method, Phase Change Materials (PCM), which can store energy as latent heat, are used. At the appropriate temperature limits, the latent heat generated during the phase change of the storage material can be stored. For the purpose of heat storage, materials which undergo phase changes at certain temperatures and whose latent heat values are high are used. Solid-solid and solid-liquid phase changes suitable for heat storage. Liquid-vapor phase change is not suitable for heat storage due to problems such as requiring storage of gas phase in pressure storage tanks. Storage volume of sensible thermal storage is less than that of latent thermal storage.

Due to increased energy costs and time shifts in energy usage, many studies have been carried out on energy storage ((Sharma et al. 2009, Sarbu and Sebarchievici, 2018, Pintaldi et al. 2015)

Li et al. (2018); have investigated composite phase change materials and solar collector / storage system experimentally and numerically. They simulated to investigate the performance of the hybrid system at different temperatures and flow rates. The results show that the composite PCM solar collector / storage system has good thermal storage performance and the average daily storage efficiency reaches 39.98%.

Tian and Zhao (2013); studied thermal collectors and the use of thermal energy storage in thermal applications. Different solar collectors were investigated in terms of optical optimization, reducing heat loss, heat recovery and different solar tracking mechanisms. Various thermal energy storage systems such as sensible heat storage, latent heat storage, chemical storage and cascade storage have also been investigated in the study. As a result of the work it has been stated that PVT solar collectors have the highest performance among the flat collectors and also the molten salts have excellent properties in thermal storage applications.

In another study of thermal energy storage materials and systems for solar energy applications, Alva et al. (2017); have investigated various solar energy thermal energy storage materials and

thermal energy storage systems that are currently in use. It has been stated that for the sensible and latent heat storage materials, the technology is commercialized and advanced. However, it is expressed that the thermochemical materials, which have high volumetric energy storage capacity and are expected to have great potential as thermal energy storage materials in the future, are still in the laboratory stage.

Utlu et al. (2014) investigated the availability of thermal energy storage for heating Yıldız Renewable Energy house in Yıldız Technical University Davut Paşa campus in Istanbul with solar collectors. They pointed out the necessity of thermal storage systems during the use of solar energy and ground source heat pumps for heating green buildings. Different methods used in heat storage were investigated and compared. The efficiency of the latent heat tanks which established by utilizing the latent heat of the phase-changing material has been investigated. In addition, thermodynamic analysis of a heating system operating with solar panels, a ground source heat pump and a latent heat storage using paraffin as a phase change material was performed.

Öztürk, (1999) reviewed the criteria to be considered in the selection of phase-change material (FDM) for latent heat technology and solar energy storage applications. Also discussed the effectiveness and applicability of latent heat storage systems and the problems and solutions proposed in latent heat storage systems. According to this study the latent heat storage method can be used in heat engines and power plants, industrial processes, residential air conditioning and commercial applications.

In the work done by Kozak and Kozak (2012), it is aimed to theoretically investigate energy storage and energy storage methods.

It is desirable that the energy is ready for use at the desired time and place. Energy storage is the capture of energy produced at one time for use at a later time. Energy is stored in many different forms.

In this study, thermal energy storage properties of Urfa stone and basalt stone were investigated experimentally in Şanlıurfa climate conditions. For this purpose, an insulated box where the stone is placed inside, an air solar collector, a fan and an experimental setup with the measuring devices have been used.

2. Material and Method

In this study, the thermal storage properties of Urfa stone and basalt stone in Şanlıurfa were investigated theoretically and experimentally with hot air obtained from a solar air collector. The

experimental setup used in the experimental study is shown in Figure 1 schematically. Solar radiation and temperature measurement points are given in the figure 1.

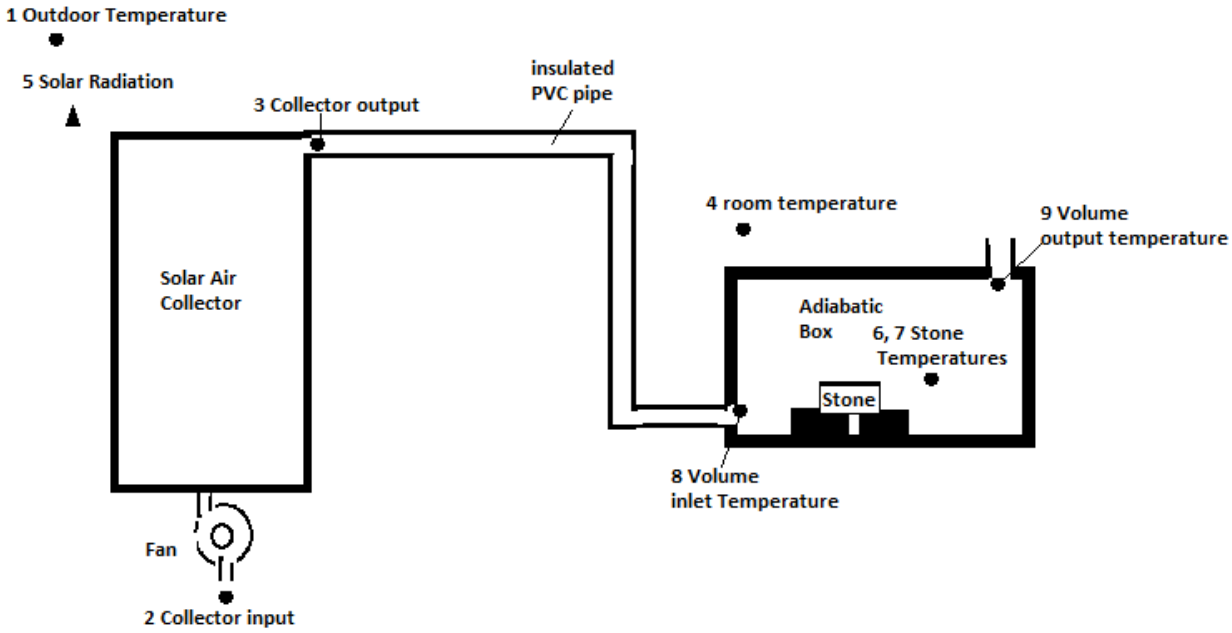

Figure 1. Experimental setup

The thermophysical properties of the natural stones of Şanlıurfa (Figure 2) used in the study are given in Table 1. Urfa stone is a natural limestone that can be easily cut and shaped and used as a building material in different applications (Turgut et al., 2008). Basalt stone is also a natural stone type that is hard and black colored from the volcanic formation of Karacadağ which is located between Diyarbakir and Şanlıurfa (Kahveci and Kadayıfçı, 2013, Günerhan 2009).

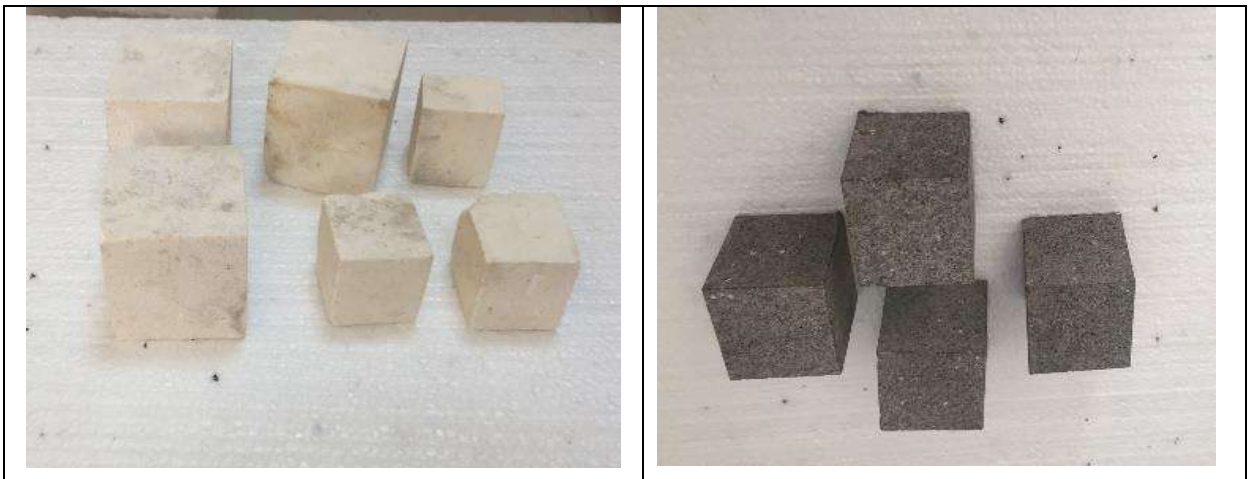

a- Urfa Stone	b- Basalt Stone

Figure 2. Natural Stones Used in the study: a- Urfa Stone, b- Basalt Stone

Table 1. Thermophysical Properties of Natural Stones (Turgut et al., 2008, Günerhan 2009.)

Material	Density (kg/m^3)	Coefficient of heat conduction W/mK)	Specific heat (J/kgK)	Coefficient of Thermal Diffusivity (10^{-6} m^2/s)	Heat Capacity (10^6 J/m^3K)
Urfa Stone	2570	1.42	1041	0.66	2.68
Basalt Stone	2800	1.513	1500	0.36	4.20

In the system established in Harran University Mechanical Engineering Department laboratory, adiabatic volume (Fig. 3-c) is shown in which the air is passed through the air solar collectors at a speed of 4 m / s (Fig.3-a). The thermal energy obtained is stored as sensible heat in natural stones. Urfa and basalt stone are cube shaped and have dimensions of 7x7x7 cm and 5x5x5 cm. 8 kg of stone was used in each experiment. Temperatures are measured by T-type thermoouples. The solar radiation coming to the surface of the solar collector is measured by a pyranometer (Figure 3-a) Temperature and radiation values are also recorded in the data-logger (Figure 3-b)

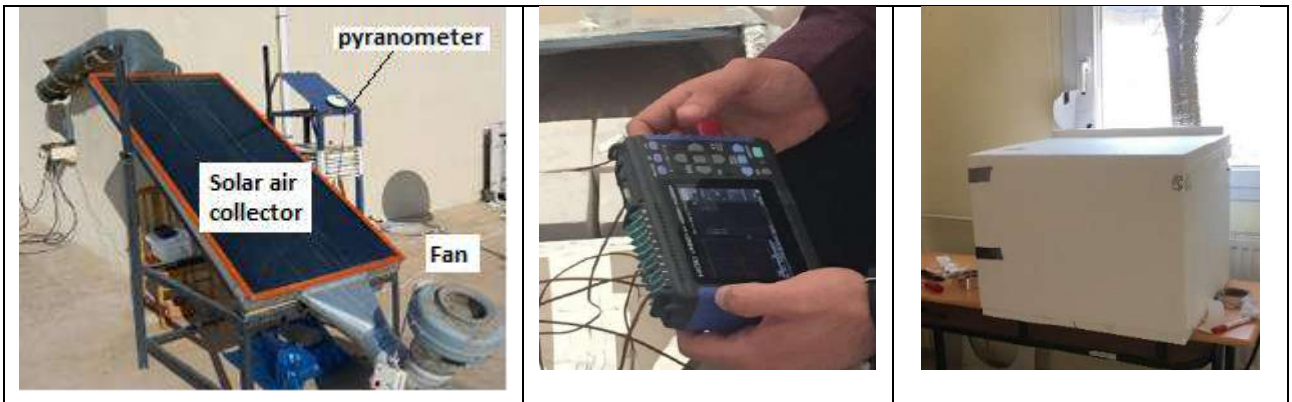

a b c

Figure 3- a: Solar Air Collector and pyranometer b: Data-logger and thermocouples c: Adiabatic Volume

3. Results and Discussions

Figure 4 shows the change in Urfa stone temperature and adiabatic volume inlet and outlet temperatures with time. It is understood that the increase of the solar radiation during the day increases the collector outlet temperature and thus the temperature of the air entering the volume and

the temperature of Urfa stone are also increased. Urfa stone temperature goes up to 42 ^{o}C. The change of adiabatic volume inlet - outlet and Urfa stone temperatures shows similarity.

The effect of solar radiation on the solar collector output temperature and hence on the volume input temperature is observed in a short time like 30 minutes and the effect on Urfa stone temperature is realized with a certain phase shift such as 1.5 hour. Urfa stone stores heat until 15:00 o'clock. After 15:00 o'clock the decrease of the solar radiation (Figure 4) decreases the temperature of the air leaving the collector and the stored heat is returned as it is lower than the temperature of Urfa stone. It is also observed that the fluctuation in the solar radiation affects the collector outlet temperature and thus the volume inlet temperature.

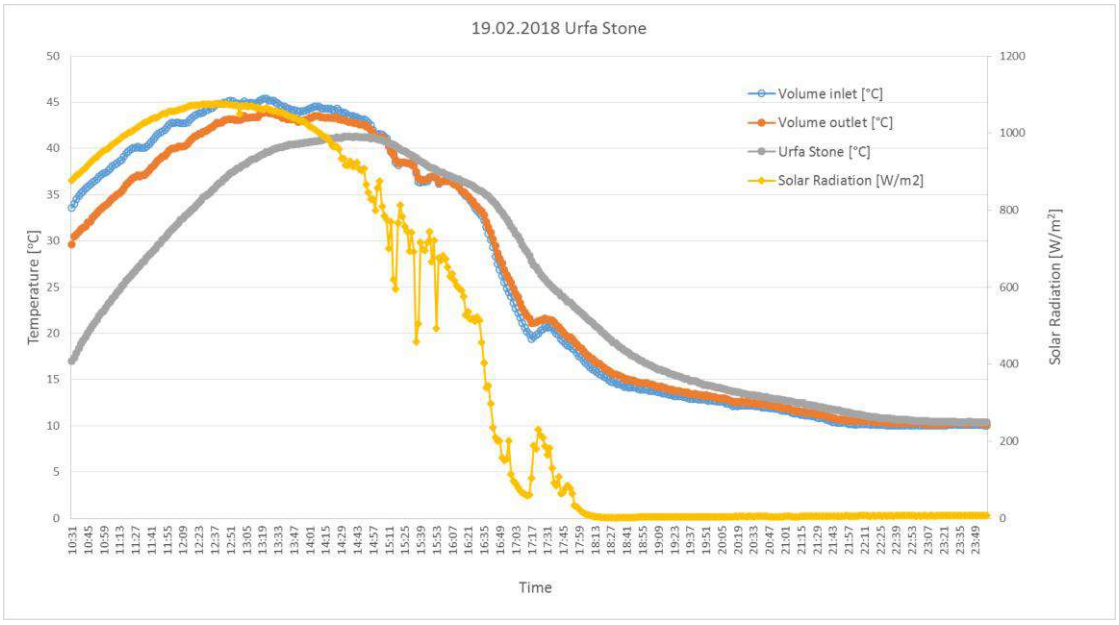

Figure 4: Urfa stone, volume inlet - outlet air temperatures and solar radiation change over time (19 February 2018)

Figures 5 and 6 show basalt stone, volume inlet - outlet temperature and solar radiation change over time for the dates of 6 and 7 February 2018. Figures show that the solar radiation and temperature show similar changes for different phase shifts. A phase shift of 30 minutes was detected at the volume inlet temperature and a phase shift of 60 minutes at the basalt stone temperature was detected. After 15:30, the basalt stone moves to the discharge position and the volume outlet temperature is higher than the inlet temperature. It is seen that the basalt stone's temperature is given to the air until late at night.

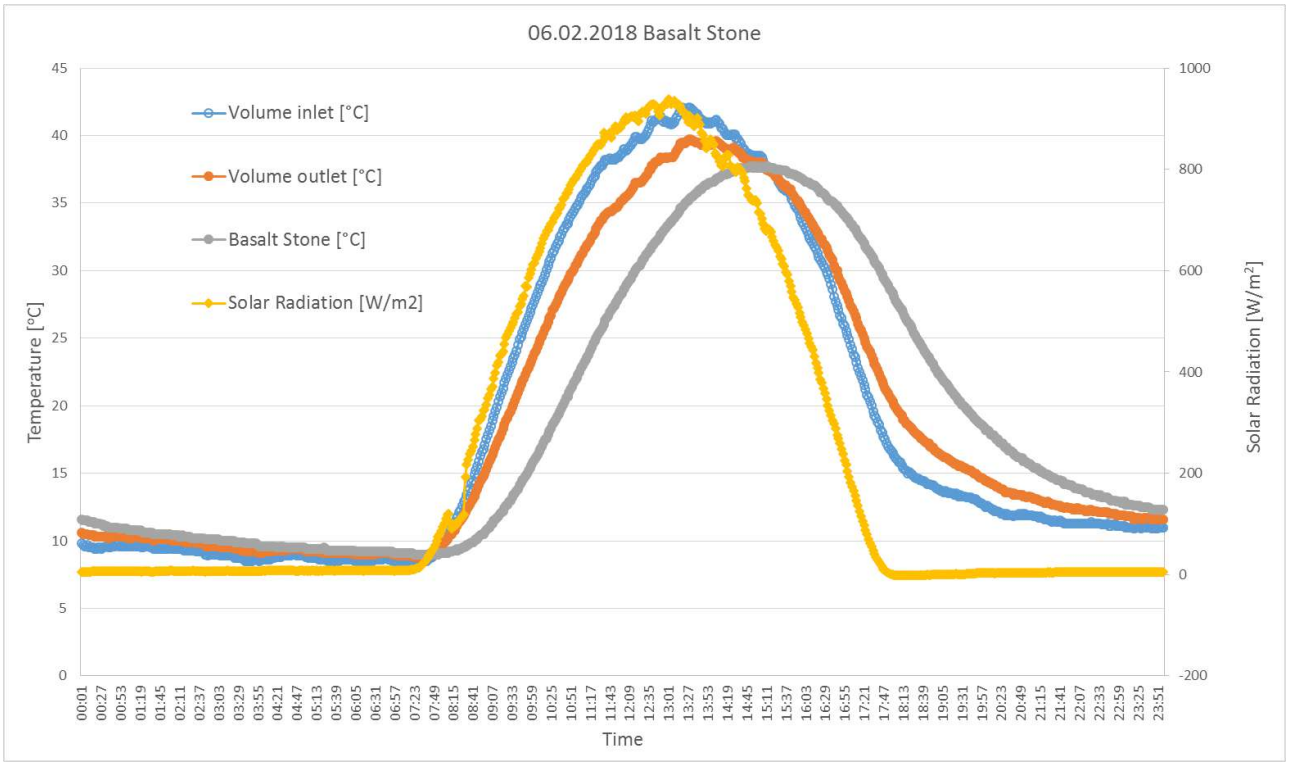

Figure 5. Basalt stone, volume inlet - outlet air temperatures and solar radiation change over time (6 February 2018)

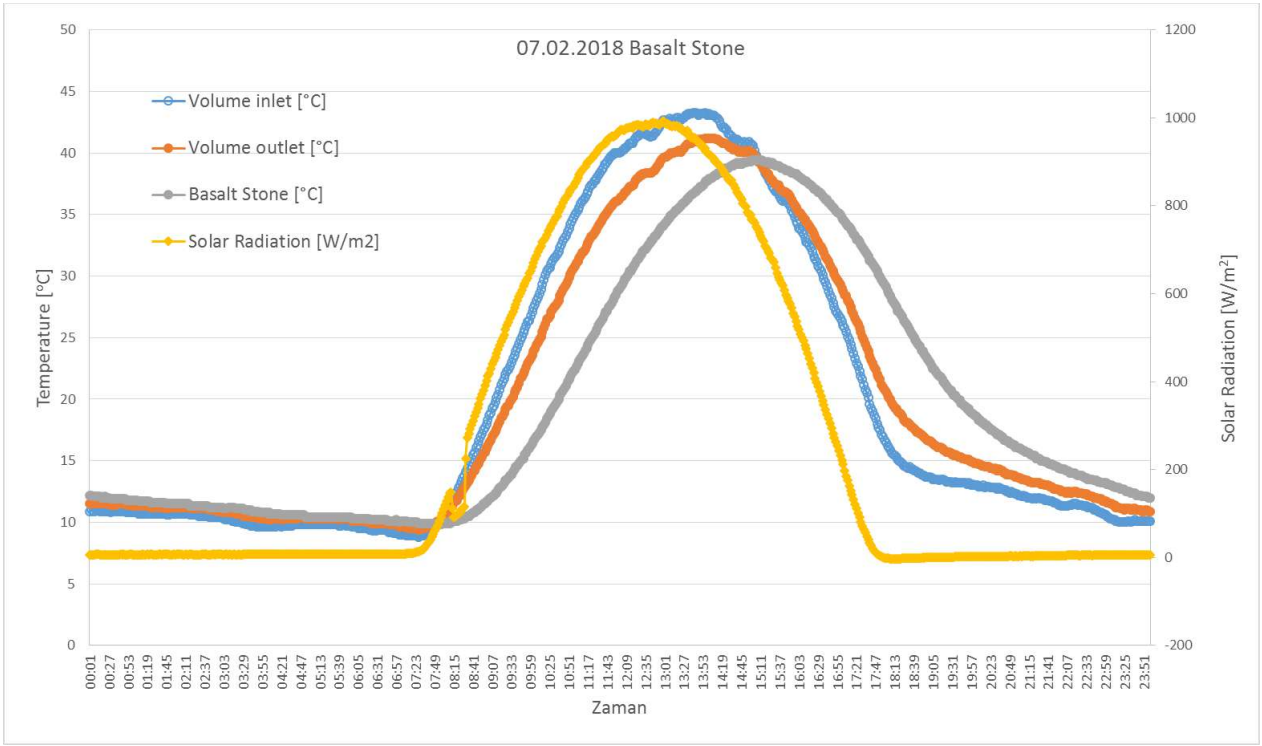

Figure 6. Basalt stone, volume inlet - outlet air temperatures and solar radiation change over time (7 February 2018)

4. Conclusions

In this study it is seen that Basalt and Urfa stone have heat storage properties and can be used as heat storage material. It has been determined that the heat storage capacity of basalt stone is higher than that of Urfa stone and also the efficiency of thermal storage is high in sunny days It was observed that the stone temperatures were up to 50°C depending on the solar radiation and the inlet temperature.

It is understood that the phase shift in the basalt stone is 30 minutes shorter than the Urfa stone. Therefore, basalt stone warms up earlier than Urfa stone. Urfa stone and basalt stone have been found to give heat until late at night and to increase the temperature of the air.

When the experimental results are evaluated, it is understood that basalt stone and Urfa stone in solar air collectors are suitable as thermal storage material. The natural basalt stone can be used as an additional energy source either directly in the heating of the place in winter conditions.

In this case, in order to obtain the most efficient performance in the heating system, it is necessary to install the automation system and good heat insulation of pipes and ducts

In summer conditions, especially solar energy drying systems, daytime heat stored in natural stones can be used as uninterrupted energy source by discharging in night hours.

References

Alva, G., Liu, L., Huang, X., Fang, G. (2017). Thermal energy storage materials and systems for solar energy applications *Renewable and Sustainable Energy Reviews*,68, 693–706

Günerhan H (2009) *Mühendis ve Makina* - Cilt: 45 Sayı: 530.

Kahveci, A.E., Kadayıfçı, A. (2013). Diyarbakır Yöresi Bazalt Taşının Yapısal Özelliklerinin İncelenmesi, *SDU International Technologic Science* , 5(3),56-69.

Kozak, M., Kozak, Ş. (2012). Enerji Depolama Yöntemleri, *SDU International Technologic Science*, 4(2), 17-29.

Li, B., Zhai, X., Cheng, X. (2018). Experimental and numerical investigation of a solar collector/storage system with composite phase change materials *Solar Energy* 164 65–76

Öztürk H.H. (1999). http://www.mmoistanbul.org/yayin/tesisat/100/2/

Sarbu, I., Sebarchievici , C. (2018). A Comprehensive Review of Thermal Energy Storage, *Sustainability*, 10, 191; doi:10.3390/su10010191.

Sergio Pintaldi, S., Perfumo,C., Sethuvenkatraman,S., White, S., Rosengarten, G. (2015). A review of thermal energy storage technologies and control approaches for solar cooling, *Renewable and Sustainable Energy Reviews*, 41, 975-995.

Sharma, A., Tyagi, V.V., Chen, C.R., Buddhi, D. (2009). Review on thermal energy storage with phase change materials and applications, *Renewable and Sustainable Energy Reviews,13,* 318–345.

Tian, Y., Zhao, C.Y. (2013). A review of solar collectors and thermal energy storage in solar thermal applications *Applied Energy,* 104,538–553

Turgut, P., Yesilnacar, M.İ., Bulut, H. (2008). Physico-thermal and mechanical properties of Sanliurfa limestone, Turkey *Bulletin of Engineering Geology and the Environment*, 67, 485–490.

Utlu Z ve Ark., 2014. *Tesisat Mühendisliği* - Sayı 144 - Kasım/Aralık 2014

Effect of Ethyl Acetate-Gasoline Blends on Energy (Thermal) Balance of an SI Engine

Abdülvahap ÇAKMAK [1*], Murat KAPUSUZ [2], Orhan GANİYYEV[3], Hakan ÖZCAN[2]

[1]Samsun University, Kavak Vocational School, Department of Motor Vehicles and Transportation Technologies, Samsun, TURKEY

[2] Ondokuz Mayıs University, Department of Mechanical Engineering, Samsun, TURKEY

[3]UBOC Oil Company, Baku, AZERBAIJAN

[*] **Corresponding Author:** a.cakmak.tr@gmail.com

Abstract

In this present study, the effect of ethyl acetate as oxygenated fuel additive on thermal balance of an SI engine was performed by evaluating experimental data. Experiments were conducted at 311 kPa brake mean effective pressure and seven different engine speed with three test fuels; unleaded gasoline, E5 and E10. Fuel power, brake power, exhaust power, engine cooling power and other total uncounted power were calculated. The results show that there is no obvious effect of E5 and E10 on thermal balance of the SI engine. However, for some brake effective power output E5 and E10 test fuels increase the fuel input power. This results in increase brake specific fuel consumption and a decrease in effective efficiency.

Keywords: Energy Analysis, Thermal Balance, SI Engine, Ethyl Acetate

1. Introduction

More than half of world's energy is consumed in gasoline and diesel engines used in transportation (Shafiee and Topal, 2009). The use of alternative fuels is inevitable due to the limited availability of fossil energy sources, the continuous increase in oil prices and environmental concerns. (Yusri et al., 2016). However, as much as the use of alternative fuels is a substantial matter, evaluation of fuels with maximum efficiencies in current internal combustion engines is an important issue.

Internal combustion engines are machines that convert heat energy resulting from combustion of different fuels in cylinders into mechanical energy (Safgönül et al., 2013). In this energy conversion process, 25-45% fuel energy is converted to effective power, while the remaining energy is dissipated by exhaust gas, engine coolant, frictions and engine auxiliaries (Heywood, 1988). To increase the power output and reducing fuel consumption of any engine it is necessary to minimize the heat losses or frictions. Thanks to thermal analysis it can be determined the heat losses rates with respect to engine operating condition and fuel used. The thermal efficiency of the engine can be increased by converting some of the heat energy dissipated by exhaust gases and engine coolant system into effective power (Li et al., 2016). However, the amount of energy that can be transformed into effective work is less (Heywood, 1988). Nevertheless, in order to increase the engine efficiency, many researches have been done many researches on low heat rejection engines since the last three decades. (Li et al., 2016).

NOx emissions emitted from the internal combustion engine can be controlled by water injection in the suction air or direct water injection in cylinders (Pulkrabek, 1997). This emission control technique is adapted to different engines and investigated by many researchers. Ozcan and Soylemez (2006) experimentally investigated the effect of water injection on thermal balance of an LPG fuelled SI engine. It was determined that when water injection rate was equal to half of fuel flow rate, the thermal efficiency of the engine increased by 2.7%. An experimental investigation of butanol as an alternative fuel was conducted by Yusri et. al. (2016). Experiments were performed on four cylinders, four-stroke spark ignition engine using 2-butanol- gasoline fuel blends at the half throttle opening position. The results showed that blends of 2-butanol of 10% and 15 % by volume base in gasoline, resulted in an increase in engine thermal efficiency and exhaust heat loses. When thermal analysis of a diesel engine fuelled with ethanol-diesel fuel blends was carried out, it was determined that blended fuels decreased heat losses and increased effective power (Ajav et al., 2000). The effect of adding hydrogen to the gasoline-air mixture on a spark ignition engine studied by Yüksel and Ceviz, 2003. Their results showed that addition of hydrogen to gasoline reduced heat loss to engine cooling system and uncounted losses, while heat loss by exhaust gas did not change significantly.

The performance and thermal balance of a turbocharged SI engine operating on natural gas have been studied by Gharehghani et. al. (2013). According to results of the study it was determined that using natural gas as a fuel in turbocharged engine led to 4.5% higher thermal efficiency than gasoline.

To reduce harmful exhaust emissions emitted from the spark ignition engines, enhance the octane rating of the fuel and usage of renewable fuel, many different oxygenated additives such as ethanol, methanol, butanol, ethyl tert-butyl ether (ETBE), methyl tert-butyl ether (MTBE) are added to base gasoline. However, alcohols and ethers are not problem free oxygenated fuels. Alcohol-gasoline blended fuels may take place phase stability problem especially at low temperature. The blending of alcohols with gasoline increases the Reid vapor pressure of the mixed fuel (Da Silva et al., 2005). Moreover, the production cost of ethers is high and they are high miscibility in water. Therefore, the search for renewable fuel have been attached more attention.

For the reasons mentioned above, ethyl acetate could be considered as alternative renewable oxygenated fuel. Ethyl acetate has some important superiors over alcohols and ethers such as low Reid vapor pressure, high octane rating and good phase stability (Dabbagh et al., 2013).

Although there are many studies in existing literature that investigate the effect of different alternative fuel on thermal balance on an SI engine (Ajav et al., 2000; Yusri et al., 2016; Modi and Gosai, 2010; Yüksel and Ceviz, 2003; Abedin et al., 2014; Ciniviz, 2010), to the best author's knowledge there is not any study on concerning the investigation of the effect of ethyl acetate on SI engine's thermal balance. Therefore the purpose of this experimental and computational study is to scrutinize thermal balance of four-stroke spark ignition engine operating on ethyl acetate-gasoline blends.

2. Material and Method

For this study, commercial unleaded gasoline was used as reference fuel and purchased from a local petrol station. Ethyl acetate was obtained in 99.5% purity from TEKKİM, a local chemical company. Firstly, unleaded gasoline (G) was blended with ethyl acetate in a ratio of 5% by volume and 10% was named E5 and E10. Secondly, the lower heating value and density of the E5 and E10 fuels were measured in our laboratory by following the ASTM D 240 and ASTM D 4052 standards, respectively. The measured fuel properties were listed in Table 1.

Experiments were performed on a four-stroke, water-cooled and unmodified spark ignition engine was operated with unleaded gasoline, E5, and E10. The detailed characterization of the test engine and the measurement system are listed in Table 2. The schematic view of the experimental setup is given in Figure 1. The water-cooled Eddy current dynamometer was used to load the engine.

Engine experiments were conducted at 75% load (314 kPa Brake Mean Effective Pressure) and 1200-1800 rpm with an increment of 100 rpm. In these test conditions, throttle valve position was fixed to obtain the same brake power for each test fuel use. All tests were performed under constant spark timing (10 CA bTDC) and compression ratio (8:1). During the experiments, all data were taken after steady-state conditions were reached and all measurements were repeated at least three times at each test point and the average values were used to minimize the systematic error. The calculated uncertainties in this study were determined and the results were listed in Table 3.

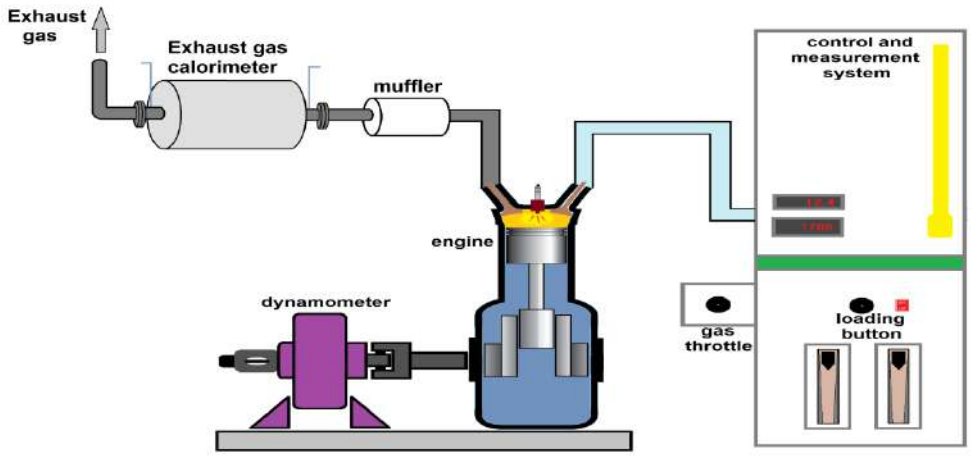

Figure 1. Experimental setup.

Table 1. Measured fuel properties.

Property	Gasoline	E5	E10
Density (kg/m^3) @ 20℃	723	732	741
Lower Heating Value (kJ/kg)	43000*	41911	40848
Energy Density (kJ/L)	31089	30679	30268

*From the literature (Pulkraberk,1997)

Table 2. Technical characteristics of the experimental system.

Type	Single cylinder, water cooled, four stroke
Dimensions: bore /stroke, mm	87.5/ 110
Compression ratio	8, CR variation: 6:1-10:1
Cylinder volume, cm^3	661
Maximum brake power	4.5 kW @ 1800 rpm
Spark timing	10 CA bTDC, Spark variation: 0-70 CA bTDC
Dynamometer	Type: Eddy current, water cooled, with a loading unit
Speed, rpm	1500 rpm, Speed range: 1200-1800 rpm

Air flow transmitter	Pressure Transmitter, Range (-) 250 mm WC
Fuel flow transmitter	DP transmitter, Range 0-500 mm WC
Piezo sensor	PCB Piezotronics; Combustion: Range 350Bar

Table 3. Calculated uncertainties.

Calculated Parameter	Uncertainties (%)
Brake Power	±0,61
Brake Specific Fuel Consumption	±1,52
Thermal Efficiency	±0,66
Fuel Energy Rate	±0,25
Heat Loss Rate by Cooling System	±1,99
Heat Loss Rate by Exhaust Gas	±2,09
Uncounted Energy Rate	±2,87

3. Thermal Balance of the SI Engine

As shown in Figure 2 the engine was considered as an open thermodynamic system. At steady-state operating conditions fuel enters in control volume while effective power, heat loss to the cooling system, uncounted heat loss and exhaust gases leave the control volume at a constant rate. The kinetic energies of incoming and outgoing gases into the control volume and the enthalpy of air entering the cylinder are neglected in the calculations. As illustrated in the figure, only the fuel energy enters selected volume and the fuel energy is assumed to be converted to heat energy with complete combustion.

The general energy balance for control volume can be presented as follow (Cengel, 2015):

$$\sum_{in} \dot{E} - \sum_{out} \dot{E} = dE_{system} \Big/ dt = \underbrace{0}_{\text{steady state}} \quad (1)$$

and open form of equation (1) can be obtained by substituting energy components in Eq.(1):

$$\dot{E}_f = BP + \dot{Q}_{exh} + \dot{Q}_{col\_w} + \dot{Q}_{unc} \quad (kW) \quad (2)$$

where $\dot{E}_f$ is fuel power, BP is effective engine power, $\dot{Q}_{exh}$ is exhaust power, $\dot{Q}_{col\_w}$ is engine cooling power and $\dot{Q}_{unc}$ is uncounted heat power, in unit of kW.

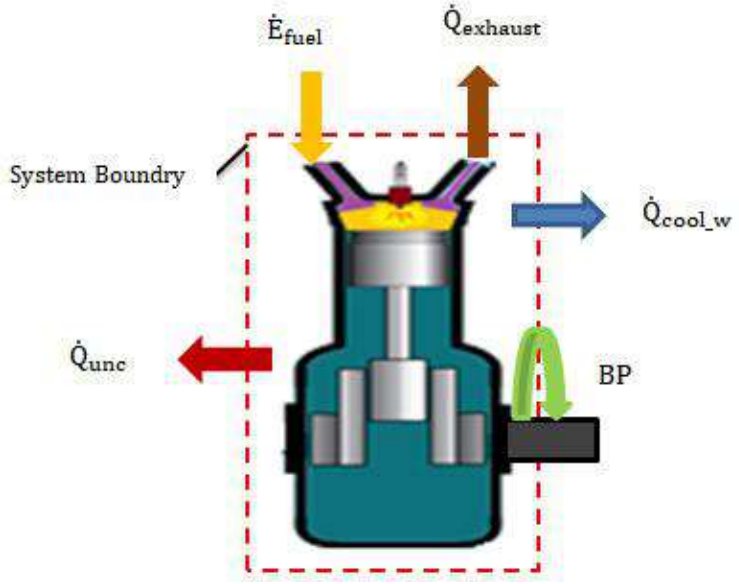

Figure 2. The test engine as an open thermodynamic system.

The fuel power is calculated by below equation:

$$\dot{E}_f = \dot{m}_f \cdot LHV_f \quad (kW) \tag{3}$$

where, LHV_f (kJ/kg) is the lower heating value and $\dot{m}_f$ (kg/s) is the mass flow rate of the fuel, respectively. Effective engine power is determined by Eq. (4).

$$BP = \frac{2 \cdot \pi \cdot n \cdot T}{60000} \quad (kW) \tag{4}$$

where n (rpm) is engine speed and T (Nm) is the engine torque output. The heat loss per unit time by the exhaust gas is determined as below (Çakmak and Bilgin, 2017):

$$\dot{Q}_{exh} = \dot{m}_{c\_w} \cdot c_w \cdot \frac{(T_{c\_w\_out} - T_{c\_w\_in})}{(T_{exh\_in} - T_{exh\_out})} \cdot (T_{exh\_in} - T_{env}) \quad (kW) \tag{5}$$

where, $\dot{m}_{c\_w}$ (kg/s) and c_w $(kJ/kg/K)$ are mass flow rate and specific heat of the cooling water, respectively. $T_{c\_w\_out}$ (°C) and $T_{c\_w_{in}}$ (°C) denote exhaust calorimeter water output and input temperature, respectively. T_{exh_in} (°C) and T_{exh_out} (°C) are the calorimeter input and output temperature of the exhaust gas and T_{env} (°C) is the environment temperature. The heat transfer from the cylinder wall to engine coolant per unit time (engine cooling power) was calculated Eq. (6).

$$\dot{Q}_{col\_w} = \dot{m}_{cw\_e} \cdot c_w \cdot (T_{out} - T_{in}) \ (kW) \tag{6}$$

where $\dot{m}_{cw\_e}$ is engine coolant mass flow rate (kg/s), c_w is the specific heat of the cooling water, T_{out} (°C) and T_{in} (°C) are the engine coolant output and input temperature, respectively.

The uncounted heat losses per unit time (uncounted heat loss power) are obtained as follows:

$$\dot{Q}_{unc} = \dot{E}_f - BP - \dot{Q}_{exh} - \dot{Q}_{col\_w} \quad (kW) \tag{7}$$

Uncounted heat losses consist of the heat rejected to engine lubricant oil and heat transfer by radiation from the engine's surface (Pulkrabek, 1997; Özcan and Söylemez, 2006). Brake thermal efficiency and brake specific fuel consumption of the test engine calculated by Equation (8) and (9), respectively.

$$\eta_{th} = \frac{BP}{\dot{E}_f} \cdot 100 \quad (\%) \tag{8}$$

$$BSFC = \frac{\dot{m}_f}{BP} \cdot 3600 \quad (kg/kWh) \tag{9}$$

4. Results and Discussions

In internal combustion engines, roughly 25-40% of the fuel energy entering the cylinder is converted into effective engine power, 25-45% is discharged from the cylinder by exhaust gases, 10-30% is transferred to engine cooling system and 10-35% is transformed other uncounted energy (Pulkrabek, 1997).

Figure 2 shows the of fuel energy (fuel power) to produce the same brake power for all test fuels. As seen in the figure, in the case of E5 and E10 use fuel power increased due to higher density and lower heating value of the fuel blends relative to gasoline. It was determined that E5 and E10 caused an average increase in fuel power by 2.62% and 4.61% compared to gasoline, respectively. This resulted a reduction in brake thermal efficiency in case of fuel blends operation. Also, it can note that fuel power increased with the increase the engine speed at constant engine load due to more fuel entering the cylinder, as expected.

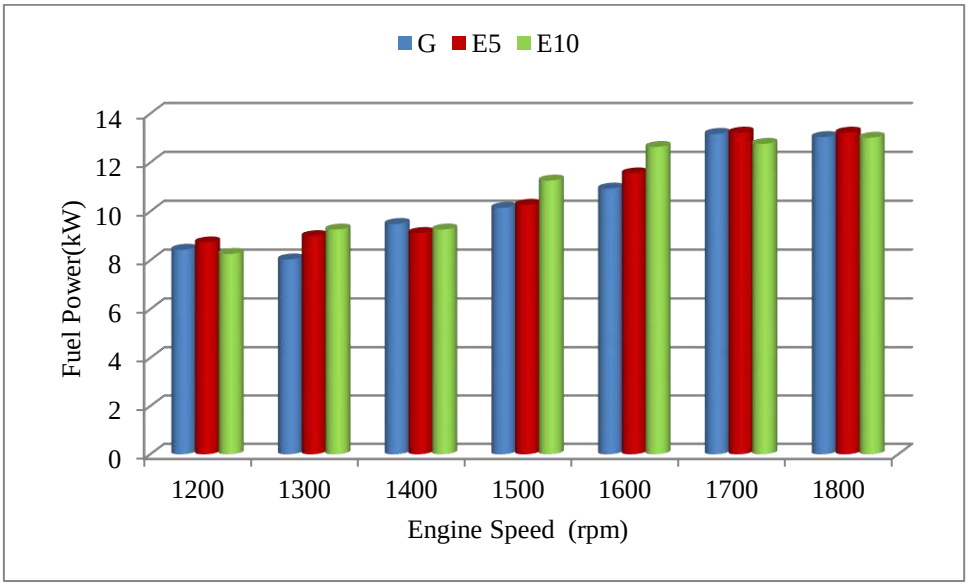

Figure 2. Fuel power as a function of test fuels and engine speed.

Figure 3 indicate the ratios of each power component to fuel power for gasoline operation. It can be seen from the figure that exhaust power changed linearly with engine speed. As increasing engine speed, fuel energy that entered cylinder increased and hence high exhaust temperature occurred. The high exhaust temperature led to more heat loss in the exhaust flow (Duan et al., 2017). However, since the engine speed is low (1200-1800 rpm) exhaust power was the lowest power components. About 20% of the fuel energy was carried away from the cylinder by exhaust gas. Besides, it is clearly that brake power and cooling power were presented similar changes. But cooling power ratio was higher than the effective power ratio at all engine speed. At high engine loads, coolant power can amount to about half of the brake power while it can increase to about twice the brake power at low load (Pulkrabek, 1997). It was determined that 28% of fuel energy was converted to brake power and about 37% of the fuel energy was carried away by engine coolant. The reason for this was the fact that at low engine speeds the heat transfer increased due to a longer duration for engine cycle (Heywood, 1988; Pulkrabek, 1997). Overall, it calculated that only 23-28% of fuel energy was converted to effective engine power, 27-37% of fuel energy dissipated to engine coolant system, 10-17% of fuel energy is carried away by exhaust gas and the 23-35% of fuel energy was lost in uncounted losses such as friction losses and heat transfer by radiation. It can be seen from the Figure 4 and Figure 5 similar power ratios were obtained for the E5 and E10 operation therefore no further explanation was made.

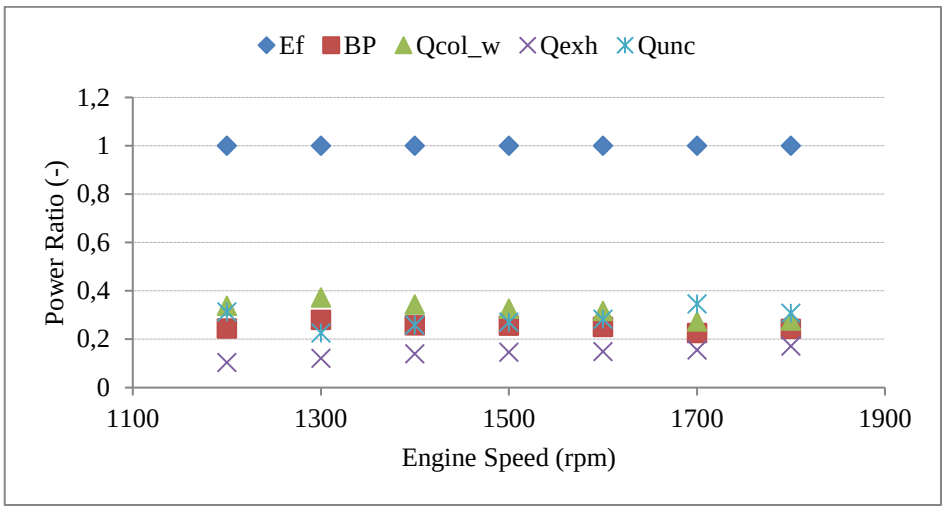

Figure 3. Power ratios for gasoline operation.

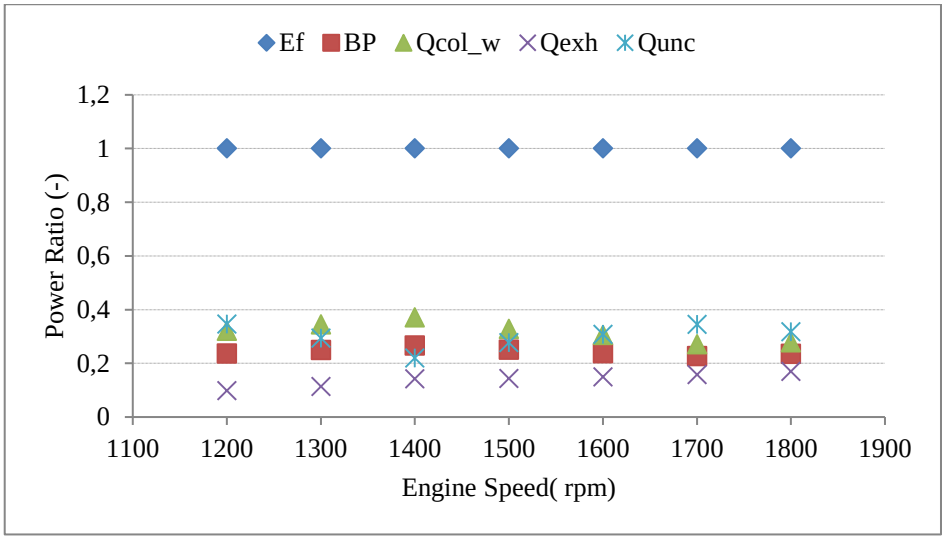

Figure 4. Power ratios for E5 operation.

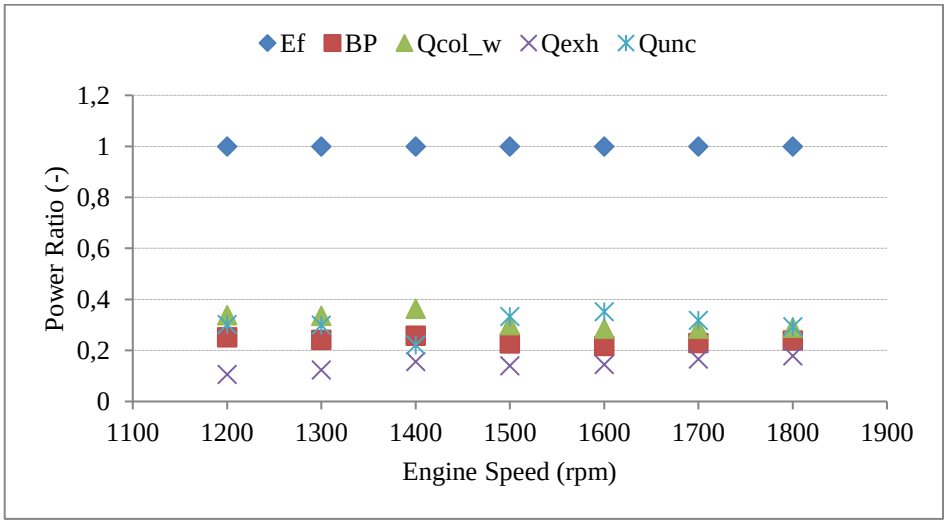

Figure 5. Power ratios for E10 operation.

Figure 6 shows brake specific fuel consumption (BSFC) for the test fuels at 1500 rpm. It was clearly that E5 and E10 increased the BSFC due to lower heating value and higher density of ethyl acetate compared to gasoline. E5 and E10 led to 5% and 18% higher BSFC than that of gasoline, respectively. This also caused a decrease in brake thermal efficiency. Brake thermal efficiency for G, E5 and E10 operation was determined as 25.7%, 25.1% and 22.8%, respectively.

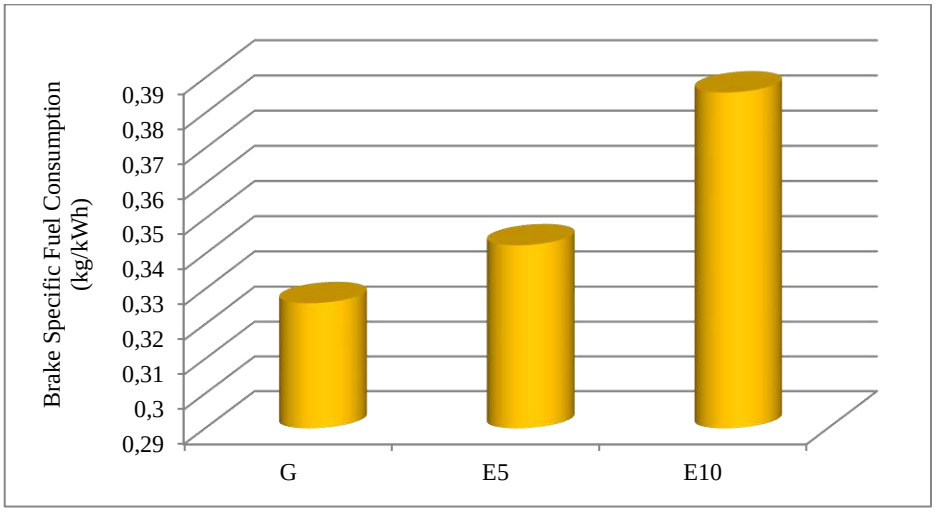

Figure 6. BSFC values for test fuels at 1500 rpm.

5. Conclusions

This study present a thermal balance on a SI engine fuelled with base gasoline, E5 and E10. Ethyl acetate as a potential oxygenated fuel investigated in the test engine by performing energy analysis where in the main results showed that ethyl acetate increased fuel consumption while reduced the brake thermal efficiency. Additionally, it was determined that no significant differences found for heat losses between test fuels.

References

Abedin, M. J., Masjuki, H. H., Kalam, M. A., Sanjid, A., Rahman, S. A., Fattah, I. R. (2014). Performance, emissions, and heat losses of palm and jatropha biodiesel blends in a diesel engine. Industrial crops and products, 59, pp. 96-104.

Ajav, E. A., Singh, B., Bhattacharya, T. K. (2000). Thermal balance of a single cylinder diesel engine operating on alternative fuels. Energy conversion and management, 41(14), 1533-1541.

Çakmak, A., Bilgin, A. (2017). Bir dizel motorda mısır yağı biyodizeli kullanımının termodinamik analizi. Gazi Üniversitesi Fen Bilimleri Dergisi Part C: Tasarım ve Teknoloji, 5(2), pp. 87-97.

Çengel, Y. A. (2015). Termodinamik: mühendislik yaklaşımıyla, Palme Yayıncılık.

Ciniviz, M. (2010). Performance and energy balance of a low heat rejection diesel engine operated with diesel fuel and ethanol blend. Transactions of the Canadian Society for Mechanical Engineering, 34(1), 93.

Dabbagh, H. A., Ghobadi, F., Ehsani, M. R., Moradmand, M. (2013). The influence of ester additives on the properties of gasoline. Fuel, 104, pp.216-223.

Da Silva, R., Cataluna, R., de Menezes, E. W., Samios, D., & Piatnicki, C. M. S. (2005). Effect of additives on the antiknock properties and Reid vapor pressure of gasoline. Fuel, 84(7-8), 951-959.

Duan, X., Fu, J., Zhang, Z., Liu, J., Zhao, D., Zhu, G. (2017). Experimental study on the energy flow of a gasoline-powered vehicle under the NEDC of cold starting. Applied Thermal Engineering, 115, pp. 1173-1186.

Gharehghani, A., Koochak, M., Mirsalim, M., Yusaf, T. (2013). Experimental investigation of thermal balance of a turbocharged SI engine operating on natural gas. Applied Thermal Engineering, 60(1-2), pp. 200-207.

Heywood, J. B. (1988). Internal combustion engine fundamentals.

Holman, J. P., Gajda, W. J. (2001). Experimental methods for engineers. (Vol. 2), New York: McGraw-Hill.

Li, T., Caton, J. A., Jacobs, T. J. (2016). Energy distributions in a diesel engine using low heat rejection (LHR) concepts. Energy conversion and Management, 130, pp.14-24.

Modi, A. J., Gosai, D. C. (2010). Experimental study on thermal barrier coated diesel engine performance with blends of diesel and palm biodiesel. SAE International Journal of Fuels and Lubricants, 3(2010-01-1519), pp. 246-259.

Özcan, H., Söylemez, M. S. (2006). Thermal balance of a LPG fuelled, four stroke SI engine with water addition. Energy conversion and management, 47(5), pp. 570-581.

Pulkrabek, W. W. (1997). Engineering fundamentals of the internal combustion engine (No. 621.43 P8).

Safgönül, B., Ergeneman, M., Arslan, H. E., Soruşbay, C. (2013). İçten yanmalı motorlar, Birsen Yayınevi.

Shafiee, S., Topal, E. (2009). When will fossil fuel reserves be diminished?. Energy policy, 37(1), pp. 181-189.

Yüksel, F., Ceviz, M. A. (2003). Thermal balance of a four stroke SI engine operating on hydrogen as a supplementary fuel. Energy, *28*(11), pp.1069-1080.

Yusri, I. M., Mamat, R., Azmi, W. H., Najafi, G., Sidik, N. A. C., Awad, O. I. (2016). Experimental investigation of combustion, emissions and thermal balance of secondary butyl alcohol-gasoline blends in a spark ignition engine. Energy Conversion and Management, 123, pp.1-14.

Experimental Research on Emissions of an SI Engine Under Oxygen-Enriched Intake Air

Abdülvahap ÇAKMAK [1*], Murat KAPUSUZ [2], Hakan ÖZCAN[2]

[1]Samsun University, Kavak Vocational School, Department of Motor Vehicles and Transportation Technologies, Samsun, TURKEY

[2] Ondokuz Mayıs University, Department of Mechanical Engineering, Samsun, TURKEY

[*]**Corresponding Author:** a.cakmak.tr@gmail.com

Abstract

Internal combustion engines are the major contributor to local and global air pollution. The main pollutants emitted from the internal combustion engines are hydrocarbons (HC), carbon monoxide (CO), carbon dioxide (CO_2), nitrogen oxides (NOx) and particulate matters (PM). Each of these emissions has a significant impact on human health and environment that is why stringent emissions regulations have enacted over the world. With the present emissions reduction technologies it is not possible to meet future emissions regulations. Therefore, search for emissions control techniques still dominate concern research area of the engineers and scientists. The current experimental study focuses on emissions analysis of a Spark Ignition engine with oxygen-enriched intake air as pre-combustion emissions control technique. Experiments are performed on a test unit at different engine speeds and full load for 21% v/v (standard condition), 24% v/v and %27 v/v oxygen concentrations. The results showed that the oxygen-enrichment technique has established a promising way of reducing CO and HC emissions. However, NOx emissions increased dramatically. From this point of view it can be concluded that oxygen-enrichment air technique is not suitable emission reduction method alone. It is necessary to use NOx control devices with that pre-combustion emissions reduction technique

Keywords: SI Engine, Emissions, Oxygen-Enriched Air, Air Pollution

1. Introduction

Air pollution is a global problem and has many harmful effects on human health. Internal combustion engines are a significant source of air pollution. Air pollution from internal combustion engine can be classified as primary and secondary pollution. Primary pollution is emitted directly atmosphere and secondary emissions are generated in the atmosphere by chemical reactions (URL 1). All pollutant has many adverse effects on human boy and environment. Therefore reducing emissions that come from internal combustion engines is an important step to improve air quality. Today, emissions reduction from engines is achieved by use of some engine technology, fuel formulation and exhaust treatment devices. However, the introduction of more stringent emissions standards requires further improvements in reducing emissions. Therefore, extensive studies have been performed on emissions from internal combustion engines. In general the studies existing in literature focuses on engine operating system and fuel technologies to reduce exhaust emissions (Behçet et al. 2015; Clenci et al. 2014; Hu et al. 2009; Maiboom, Tauzia, and Hétet 2008; Nabi, Akhter, and Shahadat 2006). Moreover, the effect of oxygen enriching of intake air on emissions mostly has been studied for diesel engines (Abdelaal, Rabee, and Hegab 2013; Assanis et al. 1990; Baskar and Senthil Kumar 2017; Baskar and Senthilkumar 2016; Li et al. 2013; Liang et al. 2013; Rajkumar et al. 2010; Sekar et al. 1990; Seong and Boehman 2011; Song et al. 2004; Zannis et al. 2007; Zhang, Chen, Li, et al. 2013; Zhang, Chen, Shen, et al. 2013). Zhang et al. (2013) performed an experimental study on a turbocharged direct injection diesel engine by using oxygen enriched air and EGR techniques for producing lower smoke and NOx emissions. They concluded that the optimal NO-smoke emissions achieved at engine operating condition: 1600rpm, full engine load, 30-40% EGR rate, 21.5-22.5% oxygen concentration; at 2200 rpm 20-45% EGR rate and 22-24% oxygen levels. Baskar and Senthilkumar (2016) conducted an experimental test on a single cylinder diesel engine to investigate the effect oxygen enrichment emissions and performance parameters by increasing oxygen levels from 21% to 27%. Their result showed that combustion process and engine performance was improved. CO, HC and smoke emissions substantially decreased by 55%, 40% and 60%, respectively. A few of the studies existing in the literature focus on the effect of oxygen enriching of intake air on emissions of an SI engine. Porpatham et al. (2018) conducted an experimental study on biogas fueled SI engine's performance, emissions and combustion characteristics under the influence of 21%, 22% and 23% oxygen levels. They found that a significant improvement in brake thermal efficiency and brake power under oxygen enriched conditions. However, at higher oxygen levels NOx emissions increased while HC and CO emissions decreased.

From the literature survey, it is evident that there is a need to further investigate the effect of oxygen enriching of intake air on emissions of an SI engine. In order to contribute to filling in this knowledge gap, the present experimental study aims to investigate the effects of oxygen-enrichment intake air as pre-combustion emissions control technique on the main exhaust emission of SI engine.

2. Material and Method

In this experimental study the unleaded commercial gasoline (95 octane) was purchased from a local petrol station and was used. A schematic view of the experimental setup is shown in Figure 1. As seen in Figure 1, the experimental setup consisting of an SI engine, eddy current dynamometer, control and measurement unit, air compressor, oxygen generator, oxygen storage tank, oxygen monitoring device and exhaust gas analyzer. The test engine is a single cylinder, four-stroke and water-cooled SI engine. Detailed specification of engine and measurement system is shown in Table 1. Experiments were performed with a various engine speed of 1200 rpm, 1400 rpm, 1600 rpm and 1800 rpm at full load. In experiments oxygen concentration of intake air was fixed at 21%, 24% and 27% in order to investigate the changes in exhaust emissions. An oxygen generator was used to increase the oxygen concentration of the intake air. As shown in Figure 1, the room air was pressurized at the 6-7 bar by an air compressor and supplied to the oxygen generator. Then, oxygen and nitrogen are separated from the air by the oxygen generator which working principle based on a continuous cycle of pressurization adsorption and depressurization desorption. The oxygen with 40-50 % purity was stored in the oxygen tank. Any desired oxygen concentration of intake air was obtained by adjusting the oxygen flow rate via a mechanical valve while continuously monitoring oxygen concentration by oxygen measurement device. Measurements of CO, HC, CO_2 and NOx emissions were made using an YT 5003 model exhaust gas analyzer of KTEST. Exhaust emissions were measures as raw emissions that are without using any aftertreatment device like a three-way catalyst. Technical specifications such as measurement ranges and accuracy of the exhaust gas analyzer are given in Table 2. All tests were performed at steady state conditions and all measurements were repeated ten times at each test point and the average values were used to minimize the systematic error.

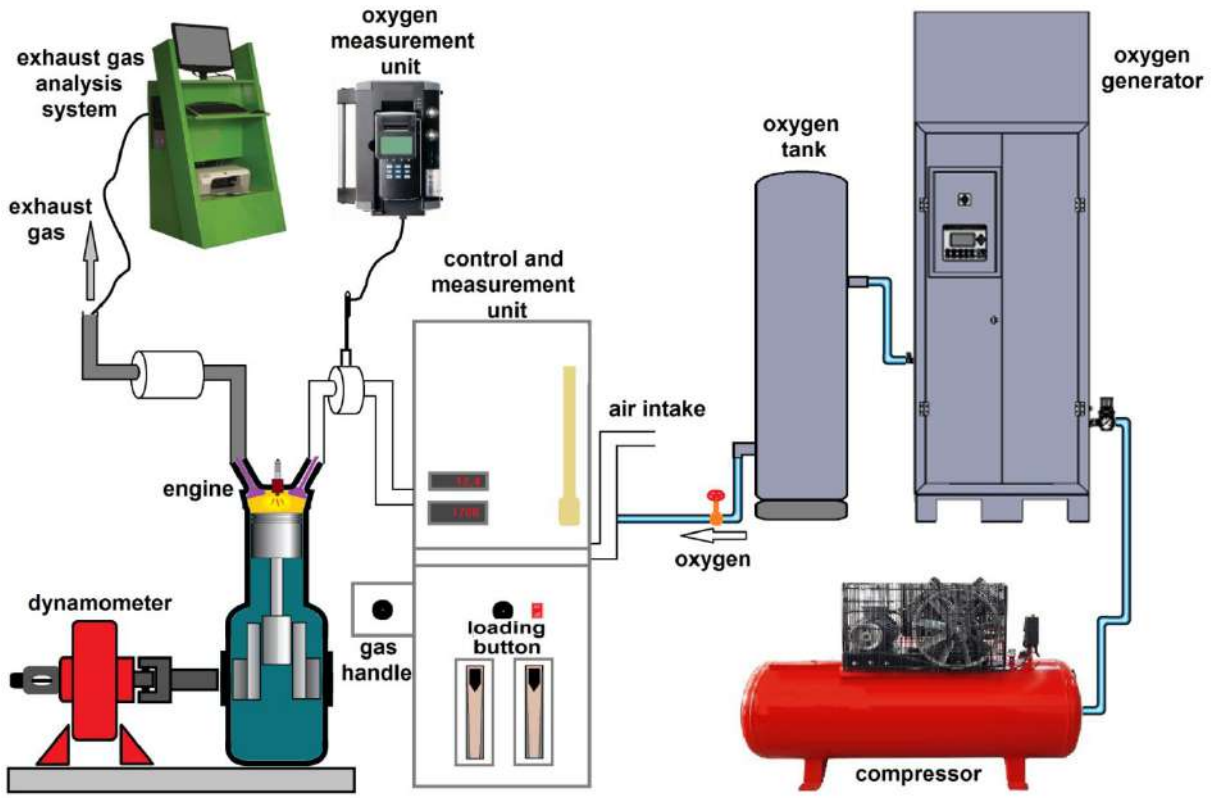

Figure 1. Schematic view of the experimental setup

Table 1. Detailed specification of engine and measurement system

Type	Single cylinder, water cooled, four stroke
Dimensions: bore /stroke, mm	87.5/ 110
Compression ratio	8, CR variation: 6:1-10:1
Cylinder volume, cm^3	661
Maximum brake power	4.5 kW @ 1800 rpm
Spark timing	10 CA bTDC, Spark variation: 0-70 CA bTDC
Dynamometer	Type: Eddy current, water cooled, with a loading unit
Speed, rpm	1500 rpm, Speed range: 1200-1800 rpm
Air-flow transmitter	Pressure Transmitter, Range (-) 250 mm WC
Fuel flow transmitter	DP transmitter, Range 0-500 mm WC

Table 2. Measurement ranges and accuracy of the exhaust gas analyzer

Emissions	Measuring Range	Accuracy
CO	0-10 % vol.	±3%
CO_2	0-20 % vol.	±3%
HC	0-5000 ppm	±25 ppm
NOx	0-4000 ppm	±8 ppm

6. Results and Discussions

In this section changes in emissions; CO, HC, CO_2 and NOx under oxygen enrichment conditions were compared and discussed in detail with the standard condition. Figure 2 presents the effects of oxygen concentrations on CO emissions. The main cause of CO formation in an internal combustion engine is incomplete combustion due to a rich mixture, poor air-fuel mixing and less combustion time (Pulkrabek, 2014). As seen in Figure 1 CO emissions increased with increasing engine speed at full engine load for all oxygen concentrations. This is an expected result since completeness of the combustion decreased due to the rich mixture and shorter combustion duration at high engine speeds. However, by increasing oxygen concentrations CO emissions decreased since the engine operated overall lean mixture and resulted in low CO emissions. As a result, CO emissions decreased averagely by 44.1% and 92.6% for 24% and 27% oxygen concentration, respectively, compared to 21% oxygen concentration.

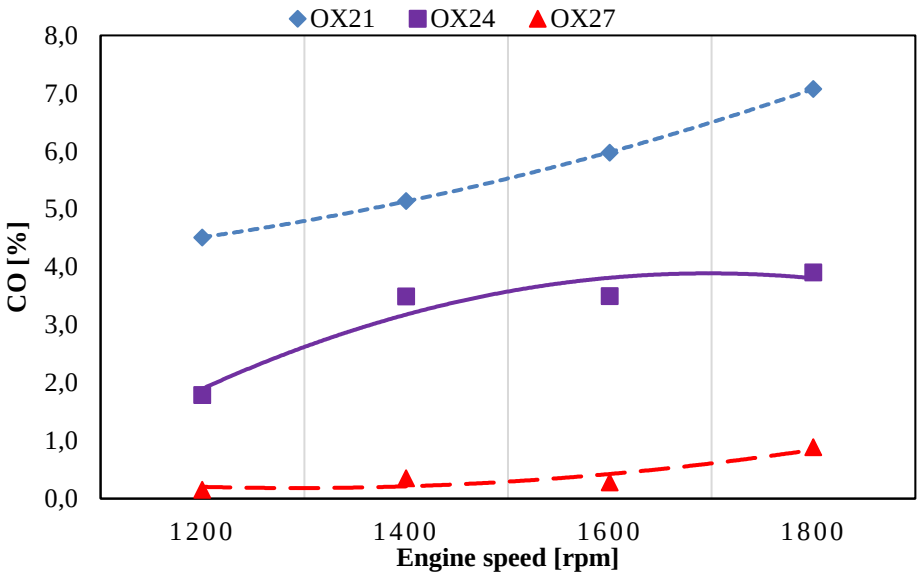

Figure 2. Effects of oxygen concentrations on the CO emissions

The variation of HC emission with oxygen concentration is shown in Figure 3. It can be observed that HC curves presented different behavior at each oxygen concentration since there are several mechanisms that contribute to the formation of HC emission (Heywood, 1988). In lower oxygen concentration there is not enough oxygen to form a homogeneous mixture for combustion and it prevents the conversion of all hydrocarbon molecules to CO_2 and H_2O. However, increasing the oxygen concentrations accelerated the fuel oxidation and resulting in better combustion. Other causes of low HC emissions for high oxygen concentrations could be less expansion quenching and more combustion of unreacted fuel originated from the crevice volumes. Overall, a significant reduction in HC emissions level was achieved by oxygen enrichment of intake air. Increasing oxygen

concentration showed average reductions of 35.2% and 54.2% HC emission for 24% and 27% oxygen concentration, respectively, compared to standard oxygen concentration.

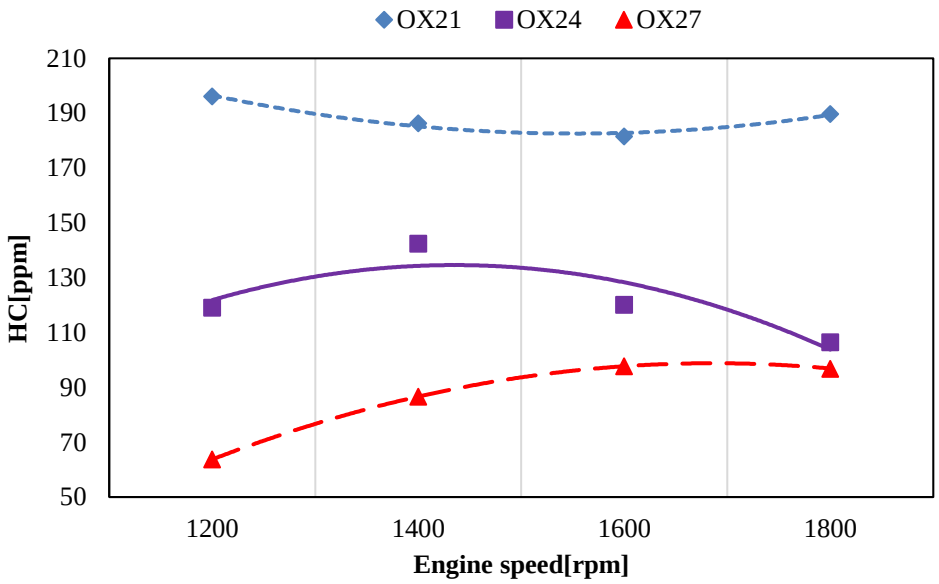

Figure 3. Effects of oxygen concentrations on the HC emissions

The effect of oxygen concentrations on CO_2 emissions is shown in Figure 4. It is seen that CO_2 emissions increased with increased oxygen concentration. This increment is an expected result since the high oxygen concentration enhances fuel oxidation. Also, it is can be seen that CO_2 curves for all oxygen concentration presented the same trend. CO_2 emissions level reached its maximum value at medium engine speeds wherein combustion efficiency is the highest. But, at high engine speeds reduction of combustion duration and dissociation of CO_2 led to a decrease in CO_2 emissions. The results showed an average increment of 24.6% and 55.2% of CO_2 emissions for 24% and 27% oxygen concentration, respectively, compared to 21%oxygen concentration.

CO_2 is not a toxic gas and it is not classified as a pollutant engine emission (Wu et al. 2011). It is also worth noting that CO_2 is a desired emission in terms of energy conversion in combustion systems. Because CO_2 emissions are the indicator of the completeness of combustion. However, it is one of the greenhouse gas emissions. Due to its contribution to global warming, using renewable fuels and reducing fuel consumption is accepted as a solution to alleviate its effects.

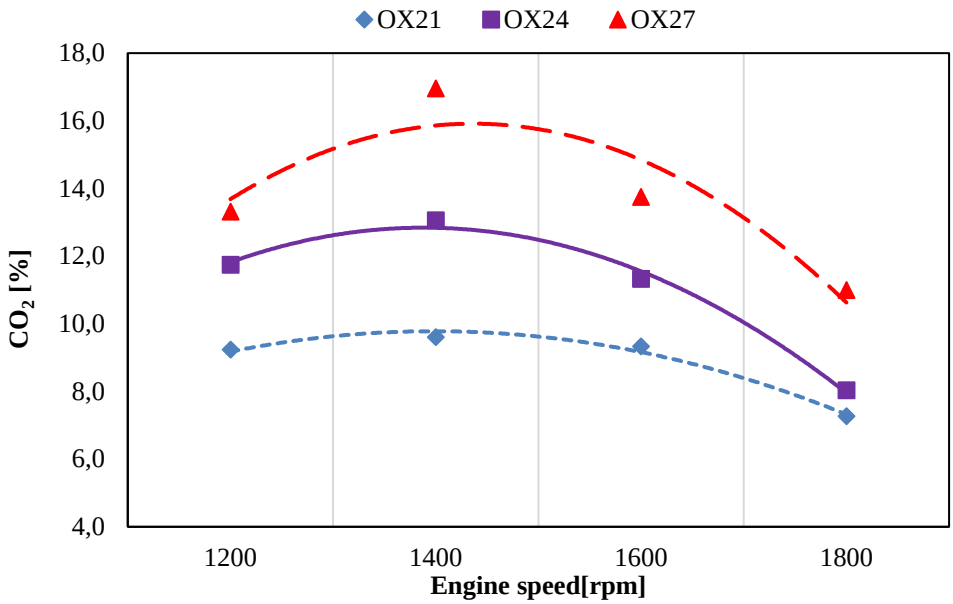

Figure 4. Effects of oxygen concentrations on the HC emissions

The effect of oxygen concentrations on NO_X emissions is shown in Figure 5. NOx is one of the very undesirable exhaust emissions since it causes the destruction of the ozone layer and to form photochemical smog (Pulkrabek, 2014). As seen in Figure 5, NOx emissions increased dramatically with increasing oxygen concentration. When increasing oxygen concentration to 27%, NOx emissions rose up to 22300 ppm. Oxygen concentration, combustion time and combustion temperature has a strong effect on NOx emissions. High oxygen concentration ratios generated higher levels of NOx than standard oxygen ratio. The explanation behind the increment of NOx with oxygen enrichment is that better combustion occurred resulting in higher level of NOx emissions. This is consistency because NOx emissions increased while CO and HC emissions concentration decreased by increasing oxygen concentration. Because of less residence time in the combustion chamber at high engine speeds NOx emissions level decreased. Emissions results showed averagely increment of 617.8% and 2022.4% of NO_X emissions for 24% and 27% oxygen concentration, respectively, compared to 21%oxygen concentration.

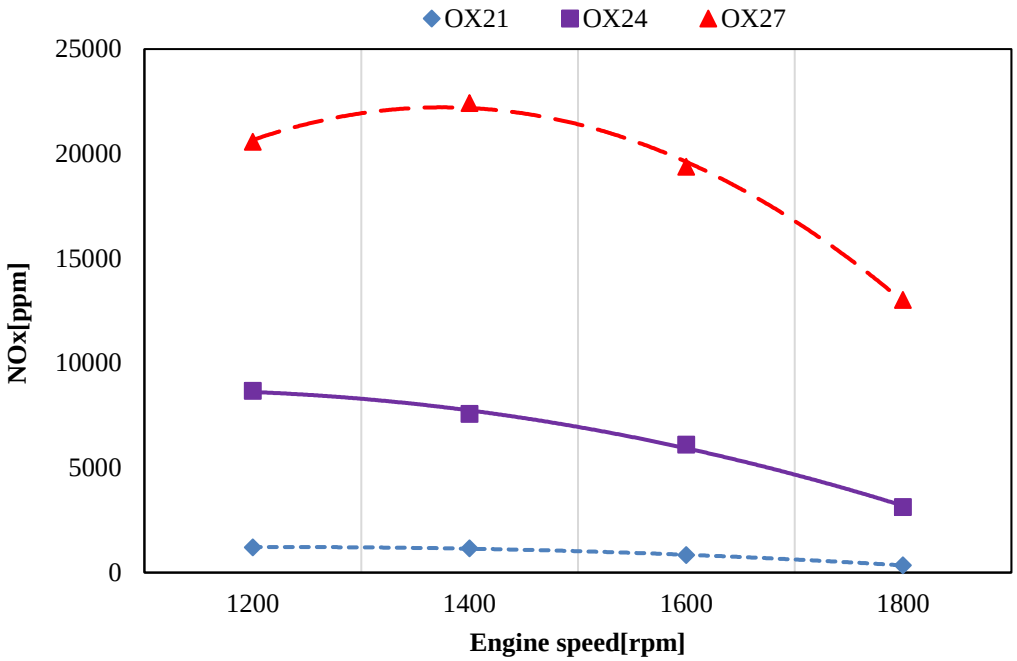

Figure 5. Effects of oxygen concentrations on the NO_X emissions

4. Conclusions

This study focused on the effects of the oxygen concentration of intake air on main gaseous emissions from an SI engine. The experiments were carried out at the oxygen concentration of 21%, 24% and 27% at full engine load. Based on the results of this experimental work, the following conclusions were drawn:

- Increasing oxygen concentration of intake air resulted in more complete fuel combustion.
- Levels of CO and HC emissions in the exhaust gas reduced effectively with increasing oxygen concentration.
- Due to improved combustion with oxygen enrichment CO_2 emissions increased.
- It was observed a significant increase in NOx emissions for both high oxygen concentrations.

The major problem with the increasing oxygen enrichment is the increasing NO_X emissions on a level that is not acceptable. Therefore, high NOx emissions seem to be the main obstacle to the application of the oxygen enrichment as pre-combustion emissions control technique for SI engines. It concluded that oxygen enrichment is not appropriate emissions control method on its own and it requires utilizing aftertreatment technologies, such as lean NO_X traps (LNT) or selective catalytic reduction (SCR) in order to meet emissions standard.

References

Abdelaal, Mohsen M., Basem A. Rabee, and Abdelrahman H. Hegab. 2013. Effect of Adding Oxygen to the Intake Air on a Dual-Fuel Engine Performance, Emissions, and Knock Tendency. *Energy* 61: 612–20. http://dx.doi.org/10.1016/j.energy.2013.09.022.

Assanis, D. N. et al. (1990). Simulation Studies of Diesel Engine Performance with Oxygen Enriched Air and Water Emulsified Fuels. *ASME Energy sources Technology Conference and Exhibition*.

Baskar, P., and A. Senthil Kumar. (2017). Experimental Investigation on Performance Characteristics of a Diesel Engine Using Diesel-Water Emulsion with Oxygen Enriched Air. *Alexandria Engineering Journal* 56(1): 137–46. http://dx.doi.org/10.1016/j.aej.2016.09.014.

Baskar, P., and A. Senthilkumar. (2016). Effects of Oxygen Enriched Combustion on Pollution and Performance Characteristics of a Diesel Engine" *Engineering Science and Technology, an International Journal* 19(1): 438–43. http://dx.doi.org/10.1016/j.jestch.2015.08.011.

Behçet, Rasim, Hasan Oktay, Abdulvahap Çakmak, and Hüseyin Aydin. (2015). Comparison of Exhaust Emissions of Biodiesel-Diesel Fuel Blends Produced from Animal Fats. *Renewable and Sustainable Energy Reviews* 46: 157–65.

Clenci, Adrian Constantin et al. (2014). A CFD (Computational Fluid Dynamics) Study on the Effects of Operating an Engine with Low Intake Valve Lift at Idle Corresponding Speed. *Energy* 71: 202–17.

Heywood, J. B. (1988). *Internal Combustion Engine Fundamentals.*

Hu, Erjiang et al. (2009). Experimental Investigation on Performance and Emissions of a Spark-Ignition Engine Fuelled with Natural Gas–hydrogen Blends Combined with EGR. *International Journal of Hydrogen Energy* 34(1): 528–39. https://www.sciencedirect.com/science/article/pii/S036031990801392X (September 8, 2018).

Li, Hu et al. (2013). Assessing Combustion and Emission Performance of Direct Use of SVO in a Diesel Engine by Oxygen Enrichment of Intake Air Method. *Biomass and Bioenergy* 51: 43–52.

Liang, Youcai, Gequn Shu, Haiqiao Wei, and Wei Zhang. (2013). Effect of Oxygen Enriched Combustion and Water-Diesel Emulsion on the Performance and Emissions of Turbocharged Diesel Engine. *Energy Conversion and Management* 73: 69–77. http://dx.doi.org/10.1016/j.enconman.2013.04.023.

Maiboom, Alain, Xavier Tauzia, and Jean-François Hétet. (2008). "Experimental Study of Various Effects of Exhaust Gas Recirculation (EGR) on Combustion and Emissions of an Automotive Direct Injection Diesel Engine." *Energy* 33(1): 22–34. https://www.sciencedirect.com/science/article/pii/S0360544207001399 (September 8, 2018).

Nabi, Md Nurun, Md Shamim Akhter, and M. Md Z Shahadat. (2006). Improvement of Engine Emissions with Conventional Diesel Fuel and Diesel-Biodiesel Blends. *Bioresource Technology* 97(3): 372–78.

URL 1. *Clean Vehicles*. https://www.ucsusa.org/clean-vehicles/vehicles-air-pollution-and-human-health/cars-trucks-air-pollution#.W5OoL3VMS01 (May 1, 2018).

Porpatham, E., A. Ramesh, and B. Nagalingam. (2018). Experimental Studies on the Effects of Enhancing the Concentration of Oxygen in the Inducted Charge of a Biogas Fuelled Spark Ignition Engine. *Energy* 142: 303–12. https://doi.org/10.1016/j.energy.2017.10.025.

Pulkrabek, W. W. (2014). *Engineering Fundamentals of the Internal Combustion Engine*. Pearson New International Edition. Pearson Higher Ed.

Rajkumar, K, Govindarajan, P (2010). Experimental Investigation of Oxygen Enriched Air Intake on Combustion Parameters of a Single Cylinder Diesel Engine" *International Journal of Engineering Science and Technology* 2(8): 3621–27.

Sekar, R. R. et al. (1990). Diesel Engine Experiments with Oxygen Enrichment, Water Addition and Lower-Grade Fuel. *Energy Conversion Engineering Conference, 1990. IECEC-90. Proceedings of the 25th Intersociety*.

Seong, H. J., Boehman A. L.. (2011). Impact of Intake Oxygen Enrichment on Oxidative Reactivity and Properties of Diesel Soot. *Energy and Fuels* 25(2): 602–16.

Song, Juhun, Vince Zello, André L. Boehman, and Francis J. Waller. (2004). Comparison of the Impact of Intake Oxygen Enrichment and Fuel Oxygenation on Diesel Combustion and Emissions. *Energy and Fuels* 18(5): 1282–90.

Wu, Xuesong et al. (2011). Dual-Injection: The Flexible, Bi-Fuel Concept for Spark-Ignition Engines Fuelled

with Various Gasoline and Biofuel Blends. *Applied Energy* 88(7): 2305–14. https://www.sciencedirect.com/science/article/pii/S0306261911000432 (September 8, 2018).

Zannis, T. C. et al. (2007). Theoretical Study of DI Diesel Engine Performance and Pollutant Emissions Using Comparable Air-Side and Fuel-Side Oxygen Addition. *Energy Conversion and Management* 48(11): 2962–70.

Zhang, Wei, Zhaohui Chen, Weidong Li, et al. (2013). Influence of EGR and Oxygen-Enriched Air on Diesel Engine NO-Smoke Emission and Combustion Characteristic. *Applied Energy* 107: 304–14. http://dx.doi.org/10.1016/j.apenergy.2013.02.024.

Zhang, Wei, Zhaohui Chen, Yinggang Shen, et al. (2013). Influence of Water Emulsified Diesel & Oxygen-Enriched Air on Diesel Engine NO-Smoke Emissions and Combustion Characteristics. *Energy* 55(x): 369–77. http://dx.doi.org/10.1016/j.energy.2013.03.042.

A Design and Prototype Production for A Feeding Focal Point to Feed Stray Animals

Cansu TUTKUN[1], Muhammed BADUR[2], Hamit Emre KIZIL[3], Murat ÇOLAK[4]*,

Hüseyin DEMİRTAŞ[4], Erkan ÇAM[4]

[1]Bayburt University, Vocational College of Health Care Services, Child Development Program, Bayburt, Turkey

[2]Bayburt University, Vocational College of Health Care Services, Department of Medical Services and Techniques, Bayburt, Turkey

[3]Bayburt University, Vocational College of Health Care Services, Bayburt, Turkey

[4]Bayburt University, Engineering Faculty, Mechanical Engineering Department, Bayburt, Turkey

* **Corresponding Author:** mcolak@bayburt.edu.tr

Abstract

The first two articles of the Universal Declaration of Street Animals mentions about the fact that all animals are equal in life at birth and that they have the right to exist and deserve respect. In addition, it is emphasized that every animal in need of a human support has the right to be fed and cared properly. As for the law issued in Turkey in 2004 with regard to animal protection, it is indicated that stray animals just like those having a home must be supported, fed, sheltered and their hygiene, health and security problems must be taken into consideration. In this sense, the current study aims at designing focal points for feeding in order to make the community aware. As a result of the design, a prototype production was made through a 3D printer and the system called DOSTLUK (Friendship) was placed as a trial work in a place where stray animals are abundant in the city of Bayburt. At the end of the field work, the design was analyzed and the deficiencies determined were revised and the system of DOSTLUK was mounted to the areas where stray animals are abundant in the city of Bayburt. In this way, stray animals would be fed actively, the food loss would be minimum and they would be supported in terms of food and water. In the study, the 3D computer aided design was comprised of design, prototype production, mounting and field application. It is aimed to spread the system of DOSTLUK throughout the country by means of other universities and it is expected that an awareness be made toward stray animals.

Keywords: Stray animals, Feeding focal point, Design, Prototype production..

1. Introduction

In order to make the natural balance sustainable, people, animals and plants should be considered as a whole. For the integrity to continue in a healthy way, the natural balance of all living things in a natural equilibrium is necessary due to the existence of the natural balance. As a result of the biological competence of human beings, each of the other living species that shares the Earth has responsibilities to act in harmony with his own biology, to protect them, and to ensure animal welfare and animal welfare. (Abanoz, 2008; Pinguet, 2008; Savaş, Yurtman ve Tölü, 2009; Sungurbey, 1999). In this respect, animal rights; defined as rights that allow animals to be treated humanely in order to sustain their lives in a healthy way. (Aksulu, 2013; Arıkan, 2014; Berksoy, 2007; Çelik, 2014; Serres, 1994; Tamzok, Kük ve Çobanoğlu, 2013). The first two articles of the Universal Declaration of Animal Rights refer to the fact that all animals are born equal in life, the right to exist and the right to be respected.. It is also emphasized that every animal that needs the support of a person has the right to proper nutrition and care. In Turkey, issued in animal protection law in 2004, " Also of stray animals, supporting life as owned animals, nutrition and shelter and hygiene, which should take into account the health and safety 'are specified. (AB Bakanlığı, 2011; Pinguet, 2008; Sungurbey, 1999).

It is known that respecting the right to life of animals has many positive effects for both animals and people. In animal studies, in recent years, it has been stated that animal love positively changes and improves human life. Children growing with love of animals; learning love, respect and commitment, and taking responsibility, more physical activity, away from harmful habits,the development of empathy skills, to be patient and they have learned to strive to achieve their wishes has been seen It is also stated that life helps to learn more clearly the facts. In a study on the subject, it has been determined that touching an animal will cause a sense of well-being in the physical and mental sense of human being, and will reduce anxiety and tension. (Beck & Katcher, 2003; Çelik, 2014; Holson, Scallet, Ali & Turner, 1991; Tipper, 2011; http://www.alopsikolog.net/).

In the dimension of protection of animals; the problems of stray animals in our country and in other countries are serious. Intensifying efforts to solve these problems should be the ethical responsibility of the human. (Tamzok vd., 2013). The feeding of stray animals, which are accepted as part of the social fabric, is a very important issue. Especially in autumn and winter, the animals in the streets have difficulty in finding food and drinks. Along with starvation and thirst, bad weather conditions adversely affect the body of stray animals and these animals have dietary requirements in order to endure the such a this circumstances (http://bipati.co/genel/sokak-hayvanlarinin-

hayatini-kurtaracak-25-eylem/). In this respect, Turkey's conditions, scheduling any live under the name of protecting ecosystems located in the city should be made. Considering the stray animals in these plans, certain living spaces in the city should be created. They can also provide suitable living and living areas for them to live in a common area with people under certain conditions of care and health. (Ürgüplü, 2013). In Turkey and some countries, different examples have been performed in order to appropriate nutrition areas of stray animals

Figure 1. Feeding areas for stray animals (hayvansevgisi.blogspot.com).

Figure 2. Feeding areas for cats, dogs and birds (behance.net, 2012).

As shown in Figures 1 and 2, feeding units designed for stray animals can be placed in appropriate areas of the city. Another example of feeding the animals in appropriate and hygienic conditions were carried out by Muhammad BADUR, a student of the Vocational School of Health Services of Bayburt University. Badur started to make feeding units for street animals since May

2017. Badur placed the feeding apparatus made with plastic pipes in certain areas of the streets in the city center of Bayburt. Then he started to feed the stray animals regularly by dropping the food into the feeding apparatus. (Figure 3)

Figure 3. Image of the Friendship apparatus field application

2. Material and Method

The performance analyzes of the apparatus, which are designed for design studies, were carried out in the center of Bayburt. In the production of friendship apparatus; 500x110 mm pinch pipe, 1 bracket, spray paint, cable tie and foam for connection are used. The bracket is cut into the mouth of the animal and softened with sharp edges and is connected to the pipe with a length of 500 mm. Then they are painted with various colors and left to dry. The apparatus, which is ready for installation, has been placed in suitable places of the city where stray animals are dense for field observations. The Friendship Apparatus is fixed with a cable tie at the appropriate angle without damaging the tree and is supported with Styrofoam and ready to pour the food. Finally, the Friendship Apparatus fills dry food and is offered to the use of street animals. However, some problems have been observed in the manufacture and use of the Friendship apparatus. As a result of field observations in the existing design of the Friendship Apparatus; it is thought that design should be developed, especially the subjects given below;

- Not suitable for mass production,
- Appearance of the animals in the apparatus while eating the food of the stray animals because of the narrow mouth of the apparatus,
- Problems in installation,
- inadequate nutrition

Therefore, it is aimed to develop a new design in order to minimize the loss of food, to provide a more effective feeding of stray animals and to eliminate the deficiencies observed in the current design.

In the field applications of friendship apparatuses, design studies were carried out in order to ensure more efficient feeding of street animals. For the design studies, the missing aspects of the existing apparatus, the advantages of the new design, the preparation of the new design, the planning process and its components, the planning problems, the basic features of the new design that can be the most suitable, and the determination of the operations to be applied are taken into consideration. Solid works 3D computer aided design program is used in design studies. Friendship apparatus design; Food tray mold, Filling and feeding hopper and Cap will be evaluated in 3 sections. (Figure 4.)

Figure 4. Solid model image of friendship components.

The apparatus is divided into 3 parts in order to be able to manufacture in accordance with mass production. In addition, the production of the components produced as standard is considered necessary in terms of cost and manufacturing. In addition to this, it is necessary to make revision on the mold tray in order to eliminate the deficiencies in the current design. For this reason, revision studies were carried out on Feed tray pattern depending on the analysis of design problems. Figure 5 shows the sample design studies for the revision.

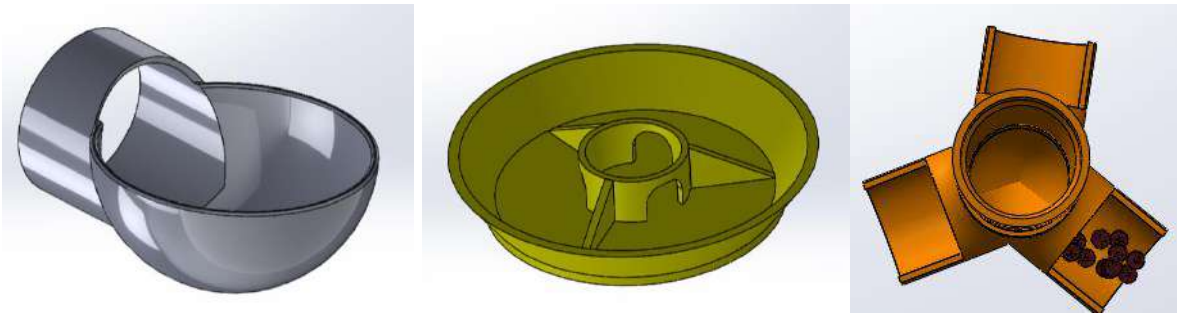

Figure 5. Sample solid model images from the Mama tray pattern design revision studies.

2.1. Prototype Manufacturing

Prototype production was carried out in order to perform performance analysis of food tray design studies in field applications. For this purpose, firstly, the related design was printed with a 3D printer. For other components, cover materials and pinch pipes with dimensions of 110 mm and 500 mm shall be taken ready and assembled. Figure 6 shows the installation images of the relevant design.

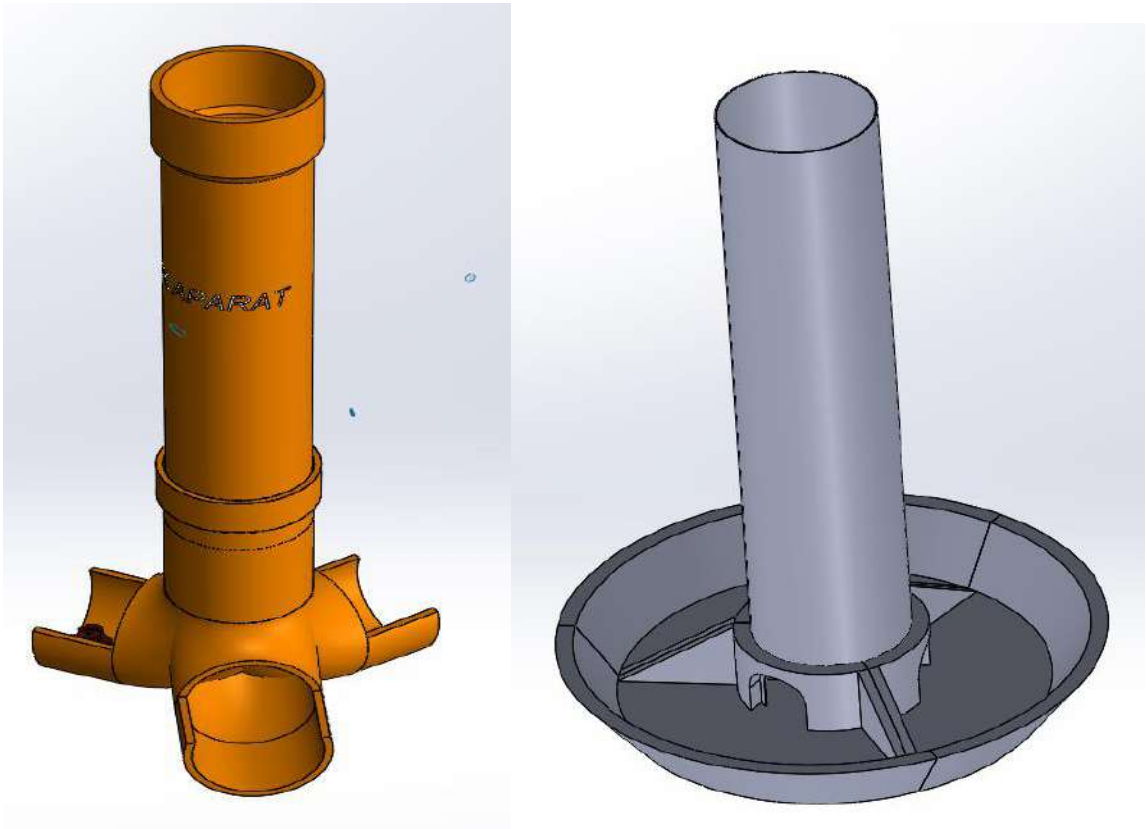

Figure 6. Sample solid model images from the revision works of the food tray mold design.

3. Results and Discussion

In order to analyze their performances, field apparatuses have been subjected to tests. A 'Performance Observation Form' was created by the researchers for these tests. In the form of observations, there were substances for "daily food consumption for each apparatus, and for the loss of food lost around the apparatus" for analyzing the shortcomings of the current design and the performance of the new design. The researchers carried out daily observations and identified deficiencies and errors caused by design. When the obtained results are evaluated, it is seen that all the problems observed in the first design can be eliminated as a result of alternative designs. As a result of field tests, it is understood that street animals can eat food more easily in new design apparatuses, animals do not lose their food during feeding and it is possible that the related design can be passed to mass production. At this stage, the selection process between 3 alternative designs; It is thought to show relative variability depending on the aesthetics and cost. Mass production works are not completed yet and it is possible to list the operations planned to be followed for mass production of related apparatus as follows.

- Model preparation for the food tray
- Preparing the diecast according to the model
- Aluminum casting into molds
- Grinding and cleaning operations
- Assembly of friendship components
- Installation for field application

Selection of aluminum material of the casting part; It is suitable for mass production, corrosion resistance and high strength. Only the food tray mold will be manufactured for the apparatus, the other parts will be provided as ready.

4. Conclusions and Recommendations

There are various feeding units developed in Turkey and abroad for the feeding of street animals. In this study, design and prototype manufacturing studies were carried out to eliminate the shortcomings observed in the application of the focal point called Friendship Apparatus. The prototypes of alternative designs were realized and their performances were analyzed in field applications. When the results were evaluated, it was seen that all the problems observed in the first design could be eliminated as a result of alternative designs. It is understood that the alternative designs developed can be selected according to the aesthetics and cost and that each design is suitable for mass production by casting method.

Depending on the principle that the right of every animal should be respected, joint protocols with the Ministry of Food, Agriculture and Livestock, municipalities, various foundations and non-governmental organizations for nutritional focal points developed within the scope of this study can be expanded and expanded. In order to be able to use these apparatus effectively and sustainably, social media studies can be done to inform the public. Trainings can be organized to provide awareness about street animals as well as information about the use of the apparatus.

Acknowledgement

This research was supported by Scientific Researches Unit of Bayburt University as Scientific Research Project coded 2018 / 01-69001-08.

Kaynaklar

Abanoz, N. (2008). Çağdaş Toplumlarda Hayvan Hakları ve Refahı. Yüksek Lisans Tezi. Atılım Üniversitesi, Sosyal Bilimler Enstitüsü, Ankara.

Aksulu, M. (2013). *Yeni toplumsal hareketler: Türkiye'de hayvan hakları savunuculuğu ve sosyal medya.* Yüksek Lisans Tezi, Maltepe Üniversitesi Sosyal Bilimler Enstitüsü, İstanbul.

AB Bakanlığı. (2011). Hayvan Hakları, Hayvanların Korunması ve Refahı. https://www.ab.gov.tr/files/Tar%C4%B1m%20ve%20Bal%C4%B1k%C3%A7%C4%B1l%C4%B1k%20Ba%C5%9Fkanl%C4%B1%C4%9F%C4%B1/hayvan_haklari__hayvanlarin_korunmasi_ve_refahi.pdf adresinden erişilmiştir.

Arıkan, E. (2014). Hayvan Refahı, Hayvan Hakları, Hayvan Hukuku. Yüksek Lisans Tezi. Galatasaray Üniversitesi, Sosyal Bilimler Enstitüsü, İstanbul.

Beck, A. M., & Katcher, A. H. (2003). Future directions in human-animal bond research. *American Behavioral Scientist, 47*(1), 79-93.

Berksoy, İ. (2007). *Özel Hukukta Hayvan Hakları*. Yüksek Lisans Tezi. Marmara Üniversitesi Hukuk Fakültesi, İstanbul.

Çelik, M. (2014). Çocuk ve Gençlerde Hayvan Sevgisinin Önemi. https://psikolik.wordpress.com/2014/01/08/cocuk-ve-genclerde-hayvan-sevgisinin-onemi/ adresinden erişilmiştir.

Holson, R.R., Scallet, A.C., Ali, S.F. & Turner, B.B. (1991). "Isolation stress" revisited: Isolation-rearing effects depend on animal care methods. Physiology & Behavior, 49(6),

Pinguet, C. (2008). İstanbul'un Köpekleri. (Çev: Saadet Özen). İstanbul: Yapı Kredi Yayınları.

Savaş, T., Yurtman, İ.Y., & Tölü, C. (2009). Hayvan hakları ve hayvan refahı: Felsefi bakış - nesnel arayışlar. *Hayvansal Üretim 50*(1), 54-61.

Serres, M. (1994). *Doğayla Sözleşme*. (Çev: Turhan Ilgaz). İstanbul: Yapı Kredi Yayınları.

Sungurbey, İ. (1999). *Hayvan Hakları*. İstanbul: İ.Ü. Basımevi ve Film Merkezi.

Tamzok, H., Kük, M. ve Çobanoğlu, N. (2013). Hukuki Ve Etik Boyutlarıyla Sokak Hayvanları. *Ankara Üniversitesi Sosyal Bilimler Enstitüsü Dergisi, 4*(1), 245-280.

Tipper, B. (2011). A dog who ı know quite well: Everyday relationships between children and animals. *Children's Geographies, 9(*2), 145–165.

Ürgüplü, G. (2013). Derin Ekoloji Bağlamında Kentte Sokak Hayvanlarıyla Birlikte Yaşamak Olgusunun İncelenmesi. Yüksek Lisans Tezi. İstanbul Teknik Üniversitesi, İstanbul.

URL-1: http://www.alopsikolog.net/, (Erişim Tarihi: 08 Nisan 2018).

URL-2: http://bipati.co/genel/sokak-hayvanlarinin-hayatini-kurtaracak-25-eylem/, (Erişim Tarihi: 08 Nisan 2018).

URL-3: https://www.behance.net/, (Erişim Tarihi: 08 Nisan 2018).

URL-4: http://hayvansevgisi.blogspot.com/, (Erişim Tarihi: 08 Nisan 2018).

Mechanical Behavior Of Nettle Fiber Filled Polylactic Acid Composites

Mustafa ASLAN[1] ,Ashkan EZZATKHAH.B[2] ,Ümit ALVER[3], Kenan BÜYÜKKAYA [4]

[1]*Karadeniz teknik university, Engineering, Metallurgy and Materials, Trabzon, Turkey; maslan@ktu.edu.tr*
[2]*Karadeniz teknik university, Engineering, Metallurgy and Materials, Trabzon, Turkey; ezzatkhah@gmail.com*
[3]*Karadeniz teknik university, Engineering, Metallurgy and Materials, Trabzon, Turkey; ualver@ktu.edu.tr*
[4]*Giresun university, Technical Sciences Vocational School, Giresun, Turkey; kenan.buyukkaya@giresun.edu.tr*

Abstract

Stinging nettle (Urtica dioica L.) is a bast fibre plant ideally suited to cultivation in Turkey, producing fibres of remarkable high tensile strength and fineness. Only limited number of study is available on literature about nettle fibres and nettle-filled plastics. Experiments conducted based on two different nettle grass were used in this study. One grows at 3500m of high altitude and the other grows at sea level in Giresun province. The short nettle fibers were mixed with polylactic acid by extruded method and followed with pressure molding for composite manufacturing. In both of the samples, 20%wt of fiber content was added to PLA polymers without any coupling agent material. It was found that the tensile and flexural properties of the PLA composites filled with high altitute nettle fibres show higher than those of composites made with nettle fibres grown at lower alttitutes. The average bending modulus of composites made with nettles grown at the sea level is 3304 GPa and the bending strenght average is of 26 MPa, while the bending modulus of the nettle fibres at high altitude increased to 3698 GPa and the bending strenght is of 25 MPa.

Keywords: Nettle, Mechanical behavior, Fiber, Polylactic acid, Growing Altitude

ÖZET

Isırgan otu (Urtica dioica L.), Türkiye'de ekimi için ideal olan, kayda değer yüksek çekme mukavemeti ve incelikte lifler üreten bir basit lifli bitkidir. Isırgan otu lifleri ve ısırgan dolgu plastikler hakkında literatürde sınırlı sayıda çalışma mevcuttur. Bu çalışmada iki farklı ısırgan otu temel alınarak yapılan deneyler kullanılmıştır. Biri Giresun ilinde 3500m yükseklikte yetişmekte, diğeri deniz seviyesinde yetişmektedir. Kompozit üretimi için, kısa ısırgan lifleri, ekstrüde edilmiş yöntemle polilaktik asit ile karıştırıldı ve bileşik basınçlı kalıplama metodu ile üretildi. Her iki numunede, herhangi bir bağlayıcı madde malzemesi olmaksızın PLA polimerlerine ağırlıkça% 20 oranında fiber muhtevası eklenmiştir. Yüksek rakımda yetiştirilen ısırgan lifleri ile güçlendirilmiş PLA kompozitlerinin çekme ve eğilme özelliklerinin, düşük rakımlarda yetiştirilen ısırgan lifleri ile yapılan kompozitlerden daha yüksek olduğu bulunmuştur. Deniz seviyesinde yetiştirilen ısırganlar ile yapılan kompozitlerin ortalama çekme modülü ve mukavemeti ortalama 3304 GPa ve26 MPa iken, yüksek rakımda yetiştirilen ısırgan liflerden üretilen kompozitlerin eğilme modülü ve mukavemeti ise ortalama 3698 GPa ve 25 MPa olarak belirlendi.

Anahtar kelimeler: : Isırgan, Mekanik davranış, Elyaf, Polilaktik asit, Yetişme rakımı

1. INTRODUCTION

Processing of natural fiber reinforced composites is an emerging area in the field of composites science and engineering. The natural fibers have low density, low-cost, comparable mechanical properties, and most importantly, these are biodegradable and environment friendly. Natural fibers like sisal, flax, nettle, and banana have a number of technical and ecological advantages over synthetic fibers like glass fiber (Huda et al. 2007; Lee et al. 2006; Mohanty et al. 2000) [1]. Though, synthetic fiber reinforced polymer composites are extensively used in many applications. But due to recent issues like rising costs of petroleum-based polymer composites and their negative impact on environment and focus on sustainable development, natural fiber reinforced composites have found a niche in the global market.

Nowadays, with the acceleration of the biomaterial studies, composite materials are produced which are less harmful to nature and can be degraded in a short time. Some of the fillers and reinforcement materials used in these works are made of natural materials. Examples of these natural materials are nettle (Urtica dioica L.), hazelnut shell (Hazelnut shell), etc. Since ancient times, it has played an active role as a food source, in obtaining fiber and in making pharmaceuticals. It is also widely used in the textile industry. The fibers were obtained from nettle (Urtica dioica), the annual plant species, and were not subjected to any chemical treatment during and after the preparation. The traditional method was used to obtain fiber from the nettle, and the separation was carried out in the form of a manual stripping so that the fibers were not mechanically damaged while leaving the woody structure. In this way, it is aimed to prevent the mechanical damages that may occur as a result of the literature. [2]

Nettle fibers are fully biodegradable like hemp, kenaf, and coir fibers and require less energy to produce. The nettle fibers have excellent thermal and mechanical properties as compared to many other natural fibers. Nettle fiber was investigated for reinforcing plastic aircraft panels and other machine components (Summerscales et al. 2010) [3] . The polymer composites used in various applications may be exposed to different environmental conditions such as under water and soil applications, exposure to sunlight and low temperatures (Agarwal et al. 2010; John et al. 2008) [4] . In this study, we aim to investigate the effect of two types of nettle fibres grown in different altitudes on mechnical performance of fibre reinforced polymer composites. The short stinging fibers were mixed with polylactic acid by the extrusion method and followed with pressure molding for compound composite sample. As a result of our researches and various experiments, we observed that different niches grown in different altitudes exhibit different mechanical behaviors.

2. MATERIALS AND METHOD

2.1 Materıals

Poly-lactic acid (PLA) with the brand of NatureWorks PLA type 3052D was supplied from Oo-kuma Company, Turkey. This type of PLA has a glass transition temperature and melting temperature of 60 °C and 180 °C, respectively. The PLA have a density of 1.24 gr/cm3 and tensile and fibres used modified with silane coupling agent were supplied from Spinteks, Turkey. The nettle we used in this study was taken from two different regions of Giresun. One of the samples was taken from the area of 350 altitudes and the other from 2000 altitudes. In both samples, 20% by weight of fiber content was added to PLA polymers without any binding agent material. Prior to composite production, nettle fibres of 3 mm length at 100 °C for 24 h and PLA granules at 60 °C for 6 h were dried in oven to remove most of the absorbed humidity.

Figure 1. Nettle fibers and nettle fibre filled PLA granules

2.2 Composite preparation

The composites were prepared by single-screw extruder (RONDOL 3212). In the first step, PLA resin was homogenized in the 20% nettle fibres with following heat and screw speed parameters. The extruder had three heating zones, and the temperature profiles of the barrel were 190-220-240 °C from the hopper to the die. The screw velocity was set at 75 rpm. The extruded nettle fibres with PLA granules was subsequently cooled down in a water cabin and then long composite pstrands were pelletized to smaller sizes. Figure 1 shows nettle fibres and nettle fibre filled PLA pellets. Afterwards, the press consolidation technique was applied to prepare the test panels. The panels for test samples (Figure 2) were produced under pressure of 45 MPa and the temperature of 190 °C for 5 minutes. After panels were cooled in their mould, the specimens were visually inspected for air bubbles, and those with defects were discarded.

Figure 2. Composite test specimens

2.3. Composite Testing

Tensile and flexural test experiments were carried out on a MTS (Criterion Model 45) brand universal testing machine according to ASTM D790 and ASTM D683 standards, respectively. The speed of cross head for both tests is of 5 mm/min. In tension test, elongation (strain) of the specimen was measured over a 25 mm gage length using an extensometer. In flexural testing, span length was determined as 16 times the thickness of the specimen (approximately 80 mm), as mentioned in the flexural properties standard. Morphology of the fractured composites after tensile testing was observed using a scanning electron microscope (SEM) (ZEISS EVO LS10, Germany) under an accelerating voltage of 5Kv and 250x magnification. A gold layer of a few nanometers in thickness was coated onto the fracture surfaces.

3. RESULTS

3.1. Mechanical Properties

According to the results of the tensile and bending tests performed, pure PLA, stinging nettle grown at altitude of 200 and nettle grown at altitude of 350 were subjected to different tests. In the tensile test, the Young's modulus of nettle was increased at 2000 altitudes, whereas the tensile strength of pure nettle was higher than the other reinforced composites. In the bending test, the nettle grown at high altitude showed higher resistance to load (Figure 3).

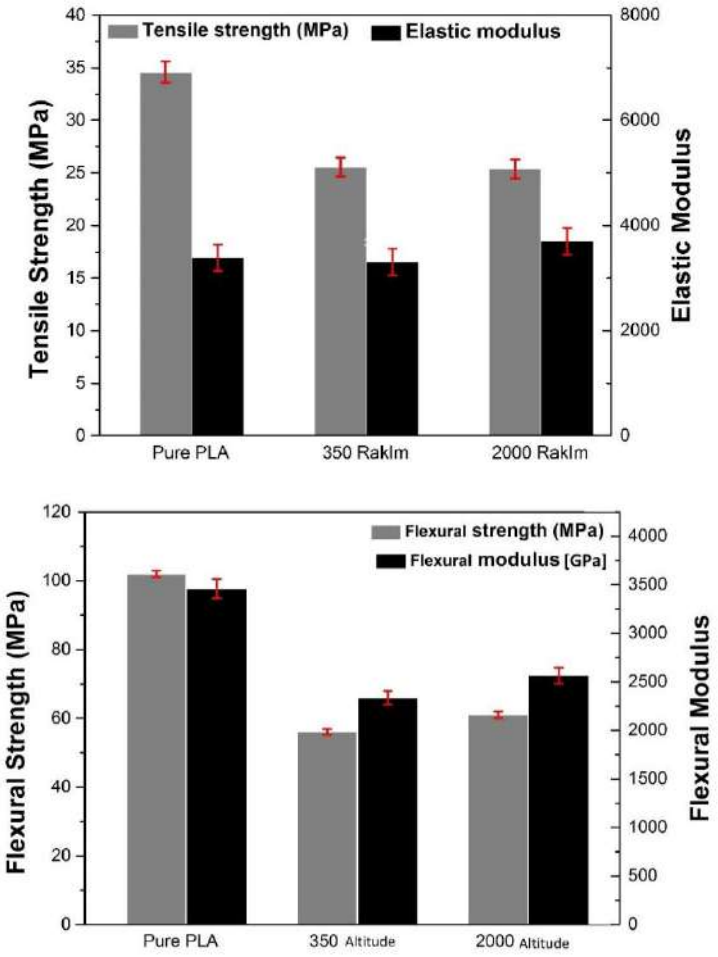

Figure 3. Tensile and flexural properties of pure PLA and PLA composites reinforced with nettle fibres grown at low and high altitudes.

Tablo 1 shows that tensile and flexural properties of both PLA composites reinforced with nettle fibres grown at low and high altitutes. Although tensile strength and tensile strain, deflection in bending are lower in PLA composites reinfroced with nettle fibres grown higher altitute of composites the tensile modulus and flexural strength and flexural modulus were higher in composites with fibres grown higher altitute. The tensile modulus increased from 3304 MPa to 3698 MPa by 10% increase while flexural modulus increase from 2336 to 2565 MPa by 9% increase with the higher growing altitude level. The tensile strength values are similar level for both altitude levels while the flexural strength value is of 61 MPa at the higher altitude level. As a similar study applied by Fischer et al., on nettle fiber reinforced poly(lactic acid), they produced nettle-reinforced poly(lactic acid) (PLA) with fiber content of 20–40 wt% to assess the technical potential of this material compared to 30 wt-% nettle/polylactic acid. The tensile strength could only be increased in case of 30 wt-% nettle/poly(lactic acid) from 52 of the pure PLA to 59 MPa. Other similar study of Kumar et al., they investigated tensile behavior of nettle fiber reinforced PLA composites. They exposed to composite

samples in various environments and found that the samples affected by varying magnitudes when subjected to selected conditions for different exposure times. [5]

Table 1. The tensile and flexural of with nettle fibre reinforced PLA composites.

	350 altitude	2000 altitude
Fibre Content (wt%)	20	20
Tensile Modulus(GPa)	3304±117	3698±135
Tensile Strength (MPa)	26±4.08	25±2.57
Tensile Strain (%)	0.69±0.023	0.66±0.07
Flexural Strength (MPa)	55,85±0.9	61,2±1.1
Flexural Modulus (GPa)	2336±71	2565±80
Deflection in Bending [mm]	2.49±0.12	2.26±0.98

3.2. Morphology

Fracture surface analysis of the composite samples applied in tension were not clearly showed any specific difference in terms of fiber breaking and displacement at the fiber matrix interface. The composite samples was damaged in a ductile manner with a slow and steady crack growth even though the damage in the PLA samples was brittle. This behavior confirms that the composites reinforced by the nettle fiber absorb more energy while breaking. SEM micro photos of the pure nettle fiber SEM micrograph and the necrosis of the nettle fiber-PLA composite samples are given in Figure 4 a, b, c.

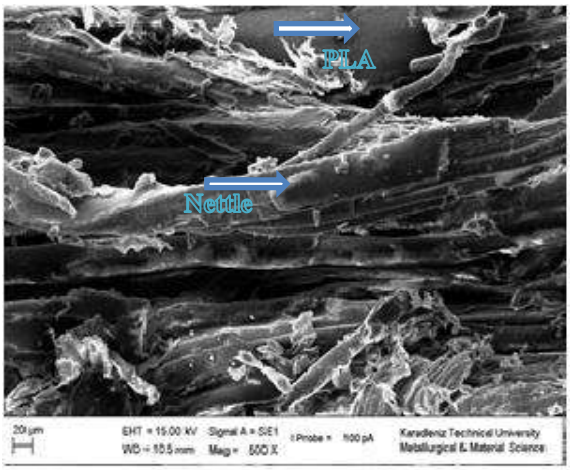

4.a

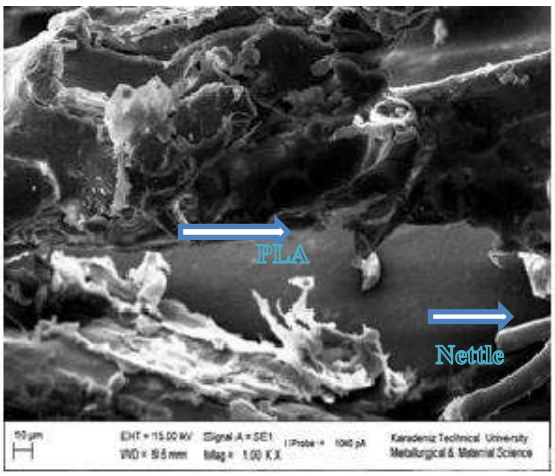

4.b

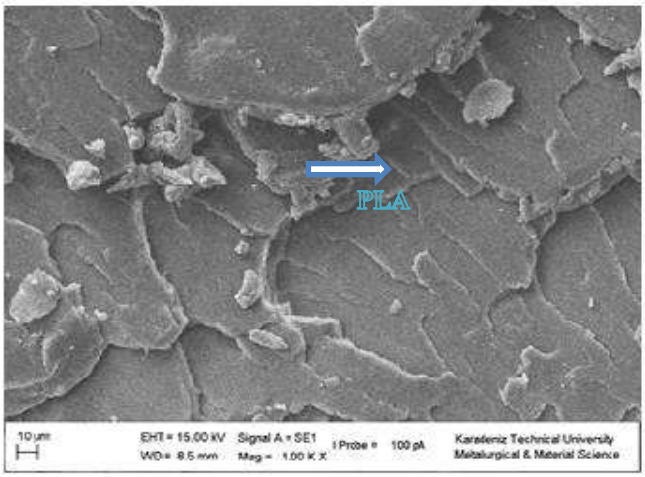

4.c

Figure 4. a. 2000 altitude nettle pla composite **b.** 350 altitude nettle pla composite **c.** Pure PLA

4. CONCLUSIONS

This study showed that as a reinforcing additive to the PLA matrix, a composite with good mechanical properties can be produced successfully with the addition of nettle fiber. According to the results, the fiber obtained from the high altitude showed higher strength and elasticity results compared to the low altitude sample. However, the addition of the stinging nettle has resulted in a reduction of strength, and elasticity of the composites compared to those of pure PLA. For understanding potential of nettle fibers in composites the chemical content and morphological characteristics of stinging nettle should be investigated in terms of different environments.

REFERENCES

1. Müssig J., industial applications of natural fibers:structure, properties and technical applications/ edited by, 447 (2007), Bremen /Germany

2. Büyükkaya K., Isırgan Lifi-Fındıkkabuğu Unu İle Güçlendirilmiş Hibrit Kompozitlerin Mekanik Davranışının İncelenmesi (2017) 2810Merkez/GİRESUN

3. Composites Part A: Applied Science and Manufacturing Volume 41, Issue 10, October 2010, Pages 1336-1344

4. Nitin Agarwal, Ethan S. Lippmann, Eric V. Shusta, Identification and expression profiling of blood–brain barrier membrane proteins, J. Neurochem. (2010) 112, 625–635.

5. Pramendra Kumar Bajpai , Dharmendra Meena , Shrey Vatsa & Inderdeep. Tensile Behavior of Nettle Fiber Composites Exposed to Various Environments, Journal of Natural Fibers, 10:244–256, 2013

Creation Of 3d Cad Model Of Femoral Component Using Reverse Engineering And Manufacturing With Rapid Prototyping

Mehmet Sami GÜLER[1]*, Erkan BAHÇE[2], Derya KARAMAN[2]

[1] Ordu University, Vocational School of Technical Sciences, Ordu/TURKEY

[2] Inonu University, Mechanical Engineering, Malatya/TURKEY

* **Corresponding Author:** mehmetsamiguler@yandex.com

Abstract

Developing computer-aided technologies have opened new perspectives for design and production in the biomedical field. With this technology, reverse engineering and rapid prototyping applications for biomedical analysis in orthopedics, prosthetic manufacturing and surgical operations for simulations are becoming more and more important nowadays. The aim of this study is to obtain the CAD model by engineering method contrary to hip femur joint and to investigate contribution to surgical operations by producing with rapid prototyping. For this study, a 3D scan of the patient's hip femur was performed with an angle interval of 1º in order to be sensitive to the CAD model. After the obtained image was processed in the MIMICS program, a 3D solid model was created in the CAD environment. The obtained CAD model was prototyped with 3-D printer using SIMPLIFY program. When the geometric shape and curvatures were compared with computerized tomography, it was determined that there was a similarity of 2µ sensitivity when the hip femur component manufactured with rapid prototyping was compared with literature. With this study, it was made possible to obtain data such as the size of the deformity formed in the bone, the determination of the implant in the appropriate size to the patient and the creation of the appropriate cuts before the surgical operation. This is thought to reduce the complications that may occur during hip joint surgery operations.

Keywords: Hip Femur Joint, CAD, Rapid Prototyping, 3D Printers

1. Introduction

It is an important issue in product design process that emphasizes reverse engineering, methods and predictions. Today, we are encountering applications in all the studies we can encounter. Reverse engineering, which has become a common point of engineering and medical field, is widely used in biomedical field.

In the field of biomedicine, reverse engineering provides individual measure of the individual and is based on realism and time saving. It is mostly used as an aid to the study of geometric structure of the bone and prosthesis design (Lin et al., 2005). Based on the collected data using medical imaging methods, 3D geometric models of the patient's bones are created. The resulting models help the treatment of the patient to be shorter and more effective. The greatest utility for realizing these functions are 3D printers.

Three-dimensional (3D) printers are a technique used in the manufacture of 3D structures from medical imaging of patients, such as computed tomography (CT) and magnetic resonance imaging (MRI). Identification of damaged areas in this way provides advantages such as the handling of structures that may be harmonious to the body, treatment of the patient by embodying the method. The presentation of these opportunities together with the developing technology is very effective in the field of health. With its widespread use, it creates new areas. One of them is fast prototyping. Rapid prototyping is a term used for rapid manufacturing of physical parts based on three-dimensional (3D) computer-aided design data. The desired product is produced in a short time and in a correct way.

When the literature survey on the works done in the field of reverse engineering was made, it was seen that many engineering applications were made. Looking at the work done, Sahin and colleagues obtained a 3-D structure for the reconstruction of damaged teeth using a reverse engineering method (Sahin at al., 2017). Mustafa Bozdemir designed a gun brass and made it with a 3D printer in order to remove the negativity such as hand fatigue from the middle of the gun hold (Bozdemir,2018). Çelebi and colleagues emphasized that treatment would be more efficient by designing the prosthesis according to the body structure of the patient instead of the damaged skull bone (Çelebi et al.,2017). Derya Celik and Kerim Cetinkaya have realized the applications in the field of reverse engineering by making three dimensional printer (Celik and Cetinkaya,2016).

In this study, to determine a more appropriate and efficient treatment method of patients with hip joint disease, 3D imaging of the patient's computerized tomography (CT) image will be obtained from the 3-dimensional printer.

2. Material and Method

In this study, rapid prototyping of the hip joint was performed to obtain information about the patient with hip joint disease. To obtain 3-dimensional bone structure of a male patient from a private hospital, MIMICS (Materialize's Interactive Medical Image Control System), an image processing program, was used. MIMICS is a computer software (MIMICS 2017) that makes 2-D tomography and MRI readings in 3D format by reading them in DICOM format (Digital Imaging and Communications in Medicine).

The patient's hip joint CT image was edited with the mimics program (Figure 1). Since we wanted to produce the femur part of the hip joint, the upper pelvic bone and the surrounding particles were cleaned. Then, for the desired solid model of bone structure, the spaces in each image layer were filled with mask command.

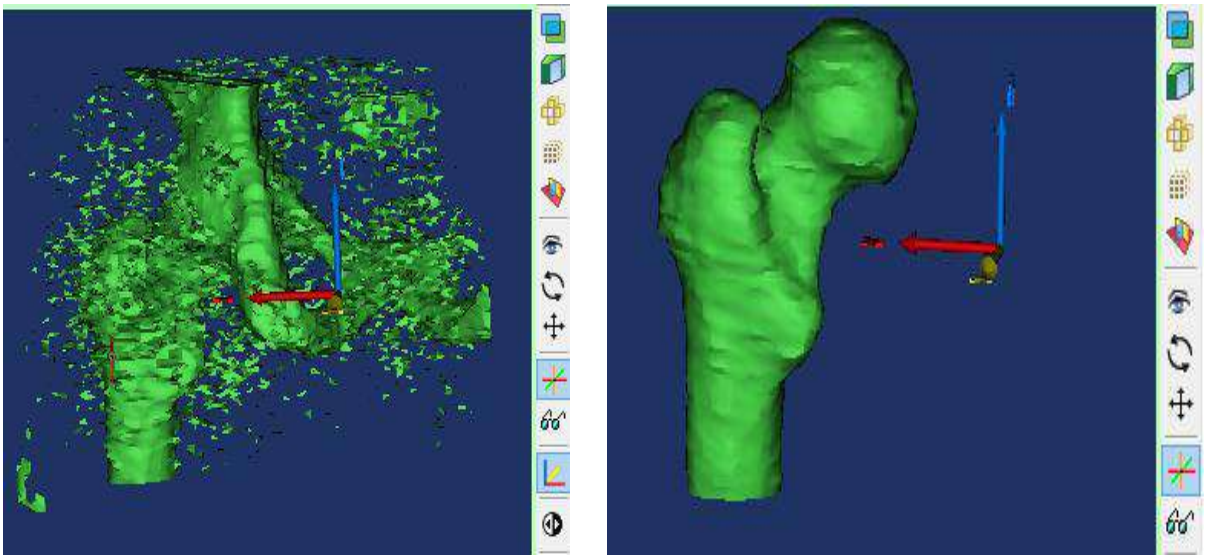

a) Unprocessed image of CT images b) Processed image of CT images

Figure 1. 3D shape of hip femur joint

The generated CAD model was calculated for STL format and transferred to the 3D printer software (Figure 2).

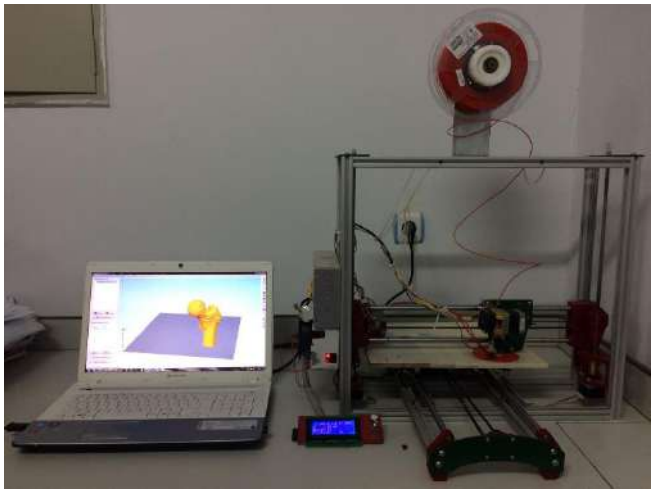

Figure 2. 3-D printer operating with FDM

A three-dimensional printer type using the commonly used Fused Deposition Modeling (FDM) method was used. The nozzle part of this printer type is heated to melt the filament. By moving the extruder and the table with the stepper motors, the design becomes physical.

Polymer materials (plastics) are used in Fused Deposition Modeling method. Materials known as thermoplastics and shaped by heating are suitable for the FDM method. These materials can be filamented and have many color options. The most known filament materials are ABS, PLA and PA.

The FDM-based 3D printer used in this study can be reduced to a layer thickness of 200 micrometers (Figure 2). For this reason, it is possible to obtain a smoother surface by carrying out some chemical and mechanical cleaning operations with FDM parts if needed. Print with biocompatible filament.

3. Results and Discussion

Three-dimensional printers ensure that many products in human life are produced. In particular, they play an important role in meeting the demanded size and materials in the field of biomedicine. Nowadays, the concept of personalization in the health field is compatible with the three-dimensional printer. It enables many surgical applications such as orthotic prosthesis and orthosis.

In this study, a low-cost hip femur joint with high sensitivity was prototyped in a short time.

Hip prostheses are a surgical operation where painful hip joints are replaced with artificial hip joint components replaced with worn joint surfaces. Hip prostheses made of metal and polyethylene materials wear over time due to human life movements and cause serious pain. If these problems are not solved, the service life of the prosthesis is reduced. Patients suffering from severe pain are exposed to revision operations by applying to doctors. This means more bone loss and cost. There are many

studies on the material and geometrical properties of the prosthesis in order to overcome these problems. For this reason, the first operation is very important.

With this study done, it is expected to help the doctor and the treatment of the patient before the operation. For surgical operation, bone cutting areas and bone prosthesis measurements can be determined. This will increase the success rates of hip prosthesis operations and increase the duration of prosthesis use.

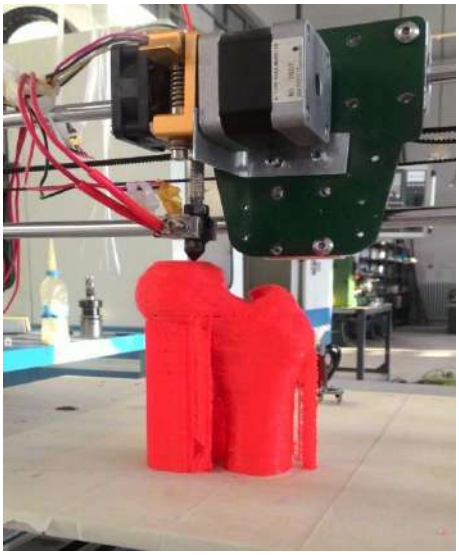

a. 3-B printer manufacture

b. Example manufactured

Figure 3. Hip joint prototyping

We have examined the usability of three-dimensional printers that are widely used in the work we do every day and are developing every day. It was produced by obtaining 3-dimensional structure from hip arthroplasty information of patients with hip joint disease. The advantages to patient and doctor in this way are as follows;

- Determination of the size of the bone deformity,
- Identification of the implant to the patient
- Establishing appropriate incisions for the patient
- High precision prototyping at low cost
- Increased life span of hip joint prostheses
- Easier explanation of patient operation

References

Bozdemir, Mustafa. "Silah Kabzasinin 3b Yazicilarla Tasarim Ve Imalati." International Journal of 3D Printing Technologies and Digital Industry 2.1: 57-68.

Çelebi, Ahu, Halil Tosun, and Ali Çağlar Önçağ. "Hasarli Bir Kafatasinin Üç Boyutlu Yazici Ile İmalati Ve İmplant Tasarimi." International Journal Of 3D Printing Technologies And Digital Industry 1 (2017): 27-35.

Çelik, Derya, And Kerim Çetinkaya. "Üç Boyutlu Yazici Tasarimlari, Prototipleri Ve Ürün Yazdirma Karşilaştirmalari." İleri Teknoloji Bilimleri Dergisi 5.2 (2016).

Şahin T., And Gökçe . "Hasarlı Dişlilerin Tersine Mühendislik Yaklaşımıyla Yeniden Oluşturulması." 485-495.

Lin, Yan-Ping, Cheng-Tao Wang, And Ke-Rong Dai. "Reverse Engineering In CAD model reconstruction of customized artificial joint." Medical Engineering and Physics 27.2 (2005): 189-193.

A Study on the Electroless Nickel Coating on the Copper Powder Particles by Chemical Route

Hüseyin İPEK[1], Onur GÜLER[1]*, Hamdullah ÇUVALCI[1]

[1]Karadeniz Technical University, Department of Metallurgical and Materials Engineering, Trabzon, Turkey

*** Corresponding author:** onurguler@ktu.edu.tr

Abstract

The use of copper-nickel powders has become increasingly widespread due to the oxidation problem of copper and the high cost of the silver especially for the electronics industry. The main purpose of this study was the execution of the nickel coating on the copper powder particles through the chemical route. Copper powders oxidation layer were cleaned with 50 % hydrochloric acid and 50 % ethyl alcohol solution. Cleaned copper powders were added in a bath which is composed of 0.1 molar Nickel (II) sulfate solution ($NiSO_4$) and 0.45 molar Sodium hypophosphite ($NaPO_2H_2$). The coating temperature, pH and mixing speed were selected as 80 °C, 5 and 500 rpm, respectively. After the produce of the nickel coated copper powders, the nickel coating layer, the thickness of the nickel layer on the copper powders and the size of final coated powders was investigated with a scanning electron microscopy (SEM). It was found that nickel coating layer was synthesized successfully on the copper particles at the different thickness.

Keywords: Electroless nickel coating, copper powders, chemical route, coating thickness.

1. Introduction

Electroless plating process is a method comprising reducing metal ions in a coating solution onto the metal ions to be coated and forming a film-like coating. A cation of the metal to be deposited is attracted by the receiving electrons on the surface of the metal to be coated, and the oxidation of the reducing agent is observed by electron transfer to the surface (Sudagar, et al., 2013 and Brenner and Riddell, 1946). If the materials to be coated have poor corrosion and corrosion resistance, it is highly desirable to coat these metals with abrasion and high resistance to chemicals by electroless plating. The difference between the electrolytic plating and the electroless plating process is the reduction of the coating material onto the material to be autocatalytically coated without the use of plating plates which are necessary for electrolysis in the electroless plated coating (Brenner and Riddell, 1947 and Würtz and Ann, 1844). Electroless nickel plating is widely preferred in engineering applications due to the superior corrosion and abrasion resistance of nickel. Besides, electroless nickel coating thickness is higher than that of electrically coatings. Because copper powder is relatively inexpensive, it is an indispensable material in places where high conductivity is required. However, due to the very low copper oxidation resistance, the adverse effect of oxidation on the desired properties is a major problem. so that the oxidation and abrasion resistance of the copper powder can

be coated with a high-resistance material to increase the resistance and stiffness of the copper (Xue, et al., 1997).

In this study copper powders will be electroless coated with nickel in order to minimize the oxidation problem of copper powders and to increase abrasion resistant materials by increasing their hardness.

2. Experimental

The copper powders as a substrate powders for coating with an average particle size of about 65 μm and chemical purity of higher than 99.0% (Alfa Aesar Company, Karlsruhe, Germany) was first dispersed in a solution including HCl and ethanol (Tekkim Chemical Industry, Bursa, Turkey) with ratio of 1:1. This process were done in order to remove oxide layer on the copper powders before electroless coating process. After this, the obtained copper powders from the solution were cleaned with distilled water and ethanol to remove the chemical products in the solution. An aqueous solution including distilled water, nickel sulfate and sodium hypophosphite was prepared in a separate vessel. Nickel sulfate and sodium hypophosphite had molar ratio in the electroless coating bath of 0.1:0.45 M, respectively. The temperature of the coating bath was 85 ^{o}C while pH was 3.5. After the coating process, the copper powders were separated from the solution and washed with ethanol three times to remove chemical products. The nickel coated copper powders were dried in a stove at 60 ^{o}C for 5 h. The temperature of the coating solution were fixed to 60 ^{o}C while the rotation speed of the mixture for the coating solution were choosen 600 rpm. The coating process was performed for 30 min. After the obtaining of the electroless nickel coated copper powders were pressed under 500 MPa to investigate the microstructure of the sample. Fig. 1. shows the workflow diagram for this stdy. The manufactured bulk samples were grinded with SiC papers numbered 200, 400, 600, 800 and 1200 respectively. And then, the samples were polished with aluminum solution. To examine the microstructure, the samples were etched with a solution including the ammonium hydroxide of 25 ml, hydrogen peroxide (3%) of 10 ml and distilled water of 25 ml. The investigation of the powders morphology were carried out with a scanning electron microscopy (SEM, Zeiss Evo LS10). The powder sizes were measured with a powder size measuring device (Malvern 2000, Mastersizer) before and after coating.

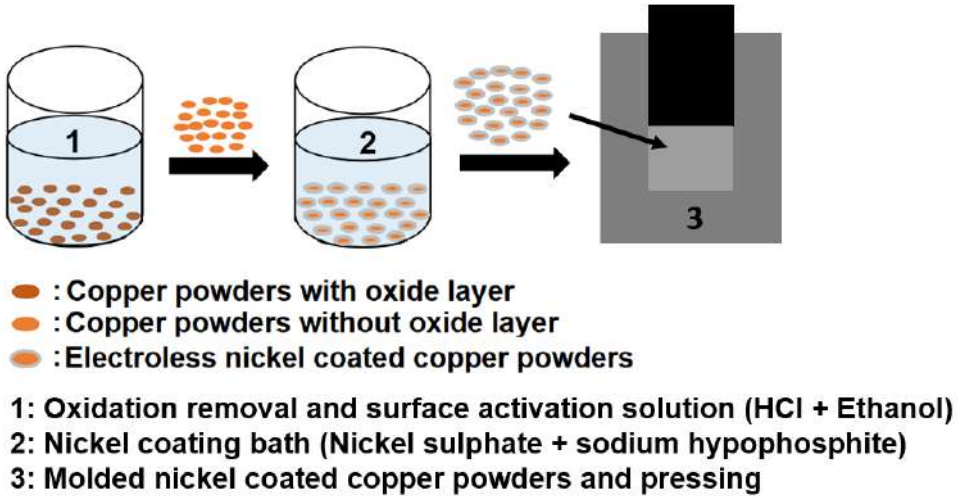

Figure 1. Flow process diagram about the coating and pressing in this study

3. Results and Discussion

In this chapter, the obtained results about the powders size and morphology after the electroless nickel coating on the copper powders were given. With this regard, Fig. 2. shows that the powder size after the electroless nickel coating on the copper powders. As can be seen from this figure, the average size of the powders were increase with the coating of the nickel on the copper powders. Initial copper powders size was about 65 μm while the average size of the electroless nickel coated copper powders was about 80 μm.

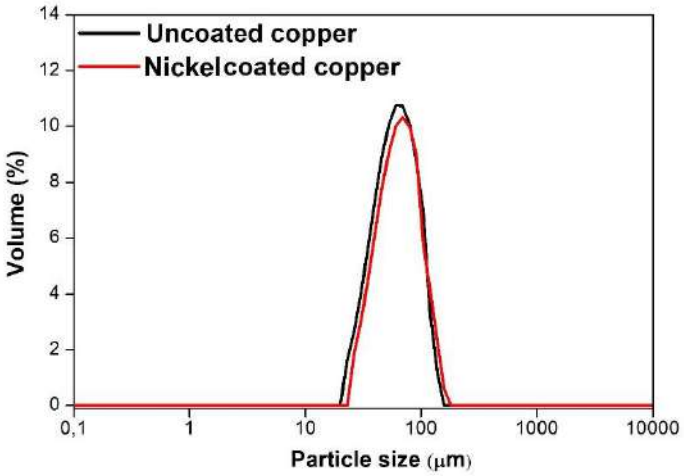

Figure 2. The powder size distribution of the uncoated and electroless nickel coated copper

Fig. 3. shows the SEM images of the uncoated and electroless nickel coated copper powders' morphologies. As can be understood from this figure, nickel was coated on the copper powders

uniformly. Any cracked or porosity can't be seen on the coating on the copper powders. The initial copper powders has spherical shape and nickel coated copper powders has still same shape because the coating is homogenous on the copper powders.

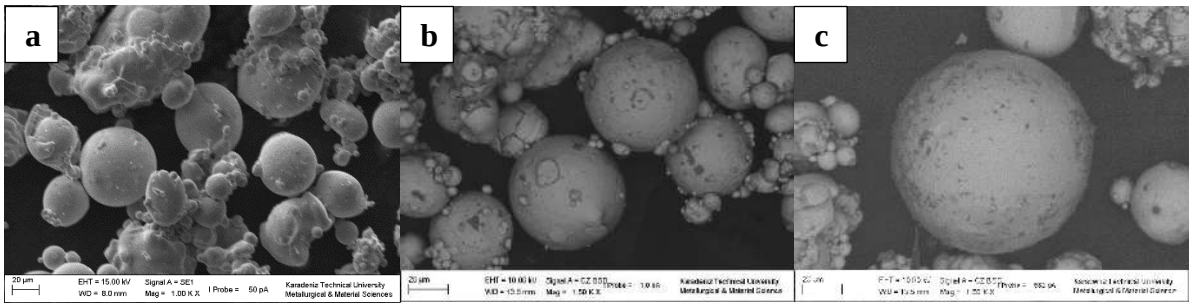

Figure 3. The uncoated (a) and electroless nickel coated copper powders (b, c) morphologies

The obtained microstructure of the bulk samples produced from uncoated and electroless nickel coated copper powders were given in Fig. 4. As can be seen, the nickel placed around the copper powders uniformly after the coating process. Red lines mean the nickel region in the microstructure of the bulk samples produced from nickel coated copper powders. The nickel region is on grain boundaries as can be seen in the figure. Besides, every grain of the copper is surrounded with nickel.

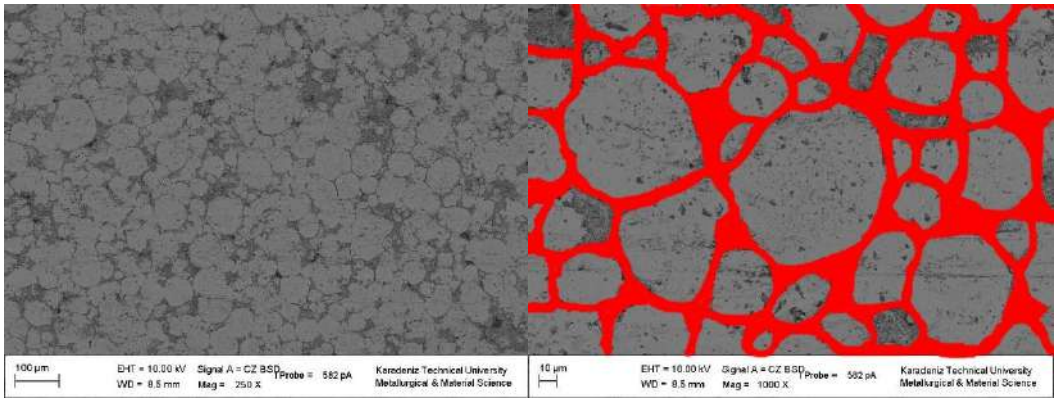

Figure 4. The microstructures of bulk samples produced from nickel coated powders

4. Conclusions and Suggestions

The aim of this study was the produce of electroless nickel coated copper powders and bulk samples following by the investigate of the quality of the nickel coating on the powders. The electroless nickel coating was obtained successfully on the copper powders during the study. Any

free nickel particles was not seen around the copper powders after the electroless coating process. Besides, nickel coating was determined uniformly dispersed onto the copper powders. The bulk samples manufactured from nickel coated copper powders by powder metallurgy showed that every copper powders were surrounded with nickel region on the grain boundaries of the copper particles. The nickel coating thickness was about 5 μm on the each copper powder.

References

Sudagar, J., Lian, J. and Sha, W., (2013). Electroless nickel, alloy, composite and nano coatings – A critical review, *Journal of Alloys and Compounds*, 571,183–204.

Brenner, A. and Riddell, G.E., (1946). *J. Res. Nat. Bureau Stand.*, 37, 31–34.

Brenner, A. and Riddell ,G.E., (1946). *Proc. Am. Electropl. Soc*., 33, 16–19.

Brenner, A. and Riddell, G.E., (1947). *Proc. Am. Electropl. Soc*., 34, 156–159.

Brenner, A. and Riddell, G.E., (1947). *J. Res. Nat. Bureau Stand.*, 39, 385–395.

Würtz, A. and Ann., (1844). *Chim. Phys.*, 11, 250–252.

Xue, Y.Q., Gao, B.J. and Gao, J.F., (1997). *J. Colloid Interf. Sci.* 191, 81.

The Effect of Printing Parameters on the Shear Strength of the 3D Printed PLA Samples

Hüseyin İPEK[1], Onur GÜLER[1]*, Kutay ÇAVA[1], Mustafa ASLAN[1]

[1]Karadeniz Technical University, Dept. of Metallurgical and Materials Engineering, Trabzon, TURKEY

*** Corresponding author:** onurguler@ktu.edu.tr

Abstract

In this study, the shear strength performance of the 3D printed poly-lactic-acid (PLA) printing properties was investigated. 3D Printing technology is novel and progressing method which is a useful technique from medicine to the mechanic. The basic disadvantage of the 3D printed objects is the mechanical strength. The mechanical strength of the 3D printed objects depends on the printing parameters. It is possible to improve the strength values with the printing parameters. Some of the parameters could be recommended by the filament suppliers or slicer programs. And the recommended parameters could be good enough for now. But it is insufficient in near future because of the size of the printed objects. Nowadays, printed objects are the relatively small size of about 20-30 cm (max.). But the printed objects probably will be formed bigger, more complicated and multi-parts. And it means, printing parameters should be recover for each 3D printer filament.

With the scope of the study, PLA based samples were produced with 3D printing method. Producing occurred at different printing parameter as printing speed, layer thickness and nozzle temperatures. And shear strength of the each sample was investigated.

Key Words: 3D printers, PLA, Shear strength

1. Introduction

The use of 3D printing that is also known as additive manufacturing is becoming increasingly widespread in recent years. This process consists of production steps using various materials (various thermoplastic filaments, powdered metals, etc. (Kietzmann et al., 2015). Recently, it is frequently resorted to the use of additive manufacturing (AM) to produce materials with properties not found in natural materials (Kadic, et al., 2012, Schittny, et al., 2013, Meza, et al., 2014, Zheng, et al., 2012, Amendola, et al., 2015, Farina, et al., 2016).

Multiscale additive manufacturing (AM) processes have provided considerable advantages in time for material production and for various micro rapid prototypes of nozzles, microfilters and composite materials (Ferreira, et al., 2017, Kruth, et al., 1998).

But, rapid prototyping methods for the making a design of a new material designs are not well known (Levy, et al., 2003, Lu, et al., 2009).

From this point of view, it is necessary to keep working at the shortest possible time so that such techniques can be used in real life (Farina, et al., 2016, Huang, et al., 2013). These methods are produced by transferring computer-aided models to material layers (Huang, et al., 2013, Gibson, et al., 2014). At this point, designers and manufacturers are able to get rid of the molding and machining processes and produce fast and cheap prototype materials (Kruth, et al., 1998, Levy, et al., 2003, Huang, et al., 2013, Anderson, et al., 2014).

The most important disadvantage of this technique is that the 3D printing materials cannot be used in load bearing applications due to the fragility of the manufactured materials (Bergemann, et al., 2016), however, in design, the formation of completely interconnected pores between the layers may play a role in preventing this problem (Lam, et al., 2002). Rapid prototyping is the most advantageous method among these techniques because it improves the flexibility of stacked products (Yan, et al., 1996).

The 3D printing technique is highly preferred because of the speed and quality it provides in the production of parts with complex shapes and sizes (Rengier, et al., 2010). In addition to rapid production, it also offers many advantages because of its low cost and low material wastage (Berman, et al., 2012). The disadvantages that can be founded are the difficulty experienced in the production of porous products and the suppression effect on the x-y axis (Pham, et al., 1998, Klift, et al., 2016).

The nozzle in the 3D printing system is co-located with the heaters holding the filament made from the material to be printed at the appropriate temperature (for melting of the filament). The heaters in the nozzle system allow the filament to melt and form layers of nozzles through a gap in the width of the nozzle (Hager, et al., 2016). 3D printing technology addresses a wide range of applications (metals, plastics, powders, fibers, ceramics, etc.). Furthermore, printed structures to be employed in a various applications as micro-sensors and actuators, fuel nozzles, scaffolds for cellular growth, home furniture objects, jewels and footwear (Gibson, et al., 2014, Siochi, et al., 2015, Zhang, et al., 2012, Invernizzi, et al., 2016, Bandyopadhyay, et al., 2016, Jiang, et al., 2016).

Thermoplastic materials such as ABS (Acrylonitrile Butadiene Styrene) or PLA (Poly lactic Acid) are usually used in 3D printing technology. ABS that is produced from maize starch and has the biodegradability feature is more preferred because it is a more environmentally friendly and sustainable variety of polymer material (Hager, et al., 2016). But, this type of polymer must be subjected to thermal, mechanical and chemical processes in order to produce suitable specialty materials, despite the biopolymer characterization. so it is not suitable for use in natural forms (Ren, et al, 2003). PLA can be used as matrix structure by using additives like biodegradable material like ABS and without any treatment and it is mostly preferred as polymer material in engineering applications (Kaya, et al., 2018).

As is known, the fiber matrix interaction is more critical than the properties of the polymer matrix or additive material. Therefore, the surface chemistry of fiber and matrix is very important (Rao, et al., 1991, Herrera-Franco, et al., 1992, Narkis, et al., 2004, Luo, et al., 2012, Graupner, et al., 2014).

Thanks to the development of AM technology, the manufacture of cage structures used in engineering applications can be achieved both quickly and inexpensively and in desired characteristics (Lin, et al. 2015, Yang, et al., 2015, Kaur, et al., 2017, Fu, et al., 2013).

The low-cost production of open source 3D printers has become indispensable for mass production. Therefore, for sustainable development plans, the use of this technology is increasing day by day, as work progresses unabated (Pearce, et al., 2015).

PLA is a thermoplastic bio-resorbable polymer in medical applications for bone reconstruction. Some works found out the need to reinforce PLA matrix. 3D-printing is a rapidly developing method for producing bone tissue engineering scaffolds, that allows minimizing time of material manufacturing at high temperatures to avoid thermos-degradation of PLA (Senatov, et al., 2017).

With this regards, the aim of this study is to investigate of the effect of the printing parameters on the shear properties of the PLA polymer materials.

2. Experimental

The materials tested in this study were poly-lactic-acid (PLA) filament (Ultimaker PLA metallic silver RAL 9006) which were used to produce samples in an Ultimaker® 3 of 3D-printer, respectively. The melting flow rate (MFR) value of PLA which were used in this study is 6,09 g/10min (210 ˚C, 2.16 kg). The melting temperature is 145-160 ˚C and the glass transition temperature is 60 ˚C of the PLA filament. These specimens and selected dimensions for specimen types are shown in Fig. 1. The specimen type were printed at a thickness of 10 mm (0.393 inches). The shear and tensile specimen were first created in Solidworks®, exported in stereo lithography (STL) format, and then imported into 3D printer respective slicer software (Cura) to create the G-code used to print specimens. The test specimens of the test specimens were divided into two with and without a perimeter figure (Fig. 1). Besides, technical drawing of the samples were given in Fig. 2.

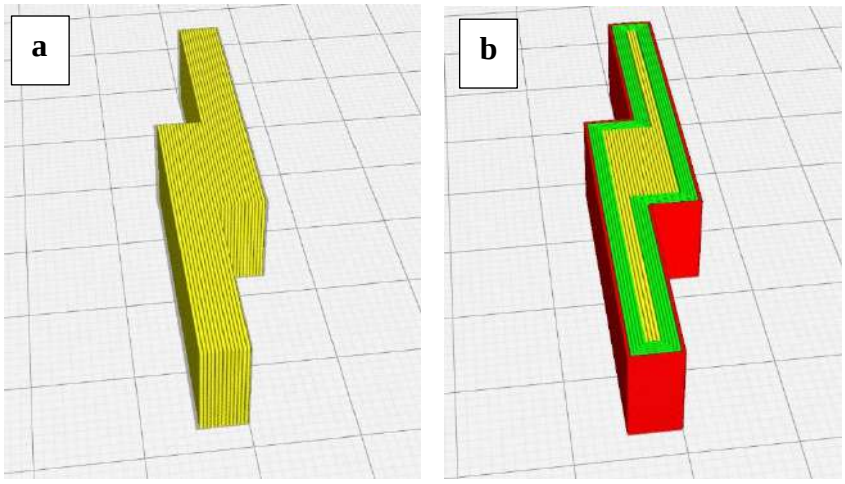

Figure 1. The produced samples (a) with perimeter and (b) without perimeter

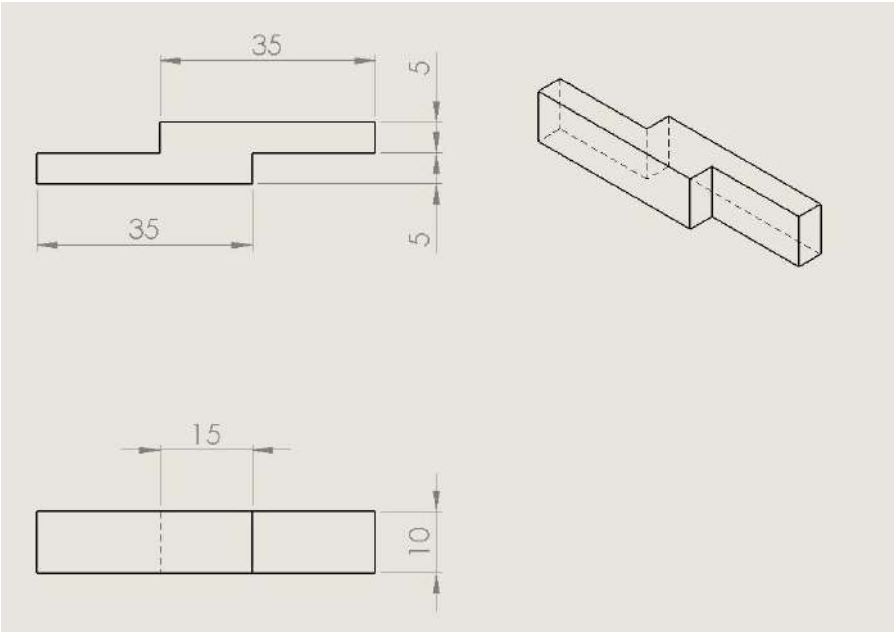

Figure 2. Technical drawing of the 3D printed samples in this study

The Ultimaker® 3 used a default slice height of 0.1 mm (0.004 in) and an extrusion width of 0.4 mm (0.016 in). The slice height, extrusion width, air gap (the space between the bead of material), printer environmental temperature (the temperature of the air around the part and the bed temperature), build temperature (the temperature of the liquefier) and nozzle size (width of the hole through which the material is extruded), were all held to constant values. The entire list of constant or default values used during this study are shown in Table 1 for printer. In order to completely understand the design space used by the printer, the layer extrusion path, otherwise known as raster orientation and the part build orientation were selected as [0/90] and flat (XY Plane).

Table 1. The parameters to produce in this study.

	With Perimeter			Without Perimeter			Without Perimeter			Without Perimeter			Without Perimeter		
Slice height (mm)	.1	.2	.3	.1	.2	.3	.1	.2	.3	.1	.2	.3	.1	.2	.3
Extrusion Width (mm)	0.4														
Nozzle size (mm)	0.4														
Fill (%)	100														
Print Temperature (°C)	200			200			190			210			230		
Bed Temperature (°C)	60														
Print Speed (mm/s)	40			40			25			25			25		

The specimens were tested at a rate of 1.5 mm/min for test method at room temperature (~23 °C). Custom modifications were made to load the specimens in a MTS model 45. Electro mechanical universal testing machine equipped with a 10 kN load cell. Load values were recorded by MTS® TestWorks4™ software at a rate of 20 Hz.

3. Results and Discussion

The results obtained by shear tests of PLA materials produced with 3D printer at various parameters are given in graphical form. Figure 1 shows the shear strength values of materials produced as with and without perimeter using a nozzle printing temperature of 200 ^{o}C according to the layer thicknesses. As can be seen, when the printing speed is 40 mm / s, the shear strength values are gradually reduced with increasing layer thickness. The increase in printing speed causes the formation of voids in the structure due to the fact that the material does not have time to get out of the nozzle during printing and to settle between the layers. The voids in the structure decrease the shear strength values by causing them to be separated from the sample layers during slip under load. However, when the printing speed is 25 mm / s, filling the voids that may form in the structure with the molten material reduces the pore formation, so that the strength values do not change much. Also, from Figure 1, it is seen that in the samples with a printing speed of 25 mm / s, the variation of the shear strength values is very small although the layer thickness is increased. As the layer thickness increases, both the increase of the voids and the increase of the roughness between the layers leads to the breakage of the specimens by making the notch effect during the application of the load which will provide the slip. However, at a printing speed of 25 mm / s, the increase in the thickness of the layer almost eliminates the effect of the decrease in strength.

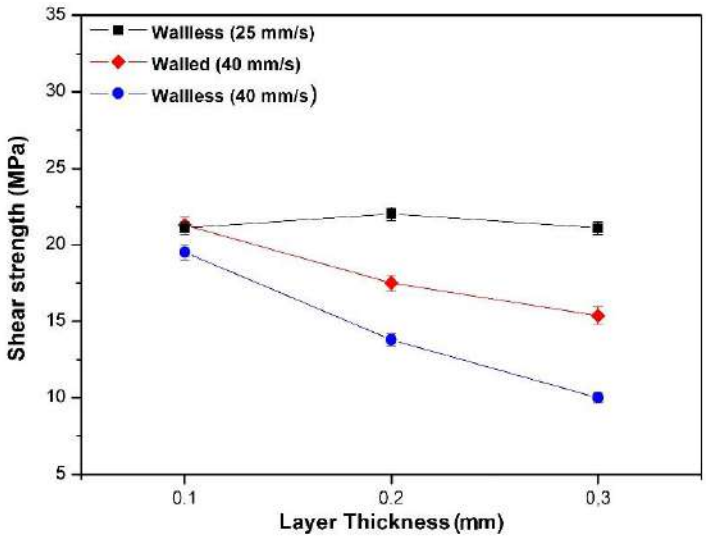

Figure 1. The variation of the shear strength with the layer thickness according to printing speed

Fig. 2 shows the shear strengths of PLA materials produced at different layer thicknesses and at different printing temperatures at a printing speed of 25 mm / s. As can be seen, the highest shear

strength is found in PLA samples produced at a layer thickness of 0.1 mm and at a printing speed of 230 °C, while the lowest shear strength is determined in specimens produced at 190 °C printing speed and in 0.3 layer thickness samples. If the pressing temperature is 190 °C and the layer thickness is 0.3 mm, the shear strength decreases considerably. Although a temperature of 190 °C is sufficient for the melt of the PLA filament material, it has been determined that the material in the nozzle is not sufficient to provide interfacial bonding during melt extrusion. If the layer thickness is more than 0.1 mm, this effect shows itself to a considerable extent with the formation of interlayer spaces during printing. It is clear that if the printing temperature is 200, 210 and 230 °C, the increase in layer thickness and the decrease in shear strength values are very low.

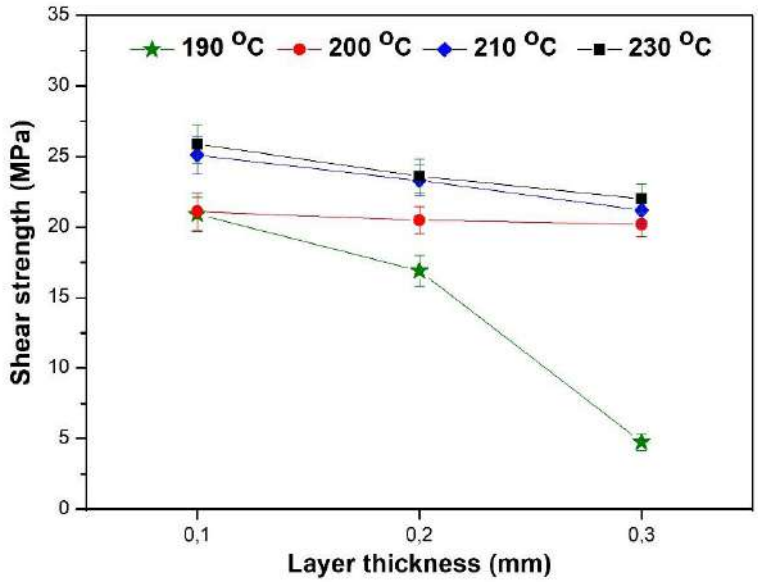

Figure 2. The variation of the shear strength with the layer thickness according to printing temperature

Fig. 3 shows the fracture surfaces obtained after determining the shear strength of the specimens tested with respect to shear rate change and with and without perimeter absence in this study. Fig. 3 (a) shows the fracture surface of specimens produced without a perimeter at a printing speed of 25 mm / s. As can be seen, there is no complete separation in the post-fracture sample and the fracture between the layers has occurred as a whole. In addition, the pore formation in the sample structure is much less than in the samples with the wall and the higher rate of printing (Fig. 3 a and b). This has resulted in a higher slip resistance. Fig. 3 (b) shows the fracture surface of specimens produced at a printing speed of 400 mm / s and wall. As you can see, some of the layers were separated from the other layers, and the fracture occurred as a whole. The fact that the separation of the layer occurs at the edge of the sample shows that the wall part is completely broken after the slip has gone. In this

case, it can be said that the wall part carries the load and resists the sliding. Fig. 3 (c) shows the fracture surface from the shear slip occurring in the specimens without a wall and at a printing speed of 25 mm / s. As you can see, the slippery fracture has formed in layers. As previously mentioned, the impression rate of 40 mm / s promotes the formation of voids between the layers, which leads to the separation of the sample into layers during slipping. Fig. 4 shows the fracture surfaces of samples produced at 190 ^{o}C print speed and different layer thicknesses after slipping. As the layer thickness increases, the formation of voids in the sample structure becomes apparent (Figures 4 a, b, c). As explained earlier, the print speed of 190 ^{o}C is not sufficient to ensure inter-layer bonding, but the layer thickness of 0.3 leads to higher levels of interlayer spacing, which leads to the layers easily slipping over each other after the slip. Fig. 4 (c) clearly shows this situation. For this reason, the shear strength of the samples showed a sudden decrease when the printing temperature was 190 ^{o}C and the layer thickness was 0.3 mm.

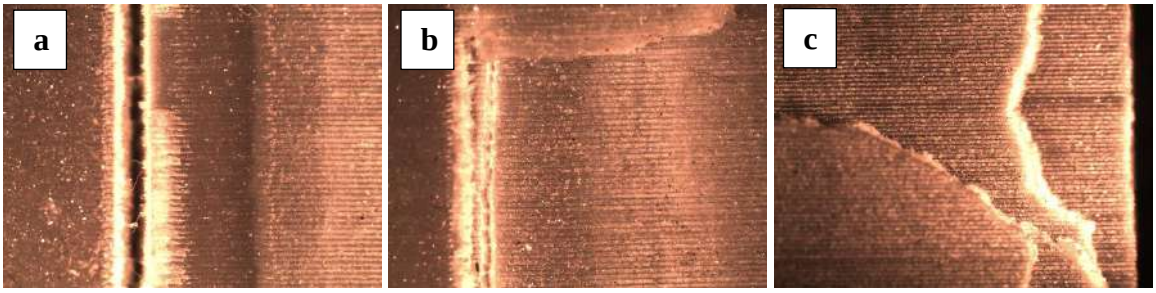

Figure 3. The fracture surfaces of the samples which were printed with the layer thickess of 0,1 mm and at the printing speed of (a) 25 mm/s (without perimeter), (b) 40 mm/s (with perimeter) and (c) 40 mm/s (without perimeter)

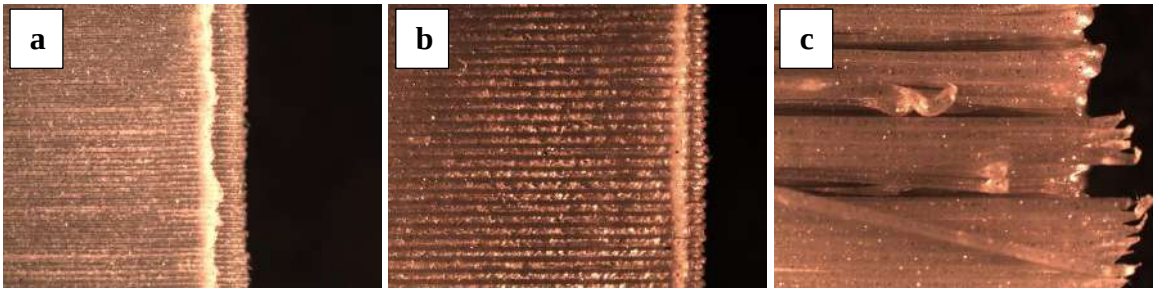

Figure 4. The fracture surfaces of the samples produced with the printing speed of 25 mm/s (without perimeter), at the temperature of 190 ^{o}C and with the layer thickness of (a) 0,1 mm, (b) 0,2 mm and (c) 0,3 mm

4. Conclusions and Suggestions

In this study, the effect of the parameters applied during production of PLA materials by 3D joint production was investigated and the effect of fracture surfaces was supported after slip tests. The findings of the study are summarized as follows:

In the scope of the study, the highest shear strength between the PLA materials produced at different printing speeds and layer thicknesses, with and without perimeter, was determined as 22 MPa without perimeter and with materials produced at 25 mm / s printing speed; the lowest shear strength was found in samples produced without a perimeter at a printing speed of 40 mm / s. The increase in layer thickness did not cause a decrease in the shear strength of the materials when the samples were produced at a printing speed of 25 mm / s and without a perimeter. In this context, shear strength values of the samples produced without a perimeter and at a printing speed of 25 mm / s were observed to be about 22 MPa in samples having a layer thickness of 0.1, 0.2 and 0.3 mm. The increase in layer thickness led to a decrease in the shear strength values when the printing speed was 40 mm / s without and with perimeters. When the effect of the printing temperature and the layer thickness on the shear strength values is investigated, it causes the shear resistance to decrease considerably with the printing temperature of 190 ^{o}C and the increase of layer thickness at the same time. Accordingly, the shear strength of the same specimens was reduced to approximately 4 MPa when the layer thicknesses were 0.3 mm, while the shear strength was determined to be approximately 20 MPa at 190 ^{o}C pressure and 0.1 mm layer thickness. In addition, when the fracture surfaces of the specimens produced in the study were examined, it was seen that the specimens produced by the wall caused the slip resistances to fall significantly in the case of separation of the walls from the specimen structure, and the layers were stratified over each other. It has been understood that when the printing temperature increases and the printing speed is 25 mm / s, the layers are tightly held together and the shear strength values are high due to the reduction of the void formation in the structure.

References

Kietzmann, J., Pitt, L. and Berthon, P., 2015. Disruptions, decisions, and destinations: Enter the age of 3-D printing and additive manufacturing. *Business Horizons*, 58(2), 209-215.

Kadic, M., et al., 2012. On the practicability of pentamode mechanical metamaterials. *Applied Physics Letters*, 100(19), 1910-1.

Schittny, R., et al., 2013. Elastic measurements on macroscopic three-dimensional pentamode metamaterials. *Applied Physics Letters*, 103(23), 23190-5.

Meza, L.R., Das, S., and Greer J.R., 2014. Strong, lightweight, and recoverable three-dimensional ceramic nanolattices. *Science*, 345(6202), 1322-6.

Zheng, X., et al., 2012. Design and optimization of a light-emitting diode projection micro-stereolithography three-dimensional manufacturing system. *Rev Sci Instrum*, 83(12), 125001.

Amendola, A., et al., 2015. On the additive manufacturing, post-tensioning and testing of bi-material tensegrity structures. *Composite Structures*, 131, 66-71.

Farina, I., et al., 2016. Surface roughness effects on the reinforcement of cement mortars through 3D printed metallic fibers. *Composites Part B: Engineering*, 99, 305-311.

Ferreira, R.T.L., et al., 2017. Experimental characterization and micrography of 3D printed PLA and PLA reinforced with short carbon fibers. *Composites Part B-Engineering*, 124, 88-100.

Kruth, J.P., M.C. Leu, and T. Nakagawa, 1998. Progress in Additive Manufacturing and Rapid Prototyping. *CIRP Annals*, 47(2), 525-540.

Levy, G.N., R. Schindel, and J.P. Kruth, 2003. RAPID MANUFACTURING AND RAPID TOOLING WITH LAYER MANUFACTURING (LM) TECHNOLOGIES, STATE OF THE ART AND FUTURE PERSPECTIVES. *CIRP Annals*, 52(2), 589-609.

Lu, M.-H., L. Feng, and Y.-F. Chen, 2009. Phononic crystals and acoustic metamaterials. *Materials Today*, 12(12), 34-42.

Farina, I., et al., 2016. On the reinforcement of cement mortars through 3D printed polymeric and metallic fibers. *Composites Part B: Engineering*, 90,76-85.

Huang, S.H., et al., 2013. *A*dditive manufacturing and its societal impact: a literature review. *International Journal of Advanced Manufacturing Technology*, 67(5-8), 1191-1203.

Gibson, I., D. Rosen, and B. Stucker, 2014. Additive Manufacturing Technologies: 3D Printing, Rapid Prototyping, and Direct Digital Manufacturing. Springer, New York.

Anderson, I., 2017. Mechanical Properties of Specimens 3D Printed with Virgin and Recycled Polylactic Acid. *3d Printing and Additive Manufacturing*, 4(2), 110-115.

Bergemann, C., et al., 2016. Continuous cellularization of calcium phosphate hybrid scaffolds induced by plasma polymer activation. *Materials Science & Engineering C-Materials for Biological Applications*, 59, 514-523.

Lam, C.X.F., et al., 2002. Scaffold development using 3D printing with a starch-based polymer. *Materials Science and Engineering C: Materials for Biological Applications*, 20(1/2), 49-56.

Yan, X. and P. Gu, 1996. A review of rapid prototyping technologies and systems. *Computer-Aided Design*, 28(4), 307-318.

Rengier, F., et al., 2010. 3D printing based on imaging data: review of medical applications. *International Journal of Computer Assisted Radiology and Surgery*, 5(4), 335-341.

Berman, B., 2012. 3-D printing: The new industrial revolution. *Business Horizons*, 55(2), 155-162.

Pham, D.T. and R.S. Gault, 1998. A comparison of rapid prototyping technologies. *International Journal of Machine Tools and Manufacture*, 38(10), 1257-1287.

Klift, F.V.D., et al., 2016. 3D Printing of Continuous Carbon Fibre Reinforced Thermo-Plastic (CFRTP) Tensile Test Specimens. *Open Journal of Composite Materials*, 6(1), 10.

Hager, I., Golonka, A. and Putanowicz, R. 2016. 3D Printing of Buildings and Building Components as the Future of Sustainable Construction?. *Procedia Engineering*, 151, 292-299.

Siochi, E.J. and Harrison, J.S., 2015. Structural nanocomposites for aerospace applications. *MRS Bulletin*, 40(10), 829-835.

Zhang, J., et al., 2012. Hybrid composite laminates reinforced with glass/carbon woven fabrics for lightweight load bearing structures. *Materials & Design*, 36, 75-80.

Invernizzi, M., et al., 2016. UV-Assisted 3D Printing of Glass and Carbon Fiber-Reinforced Dual-Cure Polymer Composites. *Materials*, 9(7).

Bandyopadhyay, A. and S. Bose, 2016. *Additive manufacturing.*

Jiang, Q., et al., 2016. Modeling rock specimens through 3D printing: Tentative experiments and prospects. *Acta Mechanica Sinica*, 32(1), 101-111.

Rao, V., et al., 1991. A Direct Comparison of the Fragmentation Test and the Microbond Pull-out Test for Determining the Interfacial Shear Strength. *The Journal of Adhesion*, 34(1-4), 65-77.

Herrera-Franco, P.J. and Drzal L.T., 1992. Comparison of methods for the measurement of fibre/matrix adhesion in composites. *Composites*, 23(1), 2-27.

Narkis, M., Chen E.J.H. and Pipes R.B., 2004. Review of methods for characterization of interfacial fiber- matrix interactions. *Polymer Composites*, 9(4), 245-251.

Luo, S. and Netravali A.N., 1999. Interfacial and mechanical properties of environment-friendly “green” composites made from pineapple fibers and poly(hydroxybutyrate-co-valerate) resin. *Journal of Materials Science*, 34(15), 3709-3719.

Graupner, N., et al., 2014. Fibre/matrix adhesion of cellulose fibres in PLA, PP and MAPP: A critical review of pull-out test, microbond test and single fibre fragmentation test results. *Composites Part a-Applied Science and Manufacturing,* 63, 133-148.

Ren, X., 2003. Biodegradable plastics: a solution or a challenge?. *Journal of Cleaner Production,* 11(1), 27-40.

Kaya, M., et al., 2018. Effect of Fibre Content on The Mechanical Properties of Basalt Fibre Reinforced Polylactic Acid (PLA) Composites. *TEKSTİL VE KONFEKSİYON,* 28(1), 81-90.

Lin, D., et al., 2015. 3D stereolithography printing of graphene oxide reinforced complex architectures. *Nanotechnology*, 26(43), 43400-3.

Yang, Z., et al., 2015. Designing 3D graphene networks via a 3D-printed Ni template. *RSC Advances.* 5(37), 29397-29400.

Kaur, M., et al., 2017. 3D printed stretching-dominated micro-trusses. *Materials & Design,* 134, 272-280.

Fu, Z., et al., 2013. Three-dimensional printing of SiSiC lattice truss structures. *Materials Science and Engineering: A.* 560, 851-856.

Pearce, J.M., 2015. Applications of Open Source 3-D Printing on Small Farms, *Organic Farming.* 1(1), 2015., 19-35

Senatov, F.S., et al., 2016. Low-cycle fatigue behavior of 3d-printed PLA-based porous scaffolds. *Composites Part B-Engineering,* 97, 193-200.

Kinetics of Water Absorption in Polypropylene / Hazelnut Shell Powder Composites

Kenan BÜYÜKKAYA

[1]*Giresun University Vocational School of Technical Sciences, Gazipaşa Yerleşkesi,28100 Merkez/GİRESUN*

ABSTRACT

The kinetics of the long cyclic water absorptions at room temperature of the composites formed by using hazelnut shell powder were investigated.

The grain size of the hazelnut powder used in the study is 75-150, 150-250, 250-425 and the volume ratios are 0, 17, 20, 24 and 27%. The water absorption of composites has changed regularly with the increase of the quantity of hazelnut shells with hydrophilic character. The pure PP showed high resistance to water absorption and absorbed water in large quantities at the saturation point.

Initially an anomalous fick diffusion was observed but as the amount of hazelnut kernels increased a normal fick diffusion behavior was observed and the results were evaluated within the scope of this law. It was observed that the absorption (S) and permeability (P) coefficients of composites changed regularly with the amount of hazelnut shells added.

Key words: Polypropylene composite, hazelnut shell powder, water absorption, diffusion kinetics

.

INTRODUCTION

Polymer composites are more and more widely used. Especially reinforced polymer composites are preferred in many structural applications due to their advantages such as low prices, chemical resistance, mechanical properties, lightness, easy production and vibration absorption. [1-3]. Natural materials and natural wastes form part of the fillers and reinforcement materials used in the production of these composites. Some examples of these natural materials are wheat and rye husks and various tree dusts. [4,5].

Studies on water absorption of PP-based composites containing various organic (cellulosic) fillers have been conducted recently [6–9]. In these studies, a significant increase in water absorption of PP was determined by the addition of these fillers, due to the hydrophilic character of organic fillers and their absorption of water. Although PP / inorganic composites have been widely used in various environments and for long periods of time, studies on the kinetics of water absorption of these composites have been limited in the literature.

There are very few researches on the use of hazelnut shell in composites and the properties of these composites. In one of these studies, Balart et al. [10] investigated the effects of the plasticizer involved in the hazelnut shell / PLA composites and reported that the plasticizer reduced the composite's breaking sensitivity and improved thermal stability. Çöpür et al. [11] performed an optimization study in MDF production by mixing hazelnut shell with hazelnut husk and reported that the hazelnut shell can be used at a maximum of 10%.

In this study, the kinetics of long - term water absorption behaviors of the PP / hazelnut shell powder composites and additives used during the formation of the composite were investigated. The effects of wax and antioxidants added during the production of the composite on the water uptake behavior were determined.

In our country the shell of the hazelnut, which is mainly grown in the Black Sea Region, is generally used as fuel. Although it varies year to year, approximately 48% of this product, which has an average production of 592 thousand tons, is shell [12,13]. To find a industrial use to this material, which has a yearly supply of about 300 thousand tons, instead of burning it is one of the socio-economic objectives of this study.

2. Material and Method

2.1 Materials

In the experimental study, PP-MH418 coded product which is used as matrix material in the production of PP / HNSF composites and defined as ETOPLEN commercial name is supplied from

Petkim. The hazelnut shell obtained from hazelnut processing factories was made into powder in local flour mills. In order to reduce the effect of the size, it was sieved on the laboratory sieves and divided into different sizes. The hazelnut shell powder of 150-250µ size was dried for 4 hours before the preparation of the samples in order to minimize the negativities that moisture may generate during the production of the composite.

Product coded as OX.PE WAX LE262 (polyethylene wax) produced by Innospec Leuna is supplied from Eral Turkey and used to easily process the polymer composite.

In the study, Irganox 1010 (tetrakismethylene-(3,5-di-t-butyl-4-hydroxyhydrocinnamate) methane) antioxidant produced by CIBA is supplied from CIBA Turkey in order to protect the polymers from oxidation.

2.2 Preparation of the Samples

Before the composites were prepared, the reinforcing material was dried in 100 ºC oven for 4 hours. Using a Mikrosan MTV 30 extruder with screw diameter = 30 mm, L / D = 25, PP and hazelnut shell powder were mixed. Sleeve temperatures were set to 160, 170, 180 and 185°C respectively from feed section to mold section. HSNF was added to PP/ hazelnut shell powder composites in a volume ratio of φ_f = % 0, 17, 20, 23,5 ve 27 and grain size of 75-150,150-250, 250-425 µm. In order to be able to process the mixture easily, 1% wax was added and 0.1% antioxcidant was added to protect the composite against oxidation. Screw rotation was 25 rpm. and the pressure was determined as 6 bar. The extrudated material was immediately cooled in water, cropped and dried in an 80°C oven for 48 hours. In order to produce composite test samples from dried granules, Super Master SM-60HC injection machine was used. Processing parameters were chosen as max sleeve temperature of 210°C, injection pressure of 800-1000 bar, mold pressure of 40°C and 25 seconds of standby time in mold.

2.3. Water Absorpsion Tests and Measurements

Water absorption experiments were carried out in accordance with EN 2378 standard and for each group, at least five test samples of 4 mm thickness (*b*), 13 mm width (*w*) and 127 mm length (*l*) were used. Control samples were dried in an 80°C oven for 48 hours. Samples taken out of the oven were rapidly weighed in a XB 220A SCS coded analytic scale with 0.1 mg precision by Precisa to determine the first weight (W_0) before water absorption test. After measurement, the control samples were placed in glass containers filled with distilled water. Samples removed from this bath at the specified time periods were gently wiped with a dry napkin and weighed with scales. Due to the fact that the weighing process was completed in approximately 15 s, errors that could be caused by the evaporation of the absorbed water during the weighing of the control samples were neglected. In order to determine the long-term water absorption behavior of the composites, the weighing and measurement processes were continued for 13000 hours.

Diffusion coefficients, k, n parameters were determined according to the diffusion law. Depending on these results, the permeability coefficients of the composites and the dimensional change rates due to the water absorption were calculated.

2.4.Diffusion

Water absorption behavior in a polymer system can be classified into three different categories: Fick diffusion (Case I), polymer relaxation controlled diffusion (Case II) and abnormal (non-Fickian) diffusion. Diffusion parameters can be calculated using correlation 2.

$$\log\left(\frac{M_t}{M_\infty}\right) = \log k + n \log t \,. \qquad (2)$$

here M_t, is the amount of water absorbed at t moment, *k* ve *n* coefficients are the diffusion parameters. Equality related to the second Fick cantos for single dimensional diffusion:

$$\frac{\partial C}{\partial t} = D_x \frac{\partial^2 C}{\partial x^2} \quad (3)$$

here C is local concentration of the diffusion , t is diffusion time; D_x is diffusion coefficient on x-direction vertical to plate surface. While the D_x in Equation 3 is single dimensional (x-direction), the control samples are three dimensional and limited in size. Therefore, the diffusion occurring at the other edges of the control samples was included to calculation with Equation 4.

$$D = D_x \left(1 + \frac{b}{l} + \frac{b}{w}\right)^{-2}, \quad (4)$$

here D is isotropic diffusion coefficient [16]. For the control samples used in this study, the correction coefficient at the right side of Equation 4 was found 0.558.

Diffusion coefficient (D), is an important kinetic parameter for Fick diffusion (Case I). When the concentration on the surfaces of a polymer sheet is held constant, that is, when the sheet is immersed in a sufficiently large water bath, the amount of water absorbed by the sheet at t moment can be expressed as in Equation 5,

$$\frac{M_t}{M_\infty} = 1 - \frac{8}{\pi^2} \sum_{i=0}^{\infty} \frac{1}{(2i+1)} \exp\left(-\frac{D(2i+1)^2 \pi^2 t}{b^2}\right) \quad (5)$$

According to Equation 5, the weight of the water absorbed by the slab increases linearly with the square root of the dip time ($\sqrt{t}$) and then slows down to reach a balance plateau (saturation) [24]. In the first stage of the diffusion coefficient ($0.00 < M_t/M_\infty \leq 0.55$) D_1 can be calculated using Equation 6.

$$\frac{M_t}{M_\infty} = \frac{4}{h}\sqrt{\frac{D_1 t}{\pi}} \; . \quad (6)$$

3. RESULTS AND DISCUSSION

3.1.Water Absorption Behavior

The characteristic water absorption behavior of the pure PP and PP / hazelnut shell powder composites is given in Figure 1.

While the water absorption rate of the composite was approximately linear until peak (saturation) point, it was determined that the velocity had decreased significantly after the peak, but the linear behavior continued. When the water intake behavior of composites containing 20% HNSF was

examined, it was found that the amount of water absorbed in the 3384 hours until the saturation point was 1.67%, whereas the amount of water absorbed later in 11616 hours was 0,31%. These results also proved that water intake increased proportionally with the amount of the additive added and water absorption after saturation continued, albeit low, depending on the amount of additive. Kochetkov et al. [16] reported that the tendency of epoxy / glass sphere composites to take water at room temperature persist, in their study of more than a decade. In the studies conducted, it was reported that PP composites with different thicknesses also had similar behavior [15,16]. Water absorption behavior after the saturation point can be explained by the water damage. In their study, some researchers reported that in equilibrium (at saturation point) a balance between the osmotic pressure of water and the elastic forces of the polymer was formed and subsequent water absorption was related to the weakening of the bonds in the polymeric structure [17,18].

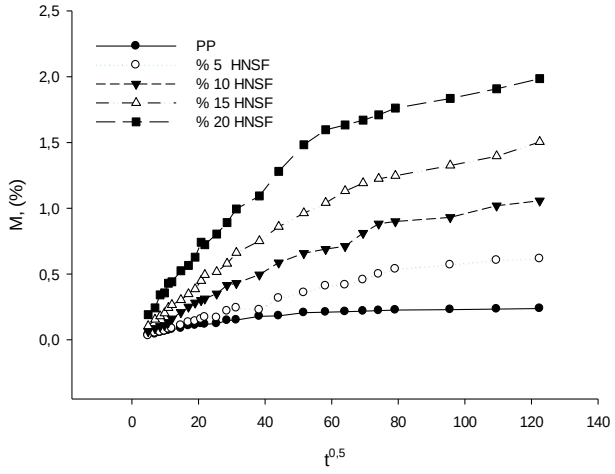

Figure 1. Water absorption (*M–t*) graphics of PP, PP/ hazelnut shell powder composites

Water absorption test results of PP / hazelnut shell powder composites are listed in Table 2. Pure PP (HNSF.00) reached the saturation point by absorbing approximately 0.16% of water by weight after approximately 5496 hours (Fig. 1). Long saturation time and low water absorption indicate that the PP has a high resistance to water absorption due to its hydrophobic character. PP/hazelnut shell powder composites containing φ_f = 0, 5, 10, 15 and 20% respectively reached saturation after approximately 5496 hours, 5118 hours, 4429 hours, 4104 hours and 3384 hours and absorbed approximately 0.16%, 0.85%, 1,01%, 1,13% and 1,67% water on their saturation poins (Fig. 1). Compared to pure PP composites, PP/HNSF composites containing 5, 10, 15 and 20% more hazelnut shell powder respectively, absorbed approximately 3,70, 6,36, 9.06, 11,95 times more water after 13000 hours. These results show that the amount of water absorbed increases regularly by the addition of hazelnut shell flour, while the saturation period decreases regularly. As previously stated, the total amount of water absorbed was maximum 1,98% due to the fact that the ratio of the additive with hydrophilic character was lower than the literature. When the absorption rates on the studies

made on room temperature with PP matrix and composites including more additives (50%) in literature are investigated, the difference with our study was found to be 15 times.[19].

3.1.1. The Effects of Particle Size of HNSF to Water Absorption Behavior

In this study, water absorption behavior of the composites prepared using three different grain sizes show difference. % water intake amounts decreased parallel to increase in grain size. As shown in Table 4, increasing the grain size of HNSF decreased the amount of water absorbed at the end of 13000 hours. Decrease rates have been +3,4%, -11.6%, -8%, -13,7% respectively on composites with 75-150 and 250-425 particle size and %5 -%20 additives.It is thought that the primary factor affecting the water intake rates of the composite is the surface area.Bouafif et al. demonstrated the water intake behavior of the composite they built using 24, 42 and 65 mesh with different grain sizes and 35% by weight HDPE/tree particles. In the study, it was determined that the size of the material that took in the least amount of water was 65 mesh [20].

Table 2. Water absorption test results of PP / Hazelnut shell powder composites with different grain size and content.

Composites (Symbol)	M_{1300} (% by weight)
PP	0,17
FKT.75-150 % 5	0.58
FKT.75-150 %10	1.03
FKT.75-150 %15	1.51
FKT.75-150 %20	1.96
FKT150-250 % 5	0,58
FKT150-250 %10	0,95
FKT150-250 %15	1,44
FKT150-250 %20	1,78
FKT250-425 %5	0,60

FKT250-425%10	0,91
FKT250-425%15	1,39
FKT250-425%20	1,69

3.2.Diffusion

According to Marom [21], water absorption of polymer composites consists of three mechanisms: (i) the progression of water molecules through free volumes between the polymer chains due to the difference in concentration (ii) the capillary penetration of water through the interfaces (iii) the capillary penetration of water through the microcracks.

Water absorption behavior in a polymer system can be classified into three different categories: Fick diffusion (Case I), polymer relaxation controlled diffusion (Case II) and abnormal (non-Fickian) diffusion.

Kinetic behavior is accepted as Fickian when n=5, relaxation controlled when n=1/1 or abnormal when 0.5<n<1.

The kinetic processes of water absorption in lignocellulose reinforced thermoplastics typically show Fick diffusion behavior [22].

As shown in Figure 3, log *k* and *n* parameters were calculated from the points where the average curves cut the log (M_t/M_∞) axis and the slopes of these curves, respectively, and are given in Table 3 together with the diffusion coefficients. With the addition of hazelnut shell powder, while the exponent *n* values of composites came close to 0.5, *k* coefficient decreased. Because of the fact that composites' exponent *n* values are close to 0.5, it was concluded that water absorptions of composites fit the classical Fick diffusion model. Therefore, the data obtained from the study were evaluated according to classical Fick diffusion.

As given in Table 3, the exponent *n* of the composites increase slightlywith the increase in hazelnut shell powder. This result shows that if more hazelnut shell flour is added, the diffusion kinetics of the composites can change through abnormal, state II or super state II. Drozdov et al. [23] reported that even though the water absorption of the pure vinyl ester resin at room temperature conformed to the Fick diffusion, diffusion status corresponded to abnormal diffusion due to clay incorporation and increasing the proportion of clay added.

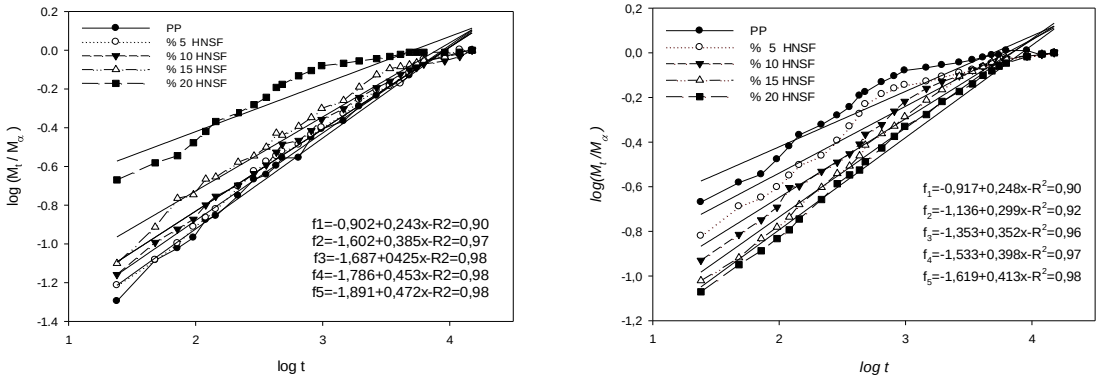

Figure 5. Diffusion status curves of PP / hazelnut shell flour composites.

D , values of PP/ hazelnut shell flour composites are given in Table 3. It can be observed that as the amount of the hazelnut shell flour increase *D* value also increases regularly. Crank [24] concluded in his work that both polymer relaxation and internal stresses simultaneously affect the diffusion coefficient and mechanical properties of polymer sheets.

The diffusion coefficients obtained in this study were consistent with the diffusion coefficients of the PP composites based on tree powders added in various rates, that were made in different air conditioned environments and reported to vary between 1,67- 58 x 10^{-13} [25-28]. Diffusion coefficients and water absorption at the saturation point of the PP composites have been reported to increase with the amount of filler added.

Table 3. Diffusion and permeability values of PP / hazelnut shell powder composites. Diffusion parameters *k*, *n*, and diffusion coefficient *D*.

Composites	*k*	*n*	*D*
	(g g^{-1} s^{-n} 10^{-2})		(m^2 s^{-1} 10^{-13})
PP	12,5	0,243	3,95
FKT.50-150 % 5	2,5	0,385	0,67
FKT.50-150 %10	2,0	0,425	0,81
FKT.50-150 %15	1,6	0,453	1,04
FKT.50-150 %20	1,2	0,472	1,10
FKT150-250 % 5	6,2	0,322	2,47
FKT150-250 %10	4,5	0,359	1,71
FKT150-250 %15	2,8	0,408	1,43
FKT150-250 %20	2,1	0,432	1,05

FKT250-425 %5	7,3	0,299	2,49
FKT250-425%10	4,4	0,352	1,56
FKT250-425%15	2,9	0,398	1,36
FKT250-425%20	2,4	0,413	1,03

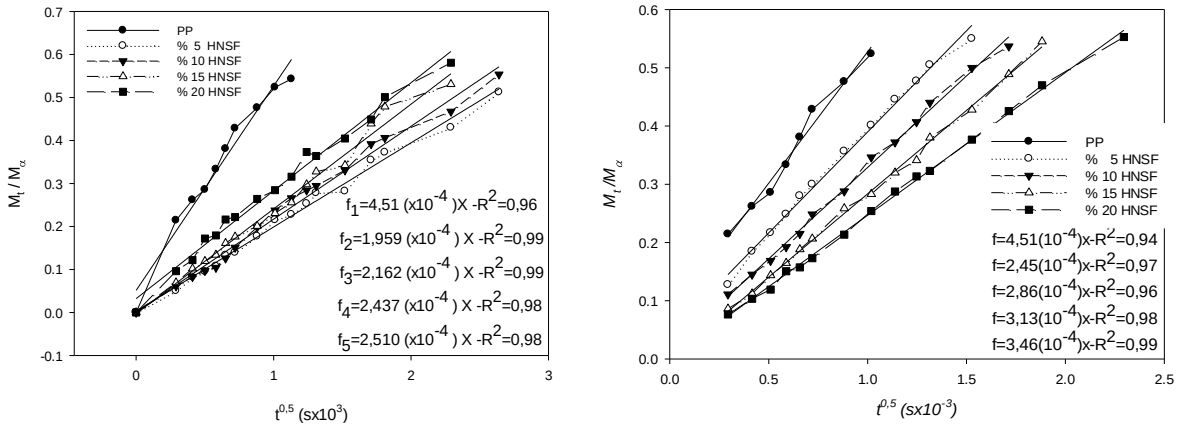

Figure 6. M_t/M_∞ *vs.* $t^{0.5}$ graphics of PP/ hazelnut shell flour composites for first stage: 0.00-0.55 range.

3.4. Permeability

As a result of water absorption, serious water damage can occur throughout the entire composite structure, such as split interfaces and cuts. As a result, the presence of damages caused by hydrophilic fillers and water in the polymer structure affects water absorption kinetics. Water permeability for a composite can be found with the correlation given:

$$P = D.S \qquad (7)$$

here P is permeability coefficient, D is Fick diffusion coefficient, S is sorption coefficient [28]. Permeability coefficient (P) is the stable transition rate of the permenant molecules (water) across a layer of limited thickness. Diffusion coefficient (D) expresses how fast the water molecule moves along a polymer mass. Sorption coefficient (S), is the mass of water absorbed per polymer mass at saturation point. As given in Table 4, the P value of PP was found to be quite low; but this value has increased significantly by increasing the amount of hazelnut shell flour added.

Composites (Symbol)	D ($m^2\ s^{-1}\ 10^{-13}$)	S ($g\ g^{-1}10^{-3}$)	P ($m^2\ s^{-1}\ 10^{-15}$)

PP	3,95	1,66	0,65
FKT.50-150 % 5	2,71	6,15	1,66
FKT.50-150 %10	1,86	10,57	1,96
FKT.50-150 %15	1,64	15,05	1,56
FKT.50-150 %20	1,10	19,85	2,18
FKT150-250 % 5	2,57	5,83	1,49
FKT150-250 %10	1,71	9,65	1,65
FKT150-250 %15	1,43	13,58	1,94
FKT150-250 %20	1,05	17,63	1,85
FKT250-425 %5	2,49	5,45	1,35
FKT250-425%10	1,56	8,90	1,38
FKT250-425%15	1,36	12,63	1,71
FKT250-425%20	1,01	14,29	1,44

4. Results and Discussion

As a result of its hydrophobic character, PP was found to be highly resistant to water absorption. By increasing the amount of hazelnut shell flour, water absorption of PP / hazelnut shell flour composites increased regularly while saturation time was shortened.

It was determined that the water intake behavior of pure PP was approximate to the fick law, but as the amount of additives increased, water absorption kinetics of the PP / hazelnut shell flour composites matched the Fick diffusion mechanism.

The grain size of the hazelnut shell powder affected the rate of water intake. There is a 14% difference in water intake between the smallest grain size composite and the largest grain size composite. Small-grained composites are considered to have a higher surface area and therefore intake water faster.

As a result of this study, it is thought that these composites can be used easily in wet environments where the dimensional stability is not very sensitive when it is considered that the hazelnut shell, which is added to the composites at a maximum of 20%, does not get high moisture, and the additives added during the process decrease the *total* humidity rate.

It is hoped that the produced composite can be used instead of wood in some structural applications so that it will provide significant gains in terms of environment and recovery of waste to the economy. Supporting this composite, which is environment-friendly in this aspect, will also mean supporting sensitivities in this topic.

REFERENCES

[1] J.E. Mark; Polymer Data Handbook, Oxford University Inc.(1999)

[2] R.M.Gill "Carbon Fibers in Composite Materials" The Plastic Institute, U.S.A 1972

[3] Schulz H. Statical and dynamical behavior of machine tool frames made of polymer concrete. Fourth int. Congress, Darmstad; 1984.p. 19-21

[4] Wenjing Guo, Fucheng Bao, Zheng Wang Biodegradability of wood fiber/poly(lactic acid) compositesJournal of Composite Materials, vol. 47, 28: pp. 3573-3580.

[5] Andrzej K. Bledzki, Abdullah A. Mamun, Jürgen Volk ''Physical, chemical and surface properties of wheat husk, rye husk and soft wood and their polypropylene composites'' Composites Part A: Applied Science and Manufacturing, Volume 41, Issue 4, April 2010, Pages 480-488

[6] Espert A, Vilaplana F, Karlsson S, *Composites* A35:1267–1276, 2004.

[7] Panthapulakkal S, Sain M, *J Compos Mater* 41:1871–1883, 2007.

[8] Steckel V, Clemons CM, Thoemen H, *J Appl Polym Sci* 103:752–763, 2007

[9] Beg MDH, Pickering KL, *Composites* A39:1565–1571, 2008.

[10] J.F. Balart, V. Fombuena, O. Fenollar, T. Boronat, L. S_anchez-Nacher , Processing and characterization of high environmental efficiency composites based on PLA and hazelnut shell flour (HSF) with biobased plasticizers derived from epoxidized linseed oil (ELO), Composites Part B 86 (2016) 168-177

[11] Y.Çöpür, C. Güler, C. Taşcıoğlu, A. Tozluoğlu,Incorporation of hazelnut shell and husk in MDF production, Short Communication, Bioresource Technology 99 (2008) 7402–7406

[12] Ayfer M. "Turkish Hazelnut Types " Ankara 1986

[13] Giresun Commodity Exchange Data 2009

[14] Kochetkov VA, Maksimov RD, *Polym Eng Sci* 37:952–958, 1997

[15] Adhikary KB, Pang S, Staiger MP, *Chem Eng J* 142:190–198, 2008.

[16] Siriwardena S, Ismail H, Ishiaku US, *J Reinf Plast Compos* 22:1645–1666, 2003.

[17] Berens AR, *Polymer* 18:697–704, 1977.

[18] Bagley E, Long FA, *J Am Chem Soc* 77:2172–2178, 1955

[19] Adhikary KB, Pang S, Staiger MP, *Chem Eng J* 142:190–198, 2008.

[20] Bouafif H, Koubaa A , Perré P, Cloutier A, Effects Of Fıbre Characterıstıcs On The Physıcal And Mechanıcal Propertıes Of Wood Plastıc Composıtes, Fpcm-9 (2008) The 9th International Conference On Flow Processes İn Composite Materials Montreal (Québec), Canada

[21] Marom G, The role of water transport in composite materials. In: Comyn J (ed) Polymer permeability. Chapman & Hall, Great Britain, pp 341–374, 1985

[22] Ashley RJ, Permeability and plastics packaging. In: Comyn J (ed) Polymer permeability. Chapman & Hall, London, pp 269–308, 1985.

[23] Drozdov AD, Christiansen JC, Gupta RK, Shah AP, *J Polym Sci* B41:476–492, 2003.

[24] Crank J, Park GS, Methods of measurement. In: Crank J, Park GS (eds) Diffusion in polymers. Academic Press, London, pp 1–39, 1968.

[25] Espert A, Vilaplana F, Karlsson S. Comp Part A 2004;35:1267-1276.

[26] Cheng Q, Shaler S. Eur J Wood Prod; 2009:1e6.

[27] Najafi SK, Kiaefar A, Hamidi E, Tajvidi M. J Reinf Plast Comp 2007;26(3): 341e8.

[28] Rangaraj SV, Smith LV. J Therm Comp Mat 2000;13:140-161.

Role of EU Grant Projects in the Technological Renewal of Vocational Schools and Erzincan Vocational School Example

Murat ÇETİN

Erzincan University, Faculty of Engineering, Mechanical Engineering, Erzincan, Turkey
mcetin@erzincan.edu.tr

Abstract

When the education levels of the vocational higher education schools that provide associate degree education in our universities examined in terms of technological development, it is seen that the technological renovation of vocational higher education schools is not at the required speed. On the other hand, the sectors have to be in a very rapid technological change in order for the Turkish economy to integrate to compete with global markets. It seems that the sectorial technological change education institutions, which the education institutions cannot bring to the required level of qualified, qualified and skilled labour, are not able to adapt. These training programs need to plug in technological innovations very well and continuously need be renew themselves technologically. One of the most important resources of this innovation is the utilization of project schemes, which provide financial support, especially the EU grant project schemes. 1.7 million students are trained in 215 different areas in vocational schools which constitute about 30% of the Turkish higher education system. In this study, the projects supported by the EU grant schemes presented on the benefits of the renovation of the technical equipment of the schools and recommendations on the sample of Erzincan Vocational School.

Key words: Vocational School; Project; Education; Technological Innovation

1. Introduction

Turkey, with its young population is the country with an important human potential for a successful future. Turkey's young population, first, middle and higher education makes it mandatory regulations dealt with in a wide range of activities on the development of vocational education. On the basis of university-industry cooperation, the qualification of vocational education starting from the secondary education institutions is the first step and the labor force profile that the sector needs is shaped in the secondary education institutions. In today's vocational technical education, university-sector cooperation has an increasing prevalence due to the change in technological speed. According to the process of structuring these studies according to programs of participation process of the European Union, it is seen that the projects carried out in secondary education and university units produce studies on increasing quality and quantity in vocational technical education. These studies also make university-industry collaboration in the region attractive. At the same time, the decision maker is actively involved in this cooperation as the relevant public institutions. Vocational Schools are higher education institutions providing education and training with a two year associate degree aiming to raise qualified human power for specific professions to meet the sectoral needs. In vocational education in college, the vocational colleges that educate human power have a more conscious basis. Therefore, vocational education in vocational colleges plays an important role in the secondary education of their students, and more importantly, beyond the vocational education, the point of view of life, communication and interaction with the environment is gaining importance. Theoretical knowledge given in university education is given a large amount of practical training and the integration of the students with the students and finally the employment compatible with the profession is realized. In addition, the sector's needs and the quality of the labor force are determined, and the locomotive characteristic of the university is of great importance. Vocational Schools are the most important educational institutions that provide the necessary qualified intermediate staff and graduated students are employed as qualified midterm personnel between engineers or specialists and workers in the sector with the title of Technician and Professional Personnel. The main objective of the vocational colleges is to educate the skilled intermediate human power which is the necessity of the industry and the service sector for the professions. However, vocational colleges also have the aim of producing information through scientific research, disseminating information, transforming it into knowledge product and technology. Vocational training is defined as the type of training that gives individuals knowledge, skills and work habits related to a particular occupation in their work life and develops their skills in various aspects. Vocational education is the result of educational activities that enable an individual to demonstrate his qualitative power and functioning according to

the economic conditions of that country in each country. The main objective of vocational training is to meet the demands of the labor force and qualified labor force demanded by the sectoral sectors. In this sense, vocational and technical education; It is a process which gives knowledge, skills and attitudes related to a certain profession area to meet the needs of society and individuals and which enables the individual to become stronger in social and economical direction by developing his abilities. Vocational training aims at defining individuals as a profession in industry, agriculture, commerce and other service areas, in the development of the profession, in the system integrality of the principles to be applied in the formal, widespread and apprenticeship training for occupational change(1,2).

2. EU Grant Projects and Sector Cooperation

European union; democracy, human rights and market economy by establishing partnerships with countries that share the same core values, economic and social developments provide financial contribution with various financial instruments. These countries are countries that are trying to become members of the European Union or are in the process of membership, and countries in the process are receiving financial support under the pre-accession assistance (IPA) issue as they are considered candidate countries. Grant schemes provide institutions with the opportunity to design and implement projects for their own needs while increasing the level of participation and capacity at the same time. Institutions receiving EU financial support; It contributes to the design and implementation of public policies in various fields, from health, education, infrastructure and rural development. Projects supported by various sources; is a policy instrument that allows for better identification of needs, alignment with national priorities, improvement of participatory planning, improvement of planning concept from top to bottom, promotion of local partnerships and cooperations, increase of project capacity and transparency. On the other hand, projects; It increases transparency as it involves stages such as competitive nature, election criteria, independent appraisal, and public announcement of winners. In addition, participation and collaboration with the required structure contributes to accountability by clearly showing the duties and responsibilities of the personnel at each stage. For example, the increase in the grant and the development of the project consciousness contributes to the recognition of the EU by the society and to the recognition and disappearance of the prejudices. At the same time the donations contribute to the economic growth of the target group and the positive effects of the secondary stakeholders. Projects, it contributes to the development of human capital and the increase in the educated labor force which can use modern technologies and access to modern technologies. In addition, such projects support sectoral

employment growth by creating consciousness in the society at the point of competing and improving the institutions and therefore the individuals. Training projects provide employment sustainability by raising the level of human capital accumulation and the level of employment of the individuals who have achieved knowledge and equipment. The projects determine the local and regional priorities, the need for resources in the region, the applicability of the relevant plans and policies. Achieving the successes and sustainability of the projects will increase the business viability and investment cost of the project beneficiaries by establishing business in the business enlargement or indirect beneficiaries, increasing the quality due to entrepreneurship and competition(3).

Today, as change takes place very quickly, countries struggle hard in the fields of education, health and economy to raise their welfare levels. At the center of this struggle is the ideal of a highly educated society that produces development-based knowledge and technology. Universities, in addition to the education and training activities and the training of the personnel that the region needs, are also involved in the research and development activities to produce the knowledge that the region, the country or the world will need. Universities for high welfare of society; producing information, having knowledge, renewing existing information, and converting new information into new technological product. Sectoral structures, small and medium-sized enterprises (SMEs), which are diversified with their working fields, are of great importance in all countries as well as increasing employment in our country, especially at local and regional level. Universities can contribute to the establishment of the scientific infrastructure of the sectors by producing solutions to sector problems by carrying out applied researches with organizations such as the Chamber of Commerce Industry and the Chamber of Craftsmen in their cities. As a result of the cooperation of the universities with the institutions, concrete projects related to the region have been realized and the projects that have been brought together by the potential project partners and the projects that have been accomplished are of great importance. Academic-level project outputs at universities generate social and economic value by using them on the commercial field or forming the basis of other projects. Projects made with grant schemes have features that can raise awareness as a mechanism to support regional policy instruments or existing tools. Capacity building with EU grant-backed development programs and regional projects coordinated by different ministries has strengthened the network structure to include all actors from place to place. Projects; every sector of the economy in our country provides opportunities for the rehabilitation of equipment and equipment for both schools and sectors while contributing to vocational training needs through the use of new technologies(4).

3. The Role of Projects in Technological Renewal and the Example of Erzincan Vocational School

The power of countries depends on the continuity of their ability to raise younger generations as creative, productive and responsible individuals in the business world and future society. Achieving this in our country is possible only if all sectors of society can work together with dedication in the targets and strategies. Strengthening technological sub-structures of projects with vocational colleges and universities play an important role in informing educators according to new technology, determining local labor market needs, raising workforce in areas where industry needs and reducing unemployment. In the projects aiming to equip the laboratories with necessary equipments; cooperation with industry firms and dealers is important. Fully equipped laboratories established with such project supports provide education for an average of 30-40 students each year. While school laboratories are equipped with special equipment for technological training and practical training is being carried out, the trainees have the opportunity to renew themselves in entrepreneurial spirit and quality systems using high-tech production systems. Especially in the underdeveloped provinces, the universities are the most effective and innovative institution that will increase the potentials from economic and social point of view. In this context; Erzincan Vocational School, which is a model training unit for our region and region, is in communication, interaction and cooperation with all sectors of industry and society. These communication, interaction and cooperation countries are being updated considering the universal need for qualified human resources in the framework of university-local government-industry collaboration. Erzincan Vocational High School offers seminars and conferences where industrial students, internships, employment, sectoral vocational training and consultancy requirements are met while the successful businessmen in our city meet with our students. On the other hand, various collaborations with the Chamber of Commerce, Chamber of Craftsmen and NGOs on EU grants and SODES projects have been carried out and various vocational trainings have been organized for collecting and unemployed. Erzincan University Vocational School has completed 3 EU Grant Projects between 2006-2016 and has managed and managed the project as a partner of 3 EU Grant Projects. In addition, he has undertaken 1 SODES project which has undertaken and owns 2 vocational training projects in common within the scope of SODES projects. Since 2006, it has been actively involved in the application of 11 projects submitted under the EU Pre-Accession Financial Assistance Instrument (IPA), which are supported by lifelong learning, support for women's employment, support for younger employment and support for innovative methods registered employment. Table 1 and Table 2 show the

distributions of AB and SIDES projects, which are owned and partnered by Erzincan Vocational School.

Table 1. Projeler of Erzincan Vocational High School

Years	Beneficiary	Program Title	Title Project Name	Budget
2006-07	Erzincan Vocational School	Local Development Initiatives	Educated Mechanic, Clean Vehicle and Clean Environment	70500(Avro)
2006-07	Erzincan Vocational School	Local Development Initiatives	Computer Aided (CNC Machining Systems Training)	93555(Avro)
2016-17	Erzincan Vocational School	Supporting Young Employment in Sectoral Investment Areas II	Innovations in Auto Repairs, Young Generation and New Horizons	246805(Avro)
2013-14	Erzincan Vocational School	SODES	Automotive Electronics and Diagnostic Education Project	79.900 TL
Total				**410.860 EURO / 79.900 Turkish Lira**

As a result of these vocational trainings, approximately 275 disadvantaged target groups have been trained and contributed to their employment in sectoral areas. Such project studies have improved the institutionalization and functionalities of civil organizations and have made great achievements in terms of the success of the projects, the modeling of the project activities and the renewal of the projects in the future. Depending on the achievement of these goals, institutionalization in our city, changes in management models and innovations have increased. As the result of the project activities; The University-Industry Cooperation is mutually preoccupied and an increase in the co-operation of the parties was observed. Erzincan Vocational School has been the driving force of this cooperation and the influence of vocational colleges on institutions in cities is high especially for cooperation of universities in undeveloped provinces. Since 2006 Erzincan University Erzincan Vocational School has been the most effective institution providing sustainability in the development process of our city(4).

Table 2. Projects of Erzincan Vocational School is as a partner

Years	Beneficiary	Program Title	Title Project Name	Budget
2010-11	Erzincan Province Special Administration	Support for Women's Employment	Let Women Hands Touch, Let the Country Be Fruitful	228 807 Euro
2010-11	Erzincan Social Assistance and Solidarity Foundation	Support for Women's Employment	Second Spring in Erzincan	320.521 Euro

2010-11	Erzincan Old Age Protection and Development Association	Support for Women's Employment	Home, Elderly, Patient and Child Care Personnel Training	205.575 Euro
2012-13	Erzincan Oto Tamirciler Odası	SODES	Certified Auto Repairing and Vocational Training	100.000 Turkish Lira
Total			754.903 Euro / 100.000 Turkish Lira	

It is observed that Erzincan Vocational School is trying to strengthen vocational education within the scope of European Union supports and shows importance and sensitivity in terms of qualitative and quantitative improvement of vocational education. The most noteworthy of these efforts is the university-sector cooperation, especially the joint EU grant projects. The establishment of a modern, exchangeable and quality vocational-technical education system that will be able to respond to the demands of the labor market and sectors and to create an integrity between primary, secondary and higher education associate degrees is of great importance for the future. When cooperation between the sector and the university is evaluated, it is very important for Erzincan University Vocational School to work in partnership with the business world of our university. These projects were carried out intensively in Erzincan Vocational School automotive technology program. Cooperation is very important in terms of sustainability of the projects and our partners are professional chambers of Erzincan Chamber of Commerce and Erzincan Union of Craftsmen and Artisans Chambers. Erzincan University Vocational School; continues to work with social initiatives with the formation of a trusting, encouraging and courageous structure that will enable the public institutions, educational institutions, local governments, professional organizations and non-governmental organizations in our province to be active in the future project activities. These projects, which were successfully completed at our school, made a big contribution to our school as our technological equipment and equipment(4,5). Table 3 shows the Erzincan Vocational School's project support and machine-and-equipment for machine and automotive technology programs.

Table 3. Equipments provided by Erzincan Vocational College Projects

Years	Project Name	Receiving Equipment	Estimated value
2006-07	Educated Mechanic, Clean Vehicle and Clean Environment	1 pcs Bosch BEA 370 Emission Device, 1 pcs Bosch FSA 751- KTS 650 fault finding device, 1pcs gasoline engine, 1 pcs diesel engine, 1 pcs Carbon cleaner device, 2 pcs Tool set (120 pieces), 1 pc Diesel injector testing and setting device, 1pcs photocopy machine, 1 pcs laptop computer, 1 pcs printer, 1 pcs desktop computer, 2 pcs projectors	37400 Euro

2006-07	Computer Aided (CNC Machining Systems Training)	1pcs CNC Lathe, 1 CNC Milling Machine, 1 pcs photocopy machine, 1 pcs laptop computer, 12 pcs desktop computers, 2 pcs projectors	52000 Euro
2013-14	Automotive Electronics and Diagnostic Education Project	1pcs photocopy machine, 1 pcslaptop computer 1 pcs desktop computer,	9000 Turkish Lira
2016-17	Innovations in Auto Repairs, Young Generation and New Horizons	5 pcs Tool set (120 pieces), 1 gas welding machine, 1 pcs battery charger, 3 pcslaptop computers, 2 pcs desktop computers, 1 pcs diesel motor car 2016 model (training, application and experimental research vehicle)	32000 Euro
Total		121.400 Euro +9000 Turkish Lira	

4. Results

Vocational technical training is an expensive education due to the requirement of various technological tools, hardware, software, laboratories and constant renewal. The speed with which technological developments emerge is more than the speed at which educational institutions are able to understand the value of these new tools in their learning processes and to be able to make informed practices. Since technological tools and equipment are obsolete over time and technologically obsolete, continuous renewal of all equipment requires a serious resource. The most important resource to be used in hardware updating of laboratories for technological innovations is that the program is being utilized from various project supports. This resource problem solution is possible by preparing projects and submitting them to different units. In addition to improving and restructuring laboratory conditions, the projects should contribute to the organization of trainings in order to ensure that the students receiving technical and vocational training have the qualifications and equipment to meet the expectations of the industry. As a result, it is imperative that each educational unit or whole education system has a mission and vision related to educational technology. In this mission and the vision, the parameters that determine the technology target should be made on the basis of the desired targets to be changed in the education system, not with the unplanned and remote control solutions. The systematic approach to renewing education technology, the need for analysis, strategy and solution proposals should be in accordance with the grant projects and the project objectives and the school objectives should overlap. It must be taken into account that society and people-centered processes are all characterized by a sustainability-based structure at all stages of decision-making. It is of great importance for the success of the social projects of the educational projects that the local partners have the same feeling and common sense for success, since the local communities do not accept the policies that they do not care about and can not digest.

5. References

1. Alkan, C., Doğan, H., Sezgin, İ.,(1996), Principles of Vocational Technical Education(Turkish). Gazi Büro Kitabevi. Ankara.
2. Higher Education Law(Turkish), official gazette dated 04/11/1981 and numbered 17506.
3. http://ec.europa.eu/regional policy/en/funding/ipa/)., for Pre-Accession Assistance (IPA).
4. Çetin M., Orman K., "Erzincan Reflections of EU Grant Projects and Looking to the Future", International Congress on Intercultural Dialogue and Educatıon., BURSA., 2009.
5. Cetin. M., EU education project of effects on auto mechanics in terms of health, safety and environmental sensitivity., Energy Education Science and Technology Part B: Social and Educational Studies.,Volume(issue) 4(1): 87-96., 2012.

Experimental and Analytical Investigation of Friction and Wear Properties of Graphene Oxide Filled PP Polymer Nanocomposites

Salih Hakan YETGIN[1*], Hüseyin UNAL[2]

[1]Dumlupınar Üni., Simav Technology Faculty, Department of Mechanical Engineering, Kütahya, Turkey, shyetgin@gmail.com
[2]Sakarya Üni., Technology Faculty, Department of Metallurgy and Materials Engineering, Sakarya, Turkey, unal@sakarya.edu.tr

[*]**Sorumlu Yazar:** shyetgin@gmail.com

Abstract

In this study, the effects of applied load and sliding speed on the friction and wear behaviors of polypropylene (PP) nano-composite with the addition of 0.5% by weight graphene oxide were investigated experimentally and analytically. The friction and wear tests of the PP nano-composite were carried out with the pin-on-disc wear test system against the AISI 1040 steel under dry environment conditions. The regression analysis was carried out to develop an equation in which the friction and wear behavior of the PP nano-composite material is expressed in terms of applied load and sliding speed. At both low and high sliding speed, the friction coefficient of PP nano-composites increased with the increase in applied load. Moreover, the wear rate of increased with the increment of applied load and sliding speed values. As a result of the regression analysis, it was determined that Gaussion and Lorentzian mathematical models are suitable for the friction coefficient results and Lorentzian mathematical model is suitable for the wear rate results.

Keywords: Friction, Wear, Regression analysis, Graphene oxide, Polypropylene

1. Introduction

In recent years, polymeric composites have become widely used engineering materials for use in automotive, electronics, construction, home furnishings and similar industries. The most important advantage of these materials is their low density and high strength/weight ratio. However, their usage areas are limited due to their low mechanical properties, low thermal and electrical properties. Different types of additives and reinforcing agents are added to polymer materials to improve its mechanical and tribological and other properties. Traditionally, micro-size fillers and reinforcements have been used to improve the mechanical and tribological properties of the polymer matrix materials. In recent years, carbon-based nanoparticles (carbon nanotube and graphene oxide) have become the most important material group for improving the tribological properties of polymers because of their superior thermal, electrical, mechanical properties and large surface area [1-3]. Many studies have been carried out on the mechanical [4-10] and tribological [11-15] properties of carbon nanotube (CNT) and graphene reinforced polymer composites. Dong et al. [16] studied the effect of multi-wall carbon nanotube (MWCNT) additives on the friction and wear properties of nano-composites. As a result of the study, MWCNT reinforcement decreased the coefficient of friction and wear rate of the nano-composites. Li et al. [17] studied the tribological properties of graphene oxide reinforcement in

the nitrile rubber under dry and aqueous media conditions. As a result of the study, they determined that both the friction coefficient and the wear rate decreased with the addition of graphene oxide reinforcement into the nitrile rubber compound. Golchin et al. [1] have investigated the tribological properties of multi-walled carbon nanotubes (MWCNT) and graphene oxide reinforcement added into the Ultra High Molecular Weight Polyethylene (UHMWPE) polymer. As a result of the study, they have reported that the friction coefficient and wear rate values decreased with the addition of multi-walled carbon nanotubes and graphene oxide into the UHMWPE polymer. Liu et al. [18] studied the tribological properties of thermoset polyimide (PI)/graphene oxide nano-composites. Experimental studies have indicated that the friction and abrasion properties of the polyimide polymer are improved by the addition of graphene oxide. The reason for this is attributed to the uniform transfer film layer formed and the increased load-carrying capacity. Padenko et al. [19] investigated the friction and wear properties of functionalized graphene reinforced poly-tetra-fluoro-ethylene (PTFE) polymer at 0-4% by weight. As a result of the study, it has been determined that the friction coefficient decreases with the addition of graphene oxide reinforcement into the PTFE polymer. They determined that the wear rate increased upto 1% graphene oxide reinforcement addition into the PTFE and decreased after this addition. The reason for this explained by transfer film layer. They have indicated that they have important influence on the friction and abrasion properties of the resulting transfer film layer. Yingfeian et al. [20] investigated the friction and wear properties of UHMWPE polymer composites with graphene oxide reinforcement content. In addition, the study also analyzed the results obtained with ANOVA. As a result of the study, it was stated that the friction coefficient increased slightly and the wear rate decreased with the addition of graphene oxide reinforcement into the UHMWPE polymer. Song et al. [2] have examined that the effect of applied load and sliding speed on the tribological properties of poly-ether-ether-ketone (PEEK) composites with multi-walled carbon nanotube, graphene oxide nano-sheet and c-aminopropyl trimethoxysilane-modified graphene oxide (GO-Si) nano-sheets. As a result of the study, it was stated that the friction coefficient and wear rate decreased until 2.94N applied load and then increased after this load value. In addition, the friction coefficient and wear rate increased after the sliding speed of 0.0628m/s. Tai et al. [21] investigated the mechanical and tribological properties of graphene oxide reinforced UHMWPE polymer composite. As a result, the addition of graphene oxide reinforcement into the UHMWPE polymer, the friction coefficient increased while the wear rate decreased. In addition to experimental studies, mathematical relationships between process conditions (such as load, sliding distance, ambient conditions) and polymer to understand and interpret wear behaviors should also be investigated. Mishra [22] statistically examined the wear behaviors of sugarcane bagasse reinforced polymer composites. Liu et al. [23] studied the effects of parameters such as sliding distance, contact

pressure, and sliding speed on wear behaviors of polyamide (PA) and UHMWPE polymers by statistical analysis. Sagbas et al. [24] have also investigated the effects of load and sliding speed on friction and wear behavior of poly-oxy-methylene (POM) polymer with a mathematical model. It is important to know the effects of process conditions and their interactions on friction and wear behavior in order to expand the application areas of polymer materials. It is expected that such information will contribute to the understanding of polymers' friction and wear behavior, optimize the use of materials, and at the same time help to develop new materials.

In this study, mathematical models and experimental data were used to estimate the wear performance of 0.5wt.% graphene oxide reinforced polypropylene polymer nano-composite. The tribological tests were carried out by using a pin-disc wear test rig under dry sliding conditions. The effects of graphene oxide reinforced PP polymer nano-composite on the sliding speed and applied load were investigated. Wear tests were carried out at between 10-40N load and 0.4-1.6m/s sliding speed under dry sliding condition. Experimental results and mathematical equations such as paraboloid, Gaussian and Lorentzian were used to correlate wear behaviors of graphene oxide reinforced PP polymer nano-composite.

2. Material and Method

In this work, polypropylene polymer (PP3374E3 commercial code) with a density of 0.91 g/ cm^3 was used as the matrix material. Thermally expanded graphene oxide was used as a reinforcement material in the PP polymer matrix. It was supplied by Nanografen Co. in Turkey. Figure 1 shows the production scheme of 0.5% graphene oxide reinforced PP nano-composite. Prior to the production of the nano-composite, the graphene oxide was mixed with distilled water in an ultrasonic mixer to separate the layers. The obtained mixture was mixed with the PP polymer and dried at 100 ^oC for 2 hours before the extrusion process. PP nano-composite granules with 0.5wt.% graphene oxide were produced in a twin screw extruder (NRII-75-Werner Pfleiderer model) at a temperature range of 185-210^oC. Wear test samples were molded by using an injection molding machine. Injection temperatures of the injection machine heater were determined to be 190-220^oC. The mold temperature is fixed at 30°C. The surface morphology of the pre-and post-solution graphene oxide reinforcement was investigated by a scanning electron microscope (SEM) (FEI-NanoSEM 650 model).

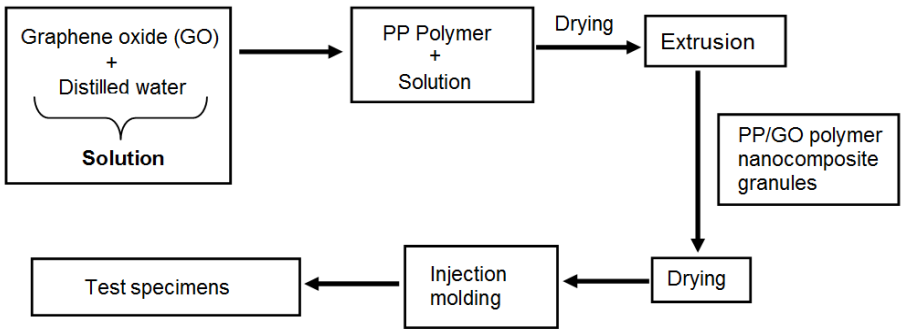

Figure 1. Production process of graphene oxide reinforced PP nano-composite

Wear tests were performed at room temperature using a pin-on-disc wear test rig under dry sliding conditions. Cylindrical pin specimens with a diameter of 6 mm and a length of 40 mm were tested against AISI 1040 steel disc. Figure 2 shows the pin-on-disc wear test rig which is designed for this study. Before each test, pin and disc surfaces were cleaned with alcohol and then dried. In Table 1, the experimental conditions (applied load, sliding speed and ambient temperature) are given. Before and after each wear test, the weights of the pins were measured and the weight loss (Δm) was determined. The wear rates (Ko) of the test specimens were calculated using the following formula.

$$K_o = \frac{\Delta m}{L * \rho * F} \ (\mathrm{m}^2/\mathrm{N}) \qquad (1)$$

where; Δm is the weight loss (g), L is the sliding distance (m), ρ is the density of the material (g / cm^3), F is the applied load (N).

During the wear test, friction force was measured by a load cell sensor mounted on the loading arm on pin-disc wear tester. The friction force readings were taken as the average of 10 readings every one second during testing time. The coefficient of friction values (μ) were directly obtained from the equipment that records the μ value by using the following relation: $\mu = F_s/F_N$. Where, Fs is the frictional force and F_N is the applied load on the wear test specimen.

Figure 2. Pin-on-disc wear test rig

Table 1. Wear test conditions

Parameters	**Test conditions**
Applied load (N)	10, 20, 30, 40
Sliding speed (m/s)	0.4, 0.8, 1.2, 1.6
Sliding distance (m)	1000
Temperature (^{o}C)	23
Humudity (%)	61

The paraboloid, Gaussian and Lorentzian mathematical equations (Table 2) were used to estimate friction coefficient and wear rate changes depending on applied load and sliding speed. The a, b, c, xo and yo constants given in Equation are the specific constants of the PP nano-composite depending on the wear test conditions. These constants were obtained by Sigma Plot 13.0 software using the equations given in Table 2.

3. Results and Discussion

Figure 3 shows SEM images of the pre-and post-solution graphene oxide layers. Thermal expansion has a worm-like structure that causes the separation of oxygen functional groups from the surface of the graphene sheets, separation of the layers from each other, and accordion-like expansion [25].

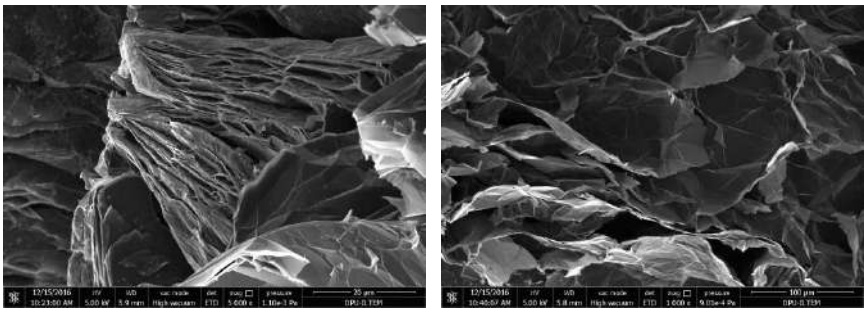

Figure 3. SEM images of the pre-and post-solution graphene oxide layers

Figure 4 shows the changes in the friction coefficient of PP nano-composite depending on the applied load and sliding speed. At all sliding speed, the friction coefficient increases with the increase in applied load. As the load increased from 10N to 40N, the friction coefficients at the sliding speeds of 0.4, 0.8, 1.2 and 1.6 m/s were increased by 33%, 38%, 39% and 46%, respectively. As seen in the

counter diagram, the friction coefficient values with applied load are more affected than sliding speed. Lee et al. [26] studied the tribological properties of CNT reinforced polyamide-66 (PA-66) polymer composites and found that the coefficient of friction did not change much due to low heat accumulation at low sliding speeds. However, when the sliding speed increases, the thermal conductivity plays an important role in determining the tribological properties due to the increasing temperature of the sliding surface of the pin and disc material. Similar results were obtained by Khun [12].

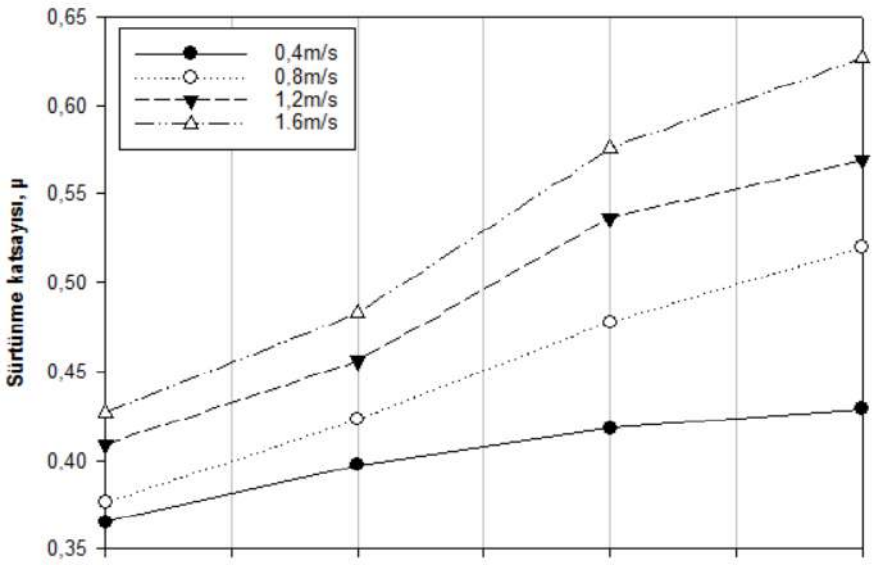

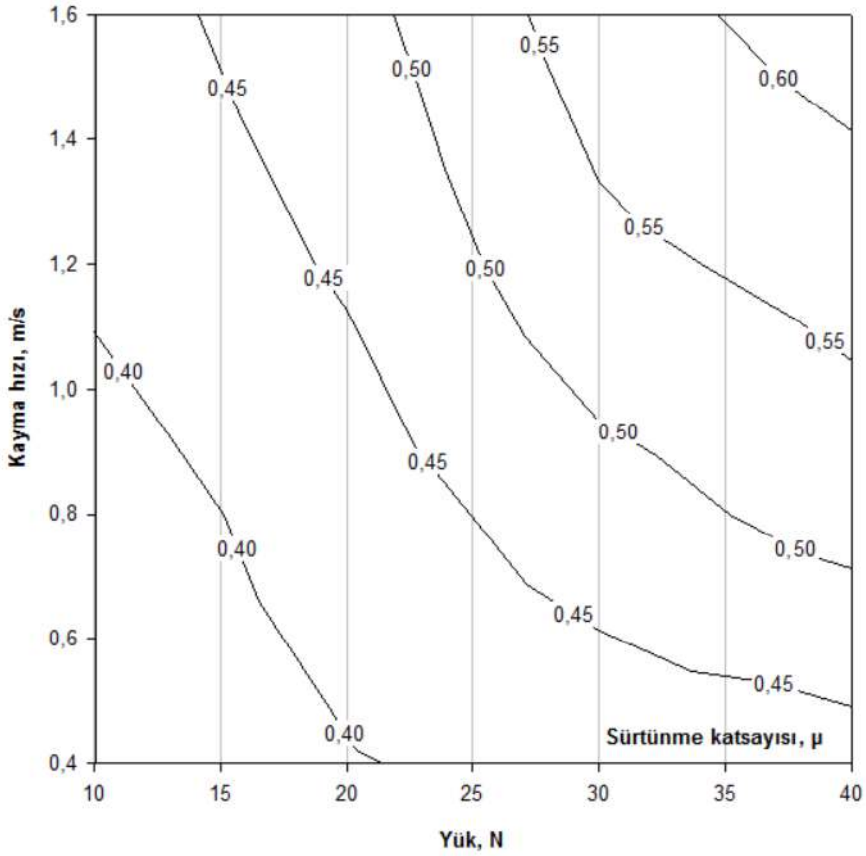

Figure 4. The counter diagram of coefficient of friction of PP nano-composite with 0.5wt.% graphene oxide reinforcement, depending on sliding speed and applied load.

Figure 5 shows the experimental and predicted results of the change in friction coefficient of PP nano-composite material depending on the applied load at 0.4m/s sliding speed. In this figure, the Paraboloid, Gaussian and Lorentzian mathematical equations are used to obtain the counter diagram of the friction coefficient as a function of sliding speed and applied load. For this, the the experimental data in Fig. 4 were used. The correlation coefficients (R^2) of the Paraboloid, Gaussion and Lorentzian mathematical equations were 92.39%, 95.71% and 95.79%, respectively. As shown in Figure 5, the best correlation coefficient is obtained for Gaussian and Lorentzian mathematical equations.

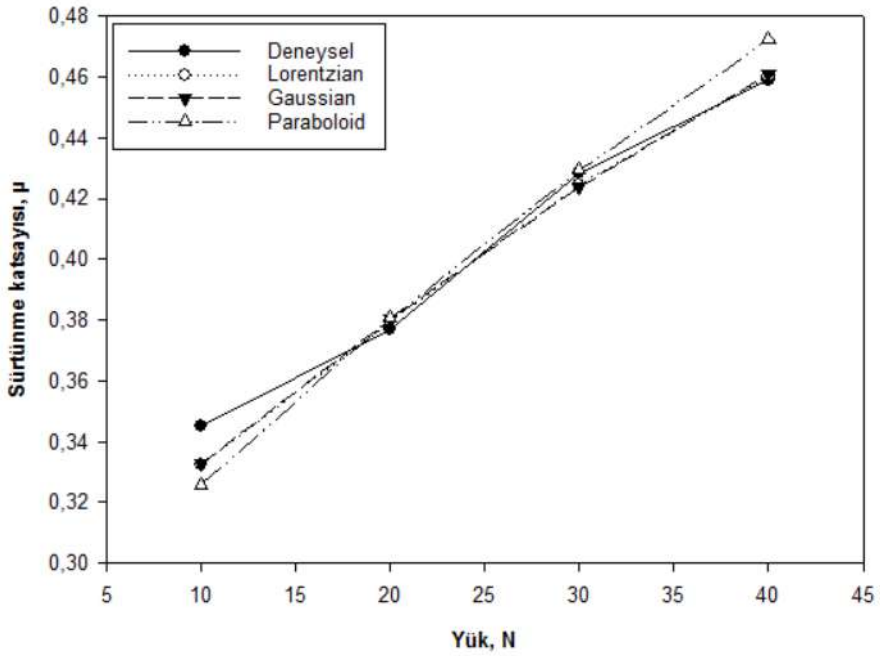

Figure 5. The experimental and predicted changes in friction coefficients of PP nano-composite material with 0.5wt.% graphene oxide depending on the applied load (sliding speed: 0.4m/s)

Figure 6 shows that the wear rate graph and the counter diagram of PP nano-composite reinforced with 0.5% graphene oxide depending on applied load and sliding speed. As seen in Figure, the wear rate increases with the increment of sliding speed. The change in friction coefficient and wear rate depending on sliding speed is closely related to the friction-induced heat at the friction interface at high sliding speeds [2]. In this case, the degradation and decomposition of the PP matrix and various additives accelerate and as a result, the wear of the PP polymer nano-composite becomes more severe as the sliding speed increases. Moreover, in the load range of 10-40N, it was observed that the wear rate increased depending on the applied load. Khun [12] and Cai [14] obtained similar results in their studies. As can be seen in Figure 6, wear rates can be predicted in the contour diagram obtained from the experimental results, depending on the applied load and sliding speed of PP nano-composites reinforced with 0.5wt.% graphene oxide.

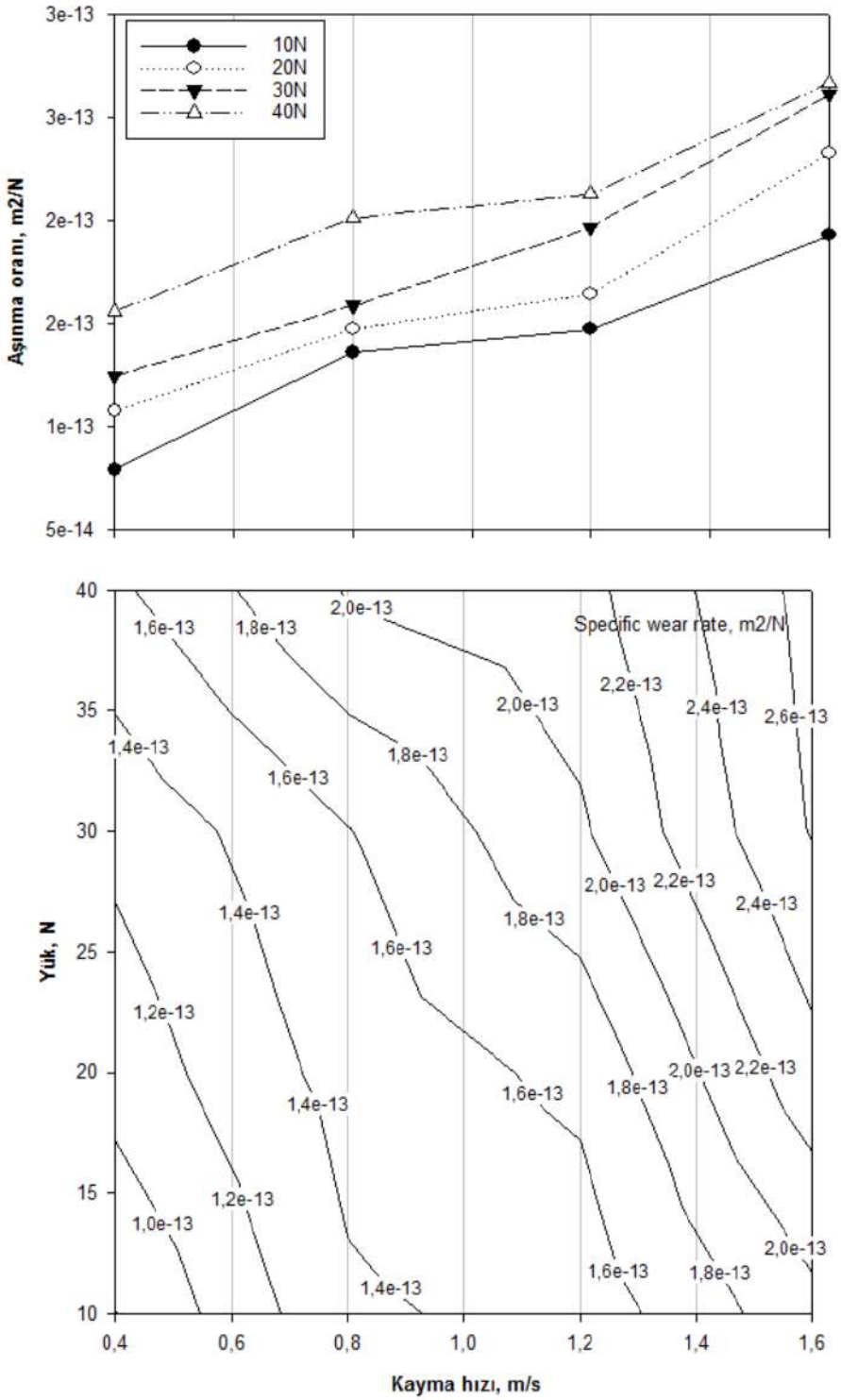

Figure 6. The wear rate graph and counter diagram of PP nano-composite filled with 0.5wt.% graphene oxide

Figure 7 compares the wear rates obtained from the experimental works and the wear rates obtained using Paraboloid, Gaussian and Lorentzian mathematical equations under the load of 30N.

The correlation coefficients (R^2) of Paraboloid, Gaussion and Lorentzian mathematical equations were 96.04%, 96.48% and 97.86%, respectively. As can be seen in Figure 7, the wear rate results obtained with Lorentzian equations are the closest result to experimental work.

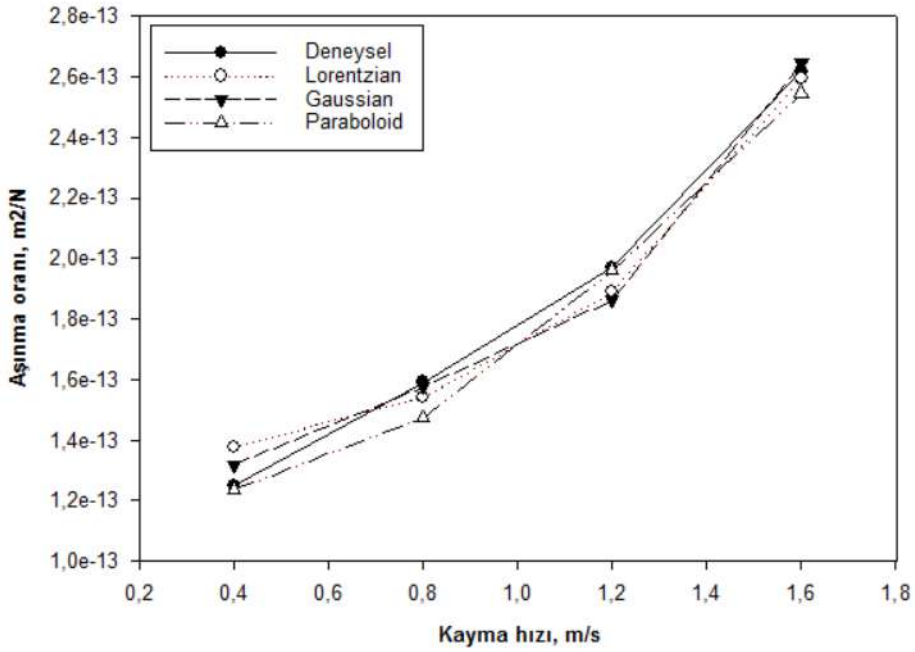

Figure 7. Experimental and predicted change in wear rates of PP nano-composite filled with 0.5wt.% graphene oxide (applied load: 30N)

4. Results

In the experimental study, the following conclusions can be drawn depend on experimental friction and wear results and regression analysis results.

1. The coefficient of friction for graphene oxide filled PP composites increased with increasing in applied load and sliding speed.
2. The best effective parameter for coefficient of friction is applied load.
3. The specific wear rate increased with the increment of applied load for graphene oxide filled PP composites
4. The average specific wear rate were obtained with a value of 10^{-13} m^2/N for graphene oxide filled PP composites
5. The best correlation factor of coefficient of friction with a value of %95.71 and %95.79 were obtained by Gaussion ve Lorentzian mathematical equations, respectively.
6. The best correlation factor for specific wear rates with a value of %97.86 were obtained by Lorentzian mathematical equations.

Table 2. Mathematical equations used in predicting the coefficient of friction and wear rate of graphene oxide filled PP nanocomposite

Equation	Formulas	Coefficient of friction Constant values used in regression analysis					Wear rate Constant values used in regression analysis				
		a	***b***	***c***	X_0	Y_0	***a***	***b***	***c***	X_0	Y_0
Paraboloid	$f = y_0+(ax)+(by)+(cx^2)+(x_0y^2)$	$6{,}32E^{-03}$	$1{,}41E^{-01}$	$-2{,}88E^{-05}$	-	$2{,}12E^{-01}$	$2{,}09E^{-15}$	$5{,}90E^{-14}$	$3{,}49E^{-17}$	-	$3{,}74E^{-14}$
Gaussian	$f=a\cdot\exp^{-0.5[((t-x0)/b))2+((T-y0)c)2]}$	0,7312	63,24	2,644	68,42	2,645	$3{,}74E^{-13}$	9,09	$5{,}46E^{-01}$	$4{,}00E^{+01}$	1,60
Lorentzian	$f=a/[1+((t-x0)/b)^2\cdot[1+((T-y0)/c)^2]$	$6{,}66E^{-01}$	$6{,}58E^{+01}$	2,93	5,40	2,21	$4{,}19E^{-13}$	$1{,}00E^{+01}$	$6{,}00E^{-01}$	$4{,}00E^{+01}$	1,60

References

1. Golchin, A. A. W., and Nazanin, E., (2016). An investigation into tribological behaviour of multi-walled carbon nanotube/graphene oxide reinforced UHMWPE in water lubricated contacts. *Tribology International*, 95, 156-161.
2. Song, H., Na, L., Yanjie, L., Chunying, M., and Zhen, W., (2012). Preparation and tribological properties of graphene/poly(ether ether ketone) nanocomposites. *Journal of Materials Science*, 47, 6436–6443.
3. Zhang, M. Q., Rong, M. Z., Yu, S. L., Wetzel, B., and Friedrich, K., (2002), Effect of particle surface treatment on the tribological performance of epoxy based nano-composites. Wear, 253, 1086–1093.
4. Hargitai, H., and Török, D., (2014). Mixing Efficiency Study of Nano and Micro Filled PP Systems. *Acta Technica Jaurinensis*, 7(4), 344-355.
5. Feng, Q., Yongbo, H., Xiaoyun, L., Bo, W., and Ming, W., (2015). Functionalized graphene sheets filled isotactic polypropylene nanocomposites. *Composites Part B: Engineering*, 175-183.
6. Xubing, F., Yan, L., Xingke, Z., Dajiang, Z., and Guisheng, Y., (2015). A commercial production route to prepare polymer-based nanocomposites by unmodified multilayer graphene. *Journal of Applied Polymer Science*, 1-12.
7. Woo-Seok, K., Kyong, Y. R., and Soo-Jin, P., (2016). Thermal, impact and toughness behaviors of expanded graphite/graphite oxide-filled epoxy composites. *Composites Part B: Engineering*, 94(1), 238-244.
8. Bettina, D., Karen-Alessa, W., Daniel, H., Rolf, M., and Bernhard, S., (2013). Flame retardancy through carbon nanomaterials: Carbon black, multiwall nanotubes, expanded graphite, multi-layer graphene and graphene in polypropylene. *Polymer Degradation and Stability*, 98(8), 1495-1505.
9. Sen-Sen, D., Fei, L., Hong-Mei, X., Yuan-Qing, L., Ning, H., and Shao-Yun, F., (2016). Tensile and flexural properties of graphene oxide coated-short glass fiber reinforced polyethersulfone composites. *Composites Part B: Engineering*, 99, 407-415.
10. Ji-Zhao, L., Qiang, D., Gary, C. P. T., and Chak-Yin, T., (2016). Tensile properties of graphene nano-platelets reinforced polypropylene composites. *Composites Part B: Engineering*, 95, 166-171.
11. Sakka, M. M., Antar, Z., Elleuch, K., and Feller, J. F., (2017). Tribological response of an epoxy matrix filled with graphite and/or carbon nanotubes. *Friction*, 5(2), 171–182.
12. Khun, N. W., He, Z., Lee, H. L., and Jinglei, Y., (2015). Mechanical and Tribological Properties of Graphene Modified Epoxy Composites. *KMUTNB Int. Journal Applied Science Technology*, 8(2), 101-109.
13. Li, Q., Yongkang, C., Yongzhen, Y., Lihua, X., and Xuguang, L., (2013). A Study of Surface Modifications of Carbon Nanotubes on the Properties of Polyamide 66/Multiwalled Carbon Nanotube Composites. *Journal of Nanomaterials*, 1-8.
14. Cai, C., Wang, W., and Zhang, J., (2016). The effect of surface functionality of carbon nanotubes on mechanical and tribological behaviours of carbon fibre-filled styrene–butadiene rubber composite. *Journal of Thermoplastic Composite Materials*, 29(9), 1167–1175.
15. Nie, W. Z., (2011). The effect of carbon nanotubes on the tribological behaviors of PEEK composites. *Advanced Materials Research*, 295-297, 140-143.
16. Dong, B., Yang, Z., and Huang, Y., (2005). Study on tribological properties of multi-walled carbon nanotubes/epoxy resin nanocomposites. *Tribology Letters*, 20(3-4), 251–254.
17. Li, Y., Qihua, W., Tingmei, W., and Guangqin, P., (2012). Preparation and tribological properties of graphene oxide/nitrile rubber nanocomposites. *Journal of Materials Science*, 47, 730–738.
18. Hong, L., Yuqi, L., Tingmei, W., and Qihua, W., (2012). In situ synthesis and thermal, tribological properties of thermosetting polyimide/graphene oxide nanocomposites. *Journal of Materials Science*, 47(4), 1867–1874.
19. Padenko, E., Van Rooyen, L.J, Wetzel, B., and Karger-Kocsis, J., (2016). "Ultralow'' sliding wear polytetrafluoro ethylene nanocomposites with functionalized graphene. *Journal of Reinforced Plastics and Composites*, 1–10.

20. An, Y., Zhixin, T., Yuanyuan, Q., Xingbin, Y., Bin, L., Qunji, X., and Jinying, P., (2014). Friction and Wear Properties of Graphene Oxide/Ultrahigh-MolecularWeight Polyethylene Composites Under the Lubrication of Deionized Water and Normal Saline Solution. *Journal of Applied Polymer Science*, 1-11.
21. Tai, Z., Yuanfeng, C., Yingfei, A., Xingbin, Y., and Qunji, X., (2012). Tribological Behavior of UHMWPE Reinforced with Graphene Oxide Nanosheets. *Tribology Letters*, 46, 55–63.
22. Punyaprıya, M., (2012). Statıstıcal Analysıs For The Abrasıve Wear Behavıor of Bagasse Fıber Reınforced Polymer Composıte. *International Journal of Applied Research in Mechanical Engineering (IJARME)*, 2(2), 7-11.
23. Liu, C., Ren, L., Arnell, R. D., and Tong, J., (1999). Abrasive Wear Behavior of Particle Reinforced Ultrahigh Molecular Weight Polyethylene Composites. *Wear*, 225, 199–204.
24. Sagbas, A. F., and Kahraman, U. E., (2009). Modelıng and Predıctıng Abrasıve Wear Behavıour of Poly Oxy Methylenes Usıng Response Surface Methodolgy and Neural Networks. *Metalurgıja*, 48(2), 117-120.
25. Saner, B., Fatma, D., and Yuda, Y., (2011). Utilization of multiple graphene nanosheets in fuel cells: 2. The effect of oxidation process on the characteristics of graphene nanosheets. *Fuel*, 90(8), 2609-2616**.**
26. Lee, S. M., Shin, M. W., and Jangn, H., (2014). Effect of carbon-nanotube length on friction and wear of polyamide 6,6 nanocomposites. *Wear*, 320, 103–110.

Investigation of Tribological Properties of Polytetrafluoroethylene (*PTFE*) and Wax Filled Carbon Fiber/PA6 Polymer Composites Under Dry Sliding Conditions

Mehmet TAŞKIRAN[1], Salih Hakan YETGIN[2*]

[1]Dumlupınar Üniversity, *Institute of Science and Technology*, Kütahya, Turkey.
[2]Dumlupınar Üniversity, Simav Technology Faculty, Department of Mechanical Engineering, Kütahya, Turkey.

[*]**Sorumlu Yazar:** shyetgin@gmail.com

Abstract

The friction and wear performance of Polyamide 6 (PA6), 20%wt. carbon fiber filled Polyamide 6 (PA6-20CF), 5%wt. polytetrafluoroethylene (*PTFE*) filled carbon fiber/Polyamide 6 (PA6-20CF-5PTFE) and 5%wt. polytetrafluoroethylene (*PTFE*)/2%wt wax filled carbon fiber/Polyamide 6 (PA6-20CF-5PTFE-2Wax) polymers comparatively evaluated under dry sliding conditions. The sliding experiments were carried out on a pin-on-disc tribometer. The contact configuration used a polymer pin on a rotating steel disc. Wear tests were carried out at room temperature under 10, 20 and 30N loads and at 0.4, 0.8 and 1.2 m/s sliding speed. The results show that the coefficient of friction for PA6 composites increases with the increase in load and sliding speed values. The coefficient of friction and specific wear rate for PA6-20CF-10PTFE polymer is obtained lower than that of PA6 and PA6-20CF polymers.

Keywords: Friction, Wear, PA6, Carbon Fiber, PTFE, Wax

1. Introduction

Polymer and their composites are widely used in engineering applications such as automotive and aerospace as alternative to traditional metal materials due to their good mechanical and tribological properties, excellent thermal performance, and also lightweight [1-3]. Polyamide 6 (PA6) is a semi-crystalline thermoplastic polymer used for numerous engineering applications because of its high strength and wear resistance [4-5]. However, its heat distortion temperature is low, and it absorbs water easily for the presence of amide groups in the molecular chain, which deteriorates its mechanical properties, dimensional stability and coefficient of friction under dry sliding conditions [4].

It is well known that solid lubricants such as polytetrafluroethylene (PTFE), ultra-high molecular weight polyethylene (UHMWPE), carbon fiber, graphite, graphene, molybdenum disulfide (MoS_2), Wax and metallic powders are widely used to improve the tribological properties of polymer materials [2, 6-17]. Carbon fiber (CF) that used as reinforcements and/or solid lubricant attracted most attention in tribological research, combining high strength and modulus, low weight, excellent heat stability, good thermal conductivity and lubricating ability [10, 13, 18, 19]. PTFE polymer which one of the industrial materials is the most important and promising solid lubricants in controlling friction, wear or both in polymer composites. The low coefficient of friction of PTFE resulted from the ability of its extended chain linear molecules, –(CF2–CF2)n–, to form low shear strength films upon its surface and mating counterfaces during sliding [18, 20, 21]. Moreover, by the external force, with the lower PTFE content, PTFE debris dragged out from the matrix were easily deformed and formed a continuous and smooth transfer film because of its low surface energy and poor creep resistance. At the same time, the lubrication properties of PTFE are the result of its high softening point. Its static and dynamic coefficient of friction are smaller than that of any other solid lubricant [9, 11]. Molybdenum disulfide's (MoS_2) lubrication capacity, i.e. easy cleavage and low friction characteristics, is intrinsic to its crystal layered structure. Each crystal layer consists of two layers of sulphur atoms separated by a layer of molybdenum atoms. The atoms lying on the same crystal layer are closely packed and strongly bonded to each other, the layers themselves are relatively far apart, and the forces, e.g. van der Waals, that bond them are weak [2]. Graphite is a potential candidate of lubricants, which could also form a transfer film on the sliding counterpart [17, 22]. As one of the three forms of carbon, graphite had a layer structure (carbon layer) in which the atoms were arranged in a hexagonal unit cell within each layer. These layers are linked by

weak van der Waals bonds, which can be easily broken by shear force under sliding conditions. With the addition of graphite, the quantity of the graphite on the sliding surface increased directly [11].

Many researchers studied the tribological properties of polymers containing solid lubricants such as PTFE, UHMWPE, carbon fiber, MoS_2 to reduce the coefficient of friction of the composites and maintain good wear performance. Neis et al. [23] have investigated the tribological properties of PA6, MoS_2 filled PA6 and solid lubricant filled PA6 polymers. Du-Xin et al. [19] have investigated the effects of additives such as PTFE and ultra high molecular weight polyethylene (UHMWPE) used as solid lubricants on the tribological properties of 15% glass fiber filled PA6 polymer. At 40N load and 200rpm sliding speed, it was determined that PTFE filler were significantly improved the tribological properties while UHMWPE did not affect the friction and wear properties. In the study also examined the effects of load and slip speed on tribological properties. Sudhir and Panneerselvam [5] studied the mechanical and abrasive wear behaviors of glass fiber filled PA6 polymer composites. The study also examined the effect of the load (5, 10, 15 and 20N) at the 500m sliding distance. As a result of the study, the specific wear rate decreased with increasing glass fiber content and the lowest value was achieved with 30% glass fiber reinforcement. It has been determined that weight loss increases with increased load. Bolvari et al. [24] have investigated the tribological properties of aramid fiber/PA6 polymer composites with and without PTFE under 30 N load and 1 m/s sliding distance. In the study, the amount of aramid fiber was used between 5 and 30%. The friction coefficient of aramid fiber/PA6 composites was found to be around 0.6, and the addition of PTFE reduces the friction coefficient by 50%. It has been stated that the transfer film layer formed by the PTFE reduces the friction coefficient and also minimizes loss of aramid fiber. Kang and Chung [25] have investigated the mechanical and tribological properties of the mineral oil and wax filled PA6 polymer. They reported that the friction coefficient of the 6% oil filled PA6 polymer decreased from 0.18 to 0.12 at a pressure of 2.5 MPa and a sliding speed of 1 m/s. It has been determined that the wax-filled PA6 polymer has a lower coefficient of friction than the oil-filled one. It has been stated that the coefficient of friction decreases to 0.08 depending on the increasing sliding speed and the pressure. Wang et al. [16] have investigated the friction and wear properties of molybdenum disulfide (MoS_2) and the chopped carbon fiber filled PA1010 polymer. The wear tests were carried out at a sliding speed of 0.42 m/s and different loads up to 300N. As a result of the study, MoS_2 filler decreases the friction coefficient at low loads but increases the wear rate and carbon fiber decreases the wear rate. When the

components of the transfer film were examined, MoO_3, FeS, $FeSO_4$ and $Fe_2(SO_4)_3$ were formed. FeS, $FeSO_4$ and $Fe_2(SO_4)_3$ increase adhesion between the disc surface and the transfer film. Avalle and Romanello [6] have investigated the effects of graphite, PTFE, silicon, MoS2 and carbon nanotube (CNT) fillers on tribological properties of thermoplastic polyurethane (TPU) and PA polymer. It has been reported that the PTFE improves the tribological properties without affecting the mechanical properties and silicon is suitable for both TPU and PA polymers. Zhang et al. [11] have investigated the tribological properties of PTFE and graphite filled poly (phthalazinone ether sulfonketone) (PPESK) polymer at different load and sliding speed. It has been determined that the tribological properties of 5-25% PTFE and 5-30% graphite filled polymers improved at room temperature. The lowest coefficient of friction and wear rate were obtained when the amount of additive was greater than 20%. Rodrigez et al. [9] studied the tribological properties of polyetheretherketone (PEEK) polymer, 10% carbon fiber+10% graphite filled PEEK and 10% carbon fiber+10% graphite+10% PTFE filled (PEEK). Graphite and PTFE fillers reduced the coefficient of friction while the lowest coefficient of friction was obtained at 10% carbon fiber+10% graphite+10% PTFE filled PEEK polymer sample. This is due to the fact that the PTFE additive has self-lubricating properties and the formation of the transfer film layer in the counter-disk.

In the present study, the tribological behaviour of the solid lubricants such as PTFE and wax filled carbon fiber/PA6 polymer matrix under a variety of load and sliding speed were investigated by means of a pin-on-disc tribometer.

2. Material and Method

In this work, polyamide 6 (PA6) polymer with a density of 1.12 g/cm^3 was used as the matrix material. The carbon fiber and PTFE that using as reinforcing elements were obtained from DowAksa (Turkey) and MicroTechnic Plastics Gmbh (Miltenberg/Almanya), respectively. A twin-screw extruder (screw diameter 26 mm, L/D ratio 46) with 11 temperature zones was used to produce 20% carbon fiber filled PA6 (PA6+20CF) and 10% PTFE filled 20% carbon fiber/PA6 polymer (PA6+20CF+10PTFE) granules. The temperature distribution is set to be 80-80-120-220-220-230-230-235-235-240-240^{o}C from the feed to extruder. The filaments in the form of a 2 mm cylindrical rod were granulated after being passed through a water bath. And then, granules were dried at 100 °C for 4 hours. The test samples according to the standards are produced by injection molding (Haste-Borche Model) method. In the

production, injection pressures of 110 bar and injection temperatures of 250-255-260-265-270-270°C were used. Wear tests were performed at room temperature using a pin-on-disc system under dry sliding conditions. Cylindrical pin specimens with a diameter of 6mm and a length of 40mm were tested against 1040 steel discs. Figure 1 shows the pin-on-disc wear device designed for this study. Before each test, pin and disk surfaces were cleaned with alcohol and then dried. The weights of the pins were measured before and after each wear test and the weight loss (Δm) was determined. The wear rates (K_o) of the test specimens were calculated using Equation 1:

$$K_o = \frac{\Delta m}{L * \rho * F} \ (m^2/N) \quad (1)$$

Δm is the weight loss (g), L is the sliding distance (m), ρ is the density of the material (g/cm^3), F is the applied load (N).

Figure 1. Pin-on-disc wear device

3. Results and Discussion

Figure 2 shows the tensile fractured surface of PA6+20CF, PA6+20CF+5PTFE and PA6+20CF+5PTFE+2Wax polymer composites. The fracture surface of PA6 polymer is not smooth, and some small cavitations can be seen from Fig. 2-a. As a kind of fiber with high strength and high modulus, carbon fiber functions as the major stress concentration point. Some carbon fibers were detached from the polymer matrix to some extent shown by the arrow in Fig. 2, which may be reasoned by the poor interfacial adhesion between the fibers and polymer matrix when hard tensile stress was focused on the fibers.

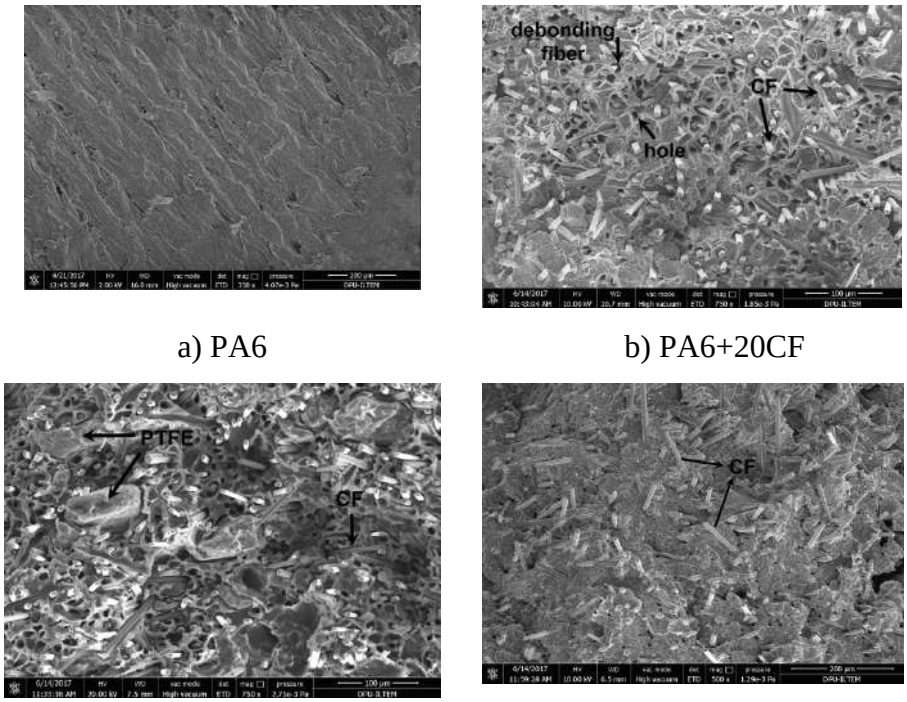

a) PA6 b) PA6+20CF

c) PA6+20CF+5PTFE d) PA6+20CF+5PTFE+2Wax

Figure 2. SEM images of PA6 and its composites

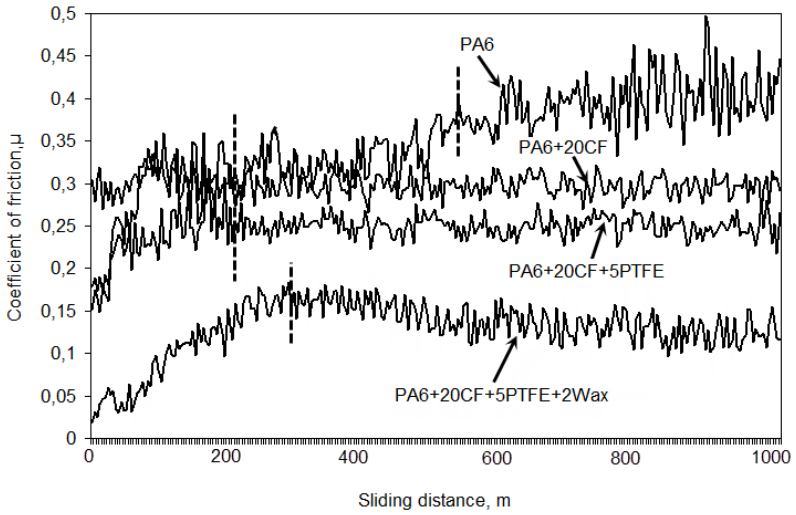

Figure 3. Coefficient of friction-sliding distance curve of PA6 and PA6 composites

The coefficient of friction are shown as a function of the sliding distance for PA6 and PA6 composites at 10N load and 0.4m/s sliding speed in Fig. 3. It can be seen that the change in the coefficient of friction of PA6 polymer materials occurred in two stages as running-in period and steady-state period. Samyn ve Schoukens [10] have explained that this situation is due to geometric effect, deformation and transfer film layer formation. It can be observed that

the running-in period for CF, PTFE and wax filled PA6 polymer composites is shorter than that of the PA6 polymer. At the same time, there are a lot of peaks on the friction curves of PA6 polymer and the intensity of coefficient of friction peak decreased with addition of CF, PTFE and wax. After running-in period, the coefficient of friction became steady about 550m for PA6 polymer, 200m for CF+PTFE filled PA6 polymer composites and 300m for CF+PTFE+wax filled PA6 polymer composites. Luo et al. [26] and Zhou et al. [4] explained that the reduction in the coefficient of friction is due to the self-lubrication behaviors of carbon fiber, PTFE and wax, and formation of the transfer film on the counter-surface under dry sliding conditions. The same trend are obtained by Luo [26] and Zhang et al. [11].

The coefficient of friction of PA6 polymer and CF, PTFE and wax filled PA6 polymer composites under dry sliding at different loads and sliding speed are given in Figure 4 and Figure 5, respectively. As one can see from Fig. 4 that the coefficient of friction increases with the increase of load for both PA6 and its composites. The coefficient of friction of PA6, PA6+20CF, PA6+20CF+5PTFE and PA6+20CF+5PTFE+2wax polymer composites increased by 8.8%, 14.5%, 15.2% and 42.9% with increase load, respectively. With the increasing load, the contact temperature between the polymer composite and the counterface will generally increase due to the frictional heat, which results in two competitive effects on the friction coefficient. On the one hand, the shear strength of the matrix material decreases which is benefit to reduce the friction coefficient. On the other hand, the matrix soften at higher temperature which results in an increase in the real contact area and then the higher friction coefficient obtained. Therefore the final friction coefficient of the polymer will be determined by these two competitive aspects [19]. When Figure 5 was examined, it was observed that the coefficient of friction increased due to the increased sliding speed. This increase was 6.8% for PA6 polymer, 10.7% for PA6+20CF polymer, 13.8% for PA6+20CF+5PTFE polymer and 37.3% for PA6+20CF+5PTFE+2Wax polymer. The effect of sliding velocity on friction coefficient of materials mainly attributes to the generation of friction heat. The accumulation of friction heat promotes a glass-to-viscoelastic-to-viscous flow state transition. When the velocity increases over a critical value, the composite is in viscous flow state, and the viscosity and shear strength of the surface material decrease [19]. At 1.2m/s sliding speed and 40N load, the coefficient of friction of PA6+20CF, PA6+20CF+5PTFE and PA6+20CF+5PTFE+2Wax polymers are 8.1%, 29.8% and 94.2% lower than that of PA6, respectively. Consequently, for the range of applied

loads and sliding speeds, the lowest coefficient of friction values are obtained when the combination of the PTFE and wax filler added to the PA6 polymer.

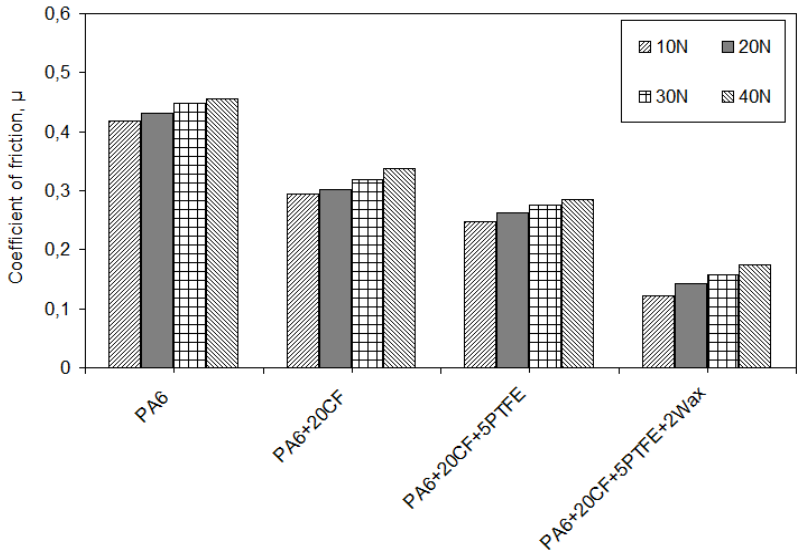

Figure 4. Coefficient of friction of the PA6 polymer composites under different loads (Sliding speed: 0.4m/s).

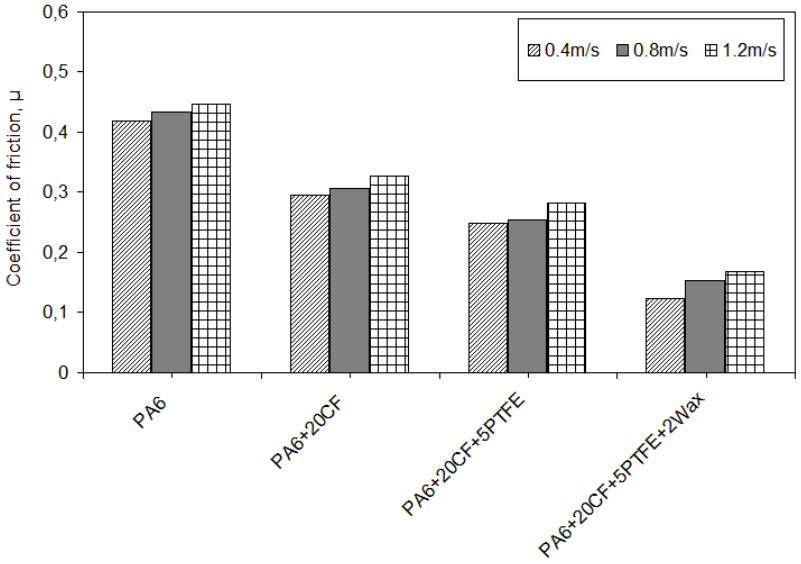

Figure 5. Coefficient of friction of the PA6 polymer composites under different sliding speeds (Load: 10N).

The effect of CF, PTFE and wax on the wear rate of the PA6 and PA6 composites under 10-40N loads and 0.4-1.2m/s sliding speeds are illustrated in Fig. 6 and Fig.7. It is clear from these figures that wear rate increased with increasing both load and sliding speed. Zhou et al.

[4] and Luo et al. [26], explained that a large number of carbon fibers were separated from the polymer matrix due to increased adhesion force and plough, and that the polymer matrix was transferred away by the severely micro-ploughing and micro-cutting, thereby the wear resistance of the composites worsening with the increasing of the applied load. At the same time, it is believed that the increase in coefficient of friction and wear rate is due to rise in surface temperature and the surface layer reaching the softening points of the polymer resulting for high wear rates [19]. Similar result are obtained by Zhang et al. [11] and Zhou et al [4] and Kang and Chung [25]. In general, the wear rate for PA6, PA6+20CF and PA6+20CF+5PTFE polymers composites were in the order of 10^{-13} m^2/N while the wear rate for PA6+20CF+5PTFE+2Wax in the order of 10^{-14} m^2/N. In the sliding speed and load range of this investigation, the lowest wear rate is for 20CF+5PTFE+2Wax filled PA6 polymer composites with a value of $3.13725E^{-14}$ m^2/N at 0.4m/s sliding speed and 10N load. The highest wear rate is for PA6 polymer with a value of $2.7604E^{-13}$ m^2/N at 1.2m/s sliding speed and 40N load. At 0.8m/s sliding speed and 30N load, the wear rates of PA6+20CF, PA6+20CF+5PTFE and PA6+20CF+5PTFE+2Wax polymers are 15.3%, 60.1% and 289.2% lower than that of PA6, respectively.

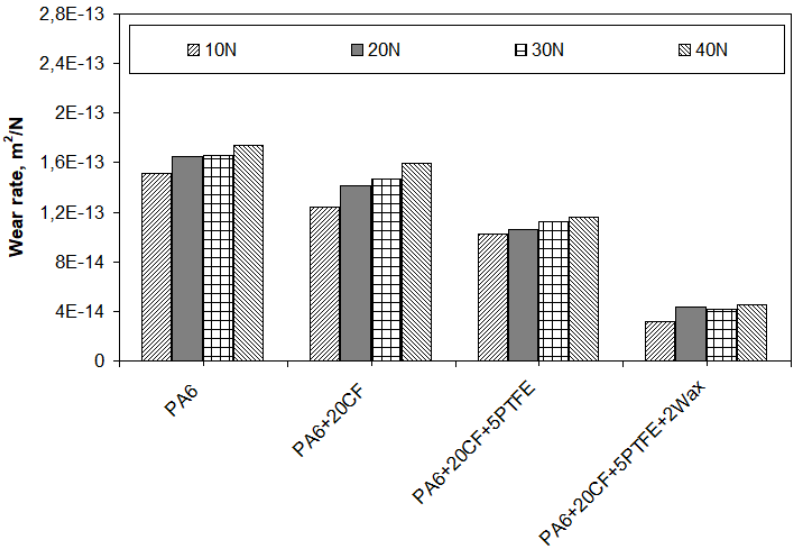

Figure 6. Wear rate of the PA6 polymer composites under different loads (Speed: 0.4m/s).

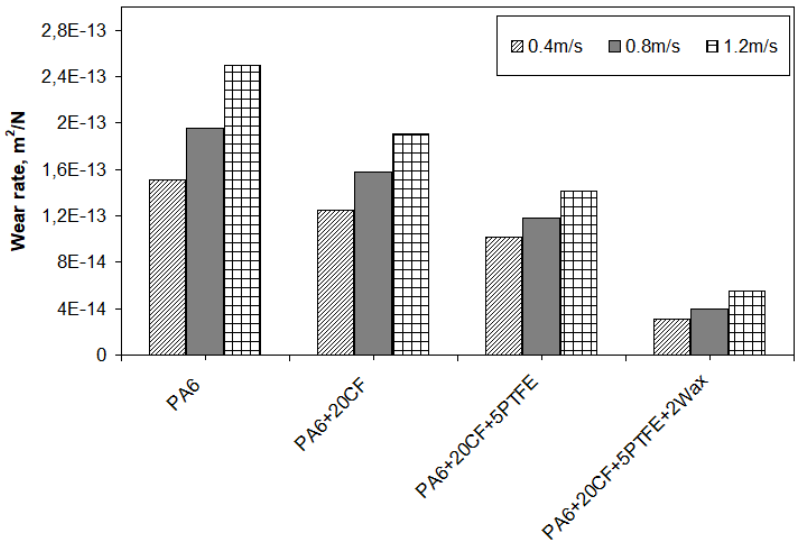

Figure 7. Wear rate of the PA6 polymer composites under different sliding speeds (Load: 10N).

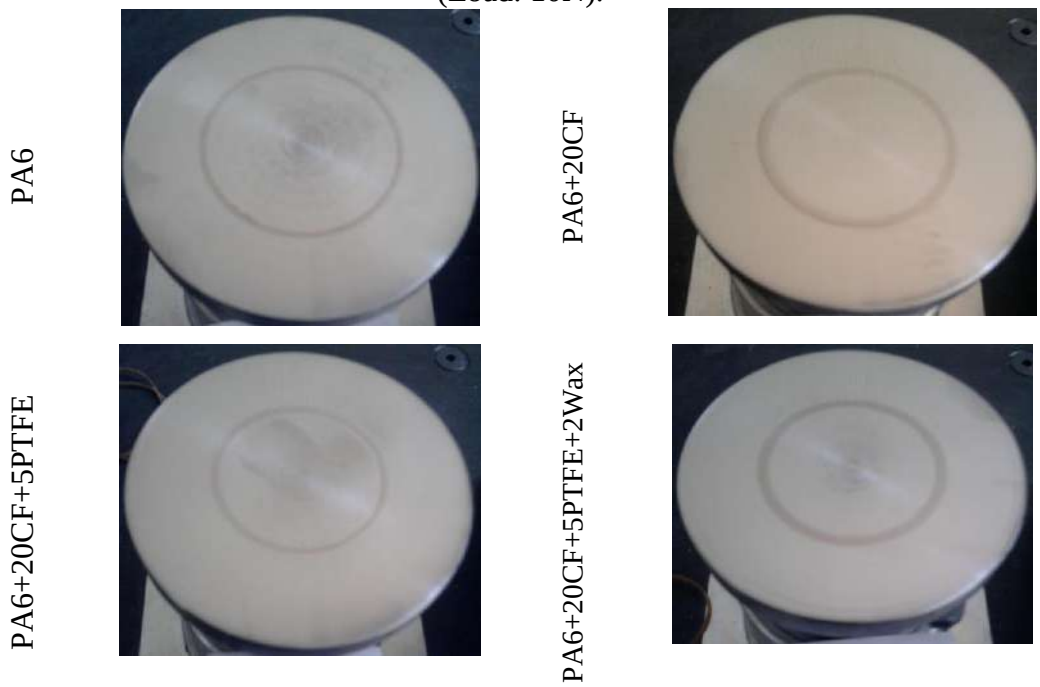

Figure 8. Macro pictures of disc surface of PA6 and PA6 polymers

Macro pictures of disc surface of PA6 and PA6 polymers are given in Fig. 8. For polymers and their composites, the characteristics of the transfer film might play dominant role in determining the tribological properties [27]. Therefore, the friction coefficient of the composites was decreased because of the emergence of the transfer film, which reduced the direct contact between matrix and counterpart. It is well known that PTFE could be easily dragged out from the matrix to form a third-body transfer film when sliding against steel

counterparts. The reduction of friction at low PTFE contents was due to the increasing efficiency of creating a lubricating transfer film of PTFE on the steel counter surface [11]. In a further work, Kang et al. [17] studied the tribological properties of oil and graphite filled PA6 polymer. It was determined that the oil filled samples had much lower wear rates than the graphite filled samples. They reported that the transfer film layer formed on the disk surface protected the PA6 polymer from the disk surface and improved the tribological properties.

4. Results

1. The coefficient of friction of PA6 and PA6 composites increased with load and sliding speed.
2. The lowest coefficient of friction values are obtained for PA6+20CF+5PTFE+2Wax polymers.
3. The wear rate of PA6 and PA6 composites increased with increasing load and sliding speed.
4. The wear rate for PA6, PA6+20CF and PA6+20CF+5PTFE polymers composites were in the order of 10^{-13} m^2/N while the wear rate for PA6+20CF+5PTFE+2Wax in the order of 10^{-14} m^2/N.
5. The coefficient of friction and wear rate of PA6 composites was affected by formation of the transfer film on the counter-surface.

Acknowledgements

The authors would like to thank Kütahya Scientific Research Projects (BAP- Project No: 2016-90) for production of PA6 and PA6+20CF polymer.

References

1. Fuzhi, S., Qihua, W., and Tingmei, W., (2016). The effects of crystallinity on the mechanical properties and the limiting PV (pressure x velocity) value of PTFE. *Tribology International*, 93, 1–10.
2. Valeria, P., Maria, J. C., Dávid, F., Joseph, K.-K., and Patricia, M. F., (2010). Changes in tribological performance of high molecular weight high density polyethylene induced by the addition of molybdenum disulphide particles. *Wear*, 269, 31-45.

3. Fengxia, D., Guoliang, H., Fengxiang, C., Fengyuan, Y., Liang, L., and Jianzhang, W., (2016). The lubricity and reinforcement of carbon fibers in polyimide at high temperatures. Tribology International, 101, 291-300.

4. Zhou, S., Qiaoxin, Z., Chaoqun, W., and Jin, H., (2013). Effect of carbon fiber reinforcement on the mechanical and tribological properties of polyamide6/polyphenylene sulfide composites. Materials & Design, 44, 493-499.

5. Sudhir, K., and Panneerselvam, K., (2016). Two-body Abrasive Wear Behavior of Nylon 6 and Glass Fiber Reinforced (GFR) Nylon 6 Composite. *Procedia Technology*, 1129 – 1136

6. Avalle, M., and Romanello, E., (2018). Tribological characterization of modified polymeric blends. *Procedia Structural Integrity*, 8, 239-255.

7. Zalaznik, M., Kalin, M., Novak, S., and Jakša, G., (2016). Effect of the type, size and concentration of solid lubricants on the tribological properties of the polymer PEEK. Wear, 364–365, 31-39.

8. Yi-Lan, Y., Du-Xin, L., Gao-Jie, S., and Xin, D., (2014). Investigation of the influence of solid lubricants on the tribological properties of polyamide 6 nanocomposite. *Wear*, 311, 57–6458.

9. Rodriguez, V., Sukumaran, J., Alois K. S., and Baets, P. D. (2016). Influence of solid lubricants on tribological properties of polyetheretherketone (PEEK). *Tribology International*, 103, 45-57.

10. Samyn, P., and Schoukens, G., (2009). Thermochemical sliding interactions of short carbon fiber polyimide composites at high pv-conditions. *Materials Chemistry and Physics*, 115, 185-195.

11. Zhang, X., Liao, G., Jin, Q., Feng, X., and Jian, X., (2008). On dry sliding friction and wear behavior of PPESK filled with PTFE and graphite, Tribology International 41, 195–201.

12. Xian, G., Walter, R., and Haupert, F., (2006). Friction and wear of epoxy/TiO2 nanocomposites: Influence of additional short carbon fibers, Aramid and PTFE particlesd. *Composites Science and Tecnology*, 3199-3209.

13. Xian, G., and Zhang, Z., (2005). Sliding waer of polyetherimide matrix composites I. Influence of short carbon fibre reinforcement. *Wear*, 776-782.

14. Shalwan, A., and Yousif, B. F., (2013). In State of Art: Mechanical and tribological behaviour of polymeric composites based on natural fibres. *Materials & Design*, 48, 14-24.

15. Franke, R., Haase, I., Lehmann, D., Hupfer, B., and Janke, A., (2007). Manufacturing and tribological properties of sandwich materials with chemically bonded PTFE-PA 66 and PA66/GF. *Wear*, 262, 958-971.

16. Wang, J., Gu, M., Songhao, B., and Ge, S., (2003). Investigation of the influence of MoS2 filler on the tribological properties of carbon fiber reinforced nylon 1010 composites. *Wear*, 255. 774-779.

17. Kang, S. C., and Chung, D. W., (2003). Improvement of frictional properties and abrasive wear resistance of nylon/graphite composites by oil impregnation. *Wear*, 254, 103-110.

18. Yousong, S., Qiang, Z., Lei, G., Xianghui, Z., Yongqi, C., and Peng, Z., (2016). xperimental study on tribological properties of carbon/polytetrafluoroethylene hybrid fabric reinforced composite under heavy loads and oil lubrication. *Tribology International*, 94, 82–86

19. Du-Xin, L., Yi-Lan, Y., Xin, D., Wen-Juan, L., and Ying, X., (2013). Tribological properties of solid lubricants filled glass fiber reinforced polyamide 6 composites. *Materials & Design*, 46, 809-815.

20. Khedkar, J., Negulescu, I., and Meletis, E. I., (2002). Sliding wear behavior of PTFE composites. *Wear*, 252(5-6), 361-369.

21. Takeichi, Y., Wibowo, A., Kawamura, M., and Uemura, M., (2008). Effect of morphology of carbon black filler on the tribological properties of fibrillated PTFE. *Wear*, 264, 308-315.

22. Myshkin, N. K., Petrokovest, M. I., and Kovalev, A. V., (2005). Tribology of polymers: adhesion, friction, wear, and mass-transfer. *Tribology International*, 38(11-12), 910-921.

23. Neis, P. D., Ferreira, N. F., Poletto, J. C., Sukumaran, J., Andó, M., and Zhang, Y., (2017). Tribological behavior of polyamide-6 plastics and their potential use in industrial applications. *Wear*, 376–377, 1391-1398.
24. Bolvari, A., Sherry, G., Rob, J., and Ellis, C. M., (1997). Wear and friction of aramid fibre and PTFE filled composites. *Wear*, (203-204), 697-702.
25. Kang, S. C., and Chung, D. W., (2000). The synthesis and frictional properties of lubricant-impregnated cast nylons. *Wear*, (239), 244-250.
26. Luo, W., Liu, Q., Li, Y., Zhou, S., Zou, H., and Mei, L., (2016). Enhanced mechanical and tribological properties in polyphenylene sulfide/polytetrafluoroethylene composites reinforced by short carbon fiber. *Composites Part B: Engineering*, 91, 579-588.
27. Wang, Q. H., Xu, J. F., Shen, W. C., and Xue, Q.J., (1997). The effect of nanometer SiC filler on the tribological behavior of PEEK,. *Wear*, 209 (1-2), 316-321.

Investigation of Mechanical Properties of AA2024 Based Hybrid Nanocomposites Reinforced with Hex-BN and B_4C Nanoparticles

Aykut ÇANAKÇI[1], K. Alp ARPACI[2], Hamdullah ÇUVALCI[3], Fatih ERDEMİR[4] ve Müslim ÇELEBİ[5]

1Karadeniz Technical University, Department of Metallurgy and Material Engineering, Trabzon, Turkey, email: aykut@ktu.edu.tr
2Karadeniz Technical University, Department of Metallurgy and Material Engineering, Trabzon, Turkey, email: alpkursat19@gmail.com
3Karadeniz Technical University, Department of Metallurgy and Material Engineering, Trabzon, Turkey, email: hcuvalci@ktu.edu.tr
4Karadeniz Technical University, Department of Metallurgy and Material Engineering, Trabzon, Turkey, email: ferdemir@ktu.edu.tr
5Karadeniz Technical University, Department of Metallurgy and Material Engineering, Trabzon, Turkey, email: muslimcelebi@ktu.edu.tr

*Sorumlu Yazar: alpkursat19@gmail.com

Abstract

Metal based hybrid nanocomposites have been largely used in engineering application due to their beneficial properties such as high strength to weight ratio, lighter weight, lower cost, and good wear behavior. In this study, the mechanical properties of AA2024/B_4C/hex-BN hybrid nanocomposites have been examined. The boron carbide nanoparticle content was changed from 0wt.% to 3wt.% while the hex-BN content was kept constant at 3wt.% Scanning Electron Microscope (SEM) was used for microstructural evolution of materials. The hybrid nanocomposites were produced by powder metallurgy method which is widely preferred because of its higher volume production, ease of operation, low cost and attractive manufacturing process. The result showed that the density values decreased with increasing boron carbide nanoparticle content, while the porosity increased with increasing boron carbide nanoparticle content. It was showed that the hardness of the hybrid nanocomposites enhanced dramatically with high boron carbide nanoparticles concentration. It was also observed that the tensile strength of hybrid nanocomposites raised with increasing boron carbide nanoparticle content.

Keywords: h-BN, tensile strength, B_4C, nanocomposite

1. Introduction

Hybrid nanocomposites are Metal Matrix Composites (MMCs) that have been developed because the traditional material cannot meet requirements in applications that need high strength and stiffness (Onat et al., 2007). Metal matrix nanocomposites show very good resistance to low density, diverse composition and geometry, with very good performances at high temperature, abrasion, oxidation, corrosion and fatigue strength. Because of these properties, the use of composite materials is increasing day by day in fields such as automotive, railways, marine, aviation, medicine, space and sport (Cornie et al., 1986).

2024 Aluminum Alloy (AA2024) has the highest hardness, elasticity modulus and strength in aluminum alloys (Kaçar et al., 2003). Hexagonal boron nitride (hex-BN) as a good lubricant is called white graphite because of its graphite resemblance (Pease, 1950; Pease, 1952; Geick et al., 1966; Paine and Narula, 1990; Gardinier, 1988). Boron carbide is the third hardest

material after diamond and cubic boron nitride. It has properties such as low density, high hardness and elasticity modulus. Therefore, composite materials produced with B_4C are used as armor materials in applications requiring high temperature and abrasion resistance (Jones et al., 1999).

The powder metallurgy method is used for producing MMCs conventionally, but uniform distribution of reinforced materials is difficult with this technique. Therefore, high energy milling is an alternative method of MMCs production (Ravindran et al., 2013). In this work, AA2024 based hybrid nanocomposites reinforced with hex-BN/B_4C nanoparticles were produced using high energy ball mill.

The purpose of the present study, therefore, was to: (a) produce and characterize hex-BN and B_4C nanoparticle reinforced AA2024 based hybrid nanocomposites; (b) investigate the effect of B_4C nanoparticle content on microstructure, density and porosity; (c) examine the effect of B_4C nanoparticle content on hardness and tensile strength.

2. Materials and Methods

2.1. Raw Materials

As received AA2024 powders (d50:110 μm) with a chemical composition of (in wt.%) 4.85 Cu, 1.78 Mg, 0.312 Mn, 0.005 Ti and 0.138 Zn, 92.114 Al (Gundogdu Exhoterm Company), B_4C (d50:45μm) (Alfa-Aesar) and hex-BN powders were used as starting materials to fabricate AA2024/hex-BN-B_4C hybrid nanocomposites. The particle sizes of as received and milled powders were investigated using a particle size analyzer (Malvern, model‘Mastersizer Hydro 2000e’).

2.2. Composite Fabrication

The ball milling process was conducted in a planetary ball mill (Retsch PM 200) using tungsten carbide containers and balls at the room temperature. AA2024, nano B_4C and nano hex-BN powders were milled for 1 h with the following parameters: ball to powder weight ratio: 5:1; ball diameter: 10 mm; speed: 400 rpm. Methanol as the process control agent was added to prevent excessive cold welding and the formation of intermetallic compounds during the ball milling process. In this study, 7 different hybrid nanocomposites samples were

produced. Components and percentages used in hybrid nanocomposite materials production are given in Table 1.

Table 1. The percent composition of the samples to be produced.

Sample code	B_4C (wt.%)	Hex-BN (wt.%)	AA2024
A0	0.0	3.0	Balance
A1	0.25	3.0	Balance
A2	0.50	3.0	Balance
A3	1.0	3.0	Balance
A4	1.5	3.0	Balance
A5	2.0	3.0	Balance
A6	3.0	3.0	Balance

Figure 1. (a) Elements used in mechanical alloying process, (b) Hot press machine

Following this process, the pressing step was passed. Hydraulic, mechanical and pneumatic presses are usually used for this process. In this work, a uniaxial hydraulic press with a load of 250 MPa is used for pressing. All powder mixes are uniaxially pressed at a pressure of 250 MPa, cold for 180 seconds. After that, the samples were sintered in a vacuum at 560 ℃ for 3 hours. After the milled powders were sintered at 560 ℃they were pressed under 250 MPa pressure on argon gas atmosphere to obtain bulk samples (Figure 1).

2.3. Mechanical Testing

Hardness values of the samples were determined by the Brinell method using a 31.25 kg load and 15 s indentation time on the Brinell hardness machine and the hardened steel ball used in this process have a diameter of 2.54 mm.

An MTS model 45 electromechanical test instrument was used to conduct tensile test, the experiment was conducted at room temperature on plate specimens with a cross-head speed of 0.5 mm min^{-1}.

2.4. Characterization

In order to find the presence and distribution of reinforcement, and interfacial integrity between matrix and reinforcement, we conducted microstructural characterization, using A Zeiss Evo LS10 scanning electron microscope (SEM). The dimensional measurement determines the density of hybrid nanocomposite samples. While the rule of mixture is the way theoretical densities of hybrid composites were determined. The porosity was calculated by using the theoretical and experimental densities.

3. Results and Discussion

3.1. Microstructural Evolution

Figure 2 shows morphologies of the hybrid nanocomposite samples (a) which include A0, (b) A1, (c) A2, (d) A3, (e) A4, (f) A5 and (g) A6.

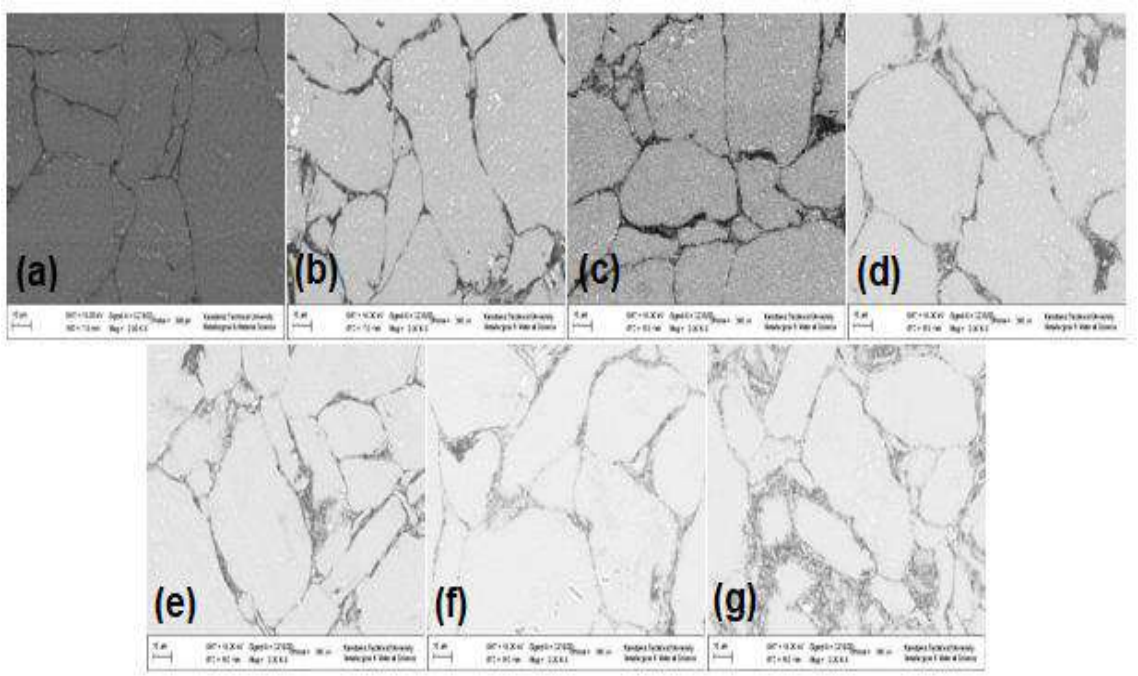

Figure 2. Microstructure images of AA2024 / 3hex-BN-B4C hybrid nanocomposites (a) A0, (b) A1, (c) A2, (d) A3, (e) A4, (f) A5 and (g) A6.

The reinforcement of hex-BN and B_4C distributions were generally homogeneous in the matrix.

3.2. Density and Porosity

The theoretical density, experimental density and porosity values of AA2024 based hybrid nanocomposite samples that were reinforced with hex-BN and B_4C nanoparticles are given in Figure 3. The experimental density values of the hybrid nanocomposite samples decreased linearly with increasing B_4C nanoparticle content due to low density of boron carbide. While the density of A0 sample was 2.69 gr/cm^3, it was decreased to 2.59 gr/cm^3 at A6 sample which is about 3.7% lower than A0 sample. Although a linear decrease can be also seen in the experimental densities, the values are much lower than those of the theoretical ones. The density measurements also showed that a great number of porosities were formed inside the hybrid nanocomposite samples. While the % porosity of A0 sample was 2.71%, it was increase to 6.06% at A6 sample which is about 3.4% higher than A0 sample. The density of samples decreased but the amount of porosity increased with the increasing B_4C nanoparticle content.

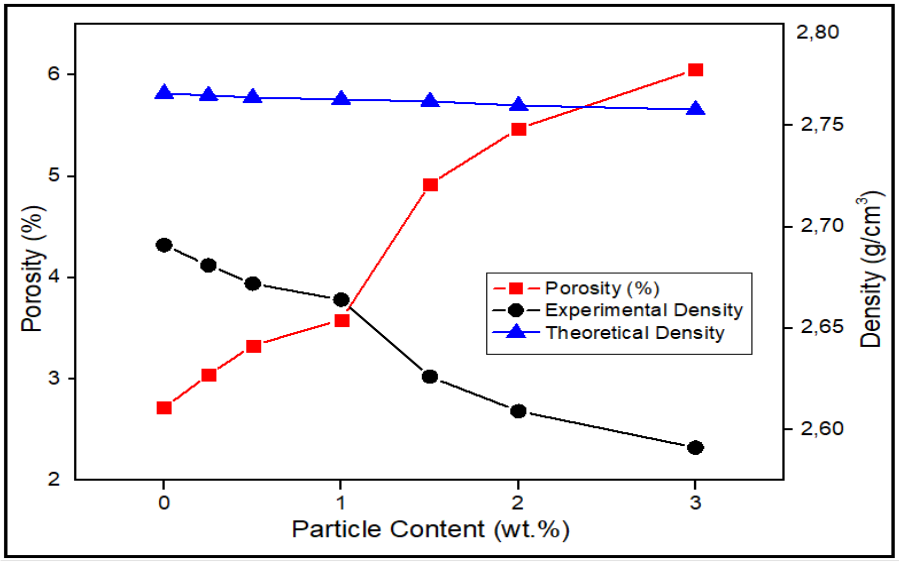

Figure 3. Change in theoretical density, experimental density and porosity of the AA2024/3hex-BN-B_4C hybrid composite group with the reinforcement ratio

3.3. Hardness Measurement

Brinell hardness measurements of AA2024 based hex-BN/B_4C nanoparticle reinforced hybrid nanocomposite samples were performed at different B_4C ratios. Five measurements were made for each sample and the average of the measurement results was taken as the hardness value. The variation of hardness values of hex-BN and B_4C reinforced AA2024 based samples was given in Figure 4 showed that as the B_4C ratio increased, the hardness of the samples increased. The hardness of the A0 (0wt.% boron carbide) was 74 HB, a gradual increase of hardness as function of particle content until it reaches 100.62 HB for A5 (2wt.% B_4C). This is due to the high hardness property of the B_4C. For A6 (3wt.% B_4C), a sudden decrease of hardness to 92.94 HB, which might be attributed to the high porosity of this sample (Figure 3).

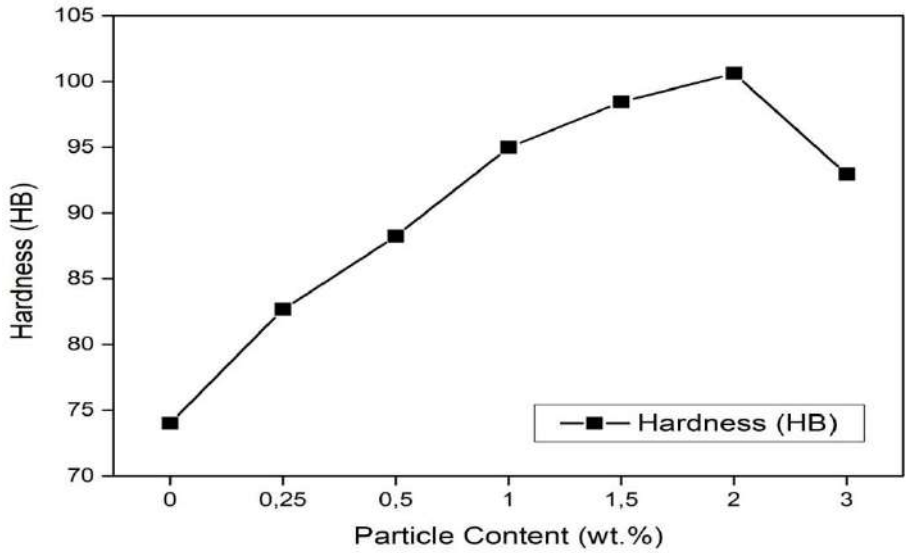

Figure 4. Hardness values of AA2024/3hex-BN-B_4C nanocomposites group

3.4. Tensile Strength

The results of the tensile strength tests are given in Figure 5, which shows the variation of tensile strength with the weight fraction of B_4C particles. The variation of tensile strength values of hex-BN and B_4C reinforced AA2024 based samples was given in Figure 5 which shows the tensile strength of the A0 (0% wt. boron carbide) was 160 MPa, a gradual increase of strength as function of particle content until it reaches 225.5 MPa for A5 (2wt.% B_4C). This is due to the homogeneous distribution of the reinforce materials. For A6 (3wt.% B_4C), a sudden decrease of tensile strength to 167.3 MPa, which might be attributed to B_4C and hex-BN aggregation.

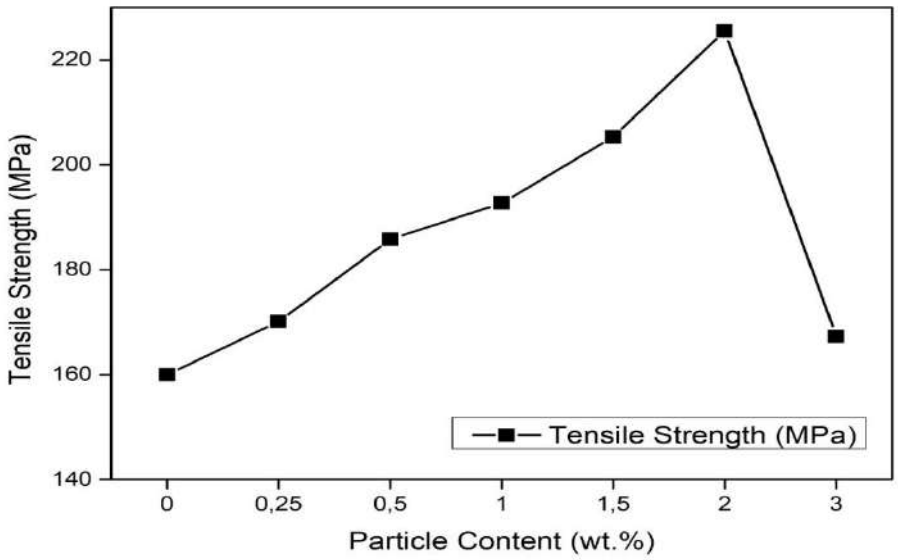

Figure 5. The tensile strength values of AA2024/3hex-BN-B_4C hybrid nanocomposite group

4. Conclusions

Conclusions are drawn as follows:

- Microstructural examination showed that the reinforcement of hex-BN and B_4C distributions were generally homogeneous in the matrix.
- The highest hardness value belonged to the A5 sample reinforced with 2wt.% B_4C because of high hardness property of the B_4C. But over 2wt.%, the porosity of the material makes the hardness value fall.
- The density of samples was decreased with increasing B_4C nanoparticle content but the porosity of the samples was increased with increasing B_4C nanoparticle content.
- A6 had the highest porosity and the lowest density values because it had the maximum B_4C content among the other samples.
- Similar to hardness, tensile strength raises until it gets the highest value for A5 sample reinforced with 2wt.% of B_4C, thanks to its homogeneous distribution. For A6 sample, the tensile strength drops because of B_4C and hex-BN aggregation.

References

Onat, A., Akbulut, H., and Yilmaz, F. (2007). Production and Characterisation of Silicon Carbide Particulate Reinforced Aluminium–Copper Alloy Matrix Composites by Direct Squeeze Casting Method. Journal of Alloys and Compounds, 436(1-2), 375-382.

Cornie, J. A., Chiang, Y. M., Uhlmann, D. R., Mortensen, A., and Collins, J. M. (1986). Processing of Metal and Ceramic Matrix Composite. American Ceramic Society Bulletin, 65(2), 293-304.

Kaçar, H., Atik, E., and Meriç, C. (2003). The Effect of Precipitation-Hardening Conditions on Wear Behaviours at 2024 Aluminium Wrought Alloy. Journal of Materials Processing Technology, 142(3), 762-766.

Pease, R. S. (1950). Crystal Structure of Boron Nitride. Nature, 165(4201), 722.

Pease, R. S. (1952). An X-Ray Study of Boron Nitride. Acta Crystallographica, 5(3), 356-361.

Geick, R., Perry, C. H., and Rupprecht, G. (1966). Normal Modes in Hexagonal Boron Nitride. Physical Review, 146(2), 543.

Paine, R. T., and Narula, C. K. (1990). Synthetic Routes to Boron Nitride. Chemical Reviews, 90(1), 73-91.

Gardinier, C., F. (1988). Physical Properties of Super Abrasives. American Ceramic Society Bulletin, 67(6), 1006-1009.

Jones, B. R., Prunier Jr, A. R., and Pyzik, A. J. (1999). Brake or Clutch Components Having a Ceramic-Metal Composite Friction Material. U.S. Patent No. 5,957,251. Washington, DC: U.S. Patent and Trademark Office.

Ravindran, P., Manisekar, K., Kumar, S. V., and Rathika, P. (2013). Investigation of Microstructure and Mechanical Properties of Aluminum Hybrid Nano-Composites with the Additions of Solid Lubricant. Materials & Design, 51, 448-456.

Weld Microstructure And Mechanical Properties of DP 800 and IF 7314 Steels by Using Resistance Spot Welding

Fatih Hayat[1], Cihangir Tevfik Sezgin[2*], Merter Çoban[3], Tayfun Morkoç[4]
[1]Karabük University, Engineering Faculty, Metallurgy and Materials Engineering, Karabük, Turkey, fhayat@karabuk.edu.tr
[2]Kastamonu University, Cide Rıfat Ilgaz MYO, Welding Technology, Kastamonu,Turkey; ctsezgin@kastamonu.edu.tr
[3]Karabük University, Engineering Faculty, Metallurgy and Materials Engineering,Karabük,Turkey, mertercoban@hotmail.com
[4]Karabük University, Engineering Faculty, Metallurgy and Materials Engineering, Karabük, Turkey, tayfunmorkoc@hotmail.com

[*] **Corresponding Author:** ctsezgin@kastamonu.edu.tr

Abstract

In this study, weldability of DP 800 Steel and IF 7314 Steel by using resistance spot welding (RSW) was investigated. The sample was prepared for be observed by optical microscope. After all operations microstructure of heat affect zone (HAZ), fussion zone was observed with optical microscope. Microhardness was observed . Tensile strength test was apllied to welded steel. It was observed that welding was successful.

Keywords: DP 800, resistance spot welding, microstructure, weldability, IF 7314

1. Introduction

Steel is a very wide range of uses such as automotive industry to the white goods industry from construction to the aviation industry. Especially the most important materials of the automotive industry are made of steel. Nowadays, car manufacturers have to consider the environmental regulation and need to reduce the global vehicle weight. On the other hand, they are expected to produce best protection in case of an accident (Huin et. al.,2016). One of these steels is IF (interstitial free) steels.

They feature the best formability of conventional high-strength steels as a result of their r-values, high work hardening and high fracture elongation. The base material is designed using a basic vacuum-decarburized IF analysis stabilized with Ti and/or Nb. The individual strength classes are achieved by adding solid-solution-strengthening alloys (Voestalpine, 2016).

Advanced high strength steels (AHSSs) play an important role for manufacturing light weight vehicles (Wang et.al, 2016; Xu et.al. ,2012;Wang et.al, 2016). DP steels are one of the commonly used AHSS. Dual phase steels are of AHSS family with strength and ductility properties. Dual-phase steels, where a combination of high tensile strength and ductility are combined, have become attractive due to advantages such as reducing the vehicle weight in the automotive industry, as well as manufacturing characteristics such as formability and weldability (Sarwar et.al., 2007; Prodromos, 2006; Gündüz, 2009). Double-phase steels are generally characterized by a microstructure consisting of 20-25% hard martensite phase in a soft ferrite matrix (Özer et.al., 2015). The volume fraction of hard martensite islands determines the strength of DP steel whereas the ductile ferrite matrix provides good formability (Niobelcon, 2018).

Today, in the automotive sector, improving vehicle safety and vehicle lightening efforts have led researchers to different manufacturing methods. The welding is one of them. Thanks to the welding, fasteners such as rivets and bolts are not used, making the vehicles lighter. Although it is not a new method of joining tools, the most important method of joining is the resistance spot welding(RSW) method. It is a combination of local melts resulting from heat transfer between the two electrodes by applying low voltage high current (AC or DC). An average of 4,000 to 6,000 resistance spot welds are applied to the sedan vehicle bodies produced today (Doruk et.al. ,2016). According to other welding methods, 85% resistance point welding is used in the formation of the vehicle body (Doruk et.al. ,2016). Being fast manufacturing method, low workmanship and low cost are the most important reasons for being preferred.

For these reasons, the effect of microstructure, tensile and hardness on the mechanical properties of DP 800 steel and IF 7314 steels in point resistance welded joints was investigated.

2. Material and Method

In this study, spot welding of IF 7314 steel was made with dual phase DP 800 steel. For this purpose, the pieces were cut at the guillotine with dimensions of 100 x 30 x 3 mm. After welding, the samples were cut in the disc (Cutting Machine) with Dispersion Oil and water. The samples were put in bakalite resin. Then, the sandpaper numbered as 200, 400, 600, 800, 1000, 1200, 2000 and 2500 was used respectively. It was then polished with diamonds paste and then etched with nital solution, dried with methanol. And then, microstructure images were taken at 50x, 100x, 200x, 500x, 1000x magnification.

Morover tensile strength test was carried out to the samples. Welding parmeters was shown in Table 1.

Table 1. Welding parameters

Ampers (kA)	Cycle
6	20
8	10
8	20
8	30
10	20
12	20

Chemical composition of both of steels were shown in Table 2. Mechanical properties of steels was seen in Table 3.

Table 2. Chemical compositions of steels

Steel	C	P	S	Mn	Si	Al	Cu
DP 800	0,14	0,0014	0,004	1,7	0,24	0,04	-
IF7314	0,08	0,03	0,03	0,4	-	-	-

Table 3. Mechanical properties of steels

Steels	Young Module (MPa)	Tensile Strenth (MPa)	Elongation (%)

DP 800	490	850	17
IF7314	210	290	38

3. Results and Discussion

3.1. Microstructure

Microstrcture of fussion zones were shown in Figure 1.

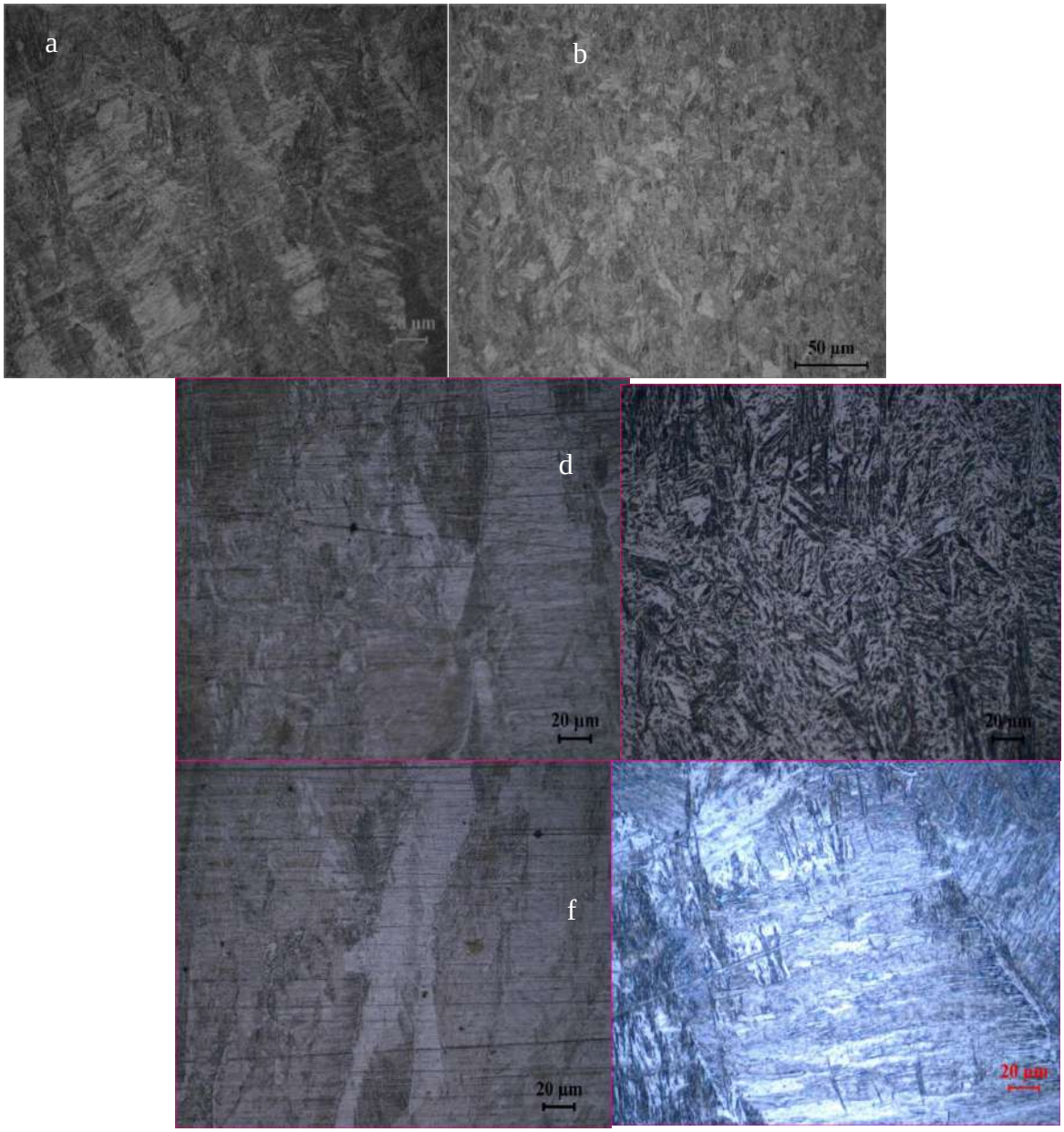

Figure 1. a)6 kA, 20cycle Fussion zone b) 8 kA, 10cycle Fussion zone c) 8 kA, 20cycle Fussion zone d) 8 kA, 30cycle Fussion zone e) 10 kA, 20cycle Fussion zone d)12 kA, 20cycle Fussion zone

Figure 1 shows microstructure of fussion zone for each welding operation. At 8 kA, 30cycle operation, the black and rod shape could be expected as martensite. This structure was occured at 8 kA, 30cycle was more than microstrucuture of other operations. Cooling rate in weld metal was pretty high. This situation could block diffusion of carbon (Elitaş and Demir, 2018). So it could cause to occure martensite in fussion zone. IF steel was low alloy steel. DP steel was also low alloy steel it included alloy element more than IF steel. May be a chemical mix occured in fussion zone because of high temperature.

3.2. Microhardness

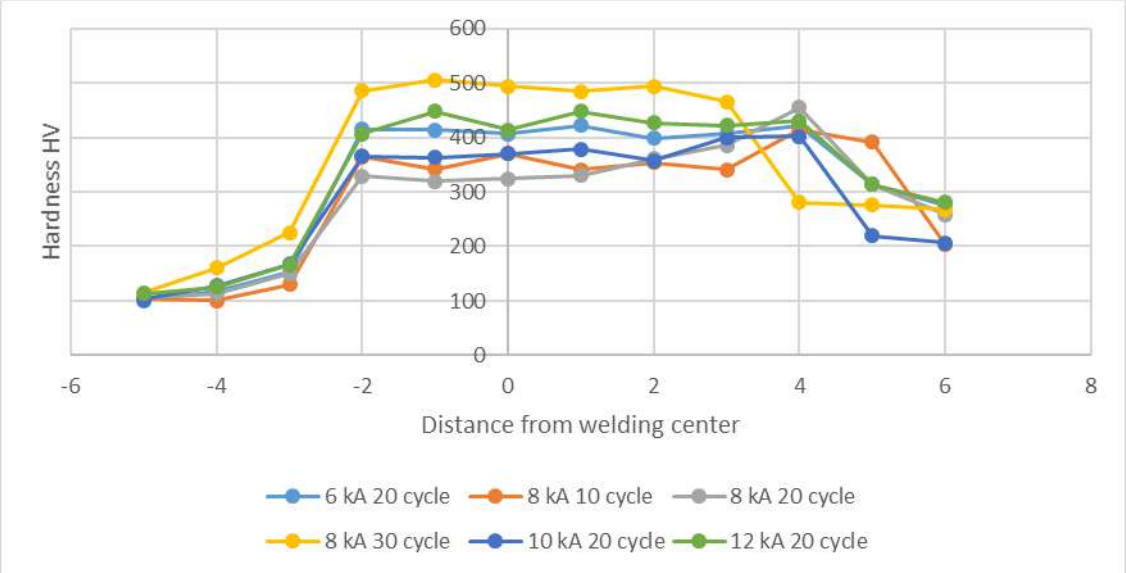

Figure 2. Microhardness results

Microhardness results was shown in Figure 2. At the same power when the cycle time was more and more hardness of fussion zone increased. The highest hardness values was seen at 8 kA 30 cycles RSW operation. Normally IF steel joinings didn't have as high as hardness. After welding with RSW, hardness of IF steel was approximately between 160 and 190 HV (Hayat et.al., 2009). It was thought that a chemical mix occured in fussion zone because of

high temperature. High temperature cause diffusion of alloy element of DP into the fussion zone such as Mn, C, Si.

The lowest hardness values were observing at base metals for each operations. Hardness of base metal of IF 7314 was lower than DP 800. Hardness of heat affect zone (HAZ) was higher than base metals. It was thought that martensite could be formed in HAZ like fussion zone. The highest hardness values were observing at fussion zone for each operations. Martensite volume fraction of DP 800 steel is higher than IF 7314 steel. Rapid cooling after welding process may increase martensite volume fraction in fussion zone. So increasing martensite volume fraction can cause these high hardness volume.

3.3. Tensile Strength Test

Tensile strength test results was shown in Table 4. Both of maximum stress and elongation values were too close for each operation. Maximum elongation was seen at operation 10 kA-20 cycle. But all stress and elongation results was lower than both of two base metals. The highest tensile strength value was observed at 8 kA- 30 cycle operation. Tensile strength value showed an increase within increasing weld time at 8 kA. But it can't say that for same cycle with different welding current. After 8 kA- 20 cycle, welding current increased but maximum stresses decreased.

Table 4. Tensile Strength Test Results

Operation	Max Stress (MPa)	Elongation (%)
6 kA-20 cycle	116	6,5
8 kA- 10 cycle	116	8
8 kA- 20 cycle	118	7,5
8 kA- 30 cycle	128	5,4
10 kA- 20 cycle	115	8,7
12 kA- 20 cycle	114	6,7

4. Results and Discussion

- At 8 kA, 30cycle operation, the black and rod shape could be expected as martensite. This structure was occured at 8 kA, 30cycle was more than microstrucuture of other operations.The hardest zone was observed at fussion zone of metal was welded at 8 kA 30 cycle.
- It was thought that a chemical mix occured in fussion zone because of high temperature. So it could cause to occure martensite. And martensite caused as high as hardness in fussion zone.
- Tensile strength value showed an increase within increasing weld time at 8 kA. But it can't say that for same time different welding current. Although welding current increased after 8 kA- 20 cycle, maximum stresses decreased. Maximum strain was observed at sample welded with 10 kA 20 cycle.

References

Demir, B., (1997), Çift fazlı çelik üretimi, çift fazlı çeliklerde martenzit hacim oranı ve morfolojisinin çekme özellikleri üzerine etkisi", Master Thesis, Gazi Üniversitesi, Ankara, Turkey.

Doruk, E., Pakdil, M., Çam, G., Durgun, İ., Kumru, U. C., 2016. Otomotiv Sektöründe Direnç Nokta Kaynağı Uygulamaları, Mühendis ve Makina, 673, 48-53.

Elitaş,M., Demir B., (2018). The effect of parameters on tensile properties of RSW junctions of DP1000 sheet metal, Engineering, Technology and Applied Science Research, 8(4), 3116-3120.

Gündüz S., (2009), Effect of chemical composition, martensite volume fraction and tempering on tensile behaviour of dual phase steels, Materials Letters, 63, 2381–2383.

Hayat F., Demir B., Acarer M., Aslanlar M. (2009). Effect of weld time and weld current on the mechanical propertiesof resistance spot welded IF (DIN EN 10130–1999) steel. Kovove Mater, 47, 11–17

Hui, T., Dancette S., Fabrègue D., Dupuy T., (2016), Investigation of the Failure of Advanced High Strength Steels Heterogeneous Spot Welds Metals 6, 111.

Özer M., Kaya H., Uçar M., (2015), Çift fazlı çelikler ve nokta direnç kaynağı uygulamaları, Metal Dünyası, 23

Pradhan, R., (1993). "Continous Annealling Steel", ASM Metal Handbook Heat Treating Volume 4, The Materials Information Company, A.B.D., 135-160.

Prodromos P., (2006). Mechanical Properties of Dual-Phase Steels", doctorate thesis, Technischen Universitat Müncheneingereicht und durch die ,Fakultatfür ,Maschinenwesen,Germany.

Sarwar M., Ahmad E., Qureshi K.A., Manzoor T., (2007). Influence of epitaxial ferrite on tensile properties of dual phase steel, Materials and Design, 28, 335–340.

Wang J., Yang L., Sun M., Liu T., Li H., (2016). Effect of energy input on the microstructure and properties of butt joints in DP1000 steel laser welding, Mater. Des. 90, 642–649.

Xu W., Westerbaan D., Nayak S.S., Chen D.L., Goodwin F., Biro E., Zhou Y., (2012). Microstructure and fatigue performance of single and multiple linear fiber laser welded DP980 dual-phase steel, Mater. Sci. Eng. A, 553, 51–58.

Wang X.P., Zhang Y.Q., Jian-Bin J.U., Zhang J.Q., Yang J.W. (2016), Characteristics of welding crack defects and failure mode in resistance spot welding of DP780 steel, J. Iron Steel Res., 23 (10), 1104–1110.

URL1:http://www.voestalpine.com/stahl/en/content/download/4680/file/Datasheet_HFIF_1608_EN.pdf?inLanguage=eng-GB

URL2:http://www.niobelcon.com/NiobelCon/resources/Advanced-metallurgical-concepts-for-DP-steels-with-improved-formability-and-damage-resistance.pdf

Determination of Magnesium Production Parameters by Metalothermic Reduction Method

Yahya BAYRAK[1], Ahmet EKERİM[1]

[1]Yıldız Technical University, Department of Metallurgy and Material Science Engineering, İstanbul, Turkey

yahyabayrak@gmail.com

Abstract

In magnesium production via metallothermic reduction; silicon (Si) or ferro-silicon (Fe-Si) is the first to come to mind as a reducing material. Beside this, aluminum (Al) and very rarely carbon (C) are used. Furthermore, even if calcium carbide (CaC2) is present as another reducing agent in the literature, commercial use of it is not feasible because the purity of the produced metal is lower than the others. In this study, reduction of magnesium oxide (MgO) was carried out using aluminum metal chips as the reducing agent. A mixture of MgO and Al was prepared by stoichiometry ratio of Al/Mg equals to 1/1, and CaO-containing slag was also added as a fluxing agent. This mixture was pressed into a mold under constant force (100Bar). Reduction experiments were carried out in an electric arc furnace under an argon atmosphere. Reduction process was carried out in 1, and 1.5 minutes by applying currents of 400, 500 and 600 Amperes. The chemical properties of the obtained magnesium wase characterized by XRF and XRD analysis.

Keywords: Magnesium oxide 1, Metallic magnesium 2, Reduction 3, Magnetherm process 4.

1. Introduction

Magnesium has a dense hexagonal crystal structure and it has two valance electrons. Its melting and boiling point are 650 ± 2 ºC and 1107 ± 10 ºC respectively. Magnesium has a very low density (1.738 g/cm^3) when it is compared to other structural metals (Andreassen ve ark., 1997).

Due to its features, magnesium has a several applications in lots of fields such as aircraft, rockets, the desulphurisation and nodularization of iron and steel, corrosion applications, production of Al-Mg alloys, some chemical applications and replace to denser materials, not only steels, cast irons, and copper-based alloys in automobile industry (Emley,1966; Ding-Fei ve ark., 2011; Rong-Ti ve ark., 2003).

Magnesium (Mg) and its alloys will become more popular because of their favorable combination of tensile strength, elastic modulus, low density, high strength-to-weight ratios, high damping capacity (Brown,2009), high specific strength, good thermoformability, and high performance of electromagnetic shielding (Brown, 2009; Rongtı, 2003).

There are two major process routes for magnesium production in industry. One is to recover magnesium chloride from the raw materials and converts it to metal through molten salt electrolysis; the other is to reduce magnesium oxide at high temperature using reducing agents, such as ferrosilicon, aluminum or carbon. The raw materials for production of magnesium used in these process are sea water, lake brines, camallite, dolomite, serpentine and magnesite (Li ve ark., 2009; Tıan ve ark., 2014; Morsi ve Ali, 2014).

Although the silicotermic reduction method in pidgeon process is widely used over the world, we have used the aluminatermic reduction method in the Magnetherm process.

The main characteristic technology of magnetherm process is the heating and production furnace in which the heating takes place with electrodes using alternating current. Flax, dolomite or magnesite and reduction agents such as silicon or aluminum, is added in furnace for producing magnesium. The process operates within a temperature range of 1,300–1,700°C (Friedrich, Mordike; 2006).

In aluminatermic reduction process, aluminum is used as the reduction material for the production of magnesium. In the main reaction is shown in Eq. (1) (Friedrich, Mordike; 2006).

$$3MgO_{(s)} + 2CaO_{(s)} + 2Al_{(l)} \rightarrow 3Mg_{(g)} + 2CaO * Al_2O_{3(S)} \quad (1)$$

P = 1 atm ; T = 1,300°C or P = 10 mm Hg ; T = 900°C

The process is based on the use of Dolomite and magnesite that have undergone calcination, and aluminum scrap as reduction material. The furnace works according to the working principles of the DC transferred arc plasma furnace. This process is supposed to work at atmospheric pressure and under argon atmosphere at temperatures of about 1,500°C (Friedrich, Mordike; 2006).

In this study, it was aimed to determine optimum experimental conditions for magnesium production. For this purpose, the current values and the experiment period have been changed and the conditions have been examined.

2. Experimental Procedure

MgO, CaO and Al2O3 powders were purchased from MERCK and used as received. As reducing agent, Aluminum shavings were used with the chemical composition given in the Table 1. The composition of the aluminum shavings was obtained from S1 TITAN 600 BRUKER XRF analyzer

Table 1. Chemical composition of the aluminum shavings.

Al	Mg	Fe	Si	Cu	Zn	Mn	Ti
98,71	0,48	0,43	0,22	0,05	0,04	0,04	0,01

Initially, CaO-Al2O3-MgO mixture was prepared as a flux. The stoichiometric ratios of the flux mixture were set to be 60-35-5, respectively. Then the mixture was mixed for 30 minutes at 30rpm

MgO powder and the previously prepared flux were mixed with the ratio of 1:1 and aluminum shavings were add with the elemental ratio of Al/Mg 1:1 as well. All the blend was mixed in a plastic bowl for 30 minutes. After that, the mixture was moistened (15% H_2O) and pressed at 100 bar pressure for 30 seconds. Then, the pressed samples were dried for 8 hours at 105 ° C. The pressing mold and the sample are given in Figure 1.

Figure 1. presleme kalıbı ve preslenmiş numune örneği.

Experiments were carried out in an atmosphere controlled electric arc furnace and the schematic appearance of the furnace is given in Figure 2. Experiments were carried out at three different current values of 400-500-600 amperes and two different times of 1-1.5 min. Experiments were also carried out in an argon atmosphere.

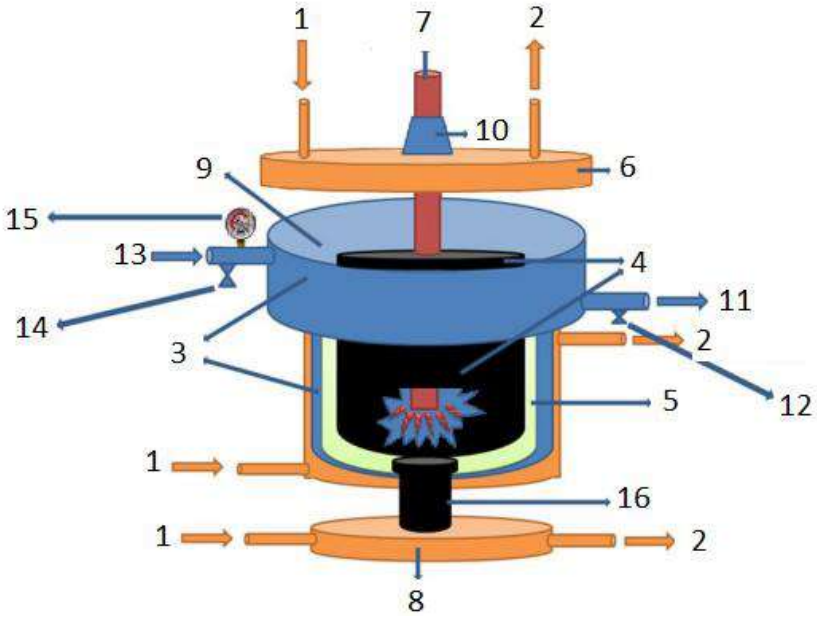

Figure 2. Schematic appearance of the electric arc furnace. Parts of the experimental setting; 1 water entrance, 2 water exist, 3 stainless steel body, 4 graphite pot, 5 alumina refractory, 6 upper cover, 7 graphite electrode, 8 conductive table(Cu), 9 Mg(steam) condensation zone, 10 metal sealing, 11 vacuum 10^{-1}atm, 12 vacuum valve, 13 argon gas enter, 14 argon shut off valve, 15 vacuum gage, 16 graphite conductor.

As can be seen in Figure 2, the experiments were carried out in a stainless steel chamber (3) with stainless steel cover (6). Graphite electrode (7) and graphite crucible (4) were used as

electrode and pot material to applied an electric arc. First, the graphite electrode was connected to the water-cooled copper electrode holder and then the electrode holder was fixed to the top cover by a metal bellows (10). Plastic sealing was also used for vacuum sealing. The graphite crucible was fixed by screwing it to the conductive table (8) with a molybdenum reinforced graphite conductivity provider (16). Also, a refractor (5) is placed between the stainless steel body and the graphite crucible for both electrical and thermal insulation. To protect the system from high temperatures, the electrode holder, the top cover, the conductive plate and a part of the stainless steel body were cooled with water (1-2).

The pressed and dried samples were adjusted to be 36 grams and it was put into the graphite crucible. Vacuum operation (13) was performed after the cover and electrode were placed. The cover and electrode were fixed to the body with screws after vacuuming. When the vacuum indicator showed 680 mmHg pressures, the vacuum valve was turned off and argon gas was vented to the system. This process was repeated 3 times to evacuate the oxygen. As a final step, the system was fixed at 740 mmHg pressure and the experiment was started.

Magnesium oxide was reduced by aluminum and then magnesium was evaporated at about 1550°C. Magnesium in the vapor phase was condensed by hitting multiplying to the condensation zone as it moves upward in the system. After the test, magnesium powder in the condensation zone was removed and weighed after the system was completely cooled. Amount of the unreduced MgO and slag was weighed to calculate the efficiency of the reduction process.

Then, to determine the degree of purity of the powders, XRD analysis was performed by using PANalytical X'Pert Pro XRD device and to analyze the amount of carbon coming from the graphite crucible and the electrode, Carbon analysis was performed with Behr CS50 HT.

3. Results and Discussion

XRD analyzes were performed to determine the degree of purity of the magnesium powder and the chemical composition of the slag, and the results are given in Figure 3.

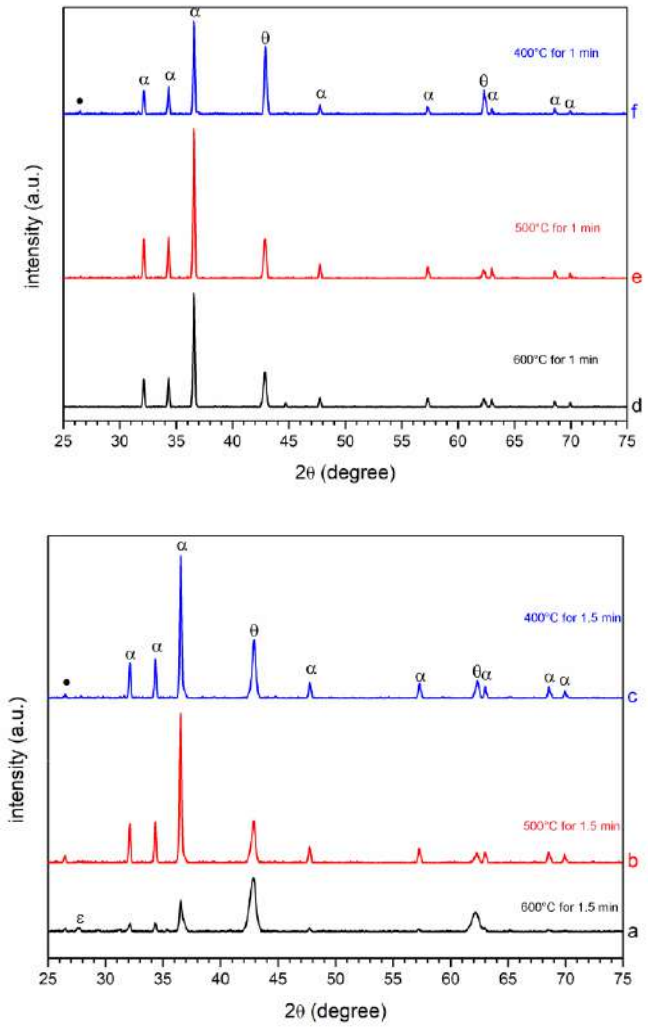

Figure 3. Analysis results of magnesium powders.

From the phases shown in Figure 3, α phase represents the metallic magnesium phase, θ phase represents the MgO phase, ε phase represents the $MgCl_2$ phase and • phase represents graphite phase.

The XRD analysis results showed; it was appeared that nearly all of the powders produced were close to pure magnesium and a small fraction of it is oxidized. It was observed that the degree of oxidation was close to each other in all of the test results, whereas in the test No. A (600 Amperes and 1.5 minutes), it was observed that magnesium was oxidized more than the others. This situation is thought to be due to oxygen leaks in the system during cooling process after arc, rather than changes in experimental conditions. In addition, reducing agent (aluminum) did not evaporate, instead it oxidize by reducing MgO to Mg because of increasing the temperatures during arc processing,. In addition, XRD results show that magnesium powder

contains trace of carbon or graphite powders. Apart from that, no other impurities were found in the Mg powder.

Since the XRD analysis does not reveal the amount of carbon completely, additional carbon analysis was carried out to determine the carbon content and degree of purity of the powders as shown the results in Table 3. These results were plotted for a better comparison in Figure 4.

Table 3. % Carbon content of magnesium powders.

Time(mins)		1,5			1	
Current (A)	600	500	400	600	500	400
Expt. No	a	b	c	d	e	f
Carbon (%)	13.82	7.16	5.21	7.28	4.92	4.21

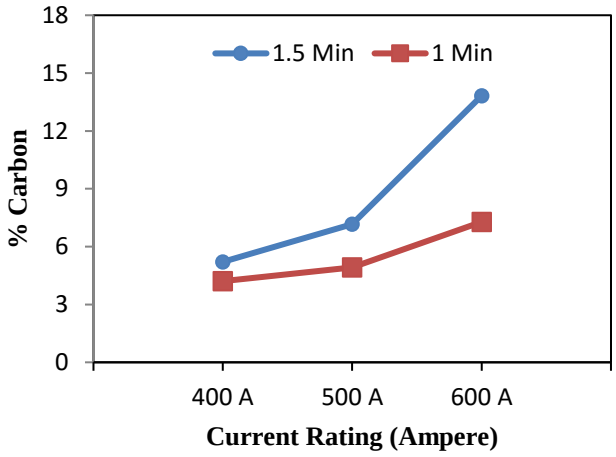

Figure 4. % Carbon amount graph of magnesium

As can be seen in Figure 4, the amount of carbon in the products increased with increasing the applied current rates. This situation was similar in both experiments at 1 and 1.5 minutes. It was observed that the amount of carbon measured was too high at high current rates, especially for the 600 Amperes and the 1.5 minute test. The reason for this situation is that the crucible and electrodes are graphite, and their interaction with the blend at high arc current rates might causes disintegration of the graphite itself.

Table 4. % Efficiency values of magnesium powders.

Time(mins)		1,5			1	
Current (A)	600	500	400	600	500	400
Expt. No	a	b	c	d	e	f
Efficiency %	73	54,78	39,16	61,73	7	29,79

The efficiency values of the magnesium powders were given in Table 4. These values were graphically shown in Figure 5 as well.

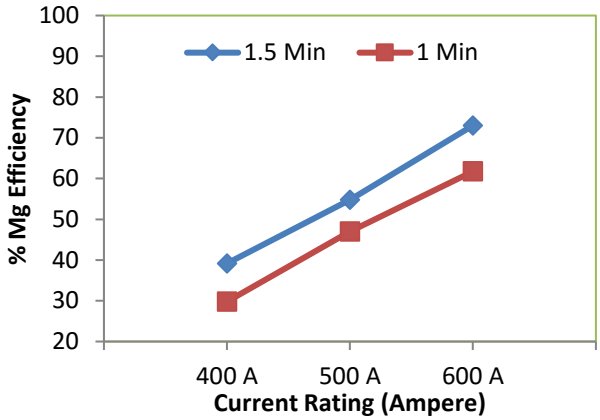

Figure 5. % Efficiency value graph of produced magnesium.

As can be seen in Figure 5, , the efficiency of magnesium also increases with increasing the current rate. This value reached its highest value in 1.5 minutes and 600 amperes. Nevertheless, the maximum efficiency value remained below 80%. Experiments at 600 amperes, when the duration increased from 1 minute to 1.5 minutes, the efficiency were increased for 18.26%. These ratios were reached 16.55% at 500A and 31.45% at 400A. In addition, for the experiments at 1.5 minutes, when the current rate increased from 400 A to 600 A, the efficiency increased by 86.4%, this rate has been 107,2% for 1 minute. In addition, for the experiments at 1.5 minutes, when the current rate increased from 400 A to 600 A, the efficiency increased by 86.4%, which was 107.2% for 1 minute.

4. Conclusion

It was observed that the efficiency increases with increasing the current rates in the experiments performed. Applying longer arc current also increased the reduction efficiency. However, as the applied current rates increased, the carbon contamination lowered the quality of product, Mg.. While the highest efficiency values were obtained at 600 amperes, the amount of carbon contained in the powder was also the highest. Considering the energy consumption

as well as the contamination, the optimum conditions were determined in this study as 500 A current rate and 1.5 min arcing duration.

5. References

Ding-Fei, Z., Fu-Gang, Q., Wei, L., Guo-Liang, S., and Xia-Bing, Z.: Trans. Nonferrous Met Soc. China, 2011, vol. 21, pp. 703–09.

Brown, R.E., (2009), "Magnesium in the 21st century", Adv. Mater. Processes, 167, 31-3.

Morsi, I.M., Ali, H.H., International Journal of Mineral Processing, 127 (2014) 37–43

Andreassen, K., Aune, T. K., Haugerod, T., N. O. Hoy-Petersen, D. Oymo, O. Skane, T. Vralstad, in Handbook of Extractive Metallurgy, Volume II (Ed. by Fathi Habashi), Wiley-VCH, Weinheim, 1997, pp. 981-982.

Emley, E.F.,: Principles of Magnesium Technology. Pergamon Press, London (1966).

Rong-Ti, L.I., Wei, P., and Sano, M.: Metall. Mater. Trans. B, 2003, vol. 8B, pp. 433–37.

Tıan, Y., XU, B.-Q. and et al. Metallurgıcal And Materıals Transactıons B, 45B(2014), 1936-1941.

Friedrich, H.E., Mordike. B. L., Magnesium Technology, Springer-Verlag Berlin Heidelberg 2006, Germany

Li, R.B., Wei, J.J., Guo, L.J., and Zhang, S.J., (2009, December,) Numerıcal Sımulatıon Of Magnesıum Productıon By The Pıdgeon Process Part I: A New Model For Magnesıum Reductıon Process In A Horızontal Retort, Seventh International Conference on CFD in the Minerals and Process Industries CSIRO, Melbourne, Australia.

Hazelnut Husk and Qualified Assessment

Mükrimin Şevket GÜNEY[1*], Özlem TUNÇ DEDE[2], Faruk GÜNER[3]

[1] Giresun University, Faculty of Engineering, Mechanical Engineering Department, Giresun, Turkey; guney80@gmail.com

[2] University, Faculty, Giresun University, Faculty of Engineering, Environmental Engineering Department, Giresun, Turkey; ozlem@tuncdede.com

[3] Giresun University, Faculty of Engineering, Mechanical Engineering Department, Giresun, Turkey; faruk.guner@giresun.edu.tr

[*] **Corresponding Author:** guney80@gmail.com

Abstract

The idea of obtaining biomass energy and using it as an additive with appropriate conversion methods is increasingly being evaluated on every platform and opportunity. Husk of hazelnut is estimated to be around 120,000 tons per year. It makes a considerable amount as biomass. In that context, more quality assessment is becoming more important. When hazelnut husks are examined elementally, they have on average about 40% carbon, about 5% hydrogen, about 1% nitrogen, about 45% oxygen, about 5 to 8% ash and trace amounts of sulfur. When the chemical structure is examined, it contains about 35% cellulose, 20% hemi cellulose and about 35% lignin. Lower heating value of hazelnut husk is estimated over 4000 kcal/kg. In this study, the elemental and structural content of hazelnut husk were presented and moreover more qualified evaluation methods are emphasized.

Keywords: Efficient, hazelnut, husk, utilization.

1. Introduction

Agricultural wastes are produced in larger amounts in the world. The idea of using agricultural wastes directly and/or as an additive material by means of appropriate conversion methods to acquire energy or an industrial product is increasingly being evaluated on every platform and opportunity. Among the agricultural products, hazelnut is one of the most important sources of income in Black Sea Region (Çimen, 2007; Çuhadar 2005).

Approximately 75% of the total hazelnut production in the world is supplied from north coasts of Turkey. Hazelnut shell and hazelnut husks are the main wastes of hazelnut processing plants (Çimen, 2007; Çuhadar, 2005; Guney, 2013).

In Turkey, approximately 120.000 tons dry basis of hazelnut husks are formed every year as a waste. It has a lignocellulosic structure and the elemental analysis showed that it contains 40% carbon, 5% hydrogen, 45% oxygen, trace amount of nitrogen and sulphur and 5-8% ash. The chemical analysis verified the data given in the literature that hazelnut husks has approximately 30% cellulose and 10% moisture and also 35% of lignin (Çöpür, 2007; Çuhadar, 2005; Guney 2013).

2. Material and Method

Hazelnut husk is a ligno-cellulosic structure and contains three major constituents: Cellulose, hemicellulose and lignin. Ligno-cellulosic material is not easily digestible by human. Ligno-cellulosic materials requires pretreatment (enzymatic hydrolysis, acid hydrolysis or hydrothermal hydrolysis) in order to obtain simple sugars needed during fermentation processes. Cellulose ($C_6H_{10}O_5$) is a solid material which is the main constitute of wood, approximately 60% of the composition of wood. Cellulose can break down to cellulose to a cellobiose ($C_{12}H_{22}O_{11}$) and glucose ($C_6H_{12}O_6$) by hydrolysis. Hemicellulose has nearly the similar structure with cellulose. The heating value of cellulose and hemicellulose is higher than 4000 kcal/kg. Lignin is the noncarbohydrate substance of wood. It is a highly polymeric material and has complex aromatic structure with higher molecular weight (about 10,000). The gross heat of combustion value of lignin is higher than 5000 kcal/kg. (Çuhadar 2005; Guney, 2013; White, 1987).

3. Results and Discussion

Hazelnut husk as an agricultural residue can be utilized in different ways:

- Applying to soils to improve physical properties due to high organic matter content
- Using for agricultural purposes and plant growing (exp. strawberry production)
- Using for house heating (burning in stoves directly, as a pellet or briquette)
- Activated carbon production
- Energy production
    - Biochemical conversion: Digestion, fermentation, enzymatic or acid hydrolysis
    - Thermochemical conversion: Combustion, pyrolysis, gasification, liquefaction

Hazelnut wastes are mostly used for heating purposes in Turkey. Hazelnut shells are used as main solid fuel with automatic loading systems especially in bread bakeries. Similarly, hazelnut husks can be used mainly during initial operation in bread bakeries. However, they are utilized in plywood, linoleum and paint industry in USA, Italy and Germany. Hazelnut husks are used as a fuel in about 300 heating plants for household in Viterbo, near Rome in Central Italy. The cost of husk is nearly US$0.03 (50 liter/kg). The other biomass wastes (wine residues, olive residues, etc.) are also available at the same cost. Some structural properties of hazelnut husk from different sources obtained in the literature were given in Table 1.

Table 1. Some structural properties of hazelnut husk from different sources in the literature

Elemental Analysis	C %w	H %w	N %w	S %w	O %w	Ash %w	References
	42.7	5.2	0.9	-	45.4	5.8	Çuhadar, 2005
	40.4	-	1.26	-	-	-	Çimen, 2007
	35.2	-	1.34	-	-	-	Dede, 2012
	42.61	5.51	1.13	0.14	50.61	5.27	Ceylan and Topçu, 2014
	-	-	-	-	-	8.22	Çöpür, 2007
Chemical composition	Cellulose %w	Lignin %w	Hemicellulose %w	Moisture %w	Volatile matter %w	Holo-cellulose %w	
	34.5	35.1	20.6	7.24	73.86	-	Ceylan and Topçu, 2014
	34.5	35.1	-	-	-	55.1	Çöpür, 2007
Functional groups	O–H stretching Aliphatic C–H C=O (ketone and/or carboxylic acid) C=C Amidic C=O, amide II band COOH (C–O and O–H of COOH) C–O stretching of polysaccharide						Çimen, 2007

References

Çuhadar, C. et al., (2005). Production and Characterization of Activated Carbon from Hazelnut Shell and Hazelnut Husk, Middle East Technical University, Institute of Science, Ankara.

Çimen, F. et al., (2007). Characterization of humic materials extracted from hazelnut husk and hazelnut husk amended soils. Biodegradation, 18, 295–301.

Dede, O.H. et al., (2012). The use of hazelnut husk and biosolid in substrate preparation for ornamental plants. African Journal of Agricultural Research, 7(43), 5837-5841.

Ceylan, S. and Topçu, Y., (2014). Pyrolysis kinetics of hazelnut husk using thermogravimetric analysis. Bioresource Technology, 156, 182-188.

Çöpür, Y. et al. (2007). Some chemical properties of hazelnut husk and its suitability for particleboard production. Building and Environment, 42, 2568–2572.

Guney, M.S., (2013). Utilization of hazelnut husk as biomass. Sustainable Energy Technologies and Assessments, 4, 72–77.

White, R.H., (1987). Effect of lignin content and extractives on the higher heating value of wood, Wood and Fiber Science, 19(4), 446–452.

Investigation of the Heat Transfer and Flow Characteristic According to Placement Angles of Semi Spheres In Converging-Diverging Channels

Koray KARABULUT[1*], Dogan Engin ALNAK[2], Ferhat KOCA[2]

[1]Sivas Cumhuriyet University, Electric and Energy Department, Sivas Vocational High School, Sivas, Turkey
[2]Sivas Cumhuriyet University, Automotive Engineering Department, Technology Faculty, Sivas, Turkey

[*]**Corresponding Author:** kkarabulut@cumhuriyet.edu.tr

Abstract

Applications on thermal analysis and technologies of electronic circuits attract intensive attention so as to increase performance by supplying efficient cooling in the literature. In this work, heat transfer and flow characteristic of semi spheres by placing at different angles of 10º, 20º, 30º and without angle in converging-diverging channels were numerically investigated. The boundary conditions were determined as three dimensional, incompressible, fully developed and laminar flow for converging-diverging channel having eight semi-spheres with different angles. The continuity, Navier-Stokes and energy equations were solved numerically by using Ansys-Fluent-17.0 software program. Air was taken as working fluid. Air inlet temperature to the channel and surface temperatures of the spheres are 300 K and 350 K, respectively. The effects of different placements of semi-spheres as angle on the heat transfer and pressure loss coefficient increment in the case of different Re numbers of 100, 200, 400 and 800 were searched. The results were presented as variations of average Nusselt number, outlet temperature, heat flux and pressure loss coefficient values of the air according to different Re numbers. However, temperature and velocity contours, velocity vectors and also local Nu number and heat flux values for each of semi spheres were investigated. The obtained results indicate that location angles of the semi-spheres in the converging-diverging channel have a great importance by providing of flux and mixing of the fluid among spheres in the cooling process. The highest mean Nu number value was also acquired for the angle with 30º at Reynolds number of 800.

Key Words: Semi sphere, Converging-diverging channel, Numerical analysis.

1. Introduction

Converging-diverging channels are used for increasing heat transfer of industrial applications due to effective dispersion and mixing by flow separation among objects (Wang and Chen, 2002). Particularly, the flow in converging-diverging channels resembles to cooling process of many electronic devices exerted at the present time. However, heat transfer has a great important role in the design of various heat exchangers, nuclear reactors, solar collectors, heaters, coolers, internal-combustion engines, combustion chambers, electric machines etc. It is required that the heat transfer is taken the highest values in order to design of compact devices. Nowadays, various type heat exchanger designs have been improved. Heat transfer coefficient belonging to surface geometry of these heat exchangers and flow properties with pressure loss coefficient should be determined. One of the heat transfer increment methods is

continuous renewed of boundary layer. For this aim, shifted plate serials have been investigated in literature and it has been shown that the heat transfer coefficients can be increased.

One of the developed methods for enhancement of heat transfer surface area and the most important for improving of heat transfer coefficient by forming flow mixture section is communicating converging diverging channels. By means of these channels, enhancement in heat transfer can be carried out by increasing surface area in unit volume and especially by composing mixture section. Pressure drop also increases with increasing heat transfer at flow on these surfaces. Therefore, main goal for using of these surfaces is that when it is provided maximum enhancement in heat transfer, increment in pressure drop is obtained by minimizing of flow rate. The main purpose should be become to determine optimum values which increase the system performance.

Converging-diverging channels as periodic has become subject of interest for many researchers. Sparrow and Prata, 1983 investigated flow and heat transfer with Reynolds number between 100 and 1000 at converging-diverging conic channels with unconnected as periodic both experimental and numerical. It was shown in study that pressure loss was little more according to flat tube and Nusselt number as depending on Prandtl number. It was seen that Nusselt number was less than flat tube for Pr<1, it was little more according to flat tube for Pr>1 in study. Patankar et al., 1977 studied flow and heat transfer under fully developed flow conditions in rectangular cross-section channels that were periodically variable cross section in flow direction. It was found that the uniform wall temperature was similar due to the fact that the velocity and temperature profiles changed periodically in the modules. It was determined that the temperature area in a given wall heat flux periodically repeated itself. Niceno and Nobile, 2001 numerically researched fluid flow and heat transfer for sinusoidal and arc shaped wavy converging-diverging channel. Wang and Vanka, 1995 numerically examined flow and heat transfer in periodic sinusoidal channels. Their studies showed that heat transfer was increased in such channels but the increase in pressure loss was less than the increase in Nusselt number. Stone and Vanka, 1999 studied developing flow and heat transfer in a wavy passage by using numerical method. Natarajan and Mokhtarzadeh-Dehghan, 2000 investigated the periodic flow both experimentally and numerically in a model of a corrugated channel in order to understand of blood stended arteries. Chunhua et al., 2010; Pankaj et al., 2014 experimentally examined periodically interrelated axial vortex generators. They made comparison in their work for the appropriate fin types in the vortex generators. Chunhua et al., 2012; Sohankar, 2007 calculated the effects of vortex generators on heat transfer by using a

three-dimensional numerical method. They came to the conclusion that by using the vortex generators, the Nusselt number can be increased significantly. Karabulut et al., 2018 researched the effects of location of semi spheres as multiple serials, placement angle and positions of spheres according to each other on the pressure drop and heat transfer enhancement for case of different Re numbers. The obtained results showed that the positions of spheres had a great importance in the case of placement as multiple serials of semi spheres. Chandra et al., 2015 investigated the heat transfer performance and fluid flow in three-dimensional converging-diverging microchannel of circular cross section, numerically. For this aim, in proposed microchannels, they studied the effect of Reynolds number, converging-diverging angle and cross-section length on pressure drop and heat transfer. The obtained results indicated that the flow in the converging-diverging cross-section caused stronger recirculation and flow separation, which decreases with decreasing the converging-diverging angle and increases with increasing aspect ratio. Pehlivan, 2013 experimentally studied heat transfer and pressure drop characteristics of air flow in corrugated channels. Experiments were carried out for uniform wall heat flux and Reynolds number varied from 2000 to 9000. Four different types finned plates were used as two sharp and two rounded corrugation peak in the experiments. Channel height effects on heat transfer and pressure drop were searched. It was seen that the increase of corrugated angle and channel height increased the heat transfer.

When investigated the studies indicated in literature, it is seen that heat transfer and flow structure of converging-diverging channels having different angle placements as semi-spheres like at this work have not already been investigated. In this work, it was studied with original geometry and angle placements for converging-diverging channels. Therefore, in the presented study, particularly in electronic devices in order to supply the more effective cooling which decreases thermal stresses and prevents undesirable results due to mechanic faults, the heat transfer, pressure drop and flow structures of converging diverging channels composed of eight semi spheres with different angles were searched. Besides, the contour distributions of temperature and velocity and velocity vectors along the channel were examined and the effects of semi spheres and their various angles on temperature, velocity and flow structure characteristics were evaluated. However, variations of the mean Nusselt number, heat transfer rate and fluid outlet temperature according to different Reynolds numbers and semi sphere angles were numerically investigated and compared with semi sphere without angle in the converging diverging channels. Besides, mean Nusselt numbers and heat flux values for each of eight semi spheres were researched and pointed out as table at different Re numbers.

Continuity, Navier-Stokes and energy equations were solved together to calculate heat transfer at channels. These basic conservation equations describing the problem were solved with computer program of Ansys FLUENT-17.0 finite element method based.

2. Numerical Method

Numerical study was conducted three dimensional, laminar, steady, incompressible fluid flow and constant fluid properties by using finite volume method of FLUENT 17.0 software program. Body forces and viscous dissipation and heat radiation are ignored due to the weak temperature gradients in the flow.

The finite volume method depends on the basis of dividing the geometry which will be solved in parts to find a solution for each of these sections and then by uniting these solutions to obtain a general solution of the problem. This method employs a method which depends on the control volume for turning heat flow equations into algebraic equations which can be solved numerically. In other words, this method depends on the basis of taking the integration of heat flow equations in each control volume. The result of this integration supplies equations which identify each control volume coming into existence. In order to arranging the most proper grid model, a fine grid should be composed in sections where the change in variables such as velocity, pressure and temperature is bigger. A grid independence test was carried out by comparing the results of different grid meshes as shown in Table 1 for Re=100. The test points out that 985458 grids are sufficient (< 0,1% difference compared with 2854420 elements). The grid distribution is shown in Fig. 1 with 985458 elements for placement without angle. A structured grid is implemented around the semi spheres. Convergence of the computations is stopped for the continuity and the momentum equations when residues are less than 10^{-6} and for the energy equation when residues are less than 10^{-7}.

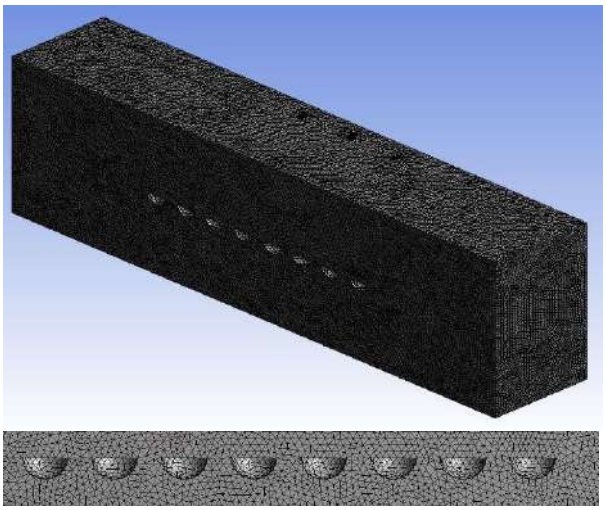

Figure 1. Mesh structure applied to models.

Table 1. Grid independence test of the model.

Number of elements	Nu_m	f	q_{out} (W/m^2)	T_{out} (K)
185465	11,7452	1,7854	145,854	315,0125
985458	11,0157	1,794902	146,754	315,4630
2854420	11,0158	1,794854	146,755	315,4634

The resulting equations are expressed as follows (Fluent, 2003)

Continuity equation

$$\frac{\partial u}{\partial x}+\frac{\partial v}{\partial y}+\frac{\partial w}{\partial z}=0 \tag{1}$$

Momentum equation

x momentum equation

$$\rho\left(u\frac{\partial u}{\partial x}+v\frac{\partial u}{\partial y}+w\frac{\partial u}{\partial z}\right)=-\frac{\partial p}{\partial x}+\mu\left(\frac{\partial^2 u}{\partial x^2}+\frac{\partial^2 u}{\partial y^2}+\frac{\partial^2 u}{\partial z^2}\right) \tag{2}$$

y momentum equation

$$\rho\left(u\frac{\partial v}{\partial x}+v\frac{\partial v}{\partial y}+w\frac{\partial v}{\partial z}\right)=-\frac{\partial p}{\partial y}+\mu\left(\frac{\partial^2 v}{\partial x^2}+\frac{\partial^2 v}{\partial y^2}+\frac{\partial^2 v}{\partial z^2}\right) \tag{3}$$

z momentum equation

$$\rho\left(u\frac{\partial w}{\partial x}+v\frac{\partial w}{\partial y}+w\frac{\partial w}{\partial z}\right)=-\frac{\partial p}{\partial z}+\mu\left(\frac{\partial^2 w}{\partial x^2}+\frac{\partial^2 w}{\partial y^2}+\frac{\partial^2 w}{\partial z^2}\right) \tag{4}$$

Energy equation

$$u\frac{\partial T}{\partial x}+v\frac{\partial T}{\partial y}+w\frac{\partial T}{\partial z}=\left(\frac{k}{\rho c_p}\right)\left(\frac{\partial^2 T}{\partial x^2}+\frac{\partial^2 T}{\partial y^2}+\frac{\partial^2 T}{\partial z^2}\right) \tag{5}$$

In above equations, u, v and z are the velocity components, p is the pressure, μ is the dynamic viscosity, ρ is the density of the fluid, T is the temperature of the fluid, k is the thermal conductivity, υ kinematic viscosity and c_p is specific heat.

Reynolds number

$$Re = \frac{V_m . D_h}{\nu} \tag{6}$$

Here, D_h is the hydraulic diameter of the channel, V_m is the mean velocity.

$$D_h = \frac{4A_c}{P} = \frac{4(H.W)}{2(H+W)} \tag{7}$$

h is the heat convection coefficient.

Pressure drop can be calculated as below

$$\Delta P_L = f . \frac{L}{D_h} . \frac{\rho . V_m^2}{2} \tag{8}$$

ΔP_L is the pressure drop at the flow direction in the channel, f is the pressure loss coefficient (friction factor).

Boundary condition and Nusselt number are given as follows

$$-k\left(\frac{dT}{dn}\right)_{surface} = h\left(T_{cf} - T_{\infty}\right) \text{ and } Nu = \frac{h.D_h}{k} \tag{9}$$

f, friction factor between plates can be calculated with Eq. (10) as analytical.

$$f = \frac{96}{\mathrm{Re}} \tag{10}$$

3. Geometric Model

A rectangular channel and four different models composed of semi spheres with three different angles of 10^o, 20^o, 30^o and without angle (0^o) located in converging diverging channels are exhibited in Fig. 2. Here, the flow is toward the inside of the channel. The geometric boundary conditions and rectangular channel used in numerical calculations are shown in Figure 3. The bottom, top, and side parts are solid surfaces defined as walls when the left side of the channel is given as velocity inlet. The cross-sectional area on the right side of the duct is defined as the pressure outlet. There is no need to define the pressure at the exit because the velocity is defined in the inlet according to Patankar and Prakash, 1981. At the same time, channel was divided into two from the middle to simplify the calculation and symmetric boundary condition is valid. The surfaces of the semi spheres were heated up to 350 K and air inlet temperature to channel was 300 K. The Reynolds numbers for inlet velocities are 100, 200, 400 and 800.

Channel shape	: Rectangular
Channel heigth (H)	: 120 mm
Channel length (L)	: 243 mm
Channel element shape	: Semi-sphere
Channel element angle (Φ)	: 0^o, 10^o, 20^o and 30^o
Channel element diameter (D)	: 20 mm
Distance between the channel elements (l)	: 30 mm
Reynolds number	: 100, 200, 400, 800
Fluid (air) temperature (T_c)	: 300 K
Sphere surface temperature (T_{cf})	: 350 K

This study was performed under the stated assumptions:

i) Flow is three dimensional, steady and laminar;

ii) The used fluid is incompressible and air;

iii) Aluminium was used as channel and channel element material (semi sphere);

iv) Thermal properties of the fluid are constant;

v) There is no heat generation for both fluid and solid material.

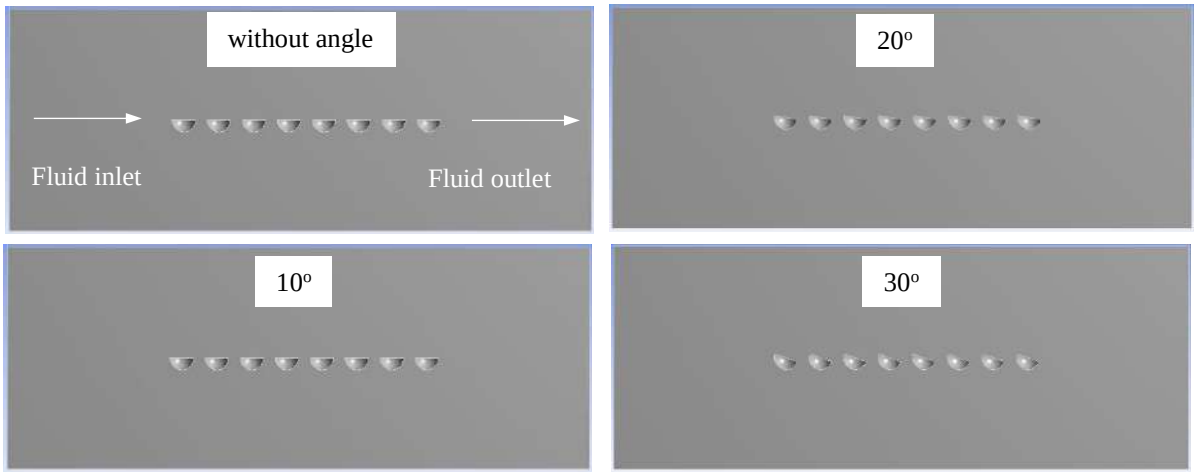

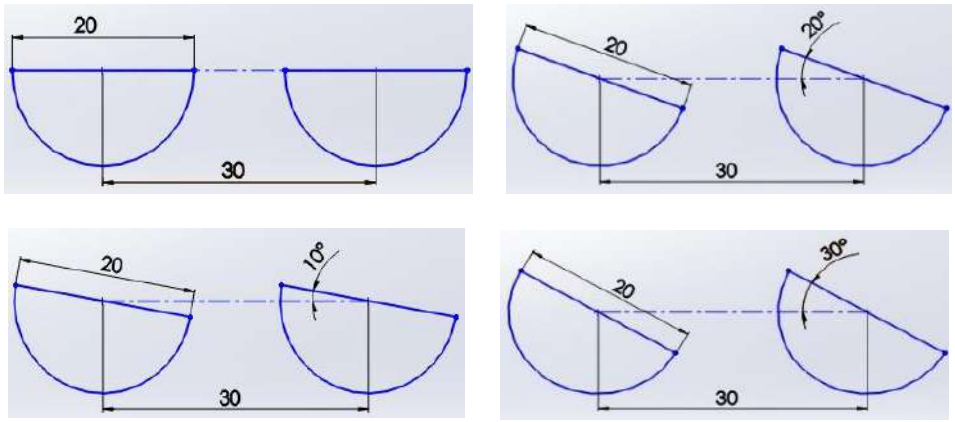

Figure 2. Models used in numerical calculations.

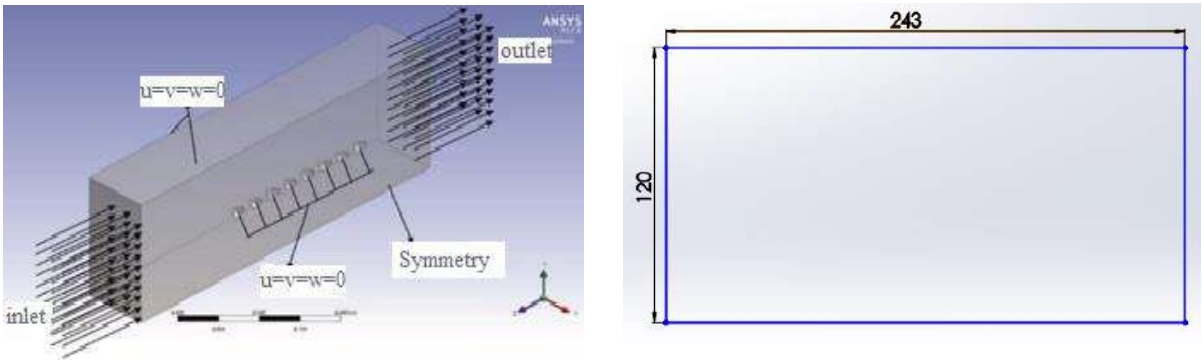

Figure 3. Boundary conditions and rectangular channel used in numerical calculations.

4. Evaluation of the Results

The results of the f-friction factor variation of the presented numerical study with the Re number for parallel plate are shown both in Figure 4 and Table 2 by comparing analytical (Eq. 10) and numerical results obtained from Erdinc, 2014. It is seen that the results are very compatible with each other and therefore it is considered that the numerical study is correct and acceptable.

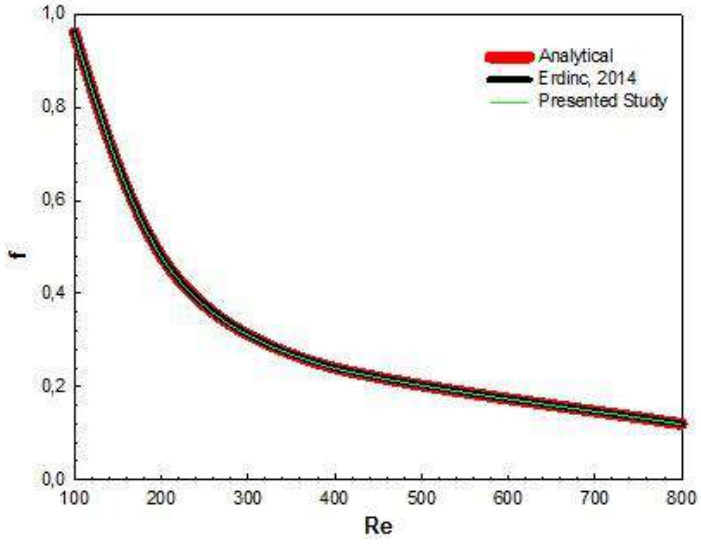

Figure 4. Comparing the results obtained for f-friction factor.

Table 2. Comparing of numerical results obtained for f.

Re	f=96/Re (Analytical)	f (Erdinc, 2014)	f (Presented study)
100	0,96	0,960159	0,9579
200	0,48	0,481034	0,4789
400	0,24	0,240616	0,2394
800	0,12	0,120082	0,1197

Fluid movements among the converging-diverging channels composing of semi-spheres are shown in Fig. 5 by means of velocity vectors at the different sphere angles and Re=400. When the fluid can not go toward converging-diverging channels for the case of without angle, it moves to gaps among the semi-spheres with increasing of the angle of the sphere. Therefore, it is important to determine optimum sphere angle in order to enable best fluid motion and mixing. However, for this aim, the sphere has been selected as semi. So, the fluid can be directed among intervals of converging-diverging channels.

The variation of the friction factor (pressure loss coefficient) with Re number are given in Fig. 6 for different semi-sphere angles of 0^o, 10^o, 20^o and 30^o. While the minimum friction

factor value is obtained for the case of without angle (0^o), it increases with increasing of location angles of spheres due to flow obstruction. Hence, pressure drop shows increment. However, the highest friction factor value changes between angles of 20^o and 30^o depending on the Re number. Besides, the friction factor reduces with the enhancing of Re number as can be seen in Fig. 6.

Outlet temperature variation of the fluid from the channel having different semi-sphere location angles for different Reynolds numbers are pointed out in Fig. 7. The outlet temperature values are much close to each other for the converging-diverging channels with different angles, the fluid outlet temperature value is higher at the channel with 30^o angle. This result states that the passing and mixing of the fluid among semi-spheres are intense for 30^o angle, which cause to enhance the heat transfer from spheres to fluid. However, the lowest value of the outlet temperature is attained for the channel with 0^o angle where the fluid motion among the converging-diverging channels is less.

The variation of the mean Nu number of semi-spheres with different angles depending on the Re number is represented in Fig. 8. The Nu numbers of semi-spheres with 20^o and 30^o angles are higher than that of 10^o and 0^o (without angle) because of the higher mixing and motion rates. However, the lower Nu number value is acquired for 30o angle when comparing with 20^o due to occurred flow distribution as shown in Fig. 5 depending on the angle positions of the spheres for Re=400. Besides, because the fluid enters into spheres at the Reynolds number of 800 for the angle of 30^o, the increment of the Nu number is more than 20^o. Therefore, this result indicates that the Reynolds number as well as placement angle affects flow structure and heat transfer.

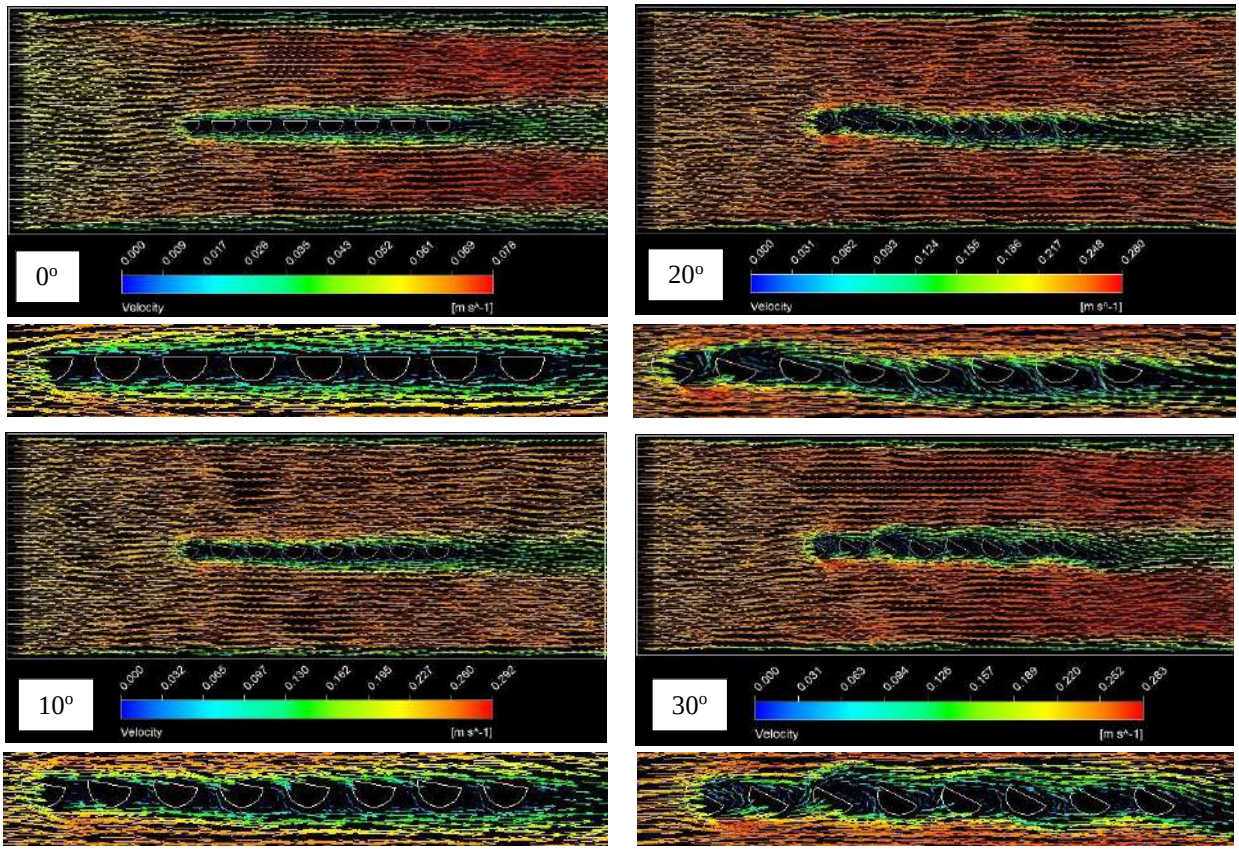

Figure 5. Exhibition of the velocity vectors of the flow along the channel for different sphere angles and Re=400.

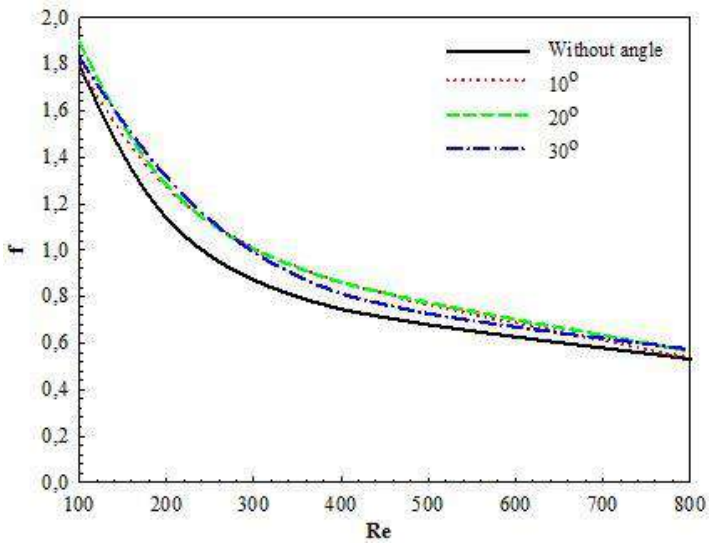

Figure 6. Variation of f-friction factor versus Re number.

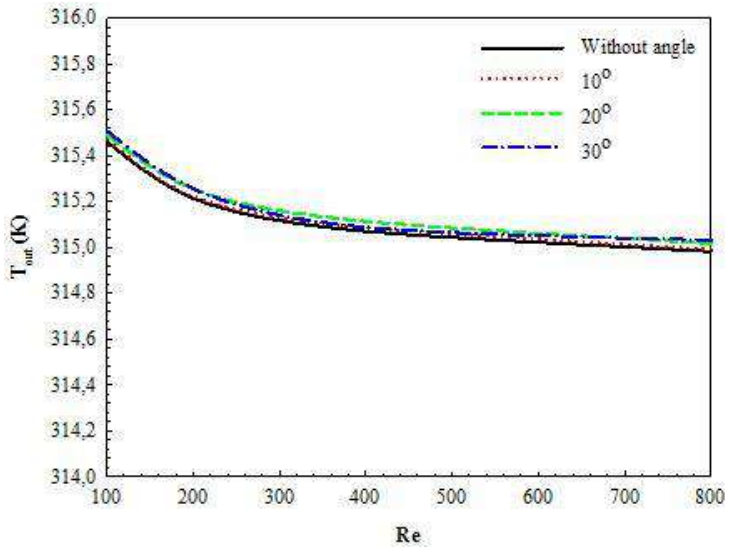

Figure 7. Outlet temperature variation of fluid from the channel according to Re number.

Figure 9 shows the heat flux value variation at the outlet of the channel for different Re numbers and semi-sphere angles of 0°,10° 20° and 30°. While the heat transfer amount from semi-spheres to air increases with increasing of Re number, the high heat flux values are obtained for converging-diverging channels with 20° and 30° semi-sphere angle.

Temperature and velocity contour distributions of converging-diverging channels having semi-spheres with angles of 0°, 10°, 20° and 30° are exhibited in Fig. 10A and B, respectively. As can be seen in contour distribution, because the converging-diverging channel with 0° angle has low fluid passing ability, the temperature around the spheres are high. However, fluid motion and mixing among the spheres increase with increasing of sphere location angle and so temperature gradient enhances along the channel (Fig. 10A). This case ends up with heat transfer increase from spheres to fluid. Besides, the decrease of the fluid movement among the semi-spheres is clearly seen from the velocity contours for each semi-spheres angles (Fig. 10B). The fluid velocity decreases among the spheres because of decreasing of the amounts of fluids coming from the top and bottom of the semi-spheres. But, it is provided to pass fluid among spheres by increasing the sphere angle.

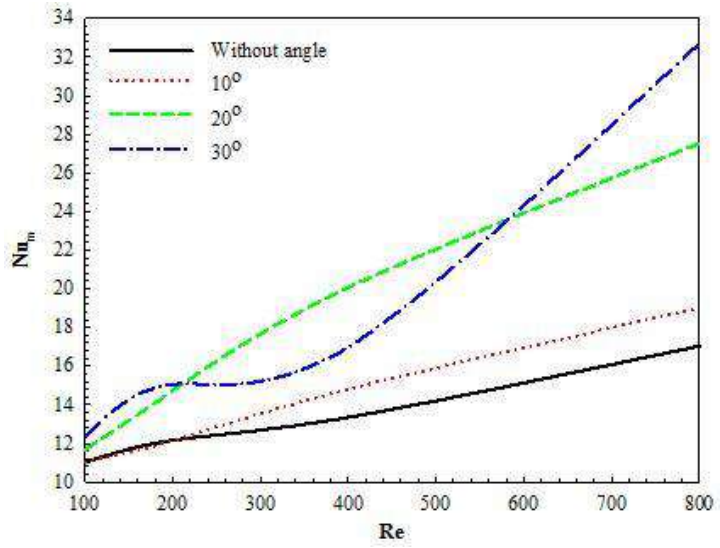

Figure 8. Mean Nu number variation depending on the Re number.

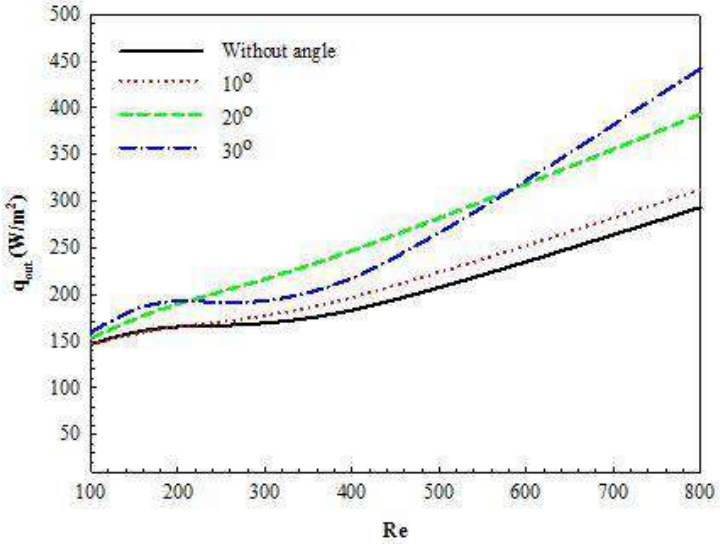

Figure 9. Heat flux variation versus Re number at the channel outlet.

Local Nu number and heat flux values for each of eight semi-spheres with 20° angle for different Re number values are shown in Table 3. The values of the Nu_L and heat flux are high for the first semi-sphere where the temperature difference among the air and spheres is maximum and they decrease along the other spheres. However, local Nu number and heat flux values increase with increasing of Re number.

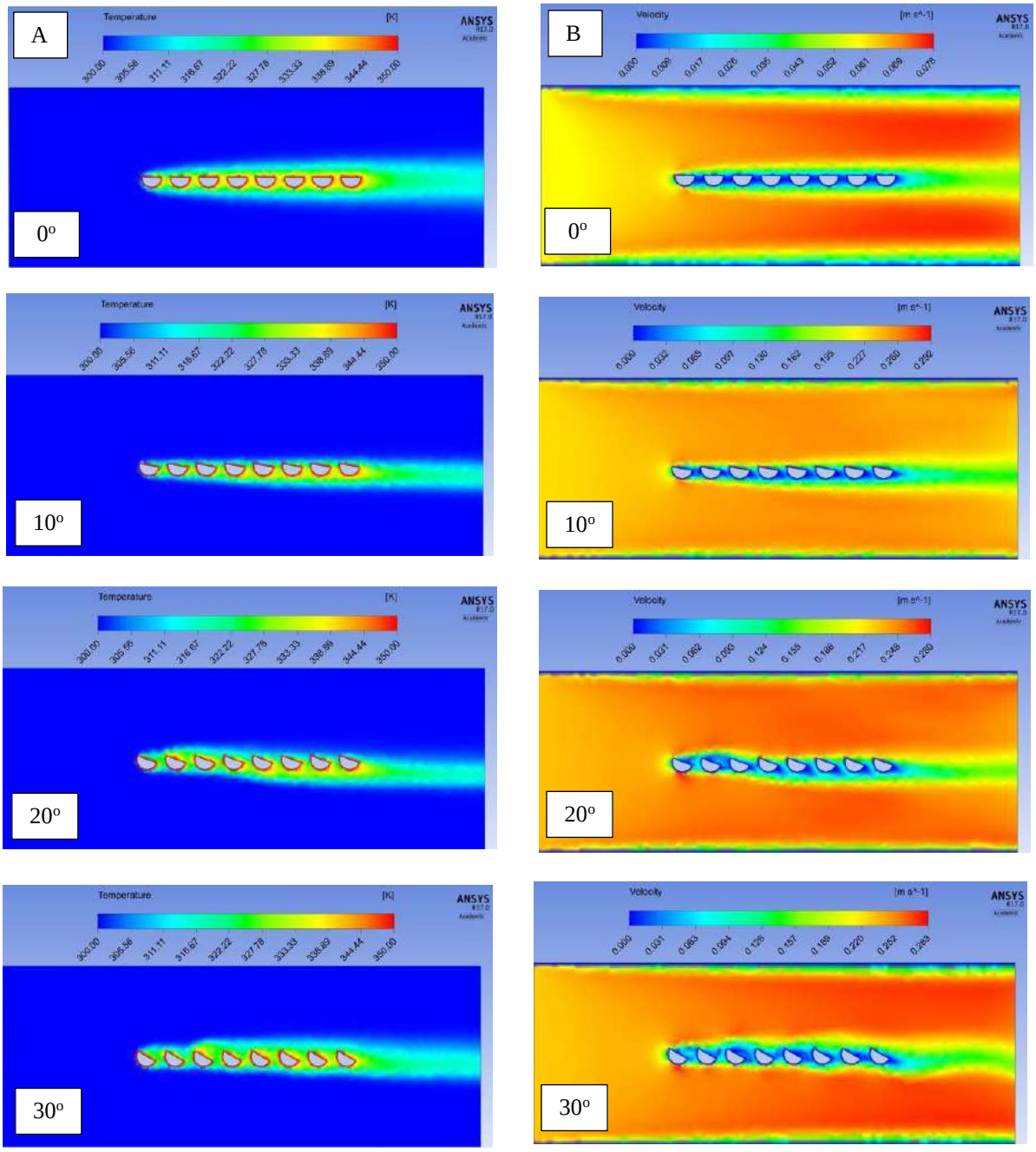

Figure 10. Contours of A-Temperature, B-Velocity for 0º, 10º, 20º and 30º angles at Re=400.

Table 3. Local Nu number and heat flux values for each of semi-sphere with 20° at the channel.

Sphere Line	Re=100 Nu_L	Re=200 Nu_L	Re=400 Nu_L	Re=800 Nu_L	Re=100 q (W/m^2)	Re=200 q (W/m^2)	Re=400 q (W/m^2)	Re=800 q (W/m^2)
1.	20,76293	25,83849	32,95508	41,51283	431,788	561,157	733,967	939,399
2.	12,63721	15,3379	21,72084	30,24858	262,804	333,106	483,761	684,499
3.	11,40085	13,89236	18,56702	31,30018	237,093	301,712	413,52	708,295
4.	10,46013	13,16159	15,27029	25,10818	217,53	285,841	340,096	568,176
5.	9,965172	12,82913	16,68456	28,00107	207,237	278,621	371,594	633,64
6.	9,434778	12,34078	17,31126	21,94255	196,206	268,015	385,552	496,541
7.	9,342648	12,17165	18,60774	20,76253	194,291	264,342	414,426	469,837
8.	9,486689	12,2641	19,48242	21,36888	197,286	266,35	433,907	483,559

5. Conclusions and Suggestions

Electronic equipments containing resistors, capacitors, microchips and others are susceptible to failure from overheating which cause to increase thermal stresses of the system.

The temperature of an electronic equipment is affected by the ambient temperature of the environment, the heat produced by the component and the efficiency of heat removal provided by the thermal system. Component temperature can be decreased by improving any of these factors. A more efficient component will give off less heat; an advanced thermal system is capable of quickly removing heat. For this aim, one of the developed methods is to increase the heat transfer surface area and the most importantly, to improve the heat transfer coefficient by forming the mixing area by means of communicating converging-diverging channels. Thanks to these channels, it is possible to improve the heat transfer by increasing the surface area in the unit volume and especially by forming the mixing region.

In the present work, the effects of the converging-diverging channels for four different angle designs composed of eight half-spheres on the heat transfer, fricton factor (pressure loss coefficient) and flow structure are numerically investigated as three dimensional for steady, fully developed and laminar flow by using the Ansys Fluent-17.0 computer program at calculation of the basic equations.

When examined the friction factor for the channels, as the minimum friction factor value is obtained for the case of without angle, it increases with increasing of sphere location angles due to formation obstruction to flow of fluid. The highest friction factor value changes between angles of 20° and 30° depending on the Re number. However, the lowest value of the outlet temperature is attained for the channel with 0° angle where the fluid motion among the

converging-diverging channels is less. The highest mean Nu number value is also acquired for the angle with 30^o at Reynolds number of 800. This result indicates that the Reynolds number as well as placement angle affects flow structure and heat transfer.

As a conclusion, the main purpose of usage of the converging-diverging channels is to provide the circulation of the fluid among the elements by mixing of the fluid. Thus, as it is in this study, the mixing of the fluid coming from the top and bottom section of the spheres and circulation among the semi-spheres are important factors for increase of the heat transfer. Besides, it should be pay attention to the location, angles and numbers of the spheres.

Acknowledgment

The authors would like to thank Scientific Research Projects Coordination Unit of Sivas Cumhuriyet University (Sivas/Turkey) for their financial support to this research under project number TEKNO-006.

Nomenclature

A	cross-section area, m^2
c_p	specific heat, J. $kg^{-1}.K^{-1}$
D	channel element diameter, mm
D_h	hydraulic diameter, m
f	friction factor
h	heat transfer coefficient, $W.m^{-2}.K^{-1}$
H	height of channel, mm
k	thermal conductivity, $W.m^{-1}.K^{-1}$
l	distance between the channel elements, mm
L	length of channel, mm
p	pressure, $N.m^{-2}$
Δp	pressure drop, $N.m^{-2}$
Nu	Nusselt number, dimensionless
Re	Reynolds number, dimensionless
V	inlet velocity to channel, $m.s^{-1}$

T	temperature, K
u, v, w	velocity components of x,y,z directions, $m.s^{-1}$
W	width of channel, mm
x, y, z	cartesian coordinates, m

Greek Symbols

μ	dynamic viscosity, kg. $s^{-1}.m^{-1}$
ρ	density, kg. m^{-3}
Φ	channel element angle, degree
ν	kinematic viscosity, $m^2.s^{-1}$

Subscripts

c	fluid
cf	sphere surface
L	local
m	mean
∞	ambient

References

Wang, C. C., Chen, C. K. (2002). Forced convection in a wavy-wall channel. *International Journal of Heat and Mass Transfer*, 45(12), 2587-2595.

Sparrow, E. M., Prata, A. T. (1983). Numerical solutions for laminar flow and heat transfer in a periodically converging-diverging tube with experimental confirmation. *Numerical Heat Transfer*, 6(4), 3219-3230.

Patankar, S. V., Liu, C. H. and Sparrow, E. M.. (1977). The periodic thermally developed in ducts with streamwise periodic wall temperature or heat flux. *International Journal of Heat and Mass Transfer*, 21(5), 557-666.

Niceno, B., Nobile, E. (2001). Numerical analysis of fluid flow and heat transfer in periodic wavy channels. *International Journal of Heat and Fluid Flow*, 22, 156-167.

Wang, G., Vanka, S.P. (1995). Convective heat transfer in periodic wavy passages. *International Journal of Heat and Mass Transfer*, 38(17), 3219-3230.

Stone, K., Vanka, S. P. (1999). Numerical Study of developing flow and heat transfer in a wavy passage. *Transactions ASME Journal of Fluids Engineering*, 121, 713-719.

Natarajan, S., Mokhtarzadeh-Dehghan, M. R. (2000). A numerical and experimental study of periodic flow in a model of a corrugated vessel with application to stented arteries. *Medical Engineering & Physics*, 22(8), 555-566.

Chunhua, M., Chengying, Q., Xiangfei, K., Jiangfeng, D. (2010). Experimental study of rectangular channel with modified rectangular longitudinal vortex generators. *International Journal of Heat and Mass Transfer*, 53(15-16), 3023-3029.

Pankaj, S., Gautm, B., Subrata, S., (2014). Comparision of winglet-type vortex generators periodically deployed in a plate-fin heat exchanger-a synergy based analysis. *International Journal of Heat and Mass Transfer*, 74, 292-305.

Chunhua, M., Chengying, Q., Wang, E., Tian, L., Qin, Y. (2012). Numerical investigation of turbulent flow and heat transfer in a channel with novel longitudinal vortex generators. *International Journal of Heat and Mass Transfer*, 55(23-24), 7268-7277.

Sohankar, A. (2007). Heat transfer augmentation in a rectangular channel with vee-shaped vortex generator. *International Journal of Heat and Fluid Flow*, 28(2), 306-317.

Karabulut, K., Alnak, D. E., Koca, F., Ozalp, C. (2018). Numerical analysis of flow and heat transfer for semi spheres placed as multiple serials in a channel. *European Mechanical Science*, 2(3), 76-82.

Chandra, A. K., Kishor, K., Mishra, P. K., Siraj, Alam. (2015). Numerical simulation of heat transfer enhancement in periodic converging-diverging microchannel. *Procedia Engineering*, 127, 95-101.

Pehlivan, H. (2013). Experimental investigation of convection heat transfer in converging-diverging wall channels. *International Journal of Heat and Mass Transfer*, 66, 128-138.

FLUENT User's Guide. (2003). Fluent Inc. Lebanon, NH.

Patankar, S. V. and Prakash, C. (1981). Analysis of the effect of plate thickness on laminar flow and heat transfer in ınterrupted plate passages. *International Journal of Heat and Mass Transfer*, 24(11), 1801-1810.

Erdinc, M.T. (2014). *Birbirleriyle Bağlantılı Daralan ve Genişleyen Kanallarda Akış ve Isı Geçişinin Sayısal Olarak İncelenmesi.* Master Thesis, Osmaniye Korkut Ata University, Institute of Science, Osmaniye.

FOOD ENGINEERING

ORAL PRESENTATIONS

Antibacterial and Antioxidant Potential of Linden (*Tilia rubra* subsp. *caucasica*) and Primrose (*Primula* sp.) Extracts

Cavidan DEMİR GÖKIŞIK[1*], Sinem AYDIN[2]

[1]Giresun University, Faculty of Engineering, Departman of Food Engineering, Giresun, Turkey; cdrdemir@hotmail.com

[2]Giresun University, Faculty of Science and Arts, Department of Biology, Giresun, Turkey; ozdogansnm@mynet.com

*__Corresponding Author__: cavidan.gokisik@giresun.edu.tr

Abstract

In this research, antibacterial and antioxidant activities of the extracts of *T. rubra* subsp. *caucasica* and *Primula* sp. were surveyed. Antibacterial activity of the extracts was performed by the disc diffusion method and micro broth dilution methods. Inhibition zones of the extracts were ranged from 6 to 14 mm. Antioxidant activity was determined by determination of total phenolic and flavonoid contents, DPPH radical scavenging activity, ABTS radical scavenging activity and total antioxidant capacity. The highest phenolic content was determined in ethanol extract of *T. rubra* subsp. *caucasica* and the lowest flavonoid content was determined in the ethanol extract of *Primula* sp. Extracts of *T. rubra* subsp. *caucasica* had higher DPPH and ABTS radical scavenging activity than the extracts of *Primula sp.* These results suggest that the extracts of *T. rubra* subsp. *caucasica* and *Primula* sp. might be an alternative to synthetic antibacterial and antioxidant agents.

Keywords: Antioxidant, antimicrobial activity, plant

1. Introduction

Increasing antibiotic resistance and the need of brand antibacterials has long been known. A main challenge in health care is the requirement for new, effective drugs to cure bacterial infections. Antimicrobial-resistant in bacterial species arise from many factors such as inappropriate use of antibiotics, excessive utilize of these agents for growth enhancers in animal feed. Because of these troubles, there is an urgent demand for developing of alternative drugs to treat such infectious diseases (Elisha et al., 2017).

Plants possess an incredible ability to produce various secondary metabolites such as terpenoids, saponins, steroids, alkaloids, glycosides, flavonoids, tannins, quinones and coumarins. These biomolecules are efficient in the combating with bacterial infections (Elisha et al., 2017).

An antioxidant might be defined as any substance that delays or inhibits oxidative damage to a target molecule. Oxidative stress cause a great deal of chronic diseases. Free radicals and other reactive oxygen species leads many illnesses such as asthma, inflammatory arthropathies, diabetes, Parkinson's and Alzheimer's diseases and atherosclerosis (Badakhshan et al., 2012.

Many medicinal plants has been explored for their antioxidant capacities. Natural antioxidants which present in raw plant extracts or their chemical constituents are very efficient to hinder the devastating processes caused by oxidative stress. Eventhough the toxicity property of some medicinal plants have not been thoroughly studied, it is usually accepted that medicines derived from plants are safer when compared with synthetic antioxidants (Saeed et al., 2012).

Primrose sp. have a very long history of medicinal use and has been particularly employed used in treating conditions involving spasms, cramps, paralysis and rheumatic pains. The plant contains saponins, which have an expectorant effect, and salicylates which are the main ingredient of aspirin and have anodyne, anti-inflammatory and febrifuge effects. The roots and the flowering parts of *Primrose* sp. are anodyne, antispasmodic, astringent, emetic, sedative and vermifuge. An infusion of the roots is a good remedy against nervous headaches (naturalmedicinalherbs web, 2018).

The genus *Tilia rubra* subsp. *caucasica* is a member of the family *Tiliaceae*. The different parts of Tilia are consumed as medical. The flowers of *Tilia* species are utilized for treatment of various diseases such as microbial infections, antiemetic and strengthening effects, increasing urine and decreasing tension. Moreover, Linden flowers are widely used in folk medicine (Ozbucak et al., 2013).

In this study, it was aimed to investigate antibacterial and antioxidant properties of Primrose sp. and *Tilia rubra* subsp. *caucasica* collected from Giresun.

2. Materials and Method

2.1. Plant Collection

Primula sp. and *Tilia rubra* subsp. *caucasica* were collected from Gökçeali Village, Piraziz District in Giresun.

2.2. Microorganisms

Salmonella enterica ATCC 14028 and *Staphlococcus aureus* ATCC 25923 were obtained from Giresun Province Control Laboratory; *Bacillus cereus* 702 ROMA were acquired from Rize University Department of Molecular Biology; *Enterobacter aerogenes* CCM 2531 and *Bacillus subtilis* IMG 22 were obtained from Fırat University Department of Biology; *Gordonia rubripertincta* (laboratory isolate) was acquired from Yeditepe University Department of Genetic and Bioenginneering; *Escherichia coli* ATCC 35218 was obtained from Giresun University.

2.3. Extract Preparation

20 g of the powdered sample (*Primula* sp. and *T. rubra* subsp. *caucasica)* were extracted with Soxhlet apparatus utilizing 200 mL ethanol and ethyl acetate solvents, separetely. The extraction process followed by filtration with Whatman filter paper no 1. The filtered extract concentrated in vacuo at 40 ˚C using a rotary evaporator. Extracts were kept at -80 ˚C for other tests (Kumar et al., 2012).

2.4. Antibacterial activity

Crude extracts were dissolved with DMSO at 30 mg/mL. Then, they were sterilized by using 0.45 µm pore sized filter. The discs were put into agar plates and filled with 25 µL ethanol extract of *Primula* sp., 25 µL ethyl acetate of *Primula* sp., 25 µL ethanol extract of *T. rubra* subsp. *caucasica*, 25 µL ethyl acetate of *T. rubra* subsp. *caucasica*, 25 µL DMSO.

Ciprofloxacin disc was utilized as standard antibacterial agent. Plates were then incubated for 24h at 37 °C. The clear zone of inhibition was observed and measured in mm (Murray et al., 1995; Saric et al., 2009).

2.5. Determination of Minimum Inhibition Concentration (MIC)

Lichen extracts were prepared at 30 mg/mL concentration. The MIC were detected by using the procedure of Yiğit et. al. (Yiğit et el., 2009).

2.6. Determination of Antioxidant Activity of The Plant Extracts

2.6.1. Total Phenolic Content

Amounts of total phenolic compounds in the tested extracts were determined using the Folin-Ciocalteu solution according to the method described by Slinkard and Singleton (1977). Gallic acid was used as a standard in the study. The results were given in µg Gallic Acid Equivalent (GAE)/mL. The tests were carried out three times (Slinkard and Singleton, 1977).

2.6.2. Total flavonoid content

Total flavonoid contents in the plant extracts were studied with the procedure of Zhishen et al. (1999). Catechin was used as a standard. The total flavonoid amount was determined as µg Cateschin Equivalent (QE)/mL sample from the standard graphical equation of catechin. The tests were performed in triplicate (Zhishen et al., 1999) .

2.6.3. ABTS radical scavenging activity

The ABTS radical scavenging activity of ethanol and ethyl acetate extracts of *Primula* sp. and *T. rubra* subsp. *caucasica* were performed according to the method developed by Arnao et al. (2001). BHT and rutin used as standards. The tests were carried out three times (Arnao et al., 2001). The results are calculated from the following equation:

$$\%\ Activity: \left[\frac{A0-A1}{A0}\right] X100 \qquad (1)$$

A_0=Absorbance of control

A_1= Absorbance of sample

2.6.4. DPPH radical scavenging activity

The DPPH radical scavenging activity of ethanol and ethyl acetate extracts of *Primula* sp. and *T. rubra* subsp. *caucasica* were measured by utilizing the method of Brand-Williams et al. (1995). Extracts were prepared at 250-1000 µg/mL concentrations. The percentage inhibition was established by comparing the results of the test and the control. The tests were carried out three times (Brand-Williams et al., 1995). Percentage of activity was calculated using the following formula:

$$\% \, Activity: \left[\frac{A0-A1}{A0}\right] X100 \quad (2)$$

A_0=Absorbance of control

A_1= Absorbance of sample

2.6.5. Total Antioxidant Capacity

Total antioxidant capacity of the extracts were defined by the method of Prieto et al. (1999). Absorbance was measured at 695 nm. The results were calculated as µg ascorbic acid/mL from ascorbic acid standard graphical equation. The tests were carried out three times (Prieto et al., 1999).

3. Results and Discussion

3.1. Antibacterial Activity

Inhibition zones of ethanol and ethyl acetate extracts of *T. rubra* subsp. *caucasica* ve *Primula* sp. are given in Table 1. While the highest activity was observed in ethanol extract of *T. rubra* subsp. *caucasica* against *E. coli*. While inhibition zones of the extracts of *T. rubra* subsp. *caucasica* were ranged from 6 to 14 mm; inhibition zones of the extracts of *Primula sp.*

were ranged from 6-13 mm. All the extracts exhibited lower activity than ciprofloxacin. Inhibition zones lower than 6 mm considered as no activity.

Table 1. Inhibition zones of te plant extracts (mm)

Bacteria	EET	EAT	EEP	EAP	DMSO	Cipro
B. subtilis	11	9	7	6	-	26
B. cereus	10	7	9	6	-	24
G. rubripertincta	11	6	6	6	-	27
S. aureus	11	7	6	6	-	24
E. coli	14	9	13	8	-	35
E. aerogenes	17	11	9	6	-	29
S. enterica	-	-	-	-	-	35

-: No Activity; EET: Ethanol extract of *T. rubra* subsp. *caucasica;* EAT: Ethyl acetate extract of *T. rubra* subsp. *caucasica;* EEP: Ethanol extract of *Primula* sp.; EAP: Ethyl acetate extract of *Primula* sp.

MIC values of the extracts are given in Table 2. Lower MIC values shows higher activity. The least MIC value was found in the ethanol extract *Primula* sp. against *B. cereus* and *E. aerogenes*.

Table 2. MIC values of the plant extracts (µg/mL)

Bacteria	EET	EAT	EEP	EAP
B. subtilis	512	1024	-	-
B. cereus	512	-	256	-
G. rubripertincta	512	-	-	-
S. aureus	512	-	-	-
E. coli	>1024	>1024	>1024	>1024
E. aerogenes	1024	1024	256	-

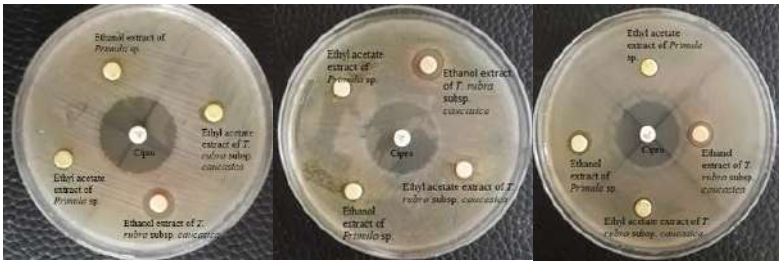

G. rubripertincta *B. subtilis* *B. cereus*

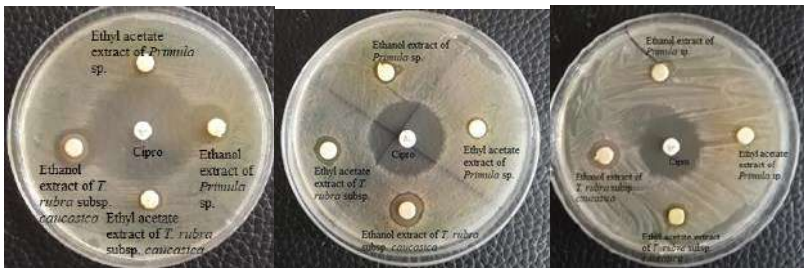

E. coli *E. aerogenes* *S. aureus*

Figure 1. Antibacterial effect of the plant extracts against bacteria

Some studies were conducted about antimicrobial activity of *T. rubra* subsp. *caucasica* and different *Primula* species. For example, Başbülbül et al. (2008) studied antimicrobial activity of ether, ethanol and water extracts of *Primula veris* and it was found that extracts had activity against *Enterococcus faecalis, Bacillus cereus* and *Pseudomonas fluorescens* (Başbülbül et al., 2008). Aslam et al. (2015) stated that ethanol extracts of *Primula denticulata* had antibacterial activity against *Escherichia coli*, *Staphylococcus aureus*, *Klebsiella pneumoniae* and *Salmonella typhi* (Aslam et al., 2015). Özbucak et al. (2013) found that ethanol extract of *T. rubra* subsp. *caucasica* had antibacterial activity against *E. coli*, *S. aureus*, *Pseudomonas aeruginosa* and *Bacillus subtilis* (Özbucak e al., 2013).

3.2. Antioxidant Activity

Total phenolic content, total flavonoid content and total antioxidant capacity of ethanol and ethyl acetate extracts of *T. rubra* subsp. *caucasica ve Primula* sp. are illustrated in Table 3. While the lowest total phenolic content and total antioxidant capacity were determined in ethanol extract of *T. rubra* subsp. *caucasica*; the lowest total phenolic content and total antioxidant capacity were determined in ethyl acetate extract of *Primula* sp. Total flavonoid content of the extracts increases in the following order: ethyl acetate extract of *T. rubra* subsp.

caucasica >ethanol extract of *T. rubra* subsp. *caucasica* >ethyl acetate extract of *Primula* sp. >ethanol extract of *Primula* sp.

Table 3. Total phenolic content, total flavonoid content and total antioxidant capacity of the extracts

Plant Extract	Total Phenolic Content (µg GAE/mL)	Total Flavonoid Content (µg QE/mL)	Total Antioxidant Capacity (µg AAE/mL
EET	237.90±0.010	96.61±0.012	87.02±0.032
EAT	72±0.004	98.69±0.004	40.37±0.019
EEP	143.90±0.003	44.65±0.003	44.52±0.006
EAP	23.63±0.015	90.26±0.002	38.25±0.015

EET: Ethanol extract of *T. rubra* subsp. *caucasica;* EAT: Ethyl acetate extract of *T. rubra* subsp. *caucasica;* EEP: Ethanol extract of *Primula* sp.; EAP: Ethyl acetate extract of *Primula* sp.

DPPH and ABTS radical scavenging activities of the extracts are demonstrated in Table 4. Ethanol extract of *T. rubra* subsp. *caucasica* exhibited higher activity than standards (BHT and Rutin). Ethanol extract of both of the plant extracts exhibited higher activity than ethyl acetate extracts of the plants. DPPH radical scavenging activity increases in the following order: Rutin>BHT> ethyl acetate extract of *T. rubra* subsp. *caucasica*>ethanol extract of *T. rubra* subsp. *caucasica* > ethanol extract of *Primula* sp.>ethyl acetate extract of *Primula* sp. Activities increases with the increasing concentration.

Table 4. DPPH and ABTS scavenging activities of the extracts (% inhibition)

Plant Extract	Concentration (µg/mL)	DPPH radical scavenging activity (% inhibition)	ABTS radical scavenging activity (% inhibition)
EET	250	69.10±0.003	95.62±0.002
	500	72.55±0.007	99.01±0.0009
	750	74.16±0.001	99.26±0.0004
	1000	76.18±0.002	99.45±0.0008
EAT	250	73.11±0.002	26.97±0.008
	500	78.34±0.004	55.43±0.032

	750	82.57±0.007	70.30±0.022
	1000	83.38±0.010	82.17±0.027
EEP	250	60.57±0.006	33.87±0.047
	500	66.33±0.001	64.15±0.008
	750	73.86±0.0003	83.54±0.003
	1000	75.22±0.001	94.21±0.009
EAP	250	21.52±0.006	7.30±0.01
	500	27.29±0.004	18.38±0.010
	750	35.57±0.002	26.50±0.014
	1000	49.47±0.004	35.81±0.018
BHT	250	84.62±0.007	93.48±0.04
	500	86.39±0.004	93.92±0.006
	750	89.49±0.009	94.43±0.004
	1000	90.50±0.007	96.65±0.008
Rutin	250	88.17±0.005	78.54±0.048
	500	88.59±0.009	81.94±0.019
	750	90.21±0.005	85.26±0.010
	1000	92.25±0.002	87.63±0.006

To the best of our knowledge, there is no study related with antioxidant activity of *T. rubra* subsp. *caucasica* but there are studies about antioxidant activity of different *Primula* species. Demir et al. (2014) studied water and ethanol extracts of *Primula vulgaris* and it was concluded that extracts are effective DPPH scavenging, superoxide anion radical scavenging and metal chelating on ferrous ions activities (Demir et al., 2014).

References

Elisha, I. L., Botha, F. S., McGaw, L. J., and Eloff, J. N. (2017). The antibacterial activity of extracts of nine plant species with good activity against *Escherichia coli* against five other bacteria and cytotoxicity of extracts. BMC Complementary and Alternative Medicine, 17, 133-143.

Badakhshan, M., Subramanian, L. J., Lachimanan,Y. L., Yeng, C., and Sreenivasan, S. (2012). Antioxidant activity of methanol extracts of different parts of *Lantana camara*. Asian Pacific Journal of Tropical Biomedicine, 2(12), 960-965.

Saeed, N., Khan, M. R., and Shabbir, M. (2012). Antioxidant activity, total phenolic and total flavonoid contents of whole plant extracts *Torilis leptophylla* L. BMC Complementary and Alternative Medicine, 12, 221-233.

Natural medicinal herbs, http://www.naturalmedicinalherbs.net/herbs/p/primula-vulgaris=primrose.php web adresinden 27.09.2018 tarihinde edinilmiştir.

Özbucak, T. ,B., Akçin Ö. E., and Ertürk, Ö. (2013). The change in ecological, anatomical and antimicrobiological properties of the medicinal plant *Tilia rubra* DC. subsp. *caucasica* (Rupr.) V. Engler along an elevational gradient. Pakistan Journal of Botany, 45(5), 1735-1742.

Kumar, S., Dhankhar, S., Arya, V. P., Yadav, S., and Yadav, J. P. (2012). Antimicrobial activity of *Salvadora oleoides* Decne. against some microorganisms. Journal of Medicinal Plants Research, 6 (14), 2754-2760.

Murray, P. R., Baron, E. J., Pfaller, M. A., Tenovar, F. C., and Yolke, R. H. 1995. Manual of Clinical Microbiology. ASM Press, Washington D.C.

Saric, C. L., Cabarkapa, S. I., Beljkas, M. B., Misan, C. A., Sakac, B. M., and Plavsic, V. D. (2009). Antimicrobial activity of plant extracts from Serbia. Food Processing Quality and Safety, 1 (2), 1-5.

Yiğit, D., Yiğit, N., Aktaş, E., and Özgen, U. (2009). Ceviz (*Junglans regia* L.)'in antimikrobiyal aktivitesi. Türk Mikrobiyoloji Cemiyeti Dergisi, 39 (1-2), 7-11.

Slinkard, K., and Singleton, V. L. (1977). Total phenol analysis: Automation and comparison with manual methods. American Journal of Enology and Viticulture, 28, 49-55.

Zhishen, J., Mengcheng, T., and Jianming, W. (1999). The Determination of flavonoid contents in mulberry and their scavenging effects on superoxide radicals. Food Chemistry, 64, 555-559.

Arnao, M. B., Cano, A., and Acosta, M. (2001). The hydrophilic and lipophilic contribution to total antioxidant activity. Food Chemistry, 73, 239-244.

Brand-Williams, W., Cuvelier, M., and Berset, C. (1995). Use of a free radical method to evaluate antioxidant activity. Lebensmittel-Wissenschaft und Technologie - Food Science and Technology, 28, 25-30.

Prieto, P., Pineda, M., and Aguiler, M. (1999). Spectrophotometric quantition of antioxidant capacity through the formation of a phosphor molybdenum complex: Specific application to the determination of Vitamin E. Analytical Biochemistry, 269, 337-341.

Başbülbül, G., Özmen, A., Bıyık H. H., and Şen, Ö. 2008. Antimitotic and antibacterial effects of the *Primula veris* L. flower extracts. Caryologia, 61(1), 88-91.

Aslam, K., Nawchoo, I. A., and Ganai, B. A. (2015). In vitro antioxidant, Antibacterial activity and phytochemical studies of *Primula denticulata*-an important medicinal plant of Kashmir Himalaya. International Journal of Pharmacological Research, 5(3), 49-56.

Demir, N., Güngör, A. A., Nadaroğlu, H., and Demir, Y. (2014). The antioxidant and radical scavenging activities of primrose (*Primula vulgaris*). European Journal of Experimental Biology, 4(2), 395-401.

Bioactive Components in Fruit and Vegetable Products

N.Şule ÜSTÜN [1*], Mustafa EVREN [2]

[1] Ondokuz Mayıs University, Faculty Of Engineering, Department. of Food Engineering,, Samsun, Turkey; sustun@hotmail.com

[2] Ondokuz Mayıs University, Faculty Of Engineering, Department. of Food Engineering,, Samsun, Turkey; mustafaevren @hotmail.com

[3] University, Faculty, Department, City, Country; e-mail

[*] **Corresponding Author:** sustun@hotmail.com

Abstract

Differences in dietary patterns and food preferences depending on the scientific developments and the awareness of consumers in recent years increase the tendency to the functional foods that have positive effects on health. The thought that the use of food additives will cause health problems have directed both the industry and consumers to natural production and consumption and accordingly bioactive components and their potential uses in functional food production have been studied. It has been reported that some food components, which are naturally found in foods and are known as bioactive compounds, are effective in weight control by various mechanisms such as inhibiting enzymes involved in the digestive system, increasing thermogenesis, preventing adipocyte differentiation, increasing lipid metabolism and reducing appetite and are being studied as a new approach in the prevention of obesity. Plant extracts are used in the food, pharmaceutical and cosmetic industries. Functional foods are foods that are produced by the addition of bioactive substances obtained from completely natural foods to the foods that are consumed in daily life and which are not synthetic. Many traditionally produced fruit and vegetable products contain bioactive components that increase the importance of these products in terms of health. In this review, bioactive components found in fruit and vegetable products, their benefits on human health and the effects of food processing on bioactive components will be examined.

Keywords: Bioactive compounds, fruit and vegetables, functional foods, food processing, traditional foods.

1. Introduction

Foodstuffs can be functionalized by the addition of phytonutrients, bioactive peptides, omega 3 polyunsaturated fatty acids, probiotics and/or prebiotics (Evren ve ark., 2017). Functional foods are foods that are produced by the addition of bioactive substances obtained from completely natural foods to the foods that are consumed in daily life and which are not synthetic (Erdoğan Bayram ve ark., 2013). The day by day increment of certain chronic diseases such as cardiovascular and cancer highlightens the importance of nutrition on health. This changes the consumer's eating habits and leads them to pursue some benefits beyond being fed from the foods. In this case, in order to achieve a healthier life, besides meeting energy and essential nutrients, it is necessary to provide healthcare-related items that provide beneficial effects on human physiology and metabolic functions, achieve beneficial effects such as reduction of disease risk, thus functioning to prevent diseases and achieve healthier life, so the tendency towards food or bioactive components of these foods is steadily increasing (Özcan ve ark., 2015).

2. Bioactive Components

In order for food to be functional, it has to have factors such as bioactive compounds, probiotic microorganisms and prebiotic substances, and these factors must be sufficiently transmitted to the relevant region of the body. The effect of the bioactive compound should not be confused with eliminating the symptoms of the disease caused by the deficiency, but should be due to the benefit it provides other than its basic function (Erbaş, 2006). Even if we consider that conventional drying technology leads to significant loss of bioactive compounds, dried fruit may be a valuable resource not only for energy, dietary fiber and minerals, but also for antioxidant activity (Jesionkowska ve ark., 2009). Dietary antioxidants are compounds that occur as intermediates in the reaction of the body (physiological or pathological) or that stabilize externally taken free radicals (O*, NO*, v.b.) by giving an electron to their unpaired electron (Erbaş, 2006). Phenolic compounds are secondary metabolites of fruits and vegetables that are responsible for the color, taste and aroma of fruits and vegetables. As a result of many studies, these bioactive compounds have been shown to have significant positive effects on health. These effects include delaying and/or preventing cell damage and destruction resulting from oxidation, and radical scavenging activities (Meral, 2016). The antioxidant compounds, called polyphenols, are the richest bioactive compounds and their consumption of 1 g per day

in the diet is 10 times more than vitamin C consumption. For this reason polyphenols have been accepted as strong antioxidants (Kasnak ve Palamutoğlu, 2015). Anthocyanins are bioactive compounds giving plants a range of colors ranging from red to blue depending on the pH of the vacuole in which they localized and many studies have shown that in addition to acting as antioxidants and fighting free radicals, anthocyanins may offer anti-inflammatory, anti-viral, anti-cancer and immune system strengthening benefits (Işık ve ark., 2016).

3. Fruit and Vegetables Including Bioactive Components

Fruits and vegetables contain phytochemicals with different bioactive properties such as antioxidative activity. While the use of artificial antioxidants has been decreasing steadily, interest in natural antioxidants has been increasing in recent years and it is becoming more important to obtain them from plant materials (Tavman ve ark., 2009). In a prospective study of the relationship between vegetable-fruit consumption and stroke incidence according to their colors fruits and vegetables were separated into four groups as green, yellow-orange, red-purple and white and white vegetables and fruits were associated with stroke risk (Bellikci Koyu ve ark., 2016). The berry fruits are a source of many bioactive and phytochemical substances that are important for human health. Especially the anthocyanin rich red and purple fruits and vegetables such as raspberries, blackberries, pomegranates, strawberries, cherries, berries, plums, grapes, cabbage have been widely studied and have shown to be very effective in the prevention and emergence of CVDs and some types of cancers causing early deaths (Tokbaş, 2009).

Pomegranate fruits, flowers, bark and leaves have positive effects on fighting against serious diseases such as diabetes and cancer, reduce blood pressure, contain bioactive components which can be antimicrobial effective (Duman ve ark., 2017). The pomegranate contains the bioactive components anthocyanins, ascorbic acid and β-carotene (O'Grady ve ark., 2014). Kamkat (Fortunella margarita Swing.) can be evaluated by processing into products like candy, marmalade, liqueur, wine besides fresh consumption. Essential oils and bioactive components derived from the peel are used in the perfumery, pharmaceutical and food industries (Yıldız ve ark., 2015). Mandarin is a rich source of phytochemicals (vitamin C, phenolic acid and flavonoid substances) useful for human metabolism. Although similar to other citrus species in terms of the bioactive substances it contains, it was stated that the predominantly flavonoids in mandarin were narirutin and hesperidin,and the phenolic acids were caffeic, p-coumaric, ferulic, sinapic, p-hydroxybenzoic and vanilic acid (Fengmei ve ark.,

2011). Persimmon (Diospyros kaki L.) may be a potential fruit with functional properties because it is rich in dense bioactive compounds such as tannins, carotenoids, ascorbic acid (Karaman ve ark., 2014). The health benefits of black grape are due to the phenolic compounds they contain and these compounds are the most important natural antioxidants. The antioxidant compounds of grape are phenolic substances such as anthocyanins, flavonols, malvidin 3-O-(6-O-p-coumarin glucosido)-5-glucoside and procyanidin B2 3-O-gallate. The total phenolic substance concentration and the antioxidative activity show a proportional change (Gülcü ve ark., 2008). Procyanidin B1 and B2, (-) - epicatechin, epigallocatechin gallate and gallic acid were identified as bioactive compounds in the hawthorn (Crataegus orientalis) (Çoklar ve Akbulut, 2016). Eriobotrya, also known as "Yenidunya", grown in the Mediterranean region in our country, contains bioactive components (Erkölencik, 2016). It has been reported that apple bark (according to varieties), blackcurrant, raspberries and blackberries contain significant levels of bioactive components (Işık ve ark., 2016).

Vegetables contain significant amounts of chlorophyll and carotenoid pigments, but also rich in bioactive phenolic compounds such as flavonoids, phenolic acids, stilbenes, kumarins, tannins and also vitamin C. Combined phytochemicals in plant foods act through various mechanisms such as antioxidant activity, cell renewal, tumor suppression (Şat ve Öz, 2015). In the production of lycopene, residuals from the production of tomato products are widely used in the food industry. These residues are very rich in bioactive and functional components (Yavuz ve ark., 2016). Sulfurous compounds which are a type of glycoside from bioactive compounds and known as glucosinolates are secondary plant metabolites containing S and N, which are generally found in plants of the family Brassicaceae (Brassicaceae). Vegetables that we consume very often in our daily life, such as broccoli, Brussels sprouts, white cabbage, purple cabbage, cauliflower, radish, which are in the Cruciferae family, are rich sources of glucosinolates (Fadhıl, 2015).

4. Results

In recent years, due to the tendency of consumers to change their eating habits because of health problems all over the world, the trend towards functional foods or the bioactive components of these foods is steadily increasing. However, the presence of many bioactive components in plants, inadequate activity and toxicity studies, inadequate control and easy access to plants reduce the safety of plants.

In functional food production for enrichment strategies with bioactive compounds, innovative approaches to food ingredients, chemical and physical factors, production methods and storage conditions are needed.

References

Bellikci Koyu, E., Kaner, G., and Akal Yıldız, E., (2016). İnme ve beslenmenin inme üzerine etkisi. Gümüşhane Üniversitesi Sağlık Bilimleri Dergisi (GÜSBD), 5(4): 112-118.

Çoklar, H., and Akbulut, M., (2016). Alıç (*Crataegus orientalis*) meyvesinin antioksidan aktivitesi ve fenolik bileşiklerinin ekstraksiyonu üzerine farklı çözgenlerin etkisi. Derim, DOI:10.16882/derim.2016.267908, 33 (2):237-248

Duman, A.D., Gültekin, Ş., Biçer, A., Uslu, K.Y., Atasayar, A.Ö., Yecan, Y.E., Çömez, N., Güney Gökçeoğlu, B., Özçelik, M., and Mirioğlu, S., (2017). Nar ekşisi ve soslarının etik açıdan değerlendirilmesi. 1. Tarım ve Gıda Etiği Kongresi, Ankara, 361-368.

Erbaş, M., (2006). Yeni bir gıda grubu olarak fonksiyonel gıdalar. Türkiye 9. Gıda Kongresi; 24-26 Mayıs, Bolu, 791-794.

Erdoğan Bayram, S., and Ömer Lütfü Elmacı, Ö.L., (2013). Gübrelemenin meyve ve sebzelerin fonksiyonel özellikleri üzerine etkileri. Adnan Menderes Üniversitesi Ziraat Fakültesi Dergisi, 10(1): 25- 31.

Erkölencik, M.F., (2016). Farklı Malta Eriği çeşitlerinin biyoaktif ve aromatik özelliklerinin belirlenmesi. Namık Kemal Üniversitesi, Fen Bilimleri Enstitüsü, Yüksek Lisans Tezi, 66s.

Evren, M., Güler, B., and Tutkun Şıvgın, E., (2017). Probiyotik gıdaların fonksiyonel özellikleri. 1. Tarım ve Gıda Etiği Kongresi, Ankara, 407-414.

Fadhıl, Z.H.F., (2015). Çeşitli sebze sularının farklı probiyotik bakteriler için prebiyotik etkilerinin ve antioksidatif aktivitelerinin belirlenmesi. Selçuk Üniversitesi, Fen Bilimleri Enstitüsü, Yüksek Lisans Tezi, 108s.

Fengmei, Z., Liangbin, H., Guihua, X., and Quanxian, C., (2011). Changes of some chemical substances and antioxidant capacity of mandarin orange segments during can processing. Procedia Environ. Sci., 11, Part C, 1260–1266.

Gülcü, M., Demirci, A.Ş., and Güner, K.R., (2008). siyah üzüm; zengin besin içeriği ve sağlık açısından önemi. Türkiye 10. Gıda Kongresi, 21-23 Mayıs, Erzurum, 179-182.

Işık, B.Ş., Altın, G., and Özçelik, B., (2016). Antioksidan özelliklere sahip doğal boyalar. Gıda Metabolizma & Sağlık: Biyoaktif Bileşenler ve Doğal Katkılar Kongersi, 28 Kasım, İstanbul, 91-95.

Jesionkowska K, Sijtsema SJ, Konopacka D, and Symoneaux R. (2009). Dried fruit and its functional properties from a consumer's point of view. J Hortic Sci Biotech., ISAFRUIT Special Issue: 85–88.

Karaman, S., Toker, O.S., Çam, M., Hayta, M., Doğan, M., and Kayacier, A., (2014). Bioactive and physicochemical properties of persimmon as affected by drying methods. Drying Technology, 32, 258–267.

Kasnak, C., and Palamutoğlu, R., (2015). Doğal antioksidanların sınıflandırılması ve insan sağlığına etkileri. Türk Tarım-Gıda Bilim ve Teknoloji Dergisi, 3 (5) 226-234.

Meral, R., (2016). Farklı ısıl işlem uygulamalarının fenolik bileşenler üzerine etkisi. Yüzüncü Yıl Üniversitesi Fen Bilimleri Enstitüsü Dergisi/ Journal of The Institute of Natural & Applied Sciences 21 (1):55-67.

O'Grady, L., Sigge, G., Caleb, O.J., and Opara, U.L., (2014). Effects of storage temperature and duration on chemical properties, proximate composition and selected bioactive components of pomegranate (Punica granatum L.) arils, Lwt-Food Science and Technology, 57, 508-515.

Özcan, T., Delikanlı, B., and Akın, Z., (2015). Soya biyoaktif bileşenleri ve sağlık üzerine etkisi. Türk Tarım – Gıda Bilim ve Teknoloji Dergisi, 3(6): 350-355.

Şat, İ.G., and Öz, Ö., (2015). Haşlama ve kurutmanın bazı sebzelerin bileşimi üzerine etkisi. Adıyaman Üniversitesi, Mühendislik Bilimleri Dergisi, 3, 54-62.

Tavman, Ş., Kumcuoğlu, S., and Akaya, Z., (2009). Bitkisel ürünlerin atıklarından antioksidan maddelerin ultrason destekli ekstraksiyonu. Gıda, 34 (3): 175–182.

Tokbaş, H., (2009). Karadut meyvesinin (*Morus nigra L.*) reçel ile marmelata işlenmesi ve ürünlerin antioksidan özelliklerinin belirlenmesi. GaziOsmanpaşa Üniversitesi, Fen BilimleriEnstitüsü, Gıda Mühendisliği Anabilim Dalı, Yüksek Lisans Tezi, 141s.

Yavuz, M., Özel, N., Gülkirpik, E., and Özçelik, B., (2016). Süperkritik karbondioksit ekstraksiyomu ile bitkisel atıklardan renklendirici üretimi. Gıda Metabolizma & Sağlık: Biyoaktif Bileşenler ve Doğal Katkılar Kongersi, 28 Kasım, İstanbul, 192-198.

Yıldız Turgut, D., Gölükcü, M., and Tokgöz, H., (2015). Kamkat (*Fortunella margarita* Swing.) meyvesi ve reçelinin bazı fiziksel ve kimyasal özellikleri. Derim, 32 (1):71-80.

Different Green Extraction Methods for Polyphenols

Zeliha KAYA[1], Duygu BALPETEK KULCU[1], Ilkay KOCA[2]

[1]*Giresun University, Engineering Faculty, Food Engineering Department, Giresun, Turkey;zeliha.kaya@giresun.edu.tr; duygu.balpetek@giresun.edu.tr*

[2]*Ondokuz Mayis University, Engineering Faculty, Food Engineering Department, Samsun, Turkey; itosun@omu.edu.tr*

* **Corresponding Author:** zeliha.kaya@giresun.edu.tr

Abstract

Plant phenolics are considered to be special bioactive compounds because of their important benefits to human health. Therefore, interest in plant products is increasing day by day. Nowadays, for phenolic extraction, there are many alternative methods such as supercritical fluid extraction (SCF), microwave-assisted (MAE) extraction, ultrasound-assisted (UAE) extraction, pressurized liquid extraction (PLE), accelerated solvent extraction (ASE) as well as conventional extraction methods. Comparing with the conventional methods, the advantages of these techniques are low solvent usage, time and energy saving, lower operating costs and high extraction yield. Due to the non-toxicity of the solvents used (CO_2), SCF is regarded as sustainable and environmentally friendly. Therewithal, SCF provides a rapid and highly selective extraction, but it is costly. MAE reduces cost, extraction time and solvent consumption comparing with the conventional methods. Its extraction efficiency and reproducibility are high. But the operating conditions must be carefully selected to avoid thermal degradation. It's also a suitable method for polar molecules and solvents with high dielectric constant. UAE is a rapid, versatile, simple, safe, eco-friendly method, and its cost is convenient. It provides time and energy saving and it reduces the consumption of expensive organic solvents. The use of high temperature and pressure in PLE increases extraction efficiency and saves time and solvent, but the pressure requires costly equipment. ASE is an expensive technique, but it's preferred because of the very low solvent requirements of liquid solvent extraction techniques. In this review, the extraction techniques used for polyphenols, their advantages and disadvantages are mentioned.

Keywords: Supercritical fluid extraction, microwave-assisted extraction, ultrasound-assisted extraction, pressurized liquid extraction

1. Introduction

The polyphenols are one of major group of secondary plants components synthesized by fruits, vegetables, teas, cocoa and other plants. In plants, polyphenols are generally related in defense against varied types of stress (UV light, parasites, pathogens, chilling, pollution etc.). They subscribe substantially to the organoleptic properties of vegetables and fruits (Kabera et al., 2014; Mojzer et al., 2016). They have certain health benefits. They are described by the antioxidant, anti-inflammatory, antidiabetic, antibacterial, positive ocular and anti-carcinogenic. They have preservative effects against cardiovascular and neurodegenerative disorders, hepatic injury. They also help prevent cytotoxic effects of oxidized low-density lipoprotein (LDL) and as a result atherosclerosis (Ghasemzadeh and Ghasemzadeh, 2011; Routray and Orsat, 2013; Kabera et al., 2014; Shahidi and Ambigaipala, 2015; Mojzer et al., 2016). These health effects support the consumption of fruits and vegetables, and they promote use of food industry wastes as extracts of phenolic compounds, which can be used for the enrichment of other food products and for the production of nutraceutical additives (Routray and Orsat, 2013).

Extraction is a fundamental process for the isolation and recovery of bioactive compounds from plants using selective solvents by standard procedures. Converts the real matrix to a sample suitable for subsequent analytical procedure.The soluble plant metabolites, leaving behind the insoluble cellular residue (Azwanida, 2015; Belwal et al., 2018). Sample preparation in ancient times was carried out by various extraction methods such as boiling, maceration, infusion, digestion and infiltration (Fig. 1). These extraction techniques have been reported as the earliest techniques that have emerged in the 11th century and are still used up to now, and they constitute the basic principles of advanced extraction techniques. Continuing to the modernization and growth of the industrial era, during the 18th century developed an extraction technique "Soxhlet Extraction", it has emerged as an advanced form of digestive and brewing method (Belwal et al., 2018). Conventional extraction techniques are safe and simple, but their extraction efficiency is poor. Because the extraction times are long and the extraction temperatures are high, this leads to the degradation of the thermolabile compounds and also the reduction of the target compounds. It is also a disadvantage in the conventional extraction techniques that organic solvents, which are generally harmful to the environment and have a high purchase and disposal cost, are consumed. For this reason, the development of a more effective and environmentally friendly extraction technique has received great interest. In the last decade, many new extraction techniques have been investigated, such as microwave

assisted extraction, ultrasound assisted extraction, pulsed electric field extraction, supercritical fluid extraction and enzyme assisted extractions, for overcome the deficiencies of conventional extraction methods (Vazquez-Roig and Picó, 2015; Wu et al., 2017). 'Green extraction', a new extraction term, is being developed for the purpose of researching and designing new processes requiring less energy. When safe and high quality extracts are obtained with these techniques, non-hazardous alternative solvents and edible natural products are used (da Silva et al., 2016).

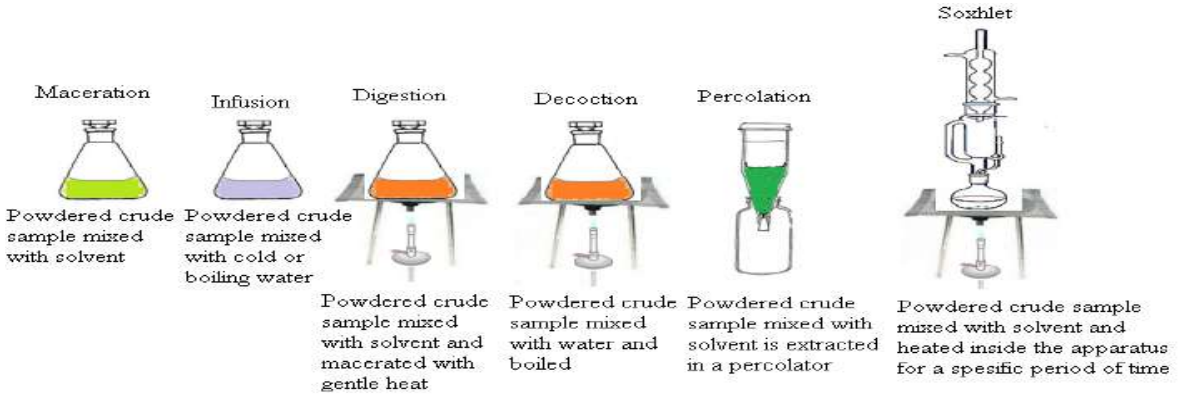

Figure1. Some conventional extraction techniques and their mechanism of extraction (Belwal et al., 2018)

Green extraction techniques have their own advantages and limitations (Pasrija and Anandharamakrishnan, 2015). This review aims to discuss the various new techniques for extraction of polyphenols with their merits and demerits.

2. Polyphenols

Phenolic compounds are well-known phytochemicals found in all plants. They have multiple biological effects, including antioxidant activity. Phenolic compounds can be classified according to the number of phenol rings that they contain and the structural elements that bind these rings to one another (Table 1) (El Gharras, 2009).

Table 1. Classes of phenolic compounds from natural sources (Ajila et al., 2011)

Class	Structure
Simple phenolics, benzoquinones	C_6
Hydroxybenzoic acids	C_6-C_1
Hydroxycinnamic acids, phenylpropanoids	C_6-C_3
Naphthoquinones	C_6-C_4
Xanthones	C_6-C_1-C_6
Flavonoids, isoflavanoids	C_6-C_3-C_6
Lignans, neolignans	$(C_6$-$C_3)_2$
Bioflavonoids	$(C_6$-C_3-$C_6)_2$

Lignin	$(C_6\text{-}C_3)_n$
Condensed tannins	$(C_6\text{-}C_3\text{-}C_6)_n$

Polyphenols contain as many as 10,000 diacids which are defined to date (Mojzer et al., 2016). For this reason the terminology and classification of polyphenols is quite complicated (Kabera et al., 2014). Although the chemical structures of all polyphenols are similar, there are some distinct differences (Kabera et al., 2014). It is possible to distinguish two classes of polyphenols based on these fundamental differences. These are flavonoids and non-flavonoids, such as tannins (Kabera et al., 2014).

The classification of plant phenolics is done as follows: (1) a few hydroxylic groups. Thus they can be separated into 1-, 2- or more atomic phenols. Phenolic compounds containing more than one OH group in the aromatic ring are called polyphenols; (2) chemical composition: mono-, di, oligo- and polyphenols; (3) substitutes in carbon skeleton, a number of aromatic rings and carbon atoms in the side chain. With reference to, phenolic compounds are divided into four essential groups. These are phenolics with an aromatic ring, with two aromatic rings, quinones and polymers (Kabera et al., 2014).

Structurally, polyphenols can be classified into two main groups as flavonoids and non-flavonoids (Kabera et al., 2014). Flavonoids are the largest group and its basic structure (a diphenylpropane skeleton or flavan nucleus, C6–C3–C6) contains two benzene rings (A and B) that are linked through three carbon atoms that often form an oxygenated pyran heterocyclic ring (C) (Fig. 2) (Valenzuela et al., 2016).

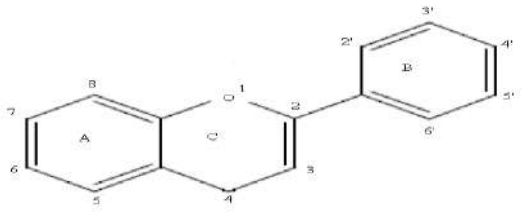

Figure 2. Phenol structure (Ghasemzadeh and Ghasemzadeh, 2011)

The other class is nonflavonoid phenolics and it includes, also comprises six subclasses: Phenolic alcohols, phenolic acids, stilbenes, coumarins, chalcones, and lignans (Valenzuela et al., 2016).

Flavonoids are the most common phenolics. They are found in renewable and non-renewable plants and have many functions. For example, coloring of flowers. The production of these blue, yellow, red color pigments in the flowers helps the plants to attract pollinator animals. These are water-soluble pigments and are found in the vacuoles of the plant cell

(Kabera et al., 2014). The flavonoids contains flavonols, flavones, iso-flavonols, anthocyanidins, anthocyanins, catechins and proanthocyanidins. All flavonoids have three-ringed structures and they are reproduced from the aromatic amino acids, phenyalanine and tyrosine. The diversity of flavonoids is due to the prenylation, alkalinization, and glycosylation reactions that change the structure of the basic molecule, and also the scale and pattern of hydroxylation (Khoddami et al., 2013).

Phenolic acids are one of the main phenolic groups in plants. They are usually found in the form of esters, glycosides and amides, which are rarely found in free form. The diversity among the phenolic acids is due to the number and location of the hydroxyl groups present in the aromatic ring. Phenolic acids have two basic structures as hydroxybenzoic and hydroxycinnamic acid. Ferric, p-cumaric, caffeic and sinapic acids as hydroxycinnamic acid varieties, gallic, syringic, vanillic and protocatechuic acids as hydroxybenzoic acid varieties (Khoddami et al., 2013).

Another important phenolic class is cell wall phenolics. These can be divided into two basic classes: lignins and hydroxycinnamic acids. These compounds are found in the cell wall and protect plants from stresses such as infection, injury and UV radiation during the development of them (Khoddami et al., 2013).

Tannins are phenolics that precipitate proteins. They can form complexes with starches, proteins, minerals, cellulose and are generally water-soluble (Kabera et al., 2014). Two basic classes can be distinguished, namely, hydrolyzable and condensable tannins. Potential for making oxidative linkages with other plant molecules is quite high (Khoddami et al., 2013; Kabera et al., 2014). Gallotannin or tannic acid is exemplified by the hydrolyzable tannins present in the fruit. Proanthocyanidins from condensed tannins are the main phenolic compounds found in grapes (El Gharras, 2009).

Polyphenols are widely deployed in plants, such as vegetables, fruits, olive oil, tea, tobacco and etc. (Ignat et al., 2011). Some sources of polyphenols are shown in Table 2.

Table 2. Dietary sources of polyphenols (Ignat et al., 2011)

Phenolic compounds	**Dietary sources**
Phenolic acids	
Hydroxycinnamic acids	Apricots, blueberries, carrots, cereals, pears, cherries, citrus fruits, oilseeds, peaches, plums, spinach, tomatoes, eggplants
Hydroxybenzoic acids	Blueberries, cereals, cranberries, oilseeds
Flavonoids	
Anthocyanins	Bilberries, black and red currants, blueberries, cherries, chokecherries, grapes, strawberries
Chalcones	Apples
Flavanols	Apples, blueberries, grapes, onions, lettuce

Flavanonols	Grapes
Flavanones	Citrus fruits
Flavonols	Apples, beans, blueberries, buckwheat, cranberries, endive, leeks, lettuce, onions, olive, pepper, tomatoes
Flavones	Citrus fruits, celery, parsley, spinach, rutin
Isoflavones	Soybeans
Xanthones	Mango, mangosteen
Tannins	
Condensed	Apples, grapes, peaches, plums, mangosteens, pears
Hydrolysable	Pomegranate, raspberries

3. Some Novel Techniques for Polyphenols Extraction

Phenolics are very unstable compounds, so they are very susceptible to deterioration. Various factors such as light, oxygen, temperature, solvents and the presence of enzymes influence their stability (Junior et al., 2010).

The most common methods used in phenolic extraction prior art were conventional methods. However, negative extractions such as long extractions, high extraction temperatures, and the presence of light and oxygen have been shown to cause degradation and loss of phenolic compounds. Deterioration can be caused by both internal and external factors, and light, air and temperature are the most important factors that accelerate deterioration (Junior et al., 2010).

Green extraction methods offer great advantages for the recovery of highly reactive phenolic molecules. Here we review several novel techniques to extract plant phenolic compounds.

3.1. Microwave-assisted extraction

Microwaves have been used for many years in studies on secondary plant metabolites. Microwaves are non-ionizing radiation at frequencies between 300 MHz and 300 GHz. Microwaves stimulate molecules with dipoles to warm up the sample. With this warming, the plant cells lose moisture by evaporation and the resulting vapor causes the active components in the cells to be released. Apart from dipole materials of the plant cell, such as water molecules, the dipole rotation of the solvent molecules under the rapid change of electric field have an significant role in microwave-assisted extraction (MAE). From the order of radiation, the wave electronic module changes too much and solvent molecules are stimulated to align themselves with the electrical phase in the normal phase. During this alignment, the sample warms up due to friction forces and vibrations (Gupta et al., 2012; Khodammi et al., 2013). The greater the dielectric constant of the solvent (Table 3), the faster

the heating is. As a result, unlike conventional conductive heating methods, microwaves heat the entire sample at the same temperature. The advantage of using microwaves in extraction is the breakdown of weak hydrogen bonds by molecules' dipol movement (Gupta et al., 2012).

Table 3. Some properties of solvents commonly used in MAE (Khodammi et al., 2013)

Solvent	Boiling Point (°C)	Dielectric constant	Dissipation factor
Acetonitrile	81.60	37.50	620
Water	100	78.30	1570
Ethanol	78.5	24.30	2500
Acetone	56.2	20.70	5555
Methanol	64.6	32.60	6400
2-Propanol	98	19.90	6700

Polyphenols can absorb microwaves due to the hydroxyl groups they contain. For this reason MAE can be used for the extraction of these compounds. Aqueous acetone, ethanol and mixtures thereof are used in the phenolic extraction with the MAE technique (Khodammi et al., 2013).

There are two commercially available MAE systems (Figure 3). These are called open and closed microwave systems. The closed system is usually used at high temperature extractions. The open system is used at the maximum temperature determined by the boiling point of the solvents at atmospheric pressure.

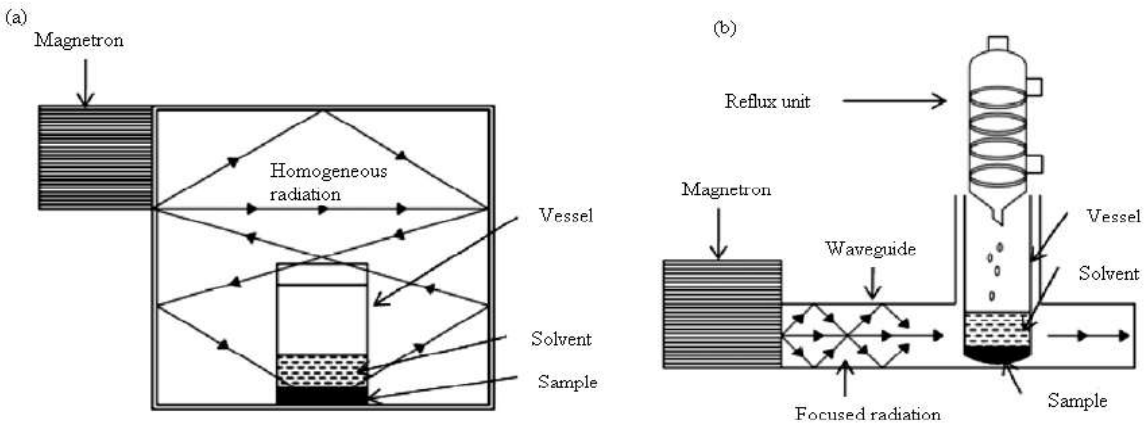

Figure 3. (a) Closed type microwave system and (b) open type microwave system (Chan et al., 2011)

MAE is considered a good alternative to traditional extraction techniques due to advantages such as reduced extraction time, reduced solvent usage, improved extraction yield, process stability and low cost. Considering its economic and practical aspects, it can also be compared with modern techniques. For example, an additional filtration or centrifugation is

required to remove solid residues in MAE as compared to supercritical extraction. Furthermore, the efficiency of microwaves can be very poor when the target compounds are not solvent polar, but are volatile at all. MAE is not suitable because it causes degradation at high temperatures in some compounds such as tannins and anthocyanins (Azwanida, 2015).

3.2. Ultrasound-assisted extraction (UAE) or sonication extraction

Sound waves are mechanical vibrations with frequencies higher than 20 kHz. Sound waves act as expansion and compression cycles in matter. As the molecules are separated from each other by expansion, they come together with compression. Ultrasonically mechanically allows solvents to penetrate the cells more and increases mass transfer. Ultrasound application breaks up the cell wall in the extraction process, allowing the contents to be released more easily, thereby increasing the efficiency of extraction (Wang and Weller, 2006). For an effective and successful ultrasound-assisted extraction (UAE), the characteristics of plants such as particle size, moisture content, and solvent that can be used for extraction should be considered. Factors affecting the UAE process include reactor selection (ultrasonic bath or probe/horn type), applied ultrasonic power and intensity, operating frequency, extraction time and temperature, solvent type, ratio and properties. Table 4 lists some of the key factors for designing UAE systems (Tiwari, 2015).

Table 4. Factors influencing ultrasound-assisted extraction (Tiwari, 2015)

External factors	**Key facts**
Amplitude or ultrasound intensity, or ultrasonic power	High amplitude causes probe erosion High amplitude enhances agitation High amplitude reduces formation of cavitation High intensity can promote degradation of extracted compounds
Ultrasonic frequency	Frequencies used restricts the formation of cavitation bubbles which should be selected in conjunction with the ultrasonic intensity to obtain desired cavitation Most ultrasonic systems operate at a given frequency Higher extraction yields are reported in low frequency range (20-40 kHz)
Extraction temperature	High temperature aids in disruption of interaction of solvent and matrix High temperature enhances solvent diffusion rates Low temperature enhances cavitation
Extraction time	Long extraction time enhances extraction yields Long extraction time may induce undesirable changes in the extracted compound.
Solvent properties	Viscous solvent reduces cavitation Volatile solvent may evaporate if extraction is carried out at higher temperature for long duration Polarity and solubility of target compound in the solvent Vapor pressure and surface tension influences cavitation
Matrix	Particle size

Solvent matrix interaction
Ratio of solvent to matrix

Probe and bath systems are the most common methods used to apply ultrasonic waves (Fig 4) (Khoddami et al., 2013). The ultrasonic probe is immersed in the direct solution and provides at least 100 times higher ultrasonic power than the bath. The probe is a powerful system for extraction but can also cause degradation. The amplitude control in the probes allows the vibrations to be adjusted to the desired level and another factor to be controlled is the temperature (Picó, 2013).

Ultrasonic baths are devices that transmit high-energy and high-frequency sound waves to a container filled with water. They are not very powerful tools. Classic bathrooms generally operate at 40 kHz frequency and temperature can be controlled (Picó, 2013).

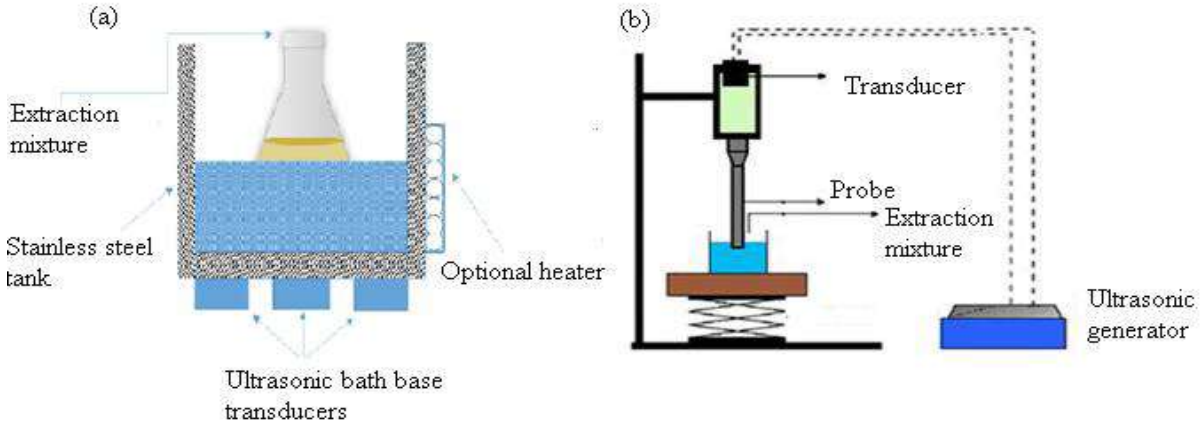

Figure 4. Operational schematic principle of a) ultrasonic bath (Ameer et al., 2017) b) ultrasonic probe systems (Gupta et al.,2012)

According to traditional extraction techniques, the UAE is a cheap, simple and effective technique. The extraction efficiency is high. As it can be used at low temperatures it allows the extraction of thermolabile compounds. It is also cheaper and simpler technique compared to other new techniques such as microwave assisted extraction. Many solvents can be used in the UAE technique. But the nature of the plant matrix is also important in the ultrasound extraction efficiency. For example, the presence of a dispersed phase weakens the ultrasonic wave and causes it to only affect a limited area (Wang and Weller, 2006). The use of ultrasonic energy in excess of 20 kHz can lead to the formation of free radicals through active phytochemicals (Azwanida, 2015).

3.3. Pressurized liquid extraction

Pressurized liquid extraction (PLE) is a preferred process in many applications due to its easy application, short extraction time, low sample requirement and high performance (Setyaningsih et al., 2016). This method has several names like pressurized fluid extraction (PLE), accelerated fluid extraction (ASE), and enhanced solvent extraction (ESE) (Azmir et al., 2013).

PLA uses organic solvents at temperatures above the boiling point and high pressure. The high pressure provides more contact between the solvent used in the extraction and the solid matrix, the higher temperature increases the solubility of the compounds by breaking the phenolic-matrix bonds. Therefore, the extraction efficiency depends on temperature, pressure, time and solvent. In addition to solvent selection, the solvent-sample ratio to be used in extraction is important (Setyaningsih et al., 2016).

PLE is a simple extraction system such as gas chromatography (GC) or liquid chromatography (LC), where solvents can be used at high temperatures and pressures for analytical separation and determination (Fig 5). The separation of the analytes from the matrix in extraction is strongly influenced by the polarity and other physical properties of the solvent. The surface tension and viscosity of the solvent are reduced at high pressures and temperatures, thus allowing the solid samples to be more effectively populated, easier extraction and reduced solvent use (Vazquez-Roig and Picó, 2015).

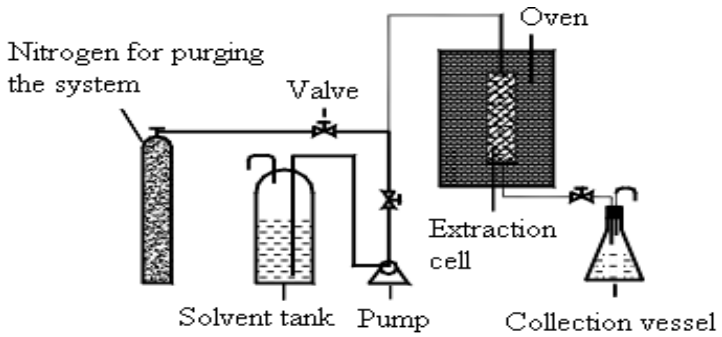

Figure 5. Schematic diagram of an PLE system (Wang and Weller, 2006)

Increased pressures at 300-5000 psi are used to keep the extraction solvent in liquid form. Alcohols such as methanol, ethanol, alkanes such as hexane, heptane, halogens such as dichloromatene and heterocyclic ethers such as dioxane are environmental friendly solvents

used in this process. Water is also used as a solvent to reduce the use of organic solvents. The advantages of water are that it is flammable and non-toxic, it is a cheap and easily recyclable solvent. It is a more useful solvent at elevated temperatures even if it is insufficient in the extraction of analytes at low temperatures (Vazquez-Roig and Picó, 2015).

Pressurized hot water extraction (PHWE) is a green method used by high temperature and high pressure conditions to keep water in a liquid state. High temperature changes the properties of water, reducing polarity and lower polarities increase the solubility of compounds. However, degradation of compounds may occur due to increased hydrolysis and oxidation kinetics with temperature. The corrosion of the PHWE system is also an important problem because the high temperature values achieved in the extraction can lead to leaks and different problems (Vazquez-Roig and Picó, 2015).

3.4. Supercritical Extraction

Supercritical fluid extraction (SCF) is a good alternative to conventional extraction because of its low solvent consumption and low operating temperature. In this technique, the normally used liquid phase is replaced by a supercritical fluid above its critical temperature. A wide variety of supercritical fluids is present, but carbon dioxide is a frequently used fluid because it has relatively low critical temperature (31.1 °C) and pressure (73.8 bar). At the same time, CO2 is a low cost, safe and easy to use solvent. An organic solvent may be added to the supercritical fluid to modify the solvent properties (Sticher, 2008).

The supercritical fluid carries the properties of both liquids and gases. Supercritical fluids have some advantages. For example, the dissolving power of the supercritical fluid depends on the density and can be changed by temperature and / or pressure. Supercritical fluid has a higher diffusion coefficient, lower viscosity and surface tension, thus providing better mass transfer. A supercritical fluid extraction (SCF) system is shown in Figure 6 (Wang and Weller, 2006).

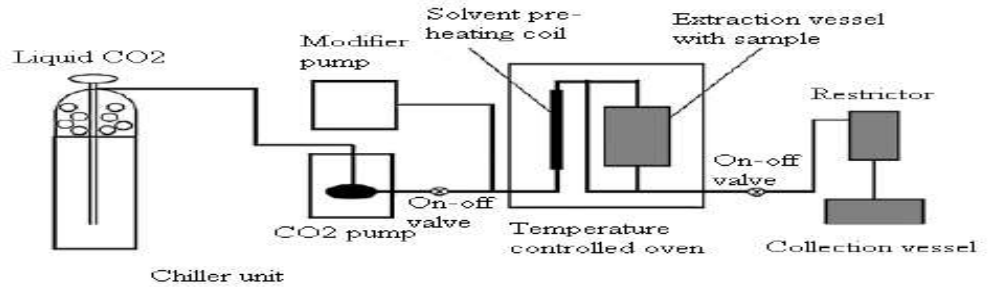

Figure 6. Schematic diagram of the basic components of an off-line SCF system (Sticher, 2008)

SCF is very advantageous in selective extractions and disintegration, but its use is limited as it has disadvantages such as high costs and harsh operating conditions (Wang and Weller, 2006). Table 5 shows some advantages and disadvantages of SCF.

Table 5. Advantages and disadvantages of SCF-CO_2 extraction processes (Bubalo et al., 2018)

Advantages	**Drawbacks**
Solvent-free products	High pressures
Gentle treatment of heat-sensitive materials (its moderate critical temperature of 31.2 ◦C is a key issue for the preservation of bioactive compounds in extracts)	High investment cost (requires a careful business plan contemplating the cost/effective analysis of the desired compounds to be extracted)
CO_2 as solvent does not cause environmental problems and is physiologically harmless, germicidal and not flammable	Phase equilibrium of the solvent/solute system is complex, making design of extraction conditions difficult
CO_2 is a generally recognized as safe (GRAS) solvent	High polar substances (sugars, amino acids, inorganic salts, proteins, etc.) are insoluble
Due to low viscosity and relatively high diffusivity, supercritical CO_2 have enhanced transport properties than liquids, can diffuse easily through solid materials and can therefore give faster extraction rates.	The use of high pressures leads to capital costs for plant, and operating costs may also be high so the number of commercial processes utilizing supercritical fluid extraction is relatively small, due mainly to the existence of more economical processes
CO_2 is inexpensive solvent	
Fragrances and aromas remain unchanged	
Selective extraction and fractionated separation	
Pure extracts by means of few process steps	
Changeable solvating power (possibility of modifying the density of the fluid by changing its pressure and/or temperature)	
High solubility for non/low polar substances (for example volatile compounds)	
Possibility of direct coupling with analytical chromatographic techniques such as gas chromatography (GC) or supercritical fluid chromatography (SFC)	

3.5.High Hydrostatic Pressure Extraction

Another new technique used to extract phenolic compounds from plants is High Hydrostatic Pressure Extraction (HHPE). This method uses superhigh hydraulic pressure (1000-8,000 bar) which is not thermal. The applied pressure improves the transientity of plant cells and allows the spread of cell components according to mass transfer and phase behavior theories. The main disadvantage of techniques such as HHPE are expensive equipment requirements. However, because high purity extract can be obtained in extraction of highly demanded products such as antioxidants and extraction efficiency is high, these processes are

used. HHPE can also cause cell deformation and protein denaturation due to the large pressure difference (Khodammi et al., 2013).

3.6.Other Extraction Methods

The pulsed electric field (PEF) process is a low-energy and non-thermal technology to facilitate cell membrane degradation and increase mass transfer. PEF technology is based on a short-term electrical application with pulse electric field strength from 100 to 300 V/cm to 20–80 kV/cm. In PEF, the cell membrane is electrically punctured and its semi-permeability is temporarily or permanently lost. Thus, selective recovery of valuable components from different matrices is ensured (Barba et al., 2015).

The high-voltage electrical discharge technique is another non-thermal technique. In this process, energy is dipped directly into an aqueous solution by a plasma channel formed by a current of high voltage electrical discharge between two immersed electrodes. The intensity of the electric field triggers the avalanche of the electron that initiates the propagation of the positive streamer within the negative electrode. Bubble cavitation, turbulence and pressure shock waves are secondary phenomena, which increase cell destruction, facilitating the release and extraction of compounds (Soquetta et al., 2018).

The sequential alkaline extraction technique is another method used to remove bound and free phenolics from plants. Free phenolics in water and organic solvents used in a water bath under nitrogen atmosphere is extracted in 20 minutes. The solid residue is hydrolyzed with NaOH under N_2 for 1 hour at room temperature in the dark. The alkaline extract is treated with HCl until pH 2, centrifuged, and the extract is used for the detection of bound phenolics (Khodammi et al., 2013).

Another technique suitable for phenolic compound extraction is enzymatic treatment of plants. It is known that phenolics in plants are bound to plant cell wall polysaccharides with substantially hydrophilic and hydrophobic bonds. Addition of enzyme accelerates the extraction process by breaking these bonds (Khodammi et al., 2013). Factors such as enzyme composition and concentration, solid-liquid ratio, particle size of plant materials and time to hydrolysis are the main factors affecting this process. This technique is considered as an environmentally friendly technique for the extraction of bioactive compounds and oil due to the use of water instead of organic chemicals as solvents (Azmir et al., 2013).

3.7. Comparison of green extraction techniques

Ultrasound-assisted, microwave-assisted, supercritical fluid and PLE extractions are very promising and widely using techniques for the extraction of phenolics from plants and waste. These techniques have advantages and disadvantages compared to each other. For example, while MAE needs a short time, UAE is one of the cheapest techniques. The advantages and disadvantages of these commonly used techniques are summarized in Table 8.

Table 8. Comparison of 4 green extraction techniques (Eskilsson and Björklund, 2000; Sticher, 2008)

	MAE	**PLE**	**SCF**	**UAE**
Extraction time	3–30 min	5–30 min	10–60 min	10–60 min
Sample size	1–10 g	1–30 g	1–5 g	1–30 g
Solvent usage	10–40 ml	10–100 ml	2–5 ml (solid trap) 5–20 ml	30–200 ml
Pressure Applied	Variable (PMAE), Atmospheric (FMAE)	1-10 MPa	25-45 MPa	Atmospheric
Investment	Moderate	High	High	Low
Advantages	-Fast and multiple extractions -Low solvent volumes -Elevated temperatures	-Fast extractions -Low solvent volumes -Elevated temperatures -No filtration required -Automated systems	Fast extractions -Minimal solvent volumes -Elevated temperatures -Relatively selective towards matrix interferences -Automated systems -No clean-up or filtration required -Concentrated extracts	Multiple extractions
Disavantages	-Clean-up step needed -Extraction solvent must be able to absorb microwaves - Waiting time for the vessels to cool needed down	-Clean-up step needed	-Many parameters to optimize, especially analyte collection	-Clean-up step needed -Large solvent volumes -Repeated extractions may be required

4. Conclusion

Today, as a result of various industrial processes, the residual plant waste is a valuable source for the plant polyphenols, which is a natural antioxidant source. Traditional methods are considered to be more laborious and non-environmentally friendly due to the high sample, time, organic solvent and energy requirements compared to the alternative methods developed recently. In line with the rules set by international regulatory agencies and institutions worldwide, research into greener extraction techniques that are more environmentally friendly and sustainable for extracting polyphenolic compounds from plants are continuing. Green extraction techniques increase the extraction efficiency by reducing carbon dioxide emission and the use of toxic solvents. In general, these techniques are fast, sustainable, economic and

environmentally friendly. However, the natural structure of the plant matrices and the relevant analyte may affect the extraction kinetics and yield in green techniques. The use of green extraction techniques and combinations as an alternative to conventional techniques is very promising in terms of increasing the extraction efficiency and protecting the environment.

As a result, extraction methods are renewed with each passing day and develops to have less negative impact on the environment. In recent years, the methods found to be effective, microwave-assisted, ultrasound-assisted, ohmic-supported, accent electric field-supported, high-pressure supported and supercritical fluid extraction was observed. Alternative methods can be used in combination with conventional methods. Combined use in this way allows time consuming, low solvent consumption and high quality end products to be obtained according to the studies using only conventional extraction methods. Alternative methods in the research phase will be developed and the effects will be seen better.

References

Ajila, C.M., Brar, S.K., Verma, M., Tyagi, R.D., Godbout, S., Valéro, J.R. (2011). Extraction and analysis of polyphenols: Recent trends. Critical Reviews in Biotechnology, 31, 3, 227-249.

Ameer, K., Shahbaz, H.M., Kwon, J-H. (2017). Green extraction methods for polyphenols from plant matrices and their byproducts: A review. Comprehensive Reviews in Food Science and Food Safety, 16, 2, 295-315.

Azmir, J., Zaidul, I.S.M., Rahman, M.M., Sharif, K.M., Mohamed, A., Sahena, F., Jahurul, M.H.A., Ghafoor, K., Norulaini, N.A.N., Omar, A.K.M. (2013). Techniques for extraction of bioactive compounds from plant materials: A review. Journal of Food Engineering 117, 426-436.

Azwanida, N.N. (2015). A Review on the extraction methods use in medicinal plants, principle, strength and limitation. Med Aromat Plants, 4,3.

Barba, F.J., Parniakov, O., Pereira, S.A., Wiktor, A., Grimi, N., Boussetta, N., Saraiva, J.A., Martin-Belloso, O., Witrowa-Rajchert, D., Lebovka, N., Vorobiev, E. (2015). Current applications and new opportunities for the use of pulsed electric fields in food science and industry. Food Research International, 77, 773-798.

Belwal, T., Ezzat, S.M., Rastrelli, L., Bhatt, I.D., Daglia, M., Baldi, A., Devkota, H. P., Orhan, I. E., Patra, J.K., Das, G., Anandharamakrishnan, C., Gomez-Gomez, L., Nabavi, S.F., Nabavi, S. M., Atanaso, A.G. (2018). A critical analysis of extraction techniques used for botanicals: Trends, priorities, industrial uses and optimization strategies. Trends in Analytical Chemistry, 100, 82-102.

Bubalo, M.C., Vidović, S., Redovniković, I.R., Jokić, S. (2018). New perspective in extraction of plant biologically active compounds by green solvents. Food and Bioproducts Processing, 109, 52-73.

Chan, C-H., Yusoff, R., Ngoh, G-C., Kung, F.W-L. (2011). Microwave-assisted extractions of active ingredients from plants. Journal of Chromatography A, 1218, 6213-6225.

Da Silva, R.P.F.F., Rocha-Santos, T.A.P., Duarte, A.C. (2016). Supercritical şuid extraction of bioactive compounds. Trends in Analytical Chemistry, 76, 40-51.

El Gharras, H. (2009). Polyphenols: Food sources, properties and applications-a review. International Journal of Food Science and Technology, 44, 12, 2512-2518.

Eskilsson, C.S., Björklund, E. (2000). Analytical-scale microwave-assisted extraction. Journal of Chromatography A, 902, 227-250.

Ghasemzadeh, A., Ghasemzadeh, N. (2011). Şavonoids and phenolic acids: Role and biochemical activity in plants and human. Journal of Medicinal Plants Research, 5, 31, 6697-6703.

Gupta, A., Naraniwal, M., Kothari, V. (2012). Modern extraction methods for preparation of bioactive plant extracts. International Journal of Applied and Natural Sciences (IJANS), 1, 1, 8-26.

Ignat, I., Volf, I., Popa, V.I. (2011). A critical review of methods for characterisation of polyphenolic compounds in fruits and vegetables. Food Chemistry, 126, 1821-1835.

Junior, M.R.M., Leite, A.L., Romanelli, N., Dragano, V. (2010). Supercritical şuid extraction and stabilization of phenolic compounds from natural sources- review (Supercritical extraction and stabilization of phenolic compounds). The Open Chemical Engineering Journal, 4, 51-60.

Kabera, J.N., Semana, E., Mussa, A.R., He, X. (2014). Plant secondary metabolites: biosynthesis, classification, function and pharmacological properties. Journal of Pharmacy and Pharmacology, 2,7, 377-393.

Khoddami, A., Wilkes, M.A., Roberts, T.H. (2013). Techniques for analysis of plant phenolic compounds. Molecules,18, 2328-2375.

Mojzer, E.B., Hrnčič, M.K., Škerget, M., Knez, Ž., Bren, U. (2016). Polyphenols: Extraction methods, antioxidative action, bioavailability and anticarcinogenic effects. Molecules, 21, 901, 2-38.

Rasouli, H., Farzaei M.H., Khodarahmi, R. (2017). Polyphenols and their benefits: A review, International Journal of Food Properties, 20:sup2, 1700-1741.

Pasrija, D., Anandharamakrishnan, C. (2015). Techniques for extraction of green tea polyphenols: A review. Food Bioprocess Technol., 8, 935-950.

Picó, Y. (2013). Ultrasound-assisted extraction for food and environmental samples. Trends in Analytical Chemistry, Volume 43.

Setyaningsih, W., Saputro, I.E., Palma, M., Barroso, C.G. (2016). Pressurized liquid extraction of phenolic compounds from rice (Oryza sativa) grains. Food Chemistry, 192, 452-459.

Shahidi, F., Ambigaipala, P. (2015). Phenolics and polyphenolics in foods, beverages and spices: Antioxidant activity and health effects-A review. Journal of Functional Foods, 18, 820-897.

Soquetta, M.B., Terra, L.M., Bastos, C.P. (2018) Green technologies for the extraction of bioactive compounds in fruits and vegetables, CyTA - Journal of Food, 16,1, 400-412.

Sticher, O. (2008). Natural product isolation. Nat. Prod. Rep., 25, 517-554.

Tiwari, B.K. (2015). Ultrasound: A clean, green extraction technology. Trends in Analytical Chemistry, 71, 100-109.

Valenzuela, J.C., Vergara-Salinas, J.R., Perez-Correa, J.R. (2016). Advances in technologies for producing food-relevant polyphenols, CRC Press.

Vazquez-Roig, P., Picó, Y. (2015). Pressurized liquid extraction of organic contaminants in environmental and food samples. Trends in Analytical Chemistry, 71, 55-64.

Wang, L., Weller, C.L. (2006). Recent advances in extraction of nutraceuticals from plants. Trends in Food Science and Technology, 17, 300-312.

Wu, K., Ju, T., Deng, Y., Xi, J. (2017). Mechanochemical assisted extraction: A novel, efficient, eco-friendly technology. Trends in Food Science and Technology, 66, 166-175.

Functional Plant Based Milk Drinks

Binnur KAPTAN[1*]

[1] *Namık Kemal University, Faculty of Agriculture, Department of Food Engineering, Tekirdag, Turkey; bkaptan@nku.edu.tr*

[*] **Corresponding Author:** *bkaptan@nku.edu.tr*

Abstract

Nowadays, nutritional situations such as food intolerance, allergies, lifestyle such as vegan and vegetarianism and inadequate absorption cause consumers to demand towards choosing functional healthy and diversified food products. Over the years, people, who can not consume animal origin milk have searched for ways to produce milk and dairy products from plant sources, although nutritional values are not the same as those of animal origin. Milk that is not of animal origin such as plant-based milk alternatives are preferred by consumers due to their high level of functional properties and their consumption is increasing. Plant milk-based beverages are functional and probiotic food, because they include components such as soluble fiber, phytoestrogens and phenolics which are beneficial for nutrition and health. Consumption of plant- based milk alternative drinks has increased in recent years, due to the prevention or treatmet of cow's milk allergy, a part of vegetarian diets, or as a result of the recommendations of alternative medicine experts. Also, plant-derived milks have beneficial nutrients that encourage the growth of probiotic cultures. The conscious for the positive effects of probiotic and functional foods on human health has increasingly among consumers. In this review, studies on plant-based probiotic fermented milk drinks are presented.

Keywords: Plant-based milk, Functional food, Probiotic drinks.

1. Introduction

The fact that lactose intolerance and casein allergies becoming widespread have been the result of research on plant-based milk alternatives. Over the years, people who cannot consume animal milk have sought ways to produce plant-based milk and products, although their nutritional values are close but not the same as those of animal origin. Plant-based milks are preferred by the consumers due to their high functional properties and the consumption of these milk are increasing. In addition, plant-based milk is a very good choice for those who have lactose intolerance, milk allergies, phenylketonuria and cholesterol as it does not contain animal protein, lactose and cholesterol, and it is also a good choice for vegetarians as it does not contain animal-based components. Plant-based milk is very diverse in terms of macro (carbohydrate, protein, fat) and micro (vitamins and minerals) components, but the most important microelement to focus on is calcium. Plant-based milks are used instead of animal milk in various cultures for hundreds of years and obtained through many different ways. The content of these products varies based on their types and they are regarded as milk although they are actually not. In the market, there are different plant-based milks enriched by the addition of calcium and vitamins (especially vitamin B_{12}). The most popular of these are almond milk, coconut milk, soy milk and rice milk. There are also other types such as oat milk, wheat milk, and hazelnut milk. Plant-based milks are obtained by the soaking, grinding and filtering the plants. Functional compounds of plant-based milks and their beneficial effects on health are given in Table 1, and their nutritional components are given in Table 2.

Table 1. Functional compounds of plant-based milk and beneficial effects on health

Milk Type	Functional Components	Health Benefits	References
Soy Milk	Isoflavones Phytosterols	Protective effect against cancer, cardiovascular disease and osteoporosis, and a lowering effect on cholesterol level.	Omoni and Aluko 2005, Fukui et al. 2002
Peanut Milk	Phenolic compounds	Protective effect against coronary heart disease, stroke and various cancers.	Wien et al. 2014, Settaluri et al., 2012
Oat Milk	b-glucan	Lowers the LDL cholesterol levels and effective against cardiovascular diseases.	Queenan et al., 2007; Othman et al., 2011

Almond Milk	β-tocopherol and polyphenolic compounds	Reduces cardiovascular disease risk, reduces glycemia, reduces oxidative damage, and cholesterol concentrations in blood.	Ahrens et al., 2005, Plat and Mensink, 2005; Berryman et al., 2015
Walnut milk	Essential fatty acids and tocopherols	It lowers the LDL cholestrol and increases the HDL cholestrol and provides protection against cardiovascular diseases.	Pereira et al., 2007 Pereira, 2008, Li et al., 2007
Rice milk	phytic acid, tannins and polyphenols	Antihypertensive and effective in stimulating immunity.	Ghosh et al., 2014 Nocerino et al., 2017
Coconut milk	Lauric asit, vitamin C and E	Antibacterial, antiviral and antifungal effects on microorganisms.	Belewu and Belewu 2007, Seow and Gwee 1997

2. Functional of Plant-Based Milks

2.1. Soy Milk

Soy milk is obtained by extracting soybeans with water. The popularity of soymilk is increasing all over the world (Haumann 1984). Soy milk is a plant-based milk rich in isoflavone, omega-3 fatty acid, dietary fibers, vitamin C, carotenoids, protein and oligosaccharides, also containing Vitamin B and iron (Yang and Li 2010). In addition, soy milk does not contain cholesterol (Wang et al., 2003) and is a good source of monounsaturated and polyunsaturated fatty acids that are regarded as beneficial for cardiovascular health. Isoflavones are active components responsible for the beneficial effects of the soya bean. Isoflavones are well known for their protective effect against cancer, cardiovascular diseases and osteoporosis (Omoni and Aluko 2005). In addition to isoflavones, it is well known that soy proteins provide the therapeutic benefits for having the best proportions of amino acids in plant proteins. As it does not contain lactose (Liu K. 2004), soy milk, an alternative product that can be consumed by people with lactose intolerance, is an alternative that vegetarians and vegans can consume.

It has been reported that soy milk drinks can be produced probiotically and lactic acid bacteria of soybean have a suitable composition for the growth of Bifidobacteria (Wang et al., 2002, Chou and Hou, 2000). Maftei et al., (2013). It has been stated that, to obtain fermented soy-milk probiotic drinks based, *Lactobacillus casei* ssp. paracasei can be used. In many studies, it was mentioned that fermented soymilk can be supplemented with probiotic and prebiotic content, especially with oligofructose and inulin (Wang et al., 2002, Fuchs et al.,

2005). Liu et al. (2005) demonstrated that soy milk kefir has antimutagenic and antioxidant activity and can be considered among the more promising food components in terms of preventing mutagenic and oxidative damage. Kesenkaş et al. (2011) found the highest ascorbate autoxidation rate in kefir produced from soy milk compared to that in kefir produced from cow's milk.

Table 2. Nutritional components of plant-based milk

Values in 240 mL milk	Calories(kcal)	Protein (g)	Fat (g)	Carbohydrates (g)
Soy Milk	80	7	4	4
Rice milk	130	1	2	27
Oat Milk	80	2.5	4	16
Almond Milk	40	1	3	2
Coconut milk	80	<1	5	7
Peanut milk	124	1.4	6	14
Walnut milk	427.8	4.84	51.19	6.74

2.2. Walnut Milk

Walnut fruit is very rich in terms of essential fatty acids and tocopherols. Linoleic acid, oleic, linolenic, palmitic and stearic acid protect against cardiovascular diseases by decreasing LDL cholesterol and increasing HDL cholesterol. In addition, walnut fruit is a very important factor in the nutritional diet due to its components such as herbal proteins, fibers, melatonin, plant sterols, folate, tanin and polyphenols (Pereira et al., 2007; Pereira, 2008; Li et al., 2007). Walnut fruit with remarkable nutritional composition, contains vitamins such as vitamin A, Thiamin (B_1), Riboflavin (B_2) and Niacin (B_6) which are important nutrients in the B group as well as minerals such as phosphorus, potassium, magnesium, iron, sodium, calcium (Patel 2005; Cosmulescu et al., 2009).

In recent years, walnut has been used for the fermentation of walnut milk using various lactic acid bacteria (LAB) to produce probiotic drinks (Hou et al., 2008; Jing, 2006; Wang, 2010). It was determined that kefir grains have the potential to be used as a starter culture in probiotic functional fermented walnut milk drink production (Cui et al., 2013). In a study on fermented walnut milk production supplemented with red jujube and fermented using Lactobacilli, fermentation temperature and duration, sucrose content and walnut ratio were

determined as optimal parameters and a flavored drink with good nutritional properties were produced (Hou, Xing and Liu, 2008).

2.3. Coconut Milk

It has been reported that coconut milk contains fiber, vitamins C, E, B_1, B_3, B_5 and B_6, and minerals including iron, selenium, sodium, calcium, magnesium and phosphorus (Seow and Gwee 1997). Coconut contains significant amounts of fat, mostly fatty acids known as lauric acid, a medium chain saturated fatty acid. Lauric acid is converted into a highly beneficial compound called monolaurin which is antibacterial, antiviral and antifungal against microorganisms causing diseases in the body.

Coconut milk is one of the most popular source of plant-based milks, and although its protein and carbohydrate content is compared to that of the cow's milk, coconut milk's healthy (medium chain triglycerides) fat content is eight-fold. Lauric acid, which forms half of the walnut milk fat content, improves metabolism with its antibacterial properties. Cream coconut milk is produced similar to other plant-based milk production methods. Coconut meat (the white part) is grated and immersed in hot water. The creamy part on the top is removed, the remaining part of the liquid coconut milk is filtered through the filter cloths, and the solid parts are separated. Coconut milk has a similar content to that of soy milk's. Especially, its fatty acid composition is rich. It is an alternative for those who cannot consume soy milk. It does not contain gluten. It is important in vegan diet. It is thought that consumption of coconut milk and other coconut-derived foods may help to protect the body from infections and viruses. Research also shows that these fats improve cholesterol levels and improve cardiovascular health. Coconut milk prevents dehydration and fatigue. Unlike the cow's milk, coconut milk does not contain lactose, so it can be used instead of milk by those with lactose intolerance. It is a popular choice for vegetarians and provides an excellent base as an alternative to puree, milkshake or dairy products. The use of coconut milk, a juice extract of solid coconut endospermine, provides another alternative in food product development. Using a combination of coconut milk, researchers have produced plant-based milk products.

Other products that can be produced from coconut milk are fermented coconut milk produced using lactic acid bacteria. Coconut kefir is important for the preservation of bone structure as it contains calcium. It helps the body to relax. It provides protection for the body due to its amino acid content. It prevents the infections in the body. It creates mobility in the intestines. It protects the intestines from infections. It is very beneficial for nervous system

disorders. It reduces excessive stress in people. Reduces blood pressure and relieves blood circulation.

2.4. Peanut Milk

Peanut milk which has a high protein content is produced by mixing peeled and ground peanuts with water and filtering it. The milk-like product is then homogenized, sterilized in the same manner as fresh milk, supplemented with vitamins and minerals, and sometimes flavored. In order to have a longer shelf life, it can be spray dried and reconstituted when dissolved in water. Peanut and peanut milk products are rich in protein and minerals and have nutritional properties for young people and the elderly due to acidic fatty acids such as linoleic and oleic. In low-starch diets, they are commonly used by overweight people and vegetarians. In addition, peanut milk has a growing awareness in people with health consciousness about the nutritional benefits of herbal proteins in their diets due to low fat and low cholesterol

Studies have focused on the fermentation of peanut milk to provide probiotic and therapeutic properties. A fermented peanut milk was successfully prepared by fermenting *Lactobacillus bulgaricus* and *Lactobacillus acidophilus*, adding flavors, sugar and fruit (Beuchat and Nail 1978). In a study focused on to determine the chemical and sensory properties of peanut milk by fermenting separately and in combination with *Lactobacillus delbrueckii* ssp. *bulgaricus* and *S. salivarius* ssp. *thermophilus*, it was found that using *S. salivarius* ssp. *thermophilus* was more effective than using *Lactobacillus delbrueckii* ssp. *bulgaricus* in the total elimination of the unwanted hexanal aromatic compounds. A significant increase in the creamy flavor was observed as a result of the fermentation. Hexane levels responsible for undesirable taste of peanut oil are effectively reduced by fermentation (Lee and Beuchat, 1992).

2.5. Almond Milk

Almonds (*Prunus dulcis*) are rich in nutrients such as monounsaturated fats, magnesium, protein and vitamin E, as well as fiber and phytochemicals (Cassady et al., 2009). Long-term consumption of almonds helps regulate body weight (Fraser et al., 2002; Sabate 2003). It also controls blood sugar fluctuations (Jenkins et al., 2002; Jenkins et al., 2006). It has plasma lipid lowering properties when taken after meals (Sabate et al., 2003; Foster et al., 2012). It was

found that it decreases cardiovascular disease risks, its low simple sugar content reduces glycemia and oxidative damage (Ahrens et al., 2005).

Almond has been shown to inhibit antioxidant, anti-inflammatory, trypsin and amylase activity (Garrido et al., 2008). Studies have suggested that phytosterols lower the blood concentrations of LDL cholesterol and thus reduce the risk of cardiovascular diseases as a result of almond consumption (Plat and Mensink, 2005; Berryman et al., 2015). Almond can increase the bioavailability of iron in the diet, in addition to high β-tocopherol and polyphenolic components (Chen et al., 2006). Despite the fact that about 50% of the almond composition is fat, it was shown that intake of 7 g per day reduces the low-density lipoprotein cholesterol concentration by 1% (Sabate et al., 2003) and can be consumed up to 84 g per day without weight gain (Chen et al., 2006). It was found that it has a low glycemic index (does not negatively affect the insulin sensitivity) (Chen et al., 2006) and prebiotic effects, as it stimulated the growth of gastrointestinal Bifidobacteria and *Eubacterium rectale* (Mandalari et al., 2008).

Almond milk is a colloidal dispersion obtained by grinding almonds with water. In recent years, almond milk has emerged as an alternative beverage in the US, European and Australian markets with no dairy ingredients. Almond milk has human health benefits especially for those who have lactose intolerance (Dhakal et al.,2014). Almond milk is regarded as a healthy food due to its plant-based unsaturated fatty acids and other useful plant compounds including vitamin, fibers and antioxidant contents (Jalali-Khanabadi et al., 2010). Almond milk is rich in essential and non-essential nutrients such as α-tocopherol, essential fatty acids, dietary fibers and a wide variety of other phytochemicals.

Almond milk is a good source of vitamin compared to other plant-based milks, especially for vitamin E, which cannot be synthesized by the body, and should be taken with dietary or supplemental substances (Burton and Ingold 1989; Niki et al., 1989). As almond milk is a quality calcium and fat source and a low-calorie nutrient, it has better nutritional properties than other plant-based milks (Sethi et al., 2016). Almond milk helps prevent high blood pressure and heart problems. As it contains omega fatty acids found in fish, it is very effective on the heart. Almond milk can be considered as a good food matrix to obtain healthy fermented products. Indeed, if the fermentation process is potentially carried out by probiotic bacteria, the developed fermented product may be useful as a means of preventing certain immuno-regulating diseases such as allergies. Almond milk fermented with probiotic bacteria has potentially positive immunomodulatory effects on macrophages. In particular, when this plant-based milk was fermented with standard yogurt bacteria *B. longum* CECT 4551, *L. rhamnosus* CECT 278 and *B. longum*, the energy metabolism of intestinal epithelial cells was positively affected. Almond

milk fermented with probiotic bacteria may be beneficial for human intestinal health and thus may be useful in controlling cow milk allergies and/or intolerances (Bernat et al., 2015). The results also show an improvement in fermentation-related bioactivity in almond milk.

2.6. Rıce Mılk

Mineral content, starch quality, glycemic index and antioxidant activity have made rice important among the grains. Rice contains 80% carbohydrates, 7-8% protein, 3% fat and 3% fiber. As the positive properties of rice, high digestibility, high biological value of amino acids, high amounts of fatty acids and selenium, and antihypertensive effects have been scientifically verified. Therefore, rice is described as a functional food (Ghosh et al., 2014).

Rice milk is made from ground rice and water. As in other alternative plant-based milks, it usually contains additives to improve the consistency and shelf stability. Rice milk is naturally rich in calcium. It is the least allergenic of milk alternatives. It is a good choice for sensitive people with lactose intolerance, soy, gluten or peanut allergy.

The development of extracts and fermented beverages obtained from rice can provide a low-cost product with nutritional and functional qualities. The addition of natural or single or multiple starter cultures in rice fermentation increases the release of different metabolites and enzymes that increase nutritional and therapeutic potential in a controlled fermentation (Ghosh et al., 2014; Satish et al., 2013). The fermentation of rice milk is effective in the formation of taste, odor, appearance and aroma depending on the fermentation time (Charalampopoulos et al., 2002; Ghosh et al., 2015a, 2015b).

Fermentation enriches the content of different essential amino acids, vitamins, minerals, prebiotics, probiotic organisms and antinutrients (phytic acid, tannins and polyphenols) which are degradation products. Thus, nutritional, energy content and therapeutic potential are increased (Amudha et al., 2011). It has about 2% calories like cow milk. Unlike other plant-based milk products, rice flour has little or no fiber. In particular, rice milk is a better alternative to soy milk for babies allergic to cow's milk (Tzifi et al., 2014). Clinical studies have reported that rice milk fermented with *L. paracasei* CBA L74 L. was effective in preventing common infectious diseases (CIDs) in children in kindergardens through the induction of innate and acquired immunity (Nocerino et al., 2017). Higher biological activity was detected in rice milk kefir produced by fermenting rice milk with 10% kefir grain at 24-26^{0}C for 24-48 h. Antibacterial activity on E. coli, B. subtilis, P. fluorescens and S. aureus was observed. In addition, rice-milk kefir was found to higher antioxidant activity (Sirirat and Jelena, 2010).

These findings suggest that rice-milk kefir may be considered among the more promising food components in terms of preventing oxidative damage (Chen et al., 2013).

2.7. Oat Milk

The oat contains relatively high protein content, unsaturated fatty acids and antioxidants. In addition, oat milk has a high dietary fiber content containing the mixed bonds of (1 → 3) -β-D and (1 → 4) -β-D-glucan (Salmeron et al., 2009). It is effective to lower LDL cholesterol level and effective against cardiovascular diseases (Queenan et al., 2007; Othman et al., 2011). Over the past two decades, there is a growing interest in the inclusion of oat into the human diet, mainly due to the functional dietary β-glucan. (Brennan and Cleary 2005). Oat provide suitable substrates for LAB growth and improve the functionality of colonic bacterial microorganisms due to the specific nondigestible components of the grain matrix that characterize the prebiotics. (Charalampopoulos et al., 2002). Cereals are suitable substrates for microorganisms such as lactic acid bacteria (LAB) and Bifidobacteria, and some studies have shown the utility of microorganisms to ferment grain substrates (Angelov et al., 2005, 2006; Kedia et al., 2008; Gupta et al. 2010). Mártensson et al. (2000) determined that oat-based products are suitable for growing probiotic strains for lactic acid fermentation.

Oat-basedfermented drink is an alternative plant-based, milk-free vegetarian product, however it is an alternative to both dairy and soy beverages and is recommended for a healthy lifestyle, whether vegetarian or not. Lee et al. (2016) have reported that flavor profiles of fermented oats inoculated with L. paracasei can vary significantly during fermentation, and this bacterium can be used to improve the quality of oat-based products and develop oat-based functional foods such as oat-based probiotic beverages.

3. Conclusion

Cow's milk is one of the most commonly consumed milk, but many people have started looking for alternatives. So lactose-free milk made with plants and water are successful alternatives. They are good for your health and they have good taste.

Milks which are not of animal origin such as grains and cereals are preferred by the consumers due to their high functional properties and the consumption of these milk are increasing. Plant-based milk drinks have functional and probiotic properties as they contain

ingredients such as soluble fiber, phytoestrogens and phenolics which are nutritional and have health benefits.

Plant-based milk alternatives are generally acceptable for healthy food markets. Technological interventions and styling techniques have to be developed and explored extensively to develop a complete drink as a nutritional supplement. Plant-based milk is different from each other according to their nutritional values. Therefore, it is an important step to combine two or more types of plant-based milks into a product with a high nutritional value.

References

Ahrens, S., Venkatachalam, M., Mistry, A. M., Lapsley, K., and Sathe, S. K. (2005). Almond (*Prunus dulcis L.*) protein quality. Plant Food Hum Nutr 60:123–128.

Amudha, K., Sakthivel, N., and Mohamed, Y. M. (2011). Rice—a novel food with medicinal value Agri Rev, 32: 222-227.

Angelov, A., Gotcheva, V., Kuncheva, R., and Hristozova, T. (2006). Development of a new oat-based probiotic drink. International Journal of Food Microbiology, 112 (1), 75e80. http://dx.doi.org/10.1016/j.ijfoodmicro.2006.05.015.

Angelov, A., Gotcheva, V., Hristozova, T., and Gargova, S. (2005). Application of pure and mixed probiotic lactic acid bacteria and yeast cultures for oat fermentation. J Sci Food Agric 85 (12): 2134–41.

Belewu, M. A., and Belewu, K. Y. (2007). Comparative physicochemical evaluation of tiger nut, soybean and coconut milk sources. Int J Agric Biol 9(5):785–787

Bernat, N., Cháfer, M., Chiralt, A., Laparra, J. M., and González-Martínez, C. (2015). Almond milk fermented with different potentially probiotic bacteria improves iron uptake by intestinal epithelial (Caco-2) cells. Int J Food Studies 4:49–60.

Beuchat, L. R., and Nail, B. J. (1978). Fermentatıon of peanut milk with. Journal of Food Science, 43(4), 1109-1112. doi: 10.1111/j.1365-2621.1978.tb15246.x

Berryman, C. E., West, S. G., Fleming, J. A., Bordi, P. L., and Kris-Etherton, P. M. (2015). Effects of daily almond consumption on cardiometabolic risk and abdominal adiposity in healthy adults with elevated LDL-cholesterol: a randomized controlled trial. Journal of the American Heart Association, 4, e000993.

Brennan, C. S., and Cleary, L. J. (2005). The potential use of cereal (1→ 3, 1→ 4)-β-D-glucans as functional food ingredients. Journal of Cereal Science 42 1–13.

Burton, G. W., and Ingold, K. U. (1989). Vitamin E as an in vitro and in vivo antioxidant. Ann N Y Acad Sci 570:7–22.

Cassady, B. A., Hollis, J. H., and Fulford, A. D. (2009). Considine RV, Mattes RD.Mastication of almonds: effects of lipid bioaccessibility, appetite, and hormone response. Am J Clin Nutr, 89: 794–800.

Charalampopoulos, D., Wang, R., Pandiella, S. S., and Webb, C. (2002). Application of cereals and cereal components in functional foods: a review. International Journal of Food Microbiology 79 131–141.

Chen, C. Y., Lapsley, K., and Blumberg, J. (2006). A nutrition and health perspective on almonds. Journal of the Science of Food and Agriculture, 86 (14), 2245-2250. doi:10. 1002/jsfa.2659.

Chen H. J., Xiao-qian, L. I. U., Li-chen, M. I. A. O., and Mei, J. I. A. N. G. (2013). The Fermentative Beverage of Rice Milk College of Food Science and Technology,Nanjing Agricultural University, Nanjing, Jiangsu, 210095, China.

Chou, C. C., and Hou, J. W. (2000). Growth of bifidobacteria in soymilk and survival in the fermented soymilk drink during storage. International Journal of Food Microbiology 56: 113–121.

Cosmulescu, S., Bacıu, A., Achım, G., Botu, M., and Trandafır, I. (2009). Mineral composition of fruits in different walnut (*Juglans regia* L.) cultivars. Not. Bot. Hort. Agrobot. Cluj 37 (2), 156-160.

Cui, X. H., Chen, S. J., Wang, Y., and Han, J. R. (2013). Fermentation conditions of walnut milk beverage inoculated with kefir grains. LWT - Food Science and Technology, 50(1), 349-352. doi: https://doi.org/10.1016/j.lwt.2012.07.043.

Dhakal, S., Liu, C., Zhang, Y., Roux, K. H., Sathe, S. K., and Balasubramaniam, V. (2014). Effect of high pressure processing on the immunoreactivity of almond milk. Food Res. Int. 62, 215–222.

Foster, G. D., Shantz, K. L., Vander Veur, S. S., Oliver, T. L., Lent, M. R., Virus, A., and Gilden-Tsai, A. (2012). A randomized trial of the effects of an almond-enriched, hypocaloric diet in the treatment of obesity. The American Journal of Clinical Nutrition, 96(2), 249–254. http://doi.org/10.3945/ajcn.112.037895

Fraser, G. E., Bennett, H. W., Jaceldo, K. B., and Sabate, J. (2002). Effect on body weight of a free 76 Kilojoule (320 calorie) daily supplement of almonds for six months. J Am Coll Nutr, 21: 275–283.

Fuchs, R. H. B., Borsato, D., Bona, E., and Hauly, M. C. O. (2005). ‘‘Iogurte’’ de soja suplementado com oligofrutose e inulina. Cieˆncia e Tecnologia de Alimentos 25: 175–181.

Fukui, K., Tachibana, N., and Wanezaki, S. (2002). Isoflavone free soy protein prepared by column chromatography reduces plasma cholesterol in rats. J Agric Food Chem 50 (20):5717–5721

Garrido, I., Monagas, M., Gómez-Cordovés, C., and Bartolomé B. (2008). Polyphenols and antioxidant properties of almond skins: influence of industrial processing. J Food Sci, 73:C106-C115.

Ghosh, K., Maity, C., Adak, A., Halder, S., Jana, A., Das, A., Parua, S., Das Mohapatra, P., Pati, B., and Mondal, K., (2014). Ethnic Preparation of Haria, a Rice-Based Fermented Beverage, in the Province of Lateritic West Bengal, India. Ethnobotany Research And Applications, 12, 039-049. doi:http://dx.doi.org/10.17348/era.12.0.039-049

Ghosh, K., Ray, M., Adak, A., Dey, P., Halder, S. K., Das, A., Jana, A., Mondal, S. P., Das Mohapatra, P. K., Pati,B. R., and Mondal, K. C. (2015a). Microbial, saccharifying and antioxidant properties of an Indian rice based fermented beverage Food Chem, 168: 196-202. https://doi.org/10.1016/j.foodchem.2014.07.042

Ghosh, K., Ray, M., Adak, A., Halder, S. K., Das, A., Jana, A., Parua, M. S., Vágvölgyi, C., Das Mohapatra, P. K., Pati, B. R., and Mondal, K. C. (2015b). Role of probiotic Lactobacillus fermentum KKL1 in the preparation of a rice based fermented beverage Bioresour Technol, 188:161-168. DOI:10.1016/j.biortech.2015.01.130

Gupta, M., and Bajaj, B. K. (2017). Development of fermented oat flour beverage as a potential probiotic vehicle. Food Bioscience, 20: 104-109. doi: https://doi.org/10.1016/j.fbio.2017.08.007.

Haumann, B. F. (1984). Soymilk: New processing, packaging. Expand markets. J. Am. Oil Chem. Soc. 61: 17884.

Hou, Y. X., Xing, J. H., and Liu, L. (2008). Study on the fermented beverage of walnut and red jujube. Journal of Henan University of Technology, 29(6) 72-74

Jalali-Khanabadi, B. A., Mozaffari-Khosravi, H., and Parsaeyan, N. (2010). Effects of almond dietary supplementation on coronary heart disease lipid risk factors and serum lipid oxidation parameters in men with mild hyperlipidemia. J. Altern. Complement. Med. 16, 1279–1283.

Jenkins, D. J., Kendall, C. W., Marchie, A., Parker, T. L., Connelly, P. W., Qian, W., Haight, J.S., Faulkner, D., Vidgen, E., Lapsley, K.G., and Spiller, G. A. (2002). Dose response of almonds on coronary heart disease risk factors: blood lipids, oxidized low-density lipoproteins, lipoproteina), homocysteine, and pulmonary nitric oxide: a randomized, controlled, crossover trial. Circulation 106: 1327–1332.

Jenkins, D. J., Kendall, C. W., Josse, A. R., Salvatore, S., Brighenti, F., Augustin, L. S., Ellis, P. R., Vidgen, E., and Rao, A. V. (2006). Almonds decrease postprandial glycemia, insulinemia, and oxidative damage in healthy individuals. J Nutr, 136: 2987–2992. DOI:10.1093/jn/136.12.2987

Jing, S. Q. (2006). Study on the fermented beverage of walnut by lactic acid bacteria. Food and Fermentation Industries, 32(7), 157-159

Kedia, G., Vázquez, J. A., and Pandiella, S. S. (2008). Enzymatic digestion and in vitro fermentation of oat fractions by human lactobacillus strains. Enzyme Microb Technol 43(4),355–61.

Kesenkas, H., Dinkci, N., Seckin, K., Kinik, O., and Gonc, S. (2011). Antioxidant properties of kefir produced from different cow and soy milk mixtures. J. Agric. Sci. 17:253–259.

Lee, C., and Beuchat, L. R. (1992). Chemical, physical and sensory characteristics of peanut milk as affected by processing conditions. J Food Sci. 57(2), 401–405

Lee, S. M., Oh, J., Hurh, B. S., Jeong, G. H., Shin, Y. K., and Kim, Y. S., (2016). Volatile Compounds Produced by Lactobacillus paracasei During Oat Fermentation. Journal of Food Science, 81: 2915–2922. doi:10.1111/1750-3841.13547.

Liu, K. (2004). Soybeans as functional foods and ingredients. Champaign, Illinois, USA: AOCS Press.

Li, L., Tsao, R., Yang, R., Kramer, J. K., and Hernandez, M. (2007). Fatty acid profiles, tocopherol contents, and antioxidant activities of heartnut (Juglans ailanthifolia Var.cordiformis) and Persian walnut (Juglans regia L.). J Agric Food Chem, 55 (4): 1164-69. DOI: 10.1021/jf062322d.

Liu, J. R., Chen, M. J., and Lin, C. W. (2005). Antimutagenic and antioxidant properties of milk-kefir and soymilk-kefir. J Agr. Food Chem, 53:2467–2474. DOI:10.1021/jf048934k.

Maftei, N. M., Aprodu, I., Dinică, R., and Bahrim, G. (2013). New fermented functional product based on soy milk and sea buckthorn syrup. CyTA - Journal of Food, 11(3), 256-269. doi: 10.1080/19476337.2012.730554.

Mandalari, G., Nueno-Palop, C., Bisignano, G., Wickham, M. S. J., and Narbad, A. (2008). Potential prebiotic properties of almond (*amygdalus communis* L.) seeds. Applied and Environmental Microbiology, 74 (14), 4264-4270. doi:10.1128/AEM.00739-08.

Mårtensson, O., Öste, R., and Holst, O. (2000). Lactic Acid Bacteria in an Oat-based Non-dairy Milk Substitute: Fermentation Characteristics and Exopolysaccharide Formation. LWT Food Science and Technology, 33(8), 525-530. doi: https://doi.org/10.1006/fstl.2000.0718.

Niki, E., Yamamoto, Y., Takahashi, M., Komuro, E., and Miyama, Y. (1989). Inhibition of oxidation of biomembranes by tocopherol. Ann N Y Acad Sci 570:23–31

Nocerino, R., Paparo, L., Terrin, G., Pezzella, V., Amoroso, A., Cosenza, L., and Berni Canani, R. (2017). Cow's milk and rice fermented with Lactobacillus paracasei CBA L74 prevent infectious diseases in children: A randomized controlled trial. Clinical Nutrition, 36(1), 118-125. doi: https://doi.org/10.1016/j.clnu.2015.12.004.

Omoni, A. O. and Aluko, R. E. (2005). The anti-carcinogenic and anti-atherogenic effects of lycopene a review. Trends Food Sci. Technol., 16;344-350.

Othman, R. A., Moghadasian, M. H., and Jones, P. J. (2011). Cholesterol-lowering effects of oat beta-glucan. Nutr Rev 69(6):299–309.

Patel, G. (2005). Essential fats in walnuts are good for the heart and diabetes. Journal of the American Dietetic Association. 105 (7):1096-1097.

Pereira, J. A., Oliveira, I., Sousa, A., Valentão, P., Andrade, P. B., Ferreira, I. C., Ferreres, F., Bento, A., Seabra, R., and Estevinho, L. (2007). Walnut (*Juglans regia* L.) leaves: phenolic compounds, antibacterial activity and antioxidant potential of different cultivars. Food Chem Toxicol 2007; 45: 2287-95. DOI: 10.1016/j.fct.2007.06.004.

Pereira, J.A., Oliveira, I., Sousa, A., Ferreira, I. C. F. R., Bento, A., and Estevinho, L. (2008). Bioactive properties and chemical composition of six walnut (*Juglans regia* L.) cultivars. Food Chem Toxicol, 46:2103-2111.

Plat, J., and Mensink, R. P. (2005). Plant stanol and sterol esters in the control of blood cholesterol levels: mechanism and safety aspects. American Journal of Cardiology, 96, 15d–22d.

Queenan, K. M., Stewart, M. L., Smith, K. N., Thomas, W., Fulcher, R. G., and Slavin, J. L. (2007). Concentrated oat beta-glucan, a fermentable fiber, lowers serum cholesterol in hypercholesterolemic adults in a randomized controlled trial. Nutr J 6:6.

Sabate, J., Haddad, E., Tanzman, J. S., Jambazian, P., and Rajaram, S. (2003). Serum lipid response to the graduated enrichment of a step i diet with almonds: a randomized feeding trial. American Journal of Clinical Nutrition, 77 (6), 1379{1384.

Salmeron, I., Fuciños, P, Charalampopoulos, D., and Pandiella, S. S. (2009). Volatile compounds produced by the probiotic strain lactobacillus plantarum NCIMB 8826 in cereal-based substrates. Food Chem 117(2):265–71.

Satish, K. R., Kanmani, P., Yuvaraj, N., Paari, K. A., Pattukumar, V., and Arul, V. (2013). Traditional Indian fermented foods: a rich source of lactic acid bacteria. Int J Food Sci Nutr, 64(4): 415-428. DOI: 10.3109/09637486.2012.746288.

Seow, C. C., and Gwee, C. N (1997). Coconut milk: chemistry and technology.Int. J. Food Sci. Technol, 32: 189-201

Sethi, S., Tyagi, S. K., and Anurag, R. K. (2016). Plant-based milk alternatives an emerging segment of functional beverages: a review J Food Sci Technol (September 2016) 53(9):3408–3423 DOI 10.1007/s13197-016-2328-3.

Settaluri, V. S., Kandala, C. V. K., Puppala, N., and Sundaram, J. (2012) Peanuts and their nutritional aspects—a review. Food Nutr Sci 3:1644–1650.

Sirirat, D., and Jelena P. (2010). Bacterial inhibition and antioxidant activity of kefir produced from thai jasmine rice milk. Biotechnology, 9: 332-337. DOI:10.3923/biotech.2010.332.337.

Tzifi, F., Grammeniatis, V., and Papadopoulos, M. (2014). Soy- and rice-based formula and infant allergic to cow's milk Endocr Metab Immune Disord Drug Targets, 14 (1), 38-46 **DOI**:10.2174/1871530314666140121144604.

Wang, Y. C., Yu, R. C., and Chou, C. C. (2002) Growth and Survival of Bifidobacteria and Lactic Acid Bacteria during the Fermentation and Storage of Cultured Soymilk Drinks. Food Microbiol. 19: 501-508. https://doi.org/10.1006/fmic.2002.0506

Wang, Y. C., Yu, R. C., Yang, H. Y., and Chou, C. C (2003) Sugar and acid contents in soymilk fermented with lactic acid bacteria alone or simultaneously with bifidobacteria. Food Microbiology 20(3), 333-338. https://doi.org/10.1016/S0740-0020(02)00125-9

Wang, G. (2010). Preparation of walnut milk fermented by lactic acid bacteria. Food Engineering, 1: 17-18

Wien, M., Oda, K., and Sabate´, J. (2014) A randomized controlled trial to evaluate the effect of incorporating peanuts into an American Diabetes Association meal plan on the nutrient profile of the total diet and cardiometabolic parameters of adults with type 2 diabetes. Nutr J 13:10. doi:10.1186/1475-2891-13-10.

Yang, M., and Li, L. (2010) Physicochemical, textural and sensory characteristics of probiotic soy yogurt prepared from germinated soybean. Food Technol. Biotechnol. 48 (4) 490–496

Modified glucans as potential food ingredients

Enes DERTLİ [1*]

[1] Bayburt University, Faculty of Engineering, Department of Food Engineering, Bayburt, Turkey; edertli@bayburt.edu.tr

[*] **Corresponding Author:** edertli@bayburt.edu.tr

Abstract

Lactic Acid Bacteria (LAB) are capable of producing homopolymeric glucans that consist of glucose units with different glycosidic linkages. So far several glucans with different structures have been identified and named depending on their structures such as alpha-glucan, alternan and reuteran. This unique glucans were shown to be important for the physicochemical properties of food products including their rheological and textural characteristics. Recently their prebiotic potential have also gained special interest. Another important potential of these glucans is originated from their modification either by enzymatic or physical applications to obtain novel oligo/polysaccharides. These modified glucans can act as food ingredients with potential hydrocolloids and prebiotics. This study aimed to reveal the recent developments about modified glucans and their applications.

Keywords: exopolysaccharides (EPS), Glucans, modified glucans

1. Introduction

There is an increasing demand in food science and technology to use natural components in order to meet the requirements of the use of food additives to obtain physicochemically stable food products. In addition, components with Generally Recognised as Safe (GRAS) status are of special interest among the selected natural components (Siro et al., 2008). One of the main food additives of the food industry in the food hydrocolloids that are used for the prevention of the syneresis in food products and several different products especially carbohydrate originated compounds are used in food industry for these purposes (Funami et al., 2005). Recently another carbohydrate group produced by Lactic Acid Bacteria (LAB) defined as exopolysaccharides (EPS) gained special interest to fulfil the requirements of the used of hydrocolloids from different sources (Freitas et al., 2011). Together with LAB, products of LAB are also at GRAS status which increase their potential to be used in food industry. Structurally LAB are able to produce two different EPS which are defined as homopolysaccharides and heteropolysaccharides that are formed by one sugar unit and two or more types of sugar units respectively (Dertli et al., 2018). Homopolymeric EPSs of LAB are formed by glucose or fructose which result in the production of glucans and fructans, respectively. Heteropolysaccharides have a repeating unit formed by mainly glucose and galactose although different sugars such as rhamnose or mannose can also present in the repeating unit of the EPS (Ruas-Madiedo et al., 2005). Both EPSs are important for food industry but being able to produce at higher levels by LAB homopolymeric EPSs expecially glucans have a different role for food industry. Other technological functions of the glucans for food industry are they are multifunctional as they can both act as hydrocolloids and prebiotics, they are potentially non-interactive with other food components and finally they are effective at low levels that increase their potential. In this study, we have discussed the potential of glucans and modified glucans to be used as food ingredients.

2. Glucans from LAB

2.1. Structure of glucans produced by LAB

So far, structurally four different glucans were defined to be produced by LAB which are alternans, reuteran, dextran and mutan. Alternans are composed of alternating α-(1,6)- and α-(1,3)-linked glucose units whereas reuterans contain large numbers of α-(1→4)-glucosidic

bonds in their structure. Similarly, dextran contain large numbers of α-(1→6)-glucosidic bonds in its structure and finally mutans contain glucose units with mainly α-(1→3) linkages (Monsan et al., 2010). These four different structures result in unique glucans with technologically and physicochemically different components to be used in food industry.

2.2. Mechanism of glucan production in LAB

Although LAB produce glucans with different structures the genetic and biochemical mechanism of the glucan production is common in which an enzyme called glucansucrase (GTF) encoded in the genomes as one gene is responsible for this process (*gft*) and structural differences in the glucans are originated from the structure of the *gtf* gene that results in unique GTF enzymes. The biochemical mechanism of the glucan production is that GTF enzyme uses sucrose as the substrate that results in the formation of glucose and fructose and following their formation GTF enzyme attaches the formed glucose units to each other which finally results in the formation of the glucans. The GTF enzyme is formed by four subunits that are signal peptide, variable region, catalytic core and the glucan binding domain and these subunits are common in all GTF enzymes. The main components of the GTF enzyme are the catalytic core and the glucan binding domains and the latter contains conserved and less conserved domains (van Hijum et al., 2006). Understanding the genetic mechanism of the glucan production and the structure of the GTF enzyme increase the potential of GTFs to be used for further future studies.

2.3. Role of glucans in food industry

Several functions of glucans produced by LAB can be discussed such as water-binding agent, stabilizer-texture improver, emulsifying agent, viscosifier and prebiotic functions. Another important characteristics of glucans is their *in situ* production as they can interact with other food components such as proteins. Recently we have showed both the water-binding ability and prebiotic functions of a glucan type EPS produced by a LAB strain (İspirli et al., 2008). All these functions of glucans increase their potential for their usage in food industry. Several factors play roles for the techno-functional properties of glucans such as structure, production level and the final molecular weight of glucan. Therefore, modifications in the structural characteristics of glucans might affect the role of glucans to be used in food industry.

2.4. Modification of Glucans

As discussed above in order to improve the techno-functional characteristics of glucans from LAB several modification strategies such as enzymatic modification, physical modification and genetic modification of the *gtf* gene can be applied. Figure 1 shows the representative EPS structure of glucan obtained from *Lactobacillus reuteri* E25.

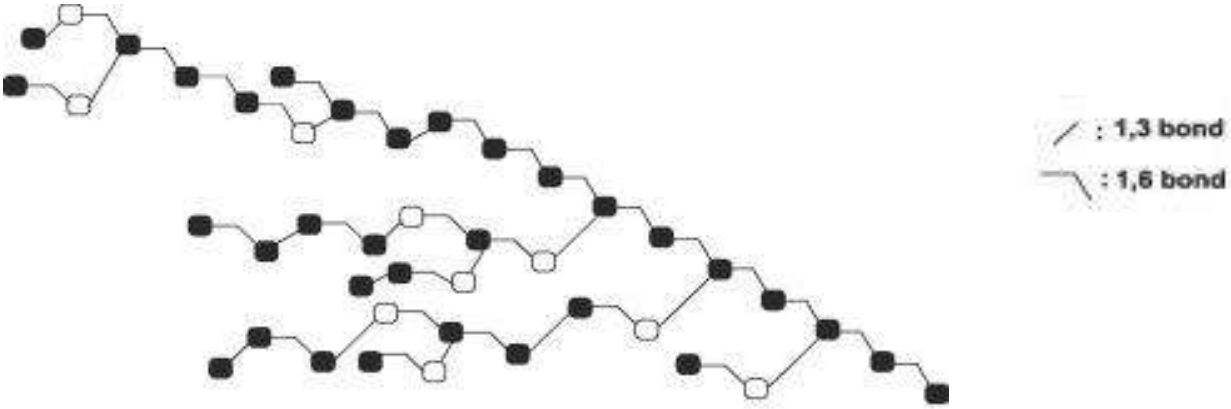

Figure 1. Schematic model of a portion of the EPS-E25 structure (Dertli et al., 2018).

As can be seen in Figure 1 glucan E25 contains α-1,6 and α-1,3 bonds and modification by enzymatic and physical methodologies target the breaking down of the glyosidic bonds and then production of new modified glucan molecules which might have improved functions related to the physicochemical and prebiotic functions of glucans. Another approach for the modification of the glucans is the genetic modification of the *gtf* gene which might result in the production of the novel glucan molecules with improved properties. For instance Miao et al., (2016) modified a glucan type EPS from *Leuconostoc citreum* strain by applications of endodextranase or ultrasonic treatment. The researchers showed that modification of the glucan type EPS improved the prebiotic functions of the glucan mostly and physical properties of the glucan altered (Miao et al., 2016). Similarly Huang et al., (2015) revealed that sonication application to the glucan with α-1,6 and α-1,3 linkages increased the shear rates of the sonicated glucan solutions suggested that the viscoelastic properties of the modified glucans were improved compared to the unmodified glucan. These findings are some examples of how glucans can be modified and how they can improve their functions especially for prebiotic roles as recently functionalization of the food products with a prebiotic component is a special issue for food technology.

In conclusion, LAB species are able to produce different types of glucans. Identification of the genetic mechanism of glucan production is a major step in order to produce novel glucan

structures. Glucans can be modified by genetic, physical and chemical (enzymatic) methodologies. Modification in glucan structures can improve the physicochemical roles of glucans. The highest increment in the role of glucans can be observed in the prebiotic functions of glucans. Glucans are one of main target of carbohydrate engineering to obtain novel modified glucans with improved technological functions.

References

Dertli, E., Colquhoun, I. J., Côté, G. L., Le Gall, G., & Narbad, A. (2018). Structural analysis of the α-D-glucan produced by the sourdough isolate Lactobacillus brevis E25. Food chemistry, 242, 45-52.

Freitas, F., Alves, V. D., & Reis, M. A. (2011). Advances in bacterial exopolysaccharides: from production to biotechnological applications. Trends in biotechnology, 29(8), 388-398.

Funami, T., Kataoka, Y., Omoto, T., Goto, Y., Asai, I., & Nishinari, K. (2005). Food hydrocolloids control the gelatinization and retrogradation behavior of starch. 2a. Functions of guar gums with different molecular weights on the gelatinization behavior of corn starch. Food Hydrocolloids, 19(1), 15-24.

Huang, C., Miao, M., Jiang, B., Cui, S. W., Jia, X., & Zhang, T. (2015). Polysaccharides modification through green technology: Role of ultrasonication towards improving physicochemical properties of (1-3)(1-6)-α-d-glucans. Food Hydrocolloids, 50, 166-173.

Miao, M., Jia, X., Hamaker, B. R., Cui, S. W., Jiang, B., & Huang, C. (2016). Structure–prebiotic properties relationship for α-D-glucan from Leuconostoc citreum SK24. 002. Food Hydrocolloids, 57, 246-252.

Monsan, P., Remaud-Siméon, M., & André, I. (2010). Transglucosidases as efficient tools for oligosaccharide and glucoconjugate synthesis. Current opinion in microbiology, 13(3), 293-300.

Ruas-Madiedo, P., & De Los Reyes-Gavilán, C. G. (2005). Invited review: methods for the screening, isolation, and characterization of exopolysaccharides produced by lactic acid bacteria. Journal of dairy science, 88(3), 843-856.

Siro, I., Kapolna, E., Kápolna, B., & Lugasi, A. (2008). Functional food. Product development, marketing and consumer acceptance—A review. Appetite, 51(3), 456-467.

van Hijum, S. A., Kralj, S., Ozimek, L. K., Dijkhuizen, L., & van Geel-Schutten, I. G. (2006). Structure-function relationships of glucansucrase and fructansucrase enzymes from lactic acid bacteria. Microbiology and Molecular Biology Reviews, 70(1), 157-176.

Partial Baking Technology: Advantages and Applications

Volkan Arif YILMAZ

Ondokuz Mayis University, Faculty of Engineering, Department of Food Engineering, Samsun, Turkey; volkan.yilmaz@omu.edu.tr

Abstract

It is not easy to maintain long-term preservation of the flavor, aroma and physical properties of bakery products after they are cooked. It is very important to maintain that these products have acceptable sensory and microbiological properties throughout their shelf life. Very high quantities of bakery products are wasted around the world because one or more of the above features can not be provided. Partial baking technology can be summarized as cutting the baking process of bakery products (usually bread) from a specified level and preserving the product with appropriate techniques and completing the baking process by the consumer before consumption. Thanks to this technology, shelf life of bakery products can be increased with minimal loss of quality, depending on the storage technique. In this way, wasting of bakery products can be avoided and significant savings can be made at the same time. Ability to consume hot and fresh bakery products to consumers whenever they want also provided through this technology. The use of this technology is becoming increasingly widespread due to the intensity of business life, the spread of ready-to-eat foods, and the decreasing time for working people to prepare meals. Number of studies about partial baking technology, including parameters of partial baking, additives, storage technique and conditions and also type of product (bread, cake, muffin etc.) were performed by the researchers. Nevertheless, with this technology, some disadvantages can be observed, including pale crust color, high crumb moisture content, thin crust, and lower specific volume at the final product.

Keywords: par-baked, bread, quality, shelf life, staling

1. Introduction

Maintaining long-term preservation of the flavor, aroma and physical properties of bakery products after they are cooked is not easy. It is very important to maintain that these products have acceptable sensory and microbiological properties throughout their shelf life. Very high quantities of bakery products are wasted around the world because one or more of the above features can not be provided.

According to FAO reports, approximately 30% of the food produced in the world every year (1.3 billion tonnes) wasted (Anonymous, 2018a). Globally, even if just ¼ of the food currently wasted could be saved, it would be enough to feed 870 million hungry people in the world. According to the European Commission's findings of 2010, approximately 30% of total bread production in EU is wasted (Anonymous, 2018b). In Turkey, bread waste was 1.8 billion loaves and the value of bread waste was 1.3 billion TL per year in 2013 (Anonymous, 2018c).

To prevent waste, industry and as well as scientists tried severals methods, including additives, improvers, packaging techniques, storage types and conditions to improve shelf life of bakery products, mainly breads. These applications had important improvements on shelf life of the products but they could not solve the staling problem and consumers sensorial expectations after couple of days of production.

Partial baking technology can be summarized as cutting the baking process of bakery products (usually bread) from a specified level and preserving the product with appropriate techniques and completing the baking process by the consumer before consumption.

2. Technique

Parbaking is a baking technique in which a bakery product is partially baked, rapidly cooled and packaged for storage. The product is baked at approximately 80% of the normal cooking time, then it is rapidly cooled or frozen.

The partial cooking sets the internal structure of the starches and proteins (the spongy texture of the bread), and kills the yeast in the product mixture if it is fermented, so that the inside is become stable, but the crust has not generated on the loaf and the other externally desirable qualities has not occurred which are not easy to preserve after full cooking.

Before consumption, a parbaked product is finished by baking it for an additional 10 to 15 minutes. The time and temperature can vary from product to product and the exact

parameters must be determined by testing. The final product is then often indistinguishable from freshly baked ones. General flow chart of partial baking process was given in Fig 1.

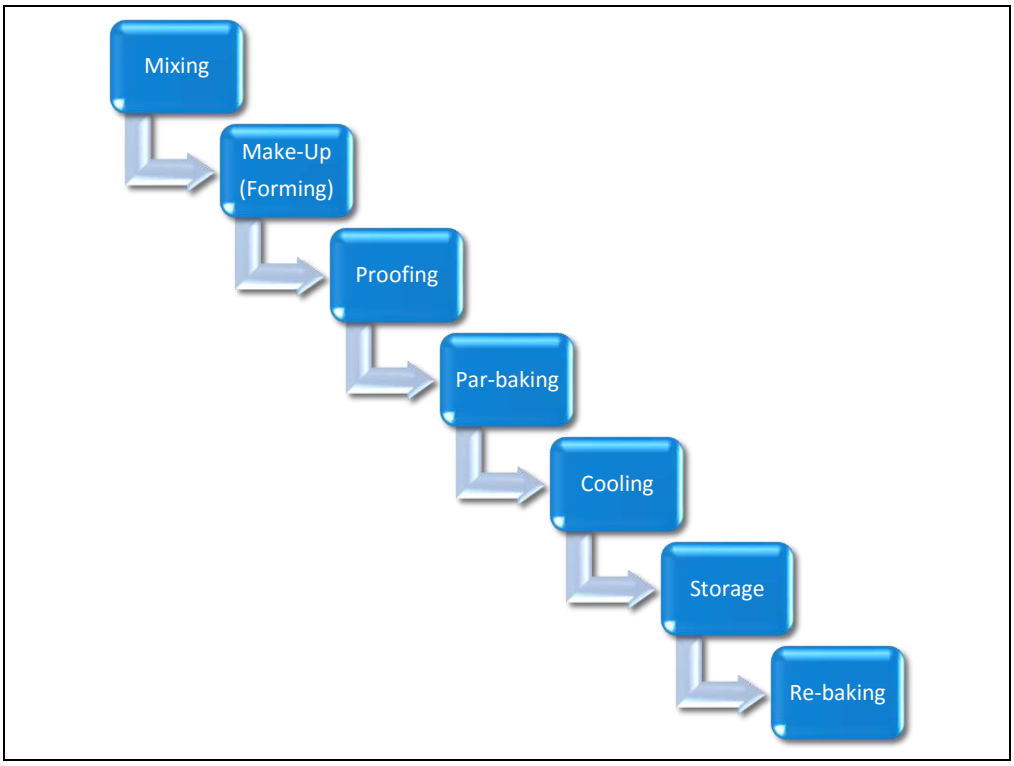

Figure 1. General flow chart of partial baking process

3. Advantages

A partially cooked product is in a more stable form against staling. It does not deteriorate like a completely baked product. Since it is packaged, it is easier to transport and can be stored until the time of consumption. As they are kept in closed containers preventing moisture loss, problems such as deterioration of product quality and weight reduction do not occur.

Producers can benefit from partial baking; they can reach to far more consumers. Since the expiration date increases significantly, the waste is reduced. The area in which traditional products are recognized and consumed can be extended and even reached the whole world. It is possible to produce much larger quantities in one produciton and save energy, time and therefore cost. As the products do not stale immediately, the product range can be greatly increased. It can be ensured that the products to be delivered to the consumers are of the same and high quality.

Those who sell partially cooked products have the following advantages: They only need a furnace to make the last cooking in their store, so they can save on machines and equipments.

Experienced baker's needs are reduced, the last cooking process can be make with simple instructions by normal workers. The producer can quickly and freshly prepare the new product in short time. In addition, commercial buyers can purchase products in larger quantities without fear of expiration.

Consumers also benefits: They can reach fresh and even hot products when they desire. They can reach various products that they have not consumed before, which are not known in their culture. Due to the standard provided in the quality of the products, they can consume better quality and safe products.

4. Applications

Studies and industrial applications of partial baking are mainly on bread types, but number of studies are focused on the application to the cakes (Karaoglu and Kotancılar, 2009), croissant, hamburger bun (Vukobratovic et al., 1999), and muffins (Schamne et al., 2010). Some of the studies about partial baking technology on formulations, mixing, par-baking, cooling, storage and re-baking steps are given below.

4.1 Mixing (Formulations)

The formulations must be carefully checked according to the process that will be used (Rosell and Santos, 2010), and some modifications should be made to par-baked formulations so as to achieve better results.

Researchers studied the addition of ingredients like; ascorbic acid and vegetable fat (Ferreira and Watanabe 1998), hydrocolloids (Mandala et al. 2008; Barcenas and Rosell, 2006a), resistant starch, pectin, inulin, fiber (Rosell and Santos, 2010), enzymes like fungal alpha-amylase, hemicellulose, protease and xylanase (Ribotta and Le Bail, 2007; Jiang et al. 2008), antimicrobial agent like calcium propionate (Karaoglu et al., 2005).

For the final product, medium strength flour which does not have a very high specific volume and tends to collapse should be used. The addition of emulsifiers acting by improving the bread texture is also recommended. Since the bread passes through two cooking stages, more water should be added as usual (Sluimer, 2005).

Hydrocolloids (guar gum, HPMC, LBG or xanthan gum) influenced the final characteristics of par-baked bread. The moisture content of the crust of such bread was 11–19% higher than that of the fresh control bread (Mandala et al. 2008).

The presence of improvers (k-carrageenan, a-amylase, sourdough and HMPC) minimized the negative effect of frozen storage and an increase in retrogradation temperature was observed by Barcenas et al. (2003).

4.2 Par-baking

In the par-baking stage, for breads, baking is carried out until the crumb of the product is formed but the crust color has still not developed, so that, the process is ended before the Maillard reaction occurs in the crust (Almeida et.al., 2016).

After partial baking, definitive size and shape of the bread should already present (Ferreira et al., 1999). According to Paid and Walker (2001), the conditions like time and temperature have significant effect on the quality characteristics of parbaked bread.

Fik and Surowka (2002) reported that the par-baking time and total baking time were depend on the type of and shape of the product and as well as on oven's thermal conditions. They also found that the optimum par-baking time was between 74 and 86% of the total baking time. Karaoglu and Kotancilar (2006) showed that the par-baking time had an important effect on the physical and technological properties of the white pan bread, like color, moisture content, softness, hydration capacity, specific volume and total titratable acidity of the bread.

4.3 Cooling

Cooling of the products is necessary after partial baking step. However, due to it does not have an established crust, par-baked bread is very vulnerable, making the structure fragile. Cooling with forced convection should be avoided as it cause great condensation on the crust (Sluimer, 2005).

Vacuum cooling is an alternative method for cooling instead of air cooling. Condensation on the crust can be avoided by vacuum cooling (Rosell, 2010). The ratio of staling of baked bread after being vacuum-cooled was almost twice that of par-baked bread cooled at ambient temperature (Le Bail et al. 2011).

4.4 Storage

Since they have a fundamental role in the technological quality of product and its staling behavior, special attention must be given to the storage conditions of par-baked products, (Rosell and Santos, 2010).

Before re-baking, the products can be stored in four different ways: room temperature, under a modified atmosphere, under refrigeration or frozen (Barcenas and Rosell, 2006a; Deschuyffeleer et al., 2011; Leuschner et al., 1997).

The main difference between storage conditions is the effect on product's shelf-life, which can vary from a few days to months.

The shelf-life of products stored at room temperature is limited (Sluimer, 2005). Without the addition of anti-microbial agents to bread samples, the microbial count increases significantly during the storage at room temperature (Karaoglu et al., 2005).

Modified atmosphere packaging of par-baked bread extends the microbiological shelf-life of this product up to few months. (Sluimer, 2005). Modified atmosphere conditions like (70% CO2 and 30% N2 in PA/EVOH//PE) was studied to partial baked baguette breads by Doulia et al. (2000). A microbiological shelf-life was reported as above 100 days at 27°C, 71 days at 35°C and only 4.6 days at the control bread.

Refrigerated storage is reported as an adequate alternative to preserve par-baked bread (Lainez et al., 2008). And also it is crucial to prevent the growth of Bacillus sp. (Leuschner et al., 1999). Storing at 7°C of the par-baked bread extents the shelf life to 9 days, while the product stored at 1°C did not present mold growth after 28 days (Lainez et al., 2008).

The most used process to preserve parbaked bread is Frozen storage. This technique allows for very long storage periods, but it is an expensive process because of the high maintenance costs of the cold chain (Lainez et al., 2008). Freezing converts the water present in a food into a nonactive compound, and in this way, together with the low temperature, freezing prevents the growth of microorganisms and it slows down the development of the enzymatic and chemical reactions responsible for deterioration (Barcenas and Rosell, 2006b).

4.5 Re-baking

Second baking stage is necessary for partial baking technology. The main objectives of these second baking are aroma development, formation of the crust, provision of a brown color and the reversal of bread staling (Leuschner et al., 1999; Sluimer, 2005).

High temperature should be kept in partial baked products to obtain an acceptable color, like 250°C and above. Also in order to maintain low water loss, the re-baking time should be kept short, like 10 minutes.

Karaoglu and Kotancilar (2006) stated that to provide crumb softness, a long re-baking time is recommended and to provide specific volume, a short re-baking time is recommended for white loaves.

5. Disadvantages

Nevertheless, with this technology, some disadvantages can be observed in the final product when compairing with normal products.

When compairing with normal cooking methods, Ferreira et al. (1999) observed a decrease in specific volume of French bread about 16%. Carr and Tadini (2003) showed that during frozen storage, crystallization of the water damaged the bread structure and it leads decreasing in the specific volume of the bread. The appearance of snow-white discoloration of the crumb can be observed in frozen storage after long time storage at the freezer (Sluimer, 2005)

Crispy bakery products can not be frozen succesfully like baguettes in which the most obvious quality problem is the separation of the crust from the rest of the product. It is reported that this problem could be solved by the migration of moisture from the crumb to the crust (Cauvain, 1998).

Crust flaking is one of the biggest problems occurring in the quality of freezed par-baked product (Ribota and Le Bail, 2007). Le Bail et al. (2005) reported that the key factor in the control of the amount of flaking is the relative humidity during fermentation and pre-cooling.

6. Conclusion

Valuable or limited bakery products are the main target to apply this technology to preserve them with long shelf life without reducing quality. Additionaly, traditional products like simit, bagel, corn bread, tortillas and panini are suitable products for this technology. With the change in life style of the population and consequent need for products that are more and more convenient, par-baked products has demonstrated great success, since it requires almost no time and effort for finalization.

References

Almeida, E.L., Steel, C.J., Chang, Y.K., 2016. Par-baked Bread Technology: Formulation and Process Studies to Improve Quality. Critical Reviews in Food Science and Nutrition 56, 70-81.

Anonymous (2018a). FAO. Global food losses and food waste – Extent, causes and prevention. Rome http://www.fao.org/docrep/014/mb060e/mb060e00.pdf. (Date of access: 22.06.2018)

Anonymous (2018b). http://www.ekmekisrafetme.com/Pages/EnglishPages/WasteWorld.aspx (Date of access: 22.06.2018)

Anonymous (2018c). http://www.tmo.gov.tr/Main.aspx?ID=1045 (Date of access: 22.06.2018)

Barcenas, M.E., Haros, M., Benedito, C., Rosell, C.M., (2003). Effect of freezing and frozen storage on the staling of part-baked bread. Food Research International 36, 863-869.

Barcenas, M.E., Rosell, C.M., (2006a). Different approaches for improving the quality and extending the shelf life of the partially baked bread: low temperatures and HPMC addition. Journal of Food Engineering 72, 92-99.

Barcenas, M.E., Rosell, C.M., (2006b). Effect of frozen storage time on the bread crumb and aging of par-baked bread. Food Chemistry 95, 438-445.

Carr, L.G., Tadini, C.C., (2003). Influence of yeast and vegetable shortening on physical and textural parameters of frozen part baked French bread. Lebensmittel-Wissenschaft Und-Technologie-Food Science and Technology 36, 609-614.

Deschuyffeleer, N., Audenaert, K., Samapundo, S., Ameye, S., Eeckhout, M., Devlieghere, F., (2011). Identification and characterization of yeasts causing chalk mould defects on par-baked bread. Food Microbiology 28, 1019-1027.

Doulia, D., Katsinis, G., Mougin, B., (2000). Prolongation of the microbial shelf life of wrapped part baked baguettes. International Journal of Food Properties 3, 447-457.

Ferreira, P. B. M. and Watanabe, E. (1998). Estudo da formula¸cao na produ¸cao de pao frances pre-assado. XIV Congresso Brasileiro de Ci^encia e Tecnologia de Alimentos, Rio de Janeiro.

Ferreira, P. B. M., Watanabe, E. and Benassi, V. T. (1999). Estudo do processo de produ¸c~ao de p~ao franc^es pre-assado. Braz. J. Food Technol. 2:91–95.

Fik, M., Surowka, K., (2002). Effect of prebaking and frozen storage on the sensory quality and instrumental texture of bread. Journal of the Science of Food and Agriculture 82, 1268-1275.

Jiang, Z., Le Bail, A. and Wua, A. (2008). Effect of the thermostable xylanase B (XynB) from Thermotoga maritima on the quality of frozen partially baked bread. J. Cereal Sci. 47:172–179.

Karaoglu, M.M., Kotancilar, H.G., Gurses, M., (2005). Microbiological characteristics of part-baked white pan bread during storage. International Journal of Food Properties 8, 355-365.

Karaoglu, M.M., Kotancilar, H.G., (2006). Effect of partial baking, storage and rebaking process on the quality of white pan bread. International Journal of Food Science and Technology 41, 108-114.

Karaoglu, M.M., Kotancilar, H.G., (2009). Quality and textural behaviour of par-baked and rebaked cake during prolonged storage. International Journal of Food Science and Technology 44, 93-99.

Lainez, E., Vergara, F., Barcenas, M.E., (2008). Quality and microbial stability of partially baked bread during refrigerated storage. Journal of Food Engineering 89, 414-418.

Le Bail, A., Ribotta, P., (2007). Thermomechanical behavior of a crumb during chilling and freezing: Potential impact on crust flaking and interaction with formulation using selected enzymes. Starch: Achievements in Understanding of Structure and Functionality, 247-+.

Le Bail, A., Leray, G., Perronnet, A., Roelens, G., (2011). Impact of the chilling conditions on the kinetics of staling of bread. Journal of Cereal Science 54, 13-19.

Leuschner, R.G.K., O'Callaghan, M.J.A., Arendt, E.K., (1997). Optimization of baking parameters of part-baked and rebaked Irish brown soda bread by evaluation of some quality characteristics. International Journal of Food Science and Technology 32, 487-493.

Leuschner, R.G.K., O'Callaghan, M.J.A., Arendt, E.K., (1999). Moisture distribution and microbial quality of part baked breads as related to storage and rebaking conditions. Journal of Food Science 64, 543-546.

Mandala, I., Kapetanakou, A., Kostaropoulos, A., (2008). Physical properties of breads containing hydrocolloids stored at low temperature: II - Effect of freezing. Food Hydrocolloids 22, 1443-1451.

Paid, Y. Y. and Walker, C. E. (2001). Influence of baking conditions on partbaked bread properties. AACC Annual Meeting, Charlotte.

Ribotta, P.D., Le Bail, A., (2007). Thermo-physical and thermo-mechanical assessment of partially baked bread during chilling and freezing process. Impact of selected enzymes on crumb contraction to prevent crust flaking. Journal of Food Engineering 78, 913-921.

Rosell, C. M. (2010). Trends in breadmaking: Low and subzero temperatures. In: Innovation in food engineering: new techniques and products, pp. 59–79.Passos, M. L. and Ribeiro,C.P., Eds.,CRC Press, Boca Raton.

Rosell, C.M., Santos, E., (2010). Impact of fibers on physical characteristics of fresh and staled bake off bread. Journal of Food Engineering 98, 273-281.

Schamne, C., Dutcosky, S.D., Demiate, I.M., (2010). Obtention and characterization of gluten-free baked products. Ciencia E Tecnologia De Alimentos 30, 741-750.

Sluimer, P. (2005). Principles of breadmaking: functionality of raw materials and process steps. The American Association of Cereal Chemists, Inc., St. Paul.

Vukobratovic, R., Simurina, O., Psodorov, D., Duric, V., Matkovic, K., (1999). Pre-baked and frozen bakery products. Flour - Bread '99, 122-129.

The Beneficial Effects Of Pickles On Human Health

Serap KAYIŞOĞLU

Namık Kemal University Tekirdağ Turkey skayisoglu@nku.edu.tr

* **Corresponding Author:** skayisoglu@nku.edu.tr

Abstract

Pickles, among the fermented foods that Turkish people likes very much to consume, are produced by naturally fermenting various vegetables and fruits. Since pickles are fermented food, they are very rich in bacteria. These bacteria make contribution to the formation of a strong intestinal flora and a strong immune system. The microorganisms in the pickle fermentation are Leuconostoc mesenteroides, Lactobacillus brevis, Pediococcus pentocaceus and Lactobacillus plantarum. The beneficial bacteria that come with pickles also support the formation of Vitamin K in the intestines. Pickles, which are rich in vitamins, minerals and antioxidants, are known to be beneficial in controlling the symptoms of allergic diseases and preventing the cancer-causing agents, within the presence of probiotic bacteria. Consumption of pickles is quite beneficial in the prevention of Ulcer disorders, the liver protection and cleansing, controlling of the values in diabetes diseases or the protection needs in the digestive system. In addition, consumption of pickles, made from vegetables and fruits with high fiber content, has been recommended, because they are found to be effective against constipation and gastric problems such as constipation and indigestion in clinical trials.

In this study, beneficial effects of pickle, which is a fermented food, on human health is pointed out and supported by the results of this study.

Keywords: Pickle, fermented foods, human health, probiotic bacteria

1. Introduction

Pickle is a product obtained by fermenting vegetables in salt water at specific concentrations with the help of their own juices and lactic acid. Pickles can be stored for a long time under the influence of lactic acid and salt. The factor that allows lactic acid fermentation to take place properly is the salt concentration in the medium. Salt concentration in pickles ranges from 2.5 to 10%, depending on the amount of sugar contained in the fruits and vegetables to be used in production (Ertugay et al., 1994). Lactic acid fermentation is the only method of preservation that retains all the natural plant ingredients while improving the quality, taste and aroma (Bamforth, 2005). Furthermore, microorganisms used for fermentation can add probiotic properties to product. The positive effects of lactic acid bacteria probiotically in the gastrointestinal tract are related to two possible mechanisms. The first is to form antimicrobial active compounds such as lactic acid and bacteriocin, and the second is to form barriers that the pathogens can not hold in the intestinal mucosa (Ehrrman et al.,2002).

2. Pickle Production Methods

The most common method of pickling production is lactic acid fermentation. In this method, the lactic acid bacteria formed by the lactic acid and the effect of the protective effect of the salt is obtained from the pickle and two different methods are encountered. The first one is the fermentation of the raw materials in acetic acid and brine, namely the acidic with brine fermentation. The second is the fermentation of the raw material in brine, namely içindeki brine fermentation In this way, the process is called; stock processing (Aktan et al. 1998; Tokatlı, 2013).

The microbial flora of the plant material, the acid and salt composition of the brine, the fermentation temperature, and the exclusion of oxygen from the process determine which microorganisms will dominate the fermentation, and also the flavor of the final product. For a good fermentation, it is essential to have a salt concentration of between 10–15%. At higher salt concentrations, lactic acid bacteria will not grow well (Kabak, 2009).

This traditional fermentation of vegetables and fruits most often involves lactic acid fermentation with many different species of lactic acid bacteria being active at different stages of the fermentation process which is then followed by yeast fermentation (Josephsen and Jespersen, 2004). The lactic acid bacteria responsible for the fermentation include Lb. plantarum, Leuconostoc mesenteroides, Lb. brevis, Pediococcus pentosaceus and Enterococcus

faecalis. Leuconostoc mesenteroides, which produces high levels of acid and gas predominates at the beginning of the fermentation, while Lb. plantarum, which is more resistant to acids, predominates subsequently, and continues the fermentation (Aktan et al., 1998).

2.1 Canned Pickles

.

Canned pickles are produced for commercial purposes. Fermentation is not applied in this method. Vegetables are placed directly in jars or tin cans, poured onto brine from acid and salt, then pasteurized. In canned pickle production, the product is usually kept in vinegar brine for prolonging the campaign period and for year-round production, and canned at intervals (Aktan et al.,. 1998; Tokatlı 2013).

2.2 Vegetables and Fruits Used In Pickles

Fruits and vegetables used in the production of pickles vary according to the regions. Most pickled vegetables are cucumber, pepper, cabbage and tomato. In addition, pickles are made from vegetables such as fresh beans, eggplants and sugar beets. Pickles are also made in many vegetables and fruits such as leek, raw melon, capers, green apples, green plums, turnip, cauliflower, apricot, medlar, okra and broccoli (Karagöz and Güllü, 2017).

2.3 Health Benefits Of Pickles

It is determined that pickles, an integral part of Turkish culinary culture, is also an important function of health, that it has an appetizing characteristic of water, and that it protects against diseases like cancer, blood and ulcer. According to experts, it has been determined that cabbage pickles prevent vascular occlusion and stomach uptake with the ulcer, cancer, heart and nervous system (Yılmaz,2010).Green plum pickles are particularly appetizing. Garlic pickles prevent the proliferation of cancer cells. Pickled beets prevent anemia and facilitates digestion. In addition, they prevent the proliferation of cancer cells. Fermented cabbage contains the active substance S-methylmethionine, which reduces the formation of tumors in human stomach. In fact, it has inhibitory effects on liver, lung, breast and colon cancers through its isotypes (Karovicova and Kohajdova, 2005).While digestibility of nutrients is increased by fermentation, detoxification and destruction of undesirable substances such as phytate, tannin and polyphenols in raw foods are realized. While digestibility of nutrients is increased by

fermentation, detoxification and destruction of undesirable substances such as phytate, tannin and polyphenols in raw foods are realized (Kabak and Dobson 2011). The pickles take this effect because they destroy toxic substances. Also; vitamins, essential amino acids and proteins by providing biosynthesis in terms of nutrition is also important (Giraffa 2004).

2.4 Useful Influence Of Probiotics

Probiotics produce much more serotonin in the intestines than those synthesized in the nervous system (Collins and Bercik 2009; Desbonnet et al., 2008).The provision of probiotics, especially for children, reduces upper respiratory tract infections, prevents unnecessary drug use and increases quality of life (Arıca et al., (2012).By strengthening the microflora in the gastro-intestinal system, probiotics help to function as a healthy gastro-intestinal tract and therefore work in harmony with the whole body (İnanç et al., 2005; Şener et al., 2008). It has also been demonstrated that probiotic bacteria have many positive effects on allergic diseases and immune system as well as antibacterial effects against pathogenic bacteria (Chandan 1997; Holzapfel and Schillinger 2002). Probiotics inhibit the growth of pathogenic microorganisms by producing bacteriocin, synthesizing organic acids such as acetic acid and lactic acid, reducing the pH of the medium and synthesizing hydrogen peroxide (Mathieu et al.,1993).Probiotics play an important role in reducing the level of cholesterol, preventing cancer, treating and preventing food allergies, treating Helicobacter pylori infections, and regulating the intestinal flora (El-Ghaish et al.,2011; Yoon et al.,2013), There is also a regulatory effect on the immune system (Saad et al.,2013). In the last decade, a number of studies have been conducted showing that probiotics and prebiotics modulate the intestinal microbiota and affect the health of the elderly positively (Yılmaz, 2015).

3. Results and Discussion

Traditional fermented products have an important place in the vast majority of population in many countries. Since fermented products have beneficial compounds, their interest has increased. Due to the increasing interest, consumption of fermented products is also increasing worldwide. For this reason, pickles are always confronted as one of the traditional products that can maintain their place in Turkish culture (Akbaş, 2006). It is very meaningful and important to focus on the production of commercial preserved pickles, industrial size, the establishment of standard production techniques and the efforts to obtain quality products (Akbaş, 2006).

References

Akbaş, L. G. (2006). Değişik Turşularda Biyojen Amin Miktarları Üzerine Araştırma. Yüksek Lisans Tezi, *Ankara Üniversitesi Fen Bilimleri Enstitüsü*, Ankara

Aktan, N., Yücel, U., Kalkan, H. (1998). Turşu Teknolojisi. *Ege Üni. Ege Meslek Yüksek Okulu Yayınları*, 23, 138 s., İzmir.

Arıca, S.G., Arıca, V., Özer, C. (2012). Çocukluk çağında üst solunum yolu enfeksiyonu tedavi ve korunmasında probiyotik kullanımı. *TJFMPC*, 2012; 6(2):22-29.

Bamforth CW (2005). Introduction. Food, Fermentation and Microorganisms, Blackwell Publishing, UK, pp. XIV-XVI.

Chandan, R. (1997). Dairy-based ingredients. American Association of Cereal Chemists, St. Paul, MN. Pp. 96-99.

Collins, S.M., Bercik, P. (2009).The relationship between intestinal microbiota and the central nervous system in normal gastrointestinal function and disease. *Gastroenterology*. 2009; 136:2003–2014.

Desbonnet, L., Garrett. L., Clarke, G., Bienenstock, J., Dinan, T.G. (2008). The probiotic Bifidobacteria infantis: An assessment of potential antidepressantproperties in the rat. *J Psychiatr Res*. 2008; 43:164–174.

Ehrmann, M.A., Kurzak, P., Bauer, J. and Vogel, R.F.(2002). Characterization of lactobacilli towards their use as probiotic adjuncts in poultry. *J. Appl. Microbiol*., 2, 966–975.

El-Ghaish, S., Ahmadova, A., HadjiSfaxi, I., Mecherfi, K.E.E., Bazukyan, I., Choiset, Y.,

Ertugay, Z., Kurt, A., Elgün, A., Gökalp, H.Y. (1994). Gıda Bilimi ve Teknolojisi. *Atatürk Üniversitesi Yayın No:671, Ziraat Fakültesi Yayın No:301, Ders Kitapları Serisi No:53*

Giraffa, G. (2004). Studying The Dynamics of Microbial Population During Food Fermantation. FEMS *Microbiology Reviews*, 28: 251-260.

Holzapfel, W.H., Schillinger, U. (2002). Introduction top re-and probiotics. *Food Res Int*, 35, 109-116.

İnanç, N., Şahin, H., Çiçek, B. (2005). Probiyotik ve prebiyotiklerin sağlık üzerine etkileri. *Erciyes Tıp Dergisi*, 27, 122-127.

Josephsen, J., and Jespersen, L. (2004). Starter cultures and fermented products. **In**: Handbook of Food and Beverage Fermentation Technology. pp. 51–88.

Kabak, B. (2009). Tursu üretimi ve fermantasyonda rol oynayan mikroorganizmalar. II. Geleneksel Gıdalar Sempozyumu, 27–29 Mayıs, Van, pp. 834–837.

Kabak, B., Dobson, A.D.(2011). An Introduction to the Traditional Fermented Foods and Beverages of Turkey. *Critical Reviews in Food Science and Nutrition*,51: 248-260.

Karagöz, Ş., Güllü, M. (2017). Türk Kültüründe Kış Hazırlıkları; Turşu Türlerinin Ve Üretim Metotlarının Değerlendirilmesi AL-FARABI International *Journal on Social Sciences* Year: 2 (2017) Vol: M Issue: May 27, 2017.

Karovicova, J., Kohajdova, Z. (2005). Lactic Asid-Fermented Vegetable Juices-Palatable and Wholesome Foods. *Chem. Pap*,59(2):143-148.

Mathieu, F., Sudirman, I., Rekhif, N. (1993). Mesenterocin 52, a bacteriocin produced by Leconostoc mesenteroides ssp. mesenteroides Fr 52. *J Appl Bacteriol*, 74, 372-379.

Saad,N., Delattre, C., Urdaci, M., Schmitter, J.M., Bressollier, P. (2013). An overview of the last advances in probiotic and prebiotic field. *Food Science and Technology*, 50(1): 1-16.

Şener, A., Temiz, A., Toğay, S.Ö., Bağcı, U. (2008). Çeşitli prebiyotiklerin Bifidobacterium animalis subsp. lactis Bb-12'nin gelişimi ve asitlik geliştirme özelliği üzerine in vitro etkileri. Hacettepe Üniversitesi Gıda Mühendisliği Bölümü, *Türkiye 10. Gıda Kongresi*, sh: 889-892, Erzurum

Tokatlı, M. (2013). Ankara Çubuk Yöresi Turşularından İzole Edilen Laktik Asit Bakterilerinin Tanımlanmaları, Teknolojik ve Fonksiyonel Özelliklerinin Belirlenmesi ve Starter Olarak Kullanılma Olanaklarının Değerlendirilmesi. Doktora Tezi, *Ankara Üniversitesi Fen Bilimleri Enstitüsü*, Gıda Mühendisliği Anabilim Dalı, Ankara

Yılmaz, S. (2010). https://samsun.tarim.gov.tr/Belgeler/Yayinlar/Kitaplarimiz/tursu_yapimi.pdf

Yılmaz, Ö.A. (2015). Yaşlılarda sağlıklı beslenme – probiyotikler Ege Tıp Dergisi / *Ege Journal of Medicine* 2015; 54: Ek Sayı / *Supplement* 16-21

Yoon, H.S., Ju, J.H., Lee, J.E., Park, H.J., Lee, J.M., Shin, H.K., Holzapfel, W., Park, K.Y., Do, M.S. (2013). The probiotic *Lactobacillus rhamnosus* BFE5264 and *Lactobacillus plantarum* NR74 promote cholesterol efflux and suppress inflammation in THP-1 cells. *Journal of the Science of Food and Agriculture*, 93: 781-787.

The Use of Mushrooms and Their Extracts and Compounds in Functional Foods and Nutraceuticals

Nebahat Şule Üstün[1*], Sanem Bulam[2], Aysun Pekşen[3]

[1]Ondokuz Mayıs University, Faculty of Engineering, Department of Food Engineering, Samsun, Turkey; sustun@omu.edu.tr

[2]Giresun University, Faculty of Engineering, Department of Food Engineering, Giresun, Turkey; sanem.bulam@giresun.edu.tr

[3]Ondokuz Mayıs University, Faculty of Agriculture, Department of Horticulture, Samsun, Turkey; aysunp@omu.edu.tr

[*] **Corresponding Author:** sustun@omu.edu.tr

Abstract

Functional foods are conventional or everyday foods consumed as part of daily diet. They exert positive effects on target function(s) beyond their nutritive value, enhancing the well-being and quality of life, and/or reducing disease risks. Nutraceuticals are defined as a food or part of a food providing medical or health benefits including the prevention and treatment of a disease. Mushrooms are considered as a delicacy with a high nutritional and functional value and accepted as functional and nutraceutical food ingredients. They are of considerable interest because of their organoleptic value, medicinal properties, and economic significance. The nutritional value of edible mushrooms is due to their high protein, fiber, vitamin and mineral contents, and low-fat levels. Besides, they include several bioactive compounds giving them the ability to exert beneficial effects at different levels. Numerous molecules of mushrooms known to be bioactive and found in fruit bodies, cultured mycelium and broth are polysaccharides, proteins, fats, minerals, glycosides, alkaloids, volatile oils, terpenoids, tocopherols, phenolics, flavonoids, carotenoids, folates, lectins, enzymes, ascorbic, and organic acids. Bioactive properties include immunomodulating, antitumour, anti-hypercholesterolemia, antibacterial, antifungal, anti-inflammatory, antiviral, anti-diabetic, and cardiovascular health promoting effects. Nowadays, mushroom extracts are commercialized as dietary supplements, mainly for antitumour activity and the enhancement of immune function. In addition, it is possible to find foods in the markets including edible wild and cultivated mushrooms and their compounds as an ingredient. This review focuses on the enhancement of biochemical and biological properties by adding mushrooms, mushroom extracts and compounds to produce value-added mushroom-related products.

Keywords: Mushroom extracts, mushroom compounds, nutritional, bioactivity, functional, nutraceutical.

1. Introduction

According to current estimates, mushrooms constitute at least 12.000 species worldwide and 2.000 of these species are reported as edible. About 35 edible mushroom species are commercially cultivated whereas nearly 200 wild species are being used for medicinal purposes (Beulah et al., 2013). Many researchers have documented that edible mushrooms are the source of a variety of nutraceutical compounds such as polysaccharides (β-glucans), dietary fibers, unsaturated fatty acids, terpenes, peptides, glycoproteins, alcohols, mineral elements and antioxidants like phenolic compounds, tocopherols, ascorbic acid (Pardeshi and Pardeshi, 2009). Mushrooms are excellent functional foods containing Se, ergothioneine, vitamin D_2, vitamin B_1 and Fe, etc. The amount and the bioavailability of any nutrient and bioactive biomolecule primarily depend on the mushroom variety (Ruiz-Rodriguez et al., 2009; Yokota et al., 2016). Higher Basidiomycetes mushrooms contain biologically active compounds in fruit bodies, cultured mycelium and cultured broth (Wasser, 2014). Thus, they might be used directly in diet and promote health, taking advantage of the additive and synergistic effects of all the bioactive compounds they included (Vaz et al., 2010; Pereira et al., 2012; Badalyan, 2014).

The presence of specific bioactive compounds makes these mushrooms valuable, from the strengthening of the immune system to the treatment and prevention of life-threatening diseases such as heart disease, hypertension, cerebral stroke and cancers. Mushrooms are also known to exhibit antiviral, antibacterial, antifungal, antiinflammatory, antitumour and immunomodulating, cardiovascular, hepatoprotective, antidiabetic, hypolipidemic, antithrombotic and hypotensive effects (Wasser and Weis, 1999a and b; Singh, 2017). The properties and mechanisms of extracts and bioactive compounds from mushrooms have already been evaluated in a human population or human cell lines and animal model or animal cell lines (Rathee et al., 2012; Roupas, et al., 2012; Giavasis, 2014a, b; Kothari et al., 2018).

Mushrooms are basically consumed for their texture and flavor. The rich source of proteins, vitamins and minerals, low in fat content (2-8%) and having unique biochemicals make mushrooms low calorie food and choice diet for those suffering from hypertension, arthrosclerosis, diabetes and obesity. Additionally, they have recently become attractive as health-beneficent food and as sources for the development of drugs (Singh, 2017). There is a wide usage of mushroom from their traditional uses to medicinal purposes (Aida et al., 2009). Modern clinical practice in Japan, China, Korea, Russia, and several other countries have relied on mushroom-derived preparations (Wasser, 2010; Chang and Wasser, 2012). Moreover, *in vitro* and *in vivo* studies on functional foods and nutraceuticals derived from edible and

medicinal mushrooms were previously conducted (Giavasis, 2014a,b; Prasad et al., 2015; Morris et al., 2016; Taofiq et al., 2016a; Rathore et al., 2017; Reis et al., 2017; Ma et al., 2018).

2. Nutraceutically Important Bioactive Compounds of Mushrooms

Recent scientific studies reported that many edible mushrooms, described before by the traditional folklore of Asian culture, especially in China, Japan, Korea and India as medicinal remedies towards a variety of disorders and diseases, contained specific bioactive compounds. These compounds were confirmed to protect against tumours and other disorders, microbes, and viruses and to lower cholesterol levels, (Ruiz-Rodriguez et al., 2009). Moreover the presence of wonder molecules like polysaccharides, low molecular weight proteins, terpenes, glycoprotein and bioactive compounds again reinforce the usage of such magic food for the better mankind (Rathore et al., 2017).

2.1. Polysaccharides

Oyster mushrooms possess bioactive compounds with hypocholesterolemic activities, such as polysaccharides, mevinolin and other statins (Gunde-Cimerman and Plemenitas, 2001). Also, proteoglycans from *Agaricus blazei* are known to have strong immuno-modulatory properties which are therapeutically important in controlling cancers and immune deficient diseases through the up-regulation of dendritic cells maturation (Kim et al., 2005). Mushroom polysaccharide extracted from *Agaricus bisporus* exhibits excellent inhibiting activity against human breast cancer (Jeong et al., 2012). Pleuran from *Pleurotus* species, lentinan from *Lentinula edodes*, schizophyllan from *Schizophyllum commune*, calocyban from *Calocybe indica*, or ganoderan and ganopoly from *Ganoderma lucidum* are various β-linked glucans isolated from mushrooms (Villares et al., 2012).

The anti fatigue activities observed in the polysaccharides extract of *Hericium erinaceus* extends the utilization of these kinds of novel polysaccharides for sports nutrition (Liu et al., 2015). These polysaccharides are known to possess various physiological activities such as antitumour, antioxidant, antiviral activities; immunomodulatory, antiinflammatory and anticarcinogenic actions (Rathore et al., 2017).

2.2. Bioactive Protein Molecules

Mushroom bioactive proteins and peptides such as lectins, mushroom immunomodulatory proteins, ribosome inactivating proteins, antimicrobial proteins, ribonucleases, and laccases are an important part of functional components with great value of pharmaceutical potential (Xu et al., 2011). Lectins are the non-immune proteins or glycoproteins binding specifically to cell surface carbohydrates and have been previously studied for their antiproliferative, antitumour, and immunomodulatory activities in *Agaricus bisporus* (Chang et al., 2007) and *Ganoderma lucidum* (Tong et al., 2008). Furthermore, there is no effect of thermal, freezing, acid, alkali and dehydration treatments on the properties of lectin protein (ABL) isolated from *A. bisporus*, hence indicating their usage as a stable immune stimulant for nutraceutical and functional food development (Chang et al., 2007).

2.3. Terpenes

Terpenes are basically a group of volatile unsaturated hydro-carbons which are responsible for the antiinflammatory activities and have been isolated from the mushrooms widely and these terpenoids are responsible for many pharmacological activities like anticancer antimalarial, anticholinesterase, antiviral, antibacterial and anti-inflammatory activities (Duru and Tel Çayan, 2015). The isolated terpenoids were monoterpenes and sesquiterpenoids, sesquiterpenoids such as flammulinol, flammulinolides, and triterpenoids such as lanostane were isolated from *Pleurotus cornicopiae*, *Flammulina velutipes* and *Ganoderma lucidum*, respectively (Rathore et al., 2017). Basically, these terpenes can be effectively utilized in developing drugs for curing Alzheimer's and other degenerative diseases.

2.4. Antioxidants

Antioxidant compounds prevent oxidative damage related to aging and diseases, such as atherosclerosis, diabetes, cancer and cirrhosis. Mushrooms that contain antioxidants or increase antioxidant enzyme activity may be used to reduce oxidative damage in humans (Yang et al., 2002). The antioxidant activities of edible and medicinal mushrooms have been associated with minerals such as Se and Zn. In addition, biomolecules such as ergothioneine, polysaccharide-protein complexes (β-D-glucans, etc.) phenolic compounds, flavonoids and, in lower amounts, peptides, carotenoids, ascorbic acid and tocopherol have been determined which are the responsible compounds isolated from the different species of mushrooms and reported to boost the immune system, have anticancerous, antihypercholesterolaemic and anti-viral activities,

and ameliorate the toxic effect of chemotherapy and radiotherapy (Ruiz-Rodriguez et al., 2009; Valverde et al., 2015). The radical scavenging activities of mushrooms have been extensively studied and documented for the species such as *Pleurotus* spp., *Agaricus* spp., *Ganoderma lucidum* and *Lentinula edodes* known for their profound antioxidant activities. *Phellinus rimosus*, *Hericium erinaceus* and *Cordyseps sinensis* can be used as nutraceuticals having natural antioxidants and healthy commercial preparations (Rathore et al., 2017).

2.5. Other Biologically Active Nutraceutical Compounds Present in Mushrooms

Some of the identified bioactive molecules in mushrooms are β-glucan, dietary fibre, proteoglycan, lectin, phenolic compounds, flavonoids, volatile oils, tocopherols, carotenoids, alkaloids, glycopeptides, folates and organic acids (Prasad et al., 2015). Because of these bioactive compounds contents, the mushrooms have antitumour, anticancer, antidiabetic, cardio-protector, hepato-protective, neuro-protective, antibacterial, antiviral, etc. functions. *Cordyceps militaris* contains a natural immunostimulating polysaccharide having potential to cure various kinds of cancers and tumours. The isolated active molecules dictyophorine A and B from *Dictyophora indusiata* account for curing neurodegenerative diseases by improving Nerve Growth Factor. *Hericium erinaceus* contains hericenones and erinancines that prevent or treat human chronic, cognitive, and neurological diseases. Furthermore, the tablet formulations of *H. erinaceus* have been extensively used for strengthening the gastrointestinal and immune function. *Phellinus rimosus* has an activity against tumour and for refreshing human body to improve longevity. *Panellus serotinus* (Mukitake) prevents the development of nonalcoholic fatty liver disease. *Pleurotus* spp., *Lentinula edodes*, *Agaricus bisporus* and *Tremella fuciformis* possess strong prebiotic activities (Aida et al., 2009; Rathore et al., 2017).

3. Therapeutical Potential of Mushroom Bioactive Compounds

The reported biological activity of some mushrooms and their active constituents were given in Table 1.

Table 1. Biological activities of biocompounds in some commonly consumed edible and medicinal mushrooms

Mushroom species	Active principle/constituent/extract	Reported biological activity
Agaricus bisporus	Fibers, lectins, fucogalactan, 2-amino-3H-phenoxazin-3-one, lectin	Hypocholesterolemic, hypoglycemic, anti-aging property, anticancer, anti-inflammatory

Agaricus blazei	Glucan-protein complex, soluble polysaccharide	Activation of T lymphocytes
Amanita muscaria	Fucomannogalactan	Anti-inflammatory
Auricularia auricula-judae	Methanolic extracts, dietary fiber, acidic polysaccharides, glucan	Antioxidant, antitumour, hypocholesterolemic, antiviral, antiradiative, hypoglycemic
Boletus edulis	Extracts of fruiting bodies, lectin, polysaccharides, polyphenols, ergothioneine, BE3, BSF-A	Antitumour, immune-modulating, antibacterial, antifungal, antiviral, anti-inflammatory, antioxidant, mitogenic, neurotropic
Cantharellus cibarius	Polysaccharides, cibaric acid, phenolic compounds	Antioxidant, antimicrobial, antifungal, insecticidal, nematicidal
Cordyceps sinensis	Adenosine, cordycepin, and ergosterol	Hypoglycemic activity, anti-depressant activity, cures lung infections, antioxidant
Dictyophora indusiata	Heteroglycan, mannan, glucan	Antitumour, hyperlipidemia
Flammulina velutipes	Fibers, ethanolic extracts, flammulin, FVP2, peptide glycans, prolamin, proflamin, enokipodin J, velutin protein, alcoholic and hot water extracts of its sporophores, FIPs, RIPs	Antioxidant, anti-cancer, hypocholesterolemic, antiviral, antiallergic, anti-ageing, cytotoxic, antibacterial, antitumour, antifungal, antiallergic, anticomplementary
Ganoderma lucidum	Ganoderan A, B, C, β-glucans, lanostane triterpenoids, ganosporeric acid A, ganopoly, the polysaccharide-containing preparation, germanium, nucleotides and nucleosides, ribonucleas, ganoderic acid B, C1, E, Y, DM, ganolucidic acid A, ganodermadiol, lucidenic acid N, A, lucidadiol	Hypoglycemic, antitumour, antiviral (HIV-1), antiallergic, anti-inflammatory, cytotoxic, antihepatotoxic, anti-cancer, anticholinesterase, antioxidative free radical scavenging effects, immunomodulating, induction of apoptosis, anti-invasive
Grifola frondosa	MD-fraction, ergosterol, grifolan, lectins, α-glucan, GFP1, mannogalactofucan, heteroxylan, galactomannoglycan, xyloglucan, fucomannoglucan, heteroglucan proteins	Antioxidant, hypotensive, antitumour, hypoglycemic, immunotherapy, antidiabetic, anti-inflammatory activity, improves ovulation, antiviral
Grifola gargal	Ergothioneine	Anti-inflammatory
Hericium erinaceus	Phenol-analogous compounds, erinacine A, hericenones, HEP3	Antioxidant, ameliorative effect in Alzheimer's dementia, antitumour, hypoglycemic
Inonotus obliquus	β-glucan, triterpenes	Antitumour, antioxidant, immunomodulating, anti-inflammatory
Mushroom species	Active principle/constituent/extract	Reported biological activity
Lactarius deliciosus	Sesquiterpenoids, lectin, phenolic compounds	Antibacterial, antifungal, cytotoxic, anti-inflammatory, insecticidal, nematocidal, antioxidant
Lactarius volemus	Phenolic acids, lectin	Antioxidant
Laetiporus sulphureus	Dehydrotrametenolic acid, acetyl eburicoic acid	Hypoglycemic, anti-inflammatory
Lentinula edodes	Methanolic and water extracts, eritadenine, lentinan, oxalic acid, ethanolic mycelial extracts, eritadenine, LT2, heterogalactan, emitanin	Antioxidant, anticancer, hypocholesterolemic, immunotherapy, antimicrobial, antiprotozoal, antitumour, anti-inflammatory
Morchella esculenta	Galactomannan (α-d-glucan), proteins, enzymes, vitamins, minerals, and amino acids	Immune-modulating, antitumour, hypoglycemic, cures pneumonia, fever, cough, cold, and stomachache

Pleurotus eryngii	Ethanolic extracts, eryngiolide A, laccases, diterpenoids	Antiallergic, antiproliferative, antiviral, cytotoxic
Pleurotus ostreatus	Water and 30% ethanolic extract, lovastatin, lectin	Antioxidant, antitumour, arhterosclerotic, hypocholesterolemic, increases gastrointestinal motility, immuno-modulatory activity
Pleurotus sajor-caju	Lovastatin, proteins having polysaccharide, xyloglucan, xyloproteins	Hypocholesterolemic, cardio-protective, anti-inflammatory, antitumour
Poria cocos	β-glucans, 29-hydroxypolyporenic acid C, polyporenic acid C	Anticancer, prebiotic, anti-inflammatory
Russula delica	Lectin	Antiproliferative, antiviral
Schizophyllum commune	β-D-glucan (Schizophyllan)	Immunotherapy, antitumour
Sparassis crispa	Bioactive β-D-glucan, phenyl derivatives, chalcones, and sesquiterpenoids	Lipid peroxidation inhibition, immunomodulation
Trametes versicolor	Coriolan, a β-glucan-protein complex, krestin (PSK), glycoproteins, PSP, CVP	Hypoglycemic, immunotherapy, anticancer, antifungal, antiviral (HIV-1), liver protective
Tremella fuciformis	Heteroglycan	Hypolipidemic, hypoglycemic, immunomodulating, antitumour, antidecrepitude, antithrombus
Tricholoma spp.	Tricholomalide A, B, C	Cytotoxic, anticancer
Volvariella volvacea	Methanolic and water extracts, exopolysaccharides, glycoproteins	Antioxidant, hypotensive, hypocholesterolemic, cardio-protective

References: Lakhanpal and Rana, 2005; Zhang et al., 2007; Rathee et al., 2012; Badalyan, 2014; Rahi and Malik, 2016; Taofiq et al., 2016a; Rathore et al., 2017; Kothari et al., 2018; Ma et al., 2018.

Supplementation of products with dried mushroom powders like *Lentinula edodes* (Regula et al., 2010) and *Pleurotus* spp. (Regula et al., 2016a; b) have been confirmed to increase the blood hemoglobin concentration, liver, and kidney Fe levels in *in vivo* models. These functional foods might also have a big potential for the prevention or cure of diabetes more than in other plant species (Perera and Li, 2011).

4. Health Promoting Novel Mushroom-Derived Products

Functional food is defined as natural or formulated food that enhances a physiological performance or prevents or treats a particular disease, and is consumed as part of the normal daily diet. Nutraceutical refers to a medicinal or nutritional component of food, plant, or naturally occurring material that is used for the improvement of health, by preventing or treating a disease in the form of extract, compound, nutrient or pharmaceutic such as pills, tablets (Doyon and Labrecque, 2008; El Sohaimy, 2012). Food supplements have essentially a feed function, taking the form of medicines as pills or capsules (Howlett, 2008). Today, mushrooms are consumed in various forms, as foods, in the form of dietary supplement (DS), as a nutraceutical or medicine, usually called “mushroom pharmaceuticals”. Moreover, they are

used as natural bio-control agents in plant protection (acting as insecticides, fungicides, bactericides, etc.) and in cosmetics (due to their film forming capability, antioxidant, anti-allergic or antibacterial activities, stimulation of collagen activity among others) (Wasser, 2014; Taofiq et al., 2016b).

Most mushroom-derived preparates and substances are used as a novel class of "dietary supplements" (DS) or "nutraceutical" not as "pharmaceutical". A "mushroom nutraceutical" is a refined or partially refined extract or dried biomass from either the mycelium or the fruiting body of the mushroom, which is consumed in the form of capsule or tablets as a dietary supplement and which may enhance the immune response of human body, thereby increasing resistance to disease and in some cases causing regression of a disease state (Wasser et al., 2000; Giavasis, 2014a; Wasser, 2014). As functional foods, mushrooms represent a paradigm of integrating traditional and novelty, due to their wide spectrum of pharmacological properties. Their bioactive components can be extracted or can be concentrated as nutraceuticals, and/or as a diverse class of dietary supplements. "Functional foods" and "nutraceuticals" particularly mushrooms, are immunoceuticals with antitumour and immunomodulatory effects which target and modulate biological processes that foster the development of diseases (Morris et al., 2016). Due to the limited supply and high price of wild mushrooms, artificial cultivation has become the major source of many edible mushroom-based products on the market (Smith et al., 2002).

Despite the studies developed in the field of mushroom incorporation to foods, these products have not got into market, yet. There is still a lack of information regarding the bioaccessibility/bioavailability of the compounds and possible interactions with the food matrix. Therefore, most of the mushrooms and their compounds are mainly consumed in natural form or in dietary supplements (Reis et al., 2017).

4.1. The Use of Mushroom Extracts and Compounds in Functional Foods

As part of a healthy diet, functional foods, can be consumed not only in their natural state, but also after biotechnical modification. It is suggested that these foods will enrich a healthy diet and improve the nutritional value of other foodstuffs (Martins et al., 2016). In Table 2, some studies on functional foods derived from various mushrooms were given. By the production of these products, it was aimed to get high nutritional value, high-fibre and low-calorie novel functional foods and beverages having some functionalities such as improving the pasting properties of wheat flour, getting and increasing antioxidant, antimicrobial, antithrombotic and hypocholesterolemic properties, decreasing the potential glycemic

response, inhibition of food contaminants, avoiding food deterioration and protection from lipid peroxidation (Giavasis, 2014b; Reis et al., 2017; Ma et al., 2018).

Table 2. Studies on mushroom-based functional foods with their powders, extracts, compounds and mycelia

Mushroom species	Functional food	References
Agaricus aegerita	Cream cheese	Petrovic et al., 2015
Agrocybe aegerita	Snack food	Brennan et al., 2012; 2013
Auricularia auricula	Bread	Fan et al., 2006
Agaricus bisporus	Snack food	Singla et al., 2009
	Bread	Ahmad and Singh, 2016
	Sponge cake	Arora et al., 2017
Agaricus blazei	Yoghurt	Stojkovic et al., 2014
	Milk	Vital et al., 2017
Agaricus blazei, *Antrodia camphorata*, *Hericium erinaceus* and *Phellinus linteus*	Bread	Ulziijargal et al., 2013
Agaricus bohusii	Cream cheese	Reis et al., 2012
Boletus aereus	Pork meat product	Stojkovic et al., 2015
Boletus edulis	Beef burger	Barros et al., 2011
Cordyceps militaris	Extruded product	Zhong et al., 2017
Ganoderma amboinense, *Agaricus* spp. or *Fomes yucatensis* or mixed mushrooms	Soup and sauce	Laroche and Michaud, 2007
Laetiporus sulphureus	Chicken pate	Petrovic et al., 2014
Lentinula edodes	Baked food	Kim et al., 2011
	Noodle	Kim et al., 2008; 2009
	Frying batter	Kim et al., 2010
Pleurotus sajor-caju	Papad (An Indian snack food)	Parab et al., 2012
Schizophyllum commune	Cheese-like food	Okamura-Matsui et al., 2001
Suillus luteus and *Coprinopsis atramentaria*	Cottage cheese	Ribeiro et al., 2015
Tirmania pinoyi	Soup	Stojkovic et al., 2013

References: Giavasis, 2014b; Reis et al., 2017; Ma et al., 2018.

Moreover, some novel mushroom-based functional foods and beverages strengthening energy, vitality and immunity have been producted such as blend of burger beef with mushrooms by Sonic Drive-In, *Hericium erinaceus*-flavored ice cream by Unframed Ice Cream and functional beverage by Koios, collogen-rich beverage containing *Auricularia auricula* by Simply Auri, *Inonotus obliquus*-blended lemonade mix by Four Sigmatic and bottled tea by Sol-ti, *Ganoderma lucidum*-based bottled mushroom-chocolate beverage, cold brew drink by REBBL and probiotic-rich fermented tea by Health-Ade, and also mushroom coffee mixes by Four Sigmatic, medicinal mushroom-infused cold-brewed coffee by Love Grace, medicinal mushroom-enriched teas by Choice and cold green teas by Mudra Mushroom in recent years (URL-1, 2018).

With regard to sensory characteristics and consumer acceptance, a potential additional advantage of using mushroom polysaccharides in functional foods may be the fact that some mushroom crude extracts also contain monosodium glutamate-like components and an intense

umami taste that might improve the flavor of the final product (Tsai et al., 2006). However, bioaccessibility and bioavailability studies are required to be performed because of the changes occurred in the digestive tract (Reis et al., 2017). There is a need of *in vivo* studies to be carried out using realistic food matrices, rather than pure/crude polysaccharide solutions, before a health claim is made for the functional foods where they are added. Another concern with the food applications of mushroom polysaccharides is to determine the appropriate dose for bioactivity without any kind of toxic effect so that a food can be declared as functional (Wasser, 2011). Although some of the most studied polysaccharides such as schizophyllan and lentinan produced by mushrooms are already available and marketed as nutraceuticals (pharmaceutical formulation), their addition to food in their purified form has not been commercialized worldwide, yet (Giavasis, 2013). It is considered that some subjects of production economics, quality standardization, and stable availability need to be resolved and clinical studies on the therapeutic effects and the effective doses of functional foods need to be performed in order to allow a more global commercialization (Wasser, 2011; Giavasis, 2013).

4.2. The Use of Mushroom Extracts and Compounds in Nutraceuticals

The principal nutraceuticals found in mushrooms include: i) lipids, especially unsaturated fatty acids; ii) vitamins, such as vitamin E and vitamin C; iii) proteins, peptides and amino acids, including lectins, leucine and valine; iv) carbohydrates, especially polysaccharides (Wasser, 2014). In addition to the participation in the production of functional food, the mushroom bioactive nutraceuticals were majoringly studied and developed as dietary supplements, which could inhibit the high risking of some threaten disease and protect the body from the damage of some disadvantageous environment (Ma et al., 2018).

Medical mushrooms have been used for a long time in countries such as China and Japan, but western countries have already recognized the therapeutic properties of mushrooms. Several different polysaccharides antitumour agents have been developed from the fruiting body, mycelia, and culture medium of various medicinal mushrooms (*Agaricus bisporus*, *A. brasiliensis*, *Auricularia auricula*, *Flammulina velutipes*, Ganoderma *lucidum*, *Grifola frondosa*, *Inonotus obliquus*, *Lentinula edodes*, *Pleurotus ostreatus*, *Schizophyllum commune*, *Trametes versicolor*, and *Tricholoma matsutake*) (Prasad et al., 2015; Sokovic et al., 2016). They possess a wide range of bioactivities such as anticancerous, antibacterial, antiviral, antifungal, antidiabetic and antiinflammatory. These are also used in cardiovascular disorders. The mushrooms are usually administered orally or intraperitoneally (Sokovic et al., 2016).

Today, there are some pharmaceutical companies developing and marketing mushroom polysaccharide based extracts, drugs, and supplements for anticancer uses such as Zhejiang Fangge Pharmaceutical Co., Ltd. in China, FineCo Ltd. in South Korea, ecoNugenics, Mushroom Wisdom, MycoFormulas, Gourmet Mushrooms, Healing Edge Sciences, Inc. and Aloha Medicinal Inc. in USA, linkNUTRITION in UK, Myko San in Crotia, Pleuran, s.r.o. in Slovakia, GlycaNova AS in Norway, and Concord Mushroom Supplements in Australia (Patel and Goyal, 2012; Reis et al., 2017; URL-2, 2018).

Medicinal mushrooms are regulated by food law and not by pharmaceutical law in Germany. The main criteria that must be provided by pharmaceutical companies to the authorities before authorization are pharmaceutical quality, efficacy, and safety of the product (Lindequist, 2013). In China, there are several commercial nutraceutical products based on medicinal mushroom extracts and mushrooms biopolymers. For instance, a tonic liquor made of extracts of *Ganoderma lucidum*, *Lentinula edodes,* and *Poria cocos*, which is claimed to have anticarcinogenic, antiviral, and hypolipidemic effects, and a similar potable extract of *Cordyceps sinensis, Ganoderma lucidum*, and some medicinal herbs, which is marketed as an antiageing dietary supplement that improves cardiovascular function and reduces blood lipids. Additionally, in a traditional Chinese medicine recipe, a soup of *Auricularia auricula-judae* and *Tremella* spp. mushrooms is recommended for the treatment of hypertension and this could form the basis of a novel nutraceutical (Xu, 2001).

Today, some dietary supplements based on mushrooms are available on the market. These include i) artificially cultivated fruiting body powders, hot water or alcohol extracts of these fruiting bodies; ii) dried and pulverized preparations of the combined substrate, mycelium and primordial mushroom; iii) biomass or extracts from mycelium harvested from submerged liquid culture grown in a fermentation tank or bioreactor; iv) naturally grown, dried mushroom fruiting bodies in the form of capsules or tablets; and v) spores and their extracts (Wasser, 2014).

In the last two decades there has been an upsurge on the use of mushrooms as nutraceuticals and many edible species have been thoroughly investigated and authenticated for medicinal use. The species that have been properly analysed for medicinal value *in vivo* are *Agaricus blazei*, *A. brasiliensis*, *Cordyceps militaris*, *Flammulina velutipes*, *Ganoderma lucidum*, *Grifola frondosa*, *Hericium erinaceus*, *Lentinula edodes,* and *Pleurotus ostreatus*, (Lakhanpal and Rana, 2005; Rathore et al., 2017). In order to promote a health claim for nutraceuticals based on mushroom polysaccharides, there is a need to consider the potential influence of food processing such as heating, high-pressure and irradiation, and food physicochemical properties and composition such as pH, moisture, presence of other

biocompounds, enzymes and organic acids on the bioactivity of the medicinal biocompounds (Giavasis, 2014b).

Many commercial products derived from these mushrooms such as Lentinan from *Lentinula edodes*, Concord Sunchih and Reishi Plus from *Ganoderma lucidum*, Grifon from *Grifola frondosa* and Didanosine from *Cordyceps militaris* are available on the market (Lakhanpal and Rana, 2005). In Table 3, there are some other mushroom-based nutraceuticals and dietary supplements available in the market and their health claims. Furthermore, there have been some clinical studies on therapeutic effects of mushroom-derived nutraceuticals and dietary supplements in the literature such as *Agaricus blazei* extract, Active hexose correlated compound (AHCC), Ganopoly®, Hispidin, Hispolon, Immune Assist™, and SX-Fraction® (Reis et al., 2017).

Although recognizing the great potential of mushrooms being the basis of such formulations, some problems which affect their preparation and subsequent marketing such as safety issues, standardization, regulation, efficacy and mechanism of action, still await to be solved (Wasser, 2014). In addition there is a strong necessity of performing clinical trials for these nutraceutical products in order to be accepted by the global market (Rathore et al., 2017).

Table 3. Some commercial mushroom-based nutraceuticals/dietary supplements available on the market

Mushroom species	Product in the market	Health benefit claim
Agaricus blazei	*Agaricus blazie* capsules	Immune support supplement
Agaricus blazei, Cordyceps sinensis, Coriolus versicolor, Ganoderma lucidum, Grifola frondosa and *Lentinula edodes*	Immune Assist complete	Immunity supporter
Agaricus blazei, Cordyceps sinensis, Ganoderma lucidum and *Lentinula edodes*	CocoaMojo-cocoa powder	Immunity supporter
Agaricus blazei, Ganoderma Lucidum, Grifola frondosa, Lentinula edodes and *Pleurotus ostreatus*	Agarikon.1	Enhancement of immune system
Cordyceps sinensis	Mycoformulas Endurance™	Enhancement of intracellular energy exchange, increases oxygenation and natural endurance
Cordyceps sinensis and *Ganoderma lucidum*	Nutricafe-organic performance coffee	Increases physical endurance and helps to remove toxins from your body
Cordyceps sinensis, Ganoderma lucidum, Hericium erinaceus and *Inonotus obliquus*	Mushroom Plus	Combines some of the most popular mushrooms for an overall health boost by supporting immune system, energy levels, and cognition
Ganoderma lucidum	Pure Red Reishi - capsules Organic Reishi tablets - MRL GanoSuper - concentrated extracts for coffee	Increases the body's resistance to stress and helps it overcome all health challenges more quickly, supports the body's normal cellular immune system

Ganoderma lucidum only or combined with *Cordyceps sinensis*	GanoPoly®	Helpful for assisting recovery after illness, supports healthy nervous system and quality of sleep, promotes calmness and sense of well-being, beneficial for healthy menstrual function, supports health of the heart and blood vessels, supports a healthy immune system, protects the body against cellular damage, helps support normal cholesterol balance and blood sugar levels
Ganoderma lucidum and *Lentinula edodes*	Organic ReiShi-Gen (synergestic formulations)	Immune support supplement
Grifola frondosa	MaitakeGold 404®	Providing daily immune protection
Grifola frondosa and *Lentinula edodes*	OsteoMykon	Maintenance of bone health (indicated for osteoporosis)
Grifola frondosa and *Phellinus linteus*	Breast-Mate®	Supports healthy breast tissue
Hericium erinaceus	MycoFormulas Memory™	Memory support and daily mental clarity
Lentinula edodes	Shiitake gold - capsules	For complete physical health
Pleurotus ostreatus	Imunoglukan P4H® capsules	Immune system enhancement
Trametes versicolor	ORIVEDA® PSP-50	Immune supporter

References: Morris et al., 2016; Reis et al., 2017; URL-2, 2018; URL-3, 2018.

Despite interest in such products having grown over the years, the market in Asian countries has been exploited more. In the West, this remains a market requiring greater investment and exploitation (Giavasis, 2014a). On the European markets, products containing medicinal mushrooms are sold as food or dietary supplements and not as licensed drugs. It means that the declaration of medicinal indication is not allowed (Chang and Wasser, 2012).

5. Conclusion

Mushrooms are traditional medicines which are ignored today due to the lack of maintaining the proper standards during manufacturing, the purity system, and insufficient clinical trials. Whereas they possess bioactive molecules such as polysaccharides, terpenoids, low molecular weight proteins, glycoproteins, and antioxidants etc., which have a great role to play in boosting immune strength, lowering risks of cancers, inhibition of tumoural growth, blood sugar maintenance and much more. Therefore, it should be created awareness amongst the consumers regarding the proper utilization of this golden drug for the future. This can only be obtained by choosing the appropriate standard protocols and practices for making the drugs out of them, and comparing with available medicines around the world. Moreover, with respect to their high nutritional and therapeutic potential, mushrooms can find different applications, namely as functional foods or as a source of nutraceuticals for maintenance and promotion of health and life quality.

References

Ahmad, K., and Singh, N. (2016). Evaluation of nutritional quality of developed functional bread fortified with mushroom and dates. Clarion, 5, 23-28.

Aida, F. M. N. A., Shuhaimi, M., Yazid, M., and Maaruf, A. G. (2009). Mushroom as a potential source of prebiotics: A review. Trends in Food Science & Technology, 20, 567-575.

Arora, B., Kamal, S., and Sharma, V. (2017). Sensory, nutritional and quality attributesof sponge cake supplemented with mushroom (*Agaricus bisporus*) powder. Nutrition & Food Science. 47, 578-590.

Badalyan, S. M. (2014). Potential of mushroom bioactive molecules to develop healthcare biotech products. Proceedings of the 8th International Conference on Mushroom Biology and Mushroom Products (ICMBMP8) (pp. 373-378). New Delhi, India.

Barros, L., Barreira, J., Grangeia, C., Batista, C., Cadavez, V. A., and Ferreira, I. C. F. R. (2011). Beef burger patties incorporated with *Boletus edulis* extracts: Lipid peroxidation inhibition effects. European Journal of Lipid Science and Technology, 113, 737-743.

Beulah, G. H., Margret, A. A., and Nelson, J. (2013). Marvelous medicinal mushrooms. International Journal of Pharma and Bio Sciences, 3(1), 611-615.

Brennan, M. A., Derbyshire, E., Tiwari, B. K., and Brennan, C. S. (2012). Enrichment of extruded snack products with coproducts from chestnut mushroom (*Agrocybe aegerita*) production: Interactions between dietary fiber, physicochemical characteristics, and glycemic load. Journal of Agricultural and Food Chemistry, 60, 4396-4401.

Brennan, M. A., Derbyshire, E., Tiwari, B. K., and Brennan, C. S. (2013). Integration of β-glucan fibre rich fractions from barley and mushrooms to form healthy extruded snacks. Plant Foods for Human Nutrition, 68, 78-82.

Chang, H. H., Chien, P. J., Tong, M. H., and Sheu, F. (2007). Mushroom immunomodulatory proteins possess potential thermal/freezing resistance, acid/alkali tolerance and dehydration stability. Food Chemistry, 105(2), 597-605.

Chang, S. T., and Wasser, S. P. (2012). The role of culinary-medicinal mushrooms on human welfare with a pyramid model for human health. International Journal of Medicinal Mushrooms, 1, 95-134.

Doyon, M., and Labrecque, J. A. (2008). Functional foods: a conceptual definition. British Food Journal, 110(11), 1133-1149.

Duru, M. E., and Tel Çayan, G. (2015). Biologically active terpenoids from mushroom origin: A review. Records of Natural Products, 9(4), 456-483.

El Sohaimy, S. (2012). Functional foods and nutraceuticals-modern approach to food science. World Applied Sciences Journal, 20(5), 691-708.

Fan, L., Zhang, S., Yu, L., and Ma, L. (2006). Evaluation of antioxidant property and quality of breads containing *Auricularia auricula* polysaccharide flour. Food Chemistry, 101, 1158-1163.

Giavasis, I. (2013). Production of microbial polysaccharides for use in food. In: Microbial Production of Food Ingredients, Enzymes and Nutraceuticals, Cambridge: Woodhead Publishing.

Giavasis, I. (2014a). Bioactive fungal polysaccharides as potential functional ingredients in food and nutraceuticals. Current Opinion in Biotechnology, 26, 162-173.

Giavasis, I. (2014b). Polysaccharides from medicinal mushrooms for potential use as nutraceuticals. In: Polysaccharides Natural Fibers in Food and Nutrition, Boca Raton, Florida: CRC Press.

Gunde-Cimerman, N., and Plemenitaš, A. (2001). Hypocholesterolemic activity of the genus *Pleurotus* (Jacq.: Fr.) P. Kumm. (Agaricales s. I., Basidiomycetes). International Journal of Medicinal Mushrooms, 3(4), 395-397.

Howlett, J. (2008). Functional foods: From science to health and claims. Belgium: ILSI Europe.

Jeong, S. C., Koyyalamudi, S. R., Jeong, Y. T., Song, C. H., and Pang, G. (2012). Macrophage immunomodulating and antitumor activities of polysaccharides isolated from *Agaricus bisporus* white button mushrooms, Journal of Medicinal Food, 15, 58-65.

Kim, Y. W., Kim, K. H., Choi, H. J., and Lee, D. S. (2005). Anti-diabetic activity of beta-glucans and their enzymatically hydrolyzed oligosaccharides from *Agaricus blazei*, Biotechnology Letters, 27(7), 483-487.

Kim, S. Y., Kang, M. Y., and Kim, M. H. (2008). Quality characteristics of noodle added with browned oak mushroom (*Lentinus edodes*). Korean Journal of Food and Cookery Science, 24, 665-671.

Kim, S. Y., Chung, S. I., Nam, S. H., and Kang, M. Y. (2009). Cholesterol lowering action and antioxidant status improving efficacy of noodles made from unmarketable oak mushroom (*Lentinus edodes*) in high cholesterol fed rats. Journal of the Korean Society for Applied Biological Chemistry, 52, 207-212.

Kim, J., Lim, J., Bae, I. Y., Park, H. G., Lee, G. H., and Lee, S. (2010). Particle size effect of *Lentinus edodes* mushroom (chamsongi) powder on the physicochemical, rheological, and oil-resisting properties of frying batters. Journal of Texture Studies, 41, 381-395.

Kim, J., Lee, S. M., Bae, I. Y., Park, H. G., Lee, G. H., and Lee, S. (2011). (1→3) (1→6)-β-glucan-enriched materials from *Lentinus edodes* mushroom as a high-fibre and low-calorie flour substitute for baked foods. Journal of the Science of Food and Agriculture, 91, 1915-1919.

Kothari, D., Patel, S., and Kim, S. K. (2018). Anticancer and other therapeutic relevance of mushroom polysaccharides: A holistic appraisal. Biomedicine & Pharmacotherapy, 105, 377-394.

Lakhanpal, T. N., and Rana, M. (2005) Medicinal and nutraceutical genetic resources of mushrooms. Plant Genetic Resources: Characterization and Utilization, 3(2), 288-303.

Laroche, C., and Michaud, P. (2007). New developments and prospective applications for β-(1, 3) glucans. Recent Patents on Biotechnology, 1, 59-73.

Lindequist, U. (2013). The merit of medicinal mushrooms from a pharmaceutical point of view. International Journal of Medicinal Mushrooms, 15(6), 517-523.

Liu, J., DU, C., Wang, Y., and Yu, Z. (2015). Anti-fatigue activities of polysaccharides extracted from *Hericium erinaceus*. Experimental and Therapeutic Medicine, 9(2), 483-487.

Ma, G., Yang, W., Zhaoa, L., Peib, F., Fanga, D., and Hua, Q. (2018). A critical review on the health promoting effects of mushroomsnutraceuticals. Food Science and Human Wellness, 7, 125-133.

Martins, N., Morales, P., Barros, L., and Ferreira, I.C.F.R. (2016). The increasing demand for functional foods. In: Wild Plants, Mushrooms and Nuts: Functional Food Properties and Applications, pp. 1-13. John Wiley & Sons, Ltd.

Morris, H. J., Llaurado, G., Beltran, Y., Lebeque, Y., Bermudez, R. C., Garcia, N., Gaime-Perraud, I., and Moukha, S. (2016). The use of mushrooms in the development of functional foods, drugs or nutraceuticals. In: Wild Plants, Mushrooms and Nuts: Functional Food Properties and Applications, pp. 123-157. John Wiley & Sons, Ltd.

Okamura-Matsui, T., Takemura, K., Sera, M., Takeno, T., Noda, H., Fukuda, S., and Ohsugi, M. (2001). Characteristics of a cheese-like food produced by fermentation of the mushroom *Schizophyllum commune*. Journal of Bioscience and Bioengineering, 92, 30-32.

Pandya, U., Dhuldhaj, U., and Sahay, N. S. (2018). Bioactive mushroom polysaccharides as antitumor: An overview. Natural Product Research, 13 p.

Parab, D. N., Dhalagade, J. R., Sahoo, A. K., and Ranveer, R. C. (2012). Effect of incorporation of mushroom (*Pleurotus sajor-caju*) powder on quality characteristics of Papad (Indian snack food). International Journal of Food Sciences and Nutrition, 63, 866-870.

Pardeshi, B. M., and Pardeshi, P. M. (2009). The edible medicinal mushrooms as supportive natural nutrients: Study of nonvolatile mineral contents of some edible medicinal mushrooms from India; eastern remedies for modern western maladies. Proceedings of 5th International Medicinal Mushroom Conference (pp. 514-18). Mycological Society of China, Nantong, China.

Patel, S., and Goyal, A. (2012). Recent developments in mushrooms as anti-cancer therapeutics: A review. Biotechnology, 2, 1-15.

Pereira, E., Barros, L., Martins, A., and Ferreira, I. C. F. R. (2012). Towards chemical and nutritional inventory of Portuguese wild edible mushrooms in different habitats. Food Chemistry, 130, 394-403.

Perera, P. K., and Li, Y. (2011). Mushrooms as a functional food mediator in preventing and ameliorating diabetes. Functional Foods in Health & Disease, 1(4), 133.

Petrovic, J., Stojkovic, D., Reis, F. S., Barros, L., Glamoclija, J., Ciric, A., Ferreira, I.C., and Sokovic, M. (2014). Study on chemical, bioactive and food preserving properties of *Laetiporus sulphureus* (Bull.: Fr.) Murr. Food & Function, 5, 1441-1451.

Petrovic, J., Glamoclija, J., Stojkovic, D., Ciric, A., Barros, L., Ferreira, I. C., and Sokovic, M. (2015). Nutritional value, chemical composition, antioxidant activity and enrichment of cream cheese with chestnut mushroom *Agrocybe aegerita* (Brig.) Sing. Journal of Food Science and Technology, 52, 6711-6718.

Prasad, S., Rathore, H., Sharma, S., and Yadav, A. S. (2015). Medicinal mushrooms as a source of novel functional food. International Journal of Food Science, Nutrition and Dietetics, 04(5), 221-225.

Rahi, D. K., and Malik, D. (2016). Diversity of mushrooms and their metabolites of nutraceutical and therapeutic significance. Journal of Mycology, 18 pp.

Rathee, S., Rathee, D., Rathee, D., Kumar, V., and Rathee, P. (2012). Mushrooms as therapeutic agents. Revista Brasileira de Farmacognosia Brazilian Journal of Pharmacognosy, 22(2), 459-474.

Rathore, H., Prasad, S., and Sharma, S. (2017). Mushroom nutraceuticals for improved nutrition and better human health: A review. PharmaNutrition 5, 35-46.

Regula, J., Krejpcio, Z., and Staniek, H. (2010). Bioavailability of iron from cereal products enriched with dried shittake mushrooms (*Lentinula edodes*) as determined by iron regeneration efficacy method in female rats. Journal of Medicinal Food, 13(5), 1189-1194.

Regula, J., Krejpcio, Z., and Staniek, H. (2016a). Iron bioavailability from cereal products enriched with *Pleurotus ostreatus* mushrooms in rats with induced anaemia. Annals of Agricultural and Environmental Medicine, 23(2), 310-314.

Regula, J., Sulibursk a, J., and Siwulski, M. (2016b). Bioavailability and digestibility of nutrients from the dried oyster culinary-medicinal mushroom, *Pleurotus ostreatus* (Agaricomycetes): In vivo experiments. International Journal of Medicinal Mushrooms, 18(8), 681-688.

Reis, F. S., Stojkovic, D., Sokovic, M., Glamoclija, J., Ciric, A., Barros, L., and Ferreira, I. C. F. R. (2012). Chemical characterization of *Agaricus bohusii*, antioxidant potential and antifungal preserving properties when incorporated in cream cheese. Food Research International, 48, 620-626.

Reis, F. S., Martins, A., Vasconcelos, M. H., Morales, P., and Ferreira, I. C. F. R. (2017). Functional foods based on extracts or compounds derived from mushrooms. Trends in Food Science & Technology, 66, 48-62.

Ribeiro, A., Ruphuy, G., Lopes, J. C., Dias, M. M., Barros, L., Barreiro, F., and Ferreira, I. C. F. R. (2015). Spray-drying microencapsulation of synergistic antioxidant mushroom extracts and their use as functional food ingredients. Food Chemistry, 188, 612-618.

Roupas, P., Keogh, J., Noakes, M., Margetts, C., and Taylor, P. (2012). The role of edible mushrooms in health: Evaluation of the evidence. Journal of Functional Foods, 4, 687-709.

Ruiz-Rodriguez, A., Santoyo, S., and Soler-Rivas, C. (2009). Antioxidant properties of edible mushrooms. Functional Plant Science and Biotechnology, 3(Special Issue 1), 92-102.

Singh, R. (2017). A review on different benefits of mushrooms. IOSR Journal of Pharmacy and Biological Sciences, 12(1), Ver. II (Jan. - Feb.2017), 107-111.

Singla, R., Ghosh, M., and Ganguli, A. (2009). Phenolics and antioxidant activity of a ready-to-eat snack food prepared from the edible mushroom (*Agaricus bisporus*). Nutrition & Food Science, 39, 227-234.

Smith, J. E., Rowan, N. J., and Sullivan, R. (2002). Medicinal mushrooms: a rapidly developing area of biotechnology for cancer therapy and other bioactivities. Biotechnology Letters, 24, 1839-1845.

Sokovic, M., Ćirić, A., Glamočlija, J., and Stojković, D. (2016). The bioactive properties of mushrooms. In: Wild Plants, Mushrooms and Nuts: Functional Food Properties and Applications, pp. 83-122. John Wiley & Sons, Ltd.

Stojkovic, D., Reis, F. S., Ferreira, I. C. F. R., Barros, L., Glamoclija, J., Ciric, A., Nikolić, M., Stević, T., Giveli, A., and Soković, M. (2013). *Tirmania pinoyi*: Chemical composition, *in vitro* antioxidant and antibacterial activities and *in situ* control of *Staphylococcus aureus* in chicken soup. Food Research International, 53, 56-62.

Stojkovic, D., Reis, F. S., Glamoclija, J., Ciric, A., Barros, L., van Griensven, L. J., Ferreira, I.C., and Sokovic, M. (2014). Cultivated strains of *Agaricus bisporus* and *A. brasiliensis*: Chemical

characterization and evaluation of antioxidant and antimicrobial properties for the final healthy product-natural preservatives in yoghurt. Food & Function, 5, 1602-1612.

Stojkovic, D. S., Reis, F. S., Ciric, A., Barros, L., Glamoclija, J., Ferreira, I. C. F. R., and Sokovic, M. (2015). *Boletus aereus* growing wild in Serbia: Chemical profile, in vitro biological activities, inactivation and growth control of food-poisoning bacteria in meat. Journal of Food Science and Technology, 52, 7385-7392.

Taofiq, O., Martins, A., Barreiro, M. F., and Ferreira, I.C.F.R. (2016a). Anti-inflammatory potential of mushroom extracts and isolated metabolites. Trends in Food Science & Technology, 50, 193-210.

Taofiq, O., González-Paramása, A. M., Martins, A., Barreiro, M. F., and Ferreira, I.C.F.R. (2016b). Mushrooms extracts and compounds in cosmetics, cosmeceuticals and nutricosmetics - A review. Industrial Crops and Products, 90, 38-48.

Tong, M.H., Chien, P.J., Chang, H. H., Tsai, M. J., and Sheu, F. (2008). High processing tolerances of immunomodulatory proteins in Enoki and Reishi mushrooms. Journal of Agricultural and Food Chemistry, 56(9), 3160-3166.

Tsai, S. Y., Weng, C. C., Huang, S. J., Chen, C. C., and Mau, J. L. (2006). Nonvolatile taste components of *Grifola frondosa*, *Morchella esculenta* and *Termitomyces albuminosus* mycelia. LWT/Food Science and Technology, 39(10), 1066-1071.

Ulziijargal, E., Yang, J. H., Lin, L. Y., Chen, C. P., and Mau, J. L. (2013). Quality of bread supplemented with mushroom mycelia. Food Chemistry, 138, 70-76.

URL-1: https://www.trendhunter.com/trends/, (Date of access: 01 October 2018).

URL-2: https://linknutrition.com/collections/boosts/products/mushroom-plus, (Date of access: 01 October 2018).

URL-3: https://www.alohamedicinals.com, (Date of access: 30 September 2018).

Valverde, M. E., Hernandez-Perez, T., and Paredes-Lopez, O. (2015). Edible mushrooms: Improving human health and promoting quality life. International Journal of Microbiology, 14p.

Vaz, J. A., Heleno, S. A., Martins, A., Almeida, G. M., Vasconcelos, M. H., and Ferreira, I. C. F. R. (2010). Wild mushrooms *Clitocybe alexandri* and *Lepista inversa*: in vitro antioxidant activity and growth inhibition of human tumour cell lines. Food and Chemical Toxicology, 48, 2881-2884.

Villares, A., Mateo-Vivaracho, L., and Guillamón, E. (2012). Structural features and healthy properties of polysaccharides occurring in mushrooms. Agriculture, 2, 452-471.

Vital, A. C. P., Croge, C., Gomes-da-Costa, S. M., and Matumoto-Pintro, P. T. (2017). Effect of addition of *Agaricus blazei* mushroom residue to milk enriched with Omega-3 on the prevention of lipid oxidation and bioavailability of bioactive compounds compoundsafter in vitro gastrointestinal digestion. International Journal of Food Science and Technology, 52, 1483-1490.

Wasser, S. P. (2010). Medicinal mushroom science: History, current status, future trends, and unsolved problems. International Journal of Medicinal Mushrooms, 12, 1-16.

Wasser, S. P. (2011). Current findings, future trends, and unsolved problems in studies of medicinal mushrooms. Applied Microbiology and Biotechnology, 89, 1323-1332.

Wasser, S. P. (2014). Medicinal mushroom science: Current perspectives, advances, evidences, and challenges. Biomedical Journal, 37, 345-356.

Wasser, S. P., and Weis, A. L. (1999a). Medicinal properties of substances occurring in higher Basidiomycetes mushrooms: Current perspectives (Review). International Journal of Medicinal Mushrooms, 1(1), 31-62.

Wasser, S. P., and Weis, A. L. (1999b). Therapeutic effects of substances occurring in higher Basidiomycetes mushrooms: A modern perspective. Critical Reviews in Immunology, 19, 65-96.

Wasser, S. P., Sokolov, D., Reshetnikov, S.V., and Timor-Tismenetsky, M. (2000). Dietary supplements from medicinal mushrooms: Diversity of types and variety of regulations. International Journal of Medicinal Mushrooms, 2(1), 19 p.

Xu, Y. (2001). Perspectives on the 21st century development of functional foods: Bridging Chinese medicated diet and functional foods. International Journal of Food Science & Technology, 36, 229-242.

Xu, X., Yan, H., Chen, J., and Zhang, X. (2011). Bioactive proteins from mushrooms. Biotechnology Advances, 29(6), 667-674.

Yang, J. H., Lin, H. C., and Mau, J. L. (2002). Antioxidant properties of several commercial mushrooms. Food Chemistry, 77(2), 229-235.

Yokota, M. E., Frison, P. S., Marcante, R. C., Jorge, L. F., Valle, J. S., Dragunski, D.C., Colauto, N. B., and Linde, G. A. (2016). Iron translocation in *Pleurotus ostreatus* basidiocarps: Production, bioavailability, and antioxidant activity. Genetics and Molecular Research, 15(1), 10 p.

Zhang, M., Cuia, S. W., Cheung, P. C. K., and Wang, Q. (2007). Antitumor polysaccharides from mushrooms: A review on their isolation process, structural characteristics and antitumor activity. Trends in Food Science & Technology, 18, 4-19.

Zhong, L., Zhao, L., Yang, F., Yang, W., Sun, Y., and Hu, Q. (2017). Evaluation of anti-fatigue property of the extruded product of cereal grains mixed with *Cordyceps militaris* on mice. Journal of the International Society of Sports Nutrition, 14, 15.

Thermal Storage Food Tank Model By Renewable Energy

Tuğba GÜNGÖR ERTUĞRAL[1]

[1]Giresun Üniversity, Şebinkarahisar Applied Science Highschool, Giresun, Türkiye

* **Corresponding Author:**: tugba.gungor@giresun.edu.tr

Abstract

Phase change material (PCM) caprylic acid / 1-dodecanol binary system provides thermal stabilization in double-walled food storage tanks. The eutectic liquid between the tank walls helps to thermal stabilization by latent heat storage. The experimental results show that the caprylic acid/1-dodecanol binary system presents eutectic point. The eutectic melting temperature (Tem) is 6.52 °C and latent heat of eutectic mixture (ΔHem) is 171.06 J g^{-1}. The corresponding mass fraction of 1-dodecanol in eutectic mixture is 30%. The eutectic melting temperature and latent heat of phase change of eutectic mixture have not obvious variations after 60 and 120 thermal cycles, which proves that the eutectic mixture has good thermal stability [Zuo et al., 2011]. Phase change material (PCM) caprylic acid / 1-dodecanol binary system good thermal stability for liquid food tanks. It is very important to 6-15°C cold storage for food.

Keywords: Caprylic acid/1-dodecanol, phase change material, latent heat storage, food tank.

1. Introduction

Packaging and storage can play active role to temperature controlling of perishable products. However, standard materials for product packaging (plastic, cardboard or wood) usually have limited thermal buffering capacity. One possible approach to enhance this capacity and maintain the product at a desired temperature is thermal energy storage by phase change materials (PCM). PCM is a substance that undergoes phase transition (e.g. fusion/crystallization) at specific temperature or narrow range of temperature. It can have high enthalpy of phase transition and then is capable of storing and releasing large amounts of energy (Rentas et al., 2004). The surplus heat can absorbed by the phase transition of the material so that augmentation of the product temperature could be limited (Hoang et al., 2015). Usually, limited thermal insulation and poor thermal buffering capacity of standard food tanks.

Tank materials (fiberglass, steel, plasticetc.) protection for foodstuffs (microbiological, chemical and physical) and correction of a handikapd food safety during temperature changes by thermal energy supplied from outside. Different classes of materials; including hydrated salts, paraffin waxes, fatty acids, the eutectics of organic and non-organic compounds and polymers have considered as potential PCMs.

PCMs can divided into three main groups based on the temperature ranges over which the TES phase transition occurs:

(i) Low temperature PCMs – with phase transition temperatures below 15 °C usually used in air conditioning applications and food industry;

(ii) Mid temperature PCMs, the most popular – with phase transition temperatures in the range 15–90 °C with solar, medical, textile, electronic and energy-saving applications in building design;

(iii) High temperature PCMs with a phase transition above 90°C developed mainly for industrial and space applications.

PCMs can be classified by their mode of phase transition: gas–liquid, solid–gas, solid–liquid and solid–solid systems (Mondal, 2008).

Caprylic acid / 1-dodecanol eutectic mixture is a good PCM and phase change time is 12000 sec.(Karaipekli A. and Sarı A., 2014).

In this study, double-walled food tanks could be filled with phase change material between the two walls and that could provide thermal insulation between 6-15°C for a certain period during transportation and storage at instantaneous temperature elevations.

For this purpose, latent heat storage material caprylic acid / 1-dodecanol eutectic mixture PCM investigated. Eutectic mixture can store this heat energy as latent heat and protect the food material

in the tank by providing thermal stabilization for a certain period of time when temperature difference between the tank walls increases.

1.1. Performance Tests and Evaluation of Milk Cooling Tanks

Power requirement of the cooling system; amount of milk, desired temperature , cooling time and heat losses. Direct cooling method, average of 0.5 kW of electrical power is required to cool down to 8 °C within 3 hours of 100 liters of raw milk at 35-36 °C. Specific energy of cooling food tank can calculate with formula (1). Heat loss is dependent on ambient temperature, tank structure and facility load. Direct cooling method specific energy consumption 1.34 kWh per 100 liters milk at 10 °C ambient temperature and 100% load. (Ayık et al., 2015)

$$E_T = (E_{first} + E_{last}).n/(V_a.2) \quad (1)$$

Equation: E_T, specific energy requirement; E_{first}, first milking energy consumption; E_{last}, final wastage energy consumption; V_a, tank declaration volume; n is the number of bottles in tank emptying. (Günhan et al., 2006)

2. Material and Method

Double-walled food tank solid works 2016 modeling by caprylic acid / 1-dodecanol PCM, caprylic acid/1-dodecanol

2.1. Experimental Methods

2.1.1. Thermal Analysis

A power compensation DSC (Pyris Diamond, PerkinElmer), equipped with a mechanical cooling accessory (Intracooler II, PerkinElmer), was used for thermal analysis. Temperature calibration was done using n-decane and indium (melting points at −29.66 and 156.60 ℃, respectively) (Fig 1.). Heat flow calibration was done using indium (heat of fusion, 28.45 J g^{-1}. Nitrogen was used as the purge gas at a flow rate of 20 mL min^{-1}. Samples were subjected to three consecutive cooling and heating cycles between −40 and 60 ℃ at a scanning rate of 10℃ min^{-1}(Table 1). The last cooling and heating cycle was used for the determination of the transition temperatures and enthalpies. For the annealing experiments, the frozen samples were heated at 10 ℃ min^{-1} to the annealing temperature, held at that temperature for controlled periods of time, and then cooled back to −40 ℃ at 10 ℃ min^{-1} (Fig 2.) [Zuo et al., 2011].

2.1.2. Accelerated Thermal Cycle Test

The accelerated thermal cycle test was conducted to study the changes in melting temperature and latent heat of phase change of the caprylic acid/1-dodecanol eutectic mixture after repeated numbers of melt/freeze cycle. The experimental equipment consisted of a thermostatic chamber with a temperature controller. The caprylic acid/1-dodecanol eutectic mixture was put in a stainless steel container with a lid. The eutectic mixture was heated above the melting temperature and then cooled below the solidifying temperature. The above procedure was performed consecutively until the number of thermal cycle would be 60 and 120. Then DSC thermal analysis was performed on the cycled and uncycled eutectic mixtures (Table 2) (Zuo et al., 2011).

2.1.3. Double-walled Food Tank Solid Works Modeling

Double-walled food tank model containing caprylic acid / 1-dodecanol eutectic mixture was drawn with Solid Works 2016 (Fig. 3).

2.2. Shapes, Tables and Equations

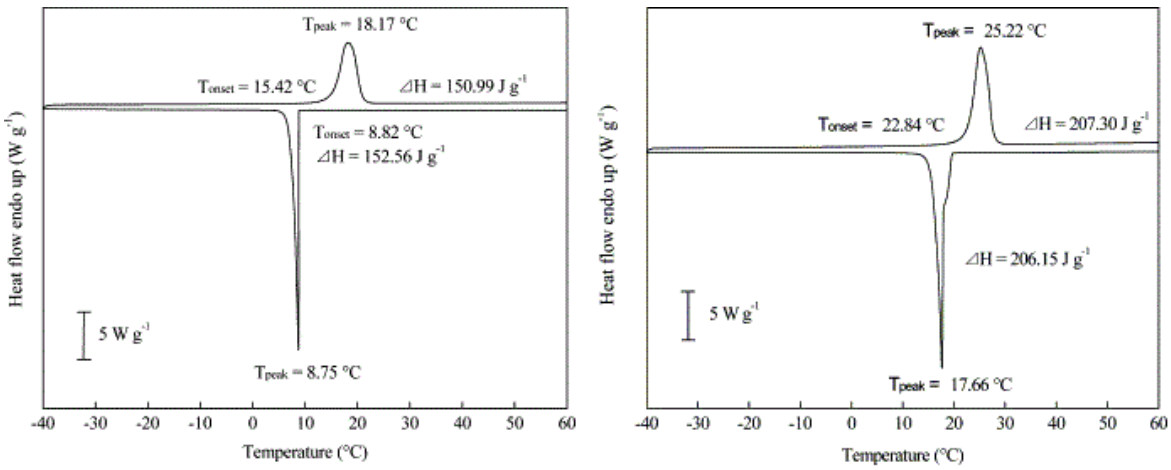

Fig. 1. DSC curves of caprylic acid (a), 1-dodecanol (b) Cooling and heating rate 10 ℃ min^{-1} (Zuo et al., 2011).

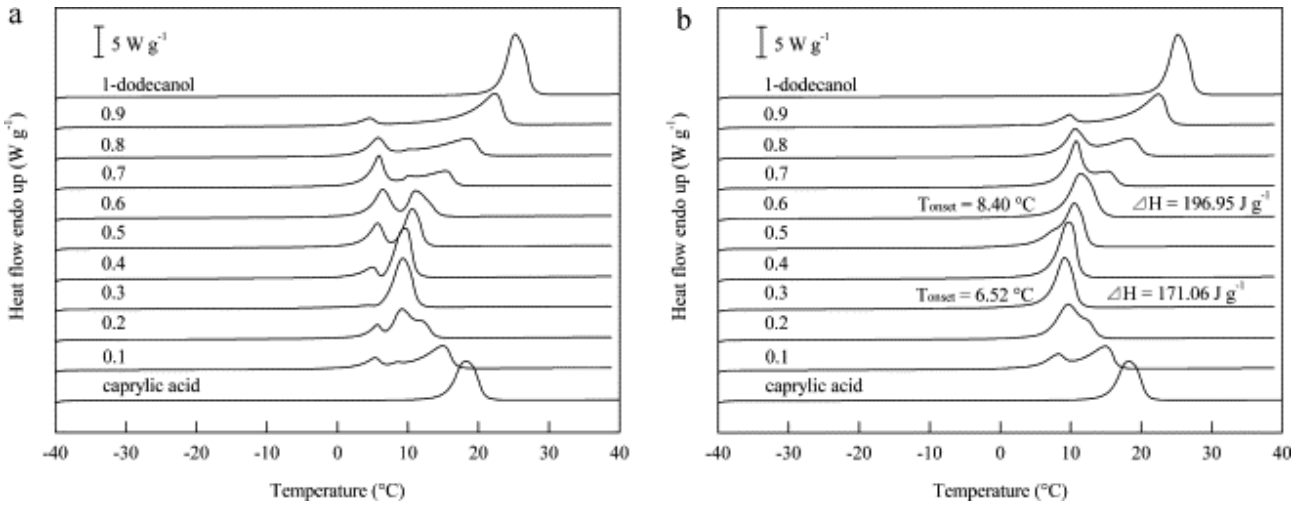

Fig . 2. DSC curves of the caprylic acid/1-dodecanol binary system as a function of the mass fraction of 1-dodecanol. Heating rate: 10 ◦Cmin−1. (a) Without annealing, (b) after annealing (Zuo et al., 2011).

.

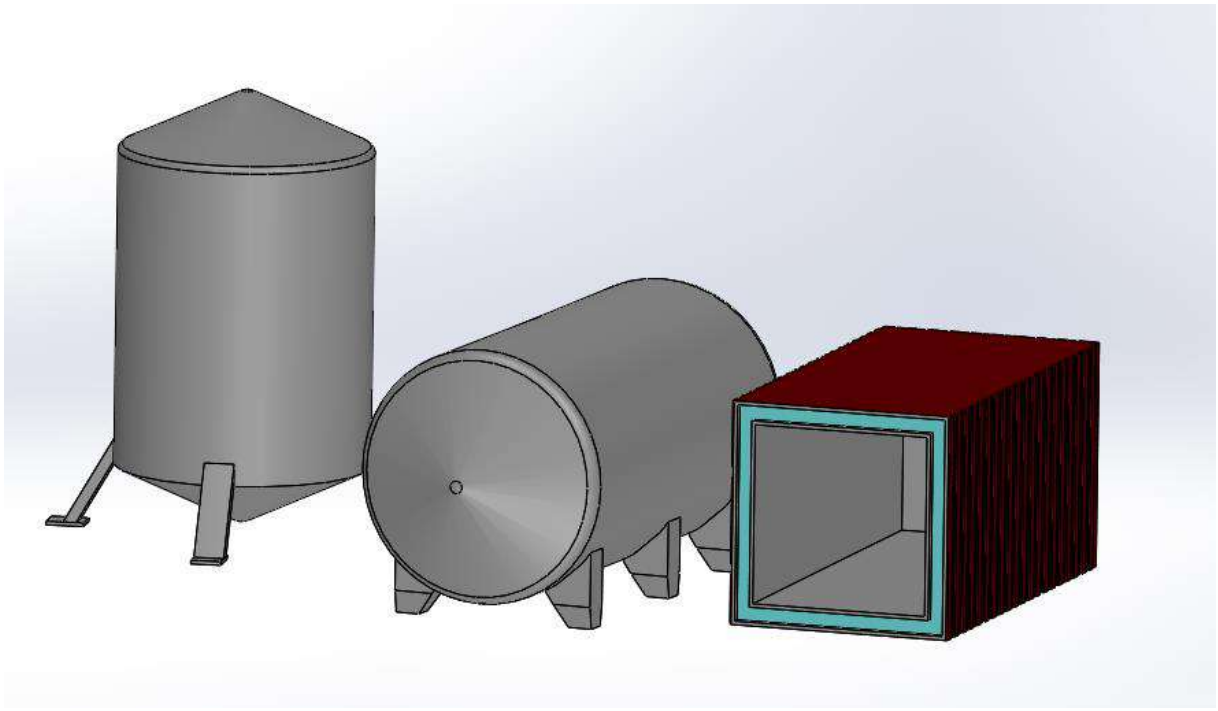

Fig. 3. PCM-filled double-walled food tank model

Table1. Peak temperatures of melting of caprylic acid, 1-dodecanol and the binary mixtures (Zuo et al., 2011).

Mass fraction of 1-dodecanol	Peak temperature T_{peak} (°C)	
	First	Second
0.00		18.17
0.10	8.29	14.91
0.20	9.65	12.68
0.30		9.15
0.40		9.72
0.50	7.29	10.52
0.60		11.41
0.70	10.81	15.15
0.80	10.62	18.29
0.90	9.86	22.47
1.00		25.22

Table 2. Thermal properties of the caprylic acid / 1-dodecanol eutectic mixture after cycles (Zuo et al., 2011).

Number of cycle	Tem (°C)	ΔHem (J/ g^{-1})
0	6.52	171.06
60	6.50	170.89
120	6.24	167.96

3. Results and Discussion

Thermal stability of caprylic acid/1-dodecanol eutectic mixture (Table 2) shows the onset melting temperature (Tem) and latent heat of melting (Hem) of caprylic acid/1-dodecanol eutectic mixture after thermal cycles. After 60 and 120 thermal cycles, the melting temperature of the eutectic mixture changes as −0.02 and −0.28 ℃, and the latent heat of melting changes as −0.17 and −3.1 J g^{-1}, respectively. Therefore, the caprylic acid/1-dodecanol eutectic mixture has good thermal stability in terms of the changes in its melting temperature and latent heat (Zuo at al., 2011).

The metastable state was identified and eliminated by thermal treatment, and the phase diagram of the caprylic acid/1-dodecanol binary system was constructed. The onset melting temperature of the eutectic mixture is 6.52 °C and the corresponding mass fraction of 1-dodecanol is 30% (Fig 2.). The latent heat of melting of the eutectic mixture is 171.06 J g^{-1}. After 60 and 120 thermal cycles, the changes in the melting temperature and the latent heat of

melting of eutectic mixture are in acceptable level (Zuo at al., 2011). Therefore, the caprylic acid/1-dodecanol eutectic mixture has potential for cold storage. For this reason, caprylic acid / 1-dodecanol PCM can be preservative by filling between the walls in double-walled tanks for food cold storage.

4. Conclusion

Caprylic acid / 1-dodecanol PCM can store average ΔH 180 Jg^{-1} heat for food industry, especially when it applied to milk, fruit juice tanks or double-walled tanks used in meat, fruit and vegetable industries (Fig. 3). When the ambient temperature rises to 8°C, it starts to change the phase and keeps the temperature over 8°C. Especially, milk and dairy products transplanted between 5-15°C and fruit juices transported and stored at 4-10°C very important to microbial load control. PCM-filled double-walled food tanks provide unfueled transport for 1 or 2 hour and that provide 2 hours non-fueled transport for a long time.

References

Ayık, M., Çilingir, İ., and Avcıoğlu, A.O. (2015)Hayvancılıkta Mekanizasyon, Ankara: Ankara Üniversitesi Ziraat Fakültesi Yayınları.

Günhan T., Demir V., and Bilgen H., (2006). Experimental Determination of Performances of Farm Type Bulk Milk Coolers. *Tarım Makinaları Bilimi Dergisi, 2 (4), 369-379*

Hoang ,H.M., Leducq D., Perez-Masia R., Lagaron J.M., Gogou E., Taoukis P., and Alvarez G., (2015). Heat transfer study of submicro-encapsulated PCM plate for food packaging application. *International journal of refrigeration 52,15 1e160*

Karaipekli A., Sarı A., (2014).Capric acid and palmitic acid eutectic mixture applied in building wallboard for latent heat thermal ener gy storage. *Journal of scientific and industrial research, 66, 470-476*

Mondal, S., (2008). Phase Change Materials for Smart Textiles-An Overview. *Applied Thermal Engineering, 28, 1536–1550.*

Rentas, F.J., Macdonald, V.W., Houchens, D.M., Hmel, P.J., and Reid, T.J., (2004). New insulation technology provides next generation containers for “iceless” and lightweight transport of RBCs at 1 to 10℃ in extreme temperatures for over 78 hours. *Transfusion 44 (2), 210e216.*

Zuo, J., Li W., and Weng L.(2011) Thermal performance of caprylic acid/1-dodecanol eutectic mixture as phase change material (PCM). *Energy and Buildings, 43, 207–210*

Usability Of Waste Position Some Tree Shells

Zehra Can[1]*, Hüseyin Serencam[2]

[1]Bayburt University, Applied Sciences, Bayburt, Türkiye; zehracan@gmail.com
[2]Bayburt Üniversity, The food Engineering, Bayburt, Türkiye; hserencam@bayburt.edu.tr

Abstract

As a natural and renewable resource, wood plays an important role in the world economy, especially in the field of construction and furniture. Environmental conditions and destruction problems of conventional chemical protectors containing metals have forced researchers to explore more environmentally friendly methods and technologies. The current practice and development of new technologies is limited by laboratory and field testing of preserving with natural products and the lack of conformity with generally defined quality standards. In this study was evaluated usability of waste position some tree shells. In the study, were prepared methanolic extracts of tree shells and determined by antioxidant and antimicrobial activity of tree shells. As a result, it was determined that tree shells have high antioxidant and antimicrobial activity. Waste position some tree shells can be using many areas and can get rid of the waste situation.

Keywords: Tree shells; antioxidant; antimicrobial; environment

1. Introduction

The crust is a protective layer that surrounds the branches, bodys and roots of the tree and is divided into two layers, the outer crust and the inner crust. The inner shell is made up of young shell cells produced by cinnamon and transmits nutrients (sugar solutions) produced on the leaves to the growth points of the tree. As the tree grows around its periphery and its floem cells age, they die slowly, pushing outward. Dead float cells are defined as crusts or shells and protect immature cells near the cambium from fungi, insects, birds and other harmful substances and serve as insulation against cold air and extreme temperature and drought. Macroscopic appearance of the shell varies according to tree species and age. For example; Although the shell thickness can reach up to 30 cm in the fleecy and Douglas fir, it is more beech and fruity. The shape of the shell can vary according to the tree species and can be flat, cracked or fibrous (Erdin ve Bozkurt, 2013).

The purpose of this work is to ensure that the idle tree shell can be used in different areas. Our study was to examine the antioxidant capacity and antimicrobial activity of tree shell.

2. Materyal and Method

2.1. Chemicals

All the reagents used were of analytical grade. Trolox was supplied by AppliChem (Darmstadt, Germany). Folin–Ciocalteu's phenol reagent and TPTZ were purchased from Fluka Chemie GmbH (Switzerland). Sodium nitroprusside, iron(III) chloride hexahydrate ($FeCl_3.6H_2O$), 2,4,6-Tris(2-pyridyl)-s-triazine (TPTZ), iron(II) sulfate heptahydrate ($FeSO_4.7H_2O$), were purchased from Sigma-Aldrich (St. Louis, MO, USA). Sodium acetate, ferric chloride, and glacial acetic acid were obtained from Merck. LC syringe filters (RC-membrane, 0.2 μm) were obtained from Sartorius Minisart RC 15, Sartorius (Darmstadt, Germany).

2.2. Extract Preparation of tree shell

The samples were extracted using the method described previously by Can (2016). The dried powdered samples (5 g) were extracted three times with 50 mL of 100% methanol for 24 h at room temperature on an orbital shaker (Heidolph Promax 2020, Schwabach, Germany). The supernatant was then used to determine the antioxidant activity tests.

2.3. Determination of total phenolic content (TPC) of tree shell

The TPC was determined using the Folin-Ciocalteau method following Slinkard ve Singleton (1971). Briefly, 680 µL of distilled water, 400 µL of 0.5 N Folin-Ciocalteu reagent, 20 µL of various concentrations of gallic acid and samples were mixed and vortexed. After a 3 minute-incubation, 400 µL of Na_2CO_3 (10%) solution was added and vortexed. Then, the mixture was incubated for 2 hours at 20 °C with interrupted shaking. After that, the absorbance of the mixture was measured at 760 nm using a spectrophotometer. Results were expressed as mg gallic acid equivalents (GAE) per g sample weight (mg GAE/g DW).

2.4. Determination of total flavonoid content (TFC) of tree shell

The TFC was determined using by Fukumoto ve Mazza (2000). Briefly, 0.5 mL samples, 0.1 mL of 10% $Al(NO_3)_3$ and 0.1 mL of 1 M $NH_4.CH_3COO$ were added to a test tube and incubated at room temperature for 40 minutes. Then, the absorbance was measured against a blank at 415 nm. Results were expressed as mg quercetin equivalents (QE) per g sample weight (mg QE/ g DW).

2.5. Condase Tannin content (CT) of tree shell

Condensed tannins were determined according to the method of small modified Julkunen-Titto (1985). An aliquot (25 µl) of each extract or standard solution (tannic acids) was mixed with 750 µl of 4% vanillin (prepared with MeOH) and then 375 µl of conc. HCl were added. The well-mixed solution was incubated at room temperature in the dark for 20 min. The absorbance against blank was read at 500 nm. (+)-Catechin was used to make the standard curve (0.05–1 mg/ml). The results were expressed as mg catechin equivalents (CE)/g extract.

2.6. Determination of antioxidant capacity (Ferric reducing antioxidant power) (FRAP) assay of tree shell

The antioxidant capacity was determined using ferric reducing antioxidant power. The FRAP assay was conducted as described by Benzie ve Strain (1996). The fresh FRAP reagent was made by adding 100 ml of 0.3 M acetate buffer pH 3.6, 10 ml of 10 mM TPTZ solution in 40 mM HCl and 10 ml of 20 mM $FeCl_3$ in a ratio of 10:1:1 and 12 ml of distilled water at 37 °C. In brief, the reaction mixture consisting of 100 µL of the sample and 3 mL of freshly prepared FRAP reagent was incubated at 37 °C for 4 min and the absorbance was measured at 593 nm aganist a control. Results were expressed as µmol $FeSO_4.7H_2O$/g DW).

2.7. Antimicrobial activity testing of tree shell

Antimicrobial activities of the sample was tested by Mueller Hinton (MH) agar well diffusion method. Bacterial suspension was prepared in 5 mL of sterile isotonic sodium chloride solution from a fresh culture (18 h) and turbidity was adjusted to 0.5 McFarland. The microbial suspension was spread on MH agar (LABM; United Kingdom) using sterile cotton swabs. The wells were opened with a diameter of 6 mm in the agar using the wide end of a blunted sterile Pasteur pipette. Each well was filled with 50 µL of sample extract, positive control (commercial Ampicillin, Gentamicin, Cefotaxime, Tetracycline or Amphotericin B solutions conveniently for each microorganisim) and negative control (DMSO). The cultures were incubated at 37°C for 24 hours. Activity was determined by visual inspection and measurement of the diameter of clear inhibition zones around the agar-wells.

3. Results and Discussion

In this study, tree shell phenolic compounds were determined as total polyphenol content, total flavonoid content, condase tannin content and for antioxidant activity FRAP methods and also antimicrobial acticity. Total polyphenol mg (GAE/g), total flavonoid mg (QE/g), condase tannin mg (CE/g) FRAP (µmol $FeSO_4 7H_2O$/g) of tree shell are presented in Table 1.

Phenolic compounds have been reported to be associated with a number of healthy promoting properties, including potential antimicrobial agents (Cowan, 1999). In this study, total polyphenolic content 321.50 mg (GAE/g sample), total flavoid content 6.60 mg (QE/ g sample), condase tannin content 4.79 mg (KE/ g sample) of tree shell. The tree shell extract ferric reducing effects that are related to the antioxidant capacity. The FRAP result showed that Table 1. It was determined that the tree shell has high antioxidant capacity.

Table 1. Antioxidant activity of tree Shell methanolic extract

Sample	Total Polyphenol mg (GAE/g sample)	TotalFlavoid mg(QE/g sample)	Condase Tannin mg(KE/gsample)	FRAP (µmol$FeSO_4.7H_2O$/g)
Tree Shell	321.50±1.04	6.60±0.23	4.79±0.03	3525.0±15.63

Agar well diffusion test results showed a positive antimicrobial activity fort he most of the methanolic extract tested aganist different bacteria Table 2. Tree shell used in the study

showed inhibitory activity against Klebsiella pneumonia, Listeria monocytogenes and Staphylococcus aureus microorganisms. The tree shell has a higher impact on shell microorganisms and inhibited Pseudomonas aeruginosa, Candida albicans and Proteus mirabilis microorganisms. In one study, new diterpenoid components were structurally isolated from the root shell of Azadirachta indica (Meliaceae) and they were reported to exhibit antibacterial activity against various gram-positive and gram-negative organisms (Ara ve ark., 1989). According to these results, it can be said that especially wood bark is natural agents showing antimicrobial properties against bacteriella and yeast.

Table 2. Antimicrobial activity of the tree shell methanolic extract by agar well diffusion

Material	**Agar Well Diffusion (mm zone diameter)**									
	S. aureus	*E. coli*	*P. aeruginosa*	*E. faecalis*	*C. albicans*	*C. Parapsilosis* **	*S.* Typhimurium	*P. mirabilis*	*K. pneumoniae*	*L. monocytogenes*
Tree Shell	4	0	0.2	0	0.1	0	0	4	3	1
Ampisilin	> 30	16 - 17	…	> 30	…	…	27	…	…	…
Gentamisin	…*	…	21-22	…	…	…	…	…	21	…
Amphoterisin B	…	…	…	…	30	…	…	…	…	…
Tetrasiklin	…	…	…	…	…	…	…	…	…	25
Sefotaksim	…	…	…	…	…	…	…	37	…	…

Referance

Ara, I., Siddiqui, B.S., Faizi, S., and Siddiqui, S. (1989). "Structurally novel diterpenoid constituents from the stem bark of Azadirachta indica (Meliaceae)." Journal of the Chemical Society, Perkin Transactions 1(2): 343-345.

Benzeie, I.F.F., and Strain, J.J. (1996). The ferric reducing ability of plasma (FRAP) as a measure of ‘‘antioxidant power”: The FRAP assay, Journal of Analytical Biochemistry 239 70-76.

Cowan, M.M. (1999). Plant products as antimicrobial agents. Clinical Microbiology Reviews. 12(4), 564-582.

Erdin, N., and Bozkurt, A.Y. (2013). Odun anatomisi, İstanbul Üniversitesi Yayınları, ISBN: 987-975-404-932-9, sayfa 4-5.

Fukumoto, L.R., and Mazza, G. (2000). Assessing antioxidant and prooxidant activities of phenoliccompounds. Journal of Agricultural Food Chemistry 48, 3597-3604.

Julkunen-Titto, R. (1985). Phenolic constituents in the leaves of northern willows: methods for the analysis of certain phenolics. Journal of Agricultural and Food Chemistry. 33(2), 213-217.

Slinkard, K., and Singleton, V.L. (1977). Total phenol analyses: Automation and Comparison with Manual Methods. American Journal of Enology Viticulture 28, 49-55.

Use of Hurdle Effect Technology in Meat Industry

Duygu BALPETEK KÜLCÜ [1*], Zeliha KAYA [1], Ümit GÜRBÜZ [2,3], Cavidan DEMİR GÖKIŞIK [1]

[1]Giresun University, Engineering Faculty, Food Engineering Department, Giresun, Turkey; duygu.balpetek@giresun.edu.tr

[2]Selçuk University, Faculty of Veterinary Medicine, Food Hygiene and Technology Department, Konya/ Turkey

[3]Kyrgyz -Turkish Manas University, Faculty of Veterinary Medicine, Department of Food Hygiene and Technology, Bishkek/ Kyrgyzstan

[*] **Corresponding Author:** duygu.balpetek@giresun.edu.tr

Abstract

Hurdle technology is a process that is applied to improve the microbiological stability and sensory quality of foods as well as the nutritional and economic characteristics of foods and also to extend the shelf life of the food. Among the hurdles used for this purpose are; aw (water activity), pH, preservative (nitrite, nitrate etc.), temperature, competitive microorganisms, and redox potential. The aim of the hurdle technology is to increase the overall quality of food by implementing barriers intelligently.

The duration of preservation is extended by eliminating microorganisms that cause deterioration in the meat and meat products or by stopping growing, preventing external factors that can cause product degradation, and disabling the enzymes present in the product. The number and type of microorganisms that is present in the meat depends on many factors. These have a very important role in the hurdle effect technology; aw, pH, temperature, oxygen and preservatives. The number of microorganisms of the meat to be processed into the product affects the preservation period of the product. A low number of microorganisms in meat and meat products is an increasing factor in the resistance of the products. The impact of hurdle in the food industry has long been known, and the field of application has been expanded by developing information on this topic. In this review, hurdle technology, that finds application and research field in food industry, has been discussed with the researches made in recent years.

Keywords: Hurdle Technology, Meat, Microbiology.

1. Introduction

Hurdle Technology is a promising method for destroying or controlling undesirable microorganisms, such as pathogens or deterioration microorganisms. Controlling these microorganisms will also provide more safety foods and / or longer shelf life (Leistner, 1985).

Hurdle technology can be seen as a method by using a combination of factors that will prevent the growth of more than one microorganism. These factors are considered as ‘hurdles" that microorganisms must overcome to sustain their vitality and activity in food. It is aimed to completely eliminate or harmless the microorganisms in the food which will be consumed by using the right combination of the hurdles (Leistner and Gorris, 1995).

Hurdle technology or combined methods consist of a mixture of two or more low-level protective methods (hurdle). In order to make the product more resistant to microorganisms, the effect of a single method is not mentioned in practice, but the synergy of the protective factors used together. Therefore, sensory changes in hurdle technology are at the lowest level. These changes are more acceptable than the products obtained with commonly used protective methods (Aguilera and Chirife, 1994).

After the benefits of the hurdle effect has been understood very well, the hurdle technology has been derived by using combined methods, and hurdles are begun to be used combined with each other to develop the microbial stability and get better quality characteristics for the foods as well as their nutritional properties and economic characteristics. Therefore, it can be said that aim of the hurdle technology is to improve the overall quality of foods by using mix of hurdles. Hurdle technology has been researched and its usage area has been expanded over the years (Leistner, 2000).

1. Hurdle Effect Technology in Food

The most important hurdles benefited in the food industry to preserve the food and provide safety of the food are acidity (pH), redox potential (Eh), water activity (aw), temperature (high or low), preservatives (e.g., sorbate, nitrite, sulfite) and competitive microorganisms (e.g., lactic acid bacteria). However, there are already described more than 60 potential hurdles for safety of foods, which improve the stability and the quality of the food products, but this list is not complete yet so number of of possible hurdles for food preservation will be increased over time (Leistner,2000).

While some hurdles (e.g., Maillard reaction products) affect only the safety and the quality of foods, some of them improve the flavor of the food products because they have antimicrobial properties. Hurdles intensity is another significant factor should be taken into consideration, because the same hurdle could have a negative or a positive impact depending on its intensity. For example, moderate chilling is useful for their shelf life but it is detrimental to some foods at the unsuitable low temperature (Evrendilek, 2010).

If the intensity of a specific hurdle in a food is very low, it should be strengthened to obtain high safety and longer shell life, but if the food quality is deteriorated, it should be lowered. By this arrangement, hurdles in foods can be kept in the optimum level considering safety and total quality of the food product (Leistner, 2000).

2. Hurdle Technology in Meat Industry

Meat is defined as the muscle of the animals which is used as food. An important term 'fresh meat' can be defined as meat has not undergone any treatment other than chilling to ensure preservation after obtained from recently processed animals and existed as vacuum-packed meat or packed in controlled-atmospheric gases (Aymerich et al., 2008).

Meat is a valuable food by having rich foodstuff that is a big disadvantage because of providing a suitable environment for proliferation of meat spoilage microorganisms and food-borne pathogens. Therefore it is necessary to apply adequate preservation technologies in order to preserve its safety and quality. Food safety and keeping it at a certain level is a top priority among authorities and consumers worldwide (Zhou, 2010).

In a study on the hot dogs, while water activity (aw) and acidity (pH) hurdle were used as the intrinsic hurdles, processing temperature (F value) hurdle and storage temperature (t value) hurdle used as the extrinsic hurdles. Researchers have stated that a significant reduction in nitrite content on meat products, such as hot dogs, is possible only by using combined treatments (hurdle technology) sensibly without nutritional, microbiological, technological or sensory problems (Jafari et al., 2007).

In a research on fresh sausages, showed that the shelf life of fresh sausages can be extended from 4 days to 32 days by combining 3 hurdle factors, consisting of vacuum packaging which reduces the potential of redox (93±5%), use of potassium sorbate as a preservative and cold preservation method at 4-8 C (Jafari, 2007).

In a study of a model system evaluating the relationship between hurdle technology and microorganism's production in meat products, the effects of various combinations of different temperatures (from 17 ºC to 27 ºC), different water activity values and sodium nitrite addition on Escherichia coli were investigated. In the study, it was determined that these hurdle factors have a complex relationship, and several hurdle factors in the hurdle technology were pointed out together (Rödel and Scheuer, 2007).

In another research, researchers applied a process by using a combination of several hurdles to shrimps for the preparation of shelf-stable, ready-to-eat shrimps. The hurdles are employed to cooked and marinated shrimps with reduced water activity (0.85 ± 0.02), packaging and γ-irradiation (2.5kGy). Microbiological analysis showed that a dose-dependent reduction in total viable count and Staphylococcus species. In non-irradiated samples a visible mold growth was seen within 15 days of storage at ambient temperature (25 ± 3°C). Researchers could not see significant change in textural properties and sensory qualities of the food product and managed to keep ready-to-eat shrimps microbiologically safe and sensory acceptable for 2 months storage at ambient temperature (Kanatt, 2006).

Researchers have found that microbiologically significant control of these products and their sensory qualities are maintained for up to 9 months when they are working with hurdle technology parameters that they produce with low water activity, irradiation and vacuum packaging in spiced mutton and spiced chicken products with intermediate-moisture that are ready for consumption (Kanatt, 2002).

Charqui is a tropical meat, exists in medium moisture environment, formulated using hurdle technology in another research with a concept described by Leistner. In this study, sodium nitrite, salt, packaging and dehydration hurdles are sequentially used to prevent deteriorating microorganisms with the choice of desirable micro biota. Salt and dehydration processes cause significant changes in the ultra-structural level of the muscle and causes changes in the texture profile of charquis (Shimokomaki, 1998).

Si-Raw is an uncooked meat (raw, smoked meat fermented with steamed rice) produced by Taiwan's aboriginal people. To prevent food poisoning or Botulism intoxication, new monitoring methods for production based on the hurdle technology have been research. New methods have been explored to reduce the aw (water activity) and pH values in the product to be able to control the microbial growth, by including sodium hypophosphite, citric acid, lactic acid bacteria inoculum or plum paste separately to meat with steamed rice and salt. The study showed that when critical points are controlled appropriately, such fermented meat products

(Si-Raw) should be safe because either low aw value or reduced aw value and reduced pH combination inhibits the development of unwanted microorganisms (Chen, 2002).

Thomas et al. developed a pork sausage which has longer shelf-life by using hurdle technology, and evaluated the quality of sausages during storage phase at ambient temperature (37 ± 1C). The used hurdles are low pH, low water activity, vacuum packaging and reheating after packaging. The vacuum packaging is also examined by dipping in potassium sorbate solution prior to packaging. Incorporation of hurdles significantly reduced emulsion stability, cooking efficiency, moisture and fat percentage, yellowness and hardness while increasing protein percentage and redness (Thomas et al., 2008).

Hurdle technology reduced quality deterioration as indicated by Ph and tyrosine values during storage. Coliform, anaerobic, lactobacillus, and Staphylococcus aureus counts were reduced by about 1 log reduction in the total number of bacteria with different inhibitors. PH, aw and reheating hurdles inhibited yeast and mold growth up to third day while dipping in an additional 1% potassium sorbate solution inhibited their development throughout 9 days of storage. Despite initially low sensory influences, treated hurdle technology sausages have acceptability in the range from "very good" to "good" for initial six days (Thomas et al., 2008).

3. Conclusion

While hurdle technology is used today in many countries and in many foods to provide maximum microorganism control, it is also important that the sensory qualities of food and the maximum preservation of its natural structure in the use of barrier factors. Increasing consumer awareness, especially in recent years, are increasingly increasing concerns, such as food residue, allergens and scammers.

For this reason, preventive chemical additives in foodstuffs and hurdle factors such as extreme ultrasound, high hydrostatic pressure, natural additives and preservatives are increasingly important for thermal processes such as pasteurization and sterilization. In the future, it will be inevitable to move towards the hurdle technologies that develop with the use of antimicrobials, preservative and new barrier factors appropriate to the natural structures of foods, which require higher technology by changing the barrier technologies applied today.

References

Aguilera, J.M., and Chirife, J. (1994). Combined methods for the preservation of foods. In Latin America And CYTED-D Project. J Food Eng., 22(1-4), 433-44.

Aymerich, T., Picouet, P.A., and Monfort, J.M. (2008). Decontamination technologies for meat products. Meat Science, 78, 114-129.

Chen, M.T., Liny, S., Tsai, H.T., and Kuo, H.L. (2002). Efficiency of hurdle technology applied to raw cured meat (si-raw) processing. Asian-aust. J. Anim. Sci., 15(11), 1646-1652.

Evrendilek, G.A. Birden fazla koruma yöntemiyle gıdaların korunması. Gıda Mikrobiyolojisi. 1. Baskı. Ankara: Efil Yayınevi; 2010. P. 351-65.

Jafari, M., and Emam-djomeh, Z. (2007). Reducing nitrite content ın hot dogs by hurdle technology. Food Control, 18(12), 1488-93.

Kanatt, S. R., Chawla, S. P., Chander, R., and Sharma, A. (2006). Development of shelf-stable, ready-to-eat (rte) shrimps (*penaeus ındicus)* using g-radiation as one of the hurdles. Lwt, 39, 621–626.

Kanatt, S. R., Chawla, S.P., Chander, R., and Bongirwar, D.R. (2002). Shelf-stable and safe intermediatemois- ture meat products using hurdle technology. J Food Protect, 65(10), 1628-31.

Leistner, L. (2000). Basic aspects of food preservation by hurdle technology. International Journal Of Food Microbiology, 55, 181–186.

Leistner, L. (1995). Principles and applications of hurdle technology. G. W. Gould (Ed.), New Methods Of Food Preservation © Springer Science+business Media Dordrecht.Charqui Meats Are Hurdle Technology Meat Products.

Leistner, L. (1985). Hurdle technology applied to meat products of the shelf stable product and ıntermediate moisture food types. Properties Of Water In Foods, 309-310.

Leistner, L., and Gorris, L.G.M. (1995). Food preservation by hurdle technology. Trends In Food Science & Techn., 6, 41-46.

Rödel, W., and Scheuer, R. (2007). Recent results on the hurdle technology - measuring of combined hurdles. Fleischwirtschaft. 87(9), 111-5.

Shimokomaki, M., Franco, B. D. G. M., Biscontini, T. M., Pinto, M. F., Terra, N. N., and Zorn, T. M. T. (1998). Charqui meats are hurdle technology meat products. Food Reviews International, 14(4), 339-349.

Thomas, R., Anjaneyulu, A.S.R.,and Kondaiah, N. (2008). Development of shelf stable pork sausages using hurdle technology and their quality at ambient temperature (37 ± 1 ºC) storage. Meat Sci., 79: 1-12.

Zhou, G.H., Xu, X.L., and Liu, Y. (2010). Preservation technologies for fresh meat – A review. Meat Sci., 86, 119-128.

β-Glucans: An Important Bioactive Molecule of Edible and Medicinal Mushrooms

Sanem BULAM[1*], Nebahat Şule ÜSTÜN[2], Aysun PEKŞEN[3]

[1]Giresun University, Faculty of Engineering, Department of Food Engineering, Giresun, Turkey; sanem.bulam@giresun.edu.tr

[2]Ondokuz Mayıs University, Faculty of Engineering, Department of Food Engineering, Samsun, Turkey; sustun@omu.edu.tr

[3]Ondokuz Mayıs University, Faculty of Agriculture, Department of Horticulture, Samsun, Turkey; aysunp@omu.edu.tr

[*] **Corresponding Author:** sanem.bulam@giresun.edu.tr

Abstract

Edible mushrooms are important for their dietary value and their biologically active and health promoting compounds such as polysaccharides, polysaccharopeptides and polysaccharide-protein complexes. Mushroom β-glucans such as β-glucan, Schizophyllan, Ganoderan, Lentinan and Pleuran are the components of the cell wall. They consist of glucopyranose molecules linked through β (1→3), β (1→4) or β (1→6) linkages. The mushroom β-glucans are not digested in human gastrointestinal tract and are thus considered as a potential source of prebiotics. β-glucans possess profound health promoting properties like speeding up the transit of bowel contents, increasing fecal bulk and frequency, consequently protecting the body from colon cancer, diverticular diseases and irritable bowel syndrome. They stimulate the immune system by having immunomodulatory, antitumour, antioxidant activities and are identified as biological response modifiers. Mushroom β-glucans differ in their nutraceutical effect due to the difference in their molecular masses, solubility, degree of polymerization, their structures and helical conformation. Various mushroom β-glucans are available as pure extracts in the market which are used as therapeutic agents, however, no commercialized functional products are available which have been enriched with mushroom β-glucans. Furthermore, it has a great potential to be used as an ingredient in the near future in various food industries, such as breakfast cereals, sport nutrition products, dairy products, bakery such as biscuits and breads, salad dressings and fat replacer. The aim of this review is to present information on β-glucans of edible and medicinal mushrooms, emphasize their benefits and the usage potential in the functional food and nutraceuticals.

Keywords: Mushrooms, β-glucan, bioactivity, functional, nutraceutical, food industry.

1. Introduction

β-glucans are polysaccharides of D-glucose monomers linked through β-glycosidic bonds. The structures of β-glucans and chemically modified β-glucans were given in Figure 1.

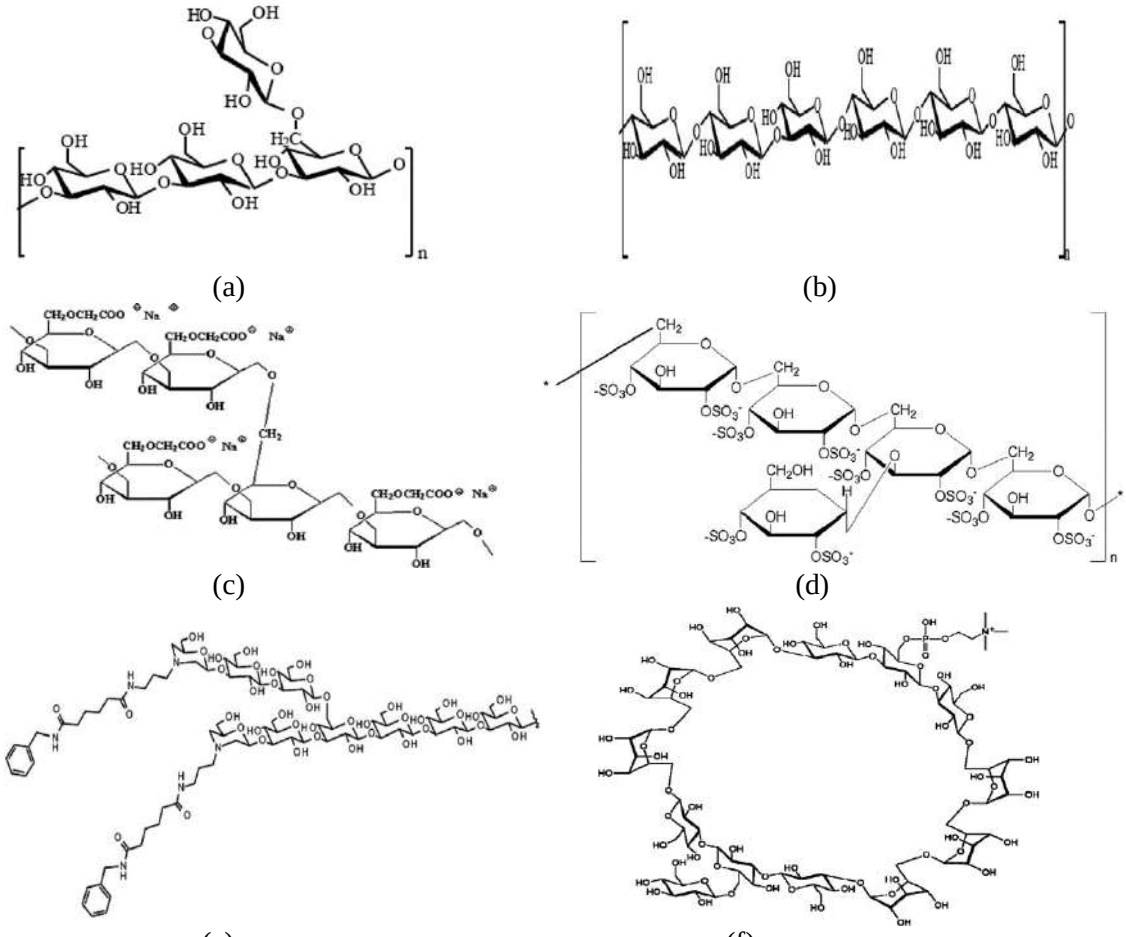

Figure 1. The structures of β-glucans and chemically modified β-glucans. (a) (1→3) β-glucans with ramifications β (1→6); (b) (1→3) β-glucans with ramifications β (1→4); (c) CM β-glucan; (d) Sulfated β-glucan; (e) Aminated β-glucan; (f) Cyclic glucan (Zhu et al., 2016).

As a kind of dietary fiber (DF), β-glucan could be found in a variety of natural sources such as yeast, mushrooms, bacteria, algae, barley and oat (Zhu et al., 2015). β-glucan exhibits a broad spectrum of biological activities including antitumour, immune-modulating (Rieder and Samuelsen, 2012), antiaging, antimicrobial, antioxidant and antiinflammatory properties. β-glucans have attracted attention because of their physical and chemical properties over the years. β-glucans from different sources and with different molecular weights have different

biological activities (Du and Xu, 2014). Fungal β-glucan has been shown to be effective as an immune system booster and an antitumour substance (Du et al., 2015). The results of clinical research indicate that the presence of β-glucan is linked to the production and activation of macrophages, NK-cells, T-cells, B-cells from the body's natural defense system (Lindequist et al., 2005).

2. Mushroom β-glucans

Mushroom β-glucan is a carbohydrate polymer derived from the cell wall of mushrooms. β-glucan is known as biological response modifier (BRM), which refers to the ability to up-regulate and down-regulate the response of biological systems (Brown and Gordon, 2003; Novak and Vetvicka, 2009).

Mushroom β-glucans such as Schizophyllan, Ganoderan, Lentinan and Pleuran are the components of the cell wall. They consist of glucopyranose molecules linked through β (1→3), β (1→4) or β (1→6) linkages. Especially in Japan and China, Pleuran from *Pleurotus ostreatus*, Lentinan from *Lentinula edodes*, Schizophyllan from *Schizophyllum commune*, Grifolan (MD-fraction) from *Grifola frondosa* and Krestin from *Trametes versicolor* (PSK and PSP) in addition to the major cancer therapies like surgical operation, radiotherapy and chemotherapy are in clinical use for the adjuvant tumour therapy (immunotherapy) (Lindequist et al., 2005; Chan et al., 2009; Novak and Vetvicka, 2009).

β-glucans are also present in many other mushrooms such as *Auricularia auricula*, *Calocybe indica* (Calocyban), *Flammulina velutipes*, *Ganoderma lucidum* (Ganoderan/ Ganopoly), *Grifola frondosa*, and *Pleurotus abalones* (Lindequist et al., 2005; Villares et al., 2012; Zhu et al., 2015).

2.1. β-glucan Amounts in Mushrooms

Important medical mushrooms containing β-glucan as bioactive compound are seen in Table 1. The β-glucan contents of the mushrooms vary between 0.22 and 0.53 g/100 g on dry weight basis. According to Manzi and Pizzoferrato (2000), *Pleurotus pulmunarius* seemed to be the richest source of fungal β-glucans and it has been reported that *L. edodes* contains high levels of β-glucans in the soluble fraction. Camelini et al. (2005) found that *Agaricus*

brasiliensis had higher (1→6)-β-glucan ratio and (1→3)-β-glucan increased with the maturation of fruiting bodies.

Table 1. Important medicinal mushrooms with β-glucans as bioactive components (Chan et al., 2009).

Mushroom species	Common name	β-glucan structure	Type of β-glucan
Agaricus blazei	Brazilian sun-mushroom, Himematsutake mushroom	Protein bound β-1,6-glucan	*Agaricus* polysaccharides
Coprinus comatus	Shaggy ink cap, lawyer's wig, or shaggy mane	β-1,3-glucan	*Coprinus* polysaccharides
Coriolus versicolor	Yun Zhi	Protein bound β-1,3;1,6-glucan	PSP (polysaccharide peptide) PSK (polysaccharide-Kureha or polysaccharide-K, krestin)
Ganoderma lucidum	Lingzhi, Reishi	β-1,3;1,6-glucan	*Ganoderma* polysaccharides, Ganopoly
Grifola frondosa	Maitake mushroom	β-1,3;1,6-glucan with xylose and mannose	Maitake D-Fraction
Lentinula edodes	Shiitake mushroom	β-1,3;1,6-glucan	Lentinan
Pleurotus ostreatus	Oyster mushroom, píng gû	β-1,3-glucan with galactose and mannose	Pleuran
Schizophyllan commune	Brazilian mushroom	β-1,3;1,6-glucan	Schizophyllan (SPG) or sizofiran

It was determined that Bracket fungi *Trametes versicolor, Piptoporus betulinus* or *Phlebia tremellosa* contained more than 50% β-glucans and in *Boletus edulis* (Bull. ex Fr., stipe part) or *Piptoporus betulinus* (Bull. ex Fr.) Karst. the amount was more than 50 g/100 g dw. In most of the wild mushrooms analysed, the β-glucan contents were significantly higher in stipes than in caps (Sari et al., 2017). Özcan and Ertan (2018) have determined that *Boletus edulis* is the highest β-glucan containing wild mushroom (13.93%). It was followed by *Cantharellus cibarius* and *Hydnum repandum* with 12.89 and 12.84% contents, respectively. Synytsya et al. (2008) working with *Pleurotus* spp. mushrooms found that the β-glucan content of the pilei was between 20.4-39.2% and the content of the stems was between 35.5-50.0%. The results of a study comparing the β-glucan content of some wild mushrooms (Sari et al., 2017) is presented in Table 2.

Table 2. β-glucan content of some wild mushrooms (not dividable in cap and stipe parts).

Mushroom species	Dry matter (%)	β-glucans (g/100g dm)	% β-glucans/ all glucans
Auricularia auricula (L.) Underwood	91.276	41.755±4.644	99.096
Fomes fomentarius (L.) Fr.	86.122	22.495±2.329	90.186
Grifola frondosa (Dicks. ex Fr.) Gray	92.783	25.991±3.643	83.761
Laetiporus sulphureus (Bull. ex Fr.) Murr.	89.627	47.006±6.517	89.345
Phlebia tremellosa (Schrad.) Nakasone & Burds.	96.547	53.555±2.452	98.572

Piptoporus betulinus (Bull. ex Fr.) Karst.	90.825	51.801±4.024	95.659
Trametes versicolor (L.) Lloyd.	87.892	60.788±11.795	99.337

2.2. Bioactive Properties of β-glucans in Mushrooms

Mushrooms polysaccharides having β-linkage have been demonstrated a boost in the human immune system and the modulation of the immunological response under certain conditions, thus they are commonly termed as biological response modifiers (BRM). As the result of the activation of the host's immune system, these polysaccharides show significant antitumour, antiviral and antimicrobial activities besides their other effects (Villares et al., 2012). A number of studies have been carried out on β-glucans that have a health-enhancing effect in various important ways such as antitumour and immunomodulatory (Table 3), antitumour, antiviral (Borchers et al., 2004; Moradali et al., 2007), cardiovascular (Wasser and Weis, 1999), liver protective, antiinflammatory (Lindequist et al., 2005), radioprotective (Pillai and Devi, 2013), antidiabetic (Kim et al., 2005), antioxidant (Deng et al., 2012), antibacterial (Beattie et al., 2010), and antiobesity activities (Zhang et al., 2013). Antitumour activity (Deng et al., 2012; Ren et al., 2012) and immunemodulating activity (Wasser, 2002) of mushroom β-glucans have been documented in the previous reviews. Basically, their health-promoting abilities are influenced by the molecular mass, branching configuration, conformation, and chemical modification of the polysaccharides (Ren et al., 2012). In terms of biological activity, β-1,3-D-glucans and β-1,6-D-glucans contained in oyster, shiitake, split gill, and himematsutake mushrooms, as well as other Basidiomycetes, are considered to be the most effective (Rop et al., 2009).

Table 3. Some mushroom β-glucans with antitumour and immunomodulatory activities (Zhang et al., 2007; Novak and Vetvicka, 2008; Kothari et al., 2018).

Mushroom species	Type of β-glucan	Character of polymer	Degree of branching
Agaricus blazei	β-glucomannan	Branched	-
Dictyophora indusiata	T-4-N, T-5-N	Branched	-
Ganoderma lucidum	Ganoderan	Branched	-
Grifola frondosa	Grifolan	Branched	0.31-0.36
Inonotus obliquus	Xylogalactoglucan	Branched	-
Laminaria spp.	Laminaran	Linear	-
Lentinula edodes	Lentinan	Branched	0.23-0.33
Pleurotus ostreatus	Pleuran (HA-glucan)	Branched	0.25
Poria cocos	Pachymaran	Linear	0.015-0.020
Schizophyllum commune	Schizophyllan	Branched	0.33
Sclerotinia sclerotiorum	Sclerotinan (SSG)	Branched	0.50

2.3. Extraction and Production of Mushroom β-glucans

The methods used to extract and produce β-glucans from various edible/medicinal mushrooms are given in Table 4.

Table 4. Production/extraction process of β-glucans from various edible/medicinal mushrooms.

Mushroom species	Production/Extraction process	References
Agaricus bisporus	Ultrasonic-assisted extraction, precipitation with ethanol, centrifugation	Tian et al., 2012
	Lyophilization, milled and submitted to successive cold and hot aqueous extraction	Smiderle et al., 2013
Agaricus brasiliensis	Sequentially extracted with 350 ml water, concentrated, dialyzed and DEAE-cellulose column chromatography	Camelini et al., 2005
	Lyophilization, milled and submitted to successive cold and hot aqueous extraction	Smiderle et al., 2013
Astraeus hygrometricus	Aqueous extraction, DEAE cellulose bag and Sepharose 6B column	Chakraborty et al., 2004
Boletus edulis	The estimation of non-starch glucans was based on the difference between glucose contents after total acidic hydrolysis of glucans and specific enzymatic hydrolysis of α-1,4-glucans	Özcan and Ertan, 2018
Boletus erythropus	Water extraction, centrifugation, DEAE Trisacryl M column and S 400 HR column	Chauveau et al., 1996
Botryosphaeria rhodina	β-glucan production were monitored in a stirred-tank bioreactor	Crognale et al., 2007
Cantharellus cibarius	The estimation of non-starch glucans was based on the difference between glucose contents after total acidic hydrolysis of glucans and specific enzymatic hydrolysis of α-1,4-glucans	Özcan and Ertan, 2018
Flammulina velutipes	Successive hot extraction with water and KOH and submitted to freeze-drying	Smiderle et al., 2006
Ganoderma lucidum	Extraction using dilute NaOH solution and Sephadex G-15 gel-filtration chromatography	Kao et al., 2012; Nie et al., 2013
Paenibacillus polymyxa	Seed culture was supplemented with carbon source to induce glucan production	Jung et al., 2007
Pleurotus eryngii	The estimation of non-starch glucans was based on the difference between glucose contents after total acidic hydrolysis of glucans and specific enzymatic hydrolysis of α-1,4-glucans	Synytsya et al., 2008
	Washing with ethanol and distilled water, extraction with boiling water, incubation with α-amylase, chemical deproteinization, dialization and lyophilization	Synytsya et al., 2009
Pleurotus ostreatus	The estimation of non-starch glucans was based on the difference between glucose contents after total acidic hydrolysis of glucans and specific enzymatic hydrolysis of α-1,4-glucans	Synytsya et al., 2008
	Washing with ethanol and distilled water, extraction with boiling water, incubation with α-amylase, chemical deproteinization, dialization and lyophilization	Synytsya et al., 2009
	Lyophilization, using of methanolic extraction, cold water, hot water, hot aqueous NaOH solutions, enzyme protease, and ethanol precipitation	Palacios et al., 2012
Ramaria botrytis	Hot water extraction followed by treating NaOH	Bhanja et al., 2014
Schizophyllum commune	Seed culture preparation, optimization of fermentation medium and schizophyllan production	Kumari et al., 2008

Termitomyces eurhizus	Hot alkaline extraction, centrifugation, DEAE cellulose bag and freeze dry	Chakraborty et al., 2006

The detection methods of β-glucan from mushrooms are summarized as: (1) enzymic method or McCleary method (Megazyme kit), (2) enzymelinked immunosorbent assay (ELISA) method, (3) fluorimetric method with aniline blue, and (4) colorimetric method with Congo red (Zhu et al., 2015).

2.3.1 Extraction and Production of β-glucans from Fruiting Bodies of Mushrooms

Kim et al. (2005) extracted β-glucan from the fruiting bodies of *Agaricus blazei* using hot water for 3 h. Bhanja et al. (2014) extracted and isolated two water-insoluble glucans from fruiting bodies of *Ramaria botrytis*. Extraction in hot or boiling water is the most common and convenient method for extracting water-soluble fungal polysaccharides (Yan et al., 2014).
Liu et al. (2014) obtained a purified β-glucan by precipitating a hot-water extract from fruiting bodies of *G. lucidum* with 20% (V/V) ethanol. The total carbohydrate content was 95.9% in prepared β-glucan.

2.3.2. Extraction and Production of β-glucans from the Mycelia of Mushrooms

Kim et al. (2009) provided a method for mass production of β-glucan from *S. commune*, comprising subjecting mycelia of *S. commune* to liquid culture with an addition of a synthetic adsorbent. In another study, a neutral polysaccharide, GLSA50-1B, was isolated from sporoderm-broken spores of *G. lucidum*, by hot-water extraction, graded ethanol precipitation, anion-exchange chromatography, and gel permeation chromatography (Dong et al., 2012). Kim et al. (2013) demonstrated generation of high β-glucan producing mutant strains of *Sparassis crispa*, additional culture optimization further increased β-glucan productivity of the mutant strains. Recently, Park et al. (2014) enhanced the β-glucan content in the sawdust-based cultivation of cauliflower mushroom (*Sparassis latifolia*) using three kinds of enzymes (chitinase, β-glucuronidase, and lysing enzyme complex) as elicitors.

2.4. Chemical Modification and Purification of Mushroom β-glucans

β-glucan is an important bioactive compound for human health, but its low solubility has led to the development of chemical modification technologies to improve bioavailability. Several methods to modify β-glucan are laid out to improve their functional and technological properties via physical and chemical crosslinking reactions (Ahmad et al., 2015). In this respect, β-glucans can be chemically modified to obtain various derivatives with potential industrial or medicinal importance (Synytsya and Novak, 2013).

Ion-exchange chromatography and gel filtration chromatograph are the most common and convenient methods for purifying polysaccharide. In general, the crude polysaccharide extracts were further applied to a Sephadex column and eluted with water (Zhu et al., 2015).

3. Studies on Mushroom β-glucan for Food and Nutraceutical Applications

3.1. Food Applications and Some Patents

There have been some studies previously conducted by enriching a product with the mushroom β-glucan agglomerated as food additive. β-glucans from *P. ostreatus* and *L. edodes* have been demonstrated satisfactory results when they were added to yogurt (Hozova et al., 2004) were used in the production of extruded snack products with low glycemic index (Brennan et al., 2013). Also chicken burgers were enriched with *P. sajor-caju*, fiber and β-glucans (Wan Rosli et al., 2011) as well as *P. ostreatus* was incorporated into sausages in an effort to lower their fat content (Chockchaisawasdee et al., 2010). In a study to produce a novel high-fibre and low-calorie functional food, Kim et al. (2011) used β-glucans from *L. edodes* as a wheat flour substitute in baked foods. These glucans improved the pasting properties of wheat flour and increased batter viscosity and shear-thinning elasticity without any adverse effect on air holding capacity or hardness. β-glucans of *Ganoderma amboinense*, *Agaricus* or *Fomes yucatensis*, or mixed mushrooms have also been tested for encapsulation of pickling liquid to be released in soups or sauces during cooking (Watanabe, 2005).

3.2. Nutraceutical Applications, Some Clinical Studies and Patents

“Mushroom nutraceuticals” is nowadays a relatively common term which refers to a refined polysaccharide, or a partially refined fruit body extract, or the dried biomass from mycelium or the fruiting body of a mushroom, which is consumed in the form of capsules,

tablets, powder, syrups, solutions as a dietary supplement with some therapeutic properties (Giavasis, 2014). Camelini et al. (2005) investigated the β-glucans of *A. brasiliensis* in different stages of fruiting body maturity and their use in nutraceutical products. The results showed that because of their important glucan contents, mature fruiting bodies of *A. brasiliensis* should be used for nutraceutical products. Cap-opened, more fragile mature fruiting bodies of *A. brasiliensis* should be selected over immature ones for the production of nutraceuticals. Synytsya et al. (2008) reported that the stems of *Pleurotus eryngii* and *P. ostreatus* could be used for the preparation of biologically active polysaccharide complexes as food supplements. Schizophyllan, produced by *S. commune* ATCC 38548 has attracted attention as immunomodulatory and anti-neoplastic agent in pharmaceutical industry in the recent years (Kumari et al., 2008). Akiyama et al. (2011) studied the effects of agaritine, a hydrazine-derivative from hot-water extract of *A. blazei* Murrill on human leukemic monocyte lymphoma (U937) cells. Agaritine induced DNA fragmentation, annexin V expression, and cytochrome C release. Caspase-3, 8 and 9 activities were gradually increased after agaritine treatment. *A. blazei* has been used as an adjuvant in cancer chemotherapy and various types of anti-leukemic bioactive components have been extracted from it (Patel and Goyal, 2012). It was proposed to mix β-glucan from mushroom with one or two substances such as ubiquinone Q10 and ferments leading to a biologically active additive for food with a wide range of action (Bragintseva et al., 2002). Suga et al. (2005) suggested converting lentinan into superfine particles, improving absorption through mucosa.

In animal experiments, β-glucans have been shown to have varying activity against sarcomas, mammary cancer, some chemically induced cancers, adenocarcinoma, colon cancer and some leukemias. Lentinan has already been shown effective in gastric carcinomas (Taguchi et al., 1985; Jeannin, et al., 1988). Furthermore, lentinan was reported to induce apoptosis in murine skin carcinoma cell-lines (Gu and Belury, 2005). Even if mushrooms and especially β-glucans have been used in Chinese medicine for decades, mechanisms need to be elucidated. However, lot of these substances have already been patented for antitumour treatments. Among them, β-glucan extracted from *Agaricus* mushroom was proposed, together with fucoidan (Hosokawa, 2003). The use of *Grifola frondosa* extract has also been patented, mixed with fucoidan and organic germanium (Sogabe, 1998).

Extracts of *L. edodes* markedly inhibited the growth of Sarcoma 180 (a retrovirus, similar to HIV which uses reverse transcriptase for its tumourpromoting activity) (Chihara et al., 1987). According to clinical studies, lentinan produces specific T-helper cell stimulation in healthy

humans as well as animals. It has also been recognized to stimulate lymphokine activated killer activity in combination with Interleukin-2 (Suzuki et al., 1990). Other patents concerning direct utilisation of β-D-glucans such as *G. frondosa* extract (Sogabe, 1996) for treating AIDS have been rare.

In 2003, an original application has been patented, proposing to use β-glucan as a gene carrier (Sakurai et al., 2003). In this patent, a hydrogen-bonding polymer with a triple-helix structure (such as schizophyllan, curdlan, lentinan, scleroglucan) was used for binding to a nucleic acid. Thus, a nucleic acid-polymer complex was obtained and could be applied as a vector. Moreover, this complex was also resistant to nuclease, allowing its use as a nucleic acid-protecting agent. PSP derived from *Coriolus versicolor* (syn. *Trametes versicolor*), a Chinese product commercially available since 1987 (Cui and Chisti, 2003), has been documented to improve the quality of life in cancer patients by providing substantial pain relief and enhancing immune status in 70-97% of patients with stomach, esophagus, lung, ovary and cervical cancers. Both PSK and PSP boosted immune cell production, ameliorated chemotherapy symptoms and enhanced tumour infiltration by dendritic and cytotoxic T-cells (Kidd, 2000). From a commercial standpoint, pleuran from oyster (*P. ostreatus*) mushrooms and lentinan from Shiitake (*L. edodes*) mushrooms are currently the most frequently used β-glucans. Both of them show positive effects on the intestines. They increase the resistance of intestinal mucosa to inflammation (Zeman et al., 2001) and inhibit the development of intestinal ulcers (Nosalova et al., 2001). Lentinan also shows a positive effect on peristalsis (Van Nevel et al., 2003).

3.3. Industrial Food Applications of Mushroom β-glucan in Functional Foods and Dietary Supplements

According to literature data, β-glucan has the potential to perform functions in the food industry such as thickening, water-holding, or oil-binding, gelling, film-making and encapsulation agent, and emulsifying stabilizer (Ahmad et al., 2012a, b; Giavasis, 2013; Zhu et al., 2016). Today, mushroom-glucans are found in the market more in the form of capsules or tablets as food supplements and to a lesser extent as ingredients in the food products (Eleftherios et al., 2014). In addition to food, β-glucans have potential applications in medicine and pharmacy, cosmetic and chemical industries, in veterinary medicine and feed production (Laroche and Michaud, 2007; Zhu et al., 2016). Besides, various mushroom β-glucans are

available as pure extracts in the market which are used as therapeutic agents. *S. commune* glucan manufactured by Bioland Technology Co. Ltd. is commercially available in the market (Zhu et al., 2016). There have been two patents on production technology of β-glucan from *S. commune*, today (Kim et al., 2008; 2009). Polysachharides such as lentinan, schizophyllan from shiitake and Schizophyllan mushrooms, PSK and PSP, the protein bound polysachharides from turkey tail mushroom, have been developed as anticancer agents in Japan and are now available worldwide (Lull, et al., 2005). There has also been a patent on application on β-glucan process, additive and food product (Cahill et al., 2003). Although some of the most studied polysaccharides produced by mushrooms (e.g. schizophyllan and lentinan) are already available and marketed as nutraceuticals (pharmaceutical formulation), their addition to food in their purified form has not been commercialized, yet (Giavasis, 2013). Nevertheless, β-glucan has a great potential to be used as an ingredient in the near future in various food industries, such as breakfast cereals, prebiotic sausage formulations, sport nutrition products, dairy products such as yogurts, bakery products such as biscuits, breads, cakes and ready-to-eat snacks, beverages, salad dressings and fat replacer that have some functionalities such as noticeable effect on physical and sensory properties, calorie-reducing and cholesterol-lowering actions and faster proteolysis, lower release of large peptides and a higher proportion of free amino acids, the glycemic response manipulation, controlling food intake and reducing 24 h energy intake and having good quality characteristics (Zhu et al., 2016).

The polysaccharides extracted from *A. brasiliensis*, *C. sinensis*, *G. lucidum*, *G. frondosa*, *L. edodes*, and *T. versicolor* are used to produce tablets for inhibiting the growth of tumours and improving the immunity (Rai et al., 2005). Several mushroom products, mainly polysaccharides such as β-D-glucans, have also proceeded successfully through clinical trials and are used as drugs to treat cancer and chronic diseases (Morris et al., 2016).

Today, it is possible to find commercial dietary supplements originated from various mushroom β-glucans in the form of powdered extracts, tablets, capsules, teas and syrups on the market. Imunoglukan P4H® from *P. ostreatus*, LentinanXP in USA/Lentinex® in Europe and Shiitake Gold and Pure Shiitake™ from *L. edodes*, Ganopoly® and Immulink MBG® from *G. lucidum*, D-fraction, MD fraction, MaitakeGold 404® nutraceutical extract and Pure Maitake™ from *G. frondosa*, Pure Turkey Tail™ from *T. versicolor* and Immune Assist™ from *A. blazei*, *C. sinensis*, *G. lucidum*, *G. frondosa*, *L. edodes* and *T. versicolor* can be given as example (Point Institute, 2013; Morris et al., 2016; Reis et al., 2017; URL-1, 2018). McCleary and Draga (2016) developed a robust and reliable method for the measurement of β-glucan in mushroom and

mycelial products. In the literature, there have been also some clinical studies on pharmacological benefits and safe doses of these mushroom β-glucan derived dietary supplements such as Lentinex® (Gaullier et al., 2011) and Imunoglukan P4H® (Jesenak et al., 2012). A scientific documentation was published to carry out the additional safety assessment for Lentinex®, an aqueous mycelial extract of *L. edodes*, as a novel food ingredient (EFSA, 2010). On the other hand, Gründemann et al. (2015) have reported that the standardisation of shiitake preparations is difficult because even preparations with similar polysaccharide and β-glucan contents have different immunological properties.

4. β-glucan Market by Food & Beverage Applications and Regions

The industries are adopting β-glucan to fortify foodstuff with high dietary fibres as consumer interests in the nutraceutical products is on escalation. Furthermore β-glucan actively impacts the metabolic parameters and help curing the chronic diseases. The worldwide development of policies for inclusion of functional ingredients in industrial products boosts the global β-glucan market. According to application segmentation, food and beverage segment was accounted more than 25% value share in 2016. Increasing demand for fibrous intake and concerns over blood cholesterol levels majorly drives the β-glucan market in food and beverage applications. In addition, β-glucan allows food product manufacturers to attract attention heart health claims in functional foods such as heart healthy biscuits, dairy products, snack bars etc., which in turn aids in driving the global β-glucan market (URL-2, 2018).

Geographically, the Europe accounted major share in the global β-glucan market in 2016. Approval of health claims by EU, related to heart health, blood glucose, cholesterol control and digestive health will be fueling the growth for β-glucan market in the region over the forecast period. In Asia Pacific, the government initiatives for awareness on cancer, women heart and maternal health are expected to drive the sales revenue of β-glucan during the forecast period of 2017-2025 (URL-2, 2018).

5. Conclusion

Although there are many findings related to the biological effects of β-glucans *in vitro* and *in vivo*, there are still some questions about structure activity and dose activity relationships.

Moreover, β-glucan content of mushroom products has not been standardised, yet. To make better use of β-glucan, food manufacturers and processors must bring attention not only to ensure sufficient concentration of β-glucan in the raw material but also to the processing methods and physicochemical properties of β-glucan, decreasing mechanical and enzymatic breakdown of the β-glucans in end-product and optimizing processing conditions. Mushroom β-glucans have potential nutraceutical properties that could be explored in the food and the pharmaceutical fields and might present different functional properties upon modification through suitable means and continuity of detailed clinical studies for the convinience of consumers.

References

Ahmad, A., Anjum, F. M., Zahoor, T., Nawaz, H., and Dilshad, S. M. (2012a). Beta glucan: A valuable functional ingredient in foods. Critical Reviews in Food Science and Nutrition, 52, 201-212.

Ahmad, A., Munir, B., Abrar, M., Bashir, S., Adnan, M., and Tabassum, T. (2012b). Perspective of β-glucan as functional ingredient for food industry. Journal of Nutrition and Food Sciences, 2, 133.

Ahmad, N. H., Mustafa, S., and Che Man, Y. B. (2015). Microbial polysaccharides and their modification approaches: A review. International Journal of Food Properties, 18, 332-347.

Akiyama, H., Endo, M., Matsui, T., Katsuda, .I, Emi, N., Kawamoto, Y., Koike, T., and Beppu, H. (2011). Agaritine from *Agaricus blazei* Murrill induces apoptosis in the leukemic cell line U937. Biochimica et Biophysica Acta, 1810, 519-525.

Beattie, K. D., Rouf, R., Gander, L., May, T. W., Ratkowsky, D., Donner, C. D., Gill, M., Grice, I. D., and Tiralongo, G. (2010). Antibacterial metabolites from Australian macrofungi from the genus *Cortinarius*. Phytochemistry, 71, 948-955.

Bhanja, S. K., Rout, D., Patra, P., Sena, I. K., Nandan, C. I. K., and Islam, S. S. (2014). Water-insoluble glucans from the edible fungus *Ramaria botrytis*. Bioactive Carbohydrates and Dietary Fibre, 3(2), 52-58.

Borchers, A., Keen, C. L., and Gershwin, M. E. (2004). Mushrooms, tumors, and immunity: an update. Experimental Biology and Medicine, 229, 393-406.

Bragintseva, L. M., Grigorash, A. I., Kovalenko, V. A., Maklanov, A. I, and Ustynjuk, T. K. (2002). RU2177699.

Brennan, M. A., Derbyshire, E., Tiwari, B. K., and Brennan, C. (2013). Integration of β-glucan fibre rich fractions from barley and mushrooms to form healthy extruded snacks. Plant Foods for Human Nutrition, 68(1), 78-82.

Brown, G. D., and Gordon, S. (2003). Fungal beta-glucans and mammalian immunity. Immunity, 19, 311-315.

Cahill, A. P., Fenske, D. J., Freeland, M., and Hartwig, G. W. (2003). Beta-glucan process, additive and food product. US patent 6749885 B2.

Camelini, C. M., Maraschin, M., Matos de Mendonça, M., Zucco, C., Ferreira, A. G., and Tavares, L. A. (2005). Structural characterization of β-glucans of *Agaricus brasiliensis* in different stages of fruiting body maturity and their use in nutraceutical products. Biotechnology Letters, 27(17), 1295-1299.

Chakraborty, I., Mondal, S., Pramanik, M., Rout, D., and Islam, S. S. (2004). Structural investigation of a water-soluble glucan from an edible mushroom, *Astraeus hygrometricus*. Carbohydrate Research, 339(13), 2249-2254.

Chakraborty, I., Mondal, S., Rout, D., and Islam, S. S. (2006). A water-insoluble (1→3)-beta-D-glucan from the alkaline extract of an edible mushroom *Termitomyces eurhizus*. Carbohydrate Research, 341(18), 2990-2993.

Chan, G. C. F., Chan, W. K., and Sze, D., M. Y. (2009). The effects of β-glucan on human immune and cancer cells. Journal of Hematology & Oncology, 2, 25.

Chauveau, C., Talaga, P., Wieruszeski, J. M., Strecker, G., and Chavant, L. (1996). A water-soluble beta-D-glucan from *Boletus erythropus*. Phytochemistry, 43(2), 413-415.

Chihara, G., Hamuro, J., Maeda, Y.Y., Arai, Y., and Fukuoka, F. (1987). Function and purification of the polysaccharides with marked antitumor activity, especially Lentinan, from *Lentinus edodes* (Berk.). Cancer Research, 30, 2776-2781.

Chockchaisawasdee, S., Namjaidee, S., Pochana, S., and Stathopoulos, C. E. (2010). Development of fermented oyster mushroom sausage. Asian Journal of Food & Agro-Industry, 3, 35-43.

Crognale, S., Bruno, M., Fidaleo, M., Moresi, M., and Petruccioli, M. (2007). Production of β-glucan and related glucan-hydrolases by *Botryosphaeria rhodina*. Journal of Applied Microbiology, 102, 860-871.

Cui, J, and Chisti, Y. (2003). Polysaccharopeptides of *Coriolus versicolor*: physiological activity, uses, and production. Biotechnology Advances, 21(2), 109-22.

Deng, C., Hu, Z., Fu, H. T., Hu, M. H., Xu, X., and Chen, J. H., (2012). Chemical analysis and antioxidant activity in vitro of a β-D-glucan isolated from *Dictyophora indusiata*. International Journal of Biological Macromolecules, 51, 70-75.

Dong, Q., Wang, Y., Shi, L., Yao, J., Li, J., Ma, F., and Ding, K. (2012). A novel water-soluble β-D-glucan isolated from the spores of *Ganoderma lucidum*. Carbohydrate Research, 353, 100-105.

Du, B., and Xu, B. J. (2014). Oxygen radical absorbance capacity (ORAC) and ferric reducing antioxidant power (FRAP) of β-glucans from different sources with various molecular weight. Bioactive Carbohydrate and Dietary Fibre, 3, 11-16.

Du, B., Lin, C. Y., Bian, Z. X., and Xu, B. J. (2015). An insight into anti-inflammatory effects of fungal beta-glucans. Trends in Food Science & Technology, 41, 49-59.

EFSA Panel on Dietetic Products, Nutrition and Allergies (NDA). (2010). Scientific opinion on the safety of "*Lentinus edodes* extract" as a novel food ingredient. EFSA Journal, 8(7), 1685.

Eleftherios, E., Vassilis, M. G., and Cleanthes, I. (2014). The potential use of mushrooms β-glucans in the food industry. International Journal of Biotechnology for Wellness Industries, 3, 15-18.

Gaullier, J. M., Sleboda, J., Øfjord, E. S., Ulvestad, E., Nurminiemi, M., Moe, C., Albrektsen, T., and Gudmundsen, O. (2011). Supplementation with a soluble beta-glucan exported from shiitake medicinal mushroom, *Lentinus edodes* (Berk.) Singer mycelium: A crossover, placebo-controlled study in healthy elderly. International Journal of Medicinal Mushrooms, 13(4), 319-326.

Giavasis, I. (2013). Production of microbial polysaccharides for use in food. In: Microbial production of food ingredients, enzymes and nutraceuticals. United Kingdom: Woodhead Publishing.

Giavasis, I. (2014). Bioactive fungal polysaccharides as potential functional ingredients in food and nutraceuticals. Current Opinion in Biotechnology, 26, 162-173.

Gründemann, C., Garcia-Käufer, M., Sauer, B., Scheer, R., Merdivan, S., Bettin, P., Huber, R., and Lindequist, U. (2015). Comparative chemical and biological investigations of β-glucan-containing products from shiitake mushrooms. Journal of Functional Foods, 18, 692-702.

Gu, Y. H., and Belury M. A. (2005). Selective induction of apoptosis in murine skin carcinoma cells (CH72) by an ethanol extract of *Lentinula edodes*. Cancer Letters, 220, 21-28.

Hosokawa, J. (2003). JP2003055234.

Hozova, B., Kuniak, L., and Kelemova, B. (2004). Application of β-glucans isolated from mushrooms *Pleurotus ostreatus* (pleuran) and *Lentinula edodes* (lentinan) for increasing the bioactivity of yoghurts. Czech Journal of Food Sciences, 22, 204-214.

Jeannin, J. F., Lagadec, P., Pelletier, H., Reisser, D., Olsson, N. O., Chihara, G., and Martin, F. (1988). Regression induced by lentinan of peritoneal carcinomatoses in a model of colon cancer in rat. Interntional Journal of Immunopharmacology, 10(7), 855-861.

Jesenak, M., Majtan, J., Rennerova, Z., Kyselovic, J., Banovcin, P., and Hrubisko, M. (2012). Immunomodulatory effect of pleuran (β-glucan from *Pleurotus ostreatus*) in children with recurrent respiratory tract infections. International Immunopharmacology, 15, 395-399.

Jung, H. K., Hong, J. H., Park, S. C., Park, B. K., Nam, D. H., and Kim, S. D. (2007). Production and physicochemical characterization of β-glucan produced by *Paenibacillus polymyxa* JB115. Biotechnology and Bioprocess Engineering, 12, 713-719.

Kao, P. F., Wang, S. H., Hung, W. T., Liao, Y. H., Lin, C. M., and Yang, W. B. (2012). Structural characterization and antioxidative activity of low-molecular-weights beta-1, 3-glucan from the residue of extracted *Ganoderma lucidum* fruiting bodies. BioMed Research International, 1-8.

Kidd, P. M. (2000). The use of mushroom glucans and proteoglycans in cancer treatment. Alternative Medicine Review, 5(1), 4-27.

Kim, Y. W., Kim, K. H., Choi, H. J., and Lee, D. S. (2005). Anti-diabetic activity of beta-glucans and their enzymatically hydrolyzed oligosaccharides from *Agaricus blazei*. Biotechnology Letters, 7(7), 483-487.

Kim, M. S., Park, Y. D., and Lee, S. R. (2008). Preparation method of beta-glucan from *Schizophyllum commune* and composition for experimental application comprising the same. US patent 0160043 A1.

Kim, M. S., Park, Y. D., and Lee, S. R. (2009). Method of using beta-glucan from *Schizophyllum commune*. US patent 0023681 A1.

Kim, J., Lee, S. M., Bae, I. Y., Park, H. G., Gyu Lee, H., and Lee, S. (2011). (1-3)(1-6)-β-glucan-enriched materials from *Lentinus edodes* mushroom as a high-fibre and low-calorie flour substitute for baked foods. Journal of the Science of Food and Agriculture, 91, 1915-1919.

Kim, S. R., Kang, H. W., and Ro, H. S. (2013). Generation and evaluation of high β-glucan producing mutant strains of *Sparassis crispa*. Mycobiology, 41(3), 159-163.

Kothari, D., Patel, S., and Kim, S. K. (2018).Anticancer and other therapeutic relevance of mushroom polysaccharides: A holistic appraisal. Biomedicine & Pharmacotherapy, 105, 377-394.

Kumari, M., Survase, S. A., and Singhal, R. S. (2008). Production of schizophyllan using *Schizophyllum commune* NRCM. Bioresource Technology, 99, 1036-1043.

Laroche, C., and Michaud, P. (2007). New developments and prospective applications for β-(1,3) glucans. Recent Patents on Biotechnology, 1, 59-73.

Lindequist, U., Niedermeyer, T., and Jülich, W. D. (2005). The pharmacological potential of mushrooms. Evidence-Based Complementary and Alternative Medicine, 2(3), 285-299.

Liu, Y., Zhang, J., Tang, Q., Yang, Y., Guo, Q., Wang, Q., Wu, D., and Cui, S. W. (2014). Physicochemical characterization of a high molecular weight bioactive β-D-glucan from the fruiting bodies of *Ganoderma lucidum*. Carbohydrate Polymers, 101, 968-974.

Lull, C., Wichers, H. J., and Savelkoul, H. F. (2005). Antiinflammatory and immunomodulating properties of fungal metabolites. Mediators of Inflammation, 2, 63-80.

Manzi, P., and Pizzoferrato, L. (2000). Beta-glucans in edible mushrooms. Food Chemistry, 68, 315-318.

McClearly, B. V., and Draga, A. (2016). Measurement of β-glucan in mushrooms and mycelial products. Journal of AOAC International, 99(2), 364-373.

Moradali, M. F., Mostafavi, H., Ghods, S., and Hedjaroude, G. A. (2007). Immunomodulating and anticancer agents in the realm of macromycetes fungi (macrofungi). International Immunopharmacology, 7, 701-724.

Morris, H. J., Llaurado, G., Beltran, Y., Lebeque, Y., Bermudez, R. C., Garcia, N., Gaime-Perraud, I., and Moukha, S. (2016). The use of mushrooms in the development of functional foods, drugs or nutraceuticals. In: Wild Plants, Mushrooms and Nuts: Functional Food Properties and Applications, pp. 123-157. John Wiley & Sons, Ltd.

Nie, S., Zhang, H., Li, W., and Xie, M. (2013). Current development of polysaccharides from *Ganoderma*: Isolation, structure and bioactivities. Bioactive Carbohydrates and Dietary Fiber, 1, 10-20.

Novak, M., and Vetvicka, V. (2008). β-glucans, history, and the present: Immunomodulatory aspects and mechanism of action. Journal of Immunotoxicology, 5, 47-57.

Novak, M., and Vetvicka, V. (2009). Glucans as biological response modifiers. Endoctrine, Metabolic & Immune Disorders Drug Targets, 9, 67–75.

Nosalova, V., Bobek, P., Cerna, S., Galbavy, S., and Stvrtina, S. (2001). Effects of pleuran (beta-glucan isolated from *Pleurotus ostreatus*) on experimental colitis in rats. Journal of the Physiological Research, 50, 575-581.

Özcan, Ö., and Ertan, F. (2018). Beta-glucan content, antioxidant and antimicrobial activities of some edible mushroom species. Journal of Food Science and Technology, 6(2), 47-55.

Palacios, I., García-Lafuente, A., Guillamón, E., and Villares, A. (2012). Novel isolation of water-soluble polysaccharides from the fruiting bodies of *Pleurotus ostreatus* mushrooms Carbohydrate Research, 358, 72-77.

Patel, S., and Goyal, A. (2012). Recent developments in mushrooms as anti-cancer therapeutics: A review. Biotechnology, 2, 1-15.

Park, H., Ka, K. H., and Ryu, S. R. (2014). Enhancement of β-glucan content in the cultivation of cauliflower mushroom (*Sparassis latifolia*) by elicitation. Mycobiology, 42, 41-45.

Pillai, T. G., and Devi, U. P. (2013). Mushroom beta glucan: Potential candidate for post irradiation protection. Mutation Research, 751, 109-115.

Point Institute. (2013). The use of mushroom-derived dietary supplements as immunomodulating agents: An overview of evidence-based clinical trials and the mechanisms and actions of mushroom constituents. Technical Report.Wisconsin: Stevens Point.

Rai, M., Tidke, G., and Wasser, S. P. (2005). Therapeutic potential of mushrooms. Natural Product Radience, 4(4), 246-257.

Reis, F. S., Martins, A., Vasconcelos, M. H., Morales, P., and Ferreira, I. C. F. R. (2017). Functional foods based on extracts or compounds derived from mushrooms. Trends in Food Science & Technology, 66, 48-62.

Ren, L., Perera, C., and Hemar, Y. (2012). Antitumor activity of mushroom polysaccharides: A review. Food & Function, 3, 1118-1130.

Rop, O., Mlcek, J., and Jurikova, T. (2009). Beta-glucans in higher fungi and their health effects. Nutrition Reviews, 67(11), 624-631.

Rieder, A., and Samuelsen, A. B. (2012). Do cereal mixed-linked β-glucans possess immune-modulating activities? Molecular Nutrition & Food Research, 56, 536-547.

Sakurai, K., Shinkai, S., Kimura, T., Tabata, K., Koumoto, K., and Gronwald, O. (2003). US2003216346.

Sari, M., Prange, A., Lelley, J. I., and Hambitzer, R. (2017). Screening of beta-glucan contents in commercially cultivated and wild growing mushrooms. Food Chemistry, 216, 45-51.

Smiderle, F. R., Carbonero, E. R., Mellinger, C. G., Sassaki, G. L., Gorin, P. A., and Iacomini, M. (2006). Structural characterization of a polysaccharide and a beta-glucan isolated from the edible mushroom *Flammulina velutipes*. Phytochemistry, 67(19), 2189-2196.

Smiderle, F. R., Alquini, G., Tadra-Sfeir, M. Z., Iacomini, M., Wichers, H. J., and Van Griensven, L. J. L. D. (2013). *Agaricus bisporus* and *Agaricus brasiliensis* (1→6)-β-D-glucans show immunostimulatory activity on human THP-1 derived macrophages. Carbohydrate Polymers, 94, 91-99.

Sogabe, T. (1996). JP8119874.

Sogabe, T. (1998). JP10033142.

Suga, T., Ogasawara, Y., Kaneko, Y., Kajiura, M., and Suga, Y. (2005). JP2005097308.

Suzuki, M., Higuchi, S., Taki, Y., Miwa, K., and Hamuro, J. (1990). Activity of Lentinan and Interleukin 2. International Journal of Immunopharmacology, 12(6), 613-623.

Synytsya, A., Míčková, K., Jablonský, I., Sluková, M., and Čopíková, J. (2008). Mushrooms of genus *Pleurotus* as a source of dietary fibres and glucans for food supplements. Czech Journal of Food Sciences, 26, 441-446.

Synytsya, A., Míčková, K., Synytsya, A., Jablonský, I., Spěváček, J., Erban, V., Kovarikova, E., and Čopíková, J. (2009). Glucans from fruit bodies of cultivated mushrooms *Pleurotus ostreatus* and *Pleurotus eryngii*: Structure and potential prebiotic activity. Carbohydrate Polymers, 76(4), 548-556.

Synytsya, A., and Novak, M. (2013). Structural diversity of fungal glucans. Carbohydrate Polymers, 92, 792-809.

Taguchi, T., Furue, H., Kimura, T., Kondo, T., Hattori, T., Itoh, T., and Osawa, N. (1985). End-point results of phase 111 study of Lentinan. Japanese Journal of Cancer and Chemotherapy, 12, 366-371.

Tian, Y. T., Zeng, H. L., Xu, Z. B., Zheng, B. D., Lin, Y. X., Gand, C. J., and Lo, Y. M. (2012). Ultrasonic-assisted extraction and antioxidant activity of polysaccharides recovered from white button mushroom (*Agaricus bisporus*). Carbohydrate Polymers, 88, 522-529.

Toyoda, S., and Kimura, M. (2004). US2004047949.

URL-1: https://alohamedicinals.com/?s=beta+glucan, (Date of access: 30 September 2018).

URL-2: http://www.credenceresearch.com/report/beta-glucan-market, Beta glucan market by source type (cereals, fungal & microbial), by application (food & beverage, pharmaceutical, cosmetics, animal feed) - growth, future prospects and competitive analysis, 2017-2025, (Date of access: 24 September 2018).

Van Nevel, C. J., Decuypere, J. A., Dierick, N., and Molly, K. (2003). The influence of *Lentinus edodes* (Shiitake mushroom) preparations on bacteorological and morphological aspects of the small intestine piglets. Archives of Animal Nutrition, 57, 399-412.

Villares, A., Mateo-Vivaracho, L., and Guillamon, E. (2012). Structural features and healthy properties of polysaccharides occurring in mushrooms. Agriculture, 2, 452-471.

Wan Rosli, W. I., Solihah, M. A., Aishah, M., Fakurudin, N. A., and Mohsin, S. S. J. (2011). Colour, texture properties, cooking characteristics and fibre content of chicken patty added with oyster mushroom (*Pleurotus sajor-caju*). International Food Research Journal, 18, 621-627.

Wasser, S. P., and Weis, A. L. (1999). Medicinal properties of substances occurring in higher Basidiomycetes mushrooms: Current perspectives (Review). International Journal of Medicinal Mushrooms, 1(1), 31-62.

Wasser, S. P. (2002). Medicinal mushrooms as a source of antitumor and immunomodulating polysaccharides. Applied Microbiology and Biotechnology, 60, 258-274.

Watanabe, M. (2005). JP2005160326.

Yan, J. K., Wang, W. Q., and Wu, J. Y. (2014). Recent advances in *Cordyceps sinensis* polysaccharides: mycelial fermentation, isolation, structure, and bioactivities: A review. Journal of Functional Foods, 6, 33-47.

Zeman, M., Nosalova, V., Bobek, P., Zakalova, M., and Cerna, S. (2001). Changes of endogenous melatonin and protective effect of diet containing pleuran and extract of black elder in colonic inflammation in rats. Biologia. 56, 659-701.

Zhang, M., Cuia, S. W., Cheung, P. C. K and Wang, Q. (2007). Antitumorpolysaccharides from mushrooms: A review on their isolation process, structural characteristics and antitumor activity. Trends in Food Science & Technology, 18, 4-19.

Zhang, Y., Xia, L., Pang, W., Wang, T., Chen, P., Zhu, B., and Zhang, J. (2013). A novel soluble β-1, 3-D-glucan salecan reduces adiposity and improves glucose tolerance in highfat diet-fed mice. British Journal of Nutrition, 109, 254-262.

Zhu, F., Du, B., Bian, Z., and Xu, B. (2015). Beta-glucans from edible and medicinal mushrooms: Characteristics, physicochemical and biological activities. Journal of Food Composition and Analysis, 41, 165-173.

Zhu, F., Du, B., and Xu, B. (2016). A critical review on production and industrial applications of beta-glucans. Food Hydrocolloids, 52, 275-288.

Indispensable Biocatalysts of Asymmetric Reduction Reactions: Pure Enzymes and whole cells

Engin ŞAHİN[1], Caner TOZLU[1*], Enes DERTLİ[1], Hüseyin SERENCAM[1]

[1] Bayburt University, Faculty of Engineering, Department of Food Engineering

[*] **Corresponding Author:** canertozlu@hotmail.com

Abstract

Asymmetric bioreduction of prochiral ketones is one of the most important and practical approaches for the synthesis of chiral secondary alcohols, which is indispensable for the synthesis of industrially significant molecules such as pharmaceuticals, agrochemicals and natural products. The interaction of chiral compounds with chiral environments is biologically different and can often lead to adverse effects of enantiomers. Therefore, the enantiomeric pure form of the obtained chiral alcohol is of major importance. The asymmetric reduction of prochiral ketones is one of the most important synthesis in organic synthesis because of the formation of optically active alcohols, which are mostly used as intermediates for the productions of drugs and other industrially important compounds. A straightforward approach to the synthesis of chiral alcohols is the asymmetric reduction of corresponding carbonyl compounds, which can be achieved by chemical or biocatalytic methods. Classic chemical methods for the enantioselective synthesis of chiral secondary alcohols have been comprehensively improved, but the synthesis of some of these compounds is still higly complex and costly. Biocatalytic reduction is a very successful and widesperead method for preparing chiral alcohols. Biocatalysts have numerous advantages compared to chemical catalysts. This study includes the differences of pure enzymes and whole-cell microorganisms as biocatalysts in asymmetric reduction of prochiral ketones and the differences of biocatalysts and chemical catalysts.

Keywords: Bioreduction, Biocatalyst, Enzyme, Asymmetric synthesis, whole cell microorganisms

1. Introduction

The asymmetric reduction of ketones is one of the most significiant, basic and convenient reactions for producing asymmetric chiral alcohols, which can be converted into various functionalities, without racemization, to production industrially important moleculas such as durugs, agrochemicals and natural products (Nakamura et al., 2003; Breuer et al., 2004; Gladiali and Alberico, 2006; Ikariya and Blacker, 2007). The catalysts for the asymmetric reduction of prochiral ketones may be classified into two class: chemical and biological methods. Both have their own features, and development of both to facilitate the suitable choice of the catalysts for special aims is essential to green chemistry. A basic approach to the procuction of chiral alcohols is the asymmetric reduction of corresponding prochiral ketones, which can be achieved by chemical or biocatalytic methods. Some chemical methods are used for that purpose in industry, however most of these methods need toxic metals and expensive metal hydrides, which require harsh reaction conditions (Blaser and ark., 2003; Ohkuma, 2010). The alternative, more environmentally friendly approach to introduce chiral centers is obtaining via biocatalytic methods. Biocatalysts have unique features when compared with chemical catalysts. Biocatalysts show very high eantioelectivity compared to chemical catalysts. For instance, high enantioselectivities can be obtained, even with the reduction of aliphatic ketones such as ethyl methyl ketone, while chemical catalysts can perform high enantioselective reductions generally when the two substituent groups of the carbonyl carbon of the ketones is different.

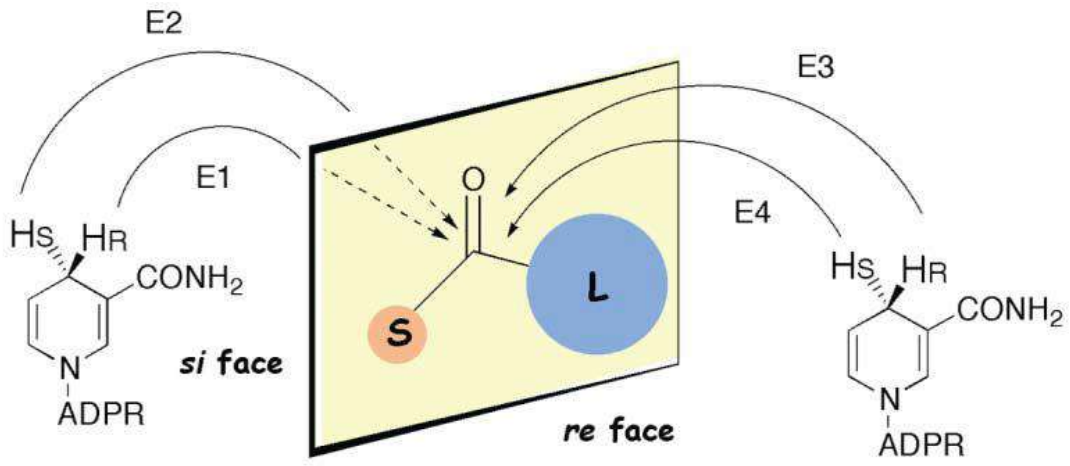

Figure 1. Selectivity in the biocatalysts

In order to exhibit catalytic activities, the enzymes require a coenzyme such as NADH or NADPH from which a hydride is transferred to the substrate carbonyl carbon. According to the structure of the enzyme and substrate, H transfer is achieved and selectivity is achieved (Figure 1) (Bradshaw et al., 1992; Nakamura et al., 1988). Biocatalytic asymmetric reductions are usually safe and the reaction conditions are mild, the solvent is water, and hazardous reagents are not necessary. For instance, ethanol and glucose are used as hydrogen sources instead of explosive hydrogen gas. Biocatalysts, microorganisms, plants, animals whole cell, or their isolated enzymes, are reproducible and can be easily decomposed in the environment (Figure 2) (Comasseto et al., 2004; Patel et al., 2004).

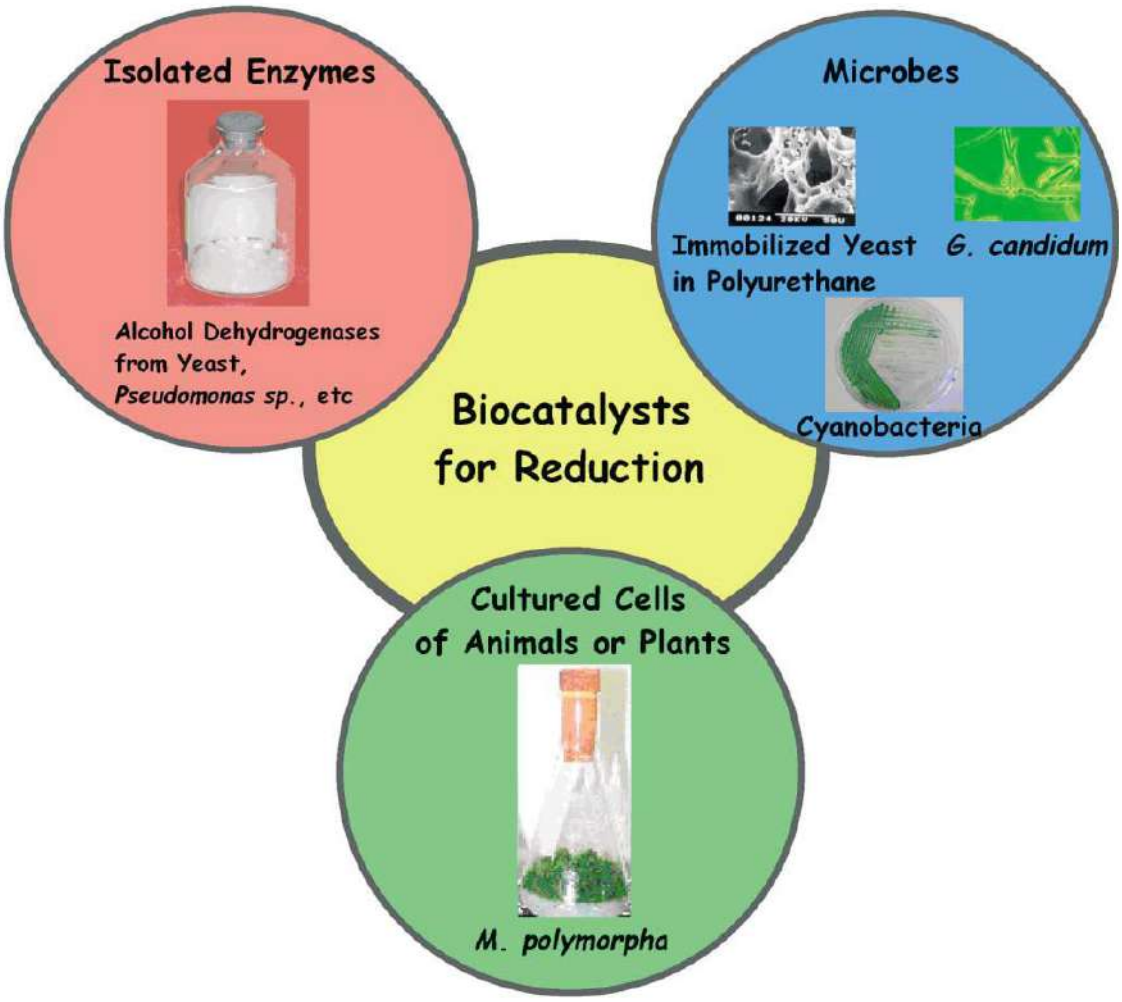

Figure 2. Types of biocatalysts used in the asymmetric reduction

Some of the biocatalysts for bioreduction, such as isolated enzymes and whole cells, are commercially available and ready to use like chemical catalysts. They are often used as

biocatalyst because they are inexpensive and easily available. Fundamentally, there are numerous advantages of using whole cell as biocatalysts instead of pure enzymes. Pure enzymes are usually very expensive and not readily accessible, there is a limited availability of enzymes and they require cosubstrates such as NADPH. However, in some cases, enzymes are much more stable within the whole cell thus extending the life of the biocatalyst. The use of whole cells is especially advantageous for perform the desired asymmetric reduction since they do not need addition of cofactors for their renewal (Murzin et al., 2005; Pollard and Woodley, 2006).

2. Results and Discussion

Biotechnology opens future probabilitys in the chemical field for the production of complex molecules and associate inexpensive crude materials with environment-friendly methods (Gao et al., 2006). As a result, the superiority of the pure enzyme and the whole cell that can be used as biocatalysts compared to each other is compared.

2.1. Advantages of Whole Cell

Using a whole cell biocatalyst is an inexpensive method compared to pure enzyme. The use of whole cells is especially advantageous for carrying out the desired reduction since they do not require addition of cofactors for their regeneration.

2.2. Disadvantages of Whole Cells

The efficiency of whole cell transformations is generally low. Because unnatural substrates are often toxic to the living organism and can be poisoned in low concentrations. If the product is stored in the cell and is not secreted, the yield is low and product recovery is difficult. In addition, when the racemic substrate is used, the chiral transport into and out of the cell affects the specificity of the selectivity.

2.3. Advantages of Pure Enzyme

The enzyme used as biocatalyst in the asymmetric reduction to give the desired product and no by-product. If there are several equivalent groups in the substrate molecule, the enzyme

distinguishes these groups and always reacts with the same region. Enzymes can distinguish between enantiomers of racemic substrates. Thus, only one of the enantiomers enters the reaction and more selective.

2.4. Disadvantages of Pure Enzyme

Pure enzymes are usually very expensive and not readily accessible, there is a limited availability of enzymes and they require expensive cosubstrates such as cofactors. Using pure enzymes is an expensive method and has little stability.

As a result, Chemical method have their own deficits such as use of toxic metal catalysts, low enantioselectivity, conversion, requirement of harsh conditions, and formation of byproducts and they use costly chiral ligands, at the same times the did not usually produce enough results for green and sustainable chemistry. When compared to pure enzymes, whole whole cells not necessary the use of external cofactors. They include multiple dehydrogenases that are able to accept a broad range of unnatural substrates. All enzymes and cofactors are well protected in their natural cellular environment. Furthermore, the use of whole cell biocatalysts in the asymmetric reduction avoids enzyme purification and cofactor addition, so it is quite cheap method.

References

Blaser, H. U., Malan C, Pugin B, Spindler F, Steiner H, Studer M. (2003) Selective hydrogenation for fine chemicals: recent trends and new developments. Advanced synthesis catalysis 345, 103–151.

Bradshaw, C. W., Hummel, W., Wong, C. H. (1992) Lactobacillus kefir alcohol dehydrogenase: a useful catalyst for synthesis, Journal of Organic Chemistry, 57, 1532–1536.

Breuer, M., Ditrich, K., Habicher, T., Hauer, B., Kesseler, M., Sturmer, R., Zelinski, T., (2004) Industrial methods for the production of optically active intermediates. Angew Chemie Int Ed, 43, 788–824.

Comasseto, J.V., Andrade, L. H., Omori, A. T., Assis, L. F., Porto, A. L. M. (2004) Deracernization of aryl ethanols and reduction of acetophenones by whole fungal cells of Aspergillus terreus CCT 4083, A. terreus CCT 3320 and Rhizopus oryzae CCT 4964. Journal of molecular catalysis. B, Enzymatic, 29, 55–61.

Gao, K., Song, Q., Wei, D., (2006) Coupling of enantioselective biooxidation of DL-1,2-propanediol and bioreduction of pinacolone via regeneration cycle of coenzyme. Applied microbiology and biotechnology, 71, 819–823.

Gladiali, S., Alberico, E., (2006) Asymmetric transfer hydrogenation: chiral ligands and applications. Chemical Society Reviw, 35, 226–236.

Ikariya, T., Blacker, A. J., (2007) Asymmetric transfer hydrogenation of ketones with bifunctional transition metal-based molecular. Accounts of chemical research, 40, 1300–1308.

Murzin, D. Y., Maki-Arvela, P., Toukoniitty, E, Salmi, T., (2005) Asymmetric heterogeneous catalysis: science and engineering. Catalysis Reviews, 47, 175–256.

Nakamura, K., Yamanaka, R., Matsuda, T., Harada, T., (2003). Recent developments in asymmetric reduction of ketones with biocatalysts. Tetrahedron: Asymmetry, 14, 2659-2681.

Nakamura, K., Yoneda, T., Miyai, T., Ushio, K., Oka, S., Ohno, A. (1988) Asymmetric reduction of ketones by glycerol dehydrogenase from Geotricum, Tetrahedron Letters. 29, 2453–2454.

Ohkuma T. (2010) Asymmetric hydrogenation of ketones: tactics to achieve high reactivity, enantioselectivity, and wide scope. Proceedings of the Japan Academy. Series B., 86, 202–219.

Patel, R. N., Goswami, A., Chu, L., Donovan, M. J., Nanduri, V., Goldberg, S., Johnston, R., Siva, P. J., Nielsen, B., Fan, J., He, W., Shi, Z., Wang, K.Y., Eiring, R., Cazzulino, D., Singh, A., Mueller, R. (2004) Enantioselective microbial reduction of substituted acetophenones. Tetrahedron: Asymmetry, 15, 1247–1258.

Pollard, D. J., Woodley, J. M., (2006) Biocatalysis for pharmaceutical intermediates: the future is now. Trends in biotechnology, 25, 66–73.

FOOD ENGINEERING

POSTER PRESENTATIONS

Alcohol Dehydrogenases (ADHs) as a Potential Promising Tool for Green Chemistry

Caner TOZLU[1*], Engin ŞAHİN[2], Enes DERTLİ[3], Hüseyin SERENCAM[4]

[1] Bayburt University, Faculty of Engineering, Department of Food Engineering
[2] Bayburt University, Faculty of Engineering, Department of Food Engineering
[3] Bayburt University, Faculty of Engineering, Department of Food Engineering
[4] Bayburt University, Faculty of Engineering, Department of Food Engineering
[*] **Corresponding Author:** canertozlu@hotmail.com

Abstract

Green chemistry is an emerging technology that can result in higher efficiency and reduce the environmental burden during chemical synthesis. One of the application areas of green technology is the use of biocatalysts in order perform chemical reactions due to the high efficiency of enzymes and their excellent regioselectivity, enantioselectivity and stereoselectivity. Among the different enzymes alcohol dehydrogenases appeared to be highly functional for the production of enantio-pure chiral secondary alcohols using different substrates. So far, alcohol dehydrogenases were identified from different sources including Lactic Acid Bacteria (LAB) and yeasts and their applications in producing different enantio-pure chiral secondary alcohols were revealed. In this work, a comprehensive approach was applied to deliver the importance of this enzyme group for the future of green chemistry.

Keywords: ADH, Biocatalyst, Enzyme, Asymmetric synthesis

1. Introduction

On account of treatment and safety, the pharmaceutical and modern chemical industry is faced with the requirement of obtaining enantiopure compounds in the production of medicinal, agricultural, and other products including antimicrobials (1). The interaction of chiral compounds, especially in biological systems, can result in different biological and opposing effects of enantiomers. Therefore, the enantiomeric purity of the product is of major importance (2, 3). The asymmetric reduction of prochiral ketones is one of the most important transformation in organic synthesis due to the structural advantage and the formation of optically active alcohols, which are usually used as intermediates for the products such as drugs, antimicrobials, fragnances, agrochemicals, and other compounds (4). Single enantiopure secondary alcohols are one of the most important chiral building blocks for many chiral pharmaceuticals, such as (S)-fluoxetine, (R)-tomoxetine, and L-chlorprenaline (5, 6). Similarly, enantiopure secondary alcohols can be important components as antimicrobial agents (7) and it is crucial to produce different reduced products and test their antimicrobial activities. The reduction reactions can be performed by traditional procedures using catalysts like metal hydrides, but racemic mixture can be obtained. Even though conventional chemical methods for the synthesis of the chiral alcohols have been comprehensively improved, the synthesis of these compounds is highly expensive, complicated, and toxic. Therefore, selective and environmentally friendly catalysts to synthesize optically pure alcohols by using isolated enzymes and microorganism are extremely attractive. Biocatalysts bearing both isolated oxido-reductases and living organism are considered as a promising catalysts due to their advantages, such as specificity, enantioselectivity, mild reaction conditions, and renewable capabilities (8) (Figure 1). Alcohol dehydrogenases (ADHs) are one of the well known biocatalysts, used as isolated enzymes or whole cells, catalyze the stereoselective reduction of prochiral ketones with remarkable chemo-, regio-, and stereoselectivity. In this study we have discussed current knowledge on the role of ADHs as biocatalysts.

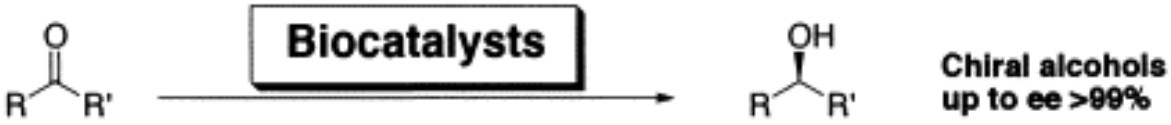

Figure 1. General overview of bioreduction of pro-chiral ketones (9)

General principles of Biocatalysis

So far, several different bioctalysts have been shown to work on bioreduction process which include isolated enzymes such as ADHs, microorganisms from different sources and cultured cells of animals and plants. All these biocatalysts were shown to act as important sources to conduct the bioreduction reactions although they have some advantages and disadvantages when comparing their efficiencies. Figure 2 shows the overview of the sources to be for the bioreduction reactions as biocatalysts.

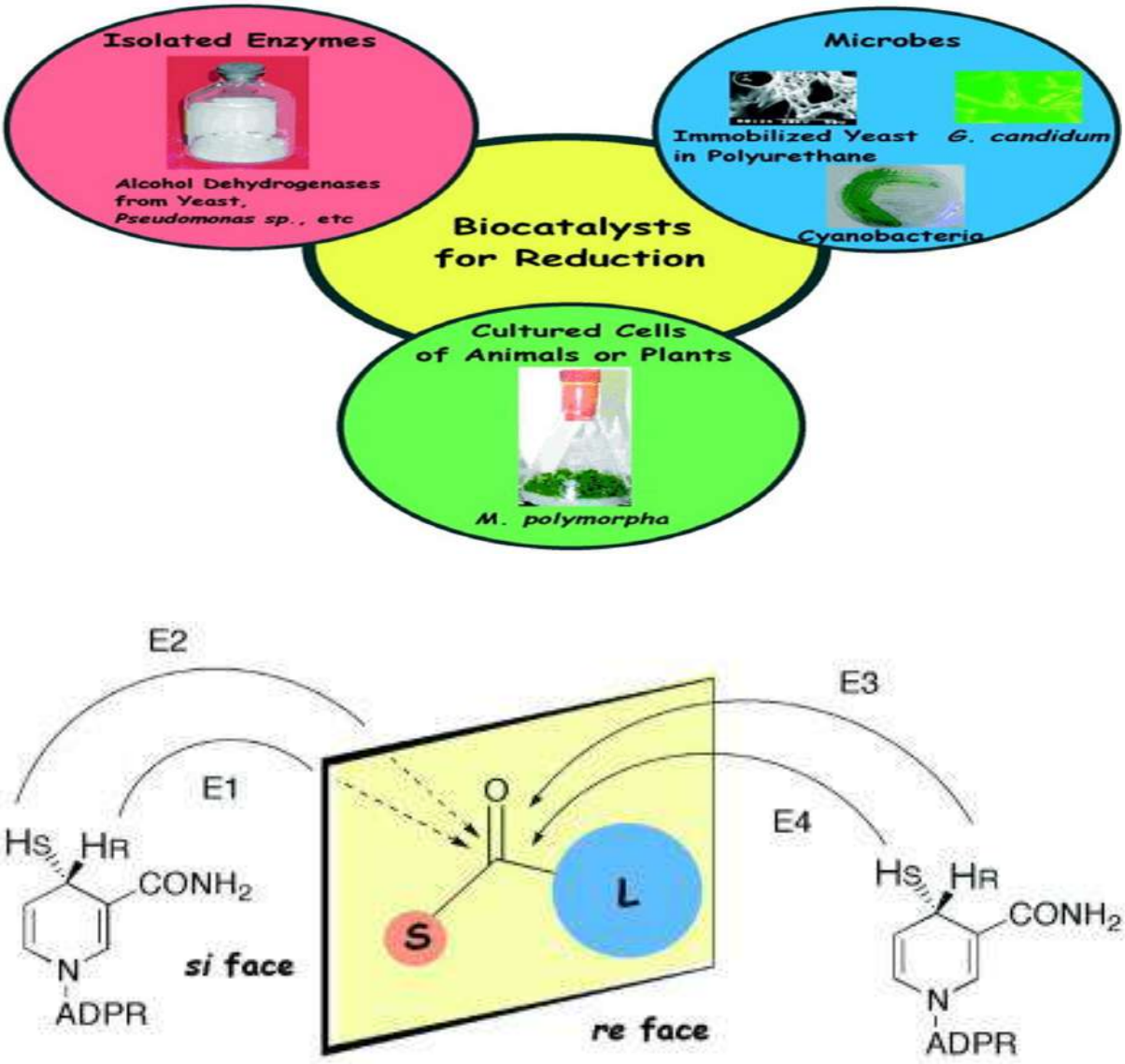

Figure 2. General overview of biocatalysts for asymmetric reductions. (9)

For instance, one of the disadvantages of using biocatalysts is the difficulty encountered in large scale synthesis; (1) workup procedures may be complicated, (2) large spaces for the cultivation of the cell may be necessary, or (3) the space–time yields are not high due to the low substrate concentrations and long reaction times. However, these disadvantages have been surmounted by improving the biocatalysts using genetic methods and by investigating the reaction conditions. ADHs are relatively small proteins that can be encoded in the genome of yeast species as well as lactic acid bacteria (LAB) species which makes the expression of ADH relatively easy and by obtaining the ADHs at high amounts the bioreduction reactions can be performed easily and the disadvantages mentioned above can be solved. Recently the immobilization techniques for the enzyme immobilization is improved and by immobilizing the ADHs they can be used more efficiently.

ADHs as efficient biocatalysts

As discussed previously chiral alcohols can be synthesized by the action of specific alcohol dehydrogenases (ADHs) which can be originated from different sources. One of the main reasons for the use of ADHs in bioreduction reactions is their potential to obtain high level of enantiomeric excesses which is a prerequiste for production of different pharmaceuticals. Another important positive role of ADHs in bioreduction reactions is their potential to obtain these chiral compounds at high yields. ADHs catalyze the

enantioselective reduction of carbonyl compounds. Several ADHs are known which have been applied in

organic synthesis. LAB are also important sources of ADHs and recently we have identified a novel ADH from a Lactobacillus brevis strain. This ADH is a small protein similar to the other ADHs from distinct LAB strains having 264 amino acids. Figure 3 shows the similarity of our recent identified ADH with the preivously identified ADHs which reveals a high level of similarity.

```
Feature 1
1EDO_A        4 VVVTGASRGIGKAIALSLGK.[3].KVLVNYAR.[20].T     FGGDV.[ 5].VEAMM.[9].IDVVVNNAG 88
query        10 ALITGSTKGIGKAIATELAR.[3].DVIINGRQ.[19].P.[2].IAADI.[ 5].QQKLF.[5].VDILINNMG 91
2D1Y_A        9 VLVTGGARGIGRAIAQAFAR.[3].LVALCDLR.[13].F     FQVDL.[ 5].RVRFV.[9].VDVLVNNAA 86
3GEG_A        5 VIVTGGGHGIGKQICLDFLE.[3].KVCFIDID.[15].Y     FHGDV.[ 5].LKKFV.[9].IDVLVNNAC 84
1AHI_A       14 AIITGAGAGIGKEIAITFAT.[3].SVVVSDIN.[19].A     CRCDI.[ 5].LSALA.[9].VDILVNNAG 97
1ZEM_A       10 CLVTGAGGNIGLATALRLAE.[3].AIALLDMN.[19].S     YVCDV.[ 5].VIGTV.[9].IDFLFNNAG 93
3E03_A        9 LFITGASRGIGLAIALRAAR.[3].NVAIAAKS.[26].A     LKCDI.[ 5].VRAAV.[9].IDILVNNAS 99
gi 75499505  18 ALITGASSGIGLTIAKRIAA.[3].HVLLVART.[19].I     FPCDL.[ 5].IDQLS.[9].VDFLINNAG 101
gi 6691663    6 ILITGASSGLGRGMAIEFAK.[3].NLALCARR.[16].H     IQIEI.[10].VFTVF.[9].LDRIIVNAG 91
gi 41615095   3 AIVTGDSRGIGKAIAERLYG.[3].KTIGIARS      N     VKTDW.[15].VLELI.[3].IRVFVHNAG 71

Feature 1                  #                          #         #   #
1EDO_A       89 .[14].WDEVIDLNLTGVFLCTQAATK.[7].GRIINIASVVG.[7].ANYAAAKAGVIGFSKTAARE.[5].INVNVVC 180
query        92 .[14].WRKFFDVMVLAGNALAKFYLP.[7].GRIIFIASEEA.[7].PQYSMTKSMNLSLAKSLSKL.[5].VTVNTIM 183
2D1Y_A       87 .[14].WRRVLEVNLTAPMHLSALAAR.[7].GAIVNVASVQG.[7].AAYNASKGGLVNLTRSLALD.[5].IRVNAVA 178
3GEG_A       85 .[14].FDYILSVGLKAPYELSRLCRD.[6].GRIINIASTRA.[7].EAYASAKGGIVALTHALAMS.[4].VLVNCIA 174
1AHI_A       98 .[13].FRRAYELNVFSFFHLSQLVAP.[7].GVILTITSMAA.[7].TSYASSKAAASHLVRNMAFD.[5].IRVNGIA 188
1ZEM_A       94 .[15].FARVLTINVTGAFHVLKAVSR.[7].GRIVNTASMAG.[7].AAYGTSKGAIIALTETAALD.[5].IRVNAIS 186
3E03_A      100 .[14].FDLXQQVNARGSFVCAQACLP.[7].PHILTLAPPPS.[9].TGYTLAKXGXSLVTLGLAAE.[5].VAINALW 193
gi 75499505 102 .[16].FERTMQLNYFGAVRLVLNLLP.[7].GQIINISSIGV.[7].SAYVASKAALDAFSRCLSAE.[5].ISITSIY 195
gi 6691663   92 .[14].NLQTAQTNFIAALAQCEAALE.[7].GHLVTISSISA.[8].TVYAATKSALTSLTEGIRID.[5].IKVSCIH 184
gi 41615095  72 .[14].IKKVYEVNVFSAILGLKKLYK.[7].SLIVFISSITA.[8].IGYVSSKAALVGLAKQLSKE.[3].IRVNAIA 162

Feature 1
1EDO_A      181 PGFIASD.[24].PENVAGLVEFLAL.[9].QAFTID 239
query       184 PGSTLTE.[39].PAEIGRFTAFVAS.[8].EALRLD 256
2D1Y_A      179 PGAIATE.[30].PEEVAEAVLFLAS.[8].AILPVD 242
3GEG_A      175 PGWINVT.[20].PKDISNMVLFLCQ.[6].ETIIVD 226
1AHI_A      189 PGAILTD.[25].PQDIANAALFLCS.[8].QILTVS 247
1ZEM_A      187 PGYMGPG.[40].INEIPGVVAFLLG.[8].VNLPIA 260
3E03_A      194 PRTVIAT.[16].PEIXADAAHAVLT.[8].QFLIDD 243
gi 75499505 196 MPLVRTP.[15].PEEAADLIVYAIV.[3].TRIATH 239
gi 6691663  185 PGFIRTE.[13].AEAGCKAIVKAIN.[3].ANSYVP 226
gi 41615095 163 PGYTETD.[24].PEDIADVVEMLIK.[6].QTIHVN 218
```

Figure 3. Amino acid similarity of ADHs from Lactobacillus brevis E25 with previously identified ADHs.

Our preliminary screening of the ADH-E25 was clearly revelaed that it is an effienct biocatalyst to perform the reaction given in Figure 4.

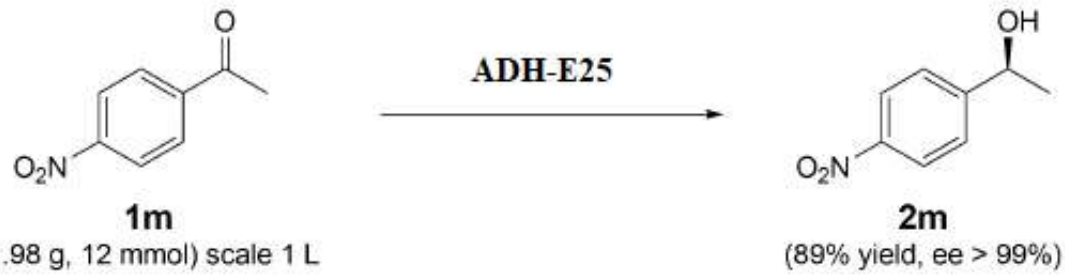

Figure 4. Production of (S)-1-(4-nitrophenyl)ethanol by the action of ADH-E25

Another important positive effect of using expressed ADH in bioreduction reactions is the non-formation of wastes which can form at high levels during the chemical reduction reactions. Also ADH as a protein has a major advantage compared to the whole cells as no additional steps such as preparation of medium for the growth of microbial cells or collection of the cells from the medium is required. The 3D model structure of ADH-E25 is given in Figure 5 which gives a clear indication of the ADH enzyme as the stucture is so similar with the identified ADH enzymes playing roles for bioreduction reactions.

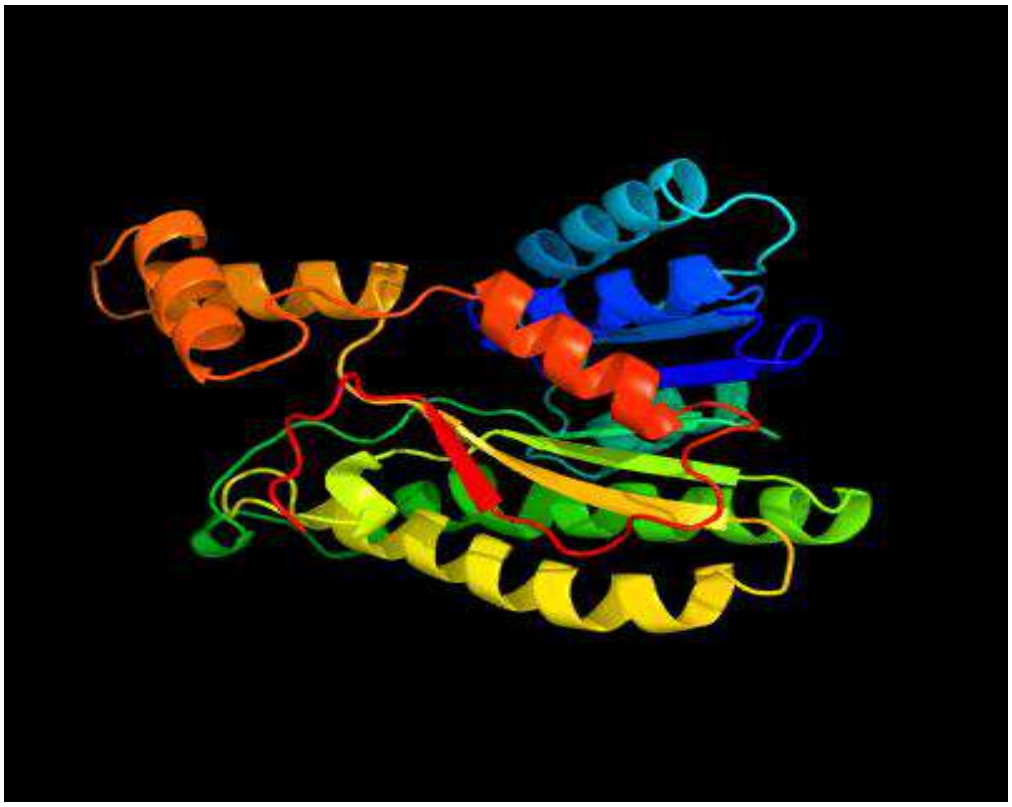

Figure 5. Schematic representation of the ADH-E25 3D model structure obtained using Phyre2.

Conclusion and Future Perspectives

- Preparation of chiral secondary alcohols is crucial for different industries including pharmaceutical industry and biocatalysts are important compounds for this purpose.
- Whole cells and expressed enzymes are efficient biocatalysts to conduct bioreduction reactions with no significant waste formation that are suitable for green chemistry.

- ADHs are one of the main enzymes to be used in bioreduction reactions efficiently.
- Recently we have identified a novel ADH from a LAB strains that is effective as a biocatalyst.
- Our future goal is to test this enzyme in different bioreduction reactions to obtain chiral secondary alcohols.

References

1. Preparation of chiral secondary alcohols is crucial for different industries including pharmaceutical industry and biocatalysts are important compounds for this purpose.
2. Whole cells and expressed enzymes are efficient biocatalysts to conduct bioreduction reactions with no significant waste formation that are suitable for green chemistry.
3. ADHs are one of the main enzymes to be used in bioreduction reactions efficiently.
4. Recently we have identified a novel ADH from a LAB strains that is effective as a biocatalyst.
5. Our future goal is to test this enzyme in different bioreduction reactions to obtain chiral secondary alcohols.
6. Rodrigues et al., Food Technol. Biotechnol.2004, 42, 295 – 303
7. Ribeiro et alBiomed. Res. Int. 2014, 2014
8. Schmid, et al., Nature 2001, 409, 258 – 268
9. Nakamura, et al., Tetrahedron: Asymmetry, 2013, 14(18), pp.2659-2681.

TEXTILE TECHNOLOGY

ORAL PRESENTATIONS

The Effect of Thickness and Density to Acoustic Parameters for Fabric Reinforced Composite Structures Produced From Rachis Material

Müslüm EROL[1*], Süreyya KOCATEPE[2], Nazım PAŞAYEV[2]

[1]Bingöl Üniversitesi, Teknik Bilimler Meslek Yüksek Okulu, Tekstil Teknolojisi Programı, Bingöl, Türkiye
[2]Erciyes Üniversitesi, Mühendislik Fakültesi, Tekstil Mühendisliği bölümü, Kayseri, Türkiye

[*] **Corresponding Author:** erolmuslum@gmail.com

Abstract

Only some of the chicken feathers obtained as a by-products in white meat production are used for protein meal production, construction industry and composite panel production for different purposes. These wastes are also harmful to the environment. The chicken feather fibers obtained by cutting and separating from rachis part are universal and have multipurpose usage. The rachis material, which predominantly forms the half of the chicken feathers, is important with its light weight, high strength and other interesting properties. In these study, porous sandwich composite structures were developed using different matrices from rachis and their acoustic properties were measured according to the impedance tube method. Sound absorption coefficients of structures made from rachis show high values at high frequencies and show low values at medium and low frequencies. When the density of material increases, there is a noticeable improvement in the sound transmission loss value of material. Acoustic parameters improved with increase of layers in material. Because of the outer layers are composite, better results at low frequencies were obtained in terms of sound transmission loss. Acoustic parameters of sandwiched structures produced with conventional sound absorbing materials such as glass wool, rock wool and felt have caused significant increases in all frequencies due to rachis composites. In terms of acoustic comfort, it is thought that the composites produced from rachis are futuristic material.

Keywords: Rachis, chicken feather, composite material, sandwiched structures, sound insulation

1. Introduction

The noise which is defined as uncomfortable noise has become an increasingly important issue because of evolving technology, mechanization, increasing of public habitats, heavy traffic and motor vehicles become indispensable elements of our social life. It is an important field of study that scientists are interested in to combat noise that affects human health negatively from psychological, physiological and psychosocial aspects. When look at the literature studies, there are many traditional materials that can be used in sound insulation. However, scientists are looking for new materials that will perform better and cost less. One of those materials can be chicken feather.

In every year, millions of tons of feathers appear a fall-out in our country and in the world. More than half of these feathers cannot be evaluated in any way, they are burnted or buried. In both cases serious damage is given to the environment. By producing a product with added value, this waste material will result in an economic gain and the health of the environment. In our studies in Erciyes University, we have produced composite materials which have a very high acoustic parameters by using special machines and processes. In this study, we analyzed how the thickness and density of composite materials produced from chicken feather rachis material affected the sound absorption and sound transmission loss value.

2. Material and Method

2.1. Material

Rachis material

The chicken feathers which were obtain from Gaziantep 'Tad Piliç' company were washed, dried and disinfected for cleaning in the Erciyes University, Textile Engineering Department Laboratories. The feathers were washed with sodium hypochlorite at 40ºC in order to remove from the dirt and grease at the first stage, than dried at 40ºC in a specially designed feather dryer and disinfected for 12 minutes at 70ºC [Paşayev et al.,2017; Paşayev, 2017; Kocatepe and Paşayev, 2018]. After the cleaning process, the chicken feathers were processed in a special machine to obtain fiber and rachis material [Paşayev and Erol., 2018].In Figure 1, obtained chicken feather fiber and rachis material can be seen.

Bonding polymer

In the production of composites, Ethylenevinylacetate (EVA) and Low Density Polyethylene (LDPE) as a powder form, Polyvinyl Acetate (PVA) and Polyacryl (PAKR) binders which dispers in water were used. This polymers were used because of we wanted to keep the process temperature as low as possible. In Table 1 and Table 2, some properties of the selected bonding materials are given.

Table 1. Some properties of the bonding materials

Properties	**Low Density Polyethylene (LDPE)**	**Ethylenevinylacetate (EVA)**
Density in 23ºC	0,92 g/cm^3	0,93 g/cm^3
Melting temperature	120ºC	80ºC
Process temperature	130ºC	90ºC

Table 2. Some properties of the bonding materials

Properties	**Polyvinyl acetate (PVA)**	**Polyacrylic (PAKR)**
Appearance	White dispersion	White dispersion
Solubility	In cold or warm water	In cold or warm water
Density in 20ºC	1,25g/cm^3	1,78g/cm^3
pH	6-7	4-5
Thermal drying	90-100	90-100

Figure 1. Fiber and rachis materials obtained from chicken feather fibers

Composite Production

Hot pressing method has been applied in the production of composites and used as press equipment of Gülnar Plastic Machines. Metal molds which has a internal dimensions of

16cmx16cmx0,5cm were used. Using these molds, samples with different bulk densities were produced by keeping the amount of raw material thickness and pressing pressure constant. The rachis material, amount of binding material and type of binding material were accepted as independent variables in the production and sample sizes were kept constant.

Experimental plans showing the mixing ratio of rachis material and binding material were prepared in Table 3 and Table 4 and samples were produced according to these plans. In Figure 2, the mold used in sample production, the composite samples can be seen.

In the composited produced by using EVA and LDPE, the amount of rachis was 33gr and 50gr, amount of binding material were twenty percent of rachis material and forty five percent of rachis materials. (Table 3).

The mixture of the rachis particles and the dry binding material was molded onto the teflon film. A teflon film was laid on top of the prepared mixture and put in to press machine. Press machine temperature was adjusted according to the process temperatures written in Table 1 and Table 2. The pressing time was determined according to the internal temperature of the structure and fixed at 120ºC as 90ºC for dry binding material.

Table 3. Plans of composite production which incledes EVA, LDPE and rachis material

Experimental number	Raw material amount, gr	Binding material, gr	Binding material type
1	33	8,25	EVA
2	50	12,5	EVA
3	33	14,85	EVA
4	50	22,5	EVA
5	33	8,25	LDPE
6	50	12,5	LDPE
7	33	14,85	LDPE
8	50	22,5	LDPE

PVA and Polyacryl (PAKR) binding materials are used in water as an emulsion. According to the results of the preliminary studies, appropriate binding material rations have determined.

For 40gr and 50gr weights of rachis material, the solution was prepared so as to be treated with binder at 30% and 50%. After the solution was mixed homogeneously together with rachis material, the mixture was molded, then pressed at 120ºC for 220sn. After cooling, the mixture was removed from the mold. In a total, 32 samples were produced as given in the production plans (Table 3 and Table 4).

Table 4. Plans of composite production which incledes PVA and Polyacryl (PAKR)

Experimental number	Raw material amount, gr	Binding material, gr	Binding material type
1	40	12	PVA
2	50	15	PVA
3	40	20	PVA
4	50	25	PVA
5	40	12	PAKR
6	50	15	PAKR
7	40	20	PAKR
8	50	25	PAKR

Figure 2. Composite production

In order to see the effect of thickness and density on the acoustic parameters in layered composites, the measurements of layers were made by combining with six different fabrics and graphs were drawn for the obtained results. For the sample production, fabrics encoded as K1, K2, K3, K4, K5 and K6 and composite plates coded as C1, C2 were used and brief information about their content are given in Table 5.

Table 5. Content of fabric codes and composite

Kod	**Malzeme içeriği**
C1	50gr rachis-12,5gr EVA
C2	50gr rachis-12,5gr EVA
K1	Chenille upholstery (17 density)
K2	Chenille upholstery (19 density)
K3	Woolen cloth
K4	Raw linen fabric
K5	Nonwoven (Cleaning fabric)
K6	Tricot fabric made from acrylic yarn

Measurement of Acoustic Parameters

The sound insulation parameters of the composite plates produced were measured with the BSWA TECH branded impedance tube (Figure 3). For this purpose, two specimens of 10cm and 3cm in diameter were cut from each produced sample.

Measurements were made according to standart of the ISO 10534-1: 1996 Acoustics-Determination of sound absorption coefficient and impedance in impedance tubes-Part1: Method using standing wave ratio ve ISO 10534-2: 1998 Acoustics-Determination of sound absorption coefficient and impedance in impedance tubes-Part2: Transfer function method.

Figure 3. Impedance tube

3. Findings and Discussion

The acoustic properties of the produced composite samples were measured and compared, the structures produced by using EVA exhibit better performance.

The change graphs of sound absorption coefficient and the sound transmission loss value of the single layer composite samples produced in Figure 4 are given. Composite samples were produced according to the test plans in Table 3 and Table 4 by using binding polymers at different densities and weights. In the curves of Figure 5, it can be seen that how the increase of sample thickness and density affects the acoustic parameters.

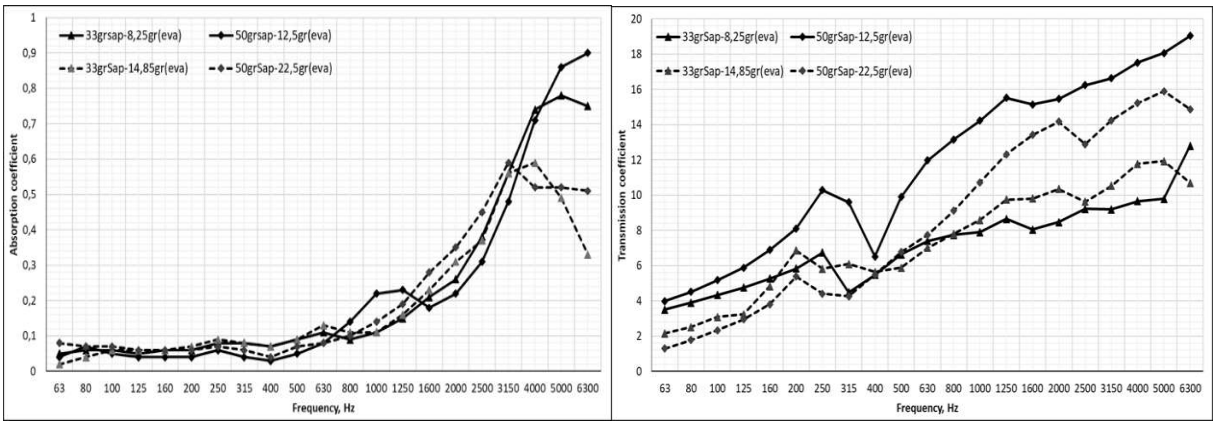

Figure 4. The effects of density and binding material to the sound absorption and sound transmission value in single-layer composite structure

When the thickness and amount of binding material are kept constant, the sound transmission loss coefficient has increased considerably due to the increase in density. This caused lower sound absorption at mid frequencies. On the other hand, as the amount of binding material used in the composite increases, the sound absorption coefficient decreases in all cases because of the pore closes. Similar results can be said in terms of sound transmission loss (Figure 4).

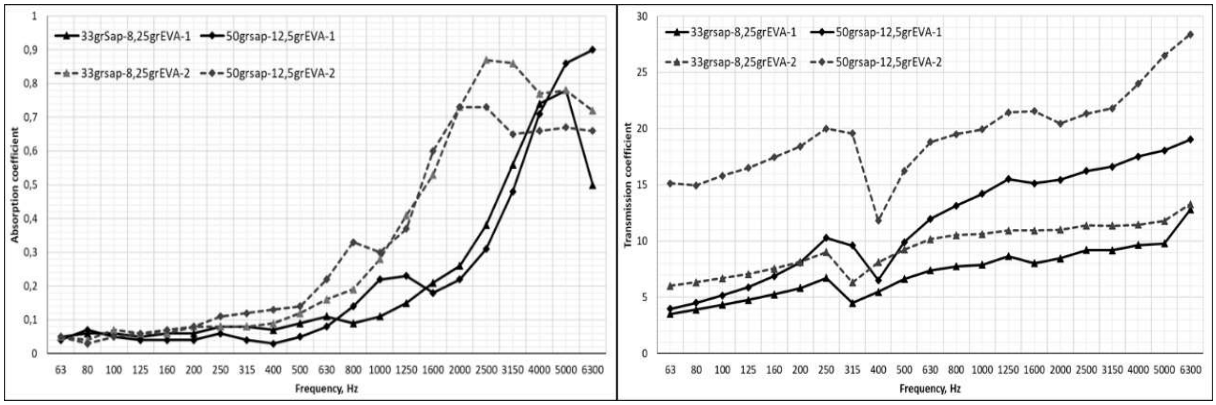

Figure 5. The effects of thickness and density to the sound absorption and sound transmission value in composite structures

As can be seen from graphs, when the thickness of sample are double layer, sound absorption values are significantly increasing in low and medium frequencies. When the thickness and density increase in all scale, the sound transmission loss value increase (Figure 5).

In Figure 6, graphs which shows how the results of the impedance tube measurements of samples coded as C1 K1, K2, K3, K4, K5, K6, are changed depending on the frequency are presented. Figure 7 shows how the sound absorption coefficient and the sound transmission loss coefficient values of the samples which are produced by adding a third composite layer to this produced two-layer structure according to the frequency.

As a results of the producing the two-layer samples which were produced with composite contain chicken feather rachis and fabrics have a different specialties, it is seen that curves of sound transmission loss of two-layered samples shows great similarity. But for the sound absorption coefficient, this situations change according to the structure and specialties of fabrics. At medium and high frequencies, it is seen that the when the knitted fabric of 1.5mm thickness produced from K6 coded acrylic yarn is used, the higher sound absorption has obtained. At the lower frequency, when the K5 coded fabric is used, the higher sound absorption has obtained in sample. In another structure used with another fabrics, close results has obtained in nearly every frequency.

When the present structure is supported by a third C2 composite layer, it is clearly visible that the curves are going the left and upward for every frequency in all samples in terms of sound absorption. It has been seen that in the structures with more voluminous and thick fabrics, much better sound absorption is achieved, especially at low and medium frequencies. Thickness, porosity and density are very important for sound absorption. When look at the curves related to the sound transmission loss, it has observed that significant increases in all samples were observed due to the increase in thickness.

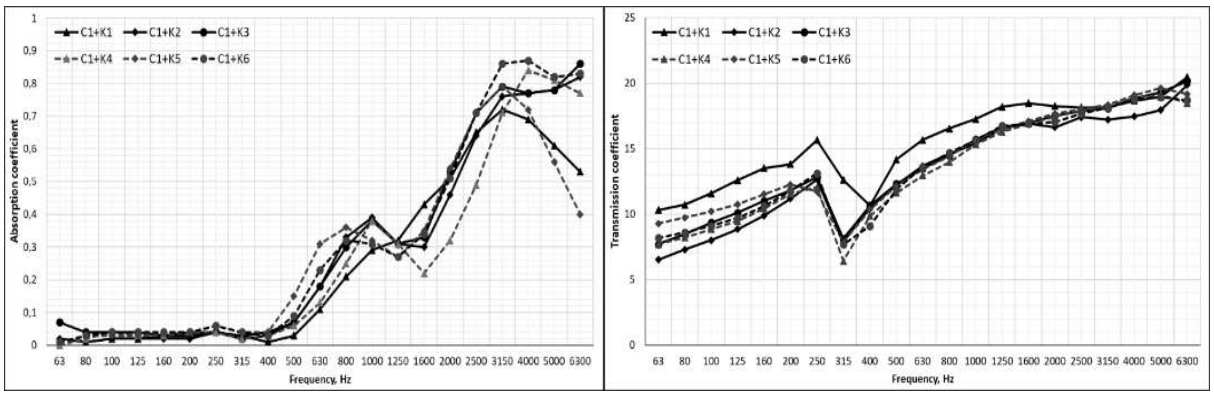

Figure 6. Effect of composites produced by combination with fabrics which have a different properties on sound absorption coefficient and sound transmission loss values

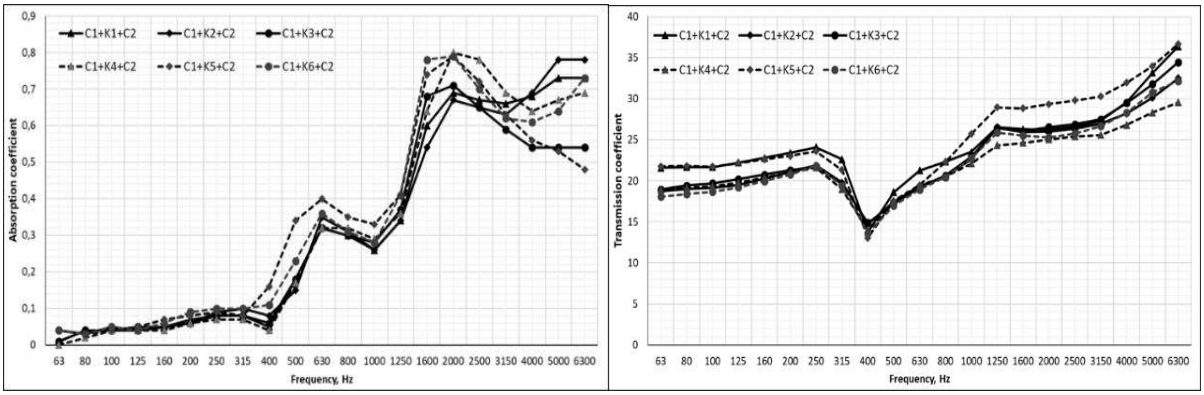

Figure 7. The effects of thickness increase on the acoustic parameters of composite structures obtained by the addition of composites in combination with the fabrics of different properties

4. Conclusions and Recommendations

It has been seen that there are significant changes in the acoustic parameters due to the variation of thickness and density of the composite plates produced according to the thermal bonding method using different binders from chicken feather rachis material. When the thickness and the amount of binding material are kept constant, the sound transmission loss coefficient has increased. This caused lower sound absorption at mid frequencies. On the other hand, as the amount of binding material used in the composite increases, the sound absorption coefficient decreases in all cases because of the pore are closed. It has been found that in a single layer structure, a low density structure at low frequencies and a high density structure at medium-high frequencies have better noise transmission loss coefficients.

When the second layer is added to a single layer composite sample with a thickness of 5mm, it is found that there is a significantly increase for sound absorption values at all low and mid frequencies. The sound absorption coefficient of 0,38 at the 2500Hz frequency rises to a high value of 0,87 when it is two layer. In the sound transmission loss coefficient, an increase was observed due to the increase in thickness and density throughout the whole scale.

It has been found that there is not important difference in sound transmission loss of the samples which produced as a two-layer at the end of the combine the chicken feather rachis and six different fabrics. But it is seen that that structure has higher performance at all frequencies from one-layer structure and the material construction is insignificant for sound transmission loss. It can be said that use of structures that are more voluminous and porous in two-layer structure gives better results at low and high frequencies in terms of sound absorption coefficient.

As a results of the combine of the present construction with a third composite layer, the sound absorption coefficient curves dramatically shift to left and right at all frequencies due to the thickness and density rise of fabrics in structures. It can be said that the properties such as thickness, weight, density and porosity of layers in layered composite structures are important properties for acoustic parameters.

Acknowledgment

The study was supported by Erciyes University Scientific Research Project Coordination with FDK-2016-6847 number Project.

References

Kocatepe, S., Paşayev, N., (2018). Tavuk Tüylerinin Lif Üretimi Açısından Yapısal Özelliklerinin Analizi, *3. International Fiber and Polymer Symposium*, (pp:127-129). BURSA

Paşayev, N., Kocatepe, S., Maraş, N., Soylak, M., Erol, M., (2017). Investigation some characteristics of chicken feather's rachis. 17th AUTEX World Textile Conference 2017. 21-29 may 2017. Corfu, Greece

Paşayev, N., (2017). Fiber production from chicken feather with industrial method. *BULLETIN of the Kyiv National University of Technologies and Design*, 110(06), pp. 107-113.

Paşayev, N., Erol, M., (2018). Ses yalıtım Amaçlı Tekstil Esaslı Sandviç Yapıların Geliştirilmesi, *3. International Fiber and Polymer Symposium*, (pp:101-103). BURSA

Statistical Analysis of Effects of Production Parameters of Sound Insulation Materials Produced From Chicken Feather Fibers on Acoustic Properties

Süreyya KOCATEPE[1*], Müslüm EROL[2], Nazım PAŞAYEV[1]

[1]Erciyes University, Faculty of Engineering, Department of Textile Engineering Kayseri, Türkiye
[2]Bingöl University, Vocational School of Technical Science, Textile Technology Program, Bingöl,

[*] **CorrespondingAuthor:**sureyya.kocatepe@hotmail.com

Abstract

In recent years, noise, which is one of the negative effects of modern life and developing technology, has become a common problem. For this reason, the issue of struggle against the noise has become increasingly important, so sound-absorbing materials are being developed to provide acoustic comfort in closed areas. Among these materials, materials developed from natural materials have a special place. In this study, nonwoven surfaces produced from chicken feather fibers which emerged as a by-product in chicken meat production via thermal binding were developed in order to provide acoustic comfort. In the study, nonwoven surface samples were obtained at different densities using different binding materials. A multi-factor experimental design was designed in the Design Exper program to determine how the produced samples affected the acoustic performance of the production parameters and the samples were produced according this plan. The acoustic parameters of the produced samples were measured in the impedance tube. Statistical analysis was applied the data obtained from the measurement. In the sample production, the binder polymer type, the thickness of the sample, the amount of fiber, the amount of binding agent and the frequency of sound were taken as independent changing parameters. The sound absorption coefficient and the sound transmission values from the acoustic values of samples were chosen as the dependent parameters. The change intervals for each of these values were determined and experiments were performed. Mathematical models expressing the relation between sound absorption coefficient and sound transmission loss values with production parameters have been obtained and interpreted.

Keywords: chicken feather fibers, sound absorption materials, nonwoven, sound insulation

1. Introduction

One of the negative aspects of modern life and technology is noise. There are increasingly ways to combat noise, which affects living standards as well as many health problems. An important groups of these methods are methods based on the use of sound absorbans or sound absorbing materials. Sound absorbing materials are commonly used to reduce noise in enclosed areas.

Among the various sound absorbing materials in market, porous sound absorbing materials produced from fibers have a special place. Nonwoven surface type textile materials which are advantageous economically and lightly as well as ecologically are also widely used. Literature studies have shown that materials made from natural fibers have better in terms of sound absorption properties [1]. In this study, chicken feather fibers which is a natural material, were used.

Research has shown that the porous internal structure of the chicken feather fibers gives a insulating properties to the fibers. In this study, it is aimed to investigate the acoustic parameters of nonwoven surfaces type insulating materials which are produced by thermal binding method based on dry-laying from chicken feather fibers.

When look the literature studies, it is seen that there are many parameters affecting the sound insulation properties of fibrous materials which has a porous. It is clear that these parameters do not affect the acoustic properties of the material at the same level. Material thickness, fiber size of the material, porosity, volumetric density, surface treatments etc. are the main parameters affecting sound insulation [2], [3], [4]. Among these parameters, as well as the importance of parameters such as material thickness and porosity in terms of material structure is, the sound frequency parameter is important in terms of parameters of emitted sound.

This study is deal with that the statistical evaluation of the acoustic properties of sound insulation materials which are produced from chicken feather. For this purpose, a multi-factorial experiment was designed and the effects of indusial factors in terms of acoustic properties were investigated.

2. Material and Method

2.1. Material

Chicken feather fibers: Chicken feather used in this study was obtained from Tad Piliç (Gaziantep), then fibers were obtained from that feather after washing, disinfection and drying process [5], [6].

Binding Materials: Powder form polyethylene and ethylene vinyl acetate and low melt bicomponent fiber (PES/PP) were used.

2.2.Method

2.2.1. Designing of experimental plan

Production of nonwoven surface samples by thermal binding was performed according to a multi-factorial experimental design in the Design Expert program. Based on the preliminary investigations, the type and amount of binding material, the sample size, the amount of fiber in sample and the sound frequency were used as independent changing parameters in the sample production. The change levels of the parameters are given in Table 1. Sound absorption coefficient and sound transmission loss are seen dependent variables from acoustic parameters of the material.

A factorial experimental design which is designed with 4 numerical, 1 categorical factor, is given in Table 2. The test plan includes 720 experiments.

Table 1. Experimental factors, change intervals and levels

				Factor levels	
Factors	**Sign**	**Factor type**	**Change levels of factors**	**Chance levels**	
				-1	**+1**
Type of binding material	A	Categorical		EVA, LDP, PE-PP(LM)	
Layer number of sample	B	Numerical	1…3	1	3
Fiber amount in sample	C	Numerical	10…20	10	20
Amount of binding material in sample	D	Numerical	30…50	30	50
Frequency of sound wave	E	Numerical	63…6300	63	6300

Table 2. Experimental design plan

No	Factors					
	A: BM	B: Layer	C:F.A	D:BM.A	E: Frequency	Y_i
1	-1	-1	-1	-1	63	
2	-1	-1	-1	1	63	
3	-1	-1	1	-1	63	
4	-1	-1	1	1	63	
5	-1	0	-1	-1	63	
6	-1	0	-1	1	63	
7	-1	0	1	-1	63	
8	-1	0	1	1	63	
9	-1	1	-1	-1	63	
10	-1	1	-1	1	63	
11	-1	1	1	-1	63	
12	-1	1	1	1	63	
13	0	-1	-1	-1	63	
…	…	…	…	…	…	

2.2.2. Production of nonwoven surface samples

At specified rations, the fiber and binding polymer material were mixed homogeneously and laid in to 16x16cm metal molds and placed in a hot press machine. Sample thickness and press pressure were fixed by means of the molds, with different volumetric density and porosity are obtained [7] (Figure 1).

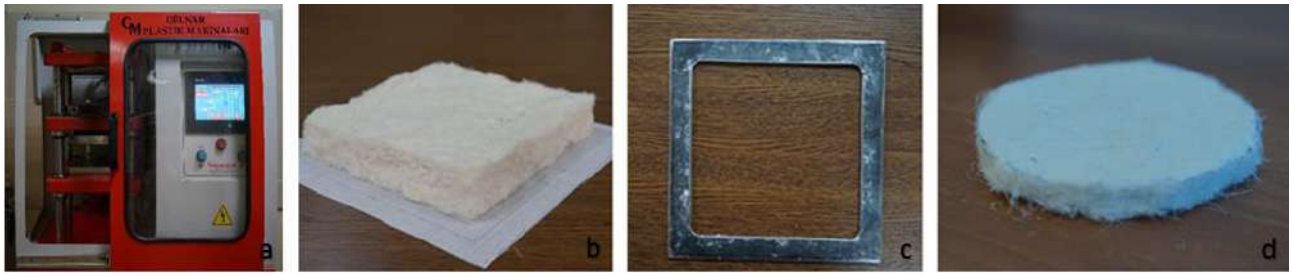

Figure 1. Production steps of nonwoven surface samples

(a-press machine, b-laid surface, metal mold, nonwoven sample)

2.2.3. Acoustic analyses of produced nonwoven surface samples

The sound absorption coefficient and the sound transmission loss values of the samples cut from the nonwoven surface samples were measured in the BSWA TECH branded impedance tube.

Figure 2. Impedance tube

3. Findings and Discussion

The acoustic properties of the samples, which were produced according to specified parameters, were measured and written to table. The summary of the experimental plan is given in Table 3.

Table 3. The summary of multi-factorial experimental plan

Design Summary								
Study Type	Factorial		**Experiments**	720				
Initial Design	Full Factorial		**Blocks**	No Blocks				
Design Model	2FI							
Response	**Name**	**Units**	**Obs**	**Minimum**	**Maximum**	**Trans**	**Model**	
Y1	CoAB		720	0.000	0.99	None	No model chosen	
Y2	TL	dB	720	0.050	66.22	None	No model chosen	
Factor	**Name**	**Units**	**Type**	**Low Actual**	**High Actual**	**Low Coded**	**High Coded**	
A	Tutkal		Categorical	EVA	BK		**Levels:**	3
B	Kat	adet	Numeric	1.00	3.00	-1.000	1.000	
C	Lif_M	gr	Numeric	10.00	20.00	-1.000	1.000	
D	Tutkal_M	%	Numeric	30.00	50.00	-1.000	1.000	
E	Frekans	Hz	Numeric	63.00	6300.00	-1.000	1.000	

The model choice for both outcome parameters (sound absorption coefficient, sound transmission loss) is given in Table 4.

Table 4. Selection of model in multi-factorial experiment plan analysis

Response: CoAB

Sequential Model Sum of Squares

Source	Sum of Squares	DF	Mean Square	F Value	Prob > F	
Mean	153.94	1	153.94			
Linear	41.88	6	6.98	204.95	< 0.0001	
2FI	2.86	14	0.20	6.66	< 0.0001	Suggested
Quadratic	9.16	2	4.58	260.14	< 0.0001	Aliased
Cubic	3.87	27	0.14	11.43	< 0.0001	Aliased
Residual	8.40	670	0.013			
Total	220.09	720	0.31			

Model Summary Statistics

Source	Std. Dev.	R-Squared	Adjusted R-Squared	Predicted R-Squared	PRESS	
Linear	0.18	0.6330	0.6299	0.6257	24.76	
2FI	0.18	0.6762	0.6669	0.6563	22.74	Suggested
Quadratic	0.13	0.8146	0.8087	0.8030	13.03	Aliased
Cubic	0.11	0.8730	0.8638	0.8552	9.58	Aliased

Response: TL

Sequential Model Sum of Squares

Source	Sum of Squares	DF	Mean Square	F Value	Prob > F	
Mean	1.114E+005	1	1.114E+005			
Linear	54674.97	6	9112.50	268.46	< 0.0001	
2FI	15809.50	14	1129.25	94.05	< 0.0001	Suggested
Quadratic	2189.13	2	1094.57	122.98	< 0.0001	Aliased
Cubic	3977.26	27	147.31	44.34	< 0.0001	Aliased
Residual	2226.10	670	3.32			
Total	1.903E+005	720	264.34			

Model Summary Statistics

Source	Std. Dev.	R-Squared	Adjusted R-Squared	Predicted R-Squared	PRESS	
Linear	5.83	0.6932	0.6906	0.6857	24793.64	
2FI	3.47	0.8936	0.8906	0.8846	9104.69	Suggested
Quadratic	2.98	0.9214	0.9189	0.9137	6803.29	Aliased
Cubic	1.82	0.9718	0.9697	0.9646	2795.61	Aliased

For the value of sound absorption coefficient, it suggests an incomplete quadratic model. Although the F and S^2 values of the model are higher than the quadratic model, incomplete quadratic model was selected. For the sound transmission loss, it is also suggested the incomplete quadratic model.

The summary of ANOVA table for sound absorption is given in Table 5. The summary of ANOVA table 6 for sound transmission loss is given in Table.

Table 5. ANOVA summary for sound absorption coefficient

Response: CoAB

ANOVA for Response Surface Reduced Quadratic Model

Analysis of variance table [Partial sum of squares]

Source	Sum of Squares	DF	Mean Square	F Value	Prob > F
Model	53.89	22	2.45	139.19	< 0.0001
A	*0.30*	*2*	*0.15*	*8.56*	*0.0002*
B	*4.52*	*1*	*4.52*	*256.74*	*< 0.0001*
C	*6.480E-003*	*1*	*6.480E-003*	*0.37*	*0.5442*
D	*0.093*	*1*	*0.093*	*5.28*	*0.0219*
E	*36.96*	*1*	*36.96*	*2099.97*	*< 0.0001*
B^2	*0.013*	*1*	*0.013*	*0.71*	*0.3988*
E^2	*9.14*	*1*	*9.14*	*519.57*	*< 0.0001*
AB	*0.069*	*2*	*0.035*	*1.97*	*0.1399*
AC	*0.10*	*2*	*0.052*	*2.98*	*0.0513*
AD	*0.021*	*2*	*0.010*	*0.60*	*0.5516*
AE	*0.019*	*2*	*9.346E-003*	*0.53*	*0.5882*
BC	*0.22*	*1*	*0.22*	*12.44*	*0.0004*
BD	*0.11*	*1*	*0.11*	*6.33*	*0.0121*
BE	*1.26*	*1*	*1.26*	*71.74*	*< 0.0001*
CD	*0.080*	*1*	*0.080*	*4.53*	*0.0336*
CE	*0.94*	*1*	*0.94*	*53.26*	*< 0.0001*
DE	*0.033*	*1*	*0.033*	*1.90*	*0.1690*
Residual	12.27	697	0.018		
Cor Total	66.16	719			

Std. Dev.	0.13	R-Squared	0.8146
Mean	0.46	Adj R-Squared	0.8087
C.V.	28.69	Pred R-Squared	0.8030
PRESS	13.03	Adeq Precision	45.963

When look at the Table 5, it is seen that the selected model is meaningful. However, some terms of the model are meaningless in the chosen experiment space. The terms ″Prob>F″ value above 0,05 are meaningless. In this respect, the values of A, B, D, E, E^2, BC, CD, DE are meaningful value. The S^2 values of the individual model terms are investigated to see which Factor is more likely to affect the value of the sound absorption coefficient. In this respect, E (sound frequency) and B (number of sample layers) are more effective as factors.

Table 6. ANOVA summary for sound transmission loss

Response: TL

ANOVA for Response Surface Reduced Quadratic Model

Analysis of variance table [Partial sum of squares]

Source	Sum of Squares	DF	Mean Square	F Value	Prob > F
Model	72673.60	22	3303.35	371.16	< 0.0001
A	*2150.98*	*2*	*1075.49*	*120.84*	*< 0.0001*
B	*13462.64*	*1*	*13462.64*	*1512.64*	*< 0.0001*
C	*12234.18*	*1*	*12234.18*	*1374.61*	*< 0.0001*
D	*563.06*	*1*	*563.06*	*63.26*	*< 0.0001*
E	*26264.11*	*1*	*26264.11*	*2951.00*	*< 0.0001*
B²	*11.92*	*1*	*11.92*	*1.34*	*0.2475*
E²	*2177.21*	*1*	*2177.21*	*244.63*	*< 0.0001*
AB	*609.75*	*2*	*304.88*	*34.26*	*< 0.0001*
AC	*2454.18*	*2*	*1227.09*	*137.87*	*< 0.0001*
AD	*647.30*	*2*	*323.65*	*36.36*	*< 0.0001*
AE	*374.88*	*2*	*187.44*	*21.06*	*< 0.0001*
BC	*901.35*	*1*	*901.35*	*101.27*	*< 0.0001*
BD	*426.01*	*1*	*426.01*	*47.87*	*< 0.0001*
BE	*5660.36*	*1*	*5660.36*	*635.99*	*< 0.0001*
CD	*236.87*	*1*	*236.87*	*26.61*	*< 0.0001*
CE	*4349.27*	*1*	*4349.27*	*488.68*	*< 0.0001*
DE	*149.53*	*1*	*149.53*	*16.80*	*< 0.0001*
Residual	6203.36	697	8.90		
Cor Total	78876.96	719			

Std. Dev.	2.98	R-Squared	0.9214
Mean	12.44	Adj R-Squared	0.9189
C.V.	23.98	Pred R-Squared	0.9137
PRESS	6803.29	Adeq Precision	120.315

As shown in Table 6, the selected model is meaningful. In here all terms of the model are meaningful except for B^2. It can be said that the factors of E (sound frequency), B (layer number of sample), C (fiber amount in sample) are more effective.

The distribution of the data is normal. The model has 0,81 value for sound absorption coefficient, has a R^2 value equal to 0,92 for sound transmission loss. This indicates that the model is sufficiently descriptive.

We can interpret from the graphs of the obtained models that how individual factors affect the acoustic parameters (Figure 3-6). When look at the graphs in Figure 3, for each binding material type, the sound absorption coefficient increases in the low and medium frequency regions as

the sound frequency value increases, but decreases in the high frequency regions (Fig.3, left). As can be seen from graphs, the acoustical parameters are not affected much by the binding material type.

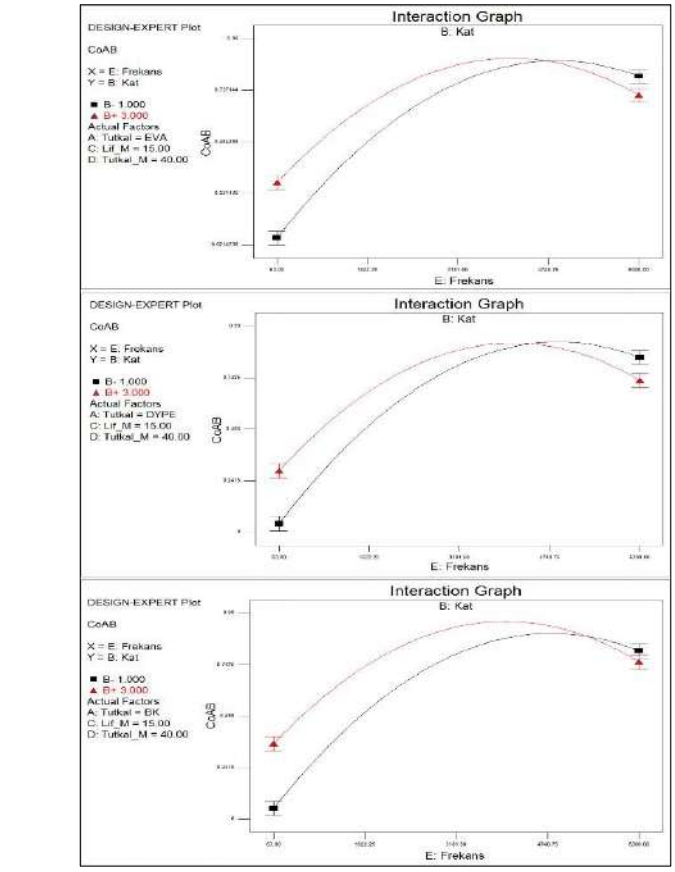

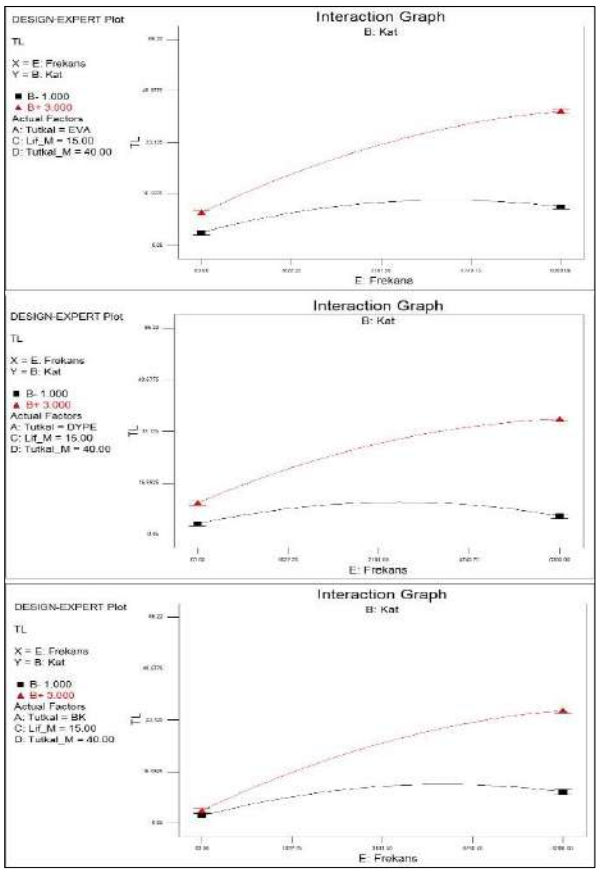

Figure 3. Effetc of binding material type on acoustic parameters

As the sample thickness increases the sound absorption coefficient increases and this shifts towards the low frequency (Fig.4, left). The same situation was seen in the curves of sound tranmission loss (Fig.4, rigt). As the thickness increases, the sound tranmission loss increases along the all frequency scale.

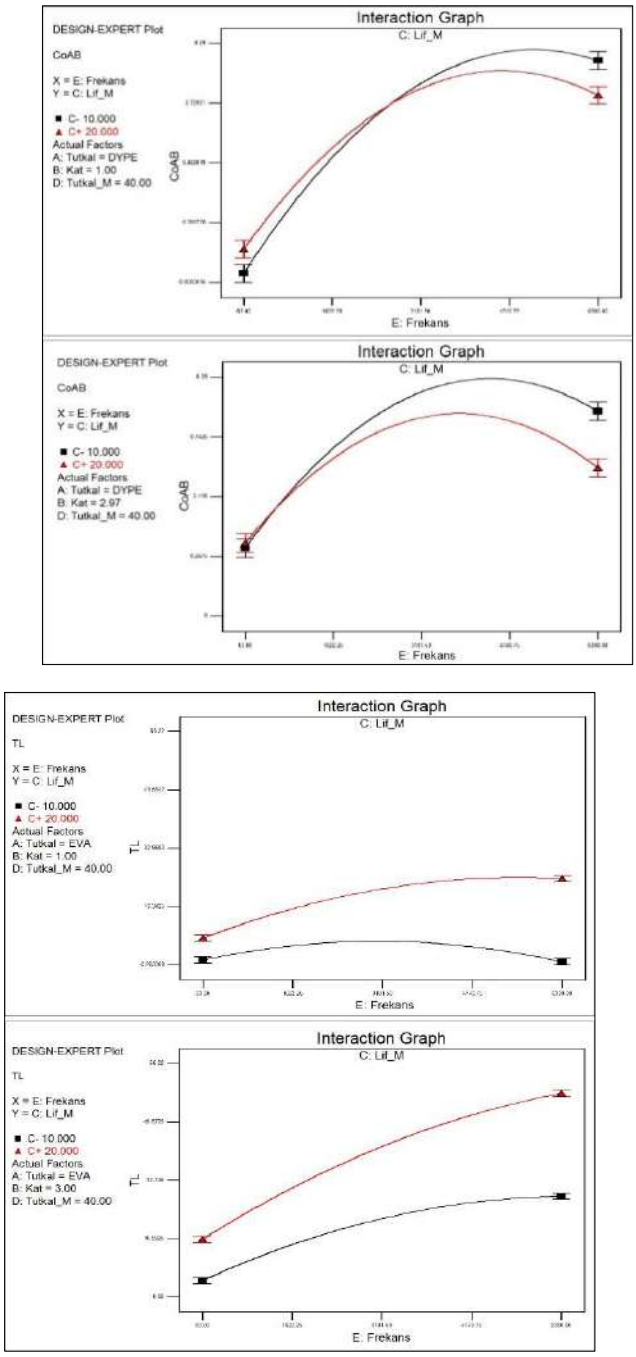

Figure 4. Effect of sample thickness on acoustic parameters

The increase of fiber amount in the sample leads to a decrease in the value of the sound absorption coefficient when the sound frequency increase (Fig., left). In fact, an increase in fiber amount means an increase in material density. This leads to a decrease in the value of the sound absorption coefficient ah high frequencies. For the values of sound transmission loss, this situation is different from it (Fig.5, right).

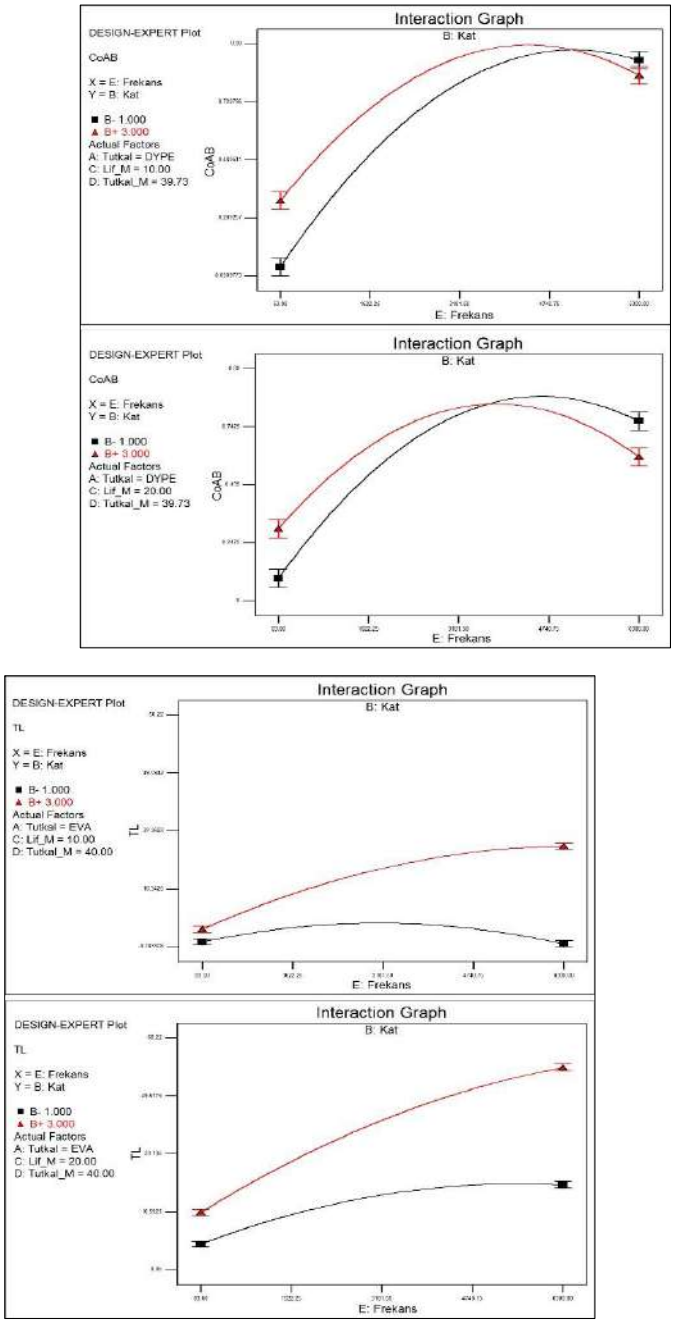

Figure 5. Effect of the fiber amount on acoustic parameters

Since the amount of binding material in samples directly affected the density of the material, fiber amount affect similarly to the values of sound absorption and sound transmission loss (Fig 6).

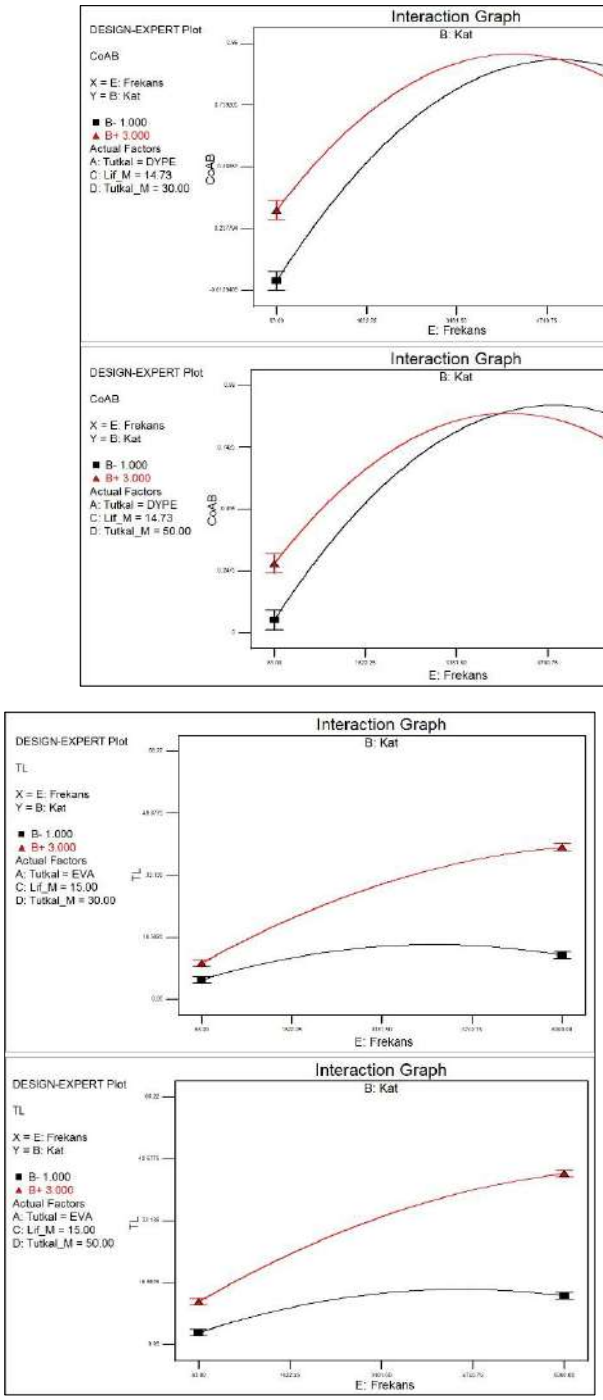

Figure 6. Effect of the amount of binding material in the sample on acoustic parameters

In the Design Expert program, the optimization issue has been resolved and study areas have been defined that allow to obtained evaluable results by determining the desired value

range for each optimization criterion. In figure 7, the change range of the sample production parameters that the sound absorption coefficient is in the range of 0,4---1,0 and the sound transmission loss is in the range of 20…70Db is given. Yellow colored areas are study areas where we can obtain these values.

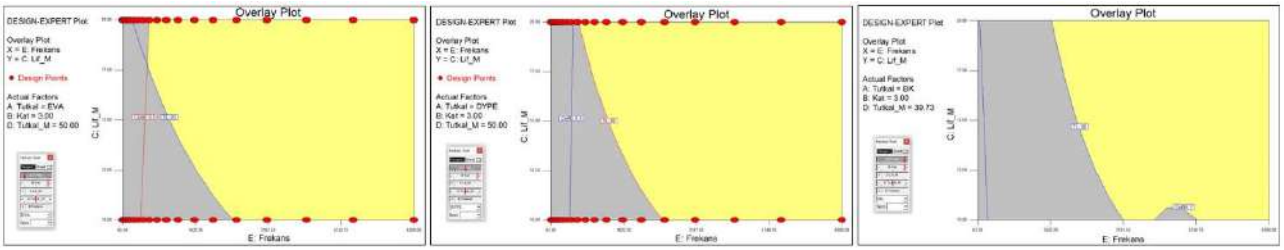

Figure 7. Study areas with factors to produce samples at acceptable quality

4. Conclusions and Recommendations

As a results of statistical analysis applied to the data obtained from the designed and realized multi-factorial experiments, parameters such as binding polymer type, sample thickness, fiber amount in sample, binding amount in sample and sound frequency, seriously affect the values of the sound absorption coefficient and sound transmission loss. According to experiment conditions, increase of fiber amount caused an increase of material density. When look at the results, it is seen that the increase of material density caused a decrease of sound transmission loss at high frequencies. In values of sound transmission, this effect caused increases. As the increases in the fiber amount effect the sample density, it decreased the value of sound absorption coefficient at high frequencies and increases the loss of sound transmission values.

It is seen from the study results, it is possible to develop acoustic materials with different sound absorption and transmission properties by changing the levels of factors.

For example, as the sample thickness increases, the values of the sound absorption coefficient increase and this increasing shift to low frequency regions. For the sound transmission loss, the increase of sample thickness caused an increase in the all frequency scales.

Acknowledgement

This study was supported by The Scientific and Technological Research Council of Turkey (TÜBİTAK) with 115M725 numbered researching project.

References

Paşayev, N., Kocatepe, S. and Maraş, N., (2018). Investigation of sound absorption properties of nonwoven webs produced from chicken feather fibers. *Industrial Textiles*. DOI: 10.1177/1528083718766843

Tascan M., (2016). Acoustical Test Methods for Nonwoven Fabrics, *Acoustic Textiles, Textile Science and Clothing Technology, Springe*r, pp:115-142.

Qui, X., (2016). *Princibles of Sound Absorbers. Acoustic Textile* RMIT University, Melbounme, VIC, Australia: (Edit: Padhve, R., Nayak, R).

Demiryürek, O., Aydemir, H., (2017). Sound Absorbing Properties of Roller Blind Curtain Fabrics. *Industrial Textiles*, 47(1), pp:3–19.

Kocatepe, S., Paşayev, S., (2018). Tavuk Tüylerinin Lif Üretimi Açısından Yapısal Özelliklerinin Analizi, *3. International Fiber and Polymer Symposium*, (pp:127-129). BURSA

N., Paşayev, (2017). Fiber production from chicken feather with industrial method. *BULLETIN of the Kyiv National University of Technologies and Design*, 110(06), pp. 107-113.

Kocatepe, S., Maraş, N., Paşayev, N., (2017). Production of Nonwoven from Chicken Feather Fibers, *XIV. International Izmir Textile and Apparel Symposium*, (pp:290-297). İZMİR

The Effects of Spinning System and Sizing Material on the Yarns' Tensile Properties

Tuba BEDEZ ÜTE[1], Pınar ÇELIK[1], Ayşegül EKMEKÇI KÖRLÜ[1], M. Bünyamin ÜZÜMCÜ[2], Hüseyin KADOĞLU[1]

[1]Ege University, Engineering Faculty, Textile Engineering Department, Izmir, Turkey
[2]Bartın University, Engineering Faculty, Textile Engineering Department, Bartın, Turkey

[*]**Corresponding Author:** tuba.bedez@ege.edu.tr

Abstract

The efficiency of weaving process depends on many parameters; the material characteristics, the sizing ingredients, the sizing operation and the yarn parameters. Sizing is a process before weaving which directly affects the performance of the weaving process. During the weaving process, as the warp yarns are subjected to abrasion with various loom components, sizing process is performed to improve the weave ability of yarns. In this process, a coating on the yarn surface is applied and protruding hairs are laid on the yarn surface. Sizing cotton warp yarns with starch is a conventional process used as standard practice in the textile industry. However some materials such as PVA and CMC are frequently used as an alternative to starch. The objective of this paper is investigating the effects of spinning system and sizing material on the yarns' tensile properties. For this purpose, compact, sirospun and ring spun yarns were produced and sized under same conditions. Tensile strength and elongation values of the yarns were tested statistically evaluated.

Keywords: warp yarns, sizing, weaving, yarn strength**.**

1. Introduction

On the weaving machine, the warp yarns are subjected to several types of friction, cyclic strain, flexing, and abrasion at various loom parts and inter yarn friction. With sizing, a coating on the yarn surface is applied and protruding hairs are laid on the yarn surface, the strength, abrasion resistance and finally weavability of the yarn will improve and this results with higher productivity and quality of the weaving process.

Effects of sizing on weavability (Faasen, 1966), causes of warp thread breakages (Dolecki, 1974, Bradburry, 1949), effects of sizing on warp breakages and different size types were investigated in various studies (Sultana et al., 2014; Ünal et al. 2003, Alay et al. 2011).

In this study the effect of sizing material and sizing process parameters on the physical and mechanical properties of the yarns, produced with different spinning systems, were investigated. For this purpose, 100% ring spun, siro spun, compact, and compact siro spun yarns were produced. In the sizing process, these yarns were sized with different sizing materials (carboxymethyl cellulose (CMC), polyvinyl alcohol (PVA),) in different concentration (4%, 6% and 8%) and temperature (20C°, 50C° and 80C°). Tensile strength, breaking elongation, yarn to yarn friction and yarn to metal friction characteristics of the yarns before and after sizing process were tested and evaluated. Optimum sizing parameters for the yarns were determined.

2.Material-Methods

In order to investigate the effects of spinning system and sizing material on the yarns' tensile properties, 100% cotton ring, siro and compact yarns were spun in yarn count of Ne 20 with the same twist coefficient (αe 4,5). Ring and siro yarns were produced in Pinter Merlin SPA 1803, compact yarns were produced in Rieter K45 spinning machines. The yarns were spliced on Saurer Schlafhorst Autoconer-X-5 winding machine at optimum opening and splicing pressure.

Table 1. Taguchi design of the sizing process for both sizing materials (CMC and PVA).

	Levels		
Trial no	A: Yarn type	B: Sizing concentration	C: Sizing temperature
1	1	1	1
2	1	2	3
3	1	3	2

4	2	1	2
5	2	2	1
6	2	3	3
7	3	1	3
8	3	2	2
9	3	3	1

Levels: Yarn type (1: ring, 2: siro, 3: compact), Sizing concentration (1: 4%, 2: 6%, 3: 8%), Sizing temperature (1: 20°C, 2: 50°C, 3:80°C)

In this study, a three-level-three-factor L9 Taguchi Orthogonal Array (OA) design was employed using Minitab statistical software to generate experimental runs by considering three independent input variables viz. Yarn type (A), Sizing concentration (B) and Sizing temperature (C) to find the optimal sizing parameters for tensile and frictional properties. Experimental design is given in Table 1. Yarn samples were sized with CMC and PVA on SS 565 CCI Tech sizing machine, according to the experimental design.

A handheld refractometer is used for measuring the bath's refractive index, to analyze the concentration of the CMC or PVA in an aqueous solution, which gives directly in Degrees Brix (symbol °Bx). Besides, a Zahn cup is used to measure the viscosity of the solution. The viscosity of the sizing solution measured by this device is expressed in Zahn numbers, that is, the time in seconds required for a definite volume of liquid to flow through the viscosimeter. Results are given in Table 2.

Table 2. Refractometre and viscosity test results.

Trial no	CMC		PVA	
	Refractometer	Viscosity	Refractometer	Viscosity
1	5 °Bx	48sec	2 °Bx	12 sec
2	5 °Bx	87 sec	2 °Bx	14 sec
3	5 °Bx	249 sec	2 °Bx	17 sec
4	6,8 °Bx	38 sec	2,5 °Bx	18 sec
5	6,8 °Bx	146 sec	2,5 °Bx	18 sec
6	6,8 °Bx	216 sec	2,5 °Bx	14 sec
7	8 °Bx	43 sec	5 °Bx	41 sec
8	8 °Bx	179 sec	5 °Bx	87 sec
9	8 °Bx	182 sec	5 °Bx	17 sec

1. Results and discussion

Yarn unevenness, number of thin places, number of thick places, number of nep and yarn hairiness of unsized yarns were tested on Uster Tester 5 and results are given in Table 3.

Table 3. IPI values of unsized yarns.

IPI values	Ring	Siro	Compact
Yarn unevenness (CV%)	10,178	10,14	10,4
Number of thin places /1000m (-%50)	0	0	0,5
Number of thick places /1000m (+%50)	2,5	2,5	4
Number of thin places /1000m (+%200)	3,5	3,5	2
Yarn hairiness (H)	4,92	4,55	3,51
Yarn hairiness (sh)	0,994	0,918	0,954

Before and after sizing process, tensile strength (cN/tex) and breaking elongation (%) of the yarns were tested on Llyod LRX. Test results are given in Figure 1-4. Unsized ring spun yarns have the lowest strength whereas the highest elongation values than siro and compact yarns.

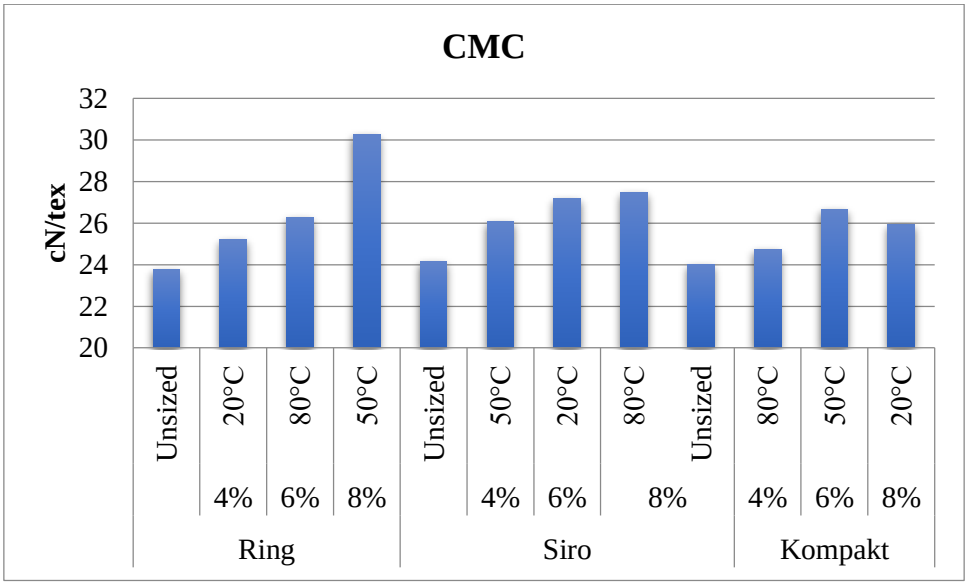

Figure 1. Tensile strength values (cN/tex) of unsized and sized (CMC) yarns.

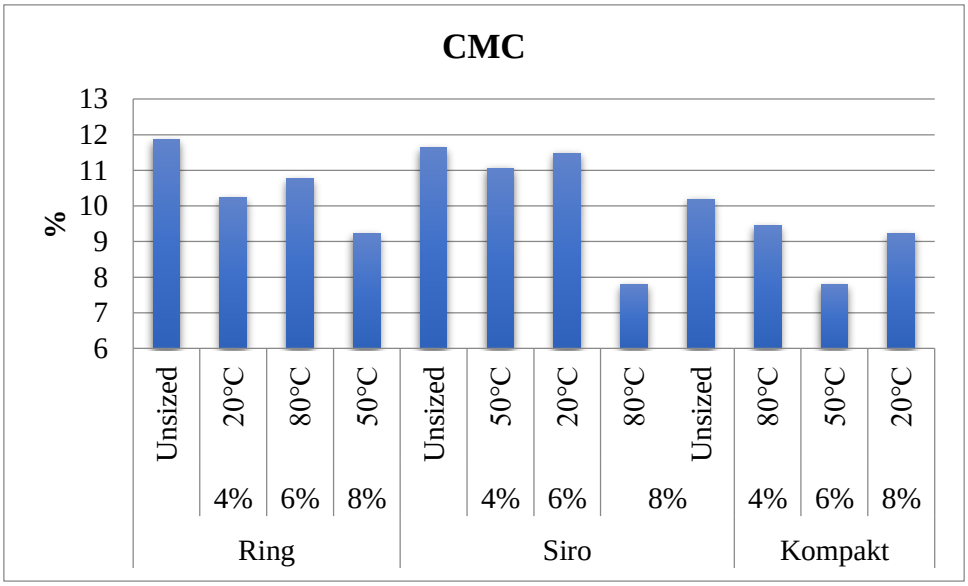

Figure 2. Breaking elongation (%) values of unsized and sized (CMC) yarns.

Figure 1 and 2 showed that, sizing process with CMC, increased the tensile strength and decreased breaking elongation values of the all types of the yarns. Ring spun yarns sized with 8% concentration and at 50°C showed the highest tenacity and it can be said that, sizing process improved the tensile properties of the ring spun yarns more than siro and compact yarns, when carboxymethyl cellulose (CMC) is used.

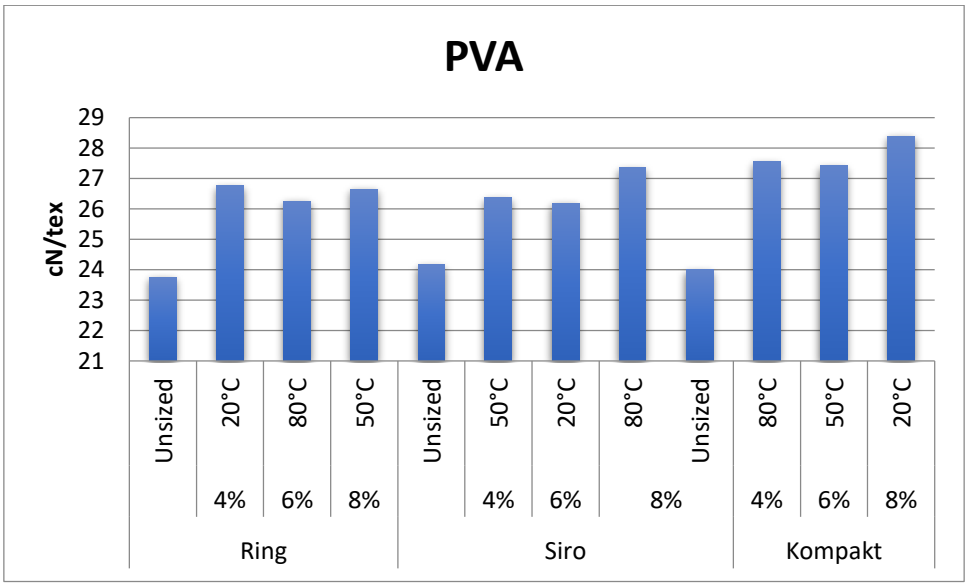

Figure 3. Tensile strength values (cN/tex) of unsized and sized (PVA) yarns.

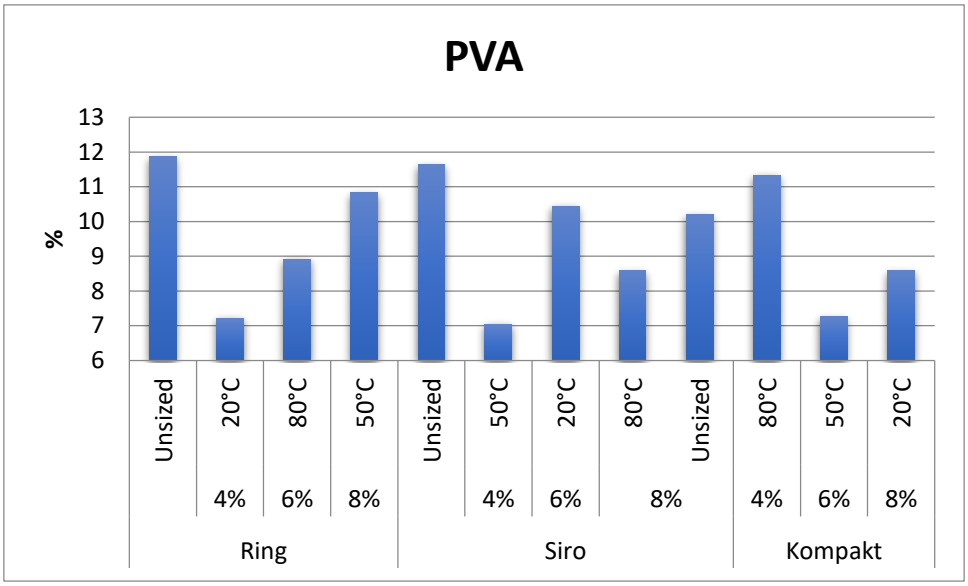

Figure 4. Breaking elongation (%)values of unsized and sized (PVA) yarns.

In a similar manner, sizing process with polyvinyl alcohol (PVA), increased the tensile strength and decreased breaking elongation values, in general (Figure 3 and Figure 4). Compact spun yarns showed the highest tenacity when sized with 8% concentration, at 20°C but highest elongation values but when sized with 4% concentration and at 80°C. The comparison of the values before and after sizing showed that, sizing process improved the tensile properties of the compact yarns more than other yarns, when PVA is used.

According to Taguchi analysis for tensile strength and breaking elongation values of the yarns, Signal to Noise Ratios (S/N) and rank based on mean values are given in Table 4 and Table 5. Besides prediction for different levels were performed for model verification. The comparison between the theoretical predictions and experimental results shows that, values are very close to each other.

Table 4. The results of Taguchi analysis (A: Yarn type, B: Sizing concentration C: Sizing temperature)

		RANK			Verification of model	
Sizing material	Yarn properties	A	B	C	Predicted	Experiment
CMC	Tensile strength (cN/tex)	3	1	2	Level: 1 3 2	
					29,4944	30,25
		2	1	3	Level: 1 1 1	

	Breaking elongation (%)				11,2967	10,23
PVA	Tensile strength (cN/tex)	1	2	3	Level: 1 2 3	
					26,2433	26,25
	Breaking elongation (%)	3	2	1	Level: 2 3 3	
					9,81	8,58

According to Taguchi analysis, sizing concentration is the most affective parameters for the yarns sized with CMC (Table 4). In terms of PVA sizing, yarn type and temperature are the most important parameters for tensile strength and breaking elongation, respectively (Table 4). The optimum sizing parameters for tensile properties are summarized in Table 5.

Table 5. The optimum sizing parameters for tensile properties.

Sizing material	Yarn properties	Yarn type	Sizing concentration	Sizing temperature
CMC	Tensile strength (cN/tex)	Ring	8	50
	Breaking elongation (%)	Siro	4	20
PVA	Tensile strength (cN/tex)	Compact	8	50
	Breaking elongation (%)	Compact	8	80

3.Conclusions

Sizing process improves the strength, abrasion resistance and finally weavability of the yarn and results with higher productivity and quality of the weaving process. In this study the effect of sizing material and sizing process parameters on the physical and mechanical properties of the yarns, produced with different spinning systems, were investigated.

The effects of the sizing parameters on the yarns' tensile properties differ for different spinning systems. For instance, when carboxymethyl cellulose (CMC) used, sizing process improved the tensile properties of the ring spun yarns more than the other yarns types, whereas sizing process is more affective for compact yarns when PVA is preferred. According to Taguchi analysis the comparison between the theoretical predictions and experimental results in order to verification of model shows that, values are very close to each other.

Acknowledgments

We would like to thank Mr. Veli Gökçil and AKSA Acrylic for their valuable helps during yarn testing. This project was funded by Ege University Scientific Research Projects (Project No: 16.MUH.045).

References

Faasen, N. J., Van, Harten, K., (1966), The effect of sizing on the weavability of cotton yarns, Journal of the Textile Institute Transactions, Volume 57, Issue 7, pp 269-285.

Dolecki, S. K., (1974), The causes of warp breaks in the weaving of spun yarns, The Journal of The Textile Institute, 65:2, pp 68-74

Bradbury, E., (1949), The effect of sizing on warp breakage, Journal of the Textile Institute Proceedings, pp 272-276.

Sultana, S., Haque, M. Z., Nur, H. P., (2014), Preparation and application of different size materials on the cotton yarn and investigating the effect of sizing on the tensile properties of cotton yarn, Bangladesh Journal of Scientific and Industrial Research, 49(1), pp 25-30.

Ünal, İ. M., Ekmekçi , A., Duran, K., (2003),. Tekstilde Kullanılan Haşıl Yardımcı Maddeleri, Tekstil ve Konfeksiyon Dergisi, Sayfa 33-37.

Alay E., Körlü E. A., (2011), Hasıl Maddesi Olarak Polivinilalkoller, Tekstil Teknolojileri Elektronik Dergisi, 5 (2) 77-82.

A Study on Characterization of Biopolymer Applied Wool Fabric

Aslı DEMİR[1*], Merve TÜREMEN[2]

[1] *Department of Textile Engineering, Ege University, Izmir-Turkey*
[2]*Ege University, Graduate School of Natural and Applied Sciences, Izmir-Turkey*

[*]**Corresponding Author:** asli.demir@ege.edu.tr

Abstract

A considerable amount of attention has been dedicated to wool fabrics. Environmentally benign and bio-based materials have been focused due to the public concern on health and environmental protection. The hydrophobic scales on the wool surfaces makes the diffusion of water and dye molecules difficult which is more pronounced during aqueous processes. Different studies have been made to find alternative processes to overcome this problem.

Today, the natural materials, like chitosan, is highly regarded to improve the properties of wool. Chitosan has gained much attention owing to its abundance, low toxicity, chemical and physical versatility. To improve chitosan coating on textiles, many methods have been applied. Plasma has been studied in recent years to impart new functionalities to the wool fibres. It modifies surface properties of fabrics without affecting their bulk properties. Also, researches have focused on modifying the wool fabric surface using sol–gel method to improve the durability of desired effects.

In this study, wool fabrics were pretreated with atmospheric plasma methods. The characterization of treatments on the wool fabric surface was made in terms of surface appearance and composition (SEM, XPS, FTIR-ATR), dyeing and hydrophilicity properties.

Keywords: Biopolymer, plasma, surface treatment, characterization

1. Introduction

Biopolymers have gained importance in terms of both scientific and industrial aspects as possible substitutes. The most promising one is the polysaccharide chitosan. Chitosan can be obtained by deacetylation of chitin in a hot concentrated NaOH solution.

In wool finishing processes, chitosan has been proposed as a substituted polymer due to its unusual combination of chemical and biological properties. The chemical properties of chitosan are caused by its polyamine character. The biological properties of chitosan are classified as biocompatibility, biodegradability, non-toxicity and antimicrobial properties. These properties enhances the potential applications in food processing, agriculture, hair and skin care products, membranes, microcapsules, biomedical and waste water treatments (Hudson,1997; Pasual et al 2001; Huang et al,2008).

As known, wool fibres have lots of excellent characteristics such as luster, elasticity, abrasive resistance, warm retention, etc. On the other hand, the presence of scales on fibre surface lead to poor wettability, dyeability and shrinkage resistance (Negri et al, 1993). In the wool treatments, chitosan overcome these problems and gives desired properties to the wool fabrics. It has been proven through some preliminary studies that chitosan treatment of wool improves fabric properties such as dyeability, antibacterial, anti-shrinkage, etc. (Huh et al, 2001; Jou et al, 2007; Wang 2015)

To improve chitosan effect on wool fabrics, the fibre surface can be modified by several methods such as plasma. Plasma is a partially ionized gas that consists of ions, electrons, and neutral particles. Plasma treatment is a dry and eco-friendly technology which represents a valid alternative to the traditional wet-chemical processes used in the textile industry. Plasma reactions can occur while the gas or parts exposed to it remain at relatively low temperatures. Also, plasma technology introduces polar groups and enhances surface roughness of fibres surface (Wang 2015; Demir et.al, 2008; Chen,2012)

Atmospheric pressure plasma treatment has gaining importance for the surface modification of textile materials since it can easily be integrated in continuous processes (Türemen,2017)

In this work, wool fabrics was treated by atmospheric plasma methods prior to chitosan application. The fibre surface morphology and chemical compositions were analysed by SEM, FTIR and XPS methods.

2. Material and Methods

2.1. Experimental

Materials

100 % wool fabric was used in the experiments. The samples were scoured with dichloromethane by using the Soxhlet extraction and thoroughly dried at room temperature.

2.2. Treatments of Wool Fabrics

Chitosan treatment

Chitosan (1%, MMW) solutions were freshly prepared by dissolving in diluted acetic acid solution. The wool fabrics were padded (100% WPU) by chitosan solution, squeezed and dried at 40 °C.

Plasma treatment

The DBD experimental setup has been extensively described elsewhere (Koçum et.al.2007). This device could be operated with rectangular and cylindrical electrodes. The distance between the electrodes was 2 mm. The samples were placed between the electrodes and passed continuously. Argon (purity of > 99.99) were used as process gas under the power 130 Watt for 60 seconds

3. Characterization techniques

Surface chemical composition was studied by XPS technique using a y a K-Alpha (Thermo Scientific) with monochromatic AlKα (1486.68 eV) X-ray source with a spot size of 300 µm and 26.04 W (12.4 kV×2.1 mA) power

The Infrared spectra of samples were determined by means of a Perkin Elmer 100 FTIR spectrometer in ATR reflection mode using a diamond/zinc selenide crystal. To ensure reproducible contact between the crystal faces and the fabric, a pressure of 80 kPa was applied to the crystal holder by means of a calibrated torque screw driver. An average of 15 scans using a resolution of 4 cm^{-1}.

The surface morphology of the fabric samples were examined using scanning electron microscopy (Phillips XL-30S) at a typical accelerating voltage of 15 kV. The samples were mounted and sputter coated with gold for 5 min prior to the observation.

To measure the kinetic friction coefficient of the fabric surface, the Frictorq instrument was used.

4. Results

4.1. XPS Analysis

XPS analysis was made to determine the changes of surface chemical composition of fibres. XPS survey scan and chemical composition of the control the chitosan-plasma treated wool fibres were presented in Figure 1. It was seen a decreased carbon content and increased oxygen content of plasma treated fabrics. The rising ratio of the O/C is caused by the etching effect of the external layer of lipids and to the insertion of oxygenated species onto the fibres surfaces(Karahan et al, 2009).

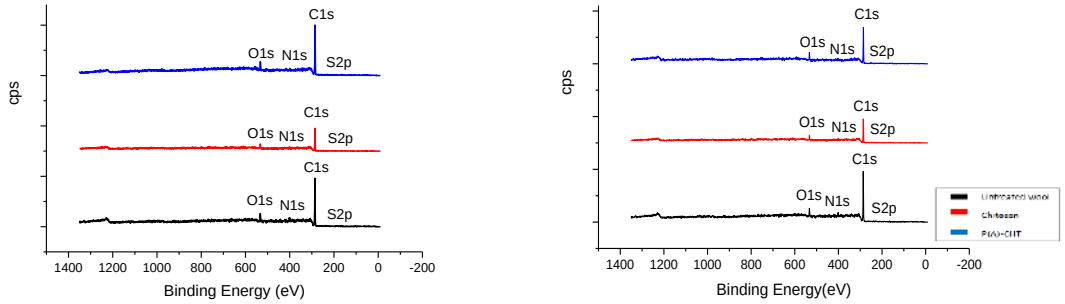

Fig.1. XPS survey spectra of the untreated and treated wool surfaces

Plasma treatment caused a decrease of carbon content due to the oxidation of surface lipids and an increase of oxygen containing functional groups. Also, the partial removal of lipid layer hydrocarbon chains on the surface and the modification of epicuticle protein matrix with fatty acid monolayer linked to it had resulted in the decrease of S content (Ristic 2010).

The C-C and C-H bonds are related with the hydrocarbon backbone of the fatty acids and side groups of the amino acids. The C-O, C-N and C-S species may be associated with the protein structure. The carbon-containing groups on wool fibre surface could be attributed to C-C (~285,75 eV), C-O/C-N (~286.9 eV). The contents of C-C and C-O/C-N groups drastically decreased and increased, respectively. The XPS results show that the plasma treatment lead to the oxidation of the underlying protein matrix, especially the disulphide bonds, with the

formation of cysteic acid residues. These changes in fibre surface and chemical composition causes improve wettability, dyeability and shrinkage resistance (Zanini et al, 2018; Naebe et al, 2010).

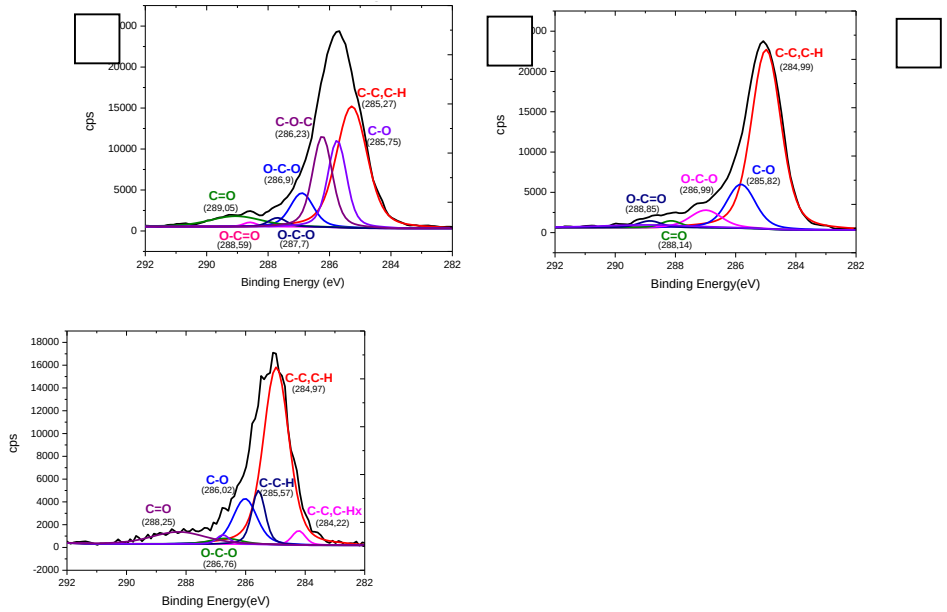

Fig.2 C1s peak core level spectra for (a) untreated (b) plasma treated (c) plasma-chitosan treated wool fabric

FT-IR/ATR (Fourier transform infrared attenuated total reflection) Analysis

The FTIR spectrum of wool was shown in Fig. 3. The bands at nearly 1630 cm^{-1} and 1514 cm^{-1} corresponded to the carboxyl and amide groups, respectively. The other bands observed at 3270 cm^{-1}, 3060 cm^{-1} and 2922 cm^{-1} being attributed to the O–H, N–H and C–H stretching modes, respectively. The main characteristic appeared between 1000 and 1700 cm^{-1} , including amide I (~1630 cm^{-1}), amide II (~1514 cm^{-1}), amide III (~1235 cm^{-1}), and SOO contraction (~1100 cm^{-1})(Hsieh et al, 2007 ; Wojciechowska et al, 1999). There is a new band at around 1040 cm^{-1} is attributed to the S-O stretching vibration of cysteic acid (Cy -SO_3H) caused by oxidation of cystine bonds (Cy –S- S -Cy) by plasma treatment. (Shikataa et al, 2004). As can be seen from the FTIR spectra of wool fabrics, the highest absorbance ratio obtained was the case of plasma-treated fabric (Kan et al, 2004).

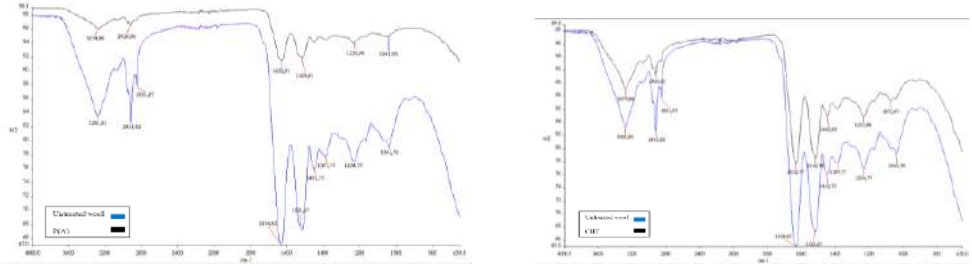

Fig 3. FTIR spectrum of P(A), CHT treated and untreated wool

SEM Analysis

In order to evaluate the coating effect of chitosan on plasma treated wool fibre surfaces, SEM observations was made. It was observed that the surface of untreated wool fibre showed characteristic sharp edges. After plasma treatment, it was observed that the wool surface generally becomes rough due to the etching effect of plasma treatment. The shape of scale edges is changed, as they become rounded (Ristic et al, 2010).

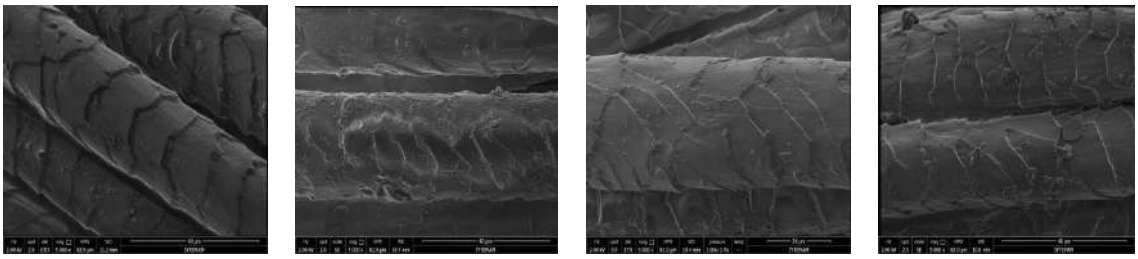

Untreated **Plasma treated (P)** **Chitosan Treated (CHT)** **P+CHT Treated**

Fig.4. SEM images of untreated and treated wool fibers

Friction Properties

Surface friction coefficients of wool fabrics are given in Figure 5 1. As shown, after the plasma treatment, the values increased with the prolonged treatment time and power. This increase is probably caused from the etching effect of atmospheric plasma (Sun et al , 2005; Kan et al 2006).

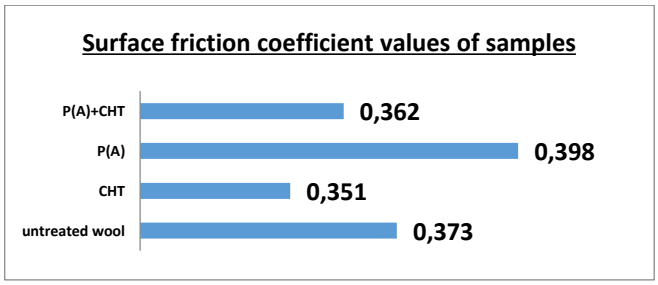

*P(A):Plasma Argon, CHT: Chitosan,

Figure 5. Surface friction coefficient results for treated samples

5. Conclusion

In recent times, the usage of natural polymers in textile industry, like chitosan, as an eco-friendly biopolymer to improve the properties of wool is gained popularity. To improve the interaction of chitosan with wool fibers, it is necessary to develop anionic groups on the wool.

The aim of this study was to investigate the effect of atmospheric plasma treatment on chitosan treated wool fabrics in terms of surface analysis.

The results showed that of plasma treatment caused an increment on surface roughness which provides better adhesion between fiber and biopolymer. The reduced scale heights of wool fibre and homogenous coating of chitosan after plasma treatment can be seen clearly from SEM images.

XPS spectra confirmed plasma and chitosan application on wool fibers by surface chemical composition including elements and functional groups. It is concluded that the changes determined on surface morphology and chemical composition of wool fibre could help to improve wettability, dyeability and shrinkage resistance.

References

Hudson, S.M Applications of chitin and chitosan as fiber and textile chemicals, Domard, A Roberts, G.A.F, Värum K.M (Eds.), Advances in Chitin Science, II,1997, pp. 590-599.

Pascual E. , . Julià, M.R The role of chitosan in wool finishing, Journal of Biotechnology, Volume 89, Issues 2–3, 2001, Pages 289-296;

Huang K.S., Chao, I.C.. Huang GS, Effects of low-molecular-weight chitosan on wool fabric, Macromolecules, Volume 4 Issue 1, 2008, pp.1-6.

Negri A. P, Cornell H. J., and. Rivett D. E, A Model for the Surface of Keratin Fibers, Textile Research Journal, 63, 109 (1993)

. Huh, M. W Kang, I. K.. Lee D. H., Kim W. S.,. Lee, D. H.,. Park, L. S., Min K. E., and Seo, K. H.,Surface characterization and antibacterial activity of chitosan-grafted poly(ethylene terephthalate) prepared by plasma glow discharge, Journal of Applied Polymer. Science, 81, 2769 (2001).

Jou, C.H. Lin, S.M.. Yun, L Hwang M.-C.,Yu D.G.,. Chou, W.L Lee, J.S.. Yang, M.C Polymers for Advanced Technologies 18 (2007) 235–239.

Wang C. X., Du M., Lv J. C., Zhou, Q. Q. Gao D. W., Liu G. L., Jin, L. M. Ren, Y. Liu, J. H., Effect of Wetting Pretreatment on Structure and Properties of Plasma Induced Chitosan Grafted Wool Fabric, Fibers Polymers (2015) 16: 404.

Demir, A., Karahan, H. A., Özdoğan E., Öktem, T., Seventekin N., The Synergetic Effects of Alternative Methods in Wool Finishing, Fibres and Textiles in Eastern Europe,200816(2):89-94

Chen, J. P., Kuo, C. Y. and. Lee, W. L, Appl. Surf. Sci., 262, 95 (2012).

Türemen,. M. Tekstil Terbiye İşlemlerinde Nanokitosan Kullanımı" Yüksek Lisans Tezi, Fen Bilimleri Enstitüsü, Ege Üniversitesi, İzmir,2017.

Koçum, C., and Ayhan, H., Design and Construction of Uniform Glow Discharge Plasma System Operating Under Atmospheric Condition, Rev. Sci. Instrum. 78, 063501, 1–5 (2007).)

Karahan A., Özdoğan E., Demir A., Koçum İ. C., Oktem T., Ayhan H., "Effects of Atmospheric Pressure Plasma Treatments on Some Physical Properties of Wool Fabrics", Textile Research Journal, vol. 79: pp. 1260 – 1265, (2009)

Ristić, N Jovančić, P Canal, C Jocić, D., Influence of Corona Discharge and Chitosan Surface Treatment on Dyeing Properties of Wool, Journal of Applied Polymer Science, Vol. 117, 2487–2496 (2010).

.Zanini, S Citterio, A Leonardi G, Riccardia C., Characterization of atmospheric pressure plasma treated wool/cashmere textiles: Treatment in nitrogen, Applied Surface Science 427 (2018) 90–96.

Naebe, M. Cookson, P G Rippon J, Brady R P, Wang, X Brack N, and Riessen G, Effects of Plasma Treatment of Wool on the Uptake of Sulfonated Dyes with Different Hydrophobic Properties Textile Research Journal,2010, Vol 80, Issue 4, pp. 312 – 324

Karahan, H.A., 2007, Atmosferik plazma kullanılarak doğal liflerin yüzey özelliklerinin değiştirilmesi üzerine bir araştırma, Yüksek Lisans Tezi, Ege Üniversitesi Fen Bilimleri Enstitüsü, İzmir, 239 s.

Kim J., Lewis D.M., 2002, The effect of various anti-setting systems in wool dyeing. Part 1: Hydrogen peroxide based systems, Coloration Technology, Vol. 118, p. 121–124.)

Hsieh S.-H., Huang, Z. K. Huang Z. Z., Tseng, Z. S. Antimicrobial and Physical Properties of Woolen Fabrics Cured with Citric Acid and Chitosan Journal of Applied Polymer Science, Vol. 94, 1999 –2007 (2004)

Wojciechowska, E Wlochowicz, A Birczyńskab, A W., Application of Fourier-transform infrared and Raman spectroscopy to study degradation of the wool fiber keratin, Journal of Molecular Structure, Volumes 511–512, 23,1999, 307-318.

Shikataa, H, T.Ryuji M S, Selective formation of polyaniline on wool by chemical polymerization, using potassium iodate, Synthetic Metals 146 (2004) 73–77

Kan C. W., Chan K., Yuen, C. W. M., Surface Characterization of Low Temperature Plasma Treated Wool Fiber , Fibers Polymers (2004) 5: 52.

Sun D. and Stylios G. K., Investigating the Plasma Modification of Natural Fiber Fabrics-The Effect on Fabric Surface and Mechanical Properties, Textile Research Journal, 75 (9), 639– 644 (2005).

Kan C. W. and Yuen, C. W. M., Low Temperature Plasma Treatment for Wool Fabric, Textile Research Journal, 76 (4), 309–314, (2006).

Entrapment of *Pinus Brutia* in Calcium Alginate Gel to Design Wound Dress

Pelin SEÇİM KARAKAYA[1*], Necdet SEVENTEKİN[1],Özlem YEŞİL ÇELİKTAŞ[2]

[1]Ege University, Faculty of Engineering, Textile Engineering, Izmir- Turkey;

[2]Ege University, Faculty of Engineering, Department of Bioengineering, Izmir- Turkey

[*]**Corresponding Author:** pelinsecim@gmail.com

Abstract

In modern aspect, successful wound healing depends on maintaining a moist environment around the wound. However, traditional dressings such as gauze and cotton are not able to maintain an optimal moist wound environment and have not biological activity on the wound healing process. Gel can accelerate the process of granulation and epithelialization and multiple studies have demonstrated that gel is beneficial for the migration, adhesion, and the growth of cells during the process of tissue regeneration. Sodium alginate (SA), which is a naturally linear anionic polysaccharide derived from algae, has been used for many different biomedical applications such as drug delivery, wound dressing etc. Due to their gel-forming properties, alginate also show promise in biomedically-relevant hydrogel systems. Generally, an SA solution will exhibit a transition to a hydrogel in the presence of polyvalent cations by forming ionic inter-chain bridges and SA hydrogels used to be prepared by dropping an SA solution into a $CaCl_2$ solution. In this study, wound dressings were prepared by gelling on the fabric apart from the dropping method. Firstly Pinus brutia extracts were obtained using ultrasound and soxhlet extraction method. The results showed that ultrasound extraction result performed better than soxhlet extraction in regards of phenolic compounds. Phenolic compounds can accelerate the wound healing process. After the extraction, the sodium alginate solution was prepared using Pinus Brutia extract and the gel was formed on the fabric by treatment $CaCl_2$ solution to obtain wound dress. Wound healing performance of the material is still being investigated in rats.

Keywords: wound dress, wound healing, gel, alginate.

1. Introduction

Wound dress which has largest share of medical textiles, is one of the significant applications. Studies carried out with using plants for wound healing purposes date back to ancient years. Nowadays natural products especially extracted from plants, due to their abundant availability, biocompatibility, nontoxicity, green approach and environmental friendly nature, are gaining popularity for their use in textiles (Shahid-ul et.al. 2013). From past to present, natural materials have been used to traditional therapy of diseases. Application of natural materials in wound healing is an interest topic due to effective treatment withno side effects (Ghayempoura et. al., 2016). The aim of this paper is to preparation of wound healing products based on the natural materials and a safe processing. Pine bark has recently a wide area of application in nutrition health and medicine. Pinus brutia extracts contain numerous phenolic compounds such as catechin, epicatechin, taxifolin and phenolic acids. Phenolic compounds responsible for the antioxidant activity and as known, antioxidants can accelerate the wound healing process. Pinus brutia as an effective natural antioxidant sources can be used in wound healing process (Celiktas et al., 2007).

Plant extracts have attracted a great deal of scientific interest due to their biologically active compounds (Celiktas et *al*., 2007). In the extraction of bioactive compounds from plants, modern extraction technique such as ultrasonically-assisted extraction (UAE) have become more popular than the conventional soxhlet extraction method (Yildiz-Ozturk et al. 2014). There has been an increasing demand for new extraction techniques with shortened extraction times, reduced organic solvent consumption, preventing pollution in analytical laboratories and reducing sample preparation costs (Hadia et al. 2013). Ultrasonically-assisted extraction (UAE) are fast and efficient unconventional extraction methods developed to extract analytes from solid matrices.

Sodium alginate, which is a natural polysaccharide derived from algae, has been used for medical applications as a wound dressing (Han et. al., 2017). Dressings made of alginate, which have various advantages in comparison with the traditional cotton and gauze dressings, have become very popular, recently. Alginate is typically used in the form of a gel in medical field, including wound healing, drug delivery and tissue engineering applications. The most common method to prepare gels from an aqueous alginate solution is to combine the solution with ionic cross-linking agents, such as divalent cations (i.e., Ca^{2+}). Gel can effectively accelerate the process of granulation and epithelialization, and multiple studies have demonstrated that gel is beneficial for the migration, adhesion, and the growth of cells during the process of tissue

regeneration. When alginate gels absorb the wound exudate, an ionexchange reaction takes place between the calcium ions in the dressing and sodium ions in serum or wound fluid.

Important parameters of the ideal wound dressing include to absorb exudates and toxic components, provide thermal isolation and a high humidity at the wound surface, allow gas exchange and be non-toxic (Ramnath et. al.).

In this study, modern wound dress was prepared with using *Pinus brutia* extract which was obtained via modern extraction method (UAE). After that, *Pinus brutia* was entrapmented in calcium alginate gel to design modern wound dress.

2. Materials and methods

2.1. Plant material

P. brutia specimens were collected from Izmir-Deliomer (N: 38º 10’ 17.0”, E: 27 º 03’ 46.7”, altitude: 120 m).in Turkey in 2008. The specimens were dried at room temperature, ground by using a conventional grinder and stored at +4 ºC. Alginate were supplied by CHT.

2.2. Materials and reagents

Folin-Ciocalteu’s reagent, 2,2-diphenyl-1-picrylhydrazyl hydrate (DPPH), sodium carbonate (Na_2CO_3) were obtained from Sigma. Ethanol and methanol were supplied by Merck. HCl, acetic acid and acetonitrile were purchased from Merck. All other chemicals were of analytical grade purity.

2.3. Extraction processes

2.3.1. Ultrasonically-assisted extraction

About 2 g of dried parts of *Pinus brutia* was transferred into a centrifuge tube containing ethanol by using ultrasonic bath (Everest Ultrasonic, Istanbul, Turkey). The ultrasonically-assisted extraction experiments were performed at 40 ºC, 40 min., % 50 power. The obtained extracts were concentrated to dryness at 55 ºC in rotary vacuum evaporator (Hahnvapor RS2005V-N) and subsequently stored at +4 ºC until biological activity assays.

2.3.2. Soxhlet extraction

50 g portion of *Pinus brutia* was extracted with 500 ml of ethanol for four cycles (about 3.5 h) using a Soxhlet (500 ml) apparatus. The extract was concentrated to dryness at 55 ºC in rotary vacuum evaporator (Hahnvapor RS2005V-N) and subsequently stored at +4 ºC until biological activity assays.

2.3.3. Total phenol content

The total phenols in the ultrasound and soxhlet extractions extracts were determined by Folin–Ciocalteu method (Akay et al. 2011). Firstly, 100 µl aliquot of the extract was made up to 10 ml with distilled water. Then 500 µl of Folin–Ciocalteu's reagent was added, and the solution was stirred with using a vortex mixer, and left to stand for 5 min. Finally, 1.5 ml of saturated sodium carbonate solution was added and stirred again for the last time and left to stand at room temperature for 1 h. The absorbance was determined at 760 nm using a Shimadzu UV-2401 spectrophotometer. Gallic acid was used as a standard [calibration curve:760 nm = $0.0946.c_{\text{gallic acid}}$(mg/ml)] and the total phenols results were expressed as mean values and were given as gallic acid equivalent (GAE) per gram of extract.

2.3.4. Free radical scavenging activity assay

The free radical scavenging activities of the extracts were determined as described in Yesil-Celiktas 2009. The extracts were dissolved in 4 ml methanol (final concentration of 250 µg/mL) and then added to 0.5 ml of 1 mM methanolic solution of DPPH. The contents were stirred for 15 s and then left to stand at room temperature for 30 min. The decrease of color was measured at 517 nm using a Shimadzu UV-2401 spectrophotometer. The radical scavenging activity (RSA) was calculated according to the equation % RSA = 100 × [1 − (AE/AD)]. AE is the absorbance of the solution containing antioxidant extract and AD is the absorbance of the DPPH• solution. The radical scavenging activity was expressed as the inhibition percentage (% I) and calculated as per the equation:

$$\text{Inhibition of percentage (\%)} = \frac{A_{DPPH} - A_{Ext}}{A_{DPPH}} \text{ x } 100$$

A_{DPPH}: absorbance of control DPPH solution at 0 min. A_{Ext}: absorbance in the presence of the sample of the extract after 30 min.

2.3.5. Total flavonoid content

The total flavonoid contents of the extracts were determined by aluminum chloride colorimetric method (Mandal and Madan 2013). 0.5 ml of the extract (final concentration 1 mg/ml in MeOH) was pipetted out in a test tube to which was added 1.5 ml of methanol, 0.1 ml of 10% aluminum chloride, 0.1 ml of 1 M potassium acetate aqueous solution and 2.8 ml of distilled water. The yellow color in solution indicated that the presence of flavonoids. The final sample solution in the tubes was left to incubate at room temperature for 30 min. Analyses were

done in duplicates and the results were defined as mg quercetin/g dry weightby comparison with quercetin standard curve [calibration curve: 415 nm = 0.0037.$c_{quercetin}$(mg/g) + 0.0027].

2.3.6. Preparation of wound dress

Alginate exhibits the ability to form gels with divalent ions, most commonly in the form of calcium ions. It is believed that sodium ions in the guluronic acid units migrate with calcium ions during the elongation of sodium alginate of calcium alginate, thus forming mutually cross-linked polymers. In this study, sodium alginate solution was prepared by adding it into *Pinus brutia* extract. The prepared solution was absorbed into cotton fabrics and after taking up the excess solution, the fabric was immersed in $CaCl_2$ solution to gel on the fabric. The samples left to dry for 4 hours were then packaged and sterilized.

3. Results and discussion

3.1. Analysis of biological activities

Phenols are essential plant constituents due to their antioxidant property. The phenolic compounds are suggested to play a preventive role against the development of cancer and cardiovascular diseases (Yildiz-Ozturk et al, 2014). In this study the total phenolic content in the extracts were determined with using Folin–Ciocalteu method. Ethanol was used as a solvent. Two extraction techniques as ultrasound (UAE) and soxhlet extraction was compared in terms of biological activities. With respect to total phenol contents, ultrasound ethanol extracts (1014.8 mg/g extract) have higher value than soxhlet extracts (813.9 mg/g extract). Additionally, Yesil-Celiktas studied the water extraction of *Pinus brutia* and the phenol content was found as 936.60 mg gallic acid/g extract (Yesil-Celiktas, 2009). From this point of view, *Pinus brutia* can be considered to be a good source of phenol. The results showed that UAE was more efficient technique than soxhlet extraction. UAE has been gaining popularity because it allows faster extraction, reduced solvent use and higher recovery. This method has been more effective in terms of yield, time and energy consumption in comparison to conventional techniques (Jaitak et al. 2009). However, the results were different in regards to total flavonoid contents where soxhlet ethanol extracts exhibited the highest content (55.1 mg/g extract) followed by ultrasound ethanol extracts (51.5 mg/g extract). Procyanidins are considered to be superior antioxidants because of the higher number of target sites for free radicals. (Yesil-Celiktas et al., 2009b). In this study, the antioxidant efficiencies of extracts for three techniques were also determined by the (DPPH) radical scavenging activity assay besides total phenol and flavonoid assays. Several studies were conducted which report excellent radical scavenger

properties of Pinus brutia extracts. O. Yesil-Celiktas et al. found out that the highest radical scavenging activities were attained with Pinus brutia (86.4 %) bark extracts in different pine species (Yesil-Celiktas et al 2009b).

In this study DPPH results of ultrasound ethanol extracts (83.4 %) performed better than soxhlet ethanol extracts (81.9 %). Ultrasound extraction technique would prefer with shortened extraction times, reduced organic solvent consumption, preventing pollution in analytical laboratories and reducing sample preparation costs.

Additionally, in another study, the *Pinus brutia* was extracted by different solvents (*n*-hexane, dichloromethane, ethyl acetate, and ethanol) and highest flavonoid compound amounts were achieved with ethanol (Yesil-Celiktas, 2009a). The results demonstrated that solvent is predominant process parameter on the composition of phenol compounds.

Antioxidants are known to accelerate wound healing process. By using the extracts obtained from ultrasound extraction, gels were formed on the textile surface to obtain wound dress. Wound healing performance of the wound dress is still being investigated in rats.

4. Conclusion

In this study phenol content of Pinus Brutia extracts was attained a large amount in with different extraction metod apart from soxhlet extraction. The high content of phenolic compounds of *Pinus brutia* extract indicates the potential to be used as a natural antioxidant in medical industry. Antioxidants can accelerate wound healing process.

Dressings made of alginate gel recently have become very popular, as they have various advantages in comparison with the traditional cotton and gauze dressings. Alginate is a biomaterial that has found numerous applications in medical textile due to its favorable properties, including biocompatibility and have the feature of gelation. From this point of view, modern wound dress was designed with using alginate gels and *Pinus brutia* extracts. Wound healing performance of this dress is still being investigated.

Acknowledgements

This work was financially supported by Ege University Scientific Research Project Office [grant number 15-MUH-051] and Scientific and Technological Research Council of Turkey (TUBITAK) 2211-C National Scholarship Program. The authors are thankful to the Novel Fluidic Technologies and Applications Laboratory at Bioengineering Department and Ege University Textile and Apparel Research & Application Center for access to the facilities.

References

Shahid-ul I., Shahid M., Faqeer M., 2013, Perspectives for natural product based agents derived from industrial plants in textile applications - a review, Journal of Cleaner Production 57, 2-18.

Ghayempoura S., Montazera M., Radb M. M., 2016, Encapsulation of Aloe Vera extract into natural Tragacanth Gum as anovel green wound healing product, International Journal of Biological Macromolecules, 93, 344–349.

Celiktas O.Y., Kocabas E.E.H., Bedir E., Sukan F.V., Ozek T. and Baser K.H.C., 2007. Antimicrobial activities of methanol extracts and essential oils of Rosmarinus officinalis, depending on location and seasonal variations. Food Chem. 100 : 553-559.

Yildiz-Ozturk E., Tag O., Yesil-Celiktas O., 2014. Subcritical water extraction of steviol glycosides from Steviarebaudiana leaves and characterization of the raffinate phase. J. of Supercritical Fluids. 95, 422–430.

Hadia B. J., Mohd M. S., Wan Aini Wan I., Shajarahtunnur J. , Mu'azuc M. A, 2013. Parametric Evaluation of Microwave-Assisted Extraction of Phenolics from C. domestica Val. ,Jurnal Teknologi, 62:3 95–98.

Han Y., Li Y., Zeng Q., Li H., Peng J., XuY., Chang J., 2017. Injectable Bioactive Akermanite/Alginate Composite Hydrogels For in Situ Skin Tissue Engineering, Journal of Materials Chemistry B, 5, 3315.

Ramnath V., Arockianathan P.M., A Review on the Recent Developments in Wound Dressing Materials, St. Joseph's Journal of Humanities and Science.

S. Akay, I. Alpak, O. Yesil-Celiktas, 2011. Effects of process parameters on supercritical CO2 extraction of total phenols from strawberry (Arbutus unedo L.) fruits: anoptimization study, J. Separation Science 34, 1925–1931.

O. Yesil-Celiktas, 2009. A comparative study of antioxidant properties of extracts obtained from renewable forestry and agricultural resources, Fresenius Environmental Bulletin 18 (8), 1507–1512.

Mandal, B., Madan, S., 2013. Preliminary phytochemical screening and evaluationof free radical scavenging activity of Stevia rebaudiana Bertoni from differentgeogaphical sources. J. Pharmacogn. Phytochem. 2 (1), 14–19.

Jaitak, V., Singh, B.B., Kaul, V.K., 2009. An efficient microwave-assisted extractionprocess of stevioside and rebaudioside-A from Stevia rebaudiana (Bertoni).Phytochem. Anal. 20, 240–245.

Yesil-Celiktas O., Ganzera M., Akgun I., Sevimli C., Korkmaz K.S., Bedir E., 2009b. Determination of polyphenolic constituents and biological activities of bark extracts from different Pinus species. J Sci Food Agric. 89, 1339–1345.

Yesil-Celiktas O., Otto F., Gruener S., Parlar H., 2009a. Determination of Extractability of Pine Bark Using Supercritical CO2 Extraction and Different Solvents: Optimization and Prediction. J. Agric. Food Chem. 57 (2), 341-347.

Evaluation of Dyeing with Natural Dyes in terms of Sustainability

Esen ÖZDOĞAN*[1], Aslı DEMİR[1], Merve TÜREMEN[2]

[1] Department of Textile Engineering, Ege University, Izmir-Turkey
[2] Graduate School of Natural and Applied Sciences, Ege University, Izmir- Turkey

*Corresponding Author: esen.ozdogan@ege.edu.tr

Abstract

Natural dyes have been used for many purposes including the coloring of textile fibers, leather, cosmetics, etc. They can be obtained from many plant parts such as, leaves, fruits, seeds, flowers, root, and insects, minerals (1-2).

The use of natural dyes to color textiles diminished after the discovery of synthetic dyes in 1856. Because of consumer demands for green products, much interest to the development of natural dyes emerged apparently. They are mostly eco-friendly, less toxic and allergenic, present better biodegradability as compared to synthetic dyes (3-6).

Recently, researchers have taken attention to environmental and socio-economic sustainability in the textile industry. Also, future demands, availability of raw materials, the standardization for large scale production of natural dyes, and economic sustainability to reach new markets have been investigated by discrete researchers(7,8).

This review study will highlights an overview of natural dyes for textiles. The general aspects of dyeing, economical and ecological points of natural dyes will be discussed in detail.

Keywords: Natural dyeing, non-toxic, herbal, renewable

1.Introduction

Natural dyes have been used since ancient times for dyeing of body, food, walls of caves, textiles, leather and objects of daily use. A large number of plant, animal, insect, mollusc or mineral sources have been identified for extraction of dyes and pigments. The art of dyeing is as old as human civilisation (Křížová, 2015).

Natural dyes were used for colouring of textiles till the 19th century when the introduction of synthetic dyes resulted in the decline in the use of natural dyes. The circumstances in textile coloration have changed. It is not only color but also some ecological factors (associated with economic factors) that have become important for consumer decisions to purchase a colored product in modern textile production (Santos et al, 2018).

Nowadays natural products especially derived from plants; on the account of their abundant availability, biocompatibility, low toxicity, green approach and environmental friendly nature are gaining popularity all around the globe for their use in textiles (Islam et al, 2013)

The present global consumption of textiles is estimated at around 90 million tonnes, and such a huge amount of required textiles materials cannot be dyed with natural dye alone. Hence, the use of eco-safe synthetic dyes is also essential. But a certain portion of coloured textiles can always be supplemented and managed by eco-safe natural dyes (Pubalina et al, 2018; Ashis Kumar and Priti, 2009)

Therefore, both qualitative and quantitative research investigations have been undertaken all over the world on colorants derived from cleaner bioresources having minimal ecological negative impacts (Mohd et al, 2017).

2.Natural Dyes

Natural dyes are derived from natural resources and based upon their source of origin, they are broadly classified as plant, animal, mineral, and microbial dyes although plants are the major sources of natural dyes (Shanmathi and Soundri, 2017). Natural dyes have been classified in a number of ways (Fig. 1). Major basis of classification of natural dyes are their production sources, application methods of them on textiles and their chemical structure (Mohd et al, 2017).

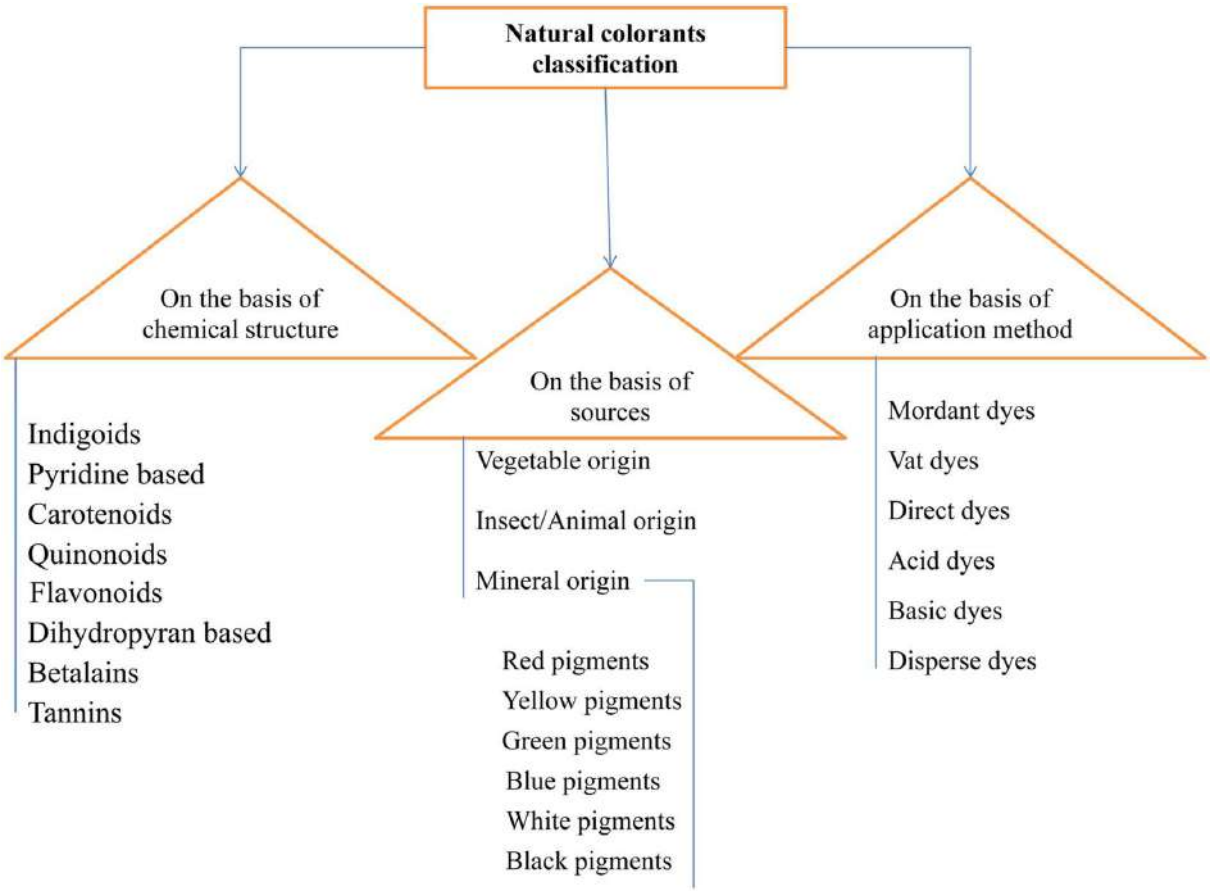

Fig. 1 Classification chart for natural colorants

Natural dyes exhibit several important properties that provide them a significant edge over synthetic dyes. Some of these advantages are as follows:

Natural dyes are not harmful to the environment. They are biodegradable and disposing them does not cause pollution. The waste generated can be used as bio-fertilizers and as a result there is no waste disposal problem.

Natural dyes are obtained from renewable sources that can be harnessed without imposing harm to the environment.

The shades produced by natural dyes are usually soft, lustrous and soothing. A wide spectrum of colours by mix and match system can be produced. A small variation in the mordant used or extraction medium or dyeing technique can bring about a drastic change in the colour.

Some natural dyes will not cause harm or health problems when ingested. Also, many natural dyes have specific properties like atibacterial, etc.

This is a labour intensive industry, thereby providing job opportunities for all those engaged in cultivation, extraction and application of these dyes on textile. Natural dyes generate sustainable employment and income for the weaker section of population in rural and sub-urban

areas both for dyeing as well as for non-food crop farming to produce plants for the natural dyes.

However, there are several limitations of natural dyes also some of which are listed below:

A larger amount of natural dyes may be needed in order to dye a specific amount of fabric as opposed to synthetic dyes. For instance, one pound of cotton may be dyed with just five grams of synthetic dye, whereas 230 grams of natural dye are needed to dye the same amount of material. Since that is the case, using natural dyes is more expensive than synthetic dyes. Industrial use of dyes from plants for dyeing of fibres is considerably limited by their high costs

Natural dyes have a significantly lower affinity to fibres, which causes the lower dye-exhaustion from bath on fibres. The dose of dyes must be at least one order of one magnitude higher and the majority of natural dyes remain in bath after dyeing, especially when trying to obtain dark shades.

Moreover, the natural dyes and pigments are contained in plants in small quantities. When dyeing a textile, we need one kilogram of dye plant for one kilogram of fibres. This creates a need to handle a large amount of biomass for obtaining them, thereby producing large quantities of waste. At the same time cost for transporting large volumes of plant material from the place of harvest to the place ofprocessing is rising. Fortunately, some dyeing plant wastes are suitable as fertiliser or fuel. Production cost of natural dyes from the direct harvest is very hight, use of plants from nature isn’t realistic.

Colour pay-off from natural dyes tend to fade quickly. More so, quality may not be more consistent than what synthetic dyes can deliver. The usage of mordant is required to fix the dye into the fabric. Clour and light fastness is low. The reproducibility of the same shade is difficult.

Another issue with natural dyes is their availability. It can be difficult to produce because the availability of raw materials can vary from season to season, place, and species, whereas synthetic dyes can be produced in laboratories all year round.

While natural dye sources are renewable, sustainability can still be an issue for natural dyes because producing them require vast areas of land.

In recent years, there has been a trend to revive the art of natural dyeing despite several limitations. This is caused by increase in environmental awareness worldwide.(Křížová, 2015; Shanmathi and Soundri, 2017; Ashis Kumar and Adwaita, 2011; Arora et al, 2017).

3. Natural Dyeing in Terms of Sustaıiability

3.1. Source

As there are about thousands of plant species which can be used in textile industry, therefore research trials are being conducted on industrial plants in order to screen and select species that are fit for modern sustainable cultivation techniques. It is to be noted that conventional farming methods for the cultivation of industrial plant species use energy, water and synthetic agrochemicals as the main inputs. For plants to be utilized in natural textile industry, a common requirement is organic certification. This means that the industrial plant species are cultivated under the conditions prescribed by organic farming. The development of organically produced fibres and dyes from abundantly available plants constitute an attractive choice for the modern green textile industry (Islam et al, 2013).

Nowadays scientific efforts are being made for the production of natural dyes with lower specific costs and new strategies for textile dyeing are being established for the industrial acceptance of natural pigments. Figure 2 shows diagram of possible sustainable production of natural products in textile manufacturing.

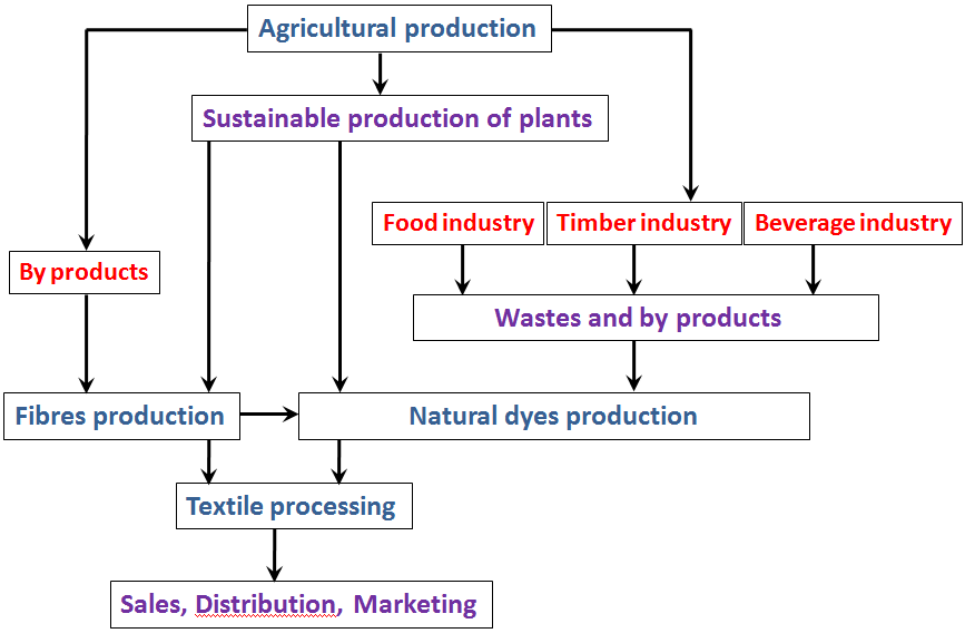

Fig.2: Concept of green and sustainable textile manufacturing using natural products

One of the ways to natural dyes leads from agricultural production through the waste products of food, beverage and timber industry. The fact is, that besides the purposeful cultivation of dye plants, there is a much more progressive option: the utilisation of colour waste from food industry and forestry production. Industrial production of food and beverages produces huge amounts of biological waste, such as molded fruits, distillation residues, pomace

and other residual by-products containing a large amount of vegetable dyes that can be used in the textile industry (Křížová, 2015).

3.2. Extraction Process

First step of extraction is preparation of the plant material ready to be extracted such as collection of plant materials, drying and grinding to make homogenous mixture and to enhance surface area for maximum contact to solvent used. After that most important step, is selection of solvent, depending on the nature of compounds to be isolated or extracted (Mohd et al, 2017).

Over the decades, the conventional extraction methods have been used for isolation of functionally active component which act as colorant. These methods include heating, overnight soaking, stirring, solvent extraction. But these methods for isolation not only take a lot of time but also need greater labor, work, care and energy along with loss of huge amount of chemicals. Such procedures may not only cause the degradation of actual matrix but also add much more value to environmental pollution which in turn deteriorate the eco system. Recently, the modern methods have been employed in order to save labor, energy, cost and time. These method involve enzyme treatment, supercritical methods, ultraviolet, ultrasonic, microwave, gamma and plasma treatment (Adeel et al, 2018; Islam et al, 2013; Ashis Kumar and Adwaita, 2011; Singh and Bharati, 2014)

It is also necessary to optimise natural dyes dyeing conditions: time, temperature, liquor ratio, dosage and type of mordant, preparation of plant material, choice of suitable fibres (Křížová, 2015).

3.3 Mordanting

After extraction processing, next step is application of natural colorants on textiles with or without the help of mordants. To get the highest substantivity of natural colorants towards textiles, some metal salts or other chemicals or compounds, so called mordants are used with colorants. A mordant has an affinity for both the colouring matter and the fibre and combining with the dye in the fibre it forms an insoluble precipitate or lake Besides metallic salt, tannins and oils are also used as mordants. Mordanting is classified on the basis of application time of mordants that are pre-, meta- and post-mordanting. (Mohd et al, 2017; Pubalina et al, 2018)

Different types of mordants yield different colours even for the same natural dye. Therefore, final colour, their brilliance and colour fastness properties are not only dependant on the dye itself but are also determined by varying concentration and skillful manipulation of the mordants.

The need to use mordants is another serious problem in the dyeing with natural dyes. The mordanting salts do not have affinity to the fibres and therefore only a small part of them is bounded with fibres. All the remnants are carried off by water after dyeing and final rinsing.

Many of metals are important micronutrients (they are necessary for the body in trace amounts), but generally, metals in soluble form (metal ions) acts on the organism as poisons.

Improving traditional mordanting processes and selecting new mordants to replace traditional heavy-metal ions must be an important part in the development of natural dyeing of textiles. Therefore a large number of researchers around the globe are working on natural colorants advancements. It can be predicted that plant-derived mordants may be a viable alternative to toxic metal salts used in textiles in the near future (Islam et al, 2013; Křížová, 2015; Ashis and Adwaita, 2011).

3.4 Dyeing

From the time, textile dyeing started in past carried out conventionally. The old technologies of dyeing consist of various steps that do not address modern demands and disregard the new possibilities offered by modern textile chemistry. The number of steps and duration of baths seem to be too high and non-productive: several hours soaking of fabrics before dyeing, multiple washing. A large consumption of water and heat is used when washing, which is necessary to eliminate non-fixed dyes, reaction products or printing pastes. Textiles were directly processed with the dye bath at high temperatures. Numerous developments in dyeing context are observed in recent decades such as evaluation of effective mordants, printing techniques and dyeing procedures. In this concept, advanced technologies or methods are trending in dyeing in recent times owing to their improved results over the conventional dyeing. Plasma treatment and ultrasonic dyeing methods are modern, advanced and sustainability compatible methods used in technologically evolved textile industry(Mohd et al, 2017) Enzymatic processing also has been used as a sustainable and eco-friendly method for textile coloration and functionalization.

Traditional dyeing technologies are based on the bath dyeing when the fabric is completely immersed into dye liquor during dyeing. It means the bath ratio of 1:50, 1:100 and more, this causesa large consumption of water. This water should be cleaned from the remains of mordants before being discharged or ideally recycled. The reduction of water consumption also means a significant saving of heat. Long time of material soaking before dyeing could be greatly reduced by wetting in a bath with suitable wetting agent as well as reducing of water

consumption is possible with the use of modern technology such as e.g. smart washing and application of dye baths with very low liquor ratio (Křížová, 2015).

4. Conclusion

Recently a lot of concern and awareness towards maintenance of ecological balance has led to revival of natural colorants. Replacement of synthetic dyes by natural dyes should be considered. Synthetic dyes, which are widely available at an economical price and produce a wide variety of colours, sometimes causes skin allergy and other harmfulness to human body, produces toxicity/chemical hazards during its synthesis, releases undesirable/hazardous/toxic chemicals etc (Ashis Kumar and Adwaita, 2011).

Availability and use of natural dyes in the current state raises big concerns about the sustainability of the concept. The organising principle for sustainability is sustainable development, which includes ecology, economics, politics, culture, social impact and human health. For successful commercial use of natural dyes for any particular fibres, the appropriate and standardized techniques for dyeing for that particular fibre-natural dye system need to be adopted. Less expensive production of natural dyes and affordable industrial application methods are needed. Also large water consumption and the amount of often unnecessary or unnecessarily long working operations should be reviewed in the context of cost savings and sustainable approach to nature.

Thus, from the point of environmental safety, natural dyes are a sustainable option only for small-scale applications and they can only complement synthetic dyes. They can be considered as best suitable on the cottage level, for small scale industries (Křížová, 2015).

References

Křížová H., (2015) Natural dyes: their past, present, future and sustainability, Recent Developments in Fibrous Material Science, Publisher: Kanina o.p.s., Editors: D. Křemenáková, J. Militký, R. Mishra

Jyoti Arora, Prerna Agarwal, Gunjan Gupta, (2017), Rainbow of Natural Dyes on Textiles Using Plants Extracts: Sustainable and Eco-Friendly Processes, Green and Sustainable Chemistry, 7, 35-47

Cristiane dos Santos, Luis Fernando Wentz Brum, Robelsa de Fátima Vasconcelos, Sérgio Knorr Velho, João Henrique Zimnoch dos Santos, (2018), Color and fastness of natural dyes encapsulated by a sol-gel process for dyeing natural and synthetic fibers, Journal of Sol-Gel Science and Technology, 86:351–364

Ashis Kumar Samanta, Priti Agarwal, 2009, Application of Natural Dyes on Textiles, Indian Journal of Fibre&Textile research, Vol. 34, p. 384-399

Shahid-ul-Islam, Mohammad Shahid, Faqeer Mohammad, (2013), Perspectives for natural product based agents derived from industrial plants in textile applications - a review, Journal of Cleaner Production 57, p. 2-18

Pubalina S., Deepali S. and Ashis Kumar S., (2018) Fundamentals of Natural Dyeing of Textiles: Pros and Cons, Current Trends in Fashion Technology & Textile Engineering, Volume 2- Issue 4, s. 1-7

Mohd Yusuf. Mohd Shabbir. Faqeer Mohammad, (2017) Natural Colorants: Historical, Processing and Sustainable Prospects, Nat. Prod. Bioprospect. 7:123–145

Ashis Kumar Samanta and Adwaita Konar, (2011), Dyeing of Textiles with Natural Dyes, https://www.intechopen.com/books/natural-dyes/dyeing-of-textiles-with-natural-dyes

Har Bhajan Singh and Kumar Avinash Bharati, (2014) Handbook of natural dyes and pigments, Woodhead Publishing India Pvt Ltd, New Delhi,

Shanmathi Swetha S., Soundri S. Geetha Margret, (2017, 11) Scope Of Natural Dyes In Present Scenario, 2. International Conference on Recent Innovations in Science, Technology, Management and Enviroment, (s. 1-23) New delhi, India

Shahid Adeel, Muhammad Hussaan, Fazal-ur Rehman, Noman Habib, Mahwish Salman, Saba Naz, Nimra Amin & Nasim Akhtar, (2018), Microwave-assisted sustainable dyeing of wool fabric using cochineal-based carminic acid as natural colorant, Journal Of Natural Fibers, DOI: 10.1080/15440478.2018.1448317

Ashis Kumar Samanta and Adwaita Konar, Dyeing of Textiles with Natural Dyes, Natural Dyes, Published by InTech, Janeza Trdine 9, 51000 Rijeka, Croatia, Copyright © 2011 InTech, Edited by E. Perrin Akçakoca Kumbasar

A Study On The Coloring Of Woolen Fabrics With Fennel Seeds

Fazlıhan YILMAZ[1*], M.İbrahim BAHTİYARİ[1]

[1]Erciyes University, Faculty of Engineering, Department of Textile Engineering Kayseri, Türkiye

[*]**Corresponding Author:** fazlihanyilmaz@erciyes.edu.tr

Abstract

The attraction of colors is a reality that has existed since ancient times. Therefore many studies on color have been made. Textile dyeing was also influenced by the color variety in the nature. In this study, fennel seed was used in the coloring process of woolen fabrics. It has been observed that different color tones can be obtained thanks to the different mordanting agents used with the fennel plant. Also, experiments were carried out without using any mordanting agent. In dyeing experiments dyeing materials were added to dye bath in the same amount of fabric weight.That is, 1:1 dyeing was performed without any previous extractions process of fennel. Wool fabric weight set to 2 gr and the liquor ratio was adjusted to 1:40. As a result of these experiments, fennel natural dye source have been found to be able to color woolen fabrics.

Keywords: Wool, natural dye, fennel, mordant, liquor

1. Introduction

Natural dyestuffs have been used widely in order to color textile materials with plants, animals or minerals (Özgüney et al., 2015). Since ancient times, dyeing has been employed to color fabrics in industry, arts, and crafts (Morimoto et al. 2011). It is known that the use of natural dyeing in textile fibers began in India and Mesopotamia in 4000 BC (Karadağ, 2007).Different herbal sources can be used as natural dye source. Here in this study the seeds of the fennel has been tested in coloration of wool fabrics.

Fennel (*Foeniculum vulgare*) is a plant belonging to the Umbelliferae (*Apiaceae*) family, known and used by humans since antiquity. It was cultivated in every country surrounding the Mediterranean Sea because of its flavour (Oktay et al., 2003). Foeniculum vulgare Mill. (Umbelliferae) is an annual, biennial or perennial aromatic herb, depending on the variety, which has been known since antiquity in Europe and Asia Minor (Özbek et al., 2003). It is also used to flavor foods, liqueurs and in the perfumery industry. Essential oils are mainly concentrated in the mericarps (fruits) and provide the unique aroma and taste (Choi and Hwang, 2004).

2. Material and Method

2.1. Material

Within the scope of the study, 100% woolen fabric, ready for dyeing, has been used. The fabric used in natural dyeings has been illustrated in figure 1.

Figure 1. Wool Fabric used in the experiments

In the natural dyeing experiments, the dried fennel seeds (Figure 2a) obtained from the local markets was grinded into small particles (Figure 2b) and then used.

Figure 2a. Dried fennel seeds

Figure 2b. The fennel seed after grinding

Copper (II) sulphate, tin (II) chloride, iron (II) sulphate, potassium dichromate and zinc chloride were used as the mordanting agent. These mordanting agents used were added to the dyeing bath at a rate of 4% in proportion to the fabric weight. In addition, dyeing was done without using mordanting agent.

2.2. Method

Dyeing of woolen fabrics with fennel seeds was carried out in laboratory type sample dyeing machines. The fabric weight was adjusted to 2 g and the milled fennel seeds at the same amount with the fabric were added to the dyeing bath at the same time. The liquor ratio was set at 1:40 and the sample was added into the dyeing tubes. In other words, after adding the fennel seed, fabric and mordanting agent to dye bath the dyeing process has been started. So mordanting and dyeing has been managed simultaneously.

The dyeing process was started at room temperature and reached to 100 ^{0}C as soon as possible and dyeing process was performed for 75 minutes at this temperature. After the dyeing process is complete, the fabric is first subjected to cold rinsing. Immediately after this step, the fabric subjected to the hot washing process and then was moved to the final rinse step and allowed to dry in room conditions in the laboratory environment.

For the evaluation of the obtained results; the CIE L*a*b* measurements of the dyed woolen fabric samples were performed on the spectrophotometer and the numerical values of these measurements are given in the Results and Discussion section of the paper.

3. Results and Discussion

Coloring experiments of woolen fabrics have been provided by fennel seeds with using 5 different mordanting agents and also without using any mordanting agents. As a result of these experiments, the colors obtained after drying at room temperature and the spectral values of these colors are presented in Table 1.

Table 1. CIE L*a*b* values of dyed samples

Mordanting Agents	**CIE L*a*b* and C* h°**				
	L*	***a****	***b****	***C****	***h°***
No mordanting	72.98	0.73	21.15	21.16	88.03
Copper (II) Sulphate	60.13	0.9	26.93	26.95	88.09
Tin (II) Chloride	79.75	-3.26	42.17	42.29	94.42
Iron (II) Sulphate	71.04	1.51	24.8	24.85	86.53
Potassium Dichromate	63.91	-0.22	18.74	18.74	90.67
Zinc Chloride	70.18	1.19	28.92	28.95	87.65

When the L* values were examined, the highest L* value was found in dyeing experiments using tin (II) chloride mordanting agent. The lowest L* value was encountered in the dyeing process using copper II sulphate. This shows that the experiment using tin (II) chloride mordanting agents resulted in the formation of a light color, while the experiment using copper (II) sulphate mordant material showed a darker color. It has been seen that woolen fabrics dyed with fennel seeds can be in yellow and tones as well as light green colors. It can be seen that when hue angles are examined, this situation can be achieved as well. In other words, hue angles are generally between 86 and 94 degrees. In this case, the angular values are close to the yellow axis and the appearance of yellow and tones is an inevitable result.

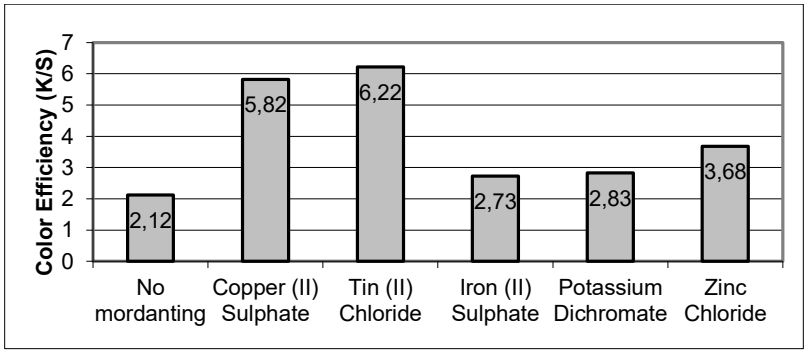

Figure 3. The Color efficiencies of thesamples dyed with different mordanting agents

The K/S values of the samples were analyzed as well.When Figure 3 is examined, it is seen that the maximum color efficiency is obtained in dyeing experiments using tin (II) chloride and this value is 6.22. The time when we look at the lowest K/S, value is 2.12. This result was achieved in dyeing process without using any mordanting agents.

4. Conclusions

In this study, it was tried to use fennel seeds as a source of natural dyestuff for woolen fabrics. Five different mordant substances were used in the experiments and also experiments

were made without using any mordanting agents. At the end of the experiments Spectral measurements of the dyed woolen fabrics were taken and presented in the relevant area. As a result of these studies, it was found that wool fabrics can be colored with fennel seeds. Thus, in addition to its different uses, it has also been determined that the fennel can be regarded as a natural dye source in the textile sector.

References

Choi, E. M., Hwang, J. K., (2004). Antiinflammatory, analgesic and antioxidant activities of fruit *Foeniculum vulgare*. *Fitoterapia*, 75, 557-565.

Karadağ, R., (2007). *Doğal boyamacılık*. Ankara: T.C. Kültür ve Turizm Bakanlığı Döner Sermaye İşletmesi Merkes Müdürlüğü, Geleneksel El Sanatları ve Mağazalar işletme Müdürlüğü. (http://www.turkelhalilari.gov.tr/icerik/Dogal_Boyamacilik.pdf).

Morimoto, Y., Ono, K., Arita, D., (2011). *Dyeing in computer graphics*. In: Akçakoca Kumbasar, E. P., (Ed.), Natural dyes. pp. 29–56 (ISBN 978-953-307-783-3), Croatia: In Tech.

Oktay, M., Gülçin, İ., Küfrevioğlu, Ö. İ., (2003). Determination of in vitro antioxidant activity of fennel (*Foeniculum vulgare*) seed extracts. *Food Science and Technology*, 36(2), 263-271.

Özbek, H., Uğraş, S., Dülger, H., Bayram, İ., Tuncer, İ., Öztürk, G., Öztürk, A., (2003). Hepatoprotective effect of *Foeniculum vulgare* essential oil. *Fitoterapia*, 74, 317-319.

Özgüney, A. T., Seçim, P., Demir, A., Gülümser, T., Özdoğan, E., (2015). Ecological printing of madder over various natural fibres. *Tekstil ve Konfeksiyon*, 25(2), 166-171.

Sound Absorption Characteristics of Textile Materials Produced from Recycled Fibers

Gonca ÖZÇELİK KAYSERİ[1*],Gamze SÜPÜREN MENGÜÇ[1], Nilgün ÖZDİL[2]

[1]Ege University, Emel Akın Vocational Training School, İzmir, TURKEY

[2] Ege University, Engineering Faculty, Department of Textile Engineering, İzmir, TURKEY

[*]**Corresponding author:** gonca.ozcelik@ege.edu.tr

Abstract

Noise has become an increasing public health problem and serious environment pollution in our daily life. Generally it is impossible to treat most of the noise problems at source and the reduction of noise emission is usually accomplished by noise isolation methods. Recently, nonwovens, as one of the most common textile products, have become important sound absorption materials. These materials are used as sound absorbers, sound diffusers, noise barriers or sound reflectors. For sustainable development of the textile industry, solutions for both decreasing waste and reducing noise have been searched for years. Since recycled materials exhibit good sound absorbing properties, these materials are becoming an interesting alternative to conventional materials for practical applications. In this study, the measurement methods of acoustic characteristics of textile materials are explained and the sound absorption properties of nonwoven fabrics produced from both pure and recycled polyester and polypropylene fibers are compared.

Keywords: sound absorption, acoustic, textile material, sustainability, recycled fibers

1. Introduction

With the increasing number of new technologies, daily noise pollution becomes one of the important negative factors affecting the comfort of life especially in big cities. Today, workplace and environmental noise pollution poses a serious threat to human health. The noise that makes communication difficult, distorts concentration and lowers the quality of life means health hazard when exposed for a long time. Headaches, fatigue, tension, body aches, sleep disturbances and other problems related to stress are the most common reactions. There are also studies showing the relationship between high blood pressure, vascular spasms and heart attack associated with prolonged exposure to noise (Wintzell, 2013; Talgar ve Kaya, 2017 ; Küçük and Korkmaz, 2012).

The classic solution to the problem of noise pollution is to remove the noise from the source, but it is not always possible to remove the noise problem in this way. For this reason, the reduction of noise emission is usually carried out by noise isolation methods. In recent times, nonwoven surfaces, as one of the most common textile products, have become an important sound absorbent material.

Sound can be defined as a pressure change in air, water, or similar elastic medium, which can be perceived by the ear as a stimulus of hearing. The human ear can sound between 20 Hz and 20,000 Hz. There are two types of sound protection such as sound absorption and sound insulation. In sound absorption, air particles rub inside the insulating material, converting part of the sound into heat energy, thus reducing the energy of the sound. Therefore, sound absorption refers to how much of the sound from the sound source is absorbed in the environment of the source (Talgar ve Kaya, 2017).

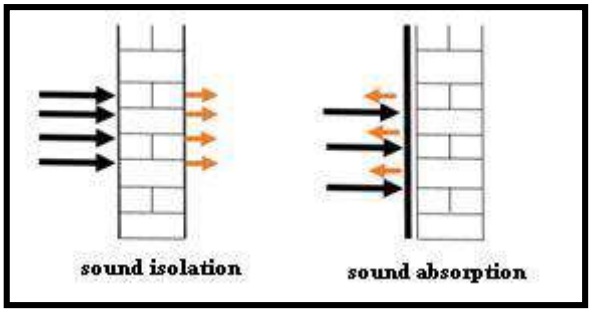

Figure 1. Sound isolation and absorption

Active and passive noise control approaches are available for noise control. Active noise control is the total noise reduction process using a secondary audio source, whereas passive noise control is provided by sound absorbers and sound insulation materials (acoustic textiles).

Active sound control is achieved by using complex digital signal processing techniques to achieve a destructive interference of sound waves (Arenes, 2016). Sound absorption is made in passive control approach and knowing acoustical properties of these porous materials is useful for proper application in products such as sound barriers, walls, road surfaces (Stanciu and et.al, 2012).

Sound absorption describes the transformation of sound energy into heat. The kinetic energy of the sound is converted to heat energy when the sound strikes the fiber. Hence, the sound disappears after striking the material due to its conversion into heat. The main reasons for the acoustic energy loss as the sound passes through the sound absorbing material are frictional losses, momentum losses and temperature fluctuation. Nonwoven textile materials are widely used for sound insulation and absorption applications due to their porous structure. To allow sound propagation through friction, the sound wave has to enter the porous material. The nonwoven surface forms a large inner surface in the form of a flexible fiber skeleton of a fabric structure. The loss of sound energy in textile materials is influenced by various physical parameters such as fiber type, fiber diameter, material thickness, density, bonding method, air resistance and porosity (Seddeq and et.al, 2012; Küçük and Korkmaz, 2012, URL-1).

Due to the reduction of natural resources and the rising costs of waste disposal, the recycling or reprocessing of textile waste is becoming increasingly important all over the world in terms of economy, environment and sustainability (Chavan RB, 2014; Eser ve ark., 2016). The use of textile surfaces produced from recycled materials has spread to a wide variety of areas and its use as sound insulation material has also become widespread.

A wide variety of studies have been carried out on the acoustic properties of textile products. In a study, nonwovens produced from recycled natural fibers blended with synthetic fibers have been tested acoustically. Also, biocomposites from agriculture wastes such as rice straw and sawdust have been investigated. The results indicated that nonwoven samples have high sound absorption coefficients at high frequencies (2000–6300 Hz), low sound absorption coefficients at low frequencies (100–400 Hz) and better sound absorption coefficients at mid (500–1600Hz) frequencies. The sound absorption coefficients at all frequency ranges improved by increased thickness of nonwovens (Seddeq and et.al, 2012). In another study, eight different nonwoven composites including different fiber types mixed with different ratios were tested. Along with sound absorption properties, thickness, weight per area, and air permeability parameters of the samples were measured. The increase in thickness and the decrease in air permeability results in an increase in sound absorption properties of the material. The samples including 70% cotton and 30% polyester resulted in the best sound absorption coefficient in the

mid-to-high frequency ranges. The increase in the amount of fiber per unit area resulted in an increase in sound absorption of the material. Addition of acrylic and polypropylene into a cotton and polyester fiber mixture increased the sound absorption properties of the composite in the low and mid-frequency ranges also (Küçük and Korkmaz, 2012).

In another study, the sound absorption characteristics of fabrics produced from 5 microfibers and a normal PES fiber were measured by reverberation chamber method. The results showed that the fabrics produced from microfibers are far superior to those of conventional fabrics of the same thickness or weight in terms of sound absorption characteristics (Na and et al., 2007).

Today, while work on new insulating materials continues intensively, the availability of recycled products in this area also comes to the forefront. Recycling technology provides environmental, social and economic benefits; with environmental awareness and increased sensitivity to sustainability, recycled materials provide significant advantages in terms of being cheap and environmentally friendly material suitable for sound insulation.

In this study, non-woven surface materials produced from conventional polyester (PES), mechanically recycled polyester (rm-PES), recycled polyester (r-PET), polypropylene (PP) and recycled polypropylene and the results were analyzed.

2. Material and Method

2.1. Material

In this study, 5 different nonwoven surface fabrics were first provided at close weights and thicknesses. These surfaces are produced from conventional polyester (PES), recycled polyester (r-PET fiber recycled from PET bottles), mechanically recycled polyester (rm-PES), polypropylene (PP), and recycled polypropylene (r-PP). The pore sizes in nonwoven fabrics were measured according to TS EN ISO 12956, the mass per unit area was determined in accordance with TS EN ISO 9864. Thickness measurements of the materials were carried out according to TS EN ISO 9863-1 using SDL Atlas fabric thickness gauge, air permeability test was conducted according to TS 391 EN ISO 9237 standard by using TEXTEST FX 100 air permeability meter at 200 Pa pressure difference and 20 cm^2 measurement area.

Table 1. Pore sizes od nonwoven fabrics

Fabric Code	Fiber types of nonwoven materials	Pore sizes (µm)
1	Conventional polyester (PES)	110
2	Recyled polyester (r-PET)	110
3	Mechanically recycled polyester (rm-PES)	110
4	Polypropylene (PP)	110
5	recycled polypropylene (r-PP)	100

2.2. Measurement of Acoustic Absorption Properties of Materials

2.2.1. Measurement of Acoustic Absorption Characteristics by Impedance Tube Method

One of the methods used for determining the sound absorption coefficients of textile surfaces is the ISO 10534-2 double microphone impedance tube method. This method is based on measuring the sound pressure difference with the help of a microphone placed in the impedance tube. In the standard arrangement used to determine the sound absorption coefficient by the impedance tube method, the sound generated by the signal generator is given to the impedance tube and the performance of the material is examined by the software.

The impedance tube measurement method works on the principle of measuring the reflected sound wave and calculating the sound absorption coefficient from the surface impedance value. The method called "Transfer Function" used in the new system impedance tubes. The advantage of this method is that the surface impedance and sound absorption coefficient values are obtained in one measurement for all frequencies.

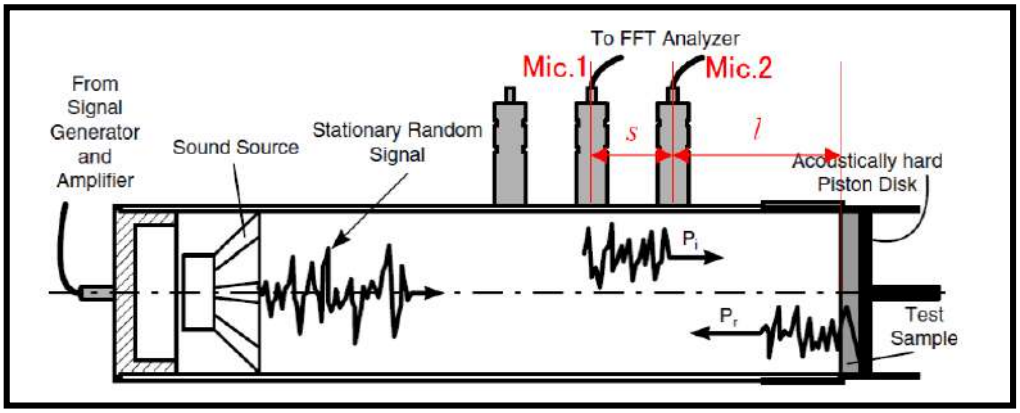

Figure 2. Impedance tube sound absorption measurement method (URL-2)

In the impedance tube arrangement schematically shown in Figure 2, firstly the signal characterizing the voice is generated by the software of test system. Then the signal passing through the amplifier is transformed into a planar progressive sound wave in the tube through the speaker. The transfer function between two microphones is a ratio of the pressure values measured separately from the two microphones. The transfer function is associated with the value of the reflection factor and the value of the sound absorption coefficient of that frequency (R) is obtained from this factor (Uzundağ, ve Tandoğan, 2013).

With the impedance tube method, the sound absorption coefficient values of the materials can be measured in the frequency range of 50 Hz to 6.4 kHz. In the study, the measurement of sound absorption coefficient by impedance tube method was carried out by 3 test samples randomly taken from nonwoven fabrics.

2.2.2. Measurement of Acoustic Absorption Characteristics by Alpha Cabinet Method

Some of the cabin examples on the market for the measurement of acoustic sound absorption characteristics are as follows.

1. Rieter Alpha Cabin Instructions; Technical note no 591,
2. Toyota engineering standard; Test Method for Acoustic Materials, no TSL0600G,
3. Renault Test method; Fibrous and Cellular Materials Sound Absorption in Diffuser Field, D491977,
4. The Design of Small Reverberation Chambers For Transmission Loss Measurements, (Uzundağ, ve Tandoğan, 2013)

Nonwoven textile products supplied within the scope of the study were tested by using Alpha Cabinet according to the Renault D49-1977-B standard. The appearance of the device for this method is shown in Figure 3.

Figure 3. Twin mini reverberation cabinets (URL-3)

Alpha Cabins receive their names from sound absorption coefficient “alpha” and their structure is like a miniature reverberation rooms (Figure 4). During the measurements, the relative humidity in the alpha cabinet was 55% and the temperature was set at 25°C. The cabinet volume was 6.44 m^3 and the total surface area was 22.2 m^2. The surface area of the test specimens was 1.12 m^2, the height of the microphone from the ground was 0.88 m, and the height of the sound source was 0.20 m. The frequency measurement range was set at 400-1000 Hz. Three Brüel and Kjaer 2669 model microphones were used.

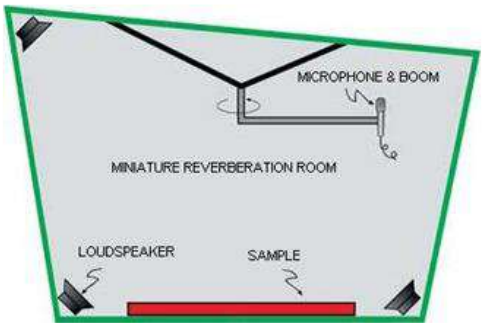

Figure 4. Alpha cabinet measurement arrangement

Before testing in Alpha cabinet, it is necessary to compare the noise levels in the cabinet with the background noise levels from the outside (motor noise, electrical noise) while the speakers are in operation.

The difference between these levels should be at least 45 dB. Alpha cabinets are quite similar to the reverberation rooms. The Sabine formula is used for the sound absorption coefficient measurements and the coefficient is calculated by taking the difference between the resonance times of the sampled and non-sampled measurements in the cabinet (Uzundağ, ve Tandoğan, 2013).

$$\alpha = \frac{0.163xV}{S}\left(\frac{1}{TR} - \frac{1}{TR_0}\right)xC \qquad \text{(Equ.1)}$$

V = cabinet volume,

S =sample area,

TR =sound receiving time with the test sample inside the cabinet,

TR_0=sound receiving time without the test sample inside the cabinet

C=cabinet correction coefficient

When studies carried out in the literature are examined, it can be concluded that impedance tube measurements and alpha cabinet measurements do not give comparable results, as also found in this study. Therefore, correlation analysis between the results is not necessary.

3. Results and Discussion

The structural properties and air permeability values of 5 different nonwoven surfaces used in the study are given in Table 2.

Table 2. Properties of nonwoven fabrics used in the study

Measured Parameter		100% PES	100% r-PET	100% rm-PES	100% PP	100% r-PP
Mass per Unit Area (g/m^2)	Mean ($\bar{X}$)	550	596	519	509	500
	Standard Deviation (S)	8,14	12,10	27,27	10,92	4,81
	CV (%)	1,48	2,03	5,25	2,15	0,96
Thickness (mm)	Mean ($\bar{X}$)	4,04	2,95	3,17	3,60	4,55
	Standard Deviation (S)	0,16	0,09	0,30	0,10	0,10
	CV (%)	3,93	2,89	9,46	2,67	2,28
Air Permeability	Mean ($\bar{X}$)	1136	1270	600	875	1536
	Standard Deviation (S)	57,71	116,40	112,13	148,66	69,14
	CV (%)	5,08	9,17	18,66	17,01	4,50

As air permeability results of nonwoven fabrics were examined, it can be seen that the surface produced from 100% r-PP material has the highest air permeability due to its porous structure. The lowest air permeability value belongs to mechanically recycled polyester surface. Since different textile materials are mechanically recycled and compressed, it has a very compact structure; less porosity and thickness. It also has comparatively less mass per unit area.

The test results obtained from the impedance tube method are given in Figure 5. According to the results, it is obtained that r-PP material has better performance, since its porous structure creates a higher friction. A decrease in r-PP material is observed at frequency values in the 315-800 Herz range. It is thought that this situation is related with the deterioration of the material structure depending on the increasing frequency. Other materials give rise to lower sound absorption characteristics than r-PP materials. The sound absorption characteristics of conventional PES and r-PET materials exhibit nearly same tendecy. Mechanically recycled material has a higher sound absorption characteristic due to its thicker structure.

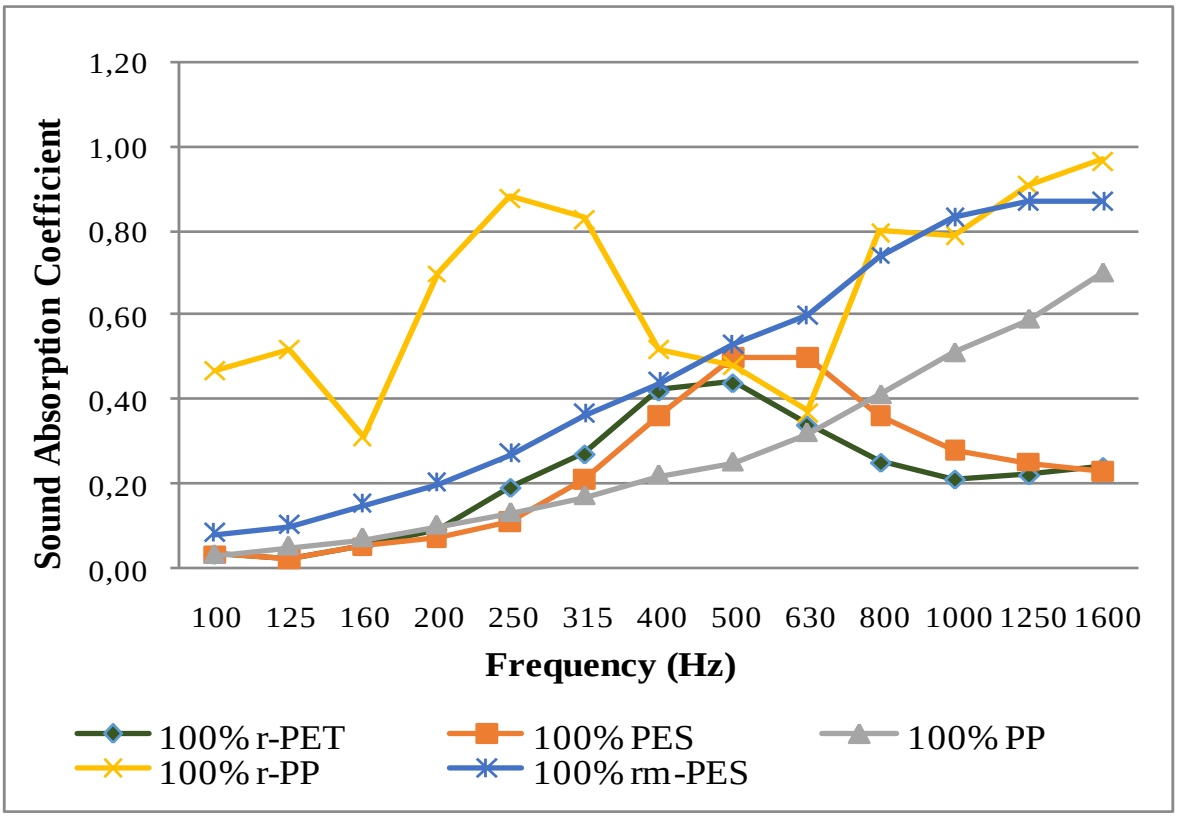

Figure 5. Sound absorption coefficients based on the impedance tube method

The acoustic absorption test results of the textile surfaces according to the alpha cabinet method are given in Figure 6.

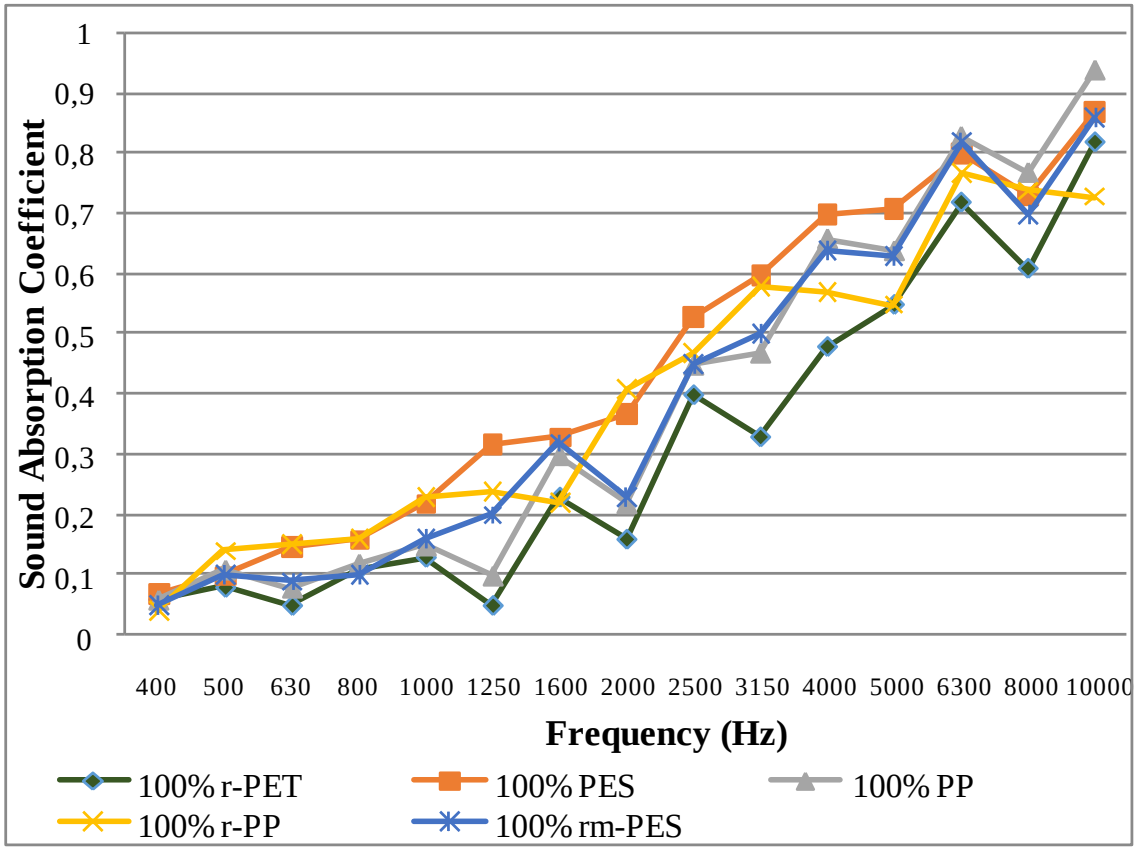

Figure 6. Sound absorption coefficients based on Alpha cabinet method

It can be seen that nonwoven surface produced from 100% PES fibers, generally has higher sound absorption feature based on Alpha cabinet method. 100% r-PET nonwoven fabric indicates the lowest sound absorption among the tested surfaces. Nonwoven fabrics produced from conventional and recycled PP fibers have similar characteristics and there is no significant difference between them in terms of acoustic insulation.

In this study, acoustic absorption coefficients were measured according to two different methods. The results obtained from the alpha cabinet and the impedance tube methods were not found parallel to each other. This difference was also pointed out by several studies in the literature. Therefore, it is very important to take into account which method is used when selecting materials for sound insulation.

4. Conclusion

Along with the growing population, noise has become one of the major problems of everyday life, affecting our quality of lives and, in some cases, our health. As the studies on reducing the noise generation continue, new solutions are being searched on systems that allow

absorbing more quantities of the present disturbing noise. Within this scope, many different technical textile materials are produced which are closely related with building construction, automotive and machinery industries. The use of these high performance products is becoming increasingly widespread in terms of technical specifications. However, in today's competitive conditions, products that can compete in terms of cost are more preferred in the market. Recycled surfaces are one of these preferred products. In addition to the price advantage, waste materials are transformed into usable products by recycling which is completely an environmentally friendly production that provides sustainability.

In this study, characteristics of conventional polyester and polypropylene nonwoven insulation materials commonly used in the market and the nonwoven fabrics produced from recycled materials were compared. When the test results are examined, it is concluded that the recycled materials used in sound insulation area have very successful competitive performance when compared with the conventional materials. Insulation materials have very good performance characteristics when used in sufficient thickness value.

Insulation materials are used especially in areas where sound insulation is desired (e.g. children's houses, hospitals, entertainment places, automotive sector etc.) and in civil engineering area. And it is a good application area for recycled materials to supply a sustainable world, to increase the environmentalist approach and to evaluate waste materials in a technical field. By the year 2017, price of 100% PP fiber in the market is about 3.0 $/kg, 1.6 $/kg for r-PP fiber, about 1.6 $/kg for 100% PES and r-PET fibers; and 1.2 $/kg for rm-PES fibers. In the scope of economy, it can be foreseen that recycling materials will provide an important advantage for both producers and consumers.

Acknowledgement

This study was supported by the BAP project of Ege University 15-MÜH-078. We would also like to thank Sarıkılıç Tekstil Sanayi ve Tic.Ltd.Şti for their material support used in the study.

References

Arenas, J. (2016). Applications of Acoustic Textiles in Automotive/Transportation. 143-163. 10.1007/978-981-10-1476-5_7.

Chavan RB. (2014). Environmental Sustainability through Textile Recycling. *Journal of Textile Science & Engineering,* ISSN: 2165-8064 JTESE, an open access journal.

Eser B., Çelik P., Çay A., Akgümüş D. (2016). Tekstil ve Konfeksiyon Sektöründe Sürdürülebilirlik ve Geri Dönüşüm Olanakları. *Tekstil ve Mühendis*, 23: 101, 43-60.

Jaatinen, J. (2011). *Alternative Methods of Measuring Acoustic Absorption, Department of Signal Processing and Acoustics*. Master of Science Thesis, Aalto University School of Electric Enginnering.

Kaya, A.İ. , Dalgar T. (2017). Ses Yalıtımı Açısından Doğal Liflerin Akustik Özellikleri, *MAKÜ FEBED*, Özel Sayı 1: 25-37.

Küçük, M., Korkmaz Y. (2012). The effect of physical parameters on sound absorption properties of natural fiber mixed nonwoven composites. *Textile Research Journal*, 82(20) 2043–2053.

Na, Y.,Lancaster J., Casali J., Cho G. (2007). Sound Absorption Coefficients of Micro-fiber Fabrics by Reverberation Room Method. *Textile Research Journal*, Vol 77(5): 330–335.

Wintzell, L. (2013). *Acoustic Textiles, The case of wall panels for home environment*, Bachelor Thesis Work, The Swedish school of Textiles, Borås, Sweden.

Reya, R., Bertób L, Albac J., Arenasd J.P. (2015). Acoustic characterization of recycled textile materials used as core elements in noise barriers. Noise Control Engr. J., 63 (5)

Stanciu, M. D., Curtu, I., Cosereanu C., Lica, D., Nastac, S. (2012). Research Regarding Acoustical Properties of Recycled Composites. *8th International DAAAM Baltic Conference*, "Industrial Engineering, Tallinn, Estonia.

Soliman, H., Aly Nermin M, Marwa A., Elshakankery M.H. (2012). Investigation on sound absorption properties for recycled fibrous materials, *Journal of Industrial Textiles*, 43(1) 56–73.

Sule, A.D., Bardhan, B.K., (2001). Recycling of Textile Waste for Environment Protection-An overwiev of some practical cases in textile industry. *Indian Journal of Fiber&Textile Research*, Vol.26, 223-232.

Standart: TS EN ISO 12956: Geotekstil ve geotekstillerle ilgili mamüller, karakteristik açıklık ölçüsünün tayini

Uzundağ, U., Tandoğan, O. (2013). *Malzemelerin Akustik Performans Testleri*, Novosim Mühendislik Hizmetleri.

URL-1:https://www.sandler.de/en/lightbox/sound-absorption/

URL-2 https://www.acoustics.asn.au/conference_proceedings/INTERNOISE2014/papers/p312.pdf

URL-3:http://proplan.com.tr/Uzmanliklar/endustriyel-ve-mimari-akustik/test-odalari-ve-kabinler

Handle Properties of Woven Pique Fabrics Produced From Mechanical Recycled Cotton Fibers

Leman ATİKER[1], Nilgün ÖZDİL[1], Arif Taner ÖZGÜNEY[1], Kadri IŞILAY[2], Turhan AVDAN[2]

[1] Ege University, Department of Textile Engineering, Bornova- Izmir, Turkey
[2] Menderes Tekstil A.Ş., Denizli, Turkey

[*]**Corresponding Author:** atikerleman@gmail.com

Abstract

Recently, there has been significant increase in textile consumption depending on the population growth and developments of life standards. It is known that there is more than 80 million tones textile and ready wear production on the global scale and such a huge material production cause very crucial environmental problems. Textile wastes can be the raw materials for the developments of new value-added products. Adequate use of natural resources for a sustainable life has become increasingly important, and as a result of this, textile industry is in the tendency of using recycled fibers. Due to recycling process, some of the physical properties of textile materials could be worsened and as an important part of clothing comfort, tactile comfort of the fabrics can be also changed. Handle characteristics of the fabrics affect the consumer purchase preferences and therefore several simple instruments have been developed for the numerical identification of fabric handle. In this study, handle related properties, such as thickness, bending rigidity, coefficient of friction, were measured in order to objectively determine the sensory properties of woven pique fabrics produced from 85% recycled cotton fibers and 15% polyester fibers.

Keywords: Recycled fiber, Mechanical recycling, Textile wastes, Sustainability, Fabric handle, Textile industry, Pique fabric.

1. Introduction

Due to the accelerated growth of the world population, developing industrialization and shift in the consumer behaviour towards fast fashion, textile production and consumption have increased considerably, leading to a higher amount of textile wastes (Ichım and Sava, 2016). The total volume of textile and fashion production at the global level is estimated to be more than 80 million tons annually, and therefore improving the environmental performances of this industry is vital (Eser and et al, 2016).

The textile waste can be divided into two categories: pre-consumer (or post-industrial) and post-consumer waste. While the pre-consumer waste is generated in the manufacturing process of fibres, yarns, fabrics, garments and carpets, the post-consumer waste consists of worn-out or outdated textile products that the owner no longer needs. Waste disposal is one of the most serious environmental problems. Both waste incineration and waste dumping in landfills have negative environmental impact. The best solution to avoid waste disposal is recycling textile waste by reusing clothing and household textiles or by mechanical processing into new generations of textiles. Recycling textile waste brings both economical and environmental benefits. Waste should be treated as a resource of raw material that saves natural resources (natural fibres like cotton, wool and crude oil used to produce synthetic fibres) (Ichım and Sava, 2016).

Cotton is the most consumed natural fibre in textile and clothing industry. Worldwide cotton production was 23 million tons in the 2016/17 season, but in the 2017/18 season it reached 25 million tons with an increase of 9.9% over the previous year. According to TÜİK data, 2,450 tons of cotton unseed production was realized in the 2017/18 season in Turkey (URL-1). However previous studies shown that water consumption, land occupation, emissions, and usage of chemicals are the most critical aspects to be evaluated during the cotton production step. Cotton growing requires substantial amounts of pesticides, insecticides, and chemical fertilizers and large amounts of water with negative impacts on environment and water resources. The landfill space required for waste disposal is substantially reduced. Recycling reduces energy and water consumption (Ichım and Sava, 2016; Esteve-Turrillas and Guardia, 2016).

Textiles should have main properties which are differs from each other with their technical structures in that it must have sufficient strength, performance characteristics and at the same time they have sensorial comfortable in sensorial aspects (Kayseri and et al., 2012). The term fabric “hand” or “handle” has been defined as the quality of a fabric or yarn assessed

by the reaction obtained from the sense of touch or the sum total of the sensations expressed when a textile fabric is handled by touching, flexing of the fingers and so on (Valatkienė and Strazdienė, 2006). It is a complex parameter and is related to the fabric properties such as flexibility, compressibility, elasticity, resilience, density, surface contour (roughness, smoothness), surface friction and thermal characteristic. The fabric hand related to the concept of comfort, style, and appearance are the most important properties of the textile end products (Özgüney and et al., 2009). Hand is often the fundamental aspect that determines the success or failure of a textile product. In textiles raw material, yarn structure, planar structure and finishing treatments affect the fabric hand (Mäkinen and et al. 2005). Fabric hand can be approached through subjective evaluation and objective measurements (Özgüney and et al., 2009).

The present work focuses on the handle properties of different patterned woven pique fabrics produced from mechanical recycled cotton fibers. A pique fabric is characterized by raised woven designs like as waffle, huck toweling, granite, honeycomb, bedcord. Lengthwise wales or cords on the face of the fabric (formed by extra warp yarns) are held in place by crosswise weft floats on the back of the fabric. Extra warp yarns (stuffer yarns) are not visible and interwoven on the face of the fabric and but lay under the cords to emphasize the quilted effect. They are made of dobby or jacquard loom. Pique patterned fabrics are generally used in home textiles especially for “pique” which is a kind of thin blanket and used in summer to cover at night coolness (URL-2).

In this study, handle related properties, such as thickness, bending rigidity, coefficient of friction, were measured in order to objectively determine the sensory properties of pique woven fabrics produced from 85% recycled cotton fibers and 15% polyester fibers. In addition, subjective handle evaluation such as softness/stiffness, smooth/rough was made to compare with the objective handle related properties of the fabrics.

2. Material and Method

2.1. Material

In this study, handle properties of woven pique fabrics produced from 85% recycled cotton 15% PES blended fibers in 6 different fabric pattern having the same warp-weft density and fabric content were investigated. Open end yarns were used for weft and warp yarns. Yarn count was Ne 6/1 for warp yarn and Ne 6/2 for weft yarns. Fabric density was 17 ends/cm for warp and 8,5 picks/cm for weft direction. Constructions of the fabrics are given in Table 1 and pictures of the fabrics are indicated in Figure 1.

Table 1. Fabric patterns used in study

Fabric Code	Fabric Pattern
1	Zigzag Pattern
2	Small Wave Pattern
3	Wave Pattern
4	2/2 Broken Twill
5	Weft Pattern Fabric
6	2/2 Panama

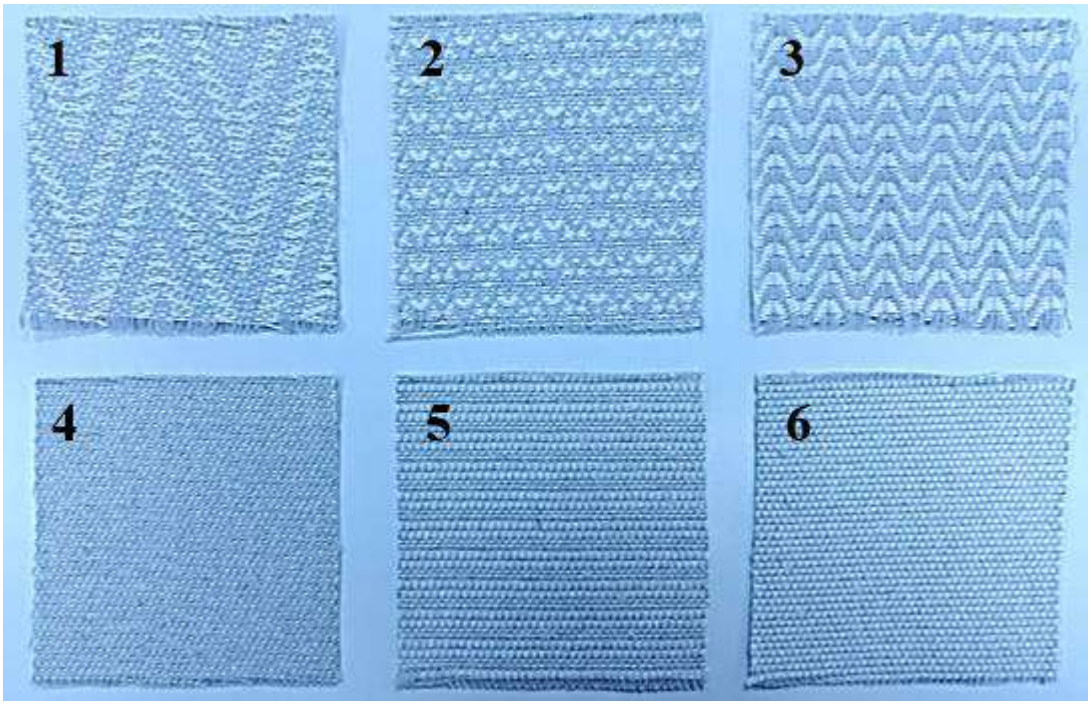

Figure 1. Woven pique fabrics in 6 different fabric pattern

2.2. Method

2.2.1. Objective Tests

All the fabrics were conditioned in standard atmosphere conditions 20 °C ±2 ve 65%±4 relative humidity before the tests. Afterwards mass per unit area, thickness, circular bending rigidity and friction coefficient were tested and the results were statistically analyzed.

Mass per unit area of the fabrics was measured according to TS 251 standard. Thickness values were tested according to TS 7128 EN ISO 5084 standard by using SDL ATLAS Digital Thickness Gauge (Fig. 2a). Stiffness test of the fabric specimens was carried out in circular bending rigidity tester, developed according to ASTM 4032 (Fig. 2b). In this method, the force which is generated while pushing a fabric specimen through a ring is measured. In order to determine the kinetic friction coefficient of the, Frictorq instrument (Fig. 3c) was used. Frictorq is based on a method to measure the coefficient of friction (μ_{kin}) of the fabrics, using a rotary principle and, therefore, measuring torque (Özgüney and et al., 2009).

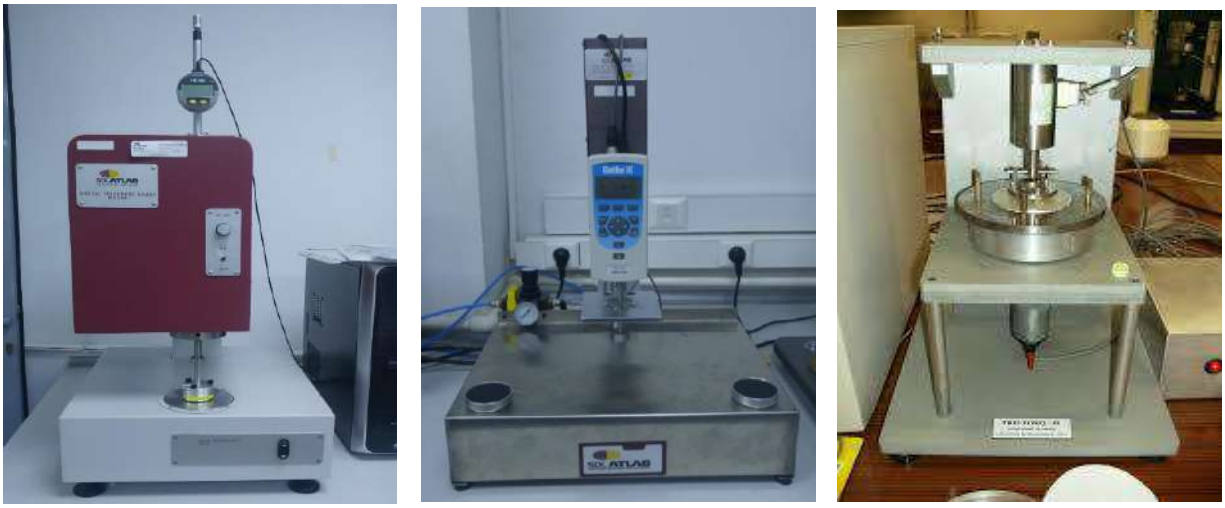

(a) **(b)** **(c)**

Figure 2. SDL Atlas Digital Thickness Gauge (a), Circular Bending Rigidity Tester (b), Frictorq Instrument (c)

In order to investigate the effect of construction type of recycling woven pique fabrics on the handle properties ANOVA tests were applied. To determine whether the variances of the fabric results are statistically significant or not, homogeneity test of variance (Levene test) was performed. According to the Levene Homogeneity test results, Student-Newman Keuls and Tamhane's T2 Post Hoc Tests were conducted. To deduce whether the parameters were significant or not, p values were examined.

2.2.2. Subjective Tests

In subjective assessments, a panel of 21 experts (researchers and students from the textile and clothing sectors) between the ages of 20 and 50 was chosen for fabric hand evaluation. Experience of the other researches shows that to control the climatic conditions where the subjective evaluation carried out is important. For that reason, the tests were performed in standard atmosphere conditions (20±2°C temperature and 65±4% relative humidity).

The specimens in 100 cm² area were prepared for subjective tests. The participants made an assessment using a 5-point scale. Before the evaluation, control fabrics with the values 1 and 5 were given to the members and they were asked to evaluate the roughness and softness attributes of the specimens. The rating numbers for the attributes were given in Table 2.

Table 2. Rating scales for the attributes

Sensory Attribute	Rating Number
Softness-Stiffness	1-Softest……..5-Stiffest
Smoothness-Roughness	1-Smoothest……..5-Rough

In the subjective assessment procedure, jury member tested the roughness evaluation by making circular movements with their two fingers on fabric surface. The smaller rate, the smooth the fabric is, likewise the bigger roughness rate, the rough the fabric is.

In the subjective assessment procedure, softness-stiffness property is associated with bending. Fabrics easily bent are described as soft where the ones resistant to bending are described as stiff. Based on the assessment technique, the jury member evaluated the fabrics by grasping it in the palm of his/her most used hand. The more the resistance, the stiffer the fabric is, likewise, the less the resistance, the softer the fabric is.

The evaluation was always performed in blind condition to minimize the effect of fabric properties on the perception. The experts individually evaluated and ranked each fabric attribute.

3. Results and Discussion

3.1. Objective Evaluation of Fabric Handle

The results of studied objective tests were given in Table 3.

Table 3. The objective test results

Parameters	Fabric Code

	1	2	3	4	5	6
Mass Unit Per Area (g/m²)	368	368	385	392	372	370
Thickness (mm)	1,30	1,32	1,31	1,18	1,19	1,10
Circular Bending Rigidity (N)	5,72	6,58	4,65	7,45	8,46	8,10
Friction coefficient (μ_{kin})	0,3424	0,3468	0,348	0,3125	0,3488	0,319

Table 4. Results of Student-Newman-Keuls test

Fabric Test	Group	N	Subset			
			1	2	3	4
Mass Unit Per Area	1	3	367,80			
	2	3	368,26			
	6	3	370,80			
	5	3	372,00			
	3	3		384,53		
	4	3			392,20	
	Sig.		,496	1,000	1,000	
Thickness	6	3	1,10			
	4	3		1,18		
	5	3		1,19		
	1	3			1,30	
	3	3			1,31	
	2	3			1,32	
	Sig.		1,000	,410	,242	
ircul ar Bend .	3	3	4,65			

	1	3	5,71	5,71		
	2	3		6,58	6,58	
	4	3			7,45	7,45
	6	3				8,10
	5	3				8,46
	Sig.		,067	,127	,127	,175
Friction Coefficient	4	3	,3125			
	6	3	,3191			
	1	3		,3424		
	2	3		,3468		
	3	3		,3488		
	5	3		,3489		
	Sig.		,138	,432		

* The mean difference is significant at the 0.05 level

Mass Per Unit Area

It is expressed as the area density of a two-dimensional object is calculated as mass per unit area and it affects the handle properties of the fabric as well as affects many fabric properties.The mass per unit area values can be seen in Figure 3.

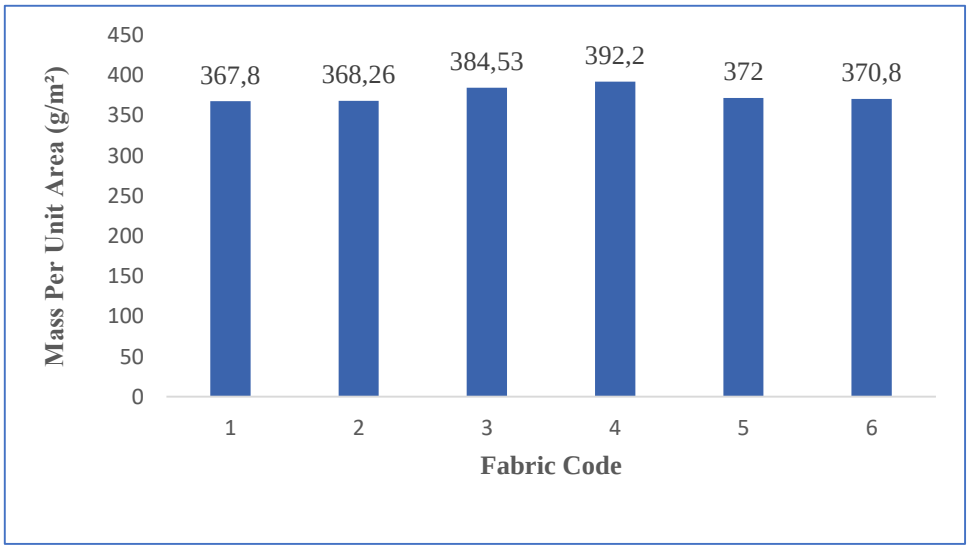

Figure 3. Fabric mass per unit area values

According to Figure 3 and statistical test results Table 4 the fabric having code number 4 has the highest value and the fabrics having code 1 has the lowest mass per unit value. Because of the long yarn floats on the fabric surface of fabric 1, this value is lower for this type of fabric. It was also seen that the differences between mass per unit areas values of the fabrics coded 1, 2, 5, 6 have not found statistically significant.

Thickness

Fabric thickness is generally evaluated by measuring the distance between two parallel plates separated by a fabric sample, with a known arbitrary pressure applied and maintained between the plates. The response of fabric thickness to applied forces normal to its plane is known as fabric compression behavior. Fabric thickness are strongly related to handle properties (Yıldız and Özdil, 2014).

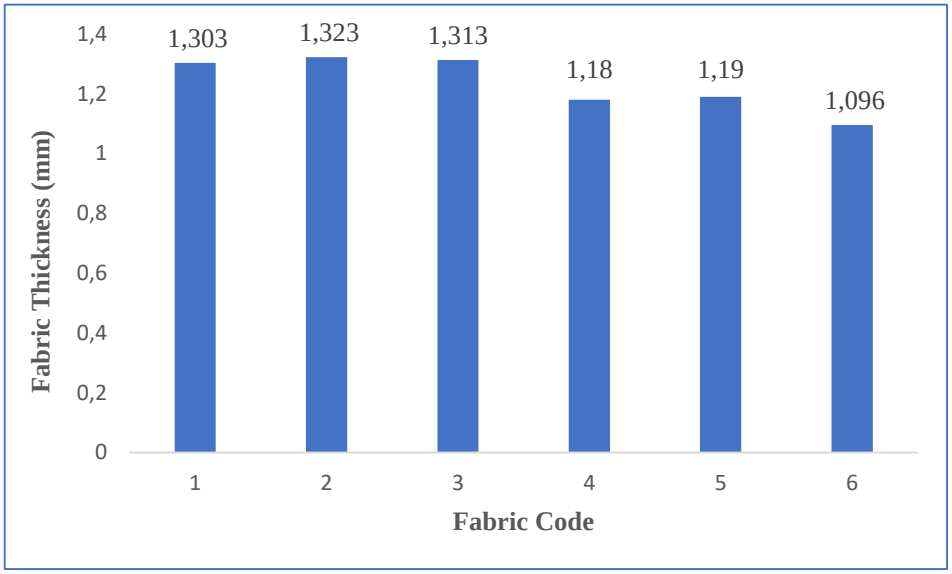

Figure 4. Fabric thickness values

The thickness values can be seen in Figure 4. When the results were evaluated in terms of fabric thickness, the fabric thicknesses vary between 1.09 mm and 1.32 mm.

According to statistical test results Table 4 and average thickness values Figure 4, fabric thickness values were grouped into 3 groups. It was revealed that, the fabric coded 6 has the lowest thickness. There was not found any significant differences between the fabrics patterned as zigzag, small wave and wave design. Because of the long floats on these fabric surfaces the structure becomes puffier.

Circular Bending Rigidity

The bending rigidity is one of the basic parameters which are decisive for the handle of textile products. A lower value of bending rigidity supports the positive impression of sensorial comfort. Bending rigidity reflects the flexibility of the fabric and higher bending rigidity values indicate greater resistance to bending motions. The higher the rigidity, the lower the fabric handle is expected to be (Yıldız and Özdil, 2014). The circular bending rigidity values can be seen in Figure 5.

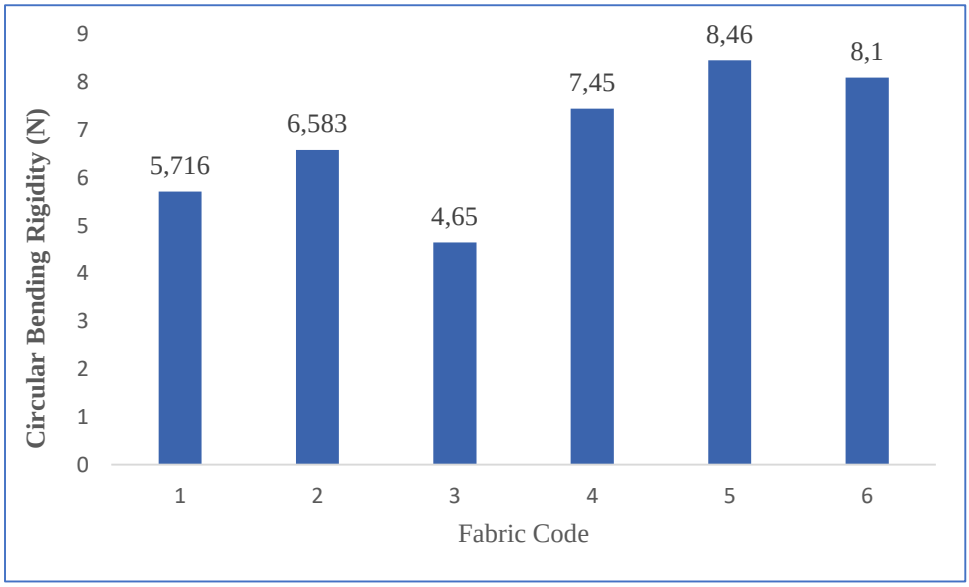

Figure 5. Circular bending rigidity values

According to statistical test results Table 4 and the average circular bending rigidity values Figure 5, fabric thickness values were grouped into 4 groups. The fabric having code number 5 has the highest value and the fabrics having code 3 has the lowest circular bending rigidity value. Due to the voluminous structure of the fabrics coded 1, 2, 3 have lower circular bending rijidity means softer fabrics.

Friction Coefficient

Traditionally, the quality and surface characteristics of fabrics is evaluated by touching and feeling by hand, leading to a subjective assessment. Therefore, one of the most important characteristics of fabrics, either for clothing or technical applications is the coefficient of friction. This is an important factor regarding the objective measurement of the so-called

parameter fabric hand. Friction coefficient is not an inherent characteristic of a material or surface, but results from the contact between two surfaces (Yıldız and Özdil, 2014).

The kinetic friction coefficient values can be seen in Figure 6.

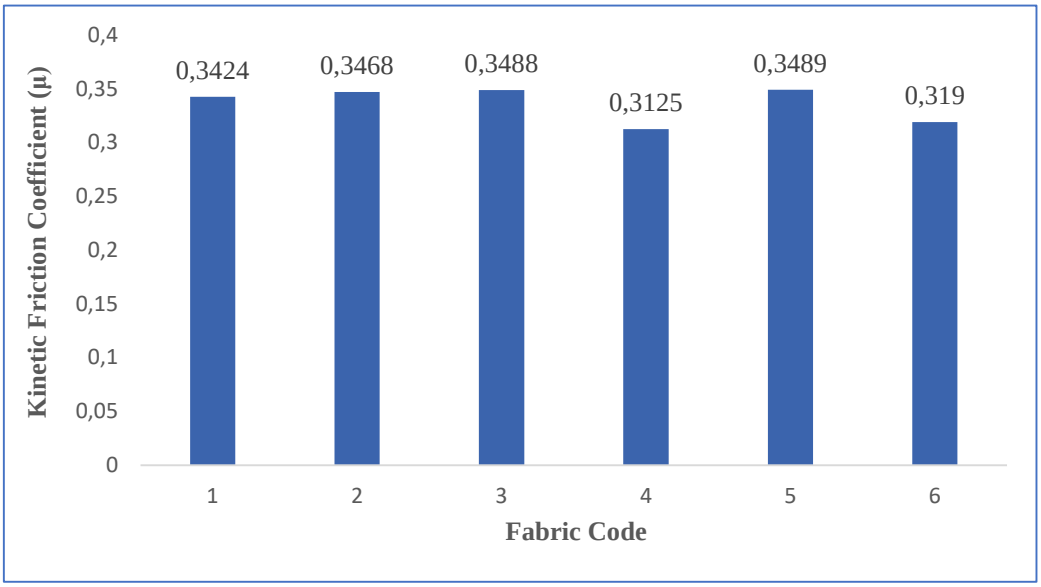

Figure 6. Kinetic friction coefficient values

According to statistical test results Table 4 and average friction coefficient values Figure 6, fabric friction coefficient values were grouped into 2 groups. The fabric coded 4 and 6 have the lower values, whether the other fabric values do not have significant differences statically. The reason is that, the small floats in the fabrics creates smoother fabric surface.

3.2. Subjective Evaluation of Fabric Handle

The mean values and standard deviations of the softness-stiffness and smooth-rough evaluations of 21 panelists were given in Table 5. Variance analysis method was used to evaluate subjective test results. The difference between rating numbers of the panelists were found statistically insignificant according to 95% confidence level.

Table 5. The subjective evaluation results

	Softness-Stiffness	Smooth-Rough

Fabric Code	Mean	Std. Deviation	Minimum	Maximum	Mean	Std. Deviation	Minimum	Maximum
1	2,47	0,78	1	4	2,76	0,81	2	5
2	3,14	0,85	2	5	3,45	0,92	2	5
3	1,47	0,60	1	3	4,64	0,55	3,5	5
4	3,59	1,09	1,5	5	2,11	0,80	1	3
5	4,57	0,57	3	5	4,73	0,51	3,5	5
6	4,33	0,65	3	5	2,76	0,93	1,5	5
Total	3,26	1,31	1	5	3,41	1,24	1	5

Table 6. Results of Student-Newman-Keuls test indicating the softness/stiffness subjective evaluations

SubjectiveValue

FabricCode		N	Subset 1	2	3	4
Student-Newman-Keuls[a,b]	3,00	21	1,4762			
	1,00	21		2,4762		
	2,00	21			3,1429	
	4,00	21			3,5952	
	6,00	21				4,3333
	5,00	21				4,5714
	Sig.		1,000	1,000	,063	,325

Means for groups in homogeneous subsets are displayed.
Based on observed means.
The error term is Mean Square(Error) = ,610.

a. Uses Harmonic Mean Sample Size = 21,000.

b. Alpha = ,05.

According to statistical test results Table 6 fabric softness/stiffness subjective evaluations values were grouped into 4 groups. It was determined that fabric having code number 5 was considered as the stiffest fabric and fabric having code number 3 as the softest. These result showed similarity with the result of objective evaluation by circular bending rigidity tester. In addition, it was seen that there were not any significant differences between the fabrics having the code (2, 4) and (5,6).

Table 7. Results of Student-Newman-Keulstest indicating the smooth/rough subjective evaluations

Subjective

FabricCode		N	Subset 1	2	3	4
Student-Newman-Keuls[a,b]	4,00	21	2,1190			
	1,00	21		2,7619		
	6,00	21		2,7619		
	2,00	21			3,4524	
	3,00	21				4,6429
	5,00	21				4,7381
	Sig.		1,000	1,000	1,000	,691

Means for groups in homogeneous subsets are displayed.
Based on observed means.
The error term is Mean Square(Error) = ,599.

a. Uses Harmonic Mean Sample Size = 21,000.

b. Alpha = ,05.

According to statistical test results Table 7 fabric smooth/rough subjective test results were evaluated similar to the frictorq test results, fabric coded 5 was considered as the most rough fabric and fabric coded 4 as the smoothest.

3.3. The Correlation Between Subjective and Objective Handle Evaluation Results

The correlation coefficient (r) between the objective circular bending rigidity values and subjective softness-stiffness values were found 0,996 (Table 8) whereas it is found 0,798 (Table 9) between objective friction coefficient values and subjective roughness results. Due to the high correlation coefficients between objective and subjective results, objective values can be used to determine the subjective handle properties.

Table 8. The correlation between subjective softness-stiffness ratings and objective circular bending rigidity values

Correlations

		Objective	Subjective
Objective	Pearson Correlation	1	,996**
	Sig. (2-tailed)		,000
	N	6	6

Subjectiv	Pearson Correlation	,996**	1

Correlations

		Objective	Subjective
Objective	Pearson Correlation	1	,798
	Sig. (2-tailed)		,057
	N	6	6
Subjective	Pearson Correlation	,798	1
	Sig. (2-tailed)	,057	
	N	6	6

Table 9. The correlation between subjective smooth-rough ratings and objective friction coefficient values

4. Conclusion

The use of recycled material is a very important factor in all respects due to the fact that it generally consumes less energy in production processes, reduces consumption of natural resources, provides sustainability, leads to less pollution and greenhouse gas emissions, and in some cases provides lower production costs.

In this study, attitude characteristics, which is one of the most important points when purchasing products of woven pique fabrics having 85% recycled cotton and 15% polyester fiber type and having 6 different pattern at the same time, were examined. As a result of the studies done, it was determined that the fabric construction had an influence on the fabric handling properties.

The fabric coded 5, which is stiffer and rougher, is not suitable to use for pique fabric, but fabrics having a puffy structure like fabric coded 1 are more preferable for use of pique fabric.

In the study, high correlation coefficients were found between the subjective and objective handle evaluation results. As a consequence it can be enounced that objective measurements can be used in comparing subjective sensorial properties of the recycling woven pique fabrics.

Acknowledgement

The authors want to give their special thanks to Menderes Tekstil A.Ş. for their support about supplying the materials used in the study.

References

Ichım M., Sava C., (2016). Study on Recycling Cotton Fabric Scraps into Yarns, Textıle Tehnıce, 3, 65-68.

Eser B., Çelik P., Çay A., Akgümüş D., (2016). Tekstil ve Konfeksiyon Sektöründe Sürdürülebilirlik ve Geri Dönüşüm Olanakları, Tekstil ve Mühendis, 23: 101, 43-60.

Esteve-Turrillas F.A., Guardia M. de la, (2017), Environmental impact of Recover cotton in textile industry, Resources, Conservation and Recycling, 116, 107–115.

Özçelik Kayseri G., Özdil N., and Süpüren Mengüç G., (2012). Woven Fabrics Chapter 9: Sensorial Comfort of Textile Materials, , InTech, Croatia, 235-266.

Valatkienė, L., Strazdienė, E., (2006). Accuracy and Reliability of Fabric's Hand Subjective Evaluation, ISSN 1392–1320 Materials Science (Medžiagotyra). Vol. 12, No. 3.

Mäkinen, M., Meinander, H., Luible, C., Magnenat-Thalmann, N., (2005, December). Influence of Physical Parameters on Fabric Hand, Proc. of the Workshop on Haptic and Tactile Perception of Deformable Objects, Hanover (HAPTEX'05), 8-16.

Özgüney A.T., Taşkın C., Özçelik G., Ünal P.G., Özerdem A., (2009). Handle properties of the woven fab rics made of compact yarns. Tekstil ve Konfeksiyon, Vol. 2, 108–113.

Yıldız E. Z., Özdil N., (2014). Subjective and Objective Evaluation of the Handle Properties of Shirt Fabric Fused with Different Woven Interlinings, Tekstil ve Konfeksiyon, 24(1), 114-122.

URL-1: http://koop.gtb.gov.tr/data/5ad06c80ddee7dd8b423eb24/2017%20Pamuk%20Raporu.pdf.

T.C. gümrük ve ticaret bakanlığı kooperatifçilikgenel müdürlüğü- 2017 yılı pamuk raporu-mart 2018.

URL-2: https://www.textileschool.com/270/major-fabric-weaving-patterns (Erişim Tarihi: 10 Haziran 2018).

Liquid Moisture Transport: Usage Of R-Pet Instead Of Conventional Pet

Mehdi HATAMLOU[1*], Gamze SÜPÜREN MENGÜÇ[2],
Arif Taner ÖZGÜNEY[1], Nilgün ÖZDİL[1]

[1]Ege Üniversity, Textile Engineering Department, Bornova-İzmir
[2]Ege Üniversity, Emel Akın Vocational Training School, Bornova-İzmir

[*] **Corresponding Author**:mhatamlou@gmail.com

Abstract

In recent years the researches on liquid moisture transport properties of fabrics have great importance. Especially for the sport garments, fabric structure should led liquid moisture to transfer from skin surface to the outer layers. For this purpose, special fibers and fabric structures were designed including channeled fibers and micro fiber productions to contribute higher capillary transport capability to the textile surface. As the literature reviewed, it could be seen that polyester fibers are used for this purpose frequently. Due to the increase in the demand of sustainable textiles, production and consumption of recycled polyester fibers are increasing recently. They are expected to have adequate mechanical properties to fulfill requirements. However their comfort properties were not investigated yet. In this study, liquid moisture transfer properties of the polyester and r-PET fabrics were investigated. For this purpose, knitted fabrics produced from 100% polyester and 100% r-PET yarns were used. Dynamic liquid transport properties of these surfaces, such as maximum wetted radius, absorption rate, wetting time and spreading speed were measured by using “SDL-ATLAS Moisture Management Tester” and the results analyzed comparatively.

Keywords: Moisture management, liquid moisture transfer, MMT, moisture management tester, maximum wetted radius, absorption rate, wetting time, spreading speed.

1. Introduction

Clothing is one of the most important and fundamental need of the humans. The first mission of the cloth is to protect the body from uncomfortable environment conditions (hot, cold, wind, injures, chemicals, etc.). However, the latest researches show that consumers meet their clothing requirements according to the their life conditions which is more dynamic and comfortable (Okur et al., 2008). As a result, changing expectations of the consumers brought the concept of 'comfort'.

An important factor on the perception of comfort is the continuous dynamic interaction of the garments along with the body movement. Because of this, physical movement, skin temperature, sweating percentage and moisture percentage on the skin etc. are continuously changing during the wearing duration. These effects cause mechanical and thermal warnings. These warnings define the users` comfort perception (Güneşoğlu, 2005).

Body generates sweat in order to adjust the body temperature. As the action is low and the environmental heat is in a normal level, there is a constant moisture transfer between the environment and the pores of the skin and the sweat is released in vapor form. While the sweating is slow, it cannot be felt. However, if the heat, which is generated due to the increased action, is not given to the environment, the skin produces sweat to keep the body temperature in 37 °C constant level. In order to evaporate the liquid sweat from the skin surface, it is necessary to take the heat energy from the body. By the way, the body temperature decreases.

Niwa (1968) stated that the ability of fabrics to absorb liquid water (sweat) is more important than water vapor permeability in determining the comfort factor of fabrics. In his study Avcı (2007) investigated socks, which were knitted with using various fiber types. It was determined that the wet behavior properties of socks are affected directly by fiber type. Marmaralı and Oğlakçıoğlu (2013) found that production parameters like raw material (fiber and yarn specialties), fabric structure (construction, density, thickness, weight, etc.) and finishing applications have important effects on the thermal comfort specialties.

In a study carried out by Süpüren et al. (2011) investigated the moisture management properties and the changes of the thermal absorptivity values of a special double-face structure and it was revealed that different moisture transport properties can be achieved by using different yarn settlements in double-face fabric construction. Wardman and Abdrabbo (2010) developed an instrument based on the image analysis technique to study the effect of oxygen plasma treatment on two polyester fiber types (polylactic acid and standard polyester) and its influence on their wetting characteristics. In a study carried out by Özdil et al. (2009), moisture

transport properties of knitted fabrics, which were knitted from cotton yarns produced with using various yarn twists and yarn counts were investigated. It was pointed out that yarn count and yarn twist has important effect on the fabric moisture transport.

Since moisture transmitting property of fabric is a key factor that affects textile and clothing comfort, many researchers have studied on this subject comprehensively. Although there are various studies in the literature on moisture management properties of natural and synthetic textile materials, recycled textile materials have not been investigated yet.

Consumption of textile fibers has increased with the overpopulation, it is reasonable to say that environmental problems of textile industry reached massive amounts in recent years. For these reasons, finding new solutions is expected from the textile industry for easing these environmental problems they have caused. In this situation, the most important topic to be focused on is extending the lifecycle of the materials used, by recycling. r-PET fibers are obtained by recycling of PET bottle wastes. Firstly, PET bottle wastes are cleaned from the other wastes; then they are broken into flakes, washed and dried respectively before spinning process of the fiber. PET flakes are converted into fibers using chemical and mechanical methods. PET is degraded into oligomer or monomer form and again a polymerization happens in chemical method. In mechanical method, PET flakes are melted and r-PET fibers are obtained by melt-spinning process (Telli ve Özdil, 2011; Telli ve Özdil, 2013; Telli ve Özdil, 2015; Anne, 2018).

These fibers have economic advantages due to the lower raw material cost. They also have lower energy consumption in production stage and low carbon emission. Because of these factors, it can be said that r-PET fibers are environmentally friendly fibers. However, in mechanical cycling method, PET flakes include too much contamination and during re-heating process molecular weight of the polymer changes (Telli ve Özdil, 2011; Oktem, 1998; Mannhart, 1998; Telli ve Özdil, 2015).

Nowadays, recycled products are being used in many areas. For instance, designers in Germany are accountable for waste production for downstream products such as clothes and interior finishing. There is a factory in Negeri Sembilan that collects mineral water bottles and recycled them into polyester fabric (Yusup, 2014; Ahmad et al., 2016). The resulting products from this polyester are uniforms for factory workers.

As it can be seen, due to the increasing conscious on sustainable materials and products, recycling of textiles is becoming more common. However, comfort characteristics of these recycled materials have not been investigated in detail. The aim of this study is to examine

moisture management properties of these fabrics produced from conventional polyester and r-PET fibers.

2. Materials And Method

Polyester and r-PET yarns were used in this experiment. Yarns were produced in Ne 20 yarn count and twist coefficients of the yarns were kept constant (αe = 3.6) for the spun yarns. The fabrics were knitted in single jersey structure by using Mesdan Knitter knitting machine.

The fabrics were conditioned in standard atmosphere conditions 20 °C ±2 ve 65%±4 relative humidity before the tests and the moisture management properties of fabrics were tested by Moisture Management Tester (MMT) which belongs to the SDL Atlas Company (Figure 1).

Figure 1. MMT- Moisture Management Tester Instrument

Some conventional methods can be employed to evaluate the fabric's simple absorbency; wicking and moisture transfer properties, whereas 6 different characteristics can be tested by moisture management tester. These properties are wetting time, absorption rate, maximum wetted radius, spreading speed, accumulative one way transport capacity and moisture management capacity (URL-1).

The specimen is held flat by top and lower sensors at a certain pressure. The computer dynamically records the resistance change between each couple of proximate metal rings individually at the top and lower sensors. A certain weight (0.15 g) of a predefined test solution (synthetic sweating, AATCC 15) is then put into the sweat gland and introduced onto the top surface of the fabric. The solution will transfer in three directions after arriving on the fabric's top surface: spreading outward on the top surface of the fabric, transferring through the fabric from the top surface to the bottom surface, and spreading outward on the bottom surface of the fabric and then evaporating (Hu et al., 2005).

The parameters measured by the instrument are given below:

Wetting time (WTt (top surface) and WTb (bottom surface)): They are the time periods in which the top and bottom surfaces of the fabric just start to be wetted, respectively, after the test commences, defined as the time in second(s) when the slopes of total water contents on the top and bottom surfaces (i.e., Ut and Ub) become greater than tan (15°).

Absorption Rate (TAR (top surface) and BAR (bottom surface)): TAR and BAR are the average moisture absorption ability of the fabric top and bottom surfaces in the pump time respectively.

Maximum Wetted Radius (MWR_{top} and MWR_{bottom} -(mm)): They are defined as maximum wetted ring radius at the top and bottom surfaces respectively, where the slopes of total water content(U_{top} or U_{bottom}) become greater than Tan (15º) for the top and bottom surfaces respectively.

Spreading Speed (SS_{top} and SS_{bottom} - (mm/sec)): It is defined as the accumulative spreading speed from the center to the maximum wetted radius.

t_{wrt} and t_{wrb} are the times to reach the maximum wetted rings on the top and bottom surfaces, respectively.

$$SS_{top} = MWR_{top/} t_{wrt} \quad and \; SS_{bottom} = MWR_{bottom/} t_{wrb}$$

Overall Moisture Management Capacity (OMMC): It is an index to indicate the overall capability of the fabric to manage the transport of liquid moisture, which includes three aspects of performances:

(1) Moisture absorption rate at bottom side: BAR

(2) One way liquid transport capability: R

(3) Moisture drying speed at bottom side, which is represented by accumulative spreading speed: BSS.

The overall moisture management capacity (OMMC) is defined as:

$$OMMC = 0.25\, BAR + 0.5\, R + 0.25\, SS_{bottom}$$

Where BAR is the absorption rate, OWTC is the one-way transport capacity, and SS_b is the spreading/drying rate. The larger the OMMC is the higher the overall moisture management ability of the fabric (Hu et al., 2005).

In order to analyze the change in surface properties of the fibers, SEM images of the fibers were also taken by using a scanning electron microscope (Hitachi TM-1000).

3. Results

Moisture management properties of the fabrics are given in Table 1.

Table 1. Moisture Management Properties of the fabrics.

	Wetting Time top(sec)	Wetting Time Bottom (sec)	Top Absorption Rate (%/sec)	Bottom Absorption Rate (%/sec)	Top Max Wetted Radius (MM)	Bottom Max Wetted Radius (MM)	Top Spreading Speed (mm/sec)	Bottom Spreading Speed (mm/sec)	OMMC
ES	2,63	2,66	70,69	78,85	30,00	28,33	5,90	6,14	0,59
-PET	5,35	5,21	66,20	66,55	23,33	23,33	3,92	3,89	0,48

After the measurements, results of fabrics produced from conventional and recycled fibers were evaluated statistically by independent samples t-test with the significance level of α= 0.05. Results of Independent Sample T-Test are given in Table 2.

Table 2. Significance values of Independent Sample T-Test.

	Significance (p)
Wetting Time top(sec)	0,000*
Wetting Time Bottom (sec)	0,001*
Top Absorption Rate (%/sec)	0,366
Bottom Absorption Rate (%/sec)	0,042*
Top Max Wetted Radius (MM)	0,045*
Bottom Max Wetted Radius (MM)	0,101

Top Spreading Speed (mm/sec)	0,049*
Bottom Spreading Speed (mm/sec)	0,049*
OMMC	0,006*

* Significant according to α=0,95 significance level

3.1. Wetting Times of Fabrics

The wetting time values of PES and r-PET fabrics are given in Figure 2.

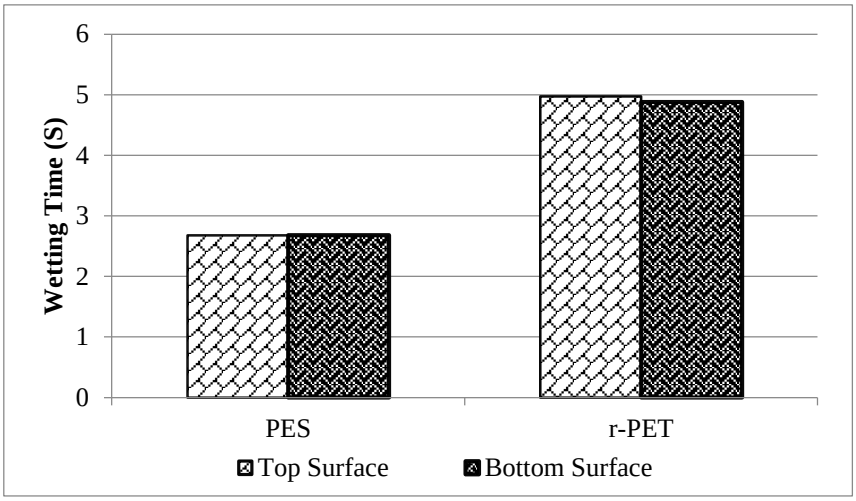

Figure 2. Wetting times of PES and r-PET fabrics

According to the results, it can be stated that, r-PET fabric has higher wetting time value than PES fabric. It is due to the lower wettability of the r-PET fibers. These fibers are produced by mechanical cycling method using bottles. Due to the contamination of PET flakes and re-heating process, molecular weight and tensile properties of the macromolecules change. For this reason, surface of the fibers become rougher. As the surface roughness increases, capillary tubes in the structure also changes. As a result, wicking and wetting property of the material changes. Damages in the surface morphology of the fibers can be seen in Figure 3.

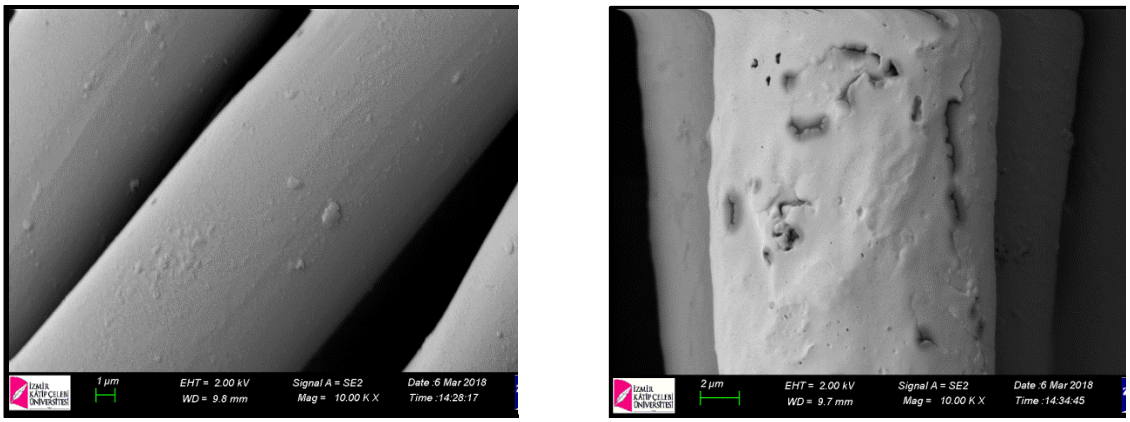

a b

Figure 3. SEM image of (a) Polyester, (b) r-PET fabric coated with 10_{nm} of gold using a 15_{kV} beam.

3.2. Absorption Rates of Fabric

Absorption rates of fabrics measured by MMT Instrument, are given in Figure 4.

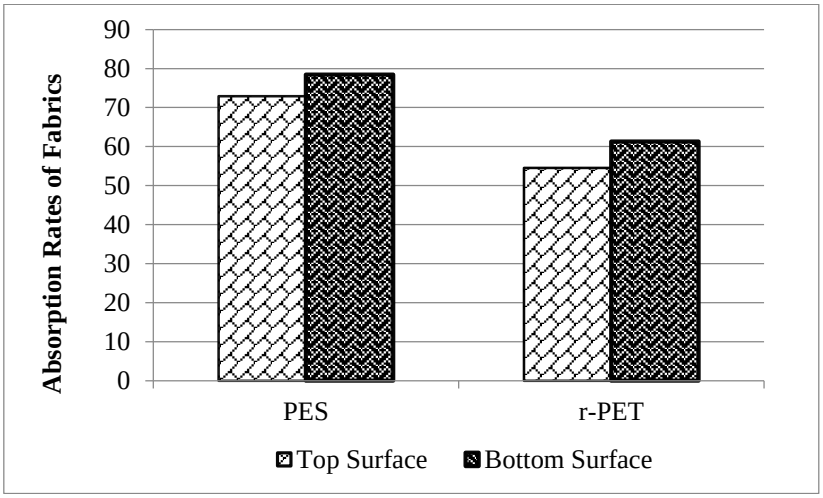

Figure 4. Absorption rates of PES and r-PET fabrics

As the absorption rates of PES and r-PET fabrics were examined, it can be seen that r-PET fabric has lower absorption capacity both on face and back sides. Absorption capacity is the average moisture absorption ability of the fabric. Therefore, due to the deformation on fiber surface capillarity decreases and absorption ability of the fabrics is found lower. PES fabric has better performance in this case. However, decrease percentage is around 25%.

3.3. Maximum Wetted Radius of Fabrics

The maximum wetted radiuses of inner and outer layers of the fabrics are given in Figure 5.

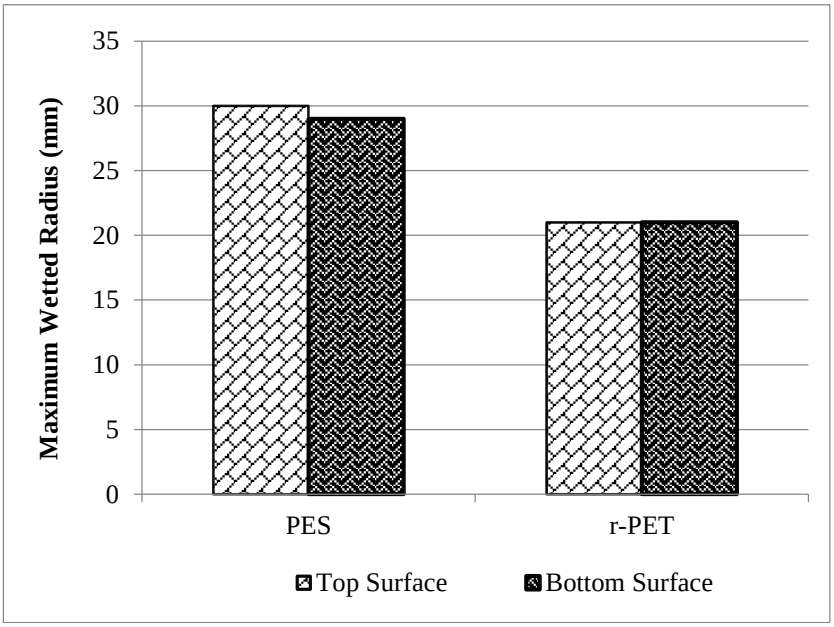

Figure 5. Maximum Wetted Radius of Fabrics

As Figure 6 was analyzed, it can be detected that r-PET fabric has lower maximum wetted radius value than PES fabric. It is again related with the changes in capillary forces, which is lower in r-PET fabric, due to the rougher surface characteristics.

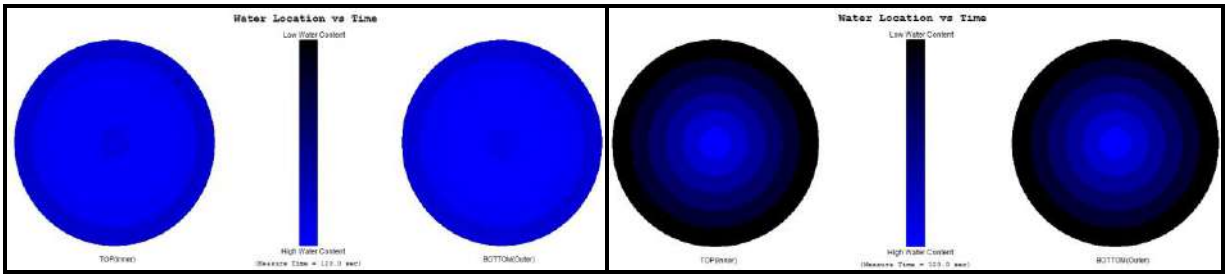

a **b**

Figure 6. The wetting radius changes in the inner/outer surfaces of fabrics (a) polyester, (b) r-PET

As the fiber surface is smoother, capillary movement of water molecules is easier. Recycled polyester fibers are mechanically deformed and surface roughness is higher, which decreases capillary forces.

3.4. Spreading Speeds of Fabrics

The spreading speeds of fabrics values of PES and r-PET fabrics are given in Figure 7.

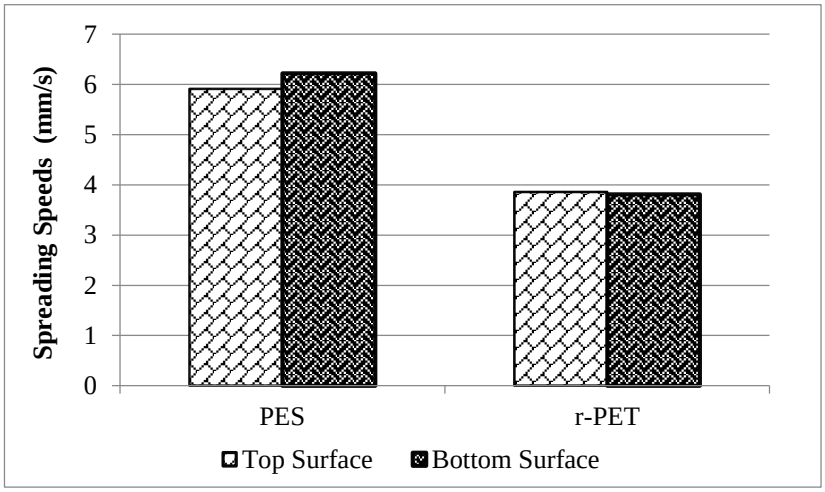

Figure 7. Spreading Speeds of Fabrics

Spreading speed is a significant property and an indicator of the speed from center to the maximum wetted radius. In this case, performance of r-PET fabric was found 35% lower than of PES fabric.

3.5. Overall Moisture Management Capacity of the Fabrics

Dynamic liquid transfer properties measured by MMT-Moisture Management Tester are graded between 1-5 levels and fabrics are classified in terms of moisture management properties by evaluating some of the measured parameters. Results (Finger Print Values) of studied fabrics are given in Figure 8.

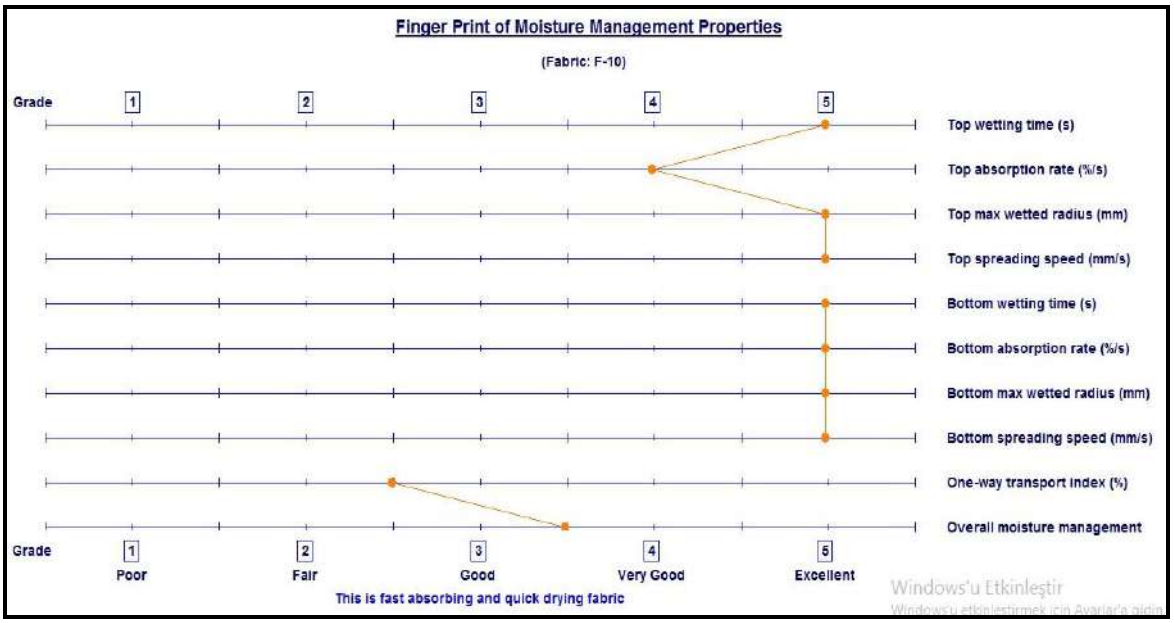

a

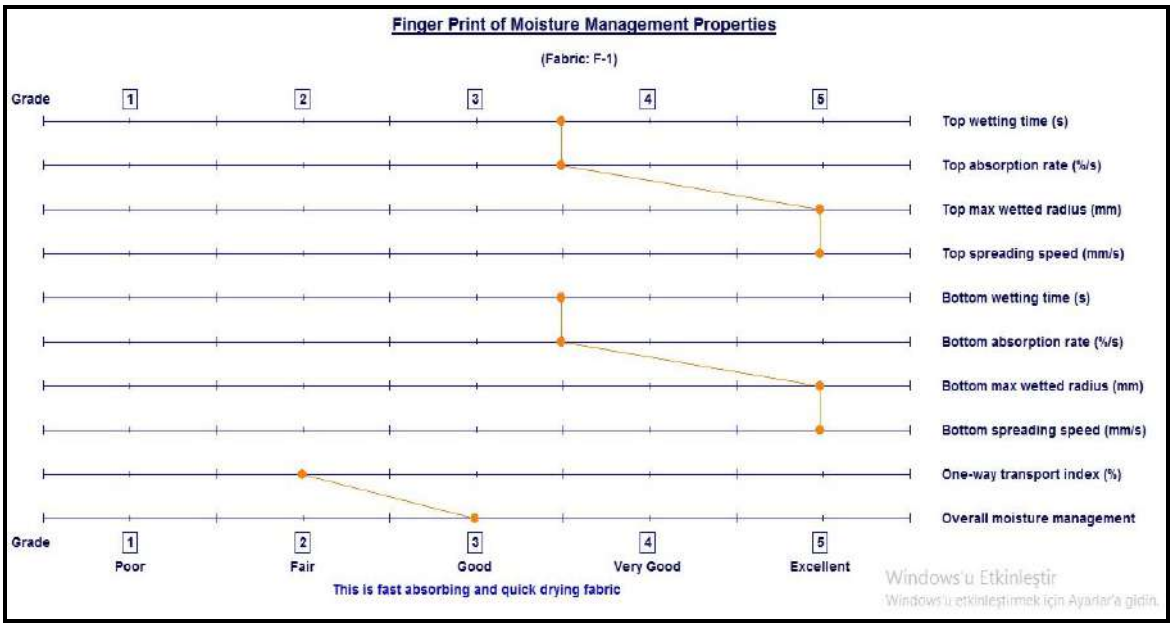

b

Figure 8. Grades of overall moisture management properties for: (a) PES fabric, (b) r-PET fabric

Polyester and r-PET fabrics are both categorized in "fast absorbing and quick drying fabrics" by the software of the instrument, since, the pumped test liquid could be transferred from the inner surface to the outer surface.

In case of OMMC values, changing between 0 and 1, which indicates multidirectional liquid transfer ability of the fabrics, are given in Table 3.

Table 3. Overall Moisture Management Capacity of the Fabrics

	PES	r-PET
OMMC Value	0,58	0,46
Evaluation	Good	Good

According to OMMC evaluation scale, the values are categorized as; 0-0,2: Very poor, 0,2-0,4: Poor, 0,4-0,6: Good, 0,6-0,8: Very good, >0,8: Excellent. Although overall moisture management capacity of polyester fabric was found higher than r-PET fabric, in scope of OMMC values of the fabrics, r-PET and polyester fabrics are both identified as "good" in terms of their overall moisture management properties. It indicates that, r-PET fabric has good moisture management characteristics to be used even in garments.

4. Conclusion

Liquid moisture management property is especially important in sportswear, where exposure to perspiration is intense. Research in this subject is more focused on high technological fibrous products such as channeled fibers and micro fibers. Recycling based researches and looking for new applications of such products is increasing worldwide.

Assessing previous studies shows that there are numerous studies on Moisture Management Properties of products produced from polyester fiber but there is a huge need for more studies on recycled products. This study aims in evaluation of comfort properties of fabrics made from r-PET and polyester.

Polyester fibers are hydrophobic fibers. Therefore, water is transferred to the outer layers from the surface of the fibers by capillary forces. Due to the mechanical and thermal effects, fiber surface are rougher in r-PET fibers. Therefore liquid water transfer properties of these fabrics were found lower than the conventional PES fabric. According to the software of the instrument, both fabrics were classified fast absorbing and quick drying fabrics category.

PES fabric has lower wetting time and higher absorption rate, maximum wetted radius, spreading speed, OMMC values than r-PET fabric. It is due to the fiber damage and rougher surface characteristics of r-PET fibers.

Conventional PES fabric has comparatively better moisture management properties. However, as recycling, sustainability and environmental pollution was considered, it should be underlined that, the fabrics produced from r-PET fibers have good moisture management properties which can give them even the opportunity to be used in sports garments.

ACKNOWLEDGEMENT

This research was supported by Ege University as 2015/MÜH/016 coded BAP Project.

REFERENCES

Ahmad, S., Mulyadi,I.M.M., Ibrahim, N., Othman, A.R., The application of Recycled Textile and Innovative Spatial Design Strategies for a Recycling Centre Exhibition Space, Procedia - Social and Behavioral Sciences 234 (2016) 525 – 535.

Anne, P., ”Why is recycled polyester considered a sustainable textile?”, http://oecotextiles.wordpress.com (Son Erişim Tarihi: 12.06.18).

Avci, H., (2007). Yeni Liflerden Mamul Çorapların Konfor Özellikleri. Yüksek Lisans Tezi, İstanbul Teknik Üniversitesi, Fen Bilimleri Enstitüsü, İstanbul, 92s.

ASTM (American Society For Testing And Materials) D 4032-94 Dairesel Eğme Test Metodu. 15. TS 391 EN ISO 9237, 1999. Tekstil-Kumaşlarda Hava Geçirgenliğinin Tayini, Türk Standartları Enstitüsü, Ankara.

Erenler, A. And Oğulata, R.T., (2013). Apre Uygulamalarının Kumaş Yumuşaklığı Üzerine Etkilerinin Araştırılması Ve Kumaş Yumuşaklığının Tahminlenmesi. 14. Ulusal & 1. Uluslararası Tekstil Teknolojisi Ve Kimyasındaki Son Gelişmeler Sempozyumu 2013, Bursa.

Güneşoğlu, S., (2005). Sportif Amaçlı Giysilerin Konfor Özelliklerinin Araştırılması. Doktora Tezi, Uludağ Üniversitesi, Fen Bilimleri Enstitüsü, Bursa, 208s.

Hu, J., Li, Y., Yeung, K-W, Wong, A.S.W., Xu, W., (2005) Moisture Management Tester: A Method To Characterize Fabric Liquid Moisture Management Properties, Textile Research Journal, 75, 57-62, 2005

ISO 11092, (1993). Tekstil-Fizyolojik Etkiler – Kararlı Şartlarda Termal Ve Su Buharı Dayanımı Ölçümü.

Mannhart, M, “Pet Siselerden Filament İplik”, Melliand Türkiye Sayısı, 3: 166-169, 1998.

Marmarali, A., Ve Oğlakçioğlu, N., (2013). Giysilerde Isıl Konfor, 11. Ulusal Tesisat Mühendisliği Kongresi Bildiri Kitabı, S1957-1963, İzmir.

Militký, J., Vik, M. And Vikova, M., (2003). Neural Networks For Air Permeability Prediction. Proceedings Of The 4th International Conference Innovation And Modelling Of Clothing Engineering Process-Imcep 2003, Slovenia-Maribor.

Moisture Management Tester- Operation Manuel.

Niwa M. (1968) : Water Vapor Permeability Of Underwear, J. Jpn. Res. Assn. Textile End Uses. Vol. 9, Pp.446 450.

Oktem, T, "Polyester Atiklarin Degerlendirilmesi", Tekstil ve Konfeksiyon, 6: 396-400, 1998.

Özdil, N., Süpüren, G., Özçelik, G., And Pruchova, J., (2009). A Study On The Moisture Transport Properties Of The Cotton Knitted Fabrics Iin Single Jersey Structure. Tekstil ve Konfeksiyon, Vol (3), S.218-223.

Özdil N., Süpüren G., Özçelik, G., (2009). Farklı Materyallerden Üretilen Örme Kumaşların Çok Yönlü Nem İletim Özellikleri, (Bölüm 2)Tekstil Teknoloji ,Yıl 14, Sayı: 157, Temmuz, S: 114-121,2009.

Özdil N., Süpüren G., Özçelik, G., (2009). Farklı Materyallerden Üretilen Örme Kumaşların Çok Yönlü Nem İletim Özellikleri, (Bölüm 1)Tekstil Teknoloji ,Yıl 14, Sayı: 156, Haziran, S: 172-186, 2009

Okur, A., Küçüka, S., Ve Kaplan, S., (2008). Giysi Termal Konforunun Belirlenmesine Yönelik Bir Yöntem Geliştirilmesi. TÜBİTAK Projesi, Proje No 107M200, 84s.

Süpüren,G.,Oğlakçıoğlu,N.,Özdil,N.,Marmaralı,A., (2011), Moisture Management And Thermal Absorptivity Properties Of Double-Face Knitted Fabrics, Textile Research Journal, 81(13), 1320-1330.

Telli, A and Ozdil, N,(2011), Lint Generation of the Yarns Produced PET Fibers, International Congress of Innovative Textiles, Corlu, Turkey, 20-22 October 2011, pp. 32-35.

Telli, A., Özdil, N., (2013), r-PET Lifleri ve Karışımlarından Üretilen Ipliklerin Özellikleri, Tekstil ve Konfeksiyon 23(1).

Telli A. and Özdil N., (2015), Effect of Recycled PET Fibers on the Performance Properties of Knitted Fabrics, Journal of Engineered Fibers and Fabrics, Volume 10, Issue 2, pp.47-60, web: http://www.jeffjournal.org.

URL-1: http://www.sdlatlas.com/html/moisture_management_tester_0.html, (Erişim Tarihi: 12 Haziran 2018).

Wardman, R. H., & Abdrabbo, A. (2010). Effect Of Plasma Treatment On The Spreading Of Micro Drops Through Polylactic Acid (PLA) And Polyester (PET) Fabrics. Autex Research Journal, 10, 320–326.

Yusup, A. R. M. (2014). Turning the tables on cast-offs. New Straits Times

Luxury Animal Fiber/Cotton Blends: Sustainable, Profitable, Niche Production

Gamze SÜPÜREN MENGÜÇ [1], Nilgün ÖZDİL [2], Faruk BOZDOĞAN [2]

[1]Ege University, Emel Akın Vocational Training School, Turkey
[2]Ege University, Faculty of Engineering, Department of Textile Engineering, Turkey

[*]**Corresponding Author:** gamze.supuren.menguc@ege.edu.tr

Abstract

Due to their distinctive properties, luxury animal fibers increase handle and thermal properties of the textile products. They are expensive; however they enable to produce textiles with high added value. On the other hand, they are natural and sustainable. For this reason, usage and application of luxury animal fibers are becoming more important. In this study, four different animal fibers including cashmere, silk, Angora rabbit fiber and wool were blended with cotton fiber. Short staple spinning system was used and Ne 30 yarns were produced. Thereafter, the yarns were knitted in single jersey structures. In order to determine whether the fabrics have sufficient mechanical properties, bursting strength of the fabrics were measured. Surface properties (pilling resistance and kinetic friction coefficient) and circular bending rigidity of the fabrics were determined and compared with the fabric produced from 100% cotton. It is thought that, although luxury animal fibers have low fiber cohesion, they can be blended with cotton fiber to a certain extent and by this way; valuable yarns and fabrics could be produced. Usage of these fibers in short staple spinning technology could be a profitable production way for the Turkish short staple spinning industry to put valuable products on the market.

Key Words: Luxury fibers, cashmere, silk, angora rabbit fiber, wool,

1. Introduction

There is an emerging demand for sustainable luxury, which a number of key industries are well placed to develop and promote to consumers. Emerging biomaterials offer new design considerations that fully engage the sustainability challenges of the twenty-first century (Fletcher ,2008; Karthik et al., 2015). For this reason, the usage of industrially used animal fibers has become more and more common. Animal fibers and specialty animal fibers are preferred by the consumers, since their natural characteristics, comfort and tactile properties (Süpüren Mengüç and Özdil, 2013).

In addition to this, luxury fibers incorporate exclusive properties to the fabrics, which make them higher value added products. Even the small quantities of these fibers improve the fabric properties in different ways according to the consumer expectations (Langley and Kennedy, 1981; Süpüren Mengüç et al., 2014). They are expensive and often blended with other fibers (Langley and Kennedy, 1981)

Speciality animal fibers need a great care during mechanical processing because of their fineness, typical surface structure and high cost. It is considered better to make its products in blend with other natural and synthetic fibers (Nagal, K., 2006).

Special animal fibers are generally spun in the long spinning system, however, they have different fineness, lengths and surface structures which cause differences in yarn production technologies. However, these valuable fibers give the opportunity to produce valuable and this technique is profitable for the spinning industry. In Turkey, most of the ring spinning mills is using short staple spinning. There are several studies on using Angora rabbit fiber and silk in blend with cotton.

Cashmere fiber, that is harvested from the Cashmere goat is very fine (12.5-19 μm) and the average length is about 35-50 mm. These fine fibers enable goats to withstand the extreme winter cold of their original habitat, the plateaux of Central Asia. Due to the smooth surface of fibers, fiber-fiber cohesion is low and that causes problems during spinning.

Silk fiber is produced by silkworm, Bombyx mori. Fiber is the only natural fiber exists as a continuous filament. Each cocoon can yield up to 1600 meters of flament. Fibers have high tensile strength. Like the other animal fibers, it is a protein fiber, however its aminoacid composition is close to that of the human skin. Due to its triangular cross-section, it has excellent light reflection property (Frank, 2001).

Angora rabbit fiber has a good potential for producing textiles with special properties. It is extremely fine, soft, antistatic, lustrous and durable, while giving high insulation and a

warmer feeling to the garments due to medulla structure in the core of the fiber (Süpüren Mengüç et al., 2014).

It has excellent luster, warmth retaining properties and flexibility, which makes it an ideal fiber for textile end uses. However, since it has little scales and crimps in comparison to other animal fibers, spinnability is very poor and it is difficult to produce a fine spun yarn (Dirgar ve Oral, 2014).

Chattopadhyay and Ahmed (2006) blended Angora rabbit fiber with cotton fibers and it was pointed out that cotton and Angora rabbit fiber blended knitted fabrics have soft feel and low shrink properties which make them suitable for women's innerwear and children's wear (Guruprasad and Chattopadhyay, 2013).

Thermal comfort properties of cotton/Angora rabbit fiber blended knitted fabrics were investigated by Oglakcioglu et al. (2009). Angora fiber content in the yarn was varied between 5% and 25%. According to the their results it was concluded that at least 25% of Angora fibers need to be added in the blend to achieve better thermal comfort properties.

.

Beside Angora rabbit fiber, silk is another luxury fiber that is widely used. Akbaş and Çelik (2016) investigated spinnability of silk fiber in open-end rotor spinning system and investigated the yarn and fabric performance. According to the results, it was concluded that, yarn hairiness and breaking elongation were increased with increasing silk ratio on yarns. In addition, air permeability and abrasion resistance of the fabrics decreased with increasing silk ratio.

Although there are several studies including Angora rabbit fiber and silk fiber with cotton, there is not a comprehensive and comparative study on blends of cotton with other luxury animal fibers. The aim of this study is to investigate handle, surface and mechanical performance of fabrics containing luxury animal fiber/cotton blends.

Figure 1. Angora rabbit Fiber (URL-1)

2. Experimental Procedures

The fibers used in the study and their properties are shown in Table 1.

Table 1. Properties of animal fibers

Construction	Fiber length (mm)	Fiber Fineness	Fiber tenacity (cN/tex)
Cashmere	59.90	14.85 µm	16.99
Wool	38.23	21.92 µm	14.23
Silk	36.78	8.16 µm	48.45
Angora rabbit Fiber	60.12	15.96 µm	19.98
Cotton	31.70	4.3 mic.index	47.00

Some animal fibers, i.e. Angora rabbit fiber, have a lack of fiber cohesion, which generates various problems such as static electricity during processing. Since it is difficult to process these fibers into yarns; blending these fibers with cotton also makes it easy to spin. Maximum blend ratio of animal fibers was kept at 30%, due to the limitations in the spinning process; 10%, 20% and 30% blend ratios of the animal fibers were used for all types of fibers.

Fibers were spun by using short staple spinning system (ring-carded) in a_e=3.6 twist coefficient and Ne 30 yarn count.

After spinning process, yarns were knitted in single jersey structures on a 28 gauge and 32'' diameter circular knitting machine in the same tightness value. The knitting process was completed with constant machine settings and the samples were kept under the standard atmospheric conditions for 24 hours for the conditioning and relaxation.

3. Experimental Results and Discussion

All test results were evaluated statistically. To determine the statistical importance of the variations, ANOVA tests were applied. To deduce whether the parameters were significant or not, p values were examined. Test results are given in Table 2. In this table, the mean values are marked with the letters 'a' to 'f'. Any levels marked by the same letter showed that they were not significantly different ('a' shows the lowest value and 'f' shows the highest value).

Table 2. Test results of the fabrics

Fabrics	Animal Fiber Content	Mass per Unit Area (g/m^2)	Thickness (mm)	Bursting Strength (kPa)	Pilling Degree	Kinetic friction coefficient (μ)	Circular Bending Rigidity (N)
100% Cotton Fabric		137,25 a	0,587 a	634,50 c	4,5 d	0,3399 c	0,84 e
	10% Wool/90% Cotton	137,14 a	0,591 a	632,67 c	4,2 c	0,3387 c	0,74 d
	20% Wool/80% Cotton	134,57 a	0,608 b	590,17 b	3,9 b	0,3461 c	0,75 d
Wool Blends	30% Wool/70% Cotton	137,90 a	0,629 b	570,17 a	3,7 a	0,3375 c	0,79 e
	10% Cashmere/90% Cotton	140,17 b	0,585 a	684,77 d	4,2 c	0,3232 b	0,75 d
	20% Cashmere/80% Cotton	142,88 b	0,586 a	638,27 c	3,9 b	0,3261 b	0,73 d
Cashmere Blends	30% Cashmere/70% Cotton	145,00 c	0,599 b	616,60 b	3,7 a	0,3303 b	0,70 c
	10% Silk/90% Cotton	145,50 c	0,592 a	850,63 f	4,0 c	0,3089 a	0,73 d
	20% Silk /80% Cotton	147,50 c	0,614 b	848,77 f	4,0 b	0,3112 a	0,73 d
Silk Blends	30% Silk /70% Cotton	153,20 d	0,649 c	832,63 f	3,8 a	0,3107 a	0,70 c
	10% Angora/90% Cotton	136,40 a	0,548 a	751,30 e	4,1 c	0,3169 b	0,70 c
	20% Angora /80% Cotton	141,40 b	0,598 b	643,27 c	4,1 c	0,3266 b	0,67 b
Angora Blends	30% Angora /70% Cotton	155,60 d	0,656 c	650,60 c	4,1 c	0,3238 b	0,64 a

3.1. Fabric Dimensional Properties

Results of dimensional properties of the fabrics are given in Figure 1 and Figure 2.

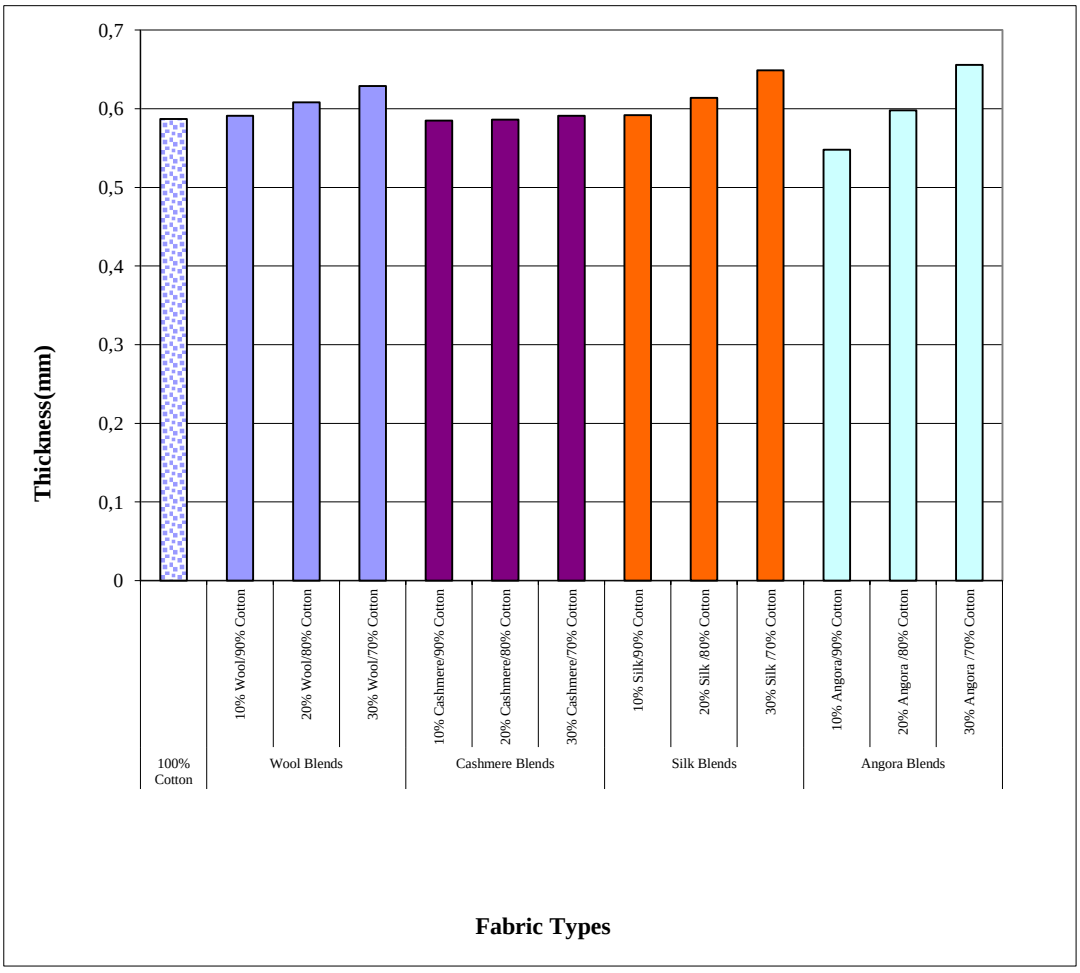

Figure 2. Fabric thickness results

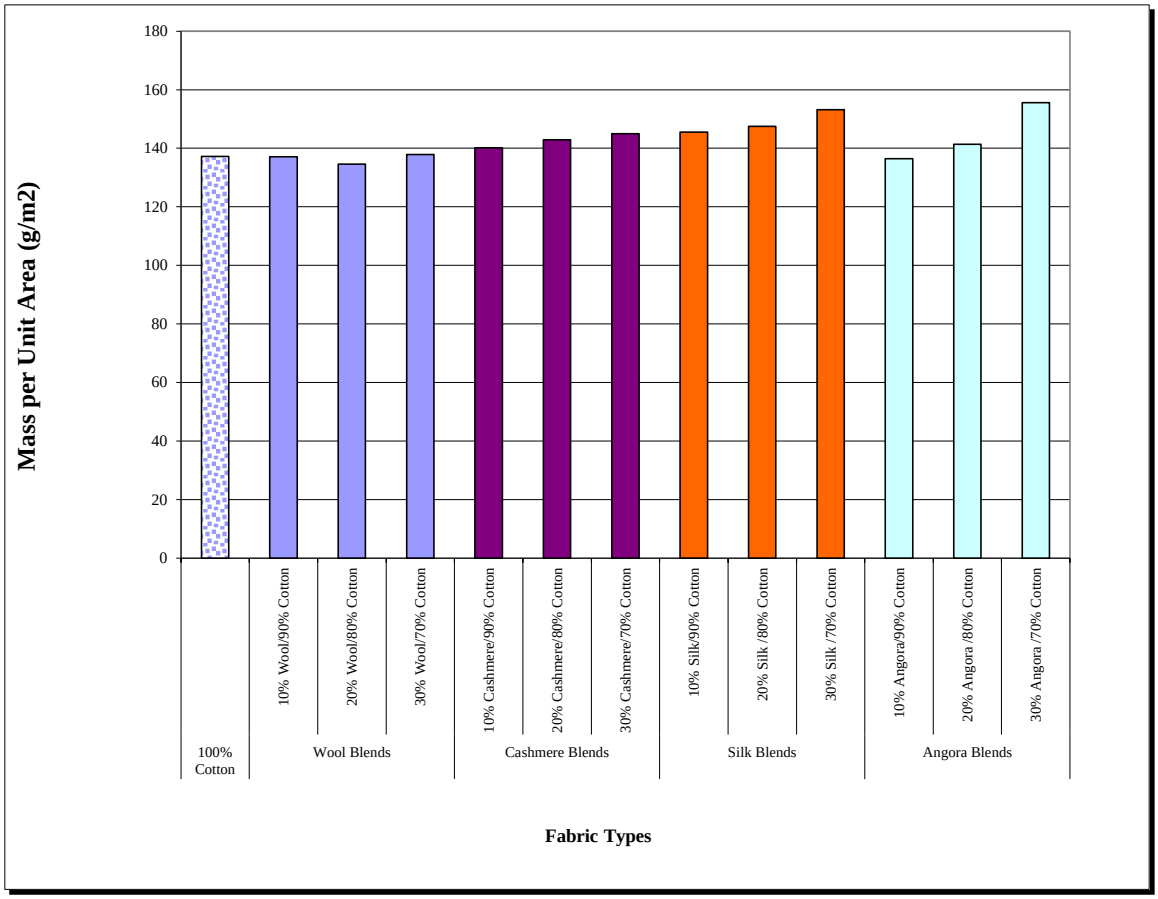

Figure 3. Mass per unit area results of the fabrics

As the dimensional properties analyzed, it can be seen that fabric thickness and weight are found parallel to each other. As the animal fiber content in fabric structure increases, weight and thickness of the fabric increase too. It is due to the relaxation shrinkage of the fabric, which is higher for the fabrics including animal fibers.

3.2. Bursting Strength Results

Bursting strength test results are given in Figure 4.

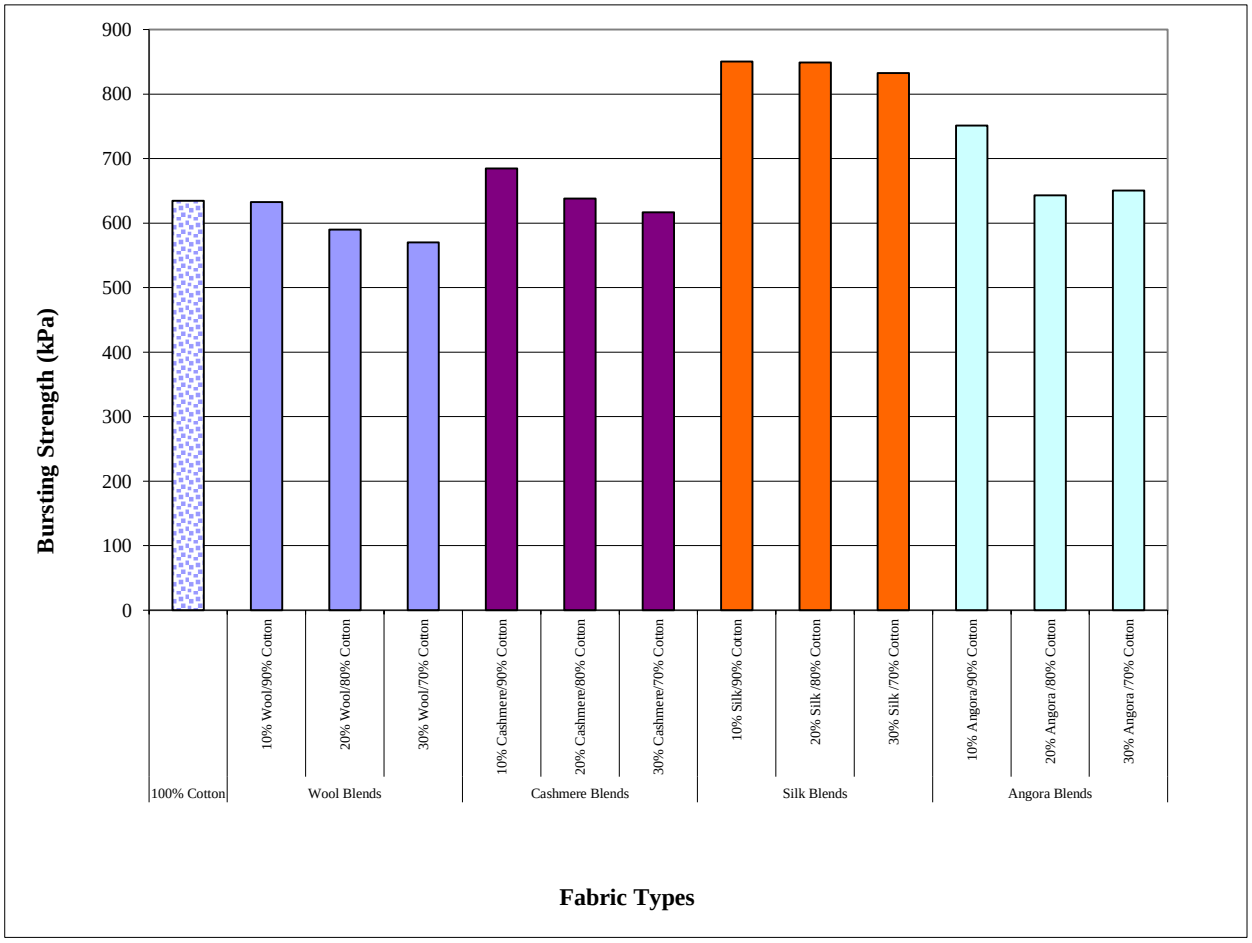

Figure 4. Bursting strength results

According to the results, it can be stated that fabrics including silk fiber have the highest bursting strength values, which is associated with the high fiber tenacity of silk fibers. All other animal fibers have lower fiber tenacity than cotton fiber. However, since all animal fiber containing fabrics have high shrinkage, their bursting strength values were found higher than cotton fabric.

In case of fiber blend ratio it was determined that, as the animal fiber content in the blend increases, mechanical performance of the fabrics decreases. This result could be explained by the lower strength values of the animal fibers as compared with cotton and increase of yarn unevenness, which is higher for the yarns including higher amount of animal fiber in the structure (Süpüren Mengüç, 2012).

3.3. Circular Bending Rigidity Results

Bursting strength test results are given in Figure 5.

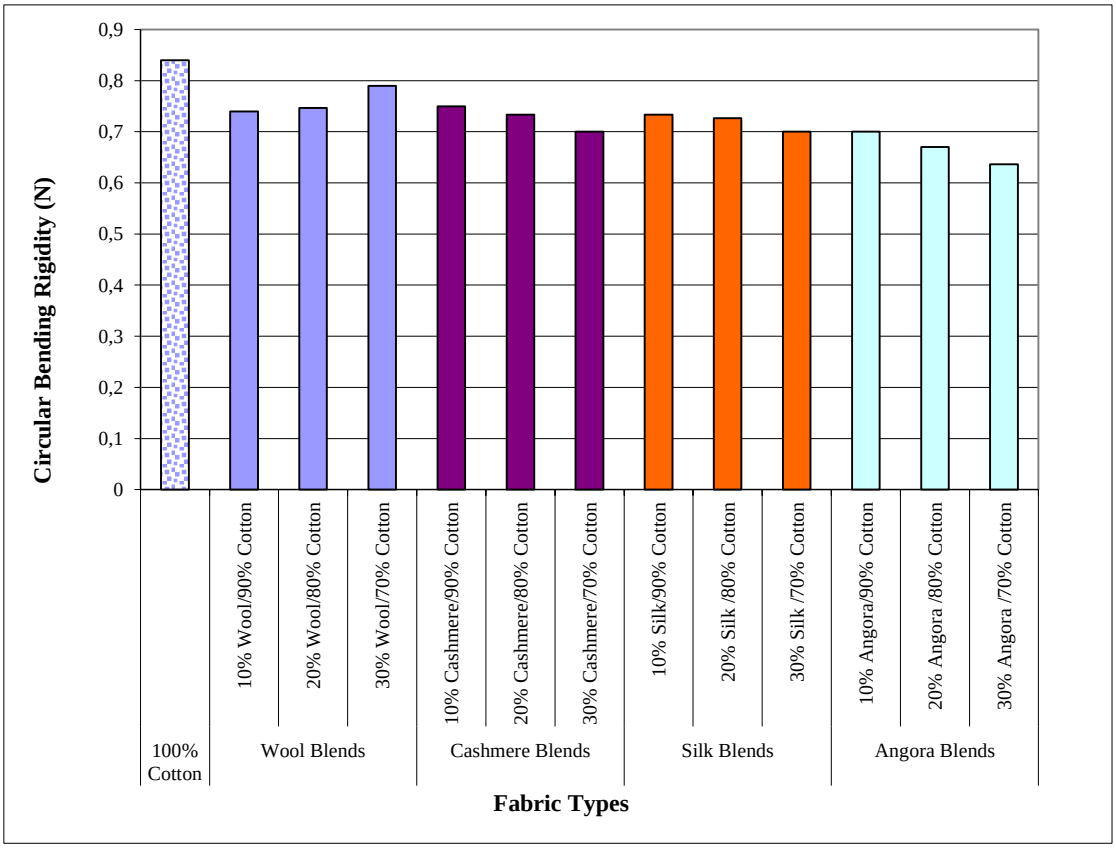

Figure 5. Circular bending rigidity results

As the circular bending rigidity results were analyzed, it was determined that due to their low circular bending rigidity values, all fabrics have very soft handle. They are all lower than the value of cotton fabric. As different fiber blends were compared, it can be seen that fabrics produced from Angora rabbit fiber gives the lowest bending rigidity value. Results of cashmere and silk fabrics are close to each other. Fabrics made of wool fibers have comparatively higher circular bending rigidity among the other animal fiber containing fabrics. For cashmere, angora rabbit and silk fibers, as the animal fiber content in the structure increases, circular bending rigidity decreases, this results in a softer handle for these fabrics. However, wool fiber is stiffer than cotton and the other animal fibers, Therefore, as wool content in yarn structure increases; fabric becomes to have higher bending rigidity.

3.4. Pilling Resistance Results

Pilling resistance test results are given in Figure 6.

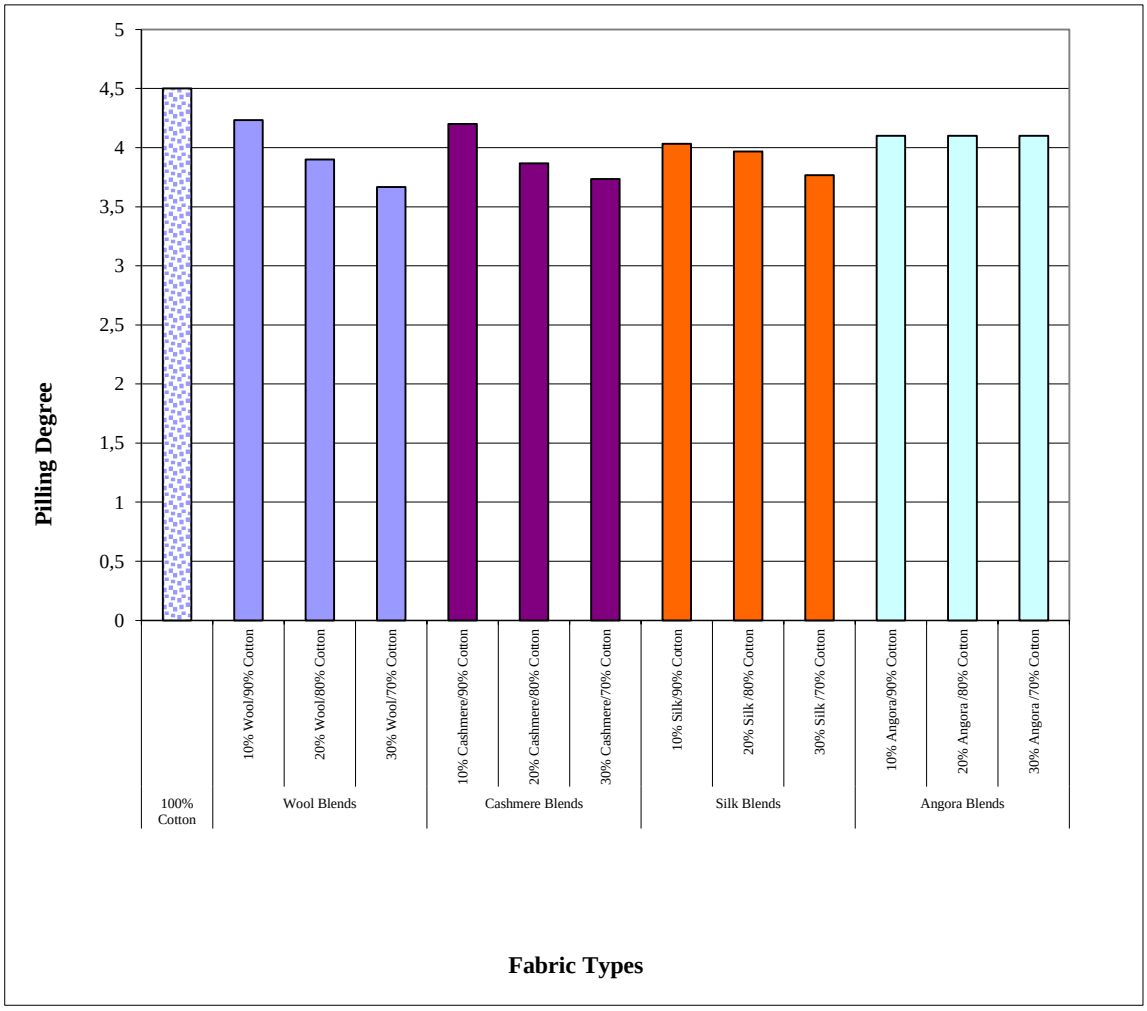

Figure 6. Pilling degree results

As the effect of animal fiber content on pilling degrees, given in Figure 6 analyzed, it can be concluded that, as the animal fiber content in the structure increases, pilling degree decreases. That means pilling tendency of the fabrics increases. It is due to the higher yarn hairiness that increases with the increasing animal fiber ratio in the blend. .

Cotton fiber is more resistant to pilling than animal fibers and adding animal fibers in the yarn structure increases yarn hairiness. For this reason pilling degree of the fabrics decreases and pilling formation increases.

3.5. Kinetic Friction Coefficient Results

In case of kinetic friction coefficient results, which is given in Figure 7, it was determined that fabrics including silk fibers have the lowest values. It is related with the finer and smooth fiber structure. Fabrics having cashmere and Angora rabbit fibers have relatively higher kinetic friction coefficient values, whereas fabrics made of wool fibers that have highest. Higher fiber

diameter and scale height of wool fiber are the main reason of this result. Wool fibers have the highest scale height as compared with the other animal fibers.

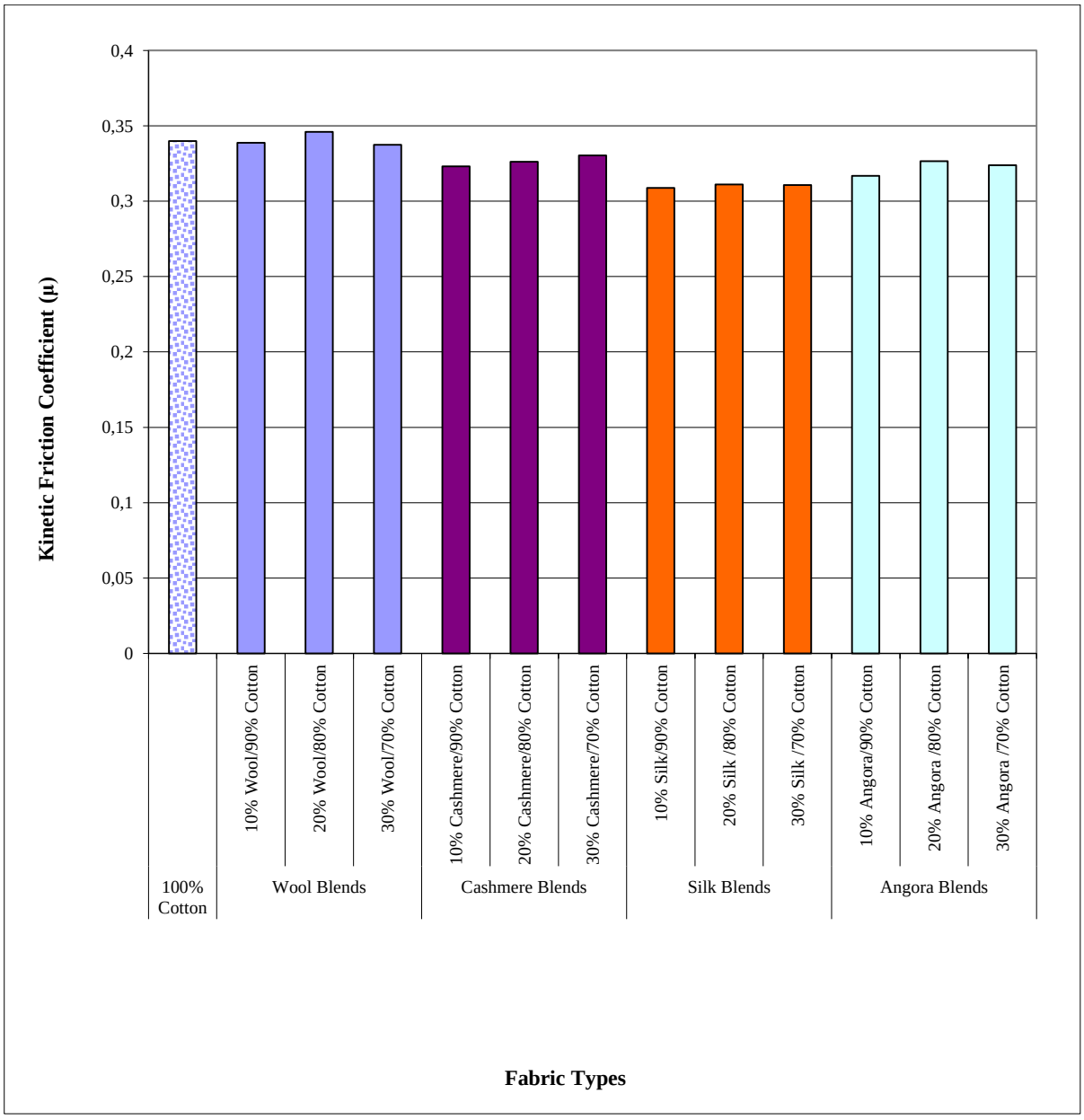

Figure 7. Kinetic Friction Coefficient Results

4. Conclusion

Turkey has a big spinning capacity and most of our mills are using short staple spinning technology. Standard basic products are easy to produce however they are not profitable. In order to compete in the global market, spinning mills should produce niche, and profitable products.

This study was planned in order to contribute to scientific knowledge about the fabrics produced from the yarns including luxury animal fibers. For this purpose, four different animal

fibers were blended with cotton and transformed into yarn form according to short staple spinning technology. Cotton was chosen, since it is the commonly used fiber, which is processed in Turkish Spinning industry.

According to the results, it was determined that fabric weight and thickness increase, due to the higher shrinkage of fabrics including animal fiber. Higher the animal fiber ratio in the yarn is, higher thickness and mass per unit area value were found.

Since the tenacity of the silk fiber is the highest, bursting strength of the fabrics produced from them is comparatively higher. Wool fiber has lowest fiber tenacity therefore wool fabrics have lowest bursting strength values. Usage of higher amount of animal fibers in the yarn structure causes increase yarn unevenness, which results in an increase in the weak points. For this reason, bursting strength of these fabrics decreases.

In case of fabric bending rigidity, Angora rabbit fibers provide the best performance among the investigated fibers. Due to the soft characteristics of animal fibers, fabric bending rigidity decreases and the fabrics becomes softer with the increasing animal fiber percentage in the yarn.

Kinetic friction coefficient results indicate that fabrics made of silk fiber has the smoothest surface, whereas 100% cotton and wool/cotton fabrics have the roughest. In addition to this, as the animal fiber content in the structure increases, pilling formation increases as well.

Acknowledgement

This research was supported by Ege University as 2016-TKUAM-001 coded BAP Project.

References

Akbaş, E., Çelik, P., (2016), A Research for Spinning Silk/Cotton Blend on Open-End Rotor Spinning System, Tekstil ve Konfeksiyon 26(2).

Dirgar, E., , Oral, O., (2014), Yarn and Fabric Production from Angora rabbit Fiber and Its End-Uses, American Journal of Materials Engineering and Technology, Vol. 2, No. 2, 26-28

Fletcher, K.,(2008), Sustainable Fashion and Textiles. Earthscan, London

Frank, R.R., (2001), Silk Mohair, Cashmere and other Luxury Fibres, Woodhead Publishing Ltd. And CRC Press LLC

Guruprasad, R., Chattopadhyay, S.K., (2013), Angora rabbit Hair Fibers: Production, Properties and Product Development, Textile Review Magazine, May

Karthik, T., Rathinamoorthy, R., Ganesan, P., (2015), Sustainable Luxury Natural Fibers-Production, Properties, and Prospects, Chapter · August Book: M.A. Gardetti and S.S. Muthu (eds.),

Handbook of Sustainable Luxury Textiles and Fashion, Environmental Footprints and Eco-design of Products and Processes,, Springer Science+Business Media Singapore 2015.

Langley K., Kennedy T., (1981), The Identification of Specialty Fibers, Textile Research Journal, 51(11), 703-709

Nagal, K., (2006), Assessment of Physical Properties of Camel and Goat Hair, Master of Home Science in Textiles and Apparel Designing, Department of Textiles And Apparel Designing College of Rural Home Science, University of Agricultural Sciences, Dharwad, 99p

Oglakcioglu, N., Celik, P., Bedez Ute, T., Marmarali, A., Kadoglu, H., (2009), Thermal Comfort Properties of Angora rabbit/Cotton Fiber Blended Knitted Fabrics, Textile Research Journal, 79 (10), 888-894,

Süpüren Mengüç, G., (2012), Bazı Özel Hayvansal Liflerden Elde Edilen İpliklerden Üretilen Kumaşların Özellikleri Üzerine Bir Araştırma, Doktora Tezi, Ege Üniversitesi Fen Bilimleri Enstitüsü, Tekstil Mühendisliği Anabilim Dalı, Bornova-İZMİR.

Süpüren Mengüç, G., Özdil, N., (2013), Hayvansal Liflerden Üretilen Giysilerin Isıl Konfor Özellikleri, 11. Ulusal Tesisat Mühendisliği Kongresi, 17/20 Nisan/İzmir

Süpüren Mengüç, G., Özdil, N., Özçelik Kayseri,G., (2014), Physical Properties of Angora rabbit Fibers, American Journal of Materials Engineering and Technology, Vol.2, No.2,11-13.

URL-1:http://impressivemagazine.com/2013/09/21/angora-rabbit-wool-resource-for-a-small-business/

BBSpecial: Thermochromic Textile Product Designs For Babies

Öykü DEGIGOĞLU[1*], Kayhan TOPLU[1], Serhat KARAKAYA[1], Arif Taner ÖZGÜNEY[2]

[1] Batı Basma Sanayi A.Ş., R&D Center, Izmir, Turkey
[2] Ege University, Department of Textile Engineering, Izmir, Turkey

[*]**Corresponding Author:** oykudegigoglu@batibasma.com.tr

Abstract

Smart textiles which generated by gaining properties such as sense and respond an effect or effect change, can be used for many purposes nowadays. Thermochromic textiles fall into the category of smart textiles that provide convenience to daily life in terms of functionality. Thermochromics that reversibly changes in color with temperature, have considerable potential for application in the field of fashion design and clothing. Due to the possibilities for developing new creative designs, thermochromic textiles are generating intense interest among the designers due to their interaction, responsiveness and ultimate functionality. One of the most common health problems in newborn babies is fever. Early recognition of this condition is vital importance, especially in 0-3 month old infants. According to the researches, it is seen that the measurement of fever, is more accurate from the forehead and armpit areas in babies. Baby clothing can be manufactured as a thermochromic textile which changes color if a baby wearing the clothing overheats above body temperature, and which thereby provides a visual indication that the baby is too hot. In this study; it has been aimed to use as a remarkable indicator which is approached aesthetically and visually, on the textile surface which changes color on a certain temperature, where especially the fever is controlled. The product designs in this collection will be a supportive medical textile product that can be recognized fever immediately. The collection that the thermochromic effect will be reflected in textile design; consist of an undershirt, a diaper shirt and a beret. Also fastness tests (acidic and alkaline perspiration, water, saliva, washing) will be done to these textile surfaces to determine the suitability for use as final product. This collection which is focused on product and design will provide innovative opportunities; using in the health sector, textile and textile desing.

Keywords: Smart textiles, smart clothes, thermochromic dyes, textile design.

1. Introduction

One of the most common problems is fever in babies. Due to immune system of the babies is not fully developed, infection disasters and high fever (pyrexia) is shown in babies more than other childhood age group (Karlı, 2015). Fever is most important symptom of the mortal infection disasters. Thus, it has known that early diagnosis is very important after the fever begins for babies that have got fever for three months (Yalçın, 2002). The fever measurements from axillary (underarm) and forehead regions are the most preferred methods in practice as well as being known to give correct results in the researches. These two methods are more suitable especially new-born babies because of they carries less risk of injury than rectal and oral methods and gives more accurate results (Yayla, 2010).

Cotton fibre that is natural, and bamboo fibre that is natural and inherently antibacterial fibre (Çarkıt, 2012; Gümüşer, 2013) gives to garments many properties such as breathing, high moisture absorption, and softness (Kurtoğlu and Şenol, 2004; Özgüney, 2016). The bamboo fibre has high moisture retention and air permeability owing to the large amount of micro-gaps and grooves in the cross section. It absorbs to sweat from the skin and prevents the fabric from sticking to the skin. The type of fibre is a factor that directly affects the warm and cold feeling. The fabric that touches the sweaty body, absorbs and then evaporates sweat quickly, therefore it gives the feeling of comfort for babies (Çarkıt, 2012).

There are many studies in textile and fashion design using thermochromic dyes (Kooroshnia, 2015; Nilsson et al., 2011; Worbin, 2010). In this study, it is aimed to create an auxiliary medical textile product that can be used in the correct and early detection of fever with designs to be created by using the color-changing property of the thermochromic dyes. In this respect, we will provide product with high value added development in technical textile field for our company. It is also aimed to create new product groups in babies' and children's wear using your existing machines and equipments. The aim of the study is to keep pace with changing technology, to increase competitive power, to provide growth and growth, and to give an innovative perspective to our products with new function and feature additions.

2. Materials and Methods

2.1. Materials

Scoured and bleached 100% single jersey knitted cotton (weight: 223 g/m^2, 19 courses/cm, 15 wales/cm) and single jersey knitted 70/30% cotton/bamboo blend (weight: 145 g/m^2, 11 courses/cm, 15 wales/cm) fabrics were used in this research. PG 4105 Thermochange

Red (TK Red, Inkuin) and PG 4110 Thermochange Magenta (TK Magenta, Inkuin) PG 4105 Thermochange Red (TK Red, Inkuin) and PG 4110 Thermochange Magenta (TK Magenta, Inkuin) as leuco dye-based thermochromic pigments, Helizarin SFT LIQ (BH, BASF) as binder, Lutexal F-HIT liq (TL, Archroma) as thickener, Luprintol Fixing Agent SE (FL, BASF) as fixing agent, Luprintol PE New (CL, BASF) as crosslinking agent, ammonia as pH catalyst and distilled water as solvent were used. Formaldehyde-free chemicals according to the Standard 100 by OEKO-TEX (Oeko-Tex, 2018) and thermochromic dye with high and low fastness properties for babies were chosen.

2.2. Methods

In order to see the effects of the thermochromic pigment on the fabric, design elements such as dots, lines, stains and textures were used. The created patterns were transferred to the printing screen and printed to fabric on the rotary screen-printing machine (Patterson and Saville, 2012). The goal of the choosing of the various design elements is observation the interaction difference between raster and lap pattern. In the raster technique, the created pattern is transferred to the fabric by the plotting method. This results in less dyeing of the printed area ratio on the fabric and reducing the effect on the color-changing region by heat. In the lap technique, the created pattern is directly transferred to the fabric. Thermochromic effect and color is better perceived owing to surface area is enlarged in the pattern. For this reason, it has been decided to design the collection according to the determined conditions with the lap patterns. In this way, the entire surface area will be printed with color and the change in visual effect will be discerned better. All patterns were designed using screen-printing method that is one of the basic methods of printing art.

Two different types of thermochromic dyes, leyko and liquid crystal, were used in the study. Chameleon EVA Masterbatch liquid crystal dye-based thermochromic pigment purchased from LCR Hallcrest (Figure 1) and PG 4105 Thermochange Red and PG 4110 Thermochange Magenta leuco dye-based thermochromic pigments purchased from Inkuin were used in this study, in order to observe the effect of thermochromic dyes in different structures.

Black background color was chosen at the printing with liquid crystal dye-based thermochromic pigment in order that perceive to color change. Printing with liquid crystal dye-based thermochromic pigment on the cotton fabric is seen in Figure 1. Study continued with leuco dye-based thermochromic pigments, because black color of the designed collection for the baby group is not suitable due to the fastnesses and is not preferred from the visual point of view.

Figure 1. Normal (left) and temperature influenced (right) state of the fabric printed with liquid crystal dye-based thermochromic pigments.

Original patterns were designed, which feels the best in effectiveness and attracts to a baby, at the surfaces that converted to concrete designs from abstract thought with single color thermochromic dyes. For example, there is smiling bee character with a thermometer in its right hand and a honeycomb symbol that planned to come under the armpit both side in the pattern design seen Figure 2. Hexagon structure of the honeycomb reminds chemical molecule icon. The collection was created with striking, cute, coloured designs that not far from pattern design for baby product (Figure 3). Created other designs for this purpose were shown in Figure 4.

Figure 2. Thermometer, bee and honeycomb patterned sample design study.

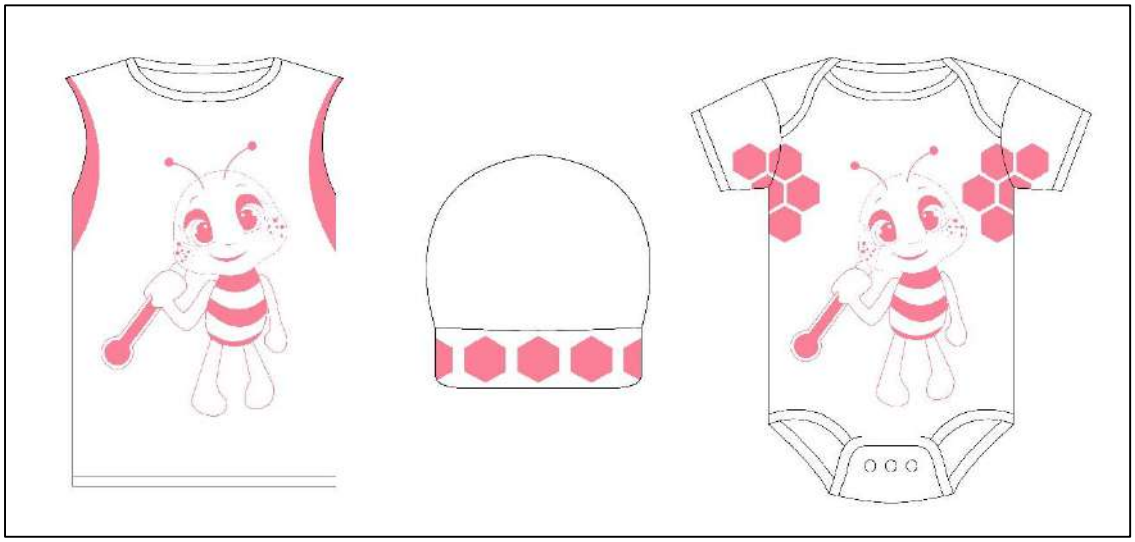

Figure 3. Collection design made up of athlete, beret and babygro.

Figure 4. Other designs.

In this study, cotton and cotton/bamboo blend fabrics were printed using screen-printing method with designed patterns. Two different leuco dye-based thermochromic pigments, red and magenta, were chosen and two different dye concentrations, 10 g/l and 40 g/l, were used.

For preparing printing paste, water, Helizarin SFT LIQ, Lutexal F-HIT liq, Luprintol Fixing Agent SE, Luprintol PE New, ammonia and TK Red or TK Magenta were added, respectively and then were mixed with mechanical agitator at 25 °C for 10 minutes. The recipes were given at Table 1. The cotton and cotton/bamboo blend fabrics were printed with prepared printing paste by sample rotary screen-printing machine (Johannes Zimmer) at 6 Pa for 6 m/s with 10 mm diameter stripper. After that, the fabrics fixed at 130°C for 2 min in a drying oven (Thermal, 420S) in order to not harden and not turn yellow of bamboo fiber.

Table 1. Recipes.

Chemical Agent	Amount of Use (g/kg)			
	Recipe 1	Recipe 2	Recipe 3	Recipe 4
Thermochromic Pigment Magenta	10	40	-	-
Thermochromic Pigment Red	-	-	10	40
Binder – BASF Helizarin SFT LIQ	160	160	160	160
Kıvamlaştırıcı – Archroma - Lutexal F-HIT liq	17	17	17	17
Fixing Agent – BASF Luprintol Fixing Agent SE	5	5	5	5
Crosslinking Agent – BASF Luprintol PE New	3	3	3	3
Ammonia	2	2	2	2
Water	X	X	X	X

In study, i. only thermochromic dye, ii. thermochromic dye on pigment dye and iii. two thermochromic dye over and over were printed on the cotton fabrics, in order to determining the color gamut and observing the effects of the colors on each other before patterns are created. In order to observe the color changes, the printed fabrics were placed on a heated magnetic stirrer (ISOLAB Laborgerate GmbH) at between 36 and 38 °C, and then temperature of the fabrics was measured with a laser infrared thermometer (Raytek ST20 Pro XB). Printing works were carried out with pastes containing 10 g/kg and 40 g/kg leuco dye-based thermochromic pigments. Color change and fastness were analysed. Sweat, water and saliva fastness, salinity fastness, wet and dry rubbing fastness and wash fastness were measured according to ISO 105 - E04, ISO GB/T 18886, ISO 105 - X12 and ISO 105 - C06, respectively.

3. Results and Discussion

As a result of the first experiment, it was seen that the design elements didn't cause a problem about the color clarity and the effect, and the color interaction values didn't change for the different design elements. It is aimed that the surface area is keep wide and effect can be noticed better due to the medical aspect of the design. After the general features of the design were determined, structural properties related to collection were decided.

It was observed that thermochromic dyes printed on yellow or grey pigment were blended in a similar manner to two color mixing and then third color appeared. This caused that thermochromic dyes were affected brighter and matt on yellow and grey, respectively. It has been seen that it is better to use the classic baby product colors as well as the matte colors and the soft color that does not contain grey for studying with the baby product. For this reason, thermochromic dyes were printed on fabrics with blue background color and without background color. The color experiments are shown in Table 2.

Table 2. Color experiments.

TK Red	Grey Pigment + TK Red	Yellow Pigment + TK Red	Blue Pigment + TK Red	TK Magenta + TK Red
TK Magenta	Grey Pigment + TK Mag.	Yellow Pigment + TK Mag.	Blue Pigment + TK Mag.	TK Magenta + TK Red

Color changes of the printed fabrics were examined different temperatures to investigate the effects of the dyes on each other. Results were shown in Table 3 and Table 4. Color change of TK Magenta and TK Red took place at <36 °C and 37 °C, respectively. When grey and blue pigment are used for background color, color change for TK Magenta and TK Red occured >36

°C and <36 °C, respectively. Thermochromic printings on pigment dyes didn't show any change at color change temperature.

When TK Red and TK Magenta over and over were printed on the cotton fabrics, color change which less than others was arisen at 36 °C. It is believed that this is due to the fact that the two overprinted thermochromic dyes could not be reached to amount of required energy for colour change. It has been found that the use of the TK Red pigment, which provides a color change at the appropriate temperature range of 36-38 °C for the detection of fever is convenient in the babies collection.

Table 3. Color changes of TK Red according to temperature.

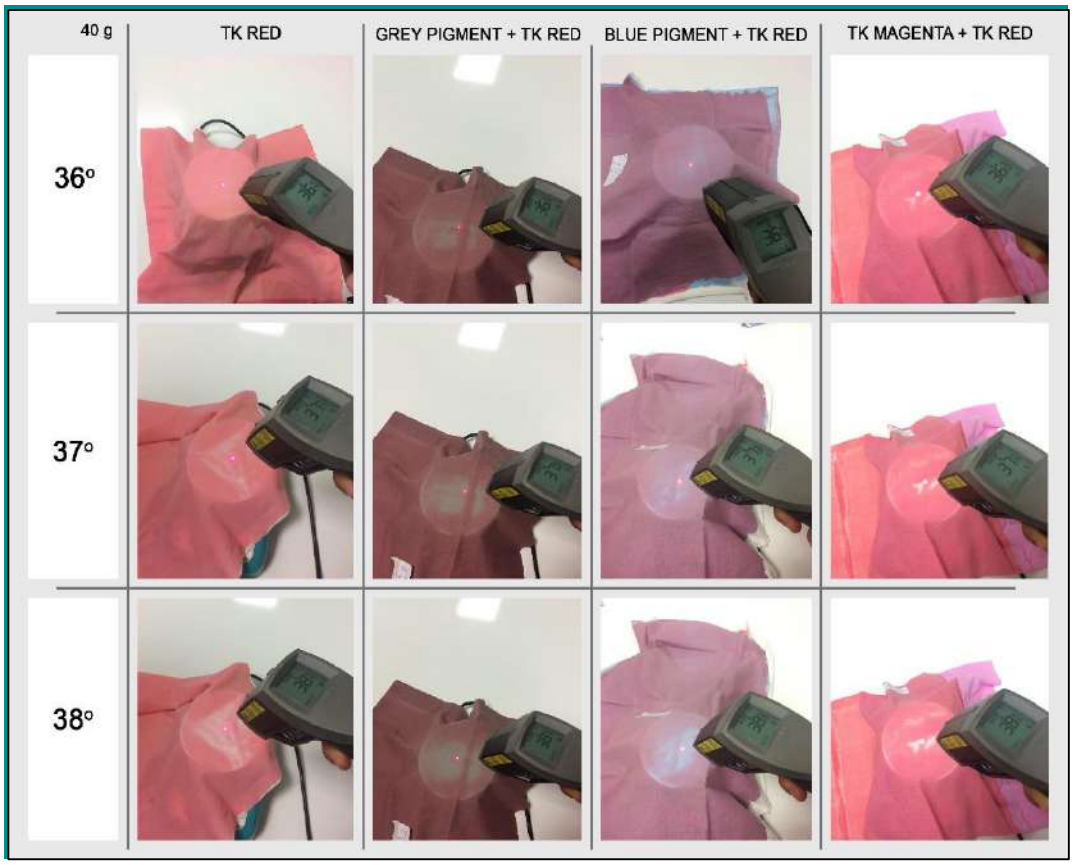

Table 4. Color changes of TK Magenta according to temperature.

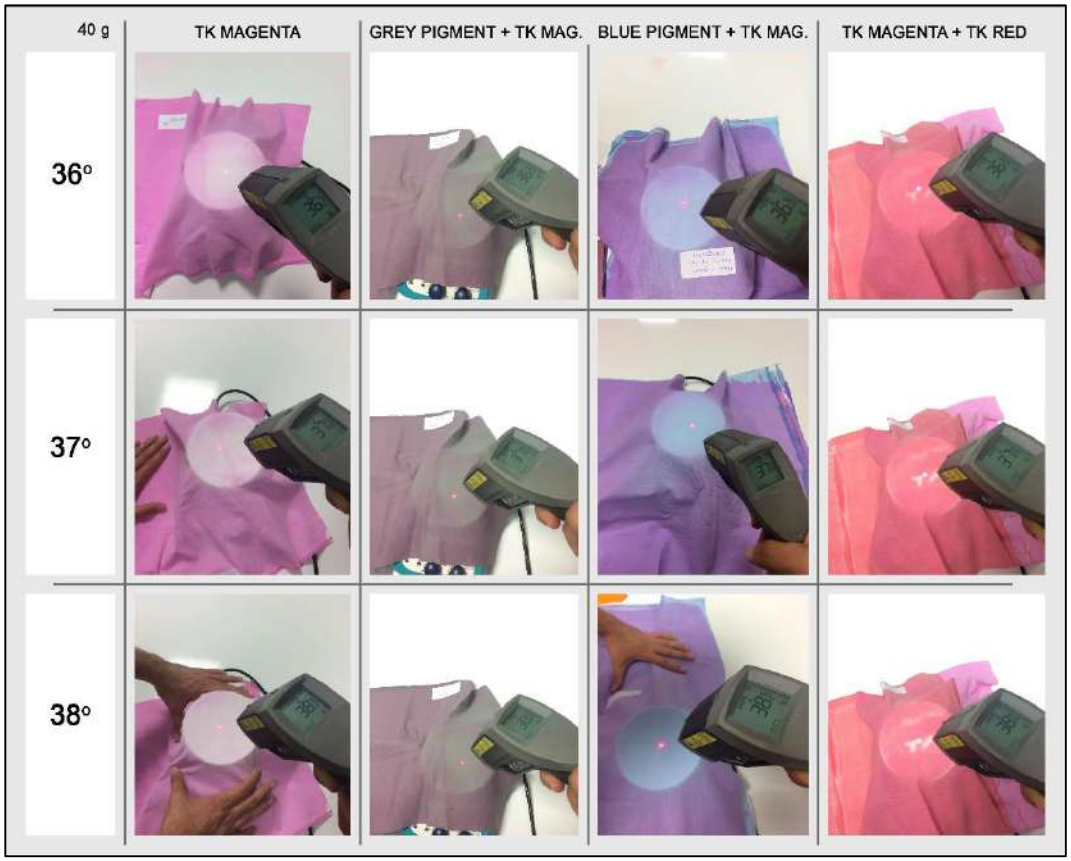

Acidic and basic sweat solutions (% 5, 10 and 20 of the fabric weight) using at perspiration fastness were sprayed on thermochromic printed fabrics that would use at baby collection with a view to evaluate the color change of the fabric when the baby is sweaty. Accordingly, it was observed that the moist areas of the fabric didn't change color at temperature range of 36-38 °C. As the amount of temperature and moisture increased, the color change rate increased in the dry areas of the fabric and didn't change in the moist areas of the fabric. It is believed that the heat energy, which comes on the fabric, is first used to evaporate moisture from the fabric and then provides the color change. The results are shown in Tables 5 and 6.

Table 5. Color changes of TK Red according to moisture (acidic) and temperature.

40 g Thermochromic Red		5%	10%	20%
ACIDIC	36 °C			
	37 °C			
	38 °C			

Table 6. Color changes of TK Red according to moisture (basic) and temperature.

40 g Thermochromic Red		5%	10%	20%
BASIC	36 °C			
	37 °C			
	38 °C			

As seen in similar studies (Kooroshnia, 2013; Meriç, 2016), it was detected that the color change could be observed more clearly when the amount of dye was increased. Fastness tests were performed for printed fabrics that contain 10 and 40 g/kg dye. When fastness results given Table 7 were analysed, significant change observed only in wet rubbing fastness. Results of the other fastness tests were found to be close to each other. It has been determined that the amount of thermochromic dyes between 10 and 40 g/kg in baby products is opportune in terms of color change and fastness.

Table 7. Results of the fastness tests.

Amount of dye	Color	Fastness					
		Dry Rubbing	Wet Rubbing	Perspiration	Water	Saliva	Wash
10 g/kg	Red	5	4-5	4-5	4-5	4-5	4-5
10 g/kg	Magenta	5	4-5	4-5	4-5	4-5	4-5
40 g/kg	Red	4	2-3	4-5	4-5	4-5	4-5
40 g/kg	Magenta	4	2-3	4-5	4-5	4-5	4-5

4. Conclusion and Recommendations

In the study, early detection of the fever was provided thanks to the color change of the areal design made with the thermochromic dye on the textile surface by heat based upon fever in the babies. The designs that supported aesthetically and visually have been created funny, cute and remarkable in terms of both family and baby. The product range of the company has been expanded with collection design working. At the same time, we will create a high value, innovative, functional and unique product group in the field of technical textiles in the name of our company with the put on market to the product. It is known that skin problems are frequently had in babies in researches.

Skin is the biggest organ of the body, and its unity is impressed by internal and external factors. Therefore, it is important to take care of the fabric and chemicals with regard to health (Altıntaş, 2016). To this end, natural fibers were preferred this study. In addition, harmless thermochromic dyes for babies and formaldehyde-free chemicals according to Standard 100 by Oeko-Tex (Oeko-Tex, 2018) were used. Test results show that the thermochromic dyes have high fastness values.

A knowledge-based process that start with identifying the problem for the goal is investigated. The design has been converted to concrete product from abstract knowledge by means of the collection, interpretation and evaluation of the data. It has benefited from many disciplines such as medicine, science, engineering, and psychology as a result of the interdisciplinary nature of design. It is aimed that the designs that created to corresponding to underarm were aesthetically both functional and visual. The color change temperature of the thermochromic dyes was chosen between 36 and 38 °C based on the critical body temperature. The color change of the garment used as an indicator with baby's sweat was also evaluated by adapting to the fact.

Acknowledgment

We would like to thanks Prof. Dr. Özlenen ERDEM İŞMAL and Assos. Prof. Dr. Leyla YILDIRIM (Dokuz Eylül Universitey Faculty of Fine Arts) for their contributions and directions.

References

Altıntaş, M. (2016). Yenidoğan Yoğun Bakım Ünitesinde Yatan Bebeklerde Cilt Sorunlarının İncelenmesi. (Yüksek Lisans Tezi). Harran Üniversitesi, Sağlık Bilimleri Enstitüsü, Hemşirelik Anabilimdalı, Şanlıurfa.

Çarkıt, G. (2012). *Bambu-Pamuk Karışımı Örme Kumaşların Özelliklerinin İncelenmesi.* (Yüksek

Lisans Tezi). Erciyes Üniversitesi, Fen Bilimleri Enstitüsü, Tekstil Mühendisliği Anabilim Dalı, Kayseri.

Gümüşer, T. (2013). Ekolojik bebek giysilerinde doğal liflerin önemi. Marmara Üniversitesi Sanat ve Tasarım Dergisi, 1(4), 2013.

Karlı, A. (2015). *Ateşli Çocuğa Yaklaşım*. s. 1-10, Ankara: Derman Tıbbi Yayıncılık.

Kooroshnia, M. (2013). Leuco dye-based thermochromic inks: recipes as a guide for designing textile surfaces. In *13th AUTEX World Textile Conference, Dresden Germany*. AUTEX World Textile Conference.

Kooroshnia, M. (2015). *Creating Diverse Color-Changing Effects On Textiles*. (Doctoral Dissertation). University of Boras, Sweden.

Kurtoğlu, N., Şenol, D. (2004). Tekstil ve Ekolojiye Genel Bakış, Karsinojen ve Allerjik Etki Yapabilen Tekstil Kimyasalları. *KSÜ Fen ve Mühendislik Dergisi, 7* (1) s. 26-31.

Majumdar, A., Mukhopadhyay, S., and Yadav, R. (2010). Thermal Properties Of Knitted Fabrics Made From Cotton And Regenerated Bamboo Cellulosic Fibres. *International Journal Of Thermal Sciences, 49*(10), 2042-2048.

Meriç, D. (2016). *Akıllı Tekstillerin Ürün Tasarımında Kullanım Olanakları ve Moda Tasarımına Yönelik Uygulamalar*. (Yüksek Lisans Tezi). Anadolu Üniversitesi, Fen Bilimleri Enstitüsü, Eskişehir.

Muhammad, A. A. and Sarwar, M. I. (2010). *Sustainable And Environmental Freindly Fibers İn Textile Fashion (A Study Of Organic Cotton And Bamboo Fibers).* (Unpublished Master's Thesis). University of Boras, Sweden.

Nilsson, L., Satomi, M., Vallgårda, A., and Worbin, L. (2011). *Understanding The Complexity Of Designing Dynamic Textile Patterns.* In Ambience'11, Where Art, Technology And Design Meet, Borås Sweden, 28-30 November 2011. CTF.

OEKO-TEX, Standard 100 by OEKO-TEX, Limit values and fastness. Retrived May 31, 2018, from https://www.oeko-tex.com/media/init_data/downloads/STANDARD%20100%20by%20OEKO-TEX%C2%AE%20-%20Standard.pdf.

Özgüney, A. T. (2016). Investigating The Effects Of Different Softeners On Pilling Properties And Durability To Washing Of Bamboo Knitted Fabrics. *Tekstil ve Konfeksiyon, 26*(3), 307-313.

Patterson, J. and Saville, S. (2012). Viscom: Design Elements and Principles. A Guide to Visual Communication Design (1st edition) içinde (35-71). Cambridge: Cambridge University Press.

Worbin, L. (2010). *Designing Dynamic Textile Patterns* (Unpublished Ph.D. Thesis). Chalmers University of Technology, Department of Computer Science and Engineering, Sweden.

Yalçın, I. (2002), Ateş, Neyzi O, Ertuğrul T. (Ed.), *Pediatri*, (3. Baskı) içinde (473-75). İstanbul: Nobel Tıp Kitabevi.

Yayla, M. E. (2010). *Çocuk Acil Servisine Başvuran 6 Ay – 5 Yaş Arası Ateşli Hastalarda Aksiller,*

Rektal ve Timpanik Ateş Ölçümlerinin Karşılaştırılması. (Aile Hekimliği Uzmanlık Tezi). T.C. Sağlık Bakanlığı, Adana Numune Eğitim Ve Araştırma Hastanesi, Çocuk Sağlığı Ve Hastalıkları Kliniği, Adana.

Yeral, A. (2017). *Annelerin Ateşli Çocuğa Yaklaşımı; Ateş Konusunda Bilgi Tutum ve Davranışları.* (Uzmanlık Tezi). Mustafa Kemal Üniversitesi, Tayfur Ata Sökmen Tıp Fakültesi, Hatay.

Comparison of The Activities Classical and Nano Chemicals on Different Finishing Processes of Cotton Fabrics

Eylen Sema DALBAŞI[1]

[1]Ege University, Engineering Faculty, Textile Engineering Department, İzmir, Turkey

Corresponding Author: sema.namligoz@ege.edu.tr

Abstract

The aim of this study is to compare the performances of classic and nano chemicals used in wrinkle resistance, water and oil repellency and softening treatments in cotton fabrics. The activity of these chemicals and the effect of the chemical concentration were examined after these processes. In addition, the durability of the chemicals against washing has also been examined. For this purpose, the wrinkle resistance, water-oil repellency and softening treatments under different conditions were applied to 100% cotton woven fabrics which have been pretreated. After the applications, the dry wrinkle recovery angles, breaking strengths, water and oil repellency values of all samples were measured and the handle evaluation of all samples were done. As a result, the performances of all classical and nano-sized products are compared. It has been found that the use of nano products was more advantageous than the classical products in terms of the effectiveness of the process.

Keywords: Nano product, WRA, Water-oil repellency, Handle evaluation

1. Introduction

Nanotechnology deals with materials 1 to 100 nm in length. A nanometer is a unit of length equal to one billionth of a metric. A nanometer can be arranged side by side but 2-3 atoms; about 100-1000 atoms come together to form an object on nanoscale scales. The nanoscales of different objects are shown in Figure 1 (Sawhney et al., 2008; Qian et al., 2004; (https://www.nano.gov, 2018).

Figure 1. Nanoscales of different objects (https://www.nano.gov, 2018)

The countries that have advanced in technology focus on nanotechnology and do serious work on programs that will enable them to take part in this revolution. World demand for nanomaterials is expected to grow, from $3,7 bilion in 2008 to $90 billion in 2020 (Figure 2) (Mariana, 2015).

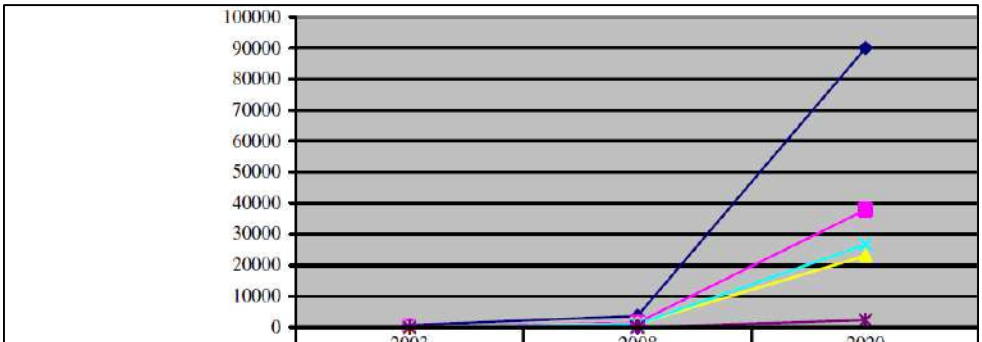

	2003	2008	2020
World Nanomaterial Demand	720	3650	90000
Americas	276	1490	37900
Western Europe	225	1067	23100
Asia Pacific	215	1035	26700
Other Regions	4	58	2300

Figure 2. World Nanomaterial Demand (million US dollars) (Mariana, 2015).

In our country, nanotechnology research has been restructured and accelerated thanks to the 6th Framework Program of the European Union. Nanotechnology has been taken as one of the priority areas in the Vision 2023 Program prepared by TUBITAK.

Focus Technology Areas:

- Nanophotonics, nanoelectronics, nanomagnetism
- Nanomaterials
- Nanocharacterisation
- Nano-scale quantum information processing
- Nanobiotechnology (http://vizyon2023.tubitak.gov.tr, 2018).

Nanotechnology is an interdisciplinary technology that controls atoms and molecules of at least 1 nm in size that provide many applications and new features such as materials science, electronics, optics, medicine, plastics, energy, textiles and the environment. Nanotechnology is used also in the textile sector to improve the performance of textile products. Textile products become multifunctional thanks to nanotechnology, which gives them different features. By using nanotechnology and nanomaterials in appropriate conditions and quantities it is possible to impart the following functions to textile products:

- Increasing resistance to mechanical, chemical, photochemical or thermal degradation,
- Improvement of water, oil and stain repellency,
- The ability to change the absorption and emission characteristics of the electromagnetic wave Development of electrical conductivity for antistatic and electromagnetic protective effects,
- Improvement of active agents (immobilized)
- Improvement of wrinkle recovery (Aktan, 2011).

Today, the main applications of nanotechnology in textiles (Figure 3) refer to; nano finishings, nano chemicals, nanocoating, nano silver (Mariana, 2015).

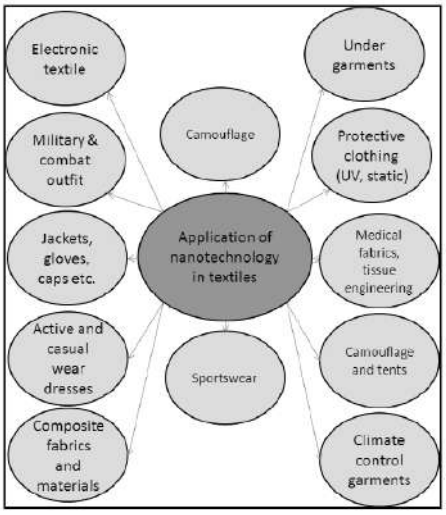

Figure 3. Some applications of nanotechnology in textiles (Patra et al., 2013)

Nano-technology applications in textile materials can be basically examined in two sections:

- To produce new textile materials in nano sizes with different functions: These products; nanofibers, nanocomposites.

- To improve the existing functions and performances of textile materials with the help of nanotechnology: This can be done in two ways:

- Nanoparticles, nanocomposites, etc. that give different properties to fiber, yarn or fabric surface to add,
- To obtain new / functional surface layers by coating with advanced technologies (plasma, sol-gel, etc.) by playing with atoms and molecules (Cireli et al, 2006).

Examples of some nanotechnology applications in the textile industry are given in Figure 4 and 5.

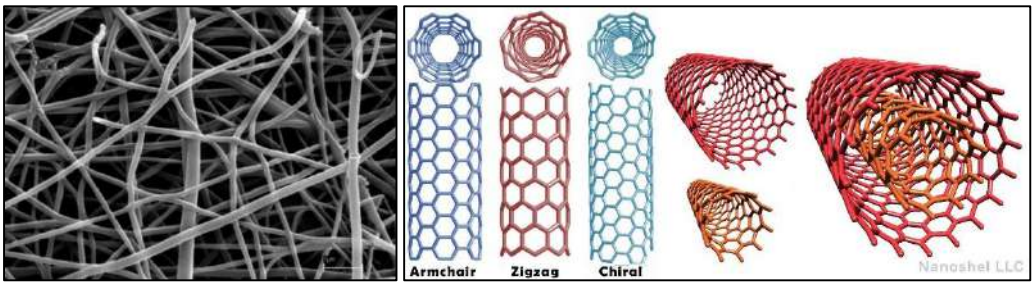

Figure 4. Nanofibers and nanotubes (https://www.nanoshel.com, 2018)

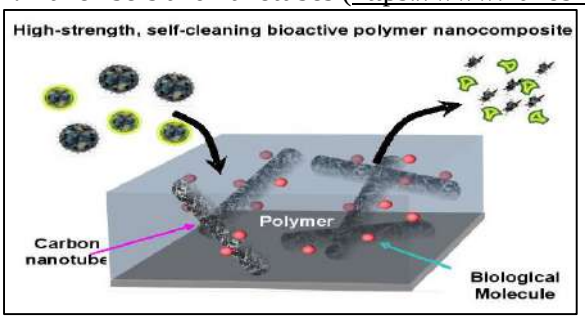

Figure 5. Nanocomposites (https://www.rpi.edu, 2018)

A number of nano finishes on textile materials have been evolved during the recent years. Conventional textile finishing methods used to impart different properties, such as water repellency and stain repellency, to the fabrics often do not lead to permanent effects, and lose their functions, after laundering or use. Also, since nanoparticles have a large surface area and a high surface energy which provide a good affinity for the fabrics and cause an increase in the durability of the desired textile functions, the strength of the treated fabrics is high (Gokarneshan et al., 2015;Kwon et al., 2002;Lee et al., 2003;Dura'n et al., 2007;Xin et al., 2004;Fei et al., 2006;Vigneswaran et al., 2006;Qi et al., 2007;Wong et al., 2006).

Some research topics for nanotechnology in textiles :

- Aesthetics (e.g., luminescence), antimicrobial, electrical conductivity
- Fire resistance, fragrance release, high strength, moisture management

- Shrink resistance, stain resistance, static protection, UV protection
- Water repellent (hydrophobic), wrinkle resistance and self-cleaning

(https://www.ic.gc.ca/textiles, 2018).

Table 1 shows the various nanomaterials used in textiles and their functions in textile finishing.

Table 1. Nanomaterials and their functions (https://www.umweltbundesamt.de, 2018)

Properties of nanotextiles	**Nanomaterial**	**Properties of nanotextiles**	**Nanomaterial**
Electroconductive/antistatic	Carbon black, copper, polypyrrol, polyaniline	Fire resistance	Carbon nanotubes, boroxosiloxane, nanoclay, antimony ash
Increased durability	Aluminum oxide, carbon nanotubes, polybutyl acrylate, silicone dioxide, zinc oxide	Controlled release of active fragrances	Silicone dioxide, nanoclay
Antimicrobial	Silver, chitosan, silicone dioxide, titanium dioxide, zinc oxide	Heat conducting or insulating properties	Carbon nanotubes, vanadium dioxide
Self-cleaning/dirt and water repellent	Carbon nanotubes, fluoroacrylate, silicone dioxide, titanium dioxide	Shielding electromagnetic radiation (IR, microradiation, radio waves)	Indium tin oxide
Moisture-absorbent	Titanium dioxide	Abrasion resistance	Carbon nanotubes
Improved dyeability	Carbon black, nanoporous hydrocarbon-nitrogen coating, silicone dioxide	UV protection, protection from fading	Titanium dioxide, zinc oxide

Examples of some nanotechnology applications in the textile finishing are given in Figure 6,7,8,9.

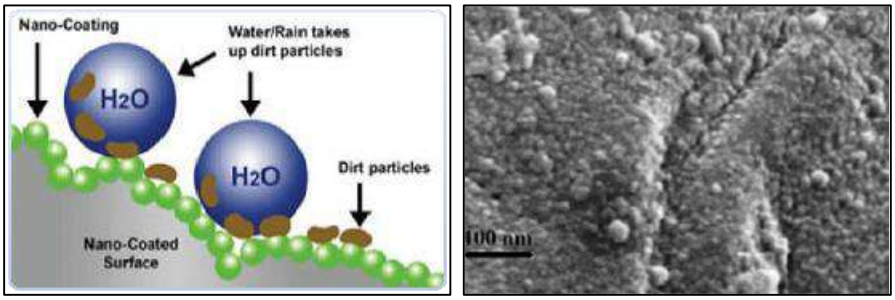

Figure 6. Nano coating/self-cleaning textile (Rezwan et al., 2017;Joshi et al., 2011)

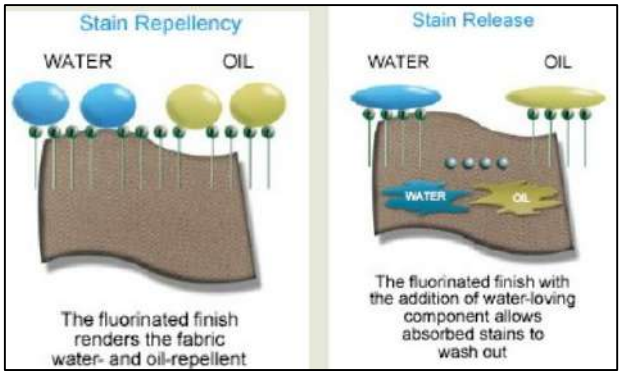

Figure 7. Stain repellent fabric (https://www.nanotex.com, 2018)

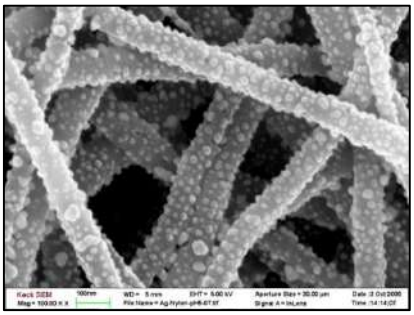

Figure 8. Antibacterial air filtration coated with silver nanoparticles (https://www.azonano.com, 2018)

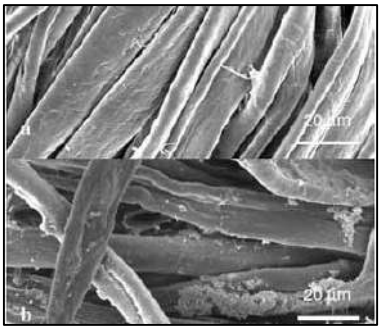

Figure 9. SEM images of cotton fibers with UV protection properties, a) untreated, b) treated with ZnO
(https://www.nanowerk.com, 2018)

2. Material and Method

2.1. Material

In Table 2, the physical properties of the 100% cotton fabric used in the experiments (desized, scoured and bleached) were given.

Table 2. The physical properties of the cotton fabric

Fiber type	100% Cotton
Fabric construction	Plain
Fabric weight (g/m^2)	146
Warp density (threads/cm)	27
Weft density (threads/cm)	19
WRA for warp	67°
WRA for weft	55°

Table 3 gave information on the chemical substances used in the experiments.

Table 3. Chemical types

Chemical type	**Structure of chemical substance**
For Wrinkle Resistance Treatment	
FIXAPRET AB-9 (BASF)	Conventional dimethyloldihydroxylethylene urea

	(DMDHEU)
RUCO-NANOLINK COM (Rudolf Duraner)	Nano functional glyoxal crosslinker
For Water and Oil Repellency Treatment	
LUROTEX TX 2504 (BASF)	Conventional fluorocarbon
RUCO-NANOGUARD GOR (Rudolf Duraner)	Nano fluorocarbon
For Softening Treatment	
SILIGEN AB-VS (BASF)	Conventional micro silicone
SILIGEN AB-**MS** (BASF)	Conventional macro silicone
RUCO-NANOFIN ISN (Rudolf Duraner)	Nanopolymeric silicone
PERSOFTAL PEN (Tanatex)	Conventional cationic softener
PERSOFTAL AKS (Lanxess)	Conventional nonionic softener

2.2. Method

Three different finishing treatments were applied to the cotton fabrics in the experimental works carried out by the impregnation method. After crease resistant and water-oil repellency treatments, the fabrics were washed 1, 5 and 10 times for testing the washing durability. The applications were realized with Rapid PA-1 (2004) marked laboratory padder for impregnation. Ataç GK 4 laboratory stenter was used for drying and curing. The samples were washed in the Wascator machine according to TS EN ISO 6330 (15A program) (TS EN ISO 6330 standard, 2012). In Tables 4 and 5, the application recipes and codes were given.

Table 4. Application recipes and codes for crease resistance and **water and oil repellency** treatment

For Crease Resistance Treatment	**Code**		
For Conventional Chemical	**C1**	**C2**	
FIXAPRET AB-9	50 g/l	80 g/l	
$MgCl_2$(Catalyst)	8 g/l	12 g/l	
For Nano Chemical	**N1**	**N2**	
RUCO-NANOLINK COM	50 g/l	80 g/l	
$MgCl_2$(Catalyst)	8 g/l	12 g/l	
For Water and Oil Repellency Treatment	**Code**		
For Conventional Chemical	**C1**	**C2**	**C3**
LUROTEX TX 2504	30 g/l	50 g/l	80 g/l
For Nano Chemical	**N1**	**N2**	**N3**
RUCO-NANOGUARD GOR	30 g/l	50 g/l	80 g/l
Impregnation conditions :	pH 4,5 (with Acetic acid) Pick up: 80% Drying: 100°C for 2 min Curing: 150°C for 5 min		

Table 5. Application recipes and codes for softening treatment

For Softening Treatment	Code	
SILIGEN AB-VS - Micro silicone, pH:5	**MIC1**	**MIC2**
	20 g/l	40 g/l
SILIGEN AB-MS - Macro silicone, pH:5	**MAC1**	**MAC2**
	20 g/l	40 g/l
RUCO-NANOFIN ISN - Nano silicone, pH:5	**N1**	**N2**
	20 g/l	40 g/l
PERSOFTAL PEN- Cationic softener, pH:5,5	**C1**	**C2**
	20 g/l	40 g/l
PERSOFTAL AKS - Nonionic softener, pH: 7	**NON1**	**NON2**
	20 g/l	40 g/l
Impregnation conditions :	Pick up: 80%	
	Drying: 100°C for 2 min	

2.3. Tests

Before the tests, the fabric samples were conditioned under standard atmosphere conditions (20°C±2°C temperature, 65%±4RH). Then, the dry wrinkle recovery angle, breaking strength, water and oil repellency tests and handle evaluation of the fabrics were performed.

Determination of Wrinkle Recovery Angle

The dry wrinkle recovery angles (WRA) of the samples were measured according to DIN 53890 standard. WRA values of the specimens in warp and weft directions were measured separately and total WRA values (warp+weft) of specimens were calculated (DIN 53890 standard, 1972).

Determination of Breaking Strength

The breaking strengths (N) of the samples were measured according to EN ISO 13934-1 standard (strip method) at Lloyd LRX Plus marked tester (EN ISO 13934-1 standard, 2013).

Determination of Water and Oil Repellency

The water repellency tests of the samples were performed according to standard AATCC 22, oil repellency tests were carried out according to standard AATCC 118 (AATCC 22 standard, 2010;AATCC 118 standard, 1997).

Determination of Handle

- **Circular Bending Rigidity Test**

The circular bending resistance of the samples according to ASTM D4032-08 was measured (ASTM D4032-08 standard, 2016).

- **Bending Resistance Test on Shirley Stiffness Tester**

The bending resistance of the samples on a Shirley stiffness tester according to ASTM D1388-08 was measured (ASTM D1388-08 standard, 2008).

➢ **Friction Coefficient Test on Frictorq Tester**

The fricton coefficient values of the samples on a Frictorq tester were measured (Lima, et al., 2003).

3. Findings and Discussion

3.1. Evaluation of WRA values

The WRA values of untreated, treated and 1, 5 and 10 washed fabrics (after the wrinkle resistance treatment) were given in Figure 10.

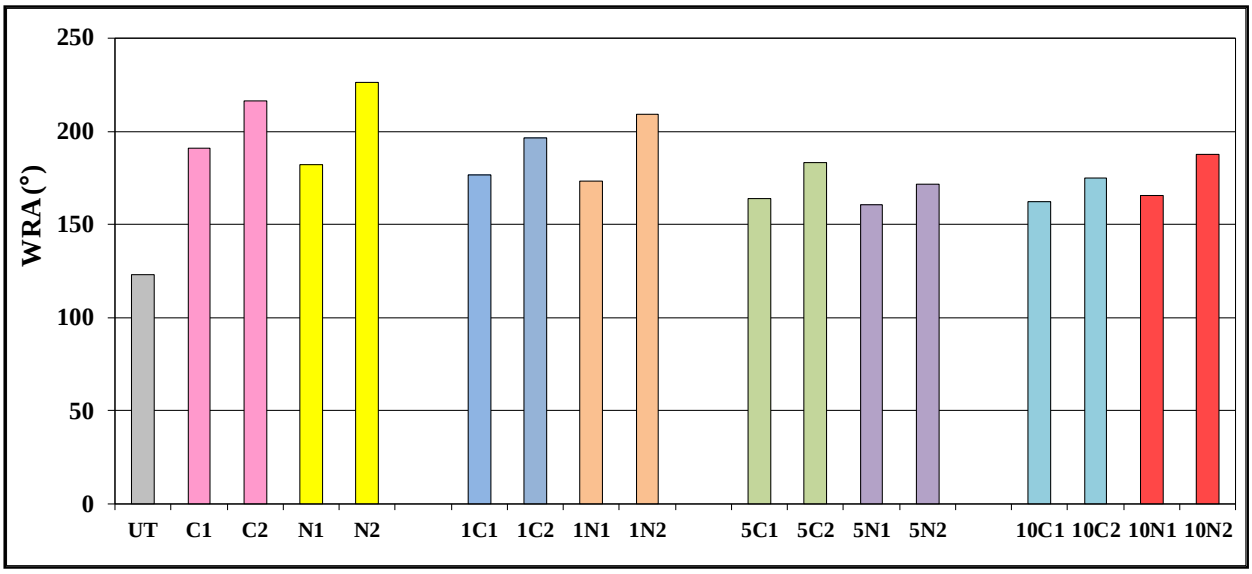

Figure 10. WRA values of the fabrics

Symbols in figures 1, 5 and 10 indicate washing numbers. After the treatment, the angle increased as the concentration of both the classical and nano products increased. However, at high concentration of nano product, the angle was higher than that of conventional product, so the concentration amount is more effective in nano products. After the washings, there were important decreases in WRA values. After one wash, the angles of the samples treated with the conventional products decreased more than the nano products. But, there is no significant difference between the WRA values after 5 and 10 washings.

The breaking strengths of untreated, treated and 1, 5 and 10 washed fabrics (after the wrinkle resistance treatment) were given in Figure 11.

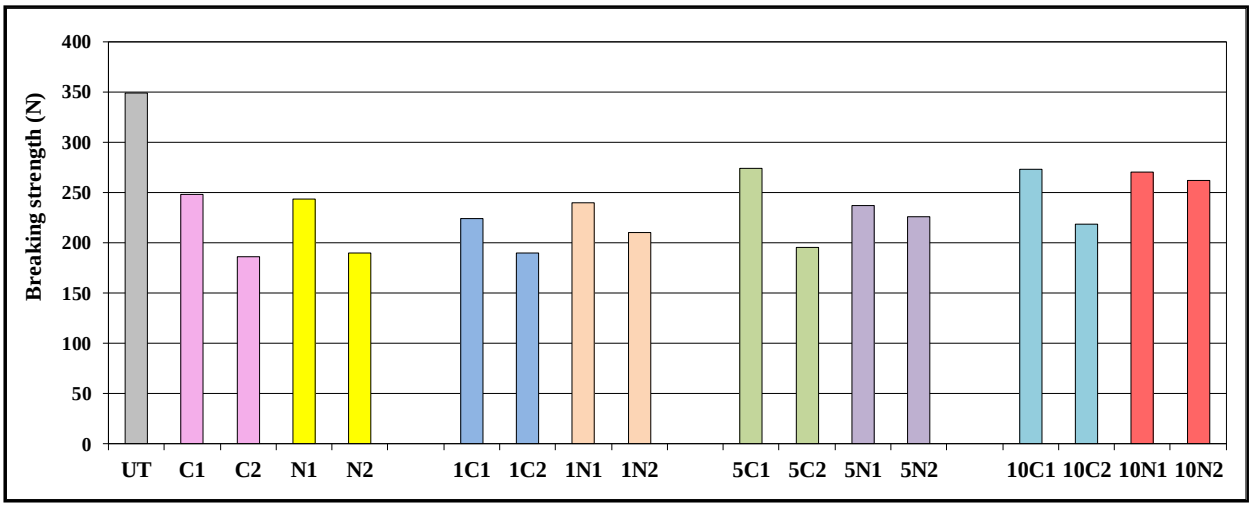

Figure 11. Breaking strengths of fabrics

In the preliminary studies, both warp and weft breaking strength measurements were done before and after the process. It has been found that the weft breaking strength values of the measurements were lower than the warp values. For this reason, it has been decided to measure the weft breaking strengths in the main experiments.

When the results in Figure 11 are examined, the breaking strength values of the samples treated with both conventional and nano products decreased as the chemical concentration increased. Moreover, the breaking strength values are independent of the chemical type, and there is a change in approximately the same ratio in both products. The decreases in breaking strength values after washing, particularly after 5 and 10 washings, are less than those of both non-washed and one-washed samples. The reason for this is that the crosslinker is washed away from the fabric and therefore the fiber-fiber adhesion begins to increase again. Because the principle of wrinkle resistance treatment is based on restricting the mobility of the fiber elements. Since the movement of the fiber elements is restricted, the fibers cannot approach each other due to the force of breaking force and cannot join together and the fibers cannot resist the breaking force all together.

3.2. Evaluation of Water and Oil Repellency Results

- **Water Repellency Results**

The water repellency values of untreated, treated and 1, 5 and 10 washed fabrics (after the water repellency treatment) were given in Figure 12.

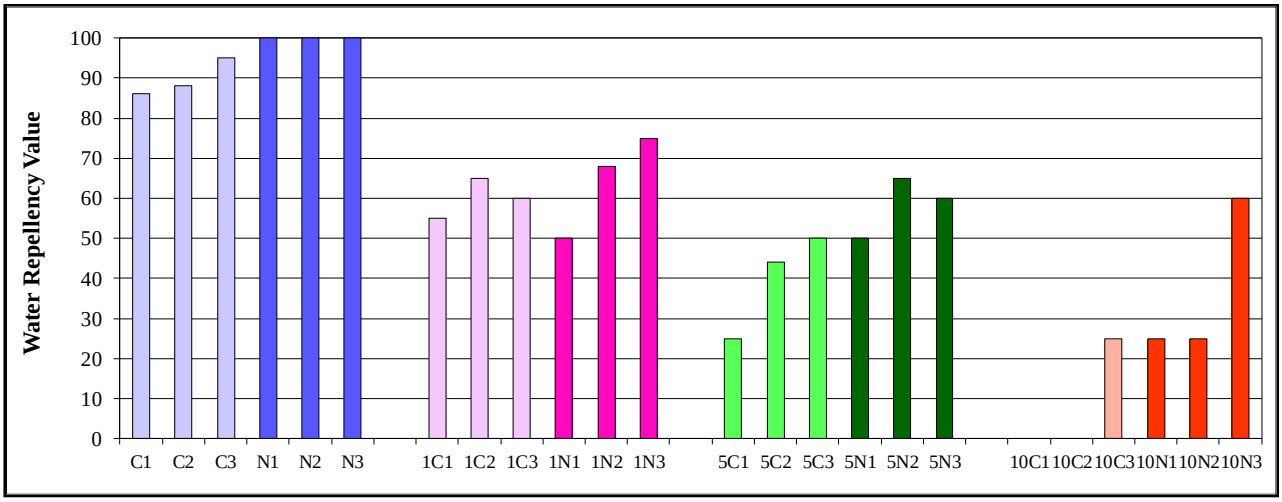

Şekil 12. Water repellency values

When we examined the water repellency values of treated and unwashed samples, the water repellency values of samples treated with nano chemicals were higher than those of conventional chemicals. While the use of classical chemicals increases the effect by increasing the concentration, even at the lowest concentration in the nano chemicals the effect is high. When the effects after washing are examined; the decrease in the effect of water repellency after 1 and 5 washes is greater in samples treated with conventional chemicals. After 10 washes, only the water-repellent effect of the nano chemical at the highest concentration continues and this effect is moderate.

➢ **Oil Repellency Results**

The oil repellency values of water-oil repellent fabrics were given in Table 6. All samples with 1, 5 and 10 washes showed no oil repellency.

Table 6. Oil repellency values

Chemical	Oil repellency values
C1	4
C2	4
C3	6
N1	4
N2	4
N3	6

The oil repellency values of both classic and nano chemicals were found to be the same in Table 6. In particular, the oil repellency values are highest at the highest concentration of 80 g/l. However, these two chemicals are not durable to washing.

3.3. Evaluation of Handle Results

- **Circular Bending Rigidity Results**

The results of circular bending rigidity of the fabrics treated with different softeners and untreated fabrics were given in Figure 13.

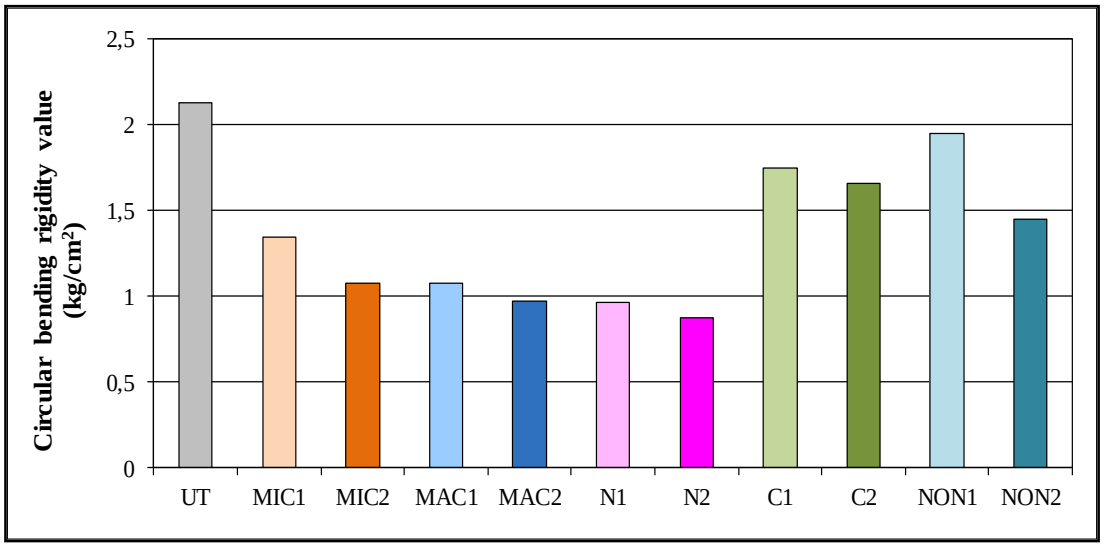

Figure 13. Circular bending rigidity results

The bending rigidity of the untreated sample is higher than those of others. Based on the results, it appears that all treated samples are provided with a soft feel. Especially, the bending strengths of fabrics treated with nano and macro silicones are the lowest. As the concentration of the softener increased, the softness effect also increased.

- **Bending Resistance Results on Shirley Stiffness Tester**

The results of bending resistance of the fabrics treated with different softeners and untreated fabrics were given in Figure 14.

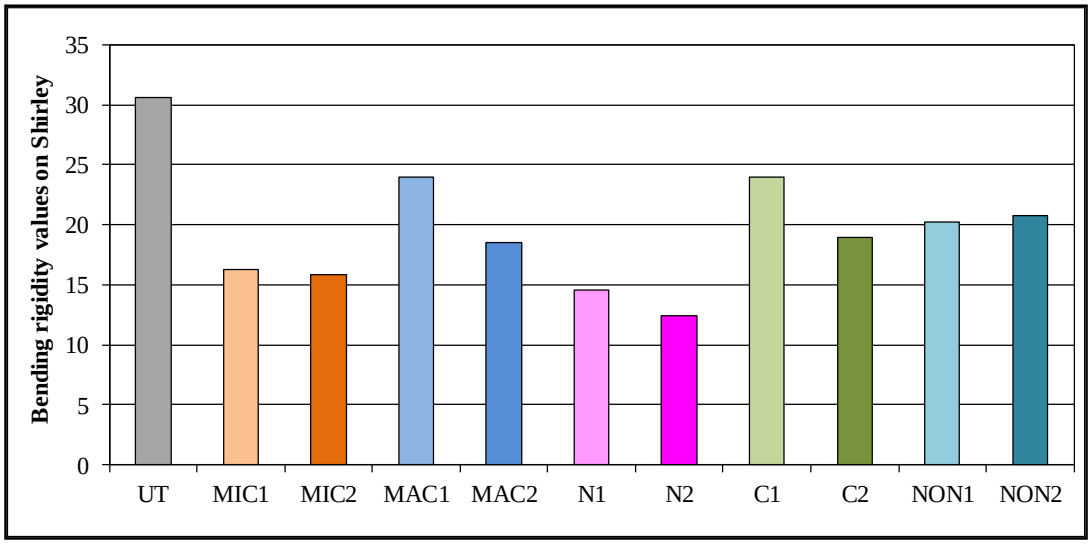

Figure 14. Bending resistance results on Shirley tester

Since the bending resistance data of the treated fabrics is lower than the untreated one, it been observed that the softness effect is obtained in all samples. However, the most softness effects were provided with nano silicone and micro silicone. The effect of concentration was seen in all samples. As the concentration of the softener increased, the effect of softness increased.

➢ **Friction Coefficient Results on Frictorq Tester**

The results of friction coefficient of the fabrics treated with different softeners and untreated fabrics were given in Figure 15.

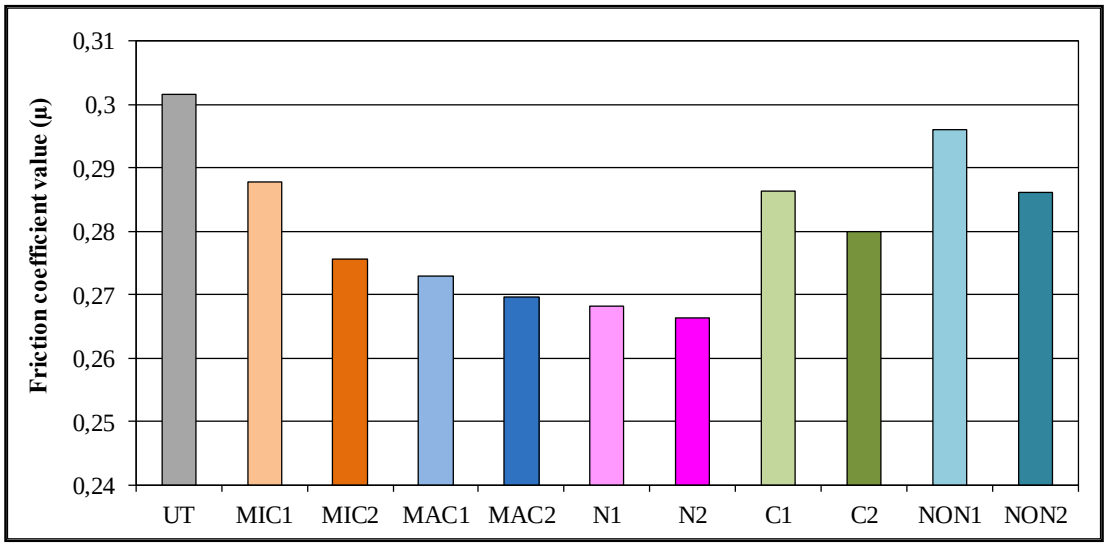

Figure 15. Friction coefficient results

When the friction coefficient results measured in Frictorq are examined; the values of all treated fabrics were lower than that of untreated one. Particularly, the fabrics treated with nano

silicone and macro silicone had the lowest friction coefficient values. As the softener concentration increases, the friction coefficient values decrease. This shows that the surface slipperiness of the fabric increases.

4. Conclusion

The aim of this study is to compare the performances of nano and conventional chemicals in with wrinkle resistance, water-oil repellency and softening treatments of cotton woven fabrics. We can summarize the results obtained as follows:

- When the results of the wrinkle resistance treatment are examined; the wrinkle recovery angles of nano chemical were higher than those of conventional ones. There is not much difference in the breaking strength values. The effect increased at high concentration. For this reason, the use of nano chemical is more advantageous than the conventional one.
- The effect of water repellency was higher in nano-treated samples than in conventional ones. Nano products are effective even at low concentration. However, the durability to washing is very low. There is no difference between oil repellency values of both conventional and nano chemicals. But, these two products are not durable to washing.
- In general, when the handle evaluation tests are examined; the softest and slippery effects were obtained by using nano, micro and macro silicones. At higher concentration, a softer effect was achieved.
- When all these results are evaluated; it has been found that the use of nano-sized product was more successful in terms of both performance and washing durability than conventional ones. For this reason; it can be said that the wide surface area of the nano products is that they occupy more space and more in the unit area than the classical micro size because they are in a small size. Moreover, the advantage of being in the nano size allows the fibers to penetrate better and the desired effect can be achieved by using less amount of material. High value-added textile products produced using nanotechnological products have an important place today and this will continue to increase for the textile industry in the future.

References

Sawhney, A.P.S., Condon, B., Singh K.V., Pang S.S., Li G., Hui D. (2008). Modern applications of nanotechnology in textiles. *Textile Research Journal*, 78(8), 731-739.

Qian, L., Hinestroza, P.J. (2004). Application of nanotechnology for high performance textiles. *Journal of Textile and Apparel, Technology and Management*, 4(1), 1-7.

URL-1: https://www.nano.gov, (Access Date: April 27, 2018).

Mariana, R. (2015). Nano technology in textile industry [PDF document]. Retrieved from Lecture Notes Online Web site: https://pdfs.semanticscholar.org/1e0a.pdf

URL-1: http://vizyon2023.tubitak.gov.tr, (Access Date: April 27, 2018).

Aktan, B. (2011). *Tekstil Atık suyunda TiO_2 Nano Partiküllerinin Oluşumu, Taşınımı ve Kimyasal Arıtımı.* MSc Thesis, Pamukkale University, Institute of Science and Technology, Denizli.

Patra, J.K., Gouda, S. (2013). Application of nanotechnology in textile engineering: An overview. *Journal of Engineering and Technology Research,* 5(5), 104-111.

Cireli, A., Kutlu, B., Onar, N., Erkan, G. (2006). Tekstilde ileri teknolojiler. *Tekstil ve Mühendis,* 13(61), 7-20.

URL-1: https://www. nanoshel.com, (Access Date: April 27, 2018).

URL-1: https://www.rpi.edu, (Access Date: April 27, 2018).

Gokarneshan, N., Suvitha, L., Maanvizhi, M. (2015). Nano finishing of cotton fabrics. *International Journal of Applied Engineering and Technology*, 5(3), 63-75.

Kwon, Y.J., Kim, K.H., Lim, C.S., Shim, K.B. (2002). Characterization of ZnO nanopowders synthesized by the polymerized complex method via an organochemical route. *Journal of Ceramic Processing Research,* 16(3), 146-149.

Lee, H.J., Yeo, S.Y., Jeong, S.H. (2003). Antibacterial effect of nano sized silver colloidal solution on textile fabrics. *Journal of Materials Science,* 38, 2199-2204.

Dura'n, N., Marcato, P.D., De Souza, G.I.H., Alves, O.L., Esposito, E. (2007). Antibacterial effect of silver nanoparticles produced by fungal process on textile fabrics and their effluent treatment. *Journal of Biomedical Nanotechnology,* 3, 203-208.

Xin, J.H., Daoud, W.A., Kong, Y.Y. (2004). A new approach to UV blocking treatment for cotton fabrics. *Textile Research Journal,* 74, 97-100.

Fei, B., Deng, Z., Xin, J.H., Zhang, Y., Pang, G. (2006). Room temperature synthesis of rutile nano rods and their applications on cloth. *Nanotechnology,*17, 1927-1931.

Vigneshwaran, N. (2006). Functional finishing cotton fabrics using zinc oxide nanoparticles. *Bulletin of Materials Science,* 29(6), 641-645.

Qi, K., Chen, X., Liu, Y., Xin, J.H., Mak, C.L., Daoud, W.A. (2007). Facile preparation of anatase/SiO_2 spherical nanocomposites and their application in self-cleaning textiles. *Journal of Materials Chemistry,* 17, 3504-3508.

Wong, Y.W.H., Yuen, C.W.M., Leung, M.Y.S., Ku, S.K.A., Lam, H.L.I. (2006). Selected applications of nano technology in textiles. *Autex Research Journal,* 6(1), 1-10.

URL-1: https://www.ic.gc.ca/textiles, (Access Date: April 27, 2018).

URL-1: https://www.umweltbundesamt.de, (Access Date: April 27, 2018).

Rezwan, M., Farhatun, N. (2017). Application of nanotechnology in the field of textile. *IOSR Journal of Polymer and Textile Engineering,* 4(1), 1-6.

Joshi, M., Bhattacharyya, A. (2011). Nanotechnology-a new route to high performance functional textiles. *Textile Progress,* 43(3), 155-233.

URL-1: https://www.nanotex.com, (Access Date: April 27, 2018).

URL-1: https://www.azonano.com, (Access Date: April 27, 2018).

URL-1: https://www.nanowerk.com, (Access Date: April 27, 2018).

TS EN ISO 6330 standard, 2012.

DIN 53890 standard, 1972.

EN ISO 13934-1 standard, 2013.

AATCC 22 standard, 2010.

AATCC 118 standard, 1997.

ASTM D4032-08 standard, 2016.

ASTM D1388-08 standard, 2008.

Lima, M., Hes, L., Martins, J. (2003, June). Frictorq, a Novel Fabric-to-Fabric Friction Tester: from Concept to Prototype. *3rd International Conference on Advanced Engineering Design*, Prague-Czech Republic.

Photochromic Textiles

E. Perrin AKÇAKOCA KUMBASAR[1*], Seniha MORSÜMBÜL[1]

[1] Ege University, Faculty of Engineering, Department of Textile Engineering, İzmir, Turkey

[*]**Corresponding author:** perrin.akcakoca@ege.edu.tr

Abstract

In this study, commercial photochromic dye capsules were applied to cotton fabric and the performance properties of the fabrics were evaluated. It has been observed that the fabrics have changed their color under UV irradiation and UV protection properties of the fabrics were improved with the application of photochromic dye capsules.

Keywords: Photochromism, Encapsulation, UV-responsive textile, UV protection.

1. Introduction

Photochromic dyes can change their molecular structure and color with UV irradiation and these dyes returns to its original state when the UV light source is removed. There are various types of photochromic dyes such as inorganic and organic photochromic dyes. However spiropyran, spirooxazine, naphthopyran, diarylethene and fulgid based photochromic dyes which exhibit photochromism according to pericyclic reactions are the most widely used dyes in the photochromic applications (Figure 1) (Corns et al., 2009; Dawson, 2010; Crano and Guglielmetti, 1999; Bamfield, 2001).

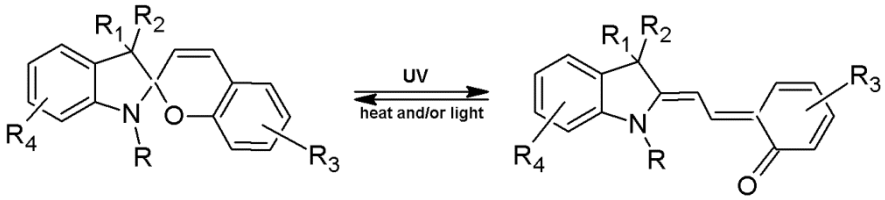

R: alkyl; R_1, R_2:alkyl (usually both methyl); R_3, R_4: H, halogen, nitro, etc.

Figure 1. Schematic representation of photochromic reaction (Bouas-Laurent and Dürr, 2001).

Photochromic dyes have been used in the optical industry for the first time and the usage possibilities of these dyes in different areas have been improved over time with the development of new technologies. Photochromic dyes have a potential to provide new fashion effects and functional properties such as UV protection, camouflage in the textile industry (Kumbasar et al., 2016). However these dyes are water-insoluble and sensitive to the environmental conditions (Billah et al., 2008; Kumbasar et al., 2016). In order to use photochromic dyes in the textile industry, these dyes are encapsulated with a polymer and then the encapsulated photochromic dyes are applied to the fabric.

Encapsulation is a coating process of a core material such as liquid droplet, solid particle or gas by a polymeric shell material. This process provides benefits such as protecting the encapsulated core from atmospheric conditions, improving the operability of the application, extending the life duration of the core material and increasing the stability. Encapsulation method, which is used in many industrial applications such as food, medicine, agriculture, is also used in many different applications in textile field such as flame retardants, odorants, phase-changing materials and liposomes (Bansode et al., 2010; Benita, 1996; Ghosh, 2006).

In the literature about textile applications, encapsulation methods such as interfacial polymerization, in-situ polymerization, emulsification-solvent evaporation and spray drying

have been used for the encapsulation of photochromic dyes. In these studies, polymers such as polystyrene, ethyl cellulose, polymethyl methacrylate, polyurethane, chitosan and melamine were used as shell materials and photochromic dyes based on diarylethene, spirooxazine and naphthopyran were used as core materials (Feczkó et al., 2011; Fan et al., 2015; Morsümbül et al., 2018).

In this study, performance characteristics of commercially produced photochromic dye capsules on textile were investigated.

2. Materials and Methods

100% cotton fabrics were used in the applications. Photochromic dye capsules (ITOFINISH UV MAGENTA) and the binder (ITOBINDER AG) were kindly provided by LJ Specialities Ltd.

The photochromic dye capsules (10, 20 and 40 g/l) were applied to the fabric by padding method (pick up: 100%) using 50 g/l binder. After the application, the samples were dried and then fixed at 150°C for 5 minutes.

UV protection factor (UPF) values of the fabrics were measured with Labsphere UV 2000F device according to standard AS/NZ 4399:1996.

Color measurements were carried out by spectrophotometer (HunterLab ProScan) before and after UV irradiation (ABET Sunlite Solar Simulator).

3. Results and Discussion

Photochromic fabric images before and after UV irradiation are shown in Figure 2. The samples have changed their color with UV light effect**.**

The color differences (ΔE) between the background (before UV irradiation) and developed colors after UV irradiation are shown in Figure 3. UPF values of the samples are also shown in Figure 3.

ΔE and UPF values of the samples have increased with the increase of the capsule concentration. UV protection values of the fabric have reached the excellent level (50+ UPF) after the application of photochromic dye capsules.

Before UV irradiation ***After UV irradiation***

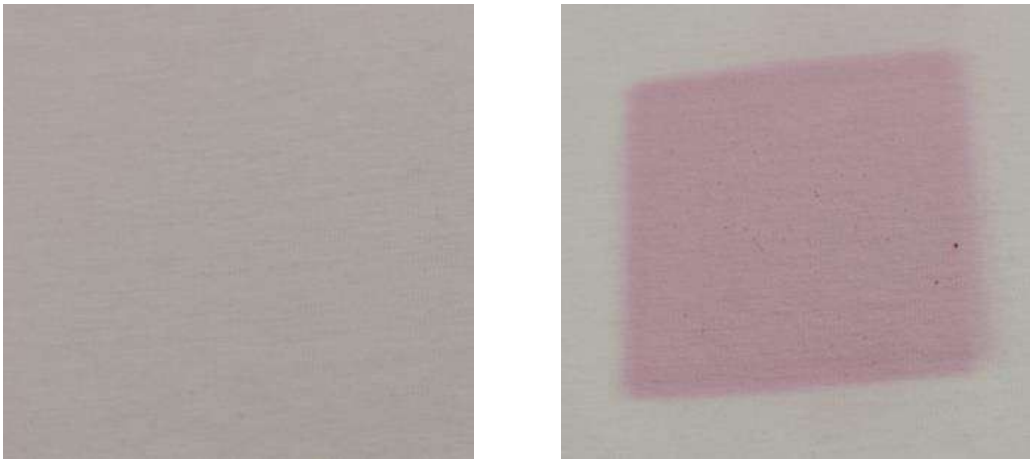

Figure 2. Images of the samples before and after UV irradiation.

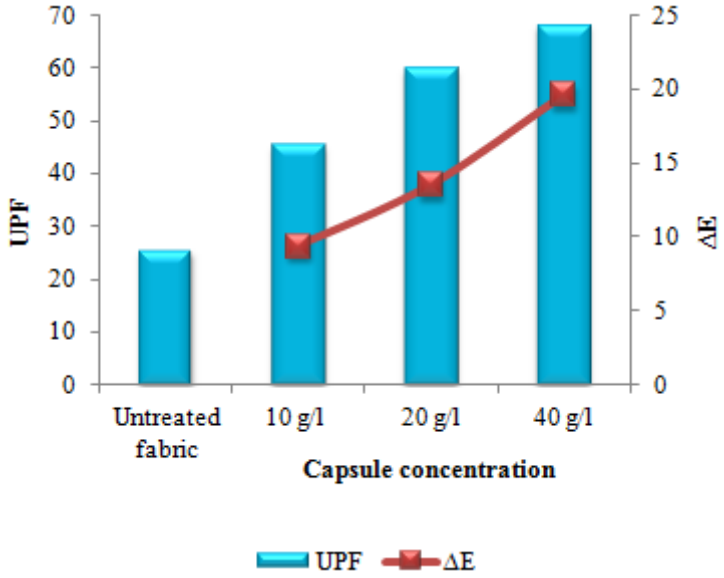

Figure 3. ΔE and UPF values of the samples.

4. Conclusion

Commercial photochromic dye capsules have been applied on cotton fabrics with binder by pad-cure process. After the applications, the fabrics were evaluated by color and UV transmittance measurements.

The samples have changed their colorless form to colored one by UV irradiation and this photochromic effect is increased with the increase of the capsule concentration. It was observed that the photochromic fabrics provide excellent protection from UV radiation (50+ UPF).

Acknowledgment

The authors would like to gratefully acknowledge Ege University, scientific research projects through the project no. 18-TKUAM-003 for financial support to this research project.

References

Bamfield, P., (2001). *Chromic Phenomena The Technological Applications of Colour Chemistry*, Cambridge, UK The Royal Society of Chemistry.

Bansode, S. S., Banarjee, S. K., Gaikwad, D. D., Jadhav, S. L. and Thorat, R. M., (2010). Microencapsulation: A Review, *International Journal of Pharmaceutical Sciences Review and Research*, 1 (2), 38-43.

Benita, S., (1996). *Microencapsulation: Methods and Industrial Applications*, New York, USA, Marcel Dekker, Inc.

Billah, S.M.R., Christie, R.M. and Shamey, R. (2008). Direct coloration of textiles with photochromic dyes. part 1: application of spiroindolinonaphthoxazines as disperse dyes to polyester, nylon and acrylic fabrics, *Coloration Technology*, 124(4), 223–228.

Bouas-Laurent, H. and Dürr, H., (2001). Organic Photochromism, *Pure Appl. Chem*., 73(4), 639-665.

Corns, S.N., Partington, S.M. and Towns, A.D. (2009). Industrial organic photochromic dyes, *Coloration Technology*, 125, 249-261.

Crano, J. C. and Guglielmetti, R. J. (1999*). Organic Photochromic and Thermochromic Compounds: Volume 1: Main Photochromic Families*, New York, Plenum Press.

Dawson, T.L., (2010). Changing colours: now you see them, now you don't, *Coloration Technology*, 126, 177-188.

Fan, F., Zhang, W. And Wang, C., (2015), Covalent bonding and photochromic properties of double-shell polyurethane-chitosan microcapsules crosslinked onto cotton fabric, *Cellulose*, 22(2), 1427-1438

Feczko, T., Varga, O., Kovacs, M., Vidoczy, T. and Voncina, B., (2011). Praparation And Characterization Of Photochromic Poly(Methyl Methacrylate) And Ethyl Cellulose Nanocapsules Containing A Spirooxazie Dye, *Journal Of Photochemistry And Photobiology A: Chemistry*, 22, 293-298.

Ghosh, S.K., (2006). *Functional Coatings by Polymer Microencapsulation*, Weinheim, WILEY-VCH Verlag GmbH & Co. KGaA.

Kumbasar, E. P. A., Çay, A., Morsunbul, S. and Voncina, B., (2016). Color build-up and UV-protection performance of encapsulated photochromic dye-treated cotton fabrics, *AATCC J. Res*, 3(2), 1-7.

Morsümbül, S., Akçakoca Kumbasar, E.P. and Çay, A., (2018), Encapsulated Photochromic Dye by Spray Drying on Cotton Fabrics, *18th AUTEX World Textile Conference*, June 20-22, Istanbul, Turkey.

Effect of Pique Pattern Printing on Thermal and Handle Properties of Fabrics

Serhat KARAKAYA[1*], Gamze SÜPÜREN MENGÜÇ[2], Arif Taner ÖZGÜNEY[3], Nilgün ÖZDİL[3], Gonca ÖZÇELİK KAYSERİ[2]

[1]Bati Basma Sanayi R& D Center, İzmir, Turkey
[2]Ege University, Emel Akın Vocational Training School, İzmir, Turkey
[3]Ege University, Faculty of Engineering, Department of Textile Engineering, İzmir, Turkey

[*]**Corresponding Author:** serhatkarakaya@batibasma.com.tr

Abstract

Fabrics woven in pique construction have different thermal and handle properties as compared with satin or plain weave fabrics. There are numerous studies in the literature concerning fabric construction and thermal insulation properties of these fabrics. In case of printing industry, pique pattern could also be given to the fabric by printing method. It could be applied to the both fabric surfaces and can be used to change handle and thermal properties of the fabrics. In this study, 4 different pique printing was applied to the plain weave woven fabric surfaces. Thermal resistance and handle properties such as roughness and circular bending rigidity of the fabrics were measured and compared.

Keywords: Pique pattern, printing, circular bending rigidity, thermal properties, roughness.

1. Introduction

Pique (pronounced "pi-kay" or "pee-kay") can refer to either a woven or a knit fabric, although it is most commonly associated with knits. In both instances, the fabric is characterized by having a visible texture due to the way the fabric is made. Woven versions are created on a dobby loom, and knits use a special kind of needle and stitch structure that forms the design (URL-1). Cotton is used in the production of these structures (URL-2).

These fabrics are produced with raised effect either in warp or weft direction and are usually characterized by cords running along the length of the fabric formed by floats or stuff yarns. They may be produced in either dobby or jacquard loom. They are generally made of spun cotton yarn. Bird's eye pique has small cord design along the fabric width using stuffer yarns. Bull's eye pique has big cord design. They have cords running across the width of the fabric. Bedford cord is a type of pique fabric, which has bold cords running along the fabric length. It is heavy and durable. It is widely used in upholstery, trousers, uniforms etc. (URL-3).

Pique's weave features cotton yarn characterised by raised parallel cords or fine ribbing. This gives the material a subtle pattern and texture – which can only be seen up close. It's breathable, durable and easily cared for and has excellent give and comfort. Its breathable nature also ensures that any wearers of pique stay cool (URL-4). Pique fabrics is used for garments such as polo shirts, jackets and hometextiles such as hand towels, curtains, blankets, pijamas etc. (Figure 1)

Figure 1. A pique hometextile (a), Jacket fabric woven in pique weave (b) Appereance of pique fabric (c) (URL-5, URL-6).

There are numerous studies in the literature concerning fabric construction and thermal insulation properties of the fabrics, which have pique structured knitted. However fabric properties of woven fabrics have not been comprehensively investigated. Rosace et al. (2016) investigated the the influence of weave structures and silica coatings obtained via sol-gel process on the thermal insulation properties of cotton samples. For this purpose three main

weave structures (plain, satin, and pique) of cotton fabric were selected. According to the results, it was found that fabrics weave and density were found to strongly influence the thermal properties. Thermal absorption progressively increased from pique to plain up to satin-weave; therefore pique provides a cooler feeling.

Pique structure has unique and well known insulation and handle properties. In order to imitate these characteristics; pique pattern can also be given to the fabric by printing method. It can be applied to both back and face fabric surfaces and can be used to change handle and thermal properties of the fabrics. The aim of this study is to investigate thermal and handle properties of pique patterned fabrics which were produced by using printing method.

In this study, 4 different pique printing was applied to the plain weave fabric surface. Thermal resistance, air permeability and handle properties such as kinetic friction coefficient and circular bending rigidity of the fabrics were measured and compared.

2. Experimental Procedures

In order to determine thermal and handle properties of the fabrics, cotton woven fabric was supplied. Properties of the fabric was given in Table 1.

Table 1. Fabric properties

Construction	Yarn Count (Ne) (Weft×Warp)	Yarn Density (Yarns/cm) (Weft×Warp)	Fabric Width (cm)
Plain Weave	30X30	30X27	160

A pique patterned fabric was supplied and in order to imitate its pattern, pique fabric was scanned with high-resolution scanner and then visual works were prepared with Adobe Photoshop CC program. Pattern with a width of 240 cm and a report length of 64 cm was created in study for embossed printing paste. The lines were drawn four different thicknesses including 0.25 mm, 0.50 mm, 1 mm and 1.5 mm (Table 2), which are used to form different height levels in printing. Thereafter, printing process was conducted on the plain weave fabric.

Table 2. Line Thickness values for the adjustment of printing height

Line thickness (mm)			
0.25	0.50	1.00	1.50

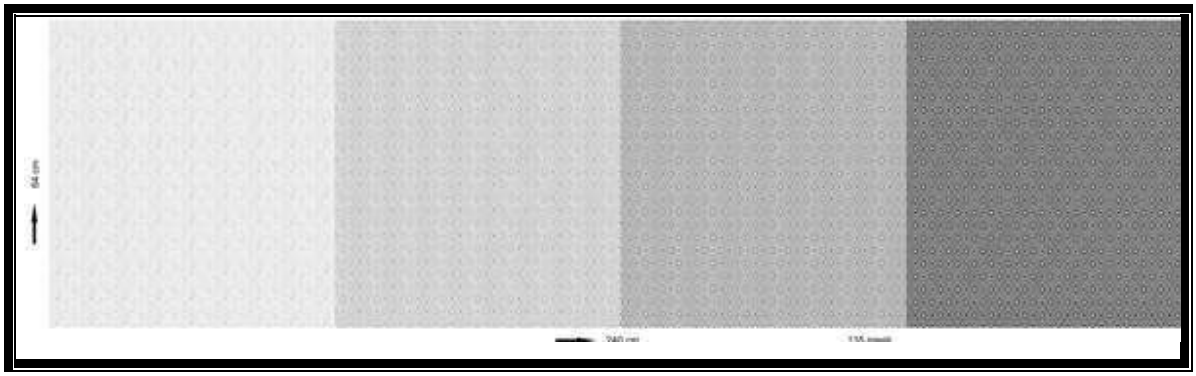

After pretreatment processes including the singeing (applied by using Osthoff-Senge model singeing machine, 100 m/min operation speed, direct beck position), desizing (enzymatic treatment), rinsing, bleaching (with hyrogen peroxide and50 m/min operation speed) and drying, pigment printing was applied on Zimmer model rotation printing machine. Printing application was given in four different printing thicknesses. These effects were obtained by changing the printing agent quantities, given in Table2. After the treatment, fabrics were conditioned under standard atmosphere conditions (20 °C±2 °C temperature, 65% ± 4% RH).

Thickness value was determined according to BS EN ISO 5084:1997 by using the pressure weight as 200 grams. It is measured by determining the distance between the pressure foot and the reference plate on where the fabric sample is placed.Thermal resistance properties of the fabrics were tested by SDL Atlas M259B Sweating Guarded Hotplate instrument (Figure 2).

Figure 2. Hotplate instrument

Hotplate conforms to ISO 11092 and this standard specifies methods for the measurement of the thermal resistance and water vapor resistance, under steady state conditions.

The Sweating Guarded Hotplate (often referred to as the "skin Model") is intended to simulate the heat and mass transfer processes which occur next to the surface of the skin. The physical properties of textile materials which contribute to physiological comfort involve a complex combination of heat and mass transfer. They are time dependant and may be considered in steady state or transient conditions.

Thermal Resistance, Rct, temperature difference between the two faces of a material divided by the resultant heat flue per unit area in the direction of the gradient. The dry heat flux may consist of one or more conductive, convective and radiant components. Rct expressed in square meters kelvin per watt, is a quantity specific to textile materials or composites which determines the dry heat flux across a given area in response to a steady applied temperature gradient (Instruction Manual).

Air permeability of the fabrics were measured by using Textest FX 3300 instrument. Circular bending rigidity of the fabrics was tested with SDL Atlas Digital Pneumatic Stiffness Tester (Fig. 3a). In order to determine the kinetic friction coefficient of the experimental fabrics, Frictorq instrument (Fig. 3b) was used.

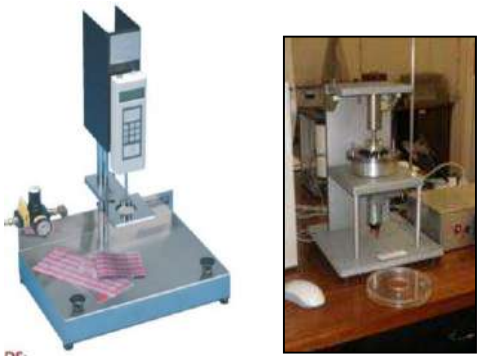

(a) (b)

Figure 3. Circular bending rigidity tester (a), Frictorq instrument (b) (URL-7, URL-8)

Frictorq Instrument is designed to measure the Coefficient of Friction, μ, in 2D flexible structures such as Frictorq woven fabrics, knitted fabrics, nonwovens and soft papers (tissue). In this model, friction coefficient is calculated from the friction reaction torque measured by means of a high sensitivity torque sensor, the normal load created by the contact sensor and a geometrical parameter (Fig. 2d).

$T = 3\,F_a\,r$ *(1)*

$Fa = \mu N$ and (2)

$N = P/3$, *(3)*

where *P* is the vertical load, the coefficient of friction is then expressed by the formula 4 (Lima et al.,2009) :

$$\mu = \frac{T}{P \cdot r} \quad (4)$$

After the measurements all test results were evaluated statistically. ANOVA and Student-Newman-Keuls tests were conducted to determine whether the effect of printing height on fabric properties are statistically significant at 95 % confidence level ($p<0.05$)

3. Experimental Results and Discussion

Results of dimensional properties of the fabrics were given in Table 3.

Table 3. Dimensional properties of the fabrics

	Mass per Unit Area (g/m^2)	**Thickness (mm)**
Unprinted Fabric	119,0	0,21
Low Height Printed Fabric	120,7	0,28
Medium Height Printed Fabric	122,7	0,30
High Height Printed Fabric	124,0	0,34
Very High Height Printed Fabric	125,0	0,34

As it can be seen from Table 3, fabric weight and thickness increase after printing processes as expected.

Thermal resistance results are given in Figure 4 and Table 4.

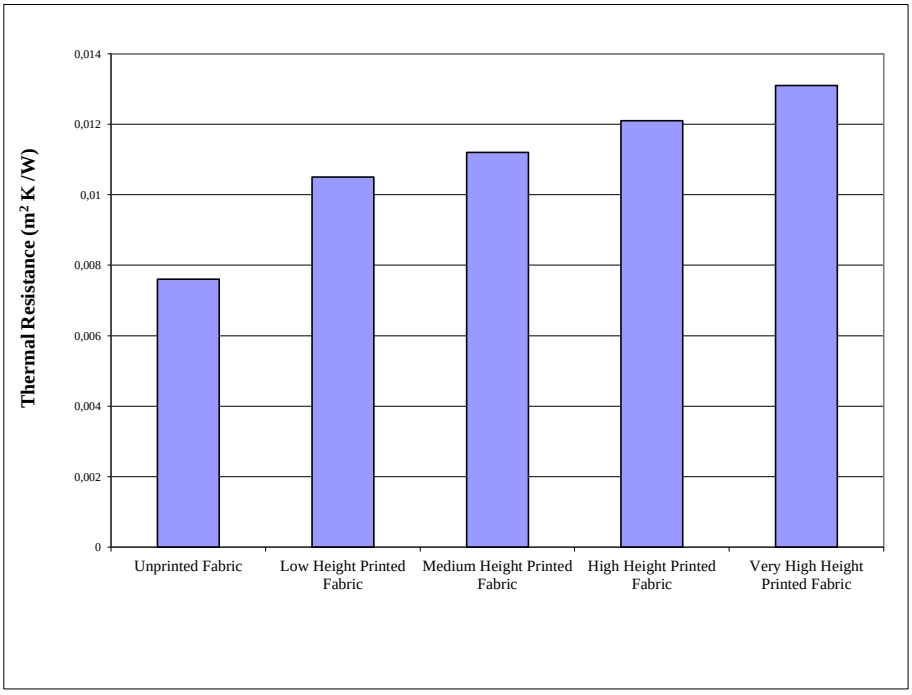

Figure 4. Thermal resistance test results

Table 4. Student-Newman-Keuls Test Results for Thermal Resistance Values

Printing Type	N	Subset 1	2	3	4	5
Unprinted Fabric	3	0,007599				
Low Height Printed Fabric	3		0,010504			
Medium Height Printed Fabric	3			0,011203		
High Height Printed Fabric	3				0,012100	
Very High Height Printed Fabric	3					0,013100
Sig.		1,000	1,000	1,000	1,000	1,000

According to the thermal resistance and statistical evaluation results, it can be concluded that, as the printing height increases thermal resistance value increases as well. It is due to the increase of still air which is entrapped between fabric and skin surface. It forms a heat barrier and increases the insulation property of the fabric.

The effect of printing height on air permeability of the fabrics is given in Figure 5 and statistical evaluation results are given in Table 5.

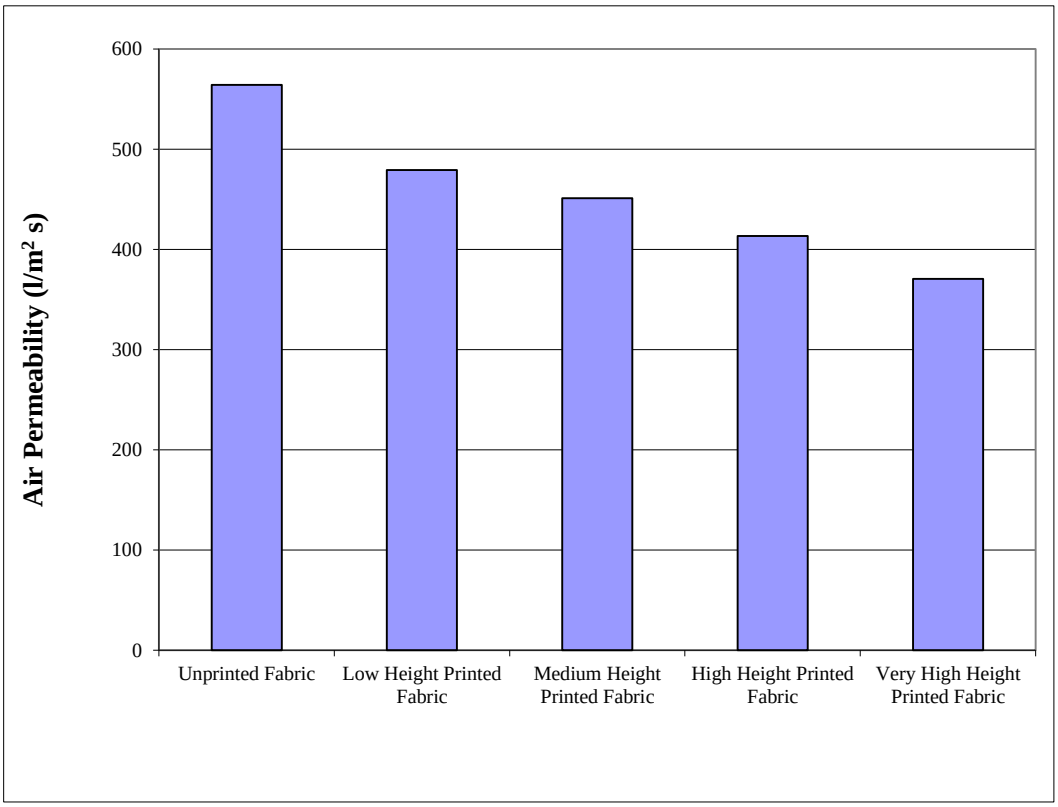

Figure 5. Air permeability test results

Table 5. Student-Newman-Keuls test results for air permeability values

Printing Type	N	Subset				
		1	2	3	4	5
Very High Height Printed Fabric	12	370,67				
High Height Printed Fabric	12		413,33			
Medium Height Printed Fabric	12			451,00		
Low Height Printed Fabric	12				479,00	
Unprinted Fabric	12					564,00
Sig.		1,000	1,000	1,000	1,000	1,000

According to the results, air permeability of the unprinted fabric is the highest, whereas the fabric having very high height printing has the lowest. It can be revealed that air permeability value decreases as the printing height decreases. This is associated with the decrease in the porosity of the fabrics. The variance between the values is found statistically significant.

Circular bending rigidity test results were given in Figure 6 and Table 6.

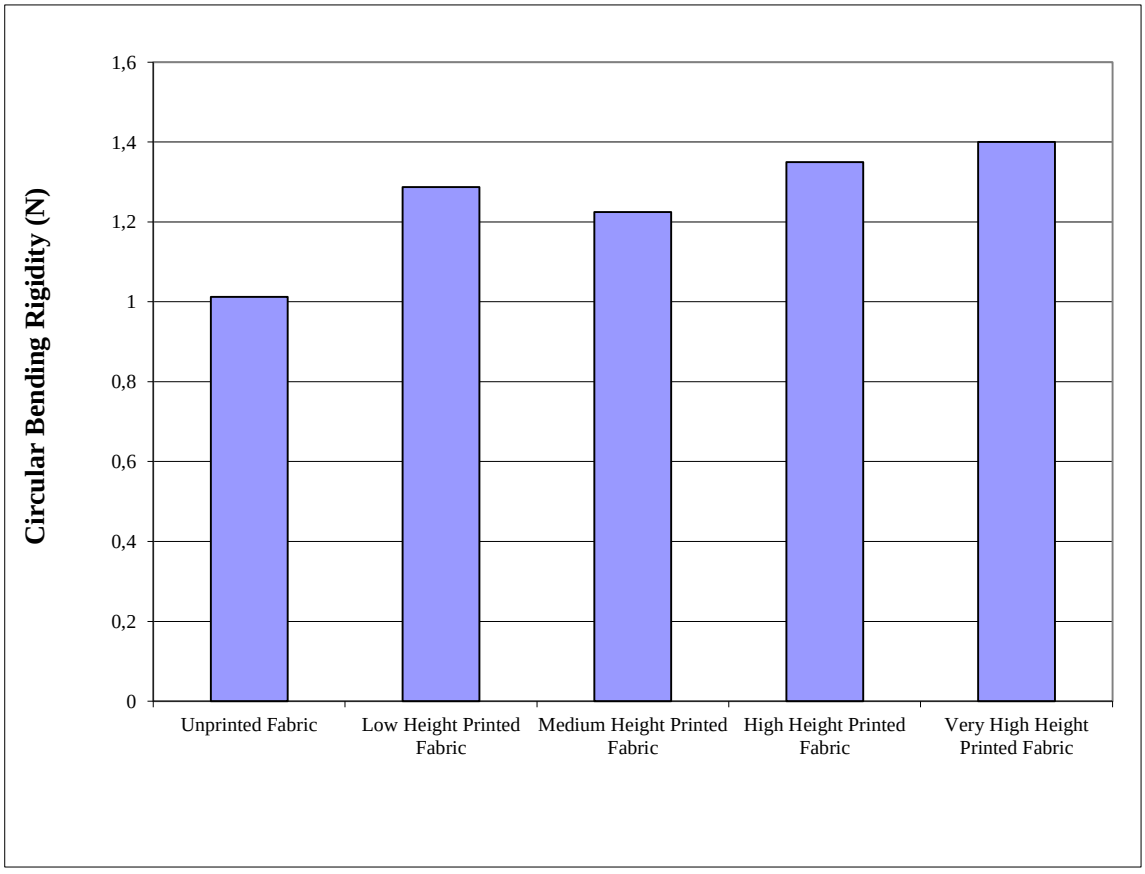

Figure 6. Circular bending rigidity test results

Table 6. Student-Newman-Keuls test results for circular bending rigidity values

Printing Type	N	Subset	
		1	2
Unprinted Fabric	4	1,0125	
Medium Height Printed Fabric	4		1,2250
Low Height Printed Fabric	4		1,2875
High Height Printed Fabric	4		1,3500
Very High Height Printed Fabric	4		1,4000
Sig.		1,000	0,115

Circular bending rigidity test results indicate that fabrics become stiffer after the printing process. Fabric bending rigidity increases with the increasing printing height. However, difference between the values was not found statistically significant. For this reason printing height affects the stiffness of the fabric to some extent in the same way.

Kinetic friction coefficient results are given in Figure 7. According to the kinetic friction coefficients and statistical evaluation results, it can be denoted that unprinted fabric has the smoothest surface and very high height printed fabric has the roughest. The higher the printing height on a fabric is applied, the higher the kinetic friction coefficient it has. Therefore, after printing treatment, it was found that fabrics become rougher.

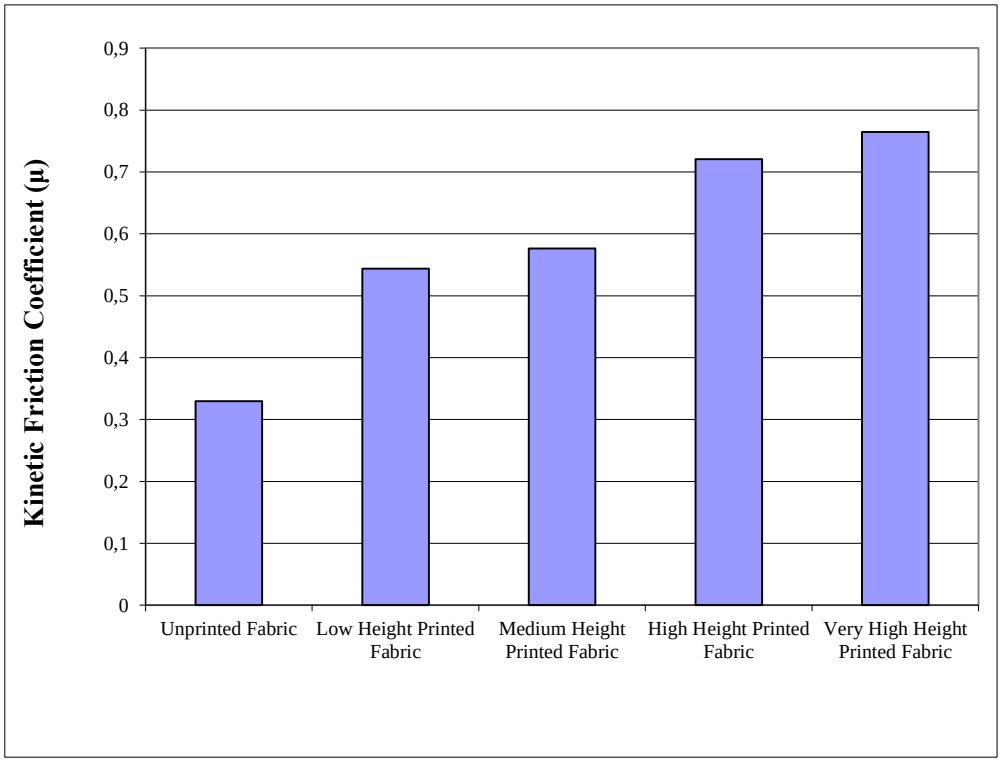

Figure 7. Kinetic friction coefficient test results

Table 7. Student-Newman-Keuls test results for kinetic friction coefficient values

Printing Type	N	Subset 1	2	3	4
Unprinted Fabric	6	0,3294			
Low Height Printed Fabric	6		0,5439		
Medium Height Printed Fabric	6		0,5766		
High Height Printed Fabric	6			0,7208	
Very High Height Printed Fabric	6				0,76447
Sig.		1,000	,091	1,000	1,000

4. Conclusion

Pique fabrics are used in many different areas such as clothing and home textile industry. This pattern can be constructed on fabric both by knitting and weaving techniques. In addition to this, it can be supplied also by printing technique.

In this study, different pique printing was applied to the plain weave woven fabric surfaces and the effect of printing height on thermal resistance, air permeability and handle properties such as kinetic friction and circular bending rigidity of the fabrics were measured and compared.

According to the results, it was found that, printed fabrics were thicker and heavier than unprinted fabrics as expected. After the printing process, fabrics become more resistant to heat transfer. Due to the increase of the printing height, volume of the entrapped air increases and fabric has better insulation property. Thermal resistance value of the very high height printed fabric was found nearly 74% higher than the unprinted fabric. Besides, air permeability of the fabrics decreases after printing, due to lower porosity for about 38%. Fabrics become stiffer after printing. However increase in circular bending rigidity is only around 34%.

According to all these results, it can be concluded that, pique printing increases insulation performance, while not increasing circular bending rigidity as much. Kinetic friction coefficient of the fabric increases. Pique pattern creates a rough surface and it gives fabric unique properties.

Although pique pattern is produced both by knitting and weaving technologies, manufacturing of this surface by printing method is a progressive approach. All types of patterns could be easily formed on fabric surface by printing method. Production is easier, cheaper and efficient. In addition to these, the fabrics have good thermal properties. For all these reasons, it can be strongly suggested for the finishing companies.

References

URL-1: https://www.leaf.tv/articles/what-is-a-pique-shirt/ (Erişim Tarihi: 10 Haziran 2018).

URL-2: http://textilescommittee.nic.in/writereaddata/files/publication/gar9.pdf (Erişim Tarihi: 10 Haziran 2018).

Subject: Fabric Studies Unit 3 - Special weaves and fabrics Quadrant 1 – e-Text, URL-3: http://content.inflibnet.ac.in/data-server/eacharya-documents/56b0853a8ae36ca7bfe81449_INFIEP_79/3/ET/79-3-ET-V1-S1__unit_3.pdf (Erişim Tarihi: 10 Haziran 2018).

URL-4: https://www.acornfabrics.com/blog/what-is-pique-fabric/ (Erişim Tarihi: 10 Haziran 2018).

URL-5: http://www.kagantextile.com/Kagan_Textile_2018_2019_CATALOGUE/?page=18 (Erişim Tarihi: 10 Haziran 2018).

URL-6: https://www.weaversbazaar.com/documents/Janet_Phillips_Masterclass_Projects.pdf ,Masterclass in Weaving with worsted wool yarns, Projects undertaken in a collaboration between Janet Phillips' Masterclass and weaversbazaar, (Erişim Tarihi: 10 Haziran 2018).

G. Rosace, E. Guido, C. Colleoni, and G. Barigozzi, (2016), Influence of Textile Structure and Silica Based Finishing on Thermal Insulation Properties of Cotton Fabrics, *International Journal of Polymer Science*, Volume 2016, Article ID 1726475, 10 pages

Instruction Manual: M259B, Sweating Guarded Hotplate Instruction Manual

URL-7: https://admin.sdlatlas.com/public/content/product_brochures/eng_M003F-ENG.pdf (Erişim Tarihi: 10 Haziran 2018).

URL-8: http://aeipro.com/files/congresos/2009badajoz/ciip09_1728_1836.2716.pdf (Erişim Tarihi: 10 Haziran 2018).

Lima, M., da Silva, L.F., Vasconcelos, R., Cunha, J., (2009), Frictorq, Design for the Objective Measurement of Friction in 2D Soft Surfaces, *XIII Congreso Internacional de Ingeniería de Proyectos Badajoz*, 8-10 de Julio de 2009

Needle Puncture Resistance of Fabric Layers used for Micrometeoroids and Orbital Debris (MMOD) Protection

Emrah TEMEL[1*]

[1] Ege University, Engineering Faculty, Textile Engineering Department, İzmir, Turkey

[*] **Corresponding Author:** emrah.temel@ege.edu.tr

Abstract

Micrometeoroids and orbital debris (MMOD) particles are the most important hazards for the astronauts performing extra-vehicular activities (EVA) in low–earth orbit. MMOD particles are micron-sized particles. Micrometeoroids are natural particles that are originating from comets and asteroids, while orbital debris particles are usually aluminum-based particles scattered from space shuttle and satellite debris.

MMOD particles travel at a speed about 10km/h in space called as hypervelocity and have vital hazards for astronauts. A spacesuit fabric composed of average 12-14 layers. Furthermore, 4-5 of these layers are stated to provide micrometeoroid and orbital debris protection. Two methods are generally used to test the MMOD resistance of these protective layers: Hypervelocity ballistic tests and hypodermic needle puncture tests. Hypodermic needles are thus ideal choices to simulate the cutting and puncture threat associated with MMOD particles.

In this study, 3 different types of fabrics used for protection against MMOD particles were investigated with needle puncture tests. Hypodermic needle puncture tests were conducted to both individual fabric layers and to different layer combinations.

For this purpose, needle puncture tests were performed on 100% para-aramid fabric, 100% meta-aramid fabric and PTFE coated glass fabric both individually and in different combinations, using 22 gauge and 26 gauge hypodermic needles.

The quasi-static needle puncture testing was performed using a modified ASTM F-1342 standard with a hypodermic needle held in a chuck replacing the puncture probe at a rate of 250 mm/min. Force measurements were performed on Zwick Universal Tensile Testing Machine using a 2500 N load cell.

Keywords: Micrometeoroid, Orbital debris, Needle puncture test, Needle puncture resistance, Spacesuit, Astronaut garment

1. Introduction

In low-earth orbit, astronauts performing extravehicular activities (EVA) are exposed to the direct threat of micrometeoroid and orbital debris (MMOD) as well as cut and puncture hazards when coming into contact with materials damaged by MMOD (Cwalina et al., 2015).

Extravehicular activity (EVA) exposes an astronaut's space suit to the meteoroid environment for short periods. To prevent meteoroid penetration of the pressure bladder and subsequent decompression of the space suit, protection must be provided to absorb meteoroid impacts (Mc Allum, 1969).

Micrometeoroids are natural particles originating from comets and asteroids while manmade orbital debris consists largely of aluminum based compounds from spacecraft and satellite debris. Micrometeoroid velocities vary widely across the solar system from 11-72 km/s while orbital debris particles in low-earth orbit travel from 1-15 km/s with an average velocity of 9 km/s. These highly energetic MMOD particles are a serious threat to spacecraft as well as EVA missions. As the desired level of MMOD protection increases, the shield weight required typically increases exponentially. Such increases in shielding weight and reduction in flexibility are undesirable for astronauts (Cwalina et al., 2015; Christiansen et al., 2009).

Hypervelocity impacts associated with ballistic missile defense intercepts can produce tens of billions of fragments in excess of several microns in size. While micron-sized (i.e., microdebris) fragments are unlikely to result in structural damage in subsequent encounters with aerospace systems, they are capable of affecting sensitive components associated with these systems. Such components include optical sensors, solar cell arrays, and communication antennae. Microdebris also affects the persistent background signatures associated with impact debris clouds (Kruse et al., 1999).

In February 2015, twenty-six (26) micrometeoroid and orbital debris (MMOD) impact features were found on a returned cover from the International Space Station (ISS). The cover was exposed to MMOD impacts for 1.63 years (from July 2013 to February 2015) before it was returned on the SpaceX CRS-6 mission. It was located at the forward port on ISS pressurized mating adapter 2 (PMA-2), as shown in Figure 1. The cover is a 2-m-diameter multilayer blanket with a beta-cloth exterior surface, which is a Teflon® coated glass fabric.

Figure 1. The cover was exposed to MMOD for 1.63 years at the forward end of PMA-2 (Orbital Debris Quarterly News, 2016).

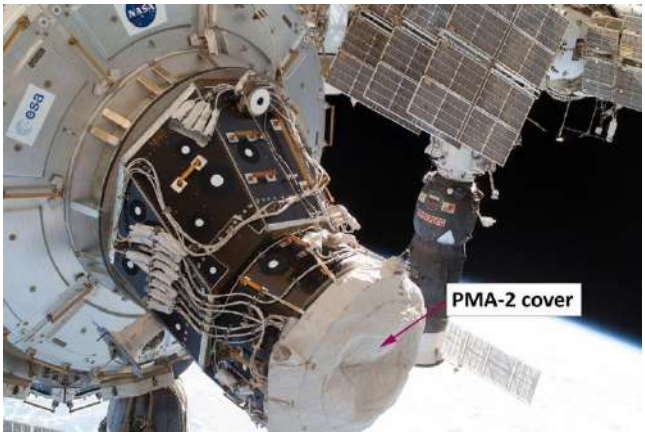

The damages were found on the cover itself as well as straps that were used to hold the cover in place on PMA-2 (Figures 2 and 3).

Figure 2. An overview of the cover including small labels indicating the location of each impact damage found in the inspection (Orbital Debris Quarterly News, 2016).

Figure 3. An impact damage (no.13) that was found on one of the hold-down straps. This damage is shown in front-light on left and through the microscope on right. The hole diameter in the outer beta-cloth layer was 0.75 mm (Orbital Debris Quarterly News, 2016).

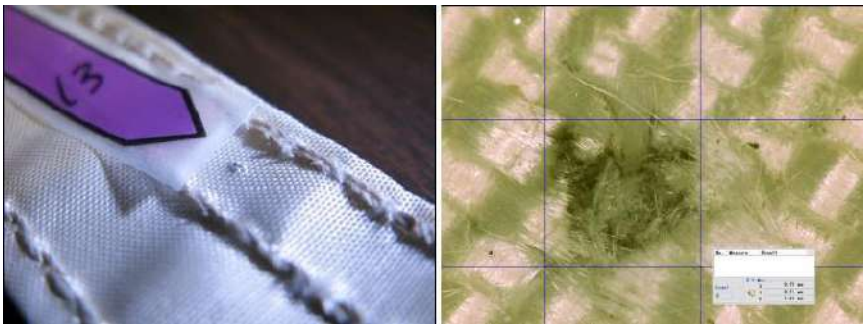

"Figure 4" lists the 10 largest damages found in the inspection and shows a histogram of all damages. The largest damage left a 1.2 mm diameter hole in the external beta-cloth layer of the cover.

None of the damages completely penetrated the cover, which has a mass per unit area of 0.46 g/cm^2.

Figure 4. Damage Size Distribution for the PMA cover inspection. The number of damages found in each size is given in this graphic (for instance, six damages that were greater than 0.3 mm but less than 0.4 mm were found), (Orbital Debris Quarterly News, 2016).

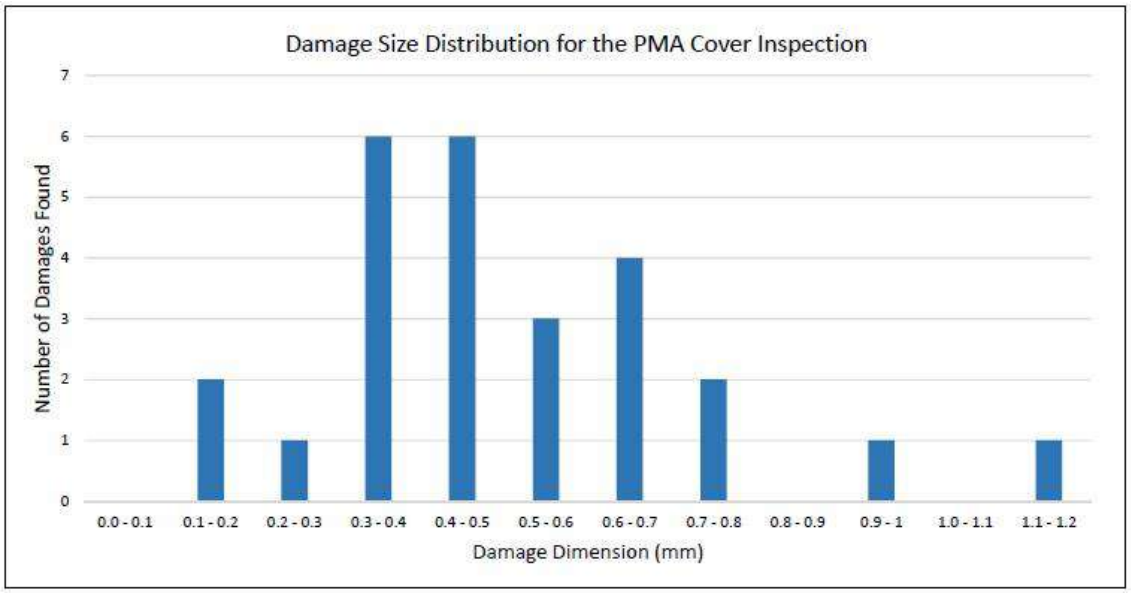

The next steps in the inspection will be to determine how deep the damages extend into the cover and to collect samples for examination in the analytical laboratories at JSC (Johnson Space Center) to determine, if possible, the composition of the impacting particle (Orbital Debris Quarterly News, 2016).

"Hypervelocity Impact Test" and "Quasi-static Hypodermic Needle Puncture Test" are the two methods for determining the micrometeoroid and orbital debris (MMOD) strength of protective layers. Furthermore, Cwalina et al. (2015) revealed that, quasi-static hypodermic needle puncture tests are ideal choices to simulate the cutting and puncture threat associated with MMOD particles (Ryan et al., 2009).

2. Materials and Methods

The quasi-static needle puncture testing was performed using a modified ASTM F-1342 standard with a hypodermic needle held in a chuck replacing the puncture probe at a rate of 250 mm/min. Force measurements were performed on Zwick Universal Tensile Testing Machine using a 2500 N load cell. Needle puncture tests were performed on 100% para-aramid fabric, 100% meta-aramid fabric and PTFE coated glass fabric both individually and in different combinations, using 22 gauge and 26 gauge hypodermic needles. Test samples are given below in Table 1.

Table 1. Description of test samples

Sample	Layers	Number of Layers	Mass per unit area (g/m^2)	Thickness (mm)
1	Para-aramid	1	135	0,24
2	Meta-aramid	1	70	0,26
3	PTFE coated glass fabric	1	660	0,35
4	PTFE coated glass fabric Para-aramid Meta-aramid	3	865	0,85
5	PTFE coated glass fabric Para-aramid x2	3	930	0,83
6	PTFE coated glass fabric Para-aramid x2 Meta-aramid x2	5	1070	1,35

Figure 5. Quasi-static Hypodermic Needle Puncture Test on Zwick Universal Tensile Testing Machine

3. Results and Discussion

The force experienced by the hypodermic needle was recorded by Universal Tensile Testing Machine. 6 different layer combinations were tested by 2 different needle gauges and average load for each lay-up is stated in Table 2.

Table 2. Hypodermic needle puncture test results

Sample code	Load (N)	
	22 gauge needle	26 gauge needle
1	0,267	0,146
2	0,052	0,016
3	2,7	1,45
4	3,006	1,63
5	3,315	1,83
6	3,398	1,88

According to the test results when the fabrics are examined individually it can be clearly seen that PTFE coated glass fabric has the highest strength to needle punctures. Subsequent to PTFE coated glass fabric, para-aramid fabric exhibits higher strength than meta-aramid fabric.

As the results were evaluated, it can be denoted that mass per unit area and coating factor have the major contribution to needle puncture strength. Since “Sample 3” has the highest mass per unit area and has also a coated fabric structure, “Sample 3” demonstrated highest needle puncture strength. However, it can be stated that increment between mass per unit area and needle puncture strength values, is not linear. Therefore, it is considered that the strength value differences are mainly caused by coating factor.

As all specimens were considered it is obviously seen that, as the number of fabric layers increases, the needle puncture strength increases. However, meta-aramid fabric does not provide a significant increase in the needle puncture strength between multi-layer structures. The increase in strength provided by meta-aramid fabric is negligible besides the increase in weight and thickness. This situation is related with the difference between the characteristics of meta-aramid fabric and para-aramid fabric. Meta-aramid has excellent thermal resistance but rather poor mechanical properties for high-performance fiber. Besides that, para-aramid provides unique combinations of toughness, extra high tenacity and modulus and exceptional thermal stability (Jassal and Ghosh, 2002).

When the effect of the needle gauge on the test results is examined, it is seen that the puncture strength of the layers decreases as the needle becomes thinner. During the puncture test, replacing speed of the needles does not change. However, the pressure applied to the fabric surface increases due to the thinning of the needle diameter. Therefore, needles can easily penetrate the fabric surface. This situation emphases reduction in needle penetration load

values. Puncture strength values of 26 gauge needle were rank among 0,016 – 1,88 N, while 22 gauge needle strength values were stated between 0,052 – 3,398 N.

Another problem with the use of narrow diameter needles (26 gauge) is measurement precision. Since the fabric layers do not withstand to narrow (26 gauge) needle punctures, no remarkable differences can be observed between strength values. It can be pointed out that using 26 gauge needle is not convenient and reliable for this study.

4. Conclusion

The current work investigated the effects of needle puncture strength of different fabric layers which are used in spacesuits. Among 3 different materials (meta-aramid, para-aramid, PTFE coated glass fabric), PTFE coated glass fabric was significantly more effective against the puncture threats of hypodermic needles than meta-aramid and para-aramid layers under quasi-static loading conditions. PTFE coated glass fabric both has higher mass per unit area, and has a coated fabric structure than aramid fabric. However, it is thought that the most important difference is caused by the coated structure of glass fabric. Coating fabrics with a suitable material can make them high resistant. For this purpose, para-aramid fabrics generally coated with STF (Shear Thickening Fluid) material in order to exhibit high puncture strength. Decker et al. (2007), revealed that needle puncture resistance of shear thickening fluid (STF) treated para-aramid fabric was found to exhibit significant improvements over neat para-aramid fabric targets of equivalent areal density (Decker et al., 2007). Cwalina et al. (2015) studied the quasi-static needle puncture resistance of STF coated para-aramid fabrics. Needle puncture test results revealed that STF coated para-aramid fabric showed 16,9 N puncture resistance, while neat para-aramid fabric in our study showed 0,267 N.

Another outcome of this study is that the use of high gauge needle (26 gauge) affects the test results negatively. Since the fabric layers do not withstand to narrow needle punctures, no remarkable differences can be observed between strength values. It can be pointed out that using 26 gauge needle is not convenient and reliable for this study.

References

Christiansen, E. L., Arnold, J., Davis, A., Hyde, J., Lear, D., Liou, J. C., Lyons, F., Prior, T., Ratliff, M., Ryan, S., Giovane, F., Corsaro, B. and Studor, B., (2009). Handbook for Designing MMOD Protection, Astromaterials Research and Exploration Science Directorate, NASA Johnson Space Center, NASA/TM–2009–214785.

Cwalina, C. D., Dombrowski, R. D., McCutcheon, C. M., Christiansen, E. L. and Wagner, N. J., (2015). MMOD Puncture Resistance of EVA Suits with Shear Thickening Fluid (STF) – Armor^{tm} Absorber Layers. *Procedia Engineering*, 103, 97 – 104.

Decker, M. J., Halbach, C. J., Nam, C. H., Wagner, N. J.and Wetzel, E. D., (2007). Stab Resistance of Shear Thickening Fluid (STF)-treated Fabrics. *Composites Science And Technology*, 67, pp. 565 – 578.

Jassal, M. and Ghosh, S., (2002). Aramid fibers – An overview, *Indian Journal of Fibre & Textile Research*, Vol. 27, pp. 290 – 306.

Kruse, G. R., Mendes, W. R., Sommers, W. J., Weed, R. A., Nash, K. D. and Mayo, D. V., (1999). Testing and Simulation of Microdebris from Impacts with Complex Targets. *International Journal Of Impact Engineering*, 23, 489 – 500.

McAllum, W. E., (1969). Development of Meteoroid Protection for Extravehicular-Activity Space Suits. *J. Spacecraft*, Vol. 6, No. 11, 1225 – 1228.

Orbital Debris Quarterly News, (2016). MMOD Impacts Found on a Returned ISS Cover, National Aeronautics and Space Administration (NASA) , Volume 20, Issue 3, pp. 4 – 6.

Ryan, S., Christiansen, E. L., Davis, B. A., and Ordonez, E., (2009). Mitigation of EMU Cut Glove Hazard from Micrometeoroid and Orbital Debris Impacts on ISS Handrails, NASA TM-2009-0012274.

The Use Of Different Clay Types For Adsorption Of Reactive Dyes From Textile Wastewater

Nuriye KERTMEN[1], Emriye Perrin AKÇAKOCA KUMBASAR[1*], Saadet YAPAR[2]

[1]Ege University, Faculty of Engineering, Textile Engineering, İzmir, Turkey
[2]Ege University, Faculty of Engineering, Chemical Engineering, İzmir, Turkey

[*]**Corresponding Author:** perrin.akcakoca@ege.edu.tr

Abstract

Adsorption method is one of the most effective methods for removing toxic organic compounds from waste water. The treatments made by the adsorption technique are economical and effective, and the water obtained after the treatment has higher quality. The adsorption method has a wide range of applications in waste water treatment. Reactive dyes in textile waste water are also toxic compounds and can be successfully removed by adsorption. The type of adsorbent used has a great influence on the quality of the water after treatment. Different organic or inorganic adsorbents can be used to remove reactive dyes. In recent years there has been an increase in the use of natural adsorbents, which are particularly cost-effective and don't threaten environmental health. Clay minerals, which humans have been familiar with since the early days of civilization, are also these adsorbents. Clay minerals; are compounds with a large surface area and chemically stable structure, and high adsorption capacity. In addition to the naturally occuring clay minerals like, kaoline, sepiolite, montmorillonite, the modified clays are also effectively used to remove dyes. In this work, studies on the adsorption of reactive dyes with different clay types have been reviewed. Studies have shown that environmentally friendly clay minerals and their modified forms are effective adsorbents for reactive dye adsorption from textile waste water. As a result, clay minerals provide important contributions to reduce water pollution, one of the most important problems of our time.

Keywords: Adsorption, Clay types, Reactive dye, Wastewater.

1. Introduction

Water is one of the most important factors affecting social and economic development in the world. The amount of industrial waste increases due to the increase in industrializationand this increase causes environmental problems and pollution and pollutes water which are one of the most basic requirements for vital activities. Wastewater is one of the types of industrial wastes that causes adverse effects on all living organisms and leads to cause of environmental pollution. The toxic organic compounds which are common components of waste water cause many diseases such as cancer, various lung diseases, skin problems and allergies (Pandey and Ramontja, 2016).

Textile industry, one of the most important industries, also releases colored and toxic waste water. The dyes in textile wastewater affect the vital activities of aquatic creatures through preventingthe light from passing through the water and poisoning as a result of their toxic components such as the metals and aromatic compounds. Therefore they are dangerous to all kind of living organisms(Liu and Zhang, 2007; Zhou et al., 2011; Yagub et al., 2014).

Today, there are over 10,000 different kinds of synthetic dyes with different chemical structures. It is known that more than 10,000 tons of dye are produced all over the world every year. It is estimated that respectively 1-2% and 1-10% of these dyes are released to the environment during production and use (Pandey ve Ramontja, 2016).

Among the dyes, reactive dyes are the most commonly used materials in the textile industry. The water-soluble reactive dyes remain in the dyeing chamber after dyeing and are dangerous in terms of environmental health. For this reason, the elimination of reactive dyes having chemically stable structure is of importantance (Joshi et al., 2004; Asgher and Bhatti, 2012; Yagub et al., 2014).

The studies show that in the last few decades there has been a huge increase in the production and use of organic pollutants and as a result there is a major pollution threat. Although there are different methods for removing organic pollutants in wastewater, cost effective and effective methods should be preferred in industrial terms (Nigam et al., 1996; Annadurai et al., 2002; Pandey and Ramontja, 2016).

Adsorption is considered as an effective and low cost technique to remove highly toxic organic compounds from waste water and the quality of treated water by adsorption is high (Rashed, 2013). The adsorption used in the removal of dyes having toxic character and the products formed by the decomposition of these dyes is a very useful treatment technique (Chen

et al., 2001; Kannan and Sundaram, 2001; Kargı and Özmıhçı, 2004; Abd El-Latif et al., 2010; Adeyemo, 2017).

In the adsorption process, the dissolved substance in a solvent mostly water is collected on the surface of the solid material used as adsorbent. Therefore, the components required to be removed from the waste water accumulate on the adsorbent.According to another definition, in the adsorption process; when the adsorbable solute in the aqueous solution comes into contact with a very porous solid having the ability to adsorband some of the solubilized compounds are collected on this porous solid. During adsorption, the compound adsorbed on the solid is identified as adsorbate and the solid matter held on is called adsorbent.Adsorbate accumulation on adsorbate is defined as adsorption (Rashed, 2013; Adeyemo et al., 2017).

The adsorbent selected is very important for the quality of wastewater treatment (Abd El-Latif et al., 2010; Menkiti and Onukwuli 2011; Adeyemo, 2017).Although organic or inorganic based adsorbents have been used for the waste water treatment, recent studies have been carried out on lower cost, natural and environmentally compatible adsorbents (Crini, 2005; Rashed, 2013; Yagub et al., 2014).

Adsorbents are divided into two groups asnatural and synthetic. Natural adsorbents (coal, clay minerals, zeolites, etc.) are cheaper and adsorption capacities of modified natural adsorbents are high (Rashed, 2013).In order to remove pollutants from the waste water, activated carbon or many organic and inorganic substances havinghigh surface area, porosityand/or functional groupsare used as adsorbents (Joshi et al., 2004).

The increase in the amount of waste water containing dyes leads to the use of more adsorbents, thus increasing the demand for lower cost and higher capacity adsorbents. In recent years, there has been much interest in low cost, easy to find, non-toxic, high cation exchange capacity, large surface area and high adsorption capacity clay minerals as an alternative to commercial adsorbents on the market (Gürses et al., 2006; Adeyemo et al., 2017).

2. Use Of Clay Minerals In Color Removal By Adsorption

Clay is one of the most important adsorbents used in color removal by adsorption such as activated carbon (Zakaria et al., 2009; Adeyemo et al., 2017).Activatedcarbon is often used to remove colored organic compounds and is the most commonly used adsorbent due to its high adsorption capacity(Joan et al., 1997; Chen et al., 2001; Markovska et al., 2001).However, activated carbon has some disadvantages such as limited availability, slow adsorption kinetics and high cost and therefore clay minerals with lower cost and higher adsorption capacity gain

importance in recent years (Abd El-Latif et al., 2010; Adeyemo et al., 2017). As in the case of the clay minerals, the abundance and the low cost of zeolites make them advantageous as adsorbent, but the success of color removal from waste water is not as high as clay (Crini, 2006).

Mankind is familiar with natural clay minerals since the first days of civilization. Clays are generally described as fine-grained minerals in the form of aqueous alumina silicate (Ngulube et al., 2017).Clay minerals have a wide application area due to their wide and structural properties, chemically and mechanically stable structures and adsorption properties of organic molecules (Özcan et al., 2007; Tülin and Gamze 2009; Adeyemo et al., 2017).Through to these properties, clay minerals are effectively used as an alternative to activated carbons for removing different types of dyes (basic, acidic, reactive) from waste water (Liu and Zhang, 2007).

The adsorption characteristics of the clays are not only due to their large surface area and the high porosity; the permanent negative charge in their structure give them the ability to adsorb positively charged compounds through these negative charges(Alkan et al., 2004; Crini, 2006).Among clay species, montmorillonites have the largest surface area and the highest cation exchange capacity (Gisi et al., 2016) and and the market price of these clays is 20 times cheaper than active carbon (Babel and Kurniawan, 2003; Crini, 2006).

Kaolinite and sepiolite are also used for adsorption. Although the existance of permanent negative charge makes the mineral advantageous for adsorption of positevely charged substances, this property is also disadvantage for the adsorption of nonionic organic compounds. Therefore the clay minerals are mostly modified to increase the adsorption capacities by the organic cations (Liu and Zhang, 2007; Gisi et al., 2016).Özdemir et al. (2004) investigated the use of modified sepiolite as an adsorbent for various azo-reactive dyes. Accordingly, sepiolite showed significant improvement in adsorption capacity when they modified the sepiolite surface with the quaternary amine compound. (Ghosh and Bhattacharyya (2002) reported the improvement of the adsorption capacity of kaolin treated with NaOH solution by removing impurities. Espantaleon et al. (2003) found that acid treated bentonite has higher adsorption capacity than unmodified bentonite. Özdemir et al. (2004) stated that sepiolit and zeolit are not suitable for adsorption of reactive dyes (Reactive Black 5, Reactive Red 239, Reactive Yellow 176) with their natural forms and and therefore should be modified with a suitable quaternary ammoniumcompound.

2.1. Adsorption Of Reactive Dyes With Different Clay Minerals

Numerous studies have been carried out on the use of different clay minerals for the adsorption from textile wastewater. According to the information obtained from these studies; clay minerals show a strong affinity for both cationic and anionic dyes (Crini, 2006).Ay et al. (2002) investigated the effect of particle size, pH, mixing time, mixing speed, initial concentration, adsorbent dose and temperature on adsorption of acidic, basic and reactive dyes (Acid Yellow N7GL, Acid Red N2RBL, Basic Red 2L, Methylene Blue, Reactive Red BB and Reactive Yellow RR) from textile waste water by using bentonite Yang and Han (2005), compared adsorption capacities of Cloisite 10A, 15A, 30B and C.I. to for Acid Red 266, Direct Red 80, Reactive Blue 19, Basic Red 2 and Disperse Red 65 dyes and at the end of the study, nanoclays were found to be quite effective in the adsorption of dyes. Özcan et al. (2007) studied the bentonite modified with dodecyl trimethyl ammonium (DTMA)for removal ofreactive dye (Reactive Blue 19) and they found that the modified bentonite is a good adsorbent. Wang and Wang (2008) compared the adsorption capacities of modified montmorillonites with different compounds and untreated montmorillonite for Congo Red dye and and that the most suitable adsorbent for Congo Red was montmorillonite modified with cetyl trimethyl ammonium bromide .Gök et al. (2010) reported that bentonite modified with diamino hexane is a suitable adsorbent for Reactive Blue 19 dye and the adsorption reached the highest level at pH 1.5 and 20 °C. Elemen et al. (2012) used clay modified with hexadecyl trimethyl ammonium bromide (HDTMA) for adsorption, and about 80% of the Reactive Red 141 dye could be removed.Gülgönül (2012) found the adsorption capacity of bentonite modified with hexadecyl trimethyl ammonium bromide for Procion Navy HEXL dye to be about 12 times higher than natural bentonite.Jamshidi et al. (2014) modified montmorillonite with diethylenetriamine (DETA) and studied on the removal of Reactive Blue 29 (RB29) dye and investigated the effect of adsorption time, pH, agitation rate and adsorbent amount on adsorption.Kaur and Datta (2014) studied on the removal of Reactive Red 2 (RR2) dye with montmorillonite.The adsorption properties of the synthesized organophilic montmorillonites were found almost independent of pH and higher than montmorillonite.Vanaamudan et al. (2014) used montmorillonite modified with cetyl trimethyl ammonium bromide (CTAB), activated with sulfuric acid and untreated montmorillonite for the adsorption of activated Reactive Blue 21 (RB21) dye and investigated the effect of time, pH and adsorbent amount on adsorption.As a result of this study, it was found that the adsorption depends on the pH, the amount of adsorbent and the duration.

Armağan et al. (2003) performed sepiolite modification and characterization with hexadecyl trimethyl ammonium bromide (HTAB) and then compared the adsorption capacities of natural and modified sepiolite for Everzol Black B, Everzol Yellow 3RS H/C, and Everzol Red 3BS.Accordingly, the modified sepiolite had ten times higher performance than natural sepiolite.(Alkan et al. (2005) studied adsorption of reactive (Acid Blue 221) and acid dyes (Acid Blue 62) with natural and calcined sepiolite and the surface area of sepiolite decreased when the calcination temperature rose above 200°C.Adsorption increased with increasing ion and temperature but it decreased with increasing pH value. (Santos and Boaventura (2008) stated that sepiolite exhibit high adsorption capacity for Basic Red 46 dyes.(Tabak et al. (2009) found that functional groups in the sepiolite structure play an active role in adsorption. They worked on adsorption of reactive dye (Reactive Blue 15) with sepiolite and they reported based on the results obtained from FTIR measurements and surface characterization tests that reactive dye was adsorbed through the channel structure in the sepiolite. (Rahman et al. (2013) used different clay minerals for adsorption of Procion Brilliant Red H-EGXL and Procion Yellow H-EXL dyes and synthetic talc had the highest adsorption capacity compared to other clay minerals. Rahman et al. (2015) compared the adsorption capacities of different clay minerals (sepiolite, kaolin and synthetic talc) for Reactive Yellow 138: 1 (Procion Yellow H-EXL) dyeing and found the highest adsorption capacities as synthetic talc, kaolin and sepiolite respectively.

Karaoğlu et al. (2010) studied color removal with kaolin and found that the adsorption time, pH, temperature, initial dye concentration (Reactive blue 221), salt concentration and acid activation of kaolin were most important factors affecting the degree of adsorption. According the this study adsorption increased with increasing initial concentration of dye, temperature and acid activation; but decreased with increasing pH. Baqir et al. (2014) activated kaolin with hydrochloric acid (HCl) and used it for the adsorption of Reactive Blue 13 dye. They also investigated the effect of time, pH and adsorbent amount on adsorption capacity. Tunç and Hanay (2016), used kaolin in their work for the removal of Remazol Brilliant Green 6B dye. The results obtained show that adsorption is more dependent on pH. At the end of the study, they proposed to use kaolin as an inexpensive, effective and environmentally friendly adsorbent as an alternative to activatedcarbon.

3. Conclusion

These studies show that environmentally friendly clay minerals are effective adsorbents for the removal of dyes from wastewater. It is also understood that the modified clay minerals show higher adsorption capacities than their unmodified forms. Numerous studies have been carried out on the use of clays for removal of different types of dyes from textile wastewater and the effect of various process parameters on adsorption.The most important parameters affecting the degree of adsorption are temperature, initial dye concentration, adsorption kinetics, type of adsorbent, adsorbent dose and pH value.It can be concluded that clay as an adsorbent with many advantages such as easy modification to obtain desired adsorption properties will maintain its importance in the near future as well as being a cost effective adsorbent.

References

Abd El-Latif, M. M., El-Kady M. F., Ibrahim, A. M., and Ossman, M. E., (2010). Alginate/Polyvinyl Alcohol-Kaolin Composite For Removal Of Methylene Blue From Aqueous Solution in A Batch Stirred Tank Reactor.*J Am Sci*, 6, 280-292.

Adeyemo, A. A., Adeoye, I. O., and Bello, O. S., (2017). Adsorption Of Dyes Using Different Types Of Clay: A Review, *Appl Water Sci*, 7, 543-568.

Alkan, M., Demirbaş, Ö., Çelikçapa, S., and Doğan, M., (2004). Sorption Of Acid Red 57 From Aqueous Solutions Onto Sepiolite, *J. Hazardous Mater.*, 116, 135–145.

Alkan, M., Çelikçapa, S., Demirbaş, Ö., and Doğan, M.,(2005). Removal Of Reactive Blue 221 And Acid Blue 62 Anionic Dyes From Aqueous Solutions By Sepiolite, *Dyes and Pigments*, 65, 251-259.

Annadurai, G., Juang, R. S., and Lee, D. J., (2002). Use of Cellulose-Based Waste For Adsorption Of Dyes From Aqueous Solutions, *Journal of Hazardous Materials*, 92, 263–274.

Armağan, B., Özdemir, O., Turan, M., and Çelik, M. S.,(2003). Equilibrium Studies On The Adsorption of Reactive Azo Dyes Into Zeolite, *Desalination*, 170, 33-39.

Asgher, M., and Bhatti, H.N.,(2012). Evaluation Of Thermodynamics And Effect Of Chemical Treatments On Sorption Potential Of (Citrus) Waste Biomass For Removal Of Anionic Dyes From Aqueous Solutions, *Ecol Eng*, 38, 79-85.

Ay, Z., Özacar, M., and Şengil, İ. A.,(2002). Bentonit İle Boyarmaddelerin Adsorpsiyonu, *SAU Fen Bilimleri Enstitüsü Dergisi*, 6, 183-187.

Babel, S., and Kurniawan, T.A.,(2003). Low-Cost Adsorbents For Heavy Metals Uptake From Contaminated Water: A Review, *J. Hazardous Mater.*, B97, 219–243.

Baqir, S. J., and Halbus, A. F.,(2014). Removal Reactive Blue Dye From Wastewater By Adsorption On White Iraqi Kaolin Clay, *Journal of Babylon University/Pure and Applied Sciences*, 7, 1947-1956.

Chen, B., Hui, C. W., and McKay, G.,(2001). Pore Surface Diffusion Modelling For Dyes From Effluent On Pith, *Langmuir*, 17, 740–748.

Crini, G., (2005). Recent Developments İn Polysaccharide-Based Materials Used As Adsorbents İn Wastewater Treatment, *Prog. Polym Sci.*, 30, 38–70.

Crini, G.,(2006). Non-Conventional Low-Cost Adsorbents For Dye Removal: A Review, *Bioresource Technology*, 97, 1061-1085.

Elemen, S., Akçakoca Kumbasar, and E. P., Yapar, S.,(2012). Modeling The Adsorption Of Textile Dye On Organoclay Using An Artificial Neural Network, *Dyes and Pigments*, 95, 102-111.

Espantaleon, A.G., Nieto, J.A., Fernandez, M., and Marsal, A.,(2003). Use Of Activated Clays In The Removal Of Dyes And Surfactants From Tannery Waste Waters, *Appl. Clay Sci.*, 24, 105–110.

Ghosh, D., and Bhattacharyya, K.G.,(2002). Adsorption Of Methylene Blue On Kaolinite, *Appl. Clay Sci.*, 20, 295-300.

Gülgönül, İ.,(2012). Evaluation Of Turkish Bentonite For Removal Of Dyes From Textile Wastewaters, *Physicochemical Problems of Mineral Processing*, 48, 369-380.

Gisi, S.D., Lofrano, G., Grassi, M., and Notarnicola, M.,(2016). Characteristics And Adsorption Capacities Of Low-Cost Sorbents For Wastewater Treatment: A Review, *Sustainable Materials and Technologies*, 9, 10-40.

Gök, Ö., Özcan, A. S., and Özcan, A.,(2010). Adsorption Behavior Of A Textile Dye Of Reactive Blue 19 From Aqueous Solutions Onto Modified Bentonite, *Applied Surface Science*, 256, 5439-5443.

Gürses, A., Doğar, C., Yalçın, M., Açıkyıldız, M., Bayrak, R., and Karaca, S.,(2006). The Adsorption Kinetics Of The Cationic Dye, Methylene Blue, Onto Clay, *Journal of Hazardous Materials*, B131, 217-228.

Kargı, F., and Özmıhçı, S.,(2004). Biosorption Performance Of Powdered Activated Sludge For Removal Of Different Dyestuffs, *Enzym Microb. Technol.*, 35, 267-271.

Kannan, N., and Sundaram, M. M.,(2001). Kinetics And Mechanism Of Removal Of Methylene Blue By Adsorption On Various Carbons- A Comparative Study, *Dyes and Pigments*, 51, 25-40.

Karaoğlu, M. H., Doğan, M., and Alkan, M.,(2010). Kinetic Analysis Of Reactive Blue 221 Adsorption On Kaolinite, *Desalination*, 256, 154-165.

Jamshidi, A., Rafiee, M., and Jahangiri-Rad, M., (2014). Adsorption Behavior Of Reactive Blue 29 Dye On Modified Nanoclay, *Trends in Applied Sciences Research*, 9, 303-311.

Joan, R. S, Wu, F. C, and Tseng, R. L.,(1997). The Ability Of Activated Clay For The Adsorption Of Dyes From Aqueous Solutions, *Environ. Technol.*, 18, 525-531.

Joshi, M., Bansal, R., and Purwar, R., (2004). Colour Removal From Textile Effluents, *Indian Journal of Fiber & Textile Research*, 29, 239-259.

Liu, P., and Zhang, L.,(2007). Adsorption Of Dyes From Aqueous Solutions Or Suspensions With Clay Nano-Adsorbents,*Separation and Purification Technology*, 58, 32-39.

Kaur, M., and Datta, M., (2014). Adsorption Behaviour Of Reactive Red 2 (RR2) Textile Dye Onto Clays: Equilibrıum And Kinetic Studies, *Eur. Chem. Bull.*, 3, 838-849.

Markovska, L., Meshko, V., Noveski, V., and Marinovski, M.,(2001). Solid Diffusion Control Of The Adsorption Of Basic Dyes Onto Granular Activated Carbon And Natural Zeolite İn Fixed Bed Columns, *J. Serb. Chem. Soc.*, 66, 463-475.

Menkiti, M. C., and Onukwuli, O.D.,(2011). Studies On Dye Removal From Aqueous Media Using Activated Coal And Clay: An Adsorption Approach, *N. Y. Sci. J.*, 4, 91-95.

Nigam, P., Banat, I. M., Singh, D., and Marchant, R.,(1996). Microbial Process For The Decolorization Of Textile Effluent Containing Azo, Diazo And Reactive Dyes, *Process Biochemistry*, 31, 435-442.

Ngulube, T., Gumbo, J. R., Masindi, V., and Maity, A.,(2017). An Update On Synthetic Dyes Adsorption Onto Clay Based Minerals: A State-Of-Art Review, *Journal of Environmental Management*, 191, 35-57.

Özcan, A., Ömeroğlu, Ç., Erdoğan, Y., and Özcan, A. S.,(2007). Modification Of Bentonite With A Cationic Surfactant: An Adsorption Study Of Textile Dye Reactive Blue 19, *Journal of Hazardous Materials*, 140, 173-179.

Özdemir, O., Armağan, B., Turan, M., and Çelik, M. S.,(2004). Comparison Of The Adsorption Characteristics Of Azo Reactive Dyes On Mezoporous Minerals, *Dyes and Pigments*, 62, 49-60.

Pandey, S., and Ramontja, J.,(2010). Natural Bentonite Clay And İts Composites For Dye Removal: Current State And Future Potential, *American Journal of Chemistry and Applications*, 3, 8-19.

Santos, S. C. R., and Boaventura, R. A. R.,(2008). Adsorption Modelling Of Textile Dyes By Sepiolite,*Applied Clay Science*, 42, 137-145.

Rashed, M.N., (2013). Adsorption Technique For The Removal Of Organic Pollutants From Water And Wastewater, Organic Pollutants – Monitoring, *Risk and Treatment*, 7, 167-194.

Rahman, A., Kishimoto, N. and Urabe, T.,(2015). Adsorption Characteristics Of Clay Adsorbents – Sepiolite, Kaolin And Synthetic Talc–For Removal Of Reactive Yellow 138:1, *Water and Environment Journal*, 29, 375-382.

Tabak, A., Eren, E., Afsin, B., and Çağlar, B.,(2009).'Determination Of Adsorptive Properties Of A Turkish Sepiolite For Removal Of Reactive Blue 15 Anionic Dye From Aqueous Solutions, *Journal of Hazardous Materials*, 161, 1087-1094.

Tülin, B.L., and Gamze, G.,(2009). Removal Of Basic Dyes From Aqueous Solutions Using Natural Clay, *Desalination*, 249, 1377-1379.

Tunç, M. S., and Hanay, Ö.,(2016). Sulu Çözeltilerden Remazol Brilliant Green 6B Gideriminde Kaolin Kullanımı, *Adıyaman Üniversitesi Mühendislik Bilimleri Dergisi*, 4, 1-10.

Vanaamudan, A., Pathan, N., and Pamidimukkala, P.,(2014). Adsorption Of Reactive Blue 21 From Aqueous Solutions Onto Clay, Activated Clay, And Modified Clay, *Desalination and Water Treatment*, 52, 1589-1599.

Wang, L.,and Wang, A.,(2008). Adsorption Properties Of Congo Red From Aqueous Solution Onto Surfactant-Modified Montmorillonite, *Journal of Hazardous Materials*, 160,173-180.

Yagub, M.T., Sen, T.K., Afroze, S., Ang, H.M, and Johnston, D.W.,(2014). Dye And İts Removal From Aqueous Solution By Adsorption: A Review, *Advances In Colloid and Interface Science*, 209, 172-184.

Yang, Y., and Han, S.,(2005). Nanoclay And Modified Nanoclay As Sorbents For Anionic, Cationic And Nonionic Dyes, *Textile Research Journal*, 75, 622-627.

Zakaria, R. M., Hassan, I., El-Abd, M. Z., and El-Tawil, Y. A.,(2009). Lactic Acid Removal From Wastewater By Using Different Types Of Activated Clay, *Thirteenth International Water Technology Conference (IWTC)*, Hurghada, 13, 403-416.

Zhou, T., Lu, W., Liu, L., Zhu, H., Jiao, Y., Zhang, S., and Han, R.,(2015). Effective Adsorption Of Light Green Anionic Dye From Solution By CPB Modified Peanut İn Column Mode, *Journal of Molecular Liquids*, 211, 909–914.

Use of Natural Fibers in Composite Reinforcement

Hatice AKTEKELİ[1*], Deniz DURAN[2]

[1]Ege University, Graduate School of Natural and Applied Sciences, Textile Engineering Department, Izmir, TURKEY

[2]Ege University, Faculty of Engineering, Department of Textile Engineering, Izmir, TURKEY

[*]**Corresponding Author:** htcaktekeli@gmail.com

Abstract

Composite materials are finding increasing application areas due to their advantages and diversity in application areas. Composite materials can be used in many different areas such as automotive, electronics, aerospace, sports equipment and construction. There are two main constituents of composite material. These are matrix and reinforcement elements. Due to the increasing demand for environment consciousness and legal regulations, the use of natural fibers as reinforcing elements in composite materials is also increasing rapidly. In the production of natural fiber reinforced composites, bast fibers, fruit and leaf fibers which are in the class of vegetable fibers of cellulosic nature are used. These ecological materials are developing because of the biodegradability and recyclability properties of natural fibers used as reinforcing material, low density, high specific strength values, as well as the renewable nature of plant-derived natural resources. Technological developments in the production and design of fiber-reinforced composite materials, such as the reduction in production cost, improvement in system efficiency and reliability, have made these materials possible to be molded into different shapes, making them candidates for replacing metals in many applications, avoiding disadvantages such as cutting and shaping of metals.

Keywords: Composite, natural fiber, environmental-friendly, renewable.

1. Introduction

'Sustainability' has become a topic that has gained importance in the whole world in recent years. The textile industry, like many other industrial fields, is looking for solutions that support sustainability in the selection of raw materials from production methods. The use of natural fibers instead of petroleum-based synthetic fibers is one of the alternatives to sustainable textile production. The use of spontaneously renewed natural materials instead of ever-decreasing oil resources has become advantageous both in environmental and economic terms (Kalaycı et al., 2016).

Increasing concerns over the environmental damage (global warming, waste) of fossil-based industrial materials in recent years and the decline in world oil reserves have led to the development and use of biomaterials and bio composites that are biodegradable, renewable, sustainable and cost- increased (Mohanty et al., 2000).

Composite materials have an important place in many engineering applications today due to their advantages and variety. It is a widely used method recently to obtain composite structures which can provide the desired properties as a result of supporting polymers which cannot meet some desired physical and / or chemical properties in application areas with textile fibers in various types and proportions (Bulut and Erdoğan, 2011).

Natural fiber reinforced composites bring many economic and environmental advantages. These materials are renewable, biodegradable, recyclable and sustainable in nature. In addition, natural fibers do not provide additional greenhouse gas loads to the environment as they use CO_2 during growth. Natural fiber reinforced composites have features such as low cost, little machine wear, low energy requirements during production and low health and safety risk. Due to the low density of natural fibers, lightness is provided in the components produced from these materials. Easy formability, acoustic and thermal insulation make natural fiber reinforced composites attractive (Yıldızhan, 2008; Ulcay et al., 2002; Karaduman, 2014).

2. What is the Composite?

The materials formed by combining these two materials in the same or different groups at the macro level in order to combine the best properties together or to create a new characteristic are called "Composite Material". In other words, to obtain superior features by correcting the weakness of each other, it may be called as materials of different kinds or materials combined with the aim (www.polerfiber.com, 2018).

Composites are generally made up of a stronger material given the name "matrix" and a name of "reinforcement element (fiber)".

From these two material groups, reinforcing material plays a role of preventing the strength and load bearing property of composite material and the matrix material plays a role in crack propagation which may occur in the transition to plastic deformation, and delays the breaking of composite material (Zor, 2018). To name a material as composite, it must carry the following properties:

- Must be man-made,
- The combination of materials with at least two separate physical and mechanical properties and a different interface,
- Mechanical properties that cannot be achieved with any individual component must be realized,
- In order to obtain optimum properties, a composite material must be formed by mixing two separate materials by distributing a material in a controlled manner into the other material,
- It is necessary that the best features of the composites are collected together (Onat, 2015).

Composites are classified according to reinforcement geometry (particle, flake and fiber) or matrix prop (polymer, metal, ceramic and carbon). In this paper, natural fiber reinforced composites will be described (Ataş, 2018).

2.1. Natural Fiber Reinforced Composites

The use of natural fibers in composite materials is rapidly increasing, as concepts such as recycling and sustainability are at the forefront. Ecological materials have been developed because of the biodegradability and recyclability properties of natural fibers used as reinforcing material, low density, high specific strength values, as well as the renewable nature of plant-derived natural resources (Doan et al., 2006).

The natural fibers which are composed of living organisms in the nature and formed from the cells are classified into two groups as animal and vegetable fibers. In the production of composite materials, bast fibers, fruit and leaf fibers which are in the class of vegetable fibers with cellulosic character are used. Fibers can be used as reinforcing element either directly in the composite or surface. Nonwoven surface structures produced by production techniques except knitting and weaving techniques are used in composite structures.

Depending on the application area, the needle punching method is frequently used especially in composites used in automotive and construction sector.

Needle Punching Method

In the needle punching method, fiber bundles are fed to the cards by air flow after opening and blending. After the carding, with the structure called camel back, the web comes to the laying and folding band and is laid on top according to the desired thickness. Needling is carried out throughout the thickness of the web which is formed by the unconnected fiber. The notched needles move the fibers from one face of the web to the other face to form a complex structure, during the needling, some of the fibers and filaments move up to the needles and another part remains in place and the fibers are pulled down with repeatedly immersed needles. In this way, mechanical bond of the fibers is carried out.

The surfaces produced by this method combine with the matrix material to bring the composite structure.

There are more details on these fibers in below (Bulut and Erdoğan, 2011).

2.1.1. Kapok Fiber

Kapok tree grows in tropical climates (India, Africa). The tree has seeds and fibers together in capsule-shaped fruit. As lightweight, it is used as filler; bed and pillow are made. Good air and heat insulation is provided due to the pores in the laminate structure. Because of its light weight and sound isolator, these features are utilized in airplanes (MEGEP, 2014). Kapok cocoon and fibers are seen in figure 1.

Figure 1. Kapok cocoon and fibers (MEGEP, 2014).

2.1.2. Kenaf Fiber

Kenaf fiber (Hibiscus Cannabinus) is a warmer climate plant obtained from plant roots. The most common is South Africa, Asia and India. Due to its fibrous structure it is widely used both in fiber and in composite production. Especially in paper manufacturing, construction materials have a large market. When kenaf fiber is evaluated from sound absorption angle, kenaf reinforced composites find use in sound insulation. Kenaf plant and fibers are seen in figure 2 (Kaya and Dalgar, 2017).

Figure 2. Kenaf plant and fibers (http://buddhajeans.com/encyclopedia/kenaf-fibre/, 2018)

2.1.3. Hemp Fiber

Cannabis fiber (Cannabis sativa) is widely used in the textile industry. In addition to having a very high acoustical character, it also has a thermal insulation feature. For this reason, hemp fiber reinforced composites find use in the construction sector. Nevertheless, the factors that would constitute a risk in human health of structures made of hemp fibers have not been determined. Hemp plant and fibers are seen in figure 3 (Kaya and Dalgar, 2017).

Figure 3. Hemp plant and fibers (www.tekstilbilgi.net/kenevir-bitkisi, 2018)

2.1.4. Bamboo Fiber

Bamboo is the fiber of the 21st century. The bamboo canes are collected from the bamboo forests of the Far East and they are converted into pulp, then separated into fibers and digested.

They are lightweight, natural and are used in composites due to their high performance and are an alternative to metals. The mechanical properties of the composite obtained are good as a result of good penetration of the matrix material into the small cavities present on the surface of the bamboo fibers obtained from low cost, ecologically produced and non-consumable sources. Bamboo fibers are seen in figure 4 (Yükseloğlu and Yöney, 2009; Karahan et al., 2006).

Figure 4. Bamboo fibers (Karahan et al., 2006).

2.1.5. Jute Fiber

Jute is the generic name given to the fibers obtained from the plant roots of the plant, which is referred to as the botanical Corchorus. Jute fibers are present in bundles of 10 or more single-fiber bundles between the cortex and the phloem layers in the trunk of the plant. It is 100% degradable in nature, recycled and environmentally friendly, and has a great prefix in jute fiber composite reinforcement due to its price advantage. Jute plant and fibers are seen in figure 5 (Karaduman, 2014).

Figure 5. Jute plant and fibers (MEGEP, 2014)

2.1.6. Pineapple Fiber

Pineapple leaf fibers, also known as PALF (Pineapple Leaf Fibers) fibers, are a natural fiber species that can be widely used both in textile products and composite structures. Pineapple (Pineapple comosus) is a perennial herbaceous plant belonging to Bromeliaceae family.

The use of remaining leaves from pineapple cultivation, usually grown in coastal areas and tropical climatic zones, for fiber production is of great importance both for the evaluation of these leaves and for the prevention of damage to the environment.

Thanks to the fact that the pineapple plant renews itself every year, with easy accessibility, recycling and easy mixing with nature, the pineapple fiber becomes an ideal material for industrial use. Pineapple leaves and fibers are seen in figure 6 (Kalaycı et al., 2016).

Figure 6. Pineapple leaves and fibers (Kalaycı et al., 2016).

2.1.7. Coconut Fiber

The fibers obtained from the outer part of the coconut which is the fruit of the palm tree grown in the tropical regions can be dried and extracted either by fiber or by pressing. The results of the studies show that these fibers have good low and high frequency acoustical properties and can be used as an alternative material for the synthetic based commercial product. Composite structures produced with these fibers offer a cheaper, lighter and brighter future compared to glass fiber and mineral based synthetic materials because of their contribution to the environment. Coconut fruit and fibers are seen in figure 7 (Kaya and Dalgar, 2017).

Figure 7. Coconut fruit and fibers (MEGEP, 2014)

2.2. Uses of Natural Fiber Reinforced Composites

Nowadays natural fiber reinforced composite materials are available for many applications from the automotive and aerospace industries to the building sector, from sporting goods to home furnishings. Due to its lightweight, economic and ecological character, these composites have a wide range of uses and they have a great advantage especially for the automotive and construction industry (Bulut and Erdoğan, 2011).

The use of natural fiber reinforced composites in the automotive industry is increasingly increasing due to increased competition and legislation that forces automotive manufacturers to recycle and reuse. Vehicles manufactured in the European Union, along with the End of Life Vehicles (ELV) legislation adopted by the European Commission in 2000, must be recyclable or biodegradable by 85% by 2015 and by 95% by 2015. Another ecological factor besides recycling is the reduction of CO_2 emissions. For this reason, it is very important to reduce the vehicle weights. With natural fiber composites, up to 30% reduction in vehicle weight is possible. In addition to ecological reasons, economic reasons also encourage the use of natural fiber composites in the automotive industry. It is economically advantageous to use natural fiber-reinforced composites as it is both cheaper than synthetic fibers used, and saves fuel with reduced vehicle weight (Bledzki et al., 2006; Karaduman, 2014).

The use of synthetic porous and fibrous acoustic materials is frequently seen, especially for sound flow and noise control applications. Products such as foam, rock wool and glass wool made from minerals have pollutant effects which are harmful to human health as well as to toxicity and environment. At the same time, it is stated that their production may be able to

deliver more carbon dioxide to the atmosphere than natural materials. However, the fact that natural fiber reinforced composites are both renewable is seen to be advantageous in areas where construction and other insulation are required, since they do not damage the environment during their production and low energy costs are considered (Kaya and Dalgar, 2017).

3. Conclusion

Composites are used in many industries due to their superior properties such as lightness, strength and economy. Fiber reinforced composites have become an important source of research and interest for the textile industry. As the concept of ecological consciousness and sustainability concept became more important in recent years besides all the features that have been mentioned, studies about natural fiber reinforced composites have accelerated.

In this article, general information about composite materials is given, advantages of natural fiber reinforced composite materials, fibers used for this purpose and applications of these composites are emphasized.

These composite materials, which have been developed by reinforcing natural fibers which give importance to both strength and durability and biocompatibility as well as sustainability and economics as well as ecological support, can be used as alternative products due to their superior properties in many different areas. Especially the automotive and construction industry has become the focus of attention.

Acknowledgement

This study was supported by BAP (Directory of Scientific Research Projects) of Ege University through the project number 2015/TKUAM/003.

References

Ataş, A., (2018). *Kompozit malzemeler ve mekaniği*. Balıkesir Üniversitesi, Mukavemet-II-Ders Notları.

Bledzki, A. K., Faruk, O., Sperber, V. E., (2006). Cars from Bio-Fibres. *Macromolecular Materials and Engineering*, 291 (5), 449-457.

Bulut, Y., Erdoğan, Ü. H., (2011). Selüloz esaslı doğal liflerin kompozit üretiminde takviye materyali olarak kullanımı. *The Journal of Textiles and Engineer*, 18(82), 28-35.

Doan, T.T.L., Gao, S.L., Mader, E., (2006). Jute/ polypropylene composites I. Effect of matrix modification. *Composites Science and Technology*, 66, 952-963.

Kalaycı, E., Avinc, O. O., Bozkurt, A., Yavaş, A., (2016). Tarımsal atıklardan elde edilen sürdürülebilir tekstil lifleri: Ananas yaprağı lifleri. *Sakarya Üniversitesi Fen Bilimleri Dergisi*, 20(2), 203-221.

Karaduman, Y., (2014). *Doğal Lif Takviyeli Sandviç Polimerik Kompozitler.* Doktora Tezi, Erciyes Üniversitesi, Fen Bilimleri Enstitüsü, Kayseri.

Karahan, A., Öktem, T., Seventekin, N., (2006). Doğal bambu lifleri. *Tekstil ve Konfeksiyon Dergisi*, 4, 236-240.

Kaya, A. İ., Dalgar, T., (2017). Ses yalıtımı açısından doğal liflerin akustik özellikleri. *The Journal of Graduate School of Natural and Applied Sciences of Mehmet Akif Ersoy University,* Special Issue 1, 25-37.

Milli Eğitim Bakanlığı, (2014). *Doğal lifler*, Tekstil Teknolojisi, http://www.megep.meb.gov.tr, (Date of access: 21 May 2018).

Mohanty, A.K., Misra, M., Hinrichsen, G., (2000). Biofibres, biodegradable polymers and biocomposites: An overview. *Macromolecular Materials and Engineering,* 24(1), 276-277.

Onat, A., (2015). *Kompozit malzemeler*. Sakarya Meslek Yüksekokulu, Makina ve Metal Teknolojileri Bölümü Metalurji Programı- Ders Notları.

Ulcay,Y., Akyol, M., Gemci, R., (2002). Polimer Esaslı Lif Takviyeli Kompozit Malzemelerin Arabirim Mukavemeti Üzerine Farklı Kür Metotlarının Etkisinin İncelenmesi. *Uludağ Üniversitesi Mühendislik- Mimarlık Fakültesi Dergisi*, 7(1), 93-116.

Yıldızhan, H., (2008). *Polimer Matrisli Kompozitlerin Mekanik Özelliklerinin İncelenmesi.* Yüksek Lisans Tezi, Süleyman Demirel Üniversitesi, Fen Bilimleri Enstitüsü, Isparta.

Yükseloğlu, S. M, Yöney, H., (2009). Bamboo fibre reinforced composite structures and their mechanical properties. *Tekstil ve Konfeksiyon Dergisi*, 4, 261-264.

Zor, M., (2018). *Kompozit malzemelerle ilgili genel bilgiler*. Dokuz Eylül Üniversitesi, Kompozit Malzeme Mekaniği – Ders Notları.

URL-1: http://www.polerfiber.com, (Date of access: 27 May 2018).

URL-2: http://buddhajeans.com/encyclopedia/kenaf-fibre/, (Date of access: 29 May 2018).

URL-3: https://www.tekstilbilgi.net/kenevir-bitkisi.html, (Date of access: 29 May 2018).

A Comparison on Physical Properties of Ring-, Compact- And Compact Siro- Spun Yarns Produced from Different Fibers

Memik Bünyamin Üzümcü[1*], Burak Sarı[2], Nida Oğlakcıoğlu[2], Hüseyin Kadoğlu[2]

[1]Bartın University,Faculty of Engineering,Department of Textile Eng., Bartın, Turkey
[2]Ege University,Faculty of Engineering,Department of Textile Eng, İzmir, Turkey

[*]**Corresponding author:** muzumcu@bartin.edu.tr

Abstract

In order to achieve novelties which will allow fabric producer to fulfill customer needs, initially they have to construct yarns which fit the purpose. For this reason modern spinning technologies, as well as ring modernizations have been developed. One of these technologies; Compact siro spinning system was constituted by using parts which allow feeding two rovings in one drafting zone of compact spinning machines. Yarns produced in this system have good properties in comparison with compact and siro-spun yarns, according to previous studies. In this study, various yarns were produced in ring, compact and compact siro spinning system by using different raw materials. The aim of this study is to determine the most suitable spinning system for each raw material in order to produce high quality yarns with them.

Keywords: Compact siro spinning, compact spinning, ring spinning, yarn properties.

1. Introduction

In order to achieve novelties which will allow fabric producer to fulfill customer needs, initially they have to construct yarns which fit the purpose. For this reason modern spinning technologies, as well as ring modernizations have been developed. Friction spinning, airjet spinning can be given as examples to these modern spinning systems. There are also spinning systems which are based on the ring spinning system and were developed with some modifications made in this system. Examples of these systems are compact, siro and core spinning systems.

The changes made in the ring spinning system were generally performed in the drafting zone of the system. In core spinning system, a feeder and an alligner for core were placed to drafting zone. The basis of the siro spinning system is to feed two rovings to the drafting zone at the same time. So, a spacer which can keep the distance between these two rovings constant and a feeder which is fit for two roving feed were placed to drafting zone.. According to the principle of compact spinning, there are parts in the drafting zone which collects fibers to the center and minimize spinning triangle.

There are several studies on foretold yarn types. Some of these studies reported that compact-spun yarns had higher strength and lower hairiness than ring-spun yarns (Cheng and Yu, 2003; Yılmaz and Usal, 2011; Krifa and Ethridge, 2007). In the same way, similar yarn characteristic differences compared to ring-spun yarns were also mentioned for siro-spun yarns (Sun and Cheng, 2000).

The compact siro system is a spinning system in which elements of both spinning systems (compact and siro) are used. That is, in this system, two rovings are fed into one drafting zone and also, compacting elements are used. Regarding this system; it was mentioned that using compact siro spinning system allowed producing higher quality wool/polyamide blended yarns in comparison with siro-spun (Ünal and Ömeroğlu, 2013), there were significant advantages of this system in terms of hairiness of worsted yarns (Çelik and Kadoğlu, 2007) and yarns produced with this system had more compact structure and smoother surface than the compact yarns (Su et al, 2015).

In this study, yarns were produced by using different raw materials with different spinning systems. By this means, the effects of the spinning systems on the different raw materials have been investigated.

2. Experimental

In this study, as described in the previous section, textile fibers of different properties were spun in different spinning systems. Ring, compact and compact-siro systems were utilized for spinning operations. Ne 20 yarns were produced with α_e 4.0 twist coefficient. The productions were made with Pinter Merlin SPA 1803 and Rieter K45 spinning machines (Figure 1) which are stationed in Ege University Textile Engineering Department's pilot spinning mill.

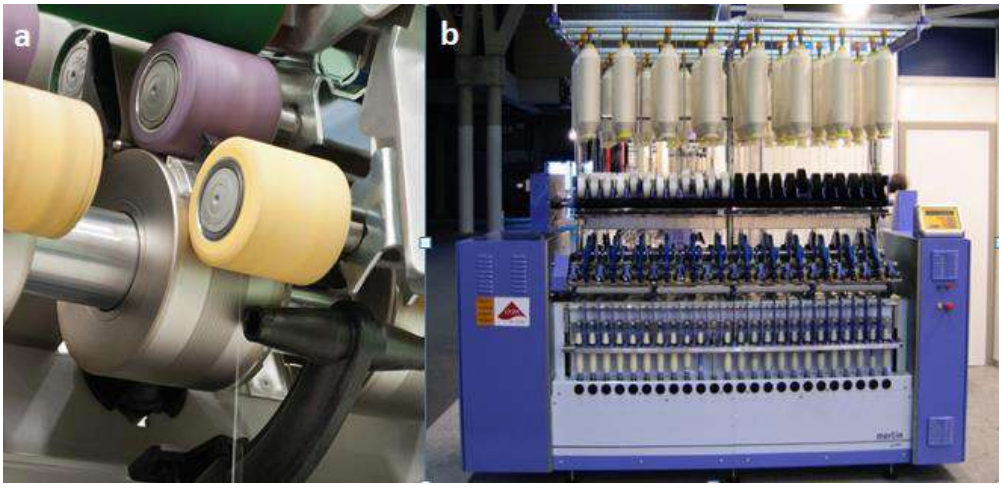

Figure 1. Rieter compact (a) and Pinter Merlin (b) spinning systems.

In this study; yarns were produced with natural, regenerated and synthetic fibers which are frequently used in textiles. Production plan is given in table 1. In addition to the 100% yarns, a blended yarn was produced in compact siro spinning system by feeding one roving of Tencel and one roving of bamboo into a drafting zone at the same time. Moreover, 100% modal and 100% micro modal ring-spun yarns were also produced in order to determine raw material effect on yarns. Lack of these materials prevented us to produce those yarns in other spinning systems.

Table 1. Production plan.

Yarn Type	Raw Material	Spinning System
1		Ring
2	Cotton	Compact
3		Compact siro
4		Ring
5	Polyester	Compact
6		Compact siro
7	Tencel	Ring

8		Compact
9		Compact siro
10		Ring
11	Bamboo	Compact
12		Compact siro
13		Ring
14	Viscose Rayon	Compact
15		Compact siro
16	Modal	Ring
17	Micromodal	Ring
18	Tencel-Bamboo	Compact siro

In the stage of determining the properties of the yarns produced, the required standards for each test were conformed. Strength tests were carried out by using Lloyd Tensile tester in Ege University Physical Textile Laboratory and unevenness tests were performed on Uster Tester 5 in the same laboratory. Statistical analyzes were performed with the data obtained as a result of the tests.

3. Results

When we examined the results, it was seen that the tensile strength of yarns produced by using compact siro system is generally higher than the other yarns. Among the yarns produced with these systems, it has been determined that those using polyester as the raw material had the highest strength. When produced with compact and compact siro spinning systems, bamboo had the lowest tensile strength. When produced with ring spinning system, viscose rayon had the lowest tensile strength. Results are shown in the graph in figure 2.

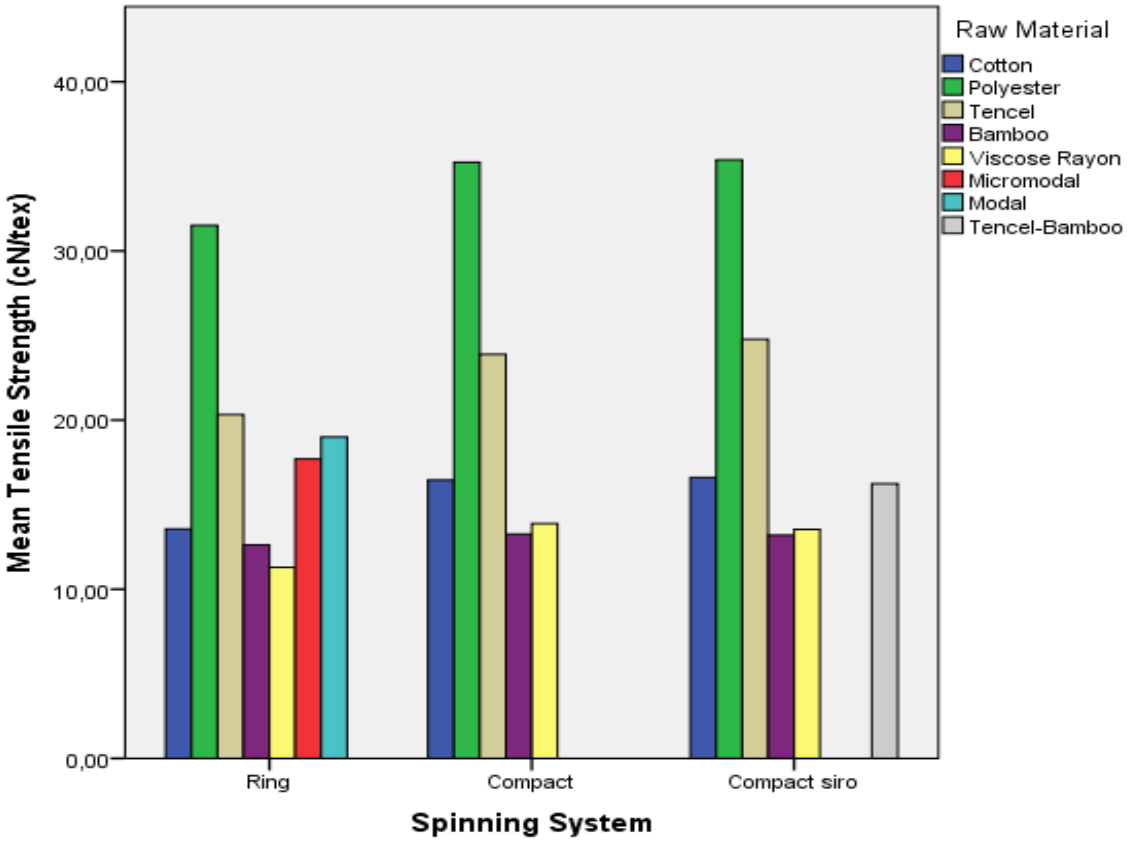

Figure 2. Tensile Strength Results

Tensile strength variations in the use of different raw materials and spinning systems were statistically analyzed. However, in these analyzes, modal, micromodal and tencel-bamboo yarns, which were not produced in other systems, were not included in the evaluation. As a result of the analyzes, it was seen that the use of different spinning systems did not cause statistically significant change ($p = 0,067 > 0,05$) in tensile strength. It was concluded that the strength differences of the yarns obtained with different raw materials were also statistically significant ($p = 0.00 < 0.05$). The results of the post-hoc tests are given in table 2.

Table 2. Post-hoc tests for tensile strength

Spinning System	N	Subsets	Raw Material	N	Subsets			
		1			1	2	3	4
Ring	75	17,8643	Viscose R.	45	12,9064			
Compact	75	20,5436	Bamboo	45	13,0231			
Compact siro	75	20,6416	Cotton	45		15,5628		

	Tencel	45	22,9947
	Polyester	45	34,0416

When the hairiness results were examined; in terms of the bending system, the lowest hairiness values were obtained by the compact siro spinning system and the highest values by the ring spinning system. The highest hairiness, in terms of raw material was found when Tencel was used as raw material, while the lowest hairiness values obtained when working with viscose rayon. It has been observed that the hairiness of viscose rayon, polyester, bamboo and tencel yarns which had the same fiber length changes in direct proportion to the roving unevenness. The highest hairiness was seen when tencel rovings, which had the highest roving unevenness (%CV = 5,63), were used. The graph of the values of hairiness is given in figure 3.

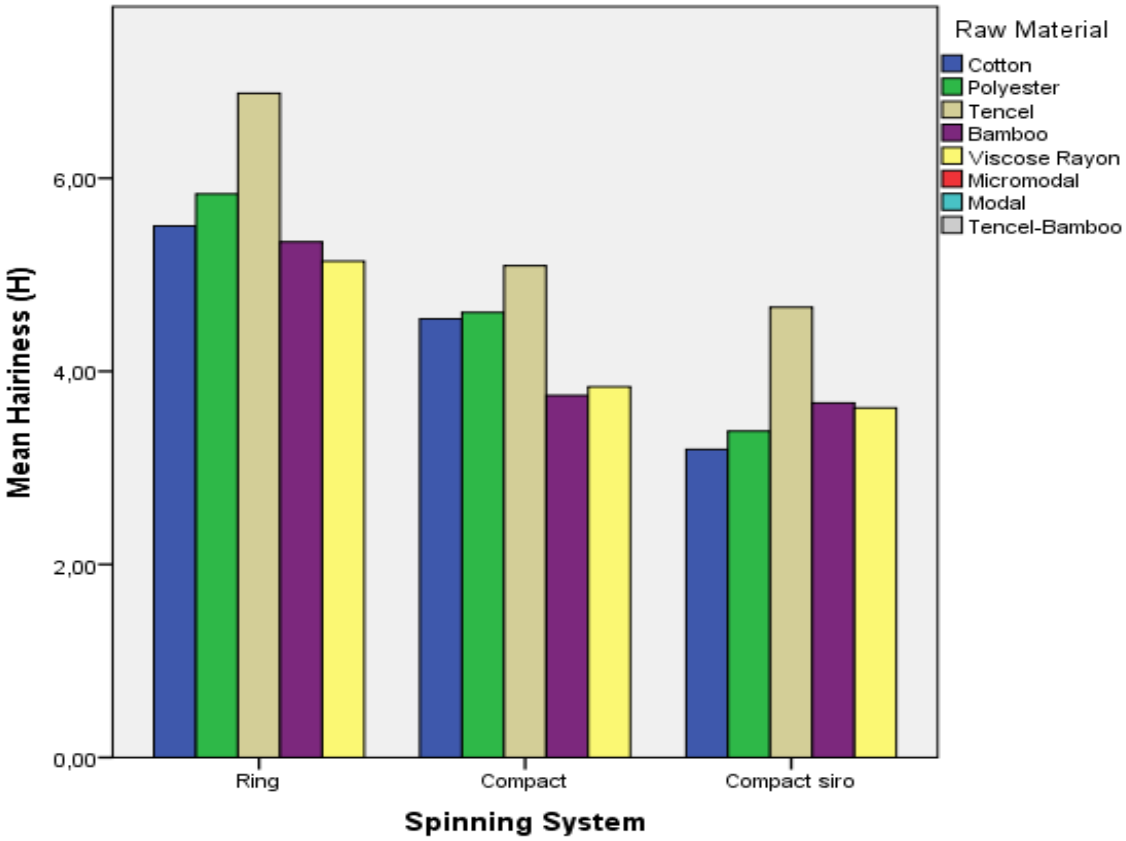

Figure 1 Hairiness (H) results

Statistical analyzes for hairiness values showed that there was statistically significant difference between the results of spinning systems ($p=0,00<0.05$) and raw materials ($p=0,00<0.05$). The results of the post-hoc tests for these variables are given in Table 3.

Table 3 Post-hoc tests for hairiness (H)

Spinning System	N	Subsets for alpha=0,05			Raw Material	N	Subsets for alpha=0,05		
		1	2	3			1	2	3
Compact siro	75	3,7053			Viscose R.	45	4,2000		
Compact	75		4,3673		Bamboo	45	4,2544	4,2544	
Ring	75			5,7407	Cotton	45	4,4133	4,4133	
					Polyester	45		4,6089	
					Tencel	45			5,5456

4. Conclusion

In this study, it was investigated that how different spinning systems and working with different raw materials would affect yarn properties. Unevenness and IPI fault values were also investigated, other than tensile strength and hairiness which were given in results section, but results of these yarn properties were inconclusive. It was thought that the reasons for this were the effects of unevenness of rovings and the machine parameters to these properties. In terms of yarn strength and hairiness, it can be said that compact siro spinning system will be more efficient for yarn productions.

References

Krifa, M. and Ethridge, M. D. (2006). Compact Spinning Effect on Cotton Yarn Quality: Interactions with Fiber Characteristics, *Textile Research Journal*. Vol 76(5), pp 388–399.

Cheng, K. P. S. and Yu, C. (2003). A Study of Compact Yarns. *Textile Research Journal*. 73(4), pp 345-349

Yılmaz, D. and Usal, M. R. (2011). A comparison of compact-jet, compact, and conventional ring-spun yarns. *Textile Research Journal*. Vol:81, Issue:5, pp 459-470

Sun, M.N. and Cheng, K.P.S. (2000). The Quality of fabric knitted from cotton sirospun yarn. *International Journal of Clothing, Science and Technology*.12 (5), pp 351-359.

Çelik, P. and Kadoğlu, H. (2007). The Effect of Spinning Method on Yarn Hairiness on Worsted Yarns. *Tekstil ve Konfeksiyon*. Volume 17, Issue 2, pp 97-103.

Ünal, S and Ömeroğlu, S. (2013). Investigation of Two-fold Yarn Properties Produced as Directly By Using Different Systems In Ring Spinning. *Pamukkale University Journal of Engineering Sciences*. Vol:19, Issue: 4, pp 164-169.

Su, X., Gao, W., Liu, X., Xie, C., Xu, B. (2015). Research on the Compact-Siro Spun Yarn Structure. *FIBRES & TEXTILES in Eastern Europe*. 23, 3(111), pp 54-57

Time-dependent Strength Change of Absorbable Surgical Sutures Held in Mucosal Medium

Deniz MİZMİZLİOĞLU [1], Emrah TEMEL [1*], Faruk BOZDOĞAN [1]

[1]Ege University, Institute of Science, Textile Engineering Department, İzmir, Turkey; denizmizmiz@gmail.com , textile.temel@gmail.com,faruk.bozdogan@ege.edu.tr

[*] **Corresponding Author:** textile.temel@gmail.com

Abstract

A suture is a biomaterial device, either natural or synthetic, used to ligate blood vessels and approximate tissues together. The goals of wound closure include obliteration of dead space, even distribution of tension along deep suture lines, and maintenance of tensile strength across the wound until tissue tensile strength is adequate. They are based either on absorbable or non-absorbable. Absorbable sutures are placed into subcutaneous tissue to eliminate dead space and into the dermis to minimize tension during wound healing. Absorbable sutures are placed into dermis and subcutaneous tissue to facilitate absorption by inflammation, enzymatic degradation or hydrolysis. Absorbable sutures provide strength support to the tissues at different locations due to their different polymer structures, and they will be absorbed by the body at the end. During surgery, which polymer-containing suture should be used is determined by considering the duration of support needed.

In this study, Poly (glycolide (75%) - co-caprolactone (25%)) copolymer-containing PGCL and Polydioxanone PDO absorbable sutures were incubated in mucosal medium up to 30 days at 37°C temperature. Tensile strength tests were applied to the specimens after 0, 10, 20, and 30 days. The time-dependent strength changes of PGCL and PDO absorbable sutures were investigated based on the test results

Keywords: Absorbable sutures, polyglycolic acid, caprolactone, polydioxanone, tensile strength.

1. Introduction

Research in the first half of the 20th century with polymers synthesized from glycolic acid and other α- hydroxyl acids were abandoned for further development because the resulting polymers were too unstable for long-term industrial uses. However, this very instability "leading to biodegradation" has proven to be immensely important in medical uses in the last three decades. Polymers prepared from glycolic acid and lactic acid has found a multitude of uses in the medical industry, beginning with biodegradable sutures first approved in the 1960 s. Since that time other medical devices, based on lactic and glycolic acid, as well as other materials, including poly(dioxanone) (PDO), poly(trimethylene carbonate) copolymers, and poly(e-caprolactone) homopolymers and copolymers, have been accepted for use medical devices. In addition to these approved devices, a great deal of research continues on polyanhydrides, polyorthoesters, and other materials (Middleton & Tipton, 2000).

A surgeon needs to use biodegradable sutures for various reasons. Foremost among them is to ensure that no second surgical intervention is needed to remove sutures from the tissue after the first surgical intervention.

Biodegradation has been accomplished by synthesizing polymers that have hydrolytically unstable linkages in the backbone. These most common chemical functional groups are esters, anhydrides, orthoesters, and amides (Middleton & Tipton, 2000).

Most of the commercially available biodegradable devices are polyesters composed of homopolymers or copolymers of glycolide and lactide. There are also products made from copolymers of trimethylene carbonate, ε-caprolactone, and polydioxanone.

Albertsson and Karlsson (2003), defined biodegradation as an event that takes place through the action of enzymes and/or chemical decomposition associated with living organisms and their secretion products. Therefore, "biodegradation of a polymer" is defined as the deterioration of its physical and chemical properties and a decrease of its molecular mass down to the formation of CO_2, H_2O, CH_4 and other low molecular-weight products under the influence of microorganisms in both aerobic and anaerobic conditions aided by abiotic chemical reactions like photo degradation, oxidation and hydrolysis (Wang et al., 2003).

Besides perfect biodegradability and biocompatibility, poly(p-dioxanone) (PPDO) has several other outstanding mechanical properties when compared with other aliphatic polyesters, such as PLA and PCL. It is one of only a few biodegradable polymers that possess both high tensile strength and excellent flexibility. Unsurprisingly, increasing attention has been paid to the synthesis, properties and applications of PDO in recent years. Based on the intensive

investigations of many researchers, PPDO has been applied successfully in the medical field, e.g., as a bone or tissue fixation device and drug delivery system. Furthermore, PPDO also has great potential for general use in such systems as films, molded products, laminates, foams, non-woven materials, adhesives, and coatings. PDO still has some unsatisfactory characteristics, such as hydrophobicity, low crystallization rate, and low melt strength, which limit its applications and processing methods (Yang et al., 2007).

PDO sutures are synthetic absorbable sterile surgical sutures which are made of Polydioxanone. PDO sutures when implanted into a living organism, it is absorbed by that organism and cause no undue tissue irritation. PDO sutures have been found to be non-antigenic, non- pyrogenic and elicit only a mild tissue reaction during absorption. This material is 55% crystalline and the glass transition temperature is -10 to 0 ºC.

Polyglycolide–caprolactone (PGCL) copolymers are suitable for wound closure materials like sutures used to hold skin, internal organs, blood vessels and other tissues of the human body together during the healing period. They must be strong, non-toxic, hypoallergenic and flexible in nature. Many complications such as infection, wound dehiscence and sinus formation occur in the wound closure line (Singh et al., 2017).

The structure of the PGCL polymer is a combination of PGA and PCL structures. *Poly(glycolide) (PGA)* is the simplest linear aliphatic polyester. PGA was used to develop the first totally synthetic absorbable suture that has been marketed as DEXON® since the 1960s by Davis and Geck. Glycolide monomer is synthesized from the dimerization of glycolic acid. The ring opening polymerization of glycolide yields high-molecular-weight materials with about 1–3% residual monomer present. PGA is highly crystalline (45–55%) with a high melting point (220–225°C) and a glass transition temperature of 35–40°C. Because of its high degree of crystallization, it is not soluble in most organic solvents; the exceptions are highly fluorinated organic solvents such as hexafluoroisopropanol. Fibers from PGA exhibit high strength and modulus and are too stiff to be used as sutures except as braided material. Sutures of PGA lose about 50% of their strength after two weeks and 100% at four weeks and are completely absorbed in 4–6 months. Glycolide has been copolymerized with other monomers to reduce the stiffness of the resulting fibers (Ratner et al., 1996a; Athanasiou et al., 1998; Ratner et al., 1996b).

In this study, two types of biodegradable sutures were degraded in mucosal medium and time-dependent strength changes of these sutures and their degradation mechanisms were investigated.

2. Material and Method

In this study, Poly(glycolide (75%) - co-caprolactone (25%)) copolymer-containing PGCL and Polydioxanone-containing PDO absorbable sutures were incubated in mucosal medium for 0, 10, 20 and 30 days at 37°C temperature. Mucosal medium is consist of: pH 4,5 phosphate buffer containing 0,1% Tween 80.

After incubation process, tensile strength tests were conducted to suture samples on Zwick Universal Tensile Testing Machine by using TS EN ISO 2062 test standard. The time-dependent strength changes of PGCL and PDO absorbable sutures were investigated based on the test results.

Biodegradation mechanisms of suture samples were also examined by FTIR spectroscopy. For this purpose, FTIR graphics were achieved by PerkinElmer FTIR Spectrometer. Moreover, weight losses have also been investigated to examine the polymer degradation process.

Figure 1. Tensile strength test on Zwick Universal Tensile Testing Machine

Figure 2. PerkinElmer FTIR Spectrometer

3. Results and Discussion

In order to determine the strength change after degradation reactions, tensile strength tests and loss of mass measurements were applied to the specimens after 0, 10, 20, and 30 incubation days. Test results are given below in Table 1 and Table 2.

Table 1. Tensile strength test results of PDO and PGCL biodegradable sutures

		PDO	PGCL
0 days	Tensile strength	93,24 N	95,9 N
	Elongation	47,62 %	31,86 %
10 days	Tensile strength	85,37 N	51,09 N
	Elongation	38,08 %	24,42 %
20 days	Tensile strength	69,07 N	4,73 N
	Elongation	34,81 %	4,47 %
30 days	Tensile strength	48,19 N	0 N
	Elongation	20,03 %	0 %

According to tensile strength and weight loss test results, a significant loss of strength and loss in weight were observed in biodegradable sutures stayed in mucosal medium up to 30 days. Before degradation process, tensile strength value of PDO sutures was measured as 93,24 N, while after 30 days of degradation, this value decreased to 48,18 N. While PGCL suture exhibited 95,7 N of tensile strength before degradation, there was no tensile strength could be observed after degradation. As a result of that, tensile strength test results of this study are highly correlated with the results of Ratner et al. (1996b) obtained in their studies.

Table 2. Loss of weight due to degradation of biodegradable materials

	Time	**Before degradation (g)**	**After degradation (g)**	**Difference (g)**	**Change (%)**
PDO	10 days	0,2366	0,2354	0,0012	0,51
	20 days	0,2335	0,2320	0,0015	0,64
	30 days	0,2348	0,2317	0,0031	1,32
PGCL	10 days	0,2451	0,2419	0,0032	1,31
	20 days	0,2432	0,2323	0,0109	4,48
	30 days	0,2441	0,2113	0,0228	13,43

When two biodegradable sutures were examined it can be stated that, PDO sutures demonstrated higher tensile strength than PGCL sutures. Similarly, when the weight loss of the sutures is examined, PGCL sutures are more degradable than PDO sutures. Therefore, PGCL showed higher weight loss values than PDO sutures. According to weight loss and tensile strength test results, it was determined that, PGCL sutures exposed to more structural deterioration than PDO sutures.

Effects of biodegradation mechanism to inner structure of PDO and PGCL biodegradable sutures were investigated by FTIR analysis. FTIR graphics are given below in Figure 3 and Figure 4.

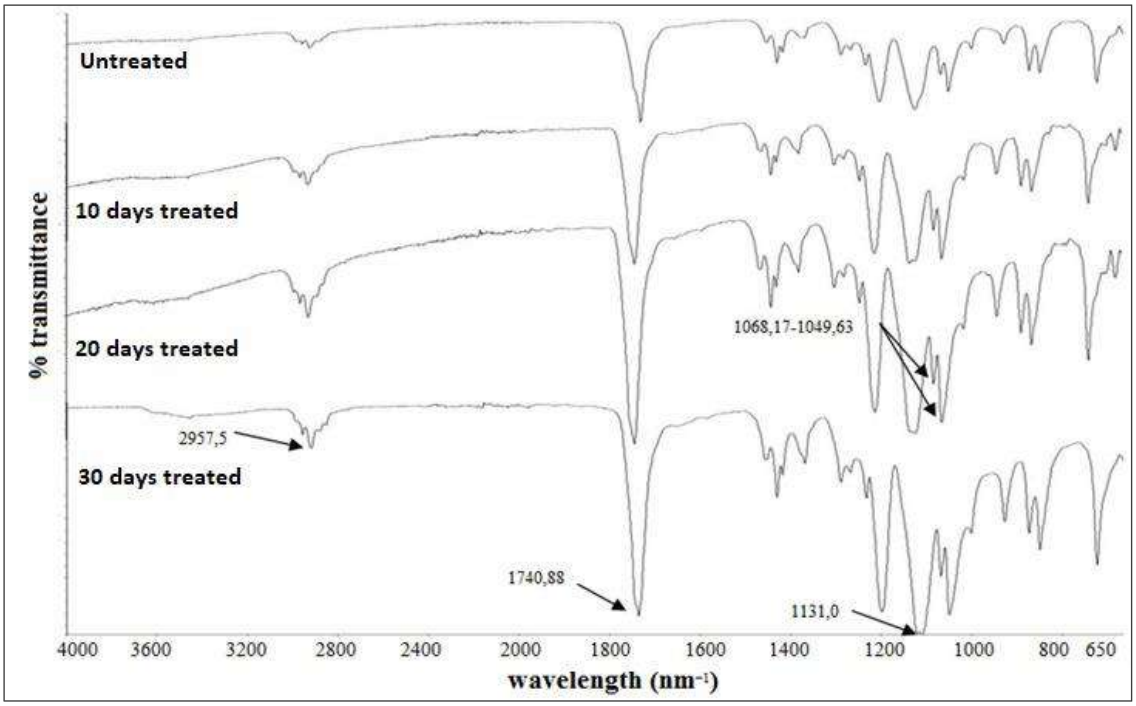

Figure 3. FTIR graphics and characteristic peaks of PDO biodegradable sutures.

FTIR spectrum is given in Figure 3 shows the characteristic peaks of PDO. According to literature review, 1735,41 cm^{-1} indicated existence of ester carbonyl group and 1131,0 cm^{-1} indicated existence of C–O–C bonds of ether groups. Vibrations peaks appear at 1068,1 and 1049,0 cm^{-1} pointed out C–O bands of esters and for aliphatic groups vibration peaks could be observed at 2919,5 cm^{-1}. The peaks at the region between 1000 and 500 cm^{-1}, i.e.; 927,2; 873,0; 849,8 and 722,0 cm^{-1} indicate the amorphous and crystalline phases of PDO polymer. The peak at 1625,0 cm^{-1} is originated from C=O stretching vibration of PDO polymer (Li et al., 2014).

When PDO degradation mechanism is analyzed, structural degradation of ester, ether and aliphatic groups were observed. The degradation in the aliphatic groups of PDO is monitored

as a shift and increase in the vibration peak between 2900 and 2950 cm^{-1} spectrum. At this point, the peak starting from 2919,5 cm^{-1} has shifted to 2957,5 cm^{-1} by the effect of degradation. The degradation of the ester carbonyl groups of PDO also can be observed as a shift and increase at the peak points in the region between 1735 and 1730 cm^{-1} on the FTIR spectrum. Degradation process caused the vibration peaks to shift from 1735,4 to 1732,0 cm^{-1}. When the deterioration in the ether groups of PDO is observed, peaks in the FTIR spectrum again demonstrated both a shift and an increase in the region between 1110 and 1135 cm^{-1}. Based on the degradation activity, vibration peak at 1131,0 cm^{-1} shifted to 1108,6 cm^{-1}.

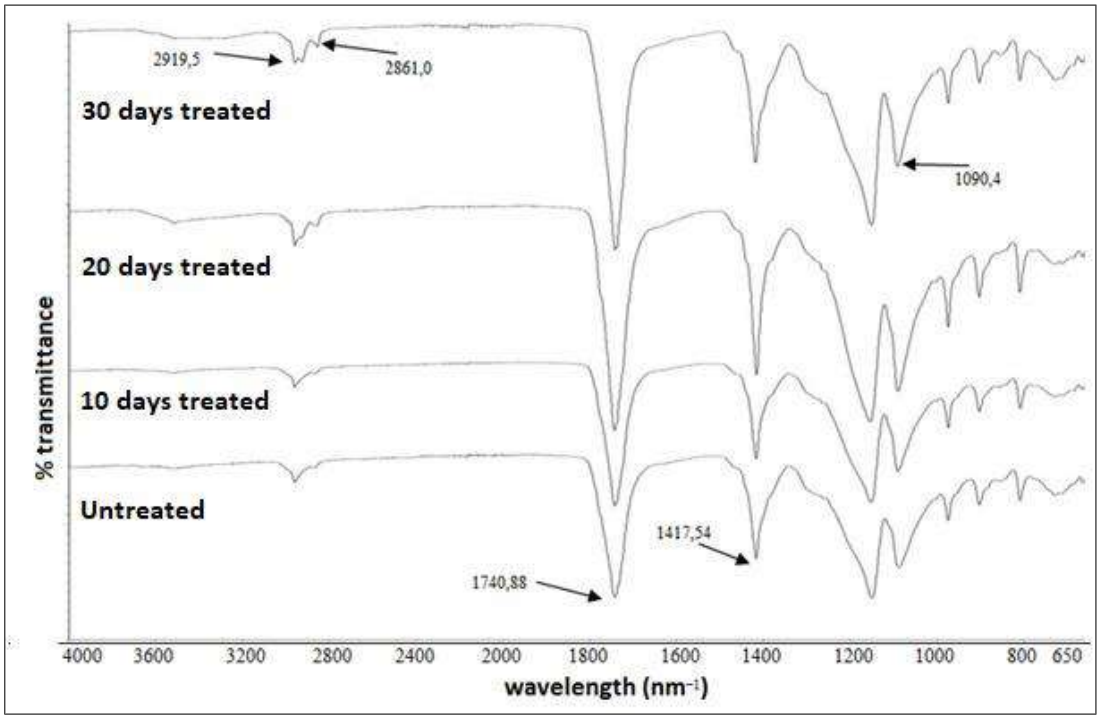

Figure 4. FTIR spectra of polyglycolide–caprolactone (PGCL)

PGCL has a co-polymer based structure containing, PGA polymer and PCL co-polymer. Therefore, both PGA and PCL characteristic peaks could be observed on FTIR spectrum. The main characteristic vibration peaks of PGCL copolymer could be summarized as follows: The absorbance peaks at 2957,5 cm^{-1} indicated CH_2 asymmetrical stretching vibration. Peak point appear at 2861 cm^{-1} pointed out CH_2 symmetrical stretching, 1740,88 cm^{-1} peak point is originated from aliphatic ester groups and 1417,54 cm^{-1} vibration is indicated CH bending. C–O bond stretching vibration could be observed at 1090,4 cm^{-1} (Singh et al., 2017).

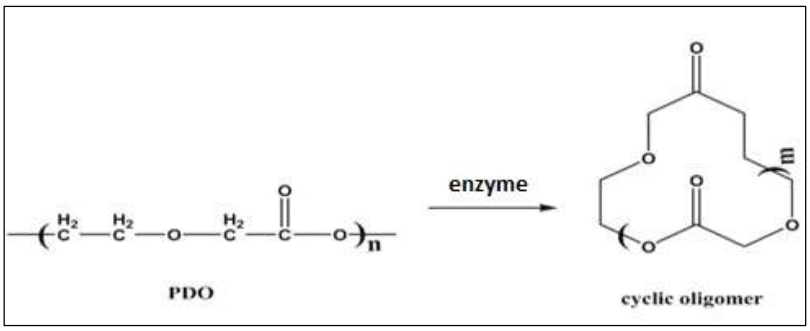

Figure 5. Chemical formulation and degradation to mechanism of poly(dioxanone) (PDO) (Banerjee et al., 2014).

When the disintegration mechanism of PGCL is examined, it is observed that structural decay occurs in CH_2 asymmetric groups and between C-O bonds. The degradation of PGCL in the CH_2 asymmetric group is observed as a shift and increase in the region between 2960 and 2915 cm^{-1} on the FTIR spectra. At this point, the peak starting from 2959,87 cm^{-1} has shifted to 2919,5 cm^{-1} by the effect of degradation. The deterioration of the C-O bond groups of PGCL is also observed as a shift and an increase in the peak points between 1090 and 1050 cm^{-1} in the FTIR spectra. Based on the degradation activity, vibration peak at 1094,4 cm^{-1} shifted to 1084,28 cm^{-1}.

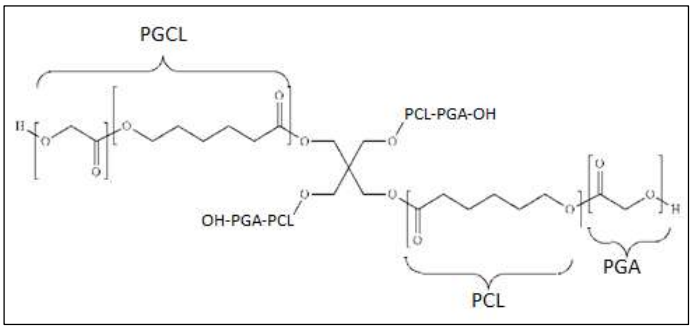

Figure 6. Chemical formulation of polyglycolide–caprolactone (PGCL) (Sharma et al., 2018).

4. Conclusion

A surgeon needs to use biodegradable sutures for various reasons. The major reason is to ensure that no second surgical intervention should be needed to remove sutures from the tissue after the first surgical intervention.

Since, PDO is more difficult to degrade according to PGCL, it can provide long term support to tissues. Therefore, PDO sutures are generally used for soft tissue approaches, i. e.; pediatric cardiovascular tissue and ophthalmic surgery expected to grow up to 6 weeks. However, PDO biodegradable sutures are not applicable in adult microsurgery, cardiovascular

and neural tissue (Yang et al., 2017). PGCL sutures are generally preferred in soft tissue applications and stitches that require absorbable suture intervention. Furthermore, it can be pointed out that PDO biodegradable sutures have more widespread application use than PGCL biodegradable sutures.

References

Athanasiou, K. A., Agrawal, C. M., Barber, F. A., & Burkhart, S. S. (1998). Orthopaedic applications for PLA-PGA biodegradable polymers. Arthroscopy: *The Journal of Arthroscopic & Related Surgery*, 14(7), 726-737.

Banerjee, A., Chatterjee, K., & Madras, G. (2014). Lipase mediated enzymatic degradation of polydioxanone in solution. *Polymer Degradation and Stability*, 110, 284-289.

Deng, K. L., Jin, W. H., Zhang, F. C., Li, C. X., Shen, H. J., Ma, X., ... & Wang, M. (2013). Preparation and Characterization of Dioxanone and Poly (dioxanone). *In Advanced Materials Research*, (Vol. 711, pp. 22-25). Trans Tech Publications.

Griffin, G. J. (1994). Chemistry and technology of biodegradable polymers. Blackie Academic and Professional.

Li, G., Li, Y., Lan, P., Li, J., Zhao, Z., He, X., ... & Hu, H. (2014). Biodegradable weft-knitted intestinal stents: Fabrication and physical changes investigation in vitro degradation. *Journal of Biomedical Materials Research*, Part A, 102(4), 982-990.

Middleton, J. C., & Tipton, A. J. (2000). Synthetic biodegradable polymers as orthopedic devices. *Biomaterials*, 21(23), 2335-2346.

Ratner, B. D., & Hoffman, A. S. (1996a). Frederick J. Schoen and Jack E. Lemons (eds.): *Biomaterial Science*. Chapter: Cardiovascular applications, pp. 64-72.

Ratner, B. D., & Hoffman, A. S. (1996b). Frederick J. Schoen and Jack E. Lemons (eds.): *Biomaterial Science*. Chapter: Cardiovascular applications, pp. 356-360.

Sharma, U., Gitlin, I., Zugates, G. T., Rago, A., Zamiri, P., Busold, R., ... & Carbeck, J. D. (2018). U.S. Patent Application No. 15/642,968.

Singh, A. K., Singh, R. K., & Tyagi, A. K. (2017). Controlled hydrolytic degradation of polyglycolide-caprolactone-based bioabsorbable copolymer. *Current Science* (00113891), 113(7).

Wang, X. L., Yang, K. K., & Wang, Y. Z. (2003). Properties of starch blends with biodegradable polymers. *Journal of Macromolecular Science*, Part C: Polymer Reviews, 43(3), 385-409.

Yang, K. K., Wang, X. L., & Wang, Y. Z. (2007). Progress in nanocomposite of biodegradable polymer. *Journal of Industrial and Engineering Chemistry*, 13(4), 485-500.

http://katsanas.com/upload/files/alcadinone_2017-11-22_16-23-23.pdf

Investigating Abrasion Resistances of Denim Fabrics Including Different Chenille Weft Yarns

Hüseyin Gazi TÜRKSOY[1], Sibel KAPLAN[2], Sümeyye ÜSTÜNTAĞ[1*], Sinem BİLGİN YÜCEL[1]

[1] Erciyes University, Engineering Faculty, Department of Textile Engineering, Kayseri, Turkey; hgazi@erciyes.edu.tr, sumeyyeustuntag@erciyes.edu.tr, sinembilgin@gmail.com

[2] Süleyman Demirel University, Engineering Faculty, Department of Textile Engineering, Isparta, Turkey; sibelkaplan@sdu.edu.tr

[*] **Corresponding Author:** sumeyyeustuntag@erciyes.edu.tr

Abstract

Denim garments have been preferred by a wide range of consumers without limitation of age, gender and social status. As it is a common garment group used in different occasions, innovative approaches are needed in production of denim fabrics to meet the further needs of consumers. In this study, chenille yarns which are usually used for home textile products due to visual and esthetic reasons were used in production of denim fabric to enhance thermal insulation properties of denim fabric.

Four different chenille yarns having different pile materials (100d/36F PET, 100d/96F PET, Ne 30 50% Viloft-50% PET, Ne 40/1 Acrylic) but the same lock materials (Ne 40/1 100% Cotton) were produced with final count of Nm 9. Denim fabric samples were produced by using these chenille yarns as weft in the fabric construction. In this study, it was focused not to show the chenille yarn fibers from fabric outer surface to create a normal denim appearance suitable for cold weather. Abrasion resistances of the denim fabrics' inner surfaces were investigated at 15000, 25000 and 35000 abrasion cycles. According to the results, it was seen that the fabrics having 50%Viloft-50%PET pile yarns have the lowest abrasion resistance values for all cycles whereas the fabrics having 100d/36F PET pile yarns have the highest abrasion resistance for 15000 and 25000 cycles. The results also revealed that pile types of chenille yarns have statistically significant influence on abrasion resistance of fabrics.

Keywords: Denim Fabric, Chenille Yarn, Pile Yarn, Abrasion Resistance.

1. Introduction

Denim is a hard and durable warp faced twill cotton fabric woven with indigo dyed warp and white filling yarns, having weights 4-16 onz/yarda. In general, cotton is the main material for denim. Cooler sensations, insufficient insulation and liquid transfer during summer and winter uses are sourced from its material and structure of the denim fabric. The mentioned disadvantages limit denim's end use areas with weather conditions. But there is a population that wants to use it in all occasions including some working and sports activities. In this study, chenille yarns which are usually used for home textile products due to the current visual and esthetic reasons were used appropriately in production of denim fabric which provides to wearable in cold weather.

Chenille yarn, which is a fancy yarn, has a soft, furry surface and a lustrous appearance (Çeven and Özdemir, 2007). Chenille yarn has a multi-component structure and consists of short lengths of spun yarn or filament that are held together by two ends of highly twisted fine strong yarn. The short lengths are called the pile and the highly twisted yarns are called the core or lock yarn. Chenille yarn can be made from many different types of fibers and yarns, most commonly cotton, viscose, acrylic, and polypropylene. The lock and pile yarn can be of the same or a different material (Ulku, Ortlek and Omeroğlu, 2003). The basic structure of a chenille yarn is shown in Figure 1.

Figure 1. The basic structure of a chenille yarn.

Chenille yarn is manufactured on a machine designed to bring the pile yarns and lock yarns together. During manufacture, the pile yarns are wrapped around a short stem of polished metal called a calliper or gauge, through which a blade passes to cut the pile yarns into short lengths. The lock yarns are pressed onto the short lengths with a rotating wheel which is also called plywood (Ulku, Ortlek and Omeroğlu, 2003).

The resulting yarn is then fed onto a traditional ring-twisting take-up mechanism. In the twisting process, the two ends of lock yarn twist and trap the short ends of pile between the lock yarns. The size of the calliper determines the diameter of the resulting yarn. The count of the lock and pile yarns, the number of the pile yarns and how many of them are fed onto the lock

yarns determines the count of the chenille yarns (Ulku, Ortlek and Omeroğlu, 2003). Basically, chenille yarn production system is shown in Figure 2.

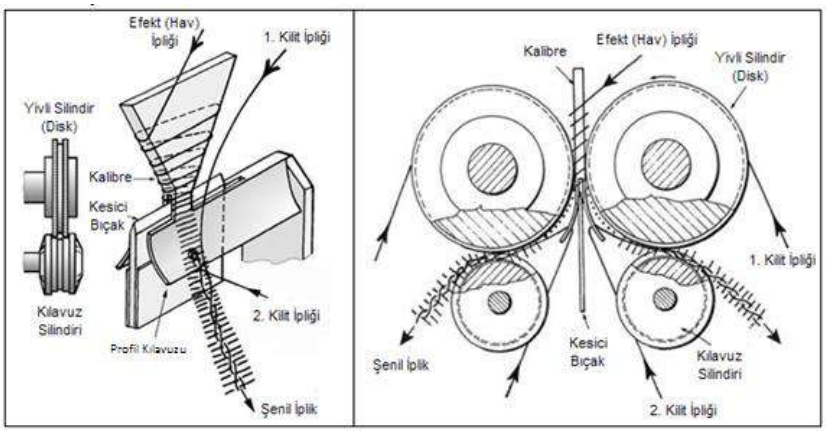

Figure 2. The production system of chenille yarn.

Chenille yarn has some disadvantages such as being delicate against machine washing and tumble drying and having low abrasion-resistance. Especially, the low abrasion resistance against rubbing and friction is a most important problem for fabrics including chenille yarn. Because chenille yarn is a combined yarn, its properties are influenced by many factors. These factors are the count of the yarn, the properties of the lock and pile yarns, twist level of the chenille yarn, pile length, fiber types, and so on (Ilhan and Babaarslan, 2007). There are a number of studies investigating abrasion resistance, dimensional and physical properties and bending behaviours of chenille woven/knitted fabrics differing in their lock and pile material, pile length, twist rate, weave construction and existence of elastane (Babaarslan and Ilhan 2005; Ceven and Ozdemir, 2006; Ceven, Tokat, Ozdemir, 2007; Kavusturan et al, 2010; Nergis, 2006; Nergis, 2007; Ortlek and Ulku, 2004; Ülkü, Ortlek and Omeroglu, 2003).

In this study, it was aimed to develop the innovative denim fabrics by using chenille yarns on proper form and structure. With this purpose, the chenille yarns with different pile yarns were used as weft yarns in the production of denim fabrics. As is known, chenille yarns which have a combined structure have low wear resistance. Therefore, the abrasion resistance of chenille yarns with different pile materials were investigated in denim fabric form. In this study, it was focused not to show the chenille yarn fibers from fabric outer surface to create a normal denim appearance suitable. That's why, the abrasion resistance test was applied only to the inner surface of the fabric.

2. Material and Method

In this study, 4 different types of chenille yarns were produced, detailed in Table 1. Ne 40 compact cotton yarns were used as lock yarns and 100d/36F PET, 100d/96F PET, Ne 30 50% Viloft-50% PET, Ne 40/1 Acrylic yarns were used as pile yarns in the production of chenille yarns. The final number of the chenille yarns is determined as Nm 9 and the calibrated pile length is 1 mm for all yarns. All chenille yarns were produced at twist level of 850 tur/m. The microscope images of produced chenille were taken by using Olympus SZ61 stereo microscope using BABSOFT image processing software.

Denim fabrics including the chenille yarns as weft were produced on a Picanol GT-Max projectile weaving machine. The weave construction, which was selected according to the target appearance, that chenille yarn can be seen from the inner side of the fabric, is given in Figure 3. An elastic commingling yarn (EC) was also used as weft yarn (one chenille yarn was inserted consecutively) besides the chenille yarns in fabric construction. The EC yarn was produced with with 78 dtex elastane and 200D/72F polyester (PET) yarn using air covering process.

Table 1. Pile yarn and microscopic images of the chenille yarns-including denim fabrics.

Code	Pile Yarn	Microscopic images
D36PET	100d/36F PET Filament	
D96PET	100d/96F PET Filament	
DVIL/PET	Ne 30 50/50% Viloft/PET	
DACRY	Ne 40/1 Acrylic	

10		X	X	X	X	Chenille
9	X	X		X	X	EC
8	X	X	X	X		EC
7	X		X	X	X	Chenille
6	X	X	X		X	EC
5		X	X	X	X	EC
4	X	X		X	X	Chenille
3	X	X	X	X		EC
2	X		X	X	X	EC
1	X	X	X		X	Chenille
	1	2	3	4	5	

Figure 3. Weave Structure/ Fabric photos in trousers form.

The abrasion resistance of the sample denim fabrics was measured by Martindale Abrasion and Pilling Tester (Figure 4) according to TS EN ISO 12947. The abrasion resistance was determined by the weight loss; the difference between the weights before and after abrasion cycles of 15000, 25000 and 35000.

Figure 4. Martindale Abrasion and Pilling Tester.

The results were evaluated for significance in differences using two-way repeated measures analysis of variance (ANOVA). The mean differences of subgroups were also compared by post hoc test of Duncan at 95 % significant level in the SPSS 17.0 statistical package.

3. Results and Discussion

In this study, the average weight loss values obtained as a result of the abrasion test was given graphically in milligrams (mg) and the results were evaluated. In addition, ANOVA and Duncan data were interpreted separately for inner side of fabrics according to statistical analysis results. The weight loss values of sample denim fabrics produced by 4 different chenille weft yarns for abrasion cycles of 15000, 25000 and 35000 are given in Figure 5. According to the results, it is seen that DVIL/PET coded fabrics has the highest weight loss value for all cycles. Moreover, D36PET coded fabric has the highest abrasion resistance for 15000 and 25000 cycles.

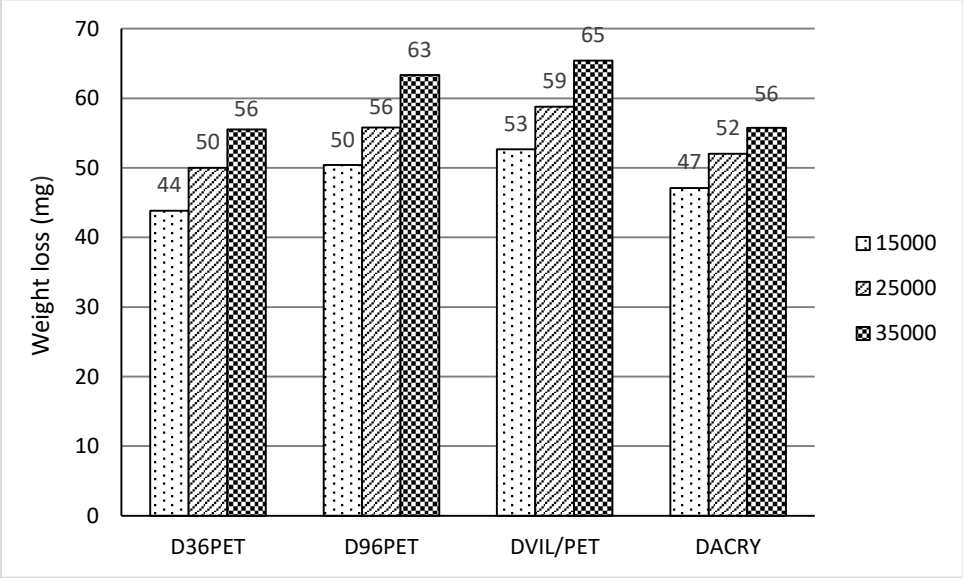

Figure 5. The weight loss values of the back side of sample denim fabrics.

The ANOVA results for the weight loss values of the inner side of the denim fabrics including chenille yarns which have different pile yarns are given in the Table 2. According to ANOVA results, it is seen that the pile type has a statistically significant effect on the weight loss values of denim fabrics. In addition, it is observed that the abrasion cycle has a significant effect on the weight loss of these fabrics.

Table 2. ANOVA results for weight loss values of the inner side of denim fabrics.

Source	Sum of Squares	df	Mean square	F	p
Corrected model	0.002[a]	11	0.000	60.370	0.000
Intercept	0.141	1	0.141	53942.918	0.000
Chenille yarn type	0.001	3	0.000	82.739	0.000
Abrasion cycle	0.001	2	0.001	202.596	0.000
Chenille yarn type * Abrasion cycle	2.791E-5	6	4.651E-6	1.777	0.132
Error	9.421E-5	36	2.617E-6		
Total	0.143	48			
Corrected total	0.002	47			

R^2 =0.949 (Adjusted R^2 = 0.933)

According to the results of Duncan analysis, the difference between the weight loss values of the inner side of the D36PET, D96PET, DVIL/PET and DACRY coded denim fabrics were found to be statistically significant. Furthermore, the highest abrasion resistance was observed in D36PET followed by DACRY, D96PET and DVIL/PET respectively. Also, it was seen that there is also a significant difference in weight loss of fabrics for all abrasion cycles (Table 3).

Table 3. Duncan test results for abrasion resistance.

Process	Subset			
Chenille Yarn Type	1	2	3	4
D36PET	0.049783			
DACRY		0.051650		
D96PET			0.056525	
DVIL/PET				0.058967
Sign.	1.000	1.000	1.000	1.000
Abrasion cycle				
15000	0.048506			-
25000		0.054169		-
35000			0.60019	-
Sign.	1.000	1.000	1.000	-

4. Conclusion

In this study, it was aimed to produce denim fabrics improved thermal properties using various chenille yarns as weft, in general. For this purpose, four chenille yarns with different pile yarns were produced. Chenille yarn has a very distinct weakness due to the instability of its construction. For this reason, chenille yarn does not have very good inherent abrasion resistance. This scope of work, the abrasion resistances of the inner face of denim fabrics produced with chenille yarns having different pile yarns were statistically investigated. As a result of the study, the difference between the abrasion resistance of the inner side of the denim fabrics having 100d/36F PET, 100d/96F PET, Ne 30 50% Viloft-50% PET, Ne 40/1 Acrylic pile yarns were found to be statistically significant. In addition, the highest abrasion resistance was observed in denim fabrics with 100d/36F PET pile yarns while the lowest abrasion resistance was observed in denim fabrics with Ne 40/1 Acrylic pile yarns. Finally, it was revealed that the abrasion resistance performances of chenille yarn being a combined yarn are influenced by the material of pile yarns.

Acknowledgement

This work was supported by the Turkish Ministry of Science, Industry and Technology (contract number 0624.STZ.2014). The authors would like to thank the Ministry for its financial support.

References

Babaarslan, O., Ilhan, I., (2005). An experimental study on the effect of pile length on the abrasion resistance of chenille fabric. The Journal of The Textile Institute, Vol. 96, No. 3, 193-197.

Çeven, E. K., and Özdemir, Ö., (2007). Using fuzzy logic to evaluate and predict chenille yarn's shrinkage behaviour. FIBRES & TEXTILES in Eastern Europe, Vol. 15, No. 3 (62), 55-59.

[1] Ceven, E. K., Tokat, S., & Özdemir, Ö., (2007). Prediction of chenille yarn and fabric abrasion resistance using radial basis function neural network models. Neural Computing and Applications, *16* (2), 139-145.

[2] Ceven, E. K., Özdemir, Ö., (2006). A Study of the basic parameters describing the structure of chenille yarns, FIBRES & TEXTILES in Eastern Europe, Vol. 14, No. 2(56), 24-28.

Ilhan, I., Babaarslan O., (2007). A theoretical approach to pile yarn-shedding mechanism of chenille yarn. The Journal of The Textile Institute, Vol. 98, No. 1, 23-30.

[3] Kavuşturan, Y., Çeven, E. K., & Özdemir, Ö. (2010). Effect of chenille yarns produced with selected comfort fibres on the abrasion and bending properties of knitted fabrics. Fibres & Textiles in Eastern Europe, 18(1), 78.

Nergis, U., B., (2006). Performance of chenille yarns with elastane. FIBRES & TEXTILES in Eastern Europe, Vol. 14, No. 3 (57).

[4] Nergis, B. U. (2007). Influence of core yarn properties on pile loss in chenille plain knitted fabrics. Indian Journal of Fiber and Textile Research, 32, 434-438.

[5] Ortlek, H. G., & Ulku, S. (2004). Factors influencing the abrasion properties of chenille yarns. *Indian* Journal of Fiber and Textile Research, 29, 353-356.

Ulku, S., Ortlek, H. G., Omeroğlu, S., (2003). The effect of chenille yarn properties on the abrasion resistance of upholstery fabrics. FIBRES & TEXTILES in Eastern Europe, Vol. 11, No. 3 (42), 38-41.

Effects of Water and Fertilizer - Saving Agrotextile Material on Biomass Production and Photosynthesis in Lettuce under Drought Stress

İlhan ÖZEN[1], Gamze OKYAY[1*], Abdullah ULAŞ[2]

[1]Erciyes University, Faculty of Engineering, Textile Engineering Department, 38039, Melikgazi, Kayseri, Turkey, iozen@erciyes.edu.tr

[2]Erciyes University, Faculty of Agriculture, Department of Soil Science and Plant Nutrition, 38039, Melikgazi, Kayseri, Turkey, agrulas@erciyes.edu.tr

[*] **Corresponding Author:** gamzeokyay@erciyes.edu.tr

Abstract

Plant growth and productivity is adversely affected by nature's various stress factors. Water deficit is one of the most limiting factors for plant growth. If plants do not receive adequate rainfall or irrigation, the resulting drought stress can reduce growth more than all other environmental stresses combined. Therefore efficient management of soil moisture is important for crop production.

The objective of the present study was to gain a better understanding of drought tolerance mechanisms and improve soil water and fertilizer management strategies using a water- fertilizer saving surface under three irrigation levels (adequate, moderate and deficit). For this purpose, we coated a nonwoven material with polymer/fertilizer mixtures and used as a source of water and fertilizer for Yedikule lettuce in greenhouse trials. Poly(ethylene terephthalate)/viscon (PET/CV) needle-punched nonwoven fabric was used as base material. Poly(vinyl alcohol) (PVOH)/ammonium sulfate (AS) and carboxymethyl cellulose (CMC)/potassium nitrate (PN) mixtures were used as the first and second coating layers, respectively. After generation of the agrotextile materials, greenhouse trials with Yedikule lettuce were carried out for determining the drought-stress response of the coated nonwovens in three different irrigation levels.

We have studied the effects of drought stress on the biomass production and photosynthesis in Yedikule lettuce. Application of agrotextile material ensured more available water and fertilizer for the plants and increased biomass production and amount of photosynthesis and could thus be an effective soil management practice.

Keywords: Agrotextile material, Water-fertilizer saving, Drought stress, Biomass production, Photosynthesis.

1. Introduction

Water availability, water use and nutrient supply to plants are the most important factors effecting plant growth and yield production. Plants often face significant challenges in obtaining an adequate supply of water and nutrient to meet the demands of basic cellular processes due to their deficiency in the soil. The water and nutrient deficiency can have a significant impact on agriculture; resulting death of plant tissue, yellowing of the leaves caused by a reduced production of chlorophyll and stunted growth (Web page, 2018). In order to eliminate these problems, various methods are developed such as controlled-release systems.

Controlled-release systems can improve the water and nutrient use efficiency of plants by increasing their water and nutrient uptake, which decreases irrigation and fertilization frequency and, therefore, substantially reduces the consumption of human resources and possible adverse effects on the environment (Yang et al., 2018). Although the relatively large number of controlled-release systems are used in agriculture, the mechanism of water and nutrient release through these systems isn't generally according to the crop demand, which is problematic in terms of both supporting proper plant growth and these systems are costly and difficult because of additional chemicals and complex synthetic routes (Morita et al., 2002; Drost et al., 2002; Tian et al., 2005; Jin et al., 2013; Yan et al., 2008; Wang et al., 2012).

A different solution in this field would be the production of innovative agrotextile materials, which is thought to address the above-mentioned problems. To this end, we generated an agrotextile material possessing both efficient water and fertilizer management together with in a simple and cheap way. Additionally, we investigated the effects of two fertilizer types (traditional and controlled release fertilizer) and two irrigation water levels (conventional and reduced) on Yedikule lettuce plant's biomass and photosynthesis.

2. Material and Method

2.1. Materials

Poly(ethylene terephthalate)/viscon (PET/CV) needle-punched nonwoven fabric was used as base material. Poly(vinyl alcohol) (PVOH)/ammonium sulfate (AS) and carboxymethyl cellulose (CMC)/potassium nitrate (PN) mixtures were used as the first and second coating layers, respectively. After generation of the agrotextile materials, greenhouse trials with Yedikule lettuce were carried out for determining the drought-stress response of the coated nonwovens in two different irrigation levels.

2.2. Preparation and Coating of PVOH/AS and CMC/PN Solution

PVOH particles were dissolved in distilled water by heating in an oil bath at 95ºC. Ammonium sulfate particles were added to the PVOH solution while dissolution proceeded. Afterwards, the PVOH/AS solution was cooled down to ambient temperature and coating was performed. Coated fabric was dried in an air-circulating oven at 80°C. CMC particles were slowly added to distilled water at 100ºC by stirring. Potassium nitrate was dissolved in distilled water at ambient temperature, added slowly to the CMC solution. The solution was left to cool down to ambient temperature and then citric acid was added. Finally, the PVOH/AS coated fabric was coated with the CMC/PN solution and subsequently cured at 80°C for 6 h.

2.3. Preparation of Soil and Germination of Seeds for Greenhouse Trial

The greenhouse experiment was established at Erciyes University's Soil Science and Plant Nutrition laboratory and conducted from 05.12.2017 to 06.02.2018. Pots were filled with pre-prepared loamy soil to a total weight of 5 kg. Then, the seeds were germinated at room temperature (25˚C - 30˚C) for 20 days. Afterwards, the coated fabrics were placed in the pots and then the lettuce plants were watered two times a week by replacing the volume of water lost by evapotranspiration for 100% irrigation pots, but the volume of water lost for the other samples (apply 50% water stress) was calculated by the average weight loss of 100% pots at the end of each irrigation.

2.4. Harvesting

Lettuces were harvested three times at about two week intervals. Samples were placed in paper bags to be transferred to the laboratory for analysis.

2.5. Analysis

Leaf Biomass Analysis

Shortly after the harvesting, leaf fresh weights (g) were taken. The samples were then dried in the oven at 75ºC for three days to attain a 5% moisture level. The dried samples were weighed to obtain the dry weight (g).

Photosynthesis Content Analysis

The relative photosynthesis content was determined by means of Portable Photosynthesis System LI-COR (LI-6400XTP). The photosynthesis measurements were performed only in

third harvest. Fully developed leaves were randomly chosen from one plant in each replication for measuring the photosynthetic activity.

3. Results and Discussion

The use of agrotextile material for the first two harvests has resulted in higher fresh weight. For all harvests, as the amount of water decreased, fresh weight decreased. However, there was less reduction in the pots using the agrotextile material. Dry weights gave similar results with fresh weights. Generally, photosynthesis results are similar irrespective of fertilizer supply and irrigation regime.

Acknowledgement

This work was supported by the Scientific and Technological Research Council of Turkey (TUBITAK), Project Number: 115M718.

References

Drost, D., Koenig, R., Tindall, T., (2002). Nitrogen use efficiency and onion yield increased with a polymer-coated nitrogen source. HortScience, 37 (2), 338–342.

Morita, A., Takano, H., Oota, M., Yoneyama, T., (2002). Nitrification and denitrification in an acidic soil of tea (Camellia sinensis L.) field estimated by delta N-15 values of leached nitrogen from the soil columns treated with ammonium nitrate in the presence or absence of a nitrification inhibitor and with slow-release fertilizers. Soil Sci Plant Nutr, 48 (4), 585–593.

Jin, S. P., Wang, Y. S., He, J. F., Yang, Y., Yu, X. H., Yue, G. R., (2013). Preparation and properties of a degradable interpenetrating polymer networks based on starch with water retention, amelioration of soil, and slow release of nitrogen and phosphorus fertilizer. J Appl Polym Sci, 128, 407–415.

Tian, X. H., Saigusa, M., (2005). Response of tomato plants to a new application method of polyolefin-coated fertilizer. Pedosphere, 15 (4), 491–498.

URL-1:https://www.nature.com/scitable/knowledge/library/plant-soil-interactions-nutrient-uptake-105289112, (Date of access: 01 October 2018).

Yan, X., Jin, Y. J., He, P., Liang, M. Z., (2008). Recent advances on the technologies to increase fertilizer use efficiency. Agric Sci China, 7 (4), 469–479.

Yang, X., Jiang, R., Lin, Y. Z., Li, Y. T., Li, J., Zhaoa, B., (2018). Nitrogen release characteristics of polyethylene-coated controlled-release fertilizers and their dependence on membrane pore structure. Particuology, 36, 158-164.

Wang, Y., Liu, M., Ni, B., Xie, L., (2012). K-Carrageenan-sodium alginate beads and superabsorbent coated nitrogen fertilizer with slow-release, water-retention, and anticompaction properties. Ind Eng Chem Res, 51 (3), 1413–1422.

TEXTILE TECHNOLOGY

POSTER PRESENTATIONS

Surface Roughness and Friction Characteristics of Denim Fabrics

Gonca ÖZÇELİK KAYSERİ[1]*, Gamze SÜPÜREN MENGÜÇ[1], Nilgün ÖZDİL[2]

[1]Ege University, Emel Akın Vocational High School, İzmir, TURKEY

[2] Ege University, Engineering Faculty, Department of Textile Engineering, İzmir, TURKEY

* **Corresponding Author:** gonca.ozcelik@ege.edu.tr

Abstract

A large number of different psychological and physiological responses of the human body along with fabric physical properties are incorporated to produce the subjective feeling of fabrics. Softness, harshness, roughness etc. are the fabric handle properties that determine these feelings. Fabric handle is a complex concept influenced by fiber, yarn, fabric and finishing processes and it is one of the most important properties affecting usage and satisfaction from the fabric. Fabric stiffness, which is difficult to quantify, has been evaluated for years as a subjective feature due to the fact that it is generated during the contact of fabric with human skin. Over time, methods and devices which are used to measure the tactile properties of the fabric have been developed using basic mechanical properties such as stress, bending, shearing and compressibility of the fabric, and the fabric handle has become objectively measurable. Friction force which refers to the resistance force exerted by the friction of a surface and the fabric and the roughness that defines the indented shapes in the vertical direction of the surface are the most important surface indicators. In this study, surface friction and roughness properties of %100 denim fabrics containing different amounts of elasthane yarn were investigated. By using Surftest SJ-310 roughness meter for the measurement of roughness and Frictorq device for the measurement of kinetic friction coefficient, surface properties of the fabrics were analyzed.
Keywords: surface characteristic, roughness, coefficient of friction, denim fabric.

1. Introduction

Friction in textiles is one of the most important factors determining the behavior of fibers in the process of yarn formation and process of yarns in the fabric formation. Friction force is a force that is created between two contacting surfaces and must be overcome in order to move the object, and in some cases the frictional force can cause negative effects (Gupta, 2008).

Friction is an important feature for all textile materials as it affects the efficiency of the operations performed and the performance of the product. In our daily life, some precautions are taken to reduce the friction forces, as well as measures to reduce the friction forces generated during the production and usage of textile materials. Coating the surfaces for various purposes and applying various finishing treatments in order to prevent the textile surfaces from wearing out of the friction can be given as examples to textile applications. It is also known that the sizing process is carried out in order to reduce the friction in the warp threads during the formation of the woven fabric and thus to increase the strength of the warp yarn. It is possible to classify the friction of textile materials as fiber friction, yarn friction and fabric friction (Balcı, 2010).

There are two reasons for surface roughness measurement. The first is to control manufacture and the second is to help ensure that the products perform well. In case of textiles, the former is related to special finishing (pressing or ironing), but the latter is related to tactile comfort and handling of fabrics (Mooneghi and et.al, 2014).

Clothing comfort is one of the major current concerns of textile and garment manufacturers. This attribute is based on the human sensory response to clothing materials and is determined by a variety of thermal, physiological and mechanical parameters. For fabrics that come into direct contact with the skin, touch and tactile properties are especially important in connection with clothing comfort. The surface characteristics contribute to the formation of the total hand value of the fabric and important parts of mechanical comfort concern tactile properties, including roughness (Semnani, 2011; Vassiliadis and Provatidis, 2004).

A surface can never be perfectly smooth and will always contain two components of surface texture, roughness and waviness. The structure at the micro level is generally termed as roughness, while the structure at the macro level is termed texture and waviness. Roughness is a surface micro-geometry which is defined as the sum of unevenness (geometric deviations) of the surface with relatively small distances. It is an important parameter influencing subjective hand feeling and connected with the behaviour of textiles layers in mutual contact. If these

deviations are large, the surface is rough; if they are small, the surface is smooth (Sirkova, 2012; Akgun 2014).

Many researchers conducted studies on the fabric roughness and relationship between roughness and yarn/fabric properties as well as the subjective perceptions. It was found that fabric roughness is associated with a number of objectively measured physical properties, such as prickle, shear stiffness, friction, bending, stiffness, thickness (Sirkova, 2012).

Studies related with surface roughness properties of polyester, cotton, and wool woven fabrics revealed that fabric constructional parameters such as fineness of filaments of yarn, yarn properties (i.e. type, count, twist level, ply number, unevenness and crimp), yarn density, type of weave pattern and fabric constructional properties (i.e. cover, porosity, thickness and balance of fabric), affect the fabric surface texture and also the surface roughness of fabrics (Akgun et.al, 2018).

The definition of surface roughness and its different evaluating methods are divided into two main groups; subjective and objective. The latter consists of contact and non-contact methods. For objective measurements, in earlier works the friction measuring data are obtained from the simple instruments and KES-F system for the tribological investigation of the textile fabrics. On the other hand, surface data obtained using optical methods and subjected to signal processing techniques have been used for the identification of the fabric structures as well (Mooneghi and et.al, 2014; Vassiliadis and Provatidis, 2004).

The accurate measurement parameter of surface roughness of woven fabric structures were investigated and was found that surface roughness properties of woven fabrics changed considerably according to measurement parameters because of the anisotropic structure of fabric surfaces (Akgun, 2015). In another study, surface roughness values of fabrics were found to be affected from yarn and fabric properties and the effects were related to fabric balance, fabric cover factor, fabric thickness and crimp values of yarns in fabric structures. Surface roughness values of fabrics decreased as yarn fineness and yarn twist levels increased but as yarn ply number decreased. Also, surface roughness values gradually decreased from open-end yarn constituting fabrics to combed yarn constituting fabrics (Akgun, 2014). The roughness and frictional properties of cotton and polyester fabrics and relationship between these properties were investigated. In a study, the roughness measurements were conducted by using Surftest and tensile tester adapted with a friction attachment. The positive and high correlation coefficient values determined between friction and roughness values showed strong relationship between the surface parameters measured in the study (Sülar, 2013). The surface frictional characteristics of the fabrics made of lyocell, bamboo, micro polyester, micro lyocell,

bamboo/charcoal, bamboo/cotton and their blends were investigated. The results revealed that the increase in cover factor gradually decreased the friction coefficient, the least friction coefficient values were obtained from lyocell fabric (Moorthy and Kandhavadivu, 2015).

2. Material and Method

In this study, the surface characteristics of denim fabrics produced from cotton and cotton/elastane core spun yarns were measured and analysed. Surface characteristics of the fabrics were measured by using three different measuring methods, such as Frictorq instrument, inclined plane method and surface roughness tester. Fabric weft and warp yarn linear densities, weight per unit area and fabric thickness values were also determined. Before the tests, all fabrics were conditioned under standard atmospheric conditions (20±2 °C temperature, 65 ± 4% RH) in the laboratory.

In Frictorq instrument, a circular fabric sample is clamped and forced to rotate around a vertical axis at a constant angular velocity while a vertical load is concentrically applied by a static upper body by means of three small contact sensors, placed in a circle at 120°. This method consists of characterising the coefficient of friction between two flat surfaces, namely textile fabrics, based on torque evaluation. Friction coefficient is proportional to the level of the dragging torque measured by a high precision reaction torque transducer (Lima and et.al, 2005).

Figure 1. Frictorq instrument and contact sensor

In inclined plane method, a block of mass *m* initially resting on an inclined plane covered with the fabric to be tested. The apparatus is arranged so that the angle of the plane θ can be continuously adjusted until the block just begins to slide. At this point, the frictional force F is equal to the component of the mass of the block parallel to the inclined plane.

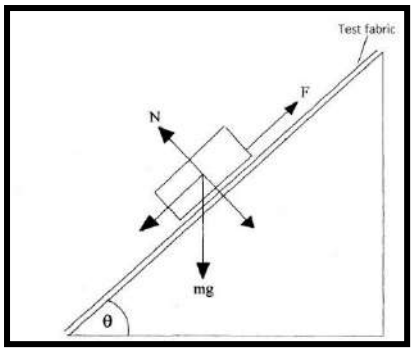

Figure 2. Inclined plane method

$$F = mg\sin\theta$$

$$N = mg\cos\theta$$

$$Friction\ coefficient = \mu = F / N$$

$$\mu = \frac{mg\sin\theta}{mg\cos\theta} = \tan\theta$$

Surftest SJ-310 roughness tester is capable of evaluating surface textures according to ISO 1997 standard. The stylus of the instrument detector unit traces the irregularities of the fabric surface and at least 20 roughness parameters can be obtained (Figure 3). From these parameters commonly used ones R_a, R_q, R_z were evaluated in this study. R_a is the most useful and common parameter for analyzing the surface structure. It is the arithmetical average of the absolute values of the profile variations (Equation 1). The sum of the maximum profile peak height and the maximum profile valley depth in one sampling length is defined as R_z (Equation 2). This parameter is approximately equal to the structural roughness of the fabric surface. The root mean square deviation of the assessed profile in one sampling length is given by R_q (Equation 3).

(a)

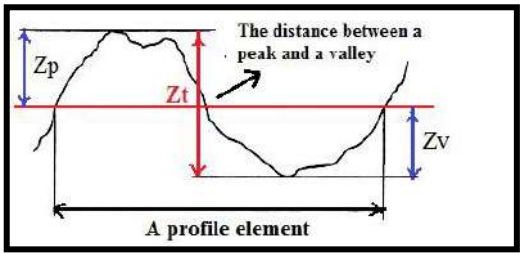

(b)

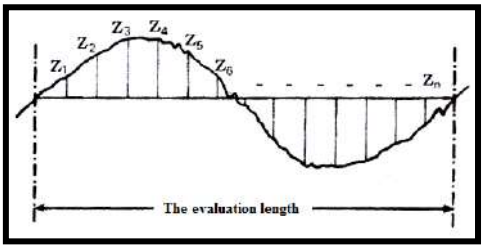

(c)

Figure 3. a) Surftest roughness instrument b) profile element (Z(x): the ordinate value, the the height of the profile in each position of x from the mean line) c) Mathematical evaluation of R_a (Mooneghi, 2014)

$$R_a = \frac{|Z_1 + Z_2 + ... + Z_n|}{n} \quad \text{(Equation 1)}$$

$$R_z = Z_p + Z_v \quad \text{(Equation 2)}$$

$$R_q = \frac{1}{l}\sqrt{\int_0^l Z^2(x)dx} \quad \text{(Equation 3)}$$

Weight per unit area of the fabrics were determined based on ISO 3801 and fabric thickness of the fabrics were measured according to ISO 5084 standard.

3. Results and Discussion

In the study 2/1 Z twill structured denim fabrics with the density of 18 yarns /cm for weft and of 27 yarns/cm for warp were used. The yarn count was 42tex for weft and 74 tex for warp yarn. In weft direction elastane core-yarns were used in different ratios and the structural parameters of denim fabrics were given in Table 1. The yarn count of the elastane used in weft yarns was 78 dtex and drafting ratio of elastane in the production of core-yarn was 5.2 %.

Table 1. The structural properties of the fabrics

Fabric code	Fabric construction-Fiber type	Weight per unit area (g/m^2)	Fabric thickness (mm)
D6	%100 cotton yarn (without elastane)	346	0,697
D2	% 33 core spun yarn (with elastane) - 67% cotton yarn	356	0,691
D4	50% core spun yarn (with elastane) - 50% cotton yarn	354	0,689
D1	67% core spun yarn (with elastane) -%33 cotton yarn	359	0,702
D3	75% core spun yarn (with elastane) - 25% cotton yarn	366	0,689
D5	100% core spun yarn (with elastane)	372	0,718
D6	100% cotton yarn	346	0,697

As can be seen from Table 1, weight per unit area values of the fabrics changes between 346 g/m^2 to 372 g/m^2 and the thickness values are in the range of 0,691 mm to 0,718 mm.

The kinetic coefficient of friction values of the fabrics measured by Frictorq instrument are given in Figure 4. As the instrument measures the surface of the fabric in macro level and the construction of the denim fabrics are the same, the difference between fabrics` coefficient of friction values are not significant. According to multiple comparison test carried out by

statistical analysis, the differences between the fabrics are found to be insignificant as well (p=.989)

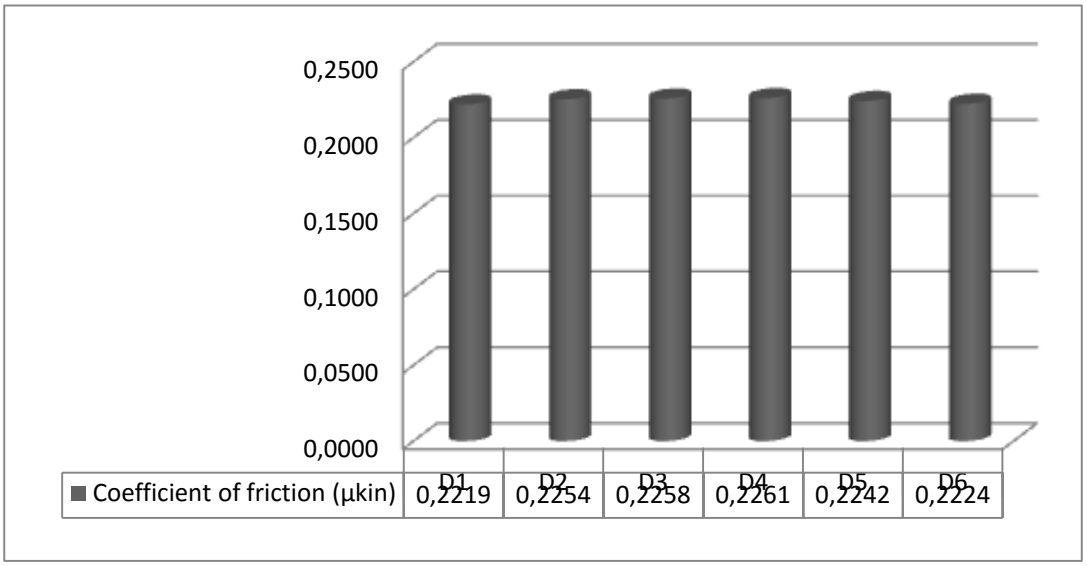

Figure 4. Kinetic coefficient of friction values of denim fabrics

In inclined plane method, the friction angle of the plane θ is measured just as the block begins to slide and tangent of the friction angle values are given in Figure 5. The lowest value was obtained with the fabric D4 and the highest value was measured by D1. However, according to multiple comparison statistical analysis, this difference was found to be insignificant (p=.0166).

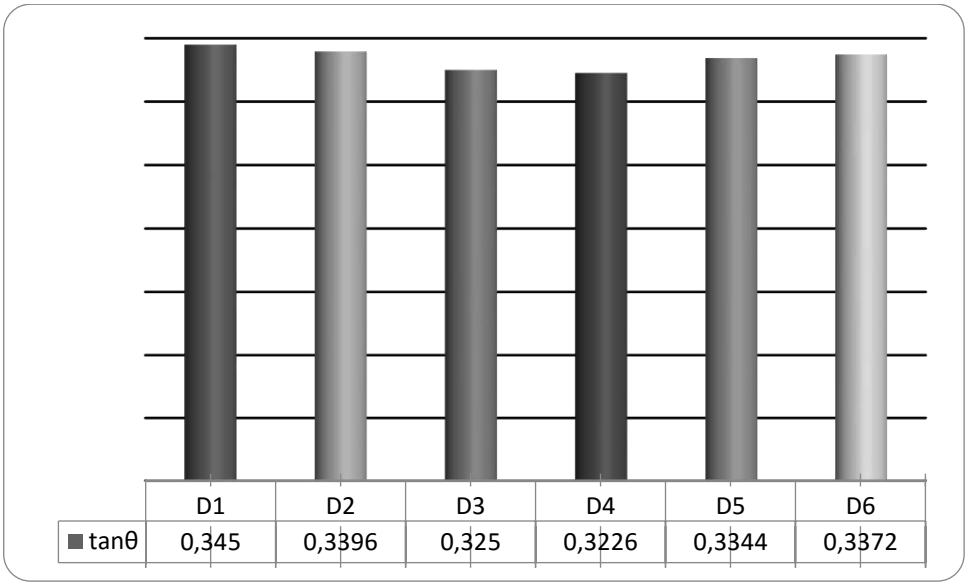

Figure 5. tan θ values of denim fabrics

In Figure 6, Figure 7 and Figure 8, the roughness parameters R_a, R_q and R_z values of the fabrics are given respectively. The roughness parameters measured in both warp and weft directions are in the same tendencies for all of the fabrics. Since fabric density in weft direction is lower as compared to warp direction, the roughness parameters are generally higher in that direction.

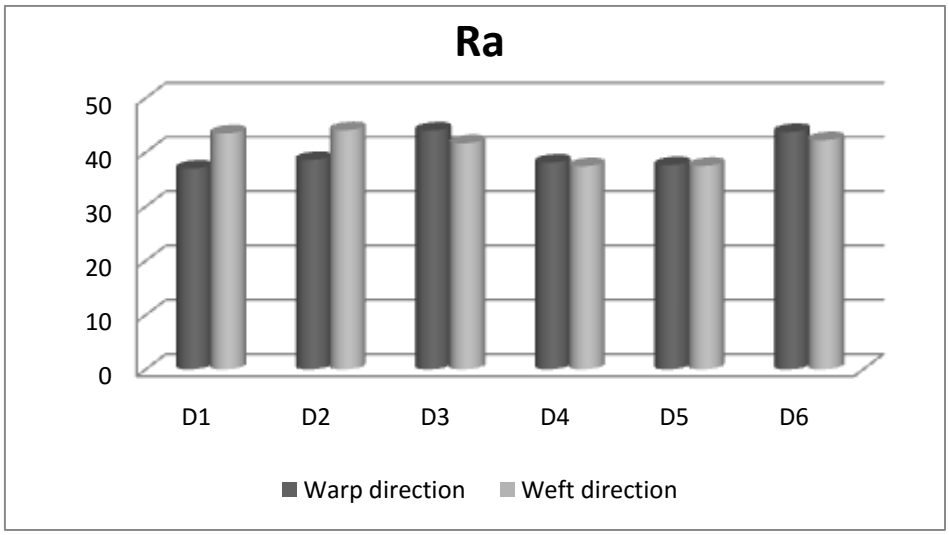

Figure 6. R_a values of the fabrics

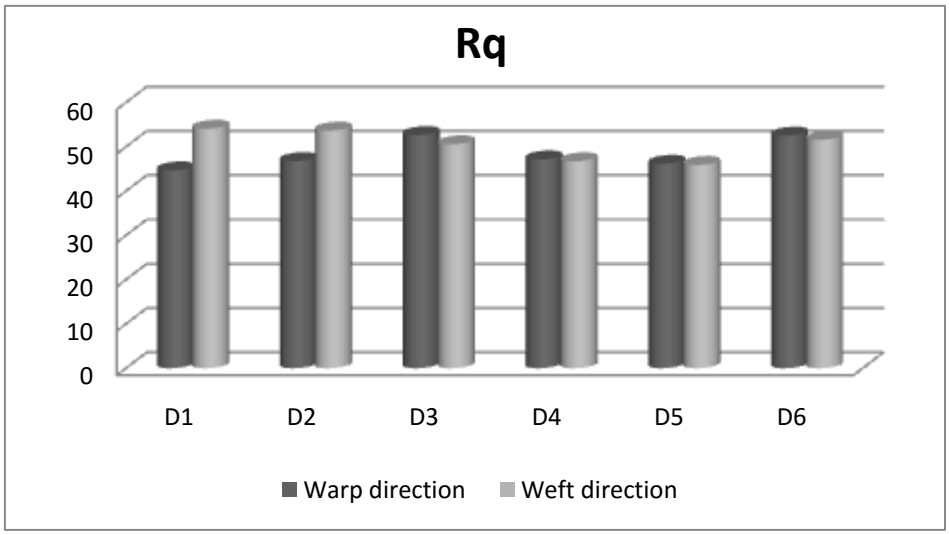

Figure 7. R_q values of the fabrics

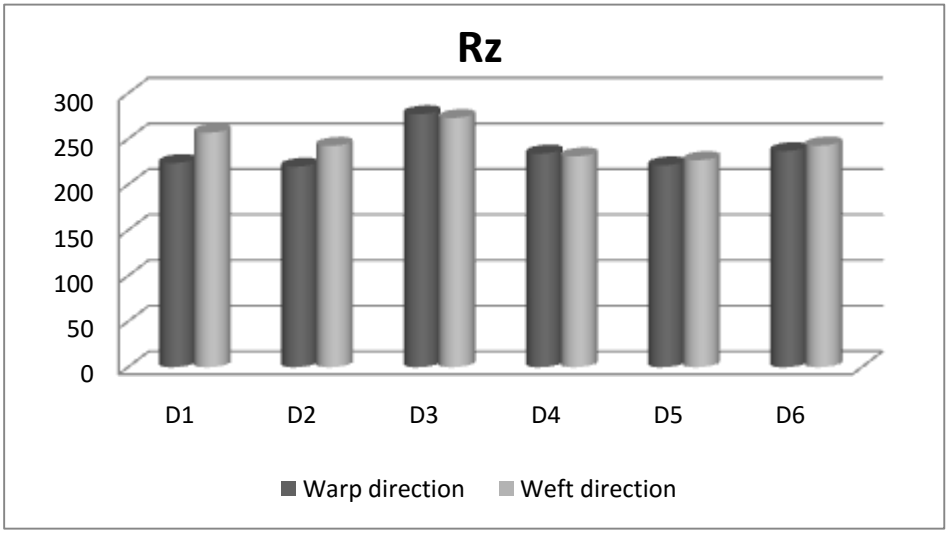

Figure 8. R_z values of the fabrics

For analyzing surface structure, generally used roughness parameter is R_a. D6 coded denim fabric is produced cotton yarn without elastane, therefore the highest roughness values are obtained with this fabric. Multiple comparison statistical analysis for all roughness parameters indicate that the differences between the fabrics are not statistically significant ($p=.218$ for R_a, $p=.237$ for R_q, $p=.348$ for R_z). Therefore, it can be stated that the effect of using elastane in warp direction is not important for the surface structure of the fabrics.

4. Conclusion

The surface properties of the fabrics supplies preliminary knowledge and resources about the performance characteristics of the fabric, the processes of the formation of the clothes, the suitability with the design model preparation stage and the sewability, as well as finishing operations of the fabrics. These parameters are very important for product development and quality assurance in garment industry.

In this study, basic surface characteristics of the fabrics affecting the tactile performances of the fabrics, roughness and friction parameters were measured by using simple measurement devices with denim fabrics containing different amounts of elastane yarns.

Friction coefficients values obtained from inclined plane and Frictorq methods are found to be quite close to each others. Considering that the weights and density values of the fabrics are the same, it is expected that the elastane ratio doesn`t have a significant effect on the fabric surface characteristics. Roughness parameters measured by Surftest instrument supplies the deviations of the fabric surface in micro scale level but nevertheless the differences between the roughness parameters of the fabrics are not statistically significant. Therefore it can be stated

that elasthane usage in the production of denim fabrics doesn`t results so divergent surface structure.

Acknowledgement

The authors give their special thanks to Ege University Scientific Research Department (Project No: 14-TKUAM-003) for their financial support.

References

Akgün M., Becerir B., Alpay H.R., (2015). Assessıng the Effect of Measurement Parameters on Surface Roughness Values of Polyester Woven Fabric Structures, *Tekstil ve Konfeksiyon*, 25(1), 66-72

Akgün M., (2014), Assessment of the Surface Roughness of Cotton Fabrics through Different Yarn and Fabric Structural Properties, *Fibers and Polymers*, 15 (2), 405-413

Akgun M., Becerir B., Alpay H.R, (2018) , Investigation of the relation between surface roughness and friction properties of polyester fabrics after abrasion, *The Journal of The Textile Institute*, 109:3, 322-337

Balcı G., Sülar V., (2016), İpliklerde Sürtünme Özelliği: Önemi ve Ölçüm Yöntemleri, *Tekstil ve Mühendis*, Sayı:73-74

Gupta B.S., (2008), Textile fiber morphology, structure and properties in relation to friction, *Friction in Textile Materials*, 3-36

Kawabata S., (1980), The standardization and analysis of hand evaluation, 2nd ed., HESC, Text. Mach. Soc., Osaka

Lima M., Hes L., Vasconcelos R., Martins J., (2005). Frictorq, A novel fabric surface tester: A progress report, *Journal of Textile Engineering*, 51(3), 40-46

Lima M., Hes L., Vasconcelos R., Martins J., (2005), Frictorq Accessing Fabric Friction with a Novel Fabric Surface Tester, *AUTEX Research Journal*, 5 (4), 194-201

Mooneghi S.A, Saharkhiz S., Varkian M.H., (2014), Surface Roughness Evaluation of Textile Fabrics: A Literature Review, *Journal of Engineered Fibers and Fabrics*, 9 (2), 1-18

Moorthy R.R, Kandhavadivu P., (2015). Surface Friction Characteristics of Woven Fabric with Nonconventional Fibers and Their Blends, *Journal of Textile and Apparel Technology and Management*, 9 (3), 1-14

Mitutoyo Surftest J-310 Manual

Sirkova B.K., (2012). Description of Fabric Thickness and Roughness on the Basis of Fabric Structure Parameters, *AUTEX Research Journal*, 12 (2), 40-43

Semnani D., Hasani H., Behtaj S., Ghorbani E., (2011), Surface Roughness Measurement of Weft Knitted Fabrics Using Image Processing, *Fıbres & Textıles in Eastern Europe*, 19, 3 (86), 55-59.

Sülar V., Öner E., Okur A., (2013), Roughness and Frictional Properties of Cotton and Polyester Woven Fabrics, *Indian Journal of Fibre & Textile Research*, 38, 349-356

Savvas G. Vassiliadis, Christopher G. Provatidis, (2004), Structural characterization of textile fabrics using surface roughness data, *International Journal of Clothing Science and Technology*, 16 (5,).445-457

Defects in Denim Washing And Solutions

Ayşegül KÖRLÜ[1]

[1]Department of Textile Engineering, Ege University, Izmir-Turkey

* **Corresponding Author:** aysegulkorlu@gmail.com

Abstract

Denim garments are very popular in the global market and will be more popular in the future. Denim products are used commonly by people of all ages, classes and genders. Because of clothing comfort and making people feel wearing "unique" garments etc. Denim washing processes give the final look of the garment. Fibre types and manufacturing methods of denim fabric effect the quality of final product.
In basic way, denim-finishing processes can be classified as below;
-Dry processes
-Wet processes
In this poster, the defects in denim washing is described and the defects are classified into three types. The sources of the defects are
-Raw material
-Process
-The others
In the end of every defect description, the solution of problems generating defect is discussed.

Keywords: Denim, denim washing, denim laundry, defect, denim finishing

1. What is Denim?

Denim is a well-known fabric usullay woven. Conventional denim is made of cotton. Recently blending of cotton with polyester, elastane, viscose and flax fibers is used for producing of denim fabric. Denim fabric is usually a thick 2/1 or 3/1 cotton twill-weave fabric with a dyed blue warp and raw white weft(Bağıran, 2017; Tortora ve Merkel, 2007).

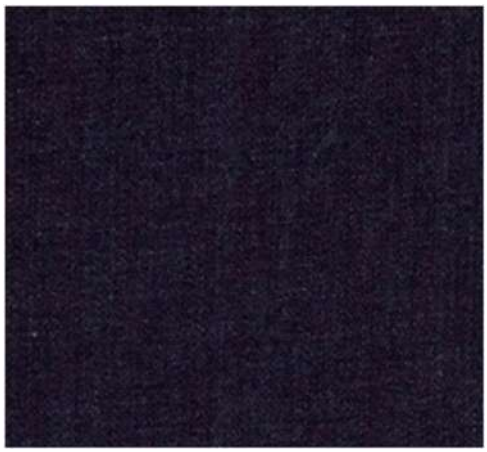

Fig. 1. Denim fabric

2. Denim Garment Washing Processes

Fibre types and manufacturing methods of denim fabric effect the quality of final product. In basic way, denim-finishing processes can be classified as below;

-Dry processes

-Wet processes

Dry processes (Fig. 2) contain grinding, tagging, breaking, laser designing etc. Wet processes (Fig. 3) are desizing, stone wash, enzyme washing, ozone treatment etc.

Fig. 2. Grinding of denim garment (Aslan, 2004)

Fig.3. Just stone-washed denim garments (Aslan, 2004)

3. Classification Of Defects in Denim Washing

The defects in denim washing are classified into three types. The sources of the defects are

-Raw material

-Process

-The others

A lot of defects can be occur in denim washing. The most common defects are described in this poster.

3.1. Defects From Raw Material

Alternating light and dark streaks: If the indigo dyeing machine stops for more than a few minutes, the yarn in the dye boxes will over-reduce. After denim washing, light streaks

appear in the garment(https://www.denimsandjeans.com/denim/manufacturing-process/latent-defects-in-denim-fabrics/1432).

Twisted legs: It is where the side seam twists around to the front of the trouser and distorts the appearance of the jeans (https://www.denimsandjeans.com/denim/manufacturing-process/common-defects-in-denim-jeans-sewing/3192).

Fig. 4 Twisted legs (https://www.denimsandjeans.com/denim/manufacturing-process/common-defects-in-denim-jeans-sewing/3192)

Recommended Solution : The grainline of the fabric must be checked. Sometimes notches are used to insure proper alignment. The cutter should not trim off the front or back with scissors to make them come out the same length. The fabric must be cut for proper skew.

3.2. Defects From Processes

Crease mark: If the denim garment was not wetted completely and evenly placed into washing machine, crease marks will form during the washing processes (Karagöz, 2009; Paul, 2015).

Fig. 5 Crease marks (Karagöz, 2009)

Recommended Solution :

- ✓ If the denim fabric contains synthetic fiber, existing crease marks on the unwashed garment should be find out.
- ✓ The garments should be totally wetted and placed evenly in the washing machine.
- ✓ Liqour ratio should be optimum for denim washing process. The amount of water in the washing machine should be checked and garments should be totally wetted before washing.
- ✓ Washed garments should be placed into dryer (Karagöz, 2009; Paul, 2015).

Backstaining problem: During the washing process removed dye from garments can be re-deposited on undyed are of the garments like pocket fabric. It is backstaining problem (Bağıran, 2017; Karagöz, 2009).

Recommended Solution :

- ✓ The quality of the cellulase enzyme should be checked in the enzymatic washing.
- ✓ Use of laccase is a useful solution for backstaining problem because of indigo degradation.
- ✓ Dispersing agent can be added in the washing bath.
- ✓ During the rinsing number of rinses and rotations in the washing machine should be increased.
- ✓ Water hardness is the important parameter. If the water is too hard,backstaining will increase.

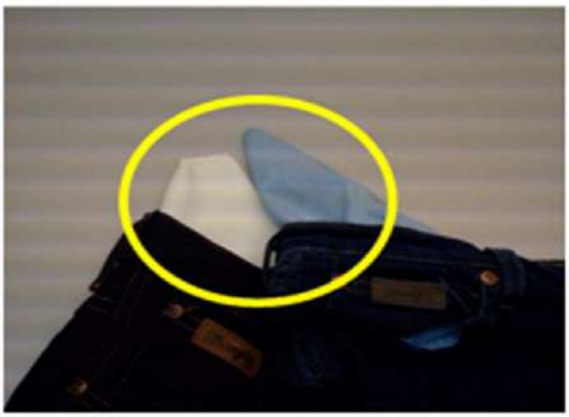

Fig. 6 Backstaining in the pocket (Karagöz, 2009)

Yellowing: It is still an important problem in denim washing because of isatin. Isatin is a by-product of indigo degradation reaction. Fenolic yellowing is an other type of yellowing because of atmospheric contaminants during storage (Bağıran, 2017; Karagöz, 2009).

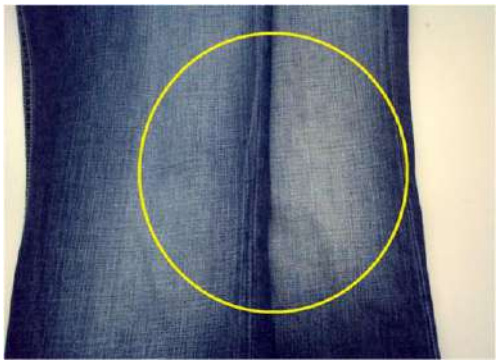

Fig. 7 Yellowing problem (Karagöz, 2009)

Recommended Solution :

- ✓ After hypochlorite bleaching neutralisation is necessary for removing residual chlorine.
- ✓ Optical brightening and softening processes should be properly controlled.
- ✓ The water used for washing should be free of hardness (Bağıran 2017; Karagöz, 2009; Paul, 2015).

3.3. The other defects

The other defects are generally occur because of accessories and thread.

Corrosion of metal parts: If the metal accessories add on the denim garment before washing, metal parts can be destroyed by the effect of water, chemicals etc.

Recommended Solution : After wet processes metal parts should add on the garment.

Label deterioration: During the washing label can be damaged because of chemicals, mechanical effects and temperature. If the proper label is used color of the label can bleed (Bağıran, 2017).

Fig. 8 Bleeding of label color(Bağıran, 2017)

Recommended Solution :

- ✓ Before washing labels should be tested.
- ✓ Good cooperation between fabric producers, garment manufacturers, laundries and chemical suppliers is essential to obtain the desired results (Bağıran, 2017; Paul, 2015).

References

Aslan, M., (2004). *Denim yıkama prosesinde enzim kullanımı*, Yüksek Lisans Tezi, Ege Üniversitesi, Fen Bilimleri Enstitüsü, İzmir.

Bağıran, İ. C., (2011). *Denim yıkamada karşılaşılan sorunlar ve bunlara yönelik çözüm önerileri*, Yüksek Lisans Tezi, Ege Üniversitesi, Fen Bilimleri Enstitüsü, İzmir.

https://www.denimsandjeans.com/denim/manufacturing-process/latent-defects-in-denim-fabrics/1432, (Erişim Tarihi: 10 Haziran 2018).

https://www.denimsandjeans.com/denim/manufacturing-process/common-defects-in-denim-jeans-sewing/3192, (Erişim Tarihi: 10 Haziran 2018).

Karagöz, G., (2009). *Denim yıkama işlemlerinde ortaya çıkan zararlar nedenleri ve çözüm olanakları*, Yüksek Lisans Tezi, Ege Üniversitesi, Fen Bilimleri Enstitüsü, İzmir.

Paul, R. (2015). Denim Manufacture, Finishing and Applications. Cambridge: Woodhead Publishing
ihi: 22 Mart 2017).

Tortora,G. P., Merkel, R. S. (2007). *Fairchild's Dictionary of Textiles*. New York: Fairchild Publication

High Strength Braiding Ropes for Different Applications

Pınar ÇELIK[1*], Tuba BEDEZ UTE[1], Hüseyin KADOGLU[1]

[1]Ege University, Engineering Faculty, Textile Engineering Department, Izmir, Türkiye

[*]**Corresponding author:** pinar.celik@ege.edu.tr

Abstract

Ropes are structures made of textile fibres. Twisting or braiding techniques are used to arrange and contain the rope elements. The tubular braids are used for ropes and other tubular products. “Braiding is a process of interlacing three or more threads diagonally to the product axis (parallel to the longest dimension of the resulting product) in order to obtain a thicker, wider or stronger product or in order to cover (overbraid) some profile.” [Kyosev, 2015]

Ropes are used in different industrial areas such as construction, maritime and mining. Although natural fibers such as cotton, linen, hemp, jute, sisal and ramie are still used in rope production, today synthetic fibers replace natural fibers for ropes. Due to the development of synthetic fibers and fiber ropes of increasingly higher quality, textile ropes can be used in many industrial applications. High strength, abrasion resistance and fatigue specifications are very important for ropes. The aim of this paper is introducing about braiding ropes, their production methods and their specifications.

Key words: Braiding, Textile ropes, High strength, Abrasion resistance, Synthetic fibers

1. Introduction

"Rope is a product obtained when three or more strands are twisted or braided or paralleled together to provide a composite cordage article larger than 4 mm in diameter." (ISO, 2001)

"Braiding is a process of interlacing three or more threads diagonally to the product axis (parallel to the longest dimension of the resulting product) in order to obtain a thicker, wider or stronger product or in order to cover (overbraid) some profile."[Kyosev, 2015]

Designing of a rope is very important for its performance. For a successful rope design, understanding the characteristics of each component in a rope and knowing how each component will perform when combined to construct a rope are key points. Ropes are commonly produced either twisted or braided. [http://www.novabraid.com/resources/rope-guide]

Ropes have been used for hunting, carrying, lifting, and climbing since prehistoric times. Ropes were made by hand using natural fibers, but now ropes are made by machines and utilize many synthetic materials to give them improved strength, lighter weight, and better resistance to rotting. Ropes are generally manufactured for using in the fishing and maritime industries today. [www.swicofil.com/ropes.html]

2. Rope Materials

Natural and synthetic fibers are used for making rope. Abaca (manila), sisal, henequen, jute, hemp, flax and cotton are the most common natural fibers for ropes. Abaca fibers are more flexible than sisal fibers due to having a large lumen of their fiber cells and this property gives some natural buoyancy. The member of the agave family, henequen yields fibers similar to sisal. The advantage of natural fibers is their biodegradability. For example, sisal and henequen are still commonly used in binder twine. In addition, abaca (manila) is used for higher-quality ropes, when consumers want a traditional product or where the impact of synthetic fibers is weaker. [McKenna et al., 2004]

After synthetic fibers (Polyamide 6, polyamide 6.6, polyester (PET), polyethylene (PE), polypropylene (PP) and high modulus and high tenacity fibers (aramid, high modulus PE)) were developed, these fibers have begun to widely used in the rope industry. One of main advantages

of synthetic fiber ropes is their lightweight. For example, high strength synthetic fiber rope also can be used in greater depths than wire. [Whitehill, Jr., 2018]

Designing of a rope is very important. All natural or synthetic fibers have different specifications, so that the materials and combination of these materials are determined according to application aim of rope usage. Aramid yarns have poor abrasion resistance; on the other hand Vectran and HMPE have ten times better abrasion resistance and polyester has a hundred times better [Whitehill, Jr., 2018]. The natural and synthetic fibers' properties have been given in Table 1 and Table 2.

Table 1 Properties of major natural rope fibres [McKenna et al., 2004].

	Cotton	Abaca	Sisal	Flax	Hemp	Jute
Density (g/cm3)	1,54	1,32	1,32	1,54	1,5	1,5
Moisture (%) 65 % rh, 20°C	7,5	7,5	7,5	7	8	12
Tenacity (mN/tex)	300	530	440	540	470	310
Strength (MPa)	460	700	580	810	705	465
Break extension (%)	7	3	3	3	1,8	2,2
Modulus (N/tex)	5	20	20	18	21,7	17,2
Modulus (GPa)	8	30	30	27	32,6	25,8
Rupture work (mN/tex)	5	5	5	8	5,3	2,7

Table 2 Properties of major synthetic rope fibres [McKenna et al., 2004].

	Nylon	PET	PE	PP	Aramid	TLCP	PBO	HMPE	Steel
Density (g/cm3)	1,14	1,38	0,95	0,91	1,45	1,40	1,55	0,97	7,85
Melting point (°C)	258*	258	140	165	decom.500	330	decom.650	150	1600
Moisture (%) 65 % rh, 20°C	5	<1	0	0	1 to 7	0	0	0	0
Tenacity (mN/tex)	840*	820	530	620	2000	2200	3700	3500	330
Strength (MPa)	960	1130	500	560	2900	3100	5700	3400	2600

Break extension (%)	20	12	20	20	3,5	3,5	3	3,5	yld at 2
Modulus (N/tex)	7**	11	4	7	60	55	180	100	20
Modulus (GPa)	8**	15	4	6	90	80	280	100	160
Rupture work (mN/tex)	80	50	50	60	35	40	55	60	yld

* Nylon 6.6–218°C for nylon 6.
** Less when wet.

3. Rope Construction

Ropes are constructions made of natural or synthetic textile fibers. The ropes can be defined as about cylindrical textile bodies whose cross-sections are small compared to their lengths and they are generally used under tension. When producing a rope, generally the structure of rope is designed according to selected yarn tenacity and breaking elongation. [McKenna et al., 2004]

The creation of high-performance rope depends on some parameters; characteristics of each component, the performance of each component when combined to a construct a rope, application area, etc. [http://www.novabraid.com/resources/rope-guide]

Twisting or braiding techniques are commonly used to arrange and contain the rope elements [McKenna et al., 2004]. The advantages of twisted ropes are easy manufacturability, relatively cheapness and disposability. It is not anticipated that twisted ropes should have very high strength or be very durable. They are generally used to tie-up packages. However, braiding ropes have high strength. On the contrary of twisting ropes, it is anticipated that braiding ropes should have very high strength or be very durable. Industrial, marine, recreation and general utility service are general usage areas. Their application areas cover everything; hawsers for mooring tankers, include clothes-lines, yachting ropes, haul lines for fishing nets, lifting slings, and a host of other applications. [http://www.novabraid.com/resources/rope-guide]

The essential steps of manufacturing are "textile yarn - rope yarn - strand" and the final stage is strand - rope which is better defined for the different rope types [McKenna et al., 2004]. Yarn is the basic component of rope and fibers or filaments are first formed into yarn. The yarn is then twisted, braided, or plaited according to the type of rope being made. The diameter of the rope is determined by the diameter of the yarn, the number of yarns per strand, and the number of strands or braids in the finished rope. [www.swicofil.com/ropes.html]

Circular braiding is a traditional technique normally employed for producing rope-like structures [Rawal, A., et al., 2015]. Braiding is a highly versatile and cost-effective method of producing structures that has been successfully used for numerous applications ranging from ropes, composites, biomedical uses, insulation to sports and recreation activities, and the list of applications of braided structures is ever-increasing. [Rawal, Saraswat, Sibal, 2015]

For cords and small ropes up to about 8mm diameter, the most popular construction is an eight-strand braided. Additionally twelve-strand is also found. When produced rope from 12mm to 96 mm diameter, twelve-strand construction is used. For above 96mm diameter ropes, the strands become too large for effective strength conversion and the structure is too loose, making it difficult to handle. [McKenna et al., 2004]

Figure 1 Tubular braids (rope). (a) Geometrical model and (b) single (upper part) and tripple (over-) braided part. [Kyosev, 2015]

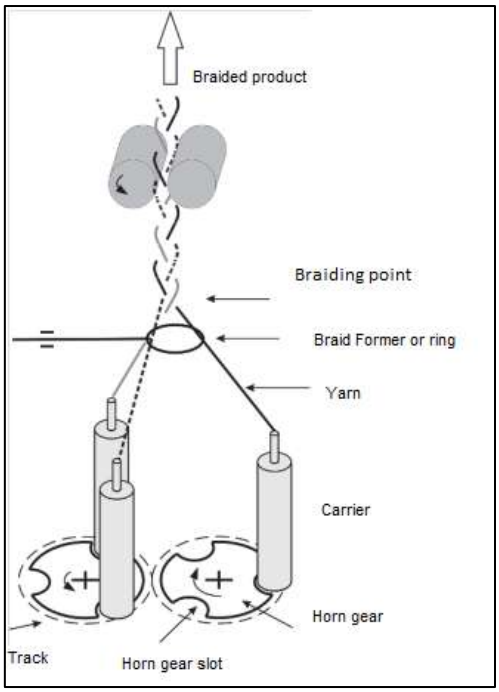

Figure 2 Principal construction of maypole braiding machine. [Kyosev, 2015]

The cycle length or pitch (cycle length/number of strands in one direction) for braided ropes is the distance from one location to where a strand reappears, making certain the axial line is straight, at a reference tension (Figure 3). Parameters such as helix angle can be determined from these measurements when the radius to the centre of a strand and the number of strands are known. For high modulus materials it is necessary to use a relatively long braid pitch length, which can result in a very soft rope.[McKenna et al., 2004]

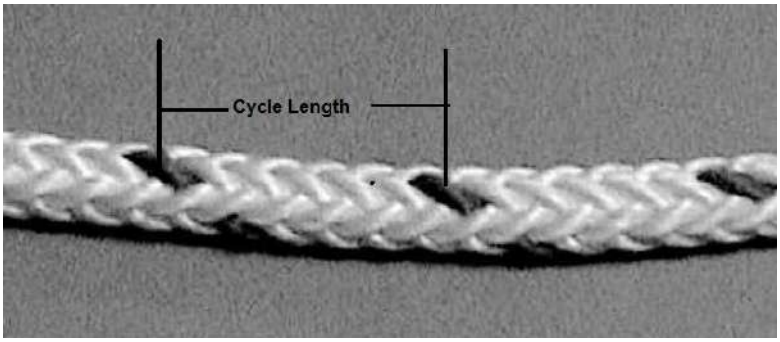

Figure 3 Cycle length (pitch) [McKenna et al., 2004]

4. The Types of Braided Ropes

Hollow single-braided rope: Hollow braids are made in a maypole fashion. Its structure can occur from the full range of low and high modulus fiber materials. The tree service work where the firmness is preferred is its popular application area. The long pitch rope is used in

many commercial applications where are important for high strength, reduced elongation and splice-ability because of its stronger, soft and pliable and can be spliced.

Double-braid (braid – on- braid) rope: Its structure consists of a braiding cover rope and a braided core. The core part and the cover part are shared the tension in the rope. Nylon, polyester, combination of these materials and polypropylene are common materials. Such ropes are generally used for mooring oil tankers to buoys in the open sea where a single line or pair of lines are used

Braided rope with jacket construction: The structure of this rope consists of a double braid rope in which a hollow braided or plaited core (high strength, high modulus material) is used to carry to load. On the outer of the rope a braided jacket (polyester) protect the rope from external abrasion. The electrical utility service is its most popular application area (Figure 3).

Solid braid rope: Its industrial applications are limited. Tie-downs, clothes-lines, flag halyards, and awning lines are its typical uses areas. [McKenna et al., 2004]

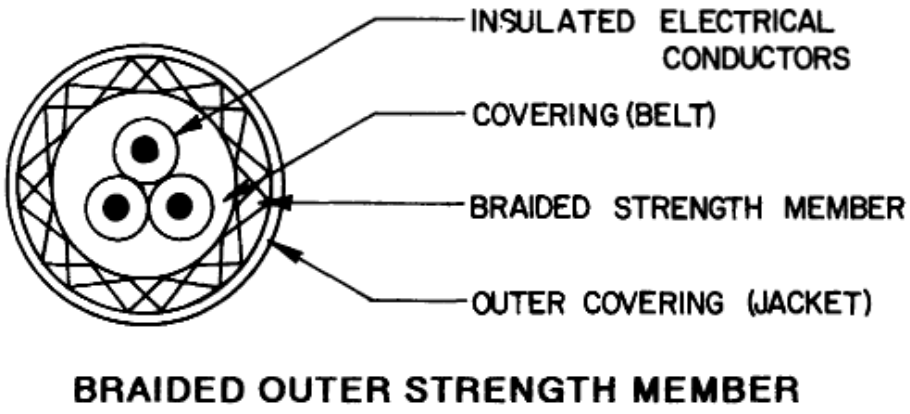

Figure 3 Braided rope with jacket construction [Bash, 2001].

5. Conclusion

In this article, braiding ropes, their production methods and their specifications have been explained. A rope is subjected to very different effects depending on its use: tension, bending, friction and mechanical damage; as well as a wide range of environmental variables such as temperature, chemical exposure, UV exposure, salt water exposure, etc.

Braided ropes are commonly made from synthetic materials. Besides material properties, braid architecture, such as biaxial or tri-axial braided structures, have important effect on the tensile behavior of the rope. Especially the braid angle is a key parameter that controls the tensile properties of braided structures. [Rawal, Saraswat, Sibal, 2015]

The level of quality control varies according to the application area of a rope. If the rope is produced for general purpose, the diameter and tensile strength of the rope can be enough. On the other hand, for high-risk applications, the inspection and testing of ropes should have been done more carefully and detailed. When any abrasion and overextension are monitored, the rope should be replaced. [www.swicofil.com/ropes.html]

Abrasion resistance is also very important for ropes. Abrasion occurs in two ways: between the rope components and between the rope and the handling equipment. Several operational factors including line speed, tension, cable to sheave alignment and bend diameter as a ratio of cable diameter, etc. effect on abrasion rate. [Bash, 2001]

Acknowledgments

This study was funded by Ege University Scientific Research Projects (Project No: 16.MUH.078).

References

Kyosev, Y., (2015). Braiding Technology for Textiles. Woodhead Publishing in association with The Textile Institute, ISBN 978-0-85709-135-2

http://www.novabraid.com/resources/rope-guide/ (Erişim Tarihi: 25 Nisan 2018)

Rope Market information and basics - yarns for ropes - Swicofil, www.swicofil.com/ropes.html (Erişim Tairihi: 25 Nisan 2018)

McKenna, H.A., Hearle, J.W. S., O'Hear, N.,(2004). Handbook of fibre rope technology. Woodhead Publishing Limited in association with The Textile Institute, ISBN 1 85573 606 3

Whitehill, Jr., A.S., High Strrength Synthetic Fiber Ropes. http://www.sssg.whoi.edu/sssg/winch_wire/UNOLS_Winch_and_Wire_Handbook/03_synthetic_fiber_ropes.pdf (Erişim Tarihi: 13 Nisan 2018)

Rawal, A., et al.,(2015). Geometrical modeling of near-net shape braided preforms. Textile Research Journal, 85(10), 1055–1064.

Rawal, A., Saraswat, H. and Sibal, A., (2015). Tensile response of braided structures: a review. Textile Research Journal, 85(19), 2083–2096.

Bash, J.F., (2001), Handbook of Oceangraphic Winch, Wire and Cable Technology, 3rd Edition.

Deep Rope Manuel 2004, Digital Version. https://ocw.tudelft.nl/wp-content/uploads/deepropemanual.pdf (Erişim tarihi: 25 Nisan 2018)

Time-dependent Strength Change of Emergency Tent Fabric after UV Exposure

Emrah TEMEL[1*], Faruk BOZDOĞAN[1], Deniz MİZMİZLİOĞLU[2]

[1]Ege University, Engineering Faculty, Textile Engineering Department, İzmir, Turkey
[2]Ege University, Institute of Science, Textile Engineering Department, İzmir, Turkey

[*]**Corresponding author:** emrah.temel@ege.edu.tr

Abstract

Emergency tent is a basic human need and a critical determinant for survival and coping in the majority of crises. There are many reasons people might need temporary shelters. Natural disasters like hurricanes, earthquakes, floods, fires, and tornados are some of them. Millions of people around the globe have had their lives disrupted by these disasters. The environmental health conditions faced by people are largely affected by the conditions where they are obliged to live in the days, weeks or months after a disaster. The quality of emergency tent available has a great impact on health and well-being. Therefore, mechanical properties of the tent fabric will be vital for sufferers. Since these tents are used under natural environment, tent fabrics have to face with natural exposures that force the mechanical strength of the fabric. One of the most important of these effects is UV exposure. It is known that fabrics lose their strength under UV light. In this study %100 cotton tent fabric was aged under UV exposure (35 w/m^2) for 0, 250 and 500 hours. After UV exposure, tensile strength, tear strength, mechanical bursting strength and air permeability tests were conducted to tent fabrics.

Keywords: Tent fabrics, UV exposure, UV aging, tensile strength, tear strength.

1. Introduction

Millions of people around the globe have had their lives disrupted by disasters. The provision of emergency shelter is a last resort when no other solution can be found for homeless people. Therefore, emergency tents must exhibit high strength against environmental conditions and exposures. Physical properties of emergency tents are directly related to the living standards of the users (Manfield, 1999; Crawford et al., 2005).

One of the most important problems faced by emergency tents is UV exposure. Tents are constantly exposed to UV exposure as they remain under the sun light during the day. Since UV radiation degrade the molecular chains of the fabric material tent fabric loses its strength over time (De et al., 2005). The phenomenon of 'weathering' of polymeric materials is usually caused by a complex series of chemical reactions initiated by the absorption of ultra-violet light which ultimately result in the deterioration of the physical properties of the polymer (Guillet, 1972).

The deterioration of polymers in outdoor weathering is caused primarily by sunlight, especially ultraviolet radiation. Sunlight reaching the earth is filtered through the atmosphere, removing shorter wave-lengths up to 280-310 nm before it reaches the surface of the earth. Beyond 380-400 nm, the light becomes visible to the human eye. Thus ultraviolet effects on polymers result primarily from wave-lengths of approximately 300-400 nm, which is ~5% of the total solar radiation reaching the earth. The sun has an approximate Boltzmann distribution of energy with a peak maximum at a wavelength of approximately 400-500 nm. However, the shorter wavelengths are not available at the earth's surface because they are absorbed by the ozone layer in the upper atmosphere. As a general rule, only light having a wavelength exceeding 300 nm reaches the earth's surface. This restricts the number of reactions which may occur (Deanin et al., 1970).

Most polymers contain functional groups which absorb ultraviolet light. Most prominent and frequently-mentioned is the carbonyl C=O group, whose ultraviolet absorptions have been observed at 270-360 nm in different compounds.

Polymers such as plastics and rubbers, consist of long molecular chains. These can vary in length, complexity and orientation, and these factors all contribute to the overall material behaviour. Specific polymers possess specific chemical groups and bonds in their structure. These different chemical groups absorb differing amounts of energy. Unfortunately most of these chemical groups have big absorbance within the UV spectrum. Furthermore, ultraviolet can cause breakdown of many polymer (http://www.drb-mattech.co.uk/uv%20degradation.html). Figure 1, demonstrates some of the typical chemical

groups and their absorption energies. Table 1, demonstrates ultraviolet wave lengths for typical commercial polymers.

Pure native cellulose absorbs UV radiation strongly between 200 and 300 nm, but only very weakly up to 400 nm. Two pathways are important in cellulose degradation: oxidation of the hydroxyl side groups (changes in the color, polarity, solubility and water absorption–desorption properties) and rupture of the glycosidic ether bonds between cellulose units (Wypych, 2015).

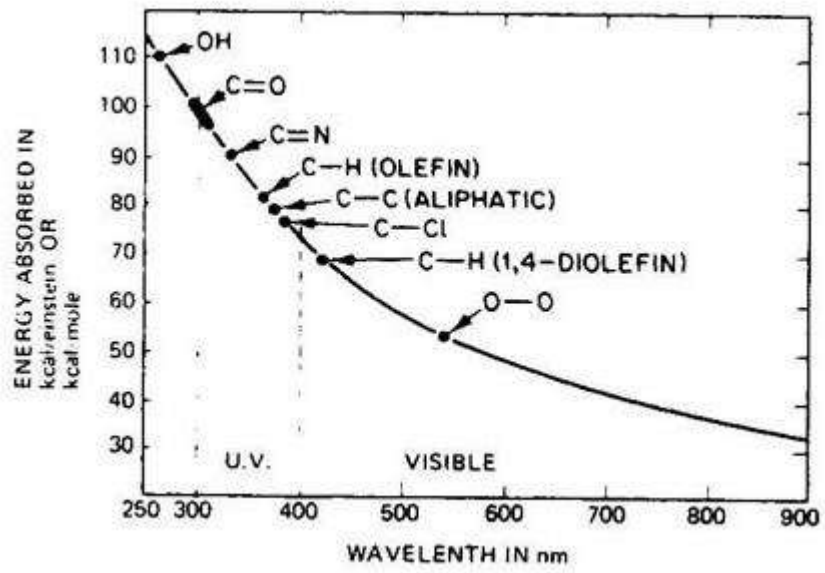

Figure 1. UV absorbtion energies and wavelengths of chemical groups (http://www.drb-mattech.co.uk/uv%20degradation.html).

Table 1. Ultraviolet wave lengths for typical polymers (Deanin et al., 1970)

Polymer	**Ultraviolet wavelength of maximum sensitivity (nm)**
Polyester	325
Polystyrene	318
Polyethylene	300
Polypropylene	310
Polymethyl Methacrylate	290-315
Polyformaldehyde	300-320

Hence the addition of energy via UV photons can produce significant absorptions of energy by the material and if the energy is sufficient can lead to breaking of the molecular bonds, effectively cutting the molecular chains. These leads to a reduction in molecular weight and subsequent loss in elastic behavior, cracking and general reduction in the mechanical properties (http://www.drb-mattech.co.uk/uv%20degradation.html).

The chemical changes caused by short-term UV-irradiation are confined to fibers at the fabric surface and UV is unable to penetrate beyond the surface to weaken the bulk fibers responsible for the mechanical strength. This has enabled the potential application of UV technology as a surface-specific treatment in several areas (Millington, 2000).

UV degradation impact of a fabric may effected by many textile properties. These parameters include mass per unit area, fiber type, yarn construction, finishing process and coloration process etc. (Kurşun & Özcan, 2010). Nevertheless, the most important factor affecting the fabric strength is UV exposure duration. Therefore, in this study tent fabrics were aged under UV exposure for different periods and investigated their mechanical properties.

2. Materials and Methods

In this study the aim is to investigate the time dependent strength change of emergency tent fabric after UV exposure. For this purpose, %100 cotton tent fabric was aged in a UV aging cabin for 250 and 500 hours. After aging process, aged fabrics and untreated tent fabric were conducted to tensile strength test, tearing strength test and air permeability test. Tensile strength and tearing strength tests were performed on Zwick Universal Tensile Testing Machine by using TS EN ISO 13934-1 and TS EN ISO 13937-2 test standards respectively. Tearing strength test was also conducted to test samples on Elmendorf Ballistic Pendulum Tear Tester by using TS EN ISO 13937-1 test standard. Air permeability test were applied on TEXTEST FX 3300 Air Permeability Tester under 200 Pa air pressure.

The detailed description of the test material is given below in Table 2.

Table 2. Description of test material

Property	**Description**
Material	%100 cotton
Weaving pattern	1x1 plain weave
Warp density	20 ends/cm

Weft density	11 ends/cm
Mass per unit area	580 g/m^2

Aging process was applied to test materials on Prowhite UV Test Box under 35 watt/m^2 light intensity for 250 and 500 hours.

3. Results and Discussion

0, 250 and 500 hours aged %100 cotton tent fabrics were conducted to tensile strength, tear strength and air permeability tests. Test results are given below in Table 3 and Table 4.

Table 3. Tensile strength test results of samples

Samples	**Tensile strength (N)**		**Elongation (%)**		**Work of rupture (Nmm)**	
	Warp direction	Weft direction	Warp direction	Weft direction	Warp direction	Weft direction
Untreated	2297,16	1263,70	22,19	9,63	21477,00	5008,00
250 hours treated	1551,31	934,40	17,94	8,62	12037,75	3172,00
500 hours treated	1330,84	777,54	17,01	7,99	10167,75	2510,75

Table 4. Tear strength and air permeability test results of samples

Samples	**Tear strength (Trouser Tear) (N)**		**Tear strength (Ballistic pendulum) (N)**		**Air permeability (l/m^2/s)**
	Warp direction	Weft direction	Warp direction	Weft direction	
Untreated	34,18	42,62	38,58	57,63	12,49
250 hours treated	23,53	26,73	29,70	39,02	12,88
500 hours treated	10,93	14,92	25,27	32,13	13,28

When the effect of the UV exposure duration on tensile strength is examined, it can be denoted that increase in exposure time results in loss in tensile strength both in warp and weft direction. It is thought that, this result is mainly depends on degradation of hydroxyl side groups and rupture of the glycosidic ether bonds between cellulose units as Wypych (2015) mentioned in his study. Wypych (2015), also stated that degradation of hydroxyl side groups cause change in material color. In Figure 2 it can be clearly seen that, the sample that was exposed to the maximum UV light was the sample that was most yellowish.

As all specimens were considered, no significant difference is observed between the elongation values of the samples except warp direction for untreated sample. Since the untreated sample was not degraded and the test was performed in warp direction, untreated sample showed very high tensile strength values. For that reason, the elongation value is thought to be high. As work of rupture values were evaluated, it can be clearly seen that, work of rupture values highly depend on tensile strength and breaking elongation values. Therefore, it can be pointed out that the shorter the sample exposed to UV degradation, the higher work of rupture value has.

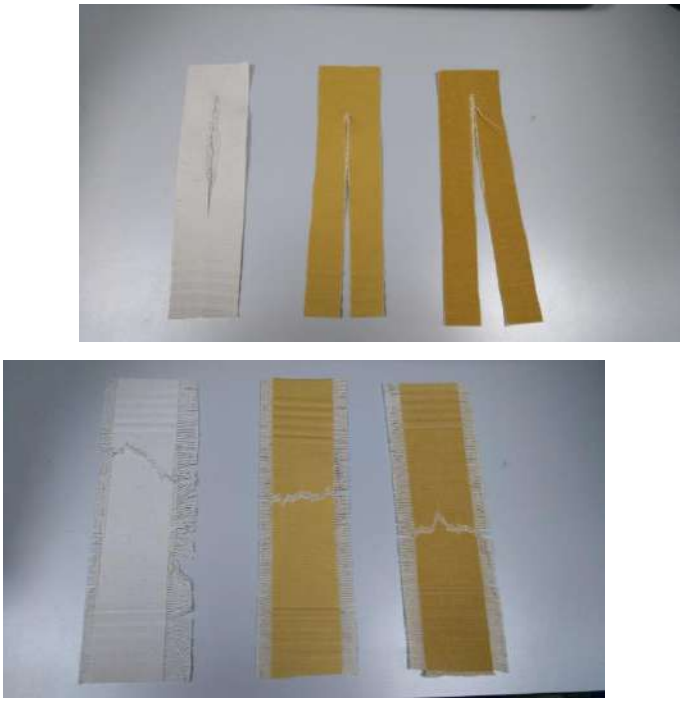

(a) (b)

Figure 2. Samples that were conducted to tearing (a) and breaking (b) strength tests after UV exposure for 0, 250 and 500 hours respectively.

When the ballistic pendulum and trousers tearing strength test results are examined, it can be stated that, the fabric the most exposed to UV degradation has the most loss of strength, as expected. This situation is also associated with degradation of hydroxyl side groups and rupture of the glycosidic ether bonds between cellulose units as mentioned above.

Figure 3. Ballistic pendulum tearing strength test

When air permeability test results examined, it was determined that samples demonstrated nearly same air permeability test values with 12-13 ($l/m^2/s$). This obtained result can be summarized as; UV degradation has no effect on air permeability.

4. Conclusion

Sunlight, especially ultraviolet radiation can cause massive degradation on polymers. Therefore, fabrics which are exposed to sunlight for a long time are under the risk of mechanical disruption. Since tents are equipments that are used under the sun, tent fabrics are also among those at risk.

In this study 100% cotton tent fabrics were aged under UV exposure in a UV cabin with $35w/m^2$ light intensity for 250 and 500 hours. After aging process mechanical strength changes were compared with untreated tent fabric. Cellulose absorbs UV radiation strongly between 200-300 nm, and this gap is involved by the ultraviolet region that reaches the world from atmosphere.

Due to cellulose UV degradation mechanism exhibits oxidation of the hydroxyl side groups and rupture of the glycosidic ether bonds between cellulose units, after 500 hours of UV aging process, tent fabric lost its half tensile strength compared to untreated fabric. In addition to this, degradation of hydroxyl side groups also cause color change from white to yellow as stated above. And this situation could be seen from Figure 2.

References

Crawford, C., Manfield, P. and McRobie, A., (2005). Assessing the thermal performance of an emergency shelter system, *Energy and Buildings*, 37, pp. 471 – 783.

De, P., Sankhe, M. D., Chaudhari, S. S. and Mathur, M. R., (2005). UV-resist, Water-repellent Breathable
Fabric as Protective Textiles, *Journal of Industrial Textiles,* Vol. 34, No. 4, pp. 209 – 222.

Deanin, R. D., Orroth, S. A., Eliasen, R. W., and Greer, T. N., (1970). Mechanism of ultraviolet degradation and stabilization in plastics, *Polymer Engineering & Science*, 10(4), 228-234.

Guillet, J. E., (1972). *Chemical Transformation of Polymers*, Elsevier.

Kursun, S., & Ozcan, G., (2010). An investigation of UV protection of swimwear fabrics, *Textile Research Journal*, 80(17), 1811-1818.

Manfield, P. (1999). A Comparative Study of Temporary Shelters used in Cold Climates, *Martin Centre*.

Millington, K. R., (2000). Comparison of the effects of gamma and ultraviolet radiation on wool keratin, *Coloration Technology*, 116(9), 266-272.

Wypych, G., (2015). Handbook of UV Degradation and Stabilization. *ChemTec Publishing*

http://www.drb-mattech.co.uk/uv%20degradation.html

Smart Textiles: A General Perspective

Merve TÜREMEN[1], Aslı DEMIR[2]

[1] Graduate School of Natural and Applied Sciences, Ege University, Izmir- Turkey
[2]Department of Textile Engineering, Ege University, Izmir-Turkey

[*]**Corresponding Author:** asli.demir@ege.edu.tr

Abstract

Smart textiles are able to sense stimuli from the environment, to react to them and adapt to them by integration of functionalities in the textile structure. The first labeled material as a "smart textile" was silk thread having a shape memory property. The input and reaction can be mainly thermally, electrically, chemically, magnetically. Smart clothing has applications in medical, space travel and the military areas where observation and activation is of importance.

Textile industry has made progression from technical performances to the smart textiles. These textiles comprise fabrics with thermo-regulators, moisture management and fabrics designed to increase competitive performance by increasing speed, mobility, and continuation.. Some more advanced materials are now being created that both react and transform, but the majority of textiles for increased physical performance are passive smart textiles.

Smart clothing incorporates an array of conducting strands interwoven with textile yarn, which enables it to become sensory and provide useful information to the wearer. On the face of it, the clothing may not look drastically different from any other.

The main principles of science are progressively employed for the manufacturing of innovative textile materials. In this study, a general evaluation of smart textiles will be made by giving some current implementations. Also, the potential developments of them in the future will be presented.

Keywords: Smart textile, responsive, stimuli, electronic textile.

1. Introduction

Smart textiles can be defined as textiles that are able to sense and respond to changes in their environment. They can monitor man and his environment and react in an appropriate way. In its simplest form it provides information about a person; the environment of the textile itself. Adequate analysis of such data may allow rapid identifi cation of health risks. This is particularly important for protection, as it provides a chance to prevent incidents and accidents from happening (Langenhove,2007;Chapman,2013)

Textile materials or systems that are able to sense an external stimulus such as electrical, thermal, chemical, magnetic or others. Especially, the potential impact of smart textiles for healthcare is of great significant. The risk assessment and diagnosis will be made more carefully, treatment and care will be more effective and faster. Because of their possibilities to large amounts of information about wearers such as posture, heart rate, pH levels or even the presence of infections, smart textiles have great potential. These kinds of data have been used for monitoring vital signs of patients and soldiers, firefighters, so on.(Haladjian,2016)

The textile material may incorporate the following functions to build up a smart textile system as folowing:

- Sensing.
- Actuating.
- Powering/generating/storing.
- Communicating.
- Data processing.
- Interconnecting.

Sensing

A smart textile should have a sensing function to feel and adopt changes in the surrounding conditions. For this aim, sensor is used which can be defined as a device providing information mostly in the form of an electrical signal. Textile integrated sensors could measure different variables, e.g. physical dimensions like pressure, stress and strain applied to the textile or biomedical dimensions such as heart rate, electrocardiogram, sweat rate and composition, arterial oxygenation (SpO2) of the monitored subject. (Schwarz,2010; Rothmaier, et al., 2008).

Actuating function

The requirements for personal mobility, healthcare, or rehabilitation require that novel functions in sensing and actuating be integrated into textiles. The actuators' assignment in smart textiles is to react to the signal coming from the sensor or data-processing unit, respectively. The type of reaction may be in form of movement, noise or substance release. For instance, actuators based on ICPs (Inherently Conducting Polymers) can generate much higher stresses with a strain than that of a natural skeletal muscle, and change their resistivity or generate an electrical signal in response to external stimuli. (Schwarz,2010; Coyle et al.,2007)

Data processing

A suitable system is necessary to record the data and to support sensors, processes it in some way, and transmits it. It should be as light, small, and easy to wear as possible. Data processing, storage and transmission circuitry in clothing via integrating sensors provide the patient's comfort, mobility and privacy. Electronic devices are still necessary to provide a computing ability(Catrysse,2004; Axisa 2005)

Power supply and storage

Smart textile materials can be labeled as "smart" not only by using such materials strategically, but also by incorporating smart wearable electronics that can perform the sensing and responding activities. Four key elements have to be considered: flexible electrical and data conductivity, flexible sensors and actuators, wireless communication, and power supply. Different power sources such as batteries and solar cells can be used for smart textile applications including electronic components of a smart garment can be in the form of AC/DC charge interface, lithium ion polymer battery and/or solar cell interface(Tang et al., 2006 ; Stoppa et al., 2014).

Communication and Interconnection

Among the components of a smart textile (or garment) and between the garment and its wearer, communication is mandatory. In the last years, smart textiles with wireless communication to monitor the bio-signals are increasing.Especially in a medical environment it is necessary to communicate on a longer distance to provide immediate help in case of risky situations(Shen 2006).

The electronic components that make up a smart textile system must be connected to each other in order to create versatile, interactive systems.Wires, cables and connectors are common physical materials used in the electronic world to connect electronics together. Wireless network sensors,, mobile devices, intelligent wearable devices and data communication networks will create an intelligent environment and help with long-distance health care . Their current abilities include physiological, biochemical, and motion sensing. SWS are used in areas ranging from 'telehealth', 'telehealthcare', 'telemedicine', 'telecare', 'telehomecare', 'e-health', 'p-health', 'm-health', 'assistive technology', or 'gerontechnology(Chan 2012; Schwarz,2010).

2. General Overvıew Of Smart Textıle Applıcatıons

The complexity and broadness of knowledge required makes smart textile research interesting but also challenging. Smart textile systems span the range of serious applications such as healthcare, fashion, sports and wellness, safety and security, automotive and transport construction, security, geo-textiles, lighting, industrial applications, defence, agro-textiles, home and interior textiles, packaging, architecture, energy, telecommunications, and displays.

Some applications of smart textiles is given below:

Medical area

The largest market for smart textiles is to be found in the medical sector, which will become an $843 million market by 2021. Using smart clothing, patients with chronic diseases, such as diabetes and heart problems, will continuously and simply monitor their health and send updates to their physician, providing more useful data and avoiding office visits(https://globenewswire.com,2016)

In smart textile applications, health and wellness is regarded as main application and usage areas. Sensors and textile based diagnostic systems are great instruments in following the situation of patients, managing risk and making diagnoses more accurately. Smart textiles have been used to develop textiles that monitor the health of infants, provide healing by light therapy, and detect physiological parameters such as heart rate and respiration for long-term patient health monitoring(Cherenack et al, 2012).

Smart textile applications may help the aging population to stay home longer, and they are used for rehabilitation of injured or disabled patients. Infant monitoring, mobile health monitoring, drug releasing textiles, surgical implants, wound care, and even human spare parts are among current medical applications. Medical applications are diverse and cover a large range of needs for textile structures from bed sheets, surgical clothing and bandages to more complex textiles such as light-emitting fabrics used for photodynamic therapy, stents, composite heart valves or blood vessels(Tao,2008)

Transportation, energy and industrial applications

The transportation industry such as automotive, railway and aerospace is an important field of smart textile applications. Thes most important target is the decreased the weight of vehicles and planes to improve their efficiency and behaviour. As rapidly developing textile manufacturing technologies, textile composites are increasingly used for 3D-composite reinforcement design and manufacturing. Thus, smart and communicative composites with embedded sensors, connected to devices, are able to control in real time and to alert in case of problems (predictive maintenance) will be a reality in the next few years. Also, energy issues are getting more important today. Smart textiles have great contributions for energy harvesting and production by flexible photovoltaic cells, wind mills, piezoelectric yarns and for energy storage as super capacitors and flexible batteries.(Tao,2008 ; Mattila, 2010)

The industrial application segment is anticipated to lead the market in the near future. There is an increasing demand for smart and interactive textiles from the transportation industry are regarded as one of the major factors for the growth of the market. New applications such as measuring the heating of seats, smart seat belts and functioning of steering wheels hold extensive potential in the automotive industry. The promising applications of smart textiles in industrial applications comprise various protection devices such as personal protective equipments used in industrial plants, manufacturing facilities(Patwary,2015).

Protection

Security and protection of people are of significance for smart textiles. Firemen's uniforms, police and military equipment, and ballistic structures with embedded multilayer textiles are some examples of where smart textile devices have found their effectiveness.

The military forces are exploring in order to increase the safety and effectiveness of them. There is a need for real time information technology on protection and survivability of the

people working in extreme hazardous situations and environmental conditions. The requirements for such situations are to monitor vital signs and ease injuries while also monitoring environment hazards such as toxic gases. Wireless communication to a central unit allows medics to conduct remote triage of casualties to help them respond more rapidly and safely (Patwary,2015;Mattila, 2010)

Military applications are one of the primary subjects for smart textiles. Soldiers are exposing too many threats in different ways. Smart textiles serve a function in camouflage clothing. Also, smart dyes can adopt the colour of the environment. Metamaterials can be used for redirecting light rays around an object and setting them back on path out the opposite end. The object has virtually become invisible and the results can be obtained on 2D structures and on wavelengths out of the visible range. (Chapman,2013).

In protective clothing, high-performance fibres including carbon and glass are too stiff and brittle to be used. Therefore, special fibers such as piezeoelectric fibers, shape memory polymers and phase changing materials have gained popularty for smart protective textile applications.

The piezoelectric effect has mostly been investigated in regard to converting mechanical energy into electric energy. Of decisive importance for the piezoelectric effect is the polarization change in the piezoelectric material under a mechanical stress. If the rate of change of stress is high, a very high electric field can be generated. Some polymers, when in the right form, can exhibit the piezoelectric effect and this can also be enhanced by the addition of inorganic particles. The thermoplastic fluoropolymer, polyvinylidine fluoride (PVDF) shows the strongest piezo effect and it can be processed into extruded fibres and films (Chapman,2013;Weng,2016)

Thermo-regulated textiles are a type of smart new textile product that contains low temperature phase-change materials (PCM). Phase change materials have an bility to change their state with a certain temperature range. These materials absorb energy during the heating process as phase change takes place, otherwise this energy can be transferred to the environment in the phase change range during a reverse cooling process. These changes occur with a large transfer of energy, which is required to drive the transition or is evolved when it is reversed. The human body cools itself very efficiently by evaporating water (sweat), which requires about 2260 kJ/kg to do so. Textiles containing phase change materials react immediately with changes

in environmental temperatures, and the temperatures in different areas of the body. By using these systems with incorporated phase change material for protective clothing, the wearer's comfort can be improved significantly and the phenomenon of heat stress could be prevented. (Chapman,2013; Mondal, 2004; Pause, 2004)

Shape memory fibres have the promise of providing textiles with sensing and actuation within the same material. The shape memory effect is the ability to recover the original shape when a material is activated with appropriate stimuli. In the field of textiles, shape memory materilas are applied in two different ways: one of them is shape memory alloys while the other is shape memory polymers. The fibres in the textile are set in one 'permanent' form, usually with a physical restraint at a high temperature. Different shape memory polymers such as shape memory polyurethane (SMPU), polyester, poly-hydroxyproline,polysilamine, etc., and some responsive hydrogels including poly(N-isopropylacrylamide), polythiophene gel are used to fabricate smart textile materials(Chapman,2013;Thakur,2017;Hu,2015; Yüce 2017)

Sports and fitness can be regarded as another main area for smart textile applications especially for consumer use. Smart textiles for sports will bring a dramatic change in the way athletes at all levels train. Monitoring of exercise performance in terms of heart rate, body temperature, motion details etc., is interesting to amateur and active sports people. Position and motion sensing can be used for monitoring training and rehabilitation. Use of electroactive polymer actuators for producing artificial muscles could be interesting for enhancing sports performance. Smart textiles for sports operate in the value chain comprising multiple actors from electronics, textile, clothing and software industries as an emeriging area of smart textiles(https://globenewswire.com,2016; Dervojeda, 2017)

3. CONCLUSION

The smart textile applications are very encouraging and developing area globally. This area has widespread support from both the research and commercial sectors. It will bring important changes in our way of life. Social networks have introduced a completely new approach to interactions among human beings. People can have a chance to carry more and more electronic systems while doing all kinds of activities in all kinds of places. The lighter and more flexible instruments to enhcance user comfort are necessary in smart textile applications. The advent of smart textiles and fashion design will bring the traditional textile sector to a level of high tech industry by developing a new skill-set and expanding the knowledge available to engineers and scientists.

References

Axisa, F., et al. “Flexible Technologies and Smart Clothing for Citizen Medicine, Home Healthcare, and Disease Prevention.” IEEE Transactions on Information Technology in Biomedicine, vol. 9, no. 3, 2005, pp. 325–336.,

Catrysse, M., et al. “Towards the Integration of Textile Sensors in a Wireless Monitoring Suit.”Sensors and Actuators A: Physical, vol. 114, no. 2-3, 2004, pp. 302–311.,

Chan, M., et al. “Smart Wearable Systems: Current Status and Future Challenges.”Artificial Intelligence in Medicine, vol. 56, no. 3, 2012, pp. 137–156.,

Chapman, R. Smart Textiles for Protection. Woodhead Publishing Limited, 2013.

Cherenack, K, and Pieterson L.V. “Smart Textiles: Challenges and Opportunities.” Journal of Applied Physics, vol. 112, no. 9, 2012, p. 091301

Chien-Lung Shen C.L., Kao T.,Huang,C.T., Lee,J.H., Wearable Band Using a Fabric-Based Sensor for Exercise ECG Monitoring, Wearable Computers, 2006 10th IEEE International Symposium,

Coyle, S, et al. “Smart Nanotextiles: A Review of Materials and Applications.” MRS Bulletin, vol. 32, no. 05, 2007, pp. 434–442.,

Dervojeda,K., Lengton,M., Koonstra,A., Smart Textiles For Sports Report on promising KETs-based products nr. 1 June 2017, , European Union, August 2017

Haladjian J, Bredies,K Brügge B., Interactex: An Integrated Development Environment for Smart Textiles, ISWC '16, September 12–16, 2016, Heidelberg, Germany

https://globenewswire.com/ Smart Textiles Markets 2016-2023 - Emerging Second Generation Smart Textiles: Sports, Health and Fashion(20.05.2018)

Hu J., Lu J. (2015) Shape Memory Fibers. In: Tao X. (eds) Handbook of Smart Textiles. Springer, Singapore

Langenhove, Louis van. Smart Textiles for Medicine and Healthcare: Materials, Systems and Applications. Woodhead Publishing, 2007.

Mattila H., Current Challenges In Smart Textile Research, 4th International Technical Textiles Congress, 16-18 May 2010 İstanbul-Turkey

Mondal, S. Phase change materials for smart textiles – An overview, Applied Thermal Engineering, Volume 28, Issues 11–12, August 2008, Pages 1536-1550

Patwary, Md Syduzzaman Sarif Ullah. “Smart Textiles and Nano-Technology: A General Overview.” Journal of Textile Science & Engineering, vol. 05, no. 01, 2015,

Pause, B. Nonwoven protective garments with thermo-regulating properties, Asian Textile Journal, 13 (4) (2004), pp. 62-64

Rothmaier, M, et al. “Textile Pressure Sensor Made of Flexible Plastic Optical Fibers.”Sensors, vol. 8, no. 7, 2008, pp. 4318–4329

Schwarz, A. A Roadmap on Smart Textiles. Taylor & Francis, 2010.

Stoppa M. and Chiolerio, A., Wearable Electronics and Smart Textiles: A Critical Review, Sensors 2014, 14, 11957-11992;

Tang, S. Lam P, and Stylios. G. K. “An Overview of Smart Technologies for Clothing Design and Engineering.” International Journal of Clothing Science and Technology, vol. 18, no. 2, 2006, pp. 108–128.

Tao, X. Smart Fibres, Fabrics and Clothing. CRC Press, 2008.

Thakur S., Shape Memory Polymers for Smart Textile Applications,, Textiles for Advanced Applications, Edited by Bipin Kumar Intech open. pp. 323-335, 2017,

Weng,W., Chen, P., He, S., Sun, X., Peng H., Smart Electronic Textiles, , Volume55, Issue21, 2016, Pages 6140-6169, Angewandte Chemie,International Edition.

Yüce, İ. Shape Memory Polymers And Shape Memory Alloys: Use In Smart Textiles, International Journal of Development Research Vol. 07, Issue, 11, pp.16730-16736, November, 2017

A Review on the use of Estabragh (Milkweed) Fibers in Nonwoven Applications

MohammadAmin SARLİ [1*], Deniz DURAN [2]

[1,2]Ege University, Engineering faculty, Textile Engineering, İzmir, Turkey

[*]**Corresponding Author** : mohammadaminsarli@mail.ege.edu.tr

Abstract

Milkweed fiber (Its native Persian name is Estabragh) is a natural fiber which is a valuable plant that is easy to grow in dry and arid climates, requires minimum water, and can be harvested for floss twice every year. These fibers possess hollow structure and the smooth surface. The hollow structure of Estabragh fibers is responsible for their low density; and incorporation of these fibers in different functional areas such as nonwovens, composites, sound absorbing materials, sport garments and medical textiles would be of interest. In this Review, Milkweed fibers studied for their potential applications as nonwoven material. Also in this review presents a good deal of information pertaining to Estabragh (Milkweed) fibers such as fiber morphology and characteristics, properties and summaries the various researches initiated with Milkweed fiber nonwovens in different field of applications like sound absorption material, soil erosion control material, medical and technical textile, filtration media, etc.

Keywords: Estabragh, Milkweed, Nonwoven.

1. Introduction

These days, traditional natural fibers, including Cotton, Hemp, Flax and Jute, have being seeing more demand internationally, while other fibers such as Hemp and Milkweed are starting to emerge into more developed nonwovens areas. One of the natural fibers increasing its role in the nonwovens industry is milkweed. Milkweed floss is a silky white seed with a resilient hollow tubes that looks similar to a straw. The presence of hollow channel along the fiber length is responsible for their lightweight and good insulation properties [1]. Because of the fibers' ecological and chemical benefits, numerous technical application fields could be considered for the eco-friendly and nonallergenic textiles made of milkweed fibers especially in production of medical goods Since morphological aspects as well as physical and mechanical properties of the milkweed fibers significantly affect their functional behavior during their end uses, here in this review paper it is aimed to summarize all the available information regarding the fibers' characteristics and properties and nonwoven applications in thermal and acoustic insulation Figure 1 represents the classifications of natural fibers from different origins.

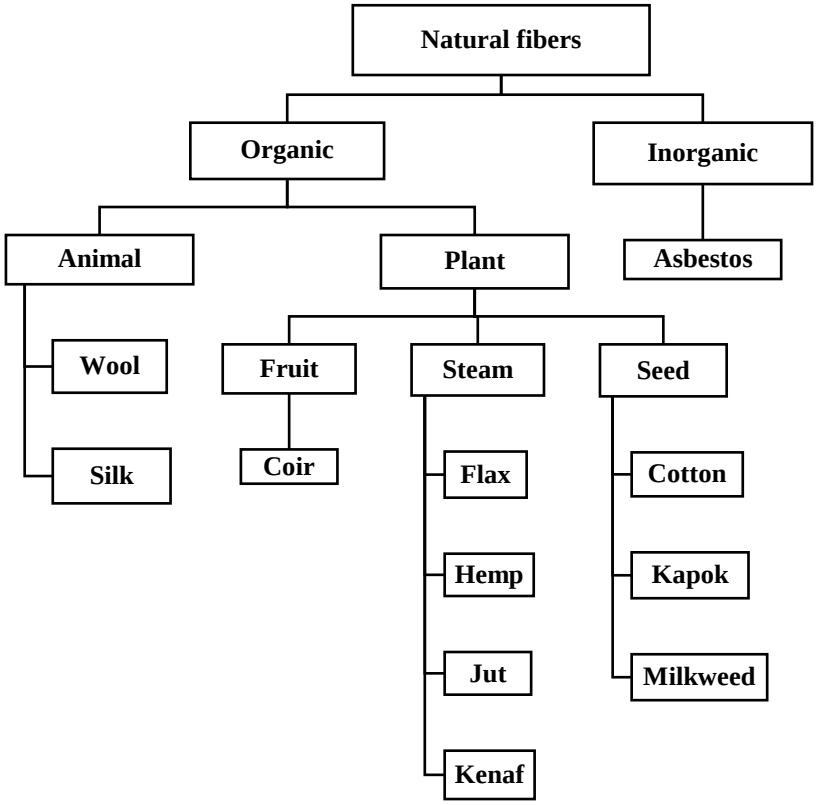

Figure 1. Natural fibers classifications [1].

2. Estabragh (Milkweed) Fibers

Milkweed is a valuable plant that is easy to grow in dry and arid climates, requires minimum water, and can be harvested for floss twice every year [2]. Its native Persian name is estabragh. It is a soft-wooded, ever green, perennial shrub [3]. In comparison to other natural or man-made fibers, the physical and mechanical properties of Estabragh fibers are similar to other naturally grown fibers such as Rux fibers, which grow in the USA and Southeast Asia, respectively. Figure 2 shows Estabragh fibers with their pods and hollow structure of Estabragh fibers [4].

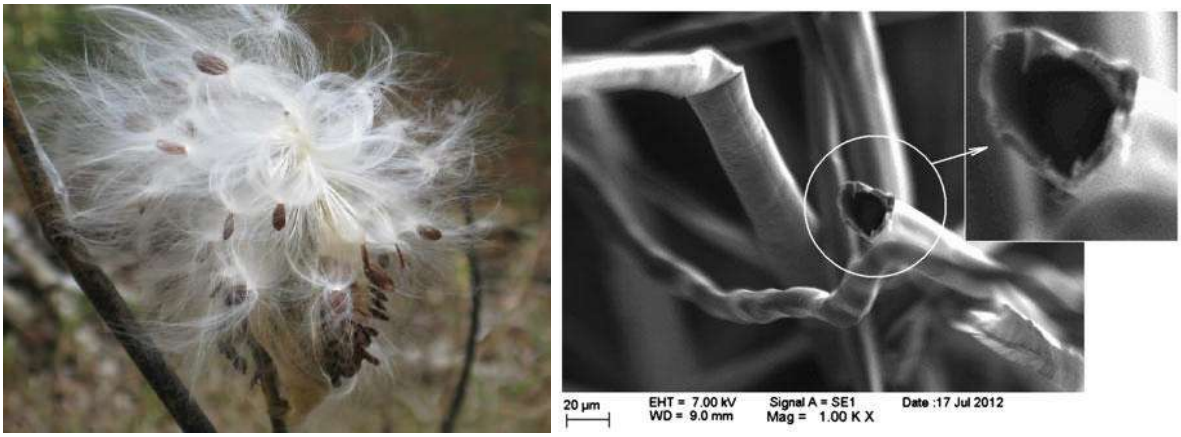

Figure 2. Estabragh fibers with their pods and hollow structure of Estabragh [4].

Milkweed floss has been reported to have hollow structure that provides large interspatial area to trap and retain oil [5]. Milkweed fiber comprise of 55% cellulose, 18% lignin [6]. Table 1 shows physical properties of milkweed fibers [7]. Milkweed floss is a unique natural fiber with a low density of about 0.9 g/cm^3 due to the presence of a completely hollow center [8]. Because of its low density, milkweed floss has been used as filling material in jackets to replace goose down [9].The fiber (floss) in the plant has been studied for use in textiles and filling materials [10].

Table 1. Properties of milkweed fibers.

Property	Milkweed (Mw)
Fiber denier (ASTM D 1577)	0.8
Fiber length, mm (ASTM D 5867)	28.9
Breaking strength, g	3.80

(ASTM D 3822)	
Tenacity, g/den	2.7
(ASTM D 3822)	
Density, g cm^{-3}	0.89
(ISO 1183)	
Moisture regain, %	10.8
(ASTM D 2495)	
Elongation at break, %	1.5
(ASTM D 3822)	

3. Application of Milkweed Fibers in Nonwovens

Nonwovens is the fastest growing sector in textile materials. They are flat, porous sheets or web structures. Nonwoven fabrics of ideal materials are used as acoustical insulation products because they have high total surface area [11].

The Milkweed fibers extracted from the Milkweed plants stems or seedpods have been identified prehistorically and utilized as the textile raw materials, especially in different regions of the United States and southern Canada. These fibers were also used for food and medical applications [12]. Milkweed floss which are widely used in textile, water safety equipment, insulation, upholstery and mattress products as a result of their softness and buoyancy. Milkweed seed floss was gathered and used as fill in “Mae West” life jackets for the World War II effort. Because of their hydrophobic nature and hollow structure, Milkweed fibers were employed as the raw material in life jacket manufacturing during the Second World War [13].

Gharehaghaji and et.al studied the mechanical damage to Estabragh fibers in the production of thermo bonded Layers. This work was designed to find the likely mechanism of Estabragh fiber failure and the effect of hollowness on the mechanical behavior. The results of a typical stress–strain curve and SEM of single Estabragh fibers show that the hollowness, variable thickness, and shape of the cross-sectional area of Estabragh fibers mainly affect the fracture phenomenon. The results show that the fiber undergoes tensile stresses deforms into a rectangular shape due to the stress concentration at the thin walls of the fibers. Furthermore, the fracture starts from the outer surface of the fiber and develops toward the inner surface in a plane perpendicular to the fiber axis. Another result is in carding process which was illustrated that fiber shortening was declined with the percentage of PET fibers increasing, while the mean tenacity shows a significant drop in the fiber. Consequently, the amount of damage in this

process was law but serious. Estabragh/PET layer shows lower bending rigidity that makes it more comfortable to use, and more useful in the sun protective clothing industry due to its higher UV protection. Finally it is illustrate that some properties of the produced layers, including moisture absorption, ultraviolet absorption, and bending length, are reported [14].

Hassanzadeh have also investigated the acoustical performance of Estabragh hollow fibers blended with polypropylene fibers in forms of needle punched nonwovens. They concluded that increasing the Estabragh fibers content in blend significantly leads to increase nonwovens sound absorbency. Numerous researches on designing the light-weight nonwovens as suitable sound absorbing materials for automotive applications are also available [15]. Mahmoud investigated the effect of hollow fibers component on acoustical performance of nonwoven structures. It was found that more sound was absorbed when the percentage of hollow fibers in the blend increased. It should be stated that using natural fiber nonwoven presents ecological benefit such as saving energy in the production process which is very important for industries [16].

A study of the insulation properties of various materials found that milkweed fiber owing to its hollow structure would possess significantly higher sound absorbency. Crews et al. investigated the potential application of milkweed fiber as insulation material. They analyzed seven identical jackets filled with various materials on a per unit weight basis and measured the thermal insulation, thickness, compression, resiliency and hand. They concluded that milkweed floss blended with down had insulative properties similar to down [17].

Hasani et al. examined the effects of different thermal bonding process variables such as Estabragh fiber ratio in blend, layer weight, needle punching density, thermal process temperature, and calendering speed on uniaxial breaking force and bending rigidity of nonwovens produced from Estabragh/polypropylene fiber blends were investigated using Taguchi method. The findings of the research showed that the blend ratio of fibers, layer weight, and the applied temperature during the thermal bonding process significantly increased the nonwoven layer resistance against axial tensile forces [18]. However, the variables like punch density and calendering speed had no significant effects on the breaking force values of the samples. In case of the samples′bending rigidity, it was found that all the variables except the calendering speed have significant effects. To the extent the bending rigidity nature of nonwoven is concerned, it was noted that the mix proportion was the most influencing component. The less number of holding point framed in the higher weighted layers realizes lessening in the resistance of the samples against bending powers [19].

Sanaz Hassanzadeh et al. evaluated the effect of needle-punching process parameters on the sound absorption properties of Estabragh/polypropylene needle-punched nonwoven [15]. They have evaluated the predictor variables like fiber blend ratio, punch density, and areal density. Their outcomes articulated that samples with higher extent of Estabragh fibers can be viewed as more effective means for noise absorption than the other proportion. This increased sound absorption capacity of the nonwoven fabric was due to the hollow structure of Estabragh fibers. In general, the geometry of fibers and their arrangement within the structure were the responsible for the acoustic performance of nonwoven structures. Hence, the physical property of the constituent fibers of a nonwoven structure was the main reason for the higher sound absorption nature of the assembly [20]

4. Conclusions

The Milkweed fibers have their own physical and mechanical properties based on the regions from which could be extracted. In other word, the appearance and chemical compositions as well as their mechanical behavior are significantly affected by the conditions of the soil and the environment The hollowness nature of Milkweeds is also responsible for the fibers lightweight and their good insulation properties than other commercially used natural fibers. Therefore, these fibers have a good potential to be used as the sound and thermal insulators. Considering this characteristic Milkweed fibers also could be used as a high potential materials with oil-cleanup capability in comparison with the commercially available synthetic materials. Capillary action through the long hollow channel of the fibers, which generally occurs due to the hydrophobic interaction between the fibers surface and the water molecules, is the main reason for the significant ability of Milkweeds in oil spills cleanup.

References

Karthik, T., (2014). *Studies on the spinnability of milkweed fibre blends and its influence on ring, compact and rotor yarn characteristics.* Ph.D. thesis, Anna University.

Nourbakhsh, A., Ashori, A., and Kouhpayehzadeh, M., (2009). *Composites, J. Reinforced Plast. Comp*, 28(17), 2143-2149.

Bahreini, Z., Kiumarsi, A., (2008). *Prog. Color Colorants Coat.*, 1, 19-26.

Nasser, R. A., Al-mefarrej, H. A., Khan, P. R., et al., (2012). Technological properties of Calotropis procera (AIT) wool and its relation to utilizations. *Am Eurasian J Agric Environ Sci*, 12, 5-16.

Kopayashi, Y., Massuo, R., and Nishiyama, M., Patent No 52, Japanesh Patent 138.

Choi, H. M., Moreau, J. P., (1993). Oil sorption behaviour of various sorbents studied by sorption capacity measurement and environmental scanning electron microscopy. *Microsc. Res. Technol.*, 25, 447-455.

Parmar, M. S., Mansi, B., and Rao, J. V., (2016). Milkweed blended fabrics and their thermal insulation and UV protection properties. *Indian Journal of Fibre & Textile*, 14.139.47.23.

Sakthivel, J. C., Mukhopadhyay, S., and Palanisamy, N. K., (2005). *J Ind Text*., 35, 63-76.

Crews, P. C., Sievert, S., and Woeppel, L. T., (1991). *Text Res J*, 61, 203-210.

Shakyawar, D. B., Dagur, R. S., and Gupta, N. P., (1999). *Indian J Fibre Text Res*, 24, 264-268.

Batra, S. K., Cook, F. L., (1992). *The Nonwoven Fabrics Handbook*, INDA Publications, Cary, NC.

Jeeshna, M.V., Manorama, S., and Paulsamy, (2009). Antimicrobial property of the medicinal shrub, Glycosmis pentaphylla. *J Basic Appl Biol*, 3, 25-27.

Knudsen, H. D., (1990). Milkweed floss fiber for improving nonwoven products. In: *Nonwovens conference proceedings* (pp. 209-212). Peachtree Corners, GA: TAPPI.

Gharehaghaji, A. A., Hayat, D. S., (2008). Mechanical Damage to Estabragh Fibers in the Production of Thermobonded Layers. *J Appl Polymer Sci*, 109, 3062-3069.

Hassanzadeh, S., Hasani, H., and Zarrebini, M., (2014). Analysis and Prediction of Noise Reduction Coefficient of Lightly-needled Estabragh/Polypropylene Nonwovens Using Simplex Lattice Design. *J Text Inst*, 105, 256-263.

Abdelfattah, A., Mahmoud, G. E., and Eman, R.M., (2011). Using Nonwoven Hollow Fibers to Improve Cars Interior Acoustic Properties. *Life Sci J*, 8, 344-351.

Crews, P. C., Sievert, S. A., and Woeppel, L.T., (1991). Evaluation of milkweed floss as an insulative fill material. *Text Res J*, 61, 203-210.

Hasani, H., Zarrebini, M., Zare, M., and Hassanzadeh, S., (2014). Evaluating the acoustic properties of Estabragh (Milkweed)/Hollow-Polyester nonwovens for automotive applications. *Text Sci Eng*. 4, 1-6.

Bahari, N., Hasani, H., Zarrebini, M., and Hassanzadeh, S., (2015). Investigating the effects of material and process variables on the mechanical properties of low-density thermally bonded nonwovens produced from Estabragh (milkweed) natural fibers. *Journal of Industrial Textiles*, 46 (3), 719-736.

Tascan, M., (2005). *Acoustical properties of nonwoven fiber network structures (Unpublished Ph.D. thesis).* Clemson University, Clemson, SC, USA.

The Usage of Natural Antimicrobials in Textiles

Tülay GÜLÜMSER[1], Ebru BOZACI[2]

[1,2] Ege University, Engineering Faculty, Textile Eng. Department, Izmir, Turkey; tulay.gulumser@ege.edu.tr, ebru.bozaci@ege.edu.tr

* **Corresponding Author:** tulay.gulumser@ege.edu.tr

Abstract

Microorganisms may grow over textiles materials due to some moisture retention capacities and their large surface areas. Antimicrobial textiles always attracted the attention of producers and consumers and the demand for that functionality has been increasing in the latest years in the medical textile field. Many antimicrobial agents have been tried and used but some of them could not be accepted because of health and environmental concerns.

Natural antimicrobial agents attract the attention of researchers and producers as the extraction and application techniques progressed. Some natural biopolymers such as chitosan and chitin which is derived from chitosan, a few natural dyestuffs, and certain essential oils can be used for this purpose.

In this study it was tried to glance at the natural antimicrobial agents in order to give an idea about the activities and application methods especially plasma surface modification method for near future.

Keywords: Antimicrobial textiles, plasma treatment, medical textiles, functional textiles.

1. Introduction

Natural fibers used in textile materials have many advantages, but because they are prone to microorganism colonization due to their large surface area and excellent moisture retention ability, consumers meet many problems. For this reason, antimicrobial finishing for textiles have been applied to textile materials from ancient times. Usage of herbs and spices to preserve mummy wrapping by ancient Egyptians is the first antimicrobial finishing of textile materials known in history (Tawiah et al., 2016; Islam et al., 2013).

In textile industry, today a lot of natural and synthetic antimicrobial agents are used as the result of R&D works made in time. The demands of such kind of products except than medical textiles increases, with the public's enhanced awareness in daily life and increasing demands seem that consumption amounts of antimicrobial agents will rise more and more. In the production of antimicrobial textiles which is the fastest growing sector of textiles, natural materials become popular day by day under the pressure of environment and health problems like other industry branches (Islam et al., 2013).

Natural biopolymers attract the attention of researchers and technologists in latest years. They use natural biopolymers in textile industry as antimicrobial agents more recently. Chitosan, sericin and alginate can be given as examples to the antimicrobial biopolymers used in textiles in latest years. Inclusion of antimicrobial agents into cyclodextrins can be possible. Important developments took place in order to apply this process. Besides the classical methods, microcapsulation and plasma method attract the attention. Plasma method with the environmental approach, savings in chemical and water usage and minimization of waste materials interests the researchers and the importance of these studies increase day by day.

2. Natural Antimicrobial Agents

2.1. Alginate

Alginate is natural polysaccharide extracted from brown seaweeds. Since it was discovered in 1800 years, alginate has been used in food, textile printing, paper and pharmaceutical industries. It also takes place in other sectors with the results of R&D works, esp. in medical textiles. In recent years, alginate has been widely used in the wound management industry as a novel material for the manufacture of 'moist healing' products. Alginate fibers are particularly useful as raw materials for the production of highly absorbent wound dressings. Advantages of alginate are: Alginate is a non-toxic material, calcium alginate fiber can act as a homeostatic agent, calcium alginate fiber absorbs a large quantity of exudates

and turns itself into a gel, which helps keep a moist interface on the wound surface, and as a natural polymer alginate is a renewable resource with unlimited supply in nature. Since alginate is a polymeric acid, it is easy for alginate fibers to carry zinc ions by forming salt with zinc ions. Zinc alginate fibers can be made by a direct extrusion of sodium alginate solution into a zinc chloride coagulation bath, or by treating calcium alginate fibers with aqueous zinc chloride solution where, after the ion exchange between calcium ions in the fiber and zinc ions in the solution, the fiber becomes a mixed calcium and zinc alginate. In order to attach silver ions onto the alginate fibers, calcium alginate fibers can be treated with aqueous solutions of silver nitrate. The silver ions in the solution exchange with calcium ions in the fiber, resulting in the formation of calcium alginate fiber containing silver ions. These fibers are highly anti-microbial. Both alginate fibers containing zinc or silver are used in medical textiles (Qin, 2008).

2.2. Chitosan

Chitosan is a derivative of chitin which is obtained from marine shells. Chitin is the second most abundant natural polymer after cellulose. Every year, approximately 100 billion tons of chitin are produced on the earth and the main usage area of chitin is the production of chitosan (Muxika et.al, 2017).

Chitosan can take place of some synthetic polymers with advantageous properties including nontoxicity, biocompatibility, biodegradability, antimicrobial activity and chemical reactivity (Şahan and Demir, 2016).

Chitosan has primary and secondary hydroxyl groups and primary amino groups in its chemical structure. As a natural biopolymer derived from the exoskeletons of crustaceans, it is used in biotechnology, wastewater treatment, pharmaceuticals, agriculture, food industry and Textiles (Türemen and Demir, 2017).

2.3. Cyclodextrins

Cyclodextrins (CDs) are cyclic oligosaccharides. Cyclodextrins are produced during enzymatic degradation of starch by the enzyme, namely cyclodextrin glycosyltransferase. The most commonly available types are α-CD, β-CD, and γ-CD having 6, 7, and 8 glucopyronase moieties, respectively. These substances, and in particular β-CD have shown huge potential in textiles, because of their ability to selectively form inclusion complexes with other substances through host−guest interactions. The complexation strength and longevity of host−guest complexes mainly depends upon the size of incoming guest molecule and the type of interaction. As the result of the toxicological evaluation, no skin irritation, sensitivity or mutagenicity were indicated. Thus the usage cyclodextrins in the controlled release of

antimicrobial agents started. It is predicted that they would present new chances in the production of functional textiles (Islam et. al., 2013).

2.4. Sericin Protein

Sericin is a natural macromolecular protein derived from silk worm, *Bombyx mori*. Sericin envelopes the fibroin fiber which forms the main silk filament content with successive sticky layers that help in the formation of a cocoon. Because sericin is an amorphous glue-like substance, it helps in the cohesion of the cocoon by gluing silk threads together. Sericin has some inherent properties, such as biocompatibility, biodegradability, antibacterial, UV resistance, oxidative resistance, and moisture absorption ability, Sericin is used different fields including pharmaceuticals, cosmetics, and textiles (Islam et. al., 2013).

In textiles especially the studies about the development of cotton antibacterial fabrics attract the attention (Kalifa et.al., 2011; Doakhan et.al, 2013).

Today about 95 % sericin is mostly discarded in silk processing wastewaters in spite of promising use of sericin in value-added products. Recovery of silk sericin from degumming liquor or cocoons could provide significant economic and social benefits. The antimicrobial modifications of sericin are in the basic research level but by promoting the studies, they can take place in medical textiles field (Islam et. al., 2013).

2.5. Natural Dyestuffs

Natural dyes have been widely used in textile coloration since ancient times. They became popular among the researchers again in the latest years. Natural dyes have an inherent antimicrobial property which is believed to be very potent. Various fibers have been dyed with some selected natural dyestuffs. As the result antimicrobial and antibacterial effects were evaluated and positive results were obtained (Tawiah et.al, 2016; Sam et.al., 1997).

Natural dyestuffs obtained from pomegranate rind, walnut tree leaves, walnut shell, bugloss plant and henna can be given as examples to the antifungal and antimicrobial materials (Joshi et.al., 2009; Yusuf et.al., 2012).

In addition to these plants, some of natural dyestuffs are obtained from fungi, algea and bacteria directly. These dyestuffs are advantageous because they are rich in color and they have ecofriendly and antimicrobial properties (Samanta and Agarwal, 2009).

2.6. Essential oils

Essential oils are a mixture of a variety of aromatic compounds which can give cologne and provide protection from a broad spectrum of microbes. Essential oils containing pleasant fragrance and different pharmaceutical effects have for centuries been applied on textiles to fulfill the psychological and emotional needs of humans. The application of essential oils for antimicrobial effect on textiles has increased in recent times because they are highly efficient when applied using the right technology. Essential oils can be used alone, in combination with others or as antibiotics. Thyme, peppermint oil, clove, cinnamon essential oils can be used for these purposes (Tawiah et.al., 2016).

3.The application Methods of Natural Antimicrobial Agents

3.1. Classical Methods

Padding, exhausting and crosslinking with these methods used in textile finishing can be examined in classical methods (Tawiah et.al., 2016).

Pad-dry-cure method is one of the oldest methods of imparting antimicrobial agents to fabrics. This method is simple but has a great disadvantage; it usually cannot achieve satisfactory durability due to the poor attractive force between the fibers and antimicrobial agent (Kim et.al.., 2010; Hebeish et.al., 2015).

Exhausting method is another one that forms poor attractive force between the textile fibers and antimicrobial agent.

In order to form covalent bonds between the natural herbal products and the textile materials, crosslinking agents are treated with textile materials by padding or exhausting methods. After these treatments, it is important to make antimicrobial activity test and some others such as washing durability, tensile strength and handle test (Tawiah et.al., 2016).

3.2. Microencapsulation

Microencapsulation is the coating of small solid particles, liquid droplets, or gas bubbles with a thin film of coating or shell material. There are many fields of application and industries using microcapsulation. Increasing research and development activities about this technology is producing a steadily increasing number of commercially successful products that utilize microcapsules (Gülümser, 2017).

Microencapsulation is an economical and eco-friendly method and additionally in manner of energy saving, it is advantageous than the other conventional processes (Sumithra and Vasugi, 2012).

This technology has become one of the most promising techniques of imparting functional finishes to textiles. Application of antimicrobial agents to the textile materials by microencapsulation attracts the attention. Many combinations are possible by choosing proper shell and core materials (Tawiah et.al., 2016).

The microencapsulation of essential oils has led to many novel applications, including children's garments, hosiery, sheets, towels, cushions, fragrant ties and shoe insoles, as a consequence not only of the pleasant smell of the essential oils released but also of the wide variety of therapeutic benefits. Besides medical purposes such as giving antimicrobial properties, some of them help with insomnia, some provide relief from respiratory problems, some stimulate mental activity (Gulumser et.al., 2015).

3.3. Plasma Surface Modification

In the complex reactions of classical textile finishing methods, high amounts of chemical, water and energy are consumed, so clean technologies that could be used in these processes gain importance day by day. Additionally, waste water load is high and there would be problems in many countries because of legal necessities.

Main characteristic of the plasma technology is the unchanging of the basic properties of the textile materials as the result of the surface modifications. In this technology no water is used, treatments are made in the gas phase, very few or no usage of chemicals, short treatment times, no wastes, energy saving, surface modifications without any damages to mechanical properties of textile products (Thorsen, 1968).

During plasma treatment, some reactive particles are formed and these particles make changes on the surface of the textile material. Surface activation, cleaning, etching, grafting and crosslinking are some of these modifications (Karahan et.al., 2007).

To give antimicrobial character to the textile material by plasma treatment s is usually made before dyeing with natural dyestuffs that are chosen because of their antimicrobial properties. In this case plasma modification is made as a pretreatment. Thus it is defined that color yield increases and antimicrobial properties develop (Ghoranneviss et.al.., 2010; Chen et.al., 2007).

3.4. Other Methods

In order to ensure the strong adhesion or bonding of natural antimicrobial agents to textile materials some other methods that change the physical properties of fibers can be used: ultra-sound technology, UV radiation, surface bridging and enzyme treatment (Tawiah et.al., 2016).

4. Results and Suggestions:

As health and hygiene issues gain importance, studies about application of antimicrobial agents to textile materials become popular. The demand for these products increase and it is also asked for the antimicrobial agents to be healthy, ecofriendly, natural and even sustainable and produced by clean technologies. When the studies made about this subject are examined, it is remarkable that the interest to the natural products increase day by day. In future the studies about this functional textiles group with high added value will be focused on natural antimicrobial agents and clean technologies that will be advantageous in manner of health and environment.

References

Chen, C., Chang, W., (2007). Antimicrobial activity of cotton fabric pretreated by microwave plasma and dyed with onion skin and onion pulp. Indian Journal of Fibre & Textile Research, 32, 122-125.

Doakhan, S., Montazer, M., Rashidi, A., Moniri, R., Moghadam, M.B., (2013). Influence of Sericin/TiO2 Nanocomposite on Cotton Fabric: Part 1. Enhanced Antibacterial Effect. Carbohydrate Polymers, 94(2),737-748.

Ghoranneviss, M., Shahidi, S., Anvari, A., Motaghi, Z., Wiener, J., Slamborova, I., (2010). Influence of plasma sputtering treatment on natural dyeing and antibacterial activity of wool fabrics. Progress Organic Coating, 70(4), 388–893.

Gülümser, T., (2017). The role of microcapsules in masking bad odors of cotton fabrics, Industria Textila, 68(4), 275-281.

Gülümser, T., Balpetek, F.G., Demir, A., (2015). Ev Tipi Yıkamalarda Kullanılan Kumaş Yumuşatıcılarının Pamuklu Ürünlerde Giyim Sırasında Kalıcılığı. Tekstil ve Konfeksiyon, 25(3), 263-269.

Hebeish, A., El-Bisi, M.K., El-Shafei, A., (2015). Green synthesis of silver nanoparticles and their application to cotton fabrics. International Journal of Biological Macromolecules, 72(0), 1384-1390.

Islam, S.U., Shaid, M., ve Mohammad, F., (2013). Green Chemistry Approaches to Develop Antimicrobial Textiles Based on Sustainable Biopolymers-A Review. Ind. Eng. Chem. Res. 2013, 52, 5245-5260.

Joshi, M., Wazed, A.S., Purwar, R., (2009). Ecofriendly antimicrobial finishing of textiles using bioactive agents based on natural products. Indian Journal of Fibre & Textile Research, 34, 295-304.

Karahan, A., Demir, A., Özdoğan, E., Seventekin, N., (2007). Plazma Teknolojisi ve Temel Özellikleri, Tekstil Teknoloji Dergisi, 128, 102-109.

Khalifa, I.B., Ladhari, N., ve Touay, M., (2011). Application of sericin to modify textile supports. J. Text. I.,103, 370-377.

Kim, H.W., Kim, B.R., Rhee, Y.H., (2010). Imparting durable antimicrobial properties to cotton fabrics using alginate–quaternary ammonium complex nanoparticles. Carbohydrate polymers, 79(4),1057-1062.

Mohd, Y., Aijaz, A., Mohammad S., Mohd, I.K., Shafat, A.K., Nikhat, M., Faqeer, M., (2012). Assessment of colorimetric, antibacterial and antifungal properties of woollen yarn dyed with the extract of the leaves of henna. Journal of Cleaner Production, 27, 42-50.

Muxika, A., Etxabide, A., Uranga, J., Guerrero, P., de la Caba, K., (2017) Chitosan as a bioactive polymer: Processing, properties and applications. International Journal of Biological Macromolecules, 105, 1358–1368.

Qin, Y., (2008). Review Alginate fibres: an overview of the production processes and applications in wound management. Polymer International, 57,171–180.

Rajendran, R., Balakumar, C., Sivakumar, R., Amruta, T., Devaki, N., (2011). Extraction and application of natural silk protein sericin from Bombyx mori as antimicrobial finish for cotton fabrics. J. Text. I., 103, 458−462.

Sam, H., Barakat, H.H., Merfort, I., Nawwar, M., (1997). Tannins from the leaves of Punica granaltum. Photochemistry, 45(4), 819-823.

Samanta AK, Agarwal, P. "Application of natural dyes on textiles" Indian J Fibre Text Res. 2009; 34: 384-389.)

Sumithra, M., Vasugi, R.N., (2012). Micro-encapsulation and nano-encapsulation of denim fabrics with herbal extracts. Indian Journal of Fibre & Textile Research, 37, 321-325.

Şahan, G., ve Demir, A., (2016). Tekstil Terbiyesinde Nano Boyutta Kitosanın Yeşil Uygulaması. Tekstil ve Konfeksiyon, 26(4).

Tawiah, B., Badoe, W., ve Fu, S., (2016). Advances in the Development of Antimicrobial Agents for Textiles: The Quest for Natural Products. FIBRES & TEXTILES in Eastern Europe, 24, 3(117), 136-149.

Thorsen, W.J., (1968). A Corona Discharge Method for Producing Shrink-Resistance Wool and Mohair Part II: Effects of Temperature, Chlorine Gas and Moisture. Textile Research Journal, 38 (6), 644-650.

Türemen, M., ve Demir, A., (2017). Pamuklu Kumaşlara Farklı Yöntemlerle Biyopolimer Uygulamasının Analizi. Tekstil ve Konfeksiyon, 27(4).

The Importance of Modeling in Design, Derince Municipality Sample Of Martyrs Memorial

Deryanur DİNÇER[1], Türker OĞUZTÜRK[2*]

[1,2]Recep Tayyip Erdogan University, Faculty of Fine Arts, Design and Architecture, Department of Landscape Architecture, Rize, Turkey; deryanur.dincer@erdogan.edu.tr; turker.oguzturk@erdogan.edu.tr

[*]**Corresponding Author:** turker.oguzturk@erdogan.edu.tr

Abstract

Computer technology is developing at a great speed today. As a reflection of these developments, it is possible to get more realistic drawings by developing every day in design programs like every other area. This feature makes the use of computer technologies more attractive. 2D drawings made during the project design phase are not enough in terms of perception of design in the application phase. With three-dimensional models, more appropriate, more realistic images can be obtained. Three-dimensional modelling technology contributes significantly to the clarification and perception of designs. In this context, the Autocad 2018, Sketchup 2018 and Lumion 6 programs were used together to determine the modelling stages of the "Martyr Monument" in the Derince Municipality Highway Underpass Park and the designs were drawn on the necessary programs. The three-dimensional modelling of the planned design was created in the computer environment.
Key Words: Design, modelling, landscape, three dimensions

1. Introduction

3D modeling is the creation of the exact same or close to reality of our designs in the virtual environment by drawing the design in computer environment with the help of computer programs of all surfaces. For this purpose, many programs can help us. With the developing technology, the number of these programs is increasing day by day and programs which respond to the needs of every profession discipline separately are developed. According to Lueptow (2000), solid modeling is the most advanced metric of an observer presentation as the most advanced modeling technique of computer aided design. The modeling is very important in the perception of the designs and in the determination of the details. We can see a design modeled in computer environment by looking at the modeling program's scene, either in cross section or in perspective. In this direction, while designing the Derince Municipality Martyr Monument, the details of the designs were determined, the method of modeling was used in determining the measurements and in the stage of decision making.

The fact that the real world is three-dimensional increases the need for three dimensions in computers. Three-dimensional images attract more attention and make visualization the closest to reality (Uğur, 2002).

2. Material and Method

2.1. Material

The material of the work; Derince Municipality Construction Plan and Landscape architecture are used in the field of Autocad, Sketchup and Lumion that are creating programs.

2.2. Method

This study consists of 6 steps. These steps are as follows:

First stage; Determination of the method to be followed in the formation of the project.

Second stage; taking the x, y, z coordinates of the important points of the field with the gps device and taking area photographs.

Third stage; processing of the obtained data in the computer environment.

Fourth stage; modeling of the data in the computer environment and deciding on the design to be implemented.

Fifth stage; taking the project renders in the created virtual environment and preparing the animations.

The sixth stage; results.

3. Findings

3.1. Workspace

Our work area is Derince Municipality Highway Altgeçit Park located on Derince-İstanbul D-100 Highway (40.7561890, 29.8309180 coordinates). The position of the study area is shown in Figure 1.

Figure 1: Workspace (Url 1).

3.2. Design Models Prepared

Six designs are prepared for the purpose of working differently in our work. The design patterns of the martyr's monument, prepared as suggestion, are shown in Figure 2.

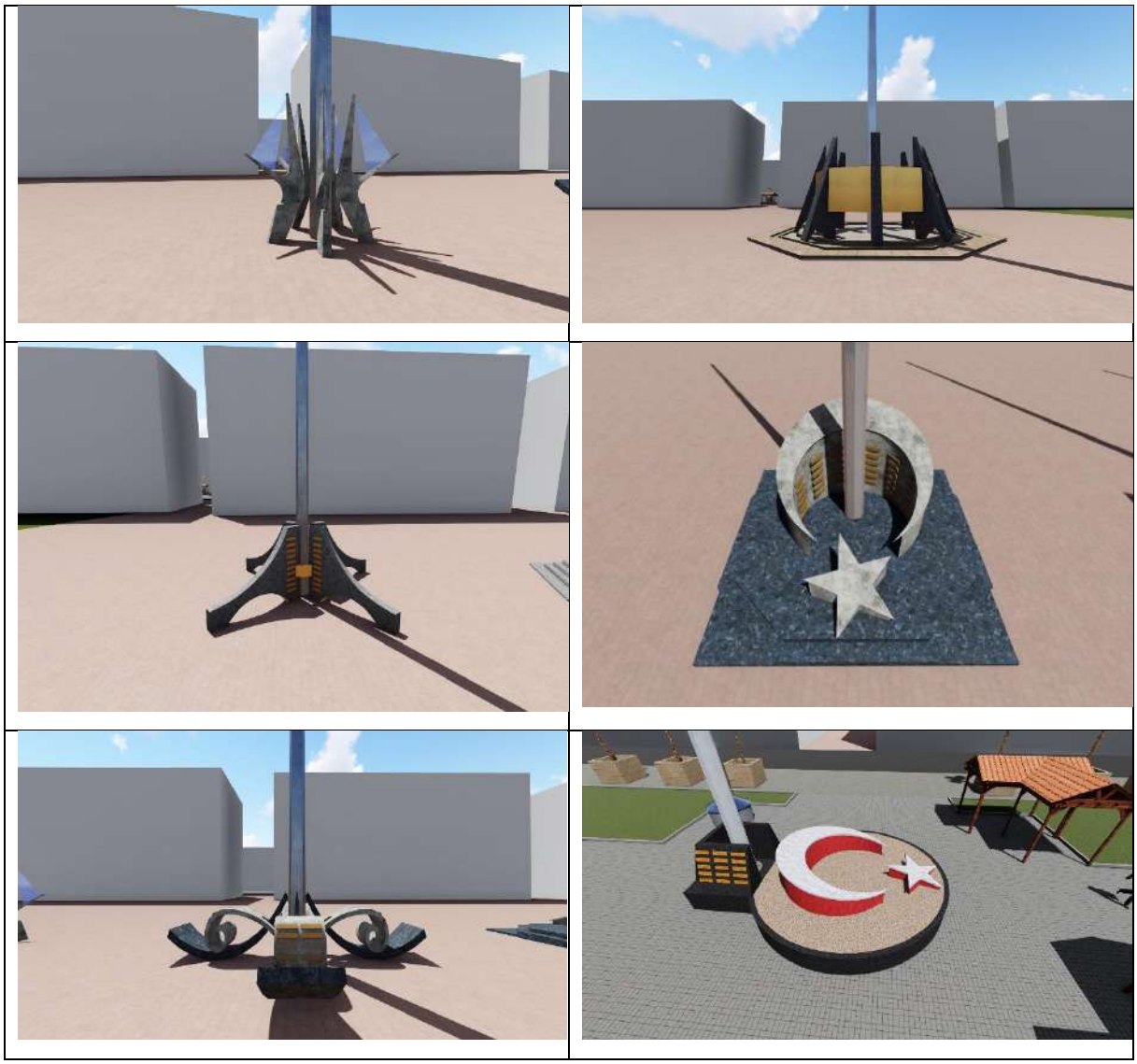

Figure 2: Recommended designs

Three-dimensional modeling technology contributes significantly to the clarification and perception of designs. In this context, when Autocad, Sketchup and Lumion 6 programs are used together, practical and realistic designs are obtained. In three-dimensional modeling of designs before implementation; it seems that the users are the most important contributors to the understanding of which recommendations are most likely to be appreciated. In this regard, it can be seen that many different examples can be presented to users. Three-dimensional modeling of the existing field seems to be able to compare the design area with the work area. The image of the selected model in the modeled study area is given in Figure 3.

Figure 3: The image of the selected model in the modeled workspace.

With 3D modeling, the types of materials used in the field can be determined. Measurements such as the width, height and thickness of these specified material types can be determined and the necessary quantities can be extracted. For example, the calculated granite covering of "Martyr Monument" is given in Figure 4.

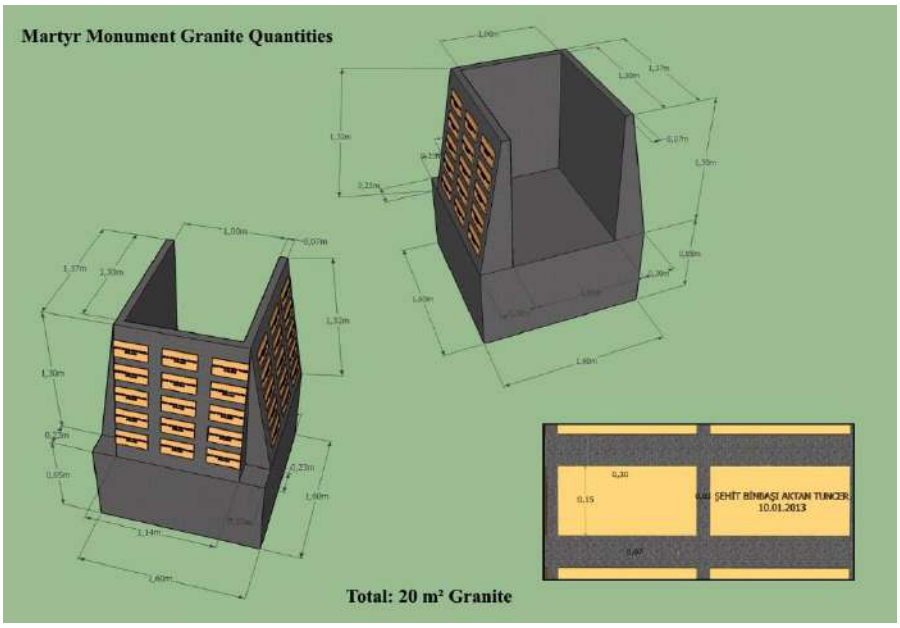

Figure 4: Granite coating quantities.

Three-dimensional modeling allows you to obtain images of the working area at night and in different climatic conditions by making the necessary render adjustments as well as obtaining images of a normal sunny day. The night and winter views of the prepared three-dimensional model are given in Figure 5.

Figure 5:. Night and winter views of the selected model.

4. Results

3D modeling is facilitating the identification of problems and details in the transition from two-dimensional design to implementation in the project. 3D modeling is important in terms of perception, interpretation and acceptance of the projects to be implemented by the users at the design stage in the projects such as the martyr monument of the 3D model. The functionality and visualization of the areas to be designed and projected are being enhanced by 3D modeling. Thanks to the modeling, many designs and projects can be easily developed for a single area. Developed designs and projects; photos and animations can be presented to the liking of users. In this respect, the most preferred and preferred designs by the users are selected and put into practice phase.

References

Lueptow, Richard M. (2000). Graphics Concepts; Prentice Hall, New Jersey.

Olgun, r., & Yılmaz, t. (2014). Peyzaj mimarlığında bilgisayar destekli tasarım ve tasarım aşamaları. Ömer Halisdemir Üniversitesi Mühendislik Bilimleri Dergisi, 3(1), 48-59.

Türkel, E. (2008). Bilgisayar destekli tasarım programlarıyla seramik ürünlerin modellenmesi ve bir pisuar uygulaması (Doctoral dissertation, DEÜ Güzel Sanatlar Enstitüsü). Uğur, A., "İnternet Üzerinde Üç Boyut ve Web3D Teknolojileri (Three Dimensional Graphics on the Internet and Web3D Technologies)", VIII. Türkiye'de İnternet Konferansı (INET-TR 2002), Bildiri No : 54, İstanbul, Türkiye, 19-21 Aralık 2002.

Uğur, A. (2002). İnternet Üzerinde Üç Boyut ve Web3D Teknolojileri (Three Dimensional Graphics on the Internet and Web3D Technologies). VIII. Türkiye'de İnternet Konferansı (INET-TR 2002), Bildiri, (54), 1-3.

Url1 https://www.google.com/maps/place/Derince,+41900+Derince%2FKocaeli/@40.7564868,29.8160694,5634m/data=!3m1!1e3!4m5!3m4!1s0x14cb47ae91250443:0x85f5a9986bc889d2!8m2!3d40.756189!4d29.830918

More Luxuriant And Aesthetic Patterned Apperal Design With Dijital Printing

Ali Uğur KÖSEOĞLU [1*], Fatma KOÇ [2], Yücel Devrim ARIK[3]

[1] Menderes Tekstil A.Ş. Design Center, Denizli, Turkey; aliugurkoseoglu@menderes.com

[2] Menderes Tekstil A.Ş. Design Center, Denizli, Turkey; design@menderes.com

[3] Menderes Tekstil A.Ş. Design Center, Denizli, Turkey; design@menderes.com

[*] **Corresponding Author:** aliugurkoseoglu@menderes.com

Abstract

Digital printing is a big advantage through eliminating traditional prin-ting limitations. Different and not ordinary designs always create interest. To overcome some difficult pattern designs is possible by dijital printing. Limitations of digital printing have been analysed at this study. Special designs have been choosen; these designs have too small repeat sizes,too high resolutions, too thin lines, complicated geometrical patterns, soft patterns, too much colour numbers and photographic patterns. Printing process has been done at MS JP-6,MS JP-7,MS JPK EVO,MS LARIO, REGGIANI RENOUR digital printing machines.Some of obtained results are: (1) Ability to print designs at high resolutions up to 600 dpi. This means two-three times more resolution than conventional printing. (2) Ability to print too thin lines down to 20-30 micron.(3) Between 0 and 256 levels density differences are used by graphic design programs for half tone colours. To obtain 90% of these levels by digital printing is possible. This ratio is 40%-50% for conventionel printing. (4) No colour registration problem, excellent dimentional accuracy. (5) Faster, easier and cheaper design improvement/revision process. (6) More designs and more colour variants can beachivedin a shorter time period. Possibility of printing small fine details, excellent softness of half tone designs and there is no colour number limitation. More luxuriant and aesthetic patterned apperal designs can be achived with digital printing

Keywords: Digital printing, Apperal, Pattern, Apperal patterns, Advantage of digital printing, Digital printing patterns.

1. Introduction

Analyse of apperal pattern design advantages through dijital printing by eliminating traditional printing limitations.

Figure 1. Clothing fabric.

2. Material and Method

One of the important factors of shaping apperal style is colours and patterns of apperals. People want to dress fine. Different and not ordinary designs always create interest. The purpose of us is to develop the aesthetic quality to the highest level. To overcome some difficult pattern designs is possible by dijital printing. We have created our pattern design samples by using graphic design programs of Adobe Photoshop, Adobe Illustrator, Ramsete, Corel Draw and by using single - pass and multi-pass digital printing machines. Printing process has been done at MS JP-6, MS JP-7, MS JPK EVO, MS LARIO, REGGIANI RENOUR digital printing machines. We have choosed special pattern designs for this study. These designs have too small repeat sizes, too high resolutions, too thin lines, complicated geometrical patterns, soft patterns, too much colour numbers and photo graphic patterns.

Figure 2. Pantone color control- Ms Lario printing machine- Wacom cintiq tablet.

3. Results and Discussion

1-Ability to print designs at high resolutions up to 600 dpi. This means two-three times more resolution than conventional printing.

2- Ability to print too thin lines down to 20-30 micron.

3- Between 0 and 256 levels density differences are used by graphic design programs for half tone colours. To obtain 90% of these levels by digital printing is possible. This ratio is 40%-50% for conventionel printing.

4- No colour registration problem, excellent dimentional accuracy.

5- Faster, easier and cheaper design improvement/ revision process.

6- More designs and more colour variants can be achived in a shorter time period.

Figure 3. Digital textile printing machine process.

The advantages for digital textile printing is immense and can have a great impacton the textile market as a whole. Today, a major drawback for mass textile printing is the design. Digital printing enables higher color definition with short designing time which is not possible with traditional printing. Furthermore, printing can be done in short runs at low investment cost both in capital equipment and in materials ; fabrics and inks. Another advantage of textile digital printing, which is receiving higher profile attention among manufacturers consumers and environmentalists is the substantial lower cost of production in terms of electricity and water consumption of over 30% savings on electricity costs and almost 95% in terms of water consumption. Savings on stock with the ability to print on demand in small quantities is an additional advantage. This is a great advantage for the fashion industry and especially for small designer collections requiring high quality printing on unique fabrics.

Figure 4. Ms Lario printing machine.

Possibility of printing small fine details, excellent softness of half tone designs and there is no colour number limitation. More luxuriant and aesthetic patterned apperal design can be achived with digital printing.

References

MS Printing Solutions. Products, MS- Lario. (Date of access: 28. 02. 2018)
Website: http://www.msitaly.com

MS Printing Solutions. News, Living The Digital Dream. (Date of access: 28. 02. 2018)
Website: http://www.msitaly.com

Evron, G. (2016). Is the Textile Digital Printing Revolution Just Around the Corner?
Website: https://www.industrialprintblog.com/blog/2016/3/29/is-the-textile-digital-printing-revolution-just-around-the-corner

Menderes Textile Photo Archive.

CONSTRUCTION MATERIALS - CONSTRUCTION TECHNOLOGY - STRUCTURE MECHANICS - BUILDING TECHNOLOGY

ORAL PRESENTATIONS

Carparking Problem in Large Cities and Ordu Provincial Example

Ahmet KÖSE[1*], Burcu KÖSE KHIDIROV[2], Bilge KÖSE[3]

[1] Ordu University, Vocational School of Technical Sciences, Construction Dept., Ordu, Turkey
[2] Mimar Sinan Fine Arts University, Faculty of Architecture, Interior Architecture Dept., Istanbul, Turkey
[3] Ordu University, Vocational School of Technical Sciences, Construction Dept., Ordu, Turkey

***Corresponding Author:** ahmetkose@odu.edu.tr

Abstract

Today, the traffic of large cities is made up of the traffic flow of visitors from private cars, urban transport, commercial vehicles, rural areas and other cities due to population growth of the cities. Passing the provincial and state highways through the city also increases the traffic load; it is becoming more and more difficult for people not to walk in a short distance, not to use public transport, and to use special vehicles.

The lack of adequate parking spaces for public institutions, work places and dwellings in urban centers, an understanding of the indefinite use of on-road and out-of-door parking, the habit of using some kind of workplace owners as their property in front of the workplace, slowing down the traffic in the city center.

It is also a fact that how much the exhaust gases disturb the floods and reduce the comfort of people in the places where vehicle traffic and vehicle traffic intersect with pedestrian traffic and vehicle traffic at crossroads.

Based on the 37th and 44th articles of the Urban Development Law No. 3194, the new parking regulation prepared by the Ministry of Environment and Urbanism was published on the official gazette numbered 30340 on 22 February 2018. This regulation has entered into force on 01.06.2018.

In this report, parking problems in Ordu province center were investigated depending on the existing transportation network, and attempts were made to produce sustainable solutions for the future without polluting the environment, air and water.

Keywords: Life comfort, Traffic, Car parking, Pollution, Ordu.

1. Introduction

Vehicle traffic of big cities today; due to the rapid population growth in the cities, comprises of private automobiles, urban transport vehicles, commercial vehicles and traffic flow of visitors from rural areas and other cities.

Image 1. Roads & usage densities of Chongqing city-China (Köse, 2013).

The life cycle of people generally continues in the form of work, transportation and rest (See Image 1). Apart from commercial vehicles, almost every family has one or two cars. Together with commercial vehicles, these are central traffic in our cities. It is also known that if the time spent on transportation within the life cycle is accounted for, the automobiles spend most of the year in a stationary state. Parking spaces are needed for these vehicles, which are increasing in number day by day and which constitute vehicle traffic in the city. This need is increasing day by day. Every vehicle owner wants the vehicle to be safe and not to suffer economic damage in the life cycle of work and rest (Haldenbilir et al., 1999; Kuntay, 2009; URL-1, 2018; URL-2, 2018).

In the cities, towns and small settlements where we live; fields where we leave our vehicles out of transportation are called parking areas or parking lots. Parking lots can be on the ground, underground, open or closed, reserved area, roadside, city, out-of-city, private or public area. The parking lot is a secure, organized and environmentally friendly place that is

outside of transportation time. It is known that people and other living things need clean fresh air and clean water to maintain their lives in a healthy and safe way. The development of vehicle traffic and parking in an unplanned way in our big cities brings with it noise, air and environmental pollution. This situation should not be overlooked when transportation plans are made in our cities. Noise, air and environmental pollution are also influencing the health and life comfort of people living in cities. Increasing number of vehicles, uncontrolled traffic, limited parking facilities, inadequate parking spaces cause the city traffic to slow down to safety problems, accidents increase. At the same time, it decreases the quality of life by increasing the loss of time and energy (Köse, 2013; Yardım, 2015; Gülhan and Ceylan 2010).

2. Methodology

The new parking lot regulation issued by the Ministry of Environment and Urbanization on 22 February 2018 and published on the Official Gazette no. 30340 and enacted on 01.06.2018 will require the revision of the Ordu Metropolitan Municipality Parking Ordinance.

In this study, Ordu Metropolitan Municipality has taken as an example the area of responsibility of the central Altınordu Municipality; Altınordu District Municipality transportation planning, parking spaces, parks, sustainable solutions for these issues are emphasized.

Parking problems in Ordu province center were investigated depending on the existing transportation network, and attempts were made to produce sustainable solutions for the future. For this aim; the parking lot regulation numbered 30320 and dated February 22, 2018; enacted by the Ministry of Environment and Urbanization on 01/06/2018; Ordu Metropolitan Municipality Parking Regulation, which was dated 11.09.2014 have been evaluated. The documents of Ordu Metropolitan Municipality and Altınordu District Municipality have been used.

2.1. Human, Transportation and Parking Relation

Most points of Ordu city centre can be reached easily by foot, by public transport and private car. People generally use private vehicles and public transport. As the vehicles used in public transport go to long distances, they become full in a short time along the line so people who are waiting at the next stops suffer from that. In this sense, preference is used as a private car. In the morning and evening hours intense traffic on Ordu-Samsun, Ordu-Giresun directions

affetcs drivers psychology in a negative way. When reaching the city center, lack of parking lots is confronted. Parking in an unsafe manner also causes economic damage to vehicles. In old or historical urban settlements, this problem is increasing more than once (Arşiv Notları-1, Arşiv Notları-2; URL-8, 2018).

It is better for people to travel through the shortest path, in the shortest time and with the least cost possible while going to work and for other activities of social life. The aim of people's comfort, confidence and ease; to prevent them from getting tired during their journey, and to work efficiently throughout the day. There is a significant relationship between quality of life and transportation in a settlement. However, the noise and air pollution caused by heavy traffic affects the comfort of people negatively. The traffic and pollution that occur during certain days of the week and especially during summer months due to tourism activities, make the city center unbearable. Whereas people want; easy access, safe parking and a peaceful city center. For this; preventing vehicles to enter urban centers by arranging central area parking lots as far as walking distance outside the center is seen as a solution (URL-1, 2018; URL-2, 2018).

2.2. Laws and Regulations

Urban development Law No. 3194 (dated 3/5/1985 and numbered 18749) is defined in article 44 as "The buildings and facilities to be separated from the parking lot and other matters shall be determined in the regulation to be ministerial. The amount, size and other conditions of the car park need and how it will be determined and paid will be specified in this regulation." the application is available. In article 37, "Parking spaces are reserved in consideration of the requirements of the zone and the zone planned in the arrangement of the development plans and the future needs. Building permission for buildings and facilities where parking is required, building permission is not permitted unless the parking lot is distinguished. After the permission to use is granted, it can not be allocated to other purposes contrary to the parking lot, plan and regulations provisions. If contrary to the provisions of this paragraph, the contradiction shall be resolved within 3 months at the latest upon notification to be made by the related administration. If the proprietor of the property does not make the necessary corrections in due time, the municipal council or the provincial administration committee decides that the service will be carried out by the relevant administration and the cost will be collected from the property owner." situation clearly stated (URL-5, 2018; URL-6, 2018).

Also related topics are stated in; The Parking Lot Regulation numbered 30320 and dated February 22-2018, enacted by the Ministry of Environment and Urbanization on 01.06.2018;

Ordu Metropolitan Municipality Parking Regulation, which was dated 11.09.2014 and entered into force with the decision number of 2014/109 and in 16.09.2014 (URL-5, 2018; URL-6, 2018; URL-7, 2018).

2.3. Parking Lots

Parking facilities; the location of the parking lot (in central areas, in intermediate areas, in the peripheries, at the second tertiary sub-centers, in areas with high traffic such as terminals, shopping malls, stadiums); duration of stay in the parking lot (short-term, medium-term, long-term parking); the type of management of car parks (private, commercial operated, public establishments, car parks operated by build-operate-transfer method); parking fees (high paid central area, moderate toll, low toll, free parking); time-dependent features (peak-to-intermediate, weekday-weekend, summer-winter); according to occupancy rate of vehicles; depending on the reasons for the trip or activity (such as sightseeing, school services, hospital car parks, entertainment, stadium car parks) (Haldenbilir et al., 1999; Kuntay, 2009; Yardım, 2015).

As it can be seen, the priority in the construction of parking lots depends on the choice of strategic features. The main concern in the design of the parking area is to provide safety. According to the places where they have parking, they are divided into on-road parking and off-street parking.

On-Road Parking: The car is parked on the sidewalk of the road. For this reason parking in this way is also called "sidewalk park". It can be shaped to suit short durations. The occupation of a single sided lane or two lanes by vehicles in this way will cause traffic congestion, especially in urban centers. Road capacity will be reduced, traffic safety and pedestrian safety will be adversely affected (See Image 2) (Yardım, 2015; Kuntay, 2009).

Image 2. On-road parking, Ordu (author's own work)

Off-Street Parking: Cars are parked in open or closed places that are designed outside the road (See Image 3). The construction of such parking spaces in city centers is very difficult. However, multi-storey car parks can be seen as a solution. For urban workers, especially those working in the business and commercial areas, the use of off-street parking should be provided wherever possible. For buildings constructed in new settlements, parking regulations should be applied and roads should not be transformed into on-road parkig lots (Yardım, 2015; Kuntay, 2009).

Image 3. Off-street parking-1, Ordu (author's own work)

2.4. The Effects of Transportation Systems

Ordu is situated in the Central Black Sea Region and on the Black Sea Coastal Road. Currently, there are passenger transportation and air transportation. Sea transportation is located in the nearest Giresun province. Locally there is a cable car from Atatürk Park to Boztepe. It is thought that the Black Sea-Mediterranean route will pass through the Mesudiye District, from Sivas and Hatay to the Mediterranean Sea. There is also connection to Central Anatolia by the road of Ünye-Akkuş-Niksar-Tokat. Fatsa-Aybastı-Tokat can also be reached by land (URL-7, 2018; URL-8, 2018).

In addition to visitors to Ordu city by land and air transportation, there is a heavy flow of traffic from outside all seasons. Especially in the city center, until the road to the environment is opened; traffic congestion, parking problems, noise and air pollution will continue. Moreover, we do not have any information about how to make transportation connections and parking of the stadium constructed in Akyazı District Durugöl Site (URL-8, 2018).

According to TÜİK data, the total number of vehicles registered in the traffic in Ordu by the end of November, 2017 was 130034. The increase compared to the previous year is 6.3%. Approximately 53.8% of the vehicles registered in the railway were automobiles, 16.4% trucks, 14.1% motorcycles, 8.3% tractors, 3.9% trucks, 2.2% minibuses, 1% are special-purpose vehicles (URL-3, 2018).

2.5. Available Parking Areas and Problems in Ordu City

In Ordu, as of 01.06.2018, the capacity of the on-road parking lots is 442 vehicles and the capacity of the off-street open-air parking lots is 1375 vehicles. Underground parking at the bottom of the Ordu Metropolitan Municipality Building is about 60 cars, under the Altınordu Municipal Building there are about 165 cars, and under the Novada Shopping Center there are about 90 cars parking spaces. Migros Shopping Center also has about 130 parking spaces (Arşiv Notları-1; Arşiv Notları-2; URL-5, 2018; URL-6, 2018; URL-7, 2018).

There are no countings in public parking lots of public buildings. However, it is observed that there is a lot of parking problems especially in hospitals. The parking problem in Boztepe, the touristic center of Ordu, was partially solved by the cable car access.

While the above numbers were given for Ordu city center, the settling areas did not participate in the account. In the districts of Şarkiye, Düz Mahalle, Zaferi Milli, Taşbaşı, Saray, Bucak, Subaşı, Yeni Mahalle and Bahçelievler; the parking lot of the central district is increasing day by day. It is a constant problem that the buildings built in these areas are used as both commercial and residential buildings and that there is no parking space for them. It is considered that the people who make the buildings should be involved in the 37th and 44th articles of the Urban Development Law and it is not known how the registration certificate is given. In the city center, the driver uses the pedestrian sidewalks as a car park, and the pedestrians remain in a difficult position to walk on the roads of vehicles. The parking lot for the disabled is rather insufficient (Arşiv Notları-1, Arşiv Notları-2).

Approximately 50 new vehicles are added to Ordu's traffic each day. Pedestrian sidewalks are also used outside the use of pedestrians due to parking problems. A cobblestone pavement, with the other floods, is causing considerable distress, causing the flow of traffic to slow down or stop. The problem still continues in new settlements. Especially in Akyazı, Durugöl, Karşıyaka, Cumhuriyet Districts, in general, the vehicles in the new construction are using the roadside as a parking area. It is known that the customers who applied for a housing contract from Akyazı neighbourhood asked the parking lot and answered "you may park on the road" from the company representatives. One of the parties to the problem is the contractors. The other stakeholder of the problem is the municipality when it is examined from the perspective of construction applications, inspection and residence permit. In this case, the new parking lot, which was prepared according to articles 37 and 44 of the Urban Development Law

in new settlements, entered into force on 01.06.2018 (Arşiv Notları-1, Arşiv Notları-2; URL-5, 2018; URL-6, 2018; URL-7, 2018; URL-8, 2018).

On the other hand; it is almost impossible to find public land within the boundaries of Altınordu District of the central Ordu in Turkey due to its geographical structure. It is very difficult to convert the land belonging to the people into national central parking lots by expropriation. However, parkings will be resolved with the zoning applications in the areas where the new residential area will be opened.

3. Conclusion

Sustainable transportation and parking should be considered together in city centers. There is a serious parking problem in the city center of Ordu in general. Long-term on-street parking; blocking occasionally traffic flow cause transportation time is prolonged, sometimes the traffic accidents and energy waste. Especially during 7.30 -8.30 hours in the morning and 16.30-18.00 hours in the evening this problem becomes much more evident.

Parking problem in Ordu should be tried to be resolved by local governments, contractors who build cities, cohabiting people and drivers through planning, common opinion and economic reconciliation. According to the new parking regulation, work should be done to solve the problem of sustainable parking for the future within the framework of revision of old settlements and implementation of zoning plans in new settlements.

When the vehicles are not being used, it is necessary to stay in a safe, orderly and environmentally friendly area. Whether or not the use of the vehicle is economical in this way is a separate matter. The important thing is that our needs and comfort are best met. The following suggestions have been made for a park integrated with a harmonious plan, integration with green, transportation systems not disturbing air traffic and visual pollution, and traffic in the city.

-Parkings to pedestrian walkways pedestrian movements are present on streets, even it is for short-term should be obstructed and severe penal sanctions should be applied.

-Short-term parkings should be directed to on-road parking areas.

-The visitor and out-of-town traffic should be directed to off-street parking lots, taking into account the length of time they are in the parking lot, if possible.

-Parking areas for work and business areas should be in a walking distance as much as possible.

-Public transportation, cycling and walking should be encouraged.

-In traffic; in places where traffic and pedestrian traffic intersect, crossing junctions must be arranged for vehicles as far as possible, pedestrian traffic should be maintained.

-Free public transport from the park areas for visitors and traffic coming from outside the city to the city center can be provided free of charge.

-The light-rail train system project on Perşembe-Ordu-Gülyalı line can be seen as one of the best solutions for the problem of Ordu city transportation and parking.

-In the framework of the new zoning plan implementation; ground floor, basement floor, underground car park and overground car park can be brought for the future.

-The parking lots in Altınordu District should be connected with the automation system; it is possible to direct drivers to free parking areas by following occupancy rates, durations, and parking violations.

-Sustainable parking policies for the future should be determined.

-A large part of the problem can be solved through urban regeneration studies.

-Major shopping malls and stadiums should be moved out of city center.

-The requirements of the "Metropolitan Municipality Parking Lot Regulations" to be prepared in accordance with the new parking regulations, which entered into force on 01.06.2018, must be fulfilled by the planners, implementers, supervisors and users.

References

Yardım, M. S., (2015). YTÜ Merkez Kampüsünde Sürdürülebilir Kampüs Otoparkı Yönetimi İçin Yaklaşımlar. Sigma Mühendislik ve Fen Bilimleri Dergisi, 33 (4), 561-575.

Gülhan, G., Ceylan, H. (2010). Otopark Sorununa Otopark Yönetimi Temelinde Yaklaşımlar: İzmir Örneği. DEÜ Mühendislik Fakültesi Mühendislik Bilimleri Dergisi, 12, 1, 63-73.

Haldenbilir, S., Murat, Y. Ş., Baykan, N., Meriç, N. (1999). Kentlerde Otopark Sorunu: Denizli Örneği. Mühendislik Bilimleri Dergisi, 5, 2-3, 1099-1108.

Kuntay, O.,(2009). Sürdürülebilir Otopark Tasarımı. Ankara: TMMOB Mimarlar Odası Ankara Şubesi.

Köse, B., (2013). Reuniting the Waterfront with People: Connecting Sustainable Urban Design Concepts & Lighting Strategies A Conceptual Recommendation. Master Degree Thesis. School of Architecture and Urban Planning of Chongqing University, Chongqing, China.

Arşiv Notları-1, ORBEL A.Ş.

Arşiv Notları-2, Ordu Büyükşehir Belediyesi UKOME Şube Müdürlüğü.

URL-1: https://www.dunya.com/kose_yazısı/sehir_ulasim_planlamasi_ve_otopark_sorunlarimiz/2961, (Ret. 30.05.2018).

URL-2:http://www.bestdergisi.com.tr/arsiv/yazi/76_büyüksehirlerin-trafik_cozumu_icin_buyuk_veri, (Ret. 30.05.2018).

URL-3: http://www.tuik.gov.tr/PreTablo.do?alt_id=1051, (Ret. 05.06.2018).

URL-4: http://www.imo.org.tr/resimler/ekutuphane/pdf/10166.pdf, (Ret. 05.06.2018).

URL-5: http://www.mevzuat.gov.tr/MevzuatMetin/1.5. 3194.pdf, (Ret. 10.03.2018).

URL-6: http://www.resmigazete.gov.tr/eskiler/2018/02/20180 222-7.htm, (Ret. 12.03.2018).
URL-7:https://www.ordu.bel.tr/uploads/yonetmelikler/2/5-%20Otopark%20Y%C3%B6netmeli%C4%9Fi %20(11.09.2014-109).pdf, (Ret. 12.03.2018).
URL-8: https://www.ordu.bel.tr/uploads/ stratejik-plan.pdf, (Ret. 15.03.2018).

Optimization of Tuned Mass Dampers using Pattern Search Algorithm

Onur Araz[1*], Volkan KAHYA[2]

[1]Gümüşhane University, Faculty of Engineering and Natural Sciences, Civil Engineering, Gümüşhane, Turkey
[2]Karadeniz Technical University, Faculty of Engineering, Civil Engineering, Trabzon, Turkey

[*]**Corresponding Author:** onuraraz29@hotmail.com

Abstract

Tuned mass dampers (TMDs) have attracted to the concern of many researchers in the field of control devices in recent years. Tuned Mass Damper is a classical engineering device consisting of a mass, a spring and a viscous damper and is directly attached to primary mass to reduce any undesirable vibration in the structure. The optimum parameters of multiple tuned mass dampers (MTMDs) for suppressing the dynamic responses of single degree-of-freedom (SDOF) system due to harmonic excitation are investigated in this study. The solution of the optimization problem is obtained using the pattern search algorithm (PSA) which has been successfully applied for several engineering problems. The parameters include the frequency spacing, damping ratio, tuning frequency ratio, mass ratio and total number. The optimization criteria is based on the minimization of the maximum value of dynamic magnification factor for displacements (DMF) of the structure with MTMD under external harmonic excitation. Equations of motion of a SDOF primary system and the attached MTMDs are first derived using the Lagrange's equations. Then, the optimum parameters for vibration reduction of SDOF primary system due to an external harmonic load are determined. The effectiveness of MTMD system designed by the presented optimization method in vibration control under harmonic excitation is demonstrated by comparison with the existing literature.

Keywords: Harmonic excitation, optimum parameters**,** multiple tuned mass dampers, vibration control.

1. Introduction

To reduce vibrations of tall buildings and other civil engineering structures excited by environmental loads, e.g. earthquake, wind and traffic loads, has been attracted great interest of many researchers. The efforts on vibration control of structures have resulted in developing various control devices. Among them, tuned mass dampers (TMDs) consisting of a mass, a spring and a viscous damper is one of the simplest, reliable and low-cost control devices.

In 1909, the first application of TMD consisting of a mass and a spring was introduced by Frahm (1909). It has a narrow operation region, and its performance reduces significantly when the exciting frequency varies. Since then, many efforts have been made to obtain the optimum parameters of TMDs. Den Hartog (1956) proposed a closed form solution to minimize the dynamic response of undamped main system under harmonic loads. Warburton (1982) derived expressions for optimum parameters for undamped system under harmonic and white noise excitations. Asami et al. (2002) gave a series solution for the H_∞ optimization and an exact solution for the H_2 optimization. Since their solution is excessively complicated, they proposed an approximate solution for practical use. Recently, several researchers employed the different optimization methods for tuning single TMD for undamped and damped systems subjected to external excitations (Ghosh and Basu, 2007; Brown and Singh, 2011; Anh and Nguyen, 2012; Yu et al., 2013; Chun et al., 2015; Dell'Elce et al., 2018).

All studies mentioned above are concerned with tuning TMD to a dominant frequency of the main system. However, single TMD is very sensitive to any change in the frequency of TMD or the main system, which is so-called the detuning. To overcome the detuning due to the frequency deviation, Xu and Igusa (1992) proposed to use multiple tuned mass dampers (MTMDs) instead of the classic single TMD. They indicated that the use of MTMDs with distributed natural frequencies in a frequency bandwidth can be more effective than that of a single TMD with the same total mass. This kind of MTMD system has also been studied by references in (Farshidianfar and Soheili 2013; Salvi and Rizzi 2016; Yazdi et al. 2016; Bekdaş and Nigdeli 2017; Zuo et al. 2017; Bozer and Özsarıyıldız 2018). The main difference in these studies is the methods and criteria adopted for obtaining the optimal design variables.

Unlike the previous studies, pattern search algorithm (PSA) is utilized to find optimum parameters of MTMDs in this paper. The optimum parameters of the MTMD system and corresponding effectiveness are obtained for different numbers of TMD units and mass ratios of the MTMD system.

2. Governing Equations

Consider a single-degree-of-freedom (SDOF) system with a MTMD shown in Fig. 1. As seen, the MTMD device attached to the primary structure is composed of a set of different TMD units. The natural frequencies of TMD units are tuned to a frequency range in the vicinity of the natural frequency of the main structure. Note that total DOFs of the coupled system is n + 1 where n is the number of TMD units. The equation of motion for the main structure with MTMD under harmonic excitation is

$$m_s\ddot{x}_s + c_s\dot{x}_s + k_s x_s + \sum_{j=1}^{n} c_j(\dot{x}_s - \dot{x}_j) + k_j(x_s - x_j) = Pe^{i\omega t} \quad (1)$$

and the vertical motion of the jth TMD is

$$m_j\ddot{x}_j + c_j(\dot{x}_j - \dot{x}_s) + k_j(x_j - x_s) = 0 \quad j = 1,2,\mathrm{L}\ ,n \quad (2)$$

where over dot denotes differentiation with respect to time t. m, c and k are the mass, damping coefficient and stiffness, respectively. Subscripts s and j denote the primary structure, the jth TMD, respectively. x_s and x_j indicate the vertical displacements.

Combining Eqs. (1) and (2), the equations of motion can be given in the following matrix form:

$$\mathbf{M}\ddot{\mathbf{X}} + \mathbf{C}\dot{\mathbf{X}} + \mathbf{K}\mathbf{X} = \mathbf{F} \quad (3)$$

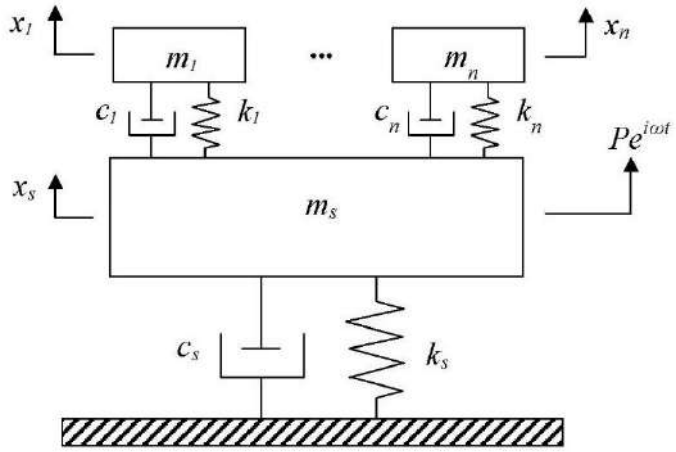

Fig. 1. Primary structure – MTMD coupled system

where **M**, **C**, **K** are the mass, damping and stiffness matrices, $\ddot{\mathbf{X}}$, $\dot{\mathbf{X}}$ and $\mathbf{X}$ are the acceleration, velocity and displacement vectors, respectively, **F** is the external force vector, that can be defined as:

$$\mathbf{M} = diag(m_s \quad m_1 \quad m_2 \quad \mathrm{L} \quad m_n] \tag{4}$$

$$\mathbf{C} = \begin{bmatrix} c_s + \sum_{j=1}^{n} c_j & -c_1 & -c_2 & \mathrm{L} & -c_n \\ -c_1 & c_1 & 0 & \mathrm{L} & 0 \\ -c_2 & 0 & c_2 & \mathrm{L} & 0 \\ \mathrm{M} & \mathrm{M} & \mathrm{M} & \mathrm{O} & \mathrm{M} \\ -c_n & 0 & 0 & \mathrm{L} & c_n \end{bmatrix} \tag{5}$$

$$\mathbf{K} = \begin{bmatrix} k_s + \sum_{j=1}^{n} k_j & -k_1 & -k_2 & \mathrm{L} & -k_n \\ -k_1 & k_1 & 0 & \mathrm{L} & 0 \\ -k_2 & 0 & k_2 & \mathrm{L} & 0 \\ \mathrm{M} & \mathrm{M} & \mathrm{M} & \mathrm{O} & \mathrm{M} \\ -k_n & 0 & 0 & \mathrm{L} & k_n \end{bmatrix} \tag{6}$$

$$\mathbf{X} = \{x_s \quad x_1 \quad x_2 \quad \mathrm{L} \quad x_n\}^{\mathrm{T}}, \quad \mathbf{F} = e^{i\omega t}\{P \quad 0 \quad 0 \quad \mathrm{L} \quad 0\}^{\mathrm{T}} \tag{7}$$

The normalized displacement amplitude or dynamic magnification factor (DMF) for the primary structure under harmonic excitation is given by

$$\mathrm{DMF} = \frac{x_1}{x_{st}} = \sqrt{\frac{1}{\mathrm{Re}(z_1)^2 + \mathrm{Im}(z_1)^2}} \tag{8}$$

where

$$\mathrm{Re}(z_1) = 1 - \beta^2 - \beta^2 \sum_{j=1}^{n} \mu_j \frac{\frac{\beta_j^2}{\beta^2} - 1 + 4\xi_j^2}{\left(\frac{\beta_j}{\beta} - \frac{\beta}{\beta_j}\right)^2 + 4\xi_j^2} \tag{9}$$

$$\mathrm{Im}(z_1) = 2\beta\xi_s + \beta^2 \sum_{j=1}^{n} \mu_j \frac{\frac{2\beta\xi_j}{\beta_j}}{\left(\frac{\beta_j}{\beta} - \frac{\beta}{\beta_j}\right)^2 + 4\xi_j^2} \tag{10}$$

where $x_{st} = P / k_s$ is the static displacement of the structure, $\beta = \omega / \omega_s$ is the frequency ratio between the external force and the structure, ξ_s is the damping ratio of the structure, $\mu_j = m_j / m_s$ is the mass ratio, $\beta_j = \omega_j / \omega_s$ is the frequency ratio, and $\xi_j = c_j / 2m_j\omega_j$ is the damping ratio of *j*th TMD. Details can be found in (Li and Ni 2007).

2. Statement of The Optimal Tuning Procedure

The tuning procedure proposed here is based on a pattern search algorithm, implemented in a MATLAB environment by the existing patternsearch function. The criteria selected for the

optimality is the minimization of the displacement response of the main system under external harmonic excitation.

Assume that the damping ratio ξ_s of the structure, the total number *n* of the TMD units contained and the mass ratio μ of the MTMD system considered are all known, and that the following ranges are selected for the control parameters: 0.8 < f_T < 1.2, 0 < β < 0.5, 0 < ξ_T < 0.4 with the search increment of each parameter set to be 0.01.

As a result of the procedure described above, the dynamic properties of the *j*th TMD unit associated with MTMD system can be determined,

$$\omega_j = \omega_T \left[1 + \left(j - \frac{n+1}{2} \right) \frac{\beta}{n-1} \right] \quad (11)$$

and

$$\omega_T = \sum_{j=1}^{n} \frac{\omega_j}{n} \quad (12)$$

$$\beta = \frac{\omega_n - \omega_1}{\omega_T} \quad (13)$$

where ω_T and β are the average frequency and non-dimensional frequency bandwidth of MTMD system, respectively.

Total mass of the MTMD system is expressed by the mass ratio defined as

$$\mu = \frac{\sum_{j=1}^{n} m_j}{m_s} \quad (14)$$

Tuning frequency ratio of the MTMD system is expressed by

$$f_T = \frac{\omega_T}{\omega_s} \quad (15)$$

where ω_s (i.e., $\omega_s = \sqrt{k_s / m_s}$) is the natural frequency of the main system.

3. Result and Discussion

To show the accuracy of proposed optimization method, some numerical results are given in the following. Here, we selected two models (i.e., TMD and MTMD) from the literature and presented the use of the PSA in the optimization of tuned mass dampers.

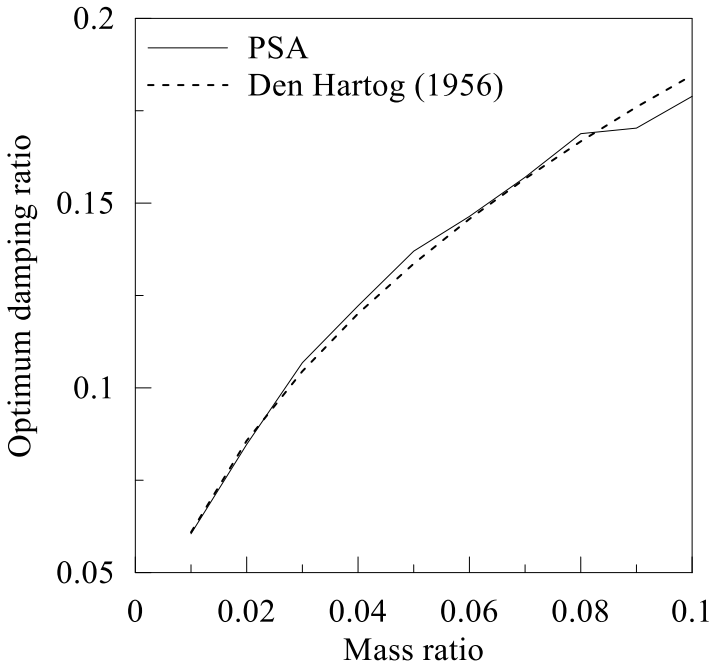

Fig. 2. Variation of the optimum damping ratio versus the mass ratio

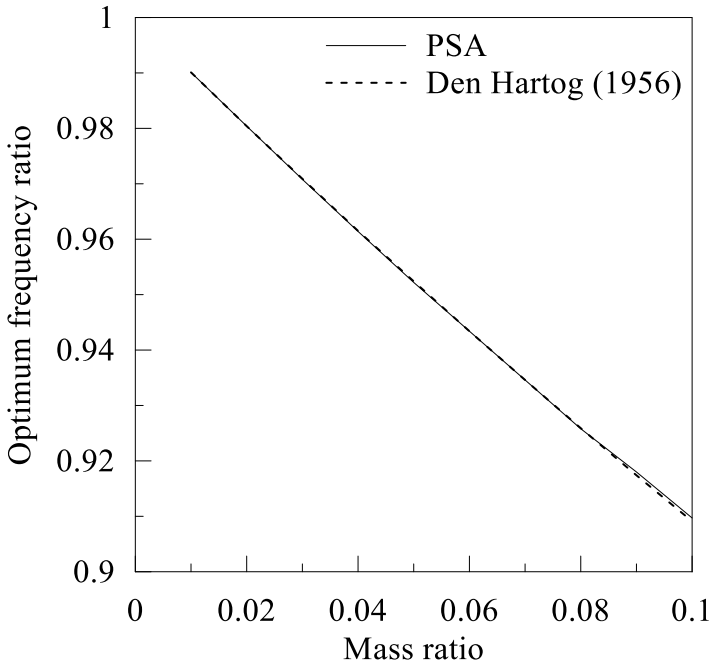

Fig. 3. Variation of the optimum tuning frequency ratio versus the mass ratio

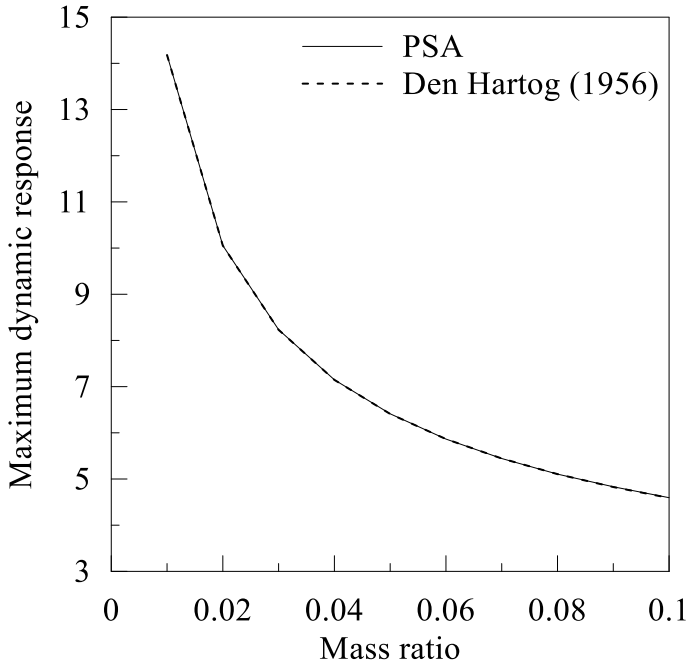

Fig. 4. Variation of the maximum dynamic response versus the mass ratio

First, undamped primary system with single TMD under harmonic external force is considered. To validate the effectiveness of results obtained in the present study, these solutions are compared with Den Hartog's optimum tuning parameters (Den Hartog, 1956). In Figs. 2-4 the variation of optimum damping ratio, optimum tuning frequency ratio and maximum

dynamic response of the primary system are plotted against the mass ratio, respectively. As seen, a good agreement is observed between the results.

Table 1. Optimum parameters of MTMD system with various numbers of TMD units for μ = 0.01.

	Present			Bandivadekar and Jangid (2012)		
n	ξ_T	β	f_T	ξ_T	β	f_T
3	0.0315	0.0864	0.9945	0.0319	0.0856	0.99441
5	0.0240	0.1117	0.9957	0.0239	0.1113	0.99571
7	0.0204	0.1239	0.9963	0.0203	0.1235	0.99631
9	0.0182	0.1312	0.9967	0.0185	0.1303	0.99663

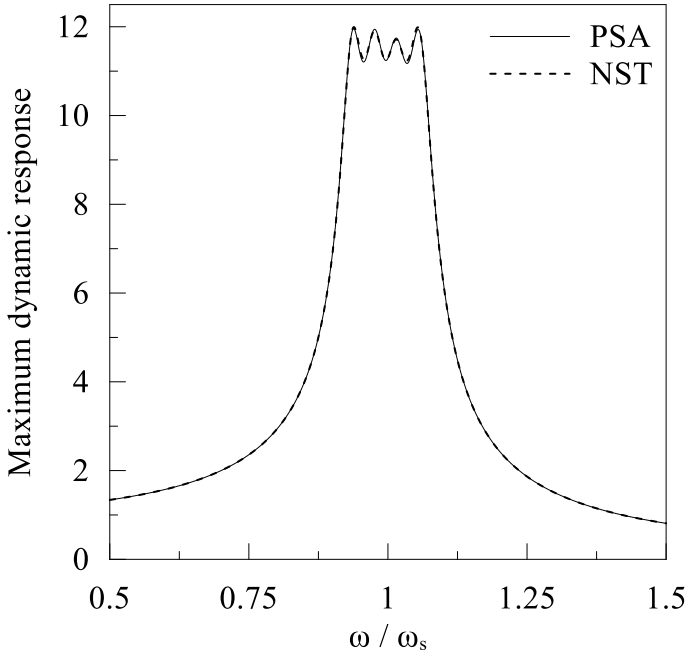

Fig. 5. Variation of response amplitude against harmonic excitation frequency for *n* = 3 and μ = 0.01

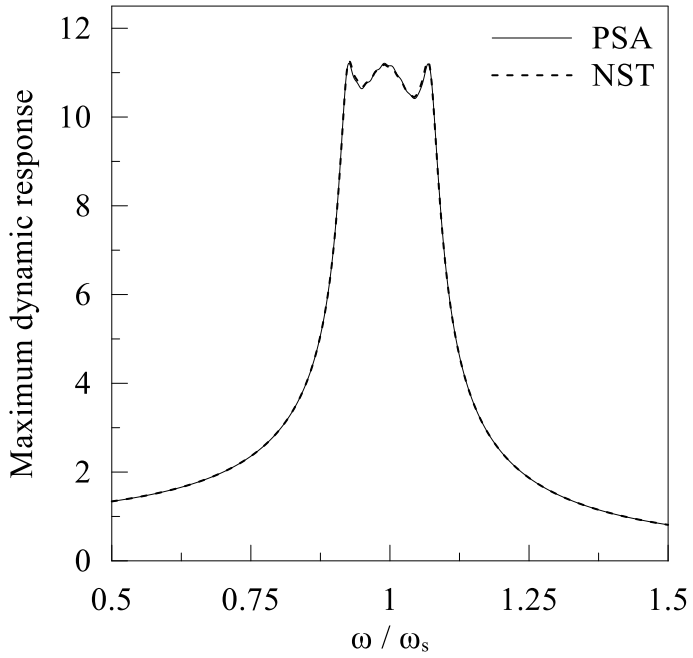

Fig. 6. Variation of response amplitude against harmonic excitation frequency for $n = 9$ and $\mu = 0.01$

As a second example, undamped primary system with various MTMD systems under harmonic external force are considered. In Table 1, the optimum parameters obtained by the present study are compared with that of the numerical searching technique (NST) proposed by Bandivadekar and Jangid (2012). The maximum relative error is found to be less than 2% for optimum damping ratio, however, it is found as 0.69% and 0.01% for optimum frequency bandwidth and tuning frequency ratio, respectively. Figs. 5 and 6 also show the frequency responses of the optimal MTMD system designed by PSA in comparison with those of the optimal MTMD system designed by NST for $n = 3$ and 9, respectively. Table 1, Figs. 5 and 6 indicate that there is a good agreement between numerical results obtained by PSA and NST.

4. Results and Discussion

The objective of this paper is to determine the optimum parameters of MTMD in order to reduce the response of primary system under harmonic external force. PSA is used to optimize the parameters of MTMD including damping ratio, tuning ratio and frequency bandwidth. Based on the above results, we can said that the present optimization method has a good accuracy to obtain optimum parameters of TMD as well as MTMD systems under harmonic excitation force. Besides,

the optimum parameters of MTMD for suppressing the dynamic response of a damped main system subjected to harmonic excitation can also be obtained using proposed method.

References

Anh, N. D., and Nguyen, N. X. (2012). Extension of equivalent linearization method to design of TMD for linear damped systems. *Structural Control and Health Monitoring*, 19, 565-573.

Asami, T., Nishihara, O., and Baz, A. M. (2002). Analytical solutions to H_∞ and H_2 optimization of dynamic vibration absorbers attached to damped linear systems. *Journal of Vibration and Acoustics*, 124, 284-295.

Bandivadekar, T. P., and Jangid, R. S. (2013). Optimization of multiple tuned mass dampers for vibration control of system under external excitation. *Journal of Vibration and Control*, 19, 1854-1871.

Bekdaş, G., and Nigdeli, S. M. (2013). Mass ratio factor for optimum tuned mass damper strategies. *International Journal of Mechanical Sciences*, 71, 68-84.

Bekdaş, G., and Nigdeli, S. M. (2017). Metaheuristic based optimization of tuned mass dampers under earthquake excitation by considering soil-structure interaction. *Soil Dynamics and Earthquake Engineering*, 92, 443-461.

Bozer, A., and Özsarıyıldız, Ş. S. (2018). Free parameter search of multiple tuned mass dampers by using artificial bee colony algorithm. *Structural Control & Health Monitoring*, 25, 1-13.

Brown, B., and Singh, T. (2011). Minimax design of vibration absorbers for linear damped systems. *Journal of Sound and Vibration*, 330, 2437-2448.

Chun, S., Lee, Y., and Kim, T. H. (2015). H_∞ optimization of dynamic vibration absorber variant for vibration control of damped linear systems. *Journal of Sound and Vibration*, 335, 55-65.

Dell'Elce, L., Gourc, E., and Kerschen, G. (2018). A robust equal-peak method for uncertain mechanical systems. *Journal of Sound and Vibration*, 414, 97-109.

Den Hartog, J. P. (1956). *Mechanical Vibrations*, New York: McGraw-Hill.

Farshidianfar, A., and Soheili, S. (2013). Ant colony optimization of tuned mass dampers for earthquake oscillations of high-rise structures including soil–structure interaction. *Soil Dynamics and Earthquake Engineering*, 51, 14-22.

Frahm, H. (1909). *Device for damped vibration of bodies*, U.S. Patent no. 989958.

Ghosh, A., and Basu, B. (2007). A closed-form optimal tuning criterion for TMD in damped structures, *Structural Control and Health Monitoring*, 14, 681-692.

Kwon, H. C., Kim, M. C., and Lee, I. W. (1998). Vibration Control of Bridges under Moving Loads. *Computers & Structures*, 66, 473-480.

Li, C. (2002). Optimum multiple tuned mass dampers for structures under the ground acceleration based on DDMF and ADMF. *Earthquake Engineering and Structural Dynamics*, 31, 897–919.

Li, H. N., and Ni, X. L. (2007). Optimization of non-uniformly distributed multiple tuned mass damper. *Journal of Sound and Vibration*, 308, 80-97.

Luu, M., Zabel, V., and Könke, C. (2012). An optimization method of multi-resonant response of high-speed train bridges using TMDs. *Finite Elements in Analysis and Design*, 53, 13-23.

Salvi, J., and Rizzi, E. (2016). Closed-form optimum tuning formulas for passive tuned mass dampers under benchmark excitations. *Smart Structures and Systems*, 17, 231-256.

Warburton, G. B. (1982). Optimal absorber parameters for various combinations of response and excitation parameters. *Earthquake Engineering and Structural Dynamics*, 10, 381-401.

Xu, K., and Igusa, T. (1992). Dynamic characteristics of multiple substructures with closely spaced frequencies. *Earthquake Engineering and Structural Dynamics*, 21, 1059-1070.

Yazdi, H. A., Saberi, H., Saberi, H., and Hatami, F. (2016). Designing optimal tuned mass dampers using improved harmony search algorithm. *Advances in Structural Engineering*, 19, 1620-1636.

Yu, H., Gillot, F., and Ichchou, M. (2013). Reliability based robust design optimization for tuned mass damper in passive vibration control of deterministic/uncertain structures. *Journal of Sound and Vibration*, 332, 2222-2238.

Zuo, H., Bi, K., and Hao, H. (2017). Using multiple tuned mass dampers to control offshore wind turbine vibrations under multiple hazards. *Engineering Structures*, 141, 303-315.

Examining Database Optimization Using Database Management System Models In A Mobile Application

Baki Gökgöz[1], Osman Duman[2], Menşure Kolçak[3]

[1,2]Gümüşhane University, Department of Computer Technology Vocational School of Torul, Gümüşhane, Türkiye
[3]Atatürk University, Faculty of Economics and Administrative Sciences, Department of Economics, Erzurum, Türkiye

[*]**Corresponding Author:**bakigokgoz@gumushane.edu.tr

Abstract

Today, with the rapid development and change experienced in information technologies, the amount of data that needs to be stored by users has reached a very large size. Horizontal scaling of large data sets is difficult to use the relational database model. As a result, NoSQL database models emerged towards the end of 2009. Large data sets can be stored with the NoSQL DBMS model. Database transactions of systems with high data communication traffic such as Facebook and twitter can be performed easily and quickly. Today, mobile devices, especially mobile phones, are used extensively. In this study, performance comparison using relational database model and NoSQL database model was done for application developed for mobile device in Android Studio environment. The results are shared and based on these results, the best method for database optimization is recommended.

Keywords: NoSQL, Mobile Application, Relational Database, Database Management Systems, SQLite, CouchBase Lite

1. Introduction

Generally, in the world of information, it is important to hide the data and to access these data quickly when there is a need. Today, with the rapid development and change experienced in information technologies, the amount of data that needs to be stored by users has reached a very large size. In 2000, social networks such as Web 2.0 technology and similar web applications have entered the life of mankind. This situation is known as the main reason for the increase of internet data.

The relational database model that stores and processes data on the Internet is used for over 40 years (Codd, 1970). The use of the relational database model is difficult when large data sets are scaled horizontally. As a result, NoSQL database models emerged towards the end of 2009. With the NoSQL DBMS model, large datasets can be stored in a single file. In this context, relational databases as well as non-relational database management systems are used in databases where processes such as reading and writing are heavily used. Non-relational database management systems (NoSQL) with performance and flexibility features have become preferred by world-renowned companies such as Google, Facebook and Amazon (Gökşen, 2015). In general, any database that is not a Relational Database Management System (RDBMS) supports things that do not have a specific order. NoSQL data warehouse does not conform to ACID specifications (atomicity, consistency, isolation, and durability), and high availability and support for large data sets can be provided in horizontally scaled environments (Tiwari, 2011).

NoSQL data models are divided into four subcategories: key-value, chart, document, and column database. The key-value accelerates database read and write operations. The diagram allows the database nodes to be navigated easily through links. The column database provides the ability to perform extensive query and data analysis on applications with associated columns aggregated in a column family (Ünalır, and others , 2015).

There are many differences between relational and non-relational databases. These differences can be summarized in three main points (Al Hinai, 2016): scaling, type of collections and consistency.

Scaling: Relational database systems are vertically scaled to accommodate more data sets. NoSQL database systems are horizontally scaled to accommodate more data sets. As the amount of data increases in relational database systems, more hardware is needed.

Type of Collections: Relational database systems use interrelated structured tables for data storage. NoSQL database systems deal with semi-structured or unstructured data sets that are

not related to each other. Depending on this situation, NoSQL database systems affect performance in a positive way (Hammes, and others, 2016).

Consistency: Consistency is a condition of ACID and CAP theorems (Brewer, 2000). All users see the consistency of the data. If any inconsistent data occurs in the operations on the database, it is necessary to undo the whole operation.

When comparing relational databases with NoSQL databases according to the nine-faceted feature, they achieved the following results (Mohamad, and others, 2014):

Transaction Reliability: Relational databases that work with ACID rules outperform NoSQL databases at this point.

Data Model: Relational databases processes are modeled mathematically. The columns are well defined and the associated data are stored in rows in the same structure. This is a well-organized data model. NoSQL uses the techniques that allow categorization to be used as a data model. The most obvious distinction is that it does not use tables as a storage structure. This is effective when managing unstructured data such as Word, pdf, images and video.

Scalability: While relational databases can be scaled vertically, NoSQL databases can be scaled horizontally. The problem that vertical growth brings with it is more hardware.

Cloud: Relational databases do not support full content in the data search and it is difficult to scale the data beyond a limit. NoSQL databases are flexible for unstructured, semi-structured, or structured data.

Big Data Handling: Since the data in the relational databases grow vertically, this can lead to new servers and performance problems. NoSQL does not have performance problems because it is designed for large data.

Data Warehouse: Data stored in relational databases is increasing over time and trying to overcome this problem through OLAP, data mining and statistical operations. NoSQL is not designed to be a data warehouse, and designers are focused on high performance and scalability.

Complexity: The data in the relational database must be transformed into tables by users. When data-table mismatch occurs, the structure of the database may become complicated. NoSQL databases do not have this problem because of their ability to store unstructured, semi-structured, or structured data.

Crash Recovery: Log files and ARIES algorithms are also used to prevent data loss that can occur in relational databases. However, this depends on the frequency of data recovery and backup in NoSQL databases.

Security: Relational databases support many security services because they are widely used. Again, there are many studies about security because relational database is used very long time.

NoSQL database systems, as opposed to relational database methods, do not have a new and long history, so new work is being done for security problems.

In this study, it was aimed to compare the performance of the CouchBase Lite NoSQL database in the Android Studio environment with the SQLite relational database used as embedded in mobile devices. CouchBase Lite, a variant of the NoSQL database used in practice, is very similar to key-value storage.

2. Methods and Materials

In this study, which aims to compare the performance of SQLite and CouchBase Lite databases, Windows 10 and 64 Bit version is used as the operating system. Android Studio 3.1.2 was used as the development environment. The code part of the work was developed in the Java programming language. The application developed for this study uses SQLite and CouchBase Lite databases. Performed database operations; adding data, listing data, updating data and deleting data. Performance comparison between relational database systems and NoSQL database systems has been made. The findings are comparatively shared in Table 1 and Table 2. In addition, the developed application interface is shown in Fig 1.

Şekil 1. Improved application interface.

3. Findings and Discussion

In this study, which is performed to determine database performance on mobile devices, transactions were performed with 10000 and 20000 records, respectively. The operations were repeated with 3 iterations and an average value was calculated.

Table 1. Performance data for 10000 records (ms).

Number of experiments	Create Database		Add Record		Bulk Data Listing	
	CouchBase Lite	SQLite	CouchBase Lite	SQLite	CouchBase Lite	SQLite

1	107	51	605	1302	7541	5245
2	101	57	513	1520	7293	5105
3	105	41	491	1321	7626	5312
Average	104,3	49,6	536,3	1381	7786,6	5087,6

Table 1. Performance data for 20000 records (ms)

Number of experiments	Create Database		Add Record		Bulk Data Listing	
	CouchBase Lite	SQLite	CouchBase Lite	SQLite	CouchBase Lite	SQLite
1	126	48	1225	3120	15321	11746
2	132	37	1003	3112	15227	12021
3	113	35	989	3225	14921	11956
Average	123,6	40	1072,3	3152,3	15156,3	11907,6

4. Results and Suggestions

In general, it has been observed that the SQLite database, which is a relational database model, is better than the NoSQL database model in terms of performance. It has been understood that the Relational Database Model will be a more optimal option for institutions when processing large amounts of data in the tomb.

Contrary to what is generally known, this study has a different conclusion. In other words, according to the literature, NoSQL database is weaker than Relational Database in terms of performance. The reason for this may be that the queries written are simple. In addition, in systems where larger data are processed, this comparison can yield better results.

References

Al Hinai A. H. (2016). A Performance Comparison of SQL and NoSQL Databases for Large Scale Analysis of Persistent Logs Department of Information Technology.

Brewer, E. A. (2000). Towards robust distributed systems (abstract). Proceedings of the Nineteenth Annual ACM Symposium on Principles of Distributed Computing - PODC '00, 7-19.

Codd, E. F. (1970). A relational model of data for large shared data banks. Communications of the ACM Commun. ACM, 13(6), 377-387.

Dayne H., Medero H., and Mitchell. H. (2014) "Comparison of NoSQL and SQL Databases in the Cloud. "Comparison of NoSQL and SQL Databases in the Cloud!: Paper 12. AIS Electronic Library (AISeL). SAIS 2014 Proceedings. http://aisel.aisnet.org/sais2014/12.

Eken, S., Kaya, F., Sayar, A., and Kavak, A. (2014). " Document-Based NoSQL Databases: MongoDB and CouchDB horizontal scalability comparison", 7. Engineering and Technology Symposium.

Gökşen, Y. (2015). “Changes in Data Sizes in Data Base Management Systems: NoSQL”, Journal of Information Technologies, 8-3.

Mohamed M, A., Altrafi O, G. and Ismail M, O. (2014). Relational vs. NoSQL Databases: A Survey. International Journal of Computer and Information Technology, 3 (3), 598-601.

Tiwari, S. (2011). Using Oracle Berkeley DB as a NoSQL Data Store . http://www.oracle.com/technetwork/articles/cloudcomp/berkeleydb-nosql-323570.html

Ünalır, T.O., İnan, E., Yöngül, B., Olca, E., Şentürk, F., and Mostafapour, V. (2015). "A Hybrid Data Architecture Recommendation for Data Intensive Information Systems”, 9th National Software Engineering Symposium.

Laboratory Applications in Construction Works-Ordu University Technical Sciences Vocational School Construction and Materials Laboratory Sample

Bilge KÖSE[1*], Ahmet KÖSE[2], Burcu KÖSE KHIDIROV[3]

[1,2]Ordu University, Vocational School of Technical Sciences, Construction Dept., Ordu, Turkey
[3]Mimar Sinan Fine Arts University, Faculty of Architecture, Interior Architecture Dept., Istanbul, Turkey

***Corresponding Author:** bilgeaydin@odu.edu.tr

Abstract

The construction sector, which includes indispensable occupation areas for the formation and development of civilizations highways, railways, ports, airports that meet our transportation needs; housing that meets our need for housing; construction, maintenance, repair of all the structures that are necessary for modern life in a wide range of contructions ranging from bridges, tunnels to supporting walls.

Desired performance on the constructions is possible with the continuity of the quality of the constructions. In this sense, construction sector; cannot be evaluated independently from the laboratory, laboratory applications. The construction laboratories serving public and private sectors for the continuity of quality in the area of construction provide the control, inspection, test services required for supervised constructions.

In this study, the importance of laboratory applications in construction works through the example of Ordu University Vocational School of Technical Sciences Construction and Materials Laboratory; evaluation of the contribution of the university to the local industry in terms of sector, taking into consideration the experimental services provided for civil engineering applications in the public and private sectors; it is aimed to examine the documents of the past and ongoing studies in the laboratory and to explain them by document scanning method. Laboratory services realized with academic discipline, provision of necessary technical support in the stages of structure production and usage has been found to increase the quality of materials production and construction works and it is envisaged that the quality of the construction sector will be increased further and the quality will be maintained.

Keywords: Construction works, Construction, Laboratory, Test, Quality, Construction sector.

1. Introduction

The construction sector, which includes indispensable occupation areas for the formation and development of civilizations housing that meets our need for housing, highways that meet our transportation needs, railways, ports, airports; bridges, tunnels, retaining all the buildings that are necessary for modern life in a wide fan design, construction, maintenance and repair. Catching quality in the construction sector, getting expected performance from the structures; it is possible to carry out the measurements and experiments on the data obtained by obtaining the necessary conditions in a controlled way and to achieve net results with systematic operation. Therefore; the construction sector, which is defined as the locomotive sector in all economies because it has developed business volume in many sectors with itself; it is not possible to evaluate them independently from the laboratories.

Ordu University Vocational School of Technical Sciences Construction and Materials Laboratory adopting the consciousness of ensuring continuity of quality in civil engineering applications, supporting the theoretical education of the work force which will step into the construction sector with the applications so provides benefits for sectoral development, provides experimental services to Ordu Metropolitan Municipality, especially the public institutions and private sector.

In addition, in the laboratory; teaching is carried out by the students of the Construction Technology Program of Technical Sciences Vocational School and the application for the courses required for implementation support; the students of the Department of Renewable Energy in Ordu University of Science Institute are facilitated in their graduate thesis studies.

2. Methodology

In this study; Ordu University, a university laboratory, through the experimental services offered by the Vocational School of Technical Sciences for the civil engineering applications in public and private sector; the contributions of the university to the regional industry from the sectoral point of view and the documents of the past and ongoing works have been evaluated and documented.

2.1. Construction and Materials Laboratory

Under Ordu Vocational School's constitution, in the beginning construction workshop applications in the form of work done, in 1993 concrete strength tests, cement and aggregate tests have been added over time. Since 1996, work carried out with concrete plants located in the city center of Ordu has continued to serve public institutions with the spread of ready-mixed concrete. The laboratory, which was revised in 2012 considering the needs of public and private sector, share of learning and scientific studies, has been regulated to provide the accreditation conditions of the Ministry of Environment and Urbanization from 2013 (See Image 1-2). Starting from this date, support for education and training, infrastructure for scientific research, meeting requests from public institutions and information exchange with the private sector (TS EN ISO/IEC 17025, 2002).

Quality control, destructive and non-destructive tests are carried out on constructions and construction materials in the laboratory. These; material strenght, crack control and corrosion control tests with ultrasonic testers in concrete and reinforced concrete structures; physical strength tests of materials such as natural stone, crushed stone (aggregate), aggregate used in fortification of sea structures and road constructions; tests of aggregates, cement tests and steel reinforcement bars from components of concrete and reinforced concrete building materials; determination of strength and durability properties of industrial steel materials and concrete design (TS EN 12620, 2003; TS EN 197-1, 2012; TS EN 196, 2009; TS EN 206-1, 2002; TS 708, 2010; TS 802, 2009).

Image 1. Construction and materials laboratory-1 (author's own work)

Image 2. Construction and materials laboratory-2 (author's own work)

2.2. Sector-Related Laboratory Work

According to the TS EN ISO/IEC 17025 standard, accreditation studies with the Ministry of Environment and Urbanization are carried out in the ongoing laboratory; instructions for the use and maintenance of laboratory machines and devices are prepared and annual calibrations are made by Turkish Standards Institute or Turkish Standards Institute and accredited laboratories (Url 1, 2018).

Work carried out in the public and private sector as much as the day-to-day work within the school-industry business association; non-destructive testing of concrete strength and reinforcement corrosion conditions, hardened concrete tests, tensile tests on concrete steel rods; tensile testing of industrial steel (sheet iron, sheet metal, round, etc.) materials; tensile, bending and abrasion tests on road pavement and surrounding elements; natural stones and concrete aggregates on the strength and endurance tests (See Image 3-4), (TS 708, 2010; TS EN ISO 6892-1, 2016; TS EN 12390-3, 2003; TS 436 EN 1340, 2010; TS EN 12504-1, 2010; TS EN 12390-5, 2002; TS EN 12390-6, 2002; TS 2824 EN 1338, 2005; TS EN 1097-1-2-6, 1999).

The laboratory has a permanent business association with public institutions and local governments. Technical support is given to the control services of the local administrations in the laboratory and quality control tests are carried out in practice.

Transactions in the laboratory in the direction of requests from public institutions and the private sector; preparation of tests, preparation of the results, preparation of the reports, and submission of official reports and reports to the tenderers.

Up to now, Ordu University has carried out quality control tests of educational buildings of about 30000 m²; abrasion and frost tests of crushed stone aggregates to be used in the construction of Ordu Orbital Road; bending, pulling and abrasion tests of concrete road covering and surrounding elements coming from Ordu Metropolitan Municipality and district municipalities; the construction of Chocolate Park constructed in Gülyalı province, concrete and steel tests with strength and durability tests of natural stone materials to be used in marine fortification; strength and durability tests of natural stone materials to be used in coastal fortification in Fatsa province; Ordu Metropolitan Municipality Rüsumat Park tests of stone and veneer materials used in the construction of landscaping; pulling tests of industrial steel materials from the industry; Ordu Credits and Dormitories Institution Male Student Dormitory concrete structure of reinforced concrete building and reinforcement corrosion by non-destructive methods are done by Ordu University Construction and Materials Laboratory (See Table 1), (Köse and Aydın, 2016; Köse and Aydın, 2017).

Image 3. Steel reinforcement bars' test (author's own work)

Image 4. Concrete preparation (author's own work)

Table 1: Tests in the laboratory for the sector between 2014-2018 (1) (author's own work)

Test Name	Company / Institution Name	Piece
Steel tensile	Metron Contruction	231
Steel tensile	Ekşioğlu Contruction	195
Steel tensile	Namık Kemal Erdoğan Contruction	39
Steel tensile	Yurt Engineering	14
Steel tensile	Ekpet-Onka Contruction	8
Steel tensile	Torunlar Contruction	4
Steel tensile	Karadeniz Tüpgaz	19
Concrete pressure strenght (cube sample)	Metron Contruction	700
Concrete pressure strenght (cube sample)	Ekşioğlu Contruction	450
Concrete pressure strenght (cube sample)	Uter Contruction	4
Concrete pressure strenght (cube sample)	Torunlar Contruction	14
Concrete pressure strenght (cube sample)	MG Concrete	6
Concrete pressure strenght (cube sample)	VG Electric	3
Concrete pressure strenght (cube sample)	Ekip Ak Engineering	7
Concrete pressure strenght (cube sample)	Yurt Engineering	55
Concrete pressure strenght (cube sample)	Torunlar Contruction	4
Concrete pressure strenght (cube sample)	Kaan Architecture	1
Concrete pressure strenght (cube sample)	Zirve Contruction	1
Curb bending strength	Ordu Metropolitan Municipality	6
Curb bending strength	Yurt Engineering	8
Curb bending strength	Aybin Contruction	3
Curb bending strength	DSC Concrete	4
Curb bending strength	Yüksel Ayaz Contruction	6
Curb bending strength	Çınar Landscaping	9
Curb bending strength	Torunlar Construction	3
Locked parquet shear strength	Uter Construction	3
Locked parquet shear strength	Ordu Metropolitan Municipality	3
Locked parquet shear strength	Bin-Aktay Construction	1
Locked parquet shear strength	MKB Construction	1
Locked parquet shear strength	DSC Concrete	12

Table 2: Tests in the laboratory for the sector between 2014-2018 (2) (author's own work)

Test Name	Company / Institution Name	Piece
Parquet shear strength	NBS Construction	30
Parquet shear strength	Kent Construction	20
Parquet shear strength	Torunlar Construction	91
Parquet shear strength	Uter Construction	21
Parquet shear strength	Yanıklar Construction	18
Natural stone pressure strenght	Namık Kemal Erdoğan Construction	5
Natural stone pressure strenght	Başak-San Construction	1
Natural stone pressure strenght	Torunlar Construction	3
Natural stone pressure strenght	Ordu Metropolitan Municipality	3
Magnesium sulphate	Nurol-Yüksel-Özka-YDA Construction	2
Magnesium sulphate	Ordu Metropolitan Municipality	3
Water content	Ordu Metropolitan Municipality	3
Water emitting	Ordu Metropolitan Municipality	6
Abrasion	Nurol-Yüksel-Özka-YDA Construction	2
Abrasion	Ordu Metropolitan Municipality	1
Los Angeles	Ordu Metropolitan Municipality	3
Eliminate analyzes	Ordu Metropolitan Municipality	3
Measurement of concrete strength (non-destructive method)	Credits and Dormitories Institution	1
Measurement of reinforcement's steel corrosion	Credits and Dormitories Institution	1

3. Conclusion

In this paper, with the Ordu University Vocational School of Technical Sciences construction and Materials Laboratory; services offered by the university for civil engineering applications in the public and private sectors were tried to be explained within the scope of the university-sector business association and the results achieved are listed below.

-The demand for performance from the buildings can be ensured by continuing the qualifications in the construction sector with laboratory applications.

-With the help of laboratory applications, technical personnel are being trained in concrete plants, R&D laboratories, private sector laboratories working for construction supervision and technical staff who can provide easier job adaptation to project application areas.

-Ordu University construction and Materials Laboratory provides inspection and testing services required for supervised constructions.

-It is observed that the quality of the material production is increased even more with the works carried out with the producers in the sector, exchange of ideas and consultancy.

-Establishment and quality awareness of establishments in the private sector and the public sector is ensured.

-All the experimental works are carried out in accordance with TS EN standards.

-If the university-industry business association is provided in a more realistic way, this business association will be beneficial to both parties as well as to a great extent for our country.

-Experimental studies on the materials used in the projects of the public sector have provided a value above the limit values given in the technical specifications of the material properties by searching for higher quality materials.

-The results obtained in scientific research projects and theses will be made available to the public and private sector as well.

-Technological support is provided for the use and application of private sector laboratory equipment.

-Dissemination of non-destructive testing technologies through the use of ultrasonic laboratory equipment; construction supervision, urban regeneration and earthquake risk should be considered together with structural safety and structural stability.

-Proliferation of well-equipped construction laboratories that enable scientific research and efficient utilization of laboratories will lead to the development of the researcher, the scientific field, the industry; it is obvious that the development will take place and economic benefit will be achieved.

References

Köse, A., Aydın, B., (2016, May). Üniversite Laboratuvarları ve Fayda: Ordu Üniversitesi Teknik Bilimler Meslek Yüksekokulu Örneği, *5th International Vocational Schools Symposium,* pg. 63-69. Prizren: University of Prizren.

Köse, A., Aydın, B., (2017, September). İnşaat Mühendisi Uygulamalarında Üniversite Sektör İş Birliği, *International Engineering Research Symposium,* pg. 34-42. Düzce: Düzce Üniversitesi.

URL-1: https://www.tse.org.tr/tr/Default.aspx, (Ret. 01.04.2018).

TS EN ISO/IEC 17025 (2002). *Deney ve Kalibrasyon Laboratuvarlarının Yeterliliği İçin Genel Şartlar.*

TS 706 EN 12620 (2003). *Beton Agregaları.*

TS EN 197-1 (2012, *Çimento.*

TS EN 196 (2009). *Çimento Deney Metotları.*

TS EN 206-1 (2002). *Beton-Özellik, Performans, Uygunluk.*

TS 708 (2010). *Çelik-Betonarme İçin-Donatı Çeliği.*

TS EN ISO 6892-1 (2016). *Metalik malzemeler - Çekme deneyi.*

TS 802 (2009). *Beton Karışım Tasarımı Hesapları.*

TS EN 12390-3 (2003). *Beton-Sertleşmiş Beton Deneyleri-Deney Numunelerinde Basınç Dayanımının Tayini.*

TS 436 EN 1340 (2010). *Zemin Döşemesi İçin Beton Bordür Taşları-Gerekli Şartlar ve Deney Metotları.*

TS EN 12504-1 (2010). *Beton-Yapıda Beton Deneyleri-Karot Numuneler-Karot Alma, Muayene ve Basınç Dayanımının Tayini.*

TS EN 12390-5 (2002). *Beton-Sertleşmiş Beton Deneyleri-Deney Numunelerinin Eğilme Dayanımının Tayini.*

TS EN 12390-6 (2002, *Beton-Sertleşmiş Beton Deneyleri-Deney Numunelerinin Yarmada Çekme Dayanımının Tayini.*

TS 2824 EN 1338 (2005). *Zemin Döşemesi İçin Beton Kaplama Blokları-Gerekli Şartlar ve Deney Metotları.*

TS EN 1097-1-2-6 (1999). *Agregaların Fiziksel ve Mekanik Özellikleri İçin Deneyler.*

Seismic Behavior Evaluation of a Cantilever Wall Considering Soil-Structure Interaction

Tufan ÇAKIR[1], Kaşif Furkan ÖZTÜRK[2*]

[1,2]Gümüşhane University, Department of Civil Engineering, Gümüşhane, Turkey, cakirtufan@hotmail.com, ozturkfurkan91@gmail.com

[*] **Corresponding Author:** ozturkfurkan91@gmail.com

Abstract

The study of the seismic response on retaining walls has gained significant attention in the last years as the seismic vulnerability of these structures represents a potential source of significant economic loss due to structural failures and environmental accidents. To investigate the dynamic behavior of retaining walls, the soil-structure interaction (SSI) should be considered since the interaction can drastically influence the dynamic behavior of the structure. The main purpose of this study is to investigate the SSI effects on seismic response of a cantilever retaining wall considering both backfill and subsoil interactions. Finite element (FE) simulation of backfill-cantilever wall-soil/foundation system has been carried out using the commercial FE software ANSYS. In the model, elastic material properties are considered for the cantilever wall. Backfill and foundation soils are modelled as an elastoplastic medium considering the Drucker-Prager yield criteria, and the backfill-wall interface behavior is taken into consideration by using interface elements between the wall and soil to allow for de-bonding. Lysmer-Kuhlemeyer type viscous boundary elements are used to simulate the wave energy absorption. Considering four different foundation soil conditions, nonlinear time history analyses are carried out in time domain to evaluate the structural response. Newmark's direct integration method is used in the analyses. The material damping of the system is represented by Rayleigh damping. The response quantities include the lateral displacements of the wall relative to the moving base, and the stresses in the wall. The results show that the SSI has a considerable effect on seismic behavior of the cantilever retaining walls.

Keywords: Cantilever wall, Soil-structure interaction, Time history analysis.

1. Introduction

Earthquakes are the significant source of seismic loading on soils for consideration of land-based structures. This is due to the damage-causing potential of strong ground motions and the fact that they represent an unpredictable and uncontrolled phenomenon in nature. The ground motion because of an earthquake may lead to permanent translational and rotational displacement, settlement and tilting of foundations and, thus, the structures supported by them (Das and Ramana, 2011).

Retaining walls, such as gravity, semi gravity, cantilever, and embedded walls generally support highway embankments, deep excavations, bridge abutments, and harbor-quays. The problems related to the vibration of soil and soil-supported and soil-retaining structures have received great attention of geotechnical engineers in recent years. Excessive seismic lateral soil/fluid pressure on retaining structures resulting from earthquakes has caused several major damages in the past. Deformations ranging from slight displacement to catastrophic failure have been observed, and seismically induced retaining wall failures have been reported during the recent major earthquakes including the 1999 Jiji, the 1999 Kocaeli, the 2004 Chuetsu, and the 2008 Wenchuan earthquakes.

The existing methods for dynamically analyzing retaining walls can be divided into three broad categories (Nazarian and Hadjian, 1979): (a) analytical limit-state analysis methods where the wall can displace and/or rotate sufficiently at its base to induce a limit or failure state in the backfill, (b) analytical linear elastic or viscoelastic methods where the wall remains fixed at its base and the backfill soil is responds in a linear elastic or viscoelastic manner, (c) numerical methods of solution, mainly finite element methods under the assumption of linear elastic or nonlinear elastoplastic soil behavior (Vrettos et al., 2016). In the first category one can mention the Mononobe-Okabe (M-O) method (Mononobe and Matsuo, 1929; Okabe, 1924), and its variants by Seed and Whitman (1970), Richards and Elms (1979), and Nadim and Whitman (1983). Numerous methods of this category have been proposed in recent years for improving the original ones. Representatives of the second category are the contributions of Matsuo and Ohara (1960), Wood (1973), Arias et al. (1981), Veletsos and Younan (1994a, 1994b, 1997), Veletsos et al. (1995), Younan and Veletsos (2000), Wu and Finn (1999), Li (1999), Jung et al. (2010), Papazafeiropoulos and Psarropoulos (2010), Kloukinas et al. (2012), Papagiannopoulos et al. (2015), and Vrettos et al. (2016). A comparison between the results of some of the two first categories of methods and those from experiments was carried out by Giarlelis and Mylonakis (2011). Representatives of the third category are the contributions of

Siddharthan and Maragakis (1989), Navarro and Samartin (1989), Siller et al. (1991), Elgamal et al. (1996), Al-Homoud and Whitman (1999), Psarropoulos et al. (2005), Ostadan (2005), Jung et al. (2010), Callisto and Soccodato (2010), Al Atik and Sitar (2010), Evangelista et al. (2010), Cakir (2013, 2014a, 2014b, 2017), Athanasopoulos-Zekkos et al. (2013). The present study deals with a solution of the third category.

Under seismic excitations, the different component of the earth retaining systems exhibit sophisticated and interdependent responses, which can be roughly summarized as follows (Rainieri et al., 2017): (a) dynamic interaction between the wall, the retained backfill, and the soil in front of the wall, (b) dynamic interaction of the subsoil with the structure. These aspects and the damping effects, natural frequencies of the interaction system, wave propagation and reflection effects, phase lags and amplifications within the backfill on the system response cannot be properly analyzed via simplified methods, such as M-O method. Accordingly, the main objective of this paper is to investigate the seismic response of an inverted T-type cantilever retaining wall considering SSI, and the status of the propagation and reflection effects of the seismic waves. In line with this aim, seismic analyses of this cantilever wall were carried out taking four different foundation soil conditions into consideration in time domain through finite element method.

2. Implementation of the Numerical Approach

For the investigation of the seismic response of backfill-inverted T-shaped cantilever wall-soil/foundation system, the general purpose structural analysis program ANSYS 13 (2010) was used. Figure 1 shows the proposed finite element model for the problem of cantilever retaining wall. The heights of the wall and backfill soil stratum are considered to be the same. The vertical stem height of the cantilever wall is H= 7 m, the wall stem has a thickness of 0.35 m at the top, and 1.05 m at the bottom, the thickness of base slab is 0.65 m, and the width of the base slab is 5.35 m. The cantilever wall system is founded on a deformable soil layer of thickness 2H. In the numerical modelling, the structural wall is modelled with 3-D reinforced concrete solid elements (SOLID65) defined by eight nodes having three translational degrees of freedom in each node. The SOLID65 is used for the 3-D modeling of solids with or without reinforcing bars. The solid is capable of cracking in tension and crushing in compression. The backfill and soil/foundation system are modelled with 3-D structural solid elements (SOLID45) with eight nodes having three degrees-of-freedom at each node: translations in the nodal x, y, z directions. The element has plasticity, creep, swelling, stress stiffening, large deflection, and

large strain capabilities. Reasonable modelling of the wall-backfill interface requires utilizing special interface elements between the wall and the adjacent soil to allow for separation. Thus, as a special interface element, nonlinear spring (COMBIN39) is used between the backfill and the wall allowing for the opening and closing of the gaps (i.e. de-bonding and bonding) to model backfill-wall interaction in this study. COMBIN39 is a unidirectional element with nonlinear generalized force-deflection capability that can be used in any analysis. The element has longitudinal or torsional capability in 1-D, 2-D, or 3-D applications. The longitudinal option is a uniaxial tension-compression element with up to three degrees of freedom at each node: translations in the nodal x, y, and z directions.

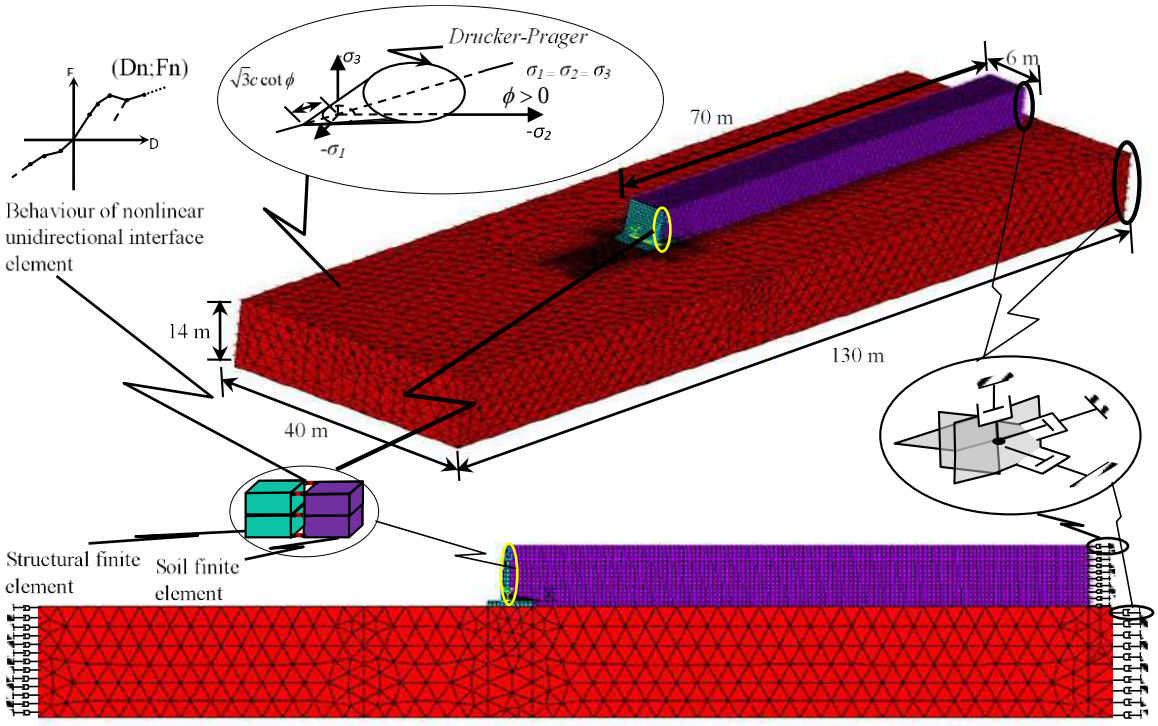

Figure 1. Geometry of the numerical modeling and the schematic plot of soil-wall interaction.

In a dynamic SSI problem, a bounded structure (which may be linear or nonlinear) consisting of the actual structure and an adjacent irregular soil if present, will interact with the unbounded (infinite or semi-infinite) soil which is assumed to be linear elastic. The most striking feature in an unbounded soil, which is never come across in a bounded medium, is, in general, the radiation of energy towards infinity, leading to so-called radiation damping even in such a linear system (Wolf and Song, 2002). There are conventionally two ways for execution of the radiation condition: one way is to enforce the condition rigorously at the soil-structure interface by using the boundary element method, and the other way is to impose a wave

absorbing boundary condition on the outer boundary of a bounded domain (Li et al., 2008). In this study, the viscous boundary model is selected considering the criterion of Lysmer and Kuhlemeyer (1969) to avoid wave distortion during seismic wave transmission through the soil medium. To represent the behavior of the semi-infinite backfill medium, the critical minimum distance from the back face of the wall is taken as 10H, a value which is believed to approximate adequately the behavior of the semi-infinite layer (Veletsos and Younan, 1994a, Psarropoulos et al., 2005). In this context, the dashpots are also placed 10H away from the wall in three dimensions to improve the accuracy of the simulation. Similarly, the artificial viscous boundaries have been placed in three dimensions on the boundaries of soil/foundation medium. Furthermore, the soil is modeled as an elastoplastic medium obeying the well-known Drucker-Prager yield criterion.

3. Seismic Loading

To shed some light on the dynamic performance of cantilever walls, a series of dynamic analysis are conducted for the system. The Young's modulus, Poisson's ratio and unit weight of the wall are 30000 MPa, 0.2 and 25 kN/m^3, respectively. The Young's Modulus, the Poisson's ratio and the unit weight, cohesion and internal friction angle of backfill soil are taken to be 100 MPa, 0.3, 18 kN/m^3, 5 kN/m^2, and 30°, respectively. To assess the seismic response of the cantilever wall supported on flexible foundation, four different foundation soil types are considered in the analyses, as shown in Table 1. HSP000 component of 1989 Loma Prieta earthquake is used in time history analyses (Figure 2). The horizontal peak ground acceleration for this record reaches 3.63 m/s^2. Furthermore, Rayleigh damping is taken into consideration in the analyses. The Newmark scheme governs the numerical time-integration.

Table 1. Mechanical and physical properties of foundation soil.

Soil System	E (kN/m^2)	G (kN/m^2)	ν	ϕ($^\circ$)	ψ($^\circ$)	γ (kN/m^3)	v_s (m/s)	v_p (m/s)
S1	500000	192308	0.30	35	0	19	318.14	595.19
S2	150000	57692	0.30	35	0	19	174.25	326.00
S3	75000	27778	0.35	35	0	18	124.23	258.60
S4	35000	12963	0.35	35	0	18	84.86	176.66

E: Young's Modulus, G: Shear Modulus, ν: Poisson' s ratio, ϕ: Internal friction angle, ψ: Dilatancy angle, γ: Weight per unit volume, v_s : Shear wave velocity, v_p : Compressional wave velocity

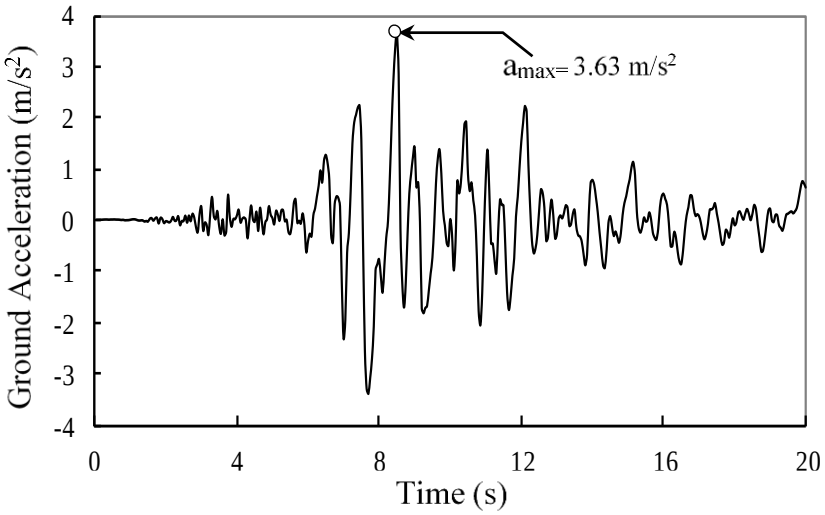

Figure 2. HSP000 component of 1989 Loma Prieta earthquake.

4. Results and Discussions

Computational results are presented in terms of the lateral displacements and stresses. Table 2 summarizes the calculated peak responses and the corresponding times where the maximum lateral top displacements and stresses occurred. Table 2 shows that SSI effect is significant on the structural response of the cantilever wall so that the peak responses and occurrence times of them are different from each other depending on the variation of soil/foundation conditions.

Table 2. Seismic analysis results.

Soil System	S1		S2		S3		S4	
Responses	t (s)	Value	t (s)	Value	t (s)	Value	t (s)	Value
u_t(m)	7.80	-0.0011	7.90	-0.0065	7.55	0.0120	7.60	0.0206
$S_{z(\text{back corner})}$ (MPa)	7.80	0.4178	7.90	2.2333	7.90	3.3934	7.95	2.6647
$S_{y(\text{back corner})}$ (MPa)	7.80	0.0620	7.90	0.3178	7.90	0.6107	7.95	0.4383
$S_{x(\text{back corner})}$ (MPa)	7.80	0.2572	8.60	-1.3209	7.90	2.5352	8.00	1.7835
$S_{z(\text{back midpoint})}$ (MPa)	7.80	0.3239	7.90	2.4391	7.90	3.3241	7.95	3.1618
$S_{y(\text{back midpoint})}$ (MPa)	7.80	0.1268	7.90	0.8349	7.90	1.3254	7.95	1.2867
$S_{x(\text{back midpoint})}$ (MPa)	7.85	0.1825	7.90	1.7382	7.90	2.8131	7.95	2.8995
$S_{z(\text{front corner})}$ (MPa)	7.80	-0.4894	7.90	-2.4530	7.90	-3.6851	7.95	-3.1207
$S_{y(\text{front corner})}$ (MPa)	7.80	-0.0230	7.85	-0.0849	7.90	-0.1238	7.90	-0.0863
$S_{x(\text{front corner})}$ (MPa)	7.80	-0.2310	7.85	-0.9015	7.90	-1.3620	7.90	-0.9751
$S_{z(\text{front midpoint})}$ (MPa)	7.80	-0.2948	7.90	-2.2883	7.90	-3.0940	7.95	-2.8238
$S_{y(\text{front midpoint})}$ (MPa)	8.55	-0.0790	7.90	-0.3677	7.90	-0.4921	7.95	-0.3465
$S_{x(\text{front midpoint})}$ (MPa)	7.80	-0.0747	7.90	-0.7565	7.90	-0.8740	7.95	-0.7185

u_t: Maximum lateral top displacement of cantilever wall; t: Time; S_z, S_y, S_x (back corner): Stresses estimated on the back face (backfill side) of the cantilever wall in *z*, *y* and *x* directions, respectively; S_z, S_y, S_x (back midpoint): Stresses estimated on the back face of the cantilever wall in *z*, *y* and *x* directions, respectively; S_z, S_y, S_x (front corner): Stresses estimated on the front face of the cantilever wall in *z*, *y* and *x* directions, respectively; S_z, S_y, S_x (front midpoint): Stresses estimated on the front face of the cantilever wall in *z*, *y* and *x* directions, respectively.

4.1. Evaluation of the Stresses

At the first stage, the numerical solution is deployed to find the stresses in the critical sections of the retaining wall. The estimated stress responses and their variations in time at the back and front faces of the cantilever retaining wall can be compared with each other to reveal the effects of SSI. As an example, the comparisons of stress time history responses in *x* direction for back face of the cantilever wall are shown in Figures 3 and 4. As these figures depict, the maximum stresses obtained at the critical section of the wall change with varying the soil conditions. For example, as shown in Figure 3, the value of peak stress, as tension, is 0.1825 MPa for S1 soil type, whereas the stresses are computed as 1.7382 MPa and 2.8131 MPa for S2 and S3 soil types, respectively. It is obvious that SSI leads to the increments of about 852% and 1441% in peak responses for S2 and S3 soil types in comparison with S1 soil type, respectively. A similar trend can be easily observed from Figure 4. Furthermore, the reversible character of stress and increments on its amplitude prove that SSI amplifies the wall vibration during seismic action.

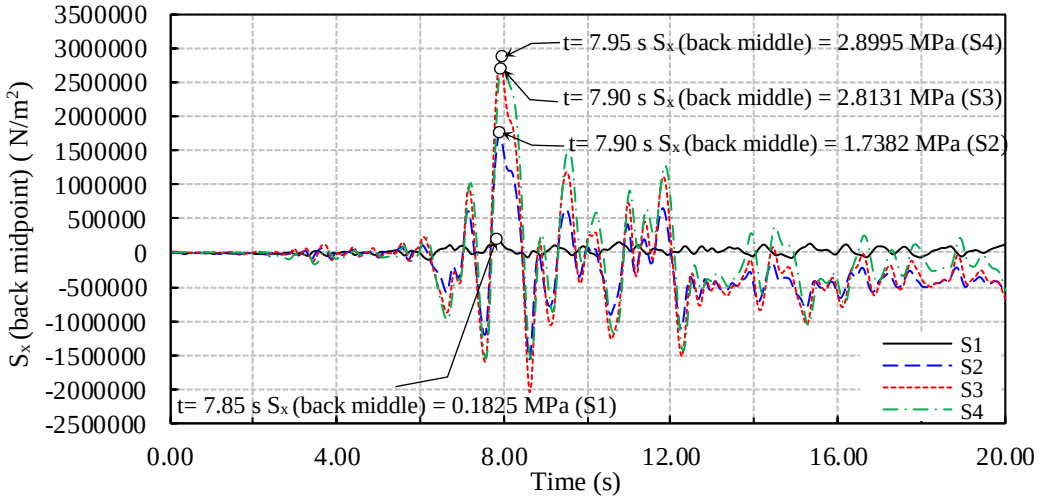

Figure 3. Stress time histories in x direction at the back midpoint of the cantilever wall.

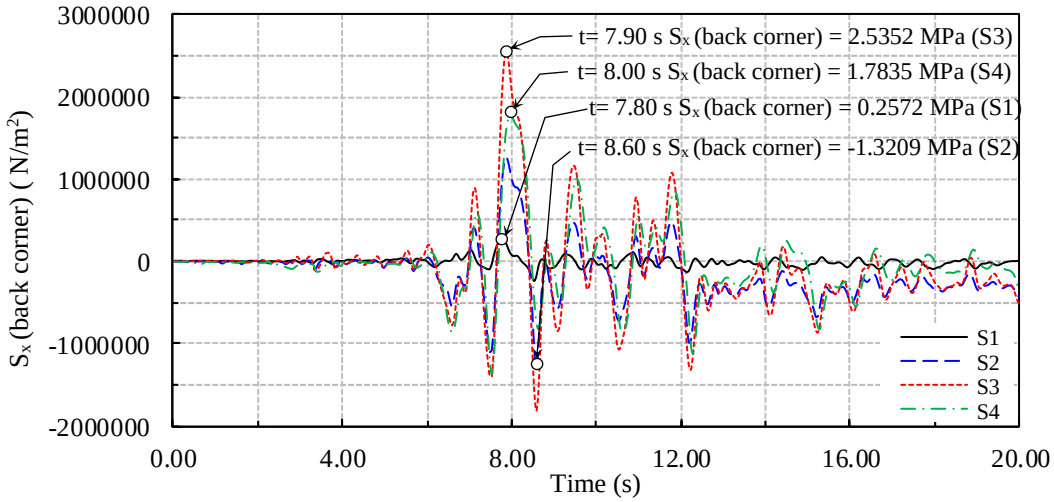

Figure 4. Stress time histories in x direction at the back corner of the cantilever wall.

The comparisons of stress time history responses in *z* direction for front face of the cantilever wall are shown in Figures 5 and 6. As the figures demonstrate, the maximum stress responses due to SSI are highly magnified. For example, as seen in Figure 5, while the peak stress, as compression, has the value of 0.4894 MPa for S1, it is calculated as 3.6851MPa for S3. This reflects a stress increment of about 653% between S1 and S3 due to SSI. Similar comparisons can be made from Table 2 and Figure 6.

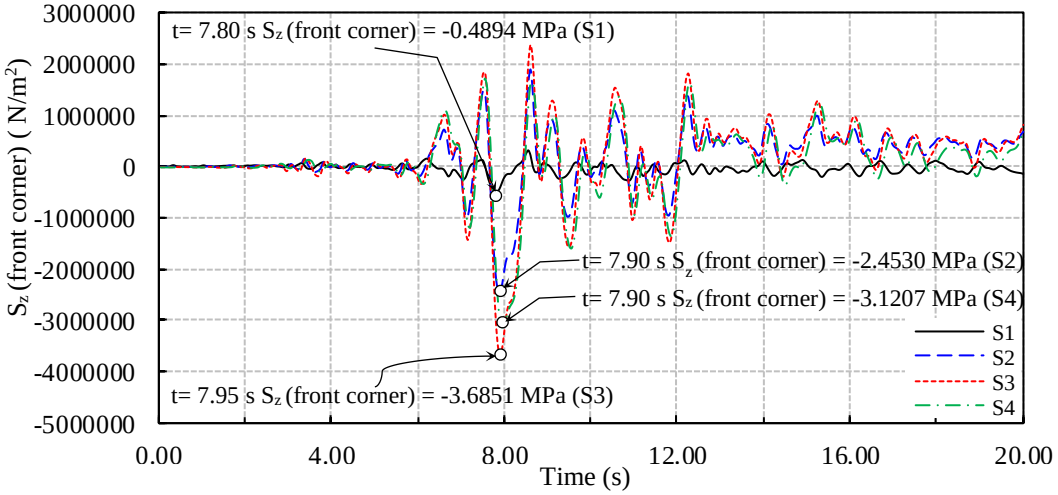

Figure 5. Stress time histories in z direction at the front corner of the cantilever wall.

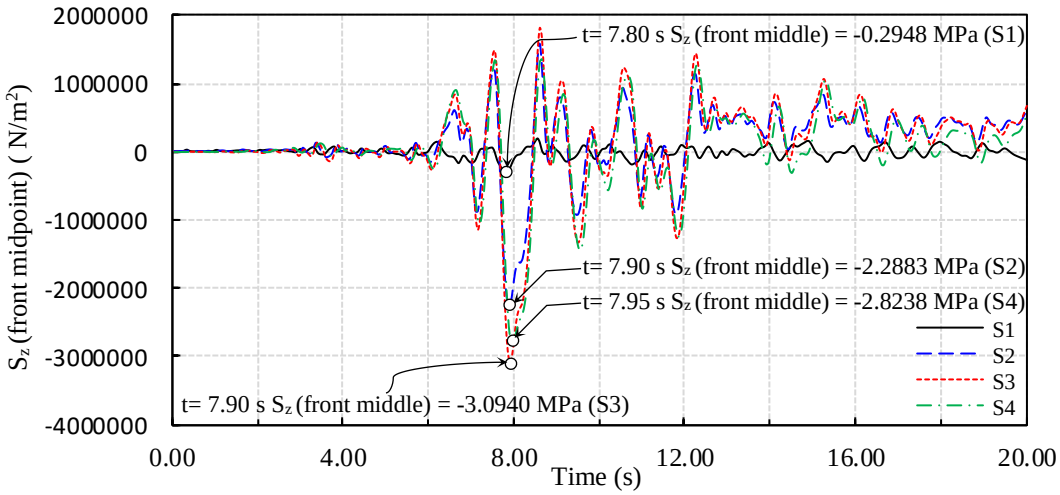

Figure 6. Stress time histories in z direction at the front middle of the cantilever wall.

4.2. Evaluation of the Horizontal Displacements

The effects of SSI on seismic horizontal displacement of the cantilever wall can be shown graphically, and discussed comparatively. Figure 7 portrays the height-wise variations of the horizontal displacements of cantilever wall for varying the foundation soil conditions. It is worth noting here that these displacements represent the relative lateral displacements of the wall with respect to the ground. While the negative displacements refer to the movements away from the backfill, the positive ones refer to the movements toward the backfill. It is observed from this figure that as the soil rigidity decreases, the displacement response tends to increase. So, the structural response is highly dependent on the SSI.

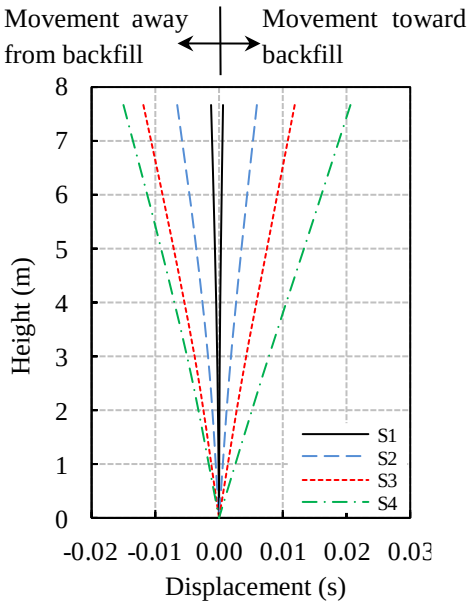

Figure 7. Height-wise variation of horizontal displacements of the cantilever retaining wall.

It is possible to assess the horizontal displacements of the wall in terms of time history using the proposed model. Accordingly, the deviations of the displacements in time are illustrated and compared in Figure 8 to clarify the changes of the horizontal top displacement values due to the SSI. It can be noted from Figure 8 and Table 2 that while the maximum horizontal displacement of the wall, as movement away from backfill, is estimated as 0.0011 m for S1, the same quantity, as movement toward backfill, is calculated as 0.0120 m for S3, and 0.0206 m for S4. It is clear that SSI has led to the dramatic increments in peak displacement responses. It is concluded that the response amplification or reduction pattern due to the deformable foundation is highly dependent on the stiffness of soil/foundation system. Furthermore, the computed time history results show that the maximum responses occur around 7.55~7.90 s.

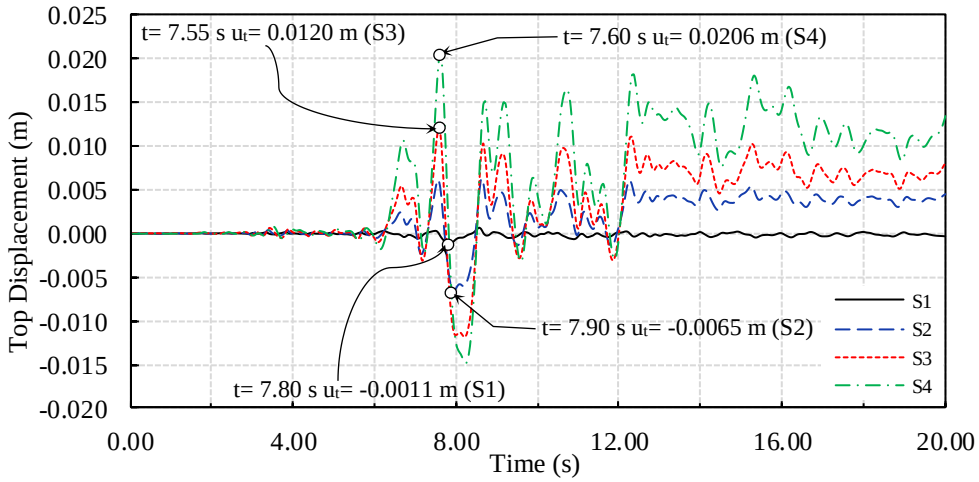

Figure 8. Calculated horizontal top displacement time histories of the cantilever retaining wall.

5. Summary and Conclusions

The first part of this paper was devoted to review briefly the researches related to the seismic behavior of retaining walls. Afterwards, the nonlinear finite element model of the backfill-inverted T-shaped cantilever retaining wall-soil/foundation system was introduced. In this process, the corresponding equations and boundary conditions were derived. Fully dynamic numerical modeling analyses were conducted to evaluate the seismic response of the inverted T-shaped cantilever retaining wall considering SSI. The effect of foundation deformability on the overall dynamic response of the system was examined by comparing the results among four

different soil types. Finally, the tables and accompanying graphs that demonstrate the effects of SSI using suitable quantities such as horizontal displacements and stresses have been presented.

The variation trends of incremental seismic stresses and horizontal displacements was considerably different for retaining wall with different foundation soil material. These assessments can be considered as a warning that especially the mechanical properties of soil are of critical importance. Not taking into account the accurate soil properties may cause underestimation or overestimation of the response, and this, in turn, may lead to unreliable seismic design of cantilever retaining walls.

References

Al Atik, L., and Sitar, N., (2010). Seismic earth pressures on cantilever retaining structures. *Journal of Geotechnical and Geoenvironmental Engineering*, 136(10), 1324-1333.

Al-Homoud, A. S., and Whitman, R. V., (1999). Seismic analysis and design of rigid bridge abutments considering rotation and sliding incorporating non-linear soil behavior. *Soil Dynamics and Earthquake Engineering*, 18, 247-277.

ANSYS 13.0., (2010). ANSYS Inc., Canonsburg, PA.

Arias, A., Sanchez-Sesma, F. J., and Ovando-Shelley, E., (1981, April). A simplified elastic model for seismic analysis of earth-retaining structures with limited displacement. *Proc. of International Conference on Recent Advances in Geotechnical Earthquake Engineering and Soil Dynamics*, (pp. 235-240). St. Louis, MO.

Athanasopoulos-Zekkos, A., Vlachakis, V.S., and Athanasopoulos, G. A., (2013). Phasing issues in the seismic response of yielding, gravity-type earth retaining walls – overview and results from a FEM study. *Soil Dynamics and Earthquake Engineering*, 55, 59-70.

Cakir, T., (2013). Evaluation of the effect of earthquake frequency content on seismic behavior of cantilever retaining wall including soil-structure interaction. *Soil Dynamics and Earthquake Engineering*, 45, 96-111.

Cakir, T., (2014a). Influence of wall flexibility on dynamic response of cantilever retaining walls. *Structural Engineering and Mechanics*, 49, 1-22.

Cakir, T., (2014b). Backfill and subsoil interaction effects on seismic behavior of a cantilever wall. *Geomechanics and Engineering*, 6, 117-138.

Cakir, T., (2017). Assessment of effect of material properties on seismic response of a cantilever wall. *Geomechanics and Engineering*,13(4), 601-619.

Callisto, L., and Soccodato, F.M., (2010). Seismic design of flexible cantilevered retaining walls. *Journal of Geotechnical and Geoenvironmental Engineering*, 136(2), 344-354.

Das, B. M., and Ramana, G. W., (2011). *Principles and Soil Dynamics* (2nd ed.), Stamford, USA: Cengage Learning.

Elgamal, A. W., Alampalli, S., and Laak, P.V., (1996). Forced vibration of full-scale wall-backfill system. *Journal of Geotechnical Engineering*, 122(10), 849-858.

Evangelista, A., Scotto di Santolo, A., and Simonelli, A.L. (2010). Evaluation of pseudostatic active earth pressure coefficient of cantilever retaining walls. *Soil Dynamics and Earthquake Engineering*, 30, 1119-1128.

Giarlelis, C., and Mylonakis, G., (2011). Interpretation of dynamic retaining wall model tests in light of elastic and plastic solutions. *Soil Dynamics and Earthquake Engineering*, 31, 16-24.

Jung, C., Bobet, A., and Fernandez, G., (2010). Analytical solution for the response of a flexible retaining structure with an elastic backfill. *International Journal for Numerical and Analytical Methods in Geomechanics*, 34(13), 1387-1408.

Kloukinas, P., Langousis, M., and Mylonakis, G., (2012). Simple wave solution for seismic earth pressures on nonyielding walls. *Journal of Geotechnical and Geoenvironmental Engineering*, 138, 1514-1519.

Li, X., (1999). Dynamic analysis of rigid walls considering flexible foundation. *Journal of Geotechnical and Geoenvironmental Engineering*, 125, 803-806.

Li, J. B., Yang, J., and Lin, G., (2008). A stepwise damping-solvent extraction method for large-scale dynamic soil-structure interaction analysis in time domain. *International Journal for Numerical and Analytical Methods in Geomechanics*, 32(4), 415-438.

Lysmer, J., and Kuhlemeyer, R.L., (1969). Finite dynamic model for infinite media. Journal of *Engineering Mechanics Division*, 95, 859-878.

Matsuo, H., and Ohara, S., (1960). Lateral earth pressure and stability of quay walls during earthquakes. *Proceedings of 2nd World Conference on Earthquake Engineering*, (pp.165-181). Tokyo, Japan.

Mononobe, N., and Matsuo, H., (1929). On the determination of earth pressures during earthquakes. *Proceedings of World Engineering Congress* (pp.179-187). Japan.

Nadim, F., and Whitman, R. V., (1983). Seismically induced movement of retaining walls. *Journal of the Geotechnical Engineering Division*, 109 (7), 915-931.

Navarro, C., and Samartin, A., (1989). Dynamic earth pressures against a retaining wall caused by Rayleigh waves. *Engineering Structures*, 11, 31-36.

Nazarian, H. N., and Hadjian, A. H., (1979). Earthquake-induced lateral soil pressures on structures. *Journal of the Geotechnical Engineering Division*, 105, 1049-1066.

Okabe, S., (1924). General theory of earth pressure and seismic stability of retaining wall and dam. *Journal of Japanese Society of Civil Engineering*, 10 (6), 1277-1323.

Ostadan, F., (2005). Seismic soil pressure for building walls: An updated approach. *Soil Dynamics and Earthquake Engineering*, **25**, 785-793.

Papagiannopoulos, G.A., Beskos, D.E., and Triantafyllidis, T., (2015). Seismic pressures on rigid cantilever walls retaining linear poroelastic soil: An exact solution. *Soil Dynamics and Earthquake Engineering*, **77**, 208-219.

Papazafeiropoulos, G., and Psarropoulos, P. N., (2010). Analytical evaluation of th dynamic distress of rigid fixed-base retaining systems. *Soil Dynamics and Earthquake Engineering*, 30, 1446-1461.

Psarropoulos, P.N., Klonaris, G., and Gazetas, G., (2005). Seismic earth pressures on rigid and flexible retaining walls. *Soil Dynamics and Earthquake Engineering*, 25, 795-809.

Rainieri, C., Dey, A., Fabbrocino, G., and de Magistris, F. S., (2017). Interpretation of the experimentally measured dynamic response of an embedded retaining wall by finite element models, *Measurement*, 104, 316-325.

Richards, R., and Elms, D. G., (1979). Seismic behavior of gravity retaining walls. *Journal of the Geotechnical Engineering Division*, 105, 449-464.

Seed, H. B., and Whitman, R.V., (1970). Design of earth retaining structures for dynamic loads. *Proceedings of the Speciality Conference on Lateral Stresses in the Ground and Design of Earth Retaining Structures* (pp.103-147). Ithaca, New York.

Siddharthan, R., and Maragakis, E. M., (1989). Performance of flexible retaining walls supporting dry cohesionless soils under cyclic loads. *International Journal for Numerical and Analytical Methods in Geomechanics*, 13, 309-326.

Siller, T. J., Christiano, P. P., and Bielak, J., (1991). Seismic response of tied-back retaining walls. *Earthquake Engineering and Structural Dynamics*, 20, 605-620.

Veletsos, A. S., and Younan, A. H., (1994a). Dynamic soil pressures on rigid vertical walls. *Earthquake Engineering and Structural Dynamics*, 23(3), 275-301.

Veletsos, A. S., and Younan, A. H., (1994b). Dynamic modeling and response of soil-wall systems. *Journal of Geotechnical Engineering*, 120(12), 2155-2179.

Veletsos, A. S., Parikh, V. H., and Younan, A. H., (1995). Dynamic response of a pair of walls retaining a viscoelastic solid. *Earthquake Engineering and Structural Dynamics*, 24, 1567-1589.

Veletsos, A. S., and Younan, A. H., (1997). Dynamic response of cantilever walls. *Journal of Geotechnical Engineering*, 123(2), 161-172.

Vrettos, C., Beskos, D. E., and Triantafyllidis, T., (2016). Seismic pressures on rigid cantilever walls retaining elastic continuously non-homogeneous soil: An exact solution. *Soil Dynamics and Earthquake Engineering*, 82, 142-153.

Wood, J.H., (1973). *Earthquake-induced soil pressures on structures*. Report EERL 73-05, Earthquake Engineering Research Laboratory, California Institute of Technology.

Wolf, J.P., and Song, C., (2002). Some cornerstones of dynamic soil-structure interaction. *Engineering Structures*, 24, 13-28.

Wu, G., and Finn, W. D. L. (1999). Seismic lateral pressures for design of rigid walls. *Canadian Geotechnical Journal*, 36, 509-522.

Younan, A. H., and Veletsos, A. S., (2000). Dynamic response of flexible retaining walls. *Earthquake Engineering and Structural Dynamics*, 29:1815-1844.

Mechanical Abrasion of Mortars Containing Clinoptilolite

Yasemin AKGÜN [1*], Ömer Fatih YAZICIOĞLU [2]

[1]Ordu University, Department of Construction, Ordu, TURKEY
[2]Ondokuz Mayıs University, Department of Civil Engineering, Samsun, TURKEY

[*] **Corresponding Author:** yakgun@odu.edu.tr

Abstract

In this study, it was investigated on the mechanical abrasion of mortars containing natural zeolite clinoptilolite. Bohme surface abrasion tests were carried out to cement mortar samples produced with different cement replacement ratio (0%, 10%, 30% and 50%). The mechanical abrasion of mortars was determined according to TS 2824 EN 1338. The results obtained from test series were compared with each other. The test results showed that, abrasion losses of mortars containing clinoptilolite were lower than portland cement mortar as approximately 15%.
Keywords: Abrasion, Clinoptilolite, Cement Mortar, Zeolite..

1. Introduction

It is known that cement is the most used and produced building material in construction sector. The cement industry is also responsible for both the high energy use as well as about 7% of the total CO_2 emissions in the world due to its production processes. For this reason, it has become quite widespread the production of blended cement by using natural or artificial pozzolanic additive material which is replaced with clinker. The application of blended cement production increases performance of mortar and concrete. At the same time, it is obtained advantages such as reducing of CO_2 emissions, energy saving and economy with this applications.

Natural zeolites have recently become widely used as additive material in blended cement productions. Because, natural zeolites are pozzolanic materials containing abundant amounts of silica and alumina. When zeolite is replaced with clinker at optimum ratio, they form additional binder components by reacts with Ca $(OH)_2$ which is a result of cement hydration. These additional binders improve strength and durability of mortar/concrete. Also, natural zeolites are preferred to synthetic zeolites because of their reserve and economic status.

The natural zeolites formed by the alteration of the vitric pyroclastic deposits are more reactive materials than the fly ash and furnace slags between mineral additives. Natural zeolites have reserve declared as hundred billions tons in the world (Chan, 1999).

Clinoptilolite is a natural pozzolan and it is one of the valuable minerals of zeolite group. The clinoptilolite is a zeolitic mineral species with chemical formula (Na_3K_3) $(Al_6Si_{30}O_{72})$ $24H_2O$, which is rich in silica and contains alkali and earth alkaline cations (Özen et. al, 2016).

Abrasion is a physical and mechanical event that is slowly occurred. The reduction in size and mass occurred by friction of abrasive materials on surfaces of objects that make contact with each other and move relative to each other is defined as abrasion loss. Generally, the amount of abrasion depends on type of material, state of abrasion surface, friction conditions and chemical effects of environment.

As a result of optimizations carried out on all of mortar/concrete components, it is known that the abrasion resistance can be increased to desired level. Therefore, it can be possible to minimize damages caused from abrasion with increasing properly of abrasion resistance of mortar/concrete in some cases such as pavement, concrete roads, factory floor surfaces, water structures, chimneys etc.

In literature, there is a little study to examine abrasion resistance on mortar or concrete samples containing clinoptilolite (Bilim, 2011; Gabriel et al, 2012; Akgün and Yazıcıoğlu,

2016). It is always an expectation that to minimize of damage caused by abrasion as a result of increase of abrasion resistance of construction materials. Therefore, the influence of clinoptilolite on the abrasion resistance of cement mortars was investigated in this study. The abrasion tests were carried out on mortar mixtures produced with different cement replacement ratio (0%, 10%, 30% and 50%). And, pozzolanic activity of clinoptilolite were determined. The results are compared with each other.

2. Material and Method

The cement used in tests is CEM I 42.5 R type of Portland cement (PC) produced in accordance with TS EN 197-1 (TSI, 2002). The clinoptilolite were used as replaced material by cement. The clinoptilolite (C) that is type of natural zeolite were obtained from Manisa/Gördes regions of Turkey. The clinoptilolite samples were finely grinded in a ball mill. The amount of clinoptilolite used in mixtures were 0%, 10%, 30% and 50% of cement weight. So, the mixtures were produced with the labels PC, C10, C30 and C50.

The CEN (The European Committee for Standardization) standard sand in accordance with EN 196-1 (TSI, 2009) was used in mortar mixtures. The sand-to-cement ratio is constantly 3 and water-to-cement ratio is constantly 0.5. It was used superplasticizer (at 1%, 1.5% and %2 ratios) complying with TS EN 934-2 (TSI, 2013) by adding to mixture water to recover of adverse effect on mortar consistency of natural zeolites in mixtures. In the production of all samples, water that does not contain organic substances and mineral salts that may be harmful is used. The flow values of mortar mixtures are about 150 ± 20 mm.

All mortar mixtures were prepared by applying the standard mixing, molding and curing procedures stated in TS 196-1. Samples was prepared in laboratory environment where temperatures are 20±2ºC and relative humidity is 60±5%. The samples taken from molds after 24 hours from their productions were kept in the curing tank at a temperature of 21 ± 1ºC until the test days.

X-Rays Fluorescence Spectrometer (XRF) analysis was performed to determine chemical composition of clinoptilolite. X-Ray Diffraction (XRD) analysis was performed to determine mineralogical composition of clinoptilolite. Some views were also obtained using a Scanning Electron Microscope (SEM).

2.1. *Test of Pozzolanic Activity*

Pozzolanic activity can be defined as the ability to react with $Ca(OH)_2$ of active silica which is in the pozzolan. At the end of this reaction the amount of portlandite ($Ca(OH)_2$) is reduced, calcium silicate hydrate (CSH) is increased.

The pozzolanic activity tests were performed on 40x40x160mm prismatic samples. In TS 25 (TSI, 2008), the pozzolanic activity test is defined as a characteristic determined in terms compressive strength of the mortar obtained by mixing natural pozzolan which is grinded at a certain fineness with water, standard sand and calcium hydroxide ($CaOH_2$). The amounts of materials required to prepare three test samples for tests on pozzolanic activity are given in Table 1.

Table 1. The amounts of materials for tests on pozzolanic activity.

Materials	**TS 25**	**The amounts for tests**
Slaked lime ($CaOH_2$)	150gr	150gr
Pozzolan	2x150x(density of pozzolan/density of $CaOH_2$)(gr)	2x150x(2.28/2.15)=318.14gr
Standard sand	1350gr	1350gr
Water	0.5x (150+pozzolan) (gr)	0.5x(150+318.14)=234.07gr

The moulds of the prepared samples were covered with a glass plate to prevent evaporation. The samples were allowed to stand at room temperature for 24 hours (23 ± 2)ºC. And then, they were left for 6 days in an drying oven at 55 ± 2°C without removing the moulds. The samples removed from the oven were left to cool until the room temperature reached. Finally, the compressive strengths of samples were performed in accordance with TS EN 196-1.

2.2. *Test of Abrasion Resistance*

Three cube moulds of 70.7 mm were used for each mixture in abrasion tests. The mortars were produced by using blended cements containing clinoptilolite. The abrasion losses by friction at the end of 28 days of the mortar samples were determined by Bohme surface abrasion tests in accordance with TS 2824 EN 1338 (TSI, 2005) (Fig. 1).

Before tests, initial volumes and initial weights of samples were determined. The abrasive force of 294 N was applied to samples placed on rotary disk of Bohme apparatus.

The samples were subjected to abrasive effect of 20 g corundum powder poured on friction path together with operation of device. Total of 16 periods that each of them is 22 cycles

were applied to samples. At the end of the test (at the end of the 352 cycles), volumetric abrasion losses (ΔV) in samples were determined.

In calculations, it was used formula at (1) which denote ΔV ($cm^3/50\ cm^2$); volumetric abrasion loss, Δm (gr); weight loss at end of 16 cycles, ρ (g/cm^3); density.

$$\Delta V = \Delta m / \rho \quad (1)$$

Figure 1. Bohme abrasion test device.

3. Results and Discussion

3.1. Some properties of portland cement, clinoptilolite and blended cements

Some properties of portland cement (PC), clinoptilolite (C), blended cements (C10, C30 and C50) are presented in Tables 2, 3 and 4. Densities of clinoptilolite is 32.37% lower than PC. Specific surface area of clinoptilolite is 27.07% higher than PC. This situation depends on mineral structure, porosity and fragilement properties of zeolite. Cumulative passing (%) of 45 μm sieve for Portland cement and clinoptilolite are 67.11% and 68.64%, respectively. Densities of blended cements have decreased with increasing of zeolite ratios. Fineness of blended cements containing zeolite has increased with increasing of zeolite ratios.

Table 2. Properties of portland cement (PC).

(wt.%)	Physical and mechanical properties of portland cement

Chemical composition					
SiO_2	19.53	Density, (g/cm^3)	3.12		
Al_2O_3	5.33	Initial set, (h)	2.50		
Fe_2O_3	3.56	Final set, (h)	4.15		
CaO	62.26	Volume expansion, mm	2.00		
MgO	0.99	Specific surface (Blaine) (cm^2/g)	3210		
SO_3	3.02	The compressive strengths	2 days	7 days	28 days
Loss of ignition	3.06	(MPa)	32.30	44.60	53.00
		Over sieve	45µm	90 µm	200 µm
		(%)	32.89	12.15	2.73

Table 3. Properties of clinoptilolite.

Chemical composition	**Clinoptilolite (wt.%)**	**Physical properties**	
SiO_2	64.70		Clinoptilolite
Al_2O_3	11.21	Density, (g/cm^3)	2.11
Fe_2O_3	1.38	Blaine (cm^2/g)	4079
CaO	2.08	Over sieve (%)	
MgO	0.79		
Na_2O	0.38	45µm	31.36
K_2O	3.78	90 µm	11.51
Loss of ignition	11.80	200 µm	2.57

Table 4. Properties of blended cements.

Physical properties	**PC**	**C10**	**C30**	**C50**
Specific surface (cm^2/g) (Blaine fineness)	3210	3408	3664	3898
Density, (gr/cm^3)	3.12	2.75	2.72	2.46

3.2 Pozzolanic Activity of Clinoptilolite

Pozzolanic activity of clinoptilolite are given in Table 5. According to Table 5. in TS 25, one of the conformity criterias for pozzolans is the 7 day compressive strength of samples prepared with lime-natural pozzolan mixture. The limit value of the compressive strength is at least 4 MPa. In test study performed for clinoptilolite, the average compressive strength value for the lime-zeolite (pozzolan) mixture samples was determined as 9.02 MPa. It has also been

emphasized that the sum of SiO_2 + Al_2O_3 + Fe_2O_3 in TS 25 should be at least 70% by mass. The value of this total was found to be 77.3% for clinoptilolite. At the same time, the specific surfaces of the pozzolans should be greater than 3000 cm^2/gr. The specific surface of pozzolan which is used in this study were found to be 4079 cm^2/gr for clinoptilolite (Table 3).

Table 5. Pozzolanic activity of clinoptilolite.

TS 25 limit values	**Clinoptilolite**
Lime-pozzolan mixture 7 days compressive strength > 4MPa	9.02 MPa
SiO_2+Al_2O_3+Fe_2O_3 wt. content >%70	%77.30
Specific surface area > 3000cm^2/gr	4079 cm^2/gr

In pozzolanic activity tests. Because of the specific surface of natural zeolite were below of portland cement fineness, the reaction which is between pozzolan and lime was increased. It is thought that, this situation was lead to an increment at value of pozzolanic activity. These value show that the zeolite used in study have an usability potential as a pozzolan.

3.3 Mineralogical Composition of Clinoptilolite

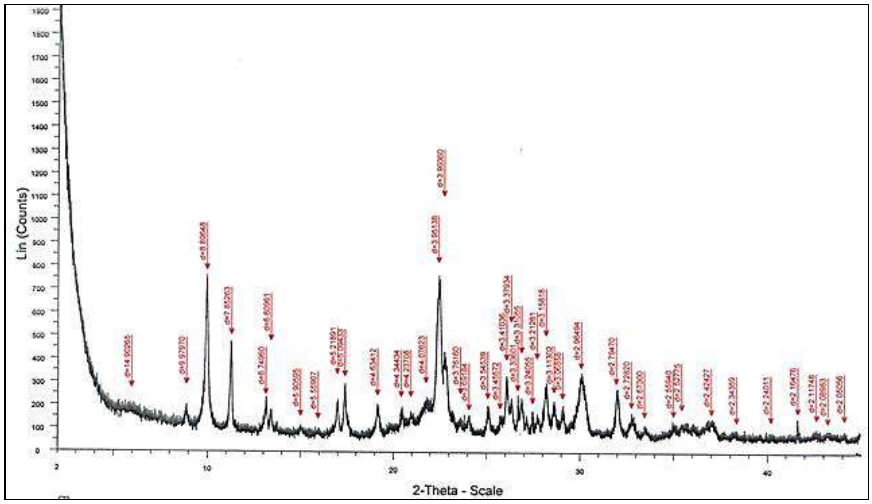

Figure 2. XRD diffraction patterns of clinoptilolite.

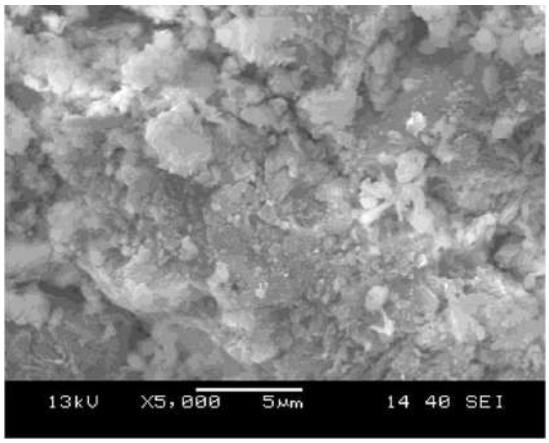

Figure 3. SEM view of clinoptilolite.

XRD diffraction pattern and SEM view are presented in Figs. 2 and 3. According to the mineral modal ratios at the mineralogical composition results determined by the X-ray diffraction analysis (XRD) of clinoptilolite sample, the sample is characterized by zeolite industrial raw material. The rate of clinoptilolite in the sample is approximately 80-85%. When the diffractogram and SEM image of zeolite is examined, it is seen that zeolite contains clinoptilolite as dominant minerals and zeolite is crystal structure. The clinoptilolite sample confirms the requirements of national and international standards for zeolite applications.

3.4 Abrasion Resistance of Mortars

Abrasion losses ΔV ($cm^3/50cm^2$) are given in Table 6. Abrasion losses variations for mortars are presented in Fig. 4.

Table 6. Volumetric abrasion losses and densities of mortar.

Mortars	**PC**	**C10**	**C30**	**C50**
Density (gr/cm^3)	2.42	2.14	2.11	1.91
ΔV ($cm^3/50cm^2$)	11.84	9.41	10.27	11.62

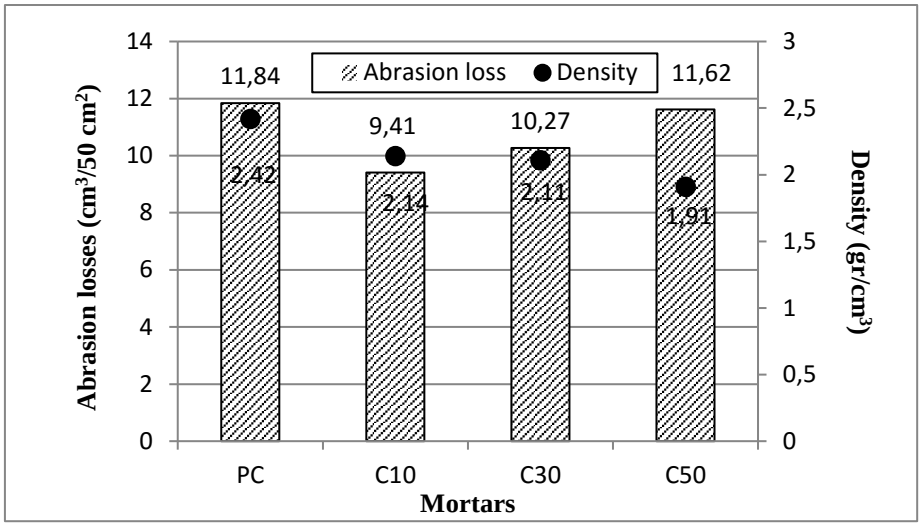

Figure 4. Abrasion loss and density variation for mortars.

The volumetric abrasion losses for mortars with blended cements containing clinoptilolite (C10, C30 and C50) were 20.52%, 13.26% and 1.86% less than mortars with PC, respectively. In other words, it has been found that the abrasion losses of mortars with blended cement are less than mortars with PC for all replacement ratios. This positive effect in abrasion resistance is probably performance increasing occurred at aggregate-cement paste interface and cement paste due to pozzolanic reactions of zeolite. Also, as clinoptilolite replacement ratio increases, the densities of mortars decrease.

4. Conclusions

1. Since the density of clinoptilolite is lower than that of Portland cement, the densities of mortars produced by blended cement containing clinoptilolite are less than that of mortars produced by Portland cement.
2. The properties of natural zeolite clinoptilolite investigated in this study such as pozzolanic activity, mineralogical structure, high silica-alumina content, high specific surface, low density are sufficient for sustainable blended cement productions.
3. The abrasion losses of mortars containing clinoptilolite were lower than that of mortars containing portland cement for all replacement ratios. The test results showed that, abrasion losses of mortars containing clinoptilolite were lower than portland cement mortar as approximately 15%.
4. A larger number of studies should be carried on zeolites named clinoptilolite obtained from different regions to reduce amount of cement and to improve of cement performance.

Acknowledgement

This study was funded by the Scientific Research Project Unit of Ordu University under Project No: TF-1521. Also, we would like to thanks to Gördes Zeolite Company for their support and assistance.

References

Akgün, Y., and Yazıcıoğlu, Ö. F., (2016). İki Farklı Doğal Zeolit Katkısının Çimento Harç Aşınma Dayanımına Etkisi, Ordu Üniv. Bil. Tek. Derg., Cilt:6, Sayı:1, 94-104.

Bilim, C., (2011). Zeolit Katkısının Harçların Aşınma Direncine Etkisi, 6th International Advanced Technologies Symposium (IATS'11), Elazığ, Turkey.

Chan, SYN. and Ji, X. (1999). Comparative study of the initial surface absorption and chloride diffusion of high performance zeolite, silica fume and PFA concretes, Cem. Concr. Compos., 21:293–300.

Gabriel C., Rajwant S. B., Yushan Y., and Junlan W., (2012). Zeolite as a wear-resistant coating, Microporous and Mesoporous Materials, vol: 151, 346–351.

Özen, S., Göncüoğlu, M. C., Liguori, B., Gennaro, B., Cappelletti, P., Gatt, G. D., Iucolano, F., and Colella, C., (2016). A comprehensive evaluation of sedimentary zeolites from Turkey as pozzolanic addition of cement- and lime- based binders", Construction and Building Materials, vol: 105, 46-61.

TS EN 197–1, (2002). Çimento - Bölüm 1: Genel Çimentolar- Bileşim, Özellikler ve Uygunluk Kriterleri. Ankara: Türk Standartları Enstitüsü.

TS EN 196–1, (2009). Çimento Deney Metotları - Bölüm 1: Dayanım Tayini. Ankara: Türk Standartları Enstitüsü.

TS EN 934-2, (2013). Kimyasal Katkılar - Beton, Harç ve Şerbet için - Bölüm 2: Beton Kimyasal Katkıları - Tarifler, Gerekler, Uygunluk, İşaretleme ve Etiketleme, Ankara: Türk Standartları Enstitüsü.

TS 25, (2008). Doğal Puzolan (Tras)-Çimento ve Betonda Kullanılan-Tarifler, Gerekler ve Uygunluk Kriterleri. Ankara: Türk Standartları Enstitüsü.

TS 2824 EN 1338, (2005), Zemin Döşemesi için Beton Kaplama Blokları-Gerekli Şartlar ve Deney Metotları. Ankara: Türk Standartları Enstitüsü.

Utilization of Type C Fly Ash and Bottom Ash in Pervious Geopolymer Concrete

Murat TUYAN[1*], H. Süleyman GÖKÇE[2]

[1]İzmir Democracy University, Faculty of Engineering, Department of Civil Engineering, İzmir, Turkey
[2]Bayburt University, Faculty of Engineering, Department of Civil Engineering, Bayburt, Turkey

[*]**Corresponding Author:** murat.tuyan@idu.edu.tr

Abstract

In this study, the utilization of Type C fly ash and bottom ash in pervious geopolymer concrete was investigated. For this purpose, Type C fly ash- and bottom ash-based pervious geopolymer concretes were produced. For comparison, a Portland cement-based pervious concrete was also produced. A coarse limestone aggregate having 5-15 mm of grain size was used for all concrete mixtures. Some physical properties (specific gravity, water absorption, density, void content and permeability) of the concrete mixtures were determined. Test results indicated that the permeability of geopolymer mixtures were higher than that of Portland cement-based concrete. Concerning the geopolymer concrete, the permeability of the bottom ash-based pervious geopolymer concrete was higher than that of the fly ash-based pervious geopolymer concrete.

Keywords: Geopolymer, Pervious Concrete, Fly Ash, Bottom Ash, Permeability.

1. Introduction

Sustainability has become a popular topic in recent years with the reduction of natural resources in the world. Pervious concrete is a building material that needs to be surveyed nowadays due to the increased environmental needs. In order to regenerate underground water, falling rainwater must leak underground. However, impervious concrete or asphalt coatings used in the cities provide rainwater to be collected at one point and transferred to the river, lake or sea with special systems. It is economically beneficial to use less water collection system to remove rainwater through the use of pervious concrete, while leakage of rain water underground provides an environmental advantage in terms of the sustainability of the source water (Delatte, 2014; Sabnis, 2015).

Pervious concrete is a special concrete that has a near zero-slump and gap graded which is usually consisted of cement, coarse aggregate, less or no sand, and water. Mixing of these components is known to produce material that is hardened and permeable allowing easy passing of water (ACI 522R, 2010).

Geopolymer binder has an important place in the alternative cementitious systems. Geopolymer binder is a material which is formed by the activation of aluminosilicate-based powder materials in the amorphous form with alkalis. Natural pozzolans (volcanic tuff, volcanic glass and trass), calcined aluminosilicates (metakaolin, calcined clay) and industrial by-product materials (blast furnace slag, fly ash) which appear as amorphous state in the nature can be used as powder material in geopolymer binder production. Theoretically, all aluminosilicate materials can be activated with alkalis and exhibit binding properties. However, the physical, chemical and mineralogical properties of the powder materials directly affect the behavior of the geopolymer binder. In this respect, knowing the properties of the powder material to be used is very important in terms of determining the performance of the geopolymer binder (Tuyan, 2017).

There are several studies on the pervious geopolymer concrete in the literature (Tho-In, 2012; Sata, 2013; Jo, 2015; Zaetang, 2015). In these studies, fly ash was usually used as aluminosilicate material. Studies on the pervious geopolymer concrete have proven that the pervious concrete can be produced with geopolymer binder. However, there is a lack of information on the bottom ash-based pervious geopolymer concrete in the literature. In this study, the utilization of Type C fly ash and bottom ash in pervious geopolymer concrete was investigated. Some physical properties (specific gravity, water absorption, density, void content and permeability) of concrete mixtures were determined. In addition, test results of the pervious

geopolymer concrete were compared with the test results of the cement-based pervious concrete.

2. Materials and Methods

2.1. Materials

Type C fly ash and bottom ash obtained from Soma Thermal Power Plant were used as an aluminosilicate binder. In addition, CEM I 42.5 R type cement were used in the study. Chemical compositions and physical properties of these binders are given in Table 1 and Table 2, respectively.

Table 1. Chemical compositions of binders

Composition (%)	Cement	Fly Ash	Bottom Ash
SiO_2	18.39	39.62	38.21
Fe_2O_3	3.24	4.06	4.78
Al_2O_3	4.20	18.95	18.51
CaO	64.53	27.67	19.68
MgO	1.32	1.95	1.39
Na_2O	0.55	0.66	0.50
K_2O	0.76	1.33	1.13
SO_3	3.46	3.83	2.49
Loss on ignition	1.42	0.97	14.12

Table 2. Physical properties of binders

Property	Cement	Fly Ash	Bottom Ash
Specific gravity	3.20	2.53	2.50
Specific surface area (cm^2/g)	3210	2460	2850
Retained on 0.090 mm (%)	0.50	18.9	17.0
Retained on 0.045 mm (%)	-	41.6	38.1

Sodium hydroxide (97% purity) and 3 module sodium silicate ($SiO_2/Na_2O \approx 3$) (8% Na_2O, 27% SiO_2 and 65% H_2O) were used as alkali activator. A crushed limestone aggregate having
5-15 mm size gradation (Table 3) was used in all of the pervious concrete mixtures.

Table 3. Size fraction of aggregate

Size (mm)	4	8	16
Passing (%)	0	37	100

2.2. Mix proportions

Mix proportions of the pervious concrete mixtures are given in Table 4. In the fly ash-based (FA) and bottom ash-based (BA) pervious geopolymer concrete mixtures; aluminosilicate material content and water/aluminosilicate material ratio were kept constant. 10% Na_2O by weight of the aluminosilicate and silicate modulus (M_s: SiO_2/Na_2O) of 1.6 were used in the pervious geopolymer concrete. In the cement-based (C) pervious concrete, 250 kg/m^3 cement was used. Water/cement ratio of the mix was used as 0.50. In all of the pervious concrete mixtures, void content was almost kept constant as 36±1% by volume of the mixture.

Table 4. Theoretical mix proportions of the pervious concrete mixtures

Component (kg/m^3)	C	FA	BA
Type C fly ash	0	240	0
Bottom ash	0	0	240
Cement	250	0	0
Aggregate 5-15 mm	1215	1215	1215
Sodium hydroxide	0	17	17
Sodium silicate	0	139	139
Additional water	125	0	0
TOTAL	1590	1611	1611

2.3. Preparation of pervious concrete mixtures

In the pervious geopolymer concrete mixtures, the alkali activator solution formed by dissolving sodium hydroxide in sodium silicate was prepared one day before cooling down to the room temperature. The alkali activator solution and aluminosilicate material were mixed with a mixer. The resulting binder paste and aggregate were mixed to obtain a homogeneous concrete mixture for two minutes in the mixer. In the cement-based pervious concrete, the water and the cement were initially mixed with a mixer, and then the cement paste and aggregate were mixed for two minutes in the mixer. Then, the mixtures were cast in the molds. Pervious

concrete mixtures were cured in water for 28 days. Finally, the specimens were removed from the curing pool and related experiments were performed.

2.4. Test methods

The fresh state properties of the paste mixtures were determined by using the flow table apparatus. The flow diameter and the flow time were measured for all of the paste mixtures.

The specific gravity of the pervious concrete was determined by the following equation:

$$\text{Specific gravity} = \frac{\text{Saturated surface dry weight in air}}{(\text{Saturated surface dry weight in air} - \text{weight in water}) \times \gamma_w} \quad (1)$$

The water absorption of the pervious concrete was determined by the following equation:

$$\text{Water absorption } (\%) = \frac{\text{Saturated surface dry weight} - \text{Oven dry weight}}{\text{Oven dry weight}} x(100) \quad (2)$$

The unit weight of the pervious concrete was determined by the following equation:

$$\text{Unit weight } (\text{kg/m}^3) = \frac{\text{Saturated surface dry weight}}{\text{Volume of the concrete specimen}} \quad (3)$$

The void content of the pervious concrete was determined by the following equation:

$$\text{Void content } (\%) = 1 - \left(\frac{\text{Unit weight}}{\text{Apparent specific gravity} \times \gamma_w}\right) x100 \quad (4)$$

where, γ_w is the density of water.

The permeability coefficient of the pervious concrete was determined by the following equation:

$$q = K \times (P \times F/e) \quad (5)$$

where, K: permeability coefficient (cm/s), P: water pressure (cm), F: cross-section (m^2), q: flow (cm^3/s), e: height of the specimen (cm).

The permeability test of the pervious concrete was performed by using the following tube given in Figure 1. The permeability test was carried out with water pressure of 1 atm.

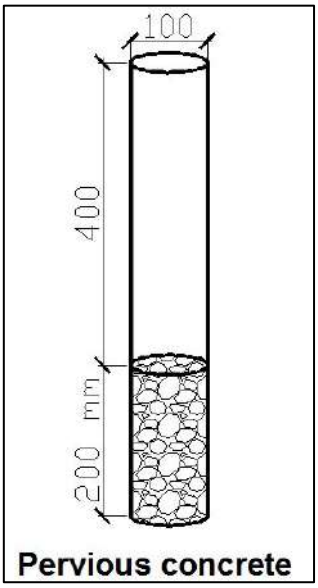

Figure 1. Schematically representation of permeability test

3. Test Results and Discussion

Fresh state properties of the paste mixtures are shown in Table 5. It can be seen from the table that although the water/binder ratio of the fly ash-based and bottom ash-based geopolymer paste mixtures was higher than that of the cement paste mixture, the flow diameter of the fly ash-based and bottom ash-based geopolymer paste mixtures were higher than that of the cement paste mixture. However, the flow time of the fly ash-based and bottom ash-based geopolymer paste mixtures were significantly higher than that of the cement paste mixture. This is due to the high cohesiveness of the alkaline solution of the geopolymer mixtures. The high cohesiveness of the geopolymer mixtures adversely affects the workability properties of these mixtures.

Table 5. Fresh state properties of the paste mixtures

Paste type	Flow diameter (cm)	Flow time (s)	Water/binder ratio
Cement	17	3	0.50
Fly ash	25	23	0.38
Bottom ash	23	26	0.38

The specific gravity of pervious concrete mixtures is given in Figure 2. Test results showed that the specific gravity of FA, BA and C mixtures was very close to each other. Although there was a significant difference between the specific gravity of the cement and the specific gravity of the fly ash and the bottom ash, the specific gravity of the pervious concrete mixtures was found almost similar. This may be due to the small amount of the paste in pervious concrete mixtures.

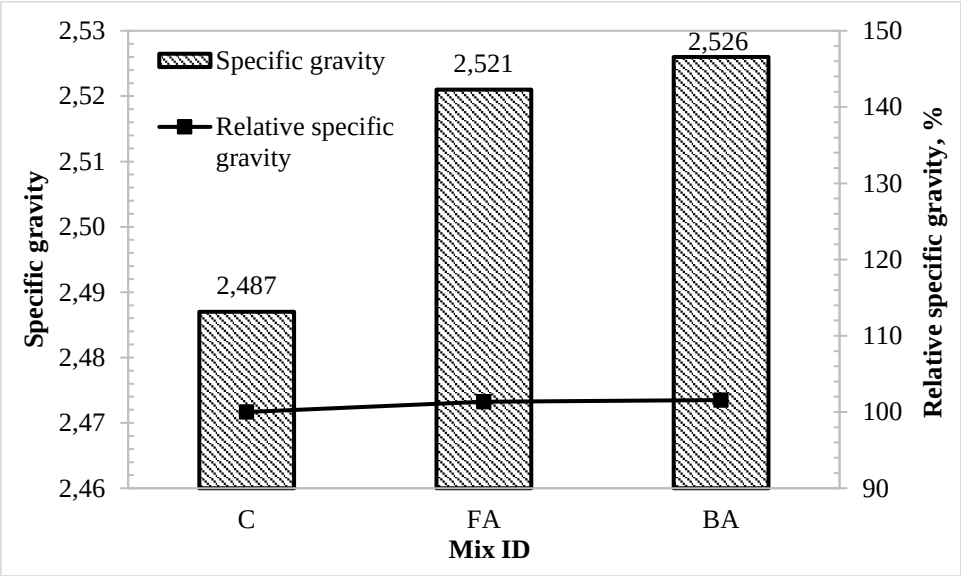

Figure 2. Specific gravity of pervious concrete specimens

The water absorption of the pervious concrete mixtures is shown in Figure 3. As can be seen in the figure, while BA mixture had the highest water absorption value, C mixture also had the lowest water absorption. The water absorption of the pervious geopolymer concrete mixtures (FA and BA) was higher (up to 33%) than that of cement-based pervious concrete mixture (C). This may be due to the high porosity of the fly ash and bottom ash paste.

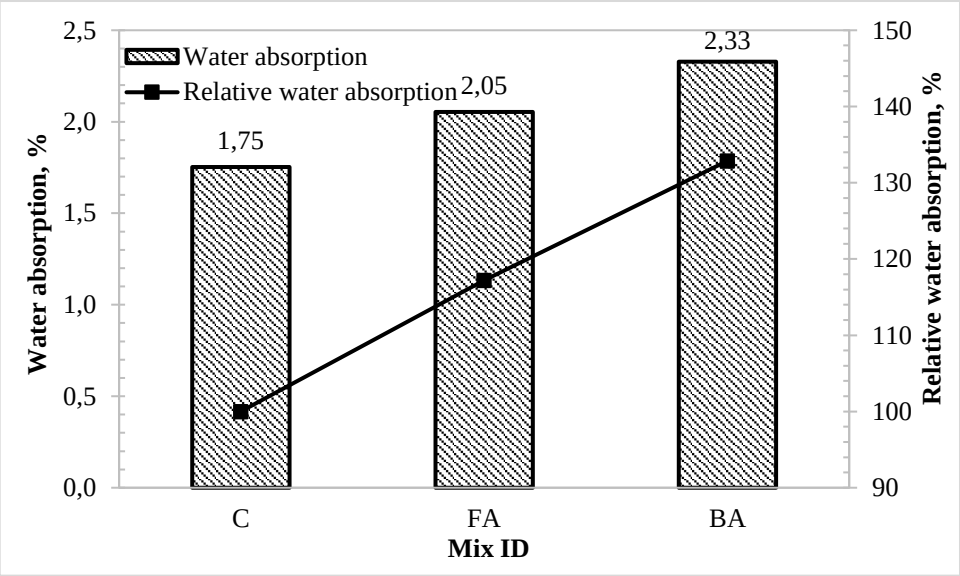

Figure 3. Water absorption of pervious concrete specimens

The unit weight of the pervious concrete mixtures is given in Figure 4. The unit weight of the pervious geopolymer concrete mixtures (FA and BA) was slightly higher than that of the cement-based pervious concrete mixture (C). As can be seen in Table 4, theoretical unit weight of the pervious concrete mixtures was very close to the measured unit weight of the mixtures. In addition to density difference of paste types, cohesiveness determines coating thickness of aggregate surface with the pastes. Thereby, such density variation can be observed in these type concrete mixtures.

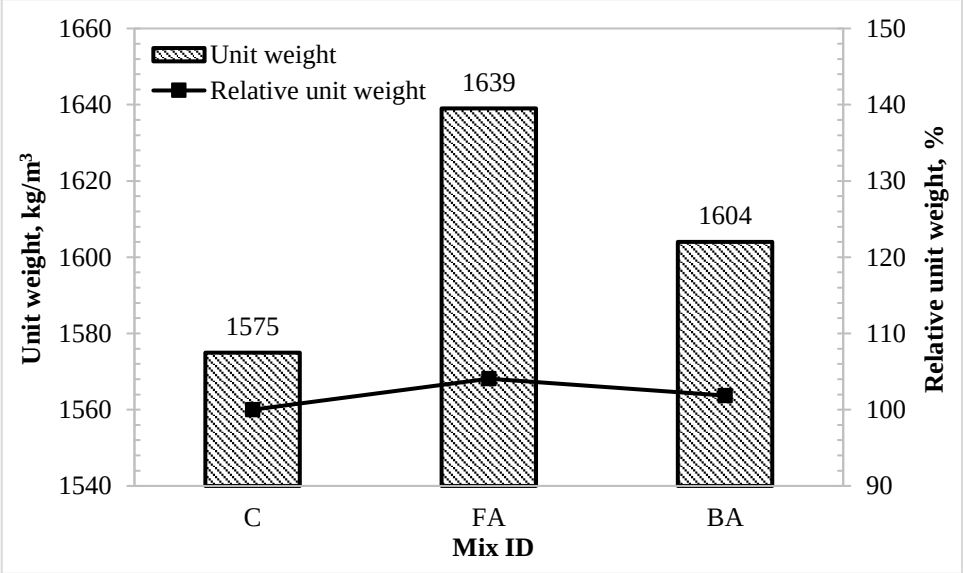

Figure 4. Unit weight of pervious concrete specimens

The void content of the pervious concrete mixtures is shown in Figure 5. The theoretical void content of the pervious concrete mixtures was almost kept constant as 36±1% in this study. As can be seen in the figure, the measured void content of the mixtures was found similar to each other. The fly ash-based pervious concrete mixture (FA) had slightly lower void content value among the mixtures.

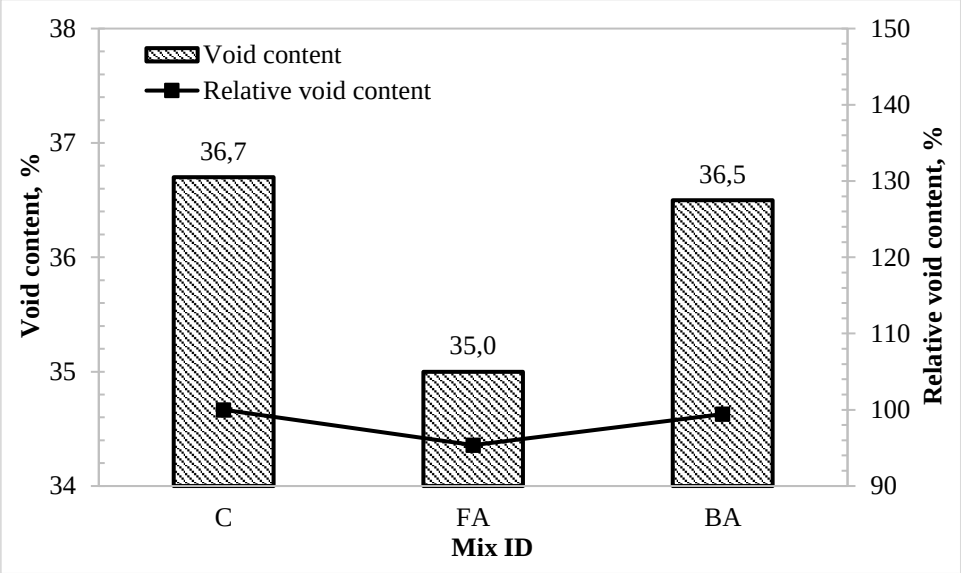

Figure 5. Void content of pervious concrete specimens

The permeability coefficient of the pervious concrete mixtures is given in Figure 6. As can be seen in the figure, the permeability coefficient of the pervious bottom ash-based geopolymer concrete (BA) mixtures was found significantly higher (34%) than those of the fly ash and cement-based pervious concrete mixtures. Because fly ash and bottom ash is more porous than the cement (Tuyan, 2017), pervious geopolymer concrete mixtures with these binders had the higher permeability coefficient than the cement-based pervious concrete mixture.

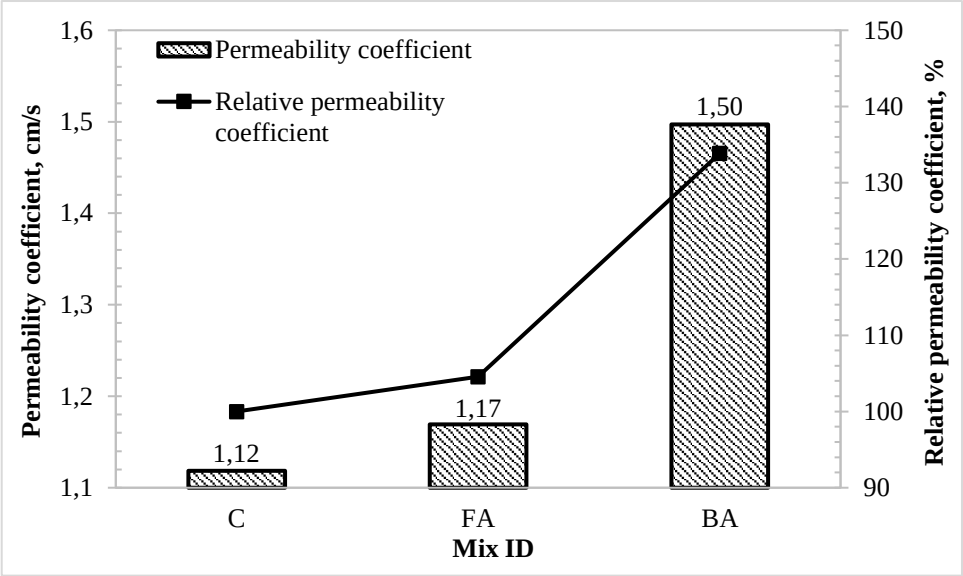

Figure 6. Permeability coefficient of pervious concrete specimens

4. Conclusions

In this study, the utilization of Type C fly ash and bottom ash in pervious geopolymer concrete was investigated. For comparison, a Portland cement-based pervious concrete was also produced. Some physical properties (specific gravity, water absorption, density, void content and permeability) of the concrete mixtures were determined. The following conclusions were drawn:

The flow diameter of the fly ash-based and bottom ash-based geopolymer paste mixtures were higher than that of the cement paste mixture. However, the flow time of the fly ash-based and bottom ash-based geopolymer paste mixtures were significantly higher than that of the cement paste mixture.

The measured specific gravity, unit weight and the void content were found similar in cement and geopolymer-based pervious concrete mixtures.

The water absorption of the geopolymer-based pervious concrete mixtures was higher (up to 33%) than that of cement-based pervious concrete mixture.

The permeability coefficient of the bottom ash-based pervious geopolymer concrete mixtures was found significantly higher (34%) than that of the cement-based pervious concrete mixture.

Experimental study has shown that the bottom ash was suitable material to use as binder in the production of geopolymer-based pervious concrete mixtures.

References

ACI. American Concrete Institute. (2008). Specification for Pervious Concrete Pavement. ACI522.1-08. ACI, Farmington Hills, MI.

Delatte, N. J., (2014). Concrete Pavement Design, Construction, and Performance, Second Edition. US: CRC Press.

Jo, M., Soto, L., Arocho, M., St John, J., and Hwang, S., (2015). Optimum mix design of fly ash geopolymer paste and its use in pervious concrete for removal of fecal coliforms and phosphorus in water. Construction and Building Materials, 93, 1097-1104.

Sabnis, G. M., (2015). Green Building with Concrete: Sustainable Design and Construction, Second Edition. US: CRC Press.

Sata, V., Wongsa, A., and Chindaprasirt, P., (2013). Properties of pervious geopolymer concrete using recycled aggregates. Construction and Building Materials, 42, 33-39.

Tho-In, T., Sata, V., Chindaprasirt, P., and Jaturapitakkul, C., (2012). Pervious high-calcium fly ash geopolymer concrete. Construction and Building Materials, 30, 366-371.

Tuyan, M. (2017). Doğal ve atık malzemelerle geopolimer harç ve beton geliştirilmesi. Doktora Tezi, Ege Üniversitesi, Fen Bilimleri Enstitüsü, İzmir.

Zaetang, Y., Wongsa, A., Sata, V., and Chindaprasirt, P., (2015). Use of coal ash as geopolymer binder and coarse aggregate in pervious concrete. Construction and Building Materials, 96, 289-295.

Flood Hydrology of Kurtun Stream

Neslihan BEDEN[1*], Hesham ALRAYESS[2], Asli ULKE KESKIN[3]

[1]Ondokuz Mayis University, Kavak Vocational School, Construction Department, Samsun, Turkey
[2,3]Ondokuz Mayis University, Engineering Faculty, Civil Engineering Department, Samsun,Turkey

[*]**Corresponding Author:** neslihan.beden@omu.edu.tr

Abstract

Flood is one of the most effective naturel disasters. The magnitude and the frequency of floods are essential for designing hydraulic structures. Floods are the most complicated problems of engineering hydrology. Therefore, the characteristics of project floods must be determined accurately in order to engineering projects, to management and to build reliable hydraulic structures. Besides changes in precipitation regimes and rapid increase in temperature and evaporation values due to climate change will lead to a gradual decline in clean water resources in the upcoming decades. Therefore, it is very important to plan the water resources to manage climate change effects such as flood, drought, extreme precipitation, extreme temperatures or evaporation. In order to use water resources efficiently, firstly the characteristics of resources must be identified realistically. water potential and flood peak discharges can be calculated by estimating rainfall and flow values correctly with using climate data and flow data.

The aim of this study is to analyze the flood hydrology of the Kurtun stream which passes through the urbanized area and forms a risk of flood, with statistical methods. For this purpose, the results obtained based on State Hydraulic Works Ahullu Stream Gauge Station data were evaluated. Observations cover the 1964-2015 period. This period is sufficient for statistical analysis. 2, 5, 10, 25, 50, 100, 200, 500-year floods are calculated and subjected to Normal, Log-Normal (2 parameters), Log-Normal (3 parameters), Gumbel, Gamma and, Log-Pearson probability distribution functions. According to the Smirnov-Kolmogorov compliance test, Log-Pearson Type-3 results are more suitable.

Key Words: Flood Hydrology, Probability Distribution Functions, Kurtun Stream,

1. Introduction

The importance of water resources has increased cause of global changes, the increase in world population, unplanned urbanization, industrial development and rapid changes in global climate events throughout the world. Hydro-meteorological processes affect the climate and human activities in a continuous manner and their impacts appear in the forms of trends or sudden jumps. Some extreme climatic phenomena as well as all kinds of large-scale water resources development projects may alter hydrological processes and may lead to abrupt changes in the hydrological time series (Xiong and Guo, 2004).

The one of the most important extreme event is the floods. Floods are characterized by high flow rates, great speeds and high-water levels. These flood characteristics must be known for all constructions to be built on the rivers. Damage from floods depends on the size of the area to be flooded and future floods. In this context, the morphology of river bed and basin hydrology should be examined for structural and non-structural measures to be taken.

In this study, flood values for different return periods belonging to the Kurtun river at the Samsun province which is the largest city of Yesilirmak basin were calculated.

2. Material and Method

2.1. Material

In this study, flood events belonging to the Kurtun river at the border of Samsun/Atakum county were calculated. In the middle part of the Black Sea coastline, Samsun province, which is located between the deltas of Yesilirmak and Kizilirmak rivers to the Black Sea, has a surface area of 9083 km^2. The study area shows typical Black Sea climate characteristics. Every season is rainy; summers are warm, and winters are relatively mild. Most precipitations are seen in autumn and winter seasons. Precipitation is usually of a frontal character. Orographic trails are also observed on the slopes of the mountain ranges extending along the Black Sea. The long-term average temperature of Samsun is 14,4°C. according to the long-term trends, there is an upward trend in average temperatures of 2,9°C/100 years. Positive anomalies are observed in average temperatures in recent years except for 2003.

The purpose of this study is; is to analyze the flood hydrology of Kurtun river passing through the settlement area of Samsun province and forming the risk of flood by statistical methods. For this purpose, the results obtained based on DSİ Stream Observation Station (AGI)

data were evaluated. It is expected that the findings of the study will support the flood protection studies in other scientific studies and study areas that can be done in the future.

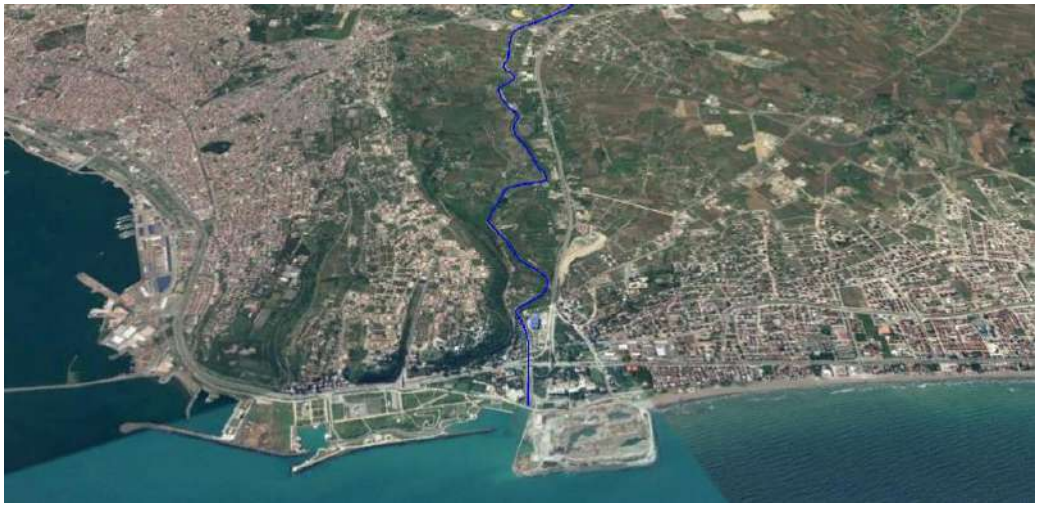

Figure 1. General view of Kurtun stream

The boundaries of the Kurtun River precipitation area begin at 1100 m elevations on the border of Kavak District and fall into the Black Sea in Samsun province center. The length of the river is 47 km. The D14A014 Kurtun Stream-Ahullu gauge station was established in 1963 and has flow observations since 1964. The Kurtun river has a 259.0 km^2 precipitation area at the gauge station location. The information of the stream gauging station in the river is given in Table 1 and the position in the basin in the station is shown in Figure 2.

Table 1. Kurtun Stream Station

Kurtun Stream Gauge Station D14A014	
Elevation	140 m
Precipitation area	259 km^2
The open date of the station	03.08.1962

Figure 1. Location of the D14A014 station

The gauge station D14A014 observations cover the 1964-2015 period. This period is sufficient for statistical analysis. It is seen that the largest flood value in 42 years between measurement years is 330 m^3/s and the smallest flood value is 5,9 m^3/s. According to the flow-frequency curve seen in Figure 2, the probability of reaching 300 $m^3/$ s nearest to the largest is around 3 %. Although this value can be used to determine the amount of water that can be recovered from water constructions, it is not appropriate to use it for flood analysis.

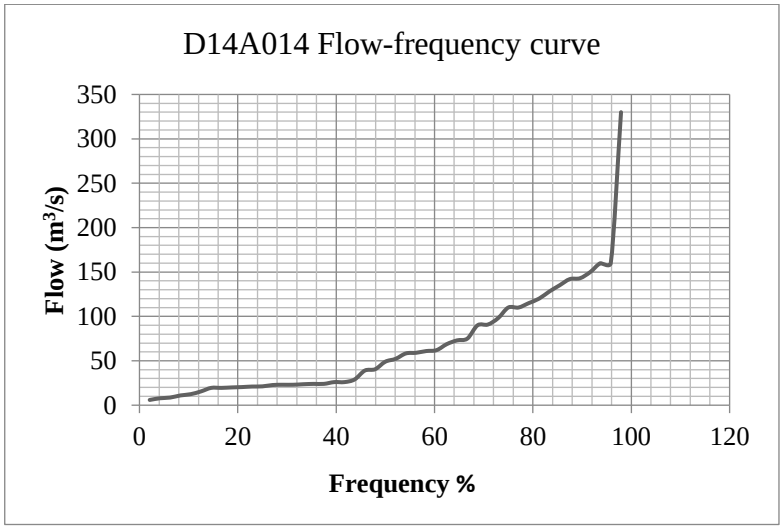

Figure 2. Flow-frequency curve of Kurtun river

Also, the trends of the annual mean and minimum flow data for the station from 1964 to 2015 are given in Figure 3.

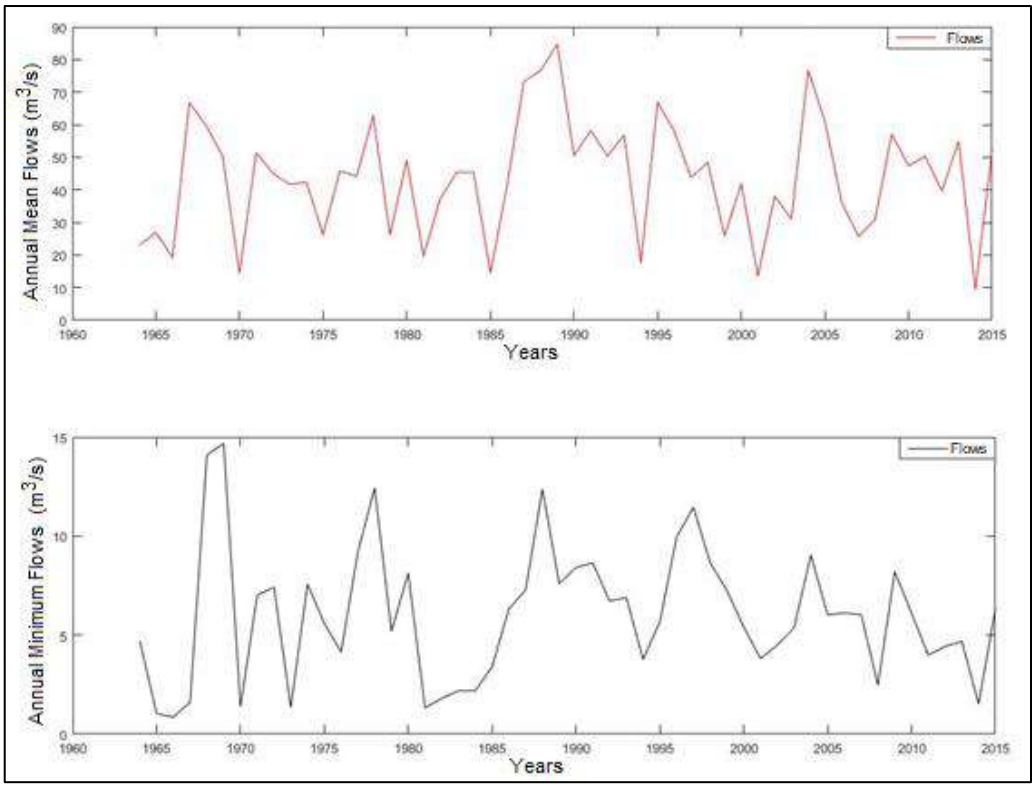

Figure 3. Annual mean and annual minimum flow values of Kurtun stream

2.2. Methods

2.2.1. Probability Distribution Functions

Normal Distribution Function

This distribution, also known as the Gaussian Distribution, has two parameters. The mean of the random variable is μ_x, and the second is the standard deviation of the random variable σ_x. The probability density function and the standard normal variance of this distribution (z) are defined in Equation 1 and Equation 2 (Bayazit ve Onoz, 2008; Bayazit ve Yegen Oğuz, 2005).

$$f(x) = \frac{1}{\sqrt{2\pi\sigma_x^{\,2}}} \exp\left[-(x-\mu_x)^2 \Big/ 2\sigma_x^{\,2} \right] \tag{1}$$

$$z = \frac{x-\mu_x}{\sigma_x} \tag{2}$$

Log-Normal Distribution Function

Since the normal distribution is easy and the properties are well known, the normal non-dispersed distributions are also made to fit the normal distribution with an appropriate

transformation. Logarithmic transformation is commonly used for this purpose, defined in Equation 3.

$$y = \ln(x - x_0) \tag{3}$$

This distribution is well suited to many variables in practice, since the random variable in a lognormal distribution can only take positive values and is a positive skew of the distribution. In the calculations related to the lognormal distribution, the normal distribution table is used for the (y) variant. In this distribution, the lognormal-2 distribution is obtained by taking x_0 as zero (Equation 4 and Equation 5) (Bayazit ve Oguz, 1994; Bayazit, 1981).

$$z = {(y - \mu_y)}/{\sigma} \tag{4}$$

$$f(x) = \frac{\exp\left[-\frac{1}{2}\left(\frac{y-\mu_y}{\sigma_y}\right)\right]}{\sigma_y (x - x_0)\sqrt{2\Pi}} \tag{5}$$

Gamma Distribution Function

The gamma distribution is also a positive skewed distribution, defined only for the positive values of the variable, such as the lognormal distribution. However, since only one parameter (β, form parameter) makes it difficult to fit the gamma distribution to the observed frequency distributions, gamma distributions of 2 and 3 parameters are also defined. The probability density function of the distribution and β are the shape parameter given in Equation 6 and Equation 7.

$$f(x) = \frac{\left(\frac{x - x_0}{\alpha}\right)^{\beta-1} \exp\left\{-\left(\frac{x - x_0}{\alpha}\right)\right\}}{\alpha\Gamma(\beta)} \tag{6}$$

$$\beta = {4}/{C_s^2} \tag{7}$$

Gamma distribution with 2 parameters is obtained by taking x_0 value as zero in gamma distribution with 3 parameters, put x / α instead of x in this distribution. Accordingly, the scale (α) parameter of the distribution and x_0 are defined in Equation 8 and Equation 9.

$$\alpha = {S}/{\sqrt{\beta}} \tag{8}$$

$$x_0 = \mu_x - S\sqrt{\beta} \tag{9}$$

The Pearson Type III distribution table is used to use the gamma distribution. This table shows the frequency factor values for various values of Cs corresponding to various surpass probabilities. The frequency factor is defined in Equation 10 (Bayazit ve Oğuz, 1994; Bayazit, 1981).

$$K_T = \frac{x - \mu_x}{\sigma_x} \tag{10}$$

Gumbel Distribution Function

The peak or minimum values of many events encountered in hydrology show similar features. For example, the peak flow in a year or extreme precipitation. It is suggested by Gumbel (1958) that the distributions of these random variables can be one of the general extreme value distributions (GEV). According to the theory of statistical values of the extremes, it is assumed that if the number of independent variables goes to infinity, it is close to one of the extreme value distributions of the distributions of the largest ones in the sample. These are Type I, II and III distributions (Bayazit ve Onoz, 2008). M_1, M_2, ..., M_N are the daily precipitation or currents. The X random variable is defined as X = max (M_i) i = 1, 2, ..., 365 per year. If the M_i values are independent, have the same distribution, and have unbounded upper bounds, the distribution of the variable X in the large values of N is the Extreme Type I (EVI) or Gumbel distribution. In the literature, Gumbel distribution is widely accepted in the literature for annual maximum flows and 24-hour maximum precipitation distribution. The Gumbel distribution function defined in Equation 11 and Equation 12.

$$f(x) = \frac{1}{a}\exp\left[-\frac{x-\xi}{a} - \exp\left(\frac{x-\xi}{a}\right)\right] \quad -\infty < x < \infty \tag{11}$$

$$F(x) = \exp\left[-\exp\left(-\frac{x-\xi}{a}\right)\right] \tag{12}$$

α and ζ are the parameters of the distribution. Median, variance and skewness coefficient of distribution are given in Equation 13-15, respectively.

$$\mu_x = \xi + 0,5772a \quad (13)$$

$$\sigma_x^2 = \frac{\pi^2 a^2}{6} \approx 1,645a^2 \quad (14)$$

$$C_{sx} = 1,1396 \approx 1,14 \quad (15)$$

Probability Distribution Functions Compliance Test (Kolmogorov-Smirnov Test)

The statistic used in the Kolmogorov-Smirnov test, which is a test used to control the theoretical distribution suitability of the frequency distribution of the observed data.

$$\Delta = \max\left|F(x_i) - F^*(x_i)\right| \quad (16)$$

In Equation 16, where $F^*(x_i)$ is the additive frequency distribution ordinates calculated by the i/N formula. $F(x_i)$ is the ordinate corresponding to the same xi values of the selected theoretical additive distribution function. According to this Δ statistic is the largest difference between observed and theoretical added distributions. The distribution of the Δ statistic is randomly independent of the distribution and depends only on the number of N elements in the sequence.

If the calculated Δ statistic is lower than Δ_α for the various values of N read from the Kolmogorov-Smirnov table, then the appropriateness of the distribution is accepted at the level of α significance, otherwise it is rejected (Bayazit ve Oguz, 1994; Bayazit, 1996).

3. Results

The Kolmogorov-Smirnov test was used in 80 %, 85 %, 90 %, 95 % and 99 % significance levels to determine which distribution of the series best fit. According to the results of the Kolmogorov-Smirnov test shown in Table 2. Log-Pearson Type-3 distribution has best fit. 5, 10, 25, 50, 100, 200, 500 years of flood forecast were calculated according to six different probability distribution functions using Kurtun Stream Observation Station data shown in Table 3. The logarithm of the maximum possible flows at various return intervals is calculated using the Log-Pearson Type-3 distribution according to the Kolmogorov- Smirnov conformance test.

Table 2. The results of the Kolmogorov-Smirnov test

					Significance Level				
	Theoretical P	Empirical P	Max. P	Observation value at P	0,80	0,85	0,90	0,95	0,99
Normal	0,728	0,438	0,166	29	Reject	Reject	Accept	Accept	Accept
Log-Normal (2 Parameters)	0,787	0,417	0,204	26	Reject	Reject	Reject	Reject	Accept
Log-Normal (3 Parameters)	0,731	0,417	0,148	26	Accept	Accept	Accept	Accept	Accept
Pearson Type- (Gamma Type-3)	0,279	0,417	0,138	26	Accept	Accept	Accept	Accept	Accept
Log-Pearson Type-3	**0,298**	**0,417**	**0,119**	**26**	**Accept**	**Accept**	**Accept**	**Accept**	**Accept**
Gumbel	0,165	0,021	0,145	5,9	Accept	Accept	Accept	Accept	Accept

Table 3. Floods values of different return periods

Distribution Type	Return Year							
	2	5	10	25	50	100	200	500
Normal	66,46	118,38	145,52	174,48	193,15	209,97	225,3	243,81
Log-Normal (2 Parameters)	48,71	94,57	133,78	193,69	245,89	304,83	370,82	469,75
Log-Normal (3 Parameters)	52,33	105,29	143,88	196,22	237,51	280,78	326,05	389,19
Pearson Type- (Gamma Type-3)	48	104,68	147,07	202,91	244,97	286,95	328,86	370,78
Log-Pearson Type-3	**44,85**	**98,78**	**148,08**	**226,85**	**297,77**	**379,2**	**472,9**	**589,76**
Gumbel	56,81	117,32	157,38	207,99	245,54	282,81	319,95	368,94

In the present study, flood events which threaten Samsun province center according to various probability distribution functions were calculated by using D14A014 station data. According to the Log-Pearson Type 3 distribution of probable maximum floods at certain periods; it is best to consider; Q_2 = 44,85 m^3/s, Q_5 = 98,78 m^3/s, Q_{10}= 148,08 m^3/s, Q_{25} = 226,85 m^3/s, Q_{50} = 297,77 m^3/s, Q_{100} = 379,2 m^3/s, Q_{200} = 472,9 m^3/s, Q_{500} = 589,76 m^3/s. Results obtained without this study provide detailed information on the hydrology of the area studied and can be used for future flood modeling studies. The resulting flood hazard poses a

significant risk to settlement areas near the river bed and necessary precautions should be taken without delay.

References

Bayazit, M. and Yegen Oguz, B., (2005). Mühendisler İçin İstatistik, Birsen Yayınevi.
Bayazit, M. and Onsoz, B., (2008). Taşkın ve Kuraklık Hidrolojisi, Nobel Basımevi.
Bayazit, M., (1981). Hidrolojide İstatistik Yöntemler, İTÜ Matbaası.
Bayazit, M., (1996). İnşaat Mühendisliğinde Olasılık Yöntemler, İTÜ Matbaası.
Bayazit, M., Oguz, B., (1994). İstatistik, Birsen Yayınevi.
Gumbel, E.J., (1958). Statistics of Extremes, New York, Columbia University Press.
Onoz, B. and Bayazit, M., (2003). The power of statistical tests for trend detection, Turkish Journal of Engineering and Environmental Sciences, 27, 247- 251.
Xiong, L., and Guo, S., (2004). Trend test and change-point detection for the annual discharge series of the Yangtze River at the Yichang hydrological station. Hydrological Sciences Journal, 49(1), 99–112.
Yesilirmak Havzasi Taskin Yonetim Plani (2015). T.C. Orman Ve Su İşleri Bakanlığı, Su Yönetini Genel Müdürlüğü, Ankara.

Strength Properties of Fly Ash and Blast Furnace Slag-Based Geopolymer Mortar

Zehra ALMAZ ÖZCAN[1], Okan KARAHAN[2*], Serhan İLKENTAPAR[2],

Uğur DURAK[2], C. Duran ATİŞ[2]

[1]Kayseri University,Tomarza M. Akıncıoğlu Vocational College, Kayseri, Turkey
[2*]Erciyes University, Engineering Faculty, Civil Engineering Department, Kayseri, Turkey

Corresponding Author: okarahan@erciyes.edu.tr

Abstract

In this study, flexural tensile and compressive strengths of alkali activated fly ash and blast furnace slag-based geopolymer mortars were presented. Class F fly ash and ground granulated blast furnace slag obtained from Çatalağzı Thermal Power Station and Iskenderun Iron–Steel Factory, respectively, were used. Sodium amountintroduced in mortar mixture and heat curing timewere investigated as the main influencing factors on the flexuraltensile strength and compressive strength of mortar. Mortar mixture parameters were 3 and 0.40 for sand-binder ratio, and water-binder ratio, respectively. The sodium metasilicate was used in this study as an alkali activator. The naturelriver sand, combination of 50% fly ash and 50% slag blend, water, and sodium metasilicate were used in the production of mortars.Sodium concentrations in mortar mixture were chosen as 4%, 6%, 8%, 10%, 12% and 14% of binder amount, in weight basis. Heat curing temperature and heat curing durations were chosen as 100°C and 24h, 72h and 168 hours, respectively. For each sodium concentration, three prismatic specimens with 40×40×160 mm dimensions were prepared using a three-cell mortar cast. After heat curing period in a laboratory oven, the samples were left to cool down to room temperature, then the flexuraltensileand compressive strengths were measured according to TS EN 1015-11. High compressive strength and flexural tensile strength, as high as 83 MPa and 12 MPa, respectively, were obtained. The highest compressive strength was measured from fly ash and slag blend geopolymer mortar containing 10% sodium amount and heat curing period for 24 hours.

Keywords: FlyAsh,Slag, Geopolymer, Alkali-activated, Strength

1. Introduction

Manufacturing of cement is harmful to nature and pollutes environment due to emerging gas from raw materials and energy used in sintering process. Cement composites do not show adequate resistance to external factors. In addition, utilizing Portland cement could be expensive and not economic, in some cases. Therefore, technical, economic and environmental concern attracts the alternative binder production other than cement (Aydın, 2010).

Developing alternative materials to Portland cement and utilization of fly ash, silica fume, ground granulated blast furnace slag (GGBFS), rice husk ash and meta-kaolin are among the subject of environmental protection and concern of global warming. In connection to the issue, geopolymer technology and geopolymer production has been suggested by Davidovits as an alternative binder to Portland cements used in concrete industry. Geopolymer technology can contribute to reduction of global warming by reducing up to 80% of CO_2 emission caused by production of cement and concrete industry (Davidovits, 1942).

It is possible that materials that contain Al_2O_3, SiO_2, CaOin its content could be converted to a strong binder in the presence of alkali activator system. While, inorganic polymer called "geopolymer" forms as a result of reaction between alkali activator and alumina silicate fly ash. Reaction between slag and alkali activator forms calcium-silicate-gel similar to Portland cement C-S-H gel (Aydın and Baradan, 2013; Pacheco-Torgal, Castro-Gomes and Jalali, 2008; Shi, Krivenko and Roy, 2006).

Interesting studies intended to produce a binder without using Portland cement were activation of industrial waste and by-products (i.e. ground granulated blast furnace slag and fly ash) in the presence of alkali activator. Materials that contain amorphous characterized ingredient such as fly ash and ground granulated blast furnace slagcan be converted to a binder through activation of an alkali activator. The most used activators were sodium hydroxide (NaOH), potassium hydroxide (KOH) and sodium water-glass ($nSiO_2Na_2O$) or potassium water-glass(nSiO2K2O) or their mixture. The best suited activator is produced by hydroxide and water soluble silicate (Aydın and Baradan, 2013; Pacheco-Torgal, Castro-Gomes and Jalali, 2008).

In the study, it is aimed to find optimal parameters and evaluate the influence of Na concentration and heat curing duration on flexural tensile strength and compressive strength of geopolymer produced with combination of 50% fly ash and 50% slag blend activated with sodium meta-silicate.

2. Materials and Method

2.1. Fly Ash

Fly ash used in the study was obtained from Catalagzi thermal power plant consuming anthracite, located northern Turkey in Zonguldak city. It is classified as class F fly ash according to ASTM C618 specification, since it contained lower than 10% CaO and higher than 70% of total SiO_2+Al_2O_3+Fe_2O_3 ingredients. Its remaining on 45 μm sieve was 28.8% and its specific gravity was 2100 kg/m^3. Pozzolanic activity index of fly ash was measured as 81% at 28 days. Chemical ingredients of fly ash were presented in Table 1.

Table 1. Chemical ingredient of Catalagzi fly ash (%).

Oxide	SiO_2	Al_2O_3	Fe_2O_3	K_2O	MgO	CaO	SO_3	LOI
Fly Ash	55.38	25.50	6.14	3.80	2.00	2.02	0.14	2.74

2.2. Ground Granulated Blast Furnace Slag

GGBFS used in the study was obtained from ISDEMIR iron-steel production plant located in Iskenderun county of Hatay city of southern Turkey. Strength activity index of GGBFS was measured as 84% at 28 days. Chemical ingredients of GGBFS were presented in Table 2.

Table 2. Chemical ingredients of GGBFS (%).

Oxi	Si	Al_2	Fe_2	K_2	Mg	Ca	SO	LO
GGBFS	39.48	10.61	1.53	0.85	7.07	33.84	1.13	2.50

2.3. Aggregate

Experimental laboratory study was carried out using natural river sand with maximum size of 4 mm. Properties obtained from experiment made on sand was given in Table 3.

Table 3. Properties of sand used

	Dry Density (g/cm³)	SSD Density (g/cm³)	Water Absorption (%)	Fineness Modulus	Fine Substance (%)	LooseUnit Weight (g/dm³)	CrampedUnit Weight (g/dm³)
Sand	2.32	2.43	4.71	3.77	1.6	1653	1761

2.4. Activator

Activation of fly ash and GGBFS was made by sodium meta-silicate ($NaSiO_3$) activator which was obtained from Tekkim Chemical Industries. Chemical ingredients of activator were given in Table 4.

Table 4. Chemical analysis result of sodium meta-silicate (%).

Specification	Purity	Sodium Oxide (Na_2O)	Silica (SiO_2)	Ferrum(Fe)	Non water soluble	pH
Values (%)	≥ 95.0	48.0–51.0	44.4–47.4	≤ 0.1	≤0.5	>12

2.5. Water

In mortar mixture preparation, drinkable tap water obtained from city water supply was used.

2.6. Mortar Mixtures and Testing

For production of three 40x40x160 mm sized prismatic specimens, three-cell mold was used. Mixture composition was 450 g binder, 1350 g sand and 180 g water for a three-cell mold. Binder was made of 50% fly ash and 50% GGBFS blend. Geopolymer mortar mixture composition for a three-cell mold was presented in Table 5.

Activator content was maintained for 4%, 6%, 8%, 10%, 12% and 14% Na amount of binder content. For each activator content fresh mixture was prepared and prismatic samples in three cell mold were produced. Each mixture was subjected to heat curing for 24h at 100°C temperature. Selected samples prepared with 8%, 10% and 12% Na concentration were also subjected to heat curing for 72h and 168h at 100°C temperature to investigate the influence of heat curing time.

Table 5. Geopolymeric mortar mixture composition for different Na concentration.

Na Ratio (%)	Metasilicate (g)	Water/Binder Ratio	Water (g)	Blast Furnace Slag (g)	Fly Ash (g)	Sand (g)
4	48	0.4	180	225	225	1350
6	72	0.4	180	225	225	1350
8	96	0.4	180	225	225	1350
10	120	0.4	180	225	225	1350
12	144	0.4	180	225	225	1350
14	168	0.4	180	225	225	1350

For fresh mixture preparation, water was put in mixture pan first. Then powder binder was put on it second. Mixer was run for 30 seconds to mix binder and water. Meta-silicate and sand was introduced into mixture pan in the second 30 seconds. Then, mixture was mixed in fast mode for 30 seconds. Mixer was stopped and mixture in the pan was cumulated in the middle of mixture during 90 seconds resting period. Later, mixtures were mixed for 60 seconds further in fast mode of mixer, then mixing was completed.

Geopolymer samples activated with sodium meta-silicate, prepared for each Na concentration and curing durations were subjected to flexural tensile strength and compressive strength. Three points loading for flexural tensile testing using 40x40x160 mm prismatic was carried out for tensile testing. Compressive strength testing was carried out on at the tip of halved-prismatic samples using 40x40 compression apparatus having 40x40 compression plate heading. Flexural strength testing was carried out on three prismatic samples produced for each mixture. Compressive strength measurements were carried out on six half-broken pieces of prismatic samples obtained from flexural tensile strength test.

3. Results and Discussion

Flexural tensile strength testing measurements carried out on geopolymer mixtures after heat curing for 24h curing durations were presented in Table 6. These values were average of three measurements. Similarly, compressive strength testing measurements were carried out on same specimens but on two halve-prismatic specimens. Averages of six specimens were presented in Table 6.

Table 6. Flexural tensile and compressive strength results of mortars containing 50% fly ash and 50%
blast furnace slag after curing at 100°C.

Na Ratio (%)	Cure Time (hours)	Metasilicate (gr)	Water/Binder Ratio	Flexural Strength (MPa)	Compressive Strength (MPa)
4	24	48	0.4	7.0	20.1
6	24	72	0.4	9.6	64.6
8	24	96	0.4	9.2	67.3
10	24	120	0.4	9.2	83.3
12	24	144	0.4	10.1	74.0
14	24	168	0.4	9.4	50.5

Table 6 shows that flexural tensile strength for mixtures activated with 4%, 6%, 8%, 10%, 12% and 14%Na amount of binder were 7.0, 9.6, 9.2, 9.2, 10.1 and 9.4 MPa, respectively. When Na concentrations were 6%, 8%, 10% and 14%, there was no difference observed in flexural tensile strength. However, the maximum flexural tensile strength was obtained from mixtures made with 12% Na concentration for 24h heat curing. Flexural tensile strength was reduced when Na concentration increased to 14%, this is explained by fast setting times observed in mixtures made with 14% Na concentration, causing compaction problem in preparing prismatic specimens. Although it is not very strong, there was a tendency observed that flexural tensile strength increases as the Na concentrations increase.

When Table 6 was evaluated in terms of compressive strength development, compressive strength measured from samples were in the range between 20 MPa to 83.3 MPa. It was also observed that there was a good tendency between Na concentration and compressive strength variation. As Na concentration increases, compressive strength of geopolymer mortar increases, however, up to a certain optimal point. Then, compressive strength decreases despite for higher Na concentration. This decrease was explained by fast setting times of geopolymer mortar made with 12% and 14% Na concentration. The highest compressive strength 83.3 MPa was obtained from mixture activated at 10% Na concentration.

As a result of evaluation of Table 6, it was decided that 10% and 12% Na concentration were seemed to be optimal values for mixtures in terms of flexural tensile strength and compressive strength values. Therefore, further investigation was carried out to evaluate influence of heat curing duration on strength properties of geopolymer mortar.

For further investigation, Na concentrations were selected as 8%, 10% and 12%, two longer heat curing times were selected as 72h (3d), and 168h (7d). Strength obtained for longer heat curing durations were compared with strength obtained for 24h heat curing duration. Strength obtained for longer heat curing time was presented in Table 7.

Table 7. Flexural tensile and compressive strength results of mortars containing 50% fly ash and 50%
blast furnace slag after curing at 100°C for 24 hours, 72 hours and 168 hours.

Na Ratio (%)	Cure Time (hours)	Metasilicate (g)	Water/Binder Ratio	Flexural Strength (MPa)	Compressive Strength (MPa)

8	24	96	0.4	9.2	67.3
10	24	120	0.4	9.2	83.3
12	24	144	0.4	10.1	74.0
8	72	96	0.4	10.1	71.0
10	72	120	0.4	10.9	71.5
12	72	144	0.4	10.9	75.7
8	168	96	0.4	10.1	76.4
10	168	120	0.4	11.9	83.0
12	168	144	0.4	11.5	74.5

Table 7 shows that increasing heat curing durations increases flexural tensile strength, however, this increment is found to be not very significant. Their values were in the order of 9 - 11 MPa.

On the other hand, increasing curing duration from 24h to 72h did not improve compressive strength significantly. Similarly, increasing heat curing time from 24h to 168h improved compressive strength for mixture containing 8% Na concentration, other mixtures did not gain further compressive strength.

It can be concluded that there was no influence of increasing heat curing duration from 24h to 168h on strength properties at 100°C temperature. This can be explained by evaporation of mixing water. During heat curing period of 24h at 100°C temperature heat curing; water, which transports the Na ions in the mixture, dries out, then, results with no or little Na movements in geopolymer mixtures causing small or no development in strength property.

4. Conclusions

As results of activating fly ash and slag blend with sodium meta-silicate, the following conclusions were made on influence of Na concentration and heat curing duration on strength properties of geopolymer mortar.

- In terms of compressive and flexural tensile strength, %10 ve %12 Na concentrations were found to be optimal values.

- Following %12 Na concentration, increasing Na concentration result with lower strength due to compaction problem of fresh mixture into mold by fast setting times of mixture.
- The highest flexural tensile strength was obtained from 10% Na concentration at 100°C temperature and for 168h curing and it was 11,9 MPa.
- The highest compressive strength was obtained from 10% Na concentration at 100°C temperature and for 24h curing and it was 83,3 MPa.
- Increase in heat curing time did not significantly improved strength values. It is concluded that optimal heat curing duration was 24h.

Acknowledgements

The authors would like to thank Erciyes University Scientific Research Unit for providing financial support for this research (FDK-2016-6270).

References

Aydın, S., (2010) *Development of a fiber reinforced composite with alkali activated ground granulated blast furnace slag*, Ph.D. Thesis, DokuzEylülUniversity, The Graduate School of Natural and Applied Sciences, İzmir, Turkey.

Davidovits, J., (1994). *High-alkali cements for 21 st century concretes. In Concrete Technology, Past, Present and Future*, Metha, P.K., Ed., pp. 383-397. American Concrete Institute, Farmington Hills, MI.

Aydın, S., Baradan, B., (2013)Effects of mineral and chemical admixtures on alkali-activated slag mortars,*Beton 2013 Ready-Mixed Concrete Exhibition* (pp. 200-209). Turkish Ready Mixed Concrete Association, İstanbul, Turkey.

Pacheco-Torgal, F., Castro-Gomes, J., Jalali, S., (2008). Alkali-Activated Binders: A review. Part 2. About Materials and Binders Manufacture, *Construction and Building Materials*, 22, 1315-1322.

Shi, C., Krivenko, P.V., Roy, D., (2006). *Alkali-Activated Cements and Concretes*, USA and Canada: Taylor and Francis.

TS EN 1015-11., (2000). *Methods of test for mortar for masonry - Part 11: Determination of flexural and compressive strength of hardened mortar*, Turkish Standard Institute, Ankara.

Wind Load Calculation of a RC Minaret According to ACI 307/98 Considering Soil-Structure Interaction

Erdem TÜRKELİ[1*]

[1]Ordu University, Vocational School of Technical Sciences, Construction Department, Ordu, Türkiye

[*]**Corresponding Author:**
erdemturkeli@odu.edu.tr

Abstract
Severe winds and strong earthquakes can be counted as the main reasons for damage or collapse of so many constructed reinforced concrete (RC) minarets. In countries like Turkey, there are so many constructed RC minarets and the construction of most of them are ongoing. During these catastrophic events, a large majority of these tall and slender structures are severely damaged or collapsed that has the result of the loss of lives and economy. Therefore, it is inevitable for us to revise the knowledge and better understand the exact behavior of these structures. The main purpose of this study is to perform wind load calculation of a representative RC minaret according to ACI 307/98 by taking soil flexibility into account. The results obtained from both analysis (with and without soil structure interaction [SSI]) are compared with each other to reach some general conclusions.
Keywords: RC Minaret, Wind, Load, ACI 307/98, Soil structure interaction.

1. Introduction

Severe winds occupy an important part for the reason of damages occurred on the minarets and total collapses. Every year, so many constructed RC minarets were reported to be suffered damage or total collapse due to severe winds (Doğangün *et.* al, 2006; Temüz, 2007; DHA, 2018). Also, according to Sezen *et.* al (2008), minarets have been built, for the most part, by experienced contractors and construction workers with no engineering knowledge and in most cases, each contractor constructs a typical minaret with the same structural and architectural features regardless of the local soil conditions or seismicity of the region. Therefore, it is very vital to consider local soil conditions in determining the wind response of RC minarets.

Some of the studies dealing with the dynamic response of RC minarets in the technical literature are given as follows: Doğangün *et.* al (2008) analyzed three representative minarets with 20, 25, and 30 m height to investigate the dynamic behavior of historical unreinforced masonry minarets by using two ground motions recorded during the 1999 Kocaeli and Düzce, Turkey earthquakes. Muvafık (2014) dealt with the field investigations and seismic analyses of a historical masonry brick minaret damaged during October 23 (Erciş) and November 9

(Edremit), 2011 Van earthquakes in Turkey. Türkeli (2014) considered the structural wind and earthquake analyses of representative RC minaret and compared and discussed the results of the analyses. Türkeli *et.* al (2015) dealt with the dynamic response of traditional and buttressed RC minarets. Pekgökgöz and Taş (2017) studied about the dynamic behavior of a RC high minaret and a form of this minaret with Tuned Mass Damper under the effect of wind forces obtained from the Rita Hurricane, harmonic ground motion and selected earthquake motions.

In this study, the wind loading of a representative RC minaret according to ACI 307/98 (ACI, 1998) was determined for the conditions with and without underlying soil. The conditions at the boundaries that are the viscous dampers were modeled using the method proposed by Lysmer and Kuhlemeyer (1969).

2. Material and Method

In this part of the study, the wind loading procedure given in ACI 307/98, the general information about the viscous boundaries and the finite element model (FEM) of the representative minaret were described in details.

2.1. ACI 307/98 Procedure

The procedure given in ACI 307/98 (ACI, 1998) is presented comprehensively as follows. Firstly, reference design wind speed is shown in Eq.(1):

$$V_R = (I^{0.5}) \cdot V \tag{1}$$

In Eq.(1), V and I are denoting basic wind load and importance factor, respectively. Also, the importance factor is given as 1.15 in ANSI/ASCE 7-95 (ASCE, 1996). The mean design wind speed $\bar{V}(z)$ is given in Eq.(2):

$$\bar{V}(z) = \frac{1.47 \cdot 0.65}{1.22} \cdot V_R \cdot \left(\frac{z}{33}\right)^{0.154} \tag{2}$$

By this way, the mean wind load $\bar{w}(z)$ is given with Eq.(3).

$$\bar{w}(z) = C_{dr}(z) \cdot d(z) \cdot \bar{p}(z) \quad (3)$$

In Eq.(3), $C_{dr}(z)$, shape parameter; $d(z)$, minaret outside diameter at height z; $\bar{p}(z)$, pressure occurred because of the mean speed of design wind at height z and z, any height on minaret. Moreover, the shape parameter $C_{dr}(z)$ is given in Eqs. (4) and (5) which is suitable for the given condition:

$$z < h - 1.5 \cdot d(h) \rightarrow C_{dr}(z) = 0.65 \quad (4)$$

$$z \geq h - 1.5 \cdot d(h) \rightarrow C_{dr}(z) = 1.00 \quad (5)$$

In Eq.(5), h and $d(h)$ are denoting the total height of the minaret and outer diameter at the top of the minaret, respectively. Also, in Eq.(6), pressure occurred due to mean design wind speed at height z is given.

$$\bar{p}(z) = 0.0013 \cdot [\bar{V}(z)]^2 \cdot 525.5 \quad (6)$$

The fluctuating load $w'(z)$ can be calculated with Eq.(7).

$$w'(z) = \frac{3.0 \cdot z \cdot G_w \cdot M_w(b)}{h^3} \cdot 1.5 \quad (7)$$

In Eq.(7), G_w and M_w are denoting the fluctuating load instantaneous wind parameter due to up-wind effects and bending moment at the base of minaret due to mean wind load, respectively. Also, G_w is determined by using Eq.(8).

$$G_w = \left[0.30 + \frac{11.0 \cdot \left(T_1 \cdot \bar{V}_{(10)}\right)^{0.47}}{(h+16)^{0.86}}\right] \quad (8)$$

In Eq.(8), T_1 is denoting the first mode natural vibration period of minaret and $\bar{V}_{(10)}$ is denoting the mean wind speed calculated with the help of Eq.(2) for 10 m. height. At the end of all calculations, the total wind load can be determined by using Eq.(9).

$$w(z) = w'(z) + \bar{w}(z) \quad (9)$$

2.2. Viscous Boundary Method (Lysmer and Kuhlemeyer, 1969)

In this study, the boundaries of soil were modelled by using viscous dampers which is proposed by Lysmer and Kuhlemeyer (1969). According to this method, the boundary condition is a pair of stresses expressed with Eq.(10) and Eq.(11).

$$\sigma = a \cdot \rho \cdot V_p \cdot \vartheta_n \quad (10)$$

$$\tau = b \cdot \rho \cdot V_s \cdot \vartheta_t \quad (11)$$

In Eq.(10) and Eq.(11), σ and τ are the normal and shear stress on the boundary, respectively. Also, v_n and v_t are the normal and tangential particle velocities of the boundary. The other parameters in the cited equations are, ρ, V_p, V_s, a and b which are denoting the unit mass, velocities of P and S waves in the boundary material, dimensionless parameters, respectively. Also, the damping coefficients of the dashpots are for normal and shear directions are given with Eq.(12) and Eq.(13), respectively.

$$c_n = a \cdot \rho \cdot l_0 \cdot V_p \quad (12)$$

$$c_t = b \cdot \rho \cdot l_0 \cdot V_s \quad (13)$$

where, l_0, is the length of the boundary to which the dashpots are attached.

2.3. FEM Model and General Information about the Representative Minaret

SAP2000 structural analysis program was utilized in producing the FEM of the minaret and the soil (Wilson, 2000). Shell elements were used in modelling the upper structure of the representative minaret. Also, the foundation and the soil under the foundation of the minaret was modelled using solid elements. Also, viscous dampers were utilized at the boundaries. All of these are shown in Fig.1.

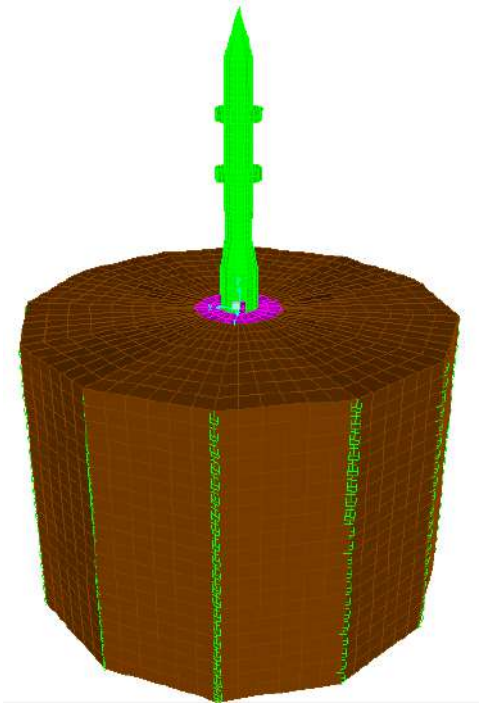

Figure 1. FEM Model of the representative minaret

The underlying soil of the representative minaret was selected from the technical literature (Livaoğlu and Doğangün, 2007). Accordingly, the mechanical properties of the soil i.e. type, Elasticity Module, Poisson's ratio and density are soft, 35000 kN/m^2, 0.4 and 1800 kg/m^3, respectively. By using a general assumption, the length of soil under the representative minaret is accepted as 2.50 times the diameter of the foundation. Also, it is assumed the soil is homogeneous in itself and the thickness of the soil is 20 m. that after this height the soil behaves as rigid (anchored to the main rock). Moreover, the representative minaret was constructed from

reinforced concrete (RC) whose unit weight, elasticity module and Poisson's ratio is 23.5 kN/m^3, 30.000.000 kN/m^2 ve 0.2, respectively.

In Fig.2, the geometrical features of the representative minaret are given.

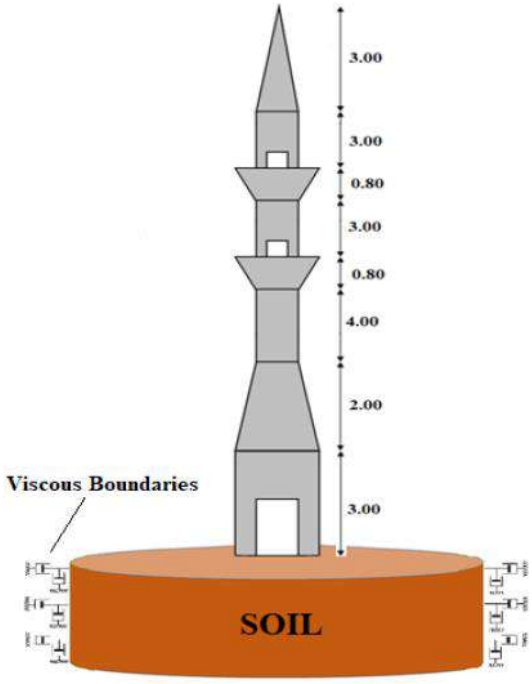

Figure 2. Geometrical features of the representative minaret

It is clear from Fig.2 that the representative minaret has a total of three door openings in the minaret, one at the ground level and the other at the level of the balconies. The door openings are considered to draw an arc of approximately 30 ° and their heights are 1.50 m. Also, the wall thickness of the minaret is constant throughout the height with the value of 0.18 m. Furthermore, the height and the diameter of the foundation is 1.0 m and 6.0 m, respectively. In addition, the representative minaret and the mosque superstructure interaction effect is not considered in this study. Furthermore, the dynamic seismic analysis of the representative minaret is not in the scope of this study. Other than these, the characteristic compressive strength of the concrete is preferred to be used as 16 MPa which is often utilized in practice.

3. Findings and Discussion

In this part of the study, the wind loading acting on a representative minaret according to ACI 307/98 with and without SSI effect is given. By this way, the effect of SSI on the wind response of a representative minaret according to ACI 307/98 can be determined.

3.1. ACI 307/98 Wind Loading Without SSI

In Table 1, the calculation of the mean design wind speed is given. It should be emphasized that the basic wind load is assumed as 45 m/s and the minaret is directly anchoraged to the ground without foundation and soil.

Table 1. The mean design wind speed

Section No	Between Heights	1. Mode Natural Period,T	V (m/s)	I	V_R (m/s)	**V(z) (m/s)**
0	0 m - 3 m	0.246	45.00	1.15	48.257	**26.125**
1	3 m - 5 m	0.246	45.00	1.15	48.257	**28.263**
2	5 m - 8 m	0.246	45.00	1.15	48.257	**30.385**
3	8 m - 11 m	0.246	45.00	1.15	48.257	**31.912**
4	11 m - 14 m	0.246	45.00	1.15	48.257	**33.120**
5	14 m - 16.6 m	0.246	45.00	1.15	48.257	**34.000**
6	16.6 m- 19.6 m	0.246	45.00	1.15	48.257	**34.881**

Also, in Table 2, the mean wind load calculated according to Eq.(3) is given.

Table 2. The mean wind load

Section No	Between Heights	$C_{dr}(z)$	d(z)	p(z)	$\bar{w}(z)$ **(kN/m)**
0	0 m - 3 m	0.65	2.500	466.26	**0.758**
1	3 m - 5 m	0.65	2.150	545.71	**0.763**
2	5 m - 8 m	0.65	1.800	630.71	**0.738**
3	8 m - 11 m	0.65	1.800	695.71	**0.814**
4	11 m - 14 m	0.65	1.800	749.35	**0.877**
5	14 m - 16.6 m	0.65	1.800	789.72	**0.924**
6	16.6 m- 19.6 m	0.65	0.900	831.18	**0.486**

In Table 3, the fluctuating load and the resultant wind load without SSI effect is presented.

Table 3. The fluctuating and the resultant wind load without SSI effect

Section No	Between Heights	$V_{(10)}$	$M_w(b)$ (kNm)	G_w	w'(z)	w(z) (kN/m)	$\bar{w}(z)$+w'(z) **(kN/m)**
0	0 m - 3 m	31.447	143.135	1.633	0.419	0.758	**1.177**
1	3 m - 5 m	31.447	143.135	1.633	0.699	0.763	**1.461**
2	5 m - 8 m	31.447	143.135	1.633	1.118	0.738	**1.856**
3	8 m - 11 m	31.447	143.135	1.633	1.537	0.814	**2.351**
4	11 m - 14 m	31.447	143.135	1.633	1.956	0.877	**2.833**
5	14 m - 16.6 m	31.447	143.135	1.633	2.319	0.924	**3.243**
6	16.6 m- 19.6 m	31.447	143.135	1.633	2.739	0.486	**3.225**

3.2. ACI 307/98 Wind Loading With SSI

In Table 4, the calculation of the mean design wind speed by considering SSI effect is presented.

Table 4. The mean design wind speed with SSI effect

Section No	Between Heights	1. Mode Natural Period,T	V (m/s)	I	V_R (m/s)	**V(z) (m/s)**
0	0 m - 3 m	0.552	45.00	1.15	48.257	**26.125**
1	3 m - 5 m	0.552	45.00	1.15	48.257	**28.263**
2	5 m - 8 m	0.552	45.00	1.15	48.257	**30.385**
3	8 m - 11 m	0.552	45.00	1.15	48.257	**31.912**
4	11 m - 14 m	0.552	45.00	1.15	48.257	**33.120**
5	14 m - 16.6 m	0.552	45.00	1.15	48.257	**34.000**
6	16.6 m- 19.6 m	0.552	45.00	1.15	48.257	**34.881**

Also, in Table 5, the mean wind load calculated according to Eq.(3) with SSI effect is given.

Table 5. The mean wind load with SSI effect

Section No	Between Heights	$C_{dr}(z)$	d(z)	p(z)	$\bar{w}(z)$ **(kN/m)**
0	0 m - 3 m	0.65	2.500	466.26	**0.758**
1	3 m - 5 m	0.65	2.150	545.71	**0.763**
2	5 m - 8 m	0.65	1.800	630.71	**0.738**
3	8 m - 11 m	0.65	1.800	695.71	**0.814**
4	11 m - 14 m	0.65	1.800	749.35	**0.877**
5	14 m - 16.6 m	0.65	1.800	789.72	**0.924**
6	16.6 m- 19.6 m	0.65	0.900	831.18	**0.486**

In Table 6, the fluctuating load and the resultant wind load with SSI effect is presented.

Table 6. The fluctuating and the resultant wind load with SSI effect

Section No	Between Heights	$V_{(10)}$	$M_w(b)$ (kNm)	G_w	w'(z)	w(z) (kN/m)	$\bar{w}(z)$+**w'(z) (kN/m)**
0	0 m - 3 m	31.447	143.135	2.249	0.577	0.758	1.335
1	3 m - 5 m	31.447	143.135	2.249	0.962	0.763	1.724
2	5 m - 8 m	31.447	143.135	2.249	1.539	0.738	2.277
3	8 m - 11 m	31.447	143.135	2.249	2.116	0.814	2.930
4	11 m - 14 m	31.447	143.135	2.249	2.693	0.877	3.570
5	14 m - 16.6 m	31.447	143.135	2.249	3.193	0.924	4.117
6	16.6 m- 19.6 m	31.447	143.135	2.249	3.770	0.486	4.256

3.3. Comparison of Wind Loads

From the comparison of Tables 2 and 5, it is clear that the mean wind load is not dependent on the soil parameters and the dynamic characteristics of the structure according to ACI 307/98. In another words, the mean wind loads calculated for all sections according to ACI 307/98 are same with and without SSI effect. However, this is not the case for fluctuating wind loads calculated according to ACI 307/98. It is clear from Tables 1 and 4 that the first mode periods and the resultant fluctuating wind loads are different for the cases with and without SSI. This is because of the reason that the parameter G_w includes the first mode period value of the

structure. In Fig.3, the resultant wind loadings for all sections with and without SSI effect according to ACI 307/98 is presented.

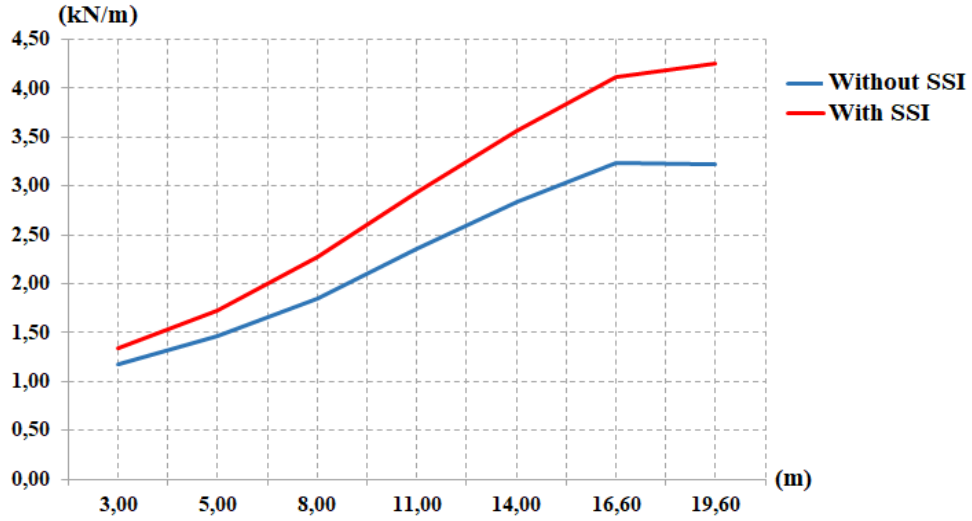

Figure 3. The comparison of total wind load for all sections according to ACI 307/98

4. Results and Discussion

This study provides a comparison for the wind loading of a representative minaret according to ACI 307/98 with and without SSI effects. In order to do that the underlying soil was produced by using viscous dampers which is a generally preferred method in modelling the interaction between the soil and structure. For all sections (*between 0-19.60 meters*), it is clear from the calculations that the wind loadings obtained from the representative minaret model that has underlying soil is higher than the ones that has no soil effect. This showed that the importance of considering the interaction between soil and the structure. Also, according to ACI 307/98, although the mean wind loads obtained are same for the representative minaret model with and without SSI effect, the fluctuating wind loads are different. This is because of the reason that the fluctuating wind load includes the effect of dynamic response of the structure i.e. the first mode period. Therefore, the total wind loads obtained for all sections are different because of the differences in fluctuating wind loads.

Acknowledgment

This study is dedicated to venerable memory of our light, great scientist and a honorable person Prof. Dr. Ing. Ahmet DURMUŞ whom we lost in 07.03.2017.

References

ACI (American Concrete Institute) (1998). ACI 307/98 with Commentary. Design and Construction of Reinforced Concrete Chimneys. ACI: Farmington Hills, MI.

ASCE (American Society of Civil Engineers) (1996). ANSI/ASCE 7-95 Minimum Design Loads for Buildings and Other Structures. ASCE: New York, NY.

Doğangün, A., Acar, R., Livaoğlu, R., and Tuluk, İ., (2006, April). Performance of Masonry Minarets against Earthquakes and Winds in Turkey. *1st International Conference on Restoration of Heritage Masonry Structures*. Cairo: Egypt.

Doğangün, A., Acar, R., Sezen, H., and Livaoğlu, R., (2008). Investigation of dynamic response of masonry minaret structures. *Bulletin of Earthquake Engineering*, 6(3), 505-517.

Livaoğlu, R., and Doğangün, A., (2007). Effect of foundation embedment on seismic behavior of elevated tanks considering fluid–structure-soil interaction. *Soil Dynamics and Earthquake Engineering*, 27(9), 855-863.

Lysmer, J., and Kuhlemeyer, R. L., (1969). Finite dynamic model for infinite media, *Journal of the Engineering Mechanics Division*, 95(4), 859-878.

Muvafik, M., (2014). Field investigation and seismic analysis of a historical brick masonry minaret damaged during the Van Earthquakes in 2011. *Earthquakes and Structures*, 6(5), 457-472.

Pekgökgöz, R. K., and Taş, G., (2017). Ayarlı Kütle Sönümleyicili Yüksek Minarelerin Dinamik Analizi. *Gazi Üniversitesi Mühendislik-Mimarlık Fakültesi Dergisi*, 32(1), 265-282.

Sezen, H., Acar, R., Doğangün, A., and Livaoğlu, R., (2008). Dynamic analysis and seismic performance of reinforced concrete minarets. *Engineering Structures*, 30, 2253-2264.

Temüz, H. T., (2007). *Minarelerin rüzgar yükleri altında davranışlarının incelenmesi ve bunların rüzgara göre hesabı*. Yüksek Lisans Tezi, Karadeniz Teknik Üniversitesi, Fen Bilimleri Enstitüsü, Trabzon.

Türkeli, E., (2014). Determination and comparison of wind and earthquake responses of reinforced concrete minarets. *Arabian Journal for Science and Engineering*, 39(5), 3665-3680.

Türkeli, E., Livaoğlu, R., and Doğangün, A., (2015). Dynamic response of traditional and buttressed reinforced concrete minarets. *Engineering Failure Analysis*, 49, 31-48.

URL-1:http://www.haberturk.com/gundem/haber/1041867-izmirde-firtina-36-metrelik-minareyi-devirdi, (Erişim Tarihi: 02 Nisan 2018).

Wilson, E.L. (2000). Sap 2000: Integrated Finite Element Analysis and Design of Structures. Computers & Structures: Berkeley, CA.

Forecasting of Annual Mean Rainfall Using Artificial Neural Network and Wavelet Components: Case of Study Sinop

Utku ZEYBEKOĞLU[1*]

[1]Sinop University, Boyabat Vocational School of Higher Education, Department of Construction, Boyabat-Sinop, Turkey

[*]**Corresponding Author:** utkuz@sinop.edu.tr

Abstract

In this study, it is aimed to forecast the annual mean precipitation using feed forward back propagation artificial neural network and wavelet transform methods. For this purpose annual mena precipitation values of Sinop meteorological station between 1966 and 2015 were used. In the first part of this study, annual mean precipitation values for the following years were tried to be forecasted by usinmg annual mean rainfall values from previous years. In the second part of the stud, the annual mean precipitation from previous years was converted to wavelet transforms and divide into sub time series. These componenets were used as inputs to the artificail neural network system to try to forecast the annual mean precipitation for the following years. More succesful results have been obatrined in artificial neural network models using wavelet transform.

Keywords: Wavelet transform; Artificial neural network; Precipitation; Forecasting.

1. Introduction

Rainfall from hydrological cycle elements is of great importance for water resources engineering. Precipitation has many effects on human life. When deficiency is expressed as drought, extreme conditions are expressed as flood. It is necessary to estimate a complex structure and the precipitation influenced by various factors. For this reason, it is very important to predict the precipitation properly when planning and using water constructions.

Artificial neural networks are widely used in predicting hydrologic cycle elements. (Wu, et al.2010, Kashid and Maity, 2012, He et al.2015) A number of artificial neural network based methods have been used in the literature to predict precipitation by researchers. Hall (1999) used artificial neural networks to predict rainfall in the United States. Partal et al (2008) has estimated the rainfall at the three stations in Turkey using artificial neural network and wavelet transform. Partal and Kişi (2007) used wavelet transform with fuzzy artificial neural network. Partal and Cıgızoglu (2009) have made precipitation prediction using wavelet transform and artificial neural network methods. Saplioglu and Çimen (2010) estimated the daily precipitation using artificial neural networks. Partal et al. (2015) combined rainfall prediction with three different artificial neural networks and wavelet transform methods. The best result is obtained by using feed forward back propagation artificial neural network. Shenify et al (2016) genetic programming has predicted precipitation using wavelet transform support vector machines and wavelet transform. Cihangir and Büyükyıldız (2018) made precipitation forecasts using three different artificial neural networks.

In this study, it is aimed to estimate Sinop meteorology station data using artificial neural networks and wavelet transform.

2. Materials and Method

2.1. Materials

In this study, annual mean precipitation heights of the Sinop meteorological station for the period 1966-2015 were used.

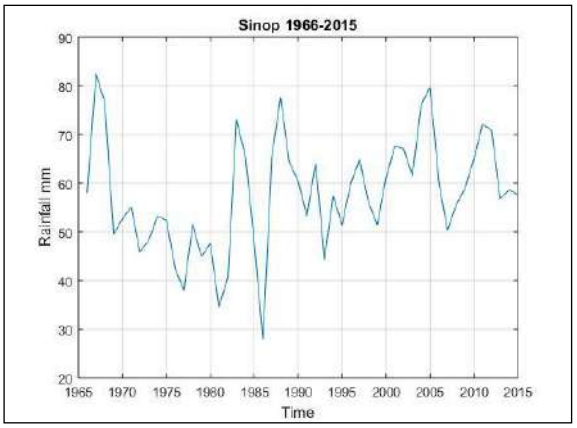

Figure 1. Annual mean precipiation of Sinop

2.2. Artificial Neural Networks

Artificial neural networks (ANN) are defined as complex systems that connect to each other with different connection geometries of artificial nerve cells that are inspired by nerve cells in the human brain. Artificial neural networks can be described as a black box that produces output in response to input. (Kohonen 1988).

ANN develops a solution system by educating itself on the examples given to it. This method does not have some predefined ideas about how the model will have a structure or work. The modeler has control over the data inputs and the irrelevant variables can be determined or can be extracted in the modeling process.

In this study, ANN method with feed forward back propagation algorithm will be used. This ANN method has three different units: input, hidden and output units. Each unit is composed of many neurons and units are connected by weight groups.

Neurons in the same section are not allowed to communicate. The forward feed backpropagation algorithm consists of two ettors. The first is a forward feed port for forwarding the external input information in the input neurons to calculate the output information signal in the output unit. The second is a backward step in which changes are made to the linking forces based on the differences between the information signals calculated and observed in the output unit. At the beginning of a training session, linking forces are assigned as random values. The learning algorithm changes the strength in each iteration until training is completed successfully. (Cığızoğlu, 2004).

A three-unit learning network consisting of an input, a secret and an output unit is shown in Fig 2. There are a large number of neurons in the input unit and a single neuron in the output unit. In input neurons, x_i, i = 1, ..., k are input values. Input values are multiplied by the first

interconnection weights w_{ij}, j = 1, ..., h in hidden neurons, and the results are summed along the i index and are inputs of hidden units.

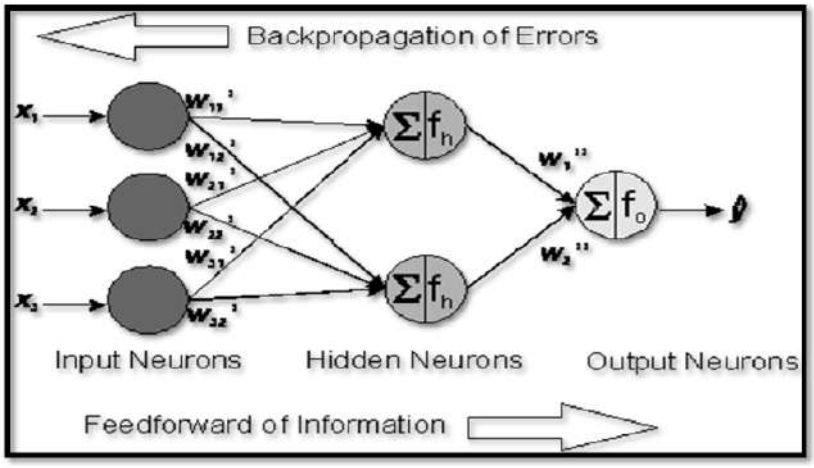

Figure 2. Feed forward back propagation ANN

$$H_j = \sum_{i=1}^{k} w_{ij} x_i \; ; \; j = 1, \dots, h \tag{1}$$

where H_j is the input of the hidden node j, and w_{ij} is the weight of the connection from the i neuron to the j neuron. Each hidden neuron produces a secret neuron output, HO_j, with the aid of a sigmoid function. HO_j is defined as:

$$HO_j = f(H_j) = \frac{1}{a + exp[-(H_j + \theta_j)]} \tag{2}$$

where Hj is the input of the neuron, $f(H_j)$ is the neuron output, and θ_j is the baseline or sagittal value. The initial value, θ_j, will be learned in the same way as weights. The output of HO_j is the input of the next unit. The input to the output neurons is as follows:

$$IO_n = \sum_{j=1}^{h} w_{jn} HO_{jn} \; ; n = 1, \dots, m \tag{3}$$

These input values are processed by the previously defined sigmoid function to obtain neural network output values. Subsequent weight adjustment or learning process is provided by

a backward advance algorithm. Output values and target values will not be the same. The mean square error between the output values and the target values is calculated. The backward forward algorithm is the iteration of the mean square error of the objective to the smallest. For this purpose, the error gradients calculated with the mean square error are distributed equally to the input weights, the input weights are updated and the process is restarted. These operations are repeated until the mean square error is reduced to a minimum or a certain number of iterations. (Cığızoğlu, 2004).

2.3. Wavelet Transform

A wavelet is a limited vibration signal that can be defined as a small piece of a waveguide. (Partal 2007) Wavelets are mathematical functions that operate on components that separate the data into different frequency components and then have a resolution that is paired with their own scale.

Wavelet transform is a method that allows the sign to be examined both in time and frequency. The sign is multiplied by a function that can be shifted in time, called a wavelet in the continuous wavelet transform, whose width can be changed. During the analysis, step-by-step traversal is provided and coefficients are obtained by multiplying the wavelet and the signal at that step in each step. The continuous wavelet transform (CWT) operation is expressed as follows.

$$CWT_x^{\psi}(\tau, s) = \psi_x^{\psi}(\tau, s) = \frac{1}{\sqrt{|s|}} \int x(t)\psi\left(\frac{t-\tau}{s}\right) dt \tag{4}$$

$$\psi_{\tau,s} = \frac{1}{\sqrt{s}}\psi\left(\frac{t-\tau}{s}\right) \tag{5}$$

Here CWT is a function of τ (displacement) and s (scale) parameters. ψ(t) is the transform function and is called the main wavelet function. x(t) is the sign to be analyzed. Subwindow functions with different widths used in the transformation are also derived from the main wavelet by scaling. The translation term refers to the location of the window used in the Short Fourier Distribution. The window is moved over the mark. Time information is provided with translation from transformation. The scale parameter (s) is defined as 1/frequency. By multiplying the wavelet function by the sign, the coefficient of wavelet transformation is obtained. Wavelength coefficients can only be calculated at selected scales and time periods.

At this point, there are fewer but more coefficients that give the frequency-scale information change over time. It is the binary scale and time step used in discrete wavelet transform. Each component thus obtained gives the time series or wavelet coefficients of the scale values in such a way that they are multiples of two and two. The wavelet function used for discrete wavelet transform is given below.

$$\psi_{m,n}\left(\frac{t-\tau}{s}\right) = s_0^{-m/s}\psi\left(\frac{t-n\tau_0 s_0}{s_0^m}\right) \quad (6)$$

where m and n are integers, the order of the wave, and the displacement parameters on the scale and time axis. S_0 refers to a constant translation step and this operation is taken as 2. τ_0 gives the value of the drift interval on the time axis and the value is taken as 1. The wavelet function generated using the folds of the second can be described as follows. (Mallat, 1989).

$$\psi_{m,n}(t) = 2^{-m/2}\,\psi(2^{-m}t - n) \quad (7)$$

The discrete wavelet transform for a time series x(t) with an i discrete step can be defined as follows ($W_{m,\,n}$, s= 2^m scale and $\tau = 2^m$ n wavelet transformation coefficients with time values).

3. Results and Discussion

In the study of the annual average precipitation belonging to the Sinop meteorological station using artificial neural network and wavelet transform, precipitation data are separated into components using discrete wavelet transform. This way it is possible to obtain components in different periods. Daubechies wavelet function is used as the main wavelet function in the study. With this method, the flow data is divided into 5 details (2-4-8-16-32) and 1 approximate component. Detail components begin at a 2-year scale and continue in multiples of 2. D1 is the component at the 2-year scale with the highest frequency resolution and D5 is the component at the 32-year scale with the lowest frequency resolution. Each component is a component representing the observed rainfall series and showing its different characteristics. Correlation coefficients between each wavelet component and observed rainfall data were calculated and presented in Table 1.

Table 1. Correlation coefficients between each wavelet component and observed rainfall data

Wavelet Component	Scale	Correlation
D1	2	0.41
D2	4	0.63
D3	8	0.40
D4	16	0.38
D5	32	0.45
APP	-	0.45

The table indicates that the highest correlated component is D2 and the lowest correlated component is D4. The correlation between the new series (D1 + D3 + D5) and the observed precipitation series obtained by the addition of the components except the components with the highest and lowest correlations was 0.69. This value is higher than the component with the highest correlation, and this series is preferred as the input of the Artificial Neural Network model. Different combinations of artificial neural network model were applied as inputs. These combinations are presented in Table 2.

Table 2. ANN input combinations

Model	Combinations	Model	Combinations
M1	P_{t-1}	W-M1	W-P_{t-1}
M2	P_{t-1},P_{t-2}	W-M2	W-P_{t-1},W-P_{t-2}
M3	P_{t-1},P_{t-2},P_{t-3}	W-M3	W-P_{t-1},W-P_{t-2},W-P_{t-3}

Models using 1 year earlier (P_{t-1},W-P_{t-1}), 2 years earlier (P_{t-1},P_{t-2}/W-P_{t-1},W-P_{t-2}), and 3 years earlier (P_{t-1}, P_{t-2}, P_{t-3}/ P_{t-1}, P_{t-2}, P_{t-3}) were used in the artificial neural network model, using wavelet transform and not using it, as seen in the table. Values between 1966 and 2000 were used for training of artificial neural network models and values for 2001-2015 were used to test artificial neural network models. The statistical values for the training and test data are given in table 3.

Table 3. Statistical information on training and testing data

Data	Mean (mm)	Standard Deviation (mm)	Skewness Coefficient (mm)
Train 1966-2000	54.85	11.94	0.22
Test 2001-2015	63.89	7.95	0.40

The correlation coefficient (R), the coefficient of determination (R^2), the mean absolute error (MAE) and the square root mean squared error (RMSE) performance criterion were chosen as the criterion for evaluating the relationship between the predicted values obtained at the test phase of the model and the observed precipitation values.

Prepared combinations were applied using various artificial neural networks. Implementation results are presented in Table 4 using the determined error assessment criteria.

Table 4. Model results

Model Structure	Model	MAE	RMSE	R	R^2	Model	MAE	RMSE	R	R^2
1-2-1	**M1**	5.91	7.86	0.59	0.35	**W-M1**	3.16	3.80	0.80	0.64
1-3-1		4.27	5.58	0.61	0.37		3.01	3.62	0.84	0.71
2-2-1	**M2**	4.98	6.57	0.69	0.48	**W-M2**	3.10	3.44	0.85	0.72
2-3-1		3.80	4.87	0.73	0.53		2.98	3.25	0.87	0.76
3-2-1	**M3**	4.90	6.33	0.70	0.49	**W-M3**	2.81	3.24	0.87	0.76
3-3-1		3.08	4.08	0.80	0.64		2.45	3.16	0.88	0.77

As seen in Table 3, annual average precipitation values were estimated using different artificial neural network models using and without wavelet transform.

In models prepared without wavelet transform, M3 input model 2 neuron and 3 neuron models gave the best results and more effective results were obtained by using M3 (3-3-1) structure. The scatter diagram of structure M3 (3-3-1) is given in Fig 2.

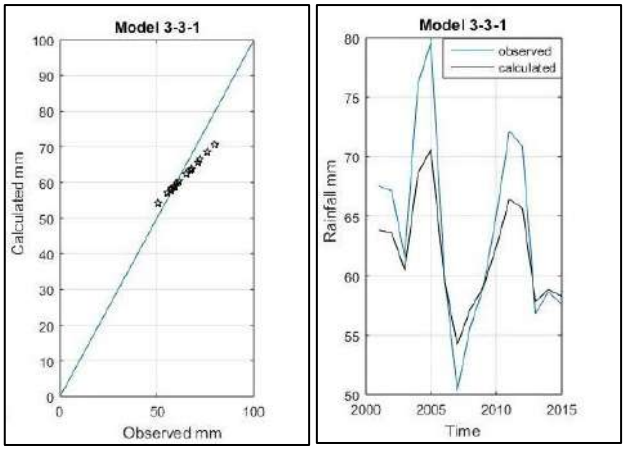

Figure 2. Diagrams of structure M3

For models prepared using wavelet transform, the W-M3 input model gives the best result. It has been determined that the results of the 2 and 3 neuron structures of this model are

close to each other. The scatter diagram and precipitation estimation results for model W-M3 (3-3-1) are given in Fig 3.

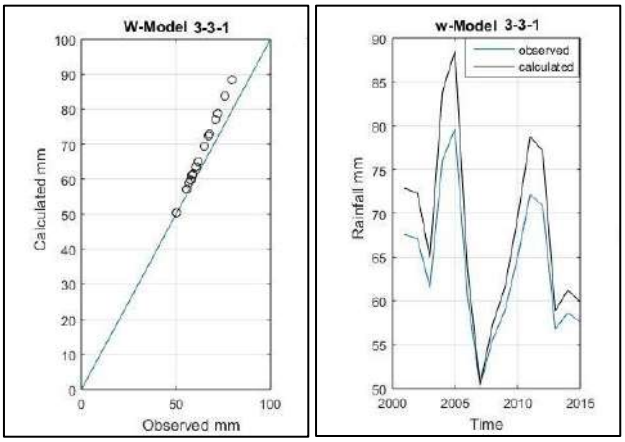

Figure 3. Diagrams of structure W-M3

4. Conclusion

In this study, it is aimed to estimate annual mean rainfall using artificial neural networks and wavelet transform methods. Firstly, the annual mean precipitation values are divided into compounds by wavelet transform at various frequencies. A new series was prepared by examining the correlation value of each component. The new series was obtained by the addition of selected components. This series is used in prediction studies using wavelet transform. On the other hand, estimating studies have been carried out without applying the wavelet transform. Models using wavelet transforms showed better results. In further studies, it is considered that different hydrological and meteorological parameters are applied by using different models.

References

Cigizoglu, H., K. (2004). Estimation and forecasting of daily suspended sediment data by multi layer perceptrons. *Advances in Water Resorces*, 27, 185-195.

Hall, T. (1999). Precipitation forecasting using a neural network. Weather Forecasting, 14, 338-345.

He,X., Guan, H., Qin, J. (2015). A hybrid wavelet neural network model with mutual information and particle swarm optimization for forecasting monthly rainfall. *Journal of Hydrology*, 527, 88-100.

Kashid, S.S., Maity, R. (2012). Prediction of monthly rainfall on homogeneous monsoon regions of India based on large scale circulation patterns using genetic programming. *Journal of Hydrology*,454-455,26-41.

Kohonen, T (1988). An introduction to neural computing. *Neural Networks*, 1,, 3-6.

Koycegiz, C., Buyukyıldız, M. (2018). Aylık toplam yağış tahmininde yapay sinir ağlarının kullanılması, *Uluslararası Su ve Çevre Kongresi*, 159-164, Bursa, Türkiye.

Mallat, S. G. (1989). A theory for multi resolution signal decomposition: The wavelet representation. *IEEE Transactions on Pattern Analysis and Machine Intelligence*, 11(7), 674-693.

Partal, T (2007). *Türkiye yağış miktarlarının yapay sinir ağları ve dalgacık dönüşümü yöntemleri ile tahmini*. Doktora tezi, İTÜ Fen Bilimleri Enstitüsü, İstanbul.

Partal,T., Kişi, Ö. (2007). Wavelet and neuro-fuzzy conjuction model for precipitation forecasting. *Journal of Hydrology*, 342, 199-212.

Partal T., Cigioglu, H. K., (2009). Prediction of daily precipitation using wavelet-neural networks, *Hydrological Science Journal*, 54(2), 234-246.

Partal, T., Cigizoglu, H.K., Kahya, E. (2008). Yağış verilerinin yapay sinir ağları ve dalgacık dönüşüm yöntemleri ile tahmini, *itüdergisi/d mühendislik*,7(3),73-85.

Partal, T., Cigizoglu, H.K., Kahya, E. (2015). Daily precipitation predictions using three different wavelet neural network algorithms by meteorological data. *Stochastic Environmental Research and risk Assessment*, 29(5),1317-1329.

Saplıoglu, K., Çimen, M. (2010). Predicting of daily precipitation using artificial neural network, *Journal of Engineering Science and Design*,1(1),14-21.

Shenify, M., Danesh, A.S., Gocic, M., Taher, R.S., Abdul Wahabb, A.W., Ghani, A., Shamshirband, S., Petkovic, D. (2016). Precipitation estimation using support vector machine with discrete wavelet transform. *Water Resources Management*, 30(2), 641-652.

Wu, C.L., Chau, K.W., Fan, C. (2010). Prediction of rainfall time series using modular artificial neural networks coupled with data-preprocessing techniques, *Journal of Hydrology*,389(1-2),146-167.

A Study on Application of Performance Analysis to New Structures

Ali DOĞAN [1], Nurullah KARACA [2*], Tülin KARADENİZ [3]

[1,2,3] Iskenderun Technical University, Faculty of Engineering and Naturel Sciences, Civil Engineering Department, Iskenderun, Turkey; ali.dogan@iste.edu.tr

[*] **Corresponding Author:** nurullah.karaca@iste.edu.tr

Abstract

In our country, the population is increasing day by day. As a result, people's need for shelter is increasing. In order to meet the increasing housing needs, various projects are being carried out. In these projects, various problems are encountered during application. In order to solve these problems, various modifications are needed. There is no obligation to perform performance analysis in new construction. Therefore, there is not enough information about the performance analysis of the build. This makes it difficult for us to understand how efficient and economical the strengthening of the new structure will be in future modifications. In this study, it was emphasized that performance analysis should be done in new projects and the necessity of providing safety or immediate use levels according to purpose of use. Even if it is a new project, it is desirable to emphasize the necessity and importance of performance analysis.

Keywords: Performance analysis, New buildings, Reinforced concrete strengthening.

1. Introduction

In our country which is located on one of earth's important seismic zones, destructive earthquakes occurred in very short time intervals and many reinforced concrete structures were damaged. The purpose of this study is to evaluate earthquake performances of low and medium height reinforced concrete buildings, which constitute a large part of the country, which has a high earthquake risk, according to the Regulation on Buildings to be Constructed in Earthquake Regions.

In the new construction, the construction of the reinforced concrete project and the regulations specified in the regulations are sufficient so that the project can be applied. However, it is also important that the project of the build has provided a performance analysis target criterion for its intended use. Because, new structures will provide the target criteria for performance analysis when they enter renovations.

At first, if the build project does not provide the performance analysis criteria, it will not be possible to perform the performance analysis as a result of the changes that will take place in the modified structure. As a result, reinforcement will be required in the structure. This is an undesirable situation in the new structure. Therefore, it is suggested to perform performance analysis in new construction. Researchers have done a lot of research on building reinforcement and building performance (Başaran, 2010; Coşgun, 2017; Doğan ve ark., 2017; İnel ve ark., 2007; Özmen 2011).

In new projects, performance analysis and providing safety or immediate use levels according to the purpose of use are important in terms of earthquake safety even if there is no modification in the construction. The project to be carried out contrasts with the directing for a project based on the 2007 earthquake directive, at least for the safety of the performance analysis. This contrast can be removed by performing a performance analysis on the newly constructed structure.

2. Material and Method

Performance-based strength and strengthening is an emerging issue in civil engineering today. The magnitude of the damage caused by the earthquakes that took place in our country and around the world necessitated the determination of the earthquake performances of existing buildings. To this end, the principles to be applied in the evaluation of the performance of existing and strengthened reinforced concrete buildings and building type structures under

earthquake effects in earthquake zones included in the 7th chapter of Turkish Earthquake Management 2007, principles to be taken as basis for strengthening decisions and reinforcement design principles of buildings which are decided to be strengthened are explained.

There are two important parameters in determining earthquake performance of constructions. Impact, demand or other name is demand and capacity. Demand is the action of earthquake, capacity is the behavior under this effect. At the moment when the capacity demands, the structure will be affected by less earthquake motion. In other words, the lower this rate, the less damage occurs.

Various methods are used to determine the damages in the buildings and to find the earthquake performance of the structure. These methods are divided into two groups of methods. These groups of methods are linear elastic and nonlinear methods.

Linear elastic methods are based on strength, and linear nonlinear methods are methods based on deformation and displacement.

In this study, analyzes were performed using linear elastic methods.

Linear methods used in seismic performance of buildings are based on strength and they are divided into two groups. These are the equivalent earthquake load method and mode combining method. There are some rules and principles that must be known in both of these methods before the account to be done with these methods is described. First, information must be collected from the station.

It is also necessary to know the extent of damage that may occur in the sections of the elements of the building before the solution is passed using the calculation methods. If the element is damaged, it will be determined according to the most damaged section of the element.

But there are two types of fracture in the structure. One is ductile and the other is brittle. For ductile fracture type, there are 3 damage limits. These are Minimum Damage Limit (MN), Safety Limit (GV) and Failure Limit (GÇ).

The minimum damage limit defines the beginning of the transverse elastic behavior of the relevant section. The safety limit defines the limit of the supersonic behavior that can safely provide the strength of the cross-section. The failure limit defines the limit of the pre-migration behavior of the cross-section. This classification does not apply to brittle damaged members.

Critical cross-section failing elements Non-reaching MN In the Minimum Damage Zone, the elements between MN and GV In the Apparent Damage Zone, the elements between GV and GC In the Advanced Damage Zone, the GC exceeding elements are located in the Failure Zone . Figure 1. shows the extent of this damage.

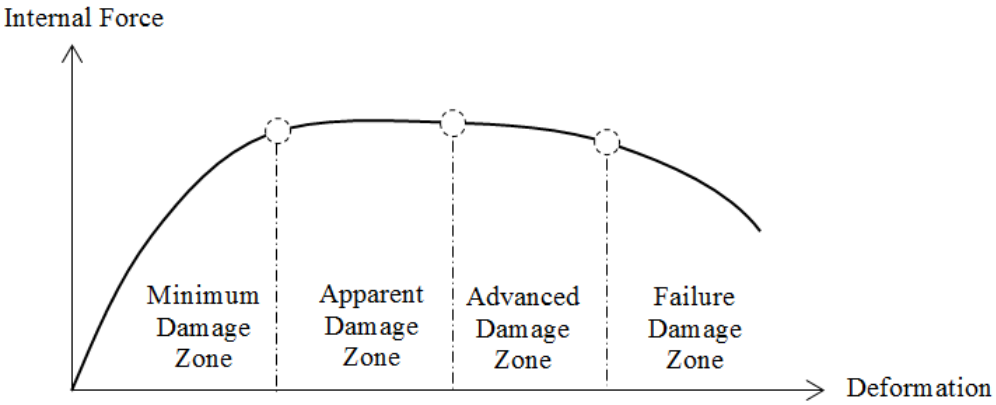

Figure 1. Damage boundary zones.

2.1. Determination of Earthquake Performances of Buildings By Linear Methods

As mentioned earlier, the linear elastic calculation methods to be used for determining the seismic performances of the buildings are the equivalent seismic load and mode joining methods. The following additional rules apply to these methods.

Equivalent seismic load method shall be applied to the building with a total height of 25 meters on the basement and a torsional irregularity coefficient ηbi <1.4, which does not exceed a total number of floors of 8 and which does not include additional external centering.

Ra = 1 will be taken in the calculation by Mode Joining Method. The internal force directions obtained in the mode dominated in this direction shall be taken as the basis of the internal forces and capacities of the elements compatible with the earthquake direction and direction applied.

Regardless of the two methods used to determine the level of damage to building elements of reinforced concrete buildings, the following principles are taken into consideration for determining the earthquake performance.

Numerical values expressed as impact / capacity ratios (r) of beams, columns, curtain members and reinforced filler walls are used in determining the damage levels of reinforced concrete ductile elements by linear elastic calculation methods.

Reinforced concrete elements are classed as "ductile" for fracture type, and "brittle" for shear type. Classification of ductile and brittle elements can be done as follows;

(a) In order that the columns, beams and curtains can be counted as ductile elements, it is necessary that the shear force Ve calculated in accordance with the bending capacity in critical sections of these elements does not exceed Vr, which is calculated according to TS-500 using existing material strength values in accordance with the information level. Ve's account shall

be made according to the sections specified in the regulation for columns, beams and curtains, but the shear force dynamic magnification coefficient βv = 1 shall be taken on the curtains. In columns, beams and curtains, the bearing moment moments will be used instead of the consolidation bearing moment moments in the calculation of Ve. If the total shear force calculated from the earthquake using Ra = 1 with vertical loads is smaller than Ve, then this shear force will be used instead.

(b) Reinforced concrete elements which do not satisfy the ductility requirements given above shall be defined as elements that are brittle.

The effect / capacity ratio of the ductile beam, column and curtain sections is obtained by dividing the section moment calculated by taking Ra = 1 under the earthquake effect into the section residual moment capacity. The direction of the applied earthquake force shall be taken into account in calculating the ratio of impacts / capacities. Cross sectional capacity ratios can be calculated as follows:

The section residual moment capacity is the difference between the bending moment capacity of the section and the moment effect calculated at the section under vertical loads. The moment effect calculated under vertical loads in beam supports can be reduced by up to 15% compared to the redistribution principle.

2) The effect / capacity ratios of column and curtain sections can be calculated as described below.

Determination of effect / capacity ratios of columns and curtains by linear elastic methods; M_A is residual moment capacity, M_D is the moment generated by the vertical loads, M_E is the moment generated under earthquake loads, M_K is the moment capacity calculated according to the material strengths, N_A is the axial force corresponding to the residual moment capacity, N_D is the axial force generated by the vertical loads, N_E is the axial force that occurs under earthquake loads, N_K is the axial force corresponding to the cross-section moment capacity, r is the effect / capacity ratio, r_s represents the limit value of the effect / capacity ratio.

The residual moment capacity M_A and the corresponding axial force N_A are defined as follows:

$$M_A = M_K - M_D \quad (1)$$

$$N_A = N_K - N_D \quad (2)$$

The effect / capacity ratio of column or curtain can be defined as follows;

$$r = \frac{M_E}{M_A} = \frac{N_E}{N_A} \leq r_s \quad (3)$$

2.2. Steps to Determine the Earthquake Performance of Buildings by Mode Joining Method

The calculation steps of determining the earthquake performances of the buildings by modal combining method can be done in the following order;

a) First, information must be collected from the station. The level of knowledge related to this is determined. (Table 1).

Table 1. Information level coefficients for buildings.

Knowledge Level	Knowledge Level Coefficient
Limited	0.75
Middle	0.90
Comprehensive	1.00

b) The carrying capacities of all structural elements are determined according to the strength of the material. Safety factors are not applied to these strength values, but existing strengths are multiplied by knowledge level coefficients.

In the definition of the earthquake effect, an elastic (non-reduced) acceleration spectrum will be used. However, for different probabilities of overturning, changes to this spectrum as noted in the directive will be taken into consideration. The Building Importance Coefficient will not be applied in the earthquake calculation.(I =1.0).

c) In the analysis, effective bending stiffness $(EI)_e$ of the cracked section will be used in reinforced concrete elements subjected to bending effect. Unless a more precise calculation is made, the following values will be used for effective bending stiffness:

$N_D / (A_c\ f_{cm}) \leq 0.10$ if it is: $(EI)_e = 0.40\ (EI)_o$ (4)

$N_D / (A_c\ f_{cm}) \geq 0.40$ if it is: $(EI)_e = 0.80\ (EI)_o$

The axial pressure force, Linear interpolation can be performed for the intermediate values of N_D. N_D will be determined by a preliminary vertical load account where the total mass compliant loads based on the earthquake calculation are taken into account and the bending stiffness's of the cracked sections $(EI)_o$ are used. The vertical load account that makes up the initial condition for the earthquake account shall be rebuilt using the effective bending stiffness $(EI)_e$ obtained as described above, in accordance with the mass loadings based on the earthquake calculation.

The same stiffness's will be used for earthquake calculation.

d) In the mode combining method, the periodic account of the system is made. Mass participation rates and mode participation factors are calculated. From here, the forces acting on the system for each mode are determined without using the earthquake load reduction coefficient and the building importance coefficient, and the shear force is calculated using the mode coupling method. The calculated shear force should not be less than the shear force β calculated by the equivalent seismic load method. By considering the earthquake direction, the internal forces calculated for each mode are combined with the mode combining method and the internal forces arising in the elements as a result of the modal analysis are calculated. However, since the values in the square root always go out positively, the internal force sign of the elements is identical to the internal force sign of the active mode (mass participation rate high mode).

e) The bending moment values obtained under the earthquake load are divided by the residual bending moment capacity to calculate the effect / capacity ratios. These values for each element are compared with the limit values in the following charts. Thus, each element is determined to be in the state of damage.

g) For all boundary conditions in reinforced concrete column-beam joints, the shear forces acting jointly and calculated shall not exceed the shear strengths given in the directives. However, the existing concrete strength determined according to the level of information will be used. If the joint exceeds the shear strength of the shear force, the column-beam joint region will be defined as the element that is brittle.

h) After the damage zones of the elements are determined, their total damage percentages occur. The level of performance of the building is determined according to the zones in which these damage percentages are located. In addition, control of relative floor drifts is carried out.

Observe the following when using boundary value charts;

Reinforced concrete columns, reinforced concrete beams and reinforced concrete beams that provide rules in directives in terms of transverse reinforcement conditions in the hull area

are considered "wrapped", while those that do not, "unwrapped" are considered. It is obligatory that the coiled fittings are arranged as "special earthquake stirrup" in the "wrapped" elements and that the cord spacing's comply with the conditions defined in the above mentioned articles.

The effect / capacity ratio of curtain walls and reinforced infilled walls that satisfy the condition of $H_w / \ell_w \leq 2.0$ is the ratio of the shear force calculated under earthquake effect to shear force strength. Here, H_w: floor height of the building, ℓ_w: expresses the height of the curtain.

The impact / capacity ratios (r) of the calculated beam, column and curtain wall sections and reinforced infilled walls will be compared to the limit values (r_s) to determine in which damage zone the elements are located. Linear interpolation will be applied for the intermediate values in the scales.

However, reinforced concrete curtains with Hw / ℓw> 2.0, (r_s) limit values will be reduced by multiplying by $[(1 + H_w / \ell_w) / 3] \geq 0.5$ coefficient.

Table 2. Impact / capacity ratios (rs) for reinforced concrete beams, which define the damage limits.

Ductile Beams			Damage Limit		
$\frac{\rho - \rho'}{\rho_b}$	Wrapped	$\frac{V_e}{b_w d\ f_{ctm}}$ (1)	**MN**	**GV**	**GÇ**
≤ 0.0	Available	≤ 0.65	3	7	10
≤ 0.0	Available	≥ 1.30	2.5	5	8
≥ 0.5	Available	≤ 0.65	3	5	7
≥ 0.5	Available	≥ 1.30	2.5	4	5
≤ 0.0	Not Available	≤ 0.65	2.5	4	6
≤ 0.0	Not Available	≥ 1.30	2	3	5
≥ 0.5	Not Available	≤ 0.65	2	3	5
≥ 0.5	Not Available	≥ 1.30	1.5	2.5	4

Table 3. Impact / capacity ratios (rs) for reinforced concrete columns, which define the damage limits.

Ductile Columns			Damage Limit		
$\frac{N_K}{A_c f_{cm}}$ (1)	Wrapped	$\frac{V_e}{b_w d\ f_{ctm}}$ (2)	**MN**	**GV**	**GÇ**
≤ 0.1	Available	≤ 0.65	3	6	8
≤ 0.1	Available	≥ 1.30	2.5	5	6
≥ 0.4 and ≤ 0.7	Available	≤ 0.65	2	4	6
≥ 0.4 and ≤ 0.7	Available	≥ 1.30	1.5	2.5	3.5
≤ 0.1	Not Available	≤ 0.65	2	3.5	5
≤ 0.1	Not Available	≥ 1.30	1.5	2.5	3.5

≥ 0.4 and ≤ 0.7	Not Available	≤ 0.65	1.5	2	3
≥ 0.4 and ≤ 0.7	Not Available	≥ 1.30	1	1.5	2
≥ 0.7	–	–	1	1	1

Table 4. Impact / capacity ratios (rs) for reinforced curtain walls, which define the damage limits.

Ductile Curtain Walls	Damage Limit		
The Curtain End Zone Wrapped	MN	GV	GÇ
Available	3	6	8
Not Available	2	4	6

After the damage zones are identified, the performance level of the structure must be determined.

2.2.1. Earthquake Performance Levels of Reinforced Concrete Buildings

The earthquake performance of the buildings is related to the state of the expected damage to the building under the effect of the earthquake applied and is defined on the basis of four different damage situations.

A) Immediate Use Performance Level

Any floor can account for up to 10% of the beams in the calculated Damage Zone for each applied earthquake direction, but all of the other bearing elements are in the Minimum Damage Zone. If so, it is assumed that the buildings in this situation are in the Immediately Use Performance Level, with the strengthening of the brittle damaged members.

B) Life Safety Performance Level

If so, the elements that are brittle damaged are considered to be in the Life Safety Performance Level of the buildings that have been strengthened and that satisfy the following conditions:

Any floor may pass up to 30% of the beams and up to the Advanced Damage Zone defined in paragraph (b) below, except for the secondary beams (not included in the horizontal load carrier system), calculated for each applied earthquake direction .

(b) The total contribution of the columns in the Forward Damage Zone to the shear force carried by each column should be less than 20%. The sum of the shear forces of the columns in the Forward Damage Zone on the top floor can be up to 40% of the sum of the shear forces of all the columns on that floor.

(c) All other bearing elements are in the Minimum Damage Zone or the Apparent Damage Zone. However, the shear forces carried by the columns exceeding the Minimum Damage Limit must not exceed 30% of the shear force carried by all the columns on that floor, in both of the upper and lower sections of any floor.

C) Pre-Failure Performance Level

Considering that all the elements that are severely damaged are in the Failure Zone, it is assumed that the Buildings that meet the following conditions are in the Pre-Failure Performance Level:

For each earthquake direction applied, no more than 20% of the beams can pass through the Failure Zone, except for the secondary (not included in the horizontal load system) beams at the end of the calculation.

(b) All other bearing elements are in the Minimum Damage Zone, the Apparent Damage Zone or the Advanced Damage Zone. However, the shear forces carried by the columns exceeding the Minimum Damage Limit must not exceed 30% of the shear force carried by all the columns on that floor, in both of the upper and lower sections of any floor. (Columns in which the strong column condition is provided at both lower and upper node points in the calculation by linear elastic method are not included in this account.)

(c) Use of the building in its present state is detrimental to life safety.

D) Failure Status

If the building does not provide the Pre-Failure Performance Level, it is in the Failure State. The use of the building is detrimental to life safety.

Performance levels according to percentage of damage in the building are given in the following charts (Table 5-6).

Table 5. 2007 According to TDY, the maximum allowable damage rates for beams.

Building Performance Level	Largest Damage Rates Allowance for Beams			
	Minimum Damage Zone	Apparent Damage Zone	Advanced Damage Zone	Failure
Immediate Use	%90	%10		
Life safety		%70	%30	
Failure Prevention		%80		%20

Table 6. 2007 According to TDY, the maximum allowable damage rates for columns.

Building Performance Level	Maximum Allowable Damage and Shear Strength Ratios for Columns			
	Minimum Damage Zone	Apparent Damage Zone	Advanced Damage Zone	Failure
Immediate Use	%100			
Life safety	Column Shearing Force Ratio.>%80 (Top Floor >%60)		Column Shearing Force Ratio <%20 (Top Floor <%40)	
Failure Prevention	Column Shearing Force Ratio >%80 (Top Floor >%60)			Column Shearing Force Ratio <%20 (Top Floor <%40)

2.3. Numerical Application

In the project of a building built in the province of Iskenderun in Hatay, various examinations and examinations were made. The construction of this project is 4 floors with a ground floor and 3 normal floors. Architectural project was first prepared. Then the mold plan was designed according to the architecture and the static-reinforced concrete projects were prepared. The mold plan was chosen hollow-tile floor slab. All columns are 30x50 cm in size. There is a lift curtain around the elevator. All mold plans are designed in the same way except for basement. With the aid of a computer program, information gathered from the building is modeled in the light. The generated model was analyzed dynamically on the computer. When these analyze was carried out, concrete class C25 used, steel grade S420 was chosen. The mode combining method is used as the analysis method.

In the first case of solution of the problem, dynamic analysis of the structure was applied. After the dynamic analysis of the structure, the structural carrier system elements were found to be sufficient and after this phase the performance analysis phase was passed. Because the building is new, comprehensive information level was selected and the life safety target criterion according to design earthquake was used because it is a housing structure.

As a result of the dynamic analysis, the building has been emigrated as a result of the building performance analysis which is sufficient as a system. In the build project, it is seen that when the problem is not seen in the X direction, that is, in the safety of the life, it is in the Y direction in the pre-crash and pre-crash performance. This data is presented via tables, as well as numerical results of performance analysis (Table 7).

Table 7. Strengthening performance summary report 1.

Strengthening Performance Summary Report		
Building Performance Evaluation		
Target Performance Level	LIFE SAFETY	
Building Performance Evaluation		
Earthquake Loading (+ X Direction)	LIFE SAFETY	√
Earthquake Loading (-X Direction)	LIFE SAFETY	√
Earthquake Loading (+Y Direction)	IMMEDIATE USAGE	√
Earthquake Loading (-Y Direction)	FAILURE	**X**

In the second case of the solution of the problem, the origin of the problem in the structure was researched and diagnosed. In the performance analysis results, it was determined that the migrant is originated from a beam (K216 beam). It was understood that this girder was the girder connecting the elevator section to the scene and the size of this weak girder was enlarged by increasing it to 25/32 denier 40/32. The analyzes were then repeated and it was found that the displacement occurred in the structure was corrected. Thus, the safety criterion is provided (Table 8).

Table 8. Strengthening performance summary report 2.

Strengthening Performance Summary Report		
Building Performance Evaluation		
Target Performance Level	LIFE SAFETY	
Building Performance Evaluation		
Earthquake Loading (+ X Direction)	LIFE SAFETY	√
Earthquake Loading (-X Direction)	LIFE SAFETY	√
Earthquake Loading (+Y Direction)	LIFE SAFETY	√
Earthquake Loading (-Y Direction)	LIFE SAFETY	√

In the second case of solution of the problem, although the safety criterion has been provided, the brittle elements have to be intervened because the structural bearing system elements PB3A, PB2A, PB05, PB07 are found to have a problem of brittle elements. In the

third case of the solution of the problem, the brittle elements were stirrup tightened. The analyze was then repeated.

In the fourth case of solving the problem, the contribution to the performance level of the column growth or the results of the analysis was investigated. In addition to the third case, column sizes were increased to 30/50 denier 30/70 and analyzes were repeated.

As a result, it can be seen from the tables that as a result of the performance analysis in the x direction, the damage of the column shear force decreases, there is no change in the y direction and the beam damage increases in both directions.

In the fifth case of the solution of the problem, only the column dimensions in the fourth case are enlarged, without beam amplification in the second case. Thus, it is desirable to investigate the effect of the enlargement of the beam (K216).

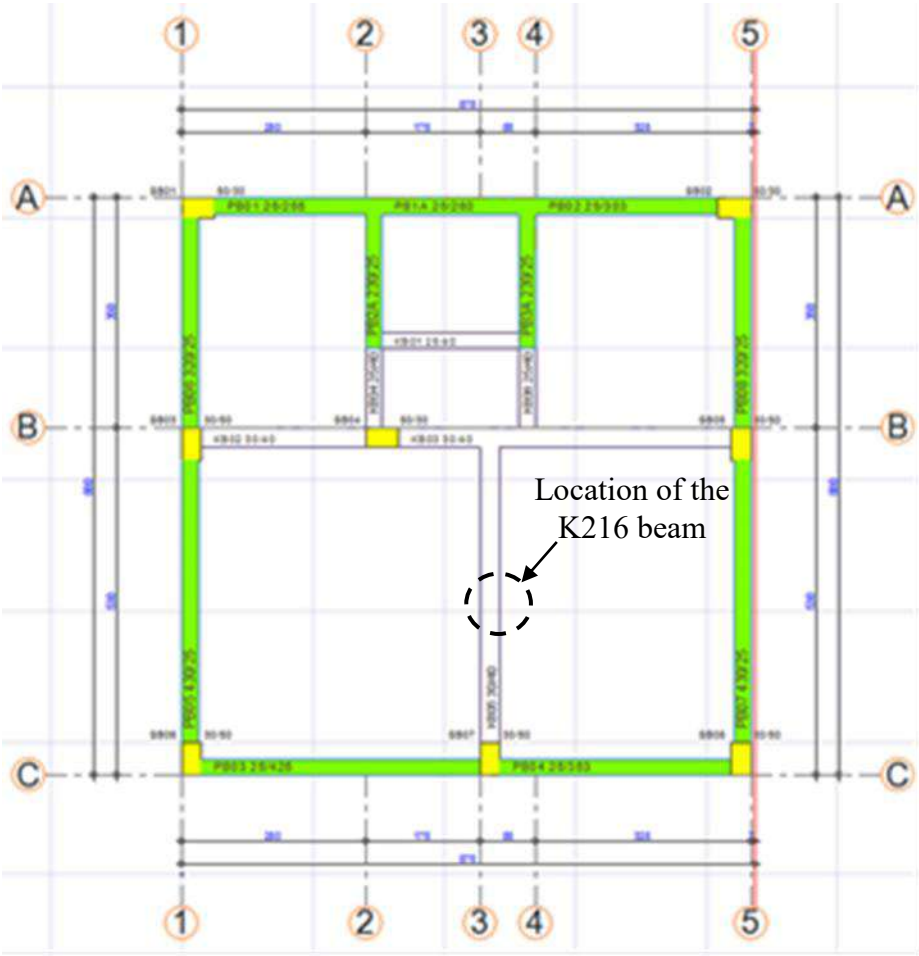

Figure 2. Building mold plan.

3. Results and Discussion

1. In the new construction, the problem should be identified first and only the problem of the problem element should be addressed.

2. The brittle elements in the structure should be stirrup tightened..

3. Increasing the column size at any time and in any way may not provide sufficient benefit for performance analysis.

4. Instead of enlarging all the columns in the structure, it is considered more economical to apply magnification to the structural system elements that are determined to be problematic as a result of performance analysis.

5. It is thought that it is necessary to perform the performance analysis in the new structures as well as in the old structures.

References

Başaran, A. B. (2010). Mevcut Bir Okul Binasının Artımsal Eşdeğer Deprem Yükü Yöntemi ile Deprem Performansının Değerlendirilmesi ve Güçlendirilmesi. Yüksek Lisans Tezi, İstanbul Teknik Üniversitesi, Fen Bilimleri Enstitüsü, İstanbul.

Coşgun, T. (2017). Yıkım Çalışması Nedeniyle Örnek Bir Yapıda Oluşan Yapısal Hasarlar ve Bu Hasarların Performans Seviyesine Etkisi. Sakarya Üniversitesi Fen Bilimleri Enstitüsü Dergisi, 21(5), 831-841.

Deprem Bölgelerinde Yapılacak Binalar Hakkında Yönetmelik, (2007, Mart). Bayındırlık ve İskan Bakanlığı, Ankara.

Doğan, A., Karaca, N., ve Karadeniz, T., (2017, Ekim). Yönetmeliklere Uygun Olarak Yapılmamış Bir Yapının 2007 Deprem Yönetmeliğine Göre Güçlendirilmesi Üzerine Bir Çalışma. 4. Uluslararası Deprem Mühendisliği ve Sismoloji Konferansı (s. 69-76). Eskişehir: Anadolu Üniversitesi

İnel, M., Bilgin, H. ve Özmen, H. B., (2007). Orta Yükseklikteki Betonarme Binaların Deprem Performanslarının Afet Yönetmeliğine Göre Tayini. Mühendislik Bilimleri Dergisi, 13(1), 81-89.

Özmen, H. B. (2011). Düşük ve Orta Yükseklikteki Betonarme Yapıların Deprem Performanslarını Etkileyen Faktörlerin İrdelenmesi. Doktora Tezi, Pamukkale Üniversitesi, Fen Bilimleri Enstitüsü, Denizli.

Optimum Design of Marine Discharge Pipeline and Diffusers by JAYA Algorithm

Nurcan ÖZTÜRK [1*]

[1] Karadeniz Technical University, Technology Faculty, Civil Engineering, Trabzon, Turkey; nurcan@ktu.edu.tr

[*] **Corresponding Author:** nurcan@ktu.edu.tr

Abstract

Pollutants in wastewater are rapidly reduced to harmless levels for the environment by means of marine discharge systems designed by considering scientific and engineering principles. The structures must be designed successfully and the cost must be optimized due to the increasing material and labor costs as well as the limited resources. In this study, the optimum design of marine discharge systems increasing prominence in recent years is performed minimum cost by using a metaheuristic algorithm known as JAYA. Parameters and variables such as discharge line diameter and length, discharge depth, size and diameter of diffuser are taken into account in the performed optimum design. In the optimization problem, the flow back state in the diffuser, the interference state between the wastewater jets and the stability of the pipeline are also examined.

Keywords: Optimization, Discharge, Minimum Cost, JAYA algorithm

1. Introduction

Marine discharge structures have been used for discharging wastewater to water media (seas, lakes, oceans). The concentration of pollutants can be drastically reduced by effectively diluting the pollutants in these wastes with marine discharges designed, built and operated properly. These structures reduce the adverse effects of pollutants on people, plants and animals using the marine environment (Tate et al. 2016).

Relations depending on diameter and flow have been developed for cost analysis of marine discharge systems. Apart from the cost of pre-treatment systems, major cost components for pipe (CTP, HDPE) lines are pipe supply, joining pipes on land, land pressure test, sea pressure test, transport of pipes at sea, connection of flanged pipes under water, grading trench floor with mounting pads, trench fill with crushed stone, manufacture and installation of sign float, detection mass, transportation, survey, engineering and consultancy services (Öztürk,2011).

While the realization of more economical designs of the past has been linked to the engineering preface, it has become commonplace to develop the optimization techniques and computers. When studies on the optimization of pipelines are examined, it is seen that different algorithms such as Teaching and Learning Based Optimization (TLBO) algorithm, multipurpose hybrid optimization algorithm, genetic algorithm, proportional differential algorithm are used (Rao, 2016; Fettaka and Thibault, 2013; Botros et al. 2004; Öztürk and Öztürk, 2018).

The JAYA algorithm is used in the literature for various purposes such as optimum design of minimum weight of steel truss structures, size and shape optimization of structures (Rao, 2016).

In this study, it is aimed to realize optimum design of a discharge pipe line with minimum cost by JAYA.

2. Material and Method

The algorithm (JAYA), “victory” in Indian language, is constantly approaching good solutions in order to achieve success, and away from bad solutions in order to get away from failure.

In this algorithm, as in other optimization algorithms, maximization or minimization of a goal function (f (x)) is targeted.

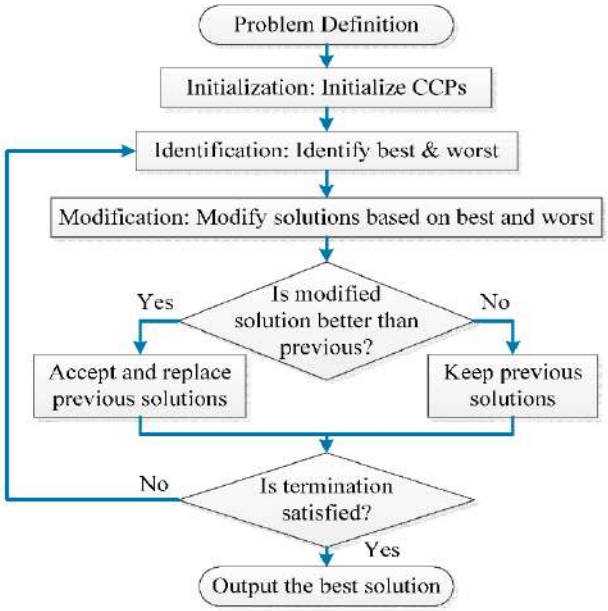

Figure 1. Flow chart of JAYA Algorithm (Rao, 2016)

The objective function consists of the cost determined by the diameter of the pipe used in the pipeline for optimum design of a discharge pipe line with minimum cost.

$$f(x) = (L_{boru} + b_{dif})\, M_{boru} \quad (1)$$

Table 1. Upper and lower limits, increments and number of available values of design variables

Design variables	Lower limits	Upper limits	Increments	number of available values
X_1	300 m	5000 m	50m	95
X_2	(110, 125, 140, 160, 180, 200, 225, 250, 280, 315, 355, 400, 450, 500, 560, 630, 710, 800, 900, 1000, 1200, 1400, 1600) mm			23
X_3	5	30	1	26

X_1 is discharge line length excluding diffuser length, X_2 is discharge pipe diameter and X_3 is number of outlets in diffuser.

3. Results and Discussion

In runs, 20 individuals were used in the algorithm and 100 independent runs with maximum objective function evaluation number 2020 were performed.

Table 2. Obtained values of design variables in optimum design

Design variables	Optimum value
X_1	700 m
X_2	450 mm
X_3	12

The statistic findings obtained from 100 independent runs of the algorithm concerning the minimum design costs and performance ratios.

Table 3. The statistic findings obtained from 100 independent runs of the algorithm concerning the minimum design costs and performance ratios

	JAYA
Lowest cost (₺)	363.245,108
Average cost (₺)	366.390,899
Highest cost (₺)	451.841,133
Standard deviation (₺)	15.488,167
Performance rate (%)	95

Table 4. The evaluation number of the objective function that the algorithm reaches to the optimum result

	JAYA
The number of best objective function evaluations	100
The number of average objective function evaluations	598,4
Highest number of objective function evaluations	2020
Standard deviation (₺)	358,2

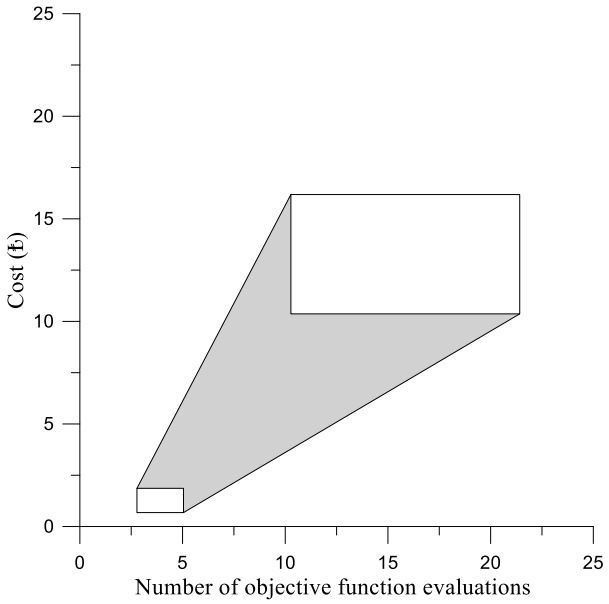

Figure 2. Average convergence graph

When the average cost values obtained from 100 parallel runs of the algorithm are examined, the lowest cost is 363.245,108₺.

The rate of success refers to the percentage of reaching the global optimum in parallel runs. In other words, the optimum result was achieved in 95 of 100 runs.

When the averages of the objective function values reached to the global optimum are examined, it is seen that the JAYA algorithm achieves the global optimum by evaluating the objective function 598.4 times on average.

4. Conclusion

At this work, the optimal design of the discharge pipe line to the sea was effectively performed by the JAYA algorithm.

Wastewater and its pollutants are diluted in the discharge environment and the necessary conditions in terms of public health and aesthetics are provided safely and economically with this design.

References

Tate, P. M., Scaturro, S. ve Cathers B., (2016). Marine Outfalls. In Springer Handbook of Ocean Engineering, Springer International Publishing, 711-740.

Öztürk, İ., (2011). Sea Outfall Plant Design. Water Foundation Publications, p. 458.

Rao, R., (2016). Jaya: A Simple and New Optimization Algorithm for Solving Constrained and Unconstrained Optimization Problems. International Journal of Industrial Engineering Computations, Vol. 7(1), 19-34.

Fettaka, S. and Thibault, J., (2013). Pipeline optimization using a novel hybrid algorithm combining front projection and the non-dominated sorting genetic algorithm-II (FP-NSGA-II). IEEE Congress on Evolutionary Computation, 697-704.

Botros, K.K., Sennhauser, D., Jungowski, K.J., Poissant, G., Golshan, H. and Stoffregen, J., (2004). Multi-objective optimization of large pipeline networks using genetic algorithm. Proceedings of the 5th Biennial International Pipeline Conference, 2005-2015.

Öztürk, N. ve Öztürk, H.T., (2018). Optimum design of marine discharge structures by Teaching Learning Based Optimization (TLBO), Technological Applied Sciences (NWSATAS), 13(3), 235-242. DOI:10.12739/NWSA.2018.13.3.2A0153.

AGRICULTURE

ORAL PRESENTATIONS

Effect of Skiffing at Different Times on Tea Quality Traits

Esra MURAT[1], Saim Zeki BOSTAN[2]

[1] Ordu University, Institute of Science, Department of Horticulture, Ordu, Turkey

[2] Ordu University, Faculty of Agriculture, Department of Horticulture, Ordu, Turkey

[*]**Corresponding Author:** szbostan@hotmail.com

Abstract

This study was carried out to determine the effect of skiffing at different times on tea quality characteristics (dry matter, total polyphenol, total ash, cellulose, extract, caffeine) at a farmer orchard in Of district (Trabzon province of Turkey) in 2015 and 2016 years. Experiment was set up out in completely randomized design with one factor and three replications. In the tea bushes, skiffing applications were made from 10 cm below the harvesting table in 8 different dates as 15 December, 1 January, 15 January, 1 February, 15 February, 1 March, 15 March and 1 April by pruning shears. The results showed that the quality traits were affected positively by skiffing applications in general.

Keywords:*Camelia sinensis*, Tea, Skiffing, Quality traits

1. Introduction

During the development season of the tea plant, the abundance of rain and the temperature must be enough for the shoots to form continuously. Otherwise, there will not be enough shoot growth and therefore the amount of product will decrease considerably (Kacar, 1987).

With the healthy growth of the tea plant, the ecological conditions are very important for obtaining quality and abundant crops (Kacar, 2010).

Also, cultural practices must be made in time to give tea plants abundant and good quality products (Mahmutoğlu, 1985a).

The most important factors affecting yield and quality are pruning, fertilization, and plant age, and climate, soil, harvesting in time and processing of harvested crop within the shortest time. Pruning is one of the cultural practices was made to controls growth and stimulates new growth, develop a sturdy framework (Mahmutoğlu, 1985 a and b).

Lighter forms of cuts given to the tea plants in between two consecutive prune years are called skiffing. Furthermore, skiffing may allow excess product load at tea factories in May to shift to other harvesting periods (Kacar, 2010).

This study was carried out to determine the effect of skiffing at different times on quality traits of fresh tea.

2. Material and Method

This study was carried out at a farmer orchard in Of district (Trabzon province of Turkey) in 2015 and 2016 years.

Experiment was set up out in completely randomized design with one factor and three replications.

In the tea bushes, skiffing applications were made from 10 cm below the harvesting table by pruning shears (Figure 1). Skiffing applications were made in 8 different dates as 15 December, 1 January, 15 January, 1 February, 15 February, 1 March, 15 March and 1 April. Tea leaves were harvested in three harvesting periods.

(a) Before skiffing (b) After skiffing

Figure 1. Skiffing application

Method for predicting tea harvest time that was stated by Yagi et al. (2010) was used. According to method, it was taken a frame (8 x 8 inches) and randomly place it on a harvestable surface (Figure 2). All the shoots and newly emerging leaves inside the frame were counted, and total number of leaves divided by total number of shoots and thus the average number of leaves per shoot was calculated. Harvest was done when the average leaf number was 3.

The dry matter, total polyphenols, total ash, cellulose, extract and caffeine analysis of fresh tea leaves that were harvested at each harvesting periods were made at the laboratory in Atatürk Tea and Horticultural Research Institute Directorate.

Figure 2. Determining of harvest time by frame

3. Results and Discussion

The results showed that the quality traits were affected by skiffing applications at different times.

Table 1. The variance analyse results for the effects of skiffing at different times on the traits at the first, second and third harvesting periods

Traits	First harvest period		Second harvest period		Third harvest period	
	F	P	F	P	F	P
Dry matter	9,0023**	<,0001	14,8607**	<,0001	5,3374**	0,0015
Polyphenol	8,8090**	<,0001	28,9246**	<,0001	10,3047**	<,0001
Total ash	8,1390**	0,0001	0,2256	0,9812	0,5272	0,8209
Cellulose	15,8997**	<,0001	1,6617	0,1764	5,3155**	0,0016
Extract	7,4619**	0,0002	8,0935**	0,0001	5,6051**	0,0012
Caffein	1,1727	0,3669	12,0543**	<,0001	10,2613**	<,0001

LSD: 0.05

**: Significant at probability level of 1%

The effects of skiffing at different times on dry matter content were found to be significant in each harvest periods (Table 2). The highest dry matter content values were determined at skiffing applications. Aşık Çuhadar (2015) determined the value of dry matter in fresh tea leaf at 22.86-27.67% on different tea clones.Kazdal (2017) determined the dry matter values of fresh tea leaf at 24.13-26.88% in the 1st period, 25.71-27.94% in the 2nd period and 25.83-26.87% in the 3rd period according to the harvesting periods.The values we have obtained in our study are similar to those in the literature.

Table 2. Dry matter contents (%) at harvesting periods with skiffing at different times

	Harvest Periods		
Skiffingdate	**First**	**Second**	**Third**
Control	23.47 c**	21.47 c**	20.71 b**
Dec. 15	28.33 a	24.14 ab	21.06 b
Jan. 1	**28.40 a**	23.21 b	20.65 b
Jan. 15	25.09 b	**24.87 a**	20.46 b
Feb. 1	25.47 b	24.67 a	20.45 b
Feb. 15	23.49 c	20.13 c	20.65 b
Mar. 1	23.47 c	20.73 c	20.37 b
Mar. 15	26.00 b	24.29 ab	**22.99 a**

Apr. 1	25.06 b	23.20 b	21.20 b
LSD	1.895	1.363	1.046

Means in the same column with different letters are statistically significant

** Significant at P= 0.01

The effects of skiffing at different times on polyphenol content were found to be significant in each harvest periods (Table 3). The highest polyphenol content values were determined at skiffing applications.Ravichandran (2004) found that the polyphenol value was increased after pruning; this value was 12.6% in pruning year, and showed a steady increase over the following years.In other studies, the polyphenol value was determined to be 9.24-13.99% (Aşık Çuhadar, 2015) and 1.31-21.67% (Turan et al., 2016), and Kazdal (2017) determined the dry matter values of fresh tea leaf at 12.59-15.84% in the 1st period, 21.66-26.14% in the 2nd period and 7.53-12.86% in the 3rd period.The results we have obtained in our study are parallel to those in the literature.

Table 3. Polyphenol contents (%) at harvesting periods with skiffing at different times

Skiffingdate	**Harvest Periods**		
	First	**Second**	**Third**
Control	12.34 d	12.34 d	16.29 bc
Dec. 15	14.44 bcd	14.44 bcd	20.04 a
Jan. 1	18.06 a	18.06 a	**21.55 a**
Jan. 15	16.64 ab	16.64 ab	16.46 bc
Feb. 1	**18.99 a**	**18.99 a**	15.98 bc
Feb. 15	12.12 d	12.12 d	20.42 a
Mar. 1	13.76 cd	13.76 cd	16.53 bc
Mar. 15	16.64 ab	16.64 ab	14.57 c
Apr. 1	15.14 bc	15.14 bc	17.10 b
LSD	2.423	2.423	2.211

Means in the same column with different letters are statistically significant

** Significant at P= 0.01

The effects of skiffing at different times on ash content were found to be significant only in first harvest period (Table 4). Ravichandran (2004) found that the ash value was 4.40% in the pruning year. In other studies, the ash value was determined to be 4.42-6.14% (Aşık Çuhadar, 2015) and 2.99-8.92% (Turan et al., 2016), and Kazdal (2017) determined the ash values at 5.07-5.37% in the 1st period, 5.04-5.37% in the 2nd period and 5.34-5.74 % in the 3rd period.The results we have obtained in our study are similar to those in the literature.

Table 4. Total ash contents (%) at harvesting periods with skiffing at different times

	Harvest Periods		
Skiffingdate	**First**	**Second**	**Third**
Control	5.49 a	5.17	5.06
Dec. 15	4.69 d	5.17	5.17
Jan. 1	4.90 cd	5.18	5.21
Jan. 15	4.94 cd	5.11	5.18
Feb. 1	5.04 bc	5.15	5.22
Feb. 15	4.94 cd	5.32	5.39
Mar. 1	5.45 a	5.30	5.32
Mar. 15	5.24 ab	5.03	4.99
Apr. 1	5.23 ab	5.19	5.23
LSD	0.280	-	-

Means in the same column with different letters are statistically significant

** Significant at P= 0.01

While the effects of different skiffing applications on total cellulose were not found to be significant at the second harvest period, the differences application were found to be significant in the first end third harvest periods (Table 5). The highest cellulose contents were obtained from control groups. Ravichandran (2004) found that the cellulose value was 13.7% in the pruning year. In other studies, the cellulose value was determined to be 8.02-16.00 % (Gürses, 1982), 18.39-22.47% (Aşık Çuhadar, 2015), 12.20-23.82% (Turan et al., 2016), and Kazdal (2017) determined the value at 14.79-16.84% in the 1st period, 14.91-16.95% in the 2nd period

and 16.85-16.28 % in the 3rd period. The results we have obtained in our study are similar to those in the literature.

Table 5. Cellulose contents (%) at harvesting periods with skiffing at different times

	Harvest Periods		
Skiffingdate	**First**	**Second**	**Third**
Control	17.00 a	12.83	18.13 a
Dec. 15	12.47 b	14.18	14.87 bc
Jan. 1	13.44 b	12.68	14.09 bc
Jan. 15	12.15 b	13.15	14.85 bc
Feb. 1	12.45 b	14.23	14.06 c
Feb. 15	13.45 b	13.61	14.87 bc
Mar. 1	12.34 b	14.14	15.51 bc
Mar. 15	10.07 c	14.91	15.73 b
Apr. 1	12.41 b	12.75	14.03 c
LSD	1.365	-	1.652

Means in the same column with different letters are statistically significant

** Significant at P= 0.01

The effects of skiffing at different times on extract content were found to be significant in each harvest periods (Table 6). While the highest extract content value in the first harvest period wasfound at control and Dec. 15, .the lowest values in the other harvest periods were found at controls. In other studies, this value was determined to be 28.36-35.88% Aşık Çuhadar (2015) and 12.40-38.81% (Turan et al., 2016), and Kazdal (2017) determined the dry matter values of fresh tea leaf at 35.58-44.91% in the 1st period, 35.65-37.52% in the 2nd period and 33.79-38.22% in the 3rd period. Our results are similar to those in the literature.

Table 6. Extract contents (%) at harvesting periods with skiffing at different times

	Harvest Periods		
Skiffingdate	**First**	**Second**	**Third**
Control	38.18 a	35.08 c	31.60 d

Dec. 15	39.59 a	34.71 c	33.48 bc
Jan. 1	35.04 b	35.03 c	34.05 b
Jan. 15	33.90 b	39.22 a	34.78 ab
Feb. 1	39.20 a	38.72 a	35.86 a
Feb. 15	34.86 b	39.72 a	32.16 cd
Mar. 1	39.45 a	36.17 bc	35.05 ab
Mar. 15	38.47 a	39.19 a	34.99 ab
Apr. 1	35.39 b	37.70 ab	33.41 bc
LSD	2.480	2.32	1.767

Means in the same column with different letters are statistically significant

** Significant at P= 0.01

The caffeine contents were found to be significant in second and third harvest periods (Table 7). Ravichandran (2004) found that the ash value was 4.40% in the pruning year. In other studies, the ash value was determined to be 4.42-6.14% (Aşık Çuhadar, 2015) and 2.99-8.92% (Turan et al., 2016), and Kazdal (2017) determined the ash values at 5.07-5.37% in the 1st period, 5.04-5.37% in the 2nd period and 5.34-5.74 % in the 3rd period.The results we have obtained in our study are similar to those in the literature.

The caffeine contents showed an irregular change according to skiffing dates. Öksüz and Demirci (1983) found that the value of caffeine varied between 0.5-3.4%. Ravichandran (2004) found that the cellulose value was 2.72% in the pruning year. Thomas et al. (2005) stated that there will be an increase in caffeine content after pruning. Aşık Çuhadar (2015) found that the value varied between 1.31-3.07%, and Kazdal (2017) determined the values at 2.22-2.50% in the 1st period, 2.20-2.62% in the 2nd period and 2.34-2.48% in the 3rd period. Our results are similar to those in the literature.

Table 7. Caffeine contents (%) at harvesting periods with skiffing at different times

	Harvest Periods		
Skiffingdate	**First**	**Second**	**Third**
Control	2.55	2.65 bc	2.38 c
Dec. 15	2.06	2.41 cd	2.46 c
Jan. 1	2.11	2.41 cd	3.09 a

Jan. 15	2.56	2.77 b	2.45 c
Feb. 1	2.22	2.52 bcd	2.75 b
Feb. 15	2.03	3.44 a	2.51 c
Mar. 1	2.27	2.66 bc	2.48 c
Mar. 15	2.15	2.31 d	2.34 c
Apr. 1	2.03	3.25 a	2.41 c
LSD	-	0.333	0.219

Means in the same column with different letters are statistically significant

** Significant at P= 0.01

According to these results;

- In general, we can say that the application of skiffing affects the quality characteristics that is to say that the skiffing practices which will be done to arrange the harvest will have a positive effect on the quality characteristics.
- In addition, it can be said that the skiffing application and the development of shoots were affected positively especially during the 2nd and 3rd shooting period, the banji formation decreased, the length of shoots increased and a more vivid appearance appeared in the tea.
- As a result, after this study which is a preliminary study on skiffing, it is beneficial to determine the changes of the criteria examined on a yearly basis and to expand and maintain the subject.

Acknowledgement

This is a part of Master Thesis. The authors would like to thank to the Ordu University Research Department (ODUBAP) (Ordu province of Turkey) for its financial support to the project of “TF-1613”, and to the Atatürk Tea and Horticultural Research Institute Directorate (Rize province of Turkey) for its laboratory analysis.

References

Aşık Çuhadar, B. (2015). Yaş ve kuru çayda, verim ve önemli kalite parametrelerine sarı çay akarı (*Polyphagotarsonemus latus* (banks, 1904)) (prostigmata: tarsonemidae)'nın etkisi. Yüksek Lisans Tezi, Ordu Üniversitesi, Fen bilimleri Enstitüsü, Bahçe Bitkileri Anabilim Dalı. Ordu.

Gürses, Ö.L. (1982). Mamül çaylarımızda ham selüloz miktarları ve kalite açısından incelenmesi. http://dergipark.gov.tr/download/article-file/78364 -(Erişim tarihi:16.03.2017).

Kacar, B. (1987). Çay Biyokimyası ve İşleme Teknolojisi. Nadir Kitap, 387 sayfa. Ankara.

Kacar, B. (2010). Çay Bitkisi Biyokimyası Gübrelenmesi İşleme Teknolojisi. Nobel Yayın, Yayın No: 1549, Fen Bilimleri: 107, Nobel bilim ve Araştırma Merkezi Yayın No: 64, 355 sayfa, Ankara.

Kazdal, N., (2017). Çayda (*Camelia sinensis*) önemli kalite özelliklerinin güneşlenme durumuna ve sürgün dönemlerine göre değişimi. Yüksek Lisans Tezi, Ordu Üniversitesi, Fen bilimleri Enstitüsü, Bahçe Bitkileri Anabilim Dalı. Ordu.

Mahmutoğlu, H. (1985a). Çay Bitkisinde Budama. Çaykur Dergisi, 1(1):22-23.

Mahmutoğlu, H. (1985b). Rize koşullarında çay bitkisinde en uygun toplama aralığının tespiti. http://biriz.biz/cay/toplamaaraligi.pdf (Erişim tarihi:05.04.2017)

Öksüz, M., Demirci, M. (1983). Türkiye'de çay atıklarından kafein üretimi. Dergi Park, http://dergipark.gov.tr/download/article-file/35100 -(Erişim tarihi:16.03.2017).

Ravichandran, R. (2004). The impact of pruning and time from pruning on quality and aroma constituents of black tea. Food Chemistry, 84(1):7–11.

Turan, M.A., Balcı M., Taşkın, M.B., Kalcıoğlu, Z., Soba, M.R., Müezzinoğlu, R., Kaya, E.C., Özer, P., Kabaoğlu, A,. Taban, S. (2016). Doğu Karadeniz Bölgesi'nde Yetiştirilen Çay Bitkisi (*Camellia sinensis* L.) Yaşlı Yapraklarının Su Ekstraktı, Toplam Kül, Toplam Polifenol, Kafein ve Ham Selüloz İçerikleri. Toprak Su Dergisi, 5 (2): (52-58).

Yagi, C., Ikeda, N., Sato, D. (2010). Characteristics of Eight Japanese Tea Cultivars. College of Tropical Agriculture and Human Resources, https://www.ctahr.hawaii.edu/site/ -(Erişim tarihi: 31.03.2017).

Investigation of Different Protease Genes In Bacteria Isolated from Different Hot Springs

Merve KIZAKLI[1*], Hakan KARAOĞLU[2], Zeynep Dengiz Balta[3]

[1]Recep Tayyip Erdogan University, Faculty of Fisheries and Aquatic Science, Department of Basic Sciences, Rize, Turkey; merve.genetik.lab@gmail.com

[2]Recep Tayyip Erdogan University, Faculty of Fisheries and Aquatic Science, Department of Basic Sciences, Rize, Turkey; hakan.karaoglu@erdogan.edu.tr

[3]Recep Tayyip Erdogan University, Faculty of Fisheries and Aquatic Science, Department of Basic Sciences, Rize, Turkey; zdbalta@hotmail.com

[*]**Corresponding Author:** merve.genetik.lab@gmail.com

Abstract

Over time, the researchers have given a great interest on studies about the discovery of bacteria living on extreme conditions and their biotechnological usage.Thermophilic enzymes are important sources for stable enzymes under harsh conditions. Proteases (EC 3.4), important group of enzymes.. They constitute more than 65% of the world-wide enzyme market because of being used for food, pharmaceutical, detergent, leather and textile industries. Proteases are highly diverse enzymes having different active sites. Thermophilic enzymes are important sources for stable enzymes under harsh conditions. In this study, the presence of different kinds of protease genes were investigated in bacteria isolated from different hot springs identified as *Anoxybacillus ayderensis*, *Anoxybacillus bogrovensis*, *Anoxybacillus contaminans*, *Anoxybacillus flavithermus*, *Anoxybacillus gonensis*, *Anoxybacillus kamchatkensis*, *Anoxybacillus kestanbolensis* by PCR. The protease genes of *Anoxybacillus flavithermus* were used as positive control.

Keywords: Protease, biotechnology, *Anoxybacillus sp.*

1. Introduction

One of the classification methods of living organisms is based on their relationship to temperature.Microorganisms are generally divided into three groups as psychrophiles, mesophiles and thermophiles.According to their adaptation to life at high temperatures, thermophilic organisms are divided into two groups, moderate thermophiles (45-65 °C) and hyperthermophiles (<85 °C).Thermophilic microorganisms are known to live at very low and very high pH values (pH 0-3 or pH 10-12) or at very high salt concentration (5-30%), where they live from the high temperatures of the volcanoes to the low temperatures of the poles (Gül Güven,2007).

Enzymes regulate the speed and specificity of thousands of reactions within the cell.They also keep their activities outside of the cell.The compound thatthe enzyme acts on is called as substrate (Burg, 2003).Today, enzymes used in industrial areas are usually supply from thermophilic microorganisms. Since, the catalytic activities of thermophilic microorganism originated enzymes are very high compared to vegetable or animal origin enzymes. Besides, they do not create unwanted by-products,they are more stable, their cost is very low and they can be supply in excess of enzyme (Wiesman, 1987; Kristjansson et al.,. 2002).

Proteases, necessary for the development and cell differentiation, are found in all living organisms. Proteases have a specific catalytic role in the hydrolysis of proteins. There have been many protease sources including plants (keratinase, papain, bromelain), animals (trypsin, chymotrypsin, pepsin, renin) and microorganisms (Mala et al., 1998; Rani et al., 2012). However, microorganisms are the most used protease sources. Because they can be produced in large amounts in a short time. Microbial proteases can be stored for long periods of time with long shelf life under suitable conditions(Guevara et al., 2001; Singhet al., 2004; Rani et al., 2012).Proteases are generally classified according to three main criteria. These criteria are the type of reaction they catalyze,chemical structure of the catalytic domain, evolutionary relationship with the stucture. Proteases are classified into four main groups: serine proteases (EC 3.4.21), aspartic proteases (EC 3.4.23), cysteine / thiol proteases (EC 3.4.22), metalloproteases (EC3.4.24)according to their functional amino acids in their active sites (Rani et al., 2012). The application areas of proteases are food industry, peptide synthesis, leather industry, removal of industrial and domestic wastes, photo industry, medical field, silk processing and farming(Nieri et al., 1998; Raghunath et al., 2010; Rani et al., 2012).

Bacterial proteases, which account for 60% of enzyme sales worldwide, have become one of the largest classes of industrial enzymes (Mala et al., 1998). There is still a big necessity to find new sources for more stable proteases with high catalytic activity. Therefore, it is aimed to invastigate the presence of different kinds of protease genes in 15 different thermophilic bacteria from hot springs by PCR-method.

2. Material and Method

Genomic DNA isolation was performed using the Promega Genomic DNA Isolation Kit following the manufacturer's recommended protocol. Bacterial protease genes were produced by PCR reaction. As the primer, primer pairs synthesized for *Anoxybacillus flavithermus* protease genes were used.Isolated bacterial genomic DNA was used as template DNA .PCR reactions were performed in a final volume of 50 µlin 200 µlof thin-walled PCR tubes. The reaction mixture consist of; 1X PCR buffer, 200 µM dNTP, 2,5 mM $MgCl_2$, 25 pmol of each primers, 10-40 ng template genomic DNA, 1 U *Taq* DNA polymerase (Karaoglu et al., 2013).

ThePCR products were cloned into pGEM-T Easy vector. It was carried out following the protocol recommended by the manufacturer of the Promega. At 10 µl of final volume;1 µl 10X Buffer, 1 µl pGEM-T Easy vector, 5 µl PCR product, 1 µl T4 DNA ligase,2 µl ddH_2O.The reaction mixture was incubated at 22 °C for 30 minutes.Ligation products were transferred to *E. coli* strain JM101 by using standard $CaCl_2$ transformation method**.**Transformation products were inoculated on LB agar containing 50 m/ml kanamycin.The cultures were incubated for 16 hours at 37 °C (Karaoglu et al., 2013).Then, isolation of plazmids were performed by the Promega Plasmid Isolation Kit.The isolated plasmids were sent for base sequence analysis to the Macrogen company.The obtained data were compared with GenBank data by using the BlastN program and the DNA sequences of the respective genes were determined (Karaoglu et al., 2013).

2. Results and Discussion

We have found out different protease genes from different themophilic bacteria.The determined gene regions are genes of ATP-dependent Zn protease FtsH, Glycoprotease, ATP-dependent protease, Lon-like ATP-dependent protease, Class III heat-shock ATP-dependent Lon protease, Zn-dependent protease, Collagenase protease, Metal-dependent protease, XkdA family, Serine protease of Rhomboid family, Phage head maturation protease. Presence of ATP-dependent Zn protease FtsH gene was detected in 6 different bacteria (Figure 1). Glycoprotease Gene, Presence of Glycoprotease Gene was detected in 10 different bacteria (Figure 2). The presence of ATP-dependent protease gene was detected in 5 different bacteria (Figure 3).Presence of Lon-like ATP-dependent protease gene genes was detected in 7 different bacteria (Figure 4).Presence of Class III heat-shock ATP-dependent Lon protease genes was detected in 3 different bacteria (Figure 5).The presence of Zn-dependent protease genes was detected in 14 different bacteria (Figure 6).The presence of Collagenase protease gene was detected in 10 different bacteria (Figure 7).The presence of Metal-dependent protease, XkdA family gene was detected in 1 different bacteria (Figure 8).The presence of Serine protease of Rhomboid familygenes was detected in 5 different bacteria (Figure 9).The presence of Phage head maturation proteasegenes was not detected in any bacteria (Figure 10).

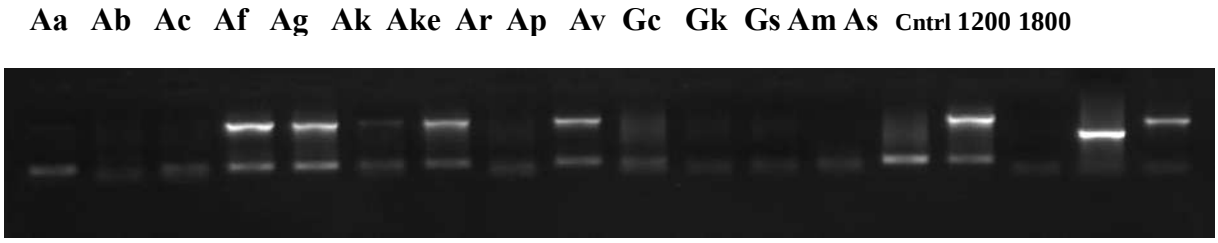

Figure 1. The peresence of ATP-dependent Zn protease FtsH gene

(The bacteria were coded as given: *Anoxybacillus ayderensis*;Aa, *Anoxybacillus bogrovensis;* Ab,*Anoxybacillus contaminans;*Ac, *Anoxybacillus flavithermus;* Af, *Anoxybacillus gönensis;* Ag, *Anoxybacillus kamchatkensis;* Ak, *Anoxybacillus kestanbolensis;* Ake, *Anoxybacillus rupiensis;* Ar, *Anoxybacillus pushchinoensis;* Ap, *Anoxybacillus voinoskiensis;* Av, *Geobacillus caldoxylosilyticus;* Gc, *Geobacillus kaustophilus;*Gk, *Geobacillus stearothermophilus;* Gs, *Anoxybacillus mongoliensis;* Am, *Anoxybacillus salavatliensis;* As.)

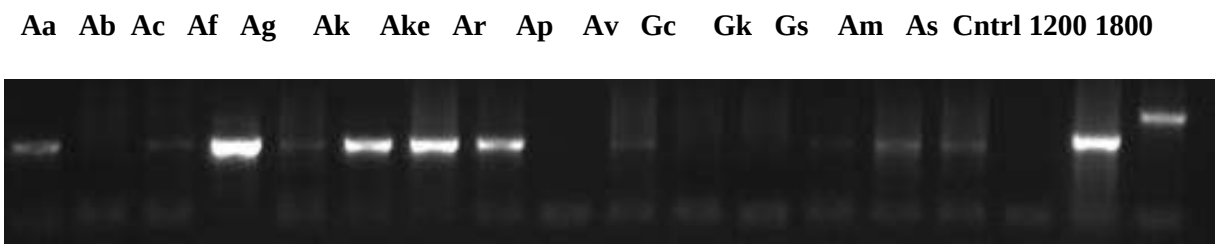

Figure 2. Presence of Glycoprotease Gene

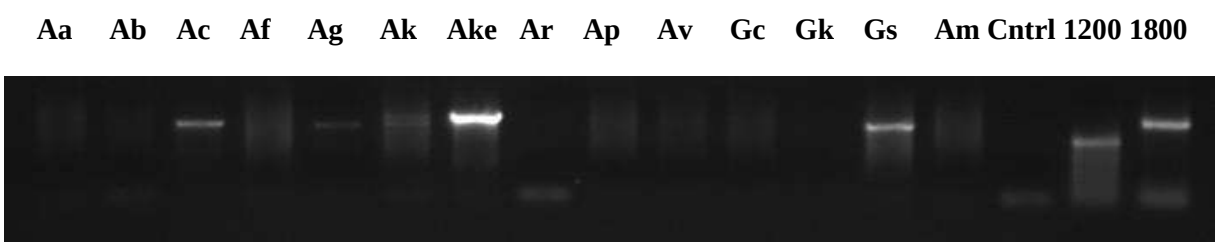

Figure 3. The presence of ATP-dependent protease gene

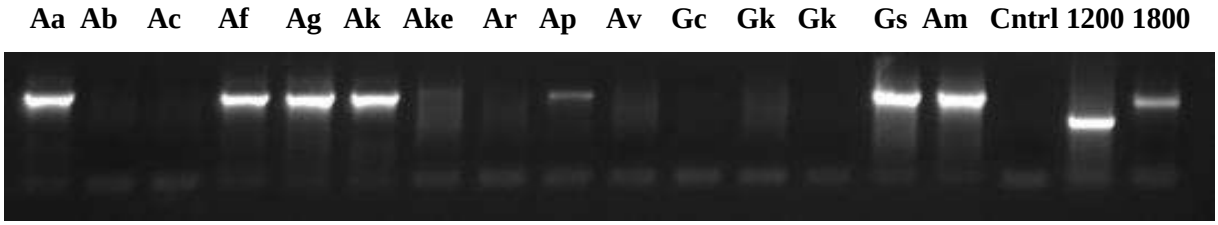

Figure 4. Presence of Lon-like ATP-dependent protease gene

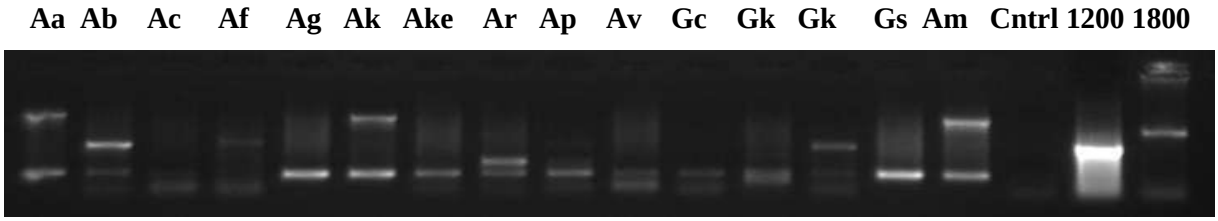

Figure 5. The presence of Class III heat-shock ATP-dependent Lon protease gene

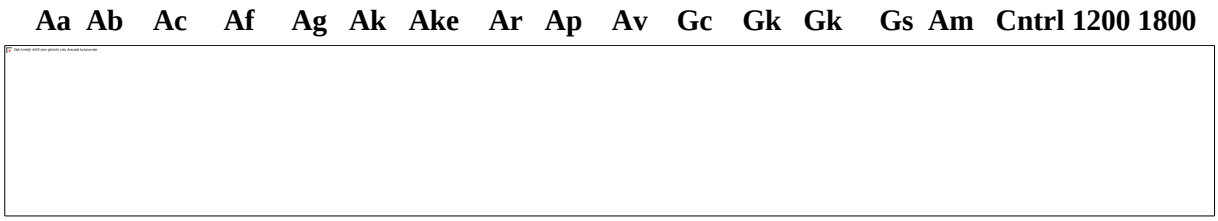

Figure 6. The presence of Zn-dependent protease gene

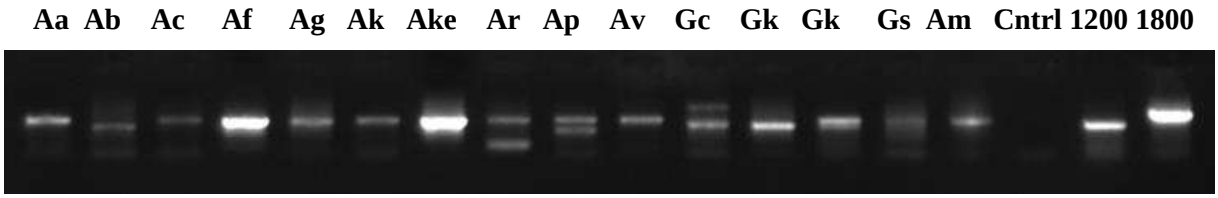

Figure 7. The presence of Collagenase protease gene

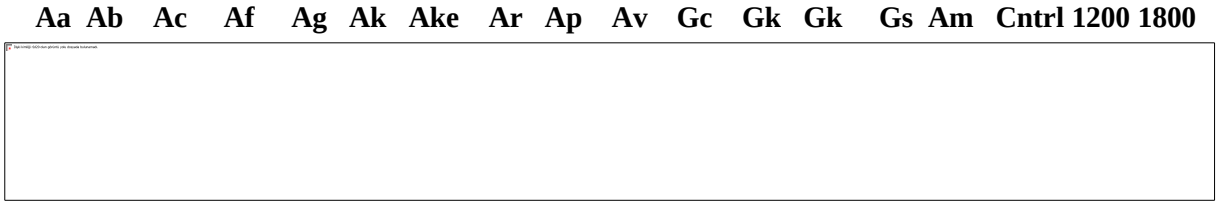

Figure 8. The presence of Metal-dependent protease, XkdA family gene

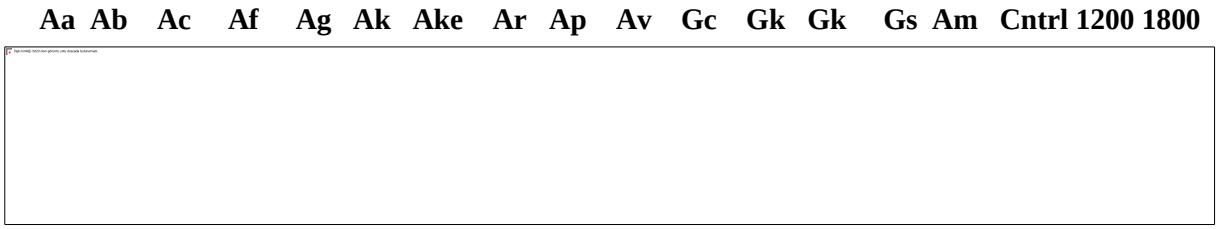

Figure 9. The presence of Serine protease of Rhomboid family gene

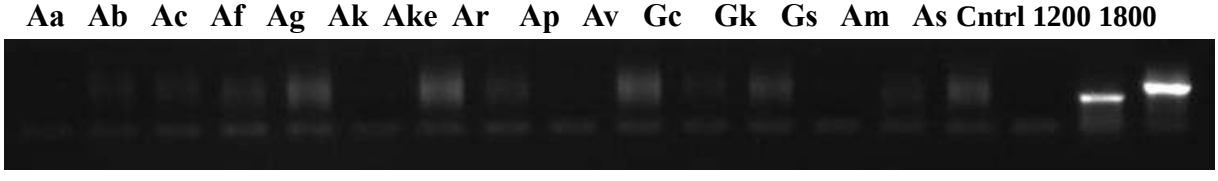

Figure 10. The presence of Phage head maturation protease

Whole genome analysis of*A. flaviermus*was performed and full sequence analysis of the genome is available in GenBank.As a result of the studies on this sequence, 10 pairs of primers have been designed to target 10 different protease genes of bacterium.We have tried to produce these protease genes by PCR method using these primers on a total of 15 thermophilic bacteria belonging to 12 *Anoxybacillus*,3 *Geobacillus* genus in our laboratory stocks.Protease genes of *A. flavithermus*bacteria were used as positive controls.The resulting genes were cloned into the pGEM-T Easy cloning vector and were sequenced. As a result of the studies done, 10 gene base sequence analysis were completed.

Acknowledgement

I am gratefull Derya EFE and Züleyha AKPINAR for their contributions. This study was supported by Rize Recep Tayyip Erdoğan University due to The Project coded as BAP.2013.103.01.3 .

References

Güven, G. (2007). Termofilik Bakteriler ve Biyoteknolojik Açıdan Önemli Bazı Enzimleri. Elektronik Mikrobiyoloji Dergisi TR, 9(1), 1-10.

Demirjian D., Moris-Varai F., Sassidy, C. (2001). Enzymes from Extremophiles. Current Opinion of ChemicalBiology, 5,144–51.

Kristjansson, M.M., Asgeırsson, B. (2002). Properties of Extremophilic Enzymes and Their Importance in Food Science and Technology. Handbook of Food Enzymology (ed. J.R. Whitaker), NY, USA, p.77-99.

Haki, GD., Rakshit, Sk. (2003).Developments in Industrially Important Thermostable Enzymes: a Review. BioresourceTecnology, 89,17–34.

Gul-Guven, R., Guven, K ,Poli, A., Nicolaus B .(2007). Purification and some properties of a beta galactosidase from the thermoacidophilic Alicyclobacillus acidocaldarius subsp rittmannii isolated from Antarctica. Enzyme and Microbial Technology, 40(6), 1570-157.

Guevara M. G., Daleo G. R., Oliva C. R.. (2001).Purification and characterization of an aspartic protease from potato leaves, Physiology Plant., 12, 321-326.

Gupta R., Q.K. Beg, Lorenz,P.. (2002).Bacterial alkaline proteases: molecular approaches and industrial applications, Application Microbiology and Biotechnology, 59, 15–3.

Mala B., Rao, Aparna M., Mohini S. Ghatge and Vasanti V. (1998). Molecular and Biotechnological Aspects of Microbial Proteases, Mıcrobıology and Molecular Bıology REVIEWS.,1, 597–635.

Raghunath T. Mahajan and Shamkant B. (2010) .Biological aspects of proteolytic enzymes: A Review, Journal of Pharmacy Research, 3(9),2048-2068.

Singh L. R, Devi T. P., Devi S. K. (2004). Purification and Characterization of a Pineapple Crown Leaf Thiol Protease, Preparative Biochemistry and Biotechnology, 34, 25–43.

Ertunga N, Colak, A, Belduz A, Canakci S, Karaoglu H and Sandalli C. (2007). Cloning, Expression, Purification and Characterization of Fructose-1,6-bisphosphate Aldolase from Anoxybacillus gonensis G2, Journal of Biochemistry, 141, 817–825.

Burg, B. (2003). Extremophiles as a source for novel enzymes. Current Opinion in Microbiology, 6, 213-218.

Karaoglu, H., Yanmis, D., Sal, A., S., Celik, A., Canakci, S., Belduz, A., O. (2013). Biochemical characterization of a novel glucose isomerase from Anoxybacillus gonensis G2T that displays a high level of activity and thermal stability. Journal of Molecular Catalysis B: Enzymatic, 97, 215–224.

Innovations Brought by Agriculture 4.0 and Its Contribution to the National Economy

Ahmet DÜRÜST[1], Hasan Alp ŞAHİN[2], Ali Kemal AYAN[3]

[1]University of Ondokuz Mayis, Facuality of Agricultere, Department of Agronomy, Samsun, Turkey; bafraofset@gmail.com

[2]University of Ondokuz Mayis, Facuality of Agricultere, Department of Animal Science, Samsun, Turkey; h.alpsahin@gmail.com

[3]University of Ondokuz Mayis, The High School of Professional of Bafra, Samsun, Turkey; akayan@omu.edu.tr

[*]**Corresponding Author:**bafraofset@gmail.com

Abstract

Developments of information and communication technology effected agriculture and also technologies of agriculture and they revealed agriculture and machine system that are wiser. Digital agriculture which is called 4.0 and bases on datas started to show up. In this regard, it makes the most of technological apportunities about optimum water utilization, damages of insect on plants and diseases soil structure, mineral need of soil, effect of climate changes on development of plant, increasing efficiency of plants.

These technologies involves lots of information and communication technologies such as GPS (global positioning system), VRT (auction – rote preferred technologies), CBS (geographical education systems), UAT (remote sensing technologies), VHS (rendement mapping system), auto arrangement and field traffic technologies, electronic measurement and control systems.

It is believed that making agriculture 4.0 large scaled productions will make lipes of people easier and increase the quality of their living.

Keywords: Agriculture 4.0, Technology, Machine system

1. Introduction

Some devastating effects of developing technologies are related to game-changing technology, especially in technology it is enlivened by extremely progress. The Fourth Industrial Revolution has been a topic of interest, especially among industries, higher education institutions, governments, and research institutions worldwide. Development is fast and important enough to affect society and the economy. Revolution is defined as the forced destruction of a government. In the context of the Industrial Revolution, it is perceived as a forced destruction of an existing technology. Not only is it seen as destructive, it also integrates very strongly with other technologies

2. Literature Summary

The history of agriculture has improved the production and upbringing of food, fiber, fuel and other goods by systematically raising humanity, plants and animals. People were hunters and gatherers before plant breeding was developed. The knowledge and skills related to the care of the soil and the growth of plants have improved the development of human society, allowing clans and tribes to remain in one place from generation to generation. Archaeological evidence of these developments indicates that 1000 years or more occurred before.

Due to agriculture, cities and trade relations developed between different regions and people. The progress of societies and cultures was ensured. It has been an important part of the economy for centuries before and after the Industrial Revolution . Sustainable development of foodstuffs in world affects the long-term survival of species. The agricultural system needs our ecosystem to maintain the green approach.

Precision engineering is the most important point in the agricultural sector in the next few years. Taiwan is one of the few countries as well as Germany, which adopts agriculture in IR 4.0. like all other businesses, crop yield will be the ultimate goal, and this can be achieved by greater environmental estimation. Predictive monitoring systems, especially those related to soil and weather conditions, will be necessary for the industry. IoT is full of potential for future farmers who adopt the correct components of Agriculture 4.0, such as smart sensors, robots, drones and satellites, hydroponics and aquaponics and others as well as solar cells . The data is important for Ziraat 4.0, which carries important information for farmers. Some initiatives provide farmers with innovative tools for capturing, monitoring, processing and performing modern equipment in digital form, software, and real-time monitoring activities. However, since agriculture is a conservative sector, it should be noted that some farmers are open to advanced technology to double their profits. A major shift in strategies is needed by policy-makers and the government to ensure that a country's middle-income model, such as Vietnam, Malaysia and Thailand, is shifted to a high-income country

3. Defınıtıon of Agrıculture 4.0 and "Dıgıtal Agrıculture" Terms

3.1. Agriculture 1.0

At the beginning of the 20th century, there was a low-productivity labor-intensive agricultural system. But he was able to feed the population. He needed a large number of small farms and one-third of the population had to be active in the agricultural production process.

3.2. Agriculture 2.0

Commonly called "Green Revolution" as recalled farming in the late 1950s, addition of nitrogen and synthetic pesticides, such as agricultural management practices, new tools, such as fertilizers and more efficient special machines began by providing opportunities to benefit from relatively cheap inputs. It was aimed to increase the potential and revenue at all levels.

3.3. Agriculture 3.0

Precision Agriculture started with the introduction of military GPS signals for the first time.

Precision Agriculture brings solutions for:

Precision Agriculture improves the accuracy of operations, managing the variations in the field rather than handling the areas as a whole . The goal is to give each plant what they need to grow optimally. This input is intended to optimize year while lowering agricultural production.

- Guidance
- Detection and Control
- Telematics
- Data management

Agriculture 3.0 can be seen as the introduction of more advanced and mature Precision Agricultural technologies progressively. S quality and to reduce cost, improve or to increase the profitability of diversified products is the main goal.

3.4. Agriculture 4.0

A new increase in precision agriculture can be observed in early 2010, based on the evolution of several technologies:

- Cheap and improved sensors and actuators
- Low cost microprocessors
- High bandwidth cellular communication

- Big data analysis

From the 2010s onwards, smart technologies are increasingly being equipped with standard features such as tractors, combine harvesters and other equipment:

- Intelligent control devices (built-in computers)
- Many sensors for machine operation and agricultural process
- Advanced automation capabilities (guidance, seed placement, spraying)
- Embedded communication technology (telematics)

4. Applıcatıons of Agrıculture 4.0 ın Fıeld Crops

Harvesters or harvesting machines in the field crop are harvested and harvested. The moisture map, protein map and fat content map of the product can also be removed (Figure 2). In Turkey, for the first time in Ankara University, Faculty of Agriculture, Agricultural Machinery Department and TAGEM in 1999, combined with a combine harvester systems, yield mapping was started. This work was continued in 2012, and today the private sector to this cooperation, Adana Commodity Exchange and Çukurova Development in Adana with the inclusion of agents from three different locations 'As for the Use of Advanced Technology in Agriculture Precision Agriculture Applications Infrastructure Development and System Creation Project' under the 3 The combine harvester is equipped with more efficiency mapping system and humidity sensor. In addition to these systems, in 2013, one of the combine combines a protein and oil sensor.

Table 1. Table.

Use Areas	Practical
Parallel movement	Many practical systems available
Soil processing	Depth adjustment system via hydraulic cylinders available
October (Cereals)	Seed drills with electronic adjustment available
Fertilization	Machines for regulating the fertilizer norm for mineral fertilizers available
Plant protection	Direct pulverization sprayer with sensor for fungicides machines present, trials that weed from the image sensor in stage
Yield mapping	Standard equipped large capacity harvesters, cotton harvesting with For some anchor plants available in silage machines (sugar beet, first practical solutions in potato and fruit harvesting there is

The use of technology in field agriculture and its practical status

In a study conducted in Turkey; In an olive garden with 84 trees, a yield map was obtained in the yield yield of olive. The soil of the olive garden is considered suitable for growing olive according to physical and chemical analyzes. However, organic matter and partly P, Mn and Zn were low. According to the results of the analysis; N, P, Mn and Zn will be required for olive production the following year. It is proposed to include these practices in the fertilization program (Bellitürk and ark., 2010-a).

4.1. Auxiliary Steering and Steering Systemsictures

In the field agriculture, the most widely used technologies in the world today are automatic steering and navigation. Thanks to this technology, the lines of in-line products can be automatically and properly created. Prevents overlapping or gaps in agricultural input applications with auxiliary steering systems. For example, it is reported that the total input loss caused by coverings and gaps in sugar beet production is 13%, while 7% is the fuel loss (Hanson, 1998).

These systems increase the productivity of the work place on the same site twice in the same place and prevent the formation of unprocessed area, extending the working time, reducing the use of input and field efficiency and increase the machine space capacity is such as issues.

There are 3 systems in the steering of tractors and equipment and manual, machine orientation and driverless systems. In the system, methods such as image processing, embedded cables, global positioning system (GPS) are used. In the manual system, all steering direction control is completely in the operator.

4.2. Sensor-Based Product Detection and Variable Rate Technologies in Fertilization in Field Crops

In the detection method, the state of the plant is measured during movement. This direct system and partial area specific measurement, calculation and fertilization are performed in a single operation. Indirectly measured parameters (chlorophyll amount of plant and bending resistance of stems etc.) are used to determine fertilizer requirement. Based on these measurements, the amount of instant fertilizer is calculated and delivered to the fertilizer distributor and the required amount of fertilizer is distributed to the area.

It is also possible to produce similar maps with unicycle or multispectral or hyperspectral cameras on an aircraft. Unmanned aerial vehicles which are capable of flying under the clouds are widely used in agriculture, especially when the air is cloudy due to remote sensing satellites.

4.3.Map Based Variable Rate Technologies in Fertilization

Map based application technologies, georeferencing of nutrients in the soil georeferentially as a result of the map and yield maps obtained as a result of the evaluation of the application maps with the GPS and smart machines are delivered to the ground.

4.4. Sensor Based Variable Rate Technologies in Disinfection

Since these systems take into account the condition of the plant, the amount of drug discarded is also related to the growth status of the plant and allows to save a lot of the drug.

4.5. Variable rate technologies in irrigation

In variable rate application, water requirement is based on land type and soil type. Based on this, after the application of water application maps, water is applied in variable rates with intelligent irrigation machines.

4.6. Variable rate technologies used in seed

They are the systems and technologies that apply the seed amounts that will best meet the current yield potentials in the land. Thanks to this technology, the amount of seed applied to the land can be changed and higher yields can be obtained.

4.7. Robot applications and driverless Technologies

The robotics-based system, which is shown as the future of agricultural technology and completely eliminates operator operation, is still under investigation and testing. Companies such as Case IH, John Deere and Kinze continue their research and development efforts to commercialize this system. The system is designed in such a way that the system is precisely

guided on a predetermined course on the field and can automatically perform agricultural activity without operator intervention.

Projects are being carried out in our country about agricultural robots. This project aims to produce a robotic farm prototype. In order to achieve this goal, a system design is made by combining existing hardware and software technologies in harmony with each other. RoboTurk (Figure 18), which is developed within the scope of the project, is equipped with sensor and image processing technologies and it is planned to collect data from the field automatically and then transmit the data to the Farm Management Information System.

Figure 1.ROBOTURK (2013)

The use of information technologies in agriculture serves our sector. We continue our researches about agricultural robots in our country and provide knowledge and experience.

5. Results and Discussion

Today's machines are now equipped with smarter technologies. For example, a machine equipped with high technology not only harvests but also collects data. Thanks to these data, the efficiency of agricultural operations can be further increased. Agricultural tractors, tools and machines are equipped with GPS, mobile computers, wireless technologies, spectrometers, infrared cameras, so instant product monitoring and instant applications have become possible.

In the future we will need more agricultural production. Meeting this need will be possible by increasing the efficiency obtained from the unit area. Since the beginning of the 1990s in the world, with the development of information technologies, a process of change that is sensitive to human, plant, animal and environment and quality and productivity factors are being passed. We should direct these supports not only to conventional machines but also to technological intelligent machines .

References

Türker, U ve Güçdemir, İ. 2013. Türkiye de yapılan Hassas Tarım çalışmalarından bir örnek.
Tarım Makinaları Bilimi Dergisi (Journal of Agricultural Machinery Science), ISSN:1306-0007, cilt 9 sayı 4. Sayfa: 257-262

FAO (2010). "The State of Food Insecurity in the World". In: Food and Agriculture Organisation of the United Nations.

Tekin, A. B., 2013. Tarım Robotları.Tarım Makinaları Bilimi Dergisi, 2013, 9 (4): 273-278

Cheng, J. D., Lin, J. P., Lu, S. Y., Huang, L. S., & Wu, H. L. Hydrological characteristics of betel nut plantations on slopelands in central Taiwan/Caractéristiques hydrologiques de plantations de noix de bétel sur des versants du centre Taïwan 53(6), 1208–1220

http://cema-agri.org/sites/default/files/CEMA_Digital%20Farming%20-%20Agriculture%204.0_%2013%2002%202017.pdf

Pierre-Philippe Mathieu, Christoph Aubrecht, Editors Earth Observation Open Science and Innovation, 2018, 261-268

Noorhana Yahya, Green Urea For Future Sustainability, 2018, 125-145

Belliturk, K., C. Saglam, B. Akdemir, C.B. Sisman, 2010-a. Determination of Spatial Variability in Olive Production Part I-Soil. Bulgarian Journal of Agricultural Sciences, Bulgaria, 16 (4).

Hanson, C. A. 1998. Analysis of operator patterns in machine operation for automatic guidance of agricultural equipment. Unpublished M.Sc. thesis. Department of Mechanical Engineering, University of Saskatchewan, Saskatoon, SK

The Effect Of The Tea Litter Compost Applications On Some Soil Properties And Plant Development

Damla BENDER ÖZENÇ[1] Selahattin AYGÜN[1] Demirhan HUT[2]

[1]Department of Soil Science and Plant Nutrition/Ordu University, Turkey
[2]Sürmene District Directorate of Food, Agriculture and Livestock, Trabzon
*Corresponding Author: (*selahattin_555@hotmail.com*)*

ABSTRACT

In our country, tea cultivation is carried out in the Eastern Black Sea Region and significant amount of waste remains during its processing. These wastes, which are not evaluated in any way, constitute an important potential for their use in plant growing media when composted.

In this study, pepperplants were grown in sandy clay loam soil mixing with different tea litter compost doses(0 %, 2 %, 4 % and 8 %). The trial was carried out with three replicates according to randomized parcels experimental design. The plants were harvested when they completed the development, the effects of applied composts on both plant growth and some properties of the soil have been investigated.

Tea litter composting applications improve both the aeration and the water availability to the soil. Aeration capacity (19.73%), easilyavailable water content (20.03%), aeration porosity (38.93%) and macropore / micropore ratio were increased.Although the pH of the trial soil was very low and the compost application did not change the pH class, it made a positive effect on the pH (4.65). While soil P (0.12%) content decreased with compost application, K (0.26%) showed increase and 4% and 8% effective doses were determined.

Root-shootfresh and dry weights and plant height of pepper plants grown in compost-applied medium increased and 4% application rate to soil was determined sufficient. Plant N and K contents (4.98%, 4.76%) were found to be sufficient and excessive depending on increase of compost amount, but plant P content decreased.

Key Words:*Capsicuum annum* L., Tea litter compost, physical properties, nutrient content

1. Introduction

Pepper is one of the most important vegetables used widely for domestic and commercial purposes. Pepper is warm and hot region vegetable.The plant has a delicate, fringe root with plenty of appearances.70% of the roots are distributed in the top 10-30 cm of the soil, while the rest are 50 cm deep and occasionally down to 100 cm.The distribution of the roots varies from 40 to 60 cm. The pepper trunk, which grows vertically and displays a grassy, gradually woody structure at the beginning, has a brittle structure that breaks quickly and can extend up to 150 cm. The best temperature for pepper is 20-30 °C. The plants maintain their vital functions up to 5 °C.Plant growth and growth at temperatures above 35 ° C are very slow. At high temperatures, growth stops altogether, fruit starts to become acrid. Good results are obtained in the peppered soil, which is very deep, permeable, good in water retention, good in soil pH; 6.0-6.5, rich in nutrition and organic matter named garden soil, for good growth and productivity in peppers.Because of roots has a delicate structure, a good cultivation can not be made in heavy clayey, airless and water holding soils. It gives the best development and yield on rich, sandy, loamy-light clay, rich soil of organic matter. (Anonymous, 2010; Keles, 2012).

The organic matter content of soils is one of the most important features in ensuring sustainability and productivity in all agricultural operations. For this purpose, with the use of many commercial substrates (such as peat, perlite, cocopeat, pumice), as a source of organic matter, many agricultural and industrial waste and residues can be used directly or after composting as long as they are not toxic. Studies on the development of pepper plant and some organic materials and inorganic fertilization studies are being carried out and continue to be done. (Majdi et al., 2012; Güngör and Yıldırım, 2013). Albaho et al. (2009) reported that different substrates prepared from peat, perlite, vermicompost and cocopeat media had significant effects on total yield, height, number of leaves, chlorophyll index of pepper. Tea litter is one of the kinds of wastes that are evolved during the transformation of wet tea leaf into black tea in tea factories. There are about 20-25 thousand tonnes of tea plant per year in the factories that process tea leaves belonging to the state in the Eastern Black Sea region. Considering factories belonging to individuals and private organizations in the region, this figure is close to 45-50 thousand tons. (Anonymous, 2014). In our country this ratio has increased by 2-3 folds to over 17% due to the fact that wet tea leaves are not collected according to the standards and the use of excess nitrogen fertilizer in tea cultivation soil. The use of tea wastes, which have a large waste potency with high organic matter, as an organic material will also provide a solution to the environmental problems that it creates.

It is reported that these wastes, which have not been assessed in any way today, may have an important potential for composting and use in the growing environment due to the characteristics they possess. Kacar (1992) stated that tea waste, which has an important organic matter, macro and micronutrient content, has positive effects on yield and soil structure. Kütük et al., (1995) reported that tea waste could be used as a plant growth medium, tea waste compost increased the amount of dry matter in turf growing, total N, K contents increased compared to farm fertilization and peat (Aşık ve Kütük, 2012); (Yilmaz and Özenç, 2012) reported that the tea waste compost was more effective on the development of corn plant than the hazelnut compost.

In this study, it was aimed to determine the growth and the fruit quality of the pepper plant grown in tea litter compost environment mixed with soil at different ratios. Thus, it is another important goal to contribute to the development of agricultural activities, which will encourage the use of tea wastes, which are released in significant quantities, in composting vegetable cultivation.

2. Materials And Methods

2.1. Material

In the study, soil with sandy clay loam taken from a depth of 0-20 cm was used as soil and organic material was compost obtained from tea refuse which is tea plant processing waste. The tea litter provided from a private factory has been subjected to composting by piling up a closed and open area. After the tea litter (about 10 cm thick) was laid, soil was laid on it (about 1 cm thick), lime and nitrogen fertilizer were spread and this process was continued until the material was finished. After each layer, compression and dampening were done and covered with nylon cover over the pile. During compost formation, the stack was subjected to moisture, temperature control, mixing and compaction. Approximately 4 months under natural conditions, composting of the material is provided. Approximately 4 months under natural conditions, composting of the material is provided. (Figure 1).

Figure 1. Composted tea litter heaps

Prior to the establishment of the experiment, some basic physical and chemical analyzes were performed to identify soil samples and compost material (Table 1). Soil, acid pH, without salt, has a high content of organic matter, and sufficient and low levels of basic nutrient content. Tea litter compost is a material that can easily mix with soil with low volume weight and the aeration and water retention capacity is within ideal limits (Verdonck et al., 1984). It contains high organic matter content, adequate pH and sufficient levels of essential nutrients.Plant material was planted with Lumbard F1 sharp pepper shrimp.

Table 1. Some properties of soil and tea litter compost used in the experiment.

	Texture	BD (gcm^{-3})	AWC (%)	AC (%)	pH	EC (dSm^{-1})	C/N	
Soil	SCL	-	-	-	4.43	2	-	
TLC	-	0.13	31.71	32.57	6.86	0.51	18	

2.2. Establishment of the Experiment

The experiment was set up with three replications, sandy clay loam, four tea litter compost mixture ratio (0%, 2%, 4%, 8%, volumetrically). For the experiment, the soil and compost were sieved from a 6.35 mm sieve. In accordance with the purpose of studying tea litter compost, mediums are prepared by mixing with soil to be 2%, 4% and 8% taking into account the amount of material mixed in 1 decare to the soil. Separately prepared mediums were filled with 4 kg soil pots in which polyethylene bags were placed, and one pepper

seedlingwas planted in each pot.The pots were irrigated at 75% of the field capacity. For basic fertilization, 100 ppm K/pot, 125 ppm P/pot from KH_2PO_4 fertilizer and 100 ppm/pot CAN fertilization were applied for nitrogen. During the experiment period, no further fertilization was done. From the planting of the seedlings (Figure 2) to the end of the fruit harvest (about 70 days), all the pots were watered as needed and the necessary cultural processes were carried out.

Figure 2. Seedling planting stage

2.3. Analysis Methods

Before harvesting the plants, the part from the soil to the end of the plant was measured and the plant size was determined. The number of fruits in each pot is determined by number and weight. Then, the plant was harvested from above the soil. In order to separate root parts of each plant from the soil in the experiment, the pots were washed separately on the sifter placed in a container and tried to prevent the root loss. After the roots were collected on the sieve, washed with pure water, and then the excess water was absorbed by the coarse drying paper, the shoots and roots were dried at 65 ° C for 48 hours and shoot and root dry weights were taken.

The soil samples taken from 0-20 cm depth were dried and then sieved from the 2 mm sieve and the properties of the test soil were determined. Field capacity according to the Klute (1986), soil pH and EC are 1: 2.5 in the soil: water mixture (U.S. Salinity Lab.Staff, 1954), soil texture hydrometer method according to (Bouyoucos, 1951), bulk density according to Blake and Hartge (1986), wet oxidation organic matter walkley-black method according to Nelson and Sommers (1982), total nitrogen according to (Bremner, 1965), available phosphorus according to (Bray and Kurtz, 1945), available potassium according to (Knudsen et al. 1982).

For the identification of organic materials and prepared media, bulk density, moisture characteristic values, percentage of easily available water and aeration capacity according to De Boodt et al. (1973); the ratio of macropor/micropore according to (Munsuz, 1982) organic matter was determined according to DIN 11542 (1978), pH and EC according to Gabriels and Verdonck (1992), P and K according to Chapman et al. (1961) were determined.

The data obtained at the end of the experiment were analyzed by analysis of variance according to the randomized experimental research design in the "JUMP" package program and LSD (Least Significant Difference) multiple comparison test was applied at the 5% significance level to determine the difference between the applications, the results are expressed in the form of letter impressions next to the means.

3. Results And Discussion

3.1. Experiment Properties

Available water content, aeration porosity and macro/microporous ratio, the aeration capacity of the sandy clay loam soil was significantly influenced ($p < 0.01$) by compost applications and didn't effect on the percentage of soil saturation (Table 2).

Table 2. Some physical properties of compost mixed soil

Medium	Sat (%)	AC (%)	AWC (%)	AP (%)	MP/MiP
Control	61.34	11.31 D	16.53 C	27.84 D	0.83 D
S + %2 TLC	64.25	13.19 C	17.91 BC	31.10 C	0.94 C
S + %4 TLC	61.18	14.89 B	20.03 A	34.92 B	1.33 B
S + %8 TLC	62.87	19.73 A	19.20 AB	38.93 A	1.63 A
LSD(p<0.01)	ns	0.6967	0.6689	0.9326	0.0263

As a result of the variance analysis made for the properties, the difference between at least in two groups mean statistically significant. The difference between the means indicated by the same letter does not significant within their group.

Sat: Saturation Percentage, AC: Aeration Capacity, AWC: Available Water Content AP: Aeration Porosity, MP / MiP: Macro/micropore ratio

As can be seen from Table 2, the compost added to the soil as a source of organic matter positively affected the important physical properties of the soil and statistically significant increases in these properties were observed when the applied compost was increased. Results were found to be consistent with the results reported with Kacar (1992), Kütük et al. (1995), Aşık and Kütük (2012); Yılmaz and Özenç (2012).

Compost applications effected some chemical properties and nutrient contents of sandy clay loam soil and caused statistically significant differences on soil reaction (pH), electrical conductivity (EC), nitrogen, phosphorus and potassium content ($p < 0.01$) (Table 3).

Table 3. Some physical properties of compost mixed soil

Medium	pH	EC (mhos/cm)	N (%)	P (%)	K (%)
Control	4.43 C	199 A	0.18 C	0.11 B	0.20 D
S + 2% TLC	4.60 B	175 B	0.21 B	0.12 A	0.23 C
S + 4% TLC	4.64 A	165 C	0.22 B	0.10 C	0.25 B
S + 8% TLC	4.65 A	153 D	0.26 A	0.03 D	0.26 A
LSD(p<0.01)	0.0118	2.1344	0.0129	0.0002	0.0003

As a result of the variance analysis made for the properties, the difference between at least two groups mean statistically significant. The difference between the means indicated by the same letter does not matter within their group.

As can be seen from Table 3, while the compost applications increased the pH, total nitrogen and extractable potassium contents of the soil, the available phosphorus and EC value of the plant in the ground decreased. The compost EC and P contents are lower than the soil, and the decrease in these properties is an expected result as the amount of the compost mixed with the soil increases. There are researches on the application of organic materials to increase the potassium content of soils. (Aşık and Kütük, 2012; Hirzel et al., 2009, Asri et al., 2013).

3.2. Plant Development

Application of tea litter compost to the soil did not have statistically effect on the number of fruit and fruit weight of the pepper plant but statistically significant differences were observed on stem, stem development and plant height (Table 4).

Table 4. Effect of tea litter compost applications on the development of pepper plant

Dose (%)	RWW (g)	RDW (g)	SWW (g)	SDW (g)	FN (adet)	TW (g)	PH (cm)
0	2.83b	1.33c	24.33b	4.33b	3.67	68.50	24.67c
2	3.53b	1.80bc	30.00b	6.67ab	4.67	95.33	32.67bc
4	5.57a	3.20a	30.00b	7.67a	5.00	92.67	37.00ab
8	5.50a	2.47ab	40.00a	9.00a	5.00	104.00	43.33a
LSD (p< 0.01)	0.5944	1.8666	3.9440 (p< 0.05)	1.0801 (p< 0.05)	ns	ns	3.8078

As a result of the variance analysis made for the properties, the difference between at least two groups mean statistically significant. The difference between the means indicated by the same letter does not matter within their group.

RWW: Root wet weight, RDW: Root dry weight, SWW: Shoot wet weight SDW: Shoot dry weight, FN: Fruit Number, TW: Total weight, PH:Plant height

As can be seen from Table 4, the highest mean root-shoot dry weight and plant height were obtained in 8% application and 4% compost application was determined to be statistically

sufficient. The tea litter compost applied to the pepper plant provided approximately 2-fold increase in the properties examined. It has been determined that the effects of organic fertilizers mixed at different ratios on the root length, plant dry weight, root wet and dry weight of the pepper plant are important (Koç, 2008). It has been determined that the tea waste compost has a positive effect on the physical, chemical and biological properties of the soil and that the plants have an effect on the peak / root ratio (Aonove et al., 1980; Allievive et al., 1992). It has been determined by researches that tea waste, hazelnut husk, urban waste compost and composted paddy mussel considerably affect the characteristics such as the rate of plant shear, number of fruits, shoot diameter, root wet weight and plant height in experimental plants. (Long et al., 2000; Stringheta et al., 1999).

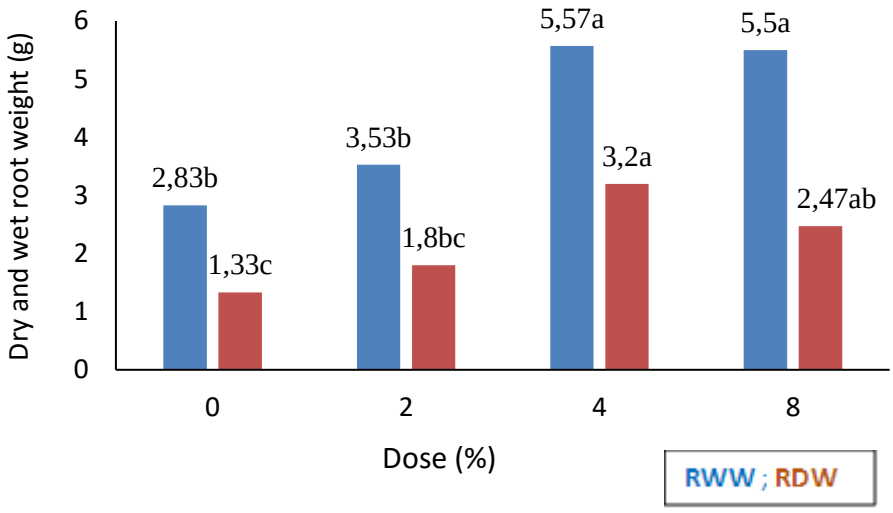

Figure 1. Effect of tea litter compost applications on dry and wet root weight

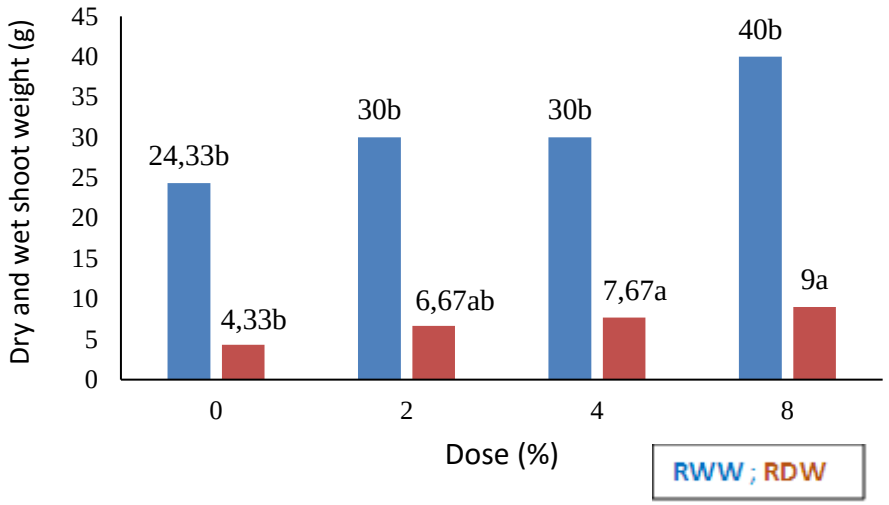

Figure 2. Effect of tea litter compost applications on dry and wet shoot weight

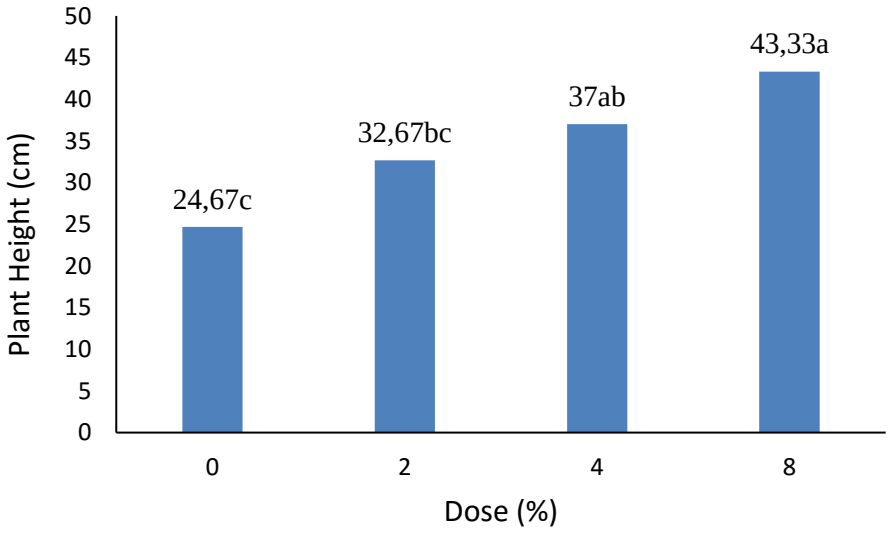

Figure 3. Effect of tea litter compost applications on plant height

3.3. Leaf N, P and K Contents

While tea litter compost applications increased the mean nitrogen and potassium contents of the pepper plant, the phosphorus content of the plant decreased with increasing application dose(Table 5).

Table 5. Some nutrient contents of the pepper plants grown in the tea litter compost kept in the root and shoot

Plant			
Dose (%)	N (%)	P (%)	K (%)
0	4.73d	0.37a	2.72d
2	4.80c	0.26b	2.98c
4	4.91b	0.25c	3.23b
8	4.98a	0.12d	4.76a
LSD	0.0133	0.0004	0.0005

With compost application mixed with soil, nitrogen and potassium intake of plant increased due to increased nutrient content. The highest N and K contents were obtained with 8% application, especially with a 75% increase in K. The contents of the plant N with compost applications determined sufficientby critical limits of Jones et al. (3.50-5%) (1991). The plant K content was reached with the compulsory limit value (3.5-4.5%) stated by the same investigator with 8% compost application.It has been stated by many researchers that composted organic materials are rich in nutrients, and it has been explained that composts can be used as soil conditioners in agriculture (Yalınkılıç et al., 1996, Kara and Erel, 1999, Alagöz et al., 2006, Polat et al., 2008) . It was stated that the highest N, P, K values were obtained with the application of herbal compost applied to the pointed pepper (Maurya and Dhar, 1983). It is stated that organic fertilizers applied to red pepper plant are statistically significant at 1% level in terms of yield and potassium content of leaf and fruit. (Kır and Mordoğan, 2006).

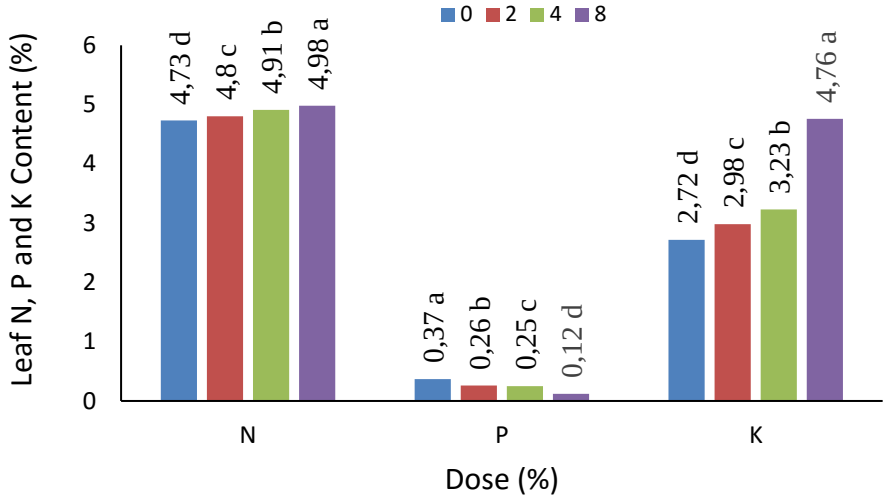

Figure 4. Effect of tea litter compost applications on leaf N, P, K of pepper plant

4. Results

It has been determined that tea litter, which constitutes an important waste potential in our region, is an effective material in improving the basic physical properties of soil when it is applied to soil by composting. It has been determined that adding soil to soil gives the most effective result on soil properties. It has also been found that the tea waste is a good source of N and K, the basic nutrients of the soil.

It has also been observed that tea litter compost on plant development brings remarkable results. Wet and dry weights ofroot-shoot, plant height, leaf N and K contents were increased and it was determined that 4% composting would be sufficient in growth parameters.

References

Alagöz Z., Yılmaz E., Ötüken F. 2006. Organik materyal ilavesinin bazı fiziksel ve kimyasal toprak özellikleri üzerine etkileri. Akdeniz Üniversitesi Ziraat Fakültesi Dergisi, 19(2): 245-254

Albaho, M., Bhat, N., Abo-Rezq, H., Thomas, B., 2009. Effect of three different substrates on growth and yield of two cultivars of Capsicum annuum. Eur. J. of Sci. Res., 28(2):227-233.

Allievi, L, Marchesini, A.,Saalrdi, C., Piano, V.and Ferrari, A. 1992. Plant quality and soil resudial fertility 6 years after a compost treatment. Bioresource Technologhy,43;85-89.

Anonim, 2010. Biber Yetiştiriciliği. GTHB Eğitim ve Yayınlar Dairesi Başkanlığı. http://www.tarimtv.gov.tr/VD236_ortu-alti-biber-yetistiriciligi.html

Anonim, 2014. Karadeniz Tarımsal Araştırma Enstitüsü Müdürlüğü Enerji Tarımı Araştırma Merkezi. Samsun

Aono, H., Yanese, Y. And Tanaka, S. 1980 Studies on the development and distribution of tearoots and their soils convervation faculty.Bulletin of the National Research İnstitute of tea, No: 16;291-319.

Aşık, B.B., Kütük, C., 2012. Çay atığı kompostunun çim alanların oluşturulmasında kullanım olanağı. U.Ü. Ziraat Fakültesi Dergisi 26(2), 47-57.

Blake, G.R., Hartge, K.H., 1986. Bulk density, Particle density. In: Methods of Soil Analysis. Part I, ASA-SSSA, Madison, WI, 363-382.

Bouyoucos, G.D., 1951. Arecalibration of the hydrometer method for making mechanical analysis of the soil. Agronomy Journal, (9);434-438.

Bray, R.H., Kurtz, L.T., 1945. Determination of total organic and available forms of phosphorus in soils. Soil Science., 45 : 39-45.

Bremner, J.M., 1965. Methods of soil analysis part II. Chemical and Microbiologial Properties. In.ed. C.A.Balack American Soc.of Agronomy.Inc.Pub.Agron Series. No:9 Madison USA.

Chapman, H.D., Pratt, P. F. and Parker, F., 1961, Methods of Analysis for Soils, Plant and Waters. Univ. OfCalifornia. Div. of Agric. Sci.

De Boodt, M., Verdonck, O., Cappaert, I. 1973. Method for measuring the water release curve of organic substrates. Proc. Sym. Artificial Media in Horticulture, 2054-2062. DIN. 11542. 1978. Torf für Gartenbau und Landwirtshaft. Germany.

Gabriels and Verdonck 1992. Reference methods for analysis of compost. In: Composting and compost quality assurance criteria., 173-183.

Güngör, F., Yıldırım, E., 2013. Effect of different growing media on quality, growth and yield of pepper (capsicum annuum l.) under greenhouse conditions. Ataturk University, Agriculture Faculty, Department of Horticulture Erzurum. Pak. J. Bot., 45(5): 1605-1608.

Kır, A. Mordoğan, N. 2006a. Değişik kompostların organik kırmızı biber (Capsicum annuum L.) yetiştiriciliğinde verim, bazı morfolojik karakterler ve potasyum içeriği üzerine etkileri. Ege Üniv. Ziraat Fak. Toprak Bölümü.

Kacar, B., Kovancı I., Atalay I.Z., 1980. Utilization of the tea waste products of tea factories inagriculture. A.Ü.Z.F. Yıllıgı 29 (1):158-173.

Kacar, B., 1987. Çayın Biyokimyası ve İşlenme Teknolojisi. Çay İşletmeleri Genel Müdürlüğü Yayını No: 6, 329 s., DSİ Matbaası, Ankara.

Kacar, B., 1992. Yapraktan Bardağa Çay. T.C. Ziraat Bankası Kültür Yayınları. No:23, T.C. Ziraat Bankası Matbaası, Ankara.

Kara, E.E., Erel, A. 1999. Tavuk gübresinin bazı toprak özelliklerine ve yulaf kuru bitki ağırlığına etkisi. Anadolu Journal of AARI, 9 (2): 91 – 104.

Keleş, D., 2012. Biber Yetiştiriciliği. GTHB Tarımsal Araştırmalar ve Politikalar Gen. Müd. Alata Bahçe Kül. Araş. İst., Erdemli.

Klute, A., 1986. Water Retention. Laboratory Methods. In:Methods of Soil Analysis, Part II, ASA-SSSA, Madison, WI, 635-662.

Knudsen, D., Peterson, G.A., Pratt, P.F., 1982. Lithium, Sodium and Potassium. Methods of Soil Analysis.,Part II.., ASA-SSSA, WI, 225-245.

Koç, F., 2008. Farklı organik gübrelerin domates ve biber bitkisinin gelişimi ile beslenmesine etkisi. Ankara Üniv. Fen Bilimleri Enstitüsü Ankara.

Kütük, C.A., Çaycı, G., Baran, A. 1995. Çay atıklarının bitki yetiştirme ortamı olarak kullanılabilme olanakları. Ankara Ünv. Ziraat Fak. Toprak Bölümü 1995.

Majdi, Y., Ahmadizadeh, M., Ebrahimi, R., 2012. Effect of different substrates on growth indices and yield of green peppers at hydroponic cultivate. Current Research Journal of Biological Sciences 4(4): 496-499.

Maurya, K. R., and N. R. Dhar. 1983. Effect of different composts on yield and composition of chilli (Capsicum annuum L.), Anales de Edafologia Agrobiologia, 1983, 42:1-2, 183-191.

Mitchell, J.P., Shennan, C., Grattan, S.R. and May, D.M.1991. Tomato fruit yields and quality under water deficit and salinity. J. Amer. Soc. Sci., pp. 116(2): 215221.

Nelson, D.W., Sommers, L.E. 1982. Total carbon, organic carbon and soil organic matter. In: Methods of Soil Analysis, Part II, ASA-SSSA, Madison, WI, 539-579.

Polat, M., Çelik, M. 2008. Ankara (Ayaş) koşullarında organik çilek yetiştiriciliği. Tarım Bilimleri Dergisi, 14 (3): 203-209.

Stringheta, A.C.O., Cordoso, A.A., Lopes, L.C., Fontes, L.E.F., 1999. Growth of chrysanthemum in substrate consisting urban solid waste compost and carbonized rice rusk. Revista Ceres, 264; 175–188.

U.S. Salinity Laboratory Staff. 1954. Diagnosis and improvement of Saline and Alkali Soils. Agriculture Handbook No.60, U.S. Depertman of Agriculture, Washington, D.C., U.S.A.

Uzun, S., Özkaraman, F., Marangoz, D., 2000. Torba kültüründe kullanılan farklı organikartıkların son turfanda olarak ısıtmasız seralarda yetiştirilen bazı sebzelerin büyüme, gelisme ve verime etkisi. OMÜ Zir. Fak. Dergisi, 2000, 15 (3): 16–21.

Yalınkılıç, M.K., Altun, L., Kalay, Z. 1996. Çay fabrikaları çay yaprağı artıklarının kompostlaştırılarak orman fidanlıklarında organik gübre olarak kullanılması.Ekoloji Çevre Dergisi, Sayı: 18, 28-32.

Yılmaz, S.,Bender Özenç, D. 2012.Fındık zurufu ve çay atığı kompostlarının mısır bitkisinin (zea mays l.) gelişimi üzerine etkileri. Ordu Ünv. Fen Bilimleri Enstitüsü Toprak Bilimi ve Bitki Besleme Anabilim Dalı. Ordu.

Good Agricultural Practices

Ali TURAN[1], Hasan KARAOSMANOĞLU[1*], N. Şüle ÜSTÜN[2]

[1]Giresun University, Vocational School of Technical Sciences, Giresun, Turkey
[2]19 Mayıs University, Department of Food Engineering, Samsun, Turkey

[*]**Sorumlu Yazar:** hasan.karaosmanoglu@giresun.edu.tr

ABSTRACT

Good agricultural practices (GAP) were born from the need to produce healthy agricultural products that will give the least damage to the environment and nature. The GAP is based on the principle of co-implementation of integrated pest management (IPM) and integrated crop management (ICM) in the commercial production of agricultural products. IPM/ICM applications are considered to be absolutely necessary for sustainable agricultural production. The implementation of hazard analysis at the crtitic control points (HACCP) is also encouragedby the GAP. With good agricultural practices, conservation of soil and water resources, preservation of natural equilibrium, prevention of environmental pollution, prevention of residue in crops and increase of productivity and reasonable profit are achieved. Therefore, it is necessary for our producers and exporters to adoptand implement the applications that will enable us to solve the major problems of agricultural exports of our country and enable us to sell more products to developed countries.

Keywords: Environmental health, integrated pest management, human health, good agricultural practices

1. Introduction

Good Agricultural Practices (GAP) arise from the need of producing healthy products with giving less harm to environment and the nature, and includes main principles developed for this purpose. GAP also aims the combined application of both Integrated Pest Management (IPM) and Integrated Crop Management (ICM) techniques. IPM, ICM applications are regarded as absolute necessities for a sustainable agricultural production. The application of Hazard Analysis in Critical Control Points (HACCP) is promoted with GAP.

Germany, Netherland, France and Greece, most of which are members of UN, take an important place in the fresh fruit and vegetable exportation of Turkey. Thus, when the subject is taken into consideration from the aspect of Turkey, the producers and exporters of the fresh fruit and vegetables especially grown for exportation are in the period of taking the EUREPGAP certificate. (At that point, the Ministry of Agriculture formed a technical commitee for the purposes of examining the EUREPGAP protocol and informing the producers and exporters. It also published a regulation.)

The first regulation of Good Agricultural Practices published at 8th of September 2004 in the Official Gazette no. 25577 was prepared for making an agricultural production giving no harm to human and animal health, saving the natural resources, providing food safety with traceability and sustainability in agriculture. According to the regulation, the producers and producer unions applying Good Agricultural Practices can have a priority to benefit from the agricultural supports.

2. Practicing

2.1. Recording

Producers who apply Good Agricultural Practices record the stages of the products from the place of production to the last consumer, in a way that they prove all of the stages are appropriate for Good Agricultural Practices and they keep these records for five years.

2.2. Fertilizing

The appropriate cultivation techniques must be applied for the effective usage of fertilizer. Fertilizing should be done in the light of the results of the analysis formed by both the nutrient need of the product and the soil. Fertilizing as mineral or organic must protect the soil fertility as well as meeting the need of production.

2.3.Irrigation

Failures in irrigation give harm to both the quality and quantity of product. Therefore, the techniques which determine the water need of product must be used not for doing excessive or inadequate irrigation. The prediction of the irrigation need is done depending on precipitation rate, water requirement of the plant, and evaporation amount. In order to get most benefit from water opportunities, the most convenient and effective irrigation system should be used. Surface irrigation application should not be preferable, because it results in excessive waste of water. Irrigating programmes are very important in decreasing the water leakage and optimizing the usage of water. (Example: Reuse of the water that leaves the plots by surface flow, which results from excessive irrigation, night irrigation, overhaul of the irrigation equipments to prevent the water loss resulted from leakage, providing the accumulation of precipitation in the soil, accumulation of rain water from greenhouses.) Producers should record the use of water for irrigation.

2.4. Plant Protection

Biological, cultural and mechanical methods should be preferable in order to protect the products from harmful weeds. In compulsary situations, pesticide applications must be done in less harmful way (volume/active matter) for environment. Producers must adopt IPM techniques. Non-chemical methods should be preferred rather than chemical ones in fighting with plant diseases and pests. In agricultural fighting practices with pesticide, producers are provided learning and encouraged applying the IPM techniques which decreases the environmental pollution. The necessary training and assistance to apply the IPM techniques should be provided by breeder organizations, research and publishing organizations, consultants and pesticide distributers.

The chemical used for agricultural fighting should be effective in protecting the product. Specific chemicals that enable controlling the harmful diseases and weeds, as well as being non-dangerous for water life, beneficial macro-organisms, workers, consumers and ozone layer should be used. If possible, chemicals which do not develop resistance in plant diseases controlled by chemicals, harmful plants and weeds must be used.

2.5. Harvesting

A staff hygene protocol which considers the possible risks to prevent the possible risks to prevent the physical, microbiological, and chemical contamination should be formed. There should be toilets and hand-washing stations near the workplaces. The workers should take basic education about hygene before harvesting. They should also inform the administration in case of a health issue that can contaminate the products.

The packaging material should be kept in appropriate storages to prevent the contamination of harmful diseases. The packaging material should be moved to storages again and not be left in the field, when the packaging is done in an open field, to prevent the risk of contamination. Reusable plastic boxes should be clean or cleared again to cleanse the foreign matter that can threaten the consumer health.

3. Conclusion

It is required that all of the organizations taking place in the food production chain should be aware of their duties and responsibilities in totally applying and supporting the GAP. If the consumer confidence is wanted to be gained in terms of agricultural products, some standards must be applied like Good Agricultural Practices and bad applications must be eliminated. All the producers can prove that they obey both the international and national rules and fulfill their commitments. It is required that the things mentioned above and alike which can be a solution to the important problems of Turkey's agricultural product exportation and allow Turkey to sell more products to develop countries should be fastly adopted and implemented by producers and exporters.

References

Anonim (2004). İyi Tarım Uygulamalarına İlişkin Yönetmelik. 08.09.2004 tarih ve 25577 sayılı Resmi Gazete.

Atış E. (2005). Tarım ve Çevre. *Türkiye'de Tarım* (s. 161-176). İzmir Ege Üniversitesi Tarım Ekonomisi Bölümü: Tarım ve Köyisleri Bakanlıgı.

Güzel (2012). Tarımda kalite uygulamaları kapsamında iyitarım uygulamarının (Gap) yerve bir örnek uygulama. Dokuz Eylül Üniversitesi, sosyal Bilimler Enstitüsü, Yüksek Lisans Tezi, İzmir.

Mızrak (2005). İyi Tarım İlkeleri. Türk Yüksek Ziraat Mühendisleri Birliği, Ankara.

WOOD MECHANICS AND TECHNOLOGY, WOOD PROTECTION TECHNOLOGIES, FOREST INDUSTRY MACHINES AND BUSINESS, FORESTRY AND SOFTWARE TECHNOLOGY

ORAL PRESENTATIONS

Evaluating the Performance of Optimal Log Bucking Decision Simulator

Ebru BİLİCİ[1*], Abdullah E. AKAY[2]

[1]Giresun University, Dereli Vocational School, Department of Forestry, Giresun, Turkey
[2]Bursa Technical University, Faculty of Forestry, Department of Forest Engineering, Bursa, Turkey

[*] **Corresponding Author:** ebru.bilici@giresun.edu.tr

Abstract

To ensure sustainable management of forest resources, the economic value of every single tree should be maximized by implementing modern methods. During timber extraction activates, bucking is the most crucial stage that effects the market value of the harvested trees. Thus, trees should be systematically cut into the optimal bucking pattern that maximizes the total economic value of timber. In many parts of the world as well as in Turkey, bucking cuts are determined by harvesting crews based on their experiences. However, it can be very difficult to quickly evaluate bucking alternatives and come up with the optimal bucking pattern. In this study, it was aimed to present the capabilities of optimal log bucking decision simulator called HW Buck. This simulator is a computerized bucking trainer which is developed to assist harvesting crews to select the optimal or near-optimal bucking cuts for hardwood logs. By using HW Buck simulator, harvesting crews can be equipped with necessary skills to determine the near-optimal bucking pattern that maximizes the economic value of a single tree. Simulator provides crews with technical knowledge about log grading, log scaling, surface defects indicators, potential internal implications, etc. HW Buck has an interactive graphic display that shows realistic representation of a stem and allows users to compare the results of the bucking decisions. The results shown that training with this simulator has great potential to reduce the gap between technological capabilities and production applications in the field.

Keywords: Bucking, HW Buck, optimization, hard woods

Introduction

After felling the tress, the process of cutting them into specific lengths is known as bucking operation. Bucking the harvested trees in an optimum way is very important to maximize the economic value of the trees (Akay et al., 2009). To gain maximum benefit from optimum bucking method, large number of alternative bucking combinations need to be evaluated while considering many decision variables (Akay et al., 2010). Some of these decision variables may include, log lengths, log quality classes, and market demand. In order to solve complex optimal bucking problems, using computer-assisted methods such as network analysis, dynamic programming, and heuristic methods must be utilized (Laroze and Greber, 1997).

Nakahata et al. (2014) conducted a study where an optimal bucking methods were applied to maximize profits, with and without taking log size into consideration. They reported that the optimal bucking approach considering log sizes can assist decision makers to determine the optimal extraction rates of younger stands with smaller DBHs. Aruga et al. (2015) developed an optimal bucking algorithm for maximizing profits, based on the previous study conducted by Nakahata et al. (2014). They tested the algorithm in clear-cutting operations on middle- and gentle-slope terrains. They stated that optimal bucking increased the profit by 2.20 and 1.50 times for middle- and gentle-slope terrains, respectively.

There are limited number of studies on the subject of optimal bucking in Turkey. Serin et al. (2010) conducted a study where, the effects of optimum bucking method on the total economic value of timber in Brutian Pine stands were investigated. They stated that optimum bucking method increased the economic value of the harvested trees by 4.7%. In another study where the effects of stem defects on optimum bucking method were investigated, it was reported that the optimum bucking method provides better results for the harvested trees with more stem defects (Akay et al., 2015). In more recently, Pak and Gülci (2017) investigated economic gain of optimum bucking method in Oriental Beech stand. They employed network analysis based Network 2000 program to implement optimum bucking method in a sample application.

It is possible to quickly evaluate bucking alternatives and come up with the optimal bucking pattern by using computer-assisted optimal bucking methods. However, harvesting crew should have appropriate training sessions in order to understand and implement these methods effectively and efficiently. HW Buck is one of well know bucking decision simulators that can assist harvesting crews to select the optimal or near-optimal bucking cuts. When

harvesting crew use this simulator they can be equipped with necessary skills to determine the bucking pattern that maximizes the economic value of a single tree. In this study, the capabilities of optimal log bucking decision simulator, called HW Buck, were presented and some of the key features were introduced.

2. History of HW Buck

The issue of potential value loss was first addressed by Pickens et al. (1992) during the bucking operation of hardwood stems in the field. They reported the potential value losses of 28-35% depending on which set of historical prices was used. According to the optimal bucking patterns, greater timber volume was received from the higher value grades and lower timber volume was from the lower value grades. Based on the previous work and experiences, Pickens et al. (1993) developed a computerized bucking decision simulator, named HW Buck, for hardwood logs (Pickens et al., 1993). The main goal of HW Buck was to help train harvesting crew to select bucking cuts that maximizes the potential value of the stem. The program was then received “1994 Hardwood Research Award” given by the National Hardwood Lumber Association referred. In early years, its features was limited because it was written for a DOS platform. Also, it was not flexible enough to consider the market conditions across the eastern hardwood region. Therefore, Pickens et al. (2006) developed the HW Buck (Figure 1) as a Windows program that provided users with advanced features and highly flexible tools to adapt for the wide range of situations that occur in hardwood log markets.

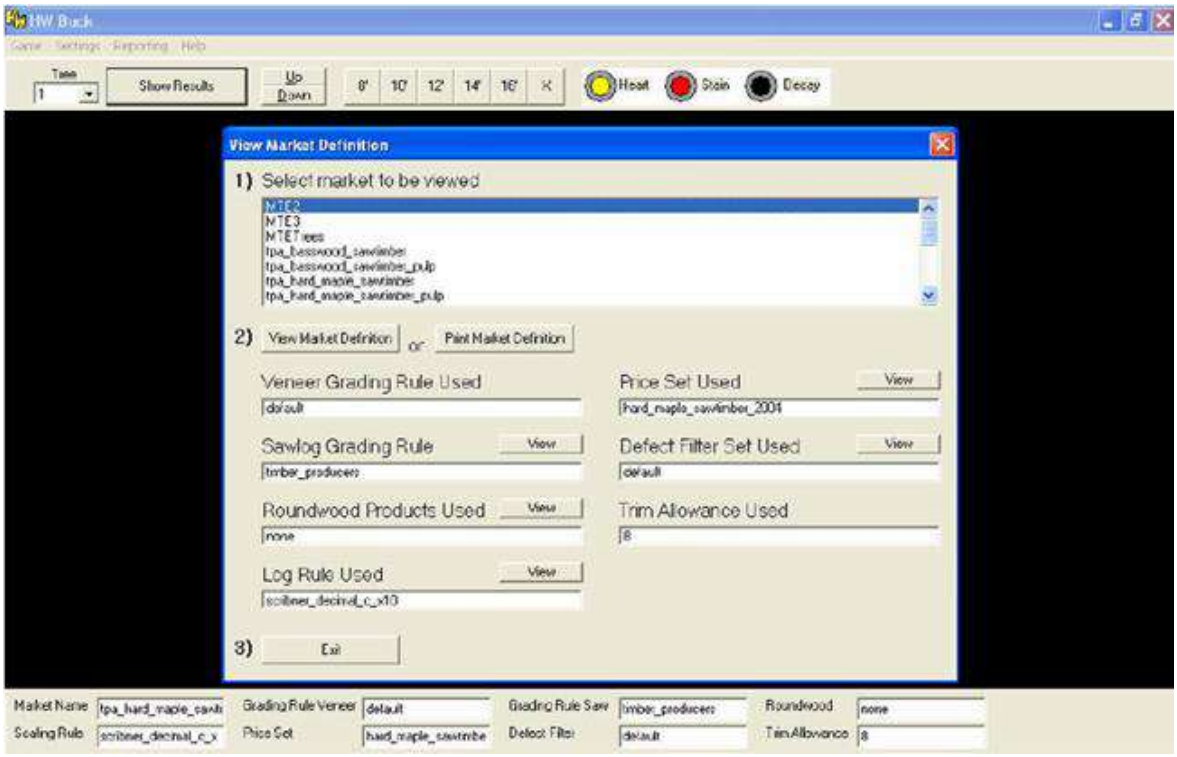

Figure 1. The interface view of HW Buck program.

3. HW Buck for Windows

3.1. Bucking Options

HW Buck for Windows has pull-down menus to facilitate navigation through the various processes. The menu called “Game” provides the commonly used options which are divided into two groups (Figure 2). At the top group there are different ways of bucking options that the user can choose from. In the “Buck With Optimal”, the user is can select a tree stem and then the stem can be rotated to check hidden defects and stem shape. The user can select bucking combination and compare with the optimal solution provided by the software (Figure 3). The HW Buck comparison page indicates bucking summary data including the log grade, bark diameter, total sweep, percent cull deduction due to sweep, and total percent cull deduction.

Figure 2. Menu called "Game" in HW Buck program.

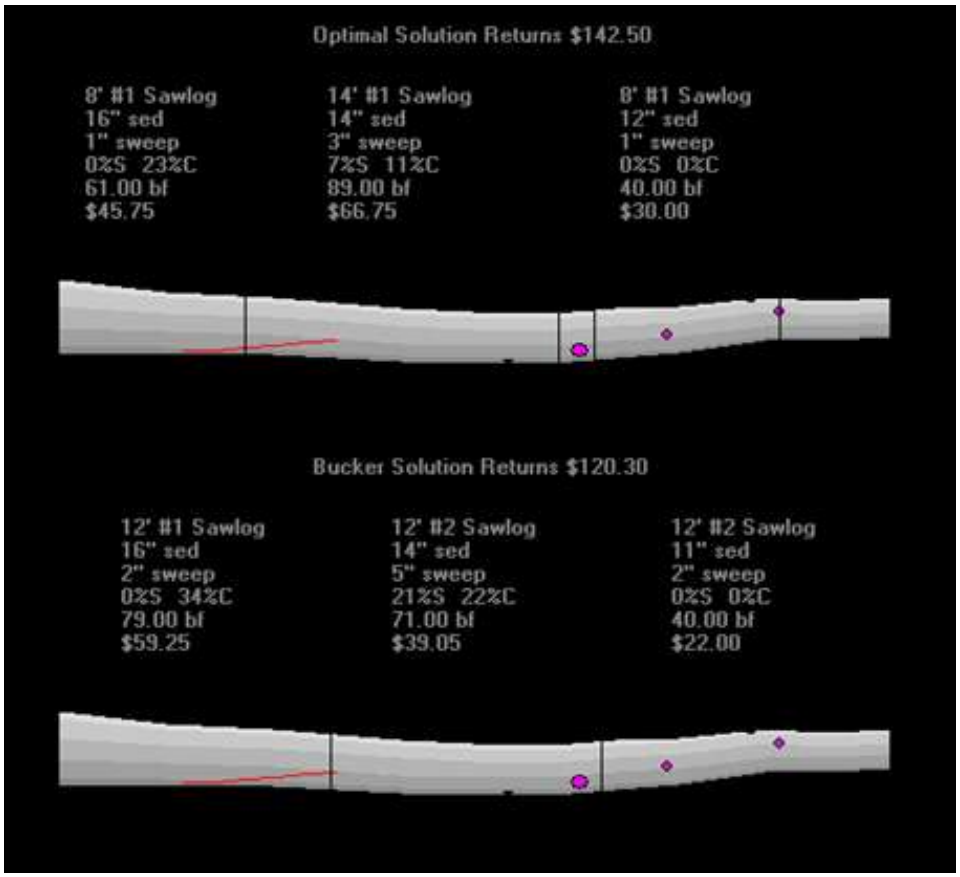

Figure 3. The HW Buck comparison page.

In the example shown in Figure 3, the trainee-chosen bucking pattern provided the totals economic value of $120.30 while optimal bucking solution improved the tree value by about 19% ($142.50). It was reported that training program was able to reduce the value lost by

buckers by about 50% by considering factors such as defect identification, grading and scaling (Pickens et al., 2006).

The other options in the top group of the Game menu, “Buck With Tracking” and “Group Buck With Tracking”, are new with the Windows version. In these options, a trainee can buck logs and evaluate the results of the bucking decisions. Using these options, harvesting crew can compete with each other without having the optimal bucking pattern displayed and develop their own bucking strategies.

3.2. Markets in HW Buck

At the bottom group “Game” menu, a user can have all the information needed to define tree bucking in a given situation by considering market demand. This information includes grading rules for sawlog and veneer, definitions for various roundwood products, log rule selection for measuring volumes, product prices for various log grade and length classes, selection of grading defects, and the required trim allowance (Figure 4). It is very important to consider alternative grading rules cause this allows users to address the range of market conditions encountered in the region. Comparing with the previous DOS version of HW Buck, Windows version provides the ability to view much of the data used when a market was previously developed (Figure 5).

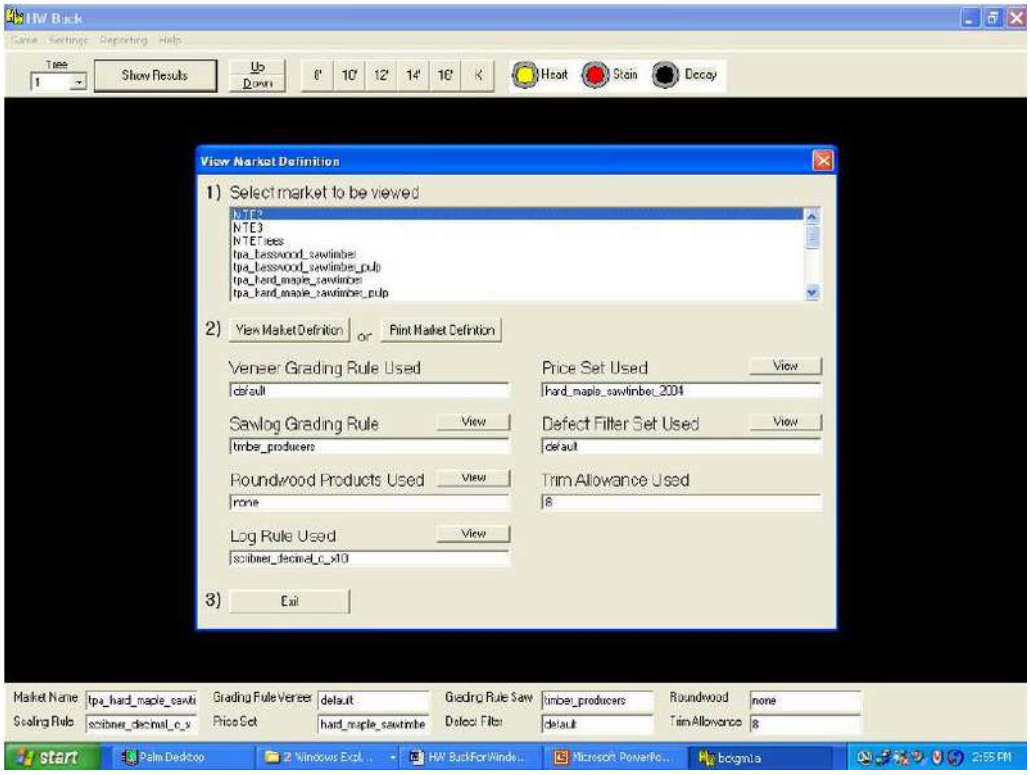

Figure 4. Input window to enter market data.

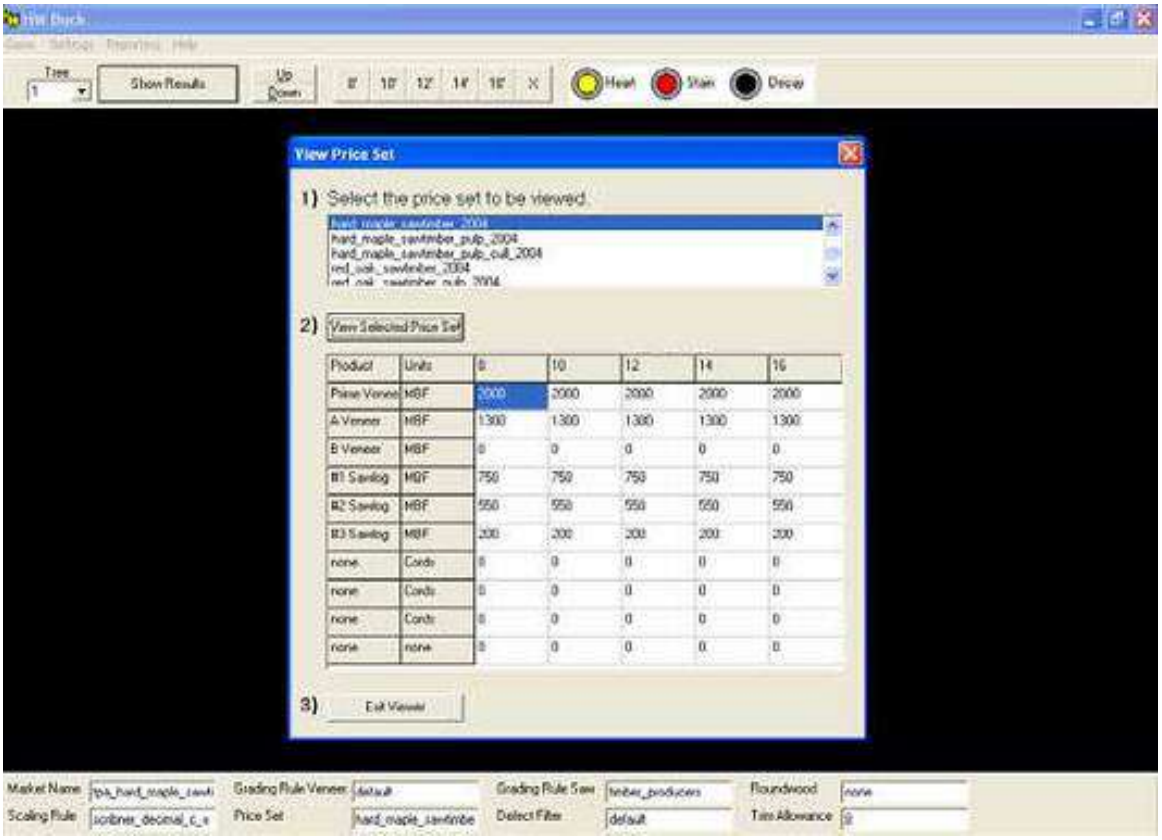

Figure 5. Previously defined data displayed in the Windows version of HW Buck.

4. Conclusions

Although current version of bucker training program improves value recovery in hardwood log bucking, there is still options to improve the performance of the HW Buck program. The first option is to acquire data on hardwood stems using remote sensing techniques, enter the data into HW Buck, and then find the optimal bucking pattern. Some of the HW Buck data such as stem shape, diameter, taper, nots, and sweep are relatively easy to collect with optical light and laser technology. The second type of information concerns the occurrence and pattern of defects along the stem. However, other type of information about stem defects such as light bark distortions, bird peck, some seams, and decay holes cannot be detected by optical light or laser approaches. In these cases, the ultrasound and x-ray techniques can be used to penetrate into the stem and to identify the occurrence and extent of defects. The down side is that these technologies are very expensive and still at the experiment stage. The second option is to train the log buckers working with harvesting crews to make better bucking decisions. By

taking training program, the harvesting crew should identify grading defects on the hardwood stems and they need to understand the log grading and scaling rules.

References

Akay, A.E., Serin, H., Pak, M. and Yenilmez, N., (2009, October). Optimum tree-stem bucking of Brutian Pine (*Pinus brutia*) Trees in Antalya, Turkey, *Third International Faustmann Symposium, "Forest Economics in a Dynamic and Changing World"*, Germany.

Akay, A.E., Sessions, J., Serin, H., Pak, M., and Yenilmez, N., (2010). Applying Optimum Bucking Method in Producing Taurus Fir (*Abies cilicica*) Logs in Mediterranean Region of Turkey. *Baltic Foresty*. 16(2), 273-279.

Akay, A.E., Serin, H., and Pak, M., (2015). How Stem Defects Affect The Capability Of Optimum Bucking Method? *Journal of the Faculty of Forestry Istanbul University*. 65(2), 38-45.

Aruga, K., Mizuniwa, Y., Uemura, R., and Nakhata, C., (2015, October). Optimum bucking method for clear-cutting operations in Nasu Forest Owners' Co-operative, Tochigi prefecture, Japan. *Proceedings of the 48th FORMEC Symposium*, Linz, Austria.

Laroze, A.J. and Greber, B.J., (1997). Using Tabu Search to Generate Stand-Level, Rule-Based Bucking Patterns, *Forest Science*. 43(2), 367-379.

Nakahata, C., Aruga, K., and Saito, M., (2014). Examining the Optimal Bucking Method to Maximize Profits in Commercial Thinning Operations in Nasunogahara Area, Tochigi Prefecture, Japan. *Croat. J. For. Eng*. 35(1): 45-61.

Pak, M. and Gülci, N., (2017). A comparative economic evaluation of bucking deciduous trees: A Case study of Oriental beech (Fagus orientalis) stands in Northeastern Turkey, *Journal of the Faculty of Forestry Istanbul University*. 67(1), 72-79.

Pickens, J.B., Lee, A., and Lyon, G.W., (1992). Optimal bucking of northern hardwoods. Northern *Journal of Applied Forestry*. 9(4), 149-152.

Pickens, J.B., Lyon, G.W., Lee, A., and Frayer, W.E., (1993). HW-BUCK computer game improves hardwood bucking skills. *Journal of Forestry*. 91(8), 42-45.

Pickens, J.B., Noble, S., Orr, B., Araman, P.A., Baumgras, J.E., and Steele, A., (2006). HW Buck for Windows: the optimal hardwood log bucking decision simulator with expanded capabilities. *Proceedings, Society of American Foresters 2005 National Convention*. 7 pp.

Serin, H., Akay, A.E., and Pak M., (2010). Estimating the Effects of Optimum Bucking on the Economic Value of Brutian Pine (*Pinus Brutia*) Logs Extracted in Mediterranean Region of Turkey, *African Journal of Agricultural Research*. 5(9), 916-921.

The Endangered Species with Natural Woody of Turkey

Elif KAYA ŞAHİN[1], Nilgün GÜNEROĞLU[2]

[1]KTÜ Orman Fakültesi, 61080 Merkez Kampüs, Trabzon (TR), elifkaya@ktu.edu.tr
[2]KTÜ Orman Fakültesi, 61080 Merkez Kampüs, Trabzon (TR), nayhan@ktu.edu.tr

* **Corresponding Author:** elifkaya@ktu.edu.tr

Abstract

Turkey has a lot of varieties of plants because it is located at the junction of three different geographical regions and climatic zones. There are approximately 12,000 plant species in our country, including 3,000 endemic species. The number of plants is increasing day by day with the discovery of a new plant.

The natural plants of Turkey are at the edge of extinction due to manmade stress and pressure on their habitats. These plants will probably stay threatened as industrialization, urbanization, overgrazing, afforestation and fires are continued.

Some of our plant species are being used for various purposes together with being under threat, and if they are not under control, they are in danger of being lost in the future.

In this study, 46 species belonging to 19 endangered families were identified in our country. *Acer undulatum, Rhododendron ponticum, Sorbus caucasica, Salix trabzonica, Zelkova carpinifolia.* Information has been provided on the sustainability of endangered species and the work to be done to reach future generations.

Keywords: Woody Plants, Endangered Species, Natural Species, Turkey

1. Introduction

Turkey, three plants have a lot of varieties of plants due to the confluence of three major geographical regions and climatic zones. The number of new plants is increasing every day. Turkey, in terms of plants, is among the richest countries in the world (Güner ve ark., 1996). There are more than 12.000 plant species in our country. Of these, 3,000 are endemic plant species.

While some of our plant species are currently under threat, they are used for a variety of purposes, and if their destruction is not controlled, they are in danger of disappearing in the future.

2. Material and Method

In this study, the importance of preserving these species by giving endangered woody species in our country is emphasized. At the end of the study, 46 species belonging to 19 families were determined.

Table 1. It detected 46 species.

▪ *Acer undulatum*	▪ *Ononis adenotricha BOISS. var. nuda*
▪ *Kalidiopsis wagenitzii*	▪ *Linum boissieri*
▪ *Fumana trisperma*	▪ *Linum hirsutum L. subsp. anatolicum (BOISS.) HAYEK var. platyphyllum*
▪ *Helianthemum germanicopolitanum*	▪ *Acantholimon caryophyllaceum BOISS. subsp. Parvifloru m*
▪ *Tanacetum munzurdaghensis*	▪ *Acantholimon confertiflorum*
▪ *Aethionema demirizii*	▪ *Polygonum samsunicum*
▪ *Aethionema papillosum*	▪ *Dionysia teucrioides*
▪ *Alyssum caricum*	▪ *Cerasus incana (PALLAS) SPACH var. Velutina*
▪ *Alyssum niveum*	▪ *Eriolobus trilobatus (POIRET) ROEMER var. Sorgerae*
▪ *Rhododendron ponticum*	▪ *Prunus kurdica*
▪ *Rhodothamnus sessilifolius*	▪ *Pyrus anatolica*
▪ *Globularia davisiana*	▪ *Pyrus salicifolia PALLAS var. serrulata BROWICZ*
▪ *Globularia dumulosa*	▪ *Pyrus serikensis*
▪ *Origanum munzurense*	▪ *Pyrus yaltirikii*
▪ *Origanum husnucanbaseri*	▪ *Sorbus caucasica*

▪ *Origanum solymicum*	▪ *Asperula pseudochlorantha*
▪ *Phlomis amanica*	▪ *Asperula sintenisii*
▪ *Thymus canoviridis*	▪ *Salix purpurea L. subsp. Leucodermis*
▪ *Thymus cherlerioides VIS. var. isauricus*	▪ *Salix rizeensis*
▪ *Thymus spathulifolius*	▪ *Salix trabzonica*
▪ *Colutea melanocalyx BOISS. ET HELDR. subsp. melanocalyx BOISS . ET HELDR.*	▪ *Thesium oreogetum*
▪ *Genista sandrasica*	▪ *Zelkova carpinifolia*
▪ *Gonocytisus dirmilensis*	▪ *Heptaptera cilicica*

2.1. *Acer undulatum*

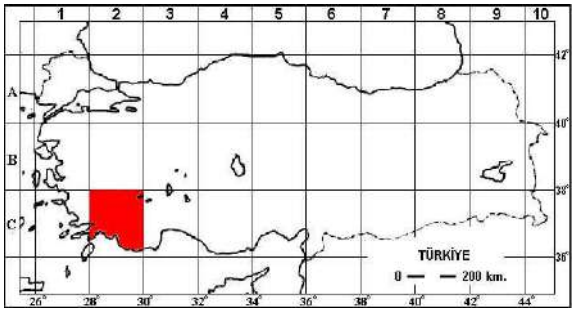

Figure 1. A Distribution in Turkey *Acer undulatum.*

Acer undulatum small, usually slow growing, is a natural endemic species in Turkey. It is only grown in Muğla's Babadağ region (Fig 1).

It ranges between 1400 and 1800 m. It is usually found on western facades and steep slopes.

The branches of these maple species are very short; first they are grayish brown and glabrous, and then gray-skinned and pubescent.

Mature leaves are 3-5 veined, the upper face is completely bright and the lower face is hairy (Ayberk ve ark., 2010; Var,2010).

2.2. *Rhododendron ponticum*

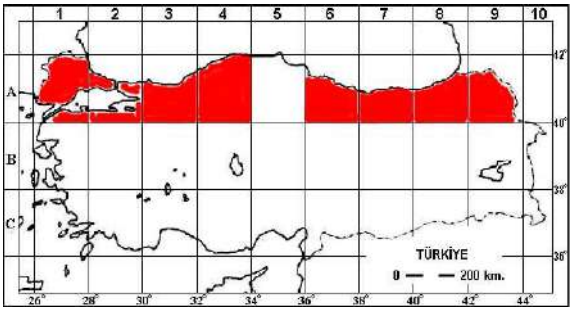

Figure 2. A Distribution in Turkey *Rhododendron ponticum.*

Usually 3-4 m tall shrub, sometimes a small tree can be a species. Leaves are evergreen, leather-like, full-edged, broadly ribbon or elliptical. May, June, flowering, purple in color. The flower stem is long and hairy.

Geographical spread of purple flowering rhododendrons Caucasus and Turkey is also locally present in Lebanon and Spain. Our country extends all along the Black Sea coasts, but the most abundant is the mountains of Northeast Anatolia (Anşin ve ark.,2006; Var,2010) (Fig.2).

2.3. *Sorbus caucasica var. Yaltirikii*

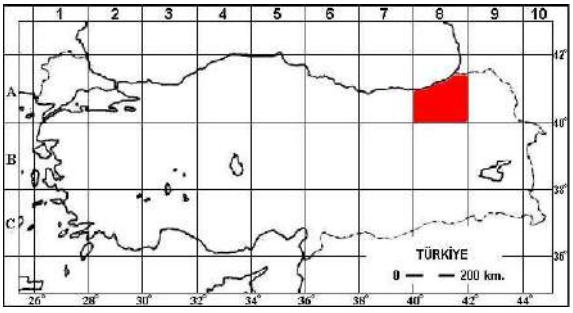

Figure 3. A Distribution in Turkey *Sorbus caucasica var. Yaltirikii.*

This species is endemic in Turkey, makes distributions in 1750 m in Rize (Fig.3). It is a small tree with a large crest up to 7 m. The shell is reddish-dark gray in color and has a fine and smooth surface. Leaf stalk is between 1-2 cm. The yellowish-green stalks are sparse or pubescent. The leaves are large or wide egg-shaped elliptical.

The edge of the leaf is 5-7 lobed. Lop edges are double-row spur gears. The upper surface of the leaves dark green and bare, yellowish-green open lower face and naked.

The flower is 15-16 mm in diameter and the leaves are dirty white.

Fruits with a diameter of 1-1,5 cm are spherical or broadly ovoid. In the ripening stage, bright orange-yellow-red fruits take a deep red color and are speckled (Eminağaoğlu ve ark.,2011).

2.4. *Salix trabzonica*

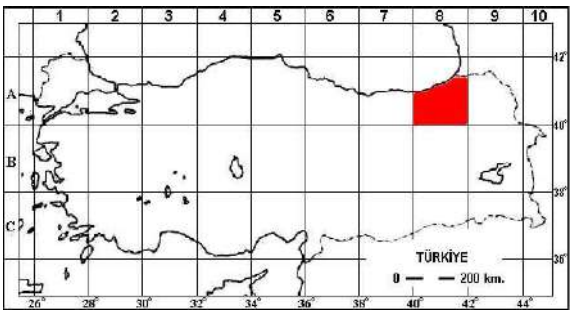

Figure 4. A Distribution in Turkey *Salix trabzonica.*

The mountain slopes of Trabzon in Turkey is a species occurring in approximately 2100 m altitude (Fig.4). The shoots are glabrous shrubs with hairless, short and thick, brown or grayish brown. Young shoots before the gushy goat hairy, later hairless.

Leaves are elliptical in shape, about 3 times the length of their length, 50-80 x 17-32 mm in diameter and tapered towards the bottom. The upper face is glabrous and dark green, the lower face is open and greyish-green in color, dense and short flattened hair, the edges are curved towards the bottom of the sheet and are finely toothed.

Leaf stem is 1-1.5 mm in length. Flowering time is July (Eminağaoğlu ve ark.,2018).

2.5. *Zelkova carpinifolia subsp. Yomraensis*

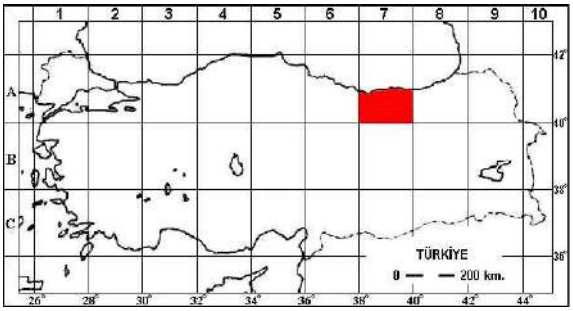

Figure 5. A Distribution in Turkey *Zelkova carpinifolia subsp. Yomraensis.*

The first step of the hornbeam Zelkova A7 Trabzon-Yomra in the region of 40 m height Z. carpinifolia sample has been identified as a new sub-species (Fig.5). This new subspecies is endemic and it is 2-3 (-5) m tall. It is found at low elevation, its leaves are smaller, its upper face is the same as Sandstone, it is sandy or rough (Geven ve ark., 2016; Var, 2010).

In our country, plants are under various pressures and some of them face difficulties in sustaining their generation as a result of these events. If we mention these (Ekim ve ark.,2000);

- **Industrialization and Urbanization:** In recent years, industrialization and urbanization events, which have shown rapid development in our country, create some danger on some narrow spread plants. Nowadays the dam, road, bridge, railway etc. substructure facilities. In addition, highway construction causes damage to some plants.
- **Expansion of agricultural and grazing Area:** Expansion of mechanization in agriculture, stepping into the field of steppe lands has accelerated the event.
- **Tourism:** Our coastal and sand dunes are occupied by an increasing number of facilities. As a result, some rare plants are damaged.

- **Extraction from Nature with the Purpose of Exportation and Domestic Use:** As is known, for a long time, some plants have been collected from nature for various purposes (medical, dental, spice, ornamental, fuel, animal feed, etc.), some are used domestically and some are sold abroad. As a result of these events, some medicinal and aromatic plants have been identified as decreases in their populations and this decrease is increasing.
- **Barren (halophytes) Areas of Improvement:** In our country, especially in Central Anatolia, the barren areas covering large areas are rapidly improved. As a result of the improvement of the habitat conditions of these species, it is highly probable that generations of these species will be lost as a result of the reclamation of these types of places mostly covered with salted plants.
- **Agricultural Struggle and Pollution:** It is known that the plant and animal species are damaged due to unconscious pesticide use which causes pollution of the soil as well as air and water pollution. The weeds that grow in the fields in terms of plants are composite plants which are very common on the earth. Therefore, it is not easy to consume these natural plants with these events. However, rare plants can be harmed by this type of struggle.
- **Silviculture:** It is necessary to be very careful in the afforestation works carried out by some organizations. This type of work, if it is done in a very rare plant, where this plant in the coming years, due to changes in the environment conditions are likely to disappear.
- **Fires:** Especially in the Marmara, Mediterranean and Aegean regions with rich endemics, the fire-sensitive maquis and red pine cuttings are very likely to be abolished by rare natural species.

3. Results and Discussion

The list of plant species that are rarely grown in our country and which are thought to be under threat in the future is important in terms of showing what they should protect their nature conservationist. In addition to various measures for the protection of nature, the most demanded view in the world in the protection of plant species is the reproduction of nature conservation areas in various statuses. Although there has been an increase in the number of National Park and Nature Conservation Areas in our country in recent years, it is difficult to say that some of them were established in places suitable for typical nature conservation purposes and they were selected for studies aiming to achieve this goal. For this reason, National Parks should be established in places with interesting flora and fauna rich in endemic species in our country.

In these areas, while endemic, rare and endangered species are preserved in their own fields, it should be ensured that the species that belong to this group in the immediate vicinity are protected and transported here. Protected areas, which have been established

mostly in forest areas so far, should be established in the future in steppe, salt marsh and even in wetlands. In recent years, very positive developments have been observed in this area.

Another point of interest about the plant species that needs to be protected is the cultivation of them in the Botanical Gardens and thus ensuring their access to the next generations.

The fact that the National Botanical Garden, which still works in accordance with the scientific objectives in our country, has not been established is one of the factors that prevent the effective conduct of the studies in this field.

References

Anşin, R., Özkan, Z. C., (2006). Tohumlu Bitkiler (Spermatophyta), Odunsu Taksonlar, KTÜ Genel Yayın No: 167, Orman Fak. Yayın No: 19. KTÜ Basımevi. Trabzon.

Ayberk, H., Cebeci, H., (2010). Scolytus rugulosus (Muller) (Coleoptera, Scolytidae)-A New Pest of Acer undulatum Pojark in Turkey. Journal of Animal and Veterinary Advances 9(17):2325-2326.

Davis, P.H., (1965-1985). Flora of Turkey and the East Aegean Islands, Vol I-IX, Edinburgh University Press, Edinburgh.

Ekim, T., Koyuncu, M., Vural, M., Duman, H., Aytaç, Z., Adıgüzel, N., (2000). Türkiye Bitkileri Kırmızı Kitabı (Eğrelti ve Tohumlu Bitkiler), Ankara.

Eminağaoğlu, Ö., Avcı, M., Ok, T., Aksoy, N. (2018). Salix L. (Ed. Ü. Akkemik) Türkiye'nin Doğal- Egzotik Ağaç ve Çalıları. Orman Genel Müdürlüğü Yayınları, Ankara. s: 592.

Eminağaoğlu, Ö., Özkaya, M.S., Akpulat, H.A., (2011). A new record for the fl ora of Turkey: Sorbus caucasica var. caucasica (Rosaceae), Turk Journal Botanik, 36 (2012) 426.

Geven, F., Adıgüzel, N., (2016). *Zelkova carpinifolia* (Pall.) C. Koch (Ulmaceae) in Turkey (Relict Tree): Floristics, Ecology, Distrubition and Threats. International Forestry Symposium (IFS 2016), 07-10 December 2016, Kastamonu/TURKEY.

Güner, A., Zielinski J., (1996). The conservation status of the turkish woody flora. Temperate Trees Under Threat, England.

Var, M., (2010). Bitki Tanıma ve Değerlendirme II Ders Notları, Trabzon. (Unpublished)

Effect of Adhesive Type on Flame Resistance, Formaldehyde Emission and Physico-Mechanical Properties of Particleboards

Uğur ARAS[1*], Hülya KALAYCIOĞLU[2], Hüsnü YEL[3], Gökay NEMLİ[2]

[1]Karadeniz Technical University, Arsin Vocational School, Department of Material and Material Processing Technology, Trabzon, TURKEY

[2]Karadeniz Technical University, Faculty of Forestry, Department Of Forest Industrial Engineering, Trabzon, TURKEY

[3]Artvin coruh University, Artvin Vocational School, Department of Material and Material Processing Technology, Artvin, TURKEY

[*]**corresponding author:** uaras@ktu.edu.tr

Abstract

Particleboard is manufactured by bonding wood particles or waste materials such as sawdust and shavings with adhesives to form a flat panel product under pressure and heat. Particleboard was invented to increase the utilization of wood and it soon became an important core material for furniture production. The adhesive properties are the most important factor affecting the quality characteristics in particleboard production. So, this study aims to determine the effect of adhesive types on flame resistance, formaldehyde emission and physico-mechanical properties. Urea formaldehyde, melamine urea formaldehyde and polymeric diisocyanate were used as adhesives. The particleboards were prepared as 550 mm x 550 mm x 18 mm and 0,650 g/cm^3 density, respectively. The boards placed in hot press at temperature of 150 °C. Time and pressure of pressing in this experiment was 7 minutes and 24 N/mm^2, respectively. Mechanical and physical properties including modulus of elasticity, modulus of rupture, internal bond strength, moisture content, density, thickness swelling, and water absorption of the samples were determined according to EN 310, EN 319, EN 322, EN 323, EN 317, and ASTM D1037 standards, respectively. Formaldehyde emission contents and the limiting oxygen İndex (LOI) levels of particleboards were determined according to in EN 717-3 and ASTM D 2863, respectively. The result showed that Isocyanate adhesive was the best resin for resulting of flame resistance and formaldehyde emission. In addition, mechanical properties and dimensional stability have increased with the use of polymeric diisocyanate.

Key World: Particleboard, flame resistance, formaldehyde emission, physico-mechanical properties, pMDI adhesive

1. Introduction

According to FAO, the amount of global sawn wood products increased by 468 million cubic metres while the amount of wood based panel production increased by 416 million cubic meters and realized an average growth of 7% (FAO, 2016). The particleboards, one of the most widely used wood composites, are made by combining materials obtained from wood or non-wood sources (lignocellulosic materials) under heat and pressure using synthetic adhesive or other suitable binder (Maloney, 1993; EPA, 2002).

The type of adhesive used in the production of wood composites has a significant effect on quality and usage area properties. The development of adhesives to be used in the production of wood composites has resulted in products that provide economical, fast and sufficient strength properties. Especially, the area of use of the products is one of the most important criterions in adhesive selection. The cost of glue is an important preference for wood composites producers (Dunky, 2017). Urea formaldehyde, developed in the 1930s, is the most preferred adhesive in the production of MDF and particleboard because of its cheap and easy production technology. However, the increase in expected resistance of wood composites and the Possibility of use in moist environments reveal the necessity of increasing performance characteristics. This has increased the use of melamine, phenol and isocyanate added adhesive in the production of wood composites. (Ormondroyd, 2015).

The use of wood and wood-based composites as building materials has increased significantly in recent years. However, it is one of the negative properties of wood-based material degradation at high temperatures. This leads to restrictions on areas of use as construction industry (Zachar et al. 2011). On the other hand, free formaldehyde emitted from wood based composites causes degradation of indoor air quality and health problems. For this reason, reducing the amount of free formaldehyde is a very important event (Zhang et al. 2015; Song et al. 2015).

The main objective was to determine the effect of adhesive type on particleboards. In this research, the LOI (Limited oxygen index) method was used fallow combustion properties. This study also relates physico-mechanical properties and formaldehyde emission of particleboards.

2. Materials and Methods

2.1.Materials

Alder (*Alnus glutinosa L.*) wood particles were used as wood material in the study. The solids content of the urea formaldehyde (UF) and melamine urea formaldehyde (MUF) adhesives used in the study was 65% and 55%, respectively, and the adhesives were supplied by Starwood İnegöl Factory. Polymeric diphenylmethane diisocyanate (pMDI) (100% solid content) was supplied by Derkim Chemistry Inc.

2.2. Method

The Alder wood samples were chipped using a hacker chipper and knife ring flaker. After these particles were screened to remove dust particles, and were dried at 105 ºC achieve 3% moisture content. A series of three-layer particleboards measuring 550 mm x 550 mm x 18 mm were produced at target density of 0,650 g/cm^3. Two boards were produced from each group. The amount of all the adhesives used were 11% (surface layer) and 9% (core layer) based on the dry weight of the wood particles. As a hardener, ammonium chloride (NH_4Cl) solution (20% solid content) was added to 1% based on the dry weight of the UF and MUF adhesives. Press pressure, pressing temperature and pressing time were 24 N/mm^2, 150 ºC and, 7 min, respectively. After pressing, the boards were conditioned at a temperature of 20 ºC and 65±5% relative humidity until stable weight was reached.

Table 1. Experimental desing.

Board types	Adhesives types
A	UF
B	MUF
C	pMDI

2.2.1. Physico-Mechanical Properties

Physical properties including mousture content (M), density (D), water absorption (WA) and thickness swelling (TS) and mechanical properties including modulus of elasticity (MOE), modulus of rupture (MOR), internal bonding strength (IB) properties of the produced boards were determined according to EN 322, EN 323, ASTM D1037, EN 317, EN 310, EN 319, respectively. The MOE, MOR and IB test were conducted with a Zwick/Roell Universal Test machine.

2.2.2. Formaldehyde Emission

Flask method was used for determination of formaldehyde emission (EN 717-3). Approximately 20 grams of samples with dimensions of 25 mm x 25 mm x 18 mm were tested for each type of boards. The samples were placed in the bottles and then kept in the oven at 40 ºC for 3 hours. Then they were cooled to about 20 degrees of ambient temperature. The amounts of free formaldehyde were determined using an UV Spectrometer and calculated according to the following formula. Three experiments were performed from each group.

2.2.3. Limited Oxygen Index (LOI)

The flammability of the investigated specimens was tested according to the ASTM D2863 standard. The LOI of the boards were detected in an oxygen index tester Dynisco Chamber. The dimensional of the test sample used is 100 mm x 15 mm x 18 mm and six samples were tested for each group.

2.2.4. Statistical Analysis

The analysis of variance with ANOVA in SPSS 20 software was used for statistical analysis of formaldehyde emission and physico-mechanical properties specimens. Groups with same letters in column indicate that there is no statistical difference ($p < 0.05$).

3. Results and Discussion

The results of physico-mechanical properties, formaldehyde emission and LOI with statistical analysis and homogeneity group values are shown in table 2 and figure 1-3 for all the boards. According to results, M values of particleboards not changed depending on adhesive types.

The D value of boards were the highest in the pMDI adhesives. raw material density, adhesive density, and the the amount of compression of the press mat are the most effective factors affecting density in the particleboards (Kelly, 1997). Therefore, the higher the solids content of the pMDI adhesives may have caused the increase in D values.

When the WA and TS values were examined, it was determined that the highest dimensional stability was found in the boards produced with pMDI adhesive. Dimensional stability od wood composite swelling could be affected by bond and adhesive properties (Boquillon et al., 2004; Pan et al., 2007).

pMDI has a significantly higher water resistance than UF because of the chemical properties of adhesives (Vick, 1999; Kordkheili and Pizzi, 2017). pMDI particleboards were higher than the 14% required for high load for use in dry conditions particleboard by the EN 312 (2010) standard for TS. On the other hand, WA and TS values were higher (poor) than requirements for UF and MUF adhesives. Hydrophobic substances such as paraffin and wax are not used in production can be shown as the reason (Nemli et al., 2004).

Table 2. Homogeneity groups of properties depending on adhesive types.

Source of properties	Adhesive type	D (g/cm^3)		WA (%)		TS (%)	
		Average	HG	Average	HG	Average	HG
Physical properties	pMDI	0,73	A	11,33	A	8,58	A
	MUF	0,69	B	113,84	B	57,73	B
	UF	0,64	B	137,72	C	58,84	B
		MOR (N/mm^2)		MOE (N/mm^2)		IB (N/mm^2)	
		Average	HG	Average	HG	Average	HG
Mechanical properties	pMDI	27,69	A	3573,33	A	1,69	A
	MUF	16,59	B	2546,67	B	0,79	B
	UF	15,78	C	2436,67	C	0,73	B
		Average	HG				
Formaldehyde emission (mg/kg)	pMDI	0,04	A				
	MUF	1,58	B				
	UF	1,70	C				
		Average					
LOI (%)	pMDI	29,50					
	MUF	29,25					
	UF	28,50					

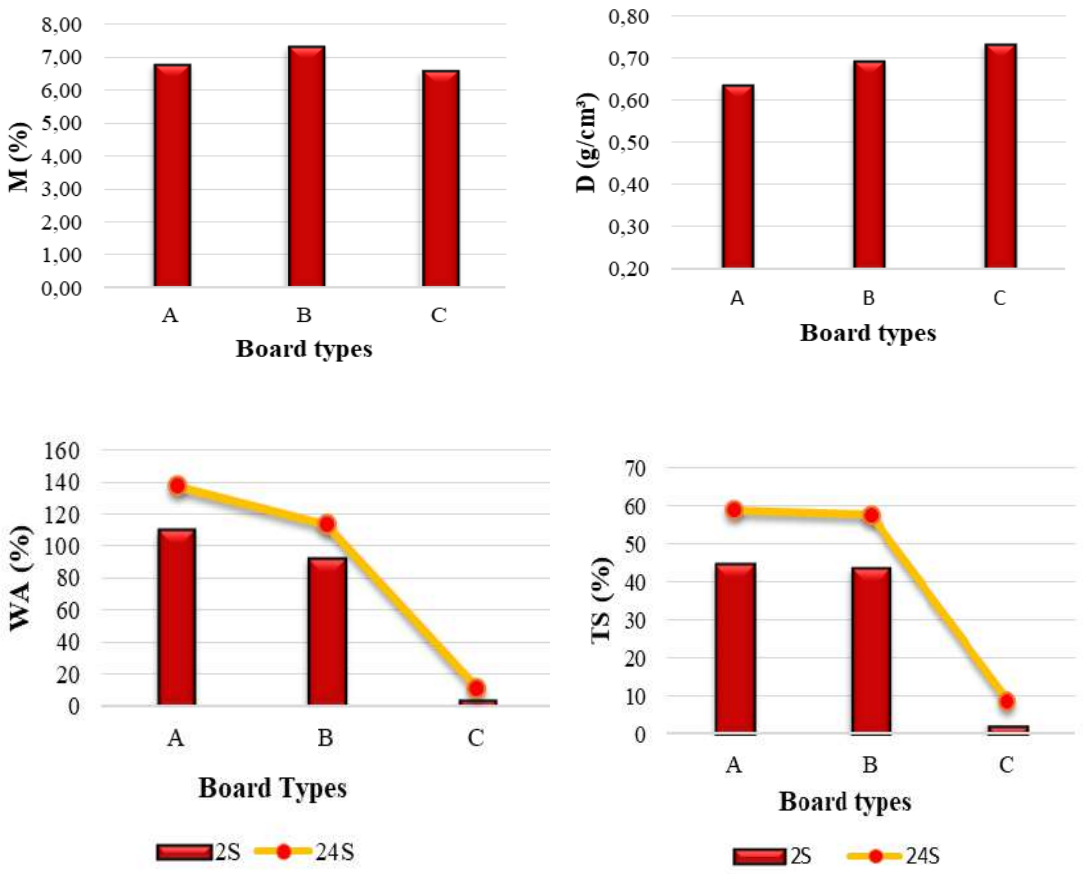

Figure 1. Effect of adhesive type on physical properties of particleboards.

Based on EN 312 (2010) standard, 20 and 3000 N/mm^2 are the minimum requirements for MOR and MOE of particleboard panels for high load for use in humidity conditions, respectively. The boards produced with the pMDI adhesive provide these requirements. The boards produced with the UF and MUF adhesives provide EN 312 P4 and P5 standard requirements, respectively. The IB data ranged from 0,73 to 1,67 N/mm^2. According to the test results, IB values were above the standard requirements in all board groups.The use of has led to a significant increase in mechanical properties. In a study using rice straw, it was pMDI determined that the MOE, MOR and IB values of particleboard increased with the use of the 4% pMDI adhesive compared to standart UF manufacturing particleboard (Li et al., 2010). UF and MUF adhesives linked to mechanically bonded (H-bond) of wood surface while pMDI adhesives form covalent bonds.the covalent bonds have higher energy astrenght than hydrogen bonds (Papadopoulos, 2006). It can be said that this difference significantly increases the strength properties.

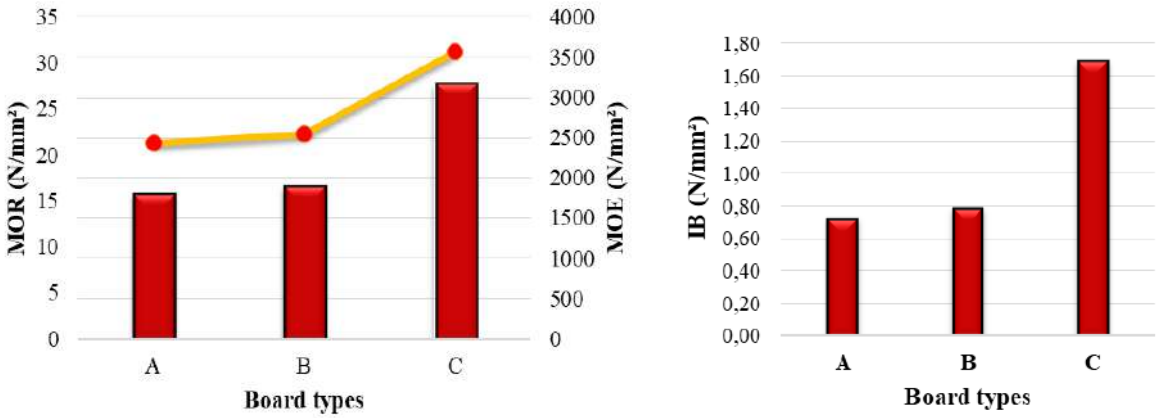

Figure 2. Effect of adhesive type mechanical properties of particleboards.

The lowest formaldehyde emission values were obtained from the boards produced using pMDI. pMDI have the characteristics of fast curing and formaldehyde-free emission properties (He and Yan, 2005). The using of MUF adhesive slightly reduced formaldehyde emissions. MUF provides high mechanical properties and low formaldehyde emission due to increasing branched methylene bonds and strong connection between the melamine molecules compared to cured UF adhesive (Tohmura et al., 2001).

LOI is a fire test in which mixture of oxygen and nitrogen gases are used to determine the minimum amount of oxygen required to combustion of the test specimen. LOI value increased by using the MUF and pMDI adhesives in this study. The highest LOI value was recorded as 29,5%. The void ratio in the board is reduced because of the use of MUF and pMDI increases the quality of bonding in boards. This reduction is clearly visible in the IB test result. The reduction in the amount of free air space of the material may cause to increase LOI values. The amount of oxygen available affect the rate of combustion (Schmid, 2017).

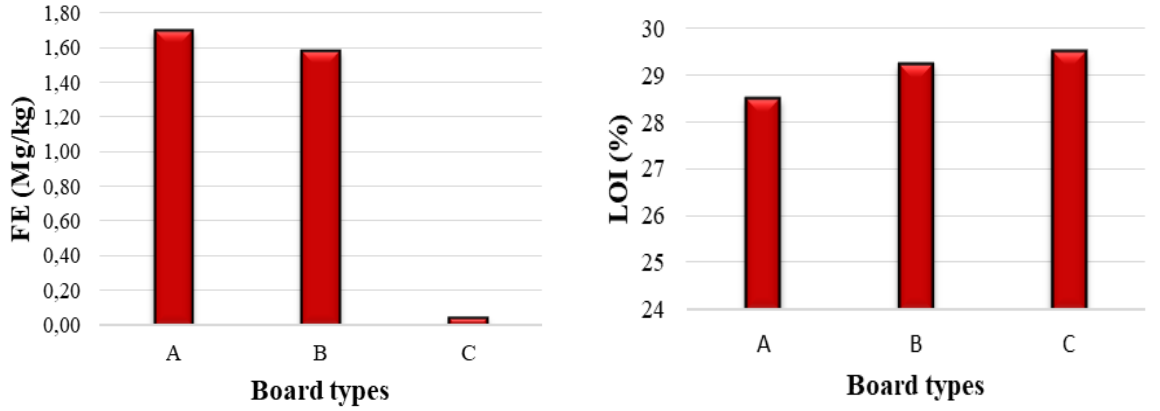

Figure 3. Effect of adhesive type formaldehyde emission and LOI properties of particleboards.

4. Conclusions

Compared with UF and MUF resin, pMDI resin had excellent bond strength for particleboard as determined by mechanical properties. Dimensional stability properties were also better for pMDI bonded board. It is possible to produce at lower temperatures due to the low curing temperature in wood composites produced with pMDI adhesive which leads to a reduction in the energy requirement. Also, if the ratio of used adhesive is reduced, the production costs will be reduced while sufficient strength is provided because of high strength properties. One of the advantages of using pMDI was no formaldehyde emission which provides a very important advantage of human health. In addition, since wood is a flammable material, fire resistance is a very important parameter especially when it is used as building material. The use of pMDI has increased the resistance to fire.

References

ASTM D1037 (2006). Standard methods of evaluating the properties of wood – based fiber and particle panel materials. American Society for Testing and Materials, Philadelphia.

ASTM D2863-10 (2010). Standard Test Method for Measuring the Minimum Oxygen Concentration to Support Candle-Like Combustion of Plastics (Oxygen Index). American Society for Testing and Materials, Philadelphia.

Boquillon, N., and SchÖnfeld, U. (2004). Properties of wheat straw particleboards bonded with different types of resin. *Journal of Wood Science*, 50(3), 230-235.

Dunky, M. (2003). Adhesives in the wood industry. In Pizzi, A., Mittal, K. L., (Ed.) *Handbook of adhesive technology* (pp. 511-575), New York Boca Raton : CRC Press.

EN 310 (1993). Wood based panels, determination of modulus of elasticity in bending and bending strength. European Committee for Standardization Brussels.

EN 312 (2010). Particleboards-specifications. European Committee for Standardization, Brussels.

EN 317 (1993). Particleboards and fiberboards, determination of swelling in thickness after immersion. European Committee for Standardization Brussels.

EN 319 (1993). Particleboards and fiberboards, determination of tensile strength perpendicular to plane of the board. European Committee for Standardization Brussels.

EN 322 (1999). Wood-based panels- Determination of moisture content. European Committee for Standardization, Brussels.

EN 323 (1993). Wood-based panels. determination of density. European Committee for Standardization, Brussels.

EN 717-3 (1996). Wood-Based panels- Determination of formaldehyde release Part 3: Formaldehyde release by the flask method. European Committee for Standardization, Brussels.

EPA 2002. Wood product Industry, Particleboard Manufacturing, https://www3.epa.gov/ttnchie1/ap42/ch10/final/c10s06-2.pdf (Erişim Tarihi: 28 Mayıs 2018)

FA0 2016. Global Forest Products Facts And Fıgures. Food and Agriculture Organizition of the United Nations, http://www.fao.org/3/I7034EN/i7034en.pdf, (Erişim Tarihi: 2 Haziran 2018)

He, G., and Yan, N. (2005). Effect of moisture content on curing kinetics of pMDI resin and wood mixtures. *International journal of adhesion and adhesives*, 25(5), 450-455.

Kelly MW. Critical literature review of relationships between processing parameters and physical properties of particleboard. Gen. Tech. Rep. FPL-10. Madison, WI: U.S. Department of Agriculture, Forest Service, *Forest Products Laboratory*, 1997, 2–50.

Li X, Cai Z, Winandy JE, Basta AH. (2010). Selected properties of particleboard panels manufactured from rice straws of different geometries. *Bioresource Technology*, 101, 4662–6.

Maloney T. M., (1993). *Modern Particleboard and Dry-Process Fiberboard Manufacturin*g. United Kingdom, Backbeat Books.

Nemli, G., Hiziroglu, S., Usta, M., & Serin, Z. (2004). Effect of residue type and tannin content on properties of particleboard manufactured from black locust. *Forest Products Journal*, 54(2), 36.

Ormondroyd, G. A. (2015). Adhesives for wood composites. In Ansell M. P., (Ed.) *Wood Composites* (pp. 47-66). Sawston UK:Woodhead Publishing.

Pan, Z., Zheng, Y., Zhang, R., & Jenkins, B. M. (2007). Physical properties of thin particleboard made from saline eucalyptus. *Industrial crops and products*, 26(2), 185-194.

Papadopoulos, A. (2007). Property comparisons and bonding efficiency of UF and PMDI bonded particleboards as affected by key process variables. *BioResources*, 1(2), 201-208.

Schmid, J., Santomaso, A., Brandon, D., Wickström, U., & Frangi, A. (2017). Timber under real fire conditions–the influence of oxygen content and gas velocity on the charring behavior. *Journal of Structural Fire Engineering*, 2017.

Song, W., Cao, Y., Wang, D., Hou, G., Shen, Z., & Zhang, S. (2015). An investigation on formaldehyde emission characteristics of wood building materials in Chinese standard tests: Product emission levels, measurement uncertainties, and data correlations between various tests. *PloS one*, 10(12)

Tohmura, S. I., Inoue, A., & Sahari, S. H. (2001). Influence of the melamine content in melamine-urea-formaldehyde resins on formaldehyde emission and cured resin structure. *Journal of Wood Science*, 47(6), 451-457.

Vick, C. B. (1999). Adhesive bonding of wood materials. Wood handbook: wood as an engineering material. Madison, WI: USDA Forest Service, Forest Products Laboratory, 1999. *General technical report FPL; GTR-113*, Pages 9.1-9.24, 113.

Younesi-Kordkheili, H., & Pizzi, A. (2017). Improving the physical and mechanical properties of particleboards made from urea–glyoxal resin by addition of pMDI. *European Journal of Wood and Wood Products*, 1-6.

Zachar, M., Mitterová, I., Xu, Q., Majlingová, A., Cong, J., & Galla, Š. (2012). Determination of fire and burning properties of spruce wood. *Drvna industrija*, 63(3), 217-223.

Zhang J, Amirou S, Essawy HA, Pizzi A, Gao Q, Li J. Hyperbranched poly(amidoamine)s as additives for urea formaldehyde resin and their application in particleboard fabrication. *BioResources*, 2015; 10: 782–792.

Comparison of Quorum Sensing Inhibition and Antimicrobial Properties of Some Commercial and Wild Mushrooms Extracted with Supercritical CO_2

Sibel YILDIZ[1], Ayşenur GÜRGEN*[1], Sana TABBOUCHE[2], Gönül SERDAR[3], Münevver SÖKMEN[4], Ali Osman KILIÇ[2]

[1] Karadeniz Technical University, Faculty of Forestry, Forest Industrial Engineering, Trabzon, Turkey.
[2] Karadeniz Technical University Faculty of Medicine, Department of Medical Microbiology, Trabzon, Turkey.
[3] Karadeniz Technical University, Faculty of Pharmacy, Department of Analytic Chemistry, Trabzon, Turkey.
[4] Konya Food and Agricultural University, Faculty of Engineering and Architecture, Department of Bioengineering, Konya, Turkey.

*Corresponding author:
aysenur.yilmaz@ktu.edu.tr

Abstract

Recently, intensive researches on the bioactive properties of mushrooms have been carried out. With the discovery of their medical properties, the consumption of mushrooms also increases day by day. In this study, quorum sensing inhibition and anti-microbial properties of some commercial and wild mushroom species were investigated. *Agaricus bisporus* cultivated mushrooms were purchased from three different commercial companies and numbered between 1-3. Additionally, *Laccaria bicolor*, *Bovista plumbea*, *Lactarius delicious*, *Boletus edulis* wild species were collected from Trabzon, Turkey. All mushrooms were extracted with supercritical CO_2 method. Antimicrobial potential of extracts was tested by agar well diffusion method against *Staphylococcus aureus* ATCC 25923, *Escherichia coli* ATCC 25922, *Enterococcus faecalis* ATCC 29212, *Pseudomonas aeruginosa* ATCC 27853, *Salmonella* Typhimurium ATCC 14028, *Klebsiella pneumoniae* ATCC 13883, *Proteus mirabilis* ATCC 7002, *Listeria monocytogenes* ATCC 43251, *Candida parapsilosis* ATCC 22019 and *Candida albicans* ATCC 10231 microorganisms. Anti-quorum sensing activity was tested on *Chromobacterium violaceum* ATCC 12472 bacteria. All wild mushroom extracts except for *B. plumbea* inhibited the violacein production of *C. violaceum*. *L. bicolor*, *A. bisporus* (1), *B. plumbea*, *A.bisporus* (2) extracts inhibited *S. aureus.* In addition, *L. bicolor* extract inhibited *K. pneumonia* and *L. monocytogenes* while *A. bisporus* (2) extract inhibited *P. aeruginosa*. Among all mushrooms, *L. bicolor* has shown remarkable results.

Keywords: Antimicrobial, cultivated mushroom, quorum sensing inhibition, wild mushroom

1. Introduction

Mushrooms, which have an important role among the non-wood forest products, have been considered as a source of powerful nutrient in human life for a long time. In addition to being cheap, they are rich in protein (Lu et al., 2018) and amino acid compositions. They are low-calorie foods because of having a low fat and high-water content. (Kalač, 2013). Mushrooms also include β-glucan, which promotes the immune system strengthening (Ohno et al., 2002), and vitamin D, that is essential for bone health (Ahlawat et al., 2016). Many mushroom species are defined as a source of functional foods and/or nutraceutical substances as they contain biological and physiologically active substances such as phenolic acids (Ferreira et al., 2009).

Wild mushroom picking has become a delightful social activity and organized by professional or amateur groups in Turkey. The most commonly produced and consumed specie of mushrooms is *Agaricus bisporus* in our country as well as in the world. In the last 10 years in Turkey, mushroom production has increased by 54% from 26,256 tons to 40,874 tons (TUIK, 2018). It has been proved through scientific studies that the active compounds contained in mushrooms have been associated their antioxidant, antimicrobial, antidiabetic etc. properties (Wu & Xu, 2015; Sevindik et al., 2018). It is thought that the further researches should be continued especially for the various species that grow in different geographies and different climatic conditions.

Recently, a new term has been added, along with medical properties of mushrooms/plants etc. that are known and frequently researched in the literature. The new term is called ‘anti-quorum sensing’. Quorum sensing is a cell-cell communication mechanism that makes it possible to distinguish low or high population intensities in the presence of bacteria. The bacteria are controlling the population level of gene expression in response to the change in cell number in the environment by this mechanism (Papenfort & Bassler, 2016). In short, this mechanism is named the ‘language of bacteria’. Anti-Quorum Sensing researches seems to be a way of preventing the communication mechanism of bacteria which are able to grow adhered to surfaces, forming complex communities termed biofilms (Alves et al., 2014). Mushrooms may be a precious resource in the search of new bioactive extracts/compounds to inhibit biofilm production. In this study, quorum sensing inhibition capabilities and anti-microbial properties of some commercial and wild mushrooms extracts were investigated and compared with each other.

2. Material and Method

2.1. Mushrooms

Wild mushrooms were collected from Trabzon province located in the north eastern part of Turkey and identified by their morphological and their ecological characteristics. *Agaricus bisporus* culture mushrooms were purchased from three different commercial companies established in Trabzon and coded between 1 and 3. Tested mushrooms and their properties are given in Table 1.

Table 1. Tested mushrooms

Mushroom		Edibility and (if) code	
Laccaria bicolor	Wild	Edible	
Bovista plumbea	Wild	Edible, not highly valued.	
Lactarius delicious	Wild	Edible	
Boletus edulis	Wild	Edible	
Agaricus bisporus	Cultivated	Edible	1
Agaricus bisporus	Cultivated	Edible	2
Agaricus bisporus	Cultivated	Edible	3

All mushrooms were dried on food dryer at 40^{o}C (Profilo, PFD1350W, Turkey), then they were ground in a basic micro fine grinder and passed through 1-millimeter sieve (IKA, WERKE MF10, Germany).

2.2. Extracts Preparation

Supercritical CO_2 extraction was applied for 10 g of mushroom powder at 250 Bar, 50 ^{o}C during 3 hours (Spe-ed SFE model 7070). CO_2 flow rate was 10 g/min and ethanol was used as co-solvent with a flow rate of 0.5 mL/min. The extracts were dissolved as 10 mg/ml in dimethyl sulfoxide (DMSO) as working solution.

2.3. Anti-Quorum Sensing Activity

Anti-quorum sensing activity was tested against *Chromobacterium violaceum* ATCC 12472 (Table 2). For this purpose, the minimal inhibitory concentration (MIC) of the different extracts was first determined in accordance to the guidelines of The Clinical & Laboratory Standards Institute (CLSI) on 96 wells plate, then the SubMic and its next lower concentration were tested for pigment production inhibition. Extract concentrations started by 5 mg/ml and

bacterial final concentration was $5x10^4$ CFU/ml. After an incubation of 24 h the well was dried at 50 ºC for 1 hour, then the pigments were dissolved in 200 µl of DMSO and leaved to dissolve for 2 hours on shaker (225 rpm). The pigment solutions were taken to a new 96 well plate and their absorbance were read at OD_{585} nm. The same test for each extract was repeated three times, twice for pigment testing and the third was used for plate count agar test. Agar counting was realized by taking 100 µl and spreading it on Mueller Hinton agar and incubating at 37 ºC for 24h.

2.4. Antimicrobial Activity

Antimicrobial activity was tested by agar well diffusion method in accordance to the guidelines of CLSI on Mueller Hinton agar (Wayne, 2012). The tested microorganisms were given in Table 2.

Table 2. Tested microorganisms, American Type Culture Collection (ATCC) number and used test

Microorganism	ATCC number	Used test
Chromobacterium violaceum	12472	Anti-quorum sensing
Staphylococcus aureus	25923	Anti-microbial
Escherichia coli	25922	
Enterococcus faecalis	29212	
Pseudomonas aeruginosa	27853	
Salmonella Typhimurium	14028	
Klebsiella pneumoniae	13883	
Proteus mirabilis	7002	
Listeria monocytogenes	43251	
Candida parapsilosis	22019	
Candida albicans	10231	

Microorganisms were obtained from Karadeniz Technical University, Department of Medical Microbiology, Faculty of Health Sciences, Trabzon, Turkey. The tested microorganisms and extracts were applied as 5 µl of 10 mg/ml solutions. Luria Bertani (LB) fluid and agar medium (LABM; United Kingdom) were used for bacterial cultures. DMSO was used as negative control and ampicillin, gentamicin, tetracycline, cefotaxime and amphotericin B were used as positive control.

Extracts with positive antimicrobial activity were tested for their minimal inhibitory concentration in accordance to the guidelines of The Clinical & Laboratory Standards Institute (CLSI) on 96 wells plate. The extract concentration started by 5 mg/ml and bacterial final concentration was $5x10^4$ CFU/ml. The last 2 well were used for growth control (bacteria without extract) and for sterility control (extract without bacteria).

3. Results and Discussions

The concentration at which the bacterial count did not change (or very little change) but the amount of pigment significantly decreased was considered as the anti-Quorum Sensing (QS) activity concentration. Two concentrations after the MIC value were tested. Optical Density (OD) at 585 nm was determined twice and the averages were added to the charts. Vanilla was used as a positive control (Figure 4). Anti-QS effect of vanilla was previously optimized and shown to be positive at around 625 µg/ml. DMSO was also tested as a negative control. Among the mushroom extracts, three wild mushroom extracts have shown anti-QS activity and their activity charts are given Figure 1-3, respectively.

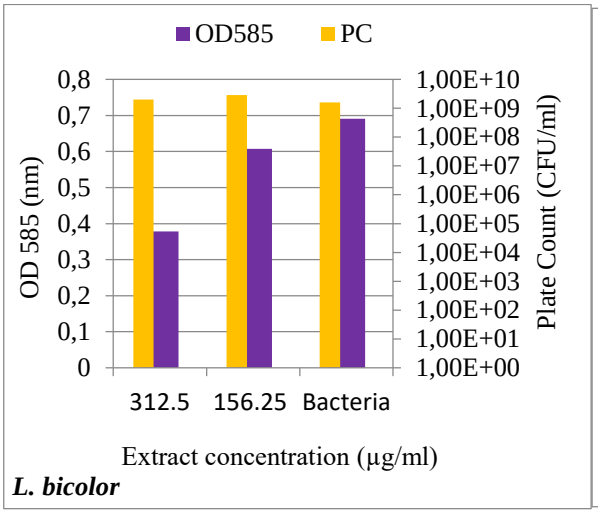

Figure 1. *L. bicolor* anti-QS activity chart

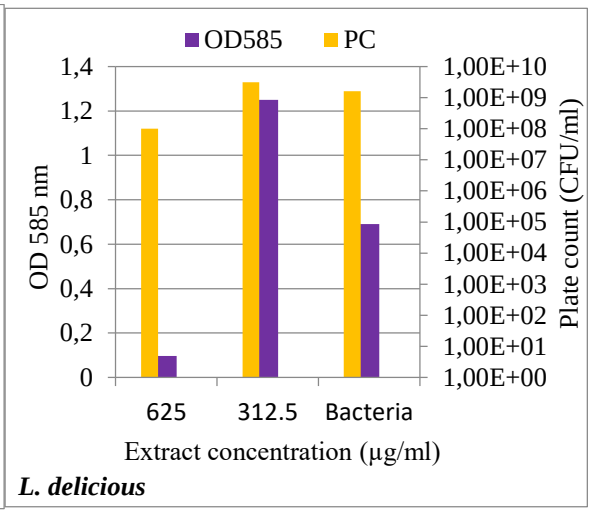

Figure 2. *L. delicious* anti-QS activity chart

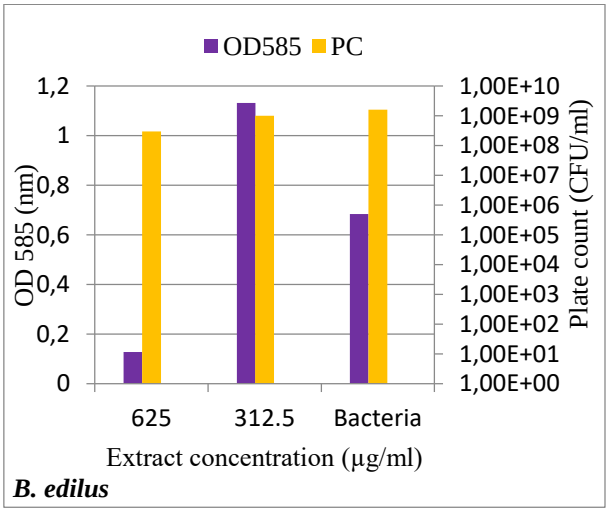

Figure 3. *B. edilus* anti-QS activity chart

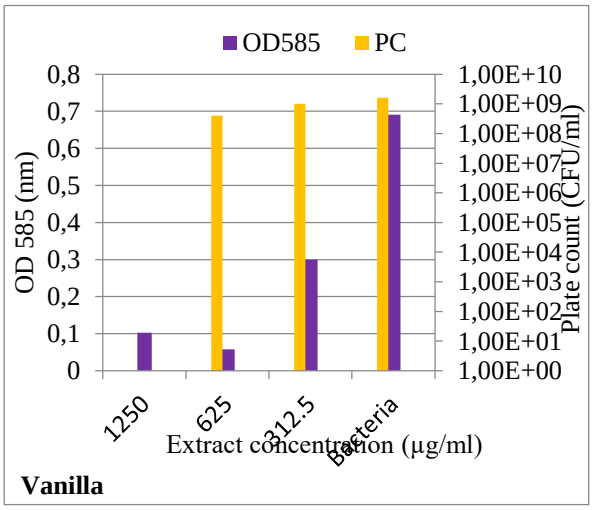

Figure 4. Vanilla anti-QS activity chart

The *Chromobacterium violaceum* is a bacterium that produces a purple pigment called violacein (Kaufman et al., 1986). If the production of the pigment stops without killing the bacteria (without decreasing the number), it can be concluded that the communication mechanisms of bacteria are blocked. In this study, three out of four wild mushrooms extracts had anti-QS effect and these mushrooms were *L. bicolor, L. delicious* and *B. edilus*, respectively. These mushrooms stopped or very markedly reduced pigment production. As shown Figure 1-3, based on the capacity to inhibit the bacterial pigment production, the activities of the mushrooms can be compared with each other as follows; *L. delicious* > *B. edilus* > *L. bicolor*. Also, anti-QS activity was not observed in any of the cultivated mushroom extracts.

In a research, *Auricularia auricular* mushroom pigments had anti-QS activity on *C. violaceum* (Zhu, H et al., 2011). Similar to the results of this study, *Tremella fuciformis* mushroom's 75% (v/v) aqueous methanol extract inhibited violacein production of *C. violaceum* (Zhu, Hu & Sun, 2008)

In a study, anti-quorum sensing activity of *Inonotus obliquus* mushroom's aqueous and ethanolic extracts was tested on *Pseudomonas aeruginosa* (Glamočlija et al., 2015). In the study, it was reported that both extracts showed anti-QS activity. Like just mentioned research, anti-QS activity of hot water extract of *Agaricus blazei* was tested on *P. aeruginosa* and anti-QS activity was observed by (Soković et al., 2014). It can be concluded that wild mushrooms are sources of anti-QS activity and that more research is needed to reveal the anti-QS activities of the mushroom species and extraction types.

Significant success has been achieved in the treatment of infections caused by the use of antimicrobial drugs. However, the development of resistance against antimicrobial drugs by some microorganisms has led to the loss of achieved achievements (Çapar, 2002). Therefore, the search for new and natural antimicrobial sources has become compulsory and it can be said that the fungi are one of these natural antimicrobial sources. Antimicrobial potential of extracts was tested by agar well diffusion method in this study. In the agar diffusion method, a suitable medium containing the test organism is used with a pit system in which the sample to be tested is present. At the end of the incubation period, if the tested sample is effective, inhibition zones are formed around the pits, where no microorganism reproduction (Figure 5)

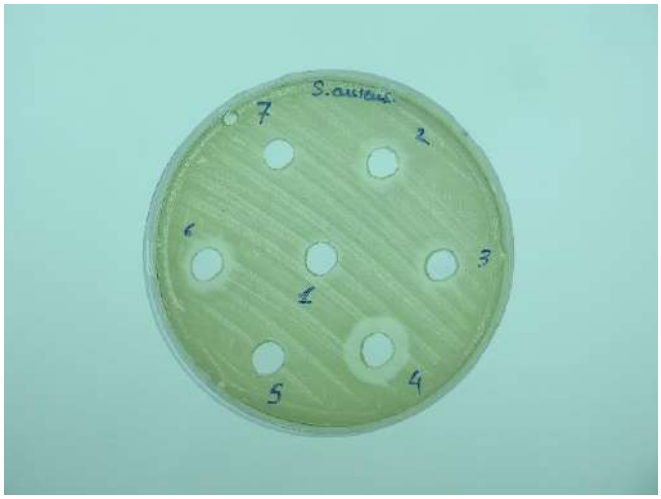

Figure 5. Agar well diffusion assay

Antimicrobial assay results (mm) of all tested mushroom extracts and positive controls (antibiotics) are given in Table 3.

Table 3. Agar Well Diffusion Results (mm)

Sample	Agar Well Diffusion Results (mm)									
	S. aureus	*E. coli*	*P. aeruginosa*	*E. faecalis*	*C. albicans*	*C. parapsilosis*	*S.* Typhimurium	*P. mirabilis*	*K. pneumoniae*	*L. monocytogenes*
L. bicolor	2	0	0	0	0	0	0	…*	2	1
A. bisporus (1)	0	0	0	0	0	0	0	…	0	0
L. delicious	0	0	0	0	0	0	0	…	0	0
A. bisporus (2)	2	0	0	0	0	0	0	…	0	0
B. plumbea	2	0	0	0	0	0	0	…	0	0
B. edilus	0	0	0	0	0	0	0	…	0	0
A.bisporus (3)	2	0	2	0	0	0	0	…	0	0
Ampicillin	> 30	16 - 17	…	> 30	…	…	27	…	…	…
Gentamicin	…	…	21-22	…	…	…	…	…	21	…
Amphotericin B	…	…	…	…	30	0**	…	…	…	…
Tetracycline	…	…	…	…	…	…	…	…	…	25
Cefotaxime	…	…	…	…	…	…	…	37	…	…

As can be seen Table 3, *L. bicolor*, *A. bisporus* (2), *B. plumbea* and *A.bisporus* (3) supercritical CO_2 extracts inhibited some microorganisms. Among the mushroom extracts, the best results were obtained from *L. bicolor* extract. Unlike the activities of other mushroom extracts, L. bicolor showed antimicrobial effect against *K. pneumoniae* and *L. monocytogene*

microorganisms. Many studies have reported in the literature about antimicrobial activity of fungi. For example, ethanol extract and four fractions of *Inonotus sanghuang* inhibited *Staphylococcus aureus*, *Bacillus subtilis* and *Bacillus cereus* (Liu et al., 2017). *A. lanipes* showed antimicrobial activity against *Micrococcus luteus, Proteus vulgari, Yersinia enterecolitica, S. aureus, B. subtilis, E. coli, C. albicans* microorganisms (Kaygusuz et al., 2017). Minimum inhibition concentration (MIC) of extracts are given in Table 4.

Table 4. Minimum Inhibition Concentration (µg/ml)

Sample	Minimum Inhibition Concentration (µg/ml)						
	S. aureus	*E. coli*	*P. aeruginosa*	*C. albicans*	*P. mirabilis*	*K. pneumoniae*	*L. monocytogenes*
L. bicolor	156.25	…	…	…	…	1250	625
A.rubescens	78.125	…	…	…	…	…	…
A. bisporus (2)	39.1	…	…	…	…	…	…
B. plumbea	78.125	…	…	…	…	…	…
A. bisporus (3)	156.25	…	1250	…	…	…	…
Ampicillin	78.125	2500	…	…	…	…	…
Gentamicin	…	…	1250	…	…	156.25	…
Amphotericin B	…	…	…	78.125	…	…	…
Cefotaxime	…	…	…	…	9.76	…	…
Tetracycline	…	…	…	…	…	…	78.125

MIC means the lowest concentration that inhibits bacterial growth. Therefore, in an antimicrobial test, it can be said that the lower the value of the concentration, the more effective the substance is. The low MIC value is also important in terms of the efficiency of the amount of used material. In this study, the lowest MIC value was obtained from *A. bisporus* (2) extract with 39.1 µg/ml. When the table is examined, the MIC value of *L. bicolor* is higher than the value of *A. bisporus* (2) MIC value, although it exhibited antimicrobial properties against the more microorganisms. In a previous study, MIC values of aqueous extracts obtained from 21 wild basidiomycete mushrooms and cultivated mushroom (*Pleurotus ostreatus)* were reported between 10 and 1524 µg/ml against microorganisms included *Listeria innocua*, *B. cereus, Campylobacter jejuni, E. coli, C. albicans*, *Aspergillus ochraceus* (Klančnik et al., 2017).

4. Conclusion

In this study, quorum sensing inhibition and anti-microbial properties of some commercial and wild mushrooms were investigated. All wild mushroom extracts except for *B. plumbea* inhibited violacein production of *C. violaceum*. *L. bicolor, A. bisporus* (1), *B. plumbea,*

A.bisporus (2) extracts inhibited *S. aureus.* In addition, *L. bicolor* extract inhibited *K. pneumonia* and *L. monocytogenes* while *A. bisporus* (2) extract inhibited *P. aeruginosa.* Among all mushrooms, *L. bicolor* has shown remarkable results. When the results of the studies in the literature and the results of our study are evaluated together, it is seen that there are many species of mushrooms to be studied, type of extraction, and different bacteria and to be tested both ani-QS and anti-microbial assays.

Acknowledgements

This work was supported by Karadeniz Technical University Scientific Research Projects Unit (FHD-2015-5373).

References

Ahlawat O., Manikandan K.,and Singh M. (2016). Proximate composition of different mushroom varieties and effect of UV light exposure on vitamin D content in Agaricus bisporus and Volvariella volvacea. *Mushroom Research,* 25(1), 1-8.

Alves M. J., Ferreira I. C., Lourenço I., Costa E., Martins A.,and Pintado M. (2014). Wild mushroom extracts as inhibitors of bacterial biofilm formation. *Pathogens,* 3(3), 667-679.

Çapar Y. (2002). Yeni ve yeniden önem kazanan infeksiyon hastalıkları. *Güncel Gastroenteroloji,* 6(1), 3543.

Ferreira I. C., Barros L.,and Abreu R. (2009). Antioxidants in wild mushrooms. *Current Medicinal Chemistry,* 16(12), 1543-1560.

Glamočlija J., Ćirić A., Nikolić M., Fernandes Â., Barros L., Calhelha R. C., Ferreira I. C., Soković M.,and Van Griensven L. J. (2015). Chemical characterization and biological activity of Chaga (*Inonotus obliquus*), a medicinal "mushroom". *Journal of Ethnopharmacology,* 162, 323-332.

Kalač P. (2013). A review of chemical composition and nutritional value of wild-growing and cultivated mushrooms. *Journal of the Science of Food and Agriculture,* 93(2), 209-218.

Kaufman S. C., Ceraso D.,and Schugurensky A. (1986). First case report from Argentina of fatal septicemia caused by Chromobacterium violaceum. *Journal of Clinical Microbiology,* 23(5), 956-958.

Kaygusuz O., Kaygusuz M., Dodurga Y., Seçme M., Herken E. N.,and Gezer K. (2017). Assessment of the antimicrobial, antioxidant and cytotoxic activities of the wild edible mushroom Agaricus lanipes (FH Møller & Jul. Schäff.) Hlaváček. *Cytotechnology,* 69(1), 135-144.

Klančnik A., Megušar P., Sterniša M., Jeršek B., Bucar F., Smole Možina S., Kos J.,and Sabotič J. (2017). Aqueous extracts of wild mushrooms show antimicrobial and antiadhesion activities against bacteria and fungi. *Phytotherapy Research,* 31(12), 1971-1976.

Liu K., Xiao X., Wang J., Chen C.-Y.O.,and Hu H. (2017). Polyphenolic composition and antioxidant, antiproliferative, and antimicrobial activities of mushroom *Inonotus sanghuang*. *LWT-Food Science and Technology,* 82, 154-161.

Lu X., Brennan M. A., Serventi L., Liu J., Guan W.,and Brennan C. S. (2018). Addition of mushroom powder to pasta enhances the antioxidant content and modulates the predictive glycaemic response of pasta. *Food Chemistry,* 264, 199-209.

Ohno N., Harada T., Masuzawa S., Miura N.N., Adachi Y., Nakajima M.,and Yadomae T. (2002). Antitumor activity and hematopoietic response of a b-glucan extracted from an edible and medicinal mushroom *Sparassis crispa* Wulf.: Fr.(Aphyllophoromycetideae). *International Journal of Medicinal Mushrooms,* 4(1).

Papenfort K.,and Bassler B.L. (2016). Quorum sensing signal–response systems in Gram-negative bacteria. *Nature Reviews Microbiology,* 14(9), 576.

Sevindik M., Akgul H., Dogan M., Akata I.,and Selamoglu Z. (2018). Determination of antioxidant, antimicrobial, DNA protective activity and heavy metals content of Laetiporus sulphureus. *Fresenius Environmental Bulletin*, 27(3), 1946-1952.

Soković M., Ćirić A., Glamočlija J., Nikolić M.,andvan Griensven L. J. (2014). *Agaricus blazei* hot water extract shows anti quorum sensing activity in the nosocomial human pathogen Pseudomonas aeruginosa. *Molecules*, 19(4), 4189-4199.

TUIK (2018). Bitkisel Üretim İstatistikleri, Başka yerde sınıflandırılmamış diğer sebzeler, 1988-2017 Retrieved from http://www.tuik.gov.tr/PreTablo.do?alt_id=1001

Wayne, P.A. (2012) Performance Standards for Antimicrobial Disk Susceptibility Tests; Approved Standard—Eleventh Edition. CLSI document M02-A11. Clinical and Laboratory Standards Institute.

Wu T.,and Xu B. (2015). Antidiabetic and antioxidant activities of eight medicinal mushroom species from China. *International Journal of Medicinal Mushrooms*, 17(2).

Zhu H., He C.C., and Chu Q.H. (2011). Inhibition of quorum sensing in Chromobacterium violaceum by pigments extracted from Auricularia auricular. *Letters In Applied Microbiology*, 52(3), 269-274.

Zhu H., and Sun S. (2008). Inhibition of bacterial quorum sensing-regulated behaviors by *Tremella fuciformis* extract. *Current Microbiology*, 57(5), 418.

The Effects of Kraft Lignin and Bark Tannin Using as Additives in Urea-Formaldehyde (UF) Adhesive on Some Properties of Medium-Density Fiberboard (MDF)

Evren ERSOY KALYONCU [1*], Derya USTAÖMER [2], Hüseyin KIRCI[3]

[1] Karadeniz Technical University, Arsin Vocational Scholl of Higher Education, Material and Material Processing Technologies, Arsin, Trabzon Turkey; eersoy@ktu.edu.tr

[2] Karadeniz Technical University, Faculty of Forestry, Department of Forest Products Engineering, Trabzon Turkey; uderya@ktu.edu.tr

[3] Karadeniz Technical University, Faculty of Forestry, Department of Forest Products Engineering, Trabzon Turkey; kirci@ktu.edu.tr

[*] **Corresponding Author:** eersoy@ktu.edu.tr

Abstract

This study evaluated the effects of kraft lignin and bark tannin using as additives in urea formaldehyde (UF) adhesive on some properties of medium density fiberboard (MDF). Lignin was produced from softwood kraft black liquor by precipitation process. Tannin was produced from Taurus cedar tree (*Cedrus libani* A. Rich.) barks by hot water extraction. Kraft lignin and bark tannin powders were added to adhesive with the two different additional rates. Furthermore, hardener was used as another experimental parameter to compare its combine effects with lignin and tannin. Some properties of these fiberboards such as water absorption (WA), thickness swelling (TS), modulus of rupture (MOR), modulus of elasticity (MOE), surface roughness parameters and color change values were determined. As a result, all values showed different trend depending on rates of kraft lignin and bark tannin powder. Also it was found that the use of hardener together with lignin and tannin had notable effects on the panel properties and gave more better results compared to results of samples without hardener.

Keywords: Medium density fiberboard (MDF), kraft lignin, bark, tannin, urea-formaldehyde (UF) adhesive

1. Introduction

The forest-products industry includes plenty of industries like lumber, pulp and paper, furniture and other wood industries (Pentti et al., 2002). During production, some of the raw material becomes wastes (Gombatz, 2007). Wastes generated during production process of forest-products industry, as by-products, can be a potentially valuable resource for the manufacture of various materials and products (Lykidis and Grigoriou, 2008).

Medium density fiberboard (MDF) is one of the widely used wood based panels instead of wood, particleboard and plywood in many applications for furniture (Stark et al., 2010). Furthermore, the use of MDF as material is preferred for mouldings, substrate for flooring, interior door skins and interior trim components (Cai et al., 2006; Youngquist et.al., 1993).

There are many parameters affecting MDF properties such as wood species, adhesives, additives and production parameters (Ayrılmış, 2008). Adhesives are the most important constituent in wood based panel industry besides wood and wood based raw materials. Phenolic and amino resins are widely used in fiberboard manufacturing (Bertaud et.al., 2012). Urea formaldehyde (UF) is the most important and mostly used adhesive for wood based panels due to its technical properties, easy application, high reactivity, good performance in the production and low price (Dunkey, 1997; Pizzi, 2003a).

The use of natural materials, also environmentally friendly adhesives as binders in wood based panels have been getting an increasing attention in recent times (Pizzi, 2006). The main natural adhesives used as wood panel binders are vegetal tannin adhesives and lignin adhesives. Tannins are natural polyphenolic compounds and large concentrations of tannins present in the wood barks (Bertaud et. al., 2012). They are extracted with different solvents such as petroleum ether, ethanol, methanol, water, sodium hydroxide or alkali (Siminonescu et al., 1988; Darkwa and Jetuah, 1996). Generally, the hot water extract of the bark contains about 60-80% of polyphenolic tannin polymers (Raffael et al., 2000).

Lignin is the second most available and renewable material after cellulose (Donaldson, 2001; Risanto, 2014; Fatehi and Chen, 2016). It is extracted from black liquor, the waste product from the kraft pulping process, traditionally by precipitation method (Luong et al., 2012). Lignin macromolecules consist of carbon rich phenolic compounds (Risanto, 2014).

Black liquor of kraft pulping and bark are the two important wastes generated during pulp and lumber production, respectively. Both of two are used in the mills to generate energy by burning (Hahn, 1982). But the economic value of the bark is much lower than that of wood and woody wastes (Lu et al., 2006).

Due to the high cost of synthetic resins, various studies have been made as a binder with tannin and lignin which have rich phenolic structures (Ndazi and Tesha, 2006). Several studies have investigated about the lignin based wood adhesives (Pizzi, 1994). Also tannins have already been used commercially for 30 years. (Pizzi, 2003b; Pizzi, 2006)

The objective of this study is to evaluate the usability of tannin extracted from waste bark and lignin precipitated from kraft black liquor as additive materials to UF resin with or without using hardener for the manufacture of medium density fiberboard (MDF). And, also it is aimed to investigate some properties such as water absorption (WA), thickness swelling (TS), modulus of rupture (MOR), modulus of elasticity (MOE), surface roughness parameters, color change of MDF panels manufactured with these additives.

2. Material and Method

In this study, commercial fibers (mixture of pine and beech) were used as raw material. Urea formaldehyde (UF) at 12% rate was used as an adhesive. Fibers were dried to 2-3% moisture content. In addition, tannin and lignin powders which produced in the laboratory were added to UF with 1-2 % by weight, separately as additives. As hardener, ammonium chloride at 1% rate was used as another experimental parameter to compare its combine effects with lignin and tannin powders. After the application of the adhesive, manually formed fiber mats were pressed using the hot press at 180 ^{o}C temperature for 7 min. Fiberboards were manufactured with 8 mm thickness and 750 kg/m^3 target density. Panel types and contents were represented in Table 1.

Table 1. Panel types and contents

Panel type	Content
T1h	Tannin 1%+hardener
T2h	Tannin 2%+hardener
L1h	Lignin 1%+hardener
L2h	Lignin 2%+hardener
T1	Tannin 1%
T2	Tannin 2%
L1	Lignin 1%
L2	Lignin 2 %

Ch	Control with hardener
C	Control without hardener

These MDF panels were conditioned at 65 ± 5% RH and 20 ± 1 °C, in accordance with TS-642-ISO 554 (1997) and dimensioned for the tests according to TS-EN 326-1 (1999).

2.1. Tannin Extraction

The bark samples of Taurus cedar tree (*Cedrus libani A. Rich.*) from Trabzon district were used for tannin powder production. The bark samples were dried to 10-12% moisture and crushed to appropriate sizes for ready to grind in a laboratory type mill. The samples prepared for extraction by grinding were taken in hot water extraction process in a water bath with bark: water ratio of 1: 8 (w/w) at 70 ° C for 1 hour. The obtained extract was first filtered through filter paper and then through a glass crucible with porosity 1. After then, the water in the filtrated solution was removed by evaporation to obtain tannin powder. (Figure 1).

Figure 1. Extracted tannin powder

2.2. Kraft Lignin Production

Lignin was produced from softwood kraft black liquor using acidification method reported by Lin (1992). Acidification has been accepted as a useful process for producing lignin in an efficient and economical way from black liquor (Sun et. al., 1999; Mussatto et. al., 2007).

Kraft black liquor was treated with 1% concentration of sulfuric acid. After this period, hot water was used to solubize the residual sugars and applied centrifuge treatment to precipitation of solid parts (Mancera et. al., 2011; Lin, 1992). After precipitation kraft lignin dried at room temperature and crushed to powder for use in adhesive (Figure 2).

Figure2. Produced lignin powder

2.3. MDF Panel Properties

All test methods of MDF samples manufactured with kraft lignin and bark tannin with or without using hardener were carried out according to related standard.

The water absorption (WA) and thickness swelling (TS) values of MDF samples were carried out to EN 317 (1993) standard. The modulus of rupture (MOR) and modulus of elasticity (MOE) values of MDF samples were carried out according to EN 317 (1993) standard. The surface roughness parameters (*R*a, *R*z) of MDF samples manufactured were measured using Time TR-100 portable surface roughness tester according to DIN 4768 (1990) standard. Color change values of the MDF samples were determined by using Konica Minolta CM-2600d spectrophotometer according to the CIE *L*a*b** system (HunterLab, 2008).

3. Results and Discussion

3.1. Water Absorption and Thickness Swelling

The water absorption (WA) and thickness swelling (TS) values of MDF samples for 24h are represented in Figure 3 and 4, respectively.

As it seen in Figure 3, the average WA values of MDF samples changed depending on the type and rate of additives. The WA values of MDF samples manufactured with or without hardener increased depending on increasing rates of tannin and lignin. The WA values of the MDF panels manufactured with additives were found higher than those of control panels. Because it is known that lignin and tannin do not have enough water resistance (Charles, 2005; Pizzi, 2003b; Pizzi, 2003c).

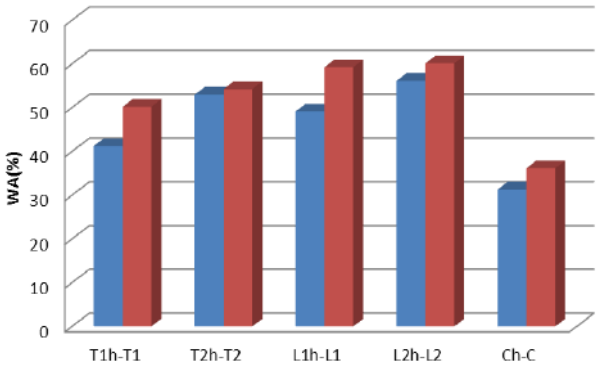

Figure 3. WA values of MDF samples

The MDF panels manufactured with lignin additive (L1-L2 groups) had slightly higher values. L2 group was found to have the highest WA values. The better results of WA were obtained with panels manufactured with tannin compared to lignin. Furthermore, better results were recorded with use of hardener.

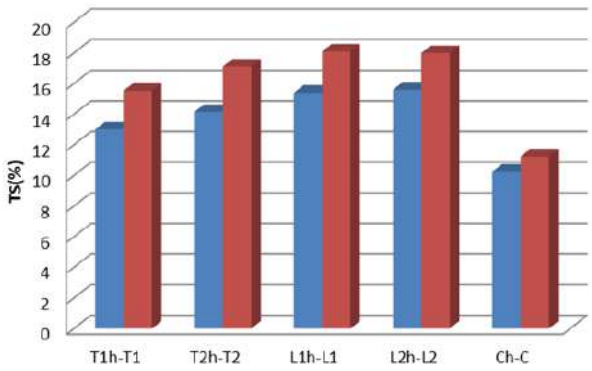

Figure 4. TS values of MDF samples

Figure 4 represents that average TS values of MDF samples showed similar trend with WA values of MDF samples. The results showed that there are distinctive effects of additives on the TS values. The lower TS values were obtained from MDF panels manufactured with tannin compared to MDF panels manufactured with lignin. However, all TS values of MDF samples manufactured with additives were found higher than those of control groups. The lowest TS value was achieved with the rate of 1% tannin and using hardener (T1h group). It is known that tannins are natural hydrophilic complexing agents (Bertaud et. al., 2012). Therefore, their structure could cause an increase on TS values. Especially, the addition of lignin resulted with more increase on the TS values. This situation is thought to concern with water-solubility of kraft lignin especially in highly alkaline environment (Lora

and Glasser, 2002; Widsten and Kandelbauer, 2008; Hemmilä et. al., 2013). Also, better results were recorded with use of hardener.

3.2. Modulus of Rupture and Modulus of Elasticity

The modulus of rupture (MOR) and modulus of elasticity (MOE) values of MDF samples were represented in Figure 5 and 6, respectively.

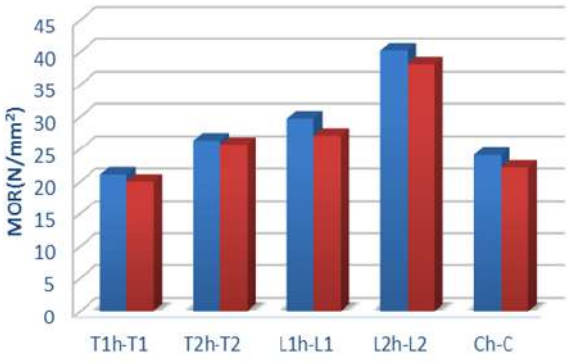

Figure 5.MOR values of MDF samples

As it seen in Figure 5, the MOR values of MDF samples changed depending on the type and rates of additives, and the use of hardener. All MOR values of MDF samples were recorded to be higher than those of control samples except for MDF panels manufactured with the rate of 1% tannin (T1h-T1 groups). The MDF panels manufactured with the rate of 2% tannin and using hardener (T2h) had slightly higher values than those of control panels. The better results were recorded with addition of lignin. MDF panels manufactured with use of lignin at the 2% rate and using hardener (L2h) gave the highest MOR value. The lowest MOR value was obtained with the MDF panels manufactured with use of tannin without hardener. Especially, the positive effect on the MOR values was observed with the use of hardener.

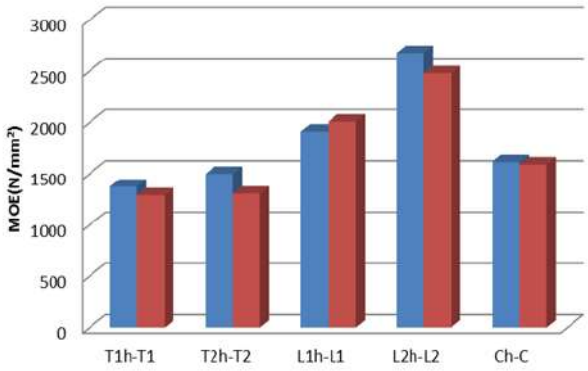

Figure 6. MOE values of MDF samples

*As i*llustrated in Figure 6, MOE values of MDF samples showed almost similar trend with MOR values. The highest MOE value was determined from the MDF panels manufactured with the rate of 2% lignin and with hardener (L2h group). Especially, the combine effect of hardener and lignin gave best result. Besides, it is seen from Figure 6 that the addition of hardener to tannin also improved the MOE values.

Evaluating both the MOR and MOE values together, the increase tendency for these values were clearly observed from Figure 5 and 6. This tendency was thought to be correlated with the addition rates of both lignin and tannin. It is known that both tannin and lignin are natural polyphenolic compounds and aids to bonding (Bertaud et. al., 2012). The increase on the MOR and MOE values of MDF samples could be attributed to the phenolic structure of tannin, lignin and UF adhesive and their effects for bonding. Therefore, increasing amount of phenolic substance in adhesive could be improved mechanical properties of MDF panel samples.

3.3. Surface Roughness Parameters

The changes in surface roughness parameters such as R_a, R_z of MDF samples are represented in 7 and 8, respectively.

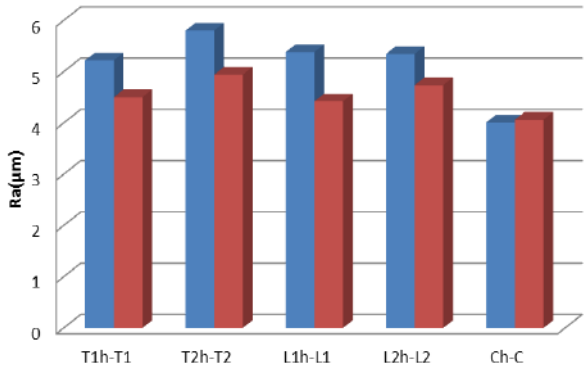

Figure 7. Ra values of MDF samples

As it seen in Figure 7, the average roughness (R_a) values of MDF panels manufactured with additives were found higher than those control panels. The use of additives caused an increase tendency for Ra values of MDF samples. Using tannin as additive, resulted more higher Ra values than using lignin. The higher Ra values were obtained with using hardener. The highest Ra value was obtained from MDF samples manufactured with the rate of 2 % tannin with using hardener (T2h group). In addition, using hardener showed negatively effect on the surface properties of MDF panels. However, the addition of lignin provided better results than the addition of tannin.

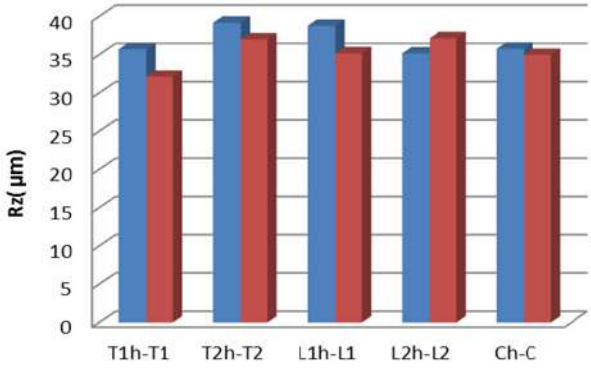

Figure 8. R_z values of MDF samples

In Figure 8, it is clearly observed that, all ten-point mean roughness (Rz) values of MDF panels changed depending on the rate and type of additives. Generally Rz values of MDF panels with additives were found higher than Rz values of control panels. The highest Rz value was obtained from MDF panel manufactured tannin and hardener (T2h group). The increasing rate of tannin with or without hardener caused increase for Rz values of MDF panels. The use of tannin and hardener together gave higher values than the use of only tannin. The similar trend

was observed with the rate of 1% lignin and using hardener (L1h and L1 groups). However, lower value was observed with the rate of 2% lignin and using hardener together (L2h group) compare to only the rate of 2% lignin (L2 group).

Evaluating both Figure 7 and 8 together; all surface roughness values (R_a, R_z) of MDF samples showed differences depending on the rate and type of additives. Surface roughness values of manufactured MDF samples were generally found to be higher than those of control groups. Besides, the highest values determined with the use of hardener. These higher values could be attributed to the use of lignin and tannin as powder form and their structural properties. The lignin and tannin powders can cause some irregularities on the panel surface, and these irregularities also affect surface parameters of final material. It is reported that the surface roughness degree is a function of production parameters and raw material properties (Hiziroglu and Kosonkorn, 2006). Besides, for lignin additive, it is reported that, the temperature is one of the important parameter for softening and plasticizing lignin (Follrich et. al., 2006; Ayrilmis and Winandy, 2009). Lignin begins to degrade at around 214 °C and also, it would be expected some softening near to 200 °C (Hodzic and Shanks, 2014). In our study, used press temperature could be lower than necessary temperature for lignin softening. This situation could be increased the surface roughness parameters.

3.4. Color Change

The color change (ΔE^*) values of MDF panel samples are given in Figure 9.

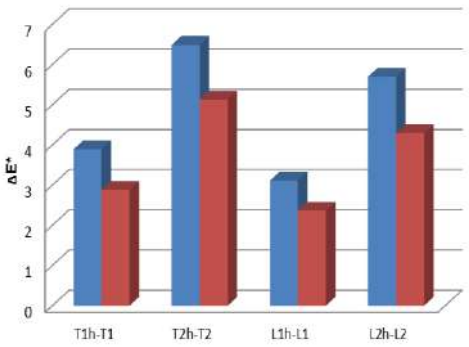

Figure 9. ΔE*values of MDF samples

As can be seen in Figure 9, ΔE^* values of MDF panel samples changed depending on the type and rates of additives and hardener. The color change (ΔE^*) values of MDF panel samples increased with increasing the rates of tannin and lignin. The higher color change values were recorded from MDF panels manufactured with tannin compare to those of MDF panels manufactured with lignin. The lower ΔE^* values were obtained from MDF panels manufactured using without hardener. The highest ΔE^* value was obtained from MDF panel manufactured with the rate of 2% tannin and using hardener (T2h group). The lowest ΔE^* value was found for MDF panel manufactured with the rate of 1% lignin (L1 group).

4. CONCLUSIONS

As conclusion, it was found that, all panel properties showed a different trend depending on addition rates of lignin and tannin powder and their combine effect with hardener. The low addition rates of tannin and lignin powder to urea formaldehyde adhesive provide an improvement on the mechanical properties (MOR and MOE) of MDF panels.

Additionally, surface parameter (R_a, R_z) values increased and smoothness of MDF panels reduced with increasing the rates of tannin and lignin powder. The color change (ΔE^*) values of MDF samples increased with increasing the rates of tannin and lignin. Generally, hardener usage lead to darkening in panel color. Additionaly, it was found that using hardener with lignin and also with tannin had notable effects on the panel properties and gave better results except for surface parameters and color change.

References

Ayrilmis, N. (2008). Effect of compression wood on dimensional stability of medium density fiberboard, Silva Fennica 42(2): 285–293.

Ayrılmıs, N.and Winandy, J. E. (2009). Effects of post heat-treatments on surface characteristics and adhesive bonding performance of medium density fiberboard, Materials and Manufacturing Processes, 24, 594-599.

Bertaud, F., Tapin-Lingua, S., Pizzi, A., Navarrete, P., Petit-Conil, M. (2012). Development of green adhesives for fibreboards manufacturing, using tannins and lignin from pulp mill residues, Cellulose Chem. Technology, 46 (7-8), 449-455.

Cai, Z., Muehl, J.H., Winandy, J.E. (2006). Effects of panel density and mat moisture content on processing medium density fiberboard, Forest Products Journal. 56(10), 20–25.

Charles, R. (2005). Handbook of Wood Chemistry and Wood Composites; Taylor and Francis: Boca Raton,

Darkwa, N.A., Jetuah, F.K. (1996). Distribution of tannins in three ecotypes of Rhizophora spp. along the coastal belt of Ghana, Ghana Journal of Forestry, 2, 25-28.

DIN 4768 (1990). Determination of values of surface roughness parameters R_a, R_z, R_{max} using electrical contact (stylus) instruments, concepts and measuring conditions. Deutsches Institut für Norming, Berlin, Germany.

Donaldson LA. (2001). Lignification and lignin topochemistry-an ultrastructural view, Phytochemistry, 57:859–873.

Dunkey, M. (1997). Urea-Formaldehyde (UF) Adhesive Resins for Wood. International Journal of Adhesion and Adhesives, 18, 95-107.

EN 317 (1993). Particleboards and Fiberboards, Determination of Swelling in Thickness After Immersion, European Committee for Standardization, Brussels, Belgium.

EN 310 (1993). Wood Based Panels, Determination of Modulus of Elasticity in Bending and Bending Strength, European Committee for Standardization, Brussels, Belgium.

Fatehi, P., Chen, J. (2016). Extraction of technical lignins from pulping spent liquors, challenges and opportunities, in Production of Biofuels and Chemicals from Lignin (Z. Fang and R.L. Smith, Jr., Eds.), Springer, Singapore, 2016, Chap. 2, pp. 35-54.

Follrich, J., Müller, U., Gindl, W. (2006). Effects of thermal modification on the adhesion between spruce wood (picea abies karst.) and a thermoplastic polymer, Holz Roh Werkst, 64, 373-376.

Gombatz, E. (2007). Managing Our Waste Series: Waste Management Big Book. Classroom Complete Press, San Diego.

Hahn T.M. (1982). Wood in our energy future, J. For. History, 26, pp. 148-153.

Hemmilä, V., Trischler, J., Sandberg, D. (2013). Lignin – An Adhesive Raw Material of the Future or Waste of Research Energy? In: Brischke, C. & Meyer, L. (Eds.) Proc. 9th Meeting of the Northern European Network for Wood Science and Engineering (WSE), (pp. 98-103) Hannover, Germany.

Hiziroglu S. and Kosonkorn P. (2006). Evaluation of surface roughness of Thai medium density fiberboard (MDF). Building and Environment, 41, 527-533.

Hodzic, A. and Shanks, R. (2014). Natural fibre composites, Materials, processes and properties, In: Woodhead Publishing Limited, Alma Hodzic and Robert Shanks (Eds). ISBN 978-0- 85709-922-8 (online), pp.10.

Hunter Associates Laboratory (2008). CIEL*a*b* color scale. Applications note insight on color, HunterLab 8 (9): 1-4.

Lin S.Y. (1992). Commercial Spent Pulping Liquors, In: Lin S.Y., Dence C.W. (eds) Methods in Lignin Chemistry, Springer Series in Wood Science. Springer, Berlin, Heidelberg.

Lora, J.H. and Glasser, W.G. (2002). Recent industrial applications of lignin: a sustainable alternative to nonrenewable materials, J. of Polymers and the Environment, 10, 39-48.

Lu, W., Sibley, J.L., Gilliam, C.H., Bannon, J.S., Zhang, Y. (2006). Estimation of U.S. bark generation and implication for horticultural industries J. Environ. Hort., 24 pp. 29-34.

Luong N.D., Binh N.T.T., Duong L.D., Kim D.O., Kim D.S., Lee S.H., Kim B.J., Lee Y.S., Nam J.D. (2012). An eco-friendly and efficient route of lignin extraction from black liquor and a lignin-based copolyester synthesis, Polym Bull, 68, 879–890.

Lykidis, C. and Grigoriou, A. (2008). Hydrothermal recycling of waste and performance of the recycled wooden particleboards, Waste Management, 28, 57-63.

Mancera C., Mansouri N., Vilaseca F., Ferrando F., Salvado J. (2011). The effect of lignin as a natural adhesive on the physic-mechanical properties vitis vinefera fiberboards, Bio-Resources, 6(3), 2851-2860.

Mussatto S.I. Fernandes M. Roberto I.C. (2007). Lignin recovery from brewer's spent grain black liquor, Carbohydr Polym., 70, 218–23.

Ndazi, B., Tesha, J., V., Karlsson, S., Bisanda, E., T., N. (2006). Some opportunities and challenges of producing bio-composites from non-wood residues, J.Mater Science, 44, 6984-6990.

Pentti, H., Anssi, N., Andreas, O., Markku, T., Johanna, V. (2002). Forest Related Perspectives for Regional Development in Europa, Brill Academic Publishers, Leiden.

Pizzi, A. (1994). Handbook of Adhesive Technology, Pizzi, A. And Mittal, K.L. (eds.), Marcel Dekker, New York.

Pizzi, A. (2003a), Phenolic Resin Adhesives, In: Pizzi, A. and Mittal, K.L. Handbook of Adhesive Technology (2nd ed.), Marcel Dekker, New York, pp. 541-571.

Pizzi, A. (2003b) Natural Phenolic Adhesives I: Tannin, In: Pizzi, A. and Mittal, K.L. Handbook of Adhesive Technology (2^{nd} ed.), Marcel Dekker, NewYork, pp. 573-587.

Pizzi, A. (2003c). Natural Phenolic Adhesives II: Lignin. In: Pizzi, A. and Mittal, K.L. (Eds.), Handbook of Adhesive Technology (2nd ed.), Marcel Dekker, New York, 589-598.

Pizzi, A. (2006). Recent developments in eco-efficient bio-based adhesives for wood bonding: opportunities and issues, Adhesion Sci. Technol., Vol. 20, No. 8, 829-846.

Raffael, E., Dix, B., Okum, J. (2000). Use of spruce tannin as a binder in particleboards and MDF. Holz als Roh- und Werkstoff, 58, 301-305.

Risanto, L., Hermiati, E., Sudiyani, Y. (2014). Properties of lignin from oil palm empty fruit brunch and its application for plywood adhesive. Makara J. Technol.17(1), 39 -43.

Siminonescu, C.L., Bulacouschi, J., Popa, U.I., Popa, M., Nuta, V. and Rusan, V. (1988). New possibilities of using alkaline extracts from vegetable biomass in adhesive systems for wood industry, Holzforschung und Holverwetung, Berlin, Germany, 40(6), 135-140.

Stark, N. M., Cai, Z. and Carll, C. 2010. Wood-based composite materials panel products, glued-laminated timber, structural materials, In: Wood Handbook: Wood as an Engineering Material. General Technical Report FPL-GTR-190, 11.1–11.28. Madison, WI: U.S. Department of Agriculture, Forest Service, Forest Products Laboratory. chap. 11, 11

Sun R.C., Tomkinson J., Bolton J. (1999). Effects of precipitation pH on the physicochemical properties of the lignins isolated from the black liquor of oil palm empty fruit bunch fi bre pulping, Polym Degrad Stab., 63(2), 195–200.

TS-642-ISO 554 (1997) Conditioning and/or Standard Atmospheres for Trial and Standard Reference Atmosphere. TSE, Ankara.

TS EN 326-1 (1999) Wood-Based Panels-Sampling, Cutting and Inspection-Part 1: Sampling Test Pieces and Expression of Test Results. TSE, Ankara.

Windsten, P. and Kandelbauer, A. (2008). Adhesion improvement of lignocellulosic products by enzymatic pre-treatment, Biotechnology Advances, 26, 379–386.

Youngquist, J.A., Myers, G.E., Muehl, J.M. (1993). Composites from recycled wood and plastics. Final Rep., U.S. Environmental Protection Agency, Project IAG DW12934608–2. Madison, WI: U.S. Department of Agriculture, Forest Service, Forest Products Laboratory. 3 p.

Comparison of GCC and PCC as Coating Material in Paper Production

Ahmet TUTUŞ[1], Mustafa ÇIÇEKLER[1]*, Ufuk KILLI[2], Muharrem KAPLAN[2]

[1]Kahramanmaraş Sütçü İmam University, Faculty of Forestry, Forest Industry Eng. Dep., Kahramanmaraş/ Turkey
[2]ADACAL Industrial Minerals I.C., Afyon/Turkey

* **Corresponding Author:** mcicekler87@gmail.com

Abstract

The aim of the coating process is to improve whiteness, brightness, opacity, surface smoothness and water resistance of paper and board. In this study, the effects of PCC and GCC on the physical and optical properties of coated papers were investigated. Writing and printing papers were produced with using bleached short (70%) and long (30%) fiber mixtures. Calcium carbonate (86.7%), starch (15%) and carboxymethyl cellulose (0.3) were used as coating materials. Precipitated (PCC) and ground (GCC) calcium carbonates were adjusted to 50% concentration with tap water. Coating suspensions were prepared with PCC and GCC mixtures and applied to paper surfaces with coating rod (no:2). The coated papers were dried at room condition and calendered under 15 bar pressure at 100˚C. The physical and optical properties of the coated papers were investigated and compared with each other. The results show that using PCC as coating material increased the optical properties of the papers and gave better results than GCC. The breaking length was found to be higher with using GCC. In terms of surface roughness, there were differences between of GCC and PCC coated papers. As a result, the use of PCC instead of GCC as a coating material has been found to improve the optical properties and the surface roughness of paper. The improvement of optical properties is costly for papermakers and this problem can be solved with using PCC as a coating materials.

Keywords: Coating, GCC, PCC, paper.

1. Introduction

After beating vegetable fibers with special tools, felting and fringing of fibers and swelling by water, the formation of hydrogen bonds by drying the sheet formed on the sieve has a definite endurance and this structure is called as paper (Eroglu ve Usta, 2004).

Writing-printing papers have 60-80 grammages and are suitable for writing and printing. The structure of the paper consists of chemical cellulose or chemical cellulose and mechanical wood pulps mixture. Coating is also applied to paper based on its usage area (Yakut, 2012).

Two methods are commonly used to improve the print quality of paper. The first is that the paper is passed through the super calender after 18 to 25% of the filler is added to the fiber suspension during the paper production. With this method, filling materials with small diameters can improve the quality of paper by improving the surface quality (Eroglu and Usta, 2004; Bucak, 2014). The second method is to give a regular structure to the surface after the production of the paper. This method is to regulate the irregularities in the surface of the paper layer by plastering just as the wall plaster does. The process of covering the surface of the paper with a plaster consisting of mineral substances and adhesives is called paper plastering or coating (Eroglu and Usta, 2004; Bucak, 2014).

It is desired that an ideal filler material should have a high whiteness, an appropriate refractive index and particle distribution, a high retention in the paper, a low density, no show chemically reactive properties, low abrasiveness and low cost (Erkan and Malayoglu, 2001). Calcium carbonate is a pigment that is very much involved in the paper industry after kaolin. It is used as filler in the paper and as a coating material on the paper surface. The particle size is usually 2-3 microns, but it can range from 7-8 microns depending on the carbonate species. The whiteness of calcium carbonates is in the range of 93-98 and is easily dispersed in water (Ozden, 1998).

Ground calcium carbonate (GCC) is obtained by grinding natural limestone with water and subjecting it to air or water separation to obtain a product of the desired particle size (Ozden, 1998). As the precipitated calcium carbonate (PCC) can be crystallized in the desired morphological properties, it can change both the chemical and physical properties of the paper when it is used as a coating mineral and as a filler. PCC is used in dying and toothpaste production, in paper industry as filler and coating material and in rubber making as filler (Eroglu and Usta, 2004; Bucak, 2014).

The aim of this study was to investigate the effects of GCC and PCC which are used both as filler pigment and as coating material in the paper industry on the physical and optical properties of the papers coated with these minerals.

2. Material and Method

2.1. Material

PCC was taken from Adacal Industrial Minerals I.C. GCC, CMC, starch and short and long fibers were supplied from the market. This study was carried out by Adacal Industrial Minerals I.C. and Kahramanmaraş Sütçü İmam University, Department of Forest Industry Engineering collaboration.

2.2. Paper Production and Coating Process

PCC and GCC used as pigment in coating process. PCC, GCC, and starch were prepared as separate suspensions at specific concentrations for coating process. The prepared suspensions were mixed to a homogeneous state in a beaker based on the ratios given in Table 1. PCC and GCC ratios were changed and 12 different coating experiments shown in same table were performed.

Table 1. Coating suspension recipes

	Pigment (%)	PCC (%)	GCC (%)	Starch (%)	CMC (%)
1	0	0	0	0	0
2	84.7	100	0	15	0.3
3	84.7	0	100	15	0.3
4	84.7	10	90	15	0.3
5	84.7	20	80	15	0.3
6	84.7	30	70	15	0.3
7	84.7	40	60	15	0.3
8	84.7	50	50	15	0.3
9	84.7	60	40	15	0.3
10	84.7	70	30	15	0.3
11	84.7	80	20	15	0.3
12	84.7	90	10	15	0.3

The bleached short (70%) and long (30%) fibers were beaten in the hollander beater to 45±5 ^{o}SR (Schopper Riegler) freeness levels according to Tappi T 200 sp-96 and ten handsheets

per tested sequence with grammages of 80 gr.m^{-2} were prepared using a Rapid-Kothen sheet former according to ISO 5269/2.

The prepared coating suspensions were applied to the paper surfaces by coating rod (no.2) three times. The coated papers were conditioned at 23±1 ºC and 65±1% relative humidity in a conditioning room and then subjected to calendering at 100 ºC under 15 bar pressures.

2.3. Determination of the physical and optical properties

Coated papers kept in the conditioning room for 24 hours were subjected to physical and optical properties in accordance with the standards given in Table 2 below.

Table 2. The physical and optical tests applied to coated paper

Physical and Optical Tests	Standards
Breaking length	TAPPI T494 om-01
Burst index	TAPPI T403 om-15
Surface Roughness	ISO 4287
Bulkiness	TAPPI T 411 om-89
Density	TAPPI T 411 om-89
Brightness	ISO 2469:2014
Whiteness	ISO 2469:2014
Yellowness	ASTM E313
Opacity	TAPPI T519 om-02

Three replicates were done for each experiment, and mean values were used to determine the physical and optical properties of the coated papers.

3. Results and Discussion

3.1. Effect of PCC and GCC Ratios on the Physical Properties

Table 3 shows test results of the physical properties of the coated paper such as breaking length, burst index, surface roughness, bulkiness and density depending on PCC and GCC ratios. The results indicated that the breaking lengths and burst indices have been significantly reduced with coating process (Fig. 1).

Table 3. The physical properties of the coated papers

	PCC (%)	GCC (%)	Breaking length (km)	Burst index (kPa.m^2/g)	Surface Roughness (ml/min)	Bulkiness (cm^3/g)	Density (g/cm^3)
1	0	0	5.83	4.06	327	1.43	0.70
2	100	0	5.55	3.85	290	1.55	0.65
3	0	100	5.68	3.90	326	1.54	0.65
4	10	90	5.25	3.78	323	1.58	0.64
5	20	80	5.25	3.68	317	1.56	0.64
6	30	70	5.19	3.50	311	1.57	0.64
7	40	60	5.81	3.56	308	1.55	0.65
8	50	50	5.49	4.03	304	1.56	0.64
9	60	40	5.68	3.90	302	1.56	0.64
10	70	30	5.55	3.83	300	1.54	0.65
11	80	20	5.34	4.03	297	1.54	0.65
12	90	10	5.37	3.87	295	1.53	0.65

When compared with non-coated writing-printing papers, the breaking length values were decreased about 4.80%, 2.57%, 9.94%, 9.94%, 10.97%, 0.34%, 5.83%, 2.57%, 4.80%, 8.40% and 7.89% and burst indices were also decreased about 5.17%, 3.94%, 6.89%, 9.35%, 13.79%, 12.31%, 0.73%, 3.94%, 5.66%, 0.73% and 4.67%, respectively. However, there are no significant effects on the bulkiness, density and surface roughness values.

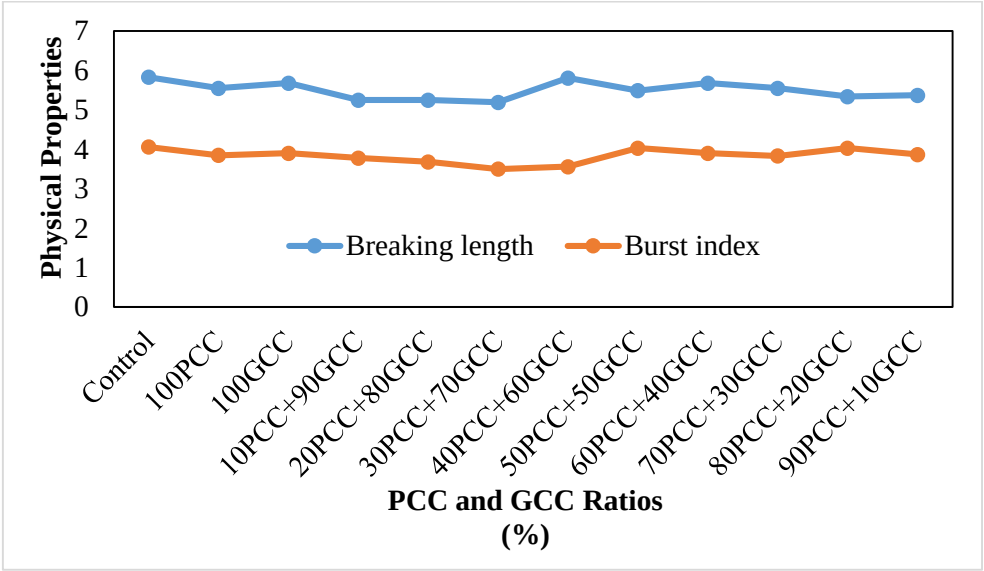

Figure 1. Physical properties of coated papers

In a study, the physical and optical properties of the paper were examined by adding PCC and GCC as fillers at certain ratios to the paper. They reported that PCC and GCC had a negative effect on the physical properties of the papers (Tutus et al., 2012).

In another study, PCC and GCC had used in newspaper, wrapping paper and writing-printing paper production as filler and the fillers were compared with each other in terms of

effects on the paper properties. According to results of this study, fillers reduced the physical properties of the papers. Because PCC has regular grain size, grain shape and size distribution, it had given the better results than GCC (Tutus et al., 2013).

3.2. The Effects of PCC and GCC Ratios on Optical Properties

Table 4 shows test results of the optical properties of the coated paper such as whiteness, brightness, yellowness and opacity depending on PCC and GCC ratios.

Table 4. The optical properties of the coated papers

	PCC (%)	GCC (%)	Whiteness (ISO)	Brightness (ISO)	Yellowness (E313)	Opacity (ISO)
1	0	0	76.69	74.71	3.31	92.89
2	100	0	82.99	81.67	1.99	96.29
3	0	100	82.07	80.59	2.29	95.92
4	10	90	81.71	80.14	2.44	95.72
5	20	80	81.61	80.13	2.30	95.63
6	30	70	81.47	80.00	2.27	95.97
7	40	60	82.05	80.59	2.23	95.93
8	50	50	82.33	80.95	2.13	95.91
9	60	40	83.00	81.17	1.79	96.24
10	70	30	83.63	81.26	2.08	96.09
11	80	20	83.99	81.73	1.90	96.33
12	90	10	84.14	81.86	1.93	96.40

There were significant increases in the optical properties such as whiteness, brightness and opacity with coating process (Fig. 2). The main reason for these increases is the high optical properties of PCC and GCC. Besides, the papers surface properties had been improved by coating process. When compared with non-coated writing-printing papers, the whiteness values were increased about 8.21%, 7.01%, 6.54%, 6.41%, 6.23%, 6.98%, 7.35%, 8.22%, 9.05%, 9.52% and 9.71% and brightness values were also increased about 9.31%, 7.87%, 7.26%, 7.25%, 7.08%, 7.87%, 8.35%, 9.50%, 8.76%, 9.39% and 11.28%, respectively.

When compared with non-coated papers, PCC and GCC has been improved the yellowness and opacity values of the writing-printing papers. However, there is no significant differences between opacity and yellowness values when PCC and GCC compared with each other.

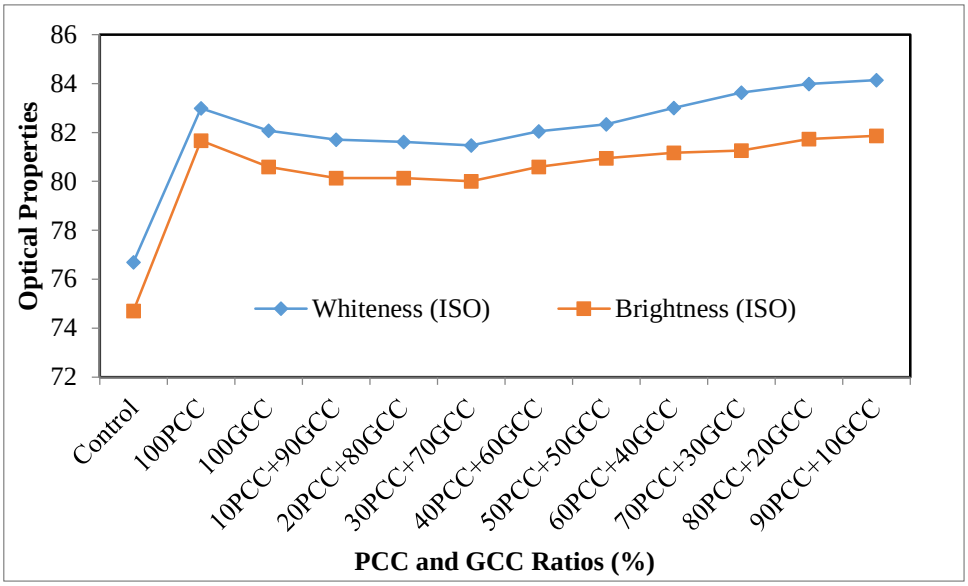

Figure 2. Optical properties of the coated papers.

Tutus et al., (2013) investigated that the effects of PCC and GCC as filler on the optical and physical properties of papers produced by recycling newspaper, packing and writing-printing papers. It was found that fillers reduced the physical properties of papers but improved optical properties such as whiteness and brightness values.

In another study, the physical and optical properties of the paper were examined by adding PCC and GCC as fillers at different ratios to the paper. It has been reported that compared to kaolin, GCC and other fillers, PCC provides better whiteness and brightness values due to its whiter and brighter structure (Tutus et al., 2012).

4. Conclusions and Recommendations

The prerequisite for print quality is that the paper surface has a homogeneous smoothness and whiteness. The coating process is needed for providing ideal printing surface. Since the ink contacts the coated layer during printing, the printability of this surface must have optimum values. Therefore, coating process is one of the most important steps of the paper industry. As a result of this study;

1. It has been determined that with using adacal PCC as coating mineral, paper surface has a more homogeneous structure and optical properties of the papers such as whiteness, brightness, yellowness and opacity have been improved.
2. It was observed that the physical properties of the papers were decreased with using PCC in coating process but these decreases were insignificant.

3. Improvements were observed in surface roughness of papers while the whiteness values which is the most important parameter for print quality has been increased with using PCC in coating process.
4. It has been also observed that using adacal PCC in coating process has better effects on the physical and optical properties of the writing-printing papers than GCC.

References

Eroglu, H. and Usta, M., (2004). *Paper and Cardboard Production Technology*, Volume I, Cellulose and Paper Industry Foundation, Trabzon.

Yakut, A., (2012). Review of New Paper Production from Recyclable Used Paper. *Installation Engineering* - Issue 127 - January / February

Erkan, Z.E., and Malayoğlu, U., (2001, October). Industrial Raw Materials and Their Properties Used in Paper-Cardboard Industry. *4 Industrial Raw Materials Symposium* (pp.250-257). Izmir: Dokuz Eylül University

Ozden, O., (1998). *Use of Starch for Coating the Paper Surface.* Doctoral Thesis. Istanbul University, Institute of Science and Technology, Istanbul.

Bucak, F., (2014). *Evaluation of Textile Residues on Paper Blank.* Master Thesis. Kahramanmaras Sutcu Imam University, Institute of Science and Technology, Kahramanmaraş

Tutus, A., Cicekler, M., Kazaskeroglu, Y., Muduroglu, M., (2012). Effects of Precipitated Calcium Carbonate (PCC) on Optical and Physical Properties of Paper. *8th International Minerals Symposium.* pp.147-152. İstanbul/Turkey

Tutus, A., Cicekler, M., Ozdemir, A., Okan, O,T., (2013). Effects of Precipitated Calcium Carbonate (PCC) on Optical Properties of Waste Paper, *International Caucasian Forestry Symposium.* pp.884-887. Artvin/Turkey.

Effects of Layer Numbers and Fiber Direction on Thermal Conductivity of Plywood

İsmail AYDIN[1], Aydın DEMİR[1*], Cenk DEMİRKIR[1]

[1]Karadeniz Technical University, Forestry Faculty, Forest Industry Engineering Department, Trabzon, Turkey

[*]**Correspondig author:** aydindemir@ktu.edu.tr

Abstract

Thermal conductivity of wood material is superior to other building materials because of its porous structure. Thermal conductivity is a very important parameter in determining heat transfer rate and is required for development of drying models in industrial operations such as adhesive cure rate. Thermal conductivity is used to estimate the ability of insulation of material. Thermal conductivity of wood material has varied according to wood species, direction of wood fiber, resin type, and addictive members used in manufacture of wood composite panels. In this study, it was examined that the effects of layer numbers and fiber direction on thermal conductivity of plywood. Scots pine (*Pinus sylvestris* L.), black pine (*Pinus nigra*) and spruce (*Picea orientalis* L.) were used as wood species in five and seven-ply-plywood manufacture. Thermal conductivity of plywood panels was determined as parallel and perpendicular to the fibers according to ASTM C 518 & ISO 8301. As a result of the study, it was found that thermal conductivity coefficient values increased with increasing layer numbers of panels. Also, the values measured parallel to the fibers of panels were higher than the values measured perpendicular to the fibers.

Keywords: Thermal conductivity, Plywood, Layer numbers, Fiber direction, Pine.

1. Introduction

Wood and wood based panels have long been used as materials in the construction industry because they have a great durability, high strength and versatility (Stevens et al., 2006). Plywood, a wood based product, is one of the most important building and furniture materials (Fateh et al., 2013). Compared with solid wood, the chief advantages of plywood are that the properties along the length of the panel are more nearly equal to properties along the width, there is greater resistance to splitting, and the form permits many applications where large sheets are desirable (Aydin and Colakoglu, 2008).

In facing the global warming trend, there is a dire need for more effective measures to sustain comfortable temperatures in living environments. To sustain an indoor temperature that is independent of outdoor temperature fluctuations, materials need to be developed that have superior thermal insulation abilities (Kawasaki and Kawai, 2006). Wood has been intensively used as residential construction material due to its natural beauty and great properties, such as high specific strength, thermal insulation, and ease of handling and processing (Kilic et al., 2006). For example, wood's low thermal conductivity and good strength make it of special interest for building construction, refrigeration, automobile applications, and cooperage, among others (Gu and Zink-Sharp, 2005; Sahin Kol and Altun, 2009).

It was stated that thermal conductivity of wooden materials was lower than others materials used in same using areas with wood in structures (Simpson and Tenwolde, 1999). Wood is one of the preferred materials in many usage areas such as construction industry, refrigerators, automobile industry, the manufacture of barrels thanks to the low thermal conductivity and high resistance (Gu and Zink-Sharp, 2005). Wood material is superior to other building materials in terms of thermal conductivity due to the porous structure of it (Ors and Senel, 1999; Gu and Zink-Sharp, 2005; Kruger and Adriazola, 2010). In another study, it was concluded that plywood sandwich panels had the characteristics of well-balanced thermal insulation and warmth keeping properties (steady- and non-steady-states), which were important for insulation performance in that they maintained temperature and relax severe temperature changes in residences exposed to diurnal and seasonal temperature changes (Kawasaki and Kawai, 2006). Thermal conductivity of wood material has varied according to wood specie, direction of wood fiber, resin type and addictive members used in manufacture of wood composite panels (Kamke and Zylkowski, 1989).

Several studies about thermal conductivity of wooden materials showed that thermal conductivity was influenced thickness of composite materials, density, moisture content, ratio of early and late wood, temperature, and flow direction of heat (Suleiman et al., 1999; Bader et al, 2007; Sonderegger and Niemz, 2009).

In this study, it was examined that the effects of layer numbers and fiber direction on thermal conductivity of plywood. For this purpose, The panels produced as five and seven ply-plywood were measured both parallel of the fibers and perpendicular of the fibers and after the formed groups were compared.

2. Material and Methods

Scots pine (*Pinus sylvestris* L.), black pine (*Pinus nigra*) and spruce (*Picea orientalis* L.) veneers having 2 mm thickness obtained by rotary cutting at laboratory conditions were used in the study. Scots pine, black pine and spruce logs were steamed for 12 h before cutting. Rotary cut veneer sheets with 50 cm by 50 cm dimensions and 2 mm thickness were obtained from logs. A rotary type peeler with a maximum horizontal holding capacity of 80 cm was used for veneer manufacturing. While the vertical opening was adjusted as 0.5 mm, the horizontal opening between knife and nose bar was 85% of the veneer thickness in the rotary peeling process. Each veneer sheet was dried to 6–8% moisture content by using a veneer dryer at 110 °C. Five and Seven-ply-plywood panels were manufactured by using phenol formaldehyde resin (PF). The adhesive mixture was applied on single surfaces of veneers at approximately 160 g/m^2. The hot press temperature, pressure and duration were 140 ^{o}C, 8 kg/cm^2 and 10 and 14 min, respectively. Two replicate panels were manufactured for all test groups.

Thermal conductivity of plywood panels was determined as parallel and perpendicular to the fibers according to ASTM C 518 & ISO 8301 (2004). Sample size required is 300x300xpanel thickness mm. Two specimens were used for each test group. The Lasercomp Fox-314 heat flow meter shown in Figure 1 was used for the determination of thermal conductivity. The top and lower layers of it was set 20 and 40 ^{o}C for all specimens, respectively. The veneer temperature during the measurement of the thermal conductivity was maintained due to this constant temperatures.

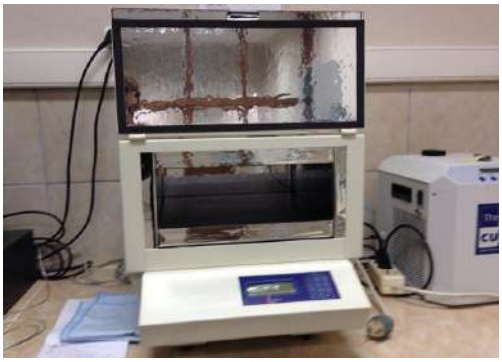

Figure 1. Lasercomp Fox-314 heat flow meter

3. Results and Discussion

The thermal conductivity mean values of plywood panels according to the layer numbers and fiber direction were shown in Figure 2.

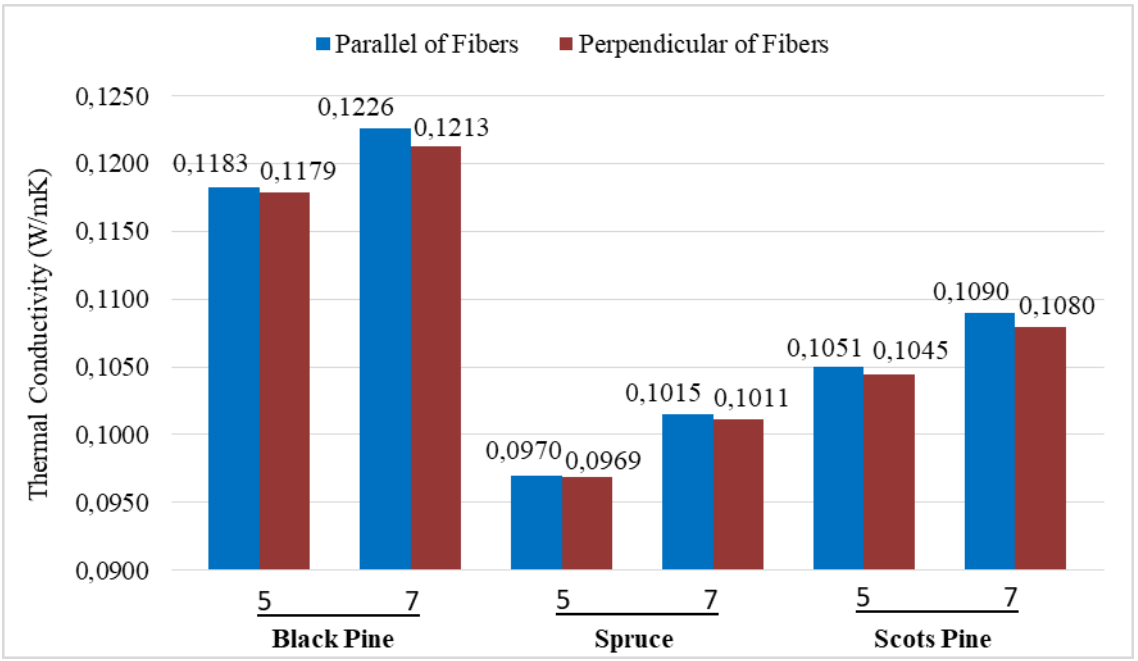

Figure 2. Effects of layer numbers and fiber direction on thermal conductivity of plywood

As can be seen from Figure 2, the highest thermal conductivity values were obtained for black pine plywood while the lowest values were obtained for spruce. This differences in the thermal conductivity values according to the wood species were due to the specific gravity differences of the material. It was stated that there is a linear relationship between specific gravity and thermal conductivity (Ors and Senel, 1999; Gu and Zink-Sharp, 2005; Sahin Kol and Altun, 2009; Sanderegger and Niemz, 2009). The reason of thermal conductivity increase

with increasing spesific gravity is lower air-filled cell spaces (Suleiman et al., 1999). Because as the air space increases, the thermal conductivity decreases (Kol et al., 2008).

As the layer numbers of panels increased, thermal conductivity values also increased. The increase in density due to panel thickness and glued layers increase is expected. Therefore, the thermal conductivity increases with the increase of the density. In addition, the values measured parallel to the fibers of panels were higher than the values measured perpendicular to the fibers. Thermal conductivity in the longitudinal direction was found to be about 2.25 to 2.75 times the transverse conductivity for solid wood. Also, thermal conductivity in the radial direction to be about 5% to 10% greater than in the tangential direction (Gu and Zink-Sharp, 2005). Since the fiber directions of the panel drafts in plywood production are prepared perpendicular to each other, the change of heat transmission, which is indicated by the fiber direction of the solid wood, should not be expected for the plywood (Demirkir, 2012).

4. Conclussions

In this study, it was aimed to investigation of effects of layer numbers and fiber direction on thermal conductivity of plywood. As a result of this study, it was found that thermal conductivity coefficient values increased with increasing layer numbers of panels. Also, the values measured parallel to the fibers of panels were higher than the values measured perpendicular to the fibers. According to wood species, the highest thermal conductivity values were obtained for black pine plywood while the lowest values were obtained for spruce. Black pine and scots pine plywood can be used where the thermal conductivity must be high. Spruce plywood can be used insulation material according to the other pine species.

Acknowledgement

The authors acknowledge the financial support of this study by TUBITAK (The Scientific and Technical Research Council of Turkey) (Project No: 112O819).

References

ASTM C, 518 (2004). Methots of Measuring Thermal Conductivity, Absolute and Reference Method. ASTM International: West Conshohocken, USA.

Aydin, I. and Colakoglu, G. (2008). Variations in bending strength and modulus of elasticity of spruce and alder plywood after steaming and high temperature drying. *Mechanics of Advanced Materials and Structures*, 15, 371-374.

Bader, H., Niemz, P. and Sonderegger, W. (2007). Untersuchungen Zum Einfluss Des Plattenaufbaus Auf Ausgew¨Ahlte Eigenschaften Von Assivholzplatten. *Holz Roh- Werkst*, 65(3), 173–181.

Demirkır, C., (2012). *Using posibilities of pine species in Turkey for structural plywood manufacturing*. PhD Thesis, Karadeniz Technical University, Natural Sciences Instute, Trabzon.

Fateh, T., Rogaume, T., Luche, J., Richard, F. and Jabouille, F. (2013). Kinetic and mechanism of the thermal degradation of a plywood by using thermogravimetry and Fourier-transformed infrared spectroscopy analysis in nitrogen and air atmosphere. *Fire Safety Journal*, 58, 25–37.

Gu, H. M. and Zink-Sharp, A. (2005). Geometric model for softwood transverse thermal conductivity. Part 1. *Wood and Fiber Science*, 37(4), 699-711.

Kamke, F. A. and Zylkowski, S. C. (1989). Effects of wood-based panel characteristic on thermal conductivity. *Forest Products Journal*, 39(5), 19–24.

Kawasaki, T. and Kawai, S. (2006). Thermal insulation properties of wood-based sandwich panel for use as structural insulated walls and floors. *Journal of Wood Science*, 52, 75–83.

Kilic, Y., Colak, M., Baysal, E. and Burdurlu, E. (2006). An investigation of some physical and mechanical properties of laminated veneer lumber manufactured from black alder (Alnus glutinosa) glued with polyvinyl acetate and polyurethane adhesives. *Forest Products Journal*, 56(9), 56-59.

Kol, H. S., Özçifçi, A. and Altun, S. (2008). Effect of some chemicals on thermal conductivity of laminated veneer lumbers manufactured with urea formaldehyde and phenol formaldehyde adhesives. *Kastamonu University Forestry Faculty Journal*, 8(2), 125-130.

Kruger, E. L. and Adriazola, M. K. O. (2010). Thermal analysis of wood-based test cells. *Construction Building Materials*, 24, 999–1007.

Ors, Y. and Senel, A. (1999). Thermal conductivity coefficients of wood and wood-based materials. *Turkish Journal of Agriculture and Forestry*,. 23(1), 239-245.

Sahin Kol, H. and Altun, S. (2009). Effect of some chemicals on thermal conductivity of impregnated laminated veneer lumbers bonded with poly(vinyl acetate) and melamine–formaldehyde adhesives. *Drying Technology*, 27, 1010–1016.

Simpson, W. and TEenwolde, A. (1999). *Physical Properties and Moisture Relations of Wood*. Wood Handbook- Wood as an Engineering Material, Chapter 3, Forest Products Laboratory, Madison, USA.

Sonderegger, W. and Niemz, P. (2009). Thermal conductivity and water vapour transmission properties of wood-based materials. *European Journal of Wood and Wood Products*, 67(3), 313-321.

Stevens, R., Es, D. S., Bezemer, R. and Kranenbarg, A. (2006). The structure-activity relationship of fire retardant phosphorus compounds in wood. *Polymer Degradation and Stability*, 91, 832-841.

Suleiman, B. M., Larfeldt, J., Leckner, B. and Gustavsson, M. (1999). Thermal conductivity and diffusivity of wood. *Wood Science and Technology*, 33(6), 465–473.

Waste Paper Recycling: Contributions to Giresun and Turkey Economies

Ahmet TUTUŞ[1], Mustafa ÇİÇEKLER[1*], Asutay KIZILTEPE[1]

[1]Kahramanmaraş Sütçü İmam University, Faculty of Forestry, Forest Industry Engineering, Kahramanmaraş, Turkey

[*]**Corresponding author:** mcicekler87@gmail.com

Abstract

Paper recycling is the process of turning waste paper into new paper products such as newspaper, corrugated boxes, tissue products and egg boxes etc. With population growth and technological developments, paper consumption rate is increasing rapidly. For this reason, recovery rate of waste paper, which is cheaper than wood cellulose and important in terms of environment, is also rapidly increasing. Due to the high amount of chemicals and water used in chemical methods and the awareness of consumers about the environment, the demand on waste paper has increased.

Approximately 15-20% of the garbage collected by the municipalities consists of paper. Waste paper recycling rate in Turkey is about 55% and this rates varies between 70-75% in Europe. Therefore, the collections of waste papers and re-evaluation in the paper sector have become an inevitable industrial activity today.

The aim of this study has to investigate contribution of Giresun province and Turkey to economies in terms of waste paper collecting and recycling.

Keywords: Giresun, waste paper, recycling, economy

1. Introduction

Paper production and consumption in Turkey has increased rapidly in the last ten years. Depending on population growth, technological development, industrialization and urbanization in our country, waste paper usage in paper production is also increasing every year. Recycling of used paper makes an important contribution both to protect the environment and to increase the variety of raw material usage.

The use of wood in the paper industry is decreasing day by day due to the inadequacy of raw materials in our country. The use of waste paper as an alternative raw material to wood in the paper industry has contributed to solving the problem of raw materials. Approximately 15% of waste paper is contained in the garbage collected by the municipalities. By using waste paper in the paper industry, large and small-sized factories can be established and at the same time, it has lots of advantages such as low raw material, energy, water usage, easy control of production technique and equipment (Tutus, 2004).

Efforts are being made to support the raw material resources of the paper industry, such as the use of fast-growing tree species, annual crops and waste paper in paper production, as well as reducing the pressure on the forests. The quantities of wood, annual plant and waste paper used in the paper industry in the world and our country in 2015 were given below in Figures 1 and 2, respectively (FAOSTAT, 2016).

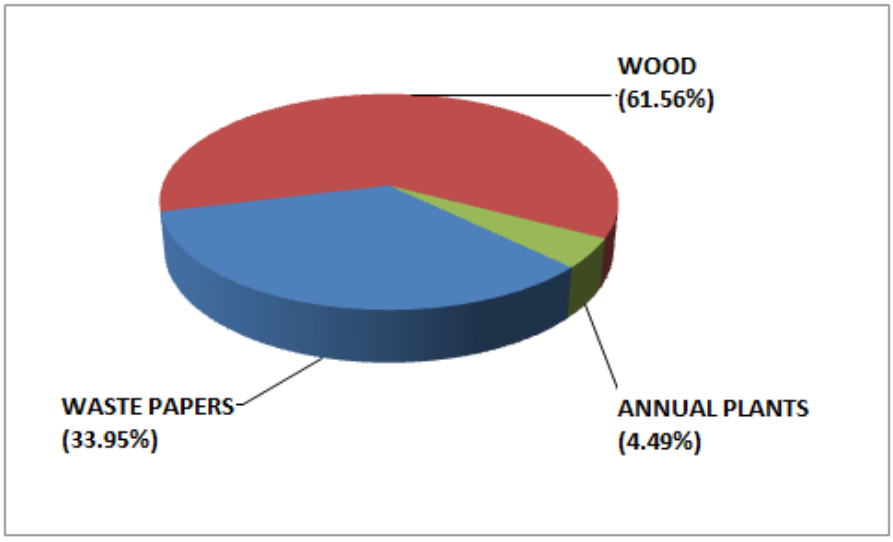

Figure 1. Raw materials and ratios used in the paper industry in the world in 2015

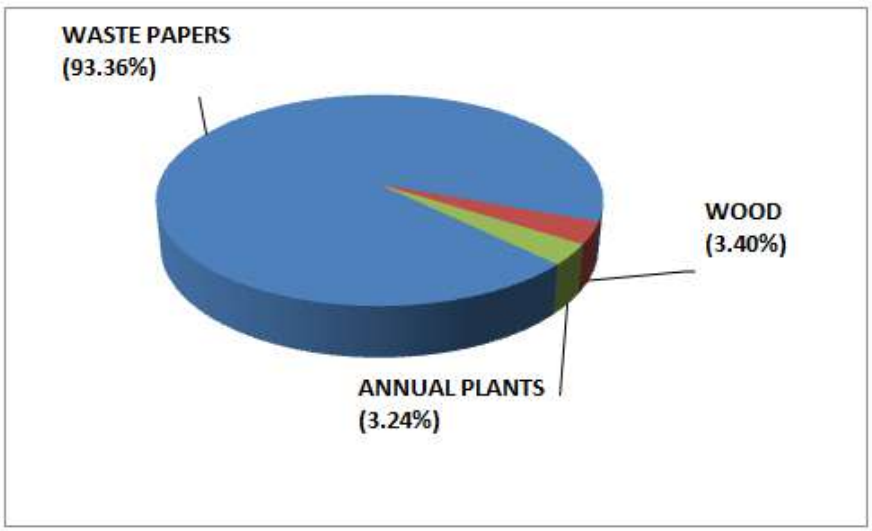

Figure 2. Raw materials and ratios used in the paper industry in Turkey in 2015

Solid wastes have a heterogeneous structure and the composition is constantly changing. The amount and quality of solid wastes produced by each country are very different from each other. This is because the socio-economic and financial structures as well as consumption habits and similar characteristics are very different from each other. In developed countries, the production of solid waste is 1.5-2 kg / person-day. While this value reaches to 3.0 kg / person-day in America, the average daily amount of solid waste per person in our country is 1.14 kg for summer season, 1.09 kg for winter season and 1.12 kg for a year. The average amount of waste per person in Giresun province is 1,12 kg /person-day for 2016 (EUROSTAT, 2014; TUIK, 2017).

In this study, the raw materials and ratios used in paper production in our country, the amount of paper and cardboard produced and consumed the collection and evaluation of waste papers and contributions to the economy of Giresun and Turkey were investigated.

2. Quantity of Paper-Cardboard Produced and Consumed in Our Country and Recycling Rates

There are currently 49 factories producing paper and cardboard in our country. World paper-cardboard production is 764 million tons. Our country is ranked 42nd with 78.3 kg/person paper-cardboard consumption, 14th with 6.326.345 tons paper-cardboard consumption, and 23rd with 4.356.823 tons paper-cardboard production in the world (FAOSTAT, 2016; SKSV, 2017).

Ranked 14th and 23rd with paper-cardboard consumption and production in the world reveals that our country mostly imports papers. This figure reflects the truth is that Turkey is a country open to the growth of the paper and cardboard industry.

Paper-cardboard and pulp production and consumption in our country, per person paper consumption and recycling rates were given separately in Tables 1, 2, 3, and 4 below (SKSV, 2017).

Table 1. Paper and cardboard production quantities in Turkey

	2013	**2014**	**2015**	**2016**	**2017**
Newsprint	836	0	0	0	0
Writing-printing papers	257.000	262.650	232.500	237.100	247.000
Wrapping papers	83.081	96.303	80.000	75.000	77.750
Corrugated papers	1.609.215	1.842.447	2.190.028	2.280.352	2.514.534
Cartons	568.407	459.550	577.291	614.989	643.342
Tissue papers	568.861	584.827	660.487	811.572	869.197
Special papers	5.000	5.000	5.000	5.000	5.000
Total	**3.092.400**	**3.250.777**	**3.745.306**	**4.024.013**	**4.356.823**

Table 2. Paper and cardboard consumption quantities in Turkey

	2013	**2014**	**2015**	**2016**	**2017**
Newsprint	435.191	390.636	346.353	261.814	224.145
Writing-printing papers	1.204.143	1.206.573	1.177.169	1.202.181	1.203.430
Wrapping papers	334.195	351.404	329.139	288.791	344.859
Corrugated papers	2.261.136	2.394.251	2.468.107	2.608.233	2.786.315
Cartons	1.000.810	1.003.515	1.026.093	1.078.303	1.180.065
Tissue papers	402.222	438.268	494.484	539.566	560.588
Special papers	19.824	21.358	23.634	25.031	26.943
Total	**5.657.521**	**5.806.005**	**5.864.979**	**6.003.919**	**6.326.345**

Paper consumption and recycling rates, which are accepted as indicators of economic development all over the world, have increased in our country depending on years, as seen in Table 3 and Table 4 below.

Table 3. Paper and paperboard consumption amounts per person in Turkey (kg)

2010	**2011**	**2012**	**2013**	**2014**	**2015**	**2016**	**2017**
68.6	69.2	70.7	73.8	74.7	74.5	75.2	78.3

Table 4. Waste paper recycling rate in Turkey (%)

2010	**2011**	**2012**	**2013**	**2014**	**2015**	**2016**	**2017**
41.8	44.4	45.1	44.8	46.4	49.2	52.2	54.0

First of all, it should be essential to realize the use of the things in the most effective and most functional manner. This may be possible with effective consumer awareness. In other words, contrary to the "use/throw" philosophy, it is necessary to try not to produce waste and garbage as much as possible. In this regard, especially in Canada, good work and public awareness programs are being carried out. In the 4 R method; 1-Reduce: Reduce the amount of garbage and waste if possible. 2-Reuse: To use the material again and again if possible. 3-Recycling: To use the most effective material in recycling process. 4-Recovery: To feed and enrich raw materials (Miner et al., 1993).

In our country and in the province of Giresun, the main sources of waste papers are collected at low cost;

- All kind of paper, cardboard and corrugated cardboard supplied from industrial establishments and major shopping centers,
- Old newspapers, cardboard boxes and magazines collected from home and work places,
- Different types of papers collected from educational institutions,
- Clippings from press, envelopes and notebook producers
- Corrugated cardboards, bag and bag making workshop residues.

3. Contributions of Waste Paper Recycling to Giresun and Country Economies

We can collect the contribution of the waste paper collection to the province and country economies under 4 headings.

1. Contribution to the Protection of the Environment
2. Contribution to the Protection of Forests
3. Contribution to Municipality
4. Contribution to Paper Production

3.1. Contribution to the Protection of the Environment

A well-organized collection system will not only relieve municipal solid waste collection loads, but will also prevent disposal in garbage dumps. In addition, the use of less wood, water, electricity and chemicals required for manufacturing is very important in terms of environmental protection if production is made using waste paper.

Improving environmental awareness in the collection of waste paper reduces the cost of transporting and disposing of solid wastes, and it is important for the health of people working in garbage dumps prior to the disposal process.

In a study carried out by Giresun Provincial Directorate of Environment and Forestry, province recyclable additive composition ratio (paper, glass, metal and plastic) was determined as 25%, of which 5% is waste paper (KCRD, 2016). If waste papers is collected in Giresun by separating it from its source, it will pour approximately 7.5 tons less garbage in one day, 225 tons less garbage in a month, 2700 tons (1080 trucks) less garbage in year.

3.2. Contribution to the Protection of Forests

In 2017, our per person annual paper consumption is 78.3 kg (SKSV, 2017).

134,937 (Provincial population) × 78.3 kg = 10 thousand 566 tons of annual paper consumption

1 ton paper is produced from 17 adult trees.

10.566 × 17 trees (1 ton of pulp) = 179.622 adult trees will be cut less.

1 ton of paper is produced from 2.5 m^3 (10.566 × 2.5 m^3 = 26.415 m^3).

26.415 m^3 × 150 TL / m^3 (the price of wood for 1 ton of paper) = 3 million 962 thousand 250 TL.

If the total amount of paper-cardboard per person (1,727 tons) in Giresun can be collected, 3 million 962 thousand 250 TL will be contributed to the protection of forests. The recycling rate in our country is 54% and will contribute at least 2 million 140 thousand TL to the provincial economy.

In Table 5 below, the amounts of wood, water and electrical energy required to produce 1 ton of paper from wood and waste paper are given. According to this table, 110% more wood raw material, about 13 times more water and 1.5 times more electricity will be harmed around the environment to produce first quality paper instead of waste paper (CEKUL, 2002).

Table 5. Quantities of wood, water and electricity required to produce 1 ton of paper from wood and waste paper

1 TON PAPER			
PAPER TYPE	WOOD	WATER	ENERGY
I. Quality Paper	2400 Kg	100 tons	7.600 kwh
II. Quality Paper	1700 Kg	80 tons	5.700 kwh
Eco-Friendly Recycled Paper	1150 Kg Waste Paper	8 tons	4.800 kwh

3.3. Contribution to Municipality

The average amount of garbage collected by the municipality in the province center (151 tons per day) is 4,534 tons/month. Approximately 5% of the garbage collected is waste paper (KCRD, 2016).

4.534 × 0.05 = 227 tons waste paper.

227 × 400 TL (1 ton waste paper sale price) = 90 thousand 800 TL.

If a regular collection network is developed on a provincial basis;

90,800 × 12 (1 year) = 1 million 89 thousand 600 TL / year will stay in the municipality.

3.4. Contribution to Paper Production

In 2017, our per person annual paper consumption is 78.3 kg (SKSV, 2017).

134,937 (Provincial population) × 78.3 kg = 10 thousand 566 tons of annual paper consumption

If half of this amount can be collected;

10566/2 = 5 thousand 283 tons of paper is collected.

1 ton of new paper is produced from approximately 1,150 kg waste paper. Approximately 4 thousand 594 tons of paper are produced from 5 thousand 283 tons waste paper.

4594 × 1100 TL (1 ton price) = 5 million 53 thousand 400 TL

If 50% of the papers collected after the use is collected, the total contribution to Giresun Economy in 1 year will be approximately 2 million 526 thousand 700 TL.

4. Conclusions and Recommendations

The paper and paperboard to be recovered by establishing a more effective waste collection network in Giresun and its provinces will provide the following contributions to the provincial economy and consequently to the country's economy.

1. Approximately 2.724 tons of waste paper will be thrown away in a year in the center of Giresun, where it will be recovered from being destroyed or destroyed and turned into paper again.
2. By collecting waste papers, the problem of environmental pollution will be reduced. In addition, contamination of the waste residues by the surrounding environment and the cost of cleaning it will be reduced.

3. Forest resources will be better protected and each ton of recycled waste paper will save 17 adult trees from cutting. Adult 1 tree meets the daily oxygen requirement of 52 people.

To collect effective and efficient waste paper in our country and in our province; inform people, to keep the level of consciousness continuously with the written and visual press, to distribute office-based paper collection bags, to place waste paper collection boxes in corridor, floors and buildings, to determine a place where collected papers are collected and piled up, to put spot and flat panel suggesting ads and words about the importance of recovering at certain locations in the city. Along with these, it has become a necessity for local managers to initiate legal sanctions such as rewarding and punishing for effective recycling.

Since the practitioner will be a human being by reviving this, it is extremely important for people to be conscious of starting from the young age. A conscious and responsible consumer who knows the value of waste paper for the environment, nature, forest and economy will reach the nearest waste paper collection box and recycle even the smallest piece of paper when necessary.

As a result, collection of waste papers, which will contribute significantly to the province and hence the country's economy, should be actively supported by municipalities, public and non-governmental organizations.

References

CEKUL, (2002). The foundation for the promotion and protection of the environment and cultural heritage, Poster, İstanbul.

EUROSTAT, (2014). Waste Generation and Treatment Database. http://epp.eurostat.ec.europa.eu/portal /page/portal/statistics/search_database, Date of access: 26.02.2017.

FAOSTAT (2016). Food and Agriculture Organization of the United Nations, http://faostat3.fao.org/download/Q/QC/E, Retrieved October 31, 2016.

KCDR, (2016). Giresun Province 2016 Yearly Environmental Status Report (KÇDR). Giresun Ministry of Environment and Urbanisation, Giresun.

Miner, R., Somehwar, A., Weigand, P., Fisher, R., Berger, H., Unnwin, J., (1193). *Characterisation of Wastes and Emissions from Mills Using Recovered Fibers. In: Secondary Fibre Recycling* (R.J. Spangenberg ed.), Tappi Press, Atlanta, pp.41-68.

Robinson, W. D., (1986). *The Solid Waste Handbook*. John Wiley and Sons. Ins. New York. (USA).

SKSV, (2017). Cellulose and Paper Industry 2014 Annual Report. Cellulose and Paper Industry Foundation Publications, İstanbul.

Taspinar, F., (2012). Integrated Solid Waste Management. *Düzce's Environmental Problems and Solution Proposals Workshop*, p:1-27, Düzce.

Toroz, I., Arikan, O., (1999). Recovery of Solid Waste in Istanbul. *Urban Management Symposium on Human and Environmental Problems'99*, February 17-19, 1999, Environmental Management and Control, Volume 3, Istanbul Metropolitan Municipality, General Directorate of Istaç, p: 263-272, İstanbul.

TUIK, (2014). Municipal Waste Data. http://www.tuik.gov.tr/VeriBilgi.do?alt_id=1019, Date of access: 25.02.2017.

Tutus, A., (2004). Contribution of the Paper Factory to the Kahramanmaraş Economy. *I. Kahramanmaras Symposium Book*, III. Vol, p: 1427-1432, 6-8 May, Kahramanmaraş.

Tutus, A., Karademir, A., (2005). Collection of Waste Paper at Our University Campus. *II. National University Campus Planning and Environmental Regulation Workshop*, p. 153-158, KSÜ, Environmental Problem Research and Application Center, Publication No: 122, Kahramanmaraş.

Investigation of Physical Properties of Plywood Treated with Fire Retardant Chemicals

Aydın DEMİR[1], İsmail AYDIN[1*]

[1]Karadeniz Technical University, Forestry Faculty, Forest Industry Engineering Department, Trabzon, Turkey

[*]**Correspondig author:** iaydin@ktu.edu.tr

Abstract

The treatment with fire retardant chemicals is the most effective process to protect wood and wood based products from fire is. Therefore, use of fire retardant chemicals has been increased. However, the fire retardant chemicals have an effect on other physical, mechanical and some technological properties of the materials treated with them. In this study, it was examined that the effect of fire retardant on physical properties of plywood. Alder (*Alnus glutinosa* subsp. *barbata*) and Scots pine (*Pinus sylvestris* L.) were used as wood species; zinc borate, monoammonium phosphate and ammonium sulfate were used as fire retardant chemicals and UF resin was used as adhesive. The veneer sheets were treated with immersion method. Physical properties of the plywood panels such as thickness swelling and water absorption, density and equilibrium moisture content of the panels were determined according to TS EN 317, TS EN 323-1 and TS EN 322, respectively. Thickness swelling and water absorption values of panels produced with the veneers treated with fire retardant chemicals were less than those of control panels for 2 h. However, there is no statistical difference in these results for 24 h. In addition, it was found that the density values of panels treated zinc borate was the highest in the all groups for Scots pine.

Keywords: Fire retardant, Plywood, Physical properties, Alder, Scots pine.

1. Introduction

Plywood is preferred as constructional material and has conventionally played an important role in light frame construction. Plywood and other wood-based materials are extensively used in the production of furniture, engineered flooring, housing, and other industrial materials (Bohm et al., 2012). However, the usage and application areas of plywood are limited since the plywood is a flammable material. Therefore, there has been much interest in the fire-retardant-treatment of wood-based panels (Cheng and Wang, 2011). The plywood panels treated with fire retardant chemicals are extensively used in usage. Especially, they are generally preferred in furniture industry and construction applications (Tanritanir and Akbulut, 1999; Winandy, 2001; Ayrilmis et al., 2006).

The wooden materials treated with fire retardant chemicals enable an applicable alternative to conventional non-combustible products where a higher level of fire safety is necessary or desirable (White and Mitchell, 1992). Boron compounds are known one of the best fire retardant chemicals due to their beneficial effects like neutral pH, protective efficiency, and less effect on mechanical strength than the others (Levan and Tran, 1990). Also, phosphorus-containing compounds like mono- and di-ammonium phosphates are considered very effective fire retardant chemicals, so they have been preferred for wooden and wood-based products for quite a long time (Grexa et al., 1999).

The fire retardant chemicals are harmless to human, animals and plants, there is also a less release of smoke and less toxis gases when burned and these are important parameters for consumers to select one of such products. It was also shown the fire retardant chemicals influence the physical, mechanical and some technological properties of the materials treated with them (He et al., 2014; Yao et al., 2012).

In this study, it was examined that the effect of fire retardant on physical properties of plywood. For this purpose, The panels produced as three ply-plywood and it was determined thickness swelling and water absorption, density and equilibrium moisture content as physical properties.

2. Material and Methods

In this experimental study, 2 mm-thick rotary cut veneers with the dimensions of 500 mm by 500 mm were obtained from alder (*Alnus glutinosa* subsp. *barbata*) and Scots pine (*Pinus sylvestris* L) logs. While the alder veneers were manufactured from freshly cut logs, Scots pine

logs were steamed for 12 h before veneer production. The horizontal opening between knife and nosebar was 85% of the veneer thickness, and the vertical opening was of about 0.5 mm in the rotary cutting process. The veneers were then dried to 6–8% moisture content with a veneer dryer. After drying, veneer sheets were treated with some fire retardant chemicals. For this aim, 5% aqueous solutions of zinc borate (ZB), monoammonium phosphate (MAP) and ammonium sulfate (AS) were used. The veneers were subjected to re-drying process at 110°C after their immersion in fire retardant solutions for 20 min.

Three-ply-plywood panels having 6 mm thickness were manufactured by using urea formaldehyde resin. The formulations of adhesive mixture used for plywood manufacturing are given in Table 1. Veneer sheets were conditioned to approximately 5–7% moisture content in a climatization chamber before gluing. The glue mixture was applied at a rate of 160 g/m^2 to the single surface of veneer by using a four-roller glue spreader. Hot press pressure was 12 kg/cm^2 for alder and 8 kg/cm^2 for Scots pine while the hot pressing time and temperature were of about 6 min and 110ºC, respectively. Two replicate panels were manufactured for each test groups.

Table 1. The formulations of UF glue mixture used for the manufacturing of plywood

Glue Type	Ingredients of Glue Mixture	Parts by weight
UF	UF resin (with 55% solid content)	100
	Wheat flour	30
	Hardener - NH_4Cl (with 15% concentration)	10

Physical properties of the plywood panels such as thickness swelling and water absorption,at 2 and 24 hours, density and equilibrium moisture content of the panels were determined according to TS EN 317 (1999), TS EN 323-1 (1999) and TS EN 322 (1999), respectively. The obtained data were statistically analyzed by using the analysis of variance (ANOVA) and Duncan's mean separation tests.

3. Results and Discussion

The density and equilibrium moisture content mean values and Duncan's test results of plywood panels according to the wood species and fire retardant chemicals were shown in Table 2. In addition, the thickness swelling and water absorption values at 2 and 24 hours and Duncan's test results were given in Table 3.

Table 2. Density and equilibrium moisture content means and Duncan's test results of plywood panels ($P < 0.05$).

Wood Species	Fire Retardants Chemicals	Density (g/cm³)		Equilibrium Moisture Content (%)	
Alder	Control	0,639	a*	8,63	b
	ZB	0,646	a	8,39	a
	MAP	0,640	a	8,57	ab
	AS	0,626	a	8,55	ab
Scots Pine	Control	0,575	a	8,89	a
	ZB	0,649	b	8,62	a
	MAP	0,600	a	8,70	a
	AS	0,599	a	8,33	a

* The mean values marked with the same symbol are statistically identical.

Table 3. Thickness swelling and water absorption means and Duncan's test results of plywood panels ($P < 0.05$).

Wood Species	Fire Retardants Chemicals	Thickness Swelling (%)				Water Absorption (%)			
		2 h		24 h		2 h		24 h	
Alder	Control	3,70	b*	9,71	a	33,71	b	48,41	a
	ZB	3,27	ab	9,40	a	32,06	a	48,10	a
	MAP	2,43	a	8,93	a	31,74	a	47,96	a
	AS	2,29	a	8,75	a	31,34	a	47,80	a
Scots Pine	Control	3,70	a	8,15	a	32,47	b	39,33	a
	ZB	3,46	a	8,72	a	28,02	a	40,80	a
	MAP	3,30	a	8,45	a	27,49	a	40,59	a
	AS	3,38	a	8,53	a	27,60	a	40,67	a

* The mean values marked with the same symbol are statistically identical.

As can be seen from Table 2, there was no statistical difference in the density values were obtained for the all groups of alder plywood. However, the mean obtained from panel treated zinc borate was statistically the highest in the all groups of Scots pine plywood. It was seen that there was generally a slight increase in the density values. The spaces in the control groups are filled with air, but the spaces of the specimens were impregnated are filled with impregnated materials. Increasing of density is expected result due to less air space (Aytaskin, 2009; Demir, 2014). There was no difference in the equilibrium moisture content means for the groups of Scots pine plywood. The mean of the control group of alder plywood was higher than the other groups of alder plywood.

As can be seen from Table 3, the thickness swelling and water absorption values of panels produced with the veneers treated with fire retardant chemicals were less than those of control panels for 2 h. Waterborne inorganic salts, such as boron compounds and phosphates, adversely affect swelling and expansion properties of wood and wood composites because of their hygroscopic characteristics and possible interaction between the deposition of boron and phosphate crystals and the monomer in the cell wall (Dundar et al., 2009). This explains some changes in the groups especially the thickness swelling and water absorption values of Scots pine for 24 h. However, there is no statistical difference in these results for 24 h. In literature, phosphate and the boron compounds did not have a significant negative effect on the dimensional stability of sandwich and LVL panels (Rosero-Alvarado et al., 2018; Dundar et al., 2009).

4. Conclussions

In this study, it was aimed to investigation of the effect of fire retardant on physical properties of plywood. As a result of this study, thickness swelling and water absorption values of panels produced with the veneers treated with fire retardant chemicals were less than those of control panels for 2 h. However, there is no statistical difference in these results for 24 h. In addition, it was found that the density values of panels treated zinc borate was the highest in the all groups for Scots pine.

It has been determined that the impregnation process generally improves the physical properties of wood materials. It was affected differently especially the swelling and water absorption of the wood materials depending on the wood species. Therefore, these changes in the strength values and the probability of moisture exchange in the usage must be taken into attention, depending on the wood species used before impregnation.

References

Ayrilmis, N., Korkut. S., Tanritanir, E., Winandy, J. E. and Hiziroglu, S. (2006). Effect of various fire retardants on surface roughness of plywood. *Build. Environ.*, 41(7), 887–892.

Aytaskin, A. (2009). *Some technological properties of wood ımptegnated with various chemical substances*, Master Thesis, Karabük University Natural Science Institute, Karabük.

Bohm, M., Salem. M. Z. M. and Srba, J. (2012). Formaldehyde emission monitoring from a variety of solid wood, plywood, blockboard and flooring products manufactured for building and furnishing materials. *J. Hazard. Mater.*, 221-222, 68-79.

Cheng, R. X. and Wang, Q. W. (2011). The influence of FRW-1 fire retardant treatment on the bonding of plywood. *J. Adhes. Sci. Technol.*, 25, 1715–1724.

Demir, A. (2014). *The effects of fire retardant chemicals on thermal conductivity of plywood produced from different wood species*. Master Thesis, Karadeniz Technical University, Natural Science Instute, Trabzon.

Dundar, T., Ayrilmis, N., Candan, Z. and Sahin, H. T. (2009). Dimensional stability of fire-retardant-treated laminated veneer lumber. *Forest Products Journal*, 59(11), 18-23.

Grexa, O., Horvathova, E., Besinova, O. and Lehocky, P. (1999). Flame retardant plywood. *Polym. Degrad. Stabil*., 64, 529–33.

He, X., Li, X., Zhong, Z., Yan, Y., Mou, Q., Yao, C. and Wang, C. (2014). The fabrication and properties characterization of wood-based flame retardant composites. *Journal of Nanomaterials*, 1-6.

Levan, S. L., Tran, H. C. (1990). *The role of boron in flame-retardant treatments*. In: Hamel M, editor. First international conference on wood protection with diffusible Preservatives. Proceedings 47355, Nashville, TN, November 28–30, p. 39–41.

Rosero-Alvarado, J., Hernández, R. E. and Riedl, B. (2018). Effects of fire-retardant treatment and wood grain on three-dimensional changes of sandwich panels made from bubinga decorative veneer. *Wood Material Science and Engineering*, 1-10. https://doi.org/10.1080/17480272.2018.1465464.

Tanritanir, E. and Akbulut, T. (1999). Plywood industry and general situation of plywood trade. *Laminart-Furniture and Decoration Journal* 9, 122–32 (In Turkish).

TS EN 317, 1999. Particleboards and fibreboards- Determination of swelling in thickness after immersion in water. Turkish Standards Institute, Ankara.

TS EN 322, 1999. Wood-based panels-Determination of moisture content. Turkish Standards Institute, Ankara.

TS EN 323-1, 1999. Wood- Based panels- Determination of density. Turkish Standards Institute, Ankara.

White, R. H., Mitchell, S. S. (1992). *Flame retardancy of wood: present status, recent problems, and future fields*. In: Lewin M, editor. Recent advances in flame retardancy of polymeric materials. Proceedings of the third annual BCC conference on flame retardance, Stamford, CT: p. 250–7.

Winandy, J. E. (2001). Thermal degradation of fire-retardant-treated wood: predicting residual service life. *Forest Product Journal*, 51(2), 47–54.

Yao, C. H., Wu, Y. Q. and Hu, Y. C. (2012). Flame-retardation characteristics and mechanisms of three inorganic magnesium compounds as fire-retardant for wood. *Journal of Central South University of Forestry and Technology*, 32(1), 18–23.

Comparison of Some Physical and Mechanical Properties in Water-Borne Acrylic Resin with Commercial UV Absorber and Tree Bark Extract Coating Systems

Özlem ÖZGENÇ[1], Süleyman KUŞTAŞ[1*],

[1] Karadeniz Technical University, Department of Forest Products Engineering, Trabzon, Turkey; oozgenc@ktu.edu.tr

[*] **Corresponding Author:** suleymankustas@ktu.edu.tr

Abstract

One of the main methods used to protect the surface of wooden material against outdoor conditions; surface treatment UV light and water contact with the wood surface. In this study, some general properties of water-borne acrylic resin based varnish systems containing 5 different tree bark extracts (maritime pine, calabrian pine, black pine, alder, fir) and commercial UV absorbers (Tinuvin 400 DW) have been investigated. The formulation ingredients were provided from BASF Turkey Representative BOYSAN company and varnish systems were synthesized in Karadeniz Technical University, Department of Forest Industry Engineering laboratory. The solids content of these varnishes were determined. Then, the varnish systems applied to the surface of the Scots pine (*Pinus sylvestris* L.) and beech (*Fagus orientalis* L.) were measured by dry-film thicknesses with a light microscope and the values of adhesion strength were determined. The solid content in the varnish systems containing the maritime pine bark extract is highest. The dry film thicknesses of varnish systems containing bark extract are higher than those of commercially available UV absorber on scots pine and beech surface. The acrylic resin varnish systems containing bark extract and commercial UV absorber on scots pine and beech surfaces have been found to be different adhesion strengths values.

Keywords: Acrylic varnish, Adhesion strength, Dry film thickness, Tree bark extract, Pull-Off test

1. Introduction

The changes in color, surface roughness and cracks occur on the wood surface exposed to outdoor conditions with light (UV, IR), damp (rain, snow, humidity, dew), mechanical forces (wind, sand, dirt) and temperature effect (Feist and Hon, 1984; Williams, 2005). As a result of these effects, some changes consist in the color, chemical and physical structure of wood (Kılıç and Hafızoğlu, 2007). Some organic components, as primarily cellulose, hemicellulose and lignin, and biological and physical factors of wood and are degraded by modification. The wood extractives are relatively less degradable, changing their concentration, color, odor and other non-mechanical properties of the wood in outdoor conditions (Feist, 1990; Pandey, 2005).

Today, different methods are applied to prevent erosion and discoloration on the wood surface due to the effect of weathering and to make the wood material more resistant to outdoor conditions (Williams, 2005). From these methods; paint, varnish, varnish, water repellent, etc. it is widely used to prevent the UV light and water from contacting the wood surface. Nowadays, different surface products applied to the wood materials used in outdoor conditions are presented to the market (Özgenç et al., 2012; Decker et al., 2004; Evans and Chowdhury, 2010).

There are some studies in the literature on the use of tree bark extracts as an organic UV absorber due to its high antioxidant effect. One of these studies; bark extract, lignin stabilizer, UV absorber and hindered amine light stabilizer (HALS), compared to the photostabilization effect on the wood surface of the acrylic polyurethane varnish. The highest photososstabilization effect after the accelerated weathering test was determined in wood samples coated with acrylic polyurethane containing bark extract and lignin stabilizer after heat treatment (Kocaefe and Saha, 2012). According to the results of another study, natural antioxidant (bark extract) and lignin stabilizer were mixed in acrylic polyurethane wood surface material alone or in combination to increase the resistance to the external environmental factors of the coating material. The color stabilization of wood samples coated with acrylic polyurethane containing bark extract on the surface is increased (Saha et al. 2011). The color stability of wood is very high in the outdoor environment when compared with wood coatings applied with 2-hydroxy-4 (2,3-epoxypropoxy) -benzophenone (HEPBP) containing UV absorber (HEPBP) and epoxy functional soybean oil. It also provides significant protection against the physical deformation of wood coatings caused by external factors such as UV radiation and rain, by the combination of UV absorber (HEPBP) and epoxy functional soybean oil (Olsson et al. 2012). Saha et al. (2013) examined the external weathering resistance of acrylic polyurethane coatings prepared

with three different UV stabilizers (UV absorber, HALS, Anti-oxidant). Yalcin and Ceylan (2017) applied polyurethane, cellulosic and water based varnish systems to wood surfaces pretreated with bark extracts of mimosa (Acacia mollissima) and quebracho (Schniopsis lorentzii). Afterwards, the durability of the modified varnish systems in outdoor was examined. It has been determined that polyurethane, cellulosic and water-based varnish systems have lower adhesion strength on the wood surfaces after pre-treatment with bark extract.

The dry-film thicknesses and surface adhesion resistance significantly affect the duration of the acrylic-based varnishes under outdoor conditions. In this study, the bark extract was obtained by alcohol-benzene method from five different tree species. The adhesion strength values were compared by evaluating dry film thicknesses and microscopic images on the scots pine and oriental beech surfaces coated acrylic based varnish systems containing five different bark extracts and UV absorbers.

2. Material and Method

2.1. Wood Materials

In this study, scots pine (*Pinus silvestris L.*) and oriental beech (*Fagus orientalis L.*) wood species were used. The scots pine and oriental beech were used in the study as defect free samples. The wood samples were prepared with dimension of 150mm (longitudinal) by 70mm (tangential) by 20mm (radial) for artificial weathering.

2.2. Tree Barks

The barks were peeled off from the 20-30-year-old alder (*Alnus glutinosa***)**, calabrian pine (*Pinus brutia*), maritime pine (*Pinus pinaster*), black pine (*Pinus nigra*) and fir (*Abies nordmanniana* L.) trees that were cut down in black sea region in the north of Turkey. TAPPI T 257 cm-12 and TAPPI T 264 cm-07standard methods were used for the preparation and chopping tree barks for extraction analysis.

2.3. Bark extraction

All tree barks were air-dried at room temperature (23 ^{O}C, 65% relative humidity) and then ground by using a laboratory scale Willey mill to obtain 40 to 60-mesh wood powder. To obtain

extractives, the bark powders were extracted in a Soxhlet extractor. The bark powder (25 g for each) was soaked in 300 mL of ethyl alcohol:benzene (1:2 v/v). The solvents from each extracts were removed by using a rotary evaporator at 50 ^{o}C and stored in sealed flasks at 4^{o}C until use.

2.4. Preparation of coating systems

Six different wood coating systems will be obtained using acrylic resin, binder, diluent, antifoam, pure water, shell extract or UV absorber (Table 1). As UV absorber, "Tinuvin 400 DW" product of BASF was used. The formulation containing the UV absorber was regarded as a control and compared with the varnish formulations containing the bark extract.

Variation code:

A: Water borne acrylic resin based coating containing fir extract
B: Water borne acrylic resin based coating containing alder extract
C: Water borne acrylic resin based coating containing calabrian extract
D: Water borne acrylic resin based coating containing maritime pine extract
E: Water borne acrylic resin based coating containing black pine extract
F: Water borne acrylic resin based coating containing UV absorber

A, B, C, D, E → Test
F → Control

Table 1. Acrylic resin based surface system formulation components (%).

No	Components	Formulation containing bark extract	Formulation containing UV absorber
1	Acrylic resin	72.5	72.5
2	Diluted water	18.88	20.88
3	Coalescent	0.67	0.67
4	defoamer	1.0	1.0
5	Thickener	0.6	0.6
6	Thickener	1.3	1.3
7	Bark extract	5.0	-
8	UV absorber	-	3.0
9	Ammoniac	0.05	0.05
		100.0	100.0

1.1. Application of varnish systems on the wood surface

The water-based wood preservative Induline SW 900 was applied as a primer layer to the side and front of the 120x70x10 mm wood samples prepared for the artifical weathering test. The prepared coating was applied in two layers using a brush for 24 hours. After surface

treatment, it was incubated for 2 weeks at a temperature of 20 ° C in a medium with 65 ± 5% relative humidity.

1.2. Determination of dry film thickness and microscopic analyzing

1 gr sample was taken from acrylic varnish prepared for testing and control purposes and the product was dried at 103 ° C. The amount of solids was calculated by taking the full dry weights of 1 gr varnish samples before and after the oven. For each varnish type, three repetitions were made. The dry film thickness is determined by ZEISS Stemi 305 light microscope and ZEISS Axiocam ERc 5s camera with 2X magnification according to EN ISO 2808 (2007) standard.

1.3. Adhesion test

For the determination of adhesion strenght, three samples of 120x70x10 mm were used and the experiments were carried out by taking two measurements from each sample according to ASTM D 4541 standards. For this purpose, steel cylinders with a diameter of 20 mm were adhered to the center of the specimens with epoxide adhesive and left to stand for 1 day at 20 ± 2 ° C temperature and 65% ± 5 relative humidity conditions for full drying of the glue. Then, the samples were placed under the drawing cylinder of the adhesion resistance measuring instrument (Erichsen Adhesionmaster 525 MC) and the steel cylinders were connected and the tests were carried out at a speed of 0.5 N / s.

The force value at break was measured at the sensitivity of ± 0,01 N and the adhesion strenght of the samples was calculated from the following equation:

$$\rho_a = \frac{F}{A}$$

ρ_a: Adhesion strenght (N/mm^2); F: Force at break (N); A: Application area (mm^2)

2. Results and Discussions

2.1. Determination of dry film thickness and microscopic analyzing

The dry film thickness values of the acrylic based varnishes containing bark extract (test) and commercial UV absorber (control) on the pine and beech wood surfaces are determined by

light microscopy and given in Table 2 (Grüll et al., 2014). The dry film thicknesses of the test samples were higher than control group (F).

Table 2. Dry film thickness on the pine and beech surfaces coated with acrylic based varnishes (μm)

Coating code	Pine	Beech
A	45.36	71.24
B	43.73	80.47
C	44.58	70.59
D	52.81	68.37
E	53.73	87.96
F	37.23	65.37

The light microscope image of pine and beech surfaces coated with acrylic based containing bark extract and commercial UV is given in Figures 1 and 2. Scots pine and beech wood species have different specific gravity and anatomical structure. Therefore, it was determined that varnish penetration was higher and dry film thickness was lower on the pine wood surface. (Ozdemir and Hiziroglu, 2007; Ozdemir and Mengeloğlu, 2009; Ozgenc, 2017).

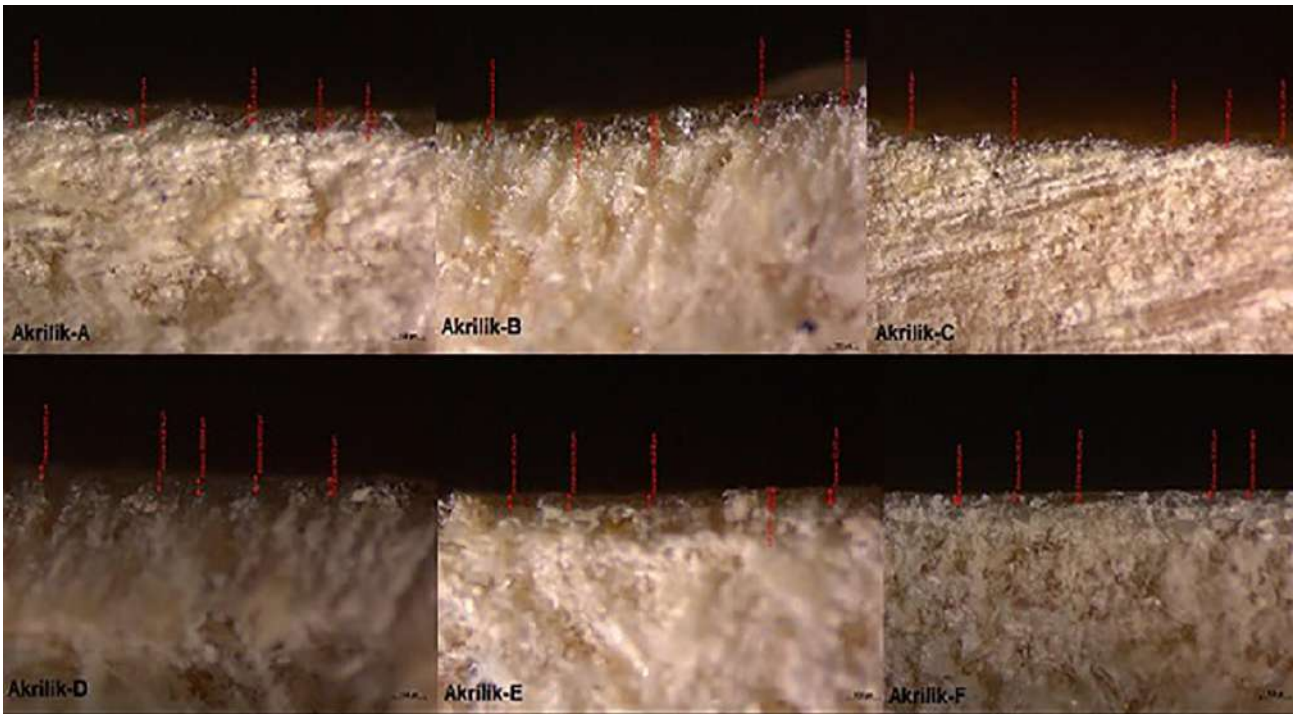

Figure 1. Microscopic image of scots pine surface coated with test and control acrylic systems.

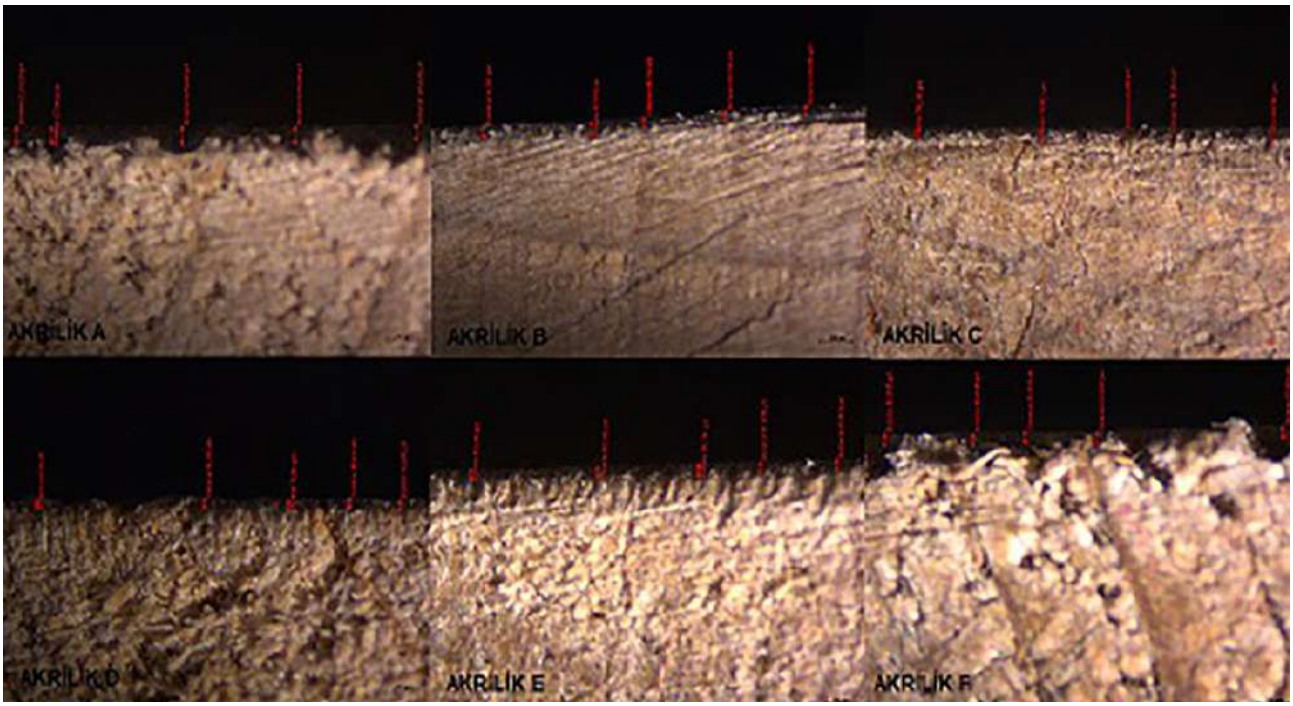

Figure 2. Microscopic image of beech surface coated with test and control acrylic systems.

2.2. Adhesion test

The adhesion strength of acrylic resin based coating systems containing bark extract and commercial UV absorber on the beech and pine wood surfaces has been found to have different adhesion strength values. The adhesion strength of the acrylic coating systems on the wood surfaces is given in Table 3.

Table 3. Adhesion Test Values of Coating Systems (N/mm2)

Coating type	A	B	C	D	E	F
Acrylic-Beech	2.64 (0.46)*	2.35 (0.24)	2.93 (0.32)	2.71 (0.88)	2.71 (0.45)	1.71 (0.41)
Acrylic-Pine	1.36 (0.19)	0.45 (0.17)	0.29 (0.09)	0.64 (0.16)	0.19 (0.09)	0.64 (0.11)

* The standard deviation values are given in parenthesis.

Compared to pine wood, acrylic based coating systems applied to beech surface have high adhesion strength. In both wood types, the adhesion resistance value of acrylic based coating containing fir (A) bark extract was higher than the coating containing commercial UV absorber. In addition, commercial UV-absorbing coating systems in beech wood have lower adhesion strength than acrylic coatings containing all barks extracts.

Studies in the literature show that the penetration of the coating system into the wood is inversely proportional to the dry film thickness. For this reason, the low dry film thickness was determined in coating systems which had good penetration on the pine wood surface. The low dry film thickness negatively affects the adhesion resistance between varnish and wood (Bardage and Bjurman, 1998; Bulian and Graystone, 2009). The results of the study support the literature; Compared to chrysanthemum, low penetration on the beech surface has created a high film thickness. Adhesion strength values were also determined to be quite high. For pine, the highest adhesion strenght was determined as an acrylic coating system with fir (A) bark extract.

Based on these results; we can say that the use of acrylic resin-based surface material, which contains bark extract (especially fir for scots pine), is often made possible by maintenance, because it is weather-resistant, environmentally friendly, easy to apply and economical. The water borne acrylic coating systems containing the bark extract, as well as being used on the wooden houses; It is also recommended to use for wooden products such as balconies, garden furniture, floor coverings, pergolas, garden fences, children's play elements, wooden flower pots These coatings is environmentally friendly because of its organic content. In addition, these organic coating systems and tree barks known as waste will be evaluated.

Acknowlegment

This study was supported by Karadeniz Technical University Scientific Research Project Unit by FUK2016-5294 project.

References

Bardage S. L. and Bjurman J. (1998). Adhesion of waterborne paints to wood. J. Coat. Technol., 70(78):39-47. DOI: 10.1007/BF02697810.

Bulian F. and Graystone J.A. (2009). Wood coatings: Theory and Practice. Elsevier, Radarweg 29, PO Box 211, 1000 AE Amsterdam, The Netherlands, The Boluvard, Landford Lane, Kidlinton, Oxford, OX5 1GB, UK, ISBN: 9780444528407.

Chang, S.-T., Wu, S.-Y., Kang, P.-L., Yang, N.-S. and Shyur, L.-F. (2001). Antioxidant Activity of Extracts from Acacia confusa Bark and Heartwood; J. Agric. Food Chem., 49, 3420-3424.

Decker, C., Masson, F., and Schwalm, R., (2004). Weathering Resistance of Water-Based UV-Cured Polyurethane-Acrylate Coatings, Polymer Degradation and Stability, 83, 309-320.

Feist, W. C. (1990). Weathering Performance of Painting Wood Pretreated with Water-Repellent Preservatives, Forest Products Journal, 40, 7/8, 21-26

Harlow, H. F. (1983). Fundamentals for preparing psychology journal articles. Journal of Comparative and Physiological Psychology, 55, 893-896.

Kernis, M. H., Cornell, D. P., Sun, C. R., Berry, A., Harlow, T., and Bach, J. S. (1993). There's more to self-esteem than whether it is high or low: The importance of stability of self-esteem. Journal of Personality and Social Psychology, 65, 1190-1204.

Kocaefe, D. and Saha S. (2012). Comparison of the protection effectiveness of acrylic polyurethane coatings containing bark extracts on three heat-treated North American wood species: Surface Degradation, Applied Surface Science, 258, 5283-5290.

Pandey, K. K., (2005). A Note onthe Influence of Extractives on the Photo-Discoloration and Photo-Degradation of Wood, Polmer Degradation and Stability, 87, 375-379.

Olsson S., Johansson M., Westin M., and Östmark E. (2012). Grafting of 2-hydroxy-4(2,3-epoxypropoxy)-benzophenone and epoxidized soybean oil to wood: Reaction conditions and effects on the color stability of Scots pine, Poly. Degr. and Stabil. 97, 1779-1786.

Ozdemir T. and Hiziroglu S. (2007). Evaluation of surface quality and adhesion strength of treated solid wood. Journal of Materials Processing Technology, 186(1-3):311-314.

Ozdemir T., Bozdogan Ö., and Mengeloglu F (2013). Effects of varnish viscosity and film thickness on adhesion strength of coated wood. ProLigno, 9(4):164-168. Online ISSN: 2069-7430

Ozgenc, O., Hiziroglu, S., and Yildiz, U., C., (2012). Weathering Properties of Wood Species Treated with Different Coating Applications, BioResources, 7, 4, 4875-4888.

Philip D. Evans and Mohammed J. A. (2010) Chowdhury, Photoprotection of Wood Using Polyester-Type UV-Absorbers Derived from the Reaction of 2-hydroxy-4(2,3-epoxypropoxy)-benzophenone with Dicarboxylic Acid Anhydrides, Journal of Wood Chemistry and Technology ,Volume 30 - Issue 2

Saha, S., Kocaefe, D., Boluk, Y. and Pichette, A., (2011). Enhancing Exterior Durability of Jack Pine by Photo-Stabilization of Acrylic Polyurethane Coating Using Bark Extract, Part I: Effect of UV on Color Change and ATR-FT-IR analysis, Progress in Organic Coatings, 70, 376-382.

Saha, S., Kocaefe, D., Krause, C., Boluk, Y. and Pichette, A., (2013). Enhancing Exterior Durability of Jack Pine by Photo-Stabilization of Acrylic Polyurethane Coating Using Bark Extract, Part II:Wetting characteristics and fluorescence microscopy analysis, Progress in Organic Coatings, 76, 504-512.

Importance of Saw Blade Geometry and Technic Conditions in Machining of Wood Materials in Circular Saw Machines

Ali ÇAKMAK[1*], Abdulkadir MALKOÇOĞLU[1]

[1]Karadeniz Technical University, Faculty of Forestry, Trabzon, Turkey.

[*]**Sorumlu Yazar:** alicakmakoem@gmail.com

Abstract

Circular saw machines are usually used for cutting of the edge flattened parts to desired dimensions and angles, sizing of panels, grooving, jointing, rebating, etc. For this purpose, it can be stated that the selection of the cutter in machining is very important in terms of product quality and efficiency. It can be indicated that the main factors affecting saw blade selection are material density and humidity, cutting edge shape and type with rake and tool angle. In this study, saw blade geometry, its selection and factors affecting the process were studied in the machining of wood materials in circular sawing machines. Also, the problems and solutions proposal encountered in the circular saws during in sizing are stated.

Keywords: Saw Blade Geometry, Saw Blade Selection, Circular Saw Machine.

1. Introduction

No cutting method or type actually cuts the materials. The process occurs as a result of force application of the blade and structural degradation of the materials. Degradations in the process are impressed by section (tangential, radial and longitudinal), different tree species, fiber orientation, moisture content and resistance properties of the wood. Same way; the construction of cutting tools and machines and their operations are closely related to the level of occurrence of defects in machining of wood materials (Davim, 2011; Wengerd, 1998; Koch, 1972; Kolmann, and Cote, 1968; Davis, 1962). The production cost of any product is quite efficient in machining. In this context, it is stated that the share of the machining in furniture production cost is 23%. (Malkoçoğlu, 2017; Malkoçoğlu and Tiryaki, 2011; Hoff et al. 1997).

Wood is one of the most precious and difficult engineering materials of the mankind. Although it is light, it is a material that has a high resistance to various effects, easily processed and consumes less energy during machining. Traditionally, it has been used as the main raw material for centuries in production of furniture, joinery, interior design, wood structures, paper, packaging, transportation, toys, various tools, etc. (Malkoçoğlu, 2018; Csanády and Magoss, 2012; Unido, 1989). Nowadays, various low priced industrial panels (MDF, chipboard, plywood and laminated wood based materials, etc.) are used instead of wood in these productions (Kaplan vd., 2018; Gottlöber et al. 2016; Gaff, 2014; Kurtoğlu and Sofuoğlu, 2013; Kurtoğlu and Sofuoğlu, 2013-2; Eroğlu, 2007; Kurtoğlu, 2000; Erdinler, 2005).

Circular saws are widely used in the machining of wood materials, especially in traditional and computerized machines in the furniture industry. There are many kinds of these in terms of the number of teeth, tooth form and material and the machining conditions. For this reason, it can be stated that the choice of saw blade is so important in terms of capacity, efficiency and end-product quality (Malkoçoğlu, 2018; Anonymous, 2017; Mitchell et al. 2005; Burdurlu and Baykan, 1998; İlhan et al. 1990)

In this study, saw blade geometry, selection and factors affecting the machining were studied in the machining of wood and wood-based materials in circular sawing machines. Also, the problems and solutions proposal encountered in the circular saws during in sizing are stated.

2. Literature

2.1. Functions of Circular Saw Machines

Circular saw machines are usually used in grooving, mortising, tenoning and cutting the length, width and thickness of surfaces and edges flattened parts to the desired dimensions and

angles in machining of wood and wood-based materials. Various machines and saw blades that have many different types and technical specifications are used for many operations. These are single or doubled circular saws. Parts are one by one in single sawed type, and one or more in doubled type depending on the size of the parts (Chabrier and Martin, 1999; Renshaw, 1999; Schajer and Wang, 1999; Burdurlu and Baykan, 1998; Lehmann and Hutton, 1997; İlhan et al. 1990) (Fig. 1).

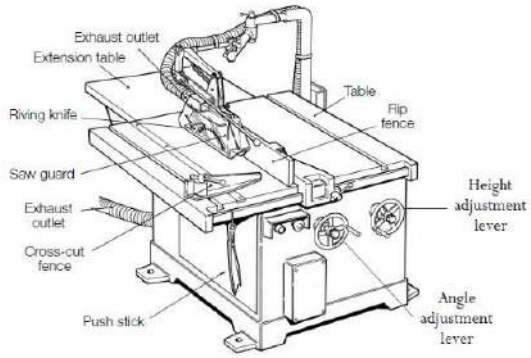

Fig. 1. Basic parts of a circular saw machine (HSE, 2018).

2.2. Factors Effecting Machining Quality

The conditions necessary for proper machining of wood materials are generally examined in three main groups (Kurtoğlu, 1981; Davis, 1962):

I. Mechanical condition of knives or cutting tools: These contain especially cutters associated with tools or machine parts (machine maintenance, cutting material and tooth form, placement of cutting tools on the machine, wedge angle and sharpness of the cutter)

II. Adjustment and operation of tools or machines: It usually occurs from four parts which directly affect the surface quality in machining (hook/rake angle, cutting depth, feed and cutting speed and tooth pitch in unit length)

III. Structure and characteristics of wood material: These are moisture content, density, growth rate of wood material or annual number of rings, latewood participation rate and wood defects.

The lack of fulfillment of the various conditions in these factors, or ignorance in the selection, directly affects the machining and hence the surface quality. According to the rules stated here with maintaining proper machining conditions.; it is ensured that the various wood material surfaces are obtained as least defects (Ratnasingam et al. 1999; Smith et al. 1990; Kurtoğlu, 1981; Koch, 1972; Koch, 1964; Davis, 1962).

The importance of factors related to cutting and feed speeds, material and cutters are emphasized based on the surface quality.

According these, it is stated that smooth surfaces are obtained with lower feed speed and higher cutting speed and machining performance increases in low rake angles. It is suggested lower rake angle (according to ASTM) for high density woods and higher rake angle for low density woods (Sofuoğlu, 2016; Söğütlü, 2010; Malkoçoğlu, 2007; Malkoçoğlu et al. 2007; Williams and Morris, 1998) (Table 1).

Table 1. Optimum hook/rake angles for some wood species in machining.

Wood Species	Hook/Rake Angle (°)*	Moisture Content (%)
Lime tree	25	6
Elm	15	6
Alder (soft)	20	6
Alder (hard)	15	6
Oak	10	6
Oriental beech	15	12
Anatolian chestnut	15	12
White alder	15	12
Scotch pine	15–20	12
Oriental spruce	15–25	12
Oriental beech	15	12

* According to ASTM

2.3. Circular Saw Machines and Machining Quality

The machining quality in circular saws can generally be stated according to the factors affecting surface quality. These are structure and characteristics of wood, geometry and technical specifications of circular saw blade (saw blade diameter, number of teeth, gullet, cutting edge type and rake angle) and machining conditions (feed and cutting speeds).

2.3.1. Structure and Characteristics of Wood

One of the most important factors in the selection of circular saw blade is making a choice according to the material to be machined in machining process. Investigations on the surface quality effect of wood moisture and density have generally indicated that smoother surfaces are obtained with better machining conditions in high density and low moisture woods. On the other hand, moisture reduces the machining quality by plasticizing the wood and compressing the wood during the process (Malkoçoğlu, 2007; Kurtoğlu, 1981; Davis, 1962).

2.3.2. Geometry and Technical Specifications of Circular Saw Blades

There are many circular saw blades that have very different brands and technical specifications in terms of material, cutter properties and processing conditions. These properties are generally the number of teeth, cutting edge type and width, rake angle, saw blade and flange diameter, saw blade thickness, material type, expansion, cooling and sound insulation slots. Flange diameter varies depending on the diameter of the circular saw. (Fig. 2).

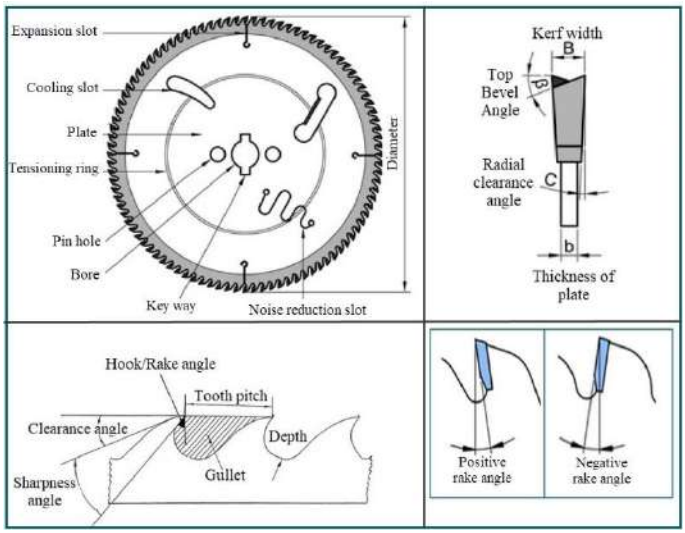

Fig. 2. Basic geometry of a circular saw blade (URL-1-2)

In the machining of wood materials in circular saw machines four tooth forms as straight, bevel, trapezoidal, conical and their combinations are commonly used (Fig. 3).

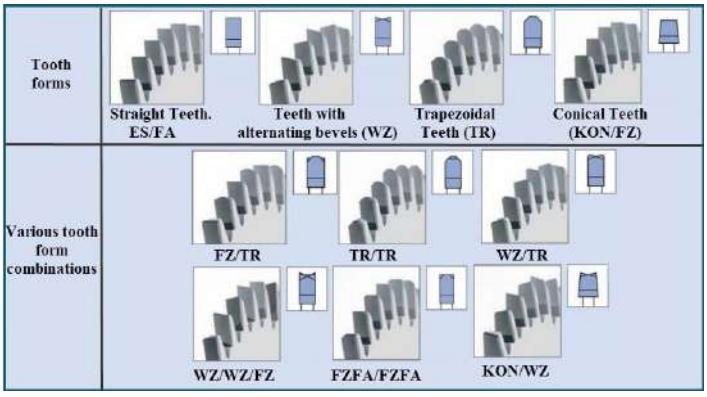

Fig. 3. Commonly used tooth forms (Bosch, 2018; Bilteks, 2018; Leitz, 2017

Straight tooth form is usually used in timber construction industry at high speeds and when an average surface quality is desired in the rip and cross cutting (transverse cutting) processes. Bevel tooth form is used in machining of glued or non-glued wood materials and veneered and laminated wood-based materials, plywood and non-ferrous metals. Trapezoidal tooth form is used in the dimensioning and grooving processes of wood-based materials. Conical tooth form is especially used in scoring saw blades for veneered and laminated wood-

based materials. Besides, these saws can also be used with various tooth form combination (Bilteks, 2018; Leitz, 2017; EDN, 2017).

Tungsten carbide (HW) and high-speed steels (HSS) cutting materials are commonly used in the dimensioning of wood materials. In addition, monocrystalline and polycrystalline (DM and DP/CVD) diamond cutters are often used in a wide range in the machining of solid woods, chipboards and fibre boards, fibre cement boards, laminate floors, fibre reinforced plastics and non-ferrous metals.

2.3.3. Machining Conditions

One of the most important factors after the selection of the saw is the choice of processing conditions. The technical specifications of the circular saws and the operations to be carried out according to the material type require different feed and cutting speed rates. Today, relationships between desired tooth pitch, number of teeth and machining conditions for circular saws are presented as table and charts (Fig. 4) (Bosch, 2018; Bilteks, 2018; Leitz, 2017).

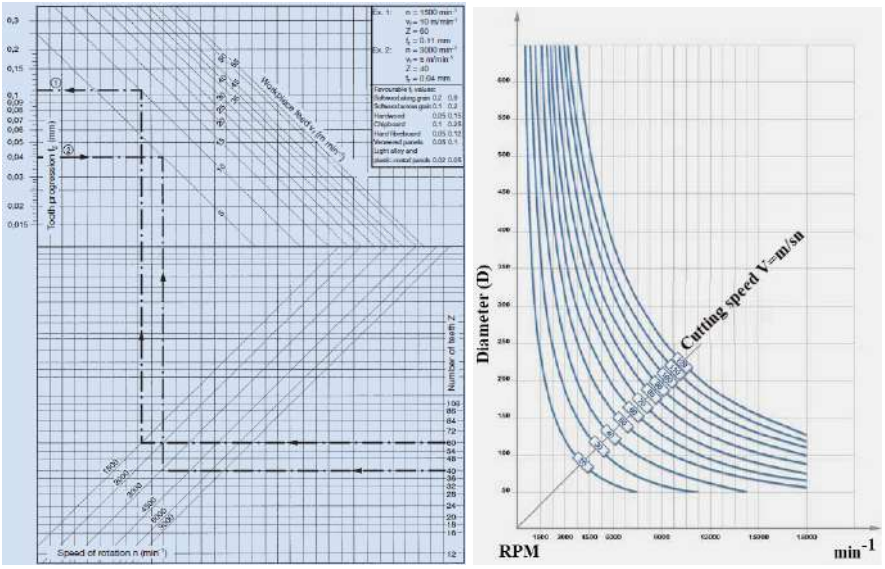

(a) (b)

Fig. 4. Relationships between RPM, feed rate, number of teeth (a) and diameter-cutting speed (b) (Bilteks, 2018; Leitz, 2017)

As shown in Figure 4, various feed rates can be selected based on the different range of RPM for number of teeth and cutting material. Thus, products of various qualities can be obtained with different tooth pitchs in relation to the capacity. At the same time cutting speed increases with the increase of saw blade diameter.

In the machining in circular saw machines more smooth surfaces are obtained in the radial direction. In addition, increasing the number of teeth and decreasing the feed speed, it is stated that smoother surfaces can be obtained and the number of teeth in dense materials should be

increased. (Sönmez and Söğütlü, 2009; Demirci and Kılıç, 2005; Kılıç and Demirci, 2003; Örs and Demirci, 1999).

3. Saw Blade Selection in Machining of Wood Materials in Circular Saw Machine

In wood machining, the "volume increase factor" in chip formation ranges from 1.5 to 7.5. This amount depends on the type of wood, moisture content and rake angle. For this reason, these factors should be considered when choosing circular saw blades (Malkoçoğlu, 2018; Sönmez and Söğütlü, 2009; Demirci and Kılıç, 2005; Kılıç and Demirci, 2003; Örs and Demirci, 1999).

In machining of wood materials in circular saw machine; the volume increase factor is lower in broad-leaved tree woods and across the grain direction in contrast to coniferous woods and the along the grain direction. Accordingly, the number of teeth should be less and the gullet should be larger in the machining with circular saws in along the grain direction. At the same time, the rake angle is higher than the circular saws used in across the grain direction. These saws are generally 180-250 mm in diameter, and the number of teeth should be chosen less in comparison with the machining in across the grain direction (Table 2 and Fig. 5) (Malkoçoğlu, 2018; Sönmez and Söğütlü, 2009; Örs and Demirci, 1999). In the machining in across the grain direction, the number of teeth should be more and the gullet must be smaller. Rake angle should be selected lower and saw diameter should be selected higher in comparison with the machining in along the grain direction (Malkoçoğlu, 2018; Sönmez and Söğütlü, 2009; Örs and Demirci, 1999).

Table 2. Some technical specifications of circular saw blades used in the machining in across and along the grain direction (Bosch, 2018; Bilteks, 2018; Oertli, 2018; EDN, 2017; Leitz, 2017)

Grain direction	Cutting material	Diameter (D) (mm)	Kerf width (SB)(mm)	Thickness of plate (TDI) (mm)	Number of teeth (Piece)	Tooth form	Hooh/Rake angle (^{0})
Along grain	HW	180- 250	1.3-4	0.9-2.8	21-40	FZ FZ/WZ	10, 15, 20
Along grain	DP	180-200	3.2	2.2	24-48	FZ	10
Across grain	HW	300-630	2.4-5.8	2.4-3.5	36-180	WZ WZ/WZ/FZ	-5, 10, 15
Across grain	DP	250-350	3.2	2.4	50-70	WZFA	10

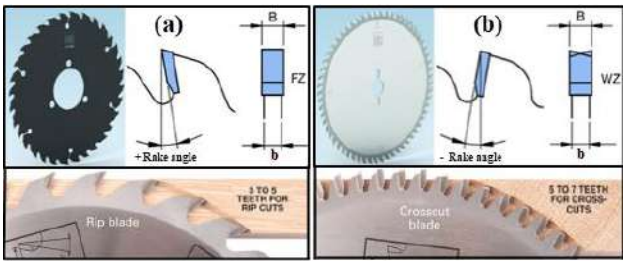

Fig. 5. Circular saw blades used in along (a) and across the grain (b) direction (Oertli, 2018; Leitz, 2017; URL-3).

The saw blade selection should be made considering the fact that the wood-based materials have various densities, glue content and coating materials. For this purpose, a great variety of saw blades are used. These have different diameters, number of teeth and tooth forms. The fact that the saw diameter is bigger, number of teeth more and feed speed less is very effective in terms of machining efficiency and surface roughness in selection of saw blade in the machining of high density materials (Table 3) (Malkoçoğlu, 2018; Sönmez and Söğütlü, 2009; Örs and Demirci, 1999).

Table 3. Some technical specifications of circular saw blades used in the machining of wood and wood-based materials (Bosch, 2018; Bilteks, 2018; Oertli, 2018; EDN, 2017; Leitz, 2017).

Process	Cutting material	Diameter (D) (mm)	Kerf width (SB) (mm)	Thickness of plate (TDI) (mm)	Number of teeth (Piece)	Tooth form	Hooh/Rake angle (^{0})
Sizing	HW	250-750	3.2-7	2.2-5	48-72	WZ FZ/TR TR/TR	10, 15, 22
Sizing	DP	300-450	4.4-4.8	3.2-3.5	60-72	TR/TR	10
Scoring	HW	100-300	3.2-6.8	2.5-4.2	24-72	KON/WZ	5
Scoring	DP	125-200	3.1-4.7	2.5-3.5	20-30	KON/WZ	10

4. Problems and Proposed Solutions Encountered with Sizing Operations

Many probles are encountered with saw blades used in sizing operations of wood and wood-based materials in circular saw machines in furniture, joinery, and wooden construction industries etc. These problems and proposed solutions are stated in Table 4.

Table 4. Problems and proposed solutions encountered with saw blades used in sizing operations (Bosch, 2018; Bilteks, 2018; Leitz, 2017).

Problems	Causes	Precautions
Sawblade wobbles	1. Thickness of tool is too low. 2. Insufficient tooth projection over tool body (sawblade jams in the cut, runs hot, tension lost). 3. Resin/chips on the flanges. 4. Flange run out tolerance too high. 5. Defective motor spindle bearing. 6. Tooth pitch and gullet too small. 7. Unbalanced sawblade. 8. Blunt cutting edges. 9. Wrong sawblade tensioning.	1. Select a sawblade with a larger kerf or a smaller diameter or increase flange diameter. 2. Select a sawblade with a higher lateral tooth projection. 3. Clean flanges. 4. Check and correct flange 5. Replace motor spindle bearing. 6. Select a sawblade with a higher tooth pitch. 7. Balance the sawblade. 8. Resharpen the sawblade. 9. Correct sawblade tensioning.
Wavy cut	1. Irregular tooth pitch or one-sided cut. 2. Irregular tooth thickness. 3. Sawblade is blunt resin build up. 4. Position of fence not parallel to feed direction. 5. One sided load from edge cutting. 6. Cutting speed too low. 7. Wrong sawblade tensioning.	1. Correct sharpening machine adjustment, resharpen the sawblade. 2. Check and correct sawblade kerf. 3. Clean and resharpen the sawblade. 4. Check and adjust position. 5. Use edging sawblades (hogger). 6. Select a larger sawblade diameter or increase RPM. 7. Correct sawblade tensioning.
Jamming of sawblade in cut	1. Slot in saw bed is too big, insufficient chip flow, causing jamming between the saw and slot. 2. Riving knife width is too thin. 3. Gullet too small.	1. Replace saw bed. 2. Replace riving knife. 3. Select sawblade with larger gullet.
Curved cut when double edging	1. Sawblades sharpened one sided. 2. Resin and glue on rollers. 3. Differences in wood thickness. 4. Too high cutting forces on one side. 5. Worn conveyor belt guide. 6. Short and uneven workpieces. 7. When machining short workpieces and when transporting piece by piece.	1. Resharpen sawblade (correct kerf of sawblade and sharpening machine adjustment). 2. Clean and, if necessary, resharpen rollers. 3. Improvements necessary at customer. 4. Optimize cutting force division. 5. Check and adjust chain guide. 6. Comply with minimum workpiece length required by the machine manufacturer‘s instructions. 7. Pay attention to angular cut off work pieces.
Exceeded tolerances of horizontally cut lamellas	1. Sawblade tensioning not suitable for horizontal application. 2. High resin builds up on tool, tool runs very hot from friction in cut. 3. Thickness and position of riving knife not adjusted to the dimensions	1. Check the sawblade tensioning. 2. Clean sawblades and check if blunt. 3. Use riving knife dimension matching the sawblade kerf. Adjust riving knife spacing to
Tear outs in workpieces coated on both sides when machining without scoring saw	1. Sawblade projection over workpiece too small or too big. 2. Tooth shape or number of teeth not suitable for the application. 3. Concentric running tolerances of the sawblade too high. 4. The flange used on the machine does not correspond to the guidelines for flange diameter and concentric running tolerances.	1. Check and adjust sawblade projection. 2. Select a sawblade suitable for the application. 3. Have the sawblade checked by service. 4. Check flanges and, if necessary, clean them. If there is a wrong ratio of sawblade diameter to flange diameter, adjust accordingly.
Tear outs on the panel coating when cutting in stacks	1. Tool is blunt. 2. Pressure beam cannot press evenly on uneven workpieces.	1. Resharpen main sawblade. 2. Check pressing force of pressure beam.
Tear outs where the tool leaves	The kerf of the scoring sawblade is too small for the main sawblade in use.	Adjust kerf of scoring sawblade to main sawblade accordingly.

5. Results and Suggestions

Saw blades should be selected in view of the fact that the factors as material, cutting tools and machine in machining of wood and wood-based materials in circular saw machines. First of all, the density of material to be processed, moisture content and grain direction must be considered in choosing of a saw blade. Accordingly, the results can be summarized as follows:

1. In high density woods and machining in the across the grain direction; the number of teeth and saw diameter should be more; the gullet should be smaller and the feed and cutting speed with the rake angle (According to ASTM) should be low.

2. In wood with high moisture content; the number of teeth should be less, the larger gullet should be selected, feed and cutting speed should be preferred lower.

3. The cutting speed should also be increased as the saw diameter increases.

4. Straight tooth form should be preferred when an average surface quality is desired in the along and across the grain direction. Bevel tooth form can be used in machining of veneered and laminated wood-based materials and non-ferrous metals. Trapezoidal tooth form can be used in the sizing of wood-based materials and conical tooth form should be considered in scoring saw blades for veneered and laminated wood-based materials.

5. According to the cutting material type; HSS and HW can be preferred for a general use in dimensioning, mortising, tenoning etc. of wood materials; HW can be used for machining of industrial panels, soft and hard woods with coated veneered panels and DP should be used in machining of industrial panels, plastics, nonferrous metals and hardwoods. However, the use of DP should be avoided in very hard knotted conifer trees.

The selection of saw blade in heterogeneous wood and wood-based materials is rather important and difficult in terms of product quality and efficiency. In this respect; considering the factors affecting the surface quality, the use of the cutter firm catalogs can be recommended for the most suitable choices.

References

Anonymous, 2017. “Weinig Group”, Weinigstraße 2/4, 97941 Tauberbischofsheim, Germany, https://www.weinig.com.

Bilteks, 2018. “Testere Ürün Kataloğu”, İTOB Organize Sanayi Bölgesi 10023 Sk. No:11 Tekeli, Menderes ,İzmir.

Bosch, 2018. “Top Precision: Daire Testereler”,

Burdurlu, E., Baykan İ., 1998. Ağaçişlerinde Kesme Teorisi ve Endüstriyel Mobilya Üretimi Makineleri, Ankara.

Chabrier, P., Martin, P. (1999): Industrial point of view on straightening and tensioning of circular saw blades. 14th Int. Wood Machining Seminar, Paris, Epinal, Cluny, 1, 137-143.

Csanády, E., & Magoss, E. (2012). Mechanics of wood machining. Springer Science & Business Media.

Davim, J.P. 2011. "Wood machining", ISTE Ltd and John Wiley & Sons, Inc., London.

Davis, E. M. 1962. "Machining and related characteristics of United States hardwoods", Technical Bulletin No: 1267, US Department of Agriculture-Forest Service, Washington, DC.

Demirci, S., Kılıç, Y. 2005. "Daire testerelerde diş sayısı ve besleme hızının ceviz (Juglans regia L.) ve mahun (Khaya sp.) odunlarının yüzey pürüzlülüğüne etkileri", İstanbul Üniversitesi Orman Fakültesi Dergisi, 55(2), 123-136.

EDN, 2017. "Catalogue 45 Circular Saw Blades", Ernst D. Neuhaus GmbH & Co. KG., Cronenberg, Germany.

Erdinler, E. S. 2005. "CAD Sistemleri ve Türkiye Mobilya Endüstrisinde Uygulanma Etkinliğinin Analizi", Doktora Tezi, Fen Bil. Enstitüsü, İstanbul Üniversitesi.

Eroğlu, F. 2007. "Ankara Mobilyacılar Sitesinde Faaliyet Gösteren Küçük ve Orta Ölçekli Mobilya İşletmelerinin Analizi ve Çözüm Önerileri", Yüksek Lisans Tezi, Fen Bilimleri Enstitüsü, Gazi Üniversitesi.

Gaff, M. 2014. "Three-dimensional pneumatic molding of veneers" BioResources, 9(3), 5676-5687.

Gottlöber, C., Wagenführ, A., Röbenack, K., Ahmed, D., Eckhardt, S. 2016. "Strategies, concepts and approaches to avoid cuttermarks on wooden workpiece surfaces", Wood Material Science & Engineering, 11(3), 147-155.

Hoff K, Fisher N, Miller S, Webb A (1997). Sources of Competitiveness for Secondary Wood Products Firms : A Review of Literature and Research Issues. Forest Prod. J. 47(2): 31±37

HSE, 2018. " Circular saw benches – Safe working practices: Health and Safety Executive", British Standards Institution, Chiswick/London.

İlhan, R., Burdurlu E., Baykan İ., 1990. Ağaçişlerinde Kesme Teorisi ve Mobilya Endüstrisi Makineleri, Ankara

Kaplan, L., Kvietková, M. S., Sedlecký, M. 2018. "Effect of the Interaction between Thermal Modification Temperature and Cutting Parameters on the Quality of Oak Wood", BioResources, 13(1), 1251-1264.

Kılıç, Y., Demirci, S. 2003. "Sarıçam ve Kestane Odunlarının Yüzey Pürüzlülük Değerlerinin Araştırılması", GÜ Fen Bilimleri Dergisi, 16(3): 553-558.

Koch P. 1964. "Wood machining processes; a volume in the wood processing series", New York: The Ronald Press Company, p. 530.

Koch, P. 1972. "Utilization of the southern pines", Department of Agriculture Forest Service. Handbook, (420), 53-463.

Kollmann, F. F., Côté Jr, W. A. 1968. "Principles of wood science and technology. vol. I. Solid Wood", Principles of Wood Science and Technology. Vol. I. Solid Wood. Springer-Verlag. Berlin.

Kurtoğlu A., Sofuoğlu S. D. 2013. Mobilya ve Ağaç İşlerinde Kullanılan Ahşap Malzemeler 1, Mobilya Dekorasyon Dergisi, Eylül-Ekim.

Kurtoğlu A., Sofuoğlu S. D. 2013-2. "Mobilya ve ağaç işlerinde kullanılan ahşap malzemeler 2: Kapı ve pencere yapımında ağaç malzemenin kullanılması", Mobilya Dekorasyon Dergisi, Kasım-Aralık, 119, 52-66.

Kurtoğlu, A. 2000. "Ağaç Malzeme Yüzey İşlemleri", Cilt 1, İstanbul Üniversitesi Orman Fakültesi, Üniv. Yayın No: 4262, Fak. Yayın No: 463, İstanbul.

Kurtoğlu, A., 1981. "Odunun işlenme özellikleri", İstanbul Üniversitesi Orman Fakültesi Dergisi, Seri: B, Cilt: 31 (2).

Lehmann, B.F., Hutton, S.G. 1997. "The mechanics of bandsaw cutting. Part II. A simulation of the cutting behaviour of bandsaws". Holz als Roh- und Werkstoff, 55: 35-43

Leitz, 2017. "Precision tables by Leitz, The Leitz-Lexicon Edition 7", GmbH & Co. KG., Germany.

Malkoçoğlu A. 2007. "Machining properties and surface roughness of various wood species planed ın different conditions", Building and Environment, vol.42, pp.2562-2567.

Malkoçoğlu A., Özdemir T., Arz N. 2007. "Mobilya ve doğrama endüstrilerinde ahşap malzemenin kullanımı ve özellikleri", Mobilya Dekorasyon Dergisi, cilt.78, ss.136-144.

Malkoçoğlu, A., 2017. "Ağaç Malzeme İşleme Teknikleri Basılmamış Ders Notları", KTÜ. Orman Fakültesi, Trabzon.

Malkoçoğlu, A., 2018. "Mobilya Endüstrisi Basılmamış Ders Notları", KTÜ. Orman Fakültesi, Trabzon.

Malkoçoğlu, A., Tiryaki, S. (2011). "Ağaç malzemelerin işlenme esasları", Mobilya Dekorasyon Dergisi, 101, 158-174.

Mitchell, P. H., Wiedenbeck, J., & Ammerman, B. (2005). Rough mill improvement guide for managers and supervisors, USDA Forest Service, Newton Square, USA.

Oertli, 2018. "Circular Saws Catalogue", Werkzeuge AG, Hofstrasse, Germany

Örs, Y., Demirci, S. 1999. "Daire Testerelerde; Diş Sayısı, Kesiş Yönü ve Besleme Hızının Ağaç Malzeme Yüzey Düzgünlüğüne Etkileri", Politeknik Dergisi, 2, 1-5.

Ratnasingam, J. Ma T.P., Perkins M.C. 1999. "Productivty in wood machining processes; a question of simple economics", Holz Als Roh-und Werktoff, 57, 51-56.

Renshaw, A. (1999) Centripetal tensioning for high speed circular saw. 14th Int. Wood Machining Seminar, Paris, Epinal, Cluny, 1, 129-135.

Schajer, G.S., Wang, S. 1999. Effect of workpiece interaction on circular saw cutting stability. 14th Int. Wood Machining Seminar, Paris, Epinal, Cluny, 1, 173-185.

Smith, P., H.O., Ma. 1990. "The global wooden furniture industry: an emphasis on the PacificRim". CINTRAFOR, Working Paper 25, University of Washington, Seattle, Washington.

Sofuoglu, S. D. 2016. "Determination of optimal machining parameters of massive wooden edge glued panels which is made of Scots pine (Pinus sylvestris L.) using Taguchi design method." European Journal of Wood and Wood Products: 1-10.

Sönmez, A., Söğütlü, C. 2009. "Biçme İşleminde Kesiş Yönü ve Daire Testere Diş Sayısının Ağaç Malzeme Yüzey Pürüzlülüğüne Etkisi", Politeknik Dergisi, 12(1).

UNIDO, 1989. "Furniture and Joinery Industries for Developing Countries", United Nations Industrial Development Organization, Vienna.

URL-1: http://www.chinasawblade.com/technical.asp (Erişim tarihi:22.05.2018).

URL-2:http://www.irwin.com/uploads/products/brochure/7_2013_CSB_eBook.pdf (Erişim tarihi:22.05.2018).

URL-3: https://makezine.com/2016/09/15/understanding-saw-blade-essentials/ (Erişim tarihi:22.05.2018).

Wengert, G. 1998. "Rx for wood machining defects: Wood processing", Department of Forestry, University of Wisconsin-Madison, Woodweb, Virginia.

Williams, D. and Morris, R., 1998. Machining and Related Mechanical Properties of 15 B.C. Wood Species, Forintek Canada Corp.

Using a Computerized Tool for Tree Cross-Cutting Operations: The Case of Yellow Pine (*Pinus sylvestris*) Stand in Giresun

Abdullah E. AKAY*, İnanç TAŞ

Bursa Technical University, Faculty of Forestry, Department of Forest Engineering, Bursa, Turkey

***Corresponding author:**
abdullah.akay@btu.edu.tr

Abstract

As the demand for forest products has increased it is now even more important to extract timber in a way that maximizes the productivity. Cross-cutting trees into proper log lengths plays important role in maximizing the economic value gained from each harvested tree. However, this operation is a complex engineering problem in which optimum cross-cutting combinations needs to be systematically searched by computer-assisted methods while considering various factors such as timber quality, log dimensions, stem defects, and market demands. In this study, a computerized tool was developed by using dynamic programming approach to solve optimum cross-cutting problems. Computer-assisted method was tested during a harvesting operation taken place in a Yellow Pine stand located in Espiye Forest Enterprise Directorate in Giresun Forestry Regional Directorate. Then, the cross-cutting pattern suggested by the computer-assisted method was compared to actual pattern generated by logger's experience based traditional method. The effects of tree diameter classes (large, medium, and small) on capabilities of computerized tool was also evaluated by statistical analysis. The results indicated that using computerized tool increased the total economic value of harvested trees by 9.23%. Statistical analysis showed that the maximum economic gain was provided by the trees with medium diameter classes (9.67%). It can be concluded that computerized tools can be effectively used to maximize the total economic income gained from harvested trees. Besides, storage time of the forest products in forest depots will be minimized since proper log lengths are generated by considering the market demand.

Key words: Computerized tools, optimum cross-cutting, timber harvesting, Yellow Pine

1. Introduction

In Turkey, the main work stages in timber extraction activities include tree felling, delimbing, debarking, cross-cutting (bucking), and hauling. It is very important to cut trees into short lengths or logs such a way that maximizes the tree value in terms of total economic gain to be obtained in the production of forest products (Akay et al., 2009a). Cutting trees into sections in a way that maximizes the total economic value of the tree is called optimum bucking (Sessions, 1988). It has been determined that the value obtained from trees can increase by more than 10% if the optimum boating method is used (Wang et al., 2007; Akay et al., 2009b).

To gain maximum benefit from optimum bucking method, log lengths should be measured accurately, log quality classes should be determined carefully, and market demand should be considered (Akay et al., 2009a). The availability of logging equipment also limiting factor in bucking operations (Yıldırım, 1989). In order to determine the most suitable bucking combination, large number of alternative bucking combinations need to be evaluated while taking all these factors into account. Such complex optimization problems can be solved by using computer-assisted methods such as network analysis, dynamic programming, and heuristic methods (Laroze and Greber, 1997). Network analysis based methods are widely used because it is more flexible and easily updatable (McKeown, 1981).

In a study conducted by Serin et al. (2010), the effects of optimum bucking method on the total economic value of timber in Brutian Pine stands were investigated. The results indicated that application of optimum bucking method increased the economic value of the harvested trees by 4.7%. Akay et al. (2015) investigated the effects of stem defects on optimum bucking method in two Brutian Pine stands. It was found that the optimum bucking method provides better results for the harvested trees with more stem defects.

Pak and Gülci (2017) evaluated economic gain of using optimum bucking method in Oriental Beech stand located in northeastern region of Turkey. To implement optimum bucking method in a sample application, network analysis based Network 2000 program was used. Network analysis method has been widely used in solving many optimization problems such as shortest path, the distance with minimum cost, and flow of maximum value (Başkent, 2004). The results indicated that the average economic value of deciduous trees were increased by 14.37% using optimum bucking method.

This study aimed to implement a stem-level optimum bucking approach by using the dynamic programming based optimum bucking method. This method was first developed by

Akay et al. (2010) and its capabilities were tested during a selective cutting of Taurus Fir stands in eastern Mediterranean region of Turkey. In this study, computer-assisted optimum cross-cutting method was presented and capabilities of the method was tested in a harvesting unit of Yellow Pine stand located in the city of Giresun in Turkey. The results from optimum bucking method were compared with the results achieved by using the traditional bucking method.

2. Material and Methods

2.1. Study Area

The study are is located in Giresun Forestry Regional Directorate, Espiye Forest Enterprise Directorate, Esenli Forest Enterprise Chief (Figure 1). The average elevation and ground slope were 1600.30 and 62%, respectively. The dominant tree species were Spruce and Yellow Pine. The optimum bucking data were measured from 30 harvested Yellow Pine trees that were randomly selected in the study area. The UTM coordinates of these trees were recorded by using handheld GPS in the field. During timber harvesting activities, chainsaw was used to fell and buck trees and then logs were transported to landing area by a farm tractor.

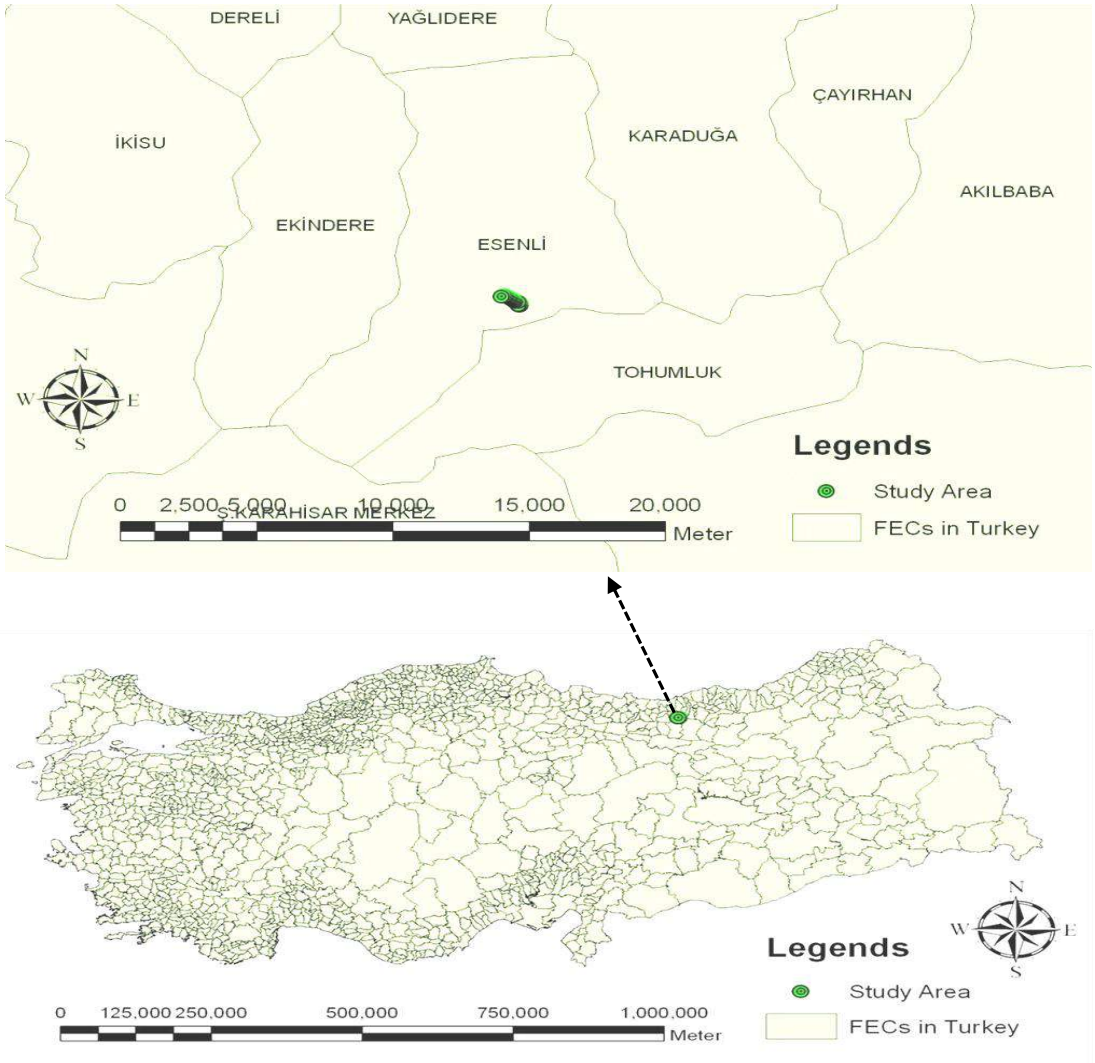

Figure 1. The study area in Esenli FEC of Espiye Forest Enterprise Directorate.

2.2. Optimum Bucking

In this study, optimum cross-cutting method developed by using Visual Basic computer programming language under Microsoft Excel was used for solving optimum bucking problems at single tree level (Akay et al., 2010). The method was employed "Node-labeling" technique which was developed based on dynamic programming approach (Sessions et al., 1988). In this approach, each node represented potential cross-cutting points and link between the nodes represented log lengths (Figure 2). The value of each link was the economic value of the log (Sessions, 1988).

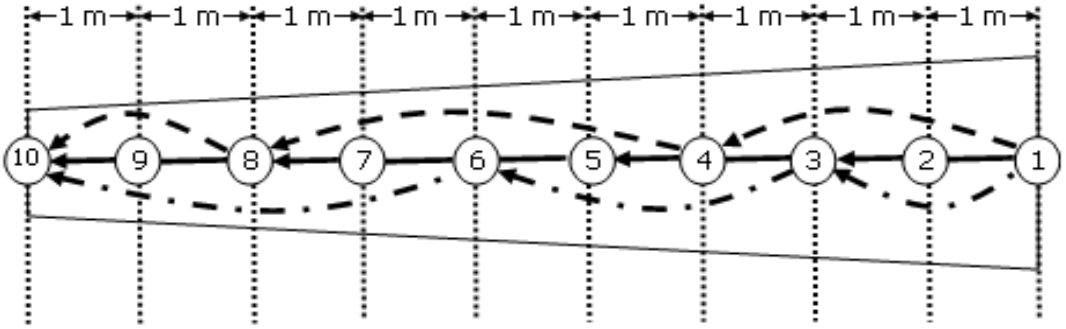

Figure 2. The tree network in optimum bucking method

In order to obtain the highest economic value from the whole tree, dynamic programming approach produces an optimum alternative which gives the maximum value among many alternative cross-cutting combinations. The minimum log length, maximum log length, and minimum middle diameter are considered as main constraints in the methodology. The economic value of the logs was computed by multiplying the unit sales price of the logs and the log volume. For the calculation of the log volumes, "Middle Surface Formula" (Huber Formula) was used, which takes into account the medium diameter and log length (Kalıpsız, 1999).

Average timber sale prices for different classes of log diameters and lengths were determined for the timber quality classes based on the information obtained from the latest bids organized at the Espiye Forest Management Directorate. The minimum length and the minimum medium diameter of the logs were taken as 2 m and 19 cm, respectively. The maximum log length that can be produced was limited to 5 m due to the limiting features of the forest road standards and the logging methods used in the study area.

2.3. Statistical Analysis

In order to investigate whether there is a statistically significant difference in the economic values of the trees produced using the existing and optimum cross-cutting methods, one-way ANOVA was applied at 0.05 significance level using SPSS 15.0 statistical software. The breast height diameter was regrouped in three classes (small: <40 cm, medium: 40-50 cm, large: > 50 cm) to examine the effect of different diameter classes on value gain of the logs that were bucked using the optimum cross-cutting method. In addition, to study the effect of different volume classes on the value gain of the logs that were bucked using the optimum cross-cutting method, the tree volumes were divided into three classes (low: <1.5 m^3, medium: 1.5-2.0 m^3, high: > 2.0 m^3).

3. Results and Discussion

The elevation, ground slope, tree diameter, and tree length information of 30 sample trees selected from the study area are given in Table 1. The average elevation and ground slope was 1600.30 meters and 64.10%, respectively. According to the results, the average tree volume was 2.15 m^3, while average tree length and the diameter was 19.73 meters and 37.43 cm, respectively. Almost all bucking combinations produced by the optimum cross-cutting method differ from combinations produced by the traditional method.

Table 1. The average size information of sample tress.

Tree No	Elevation (m)	Slope (%)	Diameter (cm)	Length (m)
1	1590	70,00	37,5	20
2	1602	65,00	34	23
3	1614	64,00	39	22
4	1612	70,00	42	24
5	1625	59,00	47	25
6	1622	65,00	45	27
7	1648	62,00	37	15
8	1653	74,00	35	22
9	1660	64,00	32	15
10	1631	60,00	33	19
11	1623	65,00	33	21
12	1612	70,00	35	19
13	1608	60,00	30	15
14	1600	70,00	29	18
15	1597	65,00	36,5	20
16	1592	60,00	44	17
17	1605	60,00	36	15
18	1604	60,00	32	17
19	1597	60,00	46	18
20	1595	65,00	32	19
21	1586	70,00	37	20
22	1582	60,00	42	23
23	1577	65,00	46	18
24	1575	60,00	33	16
25	1579	60,00	31	18
26	1570	70,00	34	16
27	1565	70,00	42	23
28	1560	55,00	49	30

29	1555	65,00	39	20
30	1570	60,00	35	17

While the average value of the trees produced using traditional cross-cutting method was 206.10 TL, the average value of the trees produced by optimum cross-cutting method was found to be 224.86 TL. Therefore, the optimum cross-cutting method increased the total economic value of the produced trees by 9.23%. In a similar study conducted by Akay (2017), the optimum bucking method increased the economic value of the average tree value by 9.44% in a Yellow Pine stand in the city of Bolu.

Although no statistically significant difference was found between the economic values of the trees bucked with the traditional cross-cutting and with optimum cross-cutting methods (p = 0.432), it was determined that the optimum cross-cutting method increased the economic value of the bucked trees. When examining the effect of different diameter classes on value gain, the maximum mean value gain was obtained from the medium diameter class (9.67%) (Table 2). This suggests that the economic contribution of the optimum sizing may increase depending on the diameter class. Among the sample trees, there were no examples of large diameter trees. In the optimal cross-cutting method, it was found that different volume classes did not have a statistically significant effect on value gain (p = 0.814). The maximum average value gain was obtained from the medium volume class (9.90%) and followed by the low (8.69%) and high (8.26%) volume classes (Table 3).

Table 2. The effects of diameter classes on tree value gain.

	Diamater Classes	N	Medium	Minimum	Maximum
Tree Value Gain (%)	Small	21	9.04	0.00	20.77
	Medium	9	9.67	5.08	15.39
	Large	--	--	--	--

Table 3. The effects of volume classes on tree value gain.

	Volume Classes	N	Medium	Minimum	Maximum
Tree Value Gain (%)	Low	14	8.69	0.00	20.77
	Medium	14	9.90	3.04	15.39
	High	8	8.26	6.55	9.97

4. Conclusions

When comparing the economical values of the trees with the traditional and optimum cross-cutting methods, the optimum cross-cutting method increased the total economic value of the harvested trees by 9.23%. In bucked trees, the value gain tended to increase by the increase in diameter classes and volume classes. This suggests that the optimal cross-cutting method gives better results at larger log sizes.

Optimal cross-cutting method has not been currently applied in the production of forest products in Turkey. The bucking operations are mostly carried out by the experience of the forest workers and away from the scientific approach. Many of the quality class parameters on the log are generally ignored. The main factor to be considered in cross-cutting is the log size and then the stem shape. However, it is estimated that the application of the optimum cross-cutting method, which provides systematic investigation of the best result and also taking into account market demands, will increase profit gained from timber production in Turkey. By considering market demands during cross-cutting process, the storage time of the logs in the forest depots will be shortened, storage and maintenance costs will be reduced, and undesired quality and volume losses will be eliminated.

Economic losses of forest products during the cross-cutting operation results in serious problems in forest industry in Turkey. If the optimum cross-cutting method is used as a decision supporting tool in the cross-cutting process, it is considered that important economic gains will be achieved in the production of forest products. As a result, the use of modern methods such as optimum cross-cutting in forestry activities will provide significant contributions in managing forest resources more effectively and efficiently.

Acknowledgement

This study is funded by The Scientific and Technological Research Council of Turkey (TUBITAK) with the project number 108O125.

References

Akay, A.E., Serin, H., Pak, M. and Yenilmez, N., (2009a, October). Optimum tree-stem bucking of Brutian Pine (*Pinus brutia*) Trees in Antalya, Turkey, *Third International Faustmann Symposium, "Forest Economics in a Dynamic and Changing World"*, Germany.

Akay, A.E., Serin, H., Pak, M., and Yenilmez, N., (2009b, October). Application of optimum bucking method in timber production activities, *I. National West Blacksea Forestry Congress*, Bartın, Turkey.

Akay, A.E., Sessions, J., Serin, H., Pak, M., and Yenilmez, N., (2010). Applying Optimum Bucking Method in Producing Taurus Fir (*Abies cilicica*) Logs in Mediterranean Region of Turkey. *Baltic Foresty*, 16(2), 273-279.

Akay, A.E., Serin, H., and Pak, M., (2015). How Stem Defects Affect The Capability Of Optimum Bucking Method? *Journal of the Faculty of Forestry Istanbul University*, 65(2), 38-45.

Akay, A.E., (2017). Potential Contribution of Optimum Bucking Method to Forest Products Industry, *European Journal of Forest Engineering*, 3(2), 61-65.

Başkent, E.Z., (2004). *Operational Research, Modelling and Natural Resources Applications*, Karadeniz Technical University, Faculty of Forestry, General Pub. No: 218, Faculty Pub. No: 36. KTÜ Print, Trabzon, 480 p.

Kalıpsız, A., (1999). *Dendrometry*, İ.Ü. Faculty of Forestry, Pub. No: 3194/354, 407 p. İstanbul.

Laroze, A.J. and Greber, B.J., (1997). Using Tabu Search to Generate Stand-Level, Rule-Based Bucking Patterns, Forest Science, 43(2), 367-379.

Mckeown, P.G., (1981). A Branch-and-Bound Algorithm for Solving Fixed Charge Problems, *Naval Research Logistics Quarterly*, 28, 607-617.

Pak, M., and Gülci, N., (2017). A comparative economic evaluation of bucking deciduous trees: A Case study of Oriental beech (Fagus orientalis) stands in Northeastern Turkey, *Journal of the Faculty of Forestry Istanbul University*, 67(1), 72-79.

Sessions, J., (1988). Making Better Tree Bucking Decisions in the Woods: An Introduction to Optimal Bucking, *Journal of Forestry*, 86(10), 43-45.

Sessions, J., Layton, R., and Guangda, L., (1988). Improving Tree Bucking Decisions: A Network Approach. *The Compiler*, 6(1), 5-9.

Wang, J., Ledoux, C.B., and Mcneel, J., (2004). Optimal Tree-Stem Bucking of Northeastern Species of China, *Forest Products Journal*, 54(2), 45-52.

Yıldırım, M., (1989), *Work Knowledge in Forestry*, İ.Ü. Faculty of Forestry, Pub. No: 3555/404, 287 p. İstanbul.

A Research on the Effects of Demographic and Socio-Economic Status Factors on Consumer Preferences in Furniture Purchase (Case of Black Sea Region)

İlker AKYÜZ[1*], Nadir ERSEN[2], Kadri Cemil AKYÜZ[1], Bahadır Çağrı BAYRAM[3]

[1]Karadeniz Technical University, Department of Forest Industry Engineering, Trabzon, Turkey;
akyuz@ktu.edu.tr

[2]Artvin Çoruh University, Department of Forestry and Forest Products, Artvin, Turkey;
nadirersen20@artvin.edu.tr

[3]Kastamonu University, Department of Forest Industry Engineering, Kastamonu, Turkey;
bcbayram@kastamonu.edu.tr

[*] **Corresponding Author:** iakyuz@ktu.edu.tr

Abstract

Consumer behavior is an issue that must be studied by businesses in terms of marketing. The stages of purchasing any product can be different for each customer. Rapidly developing economic changes lead to strategic decisions such as gain new customers, the customer retention. Home furniture is very important in Forestry Products Industry in terms of both export and domestic consumption. In this study, factors affecting consumers in the Eastern Black Sea region when purchasing furniture (before, during, and after) were investigated. In addition, strategies for acquiring new consumers for furniture businesses were presented. The data were collected by face-to-face survey method and analyzed in SPSS statistics program and the results were explained.

Keywords: Furniture, Customer, Socio-economic status, Preference.

1. Introduction

In order for a person to be regarded as a consumer in terms of marketing, the following are essential: (1) the need, (2) income and (3) spending request (Akyüz, 2006). The scope of the consumer term is quite broad and people, families, manufacturer and seller (commercial) enterprises, private and public institutions are the major consumption units. Consumer is defined as a real person who buys a marketing mix for personal desires, wants and needs and is in a purchasing capacity (Korkut and Kaval, 2015; Öztürk, 2006). Consumers prefer goods and services that provide the highest benefit and quality at the lowest cost and that suit them best. There are many factors that they pay attention when making this preference (Korkut and Kaval, 2015; Demircioğlu, 2012). For this reason, enterprises must have to take into account consumers' demands and needs, consumer behavior characteristics while producing goods and services (Korkut and Kaval, 2015).

In accordance with their preferences and desires, consumer behavior can express a range of processes related to producing and delivering goods or services to consumers (Penpece, 2006). The fact that consumer behavior is influenced by external factors such as culture, family, advisory group, socio-cultural factors, marketing environment, indicates that it has both a structure that can change and adapt (Akyüz, 2006). Determination of consumer behavior provides competitive advantages to the enterprises by developing effective market strategies and directing consumers (Gerlevik, 2012). Consumer markets are constantly changing and demographics are one of the most important changes. As the needs and demands of consumers differ, market segmentation according to demographic characteristics will be beneficial for enterprises (Akyüz, 2006). Therefore, marketers should constantly analyze consumer demands and preferences, shopping and purchasing behaviors and build their strategic decisions on this information (Öztürk, 2006).

Furniture, one of the most influential factors in the arrangement of a space, is an important factor in the design and comfort of a house. The function of furniture in our lives has not only been limited to being an object used at home, but it has become goods that establishes and transmits its own meaning structures in every period (Arpacı, 2014). For this reason, buying process of furniture is very important for consumers. The furniture sector includes (Erdinler and Koç, 2015):

(1) Manufacturers such as seating groups, kitchen, office furniture,

(2) Industrial enterprises supplying raw materials, machinery and other investment materials to these manufacturers,

(3) Contract manufacturers.

The socio-cultural, psychological, demographic and situational factors of each consumer are different from each other. These characteristics of consumers who are influential on consumer preferences are socio-demographic (age, gender, family structure, education, occupation etc.), economic (income level, general economic status etc.) and behavioral (culture, social class, motivation, perception, attitude, personality, etc.) (Burdurlu et al., 2004). This is reflected in the purchasing process and shapes the preferences of consumers (Andaç, 2008). The most influential factors for the need for furniture are (Akyüz, 1998):

(1) It is obsolescence of the existing furniture,

(2) It is the need for new furniture. Because the children in the family grow up,

(3) It is other family-related factors,

(4) It is the increase in income,

(5) It is influence of friends groups,

(6) It is outdated furniture.

Reaching the right product that is needed is possible if consumers correctly identify their needs and possibilities. Having knowledge of consumers about furniture types and furniture characteristics will help to make their preferences in the most appropriate way (Arpacı and Obuz, 2013).

1.1. Social Class

In general, status is that people are graded according to certain criteria in a social hierarchy. Social class is the process of grading people in the social hierarchy and it has a hierarchical character. Because of this feature, members of the same class have almost the same status, while members of the other classes have more or less status. Because of the similar behavior of social class members, the social class can be the basis for the market segmentation (Odabaşı, and Barış, 2002).

The most comprehensive study about the social class discrimination in Turkey was done by Zeta-Nielsen Research Company. According to this study, Turkish society is divided into six different classes named as groups A, B, C1, C2, D, and E. When the characteristics of these classes are examined, Turkish society is basically divided into three classes: upper, middle and lower. Groups A and B are the upper class, groups C1 and C2 are the middle class, and groups D and E are the lowest class. Furniture purchasing decisions also differ according to social classes. Social classes are more or less homogenous and socially hierarchical.

Similar values, lifestyles, interests and behaviors are seen in the same social class members. For example; clothing, housing, furniture, entertainment and mass media behaviors of individuals in the same social class are similar. People in different social classes have different desires and consumption values (Kalınkara, 2016).

2. Material and Method

The universe of our study constitutes 18 provincial centers located in the Black Sea Region. The number of consumers who applied the survey was found by stratified sampling according to the population sizes of 18 provincial centers and a total of 2370 surveys were evaluated.

The decision making behaviors of family members in furniture purchasing were evaluated according to different demographic characteristics. Socio-economic status groups (A, B, C1, C2, D and E) have been examined separately and socio-economic status is shortened in comments as SES.

Crosstab, frequencies, weighted averages and chi-square test were used for the results. Chi-square test results were applied on all demographic variables and significant differences were determined. The null (H_0) hypothesis which indicates that there are significant differences between consumer groups, was accepted when the P value is less than 0.05, while the alternative (H_1) hypothesis, which indicates that there are no significant differences between the consumer groups, was accepted when the P value is greater than 0.05. Table 1 gives the questions about which subjects consumers evaluate when purchasing furniture.

Table 1. Types of survey questions

Statement 1: Need for furniture and demand to purchase
Statement 2: Studies conducted before purchasing
Statement 3: Assessments regarding price before purchasing
Statement 4: Assessments regarding where to purchase
Statement 5: Assessments regarding the timing of purchasing
Statement 6: Assessments regarding color, pattern, form, design
Statement 7: Assessments regarding brand and quality
Statement 8: Assessments regarding the final decision on buying
Statement 9: Assessments regarding the usefulness after purchase

3. Findings

The distribution of demographic characteristics of the consumer groups participating in the survey was given in Table 2. As seen in Table 2, 56.1% of the consumers who participated in the survey are male and 43.9% is female. 33.5% of the respondents are low, 40.1% is in the middle and 26.4% is in the high income groups. The education levels of consumer groups are as follows: 18.9% is primary school, 11.8% is secondary school, 32.1% is high school, 34.5% is bachelor and 2.7% is postgraduate. The majority of the consumer groups participating in the survey are over the age of 31. It is seen that 35.4% of the surveyed families are in elementary family structure (4 people). The ownership status of the houses in which the families live is as follows: 61.8% is homeowner, 33.2% is rent and 4.9% is lodging building.

Table 2. Demographic characteristics of consumers

Demographic characteristics of consumers		Number (N)	Percentage (%)	Cumulative Total
Gender	Male	1330	56.1	56.1
	Female	1040	43.9	100
Income level	Low	794	33.5	33.5
	Middle	949	40.1	73.6
	High	626	26.4	100
Education status	Primary school	449	18.9	18.9
	Secondary school	279	11.8	30.7
	High school	761	32.1	62.8
	Bachelor's degree	818	34.5	97.3
	Postgraduate	63	2.7	100
Age group	18-24	125	5.3	5.3
	25-31	525	22.3	27.6
	32-38	659	28	55.7
	39-45	604	25.7	81.3
	46 and over	439	18.7	100
Number of individuals in the family	1 person	8	0.4	0.4
	2 people	257	11.4	11.7
	3 people	457	20.2	31.9
	4 people	804	35.6	67.5
	5 people	454	20.1	87.6
	6 people	223	9.9	97.4
	7 people	49	2.2	99.6
	8 people	9	0.4	100
Ownership status	Rent	784	33.2	33.2
	Homeowner	1459	61.8	95.1
	Lodging building	116	4.9	100

It was analyzed whether there are any differences between the answers given for "statement 1 (need for furniture and demand to purchase)" and all factors (demographic characteristics, male and female SES groups and total consumer SES groups). In tables, according to demographic characteristics, male and female SES groups and total consumer SES groups, Chi-square (X^2) test results of answers given by consumers were given.

The results of the X^2 test related to statement "1" were given in Table 3.

Table 3. The results of the X^2 test related to the need for furniture product and demand to purchase

Factors in Relationship		χ^2	p	df	Results
Need for furniture and demand to purchase	Gender	349.077	0.000	2	Significant
	Education	17.69	0.024	8	Significant
	Income	6.49	0.165	4	Insignificant
	Age	130.19	0.000	8	Significant
	Male SES	42.068	0.000	10	Significant
	Female SES	13.721	0.186	10	Insignificant
	Total SES	69.695	0.000	10	Significant

$p<0.05$ indicates a significant difference between the variables

When table 12 is taken into consideration, both men and women said that the demand to purchase furniture is caused by women. As the level of education in the families increases, it can be said that the ability to act together for "statement 1" increases. It has been seen that as the age increases, the demand for the purchase of furniture in the results of bilateral discussion with family members increases. As the level of income increases, the demand to purchase furniture is caused by women. For male SES groups, the following results were obtained:

(1) 31.7% of group "A" consumers said that the demand to purchase furniture is caused from their wives, while this rate for group "B" consumers decreased by 20.1%.

(2) In the middle-class consumer groups, the demand to purchase furniture is the result of bilateral discussion. To furniture purchasing demand, the rate of the shared decision making in the group "C1" is 53.2%, whereas in group "C2" this rate is 44%.

(3) It has been observed that the rate of shared decision making in lower-class consumers decreases. This rate is found to be 40.8% in group "D".

For all consumer groups, the following results were obtained:

(1) The rate that the demand to purchase furniture is caused from their partners (wife or husband) in group "D" is 32.5% and this rate is 15.7% in the E group.

(2) The rate of shared decision making was found to be highest in group “C1” and the rate is 52.8%.

The results of the X^2 test related to studies conducted before furniture purchasing was given in Table 4. There were significant differences between studies conducted before furniture purchasing and all factors.

Table 4. The results of the X^2 test related to studies conducted before furniture purchasing

Factors in Relationship		χ^2	p	df	Results
Studies conducted before purchasing	Gender	15.357	0.000	4	Significant
	Education	45.94	0.000	16	Significant
	Income	39.29	0.000	8	Significant
	Age	188.11	0.000	16	Significant
	Male SES	59.781	0.000	20	Significant
	Female SES	86.058	0.000	20	Significant
	Total SES	69.583	0.000	20	Significant

p<0.001 indicates a significant difference between the variables

When table 12 is taken into consideration, 35.8% of males and 32.8% of females stated that they made the shared decision on studies conducted before purchasing. As education levels increase in families, the rate of the shared decision making of studies conducted before purchasing also increase. This rate was found as 27.0% in primary school level, 28.9% in secondary school level and 38.7% in bachelor's degree. When income levels are examined, it appears that it is effective in children in families with higher income levels on studies conducted before purchasing. This effect is less in the middle and low income levels. For male SES groups, the following results were obtained: 43.5% of group "A" said that they made shared decision in studies conducted before purchasing and this ratio is 21.4% in group "E". For female SES groups, the following results were obtained: 45.1% of the consumers in group "B" stated that they made shared decision in studies conducted before purchasing, whereas 36.6% of the consumers in "C2" group stated that they carried out these studies by themselves. For all consumer groups, the following results were obtained: 42.9 % of the consumers in group "B" stated that they made shared decision in studies conducted before purchasing, whereas this rate is the lowest in group “E” consumers with 28.4%.

The results of the X^2 test related to assessments regarding price before purchasing were given in Table 5. There were significant differences between assessments regarding price before furniture purchasing and all factors.

Table 5. The results of the X^2 test related to assessments regarding price before purchasing

Factors in Relationship		χ^2	p	df	Results
Assessments regarding price before purchasing	Gender	232.092	0.000	3	Significant
	Education	79.49	0.000	12	Significant
	Income	44.64	0.000	6	Significant
	Age	29.79	0.000	12	Significant
	Male SES	96.747	0.000	15	Significant
	Female SES	103.387	0.000	15	Significant
	Total SES	308.987	0.000	15	Significant

p<0.001 indicates a significant difference between the variables

When table 13 is taken into consideration, 49.2% of male consumers said that they carried out assessments regarding price by themselves, whereas this rate was found to be 23.1% in female consumers. Also, 52.9% of female consumers said that they made shared decision with husband in assessments regarding price. In economic decisions, male consumers seem to dominate in the family. As education level and income level increase, the rate of the shared decision making in the family on assessments regarding price before furniture purchasing increases. The rate of the shared decision making in primary school level is 41%, whereas it is 63.5% in postgraduate level. The rate of the shared decision making was found to be 43.5% at low income level, whereas this rate was found to be 57.8% at high income level. For male SES groups, the following results were obtained: 65.7% of the consumers in group "A" stated that they made shared decision in assessments regarding price before purchasing, whereas in group “C2”, this value decreased to 36.7%. For female SES groups, the following results were obtained: 64% of the consumers in group "A" stated that they made shared decision in assessments regarding price before purchasing, whereas in group “D”, this value was 50%. For all consumer groups, the following results were obtained: 64.9 % of the consumers in group "A" stated that they made shared decision in assessments regarding price before purchasing, whereas this rate was 38.1% for group “D”.

The results of the X^2 test related to assessments regarding where to purchase were given in Table 6. There were significant differences between assessments regarding where to purchase and all factors.

Table 6. The results of the X^2 test related to assessments regarding where to purchase

Factors in Relationship		χ^2	p	df	Results
Assessments regarding where to purchase	Gender	74.147	0.000	4	Significant
	Education	66.37	0.000	16	Significant
	Income	77.93	0.000	8	Significant
	Age	128.46	0.000	16	Significant
	Male SES	111.115	0.000	20	Significant
	Female SES	58.030	0.000	20	Significant
	Total SES	157.611	0.000	20	Significant

p<0.001 indicates a significant difference between the variables

When table 13 is taken into consideration, regarding gender, 35.3% of male consumers stated that they made assessments regarding where to purchase by themselves, while for female consumers this rate was found to be 20.9%. It can be said that male consumers are more dominant in terms of assessments regarding where to purchase. With the increase of the education level, the rate of shared decision making in the family for assessments regarding where to purchase also increased. I was found that as the income level of consumers increased, they made shared decision in assessments regarding where to purchase. For male SES groups, the following results were obtained: 46.7% of respondents forming group “A” stated that they made shared decision for assessments regarding where to purchase, whereas the rate of consumers in the group "B" (50.8%) was very close to the group "A". For female SES groups, the following results were obtained: the rate of shared decision making in the family on assessments regarding where to purchase was highest for “B” consumers (52.3%). For all consumer groups, the following results were obtained: the rate of shared decision making of the groups "A and B” is higher levels than other groups.

The results of the X^2 test related to assessments regarding the timing of purchasing were given in Table 7. There were no significant differences between “assessments regarding the timing of purchasing” and “age”, whereas there is a significant difference compared to other factors.

Table 7. The results of the X^2 test related to assessments regarding the timing of purchasing

Factors in Relationship		χ^2	p	df	Results
Assessments regarding the timing of purchasing	Gender	14.027	0.003	3	Significant
	Education	63.79	0.000	12	Significant
	Income	28.47	0.000	6	Significant
	Age	14.25	0.285	12	Insignificant
	Male SES	83.537	0.000	15	Significant
	Female SES	57.793	0.000	15	Significant
	Total SES	115.267	0.000	15	Significant

p<0.05 indicates a significant difference between the variables

When table 14 is taken into consideration, 55.6% of males and 59% of females stated that they made the shared decision on assessments regarding the timing of purchasing. İslamoğlu (1990) found that men and women decided together for durable consumer goods in terms of the timing of purchasing. For assessments regarding the timing of purchasing, as the education and income level of consumers increased, the rate of the shared decision making increased. For male SES groups, the following results were obtained: the rate of shared decision making in the family in terms of the timing of purchasing were 65.7% in group “A”, 47% in group “C2” and 43.5% in group “D”. For all consumer groups, the following results were obtained:

(1) The highest rate of shared decision making in the family was found 63.4% in group “A”, whereas the lowest was found in group “D”.

(2) The highest self-decision-making rate was found group "C2", whereas the lowest was found in group "A". Group "C2" followed by group "D".

The results of the X^2 test related to assessments regarding color, pattern, form, design were given in Table 8. There were significant differences between assessments regarding color, pattern, form, design and all factors.

Table 8. The results of the X^2 test related to assessments regarding color, pattern, form, design

Factors in Relationship		χ^2	p	df	Results
Assessments regarding color, pattern, form, design	Gender	363.851	0.000	4	Significant
	Education	44.41	0.000	16	Significant
	Income	17.87	0.022	8	Significant
	Age	277.73	0.000	16	Significant
	Male SES	44.066	0.001	20	Significant
	Female SES	52.948	0.000	20	Significant
	Total SES	128.845	0.000	20	Significant

p<0.05 indicates a significant difference between the variables

When table 14 is taken into consideration, 37.4% of female consumers said that they carried out assessments regarding color, pattern, form, design by themselves, whereas this rate was found to be 10.2% in male consumers. It can be said that the female consumers are more dominant in determining the form, the pattern, the color and the design of the furniture in the family. In primary school-level, it was observed that it is effective in children in determining the form, the pattern, the color and the design of the furniture. To determining the form, the pattern, the color and the design of the furniture, as the income level of consumers increased, the rate of the shared decision making increased. As the ages of the consumers have increased, the self-decision-making rates of consumers have decreased. For male SES groups, as the level of social class decreased, the rates of shared decision making of consumers have decreased. For female SES groups, as the level of social class also decreased, the self-decision-making rates of consumers and the rates of shared decision making of consumers have decreased. For all consumer groups, the following results were obtained:

(1) The highest rate of shared decision making in the family was found in groups “A “and “B”.

(2) The highest self-decision-making rate was found in group “E”.

The results of the X^2 test related to assessments regarding brand and quality were given in Table 9. There were no significant differences between “assessments regarding brand and quality” and “gender”, whereas there is a significant difference compared to other factors.

Table 9. The results of the X^2 test related to assessments regarding brand and quality

Factors in Relationship		χ^2	p	df	Results
Assessments regarding brand and quality	Gender	3.352	0.34	3	Insignificant
	Education	34.15	0.001	12	Significant
	Income	29.09	0.000	6	Significant
	Age	21.10	0.049	12	Significant
	Male SES	51.35	0.001	15	Significant
	Female SES	51.424	0.000	15	Significant
	Total SES	68.489	0.000	15	Significant

$p<0.05$ indicates a significant difference between the variables

When table 15 is taken into consideration, as the ages, income level, and education levels of the consumers have increased, the rates of shared decision making of consumers have increased. In addition, as the ages, income level, and education levels of the consumers have increased, the self-decision-making rates of consumers have decreased. For “male SES groups”,

"female SES groups", and "all consumer groups", as the level of social class decreased, the rates of shared decision making of consumers have decreased.

The results of the X^2 test related to assessments regarding the final decision on buying were given in Table 10. There were significant differences between assessments regarding the final decision on buying and all factors.

Table 10. The results of the X^2 test related to assessments regarding the final decision on buying

Factors in Relationship		χ^2	p	df	Results
Assessments regarding the final decision on buying	Gender	133.506	0.000	3	Significant
	Education	67.85	0.000	12	Significant
	Income	39.23	0.000	6	Significant
	Age	28.88	0.004	12	Significant
	Male SES	46.443	0.000	15	Significant
	Female SES	126.088	0.000	15	Significant
	Total SES	235.473	0.000	15	Significant

p<0.001 indicates a significant difference between the variables

When table 15 is taken into consideration, 44.7% of male consumers said that they carried out assessments regarding the final decision on buying by themselves, whereas this rate was 25% in female consumers. It can be said that male consumers are more effective in making the final decision on purchasing furniture in the family. İslamoğlu (1990) emphasized that men play an important role in making final decisions on durable consumer goods. As the ages, income level, and education level of the consumers have increased, the rates of shared decision making of consumers have increased. For "male SES groups", "female SES groups", and "all consumer groups", the highest rates of shared decision making are "A" and "B" groups, respectively. In other words, as the level of social class of consumers increases, the decision making and assess of consumers together is increasing.

The results of the X^2 test related to assessments regarding the usefulness after purchasing were given in Table 11. There were significant differences between assessments regarding the usefulness after purchasing and all factors.

Table 11. The results of the X^2 test related to assessments regarding the usefulness after purchasing

Factors in Relationship		χ^2	p	df	Results
Assessments regarding the usefulness after purchasing	Gender	29.409	0.000	4	Significant
	Education	60.84	0.000	16	Significant
	Income	62.98	0.000	8	Significant
	Age	163.73	0.000	16	Significant
	Male SES	54.831	0.000	20	Significant
	Female SES	61.238	0.000	20	Significant
	Total SES	79.744	0.000	20	Significant

$p<0.001$ indicates a significant difference between the variables

When table 16 is taken into consideration, in all demographic and socio-economic variables, it was observed that it is effective in children on assessments regarding the usefulness after purchasing furniture.

4. Conclusion

It was found that the partners (husband and wife) decide together on factors such as the need to the purchase of furniture, studies conducted before the purchase of furniture, assessments regarding the timing of purchasing, and assessments regarding brand and quality. Although decision-makers are women on assessments such as form, color, pattern, design in furniture, decision-makers are men on assessments such as price, where to purchase, and the final decision on buying. Moreover, although the partners decide together on the need to purchasing, women are more dominant than men.

It was found that in factors affecting consumers when purchasing furniture, as income level and education level of the consumers increase, the rates of shared decision making of consumers increase in general.

When we examined the factors that influence the consumer's preference in terms of age, the following results were obtained:

(1) The highest rate of shared decision making in the family on factors such as the need to the purchase of furniture, studies conducted before the purchase of furniture, assessments regarding price, assessments regarding where to purchase, and assessments regarding form, color, pattern, design is in the age range 25-31.

(2) The highest rate of self-determination on the need to the purchase of furniture is in the age range 18-24.

(3) The highest rate of shared decision making on assessments such as where to purchase, and the final decision on buying is in the age range 39-45.

(4) The highest rate of shared decision making on assessments regarding the timing of purchasing is in the age range 32-38.

(5) The highest rate of shared decision making on assessments regarding brand and quality is the age group of 46 and above.

In terms of social class, the highest rate of shared decision making of consumers on all factors is in groups “A and B". That is, as the class level of consumers decreases, the rate of shared decision making of consumers decreases. One of the remarkable results is that more than 50% of the consumers in group "C2” carried out assessments regarding price on their own.

In all demographic and socio-economic variables, it was observed that it is effective in children on assessments regarding the usefulness after purchasing furniture.

References

Akyüz, İ. (1998). The study of consumers’ behavior on preferences of furniture in point of sex (Trabzon county center model). Master Thesis, Karadeniz Technical University, Graduate School of Natural and Applied Sciences, Trabzon.

Akyüz, İ. (2006). The effects of socio-cultural and socio-psychological factors on consumer behavior during furniture purchase. PhD Thesis, Karadeniz Technical University, Graduate School of Natural and Applied Sciences, Trabzon.

Andaç, T. (2008). A research on furniture consumer preference in Kayseri. Master Thesis, Kahramanmaraş Sütçü İmam University, Graduate School of Natural and Applied Sciences, Kahramanmaraş.

Arpacı, F. (2014). Furniture purchasing, using behaviors of consumers living in Ankara and their problems regarding furniture purchasing. International Refereed Journal of Marketing and Market Researches, 2(1), 1-15.

Arpacı, F., and Obuz, K. (2013). Consumers preferences related to furniture. ACADEMIC SIGHT International Refereed Online Journal of Social Sciences, 36, 1-20.

Burdurlu, E., İlçe, A. C., and Ciritcioğlu, H. H. (2004). The preference priorities of the consumers on furniture product characteristics. Hacettepe University Journal of Sociological Research. Retrieved from http://www.sdergi.hacettepe.edu.tr/burdurlu_cerceve.html.

Demircioğlu, B. (2012). Brand effect on the behavior of the consumer. Master Thesis, Kahramanmaraş Sütçü İmam University, Institute of Social Sciences, Kahramanmaraş.

Erdinler, E. S., and Koç, K. H. (2015, April). Consumer preferences and design demands in furniture. 3rd National Furniture Congress (pp.1136-1149). Konya.

Gerlevik, D. (2012). Via internet shopping' effects on consumer behaviour. Master Thesis, Atılım University, Institute of Social Sciences, Ankara.

İslamoğlu, A. H. (1990). A Research on the Roles of Family Members in the Purchasing Decisions of Durable Consumer Goods. Marketing World, 4(19), p. 21.

Kalınkara, V. (2016). Consumer behavior in purchasing home furniture. Turkey Journal of Social Studies, 20(1), 233-247.

Odabaşı, Y., and Barış, G. (2002). Consumer behavior. İstanbul: Mediacat Publishing.

Korkut, D. S., and Kaval, S. (2015). Consumer preferences in furniture selection: The example of Düzce. Düzce University Journal of Forestry, 11(1), 42-51.

Öztürk, E. (2006). Effect and importance of certificate of quality on customer purchase behaviour. Master Thesis, Marmara University, Institute of Social Sciences, İstanbul.

Penpece, D. (2006). The factors which determine the consumer behavior: The effect of culture on consumer behavior. Kahramanmaraş Sütçü İmam University, Institute of Social Sciences, Kahramanmaraş.

Table 12. Percentage distributions of statement "1" and statement "2"

Needs and demand of purchase					Studies conducted before purchasing				
Demographic and social class variables		Itself	Partner	Wife and husband	Demographic and social class variables		Itself	Partner	Wife, husband and children	Wife and husband
Gender	Male	12.9	35.9	51.2	Gender	Male	28.5	18.9	16.2	35.8
	Female	43	11	46		Female	29.2	19.7	15.9	32.8
Education	Primary school	31.8	25.8	42.4	Education	Primary school	30.8	25	17.2	27
	Secondary school	24.4	24.7	50.9		Secondary school	29.6	20.2	19.9	28.9
	High school	22.4	25.1	52.5		High school	28.6	19.3	15	35.8
	Bachelor's degree	27.2	24	48.7		Bachelor's degree	27.6	16.1	15.3	38.7
	Postgraduate	23.8	30.2	46		Postgraduate	30.2	14.3	12.7	42.9
Income	Low	27.1	22.4	50.6	Income	Low	33.1	17.9	18.1	29.7
	Middle	26.6	24.9	48.5		Middle	28.8	17.5	17	35.2
	High	24.3	28.1	47.6		High	23.4	23.7	12	39.5
Age	18-24	49.6	8.8	41.6	Age	18-24	36.8	8.8	7.2	37.6
	25-31	33	14.1	53		25-31	31.2	15.4	9.3	40.6
	32-38	27.2	24	48.8		32-38	29	17.9	13.7	39.2
	39-45	21	30.2	48.8		39-45	27.4	20.9	22.4	29.4
	46 and over	15.7	36	48.3		46 and over	25.6	26.1	20.6	27.2
Male SES	A class	7.4	51.9	40.7	Male SES	A class	10.2	30.6	13	43.5
	B class	9.3	32.8	57.9		B class	24.7	18.9	14.7	41.7
	C1 class	10.2	33	56.8		C1 class	29.2	17.2	18.8	34.2
	C2 class	17.1	35.9	47		C2 class	32.1	17.2	15.6	34.4
	D class	19.3	38.5	42.2		D class	30.6	21.9	15	32.5
	E class	23.8	28.6	47.6		E class	54.8	9.5	14.3	21.4
Female SES	A class	37.2	7	55.8	Female SES	A class	33.7	16.3	12.8	37.2
	B class	48.2	8	43.8		B class	29.5	10.7	11.6	45.1
	C1 class	46.3	9.3	44.4		C1 class	35.8	11.6	18.6	31.2
	C2 class	39.4	14.1	46.5		C2 class	36.6	19.7	25.4	16.9
	D class	41.7	12.5	45.8		D class	20.8	18.8	20.8	33.3
	E class	38.7	13.8	47.5		E class	23.3	30.1	15.8	30.1
All Consumer SES	A class	20.6	32	47.4	All Consumer SES	A class	20.6	24.2	12.9	40.7
	B class	27.4	21.4	51.2		B class	27	15.1	13.3	42.9
	C1 class	22.1	25.5	52.5		C1 class	31.1	15.2	18.8	33.3
	C2 class	21.2	31.9	46.9		C2 class	32.9	17.8	17.2	31.3
	D class	25.2	31.9	42.9		D class	29.2	21.1	16.3	32.1
	E class	37.7	15.4	46.9		E class	27	28.6	15.4	28.4

Table 13. Percentage distributions of statement "3" and statement "4"

Assessments regarding the price of furniture products					Assessments regarding where to purchase				
Demographic and social class variables		Itself	Partner	Wife and husband	Demographic and social class variables		Itself	Partner	Wife, husband and children	Wife and husband
Gender	Male	49.2	6.4	43.9	Gender	Male	35.3	13.6	14.6	36.1
	Female	23.1	22.3	52.9		Female	20.9	19.4	14.6	43.1
Education	Primary school	38.7	19.8	41	Education	Primary school	34	21.3	13.9	30.9
	Secondary school	47.3	18.1	32.9		Secondary school	35.8	16.8	16.5	29.7
	High school	39.9	11	48.4		High school	29.7	15.1	15.2	39.2
	Bachelor's degree	32.9	10.8	54.9		Bachelor's degree	23.8	14.2	13.7	46.3
	Postgraduate	23.8	9.5	63.5		Postgraduate	22.6	14.5	14.5	48.4
Income	Low	43.7	11.9	43.5	Income	Low	37.9	14.6	15.7	30.9
	Middle	39	14.9	44.9		Middle	27.7	14.8	15.4	41
	High	28.1	12.9	57.8		High	19.6	20.3	12.1	46.9
Age	18-24	36.8	16.8	45.6	Age	18-24	31.7	9.8	9.8	42.3
	25-31	34.9	11	51.6		25-31	28.4	11.6	9.9	47.2
	32-38	35.7	13.7	49.8		32-38	28.4	15.7	13.1	42.6
	39-45	39.3	16.1	43.8		39-45	28.6	20	19	32.4
	46 and over	42.6	11.1	45.9		46 and over	30.5	19.4	17.8	32.3
Male SES	A class	20.4	10.2	65.7	Male SES	A class	12.2	28	10.3	46.7
	B class	39.2	8.8	51.9		B class	25.8	8.8	14.6	50.8
	C1 class	52.5	3.8	43.2		C1 class	39	13.1	14.9	32.6
	C2 class	58.8	4.2	36.7		C2 class	43.8	10.1	13.3	32.8
	D class	53.4	11.8	34.8		D class	36	19.9	17.4	26.7
	E class	59.5	4.8	33.3		E class	45.2	14.3	19	21.4
Female SES	A class	19.8	15.1	64	Female SES	A class	12.8	17.4	17.4	52.3
	B class	23.2	13.4	61.2		B class	23.2	12.1	12.5	50.4
	C1 class	33	10.8	54.2		C1 class	25.9	12.7	14.6	43.9
	C2 class	36.6	12.7	47.9		C2 class	28.2	16.9	12.7	42.3
	D class	22.9	22.9	50		D class	18.8	27.1	10.4	37.5
	E class	15.5	37.3	46.6		E class	16.8	27.5	16.6	38.1
All Consumer SES	A class	20.1	12.4	64.9	All Consumer SES	A class	12.4	23.3	13.5	49.2
	B class	32.1	11	55.9		B class	24.6	10.4	13.7	50.5
	C1 class	45.8	6.3	47		C1 class	34.5	13	14.8	36.3
	C2 class	54.9	6.1	38.2		C2 class	41.1	11.1	13.3	34.5
	D class	46.2	14.3	38.1		D class	32.9	21	15.7	29
	E class	20.1	33.8	45.4		E class	20.1	26.7	16.5	35.7

Table 14. Percentage distributions of statement "5" and statement "6"

Assessments regarding the timing of purchasing					Assessments regarding color, pattern, form, design				
Demographic and social class variables		Itself	Partner	Wife and husband	Demographic and social class variables		Itself	Partner	Wife, husband and children	Wife and husband
Gender	Male	32	11.8	55.6	Gender	Male	10.2	29.7	26.7	33.1
	Female	25.6	14.3	59		Female	37.4	7.1	25.2	28.3
Education	Primary school	32.1	18.8	48.7	Education	Primary school	26.2	19.9	31.8	21.9
	Secondary school	29.4	17.2	51.6		Secondary school	22.9	20.8	28	27.2
	High school	31.7	11.2	56.8		High school	20	20.7	26.1	32.4
	Bachelor's degree	26.2	9.7	63.2		Bachelor's degree	21.5	18.7	22.8	35.3
	Postgraduate	15.9	14.3	65.1		Postgraduate	23.8	19	17.5	39.7
Income	Low	33.5	13.6	52.2	Income	Low	22.9	19.5	29.4	27.2
	Middle	30.1	13.1	55.7		Middle	21.8	18.7	26.4	31.9
	High	22.3	11.7	65.2		High	21.6	21.8	21.2	34.5
Age	18-24	36	17.6	45.6	Age	18-24	35.2	10.4	12	34.4
	25-31	29.1	12.8	57		25-31	30.2	14.3	11.9	41.3
	32-38	29.5	10.8	59		32-38	21.3	16.3	27.7	34.8
	39-45	27.9	13.8	57.1		39-45	19.9	23.3	32.2	24.4
	46 and over	28.5	14.1	57.2		46 and over	13	29	35.8	21.7
Male SES	A class	12	18.5	65.7	Male SES	A class	1.9	38	20.4	39.8
	B class	24.7	9.7	65.6		B class	8.5	26.4	22.5	42.6
	C1 class	31	10.4	58.6		C1 class	9.1	28.8	29.4	32.5
	C2 class	41.9	10.1	47.4		C2 class	13.6	29.5	27.9	28.2
	D class	38.5	17.4	43.5		D class	14.9	31.7	26.1	26.7
	E class	42.9	14.3	42.9		E class	19	28.6	28.6	23.8
Female SES	A class	22.1	16.3	60.5	Female SES	A class	44.2	9.3	7	39.5
	B class	29.9	6.7	61.2		B class	37.1	4	19.6	36.6
	C1 class	27.1	8.4	64.5		C1 class	37.9	7	29	23.4
	C2 class	31	8.5	60.6		C2 class	33.8	9.9	28.2	28.2
	D class	37.5	10.4	50		D class	37.5	10.4	25	20.8
	E class	19.2	22.8	57.3		E class	34.9	8.1	30.7	25.5
All Consumer SES	A class	16.5	17.5	63.4	All Consumer SES	A class	20.6	25.3	14.4	39.7
	B class	27.4	8.3	63.3		B class	22.2	16	21	39.5
	C1 class	29.8	9.8	60.4		C1 class	18	22	29.3	29.5
	C2 class	39.5	9.8	50.1		C2 class	17	25.7	28.4	28.4
	D class	38.1	15.7	44.8		D class	20.5	26.2	25.7	25.7
	E class	22.5	22	54.8		E class	34.2	9.7	30.2	25.2

Table 15. Percentage distributions of statement "7" and statement "8"

Assessments regarding brand and quality					Assessments regarding the final decision on buying				
Demographic and social class variables		Itself	Partner	Wife and husband	Demographic and social class variables		Itself	Partner	Wife and husband
Gender	Male	29.6	12.4	56.9	Gender	Male	44.7	7.1	48
	Female	28	14.9	55.9		Female	25	16.5	56.5
Education	Primary school	35.3	17	47.1	Education	Primary school	38.7	18.9	40.9
	Secondary school	29.7	12.9	55.6		Secondary school	38	12.3	48.9
	High school	28.7	13.3	57.5		High school	37.4	11	50.5
	Bachelor's degree	26.4	11.9	60.1		Bachelor's degree	33.8	7	58.3
	Postgraduate	15.9	15.9	66.7		Postgraduate	19.7	9.8	70.5
Income	Low	33.4	13.5	51.7	Income	Low	39.7	13.1	46.2
	Middle	29.7	14.3	55.3		Middle	38	11.5	49.6
	High	22	12.5	64.3		High	28.2	8.5	61.9
Age	18-24	40.8	10.4	47.2	Age	18-24	44	14.4	40.8
	25-31	30.9	12.8	54.7		25-31	32.6	13.8	52.6
	32-38	28.6	12	58.7		32-38	37.4	11.3	50.8
	39-45	28.6	15.8	54.7		39-45	33.3	9.2	56.4
	46 and over	24.9	14.8	59.1		46 and over	40.2	9	48.7
Male SES	A class	12	21.3	63.9	Male SES	A class	27.8	13.9	57.4
	B class	24.5	11.7	63		B class	37	7.5	55.1
	C1 class	31	10.8	57.5		C1 class	45.7	4.9	49.4
	C2 class	32.8	9.1	56.5		C2 class	50.2	5.9	43.3
	D class	36.6	19.3	44.1		D class	54.1	8.8	37.1
	E class	40.5	9.5	47.6		E class	50	14.3	35.7
Female SES	A class	15.1	16.3	68.6	Female SES	A class	9.3	4.7	84.9
	B class	28.1	8	60.7		B class	28.6	8.9	60.7
	C1 class	33.6	11.2	54.7		C1 class	34.1	6.1	57.9
	C2 class	26.8	15.5	57.7		C2 class	39.4	9.9	46.5
	D class	18.8	22.9	54.2		D class	21.3	34	44.7
	E class	28	19.4	52.6		E class	17.8	28.7	51.2
All Consumer SES	A class	13.4	19.1	66	All Consumer SES	A class	19.6	9.8	69.6
	B class	26.5	10	61.7		B class	33.3	8.2	57.4
	C1 class	31.7	10.9	56.8		C1 class	41.9	5.4	52.2
	C2 class	31.8	10.3	56.5		C2 class	47.9	6.4	44.4
	D class	32.4	20	46.7		D class	46.4	14.5	39.1
	E class	29.6	18.7	51.3		E class	21	27.4	49.5

Table 16. Percentage distribution of statement "9"

Assessments regarding the usefulness after purchasing furniture					
Demographic and social class variables		Itself	Partner	Wife, husband and children	Wife and husband
Gender	Male	21.6	17.6	45.1	14.7
	Female	26.6	11.2	43.3	17
Education	Primary school	26.3	14.5	36.4	22.1
	Secondary school	29.5	15.8	36.7	16.2
	High school	22.8	15.3	43.3	17.4
	Bachelor's degree	21.1	14.2	51.8	10.9
	Postgraduate	27	14.3	49.2	9.5
Income	Low	27.7	14.3	38.2	18.2
	Middle	25.4	15.4	41.3	16.4
	High	16.3	14.4	56.7	11.4
Age	18-24	38.4	9.6	40.8	0.8
	25-31	26.5	14.1	49.3	7.8
	32-38	22.1	15.4	44.4	17.4
	39-45	22.8	16.9	41.2	18.9
	46 and over	20.7	12.8	43.7	22.1
Male SES	A class	10.2	13	63	11.1
	B class	16.7	20.5	51.9	10.9
	C1 class	22.4	19.3	42.4	14.9
	C2 class	22.1	16.2	43.8	17.2
	D class	29.8	14.9	35.4	18.6
	E class	38.1	11.9	33.3	14.3
Female SES	A class	18.6	12.8	60.5	7
	B class	29.5	8	50.9	11.2
	C1 class	26.2	9.3	44.9	15.4
	C2 class	32.4	14.1	38	15.5
	D class	25	8.3	35.4	25
	E class	25.1	13.5	37	23.3
All Consumer SES	A class	13.9	12.9	61.9	9.3
	B class	22.9	14.8	51.1	11
	C1 class	23.5	15.9	42.9	15.4
	C2 class	23.6	15.9	43.2	16.7
	D class	29	13.3	35.2	20
	E class	26.7	13.7	36.6	21.7

Evaluation of Egg Shells in Wallpaper Production

Ahmet TUTUŞ[1], Ayşe ÖZDEMİR[1], Fatma BOZKURT1, Saniye ERKAN[1], Yıldız BİRBİLEN[1], Mustafa ÇİÇEKLER[1]*

[1]Kahramanmaraş Sütçü İmam University, Faculty of Forestry, Forest Industry Eng. Dep., Kahramanmaraş/ Turkey

*Corresponding author: mcicekler87@gmail.com

Abstract

Wallpaper is pasted in vertical strips over the walls of rooms, offices, restaurants, hospitals, hotels etc. to provide a decorative surface. In this study, the radiation reduction effect of waste egg shells was investigated in order to reduce the radiation, especially in offices and hospitals. Writing and printing papers were used as balance (base) paper in wallpaper production and its physical and optical properties were determined. Base papers have been coated with mixtures of precipitated calcium carbonate (PCC) and egg shell calcium carbonate (ECC) at certain rates. In order to improve water resistance of wallpaper, PVA (polyvinyl acetate) was applied on the surface of the dried wallpapers in the conditioning room. The physical and optical of the papers were investigated to compare with each other.

The results show that the whiteness values of the wallpaper increased with using PCC while decreased with using ECC. The brightness and yellowness values decreased not significantly and the physical properties of the wallpapers have decreased with coating process. As a result, waste egg shells were evaluated as a new raw material and water resistant wallpapers were produced.

Key Words: Wallpaper, ECC, PCC

1. Introduction

The wallpaper is made up of two lapped paper layers. The first one is the unprinted base (balance) paper, the other one is the printed surface paper. There are 7 different surface types on the wallpaper: paper, fiber, textile, emboss, vinyl, heavy vinyl and natural materials. There are also 3 types of base paper: paper, fiber, textile (URL-1). Wallpapers are a visual building material that is applied as proper to personal taste on interior walls. Writing-printing papers have 60-80 grammages and are suitable for writing and printing. The structure of the paper consists of chemical cellulose or chemical cellulose and mechanical wood pulp mixture. Coating is also applied to paper based on its usage area (URL-2; Yakut, 2012).

Precipitated calcium carbonate (PCC) is synthetically produced by chemical precipitation of limestone and has many outstanding properties such as high $CaCO_3$ content, low impurity ratio, diversity of crystal structure and possibility of being produced in homogeneous grain size distribution. PCC can be used as a filling material for high quality, strength paper production, as well as on surface as coating pigment (Tutus and et al., 2012; URL-3).

It is possible to obtain calcium carbonate (ECC) from egg shells after removing membranes, drying, grinding and sieving. The purity grade of the obtained ECC is approximately 93.7% (Killi, 2017; URL-4).

In this study, the usability of PCC and ECC in the wallpaper production was investigated and effects of PCC and ECC on the physical and optical properties of the wallpapers were determined.

2. Material and Method

2.1. Material

Writing-printing papers used in this study as base paper with 80 grammages were taken from Kombassan Paper Inc.; PCC as coating pigment was supplied from Adacal Industrial Minerals Inc.; carboxyl methyl cellulose (CMC), starch, glitter and PVA were bought from market.

2.2. Preparation of Coating Suspensions

PCC, ECC, and starch were prepared as separate suspensions at specific concentrations for preparing the coating suspensions. The prepared suspensions were mixed to a homogeneous state in a beaker based on the ratios given in Table 1. PCC and ECC ratios were changed and 12 different coating experiments (including non-coated paper) shown in same table were performed. To determine effects of PVA on the wallpaper properties, PVA application was also carried out on the papers which were coated under the same conditions.

Table 1. Coating suspension recipes

	$CaCO_3$ (%)	**PCC (%)**	**ECC (%)**	**CMC (%)**	**Starch (%)**	**Glitter (%)**
Control	-	-	-	-	-	-
100P	82.7	100	0	0.3	13	4
90P+10E	82.7	90	10	0.3	13	4
80P+20E	82.7	80	20	0.3	13	4
70P+30E	82.7	70	30	0.3	13	4
60P+40E	82.7	60	40	0.3	13	4
500P+50E	82.7	50	50	0.3	13	4
40P+60E	82.7	40	60	0.3	13	4
30P+70E	82.7	30	70	0.3	13	4
20P+80E	82.7	20	80	0.3	13	4
10P+90E	82.7	10	90	0.3	13	4
100E	82.7	0	100	0.3	13	4

The prepared coating suspensions were applied to the paper surfaces by coating rod (no.2) three times. The coated papers were conditioned at 23±1 ^{o}C and 65±1% relative humidity in a conditioning room and then subjected to calendering at 25 ^{o}C under 15 bar pressures.

2.3. Physical and Optical Tests

Coated wallpapers were subjected to the physical and optical properties in order to determine effects of PCC, ECC and PVA on these properties. The physical and optical tests applied to wallpaper were given in Table 2 with relevant standards.

Table 2. The physical and optical tests applied to coated paper

Physical and Optical Tests	Standarts
Breaking length	TAPPI T494 om-01
Tear index	TAPPI T414 om-12
Burst index	TAPPI T403 om-15
Thickness	TAPPI T 411 om-89
Density	TAPPI T 411 om-89
Bulkiness	TAPPI T 411 om-89
Brightness	ISO 2469:2014
Whiteness	ISO 2469:2014
Yellowness	ASTM E313
Opacity	TAPPI T 519 om-02
$Cobb_{30}$	TAPPI T 441 om-04

*Machine and cross directions averages were used for breaking length and tear index

Three replicates were done for each experiment, and mean values were used to determine the physical and optical properties of the coated papers.

3. Results and Discussion

3.1. The Physical and Optical Properties of the Wallpapers

Table 3 and 4 show test results of the physical properties of the coated wallpapers with PVA and PVA-free such as breaking length, burst and tear indices, bulkiness and density depending on PCC and ECC ratios.

Table 3. The physical properties of the PVA-free coated wallpapers

	Breaking length (km)	Burst index ($kPa.m^2/g$)	Tear index ($mN.m^2/g$)	$Cobb_{30}$ (gr/m^2)	Bulkiness (cm^3/g)	Density (g/cm^3)
Control	4.00	3.12	6.39	83	1.25	0.80
100P	3.26	2.66	4.55	105	1.15	0.87
90P+10E	3.37	2.68	5.16	105	1.34	0.75
80P+20E	3.36	2.69	5.75	103	1.39	0.72
70P+30E	3.01	2.35	5.32	101	1.52	0.66
60P+40E	3.08	2.45	5.99	100	1.47	0.68
500P+50E	3.27	2.62	4.20	93	1.51	0.66
40P+60E	3.05	2.48	5.24	100	1.46	0.68
30P+70E	3.15	2.52	5.51	98	1.61	0.62
20P+80E	3.15	2.71	5.63	96	1.60	0.62
10P+90E	3.26	2.50	5.89	111	1.60	0.63
100E	2.96	2.42	5.41	116	1.54	0.65

*P: PCC, E: ECC

Table 4. The physical properties of the coated wallpapers applied PVA

	Breaking length (km)	Burst index (kPa.m^2/g)	Tear index (mN.m^2/g)	Cobb$_{30}$ (gr/m^2)	Bulkiness (cm^3/g)	Density (g/cm^3)
Control	4.00	3.12	6.39	83	1.24	0.80
100P	3.31	2.50	5.79	84	1.29	0.78
90P+10E	3.12	2.73	6.73	85	1.41	0.71
80P+20E	3.00	2.49	4.48	98	1.51	0.66
70P+30E	3.42	2.32	5.25	84	1.52	0.66
60P+40E	3.25	2.76	4.98	87	1.53	0.65
500P+50E	3.05	2.23	4.95	88	1.53	0.65
40P+60E	3.31	2.64	5.74	87	1.55	0.65
30P+70E	3.06	2.47	4.94	83	1.55	0.65
20P+80E	3.28	2.50	5.41	88	1.59	0.63
10P+90E	3.03	2.61	4.98	93	1.62	0.62
100E	2.81	2.39	5.66	95	1.65	0.61

It has been clearly seen that the physical properties of the coated papers were significantly reduced. When fibers interact with coating pigments, the fiber-fiber bond reduces as well as paper strength (Eroglu and Usta, 2004; Karademir and et al., 2013). With PCC and ECC as coating pigment, the breaking lengths of the coated wallpapers decreased about 18.5% and 26%, respectively when compared with non-coated papers. Also, the Cobb$_{30}$ values, burst and tear indices of the wallpaper have been affected negatively (Fig. 1 and 2). In many studies, it has been found that the use of pigments such as $CaCO_3$ in the coating process has a negative effect on the physical properties of the papers. Tutus et al. (2012) found that the use of PCC (0, 20, 40, 60, 80, 100%) as filler during paper production reduced the physical properties of the paper.

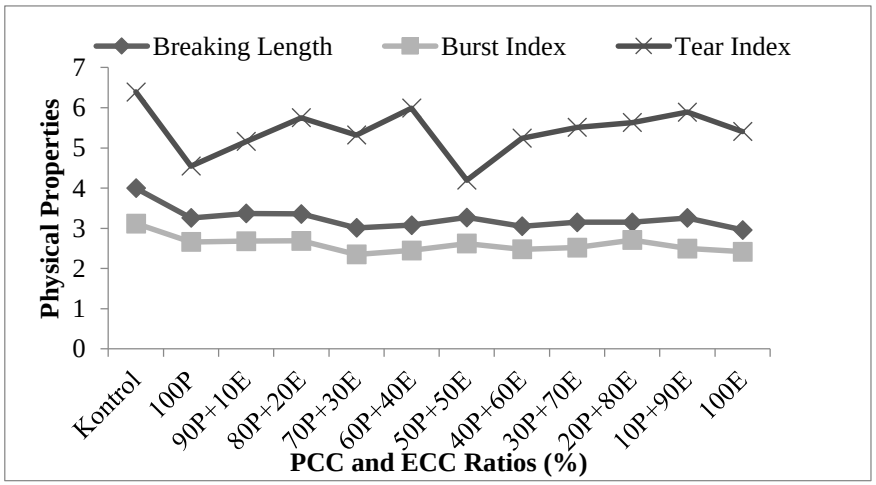

Figure 1. The physical properties of the PVA-free coated wallpapers

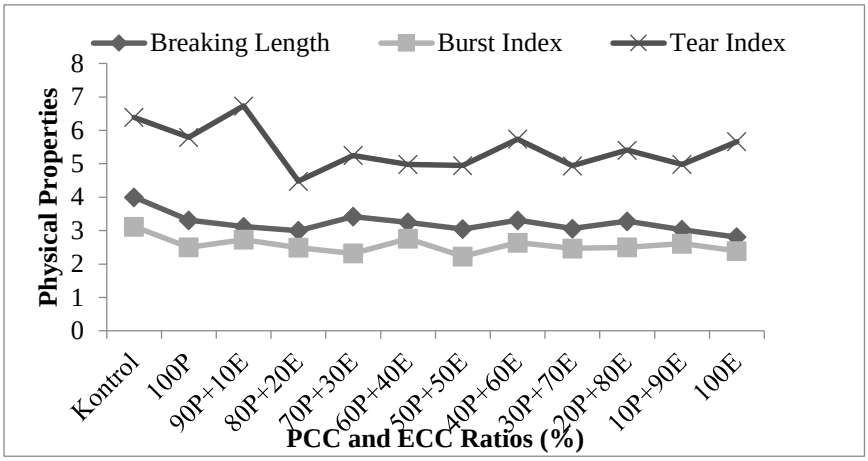

Figure 2. The physical properties of the coated wallpapers applied PVA

Tutus et al., (2013) reported that the physical properties of the waste papers were reduced with using PCC as filler in paper production. In this study they also compared the effects of PCC and GCC on optical and physical properties of the papers. Due to controlled production of PCC and its regular grain size and shape and size distribution, it has been seen that the physical properties of the papers are negligibly reduced when compared with GCC.

When PCC and ECC are compared to each other, the breaking length and burst index values are better for PCC and tear index values are better for ECC. Parallel to the increase in the ECC ratio in the coating suspension, bulkiness values increased while the density value decreased. While there was no significant effect on physical properties with the use of PVA, there was improvement in COBB value due to PVA's water repellency.

The optical properties of the coated wallpapers applied PVA and PVA-free were given in Table 5 and 6.

Table 5. The optical properties of the PVA-free coated wallpapers

	ISO Whiteness (%)	**ISO Brightness (%)**	**Yellowness (E 313)**	**ISO Opacity(%)**
Control	80.52	100.13	-29.51	96.62
100P	82.41	94.70	-16.91	97.53
90P+10E	82.71	92.86	-14.80	98.41
80P+20E	82.59	93.71	-16.33	97.32
70P+30E	82.69	92.46	-14.27	98.12
60P+40E	81.97	94.09	-17.62	97.38
500P+50E	82.71	93.54	-15.77	97.21
40P+60E	81.77	91.21	-13.92	97.07
30P+70E	81.44	92.72	-16.59	98.00
20P+80E	80.65	94.12	-20.27	97.32
10P+90E	79.81	92.41	-18.94	95.81
100E	79.74	92.84	-19.68	99.80

Table 6. The optical properties of the coated wallpapers applied PVA

	ISO Whiteness (%)	**ISO Brightness (%)**	**Yellowness (E 313)**	**ISO Opacity(%)**
Control	80.52	100.13	-29.51	96.62
100P	81.74	94.14	-18.39	97.26
90P+10E	82.15	94.45	-17.63	96.56
80P+20E	82.01	93.93	-17.71	97.97
70P+30E	81.49	92.88	-16.82	97.22
60P+40E	82.05	93.14	-16.34	98.11
500P+50E	82.07	94.82	-18.77	97.44
40P+60E	81.69	91.24	-14.06	97.44
30P+70E	81.33	94.56	-17.86	97.67
20P+80E	80.25	94.05	-20.67	98.39
10P+90E	79.55	95.35	-23.64	96.11
100E	79.86	91.70	-17.84	98.07

It has been observed that the whiteness value has increased and the brightness value has decreased with using PCC as coating pigment. With using ECC, these values have reduced. When compared with ECC, PCC provides better whiteness and brightness values due to its whiter and brighter structure. Generally, PCC and GCC have a whiter structure than paper. The whiteness value of $CaCO_3$ in PCC varies between 95% and 98% (Ozden, 1988; Koltka and Sabah, 2012). Due to its transparent structure, there is no significant effect of PVA on the optical properties of the coated wallpapers. Yoo et al. (2009) used ECC particles as coating pigments in writing-printing paper coating and investigated its effect on ink density and optical properties of the papers. As coating pigments, the addition of ECC particles has increased the ink density and optical density of blue, magenta and yellow inks, which reduces the brightness of the coated papers.

4. Conclusions and Recommendations

The physical and optical properties of the paper need to be known in order to determine its suitability for its usage area. Especially for wallpapers to be printed, it is expected that the properties such as surface smoothness, whiteness and ink absorbency are better. As a result of this study, it is seen that PCC and ECC have negative effects on the physical properties of the wallpapers applied PVA and PVA-free. Cobb value of the wallpaper applied PVA was found to be better than that of PVA-free wallpapers. In the optical properties, the whiteness increased with using PCC, but decreased with ECC. Although there is no significantly difference between

the opacity values, opaque papers have been obtained as a result of the reduction of gaps between the fibers with the use of ECC. As a result of this study;

1. ECC (60% ECC) can be used with PCC based on physical properties in wallpaper production.
2. ECC can be used up to 40% as coating pigment in wallpaper production that is the foreground of the whiteness in terms of optical properties.
3. The increase in the use of ECC is thought to be helpful in the production of wallpaper with the emboss technique.
4. The use of waste egg shells in the wallpaper production will reduce the damage to the environment and enable the production of high added value products.

References

Eroglu, H. and Usta, M., (2004). *Paper and Cardboard Production Technology*, Volume I, Cellulose and Paper Industry Foundation, Trabzon.

Karademir, A., Varlibaş H., cicekler, M.,(2013). A study on the chemical retention of $CaCO_3$ on paper production. *SDU Journal of Forestry*. 14: 48-52.

Killi U., 2017. *Production of Writing Paper from Waste Office Papers and Waste Eggshells.* Kahramanmaraş Sütçü İmam University. Faculty of Forest. Master Thesis. Kahramanmaraş.

Kolka S., Sabah, E., (2012). Paint Industry and Precipitated Calcium Carbonate (PCC). 8th International Industrial Raw Materials Symposium. November 29-30 . Istanbul/Turkey.

Yakut, A., (2012). Review of New Paper Production from Recycleable Used Paper. *Installation Engineering* - Issue 127 - January / February

Erkan, Z.E., and Malayoglu, U., (2001, October). Industrial Raw Materials and Their Properties Used in Paper-Cardboard Industry. *4 Industrial Raw Materials Symposium* (pp.250-257). Izmir: Dokuz Eylül University

Ozden, O., (1998). *Use of Starch for Coating the Paper Surface.* Doctoral Thesis. Istanbul University, Institute of Science and Technology, Istanbul.

Tutus, A., Cicekler, M., Kazaskeroglu, Y., Muduroglu, M., (2012). Effects of Precipitated Calcium Carbonate (PCC) on Optical and Physical Properties of Paper. *8th International Minerals Symposium.* pp.147-152. Istanbul/Turkey.

Tutus, A., Cicekler, M., Ozdemir, A., Okan, O,T., (2013). Effects of Precipitated Calcium Carbonate (PCC) on Optical Properties of Waste Paper, *International Caucasian Forestry Symposium.* pp.884-887. Artvin/Turkey.

Yoo, S., Hsieh. J.S., Zou. P., Kokoszka. J., (2009). Utilization of calcium carbonate particles from eggshell waste as coating pigments for ink-jet printing paper. *Bioresource Technology*. 100(24). 6416-6421.

URL-1: http://erwall.com/Duvar-Kagidi-Cesitleri.html. Date of access: 06.06.18-13:11

URL-2: https://makinecim.com/bilgi_185582_Kagit-Ve-Karton-Cinsleri-Ve-Ozellikleri-- Date of access: 6.6.18-13:15

URL-3: http://www.adacal.com.tr/adacal/urun-adacal-pcc.html. Date of access: 06.06.18-13:22

URL-4: http://www.organikpin.com/Yumurta-Nedir/Yumurta-B%C3%B6l%C3%BCmleri Date of access: 06.06.18-13:37

R&D and Technological Knowledge in SMEs: Furniture Industry in Samsun Region

Seval MUTLU ÇAMOĞLU[1]

[1] Associate Professor, Ordu University, Ünye Faculty of Economics and Administrative Sciences, Department of Economics, Ordu, Turkey

[*]**Respected Author:** smutlu28@gmail.com

Abstract

In this study, It was focused the level of R&D and technological knowledge in micro, small and medium-sized enterprises in the furniture manufacturing sector, established in Samsun. The traditional production system is usually widespread in this region. Furniture manufacturing is a labour-intensive sector that has been growing with regard to functionality, aesthetic appearance and fashion of products. The industry attracts attention due to the integration of designs and developing technologies in Turkey. The results of the field survey obtained by the furniture manufacturers constitute the findings of this study. The micro and small-scale are constituting the majority of firms in this region. The usage of technological knowledge and R&D activities were analyzed according to turnovers of these enterprises. As the turnover in the industry grows, technological knowledge is used more intensively. In the medium-sized enterprise, the difficulties related with financial and R&D are decreasing relatively small and micro sizes. It is observed that firms are following foreign technology inadequately. In particular, micro-sized firms are more far away from foreign and domestic technologies. These findings point to the need for enterprises to reach a suitable size to be more innovative and use technological knowledge. In general, SMEs in the furniture sector are quite successful in introducing new product to the market.

Keywords: R&D, Technological Knowledge, Furniture Sector, SMEs

1. Introduction

SMEs, which includes micro, small and medium-sized enterprises, is one of the key dynamics in terms of development in emerging economies. Although their size is small relatively, research and development activities in these firms are also extremely important in point of economic development. These firms are facing many challenges such as professional management, marketing, product marketization, organizational structure, providing external finance as well as technological knowledge, research and development, innovation and creativity. Globalization, in SMEs cases, requires firms to have a variety of advantages in order to survive in the market. In this sense, SMEs should offer new products to the market with high quality and provide advantage of technology (Hadjimanolis, 1999; Van de Vrande, *et al.*, 2009; Timurçin, 2010).

The share of research and development expenditures in GDP in Turkey was 0.94% as of 2016. Total R&D expenditures reached about 25 billion TL. 50% of these expenditures were for R&D personnel, 39% for current expenditures and 11% for investment expenditures. 54.2% of these expenditures were in private sector enterprises, 9.5% in government and 36.3% in higher education institutions (TUİK, 2018).

Furniture manufacturing is a labour-intensive sector that has been growing with regard to functionality, aesthetic appearance and fashion of products in globalizing world. The industry attracts attention due to the integration of designs and developing technologies in Turkey.

Furniture covers all functional and aesthetic-looking items made of wood to make daily life more comfortable and safe. It is produced by using building materials such as chipboard, fiberboard, MDF, plywood in interior or exterior spaces. A consumer from a furniture may have various expectations such as functionality, ease of use, durability, aesthetics, health (Sakarya & Doğan, 2016).

In this respect, these components to meet consumer needs require research and development process such as design, new product development, and utility model. It is possible to develop such items on SME scale in this sector.

The production value of the furniture sector in the whole world has reached about 500 billion dollars. Production location has shifted to China in the last 20 years, while European was the furniture manufacturing center, previously. Turkey in the wood based panels industry is the world's 5th and Europe's 2nd largest manufacturer (İstek, *et al.*, 2017).

The SMEs have many advantages in terms of innovation and R&D. Yelkikalan and Kalmış (2001) stated that SMEs can make more technical innovations than large enterprises with the same financial expenditure. Small and medium-sized enterprises are able to present technical ideas and practices to large-scale enterprises to further develop and process them. In addition, SMEs can perceive the consumer preferences and make the necessary changes in the production process more swiftly for working closer with the consumer. It is able to respond more quickly with the innovations to the needs that arise due to consumers' demands. Managers and employees are in closer relationship, and employees' sense of belonging increases quality and efficiency. The investment expenditures needed to increase employment are lower than large enterprises. An increase in the number of small enterprises in an industry leads to a more complete competitive market environment. In this circumstance, it has an effect that increases technical innovations and makes more efficient use of resources.

Turkish furniture sector can be observed some problems in R&D and SMEs. Çelik (2012) revealed within the framework of the sector decision-making model that the main problem in the sector are the lack of innovation and R&D activities, the deficiency of design studies and the expansion of imitations. Besides, the fact that the majority of the enterprises operating in this sector are SMEs poses problems due to the lack of capital and the high credit costs.

R&D is one of the key factors that determine the competitiveness of the country. In economic growth, factors such as physical capital in the long run are subject to the law of diminishing returns, while R&D and technology cause the fixed and increasing conditions to be valid. Innovation and creativity have important roles in terms of competitiveness. Creativity is the production of new ideas and innovation is the realization of new ideas. Differentiation of processes, new raw material usage, changes in management understanding, business facilitation are examples of innovation. The increase in creativity is also related to skilled labor employment. These are factors that prevent innovation in enterprises such as not following international developments, imitating local competitors, disrespecting the ideas of employees, not promoting patent owners, not protecting copyrights, economic instability in the country, lack of market research. Technology is the systematic application of knowledge in the processes of the industry. Technological innovations cause changes in the competitive structure, product processes and markets. To achieve competitive power requires continuing innovation activities and driving customer demands and needs to a market faster than their competitors (Timurçin, 2010; Altay, 2006).

Santamaría *et al.* (2009) stated that non-formal R&D activities such as advanced machine use, outsourced training, collaboration agreements and design are very important in industries

where low and medium technology is used. Traditional literature in technological information systems has primarily focused on large corporations. The research in this area is too limited to provide useful guidelines for the problems, opportunities, and management issues encountered by small business (Premkumar, 2003).

This study will contribute to the literature in terms of the extent to which the technological knowledge and R&D level can be reached in a regional industry where SMEs are concentrated. After examining the situation of the furniture sector in Samsun region, it is aimed to put forward the use of technology, problem areas, ways of reaching the technology and new product-design contribution in the sector.

2. Material and Methods

In this study, it is aimed to present the current situation of the R&D activities of the firms in the furniture sector in Samsun region on the SME scale. There are 267 furniture manufacturers in Samsun. It employs 1,753 people in this province (STSO, 2017). Since the sector is composed of many small enterprises, only the firms registered in Samsun Provincial Directorate of Commerce and Industry have been taken into consideration in order to represent the furniture sector. There were 77 registered furniture manufacturer firms in 2015. It was interviewed with 57 firms that agreed to conduct a survey.

In these interviews, it could be argued that these firms are able to follow technological progress in their workflow processes, the challenges in technological transportation and research and development processes, the type of new technological transportation, whether the sector offers a new product or service, whether utility model and industrial designs exist or not, the level of technological knowledge in comparison with competitors, IP rights (patent and trademark status). By examining the answers of these questions, it is aimed to reveal the level of research and development activities and technology usage in this sector.

First of all, 5 different turnover groups were created by the firms interviewed within the scope of field survey. The existence of significant relationships determined by Anova in the use of technology and R & D activities according to turnover groups. Anova, analysis of variance, applies between the turnover level and the variables including Likert-scale. It is one of parametric tests that requires data in numerical scores for each person and use F test. For variance analysis, it assumes that the population distributions are normal and variance homogeneous (Gravetter & Wallnau, 2016: 559-562).

3. Findings and Discussion

The results of the field survey obtained by firms operating in Samsun furniture sector constitute the findings of this study. Pre-prepared questionnaires have been filled out with the authorized persons in 57 firms. Firstly, socio-demographic characteristics of the mangers are given in the findings. Then, information about economic, legal, financial, production, and turnover of the firms are presented. Later, the firms involved in the research are examined by the use of technology, problem areas, and ways to reach technology, new product-design contribution according to five turnover groups.

62 percent of the managers interviewed in the firms are the owners and 23 percent are non-family. The average age of the authorized persons interviewed is 42. These people generally begin to work in the industry since their early ages. Then, they have established their own firms by specializing after learning the job. As the level of education is concerned, they usually graduate from high school. Müftüoğlu (2007) stated that the managers of the firms are engineers, technicians or skilled workers in SMEs increases success in the production processes, but this success does not seem adequate to marketing, finance and management.

This study indicates that there are firms operating in the furniture sector in Samsun since 1926. By 1982, there were only 10 firms, but after 1982, the number of firms increased every decades (see Table 1). The widespread of furniture manufacturing is influenced by the development of the construction sector in Turkey.

Table 1. Distribution of firms by year of establishment

Years	Num. of firms	%
1926-1981	10	17,5
1982-1991	12	21,1
1992-2001	20	35,1
2002-2015	15	26,3
Total	57	100,0

According to the average annual turnover of the firms; 60,7% of them are concentrated between 50,000 and 250,000 TL. Firms with annual turnover of 500 thousand TL constitute 91.1% of the firms and the average number of employees is below 15 persons (Table 2). Descriptive statistics by means and frequencies are given in Table 3 and 4. The average operating time of firms is 23 years, the average number of employees is 11, the share of paid

up debts in total turnover is 44 percent and the investment amount of firms that will enter the sector is around 500 thousand TL. The average capacity utilization rate in these firms is about 65% annually (Table 3).

Table 2. Distribution of firms according to their average annual turnover

Annual Turnover (TL)	Num. of firms	%	Num. of Employees	Turnover / Num. of Employees***
min.-50.000	11	19,6	14,00	4.653,91
50.001-100.000	20	35,7	8,30	17.528,96
100.001-250.000	14	25,0	10,64	32.705,46
250.001-500.000	6	10,7	8,33	56.894,84
500.001- max.	5	8,9	18,80	100.952,38
Total	56	100,0	10,95	30.460,35

[a] Mean, *** P<0.01

Table 3. Descriptive statistics of the firms by means

	N	Minimum	Maximum	Mean	Std. Deviation
Firms' operating period (years)	57	5,00	89,00	23,28	15,31
Number of employees	57	1	95	11,33	15,11
Total annual turnover (TL)	56	10.000	1.000.000	211.517,86	263.086,44
Share of paid up debts in total turnover (%)	56	5	80	44,32	21,64
Competing new investment amount (TL)	57	50.000	3.000.000	526.842,11	676.703,95
Annual capacity utilization rate (%)	57	20	100	65,14	16,601

Corporate characteristics of firms were evaluated with the frequency of observation. Considering the legal structure of the firms, they are more private companies. The ownership status of the firm building is 47.4% of the rent and 40.4% of the ownership. Sixty percent of the firms have used credit in the last year.

40% of the firms are producing both by order and by mass production. The majority is 47.4% only selling to the final consumer. 15.8% are for industrial users and 36.8% are for both groups. Only 9 companies receive encouragement from the government. 11 of them have TSE quality standard. 89.5% can take place in the market with its own brand.

The fact that they are at SME scale also leads to a low level of foreign trade activities. When evaluating the level of competition in the region on the basis of product and price, 28.1% of the firms stated that there are companies that operate in the same field and produce the similar

products. Besides, 26.3% of the firms stated that they implement the same price policy with their competitors.

Table 4. Descriptive statistics of the firms by frequencies

		Frequency	Percent
Legal status of the firm	Private	48	84,2
	Limited	7	12,3
	Incorporated	2	3,5
Building property status	Rent	27	47,4
	Property owner	23	40,4
	Rent and owner	7	12,3
Use of credit in the past year	Investment credit	5	8,8
	Business credit	30	52,6
Production method	Serial production	12	21,1
	Production by order	22	38,6
	Order + serial	23	40,4
Sales groups	Final consumer	27	47,4
	industrial users	9	15,8
	Both groups	21	36,8
Market groups	Only to domestic markets	45	78,9
	Only to foreign markets	1	1,8
	Both markets	11	19,3
Government Encouragement	Yes	9	15,8
Quality standard certificate	TSE	11	19,3
Branding status	Own brand	51	89,5
	The brand demanded by the customer	3	5,3
	Both of them	3	5,3

The integration level of technological development were inquired and graded by Likert-type scale (1 = very low to 5 = very high) in the workflow process. Between the technology usage and the groups that were created according to the firms' turnover, profitability, number of employees and duration of operation are analyzed with Anova. According to this, statistically significant relationship is observed only with the turnover of firms. A firm's turnover is an important indicator of sales revenue and trade volume.

According to F test results, there is a significant relationship between the level of turnover and technology usage for firm's commercial correspondence at the level of 5% and for accounting transactions and information storage, i.e. database arrangement at the level of 10%.

The usages of technology for correspondence, accounting and information storage are more important for large enterprises, while these technological developments are less important for the micro enterprises (turnover under 50.000 TL). The technology implementation for the customer tracking, computer-aided drawing and design, inventory control and computer-aided production is equally important in all enterprises. These findings indicate that as the volume of production increases, the technology is used more intensively and more emphasized at all stages of the production process. According to the score level in total; customer-driven 4.11, information storage 3.77, computer-aided drawing and design 3.64, computer-aided manufacturing 3.45, inventory control 3.41, accounting 3.36 and commercial correspondence 3.25, respectively (Table 5). Premkumar (2003) stated that the firms in small business sector are becoming increasingly dependent on information systems for their operations.

Table 5. The usages of technology according to turnover levels of firms by scores (1: very low, 5: very high)

Turnover level (TL)	Commercial correspondence **	Accounting*	Customer -driven	Computer-aided drawing and design	Inventory control	Information storage (database)*	Computer-aided manufacturing
min.-50.000	2,18[a]	2,64	4,36	3,73	3,09	2,91	3,09
	1,834[b]	1,804	1,027	1,618	1,640	1,640	1,640
50.001-100.000	3,70	3,60	4,10	3,60	3,10	3,75	3,55
	1,490	1,465	1,210	1,729	1,651	1,517	1,669
100.001-250.000	2,93	3,29	4,14	3,50	3,64	3,79	3,07
	1,817	1,729	1,460	1,743	1,646	1,626	1,900
250.001-500.000	3,17	2,83	3,33	3,67	4,17	4,50	3,50
	1,835	1,722	1,366	1,366	0,753	0,548	1,761
500.001-max	4,80	4,80	4,40	4,00	3,80	4,80	4,80
	0,447	0,447	0,894	1,732	1,789	0,447	0,447
Total	3,25	3,36	4,11	3,64	3,41	3,77	3,45
	1,740	1,634	1,231	1,623	1,581	1,501	1,683

[a] Mean, [b] Standard Deviation, ** P<0.05, * P<0.10

Table 6 examines that firms have moderate problems in various stages of production. As the scale grows, problems in finance and research-development are reduced. While research and development is a serious problem in micro-scales, this problem is eliminated at the large

scale level. The most important problem faced on the large scale within the scope of SME is to find qualified personnel.

Table 6. Problem areas according to turnover levels of firms by Likert scores (1 = very problematic, 5 = not at all problematic)

Turnover	Finance *	Marketing	Production	Personnel	Technology	Management	R&D **
min.-50.000	3,09	3,09	3,18	2,91	3,27	3,36	2,82
	1,640	1,640	1,328	1,446	1,421	1,629	1,722
50.001-100.000	4,05	3,30	3,55	3,70	3,55	3,95	4,10
	1,234	1,380	1,356	1,342	1,395	1,050	1,071
100.001-250.000	4,14	3,71	3,79	3,79	3,64	3,64	3,43
	1,292	1,490	1,424	1,477	1,550	1,499	1,604
250.001-500.000	4,17	3,83	3,00	4,00	3,33	3,33	3,33
	0,983	1,602	1,414	1,673	1,633	1,862	1,862
500.001-max	4,80	4,80	4,80	3,60	4,80	4,80	5,00
	0,447	0,447	0,447	1,673	0,447	0,447	0,000
Total	3,96	3,55	3,59	3,59	3,61	3,77	3,68
	1,321	1,464	1,359	1,449	1,423	1,375	1,503

[a] Mean, [b] Standart Deviation, ** P<0.05, * P<0.10

In Table 7 is examined how companies acquire new technologies. The transportation of the new technologies were achieved by 57.1% of firms using their own R&D activities, 35.7% using domestic technology and 7.1% using foreign technology. The rate of foreign technology usage in SMEs in this sector is extremely low. This is probably due to the labor-intensive production style at the SME level in the furniture sector.

Table 7. Ways to reach new technologies in firms

Turnover	Own R&D activities	Domestic technology	Foreign technology
min.-50.000	72,7%	18,2%	9,1%
50.001-100.000	60,0%	35,0%	5,0%
100.001-250.000	42,9%	50,0%	7,1%
250.001-500.000	66,7%	33,3%	0,0%
500.001- max	40,0%	40,0%	20,0%
Total	57,1%	35,7%	7,1%

Utility model is a technical solution for a production tool. Industrial design is an artistic and design presentation of a new and original product produced by industrial and artisans.

Utility model and industrial design should be protected by copyright law if they have new, original and applicable features for the industry (Rumyantseva *et al.*, 2016). Table 8 shows that these firms are able to offer a very high level of new products and services to the furniture sector. On the other hand, it is observed that the number of utility model and industrial design is increasing especially as the scale grows at SME level. 78.6% of these firms that were successful in introducing a new product or service to the market. In addition, 41.1% of the firms offered to the sector some utility model and industrial design. These findings indicate that furniture manufacturers on the SME scale are using moderate technology and a highly innovative-dynamic sector. Avlonitis (2007) states that sectoral adaptation of innovative products is associated with entrepreneurial behavior in SMEs, especially active entrepreneurs can make more contributions. Marcati *et. al.*, (2008) conceptualizes innovation at two abstractions levels as general innovation and original innovation. Innovation in SMEs is associated with the personality of entrepreneurs. Baumann and Kritikos (2016) found that the R&D intensity of micro-scale firms is largely based on product innovation rather than on process innovation.

Table 8. New product, model and design presentation to the sector

Turnover	Introducing a new product or service	Property of utility model and industrial design
min.-50.000	90,9%	18,2%
50.001-100.000	85,0%	50,0%
100.001-250.000	71,4%	35,7%
250.001-500.000	50,0%	50,0%
500.001- max	80,0%	60,0%
Total	78,6%	41,1%

4. Conclusions and Recommendations

In this study, the focus is on the extent to which furniture manufacturers, established in a relatively small region, are able to use technological knowledge and R&D activities. There is an intensive small-medium sized enterprises in the furniture industry in Samsun. The firms with annual turnover of 500,000 Turkish Liras constitute 91.1% of the firms and the average number of employees is fewer than 15. This indicates that the micro and small scale is constituting the

majority of firms in this sector. The level of turnover per employee, that is productivity, is increasing as the firms grows.

In this sector, family business is usually widespread in the region. The traditional production system is dominant in the form of transition from father to son, as a business management system. It is a small workshop style production in the form of relationship between master and apprentice. In this case, owner and employees do not receive adequate formal training in the relevant area. This type of production is quite common in developing countries, especially in the development efforts.

Globalization requires more competitive production. Enterprises should be able to introduce high quality new products to the market. This competitive structure highlights the importance of technological knowledge and R&D in SMEs. R&D investments in Turkey are generally not sufficient compared to other countries. R&D requires technological innovations and knowledge training.

SMEs positioned in the form of traditional production style, both managers and staff need to reach the necessary formal training. There are universities in many small cities of Turkey. However, engineering faculties are not increasing at the same extent. A local training-oriented system will enable these people to get the engineer education without moving away from the work. In fact, this situation will be effective for both accelerating regional development and becoming more professional and institutional in local SMEs. In the macro-scale, it may also prevent migration to big and industrial cities and increase local employment.

In the furniture sector, human skills can be the forefront in new product and design in the SME scale. The employees of the SMEs are closer to the consumer. Therefore, they can learn the consumer's demands and expectations faster than large-scale firms and adapt to production at lower cost. This can provide a competitive advantage in terms of innovation in the sector.

Foreign trade of the furniture sector is not adequate in this region. There should be more focus on exportation in this region where production is so intense. If necessary, government incentives should be provided in this regard.

The technological knowledge and problem areas of firms were determined by asking questions of Likert scale type. As the turnover in the industry grows, technology is used more intensively. In the medium-sized enterprise, the difficulties related with financial and R&D are also decreasing relatively small and micro levels. It points to the need for enterprises to reach an adequate size to be more innovative and use technological knowledge. On the other hand, in general, it is observed that firms are not following foreign technology sufficiently. In particular, micro-sized firms are more far away from foreign and domestic technologies.

SMEs in the furniture sector are successful in introducing new product to the market. As the scale grows, utility model and industrial design are increasing. But, micro-scale firms do not pay enough attention to patent ownership. This issue is also important in terms of intellectual property rights.

References

Altay, B., (2006). Avrupa Birliği'nde rekabet politikaları, Türkiye ve Avrupa Birliği'nin ihracatta rekabet gücünün ölçülmesi. *Afyonkarahisar, Türkiye*.

Avlonitis, G. J., and Salavou, H. E., (2007). Entrepreneurial orientation of SMEs, product innovativeness, and performance. *Journal of Business Research*, *60*(5), 566-575.

Baumann, J., and Kritikos, A. S. (2016). The link between R&D, innovation and productivity: Are micro firms different? *Research Policy*, *45*(6), 1263-1274.

Çelik, N. (2012). Türkiye'de mobilya sektörü gelişim planı için bir karar modeli önerisi. *Sosyal ve Beşeri Bilimler Dergisi*, *4*(1).

Gravetter, F. J., and Wallnau, L. B., (2016). *Statistics for the behavioral sciences*. Cengage Learning.

Hadjimanolis, A., (1999). Barriers to innovation for SMEs in a small less developed country (Cyprus). *Technovation*, *19*(9), 561-570.

İstek, A., Özlüsoylu, İ., and Kızılkaya, A., (2017). Türkiye Ahşap Esaslı Levha Sektör Analizi. *Bartın Orman Fakultesi Dergisi*, *19*(1), 132-138.

Marcati, A., Guido, G., and Peluso, A. M., (2008). The role of SME entrepreneurs' innovativeness and personality in the adoption of innovations. *Research Policy*, *37*(9), 1579-1590.

Premkumar, G. (2003). A meta-analysis of research on information technology implementation in small business. *Journal of organizational computing and electronic commerce*, *13*(2), 91-121.

Rumyantseva, T. B., Ph, S., Syryamkin, V. I., Vaganova, E. V., and Zinov, V. G., (2016). *TECHNOLOGY MANAGEMENT: Part 2. Strategic Management of Intellectual Property*. STT Publishing. 228p.

Sakarya, S. and Doğan, Ö. (2016). Orta Anadolu İhracatçı Birlikleri Mobilya 2016 Sektör Raporu, 1-36. Retrieved from http://www.turkishfurniture.org/TR,15299/mobilya-sektor-raporu-2016.html (14/06/2018).

Santamaría, L., Nieto, M. J., and Barge-Gil, A., (2009). Beyond formal R&D: Taking advantage of other sources of innovation in low-and medium-technology industries. *Research Policy*, *38*(3), 507-517.

STSO, (2017). Samsun İktisadi Rapor 2017, Samsun Ticaret ve Sanayi Odası. Retrieved from http://www.samsuntso.org.tr/upload/Dosyalar/Yayinlar/IktisadiRapor/Iktisadi-Rapor-2017.pdf *(21/06/2018).*

Müftüoğlu T., (2007). *Türkiye'de Küçük ve Orta Ölçekli İşletmeler,* Turhan Kitapevi, Ankara, p.79.

Timurçin, D., (2010). *Türkiye'de KOBİ'lerin rekabet gücü ve rekabet üstünlüğü sağlamada kümelenmenin etkisi.* Doktora Tezi, İstanbul Üniversitesi Sosyal Bilimler Enstitüsü, İstanbul, 221-222.

Van de Vrande, V., De Jong, J. P., Vanhaverbeke, W., and De Rochemont, M., (2009). Open innovation in SMEs: Trends, motives and management challenges. *Technovation*, *29*(6-7), 423-437.

Yelkikalan, N., and Kalmış, H., (2001). KOBİ'lerde Verimlilik Yönelimli Yeniden Yapılandırma Stratejileri. *Orta Anadolu Kongresi, Erciyse Üniversitesi, Nevşehir İİBF, Nevşehir*.

Assessment of Metal Contents in *Hydum rufescens, Macrolepiota procera* Mushrooms Collected from Turkey

Ayşenur GÜRGEN[1], Sibel YILDIZ[1], Uğur ÇEVİK[2], Ümit Cafer YILDIZ[1]

[1]Karadeniz Technical University, Faculty of Forest, Forest Industrial Engineering, Trabzon, Turkey.
[2]Karadeniz Technical University, Faculty of Science, Department of Physic, Trabzon, Turkey

[*]**Corresponding author:**
aysenur.yilmaz@ktu.edu.tr

Abstract

Wild-growing mushrooms have been considered as a delicious food in many countries for a long time. However, some of them can accumulate large concentrations of heavy metals, which can be dangerous to human health particularly, when the intake is high. Thanks to the climatic conditions, Turkey has also a great potential for wild edible mushroom species and several species have been consumed especially in rural areas. In this study, 13 different metals (Mg, Al, Ca, Cr, Mn, Fe, Co, Ni, Cu, Zn, As, Se, Cd) and 3 isotopes of Pb (^{206}Pb, ^{207}Pb and ^{208}Pb) contents in two different wild-growing edible mushroom species (*Hydum rufescens*, *Macrolepiota procera*) collected from Kastamonu forest in October of 2014, in Turkey were investigated. Mushroom samples were analyzed by inductively coupled plasma mass spectrometry (ICP-MS). The results showed that metal contents in *Macrolepiota procera* were higher than the metal contents in *Hydum rufescens* except Al and Mn. All of the toxic element concentrations (Cr, Cd, As) were low and below the world average in both mushroom species. Consequently, there was no any health risk associated with consumption of the analyzed wild edible mushroom species.

Keywords: Metal content, wild edible mushroom, ICP-MS, Turkey.

1. Introduction

Mushrooms are among the foods that consumption have been increasing day by day. The main reason for this increase may be due to the fact that the mushrooms are dietary nutrients (Muszynska et al., 2011). They have high water content and low-fat ratio (Manzi et al., 2001). Additionally, having a high protein content is a great way to turn off the protein deficiency (Wani et al., 2010), especially for vegetarians. In recent years, thanks to the reports of many scientists studied on the bioactive properties of mushrooms such as antioxidant (Prabu and Kumuthakalavallia, 2016), antimicrobial (Liu et al., 2017), anticancer (Muszyńska et al., 2017) etc., mushrooms have been the focus of more attention.

Some mushrooms were reported that they have ability to accumulate metals (Sevindik et al., 2015; Mleczek et al., 2016; Sun et al., 2017) in addition to their bioactive properties. They are also known as bio indicators for environmental monitoring (Garcia et al., 1998; Cocchi et al., 2006). Undoubtedly, land is the best storage material and elements such as cadmium, mercury, arsenic, etc., are also absorbed many living organisms. This type of accumulation occurred in the mushrooms can be toxic to living organisms especially at high concentrations

(Çayır et al., 2010). So, mushrooms not only include the metals necessary for our bodies but also accumulate toxic metals. To know the amount of the metal accumulation especially in the edible mushrooms is very important for learning the toxic effect on human health.

Thanks to the climatic conditions, Turkey has a great potential for wild edible mushroom and several species have been consumed especially in the rural areas. The aim of this study is to investigate the metal contents accumulated in two wild edible mushroom species (*Hydum rufescens* and *Macrolepiota procera*) collected from Kastamonu forest in Turkey.

2. Material and Methods

2.1. Mushrooms

Wild edible mushroom species were collected from Kastamonu province located in Black Sea region to the North of Turkey, (Figure 1), in October of 2014. The species of mushrooms (Figure 2 and 3), their habitats, locations (province, district and village), growing forms and regional name are given in Table 1.

Figure 1. Study area

The ecological and morphological characteristics were noted and the specimens were photographed in their natural habitat. Later, mushrooms were identified based on their morphological characteristic and then dried for future uses.

Figure 2. *Hydum rufescens*

Figure 3. *Macrolepiota procera*

Table 1. Mushroom species, their habitats and locations, growing forms and regional name

No	Mushroom species	Habitat - Location	Edibility	Growing Form	Regional name
1	*Hydum rufescens*	On soil, Kastamonu	Edible	Wild	Geyik avurdu
2	*Macrolepiota procera*	On soil, Kastamonu	Edible	Wild	Dede bürük

2.2. Samples preparation and treatment

All the mushroom samples were sliced and dried at a drying mechanism until they were completely dehydrated. Then samples were crushed for passing a 40 mm mesh sieve

Mushroom samples (0.5 g) were digested in a mixture of 5 mL of HNO_3 (65%), 2 mL of HCl (37%) in a microwave digestion system for 31 min and diluted to 50 mL volume with deionized water. The digested samples were quantitatively transferred into 100 mL polypropylene volumetric flasks and diluted to volume with ultrapure water. These samples were analyzed by inductively coupled plasma mass spectrometry (ICP-MS, A Bruker 820-MS).

2.3. Statistical analysis

The data were presented as means ± standard deviations of ten replicates for metal composition and analyzed by using Statistical Package for Social Sciences (SPSS version 23.0). The data were analyzed by ANOVA and tests of statistical significance were performed using Duncan's multiple range tests

3. Results and Discussions

The metal contents of mushrooms are presented in Table 2. Magnesium acts as a catalyst in enzymatic reactions such as the transfer, storage and use of energy. It is called 'antistress mineral' because it helps to calm down (Grubbs and Maguire, 1986). In this study, magnesium content of *Hydum rufescens* and *Macrolepiota procera* was found 1037.2±120.5 and 1052.3±110.2 mg/kg respectively. Among the all metal contents only magnesium was not found statistically significant. In a study, magnesium content of 10 wild mushrooms has reported between 755.1±7.33- 1150.7±41.45mg/kg (Ouzouni et al., 2009). In this study aluminum content of *M. procera* (37.1±2.7mg/kg) was found higher than aluminum content of *H. rufescens* (25.2±2.5 mg/kg). In the literature, the aluminum content in wild mushrooms (n = 271, 19 species) and in cultivated *Agaricus bisporus* (n = 15) was reported from 14±6.8 to 123±55 mg/kg dried weight (Müller et al., 1997). So, it can be said that the species of mushrooms affect the amount of aluminum.

Table 2. Metal contents of mushrooms (mg/kg, dry weight)

Mushroom	Mg	H.G.*	Al	H.G.	Ca	H.G.	Mn	H.G.	Fe	H.G.
Hydum rufescens	1037.2 (120.5)**	a	25.2 (2.5)	a	602.0 (45.8)	b	7.8 (0.7)	b	145.8 (15.0)	a
Macrolepiota procera	1052.3 (110.2)	a	37.1 (2.7)	b	295.3 (8.7)	a	2.6 (0.2)	a	277.8 (20.31)	b
	Co	**H.G.**	**Ni**	**H.G.**	**Cu**	**H.G.**	**Zn**	**H.G.**	**Se**	**H.G.**
Hydum rufescens	0.63 (0.051)	b	41.2 (11.3)	b	52.7 (4.4)	a	57.7 (4.3)	a	2.76 (0.06)	a
Macrolepiota procera	0.23 (0.010)	a	9.0 (1.5)	a	96.3 (6.9)	b	86.4 (6.1)	b	3.13 (0.10)	b

	Pb-206	H.G.	Pb-207	H.G.	Pb-208	H.G.	Cr	H.G.	As	H.G.	Cd	H.G.
Hydum rufescens	0.17 (0.016)	a	0.15 (0.008)	a	0.16 (0.014)	a	0.093 (0.003)	b	0.029 (0.002)	a	0.26 (0.011)	a
Macrolepiota procera	0.36 (0.033)	b	0.33 (0.030)	b	0.34 (0.033)	b	0.038 (0.002)	a	0.026 (0.002)	a	0.61 (0.035)	b

* : H.G: Homogeneity groups mean having the same superscript letter(s) are not significantly different (p>0.05) by

Duncan's multiple range test.
**: Standard deviation values are given in parentheses.

The various biological roles of calcium are necessary for processes such as structural support, cell adhesion, mitosis, blood coagulation, muscle contraction, and glandular secretion (Müller et al., 1997). In this study, calcium content of *H. rufescens* (602.0±45.8 mg/kg) was found approximately two times higher than calcium content of *M. procera* (295.3±8.7 mg/kg). Michelot et al. (1998) reported the calcium content of 92 wild specimens of mushrooms collected in France was between 174 and 7230mg/kg.

Manganese involved in bone formation, protein, fat, and carbohydrate metabolism (Institute of Medicine, 2001). Like calcium, manganese content of *H. rufescens* (7.8±0.7 mg/kg) was found approximately two times higher than manganese content of *M. procera* (2.6±0.2 mg/kg). Our manganese values were found lower than eight different species of wild edible mushrooms collected from Greek (11.3±0.6-100±5.0 mg/kg; Ouzouni et al., 2007).

Iron is one of the indispensable trace elements for people. Taking an excessive amount of iron has toxic effect (Crichton et al., 2002). In this study, iron content of *M. procera* (145.8±15.0 mg/kg) was found lower than the iron content of *H. rufescens* (277.8±20.31 mg/kg). Our results are in agreement with the literature that reported the iron content in 92 wild specimens of mushrooms collected from France (21.7- 639 mg/kg; Michelot et al., 1998).

Cobalt is an important co-factor in Vitamin-B12, which is essential element for human health (Kobayashi and Shimizu, 1999). In this study, cobalt content of *H. rufescens* and *M. procera* was found 0.63±0.051 and 0.23±0.010 mg/kg. Our cobalt values were found lower than eight wild edible mushroom species collected from forests of West Macedonia, Greece (0.65–5.74 mg/kg; Ouzouni and Riganakos, 2007).

Nickel is a moderately toxic element. (Flyvholm et al., 1984). In our study, nickel content of *H. rufescens* (41.2±11.3 mg/kg) was found approximately 4.5 times higher than manganese content of *M. procera* (9.0±1.5 mg/kg). In a previous study, nickel content of eight mushroom species of Turkish origin has been reported to be between 8.2 and 26.7 mg/kg (Mendil et al., 2004).

Copper is a necessary element in many chemical reactions for both plants and animals. This mineral, which is found in many important enzymes, has a vital importance (Ravesteyn, 1944). Copper content of *H. rufescens* (52.7±4.4 mg/kg) was found lower than that of copper content in *M. procera* (96.3±6.9 mg/kg). It was reported that the copper content of 12 different mushroom samples collected from polluted and unpolluted locations (in Tokat, Turkey) was between 12 and 181 mg/kg (Tüzen et al., 2003).

Zinc is an essential for the structure and function of myriad proteins, including regulatory, structural and enzymatic' (Frederickson et al., 2000). In this study, zinc content of *H. rufescens* and *M. procera* was found as 57.7±4.3 and 86.4±6.1 mg/kg, respectively. The zinc content of 28 species of edible mushrooms from different sites in the province of Lugo (NW Spain) was reported between 30.00 and 309.8 mg/kg (Alonso et al., 2003).

Selenium is a vital element for human because it is required in biosynthesis of important selenoenzymes (Falandysz, 2008). Selenium content of *H. rufescens* (2.76±0.06 mg/kg) was found lower than selenium content of *M. procera* (3.13±0.10 mg/kg). Selenium content of 142 mushroom samples in Finland was ranged from 0.05 to 37 mg/kg (Piepponen et al., 1983).

^{206}Pb is the end of the decay chain of ^{238}U, the uranium series or radium series. ^{207}Pb is the final step of the Actinium series from ^{235}U. ^{208}Pb is the end of the Thorium series from ^{232}Th (Wetherill, 1963). In a previous study, lead content of 238 samples of 28 species of edible mushrooms collected from different sites in the province of Lugo (NW Spain) was reported between 0.35 and 4.1 mg/kg (García et al., 2009). In our study, all lead isotopes (Pb-206, Pb-207, Pb-208) content of *M. procera* were found higher than the lead isotopes content of *H. rufescens*.

Trivalent chromium, found in most foods and nutrient supplements, is an essential nutrient with very low toxicity (Baruthio, 1992). In literature, chromium content of eight different species of wild edible mushrooms growing in Epirus (Ioannina) and West Macedonia (Grevena, Kastoria), regions of Greece were reported between 0.41 and 13.1 mg/kg (Ouzouni et al., 2007). However, in our study, chromium content of *H. rufescens* and *M. procera* was found very low levels (0.093±0.003 and 0.038±0.002mg/kg, respectively).

Arsenic is a chemical element which raises much concern in terms of the environmental effect. (Vetter, 2004). Arsenic content of *H. rufescens* and *M. procera* was found very close to the each other (0.029±0.002 and 0.026±0.002mg/kg, respectively) and the arsenic content of mushrooms was not significantly different ($p>0.05$) from each other by Duncan's multiple range test. In a previous study, the arsenic contents of 162 fruit body samples of 37 common edible mushroom taxa were analyzed and it was reported that very low [lower than 0.05 mg/kg dry matter (DM)] concentrations were found in the samples of 13 taxa, while higher (or very high) contents were quantified in other common taxa (the highest arsenic content was recorded in the fruit body of *Laccaria amethysthea* at 146.9 mg/kg DM) (Vetter, 2004).

Cadmium, is extremely toxic to humans as well as plants. Cd flow to humans is more through cereals, fruits, vegetables and other edible plant parts than through meat (muscles) (Prasad, 1995). However, like arsenic, cadmium content of our mushrooms (*H. rufescens* and

M. procera) was found very low level (0.26±0.011 and 0.61± 0.035 mg/kg, respectively). In a previous review study, cadmium contents of 88 samples of mushrooms were reported ranged in 0.28–86mg/kg (Vetter, 1994).

Consequently; all of the toxic element concentrations (Cr, Cd, As) were low and below the world average in both mushroom species (Kalač and Svoboda, 2000).

4. Conclusions

In this study; 14 different metal (Mg, Al, Ca, Cr, Mn, Fe, Co, Ni, Cu, Zn, As, Se, Cd, ^{206}Pb, ^{207}Pb and ^{208}Pb) contents in two different wild-growing edible mushroom species (*H. rufescens*, *M. procera*), collected from Kastamonu forest (in Turkey) in October of 2014 were investigated. The results showed that metal contents in *M. procera* were higher than the metal contents in *H. rufescens* except Al and Mn. In this case, it can be said that metal accumulation changes with respect to mushroom species. All the toxic element concentrations (Cr, Cd, As) were low and below the world average in both mushroom species. This result has been found satisfactory. Consequently, there was no any health risk associated with the consumption of the analyzed wild edible mushroom species. In order to explain the effect of environmental factors more sophisticated studies should be performed.

Acknowledgements

Many thanks to Prof. Dr. Ertuğrul Sesli who identified the mushroom species.

Kaynaklar

Alonso J., García M., Pérez-López M., and Melgar M. (2003). The concentrations and bioconcentration factors of copper and zinc in edible mushrooms. *Archives of Environmental Contamination and Toxicology*,44(2), 180-188.

Baruthio F. (1992). Toxic effects of chromium and its compounds. *Biological Trace Element Research*, 32(1), 145-153.

Cocchi L., Vescovi L., Petrini L.E., and Petrini O. (2006). Heavy metals in edible mushrooms in Italy. *Food Chemistry*, 98(2), 277-284.

Crichton R.R., Wilmet S., Legssyer R., and Ward R.J. (2002). Molecular and cellular mechanisms of iron homeostasis and toxicity in mammalian cells. *Journal of Inorganic Biochemistry*, 91(1), 9-18.

Çayır A., Coşkun M., and Coşkun M. (2010). The heavy metal content of wild edible mushroom samples collected in Çanakkale Province, Turkey. *Biological Trace Element Research*, 134(2), 212-219.

Falandysz J. (2008). Selenium in edible mushrooms. *Journal of Environmental Science and Health Part C*, 26(3), 256-299.

Flyvholm M.-A., Nielsen G.D., and Andersen A. (1984). Nickel content of food and estimation of dietary intake. *Zeitschrift für Lebensmitteluntersuchung und-Forschung A*, 179(6), 427-431.

Frederickson C. J., Suh S.W., Silva D., Frederickson C.J., and Thompson R. B. (2000). Importance of zinc in the central nervous system: the zinc-containing neuron. *The Journal of Nutrition*, 130(5), 1471S-1483S.

Garcia M., Alonso J., Fernández M., and Melgar M. (1998). Lead content in edible wild mushrooms in northwest Spain as indicator of environmental contamination. *Archives of Environmental Contamination and Toxicology*, 34(4), 330-335.

García M.Á., Alonso J., and Melgar M.J. (2009). Lead in edible mushrooms: levels and bioaccumulation factors. *Journal of Hazardous Materials*, 167(1), 777-783.

Grubbs R.D., and Maguire M. E. (1986). Magnesium as a regulatory cation: criteria and evaluation. *Magnesium*, 6(3), 113-127.

Institute of Medicine (2001). Dietary reference intakes for vitamin a, vitamin k, arsenic, boron, chromium, copper, iodine, iron, manganese, molybdenum, nickel, silicon, vanadium, and zinc. Retrieved from https://doi.org/10.17226/10026.

Kalač P., and Svoboda L.R. (2000). A review of trace element concentrations in edible mushrooms. *Food Chemistry*, 69(3), 273-281.

Kobayashi M., and Shimizu S. (1999). Cobalt proteins. *European Journal of Biochemistry*, 261(1), 1-9.

Liu K., Xiao X., Wang J., Chen C.Y.O., and Hu H. (2017). Polyphenolic composition and antioxidant, antiproliferative, and antimicrobial activities of mushroom *Inonotus sanghuang*. *LWT-Food Science and Technology*, 82, 154-161.

Manzi P., Aguzzi A., and Pizzoferrato L. (2001). Nutritional value of mushrooms widely consumed in Italy. *Food Chemistry*, 73(3), 321-325.

Mendil D., Uluözlü Ö.D., Hasdemir E., and Çağlar A. (2004). Determination of trace elements on some wild edible mushroom samples from Kastamonu, Turkey. *Food Chemistry*, 88(2), 281-285.

Michelot D., Siobud E., Doré J.-C., Viel C., and Poirier F. (1998). Update on metal content profiles in mushrooms—toxicological implications and tentative approach to the mechanisms of bioaccumulation. *Toxicon*, 36(12), 1997-2012.

Mleczek M., Niedzielski P., Kalač P., Budka A., Siwulski M., Gąsecka M., Rzymski P., Magdziak Z., and Sobieralski K. (2016). Multielemental analysis of 20 mushroom species growing near a heavily trafficked road in Poland. *Environmental Science and Pollution Research*, 23(16), 16280-16295.

Muszyńska B., Kała K., and Sułkowska-Ziaja K. (2017). Edible mushrooms and their in vitro culture as a source of anticancer compounds. *Biotechnology and Production of Anti-Cancer Compounds*, Springer, 231-251

Muszynska B., Sulkowska-Ziaja K., Wolkowska M., and Ekiert H. (2011). Chemical, pharmacological, and biological characterization of the culinary-medicinal honey mushroom, *Armillaria mellea* (Vahl) P. Kumm.(Agaricomycetideae): a review. *International Journal of Medicinal Mushrooms*, 13(2), 167-175.

Müller M., Anke M., and Illing-Günther H. (1997). Aluminium in wild mushrooms and cultivated *Agaricus bisporus*. *Zeitschrift für Lebensmitteluntersuchung und-Forschung A*, 205(3), 242-247.

Ouzouni P., and Riganakos K. (2007). Nutritional value and metal content profile of Greek wild edible fungi. *Acta Alimentaria*, 36(1), 99-110.

Ouzouni P. K., Petridis D., Koller W.-D., and Riganakos K.A. (2009). Nutritional value and metal content of wild edible mushrooms collected from West Macedonia and Epirus, Greece. *Food Chemistry*, 115(4), 1575-1580.

Ouzouni P.K., Veltsistas P.G., Paleologos E.K., and Riganakos K.A. (2007). Determination of metal content in wild edible mushroom species from regions of Greece. *Journal of Food Composition and Analysis*, 20(6), 480-486.

Piepponen S., Liukkonen-Lilja H., and Kuusi T. (1983). The selenium content of edible mushrooms in Finland. *Zeitschrift für Lebensmittel-Untersuchung und Forschung*, 177(4), 257-260.

Prabu M., Kumuthakalavallia R. (2016). Antioxidant activity of oyster mushroom (*Pleurotus florida* [Momt.] Singer) and milky mushroom (*Calocybe indica* P and C), *International Journal of Current Pharmaceutical Research*, 8(3), 1-4.

Prasad M. (1995). Cadmium toxicity and tolerance in vascular plants. *Environmental and Experimental Botany*, 35(4), 525-545.

Ravesteyn A.H. (1944). Metabolism of copper in man. *Acta Medica Scandinavica*, 118(1-3), 163-196.

Sevindik, M., Eraslan, C. E., and Akgül, H. (2015). Determination of Heavy Metal Content of Some Macrofungi Species. *Journal of Forestry*, 11(2), 48-53.

Sun L., Chang W., Bao C., and Zhuang Y. (2017). Metal Contents, bioaccumulation, and health risk assessment in wild edible boletaceae mushrooms. *Journal of Food Science*, doi: 10.1111/1750-3841.13698

Tüzen M., Turkekul I., Hasdemir E., Mendil D., and Sari H. (2003). Atomic absorption spectrometric determination of trace metal contents of mushroom samples from Tokat, Turkey. *Analytical Letters*, 36(7), 1401-1410.

Vetter J. (1994). Data on arsenic and cadmium contents of some common mushrooms. *Toxicon*, 32(1), 11-15.

Vetter J. (2004). Arsenic content of some edible mushroom species. *European Food Research and Technology*, 219(1), 71-74.

Wani B. A., Bodha R., Wani A. (2010). Nutritional and medicinal importance of mushrooms. *Journal of Medicinal Plants Research*, 4(24), 2598-2604.

Wetherill G. (1963). Discordant uranium-lead ages: 2. Disordant ages resulting from diffusion of lead and uranium. *Journal of Geophysical Research*, 68(10), 2957-2965.

The Effect of Fiber Orientation in The Middle Layer on Some Technological Properties of Parallel Strand Lumber (PSL)

Hasan OZTURK[1], Abdullah Ugur BIRINCI*[2], Cenk DEMIRKIR[2]

[1] Karadeniz Technical University, Arsin Vocational School, Materials and Material Processing Technologies, Trabzon, Turkey; hasanozturk@ktu.edu.tr

[2] Karadeniz Technical University, Department of Forest Products Engineering Kanuni Campus, 61080 Trabzon, Turkey; ugurbrnc61@gmail.com, cenk@ktu.edu.tr

* **Corresponding Author:** ugurbrnc61@gmail.com

Abstract

Parallel strand lumber (PSL) is a composite made of oriented wood strands that have been glued and compressed together. Its market share in the residential construction industry is considerable, being used primarily as main load bearing members such as beams and columns. In this study, it was examined that the effect of fiber orientation in the middle layer on some technological properties of PSL. Scots pine (Pinus sylvestris L.) was used as wood specie; fenol formaldehyde (FF) resin was used as adhesive. For this aim, three types of 3-layered PSL panels were produced as parallel, perpendicular and 45˚ to the fiber. Specific gravity, equilibrium moisture content, shear strength, bending strength and modulus of elasticity of PSL panels were determined according to TS EN 323-1, TS EN 322, TS EN 314-1 and TS EN 310, respectively. As a result of the study, the highest mechanical strength values were obtained from the PSL panels produced as parallel to the fiber while the lowest values were obtained from the PSL panels produced ad perpendicular to the fiber.

Keywords: PSL, Fiber Orientation, Technological Properties, Scots Pine.

1. Introduction

The products made of wood and wood in the development of human life and culture have taken an important place since and today. The molecular, chemical and microscopic properties of the wood enable it to be used for a variety of purposes. In addition to these properties, the fact that it has a fibrous structure has led to high strength and flexibility in engineering applications. In addition, it has been the reason why it is preferred in terms of isolation characteristics (Öztürk and Arıoğlu, 2006).

The use of solid wood materials in large and curved elements in one piece is not suitable both for resistance properties and economically. Due to defects in the natural structure of the wood material such as snag, rotten, crack and fiber curvature in the production of large massive solid carrier elements, the use of one piece solid wood material creates difficulties. This necessitates the removal of these defects or the use of quality materials. Since the use of solid material as a single piece in the production of curved carrier wooden elements increases the rate of waste, it also increases the cost and is not economical. In addition, due to diagonal cutting of the fiber resistance values are also reduced (Çolakoğlu, 2010). Along with the rapid population growth, urbanization and developing technology in the world, the consumption of forest products due to economic, social and cultural developments is increasing and the existing wood raw material cannot meet the needs of the industry. The increase in the use of wood materials due to industrial development in the world creates difficulties in supplying wood raw materials. As a result, it provides the rational use of wood in the most economical way (Çakıroğlu and Aydın, 2012).

The glued laminated wood materials formed as a result of the gluing of small wood materials eliminated many negative aspects of traditional wood material and became a more efficient and more functional building material. In small openings and large span gaps in structural systems, it is generally used in layered wood materials besides the use of reinforced concrete, metal and plastic materials. Nowadays, especially in structures, lattice systems, beams, columns, frames, belts and so on. in the form of glued laminated wood material is converted (Altunkaya, 2007; Hekimoğlu, 2014).

According to ASTM D5456 - 99a (2001) standard, the PSL is a material consisting of a plurality of pieces of fiber glued together and parallel to the length axis of the product. The United States is manufactured in two and one factory in Canada. It is a composite (composite) material produced in commercial timber dimensions by gluing the pieces of the coating into

large pieces and gluing them parallel to each other. The endless belt coating obtained from the coating peeling machines is cut into pieces by cutting about 20 mm wide in the form of strips. The dimensions of the covering strips are at least 600 mm long according to the relevant standard. Adhesives such as phenol formaldehyde glue, which are generally waterproof and water resistant, are used. In North America, it is generally produced from some coniferous trees and tulip tree logs (Çolakoğlu, 2010).

There are many factors that determine the technological properties of layered wood materials such as plywood, LVL, PSL. These; the ones related to the type of wood used (density, fiber structure, knot amount, moisture etc.), those related to the glue used (type of glue, amount of glue, etc.) and those related to pressing (press pressure, press temperature, press time), (Bal et al., 2015).

In this study, it is aimed to investigate the effect of fiber orientation on some technological properties in the middle layer of PSL panels from wood engineering products used in the structure. For this purpose, PSL panels produced three types of PSL panels perpendicular to the fibers, parallel to the fibers and 45˚ degrees to the fibers.

2. Material and Method

The logs used in this study were obtained from the directorates of the General Directorate of Forestry. Yellow pine (Pinus silvestris), which is one of the most widely used coniferous wood species, was chosen as tree species. When choosing the logs to be used in the production of peelings, logs with a diameter of at least 35 cm, cylindrical form, smooth fibers, no knots and no discoloration and no wood of reaction were preferred. In order to ensure that the technological properties investigated in the study are as homogeneous as possible in all the test sheets, the coatings to be used in the plate production are obtained from a single tree for each tree type. The yellow pine was steamed for 12-16 hours before the peeling process and then peeled off.

The production of the veneer was carried out at the Plywood Pilot Facility in the Department of Forest Industrial Engineering at the Karedeniz Technical University. For this purpose, a peeling machine with a length of 80 cm and a diameter of up to 40 cm was used. During the peeling process, the horizontal aperture was set as 85% of the coating thickness and the vertical opening was 0.5 mm. Produced peeling coatings; In the coating drying machine, they were subjected to drying process at a temperature of 110 ° C, which is widely used in

industrial conditions, at a temperature of 4-7%. Coatings subjected to drying; With the help of a guillotine knife, strip coatings having a width of approximately 2 mm were obtained.

Phenol Formaldehyde glue with 47% solids content was used in the production of trial panels. 4-cylinder gluing machine is used for gluing strip coating boards. The glue solution was applied to the surface of the panels to be 160 gr/m^2.

Pressing of panels; laboratory type pressing area 70x89 cm and electrically heated single-layer hydraulic press is made. Press temperature is set to 140 ° C. Press pressure is selected as 8 kg/m^2 for wood type. Pressing time, according to the method used widely in industry; each mm. thickness of 2 mm for 1 minute; The laminated wood materials produced after the pressing process are stacked in a row and without stacking stack in order to eliminate the temperature and humidity differences between the inner and outer layers. The PSL plates produced in this way have been tried to be prevented from being deformed by gradually cooling. The groups formed within the scope of the study are shown in Table 1.

Table 1. Information about the groups formed within the scope of the study

Group Name	Fiber Direction
A	Parallel
B	Perpendicular
C	45°

Specific gravity, equilibrium moisture content, shear strength, bending strength and modulus of elasticity of PSL panels were determined according to TS EN 323-1, TS EN 322, TS EN 314-1 and TS EN 310, respectively.

3. Results

The tensile-shear strength, bending strengths, elasticity modulus, specific gravity and equilibrium moisture content values are given in Table 2.

Table 2. Average values of some technological properties of the panels produced.

Group Name	Tensile-Shear Strength (N/mm^2)	Bending Strengths (N/mm^2)	Elasticity Modulus (N/mm^2)	Specific Gravity (g/cm^3)	Equilibrium Moisture Content (%)
A	4,44 0,60*	117,05 10,34*	8235 807*	0,656 0,04*	7,15 0,37*
B	1,49 0,14*	78,04 9,99*	8161 913*	0,545 0,13*	7,50 0,23*
C	1,62 0,17*	79,29 10,40*	6177 370*	0,546 0,02*	7,16 0,23*

* Standard deviation

According to Table 2, the highest values of tensile-shear strength, bending strength, modulus of elasticity and specific gravity values of the panels produced were obtained from Group A panels. Only in the modulus of elasticity; The result of group B was close to Group A. However, it was observed that the results of B and C groups gave similar values to other resistance characteristics. Equilibrium moisture content values were similar between the groups.

4. Discussion

When the results obtained in the study were examined, it was seen that the mechanical properties of the PSL panels (A) prepared in parallel with the strips of the strip coatings were higher than the other groups. The lowest mechanical resistance values were determined by the PSL panels (C), which were prepared diagonally with the fibers of the strip coatings. It is expected that the fibers of PSL panels belonging to Group A will be produced in parallel to each other and their technological properties will be similar to LVL panels. In the literature, it has been shown that LVL panels give higher tensile-shear strength values compared to other panels, because the adhesive used increased the cohesive force of wood between the smooth fibrous lamellae of LVL panels (Dallı, 2005). In this study, the specific gravity of this group was found to be high. It is reported in the literature that the tensile-shear strength is also improved as the specific gravity of wood increases (Aydın, 2004; Örs et al., 2002). In this context, the tensile-shear strength values of this group with high specific gravity values are also expected to be high. It is known that the change in the specific gravity of the panels, which vary depending on the specific gravity of the wood, has a significant effect on the adhesion resistance

and it is stated that high plate density provides high adhesion resistance (He et al., 2007; Demirkır, 2012). Considering that the increase in tensile-shear strength also improves other mechanical properties; It can be expected that the bending strength of the A group panels, which give better tensile-shear strength values, may be higher (Cırrık, 2018). It is stated that the panels, which are not properly glued and which do not have good adhesion, will show low bending strength (Demirkır, 2012).

The use of engineered wood materials is very important for the efficient and economical utilization of natural resources. The production of layered wood materials can be easily controlled. The use of dry wood material and the processing of the material after the defects are cleared during the production have great effect on the physical and mechanical properties of the product. PSL, which is a layered wood material, is an economical product and cheaper than steel beam or other engineered wood material and is generally the preference of investors for industrial and commercial buildings. PSL can be produced locally in the workplace or in construction where heavy construction is not possible. It is the ideal building material for poor soil and low maintenance costs. The use of new production techniques, types of adhesive and wood materials has begun to increase the use of these products in the construction sector and in other areas. In order to introduce this product, which is not known in our country and which is not produced in series, to the forest industry, it is necessary to make market prediction, to determine the physical, mechanical and technological properties of the mass production in order to promote the production, and to be made available as an alternative material in earthquake resistant housing construction.

References

Altunkaya, P. (2007). The facilities of using glued laminated timber structural systems in architectural field. Master Thesis, Karadeniz Technical University, , Trabzon.

ASTM D5456-99a, (2001). Standard Specification for Evaluation of Structural Composite Lumber Products, ASTM International, West Conshohocken, PA.

Aydın, İ. (2004). The effects of some manufacturing conditions on wettability and bonding of veneers obtained from various wood species, Doctoral Thesis, Karadeniz Technical University, , Trabzon.

Bal, B. C., Gündeş, Z. and Akçakaya, E. (2015). Screw Withdrawal Strength of Plywood Produced From Poplar, Beech and Eucalyptus Veneer, Kahramanmaras Sutcu Imam University Journal of Engineering Sciences, 18(2), 77-83.

Cırrık, Ö. (2018). The effect of layer orientation on some technological properties of plywood and LVL produced poplar, pine and spruce. Master Thesis, Karadeniz Technical University, , Trabzon.

Çakıroğlu, E. O. ve Aydın, İ. (2012). The Usage of Birch Wood in Plywood Manufacturing As Alternative To Beech Wood. Kahramanmaras Sutcu Imam University Journal of Engineering Sciences,, Special Issue, 50-55.

Çolakoğlu, G. (2010). Ahşap Laminasyon Teknolojisi Ders Notları. Karadeniz Technical University, , Trabzon.

Dallı, G. (2005). The research of laminated veneer lumber manufacture possibilities in Turkey and its technological properties. Master Thesis, Istanbul University, İstanbul.

Demirkır, C. (2012). Using posibilities of pine species in turkey for structural plywood manufacturing. Doctoral Thesis, Karadeniz Technical University, , Trabzon.

He, G., Yu, C. and Dai, C. (2007). Theoretical modeling of bonding characteristics and performance of wood composites. Part III. Bonding Strength Between Two Wood Elements. Wood and Fiber Science, 39(4), 566-577.

Hekimoğlu, V. (2014). Production feasibility of nanoclay added cross laminated timber manufactured by using fir and pine woods. Master Thesis, Karadeniz Technical University, , Trabzon.

Örs, Y., Çolakoğlu, G., Aydın, İ. and Çolak, S. (2002). Comparıson of Some Technıcal Propertıes of Plywood Produced From Beech, Okoume and Poplar Rotary Cut Veneers in Dıfferent Combınatıons. Journal of Polytechnic, Vol: 5 No: 3 pp. 257-265,

Öztürk, R. B. ve Arıoğlu, N. (2006). Mechanical properties of laminated wood beams produced from Turkish pinus silvestris. Journal of İTÜ, Vol: 5 No: 2 pp. 25-36

TS EN 323-1, Wood- Based panels- Determination of density, TSE, Ankara

TS EN 322, Wood-based panels- Determination of moisture content, TSE, Ankara

TS EN 314-1, Plywood-Bonding quality-part 1: Test methods, TSE, Ankara

TS EN 310, Wood- Based panels- Determination of modulus of elasticity in bending and of bending strength, TSE, Ankara

Comparison of Some Technological Properties of Plywood Produced From Beech and Plane Rotary Cut Veneers In Diffirent Combinations

Semra COLAK[1], Okan ILHAN[1*], Gursel COLAKOĞLU[1]

[1]Karadeniz Technical University, Department of Forest Products Engineering Kanuni Campus, 61080 Trabzon, Turkey

[*]**Corresponding Author:** okan.ilhan_93@hotmail.com

Abstract

Plywood is usually used in the production of the some common species such as beech, alder, poplar, spruce, pine, okume, tetra, ozigo and other tropic species. Because of the beech tree is often used species in our country brings the high cost of raw material supply. Therefore, the use of different tree species, emphasizes the necessity to manufacture plywood. In this study, the specific gravity, shear strength, bending strength and modulus of elasticity values of three-layer-plywood panels produced from beech (*Fagus orientalis*, *Lipsky*) and panels (*Platanus orientalis*) rotary cut veneers by using phenol formaldehyde glue in different combinations were determined and compared. Specific gravity, equilibrium moisture content, shear strength, bending strength and modulus of elasticity of plywood panels were determined according to TS EN 323-1, TS EN 322, TS EN 314-1 and TS EN 310, respectively. As a result; the specific gravity, shear strength, bending strength and modulus of elasticity of beech plywood panels were higher than those of panels. The mechanical strength values of plywood panels having beech veneers as outer layers were higher and those of having panels as outer layers wasthe lowest

Keywords: Plane, Beech, Plywood, Combination, Technological Properties

1. Introduction

The most important factor affecting the technological properties of plywood is the type of wood used in its production. Many types of wood can be evaluated in plywood production. However, the choice of wood species is important in the production of plywood for general, decorative or construction purposes. Okume, beech and hybrid poplar species are mostly used in the production of general purpose plywood in our country (Çolakoğlu, 2004). In our country, beech (*Fagus orientalis, Lipsky*), which has been evaluated in the plywood industry, has not been found enough in the appropriate diameter and form for the production of peeling coating in recent years, except for those imported from the Commonwealth of Independent States. However, beech plywoods are preferred in many applications. The beech logs have a homogeneous structure, a smooth surface after steaming, a homogeneous color and sufficient resistance properties. However, there are disadvantages such as red heart formation on the rock, long years to come to the cutting age and high costs for plywood production (Çakıroğlu and Aydın, 2011).

Although it is seen in the forests, the Eastern Plane Tree (*Platanus orientalis*), commonly known as the park tree, develops more rapidly than the wood species used in traditional plywood production. As it is known, the plane tree starts to form a smooth and fuller body. Although not used in a wide range of use of wood, furniture, packaging, dry material kegs and small kitchen tools are used in the construction (Derikvand et al., 2013; Örs and Keskin, 2001). There are a number of reasons for considering East Plane as an alternative tree species for plywood production. As is known, plywood is recommended for the production of rotary cut veneer logs should be at least 35 cm in diameter. Beech wood can reach this diameter in about 120 years (Toksoy et al., 2006). Not only the form of logs taken from trees, but also other features are important for plywood production. These include color, permeability, surface condition after steaming, wettability and adhesion properties. The physical and mechanical properties of the plywood, on the other hand, depend more on the properties of the wood used in its production. It is recommended that the specific weight of the wood where the coating is produced according to the purpose of use is between certain values. These values are specified for the wood to be used for building plywood specific gravity of the value of 0.41 - 0.55 gr / cm3, decorative plywood inner layers of the wood to be used in the range of 0.32 - 0.45 gr / cm3 should be specified for the coating (Çolakoğlu, 2004). With a specific gravity of 0,58 gr / cm3, the sycamore can be included in the class of wood species which can be used in plywood production in terms of specific gravity (Örs and Keskin, 2001; Demirkır et al., 2013).

In this study, it was aimed to compare some technological properties of 3 layer plywood boards produced in four different combinations using beech (*Fagus orientalis, Lipsky*) and plane (*Platanus orientalis*) peeling coatings and phenol formaldehyde (FF) glue.

2. Material and Method

Before peeling, the logs were steamed at 60-70 ° C for 20 hours. For the production of plywood slabs in accordance with the purpose of working from the steam logs, the Eastern plane (*Platanus orientalis*) and Eastern beech (*Fagus orientalis, Lipsky*) logs were peeled in 2 mm thickness with industrial peeling machine. The 50x 50 cm peeling coatings were dried in the coating dryer until they reached 4lam7% range. For the production of plywood sheets, phenol formaldehyde glue (FF) was used as the glue type with 47% solids. During the gluing process, 160 g of glue was applied to the m 2. Plywoods are produced as 3 sheets of 500x500x2 mm dimensions and 2 sheets for each group. Table 1 shows the information for the groups. In the pressing process, the hot press pressure was 12 kg / cm2, the press temperature was 140 ° C, and the pressing time was 6 minutes for each group.

Table 1. Information about the groups formed within the scope of the study.

Group	Outer layer	Middle Layer
A	Beech	Beech
B	Plane	Plane
C	Beech	Plane
D	Plane	Beech

The test plates were conditioned at 20 ° C and 65% relative humidity to ensure that they reach the balance moisture before the test. Some of the technological properties of the plywood slabs are investigated. According to TS EN 314 (1998) and TS EN 310 (1998) standards for plywood, tensile-shear strength, bending strength and elasticity module, according to TS EN 322 (1999) standards, according to TS EN 323-1 (1999) standards specific gravity values were determined.

3. Results

The tensile-shear strength, bending strengths, elasticity modulus, specific gravity and equilibrium moisture content values of the experiment plywood are given in Table 2.

Table 2. Average values of some technological properties of the plates produced.

Group Name	Pull-Shear Resistance (N/mm^2)	Bending Resistance (N/mm^2)
A	2,36 0,38*	140,17 9,25*
B	1,34 0,15*	40,15 5,75*
C	1,73 0,25*	107,47 10,95*
D	1,49 0,18*	54,42 10,86*

*Standard deviation

According to Table 2, the highest values of tensile-shear strength, bending strength, modulus of elasticity and specific gravity values of the plates produced were obtained from Group A plates. Group A boards are respectively; C, D and B groups were followed. Equilibrium moisture content values were similar between the groups.

4. Discussion

When the results obtained from the study were examined, it was seen that the mechanical properties of plywood (A) produced completely from wood were higher than the other groups. It was determined that the lowest mechanical resistance values were made by plywoods (B) which were produced completely. It was determined that the plywoods (C) whose outer layers were made of beech and the middle layer of sycamore gave the highest values after all of the slabs produced from beech. The reason for this result is that these groups have high specific gravity. It is stated that the adhesion resistance and other mechanical properties of the plywood produced from wood species with high specific gravity will be high (Bozkurt and Erdin, 1992). It is reported in the literature that the adhesion resistance increases due to the density of wood (Chow and Chunsi, 1979; Namara and Waters, 1970).

When the tensile-shear strength values of the boards produced from beech and sycamore plywood and their combinations are examined, it is known that the plywoods used in the structure according to DIN 68705-3 (2003) have a minimum bond strength of 1 N / mm². Therefore, it is seen that the sheets produced are at the value of the adhesion resistance according to the standard values. Similarly, the bending resistance values of the boards exceed the limit value of 40 N / mm² in DIN 68705-3 (2003). It is seen that all produced groups provide the specified value (34.47 N / mm2) for the bending strength in form showing the mechanical properties of the structural plywood boards prepared by APA (APA, 2010). The values obtained were determined to be 5000 N / mm2, which is determined as the lower limit value of the modulus of elasticity for plywood thicknesses between 6-12 mm according to DIN 68705-3 standard. In our country, it is a known fact that beech wood is generally used in the production of layered wood materials. In the plywood sector, the use of beech wood often brings problems such as raw material supply and cost. For this reason, it should be emphasized that the sycamore, which is one of the wood species which is close to the mechanical properties and appearance, should be used in the production of plywood. Most plywood factories in our country do not have enough information about the plane tree. Together with these works, the interest of these factories in the plane tree should be increased and the use of this wood species should be encouraged in the production of plywood. Even if not entirely from the roof, the high cost of beech can be reduced with different combinations while the plate drafts are formed. While the cost is reduced, the necessary technological features can be provided with these combinations.

References

APA, 2010. The Engineered Wood Association. Technical Topics. Form No: TT-044B, March.

Bozkurt, Y. ve Erdin, N. (1992). Yoğunluk ile Mekanik Özellikler Arasındaki İlişkiler. ORENKO'92, 1992, Trabzon, I. Cilt, s. 199-222.

Chow, S. and Chunsi, K.S. (1979). Adhesion strength and wood failure relationship in wood-gluebonds, Mokuzai Gakkaishi, 25(2), 125-131.

Çakıroğlu, O. ve Aydın, İ. (2011). Huş Odununun Kayın Odununa Alternatif Olarak Kontrplak Üretiminde Değerlendirilmesi, I. Ulusal Akdeniz Orman ve Çevre Sempozyumu, KSÜ Mühendislik Bilim Dergisi, Özel Sayı, 2012, Kahramanmaraş.

Çolakoğlu, G. (2004). Tabakalı Ağaç Malzeme Ders Notları, K.T.Ü. Orman Fakültesi, Trabzon.

Demirkır, C., Çolakoğlu, G., Çolak, S. and Aydın, İ. (2013). Çınar Ağacının Kontrplak Üretimi İçin Alternatif Bir Tür Olarak Değerlendirilmesi. Düzce Forestry Journal, 9(2), 9-13.

Derikvand, M.,Smardzewski, J., Ebrahimi, G., Dalvand, M.andMaleki, S. (2013). With drawal force capacity of motrise and loosetenon T-type furniture joints. Turk. J. Agric. For., 37, 377-384.

DIN 68705-3, (2003). Yapı Kontrplakları, Alman Standartları Enstitüsü, Verlag.

Namara, U.S. andWaters, O. (1970). Comparison of the rate of glue line strength development for oak and maple.ForestProductsJournal, 20(3), 34-35.

Örs, Y. ve Keskin, H. (2001). Ağaç Malzeme Bilgisi. Atlas Yayın Dağıtım Ltd. Şti., ISBN: 975-6574-01-1, Ankara.

Toksoy, D., Çolakoğlu, G., Aydın, İ., Çolak, S. and Demirkır, C. (2006). Technological and economic comparison of the usage of beech and alder wood in plywood and laminated veneer lumber (LVL) manufacturing.Buildingand Environment, 41(7), 872-876.

TS EN 323-1, Wood- Based panels- Determination of density, TSE, Ankara.

TS EN 322, Wood-based panels- Determination of moisture content, TSE, Ankara.

TS EN 314-1, Plywood-Bonding quality-part 1: Test methods, TSE, Ankara.

TS EN 310,Wood- Based panels- Determination of modulus of elasticity in bending and of bending strength, TSE, Ankara.

MAP AND LAND REGISTRY CADASTRE TECHNOLOGY, GEODESY AND PHOTOGRAMMETRY, GEOLOGY

ORAL PRESENTATIONS

Regional Transformation Parameters Determined with Geographic Information Systems Approach: Giresun Example

Ulku KIRICI YILDIRIM[1], YaseminSISMAN[2*]

[1]Ondokuz Mayis University, Department of Engineering, Geomatics Engineering, Samsun, Turkey; ulku.kirici@omu.edu.tr

[2]Ondokuz Mayis University, Department of Engineering, Geomatics Engineering, Samsun, Turkey; ysisman@omu.edu.tr

[*]**Corresponding Author:**ysisman@omu.edu.tr

Abstract

ED50 coordinate system is used in Turkey very long time. However this system need to be renewed with technological development, tectonic movement, the change of measurement method and measurement instruments. For this reason, the TUTGA project was established and the ITRF coordinate system was started to be used. Thus, the coordinate of the old system have to be transformation ITRF coordinate system using coordinate transformation methods. For the coordinate transformation, some mathematical relations have to be defined in both coordinate systems. In this process the common point coordinates which are known in two coordinate system are used as measurements. The coordinate transformation is determined the geometric relation of coordinate system using coordinate transformation parameters. The number of coordinate transformation parameters varies according to the transformation method to be used.

In this study, ground control points in ED50 and ITRF datum in Giresun was used. Transformation parameters were calculated using ground control points which are known the coordinates in two coordinate systems. The similarity transformation method was selected for the ED50 and ITRF coordinates in this study. Transformation parameters calculated regionally. As a result of study, the transformation parameters are applied on Giresun Map using ArcGIS software.

Keywords: Similarity transformation, Transformation parameters, Geographic information systems.

1. Introduction

An object in the earth is transformed into a numerical form by being defined in the coordinate system as one, two and three dimensions. For this process needed the coordinate system of singular defined in the World. Differences can be seen in the defined coordinate systems due to how to define, origin and axis numbers. In this way, there may be situations where different defined coordinate systems can be used in the same works. In this case coordinate transformation is required. Coordinate transformation is calculating the transformation parameters with the help of known common points in both systems. Calculated transformation parameters covered the region where the common points are located. However, as the number of data and the width are increased, the transformation parameters can be calculated for wider areas.

In this study, calculated transformation parameters for each district separately using ED-50 and ITRF coordinates known common points for 9 district of Giresun province.For this transformation, it was selected the similarity transformation which is one of the most frequently used method.Calculated transformation parameters were tested for other regions and correction values and square mean errors were found. All of these studies were done in the Matlab programming language.

2. Coordinate Systems

At the beginning of the new ages new explorations and the discovery of modern continents led to healthier drawings for cartography. Using the map is a mandatory tool for the planning and use of places in the modern and developed societies.

A datum is a reference system or an approximation of the Earth's surface against which positional measurements are made for computing locations. The reference coordinate system is defined to locate a point on the land or map (Uzun, 2003). A coordinate is a linear and angular magnitude that defines a point in a given reference system.

To define a coordinate system;

- Origin
- Orientation
- Units

are necessary to define.

The coordinate systems defined may vary according to their definition, origin and axis numbers. Different coordinate systems have been defined and used in different times in the world and in our country (Kırıcı,2016).

Coordinate systems in our country have changed and developed over time. Country triangulation network in Turkey (TUD-54) creation process has begun in the 1930s and gradually work done in 1950 was transformed into the European datum. All points and sheets are produced according to the ED-50 coordinate system. Technological developments, the fact that our country is in a geography affected by tectonic movements, destruction and various deformations the necessity of renewing the country point coordinates produced in the ED-50 coordinate system has arisen. For this purpose Turkey's National GPS network (TUTGA) was formed. Fixed GPS stations that continuously measure at some TUTGA points were installed. Thus, the TUSAGA-Active (CORS-TR) system was created and the ITRF coordinate system was started to be used.

2.1. Turkey National Vertical Datum 1954 (TUD-54)

Turkey National Triangulation Network study are based on the early 1990's(Ulusoy 1982, Şerbetçi 1999, Ayan et al. 2003). TUD-54 was formed as a result of intensive geodetic studies carried out by the Map General Command throughout in the country between 1934-1954(Fırat and Lenk 2002).

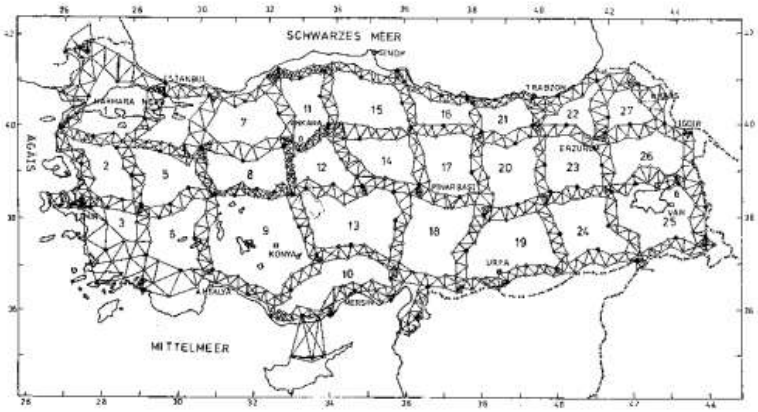

Figure 1. Turkey National Triangulation Network

Referring to Turkey's National Triangulation Network technical data, it seems to be a network connected to the European Datum (ED50). This connection was made with

observations made with 8 common points in the west before adjustment in 1954 (Ayan et al., 2003).

2.2. European Datum 1950 (ED50)

In ED-50 datum; International 1924 Hayford Ellipsoid was taken as reference ellipsoid (a=6378388m; b=6356911.9461m; f=1/297; e=0.08199188998), Greenwich Meridian was taken as prime meridian. In this system, the geoid co-ordinates with the ellipsoid and geodesic and astronomical coordinates are assumed to be based on Helmert point in Postdam / Germany (Fırat and Lenk 2002; Demirtaş, 2006).

In the ED-50 coordinate system, the upper-order network always coordinates the lower-order network. While in the designing phase, Turkey's tectonic structure has been ignored.In other words, despite the changes in the coordinates of the points, they are accepted unchangeable.However, in reality, especially where the tectonic movements are excessive, there has been an average of 2 cm of deterioration. This situation caused the need not to respond(Altıner, 1999; Ayan et al. 2003).A new geodetic network is needed and it is predicted that this network will be based on GPS technology. TUTGA was created with the intensive GPS measurements between 1997 and 1999 and updated with the revision measurements in the following years, designed to meet the need for a modern and highly accurate national network(Ayhan et al., 2002; Aktuğ et al., 2011).

2.3. ITRF

The Global Positioning System (GPS) based on satellite geodesy has begun to be used in geodesy since the late 1980s.Achieving 0.1-0.01 ppm accuracy with GPS ensures that regional and local changes in the current National Fundamental Horizontal Control Network become more visible.Thus there is a need to create a new basic geodetic network.TUTGA (Turkey National Fundamental GPS Network) was formed between Map General Command and General Directorate of Land Registry and Cadaster with the agreement signed in1996. This project have entered into practice after 1999. TUTGA is a network created in the ITRF coordinate system.

In Turkey has used the ED-50 system until 2001; but in 2001 the ITRF coordinate system was started to use in conjunction with GRS80 ellipsoid. ITRF is take the name of the

year when the update is made for example (ITRFyy) ITRF88, ITRF89, ITRF91, ITRF92, ITRF93, ITRF94, ITRF96, ITRF97, ITRF2000, ITRF2005 and ITRF2008. (Kırıcı,2016)

3. Coordinate Transformation

Coordinate transformation is the transformation of points that are known in one coordinate system transform another coordinate system (Turgut and İnal, 2003). For the coordinate transformation, some mathematical relations have to be defined in both systems.While this relation is defined, common points which are known coordinate values are needed in both systems. Coordinate transformation parameters number varies according to the transformation method to be used.Some geometric properties are preserved in both systems (Başçiftçi ve İnal, 2008).

Using transformation methods in nowadays are 2 and 3 dimension of similarity, affine and projective transformation. 2D similarity transformation was used in this study.

3.1. Similarity Transformation

In similarity transformation, before transformation and after transformation forms are similar. Since there is only one scale factor in transformation parameters, forms get smaller or bigger,thus their angle of refraction does not change.In short, the new system; by shifting initial, by generating a certain amount of rotation between the two systems and multiplying by a certain amount of scale factor are create. (Tanık, 2003; Konakoğlu 2014).

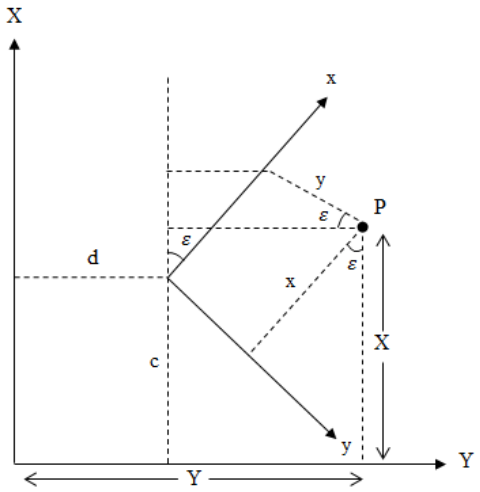

Figure 2. Two orthogonal coordinate systems to be transformed

In similarity transformation, there are a total of 4 parameters which define translation, rotation and scale. Two common points of coordinates are known are required in both systems for the transformation to be meaningful. If there are more than two common points, the transformation parameters calculated using the least square method and correction values can be written twice the number of points (Ceylan, 2009).

Similarity transformation are as follow;

x, y :Coordinate of the first system

X, Y :Coordinate of the second system

ε : Rotation angles between coordinate systems

c, d :Transformation elements

k :Scale factor

$$X = k * x * \cos\varepsilon - k * y * \sin\varepsilon + c$$
$$Y = k * x * \sin\varepsilon + k * y * \cos\varepsilon + d \quad (1)$$

It is written in the form. If it is taken from (1)

$$a = k * \cos\varepsilon$$
$$b = k * \sin\varepsilon \quad (2)$$

equality is obtained.

$$X = a * x + b * y + c$$
$$Y = a * y + b * x + d \quad (3)$$

This equation is written in matrix form as follows.

$$A = \begin{bmatrix} x_1 & -y_1 & 1 & 0 \\ y_1 & x_1 & 0 & 1 \\ .x_2 & -y_2 & 1 & 0 \\ y_2 & x_2 & 0 & 1 \\ \dots & \dots & \dots & \dots \\ \dots & \dots & \dots & \dots \end{bmatrix} X = \begin{bmatrix} a \\ b \\ c \\ d \end{bmatrix} L = \begin{bmatrix} X_1 \\ Y_1 \\ X_2 \\ Y_2 \\ X_3 \\ Y_3 \\ \dots \\ \dots \end{bmatrix} V = \begin{bmatrix} V_{X_1} \\ V_{Y_1} \\ V_{X_2} \\ V_{Y_2} \\ V_{X_3} \\ V_{Y_3} \\ \dots \\ \dots \end{bmatrix} \quad (4)$$

Root Mean Square Error (m_0) calculated as follows;

$$m_0 = \sqrt{\frac{V^T V}{2n-u}} \tag{5}$$

4. Application

In this study was chosen study area as Giresun districts. These districts are Bulancak, Dereli, Duroğlu, Keşap, Piraziz, Şebinkarahisar, Tirebolu, Espiye and Yağlıdere. Firstly, the coordinate of common points provided both ED-50 and ITRF coordinates are known in Giresun district. These points have been processed into ArcGIS program. Then transformation parameters are calculated separately for data groups. These procedure are written Matlab programming language.While transformation parameters calculated, used similarity transformation which is one of most commonly used method.

Calculated transformation parameters are tried instead of each other and calculated of correction values (V) and root mean square errors (m_0).

5. Results and Discussion

Calculated of correction values (V) and root mean square error (m_0) are tabulated.Root mean square errors (m_0) calculated separately for X and Y direction. Finding values are compared. Finally calculated transformation parameters by similarity transformation are processed into the ArcGIS program. (Figure 3)

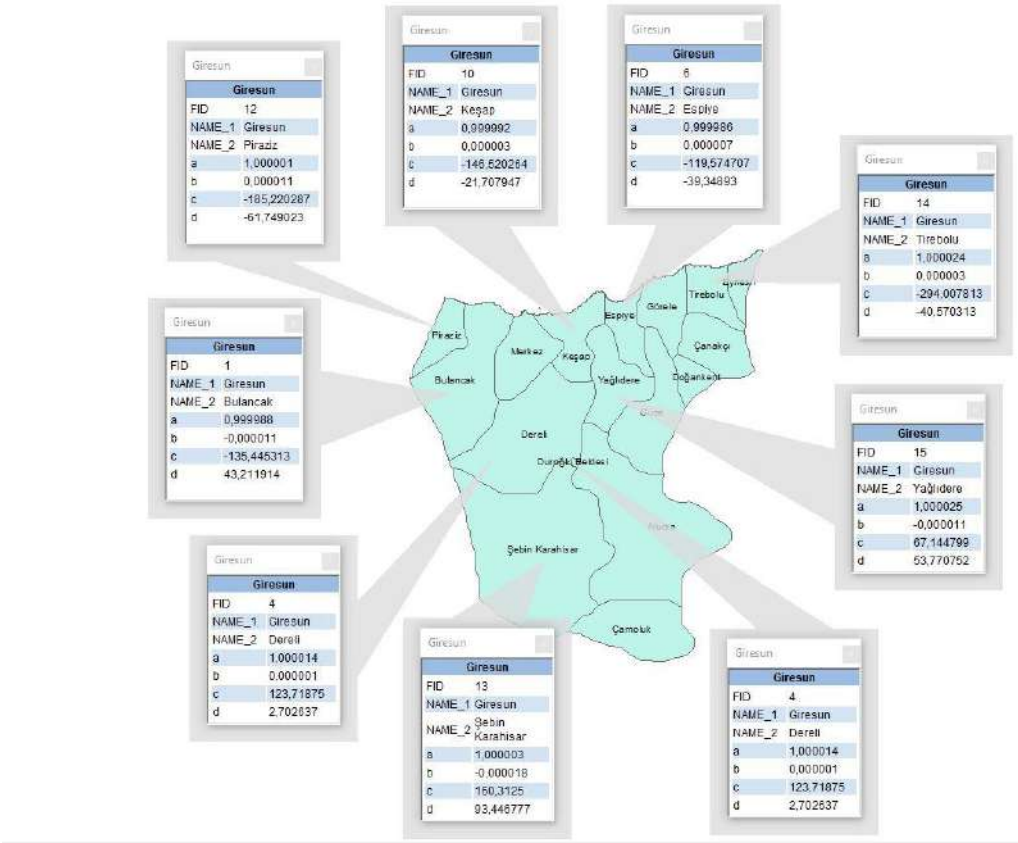

Figure 3. Transformation parameters in Giresun district

Table 1. Root mean square errors calculated in the application.

	Bulancak		Dereli		Duroğlu	
	Ydirection	Xdirection	Ydirection	Xdirection	Ydirection	Xdirection
Bulancak	-	-	24.504	336.864	24.754	336.589
Dereli	27.025	368.249	-	-	0.236	0.098
Duroğlu	21.336	288.130	0.254	0.147	-	-
Keşap	0.321	0.295	20.877	283.619	20.830	283.594
Piraziz	0.098	0.241	26.502	368.922	26.896	368.528
Şebinkarahisar	20.491	278.635	0.474	0.146	0.044	0.646
Tirebolu	0.728	0.487	21.771	296.003	21.525	296.004
Espiye	0.300	0.371	21.570	291.560	21.524	291.616
Yağlıdere	23.191	308.236	0.113	0.050	0.162	0.081

	Keşap		Piraziz		Şebinkarahisar	
	Ydirection	Xdirection	Ydirection	Xdirection	Ydirection	Xdirection
Bulancak	0.304	0.054	0.186	0.036	23.977	335.768
Dereli	26.926	368.531	27.060	368.921	0.351	0.643

Duroğlu	21.088	288.270	21.113	288.439	0.606	0.610
Keşap	-	-	0.111	0.244	20.239	283.157
Piraziz	0.224	0.045	-	-	26.018	367.512
Şebinkarahisar	20.948	278.969	21.363	279.601	-	-
Tirebolu	0.269	0.056	0.028	0.268	20.862	295.698
Espiye	0.076	0.099	0.173	0.376	20.977	291.190
Yağlıdere	22.896	308.614	22.794	308.938	0.747	0.415

	Tirebolu		Espiye		Yağlıdere	
	Ydirection	Xdirection	Ydirection	Xdirection	Ydirection	Xdirection
Bulancak	0.749	0.107	0.477	0.171	24.182	336.570
Dereli	27.518	369.398	26.929	368.359	0.120	0.340
Duroğlu	21.619	288.532	21.022	288.195	0.427	0.181
Keşap	0.180	0.246	0.032	0.035	20.889	283.634
Piraziz	1.274	0.177	0.473	0.138	26.023	368.477
Şebinkarahisar	21.481	280.848	21.109	278.625	0.092	0.564
Tirebolu	-	-	0.300	0.079	21.848	296.241
Espiye	0.268	0.561	-	-	21.676	291.558
Yağlıdere	22.951	308.974	22.920	308.592	-	-

As a result of the finding, it is seen that the transformation parameters of the districts of Bulancak, Keşap, Piraziz, Tirebolu and Espiye are close to each other. Common characteristics of these regions, it is often seen that Giresun cover the coastline and is close to each other as locations.

It is seen that the transformation parameters of the districts of Dereli, Duroğlu, Şebinkarahisar and Yağlıdere are close to each other. Common characteristics of these regions, it is often seen that middle parts of Giresun and is close to each other as locations.

This findings seem that the effective of the transformation parameters is decrease move away from the area.When the data set is increased, this work can also be done for a wider area.

References

Aktuğ B., Seymen S., Kurt M., Parmaksız E., Lenk O., Sezer S., Özdemir S., (2011), ED-50 (European Datum-1950) ile TUREF (Türkiye Ulusal Referans Çerçevesi) Arasında Datum Dönüşümü, Harita Genel Komutanlığı, Ankara.

Altıner Y, Ayan T, Deniz R, Celik RN, Ergun M, Kahveci M, Lenk O, Ocak M, Salk M, Seeger H, Türkezer A (1999) GPS Measurements in Turkey From 1990 to 1997, Third Turkish- German Joint Geodetic Days, 1- 4Haziran 1999, İstanbul

Ayan T., Deniz R., Gürkan O., Öztürk E., Çelik R.N., (2003), Ulusal Jeodezik Referans Sistemleri ve CBS, TUJK 2003 Yılı Bilimsel Toplantısı Coğrafi Bilgi Sistemleri ve Jeodezik Ağlar Çalıştayı, Konya.

Ayhan, M.E., C. Demir ,O. Lenk, A. Kılıçoğlu, B.Aktuğ, M.Açıkgöz, O.Fırat, Y.S.Şengün, A.Cingöz, M.A. Gürdal, A.İ.Kurt, M.Ocak, A.Türkezer, H. Yıldız, N. Bayazıt, M. Ata, Y. Çağlar, A.Özerkan (2002),. Türkiye Ulusal Temel GPS Ağı-1999A (TUTGA-99A), Harita Dergisi Özel Sayı, No.16, Ankara, http://www.hgk.mil.tr/dergi/makaleler/OZEL

Başçiftçi F, İnal C, (2008), Jeodezide kullanılan bazı koordinat dönüşümlerinin programlanması, S.Ü. Müh.-Mim. Fak. Derg., c.23, s.1, 27-40.

Ceylan E. , (2009), Non Sibson Yöntemi İle Lokal Koordinat Dönüşümü, Yüksek Lisans Tezi , İstanbul Teknik Üniversitesi , Fen Bilimleri Enstitüsü , İstanbul , 501071606.

Demirtaş M.Ü.,(2006), Bölgesel Koordinat Dönüşümleri, Yüksek Lisans Tezi, Yıldız Teknik Üniversitesi, Fen Bilimleri Enstitüsü, İstanbul.

Fırat, O. ve Lenk, O., (2002), "Avrupa Datumu 1950 (ED-50) ile Türkiye Ulusal Temel GPS Agı 1999 (TUTGA-99) Arasında Datum Dönüsümü", Hrt. Gn. K.lıgı, Ankara.

Kırıcı Ü., (2016), TUSAGA-AKTİF(CORS-TR) Noktaları İçin Farklı Amaç Fonksiyonlarına Göre Bölgesel Dönüşüm Katsayılarının Elde Edilmesi, Yüksek Lisans Tezi, Ondokuz Mayıs Üniversitesi, Fen Bilimleri Enstitüsü, Samsun.

Konakoğlu B., (2014), Jeodezik Dönüşümlerin İncelenmesi Ve Yazilimlarinin Geliştirilmesi, Yüksek Lisans Tezi, Karadeniz Teknik Üniversitesi, Fen Bilimleri Enstitüsü, Trabzon.

Şerbetçi M (1999) Türk Haritacılığı Tarihi (1895-1995), TMMOB Harita ve Kadastro Mühendisleri Odası, 2. Baskı, İstanbul, 1999.

Tanık, A., (2003). Dönüşümler ve Uygulamaları, Yüksek Lisans Tezi, Yıldız Teknik Üniversitesi Fen Bilimleri Enstitüsü, İstanbul.

Turgut, B., İnal, C., (2003), "Nokta Konum Duyarlıklarının İki ve Üç Boyutlu Koordinat Dönüşümüne Etkisi", TUJK Bilimsel Toplantısı , http://www.harita.selcuk.edu.tr/ arsiv/calistay2003/default.htm.

Tuşat E., Turgut B., GPS İle Bir Ağ Çalışması, Jeodezi, Jeoinformasyon ve Arazi Yönetimi Degisi 2005/2 Sayı:93.

Ulsoy E (1982) Nirengi Ağları Hakkında Genel Açıklamalar, Jeodezi Öğretimi Sempozyumu, S. 15-31, 1982, Trabzon.

Uzun Y., (2003), Üç Boyutlu Astrojeodezik Dik Koordinat Sistemlerinde Dönüşüm Modelleri ve Uyuşumsuz Ölçü Gruplarının Belirlenmesi Yöntemlerinin Karşılaştırılması, Doktora Tezi, Karadeniz Teknik Üniversitesi Fen Bilimleri Enstitüsü, Trabzon.

Yaşayan A (1978) Hava fotogrametrisinde iki boyutlu doğrusal dönüşümler ve uygulamaları, KTÜ yayın no: 102, YBF yayın no:19, Trabzon.

Accessibility of Urban Living Quality Indicators; a Case Study of Giresun

Aziz Sisman[1*], Ridvan Ertugrul Yildirim[2], Atakan KARACA[3]

[1]Ondokuz Mayis University, Faculty of Engineering, Department of Geomatics Engineering, Samsun, Turkey; asisman@omu.edu.tr

[2]Ondokuz Mayis University, Faculty of Engineering, Department of Geomatics Engineering, Samsun, Turkey; ridvan.yildirim@omu.edu.tr

[3]Ordu Metropolitan Municipality, Ordu, Turkey; atakankaraca28@gmail.com

[*]**Corresponding Author:**asisman@omu.edu.tr

Abstract

According to the United Nations, nearly half of the world's population now lives in cities and, it is predicted that 70% of the world's population will live in cities by 2050. Life quality is the major criteria in the crowded urban areas. There is no single definition of urban living quality in the literature. Despite many different definitions, the common side of these definitions is that the quality of life is a multidimensional concept that develops subjective variables and objective variables. Subjective variables can be different according to the individuals but objective variables depend on the education, income, environment, infrastructure, public service buildings, social spaces, green fields, service areas, medical services and transportation services that the city has. The most striking aspect of all these social service is accessibility. It has positive effects for the quality of life in the urban areas.
In the current study, some of urban technical infrastructures' locations such as primary and secondary schools and public medical services are examined using Network Analysis in Giresun city.

Keywords: GIS, Network Analysis, Urban Living Quality, Accessibility.

1. Introduction

The settlement systems in the developed countries are established according to a plan, thus all the settlement units from the small settlement groups to the metropolises area equipped with the social and technical infrastructure in a hierarchical structure. However, in Turkey; especially due to the immigration experienced after the 1960s, cities that had grown up with the plan to that date were exposed to uncontrolled and unplanned growth due to sudden migrations. With this unplanned and uncontrolled growth, the design of the social and technical equipment system proposed in city plans has also been distorted (Ciftci, 1999).

The development process that started in the first years of the Republic of Turkey has become a rapid urbanization process especially since the 1950's. By the 1990's, 29% of all population of the country was concentrated in the five major metropolises; İstanbul, Ankara, İzmir, Bursa, Adana (DPT, 1996 ve Ciftci, 1999). Nowadays, the internal migration movement in Turkey continues without slowing down. As a result of this situaiton, urban tissue development has impaired, urban infrastructure needs have increased and infrastructure investments have been inadequate, especially in the cities receiving immigration. It is also evident in many earthquakes that have been produced houses and other buildings unprepared for earthquakes and other disasters.

The history of the zoning legislation in our country extends to the 19th century, which called "Ebniye Nizamnamesi – 1848". After the foundation of the Republic, it is reflected in the Municipal Buildings and Roads Law in 1933 and the Zoning Law numbered 6785 entered into force in 1957. The State Planning Organization was established in 1960 and Regional Development Plans were prepared for the elimination of imbalances between regions after this period. Zoning Law numbered 6785 has been abolished in 1985 with the Zoning Law numbered 3194 has entered into force. Currently, the Zoning Law numbered 3194 is still in force and it gives direction to the urban planning and development of the country.

According to Article 6 of the Zoning Law No. 3194, the planning stages are defined in two parts in terms of their scope and objectives; these are "Regional Plans" and "Development Plans". Zoning Plans are divided in two parts as "Master Zoning Plans" and "Implementation Zoning Plans". The "Spatial Plans Preparation Regulation" which was published in the Official Gazette on 14.06.2014 and entered into force and this regulation brings the concept of "Spatial Plan" to the foreground. Spatial Plan is defined in the Regulation as "Prepared in accordance with the Zoning Law No. 3194, in terms of area they cover and their purposes, from top to

bottom in order; Spatial Strategy Plan, Environmental Plan, Master Plan and Implementation Plan".

Master Plans and Implementation Zoning Plans shape the physical structure of cities. The minimum sizes of the social and technical infrastructure areas required for the population which live in the cities are defined in the Annex of the Spatial Plans Preparation Regulation. The necessary social and technical infrastructure areas should be provided and they are not below the specified sizes defined in the regulation.

Roads, green spaces/parks, carparks, schools, healthcare facilities, and other public service areas which designed in the implementation plans are the most important of the urban social and technical infrastructure areas and these areas play an important role in establishing better living environments and enhancing the life quality of cities. The quality of urban life has become an important parameter in the concept of urbanization in recent years. The availability of a sufficient number of urban equipment and easy to access by foot or by car to them has become an indicator of the quality of urban life.

In this study, the locations of some social and technical infrastructures such as primary schools, middle schools, high schools and health centers in the study area were analyzed using Geographical Information Systems (GIS) network analysis.

2. Study Area

In the current study, the physical boundaries of the settlement area in Giresun City central district was determined as a study area. Study area was about 965 hectares, it was determined by digitizing from the current satellite image (Figure 1). The road network and the locations of the infrastructural equipment (primary schools, middle schools, high schools and health centers) has been digitized.

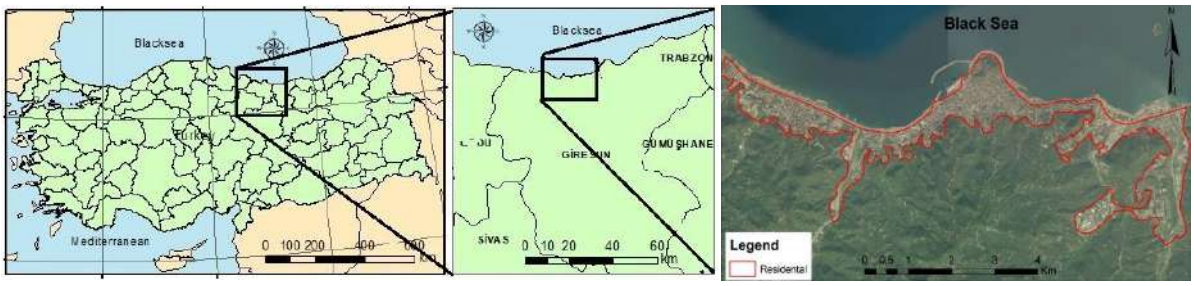

Figure 1. Resident areas of central district of Giresun.

Primary schools, middle schools, high schools and health centers located in the study area were processed with the existing road network. In the study area, 10 primary schools, 12 middle schools, 18 high schools and 14 health centers were identified (Figure 2, 3, 4, 5). It has been observed that the social facilities subject to study were evenly distributed in the working area.

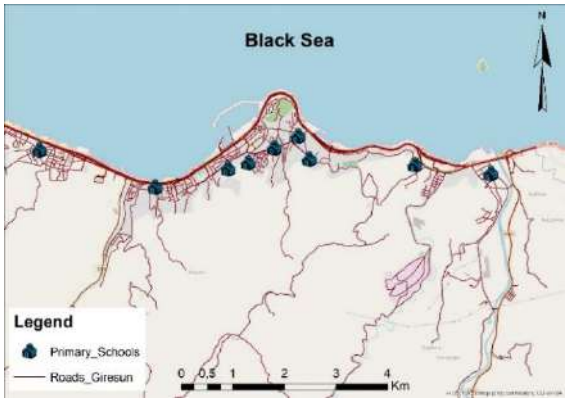

Figure 2. Primary Schools in study area

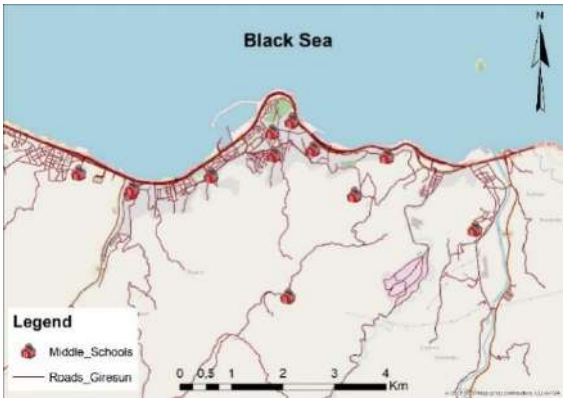

Figure 3. Middle Schools in study area

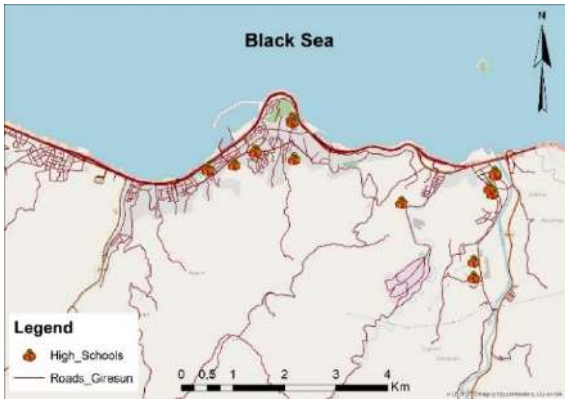

Figure 4. High Schools in study area

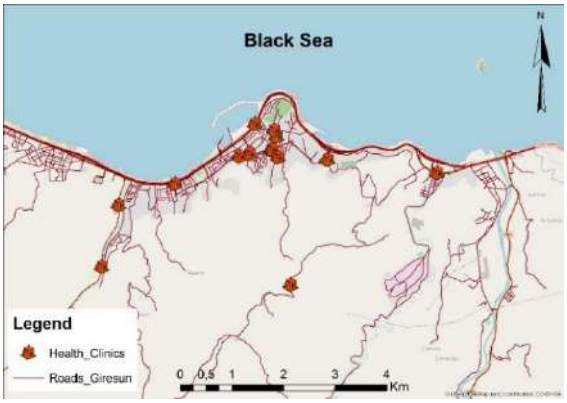

Figure 5. Health Centers in study area

When the legislation about the selection criteria of the school sites in Turkey are covered is examined, a disorganized structure is encountered. The criteria to be considered in the selection of the school place with Zoning Law No. 3194, Spatial Plans Preparation Regulation, Primary Education and Education Law numbered 222, Communiqué titled "Principles on the Establishment and Closure of the Institution of the Ministry of National Education No. 2010/2630", Minimum Design Guide to Educational Constitution (Basegmez et. al., 2017).

Article 12 of the Spatial Plans Preparation Regulation defines walking distances for social facilities.

"(1) Walking distances in zoning plans are determined by considering education, health and green spaces accessible to the population of service domain and topography, constructions, density, existing texture, natural and artificial thresholds. If the particulars specified in this section were appropriate, the minimum walking distances in the second section shall be complied with.

(2) In the zoning plans; considering the distances of 500 meters from children's garden, playground, outdoor sport places, family practice centers, kindergarten, pre-school, primary school, 1000 meters from middle school, 2500 meters from high school, service areas accessible by pedestrians can be planned." It is necessary to act appropriately in the planning stages of these listed issues. (URL 1)

3. Method

3.1. Network Analysis

Network analysis is a spatial analysis based on the links between geographical objects. The line objects used in the network analysis must be connected to each other by node points. These node points are intersection points of line networks used in real life such as, the branches of the rivers, the electric lines, the roads, the railways, the pipelines and the intersections of the telephone lines etc.

Network Analyst can solve common network problems, such as finding the least cost route across a city, finding the closest emergency vehicle or facility, or identifying a service area around a location. Network analysis is one of the analysis types performed with vector based geographic data.

Network analysis has three parts in practice;

• Route optimization

• Address matching

• Resource allocation (Erden et. al., 2003)

Common applications are route finding, route planning, identifying the closest facility by travel time or distance, calculation of service areas (e.g. areas within 10 minute's walk of a bus stop), etc. (Comber et. Al. 2008)

Network analysis is successful in situations such as where the fire brigade and ambulance stations should be located (Özkan and Sisman 2016; Yıldırım and Sisman 2016), ambulances and fire trucks reach the desired point as soon as possible, in times of emergency, where time affects life and even moment is very important.

4. Application

In this study, pedestrian access to the determined urban infrastructure facilities were examined. The pedestrian speeds according to different ages and sexes (Table 1) are specified in the standard titled "Design Rules of Urban Roads - Pedestrian Roads and Pedestrian Areas" of Turkish Standards Institution (TSE) TS 12174 (TSE, 2012). In according to this standard it is stated that it is necessary to take the normal walking speed in the range of 0,5 m/sec <v <2 m/sec and the average walking speed of the pedestrian as (v) 1.4 m/sec. In the study, a pedestrian walking speed of 1.4 m/sec was used in the network analysis. It corresponds to an average fixed speed of 1.4 m/sec, 420 m in 5 minutes, 840 m in 10 minutes.

Table 1. The pedestrian speeds according to different ages and sexes**.**

Pedestrian Type	Speed
Female with child	0,7 m/sec
Child (Between 6-10 ages)	1,1 m/sec
Female (Over 50)	1,3 m/sec
Female (Up to 50)	1,4 m/sec
Male (Over 55)	1,4 m/sec
Male (Between 40-55ages)	1,6 m/sec
Male (Up to 40)	1,7 m/sec
Teenager	1,8 m/sec

All roads and social facilities to be analyzed in the study area were transferred to ArcGIS software and network analysis was performed in accordance with the determined parameters.

a) As a result of examining the locations of primary schools at 5 and 10 minutes walking distance in 965 hectares of study area; 5 minutes walking distance covers 212 hectares, 10 minutes walking distance covers 483 hectares (Figures 6a, 6b).

Figure 6a. Primary Schools 5 min coverage area

Figure 6b. Primary Schools 10 min coverage area

b) As a result of examining the locations of middle schools at 5 and 10 minutes walking distance in 965 hectares of study area; 5 minutes walking distance covers 173 hectares, 10 minutes walking distance covers 419 hectares (Figures 7a, 7b).

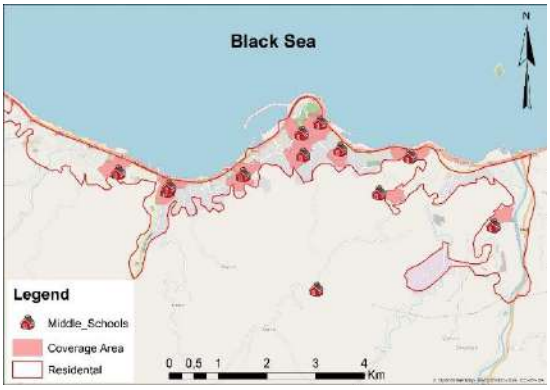

Figure 7a. Middle Schools 5 min coverage area

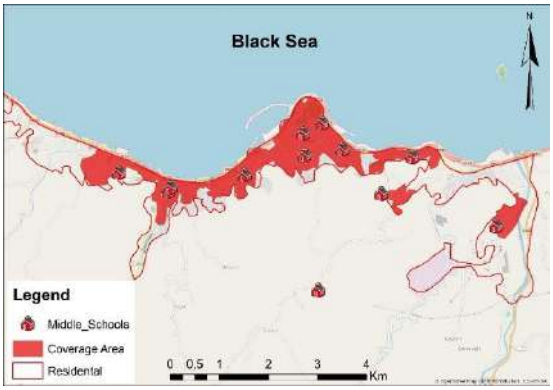

Figure 7b. Middle Schools 10 min coverage area

c) As a result of examining the locations of high schools at 5 and 10 minutes walking distance in 965 hectares of study area; 5 minutes walking distance covers 167 hectares, 10 minutes walking distance covers 360 hectares (Figures 8a, 8b).

Figure 8a. High Schools 5 min coverage area

Figure 8b. High Schools 10 min coverage area

d) As a result of examining the locations of health centers at 5 and 10 minutes walking distance in 965 hectares of study area; 5 minutes walking distance covers 192 hectares, 10 minutes walking distance covers 364 hectares (Figures 9a, 9b).

Figure 9a. Health Centers 5 min coverage area

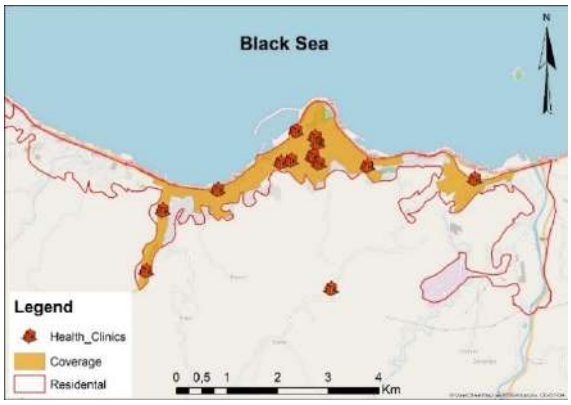

Figure 9b. Health Centers 10 min coverage area

Table 2. A summary of the coverage areas of the identified social facilities areas**.**

	5 minutes walking		10 minutes walking	
	Area (ha)	%	Area (ha)	%
Primary Schools	212	22	483	50
Middle Schools	173	18	419	43
High Schools	167	17	360	37
Healt Clinics	192	20	364	38

5. Results

It has been determined that primary, middle, high school and health centers in the study area cannot cover enough space within 5 and 10 minutes walking distance. Additionally, it has also been observed that some social facilities cover the same area, that is, they are built in close proximity.

Urban living quality has many indicators. The most important of these is the ease of access to urban facilities. In this study, access to some education and primary health care services was examined using GIS network analysis.

According to the current study; the necessity of location determination based on scientific criteria has been revealed by considering the basic access principles, while determining the location of new school, health center and other public services.

References

Başeğmez, M., Taşdemir İ., Gül, Ç. (2017). Eğitim Alanlarının Yer Seçim Kriterlerinin Belirlenmesinde Yaşanan Problemler ve Çözüm Önerileri, UCTEA, Chamber of Survey and Cadastre Engineers, 16. Turkish Scientific and Technical Map Congress, 3-6 May 2017, Ankara.

Comber A., Brunsdon C., Green E., (2008). Using a GIS-based network analysis to determine urban greenspace accessibility for different ethnic and religious groups, Landscape and Urban Planning 86,103–114

Çiftçi, Ç. (1999). Türkiye'de Büyükşehir Statüsündeki Bazı Kentlerde Sosyal Donatım Alanlarının Durumu ve Planlama İle İlişkileri. PhD Thesis. İstanbul Technical University, İstanbul.

D.P.T., (1996). İllerin Sosyo-Ekonomik Gelişmişlik Sıralaması Araştırması, Yayın No:2466, Ankara.

Erden T., Coşkun M.Z., İpbüker C., (2003). Network Analysıs and Transportatıon Problems In GIS, Harita Dergisi, 129, 16-31.

Özkan Y, Şişman A. (2016). Examining of Locations of Forest Service Fire Stations with Network Analysis Based on Critical Time, 2nd Internatıonal Researchers, Statıstıcıans And Young Statıstıcıans Congress, Ankara.

Turkish Standards Institution (TSE), (2012). Standart of TS 12174, June 2012

URL 1: http://www. Mevzuat.gov.tr (Date of access: 23 April 2018).

Yıldırım R. E, Sısman A. (2016). An Assessment the Locations of Emergency Response Units Based on Traffic Accidents; a Case Study of Samsun, 2nd Internatıonal Researchers, Statıstıcıans And Young Statıstıcıans Congress, Ankara.

Estimating Compressive Strength of Rock Using Geographically Weighted Regression

Cem YAYLAGÜL[1*], Bülent TÜTMEZ[2]

[1]TKİ (Turkish Coal Enterprise), Dodurga Control Directorate, Çorum, Turkey.
[2]Inonu University, Mining Engineering Department, Malatya, Turkey.

[*]**Corresponding Author:** bulent.tutmez@inonu.edu.tr

Abstract

Rock Engineering is utilized to analyse behaviours of rock mass/material by some experiments and numerical modelling. The determination of mechanical properties of rock has critical importance for engineering project planning. The experimental works performed in laboratory are mostly corresponded time-consuming and difficult operations. In this study, one of the most important rock mechanics parameter, the uniaxial compressive strength (UCS) is estimated by using spatial parameters (coordinates) and Schmidt Hammer Rebound measurement provided by drill-holes. As the non-destructive test measurements, the Schmidt Hammer Rebound test values are used as inputs and these values are weighted by the locational information. By this way, direct site information, spatial relationship is added in the model. The estimation of the UCS from geological information and basic index test provide additional accuracy and some possibilities for practitioners and researchers.

Key words: Rock Mechanics, Weighted Regression, Compressive Strength, Locational Information.

1. Introduction

As a branch of materials science, rock mechanics mainly focuses on physical and mechanical properties of rocks. It is difficult to specify the complexity of rocks due to the some discontinuousness and alterations. At this stage, making some estimation based on the available experimental data gains an importance (Mogi, 2007). Among the rock mechanics parameters, uniaxial compressive strength has a notable importance.

A quick and inexpensive measure of surface hardness that is widely employed for estimating the mechanical properties of rock material can be obtained by the Schmidt Hammer test (Aydin and Basu, 2005).As an effective measurement tool, the Schmidt Hammer (*SH*) is a simple and non–destructive test employed for determining surface hardness which is one of the most important mechanical properties of rocks. The SH rebound hardness is a conventional index used in rock mechanics for predicting the modulus of elasticity (*E*) and the uniaxial compressive strength (*UCS*) of rocks as suggested by the ISRM (Ulusay, 2015).

In a realistic analysis, the determination of the relationships between SH hardness and UCS also requires using locational information(Tutmez, Tercan, Kaymak, 2007). In other words, in addition to laboratory testing values, the geographic relationships recorded in the site should also be considered by a computing method. For this purpose, a weighted analysis was focused and the geographically weighted regression (GWR) modelling (Fotheringham et al. 2002) was performed. The results and performance measures showed that the areal information made some contribution to improve the model accuracy.

In the next section, the problem and the methodology will be introduced. After that, the case study and a brief discussion will be presented. In the last section conclusions will be summarized.

2. Methodology

2.1. Problem Formulation

The Schmidt Hammer Rebound testis widely used for appraising the quality of concrete and rock. It has been increasingly utilized worldwide due to its simplicity, rapidity, non-destructiveness and portability (Karakus and Tutmez, 2006). On the other hand, the UCS test is a destructive test and needs some complex equipment despite of its importance. Determining a relationship from an index measurement such as the SH value to predict the mechanical

property is a well-known method in rock mechanics. The main drawback of this approach is to disregard the site (areal) information. Actually, a geological measurement evaluation should be realized with spatial information. Therefore, a new perspective which should also include the locational information is required.

2.2. Geographically Weighted Analysis

The standard GWR model was suggested byFotheringham et al. (2002)for local estimation of the conventional multivariate regression given as follows:

$$\hat{\boldsymbol{\beta}} = (\mathbf{X}^{\mathbf{T}}\mathbf{X})^{-1}\mathbf{X}^{\mathbf{T}}\mathbf{y}\,. \qquad (1)$$

In the weighted regression models, the measurements are weighted in accordance with their distance from the kernel centre. The parameters for GWR may be estimated by solving Eq. (2)

$$\hat{\beta}(u_i, v_i) = \left[\mathbf{X}^T \mathbf{W}(u_i, v_i)\mathbf{X}\right]^{-1} \mathbf{X}^T \mathbf{W}(u_i, v_i)\mathbf{y}\ , \qquad (2)$$

where $\hat{\beta}$ represents an estimate of β, and $\mathbf{W}(u_i, v_i)$ is an n by n matrix whose off-diagonal elements are zero and diagonal elements are geographical weights of each of the n observed data for regression point i (Harris at al. 2010). Instead of $\mathbf{W}(u_i, v_i)$, $\mathbf{W}$(i)can be used as weighting scheme based on the proximity of the regression point i to the data points around i without an explicit relationship being expressed. Among the weighting schemes which express w_{ij} as a continuous function of distance d_{ij}, the Gaussian function below is employed extensively:

$$w_{ij} = \exp\left[-\frac{1}{2}\left(\frac{d_{ij}}{b}\right)^2\right] \qquad (3)$$

where d_{ij} is the Euclidean distance between the location of measurement i and the centre of the kernel j, and b is the bandwidth of the kernel.

3. Application

3.1. Data Set and Relationships

The data set provided from an andesite quarry has been considered in this study (Tutmez and Tercan, 2007). The original data set comprises of total 108 values. In addition to the laboratory measurements (SH and UCS), the drill-hole locations have been considered for weighting. Figure 1 shows the stratified sampling pattern.

In the present application, a data conditioning was not made and the potential outlier values were not eliminated. The variations and the relationships between the variables are illustrated in Figures 2 and 3. As can be noticed by Figure 2, a regular site work was performed. Figure 3 shows a small skewness and low variability for SH and two different levels (modes) for UCS, respectively. There is no strong linear relationship between the SH and the UCS values.

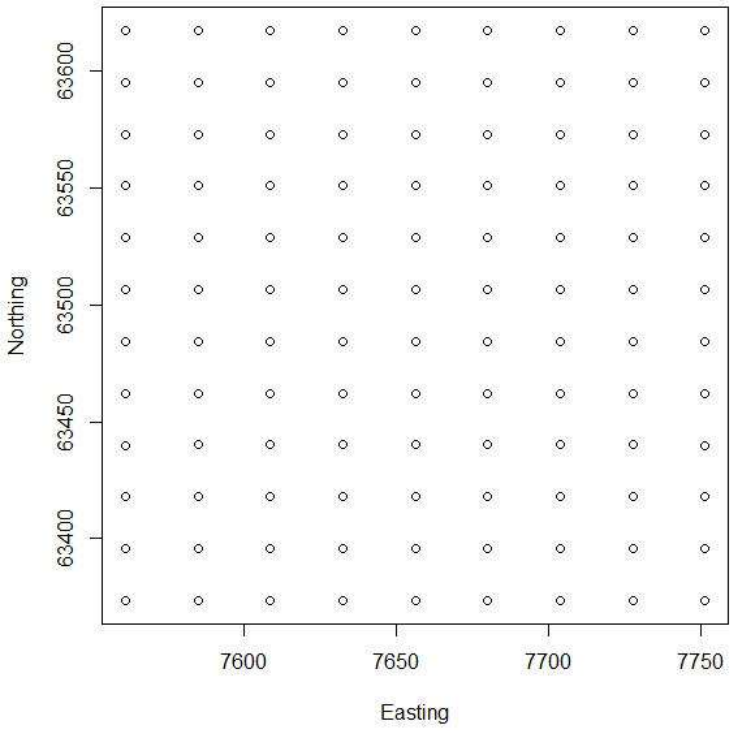

Figure 1. Sampling pattern.

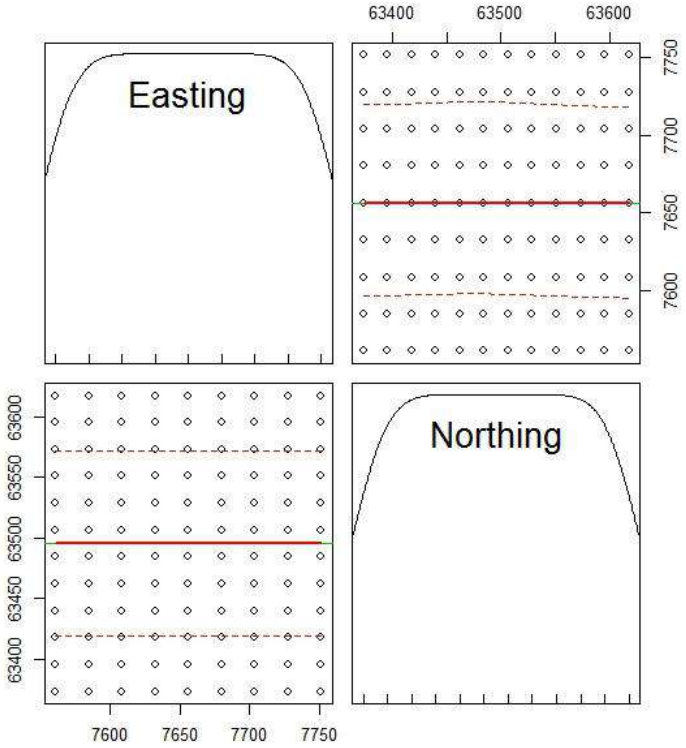

Figure 2. Locational relationships.

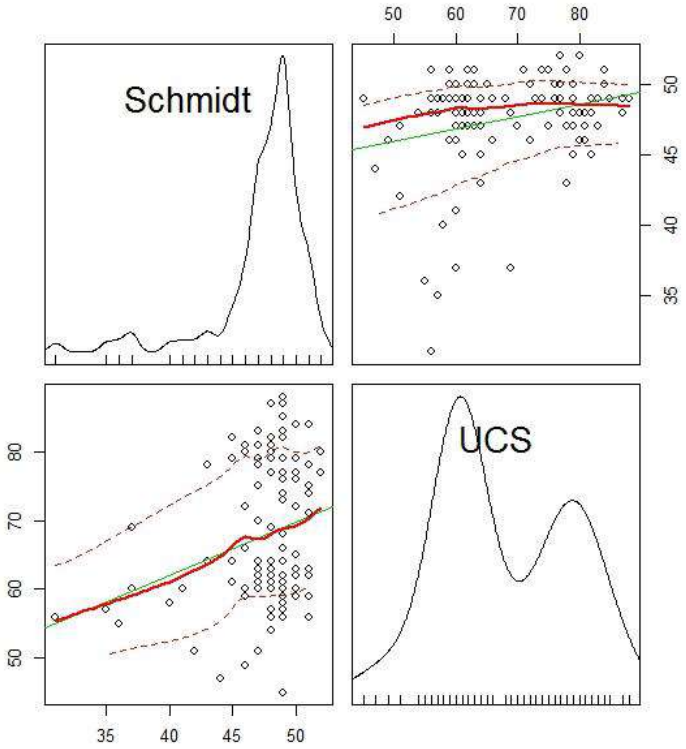

Figure 3. Relationships between model parameters.

3.2. Results and Discussion

The critical step of a GWR implementation is to determine the optimal zone of influence (bandwidth). For this purpose, Brunsdon and Comber (2015) suggested two measures such as CV and AIC indicators. Among the kernel types, the well known one, the Gaussian Kernel was selected for weighting and bandwidth optimization. In this study, a series simulation has been performed based on AIC values. The optimal fixed bandwidth has been provided via minimum AIC as 42.419 m. The outcomes of the GWR application and the conventional global regression analysis are summarized in Table 1.

Tablo 1. Results and performance measurements.

Model Parameter	Global Regression	GWR
Distance Metric	Euclidean	Euclidean
Bandwidth	-	42.419
AIC	809.825	774.8251
Correlation Coefficient	0.25	0.61

It is difficult to provide a strong relationship between SH and UCS because of heterogeneous character of rock and the motivation of the rock test methods. The SH test about surface hardness and the UCS is on the strength of the material. Differently from the suggested empirical formulas in literature, this study showed the contribution of locational (site) information on the model performance.

4. Conclusions

Predicting the compressive strength of a rock type from the index tests like Schmidt Hammer hardness measurement has critical importance due to time and cost. Unlike the conventional methods, this relationship has been constructed using site information and coordinates values. The case study showed that the use of geological information obtained some additional performance. Providing the approximate UCS from areal information and fundamental index tests can provide some possibilities for practitioners and researchers.

References

Aydin, A., Basu, A. (2005). The Schmidt Hammer in rock material characterization. Engineering Geology 81, 1-14.

Brunsdon, C., Comber, L. (2015). An Introduction to R for Spatial Analysis & Mapping. California: Sage.

Fotheringham, A.S., Brunsdon, C., Charltton, M. (2002). Geographically Weighted Regression: The Analysis of Spatially Varying Relationships. Chichester: Wiley.

Harris, P., Fotheringham, A., Juggins, S. (2010). Robust geographically weighted regression: a technique for quantifying spatial relationships between freshwater acidification critical loads and catchment attributes. Annals of the Association of American Geographers, 100(2): 286:306.

Karakus, M., Tutmez, B. (2006). Fuzzy and multiple regression modelling for evaluation of intact rock strength based on point load, Schmidt hammer, and Sonic Velocity. Rock Mechanics & Rock Engineering,39(1),45-57.

Mogi, K. (2007). Experimental Rock Mechanics.London: Taylor & Francis.

Tutmez, B., Tercan, A.E., Kaymak, U. (2007). Fuzzy modelling for reserve estimation based on spatial variability. Mathematical Geology, 39(1),87-111.

Tutmez, B., Tercan, A.E. (2007). Spatial estimation of some mechanical properties of rocks by fuzzy modelling. Computers and Geotechnics,34(1), 10-18.

Ulusay, R. (Eds.). (2015). The ISRM Suggested Methods for Rock Characterization, Testing and Monitoring. Switzerland: Springer.

Smart Cities and Transportation

Elif ALDANMAZ[1*], Aziz ŞİŞMAN[2]

[1]General Command of Mapping, Ankara, Turkey, aldanmazeliff@gmail.com

[2]Ondokuz Mayis University, Faculty of Engineering, Department of Geomatics Engineering, Samsun,Turkey, asisman@omu.edu.tr

[*]**Corresponding Author:**aldanmazeliff@gmail.com

Abstract

Smart city is a structure, which interacts between people and institutions. Contemporary cities challenge with complex problems some of them can be listed ecological, economical, financial, demographical, etc. These problems require smart solutions. Smart City Management needs simultaneous data sources such as databases, mobile crews, satellite images and sensors to make a decision.

Today, the efficient use of the transport infrastructure and answering of transportation demand has become one of the main purposes of the transportation management units in cities. For this reason, the studies to evaluating alternate solutions gained speed with a purpose of more efficient use of transportation infrastructure. Todays developing information technologies have created great chances to assemble such a technologic infrastructure, this approach introduced the Smart Transportation Systems conceptSmart Transportation Systems are used widespread and draw attention all around the world, especially in developed countries. Smart transportation system aims to improve by managing the factors that are affecting each other, with the integration of communication and information technologies. In this study, smart transport applications were investigated andsome suggestions were made for developing countries.

Keywords: Smart City, SmartTransportation Systems, GIS, Smart Applications.

1. Introduction

A city is an economic, social, political and administrative area which living space for all citizens (Akkoyunlu, 2007). It is not enough to define the city as a crowded settlement, to define it as a new economic organization and as a changed physical environment. The reason for this is that the city is also used to express a different social order that also affects people's behavior and thoughts (Kavruk, 2002).

Urbanization; the increase in the number of cities due to the economic development and the growth of cities, the increasing rate of society in the organization, specialization and interpersonal relations that cause changes in the population specific to the population accumulation process (Keleş, 1998).

A lot of factors affect development of the cities. Some of them are natural factors; such as location, climate, environment etc. others are artificial factors, such as economic, investment, politics etc.Today's cities are the basic factors that define the possibilities of communication, service and communication. On the other hand, globalization has accelerated inter-city competition and cities have assumed new economic, political and cultural roles (Işık, 1999). Nowadays, cities have become prominent units with their economy, culture, social and political structure (Aslanoglu, 1998).

2. Urbanization and Smart Cities

Around of the world despite representing only about 2% of the geographic area and accommodating over 50% of the world population, cities today produce 80% of greenhouse gas emissions and consume 80% of the total resources of the world (Yigitcanlar et al, 2018).

Developed countries and Latin America and the Caribbean have already a large proportion of their population residing in urban areas, but Africa and Asia, still mostly rural, they will urbanize faster than other regions over the coming decades. These trends are changing the landscape of human settlement, with significant implications for living conditions, the environment and development in different parts of the World (URL 1).

All over the world human population is getting increase and needs of them are also increase, however sources of the world are limited. People have to use all kind of resources efficiently. Smart city applications save more time, energy and labor, in addition it enables to

be used limited resources of the world efficiently. There are some smart city applications around the world and one of the main goal of these projects is to improve the life quality of citizens.

In this study, smart city concept is investigated and one of the most important part of the smart city is smart transport projects have been inspected for sustainable development and environment.

2.1. Smart City and Components

Smart city concept has a lot of components which are a part of day life (Figure 1). The basic factors adopted in smart cities can be listed as smart management, smart infrastructure, smart energy, smart health, smart security, smart education, smart building, smart transportationect(Kayapınar 2017).

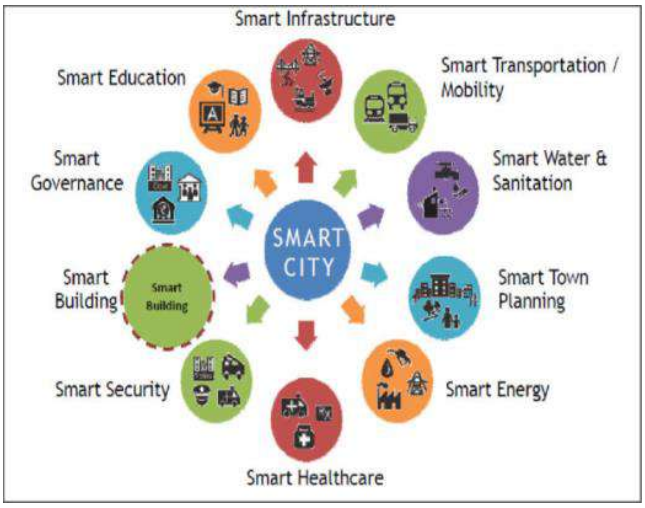

Figure 1. Smart City Component (URL 2)

2.1.1. Smart Management: Local administrations have duties in eliminating the increasing demands of citizens in the administrative administration(Kayapınar, (2017). Effective communication between different stakeholders through interoperable information and communication technology solutions, transparency in public administration and participatory decision making are ensured (Cohen, 2013).

2.1.2.Smart Infrastructure: It is expected that the existing infrastructure will not be sufficient in the near future, because of population living in cities is growing up(Kayapınar, (2017). Smart infrastructures aim to use data effectively to make full use of both existing and new city infrastructure systems (Ghafory, 2018).

2.1.3. Smart Energy: According to the Piro et al (2014), smart energy is defined as efficient management of all energy resources.Smart energy also aims to increase efficiency in renewable energy resources and to reduce the need for energy in all part of life.

2.1.4. Smart Security: Information and communication technologies make life easier and provide a more reliable environment for residents (Cohen, 2013).The safety of cities and also people can be managed smart applications, provide by information and communication technologies.

2.1.5. Smart Buildings: Internet of things (IoT) will be a basic partof smart cities.Thanks to smart buildings and IoT features in the house and offices such as heat systems, fire systems or other facilities can be controlled remote or working properly by itself.

2.1.6. Smart Transportation: The main part of smart city projects is smart transportation applications. It includes transportation systems supported by information and communication technologies. Real-time traffic information produced and shared with passengers, drivers and operators is one of the priority issues (Cohen, 2013). The smart management of traffic, vehicle parking and driving, instant follow-up of vehicles and most importantly the use of electric buses, bicycles, pedestrian road use aims to protect nature by reducing carbon consumption to zero (Kayapınar, 2017).

2.2. Smart Transportation World Applications

As all other smart city applications there are lots of smart transport project over the world. Some of them are summarized below.

2.2.1. Smart Transportation Applications in Japan

One of the smart applications in Japan is the Universal Traffic Management System (UTMS) for providing a safe, comfortable traffic environment. Radio broadcasts in the system include Advanced Mobile Information Systems (AMIS), which provides information to infrared transmitters and in-car information systems in addition to traffic signs. Fast Emergency Vehicle Preemption Systems (FAST), which allows emergency aid teams to reach the scene more quickly. Public Transportation Priority Systems (PTPS), which provides faster and more comfortable travel for people using public transport by adjusting traffic signs(Hanai, 2013).

2.2.2. Smart Transportation Applications in South Korea

Freeway Traffic Management System (FTMS) project, which provides information on traffic congestion, accidents and other incidents with electronic variable message signs on motorways (Lee, 2012). There are smart transportation applications for public transport in Bus Management System (BMS) and Bus Information System (BIS) in local administrations and integration is provided to facilitate the access of bus passengers living in different cities (Lee, 2012).

2.2.3. Smart Transportation Applications in Singapore

One of the systems with intelligent transportation is the system which allows to detect the traffic accidents, the failure of the vehicles and the return of the traffic to the normal state with Expressway Monitoring Advisory System (EMAS). Operators in the operation control center inspect cameras and help vehicles reach the scene in 15 minutes. Defective vehicles are taken free of charge to the nearest parking lot to the scene. Traffic signs are provided with electronic signs and road signs to inform other drivers (Land Transport Authority, 2014a). Green Link Determining System (GLIDE) is the centralized system that controls all traffic lights in Singapore and determines when the green lights should illuminate when the traffic flow changes (Land Transport Authority, 2014b).

2.2.4. Smart Transportation Applications in the Netherlands

Instead of getting a fixed fee from vehicles with road charging systems, GPS compatible devices have a system in which variable pricing is applied considering the location, position and time of traffic. This means that motor vehicles are encouraged to get less traffic during the busy times of traffic (Ministry of Infrastructureand Environment, 2011).

2.2.5. Smart Transportation Applications in Australia

In Australia, applications based on vehicle-vehicle and vehicle-infrastructure communication are available. The blind spot warning system, which states that there are vehicles when changing lanes in blind spots where drivers cannot see, has electronic emergency brake lights that warn drivers when they cannot see the vehicle in front of them. In addition, the advanced traffic management system, which allows traffic lights to be changed in vehicles that need to be prioritized and that compiles real-time information on the status of vehicles in traffic, the route information system indicating the weather on the route and the accident etc. projects

such as an advanced accident response system that ensures action against traffic incidents (ITS Australia, 2012).

3. Results and Discussion

Smart cities can be accepted a new way of governing with the use of technology and the consequent increase in the public administration capacity of improving the quality of life of citizens and also to keep limited resources and environment.

Providing smart cities without traffic problems in the coming years, it is necessary to use technology effectively starting from today. In addition, many infrastructural activities, especially transportation, will provide better quality and effective services in cities where spatial data infrastructure is established.

Smart cities need more new technology, more different kind of data from daily life and also need more adopted people using smart applications all part of their life.

References

Akkoyunlu, K., (2007), "Sustainable City", City and Politics: From Ancient City to World City, Compilation: Ayşegül Mengi, Ankara, İmge Publisher s.11-26.

Aslanoglu, R., (1998), City, Identity and Globalization, Asa Publisher, Bursa.

Cohen, B., (2013), "The Smart City Wheel", Smart Cities: Not Luxury Needs. ituvakıf magazine, number 77.

Ghafory, I., (2018), "Smart Infrastructure: The Key To The Future", article, Balıkesir.

Hanai, T. (2013), Intelligent Transport Systems. Tokyo: Society of Automotive Engineers of Japan.

Işık, O., (1999) "Thinking of the City", Journal of Society and Science, May-June, Skin 14, Number: 3, s. 66-79.

ITS Australia. (2012), National Intelligent Transport Systems Industry Strategy 2012-2017. Melbourne: ITS Australia

Kavruk, H., (2002), City Overview, Hizmet İş Sendikası Publishing, Ankara, s. 65.

Kayapınar Y. E., (2017), "Smart Cities And Application Examples", Environment and Urban Ministry. ituvakıf magazine, number 77.

Keleş, R., (1998), Glossary of Urbanism Terms, İmge Publisher, Ankara.

Land Transport Authority. (2014a). EXPRESSWAY MONITORING ADVISORY SYSTEM (EMAS). OneMotoring: http://www.onemotoring.com.sg/publish/onemotoring/en/on_the_roads/traffic_management/intelligent_transport_systems/emasys.html (20.03.2018) .

Land Transport Authority. (2014b). Green Link Determining (GLIDE) System . OneMotoring: http://www.onemotoring.com.sg/publish/onemotoring/en/on_the_roads/traffic _management/intelligent_transport_systems/glide.html (20.03.2018).

Lee, J.-J. (2012). Economic Growth and Transport Models Chapter 9:ITS (Intelligent Transport Systems). Seul: The Korea Transport Institute.

Ministry of Infrastructure and Environment. (2011). ITS in the Netherlands. Amsterdam: Ministry of Infrastructure and Environment.

Piro G.,Cianci I., Grieco L.A., Boggia G., Camarda P. (2014). Information centric services in Smart Cities, The Journal of Systems and Software 88 169– 188.

URL 1 (http://www.un.org/en/development/desa/population/theme/urbanization/ index.shtml), (Date of access: 20 September 2018)

URL 2 (https://www.researchgate.net/figure/Smart-City-Components-After-Murthy-2015_fig2_283291632), (Date of access: 10 September 2018)

Yigitcanlar T.,Kamruzzaman M., Buys L., Ioppolo G., Sabatini-Marques J., Moreira da Costa E., Yun J., (2018). Cities, Understanding 'smartcities': Intertwiningdevelopmentdriverswithdesiredoutcomes in a multidimensionalframeworkhttps://doi.org/10.1016/j.cities.2018.04.003

Digitization of Cadastral Sheets by Polynomial Transformation Methods

Yasemin SISMAN [1*], Ulku KIRICI YILDIRIM [2]

[1]Ondokuz Mayis University, Engineering Faculty, Department of Geomatics, Samsun, Turkey; ysisman@omu.edu.tr

[2]Ondokuz Mayis University, Engineering Faculty, Department of Geomatics, Samsun, Turkey; ulku.kirici@omu.edu.tr

[*]**Corresponding Author:**ysisman@omu.edu.tr

Abstract

A lot of non-digital cadastral maps were produced in the Turkish cartography history from the Ottoman Empire. Generally, these maps had got different coordinate system. These maps must be digitized. This digitizing problem is realized using coordinate transformation between coordinate systems. This transformation process should have high accuracy. The accuracy of the transformation is related to the common point number, distribution and solution method. The solution method of coordinate transformation generally selected as affine coordinate transformation according to article 82 of the Large Scale Map and Map Information Production Regulation. The other usable solution method is the polynomial transformation. The polynomial equations are written for the two axes (North-East or X-Y). In this process, the polynomial degree is important. The degree must be selected as optimal. For investigating the polynomial degree the significance test is applied to the polynomial coefficient.

In this study, the general information which about polynomial transformations are given and the transformation procedure is made for Giresun region. Then the application results are analyzed.

Keywords: Non-digital cadastral maps, Coordinate transformation, The polynomial transformation model.

1. Introduction

The technical structure in the construction of the country cadaster showed various changes. While the period from the Ottomans until 1934 was mostly called the written cadastral period for property and boundaries, the period from 1934 until the today is called the "Lineer Cadastral" period. Detail about legal aspects in Turkey cadastral works can be found in URL1, Coruhlu, and Demir (2008). Turkey's National Geodetic Network studies obtained in parallel with national coordinate system works Turkey's National Datum my (TUD54) started with, and soon after, the European Datum-50 (European Datum-50, ED-50) was converted into the coordinate system. Developing technologies, temporal deformations, due to the various movements of the earth's crust, the national coordinate system has been renovated as Turkey Fundamental GPS Network (TUTGA) and in the continuation of this project, the three-dimensional coordinates and velocities of the points in the country system by the TUSAGA Active project have been started to be established in the coordinate system of the International Terrestrial Reference Frame (ITRF) (Ekin, 2012; Ilvan, 2014; Sisman 2014). Cadastral maps made in various periods are legal and living documents obtained according to the technical possibilities of the period in which they were produced. Cadastral maps can be classified according to their different characteristics. One of these classifications can be done according to the coordinate system (Table 1).

Table 1. Map rates according to the coordinate systems (URL 1)

Coordinate Systems	Rate %
ITRF	24
ED-50	53
Local	14
Non-coordinate	9
TOTAL	100

As can be seen from Table 1, a large part of Turkey’s cadastral maps has the difference in coordinate system. To resolve this disparity, it is necessary to perform a coordinate transformation process for the conversion of all maps and coordinates produced until 2001 to ITRF datum. Detailed information on this transformation is given in Article 82 of the "Large Scale Map and Map Information Production Regulation", which was enacted in July 2005. However, most of these maps are not digital, there are many errors from production (wrong

measure, adversarial, border, etc.). Since the digital reconstruction of these maps is a long and labor-intensive process, it is preferable to scan the sheets and perform the transformation process using these scanned images. If non-digital maps are kept up to date, they can be digitized with the coordinates of common points by transferring them to the computer environment with today's technology (Ceylan, 2009).

Coordinate transformation is the transfer of point coordinates in one coordinate system to another coordinate system using the common point coordinates taken in common in both coordinate systems. Depending on the field of application and the type of the data used by these coordinate transformation methods, there are differences in the number of parameters and the type of evaluation of the data (Ekin, 2012; Bolat, 2011; Feizabadi et al. 2015).

In this study, the applicability of the method of polynomial coordinate transformation based on the scale of cadastral maps and the advantages and disadvantages according to similarity and affine transformation are investigated. 2^{nd} degree polynomial transformations were performed on the X and Y axes using the screen and geodetic coordinates of 10 square points taken from scanned maps of 1/500, 1/1000, 1/2000 and 1/2500 scales used in the study. Root Mean Square Error values obtained from the transformations made to compare the obtained results with Similarity Transformation, Affine Transformation, 1^{st} Degree Polynomial Transformation are calculated.

2. Coordinate Transformation

Coordinate transformation is the process of determining the value of the coordinates of a point in a coordinate system in a second coordinate system. To do this, the relationship between the two coordinate systems must be defined with the transformation parameters calculated using the coordinate values of the known coordinates in both systems. Cadastral maps are based made up of two dimensional axes (East, North) or (Y, X). In the digitization of these maps, two dimensional transformation models are applied between screen coordinates of the scanned map and actual coordinates values. Polynomial transformation can be performed for both axes as well as similarity and affine transformation, which are generally used in two-dimensional transformation.

2.1. Polynomial Transformation Method

Polynomial Interpolation is one of the most widely used techniques because main purpose is to express the work area with a single function. The relationship between two systems in a polynomial transformation can be defined by a polynomial.

$$f_{(x,y)} = \sum_{k=0}^{n} \sum_{i=0}^{k} {}_{j=k-i} a_{ij} x_i y_i \quad (1)$$

The relationship between the coordinates in two two-dimensional coordinate systems is;

$$X = a_0 + a_{10}x + a_{01}y + a_{20}x^2 + a_{02}y^2 + a_{11}xy + \cdots \ldots$$
$$Y = b_0 + b_{10}x + by + b_{20}x^2 + b_{02}y^2 + b_{11}xy + \cdots \ldots \quad (2)$$

It can be established with equations. Here, (x,y) and (X,Y) represent first and second systems coordinates, a_i and b_i polynomial transformation coefficients respectively (Conte and DeBoor, 1981). As the polynomial degree used increases, the number of unknowns in the problem increases. For this reason, the most suitable polynomial degree for the data set and application to be used should be selected. At first, it is not known that a polynomial can be used at what degree. In order to determine the appropriate polynomial, the polynomials are analyzed for the in adjustment results to be initiated from the first degree. As the polynomial degree increases, the posteriori variance value decreases. The optimal degree is a subtraction of the polynomial to which the posteriori variance begins to grow (Bolat, 2011).

Functional model written 2nd degree polynomial according to equation (2) for n common point coordinates;

$$\begin{bmatrix} X_1 + V_{X1} \\ Y_1 + V_{Y1} \\ :: \\ X_n + V_{Xn} \\ Y_n + V_{Yn} \end{bmatrix} = \begin{bmatrix} 1 & x_1 & y_1 & x_1^2 & y_1^2 & x_1^2y_1^2 & 0 & 0 & 0 & 0 & 0 & 0 \\ 0 & 0 & 0 & 0 & 0 & 0 & 0 & x_1 & y_1 & x_1^2 & y_1^2 & x_1^2y_1^2 \\ .. & .. & .. & .. & .. & .. & .. & .. & .. & .. & .. & .. \\ .. & .. & .. & .. & .. & .. & .. & .. & .. & .. & .. & .. \\ 1 & x_n & y_n & x_n^2 & y_n^2 & x_n^2y_n^2 & 0 & 0 & 0 & 0 & 0 & 0 \\ 0 & 0 & 0 & 0 & 0 & 0 & 1 & x_n & y_n & x_n^2 & y_n^2 & x_n^2y_n^2 \end{bmatrix} \begin{bmatrix} a_0 \\ a_{10} \\ a_{01} \\ a_{11} \\ a_{20} \\ a_{02} \\ a_{11} \\ b_0 \\ b_{10} \\ b_{01} \\ b_{20} \\ b_{02} \\ b_{11} \end{bmatrix} \quad (3)$$

Organized as.

$$V = AX - \ell$$

The following equation is used to solve this equation according to the indirect measurement method.

$$X = (A^T PA)^{-1} A^T P\ell \quad (4)$$

In determining the correctness obtained from the solution made in this way, the root mean square error which can be calculated by the following equation can be used as the error criterion. Here n is the number of common points and u is the unknown number (transformation parameters) (Wolf and Dewitt, 2000).

$$m_0 = \sqrt{\frac{[VV]}{n-u}} \quad (5)$$

3. Application

Cadastral sheet of 1/500, 1/1000, 1/2000 and 1/2500 scale belong to Giresun province were chosen application area for this application. The first coordinate system used in the polynomial transformation is the scanning coordinates of the non-numerical sheet, and the second coordinate system is the coordinate system in which the sheet is produced. The scan image of each sheet, the distribution of common points and the common point coordinates are given in Figure 1 and Table 2.

Table 2. The coordinate of common points

1/1000				
NN	Screen Coordinates		Grid Coordinates	
	Y(m)	X(m)	East	North
1	12.434	184.714	441600.000	4461100.000
2	12.419	216.196	441600.000	4461200.000
3	12396	247.669	441600.000	4461300.000
4	75.314	247.702	441800.000	4461300.000
5	75.345	216.212	441800.000	4461200.000
6	75.338	184.825	441800.000	4461100.000
7	138.239	347.658	442000.000	4461300.000
8	138.241	216.154	442000.000	4461200.000
9	138.253	184.715	442000.000	4461100.000
10	75.388	153.291	441800.000	4461000.000

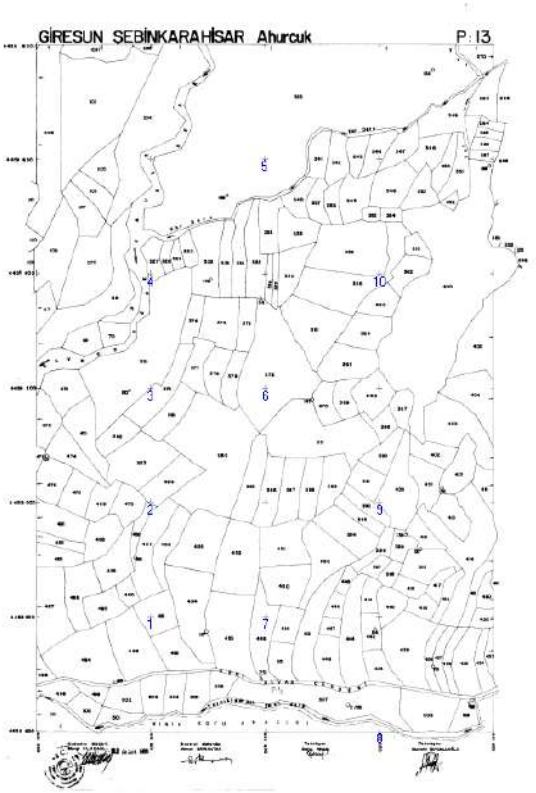

Figure 1. Distribution of common points

The 1st and 2nd degree polynomial interpolation solutions made from the coordinates obtained in this way and calculated the root mean square error given by equation (5) for each application. The results obtained were compared with the more commonly used two-dimensional similarity and affine transformation results.

4. Results and Conclusions

The root mean square error values obtained as a result of the application are given in Table 3 and Table 4.

Table 3. 1st degree polynomial interpolation transformation results

Scale	Root Mean Square Error (m)(m_0)	X direction (m) (m_0)	Y direction (m) (m_0)
1/500	0.055	0.058	0.053
1/1000	0.097	0.132	0.038
1/2000	0.132	0.145	0.119
1/2500	0.435	0.609	0.091

Table 4. 2nd degree polynomial interpolation transformation results

Scale	Root Mean Square Error (m)(m_0)	X direction (m) (m_0)	Y direction (m) (m_0)
1/500	0.063	0.068	0.057
1/1000	0.081	0.109	0.037
1/2000	0.075	0.053	0.092
1/2500	0.450	0.627	0.111

When these tables are examined, it has been found that the root mean square error values correspond to the limit values of the Large Scale Map and Map Information Production Regulations for both solutions. In addition, the root mean square error in the X direction of the 1/2500 scale sheets is found to be quite large (60,9 cm and 62,7 cm) in both solutions. This result reveals that it has been necessary to examine axes in the digitization of the sheets.

In addition, the polynomial interpolation method was compared with the two-dimensional similarity and affine transformation results, which are frequently used in application, and the results are given in Table 5 and Table 6.

Table 5. Similarity transformation results

Scale	Root Mean Square Error (m)(m_0)	X direction (m) (m_0)	Y direction (m) (m_0)
1/500	0.056	0.058	0.055
1/1000	0.103	0.129	0.067
1/2000	0.148	0.169	0.124
1/2500	0.463	0.609	0.239

Table 6. Affine transformation results

Scale	Root Mean Square Error (m)(m_0)	X direction (m) (m_0)	Y direction (m) (m_0)
1/500	0.055	0.058	0.053
1/1000	0.097	0.132	0.038
1/2000	0.132	0.145	0.119
1/2500	0.435	0.609	0.091

It is seen that the 1stDegree interpolation and the Affine transformation results are the same from each other. Also, when the results of similarity and affine transformation are

examined, it is seen that affine transformation, which should be used in accordance with the Large Scale Map and Map Information Production Regulation, is more sensitive to the transformation of maps than the similarity transformation.

In the light of these explanations, if affine transformation is used for digitizing non-digital cadastral maps and solutions exceeding the error limit value are obtained, it is concluded that the number of common points should be increased and the outlier measure analysis should be done by examining in the direction of axes.

Acknowledgement

We would like to thank the Giresun Cadastral Directorate for providing the necessary sheets in the application.

References

Bolat, S., (2011), Lokal Jeoid Belirlemede Kullanılan Enterpolasyon Yöntemleri: Samsun İli Örneği, Ondokuz Mayıs Üniversitesi, Yüksek Lisans tezi, Samsun.

Ceylan E., (2009), Non Sibson Yöntemi İle Lokal Koordinat Dönüşümü, İstanbul teknik Üniversitesi, Yüksek Lisans tezi, İstanbul

Conte, S.D., C., DeBoor (1981) Elementary Numerical AnalysisAn Algorithmic Approach, Auckland, Mc GrawHill Book, 432 p

Demir, O., and Y. E. Coruhlu. (2008). “Determining the Property Ownership on Cadastral Works in Turkey.” Land Use Policy 26 (1): 112–120. doi:10.1016/j.landusepol.2008.01.011.

Feizabadi M., Işık M. S., İpbüker C., (2015), Geomatik Mühendisliği Uygulamalarında Dönüşüm Yöntemleri, 15. Türkiye Harita Bilimsel ve Teknik Kurultayı, 25-28Mart 2015, Ankara.

İlvan, A, (2014), Mersin İli Toroslar İlçesi Örneğinde Lokal Datum Dönüşüm Parametrelerinin Belirlenmesi Üzerine Bir Çalışma, İstanbul teknik Üniversitesi, Yüksek Lisans tezi, İstanbul.

Şişman, Y., Coordinate transformation of cadastral maps using different adjustment methods, Journal of the Chinese Institute of Engineers, , 37-41, DOI: 10.1080/02533839.2014.888800.

Wolf, P. R., and B. A. Dewitt. (2000). Elements of Photogrammetry with Applications in GIS. New York: McGraw-Hill Companies.

Yetkin L.,(2012) Mekansal Verilerin Datum Dönüşümleri Ve Kadastroda Uygulamaları, T.C. Çevre Ve Şehircilik Bakanlığı Tapu Ve Kadastro Uzmanlık Tezi, Ankara.

URL-1: https://www.tkgm.gov.tr/tr/sayfa/mekansal-gayrimenkul-sistemi-megsis, (Date of access: 7Mayıs 2018).

Long Term Monitoring of Giresun Province and Perimeters by Using Remote Sensing

Mehmet Ali DERELİ [1], Nizar POLAT [2*], Mehmet Ali UĞUR [3], Mustafa YALÇIN [4]

[1]Giresun University, Engineering Faculty, Geomatics Engineering, Giresun, Turkey;
mehmet.dereli@giresun.edu.tr

[2]Afyon Kocatepe University, Engineering Faculty, Geomatics Engineering, Afyonkarahisar, Turkey;
npolat@aku.edu.tr

[3]Afyon Kocatepe University, Engineering Faculty, Geomatics Engineering, Afyonkarahisar, Turkey;
maliugur@aku.edu.tr

[4]Afyon Kocatepe University, Engineering Faculty, Geomatics Engineering, Afyonkarahisar, Turkey;
mustafayalcin@aku.edu.tr

[*]**Corresponding Author:** npolat@aku.edu.tr

Abstract

The rapid increase of the population, misuse of natural resources, contradictions about potential land use are the most important problems on the agenda of many developed and developing countries around the world. Especially providing a continuous monitoring system for the natural resources such as forests and rivers is a vital requirement today one of the efficient ways for a long term monitoring the nature is to use Remote Sensing (RS). It provides high spectral, special and temporal satellite images that allow us to observe the earth surface for a long term. The main purpose of this study is to detect the long term trend of land use/cover types of Giresun province by deriving normalized differential vegetation index (NDVI). In order to achieve this goal, the Landsat satellite data of four different years (1985, 1996, 2006, and 2017) that covers over the 30 year are obtained and the NDVI calculations are performed for these years. The land use/cover types of Giresun then detect by NDVI and NDBI. The result shows that the Giresun province is expanded.

Keywords: Remote Sensing, Landsat, NDVI, Land use/ Land cover.

1. Introduction

Today, more than 50% of people live in the cities and it is increasing from day by day. The continuously increasing urban population are caused by the challenges of rural living conditions, and some seasonal changes such as drought (Heilig, 2012; Uysal and Polat, 2015). For whatever reason, the growth of a city means more distortion of the earth's natural structure. The change in the natural cover of the land with artificial object has severe impact on the climate and ecology of the area, therefore this change will directly affect the living being. The most obvious effect of this change is increase in the residential area. Another effect is vegetation changes.

The growth in the city area and the change in the vegetation can be determined and monitored by using RS data especially satellite images. It provides high spectral, special and temporal satellite images that allow us to observe the earth surface for a long term changes by means of land use/cover types in earth surface.

The main purpose of this study is to detect the long term change of land use/cover types of Giresun province by NDVI and normalized differential built-up index (NDBI). In order to achieve this goal, the Landsat satellite data of four different years (1985, 1996, 2006, and 2017) that covers over the 30 year are obtained and the NDVI and NDBI calculations are performed for these years.

2. Material and Method

2.1. The Study Area and Data

Giresun, is a province of Turkey on the Black Sea coast. Giresun is an agricultural region and its lower areas, near the Black Sea coast, are Turkey's largest producer of hazelnuts. Like everywhere else on the Black Sea coast it rains (and often snows in winter) and is very humid throughout the year, with a lack of extreme temperatures both in summer and winter. As a result, Giresun and the surrounding countryside are covered by luxuriant flora. As soon as you get beyond the city buildings you get into the hazelnut growing area and the high pastures further in the mountains are gorgeous.

Figure 1. The Google Earth image of Turkey shows Giresun city.

For the study, the available and usable images of Landsat TM and OLI from 1985, 1996, 2006, and 2017 for the month of May are selected and downloaded from the United States Gelogical Survey (USGS) web site. The sensor and band information of the images are given in Table 1. It is important mention that the images from the USGS web site have already been geometrically registered and the geometrically corrected (USGS, 2017).

Table 1. The sensor and band information of the Landsat images used in the study

Year	Spectral Resolution	Radiometric Resolution	Temporal Resolution
1985	7 Bands (0.45-2.35)	8 bit	16 days
1996	7 Bands (0.45-2.35)	8 bit	16 days
2006	7 Bands (0.45-2.35)	8 bit	16 days
2017	9 Bands(0.433-2.30)	16 bit	16 days

2.2. NDVI

The Normalized Difference Vegetation Index is a measure of healthy, green vegetation. Because of the usage of normalized difference formulation and the highest and lowest reflectance values for vegetation, this formulation makes NDVI an effective indicator of the green vegetation in remote sensing applications. The value of this index ranges from -1 to 1. The common range for green vegetation is 0.2 to 0.8. The formulation of NDVI is as follows (Balcik, 2014; Rouse et al., 1974):

$$NDVI=\frac{(NIR-RED)}{(NIR+RED)} \quad (1)$$

In Equation 1, NIR represents the Near Inferred band where chlorophyll has highest reflectance value while RED represents the red band where chlorophyll has the lowest reflectance value. The Normalized Difference Vegetation Index is commonly used to characterize the land cover types (Uysal and Polat, 2015).

2.3. NDBI

This index highlights urban areas where there is typically a higher reflectance in the shortwave-infrared (SWIR) region, compared to the near-infrared (NIR) region. Applications include watershed runoff predictions and land-use planning. The formulation of NDBI is as follows (Zha et al., 2003)

$$NDBI=\frac{(SWIR-NIR)}{(SWIR+NIR)} \quad (2)$$

It operates with any multispectral sensor with a SWIR band between 1.55-1.75 μm and a NIR band between 0.76-0.9 μm.

3. Results and Discussion

In the application stage of the study, the first calculations are performed for NDVI in the selected years. Then the basic statistics of the NDVI are calculated (Table 2).

Table 2. The basic statistics of the NDVI images.

Year	Min	Max	Mean
1985	-0.4211	0.7857	0.6352
1996	-0.4247	0.7857	0.4841
2006	-0.9130	0.9466	0.6127
2017	-0.2509	0.6559	0.4763

According to table 2, the NDVI values vary from a mean value of 0,48 to 0,64. These changes appear mainly chlorophyll reflectance rate and the occurrence of the vegetation. The second calculations are performed for NDBI in the selected years. The built-up areas consist of both residential and un-vegetated lands. The histogram of the NDBI for the selected years is given in Figure 2.

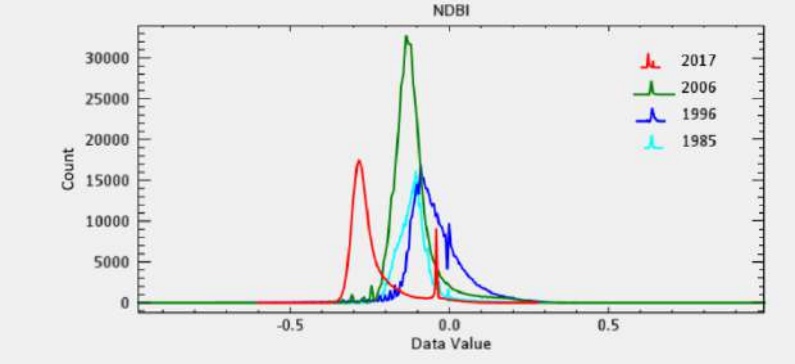

Figure 2. The histogram of the NDBI images.

From 1985 to 2017 the built-up area expands from %2,4 to % 4,3 in compliance with the study area. The generated land use/cover maps are in figure 3.

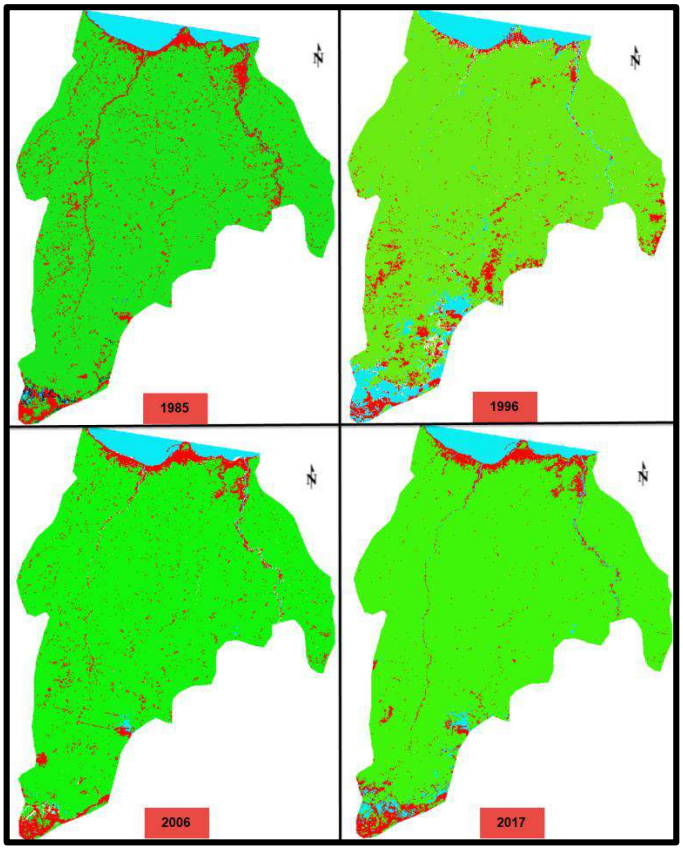

Figure 3. The generated land use/cover maps for the selected years (blue: water, green: vegetation, red: built-up area)

Built-up is changing due to the clouds and the river beds that dry up and recharge. But it is clear that the city is growing. Higher spatial resolution data should be used to determine the growth rate in the city.

3. Conclusion

This study aims to investigate the changes in land use/cover in Giresun province and its perimeters by using temporal RS satellite data. In this purpose the long term change of land use/cover types of Giresun province is investigated by deriving NDVI and NDBI indexes. In order to achieve this goal, the Landsat satellite data of four different years (1985, 1996, 2006, and 2017) that covers over the 30 year are obtained and processed. The result shows that the built-up area of Giresun province has expanded from 1985 to 2017 with a rate from %2,4 to % 4,3 in compliance with the study area.

References

Heilig, G. K., (2012). World urbanization prospects: the 2011 revision. United Nations, Department of Economic and Social Affairs (DESA), Population Division, Population Estimates and Projections Section, New York.

Zha, Y., J. Gao, and S. Ni., (2003). Use of Normalized Difference Built-Up Index in Automatically Mapping Urban Areas from TM Imagery. International Journal of Remote Sensing, (24), 583-594.

Uysal, M., and Polat, N., (2015). An Investigation of the Relationship between Land Surface Temperatures and Biophysical Indices Retrieved From Landsat Tm in Afyonkarahisar (Turkey). Tehnicki Vjesnik-Technical Gazette, vol. 22(1), ISSN 1330-3651, p. 177-181.

USGS,United States Geological Survey, (2017). USGS Global Visualization Viewer. Retrieved on 15.03.2017, from http://glovis.usgs.gov/

Rouse Jr, J. W., Haas, R., Schell, J., & Deering, D. (1974). Monitoring vegetation systems in the Great Plains with ERTS. In Third ERTS symposium, NASA SP-351, U.S. Govt. Printing Office, Washington, D.C., vol. 1, pp. 309–317

Balcik, F. B., (2014). Determining the impact of urban components on land surface temperature of Istanbul by using remote sensing indices. Environmental Monitoring and Assessment, 186(2), 859-872.

High Resolution DSM Generation with Low Cost UAV

Nizar POLAT [1], Murat UYSAL[2], Mehmet Ali DERELİ [3*]

[1]Afyon Kocatepe University, Engineering Faculty, Geomatics Engineering, Afyonkarahisar, Turkey; npolat@aku.edu.tr

[2]Afyon Kocatepe University, Engineering Faculty, Geomatics Engineering, Afyonkarahisar, Turkey; muysal@aku.edu.tr

[3]Giresun University, Engineering Faculty, Geomatics Engineering, Giresun, Turkey; mehmet.dereli@giresun.edu.tr

[*]**Corresponding Author:** mehmet.dereli@giresun.edu.tr

Abstract

Nowadays Unmanned Aerial Vehicles (UAVs) are widely used in many applications for different purposes. Their benefits however are not entirely detected due to the integration capabilities of other equipment such as; digital camera, GPS, or laser scanner. The main scope of this paper is evaluating performance of cameras integrated UAV for geomatic applications by the way of Digital Surface Model (DSM) generation in Afyon Kocatepe University Campus area. In this purpose, 5 ground control points and 12 check points are marked and surveyed with RTK. Then a photogrammetric flight plan is performed and from an altitude of 120 m, 274 aerial photographs are captured with an 80% overlap rate. After image processing, a high resolution DSM with a 50 cm pixel size was generated and the accuracy of the generated DSM was calculated as 5 cm. The outcomes of the study show that it is possible to use the UAV Photogrammetry data as map producing, surveying, and some other engineering applications with the advantages of low-cost, time conservation, and minimum field work

Keywords:UAV, SfM Point Cloud, DSM.

1. Introduction

Nowadays the documentation technologies based of advanced Geomatics tools offer a significant support in maps updating, in term of quickness, precision, cost-cutting, and in short, sustainability. The use of Unmanned Aerial Vehicles (UAV) offers almost new potentialities with high detail value, and related applications truly become progressively affordable, even where the context is not enough accessible for traditional terrestrial survey techniques (Aicardi et al., 2014).

The UAV approach can be useful to produce spatial-temporal high-resolution models, in competitive period and resources, that providing useful 3D data for many GIS monitoring applications, as georeferenced information at large-scale derived from orthoimages and DSM (Yastıklı et al., 2013). The main application of UAV survey producing spatial data for GIS modelling and analysis are the territorial, geological, urbanistic, agricultural and forestry ones (Höfle et al., 2013; Susaki, 2012). In many cases, the bare-Earth extraction can be obtained with algorithms of point clouds classification and segmentation, by filtering point along density, direction, slope, etc. In this study a high resolution DSM of Afyon Kocatepe university campus area was generated with a 50 cm pixel size and the accuracy of the generated DSM was calculated as 5 cm.

2. Material and Method

2.1. The Study Area and Data

The study area is located in Afyon Kocatepe university campus (Figure 1).

Figure 1. Study area.

For the study, DJI Phantom 4 pro UAV is used. 274 aerial photographs are captured from a 120 m altitude in an 1100 m x 500 m area. The flight path is given in figure 2.

Figure 2. The flight path of the UAV in the study area.

2.2. Image processing

The aerial photograps are processed in Pix4D mapper pro software. The main aim of process is to produce a georeferenced 3D point cloud by handling with overlapping aerial image data (Siebert and Teizer, 2014). The approach of point cloud generation from images is called as Structure from Motion (SfM). SfM runs under the same basic conditions as stereoscopic Photogrammetry. It uses overlapping images in order to get a 3d structure of interested object. The data processing is relatively easy. It starts with uploading photos from camera to computer and eliminating distorted or blurred ones.

2.3. Accuracy Analysis

In order to get root mean square error (RMSE) of Z, five new check points are used with the following equation (1).

$$\mathrm{RMSE} = \sqrt{\frac{(Z_{\mathrm{Model}} - Z_{\mathrm{Ref}})^2}{n}} \qquad (1)$$

Where Z_{model} is the value from the generated model, and Z_{ref} is the correspondent reference value from check points. n is the number of check points.

3. Results and Discussion

The generated othophoto and DSM is given in figure 3.

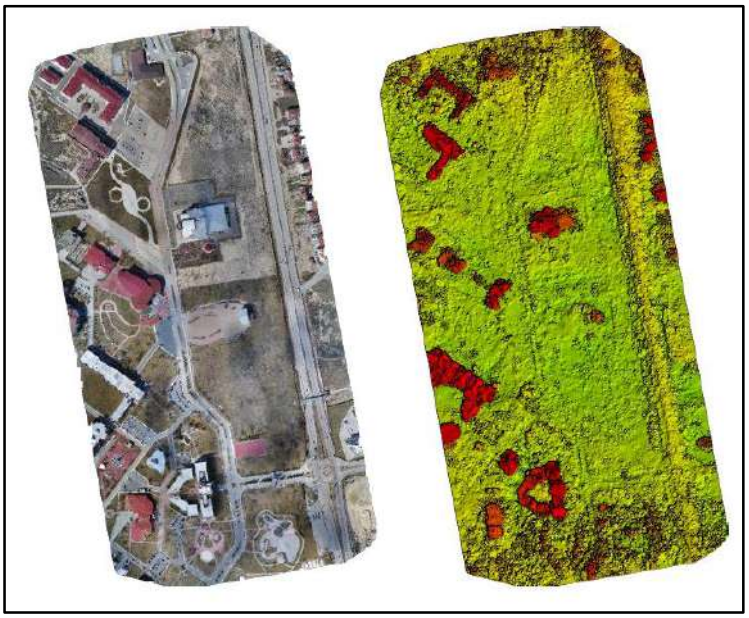

Figure 3. The generated othophoto (left) and DSM (right) for the study area.

The coordinate diffences are calculated between othophoto values and chech points. 12 check points are measured with Stonex S9 GNSS. The calculation results are given in table 1.

Table 1. The calculated RMSE for coordinates.

Check Points	X GPS	YGPS	X ortho	Yortho	D X(m)	D Y(m)
1	4298466	546313,8	4298466	546313,8	-0,003	0,023
4	4298580	546324	4298580	546324	-0,011	0
5	4298617	546470	4298617	546470,1	0,012	-0,004
6	4298416	546396	4298416	546395,9	-0,018	0,018
7	4298375	546467,9	4298375	546467,9	-0,005	0,024
8	4298244	546384,8	4298244	546384,8	-0,042	0,003
9	4298330	546275,5	4298330	546275,5	-0,017	0,028
15	4297963	546473,5	4297963	546473,5	-0,005	-0,009
16	4298093	546418,2	4298093	546418,2	-0,008	0,015
17	4298126	546558	4298126	546558	0,013	0,017
18	4297775	546566,7	4297775	546566,7	-0,019	0,036
21	4298268	546648,6	4298268	546648,6	-0,009	-0,014
				RMSE	**0,018**	**0,02**

The Z diffrences between DSM and check points are also calculted. The same 12 check points are measured with Stonex S9 GNSS. The calculation results are given in table 2.

Table 2. The calculated RMSE for Z values.

Check Points	ZGPS	ZDSM	DZ(m)
1	1047,974	1047,951	0,0229
4	1048,426	1048,397	0,0293
5	1048,698	1048,717	-0,0192
6	1047,999	1047,966	0,0333
7	1048,384	1048,334	0,05
8	1048,074	1048,059	0,015
9	1048,42	1048,44	-0,0196
15	1047,88	1047,839	0,0406
16	1047,92	1047,868	0,052
17	1048,079	1047,96	0,1186
18	1047,394	1047,38	0,0137
21	1049,168	1049,079	0,0889
		RMSE	**0,054**

3. Conclusion

This paper indicates the capability of UAVs, which is an alternative data collection technology, in a geomatic application in a small area by means of DSM generation with. Comparing with traditional manned airborne platforms, they reduce the working costs and minimize the danger of reaching to risky study sites, with sufficient accuracy. In fact, the UAV systems have lots of advantages (low-cost, real time, high temporal and spatial resolution data, etc.) which are very important for not only geomatic but also various disciplines. The application indicates that the UAV combined digital camera systems can allow to collect usable data for geomatic applications. The study shows that UAV based data can be used for DSM generation by photogrammetric techniques with a vertical accuracy of 5.4 cm. It can be stated that the UAV Photogrammetry can be used in engineering applications with the advantages of low-cost, time conservation, minimum field work, and competence accuracy. Moreover the created 3D model is satisfactory to realize topography with texture.

References

Aicardi I., Boccardo P., Chiabrando F., Facello A., Gnavi L., Lingua A., Pasquale F., Maschio P., Spanò A., 2014, A didactic project for landscape heritage mapping in postdisaster management., in Applied Geomatics.

N. Yastıklı, I. Bagci, C. Beser, 2013. The processing of image data collected by light UAV systems for GIS data capture and updating, ISPRS Archives, Volume XL-7/W2, 2013 ISPRS2013-SSG.

B. Höfle, L. Griesbaum, M. Forbriger, 2013. GIS-Based Detection of Gullies in Terrestrial LiDAR Data of the Cerro Llamoca Peatland (Peru), Remote Sensing, 5, 5851-5870.

J. Susaki, 2012. Adaptive Slope Filtering of Airborne LiDAR Data in Urban Areas for Digital Terrain Model (DTM) Generation, Remote Sensing 2012, 4(6), 1804- 1819.

Siebert, S. Teizer, J. 2014. Mobile 3D mapping for surveying earthwork projects using an Unmanned Aerial Vehicle (UAV) system. Autom Constr. 1–14.

INTERIOR DESIGN, ARCHITECTURE, LANDSCAPE, FURNITURE DESIGN, FURNITURE INDUSTRY

ORAL PRESENTATIONS

Form, Material and Symbol: Iconic Architecture in Built Environment

Burcu KÖSE KHIDIROV[1*], Bilge KÖSE[2], Ahmet KÖSE[3]

[1]Mimar Sinan Fine Arts University, Faculty of Architecture, Interior Architecture Dept., Istanbul, Turkey
[2,3]Ordu University, Vocational School of Technical Sciences, Construction Dept., Ordu, Turkey

***Corresponding Author:** burcu.kose@msgsu.edu.tr

Abstract

Iconic architecture is result of a particular point of view; and related to the notions represented. In architectural context, an iconic building stands strikingly within the city with features like concept, meaning, form, technology, material, style, and generally maintains a high level of contrast among its surroundings. The unique design, representation and specific messages of these buildings are the integrated components of the concept of "iconization"; and it is the major condition of being an iconic building to stand out in the surrounding environment. Iconic buildings reflect the cultures to establish relationships between users and construction. Since architecture is an instrument that renders cultures, social structure, history and beliefs, buildings defined as iconic possess symbolic meanings of cities. The iconic structure in the built environment can be evaluated in two parts as 'contemporary buildings iconized in historical surroundings' and 'historic buildings iconized in contemporary architectural surroundings'. In this research, the concept of iconic building will be examined in terms of form and material properties; and the contribution of these tangible features in symbolic and conceptual sense will be questioned through selected examples worldwide.

Keywords: Iconization, Built environment, Architecture, Form, Material

1. Introduction

Iconic buildings are not only outcomes of modern times, also are concepts that have always existed in the historical process. As an iconic object, they are results of specific point of views. The definition of the icon is related to the concepts it represents. When considered in the context of architecture, an iconic building stands strikingly in form and style within the city and generally maintains a high level of contrast between its surroundings. An iconic design is usually 'ground breaking' and one that sets new standards in its field. It is a design that other designers and manufacturers follow, as it becomes a bench mark for other similar products. For example, the Gherkin building in London is remarkably remarkable compared to its surroundings with its radical use of technology, material, its unique contemporary form and style. Another example of this is the Beijing National Stadium, which has been iconic in its environment with its distinctive structure, birds-nest-inspired ecological concept and steel system and materials (See Images 1 and 2).

Image 1,2. Gherkin building, London, the UK, Beijing National Stadium, Beijing, China.

According to Oxford English Dictionary, the iconic word means "an image, a figure or a presentation, a portrait, a book illustration; a solid object or sculpture; a sacred object" (Url1, 2018). In the current dictionary of the Turkish Language Institute, the iconic word is defined as "a figure, figure, or figure that symbolizes and describes a person, idea, current or anything" (Url2, 2018). Features such as use of different architectural designs, concepts, symbolic value, alternative construction techniques and materials makes a building "iconic" indeed. The uniqueness of the design idea and the buildings that are notable for its history, touristic, religious or any other reason can be called the iconic building. Many of these buildings are quite impressive and different in terms of form, size, material and construction efficiency. Niels Luning Prak says that "Architects use forms and materials as symbols. The idea of geometric shapes, materials and concepts created by architects depends on their intentions and countries. The purpose of these constructions is to reveal their socio-

cultural characteristics, religious signs and spatial characteristics" (Schulz, 1968). To describe the iconic building, Jencks (2006) expresses that the iconic building is designed to make money, to earn money, and the normal criteria are not used in the evaluation. In addition, the iconic building should give a striking new impression to spectators due to their features such as height, form or location. In some cities, iconic buildings are also used to create boulevards or squares, as reminding city icons.

In order for a building to be iconic, it must contain some integrated features such as unique design, different scale among the surrounding, spectacular representation and specific message. Cleo Broda defines iconic architecture as large-scale revolutionary designs that are familiar to community (Yvonne, 2009). Generally, iconic buildings are considerably differentiated, striking by its surroundings and designed by a recognized architect. As a result, architecture here is a vehicle that influences the appearance of the building and the location in which it is built. 'Image', 'modernity' and 'culture' affect the iconic buildings during planning process. However, in designing stage form and material are two significant element to create an iconic symbol building. In any cost, iconic buildings have contrast form and materials than their surroundings. The environment in which the building is located comes to foreground due to the presence of the large sized iconic building there.

The environment in which the building is located takes place in the foreground due to the large size of the iconic building there. For example, both Guggenheim Museums in Bilbao and New York City are successful examples of changing and strengthening the image of the surrounding by using icons (See Images 3 and 4).

Image 3,4. Guggenheim Museum in New York City, the US, Guggenheim Museum in Bilbao, Spain.

Image 5. Dancing House, Prague, Czech Republic.

There is also a touch of the construction time and its cultural feeling in iconic buildings. Dancing House is an iconic building where contemporary style is felt in terms of the form and materials used (See Image 5). The socio-cultural dimension is also very crucial to define iconic buildings. Because an iconic building is a bridge between the people and the icon, it should reflect the culture of the place where it is established. Already architecture is a tool that represents the culture, social structure, history and beliefs, iconic buildings reflect the symbolic meanings of cities.

2. Methodology

Within the scope of the method of this study, iconic buildings will be examined in two parts as contemporary ones in historical surroundings and historic ones in contemporary architectural surroundings with browsing-description method. In both categories, an 'iconic' building will be selected as an area survey and will be examined in terms of their iconic features like form and material in the context of space and architecture.

2.1.Contemporary Buildings Iconized In Historical Surroundings

When it comes to the iconization of architectural constructions, contemporary constructions of historical cities come first to the minds. The cities have a long-standing historical identity, and in this identity there is a growing urban settlement. However, expanding city scales and sizes, intense population increase through immigration, inadequacy of old buildings to meet changing demands, new technologies making new building systems possible, make constructing new buildings

obligatory. New buildings can be designed in a harmony with the surrounding area, they can be designed not to attract attention, but they can be designed as a product of new materials and technologies in complete contradiction with the historical environment - in this case an iconic contemporary structure is designed in a historical environment.

Basque Health Directorate Building designed by Coll-Barreu Arquitectos in Bilbao, Spain (2008) can be shown as an example for iconic contemporary structure in historical surrounding.

Image 6. Basque Health Directorate Building, Bilbao,Spain.

This modern and extraordinary structure is designed as a very different public building in a historical texture. This building which is second most photographed after Guggenheim Museum in Bilbao by tourists differentiated and iconified in the surrounding area. The building were raised as a single main mass, while the façades were retracted while approaching the building next to them. The buildings in the neighbouring parcels were not exceeded the upper elevation limits of the adjacent parcels and were designed in the same way as the adjacent buildings. The edges and the building were not perpendicular but joined with rounded or crack movements. Although other buildings around look so straight, linear, concrete and vertical, Basque Health Directorate Building differentiates from them through angular, crosswise, diagonal lines with transparent glass façade, and steel construction system.


Image 7, 8. Basque Health Directorate Building, Bilbao,Spain.

Building is located in the crossroad of the two most important streets of Bilbao. The restrictive city zoning rules force to repeat the existing building typology, reducing pent housing, chamfering corners and rising a tower. Therefore, this building is thought as a typical one for the area, but with a glass curtain wall system. The building provides vertical communications and general services inside a core, a prism next to the dividing wall that serves to open-plan floors.

The building is quite modern in terms of the systems and techniques used. An important feature of the building is that it is double-faced; the double-layer facade reduces the noise of heavy street traffic, thus resolving the requirements of sound insulation and fire regulations. It also reduced the heat loss of the facade and prevented the use of conventional systems for ventilation. Air circulation between the two layers provides clean air for the interior in the summer, allowing the space between the layers to be used as a balcony.

Besides, that folded element produces multiple views of the city, and changing its appearance depending on the point of view , the hour and the season. The objective of this element is introducing the mutability, the dynamic spirit of the city. Located in a very historic part of the city of Bilbao, this building has become iconic with its own image and, if necessary, with its different and striking forms and materials.

2.2.Historic Buildings Iconized In Contemporary Architectural Surroundings

Historical buildings, such as the iconic structures constructed afterwards in historical city environments, are also pre-built in the contemporary architectural circles. Old buildings can be

damaged and demolished during the historical development process of the cities. Even in some regions, this destruction is so great that sometimes the historical texture is completely destroyed; sometimes only one building remains intact and remains iconic, with new settlements and structures built around it.

An example of the historic iconic building in contemporary architectural surroundings is the Huguang Guild Hall, built in 1759 in Chongqing, China. As is well known, Chinese cities are trying to protect their historical structures, and because of the excessive population density, the necessity of shelter is in line with the fact that new and distorted structures are built up in historical textures and even in some cases they cause damage to this texture. In the vicinity of Huguang building, there are many buildings, such as modern and multi-storey car park, shopping centre.

Image 9. Huguang Guild Hall, Chongqing, China.

Huguang Guild Hall is now used as a museum, as well as opera shows in certain lounges. In the past, this building was first built with the efforts of the local tradesmen, and has gone through three major restoration and several minor repairs daily. When it was re-opened in 2006, visitors still can find the original style. The wooden building walls, doors and windows were delicately carved with themes of human figures, animals and various plants. Until today, Huguang has grown exponentially by growing clusters of different places; and there are courtyards, opera stages, rooms and gardens. Since it is built by traders who have migrated from different cities of China, there are places in different styles. The building enlarges in horizontal direction on site, has unique vivid colour, and detailed handcrafts. There are giant fires seals dividing the space into a number of small courtyards, every small courtyard can be connected by wickets, and the space is not cut off. This makes each courtyard has its own unique function and the corresponding landscape, rockery plants, small bridge over flowing stream, corridor carving painting of the unique style and characteristic spaces.

Image 10. Huguang Guild Hall, Chongqing, China.

These different styles have come together and integrated to create the unique architecture of the building. There is a delicately carved process on the wooden walls, doors and windows of the building. These subtle details, which are supposed to be local cultures, contrast with the sloppy modern and new urban texture in the world. Huguang Guild Hall once carried a glorious past of Chongqing city and it will continue to host the new another piece of brilliance today. Huguang, which still shines with its old air and nobility among the high buildings, is a successful example of the historical iconization in the contemporary environment.

3. Conclusion

In this study, the concept of iconic architecture, the scope of this concept, its components and formation patterns are revealed. After the literature survey on the subject was made, the architectural iconic situation was examined through examples.

The study emphasizes two different ways of iconization in architecture have been investigated. As it can be achieved with new and modern constructions located in historical sites, it can also be with historical buildings that have succeeded to survive in new urban fabric. If we compare these two ways of iconization, it can be said that modern buildings built in historical circles can attain

the same result as the old texture ruins. Historical buildings in contemporary urbanization differentiate them by enriching this modern texture. In today's cities, especially in the context of urban transformation which is very popular in our country, new settlements that meet the demands of the population, questions such as "what is the historic touch?", "when new and unidentified buildings are built in urban transformation, what is the contribution of the preservation of historical buildings in that area to identity?" have to be considered and such questions need to be thought carefully during the construction process

References

Jencks, C. (2006). The Iconic Building Is Here To Stay. *City Journal*. Volume 10, issue 1, pg. 1-20.

London: Routledge.

King, W. (2008). *Modern Day Iconic Buildings - What Really Makes Them Iconic.* http://ezinearticles.com/?ModernDay-Iconic-Buildings---What-Really-Makes-Them-Iconic?&id=2983327

Yvonne, C. (2009). What Makes A Building Iconic, *Malaysian Business Journal.* http://www.scribd.com/doc/43727127/What-Makes-a-Building-Iconic-2

Castells, M. (2004). *The Power of Identity (The Information Age: Economy, Society, and Culture) (Vol. 2).* Blackwell Publishing Ltd.

MacCannel. D. (2005). *Learning from the Bilbao Guggenheim*, The Fate of the Symbolic in Architecture for Tourism Piranesi, Disney, Gehry. Reno, Nev. : Center for Basque Studies, University of Nevada, Reno.

Schulz, N. C. (1968*). Intentions in Architecture*, pg. 53-58, Oslo,Norway: The M.I.T Press.

Vale, L. J. (2008). *Architecture, Power, and National Identity*, pg. 58, Routledge, Oxon.

Url 1 Iconic, Oxford Dictionaries, Ret. 01.06.2018, https://en.oxforddictionaries.com/definition/iconic

Url 2 İkonik, Türk Dil Kurumu, Ret. 01.06.2018, http://www.tdk.gov.tr/index.php?arama=gts&option=com_gts&kelime=ikonik

Three Dimensional Modelling In Landscape Architecture Teaching

Deryanur DİNÇER[1], Türker OĞUZTÜRK[2*]

[1,2]Recep Tayyip Erdogan University, Faculty of Fine Arts, Design and Architecture, Department of Landscape Architecture, Rize, Turkey; deryanur.dincer@erdogan.edu.tr, turker.oguzturk@erdogan.edu.tr

[*]**Corresponding Author:** turker.oguzturk@erdogan.edu.tr

Abstract

The visualization of the forms of designs in the minds of potential users (people) is effective in better understanding functions of the designed and created areas. Computer technology not only enhances the power of existing elements in landscape architecture but also allows the development of new design elements and presentation techniques. Within the scope of this study, the students who take three dimensional (3D) modelling lesson were asked for three dimensional drawing of a plan and then drawings made by the students were compared to each other in order to reveal whether the use of 3D modelling programs was helpful in landscape architecture teaching. At the end of the study, it is seen that students who have developed themselves in the 3D modeling program seem to be more successful in terms of reading and expressing the plans. Also, the questionnaire evaluations show that the students using computer programs achieve solutions faster, are more successful in developing alternative design proposals, are aware of making realistic presentations with a high visual quality, and are able to develop more proposals in a shorter time.

Key Words: Landscape Design, 3D Modelling, Landscape Architecture Teaching, Visualization

1. Introduction

The recent developments in computer software and hardware have greatly increased the quality and speed of computer graphics and animation processes. In this way, the interest and need for the field of computer graphics, which has begun to have an influence on every field from everyday life to various branches of science, gradually increases and this field is enhancing every day with the formation of standards and the addition of new concepts (Uğur, 1996).

Computers used in every field nowadays has naturally been started to be used for design and planning studies increasingly. Very advanced software especially used by the countries that have improved on Computer Aided Design (CAD) has emerged. As in all other sectors, when institutions engage in competition in the field of design and planning, those that use new technologies and quickly adopt innovations will survive (Benliay, 2000).

Computer graphics (three-dimensional modeling) are widely used in many areas. The most important areas are Computer Aided Design (CAD) and Computer Aided Manufacturing (CAM), Science and Scientific Visualization, Education and Training, Entertainment, Advertising, Art, Virtual Reality and Reinforced Reality and Web (Uğur, 2002).

Cinema industry has also become one of the areas in which three-dimensional model is used thanks to animations and science fiction films that were produced with massive budgets and gained recognition.

The fact that the real world is three-dimensional increases the need for three dimensions in computers. Three-dimensional images attract more attention and make visualization the closest to reality. Although three-D is difficult, it is easier to achieve the same results in real compared to 2-d. Many of today's modeling programs provide the opportunity to easily look by rotating around any axis interacting with 3D models and to obtain moving images of the model. Two dimensional drawings are inadequate when viewed from this perspective (Uğur, 2002).

Architecture is one of the technical issues in which imagination, creativity and design intelligence is at the top level. An architecture, like a painter or musician, often needs to share things he has created on his mind with others. While a painter shares his dreams drawing on the canvas, an architecture shares his dreams by making models, producing pencil drawings or technical drawings. With today's developing software and hardware technologies, computers have become a powerful alternative to models to display the imaginary worlds of architects (Uğur ve Özgür, 2003).

Architecture education has entered into a rapid change process with the development in computer and communication technologies in the last twenty years. In order to analyze the effects of this change on architecture and architectural education, application based researches are carried out.

The results of the interaction of computer technologies with architectural education are evaluated by taking into consideration the relation between utility and damage (Çetiner, 2006; Özdemir, 2008).

Landscape Architecture is one of the professions that require great care and high capability in terms of design strength and presentation characteristics. As for all work areas, these developments and their effects are very important for Landscape Architecture (Benliay, 2000).

1.1. Purpose, Importance and Scope of the Study

The exponential growth of software (computer) technology and the facilities it provides for life make software (computer) technologies important in all areas of our life and using these technologies necessary in landscape architectural education. The visualization of the designed and created areas in the minds of the potential users (people) is effective in order to better understand the design and its functions. Computer technology not only enhances the power of existing elements in landscape architecture but also allows the development of new design elements and presentation techniques. Teaching this kind of programs to landscape architecture students provides them with favorable opportunities in the field of design and presentation creating impressive and realistic images and animations of near realistic quality.

Within the scope of this study, questions about the purpose of the study were asked to Recep Tayyip Erdogan University Landscape Architecture students and it was researched whether the use of 3D modeling programs is useful in the development of landscape architectural education of the students.

2. Material and Method

2.1. Material

Material portion of our study is comprised of students have taken the course in Three Dimensional Design.

2.2. Method

Three dimensional drawings of a plan given to the students taking the 3D modeling course are requested to be drawn using the programs given below. Three dimensional design and two dimensional drawings were interpreted by comparing them with each other. It was also questioned

by the questionnaire method whether the three dimensional design contributed to the education, and it was determined what kind of contributions it provides to their designs with the help of the graphs.

Used programs;

- Autocad 2018,
- Sketchup 18,
- Lumion program is used.

This study consists of 6 steps. These steps;

First stage; Searching the literature for the purpose and importance of the study,

The second stage; Determination of the method to be followed in Three Dimensional Modeling study in Landscape Architecture Education,

Third stage; Drawing of the Autocad 2018 files related to the selected work in 2D media,

The fourth stage; The modeling of the determined projects by the students in 3D environment,

The fifth stage; Preparing and implementing questionnaires for the purpose of the study, comparing the models that the students have done,

The sixth stage; Evaluation.

3. Findings

3.1. 2D and 3D drawings of students

3.1.1. Workspace

As a study area, one house garden project plan was given to the students and they were asked to make designs related to this area and they were asked to transfer these designs to two-dimensional, three-dimensional environments. Thus, students were evaluated for their ability to master computerized drawing programs and to translate two-dimensional drawings into three-dimensional visuals.

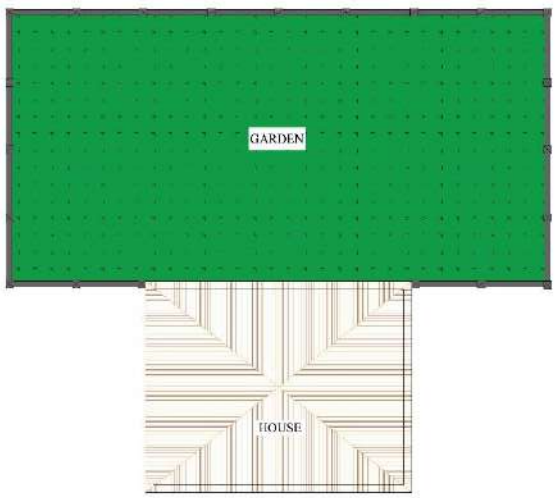

Figure 1: Study area given to students.

3.1.2. Designs and Models Made by Students

Figures 2, 3, 4 and 5 show examples of the studies made by the selected students.

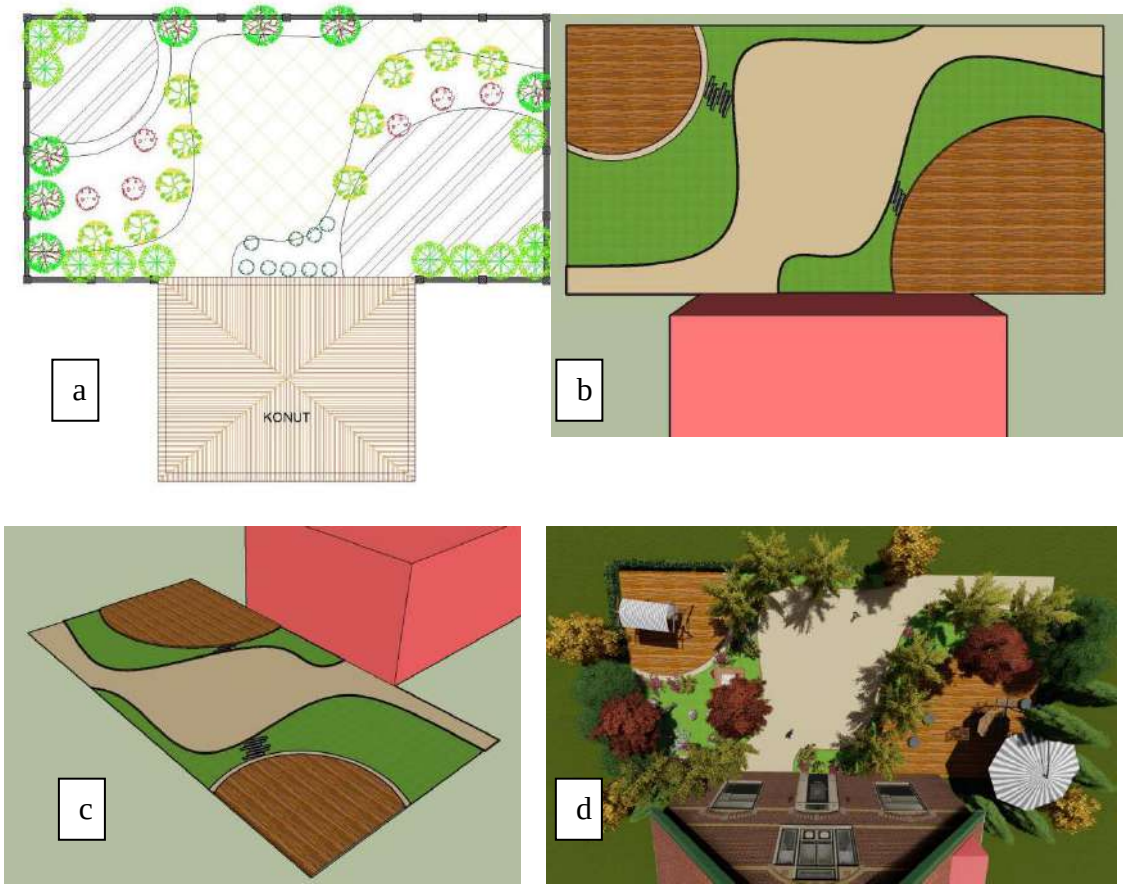

Figure 2: a) Two-dimensional drawing, **b)** Three-dimensional drawing, **c)** Three-dimensional drawing perspective, **d)** Three-dimensional drawing and Lumion

Figure 3: Three-dimensional modeling render example.

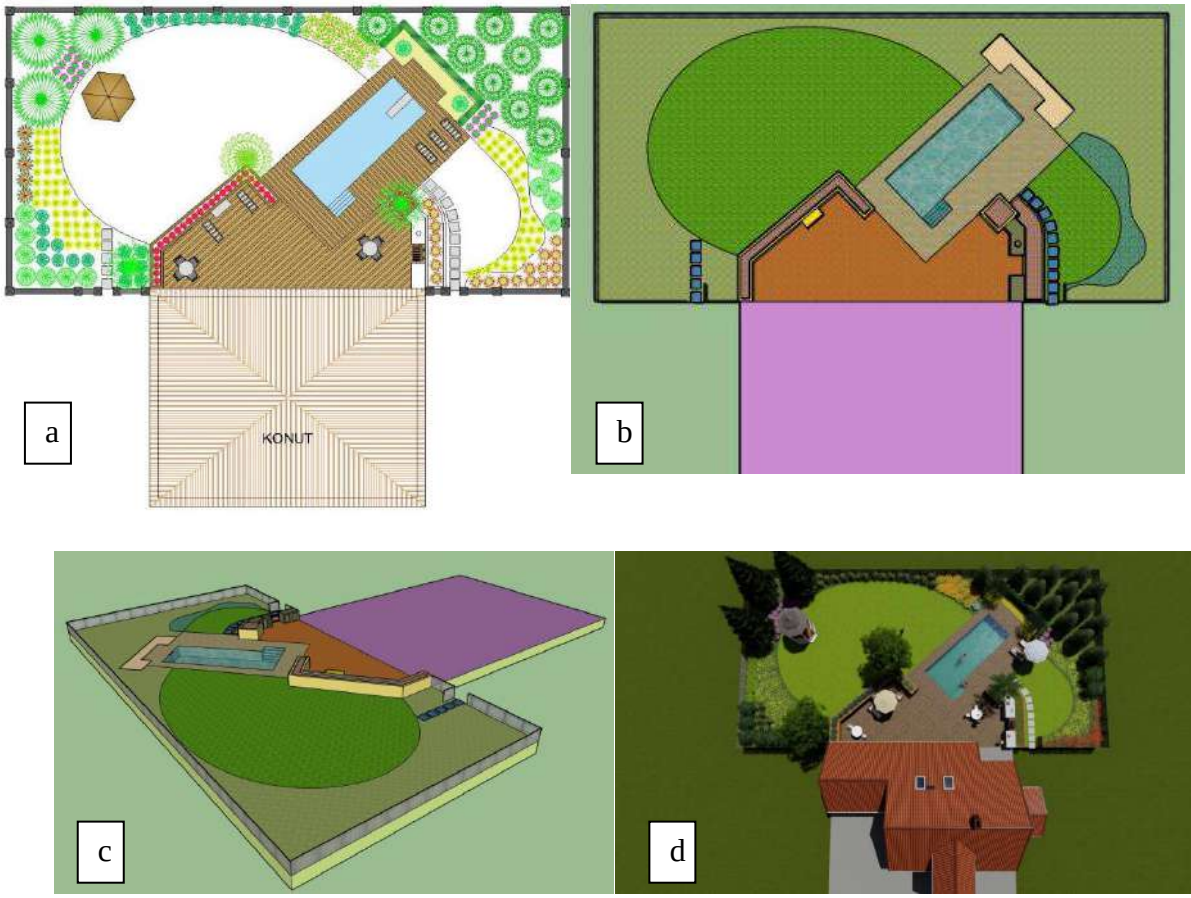

Figure 4: a) Two-dimensional drawing, **b)** Three-dimensional drawing, **c)** Three-dimensional drawing perspective, **d)** Three-dimensional drawing and Lumion

Figure 5: Three-dimensional modeling render examples.

As a result of the studies examined, it has been seen that the ability of students to master drawing programs is highly related to the way they express their visual thoughts.

3.2. Survey Studies

In order to determine the most positive feature of the three dimensional modeling in terms of the students with the questionnaires prepared for the purpose of our study, the order of the characteristics of Understandable Detail, Easy Design, Impressive images and High Perceptibility was requested from the students and the percentage points obtained after the scoring according to the ranking of all survey participants are shown in Figure 6. According to Figure 6, the most positive feature of the Three Dimensional Modeling (135 points) is Understandable Detail with a 30% share. Impressive Images (129 points) is second with 29% share, High Perceptibility (123 points) was 27% and Easy Design (63 points) was in the third and fourth place with 14% share.

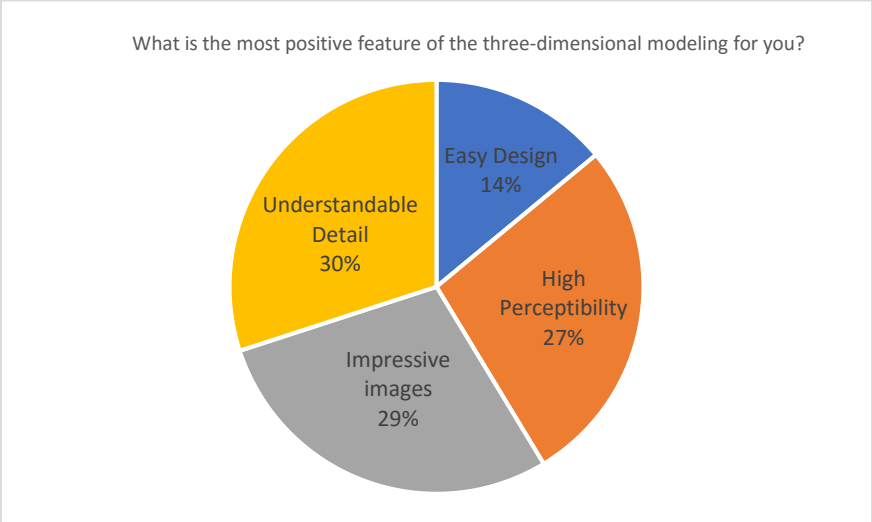

Figure 6: The most positive feature of the three-dimensional model.

The questions asked to determine in which areas the three-dimensional model is useful for students and in which areas the training contributes are shown in Figures 7-11. The obtained graphics were interpreted and the results and recommendations were reached.

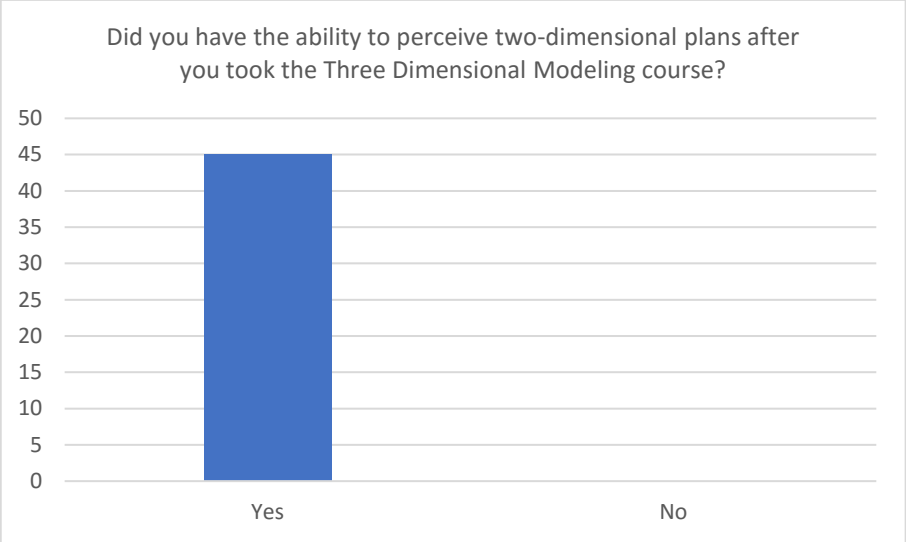

Figure 7: Contribution to the ability to perceive two-dimensional plans.

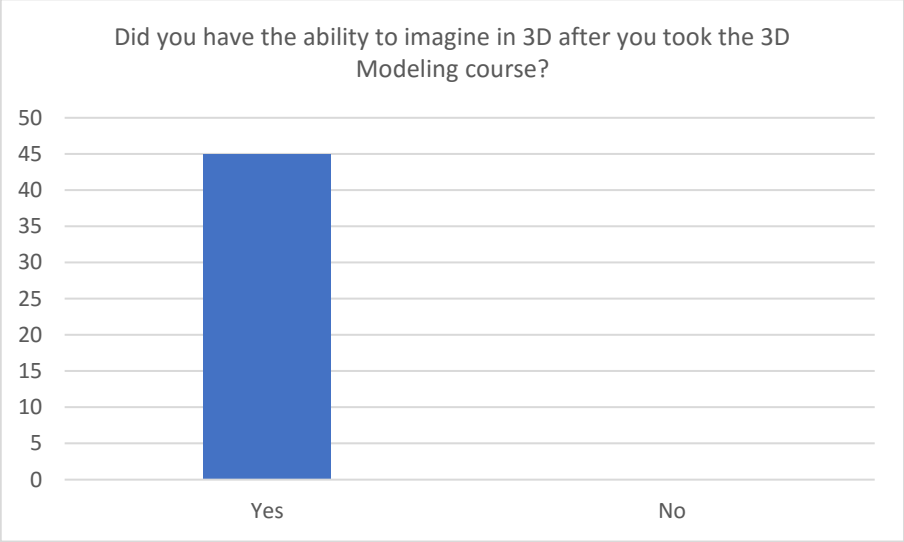

Figure 8: Contribution to three-dimensional imagination.

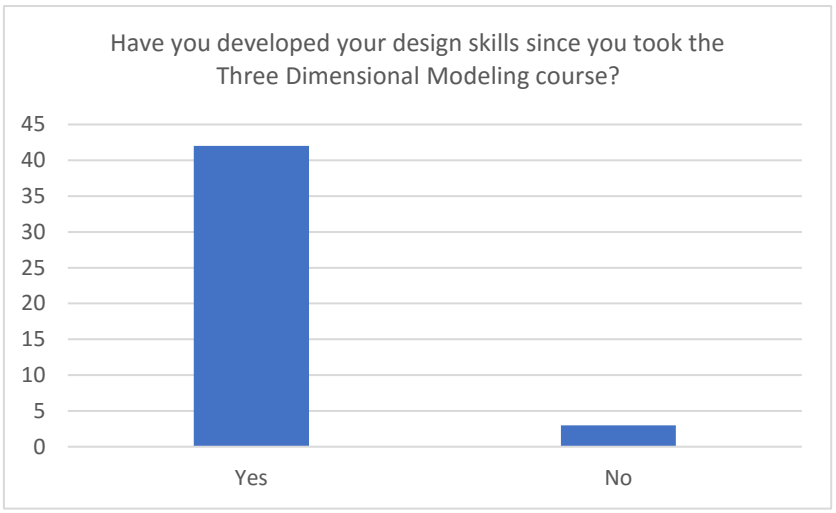

Figure 9: Contribution to design capability.

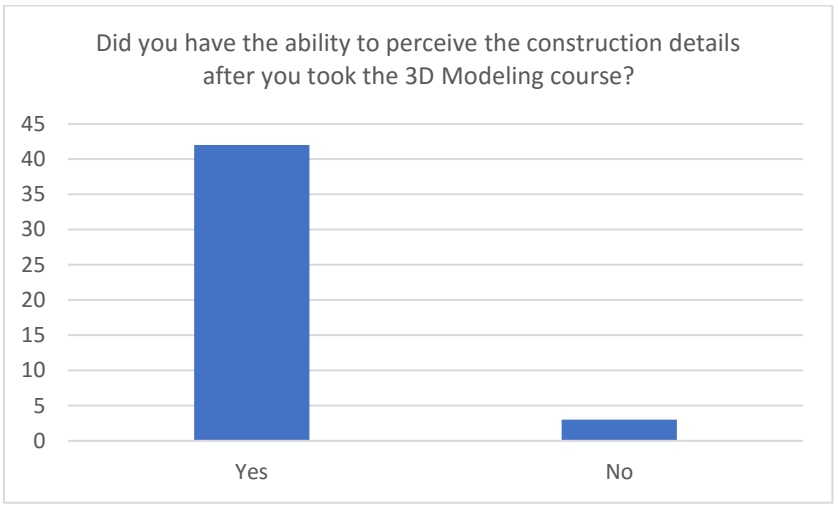

Figure 10: Contribution to the ability to perceive the scale and dimensions between drawing and reality.

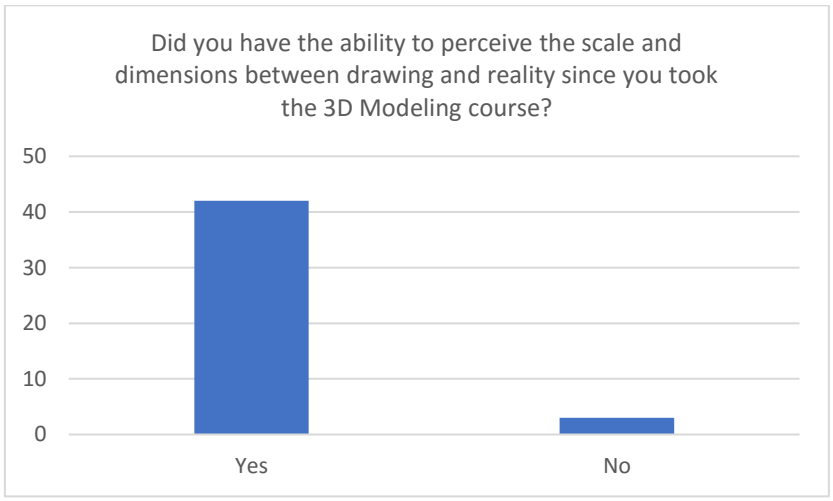

Şekil 11. Contribution to the ability to perceive the scale and dimensions between drawing and reality.

4. Results and Discussion

As a result of this study, it is seen that students do not pay attention to 2D CAD drawings (line width, double line, etc.), but these details are made automatically in the 3D Modeling programs, thus contributing to students' perceptibility. As a matter of fact, Ozdemir Işık (2017) stated that the ability to think in three dimensions and the ability to make models gradually increased after the students started using 3D Drawing programs in similar study.

When the sketches are examined, it is seen that SketchUp program does not reach sufficient visual quality alone and Lumion (Render program) program which is used later can get faster and better quality images at different angles. In his work Hamamcıoğlu Turan (2002 and 2004), visual presentations allow for the increase in the quality of work in the professional field. It is also regarded as a means of describing a model and containing descriptive information that is reduced for the purpose of clearly grasping and manipulating information about the object. The discovery of visual presentations using three-dimensional databases allows for frequent preference in perspective views.

It has been seen that the ability of the students to master the computer has the same level of success in both programs, depending on the ability to use the computer, where two-dimensional and three-dimensional drawing successes are affected at the same time.

As a result of the questionnaires directed to the students, it has been seen that the three dimensional modeling program has developed and contributed to the ability to perceive plans, to imagine three dimensions, to contribute to the development of design ability, to perceive details better, to see scale and dimensions.

As a result of this study, it is seen that the students who developed themselves in the 3D modeling program are more successful in terms of reading and expressing the plans. As a result of the questionnaire surveys, it was concluded that students who use computer programs have faster solutions and that they are more successful in developing alternate design proposals, and that they are aware of the fact that they are producing quality and realistic presentations from the visual point of view and that they can develop more suggestions in a shorter time. In Özdemir Işık's (2017) study, the introduction of technology into the architectural space, along with the ease of application of projects that are difficult and troublesome to implement, makes digital programming an architectural education highlight.

Based on these results, the use of 3D Modeling programs in Landscape Architecture training; we can say that there is a considerable contribution in the education period of the student and even in the business life after graduation.

5.Suggestions:

It is important to know and draw drawing programs in Landscape Architecture. However, it is necessary for the students to develop hand drawing skills and sketching skills. For this reason, firstly students should start to train tehmselves with traditional drawing methods and design and development infrastructure should be created and developed first. To increase the speed of use of drawing programs and the effectiveness of their use, students should also frequently find leisure time using these programs.

Computer use should be increased in the field of education and training in terms of increasing professional development and expressive power.

References

Hamamcıoğlu Turan, M., 2004. "Mimari Fotogrametri Alanındaki Çağdaş Gelişimlerin Değerlendirilmesi", Gazi Üniversitesi Mühendislik Mimarlık Fakültesi Dergisi, 19-1, 43-50.

Özdemir Işık, B., 2017. Bilgisayar destekli tasarım programlarının mimarlık eğitimine katkısı (Contrıbutıon of computer-aıded desıgn programs to archıtectural educatıon)Uluslararası Sosyal Araştırmalar Dergisi, The Journal of International Social Research, Cilt: 10 Sayı: 51 Volume: 10 Issue: 51.

Uğur, A., "İnternet Üzerinde Üç Boyut ve Web3D Teknolojileri (Three Dimensional Graphics on the Internet and Web3D Technologies)", VIII. Türkiye'de İnternet Konferansı (INET-TR 2002), Bildiri No : 54, İstanbul, Türkiye, 19-21 Aralık 2002.

Uğur, A., Özgür, E., "İnternet Üzerinde Üç Boyut ve Mimarlıkta Web3D" , IX. Türkiye'de İnternet Konferansı (INET-TR 2003), Bildiri No : 3, İstanbul,Türkiye

Benliay, A. "Bilgisayar destekli tasarım sürecinde peyzaj tasarım projelerinin sunum tekniklerinin Ankara Üniversitesi Ziraat Fakültesi dekanlık kampüsü projesi örneğinde irdelenmesi, Yüksek Lisans Tezi, Ankara Üniversitesi." Fen Bilimleri Enstitüsü, Ankara (2000).

Özdemir, B. "Bilgisayar destekli tasarım yöntemlerinin peyzaj mimarlığı açısından kullanımının yararları ve KTÜ kampüsünde bir uygulama örneği, Yüksek Lisans Tezi Karadeniz Teknik Üniversitesi." Fen Bilimleri Enstitüsü, Trabzon, Türkiye (2008).

Uğur, A., 1996, Üç Boyutlu Çizim ve Animasyon, Yüksek Lisans Tezi, İzmir, 106 s.

Hamamcıoğlu Turan, M., 2002. Applied Architectural Photogrammetry–Defensionskaserne in Minden", Unpublished Research Project Report, Minden.

R&D and Technological Knowledge in SMEs: Furniture Industry in Samsun Region

Seval MUTLU ÇAMOĞLU[1]

[1] Ordu University, Ünye Faculty of Economics and Administrative Sciences, Department of Economics, Ordu, Turkey

[*]**Corresponding Author:** smutlu28@gmail.com

Abstract

In this study, It was focused the level of R&D and technological knowledge in micro, small and medium-sized enterprises in the furniture manufacturing sector, established in Samsun. The traditional production system is usually widespread in this region. Furniture manufacturing is a labour-intensive sector that has been growing with regard to functionality, aesthetic appearance and fashion of products. The industry attracts attention due to the integration of designs and developing technologies in Turkey. The results of the field survey obtained by the furniture manufacturers constitute the findings of this study. The micro and small-scale are constituting the majority of firms in this region. The usage of technological knowledge and R&D activities were analyzed according to turnovers of these enterprises. As the turnover in the industry grows, technological knowledge is used more intensively. In the medium-sized enterprise, the difficulties related with financial and R&D are decreasing relatively small and micro sizes. It is observed that firms are following foreign technology inadequately. In particular, micro-sized firms are more far away from foreign and domestic technologies. These findings point to the need for enterprises to reach a suitable size to be more innovative and use technological knowledge. In general, SMEs in the furniture sector are quite successful in introducing new product to the market.

Keywords: R&D, Technological Knowledge, Furniture Sector, SMEs

1. Introduction

SMEs, which includes micro, small and medium-sized enterprises, is one of the key dynamics in terms of development in emerging economies. Although their size is small relatively, research and development activities in these firms are also extremely important in point of economic development. These firms are facing many challenges such as professional management, marketing, product marketization, organizational structure, providing external finance as well as technological knowledge, research and development, innovation and creativity. Globalization, in SMEs cases, requires firms to have a variety of advantages in order to survive in the market. In this sense, SMEs should offer new products to the market with high quality and provide advantage of technology (Hadjimanolis, 1999; Van de Vrande, *et al.,* 2009; Timurçin, 2010).

The share of research and development expenditures in GDP in Turkey was 0.94% as of 2016. Total R&D expenditures reached about 25 billion TL. 50% of these expenditures were for R&D personnel, 39% for current expenditures and 11% for investment expenditures. 54.2% of these expenditures were in private sector enterprises, 9.5% in government and 36.3% in higher education institutions (TUİK, 2018).

Furniture manufacturing is a labour-intensive sector that has been growing with regard to functionality, aesthetic appearance and fashion of products in globalizing world. The industry attracts attention due to the integration of designs and developing technologies in Turkey.

Furniture covers all functional and aesthetic-looking items made of wood to make daily life more comfortable and safe. It is produced by using building materials such as chipboard, fiberboard, MDF, plywood in interior or exterior spaces. A consumer from a furniture may have various expectations such as functionality, ease of use, durability, aesthetics, health (Sakarya & Doğan, 2016). In this respect, these components to meet consumer needs require research and development process such as design, new product development, and utility model. It is possible to develop such items on SME scale in this sector.

The production value of the furniture sector in the whole world has reached about 500 billion dollars. Production location has shifted to China in the last 20 years, while European was the furniture manufacturing center, previously. Turkey in the wood based panels industry is the world's 5th and Europe's 2nd largest manufacturer (İstek, *et al.*, 2017).

The SMEs have many advantages in terms of innovation and R&D. Yelkikalan and Kalmış (2001) stated that SMEs can make more technical innovations than large enterprises with the same financial expenditure. Small and medium-sized enterprises are able to present technical ideas and practices to large-scale enterprises to further develop and process them. In addition, SMEs can

perceive the consumer preferences and make the necessary changes in the production process more swiftly for working closer with the consumer. It is able to respond more quickly with the innovations to the needs that arise due to consumers' demands. Managers and employees are in closer relationship, and employees' sense of belonging increases quality and efficiency. The investment expenditures needed to increase employment are lower than large enterprises. An increase in the number of small enterprises in an industry leads to a more complete competitive market environment. In this circumstance, it has an effect that increases technical innovations and makes more efficient use of resources.

Turkish furniture sector can be observed some problems in R&D and SMEs. Çelik (2012) revealed within the framework of the sector decision-making model that the main problem in the sector are the lack of innovation and R&D activities, the deficiency of design studies and the expansion of imitations. Besides, the fact that the majority of the enterprises operating in this sector are SMEs poses problems due to the lack of capital and the high credit costs.

R&D is one of the key factors that determine the competitiveness of the country. In economic growth, factors such as physical capital in the long run are subject to the law of diminishing returns, while R&D and technology cause the fixed and increasing conditions to be valid. Innovation and creativity have important roles in terms of competitiveness. Creativity is the production of new ideas and innovation is the realization of new ideas. Differentiation of processes, new raw material usage, changes in management understanding, business facilitation are examples of innovation. The increase in creativity is also related to skilled labor employment. These are factors that prevent innovation in enterprises such as not following international developments, imitating local competitors, disrespecting the ideas of employees, not promoting patent owners, not protecting copyrights, economic instability in the country, lack of market research. Technology is the systematic application of knowledge in the processes of the industry. Technological innovations cause changes in the competitive structure, product processes and markets. To achieve competitive power requires continuing innovation activities and driving customer demands and needs to a market faster than their competitors (Timurçin, 2010; Altay, 2006).

Santamaría *et al.* (2009) stated that non-formal R&D activities such as advanced machine use, outsourced training, collaboration agreements and design are very important in industries where low and medium technology is used. Traditional literature in technological information systems has primarily focused on large corporations. The research in this area is too limited to provide useful guidelines for the problems, opportunities, and management issues encountered by small business (Premkumar, 2003).

This study will contribute to the literature in terms of the extent to which the technological knowledge and R&D level can be reached in a regional industry where SMEs are concentrated. After examining the situation of the furniture sector in Samsun region, it is aimed to put forward the use of technology, problem areas, ways of reaching the technology and new product-design contribution in the sector.

2. Material and Methods

In this study, it is aimed to present the current situation of the R&D activities of the firms in the furniture sector in Samsun region on the SME scale. There are 267 furniture manufacturers in Samsun. It employs 1,753 people in this province (STSO, 2017). Since the sector is composed of many small enterprises, only the firms registered in Samsun Provincial Directorate of Commerce and Industry have been taken into consideration in order to represent the furniture sector. There were 77 registered furniture manufacturer firms in 2015. It was interviewed with 57 firms that agreed to conduct a survey.

In these interviews, it could be argued that these firms are able to follow technological progress in their workflow processes, the challenges in technological transportation and research and development processes, the type of new technological transportation, whether the sector offers a new product or service, whether utility model and industrial designs exist or not, the level of technological knowledge in comparison with competitors, IP rights (patent and trademark status). By examining the answers of these questions, it is aimed to reveal the level of research and development activities and technology usage in this sector.

First of all, 5 different turnover groups were created by the firms interviewed within the scope of field survey. The existence of significant relationships determined by Anova in the use of technology and R & D activities according to turnover groups. Anova, analysis of variance, applies between the turnover level and the variables including Likert-scale. It is one of parametric tests that requires data in numerical scores for each person and use F test. For variance analysis, it assumes that the population distributions are normal and variance homogeneous (Gravetter & Wallnau, 2016: 559-562).

3. Findings and Discussion

The results of the field survey obtained by firms operating in Samsun furniture sector constitute the findings of this study. Pre-prepared questionnaires have been filled out with the authorized persons in 57 firms. Firstly, socio-demographic characteristics of the mangers are given in the findings. Then, information about economic, legal, financial, production, and turnover of the firms are presented. Later, the firms involved in the research are examined by the use of technology, problem areas, and ways to reach technology, new product-design contribution according to five turnover groups.

62 percent of the managers interviewed in the firms are the owners and 23 percent are non-family. The average age of the authorized persons interviewed is 42. These people generally begin to work in the industry since their early ages. Then, they have established their own firms by specializing after learning the job. As the level of education is concerned, they usually graduate from high school. Müftüoğlu (2007) stated that the managers of the firms are engineers, technicians or skilled workers in SMEs increases success in the production processes, but this success does not seem adequate to marketing, finance and management.

This study indicates that there are firms operating in the furniture sector in Samsun since 1926. By 1982, there were only 10 firms, but after 1982, the number of firms increased every decades (see Table 1). The widespread of furniture manufacturing is influenced by the development of the construction sector in Turkey.

Table 1. Distribution of firms by year of establishment

Years	Num. of firms	%
1926-1981	10	17,5
1982-1991	12	21,1
1992-2001	20	35,1
2002-2015	15	26,3
Total	57	100,0

According to the average annual turnover of the firms; 60,7% of them are concentrated between 50,000 and 250,000 TL. Firms with annual turnover of 500 thousand TL constitute 91.1% of the firms and the average number of employees is below 15 persons (Table 2). Descriptive statistics by means and frequencies are given in Table 3 and 4. The average operating time of firms is 23 years, the average number of employees is 11, the share of paid up debts in total turnover is 44 percent and the investment amount of firms that will enter the sector is around 500 thousand TL. The average capacity utilization rate in these firms is about 65% annually (Table 3).

Table 2. Distribution of firms according to their average annual turnover

Annual Turnover (TL)	Num. of firms	%	Num. of Employees	Turnover / Num. of Employees***
min.-50.000	11	19,6	14,00	4.653,91
50.001-100.000	20	35,7	8,30	17.528,96
100.001-250.000	14	25,0	10,64	32.705,46
250.001-500.000	6	10,7	8,33	56.894,84
500.001- max.	5	8,9	18,80	100.952,38
Total	56	100,0	10,95	30.460,35

[a] Mean, *** P<0.01

Table 3. Descriptive statistics of the firms by means

	N	Minimum	Maximum	Mean	Std. Deviation
Firms' operating period (years)	57	5,00	89,00	23,28	15,31
Number of employees	57	1	95	11,33	15,11
Total annual turnover (TL)	56	10.000	1.000.000	211.517,86	263.086,44
Share of paid up debts in total turnover (%)	56	5	80	44,32	21,64
Competing new investment amount (TL)	57	50.000	3.000.000	526.842,11	676.703,95
Annual capacity utilization rate (%)	57	20	100	65,14	16,601

Corporate characteristics of firms were evaluated with the frequency of observation. Considering the legal structure of the firms, they are more private companies. The ownership status of the firm building is 47.4% of the rent and 40.4% of the ownership. Sixty percent of the firms have used credit in the last year.

40% of the firms are producing both by order and by mass production. The majority is 47.4% only selling to the final consumer. 15.8% are for industrial users and 36.8% are for both groups. Only 9 companies receive encouragement from the government. 11 of them have TSE quality standard. 89.5% can take place in the market with its own brand.

The fact that they are at SME scale also leads to a low level of foreign trade activities. When evaluating the level of competition in the region on the basis of product and price, 28.1% of the firms stated that there are companies that operate in the same field and produce the similar products. Besides, 26.3% of the firms stated that they implement the same price policy with their competitors.

Table 4. Descriptive statistics of the firms by frequencies

		Frequency	Percent
Legal status of the firm	Private	48	84,2
	Limited	7	12,3
	Incorporated	2	3,5
Building property status	Rent	27	47,4
	Property owner	23	40,4
	Rent and owner	7	12,3
Use of credit in the past year	Investment credit	5	8,8
	Business credit	30	52,6
Production method	Serial production	12	21,1
	Production by order	22	38,6
	Order + serial	23	40,4
Sales groups	Final consumer	27	47,4
	industrial users	9	15,8
	Both groups	21	36,8
Market groups	Only to domestic markets	45	78,9
	Only to foreign markets	1	1,8
	Both markets	11	19,3
Government Encouragement	Yes	9	15,8
Quality standard certificate	TSE	11	19,3
Branding status	Own brand	51	89,5
	The brand demanded by the customer	3	5,3
	Both of them	3	5,3

The integration level of technological development were inquired and graded by Likert-type scale (1 = very low to 5 = very high) in the workflow process. Between the technology usage and the groups that were created according to the firms' turnover, profitability, number of employees and duration of operation are analyzed with Anova. According to this, statistically significant relationship is observed only with the turnover of firms. A firm's turnover is an important indicator of sales revenue and trade volume.

According to F test results, there is a significant relationship between the level of turnover and technology usage for firm's commercial correspondence at the level of 5% and for accounting transactions and information storage, i.e. database arrangement at the level of 10%.

The usages of technology for correspondence, accounting and information storage are more important for large enterprises, while these technological developments are less important for the micro enterprises (turnover under 50.000 TL). The technology implementation for the customer tracking, computer-aided drawing and design, inventory control and computer-aided production is equally important in all enterprises. These findings indicate that as the volume of production

increases, the technology is used more intensively and more emphasized at all stages of the production process. According to the score level in total; customer-driven 4.11, information storage 3.77, computer-aided drawing and design 3.64, computer-aided manufacturing 3.45, inventory control 3.41, accounting 3.36 and commercial correspondence 3.25, respectively (Table 5). Premkumar (2003) stated that the firms in small business sector are becoming increasingly dependent on information systems for their operations.

Table 5. The usages of technology according to turnover levels of firms by scores (1: very low, 5: very high)

Turnover level (TL)	Commercial correspondence **	Accounting*	Customer -driven	Computer-aided drawing and design	Inventory control	Information storage (database)*	Computer-aided manufacturing
min.-50.000	2,18[a]	2,64	4,36	3,73	3,09	2,91	3,09
	1,834[b]	1,804	1,027	1,618	1,640	1,640	1,640
50.001-100.000	3,70	3,60	4,10	3,60	3,10	3,75	3,55
	1,490	1,465	1,210	1,729	1,651	1,517	1,669
100.001-250.000	2,93	3,29	4,14	3,50	3,64	3,79	3,07
	1,817	1,729	1,460	1,743	1,646	1,626	1,900
250.001-500.000	3,17	2,83	3,33	3,67	4,17	4,50	3,50
	1,835	1,722	1,366	1,366	0,753	0,548	1,761
500.001-max	4,80	4,80	4,40	4,00	3,80	4,80	4,80
	0,447	0,447	0,894	1,732	1,789	0,447	0,447
Total	3,25	3,36	4,11	3,64	3,41	3,77	3,45
	1,740	1,634	1,231	1,623	1,581	1,501	1,683

[a] Mean, [b] Standard Deviation, ** P<0.05, * P<0.10

Table 6 examines that firms have moderate problems in various stages of production. As the scale grows, problems in finance and research-development are reduced. While research and development is a serious problem in micro-scales, this problem is eliminated at the large scale level. The most important problem faced on the large scale within the scope of SME is to find qualified personnel.

Table 6. Problem areas according to turnover levels of firms by Likert scores (1 = very problematic, 5 = not at all problematic)

Turnover	Finance *	Marketing	Production	Personnel	Technology	Management	R&D **
min.-50.000	3,09	3,09	3,18	2,91	3,27	3,36	2,82
	1,640	1,640	1,328	1,446	1,421	1,629	1,722
50.001-100.000	4,05	3,30	3,55	3,70	3,55	3,95	4,10
	1,234	1,380	1,356	1,342	1,395	1,050	1,071
100.001-250.000	4,14	3,71	3,79	3,79	3,64	3,64	3,43
	1,292	1,490	1,424	1,477	1,550	1,499	1,604
250.001-500.000	4,17	3,83	3,00	4,00	3,33	3,33	3,33
	0,983	1,602	1,414	1,673	1,633	1,862	1,862
500.001-max	4,80	4,80	4,80	3,60	4,80	4,80	5,00
	0,447	0,447	0,447	1,673	0,447	0,447	0,000
Total	3,96	3,55	3,59	3,59	3,61	3,77	3,68
	1,321	1,464	1,359	1,449	1,423	1,375	1,503

[a] Mean, [b] Standart Deviation, ** P<0.05, * P<0.10

In Table 7 is examined how companies acquire new technologies. The transportation of the new technologies were achieved by 57.1% of firms using their own R&D activities, 35.7% using domestic technology and 7.1% using foreign technology. The rate of foreign technology usage in SMEs in this sector is extremely low. This is probably due to the labor-intensive production style at the SME level in the furniture sector.

Table 7. Ways to reach new technologies in firms

Turnover	Own R&D activities	Domestic technology	Foreign technology
min.-50.000	72,7%	18,2%	9,1%
50.001-100.000	60,0%	35,0%	5,0%
100.001-250.000	42,9%	50,0%	7,1%
250.001-500.000	66,7%	33,3%	0,0%
500.001- max	40,0%	40,0%	20,0%
Total	57,1%	35,7%	7,1%

Utility model is a technical solution for a production tool. Industrial design is an artistic and design presentation of a new and original product produced by industrial and artisans. Utility model and industrial design should be protected by copyright law if they have new, original and applicable features for the industry (Rumyantseva *et al.*, 2016). Table 8 shows that these firms are able to offer a very high level of new products and services to the furniture sector. On the other hand, it is observed that the number of utility model and industrial design is increasing especially as the scale grows at SME level. 78.6% of these firms that were successful in introducing a new product or service to the market. In addition, 41.1% of the firms offered to the sector some utility model and industrial design. These findings indicate that furniture manufacturers on the SME scale are using moderate technology and a highly innovative-dynamic sector. Avlonitis (2007) states that sectoral adaptation of innovative

products is associated with entrepreneurial behavior in SMEs, especially active entrepreneurs can make more contributions. Marcati *et. al.,* (2008) conceptualizes innovation at two abstractions levels as general innovation and original innovation. Innovation in SMEs is associated with the personality of entrepreneurs. Baumann and Kritikos (2016) found that the R&D intensity of micro-scale firms is largely based on product innovation rather than on process innovation.

Table 8. New product, model and design presentation to the sector

Turnover	Introducing a new product or service	Property of utility model and industrial design
min.-50.000	90,9%	18,2%
50.001-100.000	85,0%	50,0%
100.001-250.000	71,4%	35,7%
250.001-500.000	50,0%	50,0%
500.001- max	80,0%	60,0%
Total	78,6%	41,1%

4. Conclusions and Recommendations

In this study, the focus is on the extent to which furniture manufacturers, established in a relatively small region, are able to use technological knowledge and R&D activities. There is an intensive small-medium sized enterprises in the furniture industry in Samsun. The firms with annual turnover of 500,000 Turkish Liras constitute 91.1% of the firms and the average number of employees is fewer than 15. This indicates that the micro and small scale is constituting the majority of firms in this sector. The level of turnover per employee, that is productivity, is increasing as the firms grows.

In this sector, family business is usually widespread in the region. The traditional production system is dominant in the form of transition from father to son, as a business management system. It is a small workshop style production in the form of relationship between master and apprentice. In this case, owner and employees do not receive adequate formal training in the relevant area. This type of production is quite common in developing countries, especially in the development efforts.

Globalization requires more competitive production. Enterprises should be able to introduce high quality new products to the market. This competitive structure highlights the importance of technological knowledge and R&D in SMEs. R&D investments in Turkey are generally not sufficient compared to other countries. R&D requires technological innovations and knowledge training.

SMEs positioned in the form of traditional production style, both managers and staff need to reach the necessary formal training. There are universities in many small cities of Turkey. However, engineering faculties are not increasing at the same extent. A local training-oriented system will

enable these people to get the engineer education without moving away from the work. In fact, this situation will be effective for both accelerating regional development and becoming more professional and institutional in local SMEs. In the macro-scale, it may also prevent migration to big and industrial cities and increase local employment.

In the furniture sector, human skills can be the forefront in new product and design in the SME scale. The employees of the SMEs are closer to the consumer. Therefore, they can learn the consumer's demands and expectations faster than large-scale firms and adapt to production at lower cost. This can provide a competitive advantage in terms of innovation in the sector.

Foreign trade of the furniture sector is not adequate in this region. There should be more focus on exportation in this region where production is so intense. If necessary, government incentives should be provided in this regard.

The technological knowledge and problem areas of firms were determined by asking questions of Likert scale type. As the turnover in the industry grows, technology is used more intensively. In the medium-sized enterprise, the difficulties related with financial and R&D are also decreasing relatively small and micro levels. It points to the need for enterprises to reach an adequate size to be more innovative and use technological knowledge. On the other hand, in general, it is observed that firms are not following foreign technology sufficiently. In particular, micro-sized firms are more far away from foreign and domestic technologies.

SMEs in the furniture sector are successful in introducing new product to the market. As the scale grows, utility model and industrial design are increasing. But, micro-scale firms do not pay enough attention to patent ownership. This issue is also important in terms of intellectual property rights.

References

Altay, B., (2006). Avrupa Birliği'nde rekabet politikaları, Türkiye ve Avrupa Birliği'nin ihracatta rekabet gücünün ölçülmesi. *Afyonkarahisar, Türkiye*.

Avlonitis, G. J., and Salavou, H. E., (2007). Entrepreneurial orientation of SMEs, product innovativeness, and performance. *Journal of Business Research*, *60*(5), 566-575.

Baumann, J., and Kritikos, A. S. (2016). The link between R&D, innovation and productivity: Are micro firms different? *Research Policy*, *45*(6), 1263-1274.

Çelik, N. (2012). Türkiye'de mobilya sektörü gelişim planı için bir karar modeli önerisi. *Sosyal ve Beşeri Bilimler Dergisi*, *4*(1).

Gravetter, F. J., and Wallnau, L. B., (2016). *Statistics for the behavioral sciences*. Cengage Learning.

Hadjimanolis, A., (1999). Barriers to innovation for SMEs in a small less developed country (Cyprus). *Technovation*, *19*(9), 561-570.

İstek, A., Özlüsoylu, İ., and Kızılkaya, A., (2017). Türkiye Ahşap Esaslı Levha Sektör Analizi. *Bartın Orman Fakultesi Dergisi*, *19*(1), 132-138.

Marcati, A., Guido, G., and Peluso, A. M., (2008). The role of SME entrepreneurs' innovativeness and personality in the adoption of innovations. *Research Policy*, *37*(9), 1579-1590.

Premkumar, G. (2003). A meta-analysis of research on information technology implementation in small business. *Journal of organizational computing and electronic commerce*, *13*(2), 91-121.

Rumyantseva, T. B., Ph, S., Syryamkin, V. I., Vaganova, E. V., and Zinov, V. G., (2016). *TECHNOLOGY MANAGEMENT: Part 2. Strategic Management of Intellectual Property*. STT Publishing. 228p.

Sakarya, S. and Doğan, Ö. (2016). Orta Anadolu İhracatçı Birlikleri Mobilya 2016 Sektör Raporu, 1-36. Retrieved from http://www.turkishfurniture.org/TR,15299/mobilya-sektor-raporu-2016.html (14/06/2018).

Santamaría, L., Nieto, M. J., and Barge-Gil, A., (2009). Beyond formal R&D: Taking advantage of other sources of innovation in low-and medium-technology industries. *Research Policy*, *38*(3), 507-517.

STSO, (2017). Samsun İktisadi Rapor 2017, Samsun Ticaret ve Sanayi Odası. Retrieved from http://www.samsuntso.org.tr/upload/Dosyalar/Yayinlar/IktisadiRapor/Iktisadi-Rapor-2017.pdf *(21/06/2018).*

Müftüoğlu T., (2007). *Türkiye'de Küçük ve Orta Ölçekli İşletmeler,* Turhan Kitapevi, Ankara, p.79.

Timurçin, D., (2010). *Türkiye'de KOBİ'lerin rekabet gücü ve rekabet üstünlüğü sağlamada kümelenmenin etkisi*. Doktora Tezi, İstanbul Üniversitesi Sosyal Bilimler Enstitüsü, İstanbul, 221-222.

Van de Vrande, V., De Jong, J. P., Vanhaverbeke, W., and De Rochemont, M., (2009). Open innovation in SMEs: Trends, motives and management challenges. *Technovation*, *29*(6-7), 423-437.

Yelkikalan, N., and Kalmış, H., (2001). KOBİ'lerde Verimlilik Yönelimli Yeniden Yapılandırma Stratejileri. *Orta Anadolu Kongresi, Erciyse Üniversitesi, Nevşehir İİBF, Nevşehir*.

Determination of Recreational Area Usage Potential of Rize Province Coastal Ridge

Banu BEKCİ[1], Merve ÜÇOK[2*], Hasan Yılmaz [3]

[1] Recep Tayyip Erdogan University, Faculty of Fine Arts, Design and Architecture, Department of Landscape Architecture, Rize, Turkey; merve.ucok@erdogan.edu.tr

[2-3] Ataturk University, Faculty of Architecture and Design, Department of Landscape Architecture, Erzurum, Turkey; hyilmaz@atauni.edu.tr

[*] **Corresponding Author:** merve.ucok@erdogan.edu.tr

Abstract

Coastal areas and shorelines are important natural resources to meet the increasing recreational needs of individuals. These areas are preferred as residential and recreational areas due to their easy accessibility, their rich resource potential and their psychological effect on the individuals. The coastal strips which have a linear structure help the spatial continuity of landscapes, textures and recreational spaces that extend into this silhouette. Due to the slope of the existing topography of the Black Sea Region, the importance of recreational use of the coastal lane is increasing and the demand for open space is in high demand. In this study, the user demands and satisfaction in the recreational areas in the coastal zone of Rize province central region were discussed and user requests were questioned by making surveys to the users of the area. According to the obtained results, when the criteria of recreational areas developed by Altman and Zube (1989) are considered and examined, it has been seen that it is preferred to perform sports with a rate of 38% in the criteria of activity and usage, to walk with 78% in the accessibility criterion, to receive fresh air with a comfort and image criterion with rate of 42% and to perform activities with family or friends groups in the sociability criterion with 42% . 190 users (44% female, 56% male) using the Rize urban shoreline do not find the area of r =, 152 * clear, 257 ** do not think that the area is well managed, r =, 262 **; r = 146 *; r =, 217 ** children playgrounds, accessory elements and open green areas are inadequate, r =, 149 * vegetation designs have no function r =, 235 ** coastal view of the coastal park is not possible due to the buildings in front of the sea facing the sea, parks. With the results obtained, proposals for recreational areas of coastal strip have been developed.

Keywords: Coastline, Rize, Recreational Area, User Satisfaction

1. Introduction

The urban parks, which offer many rescional possibilities, are open spaces which are easy-to-reach and allow the individual to get rid of the negative effects of the city. In this sense, considering the fact that the majority of the world's population lives in cities, it is seen how important parking spaces are.

The green areas, especially in the urban landscape, bring people closer to nature by bringing people together with nature through parks, gardens, sightseeing areas and recreation areas in the city (Bogenç, 2016).

Urban parks provide the aesthetic, recreational, physiological and economic benefits to the people living in the city, as well as providing environmental benefits (Chiesura, 2007) to clean the air of the city, creating a microclimate effect by filtering the wind and noise (Loures et al., 2007). In these areas, it is known that people are significantly affected by their environment and, more importantly, they affect the happiness of their environment. The reasons for this effect are mainly the characteristics and appearance of spatial elements and components that make up such environments (Sakıcı, 2014). Therefore, city parks constitute an important part of the urban ecosystem network and contribute to the ecosystem of the city. The green areas in the city have a strategic importance for the quality of life in fast urbanizing societies (Chiesura, 2007) and are considered as indicators of sustainable cities. In some studies, urban parks and open spaces are considered as places where people feel good and are encouraged to participate in physical activities (Jaafar and Tudin, 2010). Considering today's living conditions, it is seen that the physical movement capacity of the users is decreased and the active use of parking areas will have a positive effect on public health and frequent use of physical activity facilities (Stanis et al., 2009).

While the parking areas in the city have contributed significantly to the improvement and development of the deteriorated urban texture, it is one of the important uses of the city in terms of gaining identity (Bekci et al., 2013).

The basic function of the parks is to please their users. For this reason, well-managed parks should provide services that meet the needs of the users, and provide equal opportunities in society addressing all segments of the society.

Studies on visitor satisfaction for outdoor recreation experience have been important in the literature since the 1960s (Tonge et al., 2011). Recreational area users need to be satisfied with their experience in parking areas to benefit from these areas. For this reason,; it is important need to know public satisfaction from the facilities they visit and the services they use (Uysal et al., 2002). Furthermore, the perceptions and preferences of visitors about parks should be considered in the

planning and design processes of urban parks (Polat, 2012). According to Roovers et al. (2002), the characteristics of the users are a very important variable to explain the recreation activities. Cultural differences in social class, behavior and attitudes can affect customer expectations and perceptions (Kozak and Rimmington, 2000).

In order to make the life more physically and psychologically comfortable and to create more suitable environments for the needs, it is necessary to predict the needs of the users arising from the physical, physiological, psychological and social structure of the users and to shape the environment composed of the open spaces according to these needs (Aksoy, 2008). In order to meet the expectations and satisfaction of the users in higher quality areas and to increase the quality of the recreation experiences, it is increasingly becoming important to make the appropriate planning decisions in these areas (Volkan et al., 2017). In the light of all these studies, the user satisfaction in the recreational areas of the study area will be determined, the deficiencies encountered in the designs will be determined and various solutions will be developed.

.The aim is to ensure the sustainable development of the field of work and to meet the recreational needs together with the results obtained by preserving the natural and cultural landscape potential.

2. Material and Method

2.1. Study Area

Rize urban coastline, which is chosen as the study area, is located in the center of the city, which has 41 ° 1'35.06 6 K latitude, 40 ° 31'35.26 " recreation area. Study area; It has an intensive usage area of 200.000 m2 in terms of recreational activities such as picnic areas, cafeterias, sports fields, children's playgrounds, walkways, living units, landscapes and cruise spots (Figure 1). In addition, the positioning of the coastline along the settlements keeps the intensity and recreational potential of the area at a certain level.

Landscape elements such as children's playgrounds, seating units, picnic tables, fountains, sign boards and trash bins are frequently used in the use of the area according to the variety of recreational activities.

In the study, zoning plans and satellite photographs taken from Rize Municipality were used. While the regions within the study area are selected, users' need for safety, transportation, recreational activities, sport and so on. have been taken into account and the area is divided into 8 regions.

Figure 1. Study area

In Figure 1, each region is taken in order as the following; (A) Opposition to the Governorate; It is located in the western part of the coastal park, close to the parking a lot, away from recreational activities. (B) Cafes; It consists of recreational areas with different qualifications that users can reach most easily. (C) Parking; This area, which has a large hard floor surface, has a busy vehicle circulation and there are various restaurants in the part close to the sea. (D) Culture Park; cinema and fair area. (E) Play and seating area; The vegetation density of this area which has natural areas is quite high. (F) Lunapark; Various recreational vehicles for different age groups are preferred by young people and parents with children. (G) Camellias; used as a picnic area; (H) Cafes; different types of food and beverage to cater for users.

These identified regions undertake joint positive and negative characteristics together. Weaknesses are as as the followings: the proximity of the cities to the city center, being accessible from every point of the city, accommodating different recreational activities, sea view, high density of green areas, being suitable for night use, creating physical strengths, environmental pollution, lack of partial illumination, lack of indoor space, not being used in terms of active recreational activities (canoe, sailboat, swimming, etc.), incorrect budanan plant communities, being close to the traffic areas of children's playgrounds.

2.2. Data Collection and Evaluation

In the study, 4 main parameters were used to define the recreation user preferences, satisfaction evaluation and field usage frequency of the users in defining the coastal park in the urban texture. As the first parameter, the parking areas visited by the users in Rize Beach Park were evaluated according to Altman and Zube (1989) 's park criteria (activity and uses, accessibility, comfort and image, sociability) according to 4 different parameters. Each of these parameters, is evaluated according to the usage preferences such as activities and uses (for sports, reading books, children's playground, cycling), accessibility (for walking, crossing route, road circulation), comfort and image (fresh air for sunbathing, seascape, natüre) socialization (to be able to travel with friends, to do something with family or groups of friends, to meet new people).

As the second parameter, user satisfaction criteria (Yılmaz et al., 2003) were evaluated with percentage analysis method and correlation analysis. Questionnaire forms were used to evaluate these parameters. Survey studies were conducted between May and June 2018, when the recreational area uses began. The capacity of the sample size was calculated according to the formula in Özdamar (2003).

$$n = \frac{N.P.Q.Z_{\alpha}^{2}}{(N-1).d^{2}}$$

N: Number of Population Units, n: Sample size

P: Observation rate of X in the population, Q (1-P): X is not observed rate

$Z\alpha$: α= 0.05, 0.01, 0.001 to 1.96, 2.58 and 3.28

d= Sample error

. As a result of the formula, the center population of R (Population Size) 147.317 (Rize 2017 central population, URL1) was taken for the study in Rize central region. The sample size for d = 01 (sample error) was calculated as 96 persons and the study questionnaires were made to 190 field users in order to increase the sensitivity level in the results obtained in the correlation analysis.

The results of the questionnaires and tables were evaluated according to the user satisfaction. In the statistical evaluation of the data, the socio-demographic status of the users (gender, age, marital status, educational status, user group), and the parameters related to user satisfaction Spearman coefficients (r) and their significance were determined by correlation analysis between maintenance and management status, expectations etc. SPSS (Statistical Package for the Social Sciences) 16.01 program was used in the statistical analysis and some data obtained from the questionnaires were evaluated with tables and graphs by% analysis method.

3. Findings

The findings obtained from the study include (i) evaluating Rize urban coastal recreation preferences and (ii) satisfaction evaluation and (iii) evaluating the frequency of site use.

3.1. Relationships Between Rize Urban Recreation and Recreational Use Preferences

The characteristics of the recreational areas within the Rize urban coastal coastal park were evaluated according to the criteria developed by Altman and Zube (1989) (activity and usages, accessibility, comfort and image, sociability). Each of these criteria was evaluated under the different sub-headings defined for the use of the field. The results of the% analysis for this purpose are given in Table 1.

Considering the users' evaluations, the most preferred type of use in sports activity and usage criteria is 38%, while this is 15% for children's play area, 12% for cycling and 8% for book reading activity. It was seen that 27% of the users did not prefer any of the activity and usage preferences. In these reviews, 78% of walking efficiency, 9% pass route and 2% of road circulation were preferred, while 11% did not prefer any of them. In comfort and image parameters, the users use the area with a rate of 42% for fresh air and 40% for the sea view.

In the sociality parameter of the area, it is seen that 48% of the users prefer to perform the activity with their family or groups of friends.

Table 1. Relationships between Rize Coastline recreation preferences

			%	Description / Most preferred
AACTIVITY AND USES		To do sports	***38***	The study area has different recreational facilities. While there are children's playgrounds and sport areas in different areas of the area, there is no special course for cycling. In terms of activity and usage, sporting activity was the most preferred activity with 38%.
		Read books	*8*	
		For children's playground	*15*	
		For bicycle tour	*12*	
ACCESSIBILITY		To walk	***78***	Within the area, there are many ways of guiding the transportation axis. The purpose of use of persons in terms of availability is to walk with 78% and the 9% because it is a transit route.
		Since it is a transit route	*9*	
		Road circulation	*2*	
C IM		To get fresh air	***42***	Thestudy area that meets the recreational needs of the

		For sunbathing	*3*	city is the breathing point of the city. Users use 40% of the work area to get fresh air with a rate of 42% for sea views.
		For seascape	*40*	
		For the nature	*5*	
SOCIABILITY		To walk around with my friends	*39*	Users use the space with 48% their family or group of friends.
		To do something with family or groups of friends	***48***	
		To meet new people	*6*	

3.2. Satisfaction Evaluation of Rize Urban Coastal Recreation Area Users

While evaluating the satisfaction of the users of Rize urban coastal recreation area, the socio-demographic structures of the users of the area have been taken into consideration in order to distribute the user profiles in a proportional manner, and the positive and negative significant significant relationships arising from the socio-demographic structures are not included in Table 3. Some results are interpreted in the text. .

In the correlation analysis, since it has no meaningful relationship with other questions; The question “Your gender, age, marital status, education level, select your user group, the time you would prefer to use the space, the time you would like to use the space during the day” are included, and the evaluation of these questions is given as% value.

84 women (44%) and 106 men (56%) participated in the survey. There is a negative meaningful relationship with the gender factor which is evaluated within the socio-demographic structure and how much time you spend in the field and the questions you feel safe in your night use. While female users want to spend more time in the area (r = -, 145 *), they do not feel safe when using the parking area at night (r = -, 230 **).

When the age groups of the users are evaluated, as the age of the users increases, their use of space decreases (r =, 277 **), and the means of access to the area (r =, 240 **). The evaluations taken in the age factor are in parallel with the marital status of the users. As the education level of the users increases; (r =, 152 *) they do not find the area clean (r =, 152 *), do not think that the area is well managed (r =, 257 **), they find children find playgrounds, equipment elements and open green areas insufficient (r = , 262 **; r =, 146 *; r =, 217 **), they find the vegetative design dysfunctional (r =, 149 *) because of the closure of the coastal view of the buildings facing the city's sea front (r =, 235 **) It is not associated with urban parks (r =, 152 *).

Similar relationships were found between the working user and the increase in the education level of the users (r =, 158 *; r =, 162 *).

Users feel confident in areas with a high density of recreational use (r =, 152 *), and they find the reinforcement elements for their activity use insufficient (r =, 190 **).

Access to the area (r =, 200 **), with a crowded group (r =, 173 *), does not find the recreational areas they use safe (r =, 168 *), and their use in night use. they do not feel safe (r = 212).

Users who spend a long time in the area feel safe during the daytime use (r = -, 150 *), due to the closure of the coastal view of the city's other parks in the city and the facade of the city's sea front (r =, 150 *).

The question 'Do you find the area clean?' Is positively related to the (o, ö, r, ş, t, y, z,) questions (r =, 365 **; r =, 476 **; r =, 168 *; r =, 282 **; r =, 260 **; r = 147 *; r =, 198 **) and is similar to the above results..

% Analysis method was applied to the questions asked to the user in the survey conducted by the users but they were not questioned by the correlation analysis. The answers of the users to the question of “what is the most important pollution in the field”, respectively; Core shells with 52%, pollution at sea coast by 22% and pollution at green areas by 11%, followed by vandalism (10%) and incorrect plant pruning (2%).

Table 2. Rize urban coastline recreational users' satisfaction assessment

	e	f	ı	i	j	k	l	m	n	o	ö	p	r	s	ş	t	u	ü	v	y	z	w
6. What purpose do you use the area? (1: Transition, 2: To Relax, 3: For Eating, 4: As a Meeting Point, 5: For Shopping, 6: For Feeling Green Texture)	1	,071	,086	-,035	,098	,043	,089	**,152***	-,084	-,096	,002	,048	-,092	-,110	**,190****	-,001	-,135	,009	,056	,088	,117	,077
7. How often do you use this selected area? (1: Everyday, 2: 2 per week, 3: once a week, 4: every fifteen days, 5: once a month, 6: rarely)		1	-,133	**,200****	**,173***	,025	**,212****	**,168***	,039	-,079	-,031	-,059	,094	,118	,083	,007	,094	-,007	,050	,135	-,048	-,073
10. How much time do you spend in the field?(1: less than thirty minutes, 2: thirty-sixty minutes, 3: one to two and a half hours, 4: more than two and a half hours)			1	,065	,105	**-,150***	-,082	-,082	,020	-,030	,032	,084	-,011	,048	,108	-,037	-,017	-,025	,137	,028	**,150***	,041
11. What is the way of transportation to the park?(1: Pedestrian, 2: Bicycle, 3: My own vehicle, 4: Public transport)				1	,111	-,006	,069	,102	,038	**,191****	-,006	,092	-,058	,093	,005	,014	,064	,029	,109	,095	,117	-,015
12. Do you prefer to use this area individually or in a crowded way? (1: Single, 2: Group, 3: Other)					1	,008	,028	,026	-,004	-,012	-,064	-,029	-,030	,007	,112	-,041	,028	,056	-,063	,049	-,043	-,041
13. Do you feel safe in your daytime use?(1:I feel, 2: Partially, 3: I do not feel)						1	**,556****	,135	**,179***	,114	**,218****	**-,146***	,077	**,217****	-,024	,025	-,058	,076	**-,176***	**,172***	**,162***	,051
14. Do you feel safe at night use?(1:I feel, 2: Partially, 3: I do not feel)							1	**,256****	,043	,009	,120	,000	,103	**,211****	,085	,046	,006	,132	,044	**,229****	,120	**,190****
15. Is there an area where you don't feel safe?(1:A, 2:B, 3:C , 4:D , 5:E , 6:F , 7:G , 8:H)								1	,049	,073	,122	,099	-,029	,079	,087	,075	,001	,058	**,161***	,113	-,040	-,036
16. Do you find the area clean?(1:Yes, 2:No)									1	**,365****	**,476****	,014	,168*	,061	**,282****	**,260****	,046	,105	,025	**,147***	**,198****	,042
17. If your answer is no, what is the pollution that attracts the most attention? (1: Core shells, 2: Pollution on the seafront, 3: Pollution in green areas, 4: Vandalism caused by the use of accessories, 5: Wrong plant pruning)										1	**,164***	,046	-,040	,088	,133	,093	,008	-,003	-,048	,032	,121	,041
18. Do you think the area is well managed? (1:Yes, 2:No)											1	-,062	**,310****	**,192****	**,240****	**,190****	,100	**,232****	,044	**,284****	**,224****	,051
19. What are the most lacking places / details in the area?(1: Sports areas, 2: Use of water for visual and play purposes, 3: Safe areas, 4: Areas of care taken, 5: No night use, 6: Lack of accessibility, 7: Lack of suitable spaces for winter use)												1	**-,176***	**-,199****	-,001	,051	,033	,156*	**,233****	-,020	,061	**,243****
20. **Do you think children's play and sports fields are sufficient in the field?** (1: Yes, 2: No)													1	**,237****	,102	**,146***	**,184***	,138	,020	**,232****	,097	-,131
21. **Do you find the light green areas sufficient?** (1: Yes, 2: No)														1	**,173***	,096	,119	**,168***	-,063	**,148***	,007	-,104
22. Do you think the reinforcement elements (bench, lighting element, garbage bin, etc.) are sufficient? (1: Yes, 2: No)															1	**,424****	**,191****	**,368****	,125	**,293****	**,184***	,021
23. Do you find the equipment elements to be well-maintained and organized? (1: Yes, 2: No)																1	**,191****	**,276****	,092	**,252****	,125	-,044
24. Does the herbal design of the area affect you? (1: Yes, 2: No)																	1	**,215****	,025	**,184***	,117	-,017
																		1	,086	**,234****	**,146***	,050
25. Do you find plant design functional in the field? (1: Yes, 2: No)																			1	,036	-,010	-,031
26. What is your favorite spot in the field? (1: A, 2: B, 3: C, 4: D, 5: E, 6: F, 7: G, 8: H)																				1	**,618****	-,009
																					1	,109
27. **Do you find this park is related to the city parks?** (1: Yes, 2: No)																						1

The answers given to the question of "what is the most missing place in the area" are in the order of preference; 30% sports areas, 16% well maintained picnic areas and 10% need for the use of winter season

The most important reason that the coastal park is not associated with urban parks is the coastline (highway) with 49%, inadequacy of overpasses with 18%, and the closure of the coastal view of the buildings facing the sea at 9%.

"What are the designs that users want to make a new design to the field?" The question is given with the answers given in the form of 40% grass, 23% sea transport (with functionality) and 15% with plant corridors.

3.3. Evaluation of Rize Urban Coast Area Usage Frequency

The frequency of use of recreational areas is one of the most important criteria affecting field quality. Therefore, evaluations were made on weekdays and weekends, morning-lunch and evening hours when evaluating the usages. Space users prefer to use 50% of the space at any time and 45% prefer at the weekend.

54% of the users' use hours during the day were preferred in the evening and 32% in the afternoon, while morning and night hours were not preferred (3%). 53% of the users spend 1-2,5 hours in the area, 63% of the users are pedestrians, 25% are self-employed, 7% are public transport and 2% are cycling.

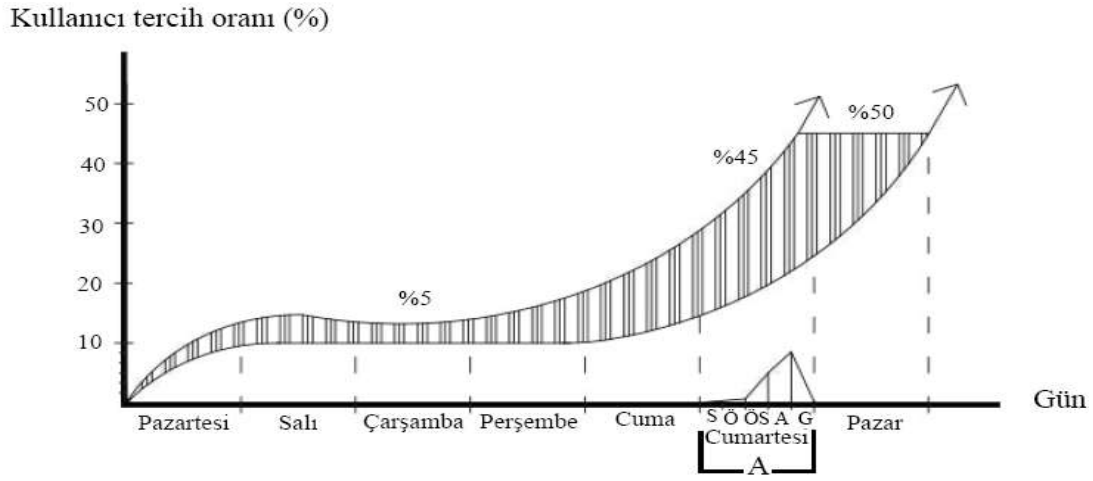

A: Graph of frequency of day use, S: 4% in the morning, D: 5% in the afternoon, PM: 31% in the afternoon, A: 54% in the evening, G: 5% at night

Figure 2. Frequency of Workspace / Time graph

3. Results and Discussion

In green spaces designed to make life more physically and psychologically comfortable and to create more suitable environments for needs, it is necessary to anticipate user needs and to shape the environment to be created in light green areas according to these needs. Therefore, user requests and needs become effective parameters in evaluating the service quality of recreational areas. These parameters also have a guiding effect on the creation of new recreational areas. It should be used to create activities within the recreational areas according to the guiding effect of the user profile and requests it creates, in terms of its contribution to the environment in terms of service or the balance of satisfaction of the users.

. Rize urban coastline recreation area offers green space uses with different characteristics to individuals as cultural landscape characters. These green areas, which are arranged to reflect the traditional texture of the city of Rize, combine different preferences with close and small areas.

The satisfaction of the green areas on individuals is related to the frequency of use, the proximity to the green areas and the level of welfare (Yılmaz et al., 2017), which are directly related to the type and characteristics of the facilities to be built. User satisfaction, service quality and level of satisfaction in the recreational regulation processes are possible with the regulation and implementation of the parameters affecting the planning processes (Onsekiz and Emur, 2008). In this study;

- Users find the equipment and equipment use in the area incompatible with the environment. Therefore, in the use of reinforcement elements at the Coastal Park, regular maintenance should be provided by developing designs suitable for natural and local textures. The natural appearance and maintenance of the reinforcements for the users as well as their safety are quite important.
- Rize Beach Park seems to be neglected and users complain about this situation due to their incorrect and sloppy usage as well as their temporal deformation besides their temporal deformation. In his study, Yavuz (2010) found that vandalism, a problem seen in urban open spaces, is effective in urban parks and consequently reduces the visual quality of parks. Therefore, care should be given to care of recreational areas and the users of the area should be made aware of this issue.
- It is seen that planting design in the study area is far from functional and aesthetic approaches. This can be done with rehabilitation studies (plant pruning-care, plant use etc.). The lack of planting design was identified by the Rize Architectural and

Aesthetics Commission and the recreational parks were covered by Vaccinium corymbosus, Citrus sp. Citrus sinensis, Citrus reticulata and Tilia cordata support are offered.

- Activities should be planned taking into account the users' area usage times and time periods.
- Water sports and beach areas should be designed by supporting the visual nature of the sea as well as active recreational uses.
- The lighting system in the area should be developed and a security need should be provided for night use.
- Pedestrian walkways and bicycle paths should be separated, and a separate course should be created for the bike.
- Children's playgrounds in urban parks are open spaces that contribute to children's recreational needs as well as their learning, and these open spaces should be designed to contribute to children's learning process (Acar, 2014).

Since a significant part of the open green areas in our cities is composed of designs containing aesthetic concerns, it is planned to be detached from nature and general cycle, ecological, free of concerns. However, the open-green areas planned by transferring large resources can be transformed into ecologically and financially sustainable design approaches (Bekci et al., 2013).

As a result, the urban or urban coastal recreation areas will be an effective and sufficient source for meeting the recreational needs of urban residents as long as they are planned in line with the cultural and natural approach.

References

Acar, H. (2014). *Learning environments for children in outdoor spaces*. Procedia-Social and Behavioral Sciences, 141, 846-853.

Aksoy, Y., Aygün, B., Turan, A. Ç., Ören, L. (2008). *Fatih İlçesinde Risk ve Afet Yönetimi Kapsamında Mevcut ve Öneri Yeşil Alanların Deprem Öncesi ve Sonrası Değerlendirilmesi Risk Yönetim Çerçevesinde Yeşil Koridor Dönüşüm Projesi*, Yürütücü: İBB/Y ve KD-İŞAT MÜDÜRLÜĞÜ, Yüklenici: BİMTAŞ A.Ş, Alt Yüklenici (Proje Yüklenici): Bahçeşehir Üniversitesi.

Altman, I., & Zube, E. (1989). *Public spaces and places*. Human Behaviour and.

Bekci, B., Bogenç, Ç., & Taşkan, G. (2013). *Karabük Üniversitesi Kampüs Alanında Yapılan Çevre Düzenleme Çalışmalarında Kullanılan Yerli ve İthal Abies sp. Türlerinin İklim Şartları ve Toprak Koşulları Karşısındaki Dayanıklılığının Araştırılması*. Karadeniz Fen Bilimleri Dergisi, 4(11), 25-34

Bekci, B., Taşkan, G., Bogenç, Ç., Dinçer D. (2013). *Ekolojik Peyzaj Tasarım Hedefinde Ergonomik Tasarım Yaklaşımları*, Balıkesir Üniversitesi 19. Ulusal Ergonomi Kongresi

Bogenç, Ç. (2016). *Dünya Mirası Safranbolu Alan Yönetim Planının Geliştirilmesine Yönelik Bir Çalışma*, T. C.Bartın üniversitesi Fen bilimleri enstitüsü Peyzaj mimarlığı anabilim dalı

Chiesura, A. (2007). *The role of urban parks for sustainable city*. Landscape and Urbun Planning, 68, 129-138.

Jaafar, N., Tudin, R. (2010). UPARQUAL: *The development of an urban park satisfaction measurement scale*.International Journal of Business and Society 11(2),17-34.

Kozak, M. and Rimmington, M. (2000). "*Tourist satisfaction with Mallorca, Spain, as an off season holiday destination*", Journal of Travel Research, Vol. 38 No. 3, pp. 2609.

Loures, L., Santos, R., Panagopoulos, T. (2007). *Urban parks and sustainable city planning – The case of Portimão. Portugal*, Wseas transactions on environment and development, 10(3), 171-18.

Onsekiz, D., & Emür, S. H. (2008). *Kent parklarında kullanıcı tercihleri ve değerlendirme ölçütlerinin belirlenmesi.*

Özdamar, K. (2003). *Modern bilimsel araştırma yöntemleri*. Eskişehir: Kaan Kitabevi.

Polat, A.,T. (2012). *Kent parklarında görsel kalite ve doğallık derecesi arasındaki ilişkilerin belirlenmesi.* Iğdır Üniversitesi Fen Bilimleri Enstitüsü Dergisi, 2(3):85-92.

Roovers, P., Hermy, M., Gulinck, H. (2002). Vis*itor Profile Perceptions and Expection in Forests From A Gradient of Increasing Urbanisation in Central Belgium*. Landscape and Urban Planing. 59:129-145.

Sakıcı, Ç. (2014). *The assessment of the relationship between various waterscapes and outdoor activities: Edirne, Turkey*. Environmental monitoring and assessment, 186(6), 3725-3741.

Stanis, S.,A., Schneider, I.,E., Anderson, D.,H. (2009). *State park visitors' leisure time physical activity, constraints, and negotiation strategies.* Journal of Park and Recreation Administration,27(3), 21-41.

Tonge, J., Moore, S.,A., Taplin, R. (2011). *Visitor satisfaction analysis as a tool for park managers: a review and case study*. Annals of Leisure Research, 14(4), 289-303.

Uysal, M., Eser, Z. I. Birkan. (2002). M*easuring Visitor Satisfaction: An Outdoor Recreational Setting*. TTRA's 33rd Annual Conference Proceedings, pp. 279-284 (CD ROM). June 23-27,Arlington, VA, USA.

Volkan, Ö., Orcid, A., & Kiliç, C. (2017). Al*tındere Vadisi Milli Parkı kullanıcılarının rekreasyonel memnuniyetini etkileyen faktörlerin belirlenmesi* Specification of factors which affect recreational satisfaction of Altındere Valley National Park users, 30–45.

Yavuz, A. (2010). *An experimental study on vandalism:* Trabzon Parks. Scientific Research and Essays, 5(17), 2463-2471.

Yılmaz, H., Yılmaz, S., & Yıldız, N. D. (2003). *Kars Kent Halkının Rekreasyonel Talep ve Eğilimlerinin Belirlenmesi/*Determination Of The Recreational Demands And Tendencies Of The People In The City Center Of Kars. Atatürk Üniversitesi Ziraat Fakültesi Dergisi, 34(4).

Yilmaz, S., Duzenli, T., & Dincer, D. (2017). *Evaluatıon Of Factors Related To Well-Beıng Effects Of Urban Green Spaces On Users.* Fresenıus Envıronmental Bulletın, 26(12 A), 174-185.

URL-1 : https://www.nufusu.com/ilce/merkez_rize-nufusu (Date of access: 1 Haziran 2017).

INTERIOR DESIGN, ARCHITECTURE, LANDSCAPE, FURNITURE DESIGN, FURNITURE INDUSTRY

POSTER PRESENTATIONS

Transforming Landscapes

Hasan YILMAZ[1], Banu BEKCİ[2], Merve ÜÇOK[3*]

[1]Ataturk University, Faculty of Architecture and Design, Department of Landscape Architecture, Erzurum, Turkey; hyilmaz@atauni.edu.tr

[2-3]Recep Tayyip Erdogan University, Faculty of Fine Arts, Design and Architecture, Department of Landscape Architecture, Rize, Turkey; merve.ucok@erdogan.edu.tr

[*] **Corresponding Author:** merve.ucok@erdogan.edu.tr

Abstract

Industrial buildings and spaces that exist in the city and that have lost their functioning life and have lost their physical life over time are left idle after finishing their activities by contributing economic, social and visual sense to the city. The recycling of these industrial areas, which are called urban lost spaces, with different forms of use, affects the sustainability of urban identity positively.

In this study, the possibilities of restoring city and urbanities after completing the functions of the industrial structures / places that left traces in the past of the city and the urban people were discussed. Various examples applied in our country and world scale have been examined on the transformation of these areas into new use areas that accommodate different types of usage to meet the recreational needs of the people. The environment with the reintroduction of these areas and the restoration of the industrial structures and environments with the protection usage balance, to gain access to the way has been emphasized. In this context, the buildings / places that left traces in the history of the city are not buried, but they will contribute to the urban identity by using the urban landscaping with the designs that will be offered to the city.

Keywords: Transforming Landscaping, Urban, Industrial Areas, Urban Image, Design

1. Introduction

Cities in our country and in the World need projects and applications for renewal, transformation, resettlement and improvement due to the reasons such as economic reasons, inadequacy in social development, overpopulation, wrong location(wrong place choice) and natural disasters. There are many examples of project applicaton in the world and in our country. These examples vary in terms of their aims, application forms, organizational models and results. With these practices, in the process of renewing the problematic areas of the cities and bringing new urban spaces to the cities, studies are being carried out not only for spatial transformation but also for social and cultural development (Şişman ve Kibaroğlu, 2009).

1.1 Concept of Conversion and Urban Transformation

Conversion describes the physical, functional, social, and economic, and ecological intervention of land use in one geography, by relating the areas, related or unrelated to the city, to cities. In other words, transformation is a phenomenon that affects and changes the macro form of the city. Since conversion involves changes over time, it also brings understanding, recognizing and comprehending the development of any city (Günay, 1999).

The conversion process can occur either spontaneously or in a planned way. The planned approaches to be adopted provide the city with a healthier reproduction process in terms of both economic sense and urban space due to the high cost of the city's spontaneous transformations (Yerliyurt ve Aysu, 2008).

According to Kap; urban transformation and renewal means an integrated vision and actions aiming make urban areas that are in the process of decaying in physical and social aspects livable and revitalized areas by activating the dynamics of the local economy.

The concepts of urban transformation and renewal which are considered within the concept of urban design appear in the same context, but in fact they are different from each other. Transformation is mainly an upper-scale concept involving urban renewal and it is not just about the physical, social and economic improvement of an existing urban space. Transformation is a phenomenon that exists together with global, economic, political and social structuring and that shapes our everyday life (Güley, 2001).

Urban renewal is a large-scale spatial intervention program which mainly involves three different types of action such as conservation, improvement and redevelopment (Yiğitcanlar, 2001).

The reasons for the necessity of transformation vary in our country and in other developing countries. These variations can be listed in terms of physical, social and technological aspects. From physical perspective; that they fill the physical lifetimes of current structural areas of today's cities, infrastructure problems, , social aspects; illegal structured areas with increasing population, unidentification of cities, when viewed technologically; such as transportation and space , this diversity can be explained by general titles. This variation can be explained under the general headings such as expired physical life of existing structural areas of today's cities, infrastructure problems, and deterioration of urban aesthetics in physical aspect; illegal structured areas with increasing population and disidentification of cities in social aspect; and transportation and spacelessness in technological aspect (Ser, 2004).

Industrial structures that have changed in parallel with technological developments since the second half of the 20th century have put forward the idea of taking production outside the cities and the evaluation of the industrial areas that have become dysfunctional in cities has come to the agenda. Utilizing these areas by transforming them into parks allows city-dwellers under the pressure of building density to perform vital activities such as living, resting, having fun, and doing exercises and increases the quality of life (Büyüköz, 2013).

In recent years, it has become popular in developed and developing countries in order to reintroduce industrial areas which have lost their economic life over time and have lost their economic life. These areas are often abandoned or left inactive after their activities are terminated while they economically, socially and visually contribute to the city which they are in during their operation. However, it is possible that these areas provide economic, visual and social contribution to the city after the operation. However, it is possible that these areas provide economic, visual and social contribution to the city after the operation (Kaya ve ark., 2015).

When the centers or historical areas of cities are faced with the appropriate interventions that will save them from becoming debris, this transformation finds its physical value and the parts exposed to collapse leave together with the remnants of the cleaned debris and are replaced with new urban designs (Kaya ve ark., 2015). Reintroducing especially industrial areas, which are inactive urban spaces, to the city and bringing them into public use is very important for the identification of industrial cities and their sustainability (Oğuz ve ark., 2010).

In this sense, the most important building units outside residential districts are industrial constructions. The study focuses on the possibilities of enabling the city and city-dwellers to regain industrial constructions/ spaces, which impressed the city and city-dwellers in the past, after they have completed their functions.

In this way, the city will have a new use after the old one and the buildings / places that impressed the history of the city will not be imbedded in history, but instead will become a building stone, even a landmark (city icon), which holds the urban identity alive.

In recent years, various competitions have been held in order to transform the industrial areas, which have completed their functions in our country, into urban spaces. Zonguldak Lavatory Area, Uşak Old Tannery Industrial Zone, Beykoz Kundura and Leather Factory, and Bursa Merinos Factory can be given as examples of theses competition projects. Various projects implemented in our country and in the world have been tried to be discussed below (URL-1).

1.2 Transformed Landscape Examples İn The World And İn Turkey

1.2.1 Examples of Transformed Landscape in the World

1.2.1.1 Qian'an Sanlihe Greenway

It is a project of rehabilitating the Luan River and its surroundings (Figure 1), which are located in China's Hebei District and which garbage and sewage was previously poured into, with ecosystem services and of providing a green field for daily life. Within the scope of this project, the concrete channel of the river was taken and swales which, soak water up and provide wildlife with habitat, were built at the side of the river road to control water floods. The plants in swales clean the water (URL-2).

Figure 1. The old and new state around the Luan River

In the plantation, local plants needing low maintenance, lush wetland weeds, self-replicating wild flowers were used.

The " resistant green river " strategy allows the water level to rise and fall in its natural course in different seasons (Fig. 2 (A)). The combination of wooden walking trails left alone and simply and

functionally designed and water-side platforms makes this green corridor a part of everyday use of people (URL-2).

The red structure of 800 meters (Figure 2 (B)), which zigzags under the canopy of the willow trees near the river, is a public art work providing shade in different places, consisting of seating and tables and keeping the project vivid with its continuity, color and functions (URL-7).

Figure 2 (A). The river formed by the resistant green river strategy, **(B).** Red structure of 800 meters

1.2.1.2 Landscape Park Duisburg-Nord

It is an old industrial area in Germany's Ruhr region which sewerage wastes were poured into until the 1990s. It was converted to a public site of 230 hectares (Figure 3), which protected the traces of industrial heritage, by being improved by herbal cleaning methods between 1990 and 2002 (URL-2).

Emsher River in the area was used as an open sewer line until the 1990s as no underground sewage system was installed due to mining activities. After the project, this artificially channeled river has been transformed into a valley (Figure 4) preventing flood and cleaning water with plants around it (URL-2). The habitat provided by the new form of the river contains a wide variety of plants and animals, including species that face the danger of extinction.

Figure 3. Emsher River

In the project, rainwater leaking from fences, water leaking from impervious surfaces and drainage water in the ground is stored. These stores are called seasonal "hard time" resources used to meet water demand resulting from evaporation in summer. The water accumulated in the reservoir is filtered and cleaned before it is pumped into the water system (URL-8).

Figure 4. An image from the Duisburg Park

The giant constructions made of steel with their crushing sizes were positioned close to each other in the field. The existing industrial plant wastes were transformed into design objects that were recycled and used frequently in the factory area. Railroads, pedestrian bridges, recreation areas, aqua parks, vegetable gardens, forests grouped by species, pioneer plants and meadows, which draw elevated circles among industrial equipment having explicit and firm designs, are examples of these different staging systems in the field (URL-8).

Etkinlikler için kullanılan Sinterpark ve ona ait çok fonksiyonlu iş merkezi, eski sığınakların içerisine saklanmış bahçeler, asansörlü izleme platformları, merkezi patlamalı ocak parkı, tırmanma duvarları (Şekil 5 (A)) ve bölünmüş bahçeler (Şekil 5 (B)) bunlardan bazılardır (URL-3). Sinterpark used for events and its multifunctional business center, gardens hidden in old shelters, elevated monitoring platforms, central bursting hearth park, climbing walls (Figure 5 (A)) and divided gardens (Figure 5 (B)) are some of these (URL-3).

Figure 5 (A). Climbing Wall, **(B).** Duisburg Park divided gardens

Piazza Metallica Figure 6 (A), one of the most important urban openings, is located in the symbolic heart of the park. This square is used as an event and gathering center. A total of 49 recycled iron plates, each one weighs 7-8 tons, were carefully placed on the ground to create a square-shaped square. The four sides of the square are surrounded by industrial structures (URL-4). The interior of a gas silo in the park is used as an operating office, while another gas tank has beenfilled with water and turned into the world's largest indoor diving center. Sturdy concrete walls have served an excellent training area for mountaineers. Chimneys and old mines are illuminated with colorful spots Figure 6 (B), to attract visitors (URL-5).

Figure 6 (A). Piazza Metallica, **(B).** Illuminated night view of the area

1.2.2 Examples of Transformed Landscape in Turkey

1.2.2.1 Seka Paper Factory

The factory where the first modern paper production has been carried out in Turkey is one of the symbols of the industrial revolution. The Seka Paper Factory (Figure 7 (A)), is located on the central coastline of Izmit (Figure 8) , the central district of Kocaeli, parallel to the D-100 highway to the north, and at the mid-point of the coastline to the south (Oral, 2007). After being transferred to Kocaeli Metropolitan Municipality, the factory has been converted to a city park (Figure 7 (B)) and its name has been changed to 'Sekapark' (Oğuz ve ark., 2010).

Figure 7 (A). Seka Paper Factory, **(B).** Seka Park

Figure 8. Sekapark's position in Kocaeli's coastal shore

The Sekapark Project was designed as a master plan with a total area of 1.210.965 square meters. Seka with its location in the city, historical background and new image has become the center of urban development that will lead the development of the whole city (Oğuz ve ark., 2010).

Figure 9 (A). Site plan for all the stages of Sekapark **(B).** Sekapark 1st Stage Application

In the area, building and building elements such as fire brigade with its different architecture, fuel silos, infrastructure and energy center structures, water reservoirs and chimneys, dough rollers, transition galleries between the buildings are protected The uniqueness of the building is another important issue that is evaluated in the issues of conservation and re-function. In this context structural and spatial elements (Figure 10) such as kite hill, organic pier, children's playgrounds and steel bullrush were included in the park.

Figure 10 (A). Kite Hill and children's playgrounds (**B).** Kite Hill and organic pier **(C).** Steel bullrush

In the context of Sekapark, the buildings belonging to the early periods projected by the German architects were held and re-used. The protected structures were given new functions such as Seka paper museum, visual arts center, exhibition hall, art workshops, cinema, theater, photography, modern dance workshops, industrial design galleries, training center, cafes and restaurants, pocket theater, library, meeting halls, wedding halls, amusement center, bowling hall, book and music stores, and gift markets (Gemici,2011).

It is seen that the plants including centennial plane and magnolia trees belonging to the existing plant stock are under protection (Figure 11), while any structures in the factory area have not been registered (Oğuz ve ark., 2010).

Figure 11. Sekapark

1.2.2.2 İzmir İzmir Air Gas Factory

The air gas factory in Alsancak (Figure 12), which has formed the basis of air gas and lighting system of the city since 1902, was restored by the İzmir Metropolitan Municipality in 2007-2008 and turned into a cultural center (URL-6).

Figure 12. Old and new form of Air Gas Factory

The foundry building of the factory was organized as cafeteria, while warehouse buildings were organized as exhibition hall and art workshops . Other registered buildings were restored to be used as reading room, sales unit and administrative building. The two-storey concrete building behind the site was also renovated. The work was realized with a budget of 1 million 650 thousand TL.

Five centennial olive trees were planted in the framework of the landscaping works, and the arrangement of the green field was done with various trees and plants (Şekil 13). The area has a car park with 122 cars, an open-air viewing area of 1800 square meters (a grassy area), squares, and five decorative pools (URL-9).

Figure 13. Views from the Air Gas Factory

3. Results and Discussion

Since there is no effective management policy on the sustainability of historical industrial constructions in our country, the sustainable reuse of these structures depends on incidental circumstances. Sometimes it is seen as a solution to remove the structures belonging to the industrial heritage under the name of urban transformation (Uyanık, 2011).

The study shows that transformation can be achieved without breaking down. Transformed industrial areas will make a positive contribution to the image of the city by hosting cultural and artistic places. It is seen that urban transformation necessitates re-creation of not only a city but also a wider region including surrounding countryside according to the social needs.

References

Gemici, B. (2011). *Eski Endüstri Alanlarının Yeniden İşlevlendirilmesinde Kentsel Kalite Ve Değer Artışına İlişkin Kullanıcı Algısı: İzmit-sekapark Örneği* (Doctoral dissertation, Fen Bilimleri Enstitüsü).

Güley, K. (2001). *Kent kimliği değişim sürecinin Gazimağusa örneğinde incelenmesi,* Yüksek lisans tezi (basılmış). Mimar

Günay, B. (1999). *Urban design is a public policy*. METU Faculty of Architecture Press.

Kaya, S., Yerli, Ö., & Döner, S. (2015). Endüstriyel Alanların Endüstriyel Parklara Dönüşümü. *Düzce Üniversitesi Bilim ve Teknoloji Dergisi*, *3*(2).

Oğuz, D., Saygı, H., & Akpınar, N. (2010). Kentiçi Endüstri Alanlarının Dönüşümüne Bir Model: İzmit/Sekapark. *Coğrafi Bilimler Dergisi*, *8*(2), 157-167.

SER, 2004. The SER Primer on Ecological Restoration, Version 2. Society for Ecological Restoration Science and Policy Working Group. http://www.ser.org/reading_resources.asp (Erişim, Ocak, 2010)

Şisman, A., & Kibaroğlu, D. (2009). DÜNYADA VE TÜRKİYE'DE KENTSEL DÖNÜŞÜM UYGULAMALARI.

Uyanık, C. (2011). Sürdürülebilirlik Bağlamında Endüstri Alanlarının Yeniden Kullanımı Ve Adapazarı Örneği. *Yüksek Lisans Tezi, Mimar Sinan Güzel Sanatlar Üniversitesi, İstanbul*.

Yerliyurt, B., & Aysu, E. (2008). Kentsel Kıyı Alanlarında Yer Alan Sanayi Bölgelerinde Dönüşüm Potansiyelinin Değerlendirilmesi; Haliç–Tersaneler Bölgesi. *MEGARON/Yıldız Teknik Üniversitesi, Mimarlık Fakültesi E-Dergisi*, *3*(3), 194-205.

Yigitcanlar, T. 2001. Kentsel yenileme olgusu ve gelisim süreci. Planlama Dergisi, 4;55-58

Büyüköz, H. (2013). Kentsel Mekanda İşlevsizleşen Sanayi Alanlarının Park Alanlarına Dönüştürülmesi. *Yüksek Lisans Tezi, Bahçeşehir Üniversitesi, İstanbul*.

URL-1: http://zonguldak.bel.tr/lavuar-alani-duzenlemesi.html, (Date of access: 1 Haziran 2017).

URL-3: http://www.landschaftspark.de/en/derpark/entstehung/index.html 2008, (Date of access: 1 Haziran 2017).

URL-4: http://www.landezine.com/index.php/2011/08/post-industrial-landscape-architecture/, (Date of access: 1 Haziran 2017).

URL-5: http://repositories.cdlib.org/cgi/viewcontent.cgi?article=1922&context=ced/places. 2008, (Date of access: 1 Haziran 2017).

URL-6: Anonim, http://tr.wikipedia.org/wiki/Havagaz%C4%B1, (Date of access: 1 Haziran 2017).

URL-7: https://www.asla.org/2013awards/062.html, (Date of access: 1 Haziran 2017).

URL-8: https://www.latzundpartner.de/en/projekte/postindustrielle-landschaften/landschaftspark-duisburg-nord-de/,(Date of access: 1 Haziran 2017).

URL-9: Anonim, www.izmir.bel.tr/Kultursanat/EtkinlikMerkezleri/TarihiHavagaziFabrikasi (Date of access: 1 Haziran 2017).


ITESDES
International Technological Sciences
And Design Symposium

How Do You Save The World Design?
"Analysis of an Artist Project about What the Design is"

Aylin GÜNGÖR[1*]

[1] Giresun University, Görele Fine Arts Faculty, Graphic Design Department, Giresun, Turkey

[*] **Corresponding Author:** aylin.gungor@giresun.edu.tr

Abstract

When we look at the design for years to describe an attitude is exhibited as a concept only remaining two-dimensional surface. However, design is a concept that function in an efficient and extends the life stages of individuals' thoughts. Design approach actually a thought, a style. Today, design, fashion, architecture, located in the automobile sector in many different areas of the packaging. This is getting really constitutes an important part of contemporary design practice. So, it is saved with the design world? So far, individuals have put forward many projects to save the world, political and social way. But today, as in individual people on the planet, it is necessary to do something on behalf of the environment and its benefits. Thus arises the importance of sustainability patients. Sustainability is essential for ecology and humanity like design. In this work, graphic design products and advertising campaigns that are created from the concepts of sustainability and design will be examined. Also, the phenomenon of saving the world was tried to be investigated by means of an artist project prepared on the basis of sustainability and design concept. Moreover, the project design aims to give the audience by not only theoretical behavior. All of this information in the light of this study; has emerged in the thinking that design is necessary for a sustainable world.

Keywords: Design, Graphic Design, Sustainability, Ecological design.

1. Introduction

Sustainable design approaches that emerged in architecture and product design in the 90s have left many different debates today. Approaches are now being produced not just on products and buildings, but on how the world can be a sustainable planet. These approaches are fed by projects produced by different disciplines and give birth to various academic knowledge.

The design is renewed every day thanks to sustainable information in the field. However, in design, information is viewed as being more of a designer-guiding quality rather than being scientifically correct. In this context, the role of the designer in developing a sustainable society is not to create "sustainable" products; in practice, to create designs that lead to more sustainable behavior. Sustainable community goals and ecological design are only possible if people are in harmony with the environment. In this study, firstly, what is the design is emphasized. In this work, firstly, what is the concept of design is mentioned. Then, the relationship between sustainability and design was examined and the reflection of the graphic design discipline in the sustainable area was explored. It is also aimed to bring sustainable behavior to people with this project by considering the exhibition created by an artist project, which is the case of saving the world.

2. Material and Method

A detailed literature search was conducted in this study. In addition, the author, as an art and design student, tried to examine the creative process of subject design, through utopian exhibition that she had done during art proficiency education.

3. What is Design?

The design word contains definitions that are still not fully understood today. The term of “design” has so many meaning layers that this causes intrinsic controversial on its own. Similar to word of “love”, meaning of design varies fundamentally on the basis of who uses this word, the person referred, and in what regard it was used. For instance, these variations in the meaning could be investigated by means of a sentence which does not seem non-sense and which includes word of “design”:

“Design is to design a design to produce a design”.

Each form of usage of this word in the sentence is grammatically correct (Heskett, 2013). But the reason for the complexity of the design is that the design practice and terminology are spread over a wide area. For example; today's design areas; It includes many disciplines such as craft design, industrial design, fashion design, graphic design. In some countries abroad, in addition to hair design, nail design, floral design, funeral design, and other areas have developed. Actually, when we look at the origin of the design concept, it can be defined as a functional system of thinking that we use to shape and express in different ways not found in nature. This functional thinking practice improves the technical and structural sense of the human being, thus saving the design concept from definitions made in two-dimensional spaces. Design is now an activity in your mind.

It is an obvious fact that all of the processes in which the world lives both positively and negatively, both environmentally and ecologically, are the result of man's design today. Only technological processes or social events are not effective in the creation of designs. For example; Think of the atom bomb as a design. The endangering damage to the environment is disaster. But at the same time it is an indication of the development of the power and war industry for the countries. There are also people's choices and decisions in the design of atom bombs. Just like the design process. The human factor is important in the decisions of design practice. In sum, designing talent manifests itself in many ways by staying right in the center of existence of humankind, as specie. No any creature in this world has similar talent which allows us to create our environment uniquely without distinguishing civilization from the nature. Design is important because it addresses one of the distinctive characteristics of being human beside the language (Heskett, 2013).

4. Sustainability

In recent years, our planet is under great threat. In this regard, significance of sustainability concept has come to prominence. Sustainability means persistence in terms of variety and productivity; and maintaining capability of survival. In the report published by the World Environment and Development Commission under title of “Our Common Future” in 1987, sustainability is capable of ensuring continuous development by providing daily needs without jeopardizing the capability of nature to meet requirements of future generations (WCED, 1987). Sustainability is a concept that people produce for the protection of nature by thinking about future generations. And this area has been in operation for years. So various

explanations have been made in terms of academic sense for the sustainability of research. According to Gilman (1992), sustainability is the functioning of society, the ecosystem, or any continuing system to function indefinitely without consuming the main sources. Ruckelshaus (1989) stated that "economic growth within the widest limits of ecology and the doctrine that development will be sustained through mutual interaction and will be preserved over time".In order to save the world, there are other things that we could do apart from design (Table 1);

Table 1: Social and individual rules that everyone knows about the environment.

What can be done socially	What can be done individually
*Thermal Power Plants must be closed.	*Using public transportation (PT) (reducing carbon emission).
*Nuclear Power Plants must be closed.	*Using bicycle from home to work.
*Using bio-diesel instead of fossil fuel.	* Reducing travels by plane.
* Electric-powered vehicles (Metro, Train, Hybrid Cars).	* Agriculture (plant tree).
*Less consumption in society (such as recycling).	* Using wind power.
* Organic consumption, transforming into compost.	* Turning off a bulb.
* What kind of individual do you want to be? (Then, raise a child like yourself).	*Seperate garbages

In general, design and sustainability concepts are adopted by the bourgeois section of the society and attached importance. Sustainability, as a recent initiative supported by the conscious section of the society, has been embraced in the virtual internet environment with great interest. Although this situation is encountered in developed countries more frequently, they could be observed globally as well. Especially, afterwards of 2000s, magazines have been focused on sustainability issue. Nevertheless, when the target audience was considered, it was observed that these publications were mostly interested in highly educated section of society

known as **"knowledge elites"**. Therefore, in this study, the concept of design was explored not only for elite individuals, but for all who constituted society. Because everyone lives in this world. No special distinction can only be made between elites. We must act together while saving the world. There is a world that live in people. Schopenhauer described this as: The motto of "*The world is my design*" is the truth valid for all living, conscious existence. However, this truth could only bring into abstract consciousness, into thought by human being. If human being really do this, then a philosophical structure strength arise from him, which make following definite and become clear: He/she knows the sun and the earth, only his/her eye that see the sun and only his/her hand that feel the earth knows. The world surrounding him/her exists at the very outside as a design – obviously, the world only exists within its relationship with other things, with someone who comprehend the design, this is him/herself (Schopenhauer, 2009).

Hence, since the purpose of the study is to acquire a behavior, they are included in the project during the thinking processes, habits and informing steps. Yet, Felix Guattari, who emphasized that ecologic issue which has recently gained importance, could not be described solely as an environmental problem suggests searching for ways prioritizing political organization success of new methods in organization methods of greens. The cause of environmental pollution was explained in 3 ecologies as follows: policy of excessive industrialization adopted by the U.S.S.R and other eastern bloc countries to catch up with the western world resulted in disaster. Environmental pollution substantively intensified in these counties. Territory of the Aral Lake has become the most polluted area of the world. The third world countries need to pollute environment so that they pay off their debts. The greater the debt, the more environmental pollution is. That is, environmental problem is not an individual problem on its own; instead, it is accumulation of industrialization, borrowing and inter-personal social exploitation (Akay, 1990).

How the world could be saved with design? Or, how design could be understood in a way that it makes sense?… Design is one of the distinguishing, basic qualities of human; it is one of the fundamental requirements determining quality of human life (Heskett, 2002). Intellectual design is a solution in the name of saving ecology and the world. "When industrial systems controlled by media adhere to science, "an intellectual ecology" is required in case the resulting eco-system is destructed. Ecosystem need to replace the term of environmental ecology; and conscience and conscious pollution need to be prevented rather than environmental pollution" (Akay, 1990).

5. Ecological Design

Ecology is as old as the existence of mankind. In sacred texts, God created nature first. Later on, he created animals and people as his wife for his life in nature. The first punishment is Adem and Havva playing the apple from the nature (picture 1). Thus the relation of mankind to nature has begun.

Picture 1: Adam and Eve are playing apples from the nature.
https://yle.fi/aihe/sites/aihe/files/migrated/blogitylefi/body_images/garden_eden.jpg

"It has also become part of the Sufi Philosophy ecology. As Mevlana said, "The world is being reborn and renewed every time. But since we have seen the world stand still, we are not aware of this renewal" (Kışlalıoğlu ve Berkes, 2017). Therefore, ecology is regarded as a scientific discipline that delves into the connection of living things. What is the relationship between the ecology and the design? Ecological design is an integrative ecologically responsible design discipline. Ecological design is defined by Sim Van der Ryn and Stuart Cowan as "any form of design that minimizes environmentally destructive impacts by integrating itself with living processes (Van der Ryn ve Cowan, 1996). In human history (Mchale, 1969), technological means have resulted in growth of human populations through fire, implements and weapons. This dramatic increase in explosive population contributed the introduction of mechanical energies in machine production and there have been improvements in mechanized agriculture, manufactured chemical fertilizers and general health measures. Although the earlier invention inclined energy adjusting the ecological balance, population growth following the industrial revolution led to abnormal ecological change. Today, design is regarded as an important element for the welfare of the people and for the salvation of nature,

independently of the ecology. When a product is sold on the market, its impact on the environment becomes inevitable. Raw materials in the structure of the product, life expectancy, user's desire for consumption or other behaviors caused, energy usage and life time to complete and become waste … But all of our commitments can be well planned in the design phase, before even more production. Nowadays, the designer can not only change the form but also change the production process and behavioral habits in the name of environmental sustainability.

The importance of design education is still not recognized in our country. It can be said that many design schools in other countries of the world are not much different from us in sustainable design. As a result, if we want to preserve ecology, we must improve both design and sustainability in our country.

6.Ecological Reflections in Graphic Design: Sustainability Impact

Sustainable design should not only mean doing the right thing to protect the environment. Sustainable design should also include aspects such as healthy growth of future generations, ecological behavior, and encouraging innovation. Especially the advertising campaigns and graphic products created in recent years have an important influence in the change of this situation. In the field of design, the discipline of graphic design is the most striking communication transfer. Therefore, it can be said that graphic design is more effective in acquiring environmental awareness and behavior for ecological continuity. For example; Tommorrow Machine, a Paris-based Swedish design studio, designed a graphic product for the infarm company under the name "microgarden kit". The Microgarden kit contains a reusable and renewable plastic layer that folds into an independent greenhouse (picture 2).

Picture 2: Microgarden kit by Tomorrow Machine
http://tomorrowmachine.se

The Microgarden uses transparent seaweed based gel as a growing medium, and it has many benefits. It allows the Microgarden to remain self-contained – which means you will never have to water the microgreens. Their roots absorb moisture from the gel. The clear gel also allows the home-farmer to see and experience the whole growing process, from when the seeds sprout to the roots growth (http://tomorrowmachine.se).

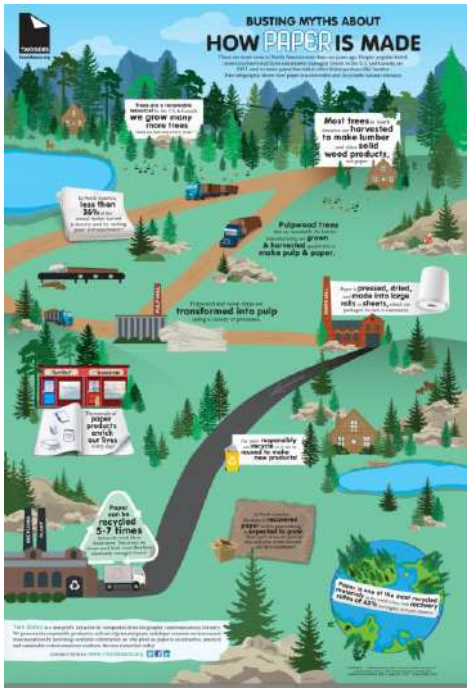

Picture 3: How Paper is Made Infographic by Two Sides
http://www.twosidesna.org/includes/files/upload/files/HowPaperIsMade-7.5x11.jpg

In addition the outdoor application "Paper Dispenser" by Saatchi & Saatchi in 2007 for World Wildlife Found regarding paper consumption is quite impressive design in terms of raphic design. South America map is seen in design and the use of green paper towels results in a blackening zone (picture 4).

Picture 4: Paper Dispenser by Saatchi & Saatchi, Client:WWF, 2007.
https://www.coloribus.com/adsarchive/outdoor-ambient/wwf-paper-dispenser-9689455/.

The environmental scientist Lester Brow summarizes the benefits of reuse in his Yearbook of the World: As the recycling rate increases, demand for all raw materials decreases. This is useful, for example, for the protection of forests; avoiding the rapid depletion of deposits at hand; to keep unexploded ore deposits for future generations (Kışlalıoğlu ve Berkes, 2017). Recycling is not only important for nature, but also for graphic design. For example; The recyclable pens that the Sprout team has created are incredible in terms of design. For a designer pencil and paper are the main materials for the manufacturing process. And the increasing pens and papers are wasting away. The Sprout team solved this problem by turning the pencil into the seed. The pens can be added to the soil when desired. Thus the pen becomes a recyclable sprout simply by becoming an article tool (Picture 5).

Picture 5: Sprout Pencil.
https://sproutworld.com.

7. Analysis of an Artist Project

Majority of today's designs are now created on the basis of directing target audience to think and to concentrate on a different point of view through receptive or interactive design. In the project created according to the phenomenon of "how could you save the world", utopian exhibition was employed. This exhibition aims individuals to gain such behavior by stressing ecologic issues. First, individuals need ticket for admission to this exhibition. Moreover, cell phones are not allowed in the exhibition area so that addictive factors could be dismissed. Visitors are required to go to the exhibition by means of public transportation instead of their personal vehicles as they keep their admission tickets. Up until now, it is evident that there are some requirements and fines with the exhibition. These are the imaginary designs to prepare and motivate individuals for appropriate behavior. For example, bringing recyclable materials while coming to the exhibition or collecting garbage if they arrive to the exhibition their personal vehicles, etc. In the name of saving the world with design, individuals who solve puzzle by asking question to others or following the codes accurately, they will be considered as saviors of the world.

In the application of the exhibition, while target audience were expecting to find a clue to save the world in the exhibition; but they will face an alien poster on the wall (Picture 6).

Picture 6: How to save the world with design ? Exhibition, 2017.

In another hall, a phone will ring uninterruptedly. This will urge visitors to answer their phones but they could not since all phones were collected from them at the entrance. In the meantime,

a poster will be on the wall in the exhibition hall about excessive technology usage. Indeed, all these activities were for bringing constituent elements of a jigsaw puzzle.

Results

In the present study, practicability of the design and its effect on sustainability were investigated in terms of its role on the target audience (all human kind) within the scope of the project to gain certain behavior. Since the target audience is rather extensive, intellectual qualifications were concentrated. The design could not be expected to be isolated from such extensive patterns because of the change in culture and humankind. Initiatives which spend efforts to adjust old formats to the new objectives since 1980s and lunatic experiments regarding what could happen in the future were exhibited in the same place together with overconfident statements. On the basis of concepts with mass production, it advanced to a new phase by proliferating to global markets. It is already obvious that computers have deep, transforming and completing impact on the current conceptualizing, representing and description tools in design although they are not completely capable of substituting them. Today, designers determine the direction of design by undertaking strategic decision making authority within the integrity of campaigns as well as future formats of designs more than ever. For example, Sony Corporation has a strategic design department one of whose extensive responsibilities is preparing potential scenarios for the future and to submit them directly to the president of the corporation. Similarly, in the present study, a strategic design process was followed and the relevant media plan was prepared. Although there are commercial potentials with meeting needs of the target audience, the extent of the exploited ecology indicates a disturbing status. At this point, there are questions to be asked: if basic requirements could become more and more easily met, then, why do all world turn to their face towards consumption focused on demonstrating effect? In this sense, design is not simply an activity directed by designers; in the mean time it is an expression of something believed by societies to as life quality at sustainable ground. Therefore, designers, in this study, reached the whole solution by a fantastic setting and by allowing audience to gain a behavior. Finally, the design is essentially important to everyone; and the world could be saved after this is adequately internalized and discussed.

References

Heskett, J. (2002). *Tasarım.* Ankara: Dost Yayınevi.

Gilman, R. (1992). Sustainability By Robert Gilman from the 1992 UIA/AIA Call for sustainable community solutions. 16 Mart 2003, http://www.context.org.

Guattari, F. (2000). *Üç Ekoloji.* İstanbul: Bağlam Yayıncılık.

McHale, J. (1969). *"An Ecological Overview",* in The Future of The Future. New York; George Braziller. 66-74.

Kışlalıoğlu, M. ve Berkes, F. (2017). *Çevre ve Ekoloji.* İstanbul: Remzi Kitapevi.

Ruckelshaus, W. D. (1989). *Toward a sustainable world.* Scientific American, *261*(3), 66-175.

California.

WCED, (1987). Our Common Future ("Brundtland Report"). http://www.un.org/documents (date of access:9 Haziran 2018).

Van der Ryn, S. ve Cowan, S. (1996). *Ecological Design.* Washington: Island Press.

A Semi Automatic Windows Which Prevent to Poison Carbon Monoxide and Other Toxıc Gases

Mehmet Senan YILMAZ[1]

[1]Bolu Abant İzzet Baysal Üniversitesi ,Gerede MYO Gerede/BOLU, TURKEY, yilmaz_m1@ibu.edu.tr

Abstract

Public health is one of the most important concepts in modern era. Various methods for the elimination of the disease or danger widespread among the people are being developed. Preventive medicine and taking measures in advance is one of the most important factors in maintaining a person's health. Poisoning is one of the most common public health problems. People are usually exposed to toxic and suffocating gas. During intoxication, it has developed a window system that will allow the window open and fresh air immediatelywindow consists of 4 main sections. These are window, motor chain mechanism, calling apparatus and alarm system. Alarm section is very sensitive. 20 second message can be recorded in the search module. And If poisoning occurs, this message can be sent to 8 different phone numbers. In this study, we will explain about new window system.

Keywords: Carbon monokside, Carbon monokside poissen (COP), Silent killer, Window, CO detector, new window system

1.Introduction

Poisoning is called by the substances that are taken by breathing or breathing to interfere with the balance of the body. Carbon monoxide is a toxic gas that is occured by burning fuels containing carbon in the structure such as gas, natural gas, gas oil, gasoline, LPG tube, coal and wood, İf not burning completely. It is known as "silent killer" due to its tasteless,, colorless, odorless and irritating properties [1]. Carbon monoxide poisoning is common in places where carbon fuels are used extensively, in mines, in garage, and in smoking places.

Carbon monoxide passes through the lungs to the blood. Carbon monoxide gas binds to hemoglobin oxygen, which is contained in red blood cells and carries oxygen to the blood, about 200 times faster and as a result, carboxyhemoglobin (COHb) is formed. So that, the blood can not carry enough oxygen to the brain because of the hemoglobin. The heart, brain and other organs will not function properly. it causes diseases and deaths.

If carbon monoxide poisoning is mild, it can be seen as headache, fatigue and exhaustion, shortness of breath, nausea, dizziness. If there is a serious level of carbon monoxide poisoning, it will result in dizziness, vomiting, loss of muscle coordination, loss of consciousness, and often death [2].The effects of CO in the blood are shown as below [8].

Table 1: According to CO level on blood, The effects of CO

Percentage of CO in blood	Clinical Findings
% 10-20	Nausea, fatigue, emotional imbalance, confusion, clumsiness
% 21-30	Headache, weakness in senses, effort dyspnea, angina, weakness of vision, slight loss of power
% 31-40	Dizziness, dizziness, nausea, vomiting, impaired vision, inability to make decisions
% 41-50	Fainting, change of consciousness, forgetfulness, tachycardia
% 51-60	Comatose, seizures, marked acidosis, death
% over 60	Death

The duration of intoxication interventionis very important. If the intervention is early, the effects can be eliminated in a short time. If the intervention period is longer, the health effects will be permanent.the following table shows effects according to poisoning times [8].

The most affected are fetuses, infants, elderly people, anemia, respiratory and cardiac insufficiency patients [1].

A wide variety of poisoning cases are encountered in our country.The most common poisoning is poisoned by carbon monoxide gas. Thousands of people are poisoned with carbon monoxide gas every year in our country and many of them result in death. Carbon monoxide poisoning is most common in winter months. The main reason is the use of coal and natural gas to heat the houses in the winter seasons.

Table 2 Percentage of findings [9].

Symptoms and Findings	**Number**	**(%)**
Nausea	23	59
Vomiting	21	53,8
Headache	17	43,8
Lassitude	10	25,6
Syncope story	8	20,5
Dizziness	6	15,4
Consciousness change	3	7,7
Shortness of breath	3	7,7
Chest pain	1	2,6
Stomachache	1	2,6

In the seasonal distribution of deaths in 2008, 76 deaths (43.43%) were seen in winter, 44 deaths (25.14%) in the spring and 41 deaths (23.43%) in autumn were carbon dioxide poisoning [3].In our country, 10154 people are poisoned by carbon monoxide in 2010 according to the data of the health ministry. The death rate was determined five people in ten million.

Table 3: Distribution of poisoning cases in Ankara between 2002-2006 by month

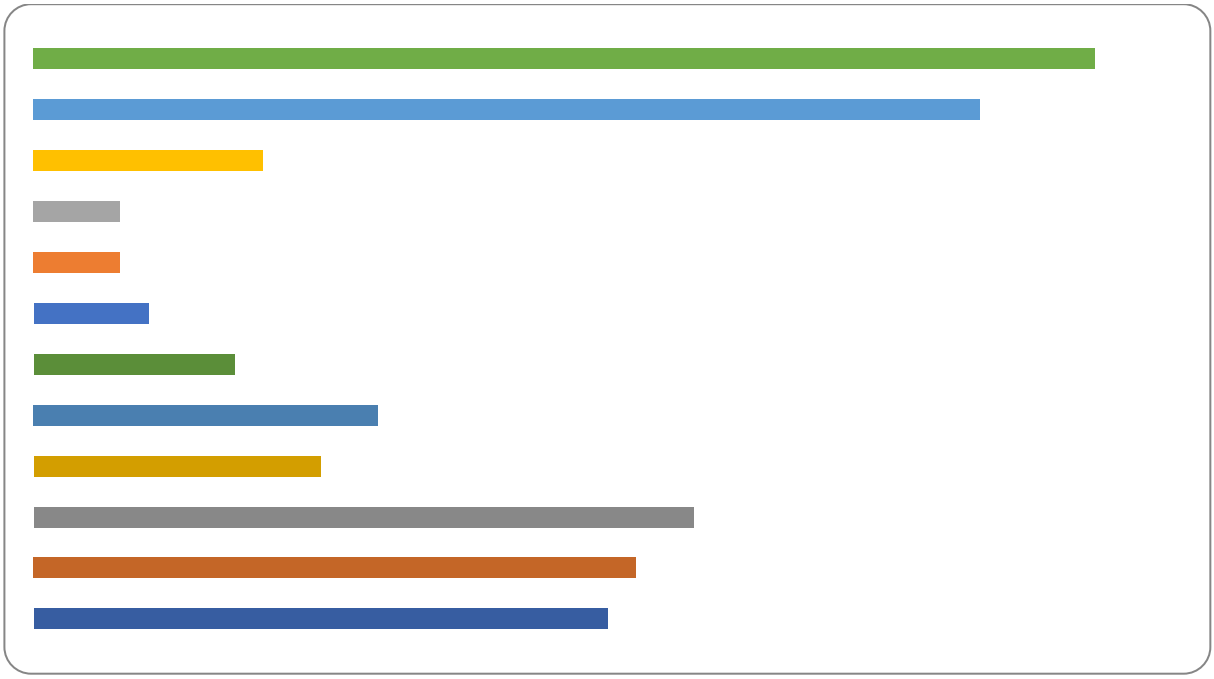

When the distribution according to cities is examined, it is seen frequently in Istanbul, Bursa and Ankara. Most deaths are seen in Bursa. In our country, carbon monoxide poisoning seen in 2011 was reported to be 80% percentage and other parts were caused by natural gas and water heater [4]. The distribution of the cases in the daytime is as follows [4].

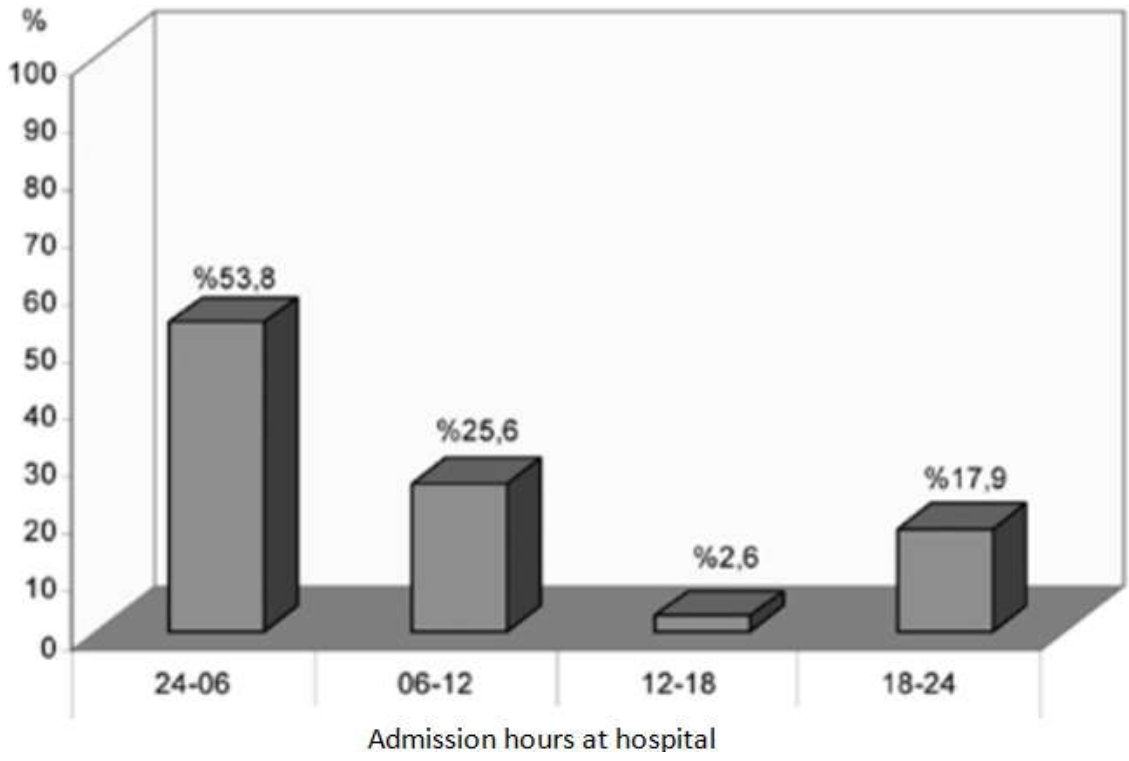

Figure 1: Application times for hospitals during CO poisoning

A total of 431 carbon monoxide poisonings were detected in almost every region according to sources reported between 1 January and 28 February 2012. In those cases, 65 people lost their lives.According to the statistics of forensic medicine institutions, 175 out of 4539 cases autopsied between 2002 and 2006 were found to be caused by carbon monoxide poisoning. In addition, in Bursa, 3065 autopsies were conducted within 5 years and 99 of the deaths were attributed to carbon monoxide poisoning. This is proportional to 2/3 " [5]. In Bursa, there were 304 cases of COP in Uludag University medical faculty emergency department policlinics which resulted in death between 1996-2006. 85.9% of these are poisonings caused by stoves [6].Between 2003 and 2005, the COP were found at 74 children (age range 1- 17, 43 girls, 31 boys) in Eskişehir [7].

2. How to Prevent Gaz Poisoning?

As explained above, many people from carbon monoxide gas are poisoned or lose their health. to reduce or prevent poisoning; a window was improved which open automaticly

This window was initially manufactured in two varieties. The first version was just a window opened after the gas was perceived. And then , a calling module was integrated at system

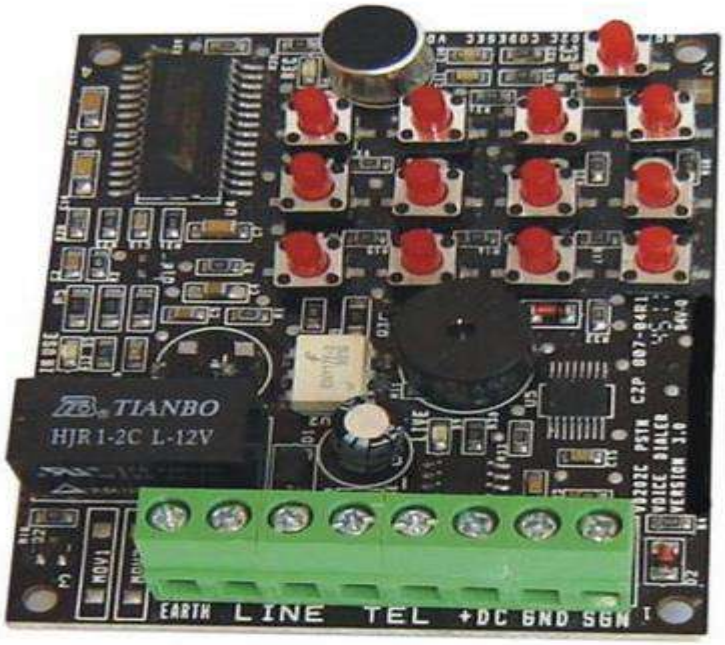

.

Figure 2: Telephone calling module

There are 4 parts of window system for poisoning; gas detector, search module and windows and chain motor mechanizm. The gas detector which the gas detects, transmits as a signal to the chain motor mechanism in the window. and the chain motor mechanism opens the window by pushing the opening part of the window and provides the entrance of fresh air. at the same time it exhausts poisoning gas. The window can be opened from 25 to 45 cm. The system works with 12 DC. 20 seconds voice can be recorded in the calling module. Recorded message can automatically dial 8 different(112, 155 and other celluler numbers) phone numbers. İn this way, the other relatives will be informed about the people who exposed to poisoning.

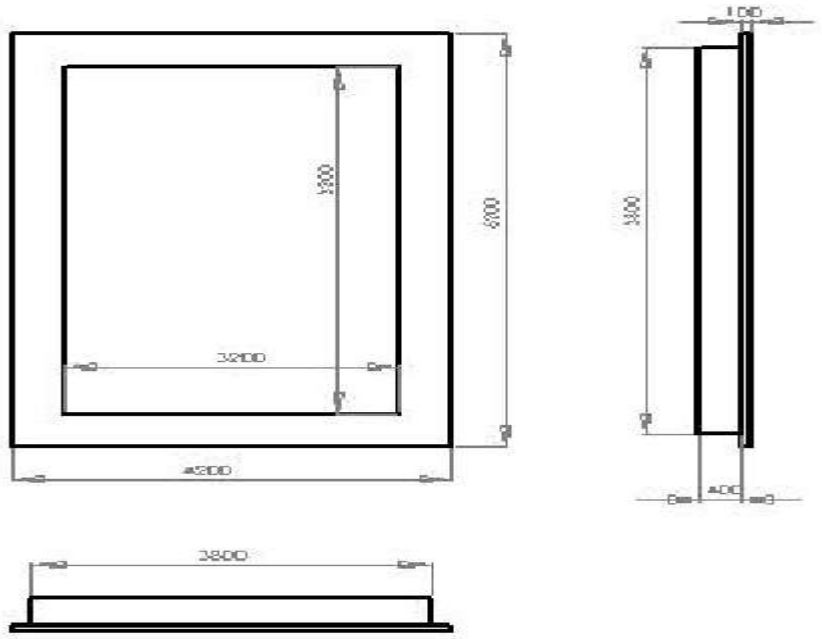

Figure 3: window section

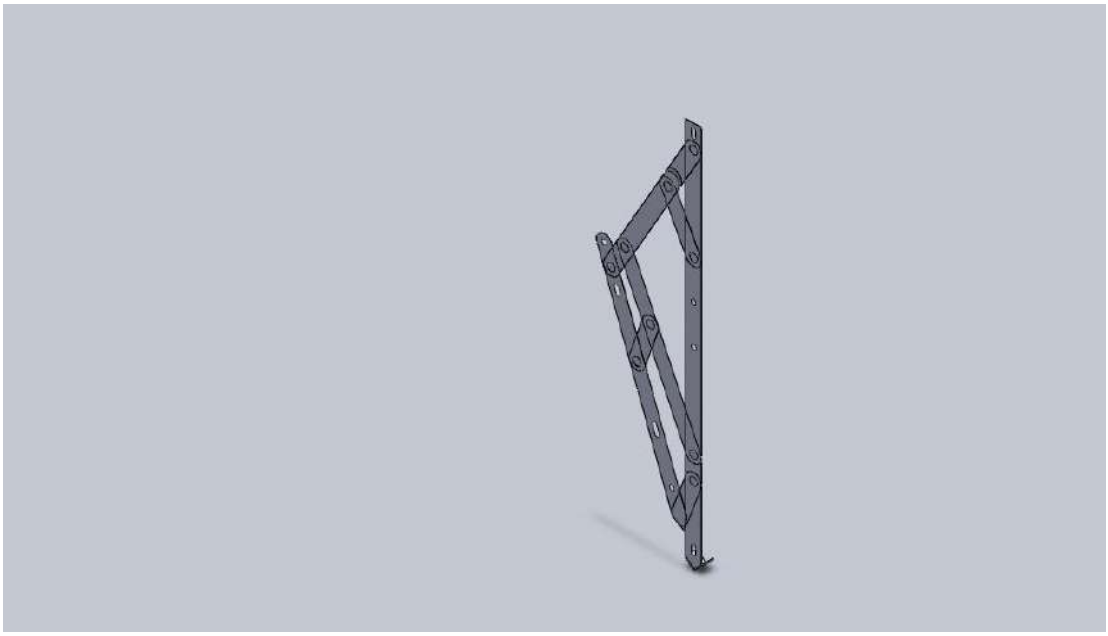

Figure 4: Hinges

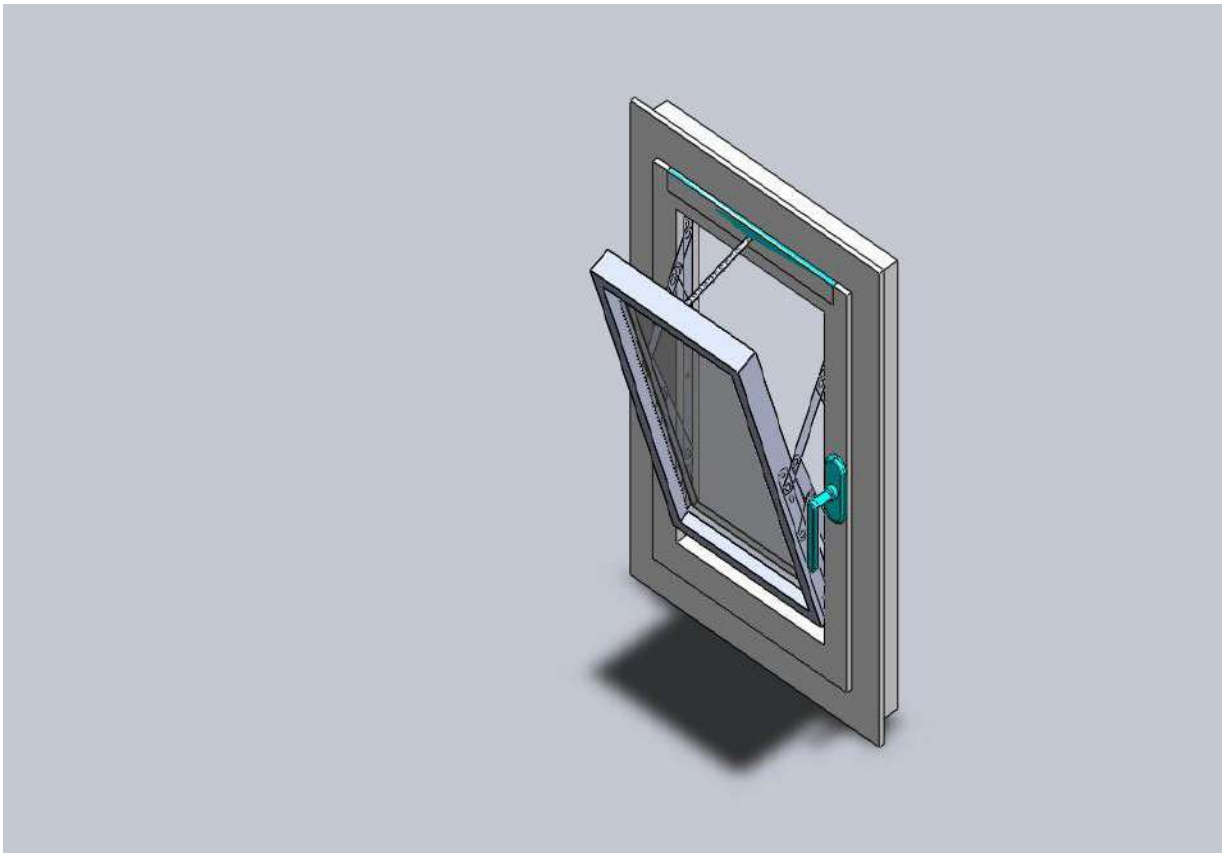

Figure 5: Assembled window

Figure 6: Alarm and electronic section

This system is called chain-on-off system. the motorized chain mechanism was used in this system.The chain window opening-closing mechanism is gray colored and works with 220 V AC. The push-pull force is around 300 Newtons. The opening distance is minimum 100 mm, maximum 450 mm. The distance can be adjusted. The opening and closing speed is 6 mm / s. It activates for 3 to 7 seconds when gas is detected. the alarm first rings after the gas is detected. At the same time, the window of the window opens 450 mm and fresh air enters. At the same time, it calls a 20 second sound record to 8 different numbers previously recorded in the search kit. Number calling frequency is 60 seconds. the window system automatically closes itself when the gas level drops to a reasonable level.

Figure 7: The section of window mounted electronic and alarm system

Figure 8: On-off mechanism. Special motor and motor spindle

Figure 9: Assembled of Windows system

The experiment were done in a room which dimentions are 2.75 meters in height, 3.5 meters in length and 2 meters in width. 3 cigarette smoke containing approximately 60 mg (3* 20 mg CO) CO was used in the experiments. For each experiment the chamber was ventilated for 2 hours. Time-distance graph is as follows

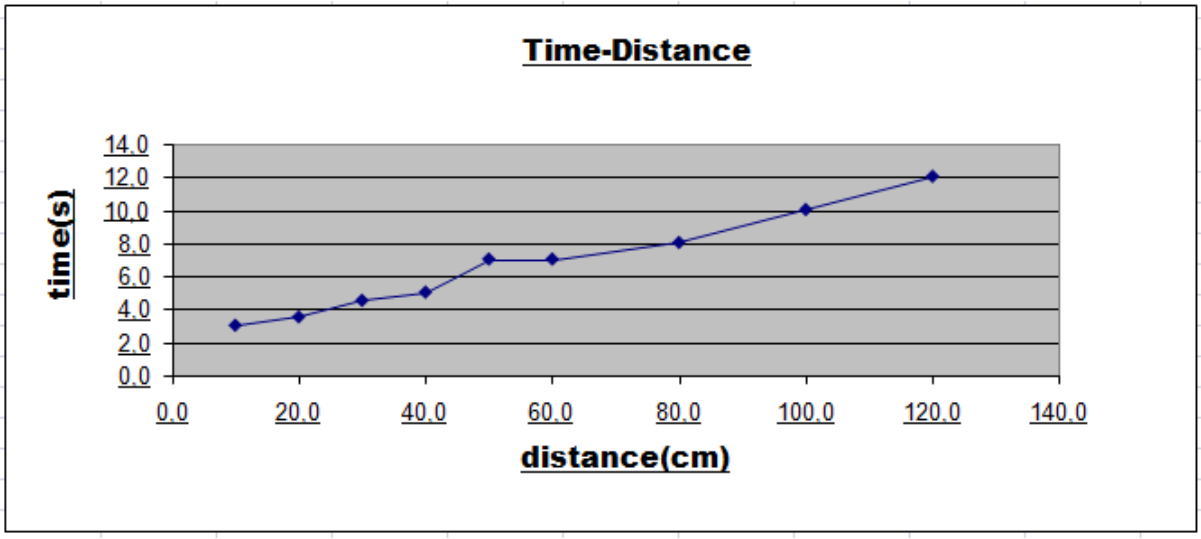

Figure 10: Time-Distance graph of window detection

3. Conclusion and Discussion

As explained above, suffocating and poisonous gases are very serious hazards and ruin health and couse economic loss. This system helps to decrease the danger of death, reducing deaths and avoiding injuries or physiological damages that can occur as a result of poisoning. Hospital expenses of many people who are poisoned and injured in dumand are very serious cost. these expenditures bring a great burden to the national economy.Besides, the deaths cause the families to be dismembered and a social trauma occurs.

The use of such a system would be an effective prevent the poisoning of people living alone and especially elderly people. As it is known, southwester is especially blowing in winter months.... It is most effective in the Aegean, Marmara and Western Mediterranean. When the southwester speed exceeds 40 knots [10] it has a very dangerous effect. The southwester causes the stove chinmey to smoke.

Due to explained above; especially in the Aegean, Marmara and Western Mediterranean regions under the influence of the southwester, and especially in cities such as Bursa, it will be a preventive precaution to prevent poisoning in the winter months.

References

1) www.carbon-monoxide-poisoning.com

2) www.bilkent.edu.tr/karbonmonksit.htm

3) Anturk, N; Başbulut, Z. Et.al “Ankara da 2002–2006 yılları arasında karbon monoksit zehirlenmeleri otopsileri” Adli Tıp Dergisi, 2008,sayı 22 s.25–30

4) Sağlık bakanlığı 2010 istatistik verileri

5) Adli tıp dergisi

6) Akköse S,Türkmen N, adli tıp dergisi, Ocak 2010,16(1)

7) Yarar, Coşkun, Ayten Yakut ve arkadaşları. The Turkish Journal of Pediatrics, 2008, 50, sayfa 235–241

8) YILMAZ, Hayri Levent ’karbon monoksit zehirlenmesi’ Çukurova Üniversitesi Tıp Fakültesi Çocuk Acil Tıp Birimi

9) Gülser, Esen Besli1, Müferet Ergüven1, Meriban Karadoğan1, Öznur Yılmaz, acil tıp dergisi, JAEM 2009 .19480

10) www.mgm.gov.tr. Meteoroloji Genel Müdürlüğü web sitesi

Examining and Reinterpreting Fashion Design Samples of Leading Designers of Futurism

Nurdan KUMAŞ ŞENOL[1], Ali Osman ELMAS[2]

[1] Giresun University, Technical College Vocational School, Giresun, Türkiye; gazi-moda@hotmail.com

[2] Giresun University, Technical College Vocational School, Giresun, Türkiye; ali.elmas@giresun.edu.tr

* **Corresponding Author:** nurdan.senol@giresun.edu.tr

Abstract

Futurism has been renowned as an Italian art current that has gained international recognition from 1909. The basic principles of the modern city life in painting and sculpture, in particular the glorification of the dynamism of new technologies such as automobiles; dynamism, future, strong lines, speed and technology. . The introduction of the futurism movement, which is regarded as futurity, has become fashionable by Giacomo Balla, who has received various manifestations on his clothes. However, the most remarkable years of the current were seen in the 1960s. In 1961, the theme of "space" in space was quickly adopted, with tour around the earth, the discovery of space, and the idea of dominating the future. Fashion designers have been involved in modern art movements and designed clothing products based on the principles and dynamics of this movement. In this study, an overview of the designs of fashion designers affected by the Futurist art were tried to be explained and re-interpreted by inspiring the work offered by the period.

Keywords: Futurism, fashion, art, design

1. Introduction

Futurism has been an art stream in Italy that has shown its effect in many different disciplines, such as painting, sculpture, music, poetry, literature, theatre, architecture, photography and cinema, just before the First World War. "Vortisizm, Constructivism (incubationalism) and suprematism other than currents such as the source of communication technique and philosophy that is the 20. Century has been an important place in the art flows (Genç, 1983:55). Transition from feudal structure to industrial society at the beginning of the century and ultranationalist ideas; In Milan, the industrial breakthroughs, especially the automobile industry, have begun to evolve. These two development artists have also influenced. The aesthetic conception of the period was formed depending on these two structures. The new form of beauty has progressed in the right proportion with the beauty of speed (Keser, 2005:143). The main source of this new level of consciousness was the Italian avant-garde art stream as a futurism. Although it reflects the country's specific conditions, it has influenced everyone from Moscow to New York, an artistic pioneer (Farthing, 2017:396).

This article, which overlooks the fashion framework of the art stream from the tradition of contemporary art, is thought to contribute to the research and designs planned to be done in the future.

Dress Fashion and Futurism

Artists of the futuristic art movement; They have gathered on the axis of changing the world and written various manifestos on everything that appears. In 1910, the Futurist emphasized the importance of the harmony of the curves and lines of modern clothing in the futuristic sense in the manifesto. According to their clothing's understanding; The clothing must be free from ornaments and pretensed, and should be designed with consideration of health and comfort elements. The Modern outfit should draw attention to the dynamism and speed of life, which must be composed of asymmetrical and dynamic fabrics (Braun, 1995). Futuristic artists have used unorthodox materials such as aluminum, glass, metal, wood in their clothing design; These materials include phosphory materials, various body painting techniques and collages. In addition, the Futurists have also suggested various ideas for clothing that lead to today's smart clothes (Özüdoğru, 2011:228).

Futuristic artists who set out from an innovative perspective to the Modern age have made a difference by contributing to many studies in the field of fashion. Giacomo Balla, one of the leading figures, believed that the clothes influenced human nature and appearance. Tullio Crali has introduced different details in women's clothing, integrating futurist elements into

their designs. In his work with his wife Rober Delunay, Sonya Delaunay suffered from a ' simultaneous ' conception in futuristic garment designs, using geometric forms, circular structures and pure colors.

Paco Rabanne (1934-), one of the leading figures of the second generation Futurist artists designers such as Pierre Cardin (1922-), Andre Courreges (1923-2006) and Emanuel Ungaro (1933-) are influenced by more than the period described as "space Age current"; The modern, simple and bold clothing they made their designs to the fashion world.

Giacomo Balla

The artist, known as the father of the futuristic fashion, has written various manifestos on the outfit, but the most vocal of them was the writings of men's clothing written in the year 1914. As the main theme in the article; You need to get rid of boring, gloomy items and they have expressed that you should go through moving colored items instead. The artist's male suit, designed in 1923, has been characterized by the characteristics of futuristic fashion that does not contain buttons, non-collar and pocket details by creating an unorthodox form (Fig. 1.).

Fig. 1. 1923, Balla, futurist team

Tullio Crali

Tullio Crali, one of the other Futurist artists, also designed clothes. In the designs of T. Crali, futuristic elements are formulated in a different way than G. Honey's design. The artist's "synthetic Jacket", designed in 1932, is without pockets and no collar; Instead of the collar,

only left-hand claps were released and this clapa was painted black to draw the emphasis on itself (Fig. 2). The jacket is also bright and has a very simplified line due to the fact that it has no pockets and no collar. The futuristic dynamism in its designs has shed light on how the futuristic midday can be applied to the outfit beyond the colors and geometric forms, unlike the Crali, G. Balla, who tries to get caught in the lines of the human body (Fig. 3). (Özüdoğru, 2013:230).

Fig. 2. 1932, Crali, futurist jacket

Fig. 3. 1933, Crali, futurist garment

Sonya Delaunay

Sonia Delaunay, Russian-American, has again revealed the fiction of complex shapes and motifs in his work, which he colored with geometric patterns and harsh colors in his atelier in Paris. Against the ordinary cuts and colors of time, he has clearly applied these thoughts to the fashion of clothing (Fig. 4). According to the artist, fashion is an artistic form of expression, in an interview he said he was not interested in fashion, he applied light and color to fabrics (Bonnie, 2007:45). Delunay has applied futuristic trials in men's and women's clothing and followed a successful line. The color research carried out with his wife was Simultaneizm current based on color contrasts; S. Delaunay was directed to the outfit design under the influence of this current. The artist has been pursuing a dynamism that shows the human body in motion in the clothes he designed, the fabrics in different tissues, the contrasting colors as well as the new cuts suggested (Stern, 2004).

Fig. 4. 1924, Delaunay, designed for Gloria Swanson mantle

Paco Rabanne

A keen advocate of new materials and techniques, Rabenne, born in Spain, created a surprise in the fashion world with its space-looking designs made of metal and plastic, all fashionable and designed by young people. has been met. The designer, which originally introduced the Industrial design experience in 1966, was named as "Body Jewel" and the pencil dresses consisting of metal, plastic squares and discs were presented in the fabric of the lower part (Fig. 5). (Dereboy, 2008:139).

While many designers have been experimenting with bright, new and modern materials, which fit into the space age stream, the most memorable is the armored mini-dresses designed by Paco Rabanne (Fig. 6). With this design, he surrounded the body with metal plates and attracted attention to contrast against the softness of the skin (Mackenzie, 2017:97). Rabbene's futuristic designs have brought many limitations to the fashion world. For example, as a dedicated jewel designer for creating dresses without using fabrics, he applied to materials such as plastic, colorful rubber, hologram leather, laser discs and optical Figer (Blackman, 2013:233). In an article published in the 1967 of Marie Claire magazine, she became a bold fashion designer to say, "My clothes are designed to be weapons for the Amazons."

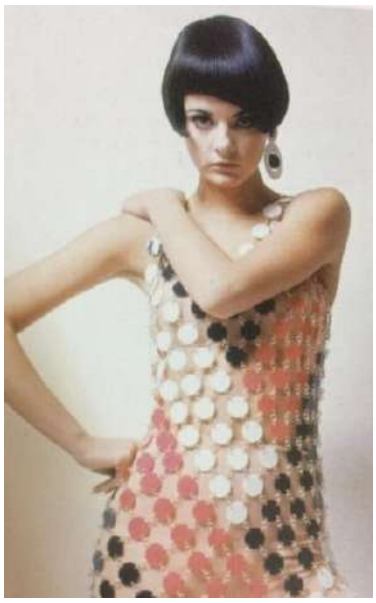

Fig. 5. 1966, Rabenne, dress

Fig. 6. 1967, Rabenne, armored dress

Andre Courreges

With the release of the mini-skirt of French fashion designer Andre courreges in 1961, lean and modern designs have survived sexual, social and modasal restrictions. In the brightest period of space studies; Attempts to go into space, launched satellites, manned space shuttle work and the first-ever foot-press designer affected by the moon; He designed his trousers from silver-effect fabrics, his jumpsuits, the lunar boots He made from PVC fabrics, the white plastic space style sunglasses, the chiffon fabric perforated cloak and the "Moon Girl" collection Attracted the attention of the world by creating (Dereboy, 2008:126). (Fig. 7). André courréges ' astronaut-style designs were of great interest at the time. His patent leather jacket design, mini skirt, boots up to the knees and short pants designs have implemented space fashion. Courréges has provided futuristic looks to the fashion world with its pure, lean, functional designs. With more white, pink, turquoise, ice-blue colors and simple, lean patterns (broad lines, squares, abstract flowers) without doubt and a revolutionary understanding, the fashion world has created a new style.

Courreges's collections included trousers and mini-size dresses, which were made with a subtle workmanship that clearly set the body lines. Modernity this couture version, completed with both square and rounded jackets A-cut mini skirts, the designer's focus point is that the clothing segments are emphasized. Their designs also feature contrasting neck parts, bright coloured and blunt-cut wigs, two-piece angular lines with metallic color buttons and edge strips, skirts that reveal legs, smooth shoes and short socks. (Fig. 8). (Fischel vd, 2013:361).

Fig. 7. 1964, Courreges, Moon Girl Collection

Fig. 8. 1969, Courreges, young appearance

Pierre Cardin

P. Cardin, who has already been widely effective until the early 1960s, has been accepted by designers who emphasize the futuristic fashion geometry. The design of the future ideal dress has been among the priorities in its life, with space-effect sewing lines, space-age technology, and the designs created by the fashion world (Dereboy, 2008:136). Among the contributions of Pierre Cardin's fashion race, he was the owner of the collection of rounded necklines, turtlenecks, short skirts and helmet-shaped hats made of men and women's clothing (Mackenzie, 2017:96). (Fig. 9.).

In an effort to bring fashion and science together, the French designer Cardin pioneered the concept of unisex clothing with its ' first space Age ' collection, which includes single-piece white braids worn under robes and tubular dresses. During the 1960s, The notebook was made of mini apron dresses worn with vinyl boots and a more commercial assortment of stylised, brightly coloured tunics (Fogg, 2014:377.). These designs are complemented by elbow-top gloves, wide belts and silver gear (Fig. 10). In the following years, the designer has assembled vinyl and metal and designed in tunics made of gabardine fabric worn with unisex zipper jackets and metallic full-size tights (Fig. 11).

Pierre Cardin's ' Cosmos ' collection, inspired by science fiction films for the big and small screen, designed by the futuristic outfits "Space Road" and "2001: Space Road Adventure", reminded us of the films. Similar uniform clothes are made for women, men and children. In Cardin's fashion world, the woolen jersey men's cosmonaut outfit has undergone a

drastic change in the boring of men's suits and the garment is finished with a large zippered tunic and shiny patent arch (Fig. 12).

Fig. 9. 1967, Cardin, Modern geometry

Fig.10. 1968, Cardin, Space age Collection

Fig.11. 1967, Cardin, tights and tunic design

Fig.12. 1967, Cardin, men's clothing

The fashion that has been styled around the futuristic ideals has rejected the old, turned down the relationship between industry and art, and has uploaded a sense of social appreciation to the genre. The futurists drew attention to the speed of life in the manifestos of their writings, embracing the machine age enthusiastically and put mass production in place of tailoring

(Braun, 1995:34). In the garment designs, it has been influenced by modernism and modern music, and has forced the boundaries of the period to exist with futuristic designs designed from different materials from vinyl to paper. However, in the future, the formal and functional proposals on the clothing of Futurism were developed with the development of technology, the number of fashion designers who made designs under the influence of the futuristic, and the clothing designed by these designers is a wide It has been addressed to the consumer audience.

Emanuel Ungaro

The French designer Ungora worked with Courreges for two seasons before opening his own fashion house with his textile artist Sonja Knapp. The first collections of the Ungaro have gone from courreges ' futurist lines and short skirts. However, Ungara used stronger and brighter colors. The designer, who opposed the official structure of the Paris fashion system, designed the gowns from the fashionable products of the fashion, apart from the satirical movement of the evening gown, which separated the first collection into daytime clothes and decorated with ping-pong balls. (Fogg, 2014:377).

The clothes in the sculpture form usually use wool gabardine fabric. The design of the futuristic elements has addressed the youth in its interpretation. He also said I am in the fashion world with its brightly coloured jackets and suits, shorts, A-cut dresses, lace-up, long boots up to the thigh, knee socks and metallic garments (Fig. 13.0-14.) (Mackenzie, 2017:97).

Fig. 13. 1960lar, Ungaro, dantel tulum

Fig. 14. 1968, Ungaro, takım elbise

2. Material and Method

This study, which encompasses the interpretation of the futuristic art movement in the fashion trends in the current garments, is an evaluation research. Evaluation surveys also include "applied research" qualities in the direction of the aim of finding out what kind of conclusions are being made in the cases where the fundamental research findings are implemented (Arseven, 1994:28). Applied research is the practice of the knowledge produced or produced (Karasar, 1991:27).

The design characteristics of the futurist garments were examined in terms of shape, form, color, decoration and fabric, and the findings were combined with the fashion trends of the day and 70 sketches were drawn in accordance with the principles and methods of design. The most important designers of the current in the fashion world of the work presented by selecting 13 designs that reflect the best design and design values of the clothes were re-interpreted in the research.

2. Findings and Comments

In this section; The works of futuristic fashion designers identified as inspiration; In terms of shape, form, fabric, ornamentation properties, sketches are prepared according to the principles and methods of design. The garments that comprise the collection were interpreted in terms of design principles and tried to demonstrate their contributions to creativity as a source of inspiration for the art of Futurism.

Design 1

Design 2

The pastel colors used in the Design 1.-2.of Balla's men's suits are quite remarkable. The designs in the form wrap are presented with both dress and trousers-blouse design. Designs in which futuristic details are collected in accessories; It also has a very characteristic appearance with hair and makeup.

Design 3.

3. Design made by considering Crali's "synthetic jacket" design ; It is described as a kind of simplified vest design. Just like Tullio Crali's designs, the emphasis on pocket and collar-based study was made in black; The model was removed and the functionality was requested to be brought to the fore.

Design 4.

Design 5

Design 4.-5. the complex shapes and geometric form structure used by Sonya Delaunay often use in two different designs, such as dress and bustier shorts. In the study, the futuristic values were determined by the design elements such as color and line, and an updated form was tried to be captured.

Design 6.

Design 7.

Inspired by the work of Courreges, one of the most important names of the second-term futuristic artists, the Design 6.-7. shoes and hair accessories were cited in the space age. The futurist details in ordinary parts are even more prominent with the colourized colors and have given a different emphasis on the design.

Design 8.

Design 9.

Design 8. and 9. The metallic world of Rabenna is interpreted from a different perspective. The designs in which the Metal color is weighted are also studied in both mini-size and maxi-size dress. The contrast of softness and stiffness in the designs is applied simultaneously. With the applied tissue work, a sense of depth has been gained.

Design 10.

Design 11.

Design with the characteristic details of Pierre Cardin's space age fashion 10. Also shoulder and hem tip; Design 11. The details of the accessories and trousers are noteworthy. The dynamism that futurist brings to the fashion world; These designs are depicted as a harmony of contrasting colors.

Design 12.

Design 13.

Designed to stick to the parts that Emanuel Ungaro uses frequently, the Design 12. asymmetrical-tipped jacket length elongated, bustier and shorts are used in lace. The design also shows that the elements of the movement of the future are gathered with knee-top boots and different hairstyles. The Design 13. is a dashed skirt worn under the blouse; It has formed a whole with the spiral structure applied to the hair of the model.

4. Results

The futuristic stream, which emerged in the early 20th century, has been deeply influenced by the world of art and fashion, although not very long-lasting. Although the first touches of the fashion were seen in the 1920s, it was the most popular period in the second half of the 1960s, which was named as the Space age. In this time period, where the famous designers of the era were not indifferent, Giacomo Balla, Tullio Crali, Sonya Delaunay, first-period futurist artists; Designers composed of Paco Rabanne, Andre coureges, Pierre Cardin and Emanuel Ungora were examined as second-term designers and presented examples of futuristic designs created by them. These designs, which started the Futurist revolution, were not adopted by the people during their time, and were regarded as the myth of modernity and the future in terms of art. This blended structure was evaluated with the characteristic characteristics of the elements and style of the futuristic style. As a result of the visual resources reached; It has been concluded that this art stream, dominated by metallic bright colors and that

the unisex styles are featured, influences the fashion industry and carries a leading role in the designs of world-renowned designers.

In the framework of the application, the elements of futuristic clothing, which are treated as inspiration to garment designs, bears the traces of the period in general. Today, along with developments in modern art approaches, the original lines of fashion design are completely changing, especially the garment designers who adopt the modernist approaches, together with the garment to address the concepts such as time, space, future They also uploaded the artistic mission to the case of dressing. As shown in the collection prepared as an example, the richness of the clothing elements of futurist, the designer; Metallic and synthetic-looking fabrics provide significant contributions to their creativity with different materials such as plastics and aluminum.

References

Arseven, Ali. D., (1994), Alan Araştırma Yöntemi: İlkeler, Teknikler, Örnekler, Tekışık Matbaası, Ankara. 04.

Blackman, C. (2013). Modanın tarihi 1900'den günümüze. (K.Kaftanoğlu, Çev.) Kerasus Yayınları, İstanbul.s.219.

Bonnie, E. (2007). A Cultural History of Fashion in the Twentieth Century: From the Catwalk to the Sidewalk. New York: Berg.

Braun, E. (1995). Three Manifestoes. Art Journal 54.1:34-41. Champsaur,

Dereboy, J.(2008). Moda ve 100 yılın Moda Tasarımcıları, Format Matbacılık, Ankara.s: 138.

Farthing, S.(2017). Sanatın tüm öyküsü.(çev.G.Aldoğan ve F. Çulcu).Hayalperest yayınevi, İstanbul.s.396.

Fischel, A.,Baggaley,A.,Gersh, C.vd. (2013).Moda Geçmişten Günümüze Giyim Kuşam ve Stil Rehberi (D. Özen, Çev.) Kaknüs Yayınları, İstanbul.

Fogg, M.(2014). Modanın tüm öyküsü. (E. Gözgü, Çev.) Hayalperest Yayınları, s.474.

Genç, A. (1983).Dada/ Entropi ve Nedensizlik Açısından Dadacı Sanat Hareketlerinin Çözümlenmesine İlişkin Bir Yöntem Araştırması, Dokuz Eylül Üniversitesi Güzel Sanatlar Fakültesi Yayımlanmamış Doktora Tezi.

Karasar, N. (1991). Bilimsel Araştırma Yöntemi: Kavramlar, İlkeler, Teknikler. Sanem Matbaacılık, Ankara.

Keser, N. (2005). Sanat sözlüğü. Ütopya Yayınevi, Ankara. s.143.

Mackenzıe, M.(2017)...izmler modayı anlamak (M. Tuna, Çev.).hayalperest Yayınları, s.124

Özüdoğru, Ş. (2013). Modern sanat akımları ve moda. İdil Dergisi. Cilt 2, Sayı 6.

Stern, R.(2005) .Against Fashion: Clothing As Art, 1850-1930. Londra: The MIT Press,20.

http://thegarconniere.telavivian.com/2013/01/09/future-perfect/futurist-suit-by-giacomo-balla-c-1918/. Date of Access: 02.02.2018.

https://tr.pinterest.com/pin/511862313868015147/. Date of access 02.02.2018.

http://www.persephonebooks.co.uk/content/persephonepost/page/67/. Date of access 02.02.2018.

http://www.vogue.fr/thevoguelist/thevoguelist/paco-rabanne-/810#people_gallery_modal. Date of access 09.02.2018.

http://fashion.telegraph.co.uk/news-features/TMG8804503/The-return-of-Courreges.html. Date of access_30.01.2018.

https://tr.pinterest.com/pin/212232201168466426/. Date of access 07.02.2018.

World War I (1914-1918) Examination of Women's Garment Fashion and Reinterpretation with Digital Programs

Nurdan KUMAŞ ŞENOL[1], Çiğdem ÖZDEMİR[2]

[1] Giresun University, Technical College Vocational School, Giresun, Türkiye; gazi-moda@hotmail.com

[2] Giresun University, Technical College Vocational School, Giresun, Türkiye; cgdm.2806@gmail.com

* **Corresponding Author:** nurdan.senol@giresun.edu.tr

Abstract

The First World War was closely influenced by the fashion industry. Many authors, artist and fashion designer has been called into the army and joined the army voluntarily, they left behind the famine and war have sought to pursue their art in the environment.. The war has slowed down the fashion sector, but many Parisian tailor has still shown products. High-fashion designers, who do not consider the changing conditions, have tried to stay independent from politics and economic changes while creating the mode; In women's fashion, much more functionality and seriousness have come to prominence in this short period.Women's fashions have been much more functional and serious in the short term. Skirts with subtle silhouettes and the effect of war, women's jackets and mantle designs, which are influenced by military uniforms, have taken their place in the history of fashion. In this article, the effects of the I. World War on apparel fashion, which occurred between the years of 1914-1918; The period features were interpreted in digital environment and the designs were made.

Keywords: fashion, clothing, high fashion, period fashions

1. Introduction

Fashion, which is a temporary periodic phenomenon adopted by consumers during a given period of time, varies in accordance with theoretical products of life periods. This change develops with the inevitable decline in all fashions, the aging face, the rising new values, the mass harmony, the adoption and presentation phases of the fashion pioneers. (Sproles,1981: 118).

The fashion, which encompasses all social activities of man, is identified by many societies with clothing and ornaments. Clothing, which is one of the most prominent indicators of social status and gender, shows how locations within social structures are perceived in different eras and how the status limits are determined (Crane, 2003: 11). That's where the high-fashion trend comes in. Turkish fully-bespoke haute couture; It is a fashion term from the French, which is designed according to the individual's special taste and is used in the meaning of a special design dress. It is usually the type of clothing prepared according to the taste of elite customers at the top income level. So the designs are made according to the person's own preferences (color, accessories, stones, etc.) (Erol, 2011: 98).

The technical changes in mass production of the near era have been filled with the desire of women to be free and equal, and the fashion innovations affected by them. We can also call it the century of technology XX. At the beginning of the century, the society tended to oppose traditions and customs. In the first decade of the century, women are usually wore one-piece dresses called the Tayyör and Princess in the style of the tayyers that worn at the end of the XIX. Women's hair as classical as the late last century and decorated straw hats were used (Komsuoğlu vd. , 1986: 13). (Picture 1.).

Picture 1. Example of applique hat decorations in 1910
(Moda geçmişten günümüze giyim kuşam ve stil rehberi, Kaknüs Yayınları, 2013, İstanbul, s.237.).

Fashion 20. In the first 14 years of the century, it continued its course in a way that was not very different from the 1800 's. Solid social structures have preserved the existence of the fashion, ensuring that the aristocratic section is a special privilege. What is the meaning of elegance is still the instructions of Paris and the Haute Couture industry has determined (Mackenzie,2017: 62).

With the beginning of World War I, the whole world has begun to change in every sense. This difficult and restrictive war period has influenced the lifestyle and hence the clothing and fashion area. The sleek and crowded outfits have become increasingly simplitic, lightens and Sportin. Women who are accustomed to the comfort of wearing uniforms prefer simple and comfortable clothes. Thus, radical changes in the fashion world have shown itself (URL 1.). The war also brought about the economic crisis. Because of the war, the male population has decreased considerably, and the increase of homosexuality among women in Western Europe has changed the sense of clothing. In this period, the style called ' ala Waiter ' which carries masculine lines is adopted (Zengingönül, 1996: 23). Short blunt hair that is common among children at the beginning of the 20th century; It has been widely adopted by women who give up the detailed and time-consuming hairstyles of pre-war years. The waiter was cut in style with the hair, the chest and back areas were closed while the arms and legs were left exposed. All forms that were contrary to women began to take place in the fashion world. (Picture 2.).

Picture 2. Actress Louse Brooks's "Ala Waiter" Hair sample
(Modanın tüm öyküsü, Hayalperest Yayınları, 2014, İstanbul, s.226.).

The evolution of transition to the Modern female silhouette took about ten years, starting just before World War I. In 1914, two pieces of women's clothing attracted attention. Blots are

made of loose and knotted woven rattan fabric (Fischel vd.,2013: 241). The gowns are emphasized to be completed with a high-level, fine-line but relatively abundant, skirt-slit and lampshade-shaped top skirt (Picture 3.). At the end of this year, the re-emergence of the plethora of ruffle skirts has pleased the producers of Jupon. The Russian influence of clothing has increased visibly. Knee-level tunics and edges of fur coats are also fashionable models that can be worn outdoors (Fischel vd.,2013: 238). (Picture 4.).

Resim 3. 1914 Years of garment samples
(Moda geçmişten günümüze giyim kuşam ve stil rehberi, Kaknüs Yayınları, 2013, İstanbul, s.232.)

Picture 4. 1914 year women's fashion dress example, Russian influence
(Moda geçmişten günümüze giyim kuşam ve stil rehberi, Kaknüs Yayınları, 2013, İstanbul, s.228.).

Thin silhouettes and skirts that are short of the impact of the war, the women's jackets, which are influenced by military uniforms in 1916, have taken place in the fashion history of mantle designs. In everyday clothes, the waist is lower, the arms are shortened, the skirts are enlarged and the body lines are left in a more comfortable form than in the past. With large pockets, arched coats, the style worn on the bulging skirts is perceived as very common and elegant. (Blackman,2013: 78). (Picture 5.).

Picture 5. Daily Clothes from Lelong, Maupas and Manby
(Modanın Tarihi 1900'den Bugüne, Kerasus Yayınları, 2013, İstanbul,78).

With the introduction of the sea in the previous century, in 1916, women wore a dress inspired by the Victorian Navy uniforms to swim. (Blackman,2013: 100). Long-lasting inlets and long socks are worn under the abundant tunics. The more useful version of the outfit as it is also seen in Picture 6 ; It has been formed by a view consisting of a jersey blouse with lace shirt and laced beach shoes and a rubber hat with tassels.

Picture 6. 1916, Sea Dress
(Modanın Tarihi 1900'den Bugüne, Kerasus Yayınları, 2013, İstanbul,100).

In France in 1917, wearing the toilet in luxury entertainment places, wearing jewelry is prohibited until the end of the war. Together with the United States, which entered the same year in the conflict, all the forces were involved. The large-scale rescue effort, which was part of the war, gave women the opportunity to develop and demonstrate their skills. One of the new voluntary organizations created during the war was the "American motorised women's Unions" (Fogg, 2014:207). The New Yorkers who sell sportswear, Abercrombie & Fitch, have produced uniforms called "Lighting Liz" for motorized units. Driving together with the invention of the car has become a way of contributing to the mobilization for women in the war. When women use trucks instead of engines, they replace the lower skirt with short pants. Women's uniforms are similar to the American army, but they are well-educated, professional, middle and high-class volunteers, dressed in custom-made uniforms. (Fischel vd.,2013: 239). The two-piece team has a similar cut to the already popular bespoke clothes. However, the fabric of the garment used wool gabardine instead of tweed, and metal accessories were used instead of buttons made of bone or leather. The jacket is worn on a olive green cotton shirt with a buttoned front pocket that has sheer collar. (Picture 7.).

Picture 7. Motorised units uniform
(Modanın tüm öyküsü, Hayalperest Yayınları, 2014, İstanbul, s.206.).

Women's clothing was influenced by men's clothing as they started working at the factory. The effects of camouflage in fashion have been clearly seen in examples such as raincoats made of waterproof, durable cotton fabric designed by Thomas Burberry. Burberry also invented the red, white, black and peach color plaits, which was registered as Gabard and Burberry Ecosound. (Picture 8.). Arched soldier uniforms have been worn by many women and have brought the fashion of the trench coat. The height of the trenchcoats worn by women who use engines or work as bodily workers in the army that finished over the knee (Fischel vd.,2013: 238) (Picture 9.).

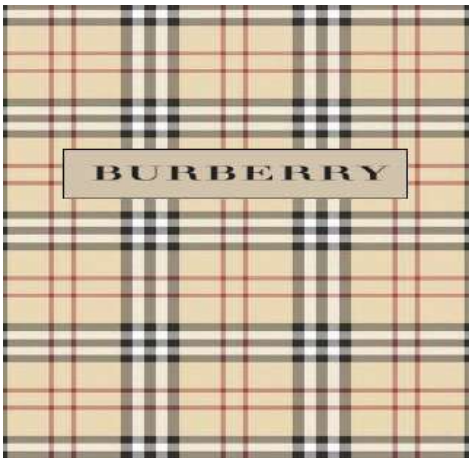

Picture 8. The Burberry Plaid

Picture 9. Trenchcoat
(Moda geçmişten günümüze giyim kuşam ve stil rehberi, Kaktüs Yayınları, 2013, İstanbul, s.238.).

The clothes of the period were reflected in the table "Sisters", which was portrayed by French painter and printmaker Edmund Dulac in 1917. A Land Army member, a nurse and an ammo worker are seen in different outfits (Picture 10.). If there is no specific uniform condition, it is often made from washable cotton fabrics that can be worn every day, with a hat or scarf to prevent hair damage (Blackman,2013: 76).

Picture 10. 1917, The painting of sisters, Edmund Dulac
(Modanın Tarihi 1900'den Bugüne, Kerasus Yayınları, 2013, İstanbul,76).

In 1917, after the United States declared war on Germany, women began to find a place in their business life instead of men who were summoned to enlist. The coats of the tram conductor and bus conductor, consisting of arched coats, boots and hats, have attracted attention as a combination of military and stylish styles. (Picture 11.). On the other hand, the women who started working in the factories along with the war are also fashionable in the 1909; They chose to wear long and more comfortable boots to the wrist (Terlikli, 2013: 78).

Picture 11. Bus ticketing
(Moda geçmişten günümüze giyim kuşam ve stil rehberi, Kaktüs Yayınları, 2013, İstanbul, s.239.)

As the battle continued with all its violence, Coco Chanel began her career as a hatter and immediately after opening a few boutiques on the Deauville coast in 1913. In 1915, she opened his first fashion house in Biarritz. In picture 12, the use of silk-jersey costumes consisting of "dress blouse" with a belt on top of the skirts has created an example of Chanel's casual wear approach.

Picture 12. 1917, Jersey Costumes , Chanel
(Modanın Tarihi 1900'den Bugüne, Kerasus Yayınları, 2013, İstanbul,120).

The clothes worn by women workers in the UK and the United States were marked by the year 1918. Arms factories and auxiliary jobs behind the front, women have been seen wearing men's clothes such as trousers, coveralls, caps and shirts. The main reason for this is that they express themselves more freely, or that they are more than a necessity and convenience than a feminist opinion. (Picture 13-14.).

Picture 13-14. 1918, Munitions workers, UK and USA
(Modanın Tarihi 1900'den Bugüne, Kerasus Yayınları, 2013, İstanbul,77).

When the World War I was over; Large, arched jackets and shorter, more fat skirts reflect the changing fashion lines. In 1918, where tights and trousers are seen quite widespread;

It is reflected in the summer styles and the silhouettes gradually become comfortable form. The skirts were worn as the precursor models of the 1920s pipe skirt style. (Picture 15.).

Picture 15. 1918, Summer Designs , Chiffons
(Modanın Tarihi 1900'den Bugüne, Kerasus Yayınları, 2013, İstanbul,77).

1918 the presence of Tango at the end of the war has been discovered, tango dance clothes have become fashionable (Dereboy, 2004: 106). After the war, women who began to be intertwined with fashion again led to the shortening of skirts, more ornaments and accessories in their shoes; The use of buckle is back in fashion, while velvet, lace, embroidery, bows, fur and badges are also used (Terlikli, 2013: 78). Everyday garments have also attracted attention to the elegant and practical garment designs. The impression of the shirt was created with the collar catches attached to the collar of the dresses. (Picture 16.).

Picture 16. 1918, Women's Daily Wear
(Moda geçmişten günümüze giyim kuşam ve stil rehberi, Kaktüs Yayınları, 2013, İstanbul, s.241.

2. Material and Method

In the year of World War I (1914-1918), this study, which covers the interpretation of women's apparel harness fashion with digital programs in line with the current trend trends, is an evaluation research. Evaluation surveys also include the "applied research" qualities that aim to demonstrate what kind of outcome the fundamental research findings are being introduced into. (Arseven, 1994: 28). Applied research is the practice of the knowledge produced or produced. (Karasar, 1991: 27).

The characteristics of garments covering the four-year period; By examining the design elements and principles in terms of fabric types and accessories, the findings obtained were combined with the fashion trends of the day and 66 pieces of sketches were drawn accordingly. The period characteristics of the most closely showing the 14 design by selecting the scope of research has been re-interpreted.

3. Findings and Comments

In this section; designated as inspiration in the years of World War I, women's clothing was designed and contributed to creativity as a source of inspiration in the scope of the period line design elements (point, line, shape, color, stain, texture, space), design principles (balance, unity, change, harmony, harmonies, movement and rhythm, rating, proportion) (Yılmaz, 2010: 7-39), reviewed and re-interpreted in terms of models, accessories and fabric properties.

Design 1. **Design 2.** **Design 3.** **Design 4.**

Design 1.

The fabric feature in World War I. was designed as a Burberry plaid in daily garment. The body-sitting mini dress is balanced with the red asymmetrical piece on the left chest and the red rectangular piece on the left leg. Accessories are also created based on the orange color in the plaid**.**

Design 2.

Designed as a daily garment, this team consists of a jacket and rider trousers that are fitted to the body through forceps and the hat is used as an accessory. Wicker was used in the fabric of the hat. As a feature of the fabric, Burberry plaid has provided unity-integrity using the same sizes as the trousers and jacket arms, and the use of triangular forms on the neck and shoulders in opposite directions has created movement and rhythm.

Design 3.

This garment is designed in the form of a daily garment; It consists of a mini vest, body and two-storey skirt. Burberry Plaid was used as a fabric type in vest. As an accessory, it is integrated with bags, hats and necks. The lines in the dashed line view used in the bottom skirt are the connector of the bag that is pinned to the skirt. The pink-brown harmony used in the neck has also adapted to the color of the lower skirt bag, which has formed unity-integrity.

Design 4.

As a type of fabric, the Burberry plaswear jacket and socks suit is designed in the form of a daily garment. The male neckline, bellows pockets and wide cuffs in the jacket are in green tones and the same green tone and tonal tone are used in hats and necks. One of the socks has created a change in the fact that the red one is black, and the tree tissues on the red socks are sorted from small to big, and the cord has formed.

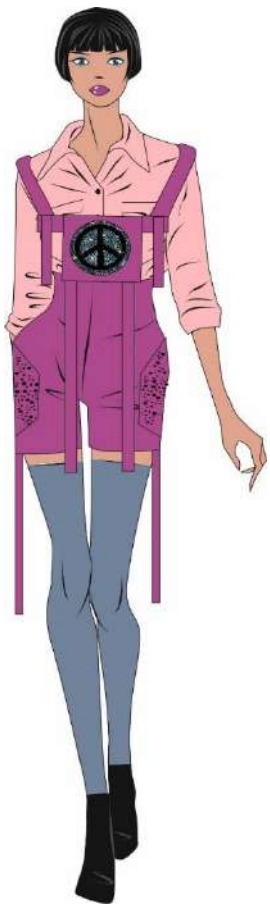

Design 5

Design 6.

Design 7.

Design 5.

Designed in the form of jump suit, this garment is attracted by the harmony of pink and shades and is integrated with grey socks. Men's collar shirts were used in the jumpsuit. The spacing between socks and jumpsuit has created an eye-relieving range in the design. The peace mark on the front of the jumpsuit has created a change in the design of the applicia. The strips on the front and sides of the jumpsuit are a balance element.

Design 6.

Designed in the form of daily garment, this jumpsuit has created a balance with triangular segments used in the triangle and rounder on the collar. The upper part of the under chest body in the form of jump suit is finished under the knee. The hat used as an accessory has ensured

harmony in the colorful form. The only hand has a glove and the other is empty. The socks are composed of dots and this harmony is integrated with the rounded form of the buttons.

Design 7.

Another jumpsuit, designed in the form of a daily garment, has formed the inner part of the outfit with lace texture and the outer part is finished with green bustier and skirt. The red ropes at the top of the boots, which tie the skirt to the middle, connecting the bustier with cross ties, completing the gloves and the hat, are the pieces of movement and rhythm above the green.

Design 8. **Design 9.** **Design 10.**

Design 8.

Designed in the form of daily garment, this döpiyes is composed of a dominant collar, short-sleeved jacket and a skirt that ends in the middle of the knee with deep slit from the right leg. The hat and the boat draw attention with the harmony of the wicker tissue, and the color

harmony was created by the use of green and purple undercoat in cold colors. The slit on the leg and the jacket were highlighted in the middle of the skirt as the spacing which caused the eye comfort. The fabric tissue was used as a pentagen from geometric forms.

Design 9.

Designed in the form of daily garment, the mini-dress with a throat body, the red color as a whole with the use of hats and socks as an example of unity, with the use of leopard tissue in socks to design movement and rhythm It is an example proportion that the triangular parts used in both sides have the same extent. Again, the hair texture used in the neck and the hat is part of the harmony.

Design 10.

This design consists of cloak and trousers designed in the form of daily garment, consisting of red, neutral colors, grey and black from warm colors. It was used as a fabric feature in the cloak. The ellipse form of the accessory used in the hair is in harmony with the elliptical forms in the shoulder pads. Strips hanging from the shoulders and trousers are the example of change.

Design 11.

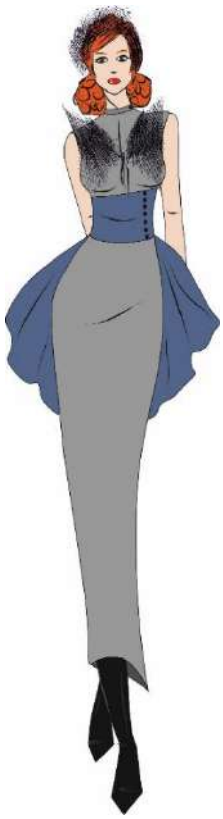

Design 12.

Design 13.

Design 14.

Design 11.

This outfit, designed in a gown form, is composed of a long skirt that leaves the shoulders open, the upper part of the elbow plunging from the elbows, and the left waist and the right leg exposed. With the use of red and lilac in a combination of hot and cold color balance, the leg slit with the middle of a leg with an example of spacing was created. It is a lilac stain on the blouse with a dark purple color on the back skirt consisting of drapelelts. The guipure in the middle of the chest and the edge of the arm also contributed to the design and thus created the change.

Design 12.

In this outfit designed in the gown form, the tulle form used on the chest and hair is in harmony because it is in the same tissue. In this design with zero sleeves, straight neckline, straight narrow dress form, the short tail draped in the waist belt and the belt is the same color. At the same time, this piece in the back is linked to the belt in the waist, forming unity-integrity.

Design 13.

This dress, designed as a gown, is a small-to-big cord of the ellipse forms of the hat used as an accessory. The upper part of the dress is composed of strapless neckline and shoulder wrap, and is decorated with small checks of fabric property. The two-piece fold on the front of the long dress, the one-piece fold on the back side is an example of balance.

Design 14.

The long narrow dress in the form of a fish skirt designed as a gown is an example of unity completions with the use of light pink, lilac and purple as color harmony. The shape of the forms used on the shoulders and neck is a pattern of harmony and is composed of dots as the fabric surface. The black glove of the design also created a balance element.

4. Results

The fact that women's clothes are more practical and aesthetical has been something that the fashionist has not been able to achieve since the 1800s. Despite the emergence of special outfits for some physical activities, many women in the early 20th century still wore a restrictive outfit for their movements. During the First World War, clothing factories and smaller workshops; It has been mobilized to produce standard uniforms for the army. During this process, they renewed their technology and became a more realistic industry. In the framework of this necessity, men's clothing parts were replaced and used frequently during the period. After the war, many women worked in jobs requiring bodily power by wearing trousers and choosing sturdy shoes. The effect of war on fashion has attracted more attention at this moment.

In particular, the way women perceive themselves, the woman's image in other people's eyes has changed during this period. Although the fashions of clothing are determined by the factors that make up their fashion every semester; The rapid change in such a realist period has been reflected in the daily garments. More functionality has been emphasized in the garments than aesthetic anxiety. The abundance of the clothes and the high waist line have attracted attention; It is also easy to move with the large cut arms.

As a result, the reduction of the civilian male population during the war forced the woman to work. This necessity, arising from necessity, has made the woman an active individual in life outside the home. As a result of these developments, women began to have a say in the community and the fashion started to change faster. In their new design, the designers gave direction to this process by continuously creating alternatives to the shaping of modern women's clothing with ideas freeing the woman's body. The garments used during World War I were inspired by these designs and the perspectives of contemporary, functional, additions-subtractions, interpretations, and the views of the design were enriched. Thus, the essence and re-interpretation of the ethnic identities, historical processes, cultural heritage has been provided today to find a place.

References

Ambrose, G., Harris, P.(2012) Görsel moda tasarımı sözlüğü.(Ç. Sirkeci, Çev.) Literatür Yayınları, İstanbul. s.184.

Arseven, Ali. D., (1994), Alan Araştırma Yöntemi: İlkeler, Teknikler, Örnekler, Tekışık Matbaası, Ankara.

Blackman, C. (2013). Modanın tarihi 1900'den günümüze. (K.Kaftanoğlu, Çev.) Kerasus Yayınları, İstanbul. s.219.

Crane, D. (2003). Moda ve Gündemleri Giyimde Sınıf, Cinsiyet ve Kimlik. (Ö. Çelik, Çev.). Ayrıntı Yayınları, İstanbul. s.11- 42.

Dereboy, E. J. (2004). Kostüm ve Moda Tarihi. Özel Güzel Sanatlar Stilistlik Ltd. Şti, Ankara.

Erol, F. (2011). Trend Öngörüsü ve Moda Dinamikleri.Mimar Sinan Güzel Sanatlar Üniversitesi, Yayımlanmış yüksek lisans tezi, İstanbul.

Fischel, A.,Baggaley,A.,Gersh, C.vd. (2013).Moda Geçmişten Günümüze Giyim Kuşam ve Stil Rehberi (D. Özen, Çev.) Kaknüs Yayınları, İstanbul.

Fogg, M.(2014). Modanın tüm öyküsü. (E. Gözgü, Çev.) Hayalperest Yayınları, s.474.

Karasar, N. (1991). Bilimsel Araştırma Yöntemi: Kavramlar, İlkeler, Teknikler. Sanem Matbaacılık, Ankara.

Komsuoğlu, Ş., İmer, A, Seçkinöz, M. vd., (1986). Resim II Moda Resmi ve Giyim Tarihi. Türk Tarih Kurumu Basımevi, Ankara. s:13.

Sproles,G.B. (1981). Analyzing Fashion Life Cycles: Principles and Perspectives, Journal of Marketing, , C. 45, S. 4, s. 118.

Terlikli, S. (2013). 1850 ve 1950 Tarihleri Arasında Batı Toplumlarında Sanat, Toplumsal Yapı ve Moda Etkileşimi. Selçuk Üniversitesi, Yayımlanmış yüksek lisans tezi, Konya.

Yılmaz, M. (2010). Görsel Sanatlar Eğitiminde Uygulamalar. Data Yayınları, Ankara.

Zengingönül, N. (1996). Giyimde Moda Akımları ve Öncü Tasarımcılar. Gazi Üniversitesi. Ankara.

http://www.giyimvemoda.com/moda-dunyasi/1900-1914-yillari-arasinda-giyim-ve-moda/161.(Date of access: 09.03.2018)

https://www.yelp.com/biz_photos/.burberry-new-york-6?select=fRpUr4zBls1My8OO25jiWg (Date of Access: 13.03.2018)

The Extraordinary Biosorption Potential of Vetiver Grass Grown in Giresun

Derya EFE[1]*, Bengü ERTAN[1]

[1]Giresun University, Espiye Vocational School, Giresun, Turkey:deryayanmis@yahoo.com

[1]Giresun University, Espiye Vocational School, Giresun, Turkey: bengu.ertan@giresun.edu.tr

* **Corresponding Author:** derya.yanmis@giresun.edu.tr

Abstract

Vetiveria zizanioides (L.) Nash belonged to the Family of Poaceae is commonly called as Vetiver grass. The plant is a perennial, dense, bunch-type grass with stiff stem and a significantly deep and strong root system. It has many biological activities antimicrobial, antifungal, antiviral, anticarconogenic, etc. activities. Besides, it is a worthwhile plant due to its hyperaccumulation potential. The long-term contamination of soil and water with synthetic dyes, caused by industrial dyes is a global problem. There are many physical and chemical technologies for the remediation of the dye contamination. However, these methods have several limitation. Therefore, there is a big interest about researches about biosorption methods that are using plants for the removal of the contaminants such as heavy metals, dyes, etc. In the current study, the biosorption potential of vetiver grass against to malachite green were evaluated. According to our results, the dried and cut stems and roots of the plant have extraordinary potantial to remediate the environment polluted with synthetic dyes. It was observed that 50 mg/l malachite green was reduced to 0.443 mg/l with the application of 0.2 gr vetiver grass. Besides, optimum conditions of 0.2 gr vetiver grass for biosorption of malachite green were determined as pH 4, 45 ^{0}C, 90 min., respectively. The used Vetiver grass has been grown in Tirebolu, Giresun for the first time by IL-CA Herbal Products and Research–Development Production.

Keywords: Remediation, extreme conditions, Vetiver grass, biosorption

1. Introduction

Malachite Green (MG), a cationic dye, is widely used in many industries including paper, leather, cotton, pulp, wool for coloring their product and in aquaculture for controlling fish parasites and diseases due to its fungicide, ectoparasiticide and disinfectant activities (Glad and El-Sayed, 2009). These industries bring out huge amount of coloured wastewater causing very serious environmental problems. MG damages aesthetic nature, transmission of sunlight into water sources such as streams, lakes and photosynthetic action of autotrophic aquatic bioata (Sudova et al., 2007). Besides, MG decreases food intake, growth and fertility rates; damages liver, spleen, kidney, heart, eye, lungs, *etc*. of organisms because of being a multi-organ toxin with teratogenic effect. MG is highly mutagenic and toxic and carcinogenic to mammalian cells (Ashtoukhy El, 2009; Sartape et al., 2017). Because of these reasons, the use of MG has banned in several countries. However, it is still extensively used in many countries because of its low cost, easy availability and efficacy (Papinutti et. al., 2006; Sartape et al., 2017). In recent years, there is a big necessity to remove MG from natural waters. There are many methods to remove synthetic dyes from contaminated waters. These methods can be divided into physical, chemical and biological methods. Physical and chemical methods such as photo degradation and photo catalytic degradation have been reported that they are very expensive and not efficient for remedation of water (Sayılkan et al., 2007). Among these methods, biological methods, especially bioadsorption techniques is very efficient to remove organic and inorganic contaminants from wastewater. The researchers have studied to evaluate the potential of many biological material such peat, de-oiled soya, rice straw, apple wood, *etc.* (Ozcan et al., 2004; Mittal et al., 2005; Jain et al., 2007; Tan et al., 2007; Gong et al., 2008).

Vetiveria zizanioides belonged to Poaceae family originates from India (Darajeh et al. 2014). This plant called as vetiver grass is a perennial, dense, bunch-type grass with stiff stem and a significantly deep and strong root system. It is a wortwhile plant because of its biological activities such as antimicrobial, antifungal, antiviral, anticarconogenic, *etc*. activities. In terms of morphological characteristics, it has a complex and lacework root system, whereby the root can penetrate much deeper in both soil and water Besides, vetiver grass is one of a few grass species with all the criteria required in removing pollutants from wastewater. Therefore it has been used to remove pollutants from water and soil in land conservation since 1980 (Danh et al. 2009; Ashraf et al. 2013; Darajeh et al. 2014; Singh et al. 2015). Its outstanding physiological and morphological characteristics have made it a suitable plant species for phytoremediation in treating various types of pollutants for water management. It has high tolerance towards

elevated concentrations of heavy metals such as As, Cd, Cu, Cr, Pb, Hg, Ni, Se and Zn (Truong et al. 2010; Vargas et al. 2016). It also has high resistance towards herbicide and pesticide (Chomchalow 2003, Truong 2001). In the light of the literatures, it was determined that there is no research to evaluate the biosorption potential of vetiver grass grown in Giresun against malachite green. In this study, it was determined the biosorption potential of vetiver grass and in terms of pH, temperature and incubation time, the optimum conditions were determined.

2. Material and Method

2.1. Preparation of plant material and dye solution

The leaves of *Vetiveria zizanioides* (L.) Nash were supplied from Il-Ca Herbal Products and Research–Development Production in Tirebolu, Giresun. The used parts of vetiver grass were kept in double distilled water to remove impurities such as dust and the colour of vetiver grass and dried in incubator at 60 °C for 12 h. The dried vetiver grass was crushed into 100 (0.15–0.08 mm) Mesh BSS particle. The prepared material was stored in room temperature to use further. The molecular formula of malachite green dye is $C_{23}H_{25}N_2Cl$ and molecular weight is 364,92). The stock solution was prepared in double distilled water as 1000 mg/L. The prepared stock solution was then wrapped with aluminum foil and stored in a dark to prevent exposure to direct light.Then, the used concentrations of malachite green such (125 mg/L, 100 mg/L, 75 mg/L, 50 mg/L, 25 mg/L, 15 mg/L, 10 mg/L, 5 mg/L) were prepared by diluting of the stock solution.

2.2. Determination of Biosorption potential of vetiver grass

The biosorption experiment was performed in 50 ml of 50 mg/l malachite green with 0.2 gr vetiver grass at room temperature with for 1 hour a rotation speed of 150 rpm. The control was established as the experiment group without vetiver grass. The analyses were performed by determination of dye concentration with UV-visible spectrophotometry at 618 nm.

2.3. Determination of optimum conditions (pH, temperature and time) for biosorption

Biosorption behaviors of vetiver grass for malachite green was investigated under reaction conditions as follows: temperature from 30 to 50 °C, pH from 2 to 8, incubation time from 10 min. to 120 min. Each of the performed experiment was established according to the optimum conditions determined from our previous experimental setup. The experiments of this

study have been carried out in three replicates. The analyses were performed by determination of dye concentration with UV-visible spectrophotometry at 618 nm.

3. Results and Discussion

Vetiver grass is a coarse perennial grass grown in the tropics, which has been proven ideal for soil conservation (World Bank 1990). The plant is widely used to protect moisture of the soil, to prevent erosion caused by slope stability in riverbanks and highways. The dense and finely structured root system of vetiver grass could create an environment ideal for microbiological processes in the rhizosphere. Moreover, it has a great potential for remediation of the contaminated environments such as soil, and surface waters. Because the extremely deep and dense roots of the plants plays a role as a biofilter by absorbing all the contaminants produced in both biotic and abiotic process (Kidney 1997). These contaminants can be metals or any of the textile dyes such as malachite green. There are many studies about phytoextraction potential of the roots of vetiver grass in Literature (Salt et al. 1995; Webb 2009; Ali et al. 2013). However, this is the first study aimed to determine bioabsorbtion potential of vetiver's leaf against malachite green.

According to the results of this study, the application of 0.2 gr vetiver grass. Besides, optimum conditions of 0.2 gr vetiver grass for biosorption of malachite green were determined as 45 ^{0}C, pH 4, 90 min., respectively. The results have given in Graph 3.1.1, 3.1.2, and 3.1.3. The obtained results have showed that the dried and cut stems and roots of the plant have extraordinary potantial to remediate the environment polluted with synthetic dyes. In the next step of the our study will be to determine optimum conditions of vetiver grass bisorption for malachite green with response surface methodology approach.

3.1. Graphs

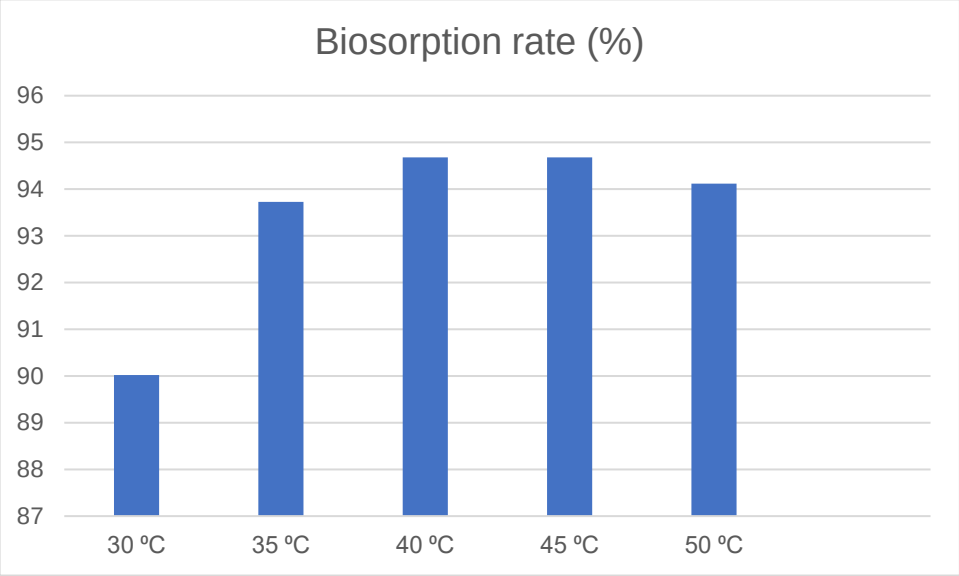

Graph 1. The effect of temperature on biosorption potential of vetiver grass of malachite green

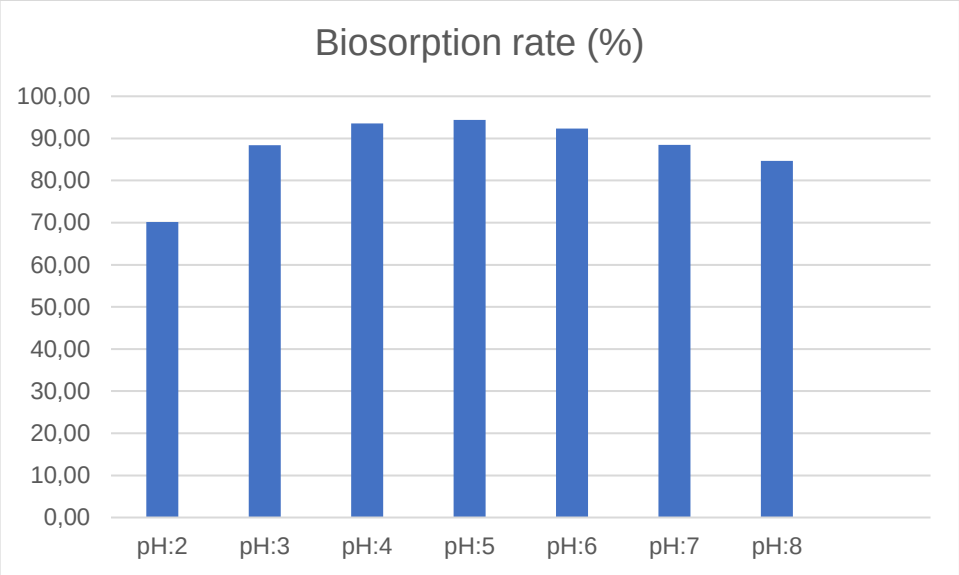

Graph 2. The effect of pH on biosorption potential of vetiver grass of malachite green

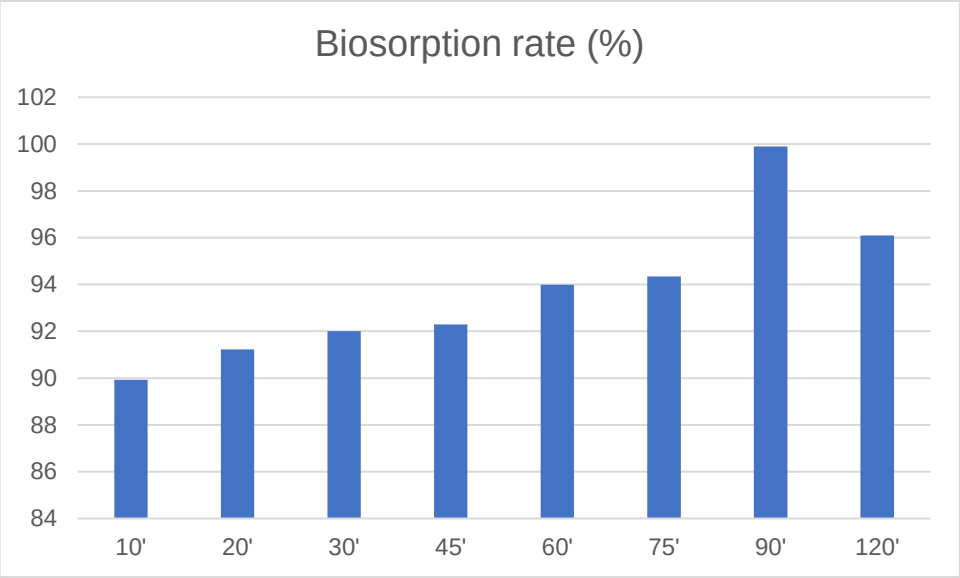

Graph 3. The effect of incubation time on biosorption potential of vetiver grass of malachite green

Acknowledgement

We are grateful to Berrin ÇAMUR and Emine ÇAMUR who helped us to supply *Vetiveria zizanioides* (L.) Nash from Il-Ca Herbal Products and R&D Production Company.

References

Ali, H., Khan, E., & Sajad, M. A. (2013). Phytoremediation of heavy metals-concepts and applications. Chemosphere, 91, 869–881.

Ashraf, M. A., Maah, M. J., Yusoff, I. (2013). Evaluation of natural phytoremediation process occurring at ex-tin mining catchment. Chiang Mai Journal of Science, 40(2), 198–213.

Chomchalow, N. (2003). The role of vetiver in controlling water quantity and treating water quality: an overview with special reference to Thailand. AU J T, 6(3), 145–116.

Danh, L. T., Truong, P., Mammucari, R., Tran, T., Foster, N. (2009). Vetiver grass, Vetiveria zizanioides: a choice plant for phytoremediation of heavy metals and organic wastes. International Journal of Phytoremediation, 11, 664–691.

Darajeh, N., Idris, A., Truong, P., Aziz, A. A., Bakar, R. A., Man, H. C. (2014). Phytoremediation potential of vetiver system technology for improving the quality of palm oil mill effluent. Advances in Materials Science and Engineering, 1–10.

El Ashtoukhy, S.Z. El. (2009). Loofa egyptiaca as a novel adsorbent for removal of direct blue dye from aqueous solution. Journal of Environmental Management, 90,2755.

Gad, H.M.H., El-Sayed, A.A. (2009). Activated carbon from agricultural by products for the removal of Rhodamine-B from aqueous solution. Journal of Hazardous Materials, 168, 1070–1081.

Gong, R., Zhong, K., Hu, Y., Chen, J., Zhu, G. (2008). Thermochemical esterifying citric acid onto lignocellulose for enhancing methylene blue sorption capacity of rice straw. Journal of Environmental Management, 88, 875–880.

Jain, R., Mathur, M., Sikarwar, S., Mittal, A. (2007). Removal of the hazardous dye rhodamine B through photocatalytic and adsorption treatments. Journal of Environmental Management, 85, 956–964.

Kidney S. (1997). Phytoremediation may take root in Brownfields. The Brownfields Report, 2(14), 1–6.

Mittal, A., Krishnan, L., Gupta, V.K. (2005). Removal and recovery of malachite green from wastewater using an agricultural waste material, de-oiled soya. Seperation and Purification Technology, 43, 125–133.

Ozcan, A.S., Tetik, S., Ozcan, A. (2004). Adsorption of acid dyes from aqueous solutions onto sepiolite. Seperation Science and Technology, 39, 301–320.

Papinutti, L., Mouso, N., Forchiassin, F. (2006). Removal and degradation of the fungicide dye malachite green from aqueous solution using the system wheat bran-fames sclerodermeus. Enzyme and Microbial Technology, 39,848-853.

Salt, D. E., Blaylock, M., Kumar, N. P. B. A., Dushenkov, V., Ensley, B. D. , Chet, I., Raskin, I. (1995). Phytoremediation: a novel strategy for the removal of toxic metals from the environment using plants. Biotechnology, 13,468–174.

Sartape,A. S., Aniruddha M., Mandhare , Vikas V. Jadhav , Prakash D. Raut , Mansing A. Anuse , Sanjay S. (2017). Removal of malachite green dye from aqueous solution with adsorption technique using Limonia acidissima (wood apple) shell as low cost adsorbent. Arabian Journal of Chemistry, 3229-3238.

Sayılkan, F., Asilturk, M., Tatar, P., Kiraz, N., Arpac,, E., Sayılkan, H. (2007). Photo catalytic performance of Sn-doped TiO_2 nanostructured mono and double layer thin films for

malachite green dye degradation under UV and vislights. Journal of Hazardous Material, 144, 140–146.

Singh, V., Thakur, L., Mondal, P. (2015). Removal of lead and chromium from synthetic wastewater using Vetiveria zizanioides. Clean-Soil, Air, Water, 43(4), 538–543.

Sudova, E., Machova, J., Svobodova, Z., Vesely, T. (2007). Negative effects of malachite green and possibilities of its replacement in the treatment of fish eggs and fish: a review. Journal of Veterinary Medicine, 12, 527–539.

Tan, I.A.W., Hameed, B.H., Ahmad, A.L. (2007). Equilibrium and kinetic studies on basic dye adsorption by oil palm fibre activated carbon. Chemical Engineering Journal, 127, 111–119.

Truong, P. and Hart, B. (2001) Vetiver system for waste-water treatment. Technical Bulletin No. 2001/21, Pacific Rim Vetiver Network, Office of the Royal Development Projects Board, Bangkok.

Truong, P. N. V., Foong, Y. K., Guthrie,M., Hung, Y. T. (2010). Phytoremediation of heavy metal contaminated soils and water using vetiver grass. Environmental Bioengineering, 11, 223–275.

Vargas, C., Pérez-Esteban, J., Escolástico, C., Masaguer, A., Moliner, A. (2016). Phytoremediation of Cu and Zn by vetiver grass in mine soils amended with humic acids. Environmental Science and Pollution Research, 23, 13521– 13530.

Webb 2009, Webb, R. (2009). Vetiver grass—a hedge against erosion. Permaculture Research Institute 4 pp. Retrieved from http://permaculturenews.org.

WorldBank. (1990). Vetiver Grass. TheWorld Bank. http://elibrary.worldbank.org/doi/book/10.1596/0-8213-1405-X.


ITESDES
International Technological Sciences
And Design Symposium